5th European Conference on Permafrost, Book of Abstract

Philip Deline, Xavier Bodin, Ludovic Ravanel

5th EUROPEAN CONFERENCE ON PERMAFROST

EUCOP5 2018

CHAMONIX MONT-BLANC

22 June - 1 July /// FRANCE

Book of Abstracts

5th European Conference on Permafrost
June 23 – July 1, 2018, Chamonix, France

Book of abstracts

5th European Conference on Permafrost

Edited by Philip Deline, Xavier Bodin and Ludovic Ravanel

Co-editors: Chloé Barboux, Reynald Delaloye, Christophe Lambiel, Florence Magnin, Paolo Pogliotti, Philippe Schoeneich

Laboratoire EDYTEM, CNRS, Université Savoie Mont-Blanc

June 2018

Recommended citation

Deline P., Bodin X. and Ravanel L. (Eds.) (2018): 5th European Conference On Permafrost – Book of Abstracts, 23 June - 1 July 2018, Chamonix, France. <hal-01816115>

Disclaimer and Copyright

Publisher

Laboratoire EDYTEM - UMR5204
Université Savoie Mont Blanc
Bâtiment « Pôle Montagne »
5 bd de la mer Caspienne
F-73376 Le Bourget du Lac cedex

Editors

Philip Deline
Xavier Bodin
Ludovic Ravanel

Preface

Five years after this trivial discussion we had about the possibility of organizing the next European Conference on Permafrost in the French Alps, we can see today how far this exciting adventure has come.

The initial step of this long route, setting up a Local Organizing Committee (LOC), has actually been the easiest one: our colleagues and friends were, obviously, very excited by the challenge. The first task of the LOC was to constitute a large panel of reputed scientists from all over the world to form the International Scientific Committee (ISC): no difficulty neither, they all accepted immediately!

Then came the time of soliciting contributions for sessions: the LOC received more than 30 proposals, of which the ISC retained 25 that cover the most significant and active fields of permafrost research and engineering. Sessions 16 and 20 were merged in a later stage, explaining why session 20 doesn't exist in the present program... Each session has to be coordinated by one of the three conveners, of which one has to be a PYRN member.

The call for abstract submission was open from August 28 to December 22 2017 and gathered 510 proposals, sent by more than 400 scientists and engineers from 30 different countries. The session conveners have had a few weeks to evaluate the abstracts and choose the format of presentation, roughly half for posters and half for orals. The session coordinators were in charge of accepting or refusing the abstract proposals, and finally of building the program of their oral slots. After the reviewing process and due to some withdrawals by colleagues prevented from participating, this Book of Abstracts of the EUCOP5 proposes 484 abstracts: 268 orals and 216 posters.

Now, a few days before the conference's opening and after months of incredibly dense exchanges between the LOC members, with the ISC members, with the session conveners, with the organizers of the side meetings and workshops, with the conference participants and with all the people that contributed for organizing, we are very delighted to deliver to the EUCOP5 attendees this Book of abstracts. To us, the high quality of the scientific program of the conference is the reflection of the vitality of the Permafrost community. Researchers from different disciplines, ages and cultures made a great job for feeding the conference with their best works and for ensuring a thorough peer-reviewing evaluation.

We hope you will appreciate the result of this collective adventure, hopefully a new significant step ahead towards a better understanding of the permafrost evolution in a changing world!

Philip Deline,
Xavier Bodin,
Ludovic Ravanel

Laboratoire EDYTEM, Université Savoie Mont-Blanc, CNRS, France

Acknowledgements

The high quality of the scientific program is to be thanked to the authors as well as to the coordinators and conveners of the 25 thematic sessions who publicized them and conducted the reviewing and selection procedures. We are very indebted to all of them, and also to our he colleagues and students that contributed to edit the abstracts.

We are very pleased to benefit from the participation of our invited speakers Dr Gustaf Hugelius, Bodin Center for Climate Research at Stockholm University (Sweden) and Dr Marcia Philips, WSL-Institut für Schnee- und Lawinenforschung SLF (Switzerland), for their keynotes lectures. We are very delighted that Wilfried Haeberli accepted to give a public conference for the inhabitants and tourists in Chamonix especially since this world renowned expert on permafrost will be the recipient of the conference with the IPA Lifetime Achievement Award for 2018 during the opening ceremony.

The International Scientific Committee has supported the Local Organizing Committee since an early stage in defining the science program and has provided timely comments on key questions on the organization. Special thanks are due for their support to Hanne H. Christiansen and Sarah M. Strand, President and Executive Director of the IPA, respectively. The International Permafrost Association Council members are also warmly thanked for their support towards the organization of this conference in France.

Finally, we acknowledge the excellent support, patience and cooperative spirit of all the Local Organizing Committee and the PhD and master students who gave their time to ensure the edition of this Book of abstracts: Chloé Barboux and Reynald Delaloye, from University of Fribourg, Switzerland; Christophe Lambiel, from University of Lausanne, Switzerland; Philippe Schoeneich and Marco Marcer, from Université Grenoble Alpes, France; Edoardo Cremonese, Paolo Pogliotti, and Umberto Morra di Cella, from ARPA Valle d'Aosta, Italy; Florence Magnin, from University of Oslo, Norway; and P.A. Duvillard, Grégoire Guillet, Guilhem Marsy and Jacques Mourey from Université Savoie Mont-Blanc, France.

Table of contents

1 - Remote sensing of permafrost landscapes

Session 1

Remote sensing of permafrost landscapes

Conveners:

- **Sabine Baumann**, Institute of Atmospherical and Physical Geography, Technical University of Munich, Germany
- **Artem Khomutov**, Earth Cryosphere Institute SB RAS, Russia
- **Ingmar Nitze**, Alfred-Wegener-Institute Helmholtz Centre for Polar and Marine Research, Potsdam, Germany (PYRN member)

A better understanding of landscape change processes over multiple spatial and temporal scales is important for predicting the impacts of climate change on permafrost terrains. For the observation of the land surface over large areas remote sensing has been proven to be a very powerful method. With ever increasing computation capacities, constantly growing archives of image data spanning several decades, and new or continued satellite constellations, completely new opportunities arise for earth observation applications. Nevertheless, until now only indicators of permafrost can be monitored from space and not the permafrost itself. Therefore, the aim of this session is to show the broad range of remote sensing applications regarding polar permafrost. Contributions on recent and upcoming advances in satellite remote sensing to different sensors and observation techniques are welcome. As the application of remote sensing on permafrost is quite a new field, we want to show the potential of this technique for permafrost monitoring. We encourage presentations on multi-platform data as well as studies using ground validation data and on remote sensing methods for observing landscape change processes in permafrost regions. This session will aim to bring together the latest development in the field of earth observation to improve the understanding of the response of highly vulnerable permafrost landscapes to rapidly changing climate conditions.

Contribution of the permafrost phenomena and processes to coastal erosion at Baydaratskaya Bay, Kara Sea

Daria Aleksyutina[1]
Nataliya Belova[1]
Anna Novikova[1]
Stanislav Ogorodov[1]
Ruslan Amanzhurov[2]
[1]*Lomonosov Moscow State University, Faculty of Geography, Russia, email aleksyutina@gmail.com*
[2]*Contemporary Geotechnologies, Moscow, Russia*

Abstract

The development of the permafrost phenomena and processes and their contribution to coastal erosion at the 10-km key plot of Ural coast of Baydaratskaya Bay are described in this article.

Keywords: Arctic, coastal erosion, thermodenudation, thermokarst

Introduction

Arctic coast is a dynamical system which is very sensitive to external changes. Coastal erosion depends on many factors. Fieldworks were conducted on 10-kilometer-long coastline located in the middle between Levdiyev and Torasavey islands in the southern Kara Sea. The area of investigation is situated at the continuous permafrost region. There are several geomorphological levels on the study area: terraces (coastal plain), laida (flood plain) and beach.

Estimation of coastal retreat rates was based on field studies including DGPS mapping of the coastal bluff edge position and analysis of high resolution space images. All variations of geological sequence and geomorphological features on the coastal plain and laida were described. Bluff's edge position was interpreted on the space images dated by August 2005, July 2012, July 2013, May 2016. DGPS surveys of cliff were performed during fieldworks in June 2013, June 2014, September 2017 and student practice (Geocryology department, Faculty of Geology, MSU) in September 2015.

Based on obtained data it was established that bluff retreat rate varies on different coast segments correlates with the features of geocryological structures of the coast. The bluffs are characterized by two main patterns of erosion retreat, depending on composition and cryogenic structure of coastal soils.

Analysis of coastal changes revealed inverse proportion between erosion rates and coast elevations. This correlation had some peculiarities for different parts of studied area, depending on geological sequence. Obtained data on erosion rates demonstrated the slowing of coastal erosion in 2012-2017 comparing to 2005-2012: annual erosion rates 1-2,5 m year $^{-1}$ and 3-4,5 m year $^{-1}$, respectively

Permafrost phenomena and processes affect the coastal zone on different scales and cause different erosion rates. Current permafrost processes observed along the studied coastal plot caused different types of erosion: I) saltatory retreat within the narrow zone strongly affected by thermokarst; II) continual retreat related to ice wedge degradation within gullying zone; III) retreat due to thermodenudation within wide zone along the bluff.

The understanding of contribution of the different permafrost processes and phenomena on coastal erosion rate will help us to simulate and predict behavior of very complex and sensitive Arctic coastal environment.

Acknowledgments

The present study was prepared with the financial support of the Russian Science Foundation project No.16-17-00034. We thank Dr. Vladislav Isaev for facilitation in field works and Digital Globe© Foundation for imagery from 2016.

Estimation of forest properties in a treeline zone using TanDEM-X and airborne laser scanning data

Sofia Antonova[1, 2]
Bernhard Höfle[1]
Christian Thiel[3]
Sabrina Marx[1]
Katharina Anders[1]
Veit Helm[4]
Julia Boike[2]

[1] *Institute of Geography, Heidelberg University, Heidelberg, Germany, sofia.antonova@awi.de*
[2] *Alfred Wegener Institute Helmholtz Center for Polar and Marine Research, Potsdam, Germany*
[3] *Institute of Geography, Friedrich-Schiller-University Jena, Jena, Germany*
[2] *Alfred Wegener Institute Helmholtz Center for Polar and Marine Research, Bremerhaven, Germany*

Abstract

The high-latitude forest-tundra transitional zone is a region which is highly vulnerable to the current Arctic warming. The local changes accompanying expected northward migration of the treeline requires systematic monitoring. We focus on an area in the east of the Mackenzie Delta in Northwest Territories, Canada, which is characterised by patches of black spruce forest. We investigate the capability of TerraSAR-X / TanDEM-X bistatic constellation for the characterisation of these forest patches. Interferometric phase and coherence from seven image pairs were used to estimate tree height and density. We compare the SAR products with standard vegetation metrics from airborne LiDAR, such as vegetation height percentiles and vegetation ratio. The preliminary analysis shows a high agreement between SAR and LiDAR data.

Keywords: Treeline; SAR; TanDEM-X bistatic mode; interferometry; coherence; airborne LiDAR.

Introduction

Northward shift of treeline is expected circum-Arctic and has been observed in numerous locations in response to Arctic warming. However, the exact processes are complex and involve various factors besides changes in the temperature regime. Structural vegetation changes within the treeline zone vary locally and influence the carbon and heat fluxes, the snow accumulation and the state of permafrost. On the large scale these changes are expected to influence albedo and, thus, the global climate. Therefore, it is important to monitor the vegetation structural properties within the treeline zone. Synthetic Aperture Radar (SAR) interferometry can be used for the forest parameters estimation. In two SAR images volumetric phase decorrelation (coherence loss) occurs in a vegetation layer due to volume scattering, i.e. input of several scatterers from different heights. Generally, more vegetation leads to stronger decorrelation, making possible the estimation of vegetation through interferometric coherence. Such approach has been used in the tropical and boreal forests (e.g. Treuhaft et al., 2015; Thiel & Schmullius, 2016). High-latitude forest-tundra transition zone, however, did not yet receive an adequate consideration by SAR remote sensing.

We use a combination of unique datasets including seven TanDEM-X bistatic pairs with large and constant baseline and airborne laser scanning (ALS) point cloud. With these data we estimate the forest properties in a treeline zone in the Canadian subarctic.

Study area

The study area is Trail Valley Creek (68°44'17" N; 133°26'26" W), located about 50 km northeast of Inuvik, Northwest Territories, Canada. Continuous permafrost underlies the area. Trail Valley Creek is located in the northern edge of the forest-tundra transition zone. According to Marsh & Pomeroy (1996), the land cover is represented by tundra (lichens, mosses, herbs and low shrubs), shrub tundra (deciduous shrubs from 0.5 to 3 m in height) and sparse forest with coniferous trees.

Data and Methods

SAR dataset

TanDEM-X (TDX) and TerraSAR-X (TSX) are twin X-band (9.6 GHz) SAR satellites flying in a close formation with the primary purpose of acquiring high quality global digital elevation model (DEM). The bistatic operational mode is based on the transmission of the signal by one of the satellites and receiving the echo by both satellites. For this study, seven co-registered single look slant range complex (CoSSC) pairs in the StripMap mode from the period 01.06 – 28.08.2015 were used. The data were processed using the Gamma radar software (Werner et al., 2000). SSC data were converted to Gamma Single Look Complex (SLC) format. Coherence images were obtained by computing the magnitude of the complex cross-correlation coefficient of a CoSSC image pair using the estimation window of 3 x 3 pixels. Coherence images were then multi-looked by factor 5 in both range and azimuth directions and co-registered to each other. Coherence images were then geocoded using Intermediate DEM (IDEM) which was provided by the German Aerospace Center (DLR) as a preliminary product of the global DEM and had a pixel size of approximately 8 m. Geocoding was done using the WGS84 ellipsoid in the Universal Transverse Mercator (UTM) projection Zone 8N. Seven geocoded coherence images were stacked and the mean coherence image was calculated and then filtered with median filter of size 3 x 3 to reduce noise. We work further only with the mean coherence image.

ALS dataset

Full-waveform airborne LiDAR data were captured in September 2016, covering an area of about 20 km x 6 km. The point density was approximately 5 points per square meter. The point cloud was transformed to a Digital Terrain Model (DTM) with 1 m cell size. Normalized vegetation heights above ground were derived by subtracting the DTM from the elevation of all ALS returns. Using this map together with high-resolution orthophotographs (Northwest Territories Centre for Geomatics) we delineated 19 forest patches of different size. Different vegetation metrics were then extracted for these patches: the 95th (p95) and 99th (p99) height percentile as well as vegetation ratio, defined as the number of ALS returns from the vegetation above the threshold of 1.5 m divided by the number of all ALS returns. The vegetation metrics were given a pixel size of SAR dataset (ca. 8 m) and also filtered with median filter of size 3 x 3.

Results

The relation between coherence and ALS metrics, averaged for each forest patch, yielded in a strong inverse correlation, varying from -0.81 to -0.88 for different ALS metrics.

On sub-patch scale, spatial patterns of coherence and ALS metrics were also highly similar. Example of coherence and p99 tree height for the one of the forest patches is shown in Fig.1. The pixel-by-pixel comparison yielded in a correlation of -0.63.

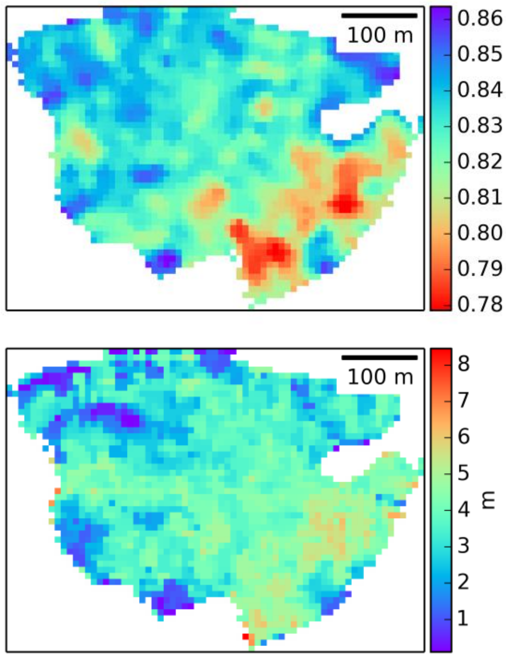

Figure 1. Upper panel: CoSSC coherence for a forest patch; lower panel: ALS p99 tree height. Similar spatial pattern is visible: the higher are trees the lower is coherence. Note the reversed color scale for the upper panel.

References

Marsh, P. & Pomeroy, J.W., 1996. Meltwater fluxes at an arctic forest-tundra site. *Hydrological Processes, 10*: 1383-1400.

Thiel, C., & Schmullius, C., 2016. The potential of ALOS PALSAR backscatter and InSAR coherence for forest growing stock volume estimation in Central Siberia. *Remote Sensing of Environment, 173*: 258-273.

Treuhaft, R., Gonçalves, F., Dos Santos, J. R., Keller, M., Palace, M., Madsen, S. N., Sullivan, F. & Graça, P. M. L. A., 2015. Tropical-Forest Biomass Estimation at X-Band From the Spaceborne TanDEM-X Interferometer. *IEEE Geoscience and Remote Sensing Letters 12* (2): 239–243.

Werner, C., Wegmüller, U., Strozzi, T., & Wiesmann, A., 2000. Gamma SAR and interferometric processing software. *Proceedings of the ERS-Envisat Symposium*, Gothenburg, Sweden, October: 1620.

Permafrost distribution in Indian Himalayas using empirical-statistical modelling and remote sensing observations – a case study of Uttarakhand region

Prashant Baral[1]
M. Anul Haq[2]
[1]NIIT University, Rajasthan, India, prashant.baral@st.niituniversity.in
[2]NIIT University, Rajasthan, India, anul.haq@niituniversity.in

Abstract

The impacts of climate change on extent of permafrost degradation in the Himalayas and its effect upon the carbon cycle and ecosystem changes are not well understood due to lack of historical ground-based observations. We have studied the permafrost distribution in Indian Himalayas using empirical-statistical modelling and remote sensing observations. Further, we look forward to modelling ground temperatures using remote sensing data and reanalysis products as input data on a regional scale and support our analysis with measured in situ data of ground temperatures. Overall, we approach to model the current state and predictable future changes in the state of permafrost in Western Himalayas and couple our results with similar research outcomes in atmospheric sciences, glaciology, hydrology and ecosystem changes in the region.

Keywords: Permafrost; Himalaya; GIS; remote sensing; rock glaciers; permafrost distribution modelling

Introduction

The area of permafrost exceeds that of glaciers in almost all Hindu Kush Himalayan (HKH) countries. However, we know very little about permafrost in the region as only a few local measurements have been conducted which is not sufficient to produce the fundamental level of knowledge of the spatial existence of permafrost (Gruber et al., 2017). We have applied empirical-statistical model and remote sensing observations for the estimation of spatial and altitudinal limits of permafrost distribution in Indian Himalayas.

Method

We have used visual interpretation of common morphological characteristics using high-resolution images for mapping, identification and classification of permafrost landforms. We have prepared a detail inventory of intact and relict rock glaciers in Uttarakhand state of India. We have analyzed the contribution of topo climatic factors in the occurrence and distribution of rock glacier. Logistic Regression modelling has been applied to establish the relationship between presence of permafrost and topo-climatic factors like Mean Annual Air Temperature (MAAT), Potential Incoming Solar Radiation (PISR), altitude, aspect and slope. The logistic coefficients for each independent variable obtained from the Logistic Regression model and rock glaciers mapped from remotely sensed data have been used to estimate the distributed probability of permafrost occurrence within a GIS environment. The ability of the model to predict permafrost occurrence was tested using the location of mapped active rock glaciers and the area under the Receiver Operating Characteristic (ROC) curve.

Table 1. Total number of all mapped and classified permafrost landforms.

Mapped Landforms			
Embryonic Rock Glaciers	981		
Rock Glaciers	Intact	Relict	Activity could not be determined
Talus — lobate	39	2	2
Talus — tongue shaped	84	18	5
Debris — lobate	107	9	3
Debris — tongue shaped	431	71	13
Total rock glaciers	661	100	23

Acknowledgments

NU Scholar Search Programme supports this study.

References

Gruber, S., Fleiner, R., Guegan, E., Panday, P., Schmid, M. O., Stumm, D., ... & Zhao, L. (2017). Inferring permafrost and permafrost thaw in the mountains of the Hindu Kush Himalaya region. *The Cryosphere*, 11(1), 81-99.

Estimating shrub height as indicator for snow depth and permafrost modelling

Annett Bartsch[1]
Barbara Widhalm[1]
Marina Leibman[2],
Ksenia Ermokhina[2,4],
Yury Dvornikov[2],
Artem Khomutov[2]
Timo Kumpula[3]
[1]*Zentralanstalt für Meteorologie und Geodynamik ZAMG, Vienna, Austria, annett.bartsch@zamg.ac.at*
[2]*Earth Cryosphere Institute, Tyumen Scientific Center SB RAS, Tyumen, Russian Federation*
[3]*University of Eastern Finland, Joensuu, Finland*
[4]*A.N. Severtsov Institute of Ecology and Evolution RAS, Moscow, Russian Federation*

Abstract

Shrub height is of relevance for snow redistribution and impacts ground temperatures. Certain land cover classes derived from satellite observations can to some extent be associated with vegetation heights but available maps are often too coarse and lack thematic content. We have tested an approach, which directly provides height information. It is based on Sentinel-2 data and has been calibrated and validated over Yamal. Results indicate the potential for large scale application.

Keywords: tundra vegetation, remote sensing, Sentinel-2

Introduction

Land cover has strong implications for the small-scale distribution of snow cover. Specifically, shrub height is required in order to identify areas with trapping of snow and subsequent impact on ground thermal conditions. Current global and circumpolar maps lack thematic detail and/or spatial resolution to appropriately represent shrubs, their types and height (Bartsch et al. 2016). In this study, we specifically investigate the capability of Sentinel-2 to estimate shrub height across large areas. It is part of the ESA DUE GlobPermafrost initiative (www.globpermafrost.info).

Data and methods

The recently launched Sentinel-2 satellite acquires optical data suitable for land cover monitoring with 10 m spatial resolution. We have selected a transect spanning from the northern tip of the Yamal peninsula (continuous permafrost) to the south into the tundra-taiga transition zone (with discontinuous permafrost) in order to test these data for shrub height retrieval. The region represents not only a gradient in vegetation zones but also sites with high heterogeneity of shrubs. Especially central Yamal is characterized by willow shrubs of up to 1.5 m height and continuous permafrost, while Southern Yamal is characterized by smaller dwarf-birch (Ukraintseva, 1997). Several studies over a CALM site and additional transects have exemplified the role of the shrubs for active layer thickness in relation to snow using in situ measurements (Leibman et al. 2015, Dvornikov et al. 2015) as well as Synthetic Aperture Radar data (Widhalm et al. 2017) from satellites in this region.

Shrub height measurements have been collected between 2014 and 2017. All available cloud-free images of summer 2016 and 2017 have been combined and seven indices derived.

Results

Figure 1 shows the mosaic over the chosen transect. The two summers have not been sufficient to obtain a complete coverage due to frequent cloudiness.

An R^2 of up to 0.72 could be obtained for the comparison to shrub heights from in situ measurements. The approach can be potentially applied over the entire Arctic to derive maps of shrub height.

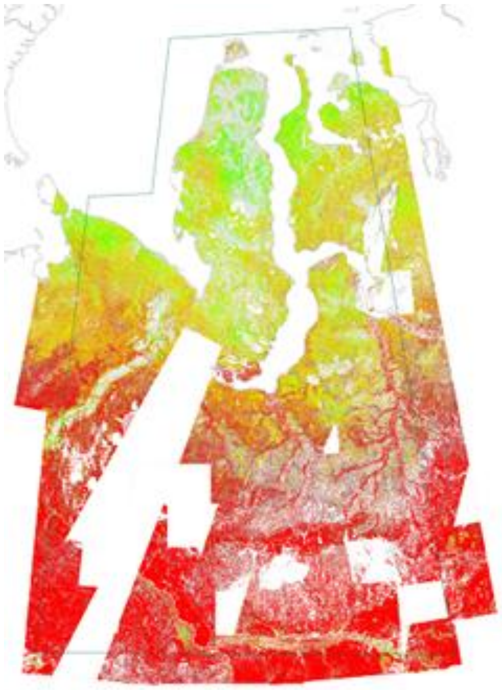

Figure 1. Shrub height derived from Sentinel-2 (2016 and 2017 acquisitions) over a transect covering the Yamal peninsula and the West Siberian Lowlands. Grey – masked, white – no data, other colors represent 0 (green) to 160cm (red – 160 cm or higher).

Acknowledgments

This work was supported by the Austrian Science Fund (FWF) under Grant [I 1401] and Russian Foundation for Basic Research Grant 13-05-91001-ANF-a (Joint Russian–Austrian project COLD-Yamal), as well as the European Space Agency project DUE GlobPemafrost, (contract number 4000116196/15/I-NB).

References

Bartsch, A.; Höfler, A.; Kroisleitner, C.; Trofaier, A. M. (2016): Land Cover Mapping in Northern High Latitude Permafrost Regions with Satellite Data: Achievements and Remaining Challenges. *Remote Sens.*, 8(12), 979.

Dvornikov, Y.A.; Khomutov, A.V.; Mullanurov, D.R.; Ermokhina, K.A.; Gubarkov, A.A.; Leibman, M.O. (2015): GIS and field data-based modelling of snow water equivalent in shrub tundra. *Fennia* 2015, 193(1), 53–65.

Leibman, M.O.; Khomutov, A.V.; Gubarkov, A.A.; Mullanurov, D.R.; Dvornikov, Y.A. (2015): The research station "Vaskiny Dachi", Central Yamal, West Siberia, Russia – A review of 25 years of permafrost studies. *Fennia*, 193(1), 3–30.

Ukraintseva, N.G. (1997): Willow tundra in Yamal as the indicator of salinity of superficial sediments. In The results of fundamental research of the Earth cryosphere in Arctic and Subarctic, 173–182. Nauka, Novosibirsk (in Russian).

Widhalm, B., Bartsch, A., Leibman, M., and Khomutov, A. (2017): Active-layer thickness estimation from X-band SAR backscatter intensity, *The Cryosphere*, 11, 483-496

Change of snow cover and its implications on arctic permafrost by using gravimetric satellite data

Sabine (Christine) Baumann[1]

[1] *Institute of Atmospherical and Physical Geography, Technical University of Munich, Germany, email: sabine.baumann@bv.tum.de*

Abstract

Data from the gravimetric satellites GRACE were used as basis for the calculation of snow water equivalent (SWE) in the polar permafrost areas. Therefore, the two models WGHM and GLDAS were applied to extract SWE from the GRACE data. Due to the good correlation between GRACE and the two models in five large arctic river catchments, the GRACE SWE data were used as input for the calculation of snow cover thickness (SCT). SCT was calculated using snow cover data from the Global SnowPack and measured snow density. The results were correlated with the change of active layer thickness from in-situ measurements.

Keywords: Snow cover; GRACE; polar permafrost; active layer thickness; SWE.

Introduction

The gravimetric satellites GRACE measure Earth's gravity and assess changes of Earth's mass. Main contributions of these changes originate from hydrological compartments as e.g. surface water, groundwater, soil moisture, or snow water equivalent (SWE). The benefit of GRACE data is to receive a direct measured signal. The data are not calibrated (as e.g. in models) or unusable due to particular Earth's surface conditions (e.g. AMSR-e). The aim of the study was to find out if it is possible to extract a SWE signal from the GRACE data. The assumption behind assumes that changes in TWS can be linked to changes in SWE if either SWE is the dominant compartment of TWS or if SWE changes proportionally with TWS.

Data and Methods

GRACE data show changes in total water storage (TWS) but cannot distinguish between different sources. Therefore, other data are necessary to extract the different compartments. Due to the spatial resolution of 200,000 km² and an accuracy of 2.5 cm w.e., mostly other global products are compared with GRACE. In this study, the hydrological model WGHM and the land surface model GLDAS were compared with the GRACE data. All data were pre-processed in the same way as the GRACE data to be comparable. They were converted into monthly 1° grid values. Time frame is from 01/2003 until 12/2013 with a total of 131 months. As a second time frame, only the winter period (November – April) was analyzed. Spatial extent was set to the large polar permafrost areas in North America and Siberia with a special focus on two river catchments in North America (Mackenzie, Yukon) and three in Siberia (Lena, Ob, Yenisei). A correlation analysis was performed between the different products both (1) pixel and (2) catchment based. The (1) pixel based correlation used absolute values and the (2) catchment based correlation the sum of monthly anomalies from the total mean for each catchment.

SWE from GRACE was extracted using the modeled data from WGHM and GLDAS by a simple subtraction. Snow cover thickness (SCT) was calculated using GRACE SWE, snow cover data from Global SnowPack (Dietz *et al.*, 2015) and measured snow density from the Calm project. These point SCT data were compared with in-situ data from active layer measurements from the Calm project. Results were compared with measured SCT data and calculated SCT data using WGHM SWE and GLDAS SWE.

Results

Results of the (1) pixel based correlation show that the correlation of GRACE vs. WGHM is higher compared to the correlation between GRACE vs. GLDAS. Additionally, it was mostly significant (5%-level) in all river catchments for the WGHM (TWS and SWE) vs. GRACE data. The values for the (2) correlation of the catchment data of GRACE vs. WGHM were, as for the pixel based correlation, higher compared to GRACE vs. GLDAS in all river catchments.

Monthly anomalies from the mean of WGHM and GLDAS in the five river catchments showed a uniform periodically annual pattern. GRACE data showed the same pattern between 2006 and 2011 but with more peak values in the beginning and the end of the study period. Therefore, a second correlation was performed for this uniform shorter period to see if the GRACE data were higher correlated with the WGHM and GLDAS data compared to the total period. The (1) pixel based correlation of GRACE vs. the two models resulted in higher values in the river catchments in North America and lower values in Russia for the short period. The (2) catchment based correlation of the shorter period improved for nearly all correlation pairs and river catchments. The winter period showed higher correlation values than the total period. GRACE correlates well with the two models, especially with WGHM TWS but also WGHM SWE.

As a result of the good correlation, GRACE SWE was extracted from WGHM and GLDAS and used as an input parameter for the SCT calculation.

Acknowledgments

I want to thank Andreas Güntner for the WGHM data and the DFG for financial support by the grant BA 4974/1-1.

References

Dietz, A. J., Kuenzer, C., & Dech, S., 2015. Global SnowPack: a new set of snow cover parameters for studying status and dynamics of the planetary snow cover extent. *Remote Sensing Letters*, 6(11): 844-853.

Potential permafrost distribution in Central Yakutia based on microwave remote sensing data

Helena Bergstedt[1]
Annett Bartsch[2,3]
Christine Kroisleitner[3,4]
[1]*Interfaculty Department of Geoinformatics, University Salzburg, helena.bergstedt@sbg.ac.at*
[2]*b.geos, 2100 Korneuburg, Austria*
[3]*Austrian Polar Research Institute, 1010 Vienna, Austria*
[4] *Zentralanstalt für Meteorologie und Geodynamik, Vienna, Austria*

Abstract

Permafrost extent is an important input variable for climate modelling. Current methods to derive permafrost extent from satellite measurements utilize coarse resolution scatterometer data. In this study we examine the possibility of improving permafrost mapping through additional information obtained from higher resolution SAR measurements. We focus on the region of Central Yakutia as it has shown to be a problematic region for mapping of potential permafrost distributions in the past.

Keywords: Scatterometer; SAR; permafrost extent; surface state

Introduction

Knowledge about permafrost extent is a critical part of climate modelling and prediction (Cheng & Wu, 2007). Different strategies to obtain a dataset suitable for the determination of the extent of permafrost based on degree days have been proposed (e.g. André et al., 2015; Gruber, 2012, Westermann et al., 2015). Interpolation, especially use of reanalysis data is essential in all cases. Purely satellite observation based methods can only account for frozen or unfrozen days (Park et al. 2016) but can be translated into potential mean annual ground temperatures (Kroisleitner et al. 2017). The accuracy differs between the microwave sensors due to resolution (25km vs 50km) and frequency (ASCAT 5.7cm, SSM/I 0.8cm). Kroisleitner et al. (2017) found Central Yakutia to be a region of high disagreement for permafrost extent between results excluding and including days of snow melt. This area also showed comparatively low performances of the empirical mean annual ground temperature (MAGT) model (Kroisleitner et al., 2017). In this study we focus on the area of Central Yakutia and compare the results of Kroisleitner et al. (2017) with freeze/thaw data based on a higher spatial resolution experimental dataset from Synthetic Aperture Radar (SAR) data (Sabel et al., 2012) to quantify the effect a higher spatial resolution has on the end results.

Data and Methods

Ground temperature data

The in situ data used in this study was obtained from the Global Terrestrial Network for Permafrost Database (GTN- P).

Surface State data

We used two radar data sets with differing spatial and temporal resolutions. The first data set was obtained from the Advanced Scatterometer (ASCAT) instrument on the MetOp satellites and is provided in a 12.5km grid (Paulik et al., 2014). The second data set was obtained from the Advanced Synthetic Aperture Radar (ASAR) instrument on the Envisat satellite and is gridded to 0.5km (Sabel et al., 2012). Both instruments operate at C-band.

Methodology

The thresholds and empirical relationships between frozen days and temperature proposed by Kroisleitner et al. (2017) are applied to the ASAR freeze/thaw data set. The results are compared and analyzed for differences concerning landscape and soil texture.

Results

The higher spatial resolution leads partially to higher performances compared to results of Kroisleitner et al.

(2017) but varies with respect to land cover which impacts thaw detection performance with SAR records.

Acknowledgments

This work was supported by the Austrian Science Fund (FWF) through the Doctoral College GIScience (DKW1237-N23).

References

André, C., Ottlé, C., Royer, A., and Maignan, F., 2015. Land surface temperature retrieval over circumpolar Arctic using SSM/I–SSMIS and MODIS data, *Remote Sensing of Environment* 162: 1-10.

Cheng, G. & Wu, T., 2007: Responses of permafrost to climate change and their environmental significance, Qinghai-Tibet Plateau, *Journal of Geophysical Research: Earth Surface*, 112.

Gruber, S., 2012. Derivation and analysis of a high-resolution estimate of global permafrost zonation, *The Cryosphere* 6: 221–233.

Kroisleitner, C. and Bartsch, A. and Bergstedt, H., 2017. Potential permafrost distribution and ground temperatures based on surface state obtained from microwave satellite data, *The Cryosphere Discussions*: 1-28.

Paulik, C., Melzer, T., Hahn, S., Bartsch, A., Heim, B., Elger, K., Wagner, W., 2014. Circumpolar surface soil moisture and freeze/thaw surface status remote sensing products (version 4) with links to geotiff images and NetCDF files (2007-01 to 2013-12). *PANGAEA*.

Sabel, D., Park, S.-E., Bartsch, A., Schlaffer, S., Klein, J.-P., Wagner, W., 2012. Regional surface soil moisture and freeze/thaw timing remote sensing products with links to geotiff images. *PANGAEA*.

Westermann, S., Østby, T., Gisnås, K., Schuler, T., and Etzelmüller, B., 2015. A ground temperature map of the North Atlantic permafrost region based on remote sensing and reanalysis data, *Cryosphere*, 9, 1303–1319.

Evolution of rock glaciers in northern Tien Shan, Central Asia, 1971 – 2016

Tobias Bolch[1]
Alexandra Strel[2]
[1] *Department of Geography, University of Zurich, 8057 Zürich, Switzerland*
[2] *Institute for Cartography, Technische Universität München, Munich, Germany*

Abstract

Rock glaciers are abundant in Tien Shan. However, only few studies investigate their reaction to climate more in detail. We used 1971 Corona, 2012 GeoEye and 2016 Pléiades data to map and investigate the velocity and surface elevation changes of the rock glaciers in central-northern Tien Shan in Kazakhstan. We identified ~50 active rock glaciers covering an area of ~18km², which is more than 40% of the glacier cover. The average surface velocity was 0.44±0.30 ma^{-1} with rates of up to 2ma^{-1}. On average the rock glaciers showed only a slight surface lowering of 0.04 ma^{-1} for 1971-2012 and of 0.06 ma^{-1} for 2012-2016. Most of the rock glaciers showed similar patters: A surface elevation gain at their fronts indicating an advance, a significant lowering in the upper probably glacier affected parts and areas of elevation gain and lowering in between caused by flow patterns and loss of subsurface ice.

Keywords: Rock glacier, digital elevation model, elevation change, velocity, Central Asia, Tien Shan

Introduction

Glaciers play a vital role in providing fresh water resources for the arid surroundings of the Tien Shan especially during summer months when the water demand is highest (Sorg et al., 2012). Several major cities such as Almaty (Kazakhstan), Bishkek (Kygyzstan) or Tashkent (Uzbekistan) and many villages are even located directly at the foothills of the Tien Shan where the share of the glacier melt to total run of is most important. However, glacier in this mountain range lost significantly area and mass during the last decades with one of the highest rates in the outer ranges of Tien Shan (Sorg et al., 2012).

Rock glaciers are abundant in Tien Shan, several rock glaciers cover an area of 1 km² or more (Bolch & Gorbunov, 2014), and in some valleys such as Ulken Almaty valley it was estimated that more than 10% of the surface ice is stored in rock glaciers (Bolch & Marchenko, 2009). All rock glaciers in northern Tien Shan originate in areas where permafrost occurrence is likely while several large rock glaciers terminate at elevations where permafrost is unlikely outside the rock glaciers themselves (Bolch and Gorbunov, 2014).

The reaction of glaciers to climate change is relatively well known However, studies about the reaction of rock glaciers are much less frequent despite the fact that they also occur in many mountain ranges and can be of significance in relation to hydrology. The rock glacier velocity shows a clear relation to climate as most of the rock glaciers experienced increasing velocities during the last years or decades (Delaloye et al., 2008). This was also measured for rock glaciers in Northern Tien Shan (Sorg et al., 2015).

One of the major difficulty to study rock glaciers using remote sensing data is that the changes in area, volume and velocity are much lower and less evident that the changes of the glaciers. Hence, high resolution imagery and digital terrain models are needed to map and investigate changes of the periglacial landforms. The aim of this study is therefore to study the evolution of the rock glaciers since the 1970s until today using high resolution imagery and to compare the rock glacier changes to the changes of the nearby glaciers.

Data and Methods

The primary data sets used in this study are high resolution imagery from 1971 (Corona KH-4B, spatial resolution ~2m), 2012 (GeoEye-1, 0.5m) and 2016 (Pleiades, 0.5m) sensors/cameras. Corona allowed to investigate the long term evolution of glaciers and rock glaciers while GeoEye-1 and Pleiades reveal the most recent short-term changes.

Pleiades and GeoEye DEMs were generated using Erdas Imagine Photogrammetry Automatic Terrain Extraction (ATE). Corona KH-4B imagery were processed using Remote Sensing Software Package Graz (RSG), developed by Joanneum Research Graz, Austria.

The RSME for the GCPs and control points were on

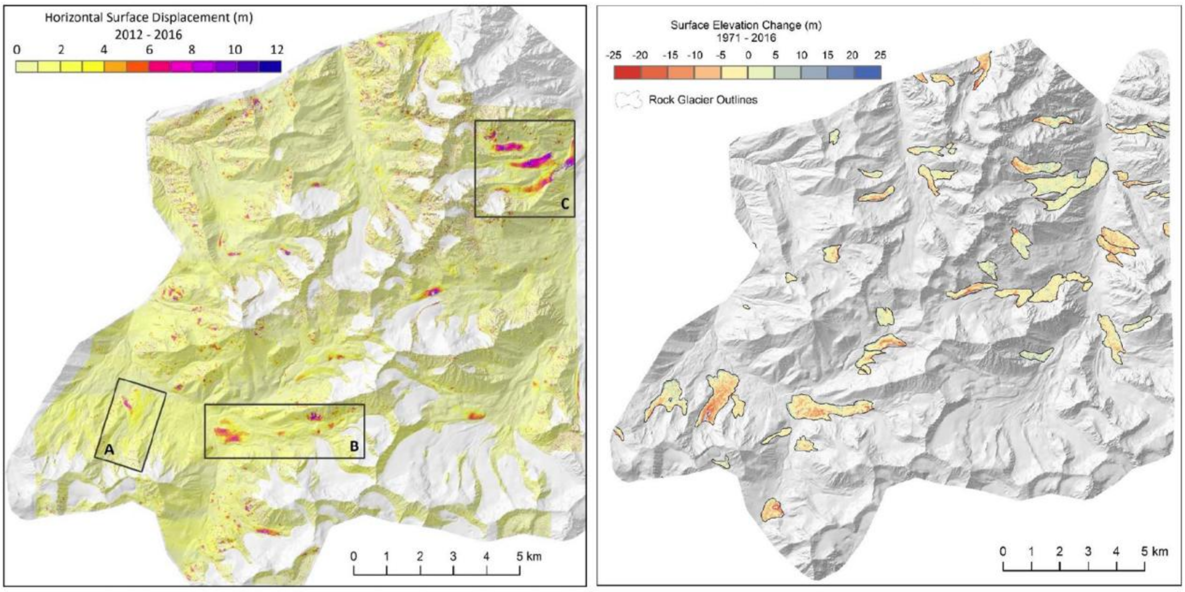

Figure 1: Surface velocity for the period 2012-2016, A: Morenny, B: Gorodetzky C: Ordzhonikidse rock glaciers (left); rock glacier surface elevation change 1971-2016 (right).

average about 2 m with the highest RSME for the z direction. The final DEMs were generated at a resolution of 5 m. Thereafter the DEMs were carefully co-registred and the DEMs subtracted. Elevation differences exceeding 3σ were considered as outliers and removed. The mean elevation difference of the stable terrains was within ±0.1 m for all DEM differences with standard deviations of the stable terrain of maximum 7.0 m (Corona-GeoEye) and minimum 2.2m (GeoEye-Pleiades). Orthoimges were generated and the rock glaciers manually delineated. Horizontal surface displacement was measured using the correlation algorithms COSI-Corr.

Results and discussion

A total of 52 rock glaciers were identified in the three investigated valleys ranging in size from 0.02 km² to 1.59 km². Overall they cover and area of about 18km², which is more than 40% of the glacier cover of the year 2016. Moraine-type rock glaciers are more common (number 36) than talus-type rock glaciers (16). Overall the identified rock glaciers were more frequent than the inventory by Bolch and Gorbunov (2014) who used mainly the lower resolution Landsat ETM+ data and did therefore only include larger rock glaciers.

The average surface velocity of the rock glaciers was 0.44 ± 0.30 m a^{-1} with rates of up to 2m a^{-1}. Highest velocities were found at Gorodetzky and Ordzhonikidse rock glaciers (Fig. 1 left). On average, the rock glaciers showed only a slight insignificant surface lowering of 0.04 m a^{-1} for the period 1971-2012 and of 0.06 m a^{-1} for 2012-2016. Most of the investigated rock glaciers showed similar distinct patters of change: A surface elevation gain at their fronts indicating an advance, a significant lowering in the upper probably glacier affected parts of the rock glaciers and areas of elevation gain and lowering in between probably caused by flow patterns and loss if subsurface ice (Fig. 1 right). Similar characteristics of surface elevation changes were found in the Swiss Alps (e.g. Müller et al. 2016).

References

Bolch, T. & Gorbunov, A.P., 2014. Characteristics and Origin of Rock Glaciers in Northern Tien Shan (Kazakhstan/Kyrgyzstan). *Permafrost and Periglacial Processes* 25(4): 320–332.

Bolch, T. & Marchenko, S.S., 2009. Significance of glaciers, rockglaciers and ice-rich permafrost in the Northern Tien Shan as water towers under climate change conditions. *IHP/HWRP-Berichte* 8: 132–144.

Delaloye, R. et al., 2008. Recent Interannual Variations of Rock Glacier Creep in the European Alps, in: Proc. of the 9th Int. Conf. on Permafrost, 343–348.

Müller, J., Vieli, A., Gärtner-Roer, I., 2016. Rock glaciers on the run - understanding rock glacier landform evolution and recent changes from numerical flow modeling. *The Cryosphere* 10(6): 2865–2886.

Sorg, A., Bolch, T., Stoffel, M., Solomina, O., Beniston, M., 2012. Climate change impacts on glaciers and runoff in Tien Shan (Central Asia). *Nature Climate Change* 2: 725–731.

Sorg, A., Kääb, A., Roesch, A., Bigler, C., Stoffel, M., 2015. Contrasting responses of Central Asian rock glaciers to global warming. *Scientific Reports* 5: 8228.

Sentinel-1 InSAR measurements of surface elevation changes over yedoma uplands on Sobo-Sise Island, Lena Delta

Jie Chen[1,2]
Frank Günther[3]
Guido Grosse[3,4]
Lin Liu[2]
Hui Lin[1]
[1]*Institute of Space and Earth Information Science, The Chinese University of Hong Kong, Hong Kong, jiechen@link.cuhk.edu.hk*
[2]*Earth System Science Programme, Faculty of Science, The Chinese University of Hong Kong, Hong Kong*
[3]*Alfred Wegener Institute Helmholtz Centre for Polar and Marine Research, 14473 Potsdam, German*
[4]*Institute of Earth and Environmental Sciences, University of Potsdam, 14476 Potsdam, German*

Abstract

Yedoma is vulnerable to thawing and degradation under climate warming, which can result in lowering of surface elevations due to thaw subsidence. Quantitative knowledge about elevation changes can help us better understand the freeze-thaw processes of the active layer and yedoma deposits. In this study, we utilize C-band Sentinel-1 InSAR measurements, characterized by frequent sampling, to study the elevation changes over ice-rich yedoma uplands on Sobo-Sise Island, Lena Delta. We observe significant seasonal thaw subsidence during summer months and inter-annual elevation changes from 2016 to 2017. Here, we demonstrate the capability of Sentinel-1 to estimate elevation changes over yedoma uplands. We observe interesting patterns of stronger seasonal thaw subsidence on elevated flat yedoma uplands when compared to surrounding yedoma slopes. Inter-annual analyses from 2016 to 2017 revealed mostly positive surface elevation changes that might be caused by delayed thaw seasonal progression associated with mean annual air temperature fluctuations.

Keywords: Sentinel-1, yedoma uplands, surface elevation changes, thaw subsidence, InSAR

Introduction

Yedoma, extremely ice-rich permafrost with massive ice wedges formed during the Late Pleistocene (Schirrmeister et al., 2011), is vulnerable to thawing and degradation under climate warming. Yedoma deposits also alternate with the thermokarst lake and basin development (Morgenstern et al., 2011). The surface elevation change, associated with the freeze and thaw cycling processes, is of importance to help us understand the response of yedoma uplands to surface disturbance and/or climatic changes.

Interferometric Synthetic Aperture Radar (InSAR) methods have been successfully used to remotely sense and quantify seasonal subsidence and inter-annual subsidence trends in permafrost regions (Liu et al., 2015). However, the space-borne C-band or L-band SAR missions prior to the Sentinel-1A/B satellites only provided a limited number of repeat images, making it difficult to fully resolve the temporal evolution of seasonal thaw subsidence and/or inter-annual variabilities. The frequent Sentinel-1 InSAR measurements (regular revisit time is 12 days; shortest is 6 days if both Sentinel-1 A and B images are acquired) provide an excellent opportunity to study seasonal and inter-annual thaw processes in permafrost regions.

The objective of this research is to demonstrate the capability of Sentinel-1 InSAR measurements to estimate surface elevation changes over yedoma uplands. We also analyzed the spatial pattern of seasonal thaw subsidence and the temporal evolution of inter-annual elevation changes.

Study site and methods

Sobo-Sise Island, located in the eastern Lena Delta, is largely dominated by yedoma uplands (Fuchs et al., 2017; Morgenstern et al., 2011). The mean annual air temperature in the region is about -12.5 ℃ and the mean annual precipitation is about 180-200 mm. The vegetation coverage is sparse and the growing season is short (Fuchs et al., 2017).

The basic principle of InSAR is to compare the phase of two complex radar images that were acquired from slightly different positions at different times. The phase differences measure the displacements along the line of sight between the two SAR acquisitions. In this study, we use four individual interferograms to calculate the accumulated seasonal subsidence during the thaw season of 2017. We also use four interferograms between the thaw season of 2016 and 2017 to conduct the averagely inter-annual elevation changes.

Results and discussion

We observe seasonal thaw subsidence up to 2-3 cm from June 23 to September 9 in 2017. Seasonal subsidence is pronounced most on top of flat yedoma uplands (Fig. 1). We also observe differences between the years, where subsidence during the thaw season of 2017 was less intense when compared with the preceding year 2016. This results in mostly a net inter-annual heave from late season 2016 to 2017 (Fig. 2), and is possibly caused by delayed thawing associated with differences in summer air temperatures. Degree days of thawing in 2016 were 812, in 2017 only 667. We also observed a shift of the warmest month from typically July to August. Mean air temperature in July 2016 was 7.8 °C and in August 7.3 °C. In 2017, July temperature was only 7.2 °C, while August was warmer with 8.3 °C. Even more pronounced were differences between September 2016 and 2017 (164 vs 63 degree days of thawing).

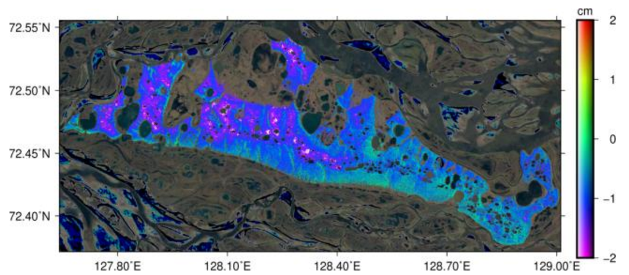

Figure 1. Map of elevation changes over yedoma uplands on SoboSise Island from June 23 to September 9 in 2017. Minus values denote subsidence.

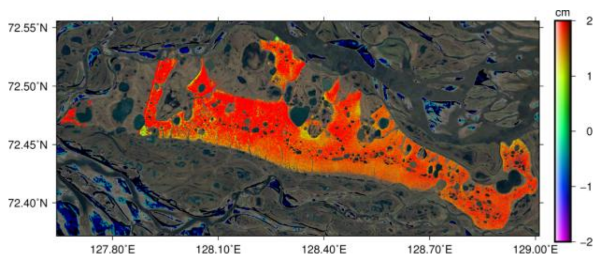

Figure 2. Map of inter-annual surface elevation changes between the thaw seasons of 2016 and 2017.

Conclusions

We explored and successfully tested the ability of Sentinel-1 InSAR measurements for quantifying both, thaw subsidence over one thawing season and the inter-annual elevation changes between two thaw seasons. In particular, the latter profits strongly from high SAR coherence values also between the years. We find that the top of yedoma uplands exhibit the highest elevation change amplitudes, suggesting that these areas are especially vulnerable for permafrost degradation through thaw subsidence processes. We also find that delayed thawing associated with air temperature fluctuations affects inter-annual elevation change magnitudes, highlighting the importance of a careful and comprehensive selection of time intervals for InSAR processing from interferogram creation.

Acknowledgments

JC, LL, and HL were supported by the Hong Kong Research Grants Council projects CUHK24300414 and G-CUHK403/15. FG and GG were supported by DAAD #57216164 within the PPP Hong Kong program and ERC PETA-CARB #338335.

References

Fuchs, M., Grosse, G., Strauss, J., Günther, F., Grigoriev, M., Maximov, G. M., & Hugelius, G. (2017). Carbon and nitrogen pools in thermokarst-affected permafrost landscapes in Arctic Siberia. *Biogeosciences Discuss., 2017*, 1-35.

Liu, L., Schaefer, K. M., Chen, A. C., Gusmeroli, A., Zebker, H. A., & Zhang, T. (2015). Remote sensing measurements of thermokarst subsidence using InSAR. *Journal of Geophysical Research: Earth Surface*.

Morgenstern, A., Grosse, G., Günther, F., Fedorova, I., & Schirrmeister, L. (2011). Spatial analyses of thermokarst lakes and basins in Yedoma landscapes of the Lena Delta. *The Cryosphere, 5*(4), 849-867.

Schirrmeister, L., Kunitsky, V., Grosse, G., Wetterich, S., Meyer, H., Schwamborn, G., . . . Siegert, C. (2011). Sedimentary characteristics and origin of the Late Pleistocene Ice Complex on north-east Siberian Arctic coastal lowlands and islands – A review. *Quaternary International, 241*(1), 3-25.

RUS Applications | Case Study: Artic lake ice dynamics monitored with Sentinel-1

Miguel Castro Gómez [1]
Tereza Šmejkalová[1]
Francesco Palazzo[1]

[1]*Serco S.p.A. Frascati (Italy), miguel.castro.gomez@serco.com*

Abstract

Since the launch of the first satellite (Sentinel-1A) in April 2014, the free and open data of the Sentinel satellites provide essential information to monitor our environment. With this massive amount of data (expected 10 petabytes of data each year with all Sentinel satellites operational), the challenge is now moving towards storage and processing capabilities. The RUS (Research and User Support for Sentinel Core Products) service provides a scalable platform in a cloud environment to facilitate the uptake of Copernicus data. In this research, we demonstrate its use on a case study to evaluate the ice cover dynamics of thermokarst lakes in Northeastern Russia.

Keywords: Copernicus; RUS; Sentinel-1; lake ice;

Introduction

With an expected rate of four Terabytes per day produced by all the Copernicus Sentinel satellites, the limits of remote sensing applications are disappearing. In 2014, the Copernicus satellites started to provide crucial data free of charge. This new generation of Earth Observation satellites greatly increases our capabilities to monitor the environment and respond to natural phenomena. The challenge is no longer data availability, but rather the analysis and exploitation of these large datasets. Storage and processing needs (mainly) are some of the barriers users have to face and solve to exploit the full potential of the Sentinel data. In addition, "knowledge barriers" prevent the use of the data by a wider community.

In this work, we present a solution to the problems outlined above and present its use through a case study on artic lake ice dynamics using Sentinel-1 time-series.

The RUS Service

To support the users in overcoming the problems related to large dataset processing, the RUS (Research and user Support for Sentinel Core Products) project (funded by EC and managed by ESA) started operations in October 2017. It provides a scalable platform in a powerful cloud environment with the storage and processing capacity needed to handle the data derived from the Copernicus Sentinel satellites. The service is offered to users at no cost through the provision of customizable Virtual Machines (VM), preinstalled with suite of Free and Open-Source Software (FOSS).

Moreover, to reduce the knowledge gap and improve the uptake of Copernicus data, the RUS service offers a dedicated Earth Observation helpdesk supported by a team of remote sensing experts and an extensive training program. The training plan includes a variety of activities. i) Face-to-face events; ii) Open Webinars organized every month; iii) E-learning platform with technical and theoretical content.

Case study

This work presents the use of RUS Copernicus to analyze lake ice dynamics (freeze-up and break-up) for a study area located in the Yedoma permafrost region of northeast Russia. The study takes advantage of the storage and processing capacity offered by the RUS service. A joint use of Sentinel-1 and Sentinel-2 data is proposed to derive a water body mask and analyze lake ice evolution.

Background information

Thermokarst lakes are a major component of permafrost landscapes and have been shown to be sensitive indicators of climate change (Surdu et al. 2015).

It has been well documented that temperatures at high latitudes rise with rate at least double the global average (Jeong et al. 2014; McBean 2005).

Dataset

For this study, the complete archive of Sentinel-1 images from November 2016 until November 2017 with the following characteristics has been used:

- Acquisition type: Interferometric Wide (IW)
- Product type: Ground Range Detected (GRD)
- Polarization: VV
- Relative orbit number: 2

In total, 30 images have been identified as suitable for this study and downloaded from the Copernicus Open Access Hub into the RUS Virtual Machines. In addition, a cloud-free Sentinel-2 image from August, 31st 2017 was used to derive a water mask.

Methodology

The proposed methodology includes the following steps. For Sentinel-2, the Normalized Difference Water Index – NDWI is derived and later used as mask to identify water bodies on Sentinel-1 images.

For Sentinel-1 images, the preprocessing includes orbit file calibration, thermal noise removal, radiometric calibration, speckle filter, terrain correction, subset and sigma0 (σ0) multi-temporal analysis.

The preprocessed SAR data will be used as an input for K-means segmentation in order to derive ice fraction time-series. The steps are adapted from the methodology proposed by Surdu et al. (2015) for ASAR and RADARSAT data. The software tools used for the analysis are SNAP and R.

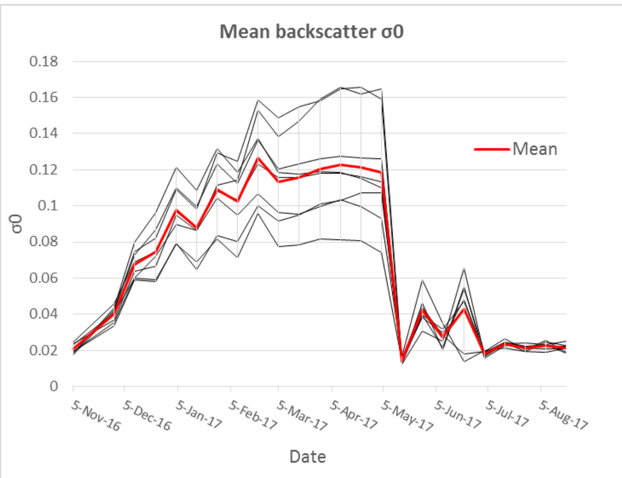

Figure 1: Mean backscatter (σ0) time series for a small subset of lakes in the study area (gray). Mean of all lakes in the subset (red).

Preliminary results

We present only intermediate results as the work is still in progress. The temporal profile of the mean sigma0 (σ0) over a subset of 8 lakes can be seen in (Fig. 1) and shows that Sentinel-1 SAR data offer a good approach for this type of monitoring activities.

Acknowledgments

RUS is operated by an international team, led by CSSI and involving Serco SPA, Noveltis, Along-Track and CS Romania.

References

Jeong, J.-H., Kug, J.-S., Linderholm, H. W., Chen, D., Kim, B.-M., Jun. S.-Y., 2014. Intensified Arctic Warming under Greenhouse Warming by Vegetation–atmosphere–sea Ice Interaction. *Environmental Research Letters* 9 (9):094007.

McBean, G., 2005. Arctic Climate: Past and Present. In *Arctic Climate Impact Assessment - Scientific Report*. Cambridge University Press.

Surdu, C. M., Duguay, C. R., Pour, H. K., Brown, L. C., 2015. Ice Freeze-up and Break-up Detection of Shallow Lakes in Northern Alaska with Spaceborne SAR. *Remote Sensing* 7 (5):6133–59.

Spatial Variation in Thermokarst Subsidence after the Anaktuvuk River Fire on the North Slope, Alaska

Go Iwahana[1]
Reginald Muskett[1]
Kazuyuki Saito[2]
Hiroshi Ohno[3]
Tokuta Yokohata[4]
Masao Uchida[4]
Robert Busey[1]
[1]*University of Alaska Fairbanks, Fairbanks, USA, giwahana@alaska.edu*
[2]*Japan Agency for Marine-Earth Science and Technology, Japan*
[3]*Kitami Institute of Technology, Japan*
[4]*National Institute for Environmental Studies, Japan*

Abstract

The consequences of permafrost degradation associated with thermokarst for surface ecology, landscape evolution, and hydrological processes have been of great scientific interest and social concern. Part of a tundra patch affected by wildfire in northern Alaska (27.5 km^2) was investigated here, using remote sensing and in situ surveys to quantify and understand permafrost thaw dynamics after surface disturbances In the first year after the fire, an average subsidence rate of 6.2 cm/year (vertical) was measured. Subsidence in the burned area continued over the following two years, with decreased rates. The mean rate of subsidence observed in our interferograms was 3.3 cm/year, a value comparable to that estimated from field surveys at two plots on average (2.2 cm/year) for the six years after the fire. Our analyses on the spatial variation in the subsidence indicated zones of highly eroding zones and showed a tendency for areas with larger slopes to experience larger subsidence.

Keywords: Thermokarst; Tundra; InSAR; Subsidence; North Slope; Alaska

Introduction

The development of thermokarst in ice-rich permafrost regions is a natural hazard, causing irreversible geomorphic changes (Haeberli & Burn, 2002). The formation of large depressions and lakes or swamps produced by thermokarst processes is observed in discontinuous and continuous permafrost zones, especially in Alaska and Northeastern Siberia. Despite the recognition of uncertainty about the fate of Arctic regions and global climate change due to permafrost degradation information about the spatial extent and rates of thermokarst processes are limited.

Liu et al. (2014) detected large-scale thermokarst subsidence in the Anaktuvuk River Fire (ARF) using InSAR. Although spatial variation in thermokarst subsidence at the regional scale was shown field information and InSAR analysis served to limit understanding of local thermokarst processes as these phenomena occur at much smaller scales. Currently InSAR techniques for quantifying thermokarst subsidence with enough spatial and temporal resolution for understanding local thermokarst processes in detail constrained by fieldwork measurements have not yet been reported for the ARF scar.

The objectives of this study are to demonstrate the ability of L-band InSAR to quantify thermokarst subsidence at spatial resolutions of an order of tens of meters with supporting evidence from field surveys and analysis of optical satellite images and to discuss the efficiency and limitations of this method as a monitoring tool for thermokarst. To this end, we investigated the northern part of the same ARF scar in detail using both optical and microwave remote sensing as well as in situ fieldwork measurements and observations.

Results and Discussion

The two-pass differential InSAR technique using ALOS-PALSAR (L-band microwave) has been shown capable of capturing thermokarst subsidence at a spatial resolution of tens of meters, with supporting evidence from field data and optical satellite images (Figure 1). Significantly large amounts of subsidence (up to 6.2 cm/year spatial average) were measured within burned areas relative to unburned nearby by three independent InSAR pairs after a tundra fire. Relatively small spatial variation (less than 0.5 cm in spatial average) was observed from two independent InSAR pairs during the pre-fire period. The obtained interferograms did not show sub-meter scale depressions along the troughs of the depression network developed by thermokarst, though they could distinguish small land areas with stable and subsiding land surface at smaller than tens of meters scale and smaller-scale detailed spatial variation of thermokarst subsidence. Post-fire interferograms were decorrelated along fire boundaries where rapid surface changes due to lateral erosion can be expected and clearly separated subsiding burned areas from stable areas of intact environment. The mean rate of subsidence observed in our interferograms from 24 Jul 2008 until 14 Sep 2010 was 3.3 cm/thawing season, with this value comparable to the rate estimated from field surveys at two plots of 2.2 cm/year for the six years after fire, on average.

Interferogram phase values show abrupt-discrete changes across the boundaries between burned and unburned areas. Fire boundaries often coincide with decorrelated areas. Inside the burned areas there are some gradual changes in phase values (e.g. slopes changes) while there are relatively uniform phase values in unburned areas. Despite the topography of the studied area being flat or showing only gentle slopes (95% of the area shows slope angles of less than 5°), the magnitude of subsidence seems to depend on the slope. There was a tendency for areas with larger slopes to experience larger subsidence. It is also worth noting that large subsidence was calculated for fragmented unburned areas, as they were small patches (most of them smaller than 1 m^2) surrounded by burned surfaces in which thermokarst had been active. This fact seems to show that thermokarst areas tend to propagate into adjacent areas by the lateral influence of thermal and/or hydrological regime shifts in the ground.

A larger magnitude of thermokarst activity on the slopes revealed by this study is in accordance with the fact that current thermokarst terrains appear as patches of depressed areas surrounded by relatively higher land underlain by ice-rich permafrost. The ground temperature is higher and thaw is deeper. Permafrost can be expected near lake basins (Plug & West, 2009) and streamlines. This results in lateral and areal expansion of drained thermokarst lake basins. This spatial variation in thermokarst is consistent with observations of an ice-rich permafrost region in eastern Siberia. For example, Sejourne et al. (2015) reported baydjarakhs as a local feature resulting from the thermokarst process observed on the banks of large thermokarst lakes and alases.

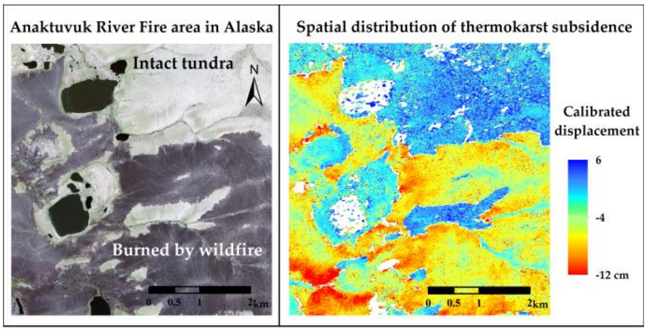

Figure 1. Surface conditions and interferometry analysis for the time interval 27 July 2009–24 July 2008. (Left) True color image by high-resolution optical sensor (QuickBird) on 3 July 2008; (Right) Spatial distribution of vertical surface movements calculated from unwrapped phases

Acknowledgments

This study was supported by the Environment Research and Technology Development Fund (2-1605) of the Ministry of the Environment, Japan (ERTDF) and the US National Aeronautics and Space Administration (NASA) NNX16AC57A.

References

Haeberli, W.; Burn, C.R. *Natural Hazards in Forests: Glacier and Permafrost Effects as Related to Climate Change*; CABI Publishing: Wallingford, UK; New York, NY, USA, 2002.

Liu, L.; Jafarov, E.E.; Schaefer, K.M.; Jones, B.M.; Zebker, H.A.; Williams, C.A.; Rogan, J.; Zhang, T. InSAR detects increase in surface subsidence caused by an arctic tundra fire. *Geophys. Res. Lett.* 2014, *41*, 3906–3913.

Plug, L. J., and J. J. West (2009), Thaw lake expansion in a two-dimensional coupled model of heat transfer, thaw subsidence, and mass movement, Journal of Geophysical Research-Earth Surface, 114.

Séjourné, A., F. Costard, A. Fedorov, J. Gargani, J. Skorve, M. Massé, and D. Mège (2015), Evolution of the banks of thermokarst lakes in Central Yakutia (Central Siberia) due to retrogressive thaw slump activity controlled by insolation, Geomorphology, 241(0), 31-40.

Spying on tundra beavers with times series remote sensing data

Benjamin M. Jones[1]
Ken D. Tape[2]
Ingmar Nitze[3,4]
Guido Grosse[1,4]
Christopher D. Arp[2]
Christian E. Zimmerman[3]

[1] *U.S. Geological Survey, Alaska Science Center, Anchorage, AK, USA, bjones@usgs.gov*
[2]*University of Alaska Fairbanks, Fairbanks, AK, USA*
[3]*Alfred Wegener Institute Helmholtz Centre for Polar and Marine Research, Potsdam, Germany*
[4]*Institute of Earth and Environmental Sciences, University of Potsdam, Potsdam, Germany*

Abstract

Landscape-scale impacts of climate change in the Arctic include increases in growing season length, shrubby vegetation, winter river discharge, snowfall, summer and winter water temperatures, and decreases in river and lake ice thickness. Combined, these changes may have created conditions that are suitable for beaver colonization of low Arctic tundra regions. We developed a semi-automated workflow that analyzes Landsat imagery time series to determine the extent to which beavers have colonized permafrost landscapes in arctic Alaska since 1999. Comparison of the potential beaver activity database with historic aerial photography from ca. 1950 and ca. 1980 indicates that beavers have recently colonized or recolonized riparian corridors in northwest Alaska. Remote sensing time series observations associated with the migration of beavers in permafrost landscapes in arctic Alaska include lake expansion and drainage, thaw slump initiation, thermo-erosional gully formation, ice wedge degradation, thermokarst shore fen development, and possibly development of taliks associated with water impoundment.

Keywords: Arctic, Beavers, Landsat, Thermokarst, Tundra, Very High Resolution Imagery

Introduction

Landscape-scale impacts of climate change in the Arctic include increases in growing season length, shrub cover and stature, winter river discharge, snowfall, summer and winter water temperatures, and decreases in river and lake ice thickness (Tape et al., In Review). Combined, these changes may have created conditions that are suitable for beaver colonization of low Arctic tundra regions. Migration of beavers in permafrost landscapes in arctic Alaska may cause permafrost degradation and thermokarst development (Tape et al., In Review).

Study Area and Methods

Recent observational evidence of beavers on the Beaufort Coastal Plain in the northwestern Canadian Arctic (Jung et al., 2017) peaked our interest (Figure 1). To systematically assess the extent to which beavers have colonized low Arctic tundra regions, we developed a semi-automated workflow that analyzes Landsat imagery time series from 1999 to 2014 (Nitze and

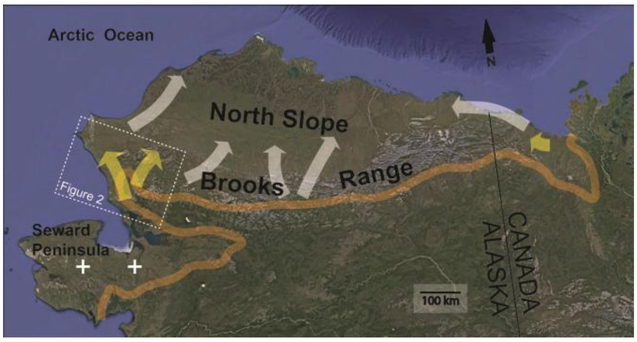

Figure 1. The low arctic tundra region of Alaska and northwestern Canada. The orange line approximates treeline, yellow arrows denote known beaver colonization routes since 1999 (Tape et al. In Review, Jung et al. 2017), plus signs show beaver activity beyond treeline on the Seward Peninsula, white box shows study area, and white arrows are potential future colonization routes.

Grosse, 2016; Nitze et al., 2017). We used multi-spectral indices trends (i.e. Tasselled Cap Brightness, Greenness, and Wetness; Normalized Difference Vegetation Index - NDVI; Normalized Difference Moisture Index -

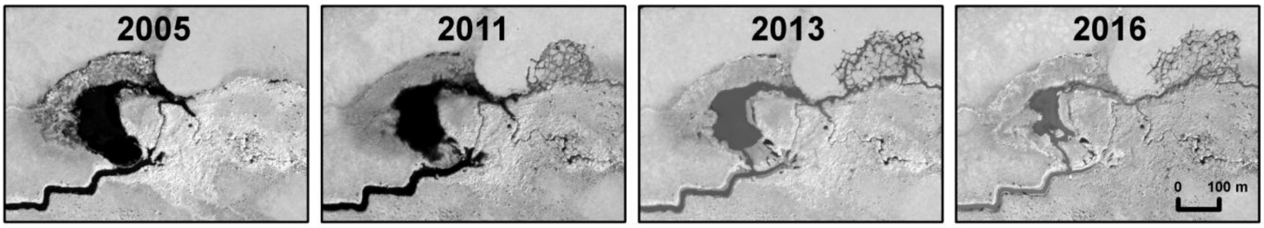

Figure 2. Very high spatial resolution image time series showing a tundra stream and lake system that was dammed by beavers in the early 2000s. Three dams are present in the 2005 image but between 2005 and 2011 the lower most dam fails as a result of thermo-erosional gullying leading to the catastrophic drainage of the lake and ice wedge degradation downstream of the outburst flood. All images courtesy of Digital Globe, Inc.

NDMI) to map changes in land surface properties (Nitze and Grosse, 2016; Nitze et al. 2017). Temporal trend analysis of each multi-spectral index, at the per pixel level, were categorized into wetting and drying trends which include per pixel probabilities (0 to 100%) of change using Random Forest supervised machine learning classification. This potential beaver activity database was then validated using very high resolution satellite imagery acquired between 2002 and 2016. Additional airborne remote sensing data from the 1950s, 1970s, and 1980s were used to assess their presence and/or absence at validated beaver locations.

Results

We identified 83 locations representing potential beaver activity in the Lower Noatak, Wulik, and Kivalina river watersheds in northwest Alaska. Seventy locations indicated wetting trends and 13 indicated drying trends. Validated locations of beaver activity in the Lower Noatak, Kivalina, and Wulik river watersheds using high-resolution satellite imagery showed that 80% of the wetting locations represented beaver activity (damming and pond formation), 11% were unrelated to beavers (no apparent dam building), and 9% could not readily be distinguished as being beaver related or not. For the drying locations, 31% represented beaver activity (pond drying due to dam abandonment or failure), 62% were unrelated to beavers (no sign of past beaver activity prior to drying), and 7% were undetermined.

Discussion and Conclusions

In the Arctic, by building dams, beavers have transformed stream reaches into wetlands likely with similar effects as at lower latitudes, such as the shift from lotic to lentic environments and increased variability in aquatic habitat. The Arctic, however, may have unique responses related to the tundra vegetation, presence of thaw susceptible permafrost soils, scarcity of water in winter, and limited biodiversity.

Very high resolution remote sensing time series observations associated with the migration of beavers in permafrost landscapes in arctic Alaska include lake expansion and drainage, thaw slump initiation, thermo-erosional gully formation, ice wedge degradation, thermokarst shore fen development, and possibly development of taliks associated with water impoundment (Figure 2). Beavering of the low Arctic will likely exacerbate ongoing permafrost terrain changes.

Acknowledgements

Funding was provided by the USGS Land Change Science and Land Remote Sensing Programs, European Research Council PETA-CARB Project, and the European Space Agency GlobPermafrost Project. Any use of trade, firm, or product names is for descriptive purposes only and does not imply endorsement by the U.S. Government.

References

Jung, T. S., Frandsen, J., Gordon, D. C., & Mossop, D. H. (2017). Colonization of the Beaufort Coastal Plain by Beaver (Castor canadensis): A Response to Shrubification of the Tundra?. The Canadian Field-Naturalist, 130(4), 332-335.

Nitze, I. & Grosse, G. (2016). Detection of landscape dynamics in the Arctic Lena Delta with temporally dense Landsat time-series stacks. Remote Sensing of Environment 181, 27–41.

Nitze, I., Grosse, G., Jones, B. M., Arp, C. D., Ulrich, M., Fedorov, A., & Veremeeva, A. (2017). Landsat-Based Trend Analysis of Lake Dynamics across Northern Permafrost Regions. Remote Sensing, 9(7), 640.

Tape, K.D., Jones, B.M., Arp, C.D., Nitze, I., Grosse, G., & Zimmerman, C.E. (In Review). Tundra be dammed: Beaver colonization of the Arctic.

Detection and quantification of lateral thermokarst lake expansion processes in periglacial landscapes based on Sentinel and RadpidEye imagery

Soraya Kaiser[1, 2]
Thomas Schneider von Deimling[1, 2]
Stephan Jacobi[1]
Richard Mommertz[1, 3]
Moritz Langer[1, 2]
[1] *Alfred Wegener Institute Helmholtz Centre for Polar and Marine Research, Potsdam, Germany*
[2] *Department of Geography, Humboldt-Universität zu Berlin, Berlin, Germany*
[3] *University of Potsdam, Potsdam, Germany*
Correspondence to: Soraya Kaiser (soraya.kaiser@awi.de)

Abstract

While there are abundant erosional features throughout the Arctic – ranging from landslides, thaw slumps or river bank to gully erosion – one of the most dynamic periglacial elements are thermokarst lakes. Due to their lateral thermal and mechanical erosion they shape their surrounding topography and hydrological network, leading to a further destabilization of permafrost soils. This study aims at the remote sensing based identification and quantification of these lateral erosion processes and their incorporation into the land surface model CryoGrid3 to estimate their effect on Arctic ecosystems and infrastructure.

Keywords: Thermokarst lake expansion; erosion rates; Sentinel; RapidEye; CryoGrid3; permafrost

Introduction

Thermokarst ponds and lakes are an abundant and widespread landform throughout the Arctic (Hinkel *et al.*, 2005). They develop in regions underlain by continuous permafrost as a consequence of soil subsidence that is triggered by the thawing of excess ground ice (Langer *et al.*, 2016; Pienitz *et al.*, 2008). When a resulting depression fills with the melt water of the degraded ice, it forms a pond that can cause – due to the waterbody's heating property and the formation of a talik beneath the basin – further thawing processes (Pienitz *et al.*, 2008). As a result of the thermal erosion, the size of the pond increases vertically and horizontally and can turn into a lake. Several studies conducted to understand thermokarst lake dynamics state that the area of the Arctic's land surface covered by these landforms is steadily growing (Jones *et al.*, 2011). Especially ponds – being the primary waterbody type (Nitze *et al.*, 2017) – underlie a strong expansion (Jones *et al.*, 2011) further shaping their surrounding landscape.

While the previous scientific work regards the dynamics of thermokarst ponds and lakes over a substantial time span, this study focuses on a detailed quantification and estimation of seasonal shoreline erosion rates, their spatial patterns and temporal variability. The retrieved information will be incorporated into the land surface scheme CryoGrid3, which simulates permafrost thawing but only regards vertical processes of soil subsidence and thermokarst development yet (Westermann *et al.*, 2016).

Methodology

Our study aims at the detection and quantification of lateral erosion and mass movement processes that occur around thermokarst lakes. For this purpose a study site in Prudhoe Bay, Alaska, is selected due to its vast natural and human-caused thermokarst features.

Figure 1: RGB image of the Prudhoe Bay Area (Alaska, U.S.A.) showing the infrastructure's close proximity to thermokarst features (Spatial Reference: WGS 84 UTM zone 6. Imagery: Planet Team, 2017)

The local infrastructure consists of gravel roads to access the production sites and pipelines for oil transport. Figure 1 shows a production site close to Prudhoe Bay and underlines the need for a better understanding of landscape changes resulting from permafrost thaw. By applying a combination of high resolution optical imagery and complementary radar and elevation data, the study aims at explaining (i) how thermokarst lakes react to changes in meteorological conditions, (ii) at investigating the spatial patterns of lake expansion (linear/ irregular) and (iii) at identifying the driving factors for lake dynamics (lake ice type, lake size, topography, vegetation etc.).

Our analysis is based on radar data of the Copernicus Sentinel 1A and B for retrieving lake ice characteristics and on multispectral imagery from the Planet Labs Incorporation's PlanetScope and RapidEye products for acquiring information about ground characteristics (soil, vegetation etc.). The (micro)topography – being an important factor concerning mass movement processes – will be analyzed on the basis of the Arctic DEM.

For representing thermokarst lake formation and expansion in the land surface scheme CryoGrid3, it is also crucial to understand the response of thermokarst dynamics to seasonal changes in meteorological conditions. We therefore analyze climate data products to identify changes in temperature, precipitation, wind speed, etc. since these parameters influence the thermal regime of the waterbodies and the susceptibility of the surrounding landscape to soil erosion.

Acknowledgments

The young investigator group PermaRisk is funded by the German Federal Ministry of Education and Research (BMBF) under the funding reference number 01LN1709A.

The RapidEye and Planetscope imagery is provided by Planet Labs Inc. within their Education and Research Program (Planet Team, 2017).

References

Hinkel, K. M., Frohn, R. C., Nelson, F. E., Eisner, W. R., Beck, R. A., 2005. Morphometric and spatial analysis of thaw lakes and drained thaw lake basins in the western Arctic Coastal Plain, Alaska. *Permafrost and Periglacial Processes* 16(4): 327-341.

Jones, B. M., Grosse, G., Arp, C. D., Jones, M. C., Walter Anthony, K. M., Romanovsky, V. E., 2011. Modern thermokarst lake dynamics in the continuous permafrost zone, northern Seward Peninsula, Alaska. *Journal of Geophysical Research: Biogeosciences* 116(3): 1-13.

Langer, M., Westermann, S., Boike, J., Kirillin, G., Grosse, G., Peng, S., Krinner, G., 2016. Rapid degradation of permafrost underneath waterbodies in tundra landscapes – Toward a representation of thermokarst in land surface models. *Journal of Geophysical Research: Earth Surface* 121(12): 2446-2470.

Nitze, I., Grosse, G., Jones, B. M., Arp, C. D., Ulrich, M., Fedorov, A., Veremeeva, A., 2017. Landsat-based trend analysis of lake dynamics across Northern Permafrost Regions. *Remote Sensing* 9(7): 1-28.

Pienitz, R., Doran, P. T., Lamoureux, S. F., 2008. Origin and geomorphology of lakes in the polar regions. *In*: W. F. Vincent & J. Laybourn-Parry (eds.), *Polar Lakes and Rivers: Limnology of Arctic and Antarctic Aquatic Ecosystems*. New York: Oxford University Press, 25-42.

Planet Team, 2017. Planet Application Program Interface. *In*: Space for Life on Earth. Retrieved from https://api.planet.com

Westermann, S., Langer, M., Boike, J., Heikenfeld, M., Peter, M., Etzelmüller, B., Krinner, G., 2016. Simulating the thermal regime and thaw processes of ice-rich permafrost ground with the land-surface model CryoGrid 3. *Geoscientific Model Development* 9(2): 523-546.

Identification and mapping of permafrost using satellite images in the mountainous regions of cryolithozone (on the example of the Elkon mountain and Olekmo-Charsky highlands in Southern Yakutia)

S.V. Kalinicheva
Melnikov Permafrost Institute SB RAS, ikoveta@rambler.ru

Abstract

The technique of identification of permafrost and taliks with use of satellite data is offered and also possibilities of mapping of their distribution in a zone of discontinuous permafrost in mountainous areas of South Yakutia, on the example of the Elkon mountain are shown. The results of the correlation analysis of satellite data with field full-scale materials are presented. For the first time, the indicator properties of the radiation temperature (thermal infrared radiation from the landscape surface) received by means of the Landsat infrared survey in channel 6 for the detection and regional mapping of permafrost are described in more detail. Algorithms for recognizing permafrost and taliks for each exposure are compiled, representing a complex indication scheme for components such as height, slope and surface exposure, vegetation and snow cover, and the radiation surface temperature.

Keywords: Landscape indication; mapping; permafrost; satellite images (remote sensing).

In the mountainous regions of the permafrost zone, the study of permafrost is complicated by a complicated dissected relief of the territory. In this connection, at the present stage of scientific and technological progress, the introduction of methods that allow remote study and research of permafrost becomes urgent. In particular, this is a method of landscape indication, the essence of which is to recognize the hidden components and properties of the landscape through physiognomic components. The relevance of this method in the study of the permafrost of mountain regions is due to the fact that the main factors (landscape components) that affect the formation of the temperature regime of rocks (on which the thawing or frozen state depends) are clearly reflected in remote sensing materials.

In this paper, we develop a technique for detecting frozen and thawed rocks using satellite imagery, which is an algorithm for complex indication of permafrost, consisting of six indicators, such as altitude, slope and relief, snow and vegetation cover, and radiation temperature (thermal infrared radiation of the surface) recorded in the thermal channel Landsat. The last parameter (indicator) is relatively new in the study of permafrost, but not well studied.

The developed technique is suitable for exploring cryolithozone in mountain regions with a dismembered relief. In view of this, parts of South Yakutia were chosen as the study area. For the first time, according to the proposed method, the study was conducted in the region of the Elkon mountain massif located in the northern part of the Aldan Shield. This method also carried out a study in the area of the Olekma-Charsky highlands. The repeated approbation of the developed technique confirmed the possibility of its use for research and mapping of permafrost rocks in the mountainous regions of the permafrost zone.

Dynamics of gas emission craters on Yamal and Gydan Peninsulas, Russia, analysis of stereo pairs of very-high resolution satellite images.

Alexander Kizyakov[1,3]
Mikhail Zimin[2]
Anton Sonyushkin[2], Yury Dvornikov[3]
Artem Khomutov[3,4], Marina Leibman[3,4]
[1] *Lomonosov Moscow State University, Faculty of Geography, Cryolithology and Glaciology Department, akizyakov@mail.ru*
[2] *ScanEx Research and Development Center*
[3] *Earth Cryosphere Institute, Tyumen Scientific Centre SB RAS*
[4] *University of Tyumen, International Institute of Cryology and Cryosophy*

Abstract

In this study, we use very-high-resolution WorldView satellite stereopairs to reveal and measure the geomorphic features that preceded and followed GEC formation on the Yamal and Gydan peninsulas. Analysis of DEMs allowed us to (a) distinguish different terrain position of the GECs (at the foot of a gentle slope, or on an upper edge of a terrace slope); (b) reveal that the formation of both Yamal and Gydan GECs were preceded by mound development; (c) determine proportions of a funnel-shaped upper part and a cylindrical lower part for each crater; and (d) measure the plan form modification of GECs.

Keywords: gas emission crater; satellite stereopair; digital elevation model; cryogenic relief.

Introduction

Newly formed, deep narrow craters were discovered in permafrost in the Yamal and Gydan peninsulas, north of Western Siberia in 2014. The first known crater (GEC-1) was discovered in the central part of the Yamal Peninsula in the summer of 2014. In 2014–2015, authors analyzed satellite images of this crater to determine the date of the crater formation as well as to provide the geomorphologic characteristics of the area prior to crater formation, immediately after it, and the state of its further development (Kizyakov *et al.*, 2015). The crater on Gydan Peninsula (AntGEC) was reported in media in summer 2014, but the site was not visited by experts until 2016. To reconstruct the relief that preceded formation of this crater and to estimate the relief changes that occurred, we, by analogy with the research done on GEC-1, processed stereopairs of satellite images of very high spatial resolution.

This paper is based on results of GEC-1 and AntGEC geomorphodynamics comparison (Kizyakov *et al.*, 2017).

Materials and Methods

Study sites

There are fragments of the IV coastal-marine plain 40–60 m high in the GEC-1 area in Central Yamal. The crater itself is located on the boundary between a khasyrey (a drained lake depression) and a slope of a terrace-like surface, modified by erosion channels and small thermokarst lakes.

The AntGEC is located in the western part of the Gydan Peninsula. It occupies the edge of III-d alluvial-marine plain 30–50 m above sea level, bordering the small flat-bottomed gully.

Remote sensing data

Digital elevation models (DEMs) with a node density of 1 m were created in order to define the morphological characteristics of the relief before and after the GEC formation. In our case, the most suitable input data source for the reconstruction of the terrain and for change detection is the stereo mode of very high spatial resolution satellite imagery. We selected multi-temporal stereopairs of very high spatial resolution satellite images, closest to the time of the GEC-1 and AntGEC formation, for further analysis.

Using the stereopairs, we created DEMs of 2013 and 2014 for each key site with 1 m grid spacing. We estimated the relative accuracies of the DEMs within 0.35-0.55 m.

Results and discussion

The AntGEC was preceded by a mound much smaller than the one preceding the formation of GEC-1 (Kizyakov *et al.*, 2015), with heights of 2 and 5–6 m, and the diameter of the base 20 and 45–58 m, respectively.

Both GECs have a similar structure, consisting of a funnel-shaped upper portion and a cylindrical lower portion. Craters are compared with each other using dimensions measured in both field survey and remote sensing. The upper edge diameter of the AntGEC and GEC-1 were the same one year after their formation: about 25–29 m.

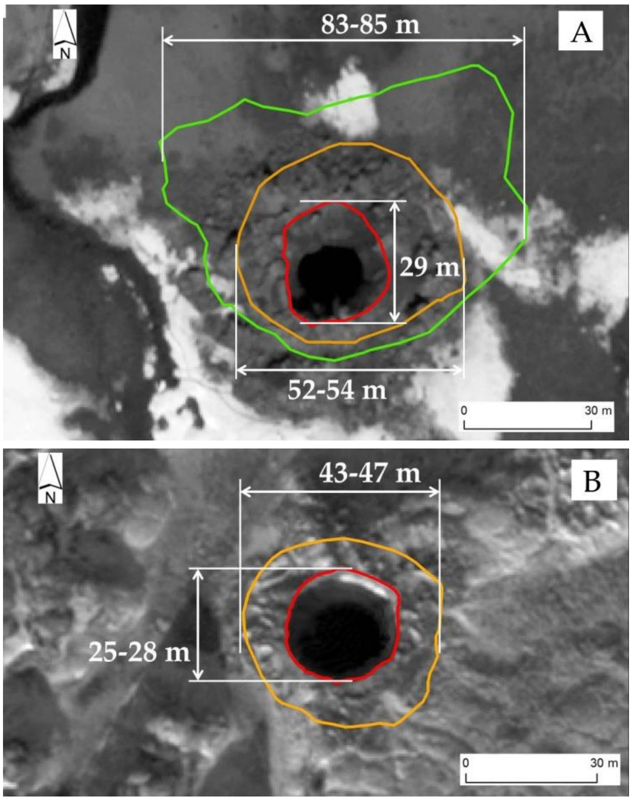

Figure 1. GEC-1 and AntGEC dynamics. (A) position of the GEC-1 upper edge: red line as of 2014-06-15, orange line as of 2015-08-31, green line as of 2016-10-19; (B) position of the AntGEC upper edge: red line as of 2014-10-11, orange line as of 2015-08-31.

Ejected material is found around both landforms. Unlike GEC-1, when calculating the difference between the 2013 and 2014 DEMs of AntGEC key site, areas of accumulation of material with a height of more than 0.9 m (the relative error of the subtraction results of DEMs) have not been identified. The absence of accumulative body can be explained as follows: the ejected material was represented by frozen sand (fairly easily eroded by meltwater and rains) and ice that melted and left traces of sand.

Craters are actively expanding due to the thaw and collapse of frozen icy walls, and are filled with water from melted ground ice, snow accumulating inside the craters in winter, and rainfalls. From 2014 to 2015, the diameter of the GEC-1 increased from 29 to 52–54 m (Figure 1, A). During the same period, the diameter of AntGEC edge increased from 25–28 m to 43–47 m (Figure 1, B). GEC-1 form an irregularly shaped lake, while the AntGEC's inner lake preserved its round shape due to both slowly retreating walls, protected by sandy scree, and the drainage of lake water into a gully nearby.

Conclusions

This study revealed commonalities and differences in the relief position and the geomorphic effects of the Yamal (GEC-1) and Gydan (AntGEC) gas-emission crater formation. Diameter of both GECs increased by 1.7-1.8 times in the first year. Yet their geomorphic position and latest observed lakes shape and size considerably differ.

The formation of both Yamal and Gydan craters was preceded by a mound. However, the dimensions of the mound, predecessor of the Gydan AntGEC was smaller than for the Yamal GEC-1. The search for mounds–predecessors that might indicate the locations of possible future gas emission craters cannot be exclusively based on mound dimensions because of their considerable variations. Indicators to characterize such predecessor mounds are still to be discovered.

Acknowledgments

This work is supported by Russian Science Foundation (RSF) grant No. 16-17-10203.

References

Kizyakov, A.I.; Sonyushkin, A.V.; Leibman, M.O.; Zimin, M.V.; Khomutov, A.V., 2015. Geomorphological conditions of the gas-emission crater and its dynamics in Central Yamal. *Kriosfera Zemli (Earth's Cryosphere)* 2: 13–22.

Kizyakov, A.; Zimin, M.; Sonyushkin, A.; Dvornikov, Y.; Khomutov, A.; Leibman, M., 2017. Comparison of Gas Emission Crater Geomorphodynamics on Yamal and Gydan Peninsulas (Russia), Based on Repeat Very-High-Resolution Stereopairs. *Remote Sensing* 9, 1023; doi:10.3390/rs9101023

Towards understanding the contribution of permafrost waterbodies to methane emissions on a regional scale using aircraft measurements and remote sensing data

Katrin Kohnert[1]
Bennet Juhls[1,2]
Sina Muster[3]
Sofia Antonova[3,4]
Andrei Serafimovich[1]
Stefan Metzger[5,6]
Jörg Hartmann[7]
Torsten Sachs[1]

[1] *GFZ German Research Centre for Geosciences, Telegrafenberg, 14473 Potsdam, Germany, katrin.kohnert@gfz-potsdam.de*

[2] *Now at: Institute for Space Sciences, Department of Earth Sciences, Freie Universität Berlin, Carl-Heinrich-Becker-Weg 6–10, 12165 Berlin, Germany*

[3] *Alfred Wegener Institute, Helmholtz Centre for Polar and Marine Research, 14473 Potsdam, Germany*

[4] *GIScience, Department of Geography, Heidelberg University, Heidelberg, 69120, Germany*

[5] *National Ecological Observatory Network, Battelle, 1685 38th Street, Boulder, CO 80301, USA*

[6] *University of Wisconsin-Madison, Dept. of Atmospheric and Oceanic Sciences, 1225 West Dayton Street, Madison, WI 53706, USA*

[7] *Alfred Wegener Institute Helmholtz Centre for Polar and Marine Research, Am Handelshafen 12, 27570 Bremerhaven, Germany*

Abstract

Waterbodies in the arctic permafrost zone are considered a major source of the greenhouse gas methane (CH_4). Spatial extrapolation of these CH_4 fluxes to a region or the circum-Arctic, however, are still associated with large uncertainties. Here, we address this issue by using a combination of airborne CH_4 flux measurements and waterbody mapping based on TerraSAR-X and Sentinel-1 data across two study areas (1000 km²) in the Mackenzie Delta, Canada. Our results indicate that permafrost waterbodies, even if they seem to be strong emitters on an individual basis, do not necessarily translate into significant CH_4 emission hot spots on a regional scale. Our results show inconsistent patterns in the correlations between waterbody types and the CH_4 flux in the two study areas and across different spatial resolutions. Technical advances enabling the determination of the CH_4 flux of individual waterbodies across a region provide a prospective direction to improve our understanding.

Keywords: airborne eddy-covariance, TerraSAR-X, Sentinel-1, lakes, ponds, CH_4

Introduction

Globally, arctic permafrost lowlands have the highest number of lakes and a large fraction of the terrestrial surface in these regions is covered by waterbodies. Arctic permafrost waterbodies are considered a major source of the greenhouse gas methane (CH_4). However, their contribution to the CH_4 budget of the arctic permafrost zone is not yet well understood, due to spatio-temporal variability of the fluxes and methodological constraints.

By using state-of-the-art technology and data products, this study aims at advancing our understanding of the role of the CH_4 emissions from waterbodies to the CH_4 budget of a region with numerous waterbodies and further to understand the role of the spatial resolution of the CH_4 measurements.

Methods

We based this study (cf. Kohnert *et al.,* submitted 2017) on results from two areas of 1,000 km² each in the Mackenzie Delta, Canada. We derived CH_4 fluxes at a resolution of 100 m from two aircraft eddy-covariance campaigns conducted in the summers of 2012 and 2013 (Kohnert *et al.,* 2017). The CH_4 fluxes were transferred into a high-resolution CH_4 flux map. We combined the flux map with two high spatial resolution (2.5 m) waterbody maps based on TerraSAR-X data from the Permafrost Region Pond and Lake Database PeRL (Muster *et al.,* 2017), cut both data sets to their mutual extent (Fig. 1) and determined the waterbody area for each waterbody within the study areas (Fig. 2). We then categorized the waterbody depths based on Sentinel-1 data utilizing differences in the backscatter signals for floating and grounded ice. Subsequently, we reduced the resolution of the CH_4 flux map to analyze if different spatial resolutions of CH_4 flux data had an effect on the detectability of relationships between waterbody coverage, number, depth, or size and the CH_4 flux.

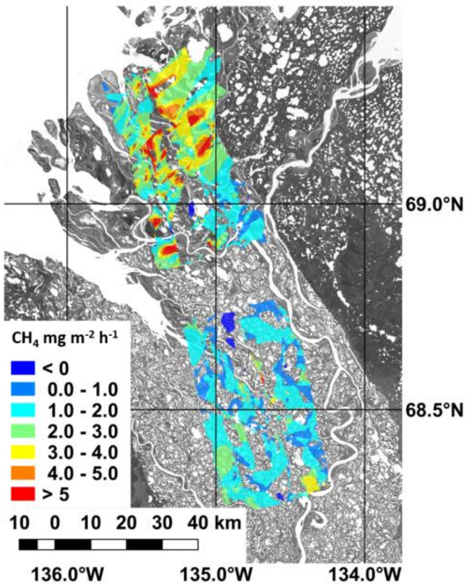

Figure 1. CH_4 fluxes across the study areas.

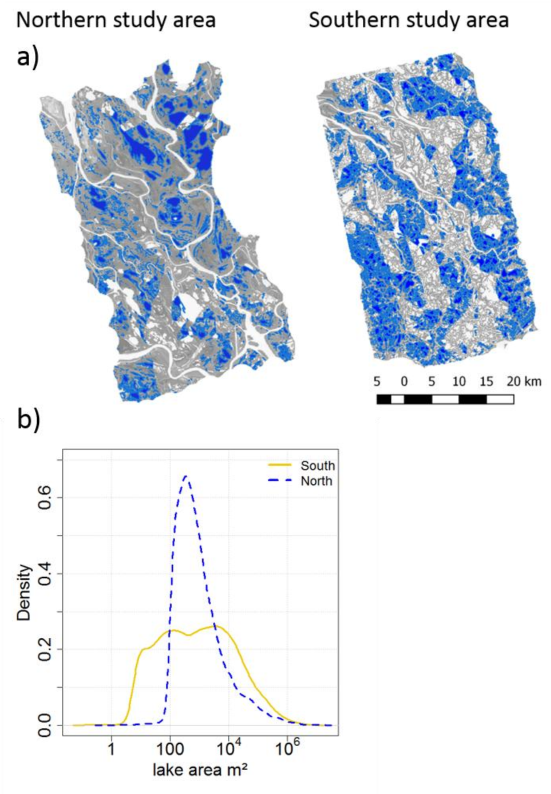

Figure 2. a) Location of included waterbodies and b) their size distribution for the northern (6,784 waterbodies) and southern (10,273 waterbodies) study area.

Results and Discussion

Our results indicate that while waterbodies may be strong emitters on an individual basis, they do not necessarily appear as significant CH_4 hot spots on a regional scale.

We did not find consistent correlations between waterbody types and the CH_4 flux in the two study areas across the different resolutions.

In the northern study area the number of small or shallow waterbodies was weakly positively correlated with the CH_4 flux, while there was no correlation in the southern study area.

The CH_4 emissions were not significantly larger above waterbodies than above terrestrial surface.

We propose determining object-level CH_4 emissions for individual waterbodies across areas similar in size to the present study in order to better understand how their spatial patterning might feed into circum-arctic or global estimates. This necessitates low measurement heights which come within reach e.g. through advances in drone technology.

Acknowledgments

This work was supported by the Helmholtz Association of German Research Centres (T.S.: grant VH-NG-821; Sina M.: grant VH-NG 203), and by the National Science Foundation (Stefan M.: grant DBI-0752017).

References

Kohnert, K., Juhls, B., Muster, S., Antonova, S., Serafimovich, A., Metzger, S., Hartmann, J. & Sachs, T., submitted 2017. *Towards understanding the contribution of waterbodies to the methane emissions of a permafrost landscape on a regional scale – A case study from the Mackenzie Delta, Canada.*

Kohnert, K., Serafimovich, A., Metzger, S., Hartmann, J., & Sachs, T., 2017. Strong geologic methane emissions from discontinuous terrestrial permafrost in the Mackenzie Delta, Canada. *Scientific Reports*, 7, 5828.

Muster, S., Roth, K., Langer, M., *et al.,* 2017. PeRL: A circum-Arctic Permafrost Region Pond and Lake Database. *Earth System Science Data*, 9, 317-348.

The Permafrost Information System PerSys – An Open Access geospatial data dissemination and visualization portal for products from ESA DUE GlobPermafrost

Sebastian Laboor[1], Guido Grosse[1], Sina Muster[1], Birgit Heim[1], Antonie Haas[1], Christian Schaefer-Neth[1], Ingmar Nitze[1], Annett Bartsch[2], Kirsten Elger[3]

[1] *Department of Periglacial Research, Alfred Wegener Institute Helmholtz Centre for Polar and Marine Research, Germany, sebastian.laboor@awi.de*
[2] *ZAMG Zentralanstalt für Meteorologie und Geodynamik, Vienna, Austria,*
[3] *Helmholtz Centre Potsdam - GFZ German Research Centre for Geosciences, Potsdam, Germany*

Abstract

The objective of the GlobPermafrost Project (2016-2019) initiated by the European Space Agency (ESA) is to better understand the global impact of changes in permafrost by providing earth observation data for the science community. For this purpose, various remote sensing products on the subject of permafrost are developed, discussed and optimized with the users of these products. The Permafrost Information System (PerSys) was developed for the user-friendly provision and visualization of these data products and is part of the Arctic Permafrost Geospatial Center (APGC). The PerSys Data Catalogue allows users to conveniently search for permafrost related datasets, obtain descriptions and previews, receive information on data prototypes and download the final published data products. The PerSys WebGIS provides detailed visualizations of the data products and their attributes and enables users to compare and combine several datasets.

Keywords: Permafrost Information System, ESA GlobPermafrost, Remote Sensing, Data Catalogue, WebGIS

Introduction

Permafrost is an important component of the Cryosphere, which is affected by rapid warming of the Arctic. The degradation and thaw of permafrost in vertical as well as lateral directions results in a reduction of permafrost in high latitudes and high altitudes. Since permafrost affects the ecosystem conditions of the about 23 million square kilometer large permafrost region, its loss has strong effects on hydrology, geomorphology, biogeochemistry, and biota. Remote sensing has become an essential tool for quantitatively detecting and monitoring changes in permafrost and associated landscapes over large regions and with repeated observations.

Remote sensing based products for the permafrost region are quickly growing in numbers. However, different storage locations, formats and observation targets pose a challenge for the usability of valuable datasets. The European Space Agency (ESA) has supported permafrost-focused remote sensing activities in two recent projects, ESA DUE Permafrost (2009-2012) and ESA DUE GlobPermafrost (2016-2019; http://www.globpermafrost.info). The ESA DUE Permafrost project with spatial coverage of the northern hemisphere developed, validated and implemented earth observation to support research communities and international organizations in their work on better understanding permafrost characteristics and dynamics. Now, the GlobPermafrost project expands on this successful approach by including both polar hemispheres as well as mountain permafrost regions.

Here we present the Permafrost Information System (PerSys), which combines a comprehensive data catalogue and a state-of-the art WebGIS within the framework of the ESA DUE GlobPermafrost project.

.

ESA GlobPermafrost Products

Products in GlobPermafrost cover different aspects of permafrost by integrating in-situ measurements of subsurface properties and surface properties, earth observation, and modelling. Currently, the GlobPermafrost team is creating prototype datasets for defined remote sensing derived products and targeting various user groups across 5 broad themes: permafrost extent, permafrost-specific land cover classes, hotspot regions of permafrost change, local sites of high research interest in the user community (“cold spots”), and mountain permafrost (see Table 1). Registered users are able to assess the usability and validity of the products and provide feedback to the GlobPermafrost team. The feedback of the user groups is used to improve the developed remote sensing products.

Table 1. GlobPermafrost products.

Product	Example Datasets
Coldspot	Bedfast (Grounded) Lake Ice from Sentinel-1A
	Land Cover Classification from TerraSAR-X
Hotspot Region of Permafrost Change	Trends of land surface change from Landsat time-series 1999-2014
Land Cover Prototype	Land Cover Prototype Wetness Level
	Land Cover Prototype Shrub Height
	Winter Backscatter Classes from Sentinel-1
	Land Cover Classification from Sentinel-1 and Sentinel-2
Mountain Permafrost	Rockglacier Inventory with Indication of the State-of-activity
	InSAR-derived Surface Deformation Map
Permafrost Extent and Properties	Ground Temperature Map of the Northern Hemisphere Permafrost Region

Permafrost Information System

To bring the resulting data products closer to the permafrost user communities, the Permafrost Information System (PerSys) has been conceptualized as an open access geospatial data dissemination and visualization portal for remote sensing derived datasets produced within the GlobPermafrost project. The prototype and final remote sensing products and their metadata will be visualized in the PerSys WebGIS and described via the PerSys Data Catalogue. The WebGIS visualization is managed via the AWI WebGIS infrastructure maps@awi (http://maps.awi.de) relying on OGC-standardized Web Mapping Service (WMS) and Web Feature Service (WFS) technologies for data display and visualization. The PerSys WebGIS projects allow visualization of raster and vector products such as land cover classification, Landsat multispectral index trend datasets, lake and wetland extents, InSAR-based land surface deformation maps, rock glacier velocity fields, spatially distributed permafrost model outputs, and land surface temperature datasets. Each of these WebGIS projects is adapted to the spatial scale of the specific products, ranging from local to hemispherical coverage. The PerSys Data Catalogue provides metadata and access to all mature-state and final-state GlobPermafrost products.

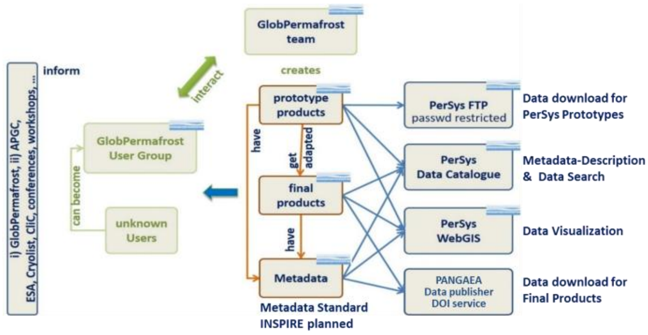

Figure 1. PerSys conception.

PerSys can be accessed through the GlobPermafrost project webpage. PerSys is also a core component of the Arctic Permafrost Geospatial Center (APGC), a geodata portal for permafrost launched within the framework of the ERC PETA-CARB project at the Alfred Wegener Institute Helmholtz Centre for Polar- and Marine Research. The APGC framework features a range of permafrost-specific geospatial data projects, including PerSys, and will allow searching for project-specific geospatial data by tags, keywords, data type and format, licence type, or by location. PerSys is available within APGC since early 2017.

In addition, the Open Access data library PANGAEA, as a certified member of The International Council for Science (ICSU), serves as permanent archive for the GlobPermafrost final products, providing permanent Digital Object Identifiers (DOIs) for each archived dataset. The ESA DUE Permafrost final products are already published in PANGAEA under DOI doi:10.1594/PANGAEA.780111.

The final GlobPermafrost remote sensing products published in PANGAEA will remain visualized in the PerSys WebGIS and catalogued, searchable and accessible via the PerSys Data Catalogue.

Acknowledgments

This work was supported by the European Space Agency project DUE GlobPermafrost (Contract Number 4000116196/15/I-NB) as well as ERC PETA-CARB #338335.

Relief and vegetation patterns in connection with permafrost features in Lena Delta (Eastern Siberia)

Nikolay N. Lashchinskiy[1]
Andrey Kartozia[2]
[1]*Central Siberian Botanical Garden SD RAS, Novosibirsk, Russia, nnl630090@gmail.com*
[2] *Sobolev Institute of Geology and Mineralogy SB RAS, Novosibirsk, Russia.*

Abstract

Two islands in Lena river delta (72˚N 126˚E) were examined by geobotanical and geomorphological ground research followed by very detailed drone images (5 cm per pixel) and digital elevation model (DEM) created by photogrammetry. Five main surfaces could be distinguished by elevation, origin and geological substrate: floodplain, first river terrace, second river terrace, third river terrace and bed rock outcrops. Four of them (except of the second terrace) were examined with drone images (5 cm per pixel) and ground research. Each surface characterized by specific set of plant communities depending on active layer deepness and microrelief features made by permafrost and ice wedges.

Keywords: Lena Delta, ice wedges, polygonal structures, shrubby tundra, tussock tundra.

Introduction

Tundra ecosystems and permafrost are highly sensitive to climate change (Anisimov et al., 2002). Warmer temperatures can have severe consequences on permafrost degradation and respectively on relief and vegetation development (Osterkamp & Romanovsky, 1999). Detailed characteristics of relief and vegetation formation in permafrost regions based on remote sensing data can provide good basis for the prognosis of permafrost ecosystems development.

Two islands in Lena river delta (72˚N 126˚E) were examined by geobotanical and geomorphological ground research followed by detailed drone images (5 cm per pixel) and digital elevation model (DEM) created by photogrammetry. First was a small island Samoylov (2 x 2 km) and second one was southern part of Kurungnakh island (about the same size as first island). Initially on the drone image all visible geomorphological and vegetation contours were determined and classified. In field vegetation was carefully described on 260 sample plots 10 to 10 meters. Vegetation data were classified and united into mapped units (complexes or associations).

Every geomorphological contour was characterized by microrelief features with their detailed morphometric characteristics, calculated from remote sensing data. In addition, slope orientation and inclination was calculated for the all microrelief features. Thickness of an active layer was measured at the end of August by metal stick in 300 points.

Results

Previously (Grigoriev, 1993; Schwamborn *at al.*, 2002) five main geomorphological surfaces were recognized in Lena delta: floodplain, sequence of three river terraces and bedrock outcrops. All of them differ by elevation, age, origin and surface geological substrate. In an area of our research there are only four of them. We grouped all our data in clusters according to these main surfaces.

On the floodplain, elevated above lowest water level about 1-2 m, active layer was deep enough (from 80 to 110 cm) to influence surface microrelief formation. Relief was mostly flat with few low ridges and channels made by the temporary streams. In terms of vegetation, there is clear sequence of plant communities representing few stages of primary succession depending on the distance from the main channel and longevity of flooding. First stage occupied an area about 10 – 15 m from the riverbank. It is sand beach without any plants and quite often with aeolian microrelif. It is flooded most part of the year and consists of pure sand. Active layer is more than 100cm. Second stage covered an area between 15 and 40 m from the riverbank. It occupied by pioneer communities of *Deschampsia borealis*, *Eriophorum scheuchzeri* and *Equisetum arvense*. Microrelief is flat and surface substrate consists of sand and fine silt. Third stage spread over the rest of floodplain. Its vegetation depends on relief forms – main area on flat surfaces covered by willow shrubs (*Salix glauca*) with sparse herbs coverage dominanted by *Equisetum arvense*; on the top of low ridges – willow shrub communities (*Salix glauca* and *S.alaxensis*) with rich herbaceous layer; in hollows there are sage fens (*Carex stans*) and *Eriophorum* fens. In depressions close to the riverbank, there are small creeks and oxbows with water vegetation. Indicator species for this surface could be few pioneers: *Cardaminopsis petrea, Descurainia sophyoides*, *Eriophorum scheuchzeri* etc.

First terrace elevated at 4 – 6 m above lowest water level. There are few big logs transported by river on this surface as a sign of periodic floods. Surface geological substrate is a mixture of fine send layers and thin layers of coarse organic detritus. Relief mostly flat with few thermocarst lakes and elongated shallow depressions (probably former channels). Active layer is from 10 to 30 cm in dependence of microrelief features. Microrelief is well developed and represented by polygonal net of ice wedges. Three main types of polygons could be distinguished by form. First – tetragonal polygons about 10 to 10 m in rows more or less parallel to the riverbank. Second – penta- or hexagonal polygons of the same size not oriented. Third – tetragonal polygons 20 to 10 meters oriented across shallow elongated drainages. Among all these types high- and low-centered polygons could be found with small water bodies inside or relatively dry tundra. Vegetation is highly complex. Polygon rims covered by moss tundra with *Hylocomium splendens var. obtusifolia* mixed with *Tomenthypnum nitens* and *Aulacomnium turgidum*. Polygon vegetation depends on water level and varies from open water with few aquatic plants to different types of water vegetation, green moss bogs and wet tundra nearly the same as on the rims. Actually all plant associations of this complex could be arranged in one successional sequence depending on water content. Indicator species for this surface could be *Carex stans*. It occurs on all surfaces but only on the first terrace is very active with high frequency and abundance.

Third terrace occurs only on Kurungnakh island. It is elevated about 30 to 50 m above the lowest water level and from the surface consists of so-called ice-complex – mixture of fine loam and syngenetic ice wedges of a big size. Relief is slightly wavy with numerous thermocarst lakes alive and dried out, pingos, creeks and valleys. Polygonal structures on the surface are nearly invisible in field but could be distinguished on drone images. They are of comparable size with polygons on the first terrace. Active layer is about 30 to 40 cm. Main vegetation type on flat drained surfaces is tussock tundra with *Eriophorum vaginatum* as main dominant. On gentle slopes shrubby tundra with *Betula exilis* is widespread and willow shrubs with *Salix glauca* grow on slopes with long lasting snow. The most diverse vegetation is in former lake depressions (alas). It is polygonal complex of water vegetation, sedge fens, green moss swamps and wet tundra. Tussock nanorelief on flat surfaces consists of tussocks from 60 up to 100 cm in diameter and 0,3 - 0,5 meter height. Because of these tussocks, it is difficult to see big polygons. No any differences in vegetation connected with big polygons. Plant indicators of this surface are main dominants of zonal tundra - *Betula exilis* and *Eriophorum vaginatum*. They are absent on floodplain and bedrock outcrops and quite rare on the first terrace.

Bedrock outcrops occurs also only on Kurungnakh island and on mainland. Their elevation could be up to 100 m above sea level. Soil is gravelly and shallow. Thickness of an active layer is not possible to measure by metal stick because on the depth of 3 – 5 cm soil underlined by continuous bedrock. General relief is hilly with slopes, hilltops and galleys. In nanorelief there are many signs of an active cryoturbations. On slopes solifluction terraces are well developed. No any polygonal structures were found. Typical vegetation here is shrubby tundra with *Dryas spp.* and lichen tundra with *Alectoria spp.*, *Cetraria spp.* and *Cladonia spp.* The main indicator plant is *Novosiversia glacialis,* which could be find only on stony or gravelly soil.

Conclusion

Specific plant associations could characterize all main surfaces in Lena delta. In its turn, vegetation depends on active layer thickness and ice wedges development. Actual vegetation diversity supported by processes of permafrost degradation and connected with microrelief formation. Different types of interconnected relief-vegetation complexes could be distinguished on drone images. This set of data is a good basis for the interpretation of satellite images with different resolution.

Acknowledgments

This work has been supported by the grant for the integrated research No. 289 (2018-2020) funded by SD RAS. We also very thankful to Igor Eltsov – director of Trofimuk Institute of Petroleum Geology and Geophysics, Novosibirsk and to Waldemar Schneider – AWI – Potsdam for the organization support of our research on different steps.

References

Anisimov, O.A., A.A. Velichko, P.F. Demchenko, A.V. Eliseev, I.I. Mokhov, and V.P. Nechaev, 2002: Effect of climate change on permafrost in the past, present, and future, Izvestiya, Atmospheric and Oceanic Physics, 38(1): 25-39.

Grigoriev, M.N., 1993. Cryomorphogenesis of the Lena River mouth. Permafrost Institute Press, Yakutsk 176 pp.

Osterkamp, T.E. and V.E. Romanovsky ,1999. Evidence for warming and thawing of discontinuous permafrost in Alaska, Permafrost and Periglacial Processes, 10, 17-37.

Schwamborn, G., V. Rachold, and M.N. Grigoriev, 2002: Late quaternary sedimentation history of the Lena Delta, Quaternary International, 89: 119-134.

CHAMONIX Mont-Blanc EUCOP5
23 June - 1st July 2018

Automated mapping of landforms in high Arctic mountains

Huw Mithan[1]
Tristram Hales[1]
Peter Cleall[2]

[1]*Cardiff University School of Earth and Ocean Sciences, huwmithan@gmail.com*
[2]*Cardiff University School of Engineering*

Abstract

Given the challenge of gathering topographic and remotely sensed data in the Arctic, we lack a basic understanding of the spatial extent of landforms. Quantifying the relationship between topography and landform process is a key challenge for periglacial geomorphologists. The effects of future climate warming on hazards and hillslope sediment fluxes depends on identifying regionally extensive periglacial landforms that are susceptible to warmer climates. To address this, we created a generalised landform classification model and used it to successfully classify landscapes in Svalbard and Alaska. We found that solifluction and scree slope development are the dominant hillslope processes acting on these landscapes and therefore should be the focus of future research.

Keywords: Landscape classification; Machine learning; Mapping; Periglacial; Scree; Solifluction.

Introduction

Being able to automate the classification of remote landscapes can provide valuable contributions to applied research (Harris *et al.*, 2001). Automated analysis of digital elevation models (DEMs) has provided a significantly improved understanding of the genesis and processes in temperate regions (Prima *et al.,* 2006). Areas of permafrost and periglacial landforms have received less research than warmer landscapes. Most classifications of the distribution of periglacial landforms tend to focus on one or a small number of processes and/or combining topographic data with climatic data and satellite-based imagery (Aalto *et al.,* 2014). I seek to develop a more generalised methodology, where I attempt to understand the spatial distribution of the major non-glacial geomorphic processes acting on a mountainous Arctic landscape.

Methods

We developed a landform classification model that uses a combination of three digital elevation model (DEM) derived topographic parameters; (i) slope gradient, (ii) relative local relief, and (iii) topographic roughness, to best model the spatial distribution of seven landforms found in mountainous arctic environments; Allochthonus material, alluvial fan, bedrock, blockfield, braided river, scree, and solifluction.

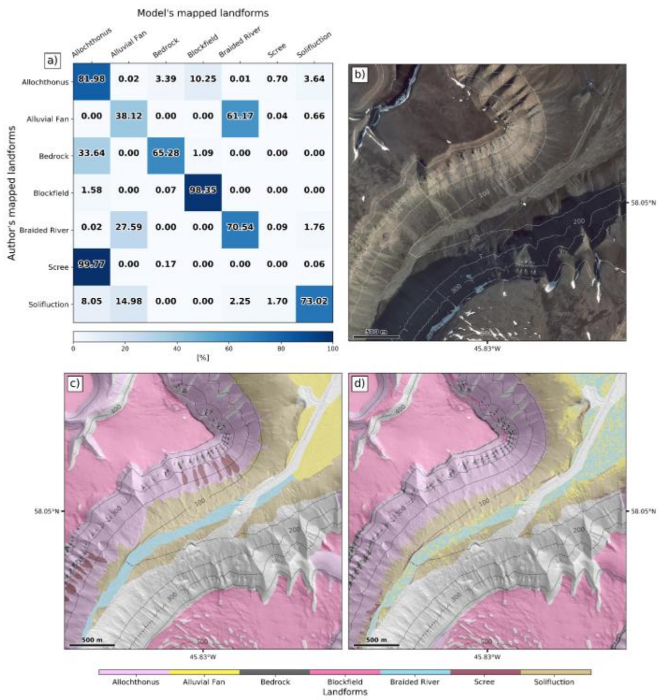

Figure 1. Endalen. a) confusion matrix, b) satellite map, and c) author's map, d) model's map. Maps underlain with hillshade. Grey areas represent no data.

We trained a linear discriminant analysis (LDA) classifier using mapped landform polygons from Endalen and Adventdalen, Svalbard. Using the extracted topographic parameter pixel values for each landform, we ran the LDA classifier on a training dataset composed of 70% of the pixel values, and validated it on the remaining 30%. Using a 10km² 5-meter DEM for Endalen (Fig. 1) and Ringdalen (Fig. 2) on Svalbard and a 10km² 5-meter DEM for Saviukviayak (Fig. 3), in Alaska, we applied the model using the parameter values extracted from Svalbard.

To evaluate the quality of the classifier we compared a geomorphology map, manually created by the authors, to the corresponding modelled map using a confusion matrix. The diagonal elements of the confusion matrix represent the percentage of correct pixel classifications in the model. The off diagonal represents the percentage of misclassifications. We assessed the general quality by using an overall accuracy score, which is the percentage of correct predictions over the number of landforms.

Results and discussion

Endalen, Ringdalen, Saviukviayak had overall accuracies of 81.69, 76.63, 17.44% respectively. Bedrock, blockfields, and solifluction were identified with a high degree of accuracy (Fig. 1), with bedrock outcrops modelled at a greater resolution than was possible to map using satellite imagery (Fig. 1). Interestingly, scree slopes were difficult to separate from the ubiquitous vegetated allochthonus slopes (Fig 3.), suggesting a similar genesis for these landforms. When we pool allochthonus and scree classifications, the overall Saviukviayak model accuracy increases to 70.32%.

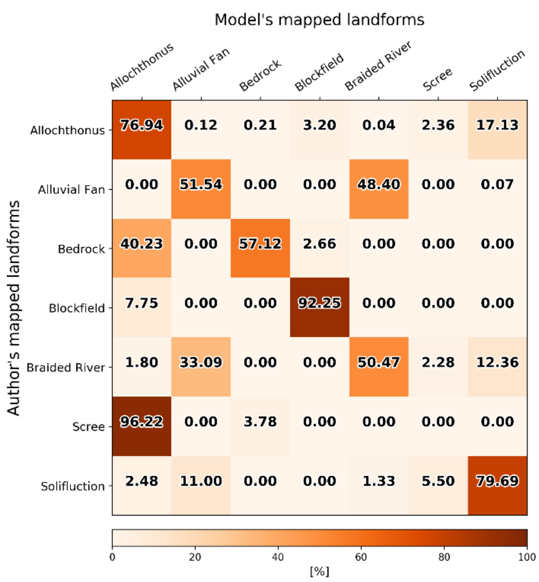

Figure 2. Ringdalen confusion matrix.

The models demonstrated that, solifluction and scree slope development are the dominant hillslope processes acting on these landscape, showing just how useful its application can be for assessing the impact of a warming arctic on the future spatial extent of periglacial/permafrost related landforms. Fluvial landforms were more consistently difficult to separate. We successfully used the classifier in Saviukviayak as in Ringdalen and Endalen, it suggesting that processes that generate similar topography, regardless of the specific geography, govern landforms in Arctic mountains. Furthermore, the success of the classification across mountains that form in different climatic and tectonic settings, although with similar lithologies, suggests that topography can provide a useful first-order tool for understanding the distribution of Arctic landforms.

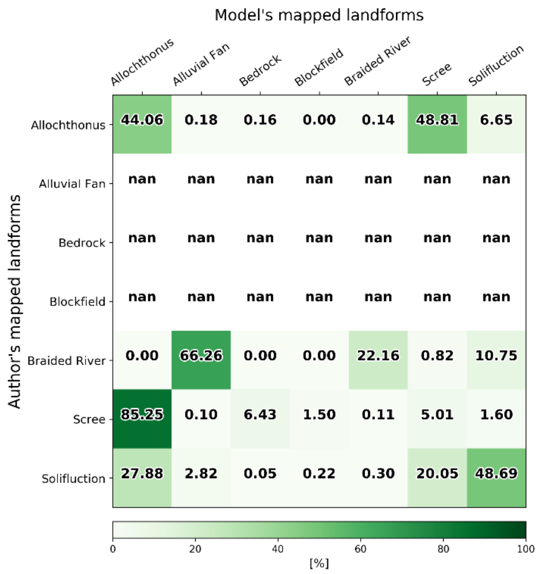

Figure 3. Saviukviayak confusion matrix. 'Nan' represents landforms not mapped by the authors.

Conclusion

Our generalised classification model successfully classified multiple periglacial landforms across different geographic regions.

References

Aalto, J., Venäläinen, A., Heikkinen, R. & Luoto, M. 2014. Potential for extreme loss in high-latitude Earth surface processes due to climate change. *Geophysical Research Letters 41*(11), pp. 3914-3924.

Harris, C., Rea, B. & Davies, M. 2001. Scaled physical modelling of mass movement processes on thawing slopes. *Permafrost and Periglacial Processes* 12(1), pp. 125-135.

Prima, O., Echigo, A., Yokoyama, R. & Yoshida, T. 2006. Supervised landform classification of Northeast Honshu from DEM-derived thematic maps. *Geomorphology* 78(3-4), pp. 373-386.

Remote sensing of landscape dynamics of the Zapolyarnoye gas field

Mikhail Dmitrievich Moskovchenko[1]
[1]Tyumen State University, simonreise@rambler.ru

Abstract

The article analyzes the landscape dynamics of Zapolyarnoye gas field (Western Siberia). Based on the analyses of Landsat images spanning more than 30 years, changes of indicator parameters (area of lakes, antropogenic disturbances, burnt lands) were estimated and compared with climate changes. The area of thermokarst lakes increased depending on the growth of precipitation. There is no evidence of extensive thermoerosion processes that indicates a low level of ground ice and the insufficient transformation of thermal regime.

Keywords: West Siberia; forest-tundra zone; landscape dynamics; Zapolyarnoye field; satellite images.

Introduction

The changes of geocryological conditions often occur under anthropogenic influence. Disturbance of vegetation leads to transformation of the thermal regime of soils, activation of thermal erosion. Therefore, it is extremely important to determine the degree of disturbance of permafrost zone landscapes in areas of intensive industrial impact.

Zapolyarnoye gas field is being developed since 2001 and nowadays it is the largest in Russia by amount of gas production (http://www.gazprom.com). It is located at Pur-Taz watershed, the north of Western Siberia (Fig.1). According to the georcyological zonation, Zapolyarnoye field is located at the south of continuous permafrost zone.

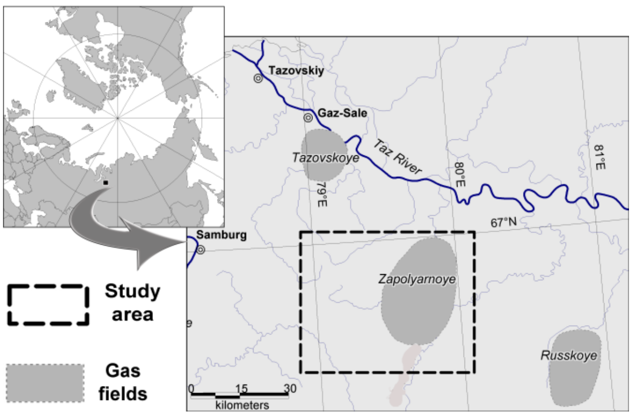

Fig.1. Study area

On the site chosen for the study most of facilities of the Zapolyarnoye field are located, as well as various types of undisturbed ecosystems. The objective of this study was to examine trends of landscape dynamics and to assess of possible future changes in geocryological condition under the anthropogenic impact and influence of climate changes.

Materials and methods

The study was carried out by remote sensing methods by processing of multispectral Landsat satellite images taken during the 1973 – 2016 mid-summer season (https://landsatlook.usgs.gov). ENVI 5.2 software package was used for the image processing. Determination of landscape dynamics was carried out using indicator objects that are easy to recognize on satellite images. We calculated the area of thermokarst lakes, burnt lands, anthropogenic disturbances. Then, the changes in the area of indicator objects were compared with the dynamics of climate parameters, such as precipitation and mean air temperature.

We were also interested in how peat fires affect vegetation and geocryological condition. The tundra fires may induce widespread thaw subsidence of permafrost terrain (Jones et al., 2015). The change in the thermal regime of soils can be estimated by the change of phytomass. Based on the assumption that the greenness of the scene is a good indicator of thermal regime stabilization, we have calculated average values of the normalized difference vegetation index (NDVI).

Results and discussion

Dynamics of lakes

The dynamics of lakes are often used to assess changes in geocryological conditions. The analysis of satelite imagery reveals a widespread decline in lake abundance and area in the Siberia; and spatial pattern of lake disappearence strongly suggest that thawing of permafrost is driving the observed losses (Smith *et al.*, 2005). It was noted that in West Siberia drainage of lakes was most active in the southern tundra and forest-tundra (Bryksina & Kirpotin, 2012).

However, the results of images processing revealed that the area of lakes in Zapolyarnoye field has increased. In 1973 lakes occupied 2.5% of the territory of the site, but in 2016 it was 3.5% (Fig.2). A comparison with the meteorological data showed that the total area of lakes (% of terrain) correlates with precipitation during the previous half-year (r = 0.57).

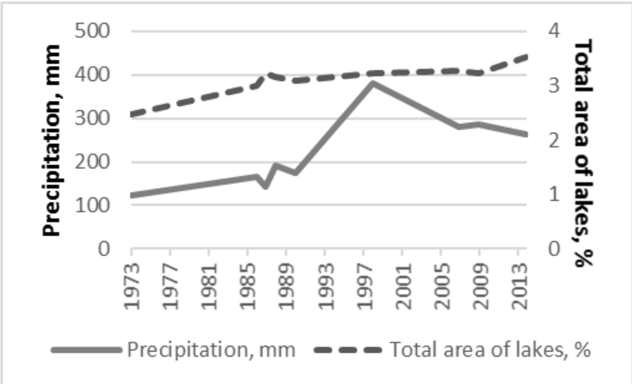

Fig.2. Area of lakes and the total amount of precipitation during the previous half-year

A more detailed examination of satellite images revealed the appearance of lakes as result of flooding of previously drained thermokarst lakes and sand pits. Thus, the changes are not generally linked to permafrost degradation processes.

Dynamics of vegetation after fires

The processing of Landsat images showed that fire is the one of the prominent disturbance factor. Overall, the satellite images show that in the period of about 45 years over 17% of this area was burned.

The rate of vegetation recovery and stabilization of thermal regime of the ground depends on the area of the fire. Large-scale fires (several thousand hectares) stay visible on the satellite images of 20 years or more. Fires significantly reduce values of the NDVI. However, our observations not show widespread permafrost degradation and associated terrain subsidence began after the tundra fires.

Anthropogenic disturbances

Satellite–based measurements of disturbance indicates that road and pipeline network, area of drill pads and gas pumping stations has grown linearly between 1990-2007. Total area of disturbances increased by 3800 ha (4.5% of the territory). Disturbances and peat fires caused to increase of dwarf birch and moss tundra area and to decrease of lichen tundra area.

Conclusions

Drainage of thermokarst lakes, which is currently inherent in the forest-tundra landscapes of Western Siberia, is almost absent on this territory. Results of this study have shown that the area of lakes showed an increasing trend (2.5% to 3,5%) from 1973 to 2016. Analysis of meteorological data suggests good correlation between lake area and increasing precipitation.

References

Bryksina, N.A. & Kirpotin S.N., 2012. Landscape-space analysis of change of thermokarst lakes area and numbers in the permafrost zone of West Siberia *Bulletin of Tomsk State University. Biology* 4 (20): 185-194.

Jones, B.M., Grosse, G, Christopher D. Arp, C.D et al.,2015. Recent Arctic tundra fire initiates widespread thermokarst development // Scientific Reports | 5:15865 | DOI: 10.1038/srep15865

Smith, L.C. Sheng Y, MacDonald G.M. Hinzman L.D., 2005. Disappearing Arctic Lakes *Science* V. 308, Issue 5727:1429. http://www.gazprom.com/about/production/projects/deposits/zm/
https://landsatlook.usgs.gov/

The Importance of L-Frequency SAR Volume Scattering On Lowland Tundra in the Arctic

Reginald R. Muskett
Geophysical Institute, University of Alaska Fairbanks, AK, USA,
rrmuskett@alaska.edu

Abstract

Geodetic methods to measure centimeter to millimeter-scale changes using aircraft- and spacecraft deployed Synthetic Aperture RADAR cannot ignore volume scattering. Backscatter and coherence at L-frequency and others possess both surface and volumetric scattering. On lowland tundra underlain by permafrost volume scattering is dominant. Measurement of the L-frequency penetration depth for evaluation of mass change (loss and transport) through permafrost thaw-degradation with erosion is necessary. Data from the NASA Ice, Cloud, and land Elevation Satellite Geoscience Laser Altimeter System (ICESat GLAS), JAXA Advanced Land Observing Satellite Phased Array type L-band Synthetic Aperture RADAR (ALOS PALSAR), aircraft-deployed NASA L-band UAVSAR and in-situ observations are employed. Collocation of ICESat GLAS exact-repeat profiles for elevation change (surface scattering) with PALSAR InSAR Line-Of-Sight changes and UAVSAR Polarimetry Cross-Pole HHVV confirms the dominance of volume scattering on lowland tundra and surface scattering on river channel deposits and rock outcrops.

Keywords: RADAR; SAR; Interferometry; Polarimetry; Arctic; Permafrost.

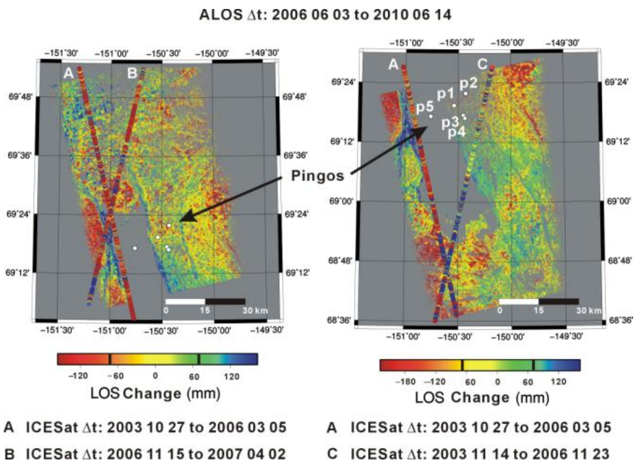

Figure 1. Colocated ALOS PALSAR Line-Of-Sight (LOS) change maps with ICESat GLAS elevation change profiles (A – C) on the Anaktovuk wildfire scar (July-Sept. 2007). Pingos are numbered P1 through P5. Black bars on the LOS scale indicate the total error, 74 mm, of PALSAR. GLAS total error is less than 20 mm.

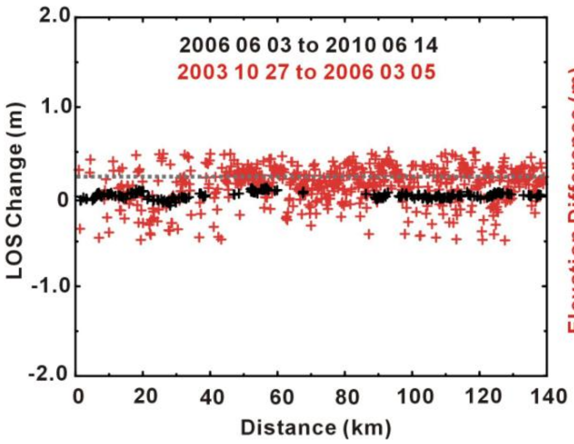

Figure 2. Colocated PALSAR LOS changes (black) to GLAS elevation changes (red) along profile A in Figure 1. Dashed line is the average snow thickness change at Umiat and Franklin Bluffs stations. GLAS elevation changes are due to surface scattering on snow whereas PALSAR LOS changes are due to volume scattering (snow, vegetation and soil volumes).

Acknowledgments

I thank the Jet Propulsion Laboratory, California Institute of Technology, NASA programs and facilities including the Arctic-Boreal Vulnerability Experiment, Earth Airborne Science Program, NASA-India SAR mission workshops, Ames Research Center, Armstrong Flight Center and Goddard Space Flight Center. I thank the National Snow and Ice Data Center for providing the Ice, Cloud and land Elevation Satellite (ICESat) Geoscience Laser Altimeter System (GLAS) datasets. I thank the Department of Energy Next-Generation Ecosystem Experiment – Arctic. I thank the Japanese Space Exploration Agency Earth Observation Center and the Alaska Satellite Facility for providing the ALOS PALSAR datasets. I thank the State of Alaska, the National Geospatial-Intelligence Agency DOD, Digital Globe, the Polar Geospatial Center University of Minnosota, the National Science Foundation and the US Department of Interior. I thank Vladimir E. Romanovsky and Go Iwahana University of Alaska Fairbanks. Funding grant NASA NNX17AC57A.

References

Muskett, R.R. (2015), ICESat GLAS Elevation Changes and ALOS PALSAR InSAR Line-Of-Sight Changes on the Continuous Permafrost Zone of the North Slope, Alaska. International Journal of Geosciences, 6 (10), 1101-1115. doi:10.4236/ijg.2015.610086 http://www.scirp.org/Journal/PaperDownload.aspx?paperID=60406

Muskett, R.R. (2017), L-Band InSAR Penetration Depth Experiment, North Slope Alaska. Geoscience and Environment Protection, 5 (3), 14-30. doi: 10.4236/gep.2017.53002.

Determine spatial distribution of methane in Arctic permafrost with an unmanned aerial system and an off-the-shelf methane sensor

Ferdinand K. J. Oberle[1]
Bruce Richmond[1]
Thomas Lorenson[1]
Peter W. Swarzenski [2]
[1]U.S. Geological Survey, Pacific Coastal and Marine Science Center, Santa Cruz, CA 95060, USA foberle@usgs.gov
[2]International Atomic Energy Agency, Monaco, 98000 Principality of Monaco

Abstract

Arctic permafrost encapsulates vast amounts of methane (CH_4) in subsurface reservoirs. Thawing permafrost opens pathways for this CH_4 to migrate to the surface. Identifying these pathways on a local scale is limited with regard to spatial coverage using traditional ground based or satellite based methane-sampling methods. Here we present an easily replicable design using only off-the-shelf cost effective methane sensor components and an Unmanned Aerial System (UAS). Our results demonstrate the high efficiency of the design and the necessity to integrate this methodology into environmental methane studies due to the high spatial variability of methane levels. On Barter Island, North Slope Alaska, we identified methane pathways through thawing coastal permafrost. These pathways represent hotspots that release significantly higher levels of methane than the surrounding areas, thus suggesting that point sampling is inadequate in characterizing methane releases and that increasing rates of permafrost thaw may result in increasing rates of trapped CH_4 emissions.

Keywords: Methane; permafrost; UAS; pathways; North Slope Alaska; sensor

Introduction

The arctic permafrost coast belongs to some of the most dramatically changing environments in the world. Despite the fact that 34% of Earth's coasts consist of permafrost (Lantuit et al. 2012), the processes that drive change along these coastlines are still poorly understood (Günther et al. 2013; Wobus et al. 2011). The combined effect of declining Arctic Ocean summer/early fall sea-ice cover, longer and warmer thawing seasons, reduced thermal insulations, and rising sea levels allow waves to hit the coast at higher elevations and more frequently (Fritz et al. 2017). Erosion rates appear to be increasing along some sections of the coast (e.g., Jones et al. 2009) with erosion rates up to 25m/year (Gibbs & Richmond 2017). This has resulted in an annual flux of 14 Tg of particulate organic carbon into the coastal ocean (Wegner et al. 2015) with equal or higher magnitude of net methane (CH_4) emissions from terrestrial permafrost (Schuur et al. 2015; Koven et al. 2011).

While it is known that thawing permafrost builds new pathways for methane emissions, the identification of these pathways using traditional ground based or satellite based methane-sampling methods has been challenging (Kohnert et al. 2017). Yet, specifically on a local scale, the identification of the pathways is pivotal for accurate methane measurements. Our first results from Barter Island, AK utilizing an off-the-shelf cost effective UAS design, show that spatial methane distribution is likely linked with areas of high permafrost thaw and meltwater runoff pathways. We also present detailed instructions on the components of the UAS to allow for easy replication of the methane sensor system.

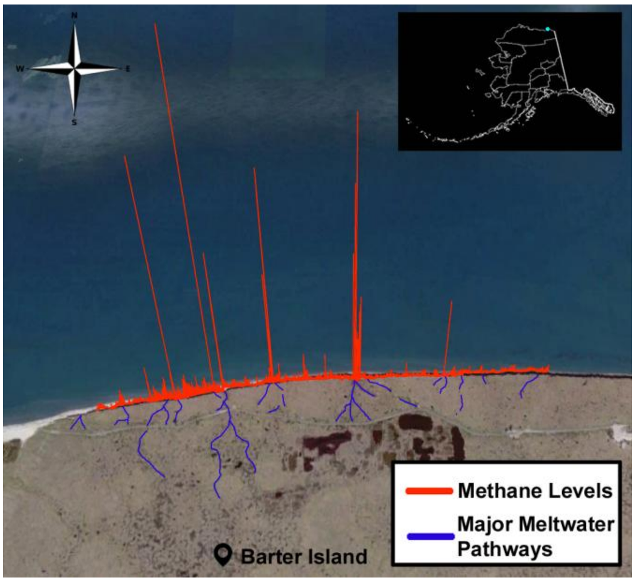

Figure 1. Methane hotspots and major meltwater pathways in a coastal permafrost environment on Barter Island, AK.

Acknowledgments

Funding for this research was provided by the U.S. Geological Survey's Coastal and Marine Geology Program and the U.S. Geological Survey's Mendenhall Program. We thank the U.S. Fish and Wildlife Services for their local support. We also thank C. Johnson with instrument deployment and data collection. A special thanks goes to the community of Kaktovik for their continued support for scientific research. Any use of trade, firm, or product names is for descriptive purposes only and does not imply endorsement by the U.S. Government.

References

Fritz, M., Vonk, J.E. & Lantuit, H. 2017. Collapsing Arctic coastlines. *Nature Climate Change* 7 : 6–7. DOI: 10.1038/nclimate3188

Gibbs, A.E. & Richmond, B.M. 2017. National assessment of shoreline change—Summary statistics for updated vector shorelines and associated shoreline change data for the north coast of Alaska. *U.S. Geological Survey Open-File Report 2017–1107* 1–21. DOI: 10.3133/ofr20171107

Günther, F., Overduin, P.P., Sandakov, A. V., Grosse, G. & Grigoriev, M.N. 2013. Short- and long-term thermo-erosion of ice-rich permafrost coasts in the Laptev Sea region. *Biogeosciences* 10 : 4297–4318. DOI: 10.5194/bg-10-4297-2013

Jones, B.M., Arp, C.D., Jorgenson, M.T., Hinkel, K.M., Schmutz, J.A. & Flint, P.L. 2009. Increase in the rate and uniformity of coastline erosion in Arctic Alaska. *Geophysical Research Letters* 36 : L03503. DOI: 10.1029/2008GL036205

Kohnert, K., Serafimovich, A., Metzger, S., Hartmann, J. & Sachs, T. 2017. Strong geologic methane emissions from discontinuous terrestrial permafrost in the Mackenzie Delta, Canada. *Scientific Reports* 7 : 5828. DOI: 10.1038/s41598-017-05783-2

Koven, C.D., Ringeval, B., Friedlingstein, P., Ciais, P., Cadule, P., Khvorostyanov, D., Krinner, G. & Tarnocai, C. 2011. Permafrost carbon-climate feedbacks accelerate global warming. *Proceedings of the National Academy of Sciences* 108 : 14769–14774. DOI: 10.1073/pnas.1103910108

Lantuit, H., Overduin, P.P., Couture, N., Wetterich, S., Aré, F., Atkinson, D., Brown, J., Cherkashov, G., Drozdov, D., Forbes, D.L., Graves-Gaylord, A., Grigoriev, M., Hubberten, H.-W., Jordan, J., Jorgenson, T., Ødegård, R.S., Ogorodov, S., Pollard, W.H., Rachold, V., Sedenko, S., Solomon, S., Steenhuisen, F., Streletskaya, I. & Vasiliev, A. 2012. The Arctic Coastal Dynamics Database: A New Classification Scheme and Statistics on Arctic Permafrost Coastlines. *Estuaries and Coasts* 35 : 383–400. DOI: 10.1007/s12237-010-9362-6

Schuur, E.A.G., McGuire, A.D., Schädel, C., Grosse, G., Harden, J.W., Hayes, D.J., Hugelius, G., Koven, C.D., Kuhry, P., Lawrence, D.M., Natali, S.M., Olefeldt, D., Romanovsky, V.E., Schaefer, K., Turetsky, M.R., Treat, C.C. & Vonk, J.E. 2015. Climate change and the permafrost carbon feedback. *Nature* 520 : 171–179. DOI: 10.1038/nature14338

Wegner, C., Bennett, K.E., de Vernal, A., Forwick, M., Fritz, M., Heikkilä, M., Łącka, M., Lantuit, H., Laska, M., Moskalik, M., O'Regan, M., Pawłowska, J., Promińska, A., Rachold, V., Vonk, J.E. & Werner, K. 2015. Variability in transport of terrigenous material on the shelves and the deep Arctic Ocean during the Holocene. *Polar Research* 34 : 24964. DOI: 10.3402/polar.v34.24964

Wobus, C., Anderson, R., Overeem, I., Matell, N., Clow, G. & Urban, F. 2011. Thermal erosion of a permafrost coastline: Improving process-based models using time-lapse photography. *Arctic, Antarctic, and Alpine Research* 43 : 474–484. DOI: 10.1657/1938-4246-43.3.474

Using remotely sensed data to identify perennial snow patches in northern Iceland

Hannah Prantl[1]
Skafti Brynjolfsson[2]
Sveinn Brynjolfsson[3]
Rudolf Sailer[1]
Johann Stötter[1]
[1]*Institue of Geography, University of Innsbruck, Hannah.prantl@uibk.ac.atl*
[2]*Icelandic Institute of Natural History, 600 Akureyri, Iceland*
[3]*Icelandic Met Office, 600 Akureyri, Iceland*

Abstract

This study uses remote sensing techniques for a large-scale identification of the perennial snow patch distribution in northern Iceland. Landsat-5/-7/-8 and Sentinel-2 images are analyzed, snow patches are classified and further compared with aerial images, orthophotos and photos from field work to validate the classification procedure. The perennial snow patch distribution of two smaller areas on Tröllaskagi peninsula are presented and compared with photos from field work. Further, the development of the changed snow patch distribution over the last five years is determined. Overall, freely, available satellite images and the method show a great potential in mapping the snow patch distribution.

Keywords: Perennial snow patches, remote sensing, optical satellite images, normalized different snow index, Iceland.

Introduction

In Iceland, less than eight percent of the surface seems to be underlain by permafrost and in the last decades the knowledge has increased (e.g. Etzelmüller et al., 2007; Farbrot et al., 2007). At most, permafrost is not directly observable and therefore, different indicators, e.g. rock glaciers, perennial snow patches (PSPs) or ice-cored moraines, are used to map the distribution of permafrost. PSPs often are associated to the distribution of permafrost and to intact rock glaciers (Furrer & Fitze, 1970; Haeberli, 1978; Stötter et al., 2012).

This study is conducted in northern Iceland, on the Tröllaskagi peninsula (65°49'13.8"N 18°51'50.4"W). About 160 glaciers, either debris free, debris covered or rock glaciers, have been mapped in the area (Björnsson, 1991).

Materials and method

The PSP classification is based on optical satellite data, in particular Landsat-5/-7/-8 and Sentinel-2 images. The results are compared with aerial images from the National Land Survey of Iceland, orthophotos from Loftmyndir ehf and photos from field work. Only few cloud free satellite images are available that cover the whole peninsula and therefore six small areas, spread over the peninsula, are brought into focus. Increasing the number of cloud free images per subarea.

After pre-processing the satellite images, the images are analyzed by calculating the Normalized Different Snow Index (NDSI) with the ratio of different bands and using different thresholds to identify snow in shadow and distinguish between snow and clouds (Dozier & Painter, 2004). In a further step, a distinction of the PSPs in i) mainly avalanche ii) mainly wind and iii) mainly permafrost induced origin is done by on the base of topographic characteristics, e.g. curvature, slope and elevation (Bühler et al., 2013).

Results and discussion

In Figure 1 the development of snow patches in Brimnesdalur over the last five years are mapped.

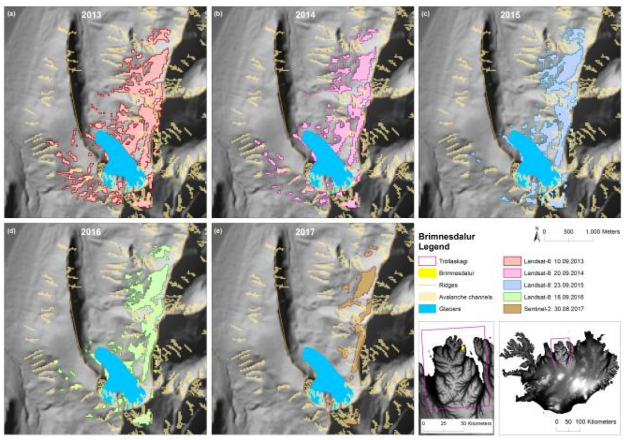

Figure 1. Development of PSPs in Brimnesdalur. The background map is a hillshade based on a digital elevation model (Loftmyndir ehf).

Avalanche channels, ridges and glacier at the head of the valley are shown. In 2013, the PSPs are widely spread and getting smaller in the last two years, e.g. in 2017 the snow patches are one third of the distribution compared to 2013.

The area of the snow patches is presented in Table 1., it was smallest in 2017, but also relatively small in 2014 and 2016.

Table1. Calculated areas of PSPs in Brimnesdalur of the last five years are listed.

Date	Area [km²]
10/09/13	1.57
20/09/14	1.07
23/09/15	1.21
18/09/16	1.04
30/08/17	0.46

An intersection of the PSPs from 2013 until 2016 determines an area of 0.64 km², but if the year 2017 is included, only half of the area is identified (0.34 km²).

Furthermore, the identified snow patches are compared with photos from field work, aerial images or orthophotos. In Figure 2 snow patches in the Kerling area of the last three years are compared with photos from field trips.

Some parts of the satellite image of 2015 are covered by clouds, however the snow patch classification is still satisfying.

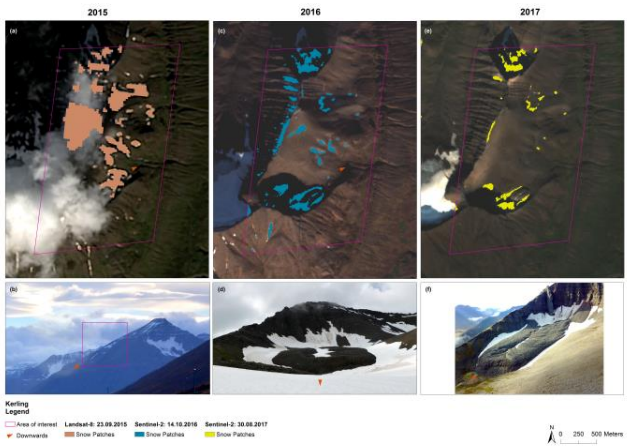

Figure 2. Comparison of PSP classification and photos from field work at Kerling. A three year time series is presented: (a) shows PSPs of 2015 based on a Landsat-8 image and (b) the comparing photo (photo taken by Skafti Brynjolfsson), (c) shows PSPs from 2016 based on a Sentinel-2 image and (d) the comparing photo (taken by Hannah Prantl) and (e) shows the PSPS of 2017 based on a Sentinel-2 image and [f] the comparing photo (taken by Jökull Bergmann).

Conclusion

Optical satellite data and topographic information show a great potential in mapping and classifying perennial snow patches. However, one problem is to get cloud free images for the study area. The results are compared with aerial images, orthophotos and photos from field work to validate the mapped snow patches and see how the analyses work. But also in this procedure step, it is difficult to get photos and images to compare the results to and further, the date of both images has to be close to each other. Otherwise, snow patches might have melted during the time gap.

Acknowledgments

This work is part of the "Permafrost in Iceland – Climate Change Impact on Permafrost Development and Resulting Mass Movement Process" project, which is funded by the Austrian Research Promotion Agency (FFG) through the Austrian Space Applications Programme (ASAP).

References

Björnsson, H. 1991. Jöklar á Tröllaskaga. *Árbók Ferðafélags Íslands*: 21-37.

Bühler, Y., Kumar, S., Veitinger, J., Christen, M., Stoffel, A. & Snehmani. 2013. Automated identification of potential snow avalanche release areas based on digital elevation models. *Nat. Hazards Earth Syst. Sci.* 13: 1321-1335.

Dozier, J., & Painter, T. 2004. Multispectral and Hyperspectral Remote Sensing of Alpine Snow Properties. *Annu. Rev. Earth Planet Sci.* 32: 465–494.

Etzelmueller, B., Farbrot, H., Guðmundsson, Á., Humlum, O., Tveito, O.E. & Björnsson, H., 2007. The regional distribution of mountain permafrost in Iceland. *Permafr. Periglac. Process.* 18: 185–1999.

Farbrot, H., Etzelmüller, B., Gudmundsson, A., Humlum, O., Kellerer-Pirklbauer, A., Eiken, T. & Wangensteen, B., 2007a. Rock glaciers and permafrost in Trollaskagi, northern Iceland. *Zeitschrift fuer Geomorphologie* 51: 1–16.

Furrer, G. & Fitze, P., 1970. Beiträge zum Permafrostproblem in den Alpen. Vierteljahrsschr. *Naturforsch. Ges. Zür.* 115: 353–368.

Haeberli, W., 1978. Special Aspects of High Mountain Permafrost Methodology and Zonation in the Alps. *Third International Conference on Permafrost*, Ottawa, Canada, July 10-13: 379–384.

Stötter, J., Zischg, A. & Sailer, R., 2012. Entwicklung des Permafrosts in Südtirol. *Permafrost in Südtirol, Innsbrucker Geographische Studien*, 45–66.

SAR Interferometry investigating Seasonal Heave and Subsidence in a Continuous Permafrost Landscape, Adventdalen, Svalbard

Line Rouyet[1]
Tom Rune Lauknes[1]
Hanne Hvidtfeldt Christiansen[2]
Yngvar Larsen[1]

[1]*Norut – Northern Research Institute, Tromsø, Norway. Corresponding email: line.rouyet@norut.no*
[2]*University Centre in Svalbard, Department of Arctic Geology, Longyearbyen, Svalbard, Norway*

Abstract

Seasonal freeze/thaw of the active layer in permafrost landscapes induces ground heave and subsidence. The amplitude of the deformation varies spatially depending on several climatic, topographic, geological, geomorphological and hydrological factors. In addition, the deformation evolves temporally in relation to the movement of the thawing/freezing front in the ground. At the regional scale, Satellite Synthetic Aperture Radar Interferometry (InSAR) provides a valuable tool to investigate the distribution, amplitude and timing of ground deformation. In this study, we applied the InSAR technique in the area in and around Adventdalen, Svalbard using TerraSAR-X (2009-2017) and Sentinel-1 (2015-2017) scenes. High resolution and long series from TerraSAR-X gives a good overview of the distribution of deformation and variability of signatures of different periglacial landforms. With Sentinel-1, time series of heave and subsidence can be retrieved and provide information about the seasonal thawing/freezing dynamics.

Keywords: Remote Sensing; SAR Interferometry; Ground deformation; Heave; Subsidence; Active Layer Dynamics

1. Introduction & Relevance

In permafrost landscapes, the seasonal freeze and thaw of the active layer induces heave during the freezing period and subsidence during the thawing period. Ground deformation related to freezing and thawing can affect the stability of infrastructure and slopes. Changes of ground thermal regime in a context of a warming climate can lead to modifications in the distribution, the amplitude and the timing of subsidence/heave (Christiansen *et al.*, 2010). In this context, it is paramount to be able to measure the ground surface over larger areas, and thus better understand the relations with climatic, topographic, geological and hydrological factors.

Satellite remote sensing provides a valuable tool to explore large and remote periglacial areas. The use of Imaging Synthetic Aperture Radar (SAR) is especially suitable for measurements in the Arctic due to its insensitivity to light and meteorological conditions, and the little vegetation on the ground. Repeat-pass SAR Interferometry (InSAR) can detect ground deformation at the millimeter scale along the radar line-of-sight (LOS) and has proven to be a valuable tool in Alpine and Arctic periglacial studies (e.g. Lui *et al.*, 2012).

Our research aims to exploit recent SAR datasets to map and investigate the seasonal evolution of ground deformation related to freeze and thaw in Adventdalen, Svalbard and study if it is consistent within individual, mapped landforms.

2. Context & Datasets

The study area includes the Adventdalen valley and adjacent valleys in Nordenskiöld Land (Central Svalbard). The area has continuous permafrost and encompasses a large range of periglacial landforms and variable ground ice conditions.

The project focuses on the exploitation of SAR series from TerraSAR-X satellite (2009-2017), as well as the recent ESA Copernicus data from Sentinel-1 mission (2015-2017). The data are highly complementary due to different frequency bands, coverages, spatial resolutions, available time periods and repeat-passes.

3. Results

3.1. Distribution of ground deformation

By multi-years averaging of SAR combinations between successive images under a chosen time interval (22 days for TerraSAR-X, 24 days for Sentinel-1), InSAR maps provide information about the spatial variation of the ground deformation on slopes (Fig.1, zoom A: rock glacier in Longyeardalen) and in the valley bottoms (Fig.1, zoom B: ice-rich eolian and alluvial frost susceptible material in Adventdalen). The results highlight the complementarity of TerraSAR-X (e.g. higher spatial resolution, see Fig.1 zoom A) and Sentinel-1 (better results on wet and fast moving sectors, see zoom B).

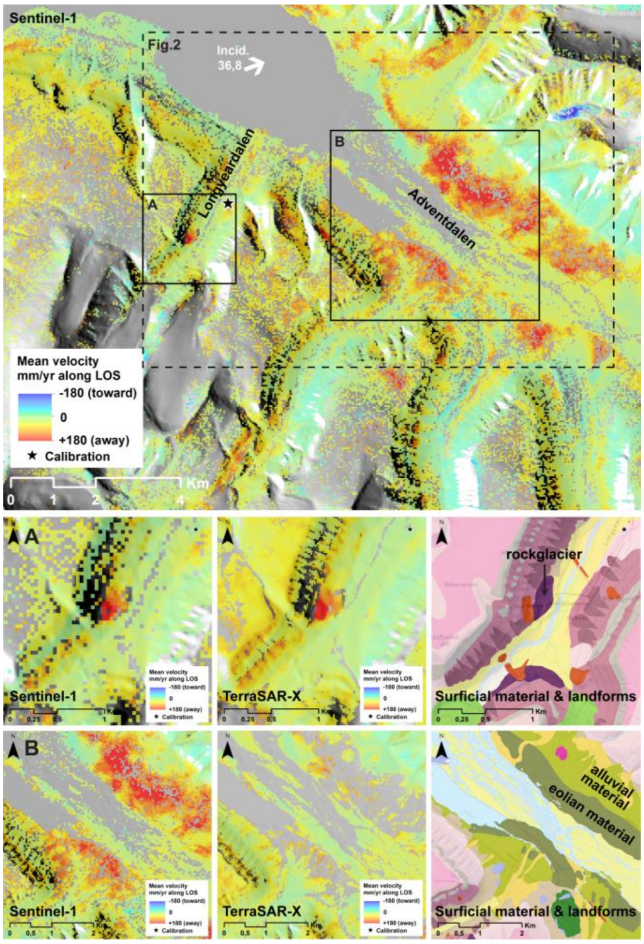

Figure 1: Multi-years InSAR surface change averages (mm/yr) using scenes during the thawing seasons. Top: Sentinel-1 surface change results. Bottom A and B: close-ups and comparison 2009-2016 TerraSAR-X, 2015-2016 Sentinel-1 and sediment & landforms (Härtel & Christiansen, 2014). White arrow: Sentinel-1 line-of-sight.

3.2. Time series of seasonal heave and subsidence

Using Sentinel-1 data in 2016 (May-November), time series can be retrieved using the Small Baseline Subsets (SBAS) method (Berardino *et al.*, 2002). Downward displacements (subsidence) are measured between May and October, and upward displacements (heave) are recorded between October and November (Fig.2).

Conclusion

The results (3.1) show potential in using InSAR for refining geomorphological mapping in complex periglacial environments. The results (3.2) highlight that InSAR can contribute to the investigation of the timing and temporal evolution of ground deformation related to freeze and thaw.

Acknowledgments

PhD project FrostInSAR (2017-2021) is funded by the Space Programme of the Research Council of Norway. TerraSAR-X data is provided by the German Aerospace Center (DLR) under the TSX-AO project contract #GEO3519.

References

Berardino, P., Fornaro, G., Lanari, R. & Sansosti, E., 2002. A new algorithm for surface deformation monitoring based on small baseline differential SAR interferograms. *IEEE Trans. On Geosci. and Remote Sens.*, 40(11). 2375-2383.

Christiansen, H.H. *et al.,* 2010. The Thermal State of Permafrost in the Nordic Area during the International Polar Year (2007-2009). *Permafrost and Periglacial Processes* 21, 156-181.

Härtel, S. & Christiansen, H.H., 2014. Geomorphological and Cryological map of Adventdalen, Svalbard. *PANGAEA*, https://doi.pangaea.de/10.1594/PANGAEA.833048.

Lui, L., Schaefer, K., Zhang, T. & Wahr, J., 2012. Estimating 1992-2000 average active layer thickness on the Alaskan North Slope from remotely sensed surface subsidence. *Journal of Geophysical Research*, 117, F01005.

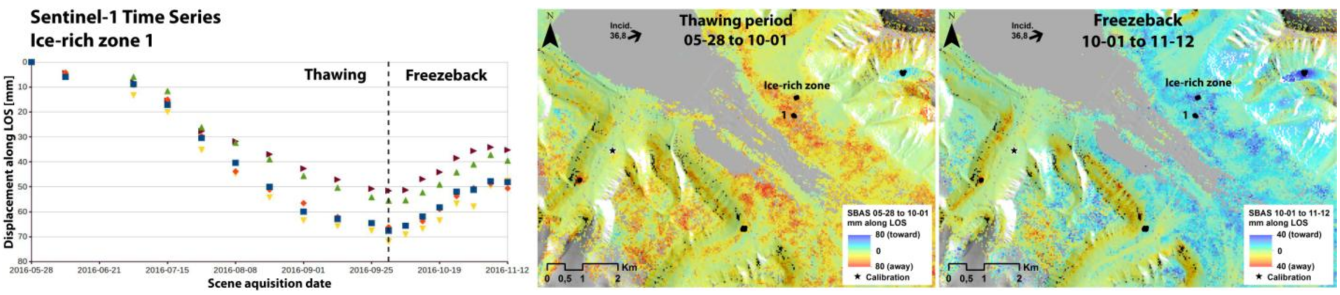

Figure 2: 2016 InSAR time series using Sentinel-1 dataset detecting heave and subsidence of up to 7 cm in parts of the valley bottom where ice-rich eolian frost susceptible sediment is located. Orange-red colors: increase in the distance sensor-to ground (subsidence or/and westward displacements); blue colors: decrease (heave and/or eastward displacements).

Evaluating DInSAR displacement products using fine-scale geomorphological mapping and field based studies along the Inuvik to Tuktoyaktuk Highway corridor, western Canadian Arctic

Ashley C.A. Rudy[1]*
Steve V. Kokelj[2]
Colin Avey[3]
Justin Kokoszka[4]
Philip Marsh[1]
Peter Morse[5]
Jurjen van der Sluijs[3]
Trevor C. Lantz[6]

[1]*Cold Regions Research Centre, Dept. of Geography, Wilfrid Laurier University, Waterloo ON, Canada, arudy@wlu.ca*
[2]*Northwest Territories Geological Survey, Yellowknife, NT, Canada*
[3]*Northwest Territories Centre for Geomatics, Yellowknife, NT, Canada*
[4]*Dept. of Geography, Simon Fraser University, Vancouver, BC, Canada*
[5]*Geological Survey of Canada, Natural Resources Canada, Ottawa ON, Canada*
[6]*Dept. of Environmental Studies, University of Victoria, Victoria, BC, Canada*

Abstract

Permafrost in Northwestern Canada, where air temperature is increasing at nearly twice the global average rate, is commonly ice rich. Therefore, the climate trend, compounded by associated changes in precipitation, ice/snow cover, wildfire regimes, and vegetation, has substantial implications for permafrost stability. Innovative monitoring strategies are needed to track long-term environmental change, assess permafrost sensitivity and improve our understanding of how intensifying permafrost processes are transforming the landscape. Differential interferometric synthetic aperture radar (DInSAR) is a remote sensing technique that can detect centimeter scale displacements in elevation. The goal of this project is to evaluate the accuracy of RADARSAT-2 DInSAR products using fine-scale geomorphological maps and field-based studies, in combination with additional remote sensing tools to explore permafrost terrain sensitivity and process.

Keywords: DInSAR, permafrost, climate change, subsidence, geomorphological maps, unmanned aerial vehicles.

Introduction

Northwestern Canada is one of the most rapidly warming regions on Earth. Changes in air temperature, precipitation, ice/snow cover, wildfire regimes, and vegetation all have substantial implications for permafrost stability. Evaluating landscape change associated with geomorphologically obvious processes such as retrogressive thaw slumping is now common, but such features are limited in extent. Conversely, terrain subsidence is expected to be the most widespread process to transform this landscape and it is likely to intensify. However, detecting and tracking this long-term environmental change beyond point measurements in the field requires innovative monitoring strategies developed from remote sensing methods.

Differential interferometric synthetic aperture radar (DInSAR) is a remote sensing technique that detects centimeter scale displacements in elevation, which can be used to evaluate permafrost sensitivity to environmental trends. In permafrost terrain, the patterns of surface displacements are attributed seasonally to heave and settlement of the active layer, and, over longer time-scales, permafrost degradation or aggradation as a result of changing local conditions or climate change. The Northwest Territories Centre for Geomatics has developed DInSAR data (2013-2016) along the Inuvik-

Tuktoyaktuk Highway (ITH) corridor, a new 138-km highway over continuous, ice-rich permafrost that traverses forest through to low-shrub tundra. Our research goal is to evaluate the accuracy of these displacement products using fine-scale geomorphological maps and field-based studies. Combined with additional remote sensing tools, DInSAR data will then be used to examine the sensitivity of different geomorphic terrain types to seasonal thaw, and how terrain dynamics vary across a climatic and permafrost ground temperature gradient.

Research Design

We will focus on 3 key areas of interest (20 km x 20 km) along the ITH where extensive ground control and field data are available. High resolution orthophotos (50 cm) acquired in 2011 will be used to identify surficial geological units and map permafrost geomorphic features including riparian areas, polygonal terrain, drained lake basins, pingos and retrogressive thaw slumps. DInSAR displacements will be compared to these maps to evaluate the magnitude of displacement variation among terrain units. DInSAR displacement data and physiographic maps will be corroborated with field data from a network of sentinel monitoring stations along the ITH, and the Trail Valley Creek Research Station. Datasets will include: A) surface displacement measured by heavemetre and from repeat unmanned aerial vehicle derived terrain models; B) near-surface ground temperatures; C) active layer thickness; D) soils and surface cover; and E) climate and snow data.

Conclusions

Together this information will support a multiscale assessment of landscape change, providing new insights on the rate and nature of change across terrain units, and will be valuable as a long-term monitoring tool to track surface displacement related to seasonal thaw and permafrost degradation. The resulting displacement maps will provide a tool for monitoring long-term terrain stability, evaluating infrastructure performance, and informing regional climate-change adaptation strategies.

Developing site specific spectral libraries for characterizing and monitoring surface features within ice-free areas of the South Shetland Islands (Antarctica)

Thomas (Fritz) Schmid[1]
Jerónimo López-Martínez[2]
Stéphane Guillaso[3]
Ana Nieto[2]
Marta Pelayo[1]
Magaly Koch[4]

[1]Centro de Investigaciones Energéticas Medio Ambientales y Tecnológicas -CIEMAT, Madrid, Spain, thomas.schmid@ciemat.es
[2]Dpt. Geología y Geoquímica, Facultad de Ciencias, Universidad Autónoma de Madrid, Madrid, Spain.
[3]Computer Vision and Remote Sensing Group, Technische Universität Berlin, Germany .
[4]Center for Remote Sensing, Boston University, Boston, USA.

Abstract

Ice-free areas of the South Shetland Islands are highly sensitive to climate change, so their mapping and monitoring is important. Advanced remote sensing techniques are ideal tools to carry out this task in areas that present limited and difficult access. Satellite-borne optical data can provide good coverage at a reasonable spectral and spatial resolution; however, complex surface characteristics within ice-free areas are difficult to distinguish. A spectral library was compiled, which contains 400 site-specific reference spectra of the most representative surface covers of the region. Image-derived spectra from multispectral optical sensors were easily labelled using the reference spectra. The potential use of the image-derived spectra is increased and can be implemented for further classification of the ice-free areas throughout the South Shetland Islands.

Keywords: Spectral library; VISNIR; Multispectral, Surface characteristics; Antarctic ice-free areas

Introduction

Nowadays, the majority of glaciers and snowfields are retreating and the permafrost is melting in the northern Antarctic Peninsula region, leading to large-scale changes in surface hydrology and affecting ecosystems (Bockheim et al., 2013). Periglacial processes and landforms together with the presence of permafrost are relevant geomorphological elements in ice-free areas of the South Shetland Islands. Since ice-free areas are highly sensitive to climate change, their mapping and monitoring is important. This can be carried out with advanced remote sensing techniques (López-Martínez et al., 2016).

The application of data from optical sensors can enhance the information obtained from these areas (Vieira et al., 2014). However, to identify and better understand the spectral features obtained with optical multispectral sensors, it is important to have reference spectra using VISNIR spectroscopy for calibration and validation purposes. The objective is to compile a site-specific spectral library to characterize and monitor surface covers within ice-free areas of the South Shetland Islands and using satellite- borne multispectral data to identify image-derived spectra.

Materials and methods

Data sources include detailed field spectroscopy and related field observations, laboratory spectroscopy and satellite-borne multispectral data for the ice-free areas of King George Island (Fildes Peninsula) and Livingston Island (Hurd Peninsula). Field data were obtained during several expeditions over the past 15 years, the most recent during the austral summer of 2016/2017.

Field and laboratory spectroscopy data were acquired with an ASD FieldSpec3 instrument under natural and controlled conditions, respectively. The data were preprocessed and then compiled into a georeferenced site-specific spectral library. Multispectral data were obtained from Sentinel-2 sensor data, acquired on 23 January 2017, to cover the areas of interest. A pre-processing of the data included radiometric, atmospheric and geometric calibration.

Spectral information was extracted from the multispectral data and a pool of image-derived spectra of specific surface covers was obtained. These spectral features were identified and validated using information from the site-specific spectral library. The library is part of a georeferenced database using a GIS support system.

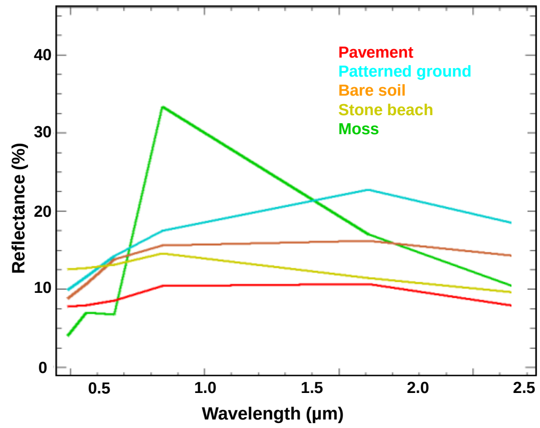

Figure 2. Image-derived spectra from Sentinel-2 data.

Results

The site-specific spectral library contains a total of 400 spectra representing gravel and sand deposits often associated to present day and Holocene raised beaches, colluvium deposits; surface pavements, stone fields and patterned ground; glacial deposits and rock outcrops; vegetated surfaces with lichens and mosses; and snow and ice covers. 115 spectra were taken in natural conditions and the remaining were taken in the laboratory in controlled conditions. Each surface cover taken in the field was selected that is representative for upscaling to the satellite resolution (Figure 1).

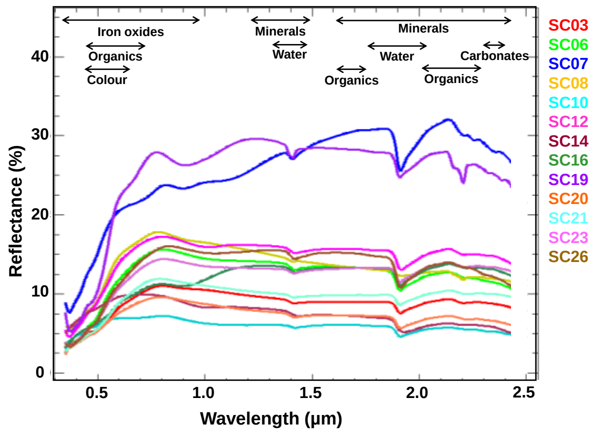

Figure 1. Soil cover spectra obtained from different locations on Fildes Peninsula (King George Island).

Examples of image-derived spectra were identified for different surface covers using Sentinel-2 (Figure 2). These spectra were identified according to field observations and were verified with the site-specific spectral library. Once the initial image derived spectra are labelled, they are then implemented in a selected classifier of preference for producing distribution maps.

Conclusion

The compilation of the spectral library is a useful tool for identifying different surface properties throughout the region. Labelled image-derived spectra using multispectral data are of advantage for classification purposes in areas that present limited and difficult access. Initially the library contains 400 spectra, but the work is ongoing with further spectra expected to be included.

Acknowledgments

This work is supported by Project CTM2014-57119-R of the Spanish R&D National Plan. The authors are very grateful to Dr. B. Oliva-Urcía and Dr. L. J. Lambán for their participation in the fieldwork as well the support provided by the Spanish logistic personnel and the Chilean Antarctic Institute.

References

Bockheim, J.G., Vieira, G., Ramos, M., López-Martínez, J., Serrano, E., Guglielmin, M., Wihelm, K. & Nieuwendam, A. 2013. Climate Warming and Permafrost Dynamics on the Antarctic Peninsula Region. *Global and Planetary Change*, 100, 215-223.

López-Martínez, J., Schmid, T., Serrano, E., Mink, S., Nieto, A. & Guillaso, S., 2016. Geomorphology and surface landforms distribution in selected ice-free areas in the South Shetland Islands, Northern Antarctic Peninsula Region. *Cuadernos de Investigación Geográfica*, 42 (2), 447-468.

Vieira, G., Mora, C., Pina, P. & Schaefer, C. 2014. A proxy for snow cover and winter ground surface cooling: mapping Usnea sp. communities using high resolution remote sensing imagery (Maritime Antarctica). *Geomorphology,* 225, 69-75.

Surface Deformation Monitoring in High-Latitude Permafrost Areas with Sentinel-1 SAR Interferometry

Tazio Strozzi and Urs Wegmüller[1]
Annett Bartsch[2]

[1]*Gamma Remote Sensing, Gümligen, Switzerland, {strozzi;wegmuller}@gamma-rs.ch*
[2]*Zentralanstalt für Meteorologie und Geodynamik, Wien, Austria, annett.bartsch@zamg.ac.at*

Abstract

Permafrost areas are subject to intense freezing cycles and characterized by remarkable surface displacement. Within the ESA GlobPermafrost project we are using Sentinel-1 InSAR data to analyze the surface displacement over several cold spots in the Arctic and Antarctica. In this contribution we will discuss the processing approach, show selected Sentinel-1 summer subsidence maps and time-series of motion with sampling intervals of 6 to 12 days, and introduce the ongoing validation activities.

Keywords: Surface deformation; Sentinel-1 SAR interferometry; Arctic; Antarctica.

Introduction

Low-land permafrost areas are subject to intense seasonal freezing and thawing cycles and, due to phase changes from ground ice to liquid water, are exposed to surface deformation processes. Thaw subsidence of the active layer at the surface in summer is followed by frost heave during refreezing in winter. Domination of one of the processes in a long term may result in significant changes of the Earth surface and can be a direct measure of permafrost change.

SAR interferometry (InSAR) has been applied in the past to measure surface deformation over permafrost during thawing seasons (Liu *et al.*, 2010; Short *et al.*; 2011; Strozzi *et al.*, 2012) and to derive remotely sensed active layer thickness (Shaffer *et al.*, 2015) using in particular satellite SAR data of the ERS-1/2 SAR, ALOS-1 PALSAR-1, TerraSAR-X and Radarsat-2 sensors. Nowadays, the Sentinel-1 mission represents the newest approach to SAR mission design with acquisitions regularly available over all polar areas every 6 to 12 days. We use Sentinel-1 SAR data to monitor subsidence in several cold spots regions in the Arctic and Antarctica (Fig. 1).

Figure 1. Study areas.

Sentinel-1 SAR Interferometry

Our investigations are based on multiple interferograms acquired during the summer season. Stacks of Sentinel-1 images are built in the two summer seasons of 2016 and 2017 in order to provide consistent series of interferograms with 6 to 12 days time intervals, which show good coherence under snow-free conditions. Yearly Sentinel-1 interferograms from the end of the summer do also show a sufficient level of coherence to link data from the two years.

Our InSAR processing sequence includes the co-registration of the single-look complex Sentinel-1 images, the computation of interferograms in series and over one year at the end of the season, the removal of the topographic-related phase with use of an external Digital Elevation Model (usually TanDEM-X), adaptive filtering, phase unwraping, computation of summer cumulative displacement maps and time series of movement via short-baseline InSAR (Werner et al., 2012), and terrain-corrected geocoding.

Results

Sentinel-1 interferograms acquired every 12 days from 14 June to 12 October 2017 were used to compute a map of the averaged displacement rates in the satellite line-of-sight direction for Teshekpuk Lake (Alaska) (Fig. 2). As suggested in Liu *et al.* (2010) floodplain areas were picked-up as reference. A temporal series of displacements on a selected location (Fig. 2) indicates that subsidence during the thawing season is occurring rather quickly, in early summer, with maximum displacements of more than 5 cm. Cross-validation with in-situ information is ongoing.

Acknowledgments

We acknowledge the European Space Agency (ESA) for support within the GlobPermafrost project.

References

Liu, L., Zhang, T. & Wahr, J., 2010. InSAR measurements of surface deformation over permafrost on the North Slope of Alaska. *Journal of Geophysical Research* 115: F03023.

Short, N., Brisco, B., Couture, N., Pollard, W., Murnaghan, K. & Budkewitsch, P., 2011. A comparison of TerraSAR-X, RADARSAT-2 and ALOS-PALSAR interferometry for monitoring permafrost environments, case study from Herschel Island, Canada. *Remote Sensing of Environment* 115(12): 3491-3506.

Schaefer, K., Liu, L., Parsekian, A., Jafarov, E., Chen, A., Zhang, T.J., Gusmeroli, A., Panda, S., Zebker, H. & Schaefer, T., 2015. Remotely sensed active layer thickness (ReSALT) at Barrow, Alaska using interferometric synthetic aperture radar. *Remote Sensing* 7 (4): 3735-3759.

Strozzi, T., Grosse, G. & Streletskiy, D., 2012. SAR Interferometry for surface deformation monitoring on permafrost areas in Alaska. *Proceedings of Earth Observation and Cryosphere Science*, Frascati, Italy, 13-16 November 2012.

Werner, C., U. Wegmüller & T. Strozzi, Deformation time-series of the Lost-Hills oil field using a multi-baseline interferometric SAR inversion algorithm with finite difference smoothing constraints, *Proceedings of the AGU Fall Meeting San Francisco (USA)*, 3-7 December 2012

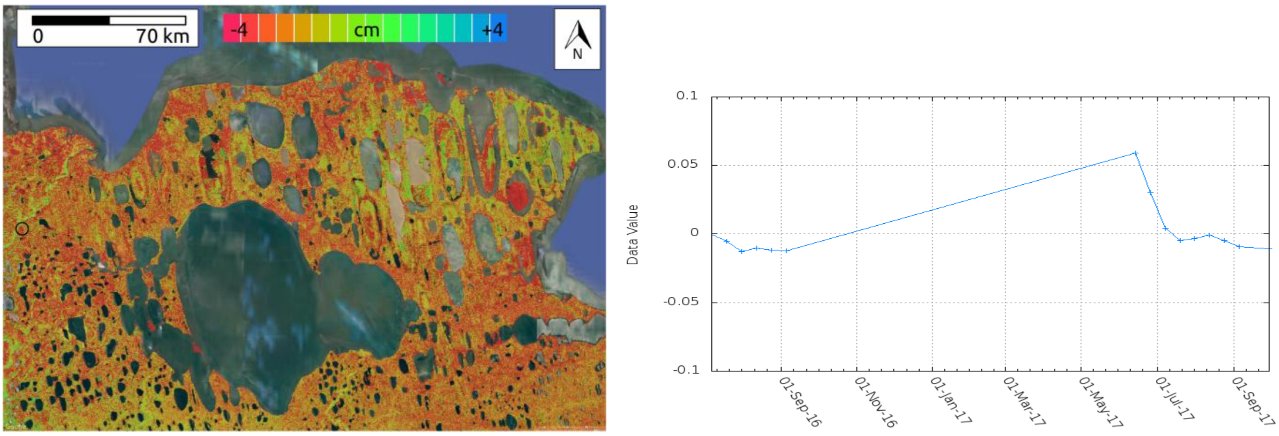

Figure 2. Subsidence map over Teshekpuk Lake (Alaska) from Sentinel-1 InSAR from 14 June to 12 October 2017 and time series of displacement in the line-of-sight direction over location "o".

Quantifying shallow and deep permafrost changes using radar remote sensing

Kanayim Teshebaeva[1]
Ko J. van Huissteden[1]
[1]*Vrije Universiteit, Department of Earth Sciences, Earth and Climate Cluster, Netherlands, k.teshebaeva@vu.nl*

Abstract

Widespread thawing of permafrost in the northern Eurasian continent cause severe problems for infrastructure and global climate. We study two potential areas in Siberian arctic, one of the test site is the Kytalyk area affected with recent inundation of the Indigirka river in July 2017 resulted in standing surface water for the period over a month. The wet soil and standing water may cause changes in active layer thickness and influence the thermal regime of the permafrost for the next decades in the region. The other test site is Yamal peninsula with recently CH_4 emitting craters which may start to contribute to emission hotspots. We hypothesize that these deeper subsurface processes also can be detected by mapping surface elevation changes using advanced SAR techniques.

We test the potential of SAR imagery to enhance detection of these features in the Siberian lowlands of the northern Eurasian continent at two test sites. We use InSAR time-series analysis to detect seasonal surface movement related to permafrost active layer changes.

Keywords: Siberian arctic, permafrost, SAR, InSAR.

Pan-Arctic Surface Water Variability by Permafrost Distribution

Erin (Dawn) Trochim[1]
Edward (Arthur George) Schuur[2]
Christina Schädel[2]

[1]*University of Alaska Fairbanks, edtrochim@alaska.edu*
[2]*Northern Arizona University*

Abstract

Surface water dynamics are an area of critical concern worldwide, in regions where permafrost exists perennially frozen ground can have unique affects in modifying where water in present on the landscape in both space and time. We contrast the ability of several global products which quantify surface water dynamics from 1985 to 2015 using Landsat data in permafrost regions. The first is the European Commission Joint Research Centre's Global Surface Water Explorer. The second is the Deltares Aqua Monitor. Both products are limited for use in permafrost regions due to data availability in parts of the Siberian plateau and Kolyma where Landsat coverage begins in 1999 and 1995 respectively. Our results summarize the trends from each of the datasets in relationship to pan-Arctic permafrost distribution. The analysis includes the general limitations of each product and identifies key areas which need to be addressed in validating these products.

Keywords: hydrology; remote sensing; permafrost; pan-Arctic

Characterization of Polar Permafrost Landscapes by Means of Multi-Temporal and Multi-Scale Remote Sensing, and In-Situ Measurements (SMART)

Tobias Ullmann[1]
Jennifer Sobiech-Wolf[2]
Christof Kneisel[1]
Wolfgang Dierking[2]
Roland Baumhauer[1]
[1] *Physical Geography, Institute of Geography and Geology, University of Wuerzburg, Am Hubland, 97074 Wuerzburg, Germany, tobias.ullmann@uni-wuerzburg.de*
[2] *Section" Earth Observation Systems", Alfred Wegener Institute for Polar and Marine Research (AWI), Bussestrasse, 27570 Bremerhaven, Germany*

Abstract

Satellite remote sensing and geophysical surveying were proven to be effective for sampling of surface and subsurface properties in permafrost landscapes. Using both techniques synergistically is the long-term goal of the project. Our approach focuses on the up- and down-scaling and coupling of space-borne remote sensing data (e.g. DEM, SAR, MSS), airborne (e.g. GPR, Laserscan, Hyperspectral), and in situ data (e.g. GPR, ERT) for the area wide detection of the active layer thickness (ALT) and the identification of interconnections between the bio-, pedo-, and hydrosphere. The contribution highlights the initial analyses of airborne GPR data (2016), TanDEM-X DEM (2011/2012), and PolSAR time series data (2016/2017) for sites in Northern-Canada. First outcomes show promising results on: (1) a remote estimation of ALT via airborne GPR, (2) high resolution and area-wide modelling of the hydrographic setting via the TanDEM-X DEM and (3) characterization of seasonal land surface variations via polarimetric Sentinel-1 data.

Keywords: Airborne; Ground Penetrating Rader; Sentinel-1; Active Layer; TanDEM-X; Canada

Introduction & Project Summary

The investigation areas are located in Northern-Canada along a north-south transect from the Richards Mountains to the Tuktoyaktuk Peninsula, including the Mackenzie Delta Region. The environmental setting comprises boreal and tundra ecozones; discontinuous and continuous permafrost, and mountainous and lowland landscapes (Burn & Kokelj, 2009). The site was object of previous studies (Ullmann *et al.*, 2014 ; Ullmann *et al.*, 2017a; Ullmann *et al.*, 2017b) and a variety of space-borne remote sensing products is/will be available (Table 1). These datasets will be used to build a comprehensive geodatabase of the environmental conditions on different spatial scales. Additionally, airborne data (Table 2) will be acquired during the flight campaign SMART in summer 2018. These data will be predominately used to link in-situ data (Table 3) with the space-borne remote sensing products. In situ field work will be conducted in 2018 and 2019 and will take use of ground-based GPR, and ERT. Both methods were proven to be effective for the characterization of the subsurface composition, including the active layer thickness (Hauck and Kneisel 2008). Additionally, the recording and mapping of the soil moisture, of the hyper-spectral surface signature, and the vegetation composition (type, height, and biomass) will be conducted. Data of space-, air-borne, and in situ mapping will then be studied in multivariate statistical analyses.

Preliminary Results

The airborne **Ground Penetrating Radar,** which will be operated during the flight campaign in 2018, was already tested for land applications over selected sites in 2016. The analyses of the recorded data showed that picking of the boundary between frozen and unfrozen ground was possible. It is expected that this method will allow determining the ALT remotely in high detail with a vertical accuracy of few centimetres. Detailed knowledge on the ALT will support a comprehensive ecosystem analysis; e.g. coupling of ALT with the slope position, or the shrub density (obtained from in-situ and space-borne data).

Further, the **TanDEM-X DEM** supported the mapping of the geomorphology and the modelling of the hydrography. Using the DEM and morphometric features, like the multi-scale topographic position indices (Lindsay *et al.*, 2015), it was possible to generate a general classification of the land form ensemble and to model the hydrographic setting. Exemplarily, the DEM was successfully applied to delineate the watersheds of the thermokarst lakes and to investigate the catchments and the potential run-off.

Further, the polarimetric **SAR data (PolSAR) of TerraSAR-X, ALOS, and Sentinel-1** were investigated for selected sites in order to test the sensitivity of the sensors to the surface properties, e.g. land cover. The results revealed that X- and C-Band PolSAR data show sensitivity to shrub and herb dominated tundra via differences in the HV channel linked to volume scattering intensities. Further, the data helped to identify the wetland vegetation via unique polarimetric signatures. Beyond this seasonal variations of the Sentinel-1 PolSAR signal were investigated and related to freezing, thawing, and flooding events.

Table 1. Space-Borne Remote Sensing Database

Sensor	Type	Resolution	Purpose
TerraSAR-X	SAR*	< 10 m	surface movements, land coverage, biomass
TanDEM-X	SAR*	< 10 m	surface movements, land coverage, biomass
TanDEM-X Mission	DEM	< 15 m	topography, hydrography, geomorphology
ALOS	SAR*	< 30 m	moisture, land coverage, surface movements
ALOS-2	SAR*	< 20 m	moisture, land coverage, surface movements
Sentinel-1	SAR*	< 15 m	surface movements, land coverage, biomass
MODIS	MSS	<500 m	land coverage, land surface temperature, biophysical parameters
Landsat	MSS	< 30 m	land coverage, land surface temperature, biophysical parameters
Sentinel-2	MSS	< 60 m	land coverage, biophysical parameters

SAR=Synthetic Aperture Radar; MSS=Multispectral Sensor System; * including polarimetric (PolSAR) and interferometric (InSAR) applications.

Table 2. Air-Borne Remote Sensing Database

Instrument	Resolution	Year	Purpose
Hyperspectral and Optical Camera	< 3 m	2013 2018	land coverage, biophysical parameters
Laser Scanner	< 3 m	2018	topography, hydrography, geomorphology
Ground Penetrating Radar	< 15 m	2016 2018	active layer thickness
Thermal Scanner	< 5 m	2018	land surface temperature

Table 3. In-Situ Geophysical Database

Instrument	Resolution	Year	Purpose
Resistivity Imaging	< 2 m	2018 2019	active layer thickness, subsurface composition
Logger Data	< 0.5 m	2018 2019	permafrost table, moisture
Ground Penetrating Radar	< 2 m	2018 2019	active layer thickness
In situ mapping	< 5 m	2012* 2013* 2018 2019	topography, geomorphology, land coverage, moisture, biophysical parameters

* Land Cover Mapping

Acknowledgments

The project "Multi-Scale Characterization of Polar Permafrost Landscapes by Airborne and Satellite Remote Sensing and In-Situ Geophysical Measurements" is funded by the Deutsche Forschungsgemeinschaft (DFG, German Research Foundation) - 329721376. The authors like to thank Joerg Hartmann, Daniel Steinhage (AWI) and Torsten Sachs (GFZ) for their support with the airborne flight campaigns.

References

Burn, C.R.; Kokelj, S.V. 2009. The environment and permafrost of the Mackenzie Delta Area. *Permafrost and Periglacial Processes*, 20: 83–105.

Hauck, C. & Kneisel, C. 2008. *Applied Geophysics in Periglacial Environments*. Cambridge Uni. Press, 240 pp.

Lindsay, J.B., Cockburn, J.M.H. & Russell, H.A.J. 2015. An integral image approach to performing multi-scale topographic position analysis. *Geomorph.* 245: 51-61.

Ullmann, T., Schmitt, A., Roth, A., Duffe, J., Dech, S., Hubberten, H.-W. & Baumhauer, R. 2014. Land Cover Characterization and Classification of Arctic Tundra Environments by Means of Polarized Synthetic Aperture X- and C-Band Radar (PolSAR) and Landsat 8 Multispectral Imagery - Richards Island, Canada. *Remote Sensing*, 6: 8565-8593.

Ullmann T., Büdel C. & Baumhauer R. 2017a. Characterization of Arctic Surface Morphology by Means of Intermediated TanDEM-X Digital Elevation Model Data. *Zeitschrift für Geomorphologie, Supplementary Issues* 61, 1: 1-23.

Ullmann, T., Banks, S.N., Schmitt, A., Jagdhuber, T. 2017b. Scattering Characteristics of X-, C- and L-Band PolSAR Data Examined for the Tundra Environment of the Tuktoyaktuk Peninsula, Canada. *Applied Science* 7, 595: 1-28.

Active layer thickness and ground temperature through assimilation of remote sensing data in permafrost models

Sebastian Westermann[1]
Kristoffer Aalstad[1]
Joel Fiddes[1]
Jaroslav Obu[1]
Bas Altena[1]
Maria Peter[1]
Laurent Bertino[2]
Moritz Langer[3,4]
Julia Boike[3]
Bernd Etzelmüller[1]

[1] *University of Oslo, Norway*
[2] *Nansen Environmental and Remote Sensing Center, Bergen, Norway*
[3] *Alfred-Wegener-Institute Potsdam, Germany*
[4] *Humboldt-University Berlin, Germany*

Abstract

We report on recent developments and breakthroughs in remote sensing of the ground thermal regime. Data assimilation techniques offer the possibility to ingest a range of remotely sensed data sets in permafrost models, thus strongly improving the results compared to simulations based on e.g. atmospheric model date. We discuss the feasibility of future "permafrost reanalysis" products, exploiting the information content of various satellite products to deliver the best possible estimate for the permafrost thermal state over a range of spatial scales.

Keywords: active layer, thaw progression, remote sensing, modeling, MODIS, Sentinel-2, data assimilation

Introduction

With current remote sensing technologies, it is not possible to directly infer thaw depths from space-borne platforms. However, operational satellites provide dense time series of a range of variables which are intimately related to the ground thermal regime and the seasonal ground thawing. Assimilation of these data sets in numerical permafrost models can strongly constrain the uncertainty and drive model results towards reality (Trofaier at al., 2017, Westermann et al., 2015a). In the SatPerm and ESA GlobPermafrost projects, such techniques have been systematically developed and explored for a range of spatial scales. Here, we focus on transient approaches based on the CryoGrid model suite which can deliver the seasonal thaw progression and ground temperature development in the uppermost meters.

Results and Discussion

First, we explore transient modeling of ground temperatures driven by remotely sensed LST, snow extent (SE) and snow water equivalent (SWE). Hereby, satellite-derived SWE clearly constitute the "bottleneck", with spatial resolutions of 25km and large uncertainties in mountain and tundra areas. Using the CryoGrid permafrost models for a site in N Siberia, we show that the simulated thaw depth is significantly less affected by shortcomings in the SWE input compared to ground temperatures, so that a satisfactory representation of thaw progression and maximum thaw depth is indeed feasible. However, information on subsurface stratigraphies including the distribution of ground ice is required to achieve this accuracy which is currently not available from remote sensing products alone. Furthermore, we demonstrate that excess ice thaw can be represented by simple modifications of the CryoGrid model physics (Westermann et al., 2016).

The availability and quality of satellite-based SWE retrievals is a strongly limiting factor, which precludes application of the method in many permafrost environments, in particular mountain and coastal areas. Aalstad et al. 2017 recently demonstrated a method based on advanced data assimilation techniques that has significant potential to overcome these limitations. It is based on back-calculating the amount and spatial distribution of SWE from the time of snow disappearance, which is accessible satellite-based products of "fractional snow-covered area" (fSCA). fSCA is derived from the surface reflectance in the VIS and NIR spectral ranges, and a whole range of satellite sensors can deliver this variable at spatial resolutions of 1km (MODIS) or even 20-30m (Sentinel-2, Landsat), thus opening fascinating opportunities for high-resolution modeling of the ground thermal state.

We present and evaluate a range of possible schemes, from "magnifying glass" - like approaches that could reproduce the measured ground temperatures at borehole sites, to larger-scale algorithms that represent the spatial variability of the thermal regime in terms of a probability density function.

Acknowledgments

We acknowledge funding by SatPerm (project no. 239918; Research Council of Norway) and ESA GlobPermafrost (www.globpermafrost.info).

References

Aalstad, K., Westermann, S., Schuler, T. V., Boike, J., Bertino, L., 2017. Ensemble-based assimilation of fractional snow covered area satellite retrievals to estimate snow distribution at a high Arctic site, *The Cryosphere*, doi:10.5194/tc-2017-109, accepted.

Trofaier, A., Westermann, S., Bartsch, A., 2017. Progress in space-borne studies of permafrost for climate science: Towards a multi-ECV approach, *Remote Sensing of Environment*, in press. Doi:10.1016/j.rse.2017.05.021.

Westermann, S., Duguay, C., Grosse, G., Kääb, A., 2015a. Remote sensing of Permafrost and Frozen Ground, in: Tedesco, M. (Ed.): *Remote Sensing of the Cryosphere*, 403 p., Wiley Blackwell.

Westermann, S., Østby, T., Gisnås, K., Schuler.T., Etzelmüller, B., 2015b. A ground temperature map of the North Atlantic permafrost region based on remote sensing and reanalysis data, *The Cryosphere*, 9, 1303-1319, doi:10.5194/tc-9-1303-2015.

Westermann, S., Langer, M., Boike, J., Heikenfeld, M., Peter, M., Etzelmüller, B., Krinner, G., 2016. Simulating the thermal regime and thaw processes of ice-rich permafrost ground with the land-surface model CryoGrid 3, *Geoscientific Model Development*, 9, 523-546, doi:10.5194/gmd-9-523-2016.

Westermann, S., Peter, M., Langer, M., Schwamborn, G., Schirrmeister, L., Etzelmüller, B., Boike, J., 2017. Transient modeling of the ground thermal conditions using satellite data in the Lena River Delta, Siberia, *The Cryosphere*, 11, 1441-1463, doi:10.5194/tc-11-1441-2017.

Spatiotemporal variation of land surface temperature in the high latitude permafrost region of China: A case study from Mohe County

Yan Lu [1,3]
Ming Guo[1,2]
Wenbing Yu[1,2]
Weibo Liu[1]
[1]*State Key Laboratory of Frozen Soil Engineering, Northwest Institute of Eco-environment and Resources, CAS, Lanzhou 730000, China*
[2]*College of Civil Engineering, Chongqing Jiaotong University, Chongqing 400074, China*
[3]*University of Chinese Academy of Sciences, Beijing 100049, China*

Abstract

Land surface temperature is a key factor relating to permafrost. Based on the RS and GIS methods, the land surface temperatures in the high latitude permafrost region of China are investigated. Especially, the cities and towns are focused. The Mohe County and its surrounding areas have been taken as study area. Spatiotemporal variation characteristics and the influencing factors of the land surface temperature over the study area in different seasons in 2015 were analyzed. There were 79.02% of the land surface without plants in winter because of abundant snowfall, and over 80% of the land surface with high vegetation cover in summer. The surface temperature of the urban area is usually higher than the surrounding areas, with a maximal temperature difference up to 6.37 ℃ in summer. In winter, the land surface temperature significantly correlated with elevation, with an averaged land surface temperature gradient of 2.27 ℃ per 100 m.

Keywords: permafrost regions; cities and towns; land surface temperature; remote sensing; temperature inversion; heat island effect

Introduction

As a major component of the cryosphere , permafrost is sensitive to global climatic change and human activities (Gruber, 2012). Compared to air temperature, land surface temperature (LST) is more suitable to reflect the up-boundary conditions of permafrost (Hachem et al., 2009; Zou et al., 2017). With the development of infrared remote sensing technology, an increasing number of LST products derived from different satellite images have been applied to global and regional permafrost distribution research (Kääb, 2008; Langer et al., 2010; Westermann et al., 2015).

So, the Xilinji Town, Mohe County of Heilongjiang Province and its surrounding areas have been taken as study area. The land use type was gained from the Landsat Satellite images based on the RS and GIS techniques. Spatiotemporal variation characteristics and the influencing factors of the land surface temperature over the study area in different seasons in 2015 were analyzed to clear the LST spatiotemporal variation characteristics in order to pave the way for further studies, such as permafrost distribution prediction and mapping.

Study Area and Methodology

The Xilinji Town, Mohe County of Heilongjiang Province and its surrounding areas have been taken as study area. Mohe County, the northern tip of China, is located in the southeastern edge of the Eurasian permafrost zone. The maximum thickness of permafrost is 50 – 100 m. The annual average air temperature is about -4.2 °C. The climate warming tendency rate is 0.34℃ per decade during the past 56 years. As the biggest town in Mohe County, the area of Xilinji town has increased from 5.74 km² in 1987 to 8.74 km² (in 2012) after the reconstructing by 1988. The urban population has grown from about 25 000 residents in 1992 to more than 41 000 in 2011. This work take advantage of two types of remote sensing data: MODIS LST products (MODLT1M) and Landsat Satellite images. Methods used for LST investigation in this study include land use type interpretation and LST retrieval.

Results and Analyses

Land use change

Table 1. Transfer Matrix of Land Use from 2000 to 2015

Land type	Water	Construction land	Unused	Forest	Lawn	Total of 2015
Water	9.23	0.62	0.00	0.16	4.44	14.45
Construction land	0.89	20.73	0.17	0.07	18.30	40.16
Unused	0.09	0.62	16.64	0.00	81.09	98.45
Forest	0.29	0.07	0.00	37.35	29.62	67.33
Lawn	1.58	6.09	1.54	14.43	445.97	469.61
Total of 2000	12.08	28.14	18.34	52.01	579.43	690.00

With the development of the county, the area of construction land and bare soil significantly increased. From 2000 to 2015, the construction land area jumped to 40.16 km² from 28.14 km², 43% increase in 15 years. This speed of urban development is much faster than most of cities and towns in permafrost regions in the world.

Spatiotemporal variation of NDVI

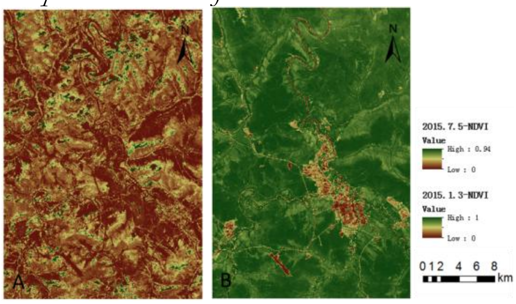

Figure 1. The spatial distribution of NDVI in the study area in winter (A) and summer (B), 2015

There were 79.02% of the land surface without plants in winter because of abundant snowfall, and over 80% of the land surface with high vegetation cover in summer.

Spatiotemporal variation of LST

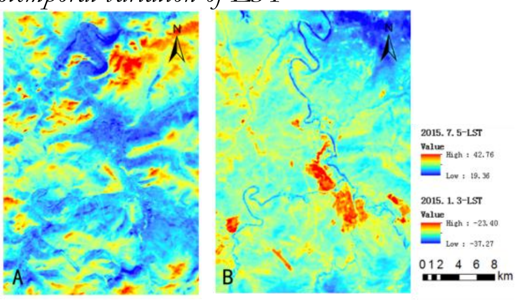

Figure 2. The spatial distribution of retrieved LST in the study area in winter (A) and summer (B), 2015

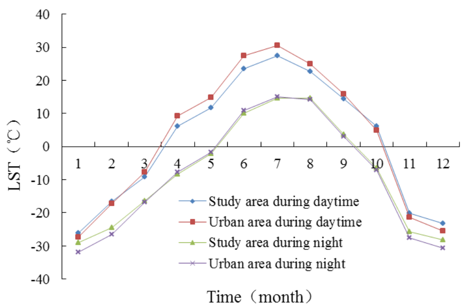

Figure 3. Monthly mean LST from MODIS products in 2015

The spatial distribution of LST obtained from two types of remote sensing data showed same trend. LST of the urban area is usually higher than the surrounding areas, with a maximal temperature difference up to 6.37 ℃ in summer. In winter, LST increase as elevation rise.

Influencing factor of LST

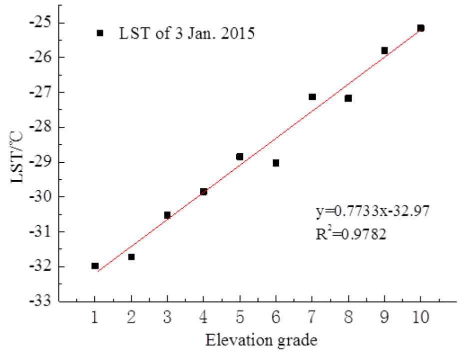

Figure 4. The relation between LST and elevation

In winter, the land surface temperature significantly correlated with elevation, with an averaged land surface temperature gradient of 2.27 ℃ per 100 m. Besides, NDVI was negatively related to land surface temperature; the surface temperature of different use types was from low to high order of water-forest-lawn-unused land-construction land.

Summary

Land surface temperature is closely relate to the distribution of permafrost. It is found that the land surface temperature of study area has significant inversion in winter and the urban heat island effect exists all year round by analyzing the remote sensing LST data, which is informative for permafrost mapping and permafrost modelling of this area. Therefore, it can be inferred that the urbanization is one of the important factor that cause permafrost degradation in urban area.

References

Gruber, S., 2012. Derivation and analysis of a high-resolution estimate of global permafrost zonation. *The Cryosphere* 6: 221-233.

Hachem, S., Allard, M., and Duguay, C., 2009. Using the MODIS land surface temperature product for mapping permafrost: an application to northern Québec and Labrador, Canada. *Permafr. Perigl. Proc* 20: 407-416.

Kääb, A., 2008. Remote sensing of permafrost-related problems and hazards. *Permafr. Perigl. Proc* 19: 107-136,

Langer, M., Westermann, S., and Boike, J., 2010. Spatial and temporal variations of summer surface temperatures of wet polygonal tundra in Siberia - implications for MODIS LST based permafrost monitoring. *Remote. Sens. Environ* 114: 2059-2069.

Westermann, S., Østby, T., Gisnås, K., Schuler, T., and Etzelmüller, B., 2015. A ground temperature map of the North Atlantic permafrost region based on remote sensing and reanalysis data. *The Cryosphere* 9: 1303-1319.

Zou D, Zhao L, Yu S, et al, 2017. A new map of permafrost distribution on the Tibetan Plateau. *The Cryosphere* 11(6): 2527.

2 - Palaeo-permafrost reconstruction, from field to simulation

Session 2

Palaeo-permafrost reconstruction, from field to simulation

Conveners:

- **Pascal Bertran**, INRAP / PACEA, Pessac, France
- **Pierre Antoine**, CNRS, LGP Meudon, France
- **Didier Roche**, CNRS, LSCE-IPSL, Gif-sur-Yvette, France
- **Charlotte Prud'Homme**, Max Planck Institute for Chemistry, Mainz, Germany (PYRN member)

Western Europe witnessed repeated phases of southward permafrost development during the Pleistocene, which impacted severely the ground and the biosphere. Although reconstructing palaeo-permafrost with accuracy is of paramount importance for a wide range of topics, including the genesis of mid-latitude landscapes, aquifer recharge, and the distribution of glacial refugia for vegetation and animals, a debate still exists about the maximal extent during the Last Glacial since field-based approaches hardly fit with simulations provided by Global Climate Models. In the mid-latitude mountain regions, the extent of permafrost on the forelands as well as the nature of glacier-permafrost interaction during the LGM are of critical importance but difficult to constrain. Fundamental information on past climatic conditions in these areas can be gained from study of the spatial pattern of the extensive mountain permafrost during the Lateglacial and Holocene. This session will highlight improvements in field mapping, proxy analyses and climate models, as well as innovative approaches such as ground temperature reconstruction through the analysis of water oxygen isotopes and dissolved noble gases in aquifers. The chronology of permafrost development and degradation also raises a lot of questions that will be addressed during this session.

Cryogenic hypothesis of the Yamal crater origin
Results of detailed studies and modeling

Buldovich S., Khilimonyuk V. , Bychkov A., Ospennikov E., Vorobyev S., Gunar A., Gorshkov E., Chuvilin E., Cherbunina M., Kotov P., Lubnina N., Motenko R., Amanzhurov R.

Lomonosov Moscow State University, Geocryology department, email : vanda@geol.msu.ru

Abstract

The article presents the results of complex research and assessment of the possibility of forming a crater on the Yamal peninsula. The origin, conditions of formation, forms and character of cryovolcanism occurrence based on the obtained data and modeling is determined. Reconstruction of the cryogenic eruption is presented.

Keywords: Yamal crater, modeling, cryovolcanism

Introduction

Multiple research work to study and estimate the possibility of crater formation on the Yamal Peninsula (N69,970965 E68,369575) was carried out in June 2015.

The authors believe in the cryogenic origin of the object with formation associated with cryovolcanism. Cryovolcanism is the formation of craters due to ground explosion and the eruption of soil material as a result of long-term freezing of water-gas saturated ground in a closed system (in a permafrost environment on the Earth and other planets).

Methods

Field works included: detailed surveys of the territory; drilling boreholes up to 20 m to study cryogenic structure and sampling for physical and mechanical properties; thermometric measurements; topographical, geochemical and geophysical works. Sampling of surface water, frozen and thawed soils was conducted, methane and carbon dioxide content was measured in boreholes with field analyzers. The content of macro components, microelements, gases in frozen soils and gases adsorbed by clay matter as well as radiological measurements were made in the laboratory. The analysis of high-resolution satellite images and aerial photographs was carried out. Modeling of processes of heat transfer in the soils was calculated by numerical simulation.

Results

The crater is located in the marginal part of the flat boggy bottom of the ancient lake basin (around 400-500 m in diameter) at III marine terrace At the moment of explosion, the crater had a diameter of about 17-20 m and the depth of at least 50 m (Leibman & Plehanov, 2014). The thickness of the frozen soils that formed the cap of the freezing talik at the time of its destruction was from 7 to 9 m.

Analysis of satellite and aerial photographs of different years (1969, 2012-2014) show that there was a large mound with average height of 8 m and diameter of 50 m. The destruction happened at the end of the winter 2014.

The cryogenic structure of frozen soils is highly variable both laterally and with depth (Khilimonyuk *et al,* 2016) and is characterized by strong dislocation of soils (cryoturbation) and the presence of injection ice (fig.1)

Fig.1 Yamal crater. Layer of injected ice inside the crater.

Particularly "warm" conditions (ground temperature near –1.0^0 C) occur at the edge of the mound while it is from –4 to –5°C in the surroundings, and from –1 to –3°C in the bottom of the lake basin.

Discussion

As a result of solving a series of thermal problems, it was established that the talik could be formed during the reduction of the lake which ensured intensive lateral freezing of the talik for 1 to 2 thousand years.

To destruct the frozen talik cap the pressure in the upper part of the talik had to be from 1 to 1.2 MPa based on the calculations.

The gas component in frozen ground and ice shows high percentage of carbon dioxide (10–20%) and dihydrogen (up to 3%) and a relatively low methane content of 2–3%. Chemical and isotopic composition does not correspond to the reservoir gas of the deposit and is of bacterial origin.

The freezing talik before the explosive destruction had a complex structure: in the lower part the mineral component (thawed soil) prevailed. Above there was a water-ground mixture with the predominance of a liquid represented by a solution of gases (mainly, carbon dioxide) in water. The gaseous cap could be formed at the top of talik. Freezing from above led to the formation of porous ice, filled with a large number of gas bubbles of different sizes.

Large amount of dissolved CO_2 in the liquid phase inside the talik can be explained by the unique mechanism of cryogenic separation of gases. During the all-round freezing of the initial talik, the moving freezing front of the soils pushed the gas and the water (partly) to the talik center. When the water froze, expulsion of the dissolved gas mixture occurred. Part of the gas formed bubbles in the ice, and highly soluble components of the gas mixture (primarily CO_2) dissolve in the liquid phase inside the talik. This mechanism can lead to a radical change in the composition of the dissolved gas in the residual talik and may cause the accumulation of a large amount of dissolved CO_2 in the thawed core of the pingo.

With increasing internal pressure and gas saturation of water, the freezing point is significantly lowered. the Freezing point of the solution saturated mainly with carbon dioxide at a pressure of 1 MPa is –1.4°C. This can have important geocryological consequences, since the freezing temperature of the talik can become lower than the mean annual temperature of frozen soils in the in the surrounding area (which is –1°C). The pressure in the lower part of the talik, according to the calculations, exceeded 1.5 MPa, which was sufficient to form stable carbon dioxide gas hydrates.

Conclusion

Cryogenic eruption was triggered by thermal contraction cracks (ice wedges) in the frozen cap and involved several stages.

In the first stage (that lasted for 5 to 10 seconds) the outgassing occurred mostly from the upper part of the talik: the gas was released through cracks and expanded adiabatically. In the second stage (hydraulic stage) that lasted for few hours, water was outpouring and degassing leading to explosive upward migration of the gas-water mixture. The last stage (from 5 to 25 hours) of unfrozen soil eruption happened when gas was released either from pore water in unfrozen soil or from decomposed carbon dioxide hydrates.

Acknowledgments

The research activities were carried out with the support of Innopraktika and OJSC “NOVATEK”.

References

Khilimonyuk, V., Ospennikov, E., Buldovich, S., Gunar, A., Gorshkov, E., 2016. Permafrost conditions of Yamal crater territory disposition. *Proceedings of the fifth conference of geocryologists of Russia,* Moscow, Russia, June 14-17: 245-255.

Leibman, M. & Plehanov, A., 2014. Yamal gas emission crater: results of a preliminary survey. *Holodok* 2: 8-15

Did permafrost modify basal conditions during the Last Glacial Maximum? The case of the Rhine Glacier, Swiss lowlands

Denis Cohen[1]
Thomas Zwinger[2]
Wilfried Haeberli[3]
Urs H. Fischer[4]

[1]*New Mexico Tech, Socorro, NM, USA, denis.cohen@gmail.com*
[2]*CSC: Center for Science, Espoo, Finland*
[3]*Department of Geography, University of Zurich, Zurich, Switzerland*
[4]*Nagra National Cooperative for the Disposal of Radioactive Waste, Wettingen, Switzerland*

Abstract

A coupled model of ice flow and permafrost is used to study how permafrost may have affected the thermal state of the base of the ice during the advance of the Rhine Glacier in the Swiss lowlands at the Last Glacial Maximum. Documented permafrost buildup north of the Alps at the Last Glacial Maximum may have delayed temperate basal conditions favorable to sliding and erosion, inhibited subglacial groundwater recharge, promoted deeper flow paths that increased fluxes of groundwater originating from the Alps in aquifers. Studying these transient conditions is important to understand the effects of permafrost on ice flow, glacial erosion, and groundwater flows, and how these could affect the safety of high-level radioactive waste repositories in the event of future ice ages.

Keywords: Rhine Glacier; basal conditions; permafrost, Last Glacial Maximum.

Introduction

During the Last Glacial Maximum (LGM), climate in the northern Swiss Plateau was cold and dry probably due to the closed humidity source of the seasonally ice-covered Atlantic Ocean and the blockage of meridional moisture from the Mediterranean Sea by the Alps in connection with a southward shift of the North Atlantic storm tracks (Florineth & Schlüchter, 1998; Luetscher *et al.*, 2015). Permafrost evidenced in that area (Andrieux *et al.*, 2016; Haeberli, 1983) may have reached a depth of around 150 meters (Delisle *et al.*, 2003). Thus, the maximum glacial advance at the LGM may have occurred over frozen ground. Here we explore how permafrost may have temporarily modified basal conditions (temperature, sliding speed) during the advance of the Rhine Glacier in the Swiss lowlands using a fully coupled numerical model of ice flow and permafrost. Knowing how long permafrost delayed temperate-bed conditions favorable to erosion and modified groundwater flow paths and fluxes is important when assessing the long-term safety of radioactive waste repositories planned in the region. The period of concern for high-level radioactive waste is 1 Ma, a time span during which repeated ice age conditions are likely to occur.

Motivation and Coupled Model

LGM paleo-climate proxies from pollen records for central Europe point towards very cold and dry conditions (Wu *et al.*, 2007; Duprat-Oualid *et al.*, 2017). Despite this climate of a cold desert, most numerical studies and geomorphological observations indicate that the bed of the Rhine glacier was largely at the pressure melting point temperature, and thus ice was able to slide over its substrate and to erode it (Cohen *et al.*, 2017). It is, however, unknown how the coeval development of permafrost at the LGM affected the basal conditions and the rates of glacial advance that led to the glacial maxima. Was the glacier bed cold or temperate when ice advanced over permafrost? Did permafrost build up to a significant depth prior to ice overriding the Swiss and German lowlands? Presumably, the glacier toe was cold and frozen to its bed but how long did permafrost delay temperate-bed conditions beneath the advancing ice lobe? To answer these important geomorphic questions, we developed a coupled model of ice-flow/permafrost interactions to simulate the temperature in the ice and in the subsurface during the advance of the Rhine Glacier at the LGM. Our simulations are two-dimensional, following a flowline that begins high up in the Hinterrhein region and extends to near the actual Rhine river in north-eastern Switzerland. We solve the unaltered Stokes equations (Gagliardini *et al.*, 2013) for the ice dynamics and the energy balance for the ice as well as the subsurface down to a depth of 5 km. We use an effective heat capacity model (Anderson *et al.*, 1973; Cutler *et al.*, 2000) for the permafrost to calculate the temperature in the subsurface. The ice and the subsurface are coupled at their interface via boundary conditions for the temperature that cannot exceed the pressure melting temperature. For cold ice below the pressure melting temperature, basal fluxes are balanced across the interface. At the pressure melting temperature, the jump in fluxes is proportional to the amount of melt water produced at the bed. The model is run for several thousand years to explore the transient evolution of the ice advance as a function of climate parameters that affect ice temperature and permafrost thickness.

Preliminary results indicate that permafrost delayed temperate-bed conditions by several hundred years, a significant fraction of the time the LGM glacier remained at or near its maximum extent, thus affecting basal conditions and the associated geomorphic process of erosion. Future simulations will include the effects of the glacier mass balance on basal conditions as these are known to affect the speed of the glacier and its thermal structure. Complex interactions between permafrost, ice flow and sliding dynamics, and climate are investigated to determine what are the primary control parameters that determine the basal conditions at the bed of the advancing Rhine glacier. These basal conditions are also likely to affect deep groundwater hydraulics at the potential sites for radioactive waste repositories.

References

Anderson, D.M., Tice, A.R. & McKim, H.L., 1973. The unfrozen water and the apparent specific heat capacity of frozen soils. In *Second International Conference on Permafrost, Yakutsk, USSR. North American contribution*: 289-295.

Andrieux, E., Bertran, P. & Saito, K. 2016. Spatial Analysis of the French Pleistocene permafrost by a GIS database. *Permafrost and Periglacial Processes* 27: 17-30. doi:10.1002/ppp.1856

Cohen, D., Gillet-Chaulet, F., Haeberli, W., Machguth, H. & Fischer, U. H., 2017. Numerical reconstructions of the flow and basal conditions of the Rhine glacier, European Central Alps, at the Last Glacial Maximum, *The Cryosphere Discussion*, doi.org/10.5194/tc-2017-204, in review.

Cutler, P.M., MacAyeal, D.R., Mickelson, D.M., Parizek, B.R. & Colgan, P.M., 2000. A numerical investigation of ice-lobe–permafrost interaction around the southern Laurentide ice sheet. *Journal of Glaciology* 46(153): 311-325.

Delisle, G., Caspers, G. & Freund, H., 2003. Permafrost in north-central Europe during the Weichselian: how deep. In *Proceedings of 8th International Conference on Permafrost,* Zurich, Switzerland, Balkema Publishers, Lisse: 187-191.

Duprat-Oualid, F., Rius, D., Bégeot, C., Magny, M., Millet, L., Wulf, S. & Appelt, O., 2017. Vegetation response to abrupt climate changes in Western Europe from 45 to 14.7 k cal a BP: the Bergsee lacustrine record (Black Forest, Germany). *Journal of Quaternary Science* 32 (7): 1008-1021.

Florineth, D. & Schlüchter, C., 1998. Reconstructing the Late Glacial Maximum (LGM) ice surface geometry and flowlines in the central Swiss Alps. *Eclogae Geologicae Helvetiae* 91: 391-407.

Gagliardini, O., Zwinger, T., Gillet-Chaulet, F., Durand, G., Favier, L., de Fleurian, B., Greve, R., Malinen, M., Martín, C., Råback, P., Ruokolainen, J., Sacchettini, M., Schäfer, M., Seddik, H. & Thies, J., 2013. Capabilities and performance of Elmer/Ice, a new-generation ice sheet model, *Geosci. Model Dev.*, **6**, 1299-1318, doi:10.5194/gmd-6-1299-2013.

Haeberli, W., 1983. Permafrost - glacier relationships in the Swiss Alps today and in the past. *Proceedings of the Fourth International Conference on Permafrost*, 415-420.

Luetscher, M., Boch, R., Sodemann, H., Spotl, C., Cheng, H., Edwards, R.L., Frisia, S., Hof, F. & Muller, W., 2015. North Atlantic storm track changes during the Last Glacial Maximum recorded by Alpine speleothems? *Nature Communication* 6: 6344.

Wu, H., Guiot, J., Brewer, S. & Guo, Z., 2007. Climatic changes in Eurasia and Africa at the last glacial maximum and mid-Holocene: reconstruction from pollen data using inverse vegetation modelling. *Climate Dynamics* 29(2-3): 211-229.

Past thermal-contraction-crack polygons in central western Poland: distribution, classification and relationship with ice-sheet recession

Marek W. Ewertowski[1]
Andrzej Kijowski[1]
Izabela Szuman[1]
Aleksandra M. Tomczyk[1]
Leszek Kasprzak[1]
[1]*Faculty of Geographical and Geological Sciences, Adam Mickiewicz University, Poznań, Poland, marek.ewertowski@amu.edu.pl*

Abstract

The examination of low-altitude aerial photographs reveals the presence of more than 400 polygonal nets in central western Poland. Polygons range from 5 to almost 70 meters in diameter. Based on the polygons' diameter and intersection angles, we identified seven main types of nets geometry. Based on ground verification, we interpreted them as past thermal-contraction-cracks, filled mostly with sand (*i.e.* sand-wedge casts). As favorable weather conditions and a proper land cover (i.e. cultivated land) are necessary for identifying polygonal nets, the observed number of polygons is probably much underestimated. The broad occurrence of former thermal-contraction-cracks' polygons indicates that continuous permafrost was widespread in central western Poland after termination of the Last Glacial Maximum (LGM). Preliminary dating of the cracks' infilling as well as polygon geometry suggest that thermal-contraction-cracking occurred in several different phases and that a time frame of a few thousand years is sufficient to form complex, mature nets.

Keywords: permafrost; thermal-contraction-cracks; polygons; patterned ground; remote sensing; GIS

Introduction

Nowadays, periglacial conditions exist over a substantial portion of the Earth's land-surface area; while in the past, the area covered by permafrost was even larger (*cf.* Ballantyne & Harris, 1994; French, 2007; Gozdzik, 1995; Kitover *et al.*, 2016; Lindgren *et al.*, 2016; Saito *et al.*, 2016; Vandenberghe *et al.*, 2014). Past periglacial features constitute therefore a unique and valuable archive, allowing for insights into past permafrost processes as well as their relationship with global and local environmental conditions (including climatic conditions), so identification of permafrost features improves the reconstructions of the Pleistocene paleoenvironment as well as our understanding of past changes in the climate. As thermal-contraction-cracks reflect climatic conditions, they are also an important source of information on ice sheet/permafrost interactions. In this context, spatial dimension as well as distribution and patterns of polygonal nets are especially important for understanding the following: (1) Coupling of ice dynamics and climate response (McCabe & Clark, 1998); (2) Broader scale paleo-environmental changes (Mandryk, 1996); (3) Validation of numerical models regarding climate/permafrost interactions (Harris *et al.*, 2009)

In this study, we investigated the remote sensing materials to detect the spatial distribution of polygonal cropmarks. Cropmarks were later verified in the field to demonstrate their periglacial origin. The main aims of this study were the following: (1) to document the spatial distribution of past polygonal nets in the central western part of Poland; (2) to classify and analyse the geometric types of polygonal nets; (3) to investigate the relationship between polygon geometry and distribution, and ice sheet recession.

Study Area

The study area is located in the central western part of Poland. In this area, the maximum ice sheet limit during the Weichselian has commonly been connected with the Leszno Phase, which occurred at around 20 ka BP (Kozarski, 1995) or 24 ka BP (Marks, 2010). The subsequent stillstand phases were the Poznan Phase (*ca.* 18.8 ka BP (Kozarski, 1995) or 20 ka BP (Marks, 2010) and Chodziez sub-phase. The study area is characterized by moraines, till plains, and outwash plains formed during the frontal recession of the Scandinavian Ice Sheet from its maximum extent (Leszno Phase) to the Poznan Phase and further to the north (Ewertowski, 2009; Ewertowski & Rzeszewski, 2006; Kasprzak, 2003; Kozarski, 1986; Kozarski, 1988; Kozarski, 1995)

Results

Numerous cropmarks were observed in the central western part of Poland. Their geometry and distribution were studied using a large number of low-altitude aerial photographs. Based on the Field verification we interpreted them as past thermal-contraction-cracks, filled most probably with aeolian sand (*i.e.* sand-wedge casts). We identified seven principal types of polygon geometry based on the angle of the cracks' intersection, their dimension and spacing. Since favorable weather conditions and proper land cover (*i.e.* cultivated land) are necessary for identifying polygonal nets, the number of polygons is likely to have been considerably underestimated.

The broad occurrence of polygons of former thermal-contraction-cracks filled with aeolian sediments (i.e. sand-wedge casts) indicated that continuous permafrost was widespread in central western Poland after the termination of LGM. However, their spatial distribution did not allow us to fully confirm the hypothesis regarding a gradual aggradation of the permafrost following the retreating ice margin. Preliminary dating of cracks' infilling as well as polygon geometry suggest that thermal-contraction-cracking occurred in several different phases, and that a time frame of a few thousand years is sufficient to form even complex and mature nets

Acknowledgments

This research project was funded by the National Science Centre (project number: N N306 599640).

References

Ballantyne, C.K., Harris, C., 1994. *The Periglaciation of Great Britain*. CUP Archive.

Ewertowski, M., 2009. Ice-wedge Pseudomorphs and Frost-cracking Structures in Weichselian Sediments, Central-West Poland. *Permafrost and Periglacial Processes* 20(4): 316-330.

Ewertowski, M., Rzeszewski, M., 2006. Using DEM to Recognize Possible Minor Stays of Vistulian (Weichselian) ice-sheet Margin in the Wielkopolska Lowland. *Quaestiones Geograficae* 25A: 7-21.

French, H.M., 2007. *The periglacial environment*. Wiley.

Gozdzik, J., 1995. Permafrost evolution and its impact on deposition conditions between 20 and 10 ka BP in Poland. *Biuletyn Peryglacjalny* 34: 53-72.

Harris, C., Arenson, L.U., Christiansen, H.H., Etzelmüller, B., Frauenfelder, R., Gruber, S., Haeberli, W., Hauck, C., Hoelzle, M., Humlum, O., 2009. Permafrost and climate in Europe: Monitoring and modelling thermal, geomorphological and geotechnical responses. *Earth-Sci Rev* 92(3): 117-171.

Kasprzak, L., 2003. *Model sedymentacji lądolodu vistuliańskiego na Nizinie Wielkopolskiej*. Wydawnictwo Naukowe UAM, Poznan.

Kitover, D.C., van Balen, R.T., Vandenberghe, J., Roche, D.M., Renssen, H., 2016. LGM Permafrost Thickness and Extent in the Northern Hemisphere derived from the Earth System Model iLOVECLIM. *Permafrost and Periglacial Processes* 27(1): 31-42.

Kozarski, S., 1986. Time scales and the rhythm of Vistulian geomorphic events in the Polish Lowland. *Czasopismo Geograficzne* 57(2): 247-270.

Kozarski, S., 1988. Time and dynamics of the last Scandinavian ice-sheet retreat from northwestern Poland. *Geographia Polonica* 55: 91-101.

Kozarski, S., 1995. *Deglaciation of Northwestern Poland: environmental conditions and geosystem transformation (~20 ka - 10 ka BP)*. Dokumentacja Geograficzna IGiPZ PAN, 1.

Lindgren, A., Hugelius, G., Kuhry, P., Christensen, T.R., Vandenberghe, J., 2016. GIS-based Maps and Area Estimates of Northern Hemisphere Permafrost Extent during the Last Glacial Maximum. *Permafrost and Periglacial Processes* 27(1): 6-16.

Mandryk, C.A., 1996. Late Wisconsinan deglaciation of Alberta: processes and paleogeography. *Quaternary International* 32: 79-85.

Marks, L., 2010. Timing of the Late Vistulian (Weichselian) glacial phases in Poland. *Quaternary Sci Rev* 44: 81-88.

McCabe, A.M. & Clark, P.U., 1998. Ice-sheet variability around the North Atlantic Ocean during the last deglaciation. *Nature* 392(6674): 373-377.

Saito, K., Trombotto Liaudat, D., Yoshikawa, K., Mori, J., Sone, T., Marchenko, S., Romanovsky, V., Walsh, J., Hendricks, A., Bottegal, E., 2016. Late Quaternary Permafrost Distributions Downscaled for South America: Examinations of GCM-based Maps with Observations. *Permafrost and Periglacial Processes* 27(1): 43-55.

Vandenberghe, J., French, H.M., Gorbunov, A., Marchenko, S., Velichko, A.A., Jin, H., Cui, Z., Zhang, T., Wan, X., 2014. The Last Permafrost Maximum (LPM) map of the Northern Hemisphere: permafrost extent and mean annual air temperatures, 25–17 ka BP. *Boreas* 43(3): 652-666.

Spatial distribution of ice-wedge pseudomorphs in the Czech Republic

Marek Křížek[1]
Tomáš Uxa[1,2]
David Krause[1]
Lukáš Vohradský[1]
[1]*Department of Physical Geography and Geoecology, Faculty of Science, Charles University, Prague, Czech Republic, marek.krizek@natur.cuni.cz*
[2]*Department of Geothermics, Institute of Geophysics, Academy of Sciences of the Czech Republic, Prague, Czech Republic*

Abstract

This work deals with the spatial distribution of Pleistocene ice-wedge pseudomorphs and morphologic features of their networks in the area of the Czech Republic.

Keywords: ice-wedge pseudomorphs; patterned ground; the Czech Republic; Central Europe

Introduction

Patterned ground is a wide group of periglacial landforms (Ballantyne, 2007; Washburn 1979), which has more or less symmetrical surficial shape, such as circle, polygon, net, or stripe. The occurrence and structure of these landforms enable to measure the variability and different quality of periglacial environment not only on a regional, but also on a local scale (Křížek & Uxa, 2013). Numerous patterned-ground types (e.g. ice-wedges, large sorted polygons) are reliable indicators of former permafrost environment (French, 2007, Murton, 2007; Murton & Kolstrup, 2003), which highlights their palaeogeographic significance. Thus, they bring an important evidence about evolution of permafrost aggradation/degradation in the past and its environmental impact. This provides important insights towards a better understanding of present-day and future changes in contemporary permafrost areas (Vandenberghe *et al.*, 2016). Recent ice wedges in polar zones are arranged in networks that cover large areas, making this group of patterned ground the most widespread periglacial landforms.

In the Czech Republic, patterned ground is located in two different environments: in the lowlands and in the mountainous areas. While in mountains can be some patterned-ground phenomena (earth hummocks and sorted circles) considered to be recently active (Křížek, 2016), the lowland patterned ground is preserved only in fossil form, mostly as ice-wedge pseudomorphs. Ice-wedge pseudomorphs have not yet been mapped systematically in this territory. They were found and described only due to accidental discoveries during construction and mining operations (Czudek, 2005). Consequently, unlike in surrounding countries (e.g. Hungary, Poland, Germany, France, Belgium etc.), their evidence from the Czech Republic is largely lacking or fragmentary (e.g. Czudek, 2005). Hence, it is timely to fill this gap and complete the existing information with new data and to amend and/or refine the existing Quaternary permafrost distribution maps at a regional or continental scale (e.g. Lindgren *et al.*, 2016, Vandenberghe *et al.*, 2014).

The aim of this work is to present a spatial distribution of ice-wedge pseudomorphs in the Czech Republic.

Methods

Mapping of ice-wedge pseudomorphs was principally based on remote sensing techniques (*sensu* Bertran *et al.*, 2014) and was validated and supplemented by published geological reports, geophysical soundings (ground penetrating radar and electrical resistivity tomography) and field logging in clay and sand pits or technical excavations.

Results and Outlook

We identified more over 700 localities in the Czech Republic where ice-wedge pseudomorphs occur in polygonal networks or individually (Figure 1), which documents that permafrost extensively covered this area during the Pleistocene. The patterns are usually found in unconsolidated sandy or gravel substrates of river terraces and in silty materials of loess covers. Two major areas of ice-wedge pseudomorphs can be distinguished: Bohemian Cretaceous Basin in the western part of the Czech Republic and Moravian Basins in the eastern part of the Czech Republic. More than 4000 polygons of ice-wedge pseudomorphs located on 50 sites were analyzed morphologically in detail (Figure 2). Their size ranges from 1.8 to 31.7 m and their mean diameter is 9.5 m. Most ice-wedge polygons are pentagonal and hexagonal.

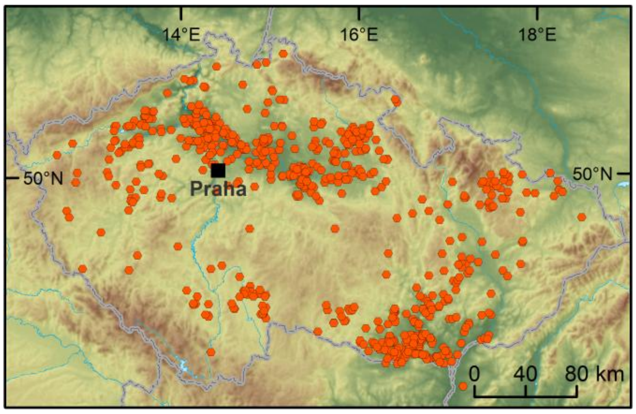

Figure 1. Sites of ice-wedge pseudomorphs in the Czech Republic.

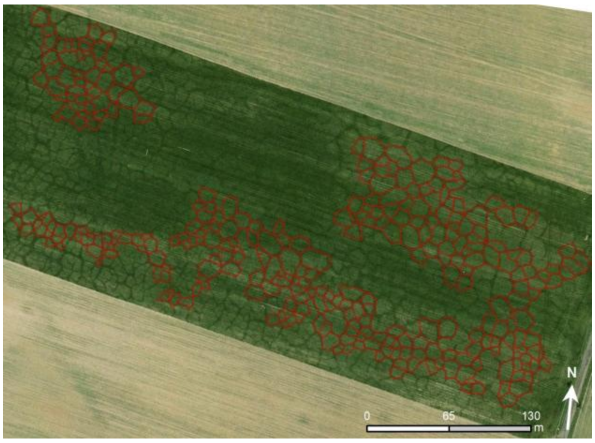

Figure 2. An example of a polygonal network of ice-wedge pseudomorphs near Kostomlaty pod Řípem (N 50°20´10´´, E 14°19´49´´).

Currently, we aim to update the database further based on the latest aerial images and field logging. We will also determine the absolute chronology of these landforms based on numerical dating, because their origin has been only tentatively estimated to the Last Glacial Maximum (Czudek, 2005).

Acknowledgments

The research is supported by the Czech Science Foundation, project number 17-21612S.

References

Ballantyne, C.K., 2007. Patterned ground. In: Elias, S.A. (ed.), *Encyclopedia of Quaternary Science*. Oxford: Elsevier, 2182–2191.

Bertran, P., Andrieux, E., Antoine, P., Coutard, S., Deschodt, L., Gardère, P., Hernandez, M., Legentil, C., Lenoble, A., Liard, M., Mercier, N., Moine, O., Sitzia, L. & Van Vliet-Lanoë, B., 2014. Distribution and chronology of Pleistocene permafrost features in France: database and first results. *Boreas* 43: 699–711.

Czudek, T., 2005. *Vývoj reliéfu krajiny České republiky v kvartéru*. Brno: Moravské zemské muzeum, 238 pp.

French, H.M., 2007. *The Periglacial Environment*. Chichester: John Wiley & Sons, 458 pp.

Křížek, M., 2016. Periglacial Landforms of the Hrubý Jeseník Mountains. In: Pánek, T. & Hradecký, J. (eds.), *Landscapes and Landforms of the Czech Republic*. Springer, 277–289.

Křížek, M. & Uxa, T., 2013. Morphology, Sorting and Microclimates of Relict Sorted Polygons, Krkonoše Mountains, Czech Republic. *Permafrost and Periglacial Processes* 24: 313–321.

Lindgren, A., Hugelius, G., Kuhry, P., Christensen, T. R. & Vandenberghe, J., 2016. GIS-based Maps and Area Estimates of Northern Hemisphere Permafrost Extent during the Last Glacial Maximum. *Permafrost and Periglacial Processes* 27: 6–16.

Murton, J.B., 2007. Periglacial Landforms/Ice Wedges and Ice Wedge Casts. In: Elias, S.A. & Mock, C.J. (eds.), *Encyclopedia of Quaternary Science*. Amsterdam: Elsevier, 436-451.

Murton, J.B. & Kolstrup, E., 2003. Ice-wedge casts as indicators of palaeotemperatures: precise proxy of wishful thinking? *Progress in Physical Geography* 27: 155–170.

Vandenberghe, J., French, H.M., Gorbunov, A., Marchenko, S., Velichko, A.A., Jin, H., Cui, Z., Zhang, T. & Wan, X., 2014. The Last Permafrost Maximum (LPM) map of the Northern Hemisphere: permafrost extent and mean annual air temperatures, 25–17 ka BP. *Boreas* 43: 652–666.

Vandenberghe, J., Woronko, B., Nieuwendam, A. & Bateman, M., 2016. Reconstruction and Modelling of Past Permafrost and Periglacial Environments. *Permafrost and Periglacial Processes* 27: 3–5.

Washburn, L.A., 1979. *Geocryology: A Survey of Periglacial Processes and Environments*. London: Arnold, 406 pp.

Thaw slurry lake deposits: paleoenvironmental indicators of long term permafrost dynamics

Scott F. Lamoureux[1]
Benjamin Amann[1]
T. Kurt Kyser[2]
Myrna J. Simpson[3]
Brent G. Pautler[3,4]
Anna J. Pieńkowski[5,6]
Catherine La Farge[7]
Christopher R. Omelon[8]

[1]*Dept. Geography and Planning, Queen's University, Kingston, ON, Canada K7L 3N6*
[2]*Dept. Geological Sciences and Geological Engineering, Queen's University, Kingston, ON, Canada K7L 3N6*
[3]*Dept. Chemistry and Dept. Physical & Environmental Sciences, University of Toronto, Toronto, ON, Canada, M1C 1A4*
[4]*Current Address: Advanced Chemistry Development Inc., (ACD/Labs), Toronto, ON, Canada M5C 1B5*
[5]*Dept. Physical Sciences, MacEwan University, Edmonton, AB, Canada T5J 4S2*
[6]*School of Ocean Sciences, Bangor University, Menai Bridge, Anglesey, UK LL59 5AB*
[7]*Dept. Biosciences, University of Alberta, Edmonton, AB, Canada, T6G 2E9*
[8]*Dept. Geology, University of Kansas, Lawrence, KS, USA, 66045*

Abstract

We evaluated unusual laminated sedimentary units from a freshwater lake in the Canadian High Arctic and determined that the likely formation mechanism was by seepage of permafrost thaw slurries into the lake, particularly during the post-1950 CE period. The thaw slurry units are diffusely laminated, show no evidence of sedimentary grading, and are enriched in Fe, Mn and $CaCO_3$. Stable isotopic signatures of the carbonate show strongly depleted $\delta^{18}O$ and the co-enrichment of redox-sensitive metals both suggest inorganic carbonate and metals precipitation in the aerobic lake water. Widespread deposition of thaw slurry units in the late 20th century is accompanied by indicators of ameliorated aquatic ecosystem conditions and increased microbial activity, all of which are consistent with observed warming in the region.

Keywords: Permafrost, sedimentology, organic geochemistry, carbonates, stable isotopes, diatoms

Introduction

Permafrost degradation resulting from climate change is currently widespread in the Arctic, but pre-instrumental permafrost proxy records are rare and determining the impact of past climate variations on permafrost remains limited. We investigated unusual sedimentary units found in a small scour lake (MV-CC) on Melville Island, NWT, Canada and found the sedimentary and geochemical properties were consistent with a permafrost thaw mechanism that is widespread in the region and forms subsurface sediment slurries. In this paper, we briefly present sedimentary data and our interpretation of the formation of what we have termed *thaw slurry* deposits.

Results and Discussion

Lake sediment core records indicate that short intervals of sedimentary laminate occur throughout the uppermost sediments of lake MV-CC. Individual laminae groups can be traced between cores located within 3 m of each other, which units showing depositional heterogeneity. The laminae are ungraded, generally coarser, and contain a slight enrichment of $CaCO_3$ (c. 1.5% compared to background values of 0.5%). Stable isotope analysis of the carbonates indicate that laminated units are strongly depleted with respect to $\delta^{18}O$, by as much as 15‰. By contrast, $\delta^{13}C$ associated with carbonates shows minimal down-core variation.

Sediment core µXRF scans further indicate enrichment of Fe, Mn, Ca and Pb in laminated units.

Geochronology provided by ^{137}Cs indicates that laminated units were formed after c. 1958 CE in all cores across the lake. Radiocarbon analyses constrain laminated units to <500 yr BP, and in long cores laminated units are absent in the post-glacial period (c. 11 ka BP). Multiple phases of laminae deposition are only evident in a single core near the lake outlet, and suggest three episodes during the past millennia.

Organic geochemistry and aquatic fossil records from the lake further indicate enhanced microbial activity in recent sediments and improved aquatic conditions during the past century, but it is unclear if the laminated units are directly associated with these aquatic changes.

Results indicate that the discrete sedimentary laminae in lake MV-CC are unlikely to be formed by conventional sedimentary processes involving fluvial or shoreline sedimentary inputs. The highly heterogeneous deposition of the laminae, and the lack of sedimentary grading and microbial remains preclude clastic or microbial formation mechanisms. The combination of enhanced carbonate and higher Fe and Mn in laminated units, together with highly depleted $\delta^{18}O$ in the laminae carbonate suggest an alternative mechanism.

Given the occurrence of similar features on the landscape in the region, we interpret the laminated units as *thaw slurry* deposits, formed by slurry seepage into the lake and accumulation in micro-topographic depressions. The geochemical properties of the laminae suggest precipitation of redox-sensitive elements (Fe, Mn) upon entry into the aerobic lake setting, along with degassing and inorganic carbonate precipitation.

The widespread occurrence of thaw slurry units in the lake since c. 1950 CE suggests an association with recent climate warming. This explanation is consistent with biogeochemical and subfossil indicators in the lake and elsewhere in the Arctic.

While our record suggests a recent unprecedented occurrence of thaw slurry deposition in MV-CC during the postglacial period, we are cautious regarding this interpretation given the high degree of spatial heterogeneity associated with the sedimentary deposits. Further work is necessary to determine a more robust chronological interpretation and if similar deposits occur in other lakes in the region.

The identification of thaw slurry units in lake MV-CC indicates the potential for paleolimnological reconstruction of past permafrost thaw events. This work will provide constraint for permafrost modelling and testing of related environmental impacts in lakes and aquatic ecosystems.

Acknowledgments

We thank NSERC and Polar Continental Shelf Program for their support. Field assistance by H. Dugan and K. Kathan are appreciated.

The role of periglacial processes in the formation of chocolate clays

Radik Makshaev[1]
Aleksandr Svitoch[1]
[1] *Lomonosov Moscow State University, Faculty of Geography, Moscow, Russia, radikm1986@mail.ru*

Abstract

The Early Khvalynian chocolate clays from key sections in the Middle and Lower Volga region were studied to obtain mineralogical and geochemical data for sediment provenance reconstruction. The results show that the main clay mineral of chocolate clays is illite. Geochemical composition of chocolate clays is characterized by high concentration of iron oxide (Fe_2O_3). The potential sediment source of illite is the Pleistocene marine complex of the East-European plain. Deglaciation after LGM and rapid melting of permafrost along with solifluction processes could predetermine the supply of illite-rich sediments to the Early Khvalynian basin. Subsequently, illite-rich sediments were deposited under oxic conditions and formed chocolate clays in the Middle and Lower Volga River valley.

Keywords: Chocolate clays; clay minerals; Early Khvalynian; Late Pleistocene; periglacial processes

Introduction

During the Late Pleistocene (15-13 ka) thick mass of clays was deposited on the territory of the Middle and Lower Volga River region. Possible causes of formation of these so-called "chocolate" clays were periglacial and permafrost processes, which occurred on the territory of the East European Plain in the Last Permafrost Maximum (LPM, 25-17 ka) (Vandenberghe et al., 2014). After LPM and Last Glacial Maximum (LGM, 15-13 ka) permafrost degradation has started in this area with intensive solifluction processes that provided a huge amount of fine-grained material. Glacial meltwater along with this fine-grained material was deposited within ancient paleodepressions in the Middle and Lower Volga River valley. At that time, the Early Khvalynian transgression, one of the largest in the Pleistocene history, began on the Caspian Sea.

Materials and methods

The aim of this study is to determine the potential role of permafrost processes in the formation of specific facies of chocolate clays. We analyzed eight samples of chocolate clays and moraine clay loam from river outcrops within Volga River region and separated them to particles of size <2 µm to analyze with X-ray diffraction (XRD). Major elements of chocolate clays were analyzed by XRF (X-ray fluorescence analysis) and SEM-EDS (Scanning electron microscope with energy dispersive x-ray spectrometer).

Results

Clay minerals

Chocolate clays consist of a number of clay minerals associations, which are presented by illite, chlorite, kaolinite and smectite. Clay minerals of the Middle Volga River valley are presented by illite (33%), kaolinite (16%), smectite (28%), chlorite (17%) and mixed layers (6%). In the Lower Volga River valley outcrop profile demonstrates a prevalence of illite (33-48%) and kaolinite (18-33%). Moraine clay loam from Upper Volga region also demonstrates the prevalence of illite (45%) and kaolinite (33%) with less concentration of smectite (22%), while chlorite in this sample is not detected.

Illite is a major clay mineral of chocolate clays in Middle and Lower Volga River valley and its maximum can be an indicator of increasing solifluction processes and intensive erosion of north moraine complexes due to huge runoff of glacial melt water during the degradation of the Late Valdai (the Late Weichselian) ice sheet. Illite formation is the result of the physical erosion and low temperatures due to huge amplitude ranges (Chamley, 1989).

Geochemical composition

Geochemical composition of these clays demonstrates high concentration of iron oxide (Fe_2O_3) ~ 9-10 %, which predetermines chocolate (dark brown) color of these clays (Table 1.). Such concentration of iron oxide can correspond to the oxic conditions of the Early Khvalynian basin during chocolate clays deposition

(Priklonsky et al., 1956). SEM images show that high amount of iron oxide is concentrated on the edge surface of clay minerals.

Table 1. Chemical composition of chocolate clays.

#Sample	Fe_2O_3	CaO	Al_2O_3	K_2O	Si_2O_3	MgO
SB-220	8.04	4.49	18.75	2.86	61.34	2.43
SB-225	11.46	2.86	22.91	3.12	70.26	1.91
SB-425	10.96	1.29	24.94	3.72	60.43	2.07
SB-450	10.03	2.03	22.64	3.47	61.61	2.02
SY-6	9.70	2.71	22.40	3.39	60.67	2.37
SY-8	8.96	2.51	21.80	3.33	61.27	2.43
SY-12	8.29	3.73	19.52	3.00	61.18	2.13
SY-15	8.85	3.63	21.89	3.32	61.13	2.18

TiO_2 , MnO, P_2O_5 elements are not included.

Conclusion

Periglacial processes played an important role in the supply of clay-rich sediments to the Early Khvalynian basin after degradation of permafrost and the Late Valdai (the Late Weichselian) glaciations 25-15 ka (Svendsen *et al*., 2004). Consequently, this fine-grained material was deposited under oxic conditions within the Early Khvalynian basin and formed chocolate clays.

Acknowledgments

This work was supported by the RSCF (Project 16-17-10103).

References

Chamley, H. 1989. *Clay Sedimentology*. Springer, Berlin. 623 pp.

Priklonsky, V.A., Gorkova, I.M., Oknina, N.A., Reutova, N.S., Chepik, V.F. 1956. *Engineering-geological properties of Khvalynian clays in the context of deposition environments*. Proceedings of Hydrogeological Problem Laboratory. USSR Academy of Sciences, Moscow, vol. 13, 152 pp. (in Russian).

Svendsen, J.I., Alexanderson, H., Astakhov, V.I., Demidov, I., Dowdeswell, J.A., Funder, S., Gataullin, et al. 2004. Late Quaternary ice sheet history of northern Eurasia. *Quat. Sci. Rev.* 23: 1229-1271.

Vandenberghe, J., French, H.M., Gorbunov, A., Marchenko, S., Velichko, A.A., Jin, H., Cui, Z., Zhang, T. &Wan, X., 2014. The Last Permafrost Maximum (LPM) map of the Northern Hemisphere: permafrost extent and mean annual air temperatures, 25–17 ka BP. *Boreas* 43: 652–666.

Evolution of paleoclimatic condition of Kara sea region (Russia) in the late Pleistocene – Holocene

Gleb Oblogov[1,2], Alexander Vasiliev[1,2], Irina Streletskaya[3], Natalia Zadorozhnaya[2,3]
[1] *Earth Cryosphere Institute of Tyumen Scientific Center (ECI TSC) SB RAS, Tyumen, Russia, e-mail: oblogov@mail.ru*
[2] *Tyumen State University (TSU), Tyumen, Russia*
[3] *Lomonosov Moscow State University, Faculty of Geography (MSU), Moscow, Russia*

Abstract

Over the past few years, the authors have compiled a database on the isotope composition of ice wedges of various ages from the Kara Sea coast (Russia). On the basis of these data, winter temperatures and temperatures of the cold period (October-May) were reconstructed for three time intervals of the late Pleistocene-Holocene: the second half of the Kargin period about 30-26 ka (MIS 3), the Sartan period about 25-12 ka (MIS 2) and the Holocene about 5-3 ka (MIS 1). During MIS 3, the decrease in average annual air temperatures compared to modern values was 2-4 °C, in MIS 2 – 6-8 °C, in MIS 1 – 1-3 °C. To illustrate the spatial distribution of paleogeographic and palaeoclimatic conditions, schematic maps were compiled.

Keywords: paleogeographic conditions; paleoreconstructions; isotope composition; the Kara Sea region; underground ice.

Introduction

Modern permafrost area bears itself features and properties that were formed during the late Pleistocene-Holocene. Current permafrost state and estimation of future changes can only be understood based on a study of the geological history and paleogeographic conditions in the past.

The goal of this paper is to reconstruct and characterize the main stages and features of the evolution of the paleogeographic (paleoclimatic) conditions of the Kara Sea region during the late Pleistocene (MIS 3-2) and Holocene (MIS 1).

Basis of reconstruction

The basis of paleoclimatic reconstructions from the isotopic composition of ground ice (mainly syngenetic ice wedges) is the relationship between the isotope composition of atmospheric precipitation (snow and liquid precipitation) and air temperatures (Dansgaard, 1964, Rozanski *et al.*, 1993, etc.). The formation of ice wedges occurs due to the ingress of snow and thawed water into the frost cracks. It is assumed that the ice retains the initial isotopic composition of atmospheric precipitations.

The collected data on the content of $\delta^{18}O$ of elementary ice wedges (i.e. formed presently) and the known temperature data on the nearest meteorological stations made it possible to construct the calibration curves for the coldest month (January, T.jan), the average temperature of the cold period (October-May, T.cold) and average winter temperature (December-February, T.wint).

The regression equations are the following:

$$T.jan = 1.12\delta^{18}O-6.43,\ R^2 = 0.745,\ \sigma = 2.6,$$

$$T.wint = 1.15\delta^{18}O-4.6,\ R^2 = 0.754,\ \sigma = 2.7,$$

$$T.cold = 0.885\delta^{18}O-2.55,\ R^2 = 0.674,\ \sigma = 2.7.$$

The confidence interval is ± 3.8 ° C.

Outcome research

To illustrate the spatial distribution of paleogeographic and palaeoclimatic conditions, schematic maps (fig.1) of the paleogeographic conditions of the permafrost area of the Kara Sea region in the late Pleistocene-Holocene were compiled. Four maps-schemes corresponding to the MIS 3, MIS 2, MIS 1 and the present were drawn up. Summer temperatures on this map were estimated from station located in the same bioclimatic zone (according to palynological data) and having close values of winter temperatures and temperatures of the cold period. Such values of summer temperatures are estimates.

The color of the maps shows the location of the regions that were continental (subaerial) region, or flooded by the sea (subaqueous regions). The basis of such constructions was the literature data on sea level changes during the late Pleistocene-Holocene (Kind, 1974, Gornitz, 2009). To reconstruct the former coastlines of the Kara Sea paleobasin, the NOAA bathymetric interactive database was used (http://www.noaa.gov/).

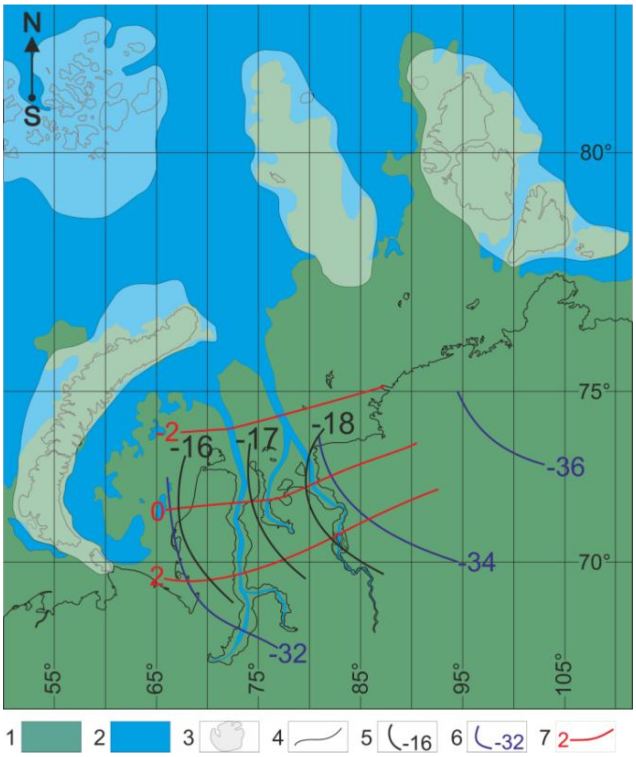

Figure 1. Schematic map of the paleogeographic pattern during MIS 2 (25-12 ka). 1- territory with subaerial conditions (land), 2 - territory occupied by the sea (subaqueous regions), 3- areas covered by glaciers, 4- modern coastline, 5- reconstructed average annual air temperatures, 6- reconstructed winter air temperatures, 7 - reconstructed summer air temperatures.

The glaciated areas are identified on the maps. The boundaries of glaciers are plotted in accordance with modern literature data (Gusev *et al.*, 2012).

Conclusions

The average paleotemperatures of January, Winter and Cold periods for the time intervals MIS 1 (5-3 ka), MIS 2 (25-12 ka), MIS 3 (30-26 ka) were calculated from the above regression equations for the Kara Sea region. The obtained temperatures were compared with modern meteorological station data averaged from 1961 to 1990 (climatic standard). In MIS 3 on the coast of the modern Kara Sea, the average temperature of the cold period was -23 to -25 °C, in January -32 to -35 °C. The decrease in the average annual air compared to modern values was 2-4 ° C.

In MIS 2, the temperature decrease at the western sector of the Russian Arctic, as compared to MIS 3, was insignificant. The temperature of the cold period decreased by only 2 °C, and the temperature of January by less 1 °C. Decrease of average annual air temperatures compared to modern values was 6-8 °C.

The transition from MIS 2 to MIS 1 is characterized by an increase in temperatures, both in the cold period and in January. The decrease in the average annual air temperatures in comparison with the modern values was 1-3 ° C.

Acknowledgments

The study was supported by grant 16-05-00612 from the Russian Foundation for Basic Research.

References

Dansgaard W., 1964. Stable isotopes in precipitation. *Tellus* 19 (4): 425-463.

Gornitz V. 2009. Sea level change, post-glacial. *In Encyclopedia of Paleoclimatology and Ancient Environments.* Springer, 1049 pp.

Gusev E.A., Kostin D.A., Rekant P.V., 2012. The problem of genesis of Quaternary formations of the Barents-Kara shelf (according to the materials of the State Geological Map of the Russian Federation, scale 1:1000000) (in Russian). *Otechestvennaya geologiya* 2: 84-89.

Kind N.V. *The geochronology of the Late Anthropogenic from isotopic data (in Russian).* Moscow. Science, 255 pp.

Rozanski K., Araguas-Araguas L., Gonfiantini R. 1993. Isotopic patterns in modern global precipitation. *Climate change in continental isotopic records. Washington, DC, USA, Amer. Geophys. Union.:* 1-36.

Holocene climate change records from sand wedge at Linggo Co, Qiangtang Plateau

Baolin Pan[1, 2], Chaolu Yi[2], Mingjian Wei [1], Zhongping Lai[3], Gang Hu[2], Guocheng Dong[2]

[1] *The Key lab resource environment and GIS, College of Resource, Environment and Tourism, Capital Normal University, Beijing, China*
[2] *Lab. of Tibetan Env. Changes and Land Surface Processes, Institute of Tibetan Plateau Research, Chinese Academy of Sciences, Beijing, China*
[3] *Key Laboratory of Salt Lake Resources and Chemistry, Qinghai Institute of Salt Lakes, Chinese Academy of Sciences, XiNing, China*

Abstract

As a type of periglacial landform, the sand wedges, usually form during dry and cold periods. One sand wedge was found, about 1.5 m high and 0.7 m wide, in the east lakeshore of Linggo Co in the central Tibetan Plateau (TP). Three optically stimulated luminescence (OSL) samples were collected from this sand wedge (SW) section, from the top, the middle, the bottom of the SW. In addition, one OSL sample was collected from the sand layer which overlies the sand wedge about 30 cm thick. We obtained ages of 0.4 ± 0.0, 1.5 ± 0.2, 1.5 ± 0.1 and 6.5 ± 0.5 ka for one sand layer and three sand wedge samples from top to the bottom of the section, respectively. The age obtained from the sand layer sample indicates that the sediments have been deposited during the Little Ice Age (LIA). The three ages from the SW from that it was active about 1.5 and 6.5 ka ago, *i.e.* during Middle and Late Holocene. During sand wedge activity, the lake level was lower than the bottom of the sand wedge and indicates a cold-dry period.

Keywords: Linggo Co, sand wedge, OSL dating, Holocene.

Introduction

In a certain sense, sand wedges(SW) are formed under conditions of cold climate, and controlled by temperature, water availability, soil texture and thickness, and the tiny terrain on the surface, ground cover (Wang *et al.,* 2003). They can be considered as an important indicator for cold-arid climate condition. So, the SW and can be used to reconstruct the paleo-climate or paleo-environment (Wang *et al.,* 2003; Cui *et al.*, 2004; Qi *et al.,* 2014). The specific aim of this research is to date the activity of a sand wedge, and discuss the climate changes during the SW formation period, at Linggo Co lake in QP, Central Tibetan Plateau (CTP).

Study area and section

Linggo Co is located on the west Tanggula Mountains in the central TP with an elevation of 5059 m a.s.l. (Fig. 1). The lake has a surface area of 95 km², a maximum water depth of more than 70 m, and is mainly supplied by meltwater from the Puruogangri ice field which is the biggest ice field in the TP, with an area of 422.6 km², ~30 km away to the east of Linggo Co (Fig. 1). On the east coast of the Linggo Co, one sand wedge was discovered during shoreline field surveys on the short wave-cut cliff, which slopes gently towards the lake, above the modern lake level. The section runs horizontally in an E–W direction, faces to the lake (Fig. 2, Fig. 3). Height of the sand wedge is about 1.5 m, the apparent maximum width and the apparent minimum width are 70 cm and 5 cm, respectively. The host sediment of the section consisted of diamicton, unfit for OSL dating. Therefore, no samples were taken from the host sediment. Other sand wedges were not found in this side of the lake. Probably, the more sand wedges maybe exist, but the outcrops of the SWs were not discovered.

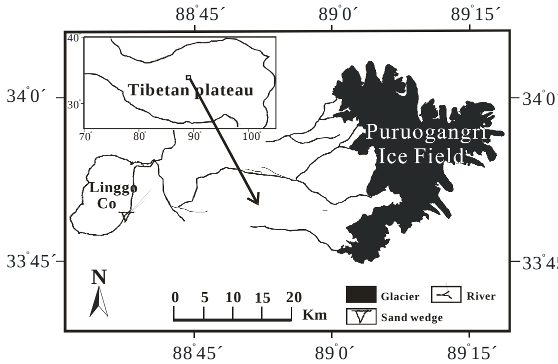

Figure 1. Location map of the Linggo Co, Puruogangri Ice Field and site of Sand wedge on the eastern coast.

Figure 2. The section of sand wedge, Linggo Co.

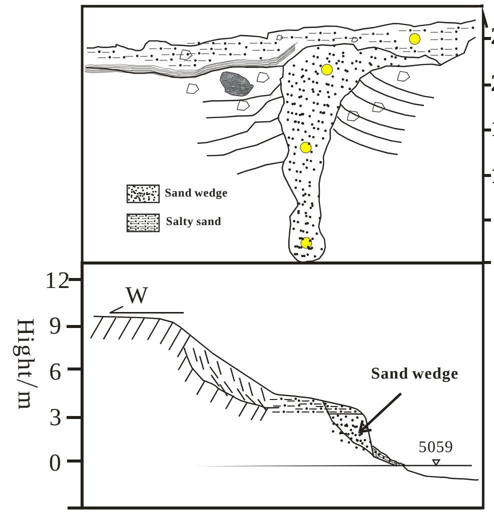

Figure 3. Schematic profile of the Linggo Co sand wedge showing sampling sections.

Materials and Methods

The OSL measurements were made using 470 nm stimulation at 130 °C for 40 s, and OSL was detected using a 7.5 mm thick U-340 filter (detection window 275–390 nm) in front of the photomultiplier tube. Irradiations were carried out using a 90Sr/90Y beta source within the RisØ reader.

In this study, the combination of the Single Aliquot Regeneration (SAR) protocol and Standard Growth Curves (SGC) methods was employed for the determination of the Equivalent doses (D_e). Fig. 4a shows the OSL decay curves for the samples LGC-SW-03. The natural and dose signals decayed to the level of the background within seconds, but the regeneration dose needed about ten seconds, demonstrated that the signals were mainly from the fast components and including the medium or slow components. The sand wedge samples exhibit a low luminescence signal (normally in the vicinity of one hundred counts/Gy for the 6 mm aliquots, integrated over the first 0.64s). The decay curve of 0-Gy regeneration shows a negligible thermal transfer signal. Recuperation was in all cases 1 % for all samples. Recycling ratios for all aliquots are in the range 0.9–1.1.

OSL ages of the sand wedge

The OSL result of the sand layer overlying the sand wedge at Linggo Co is 0.4 ± 0.0 ka, corresponding to the Little Ice Age (LIA). The ages of from upper, middle and bottom samples of the SW are 1.5 ± 0.2 ka, 1.4 ± 0.1 ka, 6.5 ± 0.5 ka, respectively. The results are in the stratigraphic order. The ages suggest that the SW was active discontinuously during the Holocene. The first wedge was smaller than the second. The overlying layer was deposited during the Little Ice Age (~0.4 ka ago).

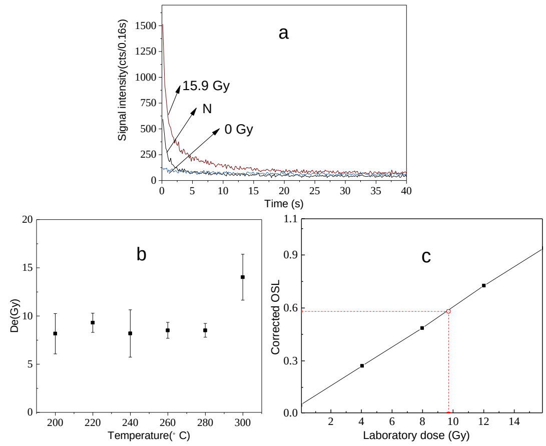

Figure 4. (a) OSL decay curves natural dose (0 Gy), natural dose (N), and regeneration dose (R4, 15.9 Gy) of sample LGC-SW-03. (b) Plots of De versus preheat temperature for samples LGC-SW-03. Each data point represents the mean of at least three aliquots. (c) OSL Standard Growth curve of the sample LGC-SW-03.

Discussion and conclusion

The sand wedge was active during the Middle and Late Holocene, which correspond to cold dry periods in the Qiantang Plateau area. During these periods, the temperature may have been lower by about ~ 5-8 ℃ than today in this area based on literature data. The lake level was least lower than the base of the sand wedge.

Acknowledgments

This study was financially supported by China NSF grants (40761010, 41301006). Thanks are given to Lei Yanbin and Ma Qingfeng for their field assistances.

References

Cui, Z. J., Yang, J. Q., Zhang, W., Zhao L., Xie, Y. Y., 2004. Discovery of a large area of ice-wedge networks in Ordos: Implications for the southern boundary of permafrost in the north of China as well as for the environment in the latest 20 kaBP. *Chinese Science Bulletin* 49(11): 1177-1184.

Qi, B. SH., Hu, D.G., Zhao, X. T., Zhang, X. J., Zhang, Y. L., Yang, X. X., Zhao, Zh., Gao, X. M., 2014. Fossil sand wedges in the northern shore of Qinghai Lake: discovery and paleoclimatic implications. *Journal of Glaciology and Geocryology* 36: 1412-1419 (in Chinese).

Wang, N. ANG., Zhang, J. M., Cheng, H. Y., Guo, J.Y., Zhao, Q., 2003. The age of formation of the mirabilite and sand wedges in the Hexi Corridor and their paleoclimatic interpretation. *Chinese Science Bulletin* 48: 1439-1445.

High-resolution quantification of earthworm calcite granules from western European loess sequences reflects stadial-interstadial climatic variability during the Last Glacial

Charlotte Prud'homme[1,2], Pierre Antoine[2], Olivier Moine[2]
Denis-Didier Rousseau[3], Kathryn Fitzsimmons[1]

[1] *Research Group for Terrestrial Palaeoclimates, Max Planck Institute for Chemistry, Hahn-Meitner-Weg 1, 55128 Mainz, Germany, c.prudhomme@mpic.de*
[2]*Laboratoire de Géographie Physique, Environnements Quaternaires et Actuels, (LGP), UMR 8591 CNRS/Universités Paris I/UPEC, 1 place Aristide Briand 92195 Meudon cedex, France*
[3]*Ecole Normale Supérieure, CERES-ERTI & LMD, 24 rue Lhomond, 75005 Paris, France and Lamont-Doherty Earth Observatory of Columbia University, Palisades, NY 10964, USA*

Abstract

Fossil granules of calcite produced by earthworms have been identified in the loess-palaeosol reference sequence of Nussloch, (Rhine Valley, Germany). They are particularly abundant in tundra gley horizons, which reflect short-term permafrost phases. These granules are characterized by a radial crystalline structure. In our study, we used this new biological indicator to characterize millennial-timescale climatic variations recorded in loess sequences, based on high resolution counting of granules in a 17-m-thick loess sequence. Increasing granule and mollusc concentrations suggest warmer climate conditions during palaeosol formation, associated with increasing biodiversity (biological activity and density of vegetation cover). Decreased granule concentrations occur within primary loess deposits, indicating a strong correlation with palaeoenvironmental conditions and demonstrating the utility of calcite granule concentration variation as a biological proxy.

Keywords: Earthworm calcite granules; Palaeoenvironmental reconstruction; Last Glacial; Western European loess; Palaeo-permafrost

Introduction

During the Last Glacial (112 to 17 ka), the European permafrost zone extended southwards to 47-44°N. Loess sequences record past permafrost conditions in the form of periglacial structures. They are mostly associated with tundra gley horizons, which formed due to hydromorphic processes in an active layer during permafrost decay.

The Nussloch loess sequence (Upper Rhine Valley, Germany) is considered one of the most complete aeolian records for the Last Glacial in western Europe (Antoine *et al.*, 2009). The middle section (~55-35 ka) is characterized by the development of arctic and boreal brown soils, whereas the upper section (~35-20 ka) is characterized by alternating primary loess (typical or laminated facies) and tundra gley horizons and by a higher sedimentation rate (up to 1mm/yr).

Fossil granules of calcite (ECG), found in loess sequences and produced by earthworms, are characterized by a radial crystalline structure. Present-day observations indicate that earthworms release their granules at the soil surface. The distribution of ECG down two 4-m-thick loess sequences in northern France correlates well with pedostratigraphy (Prud'homme *et al.*, 2015).

To further investigate the connection between ECG production and loess stratigraphy, two continuous parallel columns were sampled at high resolution (every 5 cm) in the 17-m-thick of the Nussloch P8 profile for sedimentological (~300 g each) and malacological/ECG analyses (~10 l each). Previous work analysing the stable isotope composition of the ECGs in the sequence allowed quantification of climatic parameters; precipitation during pedogenesis was 333 [159-574] mm/yr (Prud'homme *et al.*, 2017), whereas mean summer air temperature was 10±4°C during tundra gley formation, and 12±4°C during boreal brown soil formation (Prud'homme *et al.*, 2016).

The aim of this study is to compare the variability in absolute counts of ECGs continuously down the Nussloch loess profile, compared with grain size analyses. A new chronology of the Nussloch loess-sequence based on more than 40 radiocarbon dates undertaken on ECGs directly confirmed that pedogenesis took place during interstadial phases (Moine *et al.*, 2017).

Quantification of ECGs down the loess sequence

ECG counts strongly correlates with the pedostratigraphy (Fig. 1), as has already been observed in northern French sequences. However, since the sedimentation rate at Nussloch was higher, the precision of palaeoenvironmental reconstruction derived from ECG concentration is better. A strong correlation is observed between clay content and ECG concentration, with high values in palaeosols and low values in primary loess units. This observation suggests that earthworms were more active, and produced more granules during the formation of brown soils and tundra gley horizons.

Moreover, the variations of the mollusc concentration in the profile P3 of Nussloch show similar pattern as the ECG variations, especially during the Middle Pleniglacial. The increase of the molluscan diversity species indicates a densification of the vegetal cover such as steppe or shrub tundra environment during the interstadials. These observations suggest that brown soils and tundra gleys are formed under milder conditions and are associated with an increase in biodiversity.

Earthworms seem to be more sensitive to climate variations than soil horizons themselves, and provide more detailed evidence for the duration of warmer, wetter conditions. The amplitude of the ECG peak in the tundra gley horizons is larger than stratigraphical units. Thus, the activity of the earthworms precedes the development of the pedogenesis, suggesting that the increased of the temperature and humidity might start before the pedogenesis processes. Since ECG peak concentrations occur at surface (0-5 cm) of present day soils, and the concentration of ECGs in brown soils and tundra gleys differs from this pattern, we can infer that brown soils and tundra gley horizons represent accretionary soil processes. Incipient tundra gleys also occur within the Upper Pleniglacial horizons and are characterized by a large number of granules, indicating that ECGs can also be used to identify short-lived climate ameliorations. Furthermore, three drastic decreases in ECG concentration are recorded in the laminated loess units. These units, characterized by a high coarse silt content, were deposited during windy periods and correlate with major dust peaks in the Greenland NGRIP record associated with Heinrich Stadials 3 and 2.

Conclusion

The compilation of ECG concentration and grain size variations, palaeoclimate data and radiocarbon dating confirms that the ECG can be used as a new palaeoenvironmental proxy for Last Glacial continental environments. This new proxy can help us to better understand the response of terrestrial archives to millennial-timescale climate variations identified in the ice core record.

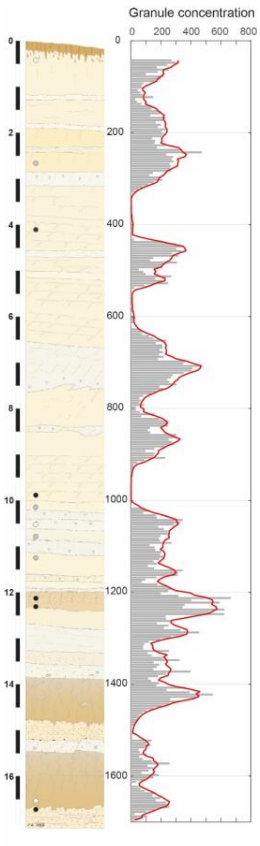

Figure 1: Variation of the ECG with the pedostratigraphy of the loess-palaeosol sequence at Nussloch (P8)

References

Antoine, P., Rousseau, D. D., Moine *et al.*, 2009. Rapid and cyclic aeolian deposition during the Last Glacial in European loess: a high-resolution record from Nussloch, Germany. *Quaternary Science Reviews* 28: 2955–2973.

Moine, O., Antoine, P., Hatté, C. *et al.*, 2017. The impact of Last Glacial climate variability in west-European loess revealed by radiocarbon dating of fossil earthworm granules. *Proceedings of the National Academy of Sciences* 114(24): 6209-6214.

Prud'homme, C., Antoine, P., Moine *et al.*, 2015. Earthworm calcite granules: a new tracker of millennial-timescale environmental changes in Last Glacial loess deposits. *Journal of Quaternary Science* 30(6): 529–536.

Prud'homme, C., Lécuyer, C., Antoine, P. *et al.*, 2016. Palaeotemperature reconstruction during the Last Glacial from δ18O of earthworm calcite granules from Nussloch loess sequence, Germany. *Earth and Planetary Science Letters* 442: 13–20.

Prud'homme, C. *et al.*, 2018. d13C signal of earthworm calcite granules: a new proxy for palaeoprecipitation reconstructions during the Last Glacial in Western Europe. *Quaternary Science Reviews* 179: 158–166.

Past 130-thousand-year frozen ground distribution north of 50°N: reconstructed advance and retreat

Kazuyuki Saito[1]
Hirokazu Machiya[2]
[1]*Japan Agency for Marine-Earth Science and Technology, ksaito@jamstec.go.jp*
[2] *Japan Agency for Marine-Earth Science and Technology*

Abstract

Simulated reconstruction of expansion and retreat of circumpolar permafrost and seasonally frozen ground distribution is attempted for the past 130 thousand years (from the Eemian/last Interglacial to the present) for north of 50ºN, using combinations of mean annual air temperature (MAAT) time series reconstructed from Greenland ice cores, coastlines and ice sheets distributions during the glacial and deglaciation period, glacial-interglacial MAAT amplitude calculated from climate model outputs, and statistical frozen ground classifications.

Keywords: Frozen ground distribution; Last interglacial; Last glacial period; Paleoclimate reconstruction.

Introduction

Changes in subsurface thermal state and consequential frozen ground distribution are interactively related to those in the eco-topo-climatic environments, which collectively condition the flora and fauna of the region. Identification of permafrost expansion in the Northern Hemisphere at the coldest period of the last glacial time was conducted by Vandenberghe *et al.* (2014).

Use of atmosphere-land-ocean-coupled numerical climate models, i.e., global climate models (GCMs), or earth system models (ESMs), for past reconstructions was demonstrated and validated against the field-based evidence by Saito *et al.* (2013, 2014, 2016). In those previous attempts, reconstructed periods were limited to those, at which GCM/ESM integrations were conducted. In this study, we attempt to depict the transience of changes at a 1 K time step, using combinations of core-derived temperature times series, spatial interpolation with GCM outputs, and statistical classification.

Glacial advance and interglacial retreat

Data and methodology

Mean annual air temperature (MAAT) time series relative to the present-day was taken from the SeaRISE project (Bindschadler, R. *et al.,* 2013). ICE6G (Argus *et al.* 2014; Peltier *et al.* 2015) were used for coastline (land/sea mask) and ice sheets distribution for the period 26ka and present-day. For the period 130ka and 26ka, the coastline and ice sheets distribution have not been reconstructed at the same resolution of ICE6G. Therefore, these distributions at an era between 130ka and 26ka were assumed to be the same as what ICE6G reconstructs at such period that has the same global sea-level (Rohling *et al.*, 2014) between 21ka and the present day.

The above MAAT anomaly time series, taken from one point of the high-latitude Northern Hemisphere, were assumed to represent the overall temporal variability during the simulated period, however, the magnitude of those variability at each grid cell was modified in such a manner as to comply with the magnitude of the glacial-inter glacial difference, namely defined by the spread of the global model-ensemble MAAT outputs between the Last Glacial Maximum (LGM; 21ka) and the mid-Holocene (6ka). The global model-ensemble was derived from five PMIP3 models (Braconnot *et al.*, 2012).

Reconstructed maps

Reconstructed expansion during the glacial period and retreat at the deglaciation are shown at the select periods for the last glacial and post-glacial periods (26ka, 14ka, 11ka, the present-day) for permafrost (CP: continuous, EP: discontinuous), and seasonally freezing ground (SF: >2-week, IF: <2-week), no freezing (NF), land ice mass, and oceans (Fig. 1). Analysis shown in Fig. 1 was done at the 1°-by-1° horizontal resolution, however, extension to a finer resolution is straightforward through the application of the downscaling procedure demonstrated by Saito et al. (2014, 2016) for northeastern Asia and south America, respectively.

a) 26ka

b) 14ka

c) 11ka

d) 0ka

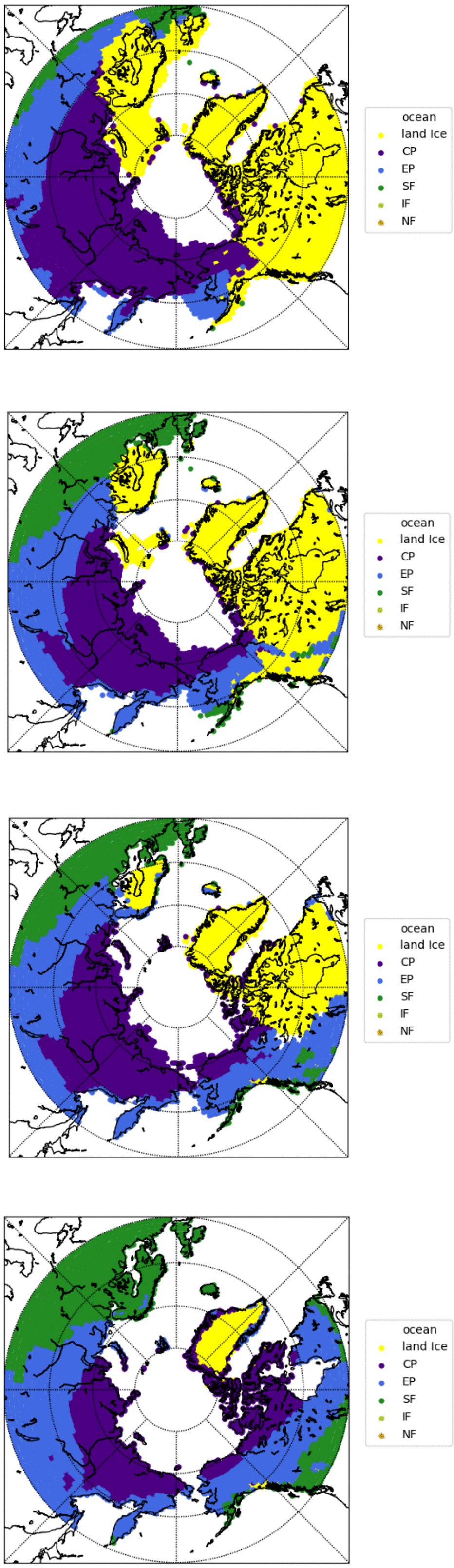

Figure 1. Changes in frozen ground distribution north of 50N for a) 26ka (thousand years before present), b) 14ka, c) 11ka, and d) present-day.

References

Argus, D.F., Peltier, W.R., Drummond, R. & Moore, A.W., 2014. The Antarctica component of postglacial rebound model ICE-6G_C (VM5a) based upon GPS positioning, exposure age dating of ice thicknesses, and relative sea level histories. *Geophys. J. Int.,* 198(1): 537-563, doi:10.1093/gji/ggu140.

Bindschadler, R. *et al.,* 2013. Ice-sheet model sensitivities to environmental forcing and their use in projecting future sea level (the SeaRISE project). *Journal of Glaciology,* 59 (214): 195-224

Braconnot, P., Harrison, S.P., Kageyama, M., Bartlein, P.J., Masson-Delmotte, V., Abe-Ouchi, A., Otto-Bliesner, B., & Zhao Y. 2012. Evaluation of climate models using palaeoclimatic data. *Nature Climate Change*, 2: 417–424. DOI: 10.1038/NCLIMATE1456.

Peltier, W.R., Argus, D.F. & Drummond, R., 2015. Space geodesy constrains ice-age terminal deglaciation: The global ICE-6G_C (VM5a) model. *J. Geophys. Res. Solid Earth,* 120: 450-487, doi:10.1002/2014JB011176.

Rohling, E. J., Foster, G. L., Grant, K. M., Marino, G., Roberts, A. P. Tamisiea, M. E. & Williams, F., 2014. Sea-level and deep-sea-temperature variability over the past 5.3 million years, *Nature,* 508: 477-482

Saito, K., Trombotto Liaudat, D., Yoshikawa, K., Mori, J., Sone, T., Marchenko, S., Romanovsky, V., Walsh, J. Hendricks, A. & Bottegal, E., 2016. Late Quaternary Downscaled Permafrost Distributions in South America: Examinations of GCM-based maps with observations. *Permafrost and Periglacial Processes*, 27: 43–55. DOI: 10.1002/ppp.1863.

Saito, K., Marchenko, S., Romanovsky, V., Hendricks, A., Bigelow, N., Yoshikawa, K. & Walsh, J., 2014. Evaluation of LPM permafrost distribution in northeast Asia reconstructed and downscaled from GCM simulations. *Boreas*, 733-749, 10.1111/bor.12038. ISSN 0300-9483.

Saito, K., Sueyoshi, T., Marchenko, S., Romanovsky, V., Otto-Bliesner, B., Walsh, J., Bigelow, N., Hendricks, A. & Yoshikawa, K., 2013. LGM permafrost distribution: How well can the latest PMIP multi-model ensembles perform reconstruction? *Climate of the Past*, 9: 1697–1714, doi:10.5194/cp-9-1697-2013.

Vandenberghe, J., French, H.M., Gorbunov, A., Marchenko, S., Velichko, A.A., Jin, H., Cui, Z., Zhang, T., Wan, X., 2014. The Last Permafrost Maximum (LPM) map of the Northern Hemisphere: permafrost extent and mean annual air temperatures, 25–17 ka BP. *Boreas* 43: 652–666. DOI: 10.1111/bor.12070.

Paleoclimate variations and impact on groundwater recharge in multi-layer aquifer systems using a multi-tracer approach (northern Aquitaine basin, France).

Marc Saltel[1]
Romain Rebeix[2,3]
Bertrand Thomas[2,3]
Michel Franceschi[4,5]
Bernard Lavielle[2,3]
Pascal Bertran[6,7]

[1] *BRGM Nouvelle Aquitaine, Parc Technologique Europarc, 24, Avenue Léonard de Vinci, 33600 Pessac, France (m.saltel@brgm.fr)*
[2] *University of Bordeaux, CENBG, 19 Chemin du Solarium - CS 10120, 33175 Gradignan Cedex, France*
[3] *CNRS (UMR 5797) CENBG, 19 Chemin du Solarium - CS 10120, 33175 Gradignan Cedex, France*
[4] *Bordeaux INP, G&E, EA 4592, 33600 Pessac, France*
[5] *University Bordeaux Montaigne, G&E, EA 4592, 33600 Pessac, France*
[6] *Inrap, 140 avenue du Maréchal Leclerc, 33130 Bègles, France*
[7] *PACEA, University of Bordeaux-CNRS, allée Geoffroy-Saint-Hilaire, 33615 Pessac, France*

Abstract

The northern Aquitaine Basin (southwest France) is a large multi-layer aquifer system that contains groundwater with strong residence time variability ranging from years to tens of thousands years. This system was studied using a multi-parameter approach involving isotopic tracers (^{14}C, ^{18}O, ^{2}H) to determine the groundwater residence time and to document climate fluctuations, while dissolved noble gases were used to estimate mean annual temperatures at the water table (NGRT, Noble Gas Recharge Temperature). Near-surface ground temperature reconstruction from 40 ka cal BP to the present was made using data collected from 5 aquifers. The coldest temperatures are recorded during late Marine Isotopic Stage (MIS) 3 and MIS 2, i.e. between 36 and 18 ka cal BP. The mean NGRT for the period 25-18 ka cal BP is estimated at 5.9 ± 0.9°C, and a strong increase towards modern values (11 to 13°C) is observed after 15 ka cal BP. The temperature drop between the Holocene and the Last Glacial ranges from 5 to 7°C, in agreement with previous NGRT studies in Europe. Since mean near-surface ground temperatures during the glacial were well above 0°C, long-term presence of permafrost in northern Aquitaine is unlikely.

Keywords: Stable isotopes, Groundwater age, Paleohydrology, Noble Gas, Late Pleistocene climate, Groundwater recharge, southwest France

Introduction

In southwest France, the Aquitaine basin is a large multi-layer aquifer system where groundwater has residence times from a few years or decades to thousands of years (Chery *et al.*, 1994) (Fig. 1). Since present groundwater is inherited from former aquifer recharge, which occurred under changing climate conditions, this residence time variability gives the opportunity to use the aquifers as paleoclimate archives for this time span (Fontes *et al.*, 1993). The purpose in the present study is to investigate this question through analyses of groundwater sampled in the northern part of the basin. A comparison with other regional proxies is then proposed.

Methods

Natural isotopic tracers have been used to determine the groundwater residence time (^{14}C), and to highlight the paleoclimate fluctuations (^{18}O, ^{2}H). Noble gas measurements (He, Ne, Ar, Kr, Xe) were used to determine the mean annual temperature at the water table (Noble Gas Recharge Temperature, NGRT).

Results and discussion

A total of 120 values of residence time from groundwater of 5 aquifers were calculated. The most recent residence times were observed near the outcrop areas. The oldest were measured in the Middle Eocene aquifer along the corridor formed by the Garonne River, which constitutes a natural drainage channel. Overall, the data shows that the aquifers in southern France were recharged continuously during the last 40 ka. This strongly suggests that permafrost, if present, was not enough widespread to have had any significant impact on aquifer recharge. Associating Noble Gases Recharge Temperature with groundwater residence times makes it possible to reconstruct paleotemperatures since 40 ka (Fig. 2). According to the data, the mean NGRT during the Holocene is 11.3 ± 1.1°C. This value is in good agreement with the mean modern temperature of near surface aquifers in southwest France. Over the period 25-18 cal. ka BP (MIS 2), the estimated NGRTs are quite homogeneous and yield a mean of 5.9 ± 0.9°C. The temperature decrease during MIS 2 relative to present is 5 to 7°C. For the MIS 3 samples (ages > 27 cal. ka BP), the NGRT rises by approximately 3°C and shows significant scattering, which reflects the alternation of short (a few hundred years long) warm interstadials and longer (in order of a millennium) cold stadials. The mean reconstructed NGRT for MIS 2 indicate that near-surface ground thermal conditions were significantly over 0°C and, therefore, not adequate for long-term permafrost development in southwest France, as already suggested by the lack of recharge gap in the aquifers. The lowest NGRT value found in Léognan (5.0 ± 0.4°C) at 23.9 ± 0.8 ka cal. BP, which may correspond to one of the coldest phase of MIS 2, also suggests that permafrost, even in favorable contexts (sporadic permafrost), was unlikely to occur during the coldest phases.

Acknowledgments

This work has been financed by Adour-Garonne Water Agency and OASU (Observatoire Aquitain des Sciences de l'Univers) through the Special Project "Organics and Inorganics Contaminants". The sampling campaign has been realised with the help of the Conseil Départemental de la Gironde and SUEZ Environment who gave us access to the wells. PB was funded by the SISMOGEL project (EDF, Inrap, University of Bordeaux).

References

Chery, L., Dusseau, P., Sourisseau, B., 1994. *Diagnostic de l'accroissement de la salinité des nappes profondes de l'Éocène moyen en Gironde*, Technical report, BRGM/RR-37998-FR, BRGM, Orléans.

Fontes, J.C., Stute, M., Schlosser, P., Broecker, W.S., 1993. Aquifers as archives of paleoclimate. *Eos Trans. AGU*, 74(2): 21-22.

Rasmussen, S.O. et al., 2014. A stratigraphic framework for abrupt climatic changes during the Last Glacial period based on three synchronized Greenland ice-core records: refining and extending the INTIMATE event stratigraphy. *Quaternary Science Reviews* 106:14–28.

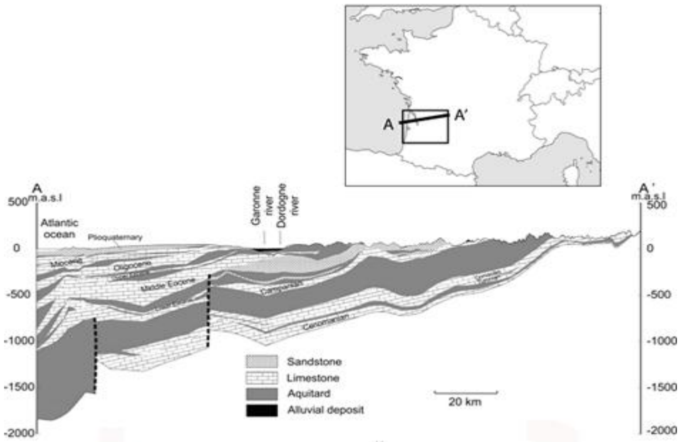

Fig. 1: Hydrogeological cross-sections of the North Aquitaine Basin.

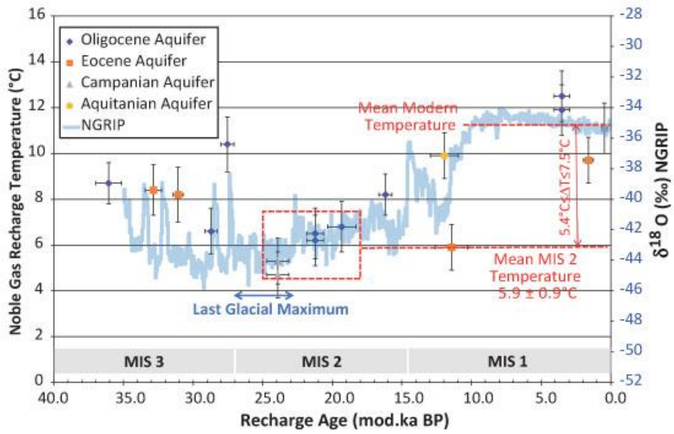

Fig 2: Noble Gas Recharge Temperatures versus groundwater recharge age. NGRIP δ18O is from Rasmussen et al. (2014).

Post-LGM landscape response to deglaciation in Val Viola, Central European Alps

Riccardo Scotti[1]
Francesco Brardinoni[1]
Giuseppe Cola[2]
Volkmar Mair[3]
[1] *Department of Biological, Geological and Environmental Sciences (BiGeA), University of Bologna, riccardo.scotti@unibo.it*
[2] *Glaciological Service of Lombardy (SGL)*
[3] *Office for Geology and Building Materials Testing, Autonomous Province of Bolzano*

Abstract

Starting from existing ^{10}Be exposure dating in Val Viola, we present the first detailed, post-LGM reconstruction of landscape response to deglaciation south of the Alpine divide. We pursue this task through Schmidt-hammer exposure-age dating (SHD) at 34 sites including moraines, rock glaciers, protalus ramparts, rock avalanche deposits and talus cones. Resulting ages indicate that favourable conditions to periglacial landform development occurred during the Younger Dryas (12.7 ± 1.1 ka), as well as in the Early and Late Holocene (10.7 ± 1.3 and 3.7 ± 0.8 ka) and suggest a ~10.000 year-long history of permafrost-related activity. Most of the mass wasting activity clusters within the Early Holocene, in correspondence of an atmospheric warming phase. By contrast, the timing of the main Val Viola rock avalanche, 7.7 ± 0.3 ka during the Holocene Thermal Optimum, suggests a possible causal linkage to permafrost degradation.

Keywords: Lateglacial; Schmidt-hammer exposure-age dating; Deglaciation; Rock glaciers; Rock avalanches; Permafrost

Introduction

Reconstructing the timing and styles of landscape response to deglaciation is critical for understanding the evolution of formerly glaciated settings (e.g., Church & Ryder, 1972). To achieve these goals it is fundamental to map the spatial organization of relict glacial and periglacial landforms, and constrain the chronology of their formation. In this study, we reconstruct the post-LGM landscape history, associated with glacial, periglacial, and mass wasting processes in Val Viola, a site located south of the main Alpine divide within the Central European Alps. To this end, starting from existing ^{10}Be dates (i.e., Hormes *et al.,* 2008), we apply SHD on 34 sites including moraines, rock glaciers, protalus ramparts, talus cones and rock avalanche deposits (Fig. 1).

Methods

We conducted a detailed mapping of glacial and periglacial landforms via fieldwork and aerial photo interpretation. Analysis of Schmidt-hammer (R)-values, which allowed obtaining the spatial distribution of calibrated ages, followed consolidated standard procedures (Matthews & Owen, 2010) and involved building four lithology-specific calibration curves based on the three recalculated ^{10}Be dates. These data were then integrated with a GIS-based reconstruction of paleo glacier extent from the Younger Dryas to the Little Ice Age.

Findings

Results show that post-LGM geomorphic response to repeated atmospheric temperature fluctuations was quite diverse across landscape components, with glacier extent conditioning the opportunity for permafrost aggradation and rock glacier formation on deglaciated terrain. The formation of the three rock glaciers considered in this study spans across 9 ka. Interestingly, the two currently intact ones i.e. supposedly still in permafrost conditions, developed roughly 7 ka apart. One (RG2) in the Early Holocene (10.7 ± 1.3 ka) and today overrides an older (12.7 ± ka) relict rock glacier (RG1), the other (RG3) in the Late Holocene (3.7 ± 0.8 ka) (Fig. 2). The former, implies a ~10.000 year-long history of permafrost-related activity, confirming recent findings on rock glacier “longevity” in South Tyrol (Krainer *et al.,* 2015). The latter suggests a Late Holocene revived phase of permafrost aggradation possibly linked to the Löbben oscillation (~3.7-3.1 ka).

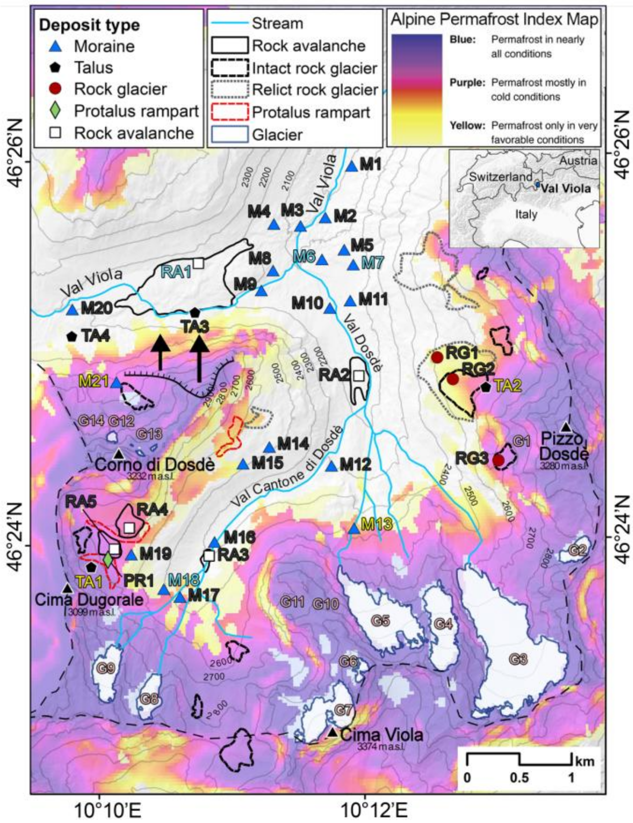

Figure 1. Map of the Upper Val Viola showing the present day permafrost distribution according to the Alpine Permafrost Index Map (Boeckli *et al.,* 2012) and the relevant study landforms. Black arrows indicate the inferred Val Viola rock avalanche trajectory (RA1).

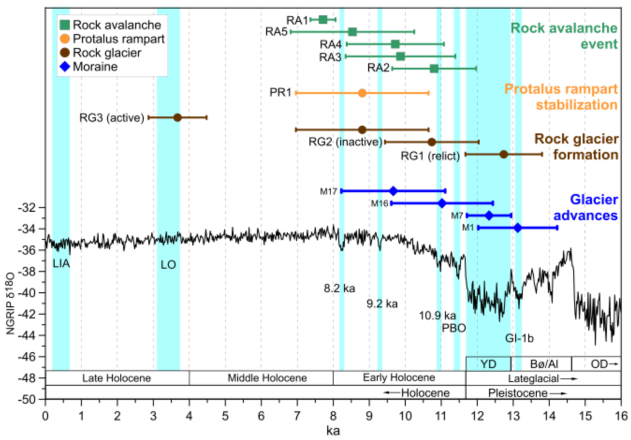

Figure 2. (Modified from Scotti et al., 2017) SHD exposure ages as a function of inferred temperature fluctuations. Bars indicate 95% confidence intervals. Cold phases are shaded in light blue, OD: Oldest Dryas, Bø/Al: Bølling/Allerød. Gl-1b: Gerzensee Oscillation, YD: Younger Dryas, PBO: Pre Boreal Oscillation, LO: Löbben Oscillation and LIA: Little Ice Age. Temperature proxy is based on NGRIP oxygen-isotope record (Rasmussen *et al.,* 2007).

Four of the five rock avalanches dated in Val Viola occurred in an atmospheric warming phase during the Early Holocene. However, the largest mass wasting event recorded, the Val Viola Rock avalanche (RA1), occurred at the apex of the Holocene Thermal Optimum (7.7 ± 0.3 ka). Considering the similarities between today's warming climate and the Middle Holocene, given that presently RA1 source area is in likely permafrost conditions (Fig. 1), by analogy, it is possible that the rocky slope became destabilized in response to permafrost degradation.

References

Boeckli, L., Brenning, A., Gruber, S. & Noetzli, J., 2012. A statistical approach to modelling permafrost distribution in the European Alps or similar mountain ranges. *Cryosphere* 6: 125-140.

Church, M. & Ryder, J.M., 1972. Paraglacial sedimentation: a consideration of fluvial processes conditioned by glaciation. *Geol. Soc. Am. Bull.* 83: 3059-3072.

Hormes, A., Ivy-Ochs, S., Kubik, P.W., Ferreli, L. & Maria Michetti, A., 2008. 10Be exposure ages of a rock avalanche and a late glacial moraine in Alta Valtellina. Ital. Alps. *Quat. Int.* 190: 136-145.

Krainer, K., Bressan, D., Dietre, B., Haas, J.N., Hajdas, I., Lang, K., Mair, V., Nickus, U., Reidl, D., Thies, H. & Tonidandel, D., 2015. A 10,300-year-old permafrost core from the active rock glacier Lazaun, southern Ötztal Alps (South Tirol, northern Italy). *Quat. Res.* 83: 324-335.

Matthews, J.A. & Owen, G., 2010. Schmidt hammer exposure-age dating: developing linear age-calibration curves using Holocene bedrock surfaces from the Jotunheimen-Jostedalsbreen regions of Southern Norway. *Boreas* 39 (1): 105-115.

Rasmussen, S.O., Vinther, B.M., Clausen, H.B. & Andersen, K.K., 2007. Early Holocene climate oscillations recorded in three Greenland ice cores. *Quat. Sci. Rev.* 26: 1907-1914.

Scotti, R., Brardinoni, F., Crosta, G. B., Cola, G., & Mair, V., 2017. Time constrains for post-LGM landscape response to deglaciation in Val Viola, Central Italian Alps. *Quat. Sci. Rev.* 177: 10-33.

Paleopedological tracers of the Late Pleistocene cryogenic environments in Europe and Western Siberia

Sergey Sedov[1], Vladimir Sheinkman[2], Vladimir Melnikov[3]

[1]Tyumen Industrial University, Russia, serg_sedov@yahoo.com
[2]Earth Cryosphere Institute of the Tyumen Science Center, RAS, Siberian Branch; Russia
[3]Tyumen State University, Russia

Abstract

Cryolithogenesis interacts with the pedogenetic processes forming a set of specific features in the solid matrix of soils. These features are preserved in the buried paleosols where they could be used as indicators (direct and indirect tracers) of the past cryogenic environment. MIS3 paleosols in the center - north of European Russia (Upper Volga basin) and Western Siberia (Middle Ob' basin) and MIS2 paleosols in low Austria are represented by hydromorphic profiles with gleyic colour pattern and sometimes Histic horizons. Conspicuously, they are developed in the well-drained geomorphic positions, where modern soils are non-gleyic. We suppose that the presence of permafrost in the Late Pleistocene was responsible for water logging and generation of reductomorphic soil environment. Macromorphological signs of cryoturbation and micromorphological evidences of coarse grain sorting and platy microstructure due to ice lens development provide additional direct indicators of cryogenic environment.

Keywords: cryogenesis, paleosols, gley, permafrost, late Pleistocene.

Introduction

Identification and reliable interpretation of the witnesses of the past permafrost development (proposed as a special branch of geosciences – cryotrassology) is of major important for reconstructing past terrestrial environments of the former cold periods. Such indicators/tracers of those events as pseudomorphs after repeated ice wedges, cryoturbations in sedimentary layers, solifluction features, lenses of segregation ice etc. are reliable but not ubiquitous direct markers.

However besides these direct evidences, soil systems could provide indirect indicators of the past cryogenic conditions. Certain pedogenetic processes although not necessarily linked to permafrost, are strongly influenced or modified in its presence. In particular icy permafrost layers could cause water saturation and thus switch on the hydromorphic soil forming processes: accumulation of peat and gleyzation in the mineral horizons, in the geomorphic positions and substrates where otherwise well-drained non-gleyic soils are formed. Therefore, we propose to use the indirect pedological indicators/tracers of former permafrost in order to complete the information about its spatial distribution and chronostratigraphic occurrence.

Materials and Methodology

We carried out comparative analysis of the late Pleistocene gleyic paleosols discovered: within the alluvial and lacustrine sequences in the center - north of European Russia (Upper Volga basin) and Western Siberia (Middle Ob' and Taz basins), and in Upper Austria in the classical loessic sequences. Correlation and pedogenetic interpretation of the studied profiles was carried out on the basis of macro- and micromorphological characteristics and radiocarbon datings of the paleosol organic materials, sometimes supported by luminescence dates of sedimentary strata

Results and Discussion

Recently well-developed paleosols formed during the MIS3 were discovered to the north from the Eurasian Loess Belt, in the north of European Russia, Upper Volga basin (Rusakov, Sedov, 2012) and North-Western Siberia, Middle Ob' basin (Sheinkman et al. 2016), and recently – in the Taz basin. The paleosols are developed within the Late Pleistocene alluvial and lacustrine sequences and produced radiocarbon dates from its organic materials within the time interval of 50–25 Ka BP (Fig. 1).

They represent hydromorphic profiles with Histic horizons or materials and gleyic colour pattern. In thin sections numerous specific ferruginous pedofeatures (concentric nodules, mottles, stripes) as well as abundant poorly decomposed plant fragments were (Fig. 2).

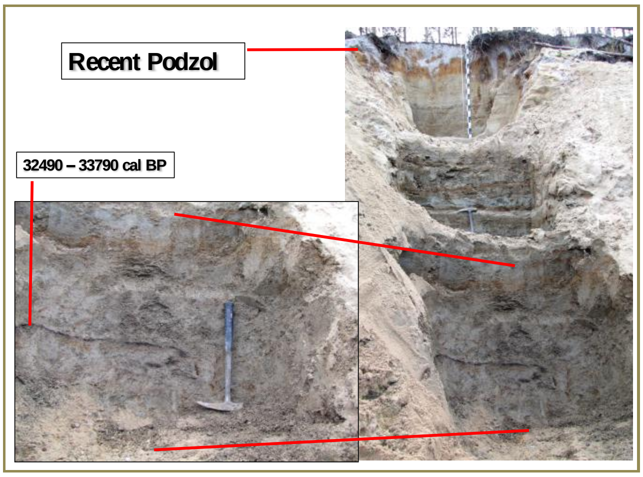

Figure 1. MIS3 gleyic paleosol in the alluvial section Belaya Gora (Vakh river, Middle Ob' basin)

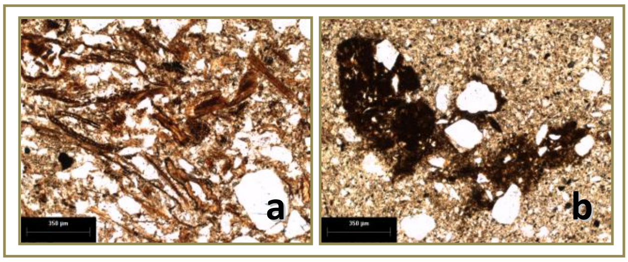

Figure 2. Micromorphology of MIS3 gleyic paleosol in the middle Ob´ basin: a – plant tissue fragments, b – ferruginous nodules. Plain polarized light.

Conspicuously they are developed in the well-drained geomorphic positions, where modern soils (Podzols and Luvisols) have only weak surficial redoximorphic (stagnic) features. These paleosols differ from synchronous Cambisols and Chernozems formed within loess sequences to the south.

In the Late Pleistocene loessic sequences of Germany and Austria strongly gleyed soils (known as Tundragley or Naßboden) correspond to the strata, developed during MIS2 including MIS3/MIS2 transition (Terhorst et al. 2015). Again, they are formed in the elevated landsurfaces providing good drainage on porous calcareous loess which hampers gleyzation. Indeed earlier (MIS3) and later (Holocene) soils of the same sequences are non-gleyic Cambisols and Luvisols. Additional evidences of permafrost in these soils are provided by morphological features of horizon fragmentation and mixing by cryoturbation and solifluction. Also in thin sections signs of cryogenic structuring, grainsize sorting, mixing of organic and mineral materials and deformation of plant debris and pedofeatures by frost processes are observed. Similar interpretation of the MIS2 incipient gleyic paleosols in the West German loessic sequences was proposed earlier by Antoine (2009).

In all presented cases we attribute strong gleization to permafrost rather than to deep seasonal freezing because only constantly frozen icy layer in the bottom of the profile could provide watter-logging and anoxic conditions throughout the year including the warmest season (when maximal microbial activity and thus gleyzation could take place). According to this interpretation we classify these paleosols as Reductaquic Cryosols. From the described spatial/temporal occurrence of the cryogenic gleyic paleosols we deduce the following: 1) Our data on gleyic MIS3 paleosols in the Upper Volga and Middle Ob' basins together with the findings of similar MIS3 gleyic paleosols in Kolyma lowlands (Zanina et al. 2011) point to a continuous zone of Reductaquic Cryosols in the Northern Eurasia during the Middle Valday/Karga interstadial (Sedov et al. 2016). This zone shifted several hundreds of km to the southwest towards the Central Europe during the MIS3-MIS2 transition. This was conditioned by the southward extension of permafrost in the beginning of the MIS2.

References

Rusakov, A. & Sedov, S., 2012. Late Quaternary pedogenesis in periglacial zone of northeastern Europe near ice margins since MIS 3: Timing, processes, and linkages to landscape evolution. *Quaternary International* 265: 126–141.

Sedov, S., Rusakov, A., Sheinkman, V. & Korkka, M., 2016. MIS3 paleosols in the center-north of Eastern Europe and Western Siberia: Reductomorphic pedogenesis conditioned by permafrost?, *Catena* 146: 38-47.

Sheinkman, V., Sedov, S., Shumilovskikh, L., Korkina, E., Korkin, S., Zinovyev, E. & Golyeva, A., 2016. First results from the Late Pleistocene paleosols in northern Western Siberia: Implications for pedogenesis and landscape evolution at the end of MIS3. *Quaternary International* 418: 132-146.

Terhorst, B., Sedov, S., Sprafke, T., Peticzka, R., Meyer-Heintze, S., Kühn, P. & Solleiro Rebolledo, E., 2015. Austrian MIS 3/2 loess–palaeosol records—Key sites along a west–east transect. *Palaeogeography, Palaeoclimatology, Palaeoecology* 418: 43–56.

Zanina, O.G., Gubin, S.V., Kuzmina, S.A., Maximovich, S.V., Lopatina, D.A., 2011. Late-Pleistocene (MIS 3-2) palaeoenvironments as recorded by sediments, palaeosols, and ground-squirrel nests at Duvanny Yar, Kolyma lowland, northeast Siberia. *Quat. Sci. Rev.* 30, 2107–2123.

Antoine, P., Rousseau, D.-D., Moine, O., Kunesch, S., Hatté, C., Lang, A., Tissoux, H., Zöller L., 2009, Rapid and cyclic aeolian deposition during the Last Glacial in European loess: a high-resolution record from Nussloch, Germany. *Quat. Sci. Rev.* 28, 2955–2973.

Reconstructing permafrost depth for high-level waste repositories in Germany

Lena Stark[1]
Jobst Maßmann[2]
[1]*Federal Institute for Geosciences and Natural Resources (BGR), Stilleweg 2, 30655 Hannover, Lena.Stark@bgr.de*
[2]*Federal Institute for Geosciences and Natural Resources (BGR), Stilleweg 2, 30655 Hannover, Jobst.Massmann@bgr.de*

Abstract

In safety assessment for high-level waste (HLW) repositories in Germany the future impact of safety-relevant processes like permafrost have to be considered for the next 1 million years. An estimation of the future development of permafrost and its maximum depth can be based on numerical simulations. Within the present study, we use the free, multi-platform numerical modeling package OpenGeoSys to investigate the permafrost depth during the last glacial maximum at generic geological settings representing hypothetical sites for HLW repositories in rock salt, claystone and crystalline rock in Germany.

Keywords: LGM, permafrost, numerical simulations, OpenGeoSys

Introduction

With the StandAG (Repository Site Selection Act) becoming effective, the site selection for a high-level waste repository in Germany restarted in 2017. The procedure of site selection is divided into several steps, which include different preliminary safety investigations. Part of these safety investigations is an assessment of processes with potential to influence the safety of a HLW repository over a period of 1 million years into the future.

One possible safety-relevant process is the development of permafrost under periglacial conditions. Permafrost can occur up to large depths and changes the thermal, hydraulic and mechanic conditions of the geosphere. Permafrost has a strong influence on groundwater chemistry, groundwater flow and thus a potential radionuclide transport. Moreover, an impact on engineered barriers with steel elements, concrete or bentonite elements may be possible. Therefore, it is important to determine how deep permafrost will develop to properly address the possible impact on the repository system.

Permafrost reconstruction

The future development of permafrost can only be extrapolated from the conditions and trends observed in the past. The climate in northern Europe has experienced several glacial periods over the past and according to the currently occurring climate cycle, it is expected that about ten warm intervals will alternate with glacial periods within the next 1 million years. Time series of climate data from the last glacial maximum (LGM) are used as an analogue for future permafrost development.

Permafrost extent during the LGM

During the LGM Germany experienced permafrost conditions a several times. As a result Pleistocene periglacial features like ice-wedge pseudomorphs, relict polygon networks or pingos are widely distributed.

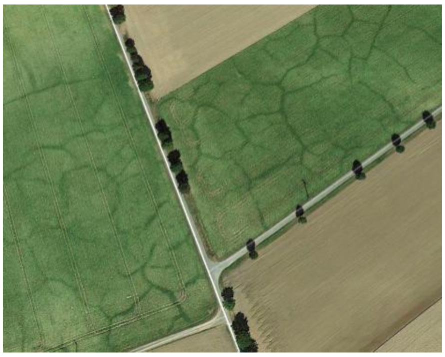

Figure 1. Aerial view of relict polygon networks (Google Earth 2017, 52°1‘9.18“N, 10°34‘54.66“E) near Isingerode, northern Germany.

Estimates of permafrost extend depend on compilations of field evidence of such features, especially ice-wedge pseudomporphs. The map below shows the permafrost extent during the LGM based on previously published maps (Kaiser, 1960; Liedtke, 2002; Lindgren *et al.*, 2016). The age determination of the wedge features relies on stratigraphic classification and/or radiocarbon or luminescence dating methods.

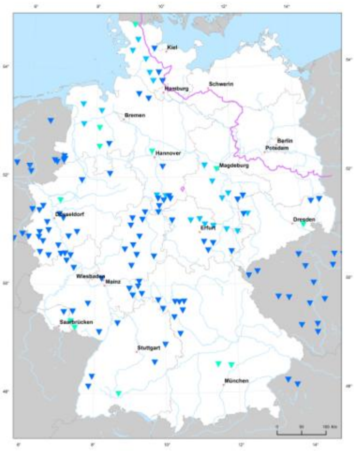

Figure 2. Permafrost extent during the LGM in Germany with permafrost evidence from (Kaiser, 1960; Liedtke, 2002; Lindgren *et al.*, 2016). Maximum ice stage of the Weichselian glacial period (Ehlers *et al.*, 2001).

Permafrost Depth

The maximum permafrost depth cannot be derived from field evidence. However, numerical simulations are a suitable tool for estimating how deep permafrost might develop in the future. Relevant input parameters for permafrost simulations depend on controlling factors like climate, topography, characteristics of the underground and the fluids contained therein or the terrestrial heat flux.

In order to use model simulations as a forecast method for the future development of permafrost an evaluation of their accuracy is necessary. Moreover the sensitivity of permafrost simulations to the used parameters and the influence of uncertainties e.g. from past climate reconstructions should be investigated. For this purpose models which are used to simulate future permafrost development should be examined regarding quality and accuracy and if they are applicable in Germany, especially by considering specific local underground conditions. Possible types of host rocks for HLW repositories in Germany are rock salt, claystone and crystalline rock. For rock salt and formations with high salinity particularly the effects of salinity on the freezing point is of importance.

OpenGeoSys enables the calculation of individual or coupled thermo-hydro-mechanical-chemical processes in porous or fractured media (Kolditz *et al.*, 2012). Recently, it has been extended to consider the influence of freezing on coupled thermo-hydro-mechanical problems (Zheng *et al.*, 2016; Zheng *et al.*, 2017; Zheng *et al.*, in press.). OpenGeoSys will be applied on a comparative study of the permafrost depth during the LGM. Different generic geological settings representing hypothetical sites for HLW repositories in rock salt, claystone and crystalline rock in Germany, will be investigated. In the first calculations, shown in this study, we will concentrate on the thermal process.

References

Kaiser, K., 1960. *Klimazeugen des periglazialen Dauerfrostbodens in Mittel- und Westeuropa.* –Universität Köln.

Kolditz, O., Bauer, S., Bilke, L., Böttcher, N., Delfs, J.O., Fischer, T., Görke, U.J.,Kalbacher, T., Kosakowski, G., McDermott, C.I., Park, C.H., Radu, F., Rink, K., Shao, H., Shao, H.B., Sun, F., Sun, Y.Y., Singh, A.K., Taron, J., Walther, M., Wang, W., Watanabe, N., Wu, Y., Xie, M., Xu, W., Zehner, B., 2012. OpenGeoSys: an open-source initiative for numerical simulation of thermo-hydro-mechanical/chemical (THM/C) processes in porous media, *Environ. Earth Sci.* http://dx.doi.org/10.1007/s12665-012-1546-x

Liedtke, H., 2002. Deutschland zur letzten Eiszeit.– In: *Nationalatlas Bundesrepublik Deutschland* - Relief, Boden und Wasser. Band 2.

Lindgren, A., et al., 2016. GIS-based Maps and Area Estimates of Northern Hemisphere Permafrost Extent during the Last Glacial Maximum. –*Permafrost and Periglac. Process.* 27: 6-16.

Ehlers, J., et al., 2011. "*Quarternary Glaciations - Extent and Chronology: A Closer Look.*" Retrieved 03.05.2017. Oxford, UK, Elsevier. Online supplement information. http://booksite.elsevier.com/9780444534477/index.php.

Zheng, T., Shao, H., Schelenz, S., Hein, P., Vienken, T., Pang, Z., Kolditz, O., and Nagel, T., 2016. Efficiency and economic analysis of utilizing latent heat from groundwater freezing in the context of borehole heat exchanger coupled ground source heat pump systems. *Applied Thermal Engineering*, 105: 314-326.

Zheng, T., Miao, X.Y., Naumov, D., Shao, H. 2017. A Thermo-Hydro-Mechanical Finite Element Model of Freezing in Porous Media—Thermo-Mechanically Consistent Formulation and Application to Ground Source Heat Pumps. In: Papadrakakis, M., Oñate, E., Schrefler, B. (Eds). *Proceedings of VII International Conference on Computational Methods for Coupled Problems in Science and Engineering, Coupled Problems*.

Zheng, T., Xing-Yuan Miao, X.Y., Naumov, D., Nagel, T. Thermo-Hydro-Mechanical Freezing Benchmark (CIF test). In Press. In: O. Kolditz, U.-J. Görke, H. Shao, W. Wang, and S. Bauer, editors. *Thermo-Hydro-Mechanical-Chemical Processes in Fractured Porous Media: Modelling and Benchmarking*: *From Benchmarking to Tutorials*. Heidelberg, Springer.

Pleistocene periglacial features near southern coast of the Finland Gulf, Russia

Irina Streletskaya

Lomonosov Moscow State University, Department of Geography, 1, Leninskie Gory, Moscow, 119991, Russia; irinastrelets@gmail.com

Abstract

Ground wedge features were investigated in Leningrad region of Russia. These features form patterned ground with polygons of different sizes and presented by primary soil, sand, and ice wedges pseudomorphs formed as result of frost cracking before 13 kyr ago. Based on cryogenic contrast coefficient, permafrost in the study area was continuous with mean annual ground temperatures at the depth of zero annual amplitude below –8 °C.

Keywords: composite wedge pseudomorphs; sand wedges; permafrost.

Introduction

The periglacial zone was widespread in Europe (Velichko, 1982; Vandenberghe *et al.,* 2014; Andrieux *et al.*, 2016). Permafrost extended south of 51° N in Poland and Ukraine during Late Pleistocene (Zielinski *et al.*, 2013). Periglacial processes were especially widespread during the Valdai (Late Weichselian) glaciation (LGM) characterized by smallest extent of ice sheets (Isarin, 1997; Vandenberghe *et al.,* 2014). Periglacial processes produced large ice, sand and primary soil wedges and polygonal forms. Remnant polygonal ground patterns control the soil cover structure in European Russia (Alifanov *et al.,* 2010).

All basic types of wedges are forming currently in high-latitude Arctic and Antarctic regions. Repeated thawing and freezing of fine-grained sediments in the permafrost zone affects relative composition of quartz and feldspar, because the two minerals have different grain size limits of cryogenic disintegration. Correspondingly, the ratio of quartz-to-feldspar percentages in coarse silt and fine sand fractions (cryogenic contrast coefficient, CCC) has implications for cryogenic weathering of sediments. CCC higher than one suggests permafrost conditions (Konishchev, 1998).

Study area and methodology

Composite wedge pseudomorphs, sand wedges and enclosing sediments were investigated in the Leningrad region, 7 km away from the southern shore of the Finland Gulf (59°49'46" N; 29°52'29" E). Three large wedges in yellow stratified sand and pebble, 2.2 to 2.7 m depth and 1.5–2.0 m width at the top, were filled with light gray, pale yellow silty sand with humus and pebble. Distances between the wedges are 45-50 m. Wedges have a bowl-shaped upper part (depth 1.0–1.5 m) and a narrow conical lower part (depth 2.5–3.5 m). The enclosing sediments at the lower part of the wedge bent down toward its center. Smaller wedge 0.7 m depth and 0.5 m width was filled with dark brown massive homogeneous sand (Fig. 1). The grain sizes and mineralogy of sediments that fill, host, and underlie the wedges were analyzed.

Formation conditions of composite wedge pseudomorphs and sand wedges

The highest CCC of 2.58 was found in the upper part of the soil wedge composed of silty sand. Silty sands in the upper parts of wedges contain about ten times greater percentages of coarse silt particles than the host sediments. Harsh cold climate was a necessary condition for frost cracking of the ground surface. The host sediments (sand with pebbles) were dated as older than 13 kyr BP by Serebrianyi & Punning (1969). Sand wedges form in the permafrost zone when deficit of moisture in the active layer promotes transportation and redisposition of sand, which fills the frost cracks in the absence of snow. The predominance of 0.05–0.01 mm particles and CCC above one suggests presence of permafrost conditions and aeolian processes. The ground temperature inferred from CCC (1.6–1.8) corresponds to –8°C, which is similar to that of present inland Antarctic regions (Shmelev, 2015). Ratios indicating active cryogenesis in the past were obtained for some samples of sands that underlie (CCC = 1.02 and 1.48) or host (1.90 and 1.02) the wedges.

Conclusions

Wedge-like structures studied in detail are filled, hosted and underlain by sediments with cryogenic contrast coefficients one, which indicates active cryogenic weathering before 13 kyr BP. Frost cracking produced primary soil and sand wedges, as well as ice wedges, and related patterned ground with polygons of different sizes. Permafrost at that time was continuous and had low mean annual temperature.

Acknowledgments

The study was supported by grant 16-05-00612 from the Russian Foundation for Basic Research and was carried out as part of the government contract "Changes in the Earth's Cryosphere under Natural and Manmade Factors" NIRAAAA-A16-16032810095-6.

References

Alifanov, V.M., Gugalinskaya, L.A., Ovchinnikov, A.Yu., 2010. *Paleopermafrost and Diversity of Soils in the East European Plain*. Moscow: GEOS, 160 pp. (in Russian).

Andrieux, E., Bertran, P., Antoine, P., Deschodt, L., Lenoble, A., Coutard, S., & collaborations, 2016. Database of pleistocene periglacial features in France: description of the online version, *Quaternaire* 27(4): 329-339.

Isarin, R.F.B., 1997. The climate in the north-western Europe during the Younger Dryas. *Nederlands Geograf. Studies* 229: 160 pp.

Konishchev, V.N., 1998. Correlation of composition and temperature of cryotic soils. *Bull. Moscow University, Ser. 5, Geogr.* 3: 9–14. (in Russian).

Serebryanyi, L.R. & Punning, J.-M.K., 1969. Palynology and radio-chronology of a buried Holocene peatland in the Gorelovo-Koyerovo area, Leningrad region. In: Neishtad, M.I., (ed.), *The Holocene*, Moscow: Nauka, 101–110. (in Russian)

Shmelev, D.G., 2015. Role of cryogenesis in the composition of Late Quaternary frozen deposits in oases of Antarctica and northeastern Yakutia. *Earth's Cryosphere (Kriosfera Zemli)* XIX (1): 41–57. (in Russian)

Vandenberghe, J., French, H.M., Gorbunov, A., Marchenko, S., Velichko, A.A., Jin, H., Cui, Z., Zhang, T., Wan, X., 2014. The Last Permafrost Maximum (LPM) map of the Northern Hemisphere: permafrost extent and mean annual air temperatures, 25–17 ka BP. *Boreas* 43 (3): 652–666.

Velichko, A.A., 1982. *Palaeogeography of Europe during the Last One Hundred Thousand Years*. Moscow: Nauka, 156 pp. (in Russian).

Zielin'ski, P., Sokołowski, R.J., Fedorowicz, S., Zaleski, I., 2013. Periglacial structures within fl uvio-aeolian successions of the end of the Last Glaciation – examples from SE Poland and NW Ukraine. *Boreas* 43: 712–721.

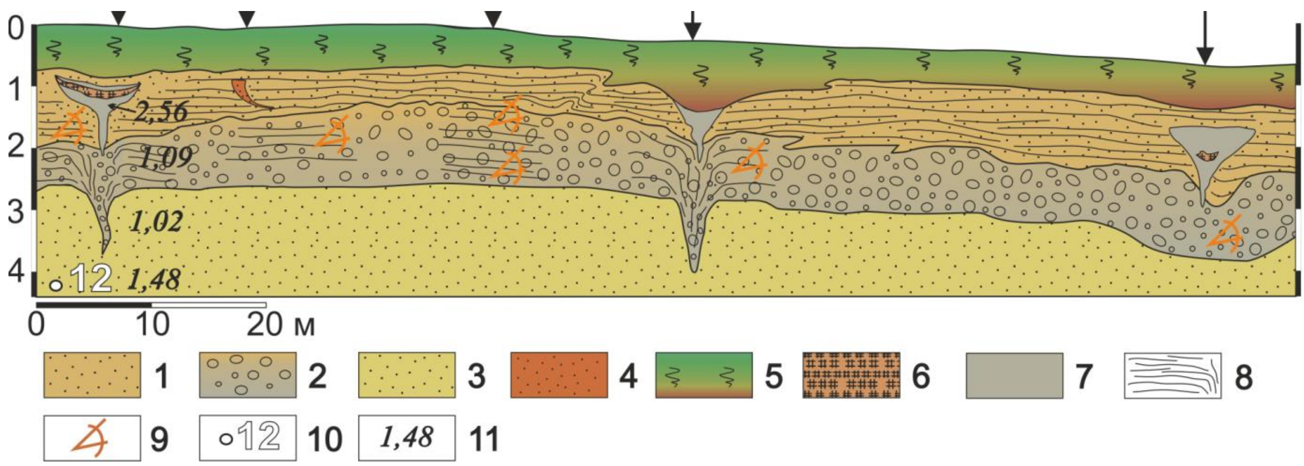

Figure 1. The profile of the study area. *1* – sand with pebbles; *2* – pebbles with lenses of coarse sand; *3* – homogeneous fine sand; *4* – inhomogeneous coarse sand; *5* – sod; *6* – humus; *7* – inhomogeneous silty sand; *8* – stratification in sand and pebble beds; *9* – oxidized sand; *10* – sampling location and sample number; *11* – cryogenic contrast coefficient. The width of wedges is not to scale.

Towards a numerical palaeo-climate interpretation of periglacial features: initial results for sorted nets

Tomáš Uxa[1,2]
Marek Křížek[1]
David Krause[1]
[1]*Department of Physical Geography and Geoecology, Faculty of Science, Charles University, Prague, Czech Republic, tomas.uxa@natur.cuni.cz*
[2]*Department of Geothermics, Institute of Geophysics, Academy of Sciences of the Czech Republic, Prague, Czech Republic*

Abstract

A novel procedure utilizing an inverse thermal modelling approach is designed to calculate palaeo-climate attributes responsible for the initiation of periglacial features indicative of the base of the palaeo-active layer. We demonstrate its performance on the example of relict sorted nets in the Krkonoše Mts., Czech Republic, and provide unique palaeo-temperature and palaeo-permafrost estimates for the Late Glacial or Early Holocene.

Keywords: palaeo-climate reconstruction; active layer and permafrost; sorted patterned ground; thermal modelling; Late Glacial and early Holocene history; Central Europe

Introduction

Periglacial features commonly form under a wide range of temperatures. Consequently, climate reconstructions utilizing these assemblages are challenging. So far, most of them have been made in a simple qualitative manner, and thus they have been frequently considered as unreliable. However, theoretical and experimental studies have demonstrated that numerous features, such as sorted patterned ground, show direct coupling between their geometry and temperature conditions at the time of their initiation. For instance, the size of sorted patterns is controlled by the frost depth in seasonally frozen regions and the thaw depth in permafrost areas, and their diameter-to-sorting depth ratio is constant, of *c.* 3.1 to 3.8 under subaerial conditions (e.g. Ray *et al.*, 1983; Hallet & Prestrud, 1986). Accordingly, temperature conditions at the time of their formation can be inferred via the sorting depth, which closely approximates former frost or thaw depth.

In this contribution, we introduce a novel procedure designed to infer palaeo-temperature and palaeo-permafrost conditions prevailing at the time of the initiation of periglacial features indicative of the base of the palaeo-active layer, which we demonstrate on the example of the Late Glacial or Early Holocene large-scale sorted nets located on the Luční pláň Plateau in the Krkonoše Mts., Czech Republic (Fig. 1).

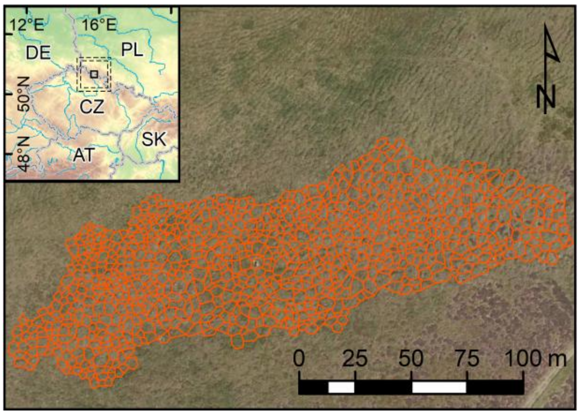

Figure 1. Location of the study area and the investigated sorted nets (orange polygons) in the Krkonoše Mts.

Methods

We employed a simple equilibrium thermal model, the Stefan equation, in an inverse form to calculate the temperature attributes associated with the sorted patterns based on the thickness of palaeo-active layer:

$$TI_A = (\xi^2 L \varrho \omega)/(2 k_T n_T) \qquad (1)$$

where TI_A is air thawing index (°C.days) multiplied by the scaling factor of 86 400 seconds per day, ξ is active-layer thickness (m), L is latent heat of fusion of water (J.kg^{-1}), ϱ is dry bulk density (kg.m^{-3}), ω is gravimetric water content (dimensionless), k_T is thermal conductivity (W.m^{-1}.K^{-1}) and n_T is thawing *n*-factor used as a transfer function between the air and surface thawing index (dimensionless).

We performed the Monte Carlo simulation with 10 000 iterations based on the equation (1) driven by best-fit distribution functions of the input data acquired by field observations and literature survey. We mapped and measured the diameters of 1 000 sorted nets using aerial photographs with a resolution of 0.25 m per pixel (Figure 1). Then we calculated their sorting depths based on the published pattern diameter-to-sorting depth ratios (Uxa *et al.*, 2017) to approximate the thickness of the palaeo-active layer. Dry bulk density and water content data were acquired by personal observations and literature survey of active sorted patterns located elsewhere (n=23 and 8, respectively). Thermal conductivity was calculated as a function of bulk density and water content after Johansen (1975) in order to reduce the dimensionality of the input data. Finally, thawing *n*-factors reported for bare-ground locations were collected from literature (n=137). Subsequently, we calculated mean annual air temperature (MAAT) using TI_A and a range of altitude-adjusted LGM annual air temperature amplitude (that is believed to be relatively constant in time) based on the three GCMs (accessible on www.worldclim.org) assuming sine temperature wave. The model outputs were subjected to a comprehensive uncertainty and sensitivity analysis.

Results

The median diameter of the investigated sorted nets is 4.15 m and the estimated median sorting depth achieves 1.18 m, which is well consistent with our electrical resistivity tomography soundings and earlier observations in excavations at the study site.

The median modelled TI_A is 285 °C.days with interquartile range of 164 °C.days to 478 °C.days. The median MAAT was calculated to be –8.3 °C with interquartile range of –10.0 °C to –6.5 °C and like for TI_A it is substantially skewed to the left and follows the gamma distribution (Figure 2). The sorted patterns likely formed under continuous to discontinuous permafrost conditions because *c.* 55 % and *c.* 44 % of MAAT is below –8.0 °C and –1.5 °C, respectively (*sensu* Gruber, 2012) (Fig. 2).

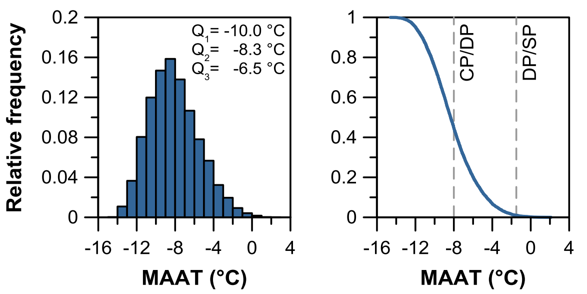

Figure 2. (Left) Mean annual air temperature and (Right) permafrost extent probabilities modelled for relict sorted nets in the Krkonoše Mts.

The modelled temperature attributes are most affected by the input active-layer thickness. Thawing *n*-factors and annual air temperature amplitude are the second-order parameters significantly affecting the results. Physical parameters of the ground also influence the model outputs substantially, but all appear to be of slightly lower importance than the above parameters, which is highly favourable for palaeo reconstructions.

Conclusions

We showed that the presented method is able to provide palaeo-temperature and palaeo-permafrost estimates for sorted patterned ground, but we believe it is applicable on other periglacial structures indicative of the base of palaeo-active layer as well. Nonetheless, testing on present-day data as well as more extensive database of the input parameters from modern analogues are needed to confirm its validity and to increase its robustness.

Acknowledgments

The investigation is supported by the Czech Science Foundation, project number 17-21612S.

References

Gruber, S., 2012. Derivation and analysis of a high-resolution estimate of global permafrost zonation. *The Cryosphere* 6: 221–233.

Hallet, B. & Prestrud, S., 1986. Dynamics of periglacial sorted circles in Western Spitsbergen. *Quaternary Research* 26: 81–99.

Johansen, O., 1975. *Thermal conductivity of soils* (Ph.D. thesis). Trondheim: University of Trondheim, 236pp.

Ray, R.J., Krantz, W.B., Caine, T.N. & Gunn, R.D., 1983. A model for sorted patterned-ground regularity. *Journal of Glaciology* 29: 317–337.

Uxa, T., Mida, P. & Křížek, M., 2017. Effect of Climate on Morphology and Development of Sorted Circles and Polygons. *Permafrost and Periglacial Processes* 28: 663–674.

Pollen, trace elements and stable isotope plots of Late Pleistocene ice wedges of Seyaha yedoma, Eastern Yamal Peninsula

A.C. Vasil'chuk[1], Yu.K. Vasil'chuk[1], N. A. Budantseva[1], J.Yu. Vasil'chuk[1]

[1]*Department of Geography, Lomonosov Moscow State University, Moscow, Russia, e-mail: alla-vasilch@yandex.ru*

Abstract

The Seyaha yedoma is located in eastern coast of Yamal Peninsula (70°10'00'' N, 72°30'30'' E). This sequence (height 22-24 m) is especially valuable for paleotemperature reconstruction because its accumulation was nearly continuous: from 30 to 11 ka BP and because of abundant syngenetic ice wedges. The previous oxygen isotope and radiocarbon results allowed aging the ice-wedge formation from 21 to 11 ka BP. The pollen plot of the large ice wedge represents three units corresponding to changes in taxa composition and their abundance. There are two trends in $\delta^{18}O$ values; from +12 to +14.2 m a.s.l. the range in $\delta^{18}O$ values is about 1.5‰, from –24.18 to –25.75 ‰, from +14.2 to +15.8 m a.s.l. there is clear upward increase in $\delta^{18}O$ values from –25.75 to –23.15 ‰. New isotope data reveal that the average January temperature was –34 to –40 °C from 23 to 15-18 ka BP. The tendency to upward increase in $\delta^{18}O$ values may be explained by increase in average winter and average January temperatures during the final stages of ice-wedge formation. There are 3 maxima of trace element content in the upper part of the ice wedge as follows: at a height of 14.6-15.2 m for Fe, Si, Mn, P, Ba, Sr, Zn, Ni, Cu, Cd, Mo, Sb, Pb; at a height of 13.5-13.8 m for Fe, Si, Mn, Zn, Ba, Sr; and at a height of 12 m for Sb, Cd, Mo, Pb.

Keywords: ice wedges, stable isotopes, Yamal Peninsula, pollen, trace elements.

Introduction

The Seyaha yedoma is located near Settlement Seyaha (Fig. 1) in eastern coast of Yamal Peninsula (70°10'00'' N, 72°30'30'' E). The site investigated in 2016.

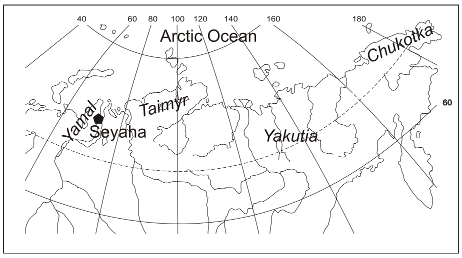

Figure 1. Location of the Seyaha yedoma.

This sequence (height 22-24 m) is especially valuable for paleotemperature reconstruction because its accumulation was nearly continuous during 20 ka: from 30 to 11 ka BP (Vasil'chuk *et al*., 2000; Vasil'chuk *et al*., 2005) and because of abundant syngenetic ice wedges.

Results

^{14}C age

The previous oxygen isotope and radiocarbon results allowed dating the formation of ice-wedges from 21 to 11 ka BP (Vasil'chuk *et al*., 2000). ^{14}C ages without inversions from the bottom part of the exposure are shown in Table 1.

Table 1. New radiocarbon ages of sediment samples.

Sample ID	Heigth, m.a.s.l.	Conventional 14C age, yr BP	Lab ID
YuV-16S/ 76	+5.0	23300 ± 640	Le-11406
YuV-16S/ 77	+3.0	24100 ± 300	Le-11407
YuV-16S/ 78	+2.0	25200 ± 420	Le-11408

Pollen

Pollen extraction using heavy-liquid separation was performed for 25 samples obtained from the main sampling profile of large ice wedge. The pollen plot was subdivided into three units corresponding to changes in taxa composition and abundance (Fig. 2). The profile is dominated by herbaceous and shrub taxa. The lower part of ice wedges (6.8-8.8 m a.s.l.) is notable for having high concentration of pollen, predominance of Betula sect. Nanae, abundance and high diversity of herb taxa. Middle part (8.8-11.1 m a.s.l.) is characterized by a low pollen concentration and high diversity of herbaceous taxa. Spores of typical tundra taxa *Lycopodium lagopus (Laest.) Zinserl. ex Kuzen* were found here. The top part of ice wedge (11.1-13.6 m a.s.l.) shows increase in percentage of boreal tree taxa (*Picea, Pinus*), maximum percentages of Poaceae and Cyperaceae, *Artemisia* and finding of *Diphasium alpinum (L.) Rothm. Lycopodiella* *innundata (L.) Holub*). There is a maximum of reworked pollen at this interval. It may be supposed that some part of boreal tree pollen is reworked.

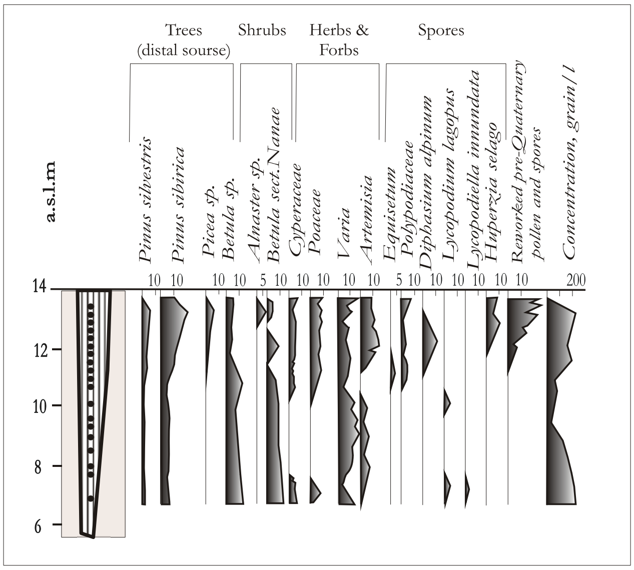

Figure 2. Selected components of pollen spectra from ice-wedge ice of Seyaha yedoma.

Table 2. Stable isotope ($\delta^{18}O$ and $\delta^{2}H$) minimum, mean, and maximum values in ice wedges of the Seyaha yedoma.

Sampl. (n)	$\delta^{18}O$, ‰			$\delta^{2}H$, ‰		
	min.	mean.	max.	min.	mean.	max.
IW profile № 1 (№ 11-58), depth 2.2-6.0 m (12-15.8 m a.s.l.)						
8	–25.75	–24.7	–23.15	–197.5	–192.0	–171.9
IW profile № 2 (№ 63-74), depth 12.0 m (6.0 m a.s.l.)						
59	–26.63	–24.9	–23.41	–203.9	–201.0	–178.9

Stable isotopes

$\delta^{18}O$ values vary from –25.75 to –23.15 ‰ in the upper part of the ice wedge (Table 2). There are two trends in $\delta^{18}O$ values; at the height from +12 to +14.2 m a.s.l. the range in $\delta^{18}O$ values is about 1.5‰, from –24.18 to –25.75 ‰, at the height from +14.2 to +15.8 m a.s.l. there is clear upward increase in $\delta^{18}O$ values from –25.75 to –23.15 ‰. The range in $\delta^{18}O$ values at +15.2 m a.s.l. is 1.49‰, from –23.41 to –24.9 ‰. The basal part of ice wedge at +6 m, is characterized by larger range in $\delta^{18}O$ values than the upper part: from –23.41 to –26.63 ‰. New isotope data reveal that the average January temperature was from –34 to –40ºC from 23 to 18 ka BP, according to the conversion equation proposed by Vasil'chuk (1991). The tendency to upward increase in $\delta^{18}O$ values may be explained by the increase of average winter and average January temperatures during the final of the ice wedge formation.

Chemical composition

There are 3 maxima of trace elements content in the upper part of ice wedge as follows: at a height of 14.6-15.2 m – for Fe, Si, Mn, P, Ba, Sr, Zn, Ni, Cu, Cd, Mo, Sb, Pb; at a height of 13.5-13.8 m for Fe, Si, Mn, Zn, Ba, Sr; and at a height of 12 m for Sb, Cd, Mo, Pb (Table 3).

Table 3. Trace element values in ice wedges of the Seyaha yedoma. Number of samples = 7.

Element	min.	mean.	max.
Si	3251.4	2514.9	3251.4
P	884.1	629.2	884.1
Mn	1620.8	983.7	1620.8
Fe	7048.2	3707.2	7048.2
Ni	40.6	30.7	40.6
Cu	38.4	25.9	38.4
Zn	131.9	90.4	131.9
As	9.23	5.1	9.23
Sr	111	92.1	111
Zr	2.23	1.6	2.23
Mo	0.46	0.23	0.46
Cd	0.45	0.25	0.45
Sb	0.11	0.10	0.11
Ba	183	152.6	183
Pb	20.1	13.0	20.1

The lower part of ice wedge is characterized by low element concentrations except for Fe, Ba, Zn; their stable concentrations both in the lower and upper parts (Table 3) is obviously due to containing in clay minerals and coming from aeolian dust inputs.

Acknowledgments

The research was financially supported by the Russian Scientific Foundation: Grant № 14-27-00083-P (isotope analyses) and Russian Foundation for Basic Research: Grant № 17-05-00794 (pollen analysis).

References

Vasil'chuk, A., Kim, J.-C., Vasil'chuk, Y., 2005. AMS ^{14}C Dating of Pollen Concentrate from Late Pleistocene Ice Wedges from the Bison and Seyaha Sites in Siberia. *Radiocarbon* 47(2): 243–256.

Vasil'chuk, Y.K., 1991. Reconstruction of the paleoclimate of the Late Pleistocene and Holocene on the basis of isotope studies of subsurface ice and waters of the permafrost zone. *Water Resources* 17(6): 640–647.

Vasil'chuk, Y.K., van der Plicht, J., Jungner, H., Sonninen, E. & Vasil'chuk, A.C., 2000. First direct dating of Late Pleistocene ice-wedges by AMS. *Earth and Planetary Science Letters* 179(2): 237–242.

Trace elements and stable isotope diagrams of Late Pleistocene ice wedges of Batagaika yedoma, Central Yakutia

Yu.K.Vasil'chuk[1]
J.Yu.Vasil'chuk[1]
N. A. Budantseva[1]
A.C. Vasil'chuk[1]

[1]*Department of Geography, Lomonosov Moscow State University, Moscow, Russia, e-mail: vasilch_geo@mail.ru*

Abstract

The subject of the study is the yedoma ice complex, which locates in the Batagaika depression, Sakha Republic, Russia. The oxygen and hydrogen stable isotope composition, and the content of the dissolved forms of minor and major elements were studied for the first time in ice-wedges of Batagaika depression, which makes the novelty of the study. The isotope composition of the two most saline ice-wedges located in the upper and lower parts of the Batagay depression indicates that they were formed in a close temperature range, the average winter temperature was close to –34/–35 °C, and the average January air temperature was –51/ –53 °C. The ice-wedge with the lowest content of all the trace elements was formed in more severe conditions, the average winter air temperature was close to -36 °C, and the average January air temperature was –54/–55 °C.

Keywords: permafrost; ice wedge; oxygen isotope; hydrogen isotope; trace elements; East Siberia, Late Pleistocene

The subject of the study is the yedoma, which is found in the Batagaika depression (67°34'49" N, 134°46'19" E), located 10 km southeast of Batagai settlement (about 17 km along the highway and about 4 km along the trail), in Verkhoyansky District of the Sakha Republic, Russia.

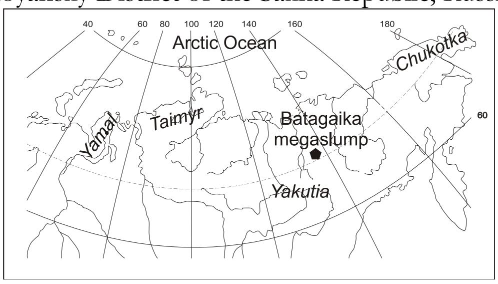

Fig. 1. Location of the study site. Batagaika yedoma in the Central Yakutia.

The site is located on the northeastern slope of the hill between the hill Kirgilyakh and the mountain Khatynnakh, its absolute height is about 290 m a.s.l.

The oxygen and hydrogen stable isotope composition and the content of the dissolved forms of minor and major elements were studied for the first time in ice-wedges of Batagaika depression. Batagai megaslump is a wide ravine with vertical walls of 50-85 m height. Ice-rich yedoma deposits are found in the wall from the surface to the depth of 75 m. In western part of the exposure yedoma deposits are subdivided into two units: the upper, 30 to 40 m thick, and the lower, 30 m thick. We observed a feather-like contact of the unit with lacustrine or taberal deposits, which are form horizontal wedge 150-200 meters long and intruding into the yedoma deposits and overlaying it. Yedoma deposits also underlay triangle-shape deposits.

The upper yedoma unit contains narrow ice wedges 1.5-2 m width. From this part, we sampled ice wedge (IW №3) from the depth of 5-10 m (or 315-320 m a.s.l.). The ice has vertical layers with high content of sandy loam. Polygons are 4-5 m width and of 1.5-3 m height. The lower part of the yedoma from the depth of 65-73 m or 252-260 m a.s.l. ice wedge (IW №2) was sampled in detail. In this lower part, the ice wedges are yellowish-gray, diagonally-vertically-layered, with few soil inclusions, which are predominantly gray in color.

From the isotopic composition of upper ice wedge (the average value of $\delta^{18}O$ for 38 samples of ice wedge (№3) is –34.23 ‰, the average value of $\delta^{2}H$ is –266.8 ‰ – (Table 1), the calculation of air paleotemperature using Vasil'chuk's (1991) formula shows that they were formed in severe winter conditions, the mean air temperature was –51/–52 °C. The isotope composition of the lower ice wedges (the average value of $\delta^{18}O$ for 59 samples of ice wedge (№2) is -35.69 ‰, and the lowest value is $\delta^{18}O$ –37.2 ‰, the average value of $\delta^{2}H$ is –276.3 ‰, and the lowest value is $\delta^{2}H$ is –290.8 ‰) shows that they were formed in even more severe winter conditions, the mean air temperature was –54/–55 °C.

We estimate the approximate age of IW profile №2 to 55-36 ka BP, and IW profile №3 to 27-12 ka BP, according to radiocarbon radiocarbon dates (Murton et al., 2017; Ashastina et al., 2017).

Table 1. Stable isotope ($\delta^{18}O$ and δ^2H) minimum, mean, and maximum values in ice wedges of the Batagaika yedoma.

Sampl. (n)	δ18O, ‰			δ2H, ‰		
	min.	mean.	max.	min.	mean.	max.
IW profile № 1 (№ 1-8), depth 68-70 m (255-257 m a.s.l.)						
8	–34.86	–34.4	–32.67	–270.2	–265.0	–247.1
IW profile № 2 (№ 9-33, 76-111), depth 65-73 m (252-260 m a.s.l.)						
59	–37.2	–35.69	–34.51	–290.8	–276.3	–267.8
IW profile № 3 (№ 34-72), depth 5-10 m (315-320 m a.s.l.)						
38	–34.83	–34.23	–33.8	–272.6	–266.8	–261.8

The isotope composition of the two most saline ice-wedges located in the upper and lower parts of the Batagaika megaslump indicates that they were formed in a close temperature range, the average winter temperature was close to –34/–35 °C, and the average January air temperature was –51/–53 °C. The ice wedge with the lowest content of all trace elements was formed in more severe conditions, the average winter air temperature was close to –36 °C, and the average January air temperature was –54/–55 ° C, and, in addition there was presumably lower wind activity. According to the data from Batagai ice wedges, the lowest values of winter paleotemperature for Arctic Siberia obtained in Batagai area. This confirmed previously designed maps of the distribution of winter temperature for different periods of late Pleistocene, where an isotope and a temperature minimum was identified (Vasil'chuk, 1992), although there was a lack of data in this area (but an analysis of the isotopic composition of the surrounding yedoma ice complexes allowed Yu.Vasil'chuk to identify the temperature minimum). The Batagay permafrost phenomenon fully confirmed the correctness of previously designed palaeotemperature maps.

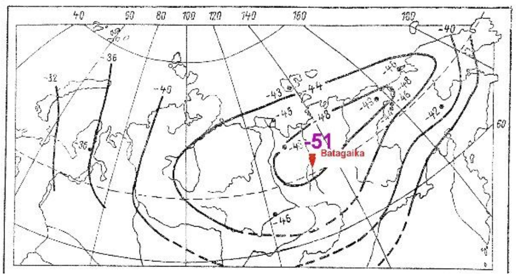

Fig. 3. The isotope data from Batagaika megaslump, which shows mean January temperature of –51 °C for the period of 30-25 ka BP. Data perfectly fitted the center of isotherm –48 °C (lowest temperature) (Vasil'chuk, 1992, p. 261).

We studied trace elements content in ice wedges in order to examine the change of concentration and distribution of environmentally available trace elements within winter and summer seasons. These data bring additional information on ice wedge development. Co content in ice wedges (Table 2) varies in the range of 0.34-8.78 µg/L, in the Batagaika River Co content was 0.99 µg/L, in the Yana River – 0.074 µg/L.

Table 2. Trace elements minimum, mean, and maximum values in ice wedges of the Batagaika yedoma, µg/L.

Sampl. (n)	Co			Ni		
	min.	mean.	max.	min.	mean.	max.
IW profile № 1 (№ 1-8), depth 68-70 m (255-257 m a.s.l.)						
3	3.35	3.62	3.88	9.20	9.95	10.70
IW profile № 2 (№ 9-33, 76-111), depth 65-73 m (252-260 m a.s.l.)						
13	0.34	1.58	3.39	2.94	5.47	11.00
IW profile № 3(№ 34-72), depth 5-10 m (315-320 m a.s.l.)						
6	1.20	3.45	8.78	3.04	9.52	23.50
Sampl. (n)	Zn			Cu		
	min.	mean.	max.	min.	mean.	max.
IW profile № 1(№ 1-8), depth 68-70 m (255-257 m a.s.l.)						
3	10.90	18.50	26.10	9.98	14.04	18.10
IW profile № 2 (№ 9-33, 76-111), depth 65-73 m (252-260 m a.s.l.)						
13	2.57	6.40	12.60	2.70	4.45	7.61
IW profile № 3 (№ 34-72), depth 5-10 m (315-320 m a.s.l.)						
6	3.14	20.24	48.40	3.18	10.79	30.70
Sampl. (n)	Mo			Ce		
	min.	mean.	max.	min.	mean.	max.
IW profile № 1(№ 1-8), depth 68-70 m (255-257 m a.s.l.)						
3	0.16	0.21	0.25	6.38	6.55	6.72
IW profile № 2 (№ 9-33, 76-111), depth 65-73 m (252-260 m a.s.l.)						
13	0.13	0.25	0.47	0.78	2.19	8.29
IW profile № 3 (№ 34-72), depth 5-10 m (315-320 m a.s.l.)						
6	0.15	0.19	0.22	1.55	8.43	24.50

Ni content in ice wedges №1-3 is 2.94-23.50 µg /L, and 4.75 µg/L in the water of the Batagaika river. Cu content in ice wedges varies from 2.7 to 30.7 µg/L, and is 7.61 µg/L in river water. Zn content in ice wedges ranges from 2.57 to 48.4 µg/L, and is 3.95 µg/L in river water. Mo content varies in ice wedges from 0.13 to 0.47 µg/L and is 0.43 µg/L. in river water. Ce content in ice wedges is 0.7-24 µg /L, and is 0.14-2 µg/L mg/L in river water.

Acknowledgments

Russian Scientific Foundation financially supported the research, grant № 14-27-00083-P.

References

Ashastina, K., Schirrmeister, L., Fuchs, M., Kienast, F. 2017. Palaeoclimate characteristics in interior Siberia of MIS 6-2: first insights from the Batagay permafrost mega-thaw slump in the Yana Highlands. *Climate of the Past* 13: 795–818.

Murton, Ju. B., Edwards, M.E., Lozhkin, A.V. et al., 2017. Preliminary paleoenvironmental analysis of permafrost deposits at Batagaika megaslump, Yana Uplands, northeast Siberia. *Quaternary Res.* 87: 314–330.

Vasil'chuk, Y.K., 1991. Reconstruction of the paleoclimate of the Late Pleistocene and Holocene on the basis of isotope studies of subsurface ice and waters of the permafrost zone. *Water Resources.* 17(6): 640–647.

Vasil'chuk, Y.K., 1992. *Oxygen Isotope Composition of Ground Ice (Application to Paleogeocryological Reconstructions).* Moscow. 1: 420 p. (in Russian).

3 - Permafrost engineering and the related risks

Session 3

Permafrost Engineering and Related Risks

Conveners:

- **Kevin Bjella**, Cold Regions Research and Engineering Laboratory – CRREL, Fairbanks, Alaska, USA
- **Guy Dore**, Université Laval, Québec, Canada
- **Elizaveta Makarycheva**, Pipeline Transport Institute – PTI, LLC, Moscow, Russia (PYRN member)

Warming permafrost is projected to weaken foundation soils and create engineering risks previously not fully appreciated. Geocryological processes such as thermokarst, frost heaving and fracturing, icing, and thermal erosion are the source of immediate danger for the engineering structures. Economic losses during the construction and exploitation procedures in the permafrost area are linked also with the other negative processes that have the specific character in cold regions. These processes are swamping, desertification, deflation, flooding, mudflows and landslides, and can lead to common risks of unsustainable development of regions. Infrastructure longevity is influenced by climate change consequences that must be calculated in insurance procedures, and this is challenging engineers to make estimates of these impacts, and also to what level the design parameters can be adjusted to maintain an acceptable level of risk and economics. Recent advancements in the use of surface based geophysics for geotechnical characterization are demonstrating that the homogeneity of the permafrost ground-ice condition can often be exploited to the benefit of infrastructure projects. Additionally, thermal modeling techniques are becoming standard engineering tools for determining the results of innovative designs, and for projecting to the future warmed condition. Presentations are invited that provide insight into the current methods for engineering on warming permafrost, and especially those that illustrate results of altered design parameters. We encourage demonstrations of innovation for maintaining or modifying founding soil conditions, innovation on the methods for characterizing the geotechnical condition, incorporation of permafrost cryostructure and geo-cryomorphology into the applied realm, assessments of risk and costs, and improved techniques for assessing, designing and constructing on warming permafrost.

High-resolution Electrical Resistivity Tomography (ERT) measurements along paved roads in permafrost regions of Mongolia

Saruulzaya Adiya[1]
Jambaljav Yamkhin[1]
Gansukh Yadamsuren[1]
Tsogt-Erdene Gansukh[1]
[1]*Institute of Geography and Geoecology, Mongolian Academy of Sciences,* saruulzaya@gmail.com

Abstract

The purpose of this study was to investigate the settlement and deformations of the embankment constructed in warm permafrost regions of Mongolia. In this investigation, five experimental sites were selected, namely R01, R02, R03, R04, and R05. High-resolution ERT measurements and drilling methods were used in this study. As the results show, frozen ground was identified at boreholes in the R02 (3.4 m), R03 (3.0 m), R05 (3.2 m) sites, while it was absent at the R04 and R01 sites. According to ERT, the upper and lower permafrost limits have resistivity values of 1022 Ω m. These permafrost limits were associated with drilling results of the boreholes. At all sites excluding the R03 site, settlement and deformations of the road surface were found with different rates between 5 cm and 30 cm. High-resolution ERT measurements clearly show the permafrost thawing, especially underneath the embankment in the R01, and R04 sites, where the permafrost thawed down to 11 m.

Keywords: ERT, paved road, permafrost, Mongolia.

Introduction

The Mongolian road network currently amounts to 12722 km, including 5354 km of paved roads, 6213 km of unpaved roads, and 1153 km of planned roads (Adhikari, 2013). Of this, approximately 1200 km of paved roads were constructed on warm permafrost with a mean annual ground temperature higher than -2.0°C (Jambaljav, 2017). Along paved roads in warm permafrost zones, significant settlement and deformations related to creep were found at many places where the embankments are unusually tin. Therefore, the stabilization of the embankments must be taken into consideration, particularly for those embankments directly underlain by the warm permafrost layer. The purpose of this study was to investigate the settlement and deformation of the embankments constructed in the Mongolia.

Five experimental sites were selected in the continuous to isolated permafrost zones (Fig. 1). These sites are referred to hereafter as R01 (Chuluut), R02 (Terkh), R03 (Khurental), R04 (Tsagaannuur), and R05 (Alag-Erdene). Furthermore, the Mongolian government is planning to construct paved road in the future at the R03 site. Along paved roads, the ice contents change significantly over short distances at the sites.

Methods

In this survey, we measured high-resolution ERT on the permafrost underneath the paved roads using the Wenner and Wenner-Schlumberger arrays. The multi-electrode resistivity technique uses a syscal R+, a switch pro and several multi-core cables. A unit of 96 electrodes was plugged into the ground at a fixed distance of 1-5 m. According to the drilling survey, the ground materials were identified with hand drilling equipment (TANAKA Japan) at all sites during the fieldwork in August 2017.

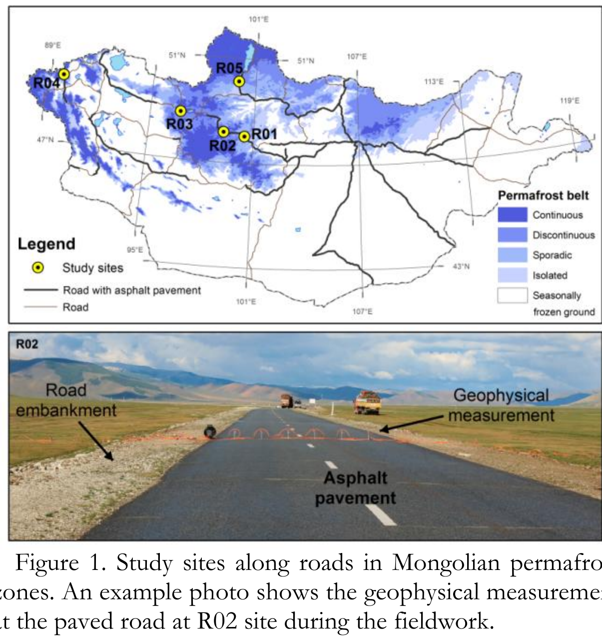

Figure 1. Study sites along roads in Mongolian permafrost zones. An example photo shows the geophysical measurement at the paved road at R02 site during the fieldwork.

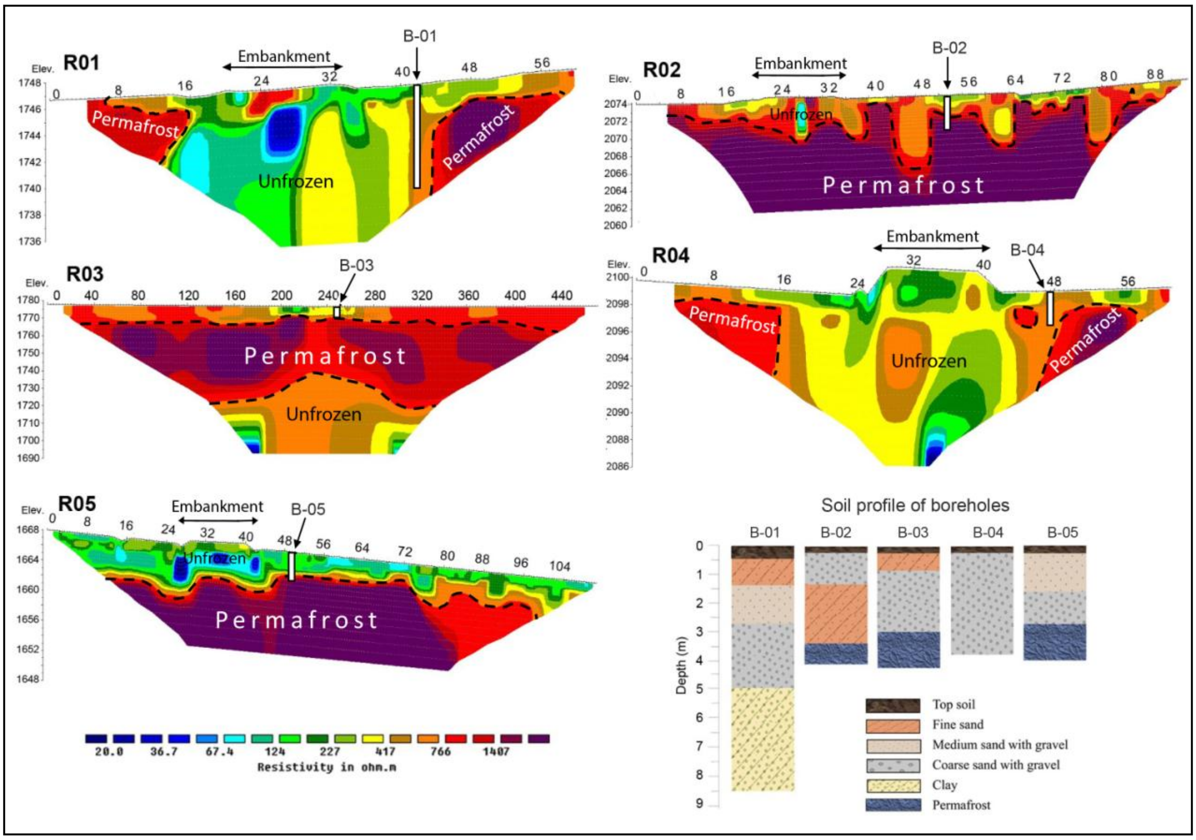

Figure 2. 2-D profile results of ERT, and soil profile of boreholes at experimental sites.

Results and Discussion

Figure 2 shows a series of five resistivity images across paved road embankments and natural ground surface, and the drilling at all sites. An 8.4 m borehole was drilled at the R01 site near the road embankment. There was no permafrost at 8.4 m, but settlements (20-30 cm) and deformations were observed on the asphalt pavement. Frozen ground was identified at several boreholes in the R02 (3.4 m depth), R03 (3.0 m depth), R05 (3.2 m depth) sites, but not at the R04. In these sites, ground temperatures ranged from -0.40°C to -1.2°C during the fieldwork.

According to ERT, the resistivity of the ground ranged from 20 Ωm to >1878 Ωm at all sites. We delineated the upper and lower permafrost limits with resistivity values of 1022 Ωm. These permafrost limits were associated with drilling results of boreholes. Besides the R03 site, the embankments of paved roads were constructed from 2012 to 2014 (Adhikari, 2013). Since that time, the permafrost underneath the embankments has been continuously thawing with different rates (Fig. 2). The R03 site lies in the area where we are planning to construct a paved road. At all sites excluding the R03 site, the settlement and deformation of the road surface were found with different rates between 5 cm and 30 cm. ERT measurements clearly show the permafrost thawing, especially the permafrost thawed down to 11 m below the embankment in the R01 and R04 sites. Ground surface was destroyed around embankments of paved roads; under these surfaces the permafrost was also thawed.

Acknowledgments

This work was supported by the Mongolian Foundation for Science and Technology. I appreciate the MERIT project's reviewer comment, which improved this extended abstract significantly.

References

Adhikari, R.B., 2013. *Sector Assistance Program Evaluation for Mongolia.* Asian Development Bank: OD Press, 89 pp.

Jambaljav, Ya., 2017. *Permafrost distribution, and changes of Mongolia.* Colorful: Ochir Press, 80 pp.

Assessing the impact of permafrost thaw on Yukon roads: Alaska Highway and Dempster Highway, YT, Canada

Fabrice Calmels[1]
Louis-Philippe Roy[1]
Christopher Burn[2]
Guy Doré[3]

[1] *Yukon College, Whitehorse, YT, Canada, fcalmels@yukoncollege.yk.ca*
[2] *Carleton University, Ottawa, ON, Canada*
[3] *Laval University, Québec, QC, Canada*

Abstract

The Yukon transportation system is under the threat of permafrost thaw. Under the initiative of Yukon Highways and Public Works (HPW), actions have been taken to anticipate and prepare for the impacts of climate change on the highways. Two corridors have been prioritized for assessment, the northern 200-km of the Alaska Highway and 465 km of the Dempster Highway. We present here the results of those multi-disciplinary studies, and a comparison in terms of the structural, geological, and geocryological setting of these two major transportation corridors.

Keywords: Yukon Highways; Adaption; Impact Assessment, Geocryology, ERT

Introduction

Passing through thaw-sensitive permafrost areas, construction and maintenance of the Alaska and Dempster Highways has always been problematic (Fig. 1). As climate scenarios project temperature increases between 2.5°C and 4°C by the 2050s, permafrost is likely to be affected. A large-scale permafrost assessment of both corridors is required to understand and prepare for the impact of permafrost thaw.

Methodology

The assessments combine desktop study and field investigation. Surficial geology maps and aerial imagery were interpreted, supplemented with geotechnical reports (Calmels *et al.*, 2015). Field investigations focused largely on areas proximal to the highway, where minimal information is currently available. New geophysical information was acquired through electrical resistivity tomography (ERT) surveys, using Wenner, dipole-dipole, and gradient arrays. Cryostatigraphic logs based on shallow drilling validated the geophysical interpretation. Laboratory analyses included soil grain characterization, cryostratigraphy, and volumetric and gravimetric ice content determinations. Finally, boreholes with variable depth were instrumented to monitor ground temperature at study sites and create permafrost monitoring arrays along the highway corridors (Idrees et al., 2015).

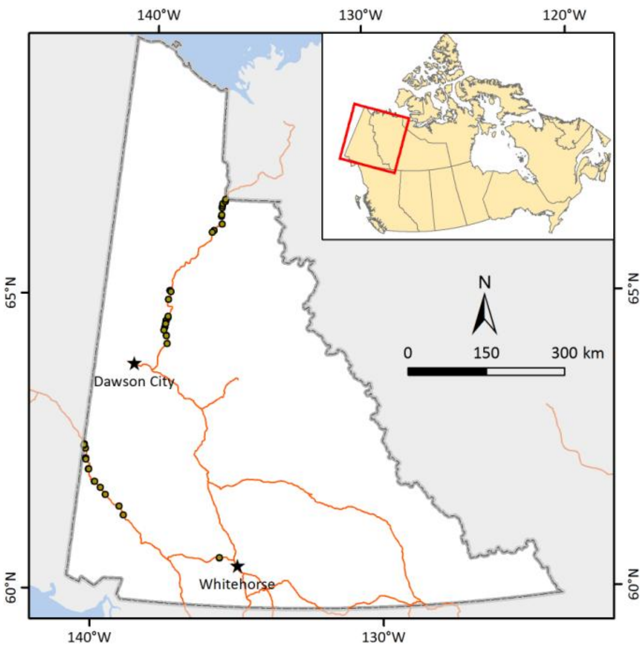

Figure 1. Locations of the study sites.

Results

The drilling (33 boreholes sampled, 20 instrumented) and geophysics (24 ERT surveys) programs along the Alaska Highway showed that less than 20% of the 200-km investigated section was located on ground with low vulnerability to permafrost thaw. Additionally, a selection of 4 highly vulnerable sections deemed suitable for remediation, and the design of 3 potential adaptation designs per site (Calmels *et al.*, 2016).

Although at a less advanced stage, the investigation along the Dempster Highway (18 boreholes sampled, 17 instrumented; and 24 ERT surveys), distributed over 17 sites, allowed for the determination of the principal type of active geohazards, such as sinkholes, and their causes. Parallelly, permanent ERT and temperature arrays have been installed to monitor the performance of adaptation techniques along a functional test culvert.

Although the two highways are located in distinct geographical areas, in both cases results indicate that the regional glacial history has influenced permafrost distribution and characteristics. Sites underlain by permafrost located within a few square kilometers of each other exhibit a wide range of ages, ground temperatures, thicknesses, and ground ice content and nature.

Acknowledgments

We are grateful to Yukon Highways and Public Works for their involvement and support of our work.

References

Burn, C., Moore, J., O'Neil, B., Hayley, D., Trimble, R., Calmels, F., Orban, S. & Idrees, M., 2015. Permafrost characterization of the Dempster Highway, Yukon and Northwest Territories. *Proceedings of the Seventh Canadian Permafrost Conference*, Québec, Canada, September 20-23.

Calmels, F., Roy, L.-P., Laurent, C., Pelletier, M., Kinnear, L., Benkert, B., Horton, B. & Pumple, J., 2015. A practical guide to permafrost vulnerability for Yukon's North Alaska Highway. *Proceedings of the Seventh Canadian Permafrost Conference*, Québec, Canada, September 20-23.

Calmels, F., Doré, G., Kong, X., Roy, L.-P., Lemieux, C. & Horton, B., 2016. *Vulnerability of the north Alaska Highway to permafrost thaw: Design options and climate change adaptation*. Northern Climate ExChange, Yukon Research Centre, Yukon College, 127 pp.

Idrees, M., Burn, C., Moore, J. & Calmels, F., 2015. Monitoring permafrost conditions along the Dempster Highway. *Proceedings of the Seventh Canadian Permafrost Conference*, Québec, Canada, September 20-23.

Transformations of the Geomorphological and Geocryological Conditions in Areas of the Arctic Zone during Climate Changes

Irina Chesnokova[1]
Emma Likhacheva[2]
Aleksandra Morozova[3]
[1] *Water Problems Institute, Russian Academy of Sciences, Moscow, Russia, ichesn@rambler.ru*
[2] *Institute of Geography RAS, Moscow, Russia, lihacheva@igras.ru*
Moscow State University, Geography Department, Moscow, Russia, aleksandra.v.morozova@yandex.ru

Abstract

The article deals with modern conditions and potential risks, related to possible further climatic change in the Arctic zone and economic development of new regions. The main attention is paid to changing geocryological and geomorphological conditions, which lead to activation of exogenous processes in the continental part of the Arctic zone. Possible changes in the ecological, geocryological and geomorphological situations of the Arctic zone regions were analyzed.

Keywords: Arctic Zone of the Russian Federation; geocryological conditions; geomorphological situation; dangerous processes; economic damage; changing climate conditions.

The Russian Arctic land zone extends from the western boundary in the Kola Peninsula to the Dezhnev Cape of the Chukotka Peninsula in the east of the country; it is presented by diverse natural conditions. The balanced economic development of the Russian Arctic zone cannot be achieved without regard to risks of global changes in the natural environment and hazards, which bring significant damage to the economy and loss of people.

The Arctic area in Russia is characterized by extreme natural conditions: low average annual air temperatures, widespread permafrost rocks that occur at a depth of from 0.3 to 2-3 m, low biological activity. The economic development of new areas and technogenic transformations of the relief is accompanied by the decay of the vegetation cover, so bringing about warmth increase in the ground, and consequently 2-3 fold increase in the depth of seasonal thawing; the conditions of discharge change, which often provide additional humidification of the ground, and even can result in the appearance of artificial reservoirs. The change in the geocryological and geomorphological conditions leads to the activation of exogenetic processes in relief formation (Chesnokova & Lokshin, 2016). These processes include: frost fissuring, ground heaving, thermokarst, solifluction, erosion, and thermoerosion, abrasion and thermoabrasion, aeolian processes.

We have analyzed the proposed changes in the geomorphologic- geocryological situations in the regions of the Arctic zone of Russia. Three subject groups have been identified, which have similar tendencies in climate changes;

I. Regions 6-8 (Krasnoyarsk Kray, Saha Republic (Yakutia), Chukotsk autonomous area). Here, a rise in temperature in frozen ground by at least 1° decreases their carrying capacity, increases the depth of seasonal thawing, their irreversible up warming, and subsidence. All these processes cause the deformation of ground and foundations, dipping of poles etc. Particularly dangerous are the consequences of the transformation of frozen ground into the thawed. Natural results of such dangerous processes are large-scale and small accidents in engineering structures.

II. Regions 4, 5, 9 (Nenets autonomous district, Yamalo-Nenets autonomous district, Komi Republic (Vorkuta-city)). Among negative consequences during climate changes, most frequently mentioned are the deterioration of engineering-geology conditions during sharp changes in the geocryological conditions. That can cause the destruction of industrial and dwelling buildings and different constructions.

III. Regions 1-3 (Murmansk district, Karelian republic, Arkhangelsk district). These are most developed areas of the Arctic zone and taking into account the existing tendencies for climate changes, deterioration of the ecological and geocryological-geomorphological situations is quite possible.

The obtained characteristics provide the general view of changes in the geomorphological- geocryological situations. The picture is more complicated. In the Sakha republic and in Chukotka the activation of geodynamic processes is defined by the seismicity of the area rather than by the changing climatic conditions. The positive affect from improving climatic conditions in regions of Group III can be leveled by the activation of anthropogenic processes with additional territory urbanization. Long-term prognoses of warming up acceleration do not provide optimism either. According to certain estimations, by 2050 the temperature of frozen rocks can rise by 3-6°C. This will cause considerable warming up of frozen rocks, their subsidence in large areas, and submergence below sea level.

Regarding the regions of the Arctic zone as territorial resources, it is necessary when developing them, to carry out complex geocryological, geomorphological, and ecological investigations on the basis of:

- Monitoring the temperature regime of permafrost rocks strata in various regional-zonal conditions;
- Prognosis of the dynamics of permafrost rocks and geocryological processes in various scenarios of global and regional climate changes;
- The assessment of the changing complexity of the geocryological conditions and of the cost of the investigations, specified by the consequences of global climate changes;
- Assessment of changes in the stability of bases and foundations of existing and projected buildings and the conditions of mineral resources maintenance
- Quantitative assessment of a risk of possible economic damage in case of realization of the scenario of global climate changing.

Acknowledgments

The investigation was carried out with financial participation of the Russian Foundation for Basic Research (grant N 16-05-00200) and of the Programme of Fundamental Research of the Presidium RAS N 53.

References

Chesnokova, I.V. & Lokshin, G. P. 2016. *Technogenic physical fields - properties of anthropogenic-geomorphological systems*. Ed. In chief Dr. E.A. Likhacheva. M.: Media-PRESS, 192 pp. (in Russian).

Geoecological risks associated with Permafrost in Russian Arctic

Vladimir Melnikov [1,2,7]
Dmitry Drozdov [1,4,7]
Vladimir Dubrovin [3]
Vladimir Romanovsky [1,5,7]
Vadim Pendin [4]
Anatoly Brushkov [6]

[1] *Earth Cryosphere Institute, Tyumen Scientific Centre, Siberian Branch, Russian Academy of Sciences, Tyumen, Russia, ds_drozdov@mail.ru*
[2] *Tyumen Scientific Centre, Siberian Branch, Russian Academy of Sciences, Tyumen, Russia*
[3] *GIDROSPETZGEOLOGIYA, Moscow, Russia*
[4] *Russian State Geological Prospecting University MGRI–RSGPU, Moscow, Russia*
[5] *Geophysical Institute, University of Alaska Fairbanks, Fairbanks, AK, USA*
[6] *Moscow State University, Moscow, Russia*
[7] *Tyumen State University, Tyumen, Russia*

Abstract

Natural and natural-technogenic geosystems in the permafrost zone are controlled by the interaction between the geological environment and the Earth's exospheres, including the technosphere. Observations are required to keep the situation under control. It is possible to consider well-studied territories of the Russian permafrost zone as "key sites" and the data describing these sites can be extrapolated on the base of geosystem approach. Corresponding map (or cartography model) should represent with predetermined precision and reliability the information on the background, current and predictive natural and technogenic conditions. Monitoring of the permafrost zone and neighbouring environment provide iterative and operative corrections of cartography models and, finally, supply developers and license holders with the information needed for the design and management. However this scheme operates badly, because investments of developers and licence holders into the permafrost studies are not sufficient while in most cases controlling ecological authorities only estimate damages but don't provide conditions to avoid them.

Keywords: permafrost; climate change; monitoring; developers and license holders; technogenesis; ecological control

Introduction

The general tendencies of climate parameter changes are unfavorable for existence and preserving of permafrost series. One can observe this fact on the example of West Siberia. Permafrost monitoring sites there form a transect crossing several nature-climatic zones from the northern taiga to the high arctic tundra. At all these sites the increase of average annual air and ground temperatures as well as snow cover thickness has been registered. In the south, this tendency leads to the ubiquitous lowering of the permafrost table and activation of the processes, while in the north - to the decrease of still being frozen ground bearing capacity on 20-30 %, that has become a surprise for owners of constructions. But this is the area, where since 1930 mineral deposits have been exploited, cities have been constructed, pipelines have being laid, more than 45 years have passed since the beginning of the intensive development of oil and gas resources. Nevertheless till now the geoecological consequences and, in general, the experience of the development of vast northern territories haven't been summarized. Meanwhile, without this analysis a rational policy for further development of the Arctic is impossible.

The problem core

According to the conditions of subsurface resources management the permafrost territory represents difficult and severe geological, geocryological, hydrogeological, geoengineering and geoecological conditions. Poor understanding of these conditions' natural-technogenic transformation and its ecological consequences determines additional exploration risks.

In the management of the Arctic regions the costs of construction can reach as high as 3-8 costs of the same in non-frozen regions. Material losses occur because of variety of design errors, low culture of construction in the Arctic region, breaches of the rules in the exploitation of regional objects, inadequate accounting for the experience of the similar territories' development.

The contribution of the latter factor often becomes the most significant as this one doesn't permit actual routines of state ecological and technical control to estimate optimally the impacts of large projects of subsoil management on the geological environment. Correspondingly, it is impossible to determine objectively the contribution of the design, construction and exploitation to the negative reactions of the nature to these projects. This problem requires substantial foundation in methodological and legal aspects.

The fundamental characteristics of an adequate conception are evident. This is a combination of (a) regional and monitoring observations, which permit an identification of natural and technogenic ecological conditions of the permafrost zone and (b) a separation of technogenic factor of occurred negative changes along with the reconstruction of specific reasons producing them.

However, the realization of the conception is not completely successful. Significant reduction of the monitoring activity in the aforementioned direction has taken place in the system of Russian geological survey comparing with the 20th Century, especially – with the Soviet period. There is no state program for the adaptation of the experience accumulated in the sphere of urban territory management in the Arctic and sub-Arctic. The activity of mining companies is concentrated practically only in the frames of license sites. Regional investigations of RAS and universities are able to reflect only the most general regularities of the Arctic permafrost zone formation and development.

Two main reasons of these conclusions: insufficient state funding and the absence of conceptual requirements to developers and licensees. Both reasons are grounded in insufficient understanding of monitoring and retrospective studies' significance for minimization of management problems in Northern territories.

Ways to solution

Territories of big deposits in the Arctic can be considered as polygons for geoecological monitoring, where the current and the former state of the art should be specified and the inferences of this knowledge should be used for the forecast of future state. But it is not in practice now.

In accordance with the tasks of "The Strategy of the Russian Federation Arctic zone development and ensuring of the state's security for the period until 2020» it is necessary to develop interdepartmental Program "Permafrost of Russia" (or "Cryolithozone of Russia"), with experts form RAS, universities, ministry research institutions and mining companies being involved into this work. This program should define a conceptual approach and a strategy for integrated regional and geoecological (hydrogeological, geo-engineering, geocryological) monitoring studies of the cryolithozone on the territories and water areas of the first- and middle-term development (types, stages and volumes of the investigations) as well as development and practical approval of progressive methods of construction. The generalization of the experience of different Arctic regions' development should form the basement of this program.

Regional works and monitoring should be extended gradually, being in advance to the expansion of economical projects into new Arctic areas. The developed areas with neighboring territories become new monitoring sites, with their informative significance being defined and changed in accordance with their economic development stage.

Acknowledgments

Supported by RAS, RFBR (№ 14-05-00956, 15-55-71004/15, 16-05-00249, 16-45-890257-ЯНАО), RSF (№ 16-17-00102); international programs TSP, CALM, GTN-P, PEEX, SWIPA, GCW; YaNAO administration.

Computer simulation of frozen ground thermal regime affected by engineering structures and cooling devices in Frost 3D Universal

Dmitri Evlanov[1]
Vladimir Gordiychuk[1,2]
Gleb V. Gribovskii[1,2]
[1] *Simmakers Ltd, simmakers@gmail.com*
[2] *Belarusian State University*

Abstract

The main features of Russian and foreign simulation software and their limitations that appeared during solving thermal problem under the permafrost conditions are considered in this poster. Frost 3D Universal, the software package for computer simulation of permafrost soils under the thermal influence of engineering constructions and cooling devices, is presented.

Keywords: permafrost, simulation software, numerical simulation, thermal analysis.

Introduction

Computer simulation of permafrost thermal regime requires numerical solution of heat equation. Since Joseph Fourier presented his paper in 1807, the heat equation and its various modifications are widely in use.

Main features of Russian *simulation software. RSN 67-87*

The well-known Russian standard RSN 67-87 (Russian Federation Gosstroy, 1987) has been previously applied successfully to all Russian simulation software and is based on the enthalpy formulation of the heat equation that provides a means to account for "water-ice" phase transitions in the ground. RSN 67-87 is still quite popular, but it should be noted that much has changed since its publication. First of all, scientific and technological progress have emerged new opportunities:

- numerical schemes (Dauzhenka & Gishkeluk, 2013) that were previously used in RSN 67-87 have been improved;

- information technologies offer new computing platforms (GPGPU, distributed computing), allowing us to significantly increase the scale of tasks and reduce the time spent on solution obtaining (Xiaohui et al, 2010).

Secondly, the software requirements have been increased due to the high demands of users:

- accounting for cooling units became extremely important;

- data visualization and workflow automation requirements have been increased.

Despite the fact that 3 decades already passed since the RSN 67-87 had been emerged, local solutions are outdated and significantly behind the modern requirements.

Main features of American and European simulations software

At the same time, western software solutions are constantly changing and incorporating new trends and opportunities in real time. It should be noted that, currently there is a number of American and European general-purpose packages for 3D numerical simulation of thermal processes, however, their employing in permafrost thermal analysis is complicated by the following:

Difficulties of considering 'water-ice' phase transitions, which in turn leads to low accuracy and cause large errors when using general-purpose software:

1) There are no specific tools for creating complicated 3D geological models;
2) There are heat pipes and cooling units to be considered;
3) Time-consuming calculations (days, weeks) due to the numerical methods, which are unoptimized for thermal processes in frozen ground.

Our solution

The practice has shown that the general-purpose software does not meet the needs of most R&D and engineering companies in the Russian Federation.

Simmakers ltd developed Frost 3D Universal software in 2014 and this is the first software package for numerical simulation of thermal processes in permafrost ground, given the issues of both western and Russian software solutions. The key advantage of Frost 3D Universal is a unique numerical scheme that provides high accuracy and makes it possible to account for phase transitions, allows to accelerate calculations ten times faster due to parallelization on graphic accelerators, and also to perform 10^7 nodes simulations for long time periods within several hours (Gishkeluk et al, 2015; Gordiychuk & Gishkeluk, 2016). Also Frost 3D Universal has a built-in set of tools for complicated geological models creation and cooling units simulation.

References

Russian Federation Gosstroy, 1987. *RSN 67-87. Engineering Surveys for Construction - Forecasting Changes in Temperature Regime of Permafrost Soils Using Numerical Methods.* MosCTISIZ, 73 pp.

Dauzhenka T.A., Gishkeluk I.A., 2013. Consistency of the Douglas – Rachford splitting algorithm for the sum of three nonlinear operators: application to the Stefan problem in permafrost soils. *Journal of Applied and Computational Mathematic0073* Vol. 2, No. 4: 100-108.

Xiaohui J.; Tangpei C., Dandan L., Qun W., 2010. Solving large-scale three-dimensional heat equations on CUDA. *3rd International Conference on Advanced Computer Theory and Engineering(ICACTE)*, Chengdu, China, August 20-22.

Gishkeluk I.A., Stanilovskaya J.V., Evlanov D.V., 2015. Forecasting of permafrost thawing around an underground cross-country pipeline. *Oil & Oil products pipeline transportation: Science & Technologies №1(17)*: 20–25.

Gordiychuk V.V., Gishkeluk I.A., 2016 Computer simulation of permafrost soil thermal regime under the thermal influence of engineering constructions. *XI international conference on permafrost, Postdam, Germany, June 20-24:* 1097.

Regionalization across of geological engineering conditions of oil, gas and condensate field Beregovoe

Galeeva (Elmira) Ildarovna[1]
Kurchatova (Anna) Nikolaevna[2]
Strokova (Lyudmila) Alexandrovna[3]
[1]*Tomsk Polytechnic University, holikaholika55@mail.ru*
[2]*Tyumen Industrial University, Earth Cryosphere Institute SB RAS, kanni@mail.ru*
[3]*Tomsk Polytechnic University, geyer@tpu.ru*

Abstract

The article describes the engineering-geological conditions of oil, gas and condensate field Beregovoe. Analysed of the results of researchs the stated data upon which the hazard identification and risk based on which the area was divided and characterize on areas across of engineering-geological conditions.

Keywords: beregovoe; regionalization; engineering-geological conditions; permafrost zone.

Introduction

Results of data processing are presented in article on the example of the Beregovoe oil and gas condensate field located in a zone of permafrost soils.

Results

Regionalization across of geological engineering conditions is performing based on the landscape differentiation of the territory.

Five types of terrain are distinguishing: A (lacustrine-marshy); B (drained lake); B (riverine); G (undulating); D (linear-ridge) (Table 1).

In accordance with SP 11-105-97 on the complexity of engineering and geological conditions, the territory is classifying as category III (complex).

The results of field work and laboratory studies of the physical and mechanical properties of soils made it possible to detail the preliminary assessment of the engineering and geocryological conditions of the deposit, based on the interpretation of the space photograph of the territory.

The main part of the route passes along the riverine type of terrain (B), which is characterizing in the upper part of the section-thawed ground of sandy-loamy composition, low activity of development of dangerous cryogenic processes. Frozen ground from the surface are distributing locally. Sandy soils are everywhere in the lower part of the section.

The most unfavorable for the construction of buildings and the laying of the pipeline are the types of terrain: A (found locally in lowlands, represented by marshes with a peat thickness of up to 2.2 m) and B (is widespread, represented by swampy areas, clayey soils with no surface runoff).Types G and D along the route don't occur.

Based on the results of the performed work is recommended to building sites lines of linear structures on well-drained dry-bottom stretches of thawed soils.

Table 1. Assessment of negative impact of engineering-geological processes depending on area type

Types of terrain	Engineering-geological processes															Sum of scores
	Dampness			Erosion			Thermo-erosion			Frost boiling			Thermokarst			
	Points															
	0	1	2	0	1	2	0	1	2	0	1	2	0	1	2	
Lacustrine-marshy			■	■			■					■			■	6
Hasyreyny			■	■			■				■			■		4
Riverine	■				■			■		■			■			3
Natural drained		■		■			■			■			■			1
Technogenic soils	■					■			■		■		■			3

References

Kudryavtsev, V.A., 1979. *Method of cryogenic plotting*. Moscow: MSU Press, 358 p.

Trofimov, V.T. & Krasilova, N.S., 2008. *Engineering-geological cards: manual*. Moscow*: KDU, 383* p.

Gafarov, N.A. *et al.,* 2010. *Use of space information in a gas industry*. Moscow: LLC Gazprom of an Expo, 132 p.

Golodkovskaya, G.A., 1983. Principles of engineering-geological typification of mineral deposits, *Questions engineering geologists and pedology*. Moscow: Press.-VOMGU 5: 355-369.

Drozdov, D.S. & Dubrovin V.A., 2016. Environmental problems of oil and gas exploration and development in the Russian arctic, *Journal Kriosfera zemli* 20: 16-27.

Permafrost temperature simulation using sequentially coupled explicit-implicit finite-difference method

Vladimir Gordiychuk[1]
[1]*Simmakers Ltd, simmakers.com, vladimir.gordiychuk@simmakers.com*

Abstract

Appliance of finite-difference method using sequentially coupled explicit-implicit scheme aiming to increase computational performance for a wide range of applied tasks in the sphere of construction design on permafrost ground is proposed.

Keywords: FDM, finite-difference method, convection-diffusion equation, heat equation, sequentially coupled explicit-implicit FDM.

Introduction

While designing constructions on permafrost ground it is necessary to predict the temperature of permafrost for the entire period of constructions building and maintenance.

Heat equation is used to describe mathematically the heat transfer processes in permafrost ground (Maksimov & Tsypkin, 1986). This equation is widely acceptable in modern CAD, where numerical methods are used to solve the heat equation. In particular, the finite element method (FEM) and the finite-difference method (FDM) can be distinguished as the most popular numerical methods for heat transfer simulation. (Vasilyev & Popov, 2009, Feulvarch et al, 2013, Vasilyev et al, 2017).

In this paper (Herein), we will consider a range of applied problems in Permafrost engineering and their solving with the help of "classical" and generally accepted approaches that has low performance. To solve such problems, we recommend using a sequential combination of explicit and implicit scheme of finite-difference method, the advantage of which is the improved computing performance.

Problem

The applied tasks in the Permafrost engineering set forth the specific requirements, such as:

1. solution of the heat equation taking into account phase transitions (permafrost ground freezing / thawing);
2. The ratio of computational domain size and minimum spatial step is about 1000:1, what requires a multi-million computational mesh for appropriate approximation;
3. high thermal diffusivity in subdomains without phase transitions (piles, concrete basements and so on);
4. simulation period is decades or even hundreds of years.

There are different forms (schemes) of the finite element method and the finite-difference method, such as explicit, implicit, etc. Each schema has pros and cons. For example, the problem of the explicit scheme is the time step limitation which is quadratically tightened as the spatial step is reduced (Voller & Prakash, 1987). The implicit scheme has limitations concerning the solution of the system of linear algebraic equations in the case of nonlinear heat equation (Idelsohn, 1994, Pham, 1995).
Due to the above facts, both explicit and implicit schemes of finite-difference method will have low computational performance. Thus, it was proposed to combine their application. It is assumed that such combined explicit and implicit scheme usage allows to increase the performance of finite-difference method in many applied problems of Permafrost engineering (Dawson et al, 1991).

Proposed method

The proposed method, in fact, aims to increase the time step of the explicit finite-difference method scheme, by avoiding the most "problem zones".

1. The initial computational domain is divided into two sub domains (A and B) due to the estimation of the maximum time step for each node in the

computational domain. Those nodes that significantly shorten the time step are referred to the B, the remaining nodes are referred to the A;

2. the time step computation is performed with an explicit finite-difference method scheme for all nodes belonging to A sub domain;
3. the time step computation is performed with an implicit finite-difference method scheme for all nodes belonging to the B sub domain. In this case, the system of linear equations solution will be implemented taking into account already known values obtained in the previous step, i.e. the number of variables will be small.

The performance of the proposed method depends on division of the initial computational domain into A and B sub domains. The expansion of B sub domain, on the one hand, allows us to increase the time step of the explicit scheme but, on the other hand, requires more computing performance to solve the system of linear equations.

References

Maksimov, A.M. & Tsypkin, G.G. 1986. A mathematical model for the freezing of water-saturated porous medium. *USSR, Computational Mathematics and Mathematical Physics, vol. 26, no. 6:* 91 – 95.

Thomas, H.R., Cleall, P., Li, Y.C., Harris, C., Kern-Leutschg, M., 2009. Modelling of cryogenic processes in permafrost and seasonally frozen soils. *Geotechnique, vol. 59, no. 3:* 173 – 184.

Vasilyev, V.I. & Popov, V.V., 2009. Numerical solution of the soil freezing problem. *Math. Models Comput. Simulations, vol.1, no. 4:* 419 – 427.

Vasilyev V.I. & Vasilyeva M.V. & Sirditov I.K. & Stepanov S.P. & Tseeva A.N., 2017. Mathematical Modeling of Temperature Regime of Soils of Foundation on Permafrost. *Vestn. Mosk. Gos. Tekh. Univ. im. N.E. Baumana, Estestv. Nauki [Herald of the Bauman Moscow State Tech. Univ., Nat. Sci.], no. 1:* 142–159.

Feulvarch, J. M. Bergheau, and J. B. Leblond, 2009. An implicit finite element algorithm for the simulation of diffusion with phase changes in solids. *International Journal for Numerical Methods in Engineering, vol. 78, no. 12:* 1492–1512.

Feulvarch, E., Roux, J.-C., Bergheau J.-M., 2013. Theoretical Framework of a Variational Formulation for Nonlinear Heat Transfer with Phase Changes. *Mathematical Problems in Engineering, vol. 2013, Article ID 257104, 6 pages.*

Rolph, D., W & Bathe, K.-J., 1982. An efficient algorithm for analysis of nonlinear heat transfer with phase changes. *International Journal for Numerical Methods in Engineering. vol. 18, issue. 1:* 119 – 134

Idelsohn, S. & Storti, M. & A. Crivelli, L., 1994. Numerical methods in phase-change problems. *Archives of Computational Methods in Engineering. 1*: 49-74.

Pham, Q. T., 1995. Comparison of general-purpose finite-element methods for the Stefan problem. *Numerical Heat Transfer, Part B, vol. 27, no. 4*: 417–435.

Dawson C. N. & Du Q. & Dupont T. F., 1991. A finite difference domain decomposition algorithm for numerical solution of the heat equation. *Math. Comp. 57:* 63-71

Voller, V. R., & Prakash, C., 1987. A fixed grid numerical modelling methodology for convection-diffusion mushy region phase-change problems. *International Journal of Heat and Mass Transfer, 30(8)*: 1709-1719.

The comparison of numerical and analytical solution of the Stefan problem

Gleb V. Gribovskii[1,2]
Yury V. Ramanouski[1]

[1]*Simmakers Ltd, gleb.gribovskiy@simmakers.com*
[2]*Belarusian State University*

Abstract

This work deals with comparing analytical solution of the Stefan problem for soil freezing with numerical solution performed by simulation software. As a result, there have been received max errors of calculated temperature, the depth of water-ice phase transition in ground and computational time.

Keywords: permafrost, Stefan problem, simulation software, numerical simulation, phase transition.

Introduction

Nowadays, it is widely acceptable to perform numerical computation using specialized simulation software while designing the engineering structures. One of the important task during such simulation routine conducted for permafrost is to predict three-dimensional thermal state of underlying soils in course of structure maintenance, because the soil state (frozen or thawed) is responsible the stability of the construction. (Oswell & Nixon, 2015; Zhou *et al.,* 2008; Gishkeluk *et al.,* 2015; Kudriavtcev *et al.,* 2013). Another important task of such numerical computation is the correct simulation of the ice–water phase transition.

This work is dealing with the result accuracy in solving a heat problem with phase transitions in the ground. Such software packages as ANSYS 18.0 Thermal, COMSOL 5.2a and Frost 3D Universal 3.0. were selected for comparison. Simulation results were compared with the well-known Stefan problem. (Pavlov, 2001; Boucígueza *et al.,* 2007; Javierre *et al.,* 2006). This problem has a certain analytical solution (Pavlov, 2001), with which the comparison of simulation software will take place. There are following criteria: the accuracy of the temperature measurement in each node, the depth of the phase transition in comparison with the analytical solution, and time spent on numerical computation. Special attention was paid to the accuracy of the temperature in an area of the phase transition.

Problem statement

Problem statement for all simulation software solutions is the following:

- The computation domain is a column of soil (1m x 1m x 25m);
- The initial temperature of the soil is T_0 = 1.5 °C;
- On the top boundary, the first-type boundary condition is set: T_{bnd} = -27 °C;
- On all other boundaries, the second-type boundary condition is set: q=0;
- Mesh step along X-Axis and Y-Axis is 0.5m and for Z axis is 0,02m.
- The heat capacity of the soil in thawed and frozen state:
  C_t = 1.89 MJ/(m³ °C);
  C_f = 1.74 MJ/(m³ °C);
- The thermal conductivity of the soil in thawed and frozen state:
  K_t = 0.7 W/(m °C);
  K_f =0.75 W/(m °C);
- Phase transition temperature is T_{bf} = 0 °C;
- The volumetric heat capacity of phase transition is L=334 MJ/m³;
- Computational time is 300 days.

In the classical Stefan Problem, the zone of freezing (or melting) is degenerated to a point, while the curve of unfrozen water content has a jump discontinuity. For the simulation software, the phase transition has been smoothed in order to make the curve of unfrozen water.

All numerical computations were performed on Intel Core i5-2500.

Results

The depth of the phase front after 300 days will be at a depth of 1.712 meters according to the analytical solution of the Stefan problem. Comparison of the numerical and analytical solutions is shown in table 1.

Table 1. Comparison of numerical and analytical solutions of the Stefan problem.

	Max error, °C	Max ratio error, %	Depth of the phase transition, m	Time of computation, s
ANSYS	2.2931	8.05	1.578	549
COMSOL	1.5066	5.29	1.899	3976
FROST 3D	0.1350	0.47	1.739	38

In all considered software packages max error occurs around the phase transition zone. The greatest error was performed by ANSYS and the smallest one - by FROST 3D. Simulation performed by COMSOL was the most time-consuming, but more accurate than by ANSYS. FROST 3D has the highest speed of computation. In addition, FROST 3D phase transition front was the closest to the analytical solution.

Such different computational results can be explained by differences in the used numerical methods. ANSYS and COMSOL is based on implicit formulation of the finite-element method, with a problem of convergence of numerical method for solving three-dimensional problems. FROST 3D is based on explicit formulation of the finite-difference scheme that is the best solution for the considered problem in 3D.

Summary

Comparison of such software packages as ANSYS 18.0 Thermal, COMSOL 5.2a, Frost 3D Universal 3.0 with the analytical solution of the Stefan problem was considered. The comparison results showed that FROST 3D have the better convergence with the analytical solution. Good results were shown by COMSOL and ANSYS, but the COMSOL computational time was greater, in comparison to other software packages.

References

Oswell J.M. & Nixon J.F., 2015. Thermal Design Considerations for Raised Structures on Permafrost. *Journal of Cold Regions Engineering,* Vol. 29, Issue 1.

Zhou F., Li R., Zhang A. & Zhu L., 2008. Surface-coupled three-dimensional geothermal model for study of permafrost geothermal regime in a building environment. *Journal of Geophysical Research: Atmospheres*, Vol. 113, Issue D19.

Gishkeluk I.A., Stanilovskaya J.V. & Evlanov D.V., 2015. Forecasting of permafrost thawing around an underground cross-country pipeline. *Oil & Oil products pipeline transportation: Science & Technologies* №1(17): 20–25.

Kudriavtcev S., Valtseva T., Kazharskyi A., Goncharova E. & Berestianyi I. 2013. Predictive modeling of the permafrost thermal regime in Russian railroad subgrade support systems. *Journal of Sciences in Cold and Arid Regions,* Vol. 4(5): 404-407.

Pavlov A.R., 2001. *Mathematical modeling of the processes of heat and mass transmission during phase transitions: tutorial.* Yakuts: Yakutsk State University, 58 pp.

Boucígueza A. C., Lozanoa R. F. & Larab M. A., 2007. About the exact solution in two phase-stefan problem. *Engenharia Térmica (Thermal Engineering),* Vol. 6: 70-75

Javierre E., Vuik C., Vermolen F.J. & van der Zwaag S., 2006. A comparison of numerical models for one-dimensional Stefan problems. *Journal of Computational and Applied Mathematics* 192: 445 – 459.

Tsytovich N.A., 1973. *Mechanics of frozen soils.* Moscow: High School, 280 pp.

Effects of insulation due to moss layer on thawing of permafrost

Shota Homma[1], Masaya Ogawa[2], Ryo Ochiai[3], Hao Zheng[4], Shunji Kanie[4]
[1]*Graduate School of Engineering, Hokkaido University, Sapporo, Japan,* shota-10-30@eis.hokudai.ac.jp
[2]*Graduate School of Engineering, Hokkaido University, Sapporo, Japan*
[3]*Undergraduated School of Engineering, Hokkaido University, Sapporo, Japan*
[4]*Faculty of Engineering, Hokkaido University, Sapporo, Japan*

Abstract

With global warming in recent years, thawing of permafrost has been accelerated seriously. By the thawing of permafrost, topographical deformation such as landslide occurs. This deformation of the terrain gives severe damage to the infrastructure in cold regions. However, thawing process of permafrost has not been fully studied until now. This study is aimed at the elucidation of thawing process and proposing the efficient countermeasures to slope collapse by using both indoor experiment and numerical analysis. Especially in this paper, we focus on the influence due to moss layer, a vegetation layer with high thermal insulating performance, to topographical deformation. As a result, both experiment and numerical analysis indicated that the moss layer plays an important role in delaying progression of collapse.

Keywords: thawing; insulation; topographical deformation; FEM; moss layer; global warming.

Introduction

With the climatic change in recent years, thawing of permafrost has been accelerated seriously (Anisimov & Reneva, 2006). Once frozen soil thaws, the ground loses its bearing capacity. As a result, topographical deformation may occur in wide areas such as landslide or subsidence (Nelson *et al.*, 2001). This terrain deformation gives severe damage to the infrastructure in cold regions. However, the thawing process of frozen soil is not yet well understood.

This study is aimed at the elucidation of thawing process and proposes the efficient countermeasures to slope collapse by using both indoor experiment and numerical analysis. Especially in this paper, we focus on influence due to moss layer, vegetation layer with high thermal insulating performance, to topographical deformation. We conducted experiment with styrene foam as an insulating layer to observe the influence of it. In the numerical analysis, FEM was used to obtain the internal thermal distribution by simulating the same situation as indoor experiment.

Indoor Experiment

The purpose of this experiment is to clarify the influence of the thermal insulating layer on the fracture of surface. We observed the temperature change of the specimen with collapse, as well as the angle of collapsing surface.

The apparatus used for the experiment consists of acrylic plates and a heat circulation system. As a fundamental experiment, we chose glass beads with a diameter of 5mm. The making procedure of the model foundation is as follows.

First, glass beads are filled in the container and fully saturated. On the foundation, granular styrene foam is put to cover the surface. However, only the left part of the surface is covered by the styrene foam to compare its insulation ability as shown in Figure 1 and Figure 2. After those preparations, the container is kept in a cold room with a temperature of -15 °C until the foundation is completely frozen. When we observe the thawing process, the heat circulation system is set at the top of container to promote thawing.

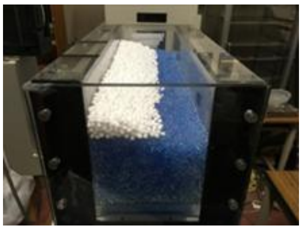

Figure 1. Bird's eye view.

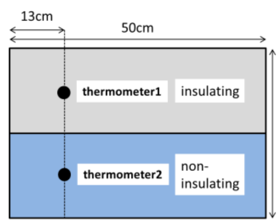

Figure 2. Plan view.

Numerical Analysis

Although the temperature change with thawing is monitored by thermometers, the number of monitoring points is limited. Then, the authors introduced Finite Element Method to simulate the temperature distribution. Figure 3 illustrates the FEM model.

The model foundation is located at the center of the model and boundary zones encircle the foundation to simulate heat transfer. The height and the length of the foundation are 12 cm and 50 cm respectively. All the elements are in squared shape of 5 mm. As an initial condition, the temperatures at all nodes are assumed as -6 °C. The conditions of outside boundaries at the top and left for convection are fixed at 60 °C according to the circulated air temperature. At the right and bottom boundaries, thermal conduction through acrylic plates is taken into consideration and the temperatures of those are kept at 20 °C as same as the room temperature during the experiment. The simulation was carried out to confirm the temperature distribution by comparing with those by the thermometers.

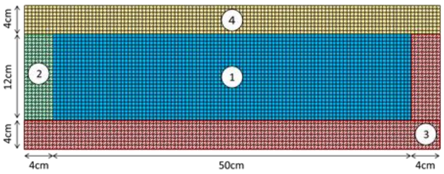

Figure 3. Analysis model.

Results and Discussion

Figure 4 shows pictures of typical experimental result. The insulation layer is placed in the back-side half of the pictures. At 6 hours after thawing, the slope with insulation layer shown by red line keeps a rather steeper angle than that without insulation illustrated by yellow one. However 16 hours passed, those angles converged to almost same, and the angles of those could be explained as the resting angle of the material.

Figure 5 shows temperature changes with time at the monitoring points. Right after the heating, they go up towards 0 °C and keep almost constant around 0 °C because of the effect of latent heat. When the frozen part is completely thawed, they go up again as the figure shows. At the positive side in the temperature after thawing, the temperature changes of the experimental result look little different from those of the analytical one because the FEM model could not consider the deformation of the foundation due to collapse. However, the authors think that the simulation of temperature distributions in thawing process could be appropriately evaluated. Figure 6 shows the temperature distributions within the model after 6 hours.

On the other hand, Figure 7 shows the changes in temperature distribution in vertical section at 8 cm inside from the left end of the region. From those figures, it is confirmed that the existence of insulation layer affects the thawing process as well as the collapse mechanism.

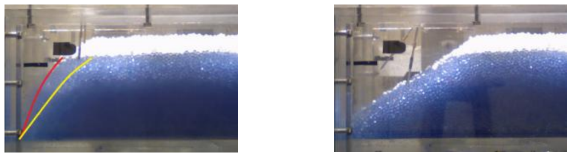

After 6 hours After 16 hours

Figure 4. Experiment pictures.

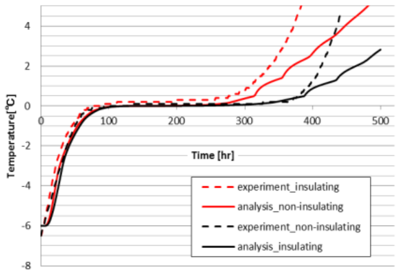

Figure 5. Temperature change.

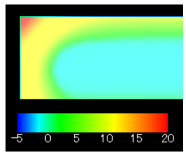

non-insulating

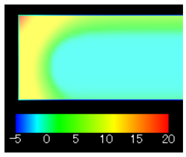

insulating

Figure 6. Temp. distributions.

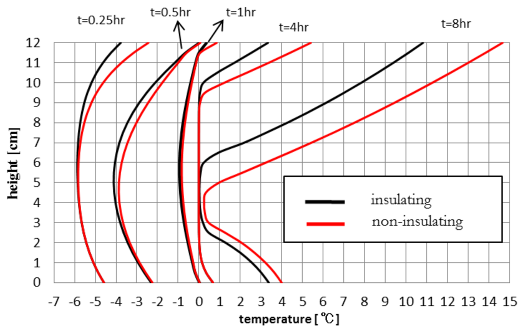

Figure 7. Temperature distributions in a vertical section.

Summary and Prospects

Experiment and analysis proved that the thermal insulation layer plays an important role in delaying the progress of thawing. Therefore repairing and protecting the moss layer is an effective measure to minimize the damage due to topographical deformation. In the near future, we plan to establish FEM model which can consider the collapsing deformation more precisely by coupling DEM or others.

References

Anisimov, O. & Reneva, S., 2006. Permafrost and changing climate: the russian perspective. *Ambio* 35.

Nelson, F. E., Anisimov, O. A., Shiklomanov, N. I., 2001. Subsidence risk from thawing permafrost, *Nature* 410: 889-890.

Geotechnical Design and Construction for Water Treatment Facilities in a Warm Permafrost

Entzu Hsieh[1]
Alexandre Tchekhovski[1]
Blake Brodland[1]
Keith Barnes[2]
Grant Hood[3]

[1]*Amec Foster Wheeler, peter.hsieh@amecfw.com*
[2]*Associate, Dillon Consulting Limited*
[3]*Senior Administrative Officer, Town of Inuvik*

Extended Abstract

The site is located in the Town of Inuvik, Northwest Territories, Canada, on the shore of to the East Mackenzie River Channel. The new development involves an expansion of the existing water treatment plant, deepening and widening the existing Duck Lake, which will be used as a settlement pond, construction of a pump station near the channel and installation of a new water intake pipeline to transfer water from the river channel to the settlement pond (Figure 1).

Field investigations were conducted including borehole drilling, ground temperature measurements, laboratory tests of thawing soils, and geothermal modeling. The results revealed that frozen soils were presented by clayey silt with various amount of gravel with mean annual temperature in a range from -1.0°C to -1.5°C. A talik with temperatures ranging between 0.3°C and 1.9°C was observed along the south and east boundary of the lake.

Based on the results of investigation, adfreeze piles using gravel slurry were determined to support the new addition of the plant. In order to reduce the potential frost heave, a bond breaker, consisting of heavy cold climate grease was applied directly to the piles and wrapped with two layers of greased polyethylene sheets. A total number of 180 piles was installed and construction monitoring was performed to monitor pile installation. Five pile locations were selected to monitor freeze-back temperatures of the slurry after pile installation and two of which were selected to carry out a long term ground temperature monitoring. Once freeze-back occurred and the adfreeze piles gained the specified capacity, construction of the water treatment plant on top of the piles was taken place.

There were approximately 100 wooden piles supporting the existing building and approximately 40 wooden piles supporting the existing water pipeline from the channel to the water treatment plant. All piles were visually inspected for rot, mechanically damage and creosote. In addition, selected piles were exposed below grade for integrity assessment via coring.

During the initial stage of the project, expansion of the lake toward the channel for the purpose to increase the raw water storage capacity was considered. An increase of the water volume would result in a considerable increase of heat flux from the lake reservoir influencing the current dimensions of the lake talik as well as to degrade the existing frozen core between the talik and East Mackenzie River Channel. A 2-dimensional geothermal model was developed to assess the potential thermal impact of the lake expansion to the existing permafrost conditions. The results suggest that the magnitude of permafrost degradation within the existing frozen core would be about 5 m to 10 m horizontally meaning that full degradation of the permafrost between the lake and the channel is unlikely. Due to environmental issues, it was determined at the final stage of the project that pumping water directly from the Channel directly to the water treatment plant was adopted rather than deepening and extending the lake as a water storage.

The inlet of the water pipeline is located about 200 m from the shoreline and secured with concrete pipe collars in the bottom of the trench. The offshore boreholes including auger holes and cone penetration tests, up to 25 m depth, were advanced along the pipeline alignment to confirm boundary of the expected talik zone under the East Mackenzie River Channel. Pore pressure dissipation tests were completed to assess the hydrostatic pore pressures at depth. Conventional open cut trench method and horizontal directional drill method were considered for the offshore section of the water pipeline. Advantages and disadvantages of the considered options are discussed in the paper.

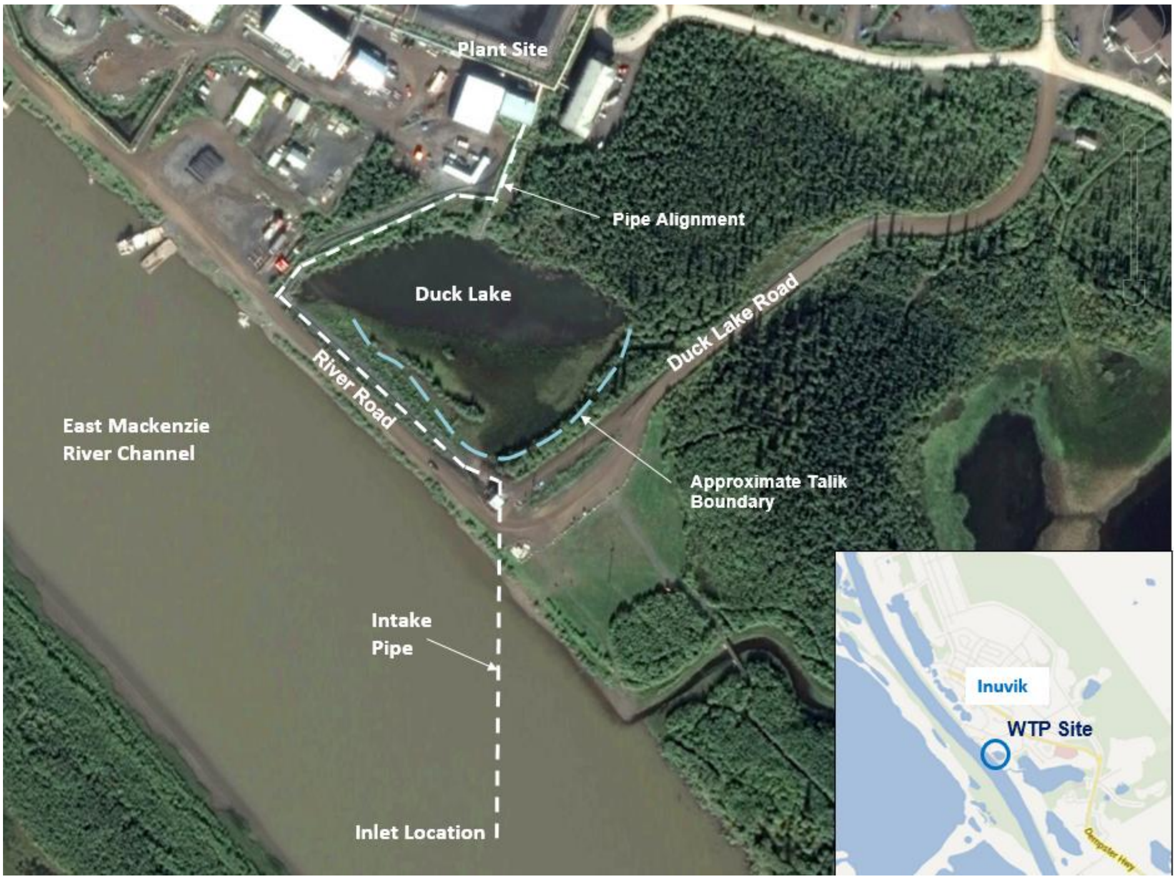

Figure 1: Inuvik Water Treatment Plant Location Plan

Multidisciplinary site investigations for improved infrastructure design in Qaanaaq, North Greenland

Thomas Ingeman-Nielsen[1]
Soňa Tomaškovičová[2]
Niels Foged[2]
[1]*Department of Civil Engineering, Technical University of Denmark, tin@byg.dtu.dk*
[2] *Department of Civil Engineering, Technical University of Denmark*

Abstract

This contribution presents a case study of permafrost geotechnical conditions in Qaanaaq, one of the northern-most communities in Greenland. Severe problems with differential settlements are observed while the community is faced with major needs for infrastructure expansion. A combination of investigation techniques, involving geotechnical drilling, electrical resistivity tomography and ground temperature monitoring were applied to characterize for the first time the geotechnical conditions in the area, to support more sustainable infrastructure development. We found that most of the town is built on relatively thaw-stable sediments. The observed problems with house foundations appear to be mainly linked to construction practices, freeze-thaw process and slope movement in the active layer, rather than the on-going permafrost degradation.

Keywords: Geotechnical investigations; electrical resistivity tomography; permafrost foundations

Introduction

The North Greenland community Qaanaaq (approx. 650 inhabitants, 77°N) was established in 1953 when the Danish authorities forcefully moved an inuit settlement from Uummannaq, during and due to the construction of the nearby Thule Air Base. Qaanaaq is located on a permafrost affected coastal slope. Houses in some parts of the community are severely affected by differential settlements and essential infrastructure is threatened by climate-induced changes. The community water supply is based on water from the river during four summer months. In winter, ice from icebergs, grounded by the sea ice, is collected and melted. In the intermediate periods (when the river is dry and the sea ice not yet stable enough to allow operation with machinery), water is stored in large tanks.

A change in seasonality has resulted in a shorter period for operating on the sea ice. Combined with population growth and a generally increased demand, an increased storage capacity and extraction capability is urgently needed.

No previous detailed geotechnical investigations have been conducted in the Qaanaaq area, in spite of the fact that the community is expanding and a 900 m gravel airstrip has been built. Here we present the initial results of systematic, extensive and multidisciplinary geotechnical investigations undertaken in the summer of 2017. The aims were to understand the geotechnical setting in Qaanaaq and document permafrost conditions and material properties, in order to determine the cause of the observed damages, and provide guidelines for future infrastructure development in the area.

The combination of methods presented in this contribution involves geotechnical drilling, Electrical Resistivity Tomography (ERT) mapping and ground temperature monitoring.

Site description

Qaanaaq is situated in an area of continuous, cold permafrost. The town extends on both banks of a river, which divides the town into an eastern part (older) and a western part (newer housing development area).

The bedrock in the area consists of Archaean-Proterozoic gneisses and amphibolites, which are overlain by late Protorozoic sandstones and conglomerates belonging to the Thule Supergroup. The rocks are cut by dolerite dykes (Dawes, 1997).

The air temperatures records from Qaanaaq document a 2 °C increase in mean annual air temperature (MAAT) over the past four decades, from -10.6 °C (average 1965 to 1979) to -8.6 °C (average 2002 to 2016) (Cappelen, 2017). The area has very little precipitation and almost no snow cover in winter, due to local wind conditions.

Geotechnical drilling

A total of 23 boreholes were drilled using a Nordmeyer DSB-3 rig and a custom-made hollow stem auger system for coring frozen fine grained sediments, and standard rotary drilling or DTH hammer for coarse material and sandstone. The boreholes were terminated at varying depth of up to 20 m b.g.s. A few of the boreholes reach the sandstone basement, which is found most shallow east of the town (at depths from 6 to 18 m b.g.s.). The sedimentary deposits consist mainly of gravels and sands, with occasional layers of silts and clays. The material is varying shades of yellowish-brown in color, with some distinct dark grey to black horizons. The coarse material is dry, with typical gravimetric water contents below 10 %. Water contents of up to 50 % are occasionally found, mainly in samples close to the permafrost table, and massive segregated ice was seldom encountered. The frozen cores of fine grained materials have not yet been classified except for visual description.

Thermal state of permafrost

Dataloggers and thermistor strings were installed in 13 of the boreholes (7 to 20 m in length). Preliminary ground temperature measurements from end of August show thaw depths in the eastern part of town in the range from 1.3 to 2.5 m (indicative of active layer thickness), with ground temperatures between -7.1 and -5.3 °C at 7 m depth. The western part of town is noticeably colder, with end of August thaw depths ranging from 0.9 to 1.8 m, and ground temperatures down to -8.5 °C at 7 m depth.

A consistent trend throughout the area, ground temperatures in boreholes at the lower part of the coastal slope are colder and exhibit a shallower thaw depth (active layer thickness) than do those in boreholes at higher elevations further from the shore. Weather this trend is coupled with variations in sediment types, hydrological processes, or other factors is not yet established.

Furthermore, the ground temperature profiles in the town area are typically warmer, but also show larger spatial variation, than ground temperature profiles measured in an undisturbed reference area east of town.

ERT surveys

Extensive mapping with Electrical Resistivity Tomography (ERT) provided information about spatial variability of ground conditions in the area. Tomograms from both sides of town reveal a high contrast three-layer resistivity structure with a low-resistive active layer, below which a highly resistive layer (5-10 kΩm) correspond to the upper part of the permafrost. At depths below 5 m a very low resistive layer (<200 Ωm) is observed throughout the area. While in other parts of West Greenland, such low-resistivity anomalies are typically indicative of partially frozen saline fine-grained marine sediments, in Qaanaaq the geotechnical drilling did not indicate wide spread occurrence of such sediments. The distinctive layers of dark sand are speculated to be the cause of the low resistive anomalies, and will be the focus of upcoming laboratory and modelling studies to investigate mineral composition, as well as thermo-mechanical and electrical properties.

Discussion and Conclusions

Our investigations have documented that Qaanaaq is constructed on a coastal slope of relatively coarse-grained sediments affected by continuous permafrost with temperatures from approximately -5 °C to -8.5 °C. The sediments are typically dry with little segregational ice. However, frost-susceptible fine-grained sediments were observed, most notably in the western part of town, where also the most issues with differential settlements occur. Foundations are typically shallow wooden foundations embedded in a gravel berm. Over the past four decades, the mean annual air temperatures have increased by approximately 2 °C in the area. Interestingly, over this period, the typical foundation depth seem to have decreased from approximately 1.7 m to around 1.2 m. Furthermore, several of the investigated berms were constructed of frost-susceptible materials with poor drainage. Thus the observed problems seem linked more to construction practices, freeze-thaw process and slope movement in the active layer, rather than the on-going permafrost degradation.

References

Dawes, P. R., 1997. The Proterozoic Thule Supergroup, Greenland and Canada: history, lithostratigraphy and development. *Geology of Greenland Survey Bulletin* 174: 1–147.

Cappelen, J., 2017. Weather observations from Greenland 1958-2016. *DMI Report 17-08*. Danish Meteorological Institute. ISSN: 2445-9127.

Applicability of the CPT cone penetrometers with regard to the soil conditions and the objectives of control on Permafrost

Isaev Oleg
Gersevanov NIIOSP, Moscow, Russia, geotechnika2017@mail.ru

Abstract

Study and control over the soil bases of buildings and structures under construction and operated ones, located on permafrost soils is a challenge that must be met by surveyors, designers, builders and building operation and maintenance services. The studies carried out in Russia and abroad showed the applicability and effectiveness of CPT application on permafrost soils, particularly when using the electrical CPT cone penetrometers equipped with additional sensors and devices.

Keywords: CPT, cone penetrometer, permafrost, applicability.

Study and control over the soil bases of buildings and structures under construction and operated ones, located on permafrost soils is a challenge that must be met by surveyors, designers, builders and building operation and maintenance services. Despite the relevance of this problem and the efforts made in recent years in Russia to develop and improve new approaches, techniques and equipment, it has not been handled yet. The current standards do not adequately illustrate the issues concerning control over soil bases, and the potential and experience of the new in-situ express methods are not sufficiently used for soils. CPT holds a special place among the in-situ express methods. The studies carried out in Russia and abroad (Blouin, S. et al. 1979; Woeller, D.J. et al. 1991; Buteau, S. et al. 2005; Fortier, R & Yu, W. 2012; Adrian B. McCallum et al. 2014; Ryzhkov, I.B. & Isaev, O.N. 2016) showed the applicability and effectiveness of CPT application on permafrost soils, particularly when using electrical probes equipped with additional sensors and devices.

The CPT cone penetrometers on permafrost may additionally include: a temperature sensor (T-CPT, RT-CPT, HT-CPT, T-CPTU); a temperature sensor and a heat element (HT-CPT); a pore pressure sensor (CPTU, T-CPTU, R-CPTU, S-CPTU); an electrical resistivity sensor (R-CPT, RT-CPT, R-CPTU); a seismic-acoustic sensor (S-CPT, S-CPTU); a gamma radiation sensor (GR-CPT); a gamma-gamma radiation sensor (GGR-CPT); a neutron-neutron radiation sensor (NNR-CPT).

Applicability of the cone penetrometers with regard to soil conditions (Table 1) depending on the type of penetrometer, degree of soil dispersion (gravel-pebble, sandy, clays) and state of soil (thawed, plastic-frozen, hard-frozen).

Applicability of the cone penetrometers with regard to objectives of control depending on the type of penetrometer and objectives of control. With the help of the cone penetrometers it is possible to control the following geotechnical parameters (Table. 2): types and varieties of soils and engineering geological sections; groundwater level; soil temperatures and thermometric wells; condition of soils; boundaries between thawed and frozen soils; salinity of soils and detection of cryopegs; corrosiveness of soils; consolidating of thawing and hardening of freezing soils; possible liquefying of thawed sands in dynamic and seismic effects; parameters of seismic microzoning of permafrost and thawed soils; physical and thermophysical properties of soils; strength and deformation properties of soils; mechanical properties of frozen soils with regard to their thawing; load-bearing capacity of foundation soils; quality of geotechnical works in foundation engineering.

Table 1. Applicability of the CPT cone penetrometers with regard to soil conditions

Probe	Dispersed soils						
	Thawed			Frozen			
	Gravel-pebble	Sands	Clays	Plastic-frozen sands	Plastic-frozen clays	Hard-frozen soils	Icy soils
Probes without heat elements							
CPT, T-CPT, R-CPT, RT-CPT, S-CPT, GR-CPT, GGR-CPT, NNR-CPT, CPTU, T-CPTU, R-CPTU, S-CPTU	C	A-B	A-B	C-D	B	C-D	C-D
Probe with a heat element HT-CPT	C	A-B	A-B	B-D	A-B	B-C	B-C

Notes: The table illustrates domestic and foreign experience on applicability (possible pushing) of an electrical probe in various soil conditions. Applicability: «A» – high, «B» – medium, «C» – low; «D» – the probe is not used.

Table 2. Applicability of the CPT cone penetrometers with regard to the objectives of control

Type of probe	Type of soil, section	Groundwater level	Soil temperature	Thermometric wells	State of soil (thawed or frozen)	Boundary between thawed and frozen soils	Cryopegs	Salinity of soil	Corrosiveness	Consolidation of thawing soils	Parameters of seismic microzoning	Possible liquefying of thawed sands	Soil density	Soil moisture	Thermophysical properties	Modulus of deformation	Modulus of shearing in small deformations	Consolidation ratio	Soil permeability	Strength properties	Properties of frozen soils in thawing	Pile bearing capacity
1	2	3	4	5	6	7	8	9	10	11	12	13	14	15	16	17	18	19	20	21	22	23
CPT	B/C	-	-	C/B	B	C	B	-	-	B	-	C	C/-	-	-	B	-	-	C/-	B	-	A
T-CPT	B	-	A	C/B	A	A	A	-	-	B	-	C	C/-	-	C	B	-	-	C/-	B	-	A
R-CPT	B/C	B	-	C/B	B	C	A	B	B	B	-	C	C/-	C	-	B	-	-	C/-	B	-	A
RT-CPT	B	B	A	C/B	A	A	A	B	B	B	-	C	C/-	C	C	B	-	-	C/-	B	-	A
HT-CPT	B	-	A	C/B	A	A	A	-	-	B	-	C	C/-	-	B	B	-	-	C/-	B	B	A
S-CPT	A/C	-	-	C/B	B	C	B	-	-	B	B	B	C/-	-	-	B	-	-	B/-	B	-	A
GR-CPT	A/C	-	-	C/B	B	C	B	-	-	B	-	C	C/-	-	-	B	-	-	C/-	B	-	A
GGR-CPT	B/C	-	-	C/B	B	C	B	-	-	B	-	C	A/B	-	-	B	-	-	C/-	B	-	A
NNR-CPT	B/C	A	-	C/B	B	C	B	-	-	B	-	C	C/-	A/B	-	B	-	-	C/-	B	-	A
CPTu	A/C	-	-	C/B	A-B	C	B	-	-	B	-	C	C/-	-	-	B	-	B	B/-	B	-	A
T-CPTu	A/C	-	A	C/B	A	A	A	-	-	B	-	C	C/-	-	C	B	-	-	C/-	B	-	A
R-CPTu	A/C	B	-	C/B	A-B	C	A	B	B	B	-	C	C/-	C	-	B	-	B	B/-	B	-	A
S-CPTu	A/C	-	-	C/B	A-B	C	B	-	-	B	B	B	C/-	-	-	B	-	B	B/-	B	-	A

Notes:

1. Applicability: "A", "B", "C" – the probe is used; "-" – the probe is not used.
2. Applicability: "A" – high, "B" – medium, "C" – low.
3. In the numerator – for thawed soils, in the denominator – for frozen soils.

REFERENCES:

Adrian B. McCallum, Andy Barwise, Roi S. Santos 2014. Is the cone penetration test (CPT) useful for arctic site investigation? *Proceedings of the ASME 2014 33rd International Conference on Ocean*, Offshore and Arctic Engineering. OMAE2014. San Francisco, USA. 5 p.

Blouin S., Chamberlain E., Sellmann P. and Garfield D. 1979. Determining subsea permafrost characteristics

Buteau, S., Fortier, R., and Allard, M. 2005. Rate-Controlled Cone Penetration Tests in Permafrost. *Canadian Geotechnical Journal*, 42 (1): pp. 184–197.Fortier, R & Yu, W. 2012. Penetration rate-controlled electrical resistivity and temperature piezocone penetration tests in warm ice-rich permafrost in Northern Quebec (Canada). *15th International Conference on Cold Regions Engineering*, Quebec, Canada. pp. 1–11.

Ryzhkov I.B. & Isaev O.N. 2016. *Cone penetration testing of soils in geotechnics*. Stockholm, Sweden: Bokforlaget Efron & Dotter AB, 408 p.

Woeller, D.J., Weemees, I., Kurfurst, P.J., and Robertson, P.K. 1991. Penetration Testing for Arctic Soil and Permafrost Conditions. *In Proceedings of the Geotechnical Engineering Congress*, Boulder, Colorado. American Society of Civil Engineers, New York. Vol. 1, pp. 76–83.

with a cone penetrometer. *Cold Regions Science and Technology*. № 1, pp. 3-16.

Study of the influence of complex geocryological conditions on the stability of roads on Taymyr Peninsula

Vladimir Alexandrovich Isakov[1]
Valery Ivanovich Grebenets[1]
Vasily Andreevich Tolmanov[1]
Aligoushad Gasan Ogly Kerimov[2]

[1]*Moscow State University, Geographical faculty, Department of Cryoliyology and Glaciology, isakov.gc@gmail.com*
[2] *NPO "Fundament", Norilsk*

Abstract

Roads in permafrost zone undergo significant deformations. Field studies were conducted in the largest industrial center of the permafrost zone (Norilsk) and causes of the destruction of transport systems were identified.

Keywords: permafrost, climate, dangerous cryogenic processes, road deformations

Introduction

Norilsk Industrial Area (NIA) is one of the largest industrial centers in the permafrost zone. Large ice content in the rocks, diverse landscapes, high snowstorm activity etc. provoke negative impact on the stability of the local transport network, which is about 1200 km long. Climate change (Malkova *et al*., 2012), observed in the recent decades, may explain enhancement of cryogenic processes, intensifying deformation of objects.

Observation and results

Examination in 2005-2017 revealed considerable road deformations in the NIA. Possible reasons of bad situation can be divided into 3 groups: 1) associated with slope processes; 2) dealt with extra-cooling; 3) developed due to heating of road foundations and adjacent areas.

The first group includes road deformations caused by solifluction, water-snow flow activity and movement of rock glaciers (Grebenets *et al*., 1998). This group of deformations within NIA is prevalent mainly at the foothills and leads to catastrophic destruction of the roadway by landslides, blockages and embankment shifts. Activation of slope cryogenic processes is aggravated by recent increase of winter snow accumulation (Malkova *et al*., 2012).

The second group includes deformations owing to supercooling of asphalt pavement, road embankments and road cut slopes induced by snow removal. Hence, ice wedges, sometimes filled with ice, are formed; conditions for frost heaving of road embankments (Isakov & Grebenets, 2017) and for the formation of "a frozen screen" are created, causing a flood of groundwater onto the surface and formation of icings up to 150-170 m long. These deformations are evenly distributed over the NIA territory. Answering the present climate trend towards increase of mean winter air temperature, one should anticipate activity of these processes decreasing to a certain extent. Nevertheless, cryogenic weathering of the roadbed is observed everywhere.

The most widespread are deformations of the third group associated with degradation of heavily iced frozen grounds at the basement and directly along transport corridors.

Deformations of this group are spread mostly in the flat terrain parts of the NIA within heavily iced soils of the Valyok lacustrine-alluvial plain. They are represented mainly by subsidence of the roadbed, by settling of the road slopes, by wave-like deformations due to thermokarst (fig.1.)

Fig.1. Deformation of roads during permafrost retreat.

The detailed study [1] showed the mechanism of their development being self-sustaining and associated with widespread fine-dispersed iced rocks and natural thermokarst hollows as well as with snow and liquid accumulation at the foot of embankments.

The activation of deformations results primarily from climate changes in the region. Increasing snow accumulation, that provokes further activation of unfavourable processes, plays decisive role in case of deformations of the first group. For the second group, relative softening of winters means weaker manifestation of deformations. For the third group, a certain relationship between winter warming and increase of both liquid and solid precipitation is deduced, but local geocryological and technogenic conditions would play a greater role.

Anknowledgements

The work is executed at financial support of the Russian Geographical Society grant №15\17: "Modern conditions and dynamics of dangerous cryogenic processes, influencing on existing and prospective transport network of the Siberia and Far East".

References

Grebenets V.I., Kerimov A.G., Titkov S.N. 1998. Dangerous movement of anthropogenic "Rock Glacier", Norilsk region Northern Siberia. //*Proc. of the 7th International Conference on Permafrost*. Yellowknife, Yellowknife, Canada, p.347-351.

Isakov V., Grebenets V. 2017. Forecast modeling the thermal behavior and cryogenic processes in road embankments constituted by fine grounds // *Proc. of Pushchino Permafrost Conference. Earth's Cryosphere: Past, Present and Future*, p.137–138.

Malkova G.V., Pavlov A.V. 2012. GIS-based assessment of contemporary climate and permafrost changes in Northern Russia // *Proc. of the Tenth International Conference on Permafrost*, p.247–251.

Modeling of ice content change in frozen grounds for road under exploitation

Isakova Daria I.[1]
Isakov Vladimir A.[1]
Grebenets Valery I.[1]
Panchenko Evgeny G.[2]
[1]*Moscow State University, Geographical faculty, Department of Cryoliyology and Glaciology*
[2]*Sergeev Institute of Environmental Geoscience, Russian Academy of Sciences*

Abstract

In the permafrost zone, the reliability of the operation of transport systems depends on many natural and technological parameters. The most important parameters of road basements are the temperature and ice content. We present a predictive model showing the ice formation of frozen grounds in the natural grounds under road basement.

Keywords: permafrost, road deformations, ice content, active layer.

Introduction

The construction of roads significantly alters the temperature conditions in the permafrost grounds. The changes may result in thawing of frozen grounds, or temperature state withstand, or even decrease in upper ground layer temperature (Isakov, 2015). When the temperature of frozen grounds decreases, some of the unfrozen water turns into ice, resulting in the ice content volume and causing the development of frost heave. The accumulation of ice at the basement of a road poses a danger due to uneven heaving and subsequent subsidence. The latter may trigger the thermokarst formation.

Results and observations

New ice formation in soils occurs mainly in two ways: in situ freezing of gravity and film water or as a result of migration of unfrozen water.

The research presented included a forecast modeling of the temperature regime at the road basement along with an estimation of the amount of unfrozen water in the soils at different temperatures, and a change in the volume of the frozen soil due to the transition of some of the unfrozen water into ice. We used a section of the motor road near Urengoy, where significant deformations were registered. Detailed investigations revealed ice layers of 0.3 m up to 1.5 m tick at the basement.

The study site is typical of discontinuous high-temperature permafrost. The temperature of frozen grounds at a depth of 10 m was -0.5 ° C before the construction began, the natural soils are ice clay loams. The configuration of the embankment, the thermal physical properties of the soils, and the meteorological data in the model were collected via of field observations. The assessment of the change in the content of unfrozen water was carried out according to the methodology set out in Russian national survey standards, the dynamics of the ground volume was based on the predicted change in the ice content under additional freezing.

The forecast modeling resulted in the ground temperature at the basement of the embankment with a height of 1.7 m to be -1.4 ° C, when the quasistationary temperature regime is reached after 50 years of operation at a depth of 10 m. Unfrozen water content on average is estimated to shrink by 20% down to 0.08 unit fraction. The ice content the top 10 m layer will increase by 3.5%. The equivalent thickness of the newly formed ice was calculated as the sum of the volumetric changes in frozen soils due to the transition of water to ice in a thickness of 10 m and is estimated to be 0.37 m. This is expected to result in the compaction of frozen soils, and some will manifest in an increase in surface under the embankment.

In winter, the soils undergo a considerable cooling to the depth of 5-7 m. The temperature of the frozen soil beneath the embankment basement reaches -15 ° C at the end of the cold season, which results in a 2-fold decrease in the content of unfrozen water and an increase in the ice content by 8% (up to 0.32 unit fraction). The equivalent thickness of the newly formed ice at the base of the embankment during winter is 0.25 m, of which 0.16 m is in the upper 2 m layer of natural grounds, which will contribute to the development of seasonal heaving and uneven subsidence.

The investigation results show that the in situ formation of ice from unfrozen water can be the cause of long-term and seasonal frost heave at the basement of road embankments. This process is particularly dangerous to the southern permafrost zone regions, where one observes high temperature of frozen grounds along with clay soils being wide spread of. Another potential hazard is related to the sections of embankments built over non frozen grounds, since these may freeze due to changes in heat exchange conditions during road construction.

Anknowledgements

The work is executed at financial support of the Russian Geographical Society grant №05\17: "Modern conditions and dynamics of dangerous cryogenic processes, influencing on existing and prospective transport network of the Siberea and Far East".

References

Isakov V.A. Temperature state of road embankments in the cryolithozone. *MSU Vestnik. Series 5: Geography, №3, 2015, 25-34 pp. (In Russian).*

Flexible and ductile pipeline: innovative structure in permafrost regions under the climate change

Shunji Kanie[1]
Hao Zheng[2]
Taichi Iwamoto[3]
[1]*Faculty of Engineering, Hokkaido University, kanie@eng.hokudai.ac.jp*
[2]*Faculty of Engineering, Hokkaido University*
[3]*Graduate School of Engineering, Hokkaido University*

Abstract

During the past half century, arctic regions have been developed as a new frontier for acquisition of natural resource as well as for improvement in their living circumstance. In the next half century, however, some change in environmental condition may be caused by the climate change, and the infrastructures in those regions should be prepared to cope with the change. Thawing of permafrost causes erosion and landslide, for example. In the case of pipelines, they are crossing over quite wide area in permafrost and subjected to large deformation due to land deformation. One of the ideas to keep their function is to make them durable with enough strength. However, it raises construction and maintenance cost of the structure. Another idea is to adopt flexible and ductile structure which allows large deformation with its flexibility. The authors introduce pipe-in-pipe filled with frozen granular material as an innovative structural material.

Keywords: Pipeline; Pipe-in-pipe; Flexible and Ductile; Frozen material.

Introduction

It has been a serious concern that land deformation in permafrost regions may be caused by the climate change in the coming tens of years. It accompanies large-size destruction in infrastructures and influences on activities of human beings. However, it is difficult to predict such deformation in advance over wide area, although energetic investigation and monitoring have been carried out. It may be possible to use high-strength material for pipeline but the construction and maintenance cost must be expensive. Then, the authors developed a pipe-in-pipe filled with granular material such as sand and it is confirmed that the pipe can flexibly bend under large bending deformation without local failure. If the filling material is saturated with water and is frozen up, the pipe bends smoothly beyond the yielding strain of material. This paper introduces the pipe-in-pipe filled with frozen granular material as well as its bending behaviors with experimental and numerical evaluation.

What is pipe-in-pipe?

Pipe-in-pipe consists of double thin-walled pipes, and the core between the pipes is filled with a filling material. Pipe-in-pipe itself has been used as a structural member with high flexural rigidity by filling the core with ceramic. Riser pipe equipped on oil drilling rigs in Arctic ocean is a typical example of use, for example.

The pipe-in-pipe, here introduced, is filled with granular material such as sand instead of ceramic. The purpose of the core material is not to increase the flexural rigidity but is to transmit stress between double pipes within the section in order to prevent local buckling known as Brazier effect as shown in Figure 1. Figure 2 shows the cross-sectional view of the pipe-in-pipe.

If it is adopted as a natural gas pipeline in permafrost, the temperature of the gas is preferably chilled under 0 degrees C because the temperature effect on the surrounding foundation is minimized to prevent thawing of permafrost. At the same time, the chilled gas freezes the saturated sand filled in the core, and it enhances the flexibility and ductility of the pipe. The authors investigated its behaviors and established a numerical model for evaluation.

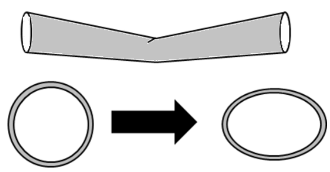

Figure 1 Bending failure due to Brazier Effect

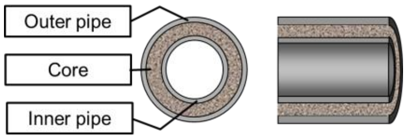

Figure 2 Cross-sectional view of pipe-in-pipe

Experiment

Testing apparatus

The testing apparatus is illustrated in Figure.3. The pipe is supported at both ends, and two loading points are located near the center of the span. Since a load cell is placed between the loading device and the actuator, the loading magnitude can be easily converted into bending moment. The loading magnitude is gradually increased over time, so that the effect of dynamic motion is negligible. A high-resolution camera records pictures at every 10 seconds while loading. Loading is ceased when the pipe is broken or the loading magnitude shows a peak value.

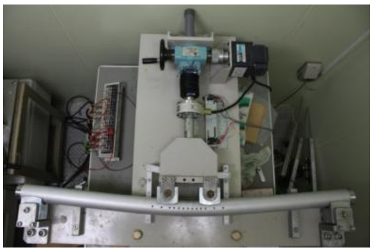

Figure 3 Testing apparatus

Test Specimens

Pipes are made of aluminum alloy with the length of 1,000 mm. The diameter of outer pipe is fixed at 50 mm, and the diameters of inner pipes are 20, 30 and 40 mm. As a filling material, we applied a fine granular sand known as Toyoura sand which average diameter is 0.2 mm. The core is filled with this material except for the hollow specimen, and the frozen specimens are chilled at -10 degrees C in a cold room.

Result and discussion

Figure 4 shows the experimental results. From this figure, it is confirmed that the pipe-in-pipe filled with granular sand can bend smoothly, and the bending curvature is much larger than that of hollow one. Furthermore, freezing the core material significantly improves the flexibility of the pipe, and it fails at almost ultimate tensile strain without local buckling. The authors have already established a numerical model to evaluate its elasto-plastic behavior and the relationship between the bending moment and the curvature is illustrated in Figure 5 with the experimental results for comparison.

(a) (b) (c)

Figure 4 Experimental results (a) Hollow, (b) Filled with sand, (c) Filled with frozen sand

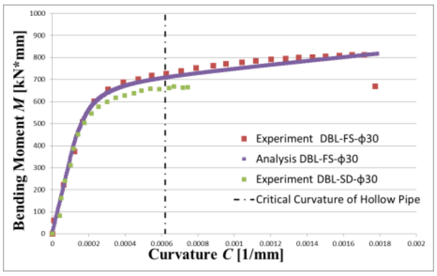

Figure 5 Relationships between the bending moment and the curvature by numerical model with the experimental results.

Conclusions

The authors verified that the pipe-in-pipe filled with granular sand can bend smoothly, and freezing the core material significantly improves its flexibility without local buckling even under large bending deformation. In addition, the numerical model successfully simulates the elasto-plastic behavior of the pipe. Although it may need further studies for practical application at real construction site, we believe the pipe-in-pipe is one of the most competitive solutions as an infrastructural material in cold regions. For example, pipeline made of this pipe can deforms under large land deformation due to thawing of permafrost and landslide.

References

Brazier, L. G., 1927. On the Flexure of Thin Cylindrical Shells and Other “Thin” Sections, *Proceedings of the Royal Society of London*, All6, 104-114

Kanie S. *et al.*, 2006. Estimation Method of Frost Heaving for Chilled Gas Pipeline Buried in Frost Susceptible Soil. *Proceeding of Pipeline conference 2006*, ASCE, 210, 33.

Kanie S. *et al.*, 2012. Development of Flexible and Ductile Pipe-in-pipe Filled with Granular Material for Cold Regions, *Proceeding of Arctic Technology Conference*, OTC23843

Kanie S. *et al.*, 2015. Numerical Analysis of Pipe-in-Pipe filled with Various Materials, *Proceeding of pipeline conference 2015*, ASCE, 412-423.

Influence of the antropogenic pond on permafrost conditions and risk for infrastructure objects in Norilsk

Aligyushad Kerimov[1]
Valery Grebenets [2]
Petr Melnikov[3]
[1] *Scientific and engineering association "Fundament", Norilsk, Russia, ali4455@rambler.ru*
[2] *Moscow State University, Geographical faculty, Moscow, Russia*
[3] *Taymirgeoradar, Norilsk, Russia*

Abstract

The situation with the reliability of buildings constructed in permafrost zone erected during the last decade. Norilsk Industrial region is characterized by maximal technogenic influence and intensification of impact on the permafrost. The natural-technogenic icing is a particular danger for the road systems. Geophysical and permafrost-lithological studies have made it possible to predict the behavior of the system "permafrost - filtration from an artificial reservoir". Measures to stabilize the situation have been developed

Keywords: icing; permafrost soils; deformations.

Introduction

During the last decade, there has been an acute situation with the reliability of objects in the permafrost zone. The development of destructive cryogenic processes often results in the destruction of buildings, threatening the normal operation of roads and pipelines (Romanovsky, 1983). In the Norilsk region (north of Siberia), the concentration of technogenic systems is quite high.

The length of the icing body is above 500-600 m, the width is 30-40 m (limited by the mechanical destruction of its front part during the snow removal of the road), maximum height - up to 3 - 5 m; an area of about 20 thousand m².

During the thawing of the ice body, excessive flooding of the terrain was noted, the relief was lowered toward the 4th microdistrict of the Talnakh district, the flow was additionally melted by the plactic-frozen base soils, and the bearing capacity of the foundations of multi-storey residential buildings was reduced.

Results and Observations

Active freezing goes in October-November in the central part (forming "permafrost bridge") and lasts almost all winter. Destruction of the ice body takes place in May - June, with regular snow removal (including mechanical destruction by ice bulldozers of ice creeping out onto the road) contribute to accelerating thawing.

The main source of water for the formation of icing is an artificial lake in the Vidnoye quarry (*Fig.1*), even in the warm season there is seepage of water through the soil-bulk body of the dam.

Fig. 1. General view of the area.

If the summer filtration is due to the difference in pressure (differences in the level of the surface of the road and the mirror of the lake inside the quarry) (lower by 4 m), in winter this factor is supplemented with cryogenic support: as the ice from the top increases, the water is squeezed into the embankment (in the fractured basalts of the base)

One of the main evidences that the icing formation contributes to the filtration and discharge of groundwater is the structural and textural features of ice: its stratification is clearly manifested, it is heavily contaminated with ground particles, sometimes wrinkled increases during the breakout of larger portions, very dense, crystalline structure.

Analysis of the engeneeric-geocryological situation showed that before the antropogenic development of the territory, the water drained along the boulder-pebble horizon and along the roof of weathered basalts.

The building process and exploitation of residential buildings with cold ventilated cellars led to the freezing of this filtration horizon; its freezing was also facilitated by regular snow removal from the roadway.

A geophysical survey was carried out on the site of investigation, maps of watered soils were compiled. The mountain massif to the depth of 25 m was investigated. The processing on a PC, using a special program, with further analysis of the amplitude-frequency characteristics was performed.

Watered areas were identified. The method was based on the analysis of the anisotropy and energy characteristics of the seismic signal.

The formation of ice (Figure 2) on the territory of the microdistrict is a dangerous process that threatens safe living and reduces the reliability of objects.

Fig. 2. Icing, near residential houses

In order to stabilize and improve the operating conditions of the facilities, engineering solutions have been proposed to minimize the process of ice formation and flooding of frozen soils on bases of residential buildings (more than 50 multi-storey houses) located lower along the terrain.

Engineering and technical solutions have been developed are as follows:
• lowering the level of the water mirror in the existing reservoir of the "Vidnyi" quarry. As a result, at a lower layer thickness, will be created conditions for the full water freezing in winter;
• installation of a drainage system to drain water into the riverbed of the existing river.

References

Romanovskiy N.N. Underground soils in permafrost zone –M.; MSU, 1983. -256p.

The fluid dynamics role of gases in the cryogenic craters formation

Alexander Khimenkov[1], Julia Stanilovskaya[2], Dmitry Sergeev[1], Alexander Vlasov[3], Dmitry Volkov-Bogorodsky[3]

[1] *Sergeev Institute of Environmental Geosciences RAS (IEG RAS), Russian Federation, a_khimenkov@mail.ru*
[2] *TOTAL S.A., France*
[3] *Institute of Applied Mechanics RAS, Russian Federation*

Abstract

The role of gas fluids migration through permafrost is stated due to the several gas emission craters formations that are located in the north of Western Siberia. These phenomena are the result of physical explosive processes. Authors consider the general sequence of the four stages and formation of the four zones of: 1 - gas fluids occurrence; 2 - gas fluids transition; 3 - gas fluids accumulation; 4 - plastic deformations. The proposed source of the gas fluids formation is decomposition of relic gas hydrates in permafrost. This assumption is based on numerous gas emissions during the wells drilling at the Bovanenkovo field. Various scenarios for the development of fluid dynamic processes in permafrost are considered. The fluid dynamic concept is also applicable for the gas emission craters formation due to free gas contained in permafrost and due to gas flows underneath the permafrost.

Keywords: gas emission crater; gas hydrates; dissociation; fluids; Yamal peninsula; frozen soils.

Introduction

In 2014-2017, a series of dry craters with vertical walls to a depth of several tens of meters was found in the north of Western Siberia. Around the craters there is a concentric spread of ice and soil over a distance of tens of meters. All this points to the explosive nature of their formation. The processes that form craters are of great destructive power and represent a new kind of geocryological hazards.

The objective of this publication is to consider a possible genesis of the Yamal craters analyzing the texture and structure of the soils composing the crater, the stages of its development, the processes accompanying dissociation of gas hydrates in permafrost, the factors causing the processes at each stage of crater formation.

Assumed reason of the Yamal crater formation is the gas hydrates dissociation, which are presumably located at a depth of 60-80 m. The cause of dissociation is local warming of frozen soils under the thermokarst lake, traces of which are found in outcrop of the crater.

The main data from different expeditions are belong to the crater located 30 kilometers south of the Bovanenkovo field (Bogoyavlenskiy *et al,* 2016; Kizyakov *et al,* 2015; Khilimonyuk *et al,* 2016, The Yamal crater. Part 2, 2016).

Stages of crater formation

Analysis of available materials (publications, video and photo shoots, interviews and speeches at conferences) made it possible to identify four stages of gas emission craters development (Fig. 1).

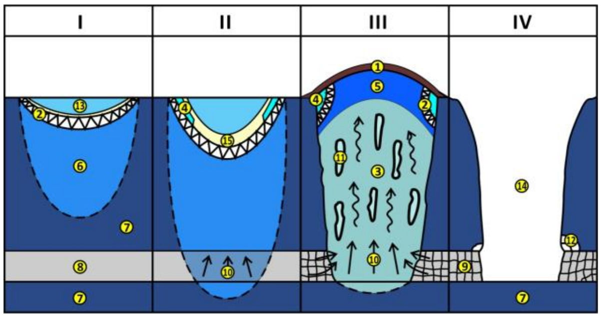

Figure 1. Stages of the Yamal crater formation:

I, II, III, IV - stage of the Yamal crater; 1 - layer 1 (cover horizon); 2 - layer 2 (white layered ice corresponding to the maximum depth of thawing under the lake); 3 - layer 3 (frozen soil saturated by gas with traces of fluid dynamics in the temperature rise zone under the lake); 4 - layer 4 (layered ice, presumably infiltration-segregation origin); 5 - layer 5 (non-penetrating permafrost table by gas); 6 - zone of temperature increase in permafrost under the lake; 7 - permafrost outside the warming effect of the lake; 8 - a layer of hydrate-bearing permafrost; 9 - zone of decompaction in the layer of hydrate-bearing permafrost, adjacent to the crater; 10 - direction of fluids movement; 11 - gas-liquid fluids; 12 - caves and caverns in the lower part of the crater; 13 - lake; 14 - crater formed after the gas emission; 15 - talik.

I stage (Fig. 1, I). A talik (15 on Fig. 1) and a zone of high temperature in comparison with the surrounding soils (6 on Fig. 1) are formed under the lake (13 on Fig. 1), containing a layer of subsurface ice (2 on Fig. 1). Temperatures of permafrost under the lake can be raised to 0-1 ° C (Khilimonyuk *et al,* 2016).

II stage (Fig. 1, II). The zone of temperature increase in frozen soils (6 on Fig. 1) reaches a layer of hydrate-bearing permafrost (8 on Fig. 1). The process of gas hydrates dissociation begins with the release of gas and supercooled water (10 on Fig. 1). Gas-water fluids, under the influence of pressure, begin to move to the least stable area, which is the zone of temperature increase under the lake, and to saturate the primary ice-soil substrate with gas.

III stage (Fig. 1, III). The decomposition of metastable gas hydrate causes an increase in pressure, which significantly exceeds the reservoir pressure. As a result, the fluids move upward and are accompanied by plastic and discontinuous deformations (3, 11 on Fig. 1).

The increase in pressure in the fluid migration zone leads to the beginning of frost heaving under the bottom of the thermokarst lake. As the lake drainages and the talik freezes, the infiltration-segregated ice (4 on Fig. 1) forms on the lower border of the talik. This mechanism leads to the formation of layers and lenses of ice, which is laid in accordance with the lake sediments containing it. Subsequent drainage in the upper part of the section forms ice-saturated layered deposits enriched with terrigenous material similar in composition to the host soils - sand, silt, clay or a combination thereof, and lenses of plant material. This is layer 1 on Fig. 1, formed over layer 4. The transition from subaquatic to subaerial state lowers the temperature of the upper layer of the soil, which increases its strength. At the same time, a frozen dome-shaped screen is formed (5 on Fig. 1). A frozen impermeable screen is an obstacle to the movement of fluids coming from below, which provides for the formation of a mound with 6 m height and 50 m diameter (Kizyakov *et al,* 2015). According to M.O. Leibman talk the mound was growing at least 70 years before destruction (The Yamal crater. Part 2, 2016). The frost heaving deforms the layers 1, 2, 4, 5 on Fig. 1.

In the primary frozen soil (5 on Fig. 1) due to fluid saturation, a stock is gradually formed, which consists of layered gas-saturated ice (3 on Fig. 1). Numerous traces of the flow of ice, soil, plastic and rupturing deformations are observed in the stock.

In the layer of hydrate-bearing frozen soils near the dissociation zone, a decompressed zone is formed (9 on Fig. 1), emphasized by L.B. Volkomirskaya using georadar as a zone of weathered soils (The Yamal crater. Part 2, 2016). In the hydrate-containing layer there is a zone of grottoes and caverns of various sizes connected together (12 on Fig. 1). Similar formations were found in the zones of gas emissions (due to decomposition of gas hydrates) in the vicinity of Bennett Island (the New Siberian Islands) and in the Sea of Okhotsk.

IV stage (Fig. 1, IV). As plastic deformations in the non-penetrating permafrost table by gas (5 on Fig. 1) reach their limit, brittle fracture deformation sets in. The gas, which is under pressure and penetrates the stock of deformed ice all the way from the hydrate-containing layer to the layer 5, breaks out together with the ground and ice. As a result, a dry crater of gas emission is formed.

Depending on the ratio of various factors, scenarios for the gas emission craters formation and, accordingly, their morphology, may differ. With a slight and short-term rise in temperature, the gas hydrates dissociation can quickly end because of self-preservation. With sufficient depth and width of the lake, the gas released during dissociation may not accumulate under the frozen screen, but be released directly into the lake. Depending on the rate of pressure growth, gas emissions can occur both: without and with the formation of the mounds of various sizes and morphologies. In those cases when the pressure release occurs gradually, the formed gas-saturated ice-ground stock remains in the permafrost.

The work was supported by the Russian Foundation for Basic Research (project 17-05-00294).

References

Bogoyavlenskiy, V., Sizov, O., Bogoyavlenskiy, I. & Nikonov, R., 2016. Remote detection of surface gas releases in the Arctic. *Journal of the Arctic: ecology and economy* 3: 4–15 (In Russian).

Khilimonyuk, V., Ospennikov, E., Buldovich, S., Gunar, A. & Gorshkov, E., 2016. Geocryological conditions of the territory of the Yamal crater location. *Proceedings of the 5th Conference of Russian Geocryologists,* Moscow, Russia, June: V. 2, 245-255 (In Russian).

Kizyakov, A., Sonyushkin, A., Leibman, M., Zimin, M. & Khomutov, A., 2015. Geomorphological conditions of the gas-emission crater and its dynamics in Central Yamal. *Journal of Earth's Cryosphere* 2: 13–22 (In Russian).

The Yamal crater. Part 2, 2016. *Workshop of the Permafrost young researchers network in Russia,* Moscow, Russia, December (In Russian).

Thermal resistance of engineering constructions soil foundation

Ilya Komarov[1]
Vitali Ananyev[2]
Dina Bek[1]
[1]*Lomonosov Moscow state University, ilya_komarov@mail.ru*
[2] *LLC SPE "Rivsmash", vvanord@yandex.ru*

Abstract

In the permafrost propagation areas, the thermal interaction between constructions and foundation soil leads to the thawing of soil and, therefore, to the loss of soil bearing capacity. The salinity of soils, which is specific for marine plains (Yamal peninsula, etc.) and North Seas' shelf areas, which can contain cryopegs, has significant negative impact on this process. On the chemical composition, cryopegs are close to marine waters, their mineralization corresponds to 10-250 g/l, and ground freezing temperature can be very low. These factors lead to the necessity of thermostabilization of foundation soil in case of choosing the construction mode with its preservation in a frozen state.

Keywords: Thermostabilization, foundation soil, bearing capacity, liquid natural gas, cryopeg, salinity.

Introduction

Currently for the soil thermostabilization cooling capacity of seasonal cooling devices, based on the cooling capacity of atmospheric air during the winter period, with the vertical and horizontal type of natural circulation. The depth of seasonal cooling devices is 10-15 meters, characteristic dimension (diameter) is 33,7-57 mm. As a coolant are used Freon – R404a with heat removal 10-15 W/lm; ammonia – R717 - the most effective coolant, considering heat transfer with heat removal 25-30 W/lm; carbon dioxide CO2 – R744, heat removal 12-18 W/lm.

The advantages of such thermostabilizers (TS) are none of energy consumption and necessity of maintenance during exploitation. The disadvantages are seasonal operating and period of installation; the relatively low rate of freezing; difficulty with freezing of high-saline soils and cryopegs.

The advantages of machine cooling with compulsory ventilation of a coolant are year-round operation; freezing of high-saline soils and cryopegs; high efficiency. The units are based on the vapor compression cooling cycle with coolant R404a and soil intercooling loop with liquid coolants like CaCl, ethylene glycol brines, etc. The disadvantages are high unit cost and significant economic expenses for the long-time operation.

Thermostabilization technique for buildings and structures soil foundations

Potential possibility of partial utilization of the liquefied natural gas and products of its rectification (ethane and propane) cooling capacity with the low boiling temperature could be one of the prospective solutions of the problem of year-round operational reliability improvement of foundation soils with high salinity and plastic frozen state.

The technological norm of liquid natural gas (LNG) storage is estimated by the value of liquefied gas in the tank storage daily evaporability, which is approximately 0.1% of the mass of the liquefied gas in one tank. These losses are formed due to heat inflows of the environment to the tank, where the liquid natural gas is kept. There is provided to use these technological outages with low freezing temperature for foundation soil thermostabilization, using for this purpose recuperative heat-exchanging facilities. In that way, in line with ensuring the competence of constructions foundation, this technology allows utilizing these outages of gas effectively, to utilize selected gas for cooling of the foundation soil through its following compaction and liquefaction. According to the estimations, daily consumption of LNG for thermostabilization of soils is approximately 0.15% by the weight of LNG in the tank.

This technology allows: to provide reliable operation of a construction all the year round and irrespective of climatic conditions; to provide much higher rate of the soil frost penetration; to minimize effect of the frost heaving (the high rate of frost penetration provides minimization of volume of water migrating to the freezing front); to freeze cryopegs with various degree of a mineralization. Besides obvious advantages of LNG utilization as a refrigerant liquid for soil thermostabilization it can lead to appearance of negative processes, such as cracking caused by emergence of big gradients of temperature near the wall of thermostabilizer tube (thermal shock) and frost cracking in interpile area, according to the different by depth or in the plan view configuration of the TS groups. For that matter, it is required to pay special attention to the determination of the optimum value of LNG-inlet temperature and the constructive solution of TS, for prevention (minimization) of these processes (Komarov et al., 2015).

The forecasting technique of TS and soil interaction, containing an estimation of temperature and the water-ionic regime of soils and cryopegs using special software is presented (Komarov et al., 2012, Pustovoit et al., 2014). For this task the typical 4-layered cross-section, formed from the surface with anthropogenic imbankment, sand layer, underlayered with the water-saturated lens of non-saline or high-saline (cryopeg) sand or high-saline sandy loam.

Climatic data was taken according to the Tambei meteorological station. Thermal and mechanical properties in the range of low freezing temperatures were taken according to the experimental data (Komarov et al., 2010)

Conclusions

Simulation results show that this technology successfully allows freezing lenses of cryopegs of high salinity. For example, for cryopeg with mineralization 90 gr/l it freezes the area of radius up to 1.5 m during the month, and for 3 m less than during four months. The most convenient period of TS installation is during the winter period, if installing in the summer period, the input temperature of coolant should be increased. This technique could be used for the thermostabilization of soil with liquid nitrogen.

References

Komarov, I.A., Mironenko, M.V., Kiyashko, N.V., 2012. Enhancement of regulatory framework on accounting estimates of thermophysical properties of soils and cryopegs, *Soil Mechanics and Foundation Engineering,* p. 25-30.

Komarov, I.A., Ananiev, V.V., Bek, D.D., 2015. Problem of utilization of the cooling capacity of natural liquid gas for the thermostabilization of ground, *Earth's Cryosphere,* p. 75-80

Komarov, I.A., Isaev, V.S., 2010. Cryology of Mars and other solar system planets, 232 p.

Pustovoit, G.P., Venkstern, A.A., Barke, VV., 2014. Program package for calculation of process of frost penetration and thawing of soil.

Thermal response of air convection embankment (ACE) over ice-rich permafrost at Beaver Creek experimental road site, Yukon, Canada

Xiangbing Kong[1],
Guy Doré[1],
Fabrice Calmels[2],
Chantal Lemieux[1]
[1]*Center for Northern Studies– Université Laval, Quebec, QC, Canada, xiangbing.kong.1@ulaval.ca*
[2]*Northern Climate ExChange, Yukon Research Center – Yukon College, Whitehorse, Yukon, Canada*

Abstract

Permafrost degradation underneath transportation infrastructure is a wide spread problem often associated with climate warming. The air convection embankment (ACE) technique has been developed in Alaska to mitigate thaw settlement of embankments caused by permafrost degradation. To test its field performance, a large-scale ACE was constructed along Alaska Highway at Beaver Creek, Yukon, Canada in 2008. Thermistor strings were installed beneath the side slope, the toe and the centerline of embankment. The temperature data collected provide valuable information on the thermal performance of ACE and a good basis for the development of a design procedure considering the effect of climate warming.

Keywords: Permafrost degradation; Air convection embankment (ACE); Alaska Highway

Introduction

Permafrost distributes widely and it underlies approximately 25% of world's land surface. Due to the construction of transportation infrastructure and on-going climate warming, the thermal equilibration of underlying permafrost is disturbed, which leads to permafrost thawing resulting in permafrost-related engineering problems, especially in ice-rich, warm permafrost regions. Permafrost degradation results in many failures, such as differential settlements, sinkholes and longitudinal cracks, which are often observed along northern roads and airstrip, like the Alaska Highway in Yukon, Canada.

Mitigation techniques, such as air ducts, heat drain, air convection embankment (ACE) and thermosyphons, have been proposed to prevent permafrost degradation from thawing, and ACE has been proved and utilized as an effective method in permafrost regions. Poorly graded aggregates are used to facilitate the air flow in ACE and air flows due to the unstable air density in winter. In summer, ACE stops working due to stable air density. The heat extraction ability of ACE heavily depends on many factors, such as thickness of rock layer, boundary conditions and sizes of stone.

Study site

To investigate the heat extraction ability of ACE, a large-scale air convection embankment was constructed in 2008 at Beaver Creek, Yukon, Canada. The thickness of the ACE layer, underlaid mainly by ice-rich silt, is about 3.3 m as shown in Fig. 1. The Beaver Creek text site is located at 620 22' 59" N, 140052'29" W, about 8 km south of the community of Beaver Creek and about 30 km south of the Canada-United States border.

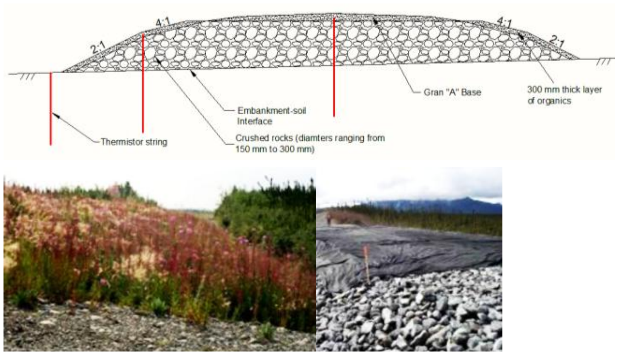

Figure 1. Air convection embankment at Beaver Creek, Yukon: a) schematic of air convection embankment (top); b) geotextile implementation (right) and organics on the west slope of embankment after 1 year of construction (left).

Results

Climate warming is observed in Yukon, Canada. The mean annual air temperature was -5.5 °C from 1971 to 2000 and -4 °C from 2001 to 2011 (Environment Canada, 2011). As a result, the thickness of the active layer underneath a conventional embankment has increased (M-Lepage, 2015).

Thermistor strings were installed in boreholes at the toe of the embankment slope, in the middle of the slope and at the centerline of the ACE embankment (see Fig. 1), and temperature data are collected since October, 2008.

Fig. 2a and 2b illustrates the average annual soil temperatures profile with depth under the centerline and the side slope from 2009 to 2013. Fig. 2a indicates that the average annual ground soil temperatures show a continuous decreasing trend from 2009 to 2013 below 2.0 m depth in the natural ground. For example, at the depth of 4.0 m, mean annual average temperature decreases from -0.34 °C in 2009 to -1.54 °C in 2013. The natural convection also has a significant cooling effect down to a depth of 10 m, while soil temperature almost stays constant at the depth of 3.0 m for the control section at this experimental site. Fig. 2b indicates that the soil temperatures mainly show an irregular variation above the depth of 3.0 m in the ground, and soils temperatures remains almost constant below the depth of 3.0 m. This observation suggests that heat extraction of ACE mainly happens underneath the traffic lanes and does not have much effect underneath the side slope of the embankment.

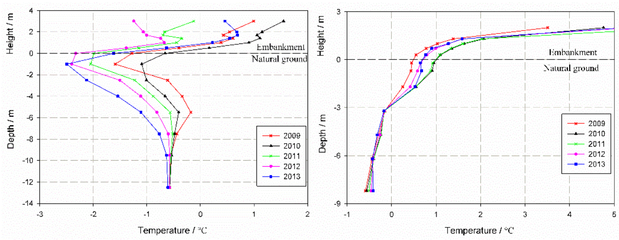

Figure 2. Average annual soil temperatures from 2009 to 2013 along: a) centerline (left); b) side slope (right).

Fig. 3 shows the ground temperature change at the depth of 2.2 m in the ground underneath the centerline. It can be seen that the soil temperature generally decreases with time from 2009 to 2013 in winter with minimum soil temperature reaching -2.5 °C in 2009 and -5.1°C in 2013. By contrast, the maximum soil temperature does not show any obvious change during the period from 2009 to 2013 in summer, and the maximum yearly temperature difference is less than 0.2 °C.

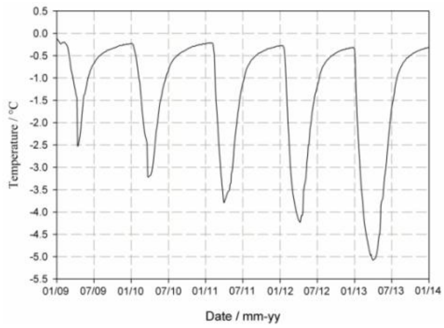

Figure 3. Ground temperature change with time at 2.2 m deep under the road centerline

Conclusion

The full width ACE layer has proven to be effective at the Beaver Creek test site in Yukon, Canada. Based on the analysis of temperature data, soil temperatures have steadily decreased during the period from 2009 to 2013. A thermal model is being built and calibrated on the test section data, and it will be used to propose a heat balance chart to assist engineers in designing air convection embankment in permafrost regions. The proposed presentation will summarize the analysis of thermal regime, and heat balance chart based on the calibrated thermal model of ACE at Beaver Creek experimental site, Yukon, Canada.

Acknowledgments

The authors would like to acknowledge the financial support of the Natural Sciences and Engineering Research Council of Canada as well as the technical and financial support of public and private partners of the permafrost engineering research program ARQULUK for this project.

References

Environment Canada, 2011. Canadian climate normals 1971–2000. Available from www.climat.meteo.gc.ca (accessed on July 4 2011).

M-Lepage, J, 2015. Experimentation of mitigation techniques to reduce the effects of permafrost degradation on transportation infrastructures at Beaver Creek experimental road site (Alaska Highway, Yukon). Master's thesis, Laval University, Canada.

Selection of equations for long-term strength calculation of frozen saline soils

Pavel Kotov[1]
Michail Tsarapov[1]
Eric Green[2]
Yulia Stanilovskaya[2]

[1] *Lomonosov Moscow State University, Geocryology department, email kotovpi@mail.ru*
[2] *Total E&PRussie, Moscow*

Abstract

Frozen saline soils are sensitive to any impact and characterized by significant changes of physical, chemical, and mechanical properties afterwards. Strength decreases in time but the equations of long-term strength cannot take into account all the factors. However, almost all existing equations were obtained for non-saline soils. The selection of the equation was carried out on the basis of spherical template indenter test on artificial samples of two soil types (fine sand, lean clay), with different salinity (from 0.07% to 1.42%), temperature (-2 °C, -4 °C,-6 °C) and water content. A total of 200 tests were conducted. The data was processed using 10 equations. As a result of the analysis, only 4 equations satisfied the selection criteria. Determined equations can be used to calculate the long-term strength of saline frozen soils depending on soil type and temperature.

Keywords: long-term strength, spherical template indenter test, frozen saline soils

Introduction

Geotechnicians calculate the bearing capacity when designing infrastructure facilities on permafrost. They need to perform a forecast of the frozen soils strength for long-term period (25-50 years). So one of the main tasks of frozen soil's mechanics is the development of methods for the prediction of long-term strength and extrapolation of its values beyond the experimental period. Ice feature is creep under load and does not have a long-term strength limit. Therefore, the strength of frozen soils in time is reduced quite strongly, and the long-term strength value is less than instantaneous strength from 2 to 15 times (Vyalov, 1986). In despite of the type of tests (compression, tension, shear, spherical indenter), the general character of the dependence of strength in time is the same (Vyalov, 2000). The general patterns in occurrence of rheological properties, with a change in temperature, time factors and stress make it possible to obtain a general method for predicting long-term strength for all frozen soils, in spite of the loading regime.

Methodology

The studies were conducted on two artificial samples (fine sand, lean clay). Artificial soil is non-saline. Solutions with different concentrations of NaCl were mixed to set different degrees of salinity (fine sand - 0,07%, 0,15%, 0,35%, 0,7%, lean clay - 0,17%, 0,35% 0,8%, 1,35%) We have prepared samples of a given water content (sand - 10% and 19%, lean clay – 20% and 35%). The density was set by layering compaction in special forms (metal ring with a diameter 7,1 cm and a height 3.5 cm) All samples had massive cryogenic texture.

Spherical template indenter test were carried out according to GOST 12248-2010 at temperatures of -2°C;-4 °C;-6 °C. All tests were carried out with a fourfold repetition. A total of 200 experiments were conducted. This test has been used in the studies of frozen soil mechanics of long-term strength (Tsytovich 1973; Roman, 2002; Zhang. 2016).

Method of selection of the equation was as follows. Parameters of the equations were calculated taking into account data of eight-hour tests. Prediction of strength was conducted for the time of the end of the experiment (192-240 hours). In total, the data were processed using 10 equations.

Results

Predicted equivalent cohesion was compared with the experimental one. Based on the tests, 90% confidence interval of the characteristic was calculated for each sample. If the predicted equivalent cohesion was not included in confidence interval, then the equation was excluded from the processing. As a result of the analysis, only 4 equations satisfied the selection criteria. (Table 1). Figure 1 shows an example of a long-term strength prediction using different equations.

The further selection of the optimal equation was to find the minimum relative error. Relative error between calculated and experimental values was evaluated according to the equation:

$$\varepsilon = \frac{(s - s_r)}{s}$$

ε - relative deviation,

s – experimental value of equivalent cohesion,

s_r – calculated value of equivalent cohesion.

Table 1. Equations for long-term strength

№	Equation	Author
1	$C_t = \dfrac{\beta}{\ln \dfrac{t + t^*}{B}}$	Vyalov (1959)
2	$C_t = \left(\dfrac{t + t^*}{T}\right)^{-\alpha}$	Vyalov (1986)
3	$C_t = \dfrac{C_0}{\left(\dfrac{t}{t_0}\right)^{\beta_0}}$	Roman (2002)
4	$C_t = C_f \left(\dfrac{t}{t_f}\right)^J$	Konovalov (2014)

Symbolic notation: C_t - equivalent cohesion at time t, t* - time unit (equal to 1 in the calculation), β, B, T, α, Co, βo, J-experimental parameters, t_o- 10^{-12}sec, C_f – first value of equivalent cohesion at time t_f

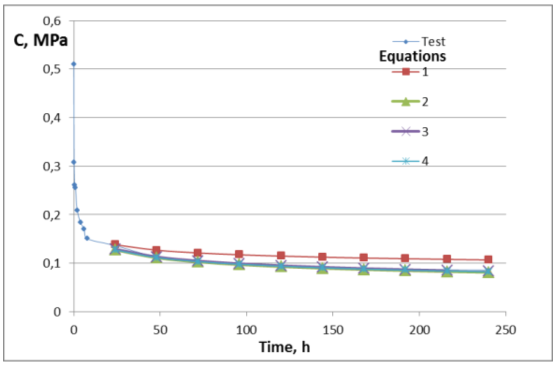

Figure 1. Experimental (Test) and predicted curves (calculated from equations (1)-(4) Table 1) of equivalent cohesion versus time for frozen lean clay (W=0,35 u.f., Dsal=1,33%, T=-6°C)

Experimental data approximated by equation (1) are better for fine sand, equation (2) at temperature -2 °C and equation (3) at temperatures -4 °C and -6 °C for lean clay.

Analysis of the applicability of the equations shows a high dependence on the temperature. Thus, the maximum relative error are observed at a temperature -2 °C (up to 30%), but at a temperature -6 °C does not exceed 15%. The influence of type soil, water content, salinity and temperature on the parameters of the predictive equations was estimated based on the obtained data.

References

GOST 12248-2010, 2011. *Soils. Laboratory methods for determining the strength and strain*. Standartinform,. 109 pp. [in russian]

Konovalov, A.A., 2014. Phase transition and longevity of frozen ground. *Cryosphere of the Earth*, v. XVIII, No. 1: 31-38 [in russian].

Roman, L.T., 2002. *Mechanics of frozen soils*. IAPC Nauka / Interperiodika, 426 pp. [in russian]

Tsytovich, N.A., 1975. *The mechanics of frozen ground*. New York: Scripta, McGraw-Hill, 448 pp.

Vyalov, S. S., 1965. *Rheological properties and bearing capacity of frozen soils*. CRREL Technical Translation No. 74, 219 pp.

Vyalov, S. S., 1986. *Rheological fundamentals of soil mechanics*. Elsevier Science Ltd., 576 pp

Vyalov, S.S., 2000. *Rheology of frozen soils*. *Stroyizdat*. 463 pp. [in russian]

Zhang Z., Zhou H., Feng W., Zhang Z. & Xiao D., 2016. A spherical template indenter for a frozen soil long-term shear strength test. *Cold Regions Science and Technology* 131:10–15.

Vulnerability of permafrost thaw and the emerging risks for the Arctic infrastructure

Hanna Lee[1]
Altug Ekici[2,3]
Benjamin Aubrey Robson[4]
Yuanchao Fan[1]
Sebastian Westermann[5]
Moritz Langer[6]

[1]*Uni Research Climate, Bjerknes Centre for Climate Research, Bergen, Norway, hanna.lee@uni.no*
[2]*Climate and Environmental Physics, Physics Institute, University of Bern, Bern, Switzerland*
[3]*Oeschger Centre for Climate Change Research, University of Bern, Bern, Switzerland*
[4]*Department of Geography, University of Bergen, Bergen, Norway*
[5]*Department of Geosciences, University of Oslo, Oslo, Norway*
[6]*Alfred Wegener Institute, Potsdam, Germany*

Abstract

We quantified the current and future land surface subsidence associated with permafrost thaw using a process-based land surface model, Community Land Model (CLM). Our results show circum-Arctic land surface subsidence under thawing permafrost and melting excess ice under future climate change scenarios. The modeling results can help suggest directions to policy-making in the circum-Arctic regions.

Keywords: subsidence, excess ice, Earth System Modeling, risk assessment

Introduction

Widespread thawing of permafrost is expected in a warmer future climate and modeling studies suggest large-scale degradation of near-surface permafrost at the end of 21st century. Rapid changes of permafrost landscapes are in particular accelerated by melting of excess ground ice and the formation of thermokarst. Various natural habitat, resources, services, as well as life and human infrastructure will be directly and indirectly affected by permafrost thaw. Concurring evidence from recent studies suggests that permafrost landscapes will undergo significant transformations, and inevitably Arctic societies and human infrastructure is directly at risk. Infrastructure damage has already been documented in the Arctic settlements and the future level of such changes must be investigated to have a clear risk management strategy.

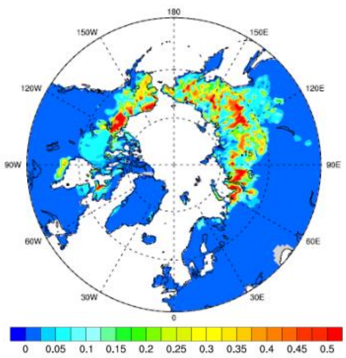

Figure 1. Circum Arctic projection of land surface subsidence due to excess ice melting in the year 2100 under the RCP8.5 climate scenario.

Methods

We quantified the current and future land surface subsidence associated with permafrost thaw using a process-based land surface model, Community Land Model (CLM). The CLM is a land surface component that has been employed in permafrost research for almost a decade and is considered one of the most advanced models with respect to permafrost among Earth System Models. As an effort to represent one of the crucial characteristics of permafrost processes within the CLM, the concept of excess ground ice was incorporated within CLM5 (Lee et al., 2014). This development requires the knowledge of the initial state of a grid cell specific excess ice content, based on existing ground ice data. We conducted 200 year transient and future simulations (1901-2100) using two different excess ice levels (medium and high) under CRUNCEP historical climate and future climate scenarios using the RCP 4.5 and RCP 8.5 scenarios.

Results

Our results show circum-Arctic land surface subsidence under thawing permafrost and melting excess ice under future climate change scenarios (Figure 1). In addition, GIS-based infrastructure datasets are overlaid on our vulnerability maps extracted from model results to set up a risk index map for the Arctic region. These results suggest vulnerable areas in the Arctic under warmer world and are critical in decision-making processes for a safer management of local societies, economic activities and any future development planned for the high latitude regions.

References

Lee, H., Swenson, S. C., Slater, A. G. & Lawrence, D. M., 2014. Effects of excess ground ice on projections of permafrost in a warming climate. *Environmental Research Letters* 9: 124006.

Methods of Main Oil Pipeline Geotechnical Monitoring in Permafrost Zone

Elizaveta (Mikhailovna) Makarycheva[1]
Vitaly (Ivanovich) Surikov[1]
Taras (Ivanovich) Kuznetcov[1]
[1]PTI, LLC The Pipeline Transport Institute, MakarychevaEM@niitnn.transneft.ru

Abstract

Permafrost processes are one of the major mechanisms of changes occurring in the natural and technical system in permafrost zone. Under rapidly changing permafrost conditions and survey of large length objects (over 2,500 km) methods of operational analysis of the situation are required. Operating companies face the issue of investments justification, design and implementation compensating or protective measures aimed at reducing the impact of such processes on engineering structures. The results of remote monitoring methods used to identify permafrost processes and hard geological conditions are explained in this paper. Use of GIS technology with 3D visualization allowed opening new possibilities for integrated analysis of geotechnical monitoring results. Integrated approach allows identifying the causes of deformations and prevent accidents.

Keywords: permafrost processes, pipelines, geotechnical monitoring, airborne laser scanning, GIS.

Introduction

In terms of underground laying oil pipeline it is impossible to avoid the impact on the permafrost. Man-induced impact in permafrost conditions both leads to activation of natural processes and to the development of their man-induced modifications. Thawing of permafrost rocks and ice monomineral inclusions under pipeline during its operation leads to the uneven ground subsidence. The consequence of such uneven subsidence is a change of design horizontal location and elevation of the pipeline and the deformation of pipe sections (Makarycheva *et al.*, 2013).

Insufficiency of geological surveys data, large length of the oil pipeline and hard natural and climatic conditions of works leads to transpose a set of tasks for obtaining initial data about the territory natural conditions and spread of processes to the sphere of geotechnical monitoring.

Operation of main pipelines under permafrost conditions requires the establishment and development of integrated analysis system.

The paper considers the use of GIS technology to identify the causes of deformation of pipe sections on the experimental site of the main pipeline.

Experimental main pipeline site is located in an area of permafrost rocks. The total length of the experimental site is 200 km. The width of the survey corridor is 75 meters to the right and to the left of the axis of the pipeline.

Methods

In order to acquire data on spread of permafrost processes along the large length pipelines remote monitoring methods are used.

Following the results of analysis of modern methods of the Earth's remote sensing, airborne laser scanning has been recognized as the most advanced and efficient method. The main factors that influenced on preferment of this technology to other ones have become its high level of plotting detail and the possibility to get data on the terrain under the vegetation canopy, which is especially important for photointerpretation of permafrost phenomena under conditions of continuous forest area (Boyko, 2009).

Airborne laser scanning allows obtaining aerial photographs for constructing a 3D model comprising, digital elevation model, shade map, slope map et al. (Dolgopolov & Kuznetcov, 2017).

In solving the task of the technical monitoring condition of the pipeline the most informative is the info acquired through pigging means. The pigging results allow determining horizontal location and elevation, detecting geometry defects and deviant bending radii of the pipeline.

Analysis causes of pipeline deformations in permafrost zone

Photointerpretation of permafrost phenomena was performed on the base of airborne laser scanning. Based on repeated observations information about permafrost phenomena dynamics was obtained. Analysis of pigging data allows identification (with a specially developed method) of pipe sections with ever decreasing bending radii.

Analysis of the causes of deformation spread is performed on the basis of geographic information systems and databases containing info acquired during ground and remote surveys of the main oil pipeline for the entire period of its operation.

After the analysis compiling a list of pipe sections with ever decreasing bending radii in areas of icy grounds and permafrost phenomena (Fig. 1).

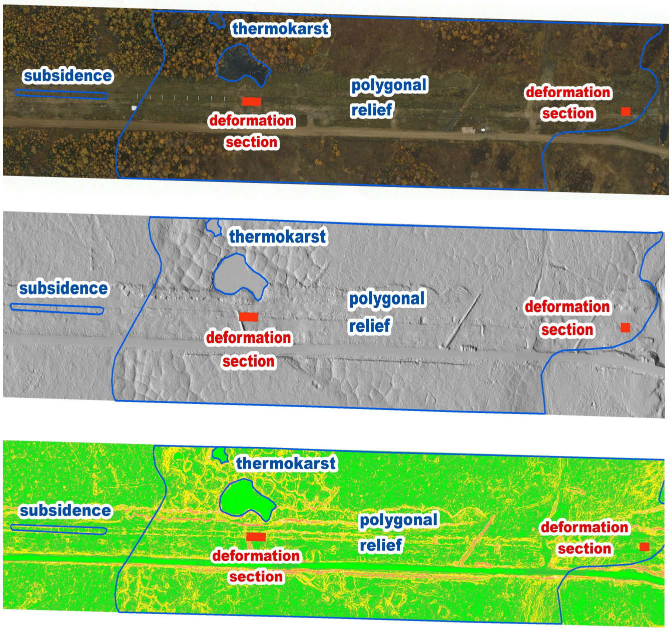

Figure 1. Example of a key site with ever decreasing bend radius of pipe sections on the aerial photograph, shade map and slope map.

Conclusions and Discussion

1. Major processes, which cause deformations of the pipeline on a key site are thermokarst and thermal ground subsidence.
2. Airborne laser scanning is the most informative method for the analysis of permafrost processes and hard geological conditions. An advantage of the method is that it allows constructing a digital terrain model, which can be analyzed visually or using digital algorithms. This method allows the identification of polygonal relief which hard identifiable by other methods.
3. Integral analysis of pigging data and airborne laser scanning results allowed to detect relation of deformations distribution with polygonal relief. The presence of deformations in areas with polygonal relief is probably due to thawing ice wedges, the presence of which is not always identifiable at the stage of survey.
4. Integrated monitoring results allow identifying the causes and feature of deformations development. Relation of pipe sections deformations with zone of geologic conditions changes was identified. The deformations of the pipeline are distributed in the area of sharp relief changes and in the area of soil condition changes (from icy dispersive soil to rocky) ones was identified on the key site of the pipeline.

References

Boyko, E, 2009. Modern methods of land surface survey in engineering and topographic surveys. Trends and problems of the development. *"Engineering researches" Magazine, #3/2009*. 58-65.

Makarycheva, E., Ugarov A. Malaeva, N. 2013. Assessment of the dynamics of exogenous geological processes according to the results of airborne-and-visual surveys of pipeline systems. *Bulletin of N.E. Bauman Moscow State Technical University. Series: Mechanic engineering, #1 (90)*. 117-124.

Dolgopolov, D, Kuznetcov, T, 2017. New opportunities for geotechnical monitoring of pipeline systems using GIS technology with 3D visualization. Proceedings of the XII International Scientific and Practical Conference. 122-123.

New data of tensile strength of frozen ground

Anna N. Maleeva[1]
Ruslan A. Belov[2]
Lidia T. Roman[1]
[1]*Lomonosow Moscow State University, malenish@yandex.ru*
[2]*Moscow State University of Railway Engineering*

Abstract

Frost cracking is a wide spread cryogenic process within the cryolithozone and territory with deep seasonal freezing which is characterized by continental climate. Frost cracking may be dangerous for civil and linear transport structures. There are several models that describe frost cracking. In all models properties of frozen ground such as tensile strength are used. When the thermal strain is more than tensile strength, frost cracks are possible. The new data about tensile strength of loam, sand and ice were obtained during the laboratory experiments. The results of experiment with loam can be described by equation of the dependence of tensile strength on temperature and water content.

Keywords: Frost cracking, tensile strength, frozen ground.

Frost cracking is a one of the main relief-forming cryogenic processes. Frost cracking is a wide spread cryogenic process within the cryolithozone and territory with deep seasonal freezing which is characterized by continental climate. Frost cracking may have a negative impact on engineering construction: urban pavements, road and railway carpet and embankment, bases of buildings, airport runway, pipelines and communication lines. Complete absence of snow and vegetation cover on these surfaces create ideal conditions for the formation of frost cracks. Usually, cracks are formed perpendicularly to the axis of the roads at a distance of 7-15 meters from each other.

Many scientists studied frost cracking and developed a few models of this process (Dostovalov, 1952; Lachenbruch, 1962; Grechishchev *et al.*, 1980; Gevorkyan *et al.*, 1987). Main natural factors and ground properties, which influence frost cracking, were determined (Romanovsky, 1977; Mackay, 2000 *et al.*).

According to S.E. Grechishchev (1980) frost cracks are formed after periods of sharp air temperature falls during winter. It induces high pulling stretch in ground massive. These stretches have not enough time to relax and frost cracks appear when the stretches surpass limit of tensile strength of ground. So one of the main characteristic of ground is tensile strength (σ).

B.P. Weinberg (1940) first measured tensile strength of ice (11.2 kg/cm^2). Later it was stated that tensile strength of ice increase from 10,5 kg/cm^2 to 12,6 kg/cm^2 with the change temperature from -10°C to -50°C (Shusherina, 1974). A few experiment to determine long-lasting strength of ice were carried out. In addition, E.P. Shusherina (1974) obtained data of tensile strength of frozen sand and clay with the change of temperature from -10°C to - 60°C and a rate of stress of 2 MPa per minute.

During experiments in laboratory of Moscow State University of Railway Engineering data of tensile strength of sand, clay and ice in temperature range from 0°C to -30°C was received. Samples of ground and ice were formed in shape similar to figure "8", through which stress transmitted equally and an even surface of rupture was formed. Rate of stress was maintained at 9 MPa per minute during the experiment ensuring destruction of sample during 20-30 seconds. As a result of processing the experimental data, an empiric equation for calculating the tensile strength as a function of temperature and water content with an error of 16% was received:

$$\sigma = 6{,}2 - 0{,}2\,\theta - 0{,}208\,W$$

where σ – tensile strength, MPa, θ – temperature, °C; W – water content, %.

Tensile strength of fine-crystalline ice change from 0.6 to 1.4 MPa and depend not only from temperature of experiment. Tensile strength of medium sand is relatively equal to tensile strength of ice and change from 0.75 to 2.65 MPa. When water content in sand rise from 16 to 20% tensile strength decreases because the water content reaches total moisture capacity. When water content in clay increases from plastic limit to liquid limit, tensile strength doesn`t depend on water content and increases linearly from 1.3 to 5.5 MPa with change of temperature from 0°C to -15°C. With a further decrease of temperature, tensile strength of clay with more water content became lower then tensile strength of sample with less water content because samples with higher water content contain micro ice lenses.

In result, a method of determining the tensile strength was developed. The method allows to obtain more exact results for fine-grained ground than for fine sand. This method isn`t recommended for medium or coarse sand. As the result of using this method was received an equation for calculating the tensile strength as a function of temperature and water content

Acknowledgments

This work was approval by RFBR grants # 15-05-04291, 16-05-01116, 18-35-00366.

References

Dostovalov, B.N., 1952. Study about conditions of frost cracking and ice-wedge in frozen soil (in Russian). *Investigation of permafrost in Yakutia*, Akad. Nauk SSSR, iss. 3, p. 162-194.

Grechishchev, S.E., Chistotinov, L.V., Shur, Y.L, 1980. *Cryogenic physic-geological processes and it`s forecast (in Russian).* Nedra. 382 pp.

Grigoryan, S.S., Krass, M.S., Guseva, E.V., Gevorkyan, S.G., 1987. *Qualimetry theory of geocryology forecast (in Russian).* Moscow University Press, 266 p.

Lachenbruch, A., 1962. Mechanics of thermal contraction cracks and ice-wedge polygons in permafrost. *Geol. Soc. Amer.*, Paper 70, 69 p.

Mackay, J.R., 2000. Thermally induced movements in ice-wedge polygons, western arctic coast: a long-term study. *Geography physique et Quatermaire*, vol. 54, n 1, p.41-68.

Romanovskij, N.N., 1977. *Formation of polygon-wedge structures (in Russian).* Akad. Nauk SSSR. Sibirskoye Otdelenie, Novosibirsk, “Nauka”, 215 p.

Shusherina, E.P., 1974. Resistance of frozen ground and ice to a rupture in the range of low temperatures (to -60°C) (in Russian). *Permafrost study (Merzlotnie issledovaniya).* Moscow University Press, iss. XIV, p. 179-189.

Weinberg, B.P., 1940. *Ice (in Russian).* Geotekhteorizdat, 214 p.

Critical shear stress of frozen and thawing soils

Julie Malenfant-Lepage[1,2,3]
Guy Doré[1,2]
Raed Lubbad[3]

[1] *Department of Water and Civil Engineering, Université Laval, Québec QC, Canada, julie.malenfant-lepage.1@ulaval.ca*
[2] *Center for Northern Studies (CEN), Université Laval, Québec QC, Canada*
[3] *Department of Civil and Environmental Engineering, Norwegian University of Science and Technology (NTNU), Trondheim, Norway*

Abstract

An important problem in erosion of frozen and thawing soils is the determination of the critical shear stress at which a soil particle is detached by flowing water. This research project proposes to adapt and apply an in-situ method used for unfrozen cohesive soils, the Cohesive Strength Meter, to frozen and thawing soils in the Arctic. Results obtained from the fieldwork done in summer 2017 in the village of Salluit, Nunavik, Canada and in the Yukon Territory, Canada show very low values of critical shear stress corresponding to a high erodibility potential. A methodology to calculate the critical slope and the maximum flow allowed to limit erosion according to the measured critical shear stress is proposed.

Keywords: drainage, permafrost, infrastructure, erosion, critical shear stress

Introduction

Currently, engineering methods for the design of drainage systems in permafrost regions are limited to a set of recommendations to reduce the risk of excessive heat transfer and soil erosion around transportation infrastructures. This research project intends to assess the critical shear stress (CSS) of frozen soils and thawing soils to obtain the maximum quantity of water that can be concentrated in one channel (e.g. ditch and culvert) to limit soil erosion. An in-situ method developed for unfrozen cohesive soils, the Cohesive Strength Meter (CSM), is applied and adapted to frozen/thawing soils in this research. The CSS of frozen/thawing soils are also fundamental properties allowing assessing bank erosion in the Arctic. CSS allows characterizing the susceptibility of a soil particle to be detached on the lower beach and subsea by wave action. It also helps quantifying the energy required to remove soils by running water on the bluff face due to precipitation (rain or snow melt) producing characteristic geomorphologic features such as gullies (Guegan, 2016). To our knowledge, the erodibility potential of permafrost and fine-grained active layer soils has not yet been studied and documented. The CSS has a high potential of application in permafrost science and engineering.

The Cohesive Strength Meter: Applicability to frozen and thawing soils

A critical problem in erosion of frozen soils is the determination of the critical shear stress, τ_c, at which a soil particle is detached by flowing water (Guegan, 2016). For unfrozen non-cohesive soils (sands and gravels), the CSS stress can be derived directly from the shield diagram using the sediment grain size and density. In contrast to non-cohesive sediments, it is presently not possible to predict the CSS of cohesive sediments from one or more easily measurable parameters, such as grain size, bulk density, or water or organic content (Dade *et al*., 1992). The cohesive bond between soil particles results from a complex combination of physico-chemical properties that control their resistance to detachment by fluid shear. The simple shield diagram can therefore not be used. Subsequently various in situ testing devices have been developed.

The CSM is a portable instrument that measures rapid in situ critical entrainment stress of surficial sediments. It is a modern, portable version of the laboratory jet test used by soil scientists for over 50 years to measure the erodibility threshold of clayey soil samples. The CSM is composed of a main instrument unit containing the computer and a reservoir of water pressurized by an external air cylinder and connected to a sensor head that will be inserted into the sediment surface (Fig. 1). Inside the sensor head, there is a nozzle, located 2 cm above the sediment surface, that can produce a water jet applying a wide range of hydraulic stresses on the soil surface. A light transmitter and receiver are also present within the test chamber 1 cm above the sediment surface to measure sediment resuspension after the jet pulse.

Figure 1. Cohesive Strength Meter MK IV from Partrac Ltd

Erosion thresholds are defined by the manufacturer (PARTRAC) as the jet pressure P_I at which average light transmission within the test chamber drops below 90% of the maximum (Fig. 2).

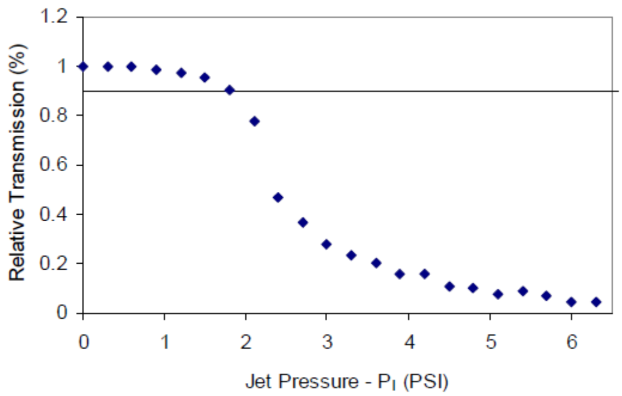

Figure 2. An example of a transmission curve from a cohesive strength meter run. A 10% reduction in transmission was used as the operation definition of erosion (Grabowski, 2014).

To convert the internal and vertical jet pressure P_I measured by the CSM in a horizontal bed shear stress value, the methodology developed by Grabowski et al. (2010) has been used in this study. Results obtained from the fieldwork done in summer 2017 in the village of Salluit, Nunavik, Canada and in the Yukon Territory, Canada show very low values of CSS corresponding to a very high erodibility potential. A methodology to calculate the critical slope and the maximum flow allowed to limit erosion according to the measured critical shear stress with the CSM is also proposed.

Conclusion

The methods developed to measure the critical shear stress of frozen and thawing soils and calculate the maximum quantity of water that can be concentrated on the ground surface to limit soil erosion can become a good working tool for engineers and scientists working in the Arctic to select the proper and cost-effective drainage system design and erosion protection techniques if required. The values obtained of critical shear stress can also become important input parameters for the coastal erosion models used in the Arctic regions.

Acknowledgments

The authors would like to acknowledge the technical and the financial support of the Sustainable Arctic Marine and Coastal Technology *SAMCoT* research program from the Norwegian University of Science and Technology, Trondheim, Norway for this project as well as the Arquluk and Sentinel North research programs from Université Laval in Canada. The first author would also like to greatly thank the W. Garfield Weston Foundation for the financial support.

References

Dade, W. B., Nowell, A. R. M. & Jumars, P. A., 1992. Predicting erosion resistance of mud. *Journal of Marine Geology* 105: 285–297.

Grabowski R. C., 2014. Measuring the shear strength of cohesive sediment in the field. In: Cook SJ, Clark LE, and Nield JM (eds), *Geomorphological Techniques*. British Society for Geomorphology, Part 1, Sec. 3.1, 1-7.

Grabowski, R.C., Droppo, I.G. & Wharton, G., 2010. Estimation of critical shear stress from cohesive strength meter-derived erosion thresholds. *Limnology and Oceanography-Methods* 8: 678-685.

Guegan, E., 2016. *Cohesive Strength Meter: Applicability to frozen (thawing) soils*. Report submitted to the Sustainable Arctic Marine and Coastal Technology *SAMCoT* WP6 research group from the Norwegian University of Science and Technology NTNU, Trondheim, Norway, 13 pp.

Geophysical methods of monitoring of permafrost on the objects of economic activity

Svet Milanovskiy [1]
Sergey Velikin [2]
Artem Cherepanov [3]
Aleksey Petrunin [1,4]
Vyacheslav Istratov [5]

[1] *Institute Physics of the Earth RAS, svetmil@mail.ru*
[2] *Vilyui Permafrost Research Station of Permafrost Institute SB RAS*
[3] *GFZ, Postdam*
[4] *Russian State Geological Prospecting University*
[5] *Radionda" Ltd.*

Abstract

Hydro units are natural laboratory for the study the interactions between climate-permafrost-aquafer. Our geophysical observations, including long-term temperature measurements, near hydro units focused on the study of seepage processes. The aim of the study is to use geophisical information for constructing reliable numerical model of interaction of human impact (hydro units) on the system "permafrost-climate-aquafer". Another part of our work is spatial electric monitoring of the permafrost state near injection wells on oil fields in Western Siberia. We present an experience of such monitoring at a multiple-well platform of an oil field. Changes of permafrost physical state near the injection well investigated using radio wave methods of cross well surveys.

Keywords: hydro unit, permafrost, seepage, geophysical monitoring, cross well survey, modelling

Introduction

The Yedoma permafrost is significant source of greenhouse gases. Increasing thawing of permafrost may have positive feedback for greenhouse effect when gases emitted to the atmosphere. Intensity of gases contribution mainly depends on the active layer thickness (ALT). The presence of artificial aquafer in permafrost environment gives an additional effect for deeper thawing than for active layer due to seepage development. The magnitude of thaw process evaluated by numerical modelling. We present monitoring geophysical data from Sitikan and Viluy hydro units and VNIMS testing ALT area of near Svetliy settlement in Western Yakutia. Special EM observation were performed near multiple-well platform of an oil field for detecting local thaw processes caused by intensive injection of hot fluid(up to 120°C) used for maintaining reservoir pressure. (Cherepanov, 2014).

Methods

Geophysical methods included surface and borehole observations. (Snegirev et al., 2003, Milanovskiy et al., 2008, Milanovskiy et al., 2015). Long-term temperature measurements organized in boreholes drilled in frozen coastal zone and in different elements of hydro unit's construction as well as in reservoir. Geophysical monitoring included Electrical Resistivity Tomography, Method of a Natural Field, Georadar, Seismic Profiling and Sounding. Down-hole observations included complex of logging studies (Resistance, Flow meter survey, Gamma logging, Neutron Gamma logging, Caliper measurement, Radio Wave Geo - Introscopy - RWGI). We also used RWGI method (Istratov &. Frolov, 2003) and its modifications for controlling condition of permafrost rock mass on different objects of oil and gas sector, located in Western Siberia. Electrical parameters of rocks - electrical resistivity (ϱ) and permittivity (ε) are more sensitive to changes in physical and mechanical properties of permafrost rock massif comparing with temperature data. Technology of spatial radio wave monitoring makes possible to determine geoelectric structure of the research site. We may classify the state of rocks in three main categories: 1) frozen rocks in stable condition; 2) rocks in the thawing state, when the process of phase transition "ice-water" is going on; 3) fully thawed rocks, in which the phase transition was completed.

Numerical Model

Numerical evaluations of originating and development of talik-zones near the dam, performed for two cross-sections: normal and orthogonal to general direction of filtration flow (quasi 3D). We solve non-steady problem of heat-mass transfer in fractured-porous saturated frozen environment. Model analyzes conditions causing origin and development of talik near reservoir, such as air temperature variations, snow cover, seasonal change of water temperature in storage basin, permeability evolution in frozen soil and inner structure of frozen massif. (Milanovskiy et al., 2011).

Results

Comprehensive environmental-geophysical monitoring including long-term regime temperature measurements and complex of logging studies, electrical, seismic, acoustic methods were used for solving of various geocryological problems in the cryosphere. It is evident that a perfect system of geophysical monitoring should include real-time observation of the permafrost state. From our data, we observe that deep talik formation in permafrost environment is in a close connection with artificial aquafer providing water head for seepage in thawing strata. After beginning of filtration, seepage zone works like intensive heat source for surrounding frozen rocks. The "domino" effect works until we have driving forces - headwater from aquafer or relief. In the last case, originally frozen rocks containing ice after thawing became seepage zone. The principal interest is the very beginning of thaw process inside frozen strata containing ice. For active layer the main factor is climate impact. From our observation, maximum thaw depth is not so much (not more than 3m). From other hand, we observe seepage processes much deeper. The model shows a significant impact of artificial aquifer. The talik forms even in case of deep permeable layer location, which do not affected by surface temperature conditions. The "domino" effect (two permeable layers divided by an impermeable one) may enhance penetration of the thawed zone with time significantly. The problem of deep thawing of permafrost near aquafer (even without seepage on deep level) is important in connection with possible instability of gas hydrates under growing temperature.

The technology of spatial geoelectric monitoring for the early diagnosis of the change in the frozen state of rocks in situ, has been developed and experimentally tested. Developed algorithms and data processing programs permit to obtain 3D distribution of effective ϱ and ε of the rocks in the inter-wellbore space. We consider the experience of new technology testing in stages of engineering design, construction and production time of multiple-well platforms of oil and gas fields in Western Siberia. The development of the thawing zone around the injection well during several years demonstrated for multiple-well platform on the oil field. The development dynamics of thawing processes in space and with time have been determined for various types of soils.

References

Cherepanov, A.O., 2014. Spatial geoelectric monitoring of permafrost state near injection wells by the example of an oil field in Western Siberia. *Geophysical Research* 12: 18-24. (In Russian).

Istratov, V.A., &. Frolov, A.D. 2003. Radio wave borehole measurements to determine *in situ* the electric property distribution in a massif. *J. Geophys. Res. – Planets*, Vol. 108, No E4: 8038-8043.

Milanovskiy, S., Petrunin, A., Velikin, S., & Istratov, V., 2011. Numerical simulation of seepage processes in permafrost near a hydro unit In: *Cold Region Hydrology in a Changing Climate* (*Proceedings of symposium H02 held during IUGG2011 in Melbourne, Australia, July 2011*) IAHS Publ. 346: 164-170.

Milanovskiy, S., Velikin, S. & Istratov V. 2008. Geophysical study of talik zones (Western Yakutia). *Proceedings of the Ninth International Conference on Permafrost* (ed. by D. L. Kane & K. M. Hinkel) (University of Alaska, Fairbanks)

Milanovskiy, S., Velikin, S., Petrunin, A., & Istratov, V., 2015. Geophysical Monitoring of Engineering Constructions in Western Yakutia and Study of Coupled Problem of Temperature and Seepage Fields in Permafrost near Hydro Unit. *Proceedings of 68th Canadian Geotechnical Conference and 7th Canadian Permafrost Conference*, *GeoQuebec2015*, Quebec City, Canada, September: 20-23, 9p.

Snegirev, A.M., Velikin, S.A., Istratov, V.A., Kuchmin A.O., Skvortsov A.G., Frolov A.D. 2003. Geophysical monitoring in permafrost areas. *Proceedings of the Eighth International Conference on Permafrost*, 21–25 July 2003, Zürich, Switzerland, Phillips M., Springman S.M., Arenson L.U. (eds.) Zurich, ICOP: 1079-1084.

Prediction of Gas Flaring Effect on Permafrost

Sergey Myshkovski[1]
Yury V. Ramanouski[2]
[1] *Simmakers Ltd., sergei.myshkovski@simmakers.com*
[2] *yuri.romanovsky@simmakers.com*

Abstract

When simulating gas flares located in permafrost regions, radiation is not the only phenomenon to consider, but global warming remains the key feature of the worst-case scenario of simulation. We describe our experiences in numerical heat analysis of soil temperature under the flare.

Keywords: gas flare, permafrost, radiative heat transfer, soil warming, numerical simulation.

Introduction

The "Zero Routine Flaring by 2030" initiative [World Bank, 2015] is aimed at reduction of global gas flaring. However, there is still a demand for numerical simulation of permafrost warming by flares.

A naïve solution is to use a 1D computational domain and specify a heat flux boundary condition with a convective heat transfer coefficient and an inward heat flux, responsible for the ground-level radiation. However, the flux must be properly estimated [Guigard *et al*., 2000], and still, the accuracy of a long-term numerical prediction is likely to be unacceptable.

Phenomena to consider

In a circumpolar region, if there is no flare or flaring has long been stopped, there might be no need to consider heat surface heat emission: It is largely balanced by solar radiation and back radiation. A hot surface emits an amount of energy, comparable to the flare radiation. This emission obeys the Stefan–Boltzmann law and continues for some time even after interrupting the flare.

The fireproof and heat insulation layers (if present) should be simulated as well.

The snow cover, until it melts, reflects some portion of flare radiation and absorbs some portion of the soil heat. Since the snow may be blackened, the reflected portion of radiation is quite small.

Finally, one should pay attention to far-field absorption of heat by the soil and even to vaporization of groundwater: The latent heat of evaporation is quite high (especially if there is some water influx) and the thermal diffusivity of a dry soil is lower than of a moist one.

Worst-case scenario

Along with the global warming, emergencies and gas flare maintenance (e.g., in case of venting gas wells) are desirable to consider.

Tips and Tricks

When modeling a single vertical flare, one may exploit the rotational symmetry about the vertical axis. In case of a horizontal flare, there is a vertical plane of symmetry. For a multi-point flare pit, there are two of such planes (mutually orthogonal).

If any kind of symmetry is exploited and a flare is not enclosed (so there is no wind protection), one should use the worst-case sector of the wind rose.

References

World Bank, 2015. *Zero Routine Flaring by 2030*. http://www.worldbank.org/en/programs/zero-routine-flaring-by-2030.

Guigard, S.E., Kindzierski, W.B., Harper, N., 2000. *Heat Radiation from Flares*. Edmonton, Alberta (Canada), 90 pp.

Temperature changes influence on slopes stability at the Baydara bay sites of Kara sea.

Nazarov Alexander[1]

[1]*Lomonosov Moscow state university, Department of geocryology, dulciolum@mail.ru*

Abstract

The big part of a Earth's surface relief can be represented as a sum of different in structure and origin slopes. Thus, the research, prediction and calculation of slopes stability is one of the actual problems of engineering geology.

Keywords: coastal retreat; slopes stability; climate change; soil mechanics; solifluction; temperature influence.

Introduction

The big part of a Earth's surface relief can be represented as a sum of different in structure and origin slopes, the prevailing part of the coastal zone also can be represents a variety of slopes. Thus, the research, prediction and calculation of slopes stability is one of the actual problems of engineering geology, the harmful influence of slope processes should be taken into account in the design and construction of structures. The slope processes that arise and develop under the action of cryogenic factors (the presence of permafrost and the freeze-thaw cycle on the slopes) are of great importance. These processes are intensively developing in the permafrost territories. In the description of slope processes, the main attention is paid to solifluction, which is the most important of slope cryogenic processes and, moreover, studied better than other processes. Also, external factors of slope development dynamics are of great importance, including instability of the temperature regime of frozen soils associated with global climate changes.

Baydara Bay is one of the largest bays of the Kara Sea, in it's southwestern part, between the Yugor and the Yamal demi-islands. The length of the lip is about 180 kilometers. The width at the entrance is 78 kilometers. It's depth is up to 20 meters. Baydara Bay is located in the eastern part of the Atlantic sector of the Arctic Ocean. The average annual air temperature in the region is negative: -7-10˚C.

The coastline of the Baydara Bay during the Holocene period changed from the markers – 30 meters to it's current position. Displacement of the coastline is due to both a constant increase in the level of the World Ocean, and the destruction of shores. Currently, the maximum displacement of the coastline by 2-3 meters in a year is due mainly to the destruction of the coast. The Baydara Bay coasts belong to the zone of continuous propagation of permafrost with a width of 150-300 meters and the temperature of the rock on the sole of the seasonal temperature range -4 ° -6 ° C (Fig.1).

Figure 1. One of the typical slopes on Baydara Bay coastline.

Cryolithozone in the Baydaratskaya Bay region is in extremely dynamic equilibrium. Virtually any technogenic impact can lead to a violation of this equilibrium, and as a result, cause degradation of the permafrost or change the intensity of the development of cryogenic processes. Solifluction - the flow of soil, oversaturated with water and rich in colloids. Solifluction occurs mainly in the polar and high mountain regions, in the areas of long-term and permafrost development, where the active layer of soil thawed to a comparatively shallow depth is periodically waterlogged by thawed and rainwater, penetration of which to depth is impeded by the underlying frost. Due to a reduction in internal friction and a simultaneous increase in weight, the water-soaked soil drains down under the influence of gravity. This is facilitated by fluctuations in the volume of earth masses during freezing and thawing, swelling of colloids, a decrease in the density of water with a temperature change of 4 to 0°C, and capillary forces. Solifluction occurs noticeably already at slope angles from 3 to 5 degrees, and the current velocity varies from several decimeters to tens of meters per year. With the phenomena of solifluction, the formation of solifluction terraces and trees, earthy rivers and trails is associated. [Geological dictionary, 1955].

For the calculation the stability of the slope, it is necessary to determine the ultimate strength characteristics of shear resistance, friction and cohesion of thawing soils. An objective assessment of the stability of slopes is possible with the correct choice of the design scheme, which most fully takes into account the existing array of impacts and the conditions in which it is located.

In September 2017 I with a group of scientists, students and engineers from Moscow State University and IGE of Russian Academy of Science performed fieldwork in Baydara Bay. In the process, monoliths of frozen soil were extracted and delivered to the laboratory of soil mechanics of IGE of Russian Academy of Science. Conductes tests were carried out for the unconsolidated and undrained scheme, also tests for triaxial compression of the soil on a consolidated and non-consolidated undrained scheme. The tests were carried out on soils at different temperatures, thus simulating the expected warming or cooling of the climate. The results of the tests make it possible to forecast the condition of the slopes and also the speed of the retreat of the banks of the Baydara Bay with appropriate climate changes.

References

Vturina. E.A. 1966. Cryogenic slope terraces. *Science*, 1966. 44-84 p.

Grechishchev S.E. et al. 1984. Fundamentals of modeling of cryogenic physical-geological processes. *Science*, 130-135 p.

Grechishchev S.E. et al. 1980. Cryogenic physico-geological processes and their forecast. *Nedra,* 233-244p.

Zhigarev L.A. 1967. Reasons and mechanism of development of solifluction. *Nauka*, 134-158 p.

Kaplina T.N. 1965. Cryogenic slope processes. *Science*, 187-202p.

Krishtovich A.N. 1955. Geological dictionary. *Gosgeoltekhizdat*, 2nd volume., 376-378p.

Root P.E. & Ziangirov R.S. 1984. Workshop on the mechanics of soils. *Science*, 140-145p.

Savelyev V.S. 1964. Solifluction. 45-49p.

Trofimov V.T., Korolev V.A., Voznesensky E.A., Golodkovskaya G.A., Vasilchuk Y.K., Ziangyrov R.S. 2005. Soil science. *Science*, 6th edition. 1024 pp.

Tsytovich N.A. 2014. Soil mechanics. *Lenand*, 5th edition. 640pp.

Cooling enhancement of a new crushed rock revetment embankment in a warm permafrost region

Fujun Niu[1]
Minghao Liu[1]
Jing Luo[1]
Zhanju Lin[1]
Guoan Yin[1]
[1] *State Key Laboratory of Frozen Soil Engineering, Northwest Institute of Eco-Environment and Resources, Chinese Academy of Sciences, Lanzhou, Gansu 730000, China, email: niufujun@lzb.ac.cn*

Abstract

Poor cooling effects of crushed-rock revetment embankments (CRRs) have been observed in warm permafrost regions along the Qinghai-Tibet Railway (QTR), which will significantly affect the roadbed's integrity and stability, and further lead to potential threat to the long-term safe operation of the railway. To solve this problem, a new embankment structure was designed, and a field experiment was carried out in a section of the QTR at Tuotuohe to examine its convection and thermal characteristics and to assess its cooling performance. The experimental results indicate that, compared with the traditional CRR, the new structure has a significantly increased cooling effect on the embankment slope. This is due to an effective prevention of side-slope warming in hot seasons and an enhanced forced convection cooling effect in cold seasons. This study provides valuable guidelines for the design and maintenance of roadbeds in warm permafrost regions.

Keywords: Cooling enhancement; crushed rock revetment embankment; slope structure; permafrost; field experiment; heat transfer; convection.

The New Embankment Structure Design

This paper describes a new embankment structure, a combination of a CRR and a prevention of side-slope warming measure. In this design, the shading board in the composite embankment (Quan *et al.*, 2006), impractical for engineering applications, was replaced by a paved soil layer with geotextile. These layers are intended to prevent the warm wind from entering the crushed-rock layer in summer, exclude solar radiation, and strengthen convective heat transfer within the rock layer in winter.

Field Experiment

Construction of the experimental embankment

The experimental section was built on the QTR at K1217+930. The newly designed embankment, completed in August 2012, was constructed by transforming an existing CRR of the QTR. The transformation process is shown in Figure 1. Based on the design of the existing embankment, two layers of crushed-rocks (marked A and B in Fig. 2b) were added to it to form a new crushed rock connective region from the toe to the crest of the slope. Then, the surface of the newly formed crushed-rock layer was paved with 0.3 m of soil interlayered with a geotextile to prevent the upper soil from falling into the pores of the crushed-rock layer. Thus, the crushed rock revetment acts as a narrow ventilated pass so that the forced convection in winter is strengthened along the slope because of a "narrow pipe" effect. The length of the experimental section is 20 m, the height of the embankment is 4 m, and the diameter of the crushed rock is 0.15–0.3 m. The experimental section was constructed on the sun-facing slope, to

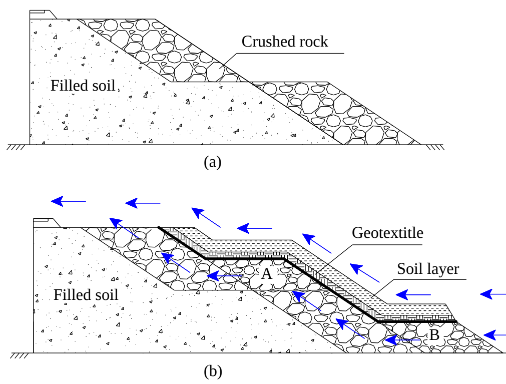

Figure2. Structural diagram of the embankment slope transformation. (a) The existing CRR; (b) the new structure. Notes: Arrows stands for air flow direction.

examine its effect in controlling solar radiation. To evaluate the cooling performance of the new embankment structure, a monitoring system for temperature and convection speed was established.

Results

Temperature variation of the embankment slope

Based on the observed temperature data, the time series of soil temperatures at a 0.5 m depth beneath the crushed-rock layer of the embankment slope is shown in Figure 2. The soil temperatures at the three positions, including the slope crest, slope toe, and middle of the slope, obviously decreased, which reveals the effectiveness of the new embankment structure in decreasing the temperature of the embankment slope. The mean annual temperatures at the three positions were reduced by 1.96 °C, 1.86 °C, and 1.88 °C, respectively, in three years after the slope transformation. The maximum temperature reduction occurred in the summer from 2013 to 2014, with magnitudes of 2.0 °C to 2.3 °C. The decrease in soil temperature weakened but continued after 2014. It is concluded that the clear cooling process in summer mainly comes from the effectiveness of the new slope structure in reducing solar radiation and preventing warm winds from entering the crushed-rock layer. Similarly, the cooling process was also observed in winter and its lowest temperature decreased with years, which was mainly caused by the enhanced convection heat transfer of the new CRR.

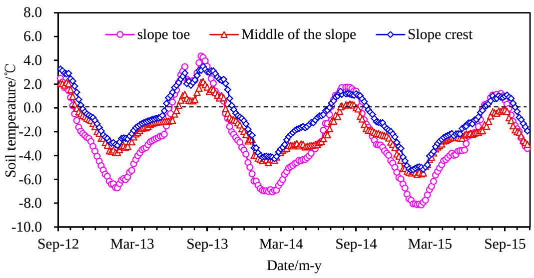

Figure 2. Time series of soil temperatures at 0.5 m depth beneath crushed-rock layer of the new embankment slope

Cooling effects comparison between the new embankment and the CRR

To examine whether the cooling effect of the new embankment structure is increased after the modification, a traditional CRR located in the Tuotuohe Basin was chosen to make a contrastive analysis. Figure 3 presents the differences in temperature of the embankment slopes (temperature beneath the crushed-rock layer) between the new structure and the traditional one. As shown, the temperature of the embankment slope was clearly lower in the new embankment than in the traditional one, with a mean annual difference of nearly 2.4 °C, demonstrating a superior cooling effect on the slope by the new design.

During cold seasons, the maximum difference in slope temperature between the new and the traditional embankment could reach 2.0 °C, which was mainly determined by the reinforced heat transfer caused by the enhanced forced-convection in the new CRR. In summer, the difference in slope temperature between the two embankments increased, with a maximum value of about 3.8 °C, which was mainly caused by the sun-shade and warm wind shield effects caused by 0.3 m of paved soil on the surface of the CRR. The differences in temperature demonstrate the effectiveness of the new slope design in increasing the thermal stability of the traditional CRR along the QTR.

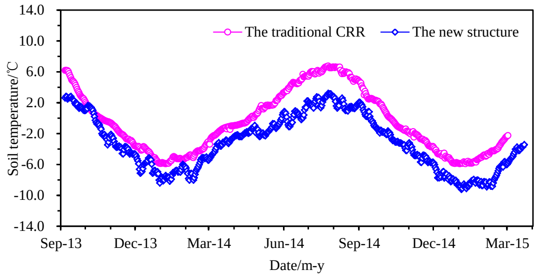

Figure 9. Temperature variations of the embankment slopes between the new structure and the traditional CRR

Conclusions

Compared with the traditional CRR, the new embankment structure produced a significantly enhanced cooling effect on the embankment slope, and thus increased embankment stability in warm permafrost regions. This is due to an effective prevention of side-slope warming in hot seasons and an enhanced forced convection cooling effect in cold seasons. Moreover, this structure plays an important role in sand-filling prevention, which is beneficial to protect the long-term cooling effect of the crushed-rock layer on side slopes. Therefore, it is hoped that the new embankment structure can be applied in railway construction or as a maintenance measure to increase the long-term stability of embankments in warm permafrost regions.

Acknowledgments

This work was supported by the National Natural Science Foundation of China (Grant no. 41601069 and 41271092), and the Foundation for Innovative Research Groups of the National Natural Science Foundation of China (Grant No. 41121061)

References

Quan, X.J., Li, N., Li, G.Y., 2006. A new ripraped-rock slope for high temperature permafrost regions, *Cold Regions Science and Technology*. 45 (1): 42–50.

An experimental study of unfrozen water content in fine grained permafrost soils

Marte Sundby Nybo[1]
Arne Instanes[2]

[1]*Norconsult AS, Vestfjordgaten 4, N-1338 Sandvika, NORWAY, marte.sundby.nybo@norconsult.com*
[2]*University Center in Svalbard (UNIS), N-9171 Longyearbyen, NORWAY, arne.instanes@unis.no*

Abstract

Accurate determination of unfrozen water content in permafrost soils are important for geotechnical analysis such as soil stability analyses, bearing capacity analysis and settlement analysis. In this article, two methods for determining unfrozen water content in fine grained permafrost soils have been investigated: modified liquid limit test and water potential test. Estimated unfrozen water content from the modified liquid limit testing is lower than from the water potential test. Revised equations for the modified liquid limit test is proposed. The water potential method gives a quick and accurate estimate of unfrozen water, and should be the preferred method for engineering purposes.

Keywords: Unfrozen water; permafrost; geotechnical engineering.

Introduction

The soil shear strength increases when pore water changes phase from water to ice. However, in fine grained soils, some of the water in the soil matrix will remain unfrozen at subzero temperatures. Unfrozen water content is an important mechanical, thermal and hydrological property of a soil, as flowing water may supply heat to the ground, reduce the soil shear strength, and induce increased settlement rates on foundations in permafrost. Thus, estimating unfrozen water contents, is important for geotechnical design considerations.

Reliable methods for determining unfrozen water content in frozen soil exist, but requires sophisticated laboratory instruments and time-consuming procedures. For engineering purposes, more efficient methods are desired. In this article, two methods for determining unfrozen water content in fine grained permafrost soils have been investigated. Firstly, liquid limit test and empirical relationships were used to create an unfrozen water content versus temperature function. Then, determination of the water potential of the tested soils was carried out and a similar function was established. Results from the methods are compared and discussed.

Methodology

Soil samples from Longyearbyen and Trondheim were investigated in geotechnical laboratories at the University Center in Svalbard (UNIS), Longyearbyen, and at the Norwegian University of Science and Technology (NTNU) in Trondheim, Norway.

Two methods were used to determine the unfrozen water versus temperature function for the tested soils: A modified liquid limit test and water potential test.

Modified liquid limit test

Tice et al. (1976) found that the unfrozen water versus temperature relationship could be expressed as a simple power law equation:

$$w_u = \alpha \, \Theta^{\beta} \qquad (1)$$

where w_u is unfrozen water content at temperature Θ, and α, β are soil parameters.

The modified liquid limit test was then used at temperatures of -1 °C (Θ=1) and -2 °C (Θ=2) for determining the soil parameters α and β:

$$w_{u,\Theta=1} = 0.346 \, w_{N=25} - 3.01 \qquad (2)$$

$$w_{u,\Theta=2} = 0.338 \, w_{N=100} - 3.72 \qquad (3)$$

The water contents in a liquid limit test with $w_{N=25}$ and $w_{N=100}$ were measured and used in the empirical relationship in equation (1) to develop the unfrozen water content versus temperature curve. The method is widely accepted for soils considered not to contain excessive amounts of soluble salts.

Water potential

The water potential method estimates the contents of liquid water in equilibrium with bulk ice, defined as unfrozen water, in the soil. The method was proposed by Istomin et al. (2015, 2017) and Istomin et al. (2017).

The test was performed using a Dewpoint PotentiaMeter, WP4C, measuring pore water potential, dependent of temperature and moisture content, and thermodynamic activity of water at atmospheric pressure. Based on experimental determination of water potential and water activity in porous media, the measured data is used in thermodynamic calculations for determining pressure- and temperature-dependent unfrozen water content. The water contents calculated by this method show good correlation with results from direct contact measurements for equilibrium water in contact with ice at given temperatures and pressures (Istomin et al., 2015, 2017).

Results and discussion

Figures 1 and 2 show the unfrozen water versus temperature curves for two sites in Longyearbyen, Svalbard. The continuous line is from the modified liquid limit tests, while the dots are from the water potential tests. As can be seen from the figures, estimated unfrozen water content from modified liquid limit testing is lower than from the water potential test.

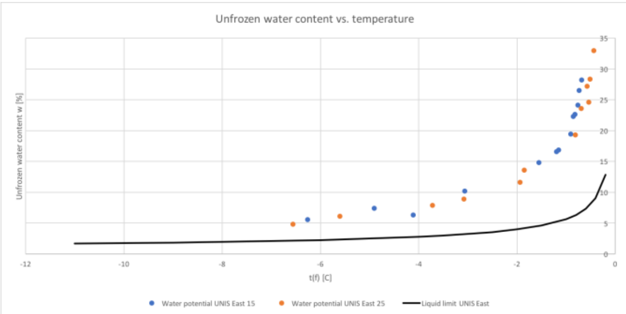

Figure 1 Unfrozen water vs temperature, UNIS East

The liquid limit determination is an empirical method that has given good results for unfrozen water content for several soils (Tice et al., 1976). However, from these tests it seems that the method does not fit very well with Norwegian soils, providing unfrozen water contents lower than the actual amount of unfrozen water. Thus, for geotechnical analysis such as creep and settlement, the estimated deformations may be too small due to underestimation of unfrozen water. Furthermore, the liquid limit method is somewhat time-consuming and cumbersome.

Nybo (2017) propose a revised version of equation (2) and (3) valid for Longyearbyen soils. The revised version, equation (4) and (5), gives a much better fit between the two testing methods, shown in figure 2.

$$w_{u,\Theta=1} = 0.7036\, w_{N=25} - 1.67 \quad (4)$$

$$w_{u,\Theta=2} = 0.657\, w_{N=100} - 4.33 \quad (5)$$

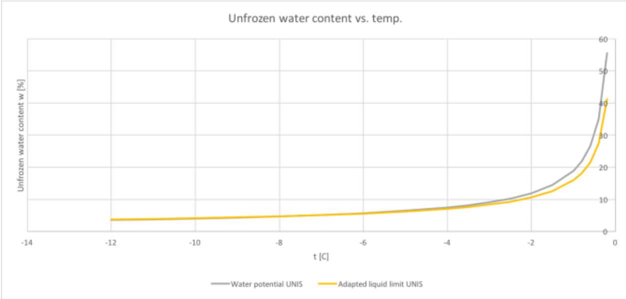

Figure 2 Unfrozen water versus temperature, UNIS East. Modified liquid limit equations.

Accurate determination of unfrozen water content in permafrost soils are important for geotechnical analysis such as soil stability analyses, bearing capacity analysis and settlement analysis. The water potential method gives a quick and accurate estimate of unfrozen water versus temperature, and should be the preferred method for engineering purposes.

Acknowledgments

The work presented in this paper is partly funded by the Research Infrastructure Program Norwegian Geo-Test Sites (NGTS), see https://www.ngi.no/eng/Projects/NGTS-Norwegian-Geo-Test-Sites, funded by the Research Council of Norway. Laboratory testing was carried out at the University Center in Svalbard (UNIS) and at the Norwegian University of Science and Technology (NTNU).

References

Istomin, V., Chuvilin, E., Bukhanov, B., and Uchida, T., 2015. A method for determination of water content in real and model porous media in equilibrium with bulk ice or gas hydrate. Technical report, Skolkovo institute of science and technology (Skoltech). Presented at Geo Québec 2015.

Istomin, V., Chuvilin, E., Bukhanov, B., and Uchida, T., 2017. Pore water content in equilibrium with ice or gas hydrate in sediments. *Cold Regions Science and Technology*, 137:60–67.

Nybo, M.S., 2017. An experimental study of unfrozen water content in fine grained permafrost soils. Master thesis TBA4900, Geotechnical Division, Department of Civil and Transport Engineering, Norwegian University of Science and Technology, Trondheim, Norway.

Tice, A. R., Anderson, D. M., and Banin, A., 1976. The prediction of unfrozen water contents in frozen soils from liquid limit determinations. Technical report, US Cold Regions Research and Engineering Laboratory. CRREL report 76-8.

Coastal protection facilities in the cryolithozone

Stanislav Ogorodov[1]
Daria Aleksyutina[1]
Nataliya Belova[1]
Alisa Baranskaya[1]
Osip Kokin[1]
Stepan Maznev [1]
[1]*Lomonosov Moscow State University, Faculty of Geography, Russia, email ogorodov@aha.ru*

Abstract

It is necessary to consider a lot of factors for the design of coastal protection structure. In this article, the features of coastal protection facilities in permafrost are described in connection with hydrodynamic conditions, ice regime, cryogenic and lithology characteristics etc.

Keywords: coastal erosion, frozen sediments, sea ice effect, industrial infrastructure, coastal protection

The coasts and shelf of the Arctic and other freezing seas of Russia are currently subject to active immediate industrial development, above all oil, gas and transport exploration. Safe operation of the infrastructure currently built both on the coasts and shelf is one of the most important tasks of the modern applied and fundamental research. The coastal-shelf zone of most of the Arctic seas has two most important features, making it different from temperate and tropical sea coasts: 1) long, sometimes up to 9-11 months, presence of sea ice; 2) presence of perennially frozen sediments, composing the coasts and the underwater sea slope. These factors are in most cases the reason of low efficiency of the traditional coastal protection infrastructure in the cryolithozone.

Sea ice as a zonal factor is an important passive and active relief-forming agent in the coastal-shelf zone of the Arctic and other freezing seas. The most dangerous process in relation to the hydrotechnical facilities is ice gouging - destructive mechanical impact of the ice of the ground, connected with the dynamics of the ice cover, formation of hummocks and stamukhas under the influence of hydrometeorologic factors and of the relief of the coastal-shelf zone. Underestimation of the ice gouging intensity can lead to damage of the engineering facilities, while excessive deepening increases the expenses of the construction.

Along with the impact of the ice cover, another important factor, crucial for geotechnical safety of the infrastructure and for geoecological safety of the surrounding landscapes and water areas is the process of cryolithogesesis. In the cryolithozone, coasts are composed by perennially frozen grounds with high ice content, which are vulnerable to the joint impact of heat and mechanical destruction (thermomechanical impact) during thermoabrasion. Depending on how severe climatic conditions of a freezing sea are, permafrost can also be found on the underwater coastal slope, and in some cases it can even be encountered far seaward from the modern coastline as relics from at least late Neopleistocene times. Other bottom sediments are either melted (unfrozen) or have temperatures around the freezing point of sea water: from −0,1 to −1,9°C.

Climate warming expressed in air temperature growth and sea ice decay leads to increased lengths of the wave fetch, greater probability of extreme storm surges along with longer dynamically active ice-free period and creates favorable conditions for more intensive thermomechanichal impact on the coasts and their faster destruction. During the displacement of the profile landwards, the underwater coastal slope is also subject to abrasion. Therefore, not only the buildings and facilities on land, but also underwater infrastructure crossing the coastline are under threat. Infrastructure exposed due to abrasion (e.g., an underwater pipeline) is inevitably damaged by sea ice, causing its deformation, and, finally, leading to a natural technogenic-induced disaster.

Engineering facilities are often built without the consideration of cryolithologic features of the coasts and shelf, with numerous technogenic impact on the topography, soils, vegetation cover and thermal regime of the frozen grounds; sediments are often directly extensively excavated from the coastal zone; lithodynamic balance in natural systems is often disturbed. Combined with the effect of increased potential of thermoabrasion caused by natural increase of the thermal and hydrodynamic impact on the coasts, such technogenic disturbances launch a trigger mechanism of enhanced destruction of the coasts and underwater slope. Consequently, additional, initially unplanned coastal protection measures, aiming at maintaining the safety of the facilities' operation are required. Their efficiency is directly connected with their account for cryolithologic and lithodynamic conditions of the coastal zone.

In this way, apart from obligatory functions of direct protection of the coasts and engineering infrastructure next to or crossing the coastline from wave action, constructions designed for coastal protection and facilities' geotechnical safety have to be built taking into consideration both the geocryological features of the coastal area and the possible dynamic load connected with sea ice impact. However, an approach based on reliable forecasts of the coastal dynamics is more appropriate both from the economical and ecological points of view. Using this approach, mutual influence of the engineering infrastructure and dangerous (sea ice, cryogenic and lithodynamic) processes is estimated during the initial phase of preparation, design and construction; as a result, the need for expensive measures of coastal protection is reduced or excluded.

Acknowledgments

The present study was prepared with the financial support of the Russian Science Foundation project No.16-17-00034.

Coupled thermo-hydro-mechanical model of artificial ground freezing process

Oleg Plekhov[1]
Ivan Panteleev[2]
Anastasiia Kostina[3]
Lev Levin[4]
[1]*Institute of Continuous Media Mechanics UB RAS, poa@icmm.ru*
[2]*Institute of Continuous Media Mechanics UB RAS*
[3] *Institute of Continuous Media Mechanics UB RAS*
[4] *Mining Institute UB RAS*

Abstract

This work is devoted to the numerical simulation of the artificial ground freezing process in the layered porous media. The model includes the heat transfer equation, the Fourier's law, the equilibrium equation, the constitutive equations for stress tensor, the geometric relation for linear strain tensor, the continuity equation and the Darcy's law. Results of numerical simulation have shown that ice wall forms non-uniformly. This can be explained by deviations of the freezing wells from vertical location as well as by difference in thermal and filtration properties of the layers.

Keywords: artificial ground freezing; numerical simulation; coupled problems; thermogravitational convection

Introduction

Artificial ground freezing is one of the universal and safe techniques for vertical shaft sinking in complex hydrogeological conditions. During the freezing process a temporary ice barrier protecting from groundwater flows is formed. The effectiveness of the obtained ice wall depends on its tightness and strength. The problem of optimal ice thickness is closely related to the adequate description of a complex thermo-hydro-mechanical process occurring during freezing.

Investigations on mass and heat transfer between frozen and unfrozen boundaries can be found in (Bronfenbrener, 2009), (Talamucci, 2003). Issues of fluid transfer in freezing soils are discussed in (Bittelli *et al*, 2004), (Konrad, 2005), (Mottagy & Rath, 2006), (Zhou & Zhou, 2010).

Despite the various works devoted to the freezing of soils, there is still no consensus on the nature of this process. Especially, this is concerned to the transition zone with simultaneous coexisting of ice and water at temperatures from 0 to -0.6 degrees of Celsius. Moreover, experimental investigations have shown that under the temperature below -15 degrees of Celsius the amount of the residual moisture in the soil is close to zero. The basic idea of this work is to propose relatively simple coupled thermo-hydro-mechanical model for three-dimensional simulation of artificial ground freezing process. Efficiency of the model is demonstrated by the numerical simulation of the ice wall formation in one of the potassium salt deposit.

Thermo-hydro-mechanical model of ground freezing and results of numerical simulation

To formulate a model the following hypothesis are assumed. The media is considered as the three-phased fully saturated material consisting of the solid skeleton, fluid and ice. All liquid transforms into ice and dry skeleton remains unchanged during the phase transition process. Developed model is restricted to isotropic linear theory of thermo-poroelasticity within which it is assumed that the media undergoes small deformations. Fluid is considered as a nearly incompressible.

The real data on temperature supply and return of the coolant circulating in the freezing column were used to specify boundary conditions (26). These data can be found in (Panteleev *et al*, 2017).

The model was used for the three-dimensional numerical modelling of the ice wall formation in the one of the potassium salt deposit. Simulation was carried out in the finite-element package Comsol Multiphysics® with the use of the academic license.

The domain of the considered problem has the shape of the cylinder with the radius of 13.25 m and the height of 265 m. The ice wall is formed by 41 freezing column. The location of the freezing wells is presented in (Panteleev *et al*, 2017). The area has been divided by finite elements with a form of rectangular prisms. The size of the finite element was varied from 9-11 centimeters near the well to 6-7 meters in the periphery. The height of the elements was no more than 6 meters. The total number of elements was about 1 million.

According to the geological data and the analysis presented in (Panteleev et al, 2017) the sedimentary cover is modelled by 14 different layers.

Results of the obtained ice wall after 300 days after the beginning of the freezing process are presented in Fig. 1.

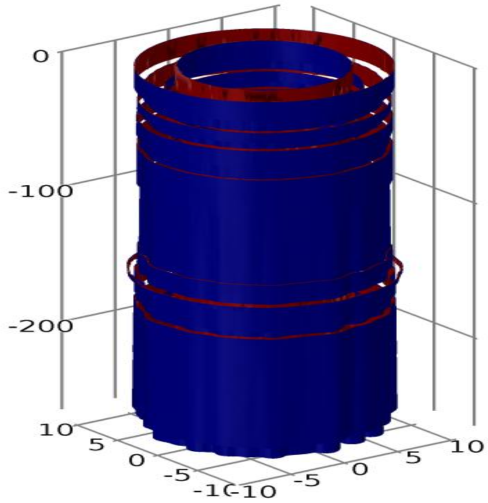

Figure 1. Ice wall obtained by numerical simulation.

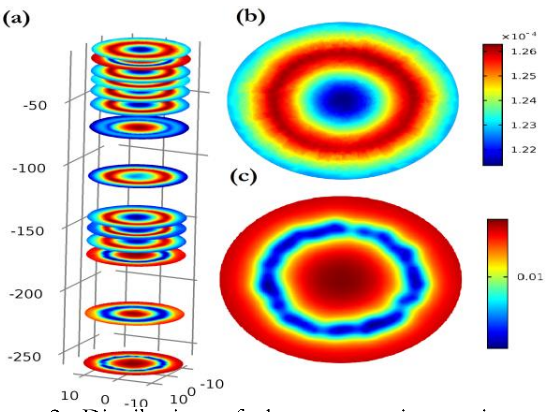

Figure 2. Distribution of the compressive strain tensor component: (a) in cross-sectional planes of every layer; (b) in cross-sectional plane of the first layer (quartz sand); (c) in cross-sectional plane of the last layer (dense clay)

The results of the numerical simulation have shown that deviation of the freezing columns from the vertical leads to the non-uniform ice wall formation. At the beginning of the process, freezing front is localized near the well. Further, an integration of the fronts of the neighboring wells is observed until the ice wall closure. After that, the size of the wall is increased and heterogeneity of the wall's boundary is preserved.

Figure 2 represents distribution of the compressive strain in cross-sectional planes for every allocated layer. The strain is distributed non-uniformly over the layer as well as over the depth of the considered area. Layers with large thermal expansion coefficients (such as sands) have maximum compressive strains inside of the ice wall (Fig. 2(b)). For clayey rocks an opposite situation is observed (Fig. 2(c)).

Conclusions

A coupled thermo-hydro-mechanical model of a fully saturated porous media is proposed. The model includes the heat transfer equation, the Fourier's law, the equilibrium equation, the constitutive equations for stress tensor, the geometric relation for linear strain tensor, the continuity equation and the Darcy's law. This model is used for numerical simulation of artificial ground freezing in one of the potassium salt deposits. Results of numerical simulation have shown that ice wall forms non-uniformly. This is explained by deviations of the freezing wells from vertical and difference in thermal and filtration properties of the layers.

Acknowledgments

This work was supported by the Russian Science Foundation (Grant No. 17-11-01204).

References

Bronfenbrener, L. & Korin, E., 1999. Thawing and refreezing around a buried pipe. *Chemical Engineering and Processing: Process Intensification* 38: 239–247.

Talamucci, F., 2003. Freezing process in porous media: formation of ice lenses, swelling of the soil. *Mathematical and Computer Modelling* 37: 595–602.

Bittelli, M., Flury, F. & Roth, K., 2004. Use of dielectric spectroscopy to estimate ice content in frozen porous media. *Water Resources Research* 40: 1–11.

Konrad, J.M., 2005. Estimation of the segregation potential of fine-grained soils using the frost heave response of two reference soils. *Canadian Geotechnical Journal* 42: 38–50.

Mottagy, D. & Rath, V., 2006. Latent heat effects in subsurface heat transport modeling and their impact on palaeotemperature reconstruction. *Geophysical Journal International* 164: 236–245.

Zhou, Y. & Zhou, G., 2010. Finite volume simulation for coupled moisture and heat transfer during soil freezing. *Chinese Journal of Geotechnical Engineering* 32: 440–446.

Panteleev, I.A., Kostina, A.A., Plekhov, O.A. & Levin, L. Yu., 2017. Numerical simulation of artificial ground freezing in a fluid-saturated rock mass with account for filtration and mechanical processes. *Sciences in Cold and Arid Regions*. 9: 363-377.

Simulation of Thermal Regime of Permafrost-Resistant Roads

Yury V. Ramanouski[1]
[1] *Simmakers Ltd., yuri.romanovsky@simmakers.com*

Abstract

Preservation of permafrost under roads, along with road de-icing/anti-icing, is considered. The suitability of so-called buried thermosyphons is discussed, and a sketch of numerical thermal analysis follows.

Keywords: permafrost roadbed, thaw subsidence, frost heave, black ice on roads, heat pump, numerical heat transfer.

Introduction

Deformation and failure of roads in permafrost regions

Roads on permafrost soils must be designed and constructed with the consideration of freeze-thaw damage. In Russia, where more than 60% of the area is covered by permafrost, road engineers choose between the 3 "principles" (methods of construction). Assume, "principle 1" is the choice. Then the road design includes artificial ground freezing (AGF). As a freezing system, one would use two-phase gravity thermosyphons.

Road slipperiness

For cold areas, in addition to the struggle with road damage from weather/climate changes, engineers aim to prevent the slipperiness caused by ice formations and snow deposits on road surface.

One of the measures against black ice, packed snow, etc., is heating road surface. As the experience of Alaskan engineers indicates (Goering, 2008; Xu & Goering, 2008; Long, 1993), the very thermosyphons can, to a certain extent, be adapted to provide such heating. For this, one needs to fully submerge the thermosyphons under the road surface, i.e. to bury their capacitors in the pavement. Since a pavement is too thin to contain a condenser, the thermosyphon needs to be bended or equipped with a flexible bellow, while the condenser should be inclined at a small angle (a positive gradient is necessary in order to let the cooling agent flow down). Thus, one obtains a system of buried thermosyphons that are passive heat pumps: the excess heat is transferred from the roadbed to the road surface.

Road anti-icing with thermosyphons

Using aboveground condensers would result in the loss of useful heat. In combination with AGF, this itself would be likely to contribute to the black ice formation. So one is forced to bury the thermosyphons anyway.

Unfortunately, the heat pumps self-start only when the temperature of the road surface is already below 0 ºC (32 ºF): it is necessary for a thermosyphon to operate that the condenser is in a slightly colder environment than the evaporator. Chemical anti-icing, even at low reagent concentration, lowers the freezing point of water and makes the discussed method of heating meaningful.

Calculating impact on road

Computational domain

In our simulations, we use a 3-dimensional domain with 2 transverse planes of symmetry and 1 longitudinal plane, which is a plane with a vertical axis of order-2 rotational symmetry. We neglect the fact that all these symmetries are, indeed, imperfect. The one remaining lateral boundary is far-field. The lower boundary is at the level of zero annual temperature amplitude, and the upper boundary passes along the exposed surface of the pavement, embankment and roadside.

Inner sources

Both evaporator and condenser can be treated as inner line sources. The sum of their heating powers is zero. If an explicit numerical method is used, the condenser heating power can be approximated by the evaporator cooling power at the previous time level. In turn, the evaporator cooling power depends on the temperature drop between the roadbed and pavement. One should also account for hydrostatic head effect that raises the boiling temperature of cooling agent.

We perform numerical thermal analysis of such inner sources, using the software package *Frost 3D Universal*®, which is specially designed to simulate the effect of thermosyphons on soils, groundwater and constructions.

Conclusions from numerical experiments

It is necessary to place a layer of thermal insulation into the bottom part of the road embankment. The thermosyphon part between the insulation layer and the pavement must be insulated, too. In that way, the heat supply, accumulated during the warm season, won't leak down from the pavement to roadbed.

Buried thermosyphons must be of advanced design (low thermal resistance, small lag on self-starting), and the quality of their installation (no air cavities) and charging (optimal kind and mass of cooling agent) must be pretty high.

References

Fedotov, G.A. & Pospelov, P.I., 2007. *Spravochnaya ehnciklopediya dorozhnika. Tom 5. Proektirovanie avtomobil'nyh dorog. [Highway Engineer's Reference Encyclopedia. Vol. 5. Design of Roads].* Moscow, 815 pp. (in Russian).

Russian Fed. Agency for Constr., 2013. *SP 34.13330.2012. Automobile roads.* Moscow, 107 pp. (in Russian).

Russian Min. of Constr., 2014. *SP 14.13330.2014. Construction in seismic areas*. Moscow, 125 pp. (in Russian).

Goering, D., 2008. Thompson Drive. In: Stevens, D.S.P. (ed.), *Guidebook to permafrost and Quaternary geology of the Fairbanks area, Alaska. Guidebook 11 (preliminary draft).* Fairbanks, Alaska, 1–4.

Xu, J. & Goering, D.J., 2008. Experimental validation of passive permafrost cooling systems. *Cold Regions Science and Technology*, 53(3): 283-297.

Long, E.L., 1993. *Method of and system for warming road surface.* Patent US5238053.

Engineering-Geocryological Mapping of the Republic of Sakha (Yakutia)

Alyona Shestakova[1,2]
Vladimir Spektor[1]
Yaroslav Torgovkin[1]
[1]*Melnikov Permafrost Institute SB RAS, Yakutsk, aashest@mail.ru*
[2]*North-Eastern Federal University in Yakutsk, Yakutsk*

Abstract

Engineering-geocryological zoning of the Republic of Sakha (Yakutia) was performed based on the analysis of the main factors controlling engineering-geocryological conditions in the region and their cartographic generalization. Zonation maps were compiled depicting topography (landforms), frost-related processes, soils and rocks, and geocryological conditions. Hydrogeological conditions and seismicity were described on schematic maps. Groups of engineering-geocryological conditions were ranked to classify areas by suitability for engineering activities.

Keywords: *Zoning; engineering-geocryological conditions; cryogenic processes; ground conditions; morphostructure; suprapermafrost water.*

The map of engineering-geocryological zoning of the Republic of Sakha (Yakutia) compiled in ArcGIS 10 is intended to provide information for the comprehensive evaluation of land-use and the planning of civil engineering works, including preliminary selection of transportation and communication routes, as well as for the assessment of geological hazards for mitigation and prevention. Engineering-geocryological zoning of Yakutia is particularly important and necessary in view of accelerated development of northern areas, including the Arctic. Compilation was based on the analysis and generalization of the main factors controlling geocryological conditions relevant for civil engineering practice. Engineering-geocryological conditions were studied to a depth of 10-20 m within which permafrost can influence or be influenced by the existing or new engineering work. This depth coincides with the zone of annual temperature variation in permafrost.

The following hierarchy of mapping taxons was used: Regions, Areas, and Districts. The mixed classification principle was selected, when each classification parameter was assigned with a different classification taxon. Regions, the highest taxons, were assigned to the largest land elements which determine the closely related *exogeneous (and permafrost) processes*. The second, lower taxonomic level – the Area – was used to depict the *soil and rock units*. The District taxon was used to show the geocryological characteristics of soils and rocks, viz. *temperature and ice content*, within the upper 10-20 m of the ground. Hydrogeological conditions and seismicity were depicted on complementary maps.

On the morphostructure scale, four regions are recognized within Yakutia. ***I. The Coastal Lowlands and Shallow Seashelf Region*** is the lowest-lying morphological feature (a negative morphostructure) distinctive in the present-day topography (Parfenov, 2001). The most hazardous processes in this region include thermokarst and wave erosion of the coasts composed predominantly of loess-like silts with peat interlayers. These materials are often more than 30-40 m in thickness. On the coasts, permafrost temperatures at the zero annual amplitude depth are often below -10°C. Thin discontinuous permafrost is likely in the shallow shelves. ***II. Central Siberian Plains and Plateaus –*** This region is characterized by a wide variety and medium intensity (Rank 2-3) of exogeneous (permafrost) processes. Karst is common in carbonate rocks. Surficial materials are also variable, with solid rocks in the plateaus and soils and soft rocks in the plains. In much of the region, permafrost temperatures at the depth of zero annual amplitude vary from -7° to -12°C. ***III. The Baikal-Stanovoy Region*** is characterized by high topography and recent tectonic activity responsible for widespread rock failures, including those induced by seismic activity, rock falls, slides and streams (Rank 4-5). Bedrock occurs at the surface in most of the region and consist of Archaean and Proterozoic crystalline rocks and subordinate Riphean and Paleozoic carbonate rocks. Intermontane depressions contain soft rocks of Mesozoic age. The region lies within the zone of discontinuous permafrost. ***IV. Verkhoyansk-Chukotka Region*** is dominated by mountains and thus rock falling and sliding are common processes here (Rank 4-5). Soft rocks are widespread with temperatures of -5°C or lower.

Acknowledgments

The work was supported by the Russian Foundation for Basic Research (project No. 17-05-41079).

References

Parfenov, L.M. (ed.), 2001. *Tectonics, Geodynamics and Metallogeny of the Republic of Sakha (Yakutia)*. Moscow: MAIK Nauka/Interperiodika, 571 pp.

Influence of urbanization on engineering properties of soils in the geocryological environment under climate change and technical loading

Dmitrii M. Shesternev
Melnikov Permafrost Institute SB RAS, Yakutsk 677010, Russia, shesdm@mail.ru

Abstract

This study examines the effects of urbanization on geocryological conditions in the southernmost permafrost zone of Russia, using the city of Chita as an example. Based on an integrated research methodology, urbanization stages are analyzed in synchrony with climatic variations during the 20th century, and the permafrost effects of urbanization are considered in detail taking into account the landscape-botanical and functional zones of the urban environment. Measures adapted to urban areas are proposed to control the interaction between engineering and natural environments within the natural-technical systems.

Keywords: southern permafrost zone; urbanization; natural environment; natural-technical system.

Introduction

Many distinguished scholars contributed to the understanding of the formation and dynamics of geological and geocryological environments for safe functioning of natural-technical systems (NTS). Fundamental and, in many respects, applied problems were investigated by E.M. Sergeev, V.T. Trofimov, P.I. Melnikov, V.P. Melnikov, V.A. Korolev, L.N. Khrustalev and many others who considered geological environment (GE) and geocryological environment (GCE) as integral parts of the natural environment. Their studies helped develop the methodological and methodical principles for urban GE and GCE studies, as well as gain a general understanding of the dynamics of engineering-geological and geocryological processes affecting the efficiency and ecological safety of NTS. However, our understanding of the dynamics and transformation of GE composition, structure, and properties in response to climate change and anthropogenic loading, as well as of the engineering and ecological effects of GCE changes in the urban areas of the southern permafrost zone is still inadequate.

Materials and methods

Materials for the writing of this work are given in the process of research within the Project of fundamental research of the Permafrost Institute ‘Cryogenic and physico-chemical processes of freezing and thawing ground, their impact on the formation and development of permafrost natural-technical systems in conditions of climate change and technogenic loading’; Government Natural Resources Ministry contract of Zabaykalsky region ‘Geological environmental studies in the Chita area with the purpose of anthropogenic impact estimation on the environment’, Fiscal topics of Transbaikal State University ‘Anthropogenic impact estimation on the geo-ecological conditions of the urbanized areas of southern permafrost (by the example of Chita)’ and ‘Anthropogenic impact estimation on the geological environment of the urbanized areas of southern permafrost in conditions of global climate change (by the example of Chita)’.

The main research methods were theoretical, experimental (laboratory and natural) and cameral methods. Application of theoretical methods was directed on establishment of change regularities of GCS and their impact on the NTS elements, experimental – on the obtaining of the quantitative and qualitative information characterizing structure changes, a structure and GCS properties, cameral - on drawing up the GCS cartographical models in the urbanized Chita area.

Elaboration and assessment of the accuracy (reliability) of results of long-term experimental studies were carried out with usage of modern computer aids, were based on the application of theoretical fundamentals of mathematical massive statistics of the engineering-geological, geocryological and hydrogeological information made by results of monitoring research of environment change in the urbanized area (Shesternev, 2011; Shesternev, Vasyutich, 2015).

Results and discussion

The orientation of parameters change of GCS structure in the course of areas urbanization is caused by integral impact of natural climate change and influence on geocryological conditions of technical loading. Allocated three stages of various intensity urbanization which time is synchronized with three periods of climate change towards its warming, caused since 1890 and until the present reduction of GCS area according from 70-80 to 20-30%, and thickness – from 30-50 to 5-10 m.

The first urbanization phase lasted 36 years (1890-1926). It began with the construction of the Trans-Siberian Railway and ended with the beginning of operation of first natural-technical systems (NTS), namely, "Railway shops of Chita" and "Chernovsk mines".

The second stage (1926-1960) is characterized by the beginning of a large-scale development of Chita and building of low-rises. The population of the city during this period grew to 170 000 people. During this period, residential, industrial, recreational, agricultural zones and transport connections within the city (natural auto-roads) were formed.

The third stage of urbanization (1960-present) is divided into two periods on a background of intensive increase in annual average air temperatures and precipitation amount. The first one (1960-1995) was characterized by a rapid growth of extensively developing industrial and residential zones. The second one (1995-present) was notable for an almost complete stagnation of industrial zone functioning, except a heat and power complex, and increase in density and number of stories of new and already existing residential built-up areas.

The efficiency of NTS operation and environmental safety in urban areas of southern permafrost regions can be reached by engineering-geological monitoring taking into account climate change and man-induced loads.

A theoretical basis for control of changes in permafrost conditions was developed by Kudryavtsev and Yershov (1969). Technical solutions are widely used for the efficient operation of linear structures within the southern permafrost region. Taking into account these works, a complex of measures regulating heat exchange in the NTS of the urbanized areas was developed. The first group of measures regulates the external heat exchange in the geocryological environment by changes in parameters of the radiation-thermal balance. This group includes two systems of measures: measures affecting the proportion of ingredients for radiation balance, and measures affecting the heat balance. The second group of measures is used to control heat exchange in geocryological environment changing the composition and properties of its soils. The recommended measures allow changing the composition of organic-mineral soils, their moisture conditions and regulating soil heat and mass exchange by changing the soil properties and thermal conditions without significant changes in their material composition. The third group of measures is oriented to transform soils of the geocryological environment using additional natural and artificial heat sources and heat sinks.

Conclusions

Thus, the research conducted made it possible to solve an actual research and practice task concerning the identification and estimation of urbanization and global climate change impacts on changes in geocryological environment of the southern part of the permafrost region. As a result:

1. The urbanization stages of different intensity have been identified, the duration of which was synchronized with periods of climate warming. Geocryological conditions of each stage and parameter change in structure of the geocryological environment have been analyzed and established.

2. The impact of key environmental factors on temperature and thickness formation of the seasonally thawed and seasonally frozen soil layers at different stages of urbanization has been estimated. Reduction of permafrost area from 70% to 15-20% has been registered. In the areas where it was characterized by a continuous development type is currently presented by a residual thaw layer, i.e. the seasonally thawed later of geocryological environment soil had transformed to a seasonally frozen type.

3. Specific features of structure and properties of the geocryological environment within the functional zones of Chita have been established according to types and technologies of functioning natural-technical systems. The control techniques of engineering-geocryological processes in urbanized areas of the southern permafrost region have been adapted.

References

Kudryavtsev, V.A. & Ershov, E.D, 1969. Principles of permafrost processes control. In: *Permafrost Research*, issue IX. Moscow State University, Moscow, 147-158.

Shesternev, D.M, 2011. Basic principles of geocryological monitoring at linear structures (with reference to the Berkakit-Tommot-Yakutsk Railway). In: Zhang, R.V.(ed). *Permafrost Engineering, Proceedings of the IX International Symposium*, Mirny, Russia, 3-7 September 2011: 253-260.

Shesternev, D.M. & Vasyutich, L.A., 2015. *Influence of urbanization on environment of Central Trans-Baikal: monograph*. Chita: Transbaikal State University, 195 pp.

Fundamental study on formation process of closed-system pingo

Ryoko Shiratori[1],
Shunji Kanie[2], Zheng Hao[2]
[1] *Graduate School of Engineering, Hokkaido University, Sapporo, Japan, rshiratori@eis.hokudai.ac.jp*
[2] *Faculty of Engineering, Hokkaido University, Sapporo, Japan*

Abstract

Topographical deformation may be caused by the climate change for the coming tens of years, and it is a duty of human beings to secure the sustainability in cold regions. One of the topographical features in permafrost is pingo, known as a mound of earth-covered ice. Although the formation process of pingo has already been explained conceptionally, physical and numerical model for the process has not yet been established. The authors focus on closed-system pingo to reveal the physical formation process through experiments with some numerical models. The purpose of this study is to discuss the fundamental conditions in environment where a closed-system pingo is formed. As our first step of the study, we introduced a very simple model with methylene blue solution, and investigated the difference in the shape of pingo by changing the environmental conditions of circumstances as well as the aspect ratio of freezing zone.

Keywords: Closed-system Pingo; Permafrost; Talik; Convection; Insulation; Aspect ratio

1. Introduction

Pingo is a mound of earth-covered ice and there are two different types of those; an open-system pingo and a closed-system pingo. Open-system pingo develops when hydraulic pressure in underground induces inflation of the ground due to freezing. On the other hand, closed-system pingo occurs when permafrost is aggrading in a water-saturated foundation, and numerous closed-system pingos in the Mackenzie Delta have developed in rapidly drained lake beds (Mackay, 1973, 1979). Closed-system pingo appears more commonly and more frequently than open-system pingo due to their geographical location (Yoshikawa K, 2013). The diameter and the height of closed-system pingo depend on the size of original talik, a saturated but unfrozen zone (Pissart and French, 1976). The authors introduced a simple model with methylene blue solution, and investigated the difference in the shape of pingo by changing the environmental conditions as well as the aspect ratio of freezing zone.

2. Geological Setting

In advance of the experiment, we referred to Ibyuk Pingo, one of the largest pingos in the world located south of Tuktoyatuk (Mackay, 1986). This closed-system pingo (Fig. 1) has 49 m in height and 300 m in diameter. The highest peak is growing at a constant rate of about 2.3 cm/yr. Ibyuk Pingo is in an area where the mean annual air temperature is about -11 ^{o}C, the mean annual ground temperature is about -8 ^{o}C, and undisturbed permafrost is located about 500 m or more in depth (Mackay, 1979).

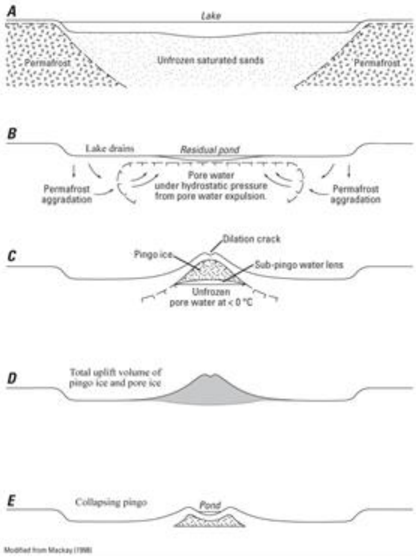

Figure 1. Illustrating the growing process of Ibyuk pingo. a) A lake existed on a basin of the saturated unfrozen sand. b) Pore water is pushed while freezing process. c) The formation of the pingo ice. d) Water necessary for growth of pingo is served though a neighboring pores. e) The fusion and the reservoir in summer. Photocopied from Mackay, J.R., [1973].

3. Experiments

3.1. Experimental method and conditions

We modeled a cylindrical talik, an unfrozen zone with the height of 150 mm and the diameter of 90 mm, filled with methylene blue solution as shown in Figure 2. The surrounding boundaries except for the top is chilled by the existing permafrost at the temperature of -10 °C. On the contrary, we put insulation of Styrofoam balls at the top boundary imitating a moss and vegetation layer. The unfrozen talik starts to freeze from the boundaries, and unfrozen portion visualized by methylene blue is confined inside of the talik. A mound of ice gradually grows with disappearance of the unfrozen part.

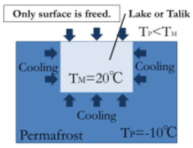

Figure 2. Cooling imitation

Figure3. Before freezing

Figure4. During freezing

3.2. *Result*

Figure 5 shows an example of a mound shape measured by contour gauge after the freezing process. In this case, a crack was found at the top similarly to Mackay model (Fig. 1). It is confirmed that the boundary conditions including insulation at the top influence on the shape of the mound as well as the aspect ratio of talik.

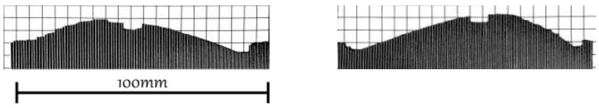

(a) X-direction (b) Y-direction

Figure 5. Formation of Pingo with indoor experiment

4. Numerical Analysis

4.1. *Effect of insulation*

In order to examine the environmental effects, we introduced an axis-symmetric FEM model to observe the temperature distribution within the talik. Figure 6 shows temperature distributions with/without insulation at the top As shown in the figure, the shapes of unfrozen portion are different to each other, and the difference causes the shape of the mound, for example.

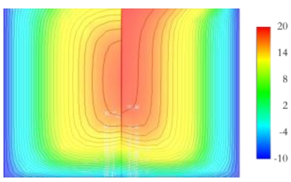

Figure 6. Temperature distribution for time change (+/-)

4.2. *Influence of Aspect Ratio*

The authors speculate that the aspect ratio of the specimen is another important factor for the formation of pingo. Figure 7 is a conceptional drawing to show the relation between the maximum height of pingo and the aspect ratio. If one anticipates the maximum value in height, some suitable value may exist as the aspect ratio. We are investigating the influence of aspect ratio on the shape of pingo by experiments as well as simulations.

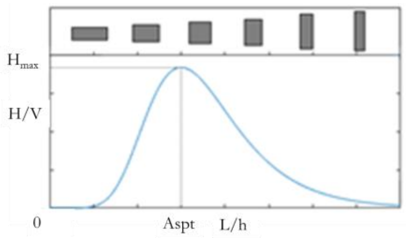

Figure 7. Anticipation Moderate Aspect Ratio

5. Summary and Future Research

The formation process of closed-system pingo was observed by indoor experiments using methylene blue solution, and it is confirmed that the boundary conditions surrounding the talik decides the shape of pingo as Mackay proposed. For the establishment of the physical model, however, we have to improve the experimental models using saturated soil foundation as well as the numerical simulation. Coupling a heat transfer analysis with a mechanical inflation model is one of the numerical solutions, for example.

By understanding the physical phenomenon in the formation of closed-system pingo, it becomes very helpful to preserve pingos in cold regions as well as its great natural environment.

References

Mackay, J.Ross. (1986). Growth of Ibyuk Pingo, Western Arctic Coast, Canada, and some implications for environmental reconstructions. Quaternary Research (Vol. 26), 68-80.

Mackay, J.Ross. (1973). The Growth of Pingos, Western Arctic Coast, Canada. Canadian Journal of Earth Sciences (Vol. 10), 979-1004.

Mackay, J.Ross (1979). Pingos of the Tuktoyaktuk Peninsula Area, Northwest Territories. Géographie physique et Quaternaire (Vol. 33), 3-61.

Pissart, A and French, H.M. (1976). Pingo investigations, north-central Banks Island,

Canadian Arctic. Canadian Journal of Earth Sciences, 937-946.

Yoshikawa, K. (2013). Treatise on Geomorphology. Reference Module in Earth Systems and Environmental Sciences (Vol. 8), 274-297.

Forecast calculation of temperature fields in grounds of the foundation of linear constructions by the example of the Bovanenkovo-Ukhta gas pipeline site

Aleksandra Sibiryakova[1]
Oleg Podchasov[2]
[1]*Lomonosov Moscow State University, Geological department, tigrenock_@mail.ru*
[2]*Lomonosov Moscow State University, Geological department*

Abstract

The aim of the research is to construct temperature fields in a cofferdam body to obtain a qualitative forecast of the conduction of frozen soils around a pipeline for 50 years, with taking into account temperature trends.

Keywords: temperature fields, forecast calculation, gas pipeline exploitation, permafrost, geophysical research

This research is devoted to the temperature fields calculation round the Bovanenkovo-Ukhta gas pipeline (Baydaratskaya Bay), put on operation in 2014.

Baydaratskaya Bay located in the southern part of the Kara Sea between the coastline of Ural coastline and Yamal Peninsula. It is one of the most largest bays of the Kara sea. It is streched from a north-west on a southeast. The length of the gulf is approximately 180 km, mouth width – 78 km, depth – up to 20 m.

The research site is located ashore of the Baydaratskaya Bay (Fig.1) within the boundaries:

NW 68° 51' 13,87" N, 66° 54' 8,79" E;

SW 68° 51' 5,47" N, 66° 54' 2,32" E;

NE 68° 50' 59,94" N, 66° 55' 33,11" E;

SE 68° 50' 51,87" N, 66° 55' 15,13" E.

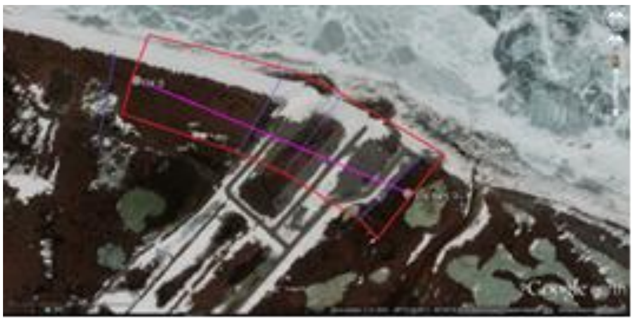

Figure 1. Research site (Google maps)

The relevance of the work lies in necessity of long-term exploitation of the gas pipeline. Ltd. "Gazprom" forms a fundamentally new gas production center on the Yamal, which in future will be a key for the development of the domestic gas industry. Pipeline route cross throughout the bottom of Baidaratskaya Bay – Gulf of the Kara Sea, a large part of the year covered by ice. In the construction, was used steel pipes encased in concrete with a diameter of 1219 mm, estimate for a pressure of 120 atm. The installation of gas pipelines with such technical parameters in conditions of permafrost under the arctic sea water and ice was carried out for the first time in the world. The necessity of the research can be confirmed by the fact that the scope of this pipeline has no analogues in the world exploitation of gas complex facilities. The uniqueness of the cryogenic structure lies in the continuous distribution of low-temperature saline permafrost with the upper part of the section. At the same time, this region is characterized by inclusions of gas and gas hydrate clusters, gas manifestations practically along the whole section of the cryogenic stratum (Badu et al., 2013).

The aim of the research is to construct temperature fields in the cofferdam body to obtain a qualitative forecast of the conduction of frozen soils around the pipeline for 50 years, with taking into account temperature trends. The simulation produced in the program developed at the Department of Geocryology of the Moscow State University (Fig. 2). The data for the predictions are taken from the reports of "Gazprom VNIIGAZ" for the year 2017 and Ltd. "Piter Gaz", and also collected by author during the field work on the Baidaratskaya Bay in September 2017.

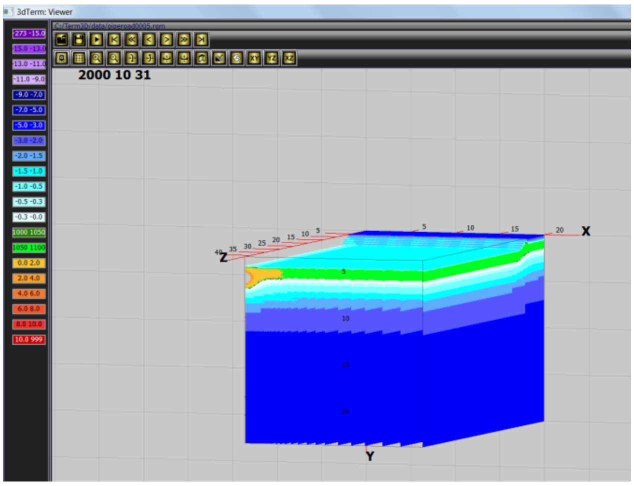

Figure 2. The model of temperature fields distribution in the body of a cofferdam

Besides, in 2017 research group of MSU students and field teachers have received geophysical data by the electrotomography method for five profiles, four ones were located within the site, and the fifth was situated along the parametric temperature boreholes in 500 meters out the north border of the area.

Author suggests the correlation of the above data with the temperature field modeling.

Comparison of the results obtained by complex methods get to researchers the ability to substantiate the forecast of the permafrost change under technogenic invasion.

Reference

Badu, Yu.B., Gafarov, N.A., Podborny, E.E., 2013. *Cryosphere of oil and gas condensate site of Yamal peninsula. Moscow:* JSC "Gazprom expo", v.2, 424 pp.

Early self-stabilization conditions of a retrogressive thaw slump, North Slope, Alaska

Eva Stephani[1, 2]
Mikhail Kanevskiy[2]
Margaret M Darrow[2]
Peppi Croft[3]
Jeremiah Drage[4]
Frank Wuttig[5]

[1]*Alaska Science Center, U.S. Geological Survey, Anchorage, Alaska, USA, estephani@usgs.gov*
[2]*Institute of Northern Engineering, University of Alaska Fairbanks, Fairbanks, Alaska, USA*
[3]*Shannon & Wilson Inc., Fairbanks, Alaska, USA*
[4]*Golder Associates Inc., Anchorage, Alaska, USA*
[5]*Alyeska Pipeline Service Company, Fairbanks, Alaska, USA*

Abstract

In 2017, we assessed climatic, surface, and subsurface conditions of a self-stabilizing retrogressive thaw slump (RTS) along the Trans-Alaska Pipeline System on the Alaska's North Slope. The RTS had walls sloping at 18-20° partially covered by vegetation. Average thaw depth in the RTS decreased by ~1.4 m between 2015 and 2017; we explained this by the fast accumulation of thawed and retransported soils that terminated active thermokarst development. However, seasonal thaw reached the top of ice wedges in some upper slope areas, suggesting that in August 2017 these zones were still actively degrading. We identified two generations of ice wedges; modern ice wedges, which have thawed completely within the RTS (except the upper slopes) and old ice wedges, which have degraded only partially within the RTS and are now protected by a layer of thawed, retransported, and refrozen soils. We distinguished seven stages of degradation and stabilization of the RTS.

Keywords: Monitoring; Ice wedge; Cryostratigraphy; Feedback effects; Linear infrastructure; Mitigation.

Introduction

While many studies have focused on the development of retrogressive thaw slumps (RTSs), the processes of their self-stabilization remain largely unstudied. Typically, stabilization occurs when there is no more ground ice to melt or when the low-angle footslope covers the ice-rich material (Burn & Lewkowicz, 1990); however, the self-stabilization mechanisms may be more complex, incorporating the interaction of local climate, surface, and subsurface conditions. In June 2015, Alyeska Pipeline Service Company (APSC) personnel made an initial assessment of an actively developing RTS along the Trans Alaska Pipeline System (TAPS) (North Slope, Alaska) that subsequently started to self-stabilize. In 2017, we assessed the climatic, surface, and subsurface conditions with the goal of better understanding RTS self-stabilization and, ultimately, developing adapted mitigation measures for affected infrastructure. Here we present the preliminary results.

Methods

We acquired air temperature data (2012–2016) from Sagwon station, located ~40 km north of the study site. In June 2015, APSC personnel probed thaw depths within the RTS (n=12). In early August 2017, we assessed local surface and subsurface conditions by: probing thaw depths (n=297); drilling with handheld coring tools (up to 5.2-m deep) on the RTS floor (n=5), slopes (n=6), and undisturbed surface (n=9); and mapping the RTS topography (n=562) and terrain conditions with a differential GPS (DGPS). We described permafrost soils and ground ice according to the methods of cryostratigraphy. We installed monitoring instrumentation, including: two digital temperature cables with telemetry, six snow depth poles, and a real-time camera. We developed a digital elevation model and thaw depth maps using kriging interpolation. We integrated data into a GIS, including high-resolution imagery to assess the RTS changes through time.

Results and discussion

In 2017, the RTS was ~1,400 m² and consisted of two coalescing lobes along the edge of the TAPS work pad. Its overall depth below the surrounding terrain was ~4.2 m, with walls sloping at 18–20°. As the overall terrain slopes towards the northwest and the pad embankment intercepts local drainage, the RTS collects surface water coming from the east and southeast. We observed ponded water at several locations on the RTS floor, and along the nearby work pad embankment, including perennial ponds identified on multiple high-resolution images. After a day of heavy rain in the field in August 2017, we also observed water flowing from the headscarp. None of the massive ice exposed in the headscarp in 2015–2016 was visible in 2017; instead, the slopes consisted of tilted soil blocks covered with broken vegetation. We observed numerous cracks.

The average thaw depth in the RTS in 2017 was 0.64 m (Fig. 1), compared to 2.07 m in 2015; the actual decrease was likely greater since measurements in 2015 were done earlier in the summer. We explain this active layer decrease primary by a significant rise of the permafrost table that followed fast accumulation of thawed and retransported soils. Average air temperatures in September–December 2015, were consistently below the 2002–2016 average. These colder air temperatures, occurring while there was no or little snow coverage, may have contributed to freeze-back of the active layer.

In late August 2017 (~19 days after drilling), the ground temperatures measured at 2 m below the ground surface within the RTS and undisturbed tundra surface were both ~−2°C, while the near-surface temperatures within the RTS, measured below ponded water, were warmer by up to ~2°C.

Field analysis of permafrost cores indicated the presence of ice wedges, although there were no troughs visible from the surface. Soils surrounding the ice wedges were mainly silts with some gravel. We observed gravel, cobbles and small boulders at the surface and in tension cracks around the RTS. We recognized wedge ice in boreholes at different elevations, indicating that the ice wedges were at least 8-m deep. We identified two generations of ice wedges: small moderately active modern ice wedges that develop in the intermediate layer (IL) of the upper permafrost, and large syngenetic ice wedges (presumably late Pleistocene) overlain by the IL. Vulnerability of ice wedges to thermokarst strongly depends on thickness of the frozen protective layer (PL) above them (Kanevskiy *et al.*, 2017). Within the undisturbed surface, modern ice wedges were protected from thawing by a ~0.20-0.25-m thick PL, which included the frozen part of the active layer, the transient layer, and modern IL. Thickness of the IL above old buried ice wedges presumably varied from 0.5 to 1.5 m.

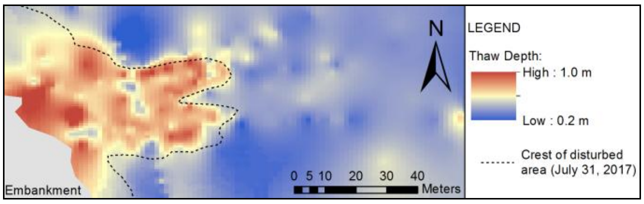

Figure 1. Thaw depth map.

Within the RTS, modern ice wedges were completely thawed (except the upper slopes) while old ice wedges were only partially degraded. We could not reach the bottom boundary of the ice wedges with host soils in any of our boreholes, including in one 5.2-m deep borehole drilled from the RTS floor. During the drilling, we encountered only three locations on the upper RTS slopes where ice-rich permafrost was degrading in early August 2017. Within the lower slopes and RTS floor, a 0.2–0.7-m thick layer of thawed, retransported, and refrozen soils protected the ice-rich permafrost containing the large and older ice wedges.

We distinguished the following stages of degradation and stabilization of RTSs: 1) undisturbed surface, where ice-rich permafrost is protected by the frozen PL; 2 to 4) degradation with high, medium, and low retreat rates that depend on thickness of thawing soil above ice-rich permafrost; and 5 to 7) initial, advanced, and progressive stabilization that are defined by thickness of the frozen PL above ice-rich permafrost and RTS re-vegetation stage. Usually several stages exist simultaneously within the same RTS, except for a very short period of initial degradation.

We will continue to monitor, conduct change detection analysis, and determine the soil properties of the cryostratigraphic units to assess the feedbacks controlling RTS self-stabilization.

Acknowledgements

The authors thank the APSC, U.S. Geological Survey, and Transport Canada for their support.

References

Burn, C.R. & Lewkowicz, A.G., 1990. Canadian landforms examples - 17 Retrogressive thaw slumps. *The Canadian Geographer* 34(3): 273-276.

Kanevskiy, M., Shur, Y., Jorgenson, T., Brown, D.R.N., Moskalenko, N.G., Brown, J., Walker, D.A., Raynolds, M.K., and Buchhorn, M. 2017. Degradation and stabilization of ice wedges: Implications for assessing risk of thermokarst in northern Alaska. *Geomorphology* 297: 20-42.

Towards Circumpolar Assessment of Climate Change Impacts on Population and Infrastructure in Arctic Permafrost Regions

Dmitry Streletskiy[1], Luis Suter[1], Nikolay Shiklomanov[1]
[1]The George Washington University, Department of Geography, Washington, D.C., USA; *strelets@gwu.edu*

Abstract

Climate change has been having profound impacts across the Arctic regions. While most studies focus on the impacts of climate change on natural systems, there are substantial impacts expected on human systems, particularly infrastructure. This study uses six CMIP5 models under RCP8.5 scenario to project climate change and its impact on various type of infrastructure in Arctic permafrost regions. The analysis provides estimates on the population, amount, and value of infrastructure at risk by climate-change. By providing estimates of the cost and spatial distribution of climate-change impacts, this study hopes to provide a metric of climate-change that will resonate with policymakers, the public, and business communities.

Keywords: permafrost, infrastructure, climate change, cost of permafrost degradation

Introduction

Permafrost degradation was observed and projected to continue in the Arctic regions. Changes in permafrost are exacerbated in areas of economic activity, such as settlements, extraction industries and transportation hubs. Few studies attempted to evaluate the cost of climate-change Arctic infrastructure (Melvin et al., 2017). Moreover, there have been no assessments available of the economic costs of changing permafrost conditions at the circumpolar scale. The goal of this research is to provide assessments of the impacts of changing climatic conditions on infrastructure built on permafrost across the Arctic countries in order to facilitate mitigation and adaptation strategies and promote sustainable development in the Arctic region.

Data and Methods

The study area was defined as permafrost areas above 60° north. Six CMIP5 models were used to estimate changes in the historic and projected climatic conditions under the RCP8.5 scenario (Shiklomanov et al., 2017). Daily temperatures and precipitation for the 1970 (historic), 2010 (present), and 2050 (future) periods were used as forcing to a permafrost-geotechnical model to estimate permafrost temperature and active layer thickness, freeze-thaw cycles, thaw subsidence, and bearing capacity within each grid cell (Streletskiy et al., 2012). Other variables in the analysis included surface ground temperature, snow cover depth, duration of cold and warm periods, winter road operability, and the duration of heating periods. Publicly available geospatial datasets on various types of infrastructure (ports/airports, roads, pipelines, railways, settlements) and population were used to estimate the extent of areas where projected climate-change and changes in permafrost characteristics would have the most profound impacts on human systems. Infrastructure construction cost data were used to estimate the capital value of existing Arctic infrastructure, and infrastructure at risk to future climate-change impacts.

Results and Discussion

~7.3 million people live in the permafrost regions of the study area. The number of settlements is estimated to be 311, with sizes ranging from small indigenous villages to large industrial cities of more than 100,000 people. An extensive infrastructure network, including 59 ports and 328 airports, serves these cities.

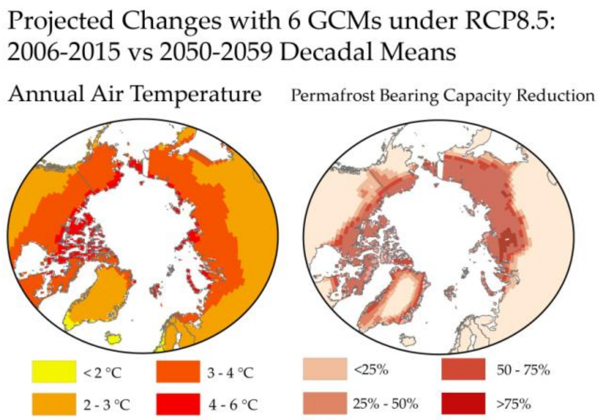

Figure 1: Projected changes in air temperature and corresponding changes in bearing capacity based on ensemble of six CMIP5 projections under RCP8.5 scenario for the Arctic regions.

While many regions in the study area rely on winter roads, there are also 30,182 km of permanent roads, 6,595 km of railroads, and 11,375 km of pipelines built on permafrost. Of this, 3,990 km of railroad and pipelines are built on ice-rich permafrost. The total capital cost of this infrastructure is conservatively estimated to be 207.7 billion USD.

Projected climate-change will affect this infrastructure, especially in Alaska and Russia (Figure 1) where projected increases in temperature and precipitation are collocated with the regions of intensive economic activity. These activities are largely based on extractive industries and depend on reliable transportation networks to bring the products to consumers outside of the Arctic regions. The value of transport infrastructure at risk is estimated to be over 5 billion USD across the Arctic region.

Summary

Under the RCP8.5 scenario, significant amounts of Arctic infrastructure will be impacted by climate-change by 2050. Knowledge about the distribution and cost of climate-change impacts on infrastructure will facilitate policymakers and businesses in planning for future climate scenarios.

Acknowledgments

The study was supported by the NSF grants PLR-1231294, ICER-1558389, OISE-1545913 to The George Washington University.

References

Melvin, A.M., Larsen, P., Boehlert, B., Neumann, J.E., Chinowsky, P., Espinet, X., Martinich, J., Baumann, M.S., Rennels, L., Bothner, A. and Nicolsky, D.J. 2017. Climate change damages to Alaska public infrastructure and the economics of proactive adaptation. Proceedings of the National Academy of Sciences (PNAS) 114(2), p.201611056.

Shiklomanov, N. I., Streletskiy, D. A., Swales, T. B. and Kokorev, V. A. 2017. Climate Change and Stability of Urban Infrastructure in Russian Permafrost Regions: Prognostic Assessment based on GCM Climate Projections. Geographical Review 107(1), 125-142. doi:10.1111/gere.12214

Streletskiy, D.A., Shiklomanov N.I., Nelson F.E. 2012. Permafrost, infrastructure and climate change: A GIS-based landscape approach to geotechnical modeling. Arctic, Antarctic and Alpine Research, 44(3), 368-380. DOI:10.1657/1938-4246-44.3.368.

Newtok Village Relocation Project – A Geotechnical and Permafrost Engineering Perspective of the New Village Site at Mertarvik

John Thornley [1]
Brenton Savikko[2]
Thomas Krzewinski[2]
Gavin Dixon[3]
Joe Hess[3]
[1]*Golder Associates Inc., john_thornley@golder.com*
[2]*Golder Associates Inc.*
[3]*Alaska Native Tribal Health Consortium*

Abstract

Over the past several decades, efforts have been focused on identifying and developing a new village location for the village of Newtok. Newtok has suffered from continued land loss, at a rate of 25 to 30 meters a year, due to loss of permafrost and erosion of the coast and has identified a new location to move the village. The new location, named Mertarvik, is located across the river from the Newtok site and offers higher ground, space for a new airport, and groundwater to accommodate the village. Recent geotechnical studies have found Mertarvik to have areas of warm, discontinuous permafrost and variable soils. Development impacts on the warm, discontinuous permafrost is a risk being considered in the engineering design of new infrastructure related to the village relocation.

Keywords: Village Relocation; Discontinuous Permafrost, Warming Permafrost.

Introduction

Numerous geotechnical studies have occurred throughout the proposed village of Mertarvik since the Newtok Traditional Council decided to relocate the village in 1994 (USACE, 2008). Concern related to the future loss of water supply and erosion due to permafrost degradation have hastened the need for this relocation. Currently, limited infrastructure exists in Mertarvik (Fig. 1) including a groundwater well and several structures. Proposed infrastructure includes roads, houses, an airport, fuel farm, water storage and distribution systems, landfill, and other related facilities. Geotechnical explorations have consisted of advancing boreholes and test pits to observe and sample the subsurface condition at proposed infrastructure sites. The results from the geotechnical explorations have been used by project planners and designers to help identify and refine locations for the proposed infrastructure. In addition, surface geophysics have been used to identify groundwater locations, and is being proposed for further refinement of the geotechnical variability, including warm permafrost extents.

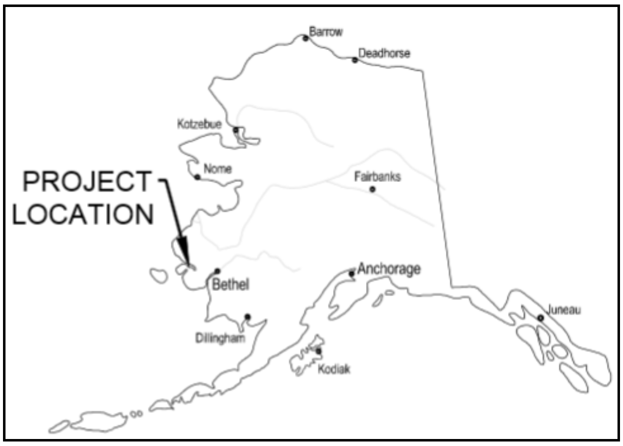

Figure 1: Project Location

Subsurface Conditions

Subsurface conditions encountered in the geotechnical explorations have varied significantly throughout the proposed community. Discontinuous permafrost was observed sporadically throughout the community, and included visible and non-visible ice within samples. In some locations, visible ice content in the samples was estimated to be as high as 50% by volume. Where measured, ground temperatures of permafrost were generally within ±1°C of 0°C (Fig. 2). Both permafrost and non-permafrost soils typically classified as frost susceptible material, with a mixture of gravel, sand, and silt present. Basalt bedrock is present in the community, but the surface is often variable and ranges from several meters below ground surface to over 10 meters below ground surface.

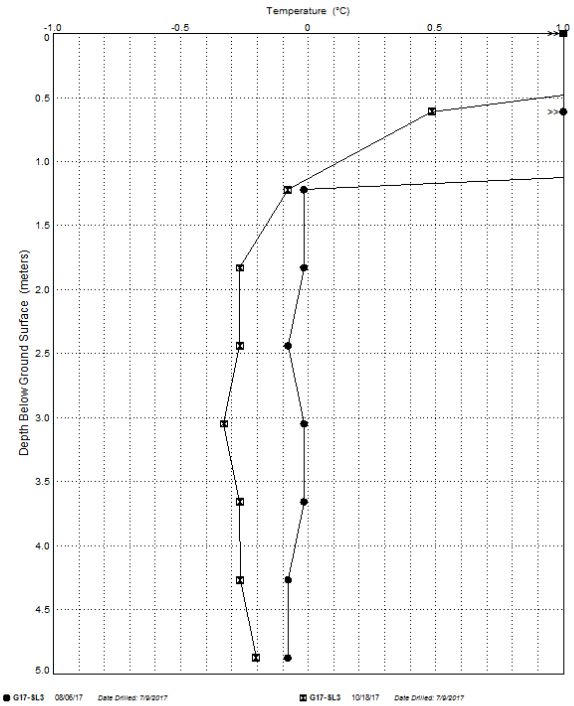

Figure 2: Example ground temperature plot displaying warm permafrost conditions. (Golder, 2017)

Project Planning

Long-term warming trends are predicted in the region, and it is anticipated that the permafrost in the community will continue to degrade with time, both from climate impacts and anthropogenic effects of the development of the community. The variability of subsurface thermal and soil conditions across the community present numerous geotechnical hazards and potential risks to the proposed infrastructure.

Project planners and designers have recognized the risk associated with the variable subsurface conditions in the project area. Geotechnical exploration findings have been considered and used to help refine site selection for critical infrastructure. An example is the proposed bulk fuel facility. The subsurface conditions encountered in the originally proposed location consisted of warm, ice rich silt. Additional sites were selected and further geotechnical explorations were conducted. The sites were ranked by geotechnical risk, and planners and designers used the information to help select a site that balanced geotechnical risk and other functions necessary for the facility.

Proposed Airport Exploration

As part of the development of the new village location, an airport runway, taxiway, and supporting infrastructure have also been evaluated. Because of the remote nature of the community, and lack of roads to much of western Alaska, airports are vital infrastructure. The findings from geotechnical exploration along the alignment have identified areas of ice-rich permafrost, which, if allowed to degrade, will cause continued need for maintenance over the life of the runway. Other airports in the region have experienced these issues and the goal is to provide improved recommendations that will reduce impacts to the underlying permafrost.

Future Subsurface Explorations

The geotechnical data collected to date has shown that highly variable subsurface conditions exist in the community. To reduce the uncertainty in subsurface conditions and limit geotechnical risk, geophysical studies are being considered in the community. Geophysical studies including ground-penetrating radar (GPR) and electromagnetic (EM) methods, combined with the existing data from geotechnical boreholes and test pits, can help identify areas of discontinuous permafrost, among other things, which can help planners and designers make more informed decisions on site selection and designs for critical infrastructure.

Acknowledgments

The authors would like to acknowledge the support provided from the elders and residents of Newtok, especially Romy Cadiente. The authors also would like to acknowledge the support of the team of field staff out collecting the field data, ANTHC representatives and support staff, and the support from the Alaska Department of Transportation and Public Facilities.

References

Golder Associates Inc., 2017. Mertarvik Geotechnical Exploration. *Draft Geotechnical Exploration Data Report*. Golder Project Number 1775079, November 2, 2017.

U.S. Army Corps of Engineers Alaska District (USACE), 2008. Mertarvik Townsite Newtok, Alaska. *Geotechnical Report*. February 2008.

Investigations of the thermoerosion process on the Tazovskiy peninsula, north of Siberia

Tolmanov Vasily A.[1]
Grebenets Valery I. [1]
Kurbatov Aleksey S.[2]
[1]*Moscow State University, Geographical faculty, Department of Cryoliyology and Glaciology*
[2] *OOO "Gazprom Dobycha Yamburg"*

Abstract

Cryogenic processes significantly affect the reliability of the northern infrastructure. The most dangerous are the processes of thermoerosion. Thermoerosion is the process of destruction of the banks or ground massives constructed by the permafrost and ground ice, by thermal and mechanical influence of the running water (Pashkin and oth., 2011; L.Duperayt et al., 2011). Tazovskiy peninsula, where the largest gas production facilities are located, is referred in Russia as "The kingdom of the thermoerosion".

Keywords: Permafrost, dangerous cryogenic processes, thermoerosion, engineering

Introduction

The geodetical level of the surface on Tazovskiy peninsula varies between 15–20 m. and 60–80 m, but the thermoerosion processes are very active. The area exposed to thermoerosion was 10–15% of the territory in the beginning of 1980th.

Tazovskiy peninsula is characterized by cold winter and short cool summer. The period of the maximum active layer thaw (ALT) is in August, when the precipitation amount is the highest, which results in the ground destruction. According to the IPCC analysis (IPCC, 2014) the trend of the temperature raise is 0.8°C/10 years. Thus, the climatic conditions and their trends lead to activation of thermoerosion.

The territory corresponds to the continuous permafrost area with the recent depth of 300–400 m. The background temperature at the depth of zero temperature amplitude was −3 –−5°Cin 1970–80th, but in recent time our observations show the temperature increase. The sediments at the surface are the upper Quaternary silty iced (the volumetric ice is up to 40–60%) sands or sandy loams. The main feature of the sediments is high level of blurring. Wide areas are formed by iced peatlands (2–3 m of depth) with polygonal ice systems serving as the positions of the future theroerosion cuts.

The active snowmelt in May–beginning of June together with increasing snowiness of the Winters also increases the processes of gullies formation. The conducted field works during the snowmelt revealed lumpy collapsing of the big ground blocks near the lateral sides of the watercourses. The blocks remained frozen, the rate of the lateral erosion was 15–20 cm/per day, the widths of the separate blocks were 1.5–2 m.

In 2000 in the central part of the peninsula on the right side of the r. Ngarka-Poylovoyaha an observed gully was 1 m depth and 1 m width. In 2006 the width of the same gully was 13 m., its depth was 5m and the length was more than 120 m. In 2009 – 19 m, 7 m and 130 m respectively; the gully was branched out. This gully (Fig. 1) was rapidly-growing, finally became the erosion-blurring complex jeopardizing the gas field infrastructure, and in 2014/15 it was filled up.

Fig. 1. Evolution of the thermoerosion system near Ngarka-Poylovoyaha river

The rate of the gully growing on the right side of the r. Nyudya-Adlyurdyepoka was up to 10 meters per year. The length of the gully was 60 m in 2006 and it was V-shaped, though in the middle of the gully the edges erosion exceeded the bottom one and t had U-shape in there. In 2016 the gully had length of 80 meters. The profile of the gully became V-shape everywhere, the gully was branched out and the steepness of the edges increased. Large ground blocks were collapsing from the edges. The volume of the gully increases by 20% in ten years. In the west part, near the Ob' river, 20–30 rapidly growing gully systems were observed around small (20 km in average) 3 rivers.

The construction and exploitation of the road systems between the deposit fields entailed the formation of linear overmoistured zones near the roads and formed new thermoerosion systems. Filling up by sand is not always effective.

Conclusion

Areas, occupied by thermoerosion processes increased by 15–20 percent in the last 40 years. It is due to climatic changes, the active exploitation of the technogenic systems on iced and easily blurred soils.

Anknowledgements

The work is executed at financial support of the Russian Geographical Society grant №15\17: "Modern conditions and dynamics of dangerous cryogenic processes, influencing on existing and prospective transport network of the Siberea and Far East".

References

A.G., Kuznetcova I.L., Lakhtina O.V., Drozdov D.C., Chekrygina S.N., Tazovskaya oblast'// In the book Geocryology of the USSR. West Siberia/ Under red. E.D. Ershov –M.: "Nedra", 1989. – P. 236-247

Pashkin E.M., Kagan A.A., Krivonogova N.F., Terminological vocabulary of engeneering geology. – M.:, "University book house". – P. 952

L.Dupeyrat, F. Costard, R. Randiamazaoro, and oth., Effects of Ice Content on the Thermal Erosion of Permafrost: Implications for Coastal and Fluvial Erosion// *Permafrost and Periglacial process.*, 22: 179-187 (2011)

Cone penetration testing of permafrost soils

Nikolay Volkov[1]
Ivan Sokolov[2]
Richard Jewell[3]

[1] *Fugro GEOINGSERVICE, Moscow, Russia, ngv@fugro.ru*
[2] *Fugro GEOINGSERVICE, Moscow, Russia*
[3] *Fugro GeoConsulting, Brussels, Belgium*

Abstract

Cone penetration testing (CPT) has great potential for geotechnical engineering in permafrost. Cone resistance q_c [MPa] and sleeve friction f_s [kPa] are measured in basic tests, and pore pressure u_2 [MPa] is measured in CPTu tests. Geotechnical engineering in permafrost requires additional data such as temperature t [°C], electrical conductivity σ [S/m], as well as pore pressure u_2 [MPa]. Interpretation of the measured CPT data allows long-term soil strength and ad-freezing shear resistance to be estimated, key parameters for foundation engineering in permafrost.

Keywords: CPT, permafrost, pile bearing capacity, long-term soil strength, electrical conductivity, temperature.

Introduction

Fugro has performed several projects using CPT technology for geotechnical site investigation in permafrost since 2014. These projects include:

- Several sites located in Salekhard and Labytnangy, Western Siberia, Russia, in 2014. Permafrost was detected at 22 locations from the CPT temperature data. The maximum penetration depth was 34 m.
- A pilot project in 2015 for Russian Railway to diagnose the condition of a railway embankment, located on permafrost near Vorkuta city, Russia (Sokolov et al., 2016).
- Salekhard College, Western Siberia, Russia in 2016 to diagnose the condition of piled foundations and the performance of thermosyphons (Volkov et al., 2017);
- On the Gydan peninsula (near Ob Bay), Western Siberia, Russia in 2017, where the soil conditions were characterized by continuous permafrost with solid frozen sand at a mean annual ground temperature around -6°C (Figure 1).

It was widely thought that permafrost conditions were not suited to CPT investigation. However, through the above projects, Fugro has demonstrated that the method is well suited in even the most challenging permafrost soil conditions and provides highly valuable data.

The measured in-situ data provides much detail on permafrost soil properties, obtained simply and economically; with different sensors providing rich data.

Figure 1. Fugro CPT truck on the Arctic coastline at Ob Bay on the Gydan Peninsula

Measured Field Data

Cone resistance and sleeve friction

An example of a CPT profile measured at the Gydan peninsula is shown on **Figure 2**. The cone resistance values for the frozen sand varied between 20 MPa and 55 MPa. The sleeve friction ranged between 100 kPa and 600 kPa. Such numbers are high and correspond to very dense sand. The active layer is clearly detected at 1 m below the ground surface; this is confirmed by cone resistance values between 1 MPa and 4 MPa, and a measured ground temperature 0°C at this depth.

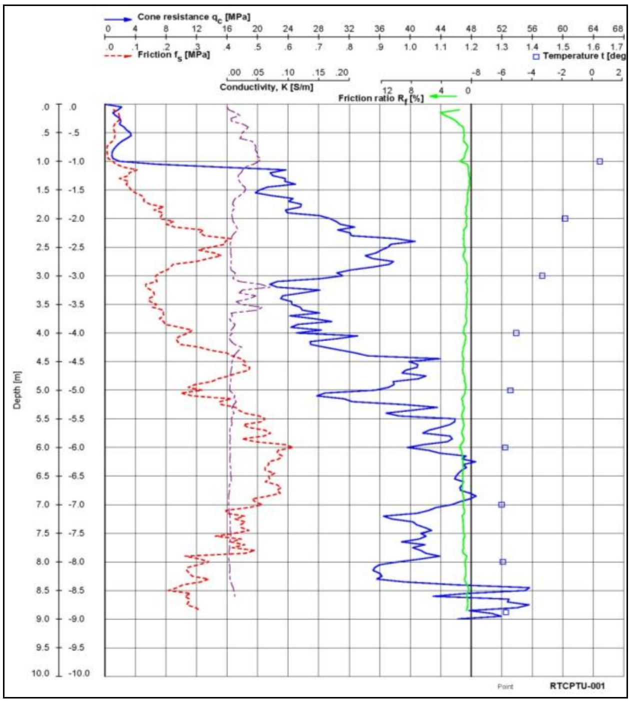

Figure 2. CPT data in non-saline frozen sand at the Gydan peninsula

Temperature

Soil temperature is a critical parameter for permafrost behavior and material properties. Measuring temperature in frozen soils by CPT has many advantages: 1) Only a very short measuring time is required; as a rule, based on Fugro experience with more than 100 measurements, a duration of 10 minutes is enough to stabilize the thermal regime and measure the in-situ soil temperature. 2) The accuracy of temperature measurement is ±0.01°C and hence very precise for permafrost studies; a typical accuracy requirement is ±0.1°C. 3) CPT provides direct measurement of soil temperature at any depth. Fugro often measures temperature at increments 1 m. However, the increments could be 5 cm or 5 m, there are no restrictions. After completion of a test, a casing can be installed into the CPT hole to provide access for continuous temperature monitoring at critical locations.

Electrical conductivity

Electrical conductivity (EC) is sensitive to ice content that reduces conductivity significantly, almost to zero. The continuous EC profile was used to discriminate soil layers, Figure 2. In addition, electrical conductivity allows soil salinity to be estimated, another critical factor for the mechanical properties of frozen soils. Electrical conductivity results obtained by CPT testing can also be applied as part of geophysics surveys, such as electrical tomography, to provide the reference 1D profile for 2D or 3D models.

Pore pressure

Pore pressure measurements also provide valuable data. The soil permeability can be estimated from dissipation tests; in the case of frozen soils, the permeability may be compared with published results (Nixon, 1991). In addition, continuous pore pressure measurements clearly identify boundaries between frozen and non-frozen soils.

CPT Data Interpretation

CPT results can be used to estimate the key mechanical characteristics in geotechnical engineering, such as deformation modulus E_f (MPa), equivalent cohesion C_{eq} (kPa) and pile bearing capacity of frozen soils according to the Appendix L of the Russian standard (SP 25.13330.2012).

Fugro has developed a new technique that processes CPT data to evaluate long-term soil strength and ad-freezing shear strength. This paper will show comparisons between:

1) Recommended values for pile tip resistance in non-saline frozen soils provided in the Russian Standard (SP 25.13330.2012) and stabilized cone resistance values measured by CPT.

2) Measured soil friction and ad-freezing shear resistance and recommended values R_{af} of pile side friction from Russian Standard (SP 25.13330.2012).

Such comparisons show good correlations between the CPT test results and recommended values in the Standards. The temperature dependence of long-term soil strength and ad-freezing shear strength shows similar trends to that found from the conventional theory for frozen soil mechanics.

References

Nixon, J.F., 1991. Discrete ice lens theory for frost heave in soils. *Canadian Geotechnical Journal* 28: 843-859.

Sokolov, I.S., Volkov, N.G. & Isaev, V.S. 2016. Cone Penetration Testing for Railways on Permafrost. *Proc. of the XI International Conference on Permafrost*, Potsdam, Germany, June 20-24.

SP 25.13330.2012 Soil bases and foundations on permafrost soils. (in Russian).

Volkov, N., Sokolov, I. & Jewell, R., 2017. Investigation by Cone Penetration Tests of Piled Foundations in Frozen Soil Maintained by Thermosyphons. *ISSN 2313-4410, American Scientific Research Journal for Engineering, Technology, and Sciences* Volume 31, No 1: 40-58.

Development of the natural and technical system during the operation of the railway (Pesets-Hanovei, Russian Federation)

Alina Sergeevna Voytenko[1]
[1]*Sergeev Institute of Environmental Geosciance RAS (IEG RAS), Voytenko-alina@mail.ru*

Abstract

The history of the problem of diagnosing the causes and preventing the deformations of the railway embankments on the territory of the Russian permafrost zone can be divided into three stages: the primary accumulation of knowledge in the first half of the twentieth century, the intensive development of long thoroughfares with the construction of a geocryological forecast and protective measures in the 1960s and 1980s, construction in the 21st century, which was mainly aimed at ensuring the development of raw materials, but not territories as such. Despite the success in the organization of geotechnical monitoring, there remain unresolved issues of assessing the dynamics and stages of the development of geocryological processes. Insufficiently studied problem remains the decision on engineering protection on the railway canvas in the terms of permafrost zone. There is a need to create methods that allow estimating the amount of annual costs and damages received from the continuing impact of engineering and geological processes on engineering structures, as well as anthropogenic load, in a changing climate.

Keywords: permafrost, engineering protection, geocryological processes, deformations of the railway track.

Characteristics of long-term dynamics of natural conditions and components of the natural-technical system

Introduction

The interaction of the components of the natural environment and the engineering structure form a natural-technical system (NTS) -a collection of natural objects and engineering structures that interact with each other and the environment and operate as a single entity (Pashkin, et al., 2011). Internal structure of the NTS, described by (Revzon, 1992) includes subsystems of the natural environment, which interact with technical elements, namely: Troptotehnicheskuyu (atmosphere); Aquatics (hydrosphere); Biotechnical (biosphere); Geotechnical (lithosphere); Historical and cultural (sociosphere).

Thus, the separation of natural-technical railroad systems affects many components of the natural environment that interact specifically with each other in the cryosphere. (Isakov, 2016). When the components of the natural-technical system interact, there is a risk of exposure to dangerous geocryological processes that are characterized by the main groups of indicators:

1. The type of interaction; 2. Level (intensity, degree) of interaction; 3. The scale of interaction; 4. The duration of the interaction.

Main results

The main phenomenon encountered in the railway canvas studied in this paper is the subsidence of the path associated with geocryological processes. At the entrance to the regionalization of the study area, a railroad embankment scheme was constructed in three types of terrain (peat-bumpy-sink, mineral-hummocky, muddy terrain type), where the permafrost is clearly represented, by which we can judge the degree and duration of exposure geocryological processes (Fig. 1) (Table 1).

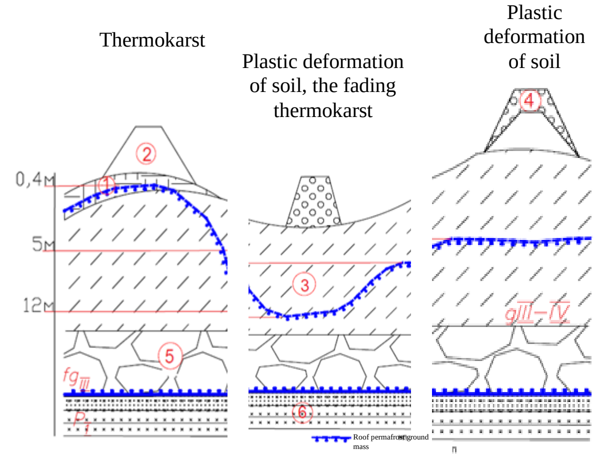

Figure 1. Variants of natural-technical systems

Table 1. Description of the NTS scheme

Number of a layer	Lithologic description
1	Peat
2	Artificial soil (sand)
3	Sand clay, clay loam
4	Artificial soil (Gravel)
5	Intermoral fluvioglacial and interglacial alluvial deposits. Sands and pebbles
6	Hard rock

Permafrost ground on each site occur at different characteristic levels: 1. - 0.4 m; 2. 5 m; 3. - 12 m. The main geocryological process studied in this territory is thermokarst. The impact of the thermokarst process is conditionally divided into three stages:

1. "Ascending" development;
2. "Fading" development;
3. The existence of a residual paleoplasm.

As a result of the obtained data, the types of terrain were identified that help to reveal the patterns of spatial distribution of geocryological phenomena and engineering-geological processes that transform the natural-technical system.

Based on the identified types of terrain, the distribution of thermokarst phenomena and the nature of deformations of the railway embankment, a map-scheme of linear zoning of the route as a natural-technical system (Fig. 2). Such a card allows:

1) to divide the territories into conditionally undisturbed and disturbed by technogenesis to isolate elements of natural-technical systems;

2) to substantiate the territorial representation of the information obtained at the sites of detailed studies;

3) to develop a scheme for geological development of the terrain in terms of trends in changing geocryological conditions and determining the leading engineering and geological processes;

4) to develop ideas on the stages of development of geocryological phenomena on the basis of comparison of data on trends in geocryological conditions, the current activity of geocryological processes and areas of geocryological phenomena formed by the results of past activity of these processes;

5) to substantiate areas suitable for monitoring the geocryological processes in disturbed and slightly disturbed (background) conditions.

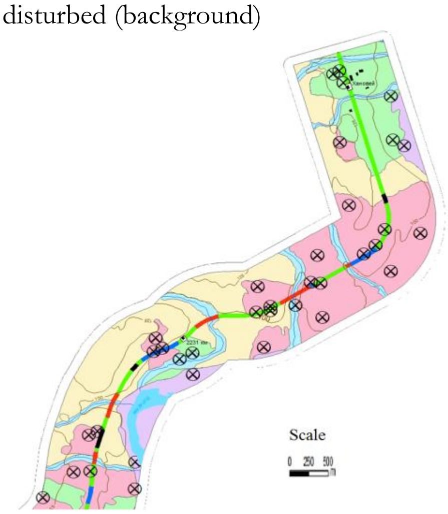

Figure 2. Ratios of location of deformations of a railway embankment with type of the area and the leading engineering-geological process.

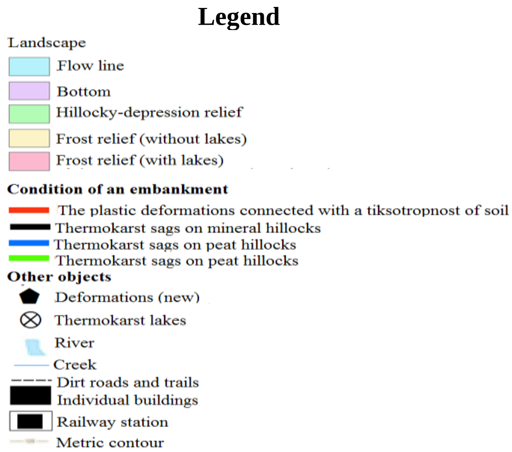

On the map presented, the deformation phenomena associated with the loss of the bearing capacity by thixotropic dilution prevail. The main basis for typifying the hilly terrain type was the predominance or absence of thermokarst lakes. The distribution of thermokarst lakes is confined to the peaty-hummocky type of terrain, since within its limits the level of occurrence of the permafrost is approximately 40-80 cm in depth, which indicates a high potential efficiency of thermokarst processes.

Conclusion

On the basis of a comprehensive specialized permafrost survey, it was established that climate change and the continuing man-made load led to the preservation of the continuous nature of the distribution of permafrost, their temperature increase and the selective thawing of the layer of frozen ground from above. This leads to a gradual attenuation of the process of thermal subsidence of the surface in the areas of the "old" thermokarst and the spatial displacement of active subsidence from the mineral hillocks to the hilly areas with a shallow depth of seasonal thawing.

As a result of the analysis of the original map-type scheme of the terrain types, the key areas of deformation of the embankment are identified, the nature of these deformations and their association with geocryological conditions is explained.

Reference

Pashkin, E.M., Kagan, A.A., Krivonogova, N.F., 2011. The terminological dictionary reference on engineering geology / under. edition of E.M. Pashkin. Moscow: KDU. - 952 pages: silt., tab.

Revzon, A.L., 1992. Mapping the state of natural-technical systems / Moscow: Nedra. -223 p.

Isakov, V.A., 2016 Influence of cryogenic processes on the stability of roads and railways: the author's abstract. dis. to the soisk. scientist. step. Cand. geog. Sciences (25.00.31) / Moscow State University.-Moscow. - 24 p.

Field observations on the thermo-mechanical process of an embankment with L-shaped thermosyphons in permafrost region

Wansheng Pei[1], Mingyi Zhang[1], Yingbing Huang[2], Jianguo Lu[1] Shuangyang Li[1]

[1] *Laboratory of Frozen Soil Engineering, Chinese Academy of Sciences, Lanzhou 730000, China*

[2]*Dongguan Geographic Information and Urban Planning Research Center, Dongguan 523129, China*

Abstract

Two-phase closed thermosyphons (TPCTs) are used as heat transfer devices in ground heat control to protect the engineering stability in cold regions, especially for the permafrost embankment engineering with wide asphalt pavement due to its heat absorption effect. In order to investigate the thermo-mechanical process of the embankment with TPCTs, a field experiment was performed in a permafrost expressway on the Qinghai-Tibet Plateau (QTP). Based on the observation data, the cooling mechanism of TPCT and deformation characteristics of the embankment were discussed. The results may benefit the application of TPCTs in the design and construction of permafrost engineering.

Keywords: L-shaped TPCT; expressway; thermo-mechanical process; permafrost region

Introduction

In permafrost regions, the mean air temperature is usually low, especially in cold seasons [1]. Thermosyphon (TPCT) is an effective technology to store the natural cool energy in the permafrost strata due to its simple structure and eco-friendly advantages [2, 3]. Meanwhile, ambient thermal energy cannot be transferred into the underlying permafrost in warm seasons due to the one-way heat transfer feature of TPCTs [3]. Thus, the embankment stability can be enhanced because the permafrost degeneration would be reduced effectively by the TPCT. At present, researchers mainly focus on the cooling effect of the embankment with TPCTs. However, literatures on the working characteristics of the thermosyphon in practical engineering are relatively few [4, 5]. In addition, the control process of TPCT on the embankment deformation is also unclear.

Therefore, the investigation on the thermo-mechanical process of embankments with TPCTs is necessary, especially for the design of proposed embankment projects.

Experimental design

A field investigation is conducted to observe the thermo-mechanical process of the embankment with L-shaped TPCT. There are five soil layers under the embankment within the depth of 30 m, including the organic matter (0-0.1 m), the silty clay layer (0.1-2.0 m), the sandy loam with gravel (2.0-5.0 m), and the weathered mudstone layer below 5.0 m. The permafrost table is at a depth of about 2 m under the natural ground surface. The mean annual ground temperature at a depth of 15 m is about -0.7 ℃. The experimental site is a typical warm and ice-rich permafrost region in the QTP.

To evaluate the thermo-mechanical stability of the embankment with L-shaped TPCTs, two experimental sections are selected, including a composite embankment installed with L-shaped TPCTs and XPS insulation board, and an embankment without any protected techniques (Fig. 1).

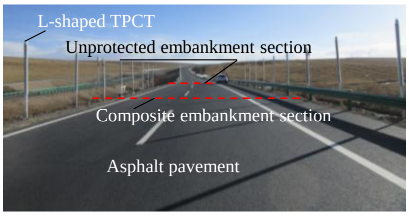

Fig. 1. Photos of the experimental embankments.

Experimental results and analysis

There are three stages for the variation of outer-wall heat flux at the evaporator section. In warm seasons (from June to October), the TPCT stops work. It operates since early October. The outer-wall heat flux reaches its maximum value in the end of December, then, it reduces with time.

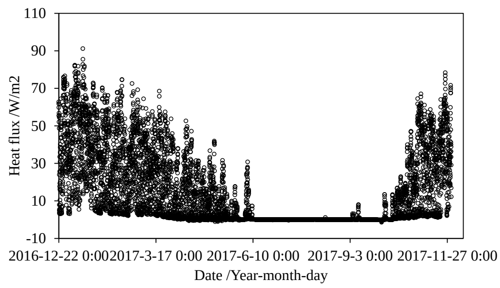

Fig. 2. Variation of the outside wall heat flux at the middle of the evaporator section of the L-shaped TPCT with time.

Meanwhile, the temperature gradient around the TPCT is also analyzed to determine the lateral thermal disturbance zone of TPCT (Fig. 3). The lateral disturbance extent changes with the working state of the TPCT (Fig. 2). From the end of January to the middle July, the disturbance zone expands to 1.5-2 m. It reduces to 0 when the TPCT stops working (from middle July to early October). Subsequently, it begins to expand from 1.0-1.5 m before the early November. After the November, the disturbance extent expands to 1.5-2.0 m again with the increasing heat flux. During the whole process, the maximum thermal disturbance zone is less than 2.0 m.

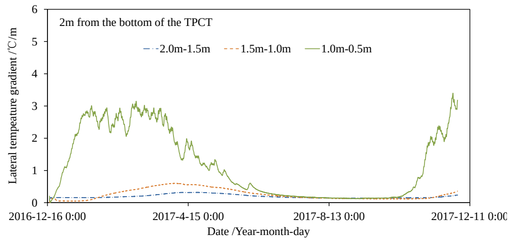

Fig. 3. Variations of temperature gradients around the TPCT.

Fig. 4 illustrates that the permafrost table (0 ℃ isotherm) under the composite embankment (Fig. 4a) is significantly higher than that under the unprotected embankment (Fig. 4b) due to the cooling performance of the L-shaped TPCT. The permafrost table moves down from Y=1.7 m in the embankment composited with TPCT and XPS to Y=0.5 m in the unprotected embankment.

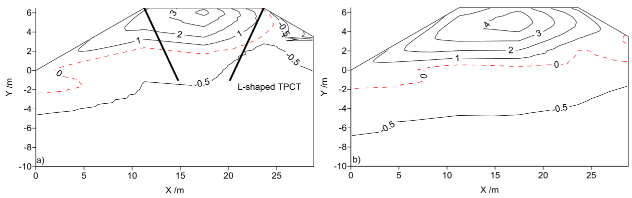

Fig. 4. Temperature distributions of two experimental embankment sections on Oct 30, 2017. (Unit: ℃)

In order to investigate the deformation control characteristics of the L-shaped TPCT, the deformation development of four depths is analyzed. Fig. 5 shows that the deformation process of active layer is different from that in the permafrost layer. For the soil in the active layer (3.5 m), there exists obvious periodic freezing-thawing fluctuation. For the soil under the permafrost table, settlement caused by the creep of permafrost is the main source of the embankment. The deformation development at the depth of 6 and 12 m is approximate. The phenomenon is caused mainly by 1) the creep of the permafrost with higher temperature is larger; and 2) the cooling ability of L-shaped TPCT can reduce the settlement of the surrounding permafrost layer.

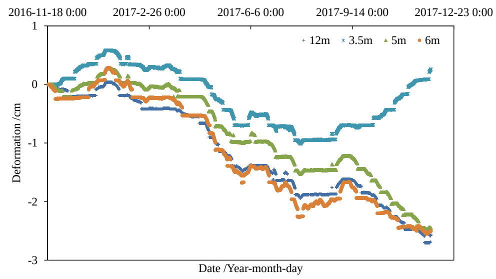

Fig. 5. Vertical deformation at different depths of the composite embankment.

Conclusions

The field test reveals the geotemperature and deformation control process of the TPCT. The results can supply reference for the design of composite embankment with TPCTs in permafrost regions to enhance their thermo-mechanical stability.

Acknowledgements

This research was supported by the National Natural Science Foundation of China (Grant Nos. 41471063, 41701070), the West Light Foundation of the Chinese Academy of Sciences (Dr. Shuangyang Li and Wansheng Pei), the 100-Talent Program of the Chinese Academy of Sciences (granted to Dr. Mingyi Zhang), and the STS Program of the Chinese Academy of Sciences (grant no. HHS-TSS-STS-1502).

References

Andersland OB, Ladanyi B, 2004. *Frozen ground engineering*. John Wiley & Sons.

Cheng GD, Jiang H, Wang KL, 2003. Thawing index and freezing index on the embankment surface in permafrost regions. *Journal of Glaciology and Geocryology*; 25(6): 603-607.

Ma W, Cheng GD, Wu QB, 2009. Construction on permafrost foundations: lessons learned from the Qinghai–Tibet railroad. *Cold Regions Science and Technology*; 59(1): 3-11.

Pei WS, Zhang MY, Li SY, et al, 2017. Geotemperature control performance of two-phase closed thermosyphons in the shady and sunny slopes of an embankment in a permafrost region. *Applied Thermal Engineering*; 112, 986-998.

Zhang MY, Lai YM, Wu QB, et al, 2016. A full-scale field experiment to evaluate the cooling performance of a novel composite embankment in permafrost regions. *International Journal of Heat and Mass Transfer*; 95, 1047-1056.

Developing a research coordination network to identify challenges of and solutions to permafrost related coastal erosion and its socioecological impact in the Arctic

Ming Xiao[1]
Vladimir Romanovsky[2]
Benjamin Jones[3]
Guangqing Chi[1]
Kathleen Halvorsen[4]
Louise Farquharson[2]
[1]*Pennsylvania State University, mxiao@engr.psu.edu*
[2]*University of Alaska Fairbanks*
[3] *United States Geological Survey*
[4]*Michigan Technological University*

Abstract

Permafrost coasts make up 34% of the world's coastlines. Observations from multiple sites across the pan-Arctic suggest that Arctic coastlines are becoming more dynamic since the early 2000s. Increases in erosion and accretion along permafrost-influenced coastlines are posing new hazards and threatening many Arctic communities. As such, there is an urgent need for the integration of knowledge, techniques, and expertise from multiple fields in order to develop frameworks that address scientific and societal challenges on permafrost coastal erosion. The Permafrost Coastal Erosion Research Coordination Network (PCE-RCN) has recently been established to identify the challenges of, and explore solutions to, permafrost coastal erosion issues. In addition, the PCE-RCN will assess the socioecological impacts of arctic coastal change by converging civil and coastal engineering, social sciences, and permafrost and climate sciences. Over the next four years, the PCE-RCN will 1) establish a diverse network of specialists comprised of researchers, stakeholders, and Arctic coastal community members, 2) identify key challenges and socioecological impacts of permafrost coastal erosion, 3) synthesize current knowledge on Arctic coastal dynamics and potential solutions, and 4) explore preliminary solutions to address the challenges of permafrost coastal erosion and its socioecological impacts.

Keywords: Permafrost, coastal erosion, social impact, research coordination network.

Introduction

The Arctic is currently subject to major and rapid changes across ecosystems, socioeconomic systems, and environmental processes. Declining sea ice extent, longer periods of open water, more frequent and severe storms, and sea level rise, coupled with warming and thawing of permafrost, fundamentally affect coastal communities, ecosystems, and industrial activity occurring in coastal settings in the Arctic. For example, more than 85% of Alaska Native villages are negatively impacted by coastal erosion and flooding; of these 184 villages, 17% have been identified as facing imminent threats to life and property, while nearly half of them have already decided to relocate (USGAO, 2009).

Permafrost coasts make up 34% of the world' s coastlines (Lantuit et al., 2012). Erosion of permafrost-influenced coastlines, as illustrated in Fig 1, is typically restricted to a three to four months period during the year. However, this period has been lengthening arctic wide. The way in which permafrost coastlines respond to this increased erosion season can be quite varied. Permafrost coasts may respond to changes occurring in the Arctic through increased erosion rates, more dramatic episodic events, and/or enhanced sedimentation and beach building. In order to develop strategies for these varying response scenarios an inter-disciplinary approach is required.

To meet the needs of the arctic community, we have established a transdisciplinary Permafrost Coastal Erosion Research Coordination Network (PCE-RCN) to identify challenges of and explore solutions to Arctic coastal permafrost erosion as well as its socioecological impacts by converging civil and coastal engineering, social sciences, and permafrost and climate sciences.

Figure 1. Example of permafrost coastal erosion in Alaska (Photo courtesy: Benjamin M. Jones)

Methodology

The project plan of developing the PCE-RCN is comprised of activities in four evolutionary phases in 4 years. The activities include:

- Year 1: Form RCN and initiate dialogues with national and international communities, including inviting diverse participants to form PCE-RCN, creating PCE-RCN website, convening the first PCE-RCN annual meeting in Alaska and identifying challenges in permafrost coastal erosion and its socioecological impacts, and outreaching to international community.
- Year 2: Broaden PCE-RCN including continuing discussion with PCE-RCN participants and broad audience, holding the second project team meeting in Alaska, identifying data sharing mechanisms among various stakeholders, and producing the 1st synthesis report on PCE-RCN.
- Year 3: Explore preliminary solutions to address the challenges of permafrost coastal erosion and its socioecological impacts, and produce international transdisciplinary special issue of Journal of Environmental Management on "Socioecological Impacts of Permafrost Coastal Erosion."
- Year 4: Explore research methodology to study permafrost coastal erosion, produce the 2nd synthesis report, and define mechanisms of continued collaboration beyond the project.

Acknowledgment

This research is funded by the United States National Science Foundation under award number 1745369.

References

Lantuit, H., Overduin, P.P., Couture, N., Wetterich, S., Are, F., Atkinson, D., Brown, J., Cherkashov, G., Drozdov, D., Forbes, D., Graves-Gaylord, A., Grigoriev, M., Hubberten, H.W., Jordan, J., Jorgenson, T., Ødegård, R.S., Ogorodov, S., Pollard, W., Rachold, V., Sedenko, S., Solomon, S., Steenhuisen, F., Streletskaya, I., Vasiliev, A., 2012. The Arctic Coastal Dynamics Database: A New Classification Scheme and Statistics on Arctic Permafrost Coastlines." Estuaries and Coasts, 35: 383–400.Jones, B. M., C. D. Arp, M. T. Jorgenson, K. M. Hinkel, J. A. Schmutz, and P. L. Flint 2009. Increase in the rate and uniformity of coastline erosion in Arctic Alaska. Geophys. Res. Lett., 36, L03503, doi:10.1029/2008GL036205.

U.S. Government Accountability Office (USGAO) 2009. Alaska native villages: Limited progress has been made on relocating villages threatened by flooding and erosion, Report to Congressional Committees GAO-09-551, U.S. Government Accountability Office, Washington, D.C., 53 p.

Experimental study on the damage deterioration of cracks of coal samples subjected to freeze-thaw cycles

Zhemin You[1]
Yuanming Lai[2]
Chong Wang[3]
Shuangyang Li[4]
[1] State Key Laboratory of Frozen Soil Engineering, Northwest Institute of Eco-Environment and Resources, Chinese Academy of Sciences. zheminyou@lzb.ac.cn
[2] State Key Laboratory of Frozen Soil Engineering, Northwest Institute of Eco-Environment and Resources, Chinese Academy of Sciences
[3] School of Civil Engineering and Mechanics, Lanzhou University
[4] State Key Laboratory of Frozen Soil Engineering, Northwest Institute of Eco-Environment and Resources, Chinese Academy of Sciences

Abstract

Combined with geological characteristics and physical and mechanics parameters of coal samples (Table 1), a set of measuring device with thick organic pipe and temperature control board was manufactured to conform to the in situ condition (Fig.1). Freeze-thaw cycles tests from up to the bottom of the coal samples were carried out, and the temperatures and the cooling rates were obtained. CT scanning tests (Fig.2) were adopted to scan the coal samples with different freeze-thaw cycles (Fig.3) and the increment of porosity can be calculated (Equation 1). As the freeze-thaw cycles increased, the CT values induced and the increment of porosity increased. The porosity of coal samples were approximately 5.04%~5.062% (Table 3) and the freeze-thaw cycles can propagate the cracks of coal samples. The objective of this project is to provide theoretical guidance to ascertain the freezing time, the temperatures of freeze-thaw and its cycles and energies for exploring coalbed methane.

Keywords: coal samples; freeze-thaw cycles; damage deterioration; crack; CT scanning; porosity

Introduction

Figures and tables

Table1. The physical parameters of coal rock

parameters	ρ	w/%	ρ	wsat	ρ	porosity
values	1.44	1.05	1.48	3.53	1.43	5.03

Table2 The thermodynamic and mechanical parameters of coal rock

Temperature/℃	λ（W·m-1·K-1）	σ_c /MPa	E/GPa	σ_t /MPa	q/MPa
20	0.31~0.34	4.86	0.35	2.03	21.08
-4	0.26~0.28	5.07	0.41	2.13	26.88
-10	0.24~0.26	5.19	0.49	1.95	30.15
-20	0.22~0.24	5.22	0.51	1.89	35.02

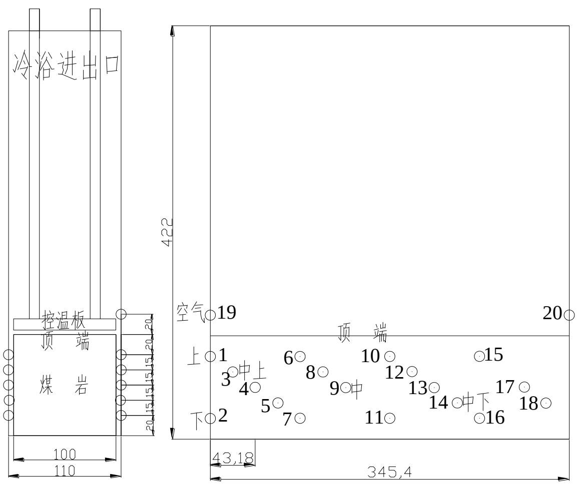

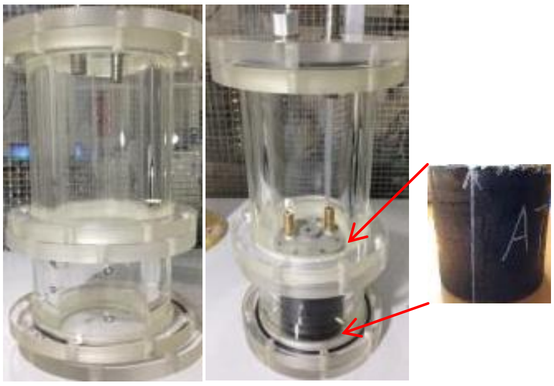

Fig.1 The diagram of the model

$$\overline{\Delta n_i} = \frac{\sum_{i=1}^{m} \Delta n_i}{m} = \frac{\sum_{i=1}^{m}\left[-\frac{1}{m_0^2}\left(\frac{H_i - H_0}{1024 + H_0}\right)\right]}{m} \quad (1)$$

Fig.2 CT scanning

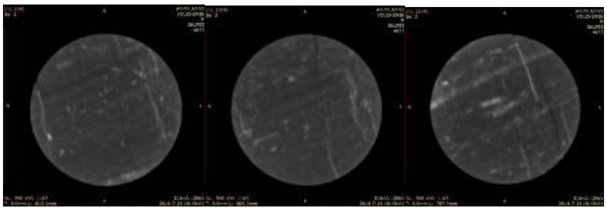

before

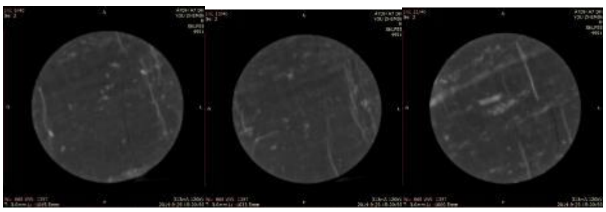

after 1 cycles

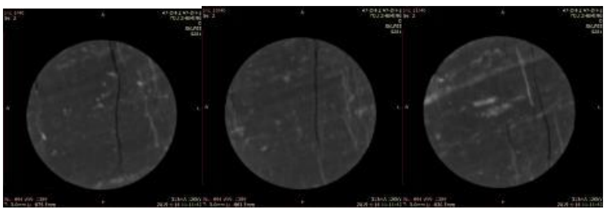

after 6 cycles

Fig.3 The CT photographs of coal rock before and after 1 and 6 freeze-thaw cycles

Table 3 The increment of porosity of coal rock (-20℃)

samples	①	②	③		④	⑤	
Δn(%)	0.01	0.047	1	6	0.035	1	6
			0.01	0.026		0.023	0.032

Note: 1,6 represent 1, 6 freeze-thaw cycle, respectively

Acknowledgments

The authors greatly appreciate the reviewers for their comments and suggestions. This research was supported by National Natural Science Foundation of China (41230630, 41471063, 41601074), Key Research Projects of the Frontier Sciences of Chinese Academy of Sciences (QYZDY-SSW-DQC015), and the 100-Talent Program of the Chinese Academy of Sciences (Granted to Dr. Mingyi Zhang).

References

Nicolsky, D.J., et al., 2009, Estimation of soil thermal properties using in-situ temperature measurements in the active layer and permafrost. Cold Regions Science and Technology, 55(1): 120-129.

Mutlutuk, M., et al., 2004, A decay function model for the integrity loss of rock when subjected to recurrent cycles of freezing-thawing and heating-cooling. International Journal of Rock Mechanics and Mining Sciences, 41(2): 237-244.

Chen, T.C. , et al., 2004, Effect of water saturation on deterioration of welded tuff due to freeze-thaw action[J]. Cold Regions Science and Technology, 38(2): 127-136.

Watanabe, K, 2002. Amount of unfrozen water in frozen porous media saturated with solution[J]. Cold Regions Science and Technology, 2002, 34(2): 103-110.

Zero curtain effect of ponded water on thermal regime of railway embankment in continuous permafrost area, the Qinghai-Tibet Plateau

Yanhu Mu[1]
Wei Ma[2]
Guoyu Li[3]
[1]*State Key Laboratory of Frozen Soil Engineering*, Chinese Academy of Sciences, muyanhu@lzb.ac.cn
[2]*State Key Laboratory of Frozen Soil Engineering, Chinese Academy of Sciences*
[3]*State Key Laboratory of Frozen Soil Engineering, Chinese Academy of Sciences*

Abstract

Impacts of ponded water on thermal regime of railway embankment in continuous permafrost area of the Qinghai-Tibet Plateau was investigated in this paper. The embankment construction in 2003 destroyed the natural drainage paths, thereby concentrating surface and subsurface water along the embankment. As great latent heat of the ponded water, a 5.5-m-thick zero curtain layer (ZCL) developed in and beneath the embankment. Although crushed rock revetments were used at the embankment in 2007, no soils cooling occurred beneath the ZCL. Thermal interaction between the embankment and the subgrade were heavily impeded by the ZCL. In August 2012, a ditch was excavated to drainage the ponded water far away from the embankment toe. After that, the ZCL cooled down rapidly and frozen totally after two cold seasons. The original permafrost table also moved upwards into the embankment.

Keywords: Ponded water; zero curtain effect; thermal regime; railway embankment; continuous permafrost

Introduction

In slope terrain, supra-permafrost water flow in summer times can causes and accelerate permafrost degradation under linear transportation infrastructure (Grandpré *et al.*, 2012; Périer *et al.*, 2015; Wang and Wu, 2017). As unreasonable layout of water retaining wall and drainage system, supra-permafrost water ponding along the Qinghai-Tibet Railway (QTR) in permafrost area are also very common. Although some control and remedial measures have been used, impacts of ponding of supra-permafrost water on thermal regime of the railway embankment are still not well evaluated at present. In this study, soil temperatures in and beneath an embankment at a depression along the QTR were measured continuously to evaluate thermal effect of ponded water on railway embankment.

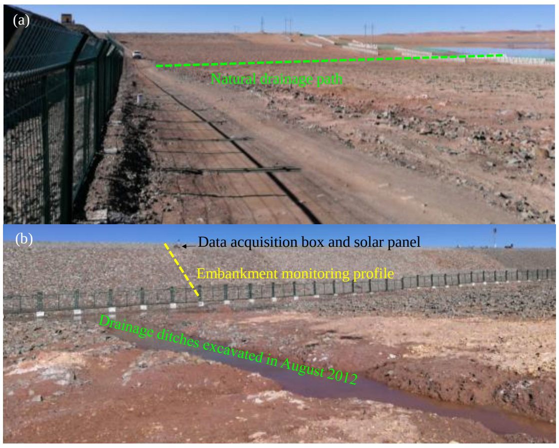

Figure 1. Photos taken at the northwest side (a) and the southeast side (b) of the embankment at the study site.

Study site and method

The study site is a segment of the Qinghai-Tibet Railway, located in continuous permafrost area of the interior of the Qinghai Tibet Plateau (35° 04′ N, E93° 01′ E, 4670 m a.s.l). Embankment construction at the site was completed in 2003. As there was a depression, the embankment had a thickness ranging from 6.4 to 8.5 m (Fig. 1).

After the embankment construction, surface and subsurface water (referred as supra-permafrost water hereafterin) were concentrated along the embankment in the depression due to the interception of natural drainage paths by the embankment (Fig. 1a). In summer times of 2007, crushed rock revetments were used cool permafrost beneath the embankment. In August 2012, a drainage ditch perpendicular to the embankment route was excavated to drainage the ponded water away from the embankment toe (Fig. 1b). An embankment monitoring profile was installed after the embankment construction (Figure 2b). A thermal cable with thermistors at 0.5 m interval was installed into a borehole drilled at the embankment centerline. Soil temperatures in and beneath the embankment were measured continuously.

Results and analysis

After the embankment construction, the thermal regime in the embankment and the subgrade can be divide into three layers (Fig. 2). Between the seasonal freezing and thawing layer (I) and the natural permafrost layer (III), a zero curtain layer (ZCL, II) developed in the embankment and the subgrade as great latent heat of ponded water. The ZCL is about 5.0~5.5 m in thickness.

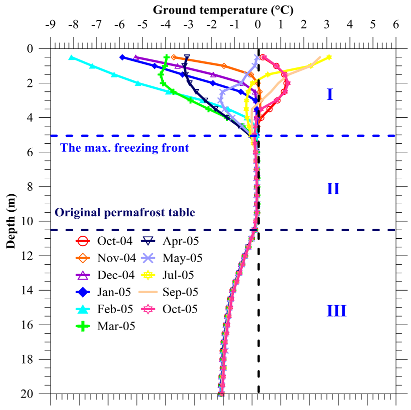

Figure 2. Soil temperature profile at the embankment centerline in 2004-2005.

Before the drainage in August 2012, soil temperatures in the ZCL maintained closet to 0 °C all the time in upper part (6.5 to 8.5 m in depth) and decreased slowly with time in the lower part (9.0 to 12.0 m in depth) (Fig. 3). Although crushed rock revetments were used in 2007, no measurable cooling occurred. After the drainage, soil temperatures in the ZCL decreased rapidly. Moreover, seasonal fluctuations of the environmental temperatures penetrated the embankment body to a depth as much as 10.5 m relative to the embankment surface.

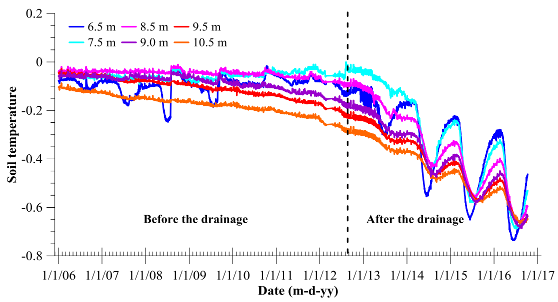

Figure 3. Time series of soil temperature in the ZCL

After two cold seasons in 2012 and 2013, the ZCL refrozen totally and thermal regime in and beneath the embankment changed to a two-layered thermal regime (Fig. 4). The original permafrost table beneath the embankment rise from the depth of 10.5 m up into the embankment body and kept stable at the depth of 5.0 m.

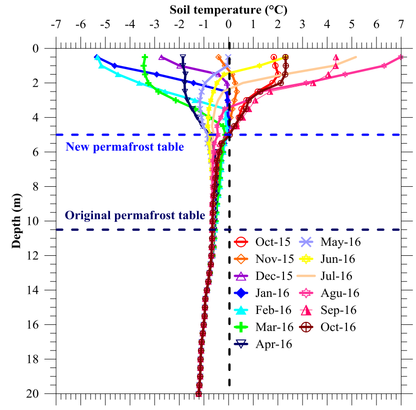

Figure 4. Soil temperature profile at the embankment centerline in 2015-2016.

Acknowledgments

The National Natural Science Foundation of China (Nos. 41772325 and 41630636) and the Foundation of State Key Laboratory of Frozen Soil Engineering (No. SKLFSE-ZY-17)support this work.

References

de Grandpré I., Fortier D., Stephani E., 2012. Degradation of permafrost beneath a road embankment enhanced by advected in groundwater. *Canadian Journal of Earth Sciences*, 49: 953-962.

Périer L, Doré G, Burn CR., 2015. Influence of water temperature and flow on thermal regime around culverts built on permafrost. *Proceedings of the 68th Canadian Geotechnical Conference and the 7th Canadian Permafrost Conference*, September, Québec City, Canada Digital release. Canadian Geotechnical Society http://www.cgs.ca.

Wang JC, Wu QB., 2017. Settlement analysis of embankment-bridge transition section in the permafrost regions of Qinghai-Tibet Railway. *Journal of Glaciology and Geocryology*, 39:79-85.

Eliminating the Frost Uplift of Foundation by Cone-shaped Pile

Zurun Yue[1]
Tiecheng Sun[2]
Tianliang Wang[2]

[1]*Shijiazhuang Tiedao University, Graduate School, Beierhuan East Rd. 17, Shijiazhuang, China, yzr1898@qq.com*
[2]*Shijiazhuang Tiedao University, Civil Eng. School, Beierhuan East Rd. 17, Shijiazhuang, China*

Abstract

In this paper the author devoted to solve the frost uplift problem of small foundations by cone-shape pile. At first, analysis is made on the theoretical mechanism of tangential frost heaving force(TFHF) and the pile-soil contact frost force. Secondary, measuring the TFHF per unit surface area of piles through laboratory tests. At least three types of soil, cohesion soil, sand and gravel, with different water content are considered. The dip angle of pile change from 5° to 12° to select the optimum value. Thirdly, simulation model is built and verified by the laboratory tests. The frost uplift effect simulation is carried out and the displacement distribution along depth of different position is analyzed. At last, the design method of cone-shape pile is to be established, the pile drilling technology and the drilling machine are studied as well.

Keywords: frost uplift; tangential frost heave force (TFHF); cone-shape pile; design technique

Introduction

Frost uplift effect is a common kind of foundation damages in frost region. During the period of construction and operation of the structures in frost region, frost uplift lead to excess upward displacement of the foundations, especially for small size foundations, such as levelling pile, pile foundation of power tower or solar panel, etc. The frost uplift force is also called as TFHF.

There are three ways to control frost uplift, reducing the frost heave properties of soil around pile, increasing the surface smoothness of pile, and employing self-anchored foundation. The self-anchored structure is an economical and reasonable way to control frost uplift of piles.

Self-anchored foundation has a variety of forms as shown in Figure 1, such as spread foundations, anchored mudsill, explosive end-enlarged pile, anchored ring pile, cone-shape pile et ac. Cone-shape pile structure with a dip angle has many advantages: efficient in controlling of the frost uplift, simple in foundation shape, and easy for construction.

In 1930s, B.O. Орлов, professor of frozen soil in former Soviet Union, proposed based on experience that frost uplift phenomenon of pile foundation can be effectively prevented when the cone angle of the pile is about 2~3°.

The patent of American (Takeda *et al.*, 1989) provide a manner of prevention of frost uplift in1989, as shown in Figure 2. In the freezing layer, the case pipe and the lubricant oil were adopted to control the uplift force of the uniform-section pile, but the cost was relatively high.

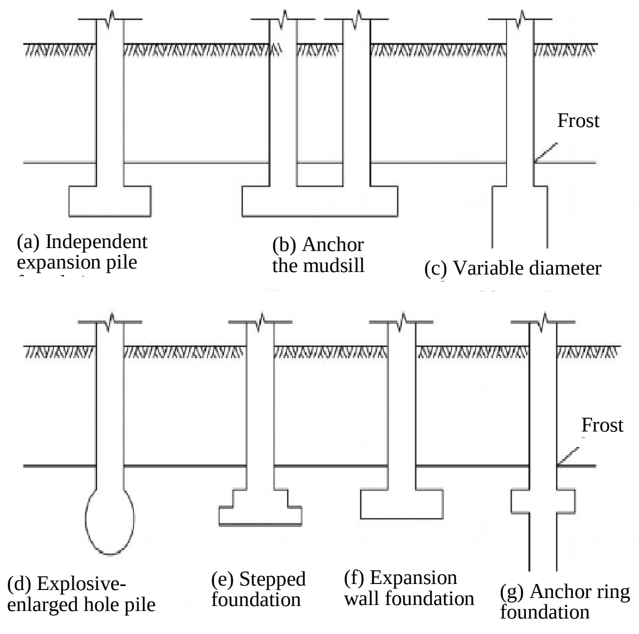

Figure 1. Types of foundations to prevent frost uplift

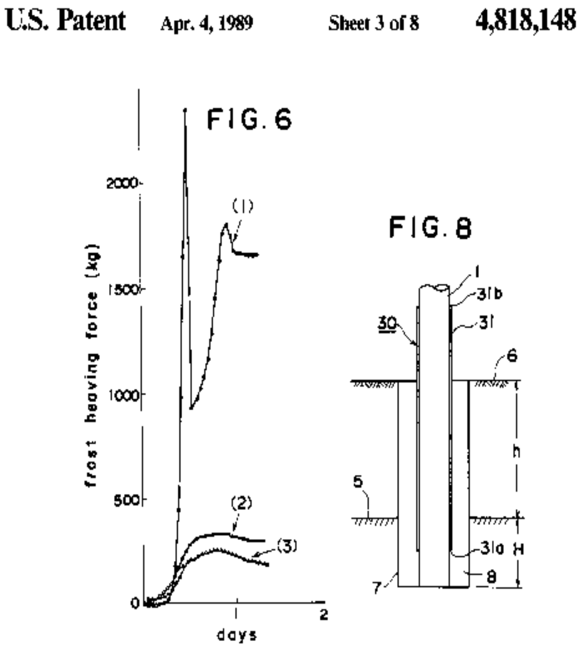

Figure 2. Another way to prevent frost uplift

Y. Zhou in Heilongjiang Low Temperature Building Science Research Institute, tested the variety of frost heaving factor along the depth and influence of cone angle on frost uplift displacement of conical pile foundation (Zhou, 1990).

L. Wang proposed that the inclined pile surface caused the crack near contact surface between soil and the pile. When dip angle is larger than 9 °, the pile foundation can eliminate the damage of frost uplift force (Wang *et al.*, 1995).

TFHF Tests

Device

The test device was designed to work in the frost cell in the laboratory. One controlling way is that a force transducer is employed to measure the total value of TFHF and no vertical displacement take place. Another controlling way is that the LVDT is employed to measure the total uplift displacement, and no vertical force take place.

By changing the material of model pile and the types of soil around the model pile, as well as the dip angel of model pile, the approach of TFHF is obtained, which is an important parameter in the cone- shape pile design. Then the design and drilling technique are studied.

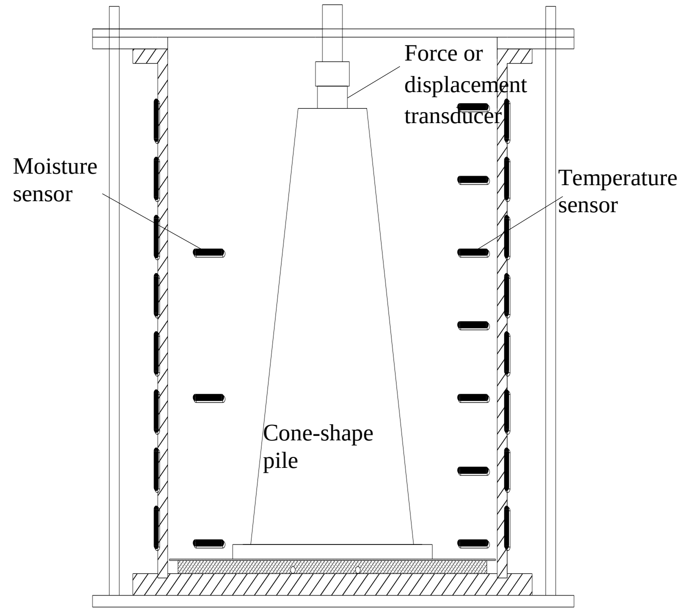

Figure 3. Cone pile test apparatus

Acknowledgments

The tests were carried out by the graduates Dejie Zhao, Xiaojian Yan, and Xin Sun. The program was supported by China National Natural Science Found. The authors wish to express their sincere thanks to them for their contribution to this study.

References

Wang, L. *et al.*, 1995. Stress analysis on tangential frost heave force of foundations with inclined surface. *Journal of Low Temperature Architecture Technology* 3:30-32 (in Chinese).

Takeda *et al.*, 1989. United States Patent, Patent numbe :4818148

Zhou, Y., 1990. The minimum angel of overcoming frost uplift force by foundations with inclined surface. *Journal of Architecture Technology* 1: 23-25 (in Chinese).

Numerical study on the cooling performance of a composite embankment in permafrost regions

Mingyi Zhang[1], Wansheng Pei[1], Zhongrui Yan[1]

[1]*State Key Laboratory of Frozen Soil Engineering, Northwest Institute of Eco-Environment and Resources, Chinese Academy of Sciences, Lanzhou 730000, China*

Abstract

In permafrost regions, a wide and dark-colored asphalt pavement of high-grade highways may cause the degradation of underlying permafrost. However, the embankments with single commonly cooling technique, e.g. two-phase closed thermosyphon (TPCT) embankment and crushed-rock embankment are not sufficient to prevent degradation of underlying permafrost because of their limited cooling capacities. Therefore, in this study, we numerically evaluated the cooling performance of a composite embankment combined with L-shaped TPCTs, crushed-rock revetments and insulation, which is used in a high-grade highway with a wide and dark-colored pavement (double lanes each direction) in permafrost regions, as well as an unprotected embankment (as a control). The numerical results indicate that the composite embankment can effectively cool the permafrost and raise the permafrost table under the high-grade highway, however the unprotected embankment cannot. Therefore, it is hoped that the composite embankment can be applied in the construction of high-grade highways in permafrost regions.

Keywords: Cooling performance; Composite embankment; High-grade highway; Numerical study; Permafrost region

Introduction

At present, a series of embankments have been used to increase the stability of underlying permafrost, of which three commonly used embankments are a two-phase closed thermosyphon (TPCT) embankment, a crushed-rock revetment embankment, and an insulation embankment [1-3]. The Qinghai-Tibet Expressway is a high-grade highway with a wide and dark-colored asphalt pavement, which will absorb much more solar energy than the existing narrow highway pavement; however, the single commonly cooling technique, e.g. TPCT embankment and crushed-rock embankment cannot satisfy the cooling requirement of high-grade highways because of their limited cooling capacities. Therefore, considering the global warming, we numerically studied the thermal characteristics of an unprotected embankment and a composite embankment including L-shaped TPCTs, crushed-rock revetments and insulation, which are used in high-grade highways with wide and dark-colored pavements (double lanes each direction) in permafrost regions.

Model description

According to the Design Specifications for Highway Alignment in China [4] and related references [3, 5], the composite embankment (Fig. 1) was designed to protect the permafrost beneath high-grade highways with wide and dark-colored pavements (double lanes each direction) in permafrost regions. The L-shaped TPCTs with a separation distance of about 3 m along the embankment direction were designed to cool the core of the embankment, the crushed-rock revetments was used to cool the side slopes, and the insulation was intended to strengthen the cooling effect by increasing the thermal resistance of the embankment. According to the different heat transfer characteristics of different media, the embankment model was divided into three zones, i.e. crushed-rock revetment zone, soil layer zone and TPCT zone. Based on the previous researches[3, 6-8], a three-dimensional coupled mathematical model was developed to simulate the heat transfer process of the composite embankment with a climate warming rate of 0.052 ℃/year [9]. An unprotected embankment with the same geometric and physical parameters was used as a control case.

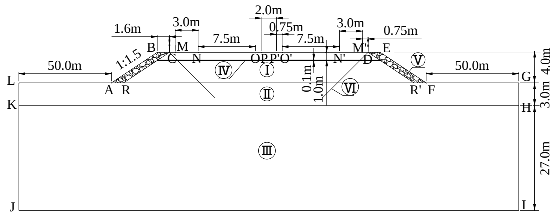

Ⅰ-embankment fill, Ⅱ-silty clay layer, Ⅲ-strongly weathered mudstone layer Ⅳ-insulation layer, Ⅴ-crushed-rock revetment, Ⅵ-L-shaped TPCT

Fig. 1 Physical model the composite embankment

Results and analysis

The centerline ground temperature of the composite embankment at the original natural ground surface is below 0 ℃ for the whole year after it has been finished for 8 years, and the lowest temperatures are below -2 ℃ in cold seasons (Fig. 2); however the temperature of the unprotected embankment is almost above 0 ℃ at the same point all the time. Furthermore, under the unprotected embankment, the permafrost table (0 ℃ isotherm) moves down continuously, and the permafrost temperature rises (Fig. 3); but under the composite embankment, not only the permafrost table rises, but also the -2.0 ℃ frozen zone still exists in the 20th year after the construction (Fig. 4). These show that the composite embankment is an effective method in protecting the underlying permafrost. It is also concluded that the cooling performance of the composite embankment on the underlying soil layers is from the composite effects of the L-shaped TPCTs, crushed-rock revetments and insulation, and cooling effect would benefit to increase the stability of the embankment in permafrost regions.

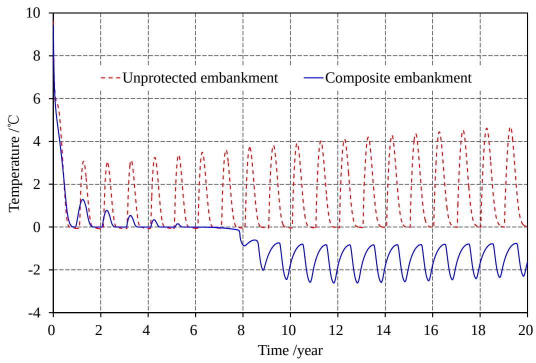

Fig. 2 Centerline temperature of the composite embankment at the original ground surface

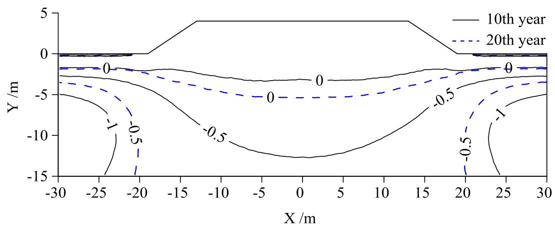

Fig. 3 Temperature distributions of the unprotected embankment on October 15, 10th and 20th years (Unit: ℃).

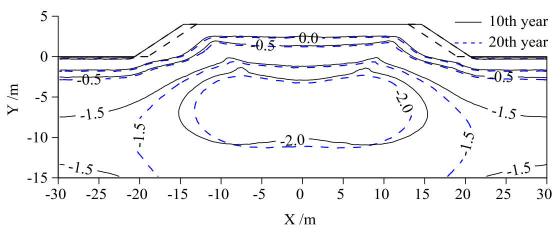

Fig. 4 Temperature distributions of the composite embankment on October 15, 10th and 20th years (Unit: ℃)

Conclusions

The composite embankment that includes L-shaped TPCTs, crushed-rock revetments and insulation is an effective method to protect underlying permafrost, and to increase embankment stability in permafrost regions. The combination of the thermal protection measures does not require any external energy supply, and thus has low environmental impacts. Therefore, this composite embankment should be considered for application to high-grade highways with wide and dark-colored pavements (double lanes each direction) in permafrost regions.

Acknowledgements

This research was supported by the National Natural Science Foundation of China (Grant Nos. 41471063, 41701070), the 100-Talent Program of the Chinese Academy of Sciences (Granted to Dr. Mingyi Zhang), and the Program of the State Key Laboratory of Frozen Soil Engineering (Grant No. SKLFSE-ZT-23).

References

[1] Cheng, G.D., 2005. A roadbed cooling approach for the construction of Qinghai-Tibet Railway. *Cold Regions Science and Technology* 42: 169-176.

[2] Xu, J., Goering, D.J., 2008. Experimental validation of passive permafrost cooling systems. *Cold Regions Science and Technology* 53: 283-297.

[3] Lai, Y.M., Zhang, M.Y., Li, S.Y., 2009. *Theory and Application of Cold Regions Engineering*. Beijing: Science Press.

[4] Ministry of Transport of the People's Republic of China, 2006. Design specification for highway alignment. Beijing: China Communications Press.

[5] Zhang, M.Y., Pei, W.S., Zhang, X.Y., Lu, J.G., 2015. Lateral thermal disturbance of embankments in the permafrost regions of the Qinghai-Tibet Engineering Corridor. *Natural Hazards* 78: 2121-2142.

[6] Zhuang, J., Zhang, H., 2000. *Heat Pipe Technology and Engineering Application*. Beijing: Chemical Industry Press.

[7] Zhang, M.Y., Lai, Y.M., Zhang, J.M., Sun, Z.Z., 2011. Numerical study on cooling characteristics of two-phase closed thermosyphon embankment in permafrost regions. *Cold Regions Science and Technology* 65: 203-210.

[8] Zhang, M.Y., Lai, Y.M., Gao, Z.H., Yu, W.B., 2006. Influence of boundary conditions on the cooling effect of crushed-rock embankment in permafrost regions of Qinghai–Tibetan Plateau. *Cold Regions Science and Technology* 44 : 225–239.

[9] Qin, D.H., 2002. *The Comprehensive Evaluating Report on the Environment Evolvement in West China*. Beijing: Science Press.

The observation of ice lenses produced in frost heave process by image processing method

Hao Zheng[1], Yuutarou Sasaki[2], Shunji Kanie[3]
[1] *Faculty of Engineering, Hokkaido University, Sapporo, Japan, zhenghao@eng.hokudai.ac.jp*
[2] *Undergraduate School of Engineering, Hokkaido University, Sapporo, Japan*
[3] *Faculty of Engineering, Hokkaido University, Sapporo, Japan*

Abstract

The freezing process of soil causes serious water migration and volume expansion which is called frost heave. In this freezing process, the pore water in the soil will be segregated into ice lenses with the help of continuous water migration to the freezing front. This ice lens is the direct reason for the changed properties of frozen soil. However, until now the research concerning the ice lenses in soil is still in observation and qualitative evaluation level, let alone the forming and growing process of ice lenses. The limited observation methods impede the research progressing in frozen soil and therefore, the authors are aiming to propose a direct observation method which can estimate the ice lenses quantitatively and real-timely, and then establish a relationship between the ice lenses and absorbed water.

.

Keywords: Ice lenses, image processing method, absorbed water, frost heave

Introduction

The recent freezing wall technology applied in Fukushima nuclear power plant to prevent the polluted nuclear waste water, drags the public attention to the artificial freezing technology again (TEPCO, 2016). In fact, the freezing technology has been widely applied in the construction of subway and tunnels for more than 50 years. Meanwhile, since nearly 70% of the earth surface will be frozen in winter (Subcommittee on Ground Freezing, 2014), the freezing soil threatens the safety of infrastructure and then affects the human's daily life remarkably. In addition, the freezing process of soil causes serious water migration and volume expansion which is called frost heave. And in this freezing process, the pore water in the soil will be segregated into ice lenses with the help of continuous water migration to the freezing front (Konrad & Morgenstern, 1984). And this ice lens is the reason for all the changed properties of frozen soil. However, until now the research concerning the ice lenses in frozen soil still relies on the indirect measuring methods such as the pulsed Nuclear Magnetic Resonance (NMR) and the Time Domain Reflectometry (TDR) (Akagawa *et al.*, 2012). Although there is some research concerning ice lenses distribution after frozen by Computed Tomography (CT), it is still hard to know the ice lenses forming and growing process real-timely (Joseph & Spital, 1981). The limited observation methods impede the research progressing in frozen soil. To improve the observation level of ice lenses, the authors introduce the image processing method to the frost heave experiments, in order to establish a procedure to monitor the ice lenses forming and growing process quantitatively and real-timely. The authors consider the observation of ice lenses as a prospective method for the research of the property changes of frozen soil.

Experiment method

In this section, we conducted an indoor frost heave experiment for the image processing. We adopted the Kaolin as the experiment material and the indoor frost heave experiment system is shown in Fig.1. The details of the experimental conditions are listed in Table 1.

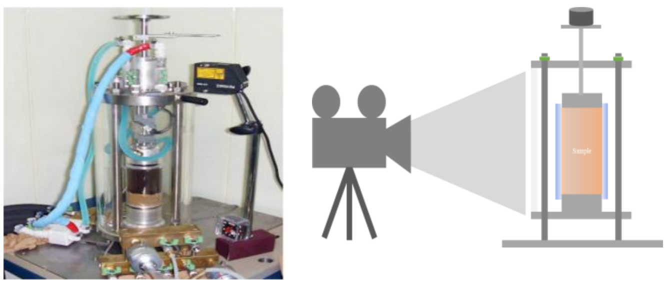

Figure 1. Indoor frost heave experiment system

During this experiment, we set a video camera to take pictures of the freezing process of the sample in order to identify the ice lenses by image processing method. The video camera used in this experiment is Sony DCR-

HC1000 which is a 1/4.7 inch 3CCD video camera with 1 million pixels. And we take the pictures every 1 minute.

Table 1. Experiment conditions

Soil	Kaolin
Height of sample	65 mm
Freezing rate	2.0 mm/hr
Thermal gradient	0.062 °C/mm

Image processing and results

After taking all the pictures of the freezing process, we apply the open-source image analysis software ImageJ to process the ice lenses pictures. The image processing conditions are listed in Table 2. In Fig. 2, the yellow box is the objective area. And Fig.3 presents the processed picture and in this figure, the red color indicates the ice lenses. Through this processed figure, we can know the ice lenses distribution clearly and it delineates an ice gird structure which can provide strong support for frozen soil. In addition, by ImageJ, we can evaluate the area of ice lenses quantitatively.

Table 2. Image processing conditions

Measured size	470 pixels ×720 pixels
Picture interval	10min
Total pictures	150
Scale	1pixel=0.98mm

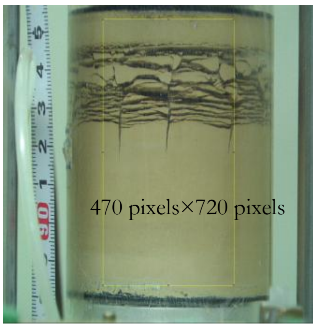

Figure 2. The measured area in the freezing sample

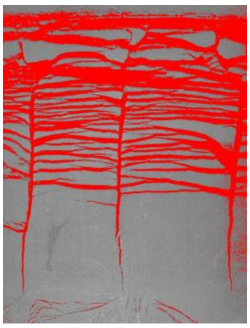

Figure 3. The processed figure (red color represents the ice lenses)

For the ice lenses area, we made a graph (Fig.4) to indicate the relationship between ice lenses area and the absorbed water amount. We note that the absorbed water amount displays a linear relationship with the ice lenses except the beginning and ending stages. This is easy to understand: at the beginning stage, ice lenses mainly come from the freezing of in-situ pore water, therefore the ice lenses area grows faster than the absorbed water. But at the ending stage, the sample was frozen including the bottom which is the entrance of water supply. Therefore, it is hard to supply water to the freezing front. Meanwhile, the unfrozen water inside the soil sample becomes ice gradually with the decreasing of temperature. Accordingly, the ice lenses area increases faster than the absorbed water again.

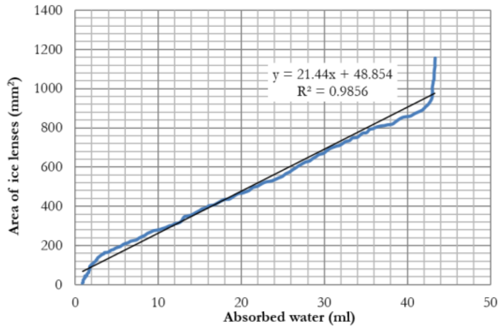

Figure 4. The relationship between absorbed water and ice lenses area

Conclusions

Through this study, we establish the basic procedure of the image processing method for the identification of ice lenses. This method can evaluate the ice lenses quantitatively with a high accuracy. By this method, we confirm the linear relationship between ice lenses area and absorbed water. This finding constructs the foundation for further ice lenses analysis which is aiming to clarify the water migration path and its distribution by the ice lenses distribution. In addition, the authors also want to explain the mechanism of improved strength of frozen soil by the research of structure of ice gird.

References

https://www4.tepco.co.jp/en/decommision/planaction/landwardwall/index-e.html

Subcommittee on Ground Freezing, 2014. Knowledge of Frozen Soil -Technology of Artificial Frozen Soil Wall. *Seppyo*, 76(2):179-192.

J.-M. Konrad and, N. R. Morgenstern, 1984. Frost heave prediction of chilled pipelines buried in unfrozen soils. *Canadian Geotechnical Journal*, 21(1):100-115.

Akagawa Satoshi, Go Iwahana, Kunio Watanabe, Evgeny M. Chuvilin, and Vladimir A. Istomin. 2012 Improvement of pulse NMR technology for determination of unfrozen water content in frozen soils. *Proceedings of the Tenth International Conference on Permafrost*, Russia, June 25-29, Vol 1:21-26.

Joseph, P. M., & Spital, R. D. 1981. The exponential edge-gradient effect in x-ray computed tomography. *Physics in medicine and biology*, 26(3), 473.

The Modelling of Solifluction Behaviour of Freezing-Thawing Soils

Bertan Bas[1]
Adil Binal[1]

[1]*Hacettepe University, Department of Geological Engineering, 06800 Beytepe-Ankara/Turkey, adil@hacettepe.edu.tr*

Abstract

In the scope of this study, a new experimental setup was designed to model the solifluction observed on the gentle slopes during the freeze-thaw process at the high altitudes in the mountain areas. The experiment is carried out with a new laboratory device, which can model slip conditions at the low temperatures. During the tests, it is aimed to observe the possible earth movements after the melting of the frozen soil specimen is brought to specific slope values (17^0, 22^0, and 26^0). These soil movements were observed by taking photographs from fixed points with the aid of the photo shooting method. Three-dimensional models of the slides and digital elevation models were created with the GIS software. At the end of the study, the relationships between the slope angle and the volume of material flowing as well as the soil temperature and soil displacement were determined.

Keywords: Solifluction, slope stability, mountain areas, laboratory modelling.

Introduction

Solifluction, which is usually seen as a result of freezing-thawing in cold climates and high altitudes, is the earth flow in the direction of the slope, which occurs when the soil layer or regolith become saturated with water in different thicknesses (Stahler, 1997). The purpose of this study is to find a relation between the soil type and the soil volume flowing and determine the effect of the temperature on the amount of material flowing.

Materials

Field works were carried out in Ilgaz, Kaçkar Mountains, Erciyes and Palandoken Mountains and laboratory studies were carried out with soil samples taken from these regions. The characteristics of the specimens were determined by performing the index and mechanical experiments of the soil samples taken from four mountain areas.

Modelling

A new device was designed to determine the degree of slope and conditions of soil became unstable and flowed. The developed device mainly consists of two main parts: the test chamber and the cooling block (Fig. 1). The aim of the device made of the artificial slope that can be formed at the desired inclination and to provide the terrain conditions in the laboratory environment as much as possible. In the cooling system, which is based on liquid cooling principle, the antifreeze can be cooled to -20^0C, and the antifreeze is circulated through the copper pipes to the top cover of the fan using circulating pump; with the help of the propellers in the inner part of the cover. The cooling unit is capable of freezing the soil sample placed in it. The soil samples used in the modelling experiments are 55 cm long, 45 cm wide, and 15 cm thick.

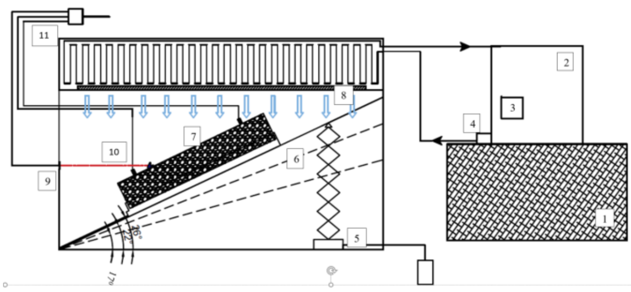

Fig. 1 The overview of the device and system developed to model solifluction (1: Cooling unit, 2: Coolant reservoir, 3: Temperature control unit, 4: Circulation pump, 5: Controlled jack system, 6: Adjustable incline table, 7: Soil sample, 8: Propeller system that blows cold air into closed system, 9: Laser meter (shown as red line), 10: Temperature and humidity sensors, 11: Transfer of laser meter, humidity and temperature values to computer).

Method

Soil samples supplied from the field were frozen and subjected to 17, 22, 26-degree slide tests in the newly developed device regarding internal friction angle obtained in the direct shear test. A temperature and a moisture sensor were placed in the frozen samples, and distance measurements were made with laser beams sent to a body fixed on the sample. In this case, when the frozen soil starts to dissolve slowly, temperature and moisture content of the sample was automatically recorded on the computer in the event of motion on the surface of the soil sample. The photographs of the sample were taken before and after tests for determining surface and volume changes (Fig 2). Then, a digital elevation map of the surface of the sample was prepared from photographs by using the Photoscan software.

Figure 2. The process of taking photographs procedure and an orthophoto of the sample.

The volume of change on the surface of the sample occurring due to the solifluction movement was determined from digital elevation model of before and after sliding tests with using ArcGIS software (Fig. 3).

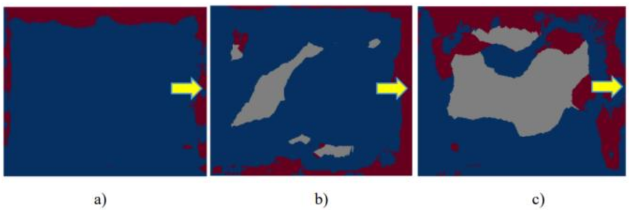

Figure 3. The volume change of Kackar soil because of solifluction. The yellow arrow shows the direction of the flow. Blue area: collapse; grey area: unchanged zone; red area: rising zone.

Results

The results of the experiments performed on the designed new device set-up are given in Table 1. The data in the table is based on the initial movement of the frozen soil and the time to the start of the movement.

Table 1. Test results

Sample-Inclination	The movement initial time (sn)	Upper part humidity value (%)	Lower part humidity value (%)	Upper part temperature (⁰C)	Lower part temperature (⁰C)	The amount of movement (mm)
Kaçkar-26⁰	5000	95,2	95,42	4,06	5,63	7
Kaçkar-22⁰	6000	96,01	97,41	6,19	6,25	7
Kaçkar-17⁰	6000	97,37	97,52	4,94	7,25	6
Palandöken-26⁰	2000	97,33	97,53	2,06	3,82	22
Palandöken-22⁰	6400	94	94,2	2,69	4,44	3
Palandöken-17⁰	8000	97,72	98,26	6,88	7,56	4
Ilgaz-26⁰	3000	95,03	96,84	2.38	2,81	4
Ilgaz-22⁰	8000	95,35	98,62	3,52	4,44	3
Ilgaz-17⁰	7000	99,6	99,94	7,69	10,31	2
Erciyes-26⁰	2000	91,09	93,2	3,14	4,07	6
Erciyes-22⁰	10000	96	97,5	7	8	5
Erciyes-17⁰	5000	96	96,5	3,63	4,51	2

Numerical changes were made in the area and volume after the slide experiment on raster maps created using the ArcGIS program. It is observed that the changes in volume are related to the grain size ratios contained in the samples, and they are presented in graphs with the slope values of 26⁰ in which the experiment was performed. It was determined that there is a significant relationship between the volume of flowing material and the fine grain ratio (Fig. 4).

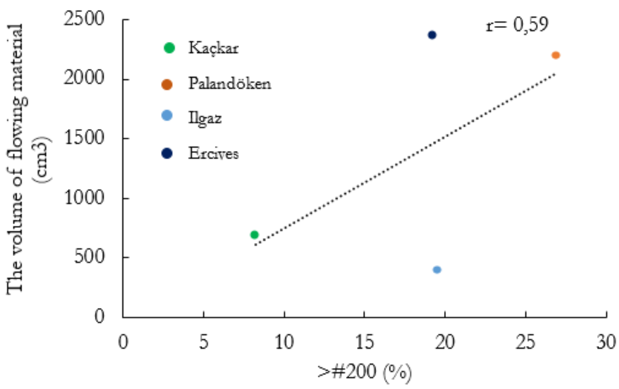

Figure 4. The result of soil slip test carried out at 26°; changes in the volume of material flowing depends on the ratio of sub-screen material (>No. 200) contained in the samples.

Acknowledgments

This study was funded by the Turkish National Scientific Committee (Project No: 114Y088).

References

Strahler, A., 1997. *Physical Geography, Science and Systems of the Human Environment*. Wiley & Sons, 369 pp.

Fractal characteristics of microstructural changes before and after warm frozen soil stabilizing

Gaochen SUN[a,b], Yingsheng Dang[a] ,Jianming Zhang[a], Cong Ding[c]

[a] State key laboratory of Frozen Soil Engineering, Northwest Insitutue of Eco-Environment and Resources, Chinese Academy of SCIENCES,Lanzhou730000, China

[b] China State Construction Engineering Corporation, Architecture Engineering Construction Operation Maintenance, Co, Ltd

[c] Shanghai Investigation, Design & Research Institute Co, Ltd

Abstract: Macro mechanics properties of warm frozen soil determined by its inner pore characteristics and its distribution. The changes of its inner pore structure, especially when add some additives, is the most direct and most significant. Thus, do the research of microstructure of stabilized warm frozen soil should pay more attention to changes in internal porosity before and after stabilizing. It's difficult to Quantitatively describe the amount of pore reduction or increase and the macroscopic mechanical properties before and after stabilizing due to the complexity and uncertainty of pore in soil. This article starts from the microscopic perspective, studied the microstructure changes of original soil and two kinds of high-performance cement-stabilized soils with the same dosage, same maintenance age and different additives. Proposed the method of dividing the pore diameter of solidified warm frozen soil by mercury intrusion test. In addition, the properties of soil pore before and after solidification of warm frozen soil were analyzed by using CURVEEXTRACT image analysis system, which is programmed and developed by MATLAB, combined with Image-Pro Plus (IPP) image analysis software. Though these above jobs, the effect of stabilizer on the warm frozen soil is verified, the relationship between fractal dimension of soil samples before and after soil consolidation and physical properties related to warm frozen soil has been established.

Keywords: Warm frozen soil stabilization; Fractal characteristics; MATLAB ; CURVEEXTRACT ; Permafrost engineering

Characteristics of Thawed Interlayer beneath Embankment of the Qinghai-Tibet Railway in Permafrost Regions and Its Effect on Embankment Settlement

Zhizhong Sun
Yongzhi Liu
Shujuan Zhang
Honglei Wang
State Key Laboratory of Frozen Soil Engineering, Northwest Institute of Eco-environment and Resources, CAS, Lanzhou 730000, China, sun@lzb.ac.cn

Abstract

The formation of thawed interlayer beneath embankment can result in embankment settlement in permafrost regions. Based on the data of ground temperatures and deformations beneath embankment observed in-situ from the Qinghai-Tibet Railway in permafrost regions from 2006 to 2013, characteristics of the thawed interlayer beneath embankment and its effect on the embankment settlement are studied. The results indicate that beneath the embankment the thawed interlayer develops widely, while it can be refrozen totally in the regions of lower mean annual ground temperature and develops further in the regions of higher mean annual ground temperature. The thawed interlayer is closely related to the embankment settlement. The increase in thickness of thawed interlayer mainly results from declining of artificial permafrost table in high-temperature permafrost regions.

Keywords: Qinghai-Tibet Railway; Embankment; Thawed interlayer; In-situ monitoring; Settlement

Introduction

The Qinghai–Tibet Railway (QTR), about 1952 km long in total, is the longest and highest in altitude railway in permafrost regions, crossing approximately 550 km of continuous permafrost regions on the Qinghai–Tibet Plateau (QTP). The thawed interlayer beneath the embankment refers to nonfreezing thawed soil layer between maximum depth of seasonal freezing and artificial permafrost table (Liu et al. 2009). Under natural fields, thawed interlayer can be called as the supra-permafrost talik accurately because it distributed widely in horizontal and vertical directions. A supra-permafrost talik can be often found under a lake, river and rock glacier in permafrost regions (Roux et al. 2017). But under embankment, the thawed soil layer was not widespread, called as thawed interlayer appropriately. The settlement resulted from thawing consolidation when permafrost thawed beneath embankment mostly occurred within the thawed interlayer, so formation of thawed interlayer can give rise to significant engineering problems, such as uneven settlement, longitudinal cracks and shoulder collapse. Now the questions, including development characteristics, change trend of thawed interlayer and its effect on embankment deformation are increasingly concerned by researchers for permafrost engineering and technicians for railway maintenance. The above-mentioned questions will be analyzed and discussed preliminarily based on in-situ ground temperature and embankment deformation from a long-term monitoring system along the QTR in permafrost regions from 2006 to 2013.

Sites description and data acquisition

In order to investigate long-term stability of embankment of the QTR, ground temperatures and embankment deformations at 40 sites along the 550 km of permafrost regions were monitored continuously (Yu et al. 2008). These monitored sites are distributed in various types of terrain including the high mountains, the high plains and the intermontane basins from the north to south of the plateau, and the elevations of sites vary from 4423 m above sea level (a.s.l) to 5080 m a.s.l, with an average elevation of about 4713 m a.s.l (Wu et al. 2011). At one representative monitoring site, ground temperatures were measured by strings of thermistors installed in four boreholes, including natural borehole, left toe borehole, left shoulder borehole and right shoulder borehole. The ground temperatures were automatically collected daily. At each monitoring site, 12 deformation monitoring points and 1 reference point were installed on the embankment surface.

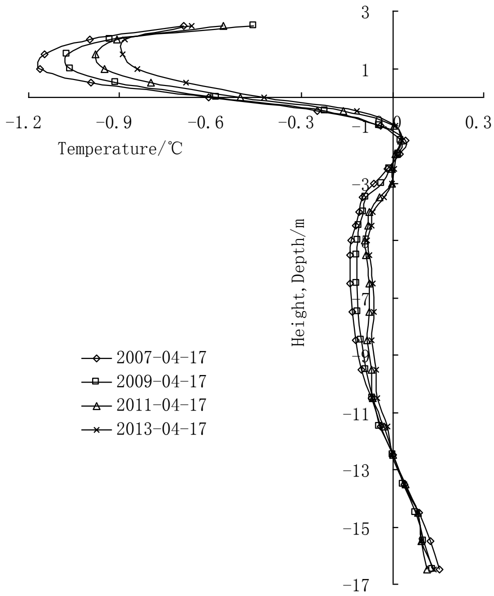

Figure 1. Ground temperature profile under the left shoulder at P44 site

Results and Analyses

The P44 site is located in the front part of alluvial-proluvial fan with swamping wetland. Frost heaving grass mound developed on the surface and vegetation coverage is 80~90%. The elevation of the site is 4807 m a.s.l and permafrost types are ice-rich and saturated permafrost with a MAGT of -0.12 ℃. The common embankment height is 2.4 m. Natural permafrost table was 2.4 m and no thawed interlayer developed under natural field. The thawed interlayer only developed beneath the left shoulder. The ground temperature curves (Fig.1) showed that maximum depth of seasonal freezing beneath the left shoulder was 4.5 m. The thickness of thawed interlayer is 2~3 m and its development is slow with time. Permafrost with temperature higher than -0.08 ℃ exist under thawed interlayer and permafrost was in a situation of temperature rising. The permafrost base is at the depth of 16 m beneath the embankment surface and permafrost thickness is approximately 12 m. The thawed soil is below the permafrost base. This P44 site is adjacent to the southern limit of permafrost along the QTR. Thermal accumulation resulting from such factors, including air temperature warming, pond condition at embankment toe, thermal storage in embankment fill and higher permafrost temperature itself may be account for the formation of the thawed interlayer. Existence of the thawed interlayer resulted in decline of artificial permafrost table beneath the left shoulder and artificial permafrost table had arrived 6.9 m beneath embankment surface. Thawing of permafrost lead to significant settlement of left shoulder and value of accumulative settlement ranged from 412 mm to 520 mm from 2006 to 2013 (Fig.2).

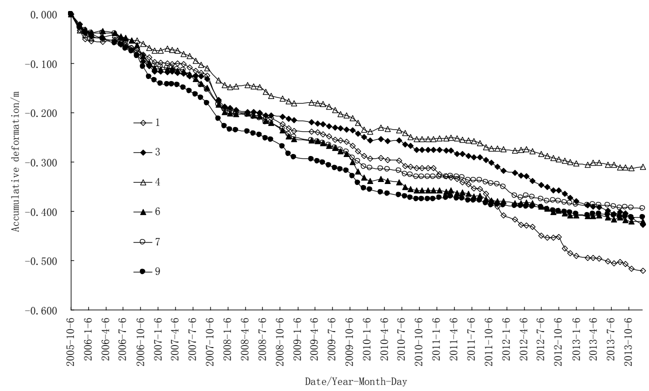

Figure 2. Embankment deformation with time at P44 site

Conclusions

In the existing monitor field, thawed interlayer developed less beneath natural field. The thawed interlayer developed more beneath embankment. The thawed interlayer is closely associated with settlement when permafrost with higher ice content below and value of embankment settlement is greater. The increase in thickness of thawed interlayer in high-temperature permafrost regions mainly results from declining of artificial permafrost tabled.

References

Liu G, Zhang JZ, Zhu DP, et al., 2009. Research of subgrade damages caused by the thaw layer and their disposal measures in permafrost regions. In Proceedings of the 8th International Symposium on Permafrost Engineering. Lanzhou University Press, Xi'an. pp 286-289.

Roux N, Costard F and Grenier C., 2017. Laboratory and numerical simulation of the evolution of a river's talik. *Permafrost and Periglacial Processes* 28: 460–469.

Wu QB, Liu YZ and Hu ZY., 2011. The thermal effect of differential solar exposure on embankments along the Qinghai-Tibet Railway. *Cold Regions Science and Technology* 66(1): 30-38.

Yu H, Wu QB and Liu YZ., 2008. The long-term monitoring system on permafrost regions along the Qinghai-Tibet Railway. *Journal of Glaciology and Geocryology* 30(3): 475-481.

Experimental study of relation between constitutive property and compressibility of pre and post stabilization of warm and ice-rich frozen soil

Zhenhua Yin[1]
[1] *State Key Laboratory of Frozen Soil Engineering, Northwest Institute of Eco-Environment and Resources, Chinese Academy of Sciences, Lanzhou730000, China, yinzhenhua1124@sina.com*

Abstract

In cold regions road engineering, warm and ice-rich frozen soil under subgrade can be reduced its compressibility by adding cement and other additives. In order to research the relation between constitutive property and compressibility of pre and post stabilization of warm and ice-rich frozen soil, the experiments of constant load and different temperatures are undertaken. The constant load is 0.1MP、0.2MP and 0.3MP and the temperature is respective -1℃, -0.5℃ and 2.0℃. Meanwhile, a structural parameter reflecting the structural change of pre and post stabilization of warm and ice-rich frozen soil is introduced. It is found that the changes of structural parameter of pre and post stabilization of warm and ice-rich frozen soil follow an obvious regularity with the compression deformation index. It provides a new way to quantitatively study the constitutive property of pre and post stabilization of warm and ice-rich frozen soil, which also has a guiding significance for the development of cold regions engineering.

Keywords: Stabilization of warm and ice-rich frozen soil; Compression test; Structural parameter; Compressive deformation

4 - Educating with Permafrost: Training the next generation permafrost specialists

Session 4

Educating with Permafrost: Training the next generation permafrost specialists

Conveners:

- **Hanne Christiansen**, University Centre in Svalbard (UNIS), Longyearbyen, Norway
- **Irina Streletskaya**, Moscow State University, Moscow, Russia
- **Ylva Sjöberg**, Stockholm University, Stockholm, Sweden (PYRN member)

Permafrost can serve as a valuable resource to teach about how scientific research is done, how the Earth system works, and about permafrost's unique impacts and challenges. It is also important and necessary to educate and train the next generation permafrost researchers and engineers, at the college level and through continuing post-graduate opportunities. For this session, the International Permafrost Association's (IPA) Standing Committee on Education and Outreach welcomes contributions on materials and activities, courses for undergraduate and graduate students, or continuing educational opportunities including the University of the Arctic (UArctic) Thematic Network on Permafrost (TNP) activities as well as the International University Courses on Permafrost (IUCP) database also in the Southern Hemisphere. A wide variety of initiatives are underway in many countries to include permafrost in the school curriculum and we encourage submissions on these efforts or on the effectiveness of these activities. We also encourage all those who are engaged in college-level activities, including those who offer a class or field course about permafrost at any university or offer international permafrost field courses, such as those organized by TNP member institutions. All those who lead post-graduate initiatives are also encouraged to contribute, such as the Permafrost Young Researchers Network (PYRN) among others.

FROZEN CANOES: Landscape and infrastructure dynamics in frozen environments undergoing Climate Change in Canada, Norway and Svalbard

Hanne H. Christiansen[1]
Christopher Burn[5]
Bronwyn Benkert[6]
Jean Cote[4]
Guy Dore[4]
Graham L. Gilbert[2,1]
Inge Hoff[3]
Arne Instanes[2]
Julie Malenfant-Lepage[4]
Elena Scibilia

[1]*Arctic Geology Department, The University Centre in Svalbard, UNIS, Norway; hanne.christiansen@unis.no*
[2]*Arctic Technology Department, The University Centre in Svalbard, UNIS, Norway*
[3]*Department of Civil and Environmental Engineering, Norwegian University of Science and Technology, NTNU, Norway*
[4]*Department of Civil Engineering, Laval University, Canada*
[5]*Geography Department, Carleton University, Canada*
[6]*Yukon Research Centre, Yukon College, Canada*

Abstract

The FROZEN CANOES INTPART project develops a joint research and educational field-based programme, combining geoscience and engineering addressing perennially and seasonally frozen ground undergoing climate change, using innovative educational knowledge from the Norwegian (UNIS & NTNU) and Canadian (Laval University, Carleton University and Yukon College) partners. Three interdisciplinary Master level field-based courses will be developed and run: at NTNU, Norway in 2019, at UNIS, Svalbard in 2020 and at Yukon College, Canada in 2021. Each course will be coordinated by an early career scientist and will have guest lecturers from the project partners. Research collaboration will be improved, as stipends are available for staff and student exchange for short stays at the other participating institutions. New teaching methods and online modules will be part of the project. The project starts summer 2018, and will be a contribution to the Thematic Network on Permafrost of the UArctic.

Keywords: Permafrost, seasonal frost, climate change, infrastructure, landscape, higher education.

Introduction

Public transportation and municipal infrastructure in the far North faces challenges to its operation and sustainability due to the changing climate. A key transition concerns geohazards related to degradation of permafrost, either through thawing of ground supporting the infrastructure, or by modifying the geotechnical properties of frozen soil as it approaches its melting point. In some areas, permafrost will be replaced by intense seasonal freezing. FROZEN CANOES provides education and research collaboration for engineers and scientists in environments spanning a range of conditions from continuous permafrost, through thawing discontinuous permafrost, to seasonally frozen ground. The specific aim is to develop synergistic approaches to understanding frozen and freezing ground and sustainability of the infrastructure built upon it.

The FROZEN CANOES project contributes to high quality research-based educational collaboration between Norway and Canada, in particular between the strong geoscience groups at UNIS, Carleton University, and Yukon College, and between the geotechnical groups at UNIS, NTNU, and Université Laval. The project partners have and have had project collaboration before within geoscience and geotechnics separately, but the combination of geoscience and geotechnics to be achieved in this application is unique.

Background and ambition

The project builds on collaboration to develop three new master level courses and four online modules. The aim is that the course package will continue to be offered at the Master degree level through the participating institutions, thereby forming a lasting legacy of FROZEN CANOES.

Early career scientists will be involved with development of the project in order to transfer research-based educational skills from the senior scientists to the next generation of scientists and engineers. Online modules will be used to prepare participants for field courses and to provide educational tools that will be more widely accessible.

Knowledge of the key science foundation for frost action, permafrost and geohazards is required to adequately address long-term geotechnical stability of infrastructure in permafrost environments. Climate change increases the uncertainty surrounding appropriate infrastructure design life in these environments. Sharing expertise between researchers in academic geoscience and engineering environments and in industry will improve our capacity to respond to future cold region issues.

The 2019-2021 university educational programme

'*Construction of roads and railways in cold climate' 7.5 ECTS course at NTNU in Norway in 2019*

The course will be an international and multidisciplinary intensive course to disseminate knowledge on road and railway construction in cold climate regions with a special focus on seasonal frost conditions in Norway and Canada. A special focus will be on seasonal frost conditions in Norway and Canada. The main learning outcome will be an innovative mindset aimed at collaborative multidisciplinary problem solving.

The course will be balanced between Canadian and Norwegian priorities, and will target Master and PhD students in engineering and the Earth Sciences. A maximum of 20-25 students can take this course. This Master level course will include two parts: (1) online modules and (2) a residential course at NTNU with several field trips.

'High-Arctic permafrost geotechnics and geohazards' 10 ECTS course at UNIS in Longyearbyen, Svalbard in 2020

With increased development in a changing Arctic, it is important to understand the engineering and geoenvironmental challenges unique to continuous permafrost settings. This Master level, 5 weeks course given for up to 20 engineering and geoscience students will last five weeks in summer 2020. Topics will include: the permafrost ground thermal regime, landforms in permafrost areas, ground ice, mechanics of freezing, frozen, and thawing soils; foundations and infrastructure design in permafrost environments, impoundments in the Arctic, slope stability and mass wasting, and risk assessments in relation to geohazards. The course will utilize the high-relief permafrost landscape and built environment in Longyearbyen through numerous field and laboratory exercises and excursions.

'Advanced Permafrost Engineering Applied to Transportation Infrastructure' One-term Canadian course Equivalent at Yukon College, Whitehorse, Canada in May

The course will contribute directly to the development of knowledge for engineers and geoscientists involved in northern transportation infrastructure design and maintenance. The course takes place in a discontinuous permafrost area. There will be room for 20 students. The course will last for 2 weeks.

This Master-level course will be organized for engineering and geoscience students. The focus will be on permafrost geomorphological dynamics and principles and methods for site investigation, design and management of roads and airstrips, and other linear structures built on permafrost. There will be field visits to sites where important permafrost and engineering features can be observed.

Who can study with the FROZEN CANOES?

The courses will be open to all qualified and interested students and be announced also through the Thematic Network on Permafrost, University of the Arctic. Students from Canada and Norway will be eligible for financial support to participate in the courses. Registration of students will be through the hosting institutions, and follow their normal application deadlines and procedures for the semester in which the FROZEN CANOES courses will run.

Acknowledgements

FROZEN CANOES is funded by the INTPART programme of the Norwegian Research Council and the Centre for Internationalization of University Studies in Norway.

International Arctic Field Student Course on Permafrost and Northern Studies (July 2017, the north of Russia)

Grebenets Valery I.[1]
Streletsky Dmitry A.[2]
Shiklomanov Nikolay I.[2]
Tolmanov Vasily A.[1]
Suter Luis E.[2]
Kharedinova Alexandra G.[1]
[1]*Moscow State University, Geographical faculty, Department of Cryoliyology and Glaciology*
[2]*George Washington University, Washington DC, USA*

Abstract

The special field student course on the study of permafrost and northern regions was organized in the lower reaches of the Ob River and in the European north of Russia in July 2017. The international group of students studied geocryological features of the regions, physico-geographical conditions in the plain and mountainous permafrost zone, as well as the economic and geographical problems in the Arctic regions.

Keywords: international student courses, study methods, permafrost, dangerous cryogenic processes, landscapes, engineering geocryology, Arctic region problems

Introduction

The department of cryolithology and glaciology at the Geographical Faculty of the Lomonosov Moscow State University holds every year the special field student courses on the investigation of Arctic permafrost. In 2007-2008, within the framework of the International Polar Year, the special field training courses were arranged for the Russian and foreign students *(fig.1.)* in the north of the Western Siberia.. In 2012-2015, students from Germany, USA, Norway, Canada and UK participated in field courses on glaciology arranged at the department of cryolithology and glaciology. The accumulated experience permitted us in collaboration with the George Washington University, USA, to arrange the International Arctic Field Student Courses on Permafrost and Northern Studies in July 2017, which were attended by 25 representatives from Russia, USA, Germany, Spain, Netherlands, UK, France, Austria and Canada..

Methodology, Results and Observations

The courses held from July 5 till July 27, 2017 involved 2 stages: (1) the field studies in the Northwestern part of the Yamal-Nenets Autunomous okrug (Salekhard, Labytnangi, Obskaya, Kharp and their tundra and mountainous area) (2) the field studies in Vorkuta and its outskirts.

The studies were focused on the investigation of the cryological features in the regions, on assessing the permafrost dynamics as affected by the climate change and technogenic impact in the permafrost zone, and on getting acquainted with socio-economic problems of Arctic regions.

The course program covered the history of territory development in Pleistocene and Holocene; The field measurement of active layer depth was regularly performed for different natural landscapes and different lithological conditions, including the CALM program. A special attention was paid to the investigation of mechanisms of the formation of various cryogenic landforms, to revealing relationship between the local landscape conditions (drainage, vegetation, slope processes, etc.) and cryological situation; as well as to the study of ice wedges. The landscape indication method of permafrost study was applied widely. A significant part of the course implied training students in thermometry using loggers and digital thermometers, in the methods of processing the data obtained; in the assessment of factors influencing the temperature regime of permafrost. Another major section was devoted to the cryoengineering investigations, i..e., the methods of engineering development, the main types of basements and technologies of building them on permafrost; the reasons of deformation of engineering structures, the methods of managing cryogenic situation in constructional purposes.

The students got comprehensively acquainted with ethnic and cultural traditions of local population.

The collaborative field studies, listening to professors' lectures and delivering scientific reports on their own, visits to local centres on science and culture, museums, as well as field trips both pedestrian and taken by bus and river ships, informal communication permitted the students from different countries to unite in an effectively working team.

Figure.1. The participants of International Arctic Field Student Course on Permafrost and Northern Studies (July 2017, the north of Western Europe, Labytnangi.

The main results of this field course are the following: (a) the students have got experience and competence in conducting landscape cryological studies in the Arctic zone; (b) the students have learnt cryological ecological engineering geocryological problems in the permafrost zone; (c) the scientific report in two volumes (245 pp) was written; (d) recommendations on tehrational use of the permafrost were given; and finally (e) the international effectively working research team was arranged capable of solving many permafrost-related problems via communication.

Frost depth measuring program in JAPAN

Koichiro Harada[1]
Kenji Yoshikawa[2]
Go Iwahana[2]
Julia Stanilovskaya[3]
Yuki Sawada[4]
Toshio Sone[5]
[1]*Miyagi University, Japan, haradak@myu.ac.jp*
[2]*University of Alaska Fairbanks, USA*
[3]*Total S.A., France*
[4]*Fukuyama City University, Japan*
[5]*Hokkaido University, Japan*

Abstract

Since 2011 winter season, an education program measuring frost depth has started in Hokkaido, northern part of Japan, where the seasonal ground freezing occurs in winter. This program is made at schools in order to emphasis their interests for earth sciences. At schools, seasonal frost depth was measured directly by students under no snow-removal condition using frost tube with blue-colored water. In 2011 season, we started this program at three schools, and the number of participated school is extended to 33 schools in 2017 winter season. The maximum frost depths in Hokkaido was more than 50 cm, but no frost depth was measured in some schools due to heavy snow. We confirmed that the frost depth strongly depends on air temperature and snow depth.

Keywords: frost tube, seasonal frozen ground, frost depth

Introduction

In 2011 winter season, we started an education program measuring frost depth in Japan. The objective of this program is to emphasis students' interests for earth sciences.

Frost depth measuring program

This program is based on the UAF's Permafrost Outreach Program operated by 'Tunnel man', using clear tube with blue-colored water. Programs were made at elementary, junior high and high schools in Hokkaido, northern part of Japan, where the seasonal ground freezing occurs in winter. At schools, a lecture was made in class and a frost tube was set at schoolyard. After that, seasonal frost depth was measured directly by students or teachers once a week at each school during ground freezing under no snow-removal condition. Snow depth around frost tube was also measured directly for discussions.

In summer time or just before frost season, we visited schools to explain the method of measurement, and the frost depth was measured by students in winter. After the end of frozen period, we visited schools again to explain measured results of each school or to compare with those of another schools in Japan, Alaska, Canada and Russia, where frost depths were measured by same method.

Processes and results

In November 2011, we started this program at three elementary schools in Hokkaido (e.g. Harada *et al.* 2012). Next year the schools measuring frost depth was 8 schools, including all elementary schools in Shikaoi Town. The number of schools having frost tube increased year by year, and extended to 33 schools in December 2017, 27 elementary schools, 5 junior high schools and one high school (Fig. 1).

The measured frost depths in Hokkaido ranged widely, from only a few to more than 50 cm. However, some schools had no frost depth due to heavy snow. We confirmed that the frost depth strongly depends on air temperature and snow depth. The lecture was made to student why the frost depth ranged widely, and the effect of snow was explained by using the example of igloo.

Figure 1. Locations of school, Hokkaido, Japan.

In order to validate the effect of snow and to compare frost depths, at one elementary school (Shikaoi Elementary School), we tried to measure frost depths under snow-removal and no snow-removal conditions in same school yards. In 2012-2013 winter season, the maximum frost depths under two conditions were 27 cm and 13 cm, respectively (the maximum snow depth was 40 cm). In 2013-2014, the depths were 23 cm and 30 cm, respectively under the maximum snow depth of 28 cm. The frost depths under snow-removal condition were 7-14 cm deeper than those under no snow-removal condition. These results show apparently that snow has a role as insulator and affects the frost depth strongly. In class, after showing these measured results, students notice this role of snow.

At one elementary school (Komaba Elementary School), frost depths were measured almost every day for four seasons, from 2013-2014 to 2016-1017 winter season (Fig. 2). The maximum frost depth was recorded in 2015-2016 season, 40 cm, and the minimum value was 15 cm in 2014-2015. The frost depth ranged widely and it was confirmed that difference of frost depth was depended on air temperature and snow depth of each year. Based on these results, we will try to estimate frost depth from these factors.

The activities of this program, attending schools and measured frost depth is shown in the following web site but only in Japanese;

http://www.myu.ac.jp/~haradak/frost_tube.html

The network of this program will be expected to expand, finally more than a hundred schools.

Acknowledgments

We are very grateful to all the students and teachers who measured frost depth in their schools. This study was supported partly by the Grant for Joint Research Program of the Institute of Low Temperature Science, Hokkaido University, Japan.

References

Harada, K., Yoshikawa, K., Iwahana, G., Sawada, Y. & Stanilovskaya, J. 2012. Measurements of frost depth in winter at the schoolyard. *Tohoku Journal of Snow and Life* 27: 21-23. (in Japanese)

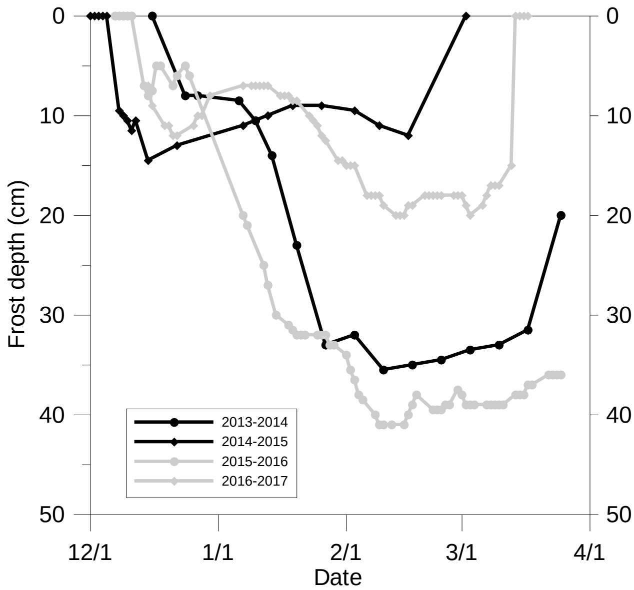

Figure 2. Measured frost depth at Komaba E.S. from 2013-2014 to 2016-2017winter season.

Engineer-geocryological scientific-educational field work of Moscow university Master of Science students at polar regions of European Russian arctic

Vladislav Isaev[1]
Andrey Koshurnikov[1]
Oleg Komarov[1]
Dmitry Sergeev[2]
[1]*Lomonosov Moscow State University, Geological Department, isaev@geol.msu.ru*
[2]*Sergeev Institute of Environmental Geoscience Russian Academy of Sciences, Geocryology laboratory*

Abstract

Engineer-geocryological scientific-educational field work of Moscow state university masters students at polar regions of European Russian arctic had been founded in 2012 and on previous step had based on the program of complex researches by the field geocryological methods.

Keywords: educational program; cryological mapping; synergy researches; temperature monitoring; DGPS mapping; geophysics survey.

Introduction

Engineer-geocryological scientific-educational field work of Moscow state university masters students at polar regions of European Russian arctic had been founded in 2012 and on previous step had based on the program of complex researches by the field geocryological methods (Melnikov & Spesivcev, 1995). The main sites of researches were situated close to Vorkuta city and the coastal site Yary on the Baydara Bay at Kara sea (Fig.1). In 2014 the field work program was changed and the main idea of it had became the training and working out of the geocryological mapping in geocriologically differ sites. It was choosing some new sites:

– the Hanovey station surrounding on the river Vorkuta high coast located in Bolshezemlskaya tundra;

– the 110 km railway station at the Sot' river valley in Polar Ural mountain area.

– the western coastal area at Baydara Bay of Kara sea with total extension close 6,5 km.

At Hanovey area it was organized the research & educational geocryological station of temperature, water resource, radiation balance, vegetation and cryological processes monitoring (Fig. 2).

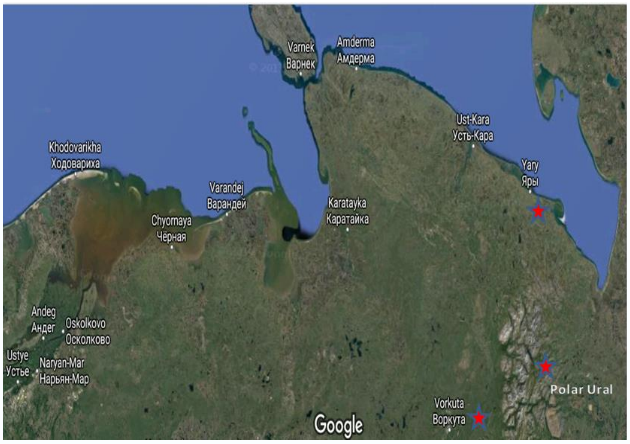

Figure 1. Field work site location.

During one-week training students are fulfilling the field work including next methods groups: Engineer-geocryologic - Engineer-geological drilling with samples eject and description, later - laboratory research; Temperature monitoring of grounds and water sources; CALM – circum polar active layer monitoring; Geophysical - Electro tomography research; Method of formation of an electromagnetic field in the near zone; Radar research; Mapping of permafrost – DGTS mapping with post work in AutoCAD; Geocryologic mapping; Landscape micromapping; Air photo mosaic mapping by drone; Ecological - Measurement of gas emission from frozen ground under the thawing process; Hydrogeological – determination of water filtration coefficient in thawing grounds by the method of the water filling in the pit; mapping of the underground water flux lines by the moisture testing of ground samples; determination of isotopes compound for the finding influence between precipitation and basic water resources leveling.

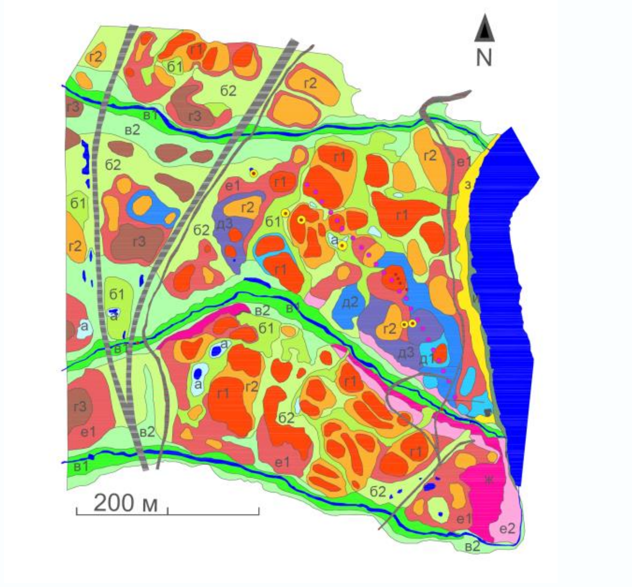

Figure 2. Hanovey site geocryological map. (a-e – landscape types determinated by geomorphology, vegetation, saturation of grounds and linear technigenic objects and water resourses)

At the Polar Ural site the one-week field work is aiming on the research of the influence of technogenic object such as railway road on the environmental conditions. It includes the same complex methods, which lets to analyze the situation and to make forecasts of possible changes in thermal fields of surrounding grounds (Fig. 3).

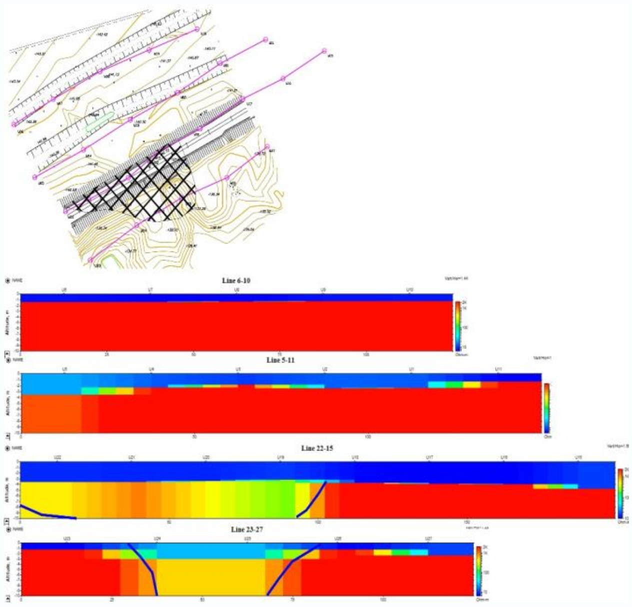

Figure 3. Results of geophisical research of the permafrost ground massif at the railway embankment area at Polar Ural research site (upper part – geodethic plan of research area, 4 – electrogeophysical sections on line 6-10;5-11; 22-15;23-27).

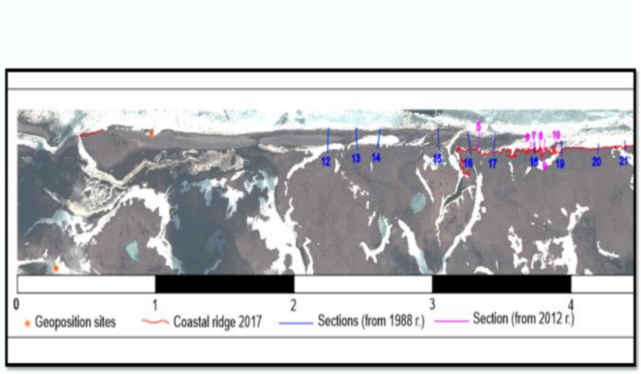

Figure 4. DGPS sections of western coastal line of Baydara bay from 1988 to 2017. (Isaev et al., 2017).

At the Baydara Bay site the one-week field work mostly concentrated on the researches of coastal processes such as thermal abrasion, thermal denudation and accumulation of salted and unsalted coastal deposits of marine and alluvial genesis. The other task is the research of the interaction of gas pipeline and cofferdam construction with coastal environment. Students are using complex geophicis methods, as well DGPS mapping and mapping by dron (Fig.4). They are drilling, sampling and researching grounds on mechanical properties, gas content and so on. Additional part of field work is connecting with hydrological survey of the sea. It includes echolocation of the coastal zone (bathymetric works).

Conclusions

In final students have to present the report with modelling of forecast of thermal field in the cofferdam massif, ground massifs around gas pipeline and railway embankment. This field work is the test of the Moscow state university masters students skills of 6th year study.

Acknowledgments

The research is supported by the SAMCoT WP6 (https://www.ntnu.edu/web/samcot/home)

References

Isaev, V. Koshurnikov, A., Pogorelov, A., Amangurov, R., Komarov, O., Gorshkov, E., Belova, N., Aleksyutina, D., Kokin, O. 2017. Field investigation and laboratory analyses; Baydaratskaya bay 2017, *SAMCoT report.*

Melnikov, V.P., Spesivcev, V.I. 1995. *Engineering-geological and geocryological conditions of Barents and Kara seashelfs*. Novosibirsk: Nauka, 198 pp.

Communicating Permafrost Research and Arctic Climate Change: a Modular Concept for Student Workshops

Katrin Kohnert[1]
Sina Muster[2]
Caroline Coch[2]
Jan Nitzbon[2]
[1]GFZ German Research Centre for Geosciences, Telegrafenberg, 14473 Potsdam, Germany, katrin.kohnert@gfz-potsdam.de
[2] Alfred Wegener Institute, Helmholtz Centre for Polar and Marine Research, 14473 Potsdam, Germany

Abstract

The Arctic not only fascinates scientists, but its landscape and remoteness also hold a large potential to fill children and teenagers with enthusiasm. We built on this circumstance to develop a modular concept for a workshop for students addressing climate change in the Arctic. The three-hour workshop consists of an input presentation, three workstations where the students learn about permafrost and research in the Arctic through conducting short experiments, using laboratory equipment, seeing expedition equipment and planning an expedition, and a final discussion round where newly gained insights are put into the broader context of global climate change.

Keywords: Students; hands-on experiments; Arctic Climate Change; interdisciplinary learning.

Framework of the workshop

The adventure of doing field research in an exotic, faraway place such as the Arctic is a riveting story that holds many great possibilities to fascinate students of all ages. We use this circumstance to transport information about Arctic permafrost and climate change research as well as scientific methods in an entertaining and interactive manner. Here, we present the modular concept (Fig. 1) of a student workshop that we have offered three times to school classes with students aged 11 to 16. We held the workshop in its presented form with three instructors each time. The workshop period is ideally three hours, but it can be adapted to a shorter or longer duration. The level of difficulty is easily adaptable to students of different ages. The workshop is set up of five modules: a scientific presentation, three different workstations, and a final discussion round. It can be accompanied by short group games or activities adapted to and embedded in a narrative related to the Arctic or a specific research field.

The workshop begins with a short (10-15 min) scientific presentation to learn about the background of Arctic climate change with variable foci such as climate research in the Arctic or permafrost. The students learn about climate change, how the Arctic is affected by it and how changes in the Arctic have an impact on the globe. We introduce them to the Arctic landscape, its inhabitants, climate, vegetation, and animals.

The students are then divided into three groups to participate in each of the workstations consisting of background information, hands-on experiments and exercises. The groups then rotate between the three hands-on workstations. We developed the workstations in such a way that the order is interchangeable, by adapting the narratives for each group and making connections to the previous and following workstation. This allows the students to get an impression of life and work on expedition in the Arctic, as well as scientific field methods. The small size of the groups and the interactive format allow the students to raise questions and start discussions. Furthermore, the workshops allow the students themselves to experience Arctic research including planning, experimenting and measuring. This way of experimental education links personal experiences with theoretical understanding, which ensures a more sustainable learning experience than simple textbooks even in short time frames.

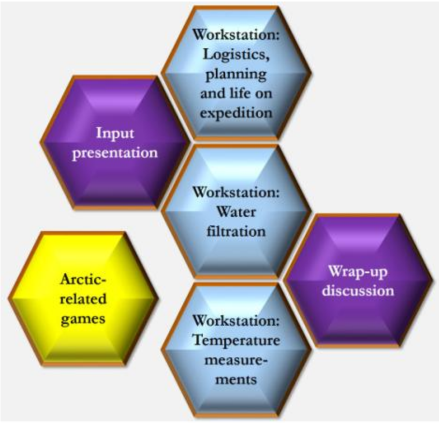

Figure 1. Modular concept of the workshops.

In the end, the workshop wraps up with a final discussion about the global and local implications of Arctic climate change. The discussion at the end of the workshop starts with a short feedback round of students regarding their experiences at the different workstations. It continues by putting their insights in a broader context of climate change in the Arctic and can lead towards discussing why and how human behavior has an impact on distant places and, in turn, how this may affect our life. Finally, it can be discussed what role our everyday life plays and which changes in human behavior could have a positive effect counteracting or mitigating climate change.

Cryolithology field courses on Svalbard, Barentsburg location

Aleksandra Naidenko[1]
Aleksandra Khairedinova [1]
Vasily Krotkov [2]
Alexander Kizyakov[1]
[1]*Lomonosov Moscow State University, Faculty of Geography, Cryolithology and Glaciology Department, naydenkosasha@gmail.com*
[2] *Lomonosov Moscow State University, Faculty of Geography, Physical Geography and Landscape Science.*

Abstract

In the context of the agreement on scientific cooperation between Federal State Budget Institution Arctic and Antarctic Research Institute (FSBI "AARI") and Faculty of Geography of Lomonosov Moscow State University there was held the field-based course for third-year students during July,24th -August,5th 2017 on the Svalbard Archipelago. Students of the Cryolithology and Glaciology Department and student of the Physical Geography and Landscape Science Department were invited by FSBI "AARI" to perform cryogenic investigations near the Barentsburg settlement on the base of Russian Science Center on the Svalbard Archipelago as a part of seasonal squad RAE-S (Russian Arctic Expedition – Svalbard) "Svalbard-2017".

Keywords: cryolithology, education; field courses; Svalbard.

Introduction

In the context of the agreement on scientific cooperation between Federal State Budget Institution Arctic and Antarctic Research Institute (FSBI "AARI") and Faculty of Geography of Lomonosov Moscow State University there was held the field-based course for third-year students during July,24th -August,5th 2017 on the Svalbard Archipelago. Students of the Cryolithology and Glaciology Department and student of the Physical Geography and Landscape Science Department were invited by FSBI "AARI" to perform cryogenic investigations near the Barentsburg settlement on the base of Russian Science Center on the Svalbard Archipelago as a part of seasonal squad RAE-S (Russian Arctic Expedition – Svalbard) "Svalbard-2017".

Objectives of the field course

Standardized methods of cryolithological studies were used to describe the territory. Along the route we've done observations including determination of relief forms, based on terrain, space images of ultra-high spatial resolution and mosaic of aerial photographs (tied to the terrain by GPS). Morphological and morphometric characteristics of cryogenic relief forms were determined. Pits and stripping have been completed to document the cryolithological structure of the surface sediment cover.

During the practice we used equipment provided by AARI, measurements were made in equipped thermometric holes (Demidov et al., 2016).

The thickness of the seasonally thawed layer was determined during the passage of pits, by measurement with a probe and sledgehammer, and also on the basis of temperature data from thermosets installed in the holes. For thermometric observations we used GeoPrecision thermocouples equipped with loggers for automated temperature measurement.

Together with RA Chernov, head of the glaciological team of the Institute of Geography of the Russian Academy of Sciences, glaciological observations were made on the glacier West Grønfjord.

Conclusions

In the process of passing the production practice, a whole range of studies has been carried out. Theoretical knowledge and obtained useful data for writing the thesis work are applied. All the planned work has been successfully completed. A plan for further investigations of permafrost and processes related to it has also been developed in the Svalbard archipelago.

Acknowledgments

This work was partly supported by RFBR grant No.16-05-00612.

We express our gratitude to the leadership of AARI: Deputy Director A.S. Makarov, deputy chief of the RAE-S Yu.V. Ugryumov - for providing the opportunity to conduct field course, providing comfortable and safe working and living conditions; employees of the wintering staff of the RAE-S - G.V. Tarasov and O.R. Sidorova for help and solving emerging organizational issues during field work.

References

Demidov N., Karaevskaya E. Verkulich S., Nikulina A., Savatyugin L., 2016. The first results of permafrost observations at the cryospheric range of the Russian Scientific Center on the Spitsbergen Archipelago (RSCS). *Problems of the Arctic and Antarctic*, 4(110): 67-79.

Citizen approach to periglacial discussion: Scholar curriculum in Chile

Voltaire Alvarado Peterson[1,2]
Sebastián Ruiz Pereira[1]
Hans Fernández Navarro[1,2]

[1] Institute of Geography, Pontificia Universidad Católica de Chile, *vcalvarado@uc.cl*
[2] School of Geography, Universidad Academia de Humanismo Cristiano, Santiago de Chile.

Abstract

Climate forcing challenges the institutional apparatus to disseminate knowledge, promulgating mid and long-term strategies on cryospheric element assessment. Despite the mountainous character of Chilean geography, there are neither clear adapting policies nor sound pedagogic strategies to approach cryoform dynamics. The present study exhorts for the need of curricular exercises of situated learning within Chilean Academy-Legislation- Citizenship articulations

Keywords: Environmental education, Situated learning, Periglacial environment, Andes, South America, Chile.

Introduction

No legislative frame exists in Chile to preserve/assess glaciers and periglacial environment in Chile (Herr, 2013). Legislative projects (strictly) on matters of periglacial environments in Chile commenced on year 2014, when a draft law intended to 'protect and preserve glacial and periglacial environments, regulating potential activities on them (Bulletin Law 9364-12). In 2015, the Central Government exercised substitutive amendments (N°1170-362) to the draft and hence changing its nature. After the modifications, article n° 1 determined glacial areas as environmental heritage of the country, representing fresh water reservoirs, which provide eco-systemic services. The confrontation between strategic reservoir and element of inherent value to be protected portraits the unintelligibility of key-concepts that further interfere in the proper assessment of mountain cryosphere elements. This problem demands the enactment of sound knowledge transmission methodologies to the interacting parts.

Methods

Situated learning provides a valuable tool for enhancing the design and implementation of learning experiences (McLellan, 1996). When considering learning as a social phenomenon that should take place in complex, social situations (Anderson et al., 1996), it demands a deepening into the circumstances that determine the continuum's resolution of optimal teaching-learning targets for effective skills to be developed. Thus, aiming at the promotion of activities that bind mountainous environments and citizens together, the present proposal explores scholar curriculum and notions of situated learning related to periglacial topics. Both elements require deeper, redefining concepts and the clearing out the institutional approach, which may drive citizenship closer to periglacial settings understanding.

Results

Natural and social science national curriculum have shared the responsibility of transmitting these elements but failed to achieve an effective dissemination due to a weak training on these areas in high-school and college professors. Such problem may further fuel conflicts of interest and pernicious management if natural resources lie below the reach of the social body.

Outlines of the national curriculum in natural and social sciences present scattered and reduced contents on permafrost and glacier education, rendering gaps of knowledge on effective measures for management and conservation. These contexts, together with a review of their interaction would allow a critical reading of the State's role on this issue and the making of an environmentally resolved citizenship, representing solid contents and political responsibility.

Curricular national frame was reviewed for Natural and Earth Sciences and History, Geography and Social Sciences (Table 1), identifying contents, learning outcomes and skills expected for primary and high-school students in their ending first year. Further, glacier conservation normative in Chile was described and discussed within this perspective.

Conclusions

From the Academy-Legislation-Citizenship articulation, the constituting results display the need for a curricular exercise of located-learning strategies focused in environmental issues and citizenship in different school levels. The problem about politics it reflects the transit between legislation and school. The articulation is expressed in key learning dispositive for the enactment of a critical attitude towards these topics. Further, chronology of normative proposals on cryic environments was revised and weaknesses were identified in relation to the insertion of appropriated contents in the educational program.

An initial data base is the curricular sequence in bought disciplines. Table 1 describes cover and focus for these issue.

Table 1. Scholar Curriculum of History, Geography and Social Science academic content on glacial/periglacial topics.

Scholar level	Subject		Academic years	Programs for review
Primary	Natural sciences	History, Geography and Social Sciences.	8	16
High-school	Natural sciences	History, Geography and Social Sciences.	4	15

References

Anderson, J. R., Reder, L. M. & Simon, H. A., 1996. Situated learning and education. *Educational researcher,* 25.4: 5-11.

Chilean Deputy Chamber, 2014. Bull. 9364-12, Leg. 362, 20-May, 2014

Herr, L., 2013. Legal Framework of the Glaciers in Chile. *Justicia Ambiental*, May-2013.133 pp.

McLellan, H, 1996. Situated learning perspectives. *Educational Technology*.

Sharing knowledge about Central Andes permafrost (South America). Chances and shortcomings.

Sebastián Ruiz Pereira[1]
Carla Tapia[2]
Hans Fernández [1]
Dario Trombotto Liaudat[2]

[1] *Programa de Doctorado en Geografía, Instituto de Geografía, Pontificia Universidad Católica de Chile (sruizp@uc.cl).*
[2] *IANIGLA (Argentine Institute of Snow Research, Glaciology and Environmental Sciences), CCT Conicet, Mendoza, Argentina.*

Abstract

Networks for the dissemination of knowledge are created for an improved transfer of information between different researchers, individuals and organizations. It is the aim of this publication to review South American experiences in sharing knowledge regarding permafrost sciences during the last years. Current context includes a more interested society and expanding young-researchers population. To enhance the process of knowledge sharing, a better communication inside the research community should be achieved first, with emphasis in young-senior researcher interactions.

Keywords: Permafrost knowledge sharing, South America networks, AASP, PYRN

Introduction

The Andean range (South America) presents multi-level challenges for cryospheric sciences, hence calling for readily strategies for sharing of new scientific knowledge. Knowledge dissemination (KD) is the active task of communicate or share the results, during or after a research project, to the potential users of knowledge, using diverse strategies to adapt the findings to a particular audience. To encourage the KD it is necessary first to analyze the regional network structure, to establish and openly display possible user targets.

KD in the Andes. A brief history.

Andean permafrost-science networks started as national and regional scientific meetings during the 1980's .The books of abstracts of the Argentine Periglacial Group (1983-1989) include several works with multidisciplinary focus on permafrost research. Later, the IGU Latin American Subcommittee on the Importance of Periglacial Phenomena (1985) recognized the importance of South American research in permafrost, through the project "Geocryology of the Americas" (1989). Is in this context, Argentine and South American Permafrost Association (AASP; www.geocriologia.com.ar) was founded as a primal network for permafrost-research sharing in South America; its activity grows over the years and now has members from 10 different countries.

KD for permafrost research started with small activities with schools and teachers, through the work with autochthonous communities in northwestern Argentina by "Miguel Lillo Institute" research group and through national park's rangers training, among others. In spite of this reasonably good background, permafrost research had to overcome several barriers in the following years, flaws that weakened the transfer network and research progress. Institutional barriers and lack acceptance of permafrost-sciences as a legitimate approach in some academic institutions were some of the reasons behind this result. Others were related to the lack of funds and policies to protect subterranean ice, that aim regionally integrate the different stakeholders. As a result, the formation of new generations of researchers was stopped during several years.

In the last years however, Andean permafrost stands as a sensitive element in terms of mining, industrialization and progressive occupation of mountain regions in South America. A better understanding of the Andean periglacial environment with ice-rich geoforms such as rock glaciers, for example resulted in the approval of a law in Argentina aimed at the protection of the subterranean Andean ice. In this law, this kind of ice is consider a potential water supply to be used in the future and at the same time, it is taken into account as a present possible water contributor and/or a modifier of the high mountain environmental system affected by global warming (Sileo et al., 2016). In Chile, mining activities in periglacial environments gained social attention but the proposal of law on glacial and periglacial protection has not yet been successful until today. A similar situation is reflected in Bolivia and Perú.

Societies claim now for clear and useful knowledge to use or protect their natural resources. As result, a new generation of young researchers and students is currently under formation and in continuous growing. The integration of these groups and the stakeholders with the senior research community should be satisfied by the strategies of an expanded KD net.

Proposal of expanded KD network

International and inter-institutional scientific networks require a process of mutual learning, between young and senior researchers, policy makers and the education system at various levels. Convenient strategies should fall within a determined topology of the KD process since organizational levels acquire diverse complexities; for instance, **multi-disciplinarily**, **trans-disciplinarily** and **inter-disciplinarily**. Today, Andean permafrost-science networks are evolving towards the integration of the discipline spectrum.

AASP structure should act as the base level of the network, that facilitates the communication between researchers. Young researchers and students should involve into the pre-existing AASP network and PYRN activities simultaneously, but also actively participate in open forums with senior-lecturers on interlinked issues belonging to a similar epistemic topology. Main aim is to close the generation gap between young and senior researchers, through knowing the extensive permafrost background. Also it helps young researchers to train their communicative skills and learn KD strategies based on senior's experiences. Collaborative research projects, based on the resolution of territorial problems with a broad participation of actors is other alternative to reinforce international networks. Interest and motivations of the involved actors will fuel the process.

References

Book of Abstracts: Reunión del Grupo Periglacial Argentino, 1983-1986. Subcomisión Latinoamericana sobre la Importancia de los Procesos Periglaciales International Geographical Union. Director: Arturo Corte. Ianigla - Cricyt – Conicet, Mendoza, Argentina.

Book of Abstracts: Geocryology of the Americas, 1989. Primera Reunión del Proyecto 197 IGCP, Unesco. Ianigla – Cricyt – Conicet, Mendoza, Argentina

Sileo, N., Dario Trombotto Liaudat, D. y Dapeña, C., 2015. Estudios preliminares del agua, nieve y hielo en la cuenca del río Vallecitos, Mendoza, Argentina. *Acta Geológica Lilloana* 27 (2): 130–145.

The legacy of Cryolithology Scientific School in Lomonosov Moscow State University

Streletskaya I.D., Grebenets V.I., Konishchev V.N., Tumel N.V.,
Rogov V.V., Shpolyanskaya N.A., Badu Yu.B., Kizyakov A.I., Zotova L.I.
Lomonosov Moscow State University, Department of Geography, 119992, Moscow, GSP-2, Leninskie Gory, Russia, irinastrelets@gmail.com

Abstract

The Department of Cryolithology and Glaciology of Geographical Faculty, Lomonosov Moscow State University was founded by Dr. Alexander Popov and is one of the oldest continuously operated equational centers in the area of permafrost science worldwide. More than 600 specialists graduated from the Department over the years. The legacy of the school of cryolithology, recent work and educational activities conducted by the Department faculty and students are briefly summarized.

Keywords: Cryolithology, Lomonosov Moscow State University, education, history of science.

The Department of Cryolithology and Glaciology of Geographical Faculty, Lomonosov Moscow State University is one of the oldest continuously operated equational centers in the area of permafrost science (Fig.1). The Department of Cryolithology and Glaciology was founded in 1945. The important stage in the history of the Department was the alliance of the two closely related, but distinct branches of the cryospheric science: Permafrost and Glaciology within one department. The goal of this merge was to bring investigation of glacier and underground ice closer and to determine the factors of their occurrence throughout the Quaternary period. Since 1964 to 1993 the Department was led by Prof. Dr. Alexander Popov who created the new branch of permafrost science, titled "cryolithology" as a systemic study of cryogenic processes and landforms they create. Dr. Popov developed a theory of cryolithogenesis, the specific type of climatically driven lithological process, which is characteristic for cold regions of the lithosphere. In a series of publications he demonstrated that freezing processes and ground ice formation are determined by geologic, climatic and thermal properties of the ground. Dr. Popov also developed genetic classification of periglacial landforms and proposed the cryogenic weathering as the major factor of loess formation. Currently, the department continues to develop fundamental scientific problems of the Cryosphere, such as ground ice genesis; the formation, structure and composition of frozen sediments; the characteristics of seasonal freezing and thawing; interactions of permafrost and glaciations. The results of this research were published in numerous papers and monographs; series of Permafrost and Cryolithological maps of various scale and presented in national and international conferences. More than 600 specialists graduated from the Department, several dozen Ph.D. and 10 D.Sc. were trained at the Department. Currently the Department gives BS, MS and PhDs degrees.

The main directions of the scientific research of the Department are 1) study of the Earth cryosphere evolution; 2) development of the palaeocryogenic reconstructions based on cryogenic, isotope, geochemical, and paleogeographic methods; 3) evolution of the mountain glaciations based on analytical and field studies; 4) study of the snow cover properties and avalanche dynamics under the changing climate; 5) geoecology of the cryosphere and forecast of hazards in permafrost and high mountainous areas.

The success of the Department of Cryolithology and Glaciology is attributed to integrating field methods, internships and field research in its curriculum. The area of field research is extremely wide: Kola Peninsula, Arkhangelsk region, Bolshezemelskaya and Malozemelskaya Tundra, Western Siberia, Novosibirskie Islands, Yano-Indigirka and Kolya Lowlands, Central Yakutia and Baikal region, Antarctic. During the last decade, the geography of field classes widened even further, and now it includes Norilsk industrial area, Salekhard, and Vorkuta. The Department of Cryolithology and Glaciology is a consolidated collective of scientists, teachers and students, well-known all around the world for its scientific and training achievements.

Figure 1. The Department of Cryolithology and Glaciology logo.

References

Popov, A.I., 2013. *Selected works, and about Him*. Moscow, Scientific World, pp. 536.

http://www.eng.geogr.msu.ru/departments/crio/

Winter field practice for the study of seasonal freezing in Central Russia

Tolmanov Vasily A.[1]
Grebenets Valery I.[1]
Maslakov Alexey A.[1]
Yurov Fyodor D.[1]
[1]*Moscow State University, Geographical faculty, Department of Cryoliyology and Glaciology*

Abstract

For more than 15 years, the Department of Cryolithology and Glaciology organises a winter field practice for 2nd year students in order to study the snow cover and seasonal freezing in Central Russia. In the course of this practice, students acquire the skills of studying frozen soils and their basic parameters: cryo-texture, temperature and lithology

Keywords: student practice, investigations of seasonal freesing

Introduction

Department of cryolithology and glaciology of the Faculty of Geography of Moscow State University organized special winter field practices on the study of seasonal freezing and snow cover in the territory of Central Russia, during the last two decades.

Seasonal freezing is the natural phenomenon, which depends on landscape, lithological and meteorological conditions (air temperature, snow accumulation).

A standard program for studying the seasonally frozen layer (SFL) does not exist, the department has developed its own program. The study of seasonal freezing has both practical and scientific significance. There are two stages of the practice: the first stage of the practice takes place at the beginning of winter period (late November - early December), when seasonal freezing of soils and formation of snow cover only begins, the second stage is carried out at the end of the winter period, just before beginning of snow melting (end of February - early March).

Practices were organized in Pushchino (south of Moscow region), Satino (Kaluga region), Zvenigorod and Krasnovidovo (west of the Moscow region)

The aim of the practice is to educate the students of the 2nd course in the skills of cryolithological research: the basic methods of studying frozen soils and their characteristics.

Methodology, results and observations

We carried out investigations, included various elements of the permafrost survey, the regularities of the seasonal-frost layer formations, its cryogenic structure, special microforms of the cryogenic relief.

Study points are located in different landscape conditions (including anthropogenically altered), which is necessary for a comprehensive study of seasonal freezing and its patterns.

A detailed description of the surrounding landscapes, relief, nature of vegetation, measurements of air temperatures in the immediate vicinity of the point were made.

Each research on the point consists of: soil pit digging, description of upper horizons of the soil massif and snow cover structure. Students fix the lower bound of frost layer, temperature of soil massif and sampling of soil, which is necessary for further laboratory studies. Particular attention in pit describing is given to the cryo-textures (*fig.1*) and their distribution along the soil profile.

Temperature loggers that fix temperature values throughout the winter period and frostmeters, that fix maximal depth of frost layer are installed in some pits. During the frostmeters installations, the students obtained drilling skills with manual and semi-automtic drill. The students determine the moisture content of the soil at the beginning and end of the winter period in the soil laboratory, need to detect migration of moisture along the profile during the development of the seasonal freezing process.

The results of the practices are follows: obtaining by students the skills of studying frozen soils, knowledge of the basic properties of frozen soils, the patterns of snow cover distribution and seasonal frost power. A special aspect of the practice was the studying problems arising in the construction of engineering objects in unstable temperature conditions.

Fig.1. Description of the cryogenic texture, photo: Tolmanov V.A.)

Practice also have significant scientific component: data, dedicated to the: change in soil conditions during seasonal freezing of soils, the conditions of occurrence and the nature of accumulation of snow cover, the effect of various natural factors on the nature of soil freezing, and the regularities in the formation of a layer of seasonal freezing in various landscape and lithological condition were obtained (*table.1*).

Table 1. Distribution of the seasonal frost layer in different landscape conditions

Winter, yrs.	The sum of negative degree-hours.	High and low floodplain and the 1st terrace above the floodplain		Watershed			
				Forest at the watershed		Trail at the watershed	
		Snow thickness, cm	Seasonal freezing, cm	Snow thickness, cm	Seasonal freezing, cm	Snow thickness, cm	Seasonal freezing, cm
1999/00	14500	30	10	23	0	17	40
2000/01	15050	Not data	Not data	30	0	10	20
2001/02	15500	28	Not data	19	0	0	28
2002/03	20500	27	16	29	10	24	62
2003/04	10500	35	0	8	0	40	6
2004/05	14600	27	20	32	35	14	40
2005/06	21500	47	28	39	60	4,5	98
2006/07	7296	32	0	27	8	Not data	Not data
2007/08	10500	20	22	17	35	9	88
2008/09	11290	31	15	30	25	12	73
2009/10	23230	34	22	36	35	14	77
2010/11	18800	26	19	35	31	16	68
2011/12	14070	44	17	19	41	32	60
2012/13	17455	57	1	48	44	41	41
2013/14	11830	17	13	10	15	11	45
2014/15	9970	37	42	28	10	30	30
2015/16	22766	Not data	Not data	8	20	8	45

Conclusions

In general, seasonal freezing in the territory of Central Russia distributed everywhere, but with different levels of intensity, heterogeneity in space, and considerable variability from year to year. The spatial and temporal patterns of the development of seasonal freezing are affected by factors, but meteorological are determining. Lithological and landscape conditions, as well, as the degree of antropogenic impact, can provide variations in the depth of the season frost layer in fairly limited spaces.

Education with Permafrost: Expanding permafrost specialists

Kenji Yoshikawa[1]
Hanne Christiansen[2]
Member of the Education and Outreach committee[3]
[1]*University of Alaska Fairbanks, kyoshikawa@alaska.edu*
[2]*University Centre in Svalbard*
[3]*International Permafrost Association*

Abstract

Permafrost can serve as a valuable resource to teach about how scientific research is done, how the earth system works, and about permafrost's unique impacts and challenges. It is also important and necessary to educate and train future permafrost researchers and engineers, at the college level and through continuing post-graduate opportunities. We, the International Permafrost Association's (IPA) Standing Committee on Education and Outreach introduce continuing educational opportunities including IPA hosting University of the Arctic (UArctic) Thematic Network on Permafrost (TNP) activities as well as the International University Courses on Permafrost (IUCP) database. A wide variety of initiatives are underway in many countries to include permafrost in the school curriculum and we encourage submissions on these efforts or on the effectiveness of these activities.

Keywords: Education and Outreach committee; University of Arctic; thematic network on permafrost; International University Courses on Permafrost; TNP; IUCP

Introduction

The Global Learning and Observations to Benefit the Environment (GLOBE) Program is an international science and education program for K-12 younger education program for the active layer monitoring. Over 110 countries participate in GLOBE and the website and activities are available in English, French, German, Spanish, and Russian, and other languages. The Frost Tube Protocol Investigation was launched in October 2017, which means that teachers (in all frost tube countries) can now enter their frost tube data to the GLOBE database. Teachers, students, or anybody interested can access this archived data and learning about soil freezing.

Many collage level permafrost summer courses were organized last several years such as, South American Geocryology, Permafrost in the Andes, and Paleo-Permafrost in Patagonia at the National University of San Juan, Argentina. Both Lomonsov Moscow State (MSU) in Russia and the University Centre in Svalbard (UNIS) offered their field courses open to international students. Many of the field courses are available at low cost but this varies from course to course today. In addition, four consecutive years, the University of the Arctic's Thematic Network on Permafrost (TNP) summer field school was held at the UNIS (2014,15), North Eastern Federal University (NEFU) Yakutsk (2016) and University of Alaska Fairbanks (UAF) in 2017. In this presentation, we focus to the UArctic activities and future participation.

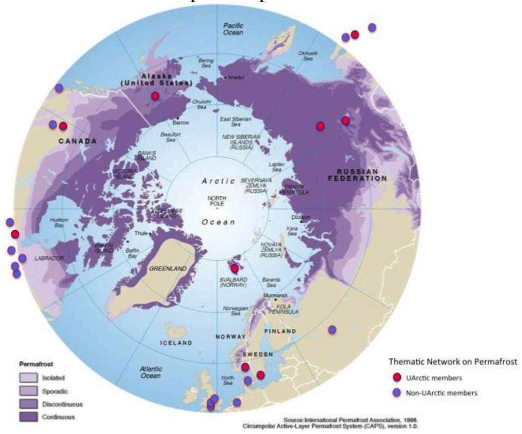

Figure 1. the member of the University of the Arctic, Themathic Network on Permafrost (TNP)

Thematic Network on Permafrost

Our work with this group is primarily with field courses and developing a model graduate curriculum. Several institutions continue to run annual summer field courses open to international students, such as Lomonsov Moscow State University (MSU). Many of the field courses are available at low cost but this varies from course to course. The EO Committee maintains a database of International University Courses on Permafrost (IUCP) which continues to list all university classroom and field-based courses which we know of.

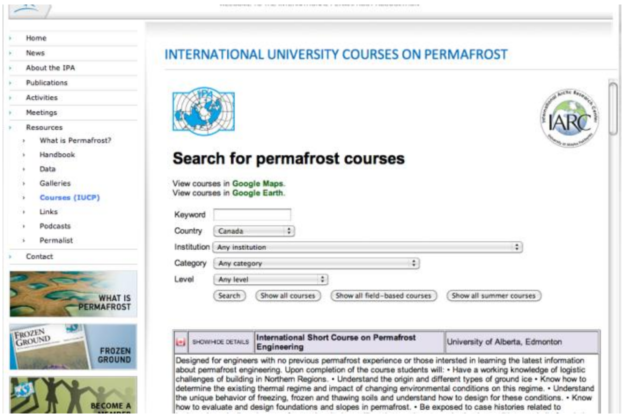

Figure 2. IUCP data base

The University Centre in Svalbard (UNIS), after holding two University of the Arctic's Thematic Network on Permafrost (TNP) summer field courses in Longyearbyen (2014, 2015), took over the responsibility of continuing to annually offer this field course as a true legacy of the Thematic Network on Permafrost Norwegian activity. These courses are now open to bachelor and graduate students. The third year of the TNP field school focused on permafrost and natural hazards in Yakutsk, Russia, as a collaboration between the University of the Arctic TNP and North Eastern Federal University. During the 3 week session, 14 students from 9 countries attended (India, China, Mongolia, Japan, Germany, UK, Norway, Russia and USA). The summer field school aims to provide students with an overview of the many different research topics related to permafrost, ranging from geoscience, engineering, and bioscience to social science. We invited 14 professors/ doctors as lecturers. We used the Central Yakutian landscape to study different landforms and to gain hands on experience with field techniques for studying permafrost. We deeply appreciate the volunteer participation of the professors and much logistical support from the Russian Academy of Science's Melenikov Permafrost Institute. We did host University of Alaska Fairbanks (UAF) at Siberian style reindeer farm near Fairbanks Alaska in 2017 and planning in Greenland in 2018 hosting by Stockholm University.

Continuing work on a model curriculum on permafrost at the Master and Doctoral level, has led to establishment of a "Master of Permafrost" program at University of Alaska-Fairbanks (UAF). The first student graduated in August 2016, with an Interdisciplinary Master of Science in International Permafrost Ecosystem Studies. We hope additional students at UAF and elsewhere follow this path using UArctic systems.

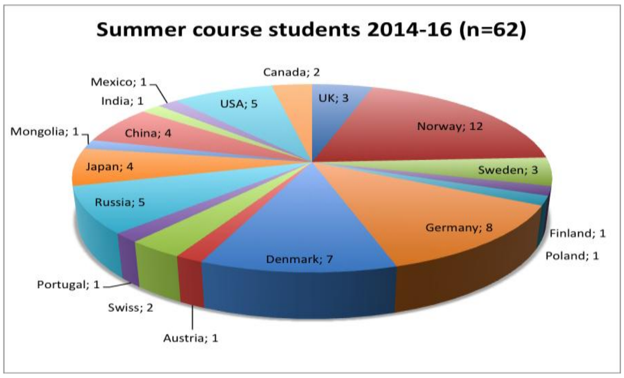

Figure 3. International Bachelor Permafrost Summer School 2014, 2015, 2016 (From 2016 UNIS takes over the responsibility to continue this course as a true legacy of the Thematic Network on Permafrost Norwegian activity)

5 - Interdisciplinary approaches to conceptualize changes and feedbacks in permafrost landscapes

Session 5

Interdisciplinary approaches to conceptualize changes and feedbacks in permafrost landscapes

Conveners:

- **Thomas A. Douglas**, U.S. Army Cold Regions Research and Engineering Laboratory, Alaska USA
- **Benjamin W. Abbott**, Brigham Young University, USA (PYRN member)
- **Yuanchao Fan**, Uni Research Climate and Bjerknes Centre for Climate Research, Bergen, Norway (PYRN member)

Climate change is altering disturbance regimes in permafrost landscapes. Dramatic shifts have been observed or are projected in the timing and severity of wildfire, hydrogeology, and permafrost degradation including active-layer deepening and thermokarst development. These changes may provide significant feedbacks to the Earth system on local to global scales that can shape future climate. Biogeophysical and biogeochemical processes of permafrost have complex interplays with other ecosystem elements such as vegetation, microorganisms, and hydrological properties. Multiple approaches and disciplines are therefore needed to make meaningful predictions about what permafrost landscapes will look like in the future at decadal to century timescales.Progress is being made toward understanding ecosystem function under historical and current disturbance regimes using remote sensing, pattern and change detection, and chronosequence approaches. Mechanistic and empirical modelling efforts are integrating this understanding to project these trajectories into the future. These approaches often vary between upland, wetland, and lake systems, limiting our ability to project potential future states at landscape and regional scales or incorporate these processes into global frameworks such as Earth System Models (ESM's). In this interdisciplinary session, we invite presentations investigating how ecosystem structure and function respond to changing disturbance regimes in permafrost landscapes. This includes studies using remote sensing, long-term or chronosequence methods, or process-oriented experiments or models. We are particularly interested in presentations addressing abrupt or nonlinear landscape change in space and time, and efforts towards global-scale assessments (including those using ESM's). A few example questions include: How to identify areas vulnerable to thermokarst based on vegetation-permafrost interactions? How will water availability and flowpaths change? What biogeochemical signals of landscape and hydrologic change can we use to quantify abrupt or nonlinear shifts? How will coupled nutrient and elemental cycles respond to physical and ecological disturbance? We specifically encourage presentations that strive to unify terrestrial and aquatic ecosystems and links with climate change at multiple spatial and temporal scales.

Numerical Simulation of Lateral Permafrost Thaw in Northwest Territories

Erfan A. Amiri[1], James R. Craig[2], M. Reza Hirmand[3], Elise Devoie[2], William L. Quinton[4]

[1]*Deparment of Civil and Environmental Engineering, University of Waterloo, Waterloo, Canada, eabedian@uwaterloo.ca*

[2]*Deparment of Civil and Environmental Engineering, University of Waterloo, Waterloo, Canada*

[3]*Deparment of Mechanical and Mechatronics Engineering, University of Waterloo, Waterloo, Canada*

[4]*Centre for Cold Regions and Water Science, Wilfrid Laurier University, Waterloo, Canada*

Abstract

During past decades, an increase in mean annual temperature in the northern hemisphere has led to an acceleration of permafrost thaw. While gradual vertical thaw plays some role in landscape evolution, the lateral thawing of permafrost beneath peat plateaus is of critical importance in the wetlands of the Taiga Plains in the Northwest Territories, Canada. Despite the importance of this phenomenon, little is known about the external and internal controls on the rate of lateral thaw and few efforts have been made to assess and quantify the relative impacts of the lateral components of the energy balance that drives thaw. Lateral thaw can take place after formation of an open talik or can be encouraged by the presence of advective heat transfer from adjacent fens. In this research, permafrost lateral thaw is investigated based upon sharp interface and continuum phase change criteria. Numerical simulations show that permafrost is thawing laterally.

Keywords: permafrost, lateral thaw, finite element model, enthalpy method, extended finite element, conductive heat transfer.

Introduction

Understanding of permafrost thaw processes in the regions with discontinuous permafrost is crucial since the mean temperature in these areas is close to permafrost thaw temperature, and a slight increase in the mean temperature can results in a severe and irreversible thaw. Previous simulation results and field observation reports show that permafrost is thawing laterally (Ling *et al.*, 2012), which is due to the dominancy of lateral heat conduction in this environment. Estimating the rate of permafrost lateral thaw requires a thorough understanding of the controlling parameters in permafrost processes. Kurylyk *et al.* (2016) studied the effect of permafrost lateral thaw on peat plateau-wetland system landscape evolution. They illustrated by field observations and simulations that the conventional models, which are restricted to vertical 1-D heat transfer, may not be sufficient for estimating permafrost thaw rates. McClymont *et al.* (2013) developed a model for estimating permafrost degradation rates in discontinuous permafrost. The results of their study show that peat plateaus—compared to fens and bog—play a substantial role in decreasing permafrost thaw rate since a layer of peat plateau that is partially saturated acts as an insulation layer due to its low thermal conductivity.

To model permafrost lateral thaw, a realistic permafrost model is required. The present research is based upon the application of a two-dimensional cross-sectional finite element model that is developed using both the extended finite element (XFEM) technique (sharp interface) and an enthalpy method (continuum slushy zone) for capturing the phase change process at the ice-water interface. Only saturated flow is considered.

Methodology

In the present work, the finite element and Newmark methods are employed for space and time domain discretization, respectively. The weak formulation of the problem is obtained by integrating the product of the governing PDE, Eqn. 1, multiplied by an admissible test function over the computational domain and implementing the Gauss-Green theorem.

$$\frac{\partial(\beta(T)T+\alpha(T))}{\partial t}-\nabla.(K(T)\nabla T)=0\,, \tag{1}$$

in which $\beta(T)$ is the average bulk heat capacity and $\alpha(T)$ is the latent heat released by the phase-change process, which are defined as

$$\beta(T) = n\left(S_w(T)\rho_w c_w + \left(1 - S_w(T)\right)\rho_i c_i\right) + (1-n)\rho_s c_s \quad (2)$$

$$\alpha(T) = n\rho_i L_f\,. \quad (3)$$

Since $\beta(T)$ and $\alpha(T)$ are temperature dependent, a fully nonlinear approach must be implemented for solving Eqn. 1. Hence, a hybrid full Newton-Raphson-Trust-Region solver is developed to tackle the nonlinearity of the problem.

Results

In this research, the estimates of lateral thaw rates quantified by the sharp interface and continuum models are compared. The study area of this research is the Scotty Creek region in the southern Northwest Territories, Canada, where discontinuous permafrost exists underneath the bogs and peat plateaus. The goal of this research is to study the processes that contribute to the long-term lateral permafrost evolution, quantify the role of the key external forcings, and investigate the response of the permafrost bodies to future seasonal temperature changes.

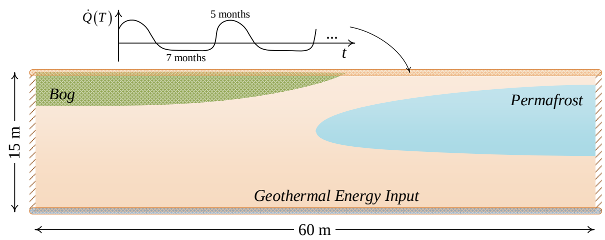

Figure 1. Permafrost region configuration with input flux from top and geothermal flux from bottom

A schematic of the configuration of the simulation region is shown in Figure 1. The energy input of the top boundary is based on in situ data collected from Scotty Creek site in the Northwest Territories. Results will demonstrate the critical controls on lateral thaw and the dependency of thaw rates upon rates of lateral advection, presence of snow, radiative forcing, geothermal gradient, and system heterogeneity. Results may later be used to inform simulation models that represent long-term landscape change.

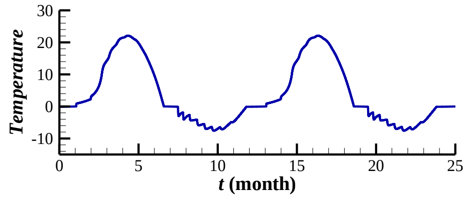

Figure 2. Temperature profile of ground (the top boundary) over two years

The preliminary results from simulating permafrost in a 60m by 30m domain by the developed continuum model is shown in Fig. 3. As is evident in the results, permafrost is thawing laterally over the solution time (100 years). The ground temperature used in the simulations is shown in Figure 2.

(a)

(b)

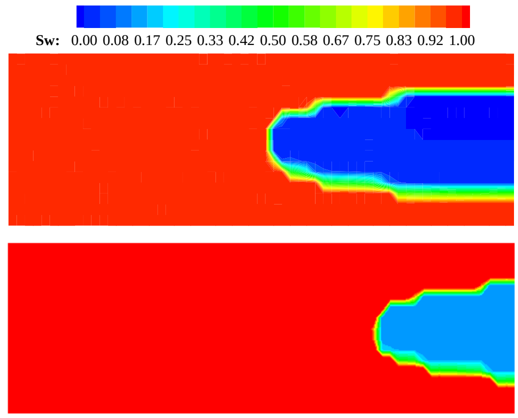

(b)

Figure 3. Water saturation profiles, (a) after 3 years, (b) after 100 years

References

Kurylyk, B.L., Hayashi, M., Quinton, W.L., McKenzie, J.M., & Voss, C.I., 2016. Influence of vertical and lateral heat transfer on permafrost thaw, peatland landscape transition, and groundwater flow. *Water Resources Research*. 52: 1286–1305.

Ling, F., Wu, Q., Zhang, T., & Niu, F., 2012. Modelling Open-Talik Formation and Permafrost Lateral Thaw under a Thermokarst Lake, Beiluhe Basin, Qinghai-Tibet Plateau. *Permafrost and periglacial processes*. 23: 312–321.

McClymont, A.F., Hayashi, M., Bentley, L.R., & Christensen, B.S., 2013. Geophysical imaging and thermal modeling of subsurface morphology and thaw evolution of discontinuous permafrost. Journal of Geophysical Research: Earth Surface. 118: 1826–1837.

Dendrochronologic reconstruction and indication of gas-emission pre-crater mound

Stanislav (P) Arefyev[1,3]
Marina (O) Leibman[2,3]
Artem (V) Khomutov[2,3]

[1]*Tyumen Scientific Centre SB RAS, Institute of the problems of Northern development, Tyumen, sp_arefyev@mail.ru*
[2]*Earth Cryosphere Institute Tyumen Scientific Centre SB RAS, Tyumen*
[3]*University of Tyumen, International Institute of Cryology and Cryosophy*

Abstract

Tree-ring width chronologies of willow (up to 95 years age) sampled from two gas-emission crater sites on Yamal and Gydan Peninsulas were analyzed. Willow samples were collected from blocks of material ejected from the pre-crater mound and *in situ* in surrounding tundra. Willow growth on the mound depends on July and August air temperature which differs from surrounding background tundra willows with growth depending only on July air temperature. The absolute willow ring accretion in different loci of GEC-1 pre-crater mound depended on the snow cover thickness, which changed during the period of mound growth. The mound elevation increased by 0.8 m in 1976-1985. This mound started to grow in 1940s. Periodic dissonances of willow ring chronology on the mound and in surrounding tundra following cycles of 6, 11 and 20-22 years. The mound eruption in 2013 coincided with the year of dissonance and the peak of solar activity cycle.

Keywords: Gas-emission pre-crater mound; tundra shrubs; annual growth rings; solar cycles; West Siberia.

Introduction

Tree-ring width chronologies (TRW) are widely used for reconstruction of natural processes (Cook & Kairiukstis, 1990), in particular in permafrost area to study permafrost dynamics, thermokarst, icings, snow cover. In the treeless tundra, shrubs 100 and more years old are used for TRW. The relationship between their ring accretion and July air temperature along with other climate parameters is established indicating climate warming (Buchwal *et al.*, 2013; Arefyev, 2015). Shrub TRW are used for the reconstruction of cryogenic landslides (Leibman *et al.*, 2000), in particular on the violation of coherence of TRW from the landslide and TRW from background tundra.

Tundra shrubs are considered as sensors-recorders of active layer conditions, snow thickness and background climatic factors in 1-3 m^2 wide locus. We used shrub TRW to reconstruct and indicate formation of mounds-predecessors of gas-emission craters (pre-crater mounds) (Arefyev *et al.,* 2017).

Study area and methods

Craters under study were found in the north of West Siberia in the central part of Yamal Peninsula (GEC-1) and in Gydan Peninsula (AntGEC) approximately at the same latitude of about 70ºN. Both eruptions occurred in the fall of 2013. GEC-1 was studied in more detail. Remote sensing data analysis showed that mound by 45-48 meters in diameter and 5-6 meters in height existed in the place of future crater.

Willow samples (Salix lanata) were collected from 6 loci of GEC-1 in August of 2015, one trunk for each locus. S1-S3 samples were collected from ejected blocks of material with vegetation residues. We reconstructed position of blocks on the existing pre-crater mound based on the distance from crater axis and vegetation status. This reconstruction was confirmed by further analysis. S1 is assigned to mound top, S2 to the edge of mound top, S3 to a steep slope of the mound. S4 sample was collected *in situ* from low undisturbed part of the slope, S5 also *in situ* from mound foot, and S6 *in situ* 50 meters away from the crater in surrounding background tundra.

Thin slices were cut in different parts of trunks: from base to 2/3 of trunk length. In each slice rings were measured under a microscope in 1-4 radii. In total, 103 radii were measured, from 10 to 31 for a loci. After cross date procedure for individual ring radii we standardized them by triangular moving average (TMA) calculation with equal weights to exclude local and age-related factors. Generalized TRW are compiled for each locus using absolute ring width (millimeters), and standardized ring width (indices). Indices were processed by STATISTICA 10.0 Software to find relationship between willow ring accretion and background climatic factors, such as monthly average air temperature and sum of precipitation.

We had found one willow shrub dated since 1918 on ejected block from AntGEC, and samples of willow from background tundra (grown since 1996). Background willow samples from other locations of Gydan Peninsula were also used for analysis.

Results and discussion

Cluster analysis showed that at GEC-1 location the oldest willow (since 1924-1935) sampled in background tundra (S6) as well as on a mound foot (S5) where willow was not affected by mound expansion until 1998. Willow has been growing since 1948-1951 on mound top and only since 1965-1976 on its slopes. According to average ring width exceeding 0.3 mm, conditions for willow growth were most favorable in surrounding background tundra and in the lower part of mound slope (S4), where shrubs were protected by 0.8-m snow cover in winter as indicated by willow height. Conditions were the least favorable on mound top, where snow was blown away by wind and trunks had gained dwarfish forms with ring width about 0.1 mm.

The first years willow ring accretion in mound top loci was close to its value in background tundra because snow cover was yet thick and conditions for willow growth were similar to surrounding background conditions. Growing up of the mound caused reduction of willow ring accretion due to decrease of snow thickness. Equality of conditions was observed in 1947, which can be taken as the start of pre-crater mound formation.

Relation of willow-ring accretion to snow thickness is very indicative at loci S3 in the upper part of mound slope. In 1976, ring width matched 0.8-m snow thickness, by 1985 it decreased to level of snowless loci on mound top. Probably, in 10 years mound grew up by 0.8 m. Thus, mound age calculated through the rate of its growth and the final mound height provides approximately the same result between 1938-1951. For mound loci S1 and S4 reliable relationship between willow ring accretion and air temperature detected not only in July as in surrounding tundra but also in August was established. This phenomenon observed in Yamal for the first time may be considered an indicator of the pre-crater mounds.

Calculation of Pearson correlation between willow TRW from background tundra and from mound shows periodical dissonance associated with stresses in root layer. The 6-year and 20-22-year ("Hale cycle") cycles associated with the effect of planetary tidal forces are detected, as well as the 11-year solar cycle ("Wolf cycle"). The eruption in 2013 coincided with the year of dissonance and the peak of solar activity cycle. Similar results were obtained for AntGEC location.

Conclusion

The most probable dates (since 1940s) and rate of pre-crater mound formation were determined in connection to solar activity cycles using dendrochronologic reconstruction. Existence of relationship between willow ring accretion on the mound and the August air temperature could indicate such pre-crater mounds.

Acknowledgments

This work is supported by Russian Science Foundation grant No.16-17-10203.

References

Arefyev, S.P., 2015. Fixing of climate warming in ring chronologies of shrubs in the north of Yamal and Gydan Peninsulas. *Journal of Siberian Federal University. Biology* 4(8): 377-393 (In Russian).

Arefyev, S.P., Khomutov, A.V., Ermokhina, K.A., Leibman, M.O., 2017. Dendrochronologic reconstruction of mound formation at the Yamal gas crater location. *Earth Cryosphere* XXI(5): 107-119 (In Russian).

Buchwal, A., Rachlewicz, G., Fonti, P., Cherubini, P. & Gärtner, H., 2013 Temperature modulates intra plant growth of Salix polaris from a high arctic site (Svalbard) *Polar biology* 36 (9): 1305-1318.

Cook, E.R. & Kairiukstis, L.A. (eds.), 1990. *Methods of dendrochronology: Applications in the environmental sciences.* Dordrecht; Boston; London: Kluwer Acad. Publ., 364 pp.

Leibman, M.O., Archegova, I.B., Gorlanova, L.A. & Kizyakov, A.I., 2000. Stages of cryogenic landslides on Yugorsky and Yamal Peninsulas. *Earth Cryosphere* IV(4): 67-75 (In Russian).

Linking geomorphological connectivity to sediment transport measurements in an Alpine glaciated basin: present dynamics and future scenarios

Anuschka Buter[1]
Francesco Comiti[2]
Andrea Andreoli[2]
Tobias Heckmann[3]
[1]*Free University of Bozen-Bolzano, anuschka.buter@natec.unibz.it*
[2]*Free University of Bozen-Bolzano*
[3] *Catholic University of Eichstätt-Ingolstadt*

Abstract

A high proportion of glaciated and permafrost areas in the Alps are retreating with consequent strong impacts on sediment cascades of mountainous catchments. A modelling approach, using a geographical information system (GIS) combined with an analysis based on graph theory, is applied to study the sediment connectivity of a glaciated catchment in the Italian Alps. The spatial distribution of sediment source, transport and deposition areas are defined for contrasting sub-catchments and related to real-time measurements of sediment fluxes. Additionally, multi-temporal digital elevation models (DEMs) are analyzed using DEMs of Difference (DoDs) and flow routing algorithms to determine sediment pathways and calculate sediment delivery ratios (SDR). The results of the project will greatly contribute to advance our comprehension of sediment connectivity dynamics driven by glacier melting and permafrost thawing, which will allow river managers to set up improved strategies for integrating flood hazard mitigation and ecological restoration in mountain river networks.

Keywords: Alpine glaciated catchment; permafrost thawing; sediment connectivity; sediment cascades; graph theory; DEMs of Difference.

Introduction

Glaciated and permafrost areas in the Alps are shrinking because of the global warming trend. Consequences regarding sediment transport are a higher availability of sediment due to loss of glacial storage and increasing instability of permafrost zones. Further, sustained high-flows due to augmented glacier melting and a higher frequency of extreme meteorological events are expected in the future (Beniston 2006). Thus, an elevated potential of sediment-loaded floods is likely, which may be a threat for people and infrastructure. Studying sediment connectivity is valuable to understand and predict these sediment management issues (Cossart & Fressard 2017; Lane *et al.* 2017).

Material and Methods

Study area

The study area, the Solda river catchment (130 km²), is located in the Italian Alps. It is characterized by a large relief (1100-3905 m a.s.l), a high glacial coverage (14% of the total area) and a complex geology including metamorphic and dolomitic rocks. Hence, it comprises a spatially highly variable erodibility. Furthermore, glacial landforms and permafrost zones are highly relevant regarding sediment transfer.

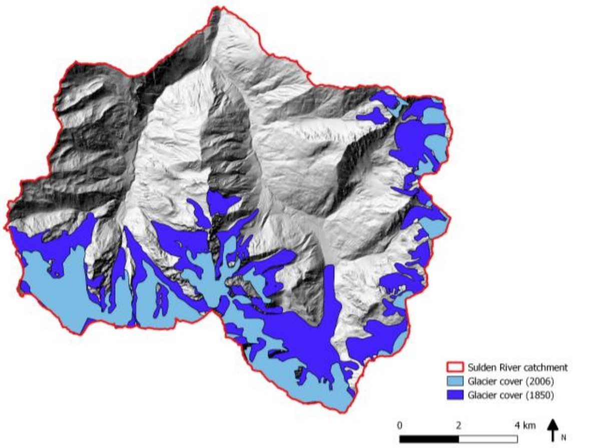

Figure 1. Catchment area with glacial cover at 1850 and 2006.

Field work

Within the fieldwork, the fluvial sediment is analyzed by direct and indirect measurements. Indirect measurements are conducted by geophones and turbidimeters. Both techniques are calibrated based on direct sampling campaigns. Indirect measurements offer the possibility to monitor sediment continuously and provide valuable data to acquire detailed insights in the processes and triggering mechanisms of fluvial sediment transport (Mao *et al.* 2014).

GIS-based modelling

A new method of analyzing sediment connectivity is based on graph theory (Heckmann & Schwanghart 2013; Cossart & Fressard 2017), which is used to define objects within a network system and their interactions (Heckmann *et al.* 2015). Sediment transport processes are considered by different spatial explicit models, integrating specific threshold parameters. The resulting registered sediment pathways contain spatial information as well as the type of process. The spatial distribution of sediment source, transport and deposition areas is defined and compared to observations of the fieldwork. The simulation of extreme events, implemented in the model, e.g. in form of a lower slope threshold for debris flows, will be considered by a sensitivity analysis.

Analysis of DoDs

Morphological budgeting and spatial definition of erosion and storage zones is conducted based on the analysis of DoDs. Additionally, a recently developed approach to combine DoDs and flow routing is applied to infer sediment pathways and calculate the SDR (Heckmann & Vericat, acc.). In most studies so far the SDR was only estimated. Consequently, this new approach can be seen as a major advancement (Heckmann & Vericat, acc.).

Conclusion and expected outcomes

There is an urgent need to analyze and understand sediment transfer processes in glaciated mountain catchments as the climatic changes have a strong impact on their geomorphology and hydrology (Beniston 2006). The project includes innovative approaches to study sediment connectivity quantitatively, but also traditional geomorphological observations and field measurements are conducted. The results are expected to have a significant effect on the development of these new methodologies. Further, knowledge about the complex system of sediment transfer processes in glaciated and permafrost areas at present-day and for potential future scenarios will increase and may be used to assess and prevent potential future threats for civilization and infrastructure.

References

Beniston, Martin, 2006. Mountain weather and climate. A general overview and a focus on climatic change in the Alps. *Hydrobiologia* 562: 3–16

Cossart, É. & Fressard, M., 2017. Assessment of structural sediment connectivity within catchments: insights from graph theory. *Earth Surf. Dynam.* 5: 253-268.

Heckmann, T. & Schwanghart, W., 2013. Geomorphic coupling and sediment connectivity in an alpine catchment - Exploring sediment cascades using graph theory. *Geomorphology* 182: 89–103.

Heckmann, T. et al., 2015. Graph theory - Recent developments of its application in geomorphology. *Geomorphology* 243: 130–146.

Heckmann, T., & Vericat, D., accepted. Computing spatially distributed sediment delivery ratios: Inferring functional sediment connectivity from repeat high-resolution Digital Elevation Models. Earth Surface Processes and Landforms.

Lane, S.N. et al., 2017. Sediment export, transient landscape response and catchment-scale connectivity following rapid climate warming and Alpine glacier recession. *Geomorphology* 277: 210–227.

Mao, L. et al., 2014. Bedload hysteresis in a glacier-fed mountain river. *Earth Surf. Process. Landforms* 39: 964–976.

Micheletti, N. & Lane, S.N., 2016. Water yield and sediment export in small, partially glaciated Alpine watersheds in a warming climate. *Water Resources Research* 52: 4924–4943.

Continued carbon loss from collapsed permafrost despite decreasing biodegradability

Leiyi Chen [1]
Futing Liu [1,2]
Benjamin (W.) Abbott [3]
Yuanhe Yang [1]
[1] *State Key Laboratory of Vegetation and Environmental Change, Institute of Botany, Chinese Academy of Sciences, Beijing 100093, China*
[2] *University of Chinese Academy of Sciences, Beijing 100049, China*
[3] *Department of Earth and Environmental Sciences, Michigan State University, East Lansing, Michigan 48824, USA*

Abstract

Carbon (C) release from thawing permafrost is potentially the largest climate feedback from terrestrial ecosystems. However, the magnitude of this feedback remains highly uncertain due to limited understanding of how permafrost collapse alters soil organic matter (SOM) biodegradability. Here, we combined elemental analysis with biomarker and nuclear magnetic resonance techniques, to explore changes in soil C concentration and its biodegradability following permafrost collapse on the Tibetan Plateau. Our results showed that permafrost collapse resulted in a 10-21% decrease in residual soil C concentration over 16 years. The relative abundance of labile SOM fractions decreased, whereas recalcitrant SOM fractions increased after 16-year collapse, leading to a significant decline in SOM biodegradability. Despite these changes in biodegradability, soil C loss continued with time since thaw, potentially due to hydrologic C export. These results demonstrate that permafrost collapse could trigger substantial C release on decadal timescales, implying that thermokarst may be a dominant mechanism exposing upland permafrost C to mineralization.

Keywords: biodegradability; carbon cycle; climate feedback; ecosystem respiration; thermokarst; upland permafrost

Introduction

Thermokarst is an abrupt permafrost thaw process that can dramatically alter the local landscape, affecting soil, vegetation, and hydrology (Jensen *et al.*, 2014). Despite of growing evidence indicating the acceleration of soil organic matter (SOM) decomposition in upland thermokarst (Schuur *et al.*, 2009), the magnitude and persistence of this effect is unknown (Abbott & Jones, 2015). Much of this uncertainty arises from the fact that SOM decomposition after permafrost thaw depends on environmental conditions as well as the quality or biodegradability of thawed SOM (Hodgkins *et al.*, 2014). Therefore, better quantifying how changes in physical conditions alter permafrost SOM biodegradability is crucial to predicting the timing and magnitude of the permafrost C feedback.

In this study, we took advantage of a thermo-erosion gully in the northeastern Tibetan Plateau to explore how permafrost collapse accompanied by soil environmental changes alters C biodegradability. We tested the hypotheses that (i) thermokarst-induced environmental variations (drying and warming) in upland regions would intensify SOM decomposition, potentially decreasing residual soil C biodegradability, and (ii) carbon dioxide (CO_2) release would decrease gradually due to this decreasing C biodegradability.

Results

Effects of upland thermokarst on soil C

Permafrost collapse caused significant changes in soil C. Albeit no change in soil C concentration in vegetated rafts during the first 7 years following collapse, a substantial decrease of 10-21% was observed at mid- and late stages ($P < 0.05$; Fig. 1). Moreover, the change in soil C concentration (ΔSOC) was negatively correlated with the time since collapse ($r^2 = 0.65$, $P = 0.03$; Fig. 1), with the maximum reduction after 16-year collapse.

Changes in residual SOM biodegradability

The thermokarst-impacted soils showed a lower signal in the O-alkyl C region (3.2% decrease in easily degraded SOM constituents), but a higher signal in alkyl C region (12.2% increase in recalcitrant compounds) at the late stage of permafrost collapse (Fig. 2). Furthermore, the ratio of Alkyl/O-alkyl was 15.8% higher in the thermokarst-impacted soil than undisturbed grassland at the late stage site ($P = 0.006$; Fig. 2), confirming a lower SOM biodegradability compared to control. The relative abundance of carbohydrates (trehalose) showed the biggest decrease at the late stage site compared to reference soil (Fig. 2). In contrast with the decrease in labile SOM fractions, suberin- and lignin-derived compounds increased by 29.0% and 15.3% (Fig. 2) at the late stage of permafrost collapse, respectively.

Soil C flux under upland thermokarst

Our results showed that R_{eco} increased significantly at the early stage of permafrost collapse (Fig. 3a). However, as gully subsidence proceeds, R_{eco} dropped back to the level of that measured in the undisturbed soils after approximately 16 years of subsidence (Fig. 3a). Different to C release via R_{eco}, TOC content within gully was always higher than that in reference water from out gully (Fig. 3b), indicating that lateral delivering C was also an important pathway of C loss which could not be ignored in thermokarst-impacted soils. Consistent with this deduction, our results revealed that TOC flux, which was based on TOC concentration and stream discharge, was also significantly higher within gully than that in reference water.

Conclusions

This study presented evidence that upland thermokarst resulted in substantial soil C loss over 16 years following collapse. The depletion of labile SOM compounds gradually slowed growing-season rates of SOM mineralization, but soil C losses continued, potentially due to non-growing season effects and hydrologic export of C. Previous researches demonstrated that non-growing season microbial respiration and mineralization of C could not be ignored and was even more important because the increase in soil temperature could substantially contribute to the SOM decomposition during the winter, when the plant C input has ceased.

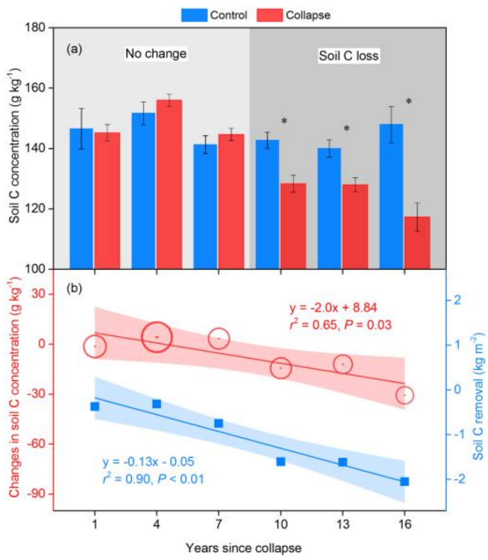

Figure 1. Changes in soil carbon (C) concentration induced by permafrost collapse. (a) Comparison of soil C concentrations between collapse (red) and control plots (blue) along the thaw chronosequence. (b) Relationships of changes in soil C concentration (ΔSOC) (red line) and organic C removal (blue line) with the years since collapse.

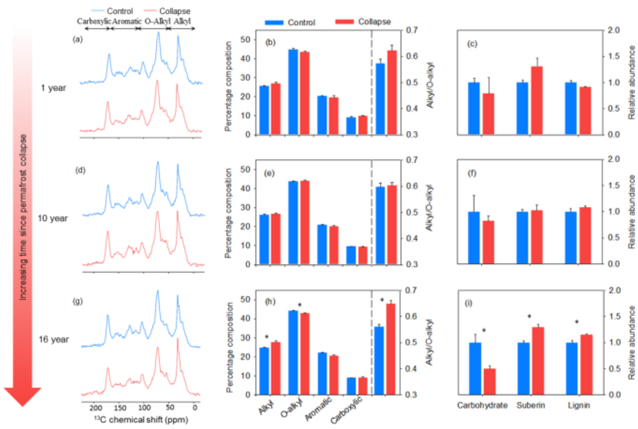

Figure 2. Comparisons of SOM biodegradability between collapse (red) and control plots (blue) along the thaw chronosequence on the Tibetan Plateau. The left, middle and right panels corresponds to the ^{13}C NMR spectra, the percentage composition of different structural units in ^{13}C NMR and relative abundance of major SOM components derived from biomarker analysis, respectively.

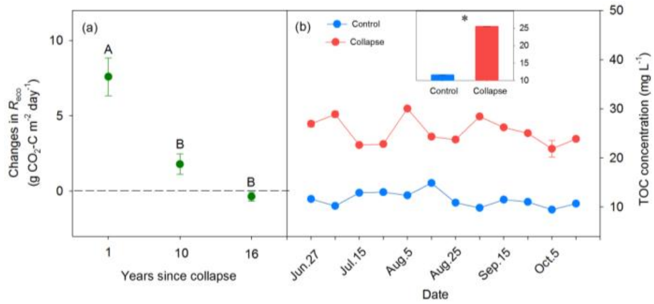

Figure 3. Two different C loss pathways in a thermo-erosion gully. The panel (a) corresponds to the changes in-situ Reco measured in July and August 2016. The panel (b) corresponds to the dynamics of total organic carbon (TOC) concentrations in the gully (collapse) and reference water (control) from June to October, 2015. Inset in panel (b) shows the comparison of seasonal average of TOC concentration within gully and out gully.

References

Abbott BW, Jones JB (2015) Permafrost collapse alters soil carbon stocks, respiration, CH_4 , and N_2O in upland tundra. *Glob Chang Biol,* **21**, 4570-4587.

Hodgkins SB, Tfaily MM, Mccalley CK *et al.* (2014) Changes in peat chemistry associated with permafrost thaw increase greenhouse gas production. *Proc Natl Acad Sci U S A,* **111**, 5819-5824.

Jensen AE, Lohse KA, Crosby BT, Mora CI (2014) Variations in soil carbon dioxide efflux across a thaw slump chronosequence in northwestern Alaska. *Environmental Research Letters,* **9**, 025001.

Schuur EaG, Vogel JG, Crummer KG, Lee H, Sickman JO, Osterkamp TE (2009) The effect of permafrost thaw on old carbon release and net carbon exchange from tundra. *Nature,* **459**, 556-559.

Coupling ground subsidence and surface wetlands

Altug Ekici[1,2,3]
Hanna Lee[1]
David M. Lawrence[4]
Sean C. Swenson[4]

[1]Uni Research Climate, Bjerknes Centre for Climate Research, Bergen, Norway, ekici@climate.unibe.ch
[2] Climate and Environmental Physics, Physics Institute, University of Bern, Bern, Switzerland
[3] Oeschger Centre for Climate Change Research, University of Bern, Bern, Switzerland
[4]Climate and Global Dynamics Division, National Center for Atmospheric Research, Boulder, Colorado, USA

Abstract

A new version of CLM with prescribed excess ice data is utilized to couple ground subsidence and surface wetland fractions in the pan-Arctic domain. Increased wetland fractions with localized extreme drainage areas are shown in the model results for the current day. Mechanistic coupling of ground subsidence events with surface hydrology allows a more natural representation of thermokarst processes in the permafrost regions.

Keywords: Earth System Model; thermokarst; subsidence; excess ice; wetland; microtopography.

Introduction

With the Arctic amplification, climate change effects are more pronounced in the high latitudes, where the landscape is constantly changing due to ground subsidence events and thermokarst lake formations. Modeling such processes in Earth system models are essential to capture the full response of permafrost ecosystems to future climate change. Even though soil thermodynamics and biogeochemistry have been advanced in the ESMs during the last decade, thermokarst – surface hydrology interactions have been a challenging drawback. Uncertainties in modeling surface wetland areas are directly related to terrestrial carbon fluxes and can lead to mismatches in soil respiration pathways either releasing CO_2 or CH_4 to the atmosphere. Such complications in modeling high latitude wetland areas are further aggravated with disappearing excess ice within the soil and subsequent ground subsidence events. Here, we present new model parameterization that represents these processes.

Methods

We used the CLM model version that was previously advanced with the inclusion of excess ice representation from Lee et al. (2014). In that version the ground subsidence is calculated with the amount of excess ice melt due to warming climate. We have now coupled this process with the surface hydrology. The subsidence levels are directly related to surface micro topography in order to represent the changing surface conditions. A sensitivity analysis of such coupling and a comparison to satellite estimates (Prigent et al., 2012) are performed to validate the model.

Results and Conclusions

The sensitivity analysis showed an inverse relationship between surface microtopography distribution and surface wetland fraction. The new coupling formulation allows such relation as well as extreme ground subsidence leading to catastrophic drainage events and drier surface conditions. A 20th century experiment with an offline land-only simulation reveals a generally increased wetland fraction overall the pan-Arctic domain. The most susceptible areas for increased wetland fractions are around western Siberia and around the Hudson Bay, while some dried up locations due to advanced subsidence events are simulated at south of Yamal Peninsula, southern banks of Hudson Bay and western coast of Alaska. The combined effects of climate forcing and ground subsidence on surface wetland fraction are scrutinized and results support the new formulation to represent temporal dynamics of surface hydrology under changing climate conditions.

Comparison to the satellite derived surface wetland dataset (Fig. 1) shows spatial agreement on larger wetland fractions in western Siberia and around the Hudson Bay. The temporal patterns during the satellite data period 1993-2007 are also comparable between the model results and the satellite dataset. (Fig. 2). This shows the strength of process-based modeling to capture the wetland area seasonality reflected by the atmospheric forcing, which is much needed for a future scenario experiment.

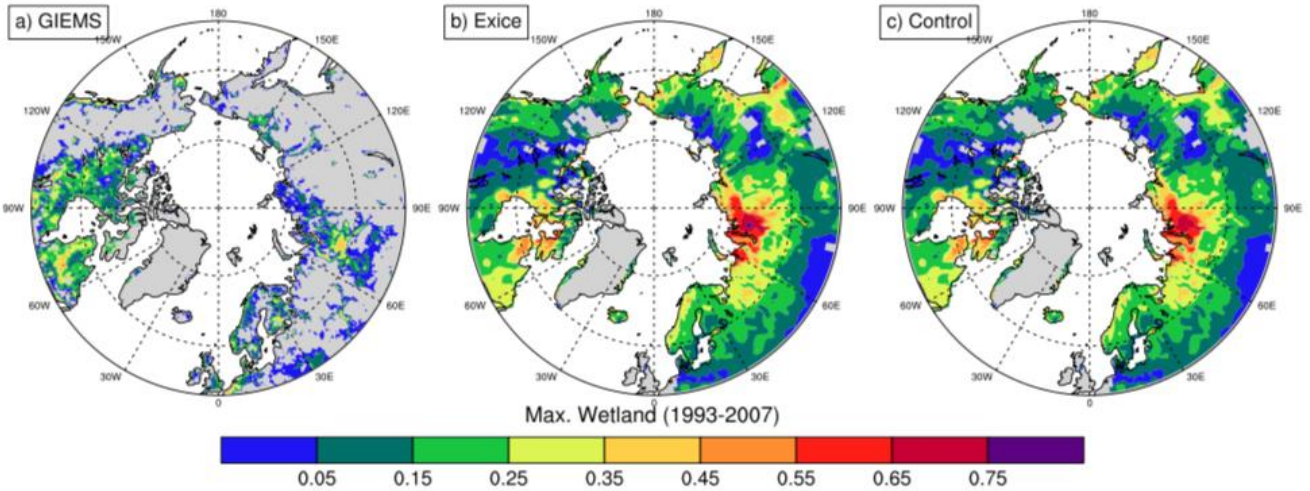

Fig. 1: Surface wetland fraction comparison from high latitude (50N) maps of surface wetlands fractions from GIEMS dataset (Prigent et al., 2012) and annual maximum fh2osfc values of Exice and Control experiments for the period 1993-2007.

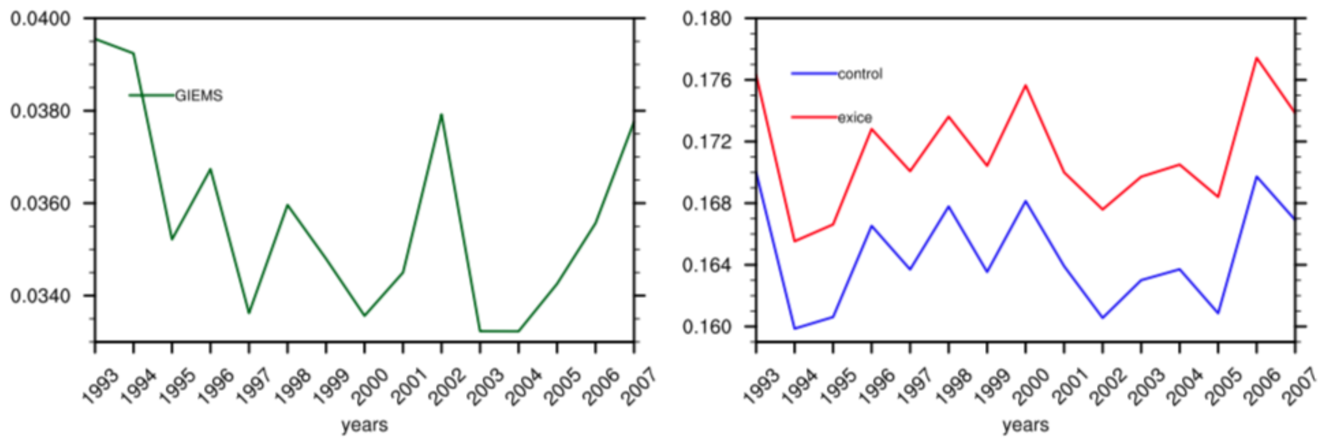

Fig. 2: Timeseries of annual surface wetlands fraction from GIEMS dataset and annual maximum fh2osfc values from Exice and Control experiments averaged for high latitude gridcells (50N) during 1993-2007.

These results emphasize the importance of representing ground ice conditions properly within ESMs in order to capture more realistic surface hydro-physical processes. This study represents the first step in a process-based representation of such hydrological processes in CLM. Further work will proceed to include soil biogeochemistry and potential changes in the natural greenhouse gas fluxes form land to the atmosphere.

Acknowledgments

We thank Dr. Catherine Prigent for providing the GIEMS dataset of satellite derived surface wetland areas to evaluate our model results.

References

Lee, H., Swenson, S.C., Slater, A.G. and Lawrence, D.M., 2014. Effects of excess ground ice on projections of permafrost in a warming climate. *Environmental Research Letters*, 9(12), p.124006.

Prigent, C., Papa, F., Aires, F., Jimenez, C., Rossow, W.B. and Matthews, E., 2012. Changes in land surface water dynamics since the 1990s and relation to population pressure. *Geophysical Research Letters*, 39(8)

Simulation of the coupled carbon-nitrogen cycle in the northern high latitudes with a land surface model

Eleanor J Burke[1]
Sarah E Chadburn[2]
[1]*Met Office, UK, Eleanor.burke@metoffice.gov.uk*
[2]*Leeds University, UK*

Abstract

Nitrogen is known to be one of the mail limiting nutrients for plant growth in the arctic tundra. As the climate changes and the permafrost thaws, the nitrogen available to plants may increase leading to enhanced plant growth. In order to enable the interactions between permafrost and the nitrogen cycle, a vertical representation of the soil nitrogen cycle was added to the JULES land surface model. JULES is the land surface component of the UK Earth System Model. This version of JULES was evaluated for a range of tundra sites. Simulations under projected future climates were carried out in order to identify the impact of including the vertical representation of the coupled carbon and nitrogen cycle on the local carbon balance.

Keywords: feedback; carbon; nitrogen; earth system models; land surface models; climate change.

Introduction

Nitrogen is one of the main limiting nutrients for plant growth in the arctic tundra. As the climate changes and the permafrost thaws the nitrogen available to plants may increase and may lead to some enhanced plant growth. In order to enable the interactions between permafrost and the nitrogen cycle, a vertical representation of the soil nitrogen cycle was added to the JULES land surface model.

JULES land surface model

This analysis is based on a version of the Joint UK Land Environment Simulator (JULES; Clark et al., 2011,). This is the land surface component of the UK Earth System Model. JULES describes the physical, biophysical and biochemical processes that control the exchange of radiation, momentum, heat, water and carbon between the land surface and the atmosphere. Several important modifications have been added into JULES to improve the representation of physical and biogeochemical processes in the cold regions.

A new representation of the nitrogen cycle has been included in order to quantify the effect of nitrogen limitation on the carbon cycle. This includes a vertical representation of organic and inorganic nitrogen in the soil. This model was evaluated at Samoylov.

Samoylov site simulations

Continuous cold permafrost underlies the study area. The active layer depth is typically less than 1 m (Boike et al., 2013). The terrace where the study site is situated is covered in low-centered ice wedge polygons, with water saturated soils or small ponds in the polygon centers. Detailed information concerning the climate, permafrost, land cover, vegetation and soil characteristics can be found in Boike et al. (2013).

Results

Figure 1 shows highly preliminary results of the vertical profile of soil inorganic nitrogen. The simulated annual maximum of the active layer is at about 0.6 m depth. The simulated inorganic nitrogen builds up at depths just below the maximum thaw depth where the soil is continuously frozen. This is similar to the observed inorganic nitrogen profile found by Beerman et al. (2016).

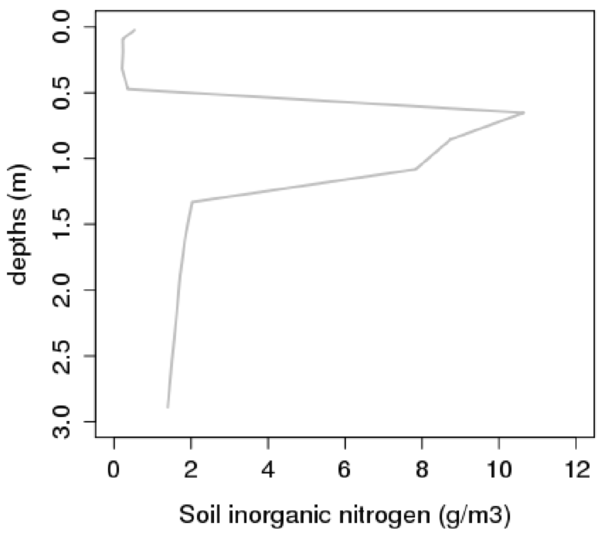

Figure 1: Samoylov: soil inorganic nitrogen (g/m3)

Conclusions

A representation of the nitrogen cycle has been included within JULES. Preliminary results suggest that the model can represent the build up of inorganic nitrogen observed at depths just below the top of the permafrost table.

Acknowledgments

E.J.B. was supported by the Joint UK DECC/Defra Met Office Hadley Centre Climate Programme (GA01101) and CRESCENDO (EU project 641816). S.E.C. was supported by the Joint Partnership Initiative project COnstraining Uncertainties in the Permafrost-climate feedback (COUP) (National Environment Research Council grant NE/M01990X/1.

References

Boike, J., Kattenstroth, B., Abramova, K., Bornemann, N., Chetverova, A., Fedorova, I., Fröb, K., Grigoriev, M., Grüber, M., Kutzbach, L., Langer, M., Minke, M., Muster, S., Piel, K., Pfeiffer, E.-M., Stoof, G., Westermann, S., Wischnewski, K., Wille, C., and Hubberten, H.-W., 2013. Baseline characteristics of climate, permafrost and land cover from a new permafrost observatory in the Lena River Delta, Siberia (1998-2011), *Biogeosciences*, 790 10, 2105–2128, doi:10.5194/bg-10-2105-2013.

Clark, D.B., Mercado, L.M., Sitch, S., Jones, C.D., Gedney, N., Best, M.J., Pryor, M., Rooney, G.G., Essery, R.L.H., Blyth, E. and Boucher, O., 2011. The Joint UK Land Environment Simulator (JULES), model description–Part 2: carbon fluxes and vegetation dynamics. *Geoscientific Model Development*, *4*(3), pp.701-722.

Beermann, F., Langer, M., Wetterich, S., Strauss, J., Boike, J., Fiencke, C., Schirrmeister, L., Pfeiffer, E.-M., and Kutzbach, L., 2016. Permafrost thaw and release of inorganic nitrogen from polygonal tundra soils in eastern Siberia, Biogeosciences Discuss., https://doi.org/10.5194/bg-2016-117.

Field incubation study of greenhouse gas release from buried soil in the Lena River Delta, Siberia

Svetlana Evgrafova[1,2]
Oleg Novikov[2]
Maria Meteleva[1]
Georg Guggenberger[3]
Dirk Wagner[4]
[1]*V.N. Sukachev Institute of Forest FRC KSC SB RAS, Krasnoyarsk, Russia, email: esj@yandex.ru*
[2]*Siberian Federal University, Krasnoyarsk, Russia*
[3]*Institute of Soil Science, Leibniz University of Hannover, Germany*
[4]*GFZ German Research Centre for Geosciences, Potsdam, Germany*

Abstract

A fundamental research question related to the impact of thawing permafrost on global change is, how fast organic matter in the thawing permafrost can be converted to CO_2 and CH_4 and released into the atmosphere. Current estimates on the degradability of thawing organic matter in permafrost are based on incubation studies which are highly artificial and probably overestimate the greenhouse gas production under *in situ* conditions. We aimed at identifying the microbial response and associated release of CO_2 and CH_4 from thawing soil that has previously been permanently frozen. We moved formerly frozen soil to the active layer. This material was either placed partly in the subsoil, to mimic the cryoturbation processes, or was exposed to the soil surface to simulate an eroded river bank. Data from the incubation experiment showed low intensity of gas emission which indicates a weak involvement of the buried soil in the present-day processes of microbial decomposition.

Keywords: permafrost-affected soils, buried organic matter, field-based incubation experiment, CO_2, CH_4

Introduction

Permafrost thawing may provoke a positive feedback to climate warming by causing increased greenhouse gas emissions. When permafrost soils thaw, ancient organic carbon is made accessible to microbial respiration, emitting greenhouse gases (GHG) like CO_2 and CH_4 (Tarnocai et al. 2009). For example, a positive feedback of methanogenic communities to warmer periods in the Late Pleistocene and Holocene has been proposed for the Lena River Delta (Bischoff *et al.*, 2013).

Numerous laboratory experiments have addressed climate change effects, especially the effects of increasing temperatures on the release of GHG. But current estimates on the degradability of thawing organic matter in permafrost are based on incubation studies that are highly artificial and probably overestimate the production of GHGs under *in situ* conditions. In this respect, the organic matter rich Holocene permafrost deposits are of particular interest, because current research indicates that they contain substantial amounts of labile organic matter, which will be the source for CO_2 and CH_4 after thaw (Schaefer et al., 2011). The basic research question is how fast this thawed organic matter can be mineralized under *in situ* conditions to CO_2 and CH_4.

To measure the microbial response and associated carbon release in gaseous forms (CO_2, CH_4) from organic matter that has been permanently frozen, we performed an *in situ* field-based incubation experiment in a rim of an ice-wedge polygon on Samoylov island in the Lena River Delta, Russia, at 72°22’N, 126°28’E.

Method description

Frozen buried soil was taken from Holocene permafrost, that had been exposed by erosion of the Lena river bank. We transferred the material partly to the top of the active layer and partly into the subsoil in a rim of an ice-wedge polygon. The intention was that formerly frozen soil was moved to the active layer, while still residing in the subsoil to mimic cryoturbation processes, or was exposed to the soil surface to simulate eroded riverbank. The experiment was installed in August 2015 (plots with buried soil covered by living groundcover of 5 cm thickness), and in August, 2016 (plots with uncovered buried soil). The experimental design is described on Figure 1.

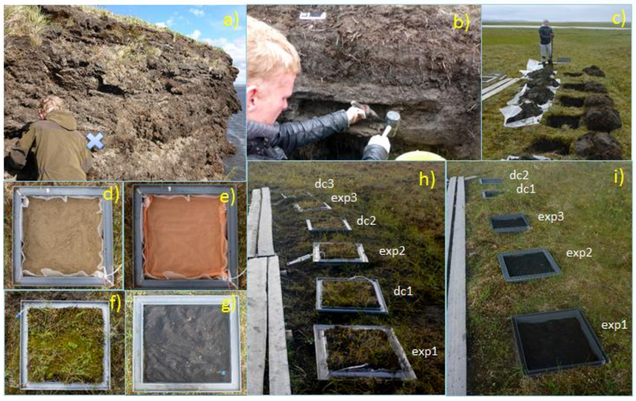

Figure 1. Field-based incubation experiment: a) Lena river bank of Samoylov island, x – sampling place; b) sampling of frozen (buried) soil; c) experimental site preparation (holes dug up to permafrost table); d) every plot was filled with carbon-free sand; e) approx. 3.5-4.5 kg of buried soil were placed in polyester bags and placed on top of sand; f) bags with buried soil covered by groundcover (5 cm thickness) - cryoturbation mimicking experiment; g) bags with buried soil exposing uncovered – eroded river bank simulation experiment; h) artificial cryoturbation experiment; exp1-3 – plots with bags filled with formerly buried soil, dc1-3 – plots with bags without formerly buried soil i.e., disturbance control; i) eroded river bank simulation experiment; exp1-3 – plots with bags filled with formerly buried soil, dc1-2 – plots with bags without formerly buried soil (disturbance control).

The buried soil had relatively much organic matter (5.67% organic C and 0.24% total N) which, according to the wide C/N ratio of 23.5, was not much microbially transformed. This is also corroborated by $\delta^{13}C$ ratio of -25.1 ‰ and $\delta^{15}N$ ratio of 1.77 ‰.

CO_2 and CH_4 released from the soil surface of both variants was obtained by the close chamber technique and quantified according to Lal (2016).

Results

In the field-based incubation experiment, emission of both GHG (Figure 2) was much higher in plots with buried soil covered by groundcover compared to plots with the exposed, uncovered buried soil. The release of gases from covered plots was mainly responding to soil temperature of the upper layer (0-5 cm). Plots where the buried soil material was placed on the soil surface showed a weak flux of CO_2, despite the fact that the organic matter was in a permanently moist state during the whole measurement period. The one-year cumulative methane efflux from plots with buried soil covered by groundcover was significantly larger than in disturbance control plots.

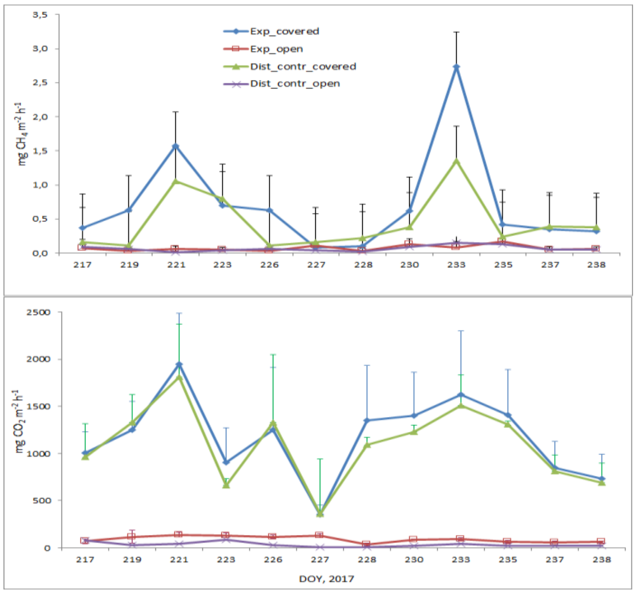

Figure 2. Time course of CH_4 (a) and CO_2 (b) evolution from soil in a field-based experiment. Legend: *Exp_covered* – mean value of plots with buried soil covered by groundcover (5 cm thickness); *Exp_open* – mean value of plots with uncovered buried soil; *Dist_contr_covered* – mean value between plots without buried soil, covered by groundcover (5 cm thickness); *Dist_contr_open* – uncovered plots without buried soil. Bars indicate standard deviations (n=3).

Conclusion

In general, the low intensity of gas emission from both variants of the incubation experiment indicates a weak involvement of the buried soil in the present day processes of microbial decomposition.

Acknowledgments

This work was supported by the Russian Government Megagrant (project no. 14.B25.31.0031) and by the Russian Foundation for Basic Research (project no. 16-04-01677-a).

References

Bischoff J., Mangelsdorf K., Gattinger A., Schloter M., Kurchatova A., Herzschuh U., Wagner D., 2013. Response of methanogenic Archae to Late Pleistocene and Holocene climate changes in the Siberian Arctic. *Global Biogeochemical Cycles* 27(2): 305-317.

Tarnocai, C., Canadell, J.G., E. A. G. Schuur, Kuhry, P., Mazhitova, G. & Zimov, S. 2009. Soil organic carbon pools in the northern circumpolar permafrost region. *Global Biogeochemical Cycles* 23 (2): GB2023.

Schaefer K, Zhang T, Bruhwiler L and Barrett A P 2011 Amount and timing of permafrost carbon release in response to climate warming. *Tellus Series B: Chem. Phys. Met.* 63 165–80.

Lal, R. (2016). *Encyclopedia of Soil Science*, Third Edition. Boca Raton: CRC Press.

Climate change and ecological interactions affecting permafrost temperature regime and ice-wedge activity in the Narsajuaq river valley, Nunavik, Canada

Samuel Gagnon[1]
Michel Allard[1]
[1]*Centre d'études nordiques (CEN) and Université Laval, Québec, Canada, samuel.gagnon,9@ulaval.ca*

Abstract

This project aims to determine how climate change may have affected active layer depth and dynamics and reduced winter ice-wedge cracking frequency. We revisited 16 sites in the Narsajuaq river valley near Salluit (Nunavik, Canada) that were extensively studied between 1989 and 1991. The top of ice wedges in 1991 had upgrowth features indicating thinning of the active layer during the cooling period 1946-1992. After digging over 100 soil pits above ice wedges across various soil types, we observed that the active layer thickness reached depths pre-dating 1946 over the past decades. In most instances, upgrowth forms had disappeared and the ice wedge tops were in decay. We also observed recent ice veins through the active layer in several pits, indicating some continuing frost cracking and ice-wedge activity. Our results also indicate that the increasing shrub cover might be accumulating more snow and decreasing ice-wedge activity in some areas.

Keywords: Ice wedge; permafrost; tundra; active layer; Salluit; Nunavik

Extended abstract

Despite the growing attention the northern regions are now receiving, field studies spanning multiple decades are scarce and consequence assessments of permafrost thawing over many years remain speculative, based on numerical models or limited to observations of short duration. This project aims to determine how climate change may have affected active layer depth and dynamics and reduced winter ice-wedge cracking frequency, which was very high at the beginning of the 1990s. To make direct measurements, we revisited 16 sites in the Narsajuaq river valley near Salluit (Nunavik, Canada) that were extensively studied between 1989 and 1991 (Allard & Kasper, 1998; Kasper & Allard, 2001). Climate warming only started around 1993 whence mean annual air temperatures started to rise from -10 °C then to about -7 °C nowadays. We thus have the unique opportunity to observe and measure changes by directly comparing recent data with data pre-dating a climate warming of known amplitude.

The top of ice wedges in 1991 had upgrowth features (shoulders) indicating thinning of the active layer during the cooling period 1946-1992. During the summer of 2016, we installed a series of high-precision extensometers capable of measuring the timing of frost cracking and width variations of the open cracks over ice wedges during the winter. Although the instrumentation changed, such a technique was also applied in 1990 to measure ice wedge activity. We also installed a weather station to measure active layer and permafrost temperatures, weather variations and snow cover thickness. In addition, we also dug over 100 soil pits and observed the depths and top features of 58 ice wedges across various soil types to observe how they physically changed due to climate warming.

We are also documenting the interaction between permafrost temperature regime, change in vegetation cover, active layer deepening and ice wedge degradation during the past 25 years. To do so, we mapped changes in surface vegetation, the nature and depth of the topsoil horizons, and active layer depths compared to 1989-1991. The ground temperature measurements will help validate a heat conduction model of the transient temperature regime of the active layer and the near surface permafrost over the period of climate variation.

Results from the 2016 and 2017 field campaigns show that the active layer thickness has increased on average by 41% since 1991. In most instances upgrowth forms had disappeared and the ice wedge tops were in decay (Table 1). Whereas 94% of the ice wedges excavated in 1991 by Kasper and Allard (2001) showed recent growth structures, only ~5% of the wedges unearthed in 2017 still showed similar stages. This indicates that the recent warming led to a deepening of the active layer important enough to cause the ice wedges to melt back to their main stage.

Table 1. Average depth of the ice-wedge stages measured in 1990-1991 and in 2017 on different sites.

Stage	Site					
	D1	D2	D4	D9	D10	G5
1991	Depth (cm)					
A	50	40	55	55	63	85-87
B	40	32	45	50	50	75-77
C	35	27-28	35-37	45	47	70
D	30	21-22	29-32		44	63-65
E	25	18	27		41-42	60
F	20		25			52
G	13		21			
2017						
A	53.0	61.3	70.7	59.2	74.0	>110

As opposed to 25 years ago, almost all of the ice wedges unearthed in 2017 had no upgrowth form. Moreover, over the past decades the active layer reached depths beyond the main stage of the ice wedges recorded in 1990-1991 on all sites, thus leaving only one-stage ice wedges.

We also observed recent ice veins through the active layer in several pits, indicating some recent frost cracking and ice-wedge activity (Figure 1). This indicates that ice wedges can still be cracking and growing in width under a still cold enough climate, but decreasing in height due to active layer deepening. The melting of ice wedge tops also left underground tunnels in sites with thick organic surface deposits. These tunnels appeared to be the precursors of erosion gullies through the collapsing of the ground when the active layer reaches into mineral deposits beneath the organic soils. Finally, larger and higher shrub populations than in 1990 were observed. Our results seem to indicate that the shrub cover might be accumulating more snow in zones of depression and decreasing ice-wedge activity in some areas.

Figure 1. Cross-section of an ice wedge without upgrowth form. There is an ice vein reaching the base of the active layer and indicating ice-wedge activity. The head of the axe is 17 cm in width.

Acknowledgments

We thank Denis Sarrazin, Alexandre Chiasson, Julie Nadeau, Sarah Gauthier and Michael Cameron for their invaluable help during the field campaign. We are also grateful to the Natural Sciences and Engineering Research Council of Canada (NSERC), Fonds de recherche du Québec Nature et technologie (FRQNT), the Arctic Development and Adaptation to Permafrost in Transition (ADAPT) research group, Center for northern studies (CEN) and ArcticNet.

References

Allard, M. & Kasper, J.N., 1998. Temperature conditions for ice-wedge cracking: field measurements from Salluit, Northern Québec. *Proceedings of PERMAFROST – Seventh International Conference*, Yellowknife, Canada, June 23-27: 5-12.

Kasper, J.N. & Allard, M., 2001. Late-Holocene climatic changes as detected by the growth and decay of ice wedges on the southern shore of Hudson Strait, northern Québec, Canada. *The Holocene,* 11:5, 563-577.

Cryolithology field courses on Svalbard, Barentsburg location

Aleksandra Naidenko[1]
Aleksandra Khairedinova [1]
Vasily Krotkov [2]
Alexander Kizyakov[1]
[1]*Lomonosov Moscow State University, Faculty of Geography, Cryolithology and Glaciology Department, naydenkosasha@gmail.com*
[2] *Lomonosov Moscow State University, Faculty of Geography, Physical Geography and Landscape Science.*

Abstract

In the context of the agreement on scientific cooperation between Federal State Budget Institution Arctic and Antarctic Research Institute (FSBI "AARI") and Faculty of Geography of Lomonosov Moscow State University there was held the field-based course for third-year students during July,24th -August,5th 2017 on the Svalbard Archipelago. Students of the Cryolithology and Glaciology Department and student of the Physical Geography and Landscape Science Department were invited by FSBI "AARI" to perform cryogenic investigations near the Barentsburg settlement on the base of Russian Science Center on the Svalbard Archipelago as a part of seasonal squad RAE-S (Russian Arctic Expedition – Svalbard) "Svalbard-2017".

Keywords: cryolithology, education; field courses; Svalbard.

Introduction

In the context of the agreement on scientific cooperation between Federal State Budget Institution Arctic and Antarctic Research Institute (FSBI "AARI") and Faculty of Geography of Lomonosov Moscow State University there was held the field-based course for third-year students during July,24th -August,5th 2017 on the Svalbard Archipelago. Students of the Cryolithology and Glaciology Department and student of the Physical Geography and Landscape Science Department were invited by FSBI "AARI" to perform cryogenic investigations near the Barentsburg settlement on the base of Russian Science Center on the Svalbard Archipelago as a part of seasonal squad RAE-S (Russian Arctic Expedition – Svalbard) "Svalbard-2017".

Objectives of the field course

Standardized methods of cryolithological studies were used to describe the territory. Along the route we've done observations including determination of relief forms, based on terrain, space images of ultra-high spatial resolution and mosaic of aerial photographs (tied to the terrain by GPS). Morphological and morphometric characteristics of cryogenic relief forms were determined. Pits and stripping have been completed to document the cryolithological structure of the surface sediment cover.

During the practice we used equipment provided by AARI, measurements were made in equipped thermometric holes (Demidov et al., 2016).

The thickness of the seasonally thawed layer was determined during the passage of pits, by measurement with a probe and sledgehammer, and also on the basis of temperature data from thermosets installed in the holes. For thermometric observations we used GeoPrecision thermocouples equipped with loggers for automated temperature measurement.

Together with RA Chernov, head of the glaciological team of the Institute of Geography of the Russian Academy of Sciences, glaciological observations were made on the glacier West Grønfjord.

Conclusions

In the process of passing the production practice, a whole range of studies has been carried out. Theoretical knowledge and obtained useful data for writing the thesis work are applied. All the planned work has been successfully completed. A plan for further investigations of permafrost and processes related to it has also been developed in the Svalbard archipelago.

Acknowledgments

This work was partly supported by RFBR grant No.16-05-00612.

We express our gratitude to the leadership of AARI: Deputy Director A.S. Makarov, deputy chief of the RAE-S Yu.V. Ugryumov - for providing the opportunity to conduct field course, providing comfortable and safe working and living conditions; employees of the wintering staff of the RAE-S - G.V. Tarasov and O.R. Sidorova for help and solving emerging organizational issues during field work.

References

Demidov N., Karaevskaya E. Verkulich S., Nikulina A., Savatyugin L., 2016. The first results of permafrost observations at the cryospheric range of the Russian Scientific Center on the Spitsbergen Archipelago (RSCS). *Problems of the Arctic and Antarctic*, 4(110): 67-79.

Thermal denudation due to climate fluctuations as a driver for relief transformation in central Yamal, Russia

Artem V. Khomutov[1,2]
Yury A. Dvornikov[1]
Marina O. Leibman[1,2]
Elena A. Babkina[1]

[1]*Earth Cryosphere Institute Tyumen Scientific Centre SB RAS, Tyumen, Russia, akhomutov@gmail.com*
[2]*University of Tyumen, International Institute of Cryology and Cryosophy*

Abstract

Since 2012 in the continuous permafrost zone of the Yamal Peninsula there have been a predominance of thermal denudation (processes associated with tabular ground ice thaw) over the active layer detachments (processes associated with transient layer thaw) is observed. This shift in the mass waste mechanism is caused by deepening of the active layer and exposure of the massive ground ice within permafrost to first seasonal and then perennial thaw due to climatic fluctuations. Tabular ground ice thaw, in addition, may lead to gas-emission crater formation.

Keywords: Thermal denudation; climate fluctuations; Yamal Peninsula; thermocirques; gas-emission craters.

Introduction and study area

In the typical tundra subzone of the Yamal Peninsula, bodies of tabular ground ice are found rather close to the surface of slopes, sometimes directly beneath the active layer. These ice bodies are characteristic of deeply dissected Quaternary plains and they affect relief formation through cryogenic slope processes. Less common and relatively smaller in size are ice wedges that penetrate into deeper sitting tabular ice bodies.

For the Central Yamal, formation of widely distributed cryogenic translational landslides (active layer detachments) with the last peak of activation in 1989 has been well studied (Leibman & Kizyakov, 2007; Leibman *et al.*, 2014). This type of landsliding results from short-term weather cooling, reduction of the seasonal thaw depth, and formation of ice lenses at the base of the active layer. When due to short-term climate fluctuations warmer summer occurs then deeper seasonal thaw causes melting of this accumulated in cool years ice and triggers translational landslides (Leibman & Egorov, 1996).

We hypothesize climatic fluctuations since the extremely warm spring of 2012 triggered cryogenic earth flows (retrogressive thaw slumps) in the tundra zone of the Yamal Peninsula. This assumption is based on our observation of a large number (more than 90) of active thermal denudation landforms of different sizes (Khomutov *et al.*, 2017) in the area around the research station "Vaskiny Dachi". The most significant thermal denudation landforms (thermocirques) are semi-circle shaped depressions remaining after massive ground ice thaw and removal of detached material downslope. Several such active thermocirques have been monitored annually since 2012-2013.

From cryogenic translational landslides to cryogenic earth flows

Direct observations from helicopters and reconnaissance field trips since 1987 as well as analysis of remote sensing data allow us to state that recently (since 2012) processes associated with tabular ground ice thaw (cryogenic earth flows) dominate over processes associated with ice formation at the active layer base (cryogenic translational landslides) in the area. This observed change is caused by deepening of the active layer and exposure of the massive ground ice (tabular ground ice or ice-wedges) within permafrost to, first, seasonal and then perennial thaw.

Changing the mechanism of slope processes from translational landsliding to earth flows is explained by the following. The warm period of 2012 started on May 25. Maximal average daily temperatures were +18,0°C on June 29, and the thaw index calculated for the period from May 25 to September 2 (date of active layer depth measurements) was 854 degree-days with 257 mm. of precipitation. The extremely warm summer 2012 season resulted in increased active layer depths. According to measurements at the Vaskiny Dachi CALM grid (data included in the GTN-P database as R5), the mean annual active layer depth by the end of the warm period was 102 cm, 15% deeper than the average for the 1993-2011. Thus in 2012 on some slopes thawing had reached the top of icy permafrost or mono-mineral tabular ground ice. As a result, cryogenic earth flows initiated on lakeshores and riverbanks and some of these features merged to form new or to re-activate stabilized thermocirques.

While translational landslide events are typically separated by several centuries and form landslide cirques, earth flows form thermocirques which, once triggered, develop until ice is either exhausted or insulated by landslide material.

Further joint monitoring of active layer and thermocirques, along with analysis of climatic parameters, has shown the following. Up to 2015 the rate of the thermocirque area expansion mostly slowed down (from 1400 to 950 sq.m/year on average) though gradual increase of their total area had been still observed. Field measurements of 2016 and 2017 demonstrated that for some thermocirques backwall the retreat rate was still high while some other thermocirques that were mostly stabilized in 2015 had been renewed by new cryogenic earth flows in the abnormally warm summer of 2016. It is apparent that the process of ground ice and ice-rich permafrost thaw is ongoing.

The area affected by thermocirques occupies less than 0.001% of the entire study area, compared to a translational landslide-affected surface of about 1% of the same area. Through a process different than translational landslide formation, earth flows develop continuously digging into the massif and producing 3-dimensional breach annually expanding.

Paragenesis of thermal denudation with gas-emission crater and lake formation

Gas-emission craters (GECs) found in Northwest Siberia in 2014 (Leibman *et al.*, 2014b) occur in an area of wide tabular ground ice distribution. Tabular ground ice observed in the GECs walls also provokes retreat of these walls. Thermociques are numerous around the GECs area. Shores of many lakes are terraced and have ancient to recent traces of thermal denudation activity. This suggests that GECs, tabular ground ice, thermocirques, and lakes are interrelated.

As monitoring has showed, lakes that formed inside the GECs were in part inundated through melting of tabular ground. After few years following GEC formation it is hard to determine what the initial process for the lake formation (thermokarst with further thermal denudation or gas emission with further thermal denudation) was, if not for the occasional discovery of newly formed GECs in this area.

Conclusions

In the Yamal Peninsula tundra processes associated with tabular ground ice thaw have been observed since 2012. Higher formation rate and different dimensions of relief transformation have been observed, though these are at a rather local level. Further climatic fluctuations, in particular extremely warm summers in the future, could lead to expansion of the area affected by thermal denudation due to the melting of deeper tabular ground ice by seasonal thawing.

Acknowledgments

This work is partially supported by the Russian Science Foundation under grant No.16-17-10203.

References

Khomutov, A.V., Leibman, M.O., Dvornikov, Y.A., Gubarkov, A.A., Mullanurov, D.R. & Khairullin, R.R., 2017. Activation of Cryogenic Earth Flows and Formation of Thermocirques on Central Yamal as a Result of Climate Fluctuations. In: Mikoš, M., Vilímek, V., Yin, Y., Sassa, K. (eds.), *Advancing Culture of Living with Landslides, Vol. 5: Landslides in Different Environments.* Springer International Publishing, 209-216.

Leibman, M.O. & Egorov, I.P., 1996. Climatic and environmental controls of cryogenic landslides, Yamal, Russia. In: Senneset K. (ed). *Landslides.* Rotterdam: Balkema Publishers, 1941-1946.

Leibman, M., Khomutov, A. & Kizyakov, A., 2014a. Cryogenic landslides in the Arctic Plains of Russia: classification, mechanisms, and landforms. In: Shan W., Guo Y., Wang F., Marui H., Strom A. (eds). *Landslides in cold regions in the context of climate change, environmental science and engineering.* Switzerland: Springer International Publishing (ISBN 978-3-319-00866-0), 143-162.

Leibman, M.O. & Kizyakov, A.I., 2007. *Cryogenic landslides of the Yamal and Yugorsky Peninsulas.* Moscow: ECI SB RAS, 206 pp. (in Russian).

Leibman, M.O., Kizyakov, A.I., Plekhanov, A.V. & Streletskaya I.D., 2014b. New permafrost feature - deep crater in Central Yamal, West Siberia, Russia, as a response to local climate fluctuations. *Geography, environment, sustainability* 7(4): 68-80.

Research of the permafrost-landscape conditions of the Karginskaya terrace in the lower reaches of the Ob River

Nikita A. Kostenkov [1]
Valery I. Grebenets[1]
Vasily A. Tolmanov[1]
Theresa Henning[2]
Ekaterina I. Bashkova[1]
[1]*Lomonosov Moscow State University, Department of Geography, Moscow, Russia, kostenkov.nikita@mail.ru*
[2] *Dresden University of Technology, Dresden, Deutschland*

Abstract

Karginskaya terrace of Western Siberia is a transitional area between the forest-tundra and tundra. These areas are marking for thawed and permafrost zones. The aim of the research was to study the permafrost-landscape conditions and cryogenic processes of different terrain types and to assess the effect of soil cover on the depth of the active layer.

Keywords: Western Siberia, permafrost, active layer.

Introduction

Karginskaya terrace occupies vast part of Western Siberia and was formed in the interglacial between Zyryan and Sartan cryochrones (Baulin et al., 1967). This territory is often referred to the South Yamal region in geocryological literature (Trofimov et al, 1989). Permafrost lays under tundra ecosystems in the lower reaches of the Ob River, whereas taliks are usually formed under forest tundra. We conducted this research of this area concerning the fulfilling the need to better distinguish thawed and frozen zones f. e. for the construction of facilities.

Methods

We conducted this research of permafrost-landscape conditions in summer 2016-2017 within 2 landscape areas: tundra (southern and typical) and forest-tundra. Our research covers areas represented by relatively flat surfaces with lakes, droughts of the drain and swampy terrain. We investigated key plots, thier geomorphic level, meso- and microrelief, biogeographic communities and influence of these factors on permafrost conditions and processes. In addition, we recorded the presence and activity of cryogenic processes and depths of the active layer within the key plots. Our group made soil-pits and transects to describe of the structure and texture of the soil layers, measure temperature and determine cryogenic structure of the active layer (AL).

Results

Our research shows that southern tundra occupies gentle slopes of the southern exposition and consists of hummocky hillock and shrub plant associations on poor tundra soils with a sandy loamy substrate.

Typical tundra landscapes are quite diverse. We subdivide them into four types. The first type is the drainage gutter, consists of two subtypes: a) shrub-moss plant association on tundra-peat soils on relatively drained small hills; b) sedge and moss plant association on watered tundra-peat soils with relatively leveled depressions.

The third type is polygonal peat bogs with ice wedges (Fig. 1).

Figure 1. Ice-wedge

The fourth type is a relatively flat surface, with elevated bumps of shrubby moss plant association, and individual drainage valleys or mown depressions with the sedge-moss plant association.

We measured depths of the active layer in the pits for each type. The depth of AL (mid-July 2017) was the maximum (up to 1.5-1.8 m) in the areas of forest vegetation and on the shores of lakes; on average, the depth of AL was 40-60 cm (in July in the hot summer of 2016, 60-80 cm). With the temperature measurements we estimated the influence of the microrelief of the terrain and the characteristics of the vegetation on the AL depth (Table 1 shows the different thermal insulation properties of vegetation types). We have drawn up a scheme of a polygon with a measured width every 5 m, and we also constructed and described a profile about 30 m in length across the polygon.

Table 1. Ground temperature under different plant types

Main type of vegetation	Ground temperature, °C	Temperature at a depth of 10 cm, °C
Betula nana, Ledum palustre	17,1	5,4
Betula nana, Sphagnum	21,5	8,3
Ledum palustre, Sphagnum	20,4	6,3
Sphagnum	24,8	9,8
Ledum palustre, Carex, Sphagnum	18,7	3,2
Larix sibirica, Salex pulchra	17,6	10,5

We determined the dimensions of thermokarst lakes, and estimated the influence of wave action and thermal abrasion on the destruction of polygonal veins.

Conclusions

In "warm" landscapes (northern taiga, southern tundra), the depth AL on the Karginskaya terrace is 1.5-2 times higher than in a typical tundra. Soil-vegetation cover (10 cm depth) reduces the heat flow to the ground by 2-6 times. At the latitude of the Arctic Circle in the lower reaches of the Ob river permafrost zones occupy 10-15% more territory than thawed areas.

Appreciation

We thank the staff of the department of cryolithology and glaciology for the help in the organization of work.

References

Baulin V.V., et al. 1967. *Geokriologicheskiye usloviya Zapadno-Sibirskoy nizmennosti* [Geocryological conditions of the West Siberian lowland]. Moscow, Nauka, 214 pp.

Trofimov V. T., Vasil'chuk Yu. K. et al., 1989. *Geokriologiya SSSR. Zapadnaya Sibir'* [Geocryology of the USSR. Western Siberia]. Moscow, Nedra, 454 pp.

Features of methane showings in disturbed cryogenic strata 280 km SE from the new Yamal crater Erkatayakha

Gleb Kraev[1,2]
Andrei Belonosov[3]
Anton Kudryavtsev[3]
Jakobus van Huissteden[2]
Dmitrii Zamolodchikov[4,5]
Evgenii Chuvilin[4]
Elizaveta Rivkina[1]
[1] *Institute of Physicochemical and Biological Challenges in Soil Science, Russian Academy of Sciences, kraevg@gmail.com*
[2] *Vrije Universiteit Amsterdam*
[3] *West-Siberian Filial, Trofimuk Institute of Petroleum Geology and Geophysics of Siberian Branch of Russian Academy of Sciences*
[4] *Lomonosov Moscow State University*
[5] *Center of Forest Ecology and Productivity, Russian Academy of Sciences*

Abstract

Greenhouse gases containing in permafrost could have currently unpredictable effect on climate, because the features of their distribution remain unknown. We monitored showings of methane in boreholes in North-Western Siberia. Comparing concentrations of methane in permafrost with the volumes of emitted methane, we show that the methane fluxes of up to 2.3 m^3 $day^{-1,}$ resulting from permafrost disturbance, vented from entrapped accumulations of methane in permafrost.

Keywords: fluxes of CH_4, salekhard formation, cryogenic transport, permeability of permafrost, methane accumulations, methane-hydrate.

Introduction

Permafrost degrades under natural and human impacts. Estimates of fluxes of greenhouse gases associated with these impacts often omit their pool in permafrost. Despite that the concentrations of methane (CH_4) found in permafrost were usually rather small (Rivkina et al., 2007), occurrence of lithological and cryogenic traps, or gas-hydrates (Yakushev & Chuvilin, 2000) could lead to spontaneous high emissions when uncovered (Kraev et al., 2017) or due to unknown reasons like in the case of Yamal craters.

Drilling operations disturb permafrost mechanically by extracting soils and altering the thermal regime likewise the processes of permafrost degradation.

We documented CH_4 pools and fluxes in drilling holes made in upper 30 m of permafrost on watersheds, lacustrine depressions and pingos on a site in North-Western Siberia.

Methods

CH_4 concentrations, cryogenic structure, and other physical properties were studied in the cores of alluvial-marine sands and sandy loams of salekhard formation, peats, and injection ice. Total of 9 holes were drilled. Permafrost samples were degassed by phase equilibration in ambient air and concentration of CH_4 was analyzed chromatographically.

Methane concentrations were measured periodically with optical detector of CH_4 in chambers, placed tightly to close empty holes during and after drilling. Readings corresponding to the time of exposition and geometry of drilling holes were documented. Several samples were collected from the holes to carry out chromatographical studies. Differences in the concentrationsof the gas in the holes divided by the time of exposition were treated as fluxes. Total volumes of CH_4 emitted from the drilling holes were estimated by integrals of diagrams of fluxes change over time.

The volumes of CH_4 fluxes from the drilling holes were compared with the volumes of CH_4 in the sediments. The average concentration of CH_4 in soils, extracted from the borehole was used to find the volume of sediments enclosing the same volume of CH_4 as the volume of gas emitted by a drilling hole. We assumed this volume of sediments forms the cylinder around the borehole, which should have degassed into the drilling hole to make up the total volume of CH_4 emitted. We used the radius of this cylinder as an indicator of the volume of sediments for better understanding of the sources of CH_4.

Results

Concentration of CH_4 in the sediments varied from 0 to 663 mmol m^{-3} of permafrost with the median value of 2 mmol m^{-3}, and the average of 52 mmol m^{-3}. The maximal value corresponded to the sample of icy lacustrine loams, extracted by borehole 8 on palsa in the lake depression. The maximal concentrations of CH_4 averaged along the core were found in the drilling hole 7 (with the median concentration of 102 mmol m^{-3}) drilled on pingo and the drilling hole 8 (88 mmol m^{-3}).

CH_4 concentrations in the boreholes changed from 0.0001 to 2.5 % vol. Long-term dynamics of change of CH_4 fluxes was similar for all monitored drilling holes. Maximal fluxes of up to 2.3 m^3 day^{-1} were recorded initially after drilling. They gradually decreased down to the levels below 10 cm^3 day^{-1} for 2-11 days disregarding the initial maximal flux. The volumes of CH_4 emitted per borehole over the period reached 0.3 m^3. Boreholes with maximal emitted volumes had the largest initial fluxes of 0.05-2.3 m^3 day^{-1}. They corresponded to the drilling holes 7, 2a (watershed), and 4 (lake depression).

The initial maximal concentration of CH_4 in the drilling hole 7 could have formed by degassing the soils in the radius of 22 cm around the borehole axis, which is nearly the radius of the borehole multiplied by 4. To reach the total emitted volume of 0.3 m^3 of CH_4, the volume of soils which should have been degassed lies in the cylinder with the radius of 1 m around the drilling hole.

The diameter of the cylinder with soils containing the volume of CH_4 equivalent to initial concentration of CH_4 in the drilling hole 2a was 2.1 m. This borehole disclosed an infiltration talik 3 m thick and permafrost with relatively low average CH_4 concentration of 0.01 cm^3 dm^{-3}. The volume of CH_4 emitted from the borehole reached 0.2 m^3 by 15 h after drilling. There should have been the CH_4 from 18.5 m around the borehole, which is hard to relate to impact of drilling. When the flux diminished to 3 l day^{-1} the drilling continued. Upon reaching 23.4 m depth the fluxes rose to 56 l day^{-1}. We believe that the CH_4 came from sediments of talik. However, there was no CH_4 in the borehole 2c drilled nearby to disclose the soils of talik.

Borehole 4 with the average flow of 26 l day-1 had initially the concentration of CH_4 in the borehole equivalent to the volume of CH_4 in the radius of 96 cm around its axis.

All other smaller volumes of CH_4 emitted from boreholes corresponded to degasation of large volumes of surrounding soils.

Conclusions

CH_4 entrapped in accumulations in permafrost could constitute significant contribution to fluxes of greenhouse gases. The distribution of accumulations is currently not understood.

Comparing the average concentration of CH_4 in soils and fluxes of CH_4 from boreholes points at following sources of emitted gas:

1. Soils surrounding the borehole, degassed from mechanical and thermal impact of drilling operations. This is supported by the growth of the flux with depth of the borehole.
2. Accumulations of CH_4 either in the traps containing high concentration of gaseous CH_4 or the methane-hydrates, small enough to be overlooked during sampling. This is supported by fading dynamics of gas emission, and the fact that emitted volumes of CH_4 often exceed the scale of disturbance.
3. Largescale traps, where the CH_4 permeates through permafrost of various iciness and taliks. This is supported by the difference between equivalent volume of soils around boreholes between boreholes in permafrost and the one disclosing the talik having higher permeability.

Acknowledgements

This study was accomplished under the framework of the program of the Presidium of the Russian Academy of Sciences "Arctic" (no. 55) with the support of the Netherlands Aerospace Center (grant ALW-GO/16-13), and the State appointment to the Center of forest ecology and productivity.

References

Kraev G.N., Schulze E.-D., Yurova A., Kholodov A., Chuvilin E. & Rivkina E., 2017. Cryogenic displacement and accumu;ation of biogenic methane in frozen soils. *Atmosphere* 8: 105-124.

Rivkina E., Shcherbakova V., Laurinavichius K., Krivushin K., Kraev G., Pecheritsyna S. & Gilichinsky D., 2007. Biogeochemistry of methane and methanogenic archaea in permafrost. *FEMS Microbiology Ecology* 61: 1-15.

Yakushev V.S. & Chuvilin E.M., 2000. Natural gas and gas hydrate accumulations within permafrost in Russia. *Cold Regions Science and Technology 31*: 189–197.

Dynamic of biotopes of Late Pleistocene and Holocene from northern tundra of Gydan of Western Siberia

Anna (Olegovna) Kuznetsova[1]
Alexey (Sergeevich) Afonin[2]
Yana (Vitalievna) Tikhonravova[1]
Maksim (Viktorovich) Narushko[1]
Elena (Adolfovna) Slagoda[1,3,4]
[1]*Institute of Earth Cryosphere, SB RAS, Tyumen, Russia, mouse132008@gmail.com*
[2]*Institute of Problems of Development of the North of the SB RAS, Tyumen, Russia*
[3]*Tyumen State University, Tyumen, Russia*
[4]*Tyumen Industrial University, Tyumen, Russia*

Abstract

Biotopes are caused by natural conditions during the accumulation of peat in the tundra. The plant remains in peat and permafrost rocks of the drained thermokarsthollow on the Gydan peninsula are studied. The botanical composition and layer by layer age of the plant remains are determined. By change of plant communities in lake-flooded and lacustrine-bog sediments the dynamics of the local natural conditions of the arctic tundra at the end of the Sartan period and the Holocene is reconstructed.

Keywords: Biotopes, peat, botanical composition, tundra, Gydan peninsula

Introduction

Biotopes are associated with natural conditions to during the accumulation of peat. The ratio and composition of various the peat-forming plants reflect the change in the conditions of their growth. On the botanical composition is influenced by summer air temperatures, humidity, radiation balance, the depths of seasonal thawing, the composition of maternal deposits and other accidental external factors, such as the impact of animals, fires, landslides, etc. Landscape and paleoclimatic conditions for their growthdetermine by the quantitative content and ratio of plants in the peat and peat soils. Data on dynamics of the Arctic tundra of Western Siberia in the Holocene are'nt enough.

Methods

In 2016 in the lower reaches of the Gyda River in the coastal ledge with high of 3 m frozen sediments with ice wedge and horizon of seasonally thawed peat were studied. The incision is located within the drained thermokarst basin within the II lacustrine-alluvial terrace in the zone of the Arctic tundra of Gydan peninsula. The surface of the khasyrey is represented the polygonal relief. The surface of the khasyrey is formed of peat with 0.2-0.8 m thickness.

The monolith of peat from surface was selected and is divided into 6 layers along visible boundaries and sand content. The remains of plant from permafrost rocks was selected on 195-197 cm depth buried near the place of growth. The botanical composition of peat and residues from frozen deposits is defined by microscopy method according special atlases-guides [Dombrovskaya et al. 1950, Katz et al. 1977] and collection of micropreparations of modern plants. The micropreparations are made from the most resistant to decomposition parts of plants by the method [Andreeva et al, 2008]. Radiocarbon dating of peat is performedSimonova (IMPP SB RAS, Tomsk).

Results

In the peat loam on 195-197 cm depth, lenses and layers (1-5 cm thick) of plant remains buried near the place of growth simultaneously with the accumulation of sediments are located. These remains consist mainly of slightly decomposed leaves of moss *Drepanocladus polygamus*, which constitute before 85%. In addition, a small amount of *Sphagnum* moss, *Carex sp.*and *Vaccinium vitis-idaea*was found. This association of plants is typical for places with high humidity, and moss *Drepanocladus polygamus* for an environment with a high content of mineral salts and calcium carbonate in water and soil. The features of the stratification of deposits and botanical composition of plants indicate on flood regime of their accumulation, probably, on the flooding of the khasyrey by hydro-carbonate floodplain waters of the Gyda River. The age of this peat layer was determined 12 232 ± 290 years ago. The accumulation of plant remains in floodplain loam and the increase of ice veins occurred in the second half of the Sartan (Table 1).

Table 1. The age of peat layers and plant residues (C^{14})

Depth, cm	layer	Age, yearsago	№ sample	Biotope
3-5	5	854±96	ИМКЭС-14C1243	Carex peat with Sphagnum and Petasítes sp.
5-8	4	2907±120	ИМКЭС-14C1232	
8-12	3	4680±108	ИМКЭС-14C1093	Eriophorum-Carex peat with Betula nana
12-20	2	4032±105	ИМКЭС-14C1244	Eriophorum-Carexpeat with Drepanocladus polygamus
20-23	1	3506±95	ИМКЭС-14C1268	
195-197	0	12232±290	ИМКЭС-14C1257	Drepanocladus polygamus peat

The surface of investigated incision is submitted to horizon of autochthonous peat with 23 cm thickness. The peat has inclined layers parallel to the surface, it the bottom border disrupted by cryoturbation. 6 layers of peat with degree of decomposition of 52-59%were isolated.

The bottom layer of peat from 20-23 cm depth consists of remains of roots of *Carex sp.*(before 77%), *Eriophorumsp.*(11%), leaves of moss *Drepanocladus polygamus* (8%), are also present remains of *Vaccinium vitis-idaea*, *Phragmítes*and *Equisétumsp*. This layer accumulated 3.5 thousand years ago (Table 1). In yellowish-brown peat on 12-20 cm depth, the remains of *Carex sp.*(before 70%) and moss *Drepanocladus polygamus* (5%) is decreasing, the amount of remains of *Eriophorum sp.*(20%) is increasing and a*Betula nana* appears. This layer of peat accumulated 4.0 thousand years ago. Peat in the interval 23-12 cm, was accumulated in moistened subaerial conditions [Khotinsky, 1977].

Peat from of 8-12 cm depth differ the content of inclined lenses of light gray fine sand. The *Carex sp.*(before 51%), *Eriophorum sp.*(24%) and small amount of *Betula nana*(14%) and remains of *Empetrumnigrum*is composed basis of the biotope. The remains of moss *Drepanocladus* have been not detected. The accumulation of this layer of peat occurred 4.7 thousand years ago in relatively dry conditions.

Yellowish-brown peat with an admixture of sandy loam in the diapason of 5-8 cm contains *Carex sp.*(to 57%), remains of *Betulanana* (to 10%) and *Petasítes sp.*(to 15%), indicating moist conditions. The layer of peat accumulated 2.9 thousand years ago.

The top layer of loose dark brown peat (3-5 cm) includes impurities of sand. In its composition are dominated *Carex sp.*(about 34%), there are remains of *Petasítes sp.*(about 15%), there are poorly decomposed leaves of moss *Sphagnum sp.*(about 14%), which indicates high humidity of khasyrey. Moss *Sphagnum* is characteristic of acidic substrates. This layer of peat accumulated 0.8 thousand years ago.

In the 0-3 cm layer is decrease in the amount residues of moss *Sphagnum* and an increase *Carexsp.*, as well as the roots of modern shrubs. Age of the layer is not defined, because contains many roots of modern plants.

Conclusions

On basis of the structure of the frozen sediments follows that after the completion of the formation sandy loams of Upper Sartan and, probably, sands Lower Holocene with threadlike roots of plants in situ, and ice wedge, the accumulation of peat was began on drained surface.

A change of species diversity of plants in the horizon of peat reflects the dynamics of biotopes. The most antique biotope - *Eriophorum-Carex*peat with impurity of birch was formed in relatively dry conditions, about 4.7 thousand years ago. Biotopes of *Eriophorum-Carex*peat and *Carex*peat were formed in the range of 4.0-3.5 thousand years ago. From the more ancient to the younger layers, the reduction of the *Betula nana*, the appearance of moss *Drepanocladus polygamus*, indicating on waterlogging, growth of moistening is traced. The inversion of radiocarbon dates inside the peat horizon is associated with flooding of surface.

The biotope formed 2.9 thousand years ago: *Carex*peat with *Betula nana*and *Petasítes sp.*indicates on existence of coastal zones of water in the khasyrey and humidified conditions of typical tundra. The biotope of *Carex*peat with *Sphagnum sp.* and *Petasítessp.*which existed 0.8 thousand years ago accumulated in the most moistened conditions. In the khasyrey on the north of Gydan, in the subboreal and subatlantic periods of the Holocene, the biotopes changed dynamically when wet and dry conditions changed.

References

Kats N. 1941. *Swamp and peat*. Moscow, 403 pp.

Andreeva V., Kalinina G., Salnikova E. 2008. *Methods of pharmacological analysis of medicinal plant material. Part 1. Acceptance rules and general test methods*.Tomsk, 56 pp.

Katz N., Katz S., Skobeleva E. 1977. Atlas of plant remains in peats. Moscow, Nedra, 376 pp.

DombrovskaiaA.,Koreneva M., Tyuremnov S. 1959. *Atlas of plant residues found in peat*. Moscow, Leningrad: Gosudarstvennoeenergeticheskoe Publ., 228 pp.

Khotinsky N. 1977. *Holocene of Northern Eurasia*. Moscow, Nauka, 200 pp.

Investigating permafrost-shrub interactions in Torngat Mountains National Park, northeast Canada

Caitlin M. Lapalme[1], Robert G. Way[1,2], Antoni G. Lewkowicz[2], Luise Hermanutz[3], Laura Siegwart Collier[3], Andrew Trant[4], Darroch Whitaker[5], Philip P. Bonnaventure[6]

[1]Labrador Institute, Memorial University, Happy Valley-Goose Bay, Canada, caitlin.lapalme@mun.ca, [2]Department of Geography, Environment and Geomatics, University of Ottawa, Ottawa, Canada, [3]Department of Biology, Memorial University, [4]School of Environment, Resources and Sustainability, University of Waterloo, [5]Parks Canada, [6]Department of Geography, University of Lethbridge

Abstract

The Torngat Mountains National Park (TMNP) is the southernmost zone of the eastern Canadian Arctic and is classified as having continuous permafrost on the IPA map. The region has warmed by 2°C since the 1990s and shrub growth has accelerated in the park with impacts on local ecology and wildlife. Owing to a lack of field information on permafrost characteristics, shrub distribution, and a limited understanding of how tall shrubs may be impacting permafrost, the Torngat Permafrost Project was launched to examine regional permafrost distribution and permafrost-shrub interactions. Field investigations of permafrost and shrubs were undertaken at four main study areas along a north-south transect in TMNP. Results suggest that permafrost is warmer, thinner and has deeper active layers in environments dominated by tall shrubs. Ground surface temperature data from ~80 locations show permafrost is widespread but also that TMNP should be classified as in the extensive discontinuous zone.

Keywords: Coastal permafrost, shrubs, permafrost-shrub interactions, eastern Canada, Labrador

Introduction

Torngat Mountains National Park (TMNP) is in the Canadian low-Arctic coastal region of northern Nunatsiavut, Labrador adjacent to the Labrador Sea (Fig. 1). Rapid regional warming has resulted in local tundra greening, increases in shrub density and height (Fraser *et al.*, 2011). There is presently no information on the regional permafrost distribution because TMNP has historically been ignored from field investigations. As such, there is only a conceptual understanding of how rapid vegetation change may impact permafrost characteristics in TMNP, and how permafrost degradation affects local ecology, hydrology and wildlife. The Torngat Permafrost Project was initiated to characterize permafrost within the boundaries of the TMNP. The objectives are: (1) to establish a permafrost monitoring network in TMNP; (2) to enhance existing ecological integrity monitoring initiatives in TMNP; (3) to quantify potential impacts of shrub growth on permafrost in TMNP; and (4) to understand how permafrost thaw may impact TMNP ecosystems and wildlife.

TMNP has a low-Arctic coastal climate with mean annual air temperatures ranging from -2°C to -10°C. Tundra and rock are the dominant land cover classes with upright shrubs comprising just ~6% of the park. The IPA map classifies TMNP as in the continuous permafrost zone but a modelling study by Way & Lewkowicz (2016) suggests the regional distribution is discontinuous. Regional warming of ~2°C and local sea ice loss has occurred in TMNP since the early-1990s.

Methods

Field investigations of permafrost thickness, freeze-thaw depth, general distribution and shrub characteristics were completed at four primary field sites between 2016 and 2017 in TMNP (Fig. 1, 2). At each site, surveys including permafrost geophysics (DC electrical resistivity tomography [ERT]), frost probing and/or instantaneous temperature profiling were completed. Vegetative cover and density and height of prostrate and tall shrubs was quantified in 1 m^2 plots along most ERT transects (Fig. 2B). A DJI Phantom 3 Pro UAV was used for study area photographs and for shrub cover calculations along survey lines. A total of 17 transects were completed with survey lengths ranging from 40 to 160 m.

Ground surface temperature (GST) loggers (n=18) were installed along ERT transects and were supplemented by GST loggers installed previously by Parks Canada between 2010 and 2017 (n=61). GST data was compared to gridded daily air temperatures covering TMNP from 2010-2017 (100 m. resolution) generated from 13 climate stations established in the general region. Three high elevation climate stations recording air temperature, GST, ground temperatures at 1 m depth and snow depth were installed in the region in July of 2017.

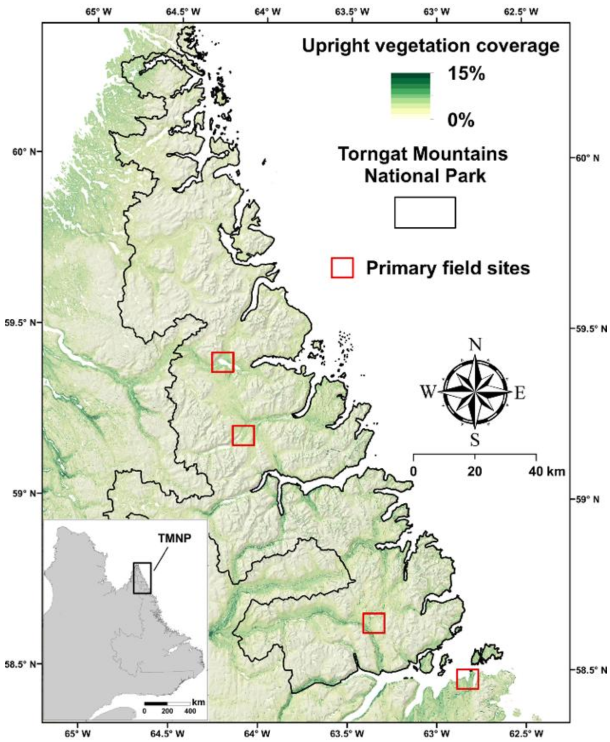

Figure 1. Upright vegetation coverage in TMNP. Field sites from North to South were Kangalaksiorvik Lake (~50 m asl), Komaktorvik Lake (~90 m asl), Nakvak Brook (~410 m asl) and Torr Bay (~20 m asl). Inset map shows location of TMNP.

Preliminary Results

Field surveys showed that tall shrubs were associated with warmer ground temperatures and thinner permafrost (inferred from ERT and instantaneous ground temperatures). In contrast, prostrate shrubs were correlated with higher near-surface resistivities and detectable permafrost. Coarse surficial geology and hydrological conditions were the main factors hindering ERT interpretation of shrub-permafrost interactions. Shrub-permafrost linkages appear to be mediated by microclimate, surficial materials, and topographic positioning. Enhanced snow accumulation is hypothesized to be the primary cause of ground temperature warming beneath tall shrubs (e.g. Way & Lewkowicz, *in press*). GST loggers (n=79) had a median of -2.3°C with a minimum value of -3.5°C and a maximum value of 1.9°C. Fifty-seven loggers had annual GSTs at or below 0°C implying the presence permafrost whereas 22 were above 0°C. Using a range of rk values (0.8-1.1) in the temperature at the top of permafrost model (Way & Lewkowicz, 2016), we estimate that permafrost is present at 70-80% of loggers sites. These results suggest that the regional distribution of permafrost in TMNP is more likely extensive discontinuous (>50% of land area) rather than continuous as depicted on most permafrost maps.

Figure 2. (A) UAV image of remote fly-in camp at Komaktorvik Lake; (B) UAV image of shrub and ERT surveys at Nakvak Brook.

Acknowledgments

We thank J. Jacobs for monitoring station data and R. Laing for supporting this research. RGW received financial support from the RCGS and NSTP. RGW and AGL received funding from NSERC and the University of Ottawa. RGW, AGL, LH, AT, PPB received funding from the W. Garfield Weston Foundation. LH received funding from ArcticNet and LSC received funding from NSERC and NSTP.

References

Fraser, R.H., Olthof, I., Carrière, M., Deschamps, A. & Pouliot, D., 2011. Detecting long-term changes to vegetation in northern Canada using the Landsat satellite image archive. *Environmental Research Letters* 6: 045502.

Way, R.G. & Lewkowicz, A.G., 2016. Modelling the spatial distribution of permafrost in Labrador-Ungava using the temperature at the top of permafrost. *Canadian Journal of Earth Sciences* 53: 1010-1028.

Way, R.G. & Lewkowicz, A.G., *in press*. Environmental controls on ground temperature and permafrost in Labrador, northeast Canada. *Permafrost and Periglacial Processes*.

Main results of 4-year gas-emission crater study

Marina O. Leibman[1,2]
Yury A. Dvornikov[1]
Artem V. Khomutov[1,2]
Alexandr I. Kizyakov[3,1]
Boris G. Vanshtein[4]

[1]*Earth Cryosphere Institute, Tyumen Scientific Center SB RAS moleibman@mail.ru*
[2]*University of Tyumen, International Institute of Cryology and Cryosophy*
[3]*Lomonosov Moscow State University, Faculty of Geography, Cryolithology and Glaciology Department*
[4]*FSBI "VNIIOkeangeologia", Department of lithology and geochemistry*

Abstract

Study of gas emission craters started in 2014 using field monitoring and sampling, laboratory testing, and remote-sensing data analysis. Documented are six craters, all in the north of West Siberia in a narrow range of latitudes. Field research covered three craters on Yamal and Gydan Peninsulas, remote sensing was applied to 4 craters and a number of pre-crater mounds. We collected samples in the crater walls, in the intra-crater lakes, other lakes and ground ice exposures. Ions, ^{18}O, ^{2}H, and ^{13}C isotopes, organic matter, methane concentration were measured in the water and ice in laboratory. All data obtained confirmed that craters were preceded by mounds, exposed tabular ground ice in their walls, and showed very high concentration of methane initially in the crater air and later in the intra-crater lake. We hypothesize that crater formation was due to methane emission resulting from ground temperature rise.

Keywords: Gas emission crater; tabular ground ice; methane clathrates; gas-inflated mounds; climate fluctuations.

Introduction

We studied gas-emission craters in the north of West Siberia, for the interest raised in the media, and real risks to population and structures that may arise from this process of unknown mechanism and controls. Documented by visits of researchers, or approved by photographs are six craters. All are located within a narrow range of latitudes around 70°N (Fig. 1).

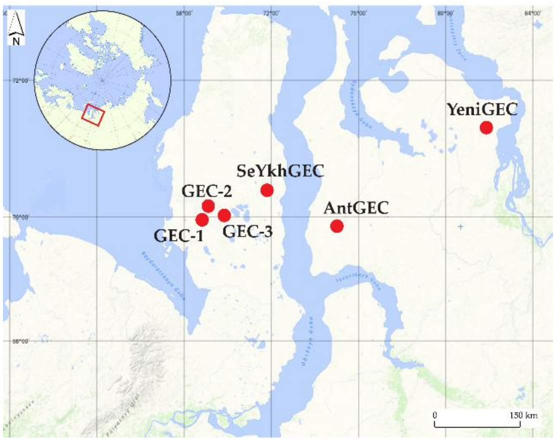

Figure 1. Scheme of the gas-emission craters location.

Four craters (GEC-1, 2, 3 and AntGEC) had appeared in the fall of 2013. YeniGEC, the northern- and easternmost, is reported to form in March 2013 but was not visited and described. SeYkhGEC was the only one observed when ejection took place in June 28, 2017. Objects under study were crater morphology and its dynamics in time; deposits exposed in its walls; parameters of the lake formed inside the crater, surrounding environments, and permafrost features; tabular ground ice in the exposures; lakes in the region; as well as vegetation, snow cover and more.

Study area and methods

The area of crater occurrence in the North of West Siberia lies in the continuous permafrost zone with thick layers of tabular ground ice as well as buried and modern polygonal ice wedges.

Geology is represented by sandy to clayey and peat sediments. There is a high content of methane in the form of both gas bubbles and clathrates in the upper 120 m of the section.

In the craters visited, edges and parapets were contoured, depth when possible measured, scattering of sediment blocks ejected from the crater measured as well. We visited GEC-1 several times in summer and winter doing measurements and sampling. For this landform dynamics of the outlines, formation of intra-crater lake and its chemistry, distribution of ice in the crater walls, differences in methane concentration in the water in summer and winter thus registering changes in time is rather well understood.

We visited GEC-2, 3 and AntGEC one-two times with limited number of measurements. We characterize SeYkhGEC features based only on photographs and video records provided by the research team (leaders A.Sinitsky and A.Baryshnikov) that was on the site soon after this crater formed. YeniGEC was only recognized on the photograph provided by V.Epifanov to be a feature of most likely the same GEC origin. Methane concentration was measured in field in GEC-1 and SeYkhGEC shortly after their discovery and showed extremely high values compared to the atmosphere in the vicinity.

Samples of ice and sediment from the crater walls and nearest exposure, as well as water from the intra-crater lakes, other lakes and ice exposures were analyzed in several laboratories for ionic composition, ^{18}O, ^{2}H, and ^{13}C isotopes, organic matter, methane concentration and other parameters. We collected samples of willow branches from the ejected blocks of turf from the pre-crater mound and in the surrounding area for tree ring analysis to date the history of mound development.

We applied remote sensing data to (1) determine the date of crater formation, only SeYkhGEC dated by direct observation; (2) to build digital elevation models of the craters and surrounding areas for several time slices; (3) to map environments to which craters were linked.

Mapping involved both remote-sensing data, special field observations and extensive permafrost study experience of the team ongoing in the region since 1987.

Results and discussion

All known craters were preceded by more or less distinct mounds 2-5 m high and about 30-50 m in diameter. Craters consisted of cylinder portion from the bottom up, and funnel-shaped upper portion. Diameter of the cylinder initially was 15-20 m. More or less developed parapet of ejected material surrounded craters. Depth was measured only at GEC-1 to be approximately 70 m. Other craters as estimated from the photographs and satellite images were much less deep. All craters observed both directly or on early photographs demonstrated thick tabular ground ice layers. At GEC-1 at earliest stage, tabular ground ice was deformed to almost vertical stratification parallel to the cylinder walls. While walls of the crater retreated, horizontal stratification appeared.

Craters of the western Yamal (Gec-1, 2, 3) exposed clayey deposits in the walls and, accordingly, in the parapet. SeYkhGEC and AntGEC exposed sandy deposits at least in the upper portion of the section.

In general, a much higher concentration of main ions (up to 2 g/l) is characteristic of intra-crater lake water as compared to other lakes, Na^+ and Cl^- dominating. Oxygen and Deuterium isotope composition of water from the crater lakes is closer to that in tabular ground ice of the crater walls. However, in time it gradually becomes heavier ($\delta^{18}O$ approximately from -20‰ in 2014 to -18‰ in 2017, and δD from -150‰ to -135‰ for the same time). Methane concentration in the intra-crater lake water (approximately 500-1000 ppm) significantly exceeds the values in the water of other lakes (15 ppm on average). Carbon and Hydrogen isotope composition in methane from the crater lake and other lakes indicates its origin to be microbial, the same as collected in the shallow gassing Yamal boreholes.

Digital elevation models of pre-crater mounds, craters and surrounding terrain reveal difference in crater localization characteristic of western and eastern "clusters". Western cluster (GEC-1, 2 and 3) are confined to lower parts of gentle slopes, shrubby, wet, and composed of clayey deposits. Eastern cluster: AntGEC is located on the bend of terrace surface to steep slope, with sparse vegetation, in sandy deposits; SeYkhGEC on the opposite is in the river valley bottom, with sandy deposits dominating.

Conclusions

We put forward a hypothesis most consistent on our opinion with data obtained: gas-emission craters form in the place of gas-inflated mounds resulting from excess gas pressure. Excess pressure appeared as a result of decomposition of methane clathrates in permafrost and ground ice due to ground temperature rise. This pressure ejected frozen sediments and ice, broken into blocks, which flew away scattering around and forming parapet. As all craters expose tabular ground ice, we consider it as an important indicator for crater prediction. The role of tabular ground ice is most likely its plasticity, impermeability for gas, and irregular structure. Methane content in the water for the first 3 years of observation remains very high and indicates the presence of its source under the bottom of the crater lake.

Acknowledgments

This work is supported by Russian Science Foundation (RSF) grant No. 16-17-10203.

Thermokarst alters soil nitrogen transformations in a typical permafrost ecosystem on the Tibetan Plateau

Chao Mao[1, 2]
Dan Kou[1, 2]
Christoph Müller[3, 4]
Yuanhe Yang[1, 2]
[1]*State Key Laboratory of Vegetation and Environmental Change, Institute of Botany, Chinese Academy of Sciences, Beijing 100093, China*
[2]*University of Chinese Academy of Sciences, Beijing 100049, China*
[3]*Department of Plant Ecology, Justus-Liebig University Giessen, Heinrich-Buff-Ring 26, 35392 Giessen, Germany*
[4]*School of Biology and Environmental Science, University College Dublin, Ireland*

Abstract

Permafrost regions store more than half of the world's soil carbon (C). Permafrost collapse (thermokarst) is expected to release an enormous amount of C, creating positive feedback to climate warming. Upon collapse, soil nitrogen (N) availability will also increase, which may stimulate plant productivity and partially offset permafrost C pool losses. Our knowledge on the dynamics of soil available N in response to thermokarst, mainly controlled by the soil N transformations, is thus crucial for understanding permafrost C-climate feedback. However, it remains unclear whether and how soil gross N transformations respond to thermokarst formation. Here we determined soil gross N transformation rates using a ^{15}N tracing method within a typical thermo-erosion gully on the Tibetan Plateau. The results showed that rates of gross N mineralization and ammonium (NH_4^+) immobilization declined with thermokarst, which were triggered by the changed soil microbial community and reduced NH_4^+ concentration under drier conditions. Likewise, denitrification was depressed under drier soil condition in thermokarst. However, heterotrophic nitrification and nitrate (NO_3^-) immobilization were accelerated, because of decreased soil moisture and increased NO_3^- concentration after thermokarst formation. Additionally, rates of autotrophic nitrification and dissimilatory NO_3^- reduction to NH_4^+ had no responses to thermokarst formation. Overall, our results demonstrate thermokarst-induced changes in soil N transformations, which may regulate the strength of permafrost C-climate feedback by altering soil N availability.

Keywords: Gross nitrogen transformations, nitrogen availability, nitrogen cycle, permafrost, thermokarst.

Introduction

Permafrost collapse (thermokarst) is expected to release large amounts of carbon (C) to atmosphere, triggering a positive feedback to climate change (Abbott & Jones, 2015). The losses of permafrost C pool will be partially offset by biomass production which is influenced by soil nitrogen (N) availability controlled by soil transformations (Finger *et al.,* 2016). However, little is known about the responses of soil N transformations to thermokarst formation.

To fill this knowledge gap, we selected a typical thermokarst landscape on the Tibetan Plateau to explore the effects of thermokarst formation on gross N transformation rates obtained through ^{15}N tracing technology.

Results

Altered soil gross N transformations after thermokarst formation

The formation of thermokarst marginally decreased soil gross N mineralization and NH_4^+ immobilization ($P < 0.1$), significantly increased soil heterotrophic nitrification ($P < 0.05$) and marginally increased soil NO_3^- immobilization ($P < 0.1$). In addition, thermokarst formation had no significant influence on autotrophic nitrification. Furthermore, denitrification was significant lower in thermokarst area than that in non-thermokarst area ($P < 0.05$).

Linking soil gross N transformations to soil physicochemical and microbial properties

Gross N mineralization increased with soil moisture but declined with F/B ($P < 0.1$; Figures 2d-e). Moreover, heterotrophic nitrification was negatively influenced by soil moisture ($P < 0.05$; Figure 2a). Furthermore, NH_4^+

immobilization exhibited an increase with soil moisture ($P < 0.05$; Figure 2f) and NH_4^+ ($P < 0.1$; Figure 2h), but had a decrease with F/B ($P < 0.05$; Figure 2g). In addition, NO_3^- immobilization was negatively associated with soil moisture ($P < 0.1$; Figure 2b), but positively correlated with NO_3^- ($P < 0.05$; Figure 2c).

Conclusions

In summary, this study revealed the diverse responses of soil N transformations to thermokarst formation. Our results revealed that the unchanged autotrophic nitrification, increased heterotrophic nitrification and decreased denitrification accelerated the accumulation of NO_3^- in thermokarst area, which implies the rising risks of NO_3^- leaching loss from permafrost ecosystems. Our results also revealed that the decreased gross N mineralization limits the production of NH_4^+ in surface soil from thermokarst, suggesting the potential adverse effect of topsoil N availability on plant growth. However, in consideration of the thermokarst-induced increases in foliar N contents and biomass production reported in previous studies (Finger *et al.,* 2016), this detrimental effect implies a boost to plant growth from N reservoirs of deep soil horizons. This deduction is confirmed by the fast soil N transformations in deep soils (Keuper *et al.,* 2012) and significant increase in aboveground biomass of deep-rooting species (Keuper *et al.,* 2017).

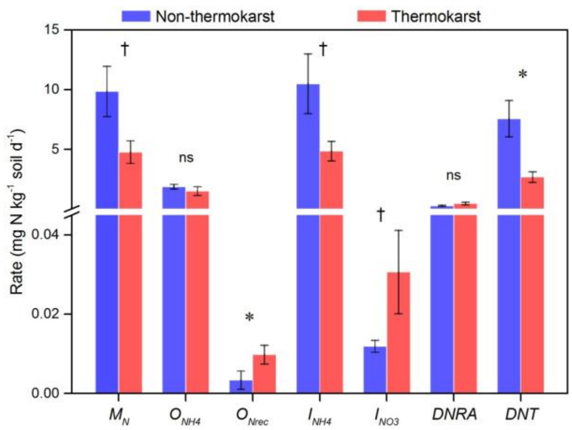

Figure 1. Comparison of gross N transformation rates between the non-thermokarst and thermokarst areas on the northeastern Tibetan Plateau. M_N, gross N mineralization; O_{NH4} (autotrophic nitrification), oxidation of NH_4^+ to NO_3^-; O_{Nrec} (heterotrophic nitrification), oxidation of organic-N to NO_3^-; I_{NH4}, immobilization of NH_4^+; I_{NO3}, immobilization of NO_3^-; *DNRA*, dissimilatory NO_3^- reduction to NH_4^+; *DNT*, denitrification. Blue and red bars represent data points in the non-thermokarst (n = 5) and thermokarst areas (n = 5), respectively. Significant differences of gross N transformation rates between non-thermokarst and thermokarst areas are determined by independent samples t-test. *: $P < 0.05$; †: $P < 0.1$; ns: no significant difference.

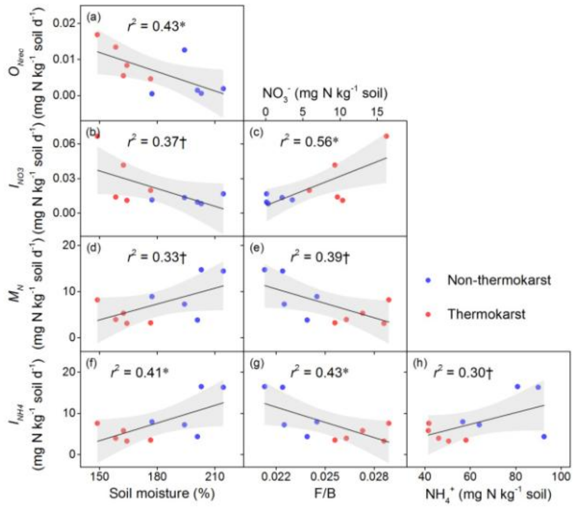

Figure 2. Relationships between gross N transformation rates and environmental, substrate and microbial properties. Blue and red solid circles represent data in non-thermokarst (n = 5) and thermokarst areas (n = 5), respectively. Solid lines represent the fitted curves and grey areas indicate 95% confidence intervals. r^2, proportion of variance explained. Significant correlations between gross N transformation rates and the corresponding variables are denoted by * ($P < 0.05$) and † ($P < 0.1$).

References

Abbott, B.W. & Jones, J.B., 2015. Permafrost collapse alters soil carbon stocks, respiration, CH_4, and N_2O in upland tundra. *Glob Chang Biol* 21: 4570-4587.

Finger, R.A., Turetsky, M.R., Kielland, K. *et al.*, 2016. Effects of permafrost thaw on nitrogen availability and plant-soil interactions in a boreal Alaskan lowland. *J. Ecol.* 104(6): 1542-1554.

Keuper, F., van Bodegom, P.M., Dorrepaal, E. *et al.*, 2012. A frozen feast: thawing permafrost increases plant-available nitrogen in subarctic peatlands. *Glob. Change Biol.* 18(6): 1998-2007.

Keuper, F., Dorrepaal, E., van Bodegom, P.M. *et al.*, 2017. Experimentally increased nutrient availability at the permafrost thaw front selectively enhances biomass production of deep-rooting subarctic peatland species. *Glob. Change Biol.* 23(10): 4257-4266.

The cartography of permafrost continuity

Frederick E. Nelson[1,2]
Kelsey E. Nyland[1]

[1]*Department of Geography, Environment, and Spatial Sciences, Michigan State University, East Lansing, MI, USA 48824* fnelson@msu.edu
[2]*Department of Earth, Environmental, and Geographical Sciences, Northern Michigan University, Marquette, MI, USA 49855*

Abstract

Maps are the primary vehicle used to communicate geographical relationships. Ironically, interest in the formal practice of *cartography*, the art and science of mapmaking, has fallen significantly during a period when the availability of mapmaking software has increased dramatically. Although there has been a significant increase in the number of geographically oriented permafrost studies over the past two decades, little discussion about competing mapping strategies, map accuracy, and the psychophysical impact of cartographic design is evident in geocryological literature. Failure to use the full potential of the tools and techniques that contemporary cartographic and spatial-analytic theory makes possible affects our ability to effectively and accurately communicate the impacts and hazards associated with thawing permafrost in the context of global change. This presentation examines recent permafrost studies involving small-scale (large area) mapping, and suggests some strategies for rectifying existing problems.

Keywords: *boundaries; cartography; frozen ground; mapping; permafrost*

Introduction

The advent of general circulation models (GCMs) more than three decades ago heralded a new era for scientific research in the polar regions. Advances in computer technology, the factor that facilitated the development of GCM modeling and continues to fuel its refinement, are also responsible for the rise of geographical information science (GISc), another branch of technological innovation that has precipitated a true revolution in the environmental sciences. Ironically, interest in the formal practice of *cartography*, the art and science of geographic visualization, fell precipitously just as GISc was ascending.

Permafrost Continuity

Using geocryological or climatic data obtained from a series of locations distributed over a region of interest, it is common practice to produce maps representing the geographic extent of permafrost. At small geographical scales (e.g., 1:5,000,000), such maps commonly depict a quasi-latitudinal zonation based on the areal continuity or dominance of permafrost. Despite frequent reference to *continuous*, *discontinuous*, and *sporadic* permafrost zones in the literature, these concepts have rarely been delimited using criteria that can be related unambiguously to the areal continuity of permafrost. Maps purporting to show the distribution of permafrost using continuity classifications have been based on highly divergent criteria in different countries and even within national borders. Despite glaring disparities in mapping criteria, the literature contains little discussion of their importance or their effects on interregional comparisons. This issue would seem to have great importance for constructing maps depicting the circumpolar or continental distribution of permafrost (e.g., AGS, 1975; CIA, 1984), but little or no discussion of mapping criteria is usually contained in such documents.

Until recently, most regional and hemispheric representations were compiled on a more or less *ad hoc* basis; rules for the placement of "boundaries," interpolation procedures, and even such primitive details as data-point locations and sources were frequently ignored. The resulting documents inspire little confidence when judged by rigorous standards, with zonal boundaries on competing representations diverging by hundreds of kilometers, even on documents with similar publication dates (Nelson, 1989; Nelson & Anisimov, 1993).

Two decades ago, the International Permafrost Association's *Circum-Arctic map of permafrost and ground-ice conditions* (Brown *et al.*, 1997) provided, for the first time, a detailed cartographic document that attempted to use consistent, replicable mapping procedures over the entire circum-Arctic region. Even so, a cursory view of this map reveals striking contrasts in mapped patterns in different regions—contrasts attributable to both geographically variable data availability and to divergent mapping criteria employed in various national "schools" of permafrost science.

Conclusions

Although geocryology has a long history of spatial representation and continues to produce maps of various permafrost-related phenomena, few publications in the field discuss competing mapping strategies, map accuracy, the psychophysical impact of cartographic design, mapping criteria, interpolation techniques, accuracy estimation, or advances in geographic visualization. Our collective failure to use the full potential of the tools and techniques that contemporary cartographic theory makes possible affects our ability to effectively communicate empirical and modeled results, as well as the potential impacts of global climate change on permafrost environments. Until our map products are constructed in ways that allow their incorporation into the larger global-change research enterprise with well-determined accuracy, permafrost research will not live up to its full potential in one of the most important scientific enterprises of our time.

This presentation discusses the concept of permafrost continuity and the criteria used to map it, demonstrates the need for standardized mapping criteria, and reviews advances in the art and science of cartography that could be applied in the mapping of permafrost.

References

AGS, 1975. *Map of the Arctic region*. New York: American Geographical Society. Scale 1:5,000,000.

Brown, J., Ferrians, O.J., Heginbottom, J.A., & Melnikov, E.S., 1997. *Circum-Arctic map of permafrost and ground-ice conditions*. Washington, D.C.: U.S. Geological Survey. Circum-Pacific Map Series CP-45. Scale 1:10,000,000.

CIA, 1984. *Permafrost regions in the Soviet Union*. Washington, D.C.: U.S. Central Intelligence Agency. Scale 1:38,400,000.

Nelson, F.E., 1989. Permafrost zonation in eastern Canada: a review of published maps. *Physical Geography* 10: 231-246.

Nelson, F.E. & Anisimov, O.A., 1993. Permafrost zonation in Russia under anthropogenic climatic change. *Permafrost and Periglacial Processes* 4: 137-148.

A scalable approach to model the ground thermal and hydrological dynamics of polygonal tundra

Jan Nitzbon [1 2 3]
Sebastian Westermann [3]
Moritz Langer [1 2]
Leo Celestin Paul Martin [3]
Guido Grosse [1 4]
Julia Boike [1 2]

[1] *Alfred Wegener Institute, Helmholtz Centre for Polar and Marine Research, Potsdam, Germany, jan.nitzbon@awi.de*
[2] *Geography Department, Humboldt University of Berlin, Berlin, Germany*
[3] *Department of Geosciences, University of Oslo, Oslo, Norway*
[4] *Institute of Earth and Environmental Science, University of Potsdam, Potsdam, Germany*

Abstract

Polygonal tundra and ice-rich permafrost landscapes are widespread across the Arctic and prone to rapid transitions due to ground subsidence, thermokarst or thermoerosion. Such small-scale processes are typically not resolved in large-scale Earth System models. Our goal with this study was to develop a scalable modeling approach that is capable of simulating the degradation of ice-wedges and the corresponding geomorphological transition from low- to high-centered polygons. For this, we employed the land surface model CryoGrid3 and improved it by adding a hydrological infiltration scheme. We simulated the lateral exchange of heat, water, and snow between polygon centers, rims and troughs by coupling multiple realizations. We proved our modeling approach to be capable of describing the evolution of ice-wedge polygons and analyzed the hydrological and climatic conditions, which are favorable for their degradation. With this, we contributed to the understanding of landscape transitions in ice-rich permafrost regions and their representation in large-scale models.

Keywords: permafrost modeling; ice-wedge degradation; polygonal tundra hydrology; thermokarst; thermoerosion; Northern Siberia

Introduction

Polygonal tundra and ice-rich permafrost landscapes are widespread across the terrestrial Arctic and feature various characteristic landforms. These landscapes are prone to rapid transitions including ground subsidence, thermokarst, thermoerosion and the degradation of polygonal tundra (Grosse & Romanovsky, 2011; Joel C. Rowland & Coon, 2015).

These processes have in common that they occur on small spatial scales, which are not resolved in large-scale Earth System models. At the same time, they can have an overall impact on the cycling of water, energy, and carbon in the entire Arctic region (J. C. Rowland et al., 2010).

Our objective with this contribution is to present a modeling approach to study the coupled thermal and hydrological dynamics of ice-rich permafrost landforms that can be upscaled in an efficient way. We focus on the application to polygonal tundra for which in recent decades degradation has been observed across the Arctic (Liljedahl et al., 2016).

Methods

Model developments

We improved the land surface model CryoGrid3 (Westermann et al., 2016) through the addition of a hydrological infiltration scheme for unfrozen ground. Additionally, we implemented the ability to exchange heat, water, and snow laterally between adjacent realizations.

Representing polygonal tundra

We represented polygonal tundra in the model by multiple realizations running in parallel, representing the polygon center, rim and trough, respectively. The same approach is suitable to describe the thermal and hydrological dynamics of other periglacial landforms (cf. Figure 1).

Forcing and validation data

Data acquired from a long-term observatory located in the Lena River delta in Northern Siberia provided the atmospheric forcing of the model and served to validate the simulations of the ground thermal and hydrological regimes.

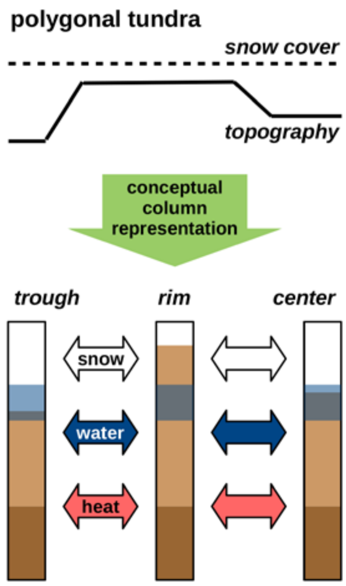

Figure 1 Representation of polygonal tundra via adjacent realizations that represent distinct landscape units. Water, snow, and heat are exchanged laterally between 1D-realizations.

Results

Degradation from low-centered to high-centered polygons

We applied the model setup to simulate the degradation of ice-wedge polygonal tundra from a low-centered to a high-centered relief. We identify conditions which are favorable for ice-wedge degradation.

Variation of the climatic and hydrological settings

We investigated the dependence of the polygon evolution on the local hydrological conditions by varying the external drainage flux and identified those conditions favorable for polygon degradation. We further studied the projected polygon evolution for different future climatic forcing scenarios.

Role of lateral exchange processes

We studied the relevance of lateral exchange of water, heat and snow for the ground thermal and hydrological regimes.

Discussion

Our model setup proved to be capable of simulating the evolution of ice-rich permafrost landscapes such as polygonal tundra for which rapid degradation processes have been observed in recent decades (Liljedahl et al., 2016). The model approach facilitates studying the coupled thermal and hydrological dynamics of different landforms and thus enables the assessment of their response to changing environmental conditions.

The ability to describe the subsidence of ground due to melting of excess ground ice is a particular strength of the model compared to other approaches. The approach does not require a 3D-representation of the landforms like in (Kumar et al., 2016; Liljedahl et al., 2016), but relies on a suitable coupling of multiple 1D-realizations with lateral exchange processes accounted for. Therefore, it is able to describe the evolution of small-scale landscape features while being scalable in an efficient way.

Conclusion

We presented a scalable modeling approach that is capable of describing the evolution of polygonal tundra and analyzed the hydrological and climatic conditions, which are favorable for the degradation of ice-wedge polygons. The scalable approach is further applicable to study the ground thermal and hydrological dynamics of other ice-rich permafrost landforms. With this, we contributed to the understanding of landscape transitions in ice-rich permafrost regions and their representation in large-scale models.

References

Journal articles

Grosse, G., & Romanovsky, V. (2011). Vulnerability and Feedbacks\rof Permafrost to Climate Change. *EOS, Transsactions, American Geophysical Union.*, *92*(9), 73–80.

Kumar, J., Collier, N., Bisht, G., Mills, R. T., Thornton, P. E., Iversen, C. M., & Romanovsky, V. (2016). Modeling the spatiotemporal variability in subsurface thermal regimes across a low-relief polygonal tundra landscape. *The Cryosphere*, *10*(5), 2241–2274.

Liljedahl, A. K., Boike, J., Daanen, R. P., Fedorov, A. N., Frost, G. V., Grosse, G., … Zona, D. (2016). Pan-Arctic ice-wedge degradation in warming permafrost and influence on tundra hydrology. *Nature Geoscience*, *9*(April), 312–318.

Rowland, J. C., & Coon, E. T. (2015). From documentation to prediction: Raising the bar for thermokarst research. *Hydrogeology Journal*, *24*(3), 645–648.

Rowland, J. C., Jones, C. E., Altmann, G., Bryan, R., Crosby, B. T., Geernaert, G. L., … Wilson, C. J. (2010). Arctic landscapes in transition: Responses to thawing permafrost. *Eos*, *91*(26), 229–230.

Westermann, S., Langer, M., Boike, J., Heikenfeld, M., Peter, M., Etzelmüller, B., & Krinner, G. (2016). Simulating the thermal regime and thaw processes of ice-rich permafrost ground with the land-surface model CryoGrid 3. *Geoscientific Model Development*, *9*(2), 523–546.

Physical and biogeochemical conditions of soils on James Ross Island, Antarctica

Daniel Nývlt[1]
Filip Hrbáček[1]
Isabel Prater[2]
Carsten W. Mueller[2]
Michaela Kňažková[1]
Barbora Kampová[1]

[1]*Department of Geography, Masaryk University, Brno, Czech Republic, Daniel.nyvlt@seznam.cz*
[2] *Lehrstuhl für Bodenkunde, TU München, Freising, Germany*

Abstract

James Ross Island represents the largest ice-free area in the Antarctic Peninsula region. More than 300 km² of the ice-free area offers unique opportunity to study soils of different origin and development stage in the region affected by ongoing climate change. In this work, we used a multidisciplinary approach for analyzing the current state of the physical and biogeochemical properties of soil across different landscapes and ecosystems of the northern part of James Ross Island.

Keywords: Antarctic soils, soil physical properties, soil organic matter, Antarctica, climate change

Introduction

Within the framework of the changing environment of marginal parts of Antarctica in connection with the present and future global climate change (IPCC, Representative Concentration Pathways (RCP) models for 2100 AD; IPCC, 2014), there is a great need to understand the effect of this change on the biological activity of Antarctic soils. Models predict a pronounced drying (reduction of moisture content in the surficial part of the active layer) of the ice-free areas of James Ross Island (JRI) due to the ongoing glacial shrinkage and enhanced active layer thawing (ATCM, 2015). It can be assumed that the change of the hydric regime will also affect the biological activity of Antarctic soils. To fully understand the possible changes in the soil environments, a multidisciplinary approach including biogeochemical analysis of soils is important. In this work we present an overview of the current results of soil research on JRI, Eastern Antarctic Peninsula (AP).

Study area

The study area is located in the northern part of JRI, which lies in the north-eastern sector of AP region (Fig. 2). The northern part of JRI called Ulu Peninsula with an area ~300 km² forms the largest ice-free area in the AP region, which composes ~8% of all ice-free land in AP region and ~1% of all ice-free areas in the whole Antarctica. The climate of JRI is classified as semi-arid cold polar with mean annual temperature at the sea level around -7.0 °C and precipitation estimated to 200–500 mm per year with a significant effect of uneven snow redistribution by wind. The ice-free area is formed mainly by bare ground, with vegetation niches limited to specific areas with sufficient liquid water, or nutrient availability.

Methods

This research is based on long term monitoring of the active layer thickness, selected in situ-measured soil parameters (temperature, moisture, and heat flux) and laboratory analyses (texture, soil thermal properties, biogeochemical composition of the soils). The areas of monitoring and sampling are distributed around the Ulu Peninsula in order to cover the variable conditions with respect to lithology, topography, vegetation or the time since the deglaciation.

Results

The studied soils on JRI were classified as Protic Cryosols (WRB). The active layer thickness varied between 40 and 120 cm in the period 2006–2016. It is

strongly dependent on lithology, which is the main driving factor affecting the soil thermal parameters. For example, the probing measurement showed variability between 60 and 110 cm in an area of 70 × 80 m, which was caused by differences in soil thermal conductivity between 0.3 W m^{-1} K^{-1} in unlithified Holocene marine sediments and 0.9 W m^{-1} K^{-1} in Cretaceous sediments (Hrbáček et al., 2017). We have also observed a strong effect of vegetation, which can cause a local decrease of the active layer thickness by 10–20 cm.
The soil texture is usually sandy loam to loam. Clay content varied in the range 2–30 % and 20–30 % in soils on volcaniclastic sediments and Cretaceous sediments, respectively. The pH values of the soils are rather neutral and range between 6.8 and 7.8, while the electric conductivity shows a higher variability from 55.7 to 259.0 µS cm^{-1}. Nitrogen contents varied between 0.280 and 2.995 mg g^{-1}, showing no depth gradient within the particular sites. Accordingly, the carbon content covered a wide range between 2.965 and 30.130 mg g^{-1} with an overall balanced proportion between organic and inorganic carbon. For both nitrogen and carbon, about 10 times higher values were observed in the areas with moss vegetation than in bare ground.

Conclusions

Current results show a large variability of soil properties across the ice-free area of JRI. The combination of geomorphological and biogeochemical approaches allow us to better understand the general soil properties, its dependence on factors such as lithology, topography or the presence of vegetation, as well as to determine the stage of soil development and content of organic matter.

Acknowledgements

Research was supported by Ministry of Education, Youth and Sports of the Czech Republic projects LM2015078 and CZ.02.1.01/0.0/0.0/16_013/0001708 and by the Masaryk University project MUNI/A/1419/2016.

References

ATCM., 2015. Information Paper 034. Antarctic trial of WWF's Rapid Assessment of Circum-Arctic Ecosystem Resilience (RACER) Conservation Planning Tool: Results of RACER workshop focused on James Ross Island. Information paper by Great Britain and Czechia., 38th Antarctic Treaty Consultative Meeting, Sofia

Hrbáček, F., Kňažková, M., Nývlt D., Láska, K., Mueller, C.W., Ondruch, J., 2017. Active layer monitoring at CALM-S site near J.G.Mendel Station, James Ross Island, Eastern Antarctic Peninsula. *Sci.Total.Environ.,* 601–602: 987–997.

IPCC, 2014. Climate Change 2014: Synthesis Report. Contribution of Working Groups I, II and III to the Fifth Assessment Report of the Intergovernmental Panel on Climate Change 5. IPCC, Geneva, Switzerland.

Divergent patterns of experimental and model derived variables of tundra ecosystem carbon exchange in response to experimental warming

Christina Schädel[1]
Charles D. Koven[2]
David M. Lawrence[3]
Gerardo Celis[1]
Jack Hutchings[4]
Marguerite Mauritz[1]
Susan Natali[5]
Elaine Pegoraro[1]
Verity G. Salmon[6]
Meghan Taylor[1]
William Wieder[3]
Edward A. G. Schuur[1]

[1]*Northern Arizona University, USA, christina.schaedel@nau.edu*
[2]*Lawrence Berkeley National Laboratory, USA*
[3]*National Center for Atmospheric Research, USA*
[4]*University of Florida, USA*
[5]*Woods Hole Research Center, USA*
[6]*Oak Ridge National Laboratory, USA*

Abstract

Warming in the Arctic in the last decades has been twice as high as for the rest of the globe and has exposed large amounts of organic carbon to microbial decomposition in permafrost ecosystem. Here, we evaluate variables associated with ecosystem carbon exchange from eight years of experimental soil warming in moist acidic tundra with the same variables derived from a modeled warming experiment using the Community Land Model (CLM4.5). Non-linear responses to experimentally induced permafrost thaw are observed for growing-season carbon fluxes while in contrast, the model predicts linear increases in carbon fluxes with every year of warming. After eight years of warming, the field showed an overall decline in ecosystem carbon uptake of 105% while the model increased carbon uptake by 130%. The field experiment revealed the importance of hydrology in carbon flux responses to permafrost thaw, a complexity that the model may fail to predict.

Keywords: Carbon fluxes; data-model comparison; tundra; net ecosystem exchange; field warming experiment;

Introduction

The representation of permafrost carbon dynamics in process-based Earth system models remains a crucial challenge. Over the last few decades, the Arctic has been experiencing rapid increases in temperature (Richter-Menge *et al.,* 2017) and frozen ground conditions are projected to become less stable and to thaw in the coming decades. Continued warming and associated changes in soil moisture conditions not only lead to enhanced microbial decomposition from permafrost soil but also enhanced plant carbon uptake (Schuur *et al.*, 2015; Mauritz *et al.*, 2017). Both processes affect the overall contribution of permafrost carbon dynamics to the global carbon cycle, yet field and modeling studies show large uncertainties and inconsistencies in regard to both uptake and release mechanisms (McGuire *et al.*, 2018). Here, we evaluate variables associated with ecosystem carbon exchange (GPP: gross primary production; R_{eco}: ecosystem respiration; and NEE: net ecosystem exchange) from eight years of experimental soil warming in moist acidic tundra (Mauritz *et al.*, 2017) with the same variables derived from a modeled warming experiment using the Community Land Model version 4.5 (CLM4.5).

Methods

We used eight years of data from an experimental field warming study that was established in the fall of 2008 (Natali *et al.*, 2011). The field site is located in upland moist acidic tundra, near Healy, Alaska. Experimental warming was established by installing snow fences that increase soil warming during the winter. Each spring, additional snow was removed to prevent a delayed spring start and extra water input.

Warming in CLM4.5 was achieved by doubling the snow thermal conductivity, which causes the same type of warming as observed in the field. We extracted environmental and biological variables from one grid cell at 65.35°N and -157.31°W, which experiences similar climatic and environmental conditions as the field site location.

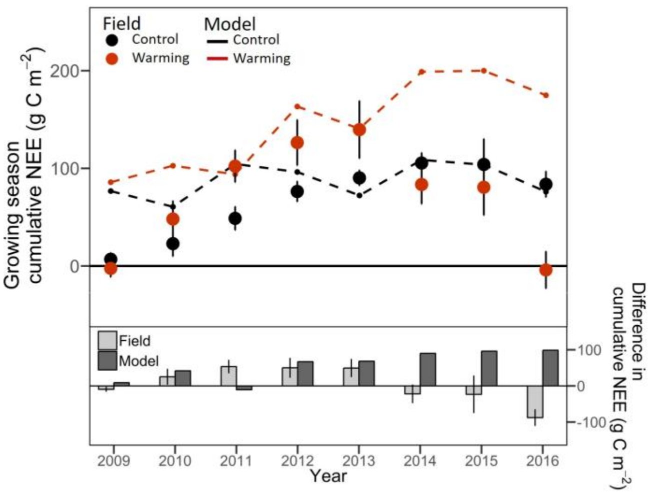

Figure 1. Growing season net ecosystem exchange (NEE) from an experimental field (dots) and modeling (lines) warming experiment. For field and modeled data, black dots and lines represent control and red represent warming. The difference in cumulative NEE is $NEE_{warming} - NEE_{control}$. Growing season ranges from May through September. Values are means and standard errors for field data, no standard errors exist for the modeling experiment.

Results and Conclusion

While soil temperatures and thaw depths show comparable increases with warming between field and model variables, water table depth shows the opposite pattern. Permafrost warming in the field causes soil subsidence and creates wetter soils while increased drainage with warming causes drier soils in the model. Non-linear responses to experimentally induced permafrost thaw are observed for growing-season GPP, R_{eco}, and NEE with higher NEE values in the warming treatment for the first few years and lower NEE values after five years of warming (Figure 1). In contrast, the model predicts linear increases in GPP, R_{eco}, and NEE with every year of warming turning the ecosystem into a net carbon sink during the growing season. After eight years of warming, the decline in NEE in the warmed sites in the field accounts for 105% while increased NEE with warming in the models causes 130% more NEE.

The field experiment revealed the importance of hydrology in carbon flux responses to permafrost thaw, a complexity that the model may fail to predict. Further parameterization of variables that drive GPP, R_{eco}, and NEE in the model will help to inform and refine future model development.

References

Harden, J.W., Koven, C.D., Ping, C.-L., Hugelius, G., McGuire, A.D., Camill, P., Jorgenson, T., Kuhry, P., Michaelson, G.J., O'Donnell, J.A., Schuur, E.A.G., Tarnocai, C., Johnson, K., Grosse, G. (2012) Field information links permafrost carbon to physical vulnerabilities of thawing. *Geophysical Research Letters*, 39, L15704.

Mauritz, M., Bracho, R., Celis, G., Hutchings, J., Natali, S.M., Pegoraro, E., Salmon, V.G., Schädel, C., Webb, E.E., Schuur, E.A.G. (2017) Non-linear CO2 flux response to seven years of experimentally induced permafrost thaw. *Global Change Biology*.

McGuire, A.D., Lawrence, D.M., Koven, C.D., Clein, J., Burke, E.J., Chen, G., Jafarov, E., MacDougall, A., Marchenko, S., Nicolsky, D., Peng, S.-S., Rinke, A., Ciais, P., Gouttevin, I., Hayes, D., Ji, D., Krinner, G., Moore, J., Romanovsky, V. et al. (2018) The dependence of the evolution of carbon dynamics in the Northern Permafrost Region on the trajectory of climate change. *in press*.

Natali, S.M., Schuur, E.A.G., Trucco, C., Hicks Pries, C.E., Crummer, K.G., Baron Lopez, A.F. (2011) Effects of experimental warming of air, soil and permafrost on carbon balance in Alaskan tundra. *Global Change Biology*, 17, 1394–1407.

Richter-Menge, J., Overland, J.E., Mathis, J.T., Osborne, E. (Eds) (2017) Arctic Report Card 2017. http://www.arctic.noaa.gov/Report-Card

Schuur E.A.G., McGuire A.D., Schädel C., Grosse G., Harden J.W., Hayes D.J., Hugelius G., Koven C.D., Kuhry P., Lawrence D.M., Natali S.M., Olefeldt D., Romanovsky V.E., Schaefer K., Turetsky M.R., Treat C.C., Vonk J.E. (2015) Climate change and the permafrost carbon feedback. *Nature*, 520, 171–179.

The impact of lateral heat and water fluxes from thermokarst lakes on tundra landscape dynamics and permafrost degradation

Thomas Schneider von Deimling[1,2]
Jan Nitzbon[1]
Soraya Kaiser[1,2]
Stephan Jacobi[1]
Moritz Langer[1,2]

[1]*Alfred Wegener Institute Helmholtz Centre for Polar and Marine Research*
[2]*Humboldt University, Berlin, Germany*
Correspondence to: Thomas Schneider von Deimling (thomas.schneider@awi.de)

Abstract

Projected future warming of the Arctic will result in pronounced degradation of permafrost and thereby trigger large-scale landscape and ecosystem changes. In this context, the formation and expansion of thermokarst lakes play a key role as thermokarst dynamics represent a mechanism for abrupt degradation of permafrost soils.

Using the process-based model CryoGrid-3 coupled to a model description of lake dynamics (FLake), we explore how the thermal and hydrological state of different permafrost landscapes is affected by an explicit consideration of the interaction between lakes and surrounding permafrost environments. Hereby we especially investigate the role of lateral fluxes in affecting the landscape heat and water budgets.

Keywords: permafrost degradation; thermokarst dynamics; abrupt thaw; lateral fluxes; permafrost modelling; CryoGrid3

Motivation

State-of-the-art land surface models used for simulating permafrost dynamics generally focus on capturing gradual thaw only (i.e. describing permafrost thaw as a vertical 1D heat conduction process). Yet observations of present-day landscape changes underline that permafrost grounds react much more dynamically to changing environmental conditions manifested e.g. in abrupt thaw features through thermokarst formation and thermal erosion. These changes may trigger significant feedbacks – from local scales by shaping landscape patterns to global scales by affecting the global carbon cycle. Therefore, the omission of abrupt thaw processes in current land surface models leads to an underestimation of projected future permafrost degradation and eventual carbon release (Schneider von Deimling *et al.,* 2015) and improved model representations of permafrost dynamics are needed.

Modelling approach

Using the permafrost model CryoGrid3 (Westermann *et al.,* 2016), we capture abrupt thaw behavior by modelling thermokarst lake formation, talik expansion under lakes, and ground subsidence due to melting of excess ice. Our model version includes a description of lake dynamics inferred from the FLake model (Mironov *et al.,* 2003; Kirillin et al., 2011). Based on Langer *et al.* (2016), we have further developed our model to also represent lateral heat and water exchange between a lake body and its permafrost soil surrounding.

Modelling analyses

In our study we focus on investigating the effect of lateral fluxes of heat and water on permafrost stability for different realizations of lake sizes and landscape coverage. We run our model for differing 21st century warming scenarios to investigate differences in permafrost degradation between climate mitigation and business-as-usual emission scenarios. Given the computational efficiency of our model, we test a large range of model parameter settings to quantify uncertainty in our simulation results. By comparing model simulations with and without describing lakes in permafrost environments, we discuss the importance of lake dynamics for affecting tundra landscape thermal regimes and future permafrost degradation.

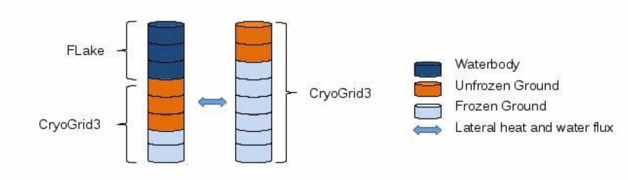

Figure 1 Sketch of model simulation design. The new model implementations account for lateral exchange of heat and water between a soil column covered by a lake (left) and its non-lake permafrost environment (right). Vertical fluxes are not shown explicitly.

Acknowledgments

The young investigator group PermaRisk is funded by the German Federal Ministry of Education and Research (BMBF, funding reference 01LN1709A).

References

Kirillin, G., Hochschild, J., Mironov, D., Terzhevik, A., Golosov, S. & Nützmann, G., 2011. FLake-Global: Online lake model with worldwide coverage, *Environ. Modell. Softw.*, 26(5), 683–684.

Langer, M., Westermann, S., Boike, J., Kirillin, G., Grosse, G., Peng, S., & Krinner, G., 2016. Rapid degradation of permafrost underneath waterbodies in tundra landscapes – Toward a representation of thermokarst in land surface models. *Journal of Geophysical Research: Earth Surface* 121(12): 2446–2470.

Mironov, D., Kirillin, G., Heise, E., Golosov, S., Terzhevik, A. & Zverev, I., 2003. Parameterization of lakes in numerical models for environmental applications, *Proceedings of the 7th Workshop on Physical Processes in Natural Waters*, pp. 135–143.

Schneider von Deimling, T., Grosse, G., Strauss, J., Schirrmeister, L., Morgenstern, A., Schaphoff, S., Meinshausen, M. & Boike, J., 2015. Observation-based modelling of permafrost carbon fluxes with accounting for deep carbon deposits and thermokarst activity, *Biogeosciences,* 12(11), 3469–3488.

Westermann, S., Langer, M., Boike, J., Heikenfeld, M., Peter, M., Etzelmüller, B., & Krinner, G., 2016. Simulating the thermal regime and thaw processes of ice-rich permafrost ground with the land-surface model CryoGrid 3. *Geoscientific Model Development* 9(2): 523–546.

Beaded streams in Alaska and Siberia: similarities and differences

Anna M. Tarbeeva[1]
Christopher D. Arp[2]
[1]*Lomonosov Moscow State University, Russia, amtarbeeva@yande.ru*
[2]*University of Alaska Fairbanks, USA*

Abstract

Beaded streams have channels consisting of pools connected by narrow runs and are common low-order watercourses throughout Arctic Alaska and Russian and Siberian taiga. The form of beaded channels has important implications for maintaining connectivity between river and lake habitats. There are two main hypotheses to explain how beaded channels form. The most accepted hypothesis states that beaded streams result from ice-wedge polygons' degradation. The other hypothesis, came from Russian Yakutia in 1927, considered that beads are ancient pools of alluvial rivers dammed due to freeze of depositional sediment in the channel. We compared results of field observations and remote sensing analysis of beaded channels in Russian Siberia and Northern Alaska to understand the most common formative processes in order to best predict how these important aquatic habitats may respond to changing conditions.

Keywords: beaded streams, fluvial geomorphology, thermokarst, permafrost, Alaska, Siberia.

Introduction

Beaded streams are typical low order watercourses in permafrost regions consisting of rounded and deepened pools connected by narrow runs. Recent studies show, that they are important for permafrost ecosystems, retaining and warming water, providing overwintering habitats and fish migration routes. Beaded channels form in permafrost due to the interaction of water flow and frozen ground. However, there is limited understanding about exact mechanisms of their formation.

Most accepted hypothesis state they result from ice-wedge polygons degradation [Hopkins at al., 1955]. However, alternative opinions also exist, arguing that widened sections of beaded channels were formed by freezing over of bedload depositional forms in channels and are inherent from the former pools preserved since warmer and more humid period [Grigoriev, 1927; Voskresensky, 1955]. Beaded streams were historically studied separately in different regions - in Arctic Alaska [Oswood et al., 1989; Arp et al., 2015] and Russian Siberia [Gubarkov & Leibman, 2010; Tarbeeva & Surkov, 2013].

We compared results of field observations and hypotheses coming from different regions to understand their formative mechanisms and potential response of changing climate.

Study Area and methods

Field studies were conducted in two regions – arctic tundra (Arctic coastal plain of Alaska) and permafrost taiga (Central Yakutia, East Siberia). Both sites are underlayed by continuous permafrost to 500 m depth, but have different ice content in sediments.

Field studies included monitoring of water levels, temperature, discharge, ice regime, measurements of water depth, describing channel morphology, geology and permafrost structure under the channels.

We also analyzed satellite imagery and digital elevation models (DEMs) to understand patterns of distribution, changes withincreasing drainage area, and relations between morphometric parameters. We compared old aerial photography (1948) and modern (2002-2011) high-resolution imagery to understand rates and patterns of channel dynamics.

Results

Morphology

Beaded streams form in different landscapes: eolian, alluvial, marine and old glacial plains. They are abundant in moderate and high ice content sediments associated with ice-wedge polygons and thermokarst lakes on the Arctic Coastal Plain. However, we found them also on the territories with low ice-content in Central Yakutia where thermokarst is not typical.

Beaded channels are usually observed on the 1-3rd order watercourses with drainage area ranging from 2 to100 sq km and gradients between 0.0005 and 0.02 m/m, where water flow has not enough power to create normal alluvial channel.

Channel morphology changes with increasing water and sediment supply. 1st order watercourses usually have straight beaded channels. 2nd and 3rd order watercourses often have a specific transitional meandering-to-beaded form resembling the shape of unconfined meandering rivers, but consisting of widened pools and connecting narrow runs. 4-5th order rivers usually have normal (alluvial) meandering channels.

Dimensions of pools of beaded channels also increase with drainage area and can reach widths up to 40 m and depth up to 4 m. There is positive relation between pool width and depth.

Thermal regime

Water in pools is well mixed during high flows and can become stratified during low flows when temperatures can reach 20°C. The deepest pools of beaded channels don't freeze entirely in winters. There is usually liquid pressured water under the ice up to 4 m depth in Yakutia and up to 1 m depth in Alaska, underlayed by lenses of taliks 3-4 m depth in Yakutia and around 1 m in Alaska. This difference presumably is cause by different depth of active layer in maritime and continental climate.

Mean annual bed temperatures in pools are positive and can reach +3°C. This shows that beaded channels are much warmer than surrounding frozen ground.

Channel Dynamics

We found no changes in number of pools and general shape on small straight beaded channels (drainage area 20-25 sq km) between 1948 and 2011. Comparison of images on beaded meandering channels (drainage area 60-90 sq km) showed, that some beads were abandoned and filled, other appeared or changed their shape. Nevertheless, no changes wereobserved in general shape of meanders. On the transitional beaded-to-alluvial channels (drainage area 200-300 sq km) we found three meanders, which were omega-shaped and close to being cut-off in 1948. At the same time, alluvial channels with developed point bars and eroded concave banks, also showed very slow dynamics. The maximum rate of banks erosion on Judy Creek with drainage area 600 sq km was 1.3 m/year.

Discussion

Common features of all beaded streams are: relatively low water flow, positive mean annual bed temperatures and thawed sediments under the pools vs. frozen ground under runs, which provide opportunity for both: thermokarst and uneven erosion in the channel. Beaded channels are observed in areas with different ice content in sediments – in ice-rich permafrost in Alaska and low ice content permafrost in Central Yakutia. Therefore, we can suppose different roles of thermokarst and uneven erosion in their formation. Beaded channels have similar formative factors, but the role of each factor is different in each case. Channels with transitional meandering-to-beaded form show the leading role of meandering process in their formation. However, such channels exhibit no evidences of present-day erosion of concave banks and sediment accumulation at the convex banks typical for normal meandering rivers, which indicate that they were formed under different conditions. Relatively stable morphology of beaded channels during last 60 years reflects balance between frozen and thawed sediments in the channels.

Acknowledgments

This research was supported by the Russian Foundation for Basic Research (RFBR), Project 17-05-01287 and the Fulbright Program (Anna Tarbeeva) and Bureau of Land Management Arctic District Office (Chris Arp).

References

Arp, C. D., Whitman M.S., Jones B.M., Grosse G., Gaglioti, B.V., Heim, K.C., *2015*. Distribution and biophysical processes of beaded streams in Arctic permafrost landscapes. *Biogeosciences. No 12 (1). 29-47.*

Grigoriev, A. A. 1927. *Geomorphology essay on Yakutia.* Leningrad: Publ. AS USSR. 52 pp. (in Russian)

Gubar'kov, A.A., Leibman, M.O. 2010. Bead-shaped channel forms as evidence of paragenesis of cryogenic and hydrological processes in the small-river valleys of Central Yamal. *Kriosfera Zemli. (Earth`s Cryosphere), 14, 1. 41-49.* (in Russian)

Hopkins D., Karlstrom T., Black R. et al. 1955. Permafrost and ground water in Alaska. *Geol. Surv., Prof. Pap. Washington, 264 F.*

Oswood, M. W., Everett, K. R*., Schell, D. M. 1989. Some physical and chemical characteristics of an arctic beaded stream. Holarctic ecology. 12. 290-295.*

Voskresensky, S.S. 1955. *Geomorphology of Siberia.* Moscow: Publ. MSU, 340 pp. (in Russian)

Interdisciplinary approaches to understanding the initiation and lateral expansion of thermokarst in peat-rich regions

Merritt R. Turetsky[1]
Jennifer Baltzer[2]
Thomas Douglas[3]
Carolyn Gibson[4]
Jean Holloway[5]
Steve Kokelj[6]
Mark Lara[7]
Antoni Lewkowicz[5]
David Olefeldt[4]
Natalie Zwanenberg[1]

[1]*University of Guelph, mrt@uoguelph.ca*
[1]*Wilfrid Laurier University*
[3]*U.S. Army Cold Regions Research and Engineering Lab*
[4]*University of Alberta*
[5]*University of Ottawa*
[6]*Northwest Territories Geological Survey*
[7]*University of Illinois*

Abstract

Thermokarst in peatlands leads to forest loss and the creation of saturated collapse scar bogs and fens. Here we synthesize across scientific approaches - including circumpolar mapping, regional comparisons, remote sensing, gradients of vegetation and geophysics, and point-level soil inventories – to address several fundamental questions about the spatiotemporal patterns of thermokarst initiation and expansion in peatlands.

Introduction

Thawing permafrost is affecting a range of ecosystem state factors and functions, including vegetation, land stability, hydrology, as well as carbon and energy feedbacks to climate. Many of these issues relate to ecohydrological processes that are complicated to predict when thaw of ice-rich permafrost triggers land subsidence and thermokarst. Thermokarst can manifest in a number of surface expressions, which all can abruptly affect large volumes of soil. Identifying what terrain types are more or less susceptible to thermokarst could support the design and siting of infrastructure, and improve our understanding of the fate of thawing permafrost carbon.

Research Questions

We are using a variety of approaches to address several fundamental questions about thermokarst initiation and expansion. Can we use underlying minerology to predict why thermokarst initiates in some places of a peatland and not others? What is the role of ice wedges in the formation and spread of collapse scar bogs? Are rates of thermokarst expansion nonlinear and how do these patterns vary with glacial history or forest cover type?

Results

We developed a circumpolar framework that assesses whether areas are predisposed to thermokarst (Fig. 1; Olefeldt *et al.*, 2016). We estimate that land predisposed to these processes cover less than a quarter of the permafrost domain. However, areas predisposed to thermokarst store nearly half of the organic carbon stored in the upper 3 meters of soil. We are now considering glacial, geomorphological, and fire legacies that influence thermokarst vulnerability in this spatial mapping.

At regional scales, we are using change detection approaches to quantify thermokarst expansion rates in different dominant forest types (i.e., spruce- versus birch-dominated forests). These studies show rapid lateral expansion of collapse scar bogs, particularly in birch forests (Baltzer *et al.*, 2014; Lara *et al.*, 2016). Point-level field measurements also support the conclusion that thermokarst features expand more rapidly in birch than in spruce forests (Zwanenberg, unpublished).

At local scales, we found no change in mineral soils between collapse scars or permafrost forests. However, we have used geophysical techniques, particularly electric resistivity tomography (ERT; Fig 2), to characterize permafrost morphology in the subsurface and to link terrain geomorphology with permafrost ice content.

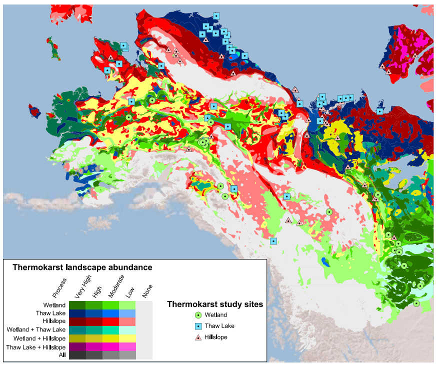

Figure 1. Map of the dominant thermokarst landscapes, distinguishing between wetland thermokarst, thaw lakes and hillslope thermokarst predisposition.

ERT suggests that a small collapse feature, the initial stage of thermokarst initiation, was associated with a melted ice wedge at 260 meters on our transect (Fig. 2). Airborne LiDAR and ground based measurements also show that degraded polygons are prevalent in this area.

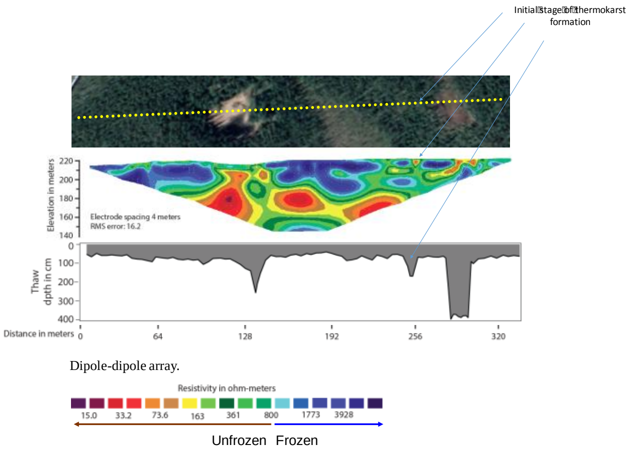

Figure 2. Electrical resistivity along a 300+ meter transect located 25 km southeast of Fairbanks in interior Alaska.

Overall our goal is to synthesize data to better understand which peatland areas are most susceptible to thermokarst at local, regional, and circumpolar scales. For example, we know thick peats protect permafrost from warming or wildfire. In discontinuous permafrost, ERT-surveys suggest that changes in the seasonally frozen layer following 2014 fire activity is minimal in sites with thick peats compared to well drained sites with coarse soils (Fig. 3; Hollaway, unpublished). However, change detection shows that fire accelerates rates of thermokarst in peatlands over decades (Gibson & Olefeldt, unpublished). Together this shows that thermokarst initiation can be slowed by thick peats, but expansion can amplify due to feedbacks between subsidence, forest mortality, and albedo. These cross-scale feedbacks (Fig. 4) can only be evaluated within an interdisciplinary framework that combines multiple measurements.

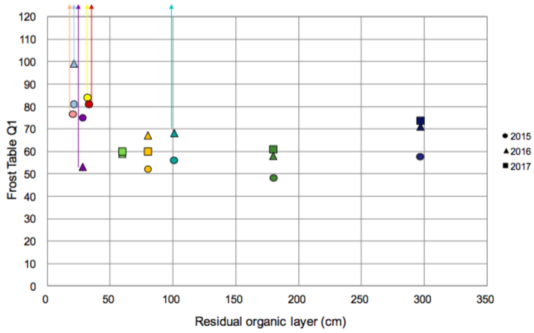

Figure 3. Change in frost table depths (2015- 2017) at sites in the southern NWT. The first quartile of the frost table depths in a site (n=60) is plotted against the residual organic layer. Unburned sites are in green. Holloway, unpublished.

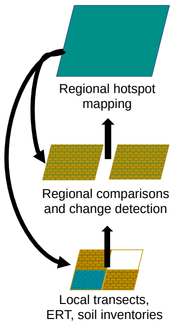

Figure 4. Conceptual diagram for examining cross-scale interactions.

References

Baltzer, J. L., Veness, T., Chasmer, L. E., Sniderhan, A. E., & Quinton, W. L. 2014. Forests on thawing permafrost: fragmentation, edge effects, and net forest loss. *Global Change Biology* 20: 824–834.

Lara, M. J., Genet, H., McGuire, A. D., Euskirchen, E. S., Zhang, Y., Brown, D. R. N., Jorgenson, M. T., Romanovsky, V., Breen, A. & Bolton, W. R. 2016. Thermokarst rates intensify due to climate change and forest fragmentation in an Alaskan boreal forest lowland. *Global Change Biology* 22: 816–829.

Olefeldt, D., S. Goswami, S., Grosse, G., Hayes, D., Hugelius, G., Kuhry, P., McGuire, A. D., Romanovsky, V. E., Sannel, A.B.K., Schuur, E.A.G., & Turetsky, M. R. 2016. Circumpolar distribution and carbon storage of thermokarst landscapes. *Nature Communications* 13043.

Estimation of methane formation and emission in dominant landscapes of typical tundra of Western Yamal

Alexander Vasiliev[1,2],
Gleb Oblogov[1,2],
Irina Streletskaya[3]
[1] *Earth Cryosphere Institute of Tyumen Scientific Center (ECI TSC) SB RAS, Tyumen, Russia, email: al.a.vasiliev@gmail.ru*
[2] *Tyumen State University (TSU), Tyumen, Russia*
[3] *Moscow State University, Faculty of Geography (MSU), Moscow, Russia*

Abstract

In this presentation, we report the main results of our estimation of methane formation and emission in dominant landscapes of typical tundra. The study area is located in Western Yamal. The landscape structure of the representative area of typical tundra was studied, and landscape map was compiled. Soils of the active layer and upper permafrost were sampled within all dominant landscapes. Methane concentration was measured for every sample, and total methane content in the active layer and upper permafrost was evaluated. The highest methane content was observed in mires and ravines. Peatlands, well-drained tundra, wet tundra, and sand fields were characterized by the lowest methane content. Thus, mires and ravines are the main sources of methane emission in typical tundra. Daily methane flux in these landscapes reaches 10 to 20 mg/m^2.

Keywords: methane, active layer dominant landscapes.

Introduction

Permafrost plays an important role in global climate change and affects biological, hydrological, and human activities in the Arctic. In this study, we estimate methane content and its emission to atmosphere in dominant landscapes of typical tundra of Western Yamal based on the field investigations.

Methodology

Prior to measurements of methane emissions, we had developed a landscape map of the representative area 1 x 1 km based on satellite imagery and field observations, and determined its landscape structure (Fig. 1).

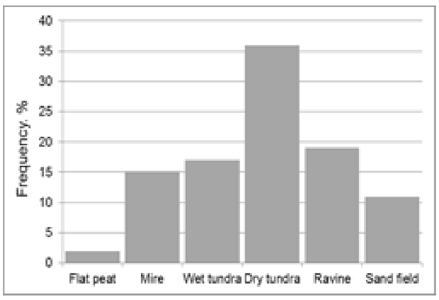

Figure 1. Landscape structure of typical tundra of Western Yamal.

It is known that emissions of methane generally peak between July and early August, with smaller emissions observed during late spring, early summer, and fall (Euskirchen et al., 2017).

Table 1. Soil conditions of the dominant landscapes

	Mire	Wet tundra	Dray tundra	Ravine	Sand field
Soil	loam	clay	clay	loam	sand
Vol. moisture content (%)	42,8	38,4	30,3	47,2	25,6
Surf. Temp. (late July) (°C)	7…8	7…9	4…7	6…8	9…11
Tot organic carbon in active layer (%)	0,68	1,26	0,45	4,50	0,34
Avg. methane content in soil (ppm)	2200	328	121	1590	86
Air methane concentration on landscape surface (ppm)	4,0	2,2	2,1	3,5	<2,0

Samples for evaluation of methane concentration were obtained from cores of boreholes drilled in late July 2016 within every dominant landscape with the exception of peatlands. In parallel, the soil conditions of active layer, including soil composition, density, volumetric moisture content, total organic carbon, were studied (Tab. 1).

Soil samples were degassed, and the gas was collected using a "head space" method. Methane content was measured using a gas chromatograph XPM.4 with plasma ionization detector in the Institute of Physical, Chemical, and Biological Problems in Soil Science RAS.

Results

High methane concentrations were detected only within the two landscapes – mires and ravines – while there is almost no methane in the active layer of all other landscapes.

Methane fluxes were measured in 200-mm-diameter plastic pipes installed within each dominant landscape. Gas samples were collected every hour during three to four hours. Field measurements showed that the highest methane emissions to the atmosphere were typical of the same two landscapes. Surface temperatures during the field experiment varied from 4 to 11 ^{o}C.

Daily methane flux in these landscapes reached 10 to 20 mg/m^2 (late July 2017), while in all other landscapes it did not exceed 2 to 5 mg/m^2.

Conclusions

Based on our studies, the highest methane emission occurs only within the two landscapes: mires and ravines, which occupy approximately 30% of typical tundra. During the peak emission, daily methane flux in these landscapes can reach 10 to 20 mg/m^2

Acknowledgments

This work was supported by RSF, grant №16-17-00102, the soil conditions were studied in the framework of the Russian Foundation for Basic Research, project no.16-05-00612.

References

Euskirchen, E.S. M.S. Bret-Harte, G.R. Shaver, C.W. Edgar, V.E. Romanovsky. 2017. Long-term release of carbon dioxide from arctic tundra ecosystems in northern Alaska. *Ecosystems*. 20: 960-974

Spatially-explicit estimation of soil nitrogen stock and its comparison with Community Land Model across Tibetan alpine permafrost

Yuanhe Yang[1]
Dan Kou[2]
[1] *State Key Laboratory of Vegetation and Environmental Change, Institute of Botany, Chinese Academy of Sciences, Beijing 100093, China; University of Chinese Academy of Sciences, Beijing 100049, China; email: yhyang@ibcas.ac.cn*
[2] *State Key Laboratory of Vegetation and Environmental Change, Institute of Botany, Chinese Academy of Sciences, Beijing 100093, China; University of Chinese Academy of Sciences, Beijing 100049, China*

Abstract

Permafrost soils store a large amount of nitrogen (N), potentially being activated under continuous climate warming, which could then alter structure and function of this warming-sensitive ecosystem. However, compared with C compartment, little is known about the pool size and spatial distributions of permafrost N stocks so far. Based on actual measurements from 519 pedons, combined with machine learning models, our results showed that soil total N density was 1.58 kg N m^{-2} to three-meter depth across the Tibetan alpine permafrost region, and the corresponding soil N storage was 1806 Tg. Our results also revealed that CLM4.5 significantly underestimated soil N stocks across the Tibetan alpine permafrost region, and the underestimation mainly occurred in the arid/semi-arid ecosystems. This data-model integration experiment highlights the necessity to improve the N module in land models to forecast changes in ecosystem function such as vegetation dynamics and nitrous oxide degassing with permafrost thawing.

Keywords: climate warming, permafrost, nitrogen cycle, Community Land Model.

Introduction

Permafrost regions, mainly distributed in cold areas with high latitude or high altitude, cover approximately 23.9% of the Northern Hemisphere. These regions have accumulated substantial soil organic matter due to slow decomposition in cold and wet environments [Schuur *et al.*, 2015]. However, climate warming is rapidly exposing permafrost soil organic matter to mineralization, potentially producing a large amount of carbon (C) dioxide from permafost regions [Schuur *et al.*, 2015]. Permafrost thaw is also expected to accelerate the depolymerization and mineralization processes of soil organic nitrogen (N), potentially releasing dissolved organic and inorganic N and hence increasing soil N availability [Keuper *et al.*, 2017]. An increase of available N could stimulate terrestrial plant growth, which is strongly N-limited in permafrost regions, altering the vegetation community structure [Keuper *et al.*, 2017]. The accumulation of available N could also alter microbiological communities that drive nitrification and denitrification processes [Mackelprang *et al.*, 2011], potentially increase the emission of nitrous oxide (N_2O) and aggravate greenhouse effects [Elberling *et al.*, 2010]. Permafrost N could also be released to aquatic ecosystems, where it could alter food webs in permafrost rivers and estuaries [Harms & Jones, 2012]. Consequently, it is crucial to evaluate the pool size and spatial distribution of soil N stocks across permafrost regions to accurately predict the alteration of the ecosystem N cycle and its ecological consequences under permafrost thaw.

In this context, we focused on the following two questions: 1) How much N is stored in the top three meters of soil across the Tibetan alpine permafrost region? 2) How realistically does CLM4.5 represent the soil N stock across the study area? To answer these questions, we collected 342 three-meter cores and 177 fifty-centimeter pits across 173 sampling sites on the Tibetan Plateau during July and August of 2013 and 2014. Based on these site-level measurements and two machine learning models (supporting vector machine (SVM) and random forest (RF) models), we estimated the pool size and spatial distribution of soil N across the Tibetan alpine permafrost region and evaluated the soil N stock simulated by CLM4.5.

Results

Size and distribution of soil N stock derived from machine learning models

The soil total N densities (STND) in the 0-50, 0-100, 0-200 and 0-300 cm depths across the study area were estimated at 0.56 (1.12 kg N m^{-3}), 0.81 (0.81 kg N m^{-3}), 1.22 (0.61 kg N m^{-3}) and 1.58 (0.53 kg N m^{-3}) kg N m^{-2}, respectively (Fig. 1). The corresponding plateau-wide soil N stocks were 644, 930, 1392 and 1802 Tg. N stored below one meter accounted for 48% of the total soil N stock in the top three meters. In addition, the soil N stocks differed among the three grassland types on the plateau, with 43%, 42% and 15% of the total soil N stock in the top three meters being stored in alpine meadow, alpine steppe and swamp meadow, respectively.

Comparison of observed and modeled soil N stocks

Our analyses based on the STND ratio and Fuzzy Numerical (FN) index revealed the spatial difference between the simulated and observed soil N stocks (Fig. 2). Specifically, soil N stocks were overestimated in part of the south plateau (CLM4.5/observation ratio > 1, Fig. 2a-b) but were underestimated in the extensive north, especially the northwest of the plateau, where a lower CLM4.5/observation ratio (< 0.6) and FN index (< 40%) (even for the deep soil layer, 3 m vs. 35 m) were dominant. Soil N stocks were similar between the observation and CLM4.5 in only 8% of the study area (FN index > 80%, Fig. 2c). Overall, these results illustrated that soil N stocks simulated by CLM4.5 exhibited large spatial biases across the Tibetan alpine permafrost region.

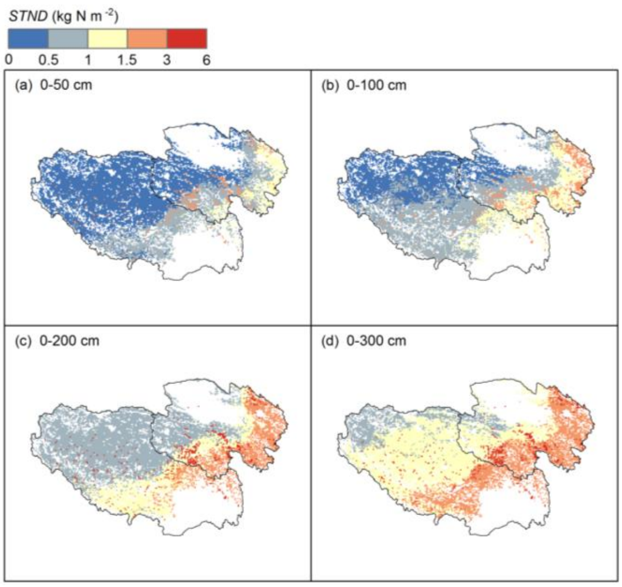

Figure 1. Spatial distributions of the estimated STND (soil total N density) across the Tibetan alpine permafrost region. Panels (a) to (d) illustrate the estimated STND in the 0-50, 0-100, 0-200, and 0-300 cm depths, respectively. The white areas in each map denote regions without alpine grasslands.

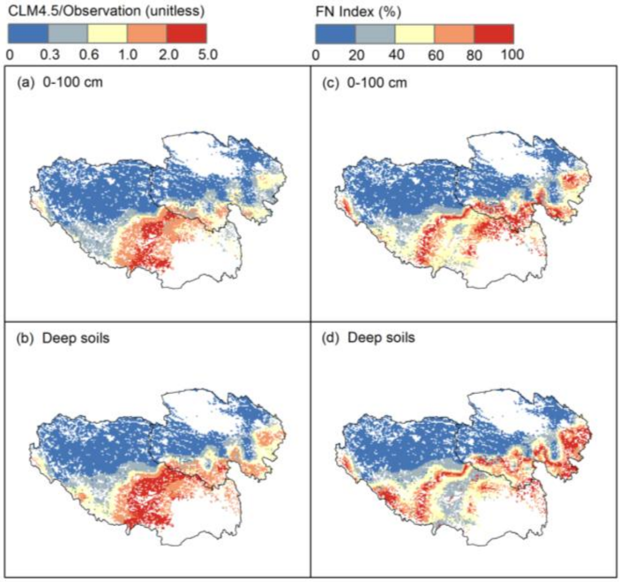

Figure 2. Maps of biases in the simulated soil total N density (STND) across the Tibetan alpine permafrost region. Panels (a) and (b) illustrate the ratio between the simulated and observed STND in the 0-100 cm depth and in deep soils (0-35 m for model vs. 0-3 m for observation), respectively. Panels (c) and (d) illustrate the Fuzzy Numerical (FN) index, reflecting the spatial similarity between simulated and observed STND in the 0-100 cm depth and in deep soils (0-35 m for model vs. 0-3 m for observation), respectively. The white areas in each map are regions without alpine grasslands.

References

Elberling, B., Christiansen, H.H. & Hansen, B.U., 2010. High nitrous oxide production from thawing permafrost. *Nat. Geosci.*, 3: 332-335.

Harms, T.K. & Jones, J.B., 2012. Thaw depth determines reaction and transport of inorganic nitrogen in valley bottom permafrost soils. *Global Change Biol.*, 18: 2958-2968.

Keuper, F., Dorrepaal, E., van Bodegom, P.M., van Logtestijn, R., Venhuizen, G., van Hal, J. & Aerts, R., 2017. Experimentally increased nutrient availability at the permafrost thaw front selectively enhances biomass production of deep-rooting subarctic peatland species. *Global Change Biol.*, 23: 4257-4266.

Mackelprang, R., Waldrop, M.P., DeAngelis, K.M., David, M.M., Chavarria, K.L., Blazewicz, S.J., Rubin, E.M. & Jansson, J.K., 2011. Metagenomic analysis of a permafrost microbial community reveals a rapid response to thaw. *Nature*, 480: 368-371.

Schuur, E.A.G., *et al.* 2015. Climate change and the permafrost carbon feedback. *Nature*, 520: 171-179.

6 - Linking terrestrial and freshwater ecosystems in the Arctic: Organic matter, nutrients and pollutants and their lateral transport from permafrost-affected soils

Session 6

Linking terrestrial and freshwater ecosystems in the Arctic: Organic matter, nutrients and pollutants and their lateral transport from permafrost-affected soils

Conveners:

- **Michael Fritz**, Alfred Wegener Institute, Helmholtz Centre for Polar and Marine Research, Potsdam, Germany (PYRN member)
- **Jorien Vonk**, Faculty of Earth and Life Sciences, Vrije Universiteit Amsterdam, Amsterdam, The Netherlands
- **Alevtina Evgrafova**, University of Koblenz-Landau, Institute of Integrated Sciences, Koblenz, Germany; University of Bern, Faculty of Science, Bern, Switzerland (PYRN member)

Permafrost soils are expected to turn from a carbon sink into a carbon source with projected climate warming. Pedogenic and hydrological processes play a crucial role in determining the rate and type of material released to the Arctic freshwater and marine ecosystems as a result of permafrost thaw. Abrupt modes of permafrost degradation (thermokarst, retrogressive thaw slumps and bank erosion of rivers, lakes and coasts) are expected to lead to higher release rates of soil organic carbon, nutrients, and toxins compared to the rates driven by gradual permafrost degradation such as active layer deepening. In this session, we welcome contributions that:

- Quantify the release of organic matter, nutrients and/or toxins from permafrost-affected soils as well as from abrupt permafrost degradation;
- Estimate permafrost-affected soil properties and environmental factors, such as soil moisture, plant productivity and species composition, that regulate SOM stabilization and degradation processes;
- Measure the bioavailability and decomposability of newly available SOM due to permafrost thaw;
- Present watershed budgets incorporating both terrestrial and aquatic organic matter fluxes;
- Assess the biogeochemical fate of thermokarst-derived carbon, nutrients and pollutants in watersheds and in the coastal zone;
- Investigate challenges pertaining to quantifying and mapping soil properties and SOM transport in permafrost regions by taking into account the spatial distribution and variability of soils.

We invite submissions that consider various biogeochemical tracers of thaw, including bulk parameters (e.g. POC, DOC, DIC), nutrients, major and trace elements, inorganic and organic pollutants, terrestrial biomarkers and isotopic compositions.

Could priming and nutrient effects from degrading permafrost alter dissolved organic matter dynamics in permafrost rivers?

Benjamin W. Abbott[1], Ethan Wologo[2], Sadie Textor[3], Sarah Shakil[4], Scott Zolkos[4], Stephanie Ewing[2], Rob Spencer[3], Michelle Baker[5], Suzanne Tank[4], Jonathan O'Donnell[6], Kimberly P. Wickland[7], Joseph Lee-Cullin[8], Jay P. Zarnetske[8], Futing Liu[9], Yuanhe Yang[9], Pirkko Kortelainen[10], Jaana Kolehmainen[10], Joshua Dean[11], Jorien Vonk[11], Robert M. Holmes[12], Gilles Pinay[13], Paul J. Mann[14], Samuel Cottingham[14]

[1]Brigham Young University, Department of Plant and Wildlife Sciences; benabbott@byu.edu; [2]Montana State University, Department of Land Resources and Environmental Science; [3]Florida State University, Department of Earth, Ocean and Atmospheric Science; [4]University of Alberta, Department of Biological Sciences; [5]Utah State University, Biology Department; [6]Arctic Network, National Parks Service; [7]USGS, Water Mission Area; [8]Michigan State University, Department of Earth and Environmental Sciences; [9]State Key Laboratory of Vegetation and Environmental Change, Institute of Botany, Chinese Academy of Sciences, Beijing; [10]Finnish Environment Institute SYKE; [11]Department of Earth Sciences, VU University Amsterdam; [12]Woods Hole Research Center; [13]National Research Institute of Science and Technology for Environment and Agriculture; [14]Northumbria University

Abstract

Permafrost degradation fundamentally alters terrestrial-aquatic connectivity by changing hydrologic flowpaths and directly delivering terrestrial material to surface water networks via thermal erosion. Dissolved organic matter (DOM) and inorganic nutrients from degrading permafrost represent a small portion of annual fluvial budgets, but it is unknown if these ancient and biodegradable compounds could stimulate mineralization of modern organic matter. We analyzed and incubated DOM from seven regions across the permafrost zone to determine sensitivity to labile carbon and nutrient priming. We found no evidence of carbon priming in bulk DOM loss nor in molecular makeup of DOM pre and post incubation. However, nitrogen and phosphorus availability limited mineralization and uptake of the added labile substrate (acetate) in the majority of sites. Despite regional differences in vegetation and soil, permafrost DOM from all sites showed striking molecular and optical similarity. We discuss implications and remaining unknowns about ancient and modern permafrost DOM interactions.

Keywords: dissolved organic matter, carbon, nutrients, priming, biodegradability, lateral flux.

Introduction

It is unknown how hydrologic fluxes of organic matter will respond to climate change, representing an important uncertainty in landscape carbon balance and habitat vulnerability in aquatic ecosystems (Laudon *et al.*, 2012; Kicklighter *et al.*, 2013; Abbott *et al.*, 2016). Permafrost degradation is causing widespread release of biodegradable dissolved organic matter (BDOM) and inorganic nutrients (Vonk *et al.*, 2013; Abbott *et al.*, 2014; Ewing *et al.*, 2015; Treat *et al.*, 2016). While permafrost BDOM is rapidly mineralized or diluted in headwater streams *(Spencer et al., 2015; Mann et al., 2015; Drake et al.*, 2015), increased delivery of BDOM and nutrients to Arctic waterways could influence the turnover and mineralization of "modern" or background organic matter moving through freshwater and estuarine systems via priming and nutrient effects (Guenet *et al.*, 2010; Rosemond *et al.*, 2015). Because these lateral carbon fluxes are substantial (*ca.* 120 $Tg.yr^{-1}$ delivered to inland waters; Abbott *et al.*, 2016), priming of modern "background" DOM by permafrost BDOM or nutrients could influence landscape and continental-scale fluxes. However, these interactions have not been quantified for most permafrost ecosystems (but see Dorado-García *et al.*, 2015).

To address these unknowns, we performed a collaborative experiment with teams from seven regions in the permafrost zone, including Alaska, Canada, Finland, Siberia, and the Qinghai-Tibet Plateau. In the early fall of 2016, each team collected water from three or more river locations spanning a range of catchment sizes. We performed incubations with and without labile carbon substrate (acetate) and nutrients (nitrogen and phosphorus) to quantify background biodegradability of DOM and potential priming and nutrient effects. We analyzed molecular and optical properties of DOM pre and post incubation using Fourier-transform ion cyclotron resonance mass spectrometry and scanning fluorescence spectroscopy.

Results and discussion

Sites had a range of nutrient concentrations and C:N:P ratios but biodegradability of background DOM was low for most sites, as expected for late-season DOM (Holmes *et al.*, 2008; Wickland *et al.*, 2012). Acetate addition had no detectable effect on background DOM mineralization or uptake. Additionally, the molecular signature of control and acetate treatments were identical, suggesting no interaction between BDOM and background fluvial DOM. Acetate disappearance in ambient nutrient concentration treatments was correlated with background nutrient concentrations, with little to no acetate uptake after four weeks in the most oligotrophic sites. Acetate was consumed within a week for all nutrient addition treatments, suggesting nutrient limitation of carbon uptake and mineralization.

The molecular and optical signatures of DOM from across the permafrost zone showed striking similarity, despite large differences in climate, vegetation, and soil. This could suggest homogenization by similar microbial processing or strong abiotic controls from physical factors such as freeze-thaw.

These findings support the emerging view that priming of DOM in freshwater systems is infrequent, but that nutrient availability may shift the metabolic function and accessibility of DOM to microbial communitites.

References

Abbott, B.W., Jones, J.B., Schuur, E.A.G. *et al.*, 2016. Biomass offsets little or none of permafrost carbon release from soils, streams, and wildfire: an expert assessment. *Environ. Res. Lett.*: 11

Abbott, B.W., Larouche, J.R., Jones, J.B., Bowden, W.B., Balser, A.W., 2014. Elevated dissolved organic carbon biodegradability from thawing and collapsing permafrost: Permafrost carbon biodegradability. J. *Geophys. Res. Biogeosciences* 119: 2049-2063.

Dorado-García, I., Syväranta, J., Devlin, S.P., Medina-Sánchez, J.M., Jones R.I., 2015. Experimental assessment of a possible microbial priming effect in a humic boreal lake. *Aquat. Sci.* 78: 191-202.

Drake, T.W., Wickland, K.P., Spencer, R.G.M., McKnight, D.M., Striegl, R.G., 2015. Ancient low–molecular-weight organic acids in permafrost fuel rapid carbon dioxide production upon thaw. *Proc. Natl. Acad. Sci.* 112: 13946-13951.

Ewing, S.A., O'Donnell, J., Aiken, G.R., Butler, K., Butman, D., Windham-Myers, L., Kanevskiy, M.Z. 2015. Long-term anoxia and release of ancient, labile carbon upon thaw of Pleistocene permafrost. *Geophys. Res. Lett.* 42: 2015GL066296.

Guenet, B., Danger, M., Abbadie, L., Lacroix, G., 2010. Priming effect: bridging the gap between terrestrial and aquatic ecology. *Ecology* 91: 2850–2861.

Holmes, R.M., McClelland J.W., Raymond P.A., Frazer B.B., Peterson B.J., Stieglitz M.. 2008. Lability of DOC transported by Alaskan rivers to the Arctic Ocean. *Geophys. Res. Lett.* 35: L03402.

Kicklighter, D.W., Hayes, D.J., McClelland, J.W., Peterson, B.J., McGuire, A.D., Melillo J.M., 2013. Insights and issues with simulating terrestrial DOC loading of Arctic river networks. *Ecol. Appl.* 23.

Laudon, H., Buttle, J., Carey, S.K. *et al.*, 2012. Cross-regional prediction of long-term trajectory of stream water DOC response to climate change. *Geophys. Res. Lett.* 39: L18404.

Mann, P.J., Eglinton, T.I., McIntyre, C.P., Zimov, N., Davydova, A., Vonk, J.E., Holmes, R.M., Spencer, R.G.M., 2015. Utilization of ancient permafrost carbon in headwaters of Arctic fluvial networks. *Nat. Commun.* 6: 7856.

Rosemond, A.D., Benstead, J.P., Bumpers, P.M., Gulis, V., Kominoski, J.S., Manning, D.W.P., Suberkropp, K., Wallace J.B.. 2015. Experimental nutrient additions accelerate terrestrial carbon loss from stream ecosystems. *Science* 347: 1142-1145.

Spencer, R.G.M., Mann, P.J., Dittmar, T., Eglinton, T.I., McIntyre, C., Holmes, R.M., Zimov, N., Stubbins, A., 2015. Detecting the signature of permafrost thaw in Arctic rivers. *Geophys. Res. Lett.* 42: 2830-2835.

Treat, C.C., Wollheim, W.M., Varner, R.K., Bowden, W.B., 2016. Longer thaw seasons increase nitrogen availability for leaching during fall in tundra soils. *Environ. Res. Lett.* 11: 064013.

Vonk, J.E., Mann, P.J., Davydov, S. *et al.*, 2013. High biolability of ancient permafrost carbon upon thaw. *Geophys. Res. Lett.* 40: 2689–2693.

Wickland, K.P., Aiken, G.R., Butler, K., Dornblaser, M.M., Spencer, R.G.M., Striegl, R.G., 2012. Biodegradability of dissolved organic carbon in the Yukon River and its tributaries: Seasonality and importance of inorganic nitrogen. *Glob. Biogeochem. Cycles* 26: GB0E03.

Dynamics of trace elements in the Arctic: role of soil organic matter

Yannick Agnan[1]
Marie (Anne) Alexis[1]
Maryse (Castrec)-Rouelle[1]

[1]*METIS, SU–CNRS–EPHE, 4 place Jussieu, F-75252 Paris, France, yannick.agnan@biogeochimie.fr*

Abstract

Mobility of trace elements potentially toxic, that are accumulated in arctic soils through both atmospheric deposition and rock erosion, is a major environmental concern for polar ecosystems and human health. Since the high latitudes are very sensitive to recent warming, the understanding of biogeochemical cycling in these remote areas requires considering the impact of climate change. Here, we investigated potential trace element leachability comparing bulk and extractable soil fractions in two distinct Arctic sites: Abisko (Sweden) on discontinuous permafrost and Toolik (Alaska, USA) on continuous permafrost. With the exception of Cu, all trace elements showed higher potential extractability, and thus leachability to the aquatic system, at Abisko. Results also indicated that dissolved organic carbon quantity was not the main driver for trace element mobility. Degree of decomposition of soil organic matter, however, seemed to be more important to control trace element dynamics.

Keywords: trace elements; organic matter; dynamics; Arctic; soil

Introduction

Arctic soils constitute reservoirs for trace elements (TE) through long-range atmospheric transport from temperate latitudes. These TE, accumulated in vegetation and organic soil horizons, add to lithogenic contribution due to rock erosion (Halbach *et al.*, 2017). Climate change, in particular permafrost thawing, may increase the pool of TE mobile to the aquatic system and available for trophic networks with potential ecosystem health concerns. Thus, biogeochemical cycles need to be better characterized in the Arctic.

Arctic soils contain half of soil organic matter (SOM) stored in global soils (Schuur *et al.*, 2015). Decomposition of SOM promotes production of dissolved organic carbon (DOC). Recent studies reported increasing DOC concentrations in Northern rivers mainly related to climate change and reactivation of arctic soils (Lepistö *et al.*, 2008). As TE are known to bind to SOM, DOC can play a role of vector for TE mobility in arctic environments.

The main objective of this study was to characterize TE in bulk and extractable arctic soil fractions and determine the role of DOC as a driver of TE mobility in arctic environments.

Materials and Methods

Soil samples were collected in two study sites: Abisko (Sweden) and Toolik (Alaska, USA). Both sites are located at 68°N latitude and characterized by organic-rich soils. Average mean temperature, however, differs between the two sites, responsible for different permafrost characteristics: −0.8 °C at Abisko on discontinuous permafrost and −8.5 °C at Toolik on continuous permafrost. Lithology is characterized by sedimentary substrate: Caledonian sandstone at Abisko and Cretaceous shale and sandstone at Toolik.

Both bulk and extractable soil fractions were considered for chemical analysis. Bulk soil samples were mineralized by H_2O_2, HNO_3, and HF before TE analysis by ICP–MS (Agilent 7500cx) and ICP–OES (Agilent 5100). Carbon and nitrogen concentrations were determined by elementary analyzer (Elementar VarioPyro Cube). SOM was characterized by solid-state ^{13}C NMR (Bruker). Extractable fractions were performed using a 0.25 mM $CaCl_2$. DOC was analyzed by DOC analyzer (Shimadzu TOC_L$_{CSH}$).

Results and Discussions

Trace elements in arctic soils

Taking into account similar tundra ecosystems, TE concentrations measured in bulk organic soil horizons were generally higher at Toolik compared to Abisko. This may result from different regional lithology. To better study the potential TE leachability to aquatic environments, ratios of TE concentrations in extractable fraction (TE_{CaCl2}) compared to those in bulk fraction (TE_{bulk}) were calculated for both sites (Fig. 1). Unlike bulk soil trends, data showed higher ratios at Abisko, with the exception of Cu. This indicates that TE leachability is higher in the warmer site, implying different driver of TE mobility.

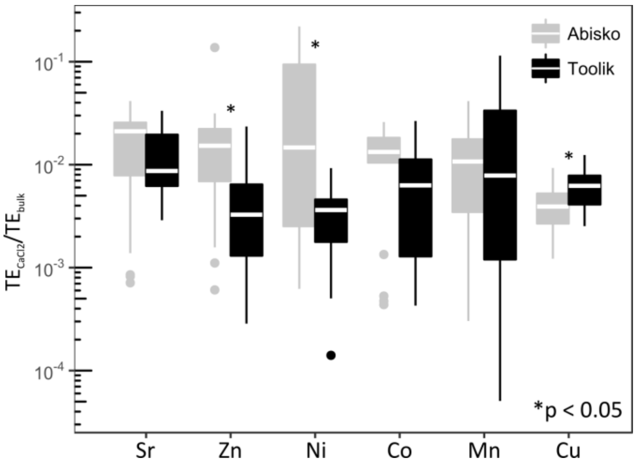

Figure 1. Ratio of TE concentrations between extractable (TE_{CaCl2}) and bulk (TE_{bulk}) fractions.

Organic matter in arctic soils

In parallel, we analyzed SOM quantity and quality. C/N ratios showed higher values at Abisko. This indicates a higher nitrogen content at Toolik, probably due to different biomass contribution (lichen/moss/grass/brush). Indeed, the ratio of functional group alkyl/O-alkyl determined by solid-state ^{13}C NMR, frequently used as decomposition indicator, showed more decomposed SOM at Absiko.

Measurements of DOC in extractable fractions showed slightly higher concentrations at Toolik. This may demonstrate the potential pool of DOC not extracted yet due to colder conditions that preserves SOM. Thus, DOC quantity cannot explain the mobilization of TE. Also, principal component analysis indicated that DOC concentration was only correlated to Sr and Cu leachability. We hypothesized that DOC quality may play an important role in TE dynamics that needs to be confirmed.

Conclusions

TE leachability and mobility were investigated in two Arctic sites. We showed that TE were more leachable in the warmer site (Abisko, Sweden), which can be attributed to a more decomposed SOM. This probably influences the DOC quality which could be a significant vector of TE mobility. We therefore assume that climate change will modify dynamics of TE in the Arctic.

Acknowledgments

We thank C. Anquetil and E. Aubry for organic and mineral analytical support and ENVEXX team for sampling support. We also thank D. Obrist, PI of the Toolik project and S. Derenne for NMR financial support.

References

Halbach, K., Mikkelsen, Ø., Berg, T. & Steinnes, E., 2017. The presence of mercury and other trace metals in surface soils in the Norwegian Arctic. *Chemosphere* 188: 567-574.

Lepistö, A., Kortelainen, P. & Mattsson, T., 2008. Increased organic C and N leaching in a northern boreal river basin in Finland. *Global Biogeochemical Cycles* 22(3): GB3029.

Schuur, E.A.G. et al., 2015. Climate change and the permafrost carbon feedback. *Nature* 520(7546): 171-179.

Sources and degradation status of particulate organic carbon in the Kolyma River watershed

Lisa Bröder[1]
Anya Davydova[2]
Nikita Zimov[2]
Negar Haghipour[3]
Timothy Eglinton[3]
Jorien Vonk[1]

[1] *Department of Earth Sciences, Vrije Universiteit Amsterdam, Amsterdam, The Netherlands, l.m.broeder@vu.nl*

[2] *Northeast Science Station, Pacific Institute for Geography, Far East Branch, Russian Academy of Sciences, Cherskiy, Republic of Sakha, Russia*

[3] *Geological Institute, Swiss Federal Institute of Technology (ETH), Zürich, Switzerland*

Abstract

Ongoing permafrost thaw potentially increases the organic matter loads of Arctic rivers. Thaw-remobilized organic carbon is mostly released in the particulate form (POC) and may either enhance or attenuate global warming, depending on its propensity for decomposition. Strong seasonality in discharge and soil hydrological flow paths in watersheds underlain by permafrost enable transport of different carbon pools with contrasting lability. To evaluate these seasonal differences, we collected POC samples from the Kolyma River mainstem and a small nearby tributary. Concentrations of POC along with carbon ($\delta^{13}C$, $\Delta^{14}C$) and hydrogen isotope analysis on bulk POC and lipid biomarkers will be used to study the contributions of different sources (contemporary terrestrial versus deeper permafrost/yedoma), as well as their degradation state. This high-resolution POC sampling combined with isotopic fingerprinting and extensive geochemical analysis will allow us to assess present-day fluvial release and fate of POC from permafrost thaw in a major Arctic watershed.

Keywords: particulate organic carbon; Kolyma; carbon isotopes; deuterium; lipid biomarkers; degradation

Introduction

Suspended particulate organic carbon (POC) is operationally defined as the fraction collected on a 0.7-µm glass-fiber filter as opposed to dissolved organic carbon (DOC), which passes through the filter. In Arctic rivers, POC is on average older than DOC and therefore more likely to originate from a permafrost thaw source (e.g., Guo *et al.*, 2007). Ancient DOC entrained in ice-rich yedoma deposits has been shown to degrade readily upon thaw/delivery to the river (Vonk *et al.*, 2013; Spencer *et al.*, 2015). For permafrost-derived POC, however, the fate is unclear: it can either be remineralized in the river, buried in the sediment or transported to the Arctic Ocean (Vonk & Gustafsson, 2013). Abrupt thaw processes such as thermokarst, river bank and coastal erosion, release several orders of magnitude more POC than DOC (e.g., Vonk et al., 2013). As these features are expected to become increasingly common throughout the Arctic (Olefeldt *et al.*, 2016), unravelling the uncertainties surrounding potential pathways for permafrost-derived POC gain ever more importance.

For this study, we focus on the Kolyma River watershed in Northern Siberia, the world's largest watershed (653 000 km²) entirely underlain by continuous permafrost (Holmes *et al.*, 2012). Like most Arctic rivers, its discharge is characterized by a strong seasonality. Highest fluxes occur during the spring flood in May-June, following river ice breakup and snow melt. As the active layer thaws, hydrological flow paths change and enable transport of different carbon pools. To evaluate seasonal differences in carbon delivery to the river, we have collected particulate matter every 4-7 days from late May to early October (Fig. 1) from the Kolyma River close to its delta near Cherskiy and from a nearby tributary (Y3, 17 km²) draining an area entirely underlain by yedoma permafrost (Pleistocene ice and organic matter rich loess deposits, Zimov *et al.*, 2006).

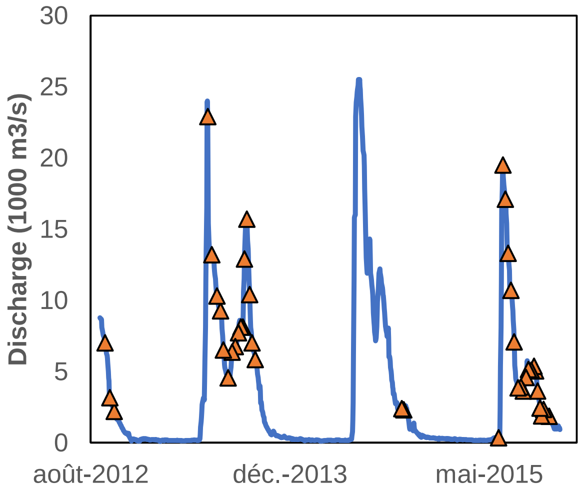

Figure 1. Hydrograph of the Kolyma River with triangles indicating when water samples were collected. Discharge data were collected by Roshydromet (Federal Service for Hydrometeorology and Environmental Monitoring, Ministry of Natural Resources and Environment, Russian Federation).

From the isotopic composition of bulk organic carbon ($\delta^{13}C$ and $\Delta^{14}C$) we obtain information about the source and age of the organic matter. Lipid biomarkers (source-specific molecular fossils) are employed to assess the contemporary and historical environment and the qualitative degradation status of the material delivered to the river. Deuterium signatures of lipid biomarkers can also reveal information about the source of the organic matter, as the cold and dry conditions during formation of yedoma deposits (last glacial period) resulted in very depleted δ^2H signatures in contrast to more enriched values in our contemporary climate (Meyer et al., 2002).

Preliminary Results

The POC concentrations for both Kolyma River and its tributary Y3 approximately follow the hydrograph with an increase of about one order of magnitude during the spring flood (~0.23 mg L^{-1} minimum just before and 2.3 mg L^{-1} maximum during the freshet for Kolyma; ~0.1 mg L^{-1} before and 0.9 mg L^{-1} during the freshet for Y3; average values of ~0.7 mg L^{-1} and 0.3 mg L^{-1}, respectively for Kolyma and Y3). A similar pattern has been observed for earlier sampling campaigns and several of the great Arctic rivers (McClelland *et al.*, 2016). Also, DOC concentrations for Kolyma and Y3 displayed a similar behavior (Mann *et al.*, 2012) of increasing concentrations with discharge.

Stable carbon isotope values ($\delta^{13}C$) range between -32.6 ‰ and -27.3 ‰ for Kolyma and -35.1 ‰ and -26.3 ‰ for Y3. They do not reveal clear seasonal trends, nor substantial differences between the Kolyma River and its tributary. Planned radiocarbon dating of bulk POC and compound-specific δ^2H analysis on lipid biomarkers (long-chained fatty acids) will help to discern the relative POC contributions from the active layer and recent vegetation in contrast to deeper yedoma permafrost (Pleistocene deposits). Furthermore, lipid biomarkers will help to assess the extent of POC degradation.

Acknowledgments

The authors would like to acknowledge founding through ERC StG THAWSOME (676982), Veni NWO (863.12.004), US-NSF Polaris Project 1044610 and the Russian Foundation for Basic Research.

References

Guo, L., *et al.*, 2007. Mobilization pathways of organic carbon from permafrost to arctic rivers in a changing climate. *Geophys. Res. Lett.* 34(13): 1–5.

Holmes, R. M., *et al.*, 2012. Seasonal and Annual Fluxes of Nutrients and Organic Matter from Large Rivers to the Arctic Ocean and Surrounding Seas. *Estuaries and Coasts* 35(2): 369-382.

Mann, P. J., *et al.,* 2012. Controls on the composition and lability of dissolved organic matter in Siberia's Kolyma River basin. *J. Geophys. Res. Biogeosciences* 117(1): 1-15.

McClelland, J. W. *et al.*, 2016. Particulate organic carbon and nitrogen export from major Arctic rivers. *Global Biogeochem. Cycles* 30(5): 629-643.

Meyer, H., et al., 2002. Palaeoclimate reconstruction on Big Lyakhovsky Island, North Siberia – Hydrogen and oxygen isotopes in ice wedges. *Permafr. Periglac. Process.* 13: 91-105.

Olefeldt, D., et al., 2015. Circumpolar distribution and carbon storage of thermokarst landscapes. *Nat. Commun.* 7: 13043.

Spencer, R. G. M., *et al.*, 2015. Detecting the signature of permafrost thaw in Arctic rivers. *Geophys. Res. Lett.* 42(8): 2830–2835.

Vonk, J. E. & Gustafsson, Ö., 2013. Permafrost-carbon complexities. *Nat. Geosci.* 6(9): 675–676.

Vonk, J. E. *et al.*, 2013. High biolability of ancient permafrost carbon upon thaw. *Geophys. Res. Lett.* 40(11): 2689-2693.

Zimov, S. A., et al., 2006. Permafrost and the Global Carbon Budget. *Science* 312: 1612–1613.

The source and fate of mercury in the snowpack of a watershed underlain by continuous permafrost near Utqiaġvik, Alaska

Thomas A. Douglas[1]
Joel D. Blum[2]

[1] *U.S. Army Cold Regions Research & Engineering Laboratory, PO Box 35170 Fort Wainwright, Alaska 99703; 907-361-9555; thomas.a.douglas@usace.army.mil*

[2] *Department of Earth & Environmental Sciences, University of Michigan; jdblum@umich.edu*

Abstract

We measured mercury (Hg) and major ion concentrations and stable isotopes of Hg and water from the snowpack through the entire spring melt runoff period for two years at a site near Utqiaġvik, Alaska. We also collected and analyzed peat and sediment cores for Hg concentrations and stable isotopes. Our research site was a small (2.5 ha) watershed underlain by continuous permafrost. Results show an "ionic pulse" of mercury and major ions in runoff during both snowmelt seasons with total dissolved Hg runoff of 14.3 (+/- 0.7) mg/ha in 2008 and 8.1 (+/- 0.4) mg/ha in 2009. This is five to seven times higher than what has been reported from other arctic watersheds. We calculate 78% of snowpack Hg was exported with snowmelt runoff in 2008 and 41% in 2009. Hg stable isotope measurements indicate the majority of the snow melt Hg originated as gaseous elemental mercury (Hg(0)) and was likely oxidized in the snowpack by reactive halogens.

Keywords: Arctic; geochemistry; snow; mercury; hydrology.

Introduction

Atmospheric mercury (Hg) is deposited to Polar Regions during springtime atmospheric mercury depletion events (AMDEs) that require reactive halogens and snow or ice surfaces. Gaseous elemental Hg (Hg(0)) is also deposited to the Arctic from the global atmospheric pool. The fate of Hg deposited to Arctic snow and ice during and following snowmelt is largely unknown. Since the Arctic is snow-covered for up to three quarters of the year a majority of the surface runoff, including any Hg, occurs during the spring freshet. In high arctic watersheds underlain by continuous permafrost there is little storage capacity during melt so most of the melt water flows over the terrain during a rapid melt event lasting 2-3 weeks. We undertook this study to track Hg and major ions in snowmelt runoff in a small high arctic catchment in northern Alaska. Our goal was to identify potential sources and sinks of Hg in the watershed.

Study site and methods

Our field site is on the Arctic coastal plain 6 km southeast of Utqiaġvik, Alaska (71.285°N, 156.575°W. 1981-2010 mean annual air temperature for the area was -11.2 °C with mean annual precipitation of 115 mm water equivalent and a total snowfall depth of 826 mm.

The watershed is underlain by continuous permafrost hundreds of meters thick and the surface topography consists of a heterogeneous mixture of high-centered, low-centered, and transitional ice wedge polygons. The watershed drains directly into Elson Lagoon which is connected to the Beaufort Sea. The watershed is representative of typical Arctic Coastal Plain wetland watersheds with low hydraulic gradients and deranged drainage networks.

Typical end of season permafrost active layer thaw depths measured at the site were 30-50 cm. which is similar to measurements since 1994 at the nearby Cold Regions Research and Engineering Laboratory (CRREL) Circumpolar Active Layer monitoring site (CALM, 2016) The area develops a classic tundra snowpack with 10-20 cm of basal depth hoar overlain by a 10 to 20 cm layer of hard wind slabs with an occasional surface layer of recent snowfall or faceted crystals. Late winter snowpack depths typically vary from 0-10 cm on windblown high centered polygon tops to 60-100 cm in low-lying drifts (Douglas and Sturm, 2004).

In late winter prior to snow melt (April) and during snowmelt runoff in May and June 2008 and 2009 we made over 10,000 snow depth measurements and 36 total snowpack water equivalent (SWE) measurements within the watershed and surrounding areas to calculate the end of winter SWE and associated Hg loading (Fig. 1). We collected snow and water samples daily from melt initiation until the snowpack was gone. Snowpack, meltwater, and stream channel water were sampled and analyzed for total dissolved Hg, major ions, and stable oxygen and hydrogen isotopes. Additional information on the study is provided in Douglas *et al.,* 2017.

Results

In 2008 and 2009 initial snowmelt runoff major ion concentrations of calcium, magnesium, sodium, potassium, sulfate, chloride, and bromide (but not nitrate) were far greater than bulk snowpack values and they decreased as discharge increased toward peak runoff. The overall trend was for initially high concentrations decreasing as discharge increased followed by increasing concentrations as discharge decreased.

Figure 1. Repeat images of the watershed channel during spring melt in 2009.

Our results suggest the preferential elution of major ions out of the snowpack during melt onset with sodium, potassium, calcium, chloride, and bromide representing the most abundant ions. This "ionic pulse" occurred in both years suggesting it is a perennial feature of the melt. The presence of bromide as a component in the enhanced meltwater signal is of significance because it has been hypothesized that $HgBr_2$, BrHgOBr, and BrOHgOBr are associated with Arctic Mercury depletion event (AMDE) chemistry by complexing and oxidizing atmospheric Hg (Raofie & Ariya, 2004).

Total dissolved mercury concentrations in pre-melt snowpack and runoff waters were greater in 2008 than 2009 by a factor of about two. This is similar in magnitude to the difference in major ion concentrations in 2008 compared to 2009. In both years initial meltwater Hg concentrations were twice or more what we measured in the snowpack prior to the melt. The highest Hg concentrations were measured in initial meltwater collected at the base of the snowpack. Runoff Hg concentrations were always greater than snowpack core pre-melt snowpack Hg concentrations.

The Hg source for the early melt runoff is predominantly melting snow with minor contributions from the underlying tundra suggesting an elution process similar to the preferential elution of major ions. We note that during both of the spring melt events the runoff Hg concentrations were consistently about four times greater than the Hg concentration of the snowpack before and during the melt period and the runoff Hg concentrations do not decrease as the snowpack converts to melt water. Based on this our approximation is that 75% of the Hg exported from the watershed during the snow melt period came from non-AMDE sources while 25% is attributable to deposition from AMDEs.

Our Hg stable isotope analyses indicate that Hg deposited directly to the snowpack as GEM (Hg(0)) and converted to Hg(II) in the snowpack comprises the majority of the mercury that remains until snowmelt and this is the Hg discharged into the surface meltwater of our Arctic coastal ecosystem. From this we surmise that the halogen rich snowpack facilitated oxidation and retention of gaseous elemental Hg.

Our results suggest enhanced Hg deposition to arctic coastal snowpacks where sea ice provides a source of reactive halogens. Projected future warming in the Arctic will produce a more dynamic sea ice regime with more first year ice and more open sea ice leads. This will enhance the source of reactive halogens and promote GEM oxidation and lead to greater Hg deposition to coastal and marine snowpacks. Any increase in AMDE Hg from the global gaseous elemental Hg pool could lead to enhanced Hg deposition to Arctic terrestrial and nearshore ecosystems.

References

Circumpolar Active Layer Monitoring Program. https://www2.gwu.edu/~calm/data/north.html.

Douglas, T. A., Sturm, M., Simpson, W. R., Brooks, S., Lindberg, S. E., Perovich, D. K. 2005 Elevated mercury measured in snow and frost flowers near arctic sea ice leads. *Geophysical Research Letters 32*, L04502; DOI 10.1029/2004GL022132.

Douglas, T.A., Sturm, M., Blum, J.D., Polashenski, C., Stuefer, S., Hiemstra, C.A., Steffen, A., Filhol, S., Prevost, R. 2017. A pulse of mercury and major ions in snowmelt runoff from a small Arctic Alaska watershed. *Environmental Science and Technology*. DOI: 10.1021/acs.est.7b03683.

Hydrochemical features of gas-emission crater lakes embedded into marine deposits

Yury (A) Dvornikov[1]
Marina (O) Leibman[1, 2]
Artem (V) Khomutov[1, 2]
Alexander (I) Kizyakov[3]
Evgeny (M) Babkin[1]
Birgit Heim[4]
Ingeborg Bussmann[4]
Irina (D) Streletskaya[3]

[1]*Earth Cryosphere Institute Tyumen Scientific Centre SB RAS, Tyumen, Russia, ydvornikov@gmail.com*
[2]*University of Tyumen, International Institute of Cryology and Cryosophy*
[3]*Lomonosov Moscow State University, Faculty of Geography, Cryolithology and Glaciology Department, Moscow, Russia*
[4]*Alfred-Wegener-Institute for Polar and Marine Research, Potsdam, Germany*

Abstract

Gas emission craters, formed in the north of West Siberia, were sampled to determine hydrochemical parameters of water and ice of enclosing and filling crater deposits. For comparison, lakes and ground ice from other exposures were analyzed as well. Comparing results of the analysis confirms that the nature of the craters lies in the emission of methane accumulated in the upper horizons of permafrost.

Keywords: Yamal, gas-emission craters, lakes, hydrochemistry.

Introduction

We present here results the analysis of water samples collected from lakes and lakes originating from filled with water gas-emission craters (GECs) in order to find specific hydrochemical features of newly formed GEC lakes. GECs found in Yamal and Gydan peninsulas (Kizyakov *et al.*, 2015, 2017) have dramatically changed the permafrost landscape. The development of such permafrost objects is accompanied by emission of methane, lateral transport of major ions, organic matter realized from thawed crater walls. Moreover, GEC lakes are nowadays characterized by specific thermal regime. Information about hydrochemical features of GEC lakes and ordinary non-GEC lakes might be helpful in the future to identify the lakes that were also formed as a result of gas emission in the West-Siberian North.

Methods

We have collected water samples in 2015-2017 winter and summer field campaigns from GEC lakes and usual lakes of Yamal and Gydan peninsulas. Water samplers were used to carry out express analyses: temperature, pH, dissolved oxygen, electrical conductivity and to collect samples for further laboratory analyses. Several parameters were determined: dissolved methane, dissolved organic carbon (DOC), major ions, stable-isotopic composition of water (O and H) and methane (C and H).

Conclusions

It is found so far that:

1) GEC lakes have much higher concentration of methane dissolved in the water which confirms the presence of methane source within the crater bottom and walls;
2) Methane is found to be mostly of biogenic origin in the GEC lakes, the same as methane extracted from tabular ground ice and water of other lakes;
3) The concentration of DOC in Yamal crater is 3-4 times higher than in other Yamal lakes;
4) The concentration of major ions is 2-3 and more times higher in Yamal and Gydan GEC lakes than in lakes of both regions on average with higher proportion of HCO_3^-;
5) At the first stage of GEC formation, the main water source for the GEC lake was thawed tabular ground ice as revealed from isotopic analysis

(Streletskaya *et al.*, 2017). Later on, the GEC lakes have filled with atmospheric precipitation changing accordingly isotopic and ionic composition of GEC lake water;

6) GEC lakes are characterized by specific thermal regime different from the one in usual Yamal and Gydan lakes: there is no thermal gradient in winter water-temperature profile in GEC lakes indicating lack of stratification in GEC-lake water, and there is thermal gradient (warmer surface and cooler bottom) in summer thus indicating stratification due to cold bottom of GEC lakes and low wind action along their small area protected by walls.

Acknowledgments

This work is supported by Russian Science Foundation (RSF) grant No. 16-17-10203.

References

Kizyakov, A.I., Sonyushkin, A.V., Leibman, M.O., Zimin, M.V., Khomutov, A.V., 2015. Geomorphological conditions of the gas-emission crater and its dynamics in Central Yamal. *Kriosfera Zemli (Earth's Cryosphere)* 2: 13-22.

Kizyakov, A., Zimin, M., Sonyushkin, A., Dvornikov, Y., Khomutov, A., Leibman, M., 2017. Comparison of Gas Emission Crater Geomorphodynamics on Yamal and Gydan Peninsulas (Russia), Based on Repeat Very-High-Resolution Stereopairs. *Remote Sensing* 9: 1023.

Streletskaya, I.D., Leibman, M.O.; Kizyakov, A.I.; Oblogov, G.E.; Vasiliev, A.A.; Khomutov, A.V.; Dvornikov, Y.A., 2017. Ground ice and its role in the formation of gas-emission crater in the Yamal Peninsula. *Moscow University Bulletin* 2: 91–99 (In Russian).

Untangling terrestrial and aquatic controls on carbon, nutrients, and microorganisms in Arctic stream networks

Rebecca J. Frei[1], Natasha Griffin[1], Benjamin W. Abbott[1], Zach Aanderud[1], Jay P. Zarnetske[2], William B. Bowden[3], Frances Iannuci[3]

[1]*Brigham Young University, Department of Plant and Wildlife Sciences, beccafrei@gmail.com;* [2]*Michigan State University, Department of Earth and Environmental Sciences; The Rubenstein School of Environment and Natural Resources, University of Vermont*

Abstract

Many longitudinal differences in dissolved organic matter (DOM) exist in permafrost river networks. Downstream decreases in DOM biodegradability, age, and bulk concentration have been observed and interpreted as signs of in-stream microbial and photochemical processing. Alternatively or additionally, longitudinal patterns could be due to systematic differences in tributaries draining upland and lowland permafrost landscapes. Because vegetation type, flowpath, residence time, and microbial community differ with landscape position, the simple mixing of different water sources could create the observed longitudinal patterns of DOM in permafrost river networks. We tested this "dilution hypothesis" by quantifying DOM biodegradability and properties, microbial community, nutrient availability, and water chemistry in 140 catchments in Arctic Alaska ranging from 1-1000 km². By comparing catchments of similar size but different landscape positions, we separated terrestrially-driven source effects from in-stream processing. We also used metagenomic methods to relate water chemistry and DOM biodegradability with microbial community.

Keywords: permafrost, river network, dissolved organic matter, metagenome, biodegradability

Introduction

As water flows from uplands to lowlands through a landscape, there are systematic changes in hydrology, vegetation, soil type, and in-stream processing. Consequently, attributing longitudinal patterns in water chemistry to terrestrial or aquatic processes requires careful constraining of hydrologic mixing (Burt & Pinay, 2005; Abbott *et al.,* 2016).

In the permafrost zone, several compelling longitudinal patterns in DOM have been observed, including downstream decreases in DOM radiocarbon age, biodegradability, and photoreactivity (Prokushkin *et al.*, 2011; Cory *et al.*, 2014; Mann *et al.*, 2015; Drake *et al.*, 2015; Vonk *et al.*, 2015). These patterns are typically attributed to in-stream processing, which would suggesting that DOM and nutrients released from degrading permafrost are quickly consumed or retained in headwaters. However, residence time in permafrost river networks is typically on the order of days to weeks, limiting the time biotic and abiotic reactions can modify DOM, even compared with laboratory rates of DOM processing at elevated temperatures (Cory *et al.*, 2013; Abbott *et al.*, 2014; Vonk *et al.*, 2015).

An alternative hypothesis for longitudinal shifts in DOM is that systematic differences in water and DOM sources moving from uplands to lowlands create longitudinal trends simply due to mixing. Hydrologic residence time and flowpath change dramatically moving from uplands to lowlands in permafrost landscapes (Zarnetske *et al.*, 2008). These hydrologic parameters are two of the fundamental controls on carbon and nutrient form and function across terrestrial-aquatic gradients (Zarnetske *et al.*, 2012; Pinay *et al.*, 2015; Abbott *et al.*, 2017). Additionally, permafrost disturbances such as thermokarst and thermal erosion change with landscape position (Bowden *et al.*, 2012; Kokelj & Jorgenson, 2013), potentially contributing to dilution of permafrost-derived DOM and nutrients in downstream reaches independent of in-stream processing.

Methods

To test this "dilution hypothesis" we sampled 140 catchments near the Toolik Field Station on the North Slope of Alaska in the early and late season in 2016 and 2017. Catchment sizes varied from 1-1000 km² and covered a range of landscape positions including alpine, upland, and lowland tundra. We stratified sampling by catchment size, including small catchments with diverse landscape positions and catchment characteristics (e.g. surficial geology, vegetation, disturbance history, and topography). Because microbial diversity can change with stream network position (Crump *et al.*, 2007; Widder *et al.*, 2014), we characterized the metagenomes of stream water and biofilms throughout the network.

We quantified DOM biodegradability with laboratory incubations and assessed DOM optical properties with scanning fluorometry.

Results and Discussion

While several longitudinal patterns were apparent among the nested watersheds, the distributed mass balance of DOM and nutrients suggested primarily conservative transport at these spatiotemporal scales. This suggests that changes in water sources account for at least a portion of observed downstream changes in DOM concentration and attributes. We note that this dilution hypothesis is not mutually exclusive with in-stream processing, and we discuss the relative importance of aquatic and terrestrial processes regarding carbon, nitrogen, and phosphorus in permafrost landscapes. We conclude that longitudinal patterns of DOM in permafrost surface water networks can only reveal lateral flux dynamics inasmuch as both the hydrology and biogeochemistry are constrained. Quantitative assessment of the ecology and hydrology of permafrost fluvial networks is needed to understand the role of terrestrial and aquatic drivers in generating and processing lateral carbon and nutrient fluxes.

References

Abbott, B. W., V. Baranov, C. Mendoza-Lera, and others. 2016. Using multi-tracer inference to move beyond single-catchment ecohydrology. *Earth Science Reviews* 160: 19–42.

Abbott, B. W., G. Gruau, J. P. Zarnetske, and others. 2017. Unexpected stability and synchrony of water quality in stream networks. *Ecology Letters*.

Abbott, B. W., J. R. Larouche, J. B. Jones, W. B. Bowden, and A. W. Balser. 2014. Elevated dissolved organic carbon biodegradability from thawing and collapsing permafrost: Permafrost carbon biodegradability. *Journal of Geophysical Research: Biogeosciences* 119: 2049–2063.

Bowden, W. B., J. R. Larouche, A. R. Pearce, and others. 2012. An integrated assessment of the influences of upland thermal-erosional features on landscape structure and function in the foothills of the Brooks Range, Alaska. *Proceedings of the Tenth International Conference on Permafrost*. Citeseer. 61–66.

Burt, T. P., and G. Pinay. 2005. Linking hydrology and biogeochemistry in complex landscapes. *Progress in Physical Geography* 29: 297–316.

Cory, R. M., B. C. Crump, J. A. Dobkowski, and G. W. Kling. 2013. Surface exposure to sunlight stimulates CO2 release from permafrost soil carbon in the Arctic. *Proceedings of the National Academy of Sciences* 110: 3429–3434.

Cory, R. M., C. P. Ward, B. C. Crump, and G. W. Kling. 2014. Sunlight controls water column processing of carbon in arctic fresh waters. *Science* 345: 925–928.

Crump, B. C., H. E. Adams, J. E. Hobbie, and G. W. Kling. 2007. Biogeography of Bacterioplankton in Lakes and Streams of an Arctic Tundra Catchment. *Ecology* 88: 1365–1378.

Drake, T. W., K. P. Wickland, R. G. M. Spencer, D. M. McKnight, and R. G. Striegl. 2015. Ancient low–molecular-weight organic acids in permafrost fuel rapid carbon dioxide production upon thaw. *Proceedings of the National Academy of Sciences* 112: 13946–13951.

Kokelj, S. V., and M. T. Jorgenson. 2013. Advances in Thermokarst Research: Recent Advances in Research Investigating Thermokarst Processes. *Permafrost and Periglacial Processes* 24: 108–119.

Mann, P. J., T. I. Eglinton, C. P. McIntyre, N. Zimov, A. Davydova, J. E. Vonk, R. M. Holmes, and R. G. M. Spencer. 2015. Utilization of ancient permafrost carbon in headwaters of Arctic fluvial networks. *Nature Communications* 6: 7856.

Pinay, G., S. Peiffer, J.-R. De Dreuzy, and others. 2015. Upscaling Nitrogen Removal Capacity from Local Hotspots to Low Stream Orders' Drainage Basins. *Ecosystems* 18: 1101–1120.

Prokushkin, A. S., O. S. Pokrovsky, L. S. Shirokova, and others. 2011. Sources and the flux pattern of dissolved carbon in rivers of the Yenisey basin draining the Central Siberian Plateau. *Environmental Research Letters* 6: 045212.

Vonk, J. E., S. E. Tank, P. J. Mann, R. G. M. Spencer, C. C. Treat, R. G. Striegl, B. W. Abbott, and K. P. Wickland. 2015. Biodegradability of dissolved organic carbon in permafrost soils and aquatic systems: a meta-analysis. *Biogeosciences* 12: 6915–6930.

Widder, S., K. Besemer, G. A. Singer, and others. 2014. Fluvial network organization imprints on microbial co-occurrence networks. *Proceedings of the National Academy of Sciences* 111: 12799–12804.

Zarnetske, J. P., M. N. Gooseff, W. B. Bowden, M. J. Greenwald, T. R. Brosten, J. H. Bradford, and J. P. McNamara. 2008. Influence of morphology and permafrost dynamics on hyporheic exchange in arctic headwater streams under warming climate conditions. *Geophysical Research Letters* 35: L02501.

Zarnetske, J. P., R. Haggerty, S. M. Wondzell, V. A. Bokil, and R. González-Pinzón. 2012. Coupled transport and reaction kinetics control the nitrate source-sink function of hyporheic zones. *Water Resources Research* 48: W11508.

Impacts of collapsing permafrost coasts: the fate of carbon, nutrients and sediments in the Arctic nearshore zone

Michael Fritz[1], Gesine Mollenhauer[2], Rafael Gonçalves-Araujo[2], George Tanski[3], Birgit Heim[1], Thorsten Riedel[2], Gregor Pfalz[1], Hugues Lantuit[1]

[1]*Alfred Wegener Institute, Helmholtz Centre for Polar and Marine Research, Potsdam, Germany, Michael.Fritz@awi.de*

[2]*Alfred Wegener Institute, Helmholtz Centre for Polar and Marine Research, Bremerhaven, Germany*

[3]*GFZ German Research Centre for Geosciences, Helmholtz Centre Potsdam, Potsdam, Germany*

Abstract

We need to consider permafrost coastal erosion as a major source of sediments, carbon and nutrients in the Arctic Ocean, especially in the nearshore zone. Marine sediments along permafrost coasts are dominated by erosion-derived terrestrial organic matter. A significant increase in matter fluxes would result in drastic impacts on global carbon cycling and related climate feedbacks, on nearshore food webs and on local communities, whose survival still relies on marine biological resources.

Keywords: coastal erosion; lateral material transport; socio-economic impact; biogeochemical cycling; Arctic Ocean; permafrost organic matter; lipid biomarkers

Introduction

Global warming is exposing permafrost along the extensive Arctic coastlines, which account for 34% of the Earth's coasts, to rapid thaw and erosion. Coastal erosion rates as high as 25 m yr^{-1} and the large organic-matter pool frozen in permafrost result in an annual release of 14.0 Tg (10^{12} gram) particulate organic carbon into the nearshore zone. This zone is the primary recipient of increasing fluxes of carbon and nutrients from thawing permafrost. We highlight the crucial role of the nearshore zone in Arctic biogeochemical cycling, as here the fate of the released material is determined to: (1) degrade into greenhouse gases, (2) fuel marine primary production, (3) be buried in nearshore sediments or (4) be transported offshore. With Arctic warming, coastal erosion fluxes have the potential to increase by an order of magnitude until 2100. Such increases would result in drastic impacts on global carbon fluxes and their climate feedbacks, on nearshore food webs and on local communities, whose survival still relies on marine biological resources (Fritz *et al.*, 2017). Determining the potential impacts of increasing erosion on coastal ecosystems is crucial for food security of northern residents living in Arctic coastal communities. Quantifying fluxes of organic carbon and nutrients is required, both in nearshore deposits and in the water column by sediment coring and systematic oceanographic monitoring. Ultimately, this will allow us to assess the transport and degradation pathways of sediment and organic matter derived from erosion.

Material and Methods

We present multi-year dissolved organic matter (DOM) fluxes from coastal erosion into the nearshore zone of the southern Canadian Beaufort Sea (Fig. 1). We further explore removal and degradation patterns of DOM based on oceanographic monitoring of coastal waters. Finally, we present accumulation rates and biogeochemical properties (e.g. carbon, nitrogen, stable isotopes) of marine sediment sequences drilled off the Yukon coast to track the pathways of the eroded material. This also involves ^{14}C radiocarbon dating of bulk carbon and marine macrofossils. It further includes biomarker analyses and carbon budget calculations based on estimating coastal, riverine, and marine endmembers.

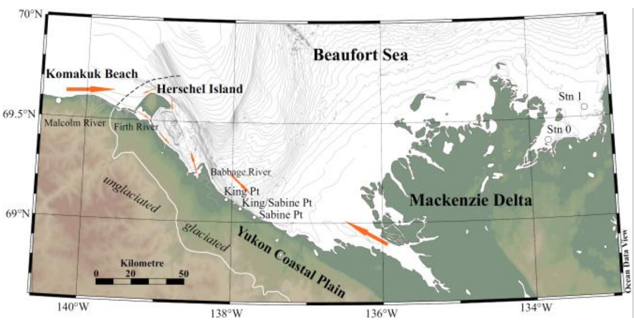

Figure 1. Overview of the study area with major currents and sediment inflows, indicated by orange arrows. The white line indicates the farthest extent of the Wisconsin glaciation.

Results and Discussion

Dissolved organic matter

Low salinity and high DOC concentrations are caused by sea-ice melt, surface runoff and material input from coastal erosion. Salinities remain mostly below 25 and DOC concentrations at or above 200 µmol L^{-1}. Elevated concentrations in the early part of the open-water season indicate the inflow of relatively DOC-rich Mackenzie River water from the east. Turbulent mixing and a stronger oceanic dominance lead to DOC concentrations mostly below 200 µmol L^{-1} in the later part of the season. Fluorescence EEMs and fluorescent components derived from PARAFAC modeling indicate that more than 70 % of the DOM is derived from terrestrial sources. CDOM indices suggest strong degradation of terrestrial DOC proximal to the coast.

Marine sediments from the surface and at depth

Organic carbon in surface sediments from the nearshore zone have been radiocarbon dated. We observe high amounts of "old" organic carbon (between 9 and 14 ka), which is much older than Mackenzie River particulate organic carbon, confirming our hypothesis that the organic carbon is mainly derived from coastal erosion. Bulk ^{14}C ages of a 12.5 m long sediment core from Herschel Basin (Fig. 1) display an overall increase from top to bottom, ranging from 6.7 ka BP to 16.1 ka BP. To distinguish between various sediment sources into Herschel Basin, an endmember model was established (Fig. 2). The model combines our ^{14}C data from marine sediments and terrestrial samples taken from Herschel Island with literature data on suspended matter from the Mackenzie River in combination with peat samples from the Yukon coast. Relative contributions from Herschel Island and the Mackenzie River were also calculated for all samples by defining endmember compositions based on the mean ratio of diploptene versus C29aß and C30aß hopanes (diploptene/(diploptene + C29aß + C30aß)). Biomarker analyses and bulk radiocarbon data show that sediments in Herschel Basin are mainly of terrigenous origin. Approximately 60 % of the organic matter in the surface sediments of Herschel Basin and the adjacent nearshore area can be assigned to eroded material from the coast. This is also based on C/N ratios and $\delta^{13}C$ signatures. Sedimentation rates are extremely high with up to 4 mm per year. Based on radiocarbon dates of marine mollusks from the core, which has a length of 12.5 m, covers the last ~5,000 years. Simple sediment budget calculations suggest that Herschel Basin receives about 720,000 metric tons of sediment and about 13,200 tons ($13.2 * 10^9$ g) of organic carbon each year.

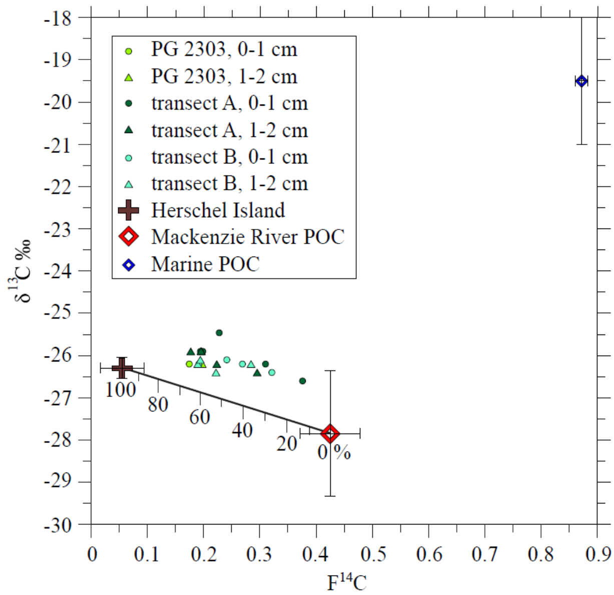

Figure 2. $F^{14}C$ endmember model. The marine POC endmember (blue diamond) and the $F^{14}C$ Mackenzie endmember (red diamond) combine data from the literature (Yunker *et al.*, 1992; Lamb *et al.*, 2006; Guo *et al.*, 2007). F14C endmember results of the surface sediments are based on the linear regression between the $F^{14}C$ Mackenzie and the $F^{14}C$ Herschel Island endmember.

We conclude that: 1) High loads of DOM in the nearshore zone are derived from surface runoff and coastal erosion. Degradation and biogeochemical cycling of DOC is particularly effective proximal to the coast; 2) Coastal erosion releases huge amounts of sediment and organic matter into the nearshore zone. Rapid burial removes large amounts of carbon from the carbon cycle in depositional settings. Flux and burial rates on the Beaufort Sea shelf seem to be significantly underestimated so far.

References

Fritz, M., Vonk, J.E., Lantuit, H., 2017. Collapsing Arctic coastlines. Nature Climate Change 7: 6-7.

Guo, L., Ping, C.L., Macdonald, R.W., 2007. Mobilization pathways of organic carbon from permafrost to Arctic rivers in a changing climate. *Geophysical Research Letters* 34: 1-5.

Lamb, A.L., Wilson, G.P., Leng, M.J., 2006. A review of coastal palaeoclimate and relative sea-level reconstructions using $\delta^{13}C$ and C/N ratios in organic material. *Earth Science Reviews* 75: 29-57.

Yunker, M.B., McLaughlin, F.A., Fowler, B.R., Brooks, G., Chiddell, G., Hamilton, C., Macdonald, R.W., 1992. Hydrocarbon determinations; Mackenzie River and Beaufort Sea. *Can. Data Rep. Hydrogr. Ocean Sci.* 9: 1-294.

Preliminary results of lateral transport of carbon in relation to active thermokarst sources in Central Yakutia (Eastern Siberia)

Christine Hatté[1], Antoine Séjourné[2,] Christophe Grenier[1], Christelle Marlin[2], Eric Pohl[1], Aurélie Noret[2], Caroline Gauthier[1], Laure Gandois[3], François Costard[2], Philippe Ciais[1], Catherine Ottlé[1], Albane Saintenoy[2], Alexander Fedorov[4], Pavel Konstantinov[4]

[1]*LSCE/IPSL – UMR 8212 (CEA/CNRS/UVSQ), Univ. Paris-Saclay, Gif sur Yvette, France, christine.hatte@lsce.ipsl.fr*
[2]*GEOPS/IPSL - UMR 8148 (UPS, CNRS), Univ. Paris-Saclay, Orsay, France*
3EcoLab - UMR 5245 (CNRS, UPS, INPT), Castanet Tolosan, France
[4]*Melnikov Permafrost Institute, Siberian Branch, Russian Academy of Sciences, Yakutsk, Russia*

Abstract

In the context of climate change, the high latitude regions with high carbon content and the presence of permafrost are especially of interest due to the perspective of positive future climate feedbacks associated with reinforced greenhouse gases emissions. However, these emissions are the atmospheric part of a more complex carbon evolution involving surface processes and lateral transport. The systems are characterized by a complex interplay of multi-scale processes (dynamical, chemical, biological) operating within different compartments (ground ice, frozen soil, hydrosphere, atmosphere) requiring intense site studies, followed by conceptualization and development of multi-dimensional modelling approaches. Our work aims to evaluate lateral transport (by water) in relation to active thermokarst sources (slumps and lakes) in a landscape unit representative of ice-rich permafrost in Central Yakutia. Preliminary results of carbon content of samples in soil (active layer and permafrost) and water (lakes, river, soil water in active layer and permafrost) are presented.

Keywords: Carbon; Transport; Arctic regions; Thermokarst; Geochemistry.

Introduction

Recent temperature increase in arctic and subarctic regions, where permafrost is present, is significantly higher than the average increase at the Earth scale and climatic simulations predict that those regions will continue to experience rapid and significant warming (IPCC, 2013). This rapid climatic change already shows clear impact on arctic regions geography, infrastructures and through carbon and water cycles, on the climate itself. The thawing of permafrost and the subsequent subsidence of the ground that is ubiquitous in these regions (i.e. thermokarst process) will spread and intensify (IPCC, 2013). On another hand, global carbon storage of terrestrial permafrost is estimated to 1,672 Pg of carbon. The carbon storage equivalent in the modern atmosphere and the estimated magnitude of the terrestrial permafrost-carbon feedback suggests that carbon releases could be in the range of 7 to 508 Pg by the year 2100.

However, present day representation of permafrost thawing in most models remains simplistic and one-dimensional. They assume that carbon is only released from the active layer of permafrost (i.e., the layer that thaws in summer and freezes in winter). These models exclude localized and abrupt releases of carbon, generated, for example, by erosion or thermokarst, deeply shaping the landscape. New regional research reveals that a large fraction of permafrost carbon is vulnerable to abrupt thaw occurring only at point locations (formation of lakes and slumps) but often causing permafrost thaw to occur deeper and more rapidly (e.g., Shuur *et al.*, 2015). Likewise, transport mechanisms between the sources of soil organic matter (SOM) and the surface waters draining the landscape also need to be incorporated into process-based models in order to understand patterns of dissolved organic carbon (DOC) accurately across space and time (Laudon *et al.*, 2011). Understanding this connection is of uttermost importance for future DOC predictions as climate change may lead to a larger proportion of accumulated organic carbon released into freshwater ecosystems (Frey et al., 2009). Furthermore, the diverse range of organic matter mineralization leading to different mineralization products from CO_2 to CH_4 is not well conceptualized, and is only at best empirically estimated and distributed.

The lateral transport within the water systems thus plays a major role requiring process characterization and parameter identification involving sediment transport and burial providing transitory carbon reservoirs (Vonk and Gustavsson, 2013).

The Syrdakh study site in Central Yakutia

The objective of the project's first phase is to focus on carbon fate involving the surface processes, while the second will consider atmospheric processes (Bouchard et al.; *present proceedings)*. The aim is to evaluate lateral transport (by water) in relation to active thermokarst sources (slumps and lakes) in a landscape unit representative of ice-rich permafrost. The main challenges to be met are: 1) constrain poorly studied organic carbon transport from localized thawing, 2) quantify the organic carbon but also classify the quality of organic matter according to the evolution degree of the sedimentological environment, 3) study the spatial and temporal heterogeneity of a larger portion of the landscape (several km),

A study region in Central Yakutia (eastern Siberia, Fig. 1A) has been selected for its representativeness as a 'natural laboratory', its relatively small scale and its heterogeneity. The chosen region is composed of ice-rich sediment of 70-80% of ice by volume (Yedoma). Thermokarst lakes, thaw slumps and river-valley thermal imprint are being monitored since 2011 (Séjourné *et al.*, 2015; Grenier *et al.*, accepted). The studied area is composed of a small river connected with different thermokarst lakes (Holocene and modern age; Fig. 1B and C).

During August and September 2017 field surveys, water from lakes and river were collected for elemental and isotopes analysis (^{2}H, ^{18}O) and characterization of particulate organic carbon and dissolved inorganic carbon (^{13}C, ^{14}C dating). Physico-chemistry parameters (temperature, pH, conductivity and CID) were measured for all water bodies. Similarly, permafrost and active-layer were sampled to analyze inorganic carbon content. Lake water and groundwater were sampled to understand their origin (e.g., mixtures, evaporation) from geochemical analyses (water stable isotopes and chemical composition of major elements). The lake and river-valley continuum (Fig. 1B) has been studied from 2012 from a thermal and hydro(geo)logical perspective including soil properties and GIS (Pohl *et al.*, *present proceedings)*. Current thermokarst evolution is monitored since 2013 (lake and thaw slump, Fig. 1C) with thermal sensors, water level sensors, topographic survey, GPR and ERT survey (Saintenoy *et al.*; Séjourné *et al., present proceedings*).

Acknowledgments

The support of Univ. Paris-Saclay SPU Carbon Fate Emerging Project and Labex-IPSL are gratefully acknowledged.

References

Frey K.E. & McClelland J.W. *Impacts of permafrost degradation on arctic river biogeochemistry*. Hydrological Processes, 2009, Volume 23, Issue 1.

Grenier C., et al. *Ground thermal impact of a small Alas Valley river in Syrdakh (Central Yakutia) in a continuous permafrost area - a comparative study of monitoring and 1D numerical analysis.* Accepted PPP.

Laudon, H., et al. *Patterns and Dynamics of Dissolved Organic Carbon (DOC) in Boreal Streams: The Role of Processes, Connectivity, and Scaling.* Ecosystems (2011) 14: 880.

Schuur E. A. G., et al. *Climate change and the permafrost carbon feedback.* Nature, 9 2015.

Séjourné A., et al. *Evolution of the banks of thermokarst lakes in Central Yakutia (Central Siberia) due to retrogressive thaw slump activity controlled by insolation.* Geomorphology 241 (34-40).

Vonk, J. & Gustafsson, Ö. *Permafrost-carbon complexities.* Nature Geoscience, Vol. 6, Sept. 2013.

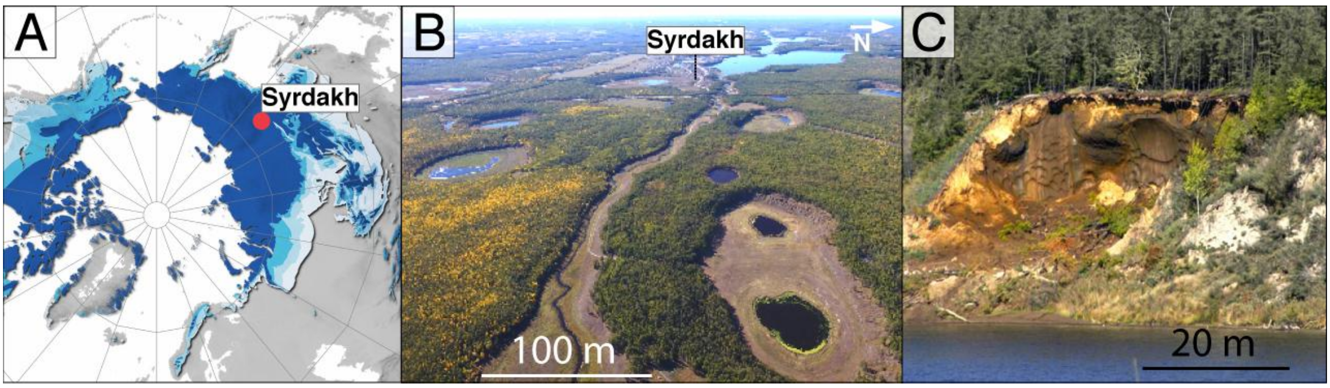

Figure 1: (A) Studied region in Central Yakutia (eastern Siberia), (B) composed of typical regional thermokarst landscape units (lake, river, forest, meadow) in an ice-rich permafrost area, (C) with zones of thaw slumps.

Local variability of mineral element distribution in permafrost terrain: implications upon thawing

Catherine Hirst[1]
Sophie Opfergelt[1]
Béatrice Lefebvre[1]
Nathan Bertouille[1]
Peter Kuhry[2]
Juri Palmtag[2]
[1]*Earth and Life Institute, Université catholique de Louvain, Louvain-la-Neuve, Belgium, sophie.opfergelt@uclouvain.be*
[2]*Department of Physical Geography, Stockholm University, Stockholm, Sweden*

Abstract

In addition to exposing organic matter to decomposition, the thawing of permafrost also exposes mineral constituents to water. To evaluate the potential to create mineral nutrient hotspots upon thawing, there is a need to better assess the local variability of mineral element distribution in permafrost terrain. Using sites in Greenland and Siberia as case studies, this study investigates the spatial variability of the soil mineral reserve, i.e. the total elemental content and the exchangeable cations, at the site scale as a function of depth. The results suggest that the lithology, the type of deposits and the topography are main factors controlling the variability of the mineral element distribution in permafrost at the site scale and between sites. These preliminary data highlight the need to account for local variability in mineral reserve, a step to improve our capacity to predict the influence of mineral nutrients on the permafrost carbon feedback.

Keywords: mineral constituents; mineral reserve; thawing permafrost; Greenland; Siberia

Introduction

In the context of thawing permafrost, there is understandably a huge ongoing effort to assess the soil organic carbon (SOC) storage and carbon emissions from permafrost regions known as the permafrost carbon feedback (Schuur *et al.*, 2015). In contrast, little attention has been paid to the mineral constituents which are increasingly exposed to weathering reactions in response to permafrost thawing and deepening of the active layer. Unlocking a frozen reservoir of mineral nutrients may boost biological activity (Jansson & Tas, 2014), thereby modifying the balance between carbon input and output in the thawing permafrost. Accurately predicting the impact of global warming on the fate of organic carbon in permafrost requires quantifying the mineral element reserve in permafrost, and assessing its local variability. More specifically, what is the role of lithology, sediment type and topography on the mineral element reserve at the site scale? This study provides preliminary data from two Arctic regions, Greenland and Siberia, to contribute towards answering this question.

Study sites

Archived permafrost samples, previously collected to study SOC storage (Palmtag *et al.*, 2015), were characterized for their mineral element content, including soil profiles from Zackenberg, Greenland and from Cherskiy and Shalaurovo, Siberia. A total of 101 soil samples are involved in this study including active layer and permafrost.

Results and discussion

The total mineral reserve

The Total Reserve in Bases (TRB = total content [Ca + Mg + K + Na] measured by ICP-AES after alkaline fusion) ranges between 235 and 572 $cmol_c.kg^{-1}$ in permafrost soils from Zackenberg (Fig.1), and between 163 and 254 $cmol_c.kg^{-1}$ in those from Cherskiy/Shalaurovo, being generally dominated by Mg, followed by Ca. The large range of TRB values can be explained by the heterogeneity of the sediment types (in Zackenberg, glacial, alluvial and deltaic in the valley and boulder fields at higher elevation; loess-derived in Shalaurovo and colluvial in Cherskiy) and the contribution from various lithologies (gneiss, granite and basalt in Zackenberg and diorite in Cherskiy; e.g., a contribution from basalt explains the high TRB value in profile Z2-11 in Fig.1).

With the aim to investigate the implications upon thawing, data from the active layer were compared with the upper permafrost layer from the same profile. Preliminary data indicate an increase in TRB values in the permafrost relative to active layer in sites derived from deltaic deposits in Zackenberg valley, but no increase in sites with boulder fields at higher elevation. This observation is verified in the Siberian sites with an increase of the TRB values in the permafrost relative to the active layer in the loess-derived deposits from Shalaurovo, but no increase in ridge crest sites from Cherskiy.

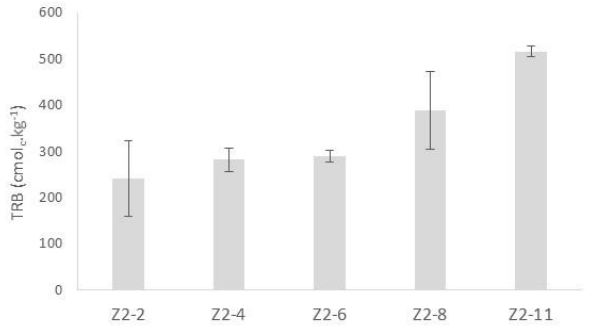

Figure 1. Evolution of the Total Reserve in Bases (TRB = $[Ca+Mg+Na+K]_{total}$) in five soil profiles from the transect Z2 in Zackenberg (transect described in Palmtag *et al.*, 2015).

The exchangeable mineral reserve

The soil cation exchange capacity (CEC, measured by by percolation with ammonium acetate 1 M at pH 7, reflecting the amount of negative charges available on organic matter and clay minerals potentially available to retain cations) ranges between 2 and 21 $cmol_c.kg^{-1}$ in permafrost terrain from Zackenberg, and 9 and 27 $cmol_c.kg^{-1}$ in those from Cherskiy/Shalaurovo, and is mainly controlled by SOC content ($R^2 = 0.75$).

The exchangeable cations are generally dominated by Ca, followed by Mg. Interestingly, the sum of the exchangeable cations is similar in Zackenberg and Cherskiy permafrost soils (11±4 and 12±1 $cmol_c.kg^{-1}$) and lower in those from Shalaurovo (6±2 $cmol_c.kg^{-1}$). The occupation of the soil exchange complex by the exchangeable cations is expressed by the Base Saturation (BS = ratio of the sum of exchangeable bases $[Ca_{exch} + K_{exch} + Mg_{exch} + Na_{exch}]$ to CEC). In this case, the BS is lower in Shalaurovo (45%) than in other soils (88% in Zackenberg, 83% in Cherskiy). The potential implication is that a higher exchangeable cation reserve would be available from Zackenberg and Cherskiy permafrost soils relative to Shalaurovo upon thawing, and these major elements would be directly available nutrients for plant uptake and microbial activity. However, the presence of carbonates in Zackenberg, confirmed by XRD, should be considered, as it likely contributes to overestimate the exchangeable Ca content.

Conclusion

Measurements at the site scale of the total mineral reserve and the exchangeable mineral reserve in permafrost soils from two main Arctic regions, Greenland and Siberia, indicate that local variability of lithology, types of deposits and topography should be considered carefully to assess the spatial variability of the mineral element reserve in permafrost terrain and the implications upon thawing. Similar measurements should be collected in different environments to better assess the controlling factors of variability, and hence contribute towards identifying areas with a potential to create mineral nutrient hotspots upon thawing, given the implications for the carbon balance.

Acknowledgments

The research is funded by the European Research Council (ERC) under the European Union's Horizon 2020 research and innovation programme (ERC Starting Grant, WeThaw, grant agreement n°714617 to S.O.). S.O. acknowledges funding from the Fonds National de la Recherche Scientifique (FNRS, Belgium, FC69480). The collection of soil profiles in Zackenberg and NE Siberia was financed by grants of the Swedish Research Council and the ESF CryoCARB project to P.K.

References

Jansson, J. K. & Tas, N., 2014. The microbial ecology of permafrost. *Nature Reviews Microbiology* 12: 414-425.

Palmtag, J. Hugelius, G. Lashchinskiy, N. Tamstorf, M. P. Richter, A. Elberling, B. Kuhry, P., 2015. Storage, landscape distribution, and burial history of soil organic matter in contrasting areas of continuous permafrost. *Arctic, Antarctic and Alpine Research* 47: 71-88.

Schuur, E. A. G. McGuire, A. D. Schädel, C. Grosse, G. Harden, J. W. Hayes, D. J., et al., 2015. Climate change and the permafrost carbon feedback. *Nature* 520: 171-179.

Composition and fate of permafrost organic carbon in the Arctic nearshore zone of Yukon, Canada

Dirk Jong[1]
George Tanski[2,3]
Lisa Bröder[1]
Hugues Lantuit[2]
Negar Haghipour[4]
Timothy Eglinton[4]
Jorien Vonk[1]

[1] Department of Earth Sciences, Vrije Universiteit Amsterdam, The Netherlands, d.j.jong@vu.nl
[2] Department of Periglacial Research, Alfred Wegener Institute, Helmholtz Centre for Polar and Marine Research, Potsdam, Germany
[3] German Research Centre for Geosciences (GFZ), Helmholtz Centre Potsdam, Potsdam, Germany
[4] Department of Earth Sciences, Swiss Federal Institute of Technology, Zürich, Switzerland

Abstract

Coastal permafrost thaw releases significant amounts of organic carbon (OC) into the nearshore zone. Degradation of this OC makes the Arctic nearshore zone a potential source of CO_2 to the atmosphere. The precise pathways of transport and degradation of particulate organic carbon (POC) from coastal permafrost erosion is however largely unknown. We collected POC and sediment samples at the Yukon Coast on multiple transects from thawing coastal permafrost to nearshore sediments, with the goal to trace the fate of POC from thawing permafrost in the coastal environment. Initial data suggest that the shallow nearshore zone plays an important role in the degradation process of this POC. Further sedimentological and geochemical results on these transects off actively eroding thaw-slumps will be presented, to shed more light on potential carbon-climate impacts of eroding permafrost coasts.

Keywords: Nearshore, Sediments, Coastal Erosion, Particulate Organic Carbon, Degradation, Pathways

Introduction

Erosion of permafrost coasts in the Arctic releases significant amounts of organic carbon (OC) into the nearshore zone, estimated up to 14 Tg yr^{-1} (Vonk *et al.*, 2012; Wegner *et al.*, 2015). Abrupt permafrost thaw, in the form of block failure at coastal bluffs or retrogressive thaw slumps (RTS) at the coast, are prominent features in Arctic coastal landscapes. The OC released from this abruptly thawing permafrost can be (1) remineralised and released as greenhouse gases carbon dioxide (CO_2) and methane (CH_4) to the atmosphere, (2) buried in nearshore sediments, or (3) transported further offshore. With the increase of Arctic coastal erosion, related to an extended open water season (Lantuit & Pollard, 2008; Overeem *et al.*, 2011), and the potential climate impact of thawing permafrost (Schuur *et al.*, 2015) it is important to quantify the transport and degradation processes of permafrost OC in the nearshore zone. Previous studies show that the dissolved fraction of OC (DOC) is highly susceptible to degradation in the water column (Vonk *et al.*, 2013). However, the degradability and transport mechanisms of the far more abundant particulate OC fraction (POC) are less well known (Tanski *et al.,* 2016). Our objective is to trace the fate of thawing permafrost POC and to quantify the transportation and degradation processes on a local scale in the nearshore zone of Yukon, Canada.

Methods

In the summer of 2017, we sampled suspended particulate matter and sediments along transects perpendicular to the coast of Herschel Island – *Qikiqtaruk* (Yukon, Canada). Sampling started at retrogressive thaw slumps onshore to approximately 700 m offshore, covering the source of the OC and its path in the nearshore zone. We measured total suspended solids (TSS) in thaw streams and sea water, and we measured mineral surface area of terrestrial and marine sediments. Additionally, we will present results of geochemical analyses on a bulk (Total Organic Carbon (TOC), $\delta^{13}C$, $\Delta^{14}C$) and molecular level (lipid biomarkers) of the sediment and the suspended particulate matter samples.

Initial Results and Discussion

Initial results on TSS concentrations and mineral surface area of sediments and TSS show that the highest TSS concentrations are found within 300 m from the shore, ranging from 100 – 1100 mg L^{-1} (n=7), compared to concentrations of around 25 – 30 mg L^{-1} (n=31) further offshore. The mineral surface area of marine sediments is lowest in the first 300 m off the coast (around 3 m^2 g^{-1} ; n=8) and increases further offshore to 9 – 17 m^2 g^{-1} (n=5). Samples from land (thaw streams, mud deposits and mud pools) have a much larger surface area (25 – 30 m^2 g^{-1}; n=5) than nearshore marine sediment. Resuspension of material by wave action was frequently observed, with sediment plumes forming offshore.

The initial results suggest that most of the finer particles with high mineral surface area remain suspended in the water column of the nearshore zone. This fraction of particles is important for the transport and degradation processes of OC, since it has a large surface area for adsorption of OC (Tesi *et al.*, 2016). In combination with high concentrations of TSS nearshore and frequent resuspension of material, this suggests that the shallow nearshore zone plays an important role in the degradation process of permafrost OC. Further geochemical analyses (TOC, $\delta^{13}C$, $\Delta^{14}C$, lipid biomarkers) on the samples will be performed to reveal to what extent the POC is degraded, where it is coming from (permafrost, recent vegetation or marine) and where it is transported. By coupling source (thaw slump OC) to sink (coastal waters and sediments) with a targeted approach on a local scale, we aim to resolve and quantify the various pathways of permafrost OC in the nearshore zone.

Acknowledgments

This project is funded through a European Research Council starting grant to J. Vonk (THAWSOME #676982) and Helmholtz Young Investigator's group "COPER" grant VH-NG-801 to H. Lantuit.

We want to thank the rangers of the *Qikiqtaruk* – Herschel Island Territorial Park for their support in the field, and the Aurora Research Institute in Inuvik for their support on logistics. We thank Dyke Scheidemann for processing the POC samples in the field, and Konstantin Klein and Kirsi Keskitalo for their help during sampling and with fieldwork preparations.

References

Fritz, M., Vonk, J. E., & Lantuit, H. (2017). Collapsing Arctic coastlines. *Nature Climate Change*, 7(1), 6-7.

Lantuit, H., & Pollard, W. H. (2008). Fifty years of coastal erosion and retrogressive thaw slump activity on Herschel Island, southern Beaufort Sea, Yukon Territory, Canada. *Geomorphology*, 95(1), 84-102.

Overeem, I., Anderson, R. S., Wobus, C. W., Clow, G. D., Urban, F. E., & Matell, N. (2011). Sea ice loss enhances wave action at the Arctic coast. *Geophysical Research Letters*, 38(17).

Schuur, E. A. G., McGuire, A. D., Schädel, C., Grosse, G., Harden, J. W., Hayes, D. J., ... & Natali, S. M. (2015). Climate change and the permafrost carbon feedback. *Nature*, 520(7546), 171-179.

Tanski, G., Couture, N., Lantuit, H., Eulenburg, A., & Fritz, M. (2016). Eroding permafrost coasts release low amounts of dissolved organic carbon (DOC) from ground ice into the nearshore zone of the Arctic Ocean. *Global Biogeochemical Cycles*, 30(7), 1054-1068.

Tesi, T., Semiletov, I., Dudarev, O., Andersson, A., & Gustafsson, Ö. (2016). Matrix association effects on hydrodynamic sorting and degradation of terrestrial organic matter during cross shelf transport in the Laptev and East Siberian shelf seas. *Journal of Geophysical Research: Biogeosciences*, 121(3), 731-752.

Vonk, J. E., Sánchez-García, L., Van Dongen, B. E., Alling, V., Kosmach, D., Charkin, A., ... & Eglinton, T. I. (2012). Activation of old carbon by erosion of coastal and subsea permafrost in Arctic Siberia. *Nature*, *489*(7414), 137-140.

Vonk, J. E., Mann, P. J., Davydov, S., Davydova, A., Spencer, R. G., Schade, J., ... & Eglinton, T. I. (2013). High biolability of ancient permafrost carbon upon thaw. *Geophysical Research Letters*, 40(11), 2689-2693.

Wegner, C., Bennett, K. E., de Vernal, A., Forwick, M., Fritz, M., Heikkilä, M., ... & O'Regan, M. (2015). Variability in transport of terrigenous material on the shelves and the deep Arctic Ocean during the Holocene. *Polar Research,* 34(1), 24964.

Degradation and composition of particulate organic carbon released from retrogressive thaw slumps in the Canadian Arctic

Kirsi Keskitalo[1]
Lisa Bröder[1]
Sarah Shakil[2]
Scott Zolkos[2]
Suzanne Tank[2]
Bart van Dongen[3]
Negar Haghipour[4]
Timothy Eglinton[4]
Jorien Vonk[1]
[1]*Department of Earth Sciences, Vrije Universiteit, Amsterdam, Netherlands, k.h.keskitalo@vu.nl*
[2]*Department of Biological Sciences, University of Alberta, Edmonton, Canada*
[3]*School of Earth and Environmental Sciences, University of Manchester, Manchester, UK*
[4]*Department of Earth Sciences, Swiss Federal Institute of Technology, Zürich, Switzerland*

Abstract

Climate warming can induce thawing and remobilisation of permafrost carbon (PF-C) in the Arctic. The organic carbon (OC) stored in permafrost soils can end up in the atmosphere as greenhouse gases if the released OC is remineralised. Abrupt permafrost thaw causes rapid collapse of permafrost in the areas of high ground-ice content (i.e. thermokarst landscapes) causing remobilisation of large amounts of PF-C. Abrupt thaw events release PF-C mainly as particulate organic carbon (POC), yet the lability of POC to biological degradation is not known. The focus of this study is to quantify degradation rates of POC released from retrogressive thaw slumps on the Peel Plateau in the Canadian Arctic.

Keywords: Arctic; particulate organic carbon; Peel Plateau; permafrost; retrogressive thaw slump.

Introduction

In the Arctic regions the temperatures have been rising twice as fast as the global average during the last decades (IPCC 2013). Northern circumpolar permafrost soils, that store around 50% of the global belowground OC, are susceptible to thaw upon climate warming (Tarnocai et al. 2009). The possible remineralisation of released PF-C to the atmosphere as greenhouse gases (CO_2 and CH_4) can further enhance warming of the climate (IPCC 2013; Vonk & Gustafsson 2013).

Aside from gradual permafrost thaw (active-layer deepening), abruptly thawing permafrost sites are becoming more common (Segal et al. 2016; Schuur et al. 2015). These so called thermokarst landscapes (e.g. eroding coastlines and river banks, retrogressive thaw slumps) cause rapid collapse of ice-rich permafrost (Vonk et al. 2012). On the Canadian Peel Plateau abruptly thawing retrogressive thaw slumps have increased in size and numbers in the past decades due to rising temperatures and higher precipitation (Kokelj et al. 2015; Segal et al. 2016). The most recent estimate of yearly OC fluxes from slumping is $82.5*10^3$ kg yr^{-1} (Ramage et al. 2017). The material released is dominantly POC yet, we currently do not know to what extent the released POC is degraded (Guo et al. 2007). Regarding the amount of remobilised OC and warming temperatures in the Arctic regions, it is important to understand the fate of PF-C after its release to be able to better predict the climate impacts of these abruptly thawing permafrost sites.

Degradation rates of particulate organic carbon from retrogressive thaw slumps

To study the vulnerability of POC to degradation in permafrost thaw streams we incubated whole water samples (corrected for DOC degradation) collected from thaw streams on the Peel Plateau in constant turbulent flow system to mimic the ambient stream conditions

(Richardson et al. 2013). In addition to the degradation assessment through laboratory incubation, we estimated degradation during transport along a spatial transect. To better understand the degradation process, POC composition was assessed with carbon isotopes ($\Delta^{14}C$, $\delta^{13}C$), lipid biomarkers and pyrolytic techniques.

Acknowledgments

We want to thank the staff of Aurora Research Institute for their support and laboratory facilities. We also want to thank Erin MacDonald and Rosemin Nathoo for their help in the field as well as Georgina Neyando, Andrew Koe and Dempster Colin for wildlife monitoring. We are also grateful to Hugues Lantuit and George Tanski for their support in the field. This study was funded with an ERC Grant (THAWSOME #676982).

References

Guo, L., Ping, C.L. & Macdonald, R.W., 2007. Mobilization pathways of organic carbon from permafrost to arctic rivers in a changing climate. *Geophysical Research Letters*, 34:1–5.

IPCC, 2013. *Climate Change 2013: The Physical Science Basis. Contribution of Working Group I to the Fifth Assessment Report of the Intergovernmental Panel on Climate Change.* Stocker, T.F., Qin, D., Plattner, G.-K., Tignor, M., Allen, S.K., Boschung, J., Nauels, A., Xia, Y., Bex V. & Midgley, P.M. (Eds.). Cambridge University Press, 1535 pp.

Kokelj, S.V., Tunncliffe J., Lacelle D., Lantz T.C., Chin K.S. & Fraser R., 2015. Increased precipitation drives mega slump development and destabilization of ice-rich permafrost terrain , northwestern Canada. *Global and Planetary Change*, 129:56–68.

Ramage, J.L., Irrgang, A.M., Morgenstern, A. & Lantuit, H., 2017. Contribution of coastal retrogressive thaw slumps to the nearshore organic carbon budget along the Yukon Coast. *Biogeosciences Discussions*. (in review).

Richardson, D.C., Newbold, J.D., Aufdenkampe, A.K., Taylor, P.G. & Kaplan, L.A., 2013. Measuring heterotrophic respiration rates of suspended particulate organic carbon from stream ecosystems. *Limnology and Oceanography: Methods*, 11:247–261.

Schuur, E.A.G., McGuire, A.D., Schädel, C., Grosse, G., Harden, J.W., Hayes, D.J., Hugelius, G., Koven, C.D., Kuhry, P., Lawrence, D.M., Natali, S.M., Olefeldt, D., Romanovsky, V.E., Schaefer, K., Turetsky, M.R., Treat, C.C. & Vonk, J.E., 2015. Climate change and the permafrost carbon feedback. *Nature*, 520:171–179.

Segal, R.A., Lantz, T.C. & Kokelj, S.V, 2016. Acceleration of thaw slump activity in glaciated landscapes of the Western Canadian Arctic Acceleration of thaw slump activity in glaciated landscapes of the Western Canadian Arctic. *Environmental Research Letters*, 11:1–12.

Tarnocai, C., Canadel, J.G., Schuur, E.A.G., Kuhry, P., Mazhitova, G. & Zimov, S., 2009. Soil organic carbon pools in the northern circumpolar permafrost region. *Global biogeochemical cycles*, 23:1–11.

Vonk, J.E., Sánchez-García, L., van Dongen, B.E., Alling, V., Kosmach, D., Charkin, A., Semiletov, I.P., Dudarev, O.V., Shakova, N., Roos, P., Eglinton, T.I., Andersson, A. & Gustafsson, Ö., 2012. Activation of old carbon by erosion of coastal and subsea permafrost in Arctic Siberia. *Nature*, 489:137–140.

Vonk, J.E. & Gustafsson, Ö., 2013. Permafrost-carbon complexities. *Nature Geoscience*, 6:675–676.

Acceleration of thermokarst alters the nature of terrestrial-aquatic linkages in glaciated permafrost terrain, western Arctic Canada.

Steve V. Kokelj[1], Jon Tunnicliffe[2], Jurjen van der Sluijs[3], Ashley Rudy[4], Robert Fraser[5], Scott Lamoureux[6], Denis Lacelle[7], Suzanne Tank[8], Sarah Shakil[8], Scott Zolkos[8], Trevor Lantz[9], Justin Kokoszka[9]

[1]*Northwest Territories Geological Survey, Government of the Northwest Territories, Yellowknife, NWT, Canada; steve_kokelj@gov.nt.ca*

[2]*School of Environment, University of Auckland, Auckland, New Zealand*

[3]*Northwest Territories Centre for Geomatics, Government of the Northwest Territories, Yellowknife, NWT, Canada*

[4]*Department of Geography, Wilfrid Laurier University, Kitchener-Waterloo, Canada*

[5]*Canada Centre for Mapping and Earth Observation, NRCan, Ottawa, Ontario, Canada*

[6]*Department of Geography, Queen's University, Kingston, Ontario, Canada*

[7]*Department of Geography, University of Ottawa, Ottawa, Ontario, Canada*

[8]*Department of Biological Sciences, University of Alberta, Edmonton, Alberta, Canada*

[9]*School of Environmental Studies, University of Victoria, Victoria, BC, Canada*

[10]*Department of Geography, Simon Fraser University, Vancouver, BC, Canada*

Abstract

An increase in the intensity of thaw slump activity is reconfiguring landscapes and altering linkages between terrestrial and aquatic systems across western Arctic, Canada. The continental distribution of slump-affected terrain reflects glacial extents and recessional positions of the Laurentide Ice Sheet. The high Arctic tundra has shown to be most sensitive to change, highlighting the influence of geological legacy and climate history on permafrost terrain sensitivity. These glaciated landscapes, maintained in a quasi-stable state throughout much of the late Holocene are transforming by climate-driven thaw. Thermokarst is converting upland sedimentary stores into major source areas, flattening topography and infilling valleys with debris deposits tens of meters thick. Emerging processes and feedbacks measured by UAV-derived digital terrain models and remote sensing imagery illustrate non-linear trajectories of change. Integration of field and mapping methods provides insight into the pathways and magnitudes of sedimentary and geochemical fluxes from terrestrial to downstream environments.

Keywords: geochemistry, ground ice, permafrost, thaw slump, thermokarst,

Introduction

Thermokarst is the fundamental mechanism of landscape change and driver of downstream effects in a warming circumpolar world. In this paper we highlight the influence of glacial and climate legacy on determining the state of permafrost and terrain sensitivity. We summarize research documenting the increase in thermokarst activity across northwestern Canada with focus on the processes and feedbacks of thaw slump activity in fluvially-incised landscapes and the downstream effects. We summarize ongoing research with focus on the distribution of thaw slump activity, evaluating the influence of thermokarst on landscape evolution and on the fine to broad-scale linkages in sediment and geochemical transfer from slopes to downstream systems, including fluvial, lacustrine and marine environments.

Research design

To examine the spatial distribution of thermokarst, its geological and climate linkages and the downstream effects this research has involved a diverse group of scientists with expertise in permafrost, geomorphology, geochemistry, sedimentology, ecology and remote sensing. General approaches included field-based permafrost, soil and surface water sampling, remote sensing, field survey and statistical modeling. Papers referenced in the extended abstract provide complete descriptions of research methods and links to related research.

Summary and highlights

Thaw slumping is a dynamic geomorphic process that can thaw thick layers of ice-rich permafrost, transfer large volumes of slope materials to downstream environments and alter landscape configuration (Fig. 1). In northwestern Canada, permafrost has preserved relict ice and glacigenic sediments, delaying a sequence of post-glacial landscape change that transformed temperate environments millennial earlier (Kokelj *et al.*, 2017). The broad-scale distribution of slump-affected terrain reflects glacial extents and recessional positions of the Laurentide Ice Sheet. Climate-driven acceleration of thaw slump activity (Segal *et al.*, 2016) is mobilizing large volumes of materials (Kokelj *et al.*, 2015), altering downstream sedimentary and geochemical regimes (Littlefair *et al.*, 2017; Rudy *et al.*, 2017), impacting water quality across a range of watershed scales. The most significant thermokarst landscape changes appear to be affecting cold, tundra environments where relict ice has been well-preserved and geomorphic potential for climate-drive thaw remains high (Segal *et al.*, 2016; Kokelj *et al.*, 2017; Rudy *et al.*, 2017).

Various remote sensing tools continue to be used that describe the distribution of thaw slumps and track change. Statistical modeling approaches that integrate landscape parameters associated with thaw slumping can improve prediction of occurrence. Future research also utilizes a range of remote sensing tools to describe the process and feedbacks contributing to the cascade of landscape and downstream effects, and to examine the influence of climate drivers on thaw slump evolution.

Large thaw slumps can displace millions of cubic metres of previously frozen material downslope, converting upland sedimentary stores into major source areas. Tracking aerial change in thaw slump disturbances provides only partial insight into landscape change and downstream impacts. The development of high-resolution digital terrain models and estimating pre-disturbance terrain surfaces enables the volume displaced by thaw-slump development to be calculated. Preliminary analysis of these data in conjunction with observed changes in aerial extent of disturbances indicates the non-linear trajectories of thaw-driven landscape change and increasing magnitudes and diversity of downstream effects. Future focus on physically-based modeling of thaw slump development can provide insight into the trajectories of landscape change, and integrating field activities with mapping of fluvial linkages will help predict the cascade of effects across watershed scales.

Figure 1. Large retrogressive thaw slump on Peel Plateau showing original disturbance feature (slump and headwall) which has grown to drain lake (rear right), vegetated upper debris tongue, upstream debris-dammed lake, secondary slumps on left side of valley, debris tongue and valley fill and valley-side erosion in foreground right.

References

Kokelj *et al.*, 2017. Climate-driven thaw of permafrost preserved glacial landscapes, northwestern Canada. *Geology* 45:371-374.

Kokelj *et al.*, 2015. Increased precipitation drives mega slump development and destabilization of ice-rich permafrost terrain, northwestern Canada. *Global and Planetary Change* 129: 56-68.

Littlefair *et al.*, 2017. Retrogressive thaw slumps temper dissolved organic carbon delivery to streams of the Peel Plateau, NWT, Canada. *Biogeosciences* 14: 5487-5505.

Rudy *et al.*, 2017. Accelerating thermokarst transforms ice-cored terrain triggering a downstream cascade to the ocean. *Geophysical Research Letters*, 44.

Segal *et al.*, 2016. Acceleration of thaw slump activity in glaciated landscapes of the western Canadian Arctic. *Environmental Research Letters*, 11.

NUNATARYUK: Permafrost thaw and the changing Arctic coast. Science for socio-economic adaptation

Hugues Lantuit[1,2]
Pier Paul Overduin[1]
Michel Fritz[1]
Leena-Kaisa Viitanen[1]

[1]*Alfred Wegener Institute Helmholtz Centre for Polar and Marine Research, Germany, Hugues.Lantuit@awi.de*
[2]*University of Potsdam, Germany*

Abstract

NUNATARYUK is a H2020 project that investigates the impacts of thawing coastal and subsea permafrost on the global climate, and develops targeted and co-designed adaptation and mitigation strategies for the Arctic coastal population

Keywords: Permafrost, Climate Change, Impacts, Coast, Community engagement

Introduction

Most human activity in the Arctic takes place along permafrost coasts. These coasts have become one of the most dynamic ecosystems on Earth because permafrost thaw is now exposing them to rapid change: change that threatens the rich biodiversity, puts pressure on communities that live there and contributes to the vulnerability of the global climate system.

The project

Aims

NUNATARYUK is a H2020 project that investigates the impacts of thawing coastal and subsea permafrost on the global climate and develops targeted and co-designed adaptation and mitigation strategies for the Arctic coastal population. NUNATARYUK brings together world-leading specialists in natural science and socio-economics to:

(1) develop quantitative understanding of the fluxes and fates of organic matter released from thawing coastal and subsea permafrost;

(2) assess what risks are posed by thawing coastal permafrost, to infrastructure, indigenous and local communities and people's health, and from pollution;

(3) use this understanding to estimate the long-term impacts of permafrost thaw on global climate and the economy.

Key numbers

NUNATARYUK involves 28 partners in 12 different countries. It is funded with 11.5 M€ for the 2017-2022 period. It is focused on three focal areas in the Arctic: The East Siberia Area, the Nordic Area (Greenland and Svalbard) and the Beaufort Sea Area. NUNATARYUK is guided by a Stakeholders' Forum of representatives from Arctic coastal communities and indigenous societies, which will create a legacy of collaborative community involvement and a mechanism for developing and applying innovative evidence-based interventions to enable the sustainable development of the Arctic.

Spatial variability of soil properties and their relationship with surrounding wetland ecosystems: a day in the life of permafrost peatland

G. Matyshak [1]
O. Goncharova[1]
A. Bobrik[1]
M. Tarkhov[1]
N. Petrzhik[1]
A. Sefilian[1]
D. Petrov[1]
M. Timofeeva[1]
I. Ryzhova[1]
A. Gravis[2]

[1]*Soil science department, Lomonosov Moscow State University, Russia, matyshak@gmail.com*
[2]*Earth Cryosphere Institute, Siberian Branch of Russian Academy of Sciences, Tyumen, Russia*

Abstract

In the north of Western Siberia (Russia), the soil properties of the one permafrost peatland were studied. It was established that most of the parameters vary widely and can differ by more than two times on this small peatland. It was established that the boundary between the peatland and wetland is a "hot spot". In this part, maximum active layer, soil temperature and moisture, and CO_2 emission were observed.

Keywords: Permafrost peatlands, cryogenic soils, carbon balance, climate change, mineralization of organic matter, soil biological activity

Introduction

Northern ecosystems are a particularly important component of global cycles of carbon and nitrogen on the planet (Natali *et al.*, 2011; Schuur *et al.*, 2008). Although climate change is expected to lead to permafrost thawing and an increase in greenhouse gas fluxes between soils and the atmosphere (Koven *et al.*, 2011), the factors governing the decomposition and transport of organic matter in the active layer have not been adequately studied (Walz *et al.*, 2017). This is especially true for peat soils in the North, since they contain up to 20% of the total carbon stock in the Earth's soils (Lal, 2008).

The aim of this work is to study the variation of soil properties within one isolated permafrost peatland and its influence on surrounding ecosystems. The tasks were to determine the range of values of soil properties within one peatland, to reveal the influence of factors and to estimate the influence of peatland on the surrounding wetland ecosystems (bogs).

The research area is located in the discontinuous permafrost zone in the northern taiga of Western Siberia, Russia (Yamalo-Nenets autonomous district (N65º18'53.2" E72º 52 '52.1"). The object of this study is a small permafrost peatland, which is a typical landscape for this area. It is 1 m high above the surrounding bog, about 30 m in diameter. It is flat with a slight slope and abrupt edge to the bogs. Typical vegetation is various lichens and mosses (*Cladonia* sp., *Sphagnum* sp.), dwarf birch (*Betula nana*), *Ledum palustre*; sedge (*Carex* sp.). The average thickness of peat is 30 cm (10 to 60 cm). The most common are peat soils.

Methods

In August 2016 and 2017, the interrelationships of vegetation, active layer depth, relief, soil temperature and moisture (0-10 cm.), CO_2 fluxes, and DOC (dissolved organic carbon) content were analyzed. Peatland was divided into 3 parts: central, middle and edge. All parameters were studied every 1 m in different directions from the center to the edge in replications.

Results

August 2016 and 2017 differed in air temperatures (more than two times). Therefore, the active layer was on average 60 cm in 2016 and 32 cm in 2017. The minimum values were at the middle part of the peatland, and the maximum thawing was in the center and on the edge. The minimum soil temperatures (0-10 cm) were observed in the middle part of the peat bog, maximum in the edge (2.3°C - 6.3°C) and (5.1°C - 9.8°C), respectively. The soil moisture significantly increased from the central part (25-42%) to the edge (42-61%). From the center to the edge of the peatland, the proportion of grasses and shrubs grows, while mosses and lichens cover does not change. The active layer thickness, soil moisture and temperature are weakly related to vegetation and are determined by a complex of factors. The most interesting is the dynamics of soils biological activity. The maximum of CO_2 emission was observed at the edge of the peatland, at the boundary with the bogs (1.5-2 times higher than on the other parts of the peatland). We assume that such variation in CO_2 emissions is due to its lateral transport in the soil and active degasation at the boundary with the bog. A maximum soil temperature and moisture and a minimum CO_2 emission were at wetland ecosystems. However, the soils of bogs have the maximum values of DOC, which significantly exceed DOC in soil of the peatland - 31100 ± 2200 mg C / kg soil and 1400 ± 300 mg C / kg soil, respectively. This is due to the low biological activity of the bogs soils and the lateral transfer of organic matter from the peatland soils. Thus, we observe a wide range of soil properties on isolated small permafrost peatland, the variation of these properties depends on its size, relief and shape. Permafrost contributes to the lateral redistribution of carbon fluxes and this determines a significant increase in CO2 emissions and the DOC concentration at the boundary of the bog and peatland.

References

Koven, C.D., Ringeval, B., Friedlingstein, P., Ciais, P., Cadule, P., Khvorostyanov, D., Krinner, G. & Tarnocai, C., 2011. Permafrost carbon-climate feedbacks accelerate global warming. *Proceedings of the National Academy of Sciences* 108: 14769-14774.

Lal, R., 2008. Carbon sequestration. *Philosophical Transactions of the Royal Society B*, 363: 815–830.

Natali, S.M., Schuur, E.A.G., Trucco, C., Pries, C.E.H., Crummer, K.G. & Lopez, A.F.B., 2011. Effects of experimental warming of air, soil and permafrost on carbon balance in Alaskan tundra. *Global Change Biology* 17: 1394-1407.

Schuur, E.A.G., Bockheim, J., Canadell, J.G., Euskirchen, E., Field, C.B., Goryachkin, S.V., Hagemann, S., Kuhry, P., Lafleur, P.M., Lee, H., Mazhitova, G.,Nelson, F.E., Rinke, A., Romanovsky, V.E., Shiklomanov, N., Tarnocai, C.,Venevsky, S., Vogel, J.G. & Zimov, S.A., 2008. Vulnerability of Permafrost carbon to climate change: implications for the global carbon cycle. *Bioscience* 58: 701-714.

Walz, J., Knoblauch, C., Böhme, L. & Pfeiffer, E-M., 2017. Regulation of soil organic matter decomposition in permafrost-affected Siberian tundra soils - Impact of oxygen availability, freezing and thawing, temperature, and labile organic matter. *Soil Biology and Biochemistry* 110: 34-43.

DOC export from Yedoma to rivers via thermo-erosional gullies and valleys in the Siberian Lena Delta

Anne Morgenstern[1], Birgit Heim[1], Olga Bobrova[2], Julia Boike[1], Antonina Chetverova[2, 3], Antje Eulenburg[1], Irina Fedorova[2], Janet Rethemeyer[4], Tatyana Skorospekhova[3], Lydia Stolpmann[1, 5], Paul Overduin[1]

[1]*Alfred Wegener Institute Helmholtz Centre for Polar and Marine Research, Potsdam, Germany, Anne.Morgenstern@awi.de*
[2]*St. Petersburg State University, St. Petersburg, Russia*
[3]*Arctic and Antarctic Research Institute, St. Petersburg, Russia*
[4]*University of Cologne, Cologne, Germany*
[5]*University of Potsdam, Potsdam, Germany*

Abstract

Thermo-erosional gullies, valleys and valley networks link inland permafrost catchments to rivers and coasts. The streams draining the catchments transport particulate and dissolved matter along these thermo-erosional landforms. In the ice and organic carbon-rich Yedoma-type Ice Complex deposits, thermo-erosional landforms are widespread and characteristic landscape elements. In this study, we investigate the relationship between stream water hydrogeochemistry (dissolved organic carbon, DOC) and geomorphological characteristics of and processes in the associated thermo-erosional landforms in the Lena Delta Yedoma deposits. Our preliminary results indicate higher DOC concentrations in stream waters affected by active thermal erosion than in surface waters running through stable valley systems, while thermokarst lakes in the drainage pathway act as DOC-reducing landscape components along the transport route.

Keywords: permafrost degradation; dissolved organic carbon (DOC); hydrogeochemistry; thermal erosion; Yedoma; Ice Complex

Introduction

The vulnerability of ice-rich permafrost deposits of the Yedoma type (Ice Complex) to thaw, in combination with its high labile organic matter stocks, make the degradation of these deposits a central component of the permafrost-carbon feedback under a warming climate. Mobilization of the carbon occurs via thawing, mineralization in situ and release into first order streams. Carbon is transformed after thaw and during transport.

Thermo-erosional landforms (valleys, gullies) and their associated streams are the main connecting pathways between inland permafrost areas and rivers and coasts. Surface and ground waters are routed along these streams, which transport particulate and dissolved matter from the catchments to the rivers and coastal waters. Regions of ice-rich permafrost, such as the Yedoma-type Ice Complex, are not only characterized by a high abundance of thermo-erosional landforms, which formed during the Holocene, but are subject to extensive degradation under current arctic warming by processes such as thermal erosion, thermokarst, and active layer deepening. Further thaw affects the morphology of thermo-erosional landforms, further impacting carbon transport and transformation in an interplay that requires more investigation.

In the Siberian Lena River Delta Yedoma-type Ice Complex deposits occur on insular remnants of a Late-Pleistocene accumulation plain that was dissected by Lena River branches and degraded by thermal erosion and thermokarst during the Holocene. This region serves as suitable exemplary study area for estimating the contribution of 1) different permafrost degradation landforms to the export of water and dissolved matter from Yedoma-type Ice Complex to the river and 2) active degradation of old permafrost versus seasonal runoff from the surface and active layer.

Methods

In the summers of 2013, 2014, 2016 and 2017 we sampled surface and soil waters from streams and their watersheds in Yedoma-type Ice Complex landscapes of the Lena River Delta and analyzed them for a range of hydrogeochemical parameters including electrical conductivity (EC), dissolved organic carbon (DOC) and stable isotopic composition (δD, δ^{18}O). The sampling sites were spread over an east-west extent of about 150 km (Fig. 1) and are characterized by diverse geomorphological and hydrological situations in terms of distance to the river branches, catchment size, discharge, degree of thermo-erosional activity, and connection to other permafrost degradation landforms (thermokarst lakes and basins). Three key sites were sampled three and four times from June to September 2013 and 2014, respectively, in order to analyze intra-seasonal changes. Six DOC samples were ^{14}C AMS dated at University of Cologne, Germany.

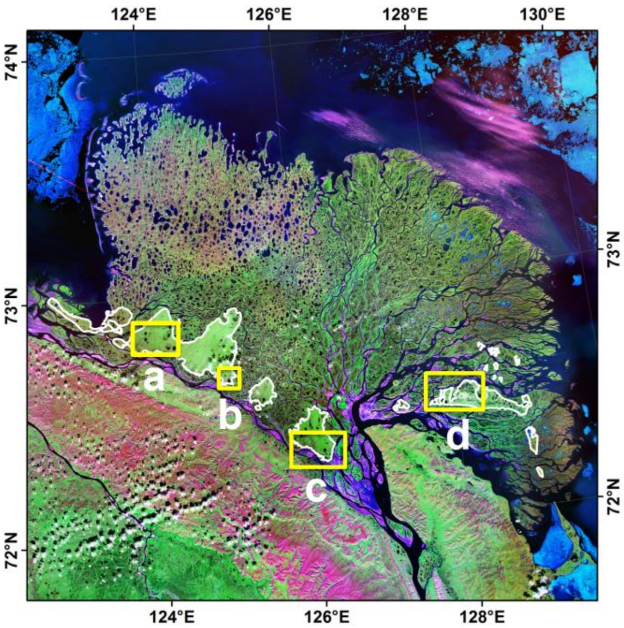

Figure 1. Sampling areas (yellow rectangles) in the Yedoma-type Ice Complex deposits (white outline) of the Lena River Delta: a) Khardang Island west, b) Khardang Island east, c) Kurungnakh Island, d) Sobo-Sise Island. (Landsat, GeoCover, 2000)

Results

The results show large variances in EC (25 to 1205 µS/cm), DOC concentrations (2.9 to 396.2 mg/l), δ18O (-29.8 to -14.6 ‰ vs. SMOW), and δD (-228.9 to -117.9 ‰ vs. SMOW) over the whole dataset, with distinct characteristics in the parameter combination for different degradation landform and water types. Highest values for DOC concentration and EC were measured for samples obtained from flow path systems related to eroding Ice Complex deposits and from Ice Complex pore waters. The temporal variability at the repeatedly sampled sites is low, which implies that there is not much change in the processes that determine the water composition throughout the summer season. The radiocarbon ages range between 514 ± 38 and 9728 ± 68 years and suggest varying sources for DOC that include recent organic carbon and degrading late Pleistocene Ice Complex.

Acknowledgments

This study was supported by the Helmholtz Association through a grant (PD-003) awarded to Anne Morgenstern.

We wish to thank all colleagues, who supported our fieldwork and laboratory analyses.

The permafrost mineral reserve: identify potential mineral nutrient hotspots upon thawing

Sophie Opfergelt[1], Elisabeth Mauclet[1], Béatrice Lefebvre[1], Arthur Monhonval[1], Nathan Bertouille[1], Aubry Vandeuren[1], Benoit Pereira[1], Catherine Hirst[1], Peter Kuhry[2], Jens Strauss[3], Guido Grosse[3], Daniel J. Conley[4]
[1]*Earth and Life Institute, Université catholique de Louvain, Louvain-la-Neuve, Belgium, sophie.opfergelt@uclouvain.be*
[2]*Department of Physical Geography, Stockholm University, Stockholm, Sweden*
[3]*Alfred Wegener Institute Helmholtz Centre for Polar and Marine Research, Potsdam, Germany*
[4]*Department of Geology, Lund University, Lund, Sweden*

Abstract

The thawing of permafrost exposes organic matter to decomposition but also mineral constituents to water. To evaluate the potential to create mineral nutrients hotspots upon thawing, an inventory of the mineral element content and its local variability in permafrost terrain is needed. Based on measurements from major Arctic regions (Alaska, Greenland, Svalbard and Siberia), it is suggested that the mineral reserve in permafrost is firstly controlled by the local lithology. More specifically, the data highlight the potential for mineral nutrient hotspots to be generated upon thawing in soils derived from deltaic deposits, but not in thermokarst deposits. Finally, we suggest that portable X-ray fluorescence (pXRF) may present a quick and low-cost alternative to total digestion and ICP-AES measurements to build a mineral element inventory in permafrost terrain at a large spatial scale.

Keywords: mineral constituents; thawing permafrost; Yedoma; Northern Circumpolar region; pXRF

Introduction

Accurately predicting the impact of climate warming on the fate of organic carbon in thawing permafrost requires quantifying the mineral element reserve in the permafrost. In contrast to organic carbon, mineral constituents from the permafrost have received little attention. These minerals are exposed to a wide range of chemical, biological and physical weathering reactions in response to permafrost thaw, both with deepening of the active layer and with thermokarst processes exposing deeper permafrost to the surface. Unlocking a frozen reservoir of mineral nutrients may boost primary productivity and plant growth, thereby modifying the balance between carbon input and output in the thawing permafrost. A mineral element inventory in permafrost terrain, which accounts for local variability, is needed to better constrain the impact for the carbon balance at larger spatial scale. With this study we provide data from major Arctic regions to initiate the build up of this inventory and investigate its local variability. Moreover, we evaluate the potential of a fast and cost-effective method like portable X-ray fluorescence to improve the resolution and spatial diversity of the mineral element inventory in the permafrost in the future.

Study sites

In order to generate a first inventory of the northern permafrost region mineral reserve, a total of 230 available samples were selected from the circum Arctic permafrost region including near-surface and deep permafrost. With this set of samples including both active layer and permafrost samples we were able to cover a wide range of parent materials. Our dataset includes near-surface permafrost soil samples from Greenland (Zackenberg), Siberia (Cherskiy, Shalaurovo), Svalbard (Adventalen), and deep Yedoma permafrost samples from Alaska (Colville, Itkillik), and from Siberia (Kytalyk, Buor-Khaya, Sobo Sise) (Fig.1).

Results and discussion

The total mineral reserve of the permafrost

The Total Reserve in Bases (TRB = total content [Ca + Mg + K + Na] measured by ICP-AES after alkaline fusion) measured in permafrost from five different regions (Alaska, Svalbard, Greenland, East Siberia, Central Siberia) and combined with available data from the literature ranges between 50 and 580 $cmol_c.kg^{-1}$. The lowest TRB values are found in Alaska (NCSS database; USDA, 1994) and is attributed to peat soils with limited content in mineral constituents. The highest TRB values are found in the Yedoma deposit from Itkillik, Alaska. We attribute this high values to the presence of carbonates (Mauclet *et al.*, this conference). High TRB values are also found in Central Siberia and in Greenland. We link this to the presence of basalt as a parent material (Bagard *et al.*, 2013; Hirst *et al.*, this conference). The low TRB values in Svalbard likely reflect the composition of the mixed sedimentary rocks of this site. Interestingly, all TRB values in permafrost from East Siberia fall in the same range, including near-surface permafrost (Cherskiy, Shalaurovo) and deep Yedoma permafrost (Buor-Khaya, Sobo Sise, Kytalyk).

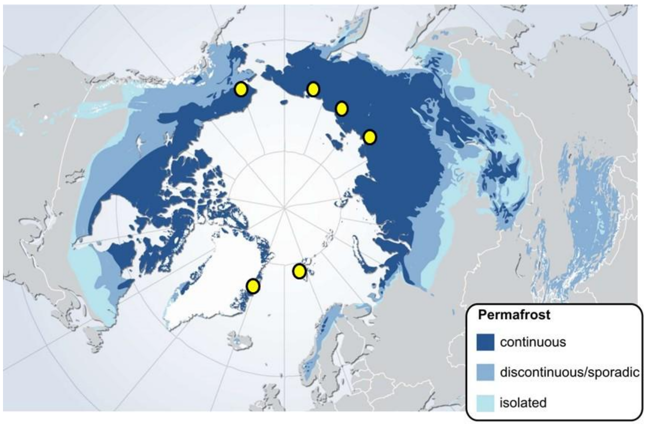

Figure 1. Location of the studied sites in the circum Arctic permafrost region (map from Brown *et al.*, 2001).

Following Hirst *et al.* (this conference), there is an increase in TRB values in permafrost relative to active layer in sites derived from deltaic deposits, but no increase in sites with boulder fields or ridge crest (Greenland, Siberia). Data from Kytalyk (Siberia) suggest that sites that experienced thermokarst in the geologic past (i.e., a drained thermokarst lake basin) show no increase in TRB in the permafrost relative to the active layer. Our hypothesis is that mineral elements have been leached from the deposit during the thermokarst stage before it became permafrost again after lake drainage.

Mineral element inventory in permafrost: testing pXRF

Alternative methods to ICP-AES to measure element content, faster, low-cost and non-destructive, such as the portable X-ray fluorescence (pXRF) are now used in the lab or in the field, including in permafrost regions (e.g., Weindorf *et al.*, 2014). For elements such as Ca, Fe, Sr, Ti, Zr, there is a strong linear relationship between the values obtained by ICP-AES and those obtained by pXRF ($R^2 > 0.85$). For other elements such as Si, Al, K, the linear relationship is lower ($0.4 < R^2 < 0.6$). For an element such as Mg, pXRF values are generally close to the quantification limits ($R^2 < 0.15$). Our observations support that the pXRF method provides an efficient way to build an inventory of the mineral elemental content of in permafrost terrain for important macronutrients such as Ca or micronutrients such as Fe.

Conclusion

This first inventory of the total mineral reserve in the northern permafrost region highlights that the potential for mineral nutrient hotspots upon thawing (i.e., higher mineral reserve in the permafrost relative to the active layer) depends on the types of deposits. In a next step we plan to test this hypothesis at a larger scale. As a hands-on recommendation, we suggest with this study that pXRF devices may represent a good alternative to the classical methods for a quick and low-cost mineral element content measurement in permafrost soils, and thereby to better understand the variability of the mineral reserve in permafrost at a larger scale.

Acknowledgments

The research is funded by the European Research Council (ERC Starting Grant, WeThaw, grant agreement n°714617 to S.O.). S.O. acknowledges funding from the Fonds National de la Recherche Scientifique (FNRS, Belgium, FC69480). The collection of soil profiles was financed by grants of the Swedish Research Council, the ESF CryoCARB project and the EU PAGE21 (contract 282700) to P.K., as well as a ERC Starting Grant (PETA-CARB, grant agreement n°338335) and Helmholtz Association's Initiative and Networking Fund (n°ERC-0013) to G.G.

References

Bagard, M.-L. Schmitt, A.D. Chabaux, F. Pokrovsky, O.S. Viers, J. Stille, P. Labolle, F. Prokushkin, A.S. 2013. Biogeochemistry of stable Ca and radiogenic Sr isotopes in a larch-covered permafrost-dominated watershed of Central Siberia. *Geochimica et Cosmochimica Acta* 114: 169-187.

Brown, J. Ferrians, Jr. O.J. Heginbottom, J.A. Melnikov, E.S., 2001. *Circum-Arctic Map of Permafrost and Ground Ice Conditions.* Boulder, CO: National Snow and Ice Data Center/World Data Center for Glaciology. Digital media.

USDA 1994. *National Soil Characterization Database*, Soil survey Laboratory, National Soil survey Center, Soil Conservation Service, Lincoln, US.

Weindorf, D.C. Bakr, N. Zhu, Y.D. McWhirt, A. Ping, C.L. Michaelson, G. Nelson, C. Shook, K. Nuss, S., 2014. Influence of ice on soil elemental characterization via portable X-ray fluorescence spectrometry. *Pedosphere* 24: 1-12.

Long-term mercury transport in High Arctic watersheds subject to permafrost degradation

Michael Pope[1]
Scott F. Lamoureux[1]
Jane Kirk[2]
Casey Beel[1]
Melissa J. Laferene[1]
Derik Muir[2]
Debbie Iqulak[3]
[1] *Queen's University, 16mp25@queensu.ca*
[2] *Environment and Climate Change Canada*
[3] *Resolute Bay, NU, Canada*

Abstract

Total mercury (THg) fluxes and seasonal hydrological transport dynamics were determined from a long-term THg water sampling (2007-2017) and hydrological program in two morphologically-similar, High Arctic watersheds (East and West River) located at the Cape Bounty Arctic Watershed Observatory, Melville Island, Nunavut. Results indicate that there are large inter-annual variations in watershed THg fluxes, in part due to the physical disturbance of near-surface permafrost and inter-annual hydroclimatic conditions. A large proportion of THg (30.5-72.5%) was particulate bound, and strong relationships were observed between THg, suspended sediment and discharge in both rivers. The timing and intensity of runoff was a dominant driver of THg flux in all years with the majority of discharge and peak THg concentrations occurring during either the brief nival freshet or uncommon late season rainfall events.

Keywords: Mercury; Hydrology; Suspended sediment; Permafrost disturbance; Canada; High Arctic;

Mercury (Hg) is a widespread toxic contaminant that is both naturally occurring and anthropogenically produced. Anthropogenic activities have been the primary driver of global Hg contamination for the last 200 years. Hg is readily volatilized into the atmosphere allowing for long-range transport of industrially-sourced Hg and its subsequent deposition onto remote Arctic landscapes (Chételat *et al.* 2015).

Hg contamination in the Arctic is significant for northern communities as it may undergo bio-amplification and accumulation through trophic levels (Evans *et al.* 2005). Many of the country foods that northerners rely on are top marine and freshwater predators such as seals and Arctic char and are therefore more susceptible to the effects of bio-accumulation of Hg. Transport of Hg from terrestrial sources to ecologically-sensitive aquatic environments is primarily achieved through the hydrological connection of streams and rivers. However, the processes that control inter-season Hg transport dynamics are poorly understood for Arctic river systems and the role of permafrost and climate change on these processes adds further challenges to characterizing the flux of Hg to downstream aquatic systems.

Long-term total mercury (THg) water sampling (2007-2017) and hydrological monitoring (2003-2017) have been carried out on two adjacent rivers at the Cape Bounty Arctic Watershed Observatory, Melville Island, Nunavut in the Canadian High Arctic. THg, suspended sediment and discharge were collected from the East River and West rivers (both ~10 km^2) and four small West River subcatchments (c. 0.1 km^2). Samples were preserved as filtered and unfiltered components and subsequently analyzed at the Canadian Center for Inland Waters at Environment and Climate Change Canada (Burlington, Ontario).

Large seasonal variations in THg concentration and particulate fractionation were observed at all study sites. Peak discharge and peak THg concentration often occurred during the nival freshet, however, uncommon heavy rainfall stormflow events also produced high THg concentrations. During both nival and rainfall events, strong daily clockwise discharge-THg hysteresis patterns were observed. These patterns were accompanied by a strong relationship between THg and suspended sediment concentration (SSC). This indicates that THg concentration is likely driven by increased sediment mobilization in the river channel rather than sub-surface or surficial runoff.

In 2007 both catchments experienced permafrost disturbances in the form of active layer detachments (1.2 & 2.7% disturbed, East and West watersheds, respectively) (Lamoureux & Lafrenière, 2017). Area and runoff-corrected specific THg fluxes were the highest in both catchments in the two years following these permafrost disturbances. Additionally, the four hillslope subcatchments with varying amounts of permafrost disturbance were also sampled in 2016 and 2017. The disturbed subcatchments showed proportionate suspended sediment and THg concentrations and these were highest in the most disturbed subcatchments.

In 2009, two large successive, late-season rainfall events substantially increased THg concentration, suspended sediment and discharge. The increase in late season runoff was responsible for the majority (~90%) of seasonal sediment and THg flux in both rivers. Long-term trends show a notable decrease in specific and uncorrected THg fluxes after 2009 indicating potential multi-year exhaustion effects of particulate bound THg in the river channel.

The High Arctic is predicted to become both warmer and wetter, likely increasing the frequency of late-season rainfall events and permafrost degradation (Bintanja & Andry, 2017). Based on the results from this study, projected permafrost degradation has important implications for the terrestrial Hg cycle and fluxes. Even localized permafrost disturbances impact water quality and THg concentrations ten years after initial disturbance. Increased rainfall is also an important mechanism for THg based on the observed response in this study. As the Arctic shifts to an increasingly pluvial dominated hydrological system, the frequency of high magnitude discharge events will increase and timing of flow will shift to conditions that are more conducive to erosion. The combination of increased surficial permafrost disturbance and stream power from a pluvial flow regime could increase the flux of Hg that is transported to downstream freshwater lakes and coastal waters.

Acknowledgments

Funding for this research was provided by NSERC, ArcticNet, Environment and Climate Change Canada, and the Government of Canada International Polar Year. Field logistics were provided by Polar Continental Shelf Program (PCSP), Natural Resources Canada. Laboratory analysis were provided by Environment and Climate Change Canada.

References

Bintanja, R. & Andry, O., 2017. Towards a rain-dominated Arctic. *Nature Climate Change*, *7*(4): 263-267.

Chételat, J., Amyot, M., Arp, P., Blais, J. M., Depew, D., Emmerton, C. A., ... & Graydon, J. (2015). Mercury in freshwater ecosystems of the Canadian Arctic: Recent advances on its cycling and fate. *Science of the Total Environment* 509: 41-66.

Evans, M. S., Lockhart, W. L., Doetzel, L., Low, G., Muir, D., Kidd, K., ... & Delaronde, J. (2005). Elevated mercury concentrations in fish in lakes in the Mackenzie River Basin: the role of physical, chemical, and biological factors. *Science of the Total Environment* 351: 479-500.

Lamoureux, S.F. & Lafrenière, M.J., 2017. More than just snowmelt: integrated watershed science for changing climate and permafrost at the Cape Bounty Arctic Watershed Observatory. *Wiley Interdisciplinary Reviews: Water*.

Composition and state of decay of soil organic matter in Cryosols of the Lena River Delta

Isabel Prater[1]
Sebastian Zubrzycki[2]
Lena Zoor[1]
Carsten W. Mueller[1]
[1]*Chair of Soil Science, TU München, Freising, Germany, i.prater@tum.de*
[2]*Center for Earth System Research and Sustainability (CEN), School of Integrated Climate System Sciences, Universität Hamburg, Hamburg, Germany*

Abstract

Permafrost-affected soils of the northern hemisphere play a crucial role in the global carbon cycle. Increasing temperatures and expanding thawing affect these soils and their capability as carbon sink. Forecasts on how soil organic matter (SOM) in permafrost-affected soils responds to enhanced warming are only possible with a more substantial knowledge on how SOM is composed and how advanced its stage of decay is. Analysis with ^{13}C CPMAS NMR spectroscopy showed that larger particulate organic matter fractions were dominated by functional groups representing primarily relatively labile SOM prone to microbial decomposition, while smaller particulate organic matter fractions contain altered SOM that is additionally stabilized by binding to mineral particle surfaces. Therefore, it could be assumed that the stability of the major part of the SOM in permafrost-affected soils is at stake when the bio-accessibility of SOM increases due to changing thawing dynamics.

Keywords: Soil organic matter, Russian Arctic, ^{13}C CPMAS NMR spectroscopy, density fractionation, decomposition.

Introduction

Constituting major reservoirs for the storage of organic carbon in the terrestrial ecosystem, permafrost-affected soils of the northern hemisphere represent a crucial storage for global soil carbon. Soils of the Arctic region face broad alterations due to enhanced warming, while subsequent deepening of the active thermal layer leads to changes of carbon stocks due to alleviated bioaccessibility of organic matter by microorganisms. In order to decipher how the stored organic matter (OM) will respond to ascending temperatures, it is indispensable to understand how OM within those soils is composed and how advanced its decomposition is.

Site and methods

To gain insight into the properties of SOM contained in permafrost-affected soils, samples from Samoylov Island, located in the Lena River Delta in the Russian Arctic, were analyzed. The investigated region is characterized by a polar climate with a mean annual air temperature of -12.5° C and an annual precipitation of around 125 mm and by 400 to 600 m thick continuous permafrost with thaw depths of about 50 cm (Zubrzycki *et al.*, 2013). Samples were obtained from four undisturbed cores according to visible soil horizons. Density fractionation was conducted to obtain free and occluded particulate OM (fPOM and oPOM) and wet sieving and sedimentation to separate the mineral soil fractions sand, silt and clay according to their size. Carbon and nitrogen contents of all fractions were determined by elemental analysis and SOM fractions were objected to 13C nuclear magnetic resonance (13C NMR) spectroscopy after sieving them by 20 µm.

Composition and state of decay

Fractionation revealed a dominance of sand- and silt-sized particles in all samples and a subordinate proportion of clay-sized particles. In most samples, the portion of fPOM exceeded the portion of oPOM independent of the depth layer. Most carbon and nitrogen is bound to the particulate organic fractions (mostly plant residues), while in some samples also clay-sized particles contribute considerably to the carbon and nitrogen stock despite their low percentage. 13C NMR spectroscopy of SOM fractions and subsequent integration debunked that the chemical shift region represented most is O/N-alkyl carbon, implying that rather fresh and only less decomposed OM is present and that this dominance is largest in the fPOM and oPOM >20 µm fractions. In oPOM <20 µm fractions the portion of alkyl C increases.

In order to better clarify the chemical composition, different methods were applied. According to Baldock *et al.* (1997), the ratio of alkyl carbon to O/N alkyl carbon enables conclusions on the stage of decomposition. This ratio confirmed overall that the decomposition is most advanced in the oPOM <20 μm fraction. Corresponding results were generated when a method introduced by Bonanomi *et al.* (2013) was utilized. The authors state that the ratio of the chemical shift regions 70-75 and 52-57 is associated with the rate of litter decay. The molecular mixing model established by Baldock *et al.* (2004) focuses on the percentage of different molecules and showed a clear dominance of carbohydrates, hence not yet altered or decomposed organic matter in the POM >20 μm fractions and a slightly more balanced distribution of compounds in the oPOM <20 μm fraction with a higher percentage of lipids.

Conclusion

These results indicate that the major part of SOM stored throughout the profiles of these permafrost-affected soils is composed of organic compounds that represent a rather early stage of SOM decay. As a consequence, we assume that the fPOM and oPOM >20 μm fractions are at stake when soil thawing enhances as these fractions are rather labile, primarily protected by freezing and therefore possibly prone to microbial decay under warmer conditions. On the other hand, the chemical composition of oPOM <20 μm fractions can be regarded as more stable as a shift towards less labile organic compounds is traceable. With ongoing changes in water regime and temperature, it can also be assumed that in the future SOC in organo-mineral complexes may play a larger role for the sequestration of carbon.

References

Baldock, J.A., Oades, J.M., Nelson, P.N., Skene, T.M., Golchin, A., Clarke, P., 1997. Assessing the extent of decomposition of natural organic materials using solid-state 13C NMR spectroscopy. *Australian Journal of Soil Research* 35: 1061-1083.

Baldock, J.A., Masiello, C.A., Gélinas, Y., Hedges, J.I., 2004. Cycling and composition of organic matter in terrestrial and marine ecosystems. *Marine Chemistry* 92: 39-64.

Bonanomi, G., Incerti, G., Giannino, F., Mingo, A., Lanzotti, V., Mazzoleni, S., 2013. Litter quality assessed by solid state 13C NMR spectroscopy predicts decay rate better than C/N and Lignin/N ratios. *Soil Biology & Biochemistry* 56: 40-48.

Zubrzycki, S., Kutzbach, L., Grosse, G., Desyatkin A., Pfeiffer, E.-M., 2013. Organic carbon and total nitrogen stocks in soils of the Lena River Delta. *Biogeosciences* 10: 3507-3524.

Spatio-temporal patterns of POC, dissolved CO_2, and CH_4 in warming permafrost: comparing results from a control and drained floodplain tundra site in NE Siberia

Sandra Raab[1]
Mathias Goeckede[1]
Jorien Vonk[2]
Anke Hildebrandt[1,3]
Linus Schauer[4]
Martin Heimann[1]

[1]*Max Planck Institute for Biogeochemistry, Department of Biogeochemical Systems, Jena, Germany, sandra.raab@bgc-jena.mpg.de*
[2]*Vrije Universiteit, Department of Earth Sciences, Faculty of Sciences, Amsterdam, The Netherlands*
[3]*Friedrich-Schiller-University Jena, Institute of Geoscience, Jena, Germany*
[4]*Bauhaus-University, Faculty of Civil Engineering, Weimar, Germany*

Abstract

Permafrost soils represent an immense carbon reservoir, which is susceptible to climate warming. Resulting changes in landscape patterns, e.g. the degradation of polygonal tundra systems, could result in modified carbon flux rates and lateral transport mechanisms. A comparative study between a dry (drained) and wet (control) site was conducted on a tundra floodplain near Chersky, Northeast Siberia. This study includes a piezometer network to monitor the groundwater level variations and to enable water sampling for water isotopes, particulate organic carbon (POC) and in-situ measurement of dissolved CO_2 and CH_4 at several key locations (groundwater of both sites and surface water from the drainage ditch and the nearby Ambolikha river). The spatio-temporal patterns of measured carbon parameters indicate differences between water types and a general seasonal increase in carbon concentration in both ground- and surface water.

Keywords: particulate organic carbon; carbon dioxide; methane; water isotopes; drainage effect; Siberia.

Introduction

Permafrost areas represent an immense carbon reservoir storing up to 1300 PgC (Hugelius *et al.*, 2014). The more permafrost thaws as a result of climate change, the more organic carbon becomes available and can be degraded and transported to the atmosphere or hydrosphere (Schuur *et al.,* 2015). As a consequence of climate warming, changes in water level, temperature and vegetation community could modify those susceptible permafrost ecosystems. Drier soil conditions are expected to become more frequent in the future, resulting in degradation of polygonal tundra landscape properties with channelled water transport pathways (Liljedahl *et al.*, 2016).

Material and methods

At the Ambolikha Site in the Kolyma floodplain near Chersky (68.75°N, 161.33°E), we sampled water from a control and a drained site. Drainage is achieved by a circle-shaped drainage ditch, constructed in 2004. The control site represents inundated conditions, whereas the drained site mimics the conditions in the dried fraction of the degraded permafrost ecosystem under future climate warming.

In 2016, 33 piezometers were installed to capture water table variations on the drained and control site. In the growing seasons of 2016 and 2017, we collected water samples at several piezometer locations to determine the isotopic composition ($\delta^{18}O$, δD) of surface water, suprapermafrost groundwater and precipitation as well as the different carbon concentrations, such as particulate organic carbon (POC), dissolved organic carbon (DOC), dissolved inorganic carbon (DIC) and their isotopic composition ($\delta^{13}C$-DIC, $\delta^{13}C$-DOC, $\Delta^{14}C$-DOC).

This study focuses on small-scale spatio-temporal patterns of dissolved CO_2, CH_4 and POC, since for these parameters the analysis for the two years is completed. Particulate material was concentrated on the filter membranes, which were dried and acidified to remove inorganic carbon. In-situ measurements of dissolved CO_2 and CH_4 were conducted using the Ultraportable Greenhouse Gas Analyzer (UGGA, Los Gatos Research) and concentrations were calculated using Henry's law.

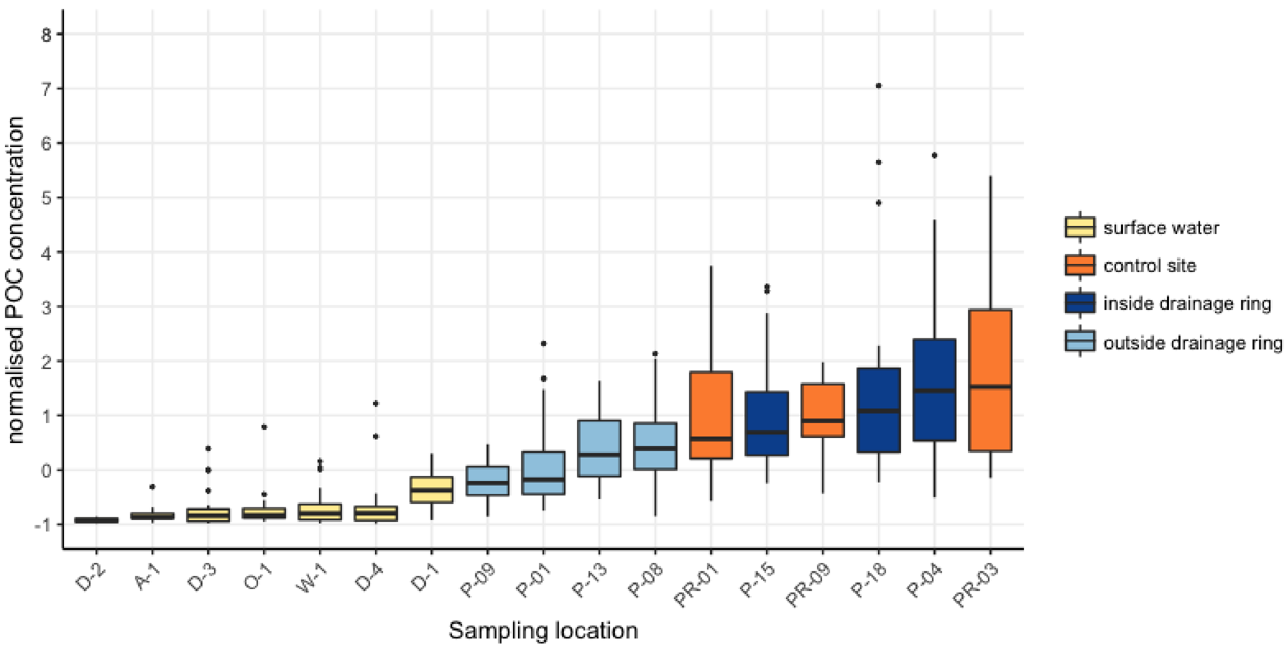

Figure 1. Normalised POC data from 2016 and 2017. Water from the control site and the inside drainage ring show highest concentrations, whereas surface water POC is lowest.

The data were normalised according to Wullaert *et al.* (2009) and ordered with the median concentration of each sampling date, to emphasise spatial differences between sampling locations and water types: (i) surface water, (ii) groundwater from the inner and (iii) outer drainage ring, (iv) control site water. Temporal data throughout the season indicate shifts in concentrations (e.g. active layer deepening).

Results and outlook

Our results from two summer field campaigns illustrate distinguishable types of water within both treatment areas (Fig. 1, e.g. POC). Highest POC concentrations are observed in water samples from the control site and the inside drainage ring. In contrast, dissolved CH_4 concentrations are dominated by water from outside the drainage ring and the control site. In 2016 CO_2 concentrations were elevated outside the drainage ditch and at the control site, whereas in 2017 data inside the drainage ditch and at the control site.

Data collected throughout the growing season 2017 showed a general increase of POC, CO_2, and CH_4 for most of the piezometer locations in the suprapermafrost groundwater over a sampling period of ca. 11 weeks.

Future research will take dissolved organic and inorganic carbon fluxes into account, as well as the carbon distribution, age and source areas to gain a deeper understanding of the carbon composition and transport mechanisms within the drainage system and to investigate the lateral carbon export.

References

Hugelius, G., Strauss, J., Zubrzycki, S., Harden, J. W., Schuur, E. A. G., Ping, C. L., Schirrmeister, L., Grosse, G., Michaelson, G. J., Koven, C. D., O'Donnell, J. A., Elberling, B., Mishra, U., Camill, P., Yu, Z., Palmtag, J., Kuhry, P. (2014): Estimated stocks of circumpolar permafrost carbon with quantified uncertainty ranges and identified data gaps. *Biogeosciences* 11(23): 6573-6593.

Liljedahl, A. K., Boike, J., Daanen, R. P., Fedorov, A. N., Frost, G. V., Grosse, G., Hinzman, L. D., Iijma, Y., Jorgenson, J. C., Matveyeva, N., Necsoiu, M., Raynolds, M. K., Romanovsky, V. E., Schulla, J., Tape, K. D., Walker, D. A., Wilson, C. J., Yabuki, H., Zona, D. (2016): Pan-Arctic ice-wedge degradation in warming permafrost and its influence on tundra hydrology. *Nature Geoscience* 9(4): 312- 318.

Schuur, E. A. G., McGuire, A. D., Schadel, C., Grosse, G., Harden, J. W., Hayes, D. J., Hugelius, G., Koven, C. D., Kuhry, P., Lawrence, D. M., Natali, S. M., Olefeldt, D., Romanovsky, V. E., Schaefer, K., Turetsky, M. R., Treat, C. C., Vonk, J. E. (2015): Climate change and the permafrost carbon feedback. *Nature* 520(7546): 171-179.

Wullaert, H., Pohlert, T., Boy, J., Valarezo, C., Wilcke, W. (2009): Spatial throughfall heterogeneity in a montane rain forest in Ecuador: Extent, temporal stability and drivers. *Journal of Hydrology* 377(1-2): 71-79.

Fate of OC in the Arctic nearshore zone: Rapid removal and degradation due to hydrodynamic and ice-related sediment transport

Boris Radosavljevic[1, 2, 4],
Nicole Couture[3],
Ulrike Herzschuh[1,2],
Hugues Lantuit[1,2],
Christian Knoblauch[5],
Michael Fritz[1]
[1]*Alfred Wegener Institute, Helmholtz Centre for Polar and Marine Research, Potsdam, Germany, boris.radosavljevic@gmail.com; [2]Institute of Earth- and Environmental Science, University of Potsdam, Potsdam, Germany; [3]Northern Canada Division, Geological Survey of Canada, Ottawa, Canada; [4]GFZ German Research Centre for Geosciences, Potsdam, Germany; [5]Institute of Soil Science, University of Hamburg, Hamburg, Germany*

Abstract

The present study investigated the fate of terrestrial carbon in shallow coastal areas. Surface sediment samples near Herschel Island, Yukon, Canada, were collected to infer sediment- and organic matter (OM) transport processes and to determine the origin and state of degradation of organic carbon. We determined total organic carbon (TOC), total nitrogen (TN), TOC:N ratios, stable carbon isotopes ($\delta^{13}C$), and grain size distributions. Sediments are predominantly silty, moderately to poorly sorted mud (<64 µm fraction). A significant correlation of TOC (mean: 1.02 % wt.) was found with mud content (silt and clay). Sediments are largely of terrestrial origin (up to 70% of the total carbon pool), yet contain up to 90% less TOC than terrestrial sediments in the area, suggesting rapid offshore transport and degradation.

Keywords: Arctic Ocean, organic carbon, stable isotopes, sediment chemistry, sediment transport, Beaufort Sea

Introduction

Fluxes from the permafrost carbon pool (1300±200 Pg of carbon in the upper 3 m) occur via permafrost degradation, microbial mineralization, river discharge, and coastal erosion (e.g. Macdonald et al., 2015; Rachold et al., 2000). Particular organic carbon fluxes into nearshore areas resulting from coastal erosion are estimated at 4.9-14.0 Tg a^{-1} (Wegner et al., 2015), corresponding to the annual amount discharged by rivers (Rachold et al., 2004). The nearshore zone (< 20 m depth) accounts for 20% of the shelf area in the Arctic (Fritz et al., 2017) and constitutes a key interface in the land to ocean transition, yet the fate of terrestrial carbon in the arctic nearshore is not fully understood.

We determined the patterns of sediment and OM distribution, identified responsible processes, and provide new information on the contribution and fate of terrestrial carbon in an arctic nearshore environment through the application of sedimentological and geochemical methods.

Study Area

Nearshore areas were sampled off Herschel Island (69°36`N; 139°04`W), in particular an embayment southeast and a shallow lagoon southwest of the island. The island is composed of perennially frozen marine and glacigenic sediments (Lantuit and Pollard, 2008), ground ice contents reach up to 60-70 % by volume in the upper 10-15 m (Pollard, 1990). Coastal retreat releases significant amounts of organic carbon to the nearshore. Organic carbon contents in island sediments range from 0.6-38.9 % wt. (Couture, 2010; Fritz et al., 2012).

Methods

Sedimentological and geochemical analyses were carried out on samples obtained using a Van Veen grab sampler during 2012 and 2013 summer expeditions by the Alfred Wegener Institute (AWI). We analyzed grain size distributions (GSDs), and bulk geochemical parameters, i.e. total organic content (TOC), nitrogen (N), and stable carbon isotope composition. Radosavljevic et al. (2016) provide a detailed methodology.

Figure 1 Location of Herschel Island in the Canadian Beaufort Sea

Results

Approximately 200 samples were analyzed (Table 1).

Table 1 Results of grain size and bulk geochemical analyses and their standard deviations (in parentheses) shown by Thetis Bay (TB) and Workboat Passage (WBP) locations.

	Location		
Parameter	TB	WBP	Overall
mean [ϕ]	5.30 (1.72)	4.44 (1.23)	5.20 (1.68)
sorting [σ_I]	2.07 (0.49)	2.09 (0.35)	2.07 (0.48)
TOC (% wt.)	1.03 (0.92)	0.97 (0.62)	1.02 (0.88)
TIC (% wt.)	1.17 (0.37)	1.65 (0.31)	1.23 (0.39)
TN (% wt.)	0.15 (0.05)	0.14 (0.02)	0.15 (0.05)
TOC:N (atomic)	11.06 (3.30)	11.63 (2.24)	11.13 (3.18)
$\delta^{13}C$ (‰)	-26.32 (0.38)	-26.55 (0.25)	-26.35 (0.37)

Discussion and Summary

The data gathered in this study show both hydrodynamic- and ice-related processes affect the spatial grain size variation. Ice processes are evident in the generally moderate to poor sorting beyond the 4 m contour. TOC concentration in nearshore sediments is ~90% lower than concentrations found in terrestrial sediments along the Yukon Coast and Herschel Island. We found a correlation with mud content since physical processes tend to focus OM in the fine fraction, where greater mineral surface area also aids sorption of OM (e.g. Blair and Aller, 2012). We conclude that while degradation occurs in the nearshore, some portion of the terrestrial carbon is transported offshore as suspended load. The isotope end member model is questionable, yet it indicates the significant contribution of terrestrial plants to benthic OM.

Acknowledgments

This work was funded by the Helmholtz Association (grant no. VH-NG-801 to H.L.). The work of M.F. was supported by the Daimler and Benz Foundation (grant no. 32-02/15). We are grateful to Yukon Government, Yukon Parks (Herschel Island Quiqiktaruk Territorial Park), and the Aurora Research Institute for their support during this project.

References

Blair, N. E. and Aller, R. C.: The fate of terrestrial organic carbon in the marine environment, Annu. Rev. Mar. Sci., 4, 401–423, 2012.

Couture, N.: Fluxes of Soil Organic Carbon from Eroding Permafrost Coasts, Canadian Beaufort Sea, PhD Dissertation, Department of Geography, McGill University, Montreal., 2010.

Fritz, M., Vonk, J. E. and Lantuit, H.: Collapsing Arctic coastlines, Nat. Clim Change, 7(1), 6–7, 2017.

Lantuit, H. and Pollard, W. H.: Fifty years of coastal erosion and retrogressive thaw slump activity on Herschel Island, Southern Beaufort Sea, Yukon Territory, Canada, Geomorphology, 95(1), 84–102, doi:10.1016/j.geomorph.2006.07.040, 2008.

Macdonald, R. W., Kuzyk, Z. Z. A. and Johannessen, S. C.: The vulnerability of Arctic shelf sediments to climate change, Environ. Rev., 23(4), 461–479, doi:10.1139/er-2015-0040, 2015.

Pollard, W. H.: The nature and origin of ground ice in the Herschel Island area, Yukon Territory, in Proceedings, Fifth Canadian Permafrost Conference, Québec, pp. 23–30., 1990.

Rachold, V., Grigoriev, M. N., Are, F. E., Solomon, S., Reimnitz, E., Kassens, H. and Antonow, M.: Coastal erosion vs riverine sediment discharge in the Arctic Shelf seas, Int. J. Earth Sci., 89(3), 450–460, 2000.

Rachold, V., Eicken, H., Gordeev, V. V., Grigoriev, M. N., Hubberten, H.-W., Lisitzin, A. P., Shevchenko, V. P. and Schirrmeister, L.: Modern terrigenous organic carbon input to the Arctic Ocean, in The organic carbon cycle in the Arctic Ocean, pp. 33–55, Springer., 2004.

Wegner, C., Bennett, K. E., de Vernal, A., Forwick, M., Fritz, M., Heikkilä, M., Łącka, M., Lantuit, H., Laska, M., Moskalik, M., O'Regan, M., Pawłowska, J., Promińska, A., Rachold, V., Vonk, J. E. and Werner, K.: Variability in transport of terrigenous material on the shelves and the deep Arctic Ocean during the Holocene, Polar Res., 34(1), 24964, doi:10.3402/polar.v34.24964, 2015.

Permafrost Thawing and Freezing – Direct Tracking with Radioisotopes

Dotan Rotem [1,2]
Yishai Weinstein [1]
Henk Kooi [3]
Yoseph Yechieli[4]
Jurgen Sultenfus[5]
Yael Kiro[6]
Yehudit Harlavan[4]
Mor Feldman[1]
Hanne H. Christiansen[2]
[1]*Department of Geography and Environment, Bar-Ilan University, Ramat-Gan, 52900 Israel* dotanrotem1969@gmail.com
[2] *Geology Department, the University Centre in Svalbard, UNIS*
[3] *Deltares, 2600 MH Delft, The Netherlands*
[4] *Geological Survey of Israel, 30 Malkei Israel St., Jerusalem, 95501 Israel*
[5] *University of Bremen, Otto Hahn Allee 1, Bremen, Germany*
[6] *Lamont-Doherty Earth Observatory, Columbia University, Palisades, NY 10964, USA*

Abstract

Permafrost in circum-polar regions has been recently undergoing thawing, with severe environmental consequences, including the expected release of greenhouse gases and global warming amplification. Although highly important, direct tracking methods of thawing do not exist. We identified a permafrost radioisotope fingerprint, and show it can be used to track thawing. Ratios of long- to the shorter-lived radium isotopes are lower in Svalbard permafrost ice than in the overlaying active layer water, which we attribute to the long residence time in the permafrost. Also, daughter-parent $^{224}Ra/^{228}Ra$ ratios are lower in permafrost than in the active layer. These fingerprints were also identified in a local stream, confirming the applicability of this tool to tracing thawed permafrost in periglacial watersheds. The permafrost Ra tracer should be applicable to other periglacial terrains, which could assist in regional quantification of the extent of permafrost thawing and carbon emissions to the atmosphere.

Keywords: radium isotopes, permafrost thawing

Introduction

More than 20% of the land surface area is underlain by permafrost. Global warming has already caused extensive permafrost degradation (Romanovsky et al. 2010), and some models predict up to 60% reduction in permafrost areal extent by the end of the 21st century. It can result in the oxidation of organic carbon and its consequent release to the atmosphere, amplifying the ongoing global warming (Schuur et al. 2013). Conventional methods of studying permafrost degradation rely on ground thermal measurements, active layer thickness monitoring, as well as modeling. While some geochemical characterization of ground ice does exist, direct methods of tracking permafrost thawing and of tracing its thawed water in local drainage systems were hardly developed (Keller et al. 2007).

In this paper, we identify a distinct radium isotope signature of permafrost ground ice, and propose its use as a tracer of permafrost thawing and possibly of intra-permafrost segregation processes.

Radium has four naturally-occurring radioactive isotopes, which are part of the U-Th decay chains, and with half-lives varying between days (^{224}Ra and ^{223}Ra), several years (^{228}Ra) and 1,600 years (^{226}Ra). All Ra isotopes are produced by the decay of thorium isotopes, which mainly reside on the sediment solids.

The main hypothesis underlying this study states that radionuclides are 'locked' in the permafrost frozen pore space, unlike in active hydrological systems, where they are both interacting with sediment grains and being flushed away by flowing water. This may result in the buildup of relatively high concentrations of ^{226}Ra, as well as in the decay in the shorter-lived isotopes, which should both lead to higher ratios of ^{226}Ra to the shorter-lived radium isotopes in permafrost ice compared with active layer water.

Study Site and Methods

The study was carried out in Adventdalen, Svalbard (780N 15.50E), in two sites south of the main river channel, both covered with 2-3 m of aeolian loess.

The top part of the permafrost (1-2.5m) was sampled by hand drill, while active layer water was sampled either from ditches or also by drilling (during winter). To have enough ground ice for the analysis of all four Ra isotopes, each permafrost profile consisted of 4-10 cores, drilled along a 1-1.5m line, with samples composed of similar depth (25-70 cm) intervals.

Processing included scraping core surfaces, crushing by hammer in a cold room (-5oC), thawing in microwave oven, adding a small volume of Ra-free tap water, centrifuging, and filtering through 3 to 0.22 µm filters.

All waters were run 5-6 times through Mn-coated fibers in order to adsorb the radium. Samples were analyzed for ^{224}Ra and ^{223}Ra by the RaDeCC, as soon as possible after thawing. After 4-5 weeks, samples were re-measured, to determine their ^{228}Th content. ^{226}Ra was determined by its radioactive daughter ^{222}Rn, after 3-week incubation of fibers in Ra-free water in 500 ml bottles. ^{228}Ra was measured by ultra-low background Canberra HPGe gamma spectrometer after ashing the fibers.

Results and Discussion

Concentration of radium isotopes were measured as activities (e.g. disintegrations per minute per liter). Since isotope activities in thawed permafrost ice could be affected by a variety of factors, both in the frozen state or during thawing in lab, we focused on isotope ratios. As hypothesized, activity ratios of ^{226}Ra to the short-lived isotopes ^{224}Ra and ^{223}Ra were higher in thawed permafrost ice than in active layer water (fig 1). Another, clear distinction between permafrost and active layer water is presented by the activity ratio of ^{224}Ra to its parent ^{228}Ra (fig 2), which is low compared with active

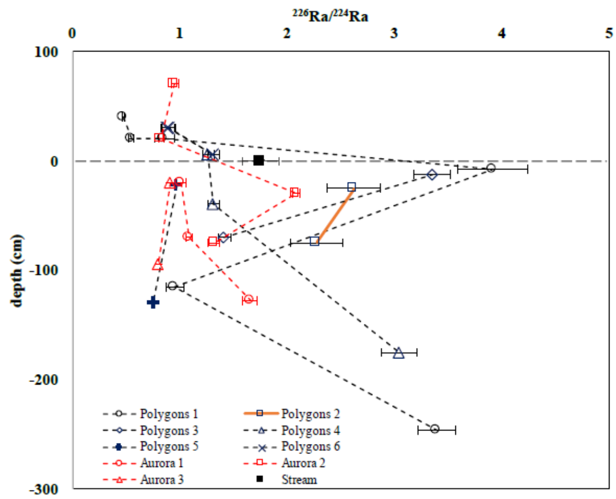

Figure 1. Ratios of $^{224}Ra/^{226}Ra$ in permafrost ice and active layer water from Adventdalen, Svalbard. The black square is the seepage water in the Polygons site.

layer water, as well as with reported groundwater from other areas. High ^{226}Ra/^{224}Ra ratio and low ^{224}Ra/^{228}Ra were also identified in a water sample obtained from a small stream draining one of the studied areas. This may indicate that this water contains a significant component derived from thawed permafrost. Although more sampling is needed, it does illustrate how radium isotopes could assist in tracing permafrost thawing through periglacial drainage systems.

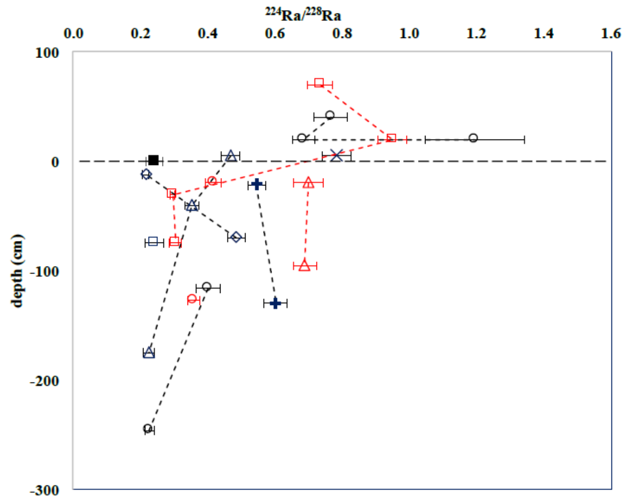

Figure 2. Daughter-parent ^{224}Ra/^{228}Ra ratios in permafrost ice and active layer water. The black square is the seepage water in the Polygons site.

Acknowledgments

We wish to express our gratitude to Dany Roehnert, Yehuda Shalem, Graham Gilbert, Gunnar Mallon, Eleanor Jones and Ebbe Norskov Bak, who assisted with the hard field and lab work, as well as to all UNIS staff. This research was funded by Israel Science Foundation Bikura grant 1487/14, and partly by an Arctic Field Grant of the Svalbard Science Forum allocated to Dotan Rotem in 2017.

References

Keller *et al.*, 2010, Stream geochemistry as an indicator of increasing permafrost thaw depth in an arctic watershed. Chemical Geology, 273(1–2), pp.76–81.

Romanovsky *et al.*, 2010, Permafrost thermal state in the polar northern hemisphere during the international polar year 2007-2009: A synthesis. Permafrost and Periglacial Processes, 21(2), pp.106–116.

Schuur *et al.,* 2013, Expert assessment of vulnerability of permafrost carbon to climate change. Climatic Change, 119(2), pp.359–374.

Viable Ancient Protists in Cryosols and Permafrost: Possible Input to the Modern Arctic Ecosystems

Anastasia V. Shatilovich[1]
Stanislav V. Gubin[1]
Alexey V. Lupachev[1]
Alexander P. Mylnikov[2]
Svetlana V. Bykova[3]
[1] *Institute of Physico-chemical and Biological Problems in Soil Science, RAS, Pushchino, Russia, nastya.shat@rambler.ru*
[2] *Institute for Biology of Inland Waters, RAS, Borok, Russia*
[3] *Institute of Ecology of the Volga River Basin, RAS, Togliatti, Russia*

Abstract

The main goal of the study was to determine the role of cryogenic mass-exchange in distribution, long-term survival and further cryoconservation of soil protists in the permafrost sediments.

Keywords: Arctic, Cryosols, protists, cryobiosis.

Introduction

Previous investigations have shown that resting cysts of soil protists can survive in permafrost for thousands of years at negative temperatures. The species diversity of ancient viable protists is assumed to be the result of constant selection going not only in permafrost sediments, but also in the modern permafrost-affected soils during long-time transition of cysts into the frozen deposits. Cryosols are subjected to the different processes of cryogenic mass-exchange that redistribute the fragments of the uppermost soil horizons with microorganisms inhabiting this material. The transition of protist cysts to the lower active layer and then into the upper layers of permafrost is considered as the period of pre-adaptation of organisms and formation of communities capable to prolonged cryobiosis and forming a natural cryobank of soil biota in the permafrost.

The main goal of the study was to investigate the patterns of diversity and abundance of viable protists' community in the permafrost sediments and in the profiles of Cryosols and to determine species that have developed adaptations to survive in consistently adverse environments.

43 samples of organic and organo-mineral material from 14 Turbic Cryosols were collected and analyzed during 2013-2016 field seasons in the region of Kolyma Lowland and arranged into five groups according to the leading cryogenic mass-exchange processes (Fig. 1): modern uppermost organogenic horizons undisturbed by cryoturbations (O+Oao); their fragments that were buried by solifluction ([Oao]); cryoturbated fragments (@); cryoturbated fragments that were accumulated in the transient layer of permafrost (⊥CR+TL); mineral horizon of Cryosol profile with no signs of cryoturbation (CR). Radiocarbon age of plant remnants that were brought into the mineral part of Cryosol profiles by solifluction and cryoturbation processes varies within 2,1-4,5 Kyr. We also compared the results for ciliates and flagellates with our previous investigations (Shatilovich *et al.*, 2009).

The taxonomical analysis of cultivable protists communities isolated from Turbic Cryosol revealed 56 species and forms of heterotrophic flagellates from 11 taxonomical groups and flagellates incertae sedis and 38 species of ciliates from 7 taxonomical groups (Fig. 1). A considerable part of the community (76% of ciliates and 68% of flagellates) maintained its viability in the dormant state in cryoturbated and buried organogenic material. Communities of ancient viable protists isolated from permafrost sediments contain 13 species of ciliates and 26 species of flagellates that is 32% and 56% respectively from the diversity of Cryosol protists community.

According to our results significant part of protists communities in Cryosols have adaptive and protective mechanisms enabling long-term cryobiosis in the inhospitable conditions of the arctic soils and permafrost. Fragments of the uppermost soil horizons that were cryoturbated, buried by solifluction or accumulated in the transient layer of permafrost appear to be the environmental niche in profiles of Turbic Cryosols that can significantly sustain protists' viability.

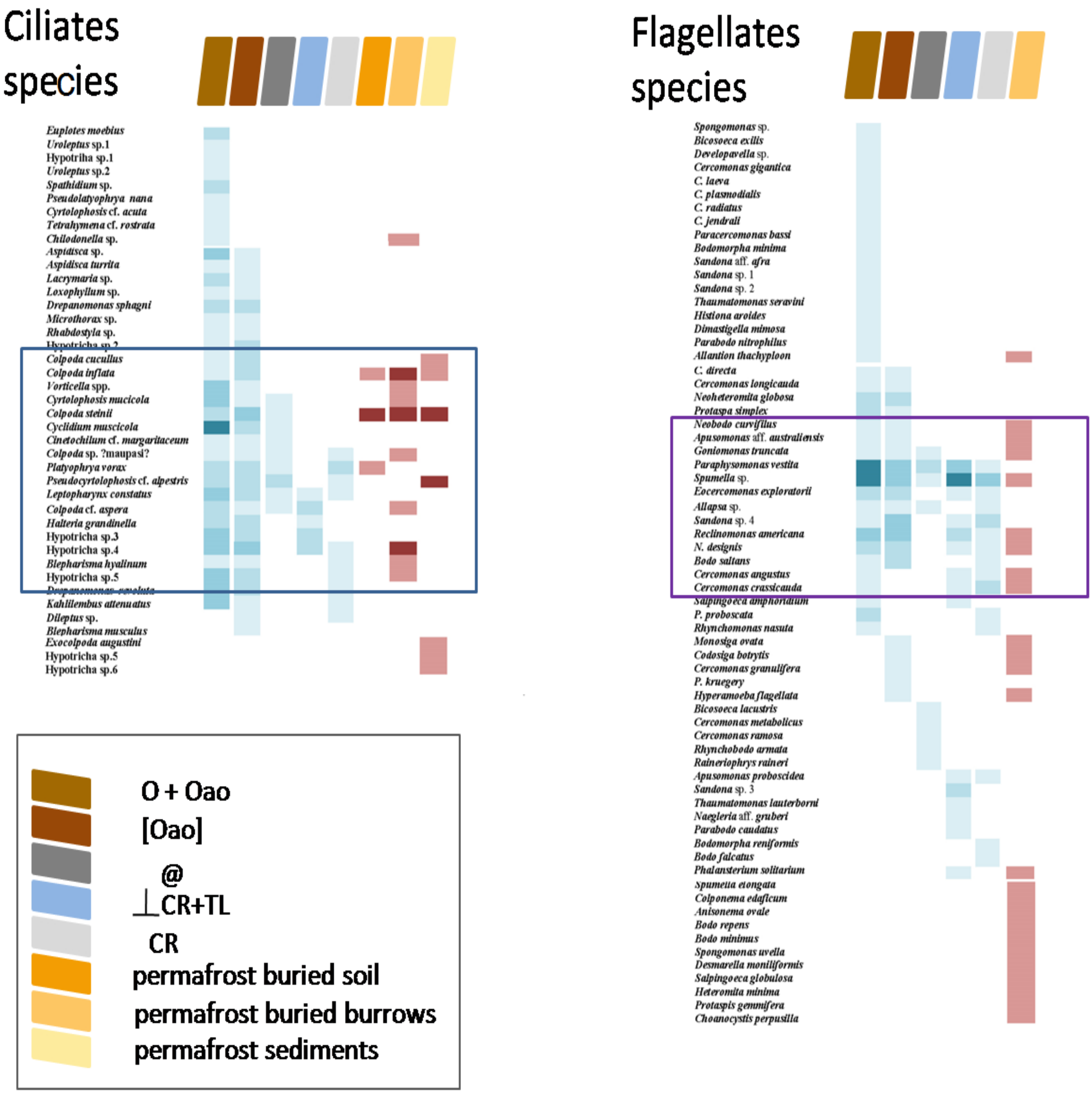

Figure 1. Occurence and frequency of ciliate (left) and flagellate (right) species in the different strata.

Acknowledgments

The research was partially supported by RFBR (17-04-01397; 17-04-00565).

References

Shatilovich, A.V., Shmakova, L.A., Mylnikov, A.P., Gilichinsky, D.A., 2009. Ancient protozoa isolated from permafrost. In: Margesin, R. (ed.), *Soil Biology*. Springer, v.16, 97–115.

A First Pan-Arctic Assessment of Dissolved Organic Carbon in Permafrost-Region Lakes

Lydia Stolpmann[1,2], Anne Morgenstern[1], Julia Boike[1], Michael Fritz[1], Ulrike Herzschuh[1], Kathleen Stoof-Leichsenring[1], Yury Dvornikov[1,3], Caroline Coch[1,2], Amy Larsen[4], Katey Walter Anthony[5], Christopher Arp[5], Benjamin Jones[6], and Guido Grosse[1,2]

[1]*Alfred Wegener Institute, Helmholtz Centre for Polar and Marine Research, Potsdam, Germany, Lydia.Stolpmann@awi.de*

[2]*University of Potsdam, Institute of Earth and Environmental Sciences, Potsdam, Germany*

[3]*Earth Cryosphere Institute Siberian Branch Russian Academy of Science, Tyumen, Russia*

[4]*Yukon-Charley Rivers National Preserve and Gates of the Arctic National Park and Preserve, National Park Service, Fairbanks, AK, USA*

[5]*Water and Environmental Research Center, University of Alaska, Fairbanks, AK, USA*

[6]*U.S. Geological Survey, Alaska Science Center, Anchorage, AK, USA*

Abstract

Permafrost-region lakes are a major component of the global carbon cycle. Many of these lakes contain large amounts of dissolved organic carbon (DOC), which may be subject to microbial or photo-degradation and result in the emission of the greenhouse gases CO_2 and CH_4. For better estimations of the total DOC pool and contribution of lake DOC to climate change, a pan-Arctic analysis of the spatial variability of lake DOC in permafrost regions is crucial but still missing. Hence, we provide an insight into the variability of DOC with lake types and regions, and an overview of the DOC concentration in permafrost-region lakes in the pan-Arctic. Our database 'PeRL-DOC v1' contains data from 1,446 water samples of 1,120 lakes in 26 arctic study sites. We here analyze the database for regional differences in DOC concentration of permafrost-region lakes, and discuss reasons for differences and similarities among and within study areas.

Keywords: Arctic Lakes; Thermokarst; Carbon Cycling; DOC.

Introduction

Next to particulate carbon from shore erosion and stream influx, dissolved organic carbon (DOC) is one of the main carbon reservoirs in permafrost-region lakes (Tranvik *et al*., 2009). Furthermore, DOC is chemically labile (Vonk *et al*., 2013) and can be rapidly mineralized by photochemical reaction or microbial activities and emitted as carbon dioxide (CO_2) and methane (CH_4) to the atmosphere (Frey & Smith, 2005). This process is an important component of the global carbon cycle and contributes to the greenhouse effect (Finlay *et al*., 2006). In recent years, lability and mobility of DOC were increasingly studied in connection to landforms and terrain properties. However, these investigations often focused on single study areas. A pan-Arctic analysis of the spatial variability of DOC concentration and reactivity in permafrost regions, particularly in lakes is still missing. Hence, the objectives of this study are to synthesize existing datasets of DOC from these regions and to provide the 'Permafrost-Region Lake DOC Database Version 1' (PeRL-DOC v1) with an overview of the concentration of DOC in permafrost region lakes in the pan-Arctic. Our synthesis includes published datasets as well as unpublished datasets from the author team to asses

(1) regional differences in DOC concentration of lakes in the Arctic, and
(2) reasons for differences and similarities of DOC concentration between or within study areas.

Study areas

In total, 1,446 freshwater samples from the water columns of 1,120 water bodies with surface areas from 0.0095 ha up to 2,120 ha in the Arctic and Subarctic were considered in our study. They include 26 study sites in northeast Siberia, northwest Siberia, northwest Canada, northeast Canada, north Alaska, west Alaska, southeast Alaska, and central Alaska.

Methodical Approach

All samples were collected during summer period; the earliest sample is from mid-May, the latest sample is from end September. For DOC measurements, high-temperature catalytic combustion with a 'Shimadzu

TOC' Analyzer was used. We digitized all lakes and ponds using high-resolution satellite imagery and the desktop geographic information system (GIS) software ArcMap. We determined lake morphological parameters, such as surface area, perimeter, and circularity index. To characterize permafrost region type we used the IPA permafrost map (Brown *et al.,* 1997) and for Alaska the high-resolution Alaska permafrost map by Jorgenson *et al.* (2008) to extract the permafrost zone, deposit type, and ground ice contents. We used various databases to extract other geological and cryolithological information for each lake, such as whether a lake is within the Yedoma region (Strauss *et al.*, 2016), within former glaciation boundaries (Ehlers & Gibbard, 2004), and what the soil carbon storage is in the region (Hugelius *et al.,* 2014). Additionally, we characterize lake basin type, presence of active shore erosion, lake connectivity, and season of sample collection (e.g. early summer, summer season, late summer/fall) for each lake.

Preliminary results

The DOC concentration of 'PeRL-DOC v1' ranges from 0 mg L^{-1} to 1,130 mg L^{-1} (Tab.1). A comparison of permafrost-region lakes and ponds from Alaska (n=1,135), Canada (n=83), and Siberia (n=228) shows higher DOC concentrations in Alaska and almost similar DOC concentrations in Canada and Siberia. The northernmost study sites North Slope, north Alaska, Cape Bounty and Bathurst Island in northeast Canada have lowest DOC concentrations in our database.

Table 1. Lake water column DOC concentrations in the study areas.

Study area	n samples/ n lakes	DOC [mg L^{-1}] range	mean	median
Northeast Siberia	158/105	1.1-33.3	9.6	9.7
Northwest Siberia	70/56	2.3-19.4	6.7	5.1
Northwest Canada	54/54	5.5-38.7	15.2	13.6
Northeast Canada	29/29	1.1-9.6	3,4	2.7
North Alaska	64/16	0-20.8	3	1.7
West Alaska	435/374	0.7-53.3	10.5	9.2
Southeast Alaska	516/366	0.8-66.7	15.6	14
Central Alaska	120/120	10.2-1,130	52.6	32.7
Total	1,446/1120	0-1,130	15.4	11.4

We found highest DOC concentrations and the biggest range in the Yukon Flats, central Alaska. Median DOC concentration of lakes in northeast Siberia and west Alaska are similar, with higher variability in west Alaska. As well as median DOC concentration of lakes and ponds in northwest Canada and southeast Alaska is similar, with higher variability in southeast Alaska. We also found no differences in the DOC concentrations of lakes in Yedoma and Non-Yedoma regions. In summary, we found a median DOC concentration of 11.4 mg L^{-1} in 'PeRL-DOC v1' with large inter- and intra-regional differences. Ongoing analyses focus on the causes for these DOC patterns.

Acknowledgments

This study is supported by a PhD stipend of the University of Potsdam to LS and the ERC PETA-CARB project. We would like to thank all colleagues being involved in sample collection and laboratory analyzes in all study areas.

References

Brown, J., et al. 1997. Circum-Arctic map of the permafrost and ground-ice conditions. *U.S. Geological Survey in Cooperation with the Circum-Pacific Council for Energy and Mineral Resources, Washington, DC, USA.*

Ehlers, J., & Gibbard, P.L., 2004. Quaternary glaciations: extend and chronology. Parts I-III. *Developments in Quaternary Science 2, Amsterdam: Elsevier.*

Finlay, J., et al. 2006. Snowmelt dominance of dissolved organic carbon in high-latitude watersheds: Implications for characterization and flux of river DOC. *Geophysical Research Letters* 33, L10401.

Frey, K.E. & Smith, L.C., 2005. Amplified carbon release from vast West Siberian peatlands by 2100. *Geophysical Research Letters* 32: L09401.

Hugelius, G., et al. 2014. Estimated stocks of circumpolar permafrost carbon with quantified uncertainty ranges and identified data gaps. *Biogeosciences* 11: 6573-6593.

Jorgenson, M.T., et al. 2008. Map of Permafrost Characteristics of Alaska. *Institute of Northern Engineering, University of Alaska Fairbanks.*

Strauss, J., et al. 2016. Database of Ice-Rich Yedoma Permafrost (IRYP). *Pangaea.*

Tranvik, L.J., et al. 2009. Lakes and reservoirs as regulators of carbon cycling and climate. *Limnology and Oceanography* 54 (6, part 2): 2298-2314.

Vonk, J.E., et al. 2013. High biolability of ancient permafrost carbon upon thaw. *Geophysical Research Letters* 40: 2689-2693.

Water and DOC fluxes from a Subarctic catchment underlain by discontinuous permafrost: insights from historical data and in-situ high resolution observations

Nikita Tananaev[1]
Laure Gandois[2]
Anatoly Prokushkin[3]
Roman Teisserenc[2]

[1]*Melnikov Permafrost Institute SB RAS, Yakutsk, Russia, nikita.tananaev@gmail.com*
[2]*EcoLab, Université de Toulouse, CNRS, INPT, UPS, Toulouse, France*
[3]*Sukachev Forest Institute, Krasnoyarsk Science Centre, SB RAS, Krasnoyarsk, Russia*

Abstract

The subarctic Graviyka River catchment was instrumented in 1938 by Roshydromet, but observations ceased in 1993. In 2014, same gauge was revisited and instrumented to obtain high-resolution data on water flows and dissolved organic carbon (DOC) concentrations. Contemporary water and DOC fluxes are calculated and compared to historical data.

Keywords: dissolved organic matter; fDOM; long–term monitoring; Northern Yenisey; permafrost hydrology.

Introduction

Long-term observations in high-latitude catchments are becoming increasingly important in the scope of the rapidly changing Arctic (Laudon *et al.*, 2017). Hydrological response of northern catchments to these changes depends on permafrost continuity and extent (Streeltsky *et al.*, 2015; Evans & Ge, 2017).

Permafrost-affected catchments stock half of the global soil organic carbon. Dissolved organic matter (DOM) concentrations in rivers draining these watersheds are elevated, and large amounts of organic carbon are exported to the Arctic Ocean (Amon *et al.*, 2012). In the context of permafrost alteration, understanding the origin of water and DOM transported by these rivers is critical. Varying importance of seasonal changes in flow paths within the active layer, and DOM origin from different sources including thawing permafrost, all have numerous implications in the perspective of establishing carbon budgets for Northern watersheds.

The objective of present narrative is twofold: (i) to describe and analyze historical hydrological dataset; (ii) to present detailed results from our ongoing monitoring campaign started in 2015.

Study Site

The Graviyka River catchment is one of the four presently active northern research basins in Russia, and the only one above the Arctic Circle (Laudon *et al.*, 2017). The Graviyka River is a right-hand tributary of the Yenisei River in the surroundings of Igarka, Krasnoyarsk Krai (67°30'02.54"N, 86°34'17.47"E). Its catchment, having an area of 323 km², is located in the transition zone between continuous and discontinuous permafrost, and between the taiga and tundra ecosystems. Periglacial landforms, as thermokarst and terminal moraine lakes, and palsas (Tananaev, 2016).

Data & Instruments

Historical data

The piled gauging station on the Graviyka R. in Igarka was maintained by Roshydromet from 1938 to 1993. Daily flow data, supplemented by scarce water chemistry and sediment data, are available for this period.

Present-day data

The Graviyka catchment in the Northern Yenisey region is studied since 2013, when regular water sampling has started close to the basin outlet to access DOC, major and trace element concentrations, stable water isotopes. The gauging station was revisited in 2014. An Exo-2 (YSI, Xylem Inc., USA) multiparameter sonde was installed at the historical gauging station location in 2015, observing water level, temperature, conductivity, pH, dissolved oxygen, and fDOM (fluorescent dissolved organic matter), a proxy for DOC, at an hourly resolution.

Results and Discussion

Historical water flows

Mean annual daily flow (MADF) for 1938–1993 is 5.08 $m^3.s^{-1}$, water flux 0.16 $km.a^{-1}$, and runoff, 15.7 $l.s^{-1}.km^{-2}$. Neither mean annual nor maximum daily flows show any significant temporal trends during this earlier period.

Water regime features four distinct periods: winter (X–V), spring freshet (VI), and summer low flow (VII–IX), interrupted by autumn floods of late September (Fig. 1). The driest decade on record falls on the 1970s, with lowest flows in 1976, aligned with a heat wave hitting Europe the same year.

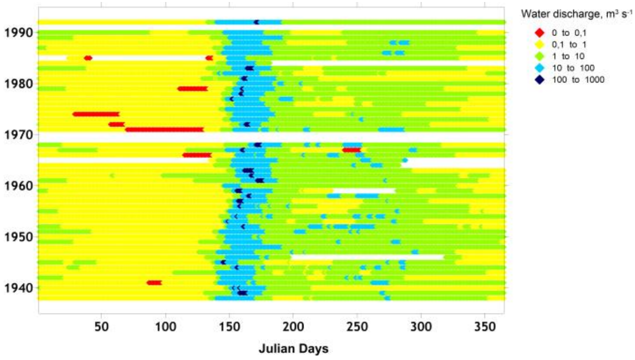

Figure 1. Daily flows of the Graviyka R. in Igarka (1938–1992)

Contemporary water & DOC fluxes

Recent observations cover period from July 2015 to present (Fig. 2), fully covering 2016 calendar year. The MADF values are comparable to previously observed, ranging from 5.02 to 7.10 $m^3.s^{-1}$. This latter value matches the historical MADF maximum of 1983.

Spring frechet peaks in the first week of June, as in mid-1940s. During spring freshet, DOC peak occurs several days before discharge peak. This peak is then strongly diluted by snowmelt. During summer storms and autumn flood, DOC peaks occur after water peaks, indicating lateral transfer, presumably from peatland, as DOC increase is accompanied by a decrease of both conductivity and pH.

In excessively dry years (2013, 2016), low DOC, high pH and negative d-excess values in July and August show potential input from heavily evaporated sources.

Based on the two years of record, we estimate the DOC export between 5 and 7 $g.m^{-2}.a^{-1}$, the lowest range corresponding to an extremely dry year (2016). Spring flood represents from 50 to 80% of both total water and DOC export. On the annual scale, the water and DOC fluxes are strongly correlated. Seasonal specificity is observed, with higher DOC to discharge ratio in autumn.

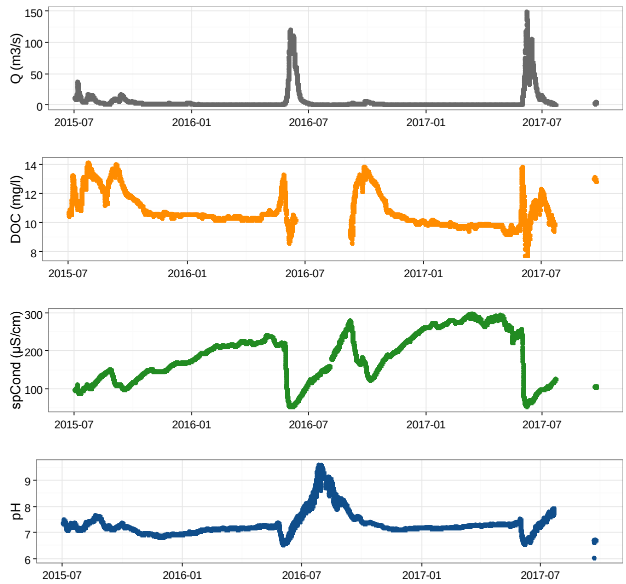

Figure 2. Hourly calculated water fluxes and DOC concentrations and measured specific conductivity and pH.

Acknowledgments

This study is partially supported by RFBR, Project No. 07-05-00943a, and by EC2CO (CNRS) project TOMCAR-Sat.

References

Amon, R.M.W., Rinehart, A.J., Duan S., *et al.*, 2012. Dissolved organic matter sources in large Arctic rivers, *Geochimica et Cosmochimica Acta* 94: 217–237.

Evans, S.G. & Ge, S., 2017. Contrasting hydrogeologic responses to warming in permafrost and seasonally frozen ground hillslopes, *Geophysical Research Letters* 44: 1803–1813.

Laudon, H., Spence, C., Buttle, J., *et al.*, 2017. Save northern high-latitude catchments. *Nature Geoscience* 10: 324–325.

Streletsky, D., Tananaev, N., Opel, T. *et al.*, 2015. Permafrost hydrology in changing climatic conditions: seasonal variability of stable isotope composition in rivers in discontinuous permafrost, *Environmental Research Letters* 9: 095003.

Tananaev, N.I., 2016. Sediment and solute fluxes at the Igarka field site, Russian subarctic. In: Beylich, A.A., Dixon, J.C., Zwolinski, Z. (eds) *Source-to-sink Fluxes in Undisturbed Cold Environments*. Cambridge: Cambridge Univ. Press, p. 144–153.

Changing biogeochemical function in thaw-disturbed freshwater networks of the Peel Plateau, western Canadian Arctic

Suzanne E. Tank[1]
Steven V. Kokelj[2]
Cara A. Littlefair[1]
Sarah Shakil[1]
Scott Zolkos[1]
Vincent St. Louis[1]
Kyra St. Pierre[1]
[1]*Department of Biological Sciences, University of Alberta, Edmonton, Alberta, T6G 2E9, Canada; suzanne.tank@ualberta.ca*
[2]*Northwest Territories Geological Survey, Government of the Northwest Territories, Yellowknife, NWT, X1A 2L9, Canada*

Abstract

The Peel Plateau is a characteristic ice-marginal glaciated landscape, typified by deposits of deep glacial tills and massive ground ice that enable catastrophic retrogressive thaw slump activity. Our work aims to understand the biogeochemical effects of permafrost thaw in this region, with a consideration of effects across slump features of various morphologies, and scales ranging from the immediate downstream-of-slump environment, to the full catchment scale. Thaw slump effects occur overwhelmingly in the particulate and inorganic phase on the Peel Plateau, with releases of particulate organic carbon that dwarf those for organic carbon in the dissolved phase, and changes to chemical weathering that cause fundamental alterations to carbon cycling at the terrestrial-freshwater interface. Our results underscore the importance of accounting for variability within and across Arctic regions when seeking to understand the biogeochemical effects of permafrost thaw.

Keywords: dissolved organic carbon; particulate organic carbon; weathering; bio-degradation, mercury; western Canadian Arctic

Introduction

Ice-marginal glaciated landscapes – which house vast quantities of Pleistocene-aged ground ice, and are therefore strongly susceptible to catastrophic permafrost thaw – are found throughout the circumpolar Arctic (Kokelj et al. 2017). This landscape type is typified by the presence of deep glacial tills, and thus differs from most locations that have been focal points for examining biogeochemical change in response to permafrost thaw. As a result, these till-dominated landscapes represent an important, but poorly understood, target for research efforts if we are to understand the range of biogeochemical effects that might be triggered by permafrost thaw across a diverse pan-Arctic system.

One region that typifies the ice-marginal glaciated landscape is the Peel Plateau, where rapid climate-induced change coupled with the presence of massive ground ice is causing permafrost thaw to manifest as large retrogressive thaw slump (RTS) features. These features can mobilize millions of cubic meters of sediment downslope, and have significant effects on downstream ecosystems (e.g., Kokelj *et al.*, 2013, Littlefair *et al.* 2017). Soils on the Peel Plateau are comprised of deep, mineral-rich glacial tills deposited during the late Pleistocene. Warming during the early Holocene caused organic matter to be incorporated into upper permafrost layers (Lacelle *et al.*, 2013), which are now separated from deeper, ice-rich Pleistocene deposits by a pronounced thaw unconformity (Burn, 1997). Our goal is to understand how permafrost degradation in this region is affecting biogeochemical cycling across the land-freshwater continuum, with a consideration of effects across various spatial scales and different thaw morphologies.

Methods

We work at a variety of spatial scales: sampling the chemical composition of headwalls, to thaw slump runoff waters, to downstream waters that incorporate variable amounts of RTS disturbance in their catchments. We also incorporate RTS features of varying size and age into our analyses, to enable us to consider how thaw slump morphology, and the variable exposure of Pleistocene- vs. Holocene-aged soils, alters the biogeochemical effect of slumping on the Peel Plateau.

Results and Discussion

The mineral-rich nature of permafrost soils on the Peel Plateau, coupled with substantial RTS-enabled sediment mobilization, causes the effects of permafrost thaw to be strongly mediated by particle- and mineral-associated processes. At a direct level, these effects are striking: particulate organic carbon concentrations increase by up to two orders of magnitude downstream of slumps, while a similar increase in weathering ions causes a fundamental alteration of the inorganic C cycle in downstream systems. However, these direct effects also have important indirect implications for biogeochemical change. For example, while RTSs release DOC of low aromaticity and high degradeability – similar to other permafrost-affected landscapes – the presence of mineral-rich suspended sediment appears to sequester DOC downstream of slumps (Littlefair *et al.* 2017). RTS activity also leads to a marked increase in methyl mercury transport, with fluxes almost entirely associated with the particulate phase. Overall, these findings from the Peel Plateau highlight the importance of assessing the effects of permafrost thaw over multiple biogeochemical constituents, and a broad diversity of Arctic landscape types.

Acknowledgments

Funding for this work was provided by the Polar Continental Shelf Program, the Natural Sciences and Engineering Research Council of Canada, and the Campus Alberta Innovates Program. We would like to acknowledge the many community members from Fort McPherson who have assisted with this work, and who have guided our access to their traditional territories.

References

Burn, C.R., 1997. Cryostratigraphy, paleogeography, and climate change during the early Holocene warm interval, western Arctic coast, Canada. *Canadian Journal of Earth Sciences* 34: 912-925.

Kokelj, S.V., Lacelle, D., Lantz, T.C., Tunnicliffe, J., Malone, L.., Clark, I.D. & Chin, K.S., 2013. Thawing of massive ground ice in mega slumps drives increases in stream sediment and solute flux across a range of watershed scales. *Journal of Geophysical Research-Earth Surfaces* 118: 681-692.

Kokelj, S.V., Lantz, T.C., Tunnicliffe, J., Segal, R. & Lacelle, D., 2017. Climate-driven thaw of permafrost preserved glacial landscapes, northwestern Canada. *Geology* 45: 371-374.

Lacelle, D., Lauriol, B., Zazula, G., Ghaleb, B., Utting, N. & Clark, I.D. 2013. Timing of advance and basal condition of the Laurentide Ice Sheet during the last glacial maximum in the Richardson Mountains, NWT. *Quaternary Research* 80: 274-283.

Littlefair, C.A., Tank. S.E. & Kokelj, S.V. 2017. Retrogressive thaw slumps temper dissolved organic carbon delivery to streams of the Peel Plateau, NWT, Canada. *Biogeosciences* 14: 5487–5505.

Impetuous CO_2 release from eroding permafrost coasts

George Tanski[1,2,3], Dirk Wagner[4], Michael Fritz[3], Torsten Sachs[1], and Hugues Lantuit[2,3]
[1]*GFZ German Research Centre for Geosciences, Helmholtz Centre Potsdam, Section 1.4 Remote Sensing, Potsdam, Germany*
[2]*Potsdam University, Institute of Earth and Environmental Sciences, Potsdam, Germany*
[3]*Alfred Wegener Institute, Helmholtz Centre for Polar and Marine Research, Potsdam, Germany*
[4]*GFZ German Research Centre for Geosciences, Helmholtz Centre Potsdam, Section 5.3 Geomicrobiology, Potsdam*

Abstract

The warming of the Earth results in extensive permafrost thaw in the Northern Hemisphere. With thaw, large amounts of organic carbon are mobilized, some of which is converted and released into the atmosphere as greenhouse gases. This in turn, facilitates a positive permafrost carbon feedback and thus further warming. Permafrost thaw and subsequent greenhouse gas release is presumed to be caused primarily by the vertical deepening of the active layer. Yet, abrupt thaw and erosion processes are neglected in carbon budgets and models. Here we show that thaw-induced lateral erosion of permafrost coasts is a major source of greenhouse gases. In addition, this greenhouse gas release is an order of magnitude relevant for the Arctic carbon cycle. With accelerating erosion rates, longer open water seasons, and warming air temperatures, this lateral flux and subsequent greenhouse gas release will increase and potentially contribute to the Earth's warming.

Keywords: Arctic Ocean, Canadian Arctic, Coastal erosion, Lateral fluxes, Biogeochemical cycling, Greenhouse gases

Introduction

Climate warming causes extensive thaw of permafrost in the Northern Hemisphere with far-reaching implications for nature and human society (Schuur *et al.*, 2015). The northern permafrost region stores vast amounts of organic carbon (~1307 Gt; Hugelius *et al.*, 2014). With permafrost thaw, large portions of this freeze-locked organic carbon pool are converted into greenhouse gases, resulting in a positive permafrost carbon feedback and thus further climate warming (Schädel *et al.*, 2014). This process is included in models as a gradual deepening of the active layer. Yet, the erosion of Arctic coasts and thermokarst processes result in rapid mobilization of deep permafrost organic carbon but are not included in the models (Schuur *et al.*, 2015). Most of the erosion-derived organic carbon is assumed to be directly buried in nearshore sediments or transported offshore, excluding turnover into greenhouse gases in the coastal zone (e.g., Vonk & Gustafsson, 2013). We hypothesize that permafrost organic carbon is subject to extensive mineralization upon erosion in nearshore waters, which result in the production of greenhouse gases in quantities significant to the Arctic carbon budget and the Earth's climate.

Methods

We mimicked the coastal erosion process in an incubation experiment by mixing permafrost with seawater under aerobic conditions for a single Arctic open-water season (~4 months) and different temperature scenarios (4°C and 16°C). Permafrost and seawater samples were taken at a continuous permafrost site - *Qikiqtaruk* – Herschel Island (Yukon Coast, western Canadian Arctic) and the adjacent coastal waters of the Beaufort Sea. Permafrost and seawater samples were kept frozen until start of the incubation experiment in the lab to avoid microbial turnover prior to incubation. Greenhouse gases (carbon dioxide and methane) were quantified systematically at certain time intervals using gas chromatography. Total and dissolved organic carbon, organic carbon/nitrogen-ratios and $\delta^{13}C$-organic carbon isotope signatures were quantified prior (T = 0) and after (T = 1) the experiment and resulting differences (Δ T = 0 : T = 1) used to detect degradation processes.

Results

Our results show that large amounts of carbon dioxide are rapidly produced within nearshore waters along eroding permafrost coast. The amounts produced within the coastal zone are comparable to carbon dioxide emissions detected from permafrost thaw on land (e.g., Knoblauch *et al.*, 2013). We found that at ambient Arctic summer temperatures (4°C scenario) the production of carbon dioxide from permafrost is almost as efficient as production without seawater added. With higher temperatures (16°C scenario) carbon dioxide production further increases by up to 115%.

Discussion

The rapid production of carbon dioxide in coastal waters is most likely caused by the turnover of the fast and labile permafrost carbon pool (Schädel *et al.*, 2014). Although organic carbon/nitrogen-ratios decrease and $\delta^{13}C$-organic carbon isotope concentrations increase only slightly, TOC and DOC contents decrease substantially in almost all incubation setups; both indicating overall degradation of organic carbon (e.g., Strauss *et al.*, 2015) and subsequent turnover into carbon dioxide (e.g., Elberling *et al.*, 2013). A simple upscaling approach based on the latest numbers on circum-Arctic sediment fluxes (up to 14 Tg yr^{-1}; Wegner *et al.*, 2015), reveals that the carbon dioxide release from nearshore zones could be significant to the Arctic carbon budget and permafrost carbon feedback loops. With expected acceleration of erosion, higher air and seawater temperatures, and longer open waters seasons (Barnhart *et al.*, 2014 and references therein), we expect a substantial increase of carbon dioxide emissions from nearshore waters along eroding permafrost coasts.

Conclusion

We conclude that lateral erosion in general and the erosion of permafrost coasts and subsequent carbon dioxide emission from nearshore waters in particular are neglected sources of greenhouse gases into the atmosphere. These emissions are important within the Arctic carbon cycle and potentially contribute to the Earth's warming.

Acknowledgements

We thank O. Burckhardt, I. Milczarek, A. Eulenburg, D. Scheidemann, and P. Overduín for their expertise and support during lab work. C. Knoblauch, S. Liebner, and A. Kiss are thanked for scientific guidance. A.M. Irrgang, E. McLeod, and S. Stettner are thanked for assisting in the field and J. Kahl for logistical support. We especially acknowledge the logistical support in Canada provided by R. Gordon and the rangers from the *Qikiqtaruk* – Herschel Island Territorial Park as well as by J. Gareis from the Aurora Research Institute.

References

Barnhart, K. R., Anderson, R. S., Overeem, I., Wobus, C., Clow, G. D., & Urban, F. E., 2014. Modeling erosion of ice-rich permafrost bluffs along the Alaskan Beaufort Sea coast. *Journal of Geophysical Research: Earth Surface* 119(5): 1155–1179.

Elberling, B., Michelsen, A., Schädel, C., Schuur, E. A. G., Christiansen, H. H., Berg, L., Tamstorf, M. P., & Sigsgaard, C., 2013. Long-term CO2 production following permafrost thaw. *Nature Climate Change* 3: 890–894.

Hugelius, G., Strauss, J., Zubrzycki, S., Harden, J. W., Schuur, E. A. G., Ping, C. L., Schirrmeister, L., Grosse, G., Michaelson, G. J., Koven, C. D., O'Donnell, J. A., Elberling, B., Mishra,U., Camill, P., Yu, Z., Palmtag, J., & Kuhry, P., 2014. Estimated stocks of circumpolar permafrost carbon with quantified uncertainty ranges and identified data gaps. *Biogeosciences* 11(23): 6573–6593.

Knoblauch, C., Beer, C., Sosnin, A., Wagner, D., & Pfeiffer, E. M., 2013. Predicting long-term carbon mineralization and trace gas production from thawing permafrost of Northeast Siberia. *Global Change Biology* 19(4): 1160–1172.

Schädel, C., Schuur, E. A. G., Bracho, R., Elberling, B., Knoblauch, C., Lee, H., Luo, Y., Shaver, M. R., & Turetsky, M. R., 2014. Circumpolar assessment of permafrost C quality and its vulnerability over time using long-term incubation data. *Global Change Biology* 20(2): 641–652.

Schuur, E. A. G., McGuire, A. D., Grosse, G., Harden, J. W., Hayes, D. J., Hugelius, G., Koven, C. D., Kuhry, P., Lawrence, D. M., Natali, S. M., Olefeld, D., Romanovsky, V. E., Schaefer, K., Turetsky, C. C., & Vonk, J. E., 2015. Climate change and the permafrost carbon feedback. *Nature* 520: 171–179.

Strauss, J., Schirrmeister, L., Mangelsdorf, K., Eichhorn, L., Wetterich, S., & Herzschuh, U., 2015. Organic-matter quality of deep permafrost carbon - A study from Arctic Siberia. *Biogeosciences* 12(7): 2227–2245.

Vonk, J. E. & Gustafsson, Ö., 2013. Permafrost-carbon complexities. *Nature Geoscience* 6(9): 675–676.

Wegner, C., Bennett, K. E., de Vernal, A., Forwick, M., Fritz, M., Heikkila, M., … & Werner, K., 2015. Variability in transport of terrigenous material on the shelves and the deep Arctic Ocean during the Holocene. *Polar Research* 34: 1–19.

Organic matter lability in High Arctic surface waters and permafrost soils

Gillian D. Thiel[1]
Julien Fouché[1,2]
Melissa J. Lafrenière[1]
Neal A. Scott[1]
Scott F. Lamoureux[1]
[1]*Department of Geography and Planning, Queen's University, Kingston, ON, Canada, gillian.thiel@queensu.ca*
[2]*Department of Biosystem Engineering (BIOSE), Gembloux Agro-Bio Tech, University of Liège (ULg), 5030 Gembloux, Belgium*

Abstract

Climate change is altering the organic matter cycle at high latitudes, which has subsequent effects on greenhouse gas emissions and water quality. This study focuses on the quantity and quality of organic matter in High Arctic surface waters and an in the active layer of permafrost soils. Specifically, it aims to identify differences in the biodegradability of organic matter between sites with varying vegetation and geomorphic characteristics as well as differences over the summer field season (July – August). Further, this study highlights the relationship between the labile organic matter fraction, quantified by incubation, and the fluorescence-absorbance properties of dissolved and water-extractable organic matter. A better understanding of the controls of organic matter lability in the High Arctic, and its relationship with more easily measurable properties such as fluorescence and absorbance, will allow for the collection of high temporal and spatial resolution data needed to develop more robust models of carbon cycling under a changing climate.

Keywords: carbon; ponds; fluorescence spectroscopy; biodegradability; active layer; permafrost disturbance

Introduction

Climate change affects organic matter cycling in the High Arctic through permafrost degradation, changes in tundra vegetation, and altered hydrological regimes (AMAP, 2017). These changing parameters affect the quantity and quality of organic matter in surface waters and the active layer of permafrost soils. Of specific interest is the quantity of labile organic matter stored in these systems, that is the organic matter readily available for microbial mineralization to CO_2 or CH_4 (Schuur *et al.*, 2008; Vonk & Gustafsson, 2013).

This study examines the lability of organic matter present in High Arctic ponds and active layer soils, through incubation experiments. Due to the high resource demands of incubation experiments, we also analyze the fluorescence and absorbance properties of pond dissolved organic matter (DOM) and water-extractable organic matter (WEOM) from soils, in an effort to develop a more efficient approach for identifying labile organic matter.

Pond dissolved organic matter

Water samples were collected from six shallow ponds in the West River watershed at Cape Bounty, Melville Island, Nunavut in 2016. Samples were collected in early to mid-July as ponds appeared, and again in early August. The ponds were located in varying geomorphic settings, including two in active layer disturbance scars formed in 2007.

Pond samples were incubated for 28 days at 20°C in the dark, with triplicate aliquots removed at 0, 2 7, 14 and 28 days for chemical and optical (fluorescence-absorbance) analyses. Chemical analyses dissolved organic carbon (DOC) concentrations, total dissolved nitrogen (TDN) concentrations, and dissolved inorganic ion (NO_2^-, NO_3^-, Cl^-, Br^-, SO_4^{2-}, K^+, Na^+, Mg^{2+}, Ca^{2+}, NH_4^+) concentrations. Labile organic matter was quantified as the loss of DOC over the incubation period which is referred to as biodegradable organic carbon (BDOC).

Results indicate that BDOC and initial chemical composition can vary significantly between ponds. Ponds with higher dissolved inorganic ion concentrations had greater BDOC concentrations. Comparison of inorganic ion concentrations with permafrost core data and measured active layer depths in 2016 suggests that inputs from subsurface flow on the permafrost table may increase DOM lability in the ponds. Furthermore, in agreement with the literature, BDOC was correlated to the specific absorption of ultraviolet light at an excitation wavelength of 254 nm

($SUVA_{254}$, n=11, $p<0.05$), indicating that $SUVA_{254}$ seems to be a relevant proxy for DOM lability (e.g. Wickland *et al.*, 2012).

Soil organic matter

In 2017, soil samples were collected in triplicate from the top 10 cm of the active layer in the five major vegetation classes at Cape Bounty. Samples were collected in early July, mid-July, and early August. Soils will be incubated for 30 days at room temperature in the dark to measure CO_2 production as a proxy for organic matter lability. Water-extractable organic matter (WEOM) will be collected from the soils before and after the incubation period. WEOM will be analyzed in the same way as the pond samples (DOC, TDN, dissolved inorganic ions, BDOC, and fluorescence-absorbance). Soils will also be analyzed for total carbon and nitrogen before and after the incubation period.

Although WEOM concentrations are generally low in soils, WEOM is often the most active fraction of soil organic matter (Chantigny, 2003). Therefore, we hypothesize that measured CO_2 production (i.e. soil organic matter lability) will increase with WEOM concentrations and lower $SUVA_{254}$ values. Additionally, it is expected that organic matter lability will vary by vegetation type due to differences in organic matter inputs, litter quality, plant and soil microbial community composition (Neff & Hooper, 2002).

The results of the soils study will contribute to the development of a more robust soil organic matter database for the High Arctic. Furthermore, understanding how soil organic matter quantity and quality varies by vegetation type will help predict future organic matter cycling in the active layer, as vegetation patterns in the High Arctic change.

Acknowledgments

Many thanks to all field researchers at the Cape Bounty Arctic Watershed Observatory in 2016 and 2017 as well as to our funding partners: NSERC, the W. Garfield Weston Foundation, the Polar Continental Shelf Program (PCSP), ArcticNet, and the Northern Scientific Training Program (NSTP). Permitting for this research was facilitated by the Nunavut Research Institute (NRI).

References

AMAP, 2017. Snow, Water, Ice, and Permafrost in the Arctic (SWIPA) 2017. Arctic Monitoring and Assessment Programme (AMAP), Oslo, Norway. xiv +269 pp

Chantigny, M., 2003. Dissolved and water-extractable organic matter in soils: a review on the influence of land use and management practices. *Geoderma* 113:357-380.

Neff, J. & Hooper, D., 2002. Vegetation and climate controls on potential CO_2, DOC, and DON production in northern latitude soils. *Global Change Biology* 8:872-884.

Schuur, E. A., Bockheim, J. Canadell, J.G, Euskirchen, E., Field, C. B., Goryachkin, S. V., Zimov, S.A., 2008. Vulnerability of permafrost carbon to climate change impacts. *Biogeosciences* 58: 701-714.

Vonk, J.E. & Gustafsson, Ö., 2013. Permafrost-carbon complexities. *Nature Geoscience* 6:675-676.

Wickland, K.P., Aiken, G.R., Butler, K., Dornblaser, M.M., Spencer, R. G. M., Striegl, R. G., 2012. Biodegradability of dissolved organic carbon in the Yukon River and its tributaries: seasonality and important of inorganic nitrogen. *Global Biogeochemical Cycles* 26:1-14.

$^{14}CO_2$ analysis of soil emissions in the High Arctic reveal the degradation of old organic matter sources in permafrost soils

Philipp Wischhöfer[1]
Anja Wotte[1]
Jan Melchert[1]
Gabriel Norén[1]
Janet Rethemeyer[1]
[1]*Institute of Geology and Mineralogy, University of Cologne, p.wischhoefer@uni-koeln.de*

Abstract

The degradability of organic matter stored within permafrost is one key parameter defining the permafrost carbon feedback. Here we present the results of CO_2 flux measurements and of in-situ ^{14}C analyses of CO_2 emitted from the active layer of a High Arctic tundra landscape. CO_2 was sampled at four sites in the Bayelva River watershed near Ny-Ålesund, Svalbard. Uncalibrated ages of the respired CO_2 of up to 880 ± 60 years BP show that microbial respiration is not only restricted to fresh organic matter sources. Variation in $^{14}CO_2$ ages of several hundreds of years for replicate samples from the different sites underlines the strong heterogeneity of the organic matter. CO_2 fluxes vary between 0.007 and 0.275 μmol CO_2 m^{-2} s^{-1}. Higher CO_2 fluxes correlate with low C/N in the upmost 20 cm of the soil, indicating predominant carbon turnover in the upper part of the active layer.

Keywords: ^{14}C, Svalbard, microbial respiration, CO_2, High Arctic, carbon cycle

Introduction

To improve estimates of the permafrost carbon feedback (Schuur et al., 2015), it is necessary to assess the decomposability of organic matter (OM) in permafrost soils. While there are several studies focusing on lower Arctic latitudes and incubation experiments (Schuur et al., 2015), information on OM quality and degradability in the High Arctic is sparse.

We thus conducted a comprehensive study in this area using in-situ $^{14}CO_2$ as well as compositional analyses of the OM that give information on the preferential microbial degradation of organic substrates.

Material and methods

Study site

Our study was performed in the Bayelva watershed, which is located 2 km west of Ny-Ålesund, NW-Spitsbergen.

As for the whole archipelago, a substantial increase of air temperatures, especially during winter times, has been observed over the past decades (Førland et al., 2011).

Sampling

Sampling took place during mid-July 2017. We chose four sites (Table 1) that differ in elevation, vegetation, water content, texture, %-C and C/N to cover the heterogeneity of the landscape.

Bulk soil was sampled from soil pits, which we dug down or close to the permafrost table. CO_2 was collected at two/three locations per site, after previously removing the vegetation, using respiration chambers coupled with molecular sieve cartridges (MSCs; Wotte & Wischhöfer et al., 2017).

A sample of atmospheric CO_2 was taken for referencing. CO_2 fluxes were determined using an infrared gas analyzer.

Analyses

The CO_2 was released from the MSCs by heating in vacuum, purified and partitioned for ^{14}C analysis with the MICADAS AMS (ETH Zurich). ^{14}C concentrations are given as $F^{14}C$ (Reimer et al., 2004).

Freeze-dried samples are currently analyzed for bulk soil parameters (C, N, total organic C, texture), water extractable OM, lipid biomarkers, and ^{14}C of bulk and water extractable OM.

Table 1. Sampling sites: LH(a) – Leierhaugen Hill (a); UDA – Upper Drainage Area; LDAa – Lower Drainage Area a

Site	Elevation (m a.s.l.)	Depth (cm)	Water content (wt.%)	TC (%)	C/N
LH	38	0-20	21.2	3.2	12.9
		20-40	10.8	1.0	16.9
		40-60	12.8	1.2	24.9
		60-70	11.1	1.1	27.5
LHAa	30	0-20	17.1	2.5	17.2
		20-40	12.7	1.6	11.7
		40-60	16.8	1.9	14.2
		60-70	18.2	3.2	21.5
UDA	33	0-20	13.8	1.4	16.1
		20-40	14.3	3.1	25.5
		40-63	13.3	2.8	20.1
LDAa	14	0-20	15.5	1.5	15.9
		20-35	13.3	1.8	23.0
		35-50	14.1	1.8	25.8

Results and discussion

The ^{14}C concentration of the emitted CO_2 varies between 1.002 and 0.897 $F^{14}C$ corresponding to >modern and 880 ± 60 years BP (Fig. 1). The $^{14}CO_2$ concentrations of replicate samples from each site show much stronger variations corresponding to age differences of up to 600 years BP than differences observed between sites. This most likely reflects the strong small-scale variability of the quality of the OM within the active layer.

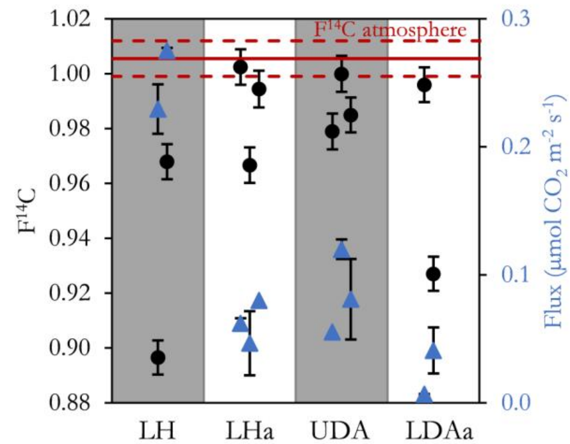

Figure 1. ^{14}C concentration ($F^{14}C$) of respired CO_2 (circles, 1-σ uncertainties) and corresponding CO_2 fluxes (triangles, standard deviation based on two measurements each).

The OM in the surface soil seems to be the major source of the respired CO_2. C/N, which is characteristic of the degradability of the OM (Schädel et al., 2014), is lowest in the surface soil at all sites and increases considerably with depth. This agrees with the increase of more recalcitrant lipids with depth (Rethemeyer et al., 2010).

CO_2 fluxes are highest at the LH site (Fig. 1) with >0.2 μmol m^{-2} s^{-1}, which has the highest carbon content, lowest C/N, and highest water content in 0-20 cm depth (Table 1). At all other sites, CO_2 fluxes are below or just above 0.1 μmol m^{-2} s^{-1} corresponding to lower carbon contents and lower degradability (higher C/N) of the OM.

References

Førland, E.J., Benestad, R., Hanssen-Bauer, I., Haugen, J.E., and Skaugen, T.E., 2011. Temperature and precipitation development at Svalbard 1900–2100. *Adv. Meteorol.* 2011.

Reimer, P.J., Brown, T.A., and Reimer, R.W., 2004. Discussion: reporting and calibration of post-bomb 14C data. *Radiocarbon* 46: 1299–1304.

Rethemeyer, J., Schubotz, F., Talbot, H.M., Cooke, M.P., Hinrichs, K.-U., and Mollenhauer, G., 2010. Distribution of polar membrane lipids in permafrost soils and sediments of a small high Arctic catchment. *Org. Geochem.* 41: 1130–1145.

Schädel, C., Schuur, E.A.G., Bracho, R., Elberling, B., Knoblauch, C., Lee, H., Luo, Y., Shaver, G.R., and Turetsky, M.R., 2014. Circumpolar assessment of permafrost C quality and its vulnerability over time using long-term incubation data. *Glob. Change Biol.* 20: 641–652.

Schuur, E. a. G., McGuire, A.D., Schädel, C., Grosse, G., Harden, J.W., Hayes, D.J., Hugelius, G., Koven, C.D., Kuhry, P., Lawrence, D.M., et al., 2015. Climate change and the permafrost carbon feedback. *Nature* 520: 171–179.

Wotte, A., Wischhöfer, P., Wacker, L., and Rethemeyer, J., 2017. $^{14}CO_2$ analysis of soil gas: Evaluation of sample size limits and sampling devices. *Nucl. Instrum. Methods Phys. Res. Sect. B Beam Interact. Mater. At.* 413: 51–56.

Biogeochemical impacts of dust deposition on Arctic soils, Kangerlussuaq, West Greenland

Maud A.J. van Soest[1]
Joanna E. Bullard[1]
N. John Anderson[1,2]
[1]*Loughborough University, m.a.j.van-soest@lboro.ac.uk*
[2]*Umeå University*

Abstract

Arctic soils are generally limited in nutrient availability. Slow turnover rates and the gradual burial of organic matter in permafrost mean that nutrients become available to plants at very slow rates. Melting and retreating glaciers produce fine dusty material and as more land surface area is exposed to wind action, local dust emissions may increase. This project is quantifying the amount and nutrient content of aeolian dust deposited on soils and the degree of soil development since deglaciation along a 30 km transect between the Greenland ice sheet and Kangerlussuaq. Results suggest that controls on permafrost, such as local topography and distance from the ice sheet, influence the extent of soil development and the quantity of dust deposited. Current work is evaluating the importance of the aeolian input as a source of nutrients to soils and the extent to which aeolian deposition could overwhelm conventional soil-forming processes.

Keywords: “Aeolian dust” “Permafrost soils” “Greenland” “Nutrients”

Introduction

The mean annual average temperature in West Greenland was 3° higher from 2007-2012 compared with 1979-2000 (Mayewski *et al.,* 2014). Melting and retreating glaciers produce fine dusty material and as more land surface area is exposed to wind action, local dust emissions are likely to increase (Bullard, 2013) potentially being an additional nutrient source for Arctic soils (Fig. 1) which are generally nutrient-poor. Rates of soil formation are likely to increase in response to climate warming, however high dust inputs might overwhelm conventional soil-forming processes.

The aim of this project is to understand how Arctic soils become colonized and productive under contemporary conditions focusing on the relative importance of soil forming processes vs dust inputs.

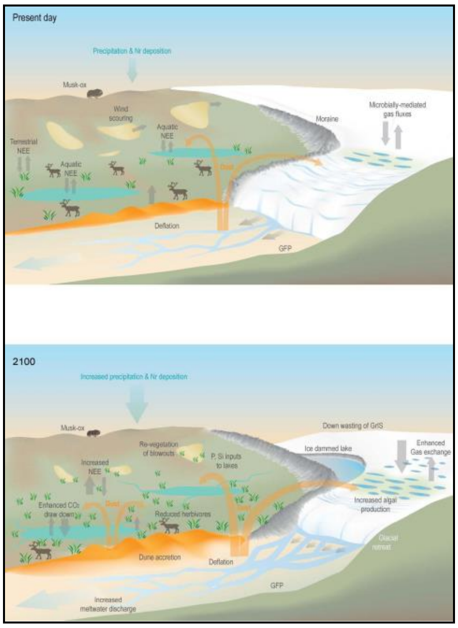

Figure 1. Possible changes in key landscape features, geomorphic and ecosystem processes in a paraglacial area between the present day and 2100 AD (Anderson *et al.,* 2017).

Study area

Kangerlussuaq is a cold and dry well-studied area in West Greenland (Fig. 2) with a mean annual temperature of –6°C and annual precipitation on average <200 mm yr.$^{-1}$. Vegetation is extremely heterogeneous with *Betula nana, Salix glauca, Vaccinium spp., Empetrum nigrum*, and various herbs and grasses as co-dominants (Anderson *et al.,* 2001).

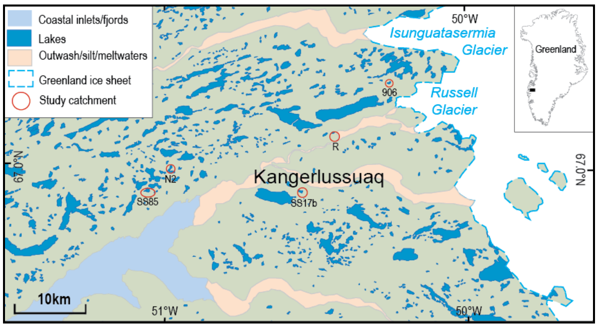

Figure 2. Study catchments near Kangerlussuaq over a 30km transect.

5 catchments were selected for fieldwork carried out in 2017 timed to coincide with seasonal variations in dustiness. Dust deposition traps were deployed in spring along an inferred gradient of dust deposition from high near the ice to near zero 30 km west. Detailed vegetation cover and soil profile descriptions were made. Soil samples were taken for physical and chemical analysis.

Preliminary results

Preliminary analysis of dust deposition rates, moisture content and soil organic matter content do suggest there is a gradient of soil characteristics with distance from the ice sheet. However, this is not a clear linear trend and there is considerable spatial variability that may be linked to microclimate, vegetation cover and local controls on time since deglaciation.

The amount of material captured in the dust traps (including organic matter) ranged from 0.1882-0.2821 g m^{-2} day^{-1} from April to end June, and from 0.0263-0.0796 g m^{-2} day^{-1} from July to late August. The highest values were as expected recorded in catchments nearest the ice sheet.

Table 1. Aeolian deposition (g m^{-2} day^{-1}) filtered from snow and dust deposition traps.

	SS85	N2	SS17b	R	906
Winter	X	0.0303	0.0040	0.0519	0.0798
Spring	X	0.1882	0.1381	0.2284	0.2821
Summer	0.0796	0.0577	0.0307	0.0310	0.0263

Winter and summer dust deposition rates are lower which is in line with the seasonal variability of dust emissions in this part of west Greenland (Bullard & Mockford, in press). Analysis is ongoing to determine the relative importance of minerogenic vs organic matter in the traps and the potential nutrient input to soils.

Acknowledgments

This work is funded by the UK Natural Environment Research Council (NE/P011578/1: NJA/JEB) and Loughborough University (MVS).

References

Anderson, N.J., Harriman, R., Ryves, D.B., Patrick, S.T., 2001. Dominant factors controlling variability in the ionic composition of West Greenland lakes *Arctic, Antarctic, and Alpine Research* 33: 418-425

Anderson, N.J., and 26 co-authors 2017. The Arctic in the 21st century: changing biogeochemical linkages across a paraglacial landscape of Greenland, *BioScience*, 67 (2): 118-133

Bullard, J.E., 2013. Contemporary glacigenic inputs to the dust cycle *Earth Surface Processes and Landforms* 38 (1): 71-89

Bullard, J.E., Mockford, T. in press. Seasonal and decadal variability of dust observations in the Kangerlussuaq area, West Greenland *Arctic, Antarctic and Alpine Research*

Mayewski, P.A., Sneed, S.B., Birkel, S.D., Kurbatov, A.V., Maasch, K.A., 2014. Holocene warming marked by abrupt onset of longer summers and reduced storm frequency around Greenland *Journal of Quaternary Science* 29: 99-104

7 - Understanding rockglacier dynamics

Session 7

Understanding rockglacier dynamics

Conveners:

- **Isabelle Gärtner-Roer**, University of Zurich, Switzerland
- **Andreas Kellerer-Pirklbauer**, University of Graz, Austria
- **Lea Hartl**, University of Innsbruck, Austria (PYRN member)

Rockglaciers are visible indicators of mountain permafrost and reflect present and former climatic conditions (local and regional characteristics) as well as local geomorphic conditions. During the last decade a growing number of studies on rockglacier dynamics have been conducted, measuring and documenting increasing ground temperatures, decreasing ice contents, increasing rates in horizontal velocities, distinct vertical changes as well as indications for landform degradation and destabilization. Despite the limited understanding of the complex thermo-hydro-mechanical behaviour of ice-rich frozen ground, many studies address the connection between rockglacier kinematics and mean annual air temperatures as well as unfrozen water effects. Based on these observations rockglaciers have been prominently appreciated as climate change indicators only recently. We invite the rockglacier community to gather at the EUCOP in 2018 in order to present and discuss recent findings, improve the understanding of ongoing processes and assess future landform developments.

Active, inactive, relict: Tracking the evolution of the Bleis Marscha rockglacier (Val d'Err, Grisons) with cosmogenic nuclide dating and finite-element modelling

Dominik Amschwand[1]
Susan Ivy-Ochs[2]
Marcel Frehner[1]
Olivia Kronig[2]
Marcus Christl[2]
[1]*Geological Institute, ETH Zürich, adominik@student.ethz.ch*
[2]*Laboratory of Ion Beam Physics, ETH Zürich*

Abstract

This work aims at reconstructing the evolution of the *Bleis Marscha* rockglacier in the Val d'Err, Grisons (Switzerland). It is a one-kilometre long, multi-unit talus rockglacier with an active upper part, a relict snout, and a furrow-and-ridge microrelief. The timing of formation of each unit is investigated with surface exposure dating with ^{10}Be and ^{36}Cl. Insights into mechanical properties and internal structure is gained with numerical finite-element modelling. The model is constrained with the horizontal surface velocity field obtained from feature-tracking of multitemporal orthorectified aerial images. The illumination-invariant orientation correlation method overcomes most of the difficulties posed by different lighting on a rugged rockglacier surface, and is a simple, yet powerful tool to capture the horizontal surface kinematics. The overarching aim is to place the development of the *Bleis Marscha* rockglacier within the Holocene climate history and to constrain the timing of glacial and periglacial processes and the relevant mechanical parameters that shaped the formerly glaciated Piz Bleis Marscha cirque.

Keywords: rockglacier; image correlation; feature tracking; numerical modelling; inverse problem

Introduction

The *Bleis Marscha* rockglacier is a talus rockglacier originating in a cirque of Piz Bleis Marscha in the Val d'Err, Grisons, Switzerland. It is more than one kilometre long, exhibits a furrow-and-ridge microrelief in the lower parts and is divided by steep front scarps into several units. Field observations such as lichen coverage and iron staining as well as results from multitemporal aerial image correlation suggests that the lower units below 2500 m a.s.l. are inactive to relict. Several previous studies have obtained exposure or luminescence dates on moraines and rockglaciers in nearby valleys, and the Holocene climate history is well established for the area (Ivy-Ochs *et al.*, 1996; Fuchs *et al.*, 2013).

Aim and methods

In the presented work, the different units of the *Bleis Marscha* rockglacier are exposure-dated with ^{10}Be and ^{36}Cl, as an aid to reconstructing the development of the rockglacier. Furthermore, the present-day dynamics is modelled with a numerical two-dimensional finite-element approach to gain insights into mechanical and material properties. The deformation above the shear zone is well captured by a linearly viscous (Newtonian) flow law (Frehner *et al.*, 2015). The model is constrained with horizontal surface velocities obtained from a feature-tracking analysis of multitemporal orthorectified aerial images with the Matlab tool "ImGRAFT" (Messerli & Grinsted, 2015).

Preliminary results

Slight differences in lighting, illumination direction or cloudiness suffice to make the rugged, bouldery surface of the rockglacier appear differently on aerial image such that a common normalized cross-correlation approach may perform poorly. The cross-correlation of orientation images is illumination invariant (Fitch *et al.*, 2002) and yields a connected displacement field all over the rockglacier. The correlation inherently fails near steep slopes, involving rotational movement of boulders, and on snow patches.

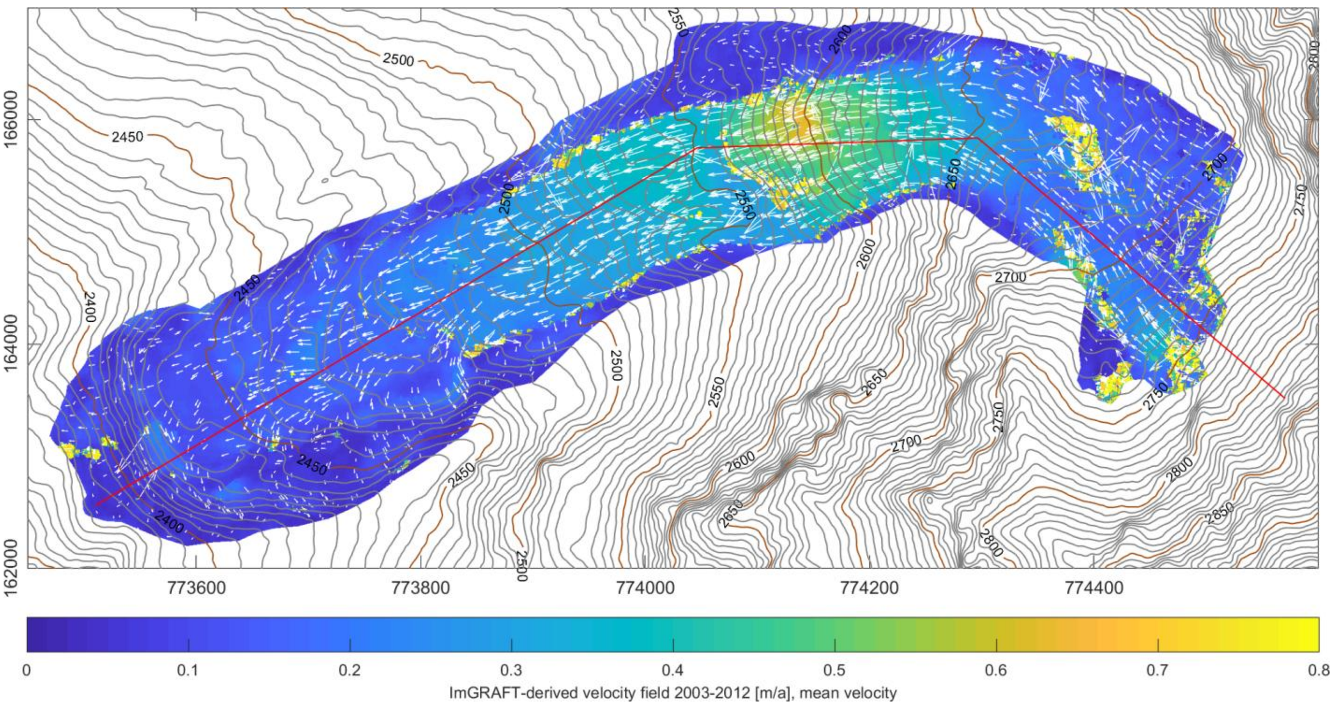

Figure 1. Horizontal surface velocity on the *Bleis Marscha* rockglacier as obtained from a feature-tracking analysis of orthorectified aerial images from 2003 and 2012. Magnitude shown by colours, direction by white arrows. The colorbar is fixed at 0.8 m/a. Higher velocities are most likely artifacts such as rotational movement of blocks at scarps or correlation problems. The red line traces the section along which the 2D numerical model is defined. Coordinates in CH1903 grid, unit in meter. Aerial images © swisstopo.

Preliminary results support the subdivision of the rockglacier into units of varying degree of activity based on field observation: the upper unit is characterized by a unidirectional downslope directed creep, with increasing velocity towards the front of the upper lobe (up to 0.8 m/a, Fig. 1). The over-steepened, failure-prone front scarp shows that this unit is overriding the lower, inactive to relict units of the rockglacier, which exhibit a more "patchy" flow field of slightly varying directions and smaller velocities (<0.4 m/a). This data is used to constrain the numerical model, reproducing the deformation on a longitudinal section along the central flowline of the rockglacier (red line in Fig. 1). The model parameters that will be tested are rockglacier thickness, effective viscosity, viscosity contrast to the low-viscosity basal shear zone and thickness of a rigid blocky mantle. In a series of numerical experiments, the influence of different parameter configurations on the modelled horizontal surface velocity is tested, and plausible configurations that reproduce the observed velocities within their error margins represent solutions to this inverse problem.

We will present a detailed analysis of the horizontal surface flow field, its relationship to the microrelief, rockglacier activity status and changes throughout the recent years.

References

Barsch, D., 1996. *Rockglaciers. Indicators for the Present and Former Geoecology in High Mountain Environments*. Springer, Berlin, Heidelberg, 331 pp.

Fitch, A. J.; Kadyrov, A.; Christmas, W. J. & Kittler, J., 2002. Orientation correlation. *Proceedings of the 13th British Machine Vision Conference,* Cardiff, England, 2-5 September:133-142.

Fuchs, M. C.; Böhlert, R.; Krbetschek, M.; Preusser, F. & Egli, M., 2013. Exploring the potential of luminescence methods for dating Alpine rock glaciers. *Quaternary Geochronology* 18:17-33.

Frehner, M.; Ling, A. H. M. & Gärtner-Roer, I., 2015. Furrow-and-ridge morphology on rockglaciers explained by gravity-driven buckle folding: A case study from the Murtèl rockglacier (Switzerland). *Permafrost and Periglacial Processes* 26:57-66.

Ivy-Ochs, S.; Schlüchter, C.; Kubik, P. W.; Synal, H.-A.; Beer, J. & Kerschner, H., 1996. The exposure age of an Egesen moraine at Julier Pass, Switzerland measured with the cosmogenic radionuclides ^{10}Be, ^{26}Al and ^{36}Cl. *Eclogae Geologicae Helvetiae, Schweizerische Geologische Gesellschaft* 89:1049-106.

Messerli, A. & Grinsted, A., 2015. Image georectification and feature tracking toolbox: ImGRAFT. *Geoscientific Instrumentation, Methods and Data Systems* 4:23-34.

Active rock glacier at sea level in Finnmark, Northern Norway?

Vetle Aune[1]
Karianne S. Lilleøren[1]
Trond Eiken[1]
Bernd Etzelmüller[1]
[1]*Department of Geosciences, University of Oslo, Norway, E-mail: k.s.lilleoren@geo.uio.no*

Abstract

In Hopsfjorden in Finnmark, northern Norway (70.8°N, 28°E), several rock glaciers are located at sea level. These appear to be active, which would imply that the northernmost coastal areas of Finnmark may be considered a part of the arctic permafrost zone. In this study, we present a thorough investigation of one these rock glaciers, including surface temperature, electrical resistivity tomography (ERT), laser scanning and photogrammetrical evaluation of surface changes.

Keywords: rock glacier; geomorphology; photogrammetry; permafrost; climate change; Northern Norway

Introduction

Permafrost is widespread in mountainous areas in Scandinavia. In northern Norway, the lower permafrost limit decreases from ca. 1000 m asl at the west coast to below 500 m asl in the more continental interiors of the area (Farbrot *et al.*, 2009). Active rock glaciers are indicators of continuous permafrost, and have previously been mapped by interpretation of aerial photos. In northern Norway, rock glaciers at sea level are abundant in the county of Troms, and have previously been acknowledged as relict features (Lilleøren & Etzelmüller, 2011).

In Hopsfjorden in Finnmark, (70.8° N, 28° E), several rock glaciers are located at sea level, and a few of these appear to be active. If any of these rock glaciers are proven active, this will be the first time active rock glaciers have been observed at this altitude in mainland Norway. Therefore, the northernmost coastal areas of Finnmark may be considered as a part of the Arctic permafrost zone instead of the mountainous permafrost zone of mainland Norway.

Similar rock glaciers terminating at or close to sea level are found in the Arctic permafrost zone, such as in the Svalbard archipelago north of mainland Norway (Farbrot *et al.*, 2005). At present, permafrost is thawing at a large scale in the Arctic, and the rock glaciers at Hopsfjorden might serve as an analogue to how the landscape in the high Arctic would act in a changing climate. In this study, there will be focus on one of these rock glaciers in Hopsfjorden.

Methods

To accomplish a change detection analysis of the rock glacier, DEMs (digital elevation models) and orthophotos based on historical aerial imagery from several years (1975, 1982 and 1992) and drone imagery (2016 and 2017) were created. An image matching analysis between the various orthophotos was conducted by using the CIAS program to detect any displacement of the rock glacier (Kääb & Vollmer, 2000; Heid & Kääb, 2012).

Surface temperature data from two consecutive years (2015-2017) were available for considerations of the current climate. The surface temperature data was measured by 14 different temperature loggers scattered around the rock glacier. In September 2017, two electrical resistivity tomography (ERT) were collected, one in the frontal part and one on top of the landform. Finally, Schmidt-hammer analysis revealed information about the relative exposure time of the rocks on and adjacent to the rock glacier.

Results and discussions

In the period 2015-2017, all temperature loggers had yearly average temperatures in the range of 2-4°C, i.e. none of the loggers indicated permafrost. The Schmidt-hammer data shows a slight increase in rebound values from the front of the rock glacier to the upper part of the glacier. This might indicate a longer exposure time of the rocks at the front compared to the rocks situated further up.

The DEM comparison showed significant vertical elevation differences and may indicate creep movement. The differences are mainly located at the front and at the lobes located on the sides of the rock glacier. The image matching between the various orthophotos show a clear pattern in the direction of the displacement (fig. 1), which is towards the front. Still, the displacements found on the rock glacier are rather small, and in many cases comparable in size to the values found adjacent to the rock glacier.

The ERT profiles revealed large resistivity differences between outside and the front of the rock glacier, indicating a frontal thickness of more than 10 m and apparent resistivities > 40 kOhm, in contrast to < 5kOhm outside the landform. The values are indicative of rock-ice mixtures, however, the rock glacier developed in quartzite, which can give quite high resistivities.

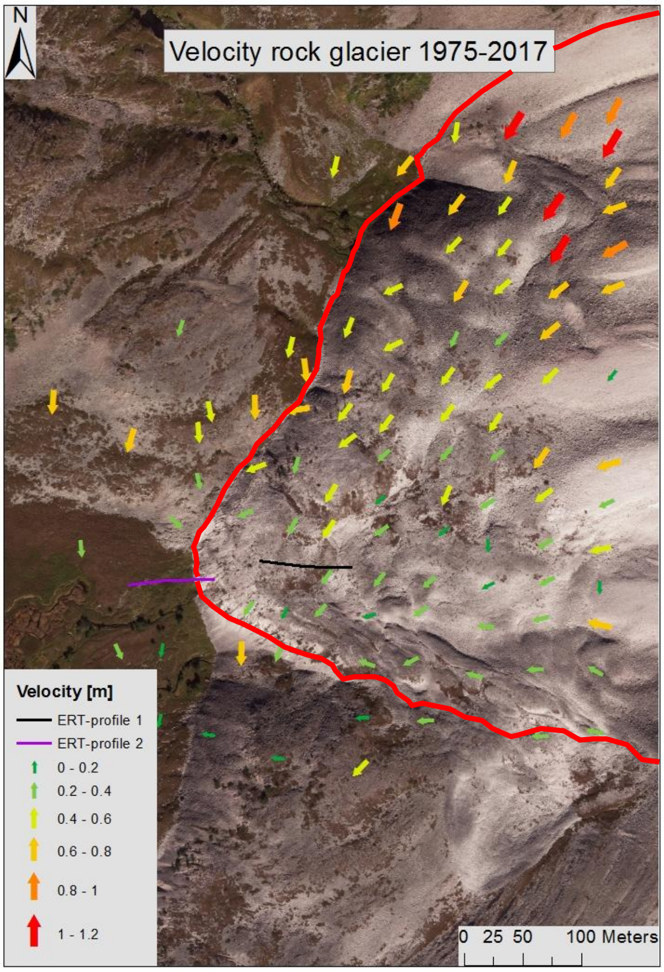

Figure 1. The arrows indicate the size and direction of the total displacement of the rock glacier between 1975 and 2017. The highest displacement values are located at the lobes at the northern part of the rock glacier.

References

Farbrot, H., Isaksen, K., Eiken, T., Kääb, A. & Sollid J. L., 2005. Composition and internal structures of a rock glacier on the strandflat of western Spitsbergen, Svalbard. *Norsk Geografisk Tidsskrift-Norwegian Journal of Geography* 59:139-148.

Farbrot, H., Isaksen, K. & Etzelmüller, B., 2009. Present and past distribution of mountain permafrost in the Gaissane Mountains, Northern Norway. *Arctic, Antarctic, and Alpine Research* 41:48-58.

Heid, T. & Kääb, A., 2012. Evaluation of existing image matching methods for deriving glacier surface displacements globally from optical satellite imagery. *Remote Sensing of Environment* 118: 339-355.

Kääb, B. & Vollmer, M., 2000. Surface geometry, thickness changes and flow fields on creeping mountain permafrost: automatic extraction by digital image analysis. *Permafrost and Periglacial Processes* 11: 315-326.

Lilleøren, K. & Etzelmüller, B., 2011. A regional inventory of rock glaciers and ice-cored moraines in Norway. *Geografiska Annaler: Series A, Physical Geography* 93: 175-191.

Twenty years of rock glaciers and periglacial slope movements analysis in the Bas-Valais (Swiss Alps)

Chloé Barboux, Maria Winterberger and Reynald Delaloye [1]
Tazio Strozzi and Rafael Caduff [2]
Christophe Lambiel and Nicolas Paillex [3]
Christian Hagin [4]
[1]*Department of Geosciences - Geography, University of Fribourg, Switzerland*
[2]*Gamma Remote Sensing, Gümligen (BE), Switzerland*
[3]*Institute of Earth Surface Dynamics, University of Lausanne, Switzerland*
[4]*Geosat SA, Sion (VS), Switzerland*

Abstract

Investigations conducted for two decades on the periglacial belt of the Bas-Valais (Swiss Alps) give a detailed overview of Alpine slope movements at a regional scale. Rock glacier inventories have first been carried out over this area in the late 1990's using aerial images and field mapping. SAR Interferometry (InSAR) has then been used to characterize moving objects related to various types of mass wasting phenomena (rock glaciers, landslides, etc.). Since then, the inventories have been regularly updated using the more recent very-high resolution SAR data. In the last 15 years, terrestrial geodetic survey (DGPS, Total station, Lidar, etc.) deployed over more than 20 sites became precious source of measurements. This study intends to combine all the results and to provide a global overview of the rock glacier and periglacial slope movements evolution during the past 20 years.

Keywords: rock glaciers; landslides; inventories; InSAR; terrestrial geodetic survey; mountain permafrost.

Introduction

For twenty years, large efforts have been carried out to analyze the evolution of slope movements over the periglacial belt of the Bas-Valais (Swiss Alps). In this study, existing data such as rock glacier inventories, terrestrial geodetic data (DGPS) and inventories of slope movements using InSAR are jointly used to produce a detailed overview of the evolution of rock glacier dynamics over the area of interest.

Rock glaciers and mass movements inventories

Rock glacier inventories have first been carried out over this area in the late 1990's using aerial images and field mapping (Delaloye and Morand, 1997; Lambiel and Reynard, 2003). InSAR with high-resolution satellite radar data of the ERS-1/2 SAR and JERS-1 sensors of the 1990's with acquisition time intervals from 1 day to several years was then considered to compile a detailed overview of complex slope movements (Barboux et al., 2014). About 1500 moving objects related to various types of mass wasting phenomena (rock glaciers, landslides, etc.) with displacement rates from a few centimeters to several meters per year were identified. Classification of the process types and validation of the spatial extent was done using optical imagery. Results were then considered in the set-up of in-situ monitoring sites (Delaloye et al., 2010).

The inventories are now regularly updated using the more recent very-high resolution SAR data. The new TerraSAR-X and CosmoSkyMed SAR data for instance, (spatial resolution ~3m), permit to better spatially characterize the displacement rates. In addition, Sentinel-1, with acquisitions available every 6 days, is suited to characterize changes of surface motion over time (Caduff *et al.*, 2017). More sophisticated processing approaches, like Persistent Scatterer Interferometry (PSI), Short Baseline Interferometry (SBAS) or offset-tracking (Strozzi *et al.*, 2002; Barboux *et al.*, 2015), are also used to quantitatively detect points moving with velocities below a few cm/yr, below several dm/yr and more than 1 m/yr, respectively.

In-situ measurements

In the last 15 years, terrestrial geodetic survey (DGPS, Total station, etc.) became precious sources of data. DGPS measurements have been performed on more than twenty sites to characterize slope movements (Lambiel and Delaloye, 2004). Campaigns are generally done annually or seasonally (i.e. either once a year generally late September, or twice a year generally late June and late September).

GNSS stations can nowadays provide real-time positioning accuracies below 1-2 meter-level. In differential GNSS mode the use of a single-phase measurement (L1) allows improving the accuracy down to the centimeter range, fulfilling the requirements for displacement tracking. Ongoing developments using bi-phase measurements (L1/L2), can even reach a millimeter range of accuracy. Some twenty L1 stations have been set up in the Bas-Valais Alps.

Evolution of rock glacier kinematics

Changes in rock glacier motion are an indicator of changes in mountain permafrost conditions (Delaloye et al., 2010). Considering all data available from the 1990's, the study shows a detailed overview of the rock glacier and periglacial slope movements over the Bas-Valais Alps so far, where about 350 active rock glaciers can be observed. First results derived from InSAR analysis show increasing velocities for about 1/10 of rock glaciers between the 90's and the 2010's, and significant deceleration. In-situ measurements, which are showing almost similar trend, are necessary to complement the InSAR data to monitor inter-annual (e.g. Fig. 1) and seasonal velocities.

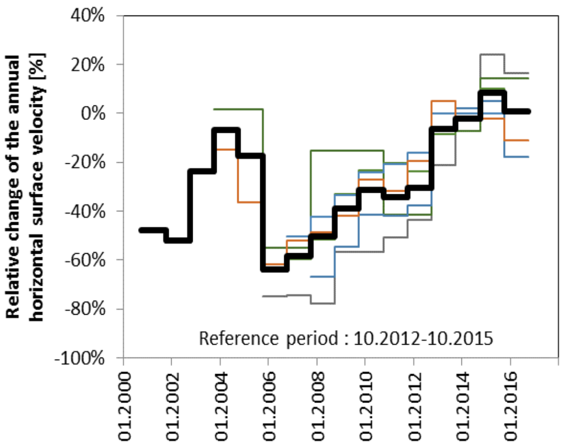

Figure 1. Relative evolution of the horizontal surface velocity of rock glaciers in the Bas-Valais region based on annual terrestrial geodetic survey. The bold line is the mean (n = 1 to 7 depending on the year).

Conclusions

InSAR is a well-established technique for the observation of moving Alpine landforms at fine spatial resolution over large areas. However, the temporal sampling is restricted, the spatial coverage is limited by layover and shadowing, decorrelation over vegetated and snow-covered areas can occur, and the measurements of the displacement are possible only along the satellite line-of-sight component. In parallel, the monitoring of mass movements using GNSS stations over few measurement points ideally complement InSAR for study of the behavior of Alpine landforms with high precision and accuracy.

Acknowledgments

We acknowledge the European Space Agency (ESA) for support within the GlobPermafrost project.

References

Barboux C., Delaloye R. & Lambiel, C., 2014. Inventorying Slope Movements in an Alpine Environment Using Dinsar, *Earth Surface Processes and Landforms*, 39(15): 2087-2099.

Barboux C., Strozzi T. Delaloye R., Wegmüller U. & Collet C., 2015. Mapping slope movements in Alpine environments using TerraSAR-X interferometric methods, *Journal of Photogrammetry and Remote Sensing,* 109: 178-192.

Caduff R., Strozzi T., Wiesmann A. & Wegmüller U., 2017. Monitoring glacial, periglacial and landslide surface motion with Sentinel-1 for the entire Swiss Alps every 6 days. *15th Swiss Geoscience Meeting*, Davos, Switzerland, November 17-18.

Delaloye R, Morand S. 1997. Du Val Ferret au Grand-Combin (Alpes Valaisannes): Inventaire des glaciers rocheux et analyse spatiale du pergélisol à l'aide d'un système d'information géographique (IDRISI). Master Thesis. University of Fribourg, 562 Switzerland

Delaloye, R., Lambiel, C. and Gärtner-Roer, I., 2010. Overview of rock glacier kinematics research in the Swiss Alps. *Geographica Helvetica,* 65, 135-145.

Lambiel C, Reynard E. 2003. Cartographie de la distribution du pergélisol et datation des glaciers rocheux dans la région du Mont Gelé (Valais). *Physische Geographie* 41, Geographisches Institut der Universität Zürich, 91-104

Lambiel C, Delaloye R. 2004. Contribution of real-time kinematic GPS in the study of creeping mountain permafrost: examples from the Western Swiss Alps. *Permafrost and Periglacial Processes* 15 : 229–241.

Strozzi T., Luckman A., Murray T., Wegmüller U. & Werner C., 2002. Glacier motion estimation using SAR offset-tracking procedures, *IEEE Transactions on Geoscience and Remote Sensing*, 40(11): 2384-2391.

Interannual and subseasonal rock glacier displacement by exploiting different SAR techniques

Aldo Bertone[1,2], Mattia Callegari[2], Giovanni Cuozzo[2], Niccolò Dematteis[1,3], Karl Krainer[4], Carlo Marin[2], Claudia Notarnicola[2], Roberto Seppi[1], Francesco Zucca[1]

[1]*University of Pavia – Department of Earth and Environmental Sciences, Pavia, Italy*
[2]*EURAC Research – Institute for Earth Observation, Bolzano, Italy*
[3]*Research Institute for Hydro-Geological Protection, National Council of Research of Italy, Torino, Italy*
[4]*University of Innsbruck - Institute of Geology, Innsbruck, Austria*

Abstract

Active rock glaciers are slow-moving, permafrost landforms that characterize high mountain periglacial terrains. Their complex movement, with interannual and subseasonal rhythms, are of interest for interpreting the evolution of the permafrost in response to meteorological and climatic variables. Given the generally remote location of the rock glaciers, we propose a methodology to monitor their interannual and subseasonal dynamics using a satellite-based approach with different types of Synthetic Aperture Radar (SAR) imagery (i.e. Sentinel 1 and TerraSAR-X), limiting the need of in-situ measurements. This proposed methodology is tested on an active rock glacier, where many in-situ measurements are available to compare the satellite results.

Keywords: rock glacier, permafrost, remote sensing, Sentinel 1, TerraSAR-X, GB-SAR.

Introduction

Rock glaciers are the most common geomorphological evidence of permafrost in alpine regions and are characterized by creeping processes that generate a downstream displacement, with velocities ranging from a few cm to more than 1 meter per year (Haeberli et al. 2006). Displacement over several years is related with climatic variables such as air temperature, and subseasonal displacement is related with shorter time-scale events such as rainfall, snow melting and other environmental factors (Kääb et al., 2007). The slope instability related to rock glacier and permafrost dynamics is monitored for a proactive management of natural hazards. Moreover, as permafrost is sensitive to climate change, observing its dynamics is a key issue in alpine environments.

Ground-based monitoring of rock glacier dynamics, such as GPS or total station, is limited by the complexity of acquiring measurements over these remote areas. For the same reasons, rock glacier dynamics at subseasonal scale are even less monitored.

Remote sensing methods based on SAR data are part of technologies at disposal to study rock glaciers at different space and time scales. In fact, SAR satellites are capable to acquire data over remote areas independently from weather conditions and with high temporal frequency (up to a few days).

In this work, we propose a satellite-based approach for monitoring rock glacier dynamics at different temporal scales. This approach aims at supporting in-situ measurements for well instrumented study areas, and at monitoring rock glaciers dynamics when in-situ measurements are not available or difficult to be carried out.

Our approach is based on the use of SAR data with different characteristics (i.e. different spatial and temporal resolution) and processed through different techniques, i.e. differential interferometry (DInSAR), multi-temporal interferometry and amplitude tracking, in order to study the annual, seasonal and subseasonal rock glacier dynamics with high precision. We tested our methodology over an active rock glacier called Lazaun and located in Val Senales (South Tyrol, Italy, fig. 1), whose internal structure is well known thanks to detailed analysis conducted in the last years (Krainer et al. 2015), but its flow pattern is still poorly investigated.

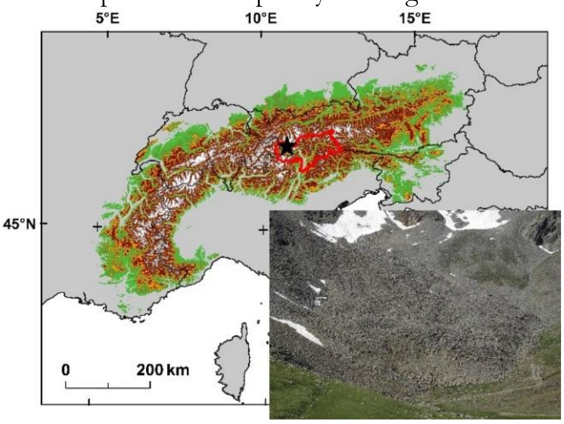

Figure 1: picture of Lazaun rock glacier and its location indicated by the black star (Val Senales, South Tyrol, Italy).

The accuracy of satellite-based products is assessed exploiting ground-based data, such as GPS and Ground-Based SAR (GB-SAR) data.

Materials and method

Subseasonal monitoring

The high acquisition time frequency of Sentinel 1 data (6 days) allowed studying the subseasonal displacement and understanding the displacement rate variation during the snow free period. Two datasets of Sentinel 1 from relative orbits 117 and 168 were used, taking into account the images from the snow free period 2017 (about mid-June to mid-October). The images were processed using Persistent Scatter (PS) technique (Ferretti et al., 2001). Interferometric techniques allowed obtaining only the displacement along the Line of Sight (LOS) of the satellite. Exploiting the combination of 117 and 168 relative orbits, displacements in two different direction can be derived.

As the Sentinel 1 images have a low spatial resolution (15 meters), to study with higher spatial accuracy the rock glacier surface dynamic, three Very High Resolution (VHR) TerraSAR-X (TSX) images acquired in summer 2017 were processed by using differential interferometry (DIn-SAR).

Interannual monitoring

Annual rock glacier displacement cannot be investigated with DIn-SAR due to decorrelation and unwrapping issues, therefore amplitude tracking technique was applied on two VHR TSX images from summer 2016 and summer 2017. In addition, exploiting the combination of the displacement along the LOS and along the satellite flight direction, we will have the possibility to further improve the accuracy of the displacement direction.

Ground-based data

A 10-days GB-SAR campaign was carried out during summer 2017 (Monserrat et al., 2014). The high acquisition time frequency (5 minutes) of this instrument enabled the comparison of daily displacement data with satellite SAR results. Moreover, seasonal and annual displacement were compared with GPS measurements conducted three times over summer on the rock glacier, in order to validate the results.

Results

DIn-SAR technique with TSX data provided high resolution displacement maps, where different velocity sectors are visible (fig. 2A). In particular, the fastest areas are located above the frontal slope and in the middle part of the rock glacier. This velocity pattern is confirmed by the GPS and GB-SAR measurements, and will be further compared with the Sentinel 1 PS results.

As the flight direction of TSX data used for amplitude tracking was roughly the same of the GB-SAR LOS, we were able to directly compare the results. In particular, annual displacement measured with amplitude tracking showed values up to 100 centimeters (2.7 mm/day), which is in the same order of magnitude of the GB-SAR velocity measurements (about 3 mm/day, fig. 2B).

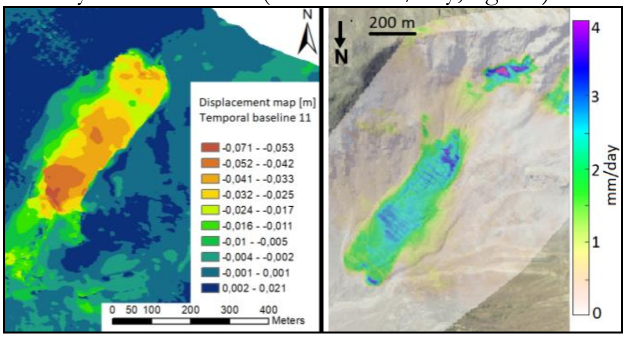

A B

Figure 2: (A) displacement map obtained by TSX DIn-SAR. (B) Daily average velocity obtained by GB-SAR.

Acknowledgments

This work was conducted within the project ALPSMOTION (ALPine Slow slope Movement moniTorIng and detectiON with remote and proximal sensing), coordinated by Eurac Research-Institute for Earth Observation and funded by the Autonomous province of Bolzano, Alto Adige, "Ripartizione Diritto allo Studio, Università e Ricerca Scientifica." The Sentinel-1 and TSX data were processed with SARscape software (SARMAP). GB-SAR instrument has been made available by University of Pavia. GPS data were provided by University of Innsbruck. TSX Data were provided by the European Space Agency, Project Proposal id 34722, © DLR, distribution Airbus DS Geo GmbH, all rights reserved.

References

Ferretti, A., C. Prati, and F. Rocca. 2001. "Permanent Scatterers in SAR Interferometry." *IEEE Transactions on Geoscience and Remote Sensing* 39(1): 8–20.

Haeberli, Wilfried et al. 2006. "Permafrost Creep and Rock Glacier Dynamics." *Permafrost and Periglacial Processes* 17(3): 189–214..

Kääb, Andreas, Regula Frauenfelder, and Isabelle Roer. 2007. "On the Response of Rockglacier Creep to Surface Temperature Increase." *Global and Planetary Change* 56(1–2): 172–87.

Krainer, Karl et al. 2015. "A 10,300-Year-Old Permafrost Core from the Active Rock Glacier Lazaun, Southern Ötztal Alps (South Tyrol, Northern Italy)." *Quaternary Research (United States)* 83(2): 324–35.

Monserrat, O., M. Crosetto, and G. Luzi. 2014. "A Review of Ground-Based SAR Interferometry for Deformation Measurement." *ISPRS Journal of Photogrammetry and Remote Sensing* 93: 40–48.

Assessing rock glacier horizontal movement in the Cordón del Plata range, Central Andes of Argentina

Jan Henrik Blöthe[1]
Christian Halla[1]
Ellen Schwalbe[2]
Dario Trombotto[3]
Lothar Schrott[1]
[1]*Department of Geography, University of Bonn, Bonn, Germany, jan.bloethe@uni-bonn.de*
[2]*Institute of Photogrammetry and Remote sensing, Technische Universität Dresden, Dresden, Germany*
[3]*Instituto Argentino de Nivología, Glaciología y Ciencias Ambientales, CCT CONICET Mendoza, Argentina*

Abstract

The semiarid central Andes of Argentina feature an extensive periglacial belt with a high density of rock glaciers and transitional ice-debris complexes, spurring a debate regarding their hydrological significance in the region. However, little is known about their state of activity, which can be used as a rough proxy for a rock glaciers' ice content. Here we investigate rock glacier activity using a feature-tracking algorithm to estimate horizontal movement from remotely sensed imagery between 2010 and 2017. First results show that active rock glaciers and transitional landforms attain maximum horizontal velocities of up to 6 m in their root zones with rates of movement generally decreasing towards their snouts. However, the Morenas Coloradas rock glacier, one of the largest in the region, also shows fast displacement of up to 2 m yr^{-1} at its front, which is supported by data obtained during field measurements.

Keywords: Rock glaciers, Andes, remote sensing, feature tracking, digital topography

Introduction

Outside Antarctica, the Central Andes of Argentina host the largest area of mountain permafrost in the southern hemisphere (Gruber, 2012). In 2010 Argentina issued a law that intends to protect the entire cryosphere, which particularly constitutes an important water reservoir in the arid regions of the Central Andes. Here, human livelihoods critically depend on Andean meltwaters that fuel the agricultural production of the region. As opposed to the clear ice glaciers in the southern Andes of Patagonia, these latitudes are predominated by rock glaciers and transitional landforms between debris-covered glaciers and rock glaciers (hereafter referred to as ice-debris complexes). This exceptionally high spatial density of rock glaciers in the central Andes has spurred controversial debates on their hydrological significance (Azócar and Brenning, 2010; Arenson and Jakob, 2010).

Close to Mendoza, one of the large population and agricultural centers of central Argentina, the frontal Cordillera of the Andes rises sharply to nearly 6000 m asl in the Cordón del Plata range that is characterized by an extensive periglacial belt. Following the implementation of the so-called "law of the glaciers", a comprehensive inventory of all glaciers, rock glaciers, ice-debris complexes and permanent snow patches was compiled for the entire country. Here we exploit this inventory for the Cordón del Plata and assess the horizontal movement of rock glaciers and ice-debris complexes to gain insights into the state of activity of these landforms. We further compare the horizontal surface movement to topographic and topoclimatic parameters.

Methods

We use a least square matching algorithm to automatically track features in remote sensing images (Planet imagery with 3x3 m and RapidEye imagery with 5x5 m ground resolution) acquired between 2010 and 2017 to derive horizontal movement of selected rock glaciers and transitional landforms in the Cordón del Plata (Schwalbe and Maas, 2017). To further constrain parameters determining the horizontal velocities, we analyze the distribution of movement with respect to topographic and topoclimatic parameters that we derive from a 12x12 m resolution digital elevation model (TanDEM-X).

Results and Outlook

The Cordón del Plata range covers ~2000 km² that feature a high abundance of rock glaciers (n= 533, Area = 66 km²) and ice-debris complexes (n= 82, 73 km²), as compared to glaciers (n= 288, 93 km²) and debris covered glaciers (n= 58, 12 km²). Preliminary results show that active rock glaciers and transitional landforms attain maximum horizontal velocities of up to 6 m averaged over the surveyed period (Figure 1).

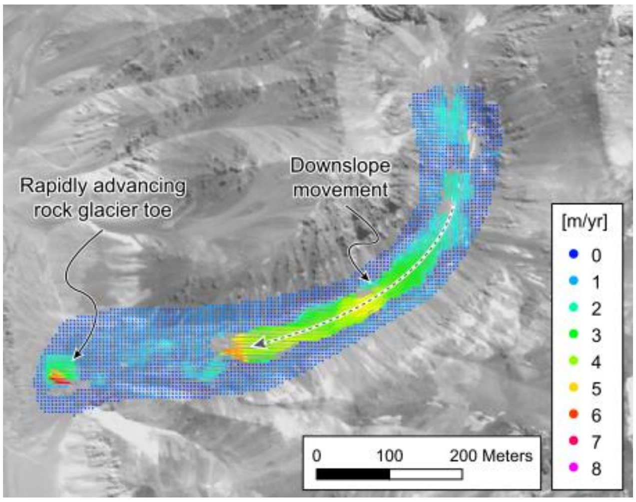

Figure 1. Horizontal surface velocities derived from remote sensing data for a rock glacier in the Cordón del Plata range, Argentina.

Ice-debris complexes generally show faster rates of movement compared to rock glaciers. Topographic analysis does not show a coherent picture: generally, higher horizontal velocities are associated with steep gradients but also coincide with higher elevations, where colder temperatures potentially allow for higher ice-contents. Nonetheless, some frontal parts of lower-lying active rock glaciers show exceptional rates of movement (Figure 1). Another example for this is the Morenas Coloradas rock glacier, a transitional complex with more than 4 km in length, where the terminal lobe reaches down as far as 3600 m asl. For the lowermost part of the Morenas Coloradas rock glacier, we derive average horizontal velocities of up to 2 m yr^{-1} from remote sensing imagery. These results are in good agreement with repeated D-GPS surveys we took out on the Morenas Coloradas rock glacier complex as well as short-term tracking of horizontal movement in high-resolution orthophotos that we derived from UAV surveys.

In future work, we will explicitly combine the analysis of surface velocities obtained from remotely sensed data with near-surface geophysical prospecting results to get further insight into the connection between internal structure and surface deformation of rock glaciers.

Acknowledgments

We thank the Deutsche Forschungsgemeinschaft (DFG) for financial support (Schr 648/3-1) and Planet Labs (www.planet.com) for providing RapidEye and Planet satellite data used for this study. We further acknowledge the provision of TanDEM-X data by the German Aerospace Center (science proposal DEM_OTHER1367).

References

Arenson, L.U. & Jakob, M., 2010. The significance of rock glaciers in the dry Andes - A discussion of Azócar and Brenning (2010) and Brenning and Azócar (2010). *Permafrost and Periglacial Processes* 21: 282–285.

Azócar, G.F. & Brenning, A., 2010. Hydrological and geomorphological significance of rock glaciers in the dry Andes, Chile (27°-33°S). P*ermafrost and Periglacial Processes* 21: 42–53.

Gruber, S. 2012. Derivation and analysis of a high-resolution estimate of global permafrost zonation. *The Cryosphere* 6: 221–233.

Schwalbe, E. & Maas, H.-G., 2017. Determination of high resolution spatio-temporal glacier motion fields from time-lapse sequences. *Earth Surface Dynamics Discussions*: 1–30.

Regional evaluation of rock glacier activity in the semi-arid Andes using optical and radar satellite imagery

Xavier Bodin[1], Thomas Echelard[2], Pascal Lacroix[3], Tazio Strozzi[4]
[1]*Univ. Grenoble Alpes, Univ. Savoie Mont Blanc, CNRS, EDYTEM, Chambéry, France,* xavier.bodin@univ-smb.fr
[2]*Cartodia, Grenoble, France*
[2]*Univ. Grenoble Alpes, IRD, CNRS, ISTerre, Grenoble, France*
[3]*Gamma Remote sensing, Switzerland*

Abstract

As evidenced by existing inventories, the semi-arid Andes (Chile and Argentina) has a high density of active rock glaciers and host some of the largest ones in the world. The movement of rock glaciers, which is crucial for understanding the effects of climate on mountain cryosphere, remains largely based on subjective interpretation of geomorphological signs visible on ortho-imagery. In order to get a regional assessment of rock glacier's activity levels, we combined two type of satellite imagery, Synthetic Aperture Radar and optical. Both SAR-derived interferograms and maps of displacement derived from optical image correlation were used to evaluate to mean activity level of more than 200 active rock glaciers. Base on this, a geospatial analysis was performed to assess the main controlling factor on the rock glaciers kinematic.

Keywords: rock glaciers; surface movements; remote sensing; SAR; image correlation; Andes.

Introduction

In the present context of Climate change, rock glaciers dynamics have potential consequences for the stability of mountain slopes (Huggel *et al.*, 2012). In the Andes, similarly to the Alps, cases of rock glacier destabilization have been observed (Bodin *et al.*, 2012). Between 29 and 34°S, more than 8000 fresh rock glaciers have been mapped by official Chilean and Argentinian authorities (IANIGLA, 2010; UGP-UC, 2011). In those inventories, the activity status of rock glaciers has been assessed based on ortho-imagery, implying subjectivity-related biases.

To overcome this limitation, we combined optical and radar satellite imagery (acquired between 2012 and 2017), from which we derived maps of SAR phase difference (TerraSAR-X) and of horizontal surface displacement (Landsat).

Study area and datasets

Our study area covers almost 3000 km², around 29-30°S, and has a median elevation of 4120 m asl. With a mean elevation of 4500 m asl, 321 rock glaciers are present, covering a total of 34 km².

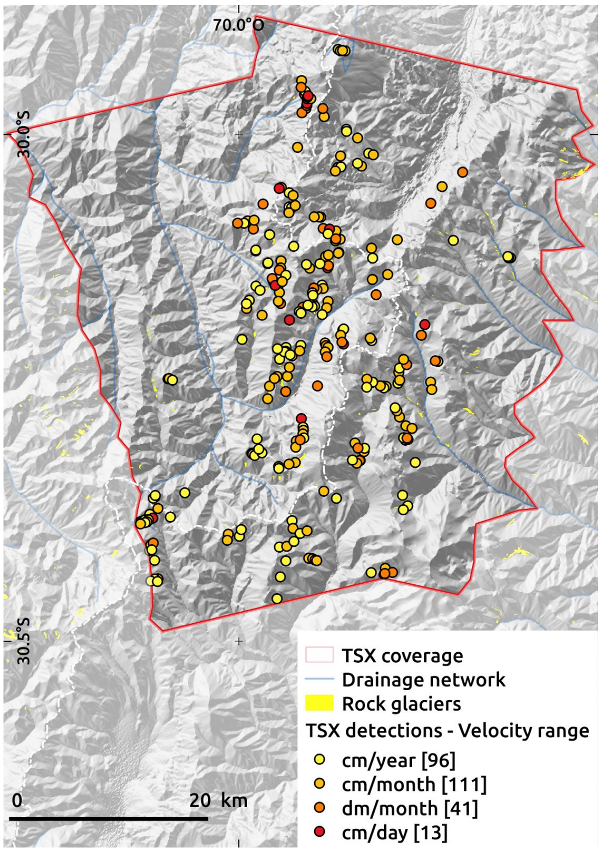

Figure 1: Velocity levels detected on rock glaciers with the interpretation of TSX-derived interferograms.

Following Barboux *et al.* (2014) procedure, we first interpreted the TSX interferograms overlaid with ortho-imagery in a GIS. Over 261 rock glaciers with SAR-derived interpretation, 54 show relatively fast surface velocity, higher than 2 m/yr (Figure 1).

Landsat images from between 2013 and 2017 were processed with image correlation technique (Zerathe *et al.*, 2016) to derive horizontal displacements over the area (Figure 2).

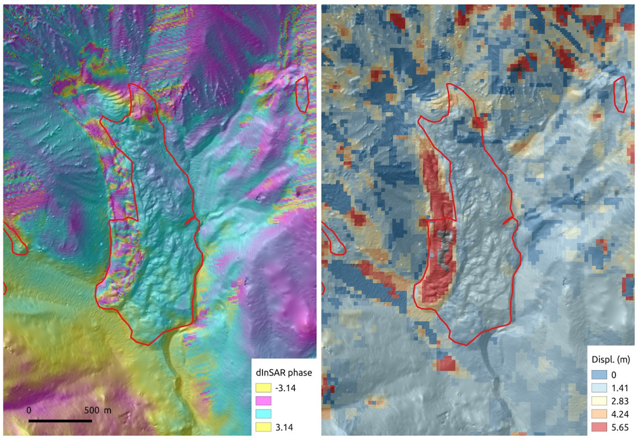

Figure 2: Comparison between SAR phase signal from a 11-day interferogram (left panel) and horizontal displacements derived from Landsat images of 2013 and 2017 (right panel) on an active rock glacier.

Results

Deriving topographic attributes from TanDEM-X 12-m DEM, no clear dependency between velocity and elevation nor slope was found. The clearest control on the rock glaciers velocity range seems to be the solar radiation, with lower values on slow rock glaciers and higher ones on the fastest (Figure 3).

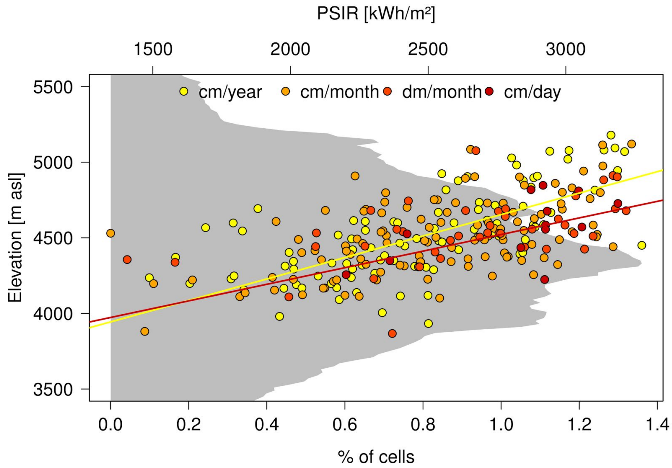

Figure 3: Hypsography of the study area and XY plot of elevation VS potential solar incoming radiation (PSIR).

Outlook

At the moment of writing this abstract, the processing of the optical imagery have not yet be fully completed. The resolution of the Landsat images (15m) is a clear limitation, though the large time span should allow producing horizontal displacement maps for the fastest rock glaciers of the study area, and to compare these maps with the TSX interpretations.

References

Bodin, X., Krysiecki, J.-M., Iribarren Anacona, P., 2012. Recent collapse of rock glaciers: two study cases in the Alps and in the Andes, in: *Proceedings of the 12th Congress INTERPRAEVENT.* Grenoble, pp. 2–3.

Huggel, C., Clague, J.J., Korup, O., 2012. Is climate change responsible for changing landslide activity in high mountains? *Earth Surf. Proc. and Landf.* 37, 77–91.

IANIGLA. *Inventario Nacional de Glaciares Y Ambiente Periglacial: Fundamentos Y Cronograma de Ejecución.* Mendoza; 2010.

UGP-UC. *Dinámica de Glaciares Rocosos En El Chile Semiárido.* Unidad de glaciología y nieves, DGA/MOP, Santiago; 2011.

Zerathe, S., Lacroix, P., Jongmans, D., Marino, J., Taipe, E., Wathelet, M., Pari, W., Smoll, L.F., Norabuena, E., Guillier, B., Tatard, L., 2016. Morphology, structure and kinematics of a rainfall controlled slow-moving Andean landslide, Peru: The Maca slow-moving Andean landslide. *Earth Surf. Proc. and Landf.* 41, 1477–1493.

Sources of uncertainty and variability in rock glacier inventories

Francesco Brardinoni[1]
Riccardo Scotti[1]
Rudolf Sailer[2]
David Tonidandel[3]
Kathrin Lang[3]
Volkmar Mair[3]

[1] *Department of Biological, Geological and Environmental Sciences (BiGeA), University of Bologna,* *francesco.brardinoni@unibo.it*
[2] *Institute of Geography, University of Innsbruck*
[3] *Office for Geology and Building Materials Testing, Autonomous Province of Bolzano*

Abstract

We report preliminary findings of a mapping test that aims to evaluate the inherent sources of uncertainty and variability associated with the compilation of a rock glacier inventory from remotely sensed imagery. In particular, we compare rock glacier inventories conducted by five operators on Google Earth (GE), and on a combination of orthophoto and LiDAR-derived shaded relief rasters (LO) in Kaiserberg Valley, Austria. Results show that: (i) the number of detected rock glaciers among operators can vary up to a factor of 3; (ii) all operators consistently mapped a larger number of rock glaciers in LO compared to GE imagery, due to the identification of additional landforms as well from the disentangling of previously merged features. Similar discrepancies in mapping outcomes are likely to affect environmental evaluations and applications that rely on rock glacier inventories.

Keywords: Rock glaciers; Geomorphological mapping; Periglacial landforms; Remote sensing

Introduction

The last decade has witnessed a blooming of rock glacier-based studies for assessing present and past spatial distribution of permafrost (e.g., Scotti et al., 2013), post-LGM landscape response to climate change (e.g., Zasadni & Kłapyta, 2016), and water storage potential (e.g., Jones et al., 2018). This revived interest for rock glaciers has been fostered by increasingly available high-resolution, remotely sensed imagery and digital topography, which are crucial for detecting and mapping such landforms. The compilation of a rock glacier inventory typically requires some expert-based image interpretation, therefore its completeness and areal extent depends not only on image quality, but also on the experience and training of the operator. This study presents preliminary results on a mapping exercise that evaluates rock glacier inventories compiled by five operators in Kaiserberg Valley, a 14-km² hanging valley located in western Kaunertal, Ötztal Alps, Austria.

Methods

Rock glacier mapping, including evaluation of the degree of activity (Barsch, 1996), was performed in two independent steps, first using Google Earth™ imagery (GE), and subsequently using higher resolution 1-m LiDAR-derived shaded relief and a 0.2-m orthophoto mosaic (LO) (Fig.1). Critical topographic attributes, such as rock glacier maximum and minimum elevations were extracted from a 1-m LiDAR DTM.

Findings

Results display high variability in the number of rock glaciers identified, which ranges from 11 to 31 in GE-based inventories, and from 22 to 40 in LO-based ones (Fig. 1). This variability reflects different mapping styles in terms of rock glacier identification i.e., whether a given lobate landform is considered a rock glacier or not, and delineation i.e., polymorphic rock glaciers vs single-lobe overlapping ones. The increase in image resolution from GE to LO produces an increase in identified rock glaciers across operators.

The greater number of landforms mapped on LO imagery chiefly derives from: (i) the identification of previously undetected rock glaciers, from a minimum of 6 to a maximum of 13, and (ii) the subdivision of single, large rock glaciers into smaller ones i.e., from no changes to 6 rock glaciers being split into 17 new ones.

Changes in rock glacier dynamic classification due to higher resolution imagery involves, on average, 37 % of the rock glacier sample, ranging from 14 % to 50 %. The most frequent classification changes concern the "intact" category, from active-to-inactive and vice versa.

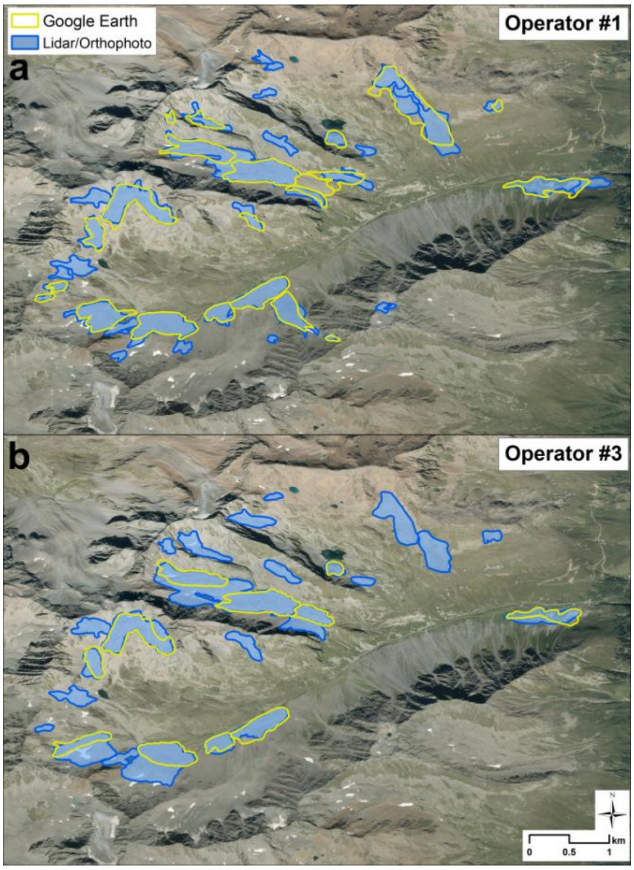

Figure 1. Sample inventory maps of rock glaciers delineated by (a) operator 1, and (b) operator 3 using Google Earth (yellow outline) and Lidar & Orthophoto (solid blue polygons).

With respect to the minimum and maximum elevation changes of rock glaciers stratified by dynamic classification, relict rock glaciers exhibit higher variability between GE and LO and across operators, compared to intact rock glaciers (Fig. 2b, c). In particular, we observe the largest discrepancies between operators for minimum and maximum elevation of relict rock glaciers mapped on GE images. By contrast, minimum elevations of intact rock glaciers mapped on LO imagery are the most consistent. Since rock glacier minimum elevation has been used as a proxy for assessing the lower limit of alpine permafrost (e.g., Boeckli *et al.,* 2012), our preliminary finding reinforces the robustness of such approach. Conversely, the high variability associated with the minimum elevation of relict rock glaciers potentially poses a question on the reliability of paleo-permafrost reconstructions, especially when based on low-resolution imagery.

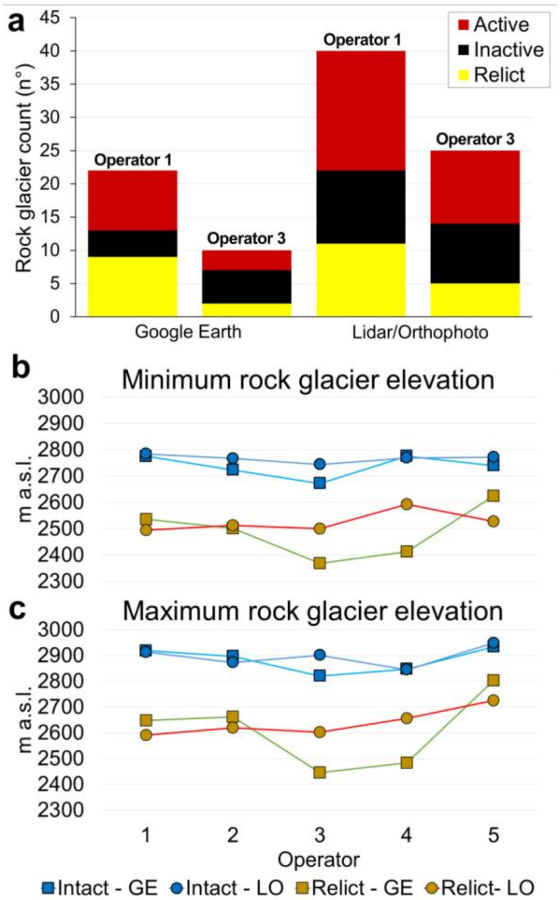

Figure 2. (a) Number of rock glaciers mapped by operators 1 and 3. Average minimum (b) and maximum (c) rock glacier elevation across the 5 operators. Data are stratified by rock glacier degree of activity and type of imagery used.

References

Barsch, D., 1996. *Rockglaciers. Indicators for the Present and Former Geoecology of High Mountain Environments.* Berlin: Springer, 331 pp.

Boeckli, L., Brenning, A., Gruber, S. & Noetzli, J., 2012. A statistical approach to modelling permafrost distribution in the European Alps or similar mountain ranges. *Cryosphere* 6: 125-140.

Jones, D.B., Harrison, S., Anderson, K. & Betts, R.A., 2018. Mountain rock glaciers contain globally significant water stores. *Scientific Reports* 8(1): 2834.

Scotti, R., Brardinoni, F., Alberti, S., Frattini, P. & Crosta, G.B., 2013. A regional inventory of rock glaciers and protalus ramparts in the central Italian Alps. *Geomorphology* 186:136-149.

Zasadni, J. & Kłapyta, P., 2016. From valley to marginal glaciation in alpine-type relief: Lateglacial glacier advances in the Pięć Stawów Polskich/Roztoka Valley, High Tatra Mountains, Poland. *Geomorphology* 253: 406-424.

Investigating the influence of temperature and liquid water on variations in rockglacier flow

Alessandro Cicoira[1]
Andreas Vieli[1]
Jérome Faillettaz[1]
[1]*University of Zurich, a.cicoira@geo.uzh.ch*

Abstract

In the past decades, seasonal and inter-annual variability in rockglacier velocities have been observed. Temperature forcing along with input of liquid water have been proposed as key processes to explain these variations in kinematics. However, the relative influence of these mechanisms have not yet been quantitatively assessed against real-world data. We investigate the processes governing variability in rockglacier flow using 1-dimensional numerical models that couple heat conduction to different creep relations and include variations in pore water pressure. We compare the modeling with borehole temperatures and surface velocity measurements from several sites of the PERMOS and PermaSense monitoring networks. We find that velocity variations cannot be explained from the influence of temperature forcing on rheology alone. Coupling variations in water input to a water pressure dependent creep relation, we are able to reproduce velocity variations both in magnitude and temporal pattern over time scales from months to several years.

Keywords: rheology; velocity variations; temperature conduction; water pressure.

Introduction

Flow velocity variability has been detected on daily, seasonal and inter-annual time scales (Wirz *et al,* 2016). Temperature forcing, through heat conduction (Kääb *et al*, 2007), along with liquid water pressure deriving from snow melt or precipitation (Ikeda *et al,* 2008) have been identified as important controls on the observed accelerations. However, the relative importance of these forcings is not fully understood yet. In this study we apply a numerical modelling approach to real-world data in order to quantify the influence of surface temperature forcing and liquid water column on rock glacier dynamics.

Data and Methods

We design a suite of 1-dimensional numerical models, based on finite-differences, to simulate the response of viscous and plastic flow to external near surface temperature forcing and water availability. For all the models, in order to solve the temperature diffusion equation and obtain the temperature field, we apply an implicit discretization (Crack-Nicholson) and constrain the model with observed temperature histories. The creep parameter, thus the strain rates, can thereafter be explicitly calculated using the proposed constitutive relations. Under the assumption of a fix bottom boundary, vertical integration results in surface flow velocities.

To investigate the influence of heat conduction on rock glacier dynamics we present a model coupling thermal diffusion, forced by permafrost superficial temperature variations, to a temperature and ice-content dependent power-law creep relation for ice-rich frozen soils (Arenson and Springman, 2005). We thereby extend previous studies (Kääb *et al*, 2007) by implementing an empirically derived creep relation and by constraining the modelling with real-world observations.

In order to consider the processes taking place in the shear horizon (accounting for about 70% of the total displacements) and include water related processes, we relate liquid precipitation and snow melt rates to the effective stresses at the base of the moving rockglacier unit. Thus, we couple the effective stresses to the deformations in the shear horizon via a pressure dependent viscoplastic relation.

For the two experiments the model inputs consist of: a reference value of the slope of the rockglacier, the thickness and other physical properties of the moving rockglacier, permafrost surface temperature measured in boreholes chains, a constant value representative of the bottom temperature, and snow melt rate and liquid precipitation time series from in situ weather stations.

Results and discussion

Applying the thermal diffusion model, we are able to reproduce the measured borehole temperatures reasonably well. This result confirms the theory that heat conduction is the main process governing rockglacier temperatures (Haeberli *et al*, 2006). In some cases non-conductive water related processes are also relevant, such as for the example of the Talik at the Rittigraben rockglacier (Fig. 1), which cannot be captured by our modelling. Nevertheless, the resulting discrepancies do not significantly influence the velocities obtained from the dynamical model.

Constraining the creep relation with the modelled temperatures we are able to simulate the correct magnitude of the observed long term average velocities, but we strongly underestimate seasonal amplitude and inter-annual variability (Fig. 1). Furthermore, the timing of the seasonal peaks is shifted. This underestimation in amplitude is confirmed by additional experiments that force the creep model with observed temperatures (including non-conductive effects on temperatures). However, these experiments reduce the discrepancies in phase.

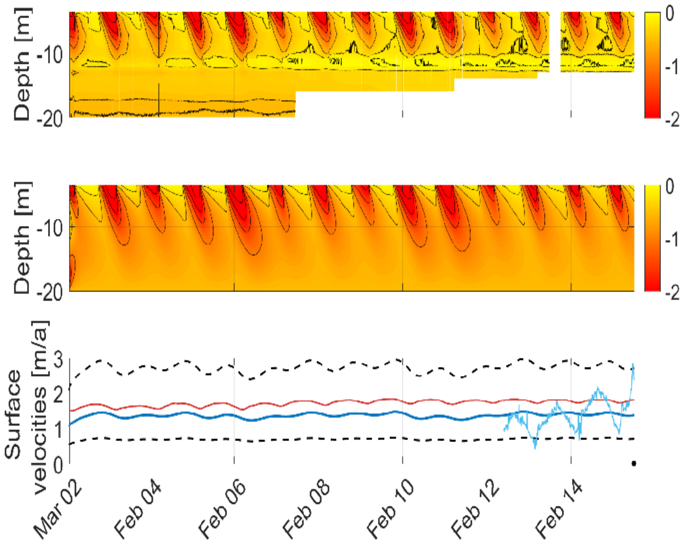

Figure 1. Results for the Rittigraben rockglacier. In the top and mid panel the measured and modelled temperature fields [°C] are plotted. Contour lines are plotted every 0.5°C differences. In the lower panel the surface velocities are shown. The blue line shows the modelled velocities when forced with modelled temperatures. The red line shows the modelled velocities when using the measured temperatures as input. The light blue line shows observed continuous velocities from *dGPS* measurements. The black dashed line express a physical range of the model parameters.

We therefore conclude that water controls rockglacier flow in other ways than through the influence of temperature dependence on viscous-creep. We hypothesize that variations in pore water pressure in particular within the shear horizon have an important effect on flow velocities.

To test this hypothesis, we include in the model the response of shear horizon strain rates to water pressure, forced by liquid precipitation and snow melt. Our preliminary results show that, using a viscoplastic rheology, we are able to reproduce velocity variations both in magnitude and temporal pattern over time scales from months to several years.

Acknowledgments

This study was possible thanks to the PERMOS and PermaSense networks. The project was founded by XSense 2 and Nano-tera.ch.

References

Arenson, L.U., Springman, S.M., (2005). Mathematical descriptions for the behaviour of ice-rich frozen soils at temperatures close to 0 °C. *Canadian Geotechnical Journal* 42(2): 431-442.

Haeberli, W., Hallet, B., Arenson, L.U., Elconin. R., Humlum, O., Kääb, A., Kaufmann, V., Ladanyi, B., Matsuoka, N., Springman, S., Mühll, D.V., 2006. Permafrost creep and rock glacier dynamics. *Permafrost and Periglacial Processes* 17: 189–214.

Ikeda, A., Matsuoka, N., Kääb, A., 2008. Fast deformation of perennially frozen debris in a warm rock glacier in the Swiss Alps: an effect of liquid water. *Journal of Geophysical Research* 113F01021.

Kääb, A., Frauenfelder, R., Roer, I., 2007. On the response of rockglacier creep to surface temperature increase. *Global and Planetary Change* 56: 172–187.

Wirz, V., Geertsema, M., Gruber, S., Purves, R.S., 2016. Temporal variability of diverse mountain permafrost slope movements derived from multi-year daily GPS data, Mattertal, Switzerland. *Landslides* 13:67–83.

Rock glacier inventories and kinematics: a new IPA Action Group

Reynald Delaloye[1], Chloé Barboux[1], Xavier Bodin[2], Alexander Brenning[3], Lea Hartl[4], Yan Hu[5], Atsushi Ikeda[6], Viktor Kaufmann[7], Andreas Kellerer-Pirklbauer[8], Christophe Lambiel[9], Lin Liu[5], Marco Marcer[10], Brianna Rick[11], Riccardo Scotti[12], Hideyuki Takadema[13], Dario Trombotto Liaudat[14], Sebastián Vivero[9], Maria Winterberger[1]

[1] *University of Fribourg, Department of Geosciences, Switzerland, reynald.delaloye@unifr.ch*

[2] *Laboratoire EDYTEM, CNRS/Université Savoie Mont-Blanc, Pôle Montagne, Le Bourget-du-lac, France*

[3] *Department of Geography, Friedrich Schiller University Jena, Germany*

[4] *IGF - Institut für Interdisziplinäre Gebirgsforschung, Österreichische Akademie der Wissenschaften, Innsbruck, Austria*

[5] *Earth System Science Programme, Faculty of Science, The Chinese University of Hong Kong, Hong Kong, China*

[6] *Faculty of Life and Environmental Sciences University of Tsukuba, Japan*

[7] *Institute of Geodesy, Remote Sensing and Photogrammetry Working Group, Graz University of Technology, Austria*

[8] *Department of Geography and Regional Science, Working Group Alpine Landscape Dynamics (ALADYN), University of Graz, Austria*

[9] *Institute of earth surface dynamics, University of Lausanne, Switzerland*

[10] *Laboratoire PACTE, Institut d'Urbanisme et de Géographie Alpine, University of Grenoble Alpes, France*

[11] *Department of Geography, University of Montana, Missoula, USA*

[12] *Departement of Biological, Geological and Environmental Sciences (BiGeA), University of Bologna, Italy*

[13] *Department of Environmental Science, Niigata University, Japan*

[14] *IANIGLA- CCT CONICET Mendoza, Argentina*

Abstract

A new IPA Action Group (2018-2020) is intending to promote the integration of permafrost creep rates (rock glacier kinematics) as a new associated parameter to the Essential Climate Variable (ECV) Permafrost within the Global Climate Observing System (GCOS) initiative supported by the World Meteorological Organization (WMO), characterizing the evolution of mountain permafrost on the global scale. The main scopes of this group are to sustain the first steps toward the organization and the management of a network dedicated to rock glacier mapping (inventorying) and monitoring all around the world and the definition of the necessary standards.

Keywords: Rock glaciers, inventories, monitoring, kinematics, standards, global network, Essential Climate Variable

Background

In mountainous terrain, frozen ground with sufficient ice content may be continuously in motion. Considerable volumes of fine- and coarse-grained debris material are involved in building up rock glaciers as a typical morphological feature of many mountain ranges in the periglacial zone. Even if there is still many discussions about the actual movement processes, rock glaciers appear to move at a rate, which is in particular depending on the temperature profile between the permafrost table and the main shear horizon at depth. Warmer permafrost conducts to higher motion rate, especially when the temperature is rising close to 0°C. Such warming may even lead to subsequent partial or complete destabilization of the rock glacier.

Rock glaciers inventories have been set up in many regions over the world for decades but without any real coordination. Rock glaciers have often been distinguished between intact (active/inactive) and relict landforms on morphological indices only, as for instance observable on aerial photography. Development in remote sensing technologies in particular, e.g. InSAR or photogrammetry, and the greater availability of appropriate satellite imagery, has recently permitted to include more detailed kinematic information within rock glacier inventories. New initiatives are rising in many regions with various methodologies, sometimes overlapping, and there is an obvious need for coordination and as far as possible for standardization.

Monitoring of rock glacier velocities provides clue information on the transfer rate of sediments along mountain slopes and on the impact of climate change on rock glacier stability. Observing or deriving a rock glacier kinematic variable on a global scale appears to be technically feasible using in particular satellite SAR interferometry, but also in combination with terrestrial geodetic surveys and photogrammetry analyses.

Objectives and scope of the Action Group

The Action Group intends to sustain the first steps toward the organization and the management of a network dedicated to rock glacier mapping (inventorying) and monitoring in all relevant mountain regions on Earth including definition of the necessary standards.

More specifically the Action Group aims to coordinate efforts to:

- define widely accepted standard guidelines for inventorying rock glaciers in mountain permafrost regions, including indications on the activity rate,

- promote the use of satellite SAR interferometry, e.g. Sentinel-1A data, for monitoring the rock glacier activity at a regional scale and define appropriate standards and guidelines,

- integrate as far as possible local-scale based monitoring data based on aerial and terrestrial geodetic surveys,

- initiate the development a world-wide rock glacier database, including kinematics,

- set up standard guidelines for selecting an appropriate number of rock glaciers per region that can be then used to assess temporal trends with decadal to intra-decadal time steps,

- build up and manage a web platform for visualization and open data access.

The Action Group is expecting that in the long run rock glacier kinematics could be recognized by the permafrost community (e.g. GTN-P) and later by the WMO as a new associated parameter to the ECVs of Permafrost. Rock glacier kinematics could be integrated in the monitoring strategy of international programs in addition to the observation of permafrost thermal state and active layer trends.

Organization of the Action Group

The basic idea of the group is to federate scientists for coordinating efforts and regrouping know-how and data on a single place (open access database) and define consensual baselines for inventorying rock glaciers and including kinematics information.

Co-authors of this abstract have agreed to take part to the scientific core group of the action in its initial stage. The core group emphasizes the need for networking and bringing international experience at participating, thus is far from being restricted in its initial form.

Timeline and expected deliverables

The Action Group will be active over a two-year period, from mid-2018 to mid-2020. It will be launched at EUCOP5 in Chamonix. Two Action Group Workshops are foreseen in 2018 and 2019, with field trips in rock glacier prone regions.

The Action Group will be closed at ICOP 2020 in Lanzhou. It expects to set up the generally accepted guidelines for inventorying rock glaciers including kinematics information and to design and establish a dedicated (pioneer) web platform allowing an open access to rock glacier inventorying and monitoring data.

Acknowledgments

Acknowledgments go to the IPA Executive Committee for having accepted to support this Action Group.

Seismologic monitoring of rock glaciers: first results on Gugla-Breithorn site (Switzerland)

Antoine Guillemot[1]
Laurent Baillet[1]
Agnès Helmstetter[1]
Éric Larose[1]

[1]*ISTerre, Univ. Grenoble-Alpes, CNRS, Grenoble (France)*

Abstract

The Gugla-Breithorn rock glacier has been surveyed since October 2015 by a seismological network, in order to estimate seismic velocity changes and to detect micro-seismicity. These two indicators are related with mechanical and meteorological variations, and thus allow a better understanding of rock glaciers dynamics along the seasons. We used ambient noise correlations to compute hourly surface waves velocities. We observed seasonal variations during the two years. During the winter period, velocities are higher, due to the freezing of surface layers that increases the whole rigidity of the medium. During the melting period, a sudden velocity decrease corresponds to the influence of melt water and the gradual destabilization of the rock glacier. Precipitations are also linked with a decorrelation of seismic responses, corresponding to a filling of the porous medium. Further processes will address mechanical properties by analysis of resonance frequency evolution.

Keywords: Rock glacier; seismology; ambient noise; micro-seismicity.

Introduction

The prevention of hazardous effects generated by permafrost degradation on mountainous steep slopes represents an increasingly important task. As ice-rich mountain permafrost areas with large amounts of potential disturbed materials, active rock glaciers are primarily concerned by these issues. With climate change and permafrost decay, ice that cements and stabilizes deep layers progressively disappears and leads to a so-called "emerging" risk, since it was quite unknown few decades ago.

Several measures have already been recorded on rock glaciers, including geodetical surveys, repeated geoelectrical campaigns and continuous recording of meteorological variables. Another technique based on seismic ambient noise and microseismic activity has been applied to measure seismic waves velocity changes inferred by mechanical changes. Many studies on landslides and volcanoes have shown that this methodology provides good results and can detect rigidity variations before failures. Such seismologic monitoring on rock glaciers could then potentially be used to find precursors of a global destabilization of theses permafrost landforms.

The following study aims to better understand rock glacier dynamics through variations in mechanical properties estimated using seismic data, which can then be linked to physical interpretations.

Methods

Located above the high perched valley of Zermatt (Valais canton, Switzerland), the Gugla-Breithorn rock glacier is from 2700 m to 3200 m high, about 130 m wide, 600 m long and up to 40 m thick in its terminal part. Most of the rock glacier has a slope smaller than 20°, but its terminal part is steeper and is moving rapidly (several meters per year), yielding hazardous issues on infrastructures below.

The continuous seismological network is composed of six seismic sensors that record vibrations on the site since October 2015. Such data have been treated by a specific signal processing that uses ambient noise correlation to provide seismic surface waves velocity changes. Other continuous surveys record meteorological variables (air temperature, rainfall, snow depth) and GPS positions on the rock glacier. These time series have been studied along the season in order to find correlations that reveal physical links between them.

Results and discussion

The two main indicators that have been computed from ambient noise correlation technique are:

- the relative surface wave velocity change dV/V (in %) with respect to a certain value averaged during a reference period. This indicator is related to a change of mechanical properties (rigidity or density) of the investigated medium;

- the correlation coefficient (CC) that quantifies the similarity of the correlation response with respect to the reference (cf. above).

These seismic data have been computed using different frequency bands filtering, that modifies the depth of the investigated medium. Low frequencies ([4-10 Hz]) data show an averaged imaging along the whole depth, whereas higher frequencies ([10-20 Hz]) deal with surface layers of the rock glacier.

Seasonal variations of dV/V at low frequencies have been estimated for the last two years. During winter period velocities are higher than during summer time, due to the freezing of surface layers that increases the whole rigidity of the medium (Fig. 1). During melting period, we observe a sudden velocity decrease (about 2%) that corresponds to the influence of melt water and the gradual destabilization of the rock glacier (red box in Fig. 1).

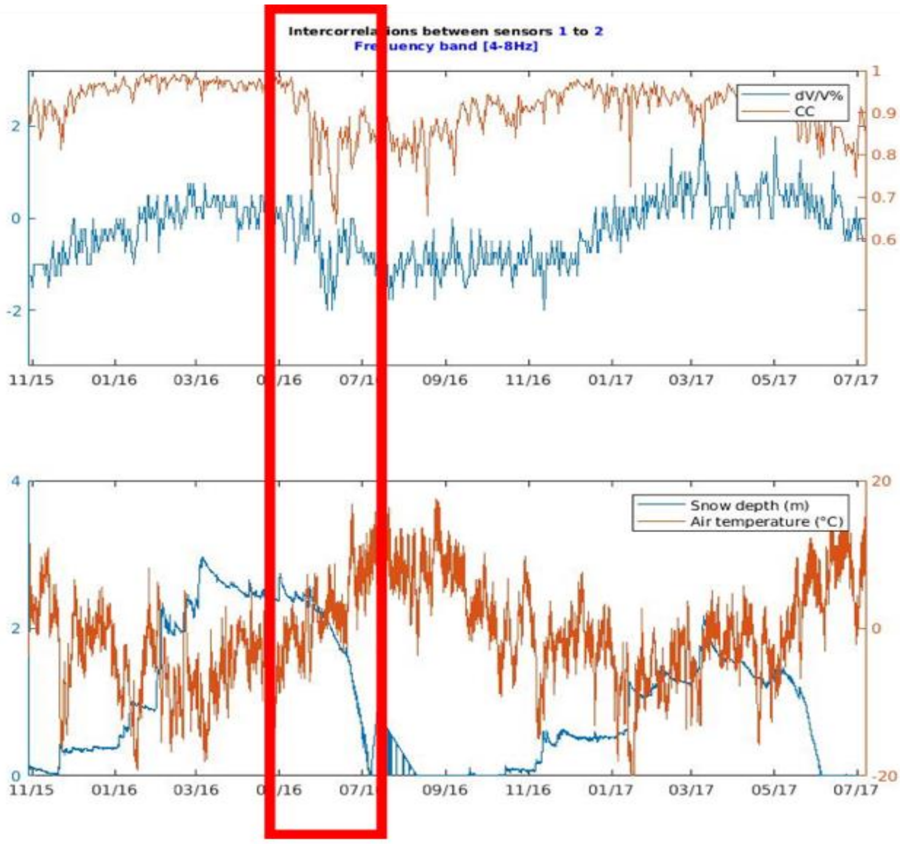

Figure 1. Above: time series of dV/V (in blue) and CC (in orange) during the whole surveyed period. Below: the corresponding series of snow depth (in blue) and air temperature (in orange). The red box shows the main melting period in 2016.

Precipitations are also linked with a decorrelation of seismic responses (shown by a CC drop), corresponding to a saturation of the surveyed porous medium.

Perspectives

Seismological monitoring of a rock glacier is a world-premiere in this field, and confirms that ambient noise correlations could improve our understanding about permafrost degradation. These observations will be combined with a mechanical model to perform Rayleigh waves sensibility kernels, and then to constrain the depth localization. Further processes will address changes of mechanical properties by analysis of resonance frequency along time. Micro-seismic activity will also be localized. A recent seismic instrumentation on Laurichard rock glacier (Hautes-Alpes, France) will provide another set of data, allowing a comparison between two sites of this permafrost landform.

Acknowledgments

We particularly thank Guillaume Favre-Bulle (CREALP) and the geological department of Valais for their valuable assistance with fieldwork, site maintenance and data retrieval.

References

Mainsant, G., E. Larose, C. Brönnimann, D. Jongmans, C. Michoud, and M. Jaboyedoff, 2012. Ambient seismic noise monitoring of a clay landslide: Toward failure prediction, *Journal of Geophysical Research*, 117, F01030.

Larose E., S. Carrière, C. Voisin, P. Bottelin, L. Baillet, P. Guéguen, F. Walter, D. Jongmans, B. Guillier, S. Garambois, F. Gimbert, C. Massey, 2015. Environmental seismology : Waht can we learn on earth surface processes with ambient noise ? *Journal of Applied Geophysics*, 116 : 62-74.

Delaloye, R., S. Morard, C. Barboux, D. Abbet, V. Gruber, M. Riedo and S. Gachet, 2012. Rapidly moving rock glaciers in Mattertal, *Jahrestagung der Schweizerischen Geomorphologischen Gesellschaft*, 21-31.

Interannual variability of rock glacier flow velocities in the European Alps

Andreas Kellerer-Pirklbauer[1], Reynald Delaloye[2], Christophe Lambiel[3], Isabelle Gärtner-Roer[4], Viktor Kaufmann[5], Cristian Scapozza[6], Karl Krainer[7], Benno Staub[2], Emmanuel Thibert[8], Xavier Bodin[9], Andrea Fischer[10], Lea Hartl[10], Umberto Morra di Cella[11], Volkmar Mair[12], Marco Marcer[13], Philippe Schoeneich[13]

[1]*Department of Geography and Regional Science, Working Group ALADYN, University of Graz, Austria, andreas.kellerer@uni-graz.at*

[2]*Department of Geosciences, University of Fribourg, Switzerland*

[3]*Institute of Earth Surface Dynamics, University of Lausanne, Switzerland*

[4]*Department of Geography, University of Zurich, Switzerland*

[5]*Institute of Geodesy, Remote Sensing and Photogrammetry Working Group, Graz University of Technology, Austria*

[6]*Institute of Earth Sciences, University of Applied Sciences and Arts of Southern Switzerland, Switzerland*

[7]*Institute of Geology, University of Innsbruck, Austria*

[8]*National Research Institute of Science and Technology for Environment and Agriculture, University Grenoble Alpes, France*

[9]*University Grenoble Alpes, Univ. Savoie Mont Blanc, CNRS, EDYTEM, 73000 Chambéry, France*

[10]*Institute for Interdisciplinary Mountain Research, Austrian Academy of Sciences, Austria*

[11]*Regional Agency for the Protection of the Environment (ARPA) - Valle d'Aosta, Italy*

[12]*Regional Office for Geology and Building Materials Testing, Autonomous Province of Bolzano, Italy*

[13]*Institute of Alpine Geography, University Grenoble Alpes, France*

Abstract

The monitoring of surface flow velocities at active rock glaciers has a long tradition in the European Alps with first surveys in the 1920s. Since the 1990s annual to seasonal flow velocity monitoring activities have been substantially expanded and partly institutionalized. In this article, we present and compare annual rock glacier surface flow velocity data from 35 rock glaciers in Austria (6), France (1), Italy (2) and Switzerland (26) spanning a time period of up to two decades. Results indicate a strong correlation of relative interannual velocity changes attributed to climate forcing.

Keywords: rock glacier monitoring, surface flow velocity, climate forcing, long-term evolution

Introduction and context

Rock glaciers are widespread periglacial landforms in the European Alps as revealed by several inventories. Monitoring of surface flow velocities at active rock glaciers has a long tradition with first terrestrial photogrammetric surveys in the Swiss and Austrian Alps already in the 1920s (Krainer *et al.*, 2012).

Since the 1990s velocity monitoring activities have been substantially expanded but also institutionalized (e.g. Delaloye *et al.*, 2010). In many cases, kinematic monitoring is carried out jointly with meteorological, hydrological and temperature monitoring in order to better understand the rock glacier-climate relationships and the reaction of rock glacier behavior to climatic changes (e.g. Kellerer-Pirklbauer & Kaufmann, 2012).

In this short contribution, we compare the relative changes of the surface velocities measured at 35 rock glaciers with at least annually-repeated data in four different Alpine countries. Similarities and differences of the movement patterns at different sites are described, while the spatio-temporal pattern of the surface velocity is compared with the climate context. This joint research effort is based on multi-annual velocity data and is a continuation of an earlier activity (Delaloye *et al.*, 2008).

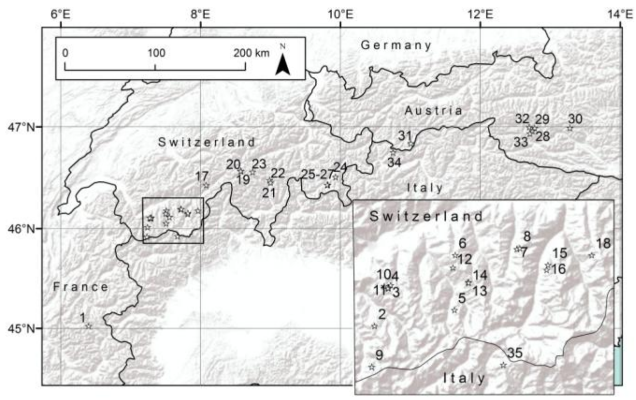

Figure 1. Location of the 35 rock glaciers in the European Alps where annual surface velocity data were used in this study. Inset map refers to S-Switzerland (numbers *cf.* Table 1).

Rock glacier monitoring sites

Table 1 lists the 35 rock glacier kinematic monitoring sites with some overview data. The sites cover a west-east distance of *c.*530 km and a north-south distance of *c.*220 km. Figure 1 depicts the monitoring locations.

Table 1. List of the rock glaciers relevant for this study

Nr.	Name	Nat.	Start	Inst.[1]	16/17[3]
1	Laurichard	FR	1984	8,9,13	115
2	Aget-Rogneux (median)	CH	2001	2	18
3	Yettes Condjà B	CH	2000	3	92
4	Yettes Condjà C	CH	2000	3	10
5	Tsarmine	CH	2004	2,3	429
6	Becs-de-Bosson / Réchy	CH	2004	2	114
7	HuHH1 / Hungerlitälli 1	CH	2001	4	91
8	HuHH3 / Hungerlitälli 3	CH	2002	4	166
9	Petit-Vélan	CH	2005	2	74
10	Lac des Vaux B	CH	2005	3	63
11	Luès Rares	CH	2006	3	36
12	Les Cliosses	CH	2006	3	25
13	Tsaté-Moiry 1	CH	2005	3	103
14	Tsaté-Moiry 2	CH	2005	3	96
15	Grosse Grabe	CH	2007	2	158
16	Gugla-Bielzug	CH	2007	2	249
17	Grosses Gufer	CH	2007	2	138
18	Gruben	CH	2012	2	81
19	Monte Prosa A	CH	2009	2	34
20	Monte Prosa B	CH	2009	2	14
21	Stabbio di Lagrario	CH	2008	6	32
22	Piancabella	CH	2008	6	16
23	Ganoni di Schenadüi	CH	2009	6	10
24	Muragl	CH	2009	4	119
25	Murtèl	CH	2009	4	14
26	Marmugnun	CH	2009	4	25
27	Chastelets	CH	2009	4	62
28	Weissenkar	AT	1997	5,1	10
29	Hinteres Langtalkar (low)	AT	1999	5,1	460
30	Dösen	AT	1995	5,1	43
31	Äußere Hochebenkar	AT	1938[2]	10	239
32	Tschadinhorn	AT	2014	5	177
33	Leibnitzkopf	AT	2010	5	321
34	Lazaun	IT	2006[2]	7,12	89
35	Gran Sometta	IT	2012	2,11	95

[1]Institutions according to the affiliation list; [2]with gaps; [3]mean annual horizontal flow velocity (cm/a) in 2016/17

Preliminary results

Rock glacier surface flow velocities in the European Alps have been relatively low in the 1980s-1990s. A first maximum was reached in 2003/04 followed by a drastic drop until *c.*2007/08. Since then, velocities increased again with new velocity maxima at most of the observed rock glaciers in 2015/16. The velocity maxima mentioned correlate with warm permafrost temperatures recorded in boreholes (e.g. PERMOS 2018) and are likely a result of the continuously warm conditions in the ground during the last years. The 35 rock glacier monitoring sites do not only differ substantially in location but also in elevation, topographical conditions and lithology. The surface velocity during the most recent monitoring year varied substantially between the rock glaciers with 10-460 cm/a (Table 1). The type of field measurement setup, the time of the measurements and the approach to calculate a "mean" annual surface velocity value differs also substantially between the sites. However, the relative change of the annual horizontal surface velocity (reference year 2016/17) shows high correlation between the sites (Figure 2).

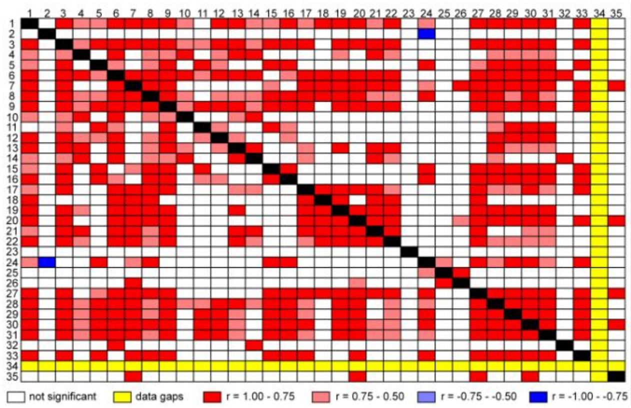

Figure 2. Correlation matrix for all 35 rock glaciers based on the relative change of the surface flow velocities (reference period 2016/17). Correlations: significant at the <0.05 level.

References

Delaloye, R., Perruchoud, E., Avian, M., Kaufmann, V., Bodin, X., Ikeda, A., Hausmann, H., Kääb, A., Kellerer-Pirklbauer, A., Krainer, K., Lambiel, C., Mihajlovic, D., Staub, B., Roer, I. & Thibert, E. 2008: Recent Interannual Variations of Rockglaciers Creep in the European Alps. *Proceedings of the Ninth International Conference on Permafrost*, Fairbanks, USA, June: 343-348.

Delaloye, R., Lambiel, C. & Gärtner-Roer, I. 2010. Overview of rock glacier kinematics research in the Swiss Alps: Seasonal rhythm, interannual variations and trends over several decades. *Geographica Helvetica* 65/2: 135-145.

Kellerer-Pirklbauer, A. & Kaufmann, V., 2012. About the relationship between rock glacier velocity and climate parameters in central Austria. *Austrian Journal of Earth Sciences* 105/2: 94-112

Krainer, K., Kellerer-Pirklbauer, A., Kaufmann, V., Lieb, G.K., Schrott, L. & Hausmann, H., 2012. Permafrost research in Austria: history and recent advances. *Austrian Journal of Earth Sciences* 105/2: 2-11

PERMOS, 2018. *Permafrost in Switzerland 2014/2015 to 2015/2016.* Noetzli, J., Pellet, C. & Staub, B. (eds.), Glaciological Report (Permafrost) No. 16-17 of the Cryospheric Commission of the Swiss Academy of Sciences (in prep).

Spatial distribution of rock glaciers and their influencing factors: a regional case study for South Tyrol, Italy

Christian Kofler[1, 2]
Stefan Steger[1]
Francesco Comiti[2]
Stefan Schneiderbauer[1]
Volkmar Mair[3]
Marc Zebisch[1]
[1]*Institute for Earth Observation, Eurac Research, Bolzano, Italy, christian.kofler@eurac.edu*
[2]*Faculty of Science and Technology, Free University of Bolzano/Bozen, Bolzano, Italy*
[3]*Office for Geology and Building Materials Testing, Autonomous Province of Bolzano-South Tyrol, Cardano, Italy*

Abstract

This paper outlines the objectives of the first stage of a PhD research. Therein, the information stored in a GIS-based inventory of rock glaciers will be related to permafrost-favoring environmental factors using multiple variable statistical procedures. The present inventory contains valuable information on the location, activity state (active/inactive/fossil), origin (talus/till-derived), shape (tongue/lobate-shaped) and size of rock glaciers in South Tyrol (Italy). The main aim is to gain insights into the influence of potential controlling factors, like topography, lithology, mean annual air temperature, perennial snowfields, avalanche debris, on rock glacier distribution, formation and status. The study will be conducted for the entire region of South Tyrol.

Keywords: Rock glacier inventory, statistical analysis, regional-scale, perennial snow

Introduction

Rock glaciers are prominent geomorphic features and indicative for mountain permafrost distribution. Their study can give valuable information on high-mountain environments such as past climate conditions or landscape development after deglaciation (Frauenfelder and Kääb, 2000; Sailer and Kerschner, 1999; Scotti et al., 2017).

Regional-scale inventories of rock glacier distribution are an important source to understand the spatial characteristics of permafrost. In addition, most rock glacier inventories that were compiled during the last decade contain also a temporal indications through the information whether a rock glacier is intact/fossil or talus/till-derived (Colucci et al., 2016; Scotti et al., 2013; Seppi et al., 2012).

The present study envisages to explore the detailed rock glacier inventory of the South Tyrolean region. This database was compiled by orthophoto and DEM interpretation, as well as applying SAR interferometry to locate the rock glaciers and to determine their activity state (Bollmann et al., 2012). We will try to identify relationships between the rock glacier distribution/status and morphological conditions, lithological units, past and present climate patterns, and periglacial features. Within this study, particular attention is paid to snow-related periglacial features in order to investigate on a regional scale the relationship between rock glaciers and avalanche activity and perennial snow fields (Humlum et al., 2007).

Methods

In a first step, a set of possible predictor variables for rock glacier presence/absence is prepared. This comprises the mapping of perennial snowfields and avalanche debris based on multi-temporal orthophoto and optical satellite imagery interpretation, the computation of a gridded map of mean annual air temperature (MAAT) and the generation of DEM-derivatives such as slope, aspect, potential incoming solar radiation and geomorphones (Jasiewicz and Stepinski, 2013).

Then, statistical relationships between the above-mentioned variables and various rock glacier characteristics (active/inactive/fossil, talus/till-derived, small/medium/large-sized) will be established and evaluated in terms of their statistical significance and geomorphic explanatory power.

It can be seen in figure 1A that in the southeastern part of South Tyrol (i.e. the area of the Dolomites), the rock glacier density is the low compared to the western and northeastern part, which are dominated by metamorphic rocks. Therefore, it is assumed that the major lithological units of the region not only influence directly on the rock glacier presence but also on other predisposing factors such as the topography. A mixed-effects model will be tested to differentiate the influence of the various predictor variables on rock glacier presence within each lithological unit.

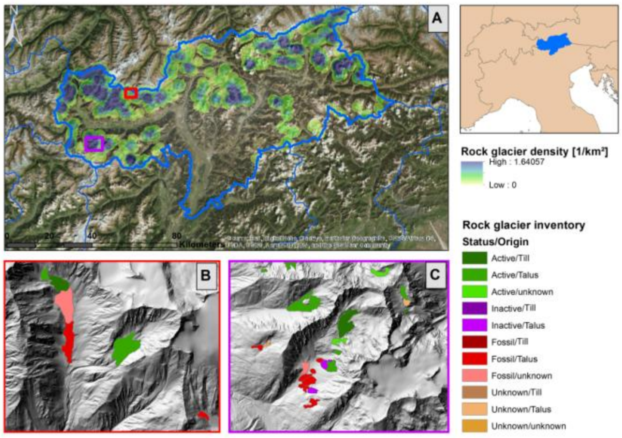

Figure 1: Overview on rock glacier distribution of South Tyrol. A: Region of South Tyrol and rock glacier density [1/km²]. B and C: Classification of rock glaciers according to activity state and origin (Data source: Autonomous Province of Bolzano, Office for Geology and Building Materials Testing)

Expected results

The presented work aims to explore the potential of an available rock glacier inventory to detect spatial relationships between different rock glacier characteristics and their forming and influencing agents.

Acknowledgments

The authors would like to acknowledge the Stiftung Südtiroler Sparkasse/Fondazione Cassa di Risparmio di Bolzano (Grant No. 2017.0160) and Eurac Research, who are jointly funding this PhD-research.

References

Bollmann, E., Rieg, L., Spross, M., Sailer, R., Bucher, K., Maukisch, M., Monreal, M., Zischg, A., Mair, V., Lang, K., Stötter, J., 2012. Blockgletscherkataster in Südtirol - Erstellung und Analyse, in: Permafrost in Südtirol, Innsbrucker Geographische Studien. University of Innsbruck, Innsbruck, Austria, pp. 147–171.

Colucci, R.R., Boccali, C., Žebre, M., Guglielmin, M., 2016. Rock glaciers, protalus ramparts and pronival ramparts in the south-eastern Alps. Geomorphology 269, 112–121. https://doi.org/10.1016/j.geomorph.2016.06.039

Frauenfelder, R., Kääb, A., 2000. Towards a palaeoclimatic model of rock-glacier formation in the Swiss Alps. Ann. Glaciol. 31.

Humlum, O., Christiansen, H.H., Juliussen, H., 2007. Avalanche-derived rock glaciers in Svalbard. Permafr. Periglac. Process. 18, 75–88. https://doi.org/10.1002/ppp.580

Jasiewicz, J., Stepinski, T.F., 2013. Geomorphons - a pattern recognition approach to classification and mapping of landforms. Geomorphology 182, 147–156. https://doi.org/10.1016/j.geomorph.2012.11.005

Sailer, R., Kerschner, H., 1999. Equilibrium-line altitudes and rock glaciers during the Younger Dryas cooling event, Ferwall group, western Tyrol, Austria. Ann. Glaciol. 28, 141–145. https://doi.org/10.3189/172756499781821698

Scotti, R., Brardinoni, F., Alberti, S., Frattini, P., Crosta, G.B., 2013. A regional inventory of rock glaciers and protalus ramparts in the central Italian Alps. Geomorphology 186, 136–149. https://doi.org/10.1016/j.geomorph.2012.12.028

Scotti, R., Brardinoni, F., Crosta, G.B., Cola, G., Mair, V., 2017. Time constraints for post-LGM landscape response to deglaciation in Val Viola, Central Italian Alps. Quat. Sci. Rev. 177, 10–33. https://doi.org/10.1016/j.quascirev.2017.10.011

Seppi, R., Carton, A., Zumiani, M., Dall'Amico, M., Zampedri, G., Rigon, R., 2012. Inventory, distribution and topographic features of rock glaciers in the southern region of the Eastern Italian Alps (Trentino). Geogr. Fis. E Din. Quat. 35, 185–197.

Investigating ages and kinematics of two rock glaciers in the Southern Alps of New Zealand

Christophe Lambiel[1]
Sebastian Vivero[1]
Stefan Winkler[2]
[1]*Institute of Earth Surface Dynamics, University of Lausanne, Lausanne, Switzerland, christophe.lambiel@unil.ch*
[2]*Institut für Geographie und Geologie, Universität Würzburg, Würzburg, Germany*

Abstract

Schmidt hammer and dGPS measurements were carried out on two rock glaciers located in the Ben Ohau range, Southern Alps, New Zealand. The increase of surface weathering towards the front suggests rather low surface deformation during the downward transfer. Both rock glaciers developed throughout the Holocene, with mean velocities of around 3 cm/y. Their kinematics is sensibly different today since no movement was measured on one of the rock glaciers, whereas the other displays velocities up to 15 cm/y. This suggests potentially strong velocity variations during the Holocene.

Keywords: Rock glacier, dating, kinematics, Schmidt hammer, dGPS, New Zealand

Introduction

Whereas rock glacier dynamics is intensely studied in the European Alps, investigations in other mountain ranges are much less frequent. This is particularly the case for the Southern Alps of New Zealand, where extremely few studies have been carried out (eg. Kirkbride & Brazier, 1995; Brazier et al., 1998). However, Sattler et al. (2016) showed that rock glaciers are widespread landforms in this mountain range. To get new insights on New Zealand rock glacier development, we initiated a study in 2016, aiming at dating and investigating the kinematics of two rock glaciers, using Schmidt hammer, dGPS and UAV.

Study site and methods

The two rock glaciers are located in the Irishman valley in the Ben Ohau range, Southern Island. Rock glacier I is a 400 m long landform and reaches an altitude of 1870 m a.s.l., thus below the lower limit of permafrost in the area, estimated at around 2000 m a.s.l. (Sattler et al., 2016). Rock glacier II is slightly smaller and front elevation is at 2000 m a.s.l. Bedrock is made of greywacke.

We used an electronic Schmidt hammer (SilverSchmidt) to obtain relative ages of rock glacier surface (Winkler & Lambiel, in press). Measurements were carried out in February 2014 on previously dated adjacent Late Glacial moraines and in January 2016 on the rock glaciers. Each site included generally 3 samples of single impacts on 50 randomly selected boulders (Figure 1).

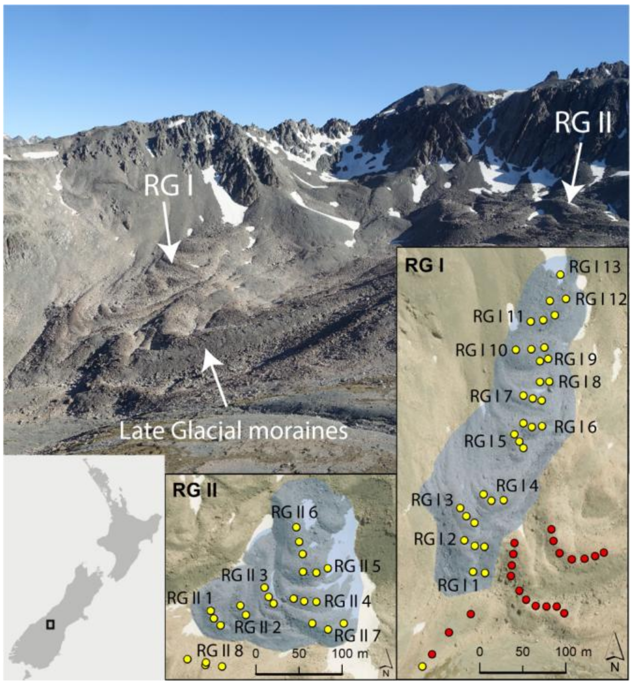

Figure 1. Location of the 2 rock glaciers investigated, with the measurement sites of 2016 (rock glaciers, yellow dots) and 2014 (Late Glacial moraines, red dots).

dGPS surveys were carried out in January 2016 and repeated in February 2017. A total of 46 points were measured on both rock glaciers. Additionally, an UAV survey was done on rock glacier II with a DJI Phantom 3 pro quadcopter in February 2017.

Results

The profiles measured on both landforms revealed a consistent and rather regular decrease of the rebound (R-) values and thus increasing weathering intensity and surface exposure ages from the roots toward the front.

Available numerical ages obtained by ^{10}Be terrestrial cosmogenic nuclide dating (Kaplan et al. 2010) allowed the calculation of a SHD calibration-curve. The maximal ages obtained are 12 kyrs for rock glacier I and 10,5 kyrs for rock glacier II, indicating a development throughout the Holocene (Figure 2). Mean Holocene velocities calculated from the obtained ages and rock glacier length are 3 cm/y for both landforms.

dGPS surveys revealed absence of movement at rock glacier I and velocities lower than 5 cm/y for the lower part of rock glacier II and up to 15 cm/y for its upper part.

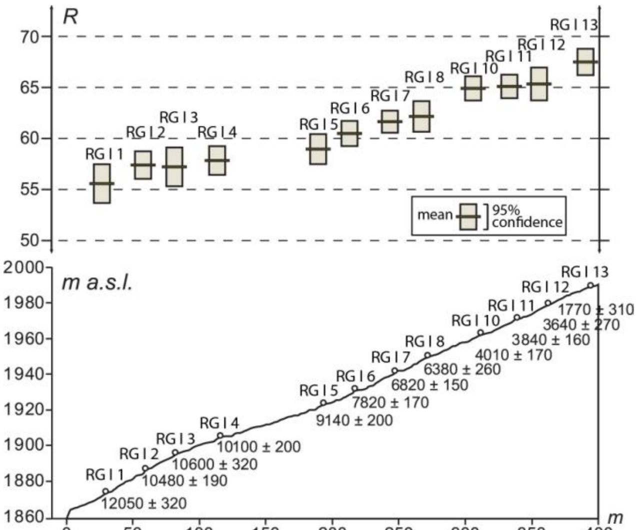

Figure 2. R-values (upper graph) and ages (bottom) obtained for rock glacier 1.

Discussion and conclusion

The significant increase of surface weathering towards the rock glacier fronts suggests a more or less passive transport of the blocks at the rock glacier surface without any major toppling. It also indicates that the ridges are rather stable during their downward migration. The ages obtained show that both rock glaciers started their development at the onset of the Holocene and that they grew up throughout this period. The relative ages of the different ridges also suggest substantial velocity variations during the Holocene. This is also expressed by current velocities. Even if caution is needed in the interpretation of the sole one-year kinematic data, rock glacier I seems to be inactive, which might be explained by its relatively low elevation. The higher altitude of rock glacier II in the permafrost belt still permits permafrost creep, in particular in its upper part.

This study is just a first step in the perspective of a desired increased focus on rock glacier kinematics and, more broadly, on the state of permafrost in New Zealand. Furthermore, improving our knowledge on rock glacier development requires reliable age control to derive long-term velocity variations.

References

Brazier, V., Kirkbride, MP., Owens, IF., 1998. The relationship between climate and rock glacier distribution in the Ben Ohau Range, New Zealand. *Geografiska Annaler A* 80: 193-207.

Kaplan MR, Schaefer J, Denton GH, Barrell DJA, Chinn TJH, Putnam AE, Anderson BG, Finkel RC, Schwartz R, Doughty AM. 2010. Glacier retreat in New Zealand during the Younger Dryas Stadial. *Nature* 467: 194-197.

Kirkbride, M. & Brazier, V., 1995. On the sensitivity of Holocene talus-derived rock glaciers to climate change in the Ben Ohau Range, New Zealand. *J. Quatern. Sci.* 10: 353-365.

Sattler, K., Anderson, B., Mackintosh, A., Norton, K., de Róiste, M., 2016. Estimating Permafrost Distribution in the Maritime Southern Alps, New Zealand, Based on Climatic Conditions at Rock Glacier Sites. *Front. Earth Sci.* 4:4.

Winkler, S. and Lambiel, C., accepted and in press. Age constraints of rock glaciers in the Southern Alps/New Zealand – exploring their palaeoclimatic potential. *The Holocene.*

Analysis of climate change on rock glaciers of the semi-arid Andes and its posible hydrological consequences

Catalina Pino Rivas[1]

Roberto Merino González[2]

[1]1Departamento de Geología, Escuela de Ingeniería y Ciencias. Facultad de Ciencias Físicas y Matemáticas, Universidad de Chile. Plaza Ercilla 803, Santiago, Chile. e-mail: catalina.pino@ug.uchile.cl

[2] Servicio Nacional de Geología y Minería, Avda Santa María 0104, Santigo, Chile. e-mail: roberto.merino@sernageomin.cl

Abstract

In the high-altitude zones of the semi-arid Andes of Chile, rock glaciers are remarkable morphological features, and representing a great area across the zones. However, their behavior is not well-understood. Therefore, identifying, locating and understand these features to implement sustainable regional planning for water resources is important. The objective of this study is to determine the volumetric variation in the active forms via the comparison of digital elevation models between 1956 –- 2017; the aim is to establish relationships between these rock glaciers and climate, geographic and/or geological conditions to demonstrate a relationship between the volumetric variation and the hydrology of the watershed, in order to improve knowledge about the hydrological role of these cryoforms. Finally, using these measures, it will be possible to develop a new classification system to identify active / inactive/ relict rock glaciers in addition to the interpretation of satellite imagery, aerial photographs and fieldwork observations.

Keywords: rock glacier; permafrost; periglacial environment; Digital Elevation Model; geomorphological mapping.

Introduction

Between 27–33°S, rock glaciers are of specific interest in high and dry mountain areas, where their abundance make them considerable solid water reservoirs (Corte, 1976; Azócar & Brenning, 2010). However, their dynamics and real contribution to the hydrologic system has not been well studied, besides the current inventories about rock glaciers present conceptual and delimitational mistakes related to their morphologies, without and adequate verification in the field. Therefore, a more precise inventory is necessary given the incompleteness of the Chilean glacier registry, as well as the omission of rock glaciers from classical glacier inventories (Janke *et al.*, 2015).

Our work will demonstrate the volumetric changes through time experienced by rock glaciers of Quebrada Caballos, in the upper basin of the Cochiguás River, in order to relate them to climatic variations existing over the same period. We will also determine the possible hydrological consequences that future variations can entail.

Study area

The area is located in the Coquimbo Region of Chile, in the southern sector of the headwaters of the Claro and Cochiguás Rivers (Fig. 1). It corresponds to a high mountain environment with altitudes between 3600 and 5000 m.a.s.l. The mean monthly temperature ranges from 5°C in the summer to -5°C in the winter. Precipitation almost exclusively occurs in winter, as snow, and varies between 25 and 300mm (New et al., 2002).

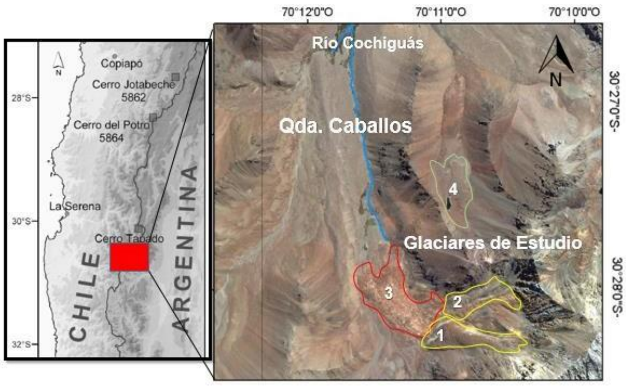

Figure 1. Area studied. Rock glaciers 1 & 2 are delimitated by a yellow line, rock glacier 3 in red and rock glacier 4 is delimitated by a green line.

Methods

Geomorphological mapping

The geomorphological assemblage was surveyed in the field with the aim of identifying and discriminating geomorphological spatial units and features, such as glacial deposits, moraines, rock glaciers, among others.

They have been mapped also by interpretation of high-resolution satellite imagery.

Development of digital elevation models from aerial photographs

We will use photogrammetric processing of stereo imagery and interpolation techniques to generate digital elevation models that allow to study volume changes between the years 1956 – 2017 on rock glaciers 1 & 2 of the study area (Fig. 1). This will be done through the aerial photographs acquired on 1956 by the Geographical and Military Institute (IGM) of Chile.

Development of DEM from surface data collection with differential GPS

Figures and tables must fit within one column or within A field campaign will be carried out in which differential GPS points will be raised, which will be used later to georeferenced and orthorectify the aerial photographs, in addition to measuring and reconstructing the surface of the rock glaciers to delimit the cryoforms.

Comparison of climatic variables with changes in volume

Based on the results obtained from the digital elevation models, we will proceed to evaluate the climatic variables for the study area in the period between 1956 – 2017. In order to attribute the volume changes to the climate change in such period.

Preliminary results

Geomorphologye

By observing the front, the surface and their shape, we have selected four rock glaciers (Fig.2) in order to stablish some common features and differences between them. We have preliminarily classified the rock glaciers 1 & 2 (Fig.2a) as active forms, due their steep fronts, evidence of ridges and furrows, imbricated clasts, and tongue-shaped. On the other hand, cryoforms 3 (Fig. 2b) & 4 (Fig. 2c) seems like an inactive and relict form, respectively. The first one shows front slopes below the angle of repose with a smooth front scarp, while the second one is characterized by collapsed structures on its surface. However, these two forms are confusing, so this must to be verified in the field.

Outlook

The results of this investigation will be obtained in the first semester of 2018, in order to have relevant conclusions about the volumetric changes of rock glaciers, their hydrological implications and their relationship with climate change, as well as contributing to the improvement in the inventory of rock glaciers in Chile, applying new methodologies and categories.

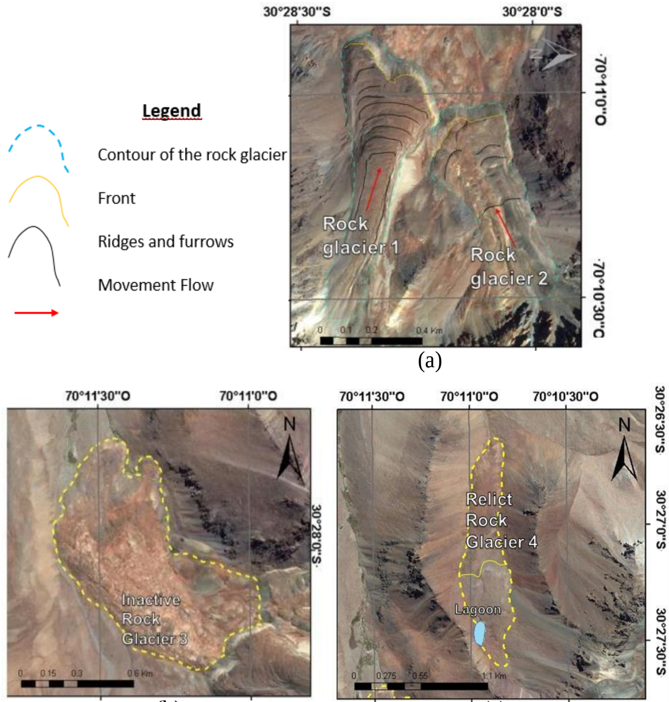

Figure 2: The four cryoforms selected and classified for this study. (a) active forms (b) inactive forms and (c) forms.

Acknowledgments

I would like to thank to the National Geology and Mining Survey of Chile (SERNAGEOMIN) for its support and funding for field campaigns; to the Geologists Association of Chile for its financial support, and finally to the School of Engineering and Sciences of the University of Chile, for all the help received and for the important financial support to attend this conference.

References

Azócar, G.F. & Brenning, A. 2010. Hydrological and geomorphological significance of rock glaciers in the dry Andes, Chile (27° - 33°S). *Permafrost and Periglacial Processes* 21: 42-53.

Corte, A. 1976. The hydrological significance of rock glaciers. *Journal of Glaciology* 17: 157-158.

Janke, J. R., Bellisario, A. C., & Ferrando, F. A. 2015. Classification of debris-covered glaciers and rock glaciers in the Andes of central Chile. *Geomorphology* 241: 98–121

Near-surface ventilation as a key for modelling the thermal regime of coarse blocky rock glaciers

Luisa Pruessner[1,2]
Marcia Phillips[3]
Martin Hoelzle[4]
Michael Lehning[3,5]
Daniel Farinotti[1,2]
[1]*Laboratory of hydraulics, Hydrology and Glaciology (VAW), ETH Zürich, Zürich, Switzerland,* pruessner@vaw.baug.ethz.ch
[2]*Swiss Federal Institute for Forest, Snow and Landscape Research WSL, Birmensdorf, Switzerland*
[3]*WSL Institute for Snow and Avalanche Research, SLF, Flüelastrasse 11, CH-7260Davos Dorf, Switzerland*
[4]*Alpine Cryosphere and Geomorphology, Department of Geosciences, University of Fribourg, Chemin du Musée 4, CH-1700 Fribourg, Switzerland*
[5]*Laboratory of Cryospheric Sciences CRYOS, School of Architecture, Civil and Environmental Engineering, Ecole Polytechnique Fédérale de Lausanne (EPFL), Lausanne, Switzerland*

Abstract

In a changing climate glaciers, rock glaciers and ice-rich permafrost are undergoing drastic changes. Due to their complex compositions with a mixture of ice and debris, rock glaciers are expected to be less sensitive to climate change than clean-ice counterparts. The active layer of rock glaciers, in fact, consists largely of debris and often large rocks thus protecting the underlying ice-rich layer from melt. The 1D physics based model SNOWPACK with a suitably adapted parameterisation of ventilation was used to represent advective airflow in the blocky active layer at three experimental sites. Snow depth dynamics and ice-content stratigraphy were shown to be the most important factors influencing the thermal regime. Our contribution presents quantitative estimates of the augmented heat flux through the blocky layer caused by ventilation of both snow and blocks.

Keywords: SNOWPACK, ventilation, rock glaciers, thermal regime, active layer

Introduction

With ongoing climate change glaciers are retreating fast, reducing expected overall run off in time (Bliss *et al.,* 2014). Rock glaciers are thought to be less sensitive to climate change (Kenner & Magnusson, 2017) and may become important freshwater resources for regions which rely on glacial runoff for water supply. For long term predictions of rock glacier evolution, their thermal regime needs to be reliably modelled.

The difficulty in modelling the thermal regime of rock glaciers lies in (a) the complexity of the processes occurring in the blocky active layer, which allows for advective modes of heat transport (Hanson & Hoelzle, 2004) due to its large interstitial pore spaces through which air can flow, and (b) their heterogeneous surface.

The advective air flow is addressed by investigating a ventilation parameterisation within the 1D physics-based model SNOWPACK (Lehning *et al.*, 1999). The parameterisation relies on only one site specific parameter, dependent on the representative pore length of the site. In this study, three sites in the Swiss Alps were considered: Murtèl-Corvatsch, Ritigraben and Schafberg.

Results and Discussion

Ventilation

Air flow through the large interstitial pore spaces in the blocky layer of rock glaciers allows for advective heat transport, which cannot be modelled explicitly in a 1D model. A parameterisation for the vertical component is utilised instead. The wind speed at the surface is attenuated into the ground, resulting in a vertical velocity gradient which is used to calculate e contribution to the effective heat conductivity of the layer.

Ventilation was shown to be important at all three test sites. Without it, the low temperatures recorded during the winter months could not be reproduced (Fig. 1). This suggests that ventilation is particularly important during the snow-covered period. Numerical experiments without ventilation show also a warming trend in the ground temperatures leading to a false indication of ice melt.

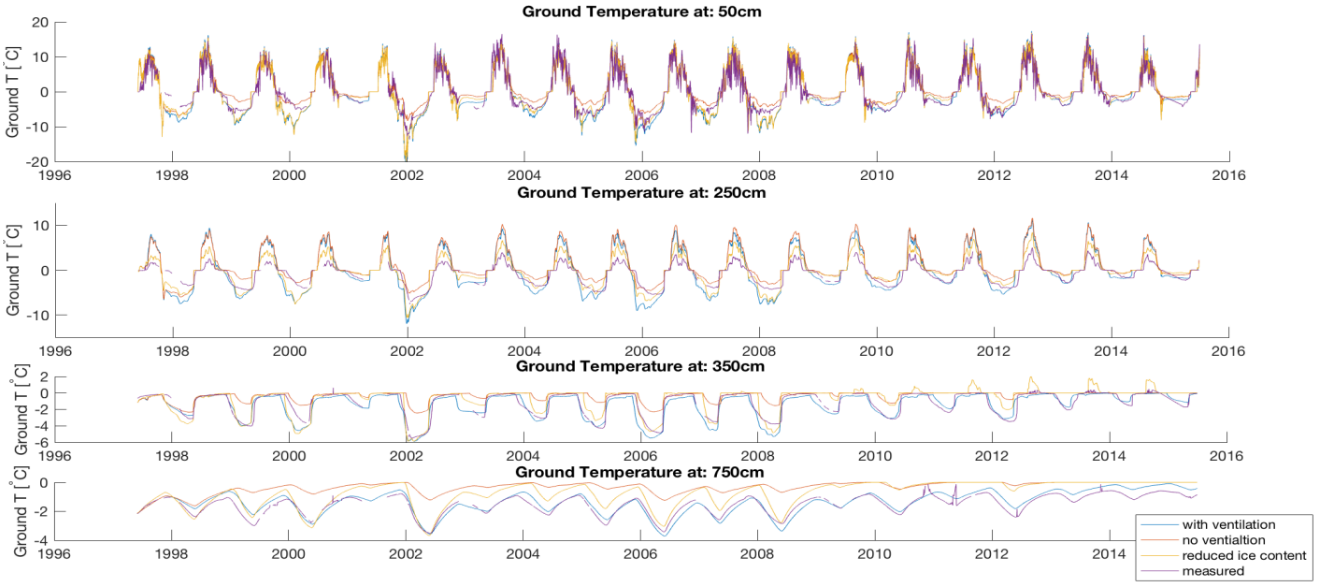

Figure 1. Modelled temperatures at depths of 0.5 m, 2.5 m, 3.5 m, and 7.5 m (from top to bottom) for the Murtèl site with the following configurations: ventilation switched on (blue) and ventilation switched off (red); ventilation switched on using a reduced ice content of 70% in the icy layer (orange). Measured temperatures are shown in purple.

Ice content

A numerical experiment done at the Murtèl test site shows that a reduced ice content can also lead to increased ground temperatures (Fig. 1). However, this effect is less pronounced than the absence of ventilation. The resulting drift in modelled ground temperatures can take up to a decade to show significant deviation from measurement data. This has important consequences for long term (decades to centuries) projections as long calibration periods may be required in the absence of reliable ice content information.

Snow height

Since snow measurements were not available directly at the Schafberg and Ritigraben sites, numerical experiments with adjusted snow heights were performed. These confirmed findings of previous studies that snow height dynamics exert strong control over ground temperatures (Haberkorn et al., 2015).

Conclusions

Three key findings have been presented here: (1) the inclusion of ventilation processes in the model are required to reproduce the low temperatures observed in winter; (2) ice content exerts a strong influence over the evolution of the thermal regime and an incorrect ice content can lead to artificial temperature drift that is hard to detect without long time series of borehole temperatures; and (3) snow height has a significant effect on ground temperatures and care needs to be taken if the measurements are not available in close proximity to the borehole.

Acknowledgments

Borehole temperature data were obtained from the PERMOS network. Meteo data at Ritigraben and Schafberg were obtained from the Swiss IMIS network.

References

Bliss, A., Hock, R., and Radić, V., 2014. Global response of glacier runoff to twenty-first century climate change. *Journal of Geophysical Research: Earth Surface* 119:717–730. doi: 10.1002/2013JF002931.

Haberkorn, A., Hoelzle, M., Phillips, M., Kenner, R., 2015. Snow as driving factor of rock surface temperatures in steep rough rock walls. *Cold Regions Science and Technology* 118:64-75. doi: 10.1016/j.coldregions.2015.06.013

Hanson, S. and Hoelzle, M., 2004. The Thermal Regime of the Active Layer at the Murtèl Rock Glacier Based on Data from 2002. *Permafrost and Periglacial Processes* 15:273–282. doi: 10.1002/ppp.499.

Kenner, R. and Magnusson, J. (2017). Estimating the Effect of Different Influencing Factors on Rock Glacier Development in Two Regions in the Swiss Alps. *Permafrost and Periglacial Processes* 28:195–208. doi: 10.1002/ppp.1910.

Lehning, M., Bartelt, P., Brown, B., Russi, T., Stöckli, U., & Zimmerli, M., 1999. SNOWPACK model calculations for avalanche warning based upon a new network of weather and snow stations. *Cold Regions Science and Technology*. 30: 145–157. doi: 10.1016/S0165-232X(99)00022- 1.

The Col du Lou event (French Alps) – an active layer detachment at the front of a destabilized rock glacier

Charles Ribeyre[1,2]
Philippe Schoeneich[1]
Marco Marcer[1,3]
Ombeline Brenguier[2]
Xavier Bodin[3]
Steffen Nielsen [4]

[1]*Université Grenoble Alpes, Institut d'Urbanisme et de Géographie Alpine, PACTE, Grenoble, France, charles.ribeyre48@laposte.net*

[2]*SAGE/ADRGT, Gières, France*

[3]*University Grenoble Alpes, Univ. Savoie Mont Blanc, CNRS, EDYTEM, 73000 Chambéry, France*

[4]*Arctic Technology Centre, Technical University of Denmark, 2800 Kgs. Lyngby, Denmark*

Abstract

On August 14 2015, two successive debris flows damaged the lower station of a chairlift in Lanslevillard, French Alps. The debris flows were triggered by two slides at the front of a rockglacier. One of them is an active layer detachment slide, the first case reported in the Alps. It occurred at the margin of a very active lobe, covered by numerous tension cracks. The reconstruction of past displacement by orthophotographs shows that the velocity has been increasing for the past ten years. Geophysical investigations suggest the presence of temperate permafrost with an important water content. The two months before the event were very hot. It is suggested that the atmospheric warming since the 2000's and the heat wave of the early summer 2015 acted as preparatory factors, whereas the event itself was triggered by a modest thunderstorm.

Keywords: rock glacier destabilization; active layer detachment; debris flow; permafrost degradation; French Alps

Introduction

On August 15 2015, two successive debris flows damaged the lower station of a chairlift at Lanslevillard in the French Alps. The event occurred after a relatively modest thunderstorm, which was not sufficient by itself to produce a debris flow of this magnitude. The uppermost source of debris consists of two slides at the front of a rockglacier. Permafrost degradation and the subsequent destabilization of the rock glacier were therefore suspected to be the main factors. Multi-method investigations were conducted, in order to better understand the processes involved and the causes of the event.

Study site

The *Col du Lou* rock glacier is situated at 2800 m a.s.l. above the village of Lanslevillard, in the Upper Maurienne valley in the French Alps (45.264946 N , 6.939622 E). It is a pebbly rockglacier, formed of flat medium sized calcschist debris. Geomorphologically, it shows smooth although distinct forms, with several lobes overhanging a steep slope.

One of the slides occurred at the side of a very active lobe that displays numerous tension cracks at its surface. The detachment area of 100 x 20 m exposed a steep, 2-3 m high scarp, corresponding to the active layer. Frozen debris was observed on the slide plane. The slide can therefore be considered as an active layer detachment slide. It is the first reported case of this kind in the Alps.

The other slide shows a long and narrow gully shape. Below the upper scar, water was flowing from the ground. The water flow played here the major role.

Methods

Investigations included detailed topographic and geomorphological field survey, instrumenting for further monitoring, and reconstruction of past displacements.

A network of marked blocks was set up in October 2015 and surveyed twice a year by DGPS. Four UTL-3 dataloggers were placed on the rock glacier for monitoring of surface temperatures at 1 h time interval.

An UAV photogrammetric survey was performed in October 2016 in order to produce a detailed DTM using

Agisoft Photoscan. The DTM served as a base for a detailed geomorphological map.

Historical aerial imagery from IGN (the French topographical survey) were used for producing orthophotos and surface displacements were calculated for each time interval by tracking of recognizable blocks.

Three geophysical measurement campaigns were conducted in September 2016 , July 2017 and October 2017. Both ERT and seismic refraction profiles were performed on the same profiles.

Results

The diachronic analysis of orthophographs shows that the surface velocities increased significantly since the late 1990's, with a strong acceleration in the last decade. Reconstructed velocities are spatially consistent with those measured by DGPS, and correspond well with the tension fractures field, showing maximal velocities along the centerline of the lobe. The front lobe shows a changing shape, indicating that slides probably occurred periodically on the front slope, although without triggering debris flows. The geophysical profiles show evidence of the presence of ice. Electrical resistivities are however much lower on the most active lower lobe than on the less active upper zones and consistent with the presence of temperate, water rich permafrost. The active layer thickness is consistent with the observed depth of the active layer in the detachment scar. Above the scar of the right-hand slide, a large depression was supposed to result from the melting of a former glacier. This is probably confirmed by the very high electrical resistivity values, indicating the presence of massive ice. Thus the melting of the ice is probably the main source of the strong water flow observed in the scar.

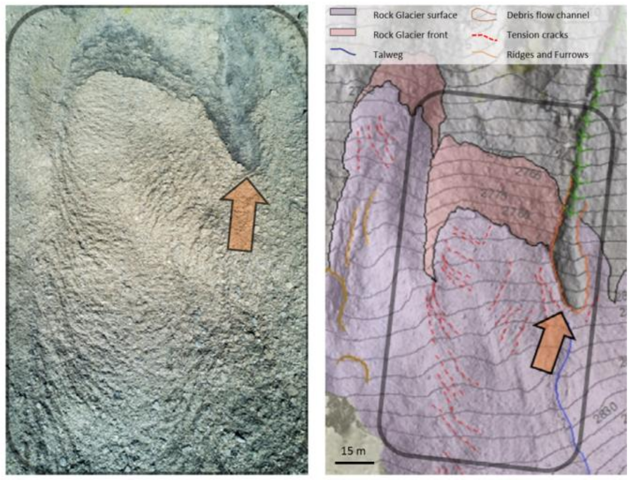

Figure 1. Geomorphological map (right) and orthoimage (left) of the most active lobe. Tension cracks are visible on the lobe. Arrows point to the active layer detachment slide.

Interpretation

The rock glacier is located at the lower boundary of the periglacial belt and may be subjected to permafrost degradation. As a consequence, the progressive acceleration of the surface velocity since the 1990's can be related to the atmospheric warming. During the early summer 2015 one of the strongest heat waves of the last decades occurred. The thunderstorm of August 15 would not have been sufficient by itself for triggering such slides but it acted as triggering factor on an already unstable body.

The main slide can be described as an active layer detachment slide. On the whole surface of the lobe, very close tension cracks completely disturb the surface. Such close cracks can be explained only by very shallow movements. We therefore suggest that the main displacements may be due to sliding of the active layer on top of the frozen permafrost body.

A field survey conducted on the whole rockglacier inventory of the french Alps showed that similar cracks can be observed on numerous fine to medium grained rockglaciers (Marcer et al., this conference). They are considered as potential indicators of a surface acceleration, and therefore as warning signs of possible destabilization phenomena.

After the collapse of the Berard rockglacier in 2006 (Bodin et al. 2016) the Col du Lou is the second case of mass movement due to rock glacier degradation in the french Alps. Both cases occurred on « pebbly » rock glaciers, which may be the most susceptible to such events.

Acknowledgments

This study was funded by the Community of Lanslevillard and the ERDF through the POIA-PermaRisk project.

References

Bodin, X., Krysiecki, J.-M., Schoeneich, P., Le Roux, O., Lorier, L., Echelard, T., Peyron, M., Walpersdorf, A., 2016. The 2006 Collapse of the Bérard Rock Glacier (Southern French Alps). *Permafrost and Periglacial Processes* 28, 209–223. DOI: 10.1002/ppp.1887

Marcer, M., Bodin, X., Brenning, A., Schoeneich, P., Charvet, R., Gottardi, F., 2017. Permafrost Favorability Index: Spatial Modeling in the French Alps Using a Rock Glacier Inventory. *Frontiers in Earth Science* 5. DOI: 10.3389/feart.2017.00105

Different dynamics of two neighbouring permafrost creeping landforms in the last 15 years

Roberto Seppi[1,6], Alberto Carton[2,6], Thomas Zanoner[2,6], Matteo Zumiani[3], Luca Carturan[2,5,6], Carlo Baroni[4,6], Maria Cristina Salvatore[4,6]

[1]*Department of Earth and Environmental Sciences – University of Pavia (roberto.seppi@unipv.it),* [2]*Department of Geosciences – University of Padova,* [3]*Geological Service – Autonomous province of Trento,* [4]*Department of Earth Sciences – University of Pisa,* [5]*Department of Land, Environment, Agriculture and Forestry – University of Padova;* [6]*Comitato Glaciologico Italiano*

Abstract

A rock glacier and a neighbouring composite landform derived from a LIA glacier, located in permafrost belt of the Adamello-Presanella Group (Eastern Italian Alps) showed a dissimilar dynamic behaviour over a long period of measurements (2001-2015). The velocity of the rock glacier increased in the last five years, while the composite landform moved with almost unchanged velocity over the investigated period. Whereas MAGST seems to be a variable controlling the displacement of both the landforms, the duration of the snow cover is significantly correlated with displacement only on the rock glacier.

Keywords: rock glaciers; creeping landforms; permafrost; LIA glacial deposits; surface dynamics; Eastern Italian Alps.

Introduction

An overall acceleration of rock glacier displacement rates has been observed in the Alps in the last decades, with many examples of partial destabilization (Delaloye *et al.*, 2012). This behaviour has been attributed to a warming permafrost, induced by the rising atmospheric temperature and regulated by water circulation in and below the permafrost layer (Ikeda *et al.*, 2008; Kenner *et al.*, 2017). Composite landforms originating from the interaction of glacial and periglacial processes have been recently described, with several examples of rock glaciers derived from the evolution of Little Ice Age (LIA) glacial deposits or closely related to them (Dusik *et al.*, 2015; Seppi *et al.*, 2015; Kellerer-Pirklbauer & Kaufmann, 2017). Compared to rock glaciers with evident periglacial origin (talus rock glaciers), the surface dynamics of these composite landforms are still poorly investigated. In this work, we compared the dynamic behaviour of two landforms with different origin, i.e. a talus rock glacier (Maroccaro rock glacier - MaRG) and a composite landform deforming LIA glacial deposits (Amola composite landform - AmCL), over the same period (2001-2015) and using the same survey techniques.

Methods

Geomorphological field investigations, documentary data (maps, photos), and remote sensing analyses (Lidar DEMs, orthophotos), enabled the characterization of the two landforms and the formulation of hypotheses on their possible origin and current evolution.

The surface dynamics of the two landforms were investigated using total station topographic surveys. Their near-surface temperature regime (Ground Surface Temperature - GST) has been monitored using mini-loggers, whereas surrounding Automatic Weather Stations provided meteorological and snow cover data. The obtained time series include 14 years of displacement rates (2001-2015) and 11 years of GST (2004-2015). Possible drivers of observed displacement rates, and differences between the two landforms, have been looked for analysing the correlation with atmospheric and ground thermal variables.

Results

Geomorphological evidence suggests that MaRG is a talus-derived rock glacier, whereas AmCL is a creeping landform originated from the deposits of a LIA glacier, composed by two ice-cored lateral moraines and a frontal area showing a rock glacier-like structure. Differencing two high resolution Lidar DEMs show elevation change patterns that support this interpretation

The average long-term (2001–2015) surface displacement of the two investigated landforms is rather low, with velocities of about 0.15 m/y for MaRG and 0.09 m/y for AmCL (Fig 1). An overall acceleration can be observed for MaRG after the 2007-‘08 hydrological year, peaking in 2014-‘15. This acceleration was not observed for AmCL. The annual displacement rates of the two landforms were highly correlated until 2007-’08, and clearly decoupled after then (Fig. 2a). The long-term vertical displacement shows prevailing lowering of the surface for both the landforms, with the exception of the frontal zone of MaRG, which is advancing (Fig. 1). The total vertical lowering is considerably larger for AmCL (Fig. 1).

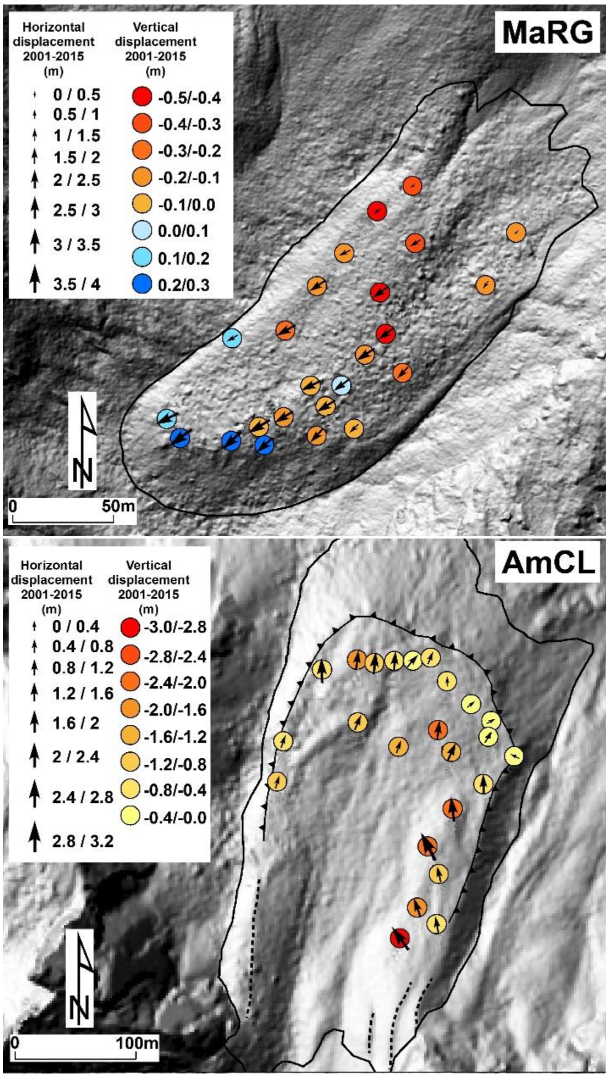

Figure 1. Total (2001-2015) horizontal and vertical displacement of MaRG and AmCL.

The GST series shows an overall increase, with maximum MAGST (Mean Annual Ground Surface Temperature) values reached in the 2014-‘15 hydrological year in both the landforms (2.8°C for AmLC and 1.2°C for MaRG). Over the whole period of observation (2004-2015), the MAGST increased on both the landforms, moving from negative to positive values on MaRG (Fig. 2b). Increasing MAGSTs led to an acceleration of the surface displacement on MaRG but not on AmCL.

The correlation analysis showed that the main control on the surface displacement of MaRG is the GFI (Ground Freezing Index), followed by the MAGST and the duration of the snow cover. The displacement of AmCL is mainly controlled by the Mean Annual Air Temperature (MAAT) and MAGST and, secondarily, by ground freezing and thawing indexes.

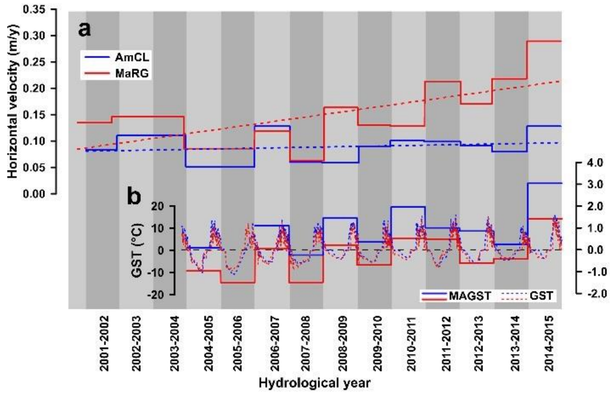

Figure 2. Average annual horizontal displacement (a) and ground surface temperature (b) of MaRG and AmCL.

References

Delaloye, R., Morard, S., Barboux, C., Abbet, D., Gruber, V., Riedo, M. & Gachet, S., 2013. Rapidly moving rock glaciers in Mattertal. *Jahrestagung der Schweizerische Geomorphologische Gesellschaft* 29: 21–31.

Ikeda, A., Matsuoka, N. & Kääb, A., 2008. Fast deformation of perennially frozen debris in a warm rock glacier in the Swiss Alps: An effect of liquid water. *Journal of Geophysical Research Earth Surface* 113: F1.

Dusik, J. M., Leopold, M., Heckmann, T., Haas, F., Hilger, L., Morche, D., Neugirg, F. & Becht, M., 2015. Influence of glacier advance on the development of the multipart Riffeltal rock glacier, Central Austrian Alps. *Earth Surface Processes and Landforms* 40: 965–980.

Kenner, R., Phillips, M., Beutel, J., Hiller, M., Limpach, P., Pointner, E. & Volken, M., 2017. Factors Controlling Velocity Variations at Short-Term, Seasonal and Multiyear Time Scales, Ritigraben Rock Glacier, Western Swiss Alps, *Permafrost and Periglacial Processes* 28: 675–684.

Seppi, R., Zanoner, T., Carton, A., Bondesan, A., Francese, R., Carturan, L., Zumiani, M., Giorgi, M. & Ninfo, A., 2015. Current transition from glacial to periglacial processes in the Dolomites (South-Eastern Alps). *Geomorphology* 228: 71–86.

Kellerer-Pirklbauer, A., & Kaufmann, V., 2017. Deglaciation and its impact on permafrost and rock glacier evolution: new insight from two adjacent cirques in Austria. *Science of the Total Environment.* In press.

Analysis of potentially hazardous rockglaciers in Aosta Valley (Italy): the Pointe d'Arpisson destabilized rockglacier

Claudio Lucianaz[1], Elena Motta[1], Fabrizio Troilo[1]
Ludovic Ravanel[2], Pierre-Allain Duvillard[2,5]
Umberto Morra di Cella[3], Paolo Pogliotti[3], Edoardo Cremonese[3]
Luca Paro[4]
[1]*Fondazione Montagna sicura, Courmayeur, Aosta valley, Italy, claudio.lucianaz@gmail.com*
[2]*Univ. Grenoble Alpes, Univ. Savoie Mont Blanc, CNRS, EDYTEM, 73000 Chambéry, France*
[3]*ARPA VdA, Saint Christophe, Aosta valley, Italy*
[4]*ARPA Piemonte, S.S. Monitoraggi e Studi Geologici, Italy*
[5]*IMSRN, Montbonnot, France*

Abstract

Here we present a research about potentially hazardous rockglaciers on Aosta Valley's territory. The research led to the finding of a destabilized rockglacier above the village of Epinel in the Cogne Valley. The rockglacier presents a downstream lobe that generates very frequent rockfalls and forms a landslide-like morphology with an evident scar upslope and a debris talus downslope. Different surveys have been carried out to investigate the rock glacier structure and behavior, which showed for example unusually high displacement rates for rock glaciers in this area.

Keywords: rock glacier, methods, rockfall, destabilization, Aosta Valley.

Introduction

This research started with the Alcotra Project *PrevRisk Haute Montagne* with the goal to identify potentially hazardous rockglaciers in Aosta Valley's territory. First of all, the starting point of the research has been the review of an output of the precedent Alcotra Project *RISKNAT* that produced the paper "Permafrost Risk areas in Aosta Valley". This study was a qualitative overview of Aosta valley's high altitude catchments basins (with high permafrost occurrence probability) based on a preliminary orthophotographs geomorphological analysis. During the year 2014 an additional study campaign was carried out to build an inventory of all the active and inactive rockglaciers of the valley using aerial photographs and remote sensed interferometric data like Permanent Scatterer Points technique in order to identify also extremely low movements. None of the rock glaciers identified in the above mentioned study showed features of strong activity or significant recent movements (> 0,5m/yr, distinctively detectable on a 5-years orthophotographs comparison), therefore a more detailed and automated GIS based research was needed on the whole region in order to possibly detect active rockglaciers. Once a significant site would be individuated, detailed studies of the area were planned to better understand the displacement behavior and the internal structure of the designated rock glacier.

PrevRisk Haute Montagne risk analysis

The first step in the analysis of the Aosta Valley rock glaciers inventory included the elimination of rock glaciers classified as non active or relict (Barsch, 1996) in the existent regional inventory. This limited the number of rock glaciers to be analyzed: from 937 bodies to 409.

Then, the analysis of risk in the rockglacier inventory has been determined by two other factors: i) the degree of activity of the different rock glaciers, preliminary assumed to be proportional to their Permafrost Occurrence Probability Index value (Boeckli *et al.*, 2012) averaged on the rock glacier digitalized surface polygon, ii) the minimum linear distance between the rock glacier polygon centroid and the nearest infrastructure.

The first factor ranked the rockglaciers by a mean permafrost index value obtained by the analysis of the Alpine Permafrost Index Map. An analysis of the classified results indicated that, by geomorphological analysis on orthophotographs, almost all rockglaciers with a mean permafrost index value lower than 0,40 showed very little signs of activity and significant displacements and were often strongly vegetated. Thus all rockglaciers under the mean 0,45 value were taken out of the risk analysis. This led to further limiting the analysis from 409 rock glaciers to 294. Those ones were subsequently ranked on the basis of the second factor, the distance from the feature to the nearest infrastructure. Finally, a detailed geomorphological analysis was performed, comprising multi-temporal Orto photographs comparisons (1988-1996-2000-2005-2012) to detect movements and to assess downslope morphology and the eventual presence of anthropic areas or infrastructures, on the first 30 results of the ranking. 11 out of the 13 potentially hazardous rockglaciers individuated in the precedent *RISKNAT* study were found in the latest analysis.

Choice of the case study

The project charter opened the possibility to select two case studies to be further investigated, but the research team decided to focus the attention to one single case study. The detailed geomorphological analysis of the 30 individuated bodies highlighted three interesting rock glaciers showing significant recent movements and some risk situations downslope: i) the Pointe Léchaud rockglacier in Val Veny (Courmayeur), ii) the Pentespetz rockglacier in Gressoney, and iii) the Pointe d'Arpisson rockglacier (Fig.1) located in the Cogne Valley, about 3 km north west from the village of Epinel.

After field observations of the three sites, the latter was chosen as the project case study as being very active (rock falls), partially destabilized, and localized on top of a basin that drains towards Epinel village.

Figure 1. The Pointe d'Arpisson rock glacier with evident signs of rockfalls in its lower part.

Field surveys on test site

Specific field surveys begun in July 2016 and led to:

i) two RTK GPS surveys,

ii) Two aerophotogrammetric drone flights,

iii) Two geophysical profiles with Electrical Resistivity Tomography technique

The above mentioned surveys led to some preliminary considerations that still need further analysis but give some interesting results: the first ortho-mosaic realized gave the opportunity to reconstruct movements of the rock glacier from 1988 to 2016 (Fig. 2). It is interesting to notice the apparent acceleration of the movements in recent years, leading to a yearly mean horizontal displacement of about 11 m on the lowest part of the rock glacier between 2014 and 2016.

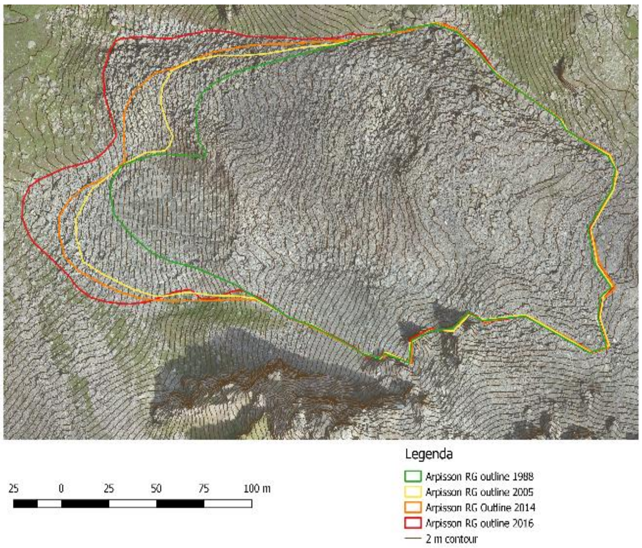

Figure 2. The Pointe d'Arpisson rockglacier surface variations from 1988 to 2016.

The second drone aerial survey gave the chance to confirm this trend: the time span between the two aero-photogrammetric surveys has been 13 months, and the second ortho-mosaic gives a yearly horizontal displacement of 12 m on the lower lobe, 7 m in the middle part and 10 m in the higher part. Those values are surprisingly high if compared to other rock glaciers in Aosta Valley, as seen for example in the two other cases that were candidate as case study, which had mean horizontal displacement rates of respectively: 2,1 m/yr (1999-2005) for the Pointe Léchaud RG, and 0.52 m/yr (1999-2005) for the Pentespetz RG.

ERT was used for its efficiency for ground ice characterization with two profiles of 48 electrodes overlapping (Hauck & Kneisel, 2008). Ground apparent resitivity was measured with ABEM SAS 4000 in Wenner configuration. The contrast between resistive and conductive terrain allows the distinction between ice debris mixtures (probably with water) and unfrozen dry debris.

References

Boeckli, L., Brenning, A., Gruber, S. & Noetzli J. 2012: Permafrost distribution in the European Alps: calculation and evaluation of an index map and summary statistics, *The Cryosphere*, 6, 807–820.

Barsch, D, 1996. *Rockglaciers, Indicators for the Present and Former Geoecology in High Mountain Environments*, Springer publishing, 319 pp.

Hauck, C., & Kneisel, C. (Eds.). (2008). *Applied Geophysics in Periglacial Environments. Cambridge* University Press. 240 pp.

Benefits of UAVs and structure from motion in the study of rock glacier kinematics: Examples from the Western Swiss Alps

Sebastián Vivero[1]
Reynald Delaloye[2]
Christophe Lambiel[1]

[1]*University of Lausanne, Institute of Earth Surface Dynamics, Lausanne, Switzerland, sebastian.viveroandrade@unil.ch*
[2]*University of Fribourg, Department of Geosciences, Fribourg, Switzerland*

Abstract

Rock glaciers are an essential component of the cryosphere in many mountain regions, where favourable climatic and geomorphological factors allow their development. Recent developments in the field of Unmanned Aerial Vehicles systems and digital photogrammetry are providing an upsurge of high-resolution data, together with the enhancement of image processing and acquisition procedures. Given the rapid change and hazardous terrain conditons where rock glacier are located, the potential to carry out detailed field observations is demanding and troublesome. To overcome this, we have been employing different UAV configurations to monitor permafrost creep and their environs. We provide the first results after two years of UAV and terrestrial geodetic surveys from fast and slow rock glaciers in the Valais Alps, Switzerland.

Keywords: Rock Glaciers; UAV; Photogrammetry; Kinematics; Swiss Alps.

Introduction

The use of Unmanned Aerial Vehicles (UAV) and digital optical cameras have revolutionised the commercial and academic sectors due to their comparably low price and high customised settings (Carbonneau & Dietrich, 2016). Concurrently, new developments in the domain of image processing and photogrammetric techniques, such as Structure-for-motion (SfM), have burgeoned during the last years (Smith *et al.*, 2016). Images acquired by different UAV platforms are usually employed for generating high-density point clouds, Digital Elevation Models (DEMs) and high-resolution orthorectified images of different landforms. These high-resolution products have been used in several domains, such as changes in river-floodplain systems and for studying glacial and periglacial processes (Piermattei *et al.*, 2016), among other applications. Until now, few studies have described the benefits of SfM-photogrammetry and UAV systems for rock glacier monitoring (Dall'Asta *et al.*, 2017). However, studies that incorporate an assessment of the accuracy based on concurrent *in situ* measurements remain uncommon. Moreover, as UAV systems are continuously changing and improving, there is still scope for optimising protocols using different UAV configurations in high and challenging terrain. In this presentation, we provide the first results after two years of repeated UAV and terrestrial geodetic surveys on two rock glaciers in the Valais Alps.

Methods

Following Lambiel & Delaloye (2004) protocols, repeated kinematic point measurements were done on Tsarmine and Les Cliosses rock glaciers, employing differential GNSS devices with the Real Time Kinematic (RTK) survey style for a rapid point acquisition over large areas. Simultaneously, repeated UAV surveys were executed for the two rock glaciers using a DJI Phantom 3 pro quadcopter and a Sensefly eBee RTK fixed-wing devices. Three orthomosaics with pixel sizes between 2 and 7 cm were produced for Tsarmine and Les Cliosses using SfM-photogrammetry processing. Co-registration and image cross-correlation were performed on the multitemporal orthomosaics for the sites. Raw IMCORR vectors were checked for consistency and filtered by direction and magnitude. Incorrectly correlated points are due to changes in the surface characteristics such as snow or shadows. IMCORR values over stable features (off rock glacier) were employed for quality assessment of the image co-registration.

Preliminary results

A good agreement between velocities derived from UAV and terrestrial measurements was obtained for the two rock glaciers. Larger velocities for the very active Tsarmine rock glacier (up to 6 m a^{-1}) contrasted with low velocities detected on Les Cliosses rock glacier (less than 0.5 m a^{-1}) during the 2016–2017 period (Fig. 1). The flow structure of Tsarmine rock glacier indicates a regular profile of increasing velocities towards the terminus. On the other hand, the flow structure of the Les Cliosses displays a more complex pattern of velocities, where the greater values are at the terminus and at the upper middle part of the landform.

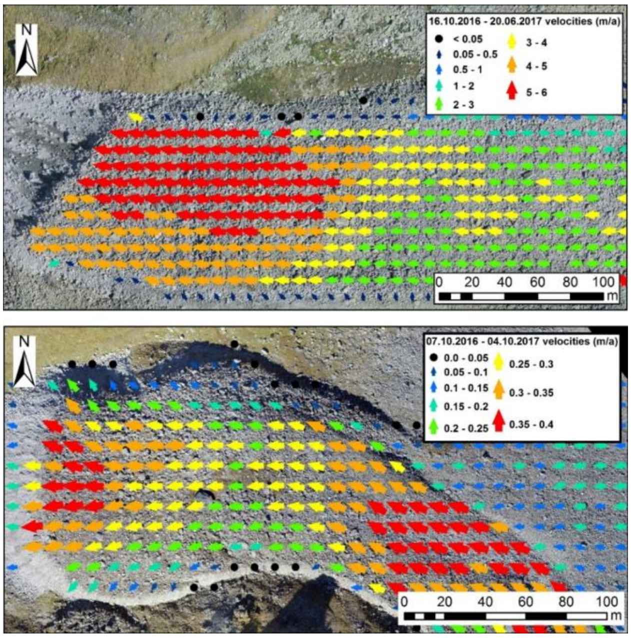

Figure 1. Horizontal rock glacier velocities derived from repeated UAV surveys on Tsarmine (top) and Les Cliosses (bottom) rock glaciers.

Conclusions and perspectives

Thanks to the very high-resolution customised UAVs surveys, rock glacier kinematics can be studied in great detail. Preliminary, comparisons between coincident terrestrial geodetic surveys (differential GNSS surveys) and UAV-derived velocities revealed a good agreement. Nevertheless, to enable the temporal and spatial variability on rock glaciers kinematics to be reliably examined, a robust quality assessment has to be undertaken, including extensive validation using ground-information from terrestrial geodetic surveys. This approach also benefits further optimisations during the UAV survey design and image processing (i.e. SfM, image co-registration and cross correlation parameters).

High-density point clouds, DEMs and high-resolution orthorectified images of different rock glaciers can be further exploited for others aspects. Rock glacier surface texture is primarily composed of different sizes of angular rocks that can have low to medium albedo; well define structures and medium to high contrast, making the use of image classification algorithms appealing.

References

Carbonneau, P. & Dietrich J., 2016. Cost-effective non-metric photogrammetry from consumer-grade sUAS: implications for direct georeferencing of structure from motion photogrammetry. *Earth Surface Processes and Landforms* 42(3): 473-486.

Dall'Asta, E., Forlani, G., Roncella, R., Santise, M., Diotri, F., & Morra di Cella, U., 2017. Unmanned Aerial Systems and DSM matching for rock glacier monitoring. *ISPRS Journal of Photogrammetry and Remote Sensing*, 127: 102-114.

Lambiel, C. & Delaloye, R., 2004. Contribution of real-time kinematic GPS in the study of creeping mountain permafrost: examples from the Western Swiss Alps. *Permafrost and Periglacial Processes*, 15: 229-241.

Piermattei, L., Carturan, L., De Blasi, F., Tarolli, P., Dalla Fontana, G., Vettore, A., & Pfeifer, N., 2016. Suitability of ground-based SfM-MVS for monitoring glacial and periglacial processes. *Earth Surface Dynamics*, 4(2): 425-443.

Smith, M., Carrivick, J., & Quincey, D., 2016. Structure from motion photogrammetry in physical geography. *Progress in Physical Geography*, 40(2): 247-275.

Investigating a destabilized permafrost landform, Ádjet rock glacier, Norway: a multi-disciplinary remote sensing approach

Harald Øverli Eriksen[1,2]
Tom Rune Lauknes[1]
Line Rouyet[1]
Ivar Berthling[3]
Ketil Isaken[4]
Heidi Hindberg[1]
Yngvar Larsen[1]
Geoffrey D. Corner[2]

[1]*Norut – Northern Research Institute, Tromsø, Norway. Corresponding email: haraldoverlieriksen@gmail.com*
[2]*Department of Geoscience, UiT-The Arctic University of Norway, Tromsø, Norway*
[3]*Department of Geography, Norwegian University of Science and Technology, Trondheim, Norway*
[4]*Norwegian Meteorological Institute, Research and Development Department, Oslo, Norway*

Abstract

62 years (1954-1016) of aerial photography, ground- and satellite-based radar data evidence the recent acceleration of a rock glacier in northern Norway. Average horizontal velocity measured from aerial orthophotos increases from ~0.5 m yr^{-1} (1954–1977) to ~3.6 m yr^{-1} (2006–2014). Displacement measurements from radar data show an increase of maximum velocity over the landform from ~2.5 m yr^{-1}, based on a 1-day measurement in 1995, to a summer seasonal mean of ~65 m yr^{-1} in 2016. Ground velocities are compared with meteorological data highlighting a relation between the acceleration and the increase of air temperature/precipitation. The results highlight the value of mutli-disciplinary remote sensing approaches for long-term monitoring of mountain permafrost.

Keywords: Remote Sensing, Permafrost Creep, Rock glacier, Destabilization, Climate change

Introduction & Relevance

Rock glaciers are creeping and ice-rich debris landforms under perennially frozen conditions. For more than a decade, significant accelerations, and in some cases even collapses, of rock glaciers have been documented in the European Alps. This development has been attributed to higher permafrost temperatures (Kääb *et al.*, 2007), increase of liquid water content (Ikeda *et al.*, 2008), and/or local overloading by debris (Delaloye *et al.*, 2013). Although a consequent amount of records and studies in the Alps, similar behavior is still poorly documented in Fennoscandinavia.

Our study exploits 62 years of remote sensing datasets from satellite, aerial and ground-based platforms to document a dramatic increase of permafrost creep over a rock glacier in Norway.

Context & Methods

The study area is located in Troms County in northern Norway in a region with a high density of rock glaciers (Lilleøren & Etzelmüller, 2011). This study focuses on the most prominent rock glacier on the southwest-facing slope of Ádjet Mountain in the Skibotn valley (Fig. 1A). It ranges in elevation from ~690 to 1080 meters above sea level, close to the regional altitudinal limit of mountain permafrost (Farbrot *et al.*, 2013).

The measurements of ground deformation have been performed by combining a large set of datasets and methods (Eriksen, 2017). Ortho-rectified aerial images acquired in 1954, 1977, 2006 and 2014 were used for feature tracking and compilation of front positions. 138 satellite TerraSAR-X scenes from 2009 to 2016 in ascending and descending geometries have been processed using Synthetic Aperture Radar Interferometry (InSAR) and SAR offset-tracking (OT) methods. InSAR has also been applied on ERS-1/2 Tandem images in 22-23th July 1995. A Gamma Portable Remote Interferometer (GPRI) acquired images every 5-min. in summers 2014 & 2015.

Results

InSAR and OT methods complementarily contribute to map the distribution of deformation over the slope using TerraSAR-X scenes (Fig. 1A). 2D surface displacement vectors were calculated by combining SAR velocities from both TerraSAR-X geometries. Fig. 1B shows projected surface-parallel yearly velocities along a profile highlighting an increase especially in the lower part. By comparing the plunge of the 2D vectors from TerraSAR-X results with the slope, areas with subsidence and uplift are identified. It shows a trend of subsidence in the upper part and alternation between uplift and subsidence in the middle and lower parts. The calculation of the longitudinal strain rate highlights pulse from extension to compression within the lower part.

Based on aerial images, average horizontal velocity increased from ~0.5 m yr^{-1} (1954–1977) to ~3.6 m yr^{-1} (2006–2014). The satellite and ground-based radar data shows acceleration up to ~11 m/yr (Fig. 1C). Meteorological data (senorge.no) shows an increase of 1.8 °C in mean annual air temperature (MAAT) and of 330 mm (55%) in mean annual precipitation (MAP) during the same period. The maximum annual modelled snow depth increased by 58 cm (56 %) (Fig. 1D).

Conclusion

The results highlight the value of multi-disciplinary remote sensing approach for documenting long-term variations of permafrost creep. The acceleration measured over Ádjet rock glacier and comparison with meteorological data suggests a destabilization of the landform related to climate change. Analysis of the spatial patterns suggests mechanical surge in the upper part and debuttressing of the lower part that can be attributed to debris overloading.

Acknowledgments

TerraSAR-X data has been provided by the German Aerospace Center (DLR) under the TSX-AO projects GEO0565/GEO0764/GEO2497, and ERS data by ESA (project AOPOL.4104).

References

Delaloye, R., Morard, S., Barboux, C., et al., 2013. Rapidly moving rock glaciers in Mattertal. In C. Graf (Ed.), *Jahrestagung der Schweizerischen Geomorphologischen Gesellschaft*, 21–31.

Eriksen, H.Ø. 2017. Combining Satellite and Terrestrial Interferometric Radar Data to Investigate Surface Displacement in the Storfjord and Kåfjord Area, Northern Norway. PhD thesis, UiT – The Arctic University of Norway.

Farbrot, H., Isaksen, K., Etzelmüller, B., & Gisnås, K., 2013. Ground Thermal Regime and Permafrost Distribution under a Changing Climate in Northern Norway. *Permafrost and Periglacial Processes, 24*(1), 20–38.

Ikeda, A., Matsuoka, N., & Kääb, A., 2008. Fast deformation of perennially frozen debris in a warm rock glacier in the Swiss Alps: An effect of liquid water. *Journal of Geophysical Research, 113*(F1).

Kääb, A., Frauenfelder, R., & Roer, I., 2007. On the response of rockglacier creep to surface temperature increase. *Global and Planetary Change, 56*(1–2).

Lilleøren, K. S., & Etzelmuller, B., 2011. A regional inventory of rock glaciers and ice-cored moraines in Norway. *Geografiska Annaler, 93*(3), 175–191.

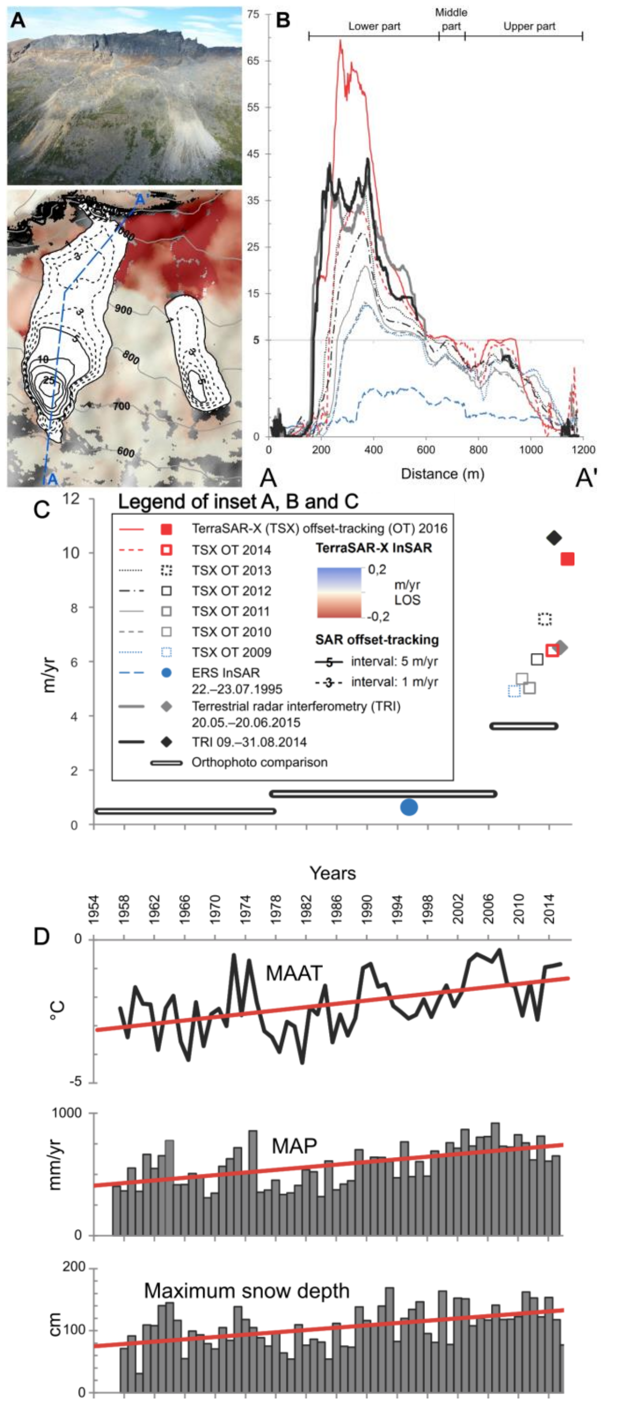

Figure 1: A. View of Ádjet rock glacier and distribution of velocity [m/yr]. B. Spatio-temporal variation of velocity along profile A-A'. C. Long-term evolution of the mean yearly horizontal velocity in the middle part of the rock glacier. D. Meteorological data 1954-2016.

8 - Coupled heat transfer and fluid flow processes in permafrost regions (including IPA Action Group InterFrost results)

Session 8

Coupled heat transfer and fluid flow processes in permafrost regions

Conveners:

- **Christophe Grenier**, Laboratoire des Sciences du Climat et de l'Environnement, LSCE/IPSL, CEA-CNRS-UVSQ, Université Paris-Saclay, Franc
- **Elena Kuzentsova**, Department of Civil and Environmental Engineering, Norwegian University of Science and Technology (NTNU), Trondheim, Norway (PYRN member)
- **Victor Bense**, Department of Environmental Sciences, Wageningen University and Research, Netherlands

Arctic and subarctic environments are particularly sensitive and susceptible to climate change effects. Key scientific questions concern the detection and evaluation of the impact of climate change on permafrost stability as well as the contribution to climate feedback through continental carbon and methane release. The role of hydrology is paramount in influencing the thermal state of permafrost landscapes.

In particular, the active layer processes, lake and river influenced zones, ground water units are the loci of such interaction. Each of these systems experience a highly complex forcing by climate resulting in water and heat redistributions involving water phase change, heat conduction and convection for saturated/non saturated conditions.

This session aims to bring together researchers focusing on theoretical and numerical modeling development, and/or laboratory and field experiments, to further our understanding of permafrost, hydrological, hydrogeological and transport processes, their interactions and evolution under the influence of climate change. Reports about the IPA Action Group InterFrost project on the inter-comparison of coupled Thermo-Hydrological models are especially welcome.

Thermal conductivity and gas permeability variations of frozen hydrate-bearing sediments during methane hydrate dissociation

Evgeny E. Chuvilin[1, 2]
Boris A. Bukhanov[1]
Sergey I. Grebenkin[1, 2]
Dinara A. Davletshina[1, 2]

[1]*Skolkovo Institute of Science and Technology (Skoltech), Moscow, Russia, email: chuviline@msn.com*
[2]*Department of Geology, Moscow State University (MSU), Russia*

Abstract

Gas hydrates in permafrost can occur in under-permafrost and intra-permafrost horizons. The intra-permafrost hydrates repeatedly recorded during deep drilling operations in cold regions. Different indirect indicators show that hydrates can locate in shallow permafrost (up to depth 200 m) under non-equilibrium conditions in a metastable state due to self-preservation effect. The relict hydrates may be responsible for methane emission and gas explosion hazard in shallow permafrost during drilling and production in gas fields of northern West Siberia. The metastable hydrates are extremely sensitive to various influences (including anthropogenic impact) and create serious geologic risks to oil and gas exploration and development and need special study. The physical (thermal and filtration) properties of frozen sediments with self-preserved gas hydrates should be investigated. The experimental results show that gas permeability and thermal conductivity of frozen hydrate-bearing sediments may change by several times during the self-preservation effect, and correlates with pore ice and hydrate ratio.

Keywords: permafrost, methane hydrate, self-preservation, thermal conductivity, gas permeability.

Introduction

The first evidence about gas hydrates in permafrost appeared almost fifty years ago, but they are remain poorly investigated (Cherskiy *et al.,* 1985; Max, 2000). The reason is primarily that gas hydrates are similar to pore ice in physical properties, and their responses are hard to discriminate by conventional geophysical (mainly seismic) studies.

The presence of gas hydrates in shallow permafrost within 150 m has been inferred from field data and some inderect indicators (Yakushev & Chuvilin, 2000). Methane gas hydrates may exist in the metastable zone (Chuvilin *et al.,* 2000) of frozen sediments above the zone of hydrate stability. They are remnant gas hydrates that formed earlier in frozen sediments under more favorable thermobaric conditions, became metastable in the course of later paleoclimatic events and permafrost evolution, and have survided due to the effect of self-preservation at negative temperatures (Ershov *et al,*. 1991; Chuvilin & Guryeva, 2008). The relict gas hydrate may be responsible for methane emission and gas explosion hazard in shallow permafrost during drilling and production in gas fields of northern West Siberia. The metastable gas hydrate formations are extremely sensitive to various influences, including the anthropogenic impact and, in their turn, affect the physical properties of frozen sediments (Bukhanov *et al.*, 2008). Permafrost gas hydrate creates serious geologic hazard and risks to oil and gas exploration and development and requires special studies. The physical (thermal and filtration) properties of frozen sediments with self-preserved pore gas hydrate can be experimentally investigated, with implication for geotechnical prediction and monitoring.

Method and results

Three different fine sand samples are used in current research. Some of them were collected from gas-saturated permafrost horizon up to 100 m depth in the north part of Western Siberia. Quarts is the predominant mineral (more 85 %) in each sandy sample. Salinity is in range 0.01-0.09 %.

Frozen methane hydrate-bearing sandy sediments were formed by hydrate formation at temperatures about -4…-6 ^{o}C. In this case, gas hydrate was growing directly on pore ice, which inhibited moisture migration and ensured uniform distribution of gas hydrate in the samples. This method allows receiving the soil samples with high hydrate saturation of pore spaces up to 60 % and more. Then investigated hydrate-contain samples are investigated at 0.1 MPa and temperature below 0 °C and measured thermal conductivity (λ_h, W/m·K) and gas permeability (K_g, mD) during the time.

Needle probe KD-2 is used for thermal conductivity measurements. Probe's length is 6 cm and diameter 1,2 mm. This analyzer is suitable for frozen hydrate-contain sediments due to small thermal effect. Temperature increasing during measuring is not more 0.5 °C. Accuracy of thermal conductivity measurements is not more 10% using benchmark materials (quartz glass, limestone, marble etc.).

The method of the gas permeability determination of frozen hydrate-containing sediments is based on measuring of gas filtration through a sediment sample in an experimental gas hydrate setup (Chuvilin & Grebenkin, 2015). It allows to determinate the gas permeability of pore materials in the range of 0.01-1000 mD.

The experimental results show that there is not complete decomposition of pore hydrate in frozen sediments due to self-preservation effect. Residual hydrate-saturated (S_h, %) can reach 10% and more (fig. 1). It is noted that during the dissociation of pore hydrates, the thermal conductivity and gas permeability of frozen sands increases. Thermal conductivity of sand-1 increases 2.5 times from 0.57 W/m·K till 1.41 W/m·K., due to S_h reducing from 40% till 15%. For frozen sand-2 thermal conductivity increases, more than 3-times, due to gas hydrate dissociation till 10%.

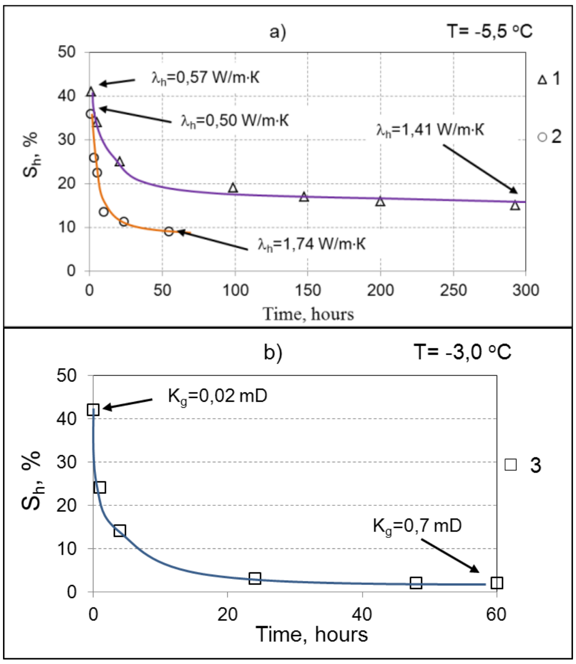

Figure 1. Thermal conductivity (a) and gas permeability (b) variations of frozen hydrate-contain fine sands (dots 1-3) during methane hydrate dissociations at 0.1 MPa.

There is a significant gas permeability of frozen sand-3 increasing (from 0.02 mD till 0.7 mD) during methane hydrate dissociation. In this case S_h reduces from 42 % till 2 %.

Conclusions

The experimental results show that values of gas permeability and thermal conductivity of frozen hydrate-bearing sandy sediments can vary several times during the process of methane hydrate dissociation under non-equilibrium conditions. The properties' variations correlate with changes of the pore ice and gas hydrate ratio, as well as structural and texture transformations of the ice-gas hydrate component due to manifestation of self-preservation of pore methane hydrates.

Acknowledgments

These researches are supported by the Russian Science Foundation (grant No. 16-17-00051) and RFBR (grant No. 17-05-00995).

References

Bukhanov, B.A., Chuvilin, E.M., Guryeva, O.M., Kotov, P.I., 2008. Experimental study of the thermal conductivity of the frozen sediments containing gas hydrate. *Proceedings of the 9th International Conference on Permafrost,* Fairbanks, USA: 205-209.

Chuvilin, E.M., Yakushev, V.S., Perlova E.V., 2000. Gas and gas hydrates in the permafrost of Bovanenkovo gas field, Yamal Peninsula, West Siberia. *Polarforschung* 68: 215-219.

Chuvilin, E.M. & Guryeva, O.M., 2008. Experimental study of self-preservation effect of gas hydrates in frozen sediments. *Proceedings of the 9th International Conference on Permafrost,* Fairbanks, USA.

Chuvilin, E.M. & Grebenkin, S.I., 2015. Gas permeability in gas-filled soils upon hydrate formation and freezing: an experimental study. *Earth's Cryosphere* 2: 59-64.

Cherskiy, N., Tsarev, V.P., Nikitin, S.P., 1985. Investigation and prediction of conditions of accumulation of gas resources in gas-hydrate pools. *Petroleum Geology* 21: 65-89.

Ershov, E.D., Lebedenko, Yu.P., Chuvilin, E.M., Istomin, V.A., Yakushev, V.S., 1991 *Reports of Academy of Science USSR* 321: 788-791 (in Russian).

Max, M.D., 2000. *Natural Gas Hydrates in Oceanic and Permafrost Environments.* Kluwer Academic Publisher, Boston.

Yakushev, V.S. & Chuvilin E.M., 2000. Natural gas and hydrate accumulation within permafrost in Russia. *Cold Regions Science and Technology* 31: 189-197.

Numerical Simulations of Groundwater Flow and Permafrost Thaw in a Discontinuous Permafrost Zone, Umiujaq, Québec, Canada

Sophie Dagenais[1]
John Molson[2]
Jean-Michel Lemieux[2]
Richard Fortier[2]
René Therrien[2]
M. Cochand[2]

[1] *Département de géologie et de génie géologique et Centre d'études Nordiques, Université Laval, Québec, QC, Canada, sophie.dagenais.2@ulaval.ca*
[2] *Département de géologie et de génie géologique et Centre d'études nordiques, Université Laval, Québec, QC, Canada*

Abstract

A two-dimensional numerical model has been developed to provide insight into coupled groundwater flow and permafrost dynamics in a degrading and discontinuous permafrost zone near the Inuit community of Umiujaq in northern Québec, Canada. The site model is 650 m long and 100-200 m deep, and includes three permafrost blocks within a 20m-thick layer of marine silt overlying a coarse sand/gravel aquifer. Groundwater flow, advective-conductive heat transport, freeze-thaw phase change with latent heat, and temperature-dependent fluid and thermal properties are included in the model. A geothermal gradient drives the system from below, while atmospheric air temperatures and winter snow cover control heat transfer across the ground surface. The model is calibrated to observed near-surface heat fluxes and to temperature profiles from 2002-2014. Results suggest that at the Umiujaq site, sub-permafrost groundwater flow plays an important role in the local thermal regime and on permafrost behaviour.

Keywords: Groundwater; permafrost; numerical modelling; climate change; cold regions hydrogeology.

Introduction

Climate warming is having a significant effect on permafrost degradation in northern Québec (Canada). As a consequence of permafrost degradation, groundwater may become an important source of drinking water for northern communities (Lemieux et al., 2016). Aquifer recharge, for example, is expected to increase, and new groundwater flow systems are expected to form.

In order to better predict permafrost evolution in these types of complex cryo-hydrogeological systems under a changing climate, coupled numerical models of groundwater flow and heat transport are becoming useful tools. In this study, a 2D cryo-hydrogeological numerical model has been developed within the Tasiapik Valley, a 2-km² watershed near Umiujaq, Nunavik, Canada. The purpose is to evaluate the effect of groundwater flow on permafrost dynamics and to predict future behavior of this cryo-system under climate change.

Cryo-hydrogeological System and Model

Based on field observations, a conceptual cryo-hydrogeological model was developed along a 2D transverse section of the Tasiapik Valley in the discontinuous permafrost zone. The model includes a 20 m thick layer of frost-susceptible marine silt, which overlies a 10 to 30 m thick semi-confined aquifer of coarse sands and gravels (Fig 1). A thin superficial layer of littoral sands lies at ground surface while the sediments are underlain by fractured basalt and arenite.

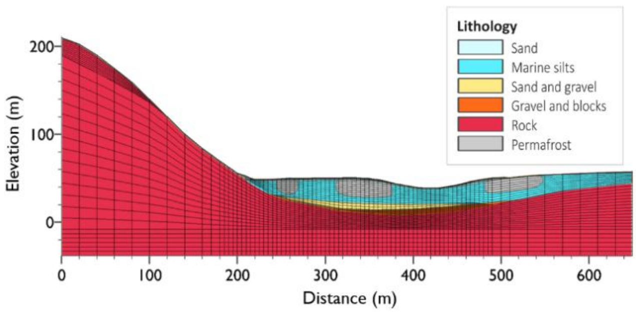

Figure 1: 2D conceptual cryo-hydrogeological model of the study site, including stratigraphy, current extent of permafrost, and finite element mesh.

The numerical simulations were run using the finite element HEATFLOW/SMOKER code (Molson and Frind, 2017), which includes coupled groundwater flow and heat transport with phase change and latent heat. Relative permeability, and fluid and material properties are temperature-dependent. The code has been validated for coupled groundwater flow and heat transport as part of the Interfrost benchmark (Ruhaak et al., 2015), and at other field sites (Shojae-Ghias et al. 2016).

In the Umiujaq 2D site model, no-flow conditions are applied at the left, right and bottom boundaries, while a mix of seasonal recharge and fixed heads are applied at the top boundary. Seasonal and long-term variations in air temperature control a thermal flux boundary applied at the ground surface, while a geothermal flux of 0.032 W/m^2 is applied at the base. The simulation begins in 1900 and extends to 2017.

Results and Interpretation

The simulated flow system and temperature distribution from 1950 to 2017 (mid-summer) are shown in Fig 2. Groundwater recharge occurs primarily through the fractured rock, which outcrops at the left (south) side of the cross-section, then flows through the semi-confined sand and gravel aquifer beneath the permafrost mounds. Most groundwater discharges through the central stream in the valley (at a distance of ~ 420 m).

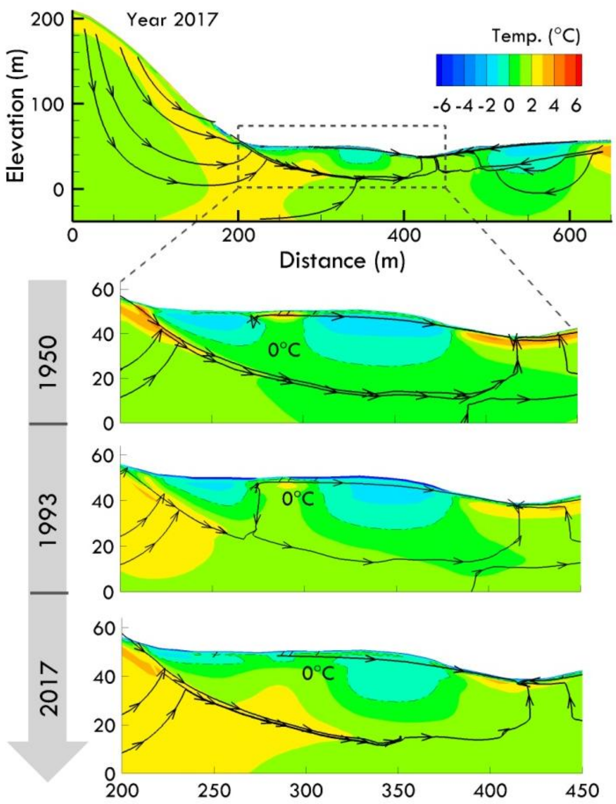

Figure 2: Simulated groundwater flow field and temperatures (in mid-summer) in 1950, 1993 and 2017.

a ... ly within the central mounds most affected by the underlying groundwater flow. The right-most permafrost mound has persisted longer as the underlying aquifer is much thinner in this area.

Conclusions

Groundwater recharge, flow, and coupled advective-conductive heat transport play important roles in controlling permafrost dynamics at the Umiujaq site. Temperature and water/ice-fraction dependent thermal properties must be included in such coupled models to accurately simulate past and future behaviour. The system is particularly sensitive to near-surface hydrogeological conditions including intrinsic and relative permeabilities and heat transfer processes at the air-ground interface.

Acknowledgments

This study was supported in part by an NSERC Strategic Project Grant and by the Québec Provincial Government (MDDELCC and FRQNT). We also acknowledge support from the Centre d'études nordiques (CEN) at Université Laval.

References

Lemieux, J.-M., Fortier, R., Talbot-Poulin, M.-C., Molson, J., Therrien, R., Ouellet, M., Banville, D., Cochand, M. & Murray, R., 2016. Groundwater occurrence in cold environments: examples from Nunavik, Canada. *Hydrogeology Journal* 24, 1497-1513.

Rühaak, W., Anbergen, H., Grenier, C., McKenzie, J., Kurylyk, B.L., Molson, J., Roux, N., & Sass, I., 2015. Benchmarking numerical freeze/thaw models, European Geosciences Union General Assembly 2015, Division Energy, Resources & Environment, *Energy Procedia*, 76, 301-310, *http://dx.doi.org/10.1016/j.egypro.2015.07.866*.

Molson, J.W., & Frind, E.O., 2017. *HEATFLOW-SMOKER User Guide*, Density-dependent flow and advective-dispersive transport of mass, thermal energy or residence time in 3D fractured porous media, Version 5.0, Université Laval & University of Waterloo.

Shojae-Ghias, M., Therrien, R., Molson J., & Lemieux, J-M., 2016. Controls on permafrost thaw in a coupled groundwater flow and heat transport system: Iqaluit Airport, Nunavut, Canada, *Hydrogeology Journal*, *http://dx.doi.org/10.1007/s10040-016-1515-7*.

Frost heave caused by the formation of ice lens in saturated soil

Dongqing Li[1]
Jiazuo Zhou[2]
Feng Ming[1]
[1] *Laboratory of Frozen Soil Engineering, Cold and Arid Regions Environmental and Engineering Research Institute, Lanzhou, China, dqli@lzb.ac.cn*
[2]*Laboratory of Geomechanics and Geotechnical Engineering, Institute of Rock and Soil Mechanics, Wuhan, China*

Abstract

Frost action had caused damage to structures with footings placed in frost susceptible soils above frozen depth. This is mainly due to water migration and formed ice lens. In this paper, A new model of coupled moisture and heat transfer was developed to describe the growth of ice lens during the freezing in a saturated soil. Movement of unfrozen water content in frozen soil is analyzed by use of the thermodynamic theory for the liquid layer near a substratum. For a simplify, water transfer in the frozen fringe and unfrozen zone is dealt with as Darcy flows. Also. the mechanism of ice lens growth process is investigated, a new ice lens is allowed to form when the neutral strength exceeds the sum of overburden pressure and tensile strength. A typical process of water migrates in a deformable, freezing saturated soil column, including the formation of ice lens, was simulated through numerical analysis software.

Keywords: frost heave; ice lenses; temperature gradient; void ratio; pore pressure.

Introduction

Temperature, water and stress interact in freezing soil. Under the effect of temperature gradient in the soil, the unfrozen water migrates from the high temperature area to the low temperature area and gathers at the freezing front, so that soil becomes deformed and frost heave happens. The stress field also changes when unfrozen water migrates in freezing soil. Because of the phase change during soil freezing, water migration affect heat transfer in return. At the same time, stress change makes the change of void ratio and pore pressure, and then affects the process of water migration.

Mathematical model

Equation of state balance and basic conceptions

Fig. 1 is a three phase diagram of saturated freezing soil. In the figure, e is void ratio, S_i is the ratio of the volume of pore ice to the volume of pore. The relative volume is with respect to the soil grain, so in the diagram the relative volume of soil grain is 1.

In freezing soil, S_i is a function of temperature (Tice et al., 1976), which can be written as:

$$S_i = \begin{cases} 1-\left[1-\left(T-T_0\right)\right]^{\alpha} & T \le T_0 \\ 0 & T > T_0 \end{cases} \tag{1}$$

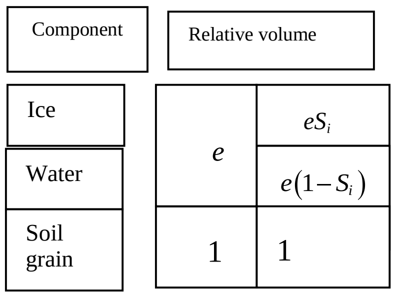

Fig. 1. Three phase diagram of saturated freezing soil

where T is temperature; a is experimental parameter; T_0 is the freezing temperature of pore water in Celsius temperature.

According to Fig. 1, the unit weight of soil can be expressed as

$$\gamma = \frac{g}{1+e}\left[\rho_s + eS_i\rho_i + e\left(1-S_i\right)\rho_w\right] \tag{2}$$

where γ is the unit weight of soil; g is the gravity acceleration; ρ_s , ρ_i and ρ_w are the density of soil grain, ice and water respectively.

In the undeformed status, the unit height of soil is $1+e_0$, and that in the deformed status is $1+e$. The relationship between strain and void ratio is

$$\varepsilon = \frac{e-e_0}{1+e_0} \tag{3}$$

Pore pressure, ice lens and new hypothesis of the separating void ratio

P_{por} is pore pressure, which can be expressed as

$$P_{por} = \begin{cases} \int_x^l (\gamma - \gamma_0) dx_0 + E_s \dfrac{e - e_0}{1 + e_0} & e < e_s \\ \sigma & e \geq e_s \end{cases} \quad (4)$$

where σ is the total stress of soil; E_s is modulus of compression; γ_0 is the initial unit weight of soil; x is the height of a certain point in soil mass; l is the height of soil mass.

Konrad and Morgenstern (1980) thought that when temperature lowers to θ_{sf} an ice lens begins to form, and when temperature lowers to θ_{sm}, the ice lens stops growing. This judge criterion for the formation of ice lenses can be expressed as

$$\theta_{sm} \leq T \leq \theta_{sf} \quad (5)$$

O'Neill (1983) thought when the pore pressure exceeds the total pressure, the ice lens forms.

$$P_{por} \geq \sigma \quad (6)$$

According to equation (5) and inequality (6), a judge criterion for the formation of ice lenses in terms of void ratio can be expressed as

$$e \geq e_s \quad (7)$$

Another opinion was that an ice lens forms when the pore pressure exceeds the sum of the total stress and the separation strength (Nixon, 1991).

$$P_{por} \geq \sigma + P_{sep} \quad (8)$$

Where P_{sep} is separation strength. According to above equations and inequality (8), we can obtain

$$e \geq e_s + \frac{P_{sep}}{E_s}(1 + e_0) \quad (9)$$

From the judge criterion for the formation of ice lenses, e_{sep} was defined as the separating void ratio, because e_{sep} is greater than e_s, inequality (9) can be expressed in another way (Zhou & Li, 2012)

$$e \geq e_s + (e_{sep} - e_s) \quad (10)$$

Comparing inequalities (9) and (10), the term $e_{sep} - e_s$ in inequality (10) can be viewed as the result of the separation strength P_{sep} (9) enlarging the separating void ratio e_{sep} in inequality (10).

Results and analysis

Recently, the model hypothesis of separating void ratio which proposes the separating void ratio as a judge criterion for the formation of ice lenses, had been used to derive a mathematical model of coupled water, heat and stress, and predict the formation of ice lenses and to calculate the amount of soil's frost heave, the equivalent water content, the pore pressure and et al. by adjusting the hydraulic conductivity in the model. Fig. 2 shows the distribution of ice lenses at different times. Ice lenses are distributed discontinuously layer by layer, which are confirmed in laboratory. At the time of 39.4h, an ice lens begins to form, and with time goes by, more ice lenses form and grow to increase the frost heave. (Zhou & Li, 2012).

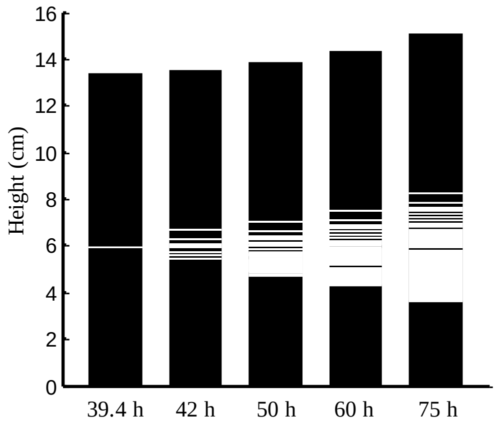

Fig. 2. Histogram of ice lenses distribution at different times with the initial soil column height of 12cm (The white parts are ice lenses).

Acknowledgments

This work is supported by the National Natural Science Foundation of China (No. 41271080 and No. 41701060).

References

Konrad, J.-M., Morgenstern, N.R., 1980. A mechanistic theory of ice lens formation in fine-grained soils. *Canadian Geotechnical Journal* 17 (4):473-486.

Nixon, J.F., 1991. Discrete ice lens theory for frost heave in soils. *Canadian Geotechnical Journal* 28 (6):843-859.

O'Neill, K., 1983. The physics of mathematical frost heave models: A review. *Cold Regions Science and Technology* 6 (3):275-291.

Tice, A.R., Anderson, D.M., Banin, A., 1976. The prediction of unfrozen water contents in frozen soils from liquid limit determinations. *Cold Regions Research & Engineering Laboratory*, U.S. Army Corps of Engineers.

Zhou J.Z., Li D.Q., Numerical analysis of coupled water, heat and stress in saturated freezing soil. *Cold Regions Science and Technology*, 2012(72):43–49.

Comparison of frontal and lateral erosion of periglacial fluvial islands

Laure Dupeyrat [1], Benoît Hurault [1], François Costard [1], Chiara Marmo [1], Emmanuele Gautier[2]
[1]*GEOPS, Geosciences Paris-Sud, Université Paris-Saclay, Orsay, France, laure.dupeyrat@u-psud.fr*
[2]*LGP, Laboratoire de Géographie Physique, Université Paris 1, Meudon, France*

Abstract

Frozen islands on the Lena floodplain present head retreats greater than on-side ones. The aim of this study is to quantify the difference of erosion between the island head and sides using the Erosion Ratio (ER). A GIS study of 19 islands of the Lena River from 1967 to 2010 provides an average Erosion Ratio (ER) equal to 4.7. We propose a model of thermal erosion for a frozen cylinder in a turbulent water flow. Thermal erosion of 19 frozen cylinders is measured for different water flows in a cold chamber. As in the field, the frontal erosion is always higher than the lateral one, with an averaged ER equal to 1.6, which decreases when temperature increases from 5 to 15°C. The higher value of ER in the field may be explained by the interaction with the neighboring islands and banks. We propose an empirical law including phase change and erosion.

Keywords: Thermal erosion ; island ; permafrost ; Lena ; physical modelling

Introduction

Periglacial rivers are affected by ice break-up, inducing a sudden rise of water level, discharge and temperature which induces thermal erosion and generates bank retreats up to 40 m. The aim of this study is to quantify the difference of erosion between the island head and sides, and to investigate the effects of the water temperature. Satellite images of fluvial islands in the Lena river have been analyzed in order to compare frontal and lateral erosion. A 2D cylindrical model of local thermal erosion of a frozen cylinder in a water flow has been developed. We have performed 6 series of repetitive measurements of local thermal erosion of a frozen cylinder in a hydraulic flume. Differences of local erosion of frozen islands were interpreted in the light of our model and experiments.

Analysis of satellite images of the Lena river

Aerial pictures (1967 (Corona): 20 m/px ; 1980 (Corona) : 15 m/px) and satellite images (1992 (Landsat 4) : 30 m/px ; 2002 (Landsat 7) : 30 m/px ; 2008 and 2010 (Spot5) : 2,5 m/px) were used to perform a follow-up of the temporal evolution of 33 islands of the Lena River (Costard & Gautier; 2007). We selected 19 islands upstream of the Yakutsk city, located in the middle of the channel in order to reduce boundary effects. We estimated the thermal erosion affecting the front and the lateral sides of these 19 islands during each period of time : The frontal erosion is always greater than lateral erosion (Fig. 1).

Figure 1. Estimation of the front, left and right erosion rate for the island 12 between 1967 and 1980. The Back point (B_{1967}) of the island is the point farthest from the center C_{1967} in the streamflow direction. The intersection of ($B_{1967}C_{1967}$) with the upstream outline of the island in 1967 (1980) defines the 1967 (1980) Front point F_{1967} (F_{1980}). The front erosion rate is calculated as (F_{1967}-F_{1980})/(1980-1967)=166/13=12.9 m/year. In the same way, the right (left) erosion rates is equal to -1.5 (5.7 m/year).

Thermal erosion of frozen cylinders

Problem statement and experiments

We have developed a model of local thermal erosion of a frozen cylinder crossing turbulent water flow. The melted sediments are instantaneously removed by the water flow and the ablation velocity is supposed to be constant (Dupeyrat *et al.*, 2011). The energy balance at the cylinder's surface between the heat brought by convection, the heat transferred by conduction in the solid and the latent heat of melting provides an estimation of the local ablation velocity Va(θ) and the Nusselt number Nu(θ) at every point a the surface of the cylinder defined by its θ angle.

We prepared 19 frozen cylinders (radius= 57 mm, height=70 mm, ice+sand, -15°C). Each cylinder was fixed in a water flow (temperature T_w=, 5 or 10 or 15°C ; velocity U_w=0.1 or 0.2 m/s). After 2 min of erosion, the cylinder was scanned with a 3D laser scanner. From the measurement of the local radius r(θ) of an horizontal section, we deduced the thermal erosion. The most eroded point (minimum r(θ)) was at the front point F (θ=0°) of the cylinder. The erosion decreased from the front (θ=0°) to the separation point (θ around 90°) and then increased again (Fig. 2).

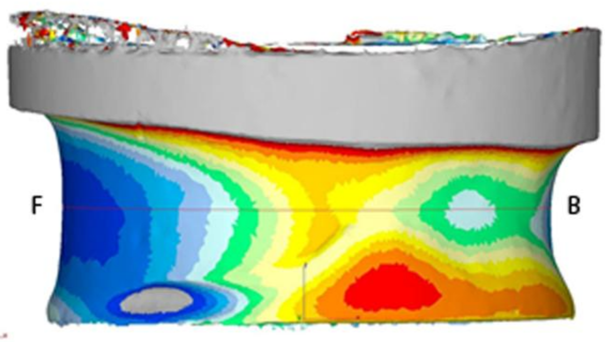

Figure 2. A frozen cylinder after erosion. During erosion, the water flow (T_w=5.6°C, U_w=0.2 m/s) came from the left. The eroded thickness is represented by colours from red (-2 mm) to dark blue (-10.5 mm) and grey (-12 mm). The upper part above water (>35 mm) is not eroded (grey). The studied horizontal section (line in red) is chosen at the location of the most eroded point (F (θ=0°)). The erosion decreases from F (-11 mm) to θ around 90° (-4 mm).

Comparison between experiments and field

The Erosion Ratio was estimated from a linear regression between the front and lateral erosion rates. Frontal erosion is always greater than lateral erosion (Fig. 3). Nevertheless, the ER gives a higher value in the field (=4.7) than in the laboratory (=1.6). In the field, the proximity of river banks or other islands prevents the lateral erosion and should increase the ER.

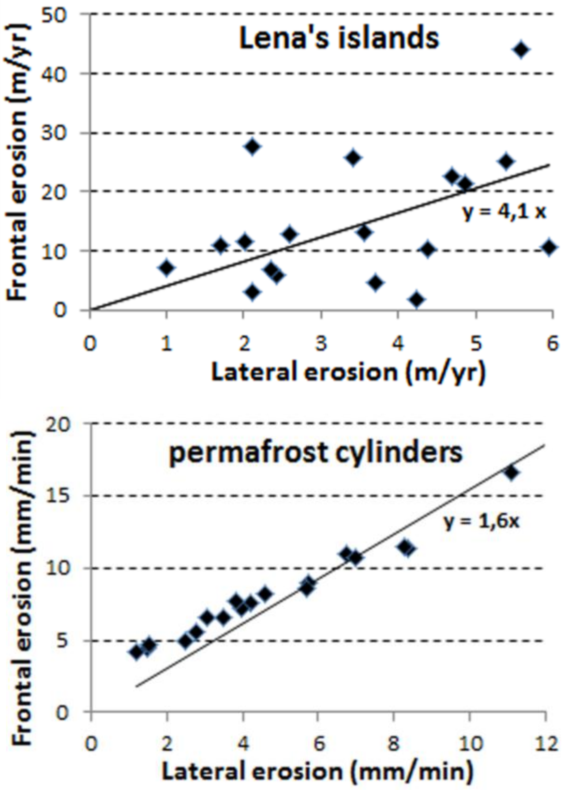

Figure 3. Comparison of the ER of the 19 Lena islands (1967 to 2010) (ER=4.7) and the 19 permafrost cylinders (ER=1.6).

Conclusions

We propose a quantification (Erosion Ratio) and a physical understanding of the greater thermal erosion at the front of islands compared to the sides in periglacial fluvial systems. The ER from the satellite image analysis of 19 islands on the Lena River from 1967 to 2010 (4.7) was higher than that derived in the laboratory experiments of 19 frozen cylinders in turbulent water flow (1.6). Boundary effects account for this discrepancy. Future work could extend this methodology to other periglacial islands.

References

Costard F. & Gautier E. 2007. The Lena river : hydromorphodynamic features in a deep permafrost zone. *Large Rivers. Geomorphology and Management. Edited by Gupta,* A, John Wiley and Sons 225-234.

Dupeyrat L, Costard F, Randriamazaoro R, Gailhardis E, Gautier E, Fedorov A. 2011. Effects of ice content on the thermal erosion of permafrost: implications for coastal and fluvial erosion. *Permafrost and Periglacial Processes* 22(2): 179-187.

Dupeyrat L, Hurault B., Costard F, Marmo C, Gautier E. 2018. In Press. Frontal and lateral thermal erosion of periglacial fluvial islands: Satellite image analysis and frozen cylinder experiments. *Permafrost and Periglacial Processes* (5) (6

Geophysical investigation and numerical modelling of heat transfer in a talik beneath the Kuuguluk River at Salluit, northern Québec, Canada

Richard Fortier[1]
Christophe Grenier[2]
Jean-Michel Lemieux[3]
John Molson[3]

[1]*Département de géologie et de génie géologique et Centre d'études nordiques, Université Laval, Québec, QC, Canada, richard.fortier@ggl.ulaval.ca*
[2]*Laboratoire des Sciences du Climat et de l'Environnement, UMR8212, Université Paris-Saclay, CEA/CNRS/UVSQ, Gif sur Yvette, France*
[3]*Département de géologie et de génie géologique et Centre d'études nordiques, Université Laval, Québec, QC, Canada*

Abstract

The Inuit community of Salluit in northern Quebec, Canada, is located in the continuous permafrost zone where finding a sustainable supply of drinking water is challenging. A well drilled in a talik beneath the Kuuguluk River is used as a source of water in this community. To assess the spatial extent of this talik, an electrical resistivity tomography survey was carried out in spring 2011. The thermo-hydraulic conditions of the riverbed have also been monitored since 2014. Following this investigation, a conceptual cryogeological model of the talik has been developed to support a 2D numerical model of conductive heat transfer. Based on the simulation results, the presence of this talik is due to the current thermal conditions along the riverbed. However, groundwater flow in the talik will have to be taken into account in a 3D numerical model to understand the formation of icing along the Kuuguluk River in winter.

Keywords: Talik; permafrost; electrical resistivity tomography, numerical modelling; conductive heat transfer; icing.

Introduction

The Inuit community of Salluit in northern Québec, Canada, uses a fractured rock aquifer in a talik beneath the Kuuguluk River as a source of drinking water (Lemieux *et al.*, 2016). To assess the vulnerability of this aquifer to climate change, a cryohydrogeophysical investigation, including electrical resistivity tomography (ERT), monitoring of thermo-hydraulic conditions of the riverbed and 2D numerical modelling of conductive heat transfer, has been undertaken. The preliminary results of this investigation are presented herein.

Cryohydrogeophysical investigation

Conceptual cryogeological model

A capacitively coupled resistivity (CCR) survey was carried out across the Kuuguluk River in April 2011 using the icing which forms each winter in the floodplain as a bridge. The electrical resistivity model derived from the inversion of the CCR survey is provided in Fig. 1. The talik beneath the riverbed appears as a zone of low electrical resistivity. It is surrounded by ice-rich permafrost characterized by high electrical resistivity. Following these results, a conceptual cryogeological model of the talik was developed (Fig. 1).

2D numerical modelling of conductive heat transfer

The numerical code Cast3M (http://www-cast3m.cea.fr/) was used to simulate conductive heat transfer in the ground with latent heat effects. Dirichlet boundary conditions were applied at the surface and Neumann boundary conditions on the sides and bottom of the 2D model (Fig. 1). The complex heat transfer at ground surface is simulated using empirical relationships between the surface and air temperatures found from monitoring of thermo-hydraulic conditions of the riverbed, floodplain, plateau and road (Fig. 2). The variability of the mean annual air temperature (MAAT) from 1885 to 2015 is also taken into account in the numerical model (Fig. 3). A training period of 35 years from 1885 to 1920 with a constant MAAT of -8.5 °C is first simulated to reach a steady-state transient thermal regime.

An example of the spatial distribution of ground temperature in the model is shown in Fig. 1 for the coldest period of the year in April 2015 at the end of the simulation period. The simulated ground temperatures at four locations in the model (at depths of 2 and 5 m beneath the riverbed and at a depth of 5 m in the plateau on the left of the model and beneath a road embankment) as a function of time over the simulation period are also given in Fig. 3.

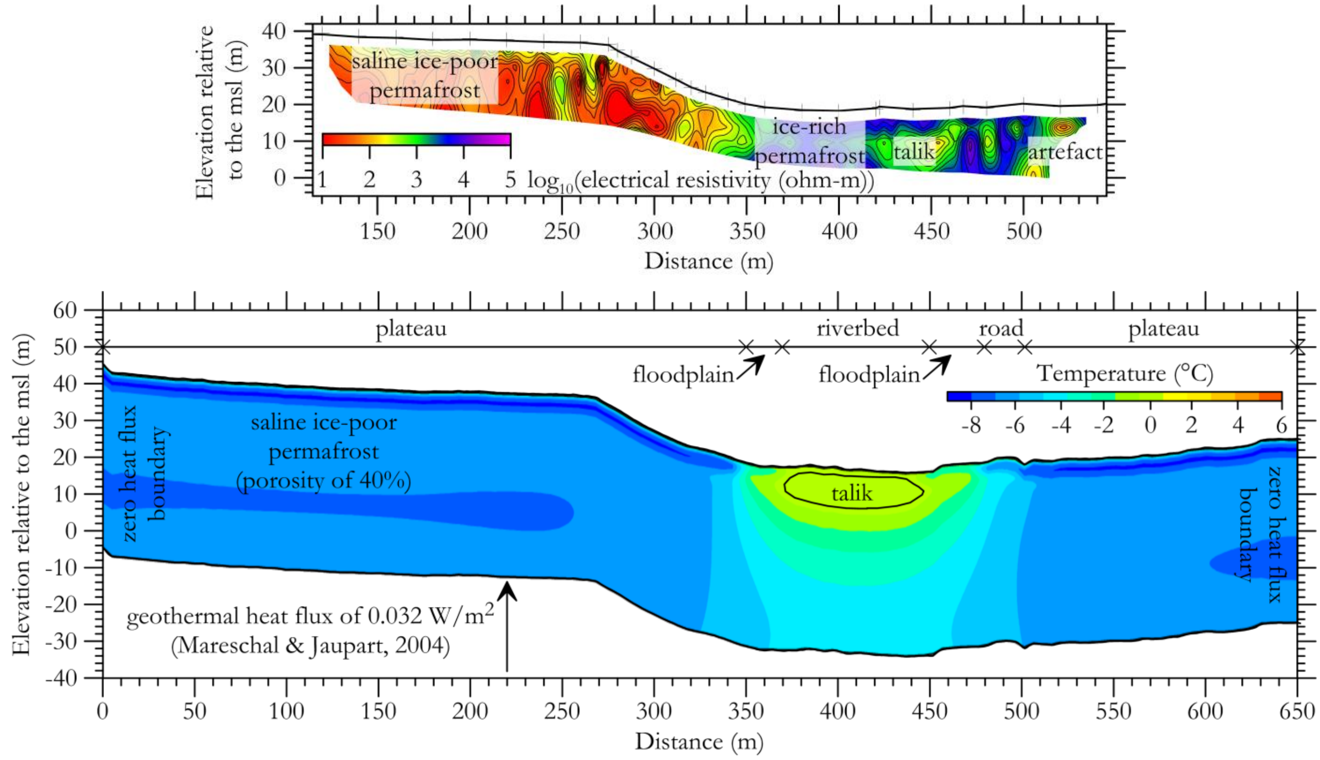

Figure 1: Upper plot: electrical resistivity model. Lower plot: conceptual cryogeological model and spatial distribution of simulated ground temperature in April of the 130th year of simulation (April 2015). Note the vertical exaggeration of 2:1.

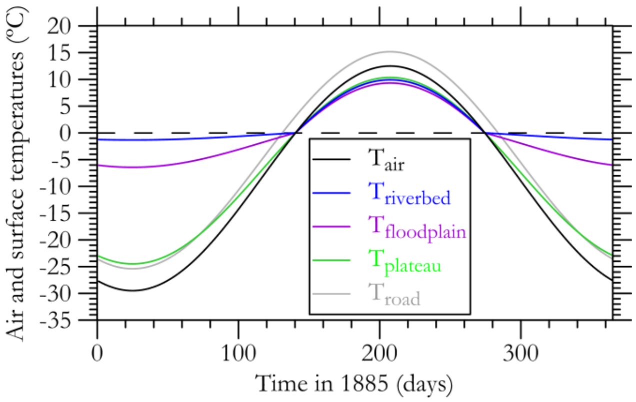

Figure 2: Simulated air and surface temperatures as a function of time in 1885 for different surface conditions (see Fig. 1). MAAT of -8.5 °C in 1885 (see Fig. 3).

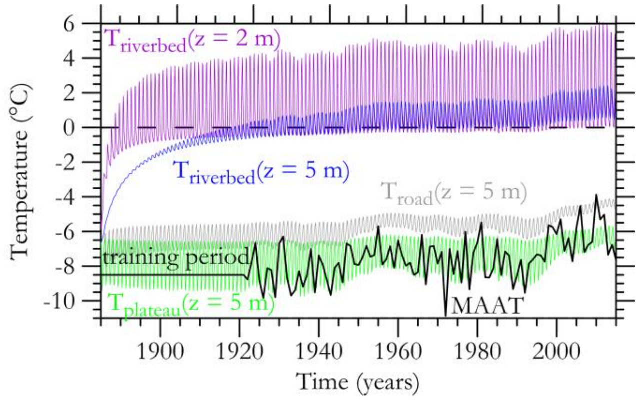

Figure 3: Simulated daily ground temperatures as a function of time for different surface conditions (see Fig. 1).

Discussion and conclusions

Based on the simulation results, the current thermo-hydraulic conditions along the Kuuguluk River and conductive heat transfer can explain the presence of the talik. The extent of the simulated talik is also consistent with that derived from the electrical resistivity model.

For a more realistic simulation, ground heterogeneity and groundwater flow in the talik should be taken into account in a 3D numerical model of coupled conductive and convective heat transfer to understand the formation of icing along the Kuuguluk River in winter.

References

Lemieux, J.-M., Fortier, R., Talbot-Poulin, M.-C., Molson, J., Therrien, R., Ouellet, M., Banville, D., Cochand, M. & Murray, R., 2016. Groundwater occurrence in cold environments: examples from Nunavik, Canada. *Hydrogeology Journal* 24-6, pp. 1497–1513.

Mareschal, J.-C., & Jaupart, C., 2004. Variations of surface heat flow and lithospheric thermal structure beneath the North American craton. *Earth and Planetary Science Letters* 223(1–2), pp. 65–77.

Validation of Cryohydrogeological codes: the InterFrost project

Christophe Grenier[1], Hauke Anbergen[2], Victor Bense[3], Quentin Chanzy[1&4], Ethan Coon[5,6], Nathaniel Collier[6], François Costard[7], Michel Ferry[8], Andrew Frampton[9], Jennifer Frederick[10], Julio Gonçalvès[11], Johann Holmén[12], Anne Jost[13], Samuel Kokh[14], Barret Kurylyk[15], Jeffrey McKenzie[16], John Molson[17], Emmanuel Mouche[1], Laurent Orgogozo[18], Romain Pannetier[9], Eric Pohl[1], Agnès Rivière[19], Nicolas Roux[1&7], Wolfram Rühaak[20], Johanna Scheidegger[21], Jan-Olof Selroos[22], René Therrien[17], Patrik Vidstrand[22], Clifford Voss[23]

[1]LSCE/IPSL, CEA-CNRS-UVSQ, Université Paris-Saclay, Gif-sur-Yvette, France, christophe.grenier@lsce.ipsl.fr
[2]Dipl.-Ing. Peter Neumann Baugrunduntersuchung GmbH & Co. KG, Eckernförde, Germany
[3]Department of Environmental Sciences. Wageningen University, Netherlands
[4]ENS Cachan, Département Génie Mécanique, Université Paris-Saclay, Cachan, France
[5]Los Alamos National Laboratories, Los Alamos, USA
[6]ORNL Climate Change Science Institute, Oak Ridge, TN, USA
[7]GEOPS/IPSL, Geosciences Paris Sud, Université Paris-Saclay, Orsay, France
[8]MFRDC, Orvault, France
[9]Department of Physical Geography, Stockholm University, Stockholm, Sweden
[10]Sandia National Laboratories, Albuquerque, NM, USA
[11]Aix-Marseille University, CNRS, IRD, CEREGE, Aix-en-Provence, France
[12]Golder Associates, Stockholm, Sweden
[13]Sorbonne Universités, UPMC Univ. Paris 6, CNRS, EPHE, Metis, Paris, France
[14]Maison de la Simulation USR 3441, Digiteo, CEA Saclay, Gif-sur-Yvette, France
[15]Centre for Water Resources Studies and Department of Civil and Resource Engineering, Dalhousie University, Halifax, NS, Canada
[16]Department of Earth and Planetary Sciences, McGill University, Montreal, PQ, Canada
[17]Département de géologie et de génie géologique, Université Laval, Québec, Canada
[18]GET, UMR 5563 CNRS-IRD-UPS, Université Toulouse, Toulouse, France
[19]PSL Research University, MINES ParisTech, Centre de Géosciences, Fontainebleau, France
[20]Federal Institute for Geosciences and Natural Resources (BGR), Hannover, Germany
[21]British Geological Survey. Nottingham, UK
[22]Swedish Nuclear Fuel and Waste Management Company, Solna, Sweden
[23]United States Geological Survey, Menlo Park, CA, USA

Abstract

Recent field and modelling studies indicate that a fully-coupled, multi-dimensional, thermo-hydraulic (TH) approach is required to accurately model the evolution of permafrost-impacted landscapes and groundwater systems. However, the relatively new and complex numerical codes being developed for coupled non-linear freeze-thaw systems require verification. This issue was first addressed within the InterFrost IPA Action Group, by means of an intercomparison of thirteen numerical codes for two-dimensional TH test cases (TH2 & TH3). The main results demonstrate that these codes provide robust results for the test cases considered. The second, ongoing phase of the InterFrost project is devoted to the simulation of a cold-room experiment based on Test Case TH2 (Frozen Inclusion). The experimental setup and monitoring results at the base of the common validation exercise are presented.

Keywords: numerical simulation; code benchmarking; thermo-hydrological coupling; permafrost; sharp interface

Introduction

Climate change has been most pronounced in high latitude regions and high altitude areas. The improvement of our understanding of the interplay between climate, hydrology and permafrost provides motivation for the development of a spatially distributed, multidimensional, fully-coupled TH approach for heat and water processes in permafrost areas. A new class of such cryohydrological codes emerged during the last decade fulfilling this intention (Walvoord & Kurylyk, 2016; Kurylyk *et al.*, 2014). However, the numerical solution of such coupled TH systems with non-linear equations and a sharp interface (freeze-thaw boundary) is challenging. Associated codes thus require some level of evaluation.

The InterFrost project (IPA Action Group) provides an open forum for such an evaluation. Validation is organized in three steps, each addressing one of the following questions: How well is the reference set of equations solved by existing codes? How realistic is the set of equations solved for fluid flow and heat transfer? How well can existing codes accommodate real world complexity?

The first step is a purely numerical issue, addressed by means of an inter-comparison of 13 codes on 2D benchmark cases with the main results presented below.

The second step is the simulation of an experiment under controlled conditions in the cold room (present status presented below). The third issue will require carefully selected field-case monitoring data.

Advancing with a group of modelers is a necessary requirement for code inter-comparison and code validation with real-world data. Promoting such a group process within the cryohydrogeological community is a major incentive of the InterFrost IPA Action Group.

Inter-comparison (TH2 & TH3 Test Cases)

Two complementary 2D test cases were developed as benchmarks for the intercomparison. Both incorporate the full complexity of TH coupling (see InterFrost web site wiki.lsce.ipsl.fr/interfrost). Evaluation of the numerical codes against these benchmarks is based on the intercomparison of simulation results through a set of performance metrics (PMs). Figure 1 presents a sketch of Test Case TH2 (initially frozen inclusion within an unfrozen domain) with 13 code simulation results for PM1 (minimum domain temperature).

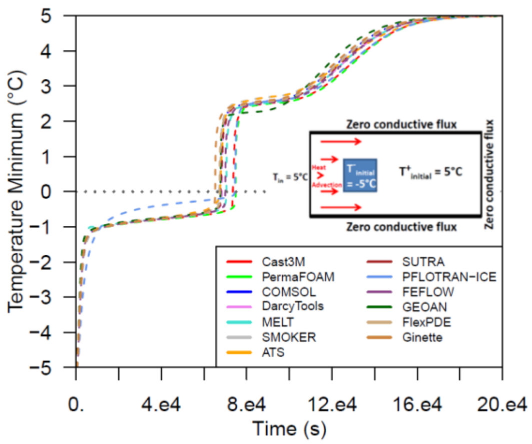

Figure 1. Result of the inter-comparison of 13 codes on TH2-PM1 (evolution of temperature minimum)

These results reflect the participant group conclusions drawn from the full inter-comparison body and are based on a critical number of participants with codes presenting a wide diversity of numerical approaches. A group of these 13 models, implementing the same equation sets and identical characteristic curves, behaved similarly for all test cases, all PMs, and over a large range of head gradients. This suggests that the codes are all solving the governing equations equally well. Discrepancies found in the intercomparison results were traced back to differences in the governing equations or simulation set-up issues. These are promising outcomes for coupled TH simulation. Interested readers may refer to the InterFrost web site, Rühaak *et al.*, (2015) and Grenier *et al.*, (in review).

Validation from experimental cases

In a need to exercise the codes' capabilities for real-world systems, Test Case TH2 was adapted for experimental conditions in the GEOPS Laboratory. The setup consists of a plexiglass box with a filter at the bottom allowing flow through. It is filled with saturated sand in which a frozen and saturated sand inclusion is placed. The box is installed in a cold room with controlled temperature conditions. Monitored parameters are: the temperature in several locations (inclusion center and down-gradient, in the air, the water and on the external wall), and water flow rates. Figure 2 provides a sketch of the setup as well as the temperature monitoring results (10_11_2017 experiment).

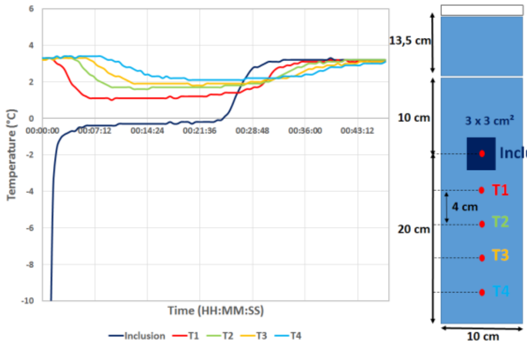

Figure 2. Experimental conditions and monitoring results

Preparatory simulations conducted with the Cast3M code indicate that conditions formerly simulated for the TH2 case may need to include additional complexity to account for actual setup conditions (e.g. the inclusion installation phase) while some calibration will be required to reproduce the observed variables. Complementary measurements (e.g. colored initial inclusion tracing the evolution of thawing water) would provide further constraints. Preliminary simulation results will be presented during EUCOP2018.

Acknowledgments

The InterFrost Action Group gratefully acknowledges the support of IPA and Labex-IPSL.

References

Grenier, C. et al., in review. Groundwater flow and heat transport for systems undergoing freeze-thaw: Intercomparison of numerical simulators. *ADWR*

Kurylyk, B.L. et al. 2014. Climate change impacts on groundwater and soil temperature in cold and temperate regions: Implications, mathematical theory, and emerging simulation tools. Earth-Sci. Rev 138: 313-334, 2014.

Rühaak W. et al. Benchmarking Numerical Freeze/Thaw Models. *Energy Procedia* 76 (2015) 301 – 310

Walvoord, M.A., Kurylyk, B.L., 2016. Hydrologic impacts of thawing permafrost – A review. *Vadose Zone J* Vol. 15, Iss. 6, 2016

Study on the development regularity of the temperature field in fractured rock mass under ming disturbance in permafrost regions

Yadong Huang[1]
Huijun Jin[2]
Xiaoying Li[3]
Ruixia He[4]
Shuhui Gao[5]

[1] *State Key Laboratory of Frozen Soils Engineering (SKFLSE), Cold and Arid Regions Environmental and Engineering Research Institute (CAREERI), Chinese Academy of Sciences (CAS), Lanzhou 730000, China; University of Chinese Academy of Sciences (UCAS), Beijing 100049, China. Presenter, Email: huangyadong@lzb.ac.cn*

[2] *SKLFSE, CAREERI, CAS, Lanzhou 730000, China; School of Civil Engineering, Harbin Institute of Technology (HIT), Harbin 150090, China; UCAS, Beijing 100049, China. Correspondent Author, Email: hjjin@lzb.ac.cn*

[3] *SKLFSE, CAREERI, CAS, Lanzhou 730000, China; UCAS, Beijing 100049, China*

[4] *SKLFSE, CAREERI, CAS, Lanzhou 730000, China*

[5] *SKLFSE, CAREERI, CAS, Lanzhou 730000, China; UCAS, Beijing 100049, China*

Abstract

Natural rock mass generally contains fractures or complex fracture networks due to geological movement and human disturbance. Fractured rock mass occurs in complex geological environment that includes temperature field, ground-water seepage field and stress field, which research began in the 1950s and lots of achievements have been obtained to date. However, the relevant research results on the seepage field and temperature field of the fractured rock mass under the condition of mining disturbance in permafrost regions are rare. In view of this, this paper regards the Gullian coal mine, in the permafrost area of northeastern China as the research object, adopts the combination of field measurement and laboratory experiment method, and simulates the distribution law of temperature field under the action of the seepage, employing finite element analysis software COMSOL.

Keywords: development regularity; temperature field; fractured rock mass; permafrost; ming disturbance.

Experimental and numerical analyses of the frost heaving mechanism and prevention technology of high-speed subgrade in seasonally frozen regions

Yuanming Lai[1]
Jianqiang Gao[1]
Mingyi Zhang[1]
Ruiqiang Bai[1]

[1]*State Key Laboratory of Frozen Soil Engineering, Northwest Institute of Eco-Environment and Resources, Chinese Academy of Sciences. University of Chinese Academy of Sciences.*

Abstract

Frost heave of subgrade in cold regions has become a key factor affecting the construction of high-speed railway. To investigate the frost heave mechanism of coarse-grained soil under consideration of "pot" effect, a series of one-side freezing experiments of coarse-grained soil were conducted in an open system with water supply firstly. The frost susceptibility of the coarse-grained soil is influenced by fines content and external water significantly, and the effect of vapor transfer on the frost heave of coarse-grained soil will become more obvious in the case of lower moisture content. Based on the test phenomena and results, a mathematical model considering vapor transfer was established to explore the coupled hydro-thermo-vapor-mechanical process. Besides, the model was validated by the test data. Finally, a heating pipe, as an anti-frost measurement, was employed to adjust the subgrade temperature and minimize or eliminate the frost heave in cold regions.

Keywords: frost heave; coarse-grained soil; "pot" effect; vapor transfer; heating pipe; subgrade temperature

Introduction

Frozen soil is a kind of soil or rock containing ice below 0°C. 50% of the Earth's land and 53.5% of China's land surface is seasonally frozen regions (Qiu *et al.*, 1994 and Xu *et al.*, 2001). Many high-speed railways have been constructed and will be constructed more in these regions. Frost heave in winter and thaw settlement in spring are the most common mechanisms causing the damages of road pavement structure. It involves complex hydro-thermo-mechanical interaction in the subgrade during freezing-thawing processes.

Experiment

One-side freezing experiments of coarse-grained soil were conducted in the freezing-thawing test chamber of State Key Laboratory of Frozen Soil Engineering, which mainly includes temperature control system, water supply system and data acquisition system (shown in Fig.1). Coarse-grained soil was made of graded crushed stones mixed with a certain amount of sieved fines. The preparation and installation of soil sample was shown in Fig.2.

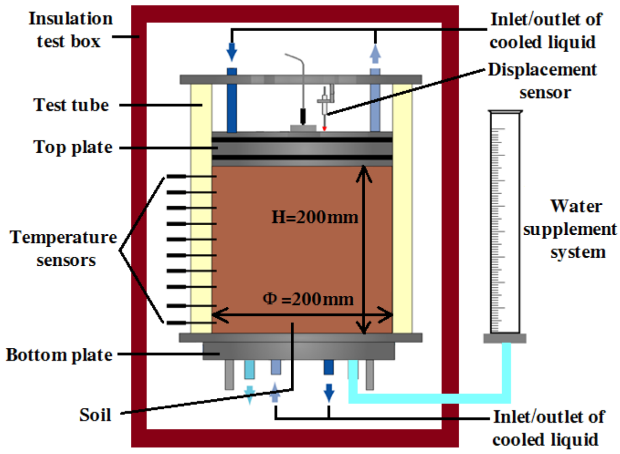

Fig.1 Schematic diagram of experimental apparatus

Numerical model description

Based on the test data, a mathematical model considering vapor transfer was established to explore the complex hydro-thermo-vapor-mechanical process. The controlled equations were listed as followed:

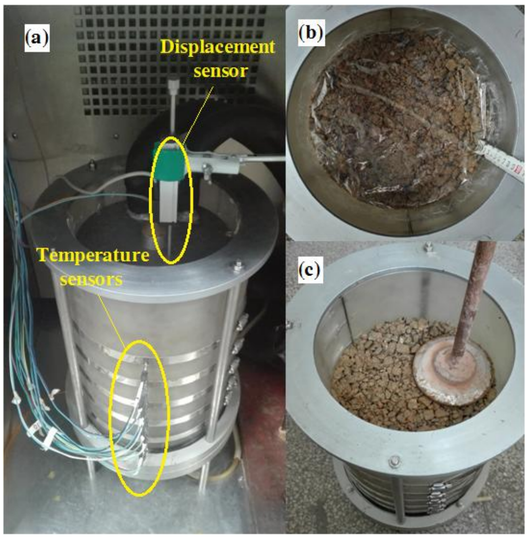

Fig.2 Preparation and installation drawings of soil sample

$$\frac{\partial\theta}{\partial t}=\frac{\partial\theta_l}{\partial t}+\frac{\partial\theta_v}{\partial t}+\frac{\rho_i}{\rho_w}\frac{\partial\theta_i}{\partial t}$$
$$=\nabla\cdot[K'_{Lh}\nabla(h+y)+K_{LT}\nabla T] \quad (1)$$
$$+\nabla\cdot[(K_{vh}\nabla h+K_{vT}\nabla T]$$

$$C_p\frac{\partial T}{\partial t}-L_i\rho_i\frac{\partial\theta_i}{\partial t}+L_w\rho_w\frac{\partial\theta_v}{\partial t}$$
$$=\nabla\cdot(\lambda\nabla T)-C_l\nabla(q_lT)-C_v\nabla(q_vT) \quad (2)$$
$$-L_w\rho_w\nabla q_v$$

The mathematical model was validated by the one-side freezing test results among temperatures profiles, moisture distributions and frost heaves. Fig.3 shows the comparison of frost heaves between calculated and measured of soil sample.

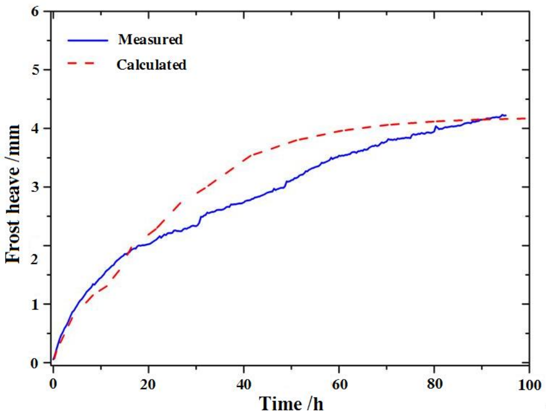

Fig.3 Calculated and measured frost heaves of the soil sample

Anti-frost measurement

The heating pipes were installed in both the side slopes of embankment, controlling the temperature of key points above 0°C, to minimize or eliminate the frost heave in cold regions. From Fig.4, it can be seen that the freezing depths can been reduced significantly.

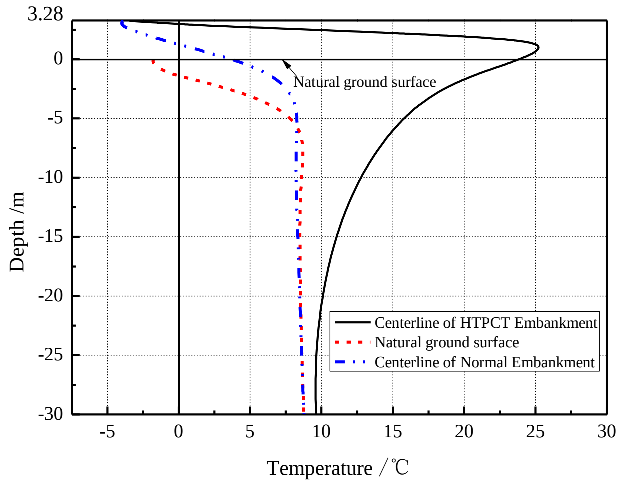

Fig.4 Variations of the temperatures with depths under the concrete track plate centerlines and under natural ground surface on March 15 after 10 years of the construction.

Conclusions

(1) The frost susceptibility of the coarse-grained soil is influenced by fines content and external water significantly.

(2) The model was validated and can account for the frost heaving mechanism of subgrade fillings.

(3) The heating pipe can protect the subgrade from frost heaving effectively.

Acknowledgments

This research was supported by the National Natural Science Foundation of China (Grant No. 41230630), Key Research Program of Frontier Sciences of Chinese Academy of Sciences (QYZDY-SSWDQC015), the 100-Talent Program of the Chinese Academy of Sciences (Granted to Dr. Mingyi Zhang), the National Natural Science Foundation of China (Grant No. 41471063).

References

Xu, X.Z., et al., 2001. *Frozen Soil Physics*, Beijing: Science Press.

Qiu, G.Q., et al., 1994. *Geocryological Glossary*. Lanzhou: Gansu Science and Technology Press.

Variations of the thermal conductivity of a silty clay during a freezing-thawing process

Jianguo Lu[1,2], Mingyi Zhang[1,2], Yuanming Lai[1,2], Xiyin Zhang[1, 3]
[1]*State Key Laboratory of Frozen Soil Engineering, NIEER, Chinese Academy of Sciences, Lanzhou 730000, China*
2. University of Chinese Academy of Sciences, Beijing 100049, China
3. School of Civil Engineering, Lanzhou Jiaotong University, Lanzhou 730000, China

Abstract

The thermal conductivity is an important parameter in calculating heat transfer. Here, the thermal conductivity was measured during a freezing-thawing process, and then calculated using three general models. The results show the thermal conductivity of soil with a large initial dry density would reduce after a freezing-thawing cycle, while opposite with a small initial dry density. For the soil with a larger initial water content, the difference of thermal conductivity between the freezing and thawing processes is larger than that of the soil with a smaller initial water content. It is concluded the variation of thermal conductivity during the freezing and thawing processes is mainly determined by the pore ratio and unfrozen water content. However, the effect of pore ratio is larger than that of unfrozen water content. Then, it shows the exponential weighted mean model is more close to the tested data.

Keywords: Thermal conductivity; Freezing-thawing process; Dry density; Pore ratio; Unfrozen water content

Introduction

Properties of soils, such as thermal conductivity, etc., significantly influence the thermal regimes of geological formations and geotechnical constructions in cold regions, e.g. plateau permafrost regions and polar regions (Xu *et al.*, 2011; Rao & Singh, 2011; Pei *et al.*, 2013) In cold regions, as the seasons alternating, the freezing-thawing process is bound to influence the thermal conductivity of soils. At the same time, the hysteresis effect of unfrozen water content between the freezing and thawing processes, which would cause the difference of ice contents at the same temperature, affects the thermal conductivity of soils. Therefore, this paper is to study the thermal conductivity of soils during a freezing-thawing process. A series of laboratory experiments were carried out to measure the thermal conductivity of a silty clay from the Qinghai-Tibet Plateau at different temperatures during a freezing-thawing process. Based on the four components of frozen soils, the expressions of the parameters during a freezing-thawing process are deduced. Additionally, the tested results were used to evaluate the three general models of thermal conductivity, i.e. weighted arithmetic mean model, weighted harmonic mean model, and exponential weighted mean model.

Experimental method

The thermal conductivity of the silty clay from the Qinghai-Tibet Plateau was tested in this study. Two kinds of dry densities, i.e. 1.75×10^3 kg/m^3 and 1.75×10^3 kg/m^3, were chosen to evaluate the effect of dry densities on the thermal conductivity of soils. The initial water content is another important factor to determine the thermal conductivity of soils, therefore, eight column soil samples with different initial dry densities and initial water contents, were made with the diameter of 63mm and the height of 72mm (Fig. 1). In order to research the effect of freezing-thawing process on the thermal conductivity of soils, the experiments were divided into two processes, i.e. cooling process and heating process. Firstly, the temperature was decreased step by step, namely, 19℃, 8℃, 0℃, -0.5℃, -1℃, -1.5℃, -2℃, -5℃, -8℃, -13℃ and -19℃. At each temperature step, the sufficient time was kept for the soil samples to reach thermal equilibrium, and then the thermal conductivities of the soil samples were measured.

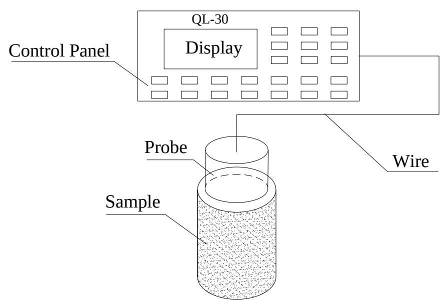

Fig. 1 Thermal conductivity experiment apparatus

Experimental results and analysis

Fig.2 shows thermal conductivities versus temperature for the soil samples with different initial dry densities during a freezing and thawing processes. This demonstrates the thermal conductivities increase with the increased initial water content. And the variations of the thermal conductivities of the soil samples with the higher initial water contents are larger than those of the soil samples with the lower initial water contents.

Based on the four components of frozen soils (gas, ice, unfrozen water, soil particles), the expressions of the parameters during a freezing-thawing process are deduced. Then, the tested results were used to evaluate the three general models of thermal conductivity, i.e. weighted arithmetic mean model, weighted harmonic mean model, and exponential weighted mean model.

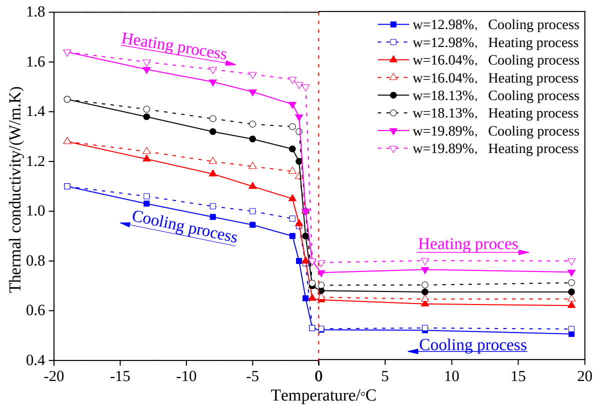

(a) $\rho_d = 1.50\times10^3\,\mathrm{kg/m^3}$

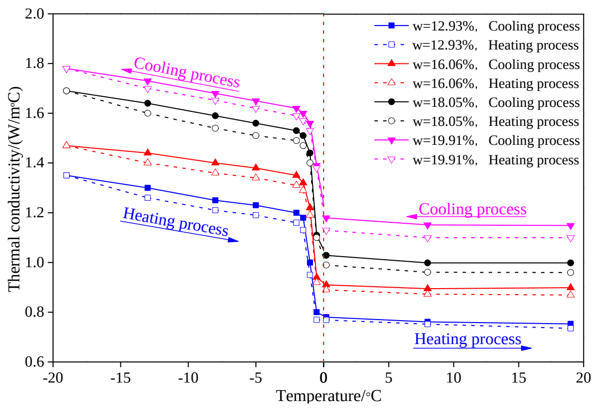

(b) $\rho_d = 1.75\times10^3\,\mathrm{kg/m^3}$

Fig. 2 Thermal conductivities versus temperature for the soil samples with different initial dry densities

A comparison between the tested results and the calculated results from the three models for the thermal conductivity of the sample with the dry density of 1.75×10^3 kg/m³ is given in Fig. 3. It is can be found that the three models can all reflect the influence of the freezing-thawing process by the change of the pore ratio and the hysteresis effect of unfrozen water content on the thermal conductivity of the soil. However, it can be found that the calculated values of the exponential weighted mean model are highly in agreement with the tested results.

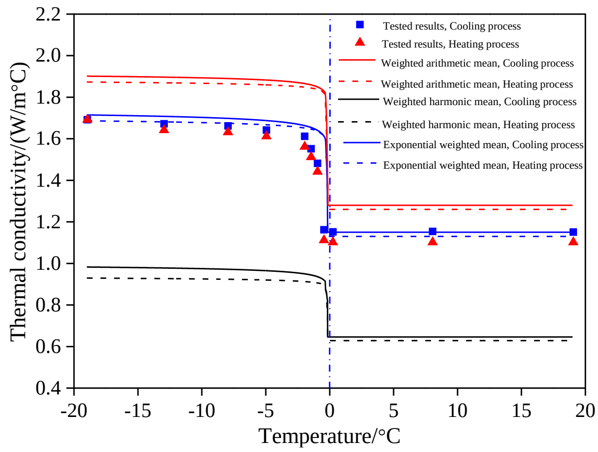

(c) 2015

Fig. 3 Comparison between tested and calculated results ($\rho_d = 1.75\times10^3\,\mathrm{kg/m^3}$)

Conclusions

The thermal conductivity of soil, with the different initial dry density and water content, changed diverse. The variations of thermal conductivity are synthetical results of the variation of pore ratio and the hysteresis effect of unfrozen water content during a freezing-thawing process. For the loose soils, the two factors make additive effects, but compensative effects for the dense soils. Furthermore, the variation of pore ratio has larger effect than the hysteresis of unfrozen water content. The three general thermal conductivity models can all be used to evaluate the thermal conductivity of soils; however, the exponential weighted mean model has a high agreement with the experimental data.

Acknowledgements

This research was supported by the National Natural Science Foundation of China (Grant No. 41471063), the 100-Talent Program of the Chinese Academy of Sciences (Granted to Dr. Mingyi Zhang), and the Program of the State Key Laboratory of Frozen Soil Engineering (Grant No. SKLFSE-ZT-23).

References

X.Z. Xu, J.C. Wang & L.X. Zhang, 2001. *Frozen soil physics*. Science Press, Beijing.

M.G. Rao & D.N. Singh, 2011. A generalized relationship to estimate thermal resistivity of soils. *Canadian Geotechnical Journal* 36(4): 767-773.

W.S. Pei, W.B. Yu, S.Y. Li & J.Z. Zhou, 2013. A new method to model the thermal conductivity of soil–rock media in cold regions: An example from permafrost regions tunnel. *Cold Regions Science and Technology* 95: 11-18.

Numerical investigation of evapotranspiration processes in a forested watershed of Central Siberia

Laurent Orgogozo[1]
Anatoly S. Prokushkin[2]
Oleg S. Pokrovsky[1,3]
Christophe Grenier[4]
Michel Quintard[5,6]
Jérôme Viers[1]
Stéphane Audry[1]

[1]GET (Géosciences Environnement Toulouse), UMR 5563 CNRS / UR 234 IRD / UPS, Observatoire Midi-Pyrénées, Université de Toulouse, 14 avenue Édouard Belin, 31400 Toulouse, France, contact: laurent.orgogozo@get.omp.eu

[2]V.N. Sukachev Institute of Forest, Siberian Branch, Russian Academy of Sciences, Akademgorodok 50/28, Krasnoyarsk, Russia

[3]BIO-GEO-CLIM Laboratory, Tomsk State University, Lenina 35, Tomsk, Russia

[4]LSCE/IPSL (Laboratoire des Sciences du Climat et de l'Environnement), UMR 8212 CNRS-CEA-UVSQ, CEA - Orme des Merisiers, 91191 Gif-sur-Yvette Cedex, France

[5]Université de Toulouse, INPT, UPS, IMFT (Institut de Mécanique des Fluides de Toulouse), Allée Camille Soula, F-31400 Toulouse, France

[6]CNRS, IMFT: F-31400 Toulouse, France

Abstract

Evapotranspiration has a major control on continental surfaces dynamics in forested boreal environments. For example, it has strong impacts on active layer thickness, mainly because of its effect on water content within the upper layers of the soil column. These are complex processes, depending not only on climate forcings (atmospheric water demand) but also on physical, geo-pedological and biological properties of the considered areas. Here we propose a numerical investigation of evapotranspiration processes in the active layer of slopes of a forested watershed in Central Siberia. The effect on actual evapotranspiration of the spatial contrasts in terms of exposure, root layer thickness and tree stand density within the watershed are simulated using a recently developed high performance computing cryohydrogeological model, permaFoam.

Keywords: Evapotranspiration; active layer thickness; cryohydrogeological modeling; high performance computing; thermo-hydrological couplings; boreal forests.

Introduction

Evapotranspiration is one of the main driving factors of landscape variability in taïga environment, as it can be seen for example through the contrast between north and south aspect slopes in the region of Tura (see Figure 1). Modifications of evapotranspiration regimes in boreal areas, either in relation with climate changes or not, may have strong impacts on continental boreal surfaces dynamics, for instance on water fluxes (*e.g.* Duan *et al.*, 2017). Thus in order to develop predictive modeling of the evolution of boreal continental surfaces under climate change, an accurate quantification of the evapotranspiration processes is required.

Figure 1: Visible contrast between north and south aspect slopes in a larch forest environment of Central Siberia.

The goal of this work is thus to develop a relevant quantification methodology for actual evapotranspiration in permafrost affected forested areas.

Modelling evapotranspiration in the Kulingdakan watershed

In order to study the relative importance of different features of the forested boreal surfaces on evapotranspiration, the thermo-hydrological dynamics of the Kulingdakan experimental watershed (*e.g.* Prokushkin *et al.*, 2011, Viers *et al.*, 2015) have been simulated under current climatic conditions using permaFoam, a high performance computing (HPC) cryohydrogeology modeling tool (Orgogozo *et al.*, 2015). The need of HPC technics in cryohydrogeology modeling is acknowledged (*e.g.* Painter *et al.*, 2013), and that is the reason why we choose to develop permaFoam in the framework of the reference open source environment for computational fluid dynamics OpenFOAM® (*e.g.* Weller *et al.*, 1998, www.openfoam.com). Based on estimated potential evapotranspirations (*i.e.* climate observations), the computation of the evapotranspirative uptakes in the active layers of the Kulingdakan watershed are performed in a temporally and spatially distributed way, taking into account both water availability and thermal status in the soils (modified from Orgogozo, 2015). Such a methodology allows the testing of the sensitivity of the actual evapotranspiration with respect to various properties of the slopes (*e.g.* exposure, root layer thickness, density of tree stand). The comparisons between observations and modeling results in terms of soil thermal regimes and water fluxes variability in the watershed allow discussing the relevance of each of the derived parameterizations of the evapotranspiration rates in the active layer.

References

Duan, L., Man, X. Kurylyk, B.L., Cai T., Li Q., 2017. Distinguishing streamflow trends caused by changes in climate, forest cover, and permafrost in a large watershed in northeastern China. *Hydrological Processes* 31: 1938-1951.

Orgogozo, L., 2015. RichardsFoam2: A new version of RichardsFoam devoted to the modelling of the vadose zone. *Computer Physcics Communications* 196: 619-620.

Orgogozo, L., Pokrovsky, O.S., Goddéris, Y., Grenier, C., Viers, J., Labat, D., Audry, S., Prokushkin, A., 2015. Thermo-hydrologic modelling of permafrost with OpenFOAM®: perspctives of applications to the study of weathering in boreal areas. *Geophysical Research Abstracts,* Vol. 17, EGU2015-9775-1, 2015, EGU General Assembly 2015.

Painter S.L., Moulton J.D., Wilson C.J., 2013. Modeling challenges for predicting hydrologic response to degrading permafrost. *Hydrogeology Journal* 21: 221–224. DOI: 10.1007/s10040-012-0917-4

Prokushkin, A.S., Pokrovsky, O.S., Shirokova L.S., Korets M.A., Viers J., Prokushkin S.G., Amon R., Guggenberger G., McDowell W.H., 2011. Sources and export fluxes of dissolved carbon in rivers draining larch-dominated basins of the Central Siberian Plateau. *Environmental Research Letter* 6: 045212, doi:10.1088/1748-9326/6/4/045212

Viers J., Prokushkin A.S., Pokrovsky O.S., Kirdyanov A.V., Zouiten C., Chmeleff J., Meheut M., Chabaux F., Oliva P., Dupré B., 2015. Zn isotope fractionation in a pristine larch forest on permafrost-dominated soils in Central Siberia. *Geochemical Transactions* 16(3). DOI 10.1186/s12932-015-0018-0

Weller, H.G., Tabor, G., Jasak, J., Fureby, C., 1998. A tensorial approach to computational continuum mechanics using object-oriented techniques. *Computer in Physics* 12(6): 620-631.

Heat transfer mechanisms of crushed rock materials

Karlis Rieksts[1]
Jean Côté [2]
Elena Scibilia (Kuznetsova)[1]
Inge Hoff[1]
[1]*Department of Civil and Environmental Engineering, Norwegian University of Science and Technology, Trondheim, Norway, karlis.rieksts@ntnu.no*
[2]*Department of Civil and Water Engineering, Laval University, Quebec city, Canada*

Abstract

Natural air convection can yield significant contribution to heat transfer in coarse open graded materials. Convection contributes to heat transfer merely during the cooling periods. Therefore, it can have both, favorable or a negative effect depending on environmental conditions. In permafrost regions extensive heat extraction during wintertime aids to maintain stable permafrost. In seasonally freezing conditions, natural air convection can give adverse effect as it can significantly increase the rate and the magnitude of frost penetration. This could results in frost heave problems when structures as roads and railways are built on top of frost susceptible soils.

The literature provides a limited amount of laboratory tests done for characterization of natural air convection in coarse mineral materials. The paper gives first a short overview of preceding laboratory tests on natural air convection and materials tested and then introduce an ongoing study for natural air convection in coarse open graded crushed materials.

Keywords: convection, crushed rock materials, intrinsic permeability.

Introduction

Natural air convection, for the last few decades, has been a topic of interest for road and railway engineers. The reason for that is the nature of convection being a temperature gradient dependent heat transfer mode. In particular, convection may give significant contribution to the overall heat transfer rate merely during the cooling periods. This in turn can give favorable effect only in permafrost conditions contributing to ground cooling and maintaining subzero temperatures under road or railway structures. The same process in seasonally freezing environment can give an adverse effect increasing frost penetration depth.

This paper presents an overview of large-scale natural air convection tests conducted in laboratory conditions during the last few decades. Description is given in a chronological sequence as they have been performed throughout the last decades. An ongoing study on natural air convection is presented afterwards.

Large Scale laboratory Experiments

Experiments by Johansen (1975)

The geometrical setup for large-scale tests was different compared to the studies that was done after Johansen (1975). The width and the length of the test box was 1.8 and 2.2 m, respectively, while the layer thickness of crushed material was 0.48 m. The heat flow was measured with nine heat flow gauges, while the temperature profiles were measured in seven horizontal cuts spaced 8 cm apart. Each of the cut contained 22 sensors.

The material tested was crushed rock with particle size ranging from 20 to 80 mm. Material was loosely packed, resulting in dry density of 1500 kg/m^3 and porosity of 0.44. The sample was subjected in total to nine different temperature gradients for upward heat flow (convection) conditions. The upper boundary conditions was set by the room temperature while the lower boundary was controlled by heat exchange plate (Johansen, 1975). Only four tests were performed with the upper boundary being impermeable. For the other five tests the upper surface was held open, thus the airflow was exposed to room conditions.

Experiments by Norwegian Geotechnical Institute (NGI) (1999)

The experimental test box had horizontal dimensions of 1x1 m and a vertical height of 0.75 m. The top and the bottom heat exchange plates where equipped with fluid circulation tubes for control of cold temperatures and electrical heating for high temperatures. Electrical input was accurately monitored during the tests allowing to calculate the total heat input. Test sample was equipped with eight thermistors placed in pairs at each 0.25 m of sample height. Thermistors were located 5 cm from the centerline. The report provides average values of each two thermistors.

Three different crushed rock materials were used: i) ballast material 25-63 mm; ii) machine crush 20-120 mm; iii) blasted rock 0-250 mm.

Experiments by Goering et al. (2000)

Goering et al. (2000) conducted his study based on the laboratory experiments already performed by NGI (1999). Test material is defined as being with fraction of 20-65 mm. In, addition only one measurement for upward heat flow has been reported in his study. The primary objective for their study was to develop a numerical model and compare it with laboratory experiments.

As reported by Goering et al. (2000), the numerical model showed a complex three dimensional air flow in the box with rising air flow in the center of the box and descending air flow in each of the corners. Therefore, the convective pattern consisted of four separate convective cells together forming a single concentrated plume.

Experiments by Côté et al. (2011)

Côté et al. (2011) based their work largely on what was done before by Johansen (1975) and Goering et al. (2000). The test setup built had few improvements. Firstly, the dimensions of the box was cubical with the inner volume of $1 m^3$. Secondly, similar to test setup by Johansen (1975) it had multiple heat flux sensors. The box was equipped with four heat flux plates (0.4x0.4 m) located at the top of the sample covering 64% of the sample top surface. The size of heat flux plates was 0.4x0.4 m. Temperature gradient was measured with vertical thermistor strings placed in the center of the sample and 0.1 m from each of the face.

Materials used by Côté et al. (2011) were natural granite cobbles with particle size ranging from 75 to 205 mm. Porosity was ranging from 0.37 to 0.41.

Experiments by Rieksts et al. (2017)

A new study on heat transfer in coarse materials is currently conducted at Norwegian University of Science of Technology as a part of a larger research program (Kuznetsova et al., 2017). The study uses a large scale heat transfer box with design based on the work by Côté et al. (2011). Slight modification regarding the heat flux measurements were made by using nine heat flux plates (0.3x0.3 m) covering 90% of the sample top surface

For setup validation, Rieksts et al. (2017) used cobbles as a test material. The general objective was to compare results with the ones obtained by Côté et al. (2011). Material with particle size ranging between 0.09 and 0.21 m was used. The porosity and d_{10} is reported as 0.36 and 0.12 m, respectively. Based on the temperature distribution and heat flux readings it was concluded that convection cell has the upward flow in one corner and downward heat flow in the opposite corner. As a next step, crushed rock material with different gradation should be tested.

Conclusions

This paper gave an overview of existing large-scale laboratory investigations for heat transfer of natural convection. Although all the laboratory experiments focused on the same physical phenomena, comparison between them is complicated. As it was proposed by Côté et al. (2011), back-calculation of intrinsic permeability based on experimental measurements can be applied for different geometrical setups with different degrees of confidence.

Acknowledgments

This research was supported by the Norwegian Research Council (NRC) under grant 246826/O70.

References

Côté, J., Fillion, M. H., & Konrad, J. M. (2011). Intrinsic permeability of materials ranging from sand to rock-fill using natural air convection tests. *Canadian Geotechnical Journal, 48*(5), 679-690. doi:10.1139/t10-097

Goering, D. J., Instanes, A., & Knudsen, S. (2000). Convective heat transfer in railway embankment ballast. *Ground freezing*, 31-36.

Johansen, O. (1975). Thermal conductivity of soils. *Ph.D. Thesis. University of Trondheim, Trondheim, Norway. US Army Corps of Engineering, Cold Regions Research and Engineering Laboratory, Hanover. N.H. CRREL Draft English Translation 637*, 291.

Kuznetsova, E., Hoff, I., & Danielsen, S. W. (2017). FROST – Frost Protection of Roads and Railways. *Mineralproduksjon, 7*(B1-B8).

NGI. (1999). Måling av varmetap i ulike steinfyllingsfraksjoner. Måling av varmetap i ballastpukk, maskinkult og sprengstein. *Norges Geotekniske Institutt (Norwegian Geotechnical Institute)*, 35.

Rieksts, K., Hoff, I., Kuznetsova, E., & Côté, J. (2017). Laboratory investigations on heat transfer of coarse crushed rock materials. *70th Canadian Geotechnical Conference.*

A Method for Calculating Heat Transfer in Water-Saturated Soils Using Temperature Measurements in Boreholes

Mikhail Semin[1]
Denis Kormshchikov[1]
Maxim Zhelnin[2]

[1]*Mining Institute of the Ural branch Russian academy of sciences, mishkasemin@gmail.com*
[2]*Institute of continuous media mechanics of the Ural branch Russian academy of sciences*

Abstract

A method for determining temperature field in artificially frozen water-saturated soils is proposed. The method can be applied for the problem of constructing shafts using artificial ground freezing, which involves drilling and installing a series of relatively closely spaced pipes and circulating a coolant through these pipes. The proposed method uses measured temperatures in control boreholes, located near the series of cooling pipes and near the future shaft. The idea of the method consists in representing the temperature field in the soil as a superposition of analytical functions satisfying the equation of thermal diffusivity in frozen and liquid areas of the soil. Then, the superposition is used for solving the inverse Stefan problem using data from control boreholes. This representation of temperature filed allows reducing the inverse problem to minimization of explicit functional using gradient descend method. The method was applied for monitoring shaft construction in Belarus.

Keywords: Artificial ground freezing; inverse Stefan problem; shaft construction, ice wall, fiber-optic temperature measurements.

Introduction

Construction of shafts in the water-bearing strata requires application of special methods to prevent waterflows in the excavation. The most commonly used and most efficient method is artificial ground freezing. It involves drilling and installing a series of relatively closely spaced pipes around the future shaft and circulating a coolant through these pipes. This method is used when other conventional methods such as dewatering, shoring and grouting are not feasible (Levin *et al.,* 2017).

The freezing continues until the formation of the frozen cylinder of necessary strength sufficient for withstanding the hydrostatic pressure of ground waters. Then the excavation of shaft begins. The formed frozen cylinder is also known as ice wall or also frozen wall.

Thermal Monitoring System

Construction of a shaft requires arrangement of temperature monitoring system. Usually, the monitoring of soil temperatures and ice wall state is conducted using water monitoring boreholes and temperature boreholes, ultrasonic inspection and numerical modeling.

The experience in construction of shafts shows that modern technologies of experimental borehole measurements don't allow precise determination of actual ice wall parameters. In the last years, the imperfection of experimental borehole measurements and calculation techniques manifested itself during the construction of shafts of Gremyachinsk mine of "EuroChem" company and Garlyk mine of "Turkmenhimiya" company.

The method proposed in the paper uses the new thermal monitoring system of soils during its artificial ground freezing while shaft sinking. The system is based on the fiber-optic temperature measurement in control boreholes. The measurement includes fiber-optical recorder for generating the signal and optical fiber cable as a linear sensor. Physically, distributed temperature measurement using optic fiber is based on Brillouin scattering.

The general scheme of the proposed monitoring system is shown in Fig. 1. The refrigeration unit provides the freezing pipes with coolant of fixed temperature and fixed mass flow. Then, the fiber-optic system measures the temperature of soil in depth. The temperature profiles in control boreholes is being preprocessed and transferring to the server and to the database. These profiles are used for mathematical modeling and prediction of temperature distribution in the whole volume of soils.

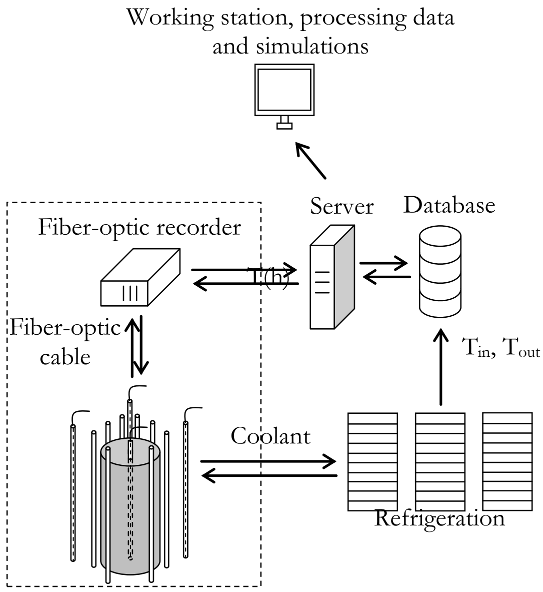

Figure 1. The general scheme of the proposed monitoring system.

Mathematical Model

The temperature profiles in control boreholes give us more detailed information about thermal processes inside the soil. They are used to calibrate the physical parameters of each soil layer No. i: heat conductivity λ_i, heat capacity c_{pi} and water content φ_i. In this sense, we consider the inverse Stefan problem. It consists in finding function $T_i(x,y,z,t)$ and parameters λ_i, c_{pi}, φ_i satisfying the following equations:

$$\frac{\partial H_i(T_i)}{\partial t} = \lambda_i(T_i)\Delta T_i$$

$$\left[\lambda_i(T_i)\mathbf{n}\cdot\nabla T_i - \alpha\left(T_{fb} - T_i\right)\right]\Big|_{\Omega_{fb}} = 0$$

$$T_i\big|_{\Omega_{out}} = T_0(h_i)$$

$$T_i\big|_{\Omega_{cb}} = T_{cb}(h_i, t)$$

$$T_i\big|_{t=0} = T_0(h_i)$$

.

This mathematical formulation is given for soil layer No. i.

Here is enthalpy, is heat conductivity, is heat exchange coefficient of freezing borehole, is temperature of coolant in freezing pipes, is temperature of salt water in control boreholes, is initial temperature of soil, is average depth of layer No. I, is the boundary of freezing pipes, is the boundary of control boreholes, is the outer boundary, is normal vector to the boundary surface

Simulation

The numerical method of determining soil temperature field using measured temperatures in control boreholes was developed. The primary task of the proposed method is to give a fast-quantitative estimation of actual thermal conditions of soils and fast prediction of its future thermal conditions.

We accomplished the necessary simplifications of the model. The following assumptions were considered:

- Isotropic and homogeneous soil within each layer and each phase.
- Vertical heat transfer is neglected.
- Temperature field has an axial symmetry at distance more than 3 pipe diameters from the freezing pipes.

The assumptions allow considering 2D problem and representing the temperature field in the soil as a superposition of analytical functions satisfying the equation of thermal diffusivity in frozen and liquid areas of the soil and the boundary conditions on freezing pipes Ω_{fb} and outer border Ω_{out}. The analytical functions include exponential integral and Fourier-Bessel series.

Then, we formulate and minimize the explicit functional $I = I(\lambda_i, c_{pi}, \varphi_i)$, which represents deviation of measured and model temperatures in control boreholes.

Acknowledgement

This research was supported by 17-11-01204 project (Russian Science Foundation).

References

Levin, L. Yu. Semin, M.A., Parshakov, O.S. & Kolesov, E.V. 2017. Method for solving inverse Stefan problem to control ice wall state during shaft excavation. *Journal of Petroleum and Mining Engineering* 16(3): 255-267.

Upscaling surface energy fluxes over the North Slope of Alaska using airborne eddy-covariance measurements and environmental response functions

Andrei Serafimovich[1]
Stefan Metzger[2, 3]
Jörg Hartmann[4]
Katrin Kohnert[1]
Donatella Zona[5, 6]
Torsten Sachs[1]

[1]*GFZ German Research Centre for Geosciences, Telegrafenberg, D-14473 Potsdam, Germany, andrei.serafimovich@gfz-potsdam.de*
[2]*National Ecological Observatory Network, Fundamental Instrument Unit, 1685 38th Street, Boulder, CO 80301, USA*
[3]*University of Colorado, Institute for Arctic and Alpine Research, 1560 30th Street, Boulder, CO 80303, USA*
[4]*Alfred Wegener Institute Helmholtz Centre for Polar and Marine Research, Am Handelshafen 12, 27570 Bremerhaven, Germany*
[5]*Department of Animal and Plant Sciences, University of Sheffield, Western Bank, Sheffield S10 2TN, UK*
[6]*Department of Biology, San Diego State University, 5500 Campanile Drive San Diego, CA 92182, USA*

Abstract

The goal of this study is to scale aircraft measured fluxes of sensible and latent heat to the North Slope of Alaska and develop high resolution flux maps. For this purpose we analyzed an eddy-covariance data set obtained by the research aircraft POLAR 5 as part of the AIRMETH-2012 campaign, and investigated the spatial patterning of energy fluxes. Environmental response functions between flux observations and corresponding biophysical and meteorological drivers were estimated using a combination of time-frequency decomposition, dispersion modeling and machine learning. The extracted relationships are then used to scale observational data across heterogeneous Arctic landscapes, thus improving the spatial coverage and representativeness of the energy fluxes. Maps of projected energy fluxes are used to asses energy partitioning in northern ecosystems and to determine dominant energy exchange processes of permafrost area.

Keywords: aircraft, eddy-covariance, sensible and latent heat fluxes, upscaling, North Slope of Alaska, permafrost.

Introduction

Arctic ecosystems are undergoing a very rapid change due to global warming and their response to climate change has important implications for the local to regional and global climate. The regional energy budget of Arctic ecosystems can be changed directly or indirectly through reduced albedo from decreased snow cover or increased albedo due to the changes in vegetation. The surface energy budget is a predominant factor in determining the climatic variability and feedback. In our study we aim to upscale aircraft-measured fluxes and develop spatially extensive, high resolution flux maps, which help to gain new insights into surface exchange processes and can be used to validate coupled atmospheric/land-surface models.

Especially, we want to answer the following questions: (i) Which surface properties of permafrost areas are the main drivers for energy fluxes? (ii) How large are land cover specific energy fluxes under certain meteorological conditions and what is the patterning of energy partitioning in northern ecosystems?

Methods

The AIRMETH-2012 (Airborne measurements of methane fluxes) campaign was carried out from 28 June - 2 July 2012 across the North Slope of Alaska. The research aircraft POLAR 5 was equipped with a turbulence probe, fast temperature and humidity sensors to measure turbulent energy fluxes. To derive the energy exchange between the surface and the atmosphere we used a modified version of the time-frequency-resolved eddy-covariance method in an early version of the edd4R eddy-covariance data processing software (Metzger *et al.*, 2017). It allows to calculate spatially resolved turbulence statistics, and sensible and latent heat fluxes for overlapping subintervals of 1,000 m length with 100 m resolution (Metzger *et al.*, 2013). To derive environmental response functions (ERF) between spatially and temporally resolved flux observations and corresponding biophysical and meteorological drivers a boosted regression trees (BRT) technique was employed. Using extracted environmental response functions and supplemental simulations of meteorological state variables from the Weather Research and Forecasting (WRF) model it was then possible to project the surface energy fluxes beyond the immediate measurement footprints across North Slope of Alaska.

Results and Discussion

For each track a separate flux projection was created, from which ensemble maps are calculated using the median operator. Figure 1 shows the spatial variability of sensible and latent heat fluxes across the North Slope of Alaska as reproduced by ERFs, without invoking typical assumptions such as closure of energy or water balances that are typically violated by field observations.

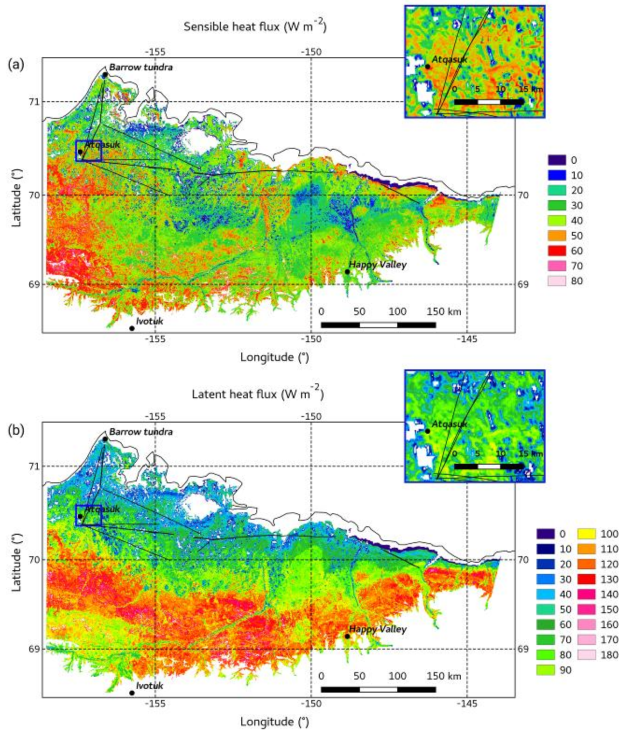

Figure 1. Median sensible (a) and latent (b) heat fluxes. Only fluxes for grid cells with standard error < 30 % are shown. The inserts show the location of the EC tower in Atqasuk. Black lines represent POLAR 5 flight tracks.

For this permafrost area downward shortwave solar radiation, potential temperature, enhanced vegetation index, water vapor mixing ratio, and land surface albedo were found to be the most important drivers for describing the energy exchange. The resulting environmental mean response functions indicate linear responses of surface heat fluxes to changes in downward shortwave solar radiation, enhanced vegetation index, land surface albedo and non-linear responses on changes of potential temperature and mixing ratio (not shown).

Information about energy partitioning and the Bowen ratio are a critical components of micrometeorological, climate, and hydrological models, and are widely used for comparing the surface energy balance of climate zones and vegetation types. Our results confirmed that under the meteorological situation during the measuring period evapotranspiration was dominating the surface energy exchange over almost the entire North Slope. Only close to the coast the evapotranspiration was restricted and sensible heat exchange prevailed. Small Bowen ratios indicated that shrub, dwarf shrub, and scrub are important regulators of water loss to the atmosphere in these ecosystems.

Acknowledgments

This work has received funding from the Helmholtz Association of German Research Centres through a Helmholtz Young Investigators Group grant to T.S. (grant VH-NG-821) and is a contribution to the European Union's Horizon 2020 research and innovation programme under grant agreement No 727890. The aircraft campaign AIRMETH was fully funded by Alfred Wegener Institute. S.M. was supported by the National Science Foundation [grant DBI-0752017]. Any opinions, findings, and conclusions or recommendations expressed in this material are those of the author and do not necessarily reflect the views of the National Science Foundation. The eddy covariance tower in ATQ is funded through the National Science Foundation (NSF) Office of Polar Programs via a grant to Donatella Zona (award number 1204263, and 1702797) and the Carbon in Arctic Reservoirs Vulnerability Experiment (CARVE).

References

Metzger, S., Junkermann, W., Mauder, M., Butterbach-Bahl, K., Trancón y Widemann, B., Neidl, F., Schäfer, K., Wieneke, S., Zheng, X.H., Schmid, H.P., Foken, T., 2013. Spatially explicit regionalization of airborne flux measurements using environmental response functions. *Biogeosciences* 10: 2193-2217.

Metzger, S., Durden, D., Sturtevant, C., Luo, H., Pingintha-Durden, N., Sachs, T., Serafimovich, A., Hartmann, J., Li, J., Xu, K., Desai, A.R., 2017. eddy4R: A community-extensible processing, analysis and modeling framework for eddy-covariance data based on R, Git, Docker and HDF5. *Geosci Model Dev* 10: 3189-3206.

Numerical simulation for adjusting sunny-shady slope effect in fine grained soil highway embankment embedding partially perforated ventilation pipe

Binxiang Sun[1]
Lijun Yang[2]
Changyang Zhang[3]
[1]*Yuanpei College, Shaoxing University, Shaoxing Zhejiang 312000, China, sbinxiang@gmail.com*
[2]*Yuanpei College, Shaoxing University, Shaoxing Zhejiang 312000, China*
[3]*Department of Civil Engineering, Shaoxing University, Shaoxing Zhejiang 312000, China*

Abstract

For the sunny-shady slope effect of the wide express highway in permafrost regions of the Qinghai-Tibet Plateau, it will be necessary to use new combined techniques. Among these, the axial-nonuniformly perforated ventilation pipes are horizontally embedded in the fine grained soil embankment of asphalt highway. This implies that two modes of heat transfer occur in perforated pipe embankment. These includes convective heat transfer between the air and the pipe wall and evaporation heat removal from the surface of the soil bared in the small holes of pipe wall. Adjusting ground asymmetrical temperatures due to the sunny-shady slope effect by means of an enhanced asymmetrical cooling effect in the fine grained soil embankment embedding nonuniformly perforated ventilation pipes is performed by simulations.

Keywords: Qinghai-Tibet Plateau; fine grained soil embankment; sunny-shady slope effect; nonuniformly perforated ventilation pipe; evaporative heat removal; numerical simulation

Introduction

Combining the warm and ice-rich permafrost and the currently proposed scenarios of climate warming on the Qinghai-Tibet Plateau, the construction of the proposed Qinghai-Tibet Express Highway will have to utilize new techniques of cooling the ground temperature (Lai *et al.*, 2004; Jin *et al.*, 2008; Ma *et al.*, 2011; Wu *et al.*, 2011). The combined techniques of lowering proactively the ground temperature with multiple cooling mechanisms may avoid damage to the express highway embankment due to the large change in the permafrost table and the sensitivity of permafrost to engineering action(Xu & Goering, 2008; Chataigner *et al.*, 2009; Lebeau & Konrad, 2009; Niu *et al.*, 2011; Qin & Zhang,2013; Dong *et al.*, 2014; Sun *et al.*, 2014).

For the sunny-shady slope effect of the wide express highway in permafrost regions, it will be necessary to use a new technique in the fine grained soil embankment of asphalt highway horizontally embedding nonuniformly perforated ventilation pipes and laid a thermal insulation layer. Convective heat transfer between the air and the pipe wall and evaporative heat removal from the surface of the soil bared in the small holes of the pipe wall are two modes of heat transfer in perforated ventilation pipe embankments. This evaporative heat removal effect by the small holes of the pipe wall in the fine grained soil embankment during summer-time is significant due to big unfrozen water content in unfrozen soils, thus being able to partially or completely balance out the sunny-shady slope effect and to ensure the thermal stability of the wide express highway embankment. In this work, adjusting the ground asymmetrical temperatures due to impacting of the sunny-shady slope effect by means of an enhanced asymmetrical cooling effect in the fine grained soil embankment embedding partially perforated ventilation pipes is performed by a numerical simulation method of nonlinear finite element.

Calculating Domains and Formulations

For the construction of the proposed Qinghai-Tibet express highway in warm and rich-ice permafrost regions, the analysis domain is assumed to consist of the express highway embankment and layered foundation soils shown in Fig. 1. Based on the Design Specifications of Highway Alignment in China, the express highway embankment structure, which is a four-lane two-way divided highway, consists of a pavement layer, a thermal insulating layer and a fine grained soil layer. So, the express highway has a wide pavement surface consisting of asphalt concrete and cement-stabilized sand-gravel layers. The partially perforated concrete ventilation pipes are horizontally embedding in the fine grained soil along the transversal direction of embankment and located above the native ground surface. These ventilation pipes are distributed at equal spacing along the longitudinal direction of highway embankment. In addition, a thermal insulation layer is placed immediately beneath the pavement layer and immediately above the fine grained soil. The underlying foundation soils consist of the active layer and the ice-rich permafrost layer.

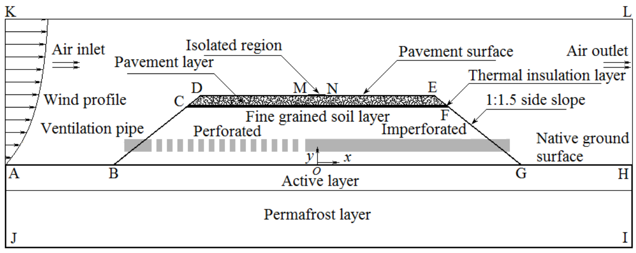

Figure 1. Computational model for the cross section of embankment embedding partially perforated ventilation pipes

Heat transfer in the solid phase zones of wide highway embankment including pavement layer, fine grained soil layer, concrete ventilation pipe, thermal insulation layer, active layer and permafrost layer is mainly dominated by heat conduction. The air motion inside the ventilation pipes and in atmospheric surface layer of the Qinghai-Tibet Plateau could fully develops into a turbulent flow. Boundary conditions and initial conditions on each edge could be obtained on the basis of measured data.

Numerical Simulation Results

Numerical simulations show that the evaporative heat removal effect by the small holes of the perforated pipe wall in the fine grained soil embankment may partially or completely adjust the ground asymmetrical temperatures due to the sunny-shady slope effect in the wide express highway embankment, as shown in Fig. 2.

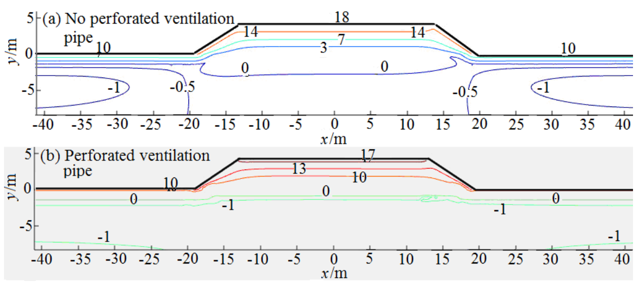

Figure 2. Temperatures for embankment without and with perforated ventilation pipes on date of Jul 15 in the 10th year

Acknowledgments

This research was supported by the National Natural Science Foundation of China (Grant Nos. 41572305 and No. 41272345). The support of the agency is gratefully acknowledged.

References

Chataigner, Y., Gosselin, L., Doré, G., 2009. Optimization of embedded inclined open-ended channel in natural convection used as heat drain. *International Journal of Thermal Sciences* 48 (6): 1151-1160.

Dong, Y.H., Pei, W.S., Liu, G., Jin, L., Chen, D.G., 2014. In-situ experimental and numerical investigation on the cooling effect of a multi-lane embankment with combined crushed-rock interlayer and ventilated ducts in permafrost regions. *Cold Regions Science and Technology* 104-105: 97-105.

Jin, H.J., Wei, Z., Wang, S.L., Yu, Q.H., Lu, L.Z., Wu, Q.B., Ji, Y.J., 2008. Assessment of frozen-ground conditions for engineering geology along the Qinghai-Tibet highway and railway, China. *Engineering Geology* 101 (3-4): 96-109.

Lai, Y.M., Zhang, S.J., Zhang, L.X., Xiao, J.Z., 2004. Adjusting temperature distribution under the south and north slopes of embankment in permafrost regions by the ripped-rock revetment. *Cold Regions Science and Technology* 39 (1): 67-79.

Lebeau, M., Konrad, J.M., 2009. Natural convection of compressible and incompressible gases in undeformable porous media under cold climate conditions. *Computers and Geotechnics* 36 (3): 435-445.

Ma, W., Mu, Y.H., Wu, Q.B., Sun, Z.Z., Liu, Y.Z., 2011. Characteristics and mechanisms of embankment deformation along the Qinghai-Tibet Railway in permafrost regions. *Cold Regions Science Technology* 67 (3): 178-186.

Niu, F.J., Lin, Z.J., Lu, J.B., Liu, H., Xu, Z.Y., 2011. Characteristics of roadbed settlement in embankment–bridge transition section along the Qinghai-Tibet Railway in permafrost regions. *Cold Regions Science and Technology* 65 (3): 437-445.

Qin, Y.H., Zhang, J.M., 2013. A review on the cooling effect of duct-ventilated embankments in China. *Cold Regions Science and Technology* 95 (11): 1-10.

Sun, B.X., Yang, L.J., Liu, Q., Wang, W., Xu, X.Z., 2011. Experimental study on cooling enhancement of crushed rock layer with perforated ventilation pipe under air-tight top surface. *Cold Regions Science and Technology* 68 (3): 150-161.

Wu, Q.B., Liu, Y.Z., Hu, Z.Y., 2011. The thermal effect of differential solar exposure on embankments along the Qinghai-Tibet Railway. *Cold Regions Science and Technology* 66 (1), 30-38.

Xu, J.F., Goering, D.J., 2008. Experimental validation of passive permafrost cooling systems. *Cold Regions Science and Technology* 53 (3): 283-297.

Permafrost conditions and groundwater flow in boreal headwater catchments, interior Alaska (USA)

Michelle Walvoord[1]
Clifford Voss[2]
Brian Ebel[2]
Burke Minsley[2]
[1]*U.S. Geological Survey, walvoord@usgs.gov*
[2]*U.S. Geological Survey*

Abstract

Permafrost distribution exerts a major control on subsurface flowpaths and fluxes of water and dissolved constituents. Our study examines linkages between permafrost conditions and groundwater flow in boreal headwater catchments, where subsurface flow is generally limited to the supra-permafrost layer. We use an integrated approach to assimilate findings from six headwater catchment sites located along a north to south gradient in the boreal region of interior Alaska (USA) with coupled heat transfer and fluid-flow modeling using the USGS SUTRA-Ice code. The study sites represent a range of shallow subsurface geology, fire history, permafrost depth and extent, and air-temperature conditions. Field characterization of soil hydraulic and thermal properties constrain sensitivity analyses designed to assess hillslope conditions conducive to active-layer thickening and talik development and to quantify rates of change. Geophysical data, including borehole nuclear magnetic resonance (NMR) and electrical resistivity tomography (ERT), provides information relevant to permafrost conditions at the study sites and identifies areas of degrading permafrost and talik development. Model simulations reproduce temporal patterns of liquid water content as shown in the NMR data and spatial patterns of permafrost as inferred from the ERT data. Groundwater flux results highlight the impact of thaw-induced changes on baseflow and terrestrial-aquatic transport of dissolved species.

Keywords: groundwater; boreal; geophysics; modeling; hillslope

Liquid-Vapor-Air Flow in the Frozen Soil

Lianyu Yu[1]
Yijian Zeng[1]
Zhongbo Su[1]

[1] *Faculty of Geo-information and Earth Observation (ITC), University of Twente, Enschede, The Netherlands, l.yu@utwente.nl*

Abstract

Accurate representing freeze-thaw (FT) process is of great importance in cold region hydrology and climate studies. With the STEMMUS-FT model (Simultaneous Transfer of Energy, Mass and Momentum in Unsaturated Soil), we investigated the coupled water and heat transfer in the variably-saturated frozen soil and the mechanisms of water phase change along with both evaporation and freeze-thaw process, at a typical meadow ecosystem over Tibetan Plateau. The STEMMUS-FT showed its capability of depicting the simultaneous movement of soil moisture and heat flow in frozen soil. The comparison of different parameterizations of soil thermal conductivity indicated that the de Vries's parameterization performed better than others in reproducing the hydrothermal dynamics of frozen soils. The analysis of water/vapor fluxes indicated that both the liquid water and vapor fluxes move upward to the freezing front and highlighted the crucial role of water vapor fluxes during soil freeze-thaw cycles. Although the soil air pressure induced liquid/vapor fluxes play a negligible role in the total mass transfer, the interactive effect of soil ice and air can be found on the spatial and temporal variations of water/vapor transfer.

Keywords: Freeze/Thaw process, frozen soil parameterizations, numerical assessment, vapor flow

Introduction

Most of freeze/thaw(FT) models differed not only in the physics representing the FT process, but also in many other ways:e.g. numerical discretization, diagnostic variables, application in different regions. These factors render the intercomparison results difficult to be interpreted and hard to identify the underlying difference among the various FT parameterizations.

Moreover, soil water and heat are strongly coupled during FT, neglecting this coupling process in most of the current models limited their capability of accurate description of soil FT physics.

In addition, how and to what extent the vapor and air flow affects the soil water and heat dynamics in frozen soils lack of a detail research.

In this paper, we aimed to i) conduct an inter-comparison of different FT parameterizations based on a fully coupled water and heat model; ii) investigate the mechanism of water and vapor transfer of FT process.

Design of numerical model experiment

CTRL1-2 were to assess the effect of different hydraulic parameterizations on the simulations; EXP1-3 were to find the optimal thermal parameterization to capture the dynamics of soil FT process.

Table 1. Numerical experimental design to assess the different FT parameterizations.

Experiment		Unfrozen Water Content		Hydraulic Conductivity		Heat Conductivity			
		Clapey + VG	Clapey + CH	VG	CH	D63	F81	T16	J75
CTRL1		√		√		√			
CTRL2			√		√	√			
CTRL1	EXP1	√		√			√		
	EXP2	√		√				√	
	EXP3	√		√					√
CTRL2	EXP1		√		√		√		
	EXP2		√		√			√	
	EXP3		√		√				√

Clapey, Clapeyron equation; VG, Van Genuchten (1980); CH, Clapp and Hornberger (1978); Heat conductivity methods: D63, De Vries *et al.* (1963); F81, Farouki *et al.* (1981); T16, Simplified De Vries (Tian *et al.*, 2016); J75, Johansen *et al.* (1975).

Results

Assessment of soil thermal conductivity parameterizations

Given the soil component, de Vries' parameterization (D63) is recommended to mimic the thermal conductivity of frozen soils. The simplified de Vries's method (T16) has the potential to be employed over Tibetan plateau when soil texture information is available.

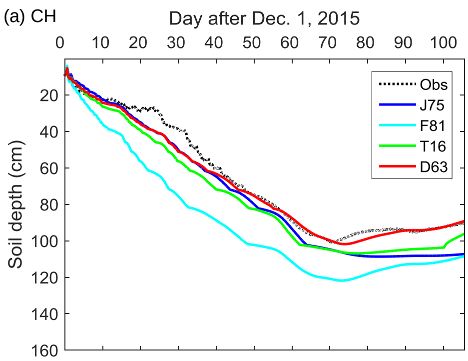

Figure 1. Comparison of observed and simulated soil freezing front using different parameterizations of thermal conductivity (see Table 1) with (a) Clapp and Hornberger and (b) Van Genuchten hydraulic schemes.

Mechanism of water and vapor transfer in frozen soils

The main findings, indicated by Figure 2, are:

1)Isothermal liquid water fluxes(Q_{LH}) move upwards to the freezing front.

2)Thermal liquid fluxes(Q_{LT}) very small, can be ignored.

3)During night time, Thermal vapor fluxes(Q_{VT}) evaporates from the freezing front and move water fluxes upwards.

4)Isothermal vapor fluxes(Q_{VH}) dominant at top 1cm soil layers, upwards.

5)Liquid/Vapor advective fluxes(Q_{LA}, and Q_{VA}) was negligible.

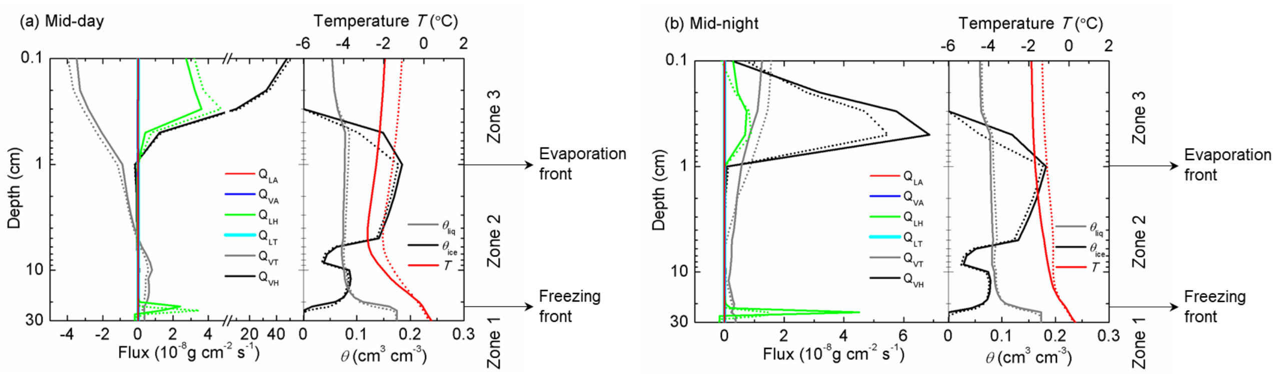

Figure 2. The simulated vertical profiles of the thermal and isothermal liquid water and vapor fluxes, soil ice content at 1200 and 0000 h of a typical freezing period during 11 and 12 Days after Dec. 1. 2015. Positive/negative values indicate upward/downward fluxes.

Acknowledgments

This work is financially supported (in part) by the NWO project "Modelling Freeze-Thaw Processes with Active and Passive Microwave Observations" (Project Number: ALW-GO/14-29).

References

Clapp, R. B., & Hornberger, G. M., 1978. Empirical equations for some soil hydraulic properties. *Water Resources Research* 14(4): 601-604.

de Vries, D. A., 1963. *Thermal properties of soils*. North-Holland Publishing Company, Amsterdam, 210-235pp.

Farouki, O. T., 1981. The thermal properties of soils in cold regions. *Cold Regions Science and Technology* 5(1): 67-75.

Johansen, O., 1975. *Thermal conductivity of soils*. University of Trondheim, , 236 pp.

Zeng, Y., Z. Su, L. Wan & J. Wen, 2011. Numerical analysis of air-water-heat flow in unsaturated soil: Is it necessary to consider airflow in land surface models? *Journal of Geophyical Research* 116: D20107.

Zeng, Y., Z. Su, L. Wan & J. Wen, 2011. A simulation analysis of the advective effect on evaporation using a two-phase heat and mass flow model. *Water Resources Research* 47: W10529.

Release of groundwater and associated carbon flux resulting from deep permafrost degradation

Elise van Winden[1]
Martine van der Ploeg[1]
Victor Bense[1]

Department of Environmental Sciences, Wageningen University, The Netherlands, [1]Elise.vanWinden@wur.nl

Abstract

Deep permafrost holds both (frozen) water and organic matter, which comes available for transport and degradation when it warms and thaws. Currently continuous permafrost areas undergo warming with deepening of the active layer and increase in the number and size of taliks in the transition towards a more discontinuous permafrost system. Both processes will propagate deep groundwater flow. As a consequence, it is expected that more organic matter will be available for transport via groundwater flow towards surface water where it can degrade and enhance CO_2 and CH_4 fluxes towards the atmosphere. Cryohydrogeological processes are central in this process whilst it is not well known how water and solutes are transported through thawing permafrost. Numerical models are hardly constrained by field- and/or laboratory measured parameters that control coupled energy- water-, and solute transport in thawing permafrost. This study aims to improve our understanding of such parameters and will carry out a series of laboratory-based experiments specifically designed to evaluate the rates of release of water and organic matter in thawing permafrost. To this end, sediment samples with known grain size, organic matter and pore ice content, will be thawed under controlled conditions. The breakthrough of meltwater and dissolved solutes will be monitored which will be related to spatial variation in pressure, moisture content and temperature inside the sample. We expect to present preliminary results from these novel laboratory experiments.

Keywords: Cryohydrogeology, Laboratory measurements, Carbon transport.

Introduction

Permafrost areas hold vast amounts of organic matter and frozen water. Future predictions suggest that warming will make these permanently frozen soils in currently cold–regions vulnerable to thaw. An increase in active layer depth leads to an increase in organic matter (OM) availability for transport to streams and rivers and degradation resulting in a release of greenhouse gasses CO_2 and CH_4. Therefore, OM degradation can lead to a positive feedback in an already warming climate. In this project we address the question as to how OM will be released and transported by the reactivation of groundwater flow and the consequent deepening of groundwater flow paths that are to be expected in areas of permafrost degradation (Bense *et al.,* 2009).

The deepened active layer may release melted pore ice, increasing the flux to streams and rivers. In addition, permafrost thaw enhances the regional nature of groundwater flow as well as groundwater storage. Consequently, timing of peak flow and magnitudes of base flow in (nearby) streams and rivers will shift is being observed in several Arctic areas (e.g., Walvoord & Striegl, 2007). This transition from polar to more temperate conditions will probably have profound socio-economic consequences when these areas are part of the source areas of important river systems such as the Yellow River (Cheng *et al.,* 2012), or Lena river.

However, the evolution of groundwater flow paths deep into permafrost areas in a warming climate are poorly understood. Even less so, we understand fluxes of dissolved organic carbon (DOC), a part of OM, associated with these flows. Field measurements for DOC changes in streams (Giesler *et al.,* 2014) and laboratory data of water and heat transfer (Watanabe *et al.,* 2012) are only sparsely available, which creates a parametrization problem for the forecasting and modeling of the subsurface release of organic matter by groundwater flow in thawing permafrost. In this research we aim to combine field-, lab- and modelling. Here we will report lab measurements mimicking field processes in order to obtain parameters that will be used to condition future model exercises.

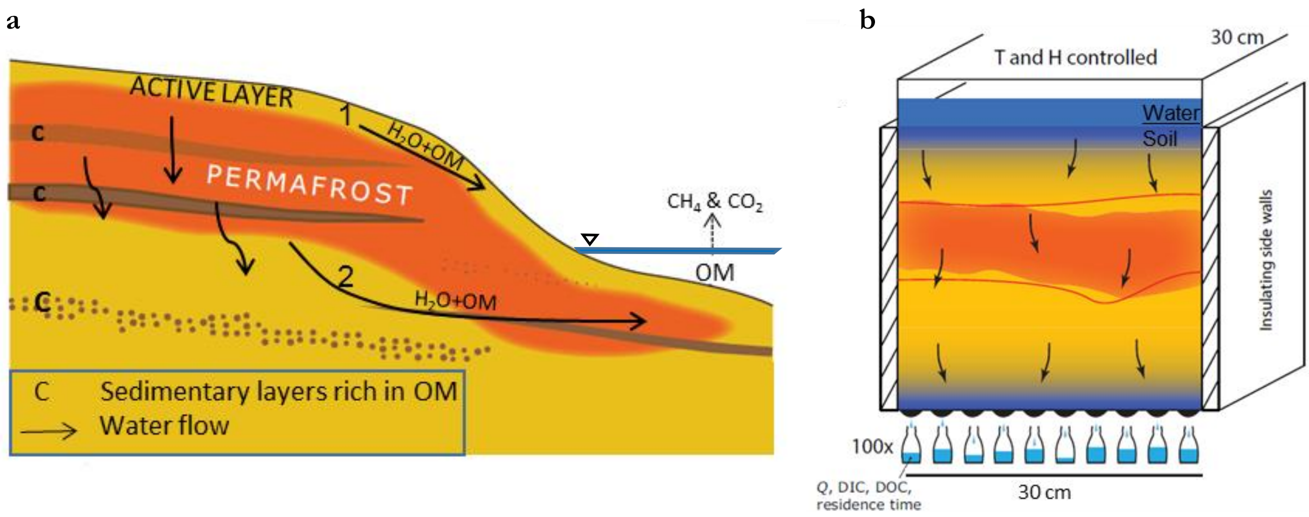

Figure 1. Water flow in an area with permafrost within the field (a) and lab set-up (b). a) Water is flowing above the (nearly) impermeable permafrost (1) and after warming trough the thawing permafrost and carbon bearing sedimentary sequence (2) transporting DOC to nearby streams. b) Lab set-up with a MCS measuring water and doc leachate by controlled thawing.

Laboratory Experiments

With the use of a multi compartment sampler (MCS) (cf. Bloem *et al.,* 2012) permafrost thawing is simulated and water and DOC leaching measured (figure 1b). Soil samples either made in the lab or taken from the field are (re)frozen. Probes for pressure, temperature and moisture content (Time-Domain Reflectometer), are installed beforehand in the permafrost sample. To simulate field conditions, a hydraulic head is created by maintaining water of a certain height and temperature on top of the soil sample, representing hydrogeological forcing. At the bottom, every 3 cm^3 square is equipped with a bottle and pressure probe to measure leaching from the 'active layer' and the thawing 'permafrost'. Then, during thawing from the top of the soil the timing of the breakthrough, discharge and its spatial variability together with the dissolved organic carbon (DOC) content is measured. Relations between the breakthrough, the DOC and the data from the spatial variation in temperature, pressure and soil moisture content are investigated.

This laboratory technique will allow to run a series of experiments using a range of sediment types in which the grain size, organic matter content and moisture content is controlled during the preparation of the soil sample. When the effect of these soil variables is known, the second step will be using field samples from different world-wide permafrost locations (e.g. North Sweden, Tibetan Plateau) for validation. The project has recently started and the preliminary results will be presented.

The outcomes are expected to create insight in parameters which can be used for permafrost hydrogeology modelling of remote field sites to get a better understanding of future climate feedback due to changes in carbon release and degradation.

References

Bense, V. F., Ferguson G. & Kooi, H., 2009. Evolution of shallow groundwater flow systems in areas of degrading permafrost. *Geophysical Research letters* 36, L22401.

Bloem, E., de Gee, M. & de Rooij, G. H., 2012. Parameterizing the leaching surface by combining curve-fitting for solute transport and for spatial solute distribution. *Transport in Porous Media* 92: 667-685.

Cheng, G. & Jin, H., 2012. Permafrost and groundwater on the Qinghai-Tibet Plateau and in northeast China. *Hydrogeology Journal* 21: 5-23.

Giesler, R., Lyon, S. W., Morth, C.-M., Karlsson, J., Karlsson, E. M., Jantze, E. J., Destouni, G. & Humborg, C., 2014. Catchment-scale dissolved carbon concentrations and export estimates across six subarctic streams in northerns Sweden. *Biogeosciences* 11: 525-537.

Walvoord, M. A., & Striegl, R. G., 2007. Increased groundwater to stream discharge from permafrost thawing in the Yukon River basin: Potential impacts on lateral export of carbon and nitrogen. *Geophysical Research Letters* 34, L12402.

Watanabe, K., Kito, T., Dun, S., Wu, J. Q., Greer, R. C. & Flury, M., 2012. Water infiltration into a frozen soil with simultaneous melting of the frozen layer. *Vadose Zone Journal* 12, 10.2136/vzj2011.0188.

The role of increasing precipitation on permafrost on the Qinghai-Tibetan plateau

Zhi Wen[1]
Mingli Zhang[2]
[1] *State Key Laboratory of Frozen Soil Engineering, Cold and Arid Regions Environmental and Engineering Research Institute, Chinese Academy of Sciences, Lanzhou Gansu 730000, China, wenzhi@lzb.ac.cn*
[2]*Lanzhou University of Technology, Lanzhou Gansu 730050, China,*

Abstract

Precipitation on the Qinghai-Tibetan plateau has increased in the past decades. To better understand the influence of increasing precipitation on permafrost on the Tibetan Plateau, thermal-moisture dynamics of the active layer was measured and permafrost variation induced by increasing rainfall was evaluated by a coupled model for liquid water, water vapor and heat transport of saturated-unsaturated soil in cold regions. The results demonstrated that increasing precipitation in summer led to the change of surface energy balance and caused subsurface soil cooling. The convective heat transfer from water infiltration reduced the temperature gradient with depth and changed near-surface heat fluxes. Our results suggest that the increase in precipitation mitigated permafrost degradation on the Tibetan Plateau.

Keywords: precipitation; water transport; permafrost; Qinghai-Tibetan Plateau; active layer

Introduction

Precipitation is one of the most important factors that controls the thermal and moisture dynamics of active layer (Wen et al., 2014). Precipitation on the Tibetan Plateau occurs mainly during May to September and the distribution of annual precipitation generally peaks in July or August. Sparse vegetation in the central Tibetan plateau make rainfall easy to infiltrate into the subsoil, affecting the thermal and moisture dynamics of active layer greatly. However, the influence of precipitation has received relatively little attention, and further study is needed. On the basis of observed temperatures and moistures of the active layer on the Qinghai-Tibetan Plateau, the thermal and moisture dynamics characteristics of the active layer were examined in this study. The impact of increasing precipitation on permafrost was investigated.

Results and analysis

Thermal-moisture dynamics of the active layer

Figure 1 shows the thermal-moisture responses of active layer to rainfall events. The observation data showed that the moisture content increased following rainfall. The soil moisture content disturbances were apparent at the 5, 15 and 25cm levels, and were clearly associated with corresponding rainfall event. The variation of the soil moisture content at the depth of 5cm reached about 15% due to the impact of rainfall event. However, the soil moisture content at the depth of 75cm remained fairly constant (Fig 1(a)).

Fig. 1(b) shows that the influence of precipitation in summer on soil temperature. Precipitation infiltration in summer led to a series of thermal feedbacks in the active layer, causing rapid cooling of the subsurface soil at the depth of 2cm, evidenced by rapid temperature drop at that depth following rainfall evens. The response of soil temperature at the depth of 50cm on rainfall also was gentle and delayed.

The heat flux depends on thermal conductivity and soil temperature gradient. The amplitude and mean value of soil temperature reduce quickly and thermal conductivity rise following rainfall events. Figure 1(c) shows the influence of rainfall on soil heat flux data. The soil heat flux had a negative correlation with rainfall. The soil heat flux at the depth of 20cm fell following rainfall events, and the daily variation amplitude of heat flux decreased. During low or no precipitation days, the soil heat flux increased and the daily variation amplitude and mean value of heat flux also increased. Light and individual rainfall event had little influence on the soil heat flux, which decreased resulting from rainfall and began to increase during sunny days.

The observation data show that the increase in soil moisture content from rainfall and decrease in soil heat flux occur concurrently. Moisture movement after rainfall not only generates convective heat transfer, which can impact the thermal regime, but also affects near-surface heat fluxes. The heat flux responds rapidly to the increase of moisture content from downward movement of rainfall. The effect on heat flux depends on the magnitude of soil moisture content variation.

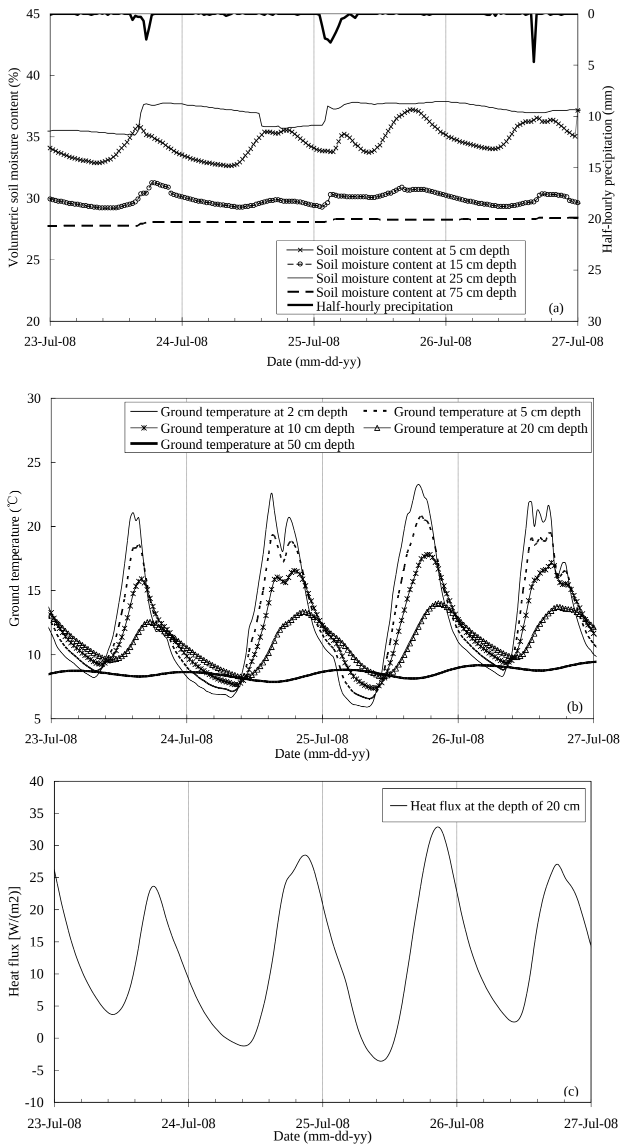

Figure 1. Active layer changes responding to individual rainfall event (a) Volumetric soil moisture content (b) Ground temperature (c) Heat flux

Response of ground surface energy balance

The influence of increasing precipitation on energy balance components is simulated by a coupled model (Zhang et al., 2016) and is shown in Figure 2. Due to the effects of precipitation and corresponding cloudy weather, the net radiation decreased with the increase in precipitation amount. The sensible heat flux also decreased significantly due to the influence of increasing precipitation events. Due to increasing precipitation, the latent heat was the dominant part in the surface energy balance. After rainfall, the land surface was relatively wet and the latent heat flux was much larger than that of sensible heat flux. As a result, the increasing precipitation affected the ground heat flux greatly. There was clear decrease of the soil heat flux with the increasing precipitation. In the rainfall period, the sensible heat flux, net radiation and ground heat flux decreased and the latent heat flux increased at the same time.

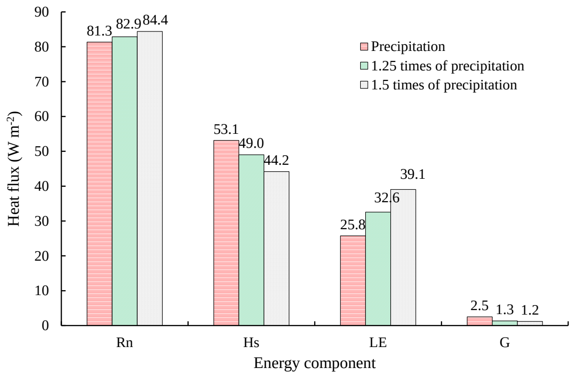

Figure 2. The influence of energy balance components

Conclusions

Based on the above analysis, some conclusions can be drawn as follows:

Precipitation affected on thermal-moisture dynamics of the active layer. Increasing precipitation in summer caused subsurface soil cooling. Soil heat flux had a negative correlation with rainfall and the increase of soil moisture content from rainfall decreased the soil heat flux. Precipitation decreased net radiation and sensible heat flux and increased the latent heat significantly. The increasing precipitation may mitigate permafrost degradation on the Tibetan Plateau.

Acknowledgements

This research project was supported by the Natural Science Foundation of China (41471061 and 41690144), the Research Project of the State Key Laboratory of Frozen Soils Engineering (SKLFSE-ZT-22), the Fund of the Cold and Arid Regions Environmental and Engineering Research Institute (HHS-TSS-STS-1502), and the Major Program of Bureau of International Cooperation, the Chinese Academy of Sciences (131B62KYSB20170012).

References

Wen, Z., Niu, F.J., Yu, Q.H., Wang, D.Y., Feng, W.J., Zheng, J.F. 2014. The role of rainfall in the thermal-moisture dynamics of the active layer at Beiluhe of Qinghai-Tibetan plateau *Environmental Earth Science* 71(3): 1195-1204.

Zhang, M.L., Wen, Z., Xue, K., Chen, L.Z., Li, D.S. 2016. A coupled model for liquid water, water vapor and heat transport of saturated-unsaturated soil in cold regions: model formulation and verification *Environmental Earth Science* 75: 701.

Thermal processes of thermokarst lakes in the eastern of Tibetan Plateau and its thermal impact on the underlying permafrost

HU Xiaoying[1,2]
SHENG Yu[1]
WU Jichun [1]
CAO Wei [1]
CHOU Yaling[3]
HE Binbin[1,2]
ZHANG Xiyan[1,2]

[1]*Northwest Institute of Eco-Environment and Resources, State Key Laboratory of Frozen Soil Engineering, Chinese Academy of Sciences Lanzhou 730000, P.R.China, xiaoyinghu@lzb.ac.cn*

[2]*University of Chinese Academy of Sciences, Beijing 100049, P.R.China*

[3]*Lanzhou university of Technology, Lanzhou 73000, P.R.China*

Abstract

A thermokarst lake in the eastern of Tibetan Plateau was regarded as a research object. Based on the measured data, the temperature variations and characteristics of thermokarst lake were analyzed. The results indicated that, compared with the natural ground, the thermokarst lake had a longer thawed time, a shorter frozen time, and a special time with water temperature being about 4℃. The annual average temperature at the bottom of lake was higher about 5.95℃ than that at the same depth of natural ground. Besides, there was a talik being about 14m depth under the lake developing with time, and the heat absorbed and released of soil under the lake were increased and decreased, respectively. The lake was the heat resource to the permafrost.

Keywords: Thermokarst lake; Thermal processes; Gradient of ground temperature; Heat exchange.

Introduction

Thermokarst lakes are widely distributed throughout the permafrost regions as a result of thawing disaster to change the topography, hydrological condition of underground and surface in permafrost regions and lead to the change of ecological environment, finally to affect the construction and operation of engineering in permafrost regions(Qiu *etal*,1994; Niu *etal*, 2011; Kokelj *etal*., 2013). This paper tried to make research the temperature characters of water and the soil underlying. Then made analysis the variations of water temperature under the thermokrast lake and soil temperature under natural ground.

Materials and methods

Experiment sites

The experiment sites(97.83°E, 34.24°N, 4725m) were located on two sides of the Gonghe-Yushu Highway in the eastern Qinghai-Tibet Plateau(Fig.1).

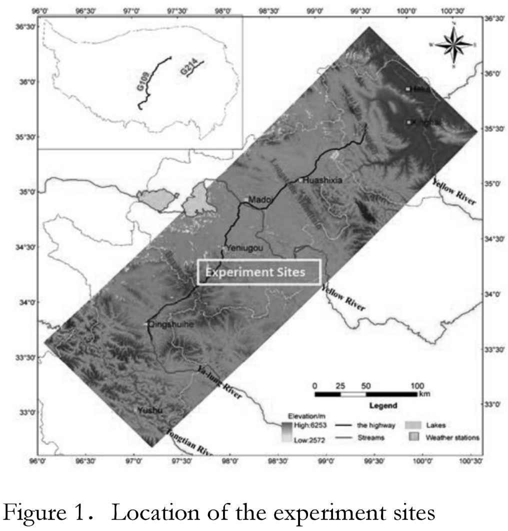

Figure 1. Location of the experiment sites

Results and analysis

Variations of temperature within 1m under two ground surface conditions

(1) Frozen stage. Its time of being frozen was about 136 days being later almost one month than the time that air temperature being under 0℃and about 20 days than that in the NG. The maximum and minimum water temperature were -0.14℃and -11.86℃,.

(2) The transition from frozen to thawed. The ice at the depth of 0.2m was changed to water for about 29 days being later and longer than that in the TL.

(3) Thawed stage. The water temperature began to be increased from 0℃and time of this stage was about 175 days. And the water temperature was about 4℃ for 37 days at the end of this stage.

(4) The transition stage from thawed to frozen. The water temperature was decreased from 4℃ to 0℃ in the 25 days after Oct 30, 2014. On the contrary, the NG was last for 24 days after the Oct 11, 2014 and the soil temperature changed about between 0.2℃ and 0℃.

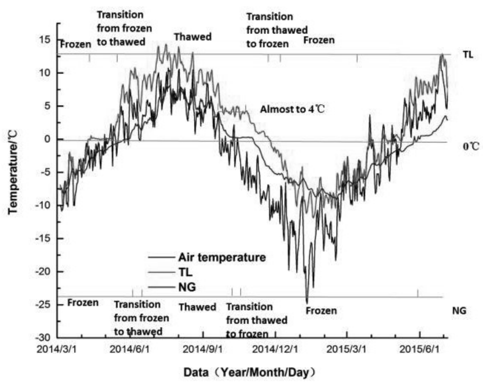

Figure 2． Temperature variations in the TL and NG

Variations of soil temperature below 1m under the two kinds of surface conditions

Below 1m, the soil temperatures in the TL were all larger than that in the NG.The average annual temperature at 10m depth of TL were 0.55℃ which was higher about 2.34 ℃ than that of TL. The maximum thawing depth of permafrost was about 14m was deeper 11.5m than that under the NG.

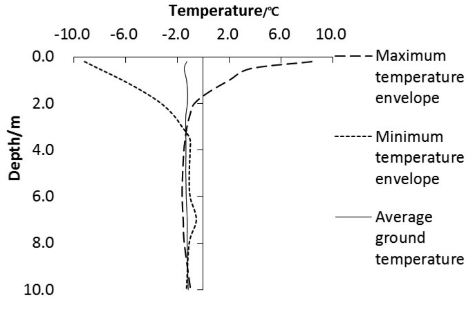

a TL

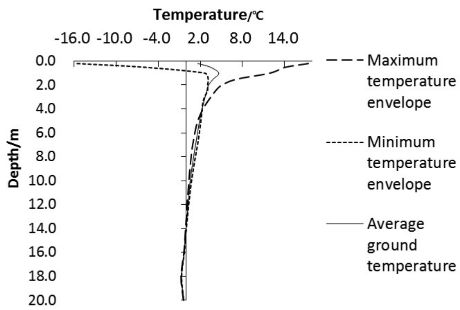

b NG

Figure3． Temperature variations below 1m

The valuation of permafrost heat flux under the TL and NG

Fig. 4 shows the maximum heat flux of permafrost under the TL was 1.54 W/m², which was greater than that under the NG where the maximum value was 0.54 (W/m²). The minimum heat flux of permafrost under the TL was -0.78W/m² which was higher than that under the NG by -2.53W/m².

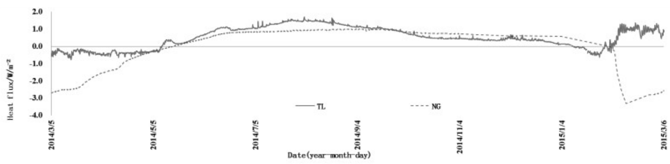

Figure 4. Heat flux of permafrost in the depth from 2.5m to 3 m under the TL and NG

Acknowledgments

The Key Deployment Project of Chinese Academy of Sciences (KZZD-EW-13), the Major Research Plan (91647103), and the National Natural Science Foundation of Innovation Group (41121061) supported this study.

References

Qiu G Q, Liu J R, Liu H X. 1994. *Geocryological Glossary.* Gansu Science and Technology Press, Lanzhou in China.

Niu F, Lin Z, Liu H, et al. 2011. Characteristics of thermokarst lakes and their influence on permafrost in Qinghai–Tibet Plateau. *Geomorphology: 222-233.*

Kokelj S V., Jorgenson M T. 2013. *Advances in thermalkarst research. Permafrost and Periglacial Processes*, 24:108-119.

Xu X Z, Wang J C, Zhang L X. 2001.*Physics of frozen soil.* Science Publish House, Beijing, China. ISBN: 7-03.

9 - Twenty years after the PACE-project: What do we know about the changing state of European permafrost?

Session 9

Twenty years after the PACE-project: What do we know about the changing state of European permafrost?

Conveners:

- **Ketil Isaksen**, Research and Development Department, The Norwegian Meteorological Institute, Oslo, Norway (PYRN member)
- **Christian Hauck**, Department of Geosciences, University of Fribourg, Fribourg, Switzerland
- **Sarah Marie Strand**, UNIS Arctic Geology Department, The University Centre in Svalbard (UNIS), Longyearbyen, Svalbard (PYRN member)

PACE (Permafrost and Climate in Europe), the European Fourth Framework project that commenced in 1997, was a major stimulus for permafrost research and monitoring in Europe. This session marks 20 years since the start of the PACE-project and therefore focuses on the state of knowledge and progress made during these two last decades of European permafrost research related to geothermal and geophysical monitoring and modelling. We invite reports on individual studies or larger initiatives investigating the present state and long-term evolution of permafrost in Europe. We especially encourage contributions focusing on the thermal response and sensitivity of permafrost to climate change and extreme weather events, as well as joint modelling and monitoring approaches. We hereby hope that the session may enhance collaboration between the monitoring and modelling communities.

Permafrost warming in different landforms and active layer thickening in central and western Svalbard

Hanne H. Christiansen[1]
Sarah M. Strand[1,2]

[1]*Geology Department, The University Centre in Svalbard, hanne.christiansen@unis.no*
[2]*Department of Geosciences, University of Oslo, Norway*

Abstract

The permafrost in Svalbard has warmed during the last nine years, as the air temperature has increased. In general, warming has been largest in bedrock sites at sea level and in a blockfield in the mountains, typically around 0.1°C/year at 10 m depth. However, a warming rate of 0.2°C/yr was recorded over the last 5 years in an ice-wedge sedimentary site in the Adventdalen valley lowland. The active layer increased on average by 0.6 cm/yr in the period from 2000 to 2017 in the UNISCALM monitoring site, and seems more controlled by winter air temperatures than summer air temperatures. The maritime climate often causes the ground to be colder than the air, which is opposite to the normal thermal offset found between the ground and the air.

Keywords: Svalbard; permafrost warming ; active layer thickness variability; landform variability.

Introduction

The permafrost thermal state and the thickness of the active layer are the most direct, important indicators and Essential Climate Variables (ECV) of permafrost change. In Svalbard, since the International Polar Year (IPY) in 2008, continuous ground thermal observations have been made in boreholes that extend through the depth of annual ground temperature variations. These boreholes are distributed in all the major periglacial landforms in central and western Svalbard (Christiansen *et al.*, 2010). Since 2000, thaw progression data have been collected through the summer periods in the UNISCALM grid in central Svalbard (Schuh et al., 2017).

All the data is stored in the Norwegian Permafrost Database (NORPERM) (Juliussen *et al.*, 2010), and selected datasets are also included in the Global Terrestrial Network on Permafrost (GTN-P) Database (Biskaborn *et al.*, 2015). This collection of ground thermal data allow us to study how individual periglacial landforms respond to the interannual meteorological variations that characterize the maritime climate in Svalbard, over almost a full decade – exactly in 9 years in summer 2017. Similarly, the active layer thaw progression data and annual active layer thaw depths can be studied in detail in combination with the meteorological record.

Svalbard permafrost observations

During the IPY, it became obvious that Svalbard had the warmest permafrost this far north (Romanovsky *et al.*, 2010).

Permafrost temperatures are recorded in boreholes in the following periglacial landforms: solifluction sheets, fluvial terraces, ice-wedge polygons, pingos, rock glaciers, weathered bedrock plateau blockfields, exposed bedrock and strandflats. The depth of annual temperature variation varies between these landforms. This variation is generally less than 10 m deep in the relatively fine-grained sediments in the valleys, whereas there are still annual variations of up to almost 3˚C at this depth in the most coarse-grained rock glaciers. The coarse-grained landforms react quicker to annual air temperature variations, whereas the same magnitude temperature reaction in more fine-grained landforms, such as e.g. pingos, can be delayed with up to 5 months.

Permafrost temperature development

The warmest permafrost temperatures at 10 m depth in summer 2008 were -3.1°C recorded in a solifluction sheet in Endalen, central Svalbard, and in bedrock with sediment cover in a strandflat on the west coast of Svalbard. In summer 2017 the warmest permafrost was -

1.9°C in the Endalen site at 10 m depth, corresponding to warming of 0.1°C/yr. The bedrock strandflat site at Kapp Linné had warmed to -2.3°C at 10 m depth, which indicates warming of 0.09°C/yr. The largest warming of 0.2°C/yr was registered in an ice-wedge polygon in Adventdalen, though this rate was only observed over the last 5 years. Minimum warming was 0.04°C/yr in a loess covered fluvial terrace over the last 9 years at 10 m depth. Also in the mountains warming of 0.1°C/yr at 10 m depth was observed in a blockfield at 677 m asl. with the summer 2017 permafrost temperature reaching -5.1°C. All periglacial landforms observed have had permafrost warming over the last nine years recorded to around 10 m depth.

Also the deeper permafrost temperatures, which we record in the Endalen solifluction site in bedrock, below 7 m of sediment, have increased by 0.08°C/yr at 19 m. In the west coast of Svalbard the bedrock in the strandflat has warmed by 0.06°C/yr and 0.07°C/yr in two boreholes at 20 m depth, and by 0.05°C/yr at 30 m depth.

Active layer thickness variation

Since the year 2000 thaw progression data have been collected in the UNISCALM site (Christiansen & Humlum, 2008). During the period from 2000 to 2017, the active layer thaw depth has varied from a minimum of 74 cm in 2005 to a maximum of 110 cm in 2008. Over the entire period, on average, the active layer thaw depth has increased by 0.6 cm/year. No direct link to summer air temperature variation has been identified, whereas winter air temperatures have been found to influence the thaw depth of the proceeding summer (Schuh et al., 2017).

Discussion

During the period from 2000 to 2016 the mean annual air temperature recorded at Longyearbyen airport has increased from -4°C to -0.1°C (data from eklima, met.no). The average mean annual air temperature for the entire period 2000-2016 was -3.3°C. The presented data show that the air temperature increase in Svalbard has caused the permafrost to warm.

It is important to note that permafrost temperatures in the instrumented boreholes, most of which are located close to sea level, are typically lower than the official air temperature recorded at sea level. This is opposite to the normally expected offsets where the mean annual ground temperatures are warmer than the mean annual air temperatures. This situation in Svalbard most likely reflects the quick air temperature increase in the area and the maritime climate.

Acknowledgments

The funding for the boreholes in Svalbard was part of the TSP NORWAY IPY project funded by the Norwegian Research Council. UNIS has supported the operation of the boreholes since the end of the TSP Norway project.

References

Biskaborn, B.K., Lanckman J.P., Lantuit H., Elger K., Streletskiy D.A., Cable W.L., Romanovsky V.E., 2015. The new Database of the Global Terrestrial Network for Permafrost (GTN-P), *Earth System Science Data. 7, 1-15, doi:10.5194/essd-7-1-2015.*

Christiansen, HH., Etzelmüller, B., Isaksen, K., Juliussen, H., Farbrot, H., Humlum, O., Johansson, M., Ingeman-Nielsen, T., Kristensen, L., Hjort, J, Holmlund, P., Sannel, A.B.K., Sigsgaard, C., Åkerman, H.J., Foged, N., Blikra, L.H., Pernosky, M.A. & Ødegård, R., 2010. The Thermal State of Permafrost in the Nordic area during the International Polar Year 2007-2009. *Permafrost and Periglacial Processes*, 21, 156-181.

Christiansen, H.H. & Humlum, O. 2008. Interannual Variations in Active Layer Thickness in Svalbard. In Kane, D.L. & Hinkel, K.M (eds.) *Ninth International Conference on Permafrost Proceedings*, Institute of Northern Engineering, University of Alaska, Fairbanks, USA, 257-262.

Juliussen, H., Christiansen, H.H., Strand, G.S., Iversen, S., Midttømme, K. & Rønning, J.S., 2010. NORPERM, the Norwegian Permafrost Database – a TSP NORWAY IPY legacy. *Earth System Science Data*, 2, 235-246. www.earth-syst-sci-data.net/2/235/2010/doi:10.5194/essd-2-235-2010.

Schuh, C., Frampton, A. & Christiansen, H.H., 2017. Soil moisture redistribution and its effect on inter-annual active layer temperature and thickness variations in a dry loess terrace in Adventdalen, Svalbard. *The Cryosphere*, 11, 635-651, doi:10.5194/tc-11-635-201

Permafrost dynamics observed in Norway and Iceland

Bernd Etzelmüller[1]
Ketil Isaksen[2]
Sebastian Westermann[1]
[2]*Department of Geosciences, University of Oslo, Norway*
Meteorological Institute of Norway, Oslo, Norway

Abstract

Since 2004 in Iceland and 2007 in southern and northern Norway, numerous instrumented boreholes add information to the PACE reference boreholes drilled in 1999/2000. The data set covers a unique series of ground thermal regime across the North Atlantic, bridging the strong maritime settings in Iceland towards dry continental setting in northern Norway. The presentation analyses 15 years of permafrost monitoring, focusing on the response to changing air temperatures, snow regime and weather patterns.

Keywords: Thermal monitoring, mountain permafrost, climate, snow cover

Introduction

Permafrost is sensitive to climate change, modulating geomorphological process rates and ultimately landscape development. In Norway, since the 1980ies many studies have been carried out to evaluate the permafrost distribution, its changing state and its relation especially to climate and snow conditions. In Iceland, permafrost boreholes first were established in 2004, while studies on permafrost landforms like palsas dominated permafrost research earlier. All this knowledge has flown into numerical models, calculating ground temperatures in space and time.

At present, we have a unique data set obtained from boreholes where we measure temperatures along both altitudinal and latitudinal gradients. In addition, at all sites we performed geophysical surveys using refraction seismic and electrical resistivity tomography, partly multi-temporal. Finally, daily gridded data sets of meteorological parameters such as air temperature, precipitation and associated snow cover are available back to 1957, allowing the evaluation of climate-ground thermal regime relations along regional gradients.

This presentation gives an overview of the thermal development of the ground in Norway and Iceland, and attempts to explain the causes of the observed patterns.

Methods and Study sites

The field sites are in Norway are concentrated in the high mountain areas of southern Norway and the northernmost counties of Troms and Finnmark. They are all situated in typical mountain settings, with bedrock covered by relatively coarse-grained regolith or moraine material. All sites are barren or only sparsely vegetated by lichen and mosses except the Iskoras site in northern Norway, which is covered by a denser vegetation cover. The geology varies in the different sites, while the glaciation history is comparable. All sites were ice-covered during the last glaciations, however, most probably under cold basal ice conditions during longer periods and thus limited erosion at least during the last ice sheet period.

In Iceland the boreholes are distributed in the center and the eastern part of Iceland. Surface cover ranged from ground moraine, via organic-rich soils to sandy regoliths, rich of volcanic ashes.

The boreholes were established during the period 2004 (Iceland) to 2007 (Norway). The depths vary between 10 and 58.5 m, and they are equipped with thermistors coupled to a logging device, with measurement accuracies between ±0.01 and ±0.2°C. For most boreholes, surface air (SAT) and ground surface temperatures (GST) are measured using miniature temperature loggers (MTL) with resolution usually better than ±0.2°C. In some areas, the sites are located close to climate stations for SAT data. At Iskoras in Finnmark an altitudinal transect of SAT/GST measurement stations allowed for investigations of lapse rates and inversion settings.

Results and discussions

In Norway the analysis of the site data confirm an overall warming of permafrost during the last decades, even if some cold years around 2010 to 2013 caused a surficial cooling, especially in southern Norway. The reason of the warming can be different for different sites. We suspect that in continental northern Norway the warming might be most associated to changes in inversion patterns and associated snow composition. In maritime settings, the increase of seasonal temperature trends mainly drives the warming. Some sites in both climate extremes have developed talliks, as observed on Iskoras (Finmark) and Hagongur (Iceland).

In Iceland, the start of the measurements in 2004 fell into the start of a short period with stagnant or cooling SAT temperatures, after a general warming trend since the 1980ies. However, the measurements the last two years shows higher SAT, together with signs of permafrost degradation.

Acknowledgments

The Research Council of Norway funded the establishment of the boreholes, while the Department of Geosciences, University of Oslo, Norway, and the Meteorological Institute of Norway, Oslo, financed the management and maintenance work after the end of the individual projects.

Long-term changes in permafrost temperature in Svalbard and Scandinavia

Ketil Isaksen[1]
Bernd Etzelmüller[2]
Rune Strand Ødegård[3]
Peter Jansson[4]
Per Holmlund[4]
[1] *Norwegian Meteorological Institute, Norway, ketili@met.no*
[2] *Department of Geosciences, University of Oslo, Norway*
[3] *Norwegian University of Science and Technology, Norway*
[4] *Department of Physical Geography, Stockholm University, Sweden*

Abstract

Here we present updated analyses from the northern part of the European PACE latitudinal transect of deep instrumented permafrost boreholes to evaluate temperature changes and their causes since 1998. The geothermal records are powerful indicators of climate change and provide benchmark data on the past and present thermal state of mountain permafrost in northern Europe and the Nordic Arctic Region.

Keywords: Mountain permafrost; long-term monitoring; active layer; thermal state; climate change

Introduction

The most direct indicators of changes in the thermal state of permafrost are permafrost temperature and active-layer thickness (ALT). Permafrost temperature measured at or below a depth where there is practically no annual fluctuation in ground temperature, i.e. the depth of zero annual amplitude (ZAA) is the best indicator of long-term change. This depth varies from a few meters in warm, ice-rich permafrost to 20 m or more in cold permafrost and in bedrock (Romanovsky *et al.*, 2017).

In this study, we present updated analyses on ground temperatures from the northern part of the PACE latitudinal transect of deep instrumented permafrost boreholes (Harris *et al.*, 2001) that extends from the continuous arctic permafrost of Svalbard to the Scandinavian alpine discontinuous permafrost zone.

Study sites

Svalbard has continuous permafrost with permafrost thickness varying from less than 150 m near sea level to more than 450 m in the mountains. In Scandinavia (Norway and Sweden) permafrost is widespread at high elevations. The northernmost borehole is located at Janssonhaugen (78°N,16°E, 270 m asl, 102 m deep), western Svalbard. It was drilled in May 1998. In Scandinavia, boreholes were drilled at Tarfalaryggen (67°N,18°E, 1550 m asl, 100 m deep), northern Sweden in March 2000 and at Juvvasshøe (61°N,08°E, 1894 m asl, 129 m deep), southern Norway in August 1999. The drill sites were located on plateaus with limited snow cover, to avoid topographical 3D-effects and influence of large snow cover variations. Borehole casing, sensors and data logging equipment were assembled according to guidelines provided by the PACE project. Data series from Janssonhaugen are complete since instrumentation of the borehole in May 1998, while at the two other sites some major data gaps exist due to instrument failure and upgrade of dataloggers. For more details, see Isaksen *et al.*, 2007.

Results and discussion

Our results show that the permafrost has warmed considerably at all sites. Previous analyses showed that significant warming was detectable down to at least 60 m depth at all sites and that warming rates at 20 m depth (near ZAA) were in the order of 0.4 - 0.5 °C per decade, with greatest warming rates on Janssonhaugen and Tarfalaryggen (Isaksen *et al.*, 2007). Our updated analyses show that that warming rates observed since the late 1990s at 20 m depth (near ZAA) are in the order of 0.2 - 0.7 °C per decade (Figure 1) with enhanced rates in Svalbard. At Tarfalaryggen, warming rates are similar to the 2007 values while on Juvvasshøe warming rates are smaller. However, permafrost temperature at 20 m in 2017 was near highest on record on Juvvasshøe; a warming that followed a period of cooling between 2010 and 2013.

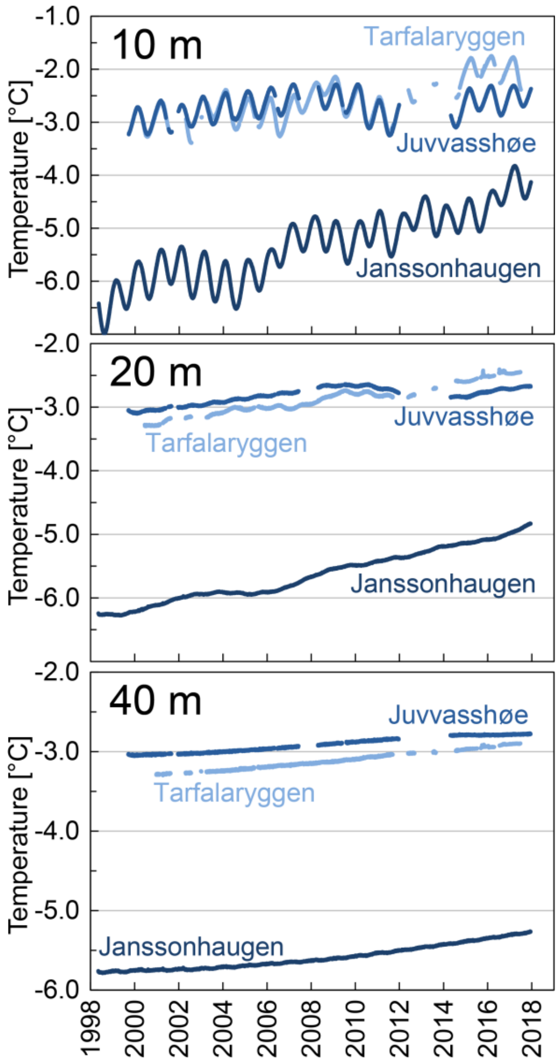

Figure 1. Observed daily ground temperatures for three selected depths (10, 20, and 40 m) at the three northernmost PACE boreholes Janssonhaugen, Tarfalaryggen and Juvvasshøe. Data series are updated from Isaksen *et al.*, 2007.

On Janssonhaugen a significant temperature increase is now measureable down to at least 80 m depth reflecting a multi-decadal warming of the permafrost surface, where the extreme warm years 2016 and 2017 clearly stand out in the observational record (Figure 2). The increase in permafrost temperatures observed in Svalbard since 1998 is among the largest observed globally, with a similar warming rate observed in the Alaskan Arctic and Canadian high arctic (Romanovsky et al., 2017). In addition, a significant increase in ALT was observed on Janssonhaugen where 2016 active-layer thickness reached its maximum (1.97 m) and increased by 15% compared to the 2000-2015 mean. Further analysis will reveal the relative influence of different factors such as surface air temperature and snow cover for the observed temperature trends at the different sites.

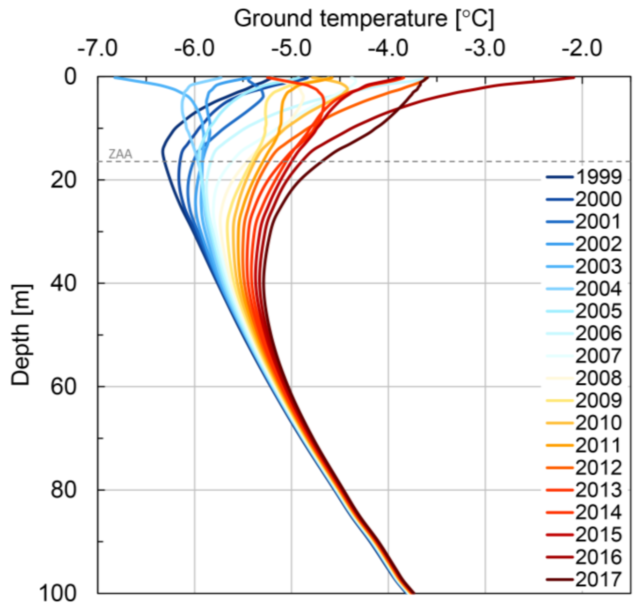

Figure 2. Mean annual ground temperature profiles on Janssonhaugen from 1999 to 2017. ZAA is marked by a grey dotted line. Data for 2017 should be considered preliminary (based on the period 1 Jan-13 Dec).

Acknowledgments

After the PACE project in 2001 the Norwegian Meteorological Institute, University of Oslo and the Stockholm University have been the main financial supporters.

References

Harris, C., Haeberli, W., Vonder Mühll, D. & King, L., 2001. Permafrost monitoring in the high mountains of Europe: The PACE Project in its global context, *Permafrost Periglacial Processes* 12: 3-11.

Isaksen, K., Sollid J.L., Holmlund, P., & Harris C., 2007. Recent warming of mountain permafrost in Svalbard and Scandinavia. *Journal of Geophysical Research* 112.

Romanovsky, V., Isaksen, K., Drozdov, D., Anisimov, O., Instanes, A., Leibman, M., McGuire, A.D., Shiklomanov, N., Smith, S., & Walker, D., 2017. Changing permafrost and its impacts. In: *Snow, Water, Ice and Permafrost in the Arctic (SWIPA) 2017*. pp. 65-102. Arctic Monitoring and Assessment Programme (AMAP), Oslo, Norway.

Long-term measurement of permafrost temperatures in the Swiss Alps

Jeannette Noetzli[1]
Reynald Delaloye[2]
Christin Hilbich[2]
Martin Hoelzle[2]
Christophe Lambiel[3]
Marcia Phillips[1]
Sarah M. Springman[4]
Andreas Vieli[5]
[1]*WSL Institute for Snow and Avalanche Research SLF, jeannette.noetzli@slf.ch*
[2]*Department of Geosciences, University of Fribourg*
[3]*Institute of Earth Surface Dynamics, University of Lausanne*
[4]*Institute for Geotechnical Engineering, ETH Zurich*
[5]*Glaciology and Geomorphodynamics Group, Department of Geography, University of Zurich*

Abstract

Reliable, robust and comparable measurements from key sites over decades are the basis for the assessment of the state of permafrost, including changes and potential adverse effects. Data collection and management over long time periods is the core task and the main challenge for long-term permafrost monitoring networks. In this contribution, we present the borehole data and recent trends measured in the scope of the Swiss Permafrost Monitoring Network PERMOS and discuss the experience gained from operating the borehole sites over more than two decades.

Keywords: permafrost temperatures; thermal state; long-term monitoring; mountain permafrost; PERMOS

From PACE to PERMOS

Reliable, robust and comparable measurements from key sites over long time periods are the basis for the assessment of permafrost state and changes as well as potential adverse effects to slope or infrastructure stability. Long-term monitoring of permafrost primarily relies on ground temperatures measured in boreholes, which are the only direct observations of the thermal subsurface condition. Thirty boreholes are currently operated at 16 sites within the Swiss Permafrost Monitoring Network PERMOS. They are complemented by distributed ground surface temperature measurements, geophysical investigations of changes in ice-content and terrestrial geodetic surveys of permafrost creep velocities (PERMOS, 2016).

PERMOS started in 2000 as an unconsolidated network of sites from research projects. The EU-funded PACE project (Permafrost and Climate in Europe, Harris *et al.*, 2003) was an important contribution towards the drilling and instrumentation of boreholes, as three of the borehole sites in the PERMOS network are part of the European borehole transect installed in the scope of PACE: Murtèl-Corvatsch, Schilthorn and Stockhorn. In parallel, strategies were established for long-term monitoring in the framework of the Global Climate Observing System GCOS.

Permafrost temperatures in the Swiss Alps

The longest temperature-time series in mountain permafrost has been measured in a 60 m deep borehole drilled in 1987 in rock glacier Murtèl on Piz Corvatsch (GR). The time series measured at Schafberg and Muot da Barba Peider cover over 20 years and Stockhorn, Schilthorn and several other sites cover 15 years. A general warming trend of permafrost in the Swiss Alps is clearly visible at 10 and 20 meters depth for the past decade (Fig. 1), with new records measured in the record year 2015 for most of the sites. Ground temperatures measured at Murtèl-Corvatsch, for example, increased by more than 0.5 °C at 20 m depth in the past 30 years. The warming is less pronounced for warmer ice-rich sites, due to the energy required for phase change at temperatures just below 0 °C. At Schilthorn for example, geoelectrical monitoring since 1999 points to a significant decrease in ice content, which is not revealed by temperature measurements. Increasing creep velocities measured on rock glaciers corroborate the warming trend (PERMOS, 2016).

The past two winters 2016 and 2017 were characterized by an exceptionally late and thin, but long-lasting snow cover. This resulted in a cooling of the permafrost at snow rich sites down to 20 m depth and a decrease in creep velocities, despite continuously high air temperatures. This has clearly demonstrated the role of the snow cover on the changes in the ground thermal regime. In contrast, only little snow accumulates on steep bedrock slopes and warming is expected to be uninterrupted there. However, limited data mostly from near-surface temperature loggers are available for steep rock slopes.

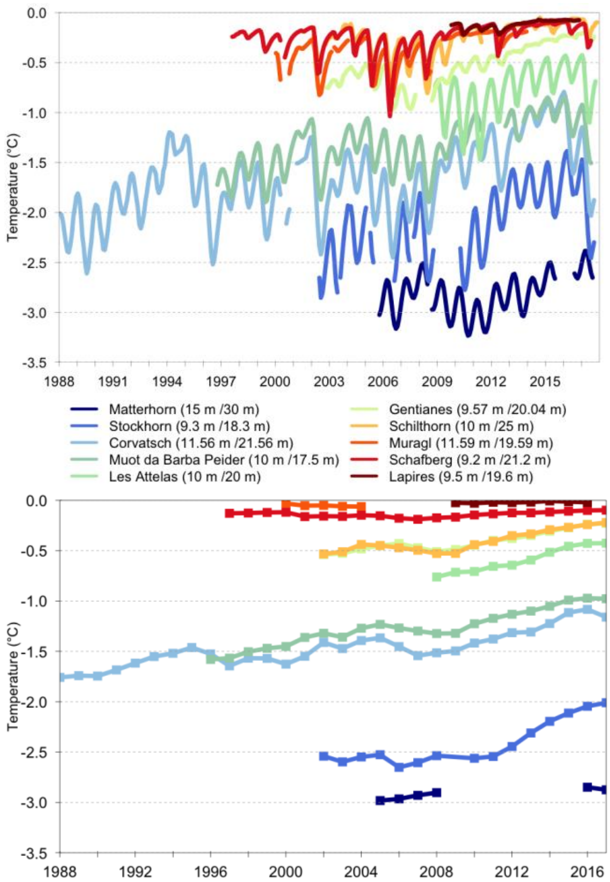

Figure 1. Borehole temperatures measured in permafrost in the Swiss Alps at 10 m (monthly means, top) and 20 m depth (annual means, bottom). Data and figures: PERMOS.

Challenges of long-term operation

Our experience with measuring permafrost temperatures over two or three decades results in the valuable time series shown above. Considerable challenges for a long-term monitoring network of mountain permafrost have also become apparent. The acquisition of reliable data at a limited number of stations in extreme environments with difficult access requires specially adapted strategies, standards and tracebility for the entire data acquisition chain: *installation* > *measurement* > *raw data* > *processing* > *archiving*.

The main difficulties relate to: i) *Harsh high mountain environments:* storms, avalanches or melt water can damage the installations, leading to data gaps. Creeping permafrost or rock slides or falls can cause thermistor chains to be blocked or shear off completely (preventing recalibration or replacement); ii) *Measurements of small and invisible changes:* drift of thermistors or measurement instabilities are sometimes hard to separate from real features and validation or calibration is difficult or even impossible. iii) *Science-driven network:* only little standardisation exists so far for the installations, station maintenance and station history, and data processing (data aggregation, gap-filling, etc.).

Best practices for borehole temperature measurements in mountain permafrost are being elaborated to tackle the challenges described above. Careful planning of borehole renovation or even redrilling is required for a sustainable PERMOS network in the coming decade. A first successful redrilling was accomplished in 2015 at Murtèl-Corvatsch to secure the temperature record in case of the expected shearing off of the thermistor chains in the near future. This additionally allowed the validation of the borehole data measured with 30-year old thermistors. A second redrilling project was completed at the Tsaté site in summer 2017.

Acknowledgments

The Federal Office for Climatology (MeteoSwiss) in the framework of GCOS Switzerland, the Federal Office for Environment (FOEN), and the Swiss Academy for Sciences (SCNAT) finance the network. Equally important are the contributions made by the academic partner institutions that are responsible for data acquisition and station maintenance: The Universities of Fribourg, Lausanne, and Zurich, ETH Zurich, the University of Applied Sciences and Arts of Southern Switzerland, and the WSL Institute for Snow and Avalanche Research SLF.

References

Harris, C., Haeberli, W., Vonder Mühll, D. and King, L.: Permafrost monitoring in the high mountains of Europe: the PACE Project in its global context. *Permafrost and Periglacial Processes*, 12(1), 3–11, doi:10.1002/ppp.377, 2001.

PERMOS 2016. Permafrost in Switzerland 2010/2011 to 2013/2014. Noetzli, J., Luethi, R., & Staub, B. (eds.), Glaciological Report (Permafrost) No. 12–15 of the Cryospheric Commission of the Swiss Academy of Sciences, 85 pp.

Analysis of winter warming events in a mountain permafrost area, Dovrefjell, southern Norway, 1868-2017

Rune Strand Ødegård[1]
Ketil Isaksen[2]
[1]*Norwegian University of Science and Technology, Norway, rune.oedegaard@ntnu.no*
[2]*Norwegian Meteorological Institute, Oslo, Norway*

Abstract

The intensity and frequency of winter warming events in a mountain permafrost area of central southern Norway (Dovrefjell/Sunndalsfjella) have been analysed. Five winter climate indices were calculated for the period 1868-2017 based on data from four meteorological stations. The results show a marked increase in the frequency and intensity of warm events during the last 30 years compared to the previous 120 years. The response of warm events on near surface ground temperature has been evaluated based on data from 11 shallow boreholes (2001-2017) and 38 mini temperature loggers (2012-2017) measuring ground surface temperature (GST).

Keywords: Mountain permafrost; ground surface temperature; episodic snowmelt; rain-on-snow.

Introduction

We have analysed the intensity and frequency of winter warming events in a mountain permafrost area of central southern Norway (Dovrefjell/Sunndalsfjella). The area of permafrost is approx. 750 km² ranging from 1400 m a.s.l. to 2300 m a.s.l. Cold season warm spells and rain-on-snow (ROS) events leads to changes in snow cover properties and may warm the permafrost and snowpack base and have the potential to damage vegetation. Refreezing creates a layer of ice in the snowpack or ground ice that increasing thermal conductivity. Such ice-layers may be difficult for animals to penetrate with their hooves, adversely affecting conditions for grazing animals such as caribou, reindeer, and musk ox (Brown *et al.*, 2017). The only large remaining wild populations of reindeer in Europe are found in the mountainous habitats of southern Norway. Table 1 show the meteorological and ground temperature data used in this study.

Data Analysis

We have used five different climate indices to detect the occurrence of winter warming events following the suggestions of Wikhamar-Schuler *et al.*, 2016. Ground temperature measurements have been used to evaluate the impact in the permafrost area. The winter season is defined here as the months November–March. The total duration of this winter season corresponds to the period during which mean monthly temperatures lie below 0°C at the Dombås station. The indices are:

(1) Warm days (WD) counts the number of warm days (WD) in a winter using a location-specific threshold temperature defined as the 90th percentile of the winter distribution for the most recent 30-yr period (1988–2017). (2) Melt days (MD) counts the number of days with a fixed threshold of 0°C. (3) Positive degree-day sum (PDD), is the sum over the winter season of temperatures values above 0°C. (4) Number of melt and precipitation days (MPD), similar to MD but with the additional constraint that precipitation >0 mm. (5) Accumulates the total winter precipitation for the MPD (MDPsum).

Table 1. Overview of data series

Station	m asl.	Period	Air T.	Prec.	GST
Dombås met.	638	1868-1915	x		
Dombås met.	638	1916-2017	x	x	
Fokstugu met.	952/973	1924-2017	x	x	
Snøheim met	1475	2001-2017	x		
Snøheim GST	1038-1505	2001-2017			x
Hjerkinn met	1012	2010-2017	x		
Kolla GST	1170-1630	2012-2017			x

Results

Fig. 1 shows the indices for the climate station Dombås (valley station) averaged over 15-year periods from 1868-2017. The results from Dombås is well correlated with station Fokstugu (mountain plateau). There is a marked increase in the number of warm events the last 30 years compared to the previous 120 years.

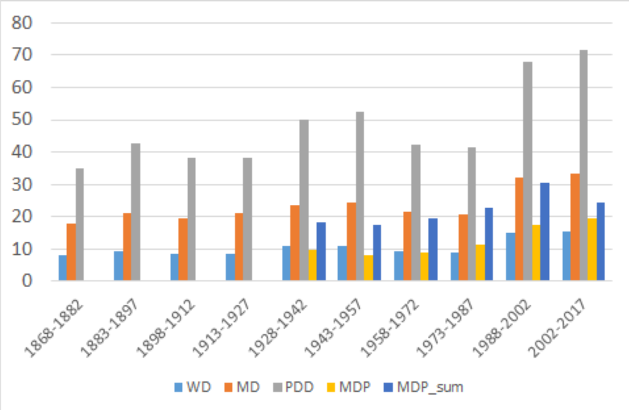

Figure 1. Winter climate indices at the meteorological station Dombås averaged over 15-year periods 1868-2017. The five indices are explained in the text.

The frequency (WD/MD) and intensity (PDD) indices show the same trend. The warm events with precipitation also show an increase (MDP/MDPsum). There is a similar trend in the mean winter air temperature. Fig. 2 and 3 show an example in mid-March 2016. The response of the near ground surface temperatures to such extreme weather events in permafrost and mountain areas is strongly modulated by snow cover, vegetation, soil type (mainly water content and porosity) and the amount of rain. Thus, the GST response at the dry and strongly wind-exposed ridge vegetation communities was of shorter duration and weaker than in snow bed sites with different soil types and more developed snow cover, vegetation cover and ground-icing. At several snow bed sites, GST stayed at or near 0 °C for two weeks or more after the event in mid March 2016, despite air temperatures below −5 °C. This was caused by water from melting snow that percolated through the snow to the cold ground surface and forming basal ice layers at the ground surface.

Acknowledgments

This study was funded by the Norwegian Environment Agency, the county council of Møre og Romsdal, Norwegian University of Science and Technology, Norwegian Meteorological Institute, University of Bergen and Bjerknes Centre of Climate Research.

Figure 2. Snow melt 14 March 2016 at 1504 m asl. during one of the most severe winter warm spells observed on Dovrefjell.

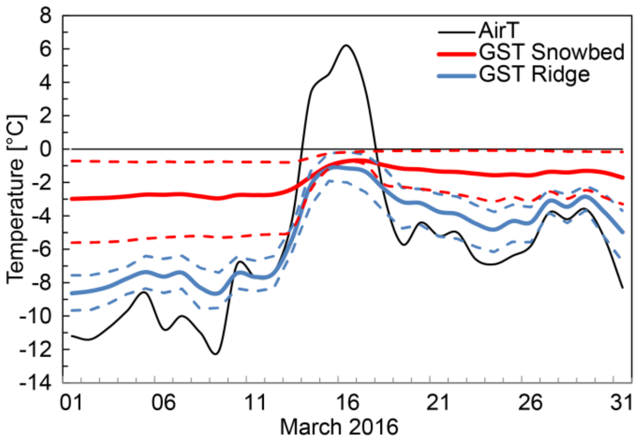

Figure 3. The response of the GST to the mid-March 2016 warm spell for 16 sites classified as snow bed and 16 sites classified as ridge vegetation communities mostly situated on permafrost. Mean values are shown in thick bold lines and the interquartile range (Q75-Q25) as dotted lines. Air temperature (black line) from Snøheim weather station.

References

Brown, R., Vikhamar Schuler D., Bulygina O., Derksen C., Luojus K., Mudryk L., Wang L., Yang D., 2017. Arctic terrestrial snow cover. Ch.3 *in*: *Snow, Water, Ice and Permafrost in the Arctic (SWIPA) 2017*, pp. 25-64, Arctic Monitoring and Assessment Programme (AMAP), Oslo, Norway.

Vikhamar-Schuler, D., Isaksen, K., Haugen, J.E., Tømmervik, H., Luks, B., Schuler, T., Bjerke, J., 2016. Changes in winter warming events in the Nordic Arctic Region. *Journal of Climate* 29.

20 year joint analysis of geophysical, energy balance, water balance and temperature time series from several Swiss and Norwegian permafrost stations – lessons since the PACE project

Guy Ramsden[1], Ketil Isaksen[2], Bernd Etzelmüller[3], Wilfried Haeberli[4], Christin Hilbich[1], Martin Hoelzle[1], Coline Mollaret[1], Cécile Pellet[1], Martin Scherler[1], Catherine Stocker-Mittaz[5], Daniel Vonder Mühll[6], Christian Hauck[1]

[1]*Department of Geosciences, University of Fribourg, Switzerland, guy.ramsden@unifr.ch*

[2]*Norwegian Meteorological Institute, Oslo, Norway*

[3]*Department of Geosciences, University of Oslo, Norway*

[4]*Department of Geography, University of Zürich, Switzerland*

[5]*Federal Office of Meteorology and Climatology MeteoSwiss, Zurich-Airport, Switzerland*

[6]*ETH Zürich, Switzerland*

Abstract

Within the European PACE project (Permafrost and Climate in Europe, 1997-2001) several new long-term permafrost stations were installed in European permafrost regions, including the Swiss Alps and Scandinavia. These installations comprised deep borehole temperature logging, snow and energy balance sensors as well as site-characterizing geophysical measurements – later, soil moisture, geoelectric as well as seismic monitoring were added and new official automatic weather stations were established at some of the sites. The now 20-year old data records were subsequently analysed and complemented by numerical heat and mass transfer simulations, also regarding scenario projections until the end of the century. Here, we summarise the findings regarding past and present permafrost evolution, and the dominant processes that are active at the different permafrost regions and landforms.

Keywords: PACE, long-term monitoring, energy balance, geophysical monitoring, modelling, permafrost evolution

Introduction

The EU-funded PACE project (Permafrost and Climate in Europe, Harris *et al.* 2001) can be seen as a milestone in European long-term monitoring efforts, as it initiated the drilling of several 100m deep permafrost boreholes in different mountain regions of Europe. Borehole drilling was conducted along a North-South oriented transect from Svalbard to the Sierra Nevada, Spain, and the obtained borehole information was in places combined with energy balance monitoring, geophysical surveying and geomorphological mapping. Besides the long-term monitoring aspect, the focus of the project was on permafrost-related process understanding, the results of which were amongst others presented in a joint review paper by Harris *et al.* (2009).

20 years after the first PACE drillings, all stations are still operational and constitute the backbone of national (e.g. Permafrost Monitoring Switzerland, PERMOS; NORPERM in Norway) and international monitoring networks (GTN-P). They also serve as validation stations for local, regional and hemispheric permafrost modelling studies (e.g. Marmy *et al.* 2016, Ekici *et al.* 2015, Gisnås *et al.* 2017). In this contribution we highlight the achievements of this monitoring network since the beginning of the PACE project, with a focus on the multi-parameter investigations that uses atmospheric and soil (geo-)physical monitoring data on the one hand and coupled hydro-thermal modelling on the other hand.

Methodology and Results

One of the main improvements of the PACE project is the initiation of operational energy balance and geophysical monitoring at the existing borehole monitoring locations. Data from continuous energy balance stations comprising radiation balance, air temperature and humidity, wind speed and direction as well as snow height exist at many of the PACE locations and can be used (a) for microclimatic analysis to analyse the driving factors for the observed permafrost evolution and (b) as input data for site-specific permafrost models.

Repeated geoelectrical monitoring began in 1999 at the station Schilthorn (SCH), Swiss Alps, and was subsequently enlarged to further permafrost stations in the Swiss Alps (Fig. 1) and Norway. The combined use of geoelectric data (electrical resistivity) and borehole temperature (cf. Fig. 2, see also Hilbich *et al.* 2011, Isaksen *et al.* 2011) allows for differentiating between heat conduction and latent heat effects in the ground, as electrical resistivity is especially sensitive to the phase transition between liquid water and ice.

Additional repeated refraction seismic measurements are used to quantify the ice content explicitly, which can then be used to compare energy balance-driven permafrost model simulations with geophysical data-driven ice content estimations (Pellet et al. 2016).

The overall permafrost evolution during the past 20 years shows significant warming of most permafrost stations in Europe (Noetzli *et al.* 2016). Hereby, the warming is most pronounced at stations having temperatures far below the freezing point, where latent heat effects have no significant effects (yet). On the contrary, active layer deepening is most pronounced for stations close to the freezing point, where additional geophysical data show that electrical resistivity, and therefore ground ice content, is strongly decreasing. This is shown exemplarily in Fig. 2 for the station Schilthorn, where the active layer thickness increased (and corresponding resistivities decreased) from 4-5m in 1999 to almost 10m in the record year 2015.

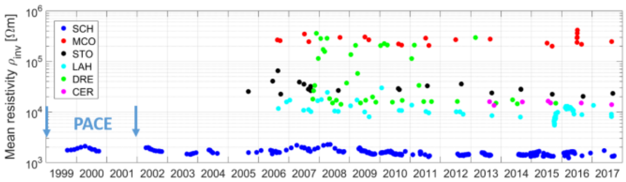

Figure 1. Time series of mean inverted electrical resistivity for several permafrost stations in the European Alps. The duration of the PACE project is indicated by the arrows.

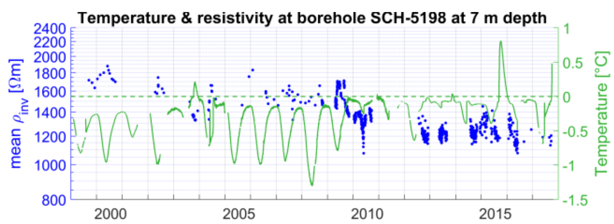

Figure 2. Time series of mean inverted electrical resistivity and borehole temperature at 7m depth at the permafrost monitoring station Schilthorn (SCH), Northern Swiss Alps.

Acknowledgments

We would like to thank the PACE community for the great collaboration during the past 20 years, and the PERMOS network for sustaining the operational monitoring in Switzerland since that time. After the PACE project the University of Oslo and Norwegian Meteorological Institute have been the main financial supporters in Norway.

References

Ekici, A. & 13 co-authors (2015): Site-level model intercomparison of high latitude and high altitude soil thermal dynamics in tundra and barren landscapes, The Cryosphere, 9, 1343-1361, doi:10.5194/tc-9-1343-2015, 2015.

Gisnås, K., Etzelmüller, B., Lussana, C., Hjort, J., Sannel, A.B.K., Isaksen, K., Westermann, S., Kuhry, P., Christiansen, H.H., Frampton, A. and Åkerman, J., 2017. Permafrost Map for Norway, Sweden and Finland. Permafrost and Periglacial Processes, 28(2), pp.359-378.

Harris, C., Haeberli, W., Vonder Mühll, D., King, L., 2001. Permafrost monitoring in the high mountains of Europe: the PACE project in its global context. Permafrost and Periglacial Processes 12 (1), 3–11.

Harris, C., & 21 co-authors (2009): Permafrost and climate in Europe: monitoring and modelling thermal, geomorphological and geotechnical responses. Earth Science Reviews 92 (3-4), 117-171.

Hilbich, C., Fuss, C., Hauck, C. (2011): Automated time-lapse ERT for improved process analysis and monitoring of frozen ground, Permafrost and Periglacial Processes 22(4), 306-319, DOI: 10.1002/ppp.732.

Isaksen, K., Ødegård,R.S., Etzelmüller,B., Hilbich, C., Hauck, C., Farbrot,H., Eiken, T., Hygen H.O., Hipp T. (2011): Degrading Mountain Permafrost in Southern Norway: Spatial and Temporal Variability of Mean Ground Temperatures, 1999–2009, Permafrost and Periglacial Processes 22(4), 361–377.

Marmy, A. & 11 co-authors (2016): Semi-automated calibration method for modelling of mountain permafrost evolution in Switzerland, The Cryosphere, 10, 2693-2719, doi:10.5194/tc-10-2693-2016.

Noetzli, J., Christiansen, H., Gugliemin, M., Romanovsky, V. E., Shiklomanov, N. I., Smith, S. L. and Zhao, L. 2016: Permafrost thermal state (in "State of the Climate in 2015"). Bull. Amer. Meteor. Soc., 97, 173–226.

Pellet C, Hilbich C, Marmy A and Hauck C (2016): Soil Moisture Data for the Validation of Permafrost Models Using Direct and Indirect Measurement Approaches at Three Alpine Sites. Front. Earth Sci. 3:91. doi: 10.3389/feart.2015.00091.

High-Arctic permafrost thermal conditions in the SVALGREEN transect

Sarah Marie Strand[1]
Hanne H. Christiansen[1]
Graham L. Gilbert[1,2]
Wesley R. Farnsworth[1,3]

[1]*The University Centre in Svalbard, Corresponding email: sarah.strand@unis.no*
[2]*University of Bergen*
[3]*UiT The Arctic University of Norway*

Abstract

Ground temperature data from Villum Research Station and Zackenberg Research Station, Northeast Greenland, and Endalen and Kapp Linné, Spitsbergen, Svalbard, are compared in the context of the SVALGREEN transect. The air temperature gradient existing across the SVALGREEN transect, which spans the Fram Strait, is generally mirrored in the permafrost thermal conditions, although the latter gradient is less extreme. Permafrost in western Svalbard is ca. 5 °C warmer than permafrost at Villum Research Station. Additionally, mean annual ground temperatures at 18 m depth at Villum and Zackenberg are within 1 °C of each other, even though Zackenberg is 800 km south of Villum. The similar permafrost temperatures are explained by a thick snowpack and short snow-free season at Villum, which buffers the area's low mean annual air temperature. Holocene glacial and sea level history influence lowland permafrost conditions in the SVALGREEN region.

Keywords: permafrost; ground temperature; Greenland; Svalbard; snow; Holocene

Introduction and background

The air temperature gradient existing across the SVALGREEN transect, which spans the Fram Strait, is one of the strongest climatic gradients in the High Arctic. By comparing the geomorphology and permafrost of Svalbard and Northeast Greenland, new insights are gained regarding landscape development and current processes in both areas. Ground temperatures are currently monitored within the SVALGREEN transect in four 20-30 m boreholes in Northeast Greenland and four 20-30 m boreholes in Svalbard (Christiansen *et al.*, 2010). The Northeast Greenland boreholes are located at Villum Research Station at Station Nord and Zackenberg Research Station. The Svalbard boreholes are located at Endalen and Kapp Linné in central and western Spitsbergen, Svalbard (Fig. 1). Northeast Greenland and Svalbard are relatively close high-Arctic locations within the SVALGREEN transect, but regional oceanic and atmospheric circulation patterns result in variations in the permafrost thermal conditions between these sites.

Geomorphological and Quaternary research indicates that permafrost development at these lowland sites was largely dependent on local deglaciation and relative sea level regression during the Holocene (Gilbert *et al.*, 2017; Gilbert, 2014). Landscape development at Villum Research Station is currently being reconstructed based on August 2016 field observations.

Study locations and results

Endalen and Kapp Linné, Spitsbergen, Svalbard

Endalen (78°10' N) is a tributary valley in central Svalbard, located near the main settlement of Longyearbyen. The Endalen borehole is located in a solifluction sheet over bedrock with moderate snow cover (30-60 cm). Kapp Linné (78°03' N) is a strandflat on the west coast of Svalbard, ca. 50 km west-southwest of Endalen. Windy conditions lead to minimal snow accumulation (<30 cm). During the 2016-2017 hydrological year (1 September to 31 August), mean annual ground temperature (MAGT) at 19 m depth in Endalen was -2.7 °C. At Kapp Linné, MAGT at 30 m depth was -3.0 °C. A major factor in western Svalbard's relatively warm permafrost and climate is the West Spitsbergen Current, which carries warm, saline Atlantic water northward. This limits sea ice formation on the eastern side of the Fram Strait, permitting ocean-atmosphere heat exchange in the winter, and increasing air temperatures during this season (Walczowski & Piechura 2011). These increased air temperatures are reflected in the permafrost temperatures.

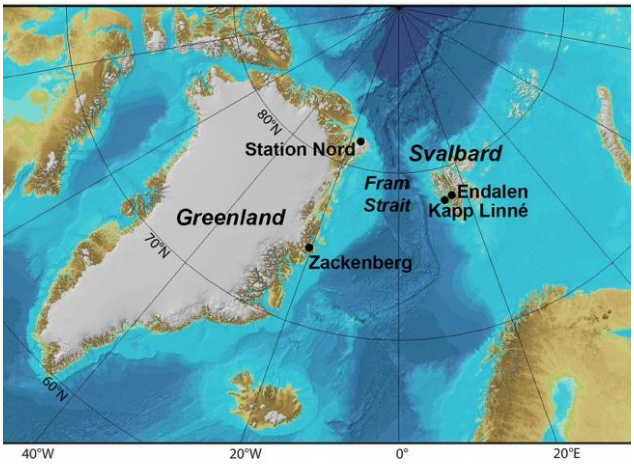

Figure 1. Map showing the SVALGREEN transect and study sites. Base map from the International Bathymetric Chart of the Arctic Ocean.

Villum Research Station at Station Nord, northern Greenland

Villum Research Station at the military Station Nord (81°34' N) is located on the Princess Ingeborg Peninsula 720 km NW of Longyearbyen, Svalbard. Mean annual air temperature (MAAT) was ca. -14 °C at Station Nord in 2016 (Villum Research Station/Asiaq, Greenland Survey) compared to -0.7 °C in Longyearbyen (Norwegian Metrological Institute). Borehole Sites 1 and 2 are located in adjacent beach ridges, and Site 2 is 9 m lower in elevation than Site 1. More snow accumulates at Site 2's downslope location. During the 2016-2017 hydrological year (20 August to 19 August, based on data availability and snow conditions at Station Nord), MAGT at 20 m depth was -7.9 °C at Site 1 and -7.1 °C at Site 2.

The coast around Station Nord has both fast ice and Arctic pack ice, though a coastal lead can open between these types of sea ice during summer.

Zackenberg, Northeast Greenland

Zackenberg (74°29' N) is ca. 800 km south of Station Nord, though ground temperatures at this location are only slightly higher. MAGT at 18 m depth was -6.8°C at Zackenberg during the 2015-2016 hydrological year. The Young Sound, just south of Zackenberg, has seasonal sea ice, but is typically ice free in the summers. 2016 MAAT at Zackenberg was ca. -7°C, between that of Longyearbyen and Villum Research Station.

Discussion and conclusions

The ground temperature data presented here demonstrate that the SVALGREEN climatic gradient is generally mirrored in the transect's permafrost thermal conditions, though this gradient is less extreme, with permafrost in western Svalbard only ca. 5°C warmer than permafrost at Villum Research Station. However, permafrost temperatures at Station Nord are still relatively high given the location's high latitude and low air temperatures. MAGT at 18 m depth at Zackenberg, 800 km south of Station Nord, is within 1 °C of 18 m MAGT at Station Nord (-6.8 °C compared to -7.8 °C). This is explained by a short snow-free period and thick snowpack (>1.3 m) at Station Nord compared to the rest of the SVALGREEN region, which is likely related to moisture availability and sea ice conditions. Snow accumulation in the landscape likely changed during the Holocene due to variation in sea ice extent, and thus these environmental conditions have impacted permafrost evolution at Station Nord.

Acknowledgments

Fieldwork at Villum Research Station during August 2016 was supported by INTERACT Transnational Access. Data from Zackenberg were provided by the Greenland Ecosystem Monitoring Programme.

References

Christiansen, H.H, Etzelmüller, B., Isaksen, K., Juliussen, H., Farbrot, H., Humlum, O., Johansson, M., Ingeman-Nielsen, T., Kristensen, L., Hjort, J, Holmlund, P., Sannel, A.B.K., Sigsgaard, C., Åkerman, H.J., Foged, N., Blikra, L.H., Pernosky, M.A. & Ødegård, R., 2010. The Thermal State of Permafrost in the Nordic area during the International Polar Year 2007-2009. *Permafrost and Periglacial Processes*, 21(2): 156-181.

Gilbert, G.L., 2014. Sedimentology and geocryology of an Arctic fjord head delta (Adventdalen, Svalbard). Master's thesis, University of Oslo, 133 pp.

Gilbert, G.L., Cable, S., Thiel, C., Christiansen, H.H. and Elberling, B., 2017. Cryostratigraphy, sedimentology, and the late Quaternary evolution of the Zackenberg River delta, northeast Greenland. *The Cryosphere* 11(3): 1265-1282.

Mernild, S.H., Hanna, E., Yde, J.C., Cappelen, J. and Malmros, J.K., 2014. Coastal Greenland air temperature extremes and trends 1890–2010: annual and monthly analysis. *International Journal of Climatology* 34(5): 1472-1487.

Walczowski, W., & Piechura, J., 2011. Influence of the West Spitsbergen Current on the local climate. *International Journal of Climatology* 31 (7): 1088-1093.

Twenty years monitoring the degradation of buried ice and permafrost at the Veleta cirque (Sierra Nevada, Spain)

Luis M. Tanarro[1], Antonio Gómez[2], Ferran Salvador[2], José J. Sanjosé[3], Marc Oliva[2], David Palacios[1], Miguel Ramos[4], Montserrat Salvà[2], Alan Atkinson[3]

[1]*Department of Geography, Complutense University of Madrid, Spain, pace@ghis.ucm.es*
[2]*Department of Geography, University of Barcelona, Spain*
[3]*Department of Graphic Expression, University of Extremadura, Cáceres, Spain*
[4]*Department of Physics, University of Alcalá, Spain*

Abstract

Sierra Nevada, located in the SE corner of the Iberian Peninsula, was the southernmost monitoring site of the PACE project (1998-2000) along a transect extending from the Mediterranean to the High Arctic. The techniques and methods used in this research unveiled the existence of relict ice and permafrost in the Veleta cirque under an incipient rock glacier and as well as in a talus slope. Since then, we have been monitoring the evolution of these frozen masses by analyzing their ground temperature conditions and their relationship with the presence of snow cover at the end of summer, as well as examining the surface dynamics of the rock glacier and the talus slopes. The results obtained during the last 20 years of monitoring have shown evidence of the accelerated degradation of the relict ice and permafrost, which has led to volume reduction and, at the same time, favoured collapses and subsidence on the rock glacier. The reason for this lies, above all, in the progressive deepening of the active layer during the warm seasons, in particular when the ground is snow-free.

Keywords: Sierra Nevada; thermal regime; buried ice; permafrost; snow cover; rock glacier.

Introduction

The Veleta peak (3,398 m a.s.l., 37° 03'N and 3° 22'W), and its northern Veleta cirque, Sierra Nevada (Spain), were the southernmost monitoring sites in Europe within the PACE project (Permafrost and Climate in Europe, years 1998-2000. The objective of this project was to study the evolution of mountain permafrost in Europe and its relation with current climate conditions in eight sites distributed along a transect from Sierra Nevada (37ºN) to Svalbard (78ºN). Sierra Nevada was the only example of semiarid subtropical mountain, and the southernmost European massif encompassing glaciers during the Little Ice Age (LIA).

Results obtained during the PACE project indicated the presence of relict ice and ground thermal regime associated to permafrost conditions in the Veleta cirque at 3,150 m, under an incipient active rock glacier, and locally in some talus slopes (Gómez Ortiz *et al.*, 2001). Most of the monitoring network implemented during the PACE project in the Sierra Nevada has been maintained for 20 years, including new approaches such as geomatic techniques for monitoring rock glacier dynamics.

The objective of this work is to present the results obtained during this long-term monitoring research.

Soil temperatures

Air temperature recorded at the Veleta peak between 2002 and 2013 averaged a mean annual air temperature (MAAT) of 0.07ºC, with an increase of 0.12ºC (Oliva *et al.*, 2016). The absolute maximum temperature was 28.6ºC and the lowest was -27.8ºC (Gómez *et al.*, 2014).

Soil thermal regime in the bedrock

A 114.5 m deep borehole recorded bedrock temperatures between September 2002 and August 2013, indicating positive temperatures along the period and showing evidence of the inexistence of permafrost conditions in the bedrock. The mean annual temperatures range between 3.2ºC, at 0.6 m depth, 2.3ºC at 20 m, and 2.5ºC at 60 m, with a seasonal frozen layer between 0.6 and 2 m depth (Oliva *et al.,* 2016).

Soil thermal regime in the rock glacier

Soil temperatures within a rock glacier were monitored since 1999 at five depths (5, 20, 50, 100 and 150 cm) showing a decrease of mean temperatures at depth, from 0.8ºC at 5 cm depth to -1.5ºC at 150 cm depth. From November to April, mean temperatures were always negative at all levels, with colder values closer to the surface. In July and August positive values were recorded, except at 150 cm depth, close to the relict ice, where negative values persisted (between -0.7º and -0.3ºC; Gómez *et al.*, 2014).

Soil thermal regime in the talus slope

The measurements of ground surface temperatures between October 2008 and August 2012 on the talus slopes suggests the inexistence of permafrost at depth. The minimum temperature of the ground during winter-spring, when the slope is snow covered, ranged between 0.01 and 0.23ºC.

Snow cover duration in late summer

Between 1998 and 2017, snow cover lasted only five years at the end of summer (1998, 2001, 2011, 2010 and 2013), being very scarce or almost inexistent in the rest, particularly in the dry years (2005 to 2009, 2015 to 2017) (Fig. 1).

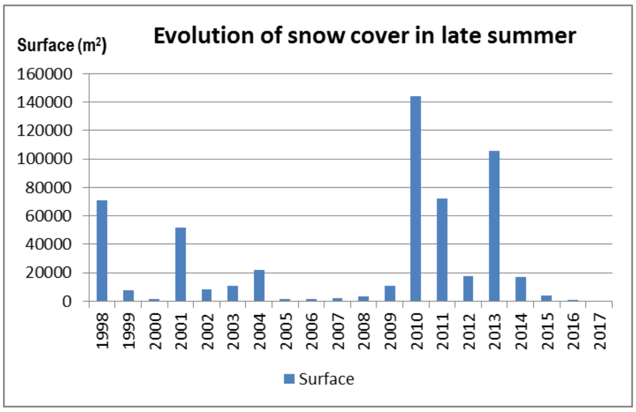

Figure 1. Snow cover surface in the Veleta cirque.

Geomorphological processes

Surface displacements of the rock glacier

Between 2001 and 2015, the rock glacier has showed different movement patterns across its surface (3815 m^2). Complementary geomatic techniques reported a total horizontal displacement of 1.59 m and surface lowering of 4.46 m (Sanjosé *et al.*, 2017). The 2004-2008 and 2014-2016 periods showed the highest sinking values, with an average around 0.45-0.50 m.

Geomorphological activity in the talus slope

Intense slope geomorphic processes mostly driven by snow melting prevailed throughout the study period, namely in 1999, 2006 and 2016, with the development of a wide variety of mass movements. Some of these landforms were ephemeral and disappeared from one year to another.

Conclusions

The MAAT has increased by 0.12ºC at the summit of Veleta peak between 2002 and 2013, where no permafrost regime exists since bedrock temperatures are relatively stable around 2-2.5ºC down to 60 m depth. By contrast, permafrost conditions have been detected within a rock glacier developed inside the Veleta cirque, in an area glaciated during the LIA. Here, increasing soil temperatures are favoring the degradation of the underlying relict ice masses, which leads to subsidence and readjustment of the surface of the rock glacier. This process is more intense in years with limited or inexistent snow cover in summer.

Acknowledgments

This study was supported by the project MOUNTAIN WARMING (CGL2015-65813-R) (Spanish Ministry of Economy and Competitiveness, SMEC), and was assisted by the High Mountain Physical Geography research group (Complutense University of Madrid). Marc Oliva is supported by the Ramón y Cajal Program of the SMEC (RYC-2015-17597).

References

Gómez, A., Palacios, D., Ramos, M., Tanarro, L.M., Schulte, L., Salvador, F., 2001. Location of permafrost in marginal regions: Corral del Veleta, Sierra Nevada, Spain. *Permafrost and Periglacial Processes* 12: 93-110.

Gómez, A., Oliva, M., Salvador, F., Salvà, M., Palacios, D., Sanjosé, J., Tanarro, L., Galindo, J., Sanz, C., 2014. Degradation of buried ice and permafrost in the Veleta cirque (Sierra Nevada) from 2006-2013 as a response to recent climate trends. *Solid Earth* 5: 979-993.

Oliva, M., Gómez, A., Salvador, F., Salvà, M., Ramos, M., Palacios, D., Tanarro, L., Pereira, P., Ruiz, J., 2016. Inexistence of permafrost at the top of Veleta peak (Sierra Nevada, Spain). *Sci. Total Environ.* 550: 484-494.

Sanjosé, J.J., Gómez, A., Sánchez, M., Salvador, F., Salvà, M., Atkinson, D.J., 2017. Técnicas geomáticas aplicadas al glaciar rocoso del corral del Veleta, durante el periodo 2001-2016. *In*: Ruiz, J., García, C., Oliva, M., Rodríguez, C., Gallinar, D. (eds.), *Ambientes periglaciares: avances en su estudio, valoración patrimonial y riesgos asociados*, Oviedo, pp. 171-179.

10 - Thermokarst lake dynamics across multiple spatial and temporal scales

Session 10

Thermokarst lake dynamics across multiple spatial and temporal scales

Conveners:

- **Josefine Lenz**, Alfred Wegener Institute Helmholtz Centre for Polar and Marine Research, Periglacial Research Unit Potsdam, Germany; University of Alaska Fairbanks, Institute of Northern Engineering, Fairbanks, AK, USA (PYRN member)
- **Frederic Bouchard**, Université Laval, Centre d'études nordiques, Québec, Canada (PYRN member)
- **Benjamin M. Jones**, Alaska Science Centre, US Geological Survey, Anchorage, AK, USA

Ice-rich permafrost degradation promotes thermokarst development and may lead to thermokarst lake initiation in vast arctic and boreal lowland regions. Potential impacts and feedback mechanisms on Arctic geomorphology, hydrology, ecology, biogeochemical cycles, energy-water balance, floral and faunal change as well as human interaction are complex. As thermokarst lakes are expected to play a key role in the widely discussed permafrost-climate feedback loop, there is an urgent need (1) to enhance the understanding of limnological, biogeochemical, physical and ecological processes and (2) to discuss their influence on the Earth system. This session highlights the role of thermokarst lake dynamics on Quaternary to modern time scales from local to global perspectives. We welcome contributions from field-based studies on lake sediments, gas measurements, monitoring programs, remote sensing, modelling, data synthesis approaches, and especially interdisciplinary efforts combining natural and social sciences in thermokarst lake research.

Introducing 'PEGS': PErmafrost and Greenhouse gas dynamics in Siberia

Frédéric Bouchard[1], Antoine Séjourné[1], François Costard[1], Christelle Marlin[1], Christine Hatté[2], Christophe Grenier[2], Daniel Fortier[3]

[1]*GEOPS/IPSL – UMR 8148 (UPS, CNRS), Université Paris-Saclay, Orsay, France, frederic.bouchard@u-psud.fr*

[2]*LSCE – UMR 8212 (CEA, CNRS, UVSQ), Université Paris-Saclay, Gif-sur-Yvette, France*

[3]*GEOCRYOLAB – Department of Geography, Université de Montréal, Montréal, Canada*

Abstract

We present a new research project related to permafrost and greenhouse gas (GHG) dynamics in Central Yakutia (Siberia). The main goal is to quantify fluxes, sources and ages of GHGs emitted from aquatic systems in response to permafrost degradation. We highlight five interconnected research axes, each defining a related 'work package' (WP). In addition to GHG dynamics, the WPs also include infrared imagery, physical modelling at different scales in permafrost simulators, paleoenvironmental reconstructions and innovative outreach. This project is funded by the international initiative "Make Our Planet Great Again" launched by the French President in June 2017.

Keywords: permafrost; thermokarst; greenhouse gases; lakes; Arctic; Siberia.

Introduction

Climate warming results in environmental impacts across the Arctic, including permafrost thawing. This can in turn release organic carbon to the atmosphere as greenhouse gas (GHG), enhancing warming (Schuur *et al.*, 2015). Considering the large quantities of carbon stored in permafrost, frozen-ground landscapes can be considered at the forefront of global climate changes.

Freshwater systems are highly diverse and ubiquitous in permafrost landscapes. Thermokarst (thaw) lakes can act as bio-geochemical 'hotspots' by releasing carbon dioxide (CO_2) and methane (CH_4) to the atmosphere. Thermokarst ecosystems have thus been identified as a major global source of GHG to the atmosphere, although the surrounding frozen soils could rather consume methane under a warmer climate (Walter Anthony *et al.*, 2014; Lau *et al.*, 2015).

Many uncertainties remain about GHG emission modelling and upscaling to the regional and global scales. There is thus an acute need to better understand the spatial and temporal evolution of lake-rich permafrost landscapes and their impacts on large-scale biogeochemical cycles, notably GHG dynamics.

Objectives

The main goal of this project called *PEGS* (PErmafrost and Greenhouse gas dynamics in Siberia) is to quantify fluxes, sources and ages of GHGs emitted from representative aquatic systems of Central Yakutia (Siberia) in response to permafrost degradation. This region is affected by thick and ice-rich permafrost. Thermokarst lakes are widespread in this region, but mostly unexplored regarding GHG dynamics. Recent work has focused on the geomorphological and hydrological evolution of thermokarst basins during the Holocene (e.g., Séjourné *et al.*, 2015; Ulrich *et al.*, 2017). Interactions between carbon exchange, surface hydrology and the atmosphere have been poorly studied until recently (Hatté *et al.*, present proceedings). This project aims at exploring the gaseous 'loop' of the carbon cycle.

The specific objectives of *PEGS* are:

1. To characterize GHG dynamics in aquatic systems of Central Yakutia using isotope geochemistry;
2. To detect CH_4 'hotspots' by infrared imagery;
3. To model GHG dynamics in response to permafrost thawing via cold-room experiments;
4. To characterize permafrost properties and thermokarst dynamics in the past based on geomorphological and paleoenvironmental surveys;
5. To disseminate knowledge via public outreach.

PEGS work packages (WPs)

A lake-rich study site near the village of Syrdakh (Sakha Republic) has been selected for its representativeness as a 'natural laboratory' in thermokarst-affected terrains. Located within the Lena River watershed near Yakutsk, it encompasses ancient agricultural fields and a small river connected with thermokarst lakes of different ages (mid-Holocene to modern). It is a highly heterogeneous landscape with varying ground-ice and organic carbon content.

WP1: GHG monitoring and characterization

We will investigate GHG dynamics in active thermokarst systems (mature lakes with thaw slump activity and recently formed shallow ponds). Stable isotope tracers and radiocarbon concentration will be analyzed from dissolved and ebullition gas samples in order to characterize their ages, sources and pathways, as done in the Canadian Arctic (Bouchard *et al.*, 2015). Water and sediment samples will also be collected to hierarchize the factors controlling dissolved carbon sources along a soil-stream-river continuum.

WP2: Methane 'hotspot' detection using infrared imagery

Methane can now be remotely detected and quantified using infrared hyperspectral imagery, even in natural environments with concentrations near atmospheric values (Gålfalk *et al.*, 2016). We will use this technology in the field and in the laboratory (WP3 below) to quantify, with high spatio-temporal resolution, methane emissions in response to permafrost thawing. This will be associated with ongoing remote-sensing studies at LSCE focused on seasonal regional emissions.

WP3: Cold-room permafrost simulations

Building on previous expertise in cold-room experimental modelling, we will investigate processes (e.g., thermokarst, thaw slump development) related to permafrost degradation in laboratory-controlled conditions. We will focus on the shielding layer and the influence of different permafrost characteristics (e.g., ice content, vertical discontinuities like ice wedges). WP3 will aim at 1) hierarchizing the parameters controlling permafrost thermal destabilization, and 2) comparing the results from cold chamber with measures from the field. At a smaller scale, we will use the infrared hyperspectral technology (WP2 above) to detect and quantify emissions of methane from permafrost samples of different carbon and ice contents. This WP will involve strong inter-lab collaborations between GEOPS and the GEOCRYOLAB at U. Montréal (Canada).

WP4: Geomorphology & paleoenvironmental reconstructions

Thermokarst basins can act as sensitive sentinels of environmental change; yet, the rich information stored in their sediments remains virtually untapped (Bouchard *et al.*, 2017). We plan to characterize permafrost properties in the area, focusing on ground-ice and organic carbon content in representative landscape units. Building on multi-proxy study of such archives from northern Canada, we will also reconstruct permafrost degradation in Central Yakutia during the Holocene by analyzing lake and soil sedimentary archives (i.e. retrieved cores). Sedimentological, geochemical and biostratigraphic data will be generated and analyzed.

WP5: Public and media outreach

Science must now be accessible and communicated to the public. This is particularly acute in the climate change realm. We aim at making a strong impact by reaching out to the society as a whole, firstly by promoting cooperation between researchers, students and the media. We wish to feed stakeholders with a clear and broad-scale understanding of permafrost thawing and related impacts (e.g., GHG emissions), and enhance large audiences with innovative tools (e.g., blogs, online fieldwork/lab movies, lab demonstrations to visiting schools). Comic strips about permafrost research were recently launched, providing a unique coverage to early-career scientists (frozengroundcartoon.com). Such an initiative will be maintained and strengthened.

PEGS is among the first 18 international projects funded by the "Make Our Planet Great Again" initiative launched by the French President in June 2017.

References

Bouchard F. *et al.*, 2015. Modern to millennium-old greenhouse gases emitted from ponds and lakes of the Eastern Canadian Arctic (Bylot Island, Nunavut). *Biogeosciences* 12: 7279-7298.

Bouchard F. *et al.*, 2017. Paleolimnology of thermokarst lakes: a window into permafrost landscape evolution. *Arctic Science* 3: 91-117.

Gålfalk M. *et al.*, 2016. Making methane visible. *Nature Climate Change* 6: 426-430.

Lau M.C.Y. *et al.*, 2015. An active atmospheric methane sink in high Arctic mineral cryosols. *The ISME Journal* 9: 1880-1891.

Schuur E.A.G. *et al.*, 2015. Climate change and the permafrost carbon feedback. *Nature* 520: 171-9.

Séjourné A. *et al.*, 2015. Evolution of the banks of thermokarst lakes in Central Yakutia (Central Siberia) due to retrogressive thaw slump activity controlled by insolation. *Geomorphology* 241: 31-40.

Ulrich M. *et al.*, 2017. Differences in behavior and distribution of permafrost-related lakes in Central Yakutia and their response to climatic drivers. *Water Resources Research* 53: 1167-1188.

Walter Anthony K.M. *et al.*, 2014. A shift of thermokarst lakes from carbon sources to sinks during the Holocene epoch. *Nature* 511: 452-456.

Activation of thermokarst in Central Yakutia during the last 25-30 years

Alexander N. Fedorov[1]
Pavel Y. Konstantinov[2]
Nikolay I. Basharin[2]
Roman V. Desaytkin[3]
Alexey R. Desyatkin[2,3]
[1]*Melnukov Permafrost Institute SB RAS, fedorov@mpi.ysn.ru*
[2]*Melnukov Permafrost Institute SB RAS*
[3]*Institute of biological problems of cryolithozone SB RAS*

Abstract

Current climatic changes have greatly affected the state of permafrost worldwide. The response of permafrost landscapes in Central Yakutia to climatic changes in recent decades is quite rapid affecting the socio-economic conditions of population and this requires serious study. Rapid, widespread thermokarst activity is observed at present. In open and anthropogenic landscapes, high-centered polygons have developed almost everywhere; thermokarst depressions and lakes are forming and growing rapidly in depth and size.

Keywords: Thermokarst, global warming, Central Yakutia.

Introduction

Central Yakutia, one of the most populated regions within the permafrost zone, is currently facing serious problems associated with the response of permafrost landscapes to climate warming. The presence of the ice complex, increasing population, changing technologies and expanding human activities make the Central Yakutia landscapes sensitive to disturbance. Human-disturbed or modified permafrost landscapes are lacking a self-preservation mechanism, since the protective layer between the upper boundary of the underground ice and the depth of seasonal thawing is practically absent and does not protect landscapes from degradation. Climate change in the past 25-30 years has led to this state.

Results

The intensive development of thermokarst in Central Yakutia is associated with an increase in soil temperature since the early 1980s, representing the climate shift, when for several years an average annual temperature was increased by almost 0.5°C. If we take into account that before 1980 the formation of the incipient thermokarst microrelief was associated with the excavation of top soil only, after 1980 the thermokarst began to develop on the meadow areas of the ice complex, which were relatively stable up to that time. The interval of time from 1980 to 1990, we define it as the preparatory period for the development of thermokarst. In these years, primary signs of thermokarst were observed, such as the formation of underground holes in the active layer and their local subsidence of the soils above them.

The strongest response of ice-rich landscapes to this process occurred in the 1990s-2000s. Widespread ground subsidence due to melting of the tops of ice wedges was observed during this period resulting in hummocky polygonal landforms. Degradation rates were quite high; the surface subsided in places by 1-2.5 m over 1990-2015. On sites of permafrost degradation, young thermokarst lakes expanded in area by 2-4 times. In some locations, the distribution areas of these lakes have reached areas of alases formed in the Holocene optimum.

Significant effects on the permafrost landscapes have been exerted by forest fires and outbreaks of the Siberian silk worm at the beginning of 2000th, induced by climate warming. Changes of the thermal regime in the disturbed areas cause ground settlements, which are already turning into thermokarst lakes. Activation of thermokarst goes inside and around settlements too. The shielding layer of the ice complex is practically absent in these conditions, and surface subsidence is everywhere observed.

The study of thermokarst development on the special monitoring sites of Yukechi, Neleger and Churapcha on the Leno-Amga interfluve of Central Yakutia allowed us to study in detail the temperature regime of the landscapes, the rate of subsidence in the individual stages of thermokarst micro- and mesorelief formation, the attenuation of the process that began, the formation of the thermokarst lake and determine the extent of degradation of the ice complex.

Conclusion

In the context of modern climate changes and increased anthropogenic impact, the permafrost landscapes of Central Yakutia are under great strain. Decreasing of agricultural and potential land area for construction, changing the water balance of landscapes due to forest fires, clear cutting and reproduction of forest-destroying insects leads to social problems during considered period. The increase in the population of settlements requires the expansion of the built-up territories. People are forced to build their homes on unstable areas where subsidence has already begun. Our task is to protect the population from the ongoing negative processes in the permafrost landscapes in order to preserve the traditional way of life and sustainable development of society in cryolithozone.

Thermokarst lake monitoring on the Bykovsky Peninsula using high-resolution remote sensing data

Theresa Henning [1]
Frank Günther [2]
Alexander Kizyakov [3]
Guido Grosse [2,4]

[1] *Technische Universität Dresden, Faculty of Environmental Science, Institute of Geography, 01069 Dresden, Germany, theresa-henning@web.de*
[2] *Alfred Wegener Institute Helmholtz Centre for Polar and Marine Research, 14473 Potsdam, Germany*
[3] *Lomonosov Moscow State University, Faculty of Geography, Department of Cryolithology and Glaciology, 119991 Moscow, Russia*
[4] *University of Potsdam, Institute for Earth and Environmental Sciences, 14476 Potsdam, Germany*

Abstract

Thermokarst lakes are a characteristic element of arctic permafrost regions and an indicator for their rapid landscape changes. Assessing their dynamics contributes to the understanding of driving processes of change, to the evaluation of impacts on landscape characteristics as well as to the estimation of the impact on the permafrost-related carbon budget. Monitoring thermokarst lake dynamics on the Bykovsky Peninsula, consisting of ice-rich Yedoma deposits, using high-resolution remote sensing imagery from 1951 to 2016, revealed a long-term tendency towards lake drainage. Approximately 17 % of the 1951 lake area was lost due to coastal erosion or the development of drainage networks. In parallel, coastal erosion driven land loss amounts to 2.3% of the peninsula. We find process interconnections between coastal erosion and lake change, as well as lake change dependency on land elevation in a developed alas-yedoma thermokarst relief.

Keywords: thermokarst, lake dynamics, yedoma, East Siberia, remote sensing

Introduction

Arctic permafrost landscapes are in equilibrium with environmental and climatic parameters. Changes in these external factors result in dynamic and rapid changes, highlighting the landscape's vulnerability. The observed increase of both, air temperatures and seasonal duration particularly affects permafrost regions with a large amount of ground ice. Degradation of ice-rich permafrost deposits, such as Yedoma Ice Complex , initiates thermokarst and subsequent lake formation. At the same time, progressing ice-wedge degradation creates pathways for lake seepage and ultimately may lead to lake drainage. Therefore, thermokarst lakes are one of the most characteristic features of permafrost regions, indicating the thaw of perennially frozen ground and portraying the expeditious alteration of permafrost lowland landscapes (Jones et al., 2011). Investigating their long-term dynamics is important for understanding the underlying driving processes, for evaluating impacts on geomorphology, hydrology, ecosystem change as well as for estimating the potential release of climate-relevant organic carbon, previously frozen in permafrost soils (Grosse et al., 2013).

As thermokarst lakes are abundant in Arctic lowlands with ice-rich yedoma permafrost, the Bykovsky Peninsula in the north of East Siberia currently exhibits more than 300 lakes larger than 1000 m² water bodies on a land surface area of 163 km².

The objective of our study is to create a time series of high resolution orthorectified imagery and to map thermokarst lakes on the Bykovsky Peninsula in four time steps, spanning an observation period of 64 years. Based on historical aerial photography and modern satellite imagery, we here report first results from detailed lake mapping that was carried out for monitoring lake expansion and lake drainage over time using the first and last dataset from 1951 and 2015, respectively. Furthermore, tendencies of drainage or expansion with respect to elevation and potential mechanisms for lake expansion and drainage were investigated.

Methods

Baseline datasets that were used comprise historical aerial photographs from 1951 that feature ahigh level of detail, as well as high resolution satellite images from

2015 (WorldView-1, WorldView-2, and RapidEye). WorldView data at 50 cm resolution consisted of two panchromatic stereo pairs that were used for digital elevation model extraction at 1 m resolution. Ground control points collected in the field and subsequent orthorectification of WorldView imagery provided a highly consistent georeferencing basis for other datasets. RapidEye data has been georeferenced and resampled to 5 m resolution. Air photo bundle block adjustment was done according to Günther et al. (2015) and air photos were resampled to 0.9 m ground resolution. After terrain correction of single air photos and mosaicking to a map geometry, lake and shoreline mapping was done manually in panchromatic imagery and automatically based on RapidEye's near-infrared band using a threshold based approach. Finally vector datasets were incorporated into GIS to measure lake area changes and coastal erosion magnitudes.

Results and discussion

Preliminary results of thermokarst lake changes over the 1951 to 2015 period revealed a net lake shrinkage tendency (Tab. 1).

Table 1. Thermokarst lake changes on the Bykovsky Peninsula from 1951 to 2015

	1951	2015
Lake quantity	577	816
Lake surface area [km²]	19.76	16.44
Land-lake-ratio [%]	11.87	10.11

In 1951, lake area was 1975.6 ha, while it decreased to 1644.4 ha until 2015. Considering the land loss of Bykovsky over the same time from 166.5 to 162.7 km² (without lagoon areas), this corresponds to an overall decrease of the peninsula's lake limnicity from 11.9 to 10.1 %. In contrast to the general lake area decrease, when focusing only lakes that are present in both datasets, the number of lakes has increased. This can be attributed to the fact that i.e. the drainage of a large lake may leave behind several smaller residual lakes. While drained large lakes were mostly located in lower elevation lake basins close to the coast, a considerably higher number of medium-size lakes drained through thermo-erosion valleys on yedoma uplands.

The initial assessment of thermokarst lake change rates focused on lakes that exist in both datasets. At this stage, we did not differentiate between growing and shrinking lakes.

Following these first order estimations, a net lake area decrease of $3.31 * 10^6$ m² was observed, corresponding to 5.2 ha lake area lost per year. Similar to lake change, coastal erosion was also investigated based on the net change area between two states of the coastline for the entire peninsula. Accordingly, mean total retreat across the entire coastline was 42.7 m, corresponding to an average rate over 64 years of 0.68 m/yr. This rate is somewhat higher than the mean erosion rate over the 1951-2007 time period found by Lantuit et al. (2011). This reflects considerably higher rates that emerged during the recent past with several all-time sea ice minima and very warm summers (Günther et al. 2015).

Conclusions

Our findings suggest that thermokarst lakes on the Bykovsky Peninsula are subject to high dynamics. Numerous lakes drained due to coastal erosion or the development of drainage networks, portraying the proneness of arctic coastal tundra lowlands to disturbances and changing environmental conditions. By monitoring thermokarst lakes on Bykovsky, a long-term tendency towards drainage was identified and this trend cannot be considered separately, but is rather the result of the interrelation of endogeneous and exogeneous forcings such as ice-wedge degradation and coastal erosion, both of which fostering accelerated permafrost degradation.

References

Grosse, G., Jones, B. & Arp, C., 2013. Thermokarst lakes, drainage, and drained basins. *In*: Shroder, J. (Editor in Chief), Giardino, R., Harbor, J. (Eds.), *Treatise on Geomorphology*, vol. 8, *Glacial and Periglacial Geomorphology*, Academic Press, San Diego, 325–353.

Lantuit, H., Atkinson, D., Overduin, P. P., Grigoriev, M., Rachold, V., Grosse, G. & Hubberten, H.-W. (2011). Coastal erosion dynamics on the permafrost-dominated Bykovsky Peninsula, north Siberia, 1951-2006, *Polar Research* 2011, 30: 7341

Günther, F., Overduin, P. P., Yakshina, I. A., Opel, T., Baranskaya, A. V. & Grigoriev, M. N. (2015). Observing Muostakh disappear: permafrost thaw subsidence and erosion of a ground-ice-rich island in response to arctic summer warming and sea ice reduction, *The Cryosphere* 9: 151-178.

Jones, B. M., Grosse, G., Arp, C. D., Jones, M. C., Walter Anthony, K. M. & Romanovsky, V. E., 2011. Modern thermokarst lake dynamics in the continuous permafrost zone, northern Seward Peninsula, Alaska. *Journal of Geophysical Research: Biogeosciences* 116 (G2).

Thermodynamic calculation of freezing temperature of gas-saturated pore water in talik zones

Vladimir A. Istomin[1,2]
Evgeny M. Chuvilin[1,3]
Daria V. Sergeeva[1]
Boris A. Buhkanov[1]
Yulia V. Stanilovskaya[4]
Erik Green[4]
Christian Badetz[4]

[1]*Skolkovo Institute of Science and Technology (Skoltech), Moscow, Russia, email: vlistomin@yandex.ru*
[2]*Scientific Research Institute of Gazprom (VNIIGAZ JSC), Russia*
[3]*Department of Geology, Moscow State University (MSU), Russia*
[4]*Total E&P Russie, Moscow, Russia*

Abstract

Nowadays, there are some unusual craters, associated with gas release from permafrost on the northern part of West Siberia (the Yamal Peninsula). One of possible mechanism is the freezing of gas-saturated talik zones and increasing gas pressure up to 1.5 - 2.0 MPa with a gas blowout and crater formation. In this case the thermodynamic technique of freezing temperature calculation of gas-saturated pore water under the gas pressure is developed. Methane, carbon dioxide and their mixtures are considered. It is shown that the solubility of gases in water should be taken into account when the pressure grows up during freezing of gas-saturated talik zones (especially when carbon dioxide is present in the gas phase). The influence of three factors on the freezing point of a gas-saturated pore water is analyzed: the external pressure created by the gas, the presence of a gas dissolved in water and the water mineralization.

Keywords: thermodynamic calculation, talik, gas saturated water, freezing temperature, pressure

Introduction

Recently, several large-diameter craters have occurred in the Yamal Peninsula, the nature of which remains unclear. Nowadays, a number of hypotheses have been proposed: the climate warming, the freezing of the sub-lakes talik zone, the decomposition of intra-permafrost relict gas hydrates, the migration of a deep gas through talik zone (Leibman *et al,* 2014; Olenchenko *et al,* 2015; Bogoyavlenskiy *et al,* 2016; Khimenkov *et al,* 2017; Buldovicz *et al,* 2017).

We assume an important role in the formation of craters is given to the processes of freezing of gas-saturated talike zone. So the current research proposes a thermodynamic analysis of the conditions of crystallization of pore water in gas-saturated soils. It includes an assessment of the influence of gas composition and pressure, and salinity of pore water on freezing temperature in gas-saturated sediments. These investigations are based on previously performed research (Isomin *et al,* 2009; Isomin *et al,* 2017).

Method and results

The thermodynamic analysis led to the dependence of freezing temperature of pore solution (moisture) on the gas pressure:

$$t_{fr} = 103.25 \cdot \ln(b) + 5.57 \cdot (1-b)^2 ,$$

$$b = a \cdot (1 - x_g) \cdot \exp\left(- \frac{\Delta V \cdot (P - P_0)}{R \cdot (t_{fr} + 273.15)} \right).$$

Where:

P - external pressure, which effects on thermodynamic system, it is gas pressure in our case, MPa; $P_0 = 0.101325$ – atmospheric pressure, MPa; t_{fr} - freezing temperature of pore water, °C; x_g - molar fraction of gases, dissolved in pore water; $x_g = \sum_i x_i$, where x_i - molar fraction of i gas in pore water;

R - universal gas constant, $R = 8.3146$ J/(mol K);

a - activity of pore water in saline solution (electrolyte solution) under atmospheric pressure P_0 (for fresh pore solution and high soil moisture content $a \approx 1$);

V_w, V_{ice} - molar volume of water and ice, cm³/mol;

$\Delta V = V_{ice} - V_w$ - difference between molar volume of water and ice, $\Delta V = 1.635$ cm³/mol.

If we put in the formula for the quantity b on the right-hand side $t_{fr} = 0$, we obtain an approximate analytical dependence of the freezing temperature of the aqueous pore mineralized solution.

On the base of developed thermodynamic method of calculation, the effect of pressure on the freezing temperature of pore water containing dissolved gases (CH_4 and CO_2) and their mixtures (Fig. 1) was calculated.

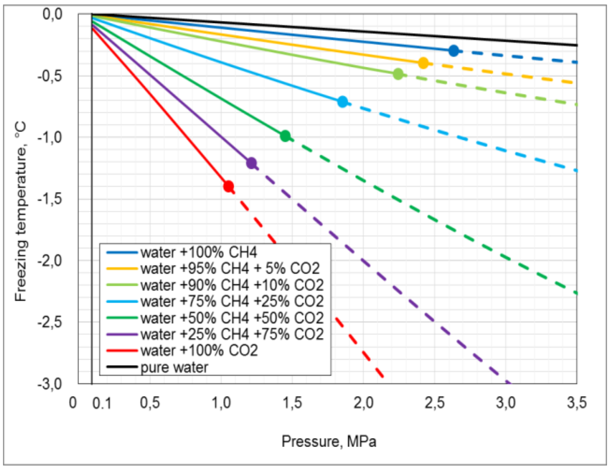

Fig. 1. Dependence of external gas pressure on freezing temperature of gas-saturated pore water. Dots are the appearance of gas hydrate phase, the dashed lines are the continuation of the "gas-gas-saturated water-ice" equilibria in the metastable region.

The performed calculations show that the freezing temperature of gas-saturated pore water in talik zones in conditions of pressure increasing can be markedly reduced even in the absence of mineralization. Thus, the freezing temperature of pore water with a high CO_2 content may drop by 1-1.5 °C below 0 °C. This allows accumulate a large amount of gas in the porous water of cold sediments at high negative temperature due to high solubility. Later, during sharp pore pressure decreasing, due to destruction of the frozen roof of talik zone, the gas will be actively allocated, creating a "champagne effect."

Conclusions

The technique of thermodynamic calculation of the freezing temperature of gas-saturated and mineralized pore solutions under the external gas pressure is presented. Different gas compositions (CH_4, CO_2 and mixtures of CH_4 with CO_2) are observed. The influence of three factors on freezing temperature of gas-saturated pore solutions are analyzed: the external gas pressure, the presence of a gas dissolved in pore water and water mineralization.

The obtained results show solubility of gases in water should be taken into account when considering the dynamics of pressure increasing during freezing of gas-saturated talik zones (especially when carbon dioxide is present in the gas phase).

Acknowledgments

This work is performed within a collaboration between Skoltech and Total.

References

Bogoyavlenskiy, V.I., Sizov, O.S., Bogoyavlenskiy, I.V. & Nikonov, R.A., 2016. Remote detection of surface gas releases in the Arctic. *Journal of the Arctic: ecology and economy* 3: 4–15 (In Russian).

Buldovicz, S.N., Khilimonyuk, V.Z., Bychkov, A.Y., Ospennikov, E.N., Vorobyev, S.A., Gunar, A.Y., Gorshkov, E.I., Chuvilin, E.M., Cherbunina, M.Y., Kotov, P.I., Lubnina, N.V., Motenko, R.G. & Amanzhurov, R.M., 2017. Cryovolcanism on the Earth: Origin of a Giant Crater in the Yamal Peninsula (Russia). *Scientific reports* 7: (in press).

Istomin, V.A., Chuvilin, E.M., Makhonina, N.A. & Bukhanov, B.A., 2009. Temperature dependence of unfrozen water content in sediments on the water potential measurements. *Earth's Cryosphere* 2: 35-43 (in Russian).

Istomin, V.A., Chuvilin, E.M., Bukhanov, B.A. & Uchida, T., 2017. Pore water content in equilibrium with ice or gas hydrate in sediments. *Cold Regions Science and Technology* 137: 60–67.

Khimenkov, A.N., Sergeev, D.O., Stanilovskaya, J.V., Vlasov, A.N. & Volkov-Bogorodsky, D.B., 2017. Gas emissions in the cryolithozone: A new type of geocryological hazards. *Journal of Georisk* 3: 58–65 (In Russian).

Leibman, M.O., Kizyakov, A.I., Plehanov, A.V. & Streletskaya, I.D., 2014. New permafrost feature: Deep crater in Central Yamal, West Siberia, Russia as a response to local climate fluctuations. *Geogr. Environ. Sustain.* 4, 68–80.

Olenchenko, V.V., Sinitsky, A.I., Antonov, E.Y., Eltsov, I.N., Kushnarenko, O.N., Plotnikov Potapov V.V. & Epov, M.I., 2015. Results of geophysical researches of the area of new geological formation "Yamal crater". *Earth's Cryosphere* 4: 94-106 (in Russian).

Different theories of thermokarst lakes evolution considered with the help of remote sensing and quantitative statistic methods

Veronika Nikolaevna Kapralova[1]

[1] *Sergeev Institute of Environmental Geoscience Russian Academy of Sciences (IEG RAS), Russia, Moscow, vkapralova@gmail.com*

Abstract

More than 25% of Earth is within a permafrost zone. Accordingly problems of permafrost and related exogenous geological processes are very important. Thermokarst is one of geocryological processes especially sensitive to anthropogenic intervention and climatic changes. It is important to study the general spatial and temporal patterns of thermokarst processes for the purpose of geotechnical risk assessment. The analysis of the spatial structure of lacustrine thermokarst plains was based on mathematical morphology of landscape methods.

Keywords: landscape pattern analysis; probability distribution; thermokarst development; mathematical morphologyof landscape; remote sensing

Introduction

Thermokarst lacustrine plains occupy vast areas in the high latitude territories. One of the important questions, regarding the thermokarst development, is to find the principles of its distribution and dynamics with the purpose of forecasting environmental changes. Many researchers studied the thermokarst processes, but proper statistical methods regarding these are yet to be developed. In particular, the analysis of quantitative aspects of thermokarst is to be considered. Various researches attempted to determine the age of thermokarst lakes, as well as the time of their occurrence.

Methods

In this work we try to investigate and compare several models of the lake development by means of modeling and remotely sensed data.

Mathematical morphology of the landscape allows investigating the patterns of the landscape mosaics as well as the ways of the quantitative analysis of those (Viktorov, 1998).

The basic model we used considers the morphological pattern of the lacustrine thermokarst plains and it is based on the mathematical relations between the key geometric parameters of the associated landscape patterns. Normally a mathematical model is based on certain assumptions and is designed as the set of quantitative expressions, describing the behavior of the key quantitative parameters of the landscape pattern, shaped by the exogenous process. The expressions contained by the model are independent and might not be derived one from each other and therefore they are not redundant but complimentary.

The first model is formulated on the basis of empirical data that were acquired from papers of Burn and other authors (Burn & Smith, 1990). We attempted elaborating the model, when the growth rate of lakes is random and constant with time. If so, at the specific moment of time the average size of the lakes should be of normal distribution.

The second model was formulated by Viktorov (Victorov, 2006), and it implies that the growth rate of lakes is proportional to their size, and at the specific moment of time, lake diameters should be of lognormal distribution. The models also accounted for different patterns of the subsequent lacustrine evolution. The models were based on the stochastic theory.

Table 1: Model of the distribution of the thermokarst lake parameter under different lacustrine thermokarst evolution scenarios

Thermokarst plain evolution scenario	Synchronous start	Asynchronous start
Lognormal growth of the lake radii	Model type 1.0 Lognormal distribution of the lake areas (radii) $f_r(x,t)=\frac{1}{\sqrt{2\pi}\sigma x\sqrt{t}}e^{-\frac{(\ln x-at)^2}{2\sigma^2 t}}$	Model type 1.1 "Logarithmic" distribution of the lake areas (radii) $F(x)\approx\frac{\ln x-\ln a}{\ln b-\ln a},\ a\le x\le b$
Quasiuniform growth of the lake radii	Model type 2.0 Normal distribution of the lake areas (radii) $f(x)=\frac{1}{\sqrt{2\pi}\sigma_0}e^{-\frac{[x-a_0]^2}{2\sigma_0^2}}$	Model type 2.1 Uniform distribution of the lake areas (radii) $F_r(x)\approx\frac{x-a}{b-a},\ a\le x\le b$

where α, σ - are distribution parameters, t – is age of lake

Also, for each of the models we considered the situation of synchronous and asynchronous start of the thermokarst processes. As a result, we came up with four distributions for lakes sizes (table 1) and we also looked for conformity of theoretical and experimental data.

Conclusion

We performed the model approval for several study areas, which are located in different Arctic regions of Russia, Canada, and USA (Alaska) (fig.1).

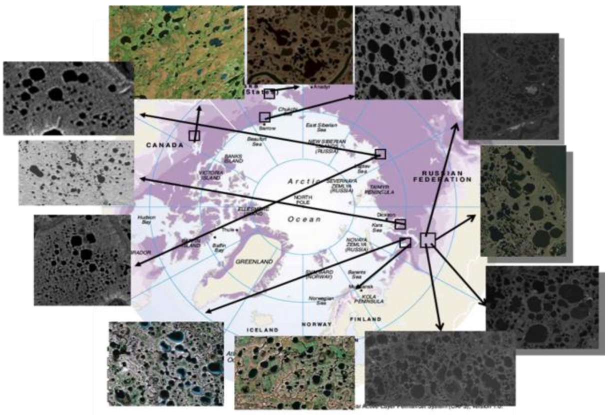

Figure.1. Study sites in different Arctic regions.

We selected the study sites based on the morphological homogeneity of those and on the availability of the remotely sensed imagery. Appropriate homogeneity of the study assumes the combination of the following conditions: 1) terrain surface is homotypic causing the appearance of the uniform pattern on the satellite or airborne image, 2) uniform lithological composition of the topsoil as well as of the underlying deposits, 3) relatively constant depth of the deposits within the study area, 4) lack of buried valleys, 5) lack of tectonic dislocations, 6) relatively uniform permafrost conditions. The model does not expect meeting the absolute uniformity, but a statistical one, which assumes random fluctuations.

We selected lakes on satellite images and evaluated the relationship of empirical and theoretical distributions of the lake areas (radii). Analysis of the results shows that the majority of sites have a lognormal distribution.

Acknowledgments

The research is done with the support of Russian Geographic Society and Russian Foundation for Basic Research Grant # 17-05-41141.

References

Burn C.R. & Smith M. W. 1990. *Permafrost and Periglacial Processes*, v. 1, 161-176.

Victorov A.S. 1998. *Mathematical morphology of landscape,* 180

Victorov A.S. 2006. *General problems of the Mathematical morphology of landscape*, 252

Carbon accumulation in thermokarst lakes: A biogeochemical comparison between boreal and tundra lake deposits in Alaska

Josefine Lenz[1, 2], Katey Walther Anthony[2], Matthias Winkel[2, 3], Susanne Liebner[3], Matthias Fuchs[1], Jens Strauss[1], Christopher Maio[4], Benjamin M. Jones[5], Guido Grosse[1]

[1]*Alfred Wegener Institute Helmholtz Centre for Polar and Marine Research, Periglacial Research Section, Josefine.Lenz@awi.de*

[2] *University of Alaska Fairbanks, Institute of Northern Engineering*

[3] *Helmholtz Centre Potsdam - German Research Centre for Geosciences*

[4] *University of Alaska Fairbanks, Department of Geosciences*

[5] *US Geological Survey, Alaska Science Centre*

Abstract

Thermokarst lakes are widespread features of changing periglacial environments. In this study, we analyze total organic carbon content (TOC), C/N, stable carbon isotopes and methane concentration in pore water from sediments of 18 tundra lakes in West Alaska and 11 boreal lakes in Central Alaska. We aim to decipher differences in carbon accumulation and sources of organic matter to assess their role in the carbon cycle. While a wide range of TOC contents was detected for West Alaska with highest TOC in lakes that initiated in drained lake basins, some boreal lakes in Central Alaska (e.g. Goldstream Lake) have surprisingly low TOC in their sediments. Similar findings in CH_4 concentration suggest that the state of permafrost, the age of the lakes and the catchment characteristics have an important influence on sources of organic carbon and, thus, affect the different potential of thermokarst lakes to contribute to the global carbon cycle.

Keywords: thermokarst lake dynamics; permafrost degradation; sedimentology; total organic carbon; methane

Introduction

Thermokarst lakes are evidence for permafrost thaw and induce deep thaw by talik development. During the thawing process, organic matter previously preserved in permafrost, is decomposed and partially mobilized as the greenhouse gases carbon dioxide and methane. In the course of lake development and shoreline expansion, both, younger near-surface and older organic matter from slumping shores are deposited in the lake basin. Lake internal bioproductivity is complementing carbon accumulation in lacustrine deposits and provides an additional source of young carbon transformed into greenhouse gases.

This study aims at identifying differences in carbon accumulation and sources for various thermokarst lake settings in Alaska to better understand the importance of permafrost conditions, hydrological systems and lake genesis for thermokarst lake carbon cycling.

Compared study sites

Tundra lakes in West Alaska

We retrieved 18 short lake cores of up to 73 cm length near the boundary of continuous-discontinuous permafrost on the Central Seward Peninsula (Fig. 1a) and in the Kobuk, Noatak, Selawik deltas (Fig. 1b) in Western Alaska. They represent dynamic lakes, which have partly developed in deltaic deposits, in ice-rich uplands, and in drained lake basins. Tundra plant communities with only sparse erect shrubs and trees dominate the vegetation.

Boreal lakes in Central Alaska

Short and long cores up to 473 cm length were retrieved from eleven thermokarst lakes in Goldstream Valley in the Fairbanks region of Central Alaska (Fig. 1c). They represent recent and Holocene lakes in a boreal river valley with discontinuous permafrost with open and closed talik systems.

Methods

We retrieved lake sediment cores in August 2016 and March 2017 using different coring systems (piston-, hammer, and vibra-corer). Cores were described, subsampled and analyzed for total organic carbon (TOC), total nitrogen (TN) and stable carbon isotopes ($\delta^{13}C$). Selected sediment samples were taken to quantify methane (CH_4) concentration in pore water and for accelerated mass spectrometry radiocarbon age determination of macrofossils.

Results and discussion

The TOC content of samples from eighteen tundra lake sediment cores ranges from 0.6 to 42 wt.%. We found highest TOC contents in lakes which initiated in drained lake basins on the Central Seward Peninsula. In addition, individual lakes in the Kobuk Delta were characterized by TOC higher than 30 wt.% whereas lowest TOC was measured in sediments of lakes developed in upland remnants in the Kobuk Delta as well as in deltaic lakes of the Selawik Delta dominated by discontinuous permafrost. Similarly, low TOC was measured for Goldstream Lake in boreal Central Alaska with a mean TOC of 2.2 wt.% averaged from 4 sediment cores. While this specific lake shows CH_4 seeps at actively expanding shorelines, its sediments have a low CH_4 concentration of 214 ppm/g in near-shore sediments and slightly higher CH_4 concentration of 772 ppm/g in its central part.

Substantial numbers of CH_4 producing microorganisms and pore water CH_4 concentrations were detected in lake sediments in West Alaska. Pore water CH_4 concentrations varied by two orders of magnitude ranging between 10 and slightly above 1000 µM (mean: 376 µM). The surface 2 cm of the lake sediments had similarly high mean CH_4 concentrations (387 µM) like the overall mean. Thus, even though all measured CH_4 concentrations were below saturation, our data suggest that thermokarst lake sediments in West Alaska are a source of CH_4 to the water column.

While sample processing is ongoing, we assume that the age of the lakes, state of permafrost (continuous vs. discontinuous) and the catchment characteristics (boreal vs. tundra) have an important influence on carbon accumulation as well as CH4 emission rates and, thus, different potential of thermokarst lakes to contribute to the global carbon cycle.

Acknowledgments

This study was supported by the National Science Foundation Arctic System Science Program (#1500931), an ERC Starting Grant (#338335) and the Initiative and Networking Fund of the Helmholtz Association (#ERC-0013). We thank the Nana Cooperation and the US Fish and Wildlife Service for supporting field work in the area of Kotzebue in Western Alaska, as well as Jim Kincaid from Northwestern Aviation and Jim Webster from Webster's Flying Service for providing field logistics.

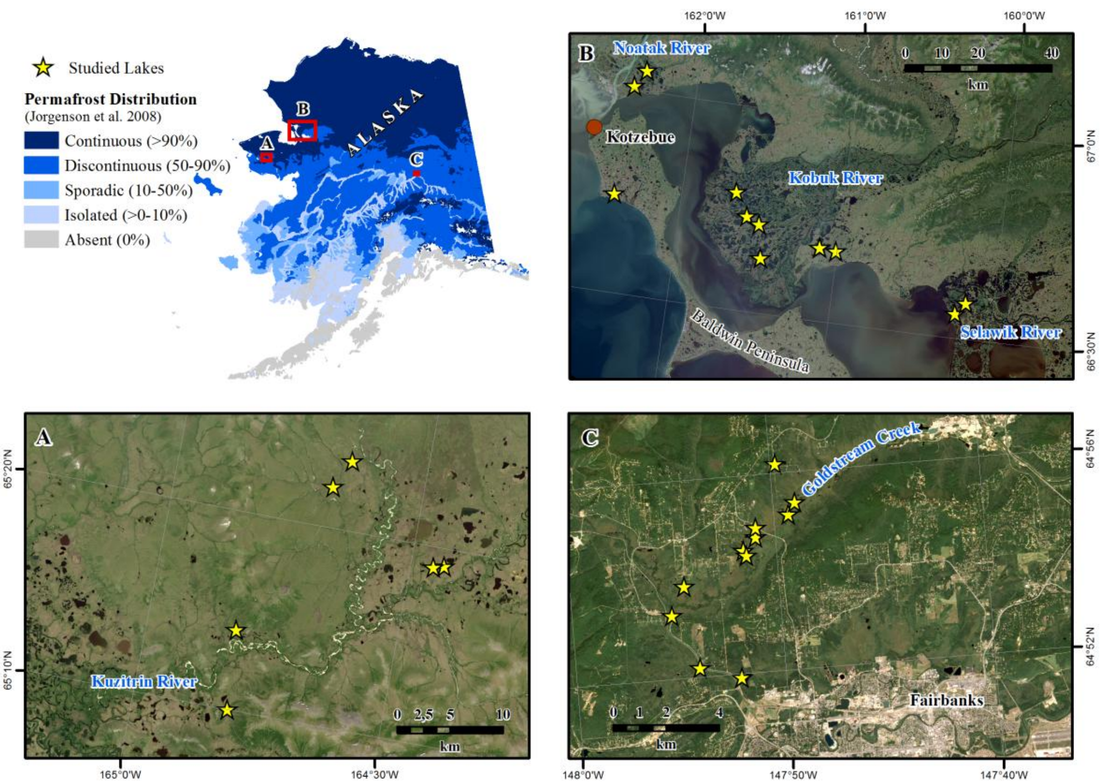

Figure 1: Studied lake sites located in continuous and discontinues permafrost region in Alaska in A) Central Seward Peninsula, B) in the Noatak, Kobuk and Selawik Deltas near Kotzebue and in C) Goldstream Valley near Fairbanks (Source: true color composites of Landsat 8 satellite images).

Lake dynamics across latitudinal permafrost transects

Ingmar Nitze[1,2], Guido Grosse[1,2], Benjamin M. Jones[3], Julia Boike[1], Vladimir Romanovsky[4,5]

[1]*Alfred Wegener Institute Helmholtz Centre for Polar- and Marine Research, Potsdam, Germany, ingmar.nitze@awi.de*

[2]*Institute of Earth- and Environmental Sciences, University of Potsdam, Potsdam, Germany*

[3]*United States Geological Survey, Anchorage, AK, USA*

[4]*Geophysical Institute, University of Alaska Fairbanks, Fairbanks, AK, USA*

[5]*Tyumen State Oil and Gas University, Tyumen, Russia*

Abstract

Earth's permafrost region, covering about one quarter of the land surface, is characterized by a large abundance of lakes, which have a strong impact on carbon, energy and water fluxes and are considered highly responsive to climate change. The monitoring of lake change in northern high latitudes, at a sufficiently high spatial and temporal resolution, is crucial for understanding the landscape's response and feedbacks to climate change. Here we report on lake change trends using dense time series of 30-m resolution Landsat satellite imagery across four continental-scale transects covering more than 2.3 million km² or 10% of the permafrost region from 1999 to 2014. Our study provides a comprehensive assessment of lake changes within these transects that capture latitudinal, altitudinal, and other environmental gradients affecting ground thermal regime, permafrost extent, and permafrost characteristics. Dynamics of more than 600,000 analyzed lakes showed a very diverse pattern, with a complex influence of multiple factors across different spatial scales.

Keywords: Lake Change, Remote Sensing, Landsat, Machine-Learning

Introduction

Lakes are an ubiquitous landscape feature in northern permafrost regions. They have a strong impact on carbon, energy and water fluxes and can be quite responsive to climate change. The monitoring of lake change in northern high latitudes, at a sufficiently high spatial and temporal resolution, is crucial for understanding the underlying processes driving lake change and its feedbacks to permafrost, ecosystems, and climate. Until recently, lake change studies in permafrost regions were often focusing on smaller regions, based on a variety of different remote sensing sensors, image acquisition periods and single snapshot observations, and localized analysis, which poses a major challenge for the comparison of lake dynamics across the permafrost domain.

Meanwhile, global surface water change products have been published (Pekel et al., 2016; Donchyts et al., 2016), however, the results for high latitudes are of rather limited quality. Improved estimates of lake changes in these regions are highly important for a better understanding of the key drivers of the thermokarst lake cycle and its potential future impact on permafrost distribution and biogechemical cycles in a changing climate.

Methods and study area

We developed an integrated and automated processing chain based on the Landsat time-series of all available peak-summer images from 1999 through 2014. We analyzed four large transects in Alaska, Eastern Canada as well as Western and Eastern Siberia with a total area of more than 2.3 million km² (Figure 1). The transects cover a wide range of permafrost conditions from Continuous to Isolated extent, different biogeographic zones, and a variety of geological conditions.

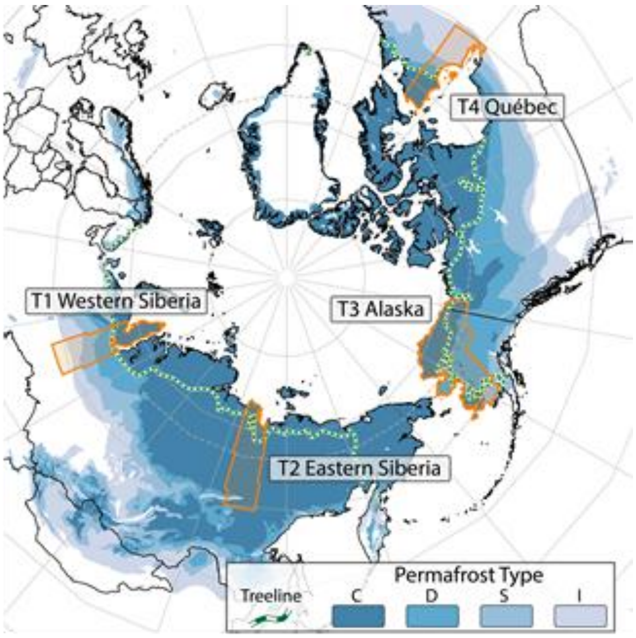

Figure 1. Overview map of study sites within the northern circum-arctic permafrost region (Brown et al., 1997).

We calculated robust Theil-Sen trends of widely used multi-spectral indices (Tasseled Cap, NDVI, NDMI, NDMI) (Nitze & Grosse, 2016), which represent the temporal trajectory of distinct surface properties, such as albedo, vegetation or moisture. For the detection and delineation of lakes, we translated the spectral trend information to semantic classes of land cover and change processes using a Random Forest supervised machine-learning classification. We extracted lake objects, and lake change information was calculated using object-based image analysis and sub-pixel analysis of the machine learning classified land cover change probabilities based on Nitze et al. (2017). Finally, we related lake change information to permafrost specific landscape properties, such as spatial extent or ground ice-content or local geology and geomorphology based on the circum-arctic permafrost map (Brown et al., 1997).

Results and Discussion

Observed changes of lakes larger than 1ha (n=643,304; water area=~120,000km²) (Table 1) were highly diverse in the Alaska and the two Siberia transects with a wide range from stability to rapid high magnitude changes, which aligned with the heterogeneous spatial patterns of surface geology, geomorphology, permafrost extent and ground-ice conditions. In contrast, the spatial dynamics of lakes in the Eastern Canada transect were coherent with the geomorphological homogeneity and followed a latitudinal gradient of increasing lake area loss from south to north. Overall lake area loss outweighed lake area gain, particularly in western Siberia with a net change of -5.41% (gross increase and gross decrease in brackets hereafter; +1.58; -7.45%) as well as in Alaska and eastern Canada with net changes of -0.62% (+3.31%; 3.96%) and -0.24% (+1.87%, -2.12%) respectively. The East Siberia transect is characterized by a positive lake area trend with a net change of +3.67% (+7.77%; -3.95%). Overall lake area loss totaled 4767 km², whereas lake growth accounted for 3030 km² leading to a net loss of 1737 km².

In discontinuous permafrost and along the continuous-discontinuous permafrost boundary in Alaska and western Siberia, lakes were highly affected by area loss, likely resulting from permafrost degradation. Several lake-rich regions, such as the Kobuk-Selawik Lowlands, Yukon flats or the southern Yamal Peninsula had a high rate of partial or complete lake drainages during the observation period. The continuous, sporadic and isolated permafrost zones did not follow any consistent patterns of lake change across the transects. The correlation of lake changes to global ice-content datasets (Brown et al., 1997) did not reveal any relationship on the continental scale. However, a more localized analysis with the same processing methodology and more detailed datasets of geology and ground conditions, revealed a measurable influence of permafrost conditions (ice-content, geology, local geomorphology) on the magnitude of lake dynamics, e.g. stronger lake dynamics in fine-grained deposits of ice-rich permafrost (Nitze et al., 2017).

Our study shows that large scale lake change patterns across latitudinal transects exist between different regions within the circum-arctic permafrost region. There is a wide array and diversity of influencing factors on the magnitude and direction of lake changes within the permafrost zone. The lack of pan-arctic permafrost datasets of sufficient detail stresses the need for more detailed and continuous datasets rather than classical maps of the permafrost domain towards a better understanding of the landscape's response on the continuously changing climate.

Table 1. Regional Lake change statistics. Changes in area percentage.

	% Net	% Growth	% Loss	# Lakes
T1 – WSib	-5.46	+1.58	-7.45	218,882
T2 – ESib	+3.67	+7.77	-3.67	69,151
T3 – Alaska	-0.62	+3.31	-3.96	158,453
T4 – ECan	-0.24	+1.87	-2.12	196,818

WSib: Western Siberia, ESib: Eastern Siberia, ECan: Eastern Canada

Acknowledgments

This study was supported by ERC PETA-CARB and ESA GlobPermafrost.

References

Brown, J., Ferrians Jr, O. J., Heginbottom, J. A., & Melnikov, E. S. (1997). *Circum-Arctic map of permafrost and ground-ice conditions*. Reston, VA: US Geological Survey.

Donchyts, G., Baart, F., Winsemius, H., Gorelick, N., Kwadijk, J., & van de Giesen, N. (2016). Earth's surface water change over the past 30 years. *Nature Climate Change*, 6(9), 810-813.

Nitze, I., & Grosse, G. (2016). Detection of landscape dynamics in the Arctic Lena Delta with temporally dense Landsat time-series stacks. *Remote Sensing of Environment*, 181, 27-41.

Nitze, I., Grosse, G., Jones, B. M., Arp, C. D., Ulrich, M., Fedorov, A., & Veremeeva, A. (2017). Landsat-based trend analysis of lake dynamics across northern permafrost regions. *Remote Sensing*, *9*(7), 640.

Pekel, J. F., Cottam, A., Gorelick, N., & Belward, A. S. (2016). High-resolution mapping of global surface water and its long-term changes. *Nature*, *540*(7633), 418-422.

Stochastic modelling and empirical verification of thermokarst hazard for unsealed roads

Timofey Orlov[1]
Alexey Victorov[1]
Dmitriy Dobrynin[2]
Olga Trapeznikova[1]
Andrey Zverev[1]
[1] *Sergeev Institute of Environmental Geoscience Ras (IEG RAS), tim.orlov@gmail.com*
[2] *A.N. Severtsov Institute of Ecology and Evolution*

Abstract

There is widespread practice of construction of linear infrastructure within Russian permafrost areas. We use stochastic modelling of lake dynamics and verify our models with high resolution remote sensing data. The study site is located in Central Yakutia region of Russia where a new unsealed road was built in 1969-1970. The main findings are the following. Areas of natural thermokarst depressions of the 1969 and 2009-2017 fit lognormal distribution. Difference between the natural logarithms for the both dates fits normal distribution. Distance between projections of lakes (appeared after the road construction) to the road fits exponential distribution. It means that lakes locating along the road fits Poisson distribution.

Keywords: stochastic modeling; thermokarst; remote sensing; linear infrastructure; permafrost thaw

Introduction

There is widespread practice of construction of linear infrastructure within Russian permafrost areas. Linear infrastructure includes: gas and oil pipelines, auto and railroads. Areas with wide spread of lake thermokarst occupy about 2 mln km^2 along Russia (Olefeldt et. al., 2016). Building new roads changes natural temperature and water exchange between ground and atmosphere, as well as among neighborhood sites. It has heating impact to frozen ground, so thermokarst starts and ground become weak, road destroyes.

So, it is very important to determine permafrost thawing and thermokarst risk for linear objects.

We use stochastic approach as the best option in case of lack of data.

The aim of this work is to develop a stochastic model of thermokarst depressions appearing and expanding along the road paved on the icy ground. The second aim is empirical verification of the model for the key site.

Stochastic modelling

Base stochastic model

We have already got a stochastic model of thermokarst lake appearance (Victorov et al. 2015). This model is based on the following assumptions: appearance of initial thermokarst depressions is a stochastic event and happens independently at non-adjacent areas. The probability of a depression appearance within a study site depends exclusively on the site area; the depression size growth under thermoabrasive action is independent for every lake. The growth is proportional to local heat accumulation and it is inversely related to the depression lateral surface area.

One of the main consequences of this model says that areas of thermokarst depressions should fit lognormal distribution for every moment we can measure. The second main consequence is that the difference between natural logarithms of the measurements should fit normal distribution.

Model of lake appearing along a linear object

We assume that thermokarst depressions are constantly appearing (i.e. asynchronous start). This stochastic process is running independently for the non-crossing strips during non-crossing periods. So, we can find an equation of the probability of the depressions to appear within a sample strip which depends exclusively on the strip length and time. The main results of this model are: density of lake location should fit Poison distribution and thus the distance between lakes projections to the road should fit exponential distribution. This means that depression appearances are independent events.

Data and methods

We selected a sample site for testing in Central Yakutia region, 165 km to southeast from Yakutsk city. Central Yakut Site has MAAT -7 °C, ground temperature -2-4°C, mean annual precipitation 260 mm and the permafrost thickness up to 300-400 m. The main site is located at terraces of the Amga river. A new unsealed road was built there in 1969-1970.

Many studies use high resolution remote sensing for analysis of lake thermokarst spreading, distribution and dynamics (Muster, S et al, 2017).

We have made two measurements of the thermokarst lakes areas based on two different sets of remote sensed data: 08.08.1969, Corona, 2.1 m/pix; modern high resolution images captured at 2009-2017 years with resolution 0,3-0,7 m/pix. Modern images were provided by:

1. R&D Centre "SCANEX"
2. Digital Globe by DigitalGlobe Foundation
3. Russian Space Systems. Research Center for Earth Operative Monitoring.

Manual digitization was used for data interpretation.

For the base model verification, we used the whole area of 253 square kilometers. We have found 310 lakes with average area about 6000 square meters in 1969 and 478 lakes with average area 7100 square meters in 2009.

At the first step we take into account lakes existed in 1969 and expanded to 2009. So, the verification is done only for 215 lakes of the site.

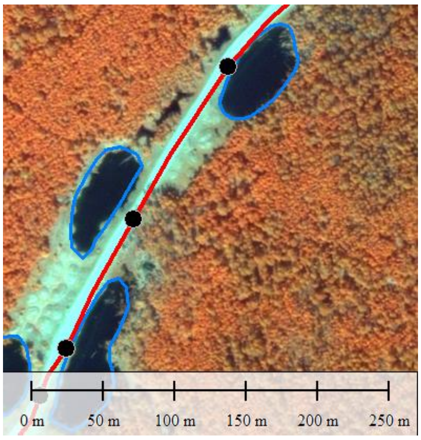

Figure 1. A fragment of the road with newly appeared depressions (Central Yakutia). Red line – road, blue contours - newly appeared depressions, black dots – projections of the depressions centers to the road.

For verification of the model of the lake appearing along a linear object we analyze the unsealed road with length 71 km. There were found 273 newly appeared depressions at its sides. The average density of the appeared depressions is 3,84 per 1 km of the road. A fragment of the road with newly appeared depressions is shown at the figure 1.

Main findings

Distribution of areas of the lakes in 1969 and 2009-2017 fit lognormal distribution.

Distribution of difference between the natural logarithms for the both dates fits normal distribution.

For newly appeared lakes in homogenous environment the distance between projections of lakes centers to the road fits exponential distribution. It means that lakes location along the road fits Poisson distribution.

The approach can be implement to the prediction of lake appearance and thermokarst hazard forecast for the unsealed roads in similar environment.

Acknowledgments

The research is done with the support of Russian Geographic Society and Russian Foundation for Basic Research Grant # 17-05-41141.

References:

Muster S., Roth K., Langer M., Lange S., Cresto-Aleina F., Bartsch A., Morgenstern A., Grosse G., Jones B., Sannel B., Sjöberg Y., Günther F., Andresen C., Veremeeva A., Lindgren P., Bouchard F., Lara M., Fortier D., Charbonneau S., Virtanen T., Hugelius G., Palmtag J., Siewert M., Riley W., Koven C., Boike, J. 2017. PeRL: Permafrost Region Pond and Lake Database, links to ArcGIS shapefiles. *PANGAEA*.

Olefeldt, D., Goswami S., Grosse G., Hayes D.J., Hugelius G., Kuhry P., Sannel B., Schuur E.A.G., Turetsky M.R.. 2016. Arctic Circumpolar Distribution and Soil Carbon of Thermokarst Landscapes, 2015. *ORNL DAAC*, Oak Ridge, Tennessee, USA.

Victorov A, Kapralova V., Orlov N., Trapeznikova O., Archipova M. 2015. Patterns of distribution of thermokarst lakes. *15th International Multidisciplinary Scientific GeoConference SGEM*. 2015. Conference Proceedings, Book1 Vol. 2, 503-510 pp

The influence of vegetation structure on the geomorphic evolution of thermokarst lakes, Old Crow Flats, Yukon

Pascale Roy-Léveillée[1]
[1] *Vale Living with Lakes Research Centre, Laurentian University, proyleveillee@laurentian.ca*

Abstract

This paper examines the effects of vegetation structure on the geomorphic evolution of thermokarst lakes in Old Crow Flats, YT, and discusses potential implications of increased shrubbiness and tree density on thermokarst lake geomorphology near treeline. For lakes in tundra and taiga, aerial photographs from 1951 and 1996 were used to estimate rates of shore recession and lake geometry was analyzed in ArcGIS. In the field, bank characteristics were monitored to determine dominant mechanisms of erosion. Lakes surrounded by taiga or tundra had similar rates of shore erosion but geometry and dominant shore erosion mechanisms differed. Climate-driven changes to the vegetation structure could lead to a decrease in the effectiveness of thermo-erosional action due to increased guarding of shorelines by tall shrubs and trees, fewer rectilinear shorelines, more lakes with irregular shapes, and, in the long term, fewer drained basins with depressed margins and raised centres after permafrost recovery.

Keywords: Thermokarst lakes, geomorphology, forest-tundra transition, vegetation structure, environmental change.

Introduction

The evolution of thermokarst lakes and how they respond to climatic trends differs based on local conditions such as permafrost, ground ice distribution, cryostratigraphy, sediment texture, and vegetation structure (e.g. Jones *et al.*, 2011; Lantz & Turner, 2015). The latter is changing rapidly in response to climatic warming, as tundra shrubbiness and tree density in the forest-tundra transition increase. The effects of such shifts in vegetation structure on the geomorphology of thermokarstic lacustrine landscapes is scarcely studied. This paper examines the effects of vegetation structure on the geomorphic evolution of thermokarst lakes in Old Crow Flats, YT, and discusses potential implications of increased shrubbiness and tree density on thermokarst lake geomorphology near treeline.

Study Area

Old Crow Flats is a 5600 km^2 wetland located in the continuous permafrost zone of northern Yukon. The area is within the forest-tundra transition, and the vegetation cover is a heterogeneous mosaic of woodlands, tall shrubs, low shrubs, and herbaceous communities (Lantz & Turner, 2015).

Thousands of thermokarst lakes and ponds are distributed through this vegetation mosaic. These water bodies cover approximately 35% of the surface area of OCF and exhibit clear signs of expansion by thermokarst processes. Some of these lakes have rectilinear shorelines oriented either NE-SW or NW-SE (Roy-Leveillee & Burn, 2015).

Methods

The distribution of lakes with irregular and rectilinear shores was examined on a vegetation map of OCF (Lantz & Turner, 2015) with land cover grouped as either tundra, including low shrubs, herbaceous vegetation, bryophytes and barren ground, or taiga, including tall shrubs, woodlands and coniferous forest. Lake geometry was analyzed in ArcGIS on two sets of 230 lakes, one from taiga and one from tundra areas. Aerial photographs from 1951 and 1996 were used to estimate rates of shore recession on a subset of representative lakes. Lakes with irregular and rectilinear shores were visited in the field to examine bank characteristics, and were monitored during ice break-up and the open water season in 2008, 2009, and 2010 to assess dominant patterns and mechanisms of shore erosion.

Results

Lakes with rectilinear shores abound in parts of OCF dominated by tundra. In areas where taiga dominates, lakes generally have irregular shapes with an average ratio of shore length to lake area five times greater than in tundra areas.

Tundra vegetation on shore banks is easily broken and removed by wave action, exposing frozen bank material to thermal erosion and unconsolidated sediment to transport by wave action and longshore currents. Trees and tall shrubs, however, can remain anchored in the sediment after subsidence of the shore banks beneath water level, and form a barrier guarding the shore from wave action and ice push. Without effective thermo-erosional action at the bank foot, heat conduction from the lake into the bank becomes the dominant process for permafrost thaw and lake expansion.

Despite differences in dominant erosion mechanisms, rates of shore recession were comparable in tundra and taiga areas. In polygonal tundra, however, rates of lake expansion increased exponentially with lake size, indicating the importance of wave action for lakes of all sizes. No clear relation was found between lake size and erosion rates in taiga lakes, indicating that other factors control rates of lake expansion.

Implications

The observed influence of vegetation structure on lake shore erosion suggests that a continued increase in the abundance of tall shrubs and trees near the forest-tundra transition may lead to a decrease in the effectiveness of thermo-erosion associated with wave action, as the 'guarding' effect of taller vegetation persisting at the bank foot increases. Consequently, oriented lakes with rectilinear shores may be progressively replaced by lakes with irregular shapes. In the long term, there may be fewer drained lake basins with depressed margins and a raised centre after permafrost recovery, as such relief also requires the redistribution of unconsolidated sediment through resuspension in the nearshore zone (Roy-Leveillee and Burn, 2016).

Acknowledgments

The research was supported by the Government of Canada IPY program, NSERC, PCSP, and NSTP. Essential logistical support was provided by the Vuntut Gwitchin First Nation Government and the Aurora Research Institute, Inuvik. Thanks to A. J. Jarvo, A.L. Frost, B. Brown, D. Charlie, E. Tizya-Tramm, K. Tetlichi, L. Nagwan, M. Frost Jr., S. Njoutli, S. Frost, and C.Z. Braul for field assistance.

References

Jones, B.M. *et al.*, 2011. Modern thermokarst lake dynamics in the continuous permafrost zone, northern Seward Peninsula, Alaska. *J. Geophys. Res. Biogeosciences* 116: G00M03.

Lantz, T.C. & Turner, K.W., 2015. Changes in lake area in response to thermokarst processes and climate in Old Crow Flats, Yukon. *J. Geophys. Res. Biogeosciences* 120: 513–524.

Roy-Leveillee, P. & Burn, C.R., 2016. A modified landform development model for the topography of drained thermokarst lake basins in fine-grained sediments. *Earth Surf. Process. Landf.* 41: 1504–1520.

Roy-Leveillee, P. & Burn, C.R., 2015. Geometry of oriented lakes in Old Crow Flats, northern Yukon, in: Proceedings of the 7th Canadian Permafrost Conference, Quebec City, Canada, September 20-23, 2015.

Reconstruction of the development of a retrogressive thaw slump on bank of a thermokarst lake in Central Yakutia using dendrochronology

A. Séjourné[1], A. Decaulne[2], F. Costard[1], A. Fedorov[3], Christophe Grenier[4], Eric Pohl[4]
[1]*Univ Paris-Sud, CNRS, Laboratoire GEOPS, UMR8148, 91400 Orsay, France, antoine.sejourne@u-psud.fr*
[2]*CNRS UMR6554, Laboratoire de Littoral, Environnement, Télédétection, Géomatique, Nantes, France*
[3]*Melnikov Permafrost Institute, RAS, Yakutsk, Russian Federation*
[4]*LSCE/IPSL – UMR 8212 (CEA/CNRS/UVSQ), Univ. Paris-Saclay, Gif sur Yvette, France*

Abstract

In the ice-rich permafrost area of Central Yakutia, the thermokarst dynamic is not fully understood. Investigations of retrogressive thaw slump using tree-rings enable studying the permafrost dynamics over a longer continuous period of time than isolated snapshots from aerial and satellite images or field studies. Our results demonstrate that trees found into the slump are tilted, recording slump development over the last 100 years. Tree-ring patterns highlight key years of major growth disturbance due to deep permafrost thawing.

Keywords: Thermokarst lake; Thaw slump; Dendrochronology; Central Yakutia

Introduction

In the continuous permafrost area of Central Siberia, Central Yakutia (CY) shows an ice-rich permafrost of 70-80% of ice by volume. As the mean annual air temperature at Yakutsk had increased by 3°C since the 1960s and thermokarst processes seem to develop rapidly since the early 1990s, this ice-rich permafrost is prone to extensive degradation. However, the correlation between thermokarst dynamics in the region and the increase in air temperature is not fully understood and thus has to be better investigated.

Along the south-facing banks of thermokarst lakes, the deep thawing of permafrost induces retrogressive thaw slumping (RTS). RTS show an expansion ranging from 0.5 and 3.16 $m.yr^{-1}$ in average for the period 2011–2013 (Séjourné et al., 2015). However, their evolution before that is unconstrained.

In CY, the development of RTS on the forested banks of thermokarst lakes induces tilting and uprooting of trees (Fig. 1; Séjourné et al., 2015). Tree-ring patterns reflect growth disturbances linked to both climate variations and/or cryogenic processes (Agafonov, 2004). Tree-ring analyses enable reconstructing landslide and snow-avalanche occurrence (Speers, 2010), but have been little used for thermokarst lake development.

Here, we reconstruct the development of RTS, their expansion rate on the banks of a thermokarst lake during the last 100 years by analyzing larch (*Larix cajendiari*) ring widths and growth disturbances, and remote sensing data.

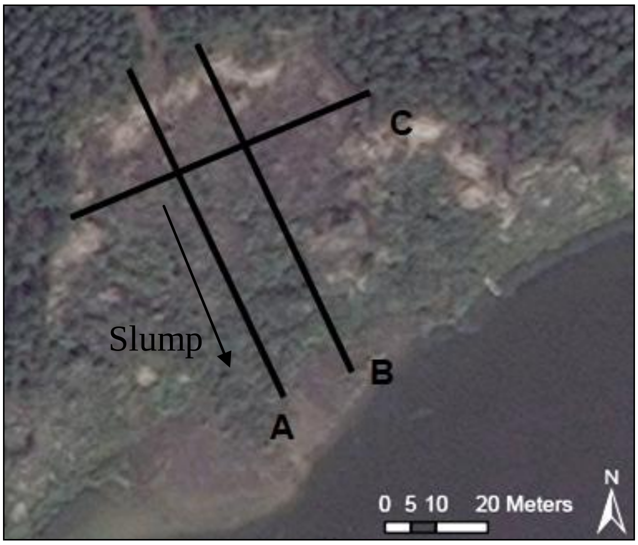

Figure 1. Locations of tree sampling across three cross-profiles into a retrogressive thaw slump in Central Yakutia.

Methods and sampling strategy

Trees affected by permafrost thawing display a pronounced tilting shape of the trunk. As a result, the trees deform the geometry of its cells to gain back their upright position resulting in an asymmetric wood production; i.e. compression wood for coniferous species (Speers, 2010). The compression wood periods would correspond to the deepening of the active layer, when the root system loses the firm support of the permafrost. The onset of compression wood can be dated by dendrochronology, offering the date (with a seasonal accuracy) of tilting, and eventually root destabilization due to slump progression.

Our strategy was to sample trees inside and outside one thermocirque to record the different compression woods marking the slump development. Samples of living and dead Siberian larches (68 cross sections of Larix Cajendiari) were collected along transversal and longitudinal profiles throughout one RTS in September 2014, 180 km east of Yakutsk (Fig. 1). Straight living trees were sampled for reference growth pattern recognition from a flat undisturbed permafrost area close by (12 trees). All trees were sampled at 1 m from the ground, providing full discs.

In the laboratory, the wood samples were prepared and analyzed according to conventional tree-ring analysis methods (Speers, 2010). Three radii were systematically measured for the reference stack (12 trees), while tree rings from discs collected in the disturbed area were measured along the upslope and the downslope radii (69 trees). All individual tree-ring chronologies were cross-dated first at the scale of the disc (tree scale) and compared with the reference stack (stand scale) to detect missing or fading rings.

A minimal chronology of deep permafrost thaw was then created for the study site, based on the visual quality of the main observed growth disturbances, i.e. eccentricity of the growth. There, we arbitrary rated each eccentricity in each sample, and only considered major disturbance with obvious compression wood. Then, growth disturbance index (GDI, with values from 0 to 100%) was calculated for each year, based on the number of responses during one single year in relation with the number of trees alive that same year t. GDI is calculated only for major growth disturbances. We recognized as key years those recording over 10% of responses (over 10% of the trees living during a single year present the exact same signal); we sub-classified the years presenting a GDI > 15% as representing a strong destabilization, and a medium destabilization when only 10-15% of trees are concerned.

Results

Our study shows that trees found into the RTS are all tilted and developed compression wood, recording the expansion of RTS. The life span of the disturbed trees lasts up to 150 years while the reference trees are 200 years old on average. According to the age structure, the trees are older near the headwall and plateau reflecting the retrogressive development of the thaw slump (Fig. 2). A similar trend is highlighted with the date of death of the trees. In the field, we observed several fallen trees, still alive as their roots are still enveloped in a mud mass into the thermocirque demonstrating that they can live several years after they collapsed due to slump movements.

GDI highlights growth disturbances in tree-ring patterns that occurred simultaneously in different trees inside and outside the thermocirque. GDI reveals seven strong years of major growth disturbances with a significant signal (at least two trees responding and >15% of the trees providing the accurate signal) in 1899, 1903, 1911, 1948, 1984, 2007 and 2013. In contrast, trees from the reference stand do not develop compression wood during those periods, as they are not deformed by root unbalance. We interpret those key years of major growth disturbances as due to deep permafrost thaw inducing tilting and/or fall of the tree associated with slump development.

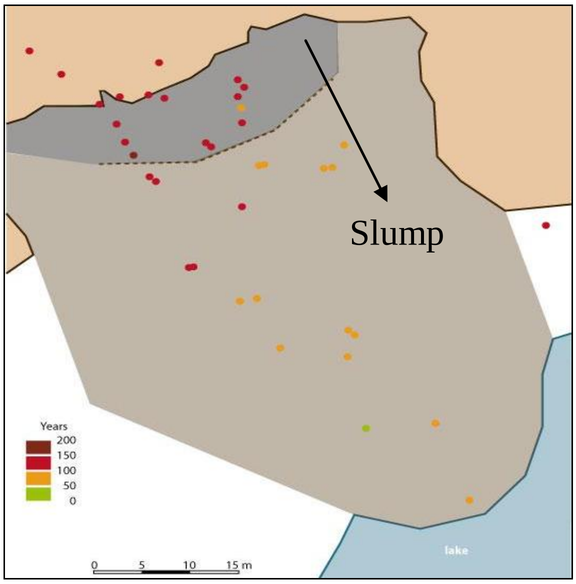

Figure 2: Age structure of the stand studied.

Conclusion

Our results demonstrate that trees found into the RTS were tilted and developed compression wood during their lifespan, recording the expansion of RTS for the last 100 years. In the next few months, the spatial distribution of trees with major and medium growth disturbances detected during these key years will be used to reconstruct the spatial extent of the retrogressive headwall.

References

Agafonov, L. et al., 2004. Thermokarst dynamics in Western Siberia: insights from dendrochronological research. *Palaeogeography, Palaeoclim., Palaeoeco.*, 209, 183-196

Séjourné A. et al.., 2015. Evolution of the banks of thermokarst lakes in Central Yakutia (Central Siberia) due to retrogressive thaw slump activity controlled by insolation. *Geomorphology* 241 (34-40).

Speers, J. H., 2010. *Fundamentals of Tree-Ring Research*. 368 pp. University of Arizona Press.

Past and present thermokarst lake dynamics in the Yedoma Ice Complex region of North-Eastern Yakutia

Alexandra Veremeeva[1]
Frank Günther[2]
Ingmar Nitze[2,3]
Guido Grosse[2,3]
Nadezhda Glushkova[4]
Elizaveta Rivkina[1]
[1]*Institute of Physical, Chemical and Biological Problems in Soil Science, Russian Academy of Sciences, Pushchino, Russia, averemeeva@gmail.com*
[2]*Alfred Wegener Institute Helmholtz Centre for Polar and Marine Research, Potsdam, Germany*
[3]*University of Potsdam, Institute of Earth and Environmental Sciences, Potsdam, Germany*
[4] *Institute of Geology and Mineralogy SB RAS, Novosibirsk, Russia*

Abstract

Thermokarst lakes are typical components of the yedoma-alas dominated relief in the coastal lowlands of North-Eastern Yakutia and formed as a result of thawing Late Pleistocene ice-rich Yedoma Ice Complex (IC) deposits. The aim of our study is to estimate thermokarst lake area changes from the early Holocene onwards based on RS data. The decrease of thermokarst lake area from the early Holocene, taking into account total alas depression areas, is as much as 81-83 %. Modern climate warming has led to a general trend of thermokarst lake area decrease. Lake drainage occurs mostly on elevated sites with high Yedoma IC fraction while lake area increase is typical for low-lying areas with a small Yedoma IC fraction. The area increase of thermokarst ponds on flat, boggy yedoma surfaces indicates ice wedge degradation in response to rising summer air temperatures and precipitation.

Keywords: North-Eastern Yakuria, Yedoma Ice Complex, Holocene, alas, thermokarst lake dynamics, RS data.

Introduction

Thermokarst lakes are typical for the yedoma-alas relief in coastal lowlands of the North-Eastern Yakutia. The yedoma-alas relief formed as a result of thawing Late Pleistocene ice-rich Yedoma Ice Complex (IC) deposits. The very high total ground ice content of up to 90 % by volume renders Yedoma IC vulnerable to observed climate warming (Günther et al., 2015). Thermokarst lakes, as a highly dynamic landscape component, reflect permafrost dynamics in response to climate change. In order to understand present spatial patterns of thermokarst lake area dynamics, it is necessary to reconstruct their changes from the early Holocene.

Study region and methods

The study region is the Kolyma Lowland tundra with an area of about 44500 km^2 that is located within the continuous permafrost zone. Radiocarbon dating of Yedoma IC and alas deposits shows that the activation of thermokarst processes and thermokarst lakes formation occured at about 13-12 kyr BP and that most alas depressions formed after thermokarst lake drainage around 10 kyr BP (Kaplina, 2009). Thus modern alas areas can be considered as thermokarst lake areas during the early Holocene. The ratio between alas and modern thermokarst lake areas thus reflects limnicity changes during the Holocene. Mapping of Quaternary deposits, represented here mostly by Yedoma IC, alas and alluvial sediments, has been done based on Landsat images (Veremeeva & Glushkova, 2016). Thermokarst lake coverage was quantified based on Landsat 8 images that have been acquired during 2013 – 2014. The Quaternary deposits map was used to distinguish lakes with thermokarst genesis from other lakes, i.e. on floodplains.

The analysis of thermokarst lake area dynamics for the 1999-2014 period of the all study region was done using the entire available Landsat archive with an automated workflow, including several processing steps, such as masking, calculation of multi-spectral indices, and object-based image analysis (Nitze et al., 2017).

Results

Thermokarst evolution from the early Holocene

We delineated regions with high, medium and low alas fraction (Fig. 1). Generally, alases occupy 72 % of the region and 17.6 % of the alas area are still covered by lakes. The decrease of thermokarst lake area from the early Holocene is similar among sites with different alas fraction area and about 81-83 %. This loss of thermokarst lake area over the Holocene can be considered as the result of a simultaneous development of thermokarst lakes and the fluvial drainage network.

Long-term historic trends (1965- 2015)

For the key site in the region of Bolshoy Oler lake (Fig. 1), based on the comparison of CORONA (21.07.1965), Landsat 7 (25.08.1999), and Landsat 8 (28.08.2015) images the trend of decrease lake area was revealed. For the recent 1999-2015 period lake area decrease has been faster (0.83 km^2 per year) when compared to the 1965-1999 period (0.7 km^2 per year).

Regions with high Yedoma IC fraction often represent flat boggy surfaces that feature a high number of small thermokarst ponds with an average diameter of 5-10 m. For another key site around Cape Maly Chukochy (Fig. 1), we investigated their dynamics using optical imagery with very high resolution of 0.5 m. A doubling in the number and areal coverage of ponds from 1972 to 2009 and a further twofold increase until 2013 has been found. This indicates ice wedge degradation in response to rising summer air temperatures, precipitation and active layer depth, which is also reflected in expanding baydzherakh fields on adjacent yedoma slopes.

Short-term trends (1999-2015)

The general modern trend for the entire region is a decrease of thermokarst lake area, predominantly caused by lake drainage (Nitze et al., 2017). Comparison of these trends with the Quaternary deposits map and a DEM revealed that lake drainage occurs mostly on elevated yedoma uplands, while lake increase dominated in low-lying territories with low Yedoma IC fraction.

Analyses of inter-annual thermokarst lake dynamics from 1999 to 2015 and comparison with meteorological data have been carried out for several groups with varying dynamic trends and relief positions. We revealed no significant connections of lake area changes to hydrometeorological parameters (air temperature and precipitation of the summer and winter periods, and the preceding 12 month period). Synchronous lake dynamics were found for lakes with increasing area and lakes that are located within the Yedoma IC distribution. While this suggests that lake increase is largely triggered by external forcing, lake decrease and lake drainage is rather determined by local preconditions such as relief position

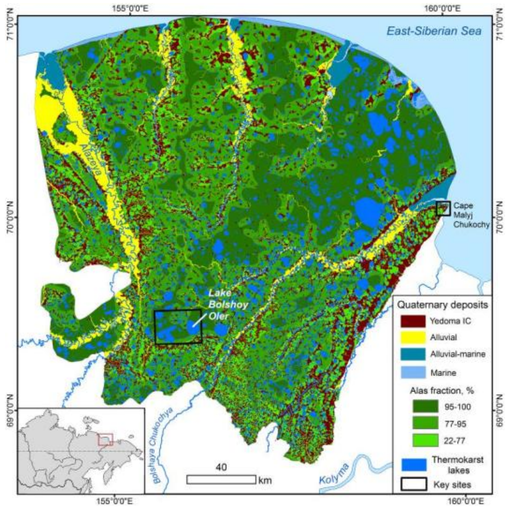

Fig.1. Alas fraction map of the study region. tundra.

and proximity to the existing erosional network. However, since lake drainage often succeeds lake expansion, both phenomena cannot be considered separately, suggesting that environmental forcings and interconnections apply to both processes.

We found a significant decrease of thermokarst lake area from the early Holocene until modern time. However, since lake shrinkage rates accelerated in the recent past, modern climate warming likely leads to a reactivation of thermokarst lake dynamics that ultimately follow a general trend of land surface levelling through continued degradation of Late Pleistocene ice-rich permafrost.

Acknowledgments

This study was supported by grant PP55 «Arctic» (AAAA-A18-118013190182-3), ERC PETA-CARB and ESA GlobPermafrost.

References

Günther, F., Overduin, P.P., Yakshina, I.A., Opel, T., Baranskaya, A.V. and Grigoriev, M.N., 2015 Observing Muostakh disappear: permafrost thaw subsidence and erosion of a ground-ice-rich island in response to arctic summer warming and sea ice reduction. *The Cryosphere* 9 (1): 151–178. Doi: 10.5194/tc-9-151-2015.

Kaplina, T.N., 2009. Alas complexes of northern Yakutia. *Kriosfera Zemli* XIII (4), 3–17 (on russian).

Nitze, I., Grosse, G., Jones, B.M., Arp, C.D., Ulrich, M., Fedorov, A. and Veremeeva, A., 2017. Landsat-Based Trend Analysis of Lake Dynamics across Northern Permafrost Regions. *Remote Sensing* 9 (7, 640): 1-28. Doi: 10.3390/rs9070640.

Veremeeva, A., Glushkova, N., 2016. Relief formation in the regions of the Ice Complex deposit occurrence: remote sensing and GIS-studies in the Kolyma lowland tundra. *Earth's Cryosphere* 20(1): 14–24, http://www.izdatgeo.ru/pdf/earth_cryo/2016-1/14_eng.pdf

Stochastic models of dynamic balance in cryolithozone landscapes and its significance for nature hazard assessment

Alexey Victorov
Sergeev Institute of Environmental Geoscience of Russian Academy of Science, vic_as@mail.ru.

Abstract

The paper deals with mathematical modelling of morphological pattern of a wide spectrum of cryolithozone landscapes, which are characterized with dynamic balance. Morphological pattern modeling was done for lacustrine thermokarst plains with fluvial erosion, alluvial plains, and plains with wide development of landslide process on the base of mathematical morphology of landscape using the random process theory. As a result, the regularities of the structure and dynamics of each landscape morphological pattern are theoretically substantiated.

Keywords: Morphological pattern; mathematical modeling; dynamic balance; landscapes of cryolithozone.

Introduction

A wide spectrum of cryolithozone landscapes has the same type of morphological pattern, which is characterized with dynamic balance. In other words all the elements of this type of morphological pattern such as thermokarst lakes, khasireis (drained thermokarst lakes), ridges and inter-ridge depressions of alluvial plains, landslide series, are under continuous changing while general parameters of the morphological pattern are stable. In case of these landscapes usual methods of analysis and stationary observation do not provide the necessary information about the trends of their evolution.

Our research shows that this type of landscapes includes lacustrine thermokarst plains with fluvial erosion, alluvial plains, and plains with wide development of landslide process.

Analysis of models

The model for lacustrine thermokarst plains with fluvial erosion.

The model for lacustrine thermokarst plains with fluvial erosion in uniform nature environment is based on the following assumptions.

1. The appearance of any thermokarst depression for any period at any selected site is a random event which probability is directly proportional to duration of the period and area of the site.
2. Appearance of a new thermokarst depression is impossible within already existing thermokarst lake.
3. Radius of an appeared thermokarst depression is a random variable being a time function; it is undependable of other lakes and the growth rate is directly proportional to heat storage in the lake water.
4. In the course of its growth, a lake can turn into a khasyrei after draining by the erosion network; probability of this does not depend on development of other lakes. If it happens the depression stops to grow.
5. The appearance of new sources of fluvial erosion within a randomly selected area is a random event and the probability of this is directly proportional to the area.

The mathematical analysis of the model shows that under rather general conditions after a long time since the thermokarst process has begun an active state of dynamic balance takes place and is characterized with the following regularities (laws):

- distribution of a number of thermokarst lakes and (separately) khasireis obeys the Poisson law within a random plot,
- lake area obeys a special distribution (the distribution of the area exponent corresponds to the integral logarithm),
- khasyrey radii obey the Reley distribution.

The model for alluvial plains

The model for alluvial plains with fluvial erosion in uniform nature environment is based on the following assumption.

1. The probability of bend straightening over some time interval depends on the duration of this interval and is independent on the behavior of other bends.

The morphological pattern of alluvial plains is characterized with dynamic balance and the following regularities (laws):

- thickness distribution of appearing and already formed segments consisting of ridges and inter-ridge depressions corresponds to exponential distribution,
- the bend orientation angle distribution corresponds to the beta distribution,
- duration distribution of the kth existing cycle of bend development corresponds to the gamma-distribution.

The model for plains with wide landslide development

The model for plains with wide landslide development in uniform nature environment is based on the following assumptions.

1. Landslide activation (more precisely a number of activations to a given moment) is a probabilistic process and statistical distribution of an activation period (time between two successive activations) is stable.

2. Landslide activations are independent from each other both for the same landslide and for different landslides.

3. The state of a land unit corresponding to a landslide depends upon time since the last activation.

The morphological pattern of plains with wide landslide development is characterized with state of dynamic balance and the following regularity (law):

Distribution of a number of landslides with different time of activation and correspondently at a different recovery stages obeys the equation

$$F_1(x) = \frac{1}{M\xi}\int_0^x [1 - F(u)]du,$$

$F(x)$ - time distribution of landslide activation periods,

$M\xi$ - average for activation periods.

Every model gives an analytical decision of the probabilistic impact assessment for an engineering construction by certain hazardous exogenous geological process.

Conclusion

Dynamic balance in criolithozone landscapes can be studied basing on models of the mathematical morphology of landscape; specific laws and analytical estimation of nature risk were obtained for engineering structures in case of dynamically balanced landscapes.

Acknowledgments

The research is done with the support of Russian Geographic Society and Russian Foundation for Basic Research Grant # 17-05-41141.

11 - Mass-wasting processes in Cold environments

Session 11

Mass-wasting processes in Periglacial environments

Conveners:

- **Costanza Morino**, The Open University, Milton Keynes, UK (PYRN member)
- **Marta Chiarle**, CNR-IRPI, Torino, Italy
- **Philip Deline**, EDYTEM, Université Savoie Mont Blanc, CNRS, Le Bourget, France

This session aims to highlight ongoing research and new findings concerning permafrost-related mass-wasting processes. Perennially frozen ground is widespread in different glacial and periglacial environments, and can affect the evolution of hillslope systems in various environments, from high arctic to alpine climates. Our understanding of slow and fast mass-wasting processes in permafrost terrains is still limited and is becoming increasingly relevant for several reasons. Slow mass-wasting processes, such as gelifluction, solifluction and frost creep, are extremely sensitive to changing climate and can reveal altering geosystem conditions in cold regions. Rapid mass-wasting processes, including landslides (in particular rockfalls and active-layer-detachment slides) and debris flows, can be triggered by permafrost-degradation in glacial and periglacial environments and could pose at risk human activities and infrastructures.

Studies from arctic, sub-arctic, alpine, high-elevation and low-latitude mountain environments are highly welcome. We invite contributions focussing on all aspects of slope processes and instabilities in permafrost terrains, including characterization, distribution, triggering factors, dynamics and evolution, magnitude and frequency, monitoring, modelling, and assessment of hazards. Contributions using innovative or well-established methods and data analysis, including field and ground-truthing measurements, monitoring techniques, remotely sensed and GIS-based analyses, experimental and numerical modelling, and laboratory studies are all encouraged.

Seismic characterization of bedload transport in a steep, glacier-fed creek

Velio Coviello[1]
Gianluca Vignoli[2]
Andrea Andreoli[1]
Anuschka Buter[1]
Michael Engel[1]
Vittoria Scorpio[1]
Francesco Comiti[1]
[1]*Free University of Bozen-Bolzano, Italy, velio.coviello@unibz.it*
[2] *CISMA S.r.l., Bolzano, Italy*

Abstract

Glacier retreat and permafrost degradation are mechanisms through which climate controls sediment transfer and landscape evolution. Prediction of bedload transport is crucial for hazard assessment but knowledge of this processes is still limited, especially at high elevations. This study presents recent research efforts devoted to obtain indirect bedload measurements through seismic monitoring in the Sulden/Solda basin, a glaciarized and permafrost catchment located in the Eastern Italian Alps. A low-cost geophone network was installed in summer 2017 along the channel, immediately downstream from the glacier front, and three months of very high frequency data (5 kHz) were collected. The joint analysis of this seismic dataset and weather data allow drawing some preliminary considerations about the potential of seismic techniques for characterizing bedload transport in periglacial environments. Daily cycles and longer-period trends in geophone data are respectively correlated with flow discharge and air temperature, suggesting a complex climatic control of sediment transport.

Keywords: permafrost degradation; sediment transport; seismic monitoring; glacierized catchment

Introduction

High mountain areas are particularly susceptible to climatic changes due to the high sensitivity of the cryosphere to melting conditions (Allen & Huggel, 2013). Climatic factors, first of all the thermal state of the ground, directly control the temporal and spatial evolution of sediment transfer in cold mountainous basins (Etzelmüller & Frauenfelder, 2009). An increasing sediment delivery and remobilization from rock walls, glacier forefields, and rock glaciers has been assumed to be produced by the joint-effect of glacier retreat and permafrost degradation (Lane *et al.*, 2017). However, quantitative estimations of the sediment transfer induced by these mass-wasting processes are still scarce.

Bedload transport capacity equations are known to overestimate the actual bedload rate in steep mountain creeks under ordinary flow conditions. Indeed, very different bedload rates can be observed at the same channel cross-section under similar hydraulic conditions, because of changes in sediment supply dictate the actual bedload fluxes. Thus, glacial creeks offer the possibility to investigate how seasonal changes in sediment supply at the basin scale – deriving from periglacial and glacial areas – affects bedload transport rates in the main channel (Comiti *et al.*, 2015).

This study presents the preliminary insights into bedload transport dynamics in proglacial environments obtained through the use seismic techniques in the upper Sulden/Solda basin, a glaciarized basin located in the Eastern Italian Alps.

Material and methods

Study area

The study area is located in the glacierized Sulden catchment (130 km²), South Tyrol (Italy). The basin ranges in elevation between 1110 and 3905 m a.s.l. and has a glacier extent of about 17.7 km² (14% of the catchment). Permafrost and rock glaciers are most probably present in this region at elevations higher than 2600–2800m a.s.l. (Boeckli *et al.*, 2012). The study area belongs to the Ortler-Campo-Cristalin, composed by metamorphic and dolomitic lithology, and is characterized by a very heterogeneous erodibility. Moreover, periglacial processes and permafrost zones make the sediment delivery of the upper Sulden basin extremely variable and dependent from climatic conditions. Meteorological data were measured at the Sulden-Madritsch automatic weather station (run by the Hydrographic Office of the Autonomous Province of

Bozen-Bolzano) located within the basin at 2825 m a.s.l., about 2 km north from the monitoring site.

Bedload seismic detection

A growing number of studies investigate the use of passive acoustic/seismic techniques to perform indirect measurements of bedload transport through the detection of ground vibrations produced by interparticle collisions or between moving particles and the channel bed, see Rickenmann (2017) and references within. These methods are very attractive, as they can provide continuous recordings without producing any interference with the investigated process. However, data analysis is complex and time-consuming, as a large amount of data need to be stored and signals produced by others seismic sources (flow turbulence, anthropic disturbances) can be confused with the ground vibration produced by bedload transport. In addition, broadband seismometers installed along the channel or instrumented check dams equipped with geophone plates are very effective in providing a detailed characterization of flow processes but have the drawback of being expensive to install.

The Sulden basin monitoring network

In early July 2017, a network composed by two vertical 10-Hz geophones was installed on the glacier forefield located at about 2500 m s.l.m. along the left bank of Sulden channel (drainage area of about 10 km^2). The two geophones were placed next to the channel, at the same cross-section, one about 3 m and the other about 5 m cross stream from the channel centre. Power is supplied via solar panels and batteries. Data were sampled at very high frequency (5 kHz) with a 16-bit AD converter and then stored in a RaspberryPi after applying a compression transforming each 10-minutes amplitude array in a 5-kB .png file. This equipment integrates a monitoring network composed by a pressure transducer measuring water stage, located right upstream the geophone network, and an instrumented check dam equipped with geophone plates and flow stage ultrasonic device, located about 15 km downstream, after the confluence with the Trafoi sub-catchment.

Results and conclusions

In this work, the effectiveness a low-cost and easy-to-install geophone network is investigated. A first seismic dataset was collected during summer 2017 and was compared with air temperature and flow discharge data. Preliminary results from the analysis of three month of continuous monitoring performed in the upper Sulden basin from July to September show how: (i) an array of single component geophones installed close to the flow path can detect both daily and longer period bedload fluctuations in a steep, glacier-fed Alpine creak; (ii) geophone signal follows the daily melt flow cycles, whereas its relationship with flow rate at a monthly scale varies, suggesting that bedload supply (in terms of rates and/or size) progressively increased (iii) there is a strong temperature control of bedload transport, as the seismic energy reach maximum values during warm periods (air temperature > 5 °C). Field evidences and direct sediment sampling campaigns performed right after the opening of a new glacier mouth, during an extremely warm week in August, confirmed those observations. Further work is needed to corroborate these findings and more information can be extracted from a larger seismic dataset that would provide insight on the temporal evolution of sediment transport in a climate change scenario. Future developments will also aim at characterizing bedload transport at the catchment scale through the use of additional seismic devices, in order to investigate incipient motion conditions and to quantify the sediment delivery of the two sub-catchments.

Acknowledgments

This research is part of GLORI (Glaciers-to-rivers sediment transfer in alpine basins) and SEDIPLAN-r+i (Sediment budgeting and planning for rivers in South-Tyrol: from hazard mitigation to environmental restoration) projects, led by the Free University of Bozen-Bolzano, and funded by the Autonomous Province of Bozen-Bolzano and the European Regional Development Fund (FESR), respectively.

References

Allen, S., & Huggel, C., 2013. Extremely warm temperatures as a potential cause of recent high mountain rockfall, *Glob. Planet. Change*, 107, 59–69.

Boeckli, L., Brenning, A., Gruber, S. & Noetzli, J., 2012. A statistical approach to modelling permafrost distribution in the European Alps or similar mountain ranges. *The Cryosphere* 6: 125–140.

Comiti, F., Dell'Agnese, A., Lucia, A., Vignoli, G., Simoni, S., Bertoldi, W., Mao, L., Macconi, P., Mazzorana, B. & Dinale, B., 2015. Bedload transport in steep glacier-fed streams: from incipient motion to floods. *Geophysical Research Abstracts*, EGU2015-7301.

Etzelmüller, B. & Frauenfelder, R., 2009. Factors controlling the distribution of mountain permafrost in the Northern Hemisphere and their influence on sediment transfer. *Arctic, Antarctic, and Alpine Research* 41: 48-58.

Lane, S.N., Bakker, M., Gabbud, C., Micheletti, N. & Saugy, J. N., 2017. Sediment export, transient landscape response and catchment-scale connectivity following rapid climate warming and Alpine glacier recession. *Geomorphology* 277: 210–227.

Rickenmann, D., 2017. Bed-Load Transport Measurements with Geophones and Other Passive Acoustic Methods. *Journal of hydraulic engineering*, 143: 1-14.

What's up on Caribou slope, Wyâshâkimî lake, Nunavik, Canada?

Armelle Decaulne[1]
Najat Bhiry[2]
[1]CNRS LETG-Nantes, Nantes, France armelle.decaulne@univ-nantes.fr
[2]Centre d'études Nordiques & Département de Géographie, Université Laval, Québec, Canada

Abstract

With an openwork structure of large clasts and a dominance of rectilinear long profiles, Caribou slope (Northern Québec, Canada) looks like a classic scree slope formation. However, details in the slope shape reveal several locations of convexities and concavities, suggesting that the distribution of debris over the talus might not be as regular as expected. Landforms of debris flows are visible, and the apical part of the talus displays fallen headwall pieces. The analysis of grain-size over the talus highlights the absence of sorting, and suggests that other reworking processes, such as snow avalanches, contribute to redistribute debris over the whole talus, building up a complex talus slope. The analysis of a first set of photos from an automatic camera that has been recording images of the slope over a full year helps at better understanding potential processes while not witnessed in this remote area of Nunavik.

Keywords: Talus; scree; rockfall; debris flows; snow avalanches; ice crust.

Introduction

Slopes in Nunavik are a major element of the landscape, even if they represent limited elevation differences. In fact, they are generally shorter than 250 m. They have attracted little interest, out of local studies motivated either by hazard and risk assessments due to snow-avalanche research in Kangiqsualujjuaq (Germain & Martin 2011; Germain, 2016; Veilleux *et al.*, 2017) or due to permafrost degradation (Jolivel, 2014). In a context of population increase in Nunavik, which leads to the extension of the fourteen villages (Plan Nord, https://plannord.gouv.qc.ca), the understanding of slope processes, triggering factors and runout distances is becoming essential. In addition, after the recent establishment of several National Parks, little-known areas are getting more and more accessible, visitors exposing themselves to potential hazards.

A meteoritic impact formed the western basin of Lake Wyâshâkimî (present-day Cree name accepted; Lac à l'Eau-Claire was used until recently). It is characterized by a circular archipelago that forms the internal islands of the lake. The study site is located on the external face of Lepage island (Fig. 1) and has been named arbitrary Caribou slope (Fig. 2) by the authors. The study area is located within the boundary of Tursujuq Narional Park.

Two previous studies on the close island Aux Foreurs highlighted a slope instability in 1933 (Bégin & Filion, 1985) and described one talus development during the Holocene (Marion *et al.*, 1995), i.e. since 5500 BP. No study has investigated the present-day slope processes in the area so far.

Figure 1. Location of Caribou slope on Lepage Island in Wiyâshâkimî Lake, Nunavik (background image from GoogleEarth).

Morphometric properties of Caribou slope

Caribou slope (56°16'48.12" N - 74°28'49.47" W) is 70 m high, with a short headwall of 10-2 m only; the eastern part has the higher headwall. The base of the slope is 240 m a.s.l. and the top of the cornice is 310 m a.s.l. The slope shortens westwards. Investigations on Caribou slope highlight the shape of the slope along longitudinal profiles (Decaulne *et al.*, in press). Long profiles are mostly rectilinear, with a mean slope gradient over 33° indicating that the talus is not yet stabilized. Grain-size measurements show that clasts are rather large, with medians ranging from 30 to 50 cm. Some boulders are very large, with a-axis up to 250 cm, and those are mostly located in the apical to median pat of the slope. Large clasts in the distal part are seldom. Lichens or mosses are abundantly present on the clasts all over the talus. Interestingly, fresh clasts, presenting no vegetation cover (no lichen, no moss, just a freshly exposed surface) tend to accumulate in the distal part, away from the runout of free-fall, and at a distance from the landforms of previous debris flows. This striking fact clearly suggests that other processes, redistributing debris over the talus, are active. The absence of sorting in the talus suggests that the building up of the talus is more complex than the development of a traditional scree slope, and that redistribution processes such as snow avalanches might be efficient there.

Findings from the automatic camera

Camera setting

To document the functioning of the talus slope year round, and to gather information on potential active slope processes and weather conditions at the site, an automatic camera Reconyx PC800 has been installed, about 3 m high on the trunk of a black spruce (*Picea mariana*), oriented toward the slope (Fig. 2). The camera records the date, the time and the air temperature at the time of the recorded photography. Eight photos were taken hourly from 8:00 am to 03:00 pm. From August 21 2016 to August 14 2017, the camera recorded 2855 photographs. On each image, we highlight several recognition points (Fig. 2), to better notice eventual changes during the year and especially during the wintertime, and to assume the snow cover thickness.

Figure 2. View of Caribou slope from the automatic camera and the different check points.

From summer 2016 to summer 2017

The slope was covered by snow continuously from October 12, 2016 to May 25, 2017; the last snow patches disappeared on June 15, 2017. The snow cover reached a thickness of about 50 cm in the distal part of the slope. During the snow covered period, diurnal temperature fluctuated from a minimum of –36°C (February 10) to a maximum of 33°C (May 13). The mean seasons, fall 2016 and spring 2017, are those with most freeze-thaw processes. On April 10 2017, the collapse of hanging snow cornices is noticed over the whole slope, resulting in a large quantity of snowballs in the distal part of the talus. This event happened after a sudden rise in temperature, reaching 26°C at 03:00 pm on April 8 2017.

This event suggests that snow avalanches are an effective geodynamic on Caribou slope. The temperature fluctuations around the freezing point during fall and spring also highlight the potential to form ice crusts over the snow cover, therefore facilitating the transfer of debris released by cryoclasty from the rockwall to the distal part of the talus by sliding on the ice crust.

Acknowledgments

Funding for this research primarily comes from LabEx DRIIHM – OHMi NUNAVIK, CRSNG, Centre d'études Nordiques and CNRS-LETG. We thank J. Lebrun, S. Veilleux, D. Sarrazin, L. Q. and C. Nowra for helpul assistance in the field during summers 2015, 2016 and 2017 and Park Nunavik staff for discussion.

References

Bégin, C., & Filion, L., 1985. Analyse dendrochronologique d'un glissement de terrain de la region du Lac à l'Eau Claire (Québec nordique). *Canadian Journal of Earth Sciences* 22: 175-182.

Decaulne, A., Bhiry, N., Lebrun, J., Veilleux, S., & Sarrazin, D., in press. Geomorphic evidence of slope dynamics on the Canadian shield throughout the Holocene – a study from lac à l'Eau-Claire, western Nunavik. *Ecosciences.*

Germain, D. & Martin, J.P., 2011. The vulnerability of northern cities to weather-related hazards: case studies from the province of Quebec, eastern Canada. In Daniels, J.A. (Ed.), *Advances in Environmental Research*, 22: 2-17.

Germain, D., 2016. Snow avalanche hazard assessment and risk management in northern Quebec, eastern Canada. *Natural Hazards* 80, 2: 1303-1321.

Jolivel, M., 2014. *Érosion du pergélisol, transport fluvial et sédimentation marine, côte est de la baie d'Hudson, Nunavik,, Canada.* PhD Université Laval. 135 p.

Marion, J., Filion, L. & Hétu B., 1995. The Holocene development of a debris slope in subarctic Québec, Canada. *The Holocene* 5: 409-419.

Veilleux, S., 2017. *Processus gravitaires et géomorphologie de versant en milieu subarctique, Umiujaq, Nunavik.* BSc. thesis, Department of Geography, University Laval.

Identification of periglacial processes and their link to rockfalls

Daniel Draebing[1]
Samuel McColl[2]
Benjamin Jacobs[1]
[1]*Chair of Landslide Research, Technical University of Munich, d.draebing@tum.de*
[2]*Massey University, Palmerston North*

Abstract

In alpine environments, rockfall represents the most important process shaping rockwalls besides glacial erosion. Periglacial and paraglacial processes influence rockfall processes. In this study, we investigate spatial patterns of permafrost, frost weathering, and assess their influence on rockfall-driven rockwall erosion. To achieve this, we use geomorphic, geophysical and geotechnical techniques on rockwalls with different glacial history and altitude. First results show that lithology controls failure on the rock sample scale, however, fracture density at the field scale increases with proximity to the glacier suggesting an increase of paraglacial influence. Permafrost is likely present in the highest rockwalls, with freezing penetration depth and snow cover increasing with ascending altitude. However, ice segregation and thermal stresses are more controlled by snow cover and moisture occurrence. These processes affect rockwall stability and we are currently processing terrestrial laserscanning data to quantify rockfall process and to identify spatial patterns.

Keywords: Permafrost Rockwalls; Frost Weathering; Thermal Stresses; Paraglacial Adjustment; Rockfall.

Introduction

In alpine environments, rockfall represents the most important processes shaping alpine rockwalls beside glacial erosion (McColl & Draebing, accepted). While different models exist that explain or simulate permafrost influence on rockwall stability or frost weathering of rockwalls, there is a lack of field data supporting the theoretical assumptions of the models and quantifying periglacial processes. Beside periglacial processes, rockwalls are concurrently adjusting to non-glacial conditions which makes it essential to assess the relative importance of all of these processes.

This study will provide first results on the spatial patterns of permafrost and frost weathering processes and resulting influence on rockwall erosion and rockfall processes. We use a space-for-time substitution approach to assess paraglacial influences, by investigating rockwalls with different distances to former glacier limits, at different altitudes. We hypothesize that rockwalls that have been more recently exposed by glacier recession and experience greater thermal stress cycles will have greater rockfall activity and erode faster.

Study Area

The study took place in the Hungerli Valley, a hanging valley of the Turtmann Valley, located in the Valais Alps, Switzerland (Fig. 1). The valley has experienced intense glaciation, but today is almost completely free from glacier processes, with only a small glacier remaining. The geology is predominantly paragneiss, consisting of quartz slate and schisty quartz slate intersected by amphibolite and aplite. The abundance of large talus slopes indicates the importance of ongoing and past rockfall processes. Past investigations in the near-by Steintaelli demonstrated the occurrence of permafrost on the ridge (Draebing *et al.*, 2017a, b), thus, permafrost occurrence is likely in adjacent rockwalls at similar altitudes.

Methods

To investigate the influence of deglaciation and periglacial processes, three rockwalls (RW1-3) located between 2590 and 2925 m a.s.l., at different distances to the glacier were investigated in 2016 and 2017 (Fig. 1). Glacial history is derived from geomorphic mapping of moraines and from historic photos. To evaluate lithologic control, discontinuities were mapped using scanline measurements. At each rockwall, two temperature loggers and two crackmeters were installed to monitor the thermal conditions and fracture kinematics in 3h-intervals. Data was processed following the approach by Draebing *et al.* (2017b) to differentiate thermal and cryogenic controls. To quantify thermal and mechanical controls, we calibrated p-wave velocities in the laboratory using rock samples from each rockwall, evaluated near-surface permafrost occurrence in the field using refraction seismic tomography (SRT; Krautblatter & Draebing, 2014), and calculated fracture density from the seismic models. Terrestrial laserscanning was applied to rockwalls ranging from the Rothorn cirque to Brändjispitz (Fig. 1) and we will difference the resulting topographic models to quantify rockslope erosion and rockfall volumes.

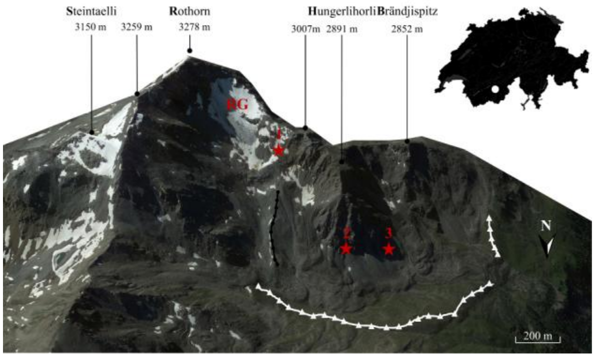

Figure 1. The research area Hungerli Valley is located in the Swiss Alps (inset map). Red stars mark location of investigated rockwalls (RWs1-3). Black Lines (LIA) and white lines (Egesen) highlight moraines. RG marks the Rothorn glacier. (photo: Google Earth, 8/7/2016)

First Results and Interpretation

The peaks of the Hungerli and RW1 were covered by cirque glaciers during the LGM and valley glaciation affected the base of RWs 2 and 3. RW 1 was additionally ice-covered during the LIA and has been ice free for less than 90 years. The lithology of the rockwalls range from aplite (RW1) to amphibolite (RW2) and schisty quartz slate (RW3). Laboratory seismic results show a low anisotropy of aplite and amphibolite in the non-frozen state (0.02-0.07) while the schisty quartz slate is highly anisotropic (0.35-0.66) due to foliation. Therefore, foliation represents planes of weakness where failures can occur. In the field, discontinuities such as fractures will additionally control failures and SRT results demonstrate that fracture density of the rockwalls increases with proximity to the glacier from 5-10 % at RW3, to 10-15% at RW2 and 10-40 % at RW1. These results indicate that discontinuities are likely to have a strong bearing on rock mass strength and suggest that RW1 is still undergoing a pronounced paraglacial adjustment to deglaciated conditions.

Temperature loggers show mean annual rock surface temperatures (MARST) above 0°C at RWs 2 and 3 which indicate an absence of permafrost. At RW1, MARST indicate that permafrost occurrence is likely (MARST < -1°C), however, SRT demonstrate the absence of permafrost within at least 6 m normal to the rock surface. Thermal modelling suggests that seasonal frost penetration is abundant and increases with altitude from 2.32-2.98 m at RW3, 2.67-2.86 m at RW2 to 3.88-3.97 m at RW1. The thermal results show that the low-lying rockwalls are affected by seasonal freezing and RW1 is additionally affected by permafrost which probably interacts with the neighboring glacier.

Crackmeters resolve thermo-cryogenic movements controlled by altitudinal- and topography-dependent snow cover and temperature. RW1 experienced 191-221 days snow-covered and showed a seasonal thermal-induced opening and closing of 0.55 mm. Ice segregation occurs but permanent fracture widening is minor (<0.1 mm). The snow cover duration was less at RW2 (69-73 days) and the fracture underwent 0.15 mm of cyclic opening from thermal contraction, with ice segregation causing 0.05 - 0.1 mm widening. At RW3, snow cover was absent and crackmeters showed a high-frequency diurnal cyclic thermal-induced opening up to 0.2 mm.

In conclusion, these data have helped to resolve location-dependent fracture kinematic patterns with potential to trigger rockfalls. We are currently quantifying rockwall erosion and rockfall processes, and will compare the results with the spatial patterns of permafrost distribution and weathering process described here.

Acknowledgments

This research was conducted within the project Alpine Rock Slopes (DR1070/1-1) funded by the German Research Foundation. We acknowledge field work support by A. Baßler, A. Brandschwede, V. Stiller, F. Strohmaier, A. Thiemann and A. Weber.

References

Draebing, D., Haberkorn, A., Krautblatter, M., Kenner, R. & Phillips, M., 2017a. Thermal and mechanical responses resulting from spatial and temporal snow cover variability in permafrost rock slopes, Steintaelli, Swiss Alps. *Permafrost and Periglacial Processes* 28: 140-157.

Draebing, D., Krautblatter, M. & Hoffmann, T., 2017b. Thermo-cryogenic controls of fracture kinematics in permafrost rockwalls. *Geophysical Research Letters* 44: 3535-3544.

Krautblatter, M. & Draebing, D., 2014. Pseudo 3D - P-wave refraction seismic monitoring of permafrost in steep unstable bedrock. *Journal of Geophysical Research* 119: 287-299.

McColl, S.T. & Draebing, D., accepted. Rock slope instability in the proglacial zone: State of the Art. In: Heckmann, T. & Morche, D. (eds.), *Geomorphology of proglacial systems - Landform and sediment dynamics in recently deglaciated alpine landscapes*.

UAV-based mapping of turf-banked solifluction lobe movement and its relation to material, thermal and vegetation controls

Jana Eichel[1]
Daniel Draebing[2]
Teja Kattenborn[1],
Johannes Senn[1]
Lasse Klingbeil[3]
Christian Eling[3]
Markus Wieland[3]

[1]*Institute of Geography and Geoecology, Karlsruhe Institute of Technology, Karlsruhe, Germany, jana.eichel@kit.edu*
[2]*Chair of Landslide Research, Technical University of Munich, München, Germany*
[3]*Institute of Geodesy and Geoinformation, University of Bonn, Bonn, Germany*

Abstract

Solifluction is a widespread periglacial process, resulting in the downslope movement of soil mass with rates of cms/year. Movement is usually determined using point measurements, however, both movement and its controls are spatially variable. To determine spatial movement patterns, we test the applicability of repeated UAV-flights (2014, 2017) and manual feature tracking on derived orthophotos at a turf-banked solifluction lobe in the Turtmann glacier foreland (Switzerland). Subsequently, we link movement patterns to material, thermal and vegetation controls. Our results show that the lower lobe tread, characterized by finest material and highest soil moisture, moves most rapidly (~ 3 cm/year), while lateral risers are mostly stable and colonized by shrub species favoring stable soil. While our UAV approach worked well to detect three-year movement rates, errors in the range of mean annual movement rates suggest that a careful research set-up is needed to detect short-term movement (<1 year).

Keywords: solifluction; biogeomorphology; periglacial processes; UAV; photogrammetry

Introduction

Solifluction is the slow downslope movement of soil mass due to needle-ice creep, frost creep, gelifluction and plug-like flow. Solifluction movement rates are comparatively low with usually cms per year, however, as it is one of the most widespread processes in periglacial environments, it is believed that solifluction contributes substantially to sediment transport and total slope retreat. In previous studies, solifluction movement was continuously monitored at a single location or discontinuously assessed using point geodetic measurements of markers or painted rocks. Therefore, spatial patterns of solifluction movement, as well as controlling factors, are poorly understood. Recent research demonstrated that these controlling factors, including material texture, soil moisture and vegetation are spatially variable and exhibit distinct spatial patterns at turf-banked solifluction lobes (Draebing & Eichel, 2017; Eichel *et al.*, 2017). Consequently, to improve the understanding of solifluction processes, its spatial variation needs to be assessed with a higher spatial resolution and linked to patterns of its controlling factors.

Our objectives are:

1) To evaluate the applicability of unmanned aerial vehicle (UAV)-based photogrammetry to detect solifluction movement
2) To quantify spatial patterns of solifluction lobe movement and link them to potential material, thermal and vegetation controls

Study area and methods

At a turf-banked solifluction lobe in the Turtmann glacier foreland, Switzerland, we conducted two UAV surveys (2014, 2017) and assessed (i) material properties, (ii) thermal regime, (iii) lobe geomorphology and (iv) vegetation using (i) Electrical Resistivity Tomography (ERT), (ii) iButton temperature loggers, (iii) geomorphic and (iv) vegetation mapping (cf. Draebing & Eichel, 2017; Eichel *et al.*, 2017). From the UAV survey in 2014, a digital elevation model and orthophoto were produced using Agisoft Photoscan (cf. Eichel *et al.*, 2017). The

2014 orthophoto was subsequently used to co-register the 2017 aerial imagery in Agisoft Photoscan based on 15 comparatively stable reference points identified in field. Manual feature tracking (> 1000 points) on both high-resolution (2 mm) orthophotos was carried out to detect lobe movement and its spatial patterns. Subsequently, spatial data on controlling factors was compared to movement patterns.

Results and Discussion

Applicability of UAV-based photogrammetry

Using UAV RGB imagery and subsequent manual feature tracking in derived orthophotos, we increase the spatial resolution of solifluction lobe movement assessment by more than an order of magnitude compared to previous approaches (>1000 points in this study vs. usually <100 points). Registration accuracy for the two orthophotos lies within 0.008 to 0.048 cm, suggesting an error in the detected movement rates of around 3.05 cm (average registration error). While our UAV approach worked well to detect longer-term movement rates, the registration errors in the range of mean annual movement rates (~ 3 cm/year) suggest that a careful research set-up (e.g. fixed ground control points for registration) is required to detect short-term movement (≤ 1 year). In addition, our results suggest limitations of previous approaches using painted rock as proxy for solifluction movements, as movement of individual rocks identified in the orthophotos is sometimes two to three times higher than observed mean lobe movement. The orthophotos provide additional information on vegetation development and growth, from which biogeomorphic studies could benefit.

Solifluction lobe movement and controls

Preliminary results show that solifluction movement mainly occurs along the longitudinal axis of the lower lobe tread, with mean movement rates of around 10 cm in three years (~ 3 cm/year). Furthermore, solifluction movement shows distinct spatial patterns, which relate to material, thermal and vegetation controls.

Highest movement at the lower lobe tread occurs where ERT results show the lowest resistivity of the uppermost 0.75 m, indicating that highest movement occurs with finest material and highest soil moisture (cf. Draebing & Eichel, 2017). This area is mainly covered by a thick mat of the ecosystem engineer dwarf shrub species *Dryas octopetala* (cf. Eichel *et al.*, 2016, 2017). Due to isolating properties of the *D. octopetala* cover, needle ice and frost creep occurrence is limited and gelifluction probably the dominant process contributing to the movement of the lower tread.

Very low movement rates are detected at the lateral risers where ERT results show high resistivities, indicating dry conditions with coarse material. Later successional plant species (*Salix* shrubs) occur which indicate stable conditions. However, some of the rocks making up the lobe risers move in an irregular fashion. This could potentially indicate a slow overturning of the lobe risers, as suggested for caterpillar-like movement.

At a mostly vegetation-free ridge feature, overall movement is slower than at the lower lobe tread, however, individual small gravel particles move over larger distances in an irregular fashion in this area, possibly indicating needle-ice creep and cryoturbation. The highest number of freeze-thaw cycles in this area and frost-adapted species (e.g. *Silene exscapa*) support this hypothesis (cf. Eichel *et al.*, 2017).

Conclusion

Using repeated UAV surveys (2014, 2017), we assess movement patterns of a turf-banked solifluction lobe with a high spatial resolution (> 1000 points). Thus, UAVs surveys are a useful method to detect solifluction movement in space but need a careful research setup to detect short-term (1 year and less) movement rates. Detected solifluction lobe movement is highest at the lower lobe tread (~ 3 cm/year) and differs between lobe tread, risers and a ridge-like feature. Differences can be related to material, thermal and vegetation controls.

Acknowledgments

This research is funded by the German Research Foundation (DI 414/22-1). The authors thank all student assistants involved in the fieldwork.

References

Draebing, D. & Eichel, J., 2017. Spatial Controls of Turf-Banked Solifluction Lobes and Their Role for Paraglacial Adjustment in Glacier Forelands. *Permafrost and Periglacial Processes* 28: 446-459.

Eichel, J., Draebing, D., Klingbeil, L., Wieland, M., Eling, C., Schmidtlein, S., Kuhlmann, H., Dikau, R., 2017. Solifluction meets vegetation: the role of biogeomorphic feedbacks for turf-banked solifluction lobe development. *Earth Surface Processes and Landforms* 42: 1623–1635.

Eichel, J., Corenblit, D., Dikau, R., 2016. Conditions for feedbacks between geomorphic and vegetation dynamics on lateral moraine slopes: a biogeomorphic feedback window. *Earth Surface Processes and Landforms* 41: 406 - 419.

The dynamics of permafrost-induced landslides in Iceland

Helgason J.K.[1], Morino C.[2], Conway S.J.[3], Sæmundsson Þ.[4], Balme M.R.[5]

[1] *Icelandic Meteorological Office, Avalanche Centre, Iceland, jonkr@vedur.is*

[2] *School of Environment, Earth & Ecosystem Sciences, The Open University, UK*

[3] *Laboratoire de Planétologie et Géodynamique de Nantes UMR-CNRS 6112, France*

[4] *Department of Geography and Tourism, University of Iceland, Iceland*

[5] *School of Physical Sciences, The Open University, UK*

Abstract

One of the most visually apparent responses of permafrost-affected mountain slopes to climate change is rapid mass movements. The influence of the changing cryosphere on the stability of rock walls is well documented, since the number of periglacial rock-falls has increased over the past century in mountain environments worldwide. However, little is known about how the dynamics of rapid mass movements involving loose deposits are conditioned by thawing ground ice. Here, we present two case studies of landslides induced by degrading permafrost in Iceland, whose source materials comprised ice-cemented talus deposits. We describe and quantify the morphometric characteristics of these landslides, which reveal different dynamic processes, and how the thawing of ground ice could have affected their emplacement. As degrading permafrost is predicted to increasingly affect mountain regions in the future, improving our knowledge on this type of landslides is important as they could be a further source of risk for local population in Iceland and other mountainous periglacial areas.

Keywords: permafrost, landslides, dynamic, ground ice, Iceland.

Introduction

Rapid mass movements, whether involving debris, snow and/or water, are a direct threat to many towns in Iceland, and nearly 200 people have died in the last century as a result of such events (Jóhannesson & Arnalds, 2001). Triggering factors of these hazardous events include heavy precipitation, rapid snowmelt, seismic activity and permafrost thaw (*e.g.*, Sæmundsson *et al.*, 2003; Decaulne *et al.*, 2005; Sæmundsson *et al.*, 2017), where the role of permafrost thaw is still poorly understood/recognised.

Permafrost degradation is known to be the cause of slope instability in periglacial environments, with rock-falls being one of the most commonly reported (*e.g.*, Gruber & Haeberli 2007). However, its role in conditioning mass movements in Iceland, and in particular landslides involving loose deposits, is not as well constrained.

Here we present the morphometric analysis of two recent landslides in Iceland that mobilised ice-cemented talus deposits. Our study contributes to progress in understanding an “unusual” type of landslide, where the ground ice cementing the source material has a major impact on the landslide’s dynamics.

Figure 1. The airborne photograph (collected in September 2015) of one of the case studies (the Móafellshyrna landslide), reporting the main geomorphological features analysed.

Case studies and methods

We studied two landslides in Iceland: the first is the Móafellshyrna landslide, located in the Tröllaskagi peninsula, northern Iceland, and the second is the Árnesfjall landslide, located in the Westfjords, north-western Iceland. Both originated on north-facing slopes in talus deposits perched on topographic benches. The Móafellshyrna landslide happened on 20th September 2012, while the Árnesfjall landslide on 14th July 2014. The Móafellshyrna landslide originated at 873 m a.s.l., travelled ~1300 m and mobilised ~500,000 m^3 of material, while the Árnesfjall landslide originated at 418 m a.s.l., travelled ~560 m and had a volume of ~130,000 m^3.

We performed morphometric analysis of the geomorphological features of both landslides, distinguishing the zones of erosion and deposition, quantifying the volumes mobilised, assessing their different rheologies and linking them to different gravitational processes. We used field observations and 1m/pixel Digital Elevation Model (DEM) from airborne LiDAR for the Móafellshyrna landslide, and 18 cm/pixel DEM from ground-based Structure from Motion photogrammetry technique for the Árnesfjall landslide.

The dynamics of the landslides

In Móafellshyrna, immediately after the failure, large blocks of ice-rich sediment and frozen deposits fell down the slope, and their remnants are still preserved as debris cones or "molards" on a flat tread surface at the foot of the talus slope below the source area (see Fig.1). We compared the reach angle and the volumes of the molards with those of normal boulders mobilised during the landslide event. The debris cones show both travel distance and volumes consistent with those of the boulders mobilised by rock-fall processes. The blocks of ice-rich sediment were deposited as intact masses at their rest position, because ground ice was still cementing them during the transport.

As the landslide moved further downslope, it exhibits coarse to fine material averaging about 2-3 m thick in a neat, straight main pathway with thicker lateral margins and different secondary lobes, a setting that can be attributed to a "debris-flow/slide phase".

The Árnesfjall landslide is characterised by distinctive curved slip surfaces visible in the major mass of debris located in the scar zone, attributable to rotational sliding. The presence of transverse elongated ridges of loose deposits, which were cemented by ground ice at the time of the failure, are further proof of rotational-sliding motion. This process was possible because the ground ice gave the loose debris a more rigid rheological behaviour. The Árnesfjall landslide also has a secondary mass that was mobilised as a debris flow, since the deposits are characterised by a straight and deep channel with lateral levees and a terminal depositional lobe.

Our study reveals that ground-ice has had a major role in the development of the landslides, not just promoting the failure and contributing to the transport with the thaw process, but also affecting the mechanical behaviour of the debris. Therefore, understanding the mobility of such large slope failures is essential for mitigating the hazard in the case of similar events in inhabited regions.

Acknowledgments

This work has been funded by a postgraduate studentship grant (NE/L002493/1) from the Central England Natural Environment Research Council Training Alliance (CENTA) and by a British Geological Survey BUFI CASE Studentship (GA/14S/024, Ref: 284).

References

Decaulne, A., Sæmundsson, P., Pétursson, O., 2005. Debris flow triggered by rapid snowmelt: A case study in the Gleidarhjalli area, northwestern Iceland. *Geografiska Annaler, Series A: Physical Geography* 87(4): 487-500.

Gruber, S. & Haeberli, W., 2007. Permafrost in steep bedrock slopes and its temperatures-related destabilization following climate change. *Journal of Geophysical Research: Earth Surface* 112(2): 1-10.

Jóhannesson, T. & Arnalds, Þ., 2001. Accidents and economic damage due to snow avalanches and landslides in Iceland. *Jökull* 50: 81-94.

Sæmundsson, Þ. *et al.*, 2017. The triggering factors of the Móafellshyrna debris slide in northern Iceland: intense precipitation, earthquake activity and thawing of mountain permafrost. *Science of the Total Environment* 621:1163-1175.

Sæmundsson, Þ., Pétursson, H., Decaulne, A., 2003. Triggering factors for rapid mass movements in Iceland. *Debris-flow hazards.* Available at: http://www.nnv.is/wp-content/uploads/2010/05/Saemundsson-ofl-2003.pdf.

Understanding slope morphology and processes on permafrost-affected mountain slopes based on very high resolution topographic surveys

Hanne Hendrickx[1]
Reynald Delaloye[2]
Jan Nyssen[1]
Amaury Frankl[1,3]

[1] *Department of Geography, Ghent University, Belgium. hanne.hendrickx@ugent.be*
[2] *Department of Geosciences, Fribourg University*
[3] *Postdoctoral Fellow of the Research Foundation Flanders (FWO)*

Abstract

Many geomorphological processes on talus slopes in alpine environments (such as debris flows, rock fall, rock glaciers and gelifluction) are related to permafrost distribution and typology. Therefore, it is expected that process dynamics will alter with climate change induced permafrost warming and degradation. In order to study this, very high resolution topographic surveys are performed with Unmanned Aerial Vehicles (UAVs), resulting in Digital Elevation Models (DEM) and ortho-photo mosaics of 0.02 – 0.05 m resolution. A detailed geomorphological map is presented, revealing where surface morphology could indicate the presence of permafrost. This will be validated next year by applying geophysical methods. Repeated measurements with the UAV will then allow detecting volumetric and horizontal displacements, assessing the geomorphological dynamics of permafrost-affected mountain slopes.

Keywords: Talus slope; geomorphology; UAVs; permafrost

Introduction

A talus slope is a common landform in mountain environments (Lambiel & Pieracci, 2008) and stores debris on a long time scale. In periglacial zones, permafrost is widespread in upper headwalls, in the talus slope itself, as well as in related debris-evacuating landforms (e.g. rock glaciers). In response to ongoing climate change, it is expected that geomorphological processes on permafrost-affected mountain slopes may change, in unfavourable situations potentially accelerating sediment transfers and causing more hazards (Rebetez *et al.* 1997; Gruber, 2004; Stoffel & Huggel 2012).

Repeated investigations and more accurate measurement techniques are required to detect morphological changes and their processes. It is therefore important to study the permafrost distribution and evolution in talus slopes and the above debris source area, and related geomorphological processes leading to sediment transfers.

Data collection

Geomorphological landforms can be identified using geomorphological mapping, interpretation of aerial photographs and fieldwork (Hendrickx *et al.,* 2015). However, to detect changes, geomorphological research needs three-dimensional data. To gain very high resolution 3D terrain models of the study area, the photogrammetric method of Structure-from-Motion (SfM) is used (Fig. 1) (Frankl *et al.,* 2015). This method allows to detect micro-topography that cannot be discerned with differential GPS measurements (dGPS) or available DEM data such as SwissAlti3D.

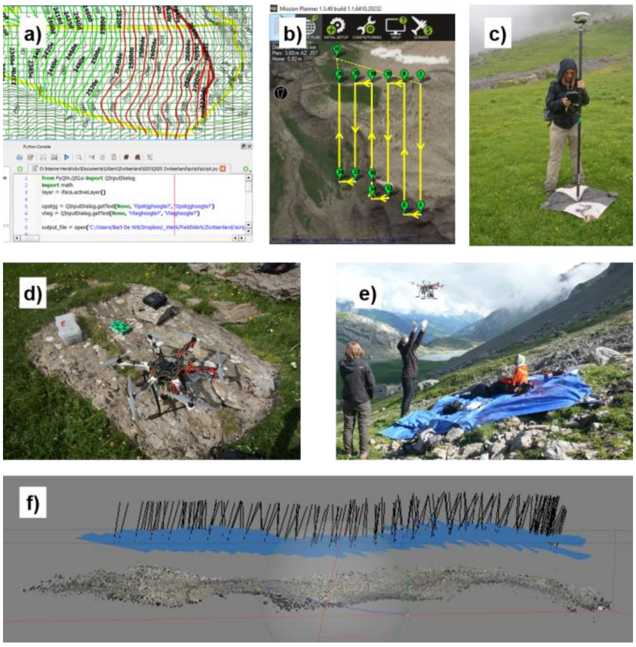

Figure 1. Workflow of the data collection, a) programming flight lines, b) Software MissionPlanner, c) Materializing Ground Control Points (GCPs), measured with RTK-GPS, d) Drone Hexacopter DJI F550, spectrum DX8 controller and 16MP Panasonic DMG-GM5, e) Fly height 70—90m, picture overlap >70%, f) Post processing in Agisoft.

Geomorphological mapping and dynamics

Preliminary results

DEMs and ortho-photo mosaics of 0.02 – 0.05 m resolution allows preparing a detailed geomorphological map of the talus slope complex. The observed surface geomorphology includes rock glaciers, gelifluction, debris flow deposits, landslides and micro-topography (Fig. 2) and will be linked to permafrost conditions using data from temperature loggers and applying geophysical methods in the future.

Figure 2. Micro-topography linked to snow (avalanches), common in the fine grained talus slopes of Col du Sanetsch, Valais, Switzerland. View the full model here: https://skfb.ly/6sK9w

Expected results

The measurements explained above, will be repeated every year, which will allow volumetric changes and horizontal and vertical displacements to be calculated. In order to validate these results, dGPS will be used. This will allow assessing the geomorphological dynamics of permafrost-affected mountain slopes.

Acknowledgments

This research was funded by a travel grant of the Research Foundation Flanders (FWO, grant number: V4.321.17N).

References

Gruber, S., 2004. Permafrost thaw and destabilization of Alpine rock walls in the hot summer of 2003. *Geophys. Res. Lett. 31*, L13504.

Frankl, A., Stal, C., Abraha, A., Nyssen, J., Rieke-Zapp, D., De Wulf, A., & Poesen, J. (2015). Detailed recording of gully morphology in 3D through image-based modelling. *CATENA*, *127*, 92–101.

Hendrickx, H., Jacob, M., Frankl, A. & Nyssen, J., 2015. Glacial and periglacial geomorphology and its paleoclimatological significance in three North Ethiopian Mountains, including a detailed geomorphological. *Geomorphology 246,* 156-167.

Lambiel, C. & Pieracci, K., 2008. Permafrost distribution in talus slopes located within the alpine periglacial belt, Swiss alps. *Permafr. Periglac. Process. 19*, 293–304.

Rebetez, M., Lugon, R. & Baeriswyl, P., 1997. Climatic change and debris flows in high mountain regions: the case study of the Ritigraben torrent (Swiss Alps*). Clim. Change 36,* 371–389.

Stoffel, M. & Huggel, C., 2012. Effects of climate change on mass movements in mountain environments. *Prog. Phys. Geogr. 36*, 421–439.

Characterizing kinematic behaviors of periglacial landforms in the eastern Kunlun Shan (China) using satellite SAR interferometry

Yan Hu[1]
Lin Liu[2]
Xiaowen Wang[3]
[1,2]*Earth System Science Programme, Faculty of Science, Chinese University of Hong Kong, Hong Kong, China, huyan@link.cuhk.edu.hk*
[3]*Earthquake Research Institute, University of Tokyo, Tokyo, Japan*

Abstract

A group of periglacial landforms were discovered in the eastern Kunlun Shan of China 20 years ago, but were ambiguously classified as rockglaciers and later gelifluction deposits. Moreover, the kinematic features of the landform had not been fully investigated or understood. Here, we use satellite SAR interferometry to quantitatively characterize the spatial and temporal changes of the surface movement of these landforms. We observe that: (1) the eastern slope is also active with a summer velocity of 20-60 cm/yr; (2) the northern lobes moved at 20 to 50cm/yr in summer, which are much larger than the previous in-situ estimation of less than 3 cm/yr near the front; and (3) both the northern lobes and eastern slope are inactive during winter. Based on these observations, we postulate that the northern lobes represent a mixed type of periglacial landform, combining the characteristics of rockglaciers and gelifluction deposits.

Keywords: Rockglaciers, gelifluction, InSAR, eastern Kunlun, periglacial landforms

Introduction

A group of tongue-shaped periglacial landforms near Jingxian Valley (35°40´N, 94° 00´E) in eastern Kunlun Shan have been reported and classified as "Kunlun-type" rockglaciers due to their unique morphology (Fig. 1) and slow creeping rates (Cui, 1980, 1985). However, the nature of the northern slopes has remained contentious and later been interpreted as gelifluction deposits (Harris *et al.*, 1998).

This study investigates the kinematic characteristics and discusses the seasonal movement variations of the landform using InSAR imagery.

Figure 1. Photograph of the lobes from the north showing the morphology of the ice-cap shaped deposits in the upper part of the landform and several lobes extending down to the valley. One lobe is outlined in red.

Methodology

Five ALOS-1 PALSAR images over eastern Kunlun Shan area have been used to generate three interferograms to measure the line-of-sight (LOS) velocities of the landform. One interferogram records the kinematic information during winter/early spring and the other two are averaged to represent the surface movement during summer.

Results and Discussion

Table 1. Comparisons of LOS velocities of the two groups of targets between summer and winter/early spring.

Target type	LOS velocity (cm/yr)	
	Summer	Winter/EarlySpring
Northern lobes	20-50	0
Eastern slope	20-60	0

The interferograms reveal that besides the northern lobes which have been identified as rockglaciers or gelifluction deposits, the eastern slope is also active during summer (Fig. 2), while during winter both two groups of targets become inactive (Fig. 3).

The seasonal acceleration in movement of rockglaciers during summer have been observed (Wirz *et al.*, 2016), and in some cases, no movement can be detected in winter (De Sanjosé *et al.*, 2014). Gelifluction processes can also trigger seasonal velocity variations. However,

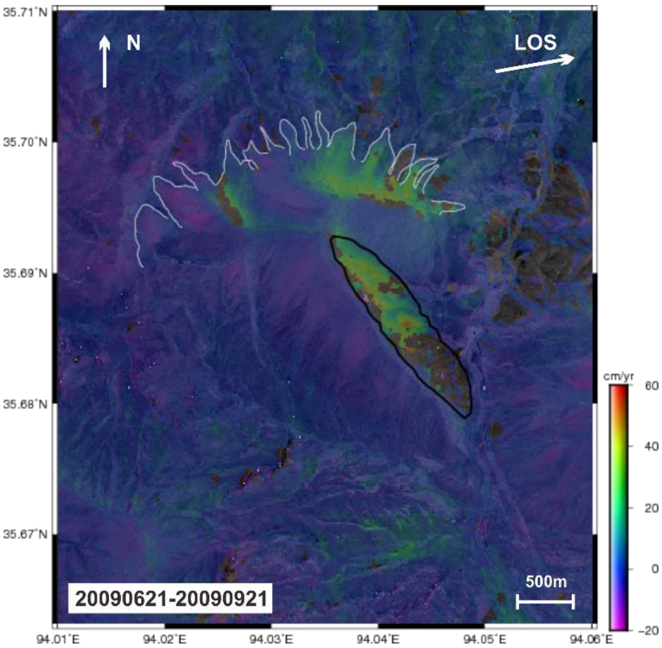

Figure 2. InSAR image showing the LOS velocities of the two groups of landforms near Jingxian Valley during summer in 2009. The northern lobes are marked by white lines and the eastern slope by black polygon.

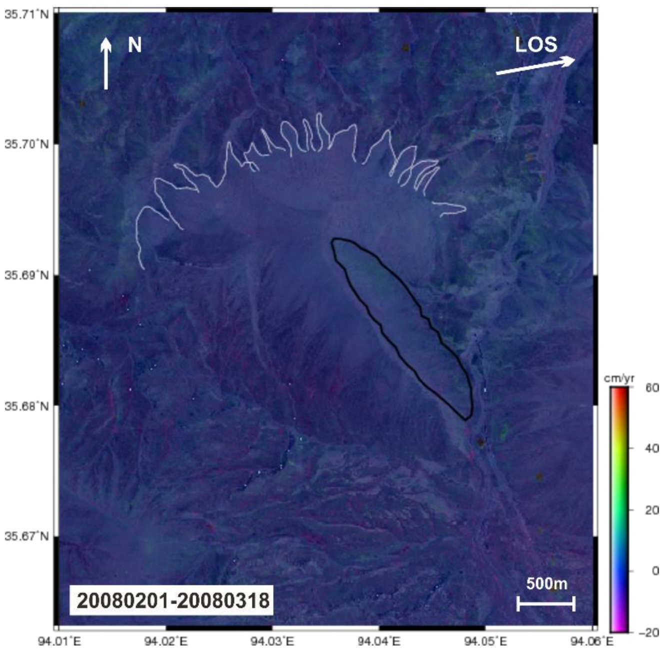

Figure 3. Similar to Figure 2, but showing the LOS velocities during winter/early spring in 2008.

creeping rates during summer are typically smaller than 20 cm/yr in cold and dry climate conditions such as Jingxian Valley (Matsuoka, 2001). Several key evidences, such as (1) the widespread and relatively fast movement and (2) the large-scale tongue-shaped morphology, suggest that the northern lobes are rockglaciers (Matsuoka *et al.*, 2005). The lack of oversteepened fronts presumably results from gelifluction processes of the fine-grained deposits covering the slopes, which smooths out the surface of the landform (Harris, 1994). The landform of the eastern slope, however, is difficult to determine due to the limited knowledge of its morphology and lithology.

Conclusion

The northern lobes and eastern slope of Kunlun Shan near Jingxian Valley show similar patterns of seasonal surface kinematic variations. However, the different morphologic characteristics of the two groups of targets indicate different types of periglacial landforms. With a relatively high surface moving speed and large geometry scale, the northern lobes are unique parts of the alpine permafrost in Eastern Kunlun Shan, representing a mixed type of rockglaciers and gelifluction deposits.

References

Cui, Z. 1980, Periglacial landforms and regional characteristics on Qinghai-Xizang (Tibet)Plateau, *Kexue Tongbao*, 11: 509–512 (in Chinese).

Cui, Z. 1985. Discovery of Kunlunshan-type rock glaciers and the classification of rock glaciers, *Kexue Tongbao*, 30(3): 365–369(in Chinese).

De Sanjosé, J. J., Berenguer, F., Atkinson, A. D. J., De Matías, J., Serrano, E., Gómez−Ortiz, A., González−García, M., and Rico, I. 2014. Geomatics Techniques Applied to Glaciers, Rock Glaciers, and Ice Patches in Spain (1991–2012). *Geografiska Annaler: Series A, Physical Geography*. 96:307-321.

Harris, S. 1994. Climatic zonality of periglacial landforms in mountain areas. *Arctic, 47*(2), 184-192.

Harris, S. A., Zhijiu, C., and Guodong, C. 1998. Origin of a bouldery diamicton, Kunlun Pass, Qinghai-Xizang Plateau, People's Republic of China: gelifluction deposit or rock glacier? *Earth Surface Processes and Landforms*. 23:943-952.

Matsuoka, N. 2001. Solifluction rates, processes and landforms: a global review. *Earth Science Reviews*. 55:107-134.

Matsuoka, N., Ikeda, A., and Date, T. 2005. Morphometric analysis of solifluction lobes and rock glaciers in the Swiss Alps. *Permafrost and Periglacial Processes*. 16:99-113.

Wirz, V., Gruber, S., Purves, R. S., Beutel, J., Gärtner-Roer, I., Gubler, S., and Vieli, A. 2016. Short-term velocity variations at three rock glaciers and their relationship with meteorological conditions. *Earth Surface Dynamics*. 4:103-123.

Mechanical modelling strategies for warming permafrost rock slopes

Michael Krautblatter[1]
Benjamin Jacobs[1]
Philipp Mamot[1]
Regina Pläsken[1]
Riccardo Scandroglio[1]
Tanja Schröder[1]
[1]*Technical University of Munich, Chair of Landslide Research, Benjamin.jacobs@tum.de.*

Abstract

This paper discusses mechanical modelling strategies for instable permafrost bedrock. Modelling instable permafrost bedrock is a key requirement to anticipate magnitudes and frequency of rock slope failures in a changing climate but also to forecast the stability of high-alpine infrastructure throughout its lifetime.

Keywords: Mechanical Modelling; Thermal Modelling; Permafrost Rockwalls; Massive Rock Slope Failure Laboratory Testing, Fatigue.

Introduction

High-alpine rock faces witness the past and present mechanical limit equilibrium. Rock segments where driving forces exceed resisting forces fall of the cliff often leaving a rock face behind which is just above the limit equilibrium. All significant changes in rock mechanical properties or significant changes in state of stress will evoke rock instability which often occurs with response times of years to 1000 years (Krautblatter and Moore, 2014; Leith *et al.*, 2014) Degrading permafrost will act to alter (i) rock mechanical properties such as compressive and tensile strength, fracture toughness and most likely rock friction, (ii) warming subcero conditions will weaken ice and rock-ice interfaces and (iii) increased cryo- and (iv) hydrostatic pressures are expected. Laboratory experiments provide estimations of the serious impact of thawing and warming rock and ice-mechanical properties (ad i and ii), which often lose 25-75% of their strength between -5°C and -0.5°C (Mellor, 1973; Dwivedi *et al.*, 2000; Krautblatter *et al.*, 2013). Approaches to calculate cryostatic pressure (ad iii) have been published and are experimentally confirmed (Murton *et al.*, 2016). However, the importance and dimension of extreme hydrostatic forces (ad iv) due to perched water above permafrost-affected rocks has been assumed (Fischer *et al.*, 2006) but has not yet been quantitatively recorded.

Parameter testing in the lab and field

This paper presents data and strategies how to obtain relevant (i) rock mechanical parameters (compressive and tensile strength and fracture toughness, lab), (ii) ice- and rock-ice interface mechanical parameters (lab), (iii) cryostatic forces in low-porosity alpine bedrock (lab and field) and (iv) hydrostatic forces in perched water-filled fractures above permafrost (field).

Modelling

We demonstrate mechanical models that base on the conceptual assumption of the rock ice mechanical (Krautblatter *et al.*, 2013) and rely on frozen/unfrozen parameter testing in the lab and field.

Continuum mechanical models (no discontinuities) can beused to demonstrate permafrost rock wall destabilization on a valley scale over longer time scales, as exemplified by progressive fjord rock slope failure in the Lateglacial and Holocene.

Discontinuum mechanical models including rock fracture patterns can display rock instability induced by permafrost degradation on a singular slope scale, as exemplified for recent a recent ice-supported 10.000 m³ preparing rock at the Zugspitze (D).

Discontinuum mechanical models also have capabilities to link permafrost slope stability to structural loading induced by high-alpine infrastructure such as cable cars and mountains huts, as exemplified for the Kitzsteinhorn Cable Car and its anchoring in permafrist rocks (A).

Over longer time scales the polycyclicity of hydro- and cryostatic forcing as well as material fatigue play an important role. We also introduce a mechanical approach to quantify cryo-forcing related rock-fatigue (Jia *et al.*, 2015, 2017).

This paper shows benchmark approaches to develop mechanical models based on a rock-ice mechanical model for degrading permafrost rock slopes.

References

Dwivedi, R.D., Soni, A.K., Goel, R.K., Dube, A.K., 2000. Fracture toughness of rocks under sub-zero temperature conditions. *Int. J. Rock Mech. & Mining Sciences* 37, 1267-1275

Fischer, L., Kääb, A., Huggel, C., Noetzli, J., 2006. Geology, glacier retreat and permafrost degradation as controlling factors of slope instability in a high-mountain rock wall: the Monte Rosa east face. *Nat. Hazards Earth Syst. Sci.* 6, 761-772.

Jia, H., Xiang, W. & Krautblatter, M. 2015. Quantifying rock fatigue and decreasing compressive and tensile strength after repeated freeze-thaw cycles. Perm. and Periglac. Process.

Jia, H., Leith, K., Krautblatter, M. 2017. Path-Dependent Frost-Wedging Experiments in Fractured, Low-Permeability Granite. Permafrost and Periglacial Processes.

Krautblatter, M., Funk, D. & Günzel, F.K., 2013. Why permafrost rocks become unstable: a rock-ice-mechanical model in time and space. *Earth Surface Processes and Landforms* 38: 876-887.

Krautblatter, M. & Leith, K. 2015. Glacier- and permafrost-related slope instabilities. Chapter 9 in Huggel C., Carey M., Clague J. & Kääb A., The High-Mountain Cryosphere, Cambridge University Press.

Leith, K., Moore, J.R., Amann, F., Loew, S., 2014. In situ stress control on microcrack generation and macroscopic extensional fracture in exhuming bedrock. *Journal of Geophysical Research-Solid Earth 119*, 594-615 10.1002/2012jb009801.

Mellor, M., 1973. Mechanical Properties of Rocks at Low Temperatures, *2nd Int. Conference on Permafrost, Yakutsk, Russia,* pp. 334-344.

Murton, J., Kuras, O., Krautblatter, M., Cane, T., Tschofen, D., Uhlemann, S., Schober, S., Watson, P. 2016. A novel experimental design for monitoring rock freezing and thawing by geoelectrical and acoustic techniques. *J. Geophys. Res – Earth Surf.*

Connectivity and sediment transfer at the front of active rock glaciers

Mario Kummert[1]
Reynald Delaloye[1]

[1]*Deptartment of Geosciences, University of Fribourg, Switzerland, mario.kummert@unifr.ch*

Abstract

When connected to torrential channels, the fronts of active rock glaciers may constitute sediment sources for gravitational transfer processes including debris flows. This contribution aims at presenting results from (i) the inventory of rock glaciers connected to torrential channel applied in a 2000 km² region in the southwestern Swiss Alps, and (ii) the observation and quantification of the erosion activity at the front of three selected rock glaciers. Such type of sedimentary connection appeared to be rather rare in the study region. The site specific study highlighted that rock glacier fronts are characterized by a gradual erosion which can lead to substantial annual transferred volumes of sediments (>ca. 1000 m^3/y and up to 7500 m^3/y). It also showed that the continuous movements of the landforms induce a continual renewal of sediments available for erosion. Rock glaciers and other moving landforms represent thus, when connected to torrent, potentially substantial active sources of sediments for the development of debris flows.

Keywords: erosion; sediment transfer; connectivity; rock glaciers; torrential channels; debris flow

Introduction

This contribution proposes to study rock glaciers as sediment sources for the development of debris flows. In periglacial environments, rock glaciers represent important sediment conveyors transporting sediment from their rooting zones to their front (Frauenfelder *et al.*, 2003, Gärtner-Roer, 2012). Rock glacier fronts are usually steep and composed of a mix of coarse sediments embedded in a matrix of finer-grained debris (Wahrhaftig & Cox, 1959). Due to the movement of the whole landform, rock glacier fronts are unstable and may represent sources of easily erodible sediments. In order to actively transfer sediments towards torrential channels, rock glaciers need to be connected to the torrents, i.e. to be located in favorable topographical conditions, for instance on steep slopes and close to a torrential channel. In such a configuration, sediments eroded from the fronts are set available for further transport. However, still very little is known about the mechanisms and the rates characterizing such sedimentary connection. In addition, several cases of rock glaciers feeding torrents with sediments have been observed (e.g. Lugon & Stoffel 2010, Delaloye *et al.*, 2013) but no regional scale inventory able to indicate the location and the number of such type of rock glacier exist. Therefore, the present study aims at better understanding the sedimentary link that may occur between rock glaciers and torrential network systems.

Approach

An inventory of all catchments in which at least one rock glacier is connected to the torrential network system was developed for a 2000 km² region in the south-western Swiss Alps. The inventory method combines the information from a DInSAR-based slope movement inventory (according to the methodology described by Barboux *et al.*, 2014) and the visual analysis of aerial images from 2007 and 2010/11 (Swisstopo) to identify cases of active sedimentary connection. This inventory also considers the connectivity between torrents and other moving landforms located in periglacial environment (e.g. push-moraines, landslides) as they also contribute to transport actively sediments downward.

In addition, the sedimentary connection between rock glaciers and torrential channels was studied into more details at three study sites located in the region, namely Dirru, Gugla and Tsarmine. At each site, the occurrence of erosion and sediment transfer processes was observed by the means of in situ webcams allowing images to be taken at hourly intervals during daytime. Additionally, multi-temporal DEMs were obtained for each site using terrestrial laser scanning in order to identify and quantify surface elevation changes related to sediment transfer activity and thus calculate sediment transfer rates. From the knowledge acquired from the site-specific study, a simplified approach to estimate the erosion rate at the front of rock glaciers based on the geometry of the frontal area and the velocity rate was developed and applied for all the slope movement previously identified within the inventory.

Results

At a regional scale, 42 catchments in which at least one moving landform is connected to the torrential network system were identified out of 659 delimited catchments and interfluve. The main criteria used to select the connected landforms are the proximity with torrents, the traces of sediment transfer activity within these torrents and the flow direction of the movement. 52 moving landforms were thus identified as connected to torrents and corresponded mainly to rock glaciers (69%), but some landslides (25%) and push moraines (6%) were also inventoried.

The results from the site-specific study showed that four main processes characterize the erosion of rock glacier fronts: rock fall, debris slide, superficial flow and concentrated flow. These processes are mainly related to either the advance of the rock glacier destabilizing the sediments lying on the frontal slope or the humidification of the sediments on the surface of the front. The occurrence of erosion at the front of rock glaciers was most frequent during the melt period, roughly between March and June. In summer and autumn, it mostly consisted of occasional rock fall whose frequency increased only during rainfall events. In winter, the front was entirely frozen, covered by snow and no erosion was observed. Debris flows represented the most intense transfer process but occurred rarely, generally in relation with the activation of water springs near the front triggering important concentrated flow.

Erosion rates between 1500 m^3/y and 7800 m^3/y characterized the front of the three studied rock glaciers. The sediments eroded from the fronts generally accumulated on the slope directly below the front, where they were occasionally remobilized by small to medium sized debris flow events. In addition to the actual occurrence of erosion processes, which depended on external climatic drivers (snowmelt, rain), the obtained values of erosion rates showed a strong relation with both the size of the frontal area and the velocity rate of the rock glacier.

Following the results issued from the study cases, the sediment transfer rates between the moving landforms and the torrents could be estimated for each connected slope movement identified in the study region. A majority of landforms was characterized by relatively low sediment transfer rate, ranging from 10 to 500 $m^3/year$ and only 15 showed sediment transfer rates of over 500 $m^3/year$.

Synthesis and conclusion

The results of this study indicate that rock glaciers can act as substantial sediment sources for torrential transfer processes. The gradual erosion of the front is mainly controlled by both weather conditions and the displacement rate of the landform and lead to the recharge of torrential channels with sediments. The sediment transfer activity is continuous in time as the rock glacier motion is constantly bringing new sediments forward. Depending on water availability, these sediments may be remobilized by debris flows. The study also showed that only specific topographic conditions lead to the occurrence of a sedimentary connection between rock glaciers and torrential channels and appear to be relatively rare. When such type of configuration exists, better assessment of the potential frequency-magnitude of debris flow events require further investigations on the identification of the channel recharge rate, which depends on the velocity, and the potentiality for enhanced water availability in the torrent.

Acknowledgments

Field data gathering have been carried out with the participation and the help of numerous persons who need to be thanked here. We also acknowledge the municipalities of Evolène and St. Niklaus as well as the *Service des forêts et du paysage du Canton du Valais* for the logistical and financial support which strongly facilitated the fieldwork operations.

References

Barboux, C., Delaloye, R., & Lambiel, C., 2014. Inventorying slope movements in an Alpine environment using DInSAR. *Earth Surface Processes and Landforms* 39: 2087–2099.

Delaloye, R., Morard, S., Barboux, C., Abbet, D., Gruber, V., Riedo, M. & Gachet, S. 2013. Rapidly moving rock glaciers in Mattertal. *Mattertal – ein Tal in Bewegung. Publikation zur Jahrestagung der Schweizerischen Geomorphologischen Gesellschaft 29. Juni – 1. Juli 2011, St. Niklaus,* Birmensdorf, Eidg. Forschungsanstalt WSL: 113 – 124.

Gärtner-Roer, I. 2012. Sediment transfer rates of two active rockglaciers in the Swiss Alps. *Geomorphology* 167-168: 45-50.

Lugon, R. & Stoffel, M. 2010. Rock glacier dynamics and magnitude-frequency relations of debris flows in a high-elevation watershed: Ritigraben, Swiss Alps. *Global and Planetary Change* 73: 202-210.

Wahrhaftig, C., & Cox, A. 1959. Rock glaciers in the Alaska range. *Geological Society of America Bulletin* 70(4): 383-436.

Quantification of Holocene nivation rates on deglaciated surfaces of James Ross Island, Antarctica

Michaela Kňažková[1]
Daniel Nývlt[2]
Filip Hrbáček[3]
[1]*Department of Geography, Masaryk University, Brno, Czech Republic, michaelaknazkova@gmail.com*
[2]*Department of Geography, Masaryk University, Brno, Czech Republic*
[3]*Department of Geography, Masaryk University, Brno, Czech Republic*

Abstract

Nivation is a broad term for a range of landscape modelling processes resulting from the occurrence of late-lying snow-patches. In this study, we aim to quantify the nivation rates on Cape Lachman, at a site consisting of an approximately 2 km long and 200 m wide semi-circular depression, where snow accumulations form on the lee slopes. The site is located on James Ross Island, Antarctica, in semi-arid polar continental climate with annual precipitation of 300–500 mm and strong effect of wind on the redistribution of snow. dGPS measurements have been carried out on 20 transects across the nivation depression with the aim to quantify the scarp retreat and slope profile change and to compare between the transects that have been affected by nivation and those who have been not. Furthermore, material samples from selected profiles were subjected to grain-size analysis to determine the ratio of fine particles removed.

Keywords: nivation processes; snow-patch erosion; James Ross Island; field survey; Antarctica.

Introduction

Nivation is a classical morphogenetical concept (Matthes, 1900) and refers to a range of processes connected with snow-patches and their role in the modelling of landscape (Thorn & Hall, 2002). Nivation processes have not been studied systematically during the recent years. Very little effort has been directed towards a quantitative description of these processes. Besides this, a general lack of any knowledge about the nivation processes in ice-free areas of Antarctica should also be mentioned.

Due to the fact that nivation processes are generally operating slowly and on a long timescale, they might be overridden by faster-working periglacial processes such as solifluction, therefore the effect of nivation alone may be hard, if not impossible to quantify. However, in cold semi-arid to arid climates with limited annual precipitation and resulting very low soil moisture levels, nivation can be considered an important factor in landscape modelling.

Study area

James Ross Island is located off the north-eastern coast of the Antarctic Peninsula in semi-arid polar climate. The average annual precipitation is approx. 300–500 mm, most of which is in the form of snow. Strong winds redistribute the snow into drifts, which can last all through the following summer. As the snow melts, fine regolith particles are carried by meltwater and accumulate in pronival alluvial fans at the foothill and the depression floor. Long-term downslope transport results in a significant remodelling of the slope profile.

The area of interest for this study is located on Cape Lachman, the northernmost part of Ulu Peninsula. Based on exposure dating of erratic boulders from Cape Lachman, it has been determined that the deglaciation of the area occurred 12.9 ± 1.2 ka ago (Nývlt *et al.*, 2014). The site itself consists of a semi-circular depression ~2 km long and 200 m wide, with two shallow lakes situated on the bottom.

Methods

Methods for this research include a field survey using dGPS measurements (Trimble GeoExplorer 6000) along 20 transects across the study area. Furthermore, surficial regolith samples (upper 10 cm) were collected from the selected transects for the purpose of grain-size analysis.

Using the dGPS data, a digital terrain model of the study site has been constructed that allows for a more thorough analysis of the affected area, e.g. calculation of the total amount of material displaced by meltwater and slope retreat over the course of the whole Holocene.

Results

Based on the shape of the slope profile and prevalent snow-patch accumulation, distinction between the profiles affected by nivation processes and those not affected has been made. Out of 20 transects, 6 have undergone changes in slope profile due to nivation. The most significant remodelling has occurred on the lee slopes, where largest accumulations of snow form during the winter. In some places, the down-wasting reached up to 10 metres due to the removal of material by meltwater. This corresponds to an average rate of 0.77±0.12 mm per year within the most significantly affected areas since the deglaciation. It should be noted that this average value would have been highly changeable throughout the Holocene in connection with the climate conditions.

Grain-size analysis of the samples supports the removal of the finest fraction and its accumulation on the depression floor in form of pronival alluvial fans. Within transects unaffected by nivation processes, the ratio of the finest fraction (<0.063 mm) remains steady along the whole profile. However, where extensive remodelling of the slope profile has occurred, the ratio of the finest fraction is twice as high in the sample from the slope apron when compared to the sample from the middle part of the slope.

Conclusions

This study suggests that nivation is an important, but slow landscape-modelling factor in the conditions of semi-arid polar climate and its average rate could be quantified even at the scale of millennia.

Acknowledgments

Research was supported by Ministry of Education, Youth and Sports of the Czech Republic projects LM2015078 and CZ.02.1.01/0.0/0.0/16_013/0001708 and by the Masaryk University project MUNI/A/1419/2016.

References

Matthes, F.E., 1900. Glacial sculpture of the Bighorn Mountains, Wyoming. United States Geological Survey, 21st Annual Report 1899–1900, 167–190.

Nývlt, D., Braucher, R., Engel, Z., Mlčoch, B., & ASTER Team, 2014. Timing of the Northern Prince Gustav Ice Stream retreat and the deglaciation of northern James Ross Island, Antarctic Peninsula during the last glacial–interglacial transition. *Quaternary Research* 82: 441–449.

Thorn, C.E. & Hall, K., 2002. Nivation and cryoplanation: the case for scrutiny and integration. *Progress in Physical Geography* 26: 553–560.

Simulating rapid permafrost degradation and erosion processes under a warming climate

Moritz Langer[1,2]
Thomas Schneider von Deimling[1,2]
Soraya Kaiser[1,2]
Stephan Jacobi[1]
Sebastian Westermann[3]
Simon Zwieback[4]
David Loibl[2]
Paul Overduin[1]
Julia Boike[1]

[1] *Alfred Wegener Institute, Helmholtz Center for Polar and Marine Research (AWI), Potsdam, Germany, moritz.langer@awi.de*
[2] *Department of Geography, Humboldt-Universität zu Berlin, Berlin, Germany*
[3] *Department of Geosciences, University of Oslo, Norway*
[4] *Department of Geography, University of Guelph, Canada*

Abstract

Amplified climate warming in the Arctic leads to thawing of permafrost, triggering large-scale landscape and ecosystems changes and thereby severely impacting the heat, water, and matter cycles of Arctic ecosystems. The induced erosion and rapid thaw processes threaten the stability of Arctic ecosystems as well as infrastructure that is important to Arctic's life and economy. In order to provide better predictions on the dynamics of Arctic permafrost landscapes we aim to develop a novel approach for simulating erosion and mass wasting processes based on a one dimensional land surface model. Preliminary results of extensive modelling exercises will be presented demonstrating the model capabilities for a test site in the Canadian Arctic.

Keywords: rapid permafrost degradation; erosion and mass wasting; landscape dynamics; land surface modeling.

Introduction

Current model approaches used to simulate the degradation of permafrost under a warming climate are highly simplistic since they only consider one-dimensional (top-down) thawing and ignore lateral processes such as soil erosion and mass wasting which are the most abundant forms of thaw in many regions. Thus, current model assessments are most likely far too conservative in their estimates of permafrost thaw impacts (Rowland & Coon, 2015). It therefore remains uncertain how climate warming and permafrost thaw will affect (i) the intensity of erosion and mass wasting processes and (ii) essential ecosystem functions, landscape characteristics, and infrastructure. It also remains unclear (iii) whether any erosion-induced landscape changes further accelerate permafrost thaw.

In order to answer these critical questions, land surface models (LSMs) require a new level of realism in order to adequately project permafrost thaw dynamics. Within the PermaRisk project, the permafrost model CryoGrid3 is extended with an erosion scheme that allows to represent lateral mass movement processes within the limited framework of one dimensional LSMs. The new model will be applied and validated at three Arctic sites in Alaska, Canada, and northern Siberia. Furthermore, 21st century climate impact projections for the key sites are scheduled as a basis for thorough risk analyses concerning potential damages to critical ecosystem functions/services and infrastructure.

We will present first simulations on rapid permafrost degradation processes with a special focus on thaw slumps at a test site in northern Canada. We expect the results to demonstrate the capabilities and the limitations of the new model.

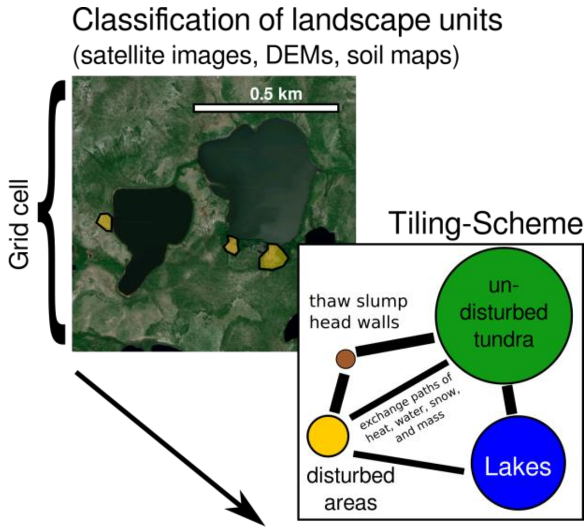

Figure 1: Conceptual illustration of the tiling scheme used to simulate thaw slumps and their interaction with surrounding landscape units.

The model concept

The CryoGrid3 land surface model (Westermann et al., 2016) makes use of a tiling scheme that allows simulating processes on a sub-grid scale (e.g. Langer et al., 2016). Tiling is an established concept for representing landscape hetero-geneities in one-dimensional LSMs. The tiling scheme divides the landscape encompassed by one grid cell (typically representing 5 to 25 km²) into landscape units that are relevant for erosion. The tilling scheme distinguish a predefined number of landscape units according to ground ice content and topography. Thereby, only the areal fraction and topological information of these land-scape units (interconnections, distances, and slopes) are stored as information in the tiles. The land surface is, thus, decomposed into virtual information allowing reduced order representation of a process that is much smaller than the nominal spatial resolution of the model.

Routines from hydrological models are currently being implemented into CryoGrid3 in order to represent lateral heat, water, snow, and mass exchange between tiles. To this end, the used rout routines are based on linear functions which are scaled according to topological indexes and shape factors consisting of distances, interface lengths, and areal fractions (Fig. 1).

Acknowledgments

The young investigator group PermaRisk is funded by a grand (01LN1709A) awarded to Moritz Langer by the Federal Ministry of Education and Research (BMBF) within the FONA program initiative.

References

Langer M., S. Westermann, J. Boike, G.B Kirillin, G. Grosse, S. Peng, and G. Krinner, 2016. Rapid degradation of permafrost underneath waterbodies in tundra landscapes - Toward a representation of thermokarst in land surface models. *J. Geophys. Res.* 121(12): 2446-2470.

Rowland, J. C., Coon, E. T., 2015. From documentation to prediction: raising the bar for thermokarst research. *Hydrogeology Journal*, 1–4.

Westermann, S., M. Langer, J. Boike, M. Heikenfeld, M. Peter, B. Etzelm□uller, and G. Krinner, 2016. Simulating the thermal regime and thaw processes of ice-rich permafrost ground with the land-surface model CryoGrid 3.. *Geoscientific Model Development* 9(2): 523-546.

.

Assessing the spatial pattern of rockfalls above the Miage Glacier, Mont Blanc Massif, and their coupling with glacial dynamics

Alex (G) McKee[1], Stuart (A) Dunning[2], Matt (J) Westoby[3]
[1]*MPhil Researcher at Newcastle University, A.G.Mckee1@newcastle.ac.uk*
[2]*Newcastle University*
[3]*Northumbria University*

Abstract

Climate change accelerates glacial retreat, thus intensifying the subsequent exposure of metastable sediment. Periglacial slopes are capable of releasing large quantities of sediment through a diverse range of mass movement processes, including rockfalls. Rockfalls are often thought to be responsible for the majority of the geomorphologic adjustment during the paraglacial period. However, the frequency of small rockfalls (<10^{-2} km^2) from steep rock walls and high-altitude rock-walls (HARWs) are relatively understudied due to low-resolution imagery and inaccessibility. The Miage Glacier, Mont Blanc Massif, provides a unique study opportunity due to its established timeline of transitioning from 'clean' ice to debris-mantled and the increasing rate of rockfalls in the last decade, which combined with Structure from Motion (SfM) and a method of dating rock scars by colour, will allow assessment of spatial rockfall patterns and their subsequent impact on glacier dynamics.

Keywords: Rockfalls; slope; climate change; glacier; sediment; rock walls.

Introduction

During the paraglacial period, when a landscape is adjusting from a glaciated to a non-glaciated state, geomorphic activity is accelerated by glacier recession and subsequent exposure of metastable sediment stores (Ballantyne, 2002). Periglacial slopes are capable of releasing vast quantities of sediment through a diverse range of mass movement processes, including rockfalls. Rockfalls are responsible for the majority of the geomorphologic adjustment during the paraglacial period (Corominas *et al.*, 2017).

Previous studies of paraglacial rock failures are subject to bias, namely: i) infrequent observation; ii) lack of reporting rockfalls that do not damage anthropogenic structures; iii) inaccurate volume estimates of rockfalls below the limit of detection (LOD) due to low-resolution imagery (Dussauge *et al.*, 2003). Consequently, small rockfalls (<10^{-2} km^2) are censored from the landscape and subsequently underrepresented in magnitude-frequency relationships.

To better understand the spatial pattern of rockfalls, it is important to attribute failure to a particular control, namely preconditioning, preparatory or triggering factors (Deline *et al.*, 2015; Allen, 2017). For example, previous studies at the Miage glacier, Italian Alps, concluded that permafrost melt, as a result of increasing annual air temperatures, was the primary trigger for the rockfalls in the area, however these studies were unable to consider smaller rockfalls (10^0 – 10^2 m^3) and the age of the failed rock.

Once a rockfall has occurred, it has the capacity to impact glacier dynamics substantially (Deline *et al.*, 2015). Dispersed and thin debris cover (<0.04 m) enhances ice melt rates through a reduction of albedo feedback, whereas a thicker debris mantle (>0.04 m) reduces ice melt by insulating the glacier from atmospheric heat and insolation (Brock *et al.*, 2010). For example, The Mer de Glace (clean ice) and Miage glacier (debris covered) retreated by 2,400m and 300m respectively since the 1820s LIA maximum (Deline *et al.*, 2015). Supraglacial rockfalls are not the only source of debris at these sites, as glacial downwasting exposes englacial debris, thus producing a similar albedo feedback effect.

Glaciers also have the ability to impact rockfall dynamics and evolution, primarily higher mobility of rockfalls on glaciers, of up to 24% greater than on soil/rock surfaces (Deline *et al.*, 2015). The longer runout distances are attributed to channelized debris, incorporation of ice and snow into the moving debris mass, and much lower coefficients of friction for snow and ice than for other materials (Deline, 2009). Previous studies of failure mobility focus on larger volumes (rock avalanches, >10^6 m^3) and little attention is given to smaller failure volumes due to varying movement processes, i.e. rockfalls and fragmental rockfalls are modelled as ballistic trajectories while rock avalanches are simulated as granular flows (Bourrier *et al.*, 2013).

The Miage Glacier, Italian Alps, provides a unique study opportunity to assess the patterns of rockfalls above glaciers and their coupling with glacial dynamics, due to its established timeline of transitioning from 'clean' ice to debris-mantled (Deline, 2005), the increasing rate of rockfalls in the last decade (Rabatel *et al.*, 2008; Ravanel & Deline, 2015) and its accessibility.

Methodology

The number and size of small rockfalls are quantified by differencing repeat Structure for Motion (SfM) models using the Multiscale Model to Model Cloud Comparison (M3C2) algorithm for cloud-to-cloud differencing (Westoby *et al.*, 2012). Pre- and post-melt season (2017), September 2016 and July 2015 (Allen, 2017) SfM datasets are available. GigaPans (high-resolution, interactive gigapixel panoramic images) are used to compare recent models to archive models generated from 2015 and 2016 imagery.

As suggested by Gallach *et al.* (2016), there is a strong relationship between rock scar colour and age at the Mont Blanc Massif due to weathering, i.e. the redder the rock, the greater its age. By calibrating modular uni-spectral (RedBand) images against a known test site (Aiguille du Midi), it was possible to establish a rock surface exposure age in order to quantify the temporal distribution of rockfall activity (Böhlert *et al.*, 2008).

By gaining meteorological, rock age, altitude and sun exposure data from the study site it will be possible to identify potential rockfall drivers by analysing spatial distributions of slope failures.

Acknowledgments

This research was supported by a Small Research Grant from Newcastle University to Dr. S. Dunning.

References

Allen, M., 2017. Landslide distributions around glaciers in high mountains, Geography PhD, Newcastle University, Newcastle upon Tyne.

Ballantyne, C.K., 2002. Paraglacial geomorphology. *Quaternary Science Reviews* 21 (18): 1935-2017.

Böhlert, R., Gruber, S., Egli, M., Maisch, M., Brandová, D., Haeberli, W., Ivy-Ochs, S., Christl, M., Kubik, P.W. & Deline, P., 2008. Comparison of exposure ages and spectral properties of rock surfaces in steep, high alpine rock walls of Aiguille du Midi (France). *Proceedings of the 9th International Conference on Permafrost*: 143 – 148.

Bourrier, F., Dorren, L. & Hungr, O., 2013. The use of ballistic trajectory and granular flow models in predicting rockfall propagation. *Earth Surface Process Landforms* 38: 435–440.

Brock, B.W., Mihalcea, C., Kirkbride, M.P., Diolaiuti, G., Cutler, M.E. & Smiraglia, C., 2010. Meteorology and surface energy fluxes in the 2005–2007 ablation seasons at the Miage debris‐ covered glacier, Mont Blanc Massif, Italian Alps. Jour*nal of Geophysical Research: Atmospheres* 115 (D9).

Corominas, J., Mavrouli, O. & Ruiz-Carulla, R., 2017. Magnitude and frequency relations: are there geological constraints to the rockfall size? *Landslides*: 1-17.

Deline, P., 2005. Change in surface debris cover on Mont Blanc massif glaciers after the 'Little Ice Age' termination. *The Holocene* 15(2): 302–309.

Deline, P., 2009. Interactions between rock avalanches and glaciers in the Mont Blanc massif during the late Holocene. *Quaternary Science Reviews* 28 (11): 1070–1083.

Deline, P., Hewitt, K., Reznichenko, N. & Shugar, D., 2015. Rock avalanches onto glaciers. In: Davies, T. (ed.), *Landslide Hazards, Risks, and Disasters*. Elsevier Inc.: 263–319.

Dussauge, C., Grasso, J.R. & Helmstetter, A., 2003. Statistical analysis of rockfall volume distributions: Implications for rockfall dynamics. *Journal of Geophysical Research: Solid Earth* 108 (B6).

Evans, S.G. & Clague, J.J., 1988, Catastrophic rock avalanches in glacial environments. In: Bonnard, C. (ed.), *Proceedings of the 5th International Symposium on Landslides* 2: 1153-1158.

Gallach, X., Ogier, C., Ravanel, L., Deline, P. and Carcaillet, J., 2017. Reconstruction of the rock fall/avalanche frequency in the Mont Blanc massif since the Last Glacial Maximum. In: *EGU General Assembly Conference* Abstracts 19: 10030.

Rabatel, A., Deline, P. & Ravanel, L., 2008. Rock falls in high-alpine rock walls quantified by terrestrial lidar measurements: A case study in the Mont Blanc area. *Geophysical Research Letters* 35 (10).

Ravanel, L. and Deline, P., 2015. Rockfall hazard in the Mont Blanc massif increased by the current atmospheric warming. *Engineering Geology for Society and Territory* 1: 425-428.

Westoby, M.J., Brasington, J., Glasser, N.F., Hambrey, M.J. & Reynolds, J.M., 2012. 'Structure-from-Motion' photogrammetry: A low-cost, effective tool for geoscience applications. *Geomorphology* 179: 300-314.

Permafrost thaw and landslide processes revealed by molards

Costanza Morino[1]
Susan J. Conway[2]
Þorsteinn Sæmundsson[3]
Jón Kristinn Helgason[4]
John Hillier[5]
Frances E.G. Butcher[6]
Matthew R. Balme[6]
Colm Jordan[7]
Tom Argles[1]

[1] *School of Environment, Earth & Ecosystem Sciences, The Open University, UK, Costanza.morino@open.ac.uk*
[2] *Laboratoire de Planétologie et Géodynamique de Nantes UMR-CNRS 6112, France*
[3] *Department of Geography and Tourism, University of Iceland, Iceland*
[4] *Icelandic Meteorological Office, Avalanche Centre, Iceland*
[5] *Department of Geography, Loughborough University, UK*
[6] *School of Physical Sciences, The Open University, UK*
[7] *British Geological Survey, Environmental Science Centre, UK*

Abstract

Molards are conical mounds of debris that compose part of a landslide's deposits. Molards 'origin could be directly linked to permafrost degradation in cold environments, but it is still unclear how they form. Here we reconstruct the entire story of the formation of molards, resulting from the decay of blocks of ice-rich sediments into cones of debris. We demonstrate that molards in cold environments indicate ground ice thaw, and can be used as a marker of permafrost degradation. We show that molards with peculiar morphometric characteristics and spatial distribution reveal different landslides' processes. We demonstrate that molards are identifiable in the field and in remote sensing data, allowing us the recognition on Earth and on Mars of candidate relict molards, which can be used as an indicator of current and past permafrost conditions.

Keywords: molards, permafrost, landslides, ground ice, Iceland.

Introduction

Molards have been described as mounds of debris occurring in landslide deposits (e.g., Goguel & Pachoud, 1972). Molards have been reported in cold environments, but their origin is still unclear. Recent studies have hypothesised a link between molards and permafrost degradation(e.g., Milana, 2016). However, no previous studies have observed the full cycle of molard evolution in the field.

We combine field and remote sensing studies of molards found in the deposits of two landslides in Iceland to constrain their complete evolution, providing observations before and after ice loss. We studied the Móafellshyrna debris slide (Tröllaskagi peninsula) and the Árnesfjall debris slide (Westfjords). Both originated from talus deposits perched on topographic benches. We analysed the distribution and geomorphic characteristics of molards on their surfaces, using high resolution Digital Elevation Models (DEMS) produced from both airborne data and ground-based Structure from Motion, in order to uncover the role of molards in the landslides' dynamic and their link to permafrost degradation.

How molards form

We surveyed both landslides immediately after their failures, in summer 2012 at Móafellshyrna and in summer 2014 at Árnesfjall. At both sites, we found pseudo-cubic and angular blocks and ridges of ice-rich sediments. We revisited the sites 2 and 3 years after the failures, respectively. We found conical molards with rounded to pointed summits in the place of the original ice-cemented blocks. No trace of ground ice was found in neither of the sites. Therefore, molards form in periglacial environments from the degradation of blocks and ridges of ice-cemented deposits into conical mounds of debris.

Molards and permafrost thaw

Mountain permafrost has been modelled at elevations above 800-900 m a.s.l. in the central-northern regions of Iceland (Etzelmüller *et al.*, 2007). The Móafellshyrna landslide (873 m a.s.l.) falls within the predicted spatial zone and altitude band for mountain permafrost. Furthermore, the ice-cemented blocks that detached here were 15-20 m thick, much larger than the expected maximum depths of annually-formed, ice-cemented ground (Matsuoka *et al.,* 1998). The Árnesfjall landslide (418 m a.s.l.) occurred on the coastline of the Westfjords, 400 m below the predicted permafrost altitude in this area. The presence of molards here is the only pragmatically detectable indicator of permafrost conditions. Hence, it is very likely that the source talus slopes of both landslides were perennially-frozen ground and that the molards indicate permafrost degradation.

Molards and landslide processes

The morphometry and the spatial distribution of molards in Móafellshyrna and Árnesfjall landslides can provide information about the failure dynamics. In Móafellshyrna, the molards are isolated and circular, they vary in size (4-7300 m^3), and lie in a sub-horizontal area at the foot of the talus slope located below the topographic bench. Their position matches that expected for rockfalls, where competent fragments detach and fall, and come to rest either within, at the foot, or beyond the base of the talus slope (Evans & Hungr, 1993). Molards in Árnesfjall are elliptical, have more homogeneous volumes (41-2300 m^3), lie on an average slope of 26.4°, and are densely clustered less than 30 m below the base of the failure scarp. This position is typical of the location of *en echelon* concave-upward rupture surfaces in debris slides. Molards in Árnesfjall derive from the degradation of densely packed, elongated ridges exposed by the rotational-sliding motion of the source material, cut by several curved planes of movement. These dynamics are reflected in their more homogeneous size and their elliptical shape, a result of the degradation of elongated cusps of ice-cemented precursor units produced by relatively coherent rotational sliding.

Molards from remote sensing

Conical mounds can be generated by many processes, but molards are always associated with a landslide. They could, however be confused with hummocky terrains found in rock avalanche deposits. However, hummocks have the following characteristics that distinguish them from molards: (i) they usually decrease in size with runout distance, unlike molards, which have heterogeneous sizes if generated by falling, or more homogeneous sizes if generated by sliding, (ii) hummocks in rock and debris avalanches can have volumes of up to millions of cubic meters, while molards in Iceland have volumes of thousands of cubic meters at most, and (iii) hummocks tend to have their long axes parallel or orthogonal to the direction of the mass movement, while we measured that molards have axes with no preferential orientation with respect to the flow if produced by fall. Hence, these characteristics can be verified from remote sensing data to reliably distinguish molards from other conical features.

We identified candidate molards in other two remote regions where continuous permafrost is thought to be present. In the first case, we report molards scattered across the surface of deposits mobilised by a rock avalanche in Greenland. In the second case, we found similar scattered conical landforms within impact ejecta originating from Hale Crater on Mars. Therefore, we have demonstrated that molards are not only readily recognisable in the field, but also via remote sensing. This allows to efficiently identify these landforms across large and remote areas, revealing the influence of ice thaw not only on Earth, but also potentially on other planets.

Acknowledgments

This work has been funded by a postgraduate studentship grant (NE/L002493/1) from the CENTA NERC and by a British Geological Survey BUFI CASE Studentship (GA/14S/024, Ref: 284).

References

Etzelmüller, B. et al., 2007. The regional distribution of mountain permafrost in Iceland. *Permafrost and Periglacial Processes* 18(2): 185–199.

Evans, S.G. & Hungr, O., 1993. The assessment of rockfall hazard at the base of talus slopes. *Canadian Geotechnical Journal* 30(4): 620–636.

Goguel, J. & Pachoud, A., 1972. Géologie et dynamique de l'écroulement du Mont Granier: dans le Massif de Chartreuse, en novembre 1248. *Bulletin du Bureau de Recherche Geologiques et Minieres* III (1): 29–38.

Matsuoka, N. et al., 1998. The role of diurnal, annual and millennial freeze-thaw cycles in controlling alpine slope instability. *Proceedings of the 7th International Conference on Permafrost,* Yellowknife, 23–27 June 1998 55: 711–717.

Milana, J.P., 2016. Molards and Their Relation to Landslides Involving Permafrost Failure. *Permafrost and Periglacial Processes* 27(3): 271–284.

Rock-face temperature at high-elevation sites: a new measuring approach

Guido Nigrelli[1]
Marta Chiarle[1]
Paolo Silvestri[1]
Andrea Merlone[1,2]
Graziano Coppa[2]
Chiara Musacchio[2]
[1]*Consiglio Nazionale delle Ricerche – Istituto di Ricerca per la Protezione Idrogeologica, Torino (Italy), guido.nigrelli@irpi.cnr.it*
[2]*Istituto Nazionale di Ricerca Metrologica – Metrologia per la Qualità della Vita, Torino (Italy)*

Abstract

The Alpine environment and in particular the cryosphere, is responding quickly and with great intensity to climate change. Temperature increase observed in the Alps urge the scientific community to study not only air temperature but also rock temperature, to deepen the knowledge about thermal properties of the potentially unstable geological materials. The metrological traceability of measurements is fundamental for data comparability in space and in time and this can be achieved by the use of calibrated instruments and with the evaluation of measurement uncertainties. Here we present some preliminary results of rock-face temperature analysis based on data acquired at high-elevation sites, by means of sensors with documented traceability to International System of Units Standards and evaluated measurement uncertainty. We found and quantified a strong difference in the hourly rate of temperature increase between air and rock. During summer rock temperature grows more than 8 times over air temperature.

Keywords: Rock, Temperature, Metrology for cryosphere, Permafrost, High-elevation sites, Alps.

Introduction

Cold mountain regions are responding quickly and with great intensity to climate change: the shrinkage of the glaciers, the permafrost degradation and the increase of the natural instability processes (NIP), are the main terrestrial indicators of climate warming (EEA 2017).

In the last 20 years in the Italian Alps, a growing number of NIP has been documented and some authors relate this trend to an increase of the near-surface air temperature (Chiarle *et al.,* 2017; Paranunzio et al., 2016; Turconi *et al.*, 2010). Air temperature (AT) increase can, for example, cause an increase of melting-freezing cycles, with volume change and rock mass damage (Nigrelli *et al.*, 2017). In NIP studies the knowledge of air temperature is not enough: it's necessary to acquire information about rock temperature (RT). RT is not yet widely measured and data are rare, compared to AT data. More importantly, RT data are often acquired by means of sensors with unknown measurement uncertainty. In this research field, the metrological traceability of measurements is actually missing but it is fundamental for data comparability in space and in time (Merlone *et al.*, 2015).

For studying RT at high-elevation sites, it is thus necessary to acquire data with a high level of accuracy, by means of calibrated sensors and inclusion of measurement uncertainty. The approach here proposed is intended as a case study for the adoption of common and standard procedures. Thanks to the close collaboration with the MeteoMet project (https://www.meteomet.org/) it has been possible to:

1. Measure RT by means of sensors with known uncertainty of measurements;
2. Increase knowledge about the thermal conditions of different types of rock;
3. Study relations between climate variability and morphodynamic processes at high-elevation site.

In this work we present the preliminary results of the analysis of the RT's that have been acquired in an experimental glacial basin (Balme, Italy), in the framework of the RiST project (project co-financed by Fondazione CRT).

The new measuring approach

To measure RT we use the MicroTemp sensors and data logger (TDL). Our approach consists of four steps:

1. Laboratory calibration (before and after use) of TDL, necessary to establish documented traceability to S.I. standards;

2. On-site test of TDL, necessary to evaluate components of measurement uncertainty other than the calibration ones;
3. Use of TDL for acquiring RT with known measurement uncertainty;
4. Use of our webcam for visual monitoring of the sites where TDL have been placed (https://bessanese.panomax.com/).

The TDL have been inserted into different types of rock at 10 cm depth (Fig. 1). The acquisition interval is every 10 minutes in summer and every 30 minutes in the other seasons (Fig. 1).

Figure 1. Inserting a TDL in a Calcschist rock.

Preliminary results

The total uncertainty of measurements is ±0.17 °C.

Firstly, we have examined RT during two summer seasons (2016 and 2017), during sunny days and when the rocks were directly exposed to the sun (no clouds, no topographic shadow). In relation to this criterion, we found 12 days that constitute our sample size. In these days we have only considered the hours when RT increases. The study involved two types of rocks: Calcschists and Prasinite rocks (Table 1).

Table 1. Descriptive statistics of the data.

	Sample (n)	Mean (°C/h)	St. dev. (°C/h)	Min÷Max (°C)	Curve f. (r^2)
AT	12	0.5	0.4	-0.2÷1.4	0.6
RT-C	12	3.83	0.49	3.08÷4.67	1.00
RT-P	12	3.89	0.27	3.41÷4.50	1.00

For a description of the acronyms see Fig 1.

We found a strong difference in the hourly rate of temperature increase between air and rock: RT grows more than 8 times over AT during summer, in sunny days with no clouds/shadows. The rate of temperature increase is shown in Fig. 2.

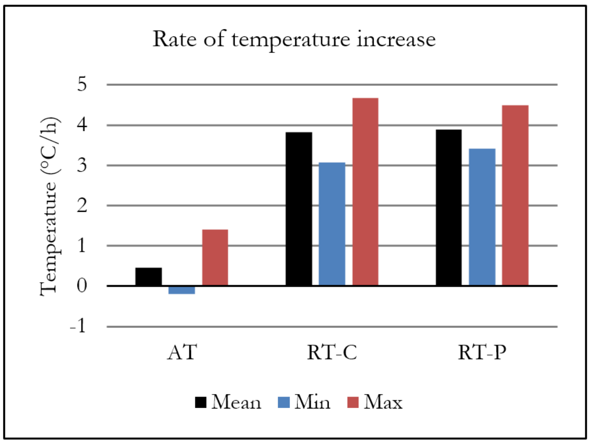

Figure 2. Rate of increase (°C/h) related to air temperature (AT, source ARPA Piemonte), Calcschists and Prasinite rock temperature (respectively RT-C and RT-P).

References

Chiarle, M. Cat Berro, D. et al. 2017. Slope instabilities occurred at high elevation in the Italian Alps in 2016: regional landscape fragility and meteorological framework.. *Geophysical Research Abstracts*, Vol. 19, EGU2017-8498.

EEA 2017. *Climate change, impacts and vulnerability in Europe 2016*. Luxembourg: Publications Office of the European Union,421 pp.

Merlone, A. Lopardo, G. *et al.* 2015. The MeteoMet project - metrology for meteorology: challenges and results. *Meteorological Application* 22: 820–829.

Nigrelli, G. Fratianni, S. *et al.* 2017. The altitudinal temperature lapse rates applied to high elevation rockfalls studies in the Western European Alps. *Theoretical and Applied Climatology* Online first.

Paranunzio, R. Laio, F. *et al.* 2016. Climate anomalies associated to the occurrence of rockfalls at high-elevation in the Italian Alps. *Natural Hazards and Earth System Sciences* 16(9): 2085–2106.

Turconi, L. Kuman De, S. *et al.* 2010. Slope failure and related processes in the Mt. Rocciamelone area (Cenischia Valley, Western Italian Alps). *Geomorphology* 114(3): 115–128.

Nivation and cryoplanation: linking two century-old hypotheses

Kelsey E. Nyland [1]
Frederick E. Nelson [1, 2]
Clayton W. Queen [1]
Brianna J. Rick [3]

[1]*Department of Geography, Environment, and Spatial Sciences, Michigan State University, kelseynyland@msu.edu*
[2]*Department of Earth, Environmental, and Geographical Sciences, Northern Michigan University*
[3]*Department of Geography, University of Montana*

Abstract

Cryoplanation terraces (CTs), staircase-like series of treads and risers in areas of moderate to high relief, have traditionally been interpreted as associated with periglacial landscapes. The formation of these features remains an enigma within periglacial geomorphology, however, there is long-standing debate about whether the dominant controls are climatic or structural. Spatial analysis of cryoplanation terrace elevation at the subcontinental scale across western Beringia and relative weathering indices applied across individual treads at the local scale provide strong evidence in support of the nivation hypothesis of CT formation. This interpretation invokes a suite of erosional processes associated with late-lying snowbanks, and ultimately points to an origin determined by climatic processes. The elevation trends of these terraces closely track the paleo-snowline defined by glacial cirques. Several measures of relative weathering across CT treads indicate that CT treads are time-transgressive surfaces.

Keywords: cryoplanation; nivation; spatial analysis; relative dating; Beringia; Alaska

Introduction

Cryoplanation terraces (CTs) are large erosional landforms consisting of sequences of scarps and treads ascending slopes and ridgecrests, often culminating in flattened summits (Fig. 1). CTs are ubiquitous in the cold, unglaciated Beringian uplands extending from the Lena River in Siberia to the Mackenzie Mountains in Canada. Over the past century, several authors have proposed process models for the development of cryoplanation landscapes, including fluvial action, nivation, solifluction, sorting and mass-movement, polygonal cracking, structural controls, and surface lowering. By the mid-20th century, cryoplanation landscapes were generally hypothesized to form under periglacial processes (Demek, 1969), although disagreement persists about the dominant controls being either climatic or structural (French, 2015).

This study examines a related hypothesis for cryoplanation terrace development first proposed by Cairns (1912): CTs are formed by *nivation*, a shorthand term for a suite of intensified weathering and transport processes associated with late-lying snow. The spatial-analytic and field investigations reported in this presentation examine evidence for and against the nivation genetic model at two different scales: (a) subcontinental, through examination of CT elevation trends across western Beringia; and (2) local, through several relative weathering indices across multiple treads at three locations.

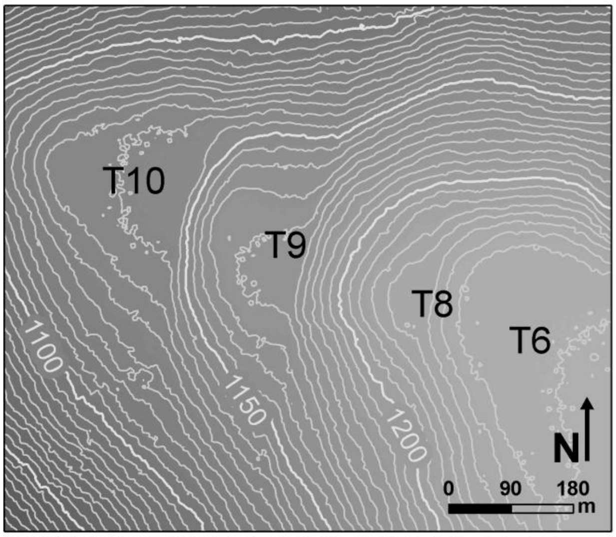

Figure 1. Topographic map showing four cryoplanation terraces near Eagle Summit, Alaska.

Methods

Subcontinental scale spatial analysis

Locational and elevational data from Reger's (1975) data set, supplemented by our own and other workers' observations were confirmed via Google Earth and used in a geostatistical analysis (Nelson & Nyland, 2017). Two data-rich transects, extending from islands in the Bering Sea eastward to Yukon Territory, were constructed to determine if CT elevation exhibits spatial structure similar to that of glacial cirques.

Relative age dating

Three locations identified by Reger were visited (Fig. 2) and four relative weathering measures performed along local transects and at control sites: 1) rock fracture distributions; 2) Cailleux roundness index; 3) Schmidt hammer rebound (rock hardness) values; and 4) weathering-rind thickness.

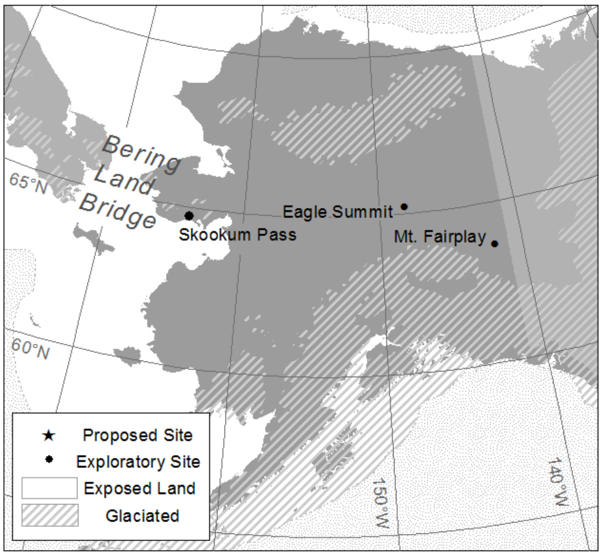

Figure 2. Map of sites where relative dating methods were applied in transects across terrace treads.

Conclusions

CT elevation rises from 175-350 m.a.s.l. on Bering Sea islands to median values greater than 1200 m near the Alaska-Canada border. These regional trends are similar to those of cirque elevation across interior and western Alaska, with consistent gradients generally less than 0.8 m km^{-1}. The similarity of these trends indicates close genetic links between glacial cirques and CTs, involving topographic position, continentality gradients, and the mass balance of localized snow accumulation.

Trends of some of the relative dating indices increase with distance outward for several tens of meters across terrace treads. A general lack of clasts in the central tread areas may be the result of non-cryogenic weathering processes dominating during warm intervals of the Quaternary. This, in turn, suggests that CT development occurs in pulses corresponding to cold climatic intervals.

Existing evidence in support of the nivation genetic model for CT formation are: (1) treads exhibit sedimentological patterns consistent with those of nivation hollows (Reger 1975); (2) scarps display statistically preferred poleward orientation (Nelson, 1998); (3) CTs develop in a "climate space" defined by gradients of temperature and precipitation similar to those of glacial cirques (Nelson and Nyland, 2017); and (4) relative weathering data indicate that terrace treads are time-transgressive surfaces.

Our future work will include absolute (cosmogenic) dating to validate and refine the trends observed in the relative dating indices and determine whether, like glacial cirques, CTs undergo cyclic development in phase with cold climatic periods.

References

Cairns, D.D. 1912. Differential erosion and equiplanation in portions of Yukon and Alaska. *Bulletin of the Geological Society of America* 23: 333-348.

Demek, J. 1969. Cryoplanation terraces, their geographical distribution, genesis and development. *Rozpravy Ceskoslovenski Akademie ved, Rada, Matematickych a Prirodnich Ved*, **79(4):** 80 pp.

French, H.M. 2015. Do periglacial landscapes exist? A discussion of the upland landscapes of northern interior Yukon, Canada. *Permafrost and Periglacial Processes* 27: 219-228.

Nelson, F.E. 1998. Cryoplanation terrace orientation in Alaska. *Geografiska Annaler: Series A, Physical Geography* 80: 135-151.

Nelson, F.E. & Nyland, K.E. 2017. Periglacial cirque analogs: elevation trends of cryoplanation terraces in eastern Beringia. *Geomorphology*, 293: 305-317.

Reger, R.D. 1975. *Cryoplanation terraces of interior and western Alaska*. PhD. Thesis, Arizona State University. 326 pp. (Tempe, Arizona).

Geomorphic mapping, geomorphometry, and cryoplanation terraces

Clayton W. Queen[1]
Kelsey E. Nyland[1]
Frederick E. Nelson[1,2]
[1]*Department of Geography, Environment, and Spatial Sciences, Michigan State University, East Lansing, MI USA, queencla@msu.edu*
[2]*Department of Earth, Environmental, and Geographical Sciences, Northern Michigan University, Marquette, MI USA*

Abstract

Cryoplanation terraces (CTs) are large landforms characterized by alternating series of treads and risers, giving the impression of giant staircases ascending ridgecrests and hillsides. CTs are well developed and abundant in unglaciated Beringia. Although disagreement exists about the origin of CTs, the dominant hypothesis is that they form through localized erosional and transportation processes associated with late-lying snowbanks. This project is concerned with identifying spatial relationships between groups of surface geomorphic features, geomorphometric parameters, and sedimentological patterns associated with cryoplanation landforms. Using these relationships, we develop a multiscale conceptual framework for the development of cryoplanation terraces. Geomorphological mapping and geomorphometry provide a starting point for parametrizing these features.

Keywords: Cryoplanation; Beringia; periglacial; geomorphometry; GIS

Introduction

Cryoplanation terraces (CTs) are large periglacial landforms characterized by alternating treads and risers ascending ridgecrests and hillsides. CTs are well developed and ubiquitous in areas of moderate to high relief within unglaciated areas of Beringia, the region bounded by the Mackenzie River in the east and the Lena River in the west, including the former Bering Land Bridge. Risers (scarps) are typically covered with clastic rubble, while the surfaces of the nearly planar treads are a mosaic of vegetation, rock debris, and small periglacial landforms. Sideslopes and associated pediment-like surfaces are in many cases covered with solifluction lobes. Cryoplanation terrace dimensions and morphology are highly variable, ranging from 3 to 76 m in height with slopes of 9-32 degrees. Treads range in length from as little as five to hundreds of meters, and have considerably gentler slopes, ranging from 1-10 degrees (Reger, 1975). Scarps and treads are differentiated by sharp breaks in slope (Figure 1). The 686 terraces inventoried by Reger (1975) in Alaska range from 3000 to 845,000 m^2 in plan view.

The genesis of cryoplanation terraces has been debated in the literature for more than a century (see discussions in Cairns 1912; Eakin 1916; Demek 1969; and Thorn & Hall 2002). Some workers have postulated that CTs are primarily a consequence of geologic structure, while others assert that nivation, a suite of weathering processes associated with concentrations of late-lying snow cover (Matthes, 1900), forms these features. However, the consensus is that not enough field-based research has been performed to definitively identify the processes involved (Thorn & Hall, 2002). This project is part of a larger effort to investigate the nivation hypothesis of CT development and seeks to partially fill that void by combining information obtained from previous descriptive studies with new field-based evidence to create a conceptual framework for terrace formation.

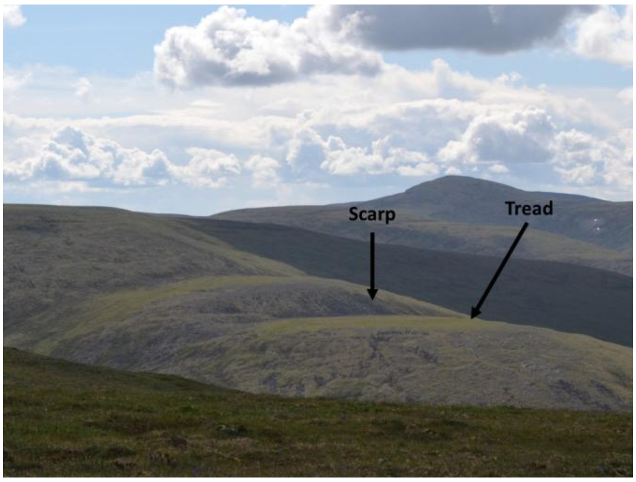

Figure 1. Cryoplanation terraces at Eagle Summit, AK. Terrace components are labeled. The tread is ~200 m long at a slope of ~1°. The scarp has a slope of ~30°.

Methodology

At the scale of individual terraces, geomorphological mapping provides a basis for spatial analysis. Repeating series of periglacial microform-sediment associations are closely related to topographic position and geomorphic processes; these "form communities" can be conceptualized as periglacial facies that yield information about erosional and depositional conditions.

Large-scale (local) mapping has been conducted at four sites distributed over a west-to-east transect across Alaska, terminating at a high-elevation site in northwestern British Columbia. Data collected from field mapping are being compared between sites to identify commonalities and differences. These data sets provide information about combinations of environmental variables that lead to the development of cryoplanation terraces.

At the landscape scale, geomorphometric analysis of landscape geometry provides a pattern-recognition tool that can be used to identify large numbers of individual terraces. At an even broader scale, hypsometric analysis can help to identify climatic and tectonic controls over geomorphic evolution in cold, unglaciated regions. With the intersection of field-based data, descriptive studies, and knowledge of processes, a theoretical framework emerges that helps to explain CT genesis.

Conclusions

Combinations of large- and small-scale analyses and results from general and specific geomorphometric analysis (e.g., Pike et al. 2008) can provide powerful tools for predicting CT locations and inferring patterns of environmental variables leading to the formation of cryoplanation terraces. The framework for terrace development discussed in this presentation will be useful by providing a set of physical, topographic, and climatic conditions necessary for CT formation.

References

Cairns, D.D. 1912. Differential erosion and equiplanation in portions of Yukon and Alaska. *Bulletin of the Geological Society of America* 23: 333-348.

Demek, J. 1969. Cryoplanation terraces, their geographical distribution, genesis and development. *Rozpravy Ceskoslovenski Akademie ved, Rada, Matematickych a Prirodnich Ved*, **79(4):** 80 pp.

Eakin, H.M., 1916. The Yukon-Koyukuk region, Alaska. *U.S. Geological Survey Bulletin* 631, 88 pp. Matthes, F.E., 1901. Glacial sculpture of the Bighorn Mountains, Wyoming. *U.S. Geological Survey*, 21st Annual Report, 1899-1900: 167-190 .

Pike, R., Evans, I.S., & Hengl, T. 2008. Geomorphometry: a brief guide. In: Hengl, T. & Reuter, H.I. (eds.) *Geomorphometry: concepts, software, applications*. Amsterdam: Elsevier, 3-30.

Reger, R.D., 1975. Cryoplanation terraces of interior and western Alaska. Ph.D. dissertation, Arizona State University.

Thorn, C.E, & Hall, K., 2002. Nivation and cryoplanation: the case for scrutiny and integration. *Progress in Physical Geography* 26: 533-550.

Contribution of Coastal Retrogressive Thaw Slumps to the Nearshore Organic Carbon Budget along the Yukon Coast

Justine (Lucille) Ramage[1,2]
Anna (Maria) Irrgang[1,2]
Anne Morgenstern[1]
Hugues Lantuit[1,2]

[1] *Department of Periglacial Research, Alfred Wegener Institute Helmholtz Centre for Polar and Marine Research, Potsdam, Germany. Justine.ramage@awi.de*

[2] *University of Potsdam, Institute of Earth and Environmental Science, Potsdam, Germany*

Abstract

We describe the evolution of coastal retrogressive thaw slumps (RTSs) between 1952 and 2011 along the Yukon Coast, Canada, and provide estimates of the contribution of RTSs to the nearshore organic carbon (OC) budget. We 1) monitor the evolution of RTSs during the periods 1952-1972 and 1972-2011; 2) measure the OC fluxes mobilized through slumping between 1972 and 2011. Our results show a 73% increase in the number of RTSs between 1952 and 2011. Between 1972 and 2011, 17% of the RTSs displaced $27.2*10^3$ m^3/yr of material, adding 0.6% to the OC flux released by coastal retreat along the Yukon Coast. Our results show that the contribution of RTSs to the nearshore OC budget is non-negligible and should be included when estimating the quantity of OC released from the Arctic coast to the ocean.

Keywords: retrogressive thaw slumps; organic carbon; erosion.

Introduction

Soil organic carbon (SOC) stocks in the Arctic are estimated to 1307 Pg; 76.4% (999 Pg) of them are stored in permafrost terrains (Hugelius *et al.*, 2014). Mass wasting processes along the Arctic coast, such as coastal retrogressive thaw slumps (RTSs), contribute to the erosion and transport of terrestrial OC to the nearshore zone (Obu *et al.,* 2016). RTSs rework sediments and mobilize carbon, nitrogen, and nutrients; as a result RTSs affect terrestrial and aquatic ecosystems.

Our study estimates the impact of thermokarst disturbances on the OC budget in coastal permafrost environments. We 1) analyse the evolution of RTSs in the area between 1952 and 2011; 2) measure the OC fluxes mobilized through slumping between 1972 and 2011.

Study area

The study area is located in the Canadian Arctic, along the westernmost coast of the Yukon Territory. It comprises a 238-km portion of the Yukon Coastal Plain, including Herschel Island (Fig. 1). The western margin of the Laurentide ice sheet shaped the topography of the Yukon Coastal Plain. Long and high moraine ridges characterize most of the previously glaciated area. Volumetric ground ice contents along the coast range from 0% to 74%. RTSs are common along the coast and mostly develop on segments with massive ground ice thicker than 1.5 m and coastal slope greater than 3.9° (Ramage *et al.*, 2017).

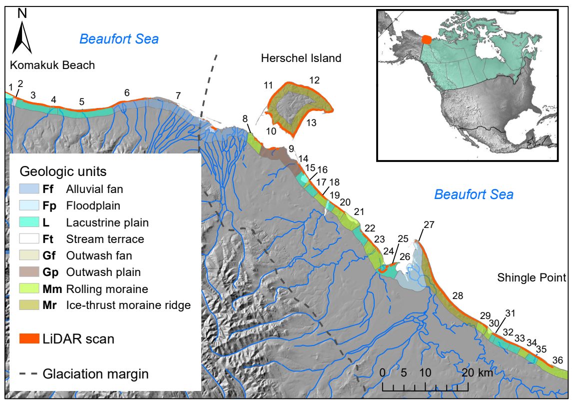

Figure 1: Study area. The coastal subset defined as the LiDAR scan is represented in red.

Methods

RTSs present in 2011 were mapped based on multispectral GeoEye-1 and WorldView-2 satellite images acquired in July, August and September 2011. RTSs present in 1952 and 1972 were mapped using a series of geocoded aerial photographs from the 1950s and 1970s obtained from the National Air Photo Library in Canada. The mapping methodology is explained in detail in Ramage *et al.* (2017).

For each RTS identified in 2011 we extracted morphological information from an airborne LiDAR dataset acquired in July 2013. We applied a regularized spline interpolation technique to model pre-slump topographies used for calculating the volume of material eroded through slumping. To obtain the volumes of eroded material subtracted the mean surface elevation values obtained from the LiDAR dataset from the mean interpolated surface elevation values.

We estimated mobilized SOC and DOC stocks and fluxes from RTSs based on the values provided in Couture (2010) and Tanski *et al.* (2016). OC values were derived from in-situ measurements and were available for each coastal segment.

Results

The number of RTSs increased by 73% between 1952 and 2011. The increase was more pronounced throughout the time period 1952 - 1972 (Table 1).

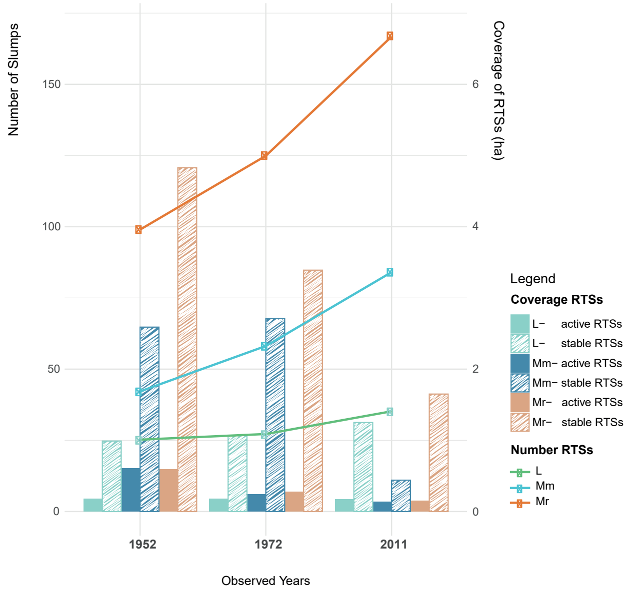

Figure 5: Evolution in the number and areal coverage of RTSs, expressed for the geologic units on which RTSs were identified in 1952, 1972 and 2011.

The 49 RTSs initiated after 1972 eroded a volume of material of $27.2*10^3$ m³/yr between 1972 and 2011. In total, 94% of the reworked material from RTSs initiated after 1972 came from those located on ice-thrust moraines. These RTSs mobilized an SOC flux of $250.1*10^3$ kg/yr (Table 3). On ice-thrust moraines, RTSs initiated after 1972 mobilized 94% of the total SOC flux (Table 3).

Table 3: Total SOC and DOC flux mobilized between 1972 and 2011 by RTSs initiated after 1972, per geologic unit (lacustrine plains, L; rolling moraines, Mm; ice-thrust moraines, Mr).

	SOC flux (kg / km / yr)	DOC flux (g / km / yr)
L	115.5	4.3
Mm	308.5	4.6
Mr	3316.6	68.6

Conclusion

The number of RTSs along the Yukon Coast increased by 73% between 1952 and 2011 and the total areal coverage of RTSs increased by 14%. We observed disparities between geomorphic units: the largest increase was on ice-thrust moraines, where the number of RTSs increased at an annual rate of 1.2 RTSs/yr. Many RTSs are polycyclic and reactivated between 1972 and 2011. RTSs reworked at least $16.6*10^6$ m³ of material within a 190-km portion of the coastal fringe. Majority of the material came from erosion of the headwall (53%) and 3% remained in the RTS floors. A large amount of the material from RTSs was eroded and transported alongshore due to coastal retreat (45%). The OC flux from 17% of the RTSs identified in 2011 represented 0.6% of the annual OC fluxes from coastal retreat in the study area. Our results show that the contribution of RTSs to the nearshore OC budget is non-negligible and should be included when estimating the quantity of OC released from the Arctic coast to the ocean.

References

Couture, N.: Fluxes of Soil Organic Carbon from Eroding Permafrost Coasts, Canadian Beaufort Sea, 155 pp, McGill University, Montreal, Canada, 2010.

Hugelius, G., er al., 2014: Estimated stocks of circumpolar permafrost carbon with quantified uncertainty ranges and identified data gaps. *Biogeosciences*, *11*(23), 6573-6593.

Obu, J., et al., 2016: Coastal erosion and mass wasting along the Canadian Beaufort Sea based on annual airborne LiDAR elevation data. *Geomorphology*.

Ramage, J.L., et al., 2017: Terrain Controls on the Occurrence of Coastal Retrogressive Thaw Slumps along the Yukon Coast, Canada. *Journal of Geophysical Research: Earth Surface*.

Tanski, G., et al., 2016: Eroding permafrost coasts release low amounts of dissolved organic carbon (DOC) from ground ice into the nearshore zone of the Arctic Ocean. Global Biogeochemical Cycles, 30(7), pp.1054-1068.

A new source of hazard risk! – GLOF caused by mass movements into the rapidly forming proglacial lakes in Iceland –

Þorsteinn Sæmundsson[1]
Costanza Morino[2]
Susan J. Conway[3]
Armelle Decaulne[4]
Ólafur Ingólfsson[5], Gro Birkefeldt Møller Pedersen[5]
Daniel Ben-Yehoshua[6], Victor Madrigal[6]

[1]*Department of Geography and Tourism, University of Iceland, Askja, Sturlugata 7, 101 Reykjavík, Iceland, steinis@hi.is*
[2]*School of Environment, Earth & Ecosystems, The Open University, Milton Keynes MK7 6AA, UK*
[3]*Laboratoire de Planétologie et Géodynamique de Nantes UMR-CNRS 6112, 2, rue de la Houssinière, BP 92208, 44322 Nantes cedex 3, France*
[4]*Laboratoire Géolittomer UMR-6554 CNRS -LETG Campus du Tertre BP 81227 44312 Nantes cedex 3 France*
[5]*Department of Geoglogy, University of Iceland, Askja, Sturlugata 7, 101 Reykjavík, Iceland*
[6]*Svarmi, remote sensing company, Hvaleyrarbraut 4-6, 220 Hafnarfjörður, Iceland*

Abstract

One of the most visible consequences of temperature rise in Iceland during the 20th and 21st centuries are fast retreat and thinning of outlet glaciers. The consequences of this rapid retreat are both unstable valley slopes above the outlet glaciers and formation of proglacial lakes. The combination of these two potentially increases the natural hazard risk of Glacial Lake Outburst Floods (GLOF) caused by mass movements onto outlet glaciers and into the proglacial lakes. This natural hazard scenario has until now gotten little attention in Iceland, but such conditions can become extremely hazardous for infrastructure and not least for the rapidly increasing tourism in the vicinity of these lakes.

Keywords: Mass movements; proglacial lakes; Glacial Lake Outburst Floods (GLOF); Iceland; mountain permafrost.

Introduction

During the last century, since the end of the Little Ice Age (LIA), glaciers have retreated in alpine and high mountain regions worldwide, often leading to the formation and growth of proglacial lakes (e.g. IPCC 2012). These lakes are either dammed by glaciers, moraine, bedrock or sandur plains. Glacial Lake Outburst Floods (GLOF) can occur in all of these lake types caused either by breaching of moraine dams, ice dams or by mass movements into the lakes (Carrivick & Tweed 2013).

The consequences of the warming trend

This warming trend has also been observed in Iceland and has caused significant changes on and around the present day outlet glaciers. According to Hannesdóttir et al. (2015) outlet glaciers draining the southeastern margin of the Vatnajökull ice cap had lost 15-50% of their 1890 volume in 2010, and their terminus had lowered about 150-270 m over the same time interval. Today the glacier retreat is rapid and in many locations new proglacial lakes have been formed in front of the retreating ice margins (e.g. Hannesdóttir et al. 2015).

Mass movements onto glaciers

During the last five decades several mass movements of various size and origin have been observed to have fall on outlet glaciers in Iceland. These mass movements occurred into two periods (Fig. 1). The former around 1970 and the second one starting around 2000 and is still ongoing. Both of these periods are characterized by warmer climate and accelerated glacial retreat. Two large mass movements have been observed during these periods. The first occurred in January 1967, when a rock slide (15 million m^3) fell on the Steinsholtsjökull outlet glacier on the northern part of the Eyjafjallajökull ice cap. The rockslide broke up the snout of the glacier and part of it fell into a proglacial lake in front of the ice margin, causing a large GLOF down the Steinsholtsdalur valley (Fig. 2). The second one occurred in March 2007, when a rock avalanche (4,5 million m^3) fell on the upper part of the Morsárjökull outlet glacier, in the southern side of the Vatnajökull ice cap (Fig. 3). The avalanche debris covered around 720.000 m^2 or 1/5 of the glacier surface (Sæmundsson et al. 2011).

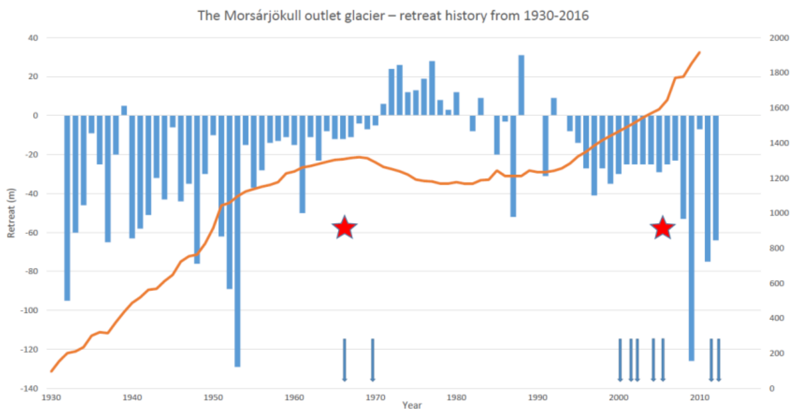

Figure 1. The retreat history of the Morsárjökull outlet glacier show the two major glacial retreat periods in Iceland from 1890-1970 and 1995 to present. The blue lines: yearly retreat/advance, brown line: total retrat, blue arrows: mass movement events on outlet glaciers in Iceland and red stars: the 1967 and 2007 events. (Modified from Sæmundsson et al. 2011).

Figure 2. A view down the Steinsholtsdalur valley.

Figure 3. The accumulation lobe of the Morsárjökull rock avalanche. Photo: Matthew Roberts 2007.

Unstable slopes, proglacial lakes, GLOF

Today the retreat and thinning of outlet glaciers in Iceland is extremely rapid and significant changes are occurring on and surrounding the glaciers. The consequences of such warming trend and rapid retreat are e.g. unstable valley slopes surrounding the outlet glaciers, both in loose sediments and bedrock, thawing of mountain permafrost (e.g. Sæmundsson et al., 2017) and not least formation of proglacial lakes in front of the rapidly retreating ice margins. Such conditions can become extremely hazardous, as seen by the above mentioned examples, for all infrastructure and the rapidly increasing tourism in the vicinity of the lakes.

References

Carrivick, J.L. & Tweed, F.S. 2013: Proglacial lakes: character, behavior and geological importance. Quaternary Science Reviews 78, 34-52.

Hannesdóttir, H., Björnsson, H., Pálsson, F., Aðalgeirsdóttir, G., & Guðmundsson, S. 2015: Changes in the southeast Vatnajökull ice cap, Iceland, between~ 1890 and 2010. The Cryosphere, 9(2), 565-585.

IPCC, 2012: Managing the Risks of Extreme Events and Disasters to Advance Climate Change Adaptation (eds Field, C. B. et al.) (Cambridge Univ. Press, 2012).

Kjartansson, G. 1967. The Steinsholtshlaup, Central-South-Iceland, on January 15th 1967. Jökull 17.

Sæmundsson, Þ., Sigurðsson, I.A., Pétursson, H.G., Jónsson, H.P., Decaulne, A., Roberts, M.J. & Jensen, E.H. 2011: Bergflóðið sem féll á Morsárjökul 20. Mars 2007. Hverjar hafa afleiðingar þess orðið? Náttúrufræðingurinn 81 (3-4), 131-141. (in Icelandic).

Sæmundsson, Þ., Morino, C., Helgason, J.K., Conway, S.J., Pétursson, H., 2017. The triggering factors of the Móafellshyrna debris slide in north Iceland: intense precipitation, earthquake activity and thawing of mountain permafrost. Sci. Total Environ. (https:// doi.org/ 10.1016 /j.scitotenv.2017.10.111.).

The collapse of LIA moraines as a consequence of the Belvedere Glacier dramatic shrinkage (Italian Alps, Monte Rosa Range)

Andrea Tamburini[1]
Gianni Mortara[2]
Walter Alberto[1]
[1] 1Imageo s.r.l, andrea.tamburini@imageosrl.com
[2] Research Institute for Geo-hydrological Protection, National Research Council (CNR IRPI), Torino, Italy

Abstract

Belvedere Glacier is one of the largest glaciers of the Italian Western Alps. At the beginning of the present millennium, the glacier gained notoriety following an exceptional surge-type movement that greatly changed its morphology. The surge ended in 2005; however, the entire basin is still experiencing geomorphic activity that is unparalleled in the Alps: ice and rock avalanches, debris flows, collapse of LIA moraines. In particular, the large deformation of the right moraine, induced by the dramatic and rapid shrinkage of the glacier, involved historical touristic trails, parts of sky runs and seriously damaged the artificial level lowering at the proglacial Locce Lake. The evolution of the LIA right moraine collapse was monitored with repeated topographic surveys, carried out with GNSS, terrestrial laser scanner and UAV (Unmanned Aerial Vehicle), which provided accurate multi-temporal 3D models. Up to 20 m lowering of the moraine crest in about three years were measured

Keywords: moraine collapse, glacier shrinkage, hazard management, touristic risk, terrestrial laser scanner, UAV.

Since the end of the Little Ice Age (LIA, *ca.* 1850) alpine glaciers have gradually decreased in surface area and volume. As a consequence of glacial debuttressing, erosion processes and landslide movements, the original shape of many LIA moraines is significantly changed (Mortara & Chiarle, 2005; Lugon *et al.*, 2000; Blair, 1994).

In recent years the dramatic increase in the rate of ice loss has significantly increased the moraine wall instability. Important collapses involved the moraines, as for instance at the Lower Grindelwand Glacier in the Swiss Alps (www.swisseduc.ch/glaciers/alps/unterer-grindelwaldgletscher/moraenenabbruch_2009), at the Bionnassay Glacier in the Mont Blanc Range, French Alps (P. Deline personal communication) and at the Forni Glacier in the Central Italian Alps (Pelfini *et al.*, 2004).

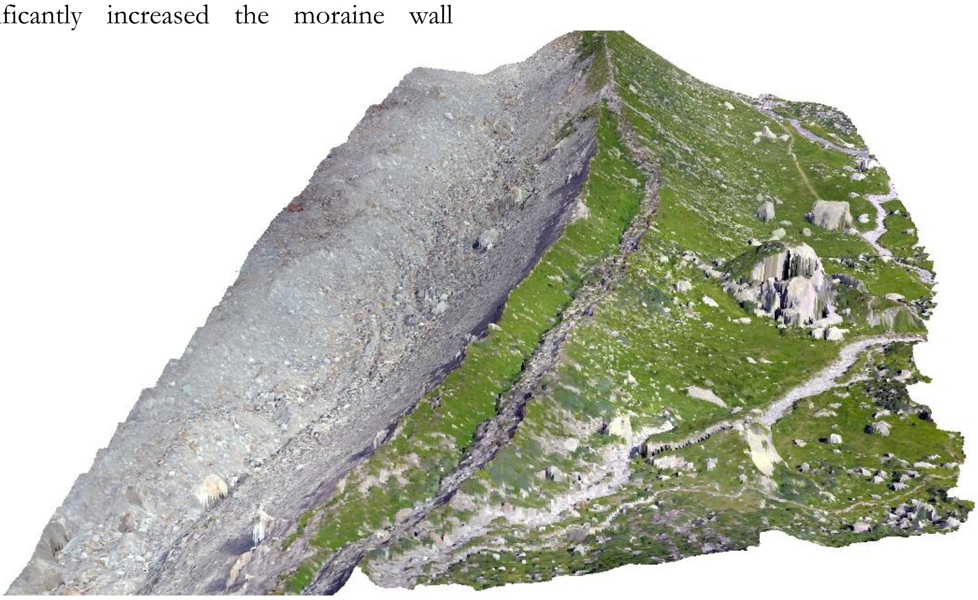

Figure 1. Belvedere Glacier: 3D photogrammetric model of the collapsing LIA moraine obtained from UAV survey (July 2017).

At Belvedere Glacier the effects of glacial shrinking related to climate change have been increased by rapid ice thickness loss after the surge occurred from 2001 to 2005 (Kaab *et al.*, 2004; Tamburini & Mortara, 2005). More than 60 m of ice were lost in the upper part of the glacier tongue resulting in a destabilization followed by the collapse of the moraine for a total length of about 500 m.

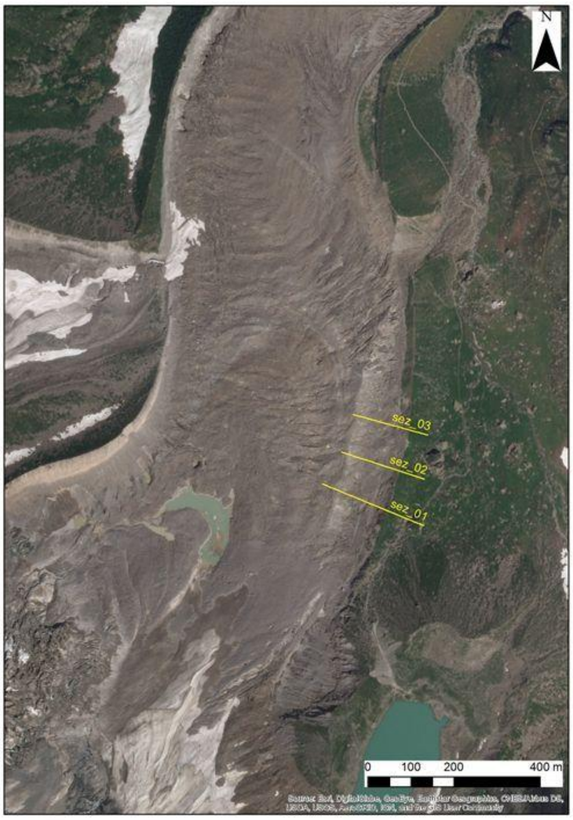

Figure 2. Belvedere Glacier: location map of multi-temporal cross sections shown in Figure 3.

References

Blair, R.W., 1994. Moraine and valley collapse due to rapid deglaciation in Mount Cook National Park, New Zealand. *Mountain Research and Development* 14(4):347-358.

Kääb, A., Huggel, C., Barbero, S., Chiarle, M., Cordola, M., Epifani, F., Haeberli, W., Mortara, G., Semino, P., Tamburini, A., Viazzo, G., 2004. Glacier hazards at Belvedere Glacier and the Monte Rosa east face, Italian Alps: processes and mitigation. *In*: *Proc. Intern. Conf. Interpraevent 2004, Riva del Garda, Italy, May 2004*

Lugon, R., Gardaz, J..M., Vonder Mühll, D., 2000. The partial collapse of the Dolent glacier moraine (Mont Blac Range, Swiss Range). *Z. Geomorph.* 122: 191-208

Mortara, G. & Chiarle, M., 2005. Instability of recent moraines in the Italian Alps. Effects of natural processes and human intervention having environmental and hazard implications. *Giornale di Geologia Applicata* 1:139-146.

Pelfini, M., Belò, M., D'Agata, C. Smiraglia, C., 2004. The collapse of an ice cored moraine along a touristic trail. *Geophysical Research Abstracts* 6: 0673.

Tamburini A. & Mortara G., 2005. The case of the Effimero Lake at the Monte Rosa (Italian Western Alps): studies, field surveys, monitoring, IHP-VI, *Technical Documents in Hydrology, 77*: 179-184.

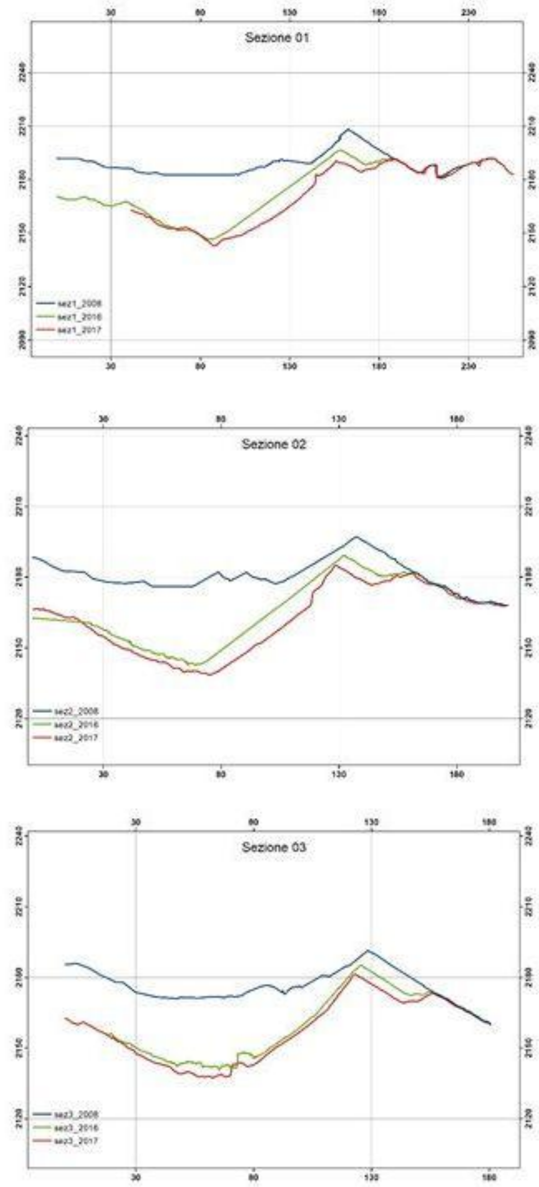

Figure 3. Belvedere Glacier: multi-temporal cross sections showing the evolution of the collapsing LIA moraine obtained from the comparison of airborne lidar (2010), terrestrial laser scanner (2016) and UAV surveys (2017). See location map in Figure 2.

Quantification of short-term dynamics of debris-flow fans in periglacial environment of Svalbard using unmanned aerial vehicle (UAV) surveys

Aleksandra M. Tomczyk[1]
Marek W. Ewertowski[1]
[1]*Faculty of Geographical and Geological Sciences, Adam Mickiewicz University, Poznań, Poland, alto@amu.edu.pl*

Abstract

Short-term dynamics were quantified for several alluvial fans located in the central part of Spitsbergen Island, Svalbard archipelago. We used time series of unmanned aerial vehicle (UAV) surveys and structure-from-motion approach to create cm-scale digital elevation models (DEMs) and orthomosaics. DEM of Differences were used to calculate volumetric changes, whereas orthomosaics were used to identify processes responsible for transformations. Our results indicate that short-term dynamics of surface of fans is very variable over time and space. In some places, no visible changes were recorded over three-year period, suggesting that landscape can be stable despite active layer presence. On the other hand, we were able to record large transformations related to freshly generated debris flows as well as collapsing of fan surfaces due to thermokarst processes.

Keywords: debris flow; mass movement; alluvial fan; Spitsbergen; RPAS; structure-from-motion.

Introduction

Landforms, whose shape resemble fans and cones are common elements in many mountain areas in all climatic zones (*e.g.* Ballantyne, 2002; Blair & McPherson, 1994; Blikra & Nemec, 1998; de Haas *et al.*, 2014; Rączkowska, 2007; Ryder, 1971; Saito & Oguchi, 2005). These depositional features develop at the mouth of small tributary catchments where there is a distinct transition from relatively steep mountain sides to less steep areas (*e.g.* valley, plains, basins; de Scally *et al.*, 2010). Understanding of fan evolution in general is important for three main reasons: (1) fans are potentially valuable archives of past environmental conditions; (2) some of low-gradient fans are used for agriculture and/or human settlement in mountain areas; Fan-related processes (e.g. sudden debris-flow activity etc.) can cause that human life is at risk and human possession may be destroyed or damaged. This is much common in relatively densely inhabited mountain areas; however, even in remote environment of Svalbard, debris-flow related hazards have occurred (*e.g.* André, 1995; Jahn, 1967; Larsson, 1982); (3) fans and fan-related processes, especially in non-vegetated polar areas, offer a potentially very good analogue, which is used for the studying and interpretation of extra-terrestrial landforms genesis.

Different processes are responsible for construction of fans and cones, including whole range from gravitational mass movements to fluvial transport and deposition (Blikra & Nemec, 1998; de Haas *et al.*, 2015; de Scally *et al.*, 2010). To understand fan evolution and its response to environmental changes it is necessary to obtain knowledge of fan morphology, processes acting on fans, and how these processes change in various temporal and spatial settings (*cf.* Clarke, 2015). However, despite the number of studies related to alluvial and colluvial fans in cold environments, our understanding of the evolution of fans in periglacial conditions is still very limited.

In this study, we focus on small fans that developed along mountain sides on Svalbard and which vary greatly in geomorphology and processes. The purpose of this study is to provide a detailed data on transformation of fan surfaces in periglacial environment. To achieve this objective, we conducted time-series of detailed topographic surveys using unmanned aerial vehicle (UAV) and quantified short-term dynamics of several debris-flow dominated fans located in the vicinity of Longyearbyen.

Study Area and Methods

The study was carried out on Spitsbergen Island, which is part of the Svalbard archipelago, located in the high-Arctic. This area is representative of central Spitsbergen as it is characterized by relatively small (compared to the coastal areas) ice cover. Svalbard is located in an area of continuous permafrost, and the thickness of the permafrost is from 100 m in the valley bottoms and near the coast to as much as 400–500 m in inland mountains (*cf.* Etzelmüller & Hagen, 2005; Humlum *et al.*, 2003). The active layer's thickness is relatively shallow, which limits the amount of debris that is potentially possible to move via mass movement processes on the fans' surface.

To assess dynamics of processes responsible for modification of fan surfaces we performed UAV surveys for several fans located in the vicinity of Longyearbyen, capital of Svalbard. Surveys were conducted using small quadcopters in 2015, 2016 and 2017. Orthomosaics and digital elevation models (DEMs) with cm-scale resolution were produced from each survey session. DEM of Differences were used to quantify volumetric changes, whereas orthomosaics were used to identify processes responsible for transformations.

Results

Our results indicate that short-term dynamics of surface of fans is very variable over time and space. In some places, no visible changes were recorded over three-year period, suggesting that landscape can be stable despite active layer presence. On the other hand, we were able to record large transformations related to freshly deposited debris flows as well as collapsing of fan surfaces due to thermokarst processes.

Acknowledgments

This work was supported by Narodowe Centrum Nauki (National Science Centre, Poland) [grant number 2016/21/B/ST10/01353].

References

André, M.-F., 1995. Holocene climate fluctuations and geomorphic impact of extreme events in Svalbard. *Geografiska Annaler. Series A. Physical Geography* 77: 241-250.

Ballantyne, C.K., 2002. Paraglacial geomorphology. *Quaternary Sci Rev* 21(18): 1935-2017.

Blair, T.C. & McPherson, J.G., 1994. Alluvial fan processes and forms, Geomorphology of desert environments. Springer, pp. 354-402.

Blikra, L.H. & Nemec, W., 1998. Postglacial colluvium in western Norway: depositional processes, facies and palaeoclimatic record. *Sedimentology* 45(5): 909-960.

Clarke, L.E., 2015. Experimental alluvial fans: Advances in understanding of fan dynamics and processes. *Geomorphology* 244: 135-145.

de Haas, T., Kleinhans, M.G., Carbonneau, P.E., Rubensdotter, L., Hauber, E., 2015. Surface morphology of fans in the high-Arctic periglacial environment of Svalbard: Controls and processes. *Earth-Science Reviews* 146: 163-182.

de Haas, T., Ventra, D., Carbonneau, P.E., Kleinhans, M.G., 2014. Debris-flow dominance of alluvial fans masked by runoff reworking and weathering. *Geomorphology* 217: 165-181.

de Scally, F.A., Owens, I.F., Louis, J., 2010. Controls on fan depositional processes in the schist ranges of the Southern Alps, New Zealand, and implications for debris-flow hazard assessment. *Geomorphology* 122(1–2): 99-116.

Etzelmüller, B., Hagen, J.O., 2005. Glacier-permafrost interaction in Arctic and alpine mountain environments with examples from southern Norway and Svalbard. *Geological Society, London, Special Publications* 242(1): 11-27.

Humlum, O., Instanes, A., Sollid, J.L., 2003. Permafrost in Svalbard: a review of research history, climatic background and engineering challenges. *Polar Research* 22(2): 191-215.

Jahn, A., 1967. Some features of mass movement on Spitsbergen slopes. *Geografiska Annaler. Series A. Physical Geography* 49: 213-225.

Larsson, S., 1982. Geomorphological effects on the slopes of Longyear valley, Spitsbergen, after a heavy rainstorm in July 1972. *Geografiska Annaler. Series A. Physical Geography* 64: 105-125.

Rączkowska, Z., 2007. *Współczesna rzeźba peryglacjalna wysokich gór Europy*, 212. IGiPZ PAN.

Ryder, J., 1971. Some aspects of the morphometry of paraglacial alluvial fans in south-central British Columbia. *Canadian Journal of Earth Sciences* 8(10): 1252-1264.

Saito, K. & Oguchi, T., 2005. Slope of alluvial fans in humid regions of Japan, Taiwan and the Philippines. *Geomorphology* 70(1): 147-162.

Daily Monitoring of a Retrogressive Thaw Slump on the Fosheim Peninsula, Ellesmere Island, Nunavut

Melissa K. Ward Jones[1]
Wayne H. Pollard[1]

[1]*Department of Geography, McGill University, Montreal, QC, Canada, melissa.ward@mail.mcgill.ca*

Abstract

The Eureka Sound Lowlands is an area of ice-rich permafrost characterized by icy marine sediments, massive ground ice and ice wedge polygons overlain by a thin active layer (57 cm). Permafrost is approximately 500 m thick and the region has a polar desert climate, with a mean annual air temperature of -19.7 °C. The landscape is sensitive to increasing summer temperatures as observed during the summer of 2012: as one of the warmest summers on record, there was a three-fold increase in thermokarst with the accelerated collapse of ice wedge polygon troughs and development of retrogressive thaw slumps. We present preliminary results of 7 weeks of daily monitoring of a thaw slump on Ellesmere Island, Nunavut. Most rapid retreat was observed on clear, warm, sunny days. Precipitation did not contribute to accelerated retreat rates as has been observed in the lower arctic.

Keywords: Permafrost; Thermokarst; Retrogressive Thaw Slump; Massive Ground Ice; Fosheim Peninsula

Introduction

With warming in the Arctic increasing faster than the rest of the globe, there is a need to understand and monitor the response of high latitude systems, however the costs and difficulty of doing fieldwork in Artic Regions has led to a limited number of studies being done, particularly in the high Arctic. Ice rich permafrost is particularly vulnerable to change, since melting ground ice causes subsidence, resulting in thermokarst (Kokelj & Jorgensen, 2013).

Retrogressive thaw slumps (RTSs) are mass wasting features that occur from the melting of ground ice. Sediments and mud slump downslope from a developed headwall with an exposed ice-rich face that regresses with continuous ice melt. Their development can be rapid, with reported headwall retreat rates including 9.6 m/yr on Herschel Island, YT (Lantruit & Pollard, 2008) and 7.2 to 26.7 m/yr in northwestern Canada (Lacelle *et al.,* 2015). We present preliminary results for a study that included the daily monitoring of a RTS on Ellesmere Island, Nunavut to fill gaps in field observations in this area.

Study Location

The Fosheim Peninsula is located in the Eureka Sound Lowlands that encompasses the central-western edge of Ellesmere Island and eastern Axel Heiberg Island. The Environment Canada Eureka Weather Station (EWS; 80°00'N, 85°55'W), has maintained daily meteorological measurements since it was established in 1947. The region is characterized by a polar desert climate with a mean annual air temperature of -19.7 °C and approximately 68 mm of annual precipitation (most of it falling as snow, Couture & Pollard, 2007).

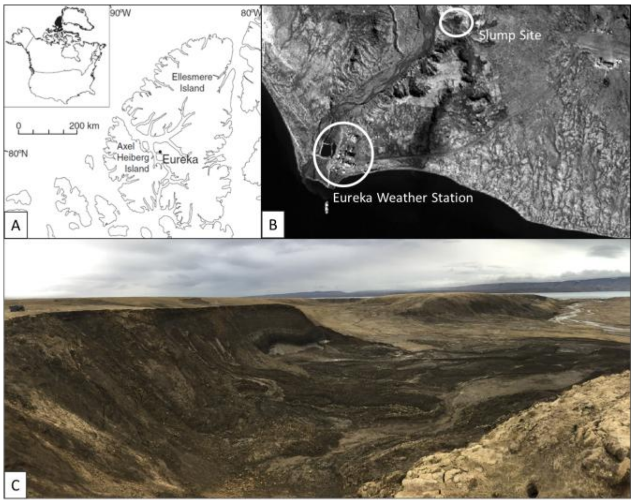

Figure 1: Location of the study Area. The RTS site is located approximately 1 km northeast of the Eureka Weather Station on Ellesmere Island, Nunavut.

Permafrost within the Fosheim is cold, continuous and over 500 m thick. The upper 20 to 30 m of permafrost of the area contains ice-wedges, massive ice and icy fine-grained marine sediments. Mean active layer depth is 57 cm (Couture & Pollard, 2007).

A RTS located approximately 1 km northeast of the EWS was monitored daily for 7 weeks (Fig. 1). This slump initiated in 2011 and has remained active since, however certain areas of the RTS have stabilized.

Methods

Survey markers were placed in 9 different locations along the headwall where ground ice was exposed. Survey markers were spaced 30 cm apart and were tracked daily between June 29th, and August 19th, 2017. Daily retreat rates and cumulative retreat were compared to meteorological data collected by the Eureka Weather Station (Fig. 2).

Results and Discussion

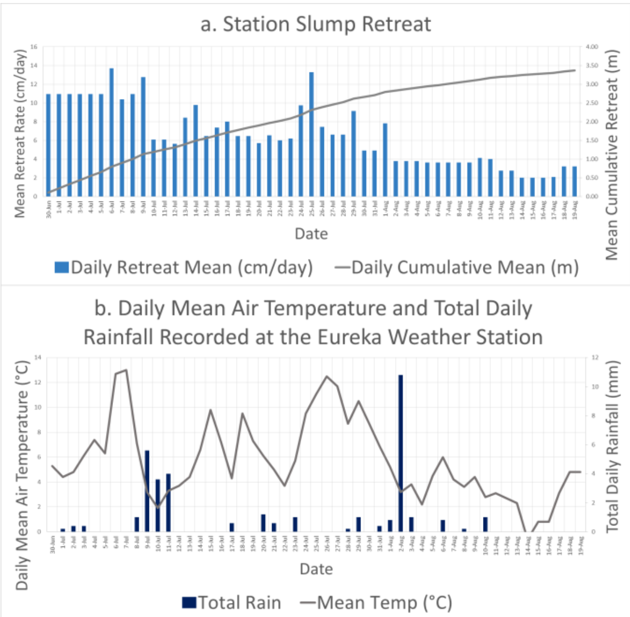

Figure 2: (a) Daily mean retreat (cm/day) and mean cumulative retreat (m) of the RTS. (b) Daily mean air temperature and total daily rainfall recorded by the EWS.

Monthly mean June, July and August air temperatures were 0.5°C, 5.5°C and 2.3°C, respectively. July was marked with fluctuations of warmer temperatures (figure 2, two of these warmer periods were above 10°C). According to station staff, this thaw season was uncharacteristically wet with more frequent rainfall events occurring in July. August is generally considered to be a period with more frequent precipitation.

Total accumulated slump retreat was 3.37 m. Max mean daily retreat was 13.7 cm, occurring on July 6th corresponding with a daily mean air temperature of 12.7°C. Retreat rates are most rapid earlier in the thaw season and generally decreased throughout the season, with pulse periods of rapid retreat. This pattern is likely attributed to the slump receiving more constant direct solar radiation earlier in the season as the position of the sun changes along the horizon over the course of the season.

Studies in the lower arctic attribute increased thaw slumping to increased precipitation rates (Kokelj *et al,* 2015). However, this trend was not observed in this study. Rainfall intensity at Eureka may not be sufficient to increase overall slumping, Max thaw season rainfall of 10.8 mm occurred on August 2nd. There was no noticeable increase in daily retreat rates: 3.8 cm and 3.6 cm were measured during the days that followed the storm event.

Acknowledgments

We would like to thank Dale Andersen and Cameron Roy for their assistance in the field. Thank you to all of the staff at the Eureka Weather Station. This research is funded by NSERC, FRQNT, NSTP, Eben Hopson Fellowship and in kind field support was provided by PCSP and ACUNS Research Support Opportunity Award.

References

Couture, N. J. & Pollard, W. H., 2007. Modelling geomorphic response to climatic change. *Climatic Change*, *85*(3), 407-431.

Lacelle, D., Brooker, A., Fraser, R.H. & Kokelj, S.V., 2015. Distribution and growth of thaw slumps in the Richardson Mountains–Peel Plateau region, northwestern Canada. *Geomorphology*, 235, pp.40-51.

Lantuit, H. & Pollard, W.H., 2008. Fifty years of coastal erosion and retrogressive thaw slump activity on Herschel Island, southern Beaufort Sea, Yukon Territory, Canada. *Geomorphology*, 95(1), pp.84-102.

Kokelj, S. V. & Jorgenson, M. T. 2013. Advances in thermokarst research. *Permafrost and Periglacial Processes*, 24(2), 108-119.

Kokelj, S.V., Tunnicliffe, J., Lacelle, D., Lantz, T.C., Chin, K.S. & Fraser, R., 2015. Increased precipitation drives mega slump development and destabilization of ice-rich permafrost terrain, northwestern Canada. *Global and Planetary Change*, 129, pp.56-68.

Dynamics of the Aget back-creeping push-moraine from 1998 to 2017

Julie Wee[1]
Reynald Delaloye[1]

[1]*Geography, Dept. Geosciences, University of Fribourg, Chemin du Musée 4, CH-1700 Fribourg, julie.wee@unifr.ch*

Abstract

Electrical resistivity measurements, which were carried out in 1998 to understand the impact of the advance of a small cirque glacier during the Little Ice Age (LIA) on pre-existing frozen debris, allowed to evidence the frozen state of an active back-creeping push-moraine, morphologically similar to an active rock glacier. These measurements were repeated in 2017 to assess the evolution of permafrost and ground ice in the push-moraine and its immediate surroundings. In combination with respectively 20-year and 15-year time series of surface temperature and displacement, data comparison indicates an overall permafrost degradation, which corroborates with the decelerating trend of the push-moraine kinematics and some local subsidence.

Keywords: permafrost, ground ice, push-moraine, glacier forefield, evolution, electrical resistivity

Introduction

In the Alps, the shrinkage of small glaciers since the Little Ice Age (LIA) has often occurred in areas located within the belt of discontinuous permafrost, that is above about 2500 m a.s.l. Permafrost conditions and ground ice – interstitial ice or buried glacier ice – are commonly encountered in the margins of these deglaciated areas, whereas they are often absent in the central zones. Such distribution dominantly reflects both thermal (e.g. warming in case of temperate-based glacier) and mechanical (e.g. build-up of push-moraines) impacts of the LIA glacier advance (Delaloye, 2004; Bosson *et al.*, 2014).

As a consequence of the glacier retreat, the heat fluxes between the ground surface and the atmosphere are more direct and ground cooling may have been expected to occur where the former glacier was temperate-based. Nevertheless, the recent 30-year strong increase in air temperature could have counterbalanced this cooling effect. Morphodynamic readjustments such as the back-creeping of formerly displaced frozen sediments (push-moraines) or the development of subsidence features (thermokarst) driven by ice melt at depth are likely to occur.

The study site and previous works

The LIA Aget glacier forefield (46°00'32" N, 7°14'20" E, western Swiss Alps) extends north-east of the Grand Aget summit from about 3000 m down to 2760 m a.s.l. (Fig. 1). The morphology of its orographic left side suggests the occurrence of an active back-creeping push-moraine whose ice content was investigated by means of geoelectrical measurements in 1998 (Reynard *et al.*, 2003). Ground ice was found in the active zone at larger depth (Ag-S06, Ag-S08), as well as in its margins (Ag-S07, Ag-S09), but not elsewhere (Ag-S03, Ag-S04). Surface temperature and surface displacement have been monitored since 1998 and 2001 respectively.

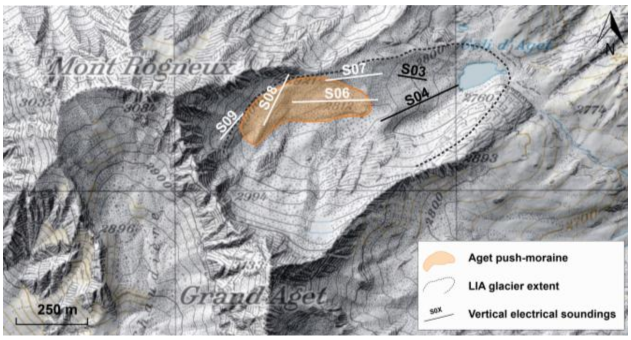

Figure 1: Location of the Aget active back-creeping push-moraine within the LIA glacier forefield and the repeated vertical electrical soundings (white: permafrost; black: no permafrost) (basemap Swisstopo).

Over the past 20 years, the mean annual ground surface temperature (MAGST) was +0.6°C, increasing by 0.15°C per decade, essentially due to warmer summers (Fig. 2). Both the high MAGST value and the temperature rise have supposedly contributed to a thermal degradation of permafrost during that time.

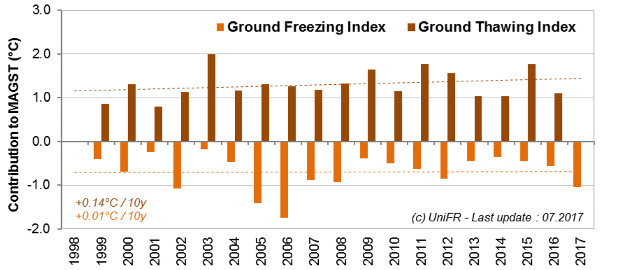

Figure 2: Contribution of the ground thawing and freezing index to the MAGST on the Aget push-moraine (mean on 7 monitoring stations).

For the last decade, displacement velocities have decreased compared to the regional trend: in particular the 2012-16 peak activity was not observed on the push-moraine in contrast with the 2003-04 event (Fig. 3). This behaviour suggests an ongoing permafrost degradation process. Therefore, electrical resistivity measurements, both the former vertical electrical soundings (VES) and resistivity mapping were repeated in 2017 to gain further insight on the driving factors contributing to the decelerating creep rate.

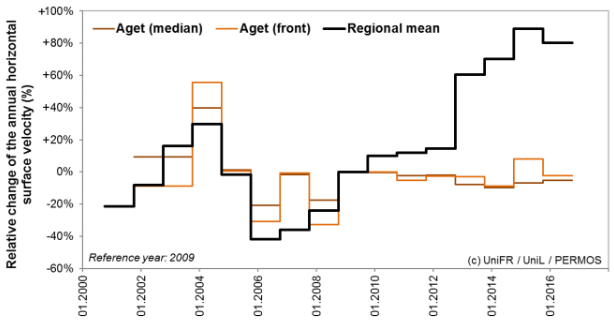

Figure 3: Relative change of the annual horizontal surface velocity (%) of the Aget push-moraine in comparison to the regional mean behaviour of active rock glaciers (n = 3-8 depending on year).

Repetition of geoelectrical measurements

VES repetition has successfully provided similar structures in 1998 and 2017 on all permafrost sites, but a significant decrease of the maximal apparent resistivity has been systematically observed (Fig. 4). On the actively back-creeping part of the push-moraine (Ag-S06 and Ag-S08) the active layer has deepened from about 5 to 7 m and the specific resistivity of the underlying frozen layer has decreased from approximately 60-70 to 40-60 kΩm. The section of the push-moraine, which is not moving, has subsided 1.9 m since 2001, reflecting a significant melt of underlying ground ice, which is accordance with the dramatic decrease in resistivity (from 30 to 10 kΩm) of the (shallower) frozen layer observed in Ag-S07. The maximal subsidence occurred in the hot summer 2003 (-27 cm), but vertical displacement has tended to diminish in the recent past.

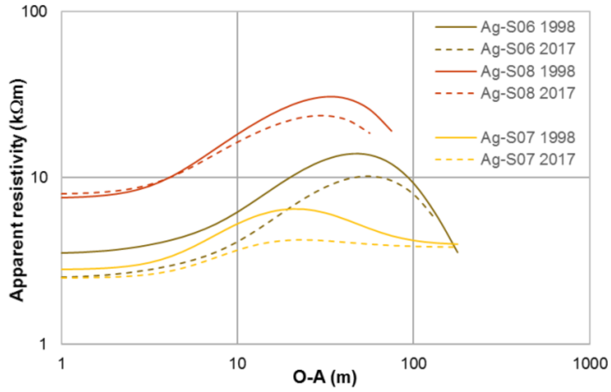

Figure 4: Modelled apparent resistivity in 1998 and 2017.

Preliminary statements

The comparative analysis of electrical resistivity values asserts a 20-year degradation of permafrost, which could explain the decelerating behaviour of the push-moraine. However, this relationship is discussable as lower resistivity means higher relative water content favouring faster creep rates. Conversely the deepening of the active layer has supposedly reduced the water column within the frozen ground above the shear horizon, contributing to lower the creep rate.

Permafrost degradation has also been observed between 1998 and 2017 in the Creux de la Lé (Sanetsch) glacier forefield, another investigated LIA glacier forefield distant of 50 km (ongoing research work), confirming the observations made at Aget.

References

Bosson, J.-B., Lambiel, C., Deline, P., Bodin, X., Schoeneich, P., Baron, L. & Gardent, M. (2014). The influence of ground ice distribution on geomorphic dynamics since the Little Ice Age in proglacial areas of two cirque glacier systems. *Earth Surface Processes and Landforms*, 40, 666-800.

Delaloye, R. (2004). *Contribution à l'étude du pergélisol de montagne en zone marginale.* GeoFocus vol. 10, Thesis, Department of Geosciences – Geography, University of Fribourg.

Reynard, E., Lambiel, C., Delaloye, R., Devaud, G., Baron, L., Chapellier, L., Marescot, L. & Monnet, R. (2003). Glacier/permafrost relationships in forefields of small glaciers (Swiss Alps). *Proceedings of the 8th International Conference on Permafrost*, Zurich; 947–952.

Retrogressive thaw slope on ice-rich permafrost under degradation: Results of a large-scale laboratory simulation

Costard Francois[1]
Séjourné Antoine[1]
Fedorov Alexander[2]
Dupeyrat Laure[1]
Marmo Chiara[1]
[1]*GEOPS, Université Paris-Sud, Orsay, France, francois.costard@u-psud.fr*
[2]*Permafrost Institut, Russian Academy of Science, Yakutsk, Russia*

Abstract

Central Yakutia (Siberia) exhibits large-scale retrogressive thaw slumps in the Yedoma ice complex area. Here we present results of a full-scale physical modelling of retrogressive thaw slumps in a cold room. For this purpose, the experimental of retrogressive thaw slumps was designed to simulate thawing on an ice-rich permafrost with various ice rich heterogeneity geometry (ice wedges, massive ice …). Preliminary results show that ice wedges increase the preferential erosion during the warming phase and supply excess water in the thawing permafrost that accelerates the thermokarst process with a basal slumping.

Keywords: permafrost, Siberia, retrogressive thaw slope, physical modeling,

Introduction

In Central Yakutia, the upper part of the permafrost regionally displays ice-rich sediments, which are up to 20–30 m thick and called the "Yedoma ice-complex" (Czudek and Demek, 1970; Soloviev, 1973). They contain ~70–80% of ice by volume and are characterized by massive syngenetic ice-wedges (≥10 m thick) which strongly favor thermokarst formation. Under global warming this ice-rich permafrost is highly vulnerable and prone to extensive degradation. Retrogressive Thaw Slumping mostly occur along the banks of thermokarst lakes (Figure 1) and are characterized by their (1) thermocirques produced by Retrogressive Thaw Slumping (RTS) and by (2) highly-degraded conical ice-wedge polygons with wide troughs referred to as "baydjarakhs". In some places around the headwall of thermocirques, the vegetation cover is disturbed and collapsed areas reflect the underlying partially melted ice-wedge network (Sejourne et al., 2015). In close association with the erosion of RTS, small mud-flows settling on the gentle slope are observed and contribute to the transport of sediments and excess water from the melting of ice wedges.

While it was assumed that the RTS are preferentially form along ice wedges due the melting of ice (Czudek and Demek, 1970), the excess supply of water from these ice wedges and their subsequent influence on thermokarst degradation has not been analyzed. The relative importance of main parameters affecting RTS are, however difficult to assess on the field. Numerous factors work simultaneously and their interdependence makes their analysis difficult. Physical modelling provides a unique tool for a more details monitoring than in the field. Here, we present results of a full-scale physical modelling of RTS in a cold room. For this purpose, the experimental RTS was designed to simulate thawing of permafrost in ice rich permafrost with various ice rich heterogeneity geometry (ice wedges, massive ice …).

Figure 1: Headwall of RTS along a thermokarst lakes in central Yakutia..

Experimental setup

Modelling was undertaken at the Laboratoire GEOPS, Université Paris-Sud, Orsay, Centre National de la Recherche Scientifique, France. For each experiment, two similar permafrost models were constructed. One with a homogeneous permafrost saturated with water, the other one with different vertical or horizontal interfaces (figure 2).

Our small-scale experiment used a rectangular box of 2.5 m, 2.5 m wide and 0.5 m deep in which a ground surface of fine sand (D50 = 200 mm; Wp(max) = 19 %) materials was saturated with water (Figure 2). The basal slope is 5° for the release of overflow during the thawing phase. For each experiment, the material was initially saturated immediately before freezing. Permafrost was created at depth (0.50 m) with an initial temperature of -15°C and then a slow warming up to -7°C. In order to evaluate the effect of permafrost heterogeneities (ice wedges, massive ice) on the development of RTS, we artificially built ice wedges with some homemade vertical ice blocks of 5 cm in thickness and regularly spaced.

Figure 2 : RTS experiment of 2.5 m x 2.5 wide and 0.5 m heigth showing on the left side an homogeneous permafrost and on the right side the same permafrost (saturated fine sand material) with ice wedges. Active thermokarst degradation due to the presence of ice wedges are observed.

The model was instrumented using 10 temperature sensors (platinum resistance thermometers Pt100) to survey the freezing and thawing front and active layer thickness vs time. During each simulation, we analyzed the development of associated thermokarst degradation landforms using a slow-motion recording with a video camera. This allows later analysis of the repeated observation of the RTS.

Here, we restricted our approach to the relative importance of the vertical (ice wedges) and horizontal heterogeneity (massive ice) of permafrost and their consequential influence on the morphology. In this experiment, we assumed that the scale effect was not a limited factor. During these experiments, various permafrost temperatures from −7·5 to −10°C and air temperature from 5 to 15°C are tested.

Experimental results

Laboratory simulations have allowed us to reproduce RTS that developed a morphology that is close to those of RTS observed in Yakutia with some morphologies similar to baydjarakhs. These results show that ice wedges increase the preferential erosion during the warming phase and supply excess water in the thawing permafrost, which accelerates the thermokarst process with a basal slumping (Figure 2). The preferential melting of the ice wedge induces a vertical incision of the water and a preferential thermal degradation on each side of the vertical heterogeneity. Different experiments clearly show the detachment and vertical sliding of individual blocks of about 20 cm large following the emplacement of the ice wedges. The evolution of these individual blocks in our cold room is similar to the baydjarakhs process. During the thawing phase, the progressive increase of the active layer depth induces a more important groundwater supply to the permafrost table and an acceleration of the slumping effect with some mudflows on the basal slope. This work confirms that ice wedges could be an important erosional process for the genesis of preferential melting.

Conclusion

The model contributes better understand the relative contribution of each parameter during the thermokarst process of RTS. Air temperature, and ice content all increase the ablation rate, whereas lower permafrost temperature (<-7°C) tends to slow down the thermokarst process. From our studies, the effect of vertical heterogeneity within the permafrost is predominant. Finally, laboratory simulations attest to the efficiency of ice wedges that control thermokarst development and RTS development. These experimental results are consistent with field observation. Further studies will consider the possible effect of various horizontal heterogeneities on the thermal erosion rate using our model. In the near future, we will use a laser-scanning instrument to precisely measure the volume of the thermal degradation for each experiment.

Acknowledgments

Financial support from Labex IPSL.

References

- Czudek, T. & Demek J., 1970. Thermokarst in Siberia and its influence on the development of lowland relief. *Quat. Res.* 1 (1), 103–120.
- Soloviev, P.A., 1973. Thermokarst phenomena and landforms due to frost heaving in central Yakutia. *Biul. Peryglac.* 23, 135–155.
- Sejourne *et a*l., 2015. Evolution of the banks of thermokarst lakes in central yakutia due to retrogressive thaw slump activity controlled by insolation. *Geomorphology* 241 (2015) 31–40.

12 - Thermal state of permafrost and active layer dynamics

Session 12

T*hermal state of permafrost and active layer dynamics: from local observations to a global permafrost assessments of permafrost system*

Conveners:

- **Jeannette Nötzli**, WSL Institute for Snow and Avalanche Research SLF, Davos Dorf, Switzerland
- **Alexey Maslakov**, Moscow State University, Moscow Russia (PYRN member)
- **Dmitry Streletsky**, The George Washington University, Washington D.C., USA (PYRN member)

This session provides a forum for presenting, discussing, assessing, and planning permafrost observational activities in both hemispheres, progress in data preservation, management and dissemination. We invite presentations addressing: (1) results of active layer and permafrost temperature monitoring at site-specific scales; (2) integration of observational data for comprehensive regional and global assessments of permafrost temperature and active layer changes; (3) use of GTN-P data for validation, modeling assimilation and reanalysis products for earth system models; (4) integration of remote sensing applications and observational data; (5) collaboration of GTN-P with other related monitoring programs. We seek contributions from those directly involved in GTN-P, as well as representatives from the broader research community who are using GTN-P data.

Two Decades Of Permafrost Monitoring In NE Asia

Andrey Abramov[1]
Alexander Kholodov[1,2]
Alexey Lupachev[1]
Alexandra Veremeeva[1]
Dmitry Fedorov-Davydov[1]
Sergey Davydov[3]
Victor Sorokovikov[1]

[1] *Institute of Physicochemical and Biological Problems in Soil Science, Russian Academy of Sciences, Pushchino, Russia, forestpro@gmail.com*
[2] *Geophysical Institute, University of Alaska Fairbanks, USA*
[3] *Northeast Science Station, Pacific Ocean Geography Institute, Far East Department, Russian Academy of Sciences, Chersky, Russia*

Abstract

More than 20 years of the active-layer thickness measurements in the different landscapes at the costal lowlands in the Eastern Siberia along with 10 years of observations in the mountain areas of Kamchatka, provide basis to explore the response of permafrost to climate changes. Changes of active layer thickness correlates well with summer air temperatures and have slight trend to increasing. The continuous ground temperatures record, started in 2007-2008 revealed similar behavior for the last 10 years. Comparison of recent data with measurements had been done in 1970's shows increase of ground temperature up to 2°C at 15 m depth. Beside the climate, the ground temperature dynamics depends significantly by the vegetation changes. For example, active growth of graminoid tussocks acts as cooling factor in early winter results in even decreasing of ground temperatures at some landscapes.

Keywords: permafrost, active layer, ground temperature, North-Eastern Siberia, Kamchatka.

Introduction

Our monitoring network including Circumpolar active layer monitoring (CALM) grids and boreholes is representative for the vast area of continuous permafrost at the North-Eastern Asia and Kamchatka peninsula. The last one is different from typical Arctic territories, as permafrost there presents in the mountains and affected locally by the processes of volcanic activity. Research sites represent most types of landscapes in this region including Arctic and alpine tundra, boreal forest and river's floodplain. In the paper we summarize the two decades of observation for main parameters of thermal state of permafrost at the Arctic lowlands, and more than 10 years for Kamchatka volcanoes.

The mean summer air temperatures dynamics at the weather stations nearby (Tiksi, Chokurdakh, Chersky) shows warming trend for 1996-2007 periods and some stabilization in later years (Fig. 1). The 2007 summer was the warmest for the last 20 years, with close temperature values in 2010 and 2014.

At Kamchatka, the weather observations are only available for Klyuchi station at the valley bottom level of 30 m a.s.l., where permafrost is absent. Summers slowly getting warmer, with stable phase in 2008-2014, minimums in 2004, 2007, 2015 and maximum in 2016.

Methods

The 19 active CALM grids are located in Arctic tundra (R28, R29A-C), typical tundra (R13, R25), southern tundra (R14, R15, R21, R22, R31), mountain tundra (R30C) and northern taiga (R18, R19, R20). Both zonal and intrazonal landscapes are represented: river plains (R17, R20), alas depressions (R13A, R15A, R29B), polygonal palsa (R16) and bog forest (R35, R36). The soils on the main part of the sites are loamy, only R16, R19 and R21 are sandy ones and R30C represents volcanic scoria practically without organic matter.

We use well described (Brown *et al.*, 2000) standard technique for active layer thickness (ALT) measurements, and the main discussion point in methodology is not simultaneous measurements on all the sites. Now, we presenting ALT data, which are normalized according to calibration graphs, discussed in details for Kolyma sites in Fedorov-Davidov *et al.*, 2004. For example, the time of reaching the maximum thaw depth for the majority of Kolyma sites is early September, it is not exact one day, but one-two week period. If the site visit occurred in August, the correction due to early measurements is in range 1-3 cm (maximum 1-3% from the mean ALT value), with only several 9-11 cm values from our experience.

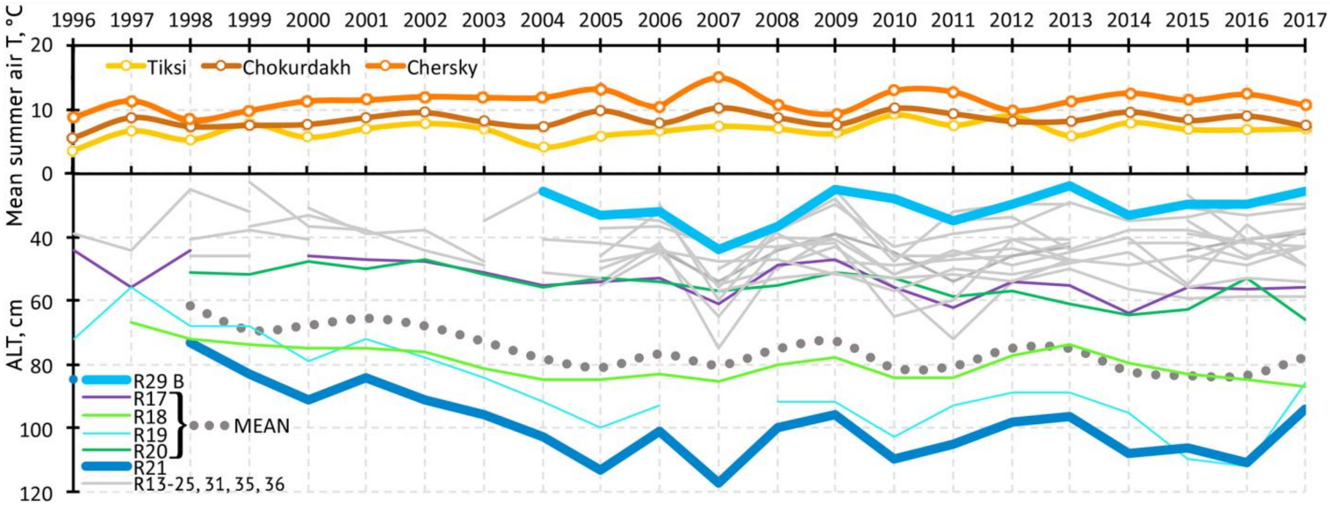

Figure 1. ALT and mean summer air temperature dynamics for NE Siberia region.

Ground temperature measurements at the moment are conducting in 13 boreholes in the North-Eastern Siberia and one more in Kamchatka. Boreholes are instrumented for continuous measurements with data loggers HOBO U12 with thermistors TMC-HD (accuracy 0.25°C, resolution 0.03°C, according to manufacturer specification).

Results and Discussion

Active layer thickness dynamics

The maximum ALT corresponds well with the warmest mean summer air temperatures (Fig.1).

Comparison of mean active layer thickness (ALT) for 1996-2017, indicate 0.2-1.8 cm/year increases for majority of sites. The minimal ALT observed at R29B site (alas at Bykovsky peninsula, Lena delta), with minimal decreasing trend. The maximal ALT is common for sandy sites like R21 (Akhmelo lake, Kolyma river). (Fig. 1).

The ALT record for Kamchatka sites seems to be more stable. As expected, the deepest active layer was observed at lowest grid (R30A, 1300 m a.s.l.) – the mean value for 2003-2012 varied in range 67-80 cm. Despite moderate mean ALT increase for 10 years (7 cm), thermo erosion processes were intensified in recent years in the vicinity of R30C site (1600 m a.s.l.).

Ground temperature dynamics

First occasional mean annual ground temperature (MAGT) measurements in the boreholes in this area dated back to 1970's. Than, continuous ground temperatures record, started in 2007-2008 revealed similar behavior. Average for 10 years warming trends varies from 0.02°C/year in boreal forest zone to 0.07 °C/year in tundra. Comparing with 1980's measurements, the MAGT increase is up to 2°C at 15 m depth. Only one borehole with long record of measurements is characterized by the stable MAGT. It is situated in the floodplain of Amboliha channel (Kolyma river). This is due to intensification of tussock growth causing snow redistribution and fast active layer freezing at the beginning of winter season.

At Kamchatka, 0.02°C/year increasing rate is observed in borehole 10-04 at 11 m depth since 2004.

Acknowledgments

This monitoring activity is supported by international CALM and TSP projects, program AAAA-A18-118013190182-3 of Russian Academy of Science and Russian science foundation project 18-44-06202.

References

Brown, J., Hinkel, K.M., & Nelson, F.E., 2000. The circumpolar active layer monitoring (CALM) program: Research designs and initial results. *Polar Geography* 24(3): 165–258.

Fyodorov-Davydov, D.G., Sorokovikov, V.A., Ostroumov, V.E., Kholodov, A.L., Mitroshin, I.A., Mergelov, N.S., Davydov, S.P., Zimov, S.A., Davydova, A.I., 2004. Spatial and temporal observations of seasonal thaw in the northern Kolyma Lowland. *Polar geography* 28(4): 308-325.

Active layer dynamics in Central Yamal, Russia due to climatic fluctuations

Elena A. Babkina[1]
Artem V. Khomutov[1,2]
Marina O. Leibman[1,2]
Damir R. Mullanurov[1]

[1]Earth Cryosphere Institute Tyumen Scientific Centre SB RAS, ea_pereval@mail.ru
[2]University of Tyumen, International Institute of Cryology and Cryosophy

Abstract

Presented are results of field monitoring and analysis of active layer dynamics. It is shown that increase in active layer depth since 2012 is associated with both air temperature and precipitation changes, in particular related to the warm period. Deeper thaw triggers cryogenic processes due to its extending to the ground ice surface, and contributes to formation of specific landforms.

Keywords: Active layer depth; climate fluctuations; Yamal Peninsula; CALM; cryogenic processes and landforms.

Introduction

Monitoring of the active layer in Central Yamal is carried out in the research station "Vaskiny Dachi" within the framework of CALM program on a 100x100 m grid (VD CALM) since 1993, on three grids 50x50 m each (VD1, VD2, VD3) since 2007, and on peatland grid 6x6 m (VD Peat) since 2014 (Leibman *et al.,* 2015).

Summer air temperature in combination with precipitation regime is the main control for the active layer depth (ALD) dynamics in time. We use the records of the weather station Marre-Sale (available at www.rp5.ru) closest to the key area for analysis.

Main environmental components: relief and microrelief, vegetation, soil texture and wetness, control spatial variations of ALD. The extreme heterogeneity of these environmental features over the area determines the considerable spatial variability of ALD.

To assess interaction between ALD and climate, we relate mean thaw depths to the thaw index for each year. Specific patterns of ALD fluctuations in space and time for the study area have been established earlier (Leibman, 2001). However, the extreme climatic events of recent years have led to significant deviations from these patterns. Here we analyze the period since 1999.

Results and discussion

Spatial variability of the active layer

As follows from monitoring data analysis, the deepest active layer is observed at VD3 grid, sandy soil and sparse vegetation. The shallowest active layer is in VD Peat grid with peat thickness up to 50 cm. The VD CALM grid records show very little trend of ALD increase between 1993 and 2011, while in 2012 to 2016 ALD increases dramatically. Through all the years of observation, one can see direct relation between ALD and the root of thaw index in degree-days, DDT (Fig. 1). Linear trend for mean thaw depths show the following: for VD3 grid it is sloping steeper than other trend lines, and at Peat plateau grid trend line slopes most gently. This follows clearly from insulating properties of the vegetation and soil cover.

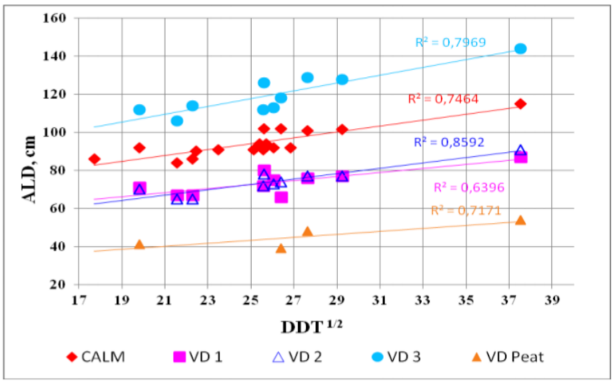

Figure 1. Relation between ALD and $DDT^{1/2}$ for Vaskiny Dachi grids in 1999-2017

Temporal variability of the active layer (VD CALM)

The perennial average of mean annual ALDs in 1993-2011 was 92 cm with a range of 81-95 cm. Since 2012 we are observing fluctuations of mean annual ALDs between 92 (2014) and 115 cm (2016).

In 2012 mean ALD was 102 cm, 16 cm deeper than in 2011 (86 cm)! Much deeper thaw depth was due to extremely warm spring. Early measurement on July 3, 2012 showed mean ALD 66 cm (77% of thaw depth reached by late August of 2010 and 2011). The warm period started on May 25, maximal average daily temperature was +18,0°C on June 29, and thaw index calculated for the period from May 25 to September 2 (date of ALD measurement) was 854 degree-days with amount of precipitation 257 mm. To compare, the same values for the warm period of the previous warmest year of 2005 were 661 degree-days and 146 mm respectively.

Abnormally deep thaw was observed also in 2013. Rather cool and dry summer of 2013 (thaw index 656 degree-days and amount of precipitation 114 mm from June 8 to September 2), and in addition very cold winter of 2012-2013 compared to 2012, indicate that these factors are likely not most important in maintaining such a high ALD this summer. We suggest that it is due to a combination of two factors. One is delayed refreezing in the fall 2012. The second is extend of thaw to the depths where saline marine clays underlay sandy and loamy active layer. Saline clay retains plasticity to a temperature of -1°C and reacts to the mechanical probing as if thawed.

Compared to previous years of 2012 and 2013, mean ALD in 2014 (92 cm) is within the range of annual means for 1993-2011 (81-95 cm). Summer season of 2014 was rather cool. The warm period started on June 6, and thaw index to the date of ALD measurement was 393 degree-days (the lowest since 1999, 314 degree-days) with amount of precipitation 115 mm. Yet 30 mm or 26% of summer total precipitation during the period between 19 and 31 August 2014 determines relatively high ALD: 87 cm by August 19 and 92 cm by August 31.

In summer 2016 air temperature achieved extreme values exceeding all observed before. Marre-Sale weather station measured 1409 degree-days in 2016, while previous maximum since 1993 was only 1057 degree-days in 2012. Air temperature above zero lasted from June 4 to October 11, being above +20°C between July 9 and 20, which is very unusual for the polar regions. Thus, ALD on VD CALM in 2016 averaged at 115 cm in a range 78 to 170 cm. This is 13% higher than mean value (102 cm) in 2012 and 2013, 25% higher than perennial average in 1993-2011. Note that in 2016 measurements were done on October 15, later than in other years, close to the date of termination of the thaw. So comparable ALD values will be several per cent less.

Summer 2017 was relatively cool and extremely dry (thaw index 697 degree-days and precipitation 47 mm). Mean ALD was less than in abnormally warm 2016, but the same as in 2012 and 2013 (102 cm).

At the same time, since warm summer of 2012 ALD reached the layer of marine saline clay underlying sand and silt in many gridnodes of the CALM grid. In the following years even under cooler summer, ALD measured by metal probe show much higher values.

Thus, the higher summer air temperature results in the deeper active layer in rainy seasons compared to dry seasons. Notable amount of summer precipitation could provide active layer deepening (more in sandy deposits than in clayey) compared to even warmer but dry summers.

We observed that in 2012 deeper thaw has reached the top of icy permafrost or mono-mineral tabular ground ice. On slopes, such impact has triggered formation of new or re-activation of stabilized thermocirques and their further development. Gas-emission craters on Yamal Peninsula which appeared in the fall of 2013 (Leibman *et al.,* 2014), and again in June 2017 could probably in part be related to abnormal increase of ALD in the years following the summer warmth extremes.

Conclusions

Climate fluctuations in 2012-2016 affected substantially increase of the ALD in various types of terrains due to combination of summer warmth and amount of precipitation.

Abnormal deepening of the active layer resulted in activation of cryogenic processes associated with ground ice thawing.

Acknowledgments

This work is partially supported by CALM program (NSF grant No.PLR1304555), Russian Science Foundation grant No.16-17-10203 and Presidential grant for scientific schools No.НШ-9880-2016.5.

References

Leibman, M.O., 2001. Procedures and results of active-layer measurements in marine saline deposits of Central Yamal. *Earth Cryosphere* V(3): 17-24 (*In Russian*)

Leibman, M.O., Khomutov, A.V., Gubarkov, A.A., Mullanurov, D.R. & Dvornikov, Y.A., 2015. The research station "Vaskiny Dachi", Central Yamal, West Siberia, Russia: A review of 25 years of permafrost studies. *Fennia* 193(1): 3-30

Leibman M.O., Kizyakov A.I., Plekhanov A.V. & Streletskaya I.D., 2014. New permafrost feature - deep crater in Central Yamal, West Siberia, Russia, as a response to local climate fluctuations. *Geography, environment, sustainability* 7(4): 68-80.

Variability in shallow permafrost temperature: results from 17 years of monitoring in the Ross Sea Region of Antarctica: latest data and trends

Megan (Ruby) Balks[1]
Annette (Gereldine) Carshalton[1]
Cathy A. Seybold[2]
Tanya (Ann) O'Neill[1]

[1]*University of Waikato, New Zealand, megan.balks@waikato.ac.nz*
[2]*NRCS, USDA, Nebraska, USA*

Abstract

Hourly temperature monitoring at a series of depths that extend into the permafrost, at nine sites in the Ross Sea region of Antarctica, are reviewed. Sites range from near sea level to 1700 m in altitude and from latitudes of 77°00'S to 78°30'S. Sites cover a range of soil and landscape positions and include both ice-cemented, and dry, permafrost. Temperatures at each site are monitored using three different probes, installed at multiple depths, an MRC probe, Campbell 107 thermistors and Vitel moisture probes, giving some means for comparison and confidence in the fidelity of probes. Data are recorded hourly and downloaded annually. We note marked inter-annual variability in mean annual temperature in both the air and the shallow permafrost. There are no apparent long-term trends in air or permafrost temperatures, though there is potentially some decadal scale variability.

Keywords: Cryosol; Dry Valleys; soil climate; permafrost; soil temperature; Gelisols.

Introduction

Soils and permafrost in the Ross Sea region of Antarctica are widely accepted as stable with soil processes acting extremely slowly in the cold, dry environment (Campbell & Claridge 1987, Denton et al 1993). However, there is evidence to suggest that the depth of the active layer may be more dynamic than is often assumed. Chinn (1979) reported both cooler and warmer years that affected both soils and streamflow. A warm summer in January 1974 resulted in extensive melting and water flow, with associated erosion, while in 1977 an "extreme" high snowfall led to cold conditions and minimal flow in the Onyx river for the following two summers (Chinn 1979). The 2000/01 summer was warmer than average in the McMurdo Dry Valleys (Barrett *et al.,* 2008, Adlam *et al.*, 2010) resulting in deeper than average active layer depths and high meltwater flows. Balks & O'Neill (2016) reported two thaw events, one at Cape Evans and one in the Wright Valley in the 2008/09 summer. Both events let to melt-out of permafrost ice and resulted in gully erosion, colluvial deposition, and fan building. To better understand the temperature dynamics of cryosols and permafrost the objective of this paper is to report the latest data from our continuous monitoring of air and soil temperatures at a range of locations in the Ross Sea region with data stretching back up to 17 years to 1999.

Methods

Nine soil climate-monitoring stations are installed in the Ross Sea region of Antarctica representing a range of latitude, altitude, soil, and microclimate situations (Fig. 1, Table 1). Multiple soil temperature probes are installed at each site to depths of 1.2m, which is into the permafrost at all sites. Above-ground monitoring includes air temperature, solar radiation, wind speed and direction, and relative humidity. The equipment used and data monitoring are described in detail in Seybold *et al.,* (2010).

Table 1. Soil climate monitoring stations.

Station	Date installed	Altitude (m)	Soil Classification USDA
Scott Base	Jan '99	38	Typic Haplorthel
Marble Point	Jan '99	50	Typic Haplorthel
Wright Valley	Jan '99	22	Nitric Anhyorthel
Victoria Valley	Jan '99	412	Typic Haplorthel
Mt Fleming	Jan '02	1700	Typic Haplorthel
Minna Bluff	Jan '03	22	Typic Haploturbel
Granite Harbour	Jan '03	5	Typic Haplorthel
Bull Pass	Jan '12	832	Typic Haplorthel
Don Juan	Jan '13	728	Typic Haplorthel

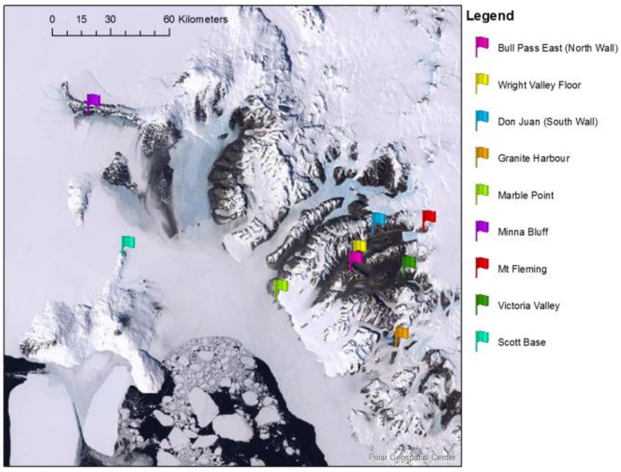

Figure 1. Location of soil climate stations in McMurdo Dry Valleys/Ross Island area.

Results & Discussion

Preliminary data analysis shows that mean annual air temperatures vary between years and that all sites have similar overall trends (Fig. 2). While there is some apparent warming in the 2003-2011, there was an apparent decline between 2011 and 2016. Soil temperatures, within the permafrost, at depths of about 1 m, show similar trends to air temperatures (Fig. 3).

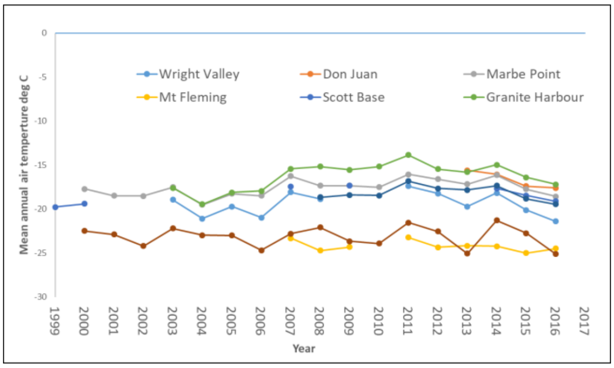

Figure 2. Mean annual air temperatures at soil climate monitoring sites.

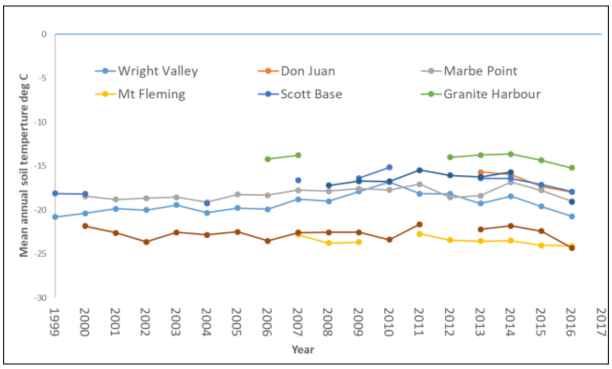

Figure 3. Mean annual permafrost temperatures at depths of about 1 m.

Acknowledgments

Thanks to Antarctica NZ for logistics support. This work was undertaken within Landcare Research FRST and MBIE projects over the years since 1999. Numerous people have helped with site installation and maintenance including; Jackie Aislabie, Ian Campbell, Ron Paetzold, Don Huffman, John Kimble, Ron Sletten, Deb Harms, Janine Ryburn, Dean Sandwell, and Chris Morcom.

References

Adlam, L.S., Balks, M.R., Seybold, C.A., & Campbell D.I., 2010. Temporal and Spatial Variation in active layer depth in the McMurdo Sound region of Antarctica. Antarctic Science 22(1)45-52. DOI 10.1017/S0954102009990640.

Balks, M.R., & O'Neill, T.A., 2016. Soil and Permafrost in the Ross Sea Region of Antarctica: stable or dynamic? *Cuadernos de Investigacion Geografica 42:415-434.*

Barrett, J.E., Virginia, R.A., Wall, D.H., Doran, P.T., Fountain, A.G., Welch, K.A., Lyons, W.B. 2008. Persistent effects of a discrete climate event on a polar desert ecosystem. *Global Change Biology 14: 1-13.*

Campbell, I.B., & Claridge, G.G.C., 1987. *Antarctica: soils, weathering processes, and environment.* Developments in Soil Science 16. Elsevier, Oxford. 368pp.

Chinn, T.H.J., 1979. Impacts of "extreme" events on the Dry Valleys area. *New Zealand Antarctic Record, 2(2):9-13.*

Denton, G.H., Sugden, G.E., Marchant, D.R., Hall, B.L., Wilch, T.I., 1993. East Antarctic ice sheet sensitivity to Pliocene climate change from a Dry Valleys perspective. *Geografiska Annaler Series A 75:155-204.*

Seybold, C.A., Balks M.R., Harms, D.S., 2010. Characterization of active layer water contents in the McMurdo Sound region, Antarctica. *Antarctic Science 22(6)633-45.*

Long-term (1996-2017) thaw subsidence above anti-syngenetic ice wedges at Illisarvik, western Arctic coast, Canada

Christopher Burn
Department of Geography and Environmental Studies, Carleton University, Canada

Abstract

Thaw subsidence varies with the ice content of near-surface permafrost. In a few settings the active layer lies above massive ice, as is common with ice wedges on hill slopes. Active-layer depth has increased near the western Canadian Arctic coast since 1983 due to climate warming, and currently is comparable to values measured in 1998 that were then considered extreme. We have measured thaw subsidence above two hillslope ice wedges annually for over 20 years (1996-2017). Continuing thaw subsidence was initiated in 2006, when the active layer reached the massive ice of the wedges. The rate has been relatively constant at up to about 35 mm/year. The active layer is no longer deepening, but incremental thaw is of the massive ice. The rate of continuing thaw subsidence is extremely high for natural, subaerial disturbances because meltwater from the ice wedges runs downslope and is not subsequently refrozen in place.

Keywords: Permafrost; thaw subsidence; ice wedges; hill slopes; climate change.

Introduction

Anti-syngenetic ice wedges occur on eroding parts of hill slopes (Mackay 1990). They grow downwards into permafrost, and are characteristically wider at the surface than syngenetic or epigenetic wedges. Anti-syngenetic ice wedges are likely as abundant as other types of ice wedges in the rolling hills of the western Canadian Arctic coastlands (Mackay 1995).

Ground subsidence has been measured above two anti-syngenetic ice wedges near the Illisarvik drained lake basin since 1996 (Fig. 1) (Mackay 1997). The ground materials near Illisarvik consist of a veneer of silty till and organic matter, about 2 m thick, above sand. Active-layer thickness in the area ranges up to about 0.7 m, and below this the till is ice rich. Solifluction lobes at the bottom of slopes, indicate that downslope movement is common in the area, as described on Garry Island, 45 km west of Illisarvik, by Mackay (1981).

Mean annual air temperature has been increasing in the Canadian western Arctic since 1970 at a rate of about 0.67 °C/decade (R = 0.634; n = 47; $p < 0.01$) (Thienpont *et al.* 2013), mostly in autumn and winter. This has led to rising temperatures in the upper 120 m of permafrost, which at Illisarvik is estimated to be over 400 m thick (Burn and Zhang 2010). The warming of permafrost is a regional phenomenon and has been accompanied by thickening of the active layer, at an average rate of 0.03 m/decade (Burn and Kokelj 2009). Mean thaw depths in the last four summers have been similar to values measured in 1998, which were then considered extreme.

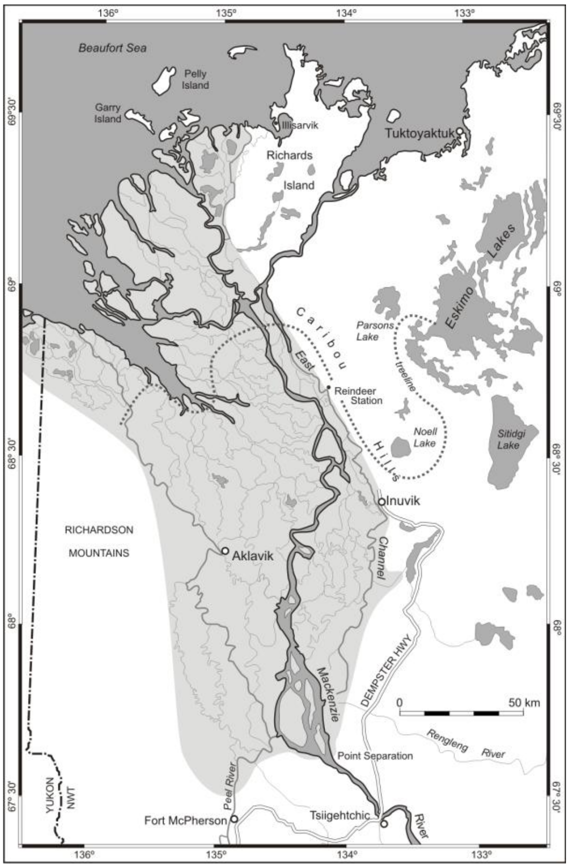

Fig. 1. Mackenzie Delta area, western Arctic Canada.

Subsidence above ice wedges

Steel benchmarks were installed in June 1996 at the two ice wedges to measure changes in elevation of the ground above them. Thaw depth has been measured at the benchmarks in August, and, in most years, late-winter snow depth. Benchmark elevations have been surveyed in mid- to late-August almost every year from 1996-2017 using a Wild NA2 level with optical micrometer and invar stadia rod. The protrusion of the benchmarks above the ground surface has been measured with a pocket tape to the nearest 0.01 m, and since 2014 to the nearest 1 mm using a 0.39 m-square stainless-steel grid placed permanently on the surface at each benchmark. The precision of the measurements of relative ground surface elevation between the troughs and adjacent polygons is ±0.01 m. Measurements of thaw depth and snow depth, both made by probing, have a similar precision.

Table 1 indicates the rate of subsidence measured in the ice wedge troughs with respect to ground in the adjacent polygons. There was little subsidence during the first decade of measurement, because the active layer developed within the sol overlying the wedge ice. Subsidence has continued each year once thaw depth reached the massive ice. The rate of thaw subsidence is high for natural conditions because meltwater may run off downslope. Meltwater may continue to drain down hillslopes during the autumn, so that by the time the active layer has frozen back, much of the melted volume has been removed.

Table 1. Year subsidence initiated, thaw depth above ice wedge (m), subsidence rate since initiation (mm/yr), and mean snow depth for (a) 1998-2004 and (b) 2009-17 (m) in troughs of two ice wedges on hillslopes at Illisarvik, western Arctic coast.

	Year	Thaw depth	Subs. rate	Snow depth-a	Snow depth-b
Wedge 1	2006	0.45	35	0.66	0.90
Wedge 2	2011	0.50	18	0.34	0.45

Snow depths in the two ice wedge troughs have increased with thaw subsidence (Table 1). The increase in trough snow depth between the mean of measurements in 1997-2004 and 2009-2017 has been 0.24 m at wedge 1 and 0.11 m at wedge 2. In contrast, the change in snow depth at the adjacent polygon centres has not been not statistically significant. These data indicate that thaw subsidence promotes deeper snow in the trough, which will warm the ground and may accelerate the thaw subsidence.

Ice wedge troughs are now widespread on hillslopes in the western Arctic but were not as visible less than a decade ago. At the time, it was recognized that ice wedges provided potential sites for thaw subsidence following construction disturbance, but it was difficult to identify specific features. How the features affect maintenance of infrastructure may become clear now that the Inuvik-Tuktoyaktuk Highway has been completed.

Acknowledgments

The research was initiated at the suggestion of the late Professor J. Ross Mackay to study deformation of anti-syngentetic ice wedges during thermal expansion of the ground. The work has been supported by: the Natural Sciences and Engineering Research Council of Canada, the Polar Continental Shelf Project; and the Aurora Research Institute, Aurora College, Inuvik. I am grateful to the many people who have provided field assistance at Illisarvik, especially Andrew Burn, Alex Elanik, Douglas Esagok, Graham Gilbert, and Alice Wilson.

References

Burn, C.R. and Kokelj, S.V. 2009. The environment and permafrost of the Mackenzie Delta area. *Permafrost and Periglacial Processes*, **20**: 83-105. DOI: 10.1002/ppp.653.

Burn, C.R., and Zhang, Y. 2010. Sensitivity of active layer development to winter conditions north of treeline, Mackenzie Delta area, western Arctic coast. In *Proceedings, 6th Canadian Permafrost Conference*, 12–16 September 2010, Calgary, AB, Paper 194. Richmond, B.C.: Canadian Geotechnical Society; 1458–1465.

Mackay, JR. 1981. Active layer slope movement in a continuous permafrost environment, Garry Island, Northwest Territories, Canada. *Canadian Journal of Earth Sciences*, **18**: 1666-1680. DOI: 10.1139/e81-154.

Mackay, JR. 1990. Some observations on the growth and deformation of epigenetic, syngenetic and anti-syngenetic ice wedges. *Permafrost and Periglacial Processes*, **1**: 15-29. DOI: 10.1002/ppp.3430010104.

Mackay, JR. 1995. Ice wedges on hillslopes and landform evolution in the late Quaternary, western Arctic coast, Canada. *Canadian Journal of Earth Sciences*, **32**: 1093-1105. DOI: 10.1139/e95-091.

Mackay, JR. 1997. A full-scale field experiment (1978-1995) on the growth of permafrost by means of lake drainage, western Arctic coast: A discussion of the method and some results. *Canadian Journal of Earth Sciences*, **34**: 17-33. DOI: 10.1139/e17-002.

Thienpont JR, Rühland, KM, Pisaric MFJ, Kokelj SV, Kimpe LE, Blais JM, Smol JP. 2013. Biological responses to permafrost thaw slumping in Canadian Arctic lakes. *Freshwater Biology*, **58**: 337-353. DOI:10.1111/fwb.12061.

Boreal forest and tundra permafrost sensitivity to soil moisture and snow depth changes

Austin Dabbs[1]
Alexander Kholodov[2]
Vladimir Romanovsky[2]
[1]*Department of Mechanical Engineering, University of Alaska Fairbanks, adabbs@alaska.edu*
[2]*Geophysical Institute, University of Alaska Fairbanks*

Abstract

Global climate changes influence the atmospheric moisture budget and the relative amounts of precipitation and evapotranspiration in addition to air temperature. Changes in the moisture budget will lead to changes in both snow depth and soil saturation. Permafrost extent and the soil temperature regime are both strongly dependent on soil moisture and snow depth due to their impact on the thermal properties of the soil and surface energy balance respectively. To assess how various ecotypes of the boreal forest would respond to these changes, we conducted a temperature sensitivity analysis using the Geophysical Institute Permafrost Laboratory Model (GIPL). GIPL simulates subsurface temperature dynamics by solving a nonlinear heat equation with phase change. In this analysis, we looked at the response of four ecotypes within the boreal forest region of Alaska; mixed, deciduous, and black spruce forests as well as willow shrubs. We also examined a tundra ecotype from Barrow, AK.

Keywords: Sensitivity; Alaska; Snow; Moisture; Model; Ground Temperature

Introduction

Permafrost is a unique feature of colder climates such as Alaska that plays an important role in ecosystems, infrastructure, and the global climate. Both soil moisture and snow depth are directly affected by changes in the atmospheric moisture budget that results from a changing global climate. Snow depth and soil moisture drastically influence the surface energy balance and ground thermal regime respectively. Through this sensitivity analysis, we were able to understand more about how permafrost temperatures in various ecotypes will respond to changes in snow depth and soil moisture.

Results

Snow depth

The variations in snow depth was done as a percent of normal variation in a range of 50-150% by factors of 10% to encompass a variety of possible changes. In addition, we conducted the analysis over a 15-year period to act as a low pass filter to remove inter-annual variability. We found that the ground temperatures in the willow shrub and tundra ecotypes were the most sensitive to the changes in snow depth at both the surface (Fig. 1) and in the upper permafrost (Fig. 2) levels. This result is primarily due to the soil moisture content of those two ecotypes. Those ecotypes were the most saturated. During the freeze up of the active layer,

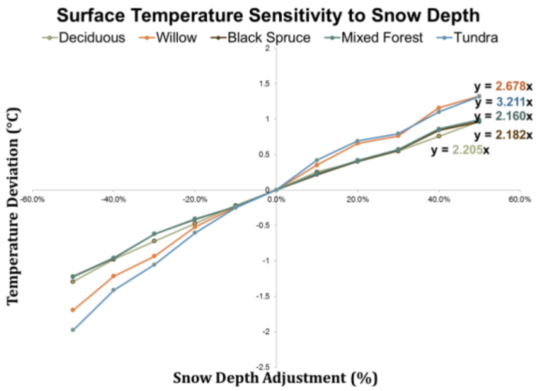

Figure 1. Modeled surface sensitivity to snow depth

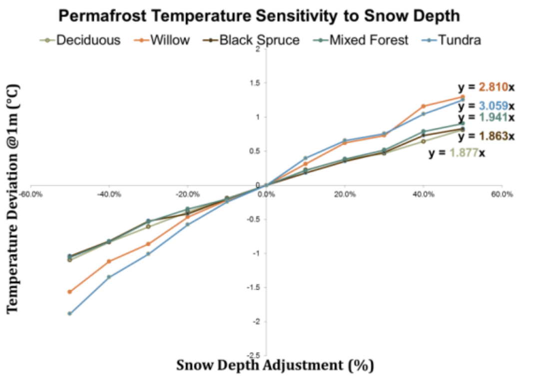

Figure 2. Modeled permafrost sensitivty to snow depth

the water within the soil undergoes a phase change and releases latent heat during the process. The snow traps some of this heat at the surface due to its insulating properties.

Due to latent heat, ecotypes with relatively saturated soils will be more sensitive to changes in snow depth. In addition to latent heat, the thermal conductivity of the soil column also plays an important role in determining the permafrost temperature sensitivity to snow depth. Ecotypes with higher thermal conductivities allowed freezing to penetrate deeper and thus release even more latent heat.

Soil moisture

For soil moisture, we varied soil moisture by factors of 5% of the normal volumetric water content in a range of plus or minus 10% of normal. As with snow depth, we did the analysis over a 15-year period. To accurately represent the effects of changing soil moisture we also varied the thermal conductivity and heat capacity of the soil as well. We developed correlations between organic layer soil moisture and both thermal conductivity and heat capacity from soil analysis done on samples from the Seward Peninsula in Alaska. For each of these samples we took measurements of volumetric water content in the lab while we took thermal conductivity measurements in the field.

We found that the tundra ecotype was extremely insensitive to changes in soil moisture while the forested ecotypes experienced a significant difference between the temperature sensitivity at the surface (Fig. 3) and at the permafrost table (Fig. 4). The tundra ecotype, which was the most sensitive to changes in snow depth, was the least sensitive to changes in soil moisture due to its preexisting soil saturation. Prior to adjustment the tundra soil column was almost completely saturated which meant that changes would result in only minor changes to the thermal conductivity of the soil column. The forested ecotypes experienced a significant drop in sensitivity from the surface to permafrost levels due to their thermal conductivities. Although the soil moisture changes were able to dramatically affect the surface temperatures, those changes did not reach to the permafrost level. This was a result of the intrinsically low thermal conductivities of forested ecotypes due to their thick organic layers.

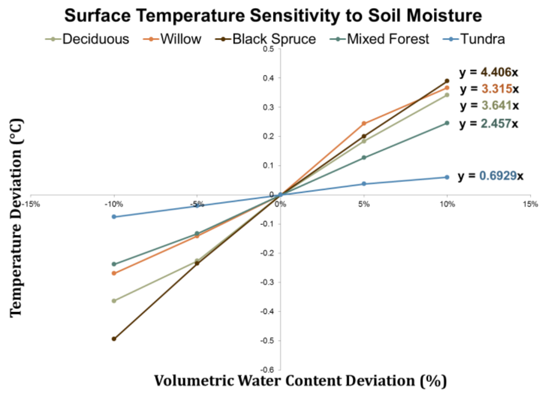

Figure 3. Modeled surface sensitivty to soil moisture

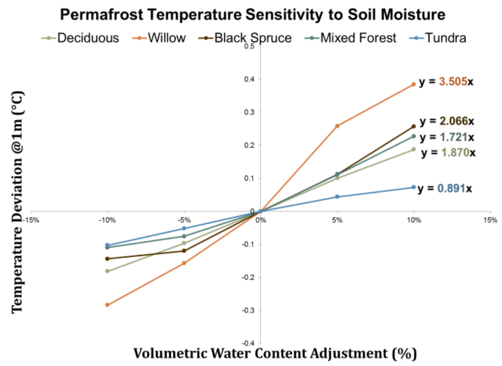

Figure 4. Modeled permafrost sensitivity to soil moisture

Acknowledgments

We would like to thank U.S. National Science Foundation (Project # 1560372) for funding "REU site: Understanding the Arctic as a system".

Ecotype-based modeling of ground temperature dynamics in the Seward Peninsula, Alaska.

Matvey V. Debolskiy[1]
Dmitry J. Nicolsky[1]
Vladimir E. Romanovsky[1]
Santosh K. Panda[1]
Reginald R. Muskett[1]

[1]*Geophysical Institute, University of Alaska Fairbanks, mvdebolskiy@alaska.edu*

Abstract

We apply an ecotype-based approach to model temporal and spatial dynamics of ground temperature in the Seward Peninsula, Alaska with the 0.5-km resolution over the 20th-21st centuries. To model soil temperature dynamics, we use a transient soil heat transfer model developed at the Geophysical Institute Permafrost Laboratory (GIPL-2). The model solves the 1-D nonlinear heat equation with phase change and is forced with a combination of the historical and future climate scenarios prepared by the Scenarios Network for Alaska and Arctic Planning for 1900-2100. We calibrate and validate the model utilizing observed air and ground temperatures as well as the snow depth data from meteostations. Overall, this study presents a series of high-resolution maps showing changes in the active layer depth and ground temperatures for the Seward Peninsula.

Keywords: discontinuous permafrost; modeling; ground temperature; ecotype-based; Alaska; Seward Peninsula; projection

Introduction

An increasing demand in assessment of the climate change-induced permafrost degradation and its consequences promotes development of high-resolution modeling products of soil temperature dynamics. This is especially relevant for areas with highly vulnerable warm discontinuous permafrost in the Western Alaska. However, substantial datasets of point-wise observations and climate forcing are required for model calibration and validation (Gisnås *et al.*, 2013; Zhang *et al.,* 2013; Nicolsky *et al.*, 2017).

The goal of this study is to develop comprehensive understanding of temporal and spatial variability of soil temperatures in discontinuous permafrost regions such as the Seward Peninsula. The resulting dataset could be used to help decision and policy makers to gain better understanding of changes in the permafrost distribution and thermal state under different scenarios in the future.

Methods

In this study, we implement a 0.5-km resolution distributed runs of GIPL2 one-dimensional model forced with the downscaled observed (CRU) and projected (RCP 4.5 and 8.5) climate scenarios. To distribute model parameters across the study area, we employ a map of 8 ecotypes by reclassifying and upscaling 30-m resolution Alaska Existing Vegetation Map by Fleming, (2015). Each considered ecotype is assigned calibrated model parameters such as the thermal properties, porosity, snow catchment rate and wind slab density.

To estimate the above-mentioned model parameters for each considered ecotype (8 total) we assimilate observations from boreholes and meteostations maintained by University of Alaska Fairbanks and other institutions. We note that observations from one or several stations could correspond to the same ecotype. The observations primarily consist of ground temperatures at various depths, air temperature and the snow depth observations in 1990-2015 period. The data assimilation algorithm we use in this study is a L_2 norm minimization with weights added to force better matching for measurements from deeper levels and prioritize data from boreholes where the air temperatures are available and modeled forcing matches the observations. In addition, we add a regularization term to keep the estimated model parameters within reasonable range of values. Mean bias for the calibrated model temperature reached as low as -0.03°C and the root mean square error (RMSE) is 1.8°C.

Results

We validate the model utilizing data collected within the NGEE-Arctic project in 2016-2017 (https://ngee-arctic.ornl.gov/). The validation process included adjusting the climate forcing to represent observed snow depth values at the boreholes locations. The mean bias for validation with unadjusted and adjusted forcing is -0.4°C and -0.04°C; RMSE is 2.5°C and 1.3°C respectively. In general, the model shows good validation results.

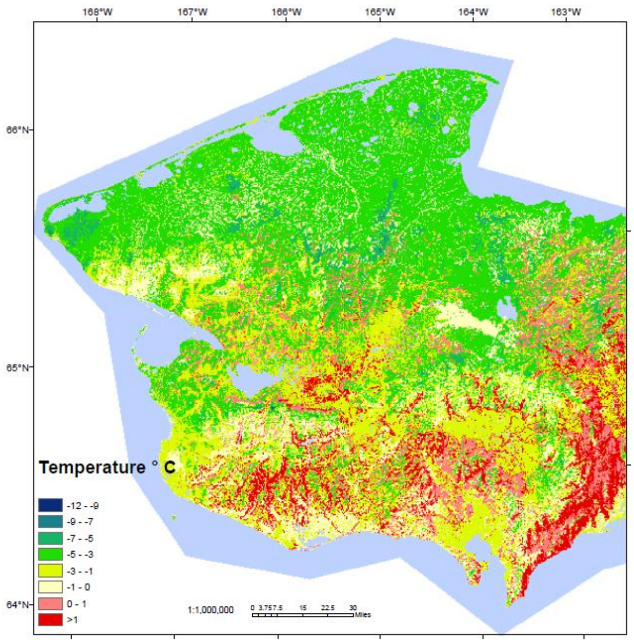

Figure 1. A decadal averaged ground temperature at the 2 m depth for 2000-2010 years.

All the modeled ecotypes show a warming trend in the soil temperatures (Table 1) even with the moderate climate warming scenario RCP 4.5. Most warming will occur in areas occupied by shrubs. Tundra areas will acquire a marginal temperature regime on average; local conditions might allow permafrost to be present.

Table 1. Spatially averaged mean annual ground temperature (°C) at 10m depth over different time periods.

Ecotype	1970-2000	2000-2030	2030-2060	2060-2090
Medium Shrub	0.2	1.1	2.3	3.0
Birch-Ericaceous Shrub	-0.4	-0.0	0.2	1.0
Sedge-Willow-Dryas Tundra	-4.6	-3.3	-1.6	-0.7
Mixed Tussock Tundra	-3.1	-1.8	-0.4	-0.0
Wet meadow tundra	-4.8	-3.3	-1.6	-0.6
Forest	0.4	1.2	2.3	3.0
'Dryas-Lichen Dwarf Shrub Tundra	-4.1	-2.7	-1.0	-0.3
Tall shrub	-0.9	0.0	1.2	2.6
Barren Land	-1.4	-0.5	0.0	0.3

At the current state Seward Peninsula shows the presence of continuous permafrost in the northern part of the Peninsula and discontinuous permafrost in the southern part (Fig. 1). South east of the peninsula is occupied by shrubby woodlands and forest with no permafrost underneath. Towards the end of 21st century most of the territory of the Seward Peninsula are likely to become unfrozen.

Discussion and Conclusions

The model can properly reproduce the observed thermal regime, which is shown by relatively good validation metrics compared to calibration metrics the validation is done only on a year-long time-series and additional data are required to properly access whether the model can reproduce climatological regimes given it is has to be forced with downscaled data from global climate models. In addition, the ecotypes are fixed in extent in our simulations, which poses the question of how overall picture will change given that dynamic vegetation is introduced.

Overall our approach shows a satisfying match between modeled and observed ground temperatures. The Seward Peninsula will experience significant warming during next century. Most of the current permafrost might be thawed and especially if it is located under shrubs.

Acknowledgments

This research was conducted with the support of NSF Office of Polar Programs ARC-1304271 grant, USGS grant G14 AP 00151 and Next-Generation Ecosystem Experiments (NGEE-arctic) project, supported by the Office of Biological and Environmental Research in the DOE Office of Science.

References

Fleming, M.D., 2015. Developing an Existing Vegetation Layer for the Western Alaska LCC Region. *U.S. Fish and Wildlife Service, WALLC*, Anchorage, AK

Gisnås, K., *et al.*, 2013. CryoGRID 1.0: Permafrost distribution in Norway estimated by a spatial numerical model. *Permafrost Periglacial Processes, 24*, 2–19.

Nicolsky, D.J., *et al.*, 2017. Applicability of the ecosystem type approach to model permafrost dynamics across the Alaska North Slope. *J. Geophys. Res. Earth Surf., 122,* 50–75, doi:10.1002/2016JF003852.

Zhang, Y., *et al.,* 2013, Modelling and mapping climate changeimpacts on permafrost at high spatial resolution for an Arctic region with complex terrain, *Cryosphere*, *7*, 1121–1137.

High Arctic microclimatic hotspot assessment, Cape Bounty, Nunavut, Canada

Madeleine C. Garibaldi[1], Philip P. Bonnaventure[1] & Scott F. Lamoureux[2]
[1]*Department of Geography, University of Lethbridge, Lethbridge, AB, Canada, madeleine.garibaldi@uleth.ca*
[2]*Department of Geography and Planning, Queens University, Kingston, ON, Canada*

Abstract

This study examines thermal heterogeneity of air, ground, and permafrost temperatures with intent to produce continuous high-resolution models for paired watersheds around the Cape Bounty Arctic Watershed Observatory (CBAWO), on Melville Island, Nunavut in the Canadian High Arctic. Air temperature varies minimally (0.16 °C difference between annual averages at sites) across the study area while ground surface temperature varies substantially, with a maximum range of 30.0 °C during winter in both watersheds. As air temperature is similar over all sites, the variability in ground surface temperatures over the topography has been shown to be a product of differential snow cover accumulation due to wind driven redistribution. Freezing n-factors ranged from 0.27 in expected high snow locations to 0.94 in expected low snow locations. The warmer ground surface temperatures allow for the existence of warmer permafrost temperatures resulting in areas of permafrost which may be more susceptible to thaw due to climatic change. These areas may also serve as sites for biological refugia and play and important role in establishing new hydrological connections and the spared of microorganism in the thaw season.

Keywords: Permafrost, High Arctic, snow, TTOP, n-factors, ground temperature.

Introduction

The spatial distribution of High Arctic ground surface and permafrost temperatures are often viewed and subsequently modelled as homogeneous, when in reality, evidence shows there can be considerable variability over short distances allotted by differential snow cover (Bonnaventure *et al.*, 2016). The assumption of homogeneity is problematic for many reasons. Perhaps most important is that this can lead to predictions of uniform permafrost warming across the High Arctic landscape regardless of the applied climate change scenario (Henry & Smith, 2001; Koven *et al.*, 2013). The current thermal heterogeneity is likely to have a profound effect on the evaluation of the landscape impacting the magnitude and distribution of permafrost warming as new thermal equilibriums are established. It is therefore essential to understand the nature of High Arctic thermal heterogeneity over multiple fields, identifying and quantifying the spatial distribution of microclimates in order to improve predictions of permafrost response to projected climate change. Areas of ground surface and permafrost where temperatures are significantly warmer than surrounding locations may serve as biological refugia (areas in which organisms can survive through periods of unfavorable conditions) and play and important role in establishing new hydrological connections.

The overall goal of this research project is to understand and model the spatial, thermal heterogeneity, generated by differential snow cover, at present conditions and under climate warming over paired watersheds in the Cape Bounty Arctic Watershed Observatory (CBAWO), Melville Island, Nunavut, in the Canadian High Arctic.

Study Area

The study area is the paired watersheds at CBAWO on the south-central coast of Melville Island, Nunavut (Fig. 1).

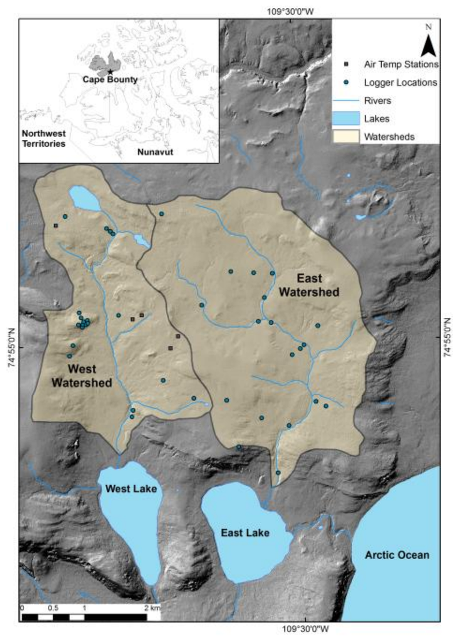

Figure 1. Study area map including locations of air temperature stations and logger locations.

Cape Bounty is a polar desert with an annual mean air temperature (AMAT) ranging between -10.0 and -12.8 °C (2005-12) and annual precipitation of ~125 mm, of which about 60 % falls as snow (Maxwell, 1981; Woo & Young, 1997). The area is underlain by continuous permafrost and has a total relief is about 100 m (Lewis *et al.*, 2012). The West and East watersheds (Figure 1) are similar in topography and vegetation. The vegetation is composed of prostrate shrub tundra communities including polar semi- desert, mesic tundra, and localized wet sedge meadows. The underlying siltstone and sandstone bedrock is overlain by unconsolidated glacial and marine sediment (Lewis *et al.*, 2012).

Methods

Ground surface temperatures were recorded using Onset Hobo™ pendant (UA-001-64; Onset, USA) loggers, deployed throughout the study area during August 2016. The primary variables considered during site selection were the topographic influences on snow cover and sites were ultimately selected to measure ground surface temperature the entire range of snow cover conditions. The variability in ground and permafrost temperatures were analyzed through the creation of continuous surface layers for each temperature field. These surfaces are generated using point data and known relations between air temperature, ground cover, and the subsurface temperatures, expressed in the temperature at top of permafrost (TTOP) model (Smith & Riseborough, 1996). n-factors at each logger site were calculated using air temperature data from the nearest air temperature station, as air temperature was assumed to be relatively uniform over the study area.

Preliminary and Anticipated Results

Across the study area, air temperature varies minimally between sites despite slight elevation changes (Table 1).

Table 1. Preliminary 2016-17 air temperature data

Station Name	Elevation (m)	Daily Min (°C)	Daily Max (°C)	Yearly Average (°C)
Mainmet	85	-46.8	11.1	-14.8
Westmet	89	-47.3	11.2	-14.7
Lower Pt	63	-47.1	11.5	-14.7
Upper Pt	67	-47.1	11.2	-14.8
Upper Goose	77	-47.2	11.0	-14.9

Ground surface temperature during 2016-17 varies substantially over the study area depending on the degree of connectivity between the ground surface and the atmosphere especially during winter (Table 2.)

Table 2. Preliminary 2016-17 ground surface temperature data for selected sites

Site Name	Daily Min (°C)	Daily Max (°C)	Yearly Average (°C)	nf
W7	-10.8	8.7	-4.8	0.33
W13	-43.5	16.8	-13.0	0.93
W19	-22.1	10.4	-8.8	0.61
E7	-43.7	14.8	-13.8	0.94
E11	-10.2	7.9	-3.8	0.27
E20	-27.8	10.5	-11.7	0.80

Areas with warmer ground surface temperatures likely also have warmer permafrost temperatures than areas with colder ground surface temperatures. Since snow is assumed to be largely responsible for the variance, locations with high snow accumulation are expected to have warmer ground surface and permafrost temperatures than locations with limited snow cover.

Acknowledgments

We thank PCSP, NSERC, and the University of Lethbridge for research support. We also thank C. Beel, C. Coch, M. Lafrenière, S. McFadden, M. Pope, G. Thiel, and J. Warburton for field support and assistance.

References

Bonnaventure, P. P., Lamoureux, S. F., Favaro, E. A., 2016. Over-Winter Channel Bed Temperature Regimes Generated by Contrasting Snow Accumulation in a High Arctic River. *Permafrost and periglacial processes* 28: 339-346.

Henry, K., & Smith, M., 2001. A model-based map of ground temperatures for the permafrost regions of Canada. *Permafrost and periglacial processes* 12(4): 389-398.

Koven, C. D., Riley, W. J., Stern, A., 2013. Analysis of Permafrost Thermal Dynamics and Response to Climate Change in the CMIP5 Earth System Models. *Journal of Climate* 26(6): 1877-1900.

Lewis, T., Lafrenière, M. J., Lamoureux, S. F., 2012. Hydrochemical and sedimentary responses of paired High Arctic watersheds to unusual climate and permafrost disturbance, Cape Bounty, Melville Island, Canada. *Hydrological Processes* 26(13): 2003-2018.

Maxwell, J. B., 1981. Climatic Regions of the Canadian Arctic Islands. *Arctic* 34(3): 225-240.

Smith, M. W., Riseborough, D. W., 1996. Permafrost monitoring and detection of climate change. *Permafrost and periglacial processes* 7(4): 301-309.

Woo, M.K, & Young, K. L., 1997. Hydrology of a Small Drainage Basin with Polar Oasis Environment, Fosheim Peninsula, Ellesmere Island, Canada. *Permafrost and periglacial processes* 8(3): 257-277.

The estimation of ground-freezing depth on the north-west of Russia on the data on thermal regime of winter season and peculiarities of snow accumulation

Vladimir Nikolaevich Golubev[1]
Denis Maksimovich Frolov[2]
[1]*Geographycal faculty of Lomonosov Moscow State University, golubev@geol.msu.ru*
[2]*Geographycal faculty of Lomonosov Moscow State University*

Abstract

Based on the data on thermal regime of winter season and peculiarities of snow accumulation regime according to the heat conductivity and phase transition formula with daily resolution the estimation of ground-freezing depth for the North-East part of European territory of Russia for the period of 1988-2015 was conducted. The comparison of estimated and observed values was performed and the correlation of equal 0.76-0.77 of them was stated.

Keywords: winter air-temperature, snow accumulation regime, ground-freezing depth.

Thermal regime of winter season and peculiarities of snow accumulation are important factors for ground-freezing depth. So, ground-freezing depth depends on winter air temperature and snow accumulation regime.

V.A. Kudriavcev (Kudriavcev, 1954) characterized warming and cooling action of snow cover on the ground depending on snow accumulation regime and on its duration and suggested an equation for estimation of ground freezing depth including snow cover thickness, its thermal properties and amplitude of yearly air temperature oscillations.

It was also stated, that intensive snowfalls in the beginning of winter season make thermos-isolating snow cover before coming of frost and prevent ground cooling and reduce freezing or increase thawing depth.

Main determining ground freezing depth parameters are winter seasonal temperature; snow cover accumulation regime and snow cover thickness as well as dampness of the soil and its other properties. Therefor the variations of these parameters were considered for the past 30 years. This was done on example of Komi (an autonomous republic of NW Russia; Syktyvkar), Syktyvkar meteorological station and Nenets Autonomous Okrug, capital Naryan-Mar meteorological station on the basis of obtained from RIHMI-WDC-website (http://aisori.meteo.ru/ClimateR) data of meteorological observations.

Variations of the ground freezing depth were estimated on the base of stepwise calculating scheme, which takes into account air temperature, thickness and averaged heat conductivity of snow cover, thickness and averaged heat conductivity of frozen and thawed ground, its dampness as well as heat of phase transition on the border of thawed and frozen ground. The results of calculations by the estimation scheme were compared with the data on observed ground temperature on the different depths on meteorological station.

The results of calculations by described estimation scheme determined general consistency of calculated ground freezing depth values with the observed ones (Fig. 1, 2). The correlation coefficient is equal to 0.76-0.77.

Figure 1. Variations of winter season observed and estimated ground-freezing depth in Syktyvkar in 1991-2015.

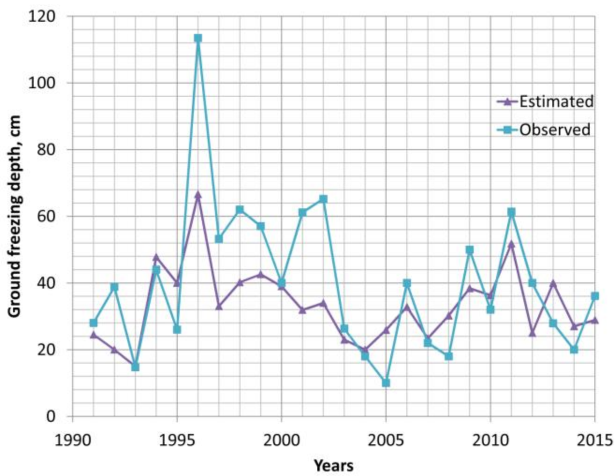

In general, for the calculating soil dampness should be taken 25% of moisture by volume. This value corresponds to 60% filling of pores by water of light clay with density of 2000 kg/m³ and porosity of 0.617.

Figure 2. Variations of winter season observed and estimated ground-freezing depth in Naryan-Mar in 1988-2008.

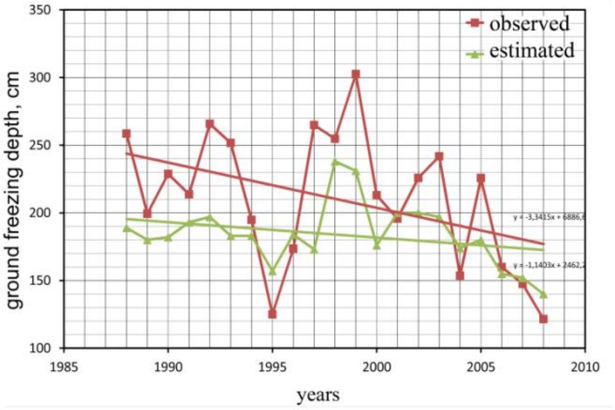

Calculation scheme

Calculation scheme considers ground freezing below the massif of frozen ground, covered with snow cover in winter season on the base of daily data on air temperature and snow cover thickness. The equation of heat balance can be written as:

$F_1 = cLV + F_2$,

F_1 – is heat outflow through snow cover and frozen ground from ground freezing interface (W/m²);

cLV – heat value for phase transition in the ground, c-ground moisture content (1-4 kg/cm*m²), (last value correspond to full filling of porous by water for light clay with density 2000 kg/m³ and porosity coefficient 0,617 (Trofimov, 2005))

L - energy of H_2O phase transition (335 kJ/kg), V-rate of movement of ground freezing interface (cm/s);

F_2 – heat outflow for cooling of thawed ground in front of ground freezing interface (W/m²).

Heat flux is expressed according to Fourier law by means of temperature gradient and heat conductivity as F=λ (grad T). Heat conductivity and heat flux through combination of two media (snow and frozen ground) according to (Mikheev & Mikheeva, 1977) can be expressed as:

$$F_1 = \lambda \frac{\Delta T}{\Delta x} = \frac{\Delta T}{\left(\frac{\Delta x_s}{\lambda_s} + \frac{\Delta x_{fg}}{\lambda_{fg}}\right)} = \frac{T_{air}}{\left(\frac{h_s}{\lambda_s} + \frac{l_{fg}}{\lambda_{fg}}\right)},$$

Here T_{air} – air temperature, h_s и l_{fg} – snow cover thickness and ground freezing depth, and λ_s и λ_{fg} – heat conductivity of snow and frozen ground.

It was supposed, that on the depth of 10 m in ground there is a point of zero annual temperature oscillation with temperature value T_0 about 3°C. That is why

$$F_2 = \lambda_{fg} \frac{\Delta T}{\Delta x} = \lambda_{fg} \frac{T_0}{10 - l_{fg}},$$

Calculations were done with the step-size of one day. For initial conditions, it was supposed that frozen ground thickness l_{fg} was equal 0.5 cm. For each time step (for each day) the rate of movement of freezing interface V and the value frozen ground thickness l_{fg} for the next day (time-step) were calculated.

According to (Pavlov, 1975) averaged heat conductivity of snow was assumed to be equal 0.18 W/m °C. According to (Trofimov, 2005) averaged heat conductivity of thawed and frozen ground was assumed to be equal 1.5 and 1.8 W/m °C correspondingly.

Acknowledgments

The authors are grateful to RFBR grants № 15-05-04461 and state topic «Mapping, modelling and assessment of risk of hazardous natural processes».

References

Trofimov, V.T. (ed.), 2005. *Soil science.* Moscow: MSU Publishing, 1024 pp. (in Russian)

Kudryavtsev, V.A., 1954. *Temperature of the Upper Horizons of Permafrost Thickness within the USSR.* Leningrad: Akad. Nauk SSSR, 183 pp. (in Russian)

Mikheev, M.A., Mikheeva, I.M., 1977. *Fundamentals of heat transfer.* Moscow: Energiya, 344 pp. (in Russian)

Pavlov, A.V., 1975. *Soil-air heat exchange in northern and middle latitudes of the USSR.* Yakutsk: Izd. AN SSSR, 302 pp. (in Russian)

Long-term temperature and active layer monitoring at geocryological key-sites in Western Siberia

Andrey Gravis[1]
Dmitry Drozdov[1,2,3]
Olga Ponomareva[1,2]
Nikolay Berdnikov[1]
[1]*Earth Cryosphere Institute, Tyumen Scientific Centre, Siberian Branch, Russian Academy of Sciences, Tyumen, Russia, ag.gravis@gmail.com*
[2]*Russian State Geological Prospecting University MGRI–RSGPU, Moscow, Russia*
[3]*Tyumen State University, Tyumen, Russia*

Abstract

Ground temperature and active layer thickness (ALT) are controlled by atmospheric temperature and other environmental factors including soil texture, drainage, snow and vegetative cover. Following the global changes in ground temperature and ALT is the main task of national programs and international TSP and CALM projects. The paper presents the results of long-term (1997-2017) ALT monitoring in Western Siberia at sites distributed from Southern tundra to Northern taiga. The analyses of active layer thickness has demonstrated ALT increase at all the observation sites from 0.5 to 3.2 cm per year in a good correlation with the summer heat and the amount of summer precipitation. ALT increase at the cryolithozone southern margin has led to the permafrost table lowering at particular sites with their area being reduced in cold, little snow years. Active layer depth has significantly increased at the sites with high spatial and temporal thaw depth variability.

Keywords: Active layer; climatic zones; monitoring; permafrost, lowered permafrost table

Introduction

Conditions and transformation of natural and natural-technogenic geosystems are mostly controlled by the interaction of the geological environment with exogenic factors. Ascending curve of the global fluctuations of the climate is traced until the present time. Established at the turn of the XX and XXI centuries a slowdown of atmospheric temperature rise hasn't appeared to be the top part of the sinusoid, as previously expected. This fact emphasizes the relevance of the continuation of landscape-geocryological observations at the key monitoring sites, which are already functioning more than 40 years.

Study Area and Methods

Monitoring key-sites are placed in 3 natural sub-zones: "Urengoy – southern tundra T'" site", "Urengoy – southern forest-tundra FT" site" and "Nadym – northern taiga F' site" (R50B, R50A, R1 sites according to CALM-protocol) (Fig. 1). The duration of ground temperature monitoring is about 40 years, of ALT monitoring – 10 years at sites R50B and R50A and 21 year - at site R1.

The ground temperatures are measured in 10m-depth boreholes at several depth levels with the periods from 6 hours to 1 year. The temperature at 8-10 m depth measured in the end of warm season is accepted as an average value: mean annual ground temperature MAGT.

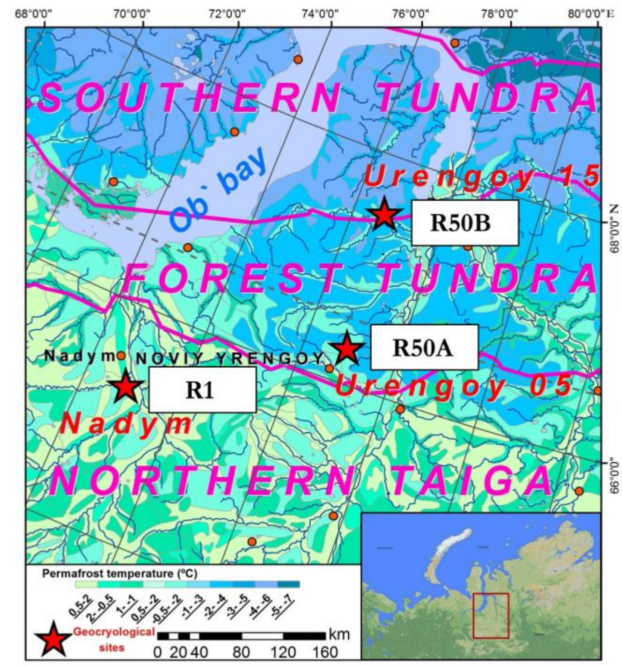

Figure 1. Ground temperature map according to the color scale bar and natural sub-zones at the study area. Locations of the key-sites.

ALT measurements are carried out according to CALM protocol by labeled metal probes on standard areas of 100×100 m size in 121 regular grid nodes at different natural landscapes (the northern site is partly disturbed by technogenic factor). Average ALT is calculated on the data measured in grid nodes excluding ones at taliks.

Results

The ground temperature at all key-sites gradually goes up with some slowdown at the turn of the XX and XXI centuries, which is correlated with the climatic trend. Under the temperatures close to 0°C the increase is less pronounced because of "zero curtain" in the thick layer of the phase transitions (Fig. 2).

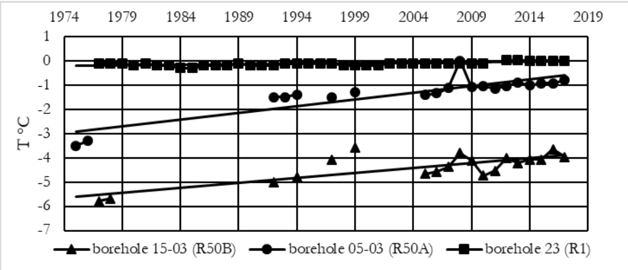

Figure 2. Permafrost temperature at 10 m depth.

The active layer thickness (ALT) also increases, but in contrast to ground temperature, the increase rate reaches its maximum at the southernmost and the most warm sites (Fig. 3). Satisfactory correlation of ALT with zone and climatic factors is obviously revealed by DDT index (day×degree thaw index – the annual sum of day-averaged positive air temperatures, Fig. 4).

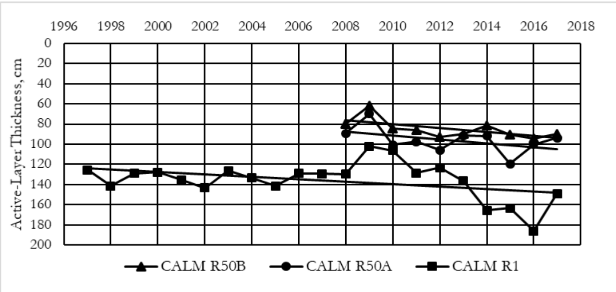

Figure 3. Annual active-layer thickness

In the southern tundra (site R50B) the thaw depth totalled 60-110 cm and under undisturbed surface stayed just unchangeable. The ground temperature changed also not so much: from -4.2 up to -3.9°C. Cold winters contribute to the permafrost stability. Significant ALT increase is caused by technogenesis around constructions and embankments and is indicated by active thermokarst.

In southern forest tundra (sites R50A) the seasonal thaw depth rarely exceeds 100-120 cm on the clay and peaty soil in the southern forest tundra. During 10 years the thaw depth has increased on 20-50% with the gradient of ~2.4 cm/yr, MAGT increase from 0…-1.2°C to 0…-0.8°C (0.025°C/yr). On sandy soils the thawing has exceeded 2 m and permafrost table lowering took place. Mean ground temperature here is estimated near 0°C.

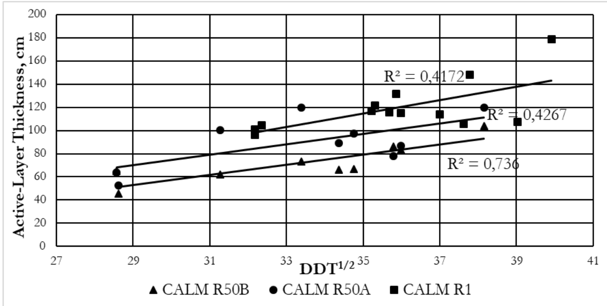

Figure 4. ALT vs $DDT^{1/2}$ for 3 CALM sites. Each data point represents annual end-of-thawing season measurements.

In northern taiga at sites R1 the near-surface permafrost was discontinuous, starting from the very beginning of the observations. The climate warming has led to ALT increase on 60 cm with the average rate 3,2 cm/yr., MAGT rising from -0.2…-0.8°C to 0…-0.3°C (0.018°C/yr.) and gradual extension of taliks, where permafrost table depth exceeds 2 m. The area of such sites extends in warm years and reduces in cold ones (2017 year is attributed to the cold ones). The horizons, having changed their state into thaw one, is specified by high lithological inhomogeneity and therefore the thaw depth is strongly differentiated spatially. Mean ground temperature for this subset of sites R1 is about 0°C.

Conclusions

During last two decades, active layer depth (ALT) has increased all over Western Siberia that has been registered at the CALM sites under study. Site-averaged active layer depth increasing trends have varied from 0.5 in southern tundra to 3.2 cm per year in northern taiga.

At the sites in northern taiga (R1) and southern forest tundra (R50A) the permafrost temperatures have approached 0°C with the permafrost table being lowered at some sites. The area of these sites reduces in the anomalously cold, low snow years.

The correlation of active layer thickness with the quantity of heat delivered into the ground in warm season decreases from north to south because of the increasing influence of the vegetative cover, which becomes richer and spatially variable.

Acknowledgments

Supported by RAS, RFBR (№ 14-05-00956, 15-55-71004/15, 16-05-00249, 16-45-890257-ЯНАО), RSF (grant № 16-17-00102), international programs TSP, CALM, GTN-P, PEEX, SWIPA, GCW, YaNAO administration, GazpromDobychaNadym, GazpromDobychaUrengoy and Northgaz companies.

Dynamics of Active Layer and thaw subsidence in Taimyr peninsula

Grebenets Valery I.[1]
Tolmanov Vasily A.[1]
Kerimov Aligoushad G.[2]
Streletskiy Dmitriy A.[3]
[1]*Moscow State University, Geographical faculty, Department of Cryolithology and Glaciology*
[2]*NPO "Fundament", Norilsk*
[3]*Georges Washington University, Washington DC, USA*

Abstract

Investigations of ALT and thaw subsidence are conducted since 2005. ALT dynamics and changes in geodetical level of the surface depends not only from positive degree days and landscapes, but also from the local moisturizing conditions and the temporal distribution of precipitation in the warm season.

Keywords: Permafrost, active layer, climate, soils, landscapes, thaw subsidence

Introduction

Active layer is characterized by its instability, dynamics, regional differences. The problems connected with thaw subsidence in the active layer are actual for natural and anthropogenic objects. It is found (Nelson, Shiklomanov, 2008) that specific of the heat-transfer in permafrost due to the external environments insufficiently accounted for an evaluation of the permafrost response to the recent and projected climate changes.

Results and discussion

The region of research is Taimyr peninsula (Norilsk, Talnakh) characterised by inclement climate. CALM observations in here are conducted since 2005. Geocryological conditions of Taimyr have large variety and complexity: from the rocks in the mountains to iced (Ii=0,3 -0,6) and high-temperature fine-grained soils. In the valleys peat covers of different thickness are widely distributed, with segregation and polygonal ice. In the typical tundra conditions the R-32 site was chosen for ALT observations and observations of thaw subsidence. We conducted new landscape investigations in 2017and found that there was a strengthening of the role of the more heat-loving plants, for example, increasing number of *Salix pultch*ra and undergrowth *Larex sibirica*, which activated transpiration.

The trend of ALT increasing for Taimyr is 0.3 cm/year. The rapid growth of ALT, following the increase of Summer temperatures and changes in the conditions of the heat transfer through the surface limited by the action of the iced transition layer of soil: in first 7 years, the increase was significant, but after it (the trend was the same) it slowed down.

Another important factor, influencing the depth of active layer is the amount of precipitation during the warm period. For example, for a record number of the positive degree-days (maximal in 66 years) in the Summer of 2013 the depth of the active layer was relatively small, due to the extreme drought. The opposite situation was observed in 2012 and 2015, (fig.1) when the highest values of seasonal melting were achieved.

Fig.1. Maps of ALT, R-32 site, 2012-2017

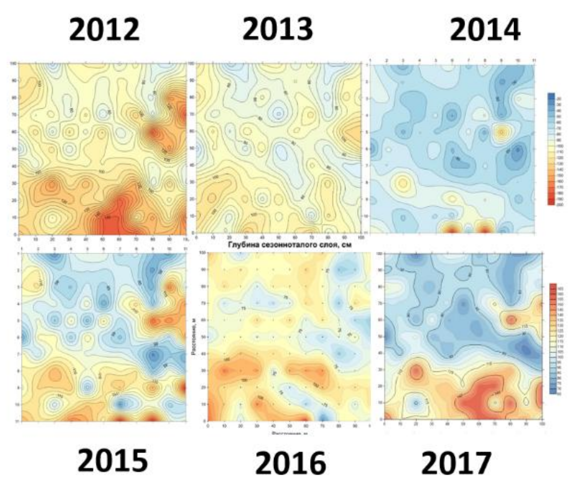

It revealed, that ALT values don't always correlate with the amount of incoming heat, the average value of ALT in 2017 was 106 cm, but the amount of positive degree days was not so large (*table 1*).

Table 1. The results of observations, siteR-32, Talnakh

Year	Amount of positive degreedays/ Amount of summer precipitations ,мм	Average values of ALT (cm)/ Deviation from mean annual values of ALT, (cm)	Changes in geodetical level of the surface, (cm)		
			1. Spot-medallions	2. Drained surface	3. Runoff hollow
2005	927/165	81,3/-12	--	--	--
2006	964 /102	90,8/-2	--	---	--
2007	1107/263	89,5/-4	-0.7	-0.69	-2.13
2008	1073/138	93,9/1	--	--	--
2009	978,4/132	91,7/-1,5	-0.73	-0.80	-2.17
2010	793/261	93/0	-0.76	-0.82	-2.18
2011	1046/235	96/3	--	--	--
2012	1173/327	104/9	-0.3	-0.76	-1.73
2013	1335/42	86/-7	-0.75	-0.75	-2.18
2014	889,1/262	94/1	--	--	--
2015	1196,4/182	102/9	-0.76	-0.73	-2.13
2016	1197,6/200	83/-10	-0.67	-0.72	-2.16
2017	1092,5/200	106/13	-0.64	-0.70	-2.16

This is due to early snow melting (mid-may), with all the heat spent on soil thawing, and the temporal distribution of the summer precipitation: 85% occurred in August.

Maximal ALT and values of thaw subsidence are fixed in the negative forms of relief, having swampy regime, minimal values of thaw subsidense are fixed in spot-madallions. In general, the level of thaw subsidense depends from ALT values, but if we have little pre-winter humidity and water-saturated soils in the summer, it may not correlate with the ALT depth.

Conclusion

Depth of the ALT in the Central part of Taimyr is very high (mean annual at the site of R-32 is 93 cm) and has a tendency to increase due to gradual continuation of the climate warming in here. Differences in ALT and in the magnitude of the displacement of the surface within different landscapes can reach 50–70%.

Acknowledgements

The research is executed by support of the NSF Project PLR-1304555

References

2008 Shiklomanov N.I., Nelson F.E., Streletskiy D.A., Hinkel K.M., Brown J., The Circumpolar Active Layer Monitoring (CALM) Program: Data Collection, Management, and Dissemination Strategies. Proceedings of the 9th International Conference on Permafrost, Institute of Northern Engineering, University of Alaska, Fairbanks, 1: 1647- 1652

Repeat terrestrial LiDAR for permafrost thaw subsidence change detection in North Alaska

Frank Günther[1]
Guido Grosse[1,2]
Mathias Ulrich[3]
Ingmar Nitze[1]
Matthias Fuchs[1]
Benjamin M. Jones[4]

[1] *Alfred Wegener Institute Helmholtz Centre for Polar and Marine Research, 14473 Potsdam, Germany, frank.guenther@awi.de*
[2] *University of Potsdam, Institute for Earth and Environmental Sciences, 14476 Potsdam, Germany*
[3] *Leipzig University, Institute for Geography, 04103Leipzig, Germany*
[4] *U.S. Geological Survey, Alaska Science Center, Anchorage, AK 99508, USA*

Abstract

The distinguishing feature of permafrost in the Arctic is the presence of a large amount of ice below the earth surface. Thermal degradation and subsequent destabilization of ground ice rich terrain cause thaw subsidence. Because these phenomena are hard to detect, they have received not much attention, despite their potentially global significance through the permafrost carbon feedback and implications for active layer thickness monitoring. Clearly, however, detailed local inventories are required to calibrate regional targeted long and short-term assessments for measuring surface deformation due to permafrost thaw. We analyze time series of repeat terrestrial laser scanning (rLiDAR) for quantification of land surface lowering on a tundra upland in the Teshekpuk Lake Special Area on Alaska´s North Slope. Here, considerable negative surface elevation changes have been detected over two years from 2015 to 2017. Spatial patterns of land elevation changes indicate that ice wedge polygon troughs are particularly prone to subsidence. This highlights the vulnerability of arctic tundra lowlands with ice-rich permafrost close to the surface.

Keywords: terrestrial LiDAR, Arctic Coastal Plain, thaw subsidence, ice wedge polygons

Introduction

Permanently frozen ground in the Arctic is being destabilized by continuing permafrost degradation, an indicator of climate change in the northern high latitudes. Accelerated coastal erosion due to sea ice reduction and an increased intensity of ground settlement through ground ice melt result in widespread geomorphological activity (Jones et al., 2013). However, particularly in the light of the enormous area underlain by ice-rich continuous permafrost, still only few observations of permafrost-thaw related landscape dynamics exist.

The objective of our study is to analyze time series of repeat terrestrial laser scanning (rLiDAR) for quantification of extensive land surface lowering through thaw subsidence on an erosional remnant of the Alaskan Arctic Coastal Plain consisting of marine silt (Farquharson et al., 2016).

Methods

We established a subsidence survey grid across the TES-1 upland over 2 km length. The survey area is equipped with benchmarks drilled and anchored deep in the permafrost. These benchmarks serve as long-term position and height reference markers for repeat terrestrial laser scanning. The set-up is generally geared towards a comparison of several measurement campaigns for quantifying recent rates of land elevation change not only with high spatial but also high temporal resolution of interannual intervals.

The first survey was done during the 2nd half of July 2015 and repeat measurements have been made during a follow-up expedition in the same season in 2017. We operated the Leica MultiStation MS50, a hybrid instrument combining high-accuracy surveying with fast laser scanning capabilities, from 26 different positions inside the survey grid that is arranged in two adjacently staggered profiles for optimum coverage. The radius of laser scans was usually in the range of 80-100m in order to ensure overlap between neighboring scans with an equidistancy of 150 m and to capture micro-topographical features resulting from permafrost thaw. The survey covers an area of 460 000 m^2: Accurate positioning of the MS50 is realized using our fixed benchmarks that have been surveyed with precise

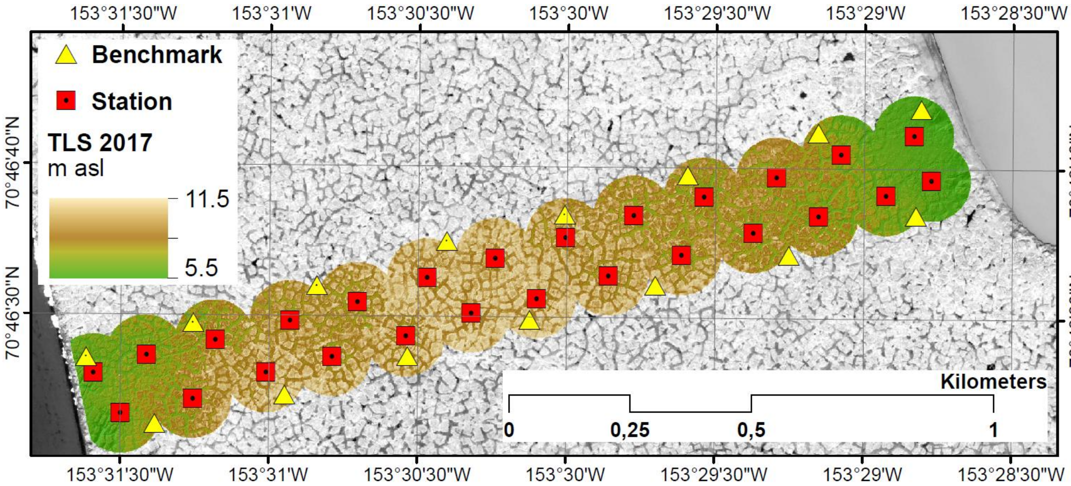

Figure 1. Map showing the 2017 LiDAR DEM stretching across the TES-1 upland between two thermokarst lakes.

local coordinate system that was then re-processed in Leica Infinity, a geodetic software package. Resulting point clouds have been interpolated to regular grids of digital elevation models (DEMs), portraying the land surface in unprecedented detail (Fig. 1).

Results and discussion

Two terrestrial LiDAR DEMs at 25 cm spatial resolution have been used to substract the older 2015 from the newer 2017 one using the geomorphic Change detection tool, an add-on for ArcGIS. Overall, 78 % of the area exhibit detectable change within accuracy thresholds determined by error surfaces that consider point heat maps, slope, and surface roughness. Out of the areas that experienced detectable change, 95 % showed negative surface elevation changes with an average of -12 cm, corresponding to a subsidence rate of -6 cm/yr. These exceptionally high values can be at least in parts explained by very high air temperatures of up to 30 °C recorded in Deadhorse/Prudhoe Bay during summer 2016, highlighting the vulnerability of near surface ground ice to pulse disturbances.

Extensive mapping of ice-wedge polygons complement our remote sensing studies and help differentiating localized elevation change. The mean polygon diameter is 22.7 ±4.9m. We noticed an increasing width of inter-polygon troughs from the upland's interior towards lake shores from 2 to 8 m. In connection with this, enhanced subsidence intensity is particularly pronounced along ice wedge networks compared to the surrounding terrain. Relating this subset of change detection to absolute elevation levels reveals enhanced subsidence with lower elevation ranges that are associated with areas close to the upland's margins where favorable drainage conditions maintain effective removal of ground ice melt water (Fig. 2).

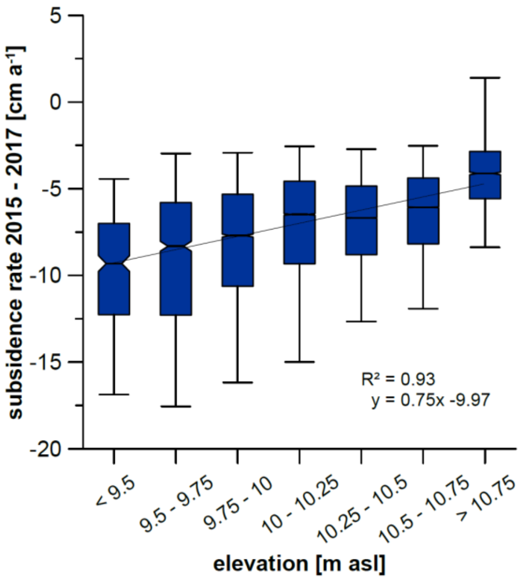

Figure 2. Graph of absolute elevation vs. subsidence rates, indicating increased surface lowering towards the upland margins with enhanced drainage conditions.

References

Farquharson, L.; Mann, D.; Grosse, G.; Jones, B. & Romanovsky, V. (2016). Spatial distribution of thermokarst terrain in Arctic Alaska, *Geomorphology*, 273, 116 – 133.

Jones, B. M.; Stoker, J. M.; Gibbs, A. E.; Grosse, G.; Romanovsky, V. E.; Douglas, T. A.; Kinsman, N. E. M. & Richmond, B. M. (2013). Quantifying landscape change in an arctic coastal lowland using repeat airborne LiDAR, *Environmental Research Letters*, 2013, 8, 045025.

Investigating the sensitivity of soil freeze/thaw dynamics to environmental conditions in the Tibetan Plateau based on observations and satellite-based model simulations

Huiru Jiang [1], Yonghong Yi [2], Wenjiang Zhang [1], Kun Yang[3]

[1]*State Key Laboratory of Hydraulics and Mountain River, Sichuan University, Chengdu 610065, China, ynjhr@163.com*

[2]*Numerical Terradynamic Simulation Group, The University of Montana, Missoula, MT, 59812, USA*

[3] *Department of Earth Science System, Tsinghua University, Beijing 100084, China*

Abstract

Climate warming has induced widespread permafrost degradation in the Tibetan Plateau (TP). It is important to better understand the soil freeze/thaw (F/T) characteristics and their sensitivity to environmental changes. In this study, we aimed to investigate the interaction between these F/T dynamics and environmental conditions such as soil moisture. We firstly ran a process model using observations of soil moisture and near-surface soil temperature at permafrost and seasonally frozen ground (SFG) sites in the central TP. Our preliminary results showed that the simulated soil temperature profile generally well agreed with in-situ observations, though with slight underestimations in winter temperature at some sites. We also found that soil moisture content played an important role in soil F/T processes by affecting the thermal conductivity. We will further extend our analysis to a regional scale so as to investigate the differences in soil F/T characteristics and their responses to environmental conditions.

Keywords: Freeze/thaw; Permafrost simulation; Soil moisture; Tibetan Plateau

Introduction

The Tibetan Plateau is underlain by the world's largest extent of alpine permafrost, where the existence of permafrost is vulnerable to climate change (Yang et al. 2010). Continuous climate warming has induced widespread permafrost degradation in the TP, and influenced the local ecological and hydrological processes (Zhao et al. 2004). Therefore, a better understanding of soil F/T characteristics and their interaction with environmental conditions is critical.

However, in-situ observations of soil temperature and moisture were relatively limited, and most were measured above the permafrost table at sites located along the Qinghai-Tibet Railway (QTR). Therefore, simulated soil profiles are important for investigating permafrost dynamics in the TP region. As for analyzing regional soil F/T dynamics at a data-sparse area, the widely-used method is using satellite-based data to drive model so as to extrapolate the soil temperature profiles.

In this study, we aimed to analyze the soil F/T characteristics and investigate their sensitivity to environmental conditions using in-situ observation and satellite-based soil heat transfer model simulations in the TP region. The study is aimed to provide a better understanding of the soil F/T dynamics and their sensitivity to environmental changes in permafrost and SFG in the TP.

Data and method

In-situ data

The in-situ observations of soil temperature and moisture from the CAMP-Tibet (CEOP Asia-Australia Monsoon Project) and the CTP-SMTMN (Central Tibetan Plateau Soil Moisture and Temperature Monitoring Network) (Yang 2013) were used in this study (Fig. 1). The CAMP network comprised 9 observation sites that located along the QTR, and crossed the permafrost region in the north and SFG area in the south. The soil temperature and moisture were measured at 9 depths from 4 to 250 cm during the period 1997-2007 with some data gaps. The CTP consisted of 56 sites in a 1.0×1.0° region around Naqu. Soil moisture and temperature were measured at 4 depths (5, 10, 20 and 40 cm) from 2011 to 2014.

Model description

We used a process model (Rawlins et al. 2013; Yi et al. 2017) to simulate soil temperature profile in the study area. This thermal model simulated soil temperature down to 50 m below ground surface by solving the 1-D heat equation with phase change. The model was first calibrated and validated using CAMP observations of near-surface soil temperature and soil moisture at the site scale. Then, in order to investigate the influence of soil moisture on soil F/T process, the model was used to simulate the soil profile at two pairs of CTP sites that located in a 0.1×0.1° region (C2, F4 and C1, F2). The near-surface soil temperature and soil properties were similar at these two pairs of sites but the soil water contents were different.

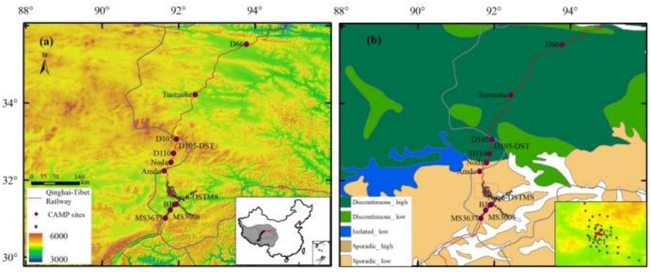

Figure 1. The terrain (a) and permafrost distribution (b) of the study area. Inset small panels in (a) and (b) showed the location of the study area and the two pairs of CTP sites (C2, F4 and C1, F2) respectively.

Results and discussion

Our preliminary results indicated that simulated soil temperature showed a good agreement with the in-situ observations at most of the CAMP sites. The model accurately simulated the soil profile at permafrost site D105 (Fig. 2) and SFG site MS308 relatively. However, it slightly underestimated the winter soil temperature of lower layers (160~250 cm) at some sites such as MS3637. This could be likely attributed to the uncertainties in the in-situ soil moisture used in model parameterization. The deviation of simulations to observations averagely ranged from -0.61 to 0.98 °C among these sites, with the RMSE ranging between 0.18 and 1.52 °C.

The simulations at CTP sites reflected the influence of soil moisture on soil F/T process. There were longer thawing zero-curtain period and deeper maximum frozen depth (MFD, averaged in 2.50 m) at CTP-C2 site, where the average soil water content at 0~40 cm was 24%. However, at CTP-F4 site, where the soil water content was lower than CTP-C2 (16%), the simulated mean MFD was 1.73 m and the zero-curtain was shorter. Similar results were also found in another pair of CTP sites (C1 and F2), and this might due to the high soil water content which influenced soil thermal conductivity.

In the future work, we plan to use more CTP sites to investigate the influence of environmental conditions on soil F/T dynamics. We will also apply the model at a regional scale by using satellite-based data input such as MODIS product of land surface temperature (LST) and enhanced vegetation index (EVI), as well as the SMAP soil moisture data, so as to investigate the sensitivity of soil F/T dynamics to environmental conditions in both permafrost and SFG areas.

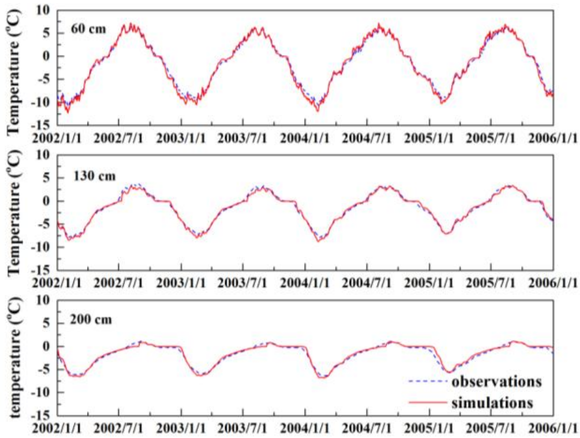

Figure 2. Daily observed (blue dash line) and simulated (red solid line) soil temperature at different layers for permafrost site CAMP-D105 during the period of 2002 to 2005.

Acknowledgments

This work was supported by the Natural Science Fund of China (41471084 and 41771112).

References

Rawlins, M.A.; D.J. Nicolsky; K.C. McDonald; and V.E. Romanovsky. 2013. Simulating soil freeze/thaw dynamics with an improved pan-Arctic water balance model. *Journal of Advances in Modeling Earth Systems* 5:659-675.

Yang, K. 2013. A Multi-Scale Soil Moisture and Freeze-Thaw Monitoring Network on the Tibetan Plateau and Its Applications. *Bulletin of the American Meteorological Society* 94:1907-1916.

Yang, M.; F.E. Nelson; N.I. Shiklomanov; D. Guo; and G. Wan. 2010. Permafrost degradation and its environmental effects on the Tibetan Plateau: A review of recent research. *Earth-Science Reviews* 103:31-44.

Yi, Y.; J.S. Kimball; R. Chen; M. Moghaddam; R.H. Reichle; U. Mishra; D. Zona; and W.C. Oechel. 2017. Characterizing permafrost soil active layer dynamics and sensitivity to landscape spatial heterogeneity in Alaska. *The Cryosphere Discussions*:1-32.

Zhao, L.; C.-L. Ping; D. Yang; G. Cheng; Y. Ding; and S. Liu. 2004. Changes of climate and seasonally frozen ground over the past 30 years in Qinghai–Xizang (Tibetan) Plateau, China. *Global and Planetary Change* 43:19-31.

CALM site in the Polar Urals (Yamal-Nenets autonomous district)

Yaroslav (Konstantinovich) Kamnev[1]
Anton (Ivanovich) Sinotsky[1]
Valery (Ivanovich) Grebenets[3]
[1] *Arctic Research Center of the Yamal-Nenets autonomous district, kamnevyk@gmail.com*
[2] *Lomonosov Moscow State University*

Abstract

In the year 2016 we created a CALM study plot close to settlement Harp. In addition to standard thawing depth measurements we conducted geology-geomorphological, botanical surveys and a complex of low-depth geophysical surveys – GPR and electro tomography.

Keywords: CALM, geology-geomorphological survey, botanical survey, GPR, electro tomography.

Introduction

The whole territory of the Yamal-Nenets autonomous district within the range of ether continues or sporadic permafrost.

Cryosphere is in the focus of researches interest for several reasons. The permafrost warming leads to a variety of geomorphological processes, thermokarst and other destructive changes. Sensitivity of the cryosphere to climate change is mainly caused by ground ice presence. Permafrost degradation, especially ground ice thawing influences the landscapes, causing mire formation and destroys the infrastructure of the Arctic territories.

Circumpolar Active Layer Monitoring (CALM) is a part of Global Terrestrial Observing System (GTOS) and Global Climate Observing System (GCOS). CALM program is focused on gathering comprehensive information on the permafrost change.

CALM study plot close to settlement Harp

In the year 2016 (Arctic Research center of the Yamal-Nenets autonomous district in collaboration with the Lomonosov Moscow State University) we created a CALM study plot close to settlement Harp (Kamnev *et. al.*, 2016). In addition to standard thawing depth measurements we conducted geology-geomorphological, botanical surveys and a complex of low-depth geophysical surveys – GPR and electro tomography.

The territory is dominated by Cretaceous sediments, overlapped with colluvia and lacustrine-alluvial deposits of Middle Pleistocene age. The lithofacies complex of surface deposits is represented by sandy loam and loam with gravel, pebbles, and boulders.

Geomorphologically the study area is represented by elevated dissected plains without linear-ridged forms. The type of terrain is piedmont, lacustrine and drained-lake, the type of landscape is forest-tundra.

According to Circumpolar Arctic Vegetation Map (Walker *et. al.*, 2005) the site is situated on the border of the Arctic zone in between forest tundra and Erect dwarf shrub tundra (S1) at the foot of the Polar Urals. The vegetation of the site is diverse. Despite the small area we could identify a row of 5 different plant communities from wet tundra to open larch forest with humifying differing from wet to dry.

The thawing depth measurements on the CALM site (size 100×100 m.) were done using standard method of probing each 10 meters (Brown *et al.*, 2000). The measuring results were biased by the type of sediments of the site – clay deposits and small coarse rocks could be regarded for the permafrost upper border during measurements. Several measurement mistakes were noticed after comparing the results with the previous year measurements following the rule that the between year difference cannot exceed 30-40 sm. In this case the results should be clarified using GPR survey.

The mean thawing depth in 2017 was 95 sm., that was 4 sm. less than in the previous year.

Low-depth geophysical surveys enrich the data collected on the site. GPR helps to detect the upper permafrost border. Electro tomography allowed to compute a pseudo 3D geoelectric model of the site, showing its' geological structure up to 12-meter depth. This will help us to trace the development of the upper part of the sequence together with the thawing depth and the landscape of the site. We plan to install a thermistor chain for monitoring the substrate temperatures on the site.

References

Kamnev, Y. & Sinitsky, A. & Grebenets, V & Petrov, B., 2016. Creating new CALM site near to town Harp. *Scientific bulletin of the Yamal-Nenets autonomous district. №4(93): 25-28p.*

Walker, D. A. & Raynolds, M. K. & Daniëls, F. J.A. & Einarsson, E. & Elvebakk, A. & Gould, W. A. & Katenin, A. E. & Kholod, S. S. & Markon, C. J. & Melnikov, E. S. & Moskalenko, N. G. & Talbot, S. S. & Yurtsev, B. A. and The other members of the CAVM Team, 2005. The Circumpolar Arctic vegetation map. *Journal of Vegetation Science, 16: 267–282*

Brown, J. & Hinkel, K. M. & Nelson, F. E., 2000. The Circumpolar Active Layer Monitoring (CALM) Program: Research designs and initial results. *Polar Geography, vol. 24, No. 3, 258 p*

Spatial and temporal controls on active layer dynamics in an Arctic mountain valley: project assumptions and preliminary results

Marek Kasprzak[1]
Petr Tábořík[2]
Jarosław Waroszewski[3]
Tadeusz Głowacki[4]
Henryk Marszałek[5]
Kacper Marciniec[1]
Michał Łopuch[1]
[1]*Institute of Geography and Regional Development, University of Wrocław, Poland, marek.kasprzak@uwr.edu.pl*
[2]*Institute of Rock Structure and Mechanics of the Czech Academy of Sciences, Czech Republic*
[3]*Institute of Soil Science and Environmental Protection, Wrocław University of Environmental and Life Sciences, Poland*
[4]*Faculty of Geoengineering, Mining and Geology, Wrocław University of Science and Technology, Poland*
[5]*Institute of Geological Sciences, University of Wrocław, Poland*

Abstract

The paper presents main assumptions and selected preliminary results of a research project focused on spatial and temporal controls on active layer dynamics in an Arctic valley, located in SW Spitsbergen. The attention is focused on areas distant from marine terraces and glacier forefields, similar to alpine environments. The study represents a comprehensive approach to the conditions of the seasonal thawing of permafrost and uses ground temperature monitoring on surfaces typified by variability of slope covers and activity of surface processes, geophysical imaging of active layer, seasonal observations of snow ablation, meteorological and hydrological measurements. All collected data will be used for spatial modelling.

Keywords: permafrost, active layer, geophysics, valley, Svalbard

Introduction

This paper is concerned with the research project focused on features of the active layer of permafrost in an unglaciated area of SW Spitsbergen. The main objective of the project is to define the spatial and temporal variation of the properties of the active layer of permafrost on the example of the Brattegg valley. In a further part of the text only a few technical details and preliminary results of the project will be given.

Methods

In summer of 2017 a system for permanent ground temperature monitoring was created in the Brattegg valley. Additionally, weather conditions and water runoff were measured (runoff at the mouth of the basin and at the mouth of glaciated, upper part the valley).

The ground temperature monitoring is based on specialized thermistor strings (Geoprecision). These devices automatically log changes of temperature at standard depths up to 1.5 m in accordance with World Meteorological Organization recommendations. The thermistors are placed in twenty different terrain situations (altitude zones, different aspects) and on different types of ground (solid rock, block cover, debris cover, solifluction lobes, patterned ground).

For better understanding of active layer behaviour and distribution, electrical resistivity tomography (ERT) and electromagnetic survey (EM) were carried out along selected profiles. At test sites geophysical measurements were conducted as time-lapse, at the beginning and in the maximum of the ablation season of 2017. The obtained inversion models were processed using RES2DINV software. Collected data, after detailed mapping of cover deposits, will be used in GIS-based modelling of active layer properties in the entire catchment area.

Study area

The study area is located in the Wedel Jarlsberg Land, in south-western Spitsbergen, in the Brattegg valley which hosts a remnant glacier on the slopes within the amphitheatre valley-head (Fig.1). The selected valley does not follow straight line, hence its slopes are exposed towards different directions, whereas its mouth is restricted by a rocky step and it is drained by a single watercourse (Brattegg river), allowing for controlling the runoff volume. The bottom of the valley can be divided into several separate morphological levels reflecting the glacial and glacial isostatic history. The valley is diverse in terms of its geological structure and was formed in crystalline rock, mainly quartzites, amphibolites and schists. Its slopes and bottom present a wide range of terrain forms (talus cones, gelifluction lobes, patterned ground) and sediments with various textures.

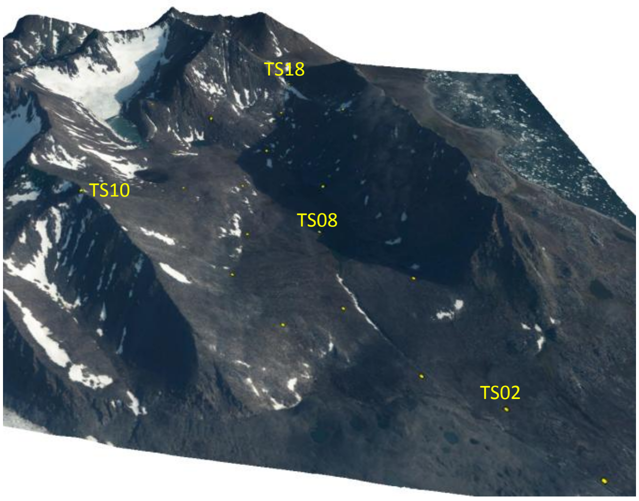

Figure 1. The SfM-based digital terrain model of the Brattegg valley with ground temperature measuring sites (TS). Source of orthopthotomaps: NPI, 2010.

Preliminary results and conclusions

The results, obtained in the summer season of 2017, indicate that in all tested sites a thickness of active layer reached at least 1.5 m (Table 1), however its properties strongly varied (Fig. 2). Thawing to greater depths could not be recorded on mounted thermistors, but was imaged using geophysical prospecting. At some sites, thawing to a depth of 4 meters is likely (Fig. 3).

Table 1. Maximum ground temperatures [°C] at selected depths measured in monitored sites (summer season 2017).

Site	Elevation [m a.s.l]	maximum temperature at depth [m]			
		0.2	0.5	1	1.5
02	23	9.43	7.81	5.75	4.0
08	73	7.25	5.93	3.87	2.62
10	582	6.5	3.18	0.5	0.12
18	303	6.5	4.06	1.5	0.31

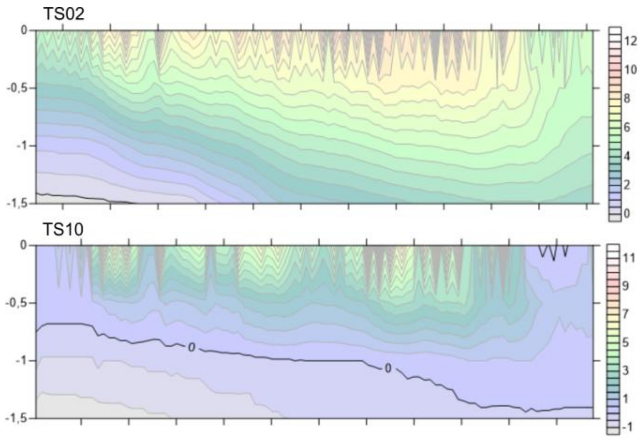

Figure 2. Examples of different thermal regime of ground in the period from 4th July to 22nd August 2017 at measurement sites TS02 and TS10 (see fig. 1)

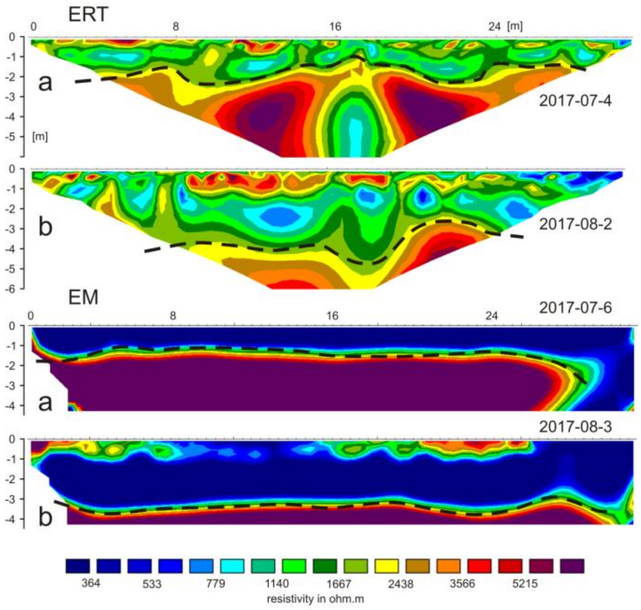

Figure 3. Examples of time-lapse geophysical measurements carried out in 2017: electrical resistivity tomography (ERT) and electromagnetic survey (EM); dashed lines – permafrost table.

The observations prove a significant increase in the depth of ground thawing compared to measurements carried out in the area 20–30 years ago. Preliminary conclusions based on terrain observations and geomorphometric modelling demonstrate a correlation between the thickness of active layer and open-work type slope deposits, slope exposure to direct solar radiation and concentration of surface/ground water outflow.

The paper is a contribution to the National Science Centre project: 'Spatial and temporal controls on active layer dynamics in an Arctic mountain valley' award no. 2015/19/D/ST10/02869.

Land cover evolution in the artificially-drained thaw lake basin (Russian European North)

Dmitry Kaverin[1]
Evgeniy Melnichuk[2]
Nikolay Shiklomanov[3]
Alexander Pastukhov[1]
[1]*Institute of Biology Komi SC RAS, Russia, dkav@mail.ru*
[2]*Company "PolarnoUralGeologia"*
[3]*The George Washington University*

Abstract

Land cover evolution accompanied with drastic changes in ground temperature regime were studied in the basin of artificially-drained thaw lake basin in the Russian European North. The studies were conducted during 1979-2011. The artificial drainage of thermokarst lake Opytnoe resulted in an initial temperature decrease in peaty-mineral bottom sediments and formation of subsurface permafrost layer all over the basin. Land cover changes in the drained lake basin develops towards the restoration of lacustrine-boggy tundra landscapes. Permafrost aggradation favored formation of peat mounds and tundra meadows, which developed on Cryic Histosols. Waterlogging affected local depressions, which led to the development of marsh meadows and willow stands on Sapric and Hemic Histosols. Shrub invasion and waterlogging favored permafrost thaw. Willow-grassy communities formed on primitive Fluvisols in the local stream's floodplain.

Keywords: lake drainage, ground temperatures, soils, vegetation changes

Introduction

The climate warming forecasted by different simulating models and temperature monitoring data can trigger thermokarst processes which dramatically change hydrology and carbon balance in sub-Arctic ecosystems (Kuhry et al., 2013). Permafrost thaw, thermokarst and water erosion are natural triggers for areal deformation of tundra lakes and their possible drainage. The evolution dynamics of thermokarst lakes can serve as a possible indicator of cryolythozone status (Yoshikawa and Hinzman, 2003). In recent decades, interest in qualitatively landscape changes in drained lake basins has increased. Large flat-bottomed thermokarst lake basins often provide ideal conditions for the formation of wetlands because of a low drainage gradient and permafrost aggradation on the basin floor (Jones et al., 2012). The soil substrate controls ice segregation and surface heave (Jorgenson and Shur, 2007), while the variable snow thickness associated with surface heave and vegetation strongly influences permafrost temperature and active-layer thickness (ALT) within the basins (Mackay and Burn, 2002). The aim of the study is to survey land cover evolution accompanied by drastic changes in temperature regime of peat-mineral grounds in the artificially-drained thaw lake basin.

Materials and Methods

The study site is represented by the basin of artificially-drained lake Opytnoe (N 67º20'; E 62º21'). It is located within the Pechora Lowland. The region is characterized by a subarctic, moderate-continental, moderate-cold climate. (MAAT is -5.7 ºC). Terrain is represented by the weakly undulating plain dissected by moraine hills and streams. Flat portions of the plain are overplayed by peatlands and dotted by heave mounds and thaw lakes. Sedge-sphagnum and sphagnum-hypnum mosses with sparse shrubs and trees dominate peatland vegetation. Histic Cryosols and Cryic Histosols dominate in the area. The basin sediment profile from the lake contained the 0.5-1.2 m thick layer of peat/mineral bottom sediments, followed by the 2-6 m. layer of sand and the 10-30 m layer of clays. Near-surface permafrost was present in sediments underling lake terrace.

The lake Opytnoe was drained in 1979. In early 1980, a SW to NE transect of fourteen 15-30 meters-deep thermometric boreholes was established across the center of the basin. Year-round ground temperatures monitoring in boreholes was conducted over the 1982 - 1995 period. Thickness of the active layer was observed in September of each year by mechanical probing down to 1.0 – 1.5 m depth. Detailed landscape and vegetation characterizations were carried out in 1980, 1982, 1985, 1993 and 2011. Climatic characteristics were obtained from the Vorkuta meteorological station. Soil survey was carried out in August 2011. Land cover changes were assessed by processing Landsat images (1984-2011).

Results and Discussion

Initially, during the Holocene Optimum, the site ecosystems had developed as a forested non-permafrost fenland. Afterwards already in permafrost period, the thermokarst lake was formed as an erosion result of ice-rich deposits of the peat plateau followed by water-logging of destructing peat horizons. After drainage, the lake basin got covered mainly with Arctophila fulva (Trin.) Anderss. and Erióphorum meadows gradually replaced by Erióphorum and Cárex communities. The natural grass stand (Calamagrostis, Cárex, Arctophila fulva (Trin.) Anderss., Erióphorum) varied by height from 0.39 to 1.5 m. Initially, flat peat bottom had no vegetation. As peat lake bottom became gradually overgrown with vegetation, bare peat area had decreased. The further evolution of meadows formed in the early 1980-ies developed according to the two main succession ways. Permafrost aggradation in elevated and dry sites favored the formation of peat mounds and tundra meadows on Cryic Histosols. Flat wet sites had been covered with marshy meadows and willow stands, which developed on Sapric and Hemic Histosols. In the lake basin, a natural watercourse was formed, where willow stands developed on primitive Fluvisols.

Artificial drainage of a thaw lake resulted in dramatic, spatially and temporally variable changes to the ground thermal regime within the basin. The ground temperature changes were controlled by atmospheric climate and landsurface evolution, which resulted in partial permafrost aggradation in the basin (Kaverin et al., 2017). In the first few years following lake drainage (1979-1987) lake-bottom sediments gradually cooled. MAGT, averaged over all strata, decreased from +1.0 to + 0.2 °C in the basin and from -1.0 to -2.2 °C on the terraces during that period. Atmospheric cooling (1985-1987) and the presence of a thick organic upper layer significantly contributed to the formation of a thin subsurface permafrost layer, which initially affected almost the entire basin area. During the relatively warm climatic sub-period (1988-1995), further growth and spread of tundra shrub vegetation over primary marshy meadows on the lake bottom resulted in progressive snow entrapment and increased ground temperatures. Near-surface permafrost completely thawed under shrub (willow) stands and marshy meadows. Permafrost was preserved and thickened under heaved peat mounds and tundra meadow surfaces, where snow was removed by wind. Basin averaged MAGTs increased from + 0.2 to + 0.5 °C and those for terrace strata from - 2.4 to -1.2 °C during this sub-period.

Acknowledgments

The study was supported by RFBR grant № 16-04-00749 "Acidic-type profile as the base control of soil-forming processes (in the context of Arctic ecosystems)", project TSP "Thermal State of Permafrost", grant PLR1304555 to the George Washington University and RFBR grant № 18-55-11003 "Towards constraining the circumarctic N2O budget".

References

Jones, M.C., Grosse, G., Jones, B.M., Anthony, K.W. 2012. Peat accumulation in drained thermokarst lake basins in continuous, ice-rich permafrost, northern Seward Peninsula, Alaska. *Journal of Geophysical Research: Biogeosciences* 117. DOI: 10.1029/2011jg001766.

Jorgenson, M.T., Shur, Y. 2007. Evolution of lakes and basins in northern Alaska and discussion of the thaw lake cycle. *Journal of Geophysical Research: Earth Surface* 112: F02S17. DOI:10.1029/2006JF000531.

Kuhry, P., Grosse, G., Harden, J.W., Hugelius, G., Koven, C.D., Ping, C.L., Schirrmeister, L., Tarnocai, C. 2013. Characterization of the Permafrost Carbon Pool. *Permafrost and Periglacial Processes* 24(2): 146-155. DOI: 10.1002/ppp.1782.

Mackay, J.R., Burn, C.R. 2002. The first 20 years (1978-1979 to 1998–1999) of ice-wedge growth at the Illisarvik experimental drained lake site, western Arctic coast, Canada. *Canadian Journal of Earth Sciences* 39(1): 95-111. DOI: 10.1139/e01-048.

Yoshikawa, K., Hinzman, L.D. 2003. Shrinking thermokarst ponds and groundwater dynamics in discontinuous permafrost near council, Alaska. *Permafrost and Periglacial Processes* 14: 151-160. DOI: 10.1002/ppp.451.

Kaverin, D.A., Melnichuk, E.B., Shiklomanov, N.I., Kakunov, N.B., Pastukhov, A.V., Shiklomanov, A.N. 2017. Long-term changes in the ground thermal regime of an artificially drained thaw-lake basin in the Russian European north. *Permafrost and Periglac Process.*: 1–11. https://doi.org/10.1002/ppp.1963.

Reconstructing temperature histories from GTN-P permafrost borehole temperature records

Fabian Kneier[1]
Pier-Paul Overduin[1]
Moritz Langer[1,2]
Boris Biskaborn[1]
Julia Boike[1]
Mikhail N. Grigoriev[3]
[1]*Alfred Wegener Institute for Polar and Marine Research, Potsdam, Germany, Fabian.Kneier@awi.de*
[2]*Humboldt-Universität zu Berlin, Germany*
[3]*Melnikov Permafrost Institute, Yakutsk, Russia*

Abstract

Local temperature histories in ice-rich permafrost areas of the Russian Arctic are either sparse or based on proxy data with potential seasonal biases. Borehole temperature reconstructions are sensitive to the temperature signal throughout the year and available in regions for which no other records exist. We reconstructed local temperature histories using two Global Terrestrial Network for Permafrost (GTN-P) permafrost boreholes of at least 65 m depth in the Laptev Sea region. Two inversion methods retrieved the history of the last 200-300 years. Distinct differences between the Lena Delta and western Laptev Sea sites were found, notably a one-century delay of warming and a three decade delay in peak warming in the western Laptev Sea. The results provide a basis for local surface temperature parameterization of climate and permafrost models. Local and regional trends deviate from the circum-Arctic average. The GTN-P network provides a partially suitable set of borehole records for circum-Arctic temperature reconstruction.

Keywords: Borehole temperature reconstruction; Arctic; Ground surface temperature (GST); Global Terrestrial Network for Permafrost (GTN-P).

Introduction

Palaeotemperature reconstructions are important palaeoclimate indicators and a valuable basis for models identifying the impact of various processes within the past and future climate system. Arctic permafrost contains large reserves of organic carbon. Temperatures in this region are therefore important as a driver for a positive feedback to the global climate. Borehole temperature reconstructions are sensitive to the temperature signal throughout the year and available in regions for which no other records exist. The objective of this study is to assess the potential in medium-to-deep (>65m) GTN-P (Global Terrestrial Network for Permafrost) borehole temperature records for the reconstruction of local temperature histories. In a case study, two inversion methods were used to retrieve the history of the last 200-300 years in the Laptev Sea region from two permafrost boreholes, and to compare them to circum-Arctic records. Lastly, the available GTN-P data is evaluated in light of the results.

Study Site

Figure 1 shows the location of the two chosen borehole sites in the tundra of the central Siberian Arctic (GTN-P IDs: 'RU 148 DE02' and 'RU 149 DE03').

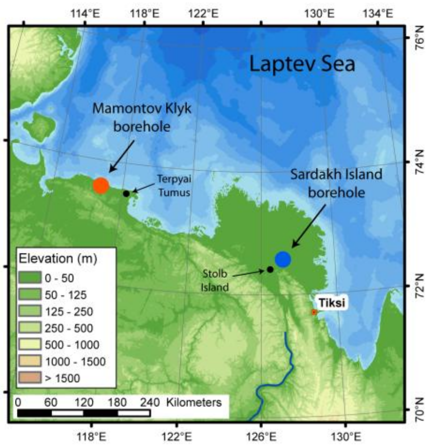

Figure 1. Laptev Sea region with the borehole locations.

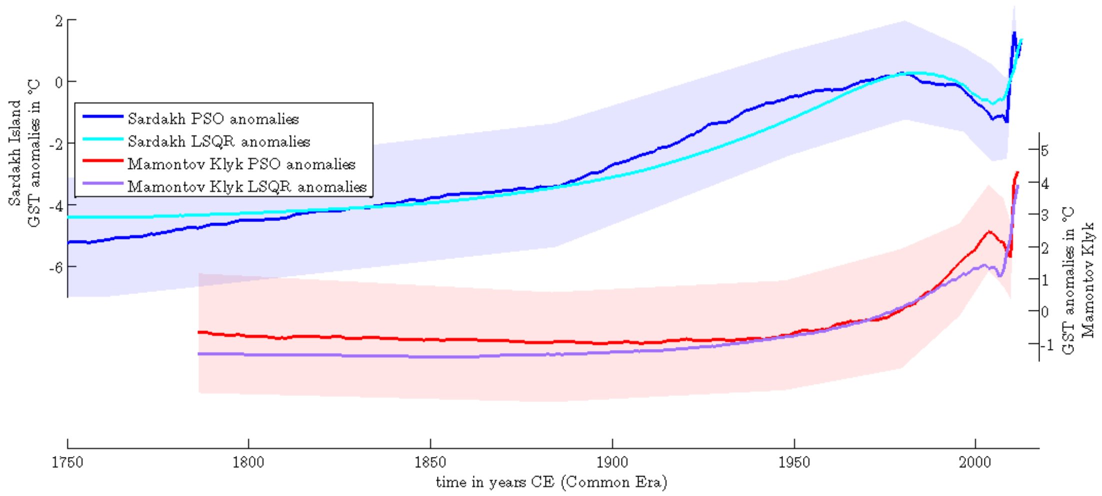

Figure 2. Anomalies of the two reconstructed ground surface temperature (GST) histories at Sardakh Island (blue) and Mamontov Klyk (red) using the least squares (LSQR) and particle swarm (PSO) inversion methods. The shaded area gives the 25th and 75th percentile in the PSO distribution. Adapted from (Kneier et al., 2017, under review).

Method

Borehole temperature reconstructions estimate temperatures prior to the start of direct observations based on geothermal heat conduction, i.e. the diffusive slow transfer of heat into the ground to different depths on different time scales. This allows reconstruction of a surface temperature history that is consistent with the observed temperature profile in the borehole. This study employed an adaption of two inversion schemes (particle swarm optimization and a least squares technique) previously applied to temperature measurements from ice core sites (Roberts et al., 2013).

Results and Discussion

Temperature histories of the last 200-300 years were retrieved from the two boreholes in the Laptev Sea region (Fig. 2).

Our results showed distinct differences in the histories between the Lena Delta and western Laptev Sea sites for both inversion methods, notably a one-century delay of warming and a three decade delay in peak warming in the western Laptev Sea. In comparison to larger scale reconstructions from the region, the local permafrost surface temperatures at Sardakh Island (central Lena Delta) resembled the circum-Arctic regional average trends. At Mamontov Klyk (western Laptev Sea) this was the case only for the most recent decade. In contrast, the Mamontov Klyk history was more similar to northern hemispheric mean trends. A rapid recent warming of synoptic scale was consistently observed at both sites. The reconstructed magnitude of temperature changes is consistent with warming greater than mean Arctic temperature trends.

In conclusion, reconstruction from permafrost boreholes provides short-scale temperature histories at two selected Arctic GTN-P sites (resolved at annual to multi-decadal scale). As local differences from the circum-Arctic average were shown to exist, the results provide a basis for local surface temperature record parameterization of climate models and of permafrost models in particular. The untapped temperature data in the GTN-P database therefore shows great promise, presented in the ability to retrieve pan-Arctic permafrost surface temperature histories of the last 200-300 years. Suitably deep GTN-P boreholes exist in the continuous permafrost region around the whole Arctic. Tapping this source would allow to obtain data from regions currently underrepresented in circum-Arctic temperature reconstruction and would further allow to retrieve information on regional temperature trend differences driving past and future permafrost warming.

References

Kneier, F., Overduin, P.P., Langer, M., Boike, J. & Grigoriev, M.N., 2017. Borehole temperature reconstructions reveal differences in past surface temperature trends for the permafrost in the Laptev Sea region, Russian Arctic *under review.*

Roberts, J.L., Moy, A.D., van Ommen, T.D., Curran, M.A.J, Worby, A.P., Goodwin, I.D. & Inoue, M., 2013. Borehole temperatures reveal a changed energy budget at Mill Island, East Antarctica, over recent decades *The Cryosphere* 7: 263-273.

Spatial and temporal trends in permafrost conditions across three discontinuous zones, Alaska Highway corridor, northwest Canada

Antoni G. Lewkowicz[1]
Sharon L. Smith[2]
Maxime A. Duguay[3]
Olivier Bellehumeur-Genier[4]
Alexandre Bevington[5]

[1]*Department of Geography, Environment and Geomatics, University of Ottawa, Ottawa, Canada; alewkowi@uottawa.ca*
[2]*Geological Survey of Canada, Natural Resources Canada, Ottawa, Canada; Sharon.smith@canada.ca*
[3]*BGC Engineering, Calgary, Canada; mduguay@bgcengineering.ca*
[4]*Geological Survey of Canada, Natural Resources Canada, Ottawa, Canada; obell034@uottawa.ca*
[5]*B.C. Ministry of Forests, Lands, Natural Resource Operations and Rural Development, Prince George, Canada; alexandre.Bevington@gov.bc.ca*

Abstract

We report on permafrost conditions from the outer limit of the isolated patches zone through to the extensive discontinuous zone within the Alaska Highway corridor, northwest Canada. Ground temperatures for permafrost sites measured at or close to the depth of zero annual amplitude in 20 shallow boreholes, range from -0.1°C in the south to -3°C near the Alaska border. The base of permafrost, estimated using ERT surveys, increases from less than 5 m at sites with ground temperatures close to 0°C, to greater than 25 m where temperatures are ≤-0.5°C. Data for a sub-set of the sites shows that they have warmed since the 1970s but there is no strong short-term trend across the entire transect. However, one borehole in the isolated patches zone and a second in the sporadic discontinuous permafrost zone have developed supra-permafrost taliks, indicating the vulnerability of permafrost to thaw in the corridor south of 61°N.

Keywords: discontinuous permafrost; ground temperature monitoring; talik; electrical resistivity tomography.

Introduction and Study Area

The thermal state of permafrost is important to global observing systems, for infrastructure and resource development planning in the Arctic and Subarctic, and in relation to potential greenhouse gas emissions caused by the breakdown of previously frozen organic matter. Here we use recent ground temperatures measured in 20 shallow boreholes, as well as electrical geophysics, to describe spatial and temporal trends in permafrost thermal state along a transect in northwest Canada.

The southeast-northwest transect runs 1550 km, covering 5° of latitude and nearly 20° of longitude, along the Alaska Highway in northern British Columbia (57.4°N 127.5°W) and the Yukon to the Alaska border (62.6°N 141°W). It traverses the entire isolated patches and sporadic discontinuous permafrost zones, as well as at least part of the extensive discontinuous permafrost zone (Heginbottom *et al.*, 1995). According to recent modelling it terminates in a localised area of continuous permafrost (Bonnaventure *et al.*, 2012).

Considerable information on the transect to the west of Whitehorse was collected in the 1970s in relation to the Alaska Highway Gas Pipeline and renewed interest in this project led to additional boreholes being drilled in 2013. Recent studies showed that permafrost has thawed over the past 50 years in the area east of Whitehorse (James *et al.*, 2013). A compilation of 2016 data from the western portion of the transect is given in Smith *et al.* (2017).

Methods

Boreholes were drilled by water-jet (7 from 2008-2016), mechanically (6 in 2013), and by steaming open boreholes first drilled mechanically in the 1970s (7 in 2011). All the boreholes are less than 10 m in depth, but 75 % reach the depth of zero annual amplitude. The sites are in the boreal forest zone, with open black spruce typically dominating the vegetation cover, but some are undergoing vegetation regrowth following disturbance along the easement of the planned pipeline.

Ground temperatures were measured every 8 hours using RBR data-loggers and multi-thermistor cables (accuracy ± 0.05°C), or every 2 hours with Onset Hobo Pro loggers and external thermistors (accuracy ± 0.2°C).

Electrical resistivity tomography (ERT) was used at 14 sites to estimate the depth to the base of permafrost. An ABEM terrameter LS was attached to 4 cables in a Wenner array, over profile lengths of 80 m (1 m electrode spacing, 12.5 m depth of investigation) or 160 m (2 m spacing, 25 m depth of investigation). Inversion of the apparent resistivities was carried out with RES2DINV software until the RMS error fell below 5 % or to the 5th iteration, whichever came first.

Results and Conclusions

Ground temperatures vary from -0.1°C in the south to -3°C near the Alaska border (Fig. 1). There is little variability in permafrost temperatures through the isolated patches and sporadic discontinuous permafrost zones south of 61°N: all are warmer than -0.3°C. Modelling shows this latitude to approximate the northern boundary of the sporadic discontinuous zone in the highway corridor (Bonnaventure *et al.,* 2012). The range of permafrost temperatures increases northwards as perennially frozen ground can be sustained beneath a wider range of surface covers, substrates and drainage conditions. For example, one of the sites in the transect north of 61°N has standing water for part of the summer, a condition that would be expected to preclude permafrost further south.

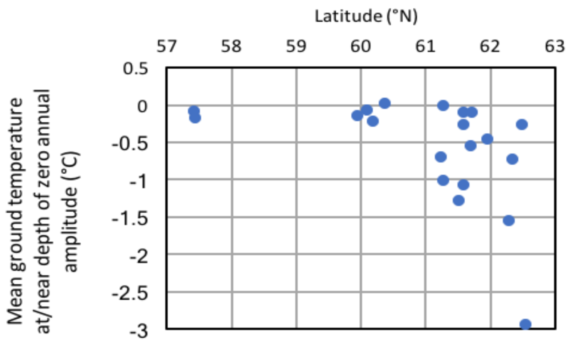

Figure 1. Mean ground temperatures at boreholes in permafrost along the Alaska Highway corridor transect. Data are from the most recent year of observations (2016 or 2014).

An inverse relationship exists between the depth of the permafrost base and ground temperature (Fig. 2). In the isolated patches and sporadic discontinuous permafrost zones, the maximum depth inferred from the ERT profiling was 20 m, whereas all sites with ground temperatures <-0.5°C had permafrost that exceeded the maximum depth of investigation (generally 25 m).

Comparisons between temperatures measured in the re-acquired boreholes and those measured manually in the 1970s indicate that permafrost has consistently warmed over the intervening decades, probably due to a warming climate. The evidence for recent ground temperature change along the transect as a whole is limited, which is not surprising given the potential for latent heat effects to slow ground warming and the short duration of the records (median 5 years). However, one undisturbed site in the isolated patches zone and a second in the sporadic discontinuous permafrost zone exhibit talik development in their temperature records, accompanied by ground surface settlement at the borehole sites. Annual ERT profiling at these sites also indicates progressive thaw.

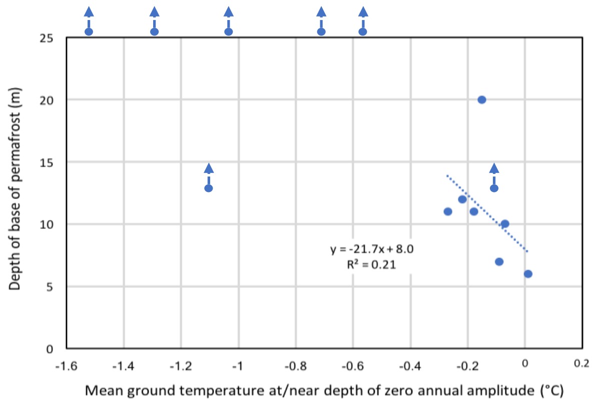

Figure 2. Relationship between mean ground temperature and depth of the base of permafrost obtained from ERT surveys. Arrows show points that exceed the maximum depth of investigation (12.5 m or 25 m). Regression line is based on 7 boreholes with a defined base of permafrost.

We conclude that most of the sites north of 61°N in the extensive discontinuous permafrost zone remain resilient to thaw. Those to the south of this boundary in the sporadic and isolated patches zones, however, are vulnerable to thaw caused by ongoing climate warming and surface disturbance, and some are actively thawing.

Acknowledgments

Financial support for this research came from NSERC, the University of Ottawa and Natural Resources Canada. We thank several Yukon First Nations for access to borehole sites and the many field assistants who helped collect data.

References

Bonnaventure, P.P., Lewkowicz, A.G., Kremer, M., Sawada, M.C., 2012. A permafrost probability model for the southern Yukon and northern British Columbia, Canada. *Permafrost and Periglacial Processes* 23: 52-68.

Heginbottom, J.A., Dubreuil, M.A., Harker, P.T., 1995. Canada-Permafrost. *In*: *National Atlas of Canada*. Ottawa: Natural Resources Canada, Map 2.1.

James, M.A., Lewkowicz, A.G., Smith, S.L., Miceli, C.M., 2013. Multi-decadal degradation and persistence of permafrost in the Alaska Highway corridor, northwest Canada. *Environmental Research Letters* 8: 045013.

Smith, S., Roy, L.-P., Lewkowicz, A.G., Chartrand, J., 2017. Ground thermal data collection along the Alaska Highway corridor (KP1559-1895), Yukon, summer 2016. *Geological Survey of Canada Open File* 8311.

Climate-driven changes in permafrost: impacts on the temperature regime of cryogenic ecosystems in the European North

Galina V. Malkova, Marat R. Sadurtdinov, Andrey G. Skvortsov, Andrey M. Tsarev, Yury V. Korostelev

Earth Cryosphere Institute, Tyumen Scientific Centre SB RAS, Tyumen, Russia, galina_malk@mail.ru

Abstract

The results of permafrost temperature regime observations in cryogenic ecosystems of the European North are described. It is shown that the temperature trends of the permafrost are several times smaller than the trends in air temperature. The trend of increase in MAAT for a 35-year period is 0.08°C/year and the MAPT trend ranges in various natural landscapes between 0.01 and 0.04°C/year, and in disturbed landscapes these trends exceed 0.06°C/year. It was found that not only the permafrost temperature was increasing, but also the ZAA decreased from 10 m in the 20th century, up to 3-5 m in recent years. In disturbed areas some isolated closed taliks began to form, and the permafrost table dropped to 4-12 m below the ground surface.

Keywords: Monitoring, climate warming, permafrost temperature, zero annual amplitude.

Introduction

The study of permafrost temperature regime is essential to assess the current state and tendencies of development of the cryogenic ecosystems under an influence of climate warming and anthropogenic impacts. The construction and operation of oil and gas facilities are accompanied by disturbance of natural ecosystems. However, the amount of available data on changes in geocryological conditions in disturbed landscapes is still very limited (Oberman, 2006; Malkova, 2010, 2011). In the Nenets Autonomous region there are currently only three active monitoring stations, Bolvansky, Kashin and Shapkina do exist. All temperature boreholes in these monitoring objects are included in the GTN-P database. In this presentation we will review the results of geocryological monitoring of cryogenic landscapes in the Russian European North during the last 35 years.

Discussion of the results

We analyzed the changes of climate in the permafrost zone of the European territory of Russia (ETR). All meteorological stations in ETR without exception show an increasing trend in mean annual air temperature (MAAT) and in the sum of positive air temperatures (thawing index) with the sum of negative air temperatures (freezing index) showing a decrease. The MAAT in the 21st century is significantly higher than the climatic norm. The displacement of MAAT isotherms of the same rank occurs from S-W to N-E and reaches in various parts of ETR about 100-200 km (Fig.1).

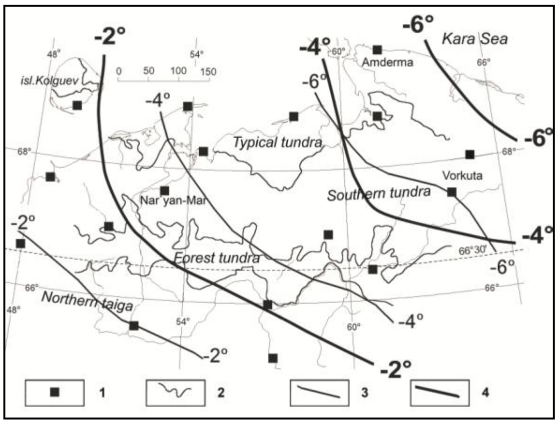

Fig. 1. MAAT (°C) on the ETR permafrost zone: 1 - the weather station; 2 – the boundaries of natural zones and subzones; 3 – MAAT during the climatic norm (average for 1960-1990 period); 4 – MAAT in the 21st century

The trend of MAAT over the past 35 years is about 0.08°C/year. The same trend is characteristic for average winter and summer air temperature. The duration of the warm period has increased over this period by about two weeks. There is a tendency of increase of annual precipitation from 350 to 450 mm and a weak tendency of increase in the snow thickness. Thus, the change of all climatic characteristics for the last 35 years should contribute to the degradation of permafrost, increase in its temperature and increase in the depth of thawing.

For the past 35 years of observations at Bolvansky and Shapkina sites, unique series of data allowing studying both rhythmic and trend changes of permafrost temperature was obtained. In 1980, the mean annual permafrost temperature (MAPT) at 10 m depth (zero annual amplitude, ZAA) in natural landscapes within the Bolvansky research area varied from -0.5 to -2.5°C depending on the location, and at Shapkina research area MAPT reached -4 °C. According to our data, during the monitoring period, MAPT at 10 m depth increased by 0.2 to 1.2°C in different landscapes. (Fig. 2).

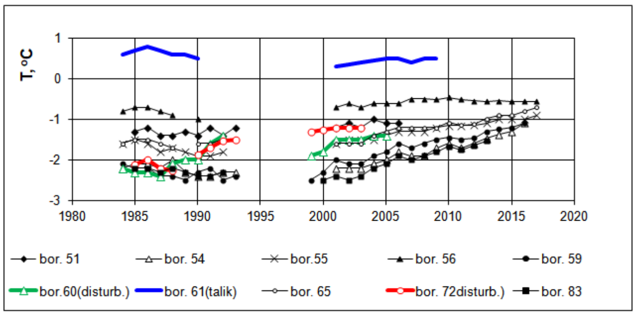

Fig. 2. MAPT at the 10 m depth. Bolvansky site

According to our calculations the greatest trends of increasing MAPT (0.04°C/year) are observed for drained tundra (bor. 59 and similar bor. 54, 83) also characterized by the lowest permafrost temperature in the area. On the polygonal peat bog (bor. 55) the MAPT increase has a trend of 0.02°C/year. The least sensitive to climate fluctuations are the edges of the lakes and hillocks, here the trend of MAPT is 0.01°C/year (bor. 56). So, the rate of MAPT increase was 2 to 8 times smaller than the trend in MAAT changes. The inertia of permafrost temperature changes is typical not only for the European North, but also for other regions of the permafrost zone (Drozdov et al., 2012; Romanovsky et al., 2010). This can be explained by the fact that when the permafrost temperature is in the range of 0 to -1°C the active phase transitions of ice start and a large fraction of the incoming heat are spent on melting of pore ice.

It was proved that there is not only the permafrost temperature at different depths is rising, but also the depth of the ZAA started to reduce in the second decade of the 21st century. In continuous permafrost zone (Bolvanskyi) the ZAA is 4-5 m now. For the discontinuous permafrost zone (Shapkina) ZAA is equal to 3-4 m, and in the sporadic permafrost zone (Kashin) ZAA is limited by the active layer depth and does not exceed 2-3 m.

Technogenic changes significantly accelerate the degradation of permafrost. When the vegetative cover is removed, the rate of MAPT increase is 0.05°C/year (Fig. 2, bor. 60), and when the peat horizon is also removed– the mean annual trend reaches 0.06°C/year (Fig. 2, bor. 72). At the beginning of the 21st century, the formation of closed taliks began in the technogenic areas. The depth of these taliks in continuous permafrost zone at present is 4-5 m, and in sporadic permafrost zone, this depth reaches 10-12 m (Sudakova et al., 2017).

Acknowledgments

This research was performed with the financial support from the grant RSF 16-17-00102 and with the technical support in the framework of international projects CALM and TSP.

References

Drozdov, D. S., Malkova, G. V., Ukraintseva N. G., Korostelev Yu. V. Monitoring of the geocryological conditions of southern tundra of the European North and Western Siberia. *10th intern. Conf. on permafrost, TICOP X: Resources and risks of regions with permafrost in a changing world.* Salekhard, 2012, vol. 3, pp. 159-164.

Malkova, G. V., Monitoring of the mean annual permafrost temperature on the Bolvansky site. *Earth Cryosphere*, vol. XIV, No. 3, 2010, pp. 22-35

Malkova, G. V., Monitoring of the permafrost temperature and active layer thickness on the Bolvansky site in the Pechora Delta. *Proceedings of the 4th conference of geocryologic in Russia, MSU 7-9 June 2011*, vol. 2, part 5: Regional and historical Geocryology. M., Publishing house University book, 2011. S. 111-118.

Oberman, N. G. Long-term trends of the natural evolution of cryolithozone of the European North-East. *Materials of Iinternational conference "Theory and practice of assessment of Earth cryosphere and prognosis of its changes"*, Tyumen, 2006., vol. 1, pp. 93 – 101.

Sudakova, M. S., Sadrtdinov M. R., Malkova G. V., Skvortsov A. G., Tsarev A. M. Application of GPR in the complex of geocryological research. *Cryosphere of the Earth*, 2017, vol. XXI, No. 3, pp. 69-82.

Romanovsky V.E., Drozdov D.S., Oberman N.G., Malkova G.V., Kholodov A.L., Marchenko S.S., Moskalenko N.G., Sergeev D.O., Ukraintseva N.G., Abramov A.A., Gilichinsky D.A., Vasiliev A.A. Thermal state of permafrost in Russia. *Permafrost and Periglacial Processes. Special Issue: IPY*, April/June 2010, Vol. 21 (2), pp. 136–155.

Active layer response to contemporary climate variations in coastal Chukotka, NE Russia

Alexey Maslakov[1], Gleb Kraev[2,3], Oleg Tregubov[4], Dmitrii Zamolodchikov[5]
[1]*Lomonosov Moscow State University, Faculty of Geography, email: Alexey.maslakov@geogr.msu.ru*
[2]*Institute of Physicochemical and Biological Challenges in Soil Science, Russian Academy of Sciences*
[3]*Vrije Universiteit Amsterdam*
[4] *Chukotka branch of NEISRI FEB RAS*
[5] *Centre for Ecology and Productivity of Forests RAS*

Abstract

Dynamics of active layer, one of the main parameters of the permafrost state, follows regional weather patterns. Compared to neighboring regions, Chukotka remains a white spot for monitoring data and recent trends in climate and permafrost dynamics. We made an update on changes in weather patterns and active layer thickness for 21st century. There is nearly no trend in regional summer warmth in 2000-2015, on the contrary with 1980-90s. Following it, thickening of the active layer have faded on the many sites, likewise in the neighboring regions: Alaska and NE Siberia. Lavrentiya and Lorino are the only exception with the trends of 7 cm per decade owing to location on icy loams. Given the activation of thermoerosion in vicinities of the plot, we suppose it is a feedback to preceding warming.

Keywords: CALM; permafrost table; seasonal thawing; active layer; Chukotka.

Introduction

Long-term ALT studies in Chukotka have already been reported for 20th century (Kotov *et al.*, 1998; Zamolodchikov *et al.*, 2004) and locally using recent data (Tregubov & L'vov, 2014). This contribution encompasses all available data from CALM sites and regular monitoring using different measurement protocol in Chukotka, NE Russia since the beginning of 21st century. We evaluate the active layer response in different landscapes of the region to contemporary climate parameters fluctuations.

Materials and methods

Monitoring sites

ALT monitoring in Chukotka dates back to 1988 when intact tundra and disturbed plots were established at Dionisiy station, 20 km SW of Anadyr (Figure 1, marked as "D"). Later in 1994-2009 there have been 5 CALM sites established on Anadyr lowland (see Figure 1): R9 Onemen, R11 Dionisiya, R45 Kruglaya and Chukotskii Peninsula: R27 Lavrentiya and R41 Lorino. Non-interrupted WMO weather monitoring stations Uelen and Anadyr are located 20-80 km from the study sites.

The sites are located 15-150 m above sea level on moist foothills and in lacustrine depressions in typical tundra on the coast of the Bering Sea. Most common soils are ice-rich loams with gravel inclusions, peats and peaty sandy loams. Sedges, willow-sedge, herb-moss-shrub and sedge-moss associations dominate in vegetation cover.

Table 1. Weather parameters in 2000-2015

	Mean air temperature, °C		Degree-days		Mean summer precipitations, mm
	July	January	Freezing	Thawing	
Anadyr	12.0	-22.6	-3375	1083	130
Uelen	6.8	-19.4	-2861	828	139

Methods

Field measurements of ALT on CALM sites followed the standard technique (Brown *et al.*, 2000), extended with several monthly measurements during summer on Lavrentiya and Lorino sites. Measurements on "Dionisiy" field station followed the Russian technical guide (Gravis *et al.*, 1979), which is similar to CALM protocol and differs only in number of measured nodes within the grid (20-40 instead of 121).

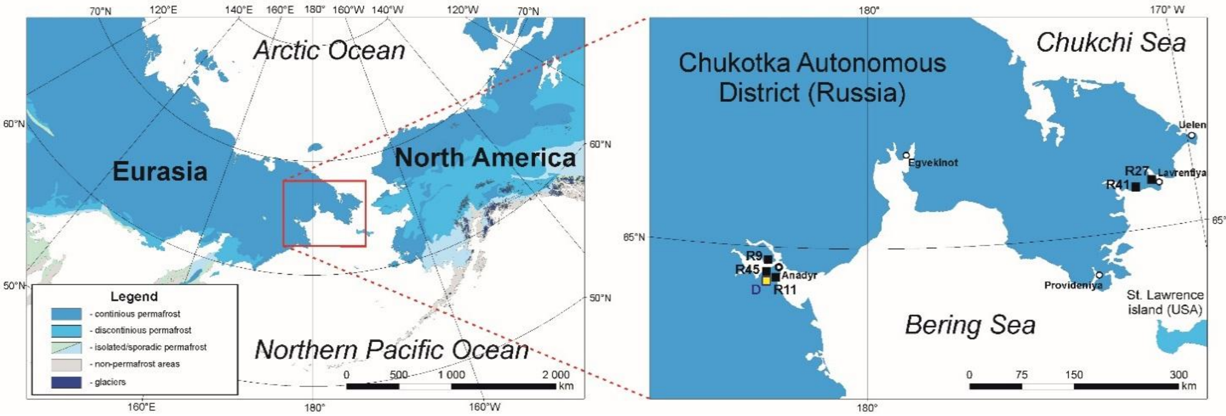

Figure 1. Active layer monitoring sites and weather stations in Chukotka (see explanations in the text)

The ALT datasets for 2000-2015, available online (www2.gwu.edu/~calm/) were analyzed statistically together with relevant weather data.

Results and Discussion

With variations from 600 to 1200°C·day warmth of summer had no pronounced trend (Figure 2). The average ALT for the coastal sites of Chukotka varied from 45 to 66 cm. There was no difference in ALT on sites between Anadyr Lowland and Chukotskiy Peninsula. However, attenuation of ALT growth is visible for the sites on Anadyr Lowland. On the contrary, ALTs in Lavrentiya and Lorino grow at rate of 7 cm per decade.

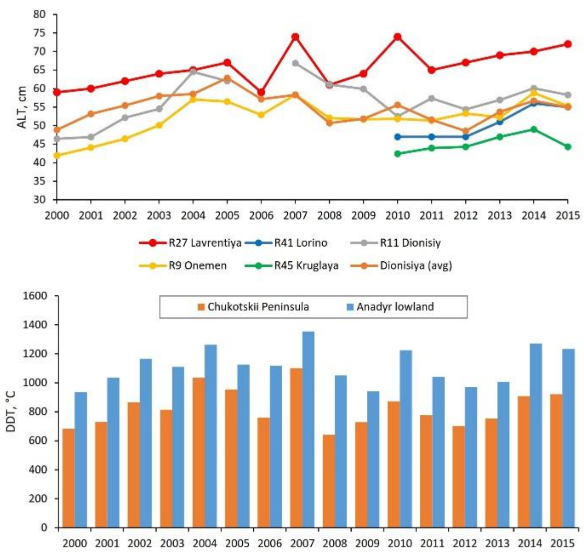

Figure 2. Thawing degree-days and ALT on various sites of Chukotka.

Thawing degree-days strongly correlated with the ALT (r=0.92 for Lavrentiya), so the reasons for discrepancy between the trends are still to be understood. Dynamics of ALT in Chukotka is similar to adjacent regions (NE Yakutia, Alaska), with stabilization in 2000s following rapid growth in 1990s. Lavrentiya and Lorino break this pattern by continuous seasonal thaw deepening. Given the activation of thermoerosion in surroundings we suppose that 1990s warming have initiated permafrost degradation.

Acknowledgments

This study was partly supported by US National Scientific Foundation (grant PLR-1304555), RFBR grant 18-35-00192 (analytical part), the Federal Appointment to Russian Academy of Sciences (project 0110-2014-0002), and by NIR AAAA-A16-116032810095-6.

References

Brown, J., Hinkel, K.M. & Nelson, F.E., 2000. The circumolar active layer monitoring (CALM) program: Research designs and initial results, *Polar geography* 24: 165–258.

Gravis, G.F., Grechishchev, S.E., Nevecherya, V.L., et al., 1979. *Technical guide on stationery studies of cryogenic physical-geological processes.* Moscow: VSEGINGEO, 72 pp. (in Russian).

Kotov, A.N., Brazhnik, S.N. & Galanin, A.V., 1998. Environmental monitoring on Onemen station. In: *Chukotka: priroda i chelovek [Chukotka: nature and people]*. Magadan, SVNTS DVO RAN, pp. 93-111. (in Russian).

Tregubov, O.D. & Lvov, A.P., 2014. Representative observations of the depth of seasonal thawing in tundra landscape. *Vestnik SVFU,* 11: 89-99. (in Russian).

Zamolodchikov, D.G., Kotov, A.N., Karelin, D.V. & Razzhivin, V.Yu., 2004. Active-layer monitoring in Northeast Russia: spatial, seasonal, and interannual variability, *Polar Geography* 28: 286-307.

Permafrost degradation, subarctic Canadian Shield

Peter D. Morse[1], Stephen A. Wolfe[1]
Taylor L. McWade[2]
Steve Kokelj[3]
[1]*Geological Survey of Canada, Natural Resources Canada, peter.morse@canada.ca*
[2] *Geography and Environmental Studies, Carleton University*
[3] *Northwest Territories Geological Survey, Yellowknife*

Abstract

Recent ground temperature and observational data for lithalsas (permafrost mounds of ice-rich, fine-grained sediments) are examined in the context of an inventory of thermokarst ponding between 1945 and 2005, subarctic Canadian Shield. Results show that many lithalsas are thermally and physically degrading, and widespread thermokarst primarily relates to lithalsa distribution. Future thermokarst development in this region of extensive discontinuous permafrost will continue to be associated with lithalsas that generally lack a protective surface organic layer.

Keywords: Canadian Shield; permafrost degradation; ground temperature; thermokarst, lithalsa.

Introduction

Permafrost degradation in ice-rich, thaw-sensitive materials can result in terrain subsidence. With ecological and hydrological implications, ground stability has societal relevance in the southern subarctic Canadian Shield as this region (nearly the size of Belgium) contains the highest population and density of infrastructure in the Northwest Territories (Fig. 1). Discontinuous permafrost, present in natural terrain beneath peatlands and forest on unconsolidated fine-grained (glacio) lacustrine sediments, is warm and in disequilibrium with contemporary climate, which has warmed since at least the mid-1960s (Morse *et al.*, 2015). Lithalsas, minerogenic permafrost mounds with cores of segregated ice and up to 8 m of relief (Fig. 2), are widespread in this area (Wolfe *et al.*, 2014). With little-to-no surface organic layer, lithalsas are likely sensitive to climate change and disturbance but the nature of permafrost degradation is not well documented. Here we present recently mapped thermokarst in the context of *in situ* ground thermal data and geomorphic observations.

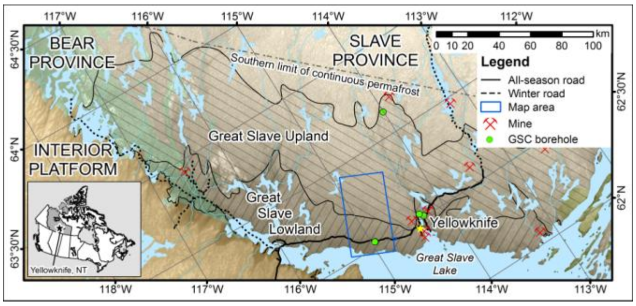

Figure 1. Great Slave Upland and Lowland regions, southern subarctic Canadian Shield. The blue rectangle represents the thermokarst map area shown in Figure 4.

Methods

Ground temperatures

The lithalsa ground temperature monitoring network consists of 9 sites throughout the region (Fig. 1) with 1 to 6 years of data (Fig. 3). Shallow boreholes (up to 11.5 m) represent the range of permafrost conditions in the region. Factory calibrated thermistor strings connected

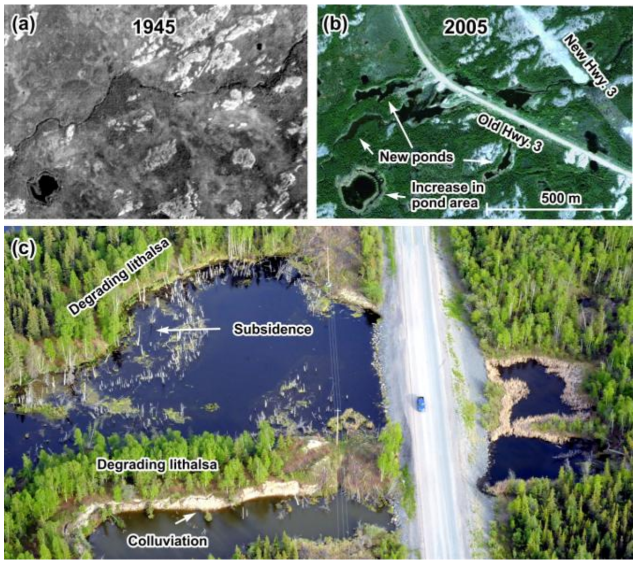

Figure 2. Thermokarst examples. Change from forested terrain (a) to thaw ponds (b). (c) Degrading lithalsas. Note submerged, standing dead birch (*Betula papyrifera*) indicating gradual subsidence, and colluviation at some lithalsa margins.

to eight channel data loggers record temperatures hourly. Thermistor temperatures are known to ± 0.1 °C, but change is resolved at 0.001 °C.

Thermokarst mapping

An inventory of thermokarst ponding (1945 to 2005) was created from historical air photos and recent satellite images (Morse *et al.*, 2017). Change from forest to water was based on differences in spectral characteristics, texture, and shape. The margin of error for an individual pond area is likely ± 50 m².

Results

Thermal degradation

Shallow borehole temperatures are generally higher than -1.5 °C and commonly isothermal or inverted on an annual basis (Fig. 3a), and temperatures below the depth of zero annual amplitude are either increasing or remain nearly static due to latent heat effects (Fig.3b). Exceptions relate to site specific conditions such as WB-5 that is located at the degrading margin of a lithalsa and shows surface cooling, but is warming at depth (Fig. 3). Such warming is physically important as ice content in these lithalsas increases with depth (Wolfe *et al.*, 2014).

Physical degradation

Thermokarst associated with lithalsas takes two main forms (Fig. 2c): (1) simple subsidence indicated by the common occurrence of ponded water with submerged stands of vertically-oriented dead trees; and (2) colluviation at the lithalsa margin into the adjacent water body. Though rare, retrogressive thaw slumps can develop with sufficient relief and ground ice.

Thermokarst, widespread throughout the study region (Fig. 4), predominantly relates to lithalsa degradation (Fig. 2). Accordingly, the distribution of thermokarst ponding is associated with fine-grained deposits and surface water sources. This mirrors the controls on lithalsa distribution reported by Wolfe *et al.* (2014).

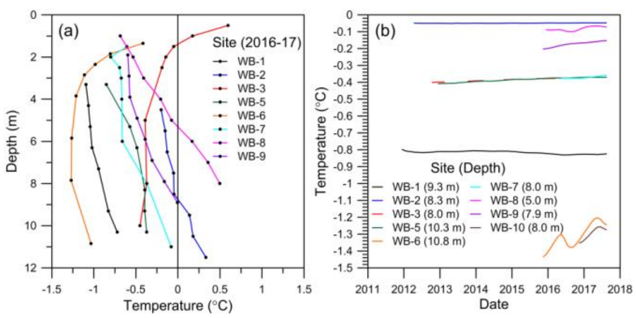

Figure 3. Ground temperature profiles (a) and trends below the depth of zero annual amplitude (b) in fine-grained materials, southern subarctic Canadian Shield.

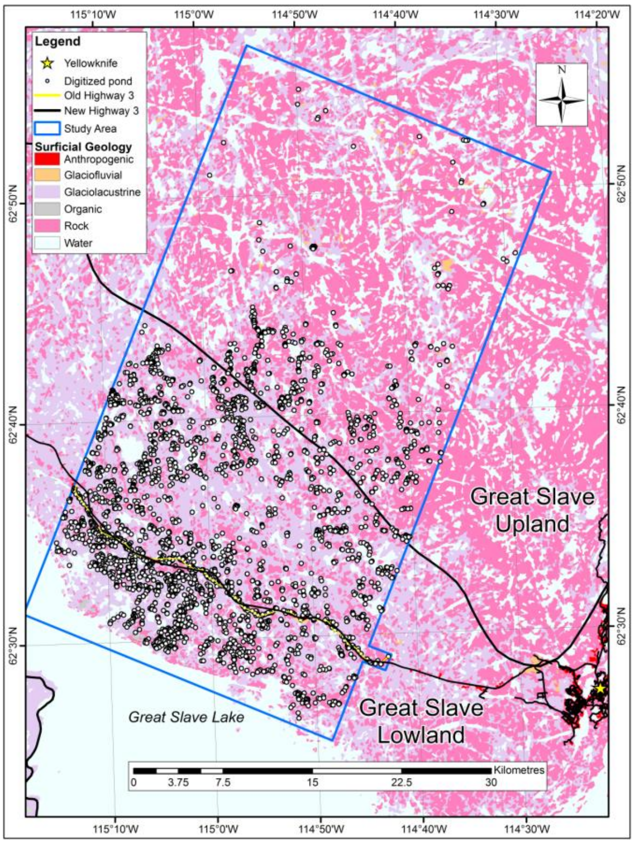

Figure 4. Thermokarst distribution, southern subarctic Canadian Shield. After Morse *et al.* (2017).

Conclusions

Lithalsas across the subarctic Canadian Shield are in a state of thermal and physical degradation. Widespread thermokarst relates directly to former lithalsa distribution. Continued thermokarst development will likely centre on these ice-rich permafrost mounds.

References

Morse, P.D., Wolfe, S.A., Kokelj, S.V. & Gaanderse, A.J.R., 2015. The occurrence and thermal disequilibrium state of permafrost in forest ecotopes of the Great Slave region, Northwest Territories, Canada. *Permafrost and Periglacial Processes* 27: 145-162.

Morse, P.D., McWade, T.L. & Wolfe, S.A., 2017. Thermokarst ponding, North Slave region, Northwest Territories. *Geological Survey of Canada, Open File 7108*. Ottawa: Geological Survey of Canada, 30 pp.

Wolfe, S.A., Stevens, C.W., Gaanderse, A.J. & Oldenborger, G.A., 2014. Lithalsa distribution, morphology and landscape associations in the Great Slave Lowland, Northwest Territories. *Geomorphology* 204: 302-313.

CHAMONIX Mont-Blanc 23 June - 1st July 2018 EUCOP5

Forecasting the degradation of deep permafrost using temperature-depth observations

Annabelle Neefjes[1], Victor Bense[1], Huijun Jin[2], Sheng Yu[2]

[1]*Wageningen University, The Netherlands, victor.bense@wur.nl*
[2]*Northwest Institute of Eco-Environment and Resources, Chinese Academy of Sciences, Lanzhou, Gansu, PR China*

Abstract

Timing of permafrost disappearance in a warming climate is a crucial control on a suite of environmental processes including the reactivation of groundwater flow, landscape development and the associated release of carbon into the atmosphere. Forecasting of permafrost demise has mainly been approached as a near-surface phenomenon from the land-surface modeling perspective, with limited consideration of heat flow processes below a few meters depth. We show, using numerical models and temperature-depth profiles of warm and vulnerable permafrost that the thermal state of deep permafrost during thaw can be obtained using relatively simple measurements of the depth at which thermal gradient is zero, the temperature at this depth and the thickness of permafrost, without the need of repeated measurements. As an example, we demonstrate that across the Source Area of the Yellow River on the Qinghai-Tibet Plateau, China it will take approximately another 80 -140 years before permafrost will be fully degraded.

Keywords: Vulnerable permafrost, monitoring, modeling

Introduction

Permafrost degradation rates have traditionally been approached by the monitoring of the permafrost active layer thickness and focussed on the complexity of coupled heat flow and hydrological processes therein. Regional assessments of the rate of the geographical shrinkage of the permafrost realm have mostly relied on the coupling between climate models generating scenarios of future air temperature trends, and land-surface models that use an energy balance approach to provide a forecast for future ground surface temperature. The latter is then used to determine permafrost extent which is commonly defined as a thermal state. Consequently, in this approach permafrost will no longer be present in areas that have ground surface temperatures above freezing for a sustained period.

It is questionable whether the existing approach to evaluate future permafrost extent has summarized above is useful when it comes to understanding the dynamics of environmental processes that are clearly dependent on the presence of permafrost below the depth of the ultimate maximum thickness of the active layer (e.g. 5 meters). These would include hydrological processes such as groundwater recharge to sub-permafrost aquifers, the release of 'deep' carbon from the subsurface, and the contribution of groundwater to sustain baseflow to rivers.

Describing deep temperature-depth profiles in warming permafrost

Numerical models can be used to evaluate the fate of the entire permafrost thickness in the currently warming climate. When heat conduction only is described these models represent the heat flow effects of freezing-thawing of water in pore space by solving the classic heat-flow equation:

$$\nabla \cdot [\kappa_a \nabla T] = C_a \frac{\partial T}{\partial t} + L_i \frac{\partial n_w}{\partial t} \quad (1)$$

in which T is temperature, κ_a is the apparent thermal conductivity, and C_a is the apparent heat capacity of the medium. The latent heat effects of freezing are represented by the last right-hand term of (1) in which L_i is the latent heat of freezing/thawing and n_w is the unfrozen water content. Hence, the latent heat term in (1) will only become active during freezing/thawing. In a scenario of progressively warmer ground surface temperatures latent heat effect will act to delay the warming of permafrost (Figure 1) which is commonly known as the zero-curtain effect.

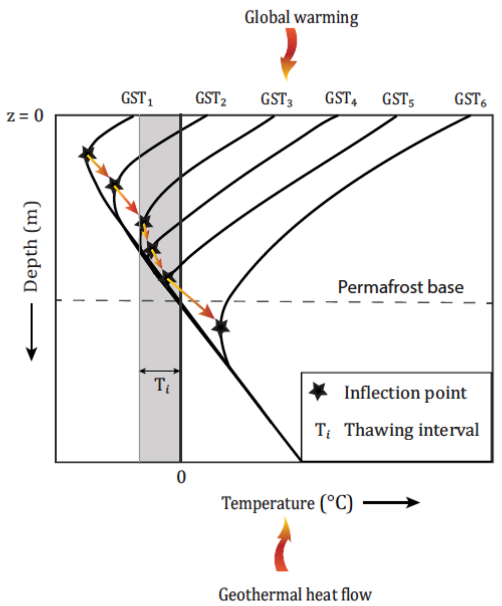

Figure 1. The development of temperature-depth profiles in a warming climate. The boundary conditions to this system are the ground surface temperature (GST), and the background geothermal heat flow. During the initial stages of warming in cold mostly continuous permafrost the propagation of the inflection point is mostly heat conduction controlled. However, latent heat effects, the width of the thawing interval (T_i) and the total porosity of the substrate will control the rate of progression with depth and temperature during permafrost thaw.

In a warming climate in which ground surface temperatures (GST) gradually rise, temperature-depth profiles develop a typical 'C'-shape as a result of a downward propagation of heat into the subsurface. At depths below where temperatures are influenced by this process, temperatures will gradually rise instead as governed by upward geothermal heat flow from deeper in the Earth's crust. Consequently, there will be a depth where the vertical temperature gradient is zero. This depth is where the 'inflection point' resides (Figure 1). Over time both the inflection point depth and the temperature at this depth will increase. The particular shape of this path in time largely depends on the thawing interval (Figure 1; T_i) which is the temperature interval just below zero (for entirely fresh water under near surface pressure) over which ice in pore space will melt into liquid water. The thawing interval is relatively wide (e.g., 1-2°C) for fine-grained sediments, for example silt-clay sedimentary material, and narrow (<1°C) for coarser grained material such as loose sand or gravel.

Measurements of the temperature and depth of the inflection point in temperature-depth profiles can in principle thus be used to monitor permafrost warming and to possibly forecast the time scale of disappearance of deep permafrost. Such measurements exist for a few deep boreholes in currently continuous permafrost. However, at these locations permafrost has not reached the stage of thawing yet. In boreholes in discontinuous permafrost that is thawing temperature changes are too slow (due to the zero-curtain effect) to be detectable in a few years time. The latter state makes it particularly difficult to evaluate the stage of thaw permafrost is in (i.e., how long ago thaw started), the thawing interval and other thermal properties that are needed to model forecast the time scale of complete permafrost thaw at those locations.

Field data and analysis

We analyzed temperature-depth (TD) data from 5 boreholes in discontinuous permafrost in the Source Area of the Yellow River that were constructed in close vicinity to each other (i.e., within a radius of about 1 km). The boreholes are up to 45 m deep which is sufficient to traverse almost the entire thickness of permafrost, whilst one borehole did not show permafrost at all. TD data from these boreholes were collected for several years in a row and do not show significant temporal change. However, comparison of the position and temperature of the inflection point in three boreholes suggests that these can be regarded as being in different stages of thaw in a similar geological environment. This is supported by analysis of temperature and depth of the inflection points in these boreholes as plotted against model simulations of the same. Further model sensitivity analysis allowed to estimate the thawing interval and porosity representative of the geological sequence encountered at these locations. Consequently, we could assess the most likely time scale of the complete disappearance of permafrost at these sites assuming purely vertical heat flow conditions and excluding the possibly accelerating effect of a reactivation of groundwater flow. In this framework of analysis, at a fourth site in the same area we conclude that although temperatures are warmer than at the other three permafrost sites thaw has probably not yet commenced due to a narrower thawing interval closer to zero in a more porous substratum.

Conclusion

We conclude that using temperature-depth profiles from boreholes in discontinuous permafrost that are placed in each other's vicinity can potentially be used to estimate those petrophysical properties (i.e., thawing interval and porosity) that would enable a reliable forecast of the timescale of degradation of the entire permafrost thickness.

Remote-sensing based global map of permafrost

Jaroslav Obu[1]
Sebastian Westermann[1]
Andreas Kääb[1]
Annett Bartsch[2]
[1]*University of Oslo, email*
[2]*Zentralanstalt für Meteorologie und Geodynamik*

Abstract

Inability to detect permafrost from space can be overcome by ground temperature modelling based on land surface temperature and ground properties. We used a TTOP model to estimate mean annual ground temperature (MAGT) for the permafrost areas of the Northern hemisphere. The permafrost occurrence probability was calculated using 200 ensemble runs with varying model adjustment factors. According to the results, the permafrost area of the Northern Hemisphere covers 16.20 × 10^6 km², which is 17.0 % of the Northern Hemisphere exposed land. The validation with borehole data yielded root mean square (RMS) of 2 °C.

Keywords: Permafrost extent; Ground temperature; Ground thermal regime; Remote Sensing; Permafrost zonation

Introduction

Permafrost cannot be directly detected from space, but many permafrost surface features and properties are observable with a variety of earth observation sensors. ESA's GlobPermafrost project develops, validates and implements different permafrost information products to support the research communities and related international organisations. Within GlobPermafrost project, we aim to produce a global map of permafrost temperatures and extent.

The thermal state of the ground cannot be directly inferred from spaceborne platforms with current remote sensing technologies. We overcome these limitations by combining the information content of several remote sensing products and reanalysis data, namely time series of remotely sensed land surface temperature (LST), snow cover information, land cover classification and wetness classes. These products are employed to force ground thermal model, which deliver ground temperatures and probability of permafrost occurrence within a grid cell.

Methods

We used a TTOP model (Smith & Riseborough, 1996) to calculate (MAGT) at 1 km spatial resolution for 2000-2016 time period. The main input are freezing and thawing degree days (FDD and TDD) that are multiplied with semi-empirical adjustment factors. We use MODIS land surface temperatures and downscaled ERA Interim reanalysis temperature to calculate FDD and TDD for the model (Westermann et al., 2015). Nf-factors are calculated from a snow cover that we calculated from ERA Interim precipitation and a T-index model (Hock, 2003). Rk-factors are defined based on ESA CCI (European Space Agency Climate Change Initiative) landcover product and tundra wetness classification. We ran 200 ensemble runs with varying nf and rk-factors, which represent subcell variability of snow and soil wetness according to land cover classification. A mean of ensemble runs was used for a MAGT at the top of the permafrost product. Permafrost occurrence probability is a fraction of model runs with MAGT < 0°C. The permafrost occurrence probability is reclassified to established permafrost zonation. The MAGT product was validated using the MAGT available for boreholes in GTN-P (Global Terrestrial Network for Permafrost) and TSP (Thermal State of Permafrost) database.

Results and Discussion

The permafrost area (MAGT below 0 °C) of the Northern Hemisphere covers 16.20 × 10^6 km², which is 17.0 % of the Northern Hemisphere exposed land. The permafrost region (continuous, discontinuous, sporadic zones and isolated patches zones) covers 24.15 × 10^6

km², which corresponds to 25.3 % of exposed land area. The validation with 750 boreholes resulted in root mean square of 2.0 °C. According to the borehole data, the difference between modelled and measured MAGT is smaller than 0.5 °C in Russia, Alaska and Mongolia. The modelled MAGT is for 1 °C too cold in Canada and China, whereas the modelled MAGT is too high in mountainous regions as Scandinavia, Greenland, Alps and Svalbard.

The overestimation of the MAGT in mountainous areas might be due to high snowfall as calculated by T-index model. Furthermore, the TTOP approach based on satellite-observed LST has a limited possibility to represent steep mountain slopes. An important source of uncertainty are validation data, since not every borehole has a MAGT depth information and thus doesn't necessarily represent top of the permafrost. In addition, borehole microloaction is does not necessarily represent the average 1 km cell properties used in the model.

Conclusions

The TTOP is a simple model that requires little input data therefore it was possible to run it for the whole Northern Hemisphere with the currently available input data and computational capacities. The spatial resolution of the modelling products and its accuracy can be crucial to provide permafrost thermal state and its extent information in areas not studied before.

References

Hock R., 2003. Temperature index melt modelling in mountain areas. Journal of Hydrology 282: 104-115.

Smith M. W. & Riseborough D. W. 1996. Permafrost monitoring and detection of climate change. Permafrost Periglac Process 7: 301-309.

Westermann S., Østby T.I., Gisnås K., Schuler T.V., Etzelmüller B. 2015. A ground temperature map of the North Atlantic permafrost region based on remote sensing and reanalysis data. The Cryosphere 9: 1303-1319.

Are there any intact rock glaciers in the Balkan Peninsula?

Alexandru Onaca[1]
Brigitte Magori[1]
Florina Ardelean[1]
Emil Gachev[2]
Petru Urdea[1]
Mircea Voiculescu[1]
Flavius Sîrbu[1]
[1]*West University of Timişoara, alexandru.onaca@e-uvt.ro*
[2]*South-West University „Neofit Rilski", Blagoegrad*

Abstract

A combined approach consisting in thermal monitoring and geophysical investigations was used to examine for the first time the presence/absence of permafrost in several rock glaciers in the Rila and Pirin Mountains (Bulgaria). The preliminary results indicate that patches of relict permafrost may occur at altitudes above 2400-2500 m in both mountain ranges.

Keywords: permafrost, rock glaciers, thermal monitoring, geophysical measurements, Rila and Pirin Mountains.

Introduction

Within the mountainous regions, rock glaciers are generally considered as the most visible expression of mountain permafrost occurrence (Barsch, 1996). These spectacular landforms were previously described in several massifs in the Balkan Peninsula but, so far, no research has been done on the possible occurrence of permafrost. The investigations were conducted in the Rila and Pirin Mountains, where the climatic conditions appear to favor the preservation of permafrost.

Study area

The Rila Mountains are the highest range in the entire Balkan Peninsula, reaching 2925 m, whereas the Pirin Mountains are the third highest in the south-eastern Europe, thanks to their 2915 m maximum elevation. Both ranges lie in the southwestern part of Bulgaria and experience a transition climate between the temperate continental and the Mediterranean. Above 2900 m, the mean annual air temperature (MAAT) drops to less than -2°C, whereas the precipitations are on average around 1000 mm/year. Similar climatic conditions can be found on the highest ridges of the Southern Carpathians where permafrost occurrence has been recently documented above 2000 m by several studies (Onaca et al., 2017). Unlike the Southern Carpathians, which are currently free of ice, the Pirin Mountains host the southernmost glaciers in Europe (Snezhnika and Banski Suhodol) along with several long-lasting snow/firn patches (Gachev et al., 2016).

Methodology

Due to restricted drilling possibilities, alternative methods (e.g., geophysical and ground surface temperature measurements) were used to get subsurface information regarding permafrost occurrence in Rila and Pirin Mountains. Since the bottom temperature of the winter snow cover (BTS) has proved to be an excellent indicator of the presence or absence of permafrost we have already conducted classical BTS measurements. A total number of 20 iButtons DS1922L were scattered on the surface of the selected rock glaciers in the Rila and Pirin Mountains to examine the near-surface thermal regime and to determine whether the microclimatic factors at the ground surface are suitable for hosting permafrost. Based on the recorded data from the ground-surface thermistors, the mean annual ground surface temperature (MAGST), ground freezing index, insulating snow cover duration and zero-curtain interval were calculated. In several cases, the summer temperatures of the springs seeping from the base of the rock glacier front were measured. In addition, geophysical measurements (electrical resisitivity tomography and ground penetrating radar) were performed in few sites.

Results and discussion

Rock glaciers are widespread in the alpine area of both Rila and Pirin Mountains, above 2200 m.

The results of geophysical and thermal measurements revealed that patches of relict permafrost may occur at altitudes above 2400-2500 m in Pirin and Rila Mountains. Based on our observations and measurements the sites where permafrost is probable to occur are characterized by openwork block layers of the rock glaciers, reduced income of solar radiation and a very efficient cooling effect of the blocky surface. BTS values lower than -3^0 C were measured, at sites where the mean annual ground surface temperature is around 0^0 C. Despite the thermal measurements were performed in similar conditions (e.g. coarse debris) a relatively high range in the BTS and MAGST values was measured, confirming that air circulation (e.g. convection, advection) within the coarse blocks could be responsible for these differences.

The geophysical and thermal measurements will continue for at least 3-5 consecutive years. However, forthcoming research on this topic is needed, since the possible permafrost patches could be the last frozen ground remnants in the Balkan Peninsula

Acknowledgements

This work was supported by a grant of Ministery of Research and Innovation, CNCS - UEFISCDI, project number PN-III-P1-1.1-PD-2016-0172, within PNCDI III.

References

Barsch, D., 1996. Rockglacier. Indicators for the Present and Former Geoecology in High Mountain Environments. Springer, Berlin, 331 p.

Gachev, E., Stoyanov, K., Gikov, A., 2016. Small glaciers on the Balkan Peninsula: State and changes in the last several years, 415: 33.54.

Onaca, A., Ardelean, F., Urdea, P., Magori, B., 2017. Southern Carpathian rock glaciers: Inventory, distribution and environmental controlling factors. Geomorphology, 293: 391-404.

Syrdakh River Database: A comprehensive collection of measurements for investigations of river-related impacts on permafrost

Eric Pohl[1]
Christophe Grenier[1]
Antoine Séjourné[2]
Albane Saintenoy[2]
Alexander Fedorov[3]
Pavel Konstantinov[3]
[1]*LSCE/IPSL, CEA-CNRS-UVSQ, Université Paris-Saclay, Gif-sur-Yvette, France, eric.pohl@lsce.ipsl.fr*
[2]*GEOPS/IPSL, Geosciences Paris Sud, Université Paris-Saclay, Orsay, France*
[3]*Melnikov Permafrost Institute, Siberian Branch, Russian Academy of Sciences*

Abstract

Climate warming and the associated transport of heat into the ground affect permafrost evolution. Especially for river systems, a large range of involved surface processes introduces high complexity. To quantify the resulting variability in associated permafrost evolution, a study site in form of a river valley between two thermokarst lakes was initiated in Central Yakutia in 2012. Thermal and hydraulic state variables are measured alongside active layer depths, and various soil properties. Most recently, Ground Penetrating Radar (GPR) and electrical resistivity measurements were conducted to complement existing active layer depth (ALD) records. Obtained measurements serve to calibrate and validate 1D and 2D hydro-thermal modeling. Above all, a striking inter-annual and spatial variability is apparent for active layer depths and soil temperatures. We present results from 2D modeling, utilizing the large data range of recorded soil temperatures and discuss the obtained results with our comprehensive database of active layer depth measurements.

Keywords: permafrost; database; Siberia; active layer depth; soil temperatures; numerical modeling.

Introduction

The impact of climate change on permafrost regions concerns a variety of processes and feedback mechanisms. The assessment, for example of resulting greenhouse gas emissions or changes in the biome composition is challenging due to complex interactions, including heat transfer and hydraulic flow. Limited data availability, especially at greater soil depths, prevents to derive a thorough picture of the current permafrost distribution and evolution. However, these data are needed as a basis to conceptualize, calibrate, and validate numerical physical models, which, in return, are the basis to assess how climate change will impact the evolution of permafrost and associated hydrological systems. While it has been widely noticed that lake systems have a significant impact on permafrost evolution, only recently river systems have attracted more attention (e.g. Roux *et al.,* 2017; companion submission: Fortier *et al.*).

The natural succession of permafrost landscapes and biomes under climatic changes are difficult to predict (e.g. Myers-Smith *et al.,* 2008) due to the complexity of interacting processes. River systems constitute a perfect example of the complexity due to their quick response to meteorological forcing and variable flow. The resulting heat transport in the presence or absence of such river systems, and its effects on active layer depth (ALD) and landscape evolution are thus of great interest.

In order to better understand the effects of climate warming on permafrost evolution, we have thus started to monitor a river system in Central Yakutia (Eastern Siberia) in 2012. Here we present an overview of the study site, the monitoring database and future prospects, along with preliminary results from an associated modeling of a 2D river-valley cross-section.

Syrdakh River - Field Site

The Syrdakh River, located in Central Yakutia, approximately 100 km northeast of Yakutsk, connects two thermokarst lakes over a distance of roughly 3 km (Fig. 1). In cooperation with the Melnikov Permafrost Institute (MPI), Yakutsk, a total of 13 HOBO 4-channels data loggers (model U12-008) were installed at various locations along and across the river valley in different settings to monitor soil temperatures at depths ranging between 1 m and 5 m. The data loggers are the same ones used at other field sites in Siberia (Konstantinov *et al.,* 2011). During each annual field campaign at the end of summer, soil pits are dug to take samples for determination of vertical gradients in volumetric water content, grain size distribution, and thermal properties. ALD are obtained through these pits as well, or through drilling and rod measurements. In 2017, five soil moisture probes were permanently installed in the active layer zone in two soil pits, two and six meters away from the main river channel, to capture the intra-annual soil moisture variability. A total of 13 thermistors to monitor air, water, and shallow (5 cm) soil temperature have been installed to capture the transfer of temperature from the atmosphere or water into the soil. Unmanned aerial vehicle (UAV) imagery and differential GPS points recorded in 2017 facilitate the generation of a digital elevation model serving for morphological analyses. Isotopic and geochemical sampling were conducted to study water provenance and interactions within the soil column.

A first systematic Ground Penetrating Radar (GPR) survey, partly complemented by electrical resistivity measurements, was conducted in 2017 (see companion submission: Saintenoy *et al.*) to capture ALD variability of various cross-sections along the river valley.

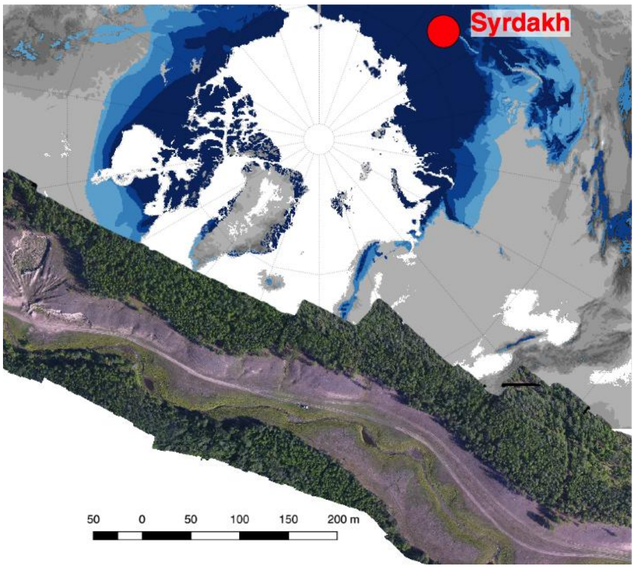

Figure 1. Syrdakh River location in continuous permafrost zone and UAV orthomosaic photo. East-West oriented river course and valley embedded in forested area.

ALD Evolution

For dissemination and application purposes, the spatially distributed data for the period between 2012 and 2017 are organized in a database. The ongoing efforts at this point concern the analysis of the complex valley ALD evolution and variability, and the development of a calibrated numerical model. Moreover, the extensive sources of measurements are suitable for a variety of future applications dealing with the active layer and permafrost zone down to 5 m depth.

ALD measurements suggest a variety of influences on ALD evolution (Fig. 2), including exposition (south vs. north), geometry of the river valley (flat vs. steep), and proximity to the river (wet vs. dry). In addition to the strong spatial variability, inter-annual variability in climate forcing and river flow adds a significant proportion of temporal variability. The modeling of the heat and water transfers along this cross-section will allow for a better understanding of the underlying complexity and the relative importance of individual factors (e.g. variability in soil thermal forcing, or soil properties).

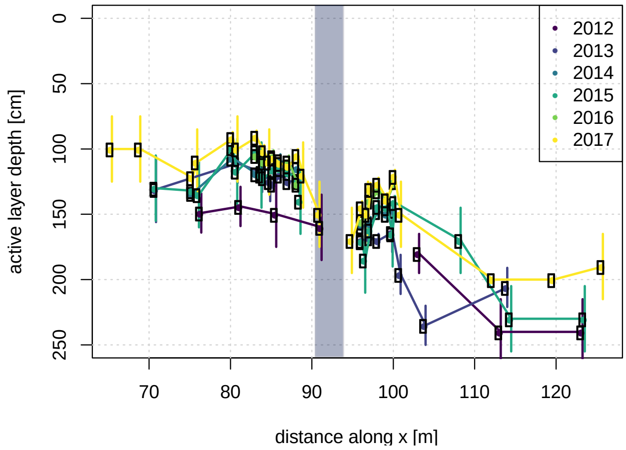

Figure 2. Active layer depth measurements at one of ten cross sections (left: north-exposed, wet; right: south-exposed, dry) for 6 years based on measurements through soil pits, bore holes, and metal rods. Blue bar indicates approximate river position. Error bars indicate measurement uncertainties.

Acknowledgements

The support of Univ. Paris-Saclay SPU Carbon Fate Emerging Project and Labex-IPSL are gratefully acknowledged.

References

Konstantinov, P., Fedorov, A., Machimura, T., Iwahana, G., Yabuki, H., Iijima, Y., and Costard, F., 2011. Use of automated recorders (data loggers) in permafrost temperature monitoring. *Earth Cryosphere*, 15(1): 23–32.

Myers-Smith, I. H., Harden, J. W., Wilmking, M., Fuller, C. C., McGuire, A. D., and Chapin III, F. S., 2008. Wetland succession in a permafrost collapse: interactions between fire and thermokarst. *Biogeosciences*, 5: 1273-1286.

Roux, N., Costard, F., and Grenier, C., 2017. Laboratory and Numerical Simulation of the Evolution of a River's Talik. *Permafrost and Periglac. Process.*, 28: 460–469.

Effect of snow layer accumulation and glacial transition in a permafrost thermal regime (Livingston Island. Antarctica)

Miguel Ramos[1,2]
Miguel Angel de Pablo[3]
Juan Javier Jiménez[1,2]
Antonio Molina[4]
Gonçalo Vieira[2]
PermaSnow team
[1]*Departamento de Física y Matemáticas, Universidad de Alcalá, Madrid, Spain, miguel.ramos@uah.es*
[2]*CEG/IGOT. Universidade de Lisboa, Portugal.*
[3]*Departamento de Geología, Geografía y Medio Ambiente, Universidad de Alcalá, Madrid, Spain.*
[4]*Centre for Astrobiology (CAB), Spanish National Institute of Aerospace Technology.*

Abstract

In polar climates, the transition from paraglacial to periglacial systems as a result of global warming has been characterized in detail. However, in this article we report the effects generated in a reverse process. We studied ground subjected to permafrost that has evolved towards a glacier environment due to local accumulation and aggradation of snow and ice. The most significant effects of thermal insulation of the ground surface layer, determined by measuring temperature distribution in the permafrost at two boreholes (15 and 25 m deep), were: a reduction in the ALT; reduced temperature dispersion at near-surface levels with respect to the MAGT; and a reduction in the difference between annual maximum and minimum soil temperatures, due to an increase in surface snow cover. Here, we report the measurements obtained on Livingstone Island (Antarctica) at two sites with different levels of surface snow cover and compare the thermal behavior observed.

Keywords: Permafrost, Thermal regime, Snow, Antarctica.

Introduction

Ground thermal regimes in polar regions where permafrost is present are studied to determine the energy balance between this system and the atmospheric boundary layer, which depends on climatic variability and the type of ground surface cover. In polar regions, where vegetation cover is scarce or non-existent, seasonal snow produces thermal insulation of the ground, which can be considered a key factor in determining the thermal behaviour of permafrost. The thermal regime of permafrost in maritime Antarctica has received increasing research attention in recent years. Since the Fourth International Polar Year (2007-08), various measuring stations have been installed on the Antarctic peninsula and nearby islands to analyse the behaviour of the active layer of permafrost (ALT), in line with the protocol of the "Circumpolar Active Layer Monitoring" (CALM) program (Vieira et al., 2010).

Our study area is located on Livingston Island (South Shetland Islands), where the Juan Carlos I Spanish Antarctic Station (Spanish initials: BAE JCI) is sited. This region has witnessed a marked rise in MAAT over the past 60 years, with variations of (~ 0.5°C/decade) since 1950, and is one of the regions where climate warming has had greatest impact worldwide. MAAT in the study area is close to the freezing point of water (-1.2ºC), any alteration in weather conditions has a profound effect on ground surface cover and the associated thermal regime. However, in recent years, a deceleration has been observed in the rise in MAAT at the study area, leading to an increase in the duration and thickness of snow cover (Turner et al., 2016). This in turn has reversed trends in the glaciers in the vicinity of the measuring stations; net mass loss has recently been replaced by a net gain. This reversal has also affected some of the lichen colonies, whereby colonization density has halted and even retreated due to the increased duration of snow cover on the bedrock (Sancho et al., 2017).

Methods

In this study, we recorded the temperature gradient in two boreholes drilled into quartzite rock subjected to permafrost (Ramos, 2009). The two sites are contiguous but present different levels of interannual snow cover and ice accumulation. One of the boreholes is sited in an area of seasonal snow on ground presenting relict geomorphological processes in the form of stone circles

(PG1). The other (PG2), is located on the margin of Hurd glacier. In 2008, this site presented a quartzite outcrop, but over the years the outcrop has become covered by several layers of interannual ice as a result of the change in climatic trends, and currently forms part of Hurd glacier (Figure 1).

This development has enabled us to monitor and compare the impact of glacier advance on the thermal state of permafrost at two sites with the same morphological, topographic and climatic characteristics. The main variable was the formation of a permanent layer of ice, with the consequent insulating effect, at one of the boreholes.

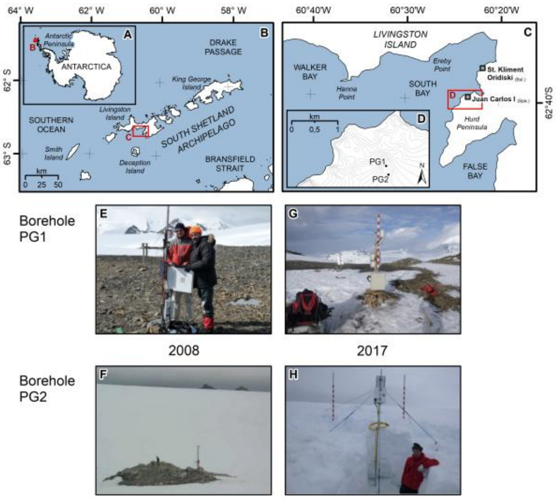

Figure 1.- Study area in the vicinity of the Juan Carlos I Spanish Antarctic Station (up). PG1 (274 m a.s.l) (medium), and PG2 (255 m a.s.l) on the margin of the glacier, after drilling in February 2008 (down-left) and in January 2017 (down-righ).

Results

The annual energy balance value for energy exchange between the ground and the atmospheric boundary layer is a function of the area between the envelopes that represent the maximum and minimum temperatures recorded during each period (Figure 2). The limits of integration of this area correspond to the temperature on the surface of the system (x = 0 m) and that at the depth of zero annual amplitude (ZAA=10±2 m), which corresponds to the depth at which the ground remains unaffected by annual temperature variations above ground. Figures 2 show the annual distribution of maximum and minimum temperatures during the study period for PG1 (25 m) and PG2 (15 m) in 2009, 2011 and 2014; shading indicates the area between the two envelopes. We can see the different evolution in the ALT and in the area between max and min temperature distribution in function of the snow/ice accumulation in PG2 respect to PG1.

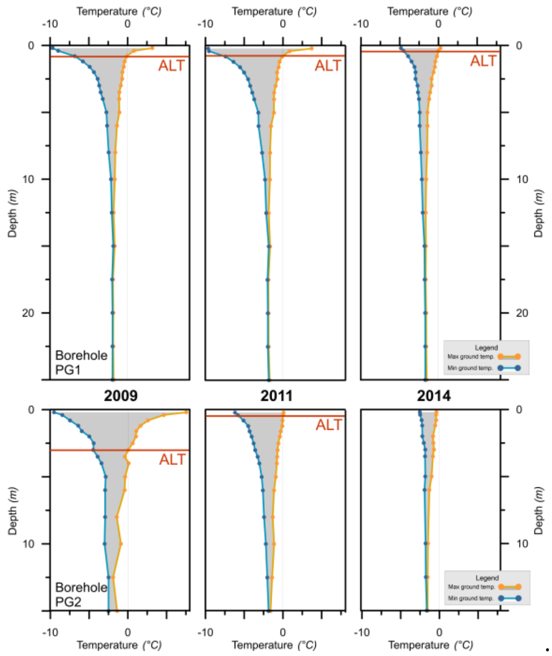

Figure 2.- Annual distribution of maximum and minimum temperatures during the study period for PG1 (25 m) and PG2 (15 m)

References

Ramos, M., Hasler, A., Vieira, G., Gruber, S., Hauck, C., 2009. Drilling and Installation of Boreholes for Permafrost Thermal Monitoring on Livingston Island in the Maritime Antarctic. *Permafrost and Periglacial Processes.* 20 (1): 57–64. DOI: 10.1002/ppp.635

Sancho, LG., Pintado, A., Navarro, F., Ramos, M., De Pablo, MA., Blanquer, J.M., Raggio, J., Valladares, F., Green, TGA.. 2017. Recent Warming and Cooling in the Antarctic Peninsula Region has Rapid and Large Effects on Lichen Vegetation. *Scientific Reports* 7. DOI: 10.1038/s41598-017-05989-4.

Turner et al. 2016. Absence of 21st century warming on Antarctic Peninsula consistent with natural variability. *Nature* 535, 411–415. DOI:10.1038/nature18645

Vieira G, et al., 2010. Thermal state of permafrost and active-layer monitoring in the Antarctic: Advances during the international polar year 2007–2009. *Permafrost and Periglacial Processes* 21: 182–197. DOI: 10.1002/ppp.685.

Ground temperature regimes and permafrost in Cierva Point (Western Antarctic Peninsula) from 2012 to 2017

Sara Ramos[1]
Gonçalo Vieira[2]
Gabriel Goyanes[2]
[1]*IGOT- Universidade de Lisboa, Portugal, sara_ramos_marin@hotmail.com*
[2]*CEG/IGOT- Universidade de Lisboa, Portugal, vieira@campus.ul.pt*

Abstract

The Western Antarctic Peninsula (WAP) has shown complex reactions to climate change in the last decades, and these are still poorly understood. In order to evaluate the changes occurring in the terrestrial environments, permafrost and active layer monitoring and modelling are essential. We evaluate the spatial distribution and thermal characteristics of permafrost in Cierva Point (Danco Coast, WAP), which will allow identifying its climate sensitivity. For that, both the ground thermal regime and the spatial distribution of permafrost are modelled using physical and GIS-based spatial models. The modelling is forced and validated with data from of eight shallow boreholes (< 4 m) and a 15 m borehole from 2012 to 2017.

Keywords: Permafrost, Active layer, temperature regime, Western Antarctic Peninsula.

Introduction

Polar permafrost is central in the Global carbon cycle and climate system (WMO, 2003). The Western Antarctic Peninsula is one of Earth's regions with strongest air temperature increase since the 1950's. However, the temperature signal is more complex than previously accounted and recent studies report a cooling in the north of the Antarctic Peninsula since 2000 (Turner et al., 2016). The complexity of the reaction of the region to climate change is still poorly understood and, in order to evaluate its consequences in the terrestrial environments dominated by the presence of permafrost, monitoring and modelling are essential.

This work is integrated in the project PERMANTAR (Permafrost and Climate Change in the Antarctic Peninsula) coordinated by CEG/IGOT - Universidade de Lisboa. The project focusses on increasing the understanding of the changes in the ice-free terrestrial environments of Western Antarctic Peninsula (WAP) and on their linkages to permafrost through systematic and long-term monitoring and modelling of ground temperature and meteorological properties.

The present research will be conducted at Cierva Point (64.10°S, 60.57°W), a highly sensitive environment to climate change. Several shallow boreholes and a deep borehole have been installed in 2012 by the CEG/IGOT and the University of Wisconsin-Madison teams at Cierva Point. The existing data series, which although discontinuous in some boreholes, allows for a very detailed analysis of the ground thermal regime and is an excellent data set for modelling the thermal regime and permafrost in the area.

Borehole data for 2012-2014 has been analysed by Wilhelm (2016) to quantify the thickness of the active layer and to model conductive energy transfer through different soil types. However, with an extra three years of data, the database has not been fully exploited, and little is known about the permafrost distribution, climate sensitivity of the area and its impacts on terrestrial ecosystem dynamics.

In this presentation we identify the spatial distribution and thermal characteristics of permafrost in Cierva Point, and assess on its climate sensitivity. For that, both the ground thermal regime and the spatial distribution of permafrost will be modelled using physical and GIS-based spatial models.

Study Area

Cierva Point (lat. 64°10'S, long. 60°57'W) is a small, ice-free peninsula on the south side of Cierva Cove located at the north end of Hughes Bay (Danco Coast, Western Antarctic Peninsula). The study area is about 1.9 km2 and is an Antarctic Specially Protected Area (ASPA), within the Antarctic Treaty, mainly due to the presence of a significant Gentoo penguin (Pygoscelis papua) rookery.

The mean annual air temperature in the area is approximately -3.2 °C and the annual precipitation ranges between 400 and 1100 mm (Wilhelm, 2016). Winter snow depths can exceed 1 m. However, during the summer most of the snow in glacier-free areas completely melts.

Methodology

The ground thermal regime and the spatial distribution of permafrost in Cierva Point are modelled, both using a physical and a spatial-based approaches.

The physical approach is based on the Temperature at the Top Temperature Of the Permafrost (TTOP) model using freezing and thawing indexes, n-factors and thermal conductivity of the ground, as factors representing ground-atmosphere interactions and providing a framework to understand the ground thermal regime and permafrost distribution. The suitability of other physical models, such as the COUP model (Scherler et al. 2013) and the H-TESSEL model, are evaluated as alternative methods to model the thermal regime of the ground.

To complement the physical modelling, a GIS-based multi-criteria methodology (see Etzelmüller et al. 2006), is used to derive an empirical permafrost distribution model. The spatial model is supported by: data from 10 boreholes from 2012 to 2017, a digital elevation model (DEM) and derived parameters such as slope, aspect, curvature, potential radiation, wetness index, a geomorphological and a landcover map derived from UAV imagery.

Acknowledgements

PERMANTAR (Permafrost and Climate Change in the Antarctic Peninsula) was funded by the Portuguese Polar Program (Fundação para a Ciência e a Tecnologia). Logistics for the field season were provided by PROPOLAR, the Instituto Antártico Argentino and the Spanish Polar Committee. Sara Ramos benefited from a grant from PROPOLAR.

References

Etzelmüller, B., Flo Heggem, E. S., Sharkhuu, N., Frauenfelder, R., Kääb, A., & Goulden, C., 2006. Mountain permafrost distribution modelling using a multi-criteria approach in the Hövsgöl area, Northern Mongolia. Permafrost and Periglacial Processes. Wiley InterScience 17: 91–104. https://doi.org/10.1002/ppp.554

Scherler, M., Hauck, C., Hoelzle, M., & Salzmann, N., 2013. Modeled sensitivity of two alpine permafrost sites to RCM-based climate scenarios. J. Geophys. Res. Earth Surface 118: 780–794. https://doi.org/10.1002/jgrf.20069

Turner, J., Lu, H.,White, I., King, J.C., Phillips, T., Scott Hosking, J., Bracegirdle, T.J.,Marshall, G.J.,Mulvaney, R., Deb, P., 2016. Absence of 21st century warming on Antarctic Pen- insula consistent with natural variability. Nature 535: 411-415. http://dx.doi.org/10.1038/ nature18645.

Wilhelm, K., & Bockheim, J., 2016. Influence of soil properties on active layer thermal propagation along the western Antarctic Peninsula. Earth surface processes and landforms. Earth Surf. Process. Landforms, 2016. https://doi.org/10.1002/esp.3926

WMO., 2003. The Second Report on the Adequacy of the Global Observing Systems for Climate, Global Climate Observing System. Geneva.

Climate warming led to the degradation of permafrost stability in the past half century over Qinghai-Tibet Plateau

Youhua Ran[1]
Xin Li[1, 2]
[1] *Cold and Arid Regions Environmental and Engineering Research Institute, Chinese Academy of Sciences, Lanzhou 730000, China, ranyh@lzb.ac.cn*
[2] *CAS Center for Excellence in Tibetan Plateau Earth Sciences, Beijing 100101, China*

Abstract

The permafrost stability degradation over Tibet in the past 50 years is evaluated base on the estimated mean annual air temperature by integrating remote sensing based land surface temperature, leaf area index, snow cover, and in situ air measurement. Results shows that the total degraded area is about 153.76×10^4 km^2, which accounting for 87.98% of the permafrost area in 1960s. The stability for 75.24% of extremely stable type, 89.56% of stable type, 90.3% of sub-stable type, 92.31% of transitional type, and 32.8% of unstable type have degraded to lower level stability. About 49.4% of unstable type and 95.95% of extremely unstable type has degraded to seasonal frozen ground. The mean elevation of extremely stable type, stable type, sub-stable type, transitional type, unstable type, and extremely unstable types have increased by 88 m, 97 m, 155 m, 185 m, 161 m, and 250 m, respectively.

Keywords: Thermal stability; Geographically weighted regression; Remote sensing; MODIS; Tibetan Plateau.

Introduction

Understanding of the degradation of permafrost stability is very important for engineering design, resource development, and environmental protection in cold regions. Monitoring and simulation show that substantial permafrost degradation is occurring on the Qinghai-Tibet Plateau (QTP). However, many previous regional studies emphasized the migration of permafrost "boundaries" change. Naturally, these boundaries are continuous, inexact representations of the permafrost distribution and permafrost degradation (Yang et al., 2010). Therefore, the objective of this study is to evaluate the degradation of permafrost stability over the QTP during the 1960 to 2010 by integrate multi-criterion remote sensing observations and an air temperature observation network.

Methods and Datasets

In this study, the degradation of permafrost stability is evaluated based on the thermal stability permafrost classification system proposed by Cheng (1984) (Table 1) and the improved mean annual air temperatures (MAAT) data over the QTP in the past half century. The MAAT in situ measurement data at 152 sites over the QTP and remote sensed data with six independent variables are combined using a Geographically Weighted Regression (GWR) model to estimate the MAAT with 1km resolution over QTP during the past five decades.

Multi remote sensing based data product include MODIS land surface temperature, the Global Land Surface Satellite (GLASS) leaf area index (LAI), smf cloud-removed MODIS fraction of snow cover (FSC) products are used in this study. The MAAT measurements at 152 stations within the QTP and the surrounding area and the mean annual ground temperature (MAGT) measurement at 142 boreholes are collected and used in this study as reference data (Fig. 1).

Figure 1. The distribution of in situ MAAT observation stations and MAGT boreholes over the QTP.

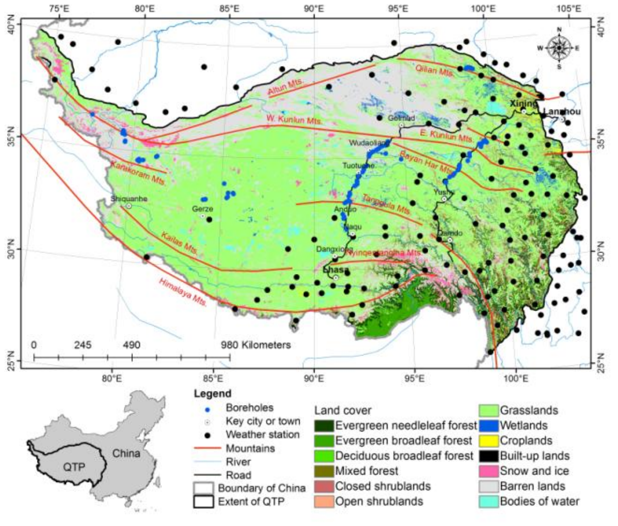

Table 1. Classification system used to assess permafrost stability (Cheng, 1984).

Code	Type	MAGT	MAAT
1	Extremely stable	<-5.0	<-8.5
2	Stable	-3.0~-5.0	-6.5~-8.5
3	Sub-stable	-1.5~-3.0	-5.0~-6.5
4	Transitional	-0.5~-1.5	-4.0~-5.0
5	Unstable	+0.5~-0.5	-2.0~-4.0
6	Extremely unstable	>+0.5	-1.0~-2.0

Preliminary results

Decadal mean MAAT estimates with a resolution of 1 km over the QTP in the past 50 years are produced using the GWR model. The mean coefficient of determination of this model is approximately 0.95. The permafrost stability map in the past five decades is then produced based on the simulated MAAT and the permafrost stability types defined in Table 1.

Thermal stability degradation

The permafrost thermal stability has degraded continuously over the past 50 years (Table 2). Specifically, the extents of the extremely stable, stable, and sub-stable types retreated from the south to the north. The extents of the transitional, unstable, and extremely unstable types extended northward correspondingly. The conversions among the thermal stability types during 1960s to 2000s can be found in Table 3. The elevation occupied by each permafrost stability type has risen continuously (Table 4).

Table 2. The area statistics of the permafrost thermal stability types over the QTP in the past 50 years (×10^4 km^2).

Type	1960s	1970s	1980s	1990s	2000s
1	12.35	8.56	8.74	5.66	3.36
2	38.59	28.30	27.64	20.91	11.53
3	34.14	34.75	34.09	31.94	24.84
4	24.73	23.95	23.59	23.39	23.55
5	44.22	43.89	43.70	46.51	48.21
6	20.73	21.05	20.54	20.16	21.63
Total area	174.76	160.50	158.32	148.57	133.10

Table 3. Transfer matrix of permafrost stability types from the 1960s to the 2000s in the QTP (%).

Type	1s	2	3	4	5	6	*SFG*
1	24.75	0.78	0.00	0.00	0.00	0.00	0.00
2	59.42	9.67	1.33	0.02	0.00	0.00	0.00
3	15.82	50.93	8.37	1.45	0.03	0.00	0.00
4	0.00	35.91	23.18	6.16	0.57	0.00	0.00
5	0.00	2.72	67.07	66.82	17.19	0.66	0.00
6	0.00	0.00	0.05	25.49	32.80	3.39	0.12
SFG	0.00	0.00	0.00	0.06	49.40	95.95	99.88

Seasonally frozen ground (SFG)

Table 4. The mean change in elevation of the permafrost thermal stability types over the QTP in the past 50 years (unit: metre).

Type	1960s	1970s	1980s	1990s	2000s
1	5240	5161	5169	5232	5328
2	5050	5052	5055	5094	5147
3	4881	4932	4937	4985	5036
4	4756	4799	4804	4859	4941
5	4614	4670	4675	4713	4775
6	4392	4503	4513	4565	4642

Validation and uncertainty analysis

The 89% of the 142 locations are consistent with the borehole survey for the permafrost extent in the 2000s. The uncertainty of the results may result primarily from the MAAT model, insufficient resolution, and the sparseness of stations, which are especially sparse in high mountain areas.

Note: This study has been submitted The Cryosphere (Ran *et al.,* 2017).

References

Cheng, G. D., 1984. Problems on zonation of high altitude permafrost. *ACTA Geographica Sinica* 39: 185–193 (in Chinese).

Ran, Y., Li, X., & Cheng, G. D. 2017. Climate warming led to the degradation of permafrost stability in the past half century over Qinghai-Tibet Plateau. *The Cryosphere Discuss* doi: 10.5194/tc-2017-120.

Yang, M., Nelson, F. E., Shiklomanov, N. I., Guo, D., & Wan, G., 2010. Permafrost degradation and its environmental effects on the Tibetan Plateau: A review of recent research. *Earth-Science Reviews* 103(1): 31-44.

Permafrost on the North Slope of Alaska may start thawing earlier than previously expected

Vladimir E. Romanovsky[1,2], Dmitry J. Nicolsky[1], Santosh K. Panda[1], Sergey S. Marchenko[1], Reginald R. Muskett[1]
[1]*University of Alaska Fairbanks, Fairbanks, AK, USA, veromanovsky@alaska.edu*
[2]*Earth Cryosphere Institute, Tyumen Scientific Centre SB RAS, Tyumen, Russia*

Abstract

In this paper we report observed changes in permafrost temperatures during the last 30 years in Alaska. The collected ground temperature data are assimilated to a high-resolution (770x770 m) stand-alone permafrost dynamics GIPL2 model that predicts active permafrost degradation on the North Slope of Alaska by the end of the 21st century and a related ground surface subsidence. At some locations, this subsidence can exceed 5 m and more.

Keywords: Permafrost temperature; modeling; talik; ground surface subsidence.

Introduction

The impact of climate warming on permafrost and the potential of climate feedbacks resulting from permafrost thawing have recently received a remarkable attention (e.g. Schaefer *et al.,* 2012; Romanovsky *et al.,* 2017). The mean annual temperature of permafrost and the thickness of the active layer (ALT) are good indicators of changing climate and therefore designated as Essential Climate Variables (ECVs) (Smith & Brown, 2009) by the Global Climate Observing System (GCOS) Program of the WMO. Climate warming promotes an increase in the permafrost temperature and ALT and affects the stability of northern ecosystems, threaten infrastructure and cause the release of carbon dioxide and methane into the atmosphere (Schuur *et al.,* 2015). The results of more than 30 years of permafrost and active layer temperature observations along an Alaskan Permafrost-Ecological Transect are presented in this paper. The same data are used to calibrate and validate a high spatial resolution model of permafrost dynamics within the North Slope of Alaska. Some results of these modeling will be presented.

Results and Discussion

Most of the research sites in our permafrost network are located along an Alaskan Permafrost-Ecological Transect. This transect spans all permafrost zones in Alaska from the southern limits of permafrost near Glennallen to the Arctic coast in the Prudhoe Bay region and further to the high Canadian Arctic. Most of the sites in Alaska show substantial warming of permafrost since the 1980s. The magnitude of warming has varied with location, but was typically from 0.5 to 3°C. However, this warming was not linear in time and not spatially uniform. While permafrost warming was more or less continuous on the North Slope of Alaska with a rate between 0.2 to 0.5°C per decade, permafrost temperatures in the Alaskan Interior started to experience a slight cooling in the 2000s that has continued during the first half of the 2010s. There are some indications that the warming trend in Alaskan Interior permafrost resumed during the last four years. Analysis of the seasonality of changes in ground temperature shows that the warming is occurring in both summer and winter, but the major part of increase occurs during the cold season. As a result, the re-freezing of the active layer takes more and more time. While the complete freeze-up of the active layer on the North Slope in the mid-1980s typically occurred in the first half of October (Romanovsky *et al.,* 2003), the typical freeze-up dates in the first half of the 2010s shifted to mid-December. In the winter of 2013-2014, an unprecedented date of freeze-up (January 15) was observed at the Deadhorse site. Thus, during the last 30 years, the average date of freeze-up increased by almost two months. If the exactly same rate of permafrost warming on the North Slope of Alaska will continue into the future the mean annual temperature at the permafrost table may reach 0°C threshold by the middle of this century (Fig. 1) and the long-term thaw of permafrost may begin.

To enhance our understanding of possible future rates and pathways of permafrost degradation and to predict the local, regional, and global consequences to human society, accurate high spatial resolution permafrost models are needed to be developed. Establishment of these models is possible only by integrating available high-resolution environmental data and by assimilation of existing field and remote sensing data and observations into these models. A high-resolution (770x770 m) stand-alone permafrost dynamics GIPL2 model is used to illustrate how changes in climate together with further industrial development of the North Slope of Alaska will affect permafrost and ecosystems in this region. Results of these modeling efforts show that under the RCP8.5 scenario by the end of the 21st century 2/3 of the permafrost area on the North Slope of Alaska may be developing taliks of various depths. This talik development process will cause the ground surface subsidence. At some locations the subsidence may be as large as 5 to 9 meters (Fig. 2) with more typical values between 0.3 and 3 meters.

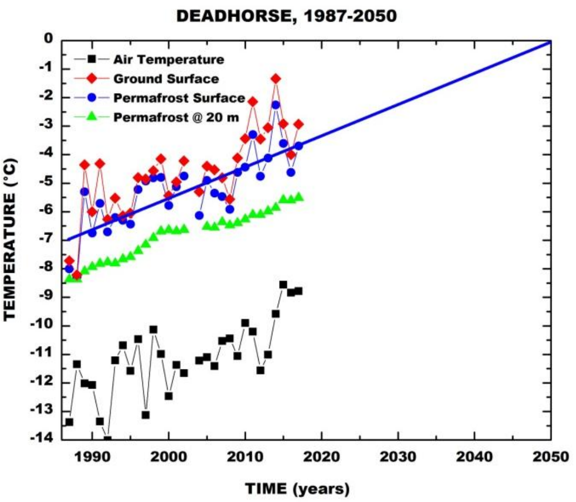

Figure 1. Mean annual temperatures of air, ground surface, permafrost surface, and permafrost at 20 m depth recorded at the Deadhorse permafrost observatory from 1987 to 2017 on the North Slope of Alaska with the linear extrapolation of permafrost surface temperature into the future.

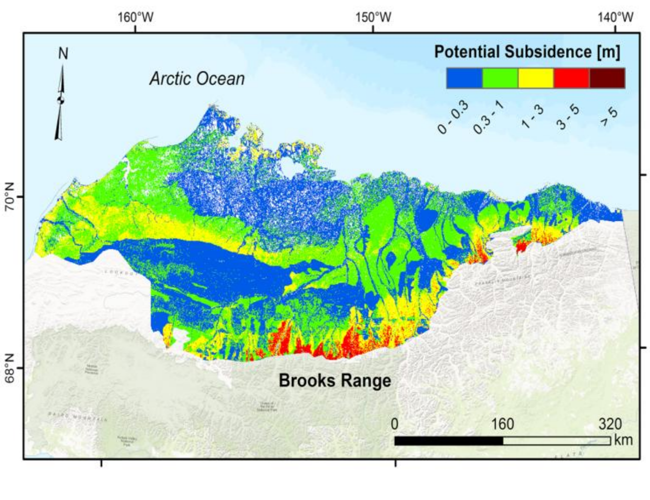

Figure 2. Thaw settlement ('subsidence') within the North Slope of Alaska between 2000 and 2090 predicted by the GIPL2 model. Simulations consisted of climate inputs based on outputs from a composite mean of five general circulation models under high-end RCP8.5 scenarios (IPCC, 2013).

References

IPCC, 2013. *Climate Change 2013: The Physical Science Basis. Contribution of Working Group I to the Fifth Assessment Report of the Intergovernmental Panel on Climate Change* [Stocker, T.F., Qin, D., Plattner, G.-K., Tignor, M., Allen, S.K., Boschung, J., Nauels, A., Xia, Y., Bex, V. & Midgley, P.M. (eds.)]. Cambridge University Press, Cambridge, United Kingdom and New York, NY, USA, 1535 pp, doi:10.1017/CBO9781107415324.

Romanovsky, V. E. et al. 2003. Temporal variations in the active layer and near-surface permafrost temperatures at the long-term observatories in Northern Alaska. In: *ICOP 2003 Permafrost: Proceedings of the 8th International Conference on Permafrost.* (Phillips, M., Springman, S. M., & Arenson, L.U. eds.) Balkema Publishers, Netherlands, pp. 989-994.

Romanovsky, V., Isaksen, K., Drozdov, D., Anisimov, O., Instanes, A., Leibman, M., McGuire, A.D., Shiklomanov, N., Smith, S., & Walker, D., 2017. [Changing permafrost and its impacts]. In: Snow, Water, Ice and Permafrost in the Arctic (SWIPA) 2017, pp. 65-102, Arctic Monitoring and Assessment Programme (AMAP), Oslo, Norway, 2017.

Schaefer, K.H. et al. 2012. Policy Implementations of Warming Permafrost, United Nations Environment Programme (UNEP), Nairobi, Kenya, 30 p.

Schuur, E.A.G. et al. 2015. Climate Change and the Permafrost Carbon Feedback, *Nature*, 520:171-179, doi:10.1038/nature14338.

Smith, S. & Brown, J. 2009. Assessment of the status of the development of the standards for the Terrestrial Essential Climate Variables - T7 - Permafrost and seasonally frozen ground.

Identification of the Active Layer Heat Exchange Mechanisms in Mountain Permafrost Conditions by using GTN-P data

Dmitrii Sergeev[1]
Irina Chesnokova [2]
[1] *Sergeev Institute of Environmental Geoscience, Russian Academy of Sciences, Moscow, Russia, sergueevdo@mail.ru*
[2] *Water Problems Institute, Russian Academy of Sciences, Moscow, Russia, ichesn@rambler.ru*

Abstract

The identification of the heat exchange mechanisms in the active layer can be obtained by direct analyzing of the ground temperature regime. The parameters of the heat waves and the time of the freezing and thawing help us to distinguish the conduction, air convection, water convection, and radiation that could be active in part of periods of seasonal cycles. This method helps to improve the ground temperature modeling.

Keywords: geothermometry; monitoring; active layer; mountain permafrost.

In various seasons, as well as in the process of freezing and thawing, temperature changes and their gradients in the ground provide enough information for identifying the processes of air and liquid convection, radiation heat transfer, and zone of phase transitions. At the same time, regime thermometric observations can be used to verify the modeling results.

As an example showing the usage of thermometric results, we refer to the comparison of seasonal temperature variations in soils of different composition in the territory of the Chara Geocryological Observatory (Sergeev *et al.,* 2007). The author carried out the measurements at various altitudes within mountain area with developed eluvial, slope, glacial and alluvial formations of different age. Combination of the obtained data with the stock data of the geotemperature monitoring, carried out by "PGO Chitageologia" and "ZabTISIZ" in 1970-80s, makes possible to analyze the territorial temperature regime formation. Such analysis shows a significant spatial spread in average ground annual temperature from one landscape to other that reaches to 8°C.

Authors compared the temperature variations in sandy-loam deposits with kurums (debris slope deposits). The main mechanisms of heat transfer in the seasonal layer on the Klyukvenniy Creek slopes (Zagryazkin Pit) are horizontal and vertical air convections, seasonal dynamics of permafrost rocks, moisture condensation on the surface of debris, radiation transfer inside he ground, and then through the contacts between fragments, conductive transfer (Fig. 1). Kurums show the maximum temperature negative shift in the active layer that reaches in some years up to -6.7°C. In winter, temperature distribution in the seasonal layer (about 2.1 m) is close to isothermal, while in summer, in a stratum of coarse clastic material, the temperature difference near the surface (conventionally accepted under the first block from the surface) and on the frozen roof amounts to 25°C.

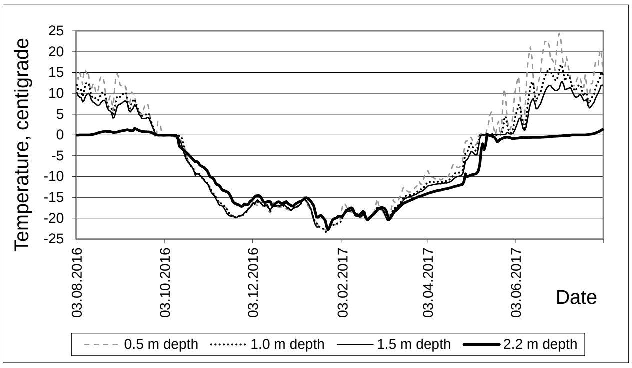

Figure 1. Air temperature variations in kurum pore space at various depths (Klyukvenniy Creek, absolute altitude is 1155 m).

Unlike kurums, temperature variations in sandy-loam stratum of fluvioglacial deposits in slope trains show that conduction is a drive mechanism of heat transfer in soil, taking into consideration the stable soil moisture in the active layer, corresponding to its complete moisture capacity (Fig. 2). Here in winter, the daily temperature cyclicity is practically not observed, in contrast to coarse-clastic formations. It is connected with phase transitions, which appear in the active layer during the most part of winter. Let's note that the temperature of the surface, covered by herb-moss vegetation, follow the air temperature, thanks to moderate thermal resistance of the snow cover, the thickness of which in the Chara basin does not exceed 0.20-0.25 m (Fig.2).

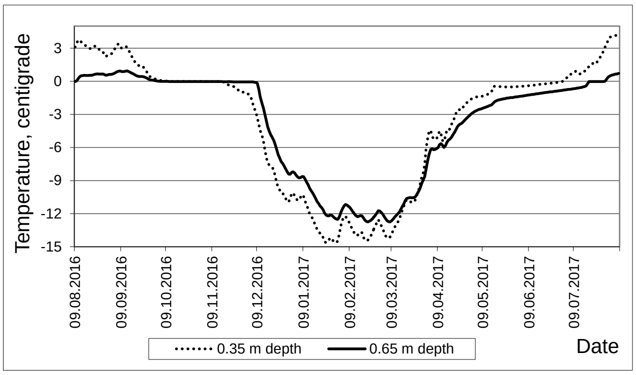

Figure 2. Ground temperature variations at different depths (Belenky Creek, absolute altitude is 728 m).

The effect of convective heat transfer due to intensive water filtration in soils is considered in the similar way (Shastkevich, 1966). The characteristic feature of such mechanism is the distinction of phases of seasonal temperature fluctuations from the common soil conditions, or even isothermal distribution of positive temperature values at significant intervals of the vertical borehole section.

The fulfilled analysis made possible to prepare a recommendation for making special geocryological maps, the legend of which should be based on leading heat transfer types in the active layer (conduction, air convection, water convection, radiation).

Most of the commonly used calculation formulas and instruments for the quantitative modeling of the temperature regime in soils cannot take into account of the convection or condensation in open soil pores, especially since these mechanisms are realized seasonally, depending upon the meteorological conditions and evolution of the structure of soils (kurums were colmated and washed during the evolution of ground water runoff). In this case it is recommended to introduce empirical amendments that may be corrected by the results of direct monitoring observations in geocryological stationaries.

Acknowledgments

The author thanks Professor V.E. Romanovsky for long-term support of geocryological monitoring works. The investigation was also carried out with financial participation of the Russian Foundation for Basic Research; grant #16-05-00200.

References

1. Sergeev D.O., Ukhova Yu..A., Stanilovskaya Yu.V., Romanovskii V.E., 2007. Temperature regime of permafrost strata and the seasonal layer in the mountains of the North Transbaikal Region (resumption of stationary observations) *Earth's Cryosphere,* V. XI, #2, p. 19-26 (in Russian)

2. Shastkevich Yu.G. , 1966. Permafrost rocks in the mountain part of the Udokan Ridge and conditions of their temperature regime formation, *In: Geocryological conditions in the Northern Transbaikalian region.* M.: Nauka, p. 24-43 (in Russian).

Temporal Variability of the Active-Layer Thickness on the North Slope of Alaska

Nikolay I. Shiklomanov[1]
Frederick E. Nelson[2]
Dmitry A. Streletskiy[1]
Anna E. Klene[3]

[1]Department of Geography, The George Washington University, USA. shiklom@gwu.edu
[2]Department of Earth, Environmental, and Geographical Sciences, Northern Michigan University, USA
[3]Department of Geography, University of Montana, USA

Abstract

The Circumpolar Active Layer Monitoring (CALM) program is a network of sites at which data about active-layer thickness (ALT) and dynamics are collected. CALM was established in the early 1990s to observe and detect the long-term response of the active layer and near-surface permafrost to changes and variations in climatic conditions. In this study we used data from 23 years (1995-2017) of extensive, spatially oriented field observations at CALM sites in northern Alaska to examine landscape-specific spatial and temporal trends in active-layer thickness.

Keywords: Active-layer thickness, Alaska, long-term monitoring, Circumpolar Active-Layer Monitoring (CALM), Global Terrestrial Network – Permafrost (GTN-P)

Study Sites

The 24 CALM sites located on Alaska's North Slope constitute a comprehensive observation network incorporating georeferenced and surveyed monitoring sites. These sites are representative of local and/or landscape level environmental conditions (e.g., topography, vegetation, soils). This approach facilitates analysis of geographical active-layer patterns and temporal trends at a range of spatial scales, from local to regional. The sites are located in two dominant North Slope physiographic provinces: the Arctic Coastal Plain and the Arctic Foothlls. They are arranged in two parallel north-south transects along the regional bioclimatic gradient. Beginning in the 1990s, the active layer has been probed manually at least once per summer at eight 1 km² grids, representative of generalized conditions found in each of the physiographic provinces, as well as at 16 1 ha plots established in relatively homogenous landscape categories the same physiographic provinces.

Methodology

Procedures involve pushing a metal rod, calibrated in cm, to the point of refusal, interpreted in most cases to be the frost table. At the 1 km² sites, the sampling protocol is based on a square array of surveyed permanent stakes separated by 100 m, yielding a 121 point array of equally spaced nodes on each grid. At the 1 ha sites the measurements were obtained by probing at 5 m intervals along the plot's two perpendicular and one diagonal transect, resulting in 71 points per plot per probing date. The date of maximum annual thaw can vary from year to year and between sites, making it difficult to detect the maximum annual active-layer thickness by mechanical probing. To insure consistency, annual thaw depth measurements at each site are performed during the same week of each year. The specific time of observations varies between sites, but falls within the mid-August to early-September interval, when thaw depth nears its maximum. All North Slope sites have data loggers for monitoring air and soil temperatures. In 2000, a spatially oriented program of monitoring frost heave and thaw subsidence using Differential Global Positioning System (DGPS) was initiated at three sites representing broad landscape units characteristic of the North Slope of Alaska.

Long-Term Active Layer Trends

Long-term trends of ALT observations, averaged over the Arctic Coastal Plain and the Arctic Foothills and corresponding trends in degree-days of thawing (DDT) are shown in Figure 1. The data are shown for each of the two North Slope transects. Both show a positive ALT trend over the 23-year period of record. These trends correspond to an increase in accumulated summer warmth, reflected by the increase in annual DDT. Despite relatively similar degree-day trends for all areas considered in this analysis, the rate of active-layer increases varied. The highest rate of active-layer increase of 0.5 cm/yr was observed at the Atqasuk site, representing the southern Coastal Plain in the western transect. The northern Coastal Plain showed the smallest rate (0.1 cm/yr) of the active-layer increase. The differences in ALT trends are attributable to variability in surface and subsurface conditions.

Trends in Thaw Settlement

Results from DGPS measurements of the vertical position of the ground surface, integrated over landscape units characteristic of the Coastal Plain and Foothills, indicate pronounced (up to 10 cm) long-term (2002-2017) thaw settlement. Subsidence resulted from soil consolidation accompanying penetration of thaw into the ice-rich stratum at the base of the active layer. However, the settlement is not monotonic but is instead predominantly achieved in years with unusually warm summers. Analysis of relations between DDT and active-layer thickness indicate that the correlations between these variables are generally better when thaw subsidence is added to the active-layer record.

Acknowledgments

The components of the CALM program operating in Alaska and Russia were partially supported by the U.S. National Science Foundation's Office of Polar Programs under grants OPP-9732051 to the University of Cincinnati, OPP-0352958 to the University of Delaware, and ARC-1002119 and PLR-1304555 to The George Washington University. Logistical support was provided by CH2M HILL POLAR SERVICES. Opinions, findings, conclusions, and recommendations expressed in this paper do not necessarily reflect the views of NSF.

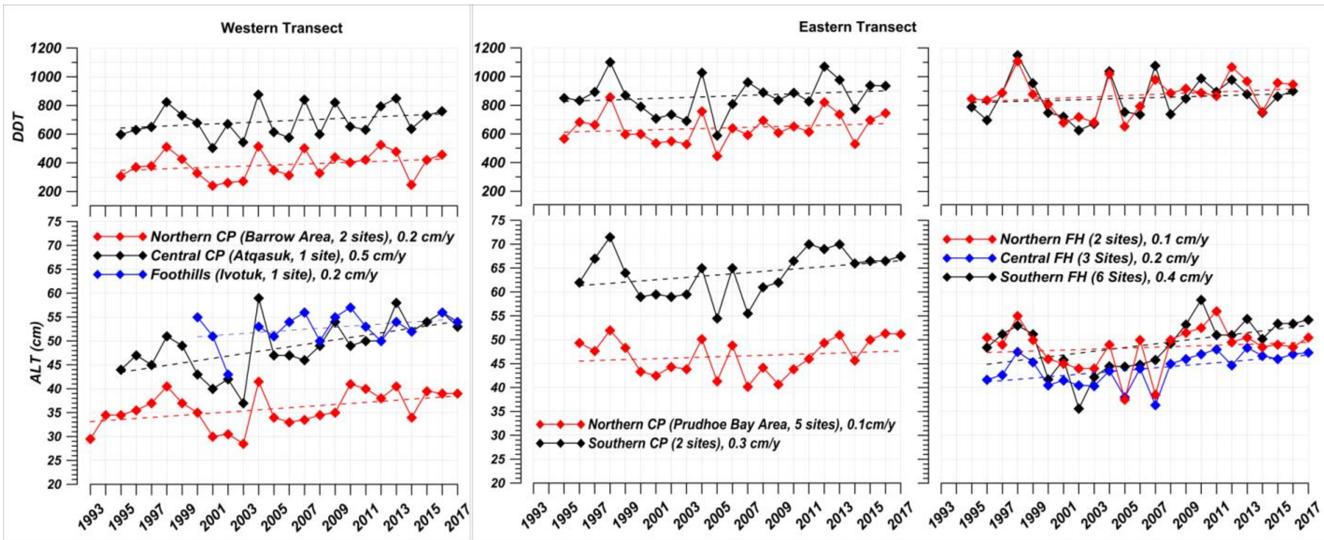

Figure 1: Long-term degree-day and active-layer thickness trends for two latitudinal transects through the North Slope of Alaska. Data are presented as averages for all CALM sites located within the two North Slope physiographic provinces: Arctic Coastal Plain (CP) and Arctic Foothills (FH). Estimates of long-term active-layer trends (in cm/year) are provided.

New data on the permafrost thermal regime near Yakutsk

Valentin Spektor[1], Alexander Kholodov[2], Georgii Maksimov[1], Susan Natali[3], Varvara Andreeva[1], Sarah Ludwig[3], Christina Minions[3]
[1]*Melnikov Permafrost Institute, Siberian Branch of Russian Academy of Sciences, Yakutsk, Russia, valentin_spektor@mail.ru*
[2]*University of Alaska, Fairbanks, AK, USA*
[3]*Woods Hole Research Center, Woods Hole, MA, USA*

Abstract

To obtain more precise data on the permafrost thermal regime in the layer of annual temperature variations, three new boreholes were equipped near Yakutsk and Pokrovsk cities. In the result, the depths of zero annual temperature variations has been corrected for different lithology and landscape conditions. New data on temperature variations at the depths of 0, 5, 10, 15, and 21 m were obtained at the basis of 6-hours measurements for the period of 2015-2017.

Keywords: thermal state; permafrost; Central Yakutia; Eastern Siberia

The problem of permafrost temperature increase is of critical importance for the densely populated and widely involved in an economic activity territory of Central Yakutia (Eastern Siberia, RF). In fact, the mean annual air temperature has increased up to −8.7 °C, with the trend of 0.07 °C per year (Skachkov, 2012). On the one hand, the rise of permafrost temperature results in increase of seasonal thaw, which is leading, especially in the presence of ice complex, to thermokarst (Fedorov & Konstantinov, 2009). On the other hand, permafrost with temperatures higher than −2 °C may transform from a solidly frozen to a plastic frozen state which inevitably leads to hazards for construction and exploitation of engineering structures (Spektor et al., 2017). According to the data of multi-year research, ground temperatures at the depth of zero annual variations in natural conditions of Central Yakutia vary from −0.5 to −6 °C depending on landscape type (Skryabin et al., 1998).

To obtain more precise data on the ground thermal state in the layer of annual temperature variations based on frequent automatic observations, in cooperation with the Project of Thermal State Permafrost, we equipped 3 new boreholes near cities Yakutsk and Pokrovsk in 2015 (Fig. 1). The boreholes are located along the submeridional section of the Lena River valley; the distance between the extreme points is ~ 100 km.

BH 15/1 (208 m a.s.l.), 27 m in depth, is located at the Tabaga cape of the Prilenskoe Plateau (N61°49.1′, E129°32.3′) in a birch-larch forest. The upper part (to the depth of 9.3 m) of the section is composed of Late Pleistocene ice complex, underlain by sands of Pleistocene, Neogene and Jurassic age.

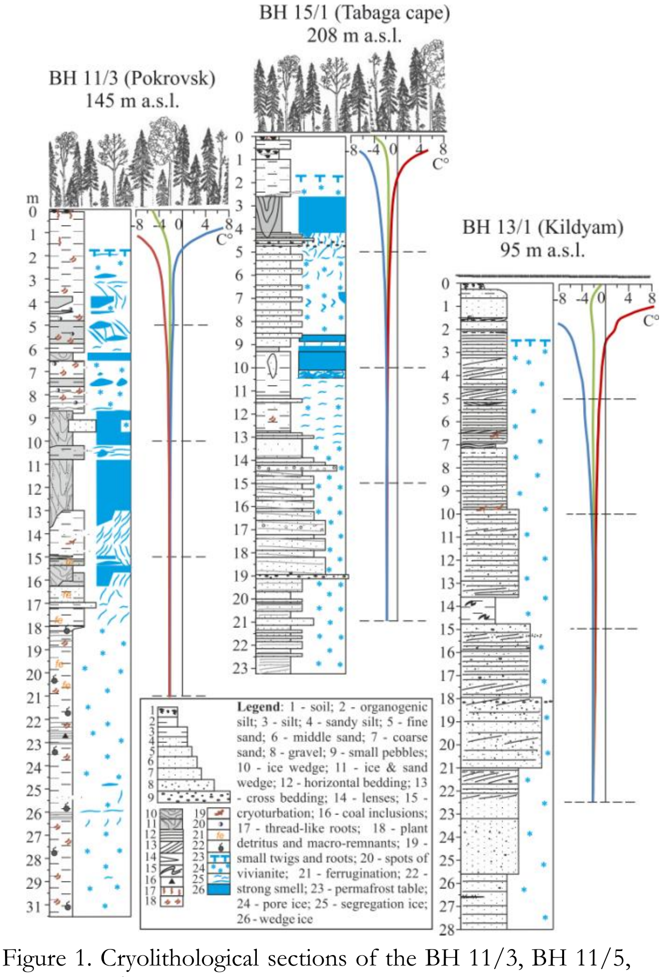

Figure 1. Cryolithological sections of the BH 11/3, BH 11/5, and BH 13/1. The graphs represent the maximum (blue lines),

minimum (red), and mean (green) ground temperatures for the period of observations.

BH 11/3 (145 m a.s.l.), 31 m in depth, is located at the Pokrovsk terrace (N61°28.4′, E129°04.7′), interalas area with a mixed larch-birch forest. Ice complex (to the depth of 17 m) and lacustrine silts underlie the surface.

BH 15/2 (95 m a.s.l.), 21 m in depth, was drilled at the surface of the first terrace above the flooplain, in the Tuimaada valley (N62°17.5′, E129°49.9′). The surface with grass meadow vegetation and scarce bushes is underlain by the Holocene alluvial sediments of the Lena River (to the depth of 18 m), lying on Jurassic sandstones (Spektor et al., 2008).

The boreholes are equipped with 4-channel loggers Hobo U12-008. Temperature sensors are placed, on average, at depths of 5, 10, 15, and 21 m. In addition, 2-channel loggers Hobo U23-003 are installed on the ground surface and in the seasonally thaw layer. The interval between measurements is 6 hours. It should be noted that the logger in the BH 15/2 had broken down temporary in 2016. Therefore, we use for analysis our data on the **BH 13/1**, which is located in 650 m, at the same surface. These data were obtained using logger thermistor chain produced in the Melnikov Permafrost Institute; the measurements had been performed several times per year in 2013, and every 12 hours in 2014-2016.

In July 2017, a terrestrial survey was done near each borehole. It included measurements of seasonal thaw depth, detailed descriptions of vegetation and upper soil horizon.

The results of temperature analysis are illustrated in the Fig. 2 at the example of the data from the BH 15/1.

The depth of zero annual temperature variations is defined where temperature variations make up less than one tenth of a degree. Main results concerning depths of seasonal thaw (DST), depths of zero annual temperature variations (DZV), and temperatures (TZV) at those depths are summarized in Table 1.

Table 1. Seasonal thaw depths and temperatures at the depths of zero annual variations.

Borehole	m a.s.l.	DST, m	DZV, m	TZV, °C
BH15/1 Tabaga	208	2.4	21	−1.72
BH11/3 Pokrovsk	145	1.9	21	−1.99
BH13/1 Kildyam	95	2.5	22.5	−2.15

The lowest (−2.15 °C) temperature, which is observed in the BH 13/1, may be due to 1) the northernmost location, 2) dense and thin snowcover at the open surface, and 3) winter temperature inversion. The highest temperature (−1.72 °C) in the BH 15/1 is likely associated with predominance of birch in the mixed forest forming a relatively thick leaf litter. Furthermore, forests, where BH 15/1 and BH 11/3 are located, favour snow accumulation, and thus have an insulating effect.

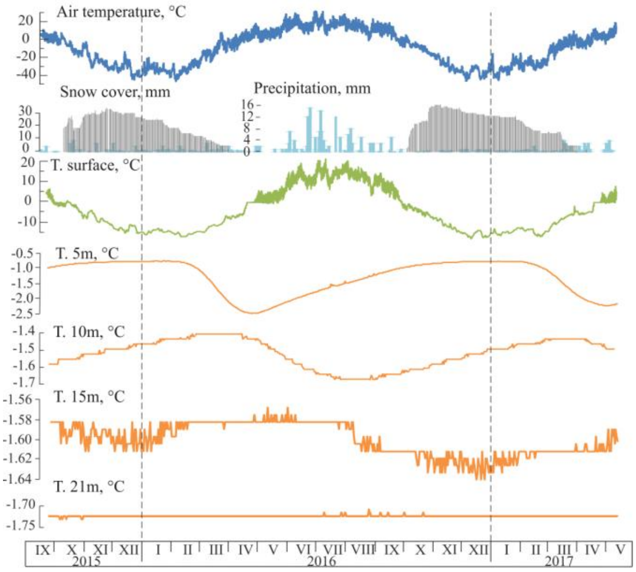

Figure 2. Interannual variability of the near-surface air temperature, ground temperatures in the BH 15/1 at the depths of 0, 5, 10, 15 and 21 m, snow cover and precipitation for the period of observations.

References

Fedorov, A.N. & Konstantinov, P.Ya. 2009. Response of permafrost landscapes of Central Yakutia on current changes of climate and anthropogenic impacts. *Geografia I Prirodnye Resursy* 2: 56-62.

Spektor, V.B., Shestakova, A.A., Torgovkin, Ya.I., Spektor, V.V. 2017. An Engineering-geological map of the Republic Sakha (Yakutia). *Engineering Geology* 2: pp. 28-37.

Spektor, V.V., Bakulina, N.T., Spektor, V.B. 2008. Relief and age of the Lena River alluvial cover at the "Yakutskii Razboi". *Geomorphologiya* 1: 87-94.

Skryabin, P.N., Varlamov, S.P., Skachkov, Yu.B. 1998. *Interannual variability of the ground thermal regime near Yakutsk*. Novosibirsk: SB RAS, 144 p.

Skachkov, Yu.B. 2012. Climate variability in Yakutia on the cusp of 20th and 21st centuries. *Proceedings of the Fourth conference of geocryologists in Russia*. Moscow State University, Russia 7-9 June 2011: 312-318.

Standards for long-term mountain permafrost monitoring

Benno Staub[1]
Jeannette Noetzli[2]
[1]*University of Fribourg, Department of Geosciences, office@permos.ch*
[2]*WSL Institute for Snow and Avalanche Research SLF*

Abstract

The strategy and methods of permafrost monitoring in the frame of the Swiss Permafrost Monitoring Network PERMOS were re-evaluated in 2017 based on 15 years of experience and following the strategic priorities 2017–2022 of GCOS Switzerland. The evaluation was performed in two workshops, where enhancements for the measurement setup were discussed and standardization of technical and organizational aspects regarding maintenance, data processing and communication was initiated. It is a considerable challenge to deliver reliable, robust and comparable measurements over decades, which requires professional instrumentation and maintenance of the stations and a well-defined data flow from the logger over data processing and archiving to analyses and visualization. For this, best practice guidelines are currently being elaborated for the observation variables ground and surface temperature, rock glacier creep and changes in ice content.

Keywords: long-term monitoring; mountain permafrost; observation strategy; best practice guidelines.

Introduction

The Swiss Permafrost Monitoring Network PERMOS documents the state and changes of permafrost in the Swiss Alps since 2000 and develop from an unconsolidated and science driven collection of permafrost research sites. PERMOS is implemented in the national and international monitoring structures (the latter as part of the Global Terrestrial Network for Permafrost GTN-P). The main objective is the systematic long-term observation of state and changes of permafrost in the Swiss Alps. Ground temperatures are measured in boreholes and near the surface, changes in ice content using electrical resistivity tomography as well as permafrost creep rates of rock glaciers. These key variables are measured at up to 30 locations in different regions and landforms. The spatially and temporally heterogeneous terrain – and hence snow and ground characteristics – ask for large samples to representatively describe mountain permafrost. At the same time the environment is harsh, rapidly changing and may pose safety issues e.g. due to rock fall or avalanches, which limites the lifetime of the measurement infrastructure. Particularly borehole installations on moving terrain are at risk when the thermistor chains are blocked or sheared off.

Evaluation 2017

The strategic priorities of GCOS Switzerland 2017-2026 define that Essential Climate Variables (ECVs, e.g. permafrost) as well as the monitoring networks and methods shall undergo a regular evaluation. The first evaluation of the PERMOS monitoring sites took place in 2007 after completion of the PERMOS pilot phase (2000–2006). A second evaluation round was initiated for 2017 to discuss and refine the monitoring strategy after more than 15 years of experience. The PERMOS Scientific Committee (SciCom) reviewed the monitoring aims and variables at two workshops and discussed possible enhancements for the measurement setup and propositions to standardize technical and organizational aspects. Moreover, the monitoring strategy was analyzed for conformity with the GCOS monitoring principles and the new GCOS implementation plan. The GCOS monitoring principles imply that new installations should focus on data-poor regions or poorly-observed parameters, a suitable period of overlap for the replacement of observing systems is required, and that the quality and homogeneity of data should be assessed as a part of routine observations.

General requirements for the Swiss permafrost monitoring

The requirements for a Swiss permafrost monitoring service for scientific as well as policy-related question are:

- *Scientific suitability and accuracy:* The observations must follow defined goals, be relevant and integrative. They describe either physical processes of interest or a related proxy, and enable answering basic questions on state and changes of permafrost. The records shall be interpretable with high certainty and uncertainties should be quantifiable.

- *Long-term feasibility*: The observations must be repeatable under the same conditions over long time periods (i.e., decades). The measurement techniques should be cost-efficient and robust in harsh high mountain environments as well as calibrated and comparable. A coherent measurement setup is future-oriented to include new findings, variables and sites from research when considered ready or appropriate.
- *Open access data:* resulting data should be open access for non-commercial use. The data should be made accessible to the public as well as submitted to international data centers.
- *Products:* useful and understandable assessment of the results obtained in the network should be delivered to scientists, practitioners, public authorities and the public in a suitable way or channel.

Chances and risks for long-term monitoring

Professionalization by standardization

The most urgent need to further develop and professionalize the PERMOS network were identified in the standardization of the key tasks of the monitoring network: the site installations and maintenance, the documentation of the instrumentation as well as the station history, and a standardized data flow from data acquisition over processing, quality control and archiving to visualization and publication. This applies to all monitoring variables. Best practice and guideline documents are being elaborated for borehole measurements, near-surface ground temperature monitoring, electrical resistivity tomography monitoring and terrestrial geodetic surveying for the monitoring of creep velocities. These guidelines will be made available on the PERMOS website www.permos.ch.

In addition to the improvement of comparability and the documentation of workflows, the standardization of key tasks aims at making the permafrost monitoring more resilient and less dependent on individual persons. Since the start of the PERMOS network, a high number of field activities involve a significant voluntary part based on few principal investigators and corresponding institutions. The dedicated community is one of the greatest strengths, but also a major risk for PERMOS. Therefore, encouraging academic junior staff to become involved in permafrost monitoring has high priority.

How to secure ground temperature monitoring over decades?

Many of the PERMOS boreholes were drilled in the frame of research projects. Several installations have now reached 10 or more years of age. Issues with deformation of the casing, blocking of thermistor chains, or the intrusion of water into the borehole arise. Several of the boreholes therefore will soon or do already require re-calibration or renewal of the thermistor chain, new logging or communication systems, or even complete re-installation with a newly drilled borehole The latter is for example the case when thermistor chains are unreliable and blocked. Re-drilling under high (financial) effort in order to secure long-term measurements furthermore bears the risk to meet differing thermal conditions than in the original borehole due to the high lateral variability in steep mountain terrain.

Priorities of sites and standards must be clearly and transparently defined in order to best allocate the available resources of the network. Sound criteria for the evaluation of the sites as well as a priority list were defined to assess the relevance of a particular installation for permafrost monitoring in general as well as for a specific region or landform. The length, quality and homogeneity of the already available data were weighted very high. Existing stations and time series have priority over new monitoring activities and sites. Only well-established monitoring techniques and instrumentation are used. Applying proven procedures and establishing best practice guidelines can optimize the long-term success of the monitoring activities.

Perspectives for long-term permafrost monitoring

The best practice guidelines developed in the frame of PERMOS can be a basis for standardizing permafrost observations in other permafrost regions. PERMOS is in exchanging experience and data with other national or international permafrost monitoring networks.

Acknowledgments

The evaluation of the PERMOS Network as well as the elaboration of best practice guidelines were based on the precious contribution of many PERMOS principal investigators and the PERMOS Scientific Committee.

Results of active layer monitoring at CALM sites with ground penetrating radar

Maria Sudakova[1]
Marat Sadurtdinov[2]
Andrei Skvortsov[2]
Andrei Tsarev[2]
Galina Malkova[2]

[1] *Earth Cryosphere Institute, Tyumen Scientific Centre SB RAS, Tyumen, Russia, Lomonosov Moscow State University, Moscow*
m.s.sudakova@yandex.ru
[2] *Earth Cryosphere Institute Tyumen Scientific Centre SB RAS, Tyumen, Russia*

Abstract

In this study we demonstrate the results of Ground Penetrating Radar (GPR) application obtained during multifaceted geocryological studies at two CALM (Circumpolar Active Layer Monitoring) sites in 2015 -2017 located in the North of the Nenets District in the delta of the Pechora River. At both sites geological cross-sections consisted of sand and peat which are a favorable material for the GPR signal propagation. At both CALM sites a correlation between annual air and ground temperatures and the thawing depth is observed. At Kashin site a correlation between annual air and ground temperatures and the moisture content is observed. At the Kumzha site thin lenses of frozen material in the active layer were observed in 2015 and 2017, but not in 2016. At the Kumzha site, maximum changes in ALT are currently observed under former roads.

Keywords: GPR, permafrost, monitoring, active layer, multi-offset GPR.

Introduction

The permafrost is a complex multicomponent media whose reaction to climate change is not always single-valued and easily predictable. Understanding of the processes in permafrost and their dependence on climatic changes are only possible through a long-term monitoring. The CALM (Circumpolar Active Layer Monitoring) program is one of these international monitoring programs which are devoted to the active layer thickness (ALT) measurements. These measurements are made once a year at the same sites over a grid of different sizes.

A recent increase in ALT at our sites in north-west Siberia made it problematic to use a traditional technique that employs a standard metal probe. If ALT on the site is increased and now is more than 1.5 m in this case the ground penetrating radar (GPR) technique can be used to estimate the ALT. GPR can also be used to obtain some additional information about soil structure, presence or absence of ice lenses and taliks, and the water content in the active layer. The effectiveness of GPR in permafrost research corresponds to a great contrast in dielectric properties of air, water and ice (frozen and unfrozen sediment). These dielectric properties of subsurface material can be measured using the GPR technique. Previous research has demonstrated the effectiveness of GPR for active layer thickness measurements (Sudakova et. al, 2017) and talik delineation (Brosten et al., 2006).

In this study we demonstrate the GPR results obtained in 2015-2017 during multifaceted geocryological studies at CALM sites on Kashin Island (CALM R24A-1) and within the Kumzha area (CALM R24A-2). These areas are located in the North of the Nenets District in the delta of the Pechora River (Figure 1). Geological cross-sections at both sites consist of sand and peat which are a favorable material for the GPR signal penetration.

At the Kashin Island site the ALT does not exceed 150 cm. At the Kumzha site ALT is more than 150 cm and a talik up to 8-9 m depth from the surface was observed in the northeastern part of this site. During the end of the 1970s, an exploration drilling site in the Kumzhinskoye field was located within the Kumzha area. Even now, traces of technogenesis still can be observed: off-road tracks, excavations, polluted soils, and other disturbances.

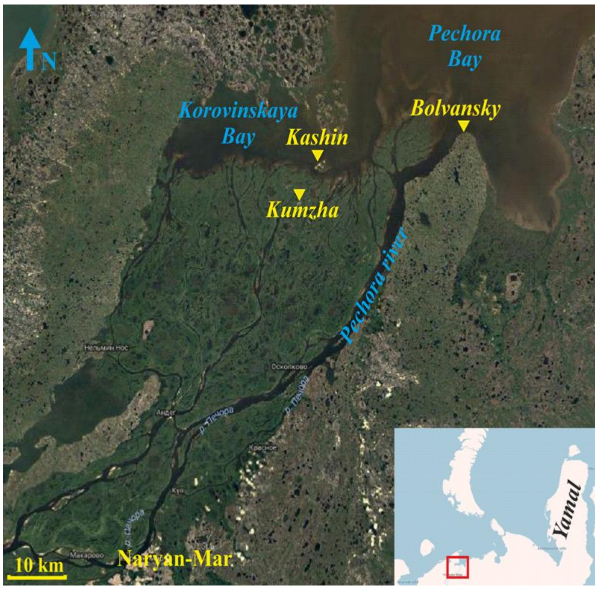

Figure 1. Kashin and Kumzha research sites map.

Methods

Research methods are chronologically listed in Table 1. In different years we used GPR profiling and a wide angle reflection with multiple offsets method, seismic refraction and reflection methods, metal stick ALT measurements, water content gravimetric measurements, and temperature measurements on the surface and in the boreholes. GPR research was conducted with "Zond-12e" radar (Radar Inc., Riga, Latvia) with a 300 MHz bowtie antenna. Electromagnetic (EM) velocities in the Kashin Island site within the active layer were recalculated into dielectric permittivity, and the permittivity into volumetric water content according to Topp's formula (Topp et al., 1980).

Table 1. Research methods we used at two CALM sites in 2015-2017.

Year	Kashin (CALM R24A-1)	Kumzha (CALM R24A-2)
2015	GPR profiling ALT direct measurements Water content gravimetric measurements Temperature measurements	GPR profiling Seismic profiling Temperature measurements
2016	GPR profiling ALT direct measurements Temperature measurements	GPR profiling Seismic profiling Temperature measurements
2017	GPR profiling ALT direct measurements Water content gravimetric measurements Temperature measurements	GPR profiling GPR wide angle (multiply offsets) survey Seismic profiling Temperature measurements

Results

The results from the Kashin Island site include maps of ALT in 2015-2017, the near-surface layer (20 cm) water content obtained by direct measurements in 2015 and in 2017, and the active layer (20 - 140 cm) volumetric water content obtained by GPR in 2015-2017. GPR results from the Kumzha site include maps of the ALT in 2015-2017 and the map of the active layer EM velocities in 2017.

At both CALM sites a correlation was observed between mean annual air and ground temperatures and the thawing depth. At Kashin site a correlation was observed between annual air and ground temperatures and the moisture content. At the Kumzha site thin lenses of frozen sediment in the active layer were observed in 2015 and 2017, although not in 2016. At the Kumzha site, the maximum changes in ALT are observed under former roads.

Acknowledgments

This work was supported by the international projects CALM and TSP, RSF grant 16-07-00102.

References

Brosten, T.R., Bradford, J.H., McNamara, J.P., Zarnetske, J.P., Gooseff, M.N., Bowden, B.W., 2006. Profiles of temporal thaw depths beneath two Arctic stream types using ground-penetrating radar. *Permafrost and Periglacial Processes* 17, 341–355.

Sudakova, M.S., Sadurtdinov, M.R., Malkova, G.V., Skvortsov, A.G., Tsarev, A.M., 2017. Application of ground penetrating radar in permafrost investigations. *Earth Cryosphere*, Vol.21, N.3, 69-82

Topp, G.C., Davis, J.L. & Annan, A.P., 1980. Electromagnetic determination of soil water content: measurements in coaxial transmission lines. *Water Resource Research*, Vol. 16, 574-582.

Extracting the time signal in surface velocity changes along 3 decades at Laurichard rock glacier (French Alps)

Emmanuel Thibert[1]
Mylène Bonnefoy-Demongeot[1]
François Finance[2]
Xavier Bodin[2]
[1] *Université Grenoble Alpes, Irstea, UR ETGR, 2 rue de la Papeterie-BP 76, F-38402 St-Martin-d'Hères, France, emmanuel.thibert@irstea.fr*
[2] *Université Grenoble- Alpes, CNRS, Université Savoie Mont-Blanc, EDYTEM, 73000 Chambéry, France*

Abstract

The Laurichard active rock glacier is the permafrost-related landform with the longest record of surface velocity in France from 1984 up to 2017 providing a spatial-temporal dataset of annual rocks displacements (13 velocity point-measurements x 26 years). The time signal from such data set is expected to be related to year-to-year changes in climate conditions. Extracting this signal is developed here in the framework of variance analysis (ANOVA) with a simple linear model. We identify that the mean velocity of the glacier (0.84 m/yr) has a year-to-year variation of ±0.24 m/yr, and the distribution of the measurements points at the rock-glacier surface provides a spatial variability of ±0.23 m/yr. The time signal extracted from the model which is the same at all point-measurements has a glacier-wide significance and provides the best possible estimate of the overall rock glacier response to climate drivers.

Keywords: Rock glacier dynamics, surface velocity, spatial and temporal variabilities, variance decomposition.

Introduction

Rock glaciers are creeping mixtures of ice and debris that exist mainly in areas of discontinuous permafrost in dry mountains (Haeberli, 1985). The thermal inertia of permafrost and the slow motion of rock glaciers lead them rather to react to long-term climatic trends. In search of that link, identifying the time response of the glacier dynamics is a prior that analyzed in this study.

Study site

The Combe de Laurichard is a well-investigated area of mountain permafrost located in the southern French Alps (Fig. 1). The main active rock glacier, RGL1 (Francou and Reynaud, 1992) extends from the rooting zone (2650 m asl.) to 2450 m asl. It is 490-m long, between 80 and 200-m wide, has an apparent thickness of 20–30 m and displays morphological features typical of an active landform.

Methods

Blocks positions and velocities

Surface velocities are derived from annual point measurements of painted rock displacements. We used in this study the initial longitudinal profile of 13 rocks set up in 1983 which provides the longest record of velocities (L1 to L13; Fig. 1; Francou and Reynaud, 1992; Bodin et al., 2009). Block positions were measured with a Total Station from 1983 to 2013, and with a geodetic differential GPS since 2012.

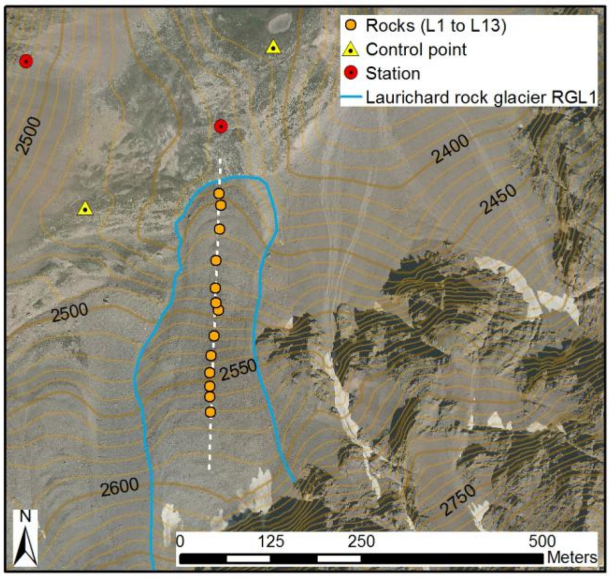

Figure 1. Location of surface velocity measurement points (painted rocks) along the longitudinal profile of Laurichard Glacier, topographic station and control points.

Variance analysis

Figure 2 plots the profiles of velocities for the 13 painted rocks between 1984 and 2017. Mean annual velocities ranging within 0.2-2.0 m/yr ±0.34 m/yr are typical for surface movements induced by deep-seated creep of ice-rich debris. A typical result one can identify from Fig. 2 is that altitude profiles, $v(z,t)$, of velocities at year t vary from year-to-year by an amount $\Delta b(t)$ that is almost constant over the entire profile. This can be written:

$$v(z,t) = \alpha(z) + \Delta\beta(t)\,, \qquad (1)$$

where $\alpha(z)$ is a specific function that can be integrated over the glacier altitude range to give the long-term glacier average velocity (0.84±0.23 m/yr). The time signal $\Delta\beta(t)$ (deviations from the mean) is the same at all point-measurements and has therefore a glacier-wide significance. Its changes (±0.24 m/yr) provide the best possible estimate of the overall rock glacier response to the climate drivers (Fig. 3). Only ±0.1 m/yr of variance remains unexplained by this linear model which is acceptable regarding measurement errors. This variance decomposition can be summed up as:

$$\langle v_{z,t} \rangle \pm 0.34 = \overbrace{0.84 \pm 0.23}^{\text{space}}\ \overbrace{\pm 0.24}^{\text{time}}\ \overbrace{\pm 0.10}^{\text{residual}}\ \text{m/yr}$$

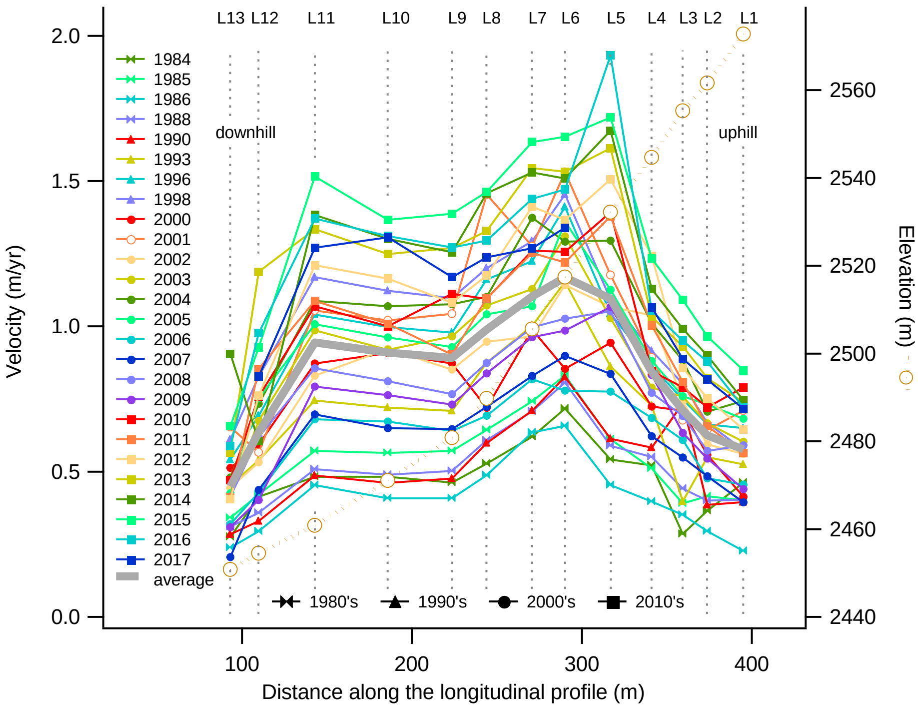

Figure 2. Annual velocities and velocity average spatial structure along the longitudinal profile from 1984 to 2017.

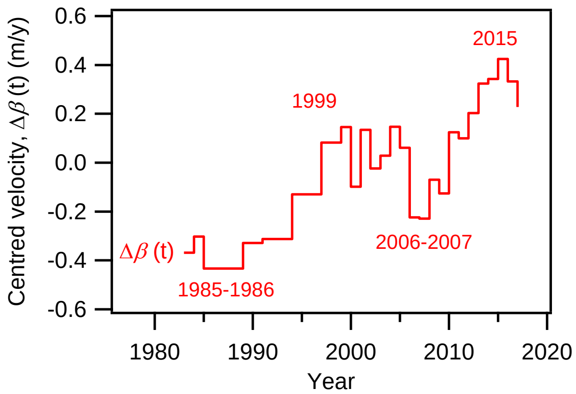

Figure 3. Velocity changes ($\Delta\beta(t)$ = deviations from the mean) resulting from the variance decomposition and representing the common time response (glacier-wide) at all measurement points. This time signal provides the best possible estimate of the glacier-wide response in surface velocity to the climate drivers.

Acknowledgments

The Ecrins National Park is deeply acknowledged for its support in funding and helping field surveys since the early 2000's.

References

Bodin X., Thibert E., Fabre D., Ribolini A., Schoeneich P., Francou B., Reynaud L., Fort M., 2009. Two Decades of Responses (1986–2006) to Climate by the Laurichard Rock Glacier, French Alps. *Permafrost and Periglacial Processes* 20, 331–344.

Francou B, Reynaud L., 1992. Ten years of surficial velocities on a rock glacier (Laurichard, French Alps). *Permafrost and Periglacial Processes* 3: 209–213.

Haeberli, W., 1985. Creep of Mountain Permafrost: Internal Structure and Flow of Alpine Rock Glaciers. Mitteilungen der VAW, ETH: Zürich; 142 pp.

Environmental controls on ground temperatures in Labrador, northeast Canada

Robert G. Way[1,2]
Antoni G. Lewkowicz[2]
[1]*Labrador Institute, Memorial University, Happy Valley-Goose Bay, Canada, robert.way@mun.ca*
[2]*Department of Geography, Environment and Geomatics, University of Ottawa, Ottawa, Canada*

Abstract

Data from 83 monitoring stations across Labrador, 17 with permafrost, were used to analyze the interrelationships of key variables in the temperature at the top of permafrost (TTOP) model. Snow depth, not mean annual air temperature, was the strongest climatic influence on temperatures at the ground surface and at the base of the annual freeze-thaw layer, and its variability strongly related to land cover class. A critical late-winter snow depth of 70 cm or more was sufficient to prevent the formation of permafrost at monitoring sites which meant that permafrost was typically absent beneath forest but present in some tundra and bedrock locations. Testing of land cover datasets for model parameterization gave errors in ground surface temperature ranging from ±0.9-2.1°C. These results highlight the importance of local field data and high-quality land cover datasets for permafrost modelling.

Keywords: TTOP; discontinuous permafrost; n-factors; snow; modelling; ground temperature

Introduction

We report on climatic and other parameters relevant to the temperature at the top of permafrost model (TTOP) (Smith and Riseborough, 2002) collected at 83 locations in Labrador (northeast Canada). Sampled environments include Subarctic boreal forest, high Subarctic Tundra and coastal Arctic mountains, and comprise of the only recent field measurements of permafrost in Labrador. This study examines relations between field observations and environmental variables, and evaluates modelling uncertainties when using gridded datasets.

Labrador includes a range of climatic zones with mean annual air temperatures varying from +1.5°C to -9°C. 60% of Labrador is forested while nearly 30% is alpine tundra, high subarctic tundra or low Arctic tundra. The remaining area is evenly divided between coastal barrens and wetlands. Regional surficial materials include glacial tills, glaciomarine sediments and exposed or concealed bedrock. Prior modelling estimated that permafrost underlies ~15% of Labrador with the lowest probabilities in southern Labrador forests (<0.1%) and the highest probabilities (>90%) in northern coastal mountains (Way and Lewkowicz, 2016; Fig. 1).

Methods

Climate monitoring stations (n=37) were established between 2012-2015 with most of these stations still active in 2017 (Fig. 1). These stations recorded shielded air temperatures, ground surface temperatures (GSTs), shallow ground temperatures (up to 125 cm depth) and snow depth using the ibutton method. GSTs were also acquired from 31 locations across an elevational transect in the Mealy Mountains (eastern Labrador) from Jacobs et al (2014). Air and GST data were also obtained for six Parks Canada monitoring locations (2010-2016) in the Torngat Mountains National Park. The entire GST dataset (83 locations) was comprised of forest (n=27), forest-tundra transitions (n=17), palsa bogs (n=5), exposed rock (n=7), low and high shrubs (n=6) and alpine or coastal tundra (n=21).

Ground temperatures were measured at ~40 sites at depths that often exceeded the position of the freeze-thaw layer, therefore corrections for sensor position were required to represent mean annual ground temperature (MAGT) equivalent to those produced with the TTOP model. Correspondingly, freeze-thaw layer depths were estimated using ground temperature gradients (°C/cm) recorded between the surface and the deepest thermistor in March and August. At seasonally frozen sites, the March freezing depth was assumed to be near the base of seasonal frost penetration while at permafrost sites, the August thaw depth was used. MAGTs were then determined by linearly extrapolating annual ground temperature gradients (°C/cm) to the estimated top of perennially frozen/unfrozen ground. Temperatures recorded near the depth of the bedrock were taken to be the MAGT (i.e., rk was assumed to be 1; Smith and Riseborough, 2002).

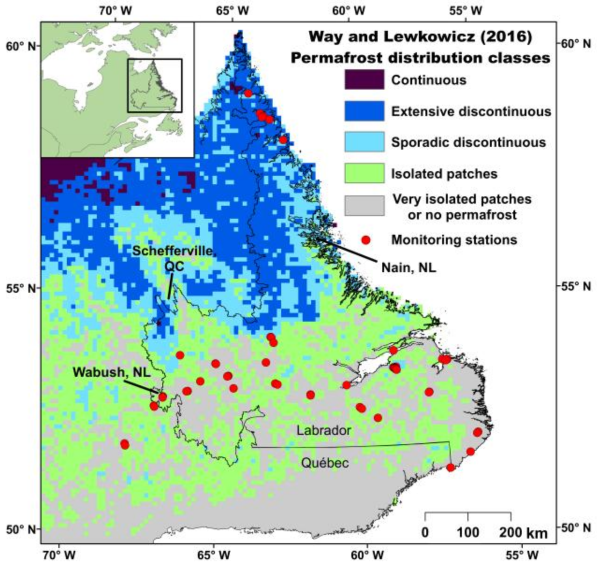

Figure 1. Monitoring stations superimposed on a regional permafrost distribution map by Way & Lewkowicz (2016).

Results and Conclusions

Differences in freezing and thawing season parameters observed at monitoring sites were strongly linked to land cover types, albeit with considerable inter-site variability for less vegetated environments. Permafrost was absent at forested and heavily vegetated locations but was generally present at tundra and rock sites (Fig. 2). The absence of permafrost beneath forest, despite the cold climate, was the result of deep snow accumulation, with most locations having twice the minimum depth of late-winter snow necessary to prevent permafrost formation (Way & Lewkowicz, *in press*). In contrast, late-winter snow depths at rock and tundra sites were typically shallow enough to permit deep frost penetration and permafrost presence, and very shallow snow depths coupled with large thermal offsets allowed permafrost to exist in palsa bogs (Fig. 2).

Comparison with other empirical field studies from permafrost environments showed that the association between late-winter snow depth and freezing n-factors is consistently curvilinear but contains considerable variability. Model tests suggest that the use of geographically-limited field datasets for characterizing these relations can result in average errors of ±1°C when applied to other regions. Further analysis of the suitability of gridded environmental datasets for parameterizing permafrost spatial modelling showed an average overall error of ±1.5°C (range: ±0.9°C to ±2.1°C). These data suggest that careful analysis of land cover datasets is needed prior to their use for spatial modelling of mean annual ground temperatures.

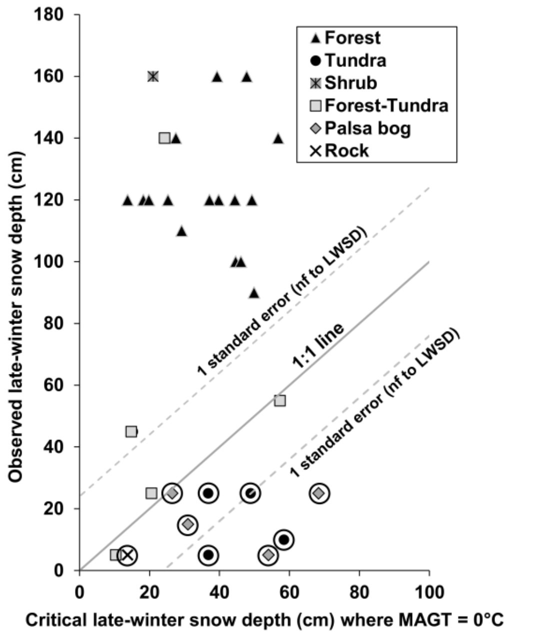

Figure 2. Late-winter snow depths recorded at monitoring stations and calculated critical late-winter snow depths for permafrost occurrence. Sites above 1:1 line should be absent of permafrost. Circled sites are those with have permafrost.

Acknowledgments

We thank D. Whitaker, J. Jacobs and L. Hermanutz for monitoring station data and field assistants A. Brooker, M. Duguay and C. Lapalme. RGW received financial support from the W. Garfield Weston Foundation, RCGS and NSTP. RGW and AGL received funding from NSERC and the University of Ottawa.

References

Smith, M.W. & Riseborough, D.W. 2002. Climate and the limits of permafrost: a zonal analysis. *Permafrost and Periglacial Processes* 13: 1-15.

Way, R.G. & Lewkowicz, A.G., 2016. Modelling the spatial distribution of permafrost in Labrador-Ungava using the temperature at the top of permafrost. *Canadian Journal of Earth Sciences* 53: 1010-1028.

Way, R.G. & Lewkowicz, A.G., *in press*. Environmental controls on ground temperature and permafrost in Labrador, northeast Canada. *Permafrost and Periglacial Processes*.

Comparing frost table depth with vegetation cover, snow, and microtopography using 3500 frost probe measurements from a shrub-tundra site

Evan James Wilcox[1]
Dawn Keim[2]
Philip Marsh[1]
[1] *Cold Regions Research Centre, Wilfrid Laurier University, Waterloo, Canada, wilc0150@mylaurier.ca*
[2] *Global Institute for Water Security, University of Saskatchewan, Saskatoon, Canada*

Abstract

Currently large-scale models simulate active layer thickness (ALT) and frost table depth (FTD) changes as uniform across the landscape, while in reality multiple factors such as microtopography, snow and vegetation cover exert a strong control on ALT and FTD at the metre scale. To assess the impact of these factors on ALT and FTD, 3500 FTD measurements were taken in a 1km² hummocky shrub-tundra headwater catchment in 2015. Results showed a seasonal shift in frost table topography between hummocks and inter-hummocks, but the magnitude of the shift differed between different vegetation covers. ALT and FTD was related to snow free date independent of vegetation cover, however vegetation cover strongly influences snow free date. These results highlight the need for the inclusion of snow and shrub distribution into large-scale models for accurate prediction of future ALT.

Keywords: frost table depth; active layer; hummocks; shrub-tundra; snow

Introduction

Climate variables control active layer thickness (ALT) and the seasonal evolution of frost table depth (FTD) at a circumpolar scale. On a local scale, "micro-scale variables" can modify ALT and FTD across a few meters (Bonnaventure & Lamoureux, 2013). The highly variable nature of ALT and FTD across such small spatial scales causes difficulties when representing it at larger scales using *in situ* measurements or modelling. However, it is necessary in order to accurately predict subsurface flow patterns, ALT response, and therefore carbon release (Painter *et al.*, 2013). In this study, the effect of snow, vegetation cover, and mineral-earth hummocks on ALT and FTD at a fine scale is evaluated using frost probe measurements.

Methods

Measurements took place within a 1km² headwater basin (68.5°N, 133.75°W) heterogeneously covered by mineral-earth hummocks with a porous organic inter-hummock zone, an end of winter snow pack ranging from 40cm to >3m, and shrub or open tundra vegetation covers (*Betula glandulosa* (Birch)*, Alnus viridis* ssp. *Fruticose* (Alder)*, Salix* spp. (Channel Shrubs) (Lantz *et al.,* 2010). FTD was measured eight times between June and August of 2015 at 10 sampling locations comprised of 40 FTD measurement points each. FTD, hummock height and frost table topography was measured in hummocks and the adjacent inter-hummock zone at 5 m intervals at each location (Fig. 1).

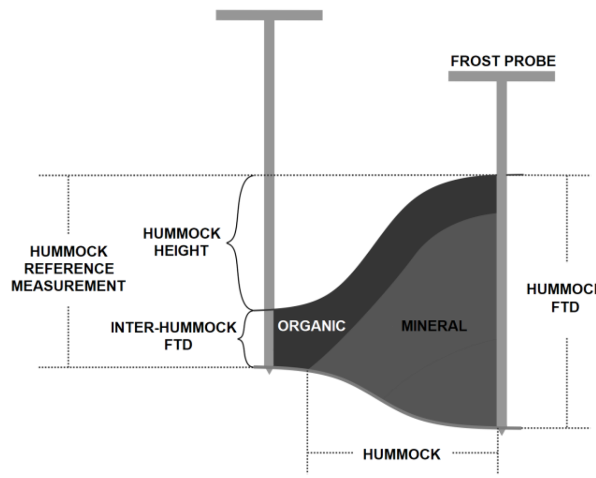

Figure 1. Frost-table depth sampling method in hummocks and adjacent inter-hummock zones.

An unmanned aerial system was used to determine snow free date for each sampling point. Dominant vegetation cover was delineated from an orthomosaic taken in Fall 2015. Scheffé multiple comparison tests were applied to ANOVA's which compared FTD to snow free date and vegetation cover to determine the influence of these variables on FTD throughout the measurement period.

Results and Discussion

While hummock FTD was consistently deeper than inter-hummock FTD during the year, the topography of the frost table shifted mid-summer. Initially the frost table beneath inter-hummocks was below the frost table of hummocks, until July when frost "bowls" began to form beneath hummocks (Fig. 2). The timing and size of bowls beneath hummocks controls the ability of hummocks to store soil water and attenuate subsurface runoff, which preferentially flows through the inter-hummock zone. Hummock bowls have been observed before and correlated to active hummock development (Kokelj *et al.,* 2007), but the spatial distribution of hummocks has not been explored in this region. With bowl depth as a proxy for hummock development, alder and birch-covered areas have better developed hummocks than tundra or stream channels, as indicated by the larger discrepancy between end of season hummock and inter-hummock FTD (Fig. 2).

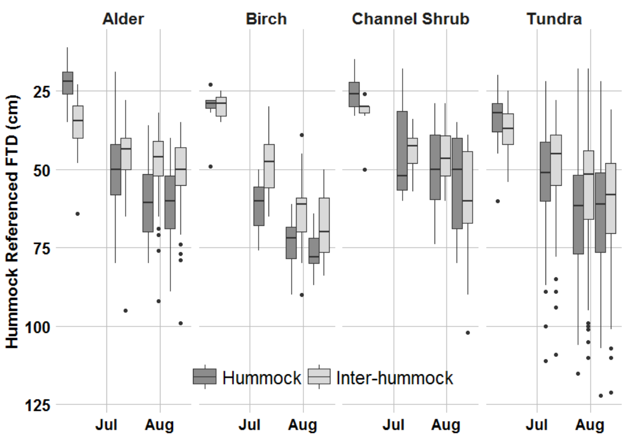

Figure 2. FTD measured from the top of the hummock. Four sampling periods were removed for easier visualization.

Snow had a significant effect on FTD, independent of vegetation cover (Table 1), however the two do not vary independently (Fig. 3). Birch covered areas became snow free weeks earlier than some alder areas (Fig. 3). Birches protruding through the snowpack, lowering albedo and conducting heat into the snowpack, possibly cause this. Alders mostly grow along hillslopes, trap drifting snow, and become buried. FTD and ALT was shallowest in stream channels, which are densely vegetated. Modeled ALT in the same basin predicted stream channels to have the deepest ALT, but the model excluded vegetation (Endrizzi *et al.*, 2011). This demonstrates the effect of dense vegetation cover on ALT.

Table 1. Mean of all FTD measurements per vegetation cover and snow-free date

		Mean Frost Table Depth & (Scheffé Group)			
Snow Free Date	May 8-11	43.1(a)	43.7(a)		
	May 11-17		34.2(b)	34.5(b)	32.9(b)
	> May 17		34.4(b)	34.8(b)	
		Birch	Tundra	Alder	Channel

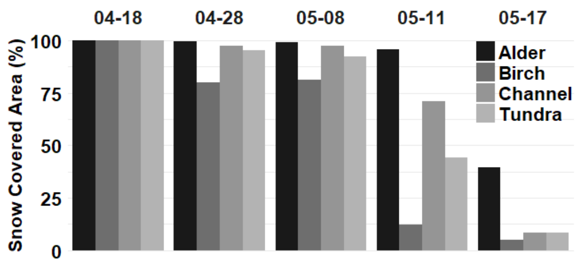

Figure 3. Snow covered area during the melt period.

Conclusions

Vegetation influences FTD and ALT through its effect on snow redistribution and melt. Snow distribution and shrub expansion patterns must be included into large-scale models in order to predict ALT. We must also focus on describing the spatial distribution of hummocks, as they exert a large control on FTD and ALT, and consequently subsurface flow.

Acknowledgments

Aurora Research Institute, Branden Walker, Tyler de Jong, Will Woodley, Andrew Ireson, NSERC.

References

Bonnaventure, P.P. & Lamoureux, S.F. 2013. The active layer: A conceptual review of monitoring, modelling techniques and changes in a warming climate. *Progress in Physical Geography* 37 : 352–376.

Endrizzi, S., Quinton, W.L. & Marsh, P. 2011. Modelling the spatial pattern of ground thaw in a small basin in the arctic tundra. *The Cryosphere Discussions* 5 : 367–400.

Kokelj, S.V., Burn, C.R. & Tarnocai, C. 2007. The Structure and Dynamics of Earth Hummocks Subarctic Forest Northwest Canada. *Arctic and Alpine Research* 39 : 99–109.

Painter, S.L., Moulton, J.D. & Wilson, C.J. 2013. Modeling challenges for predicting hydrologic response to degrading permafrost. *Hydrogeology Journal* 21 : 221–224.

Investigation on the effect of sand cover on permafrost in Tibet Plateau

Wenbing Yu[1,2]
Lin Chen[3]
Ming Guo[1]
Weibo Liu[1]
[1]*State Key Laboratory of Frozen Soil Engineering, Northwest Institute of Eco-environment and Resources, CAS, Lanzhou 730000, China, yuwb@lzb.ac.cn*
[2] *College of Civil Engineering, Chongqing Jiaotong University, Chongqing 400074, China*
[3] *Cold regions geomorphology and geotechnical laboratory, Department of Geography, University of Montreal, Montreal, H2V 2B8, Canada*

Abstract

Degradation of permafrost and desertification of land are serious in the Cryosphere of Tibet Plateau. The causal relationship between them is controversial. Drillings and field observations were conducted to state this issue at the desertification area of Tibet Plateau. Also, laboratory experiments are performed to investigate the effect of different ground surface types on ground thermal regimes, considering solar radiation and precipitation. There are 9 cases are examined in total. Factors, such as the water contents and the thickness of sand cover, the type of grass cover are considered. Field observation shows there is no permafrost beneath the old sand dunes and permafrost exists beneath the sand gravel soil. Laboratory experiments show the ground temperature, covered by grass, is cooler than that of the bare and sand covered ground. The sand cover has a function of insulation. Evidences show that desertification of land would cause degradation of permafrost.

Keywords: Tibet Plateau; Permafrost; Desertification; Field observation; Experiment

Introduction

Permafrost is a product of long-term energy exchange between ground surface and atmosphere. Desertification of land is serious under the scenarios of climate warming and human disturbance in permafrost regions on Tibet Plateau. Sand sediment of land is one of the key factors that affect permafrost. This issue has been seizing the attention of scientists. There are three conclusions on the effect of aeolian sand on permafrost: i) aeolian sand accelerate the degradation of permafrost (Huang *et al.*, 1993); ii) the thin sand layer coverage could protecting the permafrost and the thick sand coverage accelerating the thawing of permafrost (Wang *et al.*, 2002; Lv *et al.*, 2008); iii) the sand layers play a role in protecting the permafrost (Xie *et al.*,2015). In this abstract, data obtained from the field and laboratory are analyzed to state the relationship between sand sediment and permafrost at Tibet Plateau, China.

Site descriptions and methodology

Physical setting

The field data analyzed in this paper come from the Red Ridge River, Tibet Plateau, China. It is in sanded-permafrost area. Red Ridge River is an area of sand and desertification in the Qinghai Tibet engineering corridor. The river is seasonal. Only in the case of continuous rainfall, there is water flow in the river in summer. The elevation is about 4600 m. The annual mean air temperature in this area is -4.7 ^{o}C. The annual precipitation is about 340 mm. There is no snow cover in winter. Vegetation is low and extremely sparse.

Methodology

Methods used for permafrost investigation at Red ridge river area in this abstract include drilling, in-situ temperature monitoring. Thermistors were used to monitor the ground temperature. The thermistor cable was installed in a sealed PVC tube, which was inserted into the borehole after the drilling. The gap between the soil wall and the tube is filled with sand.

For the laboratory experiments, nine cases are examined in a big model experiment box. Each model is 100 cm (H) x 60 cm (D) x 55 cm (W) cm. There are insulation plates at the four sides and bottom of each model to avoid thermal interference among the models and ambient. The air temperature, radiation, and precipitation can be controlled in the box. All the experiments were performed at the same time to insure same ambient conditions. The mean air temperature is -

3.2 °C. Each period is 15 days and four periods were conducted.

Results and Analyses

Thermal profiles of the field drilling boreholes

There are 7 drilling boreholes' ground temperatures are measured in total, in which five are covered by different thickness sand and two is sand-free. Two boreholes' thermal profiles are shown herein to stand for the two kinds of ground surface type (Fig.1).

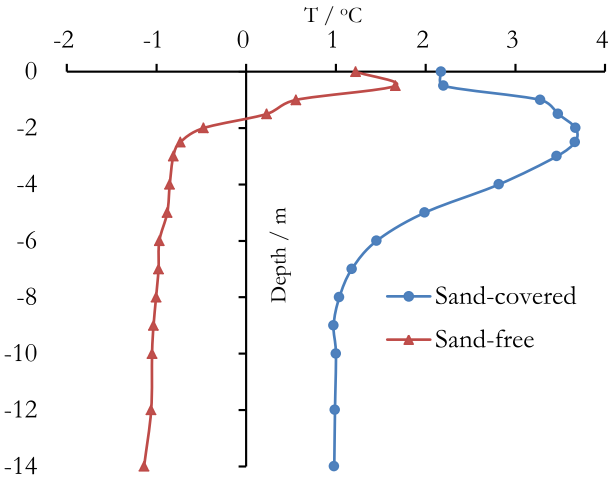

Figure 1. Thermal profiles of the field drilling holes

It shows that there is no permafrost at this site. In fact, it is as the same as the other four sand covered sites. The ground temperature is near to 1.3 °C at 14 m in depth.

Fig.1 shows the site where there is no sand cover has permafrost. Also, the other sand free site has permafrost. The ground temperature is near to -1.3 °C at 14 m in depth.

Experiments of influence of sand on heat transfer

Fig.2 presents the heat flux of different experiment cases.

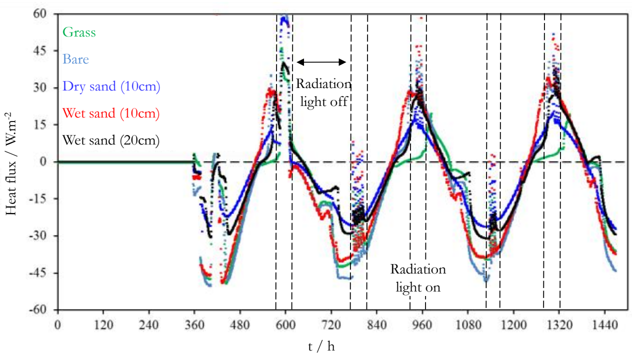

Figure 2. Heat flux of different cases

The heat flux plates (HFP01) were installed near the soil surface of each experiment model. The positive value is heat absorption, and the negative value means heat release. The total heat flux inputting /outgoing through the sand cover is smaller than other cases. The sand cover acts as a function of insulation. The heat flux of wet sand is larger than that of dry sand.

The temperatures are monitored along the depth direction of the experimental models. One depth's temperature is presented in Fig.3. It shows that grass has a strong effect of solar radiation shield. The sand covered soil is warmer than the grass covered soil.

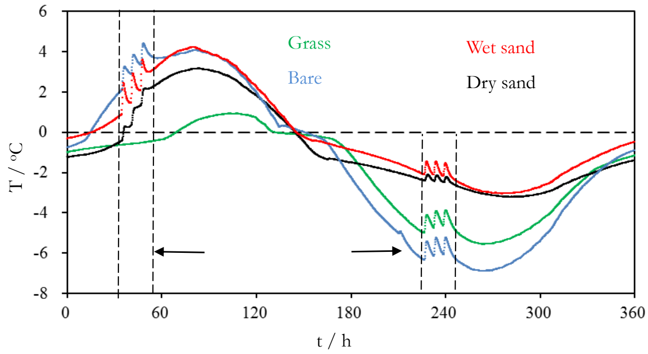

Figure 3. Temperature at 10 cm in depth

Conclusions

Field data reals that there is no permafrost under the sand cover, but it exists at the sand free sites. This proves that sand cover is not conducive to the formation of permafrost. Laboratory experiments show that permafrost will be degraded if grass is replaced by sand.

References

Huang, Y. Z. *et al.*, 1993. The Desertification in the Permafrost Region of Qinghai-Xizang Plateau and Its Influences on Enviorment. *Journal of Glaciology and Geocryology* 15: 52–57.

Lv, L. Z., *et al.*, 2008. Dual influences of local environmental variables on ground temperatures on the Interior-Eastern Qinghai-Tibet Plateau (II): sand-layer and surface water bodies. *Journal of Glaciology and Geocryology* 30(4): 546-555.

Wang, S. L.,*et al.*, 2002. Interaction between Permafrost and Desertification on the Qinghai-Tibet Plateau. *Desert Research*. 22: 33–39.

Xie S., et al., 2015. Key evidence of the role of desertification in protecting the underlying permafrost in the Qinghai–Tibet Plateau. *Scientific reports* 5:1-8.

Reaction of Cryolithozone to Climate Change in Mountainous Regions of Siberia

Mikhail Zheleznyak,
Sergey Serikov,
Aleksandr Zhirkov
Ivan Misaylov

Melnikov Permafrost Institute of SB RAS

Abstract

Currently, with the widespread climate change, a lot of attention is being paid to the study of the effect of climate on the reaction of ecosystems, including cryolithozone as one of the components of ecosystems.

To develop modern predictive models, their customization and reanalysis, accurate reference data that can be obtained only through the creation of a monitoring geocryological network is necessary.

Keywords: rock temperature, seasonally-active permafrost, temperature trend, mountainous areas, geocryological monitoring

Introduction

The Melnikov Permafrost Institute of SB RAS, with the support of the international TSP project, has developed a program with the purpose to create a monitoring geocryological network in the mountainous areas of the Aldan-Stanovoy Highlands (ASH) and the Verkhoyansk Folded Region (VFR). The longest series of observations (more than 25 years) of the temperature of rocks in the layer of seasonally-active permafrost is taking place in the ASH, where measurements were carried out from 1980. Currently, the territory is being monitored at 19 sites located in different landscape conditions.

In the VFR, monitoring observations started in 2011 and are currently being conducted at 12 sites. An estimate of the change in rock temperature at the depth of seasonally-active permafrost was performed on the basis of data from one-off observations in boreholes in different years, and at depths of 1-5 meters – by logging systems.

Result

Over a 45-year period of research in the region, we observe that the average annual air temperature tends to increase, but this growth was not the same in time and space. This period is marked by an increase in the average annual air temperature from 2.0 to 3.3 ºC (Shatz et al., 2017).

According to the data obtained in the ASH, the temperature of rocks in the range of elevations of 700-1450 meters varies from +2.0 to -6.5 °C. The thermal reaction of rocks to climate change shows a spiked core. The positive trend of rock temperature at the depth of seasonally-active permafrost here varies from 0.7 °C/10 years in zone of bald mountains and its subzone (Table 1) to absence and insignificant trend of 0.1-0.2 °C/10 years in the lower parts of “cold” exposures slopes and terraces above floodplain (Zheleznyak, 2005; Zheleznyak et al., 2014).

Table 1.Average annual temperature of rocks in the subzone of bald mountains of the ASH (1263 m)

Years	Depth of sensors, in meters				
	3,0	**7,5**	**14,0**	**20,0**	**30,0**
1980-1981	- 4,0		-3.8	-4,5	-3,6
1999-2000	-2.0			-3.2	-3,0
2007-2008	**-1,3**	**-2,6**	**-2,1**	**-2,6**	**-2.8**
2011-2012	**-1,3**	**-1,5**	**-1,0**	**-2,2**	**-2,4**
2013-2014	**-0,5**	**-1,1**	**-0,7**	**-1,9**	**-2,2**
2014-2015	**-1,0**	**-1,0**	**-0,3**	**-1,6**	**-2,1**
2015-2016	**-1,8**	**-2,4**		**-1,3**	**-1,9**

In the mountainous regions of the VFR, in altitude range of 790-1250 m, rock temperature at the depth of seasonally-active permafrost varies from -2.5 to -8.0 °C (Serikov & Zhizhin, 2014). Timeframe of the routine observations is 10 years. During this period, the last decade has witnessed a positive trend (0.3-0.4 °C/10 years) in rock temperature at the depth of seasonally-active permafrost (20-30 m). However, it should be noted that, in practically all landscape conditions, there is a negative trend of rock temperature at depths of 0.5 to 5.0 m and close to zero trend at depths of 5 to 10 m (Fig. 1).

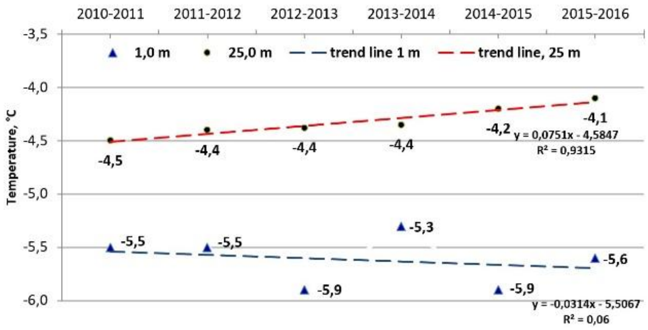

Fig. 1. Trends of average annual temperature of rocks in the intermountain space of the VFR at an altitude of 1103 m

Discussion

Characteristics and dynamics of the reaction of rocks to climate change in mountainous areas is of a variegated nature and is determined by the location of the site in the terrain, the conditions of seasonally-active permafrost on the surface, and the composition of the rocks. It should be noted that in the last decade, at the depth of seasonally-active permafrost, the temperature of the rocks in most cases tends to increase, while in the near-surface layer (1-5 m) in most landscape conditions note its decrease.

Conclusions

Inter-annual variations in air temperature due to cold (summer) or warmer (winter) individual periods, as well as the time of formation of stable snow cover are important to the inter-annual variability of rock temperature in the mountainous regions of Siberia. Thus, in the VFR, the colder 2012-2013 and the late period of snow cover formation in 2014-2015 formed the trend of lowering the average annual temperature of rocks in the active layer in virtually all landscape conditions. A similar phenomenon is noted in a significant part of the ASH.

References

Serikov, S.I. & Zhizhin, V.I., 2014. Temperatures of Rocks of Active Layer in Spurs of the Suntar-Khayata Ridge (Southern Verkhoyane). *Proceedings of World Snow Forum Session*. Irkutsk, Russia, Publishing House of Sochav Geography Institute of SB RAS, p. 24-27.

Shats, M.M. & Skachkov, Y.B., 2017. Main Trends and Consequences of Dynamics of Modern Climate of the North. *Journal of Klimat i priroda*, No. 1 (22). - p. 3-15.

Zheleznyak, M.N., 2005. *Geothermal Field and Cryolithozone in the Southeast of the Siberian Platform*. Novosibirsk. Nauka Press, 228 pp.

Zheleznyak, M., Zhirkov, A., Kirillin, A., 2014. Development of Mountainous Permafrost in the Stanovoy Highlands. *Journal of Engineering of Heilongjiang University*. Vol. 5, No. 3, September, articles 1-7.

13 - Past environments in permafrost regions

Session 13

Past environments in permafrost regions

Conveners:

- **Marc Oliva**, University of Barcelona, Catalonia, Spain
- **Michael Fritz**, Alfred Wegener Institute of Polar and Marine Research, Germany (PYRN member)
- **Stefanie Cable**, University of Copenhagen, Denmark

Permafrost regions have undergone accelerated climate and environmental changes over the last several decades. Changing landscape dynamics are affecting ecosystem conditions and human infrastructure, namely in the Arctic, where the pronounced warming has dramatic socio-economic consequences. Climate models project higher air temperatures together with increased precipitation to continue into the coming decades.

Past climate and environmental records can provide analogues to recent and future perturbations in permafrost environments to identify ice/land/ocean/atmosphere feedbacks influencing regional and global climate conditions.

Permafrost environments host a wide range of terrestrial and aquatic records, including data for past environmental and climatic changes between short (seasonal) and very long (geological) time scales. An accurate study of these records may provide the linkage between the recently observed patterns and the natural response of terrestrial ecosystems to climate variability. Additionally, understanding the history of a permafrost region can provide information on permafrost properties, such as the spatial distribution of ground ice and carbon. We welcome abstracts from terrestrial environmental archives, such as lake sediments, periglacial deposits, tree rings, ground ice, fluvial/alluvial and coastal deposits.

The main purpose of this session is to report on the state of the art and on the latest developments on understanding past environments in permafrost regions, as well as to identify gaps and areas for future research.

Seasonality matters: Past winter climate from the Canadian High Arctic

Benjamin Amann[1]
Scott Lamoureux[2]
[1]*IPREM-UMR 5254/LCABIE, Université de Pau et des Pays de l'Adour, Pau (France), benjamin.amann@univ-pau.fr*
[2]*Queen's University, Department of Geography and Planning, Kingston ON (Canada), scott.lamoureux@queensu.ca*

Abstract

Arctic winter is recognized as the most sensitive season to climate change, but assessing the sensitivity of Earth's climate to natural and anthropogenic forcings in winter is challenged by short and sparse meteorological records. Data from terrestrial paleoclimate archives, such as varved (annually laminated) lake sediments are fundamental to place climate variability into perspective. In particular, Arctic lakes with a nival (snowmelt) catchment offer the opportunity to target and reconstruct a winter signal; a key season for snow water equivalent in the catchment, consequently a key season in the preconditioning for transport and deposition of sediment in the lake during the snowmelt period. Supported by a pilot study on sedimentation process understanding, we develop a calibration model between winter temperature, snowfall and the thickness of the varve nival units of Chevalier Bay (Melville Island, Northwest Territories) to reconstruct a winter signal over the past 400 years.

Keywords: Varved sediments; Permafrost region; Snow melt; Climate change; Sedimentology; Paleoclimatology

Introduction

Permafrost environments such as those from the Canadian High Arctic are in the front line when it comes to dealing with the consequences of climate change. Amplified warming of the Arctic climate has long been demonstrated from both observations and model simulations, with a clear maximum attained in winter (Pithan and Mauritsen 2014). Although winter is considered the most sensitive season to climate change, the rate of change in near future remains insufficiently constrained by the short instrumental period.

Terrestrial environmental archives such as lake sediments are excellent natural paleoclimate archive to place this change into a longer-term context. Lake sediments provide of the only means to: (i) quantify the recent acceleration of the climate during the winter season; and (ii) assess its sensitivity to natural and anthropogenic forcings.

In this context, recent studies have emerged using sediments from Arctic lakes, especially those characterized by a nival (snowmelt) catchment. Sediment transport and deposition in these lakes are primarily governed by the length and intensity of the snowmelt runoff, and indirectly by the preceding winter temperature and snowfall conditions. Hence, these environments offer the unique opportunity to target and reconstruct a winter climate signal. Nevertheless, very few well-calibrated quantitative records exist for the Arctic (Amann et al. 2017), which clearly limits the possibility to resolve large-scale patterns of winter climate change prior the instrumental period.

Here, we present a well-calibrated quantitative temperature record for the winter season from the Canadian High Arctic covering the past 400 years; a reconstruction that is being extended over the last 2000 years.

Sedimentation process understanding

A pilot study from Cape Bounty Arctic Watershed Observatory (CBAWO, 74° 55'N, 109°35'W) is initiated with the aim to collect high-resolution (daily to 5-day) discharge and sediment load data from the catchment of West Lake for the period 2003-2010. Combined with the analysis of sediment trap material from the lake, results reveal a linear relationship between suspended sediment load in the river and sedimentation rates measured in the lake sediment trap. Also, we found that temperature and solar insolation have only a 2- to 3-day control period over the start of the snowmelt before displaying a complete decoupling from discharge and sediment transport. This decoupling indicates that snow water equivalent (SWE) controls primarily suspended sediment yield in the lake catchment.

In this context, we hypothesize that sediment transport and deposition at the lower lake bottom is directly controlled by SWE and spring snowmelt, and ultimately by temperature and related snowfall conditions during the preceding winter.

Calibration and reconstruction

The site of Chevalier Bay (50km west of CBAWO) was selected to produce a quantitative record of winter temperature and snowfall conditions. Chevalier Bay exhibits annual sedimentary structures (varves), and has a large catchment leading to high sedimentation rates (mean 2.53 mm yr-1), atypical of other studied Arctic sites (commonly 0.2 to 1 mm yr^{-1}). These features offer the great opportunity to analyze sediment properties at a seasonal resolution.

Using detailed microstratigraphic analysis from two sediment cores and supported by µ-XRF data, we separate the nival units (spring snowmelt) from the rainfall units (summer). Varve thickness for each seasonal phase was then correlated with temperature and precipitation data for each individual month and 2-to-12-month windows. Results reveal a significant correlation between the thickness of the nival units and winter temperature ($r= 0.71$, $p< 0.01$) and snowfall ($r= 0.65$, $p< 0.01$). These results indicate that higher spring sedimentation rates (i.e. thicker nival units) are associated with greater snowmelt runoff in spring, which is likely a consequence of warmer winter along with increased snowfall on the previous winter. This mechanism is consistent with large-scale climate variability studies that demonstrated the importance of local evaporation and warm spell intrusions in the increase of moisture content in the High Arctic during winter (Messori *et al.,* 2017).

Thus, we use the thickness of the nival units to predict winter temperature and snowfall back to CE 1670; a signal that is representative for a large part of the western Canadian Arctic Archipelago. This record offers a unique and novel opportunity to evaluate climate change in the Arctic (Fig. 1), and holds great potential for model implementation to make comprehensive assessments of long-term regional changes in Arctic winter; ultimately to constrain scenarios in the western Canadian Arctic region under future climate change.

References

Amann, B. *et al.,* 2017. Winter temperature conditions (1670 – 2010) reconstructed from varved sediments, western Canadian High Arctic. *Quaternary Science Reviews* 172: 1-14.

Messori, G. *et al.,* 2017. On the drivers of wintertime temperature extremes in the High Arctic. *Journal of Climate,* in press.

Pithan, F., and Mauritsen, T., 2014. Arctic amplification dominated by temperature feedbacks in contemporary climate models. *Nature Geoscience,* 7: 181-184

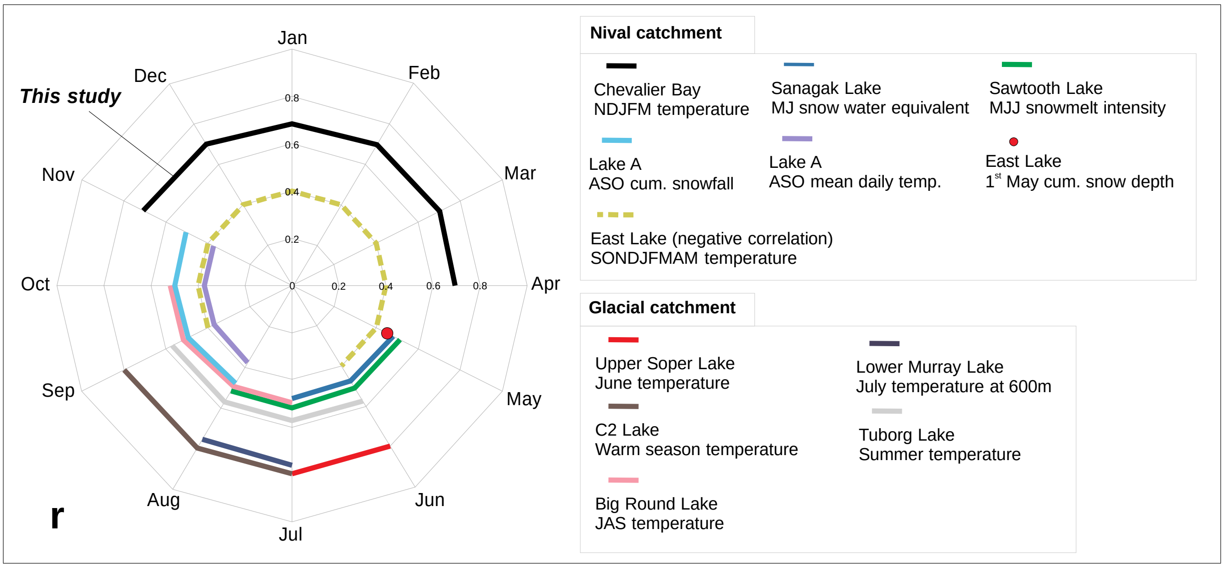

Figure 1. Overview of the correlations between sediment proxy data (mostly varve thickness) and monthly climate variables from lake records in the Canadian High Arctic. Data are from Sanagak Lake (Lamoureux *et al.,* 2006), Sawtooth Lake (Francus *et al.,* 2002), Lake A (Tomkins *et al.,* 2010), East Lake (Cuven *et al.,* 2011), Upper Soper Lake (Hughen *et al.,* 2000), Lower Murray Lake (Cook *et al.,* 2009), C2 Lake (Hardy *et al.,* 1996), Tuborg (Smith *et al.,* 2004), Big Round Lake (Thomas, E., and Briner, J., 2009)

Hard work of ground squirrels pays off 26 ka later: the last cold stage vegetation of the Yana Highlands

Kseniia Ashastina[1, 2]
Frank Kienast[2]
Svetlana Kuzmina[3]
Natalia Rudaya[4]
[1]*Friedrich Schiller University Jena, Institute for Systematic Botany, Jena, Germany, k.ashastina@gmail.com*
[2]*Senckenberg Research Institute and Natural History Museum, Research Station of Quaternary Palaeontology, Weimar, Germany*
[3]*University of Alberta, Edmonton, Canada*
[4]*Institute of Archaeology & Ethnography, Russian Academy of Sciences, Siberian Branch, Novosibirsk, Russia*

Abstract

A fossil ground squirrel nest, found in syngenetic permafrost deposits of the Batagay outcrop in the Yana Highlands provides valuable data for the palaeo-environmental reconstruction of the Last Glacial Maximum in northeast Siberia. We analyzed sedimentological data, plant macro- and micro-fossils together with insect remains in order to obtain a complete picture of the Pleistocene palaeoenvironments. Our results show that the vegetation cover experienced heavy grazing pressure; the plant fossils found within the ground squirrel nest are dominated by steppe, open ground, and pioneer species. Nevertheless, the fossil assemblage gives an intriguing evidence of tree presence in the Highlands during one of the Pleistocene climatic minima (LGM), suggesting that the vegetation cover was a mosaic of open woodlands and steppe.

Keywords: Batagay outcrop; macrofossils; LGM.

Introduction

Syngenetic permafrost sediments serve as a perfect conserve matrix for the material enclosed within. A number of analyses, *e.g.* palynological, sedimentological, ice wedge isotope composition, biomarkers, aDNA, carpological analysis, and studies of buried soils, provide valuable data for reconstruction of climatic parameters, species composition, and interactions between components of past ecosystems (*e.g.* Schirrmeister *et al.*, 2002; Kienast *et al.*, 2011; Zanina *et al.*, 2011; Willerslev *et al.*, 2014).

One of the most informative sources for palaeo vegetation reconstruction are ground squirrel nests, which are valuable treasure chests filled with seeds, leaves, fruits, and stems of vascular plants growing nearby (Gubin *et al.*, 2001; 2003). One fossil nest was found in a permafrost exposure near Batagay, the Yana Highlands, northeastern Siberia. On the contrary to numerous sea coast exposures (*e.g.* Kienast *et al.*, 2005; 2011; Schirrmeister *et al.*, 2011; Sher *et al.*, 2005), the inland Batagay permafrost outcrop provides insights into ecosystems formed under purely continental climate conditions. The aim of our work is to reconstruct palaeo-vegetation of the Yana Highlands during the LGM using carpological, palynological, and entomological analyses.

Results and Discussion

The nest was sampled from the upper part of the Yedoma Ice Complex, just 4.6 m below the ground surface; radiocarbon dating of the nest material provided an (non-calibrated) age of 26 ka BP (Ashastina *et al.*, 2017) corresponding to the LGM (*e.g.* Clark *et al.*, 2009). The palaeontological results, based on the identification of several thousand macrofossils, several hundred of chitin remains, and over 300 pollen grains, suggest that meadow steppes made up the vegetation of the Yana Highlands. The scattered occurrence of larch, proven by findings of larch needles, invites the assumption that the steppe grassland was intersected by open wood stands. The scarcity of woody plants might be not only the result of cold climate but it might also be the result of frequent disturbances of vegetation due to grazing and trampling by herbivores. This is indicated by pioneer plants we found within the ground squirrel nest like *Plantago canescens* and *Papaver* sect. *Scapiflora*.

Conclusions

The vegetation in the Yana Highlands during the LGM consisted of meadow steppe grassland comparable to scattered modern relict steppe patches in the study area. Larch stands existed in the Yana Highlands indicating relatively warm summers with an MTWA higher than 10°C during the LGM. The macrofossil-proven local presence of larch demonstrates that the study region was a northern tree refugium throughout the late Quaternary and beyond.

Acknowledgments

The research was funded by the German Science Foundation (DFG, KI 849/4-1) and FAZIT-Stiftung. We thank Dr Elena Troeva, Prof Dr Ludmila Pestryakova and their colleagues for their help with the sample logistics.

References

Ashastina *et al.*, 2017. Palaeoclimate characteristics in interior Siberia of MIS 6–2: first insights from the Batagay permafrost mega-thaw slump in the Yana Highlands. *Climate of the Past* 13(7): 795-818.

Clark *et al.*, 2009. The Last Glacial Maximum. *Science* 325: 710-714.

Gubin *et al.*, 2001. Composition of seeds from fossil gopher burrows in the ice-loess deposits of Zelony Mys as environmental indicator. *Earth's Cryosphere* 2: 76-82.

Gubin *et al.*, 2003. Reconstruction of ice complex sediment formation conditions based on study of Late Pleistocene rodent burrows. *Earth Cryosphere* 7(3): 13-22.

Kienast *et al.*, 2005. Palaeobotanical evidence for warm summers in the East Siberian Arctic during the last cold stage. *Quaternary Research* 63(3): 283-300.

Kienast *et al.*, 2011. Paleontological records indicate the occurrence of open woodlands in a dry inland climate at the present-day Arctic coast in western Beringia during the Last Interglacial. *Quaternary Science Reviews* 30(17): 2134-2159.

Schirrmeister *et al.*, 2002. Paleoenvironmental and paleoclimatic records from permafrost deposits in the Arctic region of Northern Siberia. *Quaternary International* 89: 97-118.

Schirrmeister *et al.*, 2011. Fossil organic matter characteristics in permafrost deposits of the Northeast Siberian Arctic. *Journal of Geophysical Research* 116, G00M02.

Sher *et al.*, 2005. New insights into the Weichselian environment and climate of the East Siberian Arctic, derived from fossil insects, plants, and mammals. *Quaternary Science Reviews* 24(5): 533-569.

Willerslev *et al.*, 2014. Fifty thousand years of Arctic vegetation and megafaunal diet. *Nature* 506: 47–51.

Zanina *et al.*, 2011. Late-Pleistocene (MIS 3-2) palaeoenvironments as recorded by sediments, palaeosols, and ground-squirrel nests at Duvanny Yar, Kolyma lowland, northeast Siberia. *Quaternary Science Reviews* 30(17): 2107-2123.

MAY THE FROST BE WITH YOU: AN ICE-WEDGE POLYGONS STORY.

Alexandre Chiasson[1, 2]
Michel Allard[1, 2]
Emmanuel L'Hérault[2]
[1]*Centre d'études nordiques (CEN)/ Département de géographie, Université Laval, Alexandre.chiasson.2@ulaval.ca*
[2] *Centre d'études nordiques (CEN), Université Laval*

Abstract

The Arctic regions are experiencing a rise in surface temperatures at a higher rate than the rest of the planet. Ice wedges in polygonal terrain are one of the dominant features of permafrost that are affected by the deepening of the active layer and the thawing of permafrost that result from climate warming. Our method consists of a census of ice-wedge polygons throughout the Nunavik territory by applying a TTOP model, a vegetation cover model, a snow cover model and a map of surface deposits in order to know the degree of cracking of the ice-wedge polygons. This project focuses on the evaluation of the frost-cracking of ice-wedge and tundra polygons in Nunavik. Our results show that ice-wedge polygons are localized in a variety of sedimentary environments and evolved under specific conditions during the Holocene.

Keywords: Ice-wedge; Ice-wedge polygons; Nunavik; Permafrost; TTOP model; Spatial distribution

Introduction

Ice wedges in polygonal terrain are one of the dominant features of permafrost that are affected by the deepening of the active layer and the thawing of permafrost provoked by climate warming (Kasper & Allard, 2001; Sarrazin & Allard, 2015). Despite abundant research in Nunavik on permafrost, ice-wedge polygons and on soil thermal cracking, no analysis of the spatial distribution of tundra polygons has ever been done. Furthermore, there is absolutely no knowledge of the spatial distribution of active ice wedges (i.e. actually cracking). According to several studies, the southern limit of active ice-wedge polygons is already migrating northward due to global warming.

Previous studies by Péwé (1966), Romanovskij (1973) & Mackey & Matthews (1983) mention that the mean annual air temperature (MAAT) must lay between -2°C and -6°C to allow the formation of ice-wedge polygons. However, for permafrost cracking and ice-wedge formation to occur, the ground temperature must in fact drop abruptly to temperatures below -10°C. If the temperature does not decrease rapidly enough, the material may contract without cracking (Lachenbruch, 1966; Mackay, 1984; Sarrazin & Allard, 2015).

The objective of this project is to assess the activity of frost-cracking, ice-wedge polygons and tundra polygons across the bioclimatic zones of Nunavik. Since frost-cracking is a temperature-controlled process affecting materials with different rheological properties, it is assumed that activity is related to surface climatic conditions, soil materials, vegetation type and snow cover.

Methods

In the summer of 2017, in Salluit, we dug dozens of soil pits to find out the degree of frost-cracking of the ice-wedge polygons under current climate conditions and ground temperatures. We analyzed thousands of georeferenced aerial photographs (MFFP: 42 474/ CEN: 37 500) for tundra polygon location; then we built a database and mapped our findings (Fig. 1-2). Also, we assigned basic parameters to each observed site, i.e. the probable type of ice wedge, the form of the polygons (e.g, open, closed, flat, high-center, low-center), the surficial geological material and the vegetation type.

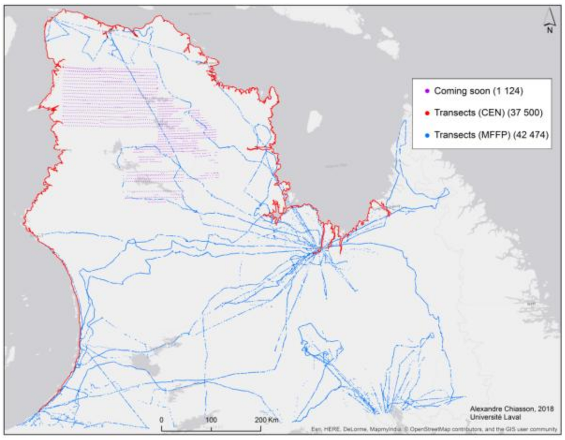

Figure 1 : Location of transects made by the MFFP between 2008-2015. Each point (68,354) represents an aerial photograph. CEN'survey lines followed the coastline.

Preliminary results

Our results show that ice-wedge polygons in Nunavik are relatively recent because of their settings (Holocene) (Fig. 3). They formed in current and raised beach deposits and on glaciogenic terrain landforms (eskers, drumlins). These deposits were put in place during or after deglaciation. In total, we identified 779 ice-wedge polygons sites.

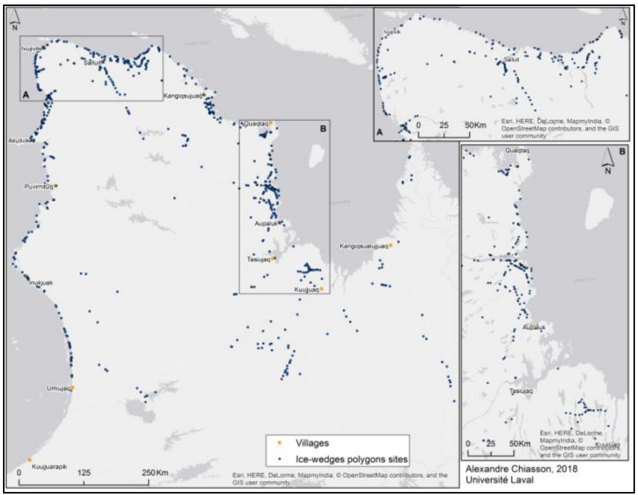

Figure 2: Ice-wedges polygons sites

In Salluit, the majority of sites with ice-wedge polygon networks were active in 2017. The ground had cracked during the previous winter (Fig. 3). Twenty percent of the located polygon sites in Nunavik are below the tree line. These ice-wedge polygons seem inactive due to the presence of a dense vegetation/snow covers.

Figure 3: The ground has cracked during the winter 2017 (Foucault River).

Next steps

We will apply the TTOP model to estimate and map the mean and minimum ground temperatures at the top of permafrost for the months of January and February 2015-2017 to identify areas that are affected by thermal regimes likely to induce cracking (Fig. 4). The buffer layer effect of the snow cover that may impede frost cracking will be calculated with an existing model of canopy cover, a model of snow cover and a surficial geology map at a resolution of 250 m. The ice-wedge polygons will be classified into four categories according to the degree of activity of the ice wedges: (1) active ice-wedge polygons, (2) sporadically active ice-wedge polygons, (3) inactive ice-wedge polygons and (4) fossil ice-wedges polygons.

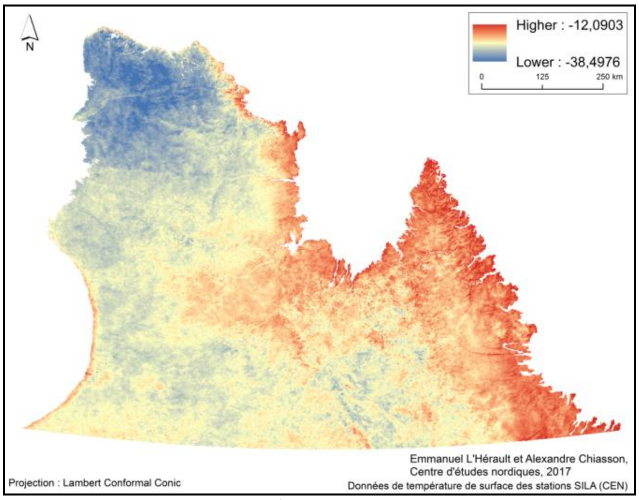

Figure 4: Temperature (° C) at the top of permafrost (February 2012).

In the summer of 2018, in Akulivik, we will also dig dozens of pits to examine whether ice-wedge polygons are still active at a more southern latitude.

Acknowledgments

We thank A. Boisson, S. Gagnon, S. Gauthier, Ministère des Forêts, de la Faune et des Parcs du Québec (MFFP) and the community of Salluit.

References

Kasper, J.N. & Allard, M., 2001. Late-Holocene climatic changes as detected by the growth and decay of ice wedges on the southern shore of Hudson Strait, northern Quebec, Canada. *Holocene*, 11(5): 563-577.

Lachenbruch, A., 1962. Mechanics of thermal contraction cracks and ice-wedge polygons in permafrost. *Geological Society of America, Special Paper 70*. 69 pages.

Mackay, J.R., 1984. The direction of ice-wedge cracking in permafrost: downward or upward?. *Canadian Journal of Earth Sciences*, 21(5): 516-524.

Péwé, T.L., 1966. Ice wedges in Alaska - classification, distribution and climatic significance. *Proceedings, 1st International Permafrost Conference, National Academy of Science - National Research Council of Canada, Publication 1287*. 76-81

Romanovskij, N.N., 1973. Regularities in formation of frost-fissures and development of frost-fissure polygons. *Biuletyn Peryglacjalny*, 23: 237-277.

Sarrazin, D. & Allard, M., 2015. The thermo-mechanical behavior of frost-cracks over ice wedges: new data from extensometer measurements. *Conference: GEOQuébec.*

Permafrost soil humic acids and their use in diagnosis of environment of Pleistocene cold periods

Maria Dergacheva[1]
Anton Uchaev[2]
Olga Nekrasova[2]
Natalia Bazhina[1]

[1]*Institute of Soil Science and Agrochemistry SB RAS, Novosibirsk, Russia, mid555@yandex.com*
[2]*Ural Federal University named after the First President of Russia B. N. Yeltsin, Yekaterinburg, Russia*

Abstract

The study, reflected in the paper, is devoted to the discussion of the specific composition, structure and properties of humic acids of cryogenic soils in order to use the obtained materials as a recent base for the diagnosis and reconstruction of environment (including the lengths of the biological activity period) of the Middle Pleistocene Tyninsky horizon formation (analogue of the cold stage of MIS 16) by the method of actualism. It was found that correlation coefficients of the main indicators of the composition and properties of modern soil humic acids between themselves and the period of biological activity lie in the range of 0.85-0.95, and that the Tyninsky horizon was formed in very cold changing conditions with a period of biological activity not exceeding 45 days.

Keywords: cryogenic soils; humic acids; middle Pleistocene; paleoenvironment reconstruction

Introduction

Humic acids occupy one of the leading places in the diagnosis of an environment state. On the one hand, they react to its change and reflect the specifics of the external environment in the features of composition, structure and properties, on the other they preserve these characteristics in time (Dergacheva, 2008). Their use for paleoenvironment diagnostic and reconstruction of warm periods of paleogeographic history (analogues of MIS odd stages) of different scale territories has already become stably used in the practice of research. At the same time, cold periods (analogues of MIS even-numbered stages) are diagnosed with the use of humic acids and their ratio with other humus components extremely rare. The reason of this lies in the lack of sufficient amounts of data on humic acids of permafrost zone soils, necessary for the creation of a recent base, without which the diagnosis and reconstruction of the paleoenvironment in the case of deep climatic cooling is impossible.

Results and discussion

The present study of humic acids and their relationship with the other humus components of cryogenic soils on the north territory within the limits 63º00'–66º30'N and 66º41'–72º00'E was undertaken to obtain recent materials for their further use in the bioclimatic reconstruction of the formation conditions of paleosols and sediments of the Middle Pleistocene cold stages on the Southern Ural territory (Russia).

In this paper the diagnostic of sediment formation conditions has been carried out on an example of the Middle Pleistocene Tynyinsky horizon (MIS 16 stage analogy). Tynyinsky horizon, the formation of which refers to the period 660–610 thousand years ago, identified in the geological sediments of the Southern Urals, has not yet been studied from the standpoint of paleopedology.

Humic acid peculiarities of cryogenic soils of different formation conditions of some regions of the territory under investigation are considered. General statistics parameters of humic acid composition and properties of cryogenic modern soils were studied and used as the recent base for paleoenvironment reconstruction of cold Middle Pleistocene period.

Humic acids were extracted from the samples of modern cryogenic soils and sediments as well as paleosols by standard methods. Additional purification with HF and/or 6n HCl was not carried out as the share and composition of humic mineral components have close connection with ecological conditions of their formation and pedogenesis.

The specificity of cryogenic soil humic acids was revealed on the basis of the study of a series main indicators of the composition, structure, and properties of humic acid: element composition and the ratio of structure-forming elements, spectral characteristics in the UV, visible and IR spectra, the ratio of the structure-forming components determined by the ^{13}C NMR method, fluorescent properties and their quantitative indicators (the first moment – M1 – and the ratio of fluorescence intensities in the blue and red regions of the spectrum – α).

Some positions have been revealed:

– Humic acids of cryogenic soils are characterized by Hydrogen predomination over Carbon. The H/C ratio in humic matters of long frozen soils is more than 1.0 (as a rule it is equal to 1.3–1.8, but can reach 2 and more), the C/N and O/C ratios are very different, the last one depends on soil particle size distribution.

– The relationship between the basic elements (H: C) and the period of biological activity is subject to the dependence $y = 2.28–0.013x$, and the share of aromatic carbon – $y = 2.99+0.41x$, where x is the period of biological activity, days.

– The close relationship of the main features of the composition and properties of humic acids with each other and with a period of biological activity is characterized by high correlation coefficients (r = 0.85–0.95).

Conclusion

The pedogenic features of Tynyinsky horizon sediments correspond to cold conditions. Extremely cold and humid period of sediment formation is fixed by the following specific characteristics of humic acids: too high H/C values and low atomic C and N portions; high portion of mineral elements in their organic-mineral derivates reaching to 50 % with Al, Fe and Mn predomination among them; very low values of M1 that does not predominant 410–420 nm. The comparison of general pedogenic features connected with the humic acid specific of modern cryogenic soils and Tynyinsky horizon paleosediments showed that its formation took place in the changing cold conditions of the environment and the period of biological activity in the coldest time was on average not more than 45 days.

References

Dergacheva M.I., 2008. Humus as a Carrier of Soil Memory. In: Targulian VO, Goryachkin SV. (ed.). *Soil Memory: Soil as a Memory of Biosphere-Geosphere-Anthroposphere Interactions*. Moscow: LKI Publ, 530-560. In Russian, English summary

Spatial distribution and morphometry of permafrost-related landforms in the Central Pyrenees and associated paleoclimatic implications

Marcelo (Vieira) Fernandes[1]
Pedro (Jesus) Palma [1]
Luís (Filipe) Lopes[1]
Jesús Ruiz Fernández[2]
Paulo Pereira[3]
Marc Oliva[4]

[1]*Centre for Geographical Studies - IGOT, Universidade de Lisboa, Portugal, marcelo.fernandes@live.com*
[2] *Department of Geography, University of Oviedo, Spain*
[3]*Environmental Management Center, Mykolas Romeris University, Vilnius, Lithuania*
[4]*Department of Geography, University of Barcelona, Spain*

Abstract

We examine the distribution of rock glaciers and protalus lobes in Aran and Boí valleys, formerly glaciated U-shaped valleys ranging from 600 to 3000 m in the Central Pyrenees. The spatial distribution of these landforms and their chronostratigraphic position within the valley allow a better understanding of the climatic and environmental conditions necessary for their development. Up to 151 permafrost-related landforms were identified in the Boí valley, including 56 rock glaciers and 95 protalus lobes. In the case of the northern Aran valley, 76 rock glaciers and 89 protalus lobes were cataloged corresponding to 165 landforms. The chronostratigraphic position of these landforms within the valley and with respect to the moraine complexes suggests the existence of three generations of permafrost-related landforms which are associated to the massive deglaciation process between the maximum glacial advance of the Last Glaciation and the Holocene.

Keywords: Central Pyrenees; Last Glaciation; Deglaciation; Permafrost; Periglacial landforms; Paleoclimate

Introduction

Present and past permafrost distribution in the Pyrenees is still under discussion. As in other mid-latitude mountain regions, rock glaciers and protalus lobes are the main indicators of permafrost conditions. In this study, we examine the distribution of these landforms in Aran and Boí valleys, formerly glaciated U-shaped valleys shaped on granite, shales and limestones at elevations ranging from 600 to 3000 m asl in the northern and southern sides of the Central Pyrenees, respectively. The spatial distribution of rock glaciers and protalus lobes and their chronostratigraphic position within the valleys allow a better understanding of the climatic and environmental conditions necessary for their development.

Methodology

Geomorphological mapping of these landforms was built using high resolution imagery (25 cm pixel) provided by the Institut Cartogràfic i Geologic de Catalunya, complemented with Basemap ESRI images and Google Earth Pro, and subsequently improved with field observations. The related–permafrost features identified by ridges, furrows and fronts were vectorized as polygons in a map generated in a GIS environment. Several parameters of each landform were measured: area, length, width, altitude, aspect and slope. This information provides accurate characterization of the spatial distribution of these landforms as well as of their morphometric properties.

Results

Up to 316 units were mapped in the study area including 132 rock glaciers and 184 protalus lobes. Boí valley concentrates 56 rock glaciers and 95 protalus lobes, whereas Aran valley includes 76 and 89 units, respectively. Most of the landforms (90%) are located inside the glacial cirques, while the rest is distributed in the slopes of the formerly glaciated valleys. The lowest rock glaciers are situated at 1744 m (Aran) and 2007 m (Boí), whereas the lowest protalus lobes are distributed at 1740 m and 2033 m, respectively. Rock glaciers show larger and wider dimensions in Boí valley than in Aran valley, with an average length of 267 m in Aran to 355 m in Boí, and a mean width of 160 and 208 m, respectively. Protalus lobes, however, are larger in Aran, with an average length of 83 m and a width of 215 m, whereas in Boí valley they have 62 and 165 m in average. The aspect shows a prevailing orientation of NW, N and NE for both cases, being almost absent in S, SE and SW aspects. The average slope landforms lies between 11 and 27º, with a maximum of 35º for rock glaciers and 29º for protalus lobes. The amplitude/length ratio reveals that rock glaciers placed at lower altitudes are more elongated.

Discussion and conclusions

The lowest features are located in MIE glaciated environments, and therefore they formed following the deglaciation. They are indicative of the lowest altitude for permafrost conditions during that time, suggesting that the temperature increase since the onset of deglaciation until nowadays has been of ca. 7-8 °C, similar to that estimated for other high mountain Mediterranean environments. A second generation of rock glaciers developed this stage on the slopes of the recently deglaciated U-shaped valleys. The deglaciation of the glacial cirques - that possibly occurred during the Younger Dryas such as in other nearby valleys - would have been also followed by the widespread formation of permafrost-related features in the bottom of the cirques. Finally, during the Holocene some glaciers formed inside the highest cirques; their disappearance was followed by the formation of rock glaciers and protalus lobes next to the cirque walls, with geomorphic evidence of permafrost creeping of some of the moraines developed during this stage (Figure 1).

The existing vegetation cover in some rock glaciers is a clear signal of their present-day inactivity, which means they formed during other more favorable climatic and geomorphological conditions. Nowadays, only one rock glacier in the study area has been reported to be active (Figure 1).

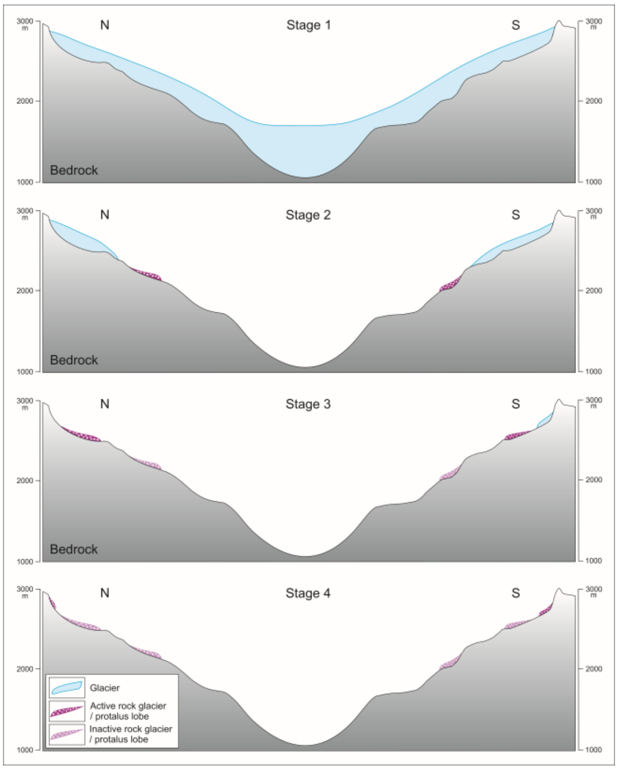

Figure 1. Sequence of environmental stages in the studied valleys: (a) Stage 1: glaciers extending over the valley bottoms during the MIE of the Last Glaciation; (b) Stage 2: formation of permafrost-related features on the slopes of the recently deglaciated valleys; (c) Stage 3: development of rock glaciers and protalus lobes inside the bottoms of the glacial cirques, (d) Stage 4: formation of new landforms next to the cirque walls.

References

Fernandes, M., Palma, P., Lopes, L., Ruiz-Fernández, J., Pereira, P., Oliva, M., 2017. Spatial distribution and morphometry of permafrost-related landforms in the Central Pyrenees and associated paleoclimatic implications. *Quaternary International*, DOI: 10.1016/j.quaint.2017.08.071.

Late Pleistocene yedoma in south-western Yukon (Canada): a remnant of Eastern Beringia ?

Daniel Fortier[1, 2]
Jens Strauss[3]
Michel Sliger[1,2]
Fabrice Calmels[4]
Duane Froese[5]
Yuri Shur[3]
[1]*Geography Department, Université de Montréal, Montréal (QC), Canada, CP6128, H3C 3J7*
[2]*Center for Northern Studies, Université Laval, Québec (QC), Canada*
[3]*Alfred Wegener Institute, Helmholtz Center for Polar and Marine Research, Potsdam, Germany*
[4]*Yukon Research Center, Whitehorse (YK), Canada*
[5]*Department of Earth and Atmospheric Sciences, University of Alberta, Edmonton, (AB), Canada*
[6]*Department of Civil Engineering, University of Alaska Fairbanks, Fairbanks (AK), USA*

Abstract

Yedoma deposits developed from the syngenetic accumulation and freezing of organic-rich and ice-rich sediments during the Late Pleistocene over vast portions of Siberia, Alaska and Yukon Territory. Cryostratigraphic investigations revealed the presence of a yedoma deposit in the Beaver Creek area of south-western Yukon. The Beaver Creek area was not glaciated during the last glacial advance and the cryostratigraphic record comprises Middle Wisconsinian up to Holocene deposits covering the Mirror Creek disintegration moraine. Reworking of glacial deposits by alluvial and solifluction processes and peat accumulation in the depression of the hummocky moraine likely occurred during the Middle Wisconsinian period and was followed during the Late Wisconsinian by the yedoma build-up. A major thaw event interrupted the syngenetic permafrost aggradation which eventually resumed as attested by the upward growth of ice wedges.

Keywords: Yedoma; Cryostratigraphy; Syngenetic Permafrost; Carbon Stock; Ice Wedge; Late Pleistocene

Introduction

During the Late Pleistocene extensive portions of Siberia, Alaska and the Yukon Territory remained largely unglaciated (Elias and Brigham-Grette, 2013). These areas were covered by yedoma deposits which developed from the syngenetic accumulation and freezing of organic-rich and ice-rich fine-grained sediments and growth of ice wedges. Strauss *et al.* (2013, 2017) estimated that yedoma deposits cover approximately 625 000 km^2 of the Northern hemisphere accounting for about 398 gigatonnes (Gt) of organic carbon (including taberal and Holocene strata). However, this estimate didn't take into account the yedoma deposits from south-western Yukon, Canada.

Last glacial maximum in North-West Canada

During the McConnell glaciation (last glacial maximum) the Cordilleran Ice Sheet covered most of north-western America and merged with the Laurentide Ice Sheet up to southwestern North-West Territories although some areas of North-Western Canada remained ice-free (Jackson *et al.*, 1991; Dyke 2004). Cryostratigraphic investigations in the Beaver Creek area, South-western Yukon, revealed the presence of yedoma deposit with ice-rich cryofacies and syngenetic ice wedges down to 10 m below the surface (Fig.1). The Beaver Creek area was not glaciated during the last glacial advance (Vermaire & Cwynar 2010).

Study site

The Beaver Creek area is located in the Wellesley basin, north of the Kluane range (Fig.2). The Wellesley basin rests at the base of the St-Elias Mountains, where a glacial lobe has spread as a piedmont glacier complex more than once during the Pleistocene (Fig.2) (Jackson *et al.* 1991).

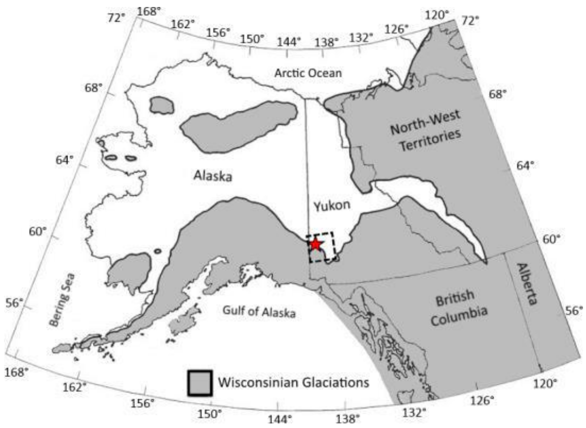

Figure 1. Localisation of the study site in relation to Eastern Beringia (unglaciated white area). The dashed square outlines the contour of Figure 2 and the red star locates the study site (figure modified from Sliger et al. 2015).

This site was glaciated during the Mirror Creek glaciation (Early Wisconsinian) but remained ice-free during the Late Wisconsinian McConnell glaciation (Fig.2)

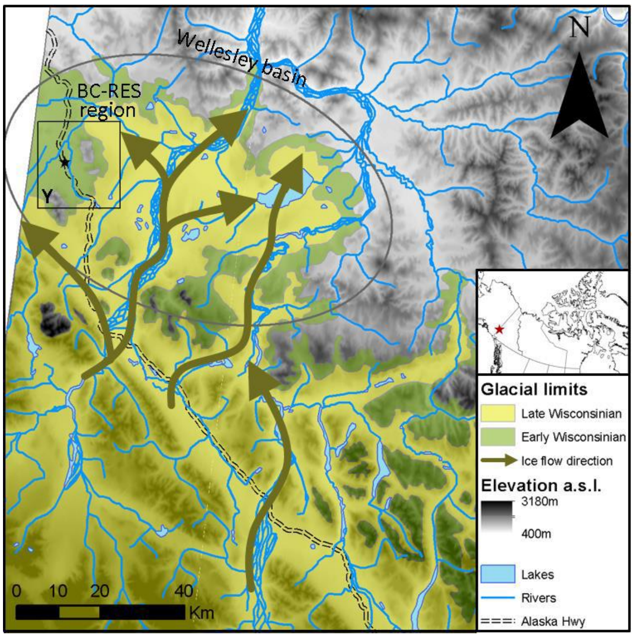

Figure 2. Glacial limits during the Wisconsinian and general ice flow direction. Star: study site location (figure modified from Sliger et al. 2015).

The Mirror Creek deglaciation left an extensive hummocky disintegration moraine deposits (Sliger *et al.* 2015). Reworking of glacial deposits by alluvial and solifluction processes and peat accumulation in the depression of the hummocky moraine likely began during the Middle Wisconsinian period and was followed during the Late Wisconsinian by the yedoma build-up. A major thaw event interrupted the syngenetic aggradation of the permafrost which later resumed as illustrated by the upward growth of the ice wedges. During the Holocene, the aeolian sedimentation and ice wedge growth decreased significantly and peat accumulation promoted the development of a carbon/ice -rich layer (*intermediate layer*).

Acknowledgments

This research was supported by Natural Sciences and Engineering Research Council of Canada, Transport Canada, and Yukon Highways and Public Works.

References

Dyke, A. S. 2004. An outline of North American Deglaciation with emphasis on central and northern Canada, *in* Ehlers, J. & Gibbard, P.L. (eds), *Quaternary Glaciations-Extent and Chronology*. Amsterdam: Elsevier, 373-424.

Elias, S.A., Brigham-Grette, J., 2013. Late Pleistocene Glacial Events in Beringia. In: Elias, S.T. (ed.), *Encyclopedia of Quaternary Science*. Amsterdam: Elsevier, 1057–1066.

Jackson, L.E. *et al.*, 1991. The Last Cordilleran Ice Sheet in Southern Yukon Territory. *Géographie physique et Quaternaire, 45*: 341-354.

Sliger, M. *et al.* 2017. Incidence of Late Pleistocene-Holocene Climate on the Concurrent Landscape and Permafrost Development of the Beaver Creek Region, Southwestern Yukon, Canada. *Proceedings of the Seventh Canadian Permafrost Conference & 68th Canadian Geotechnical Conference*, Quebec City, Canada, September 20th-23rd.

Strauss, J. *et al.*, 2017. Deep yedoma permafrost: a synthesis of depositional characteristics and carbon vulnerability. *Earth Science Reviews* 72: 75-86.

Strauss, J. *et al.*, 2013. The deep permafrost carbon pool of the Yedoma region in Siberia and Alaska. *Geophysical Research Letter* 40: 6165–6170.

Vermaire, J.C. & Cwynar. L.C., 2010. A revised late-Quaternary vegetation history of the unglaciated southwestern Yukon Territory, Canada, from Antifreeze and Eikland ponds, *Canadian Journal of Earth Sciences* 47: 75-88

Retrogressive thaw slumps: indicators of Holocene climate changes

Roxanne Frappier[1]
Denis Lacelle[2]
André E. Viau[3]
[1]*Univerisity of Ottawa, roxanne.frappier@uottawa.ca*
[2]*University of Ottawa, dlacelle@uottawa.ca*
[3]*University of Ottawa, aviau@uottawa.ca*

Abstract

The ongoing climate warming increases thermokarst activity and its impacts by inducing permafrost degradation and active layer deepening. A retrogressive thaw slump, the most dynamic thermokarst landform, was investigated in the Peel Plateau region of the Northwest Territories, Canada. It exposes a thaw layer, a relict thaw layer, and four massive ground ice units. Analyses of the stratigraphy, sedimentology, isotope geochemistry and radiocarbon dating are presented. Main conclusions are that 1) physical and chemical parameters of the exposed massive ice are characteristic of buried glacier ice that experienced water infiltration and partial refreezing, 2) the relict thaw layer represents a mid-Holocene period of maximum active layer deepening, 3) association of the region's thaw slump activity with paleoclimatic parameters reveals a specific set of conditions favorable to thaw slump activity. The conclusions contribute to the understanding of how thaw slumps fit in the climate history and terrain conditions of the region.

Keywords: Thermokarst; Permafrost; Retrogressive thaw slumps; Massive ground ice; Isotope geochemistry; Holocene

Introduction

Permafrost degradation in Arctic regions has gained attention in recent years, mostly because of the ongoing climate warming, which is enhanced in Arctic regions. In ice-rich permafrost terrain, permafrost degradation can lead to the formation of thermokarst terrain, the most impressive form being retrogressive thaw slumps. Thaw slumps frequently expose meters to tens of meters of permafrost terrain and offer an opportunity to examine the cryostratigraphy of permafrost. Combined with isotopic geochemistry and dating, and multiple proxy data, the study of cryostratigraphy allows for a better understanding of the genesis of permafrost terrain and its climatic significance, which is notably relevant in the context of the study of Holocene climate changes. The study aims to characterize the cryostratigraphy of the uppermost 5 m of permafrost at a site on the lower Peel Plateau, NWT. The region is underlain by ice-rich permafrost as inferred from the presence of nearly 200 active thaw slumps. However most of the thaw slumps (70%) are concentrated between the maximum extent of the Laurentide Ice Sheet (LIS) and a recessional limit. Past studies in the region determined the origin and age of ground ice and timing of past thaw slumping at sites near the maximum extent of the Laurentide Ice Sheet (Lacelle *et al.*, 2004; 2010); here the first site within the recessional limit of the LIS is investigated. The specific objectives are to determine the origin and age of the ground ice exposed in a retrogressive thaw slump, and the response of permafrost to Holocene climate changes.

Methods

In July 2016, observations and sampling of the thaw layer, relict thaw layer, and four massive ground ice units exposed at a thaw slump were achieved.

Filtered melted ground ice samples were analyzed for major ions, stable water isotopes ($\delta^{18}O$ and $\delta^{2}H$, or δD), and dissolved organic carbon (DOC) concentrations. Thaw layer and permafrost soil were analyzed for particle size distribution, and excess water, gravimetric water and organic carbon contents. Organic fragments extracted from the organic debris sample and wood pieces found at the bottom of the thaw layer were radiocarbon dated.

Results and main conclusions

Based on the visual aspect of the four massive ice units, the nature of the contact between them and the overlying sediments, their geochemistry, and a comparison of their geochemistry with that of the ice contained in the overlying sediments, the massive ice exposed shows evidence of both typical massive ground ice origins in northwestern Canada; buried glacier ice and segregated-intrusive ice. Considering that our site is located at the margin of the LIS, and that marginal glacier ice presents varying facies and chemical parameters, our hypothesis is that this ground ice consists of buried glacier ice that experienced water infiltration and partial refreezing.

The layer above the massive ground ice and below the thaw layer, which presents a lighter coloration, buried organic sections, and ice of low $\delta^{18}O$ values, is identified as a relict thaw layer (RTL). It dates to the Holocene thermal maximum, which represents a period of important active layer deepening and thermokarst activity that resulted in widespread paleo-thaw unconformities across northwestern Canada.

The studied site fits within the region's thaw slump activity history. Association of these thaw slumps with paleoclimatic parameters indicate that the combination of formerly glaciated continuous permafrost, hummocky rolling moraine terrain, stream-incised relief, and massive ground ice in the Richardson Mountains-Peel Plateau region, coupled with major rainfall events, represents a set of condition that is favourable to thaw slump activity (i.e. initiation and retrogression), by inducing slope instability and easy removal of slumped sediments (Kokelj *et al.*, 2017; Lacelle *et al.*, 2010).

Acknowledgments

This research was funded by the Natural Sciences and Engineering Research Council (NSERC), the Polar Continental Shelf Program (PCSP), and the Northern Scientific Training Program (NSTP).

References

Kokelj S.V., Lantz, T.C., Tunnicliffe, J., Segal, R. and Lacelle, D., 2017. Climate-driven thaw of permafrost preserved glacial landscapes, northwestern Canada. *Geology 45*(4): 371-374.

Lacelle, D., Bjornson, J., Lauriol, B., Clark, I.D., & Trouter, Y., 2004. Segregated-intrusive ice of subglacial meltwater origin in retrogressive thaw flow headwalls, Richardson Mountains, NWT, Canada. *Quaternary Science Reviews 23*: 681-696.

Lacelle, D., Bjornson, J. and Lauriol, B., 2010. Climatic and geomorphic factors affecting contemporary (1950–2004) activity of retrogressive thaw slumps on the Aklavik Plateau, Richardson Mountains, NWT, Canada. *Permafrost And Periglacial Processes 21*(1): 1-15.

Relative age dating of rock glacier surfaces in False Bay (Livingston Island, Maritime Antarctica) using the Schmidt Hammer

Cristina García-Hernández[1]
Jesús Ruiz-Fernández[1]
Marc Oliva[2]
Augusto Pérez-Alberti[3]

[1]*Department of Geography, University of Oviedo, C/Amparo Pedregal s/n, 33011, Oviedo, Spain. cristingar@hotmail.com*
[2]*Department of Geography, University of Barcelona, C/Montalegre, Barcelona, Spain.*
[3]*Department of Geography, University of Santiago de Compostela, Campus Universitario Sur, 15782, Santiago de compostela, Spain.*

Abstract

A Schmidt Hammer type "N" has been applied in False Bay (Livingston Island, Maritime Antarctica), for calculate the rebound value (and use it as a relative dating method) of three large rock glaciers with measures in the arches along a longitudinal profile from the distal sector (the front) to the proximal sector of the rock glaciers. The rebound values reveal that weathering is higher in the frontal sector of rock glaciers. Age dating based on cosmogenic isotope analysis in sample sites is currently in progress and will allow to validate the results of the Schmidt hammer measurements.

Keywords: Schmidt hammer; relative age dating; rock glacier; False Bay; Antarctica

Introduction and methods

The Schmidt hammer, originally designed (and widely used) for concrete stability testing, is an easy-to-use device which has been successfully used for several purposes related to relative dating of Holocene landforms (Goudie, 2006; Viles *et al.,* 2011).

This device records a rebound value as a result of the impact of a surface, being this value proportional to the compressive strength of the impacted structure. The lower the rebound value is, the higher the degree of weathering and, consequently, the higher the age (and vice-versa).

A Schmidt Hammer type "N" has been applied in False Bay (Livingston Island, Maritime Antarctica), for dating the surfaces of three large rock glaciers with measures in the arches along a longitudinal profile from the distal sector (the front) to the proximal sector of the glacier.

150 rebound values have been obtained in each sample site and descriptive statistics were applied to determine the mean rock hardness. The data were processed with the software R (an open source environment for statistical analysis). The rock glaciers were mapped based on aerial photographs and field work, and each sample site was located using a high precision GPS.

Results

The obtained rebound values were always lower in the rock surfaces of the distal sector (in the fronts) while the highest values have been obtained in the surfaces of the proximal sector. These rebound values reveal that weathering is in line with the age, which habitually is higher in the front glacier surfaces.

Age dating based on cosmogenic isotope analysis from surface samples of three blocks in each glacier sector (three in the distal, three in the medial and three in the proximal) is currently in progress. Absolute dating will allow to validate the results of the Schmidt hammer measurements.

Acknowledgments

This research has been conducted with the support of the Spanish Ministry of Economy, Industry and Competitiveness with the project CRONOANTAR [CTM2016-77878-P]. Cristina García-Hernández appreciates the support of Kaleidos and the Spanish Ministry of Education, Culture and Sport under doctoral fellowship [grant number MECD-15-FPU14/01279].

References

Goudie, A.S., 2006. The Schmidt hammer in geomorphological research. *Prog. Phys. Geogr.*, 30:703-718.

Viles, H., Goudie, A., Grab, S. & Lalley, J., 2011. The use of the Schmidt hammer and Equotip for rock hardness assessment in geomorphology and heritage science: a comparative analysis. *Earth Surf. Process. Landf.,* 36:320-333.

Permafrost-related threats to alpine headwater lakes: evidence from integrating contemporary research

Boris P. Ilyashuk[1, 2]
Elena A. Ilyashuk[1]
Roland Psenner[1, 2]
Richard Tessadri[3]
Karin A. Koinig[1, 2]
[1]*Institute of Ecology, University of Innsbruck, Technikerstraße 25, 6020 Innsbruck, Austria, boris.ilyashuk@uibk.ac.at*
[2]*Institute for Alpine Environment, Eurac Research, Viale Druso 1, 39100 Bozen/Bolzano, Italy*
[3]*Institute of Mineralogy and Petrography, University of Innsbruck, Innrain 52, 6020 Innsbruck, Austria*

Abstract

Degrading permafrost in periglacial environments can produce acid rock drainage (ARD) and cause severe ecological damage in areas underlain by sulfide-bearing bedrock. Comparative research design was used in the integrating contemporary study to assess and compare ARDs generated by rock glaciers and their effects on alpine headwater lakes with similar morphometric features and underlying bedrock geology, but characterized by different intensities of frost action in their catchments. We argue that ARD and its effects on lakes are more severe in the alpine periglacial belt with mean annual air temperatures (MAAT) between −2 °C and +3 °C, where groundwater persists in the liquid phase for most of the year, in contrast to ARD in the periglacial belt where frost action dominates (MAAT < −2 °C). The findings clearly suggest that the ambient air temperature is an important factor affecting the ARD production in periglacial environments.

Keywords: acid drainage, aquatic invertebrates, frost action, metals, periglacial environments, rock glacier.

Introduction

Despite the fact that changes in the mountain cryosphere are progressing rapidly, surprisingly little research has been devoted to studying the impact of meltwater from glaciated and perennially frozen areas on alpine aquatic ecosystems (e.g. Slemmons *et al.*, 2013). Extremely serious environmental problems associated with the generation of acid rock drainage (ARD) can arise in mineralized watersheds with sulfide-bearing bedrock (Thies *et al.*, 2007; Ilyashuk *et al.*, 2014). Changes in the location of glacier ice and ice-rich permafrost can greatly affect ARD in areas where the ice has been providing a cover to prevent oxidation of sulfide minerals (e.g. Todd *et al.*, 2012). As of today only a few studies exist which have been dealing with the investigation of ARD in periglacial environments.

In the present study, we hypothesized that ARD generated by a rock glacier and its effects on a lake in a crystalline-rock area are more severe in the alpine periglacial belt in which groundwater persists in the liquid phase for most of the year (MAAT between −2 °C and +3 °C; French, 2007), in contrast to the periglacial belt in which frost action conditions dominate (MAAT lower than −2 °C).

Research Design

The study area is located within a crystalline-rock watershed in periglacial environments of the upper Vinschgau valley in the Central Eastern Alps, Northern Italy. Disseminated sulfide ore minerals are widespread in the bedrock of the valley (Spötl *et al.*, 2002) and are one of the key factors in generating ARDs. The present study aimed at testing the research hypothesis by assessing and comparing ARDs generated by rock glaciers and their effects on two alpine headwater lakes (RAS and POR) with similar morphometric features and bedrock geology, but characterized by different intensities of frost action in their catchments. A third lake (SAL1), not influenced by rock glaciers, was sampled as a reference site. The ARD effects were assessed through the determination of the concentrations of metals in water, sediment, and biota of the lakes.

Results and Discussion

Chemical analysis of rock samples from the lake catchments showed that the geochemical composition of bedrock is rather similar between the lake catchments.

Chemical analysis of water samples revealed that the total concentrations of Al, Mn, Ni, and Zn are negligibly small in the circumneutral SAL1 compared to the acidic RAS and POR situated at the toes of rock glaciers. The concentrations of Mn and Ni exceed the appropriate EU limits for drinking water (The Council of the EU, 1998) ~16 and ~8 times, respectively, in the POR water and ~23 and ~15 times, respectively, in RAS. Speciation analysis performed with the Visual MINTEQ equilibrium model demonstrated that free Ni^{2+} and Mn^{2+} ions account for 88–91% of the total nickel and manganese concentrations in RAS and POR.

Geochemical analysis of surface sediments showed that the total concentrations of Cr, Cu, Ni and Zn in the deep-water sediments are significantly greater in RAS and POR than in SAL1. It is noteworthy that Ni and Zn concentrations are significantly less in POR whose catchment is governed mainly by frost action, compared to RAS, lying in the catchment dominated by melting of ground ice in the rock glacier.

The data provided evidence for the presence of natural ARDs in the catchments of RAS and POR situated at the toes of rock glaciers. However, POR and its catchment located in the periglacial environment with a MAAT below −2 °C are affected by less severe ARD than RAS and its catchment located within the periglacial belt with MAATs ranging from −2° C to +3 °C (Ilyashuk *et al.*, 2017).

Concentrations of five metals (Al, Cr, Cu, Mn, and Ni) in the chironomid body tissues are significantly greater in RAS and POR as compared to SAL1. The greatest concentration of Mn, Ni and Zn were measured in chironomids from RAS. The difference between the lakes in the metal body burdens observed in the invertebrates reflects the difference in the presence as well as in the severity of ARD.

It would be useful to test our hypothesis and obtained results on a broader set of lakes and in different mountain areas of the world.

References

French, H.M., 2007. *The Periglacial Environment.* Chichester: John Wiley & Sons, 458 pp.

Ilyashuk, B.P., Ilyashuk, E.A., Psenner, R., Tessadri, R., Koinig, K.A., 2014. Rock glacier outflows may adversely affect lakes: lessons from the past and present of two neighboring water bodies in a crystalline-rock watershed. *Environmental Science and Technology* 48: 6192–6200.

Ilyashuk, B.P., Ilyashuk, E.A., Psenner, R., Tessadri, R., Koinig, K.A., 2017. Rock glaciers in crystalline catchments: hidden permafrost-related threats to alpine headwater lakes. *Global Change Biology*, https://doi.org/10.1111/gcb.13985.

Slemmons, K.E.H., Sarosa, J.E., Simon, K., 2013. The influence of glacial meltwater on alpine aquatic ecosystems: a review. *Environmental Science: Processes and Impacts* 15: 1794–1806.

Spötl, C., Unterwurzacher, M., Mangini, A., Longstaffe, F., 2002. Carbonate speleothems in the dry, inneralpine Vinschgau Valley, northernmost Italy: witnesses of changes in climate and hydrology since the Last Glacial Maximum. *Journal of Sedimentary Research* 72: 793–808.

The Council of the EU, 1998. Council Directive 98/83/EC of 3 November 1998 on the quality of water intended for human consumption. *Official Journal of the European Communities* L330: 32–54.

Thies, H., Nickus, U., Mair, V., Tessadri, R., Tait, D., Thaler, B., Psenner, R., 2007. Unexpected response of high alpine lake waters to climate warming. *Environmental Science and Technology* 41: 7424–7429.

Todd, A.S., Manning, A.H., Verplanck, P.L., Crouch, C., McKnight, D.M., Dunham, R., 2012. Climate-change-driven deterioration of water quality in a mineralized watershed. *Environmental Science and Technology* 46: 9324–9332.

Permafrost-related threats to alpine headwater lakes: insights from paleo-ecotoxicological studies

Elena A. Ilyashuk[1]
Boris P. Ilyashuk[1, 2]
Roland Psenner[1, 2]
Richard Tessadri[3]
Karin A. Koinig[1, 2]
[1]*Institute of Ecology, University of Innsbruck, Technikerstraße 25, 6020 Innsbruck, Austria, elena.ilyashuk@uibk.ac.at*
[2]*Institute for Alpine Environment, Eurac Research, Viale Druso 1, 39100 Bozen/Bolzano, Italy*
[3]*Institute of Mineralogy and Petrography, University of Innsbruck, Innrain 52, 6020 Innsbruck, Austria*

Abstract

The exposure of fresh surfaces of sulfide-rich rocks to air and oxygenated water by retreating glaciers and degrading permafrost increases the oxidation of sulfide minerals, which is responsible for the generation of natural acid rock drainage (ARD). Applying the paleoecological analysis of morphological abnormalities in populations of a chironomid species inhabiting lakes affected by ARD through the past millennium, we tested and rejected the hypothesis that unfavorable conditions for aquatic life in the ARD-stressed lakes are largely related to the temperature increase over recent decades, responsible for the enhanced release of ARD contaminants. Our results indicate that the ARDs generated by rock glaciers in the catchments are of a long-lasting nature and the frequency of chironomid morphological deformities was significantly higher during the Little Ice Age (LIA) than during pre- or post-LIA periods, suggesting that lower water temperatures may increase the adverse impacts of ARD on aquatic invertebrates.

Keywords: acid drainage, chironomid deformities, metals, paleo-ecotoxicology, periglacial environments, rock glacier.

Introduction

The expansion and upward movement of the periglacial mountain belts in response to climate warming are usually accompanied by an increase in runoff from alpine basins and rapid formation and growth of lakes and ponds in deglaciating areas (e.g. Tartari *et al.,* 2013), which are an important component of alpine periglacial landscapes. Recent investigations in an alpine watershed with sulfide-bearing lithology have demonstrated that rock glaciers, one of the most common permafrost landforms in periglacial mountain environments, can represent potent sources of acidic, metal-rich solutes that severely disturb lake ecosystems (Thies *et al.*, 2007; Ilyashuk *et al.*, 2014). The incidence of morphological abnormalities (response at the phenotypic level) in chironomid (Diptera: Chironomidae) populations inhabiting such lakes can be as high as that recorded in chironomid populations from sites heavily polluted by trace metals of anthropogenic origin (Ilyashuk *et al.*, 2014).

In the present study, we hypothesized that, due to reduced oxidation of the sulfide-bearing minerals at lower temperatures (e.g. Schoonen *et al.*, 2000), conditions for aquatic life in lakes affected by acid rock drainage (ARD) generated by rock glaciers may have been more favorable during colder climate phases than during warmer phases in the past.

Materials and methods

To test the research hypothesis we applied paleolimnological techniques to track and compare changes over the past millennium in the incidence of morphological abnormalities in populations of the chironomid *Pseudodiamesa nivosa* from two lakes affected by ARDs generated by rock glaciers. As a reference, we sampled a third high-alpine lake, not influenced by rock glaciers and without obvious signs of ARD in the catchment. Sediment cores were obtained with a gravity corer from the deepest part of each lake. The incidence of morphological abnormalities (namely mentum gaps) in chironomid subfossil remains was used for assessing patterns and temporal trends in the ecotoxicological state of the lakes over the past millennium.

Results and discussion

The inspection of *P. nivosa* remains in surface sediments for mentum abnormalities revealed a high incidence of mentum gaps in the RAS (32−38%) and POR (7−14%) populations. In SAL1, without a rock glacier in the catchment, the frequency of mentum gaps is not higher than 1%, which is well within natural background levels for chironomid populations (Vermeulen, 1995).

The analysis of down-core sediment samples showed that a high mentum gap incidence in the RAS population (between 33% and 58%) and the POR population (7−33%) persisted throughout the past millennium. The findings provide evidence that the ARDs in the catchments of RAS and POR are of a long-lasting nature and cannot be associated with only the temperature increase over recent decades.

The highest rates of mentum gap incidence in the stressed *P. nivosa* populations of RAS (55−58%) and POR (16−33%) were recorded during the LIA, the coldest period over the last millennium in the European Alps. The rates of mentum gap incidence in RAS and POR during the LIA are approximately 1.4 and 2.3 times higher, respectively, than over the post-LIA period. Our paleoecological inferences from the lakes located in the periglacial belt are in line with the findings of Pereira *et al.* (2017) in the chronic toxicity experiments, which showed that lower temperatures can increase metal toxicity to invertebrates exposed to toxicants for a long time. Apparently, the temperature-mediated effects of exposure duration and physiological mechanisms of the chironomid response amplify the mentum gap incidences in the RAS and POR populations during cold periods, accompanied by prolonged lake ice cover and slowed down growth and development of the chironomids.

Altogether, the results of the paleolimnological analysis allowed us to track the periods of more unfavorable conditions for aquatic life in the ARD-stressed lakes, highlighting that examining chironomid mentum deformities is a valid paleo-ecotoxicological tool (Ilyashuk *et al.*, 2017).

References

Ilyashuk, B.P., Ilyashuk, E.A., Psenner, R., Tessadri, R., Koinig, K.A., 2014. Rock glacier outflows may adversely affect lakes: lessons from the past and present of two neighboring water bodies in a crystalline-rock watershed. *Environmental Science and Technology* 48: 6192–6200.

Ilyashuk, B.P., Ilyashuk, E.A., Psenner, R., Tessadri, R., Koinig, K.A., 2017. Rock glaciers in crystalline catchments: hidden permafrost-related threats to alpine headwater lakes. *Global Change Biology,* https://doi.org/10.1111/gcb.13985.

Pereira, C.M.S., Deruytter, D., Blust, R., De Schamphelaere, K.A.C., 2017. Effect of temperature on chronic toxicity of copper, zinc, and nickel to *Daphnia magna*. *Environmental Toxicology and Chemistry* 36: 1909–1916.

Schoonen, M., Elsetinow, A., Borda, M., Strongin, D., 2000. Effect of temperature and illumination on pyrite oxidation between pH 2 and 6. *Geochemical Transactions*, 1:23, doi:10.1186/1467-4866-1-23.

Tartari, G., Salerno, F., Buraschi, E., Bruccoleri, G., Smiraglia, C., 2008. Lake surface area variations in the North-Eastern sector of Sagarmatha National Park (Nepal) at the end of the 20th century by comparison of historical maps. *Journal of Limnology* 67: 139–154.

Thies, H., Nickus, U., Mair, V., Tessadri, R., Tait, D., Thaler, B., Psenner, R., 2007. Unexpected response of high alpine lake waters to climate warming. *Environmental Science and Technology* 41: 7424–7429.

Vermeulen, A.C., 1995. Elaboration of chironomid deformities as bioindicators of toxic sediment stress: the potential application of mixture toxicity concepts. *Annales Zoologici Fennici* 32: 265–285.

Ice-Wedge Thermokarst: Past, Present, and Future

Mikhail Kanevskiy[1]
Yuri Shur[2]
M. Torre Jorgenson[3,2]
[1]*Institute of Northern Engineering, University of Alaska Fairbanks, Fairbanks, Alaska, USA, mkanevskiy@alaska.edu*
[2]*Institute of Northern Engineering, University of Alaska Fairbanks, Fairbanks, Alaska, USA*
[3]*Alaska Ecoscience, Fairbanks, Alaska, USA*

Abstract

Ice-wedge thermokarst has played an important role in permafrost evolution, and numerous cycles of ice-wedge formation/degradation have occurred through the Quaternary history. Studies of ice-wedge degradation help to explain processes of past ice-wedge thermokarst and predict its future consequences. We developed a conceptual model of ice-wedge degradation/stabilization, which is based on the dynamics of the intermediate layer of the upper permafrost. This model explains high resilience of ice-wedge systems and low probability of formation of large thaw lakes in the continuous permafrost zone. Absence of the intermediate layer at the time of yedoma accumulation and increased precipitation caused very high activity of thaw-lake formation during the Pleistocene/Holocene transition.

Keywords: permafrost; yedoma; ice-wedge degradation; permafrost zones; intermediate layer; thaw-lake basins.

Introduction

Wedge ice is the most common type of massive ground ice. It can be encountered almost everywhere in the continuous permafrost zone and is very common in the discontinuous permafrost zone, especially in its inactive form. Permafrost evolution during the Quaternary time has been largely defined by alternating periods of active ice-wedge development and periods of ice-wedge degradation accompanied by formation of thaw-lake basins. Numerous cycles of ice-wedge formation/degradation that occurred during the late Quaternary have been recorded in Siberia and, to a lesser extent, in northern part of North America. Available data refer mostly to cycles that started in the late Pleistocene and included large-scale thermokarst events, which occurred during the Pleistocene/Holocene transition that caused formation of numerous thaw-lake basins (alases). These transformations have triggered fundamental geomorphic, hydrological, and environmental changes. Generally, ice-wedge degradation starts with an increase in the active-layer thickness (ALT), which affects top parts of ice wedges and eventually may lead to their complete thawing and, under certain conditions, formation of large thermokarst lakes. However, we still do not have clear understanding of rates and mechanisms of this long-term process. Our studies of modern ice-wedge thermokarst define the main stages and patterns of ice-wedge degradation, which help to explain thermokarst processes in the past and predict their consequences in the future.

Ice-wedge development and degradation in the late Quaternary

Syngenetically frozen ice-rich deposits with large ice wedges (known as yedoma or ice complex) were forming very actively within unglaciated areas during full-scale glaciations, while interglacial periods were characterized by increasing thermokarst activity. By the end of the Pleistocene, the accumulation of silt in extremely cold periglacial environments formed yedoma in the vast areas of Eurasia and North America, which were unglaciated during the last Ice Age. Since the end of the Pleistocene, a significant portion of yedoma in all permafrost zones has been destroyed by thermokarst and thermal erosion.

Dramatic changes in the yedoma environment that caused formation of large and deep thaw-lake basins started approximately 12-14 ky BP. Despite a common opinion that the climate warming resulted in a significant increase in the ALT, there is strong evidence that a wetter climate facilitated formation of a thick vegetation mat and transition from dry "tundra-steppe" ecosystem to wet tundra. These processes led to a decrease in the ALT and formation of the ice-rich intermediate layer (IL) above large ice wedges (Shur, 1988). More likely, large-scale thermokarst was not triggered solely by increased air temperatures, but rather by a significant increase in precipitation. This resulted in an accumulation of water in depressions, which led to lake thermokarst, and increased activity of thermal erosion.

Extent of yedoma degradation strongly varies among different permafrost zones (in their modern boundaries) and landscapes. In the continuous permafrost zone, more than 50% of yedoma terrain has degraded within flat lowlands (e.g., Coastal Lowlands of Northern Yakutia in Siberia and northern part of the Seward Peninsula in Western Alaska), while better drainage conditions in uplands of Siberia and Alaska generally prevented large-scale yedoma degradation (e.g., Arctic Foothills of northern Alaska). Thaw-lake basins in this zone have experienced fast peat accumulation and a new cycle of active ice-wedge development, which started immediately after drainage. Currently, the infrequent development of thaw lakes in yedoma occurs mainly in the areas with relatively warm permafrost, such as the Seward Peninsula (Shur *et al.*, 2012).

In the discontinuous permafrost zone, yedoma has been almost completely reworked by thermokarst and thermal erosion within poorly drained plains (e.g., Koyukuk and Innoko Flats in West-Central Alaska). In this zone, yedoma occurs mainly in foothills and valleys within the uplands and low mountains, where ice-rich yedoma deposits are commonly overlain by a layer of ice-poor soils (yedoma silt reworked by earlier thermokarst events). Now, this layer protects remnants of yedoma from active thermokarst even in the areas of very warm discontinuous permafrost. Modern ice-wedge development in this zone occurs sporadically (mainly in peatlands) and is not very active. In the sporadic permafrost zone, yedoma remnants probably survived through the Holocene warming in some relatively small areas but it still needs confirmation.

Conceptual model of ice-wedge degradation/stabilization

Widespread degradation of ice wedges has been observed during the last decades in Arctic regions of Eurasia and North America. Despite strong concerns that progressive ice-wedge thermokarst will eventually lead to permafrost degradation, our studies showed that ice-wedge thawing is usually a reversible process in the continuous permafrost zone. We developed a conceptual model of ice-wedge dynamics that identify the main factors affecting ice-wedge degradation and stabilization and the main stages of this quasi-cyclic process (Jorgenson *et al.,* 2015; Kanevskiy *et al.*, 2017).

According to this model, vegetation colonization and accumulation of organic matter in the troughs developing over degrading wedges leads to a reduction in soil temperatures, a decrease in the ALT, formation of the new ice-rich IL above stabilizing ice wedges, and rejuvenation of ice wedges. Thus, degradation of ice wedges in the continuous permafrost zone very seldom continues to their complete melting, and in most cases wedges recover.

Vulnerability of ice wedges to thermokarst is controlled by the thickness of the IL of the upper permafrost, which overlies ice wedges and protects them from thawing. A thickness of the IL on top of stabilized ice wedges is usually 2 to 3 times greater than that in undisturbed conditions, which makes the permafrost more resistant to external changes, such as climate change and disturbance. This mechanism explains the very low probability of formation of large thaw lakes in the continuous permafrost zone as a result of ice-wedge thermokarst.

We also presume that wedge-ice volume in the upper permafrost is crucial for formation of thermokarst lakes. In modern environments of the continuous permafrost zone, it is commonly less than 20-30% (e.g., in Holocene deposits of the Arctic Coastal Plain of northern Alaska and within the modern IL above yedoma), which is probably not sufficient. Absence of the protective IL during yedoma accumulation may explain very active degradation of large ice wedges and formation of thaw lakes during the Pleistocene/Holocene transition.

Acknowledgments

This work was supported by the National Science Foundation grants ARC 1023623 and ArcSEES 1233854.

References

Jorgenson, M.T., Kanevskiy, M., Shur, Y., Moskalenko, N., Brown, D.R.N., Wickland, K., Striegl, R., & Koch, J., 2015. Ground ice dynamics and ecological feedbacks control ice-wedge degradation and stabilization. *Journal of Geophysical Research: Earth Surface* 120 (11): 2280-2297.

Kanevskiy, M., Shur, Y., Jorgenson, T., Brown, D.R.N., Moskalenko, N., Brown, J., Walker, D.A., Raynolds, M.K., & Buchhorn, M., 2017. Degradation and stabilization of ice wedges: Implications for assessing risk of thermokarst in northern Alaska. *Geomorphology* 297: 20-42.

Shur, Y.L., 1988. The upper horizon of permafrost soils. *Proceedings of the Fifth International Conference on Permafrost,* Trondheim, Norway, August 2-5. Vol. 1: 867–871.

Shur, Y., Kanevskiy, M., Jorgenson, T., Dillon, M., Stephani, E., Bray, M., & Fortier, D. 2012. Permafrost degradation and thaw settlement under lakes in yedoma environment. *Proceedings of the Tenth International Conference on Permafrost,* Salekhard, Russia, June 25-29, Vol. 1: 383-388.

The Habitat of the Megin Mammoth: vegetation, environments and climate in Central Yakutia during the late Weichselian

Frank Kienast[1]
Natalia Rudaya[2]
Evgeny N. Maschenko[3]
Olga Potapova[4]
Albert V. Protopopov[5]

[1]*Senckenberg Research Institute and Natural History Museum, Research Station of Quaternary Palaeontology, Weimar, Germany, Frank.Kienast@senckenberg.de*
[2]*Institute of Archaeology & Ethnography, Russian Academy of Sciences, Siberian Branch, Novosibirsk, Russia*
[3] *Borissiak Paleontological Institute, Russian Academy of Sciences, Moscow, Russia*
[4]*The Mammoth Site of Hot Springs, SD, Inc., Hot Springs, SD, USA*
[5]*Yakutian Academy of Sciences, Yakutsk, Russia*

Abstract

Detailed palaeobotanical analyses of organic material found in the context of the almost complete skeleton of a mammoth at the Megin site on the Suola River bank near Nizhniy Bestyakh in the Lena River basin form the basis for the reconstruction of vegetation, habitats and climate conditions existing during the late Weichselian in Central Yakutia, Russia. The dominance of pollen from *Artemisia* and other herbaceous taxa indicate that steppe vegetation prevailed in the study area. A wide range of habitats including aquatic and riparian biotopes, grassland and groves could be reconstructed by macrofossils. Pollen and macrofossils of larch and birch prove the existence of forest patches and indicate that the study area was a northern refugium for trees. Some of the aquatic or riparian plants indicate a high MTWA. Steppe plants, halophytes and riparian pioneers indicate dry conditions; the latter are characteristic of seasonally fluctuating water level.

Keywords: Megin mammoth; palaeobotany; late Weichselian; MIS 2; Central Yakutia; mammoth steppe.

Introduction

A nearly complete skeleton of a mammoth was discovered at the Megin Site on the Suola River bank near Nizhniy Bestyakh in the Lena River basin, Central Yakutia in 2015 (Maschenko *et al.,* 2016; Potapova et al., 2016). The mammoth was found together with bone remains of other mainly open-biotope herbivores (Bison, musk ox, horse, reindeer and roe deer) and with coprolites of mammoth and woolly rhinoceros. The 8 meter sequence of syngenetic sandy Yedoma permafrost deposits was radiocarbon dated between 31,180 and 9,130 cal years BP. Radiocarbon dating of the mammoth itself resulted in an age of 17,820–17,330 cal BP indicating that the mammoth lived during the late glacial period (MIS 2). With respect to the taxonomic identification of the mammoth, radiocarbon dating, mitochondrial DNA analyses and morphometric characteristics led to contradictory results so that a definitive decision whether it is a steppe mammoth (*M. trogontherii*)or a woolly mammoth (*M. primigenius*) cannot be taken until nuclear genomic data are available (Maschenko *et al.,* 2016).

Here, we present palaeobotanical data based on plant macro-remains (61 taxa) and pollen (25 taxa) from a clump of plant material collected at the approximate Megin Mammoth skeleton level, and give implications on vegetation, environmental and climate conditions existing at the lifetime of the mammoth..

Results and Discussion

The studied organic material represents an accumulation of plant remains originating obviously from a wide variety of habitats. Animals (*Cristatella mucedo, Daphnia* spp.), algae (*Botryococcus*) and vascular plants representative of aquatic environments indicate the deposition in shallow water, e.g. at the shore of a small lake or pond.

Among submerged and emerged aquatics, several *Potamogeton* species, *Batrachium*, *Sparganium minimum* and *Ceratophyllum demersum* were found together with typical reed or, respectively, riparian plants, such as *Butomus umbellatus, Alisma, Sagittaria, Eleocharis palustris*, *Scirpus tabernaemontani, Scutellaria galericulata, Epilobium palustre, Lysimachia thyrsiflora* and a number of *Carex* species.

Some of the aquatic or riparian plants have high demands on temperature during the growing season and are restricted in their distribution by summer warmth. This is true especially for *Ceratophyllum demersum*, which occurs at a mean July temperature above 16 °C only vegetatively and requires higher temperature for flowering and fruiting. A matured *Ceratophyllum* fruit was found in the fossil plant material. Temperature during the growing season resembling or even exceeding modern conditions in Central Yakutia can therefore be assumed for the time of deposition of the plant remains.

Many of the detected riparian plants, e.g. *Alisma*, *Potentilla supina, Chenopodium* spp., *Rorippa palustris*, and *Rumex maritimus* are characteristic of uncovered, erosive, muddy shore sites getting exposed in the course of the growing season, which is an indication for seasonally fluctuating water level. Most of these littoral pioneer species are also adapted to eutrophic and brackish conditions. This is also true for a number of detected ruderal plants such as *Puccinellia hauptiana* and *Polygonum* cf. *persicaria*. Fluctuating water level and salt accumulation are inland both indicative of high evaporation and dry climate conditions.

The assumption of dry climate at the time of deposition is confirmed by numerous species characteristic of steppes and steppified meadows, which account for a quarter of all plant species recorded by macrofossils. The high percentage of pollen from *Artemisia* and other herbaceous taxa indicate that steppe vegetation prevailed in the study area. *Aster alpinus, Alyssum obovatum, Bromopsis* cf. *pumpelliana*, *Elymus*, *Festuca, Koeleria, Androsace septentrionalis, Potentilla arenosa, P. conferta*, and *Thesium refractum* are such steppe indicators. Many of the detected grasses are productive and might have provided the food base for large herbivores. Plants that usually occur at ruderal sites within steppe vegetation, e.g. Crepis tectorum, *Corispermum, Descurainia sophioides, Carex duriuscula*, *Plantago canescens*, and *Linaria acutiloba* point to frequent disturbances of the vegetation possibly caused by large herbivores (grazing, trampling, wallowing).

The high number of steppe plants indicates a largely open landscape, which however formed a mosaic of grasslands and light coniferous forest patches, which are represented by pollen of larch and birch and by macrofossils of tree and shrub species like *Larix gmelinii*, *Betula platyphylla*, *Rosa acicularis*, and *Spiraea salicifolia*. At the margin or in glades of forest patches, herbs such as the detected *Hieracium umbellatum* and *Thalictrum simplex* occurred. The palaeobotanical evidence of forest plants proves that Central Yakutia was a northern refugium for trees during the Weichselian cold stage.

The variety of habitats indicated by the plant remains reflects an environment suitable for the existence of megaherbivores providing water, food, shelter, minerals (salt in top soil) and open ground for wallowing in mud and dust. Apart from the mammal bone remains listed above, the occurrence of *Sordaria* spores indirectly point to the presence of grazers as this fungus colonizes animal dung.

References

Maschenko, E. N., Potapova, O., Protopopov, A. V., Heintzmann, P. D., … Kolesov, S., 2016. Discovery of a new skeleton of the mammoth (*Mammuthus* sp.) from the Sartanian deposits in eastern Siberia, Russia. *Journal of Vertebrate Paleontology, Program and Abstracts of the Society of Vertebrate Paleontology - 76th Annual Meeting*, Salt Lake City, Utah, USA., October 26–29: 184-185.

Potapova, O., Maschenko, E. N., Protopopov, A. V., Kienast, F., … Pavlov, I., 2016. The Sartanian Biodiversity of Central Yakutia, Russia: The Analyses of the New Late Pleistocene Megin Site. *Journal of Vertebrate Paleontology, Program and Abstracts of the Society of Vertebrate Paleontology - 76th Annual Meeting*, Salt Lake City, Utah, USA., October 26–29: 208.

Morphometry and spatial distribution of glacial cirques in the Central Pyrenees (Aran and Boí valleys)

Luís Lopes[1]
Marc Oliva[2]
Marcelo Fernandes[1]
Paulo Pereira[3]
Pedro Palma[1]
Jesús Ruiz-Fernández[4]

[1]*Centre for Geographical Studies - IGOT, Universidade de Lisboa, Portugal, luis.filipelopes@live.com.pt*
[2]*Department of Geography, University of Barcelona, Spain*
[3]*Environmental Management Center, Mykolas Romeris University, Vilnius, Lithuania*
[2] *Department of Geography, University of Oviedo, Spain*

Abstract

The morphology of glacial cirques as well as their distribution is a consequence of specific palaeoenvironmental conditions. Therefore, its characterization provides quantitative and qualitative information about the characteristics of past glaciers and climates. Within this context, using a multivariate statistical approach we have examined the distribution, morphometrical and topographical characteristics of glacial cirques in two valleys in the Central Pyrenees, located in different slope aspects of this mountain range: Aran (north) and Boí (south). A total of 186 glacial cirques have been identified: 119 in Aran and 67 in Boí. They show significant differences in terms of morphometrical and topographical properties. Glacial cirques are located at lower altitudes in Aran valley than in Boí valley, generally above 2200 m. These features are also longer and wider in Boí valley.

Keywords: Central Pyrenees; Glacial Cirques, Periglacial Processes, Paleoenvironments.

Introduction

One of the most distinctive landscape features in Mediterranean high mountain are the currently ice-free glacial cirques where periglacial processes are still active (Oliva *et al.*, 2016). The spatial distribution and dimensions of glacial cirques are consequence both of glacial erosion and of post-glacial periglacial activity (García-Ruiz *et al.*, 2000; Barr & Spagnolo, 2015).

This research examines the morphology and distribution of glacial cirques in two valleys from the Central Pyrenees: Aran and Boí valleys. Aran valley is located in the northern slope of this range and Boí valley is placed in the southern slope. Both correspond to formerly glaciated U-shaped valleys (Vilaplana 1983; Fernandes *et al.*, 2016). Aran valley (550 km^2), aligned E-W between 500-3000 a.s.l., is mostly composed of granites and slates. Boí valley (247 km^2), which flows NE-SW between 850-3000 m, is composed of granites and shales. An accurate characterization of the geographical distribution of the cirques in both valleys can allow unveiling the key variables involved in the development of glacial cirques, allowing also for paleoclimatic inferences.

Methodology

The geomorphological mapping of the cirques was conducted through photointerpretation using high resolution imagery (25 cm pixel size) provided by the Institut Cartogràfic i Geològic de Catalunya and complemented with Basemap ESRI images and Google Earth Pro. The maps were subsequently validated with topographic cartography at scale 1:5000 and field observations. The lithological information was obtained from geological maps at scale 1:50.000. Several topographical and morphometrical parameters of the glacial cirques commonly examined in the scientific literature have been measured in a GIS environment followed by a statistical and geospatial analysis.

Results

A total of 186 glacial cirques have been identified, with 119 units in Aran valley and 67 in Boí valley. The density of glacial cirques is 0.22 per km^2 in Aran and 0.27 per km^2 in Boí. The glacial cirques are generally distributed at lower altitudes in Aran than in Boí, with 8.4% of the glacial cirque floors placed below 2000 m (figure 1). Most of the glacial cirques sit between 2200-2400 m (42.9%) and decrease notoriously at higher elevations with 18.5% in the range 2400-2600 m (15.1%). Only four cirques (3.3%) have cirque floors located in terrain above 2600 m. By contrast, in Boí valley glacial cirques placed under 2000 m are inexistent and the elevation range 2200-2400 m does not concentrate most of the landforms (29.8%), which are included within the interval 2400-2600 m (47.7%). Up to 13.4% of the glacial cirques developed above 2600 m. Aran cirques show a prevailing NE aspect (32.8%), while in Boí glacial cirques do not show a clear pattern. Regarding the lithology, glacial cirques in Aran do not show a dominant bedrock type, contrasting with Boí valley, where 84% of the glacial cirques are shaped in granitic bedrock.

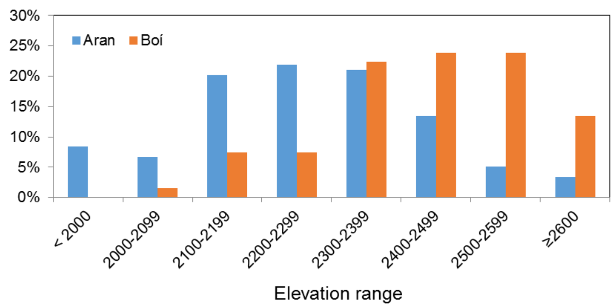

Figure 1. Distribution of glacial cirques in both valleys according to elevation range.

In Aran valley the maximum length (L) and width (W) of the glacial cirques presents an increasing trend with altitude. The longest cirques are observed within the range 2400-2500 m (mean of 646 m), while the widest are placed at 2500-2600 m (437 m). In higher cirques, both values decrease considerably (265 and 137 m, respectively). This decline is also observable in cirque amplitude (H), being relatively stable until 2600 m (values varying between 299 and 389 m) but considerably lower for cirques above this level (196 m). In Boí valley, glacial cirques show a greater length, width and amplitude at higher altitudes. The longest (870 m) and widest cirques (528 m) are located within the elevation range 2300-2400 m. On the other hand, the H presents a clear decreasing trend with increasing elevations, being maximum at 2000-2100 m (676 m) and minimum in cirques above 2600 m (319 m). But Boí cirques remain almost stable.

Discussion and conclusions

Present-day morphology of glacial cirques result from past glacial processes and post-glacial periglacial dynamics (Barr and Spagnolo, 2015). We examined two contrasting U-shaped glacial valleys in the Central Pyrenees that were largely glaciated during the Last Glaciation (Vilaplana 1983; Fernandes *et al.*, 2016). The impact of glacial and periglacial processes on these valleys with different environmental conditions (lithology, aspect, climate) has conditioned a different spatial distribution of glacial cirques, which also show different spatial and morphological characteristics.

The morphostructure of Aran valley conditioned a larger number of glacial cirques than in Boí valley, but these landforms are larger in Boí valley, where they are mostly shaped on granites and shales. The elevation of the cirques is higher in Boí valley than in Aran valley. This is conditioned by the lower elevation of the mountain ridges, where the intensity and duration of the glaciations was not enough to carve the hollows characteristic of the glacial cirques (Barr and Spagnolo, 2015). Besides, their southern exposure did not favour snow accumulation and subsequent transformation into ice, impeding the deepening of these concavities by means of glacial erosion. Most of the cirques in Aran valley have a prevailing NE aspect, with a significant number exposed to eastern aspects. The prevailing W and SW winds, as also observed in other European massifs (Barr and Spagnolo, 2015), favoured snow accumulation by wind redistribution. In other valleys of the Central Pyrenees the morphometric variables are similar to those existing in Aran and Boí valleys (García-Ruiz *et al.*, 2000). However, the dimensions of glacial cirques in both valleys are greater than in other mountain ranges in the northern sector of the Iberian Peninsula, such as the Picos de Europa and the sierras of SW Asturias (Ruiz-Fernández *et al.*, 2019).

References

Barr, LD. & Spagnolo, M., 2015. Glacial cirques as palaeoenvironmental indicators: Their potential and limitations. *Earth-Science Reviews* 151 48–78.

Fernandes, M.; Oliva, M.; Palma, P.; Ruiz-Fernández, J. & Lopes, L., 2017. Glacial stages and post-glacial environmental evolution in the Upper Garonne valley, Central Pyrenees. *Science of the Total Environment*, 584-585, 1282-1299.

García-Ruiz, JM., Gómez-Villar, A., Ortigosa, L., Martí-Bono. C., 2000. Morphometry of glacial cirques in the Central Spanish Pyrenees. Geogr. Ann., 82 A (4): 433–442.

Ruiz-Fernández, J., Poblete-Piedrabuena, MA., Serrano-Muela, MP., Martí-Bono, C., García-Ruiz, JM., 2009. Morphometry of glacial cirques in the Cantabrian Range (Northwest Spain). Z. Geomorph. N. F., 53 (1): 47–68.

Vilaplana, JM., 1983. Estudi del glaciarisme quaterni de les Altes Valls de la Ribargorça. PhD Thesis, Barcelona University, Barcelona, Spain.

East Siberian Shelf slope sediments suggest permafrost carbon mobilization duringthe last glacial termination

Jannik Martens[1,2*],
Birgit Wild[1,2],
Francesco Muschitiello[2,3,4],
Tommaso Tesi[1,2,5],
Matt O'Regan[2,3],
Martin Jakobsson[2,3],
August Andersson[1,2],
Martin Sköld[6],
Igor Semiletov[7,8,9],
Oleg V. Dudarev[7,8],
ÖrjanGustafsson[1,2]

[1]*Department of Environmental Science and Analytical Chemistry (ACES), Stockholm University, Sweden*
[2]*Bolin Centre for Climate Research, Stockholm University, Sweden*
[3]*Department of Geological Sciences (IGV), Stockholm University, Sweden*
[4]*Lamont-Doherty Earth Observatory, Columbia University, USA*
[5]*Institute of Marine Sciences, National Research Council (ISMAR-CNR) Bologna, Italy*
[6]*Department of Mathematics, Stockholm University, Sweden*
[7]*Pacific Oceanological Institute FEB RAS Vladivostok, Russia*
[8]*Tomsk Polytechnic University, Russia*
[9]*University of Alaska Fairbanks, USA*

Abstract

Arctic warming is expected to activate largepermafrost organic carbon stocks (PF-C)and stimulate their mineralization to greenhouse gases (CO_2 and CH_4). Marine geoarchivessuggest that the remobilization of PF-C was higherduring theabrupt MIS2/MIS1 transition (early Holocenefrom 11.7 ka BP) than in themodern system. This study characterizes OC fluxes to sediments (SWERUS-L2-31-PC1) of the continental slope to the East Siberian Arctic Shelf system (ESAS) from the last glacial maximum (LGM) to the present. Wemeasured carbon isotopes ($\Delta^{14}C$, $\delta^{13}C$), as well as lignin phenols, and identified PF-C from deep and old permafrost depositsas an important OC source during the post-LGMclimate warming (16.0 – 6.6ka BP). Large-scale permafrost degradation during the last deglaciation might have caused carbon cycle perturbationsthat would explain glacial-interglacial CO_2anomalies of theatmosphere.

Keywords:permafrost thaw; deglaciation; coastal erosion; Siberian shelf

Introduction

The Arctic mightact as a capacitor for global carbon cycling between glacials and interglacials. During cold episodes, e.g. the last glacial maximum (LGM),arctic environments capture carbon which is then stored frozen in permafrost deposits(PF-C) (Zimov et al., 2006). Climate warming turnspermafrost into an organic carbon(OC) source sincehigher environmental temperaturesstimulate themicrobial transformation of PF-Cto CO_2 and CH_4(Schuur et al., 2015). Permafrost thaw exposesOC by various mechanisms; most importantly by i) progressive seasonal thawing of the permafrost surface (active layer) and ii) abrupt collapse of ground ice and thermokarst of deeper compartments(Vonk and Gustafsson, 2013).

Arctic rivers and nearshore seas are the main recipients of mobilized particulate PF-C. Accordingly, marine sediments of the East Siberian Arctic Shelf system (ESAS) exhibit characteristics of pre-aged terrestrial OC (depleted $\delta^{13}C$ values, depleted $\Delta^{14}C$ values, plant-derived molecules). Sediment archives suggestthat the seaward transport of PF-C was much stronger during the Holocene temperaturemaximum (HTM)11.7– 8.5ka BP compared to modern rates(Keskitalo et al., 2017; Tesi et al., 2016). This implicates large-scaledeglacial permafrost thawing and suggests PF-C as a possible source of post-glacial (and future) atmospheric CO_2 emissions (Crichton et al., 2016). No published study has investigated PF-C fluxes to Ocean sediments during the entire MIS2/MIS1 termination.

Materials and methods

This study reconstructs the PF-C transport to the Arctic Ocean of the MIS2 (LGM) and MIS1using a sediment core (SWERUS-L2-31-PC1) from the continental rise of the ESAS. Our approach combines bulk carbon isotopes ($\Delta^{14}C$, $\delta^{13}C$) with terrestrial biomarkers (CuO-derived lignin phenols) to identify and characterize land-based carbon sources. Furthermore, bulk radiocarbon ages corrected for their residence time in the seabed ($\Delta\Delta^{14}C$) and stable carbon isotopes ($\delta^{13}C$)permit statistical source apportionments, whichwill be applied to quantify the flux of PF-C toouter Siberian Shelf sediments.

Preliminary results and interpretations

Preliminary data suggest higher fluxes of OC from permafrost depositsduring the MIS2/MIS1 deglacial (16.0 – 6.6ka BP) compared to LGM and the late Holocene. Bulk carbon isotopes ($\Delta\Delta^{14}C$, $\delta^{13}C$)resemble those of Siberian PF-C end members and lignin phenol fluxes are one order of magnitude higherduring the deglacialthan in the periods before (LGM) and after (late Holocene).A large fraction of old (^{14}C-depleted) PF-C in the MIS2/MIS1 post-glacial section indicates the release of material from deep permafrost compartments (e.g. Ice Complex deposits) that are ubiquitous in NE Siberia, and suggests that coastal erosion might have been an important OC remobilization pathway.

The core 31-PC1 archive suggests permafrost thawing and the mobilization of PF-C to the Arctic Ocean during the post-glacial temperature increase. We preliminarily infer that Siberian permafrost was stable during the LGM (MIS2) but reacted sensitively16.0 ka BP to Northern Hemispherewarming not higher than1.0°C(Shakun et al., 2012)during theHeinrich Stadial 1/Mystery Interval (17 – 15 ka BP). Understanding the mobilization of PF-C will help elucidating the role of permafrost as a pool for glacial-interglacial OC storage and thresholds for PF-C release in a warming climate.

References

Crichton, K.A., Bouttes, N., Roche, D.M., Chappellaz, J., Krinner, G., 2016. Permafrost carbon as a missing link to explain CO2 changes during the last deglaciation. *Nat. Geosci.* 9, 683–686. doi:doi:10.1038/ngeo2793

Keskitalo, K., Tesi, T., Bröder, L., Andersson, A., Pearce, C., Sköld, M., Semiletov, I.P., Dudarev, O. V., Gustafsson, Ö., 2017. Sources and characteristics of terrestrial carbon in Holocene-scale sediments of the East Siberian Sea. *Clim. Past* 13, 1213–1226. doi:10.5194/cp-13-1213-2017

Schuur, E.A.G., McGuire, A.D., Grosse, G., Harden, J.W., Hayes, D.J., Hugelius, G., Koven, C.D., Kuhry, P., 2015. Climate change and the permafrost carbon feedback. *Nature* 520, 171–179. doi:10.1038/nature14338

Shakun, J.D., Clark, P.U., He, F., Marcott, S.A., Mix, A.C., Liu, Z., Otto-Bliesner, B., Schmittner, A., Bard, E., 2012. Global warming preceded by increasing carbon dioxide concentrations during the last deglaciation. *Nature* 484, 49–54. doi:10.1038/nature10915

Tesi, T., Muschitiello, F., Smittenberg, R.H., Jakobsson, M., Vonk, J.E., Hill, P., Andersson, A., Kirchner, N., Noormets, R., Dudarev, O. V., Semiletov, I.P., Gustafsson, Ö., 2016. Massive remobilization of permafrost carbon during post-glacial warming. *Nat. Commun.* 7, 13653. doi:10.1038/ncomms13653

Vonk, J.E., Gustafsson, Ö., 2013. Permafrost-carbon complexities. *Nat. Geosci.* 6, 675–676.

Zimov, S.A., Schuur, E.A.G., Chapin, F.S., 2006. Climate change. Permafrost and the global carbon budget. *Science* (80-.). 312, 1612–1613.

Potential and challenges to use the stable isotope composition of ice wedges as winter climate archives

Hanno Meyer[1]
Thomas Opel[1,2]
Alexander Dereviagin[3]
[1]*Alfred Wegener Institute Helmholtz Centre for Polar and Marine Research, Potsdam, Germany*
[2]*Department of Geography, University of Sussex, Brighton, United Kingdom*
[3]*Geography Department, Lomonosov Moscow State University, Moscow, Russia*

Abstract

During the last years, ice wedges have been used as archives for past winter climate conditions with increasing success. Ice-wedge oxygen and hydrogen isotopes ($\delta^{18}O$ and δD) are temperature proxies that may have the potential to close existing seasonal and spatial gaps of Arctic palaeoclimate reconstructions. To fully exploit the potential of ice wedges as winter-precipitation archives it is necessary to improve the understanding of the relevant processes involved in ice-wedge growth dynamics and in the preservation of the stable isotope signals in ice veins. This paper briefly highlights the potential and reviews the current state of ice-wedge palaeoclimatology.

Keywords: Ice wedge; water isotopes; frost cracking; palaeoclimate reconstruction.

Introduction

Ice wedges are a main component of northern permafrost landscapes and are fed mainly by snowmelt that refreezes in thermal contraction cracks that open in winter (Lachenbruch, 1962). In spring, when snow melt water trickles into frost cracks, an ice vein is formed that integrates the stable-isotope signature ($\delta^{18}O$ and δD) of the preceding cold season. As in high latitudes, the stable isotope composition of precipitation is sensitive to air temperature, the integrated climate information of winter precipitation may be transferred to the ice vein. This signal can under certain circumstances be preserved over hundreds and thousands of years.

During the infill process, organic matter is often washed into the frost cracks that allow for direct AMS ^{14}C dating (Vasil'chuk et al., 2000, Meyer et al. 2010). Hence, (1) ice wedges can be studied to reconstruct past winter climate and (2) the period of formation can be determined in the best case to a sub centennial-scale level. Recent studies indicated a promising potential of ice-wedge based palaeoclimate reconstructions for more comprehensive reconstructions of Arctic past climate evolution. Despite the substantial progress in the past years (e.g., Lachniet et al., 2012; Meyer et al. 2015; Opel et al. 2017), the temporal and spatial coverage of ice-wedge based palaeoclimate reconstructions is still scarce, and only seldomly high-quality time series have been generated.

Future research directions

This paper briefly highlights the potential and reviews the current state of ice-wedge palaeoclimatology. Existing knowledge gaps and challenges are outlined and priorities for future ice-wedge research suggested. The major research directions are - to our understanding - related to a better assessment of: (1) frost crack dynamics (When and where does cracking happen?); and (2) crack infill and incorporation of the stable-isotope information into ice veins (Which material is available above the frost crack after snowmelt); (3) enhanced dating of ice-wedge sequences and age-model development (How do we generate reliable time series at high resolution?); which would then lead to (4) interpretation of new, spatially and temporally distributed ice-wedge based stable-isotope time-series.

Progress in each of these research directions will contribute to a better understanding of the palaeoclimatic potential of ice wedges, given in particular their unique cold-seasons seasonality that is not yet adequately covered by other climate archives.

References

Lachenbruch, A.H., 1962. Mechanics of thermal contraction cracks and ice-wedge polygons in permafrost. *Geological Society of America Special Papers* 70, 69 p.

Lachniet, M.S., Lawson, D.E., & Sloat, A., 2012. Revised 14C dating of ice wedge growth in interior Alaska to MIS2 reveals cold paleoclimate and carbon recycling in ancient permafrost terrain. *Quaternary Research* 78: 217-225.

Meyer, H., Schirrmeister, L., Yoshikawa, K., Opel, T., Wetterich, S., Hubberten, H.-W., & Brown, J., 2010. Permafrost evidence for severe winter cooling during the Younger Dryas in northern Alaska. *Geophysical Research Letters* 37, L03501.

Meyer, H., Opel, T., Laepple, T., Dereviagin, A.Y., Hoffmann, K., Werner, M., 2015. Long-term winter warming trend in the Siberian Arctic during the mid- to late Holocene. *Nature Geoscience* 8, 122-125.

Opel, T., Laepple, T., Meyer, H., Dereviagin, A.Y., & Wetterich, S., 2017. Northeast Siberian ice wedges confirm Arctic winter warming over the past two millennia. The Holocene 27: 1789–1796

Vasil´chuk, Y.K., van der Plicht, J., Jungner, H., Soininen, E., Vasil´chuk, A.C., 2000. First direct dating of Late Pleistocene ice wedges by AMS. Earth and Planetary Science Letters 179, 237-242.

Comprehensive studies of ground ice at central Yamal, Russia

Dmitry (Yu) Nekrasov[1]
Alexander (I) Kizyakov[1,2]
Marina (O) Leibman[2,3]
Artem (V) Khomutov[2,3]
Yury (A) Dvornikov[2]
Irina (D) Streletskaya[1]
[1]*Lomonoaov Moscow State University, Faculty of Geography, Cryolithology and Glaciology Department, Moscow, Russia*
dumucn@gmail.com
[2]*Earth Cryosphere Institute Tyumen Scientific Centre SB RAS, Tyumen, Russia*
[3]*Universuty of Tyumen, International Institute of Cryology and Cryosophy*

Abstract

In August 2017, comprehensive studies of ground ice were performed at central Yamal (Vaskiny Dachi research station). Research activities were undertaken on two sites with active thermodenudation processes and comprised the following: 1) sampling of ground ice (tabular ground ice, ice wedge ice) and enclosing ice deposits from exposures for various analyses (stable water isotope δD and $\delta^{18}O$, gaseous inclusions using headspace sampling method, gravimetric water content, major ions, radiocarbon dating, water extraction chemistry); 2) water sampling from the adjacent lake in order to understand the impact of thermocirque on the geochemistry of the lake water, 3) UAV overflights and tacheometric survey of thermocirques in order to assess the rate of edge retreat.

Keywords: tabular ground ice, ice wedges, isotopic composition, hydrochemistry, headspace, Yamal Peninsula.

Introduction

The presence of tabular ground ice very close to the surface and warm summer of 2012 has led to the activation of thermodenudation processes in central Yamal (Leibman *et al.*, 2015). In 2012-2013, several thermocirques appeared adjacent to lakes (Khomutov *et al.*, 2017) accompanied by the exposure of tabular ground ice (TGI) and ice wedges inserted into TGI, as well as large sediment input into adjacent lakes.

In August 2017, comprehensive sampling of ground ice, enclosing ice deposits, and surface (lake) water was performed in order to obtain the information on physical and chemical properties of the sampled media.

Number of samples

In total, 132 samples were collected from ground ice exposures in the scarps of active thermocirques within two sites. Samples included: 17 ice monoliths, 38 samples for stable isotopic composition (each doubled), 6 for major ions, 11 for gravimetric water content, 3 samples of buried peat for ^{14}C radiocarbon dating , 7 for water extraction chemistry, 50 for gaseous inclusions (headspace method).

Sampling methods

Ground ice samples were taken from the exposures with shovel and ice axe. Sampling locations are shown on Fig. 1. Ice monoliths were continuously stored in below zero temperatures (in coolboxes and freezers). Samples for isotopic composition were stored in plastic zip-packs and transferred to plastic containers after melting. Gaseous inclusions were sampled by placing cylinder of ice of respective size into syringes and transferred to 15 ml glass vials after melting.

Goals and Plans

During this expedition, the unique regional permafrost related information was collected. Samples are delivered to the relevant laboratories for testing. This data will be put in Yamal permafrost database and be analyzed and compared with existing results of TGI and ice wedge studies on Bovanenkovo gas field (central Yamal) and Marre-Sale research station (western Yamal).

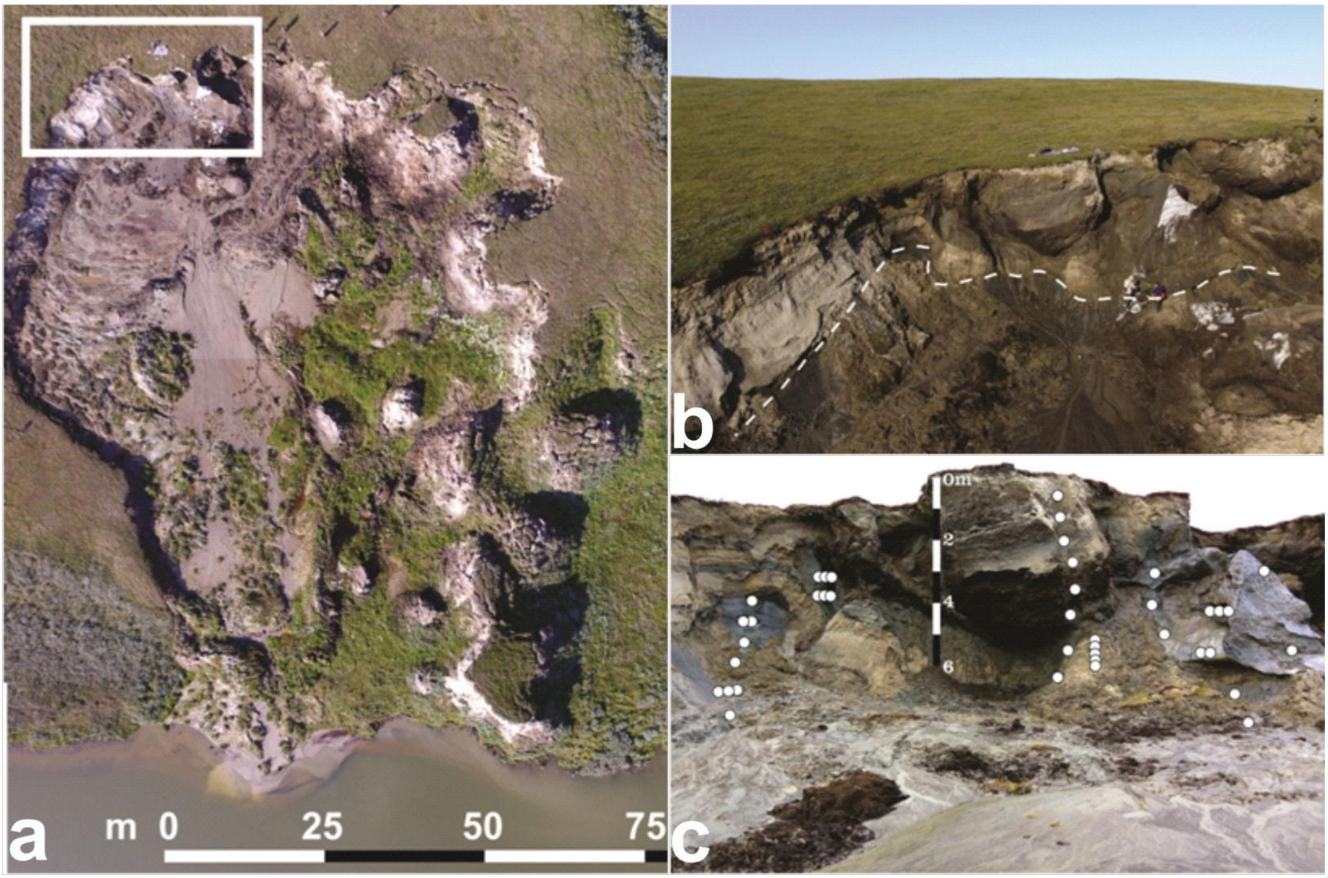

Figure 1. Overview photos of (a) Bird's eye view of Thermocirque 2 on Vaskiny Dachi research station with work area (white rectangle); (b) panorama of the exposure - dashed line delineates the orientation of the TGI, which is non-conformable with the overlying surface; (c) sampling points (white circles). Photos by A. Khomutov (a,b) and A. Kizyakov (c).

Acknowledgments

This work was partly supported by RFBR grant No.16-05-00612 and RSF grant No.16-17-10203. Expedition was organized with the participation of Interregional Expedition Center "Arctic", Salekhard, RU.

References

Leibman, M.O. Khomutov, A.V., Gubarkov, A.A., Mullanurov, D.R. & Dvornikov, Y.A., 2015. The research station "Vaskiny Dachi", Central Yamal, West Siberia, Russia – A review of 25 years of permafrost studies. *Fennia* 193(1): 3-30.

Khomutov, A.V., Leibman, M.O., Dvornikov, Y.A., Gubarkov, A.A., Mullanurov, D.R. & Khairullin, R.R., 2017. Activation of Cryogenic Earth Flows and Formation of Thermocirques on Central Yamal as a Result of Climate Fluctuations. In: Mikoš, M., Vilímek, V., Yin, Y., Sassa, K. (eds.), *Advancing Culture of Living with Landslides*, *Vol. 5: Landslides in Different Environments*. Springer International Publishing, 209-216.

Reconstructing cold climate paleoenvironments from micromorphological analysis of slope deposits (Serra da Estrela, Central Portugal)

Alexandre Nieuwendam[1]
Gonçalo Vieira[1]
Carlos Schaefer[2]
[1]*Centre of Geographical Studies – IGOT, Universidade de Lisboa, Portugal, alexandretn@gmail.com*
[2]*Department of Soils, Federal University of Viçosa, Brazil*

Abstract

This study deals with the genetical processes and paleoenvironmental significance of relict slope deposits in Serra da Estrela, Central Portugal. Data shows that 4 main processes were responsible for the emplacement of relict slope deposits: solifluction, debris flow, runoff and sliding. Well-developed frost related features are observed in different sites at 1300-1520 m and 650-700 m, and poorly to moderately developed frost structures at sites at 990-1010 m. These results suggest that solifluction process may have developed in different periods, between the Last Maximum of the Glaciation of Serra da Estrela (LMGSE) and the Younger Dryas, indicating conditions related to a periglacial environment. Debris-flow, sliding and runoff are observed at several sites between 680-1260 m and are probably related to a paraglacial period.

Keywords: paleoenvironments; micromorphology; relict slope deposits; Serra da Estrela.

Introduction

Serra da Estrela is the highest mountain in mainland Portugal (1993 m a.s.l.) and part of the Iberian Central Cordillera (Fig. 1). The mountain shows a rugged relief and a lithological diversity with several types of granitoids and metasediments. Most of the western plateau area was glaciated during the LGM and its morphology is dominated by glacial landforms. Vieira (2004) produced a detailed geomorphological map and described several sites showing stratified slope, head and debris-flow deposits. Based on the geomorphological analysis of the relationships between glacial and periglacial evidence, a first relative chronology was presented.

In this study, micromorphology is used to characterize the composition, structure, origin and depositional processes involved in the genesis of relict slope deposits. A total of 30 undisturbed samples were collected from 12 sites along an altitudinal transect between 650 and 1520 m a.s.l.

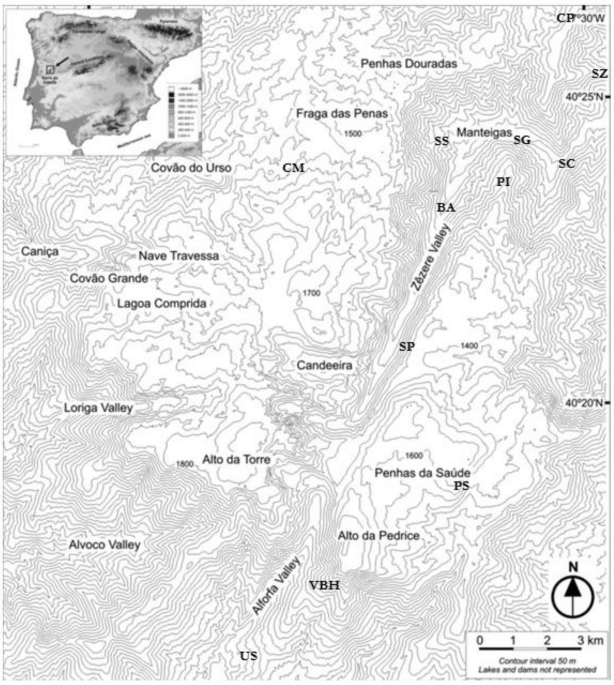

Figure 1. Location of Serra da Estrela and of the sites. PS-Penhas da Saúde (1520 m a.s.l.); CM-Covão da Malhada (1500m); SP-Sitio das Pessoltas (1300 m); VBH-Vila Belo Horizonte (1260 m); SS-São Sebastião (1010 m); PI-Poço do Inferno (1008 m); BA-Barroca de Água (1000 m); CP-Covão da Ponte (990 m); SC-Souto do Concelho (700 m); SG- São Gabriel (680 m); SZ-Sarzedo (675m); US-Unhais da Serra (650 m).

Results and Discussion

The work reported here accounts for sites mostly from the eastern plateau of the Serra da Estrela (Fig. 1). The deposits show a crude or clear stratification and most of them have a clear stratification, but in some case, it is completely absent in part of the sediments. Some accumulations display loosely stacked clasts, often with open-work arrangements. The samples were collected from units that show a matrix-supported diamictic character.

The microstructures from the samples PS, CM and SP (1520-1300 m), and US and SZ (675-650 m) are associated with solifluction, displaying well-developed structures, related to: (a) disturbance and rotation movements in the matrix (circular arrangement of grains, rounded vesicle); (b) stress induced at the matrix interface during rotation (fine-grained deposits and matrix deformations, layering grain coatings and silt caps); (c) ice segregation (vertical grains and platy microstructure); and (d) crushed grains (frost weathering) (Todisco & Bhiry, 2008). The microstructures from SS, PI and CP (1010-990 m a.s.l.) display identical microstructures, but they are poorly to moderately developed, indicating a less intensity of the frost action.

The microstructures from the samples VBH, BA, SC and SG (1260-680 m a.s.l.) show characteristics associated with debris-flow, sliding and runoff.

Debris flow microstructures at VBH, BA and SG, show moderately-developed circular arrangement of grains (rotational movement), fine grain coatings and grain dumps (translocation of particles by percolation water), coarse grain lineations and redox oncentrations (prevailing wet conditions; Todisco & Bhiry, 2008).

Runoff microstructures at VBH and SG display a banded distribution with larger grains at the bottom and smaller grains on the top indicating a velocity decrease, and poorly-developed fine grain lineations and oblique grains indicating a stream-laid deposition (Bertran & Texier, 1999).

Sliding at SC and SG deposits typically show heterogeneous fragments of sedimentary material incorporated in a dense matrix. Specific microfeatures are moderately-developed, evidencing prevailing wet conditions (fine grain coatings, grain dumps, coarse and fine grain lineations, redox concentrations) and deformation stages (circular arrangement of grains). These last samples demonstrate well-developed postdeposition frost action microstructures. SG shows structures related to ice segregation (platy microstructures and vertical grains) and frost weathering (crushed grains) and SC displays granular microfeatures that are the result of frost-induced deformations (Bertran & Texier, 1999).

You may include acknowledgments by replacing this paragraph. This section goes just before the References.

Conclusions

The relict slope deposits of the Serra da Estrela generally show an increase in cryogenic micromorphological features with altitude. PS, CM and SP (1300-1520 m a.s.l.) and US and SZ (675-650 m) display features related to a periglacial environment. SS, PI and CP (990-1010 m) and SC and SG (680-700 m) display a less intense frost action that could be related to seasonal frost. Vieira (2004) hypothesises that relict periglacial deposits in the Estrela may have developed in different phases between the Last Maximum of the Glaciation of Serra da Estrela (LMGSE – *c.* 30 ka BP) and the Younger Dryas. Debris-flow and run-off processes occur in a wider altitudinal range and are controlled by local topographical and geomorphological conditions probably related to a paraglacial period.

References

Bertran, P. & Texier, J.P., 1999. Facies and microfacies of slope deposits. *Catena* 35: 99-121.

Todisco, D. & Bhiry, N., 2008. Micromorphology of periglacial sediments from the Tayara site, Qikirtaq Island, Nunavik (Canada). *Catena* 76: 1-21.

Vieira, G., 2004. *Geomorfologia dos Planaltos e altos vales da Serra da Estrela: Ambientes frios do Plistocénico superior e dinâmica actual.* Dissertação de doutoramento, Universidade de Lisboa, Lisboa, 741 p.

Permafrost conditions in the Mediterranean region since the Last Glaciation

Marc Oliva[1] ; Manja Žebre[2]; Mauro. Guglielmin[3] ; Attila. Çiner[4] ; Gonçalo Vieira[5] ; Xavier Bodin[6] ; Nuria Andrés[7] ; Renato Colucci[8] ; Cristina García-Hernández[9] ; Phil Hughes[10] ; Carla Mora[5] ; Jordi Nofre[11] ; David Palacios[7] ; Augusto Pérez-Alberti[12] ; Adriano Ribolini[13] ; Jesús Ruiz-Fernández[9] ; Akif Sarıkaya[4] ; Enrique Serrano[14] ; Petru Urdea[15] ; Marcos Valcárcel[12] ; Jamie Woodward[10] ; Cengiz Yıldırım[4]

[1]*Department of Geography, University of Barcelona, Catalonia, Spain, oliva_marc@yahoo.com*
[2]*Geological Survey of Slovenia, Slovenia*
[3]*BICOM, Insubria University, Italy*
[4]*Eurasia Institute of Earth Sciences, Istanbul Technical University, Turkey*
[5]*Institute of Geography and Spatial Planning – CEG, Universidade de Lisboa, Portugal*
[6]*Environment Dynamics and Territories of Mountains (EDYTEM), University of Grenoble, France*
[7]*Department of Physical and Regional Geography, Complutense University of Madrid, Spain*
[8]*Department of Earth System Sciences and Environmental Technologies, ISMAR-CNR, Italy*
[9]*Department of Geography, University of Oviedo, Spain*
[10]*Department of Geography, School of Environment, Education and Development, The University of Manchester, United Kingdom*
[11]*Interdisciplinary Centre of Social Sciences, New University of Lisbon, Lisbon*
[12]*Department of Geography, University of Santiago de Compostela, Spain*
[13]*Department of Earth Sciences, University of Pisa, Italy*
[14]*Department of Geography, University of Valladolid, Spain*
[15]*Department of Geography, West University of Timisoara, Romania*

Abstract

Quaternary climate variability has conditioned the spatial distribution of glacial and periglacial processes in the Mediterranean region, and therefore the area under permafrost conditions. In this paper, we examine the evolution of permafrost regime in the Mediterranean basin since the Last Glaciation until nowadays. Glacial stages favoured the expansion of glaciers in mountain ranges and periglacial processes and permafrost at lower elevations. The temperature increase recorded during interglacial phases - such as the Holocene - conditioned the disappearance or substantial retreat of glaciers and the migration of permafrost and periglacial processes to higher elevations.

Keywords: Mediterranean region, permafrost, Last Glacial Maximum, deglaciation, Holocene.

Introduction

Present and past distribution of cold-climate geomorphological processes in the Mediterranean region is largely conditioned by the rough orography and wide spectrum of microclimatic conditions prevailing in the region. Both glacial and periglacial processes since the Last Glaciation have been almost exclusively restricted in mountain environments, as well as permafrost conditions. Here, we examine permafrost conditions in the Mediterranean region taking into account five periods: Last Glaciation, deglaciation, Holocene, Little Ice Age (LIA) and present-day.

Results and discussion

The distribution of currently inactive permafrost-derived landforms and sedimentary records indicates that the lower limit of permafrost during the Last Glaciation was ca. 1000 m lower than present (Oliva et al., 2016). Permafrost was also widespread in non-glaciated slopes above the snowline forming rock glaciers and block streams, as well as in relatively flat summit areas where meter-sized stone circles developed (Fig.1). As in most areas of the Northern Hemisphere, the deglaciation in the Mediterranean region started ca. 19-20 ka (Hughes, & Woodward, 2016). The exposed terrain by retreating glaciers was affected by paraglacial dynamics and intense periglacial processes, mostly associated with permafrost conditions. Many rock glaciers, protalus lobes and block streams formed in these recently deglaciated environments, becoming gradually inactive as temperatures rose during the Bølling-Allerød. Following the Younger Dryas glacial advance, the last major deglaciation in Mediterranean mountains took place during the Early Holocene together with a progressive shift of the periglacial belt to higher elevations (Oliva et al., 2016).

It is unlikely that widespread permafrost has existed in Mediterranean mountains during the Holocene, except sporadically in the highest massifs exceeding 2500-3000 m. The colder climate prevailing during the LIA favoured a minor glacial advance and the spatial expansion of permafrost, with the development of new protalus lobes and rock glaciers in the highest massifs. Finally, the marked warming that has occurred since the second half of the 20th century has led to glacial retreat and/or complete melting, increased paraglacial activity, migration of periglacial processes to the highest areas and degradation of alpine permafrost along with geoecological changes.

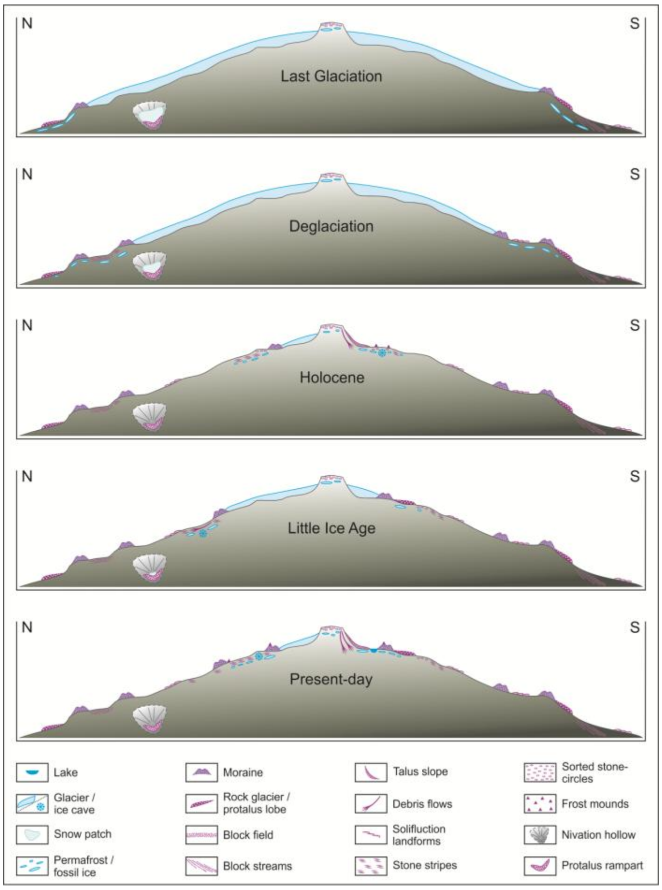

Figure 1. Geomorphological sketch of the formation of different generations of permafrost-related features in Mediterranean mountains since the Last Glaciation.

Conclusions

Today, cold-climate geomorphological processes in the Mediterranean region are restricted to the highest mountain environments. However, climate conditions prevailing during the Late Pleistocene and Holocene have conditioned significant spatio-temporal variations of the glacial and periglacial domain in these mountains, including permafrost.

Acknowledgments

Marc Oliva is supported by the Ramón y Cajal Program of the Spanish Ministry of Economy and Competitiveness (RYC-2015-17597).

References

Hughes, P.D., Woodward, J.C., 2016. Quaternary Glaciation in the Mediterranean Mountains. *Geological Society of London*, 433(1), 1-23.

Oliva, M., Serrano, E., Gómez-Ortiz, A., González-Amuchastegui, M.J., Nieuwendam, A., Palacios, D., Pérez-Alberti, A., Pellitero-Ondicol, R., Ruiz-Fernández, J., Valcárcel, M., Vieira, G., Antoniades, D., 2016. Spatial and temporal variability of periglaciation of the Iberian Peninsula. Q*uaternary Science Reviews* 137, 176-199.

Preliminary stable-isotope signals from ice wedges in the Batagai Megaslump (Verkhoyansk region, northern Yakutia)

Thomas Opel[1,2]
Julian B. Murton[1]
Kseniia Ashastina[3]
Hanno Meyer [2]
[1]*Permafrost Laboratory, Department of Geography, University of Sussex, Brighton, United Kingdom, T.Opel@sussex.ac.uk*
[2] *Alfred Wegener Institute Helmholtz Centre for Polar and Marine Research, Potsdam, Germany*
[3] *Senckenberg Research Institute and Natural History Museum, Research Station of Quaternary Palaeontology, Weimar, Germany*

Abstract

Ice wedges at the Batagai Megaslump were sampled to gain preliminary information on winter temperatures and continentality in the Verkhoyansk region (northern Yakutia) during the Pleistocene (MIS2–6). Stable-isotope values of wedges in the upper Ice Complex are more depleted than those in northern coastal regions and in central Yakutia to the south. This supports the hypothesis of higher continentality and lower winter temperatures in interior Yakutia during MIS3 than at present.

Keywords: Ice wedges; stable isotopes; past climate reconstruction, continentality; Batagai megaslump

Introduction

Interior Yakutia is the most continental region of the Northern Hemisphere. The climate has mean annual temperature ranges of >60°C (maximum >100°C). The city of Verkhoyansk is known as the pole of cold, with a minimum recorded temperature of –67.8°C.

During Late Pleistocene cold stages, interior Yakutia probably experienced even more continental climate conditions (larger temperature ranges), when sea level was lower. Ice wedges are widespread in Late Pleistocene permafrost deposits. The wedges may provide valuable climate information for the cold season due to their specific seasonality (Meyer *et al.*, 2015), because stable oxygen ($\delta^{18}O$) and hydrogen (δD) isotopes serve as proxies for past temperatures (Dansgaard, 1964). However, compared to coastal regions in the north (e.g., Opel *et al.*, 2017) as well as central Yakutia in the south (e.g., Popp *et al.*, 2006), interior Yakutia is understudied in terms of ice-wedge based palaeoclimate studies. Here we present preliminary results of a reconnaissance expedition to the Batagai megaslump.

Study site and field work

The Batagai megaslump (Ashastina *et al.*, 2017, Murton *et al.*, 2017) is the world's largest known thaw slump. It is located on a hillslope and incised more than 70 m into the taiga landscape. It provides access to Holocene and Pleistocene permafrost formations corresponding to Marine Isotope Stages (MIS) 1 to 6 or older. Four major cryostratigraphic units are differentiated, from bottom to top: (1) lower Ice complex, (2) lower sand, (3) upper Ice Complex, and (4) upper sand, which intersects the upper Ice Complex downslope.

We sampled six ice wedges corresponding to the lower sand, the upper Ice Complex and the upper sand, respectively. The lower Ice Complex was inaccessible due to dangerous outcrop conditions.

Results and discussion

The lower sand unit, most likely related to MIS 6, has a low ice content. A small ice wedge (0.5 m wide) shows a mean isotopic composition of $\delta^{18}O$: –33.1‰, δD: –256.9‰, dxs: 8.2‰ (n=8).

The ice-rich upper Ice Complex dates to MIS3 and contains much larger ice wedges. The mean stable-isotope composition of two sampled ice wedges 0.5 and 1.6 m wide ($\delta^{18}O$: –34.5‰ and –34.9‰, δD: –262.6‰ and –271.0‰, dxs: 13.8‰ and 8.1‰ (n=6 and n=12), respectively) indicates colder conditions during ice-wedge formation compared to the lower sand.

The upper sand unit (MIS3–2) comprises ice-poor sediments hosting narrow ice and composite wedges. These show more enriched stable-isotope values ($\delta^{18}O$: –32.8‰, –31.8‰ and –29.9‰, δD: –247.5‰,

–240.5‰, and –225.5‰, dxs: 15.1‰, 14.7‰ and 13.5‰ (n=4, n=2, n=8), respectively) than both the lower sand and the upper Ice Complex.

Our results roughly correspond to recently reported data for ice wedges from other altitude levels of the slump (Vasil'chuk *et al.*, 2017). Compared to ice-wedge data from north (Opel *et al.*, 2017) and central Siberia (Popp *et al.*, 2006) the ice wedges of the upper Ice Complex show more depleted isotope values, indicating lower winter temperatures and likely a higher continentality during the MIS3.

To confirm these preliminary findings and improve the temporal resolution, future studies need to (1) better constrain the chronology of the outcrop and (2) sample more ice wedges from all accessible altitude levels, including the lower Ice Complex.

References

Ashastina, K., Schirrmeister, L., Fuchs, M., and Kienast, F. 2017. Palaeoclimate characteristics in interior Siberia of MIS 6–2: first insights from the Batagay permafrost mega-thaw slump in the Yana Highlands, *Climate of the Past* 13: 795–818.

Murton, J.B., Edwards, M.E., Lozhkin, A.V., Anderson, P.M., Savvinov, G.N., Bakulina, N., Bondarenko, O.V., Cherepanova, M.V., Danilov, P.P., Boeskorov, V., Goslar, T., Grigoriev, S., Gubin, S.V., Korzun, J.A., Lupachev, A.V., Tikhonov, A., Tsygankova, V.I., Vasilieva, G.V., and Zanina, O.G. 2017. Preliminary paleoenvironmental analysis of permafrost deposits at Batagaika megaslump, Yana Uplands, northeast Siberia, *Quaternary Research* 87: 314–330.

Dansgaard, W., 1964. Stable isotopes in precipitation. *Tellus* 16: 436–468.

Meyer, H., Opel, T., Laepple, T., Dereviagin, A.Y., Hoffmann, K., Werner, M., 2015. Long-term winter warming trend in the Siberian Arctic during the mid- to late Holocene. *Nature Geoscience* 8: 122–125.

Opel, T., Wetterich, S., Meyer, H., Dereviagin, A.Y., Fuchs, M.C., Schirrmeister, L. 2017. Ground-ice stable isotopes and cryostratigraphy reflect late Quaternary palaeoclimate in the Northeast Siberian Arctic (Oyogos Yar coast, Dmitry Laptev Strait). *Climate of the Past* 13: 587–611.

Popp, S., Diekmann, B., Meyer, H., Siegert, C., Syromyatnikov, I., Hubberten, H.-W. 2006. Palaeoclimate signals as inferred from stable-isotope composition of ground ice in the Verkhoyansk foreland, Central Yakutia. *Permafrost and Periglacial Processes* 17: 119–132.

Vasil'chuk Y.K., Vasil'chuk J.Y., Budantseva N.A., Vasil'chuk A.C., Trishin A.Y. 2017. Isotopic and geochemical features of the Batagaika yedoma (preliminary results). *Arctic and Antarctic* 3: 69–96 (in Russian).

Isotopes in Wedge Ice Database (IsoWID), Phase 1

Trevor Porter[1]
Thomas Opel[2]
Nataliya Belova[3]
Nadine Budantseva[3]
Kira Holland[1]
Matthew Lachniet[4]
Hanno Meyer[5]
Dmitry Nekrasov[3]
Yana Tikhonravova[6]
Jessica Vasil'chuk[3]

[1]*Department of Geography, University of Toronto, Erindale Campus, Mississauga, Canada, trevor.porter@utoronto.ca*
[2]*Department of Geography, University of Sussex, Brighton, United Kingdom*
[3]*Faculty of Geography, Lomonosov Moscow State University, Moscow, Russia*
[4]*Department of Geoscience, University of Nevada Las Vegas, USA*
[5]*Alfred Wegener Institute Helmholtz Centre for Polar and Marine Research, Potsdam, Germany*
[6]*Earth Cryosphere Institute Tyumen Scientific Center of Siberian Branch of the Russian Academy of Sciences, Russia*

Abstract

An action group has been proposed by an international team of scientists for establishing a database of stable hydrogen and oxygen isotope ratio (δ^2H and $\delta^{18}O$) measurements from ice wedges – IsoWID (Isotopes in Wedge Ice Database). Wedge ice is a unique form of ground ice derived from snowmelt. As precipitation isotopes are tightly coupled to air temperature, the δ^2H or $\delta^{18}O$ of relict wedge ice can serve as a proxy for winter palaeotemperatures, a season rarely captured by other proxies. IsoWID will compile all future and published (including Russian literature) ice wedge isotope data, and provide a resource to the international permafrost and climate science communities for the advancement of knowledge of cold-season dynamics in periglacial regions. The IsoWID team will meet at EUCOP5 to engage the broader permafrost research community, discuss data selection criteria, database design, development and implementation, as well as project outputs and community outreach.

Keywords: wedge ice; water isotopes; database; palaeoclimate

Introduction

Ice wedges are a prominent feature of permafrost environments, and a natural archive for ancient winter precipitation in ice veins. Ice wedges integrate snowmelt that infills thermal contraction cracks in the ground that open in winter (Lachenbruch, 1962). In high-latitude regions, stable hydrogen and oxygen isotope ratios (δ^2H and $\delta^{18}O$) of precipitation and air temperature are tightly coupled (Dansgaard, 1964), a relation glaciologists use to derive long temperature histories from ice cores. More recently, this framework has been applied to well-dated wedge ice for reconstructing winter palaeotemperatures (Vasil'chuk, 1992; Meyer et al., 2015). This seasonality distinguishes wedge ice isotope datasets from ice cores (annual seasonality) and other terrestrial proxies such as tree-rings (mostly sensitive to warm-season conditions).

Existing ice wedge isotope data have broad temporal coverage (Late Pleistocene and Holocene) in the circum-Arctic (e.g., Lachniet et al., 2012; Meyer et al. 2010; Opel et al., 2017; Porter et al., 2016; Vasil'chuk, 1992). But most climate system modelers are unaware of ice wedges as source of palaeoclimate data. This is partly because a large fraction of ice wedge isotope literature is published in Russian only (e.g, Vasil'chuk, 1992) and is 'hidden' to the international community.

Over the last years, new community-driven and freely accessible palaeoclimate databases have been generated for more holistic climate reconstructions and model-data comparison (PAGES2k Consortium, 2017). However, due to very strict proxy data criteria, especially in regards to temporal resolution, many ice wedge isotope datasets have not yet been considered.

Establishing the IsoWID Database

For ice wedge isotope data to factor more prominently in climate system research, it is important to promote ice wedge isotopes to the climate science community and to make existing and future datasets available in a format that modelers can use. To this end, an international team of permafrost researchers has proposed to establish an Isotopes in Wedge Ice Database (IsoWID). IsoWID will help to stimulate inter-disciplinary exchange between the permafrost and modelling communities. The IsoWID team will meet at EUCOP5 to engage the permafrost community, discuss data selection criteria, and discuss database design and implementation. The main project objectives are:

(1) Develop a freely available database of wedge ice isotope data and metadata (spatiotemporal dimensions, sampling and dating method, age uncertainty, attribution and citation to relevant publications). The database will be freely available in an online format accessible to the climate science and permafrost research communities.

(2) Conduct a spatiotemporal analysis of IsoWID to characterise the contemporary and palaeo-isoscapes, demonstrate applications in paleoclimatology, and raise awareness of these applications through: (i) publication in scholarly journal; and (ii) presentations at international conferences that attract climate system researchers (e.g., AGU, EGU).

References

Dansgaard, W., 1964. Stable isotopes in precipitation. *Tellus* 16, 436-468.

Lachenbruch, A.H., 1962. Mechanics of thermal contraction cracks and ice-wedge polygons in permafrost. *Geological Society of America Special Papers* 70, 69 p.

Lachniet, M.S., Lawson, D.E., & Sloat, A., 2012. Revised 14C dating of ice wedge growth in interior Alaska to MIS2 reveals cold paleoclimate and carbon recycling in ancient permafrost terrain. *Quaternary Research* 78: 217-225.

Meyer, H., Schirrmeister, L., Yoshikawa, K., Opel, T., Wetterich, S., Hubberten, H.-W., & Brown, J., 2010. Permafrost evidence for severe winter cooling during the Younger Dryas in northern Alaska. *Geophysical Research Letters* 37, L03501.

Meyer, H., Opel, T., Laepple, T., Dereviagin, A.Y., Hoffmann, K., Werner, M., 2015. Long-term winter warming trend in the Siberian Arctic during the mid- to late Holocene. *Nature Geoscience* 8, 122-125.

Opel, T., Laepple, T., Meyer, H., Dereviagin, A.Y., & Wetterich, S., 2017. Northeast Siberian ice wedges confirm Arctic winter warming over the past two millennia. The Holocene 27: 1789–1796

PAGES2k Consortium, 2017. A global multiproxy database for temperature reconstructions of the Common Era. *Scientific Data* 4, doi:10.1038/sdata.2017.88.

Porter, T.J., Froese, D.G., Feakins, S.J., Bindeman, I.N., Mahony, M.E., Pautler, B.G., Reichart, G.-J., Sanborn, P.T., Simpson, M.J., & Weijers, J.W.H., 2016. Multiple water isotope proxy reconstruction of extremely low last glacial temperatures in Eastern Beringia (Western Arctic). *Quaternary Science Reviews* 137: 113-125

Vasil'chuk, Y., 1992. Oxygen Isotope Composition of Ground Ice (Application to Paleogeocryological Reconstructions). Moscow. v.1, 420 p., v. 2, 264 p. (in Russian)

Holocene permafrost evolution in marine sediments along the Eureka Sound Lowlands, NU, Canada

Cameron Roy[1], Wayne H. Pollard[1], Denis Lacelle[2]
[1]*Department of Geography, McGill University, cameron.roy@mail.mcgill.ca*
[2]*Department of Geography, University of Ottawa*

Abstract

Massive ground ice and ice-rich sediments are found extensively within marine sediments in the Eureka Sound Lowlands (ESL) of the Canadian High Arctic. Landscape models suggest thick segregated ice lenses forming as permafrost aggraded during isostatic uplift and marine regression starting 8,500 yrs. BP. We present high-resolution geochemical results from 5 distinct massive ice bodies along an elevational gradient collected in the summer of 2017. Our data reveals that there is high variability of $\delta^{18}O$ and major ions in massive ice throughout the ESL. Regression slope values between δD and $\delta^{18}O$ range from 5.4 to 8.4, indicating changes in open-system freezing conditions as permafrost aggraded during the early to mid Holocene. An improved understanding of massive ground ice processes based on geochemical characterization across the ESL has implications on interpreting the region's Quaternary landscape evolution and the processes associated with ground ice formation in raised marine sediments for this area.

Keywords: permafrost; massive ground ice; marine sediments; polar desert; Innuitian Ice Sheet

Introduction

The distribution, nature and origin of ground ice is an important component of reconstructing the evolution of permafrost landscapes. In the Eureka Sound Lowlands (ESL) of Ellesmere and Axel Heiberg islands, Pollard (2000) proposed that the development of tabular massive ice bodies was linked to Holocene marine regression with permafrost aggrading in emerging land. This study explores the origin and timing of formation of the massive ground ice within the Holocene marine limit of the ESL. The primary objectives of this research are to: i) characterize the geochemical composition of the ice bodies to determine their origin; and ii) reconstruct Holocene permafrost evolution within the Holocene marine limit. This research is timely in view of recent trends in increases thermokarst activity and landscape change in this area (Pollard *et al* 2015).

Study Area

The ESL are a flat to gently rolling area (~750 km^2) (Fig. 1). It is situated in the high Arctic polar desert climate regime, with a long-term (1947-2015) mean annual air temperature of -19.7°C and mean annual precipitation of 68 mm. Since the early 1970s, the MAAT at Eureka has increased by ~ 4°C, which is leading to permafrost instability (Pollard *et al.*, 2015).

The ESL are underlain by deep, cold and continuous permafrost (>500 m) (Pollard, 2000). Ground ice is widespread in permafrost; ranging from pore ice to tabular bodies of massive ice; the latter is associated with marine sediments that lie below the Holocene marine limit. Ice wedges are ubiquitous over much of the ESL and developed in all surficial materials. Unconsolidated Tertiary sandstone underlies the study region. Marine transgression and subsequent regression are linked to the melting of the Innuitian Ice Sheet around 8,500 yrs. BP (Simon *et al.*, 2015).

Methods

Tabular bodies of icy permafrost exposed in headwalls of four thaw slumps were cored to depths of 2.5 m across an elevational gradient below Holocene marine

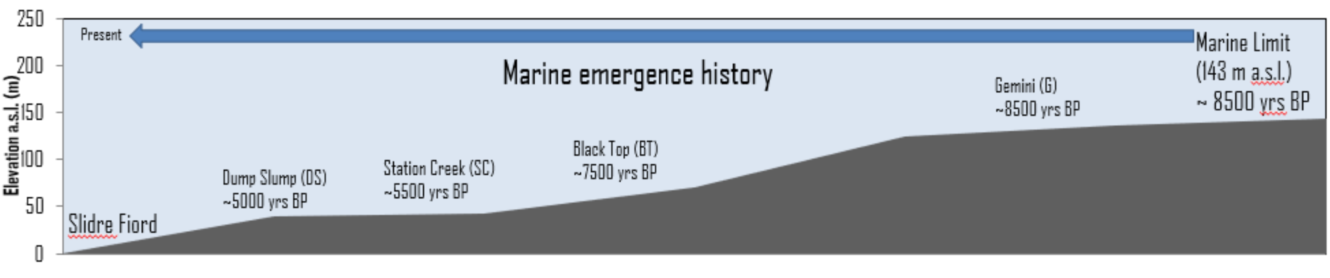

Figure 1: Massive ice exposures along an elevational gradient on the Fosheim Peninsula, with estimated time of marine emergence from Simon *et al.*, 2015.

limit. Ice wedges exposed in headwall of the same slumps were also sampled. Massive ice was overlain by variable depths (1-10 m) of sediment, ranging from clay to fine sand, depending on location.

All permafrost cores were cut into vertical 2 cm resolution, allowing for high-resolution profiles of ice content (gravimetric and volumetric), stable isotopes (δD, $\delta^{18}O$), major cations (Na^+, Mg^{2+}, K^+, Ca^{2+}) and anions (NO_3^-, SO_4^{2-} , Cl^-), with age constrained by $^{14}C_{DOC}$.

Results & Discussion

Icy permafrost below the marine limit in the ESL has a broad range of volumetric ice content (50-100%), $\delta^{18}O$ (-35 to -21‰) and δD (-268 to -165‰). Soluble ion concentrations vary on the order of 10^4; Black Top (70 m a.s.l.) has [Na^+] and [Cl^-] comparable to modern water in Slidre Fiord (>2 g/l), whereas they are <5 mg/L at Dump Slump (40 m a.s.l.) and Gemini sites (120 m a.s.l.).

Co-isotope plots (δD-$\delta^{18}O$), in combination with other measurements, are often used to help determine the origin of ground ice. At the Dump, Station Creek and Gemini sites, δD-$\delta^{18}O$ regression slopes similar to the LMWL were calculated for the entire core (7.3-8.2), whereas the Black Top site had a much lower regression slope value (5.4). However, micro-scale analysis revealed clear "freezing slopes" over variable thickness at all sites, and a correlation between $\delta^{18}O$ and soluble ions was found, which would not be the case for glacial ice. Based on this, we interpret the massive ice to be segregated in origin. The apparent "meteoric" slope values for the entire core at 3 out of the 4 sites can be attributed to: 1) the effect of freezing of water in an open system where the input rate of water is greater than the freezing rate. This may produce δD-$\delta^{18}O$ slopes with values near the LMWL since isotopic fractionation at the freezing front is limited by continued mixing (Souchez & De Groote, 1985); 2) an average of successive freezing episodes during the growth of the ice. Thus, micro-scale variations in δD-$\delta^{18}O$ slopes reflect differences in the rate of freezing and supply of an isotopically-changing input (which in the case of the ESL is meltwater of late Pleistocene to early Holocene glacial ice).

From the isotope geochemistry of the massive tabular ice, supplemented with data from ice wedges, we are able to reconstruct the aggradation of permafrost in the raised marine sediments during the early to mid Holocene. We can infer differences in freezing conditions and water supply across an elevational gradient and correlate our findings with paleoclimatic conditions from Agassiz ice cap (Lecavalier *et al.*, 2017). The rate of freezing, sediment texture and the supply of glacial meltwater from upslope around the time of marine emergence are key factors in explaining chemical and physical variability in massive ground ice in the ESL.

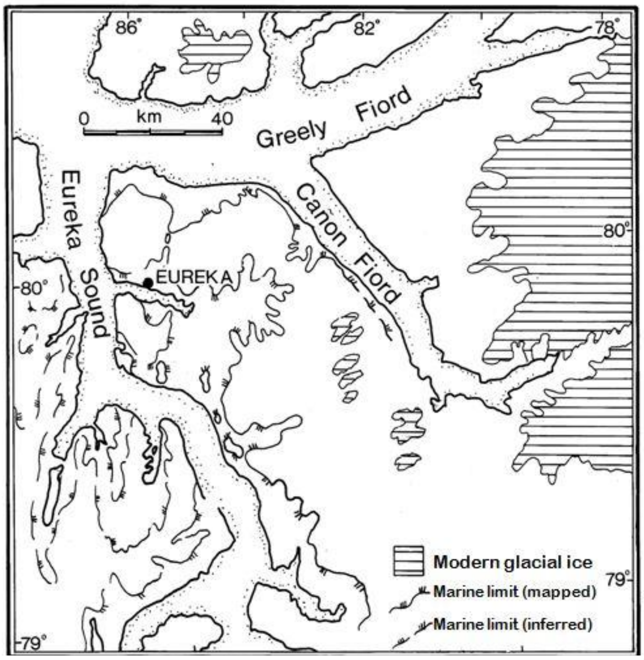

Figure 2: Map of Eureka Sound Lowlands, Nunavut, Canada

Acknowledgments

This work is supported by the Northern Scientific Training Program, the Polar Continental Shelf Program and the Natural Science and Engineering Research Council of Canada.

References

Lecavalier, B.S. *et al.*, 2017. High Arctic Holocene temperature record from the Agassiz ice cap and Greenland ice sheet evolution. *PNAS* 114: 5952-5957.

Pollard, W.H., 2000. Ground-ice aggradation on Fosheim Peninsula, Ellesmere Island, Nunavut. In Garneau M, Alt B (eds.), *Environmental Response to Climate Change in the Canadian High Arctic*, Geological Survey of Canada Bulletin 529, 325-333.

Pollard, W.H., Ward, M. & Becker, M., 2015. The Eureka Sound Lowlands; an ice-rich landscape in transition. *Proceedings of GeoQuebec*. Paper 402.

Simon, K., James, T.S. & Dyke, A.S., 2015. A new glacial isostatic adjustment model of the Innuitian Ice Sheet, Arctic Canada. *Quaternary Science Reviews* 119: 11-21.

Souchez, R.A. & de Groote J.M., 1985. dD-d18O relationships in ice formed by subglacial freezing: paleoclimatic implications. *Journal of Glaciology* 31: 229-232.

Paraglacial dynamics in the Antarctic Peninsula region since the Last Glacial Maximum

Jesús Ruiz Fernández[1]
Marc Oliva[2]
Daniel Nývlt[3]
Nicoletta Cannone[4]
Cristina García-Hernández[1]
Mauro Guglielmin[5]
Filip Hrbáček[3]
Matěj Roman[3]
Susana Fernández[6]
Jerónimo López-Martínez[7]
[1]Department of Geography, University of Oviedo, Oviedo, Spain, ruizjesus@uniovi.es
[2]Department of Geography, University of Barcelona, Barcelona, Spain.
[3]Department of Geography, Masaryk University, Brno, Czech Republic.
[4]Department of Science and High Technology, Università degli Studi dell'Insubria, Varese, Italy.
[5]Department of Theoretical and Applied Sciences, Università degli Studi dell'Insubria, Varese, Italy.
[6]Department of Geology, University of Oviedo, Oviedo, Spain.
[7]Department of Geology and Geochemistry, Universidad Autónoma de Madrid, Madrid, Spain

Abstract

The Antarctic Peninsula (AP) constitute the warmest region of Antarctica, with 98% of the surface covered by glaciers. The region shows contrasting geographic and climatic properties, which have conditioned past and present glacial activity. The number and extent of ice-free environments has gradually increased since the Last Glacial Maximum, particularly during the Early Holocene and second half of the XX century, when significantly warm climate conditions accelerated glacial retreat. Despite minor glacial advances, the long-term glacial retreat has led to major geomorphological and ecological changes. The loss of glacial ice favoured glacio-isostatic uplift of the landmasses and the consequent redefinition of the coastlines in the new exposed ice-free areas. The transition from glacial to periglacial conditions (paraglacial stage) favoured the development of rock glaciers, protalus lobes and other periglacial features. Their formation is highly dependent on the cold/warm based character of the glaciers; this fact determines the existence or inexistence of permafrost following the deglaciation, which in turn conditions the type and intensity of geomorphic processes in the newly exposed ice-free areas. Ice-free environments rich in fine particles are very favorable for the development of intense cryoturbation processes. Thus, a wide range of patterned ground are distributed across flat surfaces and gentle slopes (e.g. stone fields, stone sorted-circles, stone stripes, stone polygons, micropolygons, earth hummocks, mudboils). Solifluction landforms are abundant in gentle slopes covered by detrital deposits, whereas talus cones are common landforms at the foot of rock walls, volcanic plugs, rocky outcrops and scarps. These environments are also affected by intense alluvial dynamics as well as widespread mass wasting processes on slopes formed by unconsolidated sediments. In addition, glacial retreat triggered substantial ecological responses in the recently deglaciated environments, including vegetable and wildlife colonization and soil formation. The accurate characterization of the different paraglacial responses existing in the AP allows to better understand future environmental responses in this climatically sensitive region where climate models forecast significant climatic changes for the forthcoming decades.

Keywords: Antarctic Peninsula, deglaciation, paraglacial processes, geomorphology, permafrost, ecology.

Acknowledgments

This research has been conducted with the support of the Spanish Ministry of Economy, Industry and Competitiveness with the project CRONOANTAR [CTM2016-77878-P].

Characteristics of wave-built sedimentary archives in Buor Khaya Bay (71°N/130°E), Siberian Arctic, Russia.

Lasse Sander[1]
Rune Michaelis[1]
Svenja Papenmeier[1]
Sergey Pravkin[2]
Karen H. Wiltshire[1]

[1]*Alfred-Wegener-Institute, Helmholtz Centre for Polar and Marine Research, Wadden Sea Research Station, List/Sylt, Germany, lasse.sander@awi.de*
[2]*Arctic and Antarctic Research Institute, St. Petersburg, Russian Federation*

Abstract

Progladed sequences of beach deposits preserve valuable paleoenvironmental information on the long-term variability of sea level, climate forcing and sediment supply driving centennial to millennial coastal evolution. Buor Khaya Bay, NE Siberian Arctic, is located at the transition between the Verkhoyansk mountain range and the southern Laptev Sea and is one of the few places along the Russian arctic coast, where wide beach-ridge systems exist. The area was visited during an expedition in August 2017 in order to obtain baseline information on the potential of five different coastal sedimentary systems (barriers, spits, lagoons, beach-ridge systems), for the reconstruction of Holocene sea level and past sea-ice extent. The project is at an early stage of investigation and we present first insights into a new and promising area of investigation. Work will be continued in summer 2018.

Keywords: Beach ridges; Holocene; coastal geomorphology; relative sea level; wave climate.

Introduction

Sequences of prograded beach deposits (so-called beach-ridge systems) are a wave-built coastal geomorphological feature of global occurrence. The deposits may preserve information on the environmental conditions during their formation and have been used as archives for the reconstruction of parameters such as relative sea-level, wave climate, extreme events, sediment supply or sea-ice extent (see e.g. Funder *et al.*, 2011; Tamura, 2012; Sander *et al.*, 2016). Other coastal sedimentary systems (such as barriers and lagoons) may provide useful insights into the sedimentary record of processes determining shoreline change *e.g.* overwash frequency or extreme events. In general, only limited information on Holocene coastal evolution exists for the coast of arctic Siberia and all visited sites are previously unstudied.

Coastal geomorphology of Buor Khaya Bay

The geomorphology of the south-western shoreline of Buor Khaya Bay (cf. Fig. 1) is determined by the relief of the Verkhoyansk mountain range. Sites A and B are composed of slim and low-lying barriers that separate coastal lagoons from the open waters of the southern Laptev Sea. Site C is a wide barrier spit composed of beach ridges and is characterized by a steep storm berm. Sites D1 and D2 comprise several sets of prograded beach ridges. Apart from these sites, most of the shoreline of south western Buor Khaya Bay is dominated by bedrock cliffs.

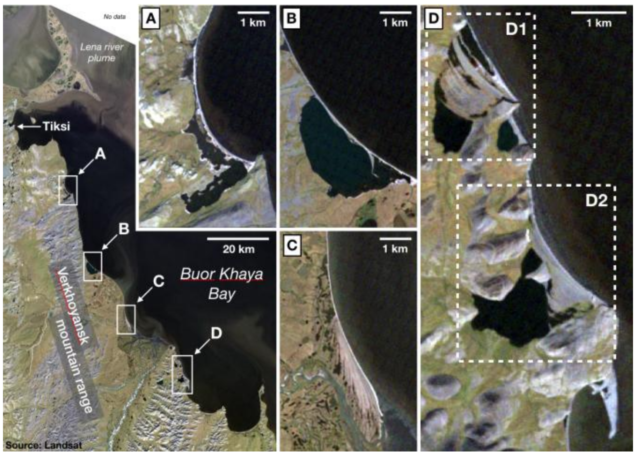

Figure 1. Overview of the south-western shoreline of Buor Khaya Bay (southern Laptev Sea) and the location of the investigated field sites. Site D is the focus area of this study.

Unraveling records of past coastal processes

Methods

All field sites were accessed by boat. At each field site, GPS-RTK elevation profiles were recorded in a cross-ridge direction, perpendicular to the modern shoreline. Data on beach morphology and the surface properties of the elevated marine deposits (grain size, vegetation, debris) were collected in the field and supported by kite aerial photography (KAP) surveys. Age control (for system D1 only) was established using the ^{14}C-dating of buried drift wood (dated at MICADAS Laboratory, Alfred-Wegener-Institute, Bremerhaven; cf. Table 1). Preparation of the campaign and the interpretation of field data are supported by Landsat satellite imagery, medium-resolution digital elevation models and archived topographical maps.

Table 1. Overview of ^{14}C samples from site D1.

Sample	Coordinate	Lab code	Age (yr)	+/- (yr)
K1	71°1.728'N/130°11.991'E	1288.2.3	3234	177
K2	71°1.670'N/130°11.656'E	1289.2.3	3540	177
K3	71°1.593'N/130°11.402'E	1290.2.3	4028	177
K4	71°1.738'N/130°11.466'E	1291.2.3	3826	177

Observations and inferences on Holocene coastal evolution

The modern shoreline at both beach-ridge sites (Fig. 2) is composed of a low gradient upper shoreface with longshore intertidal bars primarily composed of sands and gravels, and a steeply inclined beachface characterized by pebble- to cobble-sized material and the presence of ample amounts of debris (driftwood, anthropogenic debris). The steep angle of the modern berm ridge (storm berm elevation: *c.* 4m above MSL) and the presence of overtopped debris suggest the occurrence of increased water levels under high energy conditions. The fossil beach ridges have elevations of 2.5 – 4.5 m above MSL and surface deposits are composed of pebble- to cobble-sized material. Swales are mostly vegetated and locally water-logged. The surrounding headlands show clear indication of wave erosion (in the form of active and palaeocliffs) and thick layers of regolith cover the slopes. The minerogenic beach deposits are composed of gray shales. These are probably of local origin, given their high degree of similarity (color, lithology) with the weathering products from adjacent bedrock cliffs. No aeolian deposits were observed.

The elevation and composition of the beach deposits suggest a construction during (storm-)wave conditions. Both systems can be divided into distinct sets of ridges, suggesting (1) continuous progradation under conditions of high sediment availability over mid-Holocene time scales, and (2) unconformities evidencing periods of increase in allogenic perturbation or reduced sediment supply.

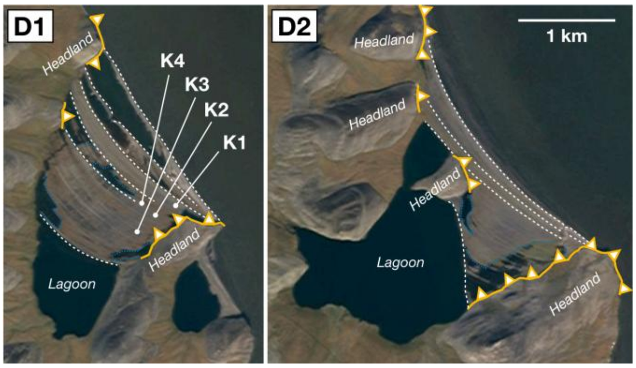

Figure 2. Field sites D1 and D2 are prograded beach-ridge systems, located in topographic depressions within the denudated relief of the Verkhoyansk mountain range. Both sites are surrounded by marine (paleo-) cliffs (yellow signature) and can be divided into different sets of ridges, separated by unconformities (dashed white lines). Arrows indicate the locations of the ^{14}C ages (K1-4; cf. Table 1).

Acknowledgments

Field work was conducted as part of the expedition "LENA 2017". We would like to express our gratitude for the indispensable logistical support of Waldemar Schneider and Volkmar Aßmann (both AWI, Potsdam). The crew of RV "Nicole" is thanked for facilitating access to the field sites as well as for their hospitality during the field campaign. Torben Gentz and Gesine Mollenhauer (MICADAS Lab, AWI Bremerhaven) conducted the radiocarbon dating.

References

Funder, S., Goosse, H., Jepsen, H., Kaas, E., Kjær, K.H., Korsgaard, N.J., Larsen, N.K., Linderson, H., Lyså, A., Möller, P., Olsen, J. & Willerslev, E. (2011): A 10,000-Year Record of Arctic Ocean Sea-Ice Variability—View from the Beach. *Science* 333: 747-750.

Sander, L., Hede, M.U., Fruergaard, M., Nielsen, L., Clemmensen, L.B., Kroon, A., Johannessen, P.N., Nielsen, L.H. & Pejrup, M. (2016): Coastal lagoons and beach ridges as complementary sedimentary archives for the reconstruction of Holocene relative sea-level changes. *Terra Nova* 28(1): 43-49.

Tamura, T. (2012): Beach ridges and prograded beach deposits as palaeoenvironment records. *Earth-Science Reviews* 114(3), 279-297.

Frozen but non-glaciated area as a characteristic feature ofthe Pleistocene development of Northwestern Siberia

Vladimir S. Sheinkman[1]
Vladimir P. Melnikov[2]
[1]*Tyumen Industrial University, Tyumen State University, Earth Cryosphere Institute of the Tyumen Scientific Center of the SB RAS, Tyumen, Russia, vlad.sheinkman@mail.ru*
[2]*Tyumen Industrial University, Tyumen State University, Earth Cryosphere Institute of the Tyumen Scientific Center of the SB RAS, Tyumen, Russia, melnikov@ikz.ru*

Abstract

Permafrost occupies a vast area ofNorthwestern Siberia. Moreover, there is numerous evidence that for a long time such indicators of strong rock freezing as polygonal ice wedges formednorth of the Middle Ob' River. Permafrost changed in thickness, its area fluctuated in size, butit always formed here during the Quaternary. However, some researchers suppose presence of ice sheets at this area during cryochrones, though to explain combined development of giant glaciers and well-expressed permafrost under conditions of Northwestern Siberiais impossible. At the base of the ice sheets, frozen grounds andunderground ice bodies have to transform, whereas they occur as unaffected forms. Surface deposits within the West-Siberian Plain underwent only active freezing happened at the background ofsea and river self-development and resulted in different forms.Our investigation has shown that some of those forms rated, at times, as glacial relics, are not of glacial origin, and no evidence of ice sheets occurs here.

Keywords: Northwestern Siberia, permafrost, glaciation, Pleistocene.

Introduction

Development of permafrost in Northwestern Siberia has been a fact that is beyond any doubt. The problem is its coexistence, in the course of the Pleistocene, with glaciation presented in various modelsby different forms.Some researchers even suppose a growth of giant ice sheets at the area of Northwestern Siberia during the Pleistocene cryochrones, though to explain the combined development of giant glaciers and well-expressed permafrost phenomena under conditions of that area is impossible. Our study,aiming at solution ofthe problem, has shown that surface deposits within the West-Siberian Plain underwent only active freezing at the background of mostly river self-development resulted in different forms. We revealed that some of those forms rated, at times, as glacial relics, are not of glacial origin, and no evidence of ice sheets occurs here.

Scientific background and obtained results

Originating in the Early Pleistocene, the permafrost phenomena exist in Northwestern Siberia so far; moreover, there is numerous evidence that for a long time such indicators of strong rock freezing as polygonal ice wedges formed north of the Middle Ob' River. The permafrost area fluctuated in size,and frozen grounds changed in thickness, but they always formed in Northwestern Siberia during the Quaternary. At the base of ice sheets the frozen grounds and, even more so, underground ice bodies have to transform, whereas they occur as unaffected forms in a state of fair preservation.

Analysis of different data on the subject shows that the problem concerns the mode of interaction between permafrost and glaciation. For a long time researchers carried out study of glaciation in Siberia on the base of the Alpine scientific concept defining high snow supply and active ice turnover to form the glaciers. Theyconsidered glaciers as so-called warm ice bodies, which lay on thawed bases and, for the most their part, on the ground outside the permafrost area. The glaciers were the formscaused by the primary snow transformation. They must grow quickly under a cooling, since the snow supply is firstly enough against sharp ablation decrease yielded by the cooling. The process went until the humid and cold (cryogygrotic) stage of the cooling will change by the dry and cold (cryoxerotic) stage. Under initial high moistening, the glaciation then can reach the sheet form over geologically short, relatively, duration of the Pleistocene cryochrones.However, such a model is only suitable in the area with climate similar to the Alpine, in order to explain forming the past ice sheets in Northern Europe moistened from the Atlantic. At the sametime, that model is not suitable in Siberia, Northwestern Siberia included, where cold and enough dry environments prevailed over the Quaternary as an effect of cryoaridization (the phenomenon showing increase in climate continentality and permafrost promoting under enhancement in cold and arid conditions).

In spite of low snow supply and active ablation (that is an attribute of continentalclimate) the Siberian glaciers exist due to big cold storage in their bodies: it keeps additional ice feeding, when thawed water repeatedly freezes on their surface. So, the Siberian glaciers, being under the initial developed cryoxerotic stage, had to react to the cooling during the Pleistocene cryochrones by slow growth. Their snow supply decreased as the cryoaridization was stronger, and during the Pleistocenecryochrones they, gradually absorbing scanty supply, could reach the valley form only. They could not advance into the area of the West-Siberian Plain and stopped in the foothill of mountains surrounding the plain. Being cooled (their temperature is significantly lower than 0°C), the Siberian glaciers obtained properties which are more characteristic for permafrost phenomena. The obtained quality requires reckoning the formed combination of the glaciers with permafrost to the specific permafrost-glacial geosystems.

The base to suppose an ice sheet in Northwestern Siberia isdistribution of stony material north of the Middle Ob' River where the Siberian Uval is situated (Fig. 1). This is a low upland (less than 300 m a. s. l.) stretched along the sub-latitudinal direction. When to look at the map, the Uvalis a ridge like to a moraine ridge; however, it is only in the form. The intrigued is presence of erratic boulders in the deposits making up that upland. Nevertheless, these depositsare everywhere composed of fluvial, mostly sandy, sediments, whereas the stony erratic materialis much dispersed debris embedded in sandy deposits only close to the surface. Sometimes, the debris washed away from the terrace body, transported to the base of the terrace and accumulated at the riverbanks (Fig. 1).

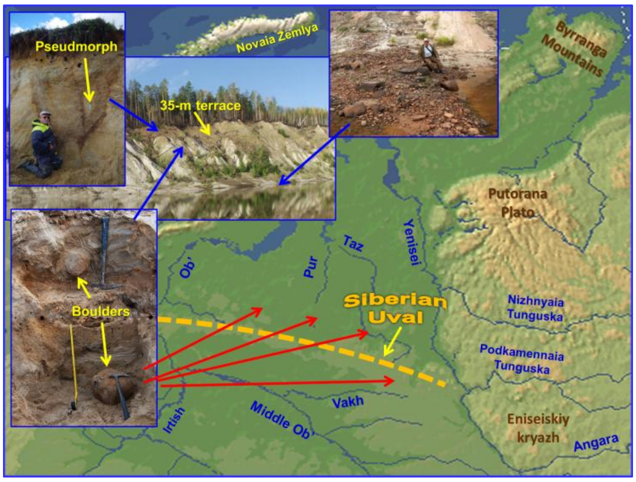

Fig. 1. Specific features of Northwestern Siberia
(Explanation in the text)

Overall, the Siberian Uval represents a system of typical river terraces, and such indicator of former strong freezing as pseudomorphs after polygonal ice wedges occurs in their bodies (Fig.1). According to the dating carried out by different ways, the wedges at the top of the terraces formed during MIS-2, and during the cold phase of MIS-5 in the central part of the terrace section. It confirms non-glaciated development of the studied area. As to the stony material imbedded in the terraces, it mostly represents fragments ofbasaltic rock carried away from the mountains at the right-hand bank of the Yenisei River. To our mind,it is a result, of river ice-floe drifttypical for self-development of many rivers in Siberia (Fig. 2).

Fig. 2.Ice drift and its results near Tomsk in 2010
(I – concrete beams relocated by ice drift at the quay of the Tom' River; II, IV – cottages and an excavator relocated by ice drift; III – ice floes effecting the quay of the Tom' Riverduring the ice-drift)

The Yenisei River is very powerful. Even at present, in the area round the mouth of its tributary Nizhnyaia Tunguska River,raising of water level during the ice drift time can rich 30 m whereas thickness of ice floes can rich 2 m. It is quite enough to captureboulders by ice floes and to move them over not high water divides. In thepast, the water divide at the left-hand bankof the Yenisei River was lower, and floods accompanied by ice drift could distribute the stony material over that divide into the upper riches of the rivers north of the Middle Ob' River.

We revealed that the Siberian Uval represents a block of sedimentary rocks elevated by tectonic processes along faults renewing in the course of the Quaternary. This block includes different sediments, which are regular for reflecting the river activity but not for any glacial geological work.

The presented work fulfilled on the base of partner projects between Tyumen Industrial University, Tyumen State University and Earth Cryosphere Institute of the Tyumen Scientific Center of the SB RAS.

Neopleistocene cryogenesis features in loess of the Lower Volga region (Russia)

Natalia A. Taratunina[1,2]
Victor V. Rogov[3]
Redzhep N. Kurbanov[2,3]
Irina D. Streletskaya[3]
Tamara A. Yanina[3]
[1]*Lomonosov Moscow State University, Faculty of geology, taratuninana@gmail.com*
[2]*Institute of Geography of the Russian Academy of Sciences*
[3]*Lomonosov Moscow State University, Faculty of geography*

Abstract

Loess-soil formations within the Pleistocene periglacial zone are widely spread. Most researchers believe that cyclical climate variations in the Pleistocene are fixed in the structure of loess-soil formations. A cryolithological analysis of mineral matter was conducted to assess the paleogeographic conditions of their formation. It is shown that processes of cryogenic transformation of deposits took place in the conditions of seasonal freezing in the Pleistocene, which contributed to the formation of the high thickness loess.

Keywords: cryolithology; loess; mineralogical, micromorphological, granulometric analyzes.

Introduction

The article presents the results of complex cryolithological analysis for sediments of two sections: Beglitza (northern coast of the Taganrog Bay) and Srednyaya Akhtuba (left bank of the Akhtuba River); both sections located on the southern periphery of the loess European area. Beglitsa section reveals the loess stratum of Late Valday with horizons of buried soils of Bryansk and Mezinsky pedological complexes; the lower part of the section is composed of liman-alluvial late-Khazarian deposits. The Srednyaya Akhtuba section reveals the reference horizon of the chocolate clays of the Khvalyn transgression, the powerful polyfacial thickness of Atelian continental sediments and three pronounced buried soils with a total thickness of about 20 m.

Results

The structure and composition of loess in both sections is very similar. In the granulometric composition coarse dust (0.025-0.05 mm) predominates (up to 60%), there is practically no fractions of more than 0.25 mm and there are only traces clay fraction (<0.001 mm) - not more than 1.5-2.5%. The granulometric composition of soil horizons (which is separating loess stratum) on the one hand is sandier, but also the clay component is greater compared with loess.

The morphology of sand particles is very diverse and reflects the conditions of the deposits formation in different horizons of loess: in some cases, well-rounded particles with slightly eroded surface; in other cases, more than half of the particles are angular with numerous chips and sharp edges that indicate a cryogenic mechanism of their destruction.

The aggregate microstructure of the loess is primarily due to gypsum and calcium carbonate. The basis of microstructure is large aggregates (1-3 mm) of varying degree of cohesion, which are separated by sinuous cracks and isometric pores of irregular shape. The aggregates are composed of particles of different size and composition. Microaggregates of the dust fraction are very interesting because a number of researchers suggest their cryogenic genesis (Konishhev, 1999; Konishhev, 1999).

The peculiarity of microstructure is tubular pores of almost perfect round shape in cross section, pore diameter 0.4-0.6 mm. Part of the channels in the transverse section have a shape close to hexagonal, which allows to link their genesis with the formation of ice-cement crystals.

Numerous crystals of calcium carbonate and inclusions of gypsum represent authigenic minerals in samples. Amorphous spots on the particles surface, concretions of siderite and new formations of magnetite and titanium-magnetite represent iron.

Mineralogy for the main loess granulometric fractions was analyzed to estimate the cryogenic effect. The coefficient of cryogenic contrast (CCC)* was calculated. Values of more than "1" allow us to assume the existence of low- power high-temperature permafrost or deep seasonal freezing during the indicated periods of the loess formation. In the Beglitza section (Fig.1) the highest values reflecting the influence of cryogenesis correspond to the Late and Middle Valday time. In the section of the Srednyaya Akhtuba (Fig.2) the highest values correspond to the Middle Valdai then MIS5d, MIS4 stages; then the Khvalynian transgression sands.

Researches showed prospects of the cryolithological analysis of mineral matter to estimate the paleogeographic conditions. This made it possible to reveal the significant role of cryogenic factors in the formation of the composition and structure of loess horizons. It was shown that processes of cryogenic transformation of deposits took place within the periglacial area in the Pleistocene that contributed to the formation of the composition and properties of loess of high thickness.

* CCC = Q1/F1 : Q2/F2, where Q1 and F1 are the content of quartz and feldspars in the fraction 0.05-0.01 mm; Q2 and F2 are the content of quartz and feldspars in the fraction 0.1-0.05 mm (Konishchev & Rogov, 1994).

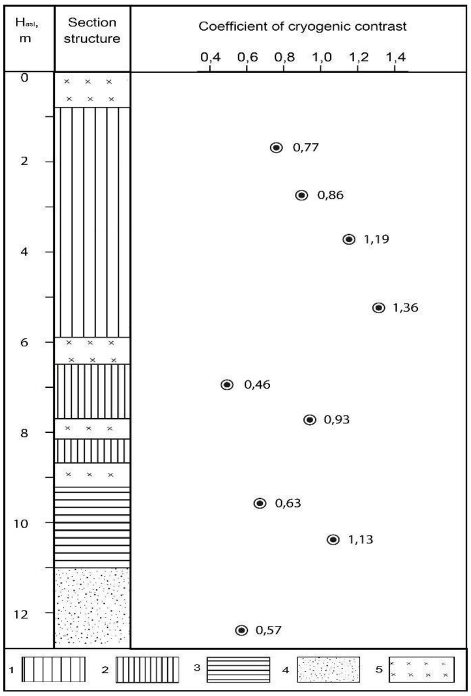

Figure 1. Distribution of CCC values for the Beglitza section: 1-pale yellow–gray loess, 2-pale yellow loess, 3- gray-yellow loess, 4-pale yellow sand, 5-soil horizons.

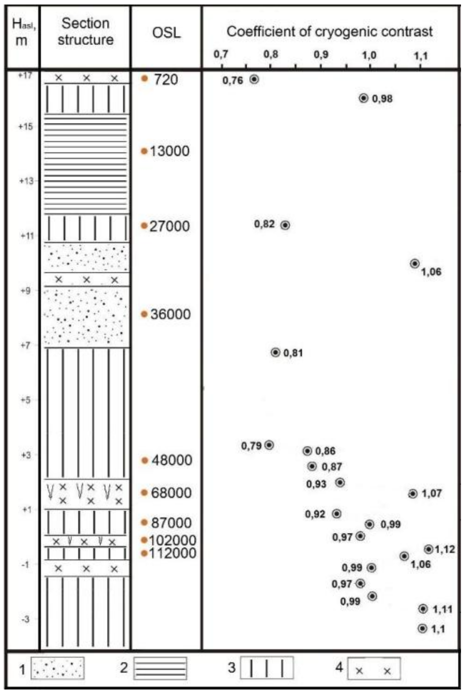

Figure 2. Distribution of CCC values for the Srednyaya Akhtuba: 1-sand, 2-cl ay, 3-loess, 4-soil (Yanina, 2017).

Acknowledgments

This study has been supported by Russian Foundation for Basic Research (Grant №18-35-00619).

References

Konishhev V.N., 1981, *Formation of the composition of dispersed rocks in the cryolithosphere*. Novosibirsk: Nauka, 197 pp.

Konishhev V.N., 1999. Evolution of rock temperature in the Arctic zone of Russia in the Upper Cenozoic. *Journal of Earth`s Cryosphere* IV, 39- 47.

Konishhev V.N., Rogov V.V. 1994. *Methods of cryolithological studies*. Moscow: MGU, 135 pp.

Minervin A.V., 1982. The role of cryogenic factors in the formation of loess. *Journal of Problemy kriolitologii* X, 41-60.

Yanina T.A., Svitoch A.A., Kurbanov R.N., Murray A.S., Tkach N.T., Sychev N.V., 2017, *Paleogeographic analysis of the results of optically stimulated luminescence dating of Pleistocene deposits of the Lower Volga area.* Vestnik of the Moscow University, Series 5, Geography. 21-29.

Genetic types and microstructure of Early Holocene ice

Yana (V.) Tikhonravova[1]
Elena (A.) Slagoda[1, 2, 3]
[1]*Earth Cryosphere Institute Tyumen Scientific Centre SB RAS, tikh-jana@yandex.ru*
[2]*Tyumen State University*
[3]*Industrial University of Tyumen*

Abstract

Genetic types of ice (ice of thawing cavities, crack ice, ice of thermoerosional niches, fast sea ice) were studied in the North-West Siberia. Their texture and structure characteristics (shape, size and orientation of ice crystals, organic and mineral inclusions, air bubbles) were determined. Difference in the microstructure of ice types depends on the freezing conditions – configuration of freezing cavities, temperature and hydrodynamic conditions of ice crystals' growth. The obtained features of ice crystal morphology helps to identify the Early Holocene ice within the massive ice and conditions of formation permafrost reconstruction.

Keywords: ice crystal morphology; ice of thawing cavities; crack ice; ice of thermoerosional niche; fast marine ice.

Introduction

The structure of massive ice and permafrost can contain the recently formed Early Holocene ice: ice of thawing cavities, crack ice, ice of thermoerosional niche, glacier ice, snowpatches, sea ice, lake and river ice (Tikhonravova *et al.*, 2017). The genesis of massive ice is identified by the ice morphology, configuration of enclosing sediments and ground ice, composition, structural and textural features of ice. Different genetic types of ice have individual combinations of macro- and microstructure due to formation conditions and conditions of ice crystals' growth (Shumsky, 1955). But the data about this genetic ice types have not been demonstrated yet.

Methods

Field observations included description of permafrost and sampling of ice monoliths. Ice thin sections were made using the petrographic method (Shumsky, 1955; Rogov, 2009). Images were taken using the Polaroid under the negative temperatures. The ice structure parameters calculated using the program "Crystal" (Tikhonravova *et al.*, 2017b).

Results

Closed-cavity ice

The closed-cavity ice has fibrous radial structure formed by cylindrical air bubbles that are elongated from the cavity walls to the center, and has one or more axial seams of the air bubbles' orientation (Fig. 1a). Ice crystals are perpendicular to the walls and to the axial seams of the air bubbles orientation (Fig. 1b).

The average crystal diameter (D) ~0.95 cm. This microstructure is determined by the slow freezing from two or more sides in closed cavities at high negative temperatures in the early winter.

Figure 1. Closed-cavity ice (horizontal cross-section).

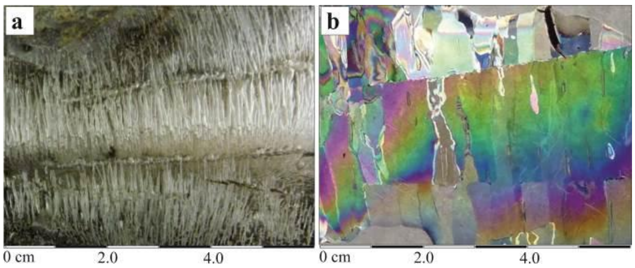

a – monolith of the ice with subhorizontal axial seams; b – ice crystal morphology under the polarized light

Crack ice

The crack ice is formed in any types of fissures except for the frost cracks. This ice has a linear shaped and inclined orientation. Differences in the microstructure depends on the configuration and time period of crack formed, rate of ice growth in the fissure etc. The crack ice contains mineral particles. Ice veins have not been obtained. Crack ice often have chaotic ice crystals orientation. If the ice has an axial seam, the elongated ice crystals are oriented from a cavity wall to the seam. Crack ice can have small internal ice cracks with small ice crystal debris and mineral particles around (Tikhonravova *et al.,* 2017b). Crack ice often has relatively big crystals (D = 1.4 cm) that are formed by slow ice growth at high negative temperatures in early winter.

Ice of thermoerosional niche

The ice of thermoerosional niche is located as horizontal lens and includes organo-mineral interbed (Fig. 2). The layered structure of such ice is formed by crystals of different shapes and sizes (D ~ 0.1-2 cm). Small isometric crystals on the top form a thin crust on the air-water boundary. Elongated vertical prismatic ice crystals are located below the ice crust. Prismatic and curved ice crystals (D = 0.55 cm) form basal cryostructure inside the mineral layer. The distribution and shape of the ice crystals similar to microstructure morphology for sea and river ices (Savel'ev, 1980; Rogov, 2009). This ice microstructure is determined by the freezing from the top of the small water reservoirs at the start of winter (Tikhonravova *et al*. 2017a).

Figure 2. Ice crystal morphology of ice inside the thermoerosional niche under the polarized light (vertical cross-section).

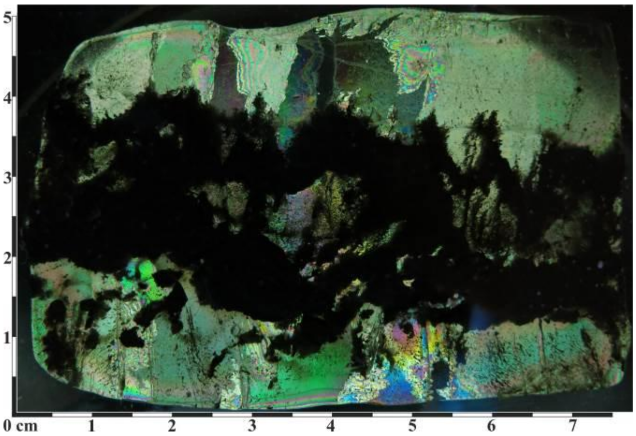

Fast sea ice

Fast marine ice is annually formed in the shallow (0.5-5.0 m sea depth) waters and characterized by bedded structure - layers with different size and shape of the ice crystals (small isometric crystals are 0.2 cm in diameter and elongated columnar crystals are 0.7-1.3 cm high), with mineral particles and air bubbles. Fast sea ice microstructure shows the stages of annual ice formation (Savel'ev, 1980). It has multilayered structure and smaller size of columnar crystals (Tyshko *et al*., 2000). Multiple layers of such ice connected to the periods of the prismatic crystal growth. This is determined by the influence of waves and flows that change the water temperature and disturb the mineral particles on the bottom during ice growth. Mineral particles are included into the ice and can act as nuclei for ice crystal formation (Tikhonravova & Slagoda, 2017).

Conclusions

The morphological and microstructure features of Early Holocene ice show the conditions and environment of their formation determined. The quantitative parameters of the ice crystal structure (Tikhonravova *et al*., 2017b; Tikhonravova & Slagoda, 2017) can be used to identify different genetic types of ice in the massive ices.

References

Rogov V., 2009. *Fundamentals of Cryogenesis*. Novosibirsk: GEO, 2003 pp.

Savel'ev, B., 1980. *The structure and composition of natural water*. Moscow: MGU, 280 pp.

Shumsky, P., 1955. *Fundamentals of structural ice sciences*. Moscow: AS USSR, 492 pp.

Tikhonravova, Y., Slagoda, E., Butakov, V., 2017a. Crystal ice structure of thermoerosional niche. *Proceedings of the conference "Scientific and production activity – a method of forming the human environment",* Tyumen, Russian, April 27-27: 278-285.

Tikhonravova, Ya., Slagoda, E., Rogov, V., Galeeva, E., Kurchatov, V., 2017b. Texture and structure of the Late Holocene ground ice in the Northern West Siberia. *Ice and Snow* 4: 553–564.

Tikhonravova, Ya. & Slagoda, E., 2017. Sea ice structure in coastal area of Baidarata Bay. *Proceedings of the conference "Natural processes in polar regions of the Earth in the global warming era"*, Sochi, Russian, October 9-11: 47-48.

Tyshko, K., Cherepanov, N., Fedotov, V., 2000 *Crystal structure of the sea ice cover*, Saint-Petersburg: Gidrometeoizdat, 66 pp.

Timing and drivers of mid- to late Holocene ice-wedge polygon development in the Western Canadian Arctic

Juliane Wolter [1]
Hugues Lantuit [1, 2]
Sebastian Wetterich [1]
Janet Rethemeyer [3]
Michael Fritz[1]
[1]*Alfred Wegener Institute Helmholtz Centre for Polar and Marine Research, Periglacial Research Section, Potsdam, Germany, email: juliane.wolter@awi.de*
[2] *University of Potsdam, Institute of Earth and Environmental Sciences, Potsdam, Germany*
[3] *University of Cologne, Institute for Geology and Mineralogy, Zülpicher Str. 49a, 50674 Cologne, Germany*

Abstract

Ice-wedge polygon formation and development from low-centred to high-centred types are thought to be either linear processes acting on long time-scales or rapid shifts between different regimes. We analyzed six sediment cores from three ice-wedge polygons on the Yukon Coastal Plain to examine the timing and drivers of these dynamics. All sites developed from shallow lakes or submerged polygon environments to low-centred polygons before rapid degradation and drying during the last century. We found that ice-wedge polygon initiation was linked to moderate climatic cooling during the mid-Holocene combined with drainage of lakes. The further conversion to high-centred polygons appeared to have been a rapid process linked to modern climatic warming. Continued warming may thus lead to increasing ice-wedge melt on larger scales and subsequent degradation of ice-wedge polygons, especially if paired with increasing geomorphic disturbances caused by thermokarst and thermo-erosion.

Keywords: coastal lowlands; permafrost degradation; tundra vegetation; plant macrofossils, Yukon Coastal Plain

Introduction

In Arctic lowlands, ice-wedge polygons are widespread features that determine carbon storage and landscape hydrology. These properties differ between high-centred polygons and low-centred polygons, from which the latter are thought to develop. It is not entirely clear, however, to which extent climate and geomorphology influence polygon development. This study investigated past landscape development in modern ice-wedge polygons, focusing on timing and triggers of possible tipping points between polygon types.

Methods

We addressed these questions by analyzing six cores from three ice-wedge polygons on the arctic coastal plain of the Yukon Territory, Canada. Grain size distribution, carbon and nitrogen contents, and stable carbon isotope signatures were determined for each 1 cm subsample. We conducted plant macrofossil analyses on 44 selected samples, and obtained radiocarbon dates for 24 of these samples. Constrained incremental sum of squares (CONISS) analysis validated by broken stick analysis and principal component analysis (PCA) aided data interpretation.

Results and Discussion

Fig. 1 shows the reconstructed landscape development together with climate reconstructions for the region. All sites showed a general development from aquatic to wetland environments. Sediment analyses and plant macrofossils supported these shifts from aquatic vegetation typical for shallow lake margins (e.g. Potamogeton, Batrachium, Menyanthes trifoliata, Charophytes, cf. Fritz et al., 2016; Wolter et al., 2017) to wetland vegetation typical for low-lying areas in ice-wedge polygons (e.g. Carex, cf. Wolter et al., 2016), and finally to vegetation typical for elevated, better drained areas in ice-wedge polygons (e.g. Betula glandulosa, Ledum decumbens, Eriophorum vaginatum, cf. Wolter et al., 2016).

In the mid-Holocene portion of our reconstruction (ca. 7000-6000 cal yrs BP) shallow lakes and partly submerged ice-wedge polygons existed at the studied sites. At two sites where high- and intermediate-centred polygons exist today, a hiatus of ca. 5000 years, accompanied by strong shifts in grain size distribution and organic carbon contents, indicated substantial disturbance during a time of stable temperatures and increased precipitation (Fig. 1). The initiation or re-initiation of ice-wedge polygon development roughly fell within the last millennium, when temperatures dropped. Lake drainage is one major factor promoting ice-wedge development. Our reconstructions suggest that all sites indeed hosted lake environments before developing into ice-wedge polygons (Fig. 1). Finally, all three polygons experienced recent degradation and drying. Low-lying surfaces were converted into elevated surfaces and the vegetation composition changed markedly. This phenomenon accompanied recent climatic warming and accelerated coastal erosion, which led to a landscape-scale increase in surface drainage.

Our findings suggest that both, climatic and geomorphic drivers caused changes to the landscape in this specific region of low-Arctic lowland tundra. The conversion of low-centred polygons to high-centred polygons likely happened during the last 100 years.

In our study, geomorphology outweighed climatic influence on ice-wedge polygon development during the late Holocene, with the possible exception of recent warming, which caused ice wedge degradation at all studied sites. The initiation of ice-wedge polygons was linked to lake drainage. The conversion of low-centred polygons into intermediate- or high-centred forms was triggered by ice-wedge degradation and changes in the local topographic gradient through geomorphic disturbance attributable to thermokarst and thermal erosion as well as coastal erosion. Stable conditions were found where no geomorphic change or disturbance was evident and a stable water balance was maintained. Our study showed that in areas with strongly impeded drainage, low-centred forms might persist for millenia, while any drainage may trigger self-enhancing degradation.

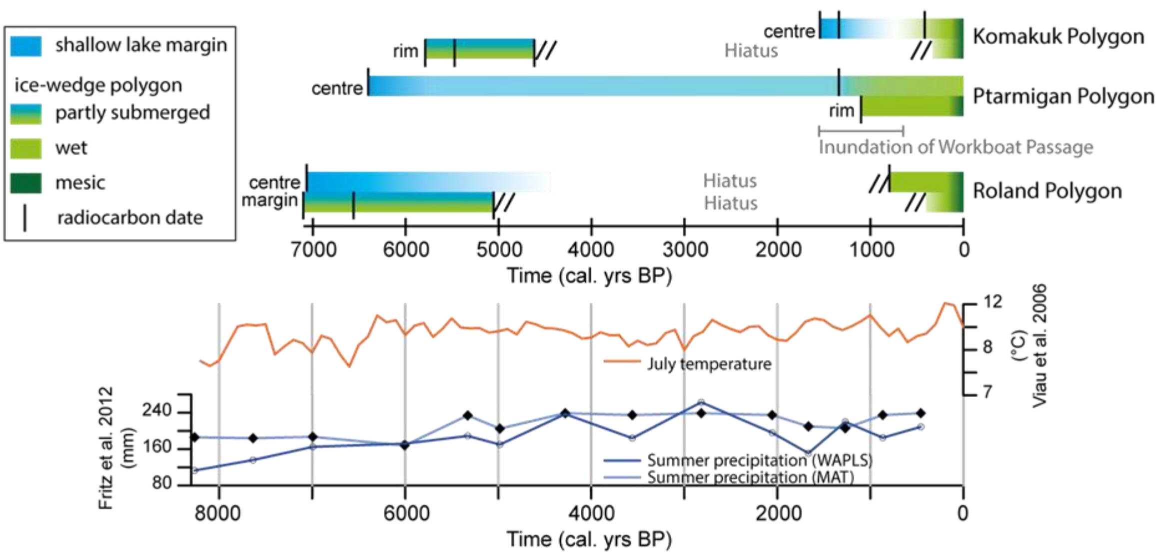

Figure 1. Environmental reconstruction for the studied ice-wedge polygons on the Yukon Coastal Plain and climate reconstructions. Black vertical lines indicate calibrated median radiocarbon ages.

References

Viau, A. E., Gajewski, K., Sawada, M. C., & Fines, P., 2006. Millennial-scale temperature variations in North America during the Holocene. *Journal of Geophysical Research: Atmospheres* 111: D09102.

Fritz, M., Wolter, J., Rudaya, N., Palagushkina, O., Nazarova, L., Obu, J., Rethemeyer, J., Lantuit, H., Wetterich, S., 2016. Holocene ice-wedge polygon development in northern Yukon permafrost peatlands (Canada). *Quaternary Science Reviews* 147: 279-297.

Wolter, J., Lantuit, H., Fritz, M., Macias-Fauria, M., Myers-Smith, I., & Herzschuh, U., 2016. Vegetation composition and shrub extent on the Yukon coast, Canada, are strongly linked to ice-wedge polygon degradation. *Polar Research* 35 (1): 27489.

Wolter, J., Lantuit, H., Herzschuh, U., Stettner, S., & Fritz, M., 2017. Tundra vegetation stability versus lake-basin variability on the Yukon Coastal Plain (NW Canada) during the past three centuries. *The Holocene* 27(12): 1846-1858.

14 - Permafrost peatlands in a changing climate – past, present and uncertain future

Session 14

Permafrost peatlands in a changing climate – past, present and uncertain future

Conveners:

- **Britta Sannel**, Department of Physical Geography, Stockholm University, Sweden
- **Ylva Sjöberg**, Department of Physical Geography, Stockholm University, Sweden; USGS Alaska Science Center, Anchorage, USA (PYRN member)
- **Sebastian Westermann**, Department of Geosciences, University of Oslo, Norway

Peatlands cover vast areas in the permafrost region and are important soil organic carbon reservoirs. Because of the characteristic thermal and hydraulic properties of peat, permafrost peatlands respond differently to ongoing and future climatic changes compared to mineral soils. Complicated feedbacks between energy, water and carbon cycles constitute a significant challenge for modelling approaches, making future projections on the fate of permafrost peatlands highly uncertain. In this session, we aim to provide an interdisciplinary platform showcasing state-of-the-art research on permaforst peatlands. We welcome presentations on a wide range of aspects and disciplines, such as landscape development and permafrost history, thermokarst features, monitoring activities, cryostratigraphy, carbon storage and cycling, numerical modelling and representation in Earth System Models.

Simulating Permafrost Peatlands under Climate Change with Laterally Coupled Tiles in a Land Surface Model

Kjetil Aas[1]
Sebastian Westermann[1]
Leo Martin[1]
Terje K. Berntsen[1]
[1]*University of Oslo, Department of Geosciences, k.s.aas@geo.uio.no*

Abstract

Here we present results from a land surface model (NoahMP) modified to include two laterally coupled tiles, and soil properties relevant for ice-rich, permafrost peatlands. The model is applied to a palsa mire location in Northern Norway, and a low-centered, ice-wedge polygon location in Northern Siberia, to test its abilities to simulate stable and thawing permafrost under very different conditions. The same basic processes, with lateral fluxes of snow, soil water and energy are required to capture important features at both locations.

Keywords: climate change; permafrost peatlands; numerical modeling; lateral fluxes.

Introduction

Permafrost peatlands represent an important, but complex component of the Earth's climate system. As a major reservoir of soil carbon which can potentially be activated by enhanced permafrost thaw, these regions are important to represent in future climate projections. However, the complex interplay between changing micro-topography due to melting excess ground ice, lateral fluxes of snow, water and energy, combined with the sensitivity of the thermal and hydraulic properties of peat to changing climatic conditions makes these regions particularly challenging to represent in large scale models.

Methods

In order to improve model representation of these regions, we have developed a version of the NoahMP land surface model (LSM) with two laterally coupled tiles. Previous work with an earlier version of this model has shown that sub-grid heterogeneities in snow accumulation can be well represented with tiles, resulting in improved representation of local meteorology and land surface conditions during the snow-melt season in high-mountain Norway (Aas *et al.*, 2017). Building upon this work, we have now developed a model version which includes lateral subsurface water and energy fluxes, as well as the previous snow redistribution. Additionally, the model has been augmented with excess ice capabilities following Lee *et al.* (2014) and Westermann *et al.* (2016), and with soil organic matter as an optional input parameters to more appropriately represent peat conditions.

The model is applied to a palsa mire location in Northern Norway, representing the warm, discontinuous margin of current Arctic permafrost region (Borge *et al.* 2017); and ice-wedge, low-centered polygons in Samoylov Island in Northern Siberia, representing cold, continuous permafrost in the current climate (Boike *et al.,* 2013). We investigate to what extent the transition from stable to degrading palsas and from low-centered to high-centered polygons, under current and warming climate conditions respectively, can be represented with this two-tile approach, and to what extent this could be achieved with the traditional horizontally independent 1D realizations.

Preliminary results

Preliminary results suggest that lateral fluxes of both snow, water and energy are important in order to represent these very different locations and their response to climate change, which highlights the need for improved representation lateral processes in future development of LSMs in Earth System Models.

References

Aas, K. S., et al. 2017. A Tiling Approach to Represent Subgrid Snow Variability in Coupled Land Surface–Atmosphere Models. *Journal of Hydrometeorology* 18, 49-63

Boike, J., et al. 2013. Baseline characteristics of climate, permafrost and land cover from a new permafrost observatory in the Lena River Delta, Siberia (1998-2011). *Biogeosciences* 10, 2105-2128

Borge, A. F., et al. 2017. Strong degradation of palsas and peat plateaus in northern Norway during the last 60 years. *The Cryosphere* 11: 1-16.

Lee, H., et al. 2014. Effects of excess ground ice on projections of permafost in a warming climate. *Environmental Research Letters* 9, 124006.

Westermann, S., et al. 2016. Simulating the thermal regime and thaw processes of ice-rich permafrost ground with the land-surface model CryoGrid 3. *Geoscientific Model Development* 9: 523-546.

Repeated tachymeter survey of peat plateau with degrading ice wedges, Pur-Taz interfluve, Russia

Evgeny M. Babkin[1]
Artem V. Khomutov[1,2]
Rustam R. Khairullin[1,3]
Yury A. Dvornikov[1]
Elena A. Babkina[1]
[1]*Earth Cryosphere Institute Tyumen Scientific Centre SB RAS, Tyumen, Russia, zbbkin@rambler.ru*
[2]*University of Tyumen, International Institute of Cryology and Cryosophy, Tyumen, Russia*
[3]*Saint Petersburg University, Saint Petersburg, Russia*

Abstract

Presented are first results of monitoring of polygonal peat plateau with ice wedges, degrading under the influence of natural cryogenic processes (thermokarst, thermal erosion) triggered by climatic fluctuations and possibly by technogenic factors. Analysis of 2016 and 2017 digital elevation models (DEMs) based on tachymeter and UAV surveys showed significant deepening of inter-polygonal troughs in 1-year period.

Keywords: ice wedges degradation; peat plateau; active layer depth; thermal erosion; thermokarst.

Introduction

Permafrost areas have widespread polygonal relief formed by a system of frost fractures with the formation of ice wedges (Dostovalov & Kudryavtsev, 1967). Since 2012, climate of the north of West Siberia is characterized by abnormally warm summer air temperature, that affects the dynamics of active layer depth and activation of cryogenic processes. The warm season of 2016 was particularly hot (Bardin *et al.,* 2016). Technogenic factors also have sufficient influence on changing the permafrost stability.

The article presents first results of the monitoring of polygonal peat plateaus with ice wedges, degrading under the influence of natural cryogenic processes (thermokarst, thermal erosion) triggered by climatic fluctuations and possibly by technogenic factors.

Study area and methods

The peat plateau is located five kilometers west of the Gaz-Sale settlement in the eastern part of Pur-Taz interfluves (Fig.1).

The monitoring site is adjacent to a road made of concrete slabs and, apparently, partly covered by road embankment and is represented by a set of convex polygons and deeply settled inter-polygonal troughs. In 2016, troughs were entirely water-filled.

To monitor dynamics of the peat plateau's surface, it was surveyed twice with tachymeter in conditional coordinates and heights system with time benchmarks in 2016 and repeatedly in 2017. In 2017 monitoring included UAV survey. Digital elevation models (DEMs) for each year were created.

The surveys have been carried out in area without direct impact of road embankment construction with the fixation of details like peat polygons' edges, trough thalwegs, flooded areas between the polygons, the polygons' topography, edges of roadway cover slabs. Peat polygons' edges did not include pieces of sod and peat already detached off the main polygon. If the piece was already lying in the water or on trough bottom, it was not considered as part of the polygon. In water-filled troughs, thalwegs were fixed under water.

The peat plateau surface is splitted by numerous intersecting frost fractures on rectangular, triangular and multangular polygons. The central part of the bulk of polygons is 0.2-0.3 m lower than edges, the surface is partially wet, supplemented by hummocks.

Within the peat plateau we can distinguish: 1) rather drained flat tops and slopes of peat polygons; 2) lowered flat tops and slopes of peat polygons, poorly-drained; 3) peripheral parts of polygons; 4) inter-polygonal troughs, partially drained, flooded in some places. On each surface type listed above, the active layer depth was measured mechanically with a metal probe.

Dynamics of peat plateau relief

Dynamics of ten peat plateau polygons covered by survey in both years was analyzed (Fig.1). Analysis of tachymeter and UAV survey data shows decrease of these polygons area and inter-polygonal troughs network expansion in 2017 compared to 2016. Each polygon area was decreased by a 4 to 43 square meters (2-11 %). Repeated survey showed that mostly flooded inter-polygonal troughs in 2016 with depth up to 3 meters were drained in 2017. Analysis of 2016 and 2017 DEMs showed that inter-polygonal troughs became deeper by 16-87 cm in average.

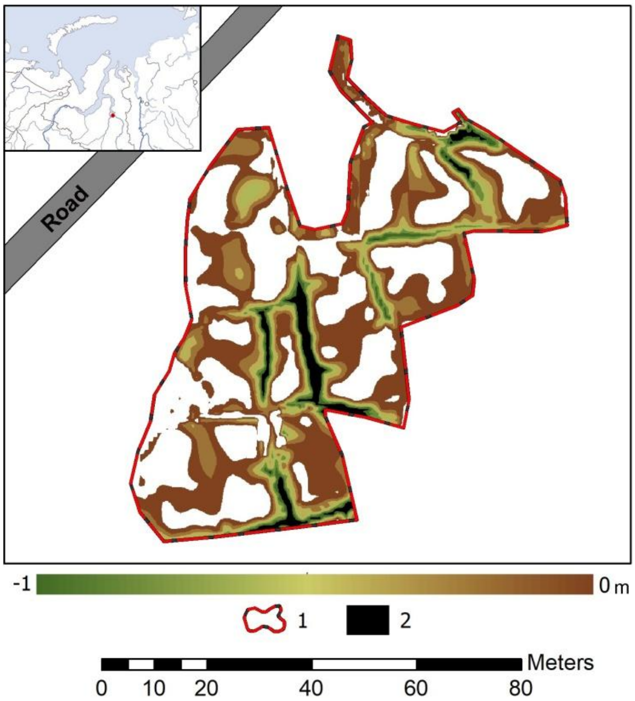

Figure 1. Difference between DEM of 2016 and 2017. 1 – area covered by surveys, 2 – no measurements.

Conclusions

Analysis of 2016 and 2017 digital elevation models based on tachymeter and UAV surveys showed significant deepening of inter-polygonal troughs up to 87 cm.

Further detailed monitoring of these peat plateau with study of heating effect of road embankment will result in better understanding of ice wedge degradation factors.

Acknowledgments

This work is partially supported by CALM program (NSF grant No.PLR1304555) and Presidential grant for scientific schools No. НШ-9880-2016.5. We thank Interregional Expedition Center "Arctic" (Salekhard) for the logistical support.

References

Dostovalov, B.N. & Kudryavtsev, V.A., 1967. *General permafrost studies*. MSU Publishing, 404 pp (In Russian)

Bardin, M.Yu., Rankova, E.Ya. & Samokhina, O.Ph., 2016. Temperature extremes of June and July. *Fundamental and applied climatology 2*: 143-148 (In Russian)

Timeline of permafrost peatland formation in subarctic Quebec (Canada)

Najat Bhiry[1], najat.bhiry@cen.ulaval.ca
Martin Lavoie[1]
[1]*Centre d'études nordiques & Département de Géographie, Université Laval, Québec, Canada*

Abstract

Several studies have shown that subarctic peatlands are influenced by allogenic factors such as climate and, autogenic processes such as peat accumulation (or Sphagnum acidification). The aggradation of permafrost in these peatlands was linked to cold periods of the Holocene. We synthesized the numerous available data concerning the periods of establishment of permafrost in peatlands located in subarctic Québec (Canada) leading to the formation of palsas and peat plateaus. There have been many studies of subarctic Québec, making it one of the most studied subarctic sites in the world. Our synthesis shows that palsas and peat plateaus started to form during the Little Ice Age, between 1450 and 1600 AD, while others began to form centuries earlier.

Keywords: Subarctic peatlands; palsas and peat plateaus; Little Ice Age; climate change; subarctic Québec

Introduction

Palsas and peat plateaus are periglacial landforms that are commonly found in subarctic minerotrophic peatlands. A palsa consists of a mound of peat rising out of a mire 1 to 7 m deep and containing a permafrost core of peat or silt. The surface of palsas and peat plateaus is dry and colonised by xeric to mesic plant species. In Québec (Canada), these landforms are concentrated in the coastal regions of James Bay, Hudson Bay, Ungava Bay (Fig. 1), the Labrador Sea, and the Gulf of St. Lawrence. These regions are part of the sporadic permafrost zone and the discontinuous permafrost zone and contain silty-sandy deposits originating from postglacial marine regression. There have been many studies of subarctic Québec, making it one of the most studied subarctic sites in the world. Studies of the ecology and long-term development of permafrost peatland over thousands of years in this region have employed a variety of methodologies from dendrochronology, stratigraphy, paleoecology and radiochronology disciplines (e.g. Allard & Séguin, 1987; Arlen-Pouliot & Bhiry, 2005; Bhiry *et al.*, 2007; Bhiry *et al.*, 2011; Fillion *et al.,* 2014).

In this paper, we report on our synthesis of available data concerning the periods of aggradation of permafrost in peatlands leading to the formation of palsas and peat plateaus in northern Québec (Fig. 1). Our aim is to construct a timeline and to determine whether some periods were more conducive to palsa and peat plateau formation than others, with a focus on the late-Holocene period.

Our hypothesis is that the majority of permafrost peatlands started to form during the Little Ice Age (~1450-1850 AD) during winters in which there was very little snowfall.

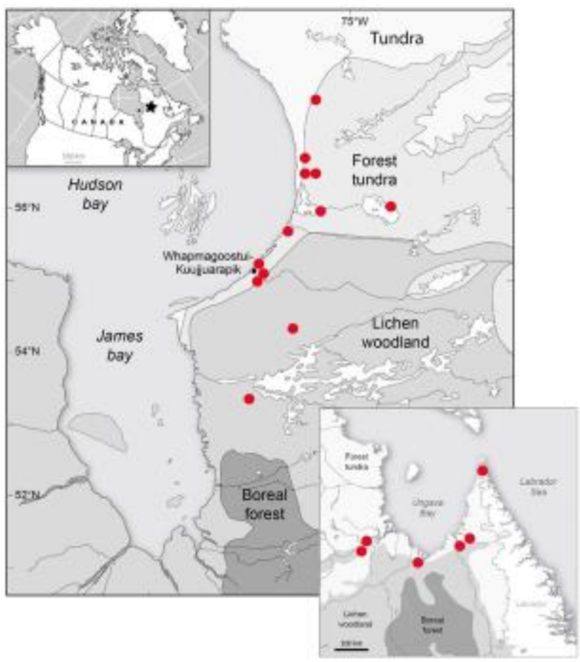

Figure 1. Location of sites in subarctic Québec with available paleoecological and radiochoronological data concerning peatland and permafrost formation.

Methods

We collated data from 24 sites, each of which contained one or more palsas or plateaus (Figure 2). The date of formation was calculated based on either ^{14}C dating of the surficial peat or by dendrochronological analysis of trees at the site.

Figure 2. Palsas field located south of the village of Whapmagoostui-Kuujjuarapik on the east coast of Hudson Bay in subarctic Québec.

Main results and interpretation

The dates at all sites ranged between 1730 BC and 1915 AD. Several palsas and peat plateaus started to form during the Little Ice Age between 1450 and 1600 AD, while others began to form centuries earlier. Very few palsas and peat plateaus were established during the Medieval Warm Period. The period of permafrost aggradation was also different for palsas located in the same field. In order to assess the relative contributions of climate factors (i.e., temperature and precipitation), the dates of onset were compared to quantitative paleoclimate data, periods of aeolian activity, and changes in water levels in northern Quebec lakes. Permafrost peatlands elsewhere in Canada, Scandinavia, and Siberia were also used as comparators. Results suggests that climate played a significant role in the evolution of the peatland. In particular, the cold conditions of the Neoglacial period and of the Little Ice Age period triggered palsas and peat plateaus formation. The recent climate warming has also contributed to the degradation of palsas (Fillion et al. 2014) (Fig. 3).

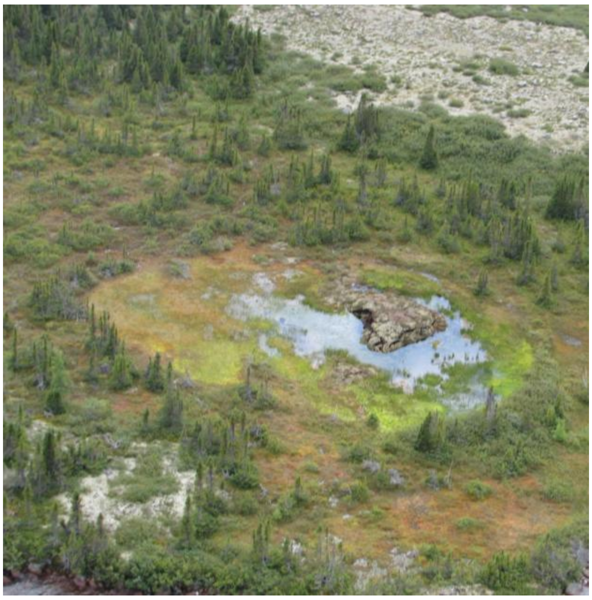

Figure 3. Collapsing of a palsa and formation of a thermokarst pond, Lac à l'Eau-Claire, subarctic Québec.

Acknowledgments

Funding for this research primarily comes from Centre d'études nordiques in frame of a trans-axial program Hudsonie21. We thank M. Desroches Bourgon for helpful in gathering of data.

References

Allard, M. & Séguin, M.K., 1987. The Holocene evolution of permafrost near tree line, on the eastern coast of Hudson Bay (northern Québec). *Canadian Journal of Earth Sciences* 24: 2206-2222.

Arlen-Pouliot, Y. & Bhiry, N., 2005. Palaeoecology of a palsa and a filled thermokarst pond in a permafrost peatland, subarctic Québec, Canada. *The Holocene* 15: 408-419.

Bhiry, N., Payette, S. & Robert, E.C., 2007. Peatland development at the arctic tree line (Québec, Canada) influenced by flooding and permafrost. *Quaternary Research* 67: 426-437.

Bhiry, N., Delwaide, A., Allard, M., Bégin, Y., Filion, L., Lavoie, M., Nozais, C., Payette, S., Pienitz, R., Saulnier-Talbot, E. & Vincent, W., 2011: Environmental change in the Great Whale River region, Hudson Bay: five decades of multi-disciplinary research by Centre d'études nordiques (CEN). *Écoscience* 18: 182–203.

Fillion, M.E., Bhiry, N. & Touazi, M., 2014. Differential development of two palsa fields in a peatland located near Whapmagoostui-Kuujjuarapik, Northern Quebec, Canada. *Arctic, Antarctic, and Alpine Research* 46: 41–55.

Recent rapid decay of palsa near Abez' settlement, northeast of European Russia

Nadine Budantseva[1]
Julia Chizhova[2]
Yurij Vasil'chuk[1]

[1]*Department of Geography, Lomonosov Moscow State University, Moscow, Russia, e-mail: nadin.budanceva@mail.ru*
[2]*Institute of Geology of Ore Deposits, Petrography, Mineralogy and Geochemistry, Russian Academy of Science, Moscow, Russia*

Abstract

The object of the study is the palsa located near Abez' settlement, the northeast of European Russia. The authors re-examined the palsa in 2001, 2016 and 2017. Since 2001 almost complete degradation of palsa is observed. The height of the palsa has reduced by more than 2 m and now does not exceed 1 m. During the period of 1960-2015, the average annual air temperature at nearby meteorological stations had been increasing by 2°C. The most probable reason for the rapid degradation of the palsa in the area of Abez' settlement is a combination of a positive climatic trend and significant draining of the mire as a result of the construction of the "Bovanenkovo-Ukhta" gas pipeline, which crosses the southern part of the massive. It is shown that the palsa in more southern region of the area ("Bugry Polyarnye" site) have no signs of degradation.

Keywords: palsa; peat; radiocarbon dates; stable carbon isotope; air temperature; degradation

Introduction

Palsa are vulnerable to climate change especially in the areas where they demarcate the outer or lower limit for permafrost. Studies of palsa dynamics in northern Europe and Canada permafrost show that palsa decay may be caused by increase of air temperature as well as by non-climatic factors such as change of hydrology, increased precipitation, etc.

According to Borge *et al.* (2017) total decrease of 33–71% in the areal extent of palsa and peat plateaus from the 1950s to the 2010s along a NW–SE transect through Finnmark observed in the last decade, is caused by air temperatures increase by 1.0 to 1.5°C.

An increase of mean annual air temperature form the 1930s to the end of 1990s together with increased snowfalls led to palsa degradation in Northern Sweden. The decay of the palsa was enormous in the dome–shaped part of the palsa complex: between 1996 and 2000 the height decreased from 2.3 m to 0.5 m. In 2000, the palsa dome had almost disappeared: only some peat blocks in a palsa pond were left (Zuidhoff, 2002).

For eastern Selwyn, western Mackenzie Mountains, NT, Canada, air temperatures appear to be important climatic drivers of palsa thaw at low elevations. Mamet *et al.* (2017) showed that over the last 25 years permafrost temperatures have increased from 0.2 to 1.3°C per decade and active layers have deepened by 8.2–17.4 cm per decade. Palsa areal extents have decreased by up to 96 % since the 1940s.

Study area and results

Palsa mire near Abez' settlement (66°31' N, 61°46' E) is located in the central part of palsa area of Bolshezemel'skaya Tundra, northeast of European Russia (Fig. 1).

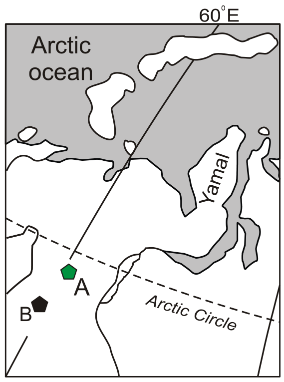

Figure 1. Map with study area: A – Abez' settlement. (B – "Bugry Polyarnye" site where palsa have no signs of degradation)

Mean annual air temperature (MAAT) in the middle of the 1960s was about –4.8°C. Permafrost associated mainly with peatlands had thickness of 10-12 m and more. Mean annual ground temperature (MAGT) often close to 0°C and MAGT within palsa 2.5-3 m high were about 1°C lower (Yevseev, 1976).

In 2001 near Abez' several palsa of different sizes and age have been studied in detail: large palsa 3-4 m high with spots of bared peat on the top, palsa with crescent form destroyed by a block erosion as well as young growing palsa in the central part of the mire (Vasil'chuk *et. al.*, 2008, 2013).

The radiocarbon dating carried out for 8 peat samples from an axial part of the palsa 3 m high showed that peat accumulation began here about 5.6 ka ago and continued for more than 2.5 ka in the eutrophic regime with average rate of accumulation 0.02-0.03 cm/year. The palsa began to form about 2.8 ka ago that marked in palsa section by transition to poorly decayed (i.e. quickly frozen) moss and moss-grass peat. The rate of peat accumulation sharply decreased to 0.004 cm/year.

Repeated studies of palsa mire near Abez' settlement in September 2016 and 2017 have shown that palsa height has considerably decreased and doesn't exceed 1 m (Fig. 2). Flat palsa surfaces were distinguished only by the color of vegetation.

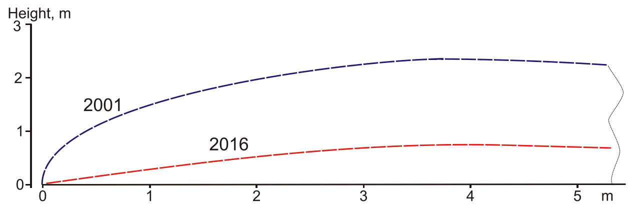

Figure 2. Mean height of palsa near Abez' settlement in 2001 and 2016-2017

Noticeable drainage of mire depression and reduction of its area as a result of trees expansion (mainly fir and birch) were also noted.

The depth profiles of $\delta^{13}C$ in peat of palsa 1 m high demonstrate that degradation of palsa wasn't followed by essential processing of a surface and mixing of peat. The profiles are characterized by so-called "turning points" which indicates the uplifting of the palsa by permafrost (Fig. 3). The same distribution of $\delta^{13}C$ values has been noted in the peat of palsa studied near Abisko in northern Sweden (Krüger *et al.*, 2014).

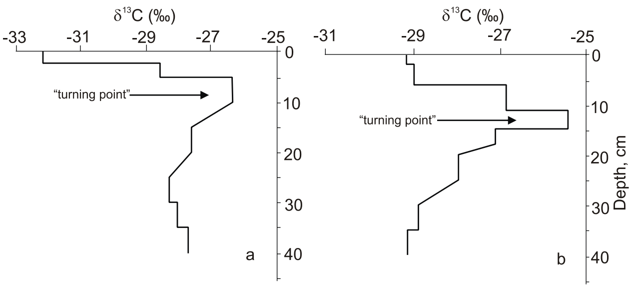

Figure 3. $\delta^{13}C$ values in the peat of palsa near Abez' settlement, 2016: a – at the top of the palsa, b – at the edge of the palsa

Probable causes of palsa degradation

Data of meteorological stations neighboring with Abez' settlement shows that MAAT increased on average on 2°C from 1960 to 2017, though steady trend of precipitation amount change was not recorded for this period.

At the same time water content of the mire considerably changed, even small water bodies disappeared. Drainage of the mire depression may be caused by construction of the "Bovanenkovo-Ukhta" gas pipeline that reached the Abez' area in 2012.

The underground way of the pipeline construction led to change of hydrological conditions and to drainage of the territory. The combination of a positive climatic trend and essential drainage of mire depression as a result of construction of the "Bovanenkovo-Ukhta" gas pipeline crossing the southern part of the mire became the most probable cause of rapid decay of palsa near Abez' settlement. It is noted that in more southern areas of Bolshezemelskaya Tundra (for example, at "Bugry Polyarnye" site) palsa almost have no signs of degradation for the period of 2001-2017.

Acknowledgments

The research was financially supported by the Russian Scientific Foundation: Grant № 14-27-00083-P

References

Borge, A., Westermann, S., Solheim, I. & Etzelmüller B. 2017. Strong degradation of palsas and peat plateaus in northern Norway during the last 60 years. *The Cryosphere* 11: 1–16.

Krüger, J., Leifeld, J. & Alewell, C. 2014. Degradation changes stable carbon isotope depth profiles in palsa peatlands. *Biogeosciences* 11: 3369–3380.

Mamet, S., Chun, K., Kershaw, G., Loranty, M. & Kershaw, G. 2017. Recent Increases in Permafrost Thaw Rates and Areal Loss of Palsas in the Western Northwest Territories, Canada. *Permafrost and Periglacial Processes* 28(4): 619–633.

Vasil'chuk, Yu., Vasil'chuk, A., Budantseva, N., & Chizhova, Ju. 2008. *Palsa of frozen peat mires.* Prof. Yu.K.Vasil'chuk (Ed.) Moscow: Moscow University Press, 571 pp. (In Russian).

Vasil'chuk, Yu., Vasil'chuk, A., Jungner, H., Budantseva, N. &, Chizhova, Ju. 2013. Radiocarbon chronology of Holocene palsa of Bol'shezemel'skaya tundra in Russian North. *Geography, Environment, Sustainability* 6(3): 38–59.

Yevseev, V. 1976. Regularities of migrational palsas distribution in the northeast of the European part of the USSR and Northwest Siberia. In Popov A.I. (ed.). Problems of Cryolithology. Moscow. Moscow University Press 5: 95–159.

Zuidhoff, F. 2002. Recent decay of a single palsa in relation to weather conditions between 1996 and 2000 in Laivadalen, northern Sweden. *Geografiska Annaler. Series A, Physical Geography* 84A(2): 103–111.

Methane emissions from high latitude peatlands: Constraining models with observations

Sarah Chadburn[1], Yuanchao Fan[2], Tuula Aalto[3], Annett Bartsch[4], Christina Biasi[5], Julia Boike[6], Eleanor Burke[7], Eddy Comyn-Platt[8], Han Dolman[9], Thomas Friborg[10], Yao Gao[3], Nic Gedney[7], Garry Hayman[8], Gustaf Hugelius[11], Ko van Huissteden[9], Mathilde Jammet[10], Hanna Lee[2], Annalea Lohila[3], Maija Marushchak[5], Frans-Jan W. Parmentier[12,13], Torsten Sachs[6], Narasinha Shurpali[5]

[1]*University of Leeds, UK, s.e.chadburn@exeter.ac.uk*
[2]*Uni Research, Bjerknes Center for Climate Research, Norway* [3]*Finnish Meteorological Institute* [4]*University of Vienna, Austria* [5]*University of Eastern Finland* [6]*Alfred Wegener Institute, Potsdam, Germany* [7]*Met Office Hadley Centre, UK* [8]*Centre for Ecology and Hydrology, UK* [9]*VU University Amsterdam, The Netherlands* [10]*University of Copenhagen, Denmark* [11]*University of Stockholm, Sweden* [12]*University of Oslo, Norway* [13]*Lund University, Sweden*

Abstract

Methane emissions from high-latitude peatlands represent a potentially important feedback mechanism with the Earth's climate. It is therefore essential to include them in Earth system models (ESM's). Here we use detailed high-frequency long-term observations at five high-latitude peatland sites, in order to cross-compare land surface schemes from two different ESM's. We firstly assess the uncertainties associated with process representations and modeling errors, and secondly constrain the model parameters by fitting to the observed data. We find that including soil carbon stocks may be the key to fitting a consistent set of parameters across different sites.

Keywords: Modeling, methane, wetlands, peatlands, broad-scale

Introduction

High-latitude peatlands usually form in water-saturated conditions, which lead to anaerobic decomposition and thus emission of methane (CH_4). CH_4 is a powerful greenhouse gas, which is produced by natural wetlands as well as anthropogenic sources (e.g. rice, agriculture). Wetland CH_4 emissions are likely to change under global warming, driven by changes in temperature, water content and shifts in wetland extent, leading to climate feedbacks. High latitude wetlands are an important CH_4 source, estimated to contribute 20-70 $TgCH_4$/yr to the global total 500-600 $TgCH_4$/yr budget (i.e. 2-20%, Saunois *et al.*, 2016, Poulter *et al.*, 2017). Furthermore, this region is experiencing a rapid warming as the climate changes. Thus it is important and timely to focus on including high latitude CH_4 emissions and feedbacks in climate models.

Several recent global land surface schemes – which are used in climate models – include process-based CH_4 models. These represent production, oxidation, emission, and the transport mechanisms of CH_4 through the soil and into the atmosphere (e.g. Riley *et al.*, 2011). These schemes build upon the original CH_4 modules in such models, which are simple functions of soil temperature, wetland area and substrate (e.g. Gedney *et al.*, 2004).

Methods

In this study we used detailed half-hourly CH_4 flux from eddy covariance flux towers to cross-validate land surface models. These measurements provide the ecosystem-scale CH_4 flux. We also used detailed profile soil carbon measurements and high-frequency soil temperature readings at multiple depths. A number of sites with such high data density available were used in this study, including several Russian permafrost sites, a peatland in Northern Sweden with limited permafrost and a peatland in Finland without permafrost. We then compared the observations with two land surface schemes, one of which contains a detailed process-based CH_4 model (CLM) and the other contains a simpler scheme based on soil temperature, carbon and wetland fraction (JULES).

Comparing the models with each other, we assessed the uncertainty associated with not considering the more detailed CH_4 processes in the model. Comparing functional relationships in the models and observations allowed us to constrain the model parameters, and to assess the largest sources of uncertainty in CH_4 emissions in these land surface schemes.

Results

We showed that using wetland fraction, measured soil temperature and soil carbon density (as a proxy for substrate) allowed us to fit a single relationship with CH_4 emissions. Such a function was reasonably applicable across all of the sites used in this study. The main difference between this and previous studies (e.g. Turetsky *et al.*, 2014) is the inclusion of the soil carbon density. Soil carbon may therefore provide the key to constraining CH_4 emissions from high-latitude peatlands.

Observed and modelled total annual CH_4 flux from five different sites and several different years is shown in Figure 1. The model was fitted to data from the Abisko site (shown in red), and the same parameters were applied across all sites. Note that the data are not gap-filled, and any missing data in the observations were also removed in the model before calculating the totals. This modelling exercise shows that such a simple scheme may be sufficient for modeling CH_4 emissions at coarse scales. However, this depends on simulating wetland fraction and soil carbon correctly, which is a major challenge for land-surface modeling.

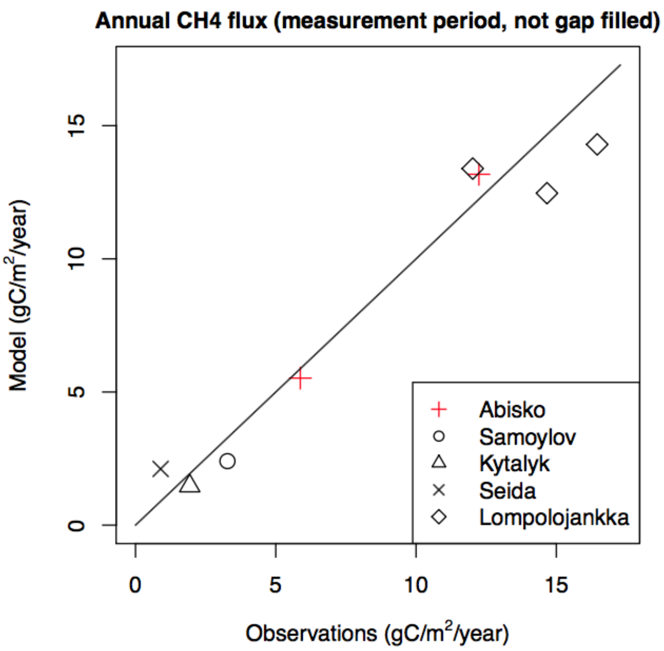

Figure 1. Annual CH_4 emissions for each year for five different sites, modeled using the same set of parameters for every site, in a simple model of wetland fraction, soil temperature and soil carbon. The model parameters applied across all sites were fitted using the Abisko site, shown in red.

Acknowledgments

The authors acknowledge support from the following projects: COUP (Constraining uncertainties in the permafrost-climate feedback, Natural Environment Research Council (NERC) grant NE/M01990X/1); CLIFFTOP (Climate feedbacks from wetlands and permafrost thaw in a warming world, NERC grant NE/P015050/1); CoMIP (Collaborative Earth System Model development and intercomparison on permafrost processes, Research Council of Norway KLIMAFORSK project no. 261806).

References

Gedney, N., Cox, P. M., & Huntingford, C., 2004. Climate feedback from wetland methane emissions. *Geophys. Res. Lett.* 31: L20503

Riley, W. J., Subin, Z. M., Lawrence, D. M., Swenson, S. C., *et al.*, 2011. Barriers to predicting changes in global terrestrial methane fluxes: analyses using CLM4Me, a methane biogeochemistry model integrated in CESM. *Biogeosciences* 8: 1925-1953

Poulter, B., Bousquet, P., Canadell, J. G., Ciais, P., *et al.*, 2017. Global wetland contribution to 2000–2012 atmospheric methane growth rate dynamics. *Environ. Res. Lett.* 12: 094013

Saunois, M., Bousquet, P., Poulter, B., Peregon, A., *et al.*, 2016. The global methane budget 2000–2012. *Earth Syst. Sci. Data* 8: 697-751

Turetsky, M. R., Kotowska, A., Bubier, J., Dise, N. B., *et al.*, 2014. A synthesis of methane emissions from 71 northern, temperate, and subtropical wetlands. *Glob. Change Biol.* 20: 2183–2197

Advancing permafrost carbon climate feedback – improvements and evaluations of the Norwegian Earth System Model with observations

Casper (Tai) Christiansen[1]
Sebastian Westermann[2]
Dave Risk[3]
Hanna Lee[1]
[1]*Uni Research Climate, Bjerknes Centre for Climate Research, Norway, casper.christiansen@uni.no*
[2]*University of Oslo, Norway*
[3]*St. Francis Xavier University, Canada*

Abstract

The response of permafrost-affected soils to Arctic warming represents a major source of uncertainty in projecting carbon (C) cycle climate feedbacks as permafrost C can become a significant additional source of greenhouse gas to the atmosphere. Accurate climate predictions from Earth System Models (ESMs) are dependent on a sound representation of the biogeochemical processes in permafrost soils. However, limited observational data on permafrost C release over a range of soil hydrological environments currently limit development of biogeochemical process-level models, and prevent robust evaluation of model simulations. In this project, we seek to integrate efforts across often-distinct research areas such as field-based observations, statistical data synthesis and model parameterization, and Earth System Modelling (ESM) development and evaluation. We do this by obtaining high frequency observational data from a palsa peatland in Northern Norway (Iskorasfjellet; 69º N), and use these data to evaluate the performance of the Norwegian ESM (Nor-ESM).

Keywords: Peatland; Methane; Earth System Modelling; Climate Change; Carbon Cycling; Observations

Introduction

Permafrost is a key element of the cryosphere, which dominates a quarter of the landmass in the northern hemisphere. Permafrost soils contain over 1600 Pg of carbon (C), which constitutes approximately half of global soil C storage and double that of the atmosphere (Tarnocai et al. 2009; Zimov et al. 2006). Projected climate warming will likely thaw permafrost and accelerate the release of permafrost C to the atmosphere (Lawrence et al. 2012; Schuur et al. 2009), but a major uncertainty is how this C is released – i.e. as either CO_2 or CH_4.

The rate of C turnover and CO_2 release is generally faster under dry aerobic conditions; whereas, under wetter anaerobic conditions soil C turnover is slower, but produces CH_4 that has 25 times greater global warming potential than CO_2 over a 100 year time scale (IPCC 2013; Lee et al. 2012). Therefore, changes in soil hydrological conditions during permafrost thaw are likely to have a large influence on both the total rate of permafrost C release and its potential to affect the future climate. Specifically, two questions remain unresolved: 1) will permafrost thaw release C primarily as CO_2 or CH_4; and, 2) what is the magnitude of the climate-related feedbacks that we can expect from permafrost C release?

The coupled dynamics of permafrost hydrology and biogeochemical processes that result in permafrost C release in the forms of CO_2 and CH_4 are generally not realistically simulated by the Earth System Models (ESMs) used in the recent CMIP5 framework (Todd-Brown et al. 2013; Koven et al. 2013). Results so far indicate a need for greater quality observations for model parameterization and evaluation, especially at high latitudes (Koven et al. 2013) to achieve better model simulations.

Methods

In CLM4.5BGC (the terrestrial module of the Norwegian ESM, Nor-ESM) the developers aimed to improve representation of the complex biogeophysical and biogeochemical interactions characterized in permafrost soils. These developments enable simulations of changing hydrological states during permafrost thaw and the subsequent fate of permafrost C under various hydrological conditions. However, despite novel improvements in the Nor-

ESM, the current level of model evaluation has only been conducted from a collection of surface flux measurements of CH_4, and not subsurface data that could show where CO_2 and CH_4 are produced and oxidized in vertical soil profiles under varying conditions of the soil environment.

In the this project, we aim to improve our process-level understanding of tundra soil profile greenhouse-gas dynamics, and advance our ability to project permafrost carbon-climate feedback potentials under various climate change scenarios. In order to achieve this, we have established a field site along a hydrological and permafrost thaw gradient within a palsa peatland in Northern Norway (Iskorasfjellet; 69º N; discontinuous permafrost zone). Throughout the year, we record high temporal frequency automated measurements of soil profile CO_2 and CH_4 dynamics, as well as surface-atmosphere fluxes and various microclimatological parameters.

Continuous subsurface measurements of CO_2 and CH_4 under different hydrological conditions is extremely rare due to methodological difficulties and sensor availability. However, CH_4 production and oxidation in saturated and unsaturated permafrost zones are sensitive to environmental conditions in subsurface soil profiles. Therefore, the observations we conduct in FEEDBACK is a unique contribution to both observations and modeling research-communities working on permafrost carbon dynamics.

References

I.P.C.C., 2013. *Climate Change: The Physical Science Basis. Contribution of Working Group I to the Fifth Assessment Report of the Intergovernmental Panel on Climate Change.* Cambridge, Cambridge University Press, 1535 pp.

Koven, C.D., Riley, W.J., Stern, A., 2013. Analysis of Permafrost Thermal Dynamics and Response to Climate Change in the CMIP5 Earth System Models. *Journal of Climate* 26: 1877-1900.

Lawrence, D.M., Slater, A.G., Swenson, S.C., 2012. Simulation of Present-Day and Future Permafrost and Seasonally Frozen Ground Conditions in CCSM4. *Journal of Climate* 25: 2207-2225.

Lee, H., Schuur, E.A.G., Inglett, K.S., Lavoie M., Chanton, J.P., 2012. The rate of permafrost carbon release under aerobic and anaerobic conditions and its potential effects on climate. *Global Change Biology* 18: 515-527.

Schuur, E.A.G. *et al.*, 2009. The effect of permafrost thaw on old carbon release and net carbon exchange from tundra. *Nature* 459: 556-559.

Tarnocai, C. *et al.* (2009) Soil organic carbon pools in the northern circumpolar permafrost region. *Global Biogeochemical Cycles* 23: GB003327.

Todd-Brown, K.E.O. *et al.*, 2013. Causes of variation in soil carbon simulations from CMIP5 Earth system models and comparison with observations. *Biogeosciences* 10: 1717-1736.

Zimov, S.A., Schuur, E.A.G., Chapin, F.S., 2006. Permafrost and the global carbon budget. *Science* 312: 1612-1613.

Evolution of dissolved organic matter origin and methanogenesis processes in degrading palsa of North Siberia

Laure Gandois[1], Alison Hoyt[2], Christine Hatté[3], Nikita Tananaev[4], Karla Martinez Cruz[5], Armando Sepulveda-Jauregui[5], Oscar Alejandro Gerardo Nieto[6], Frederic Thalasso[6], Léa Cabrol[7], Roman Teisserenc[1], Maialen Barret[1]

[1] *EcoLab, Université de Toulouse, CNRS, INPT, UPS, Toulouse, France, laure.gandois@ensat.fr*
[2] *Max Planck Institute for Biogeochemistry, Hans-Knöll-Straße 10, Jena, Germany*
[3] *LSCE, UMR8212 CEA/CNRS/UVSQ, Université Paris Saclay, Gif-sur-Yvette, France*
[4] *Melnikov Permafrost Institute, Siberian Branch, Russian Academy of Sciences, Yakutsk, Russia*
[5] *Universidad de Magallanes, Magallanes, Chili*
[6] *Cinvestav, Mexico, Mexico*
[7] *MIO, Marseille, France*

Abstract

Permafrost peatlands are important carbon stocks currently experiencing rapid evolution in relation to permafrost thaw. The degradation of palsa mounds locally induces ecosystem shifts and the formation of new peatlands. This study investigates, in a discontinuous permafrost area of North Siberia, both the evolution of the origin and composition of dissolved organic matter (DOM), as well as the CH_4 cycle, along a thaw gradient. Strong patterns are observed along the thaw gradient. The contribution of permafrost to DOM decreases with time after thaw. This is accompanied by the evolution of DOM composition, with an increased contribution of microbial DOM. As evidenced by combined isotopic and 16S rRNA analysis, a shift from hydrogenotrophic to acetoclastic CH_4 production occurs along the thaw gradient.

Keywords: Permafrost peatlands, Siberia, Dissolved Organic Matter, Methanogenesis, Isotopic Analyses, 16S rRNA

Introduction

Palsa peat mounds are typical of the margin between the Artic and sub-Arctic regions. In recent decades, they are degrading with the thawing of permafrost. This implies ground subsidence, modifications of hydrological pathways and complex ecological shifts of vegetation and microbial communities, with the formation of new peatlands (Liebner et al. 2015; McCalley et al. 2014). Along these ecosystem transitions, the origin of carbon potentially available to microorganisms evolves. Carbon can be old sequestered carbon released from permafrost or recently fixed from the atmosphere by vegetation through photosynthesis, with very different implications for climate change feedbacks. In thawing permafrost landscapes, a complex link exists between organic matter origin and availability and the microbial community structures. We investigate the evolution of dissolved organic matter (DOM) origin and characteristics, as well as CH_4 production pathways along a palsa thaw gradient in a discontinuous permafrost area of North Siberia.

Study sites and Methods

Study Site

The study area is located in a discontinuous permafrost area of Siberia affected by permafrost degradation (Igarka, the Graviyka River catchment (67°27'11"N, 86°32'07"E)).

Methods

Thawing palsa ponds of various sizes (with the hypotheses of size representing time since thaw), larger thermokarst lakes, and streams draining the peatland complexes. In the newly formed peatlands, we collected porewater profiles. The origin and quality of DOM was determined by combining isotopic ($\delta^{13}C$, ^{14}C) and optical (specific UV absorbance (SUVA) and fluorescence Index (FI)) analysis. We investigated the methanogenic and methanotrophic pathways using measurements of CH_4 concentrations, isotopic ($\delta^{13}C$ and δ^2H) composition, in situ emissions fluxes as well as microbial community structures (16S amplicon sequencing).

Results and Discussion

Dissolved Organic Matter composition and origin

In degrading palsa, the composition and origin of DOM evolves along the thaw gradient. The highest DOC concentrations are measured in the smallest thermokarst ponds (Figure 1). Dissolved organic matter has mostly terrestrial origin (low FI, high SUVA) and shows previous microbial processing. (relatively high $\delta^{13}C$ values). In larger thawing ponds, lower DOC concentrations are paired with a higher FI, lower SUVA and $\delta^{13}C$-DOC values, indicating a greater contribution of nonaromatic compounds and microbial DOM. The ^{14}C content of DOM also shows a strong evolution along the gradient. The bulk age of DOM increases in small ponds and in deep layers, reflecting the permafrost DOM contribution. In the smallest ponds, permafrost DOM constitutes from 40 to 60 % of DOM, and this proportion decreases with pond size to less than 10%. When measured, ^{14}C of dissolved CH_4 and CO_2 matches ^{14}C of DOM in pore water profiles. In larger thermokarst lakes, only modern DOM, CO_2, CH_4 are detected, with an estimated range of age from 5 to 10 years, with the notable exception of collapsing palsa banks, where permafrost carbon constitutes 40 % of dissolved CO_2 and CH_4.

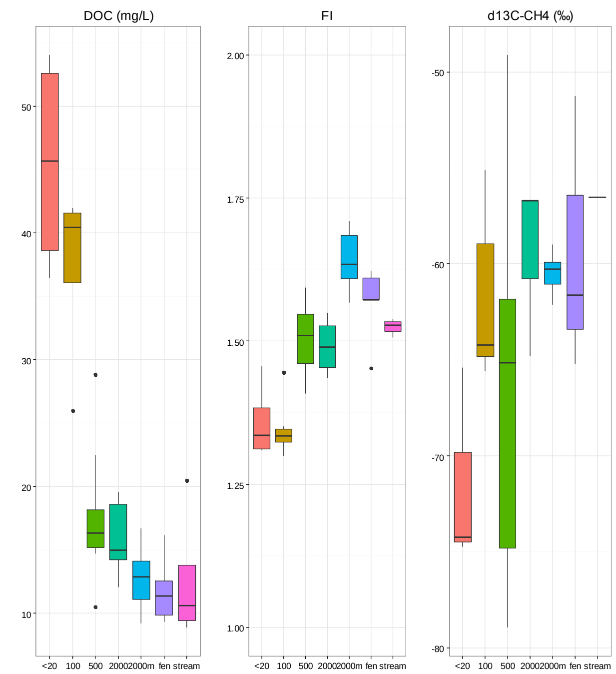

Figure 1. DOC concentrations, FI and $\delta^{13}C$-CH_4 from porewater sampled following a palsa thaw gradient (from <20 to 2000 m^2), newly formed peatland in a mineral soil context (2000m),fen and stream draining the thawing palsa complex.

Methane cycling

Although no significant trends are observed in CH_4 concentration and fluxes, methane cycling strongly evolves along pore water profiles and the thaw gradient. In small ponds, low isotopic signatures are measured in pore water indicating the importance of the hydrogenotrophic pathway for methane production (Figure 1). This is confirmed by the predominance of *Methanobacterium* in archaea communities. Along the thaw gradient, the $\delta^{13}C$ of CH_4 of shallow pore water samples increases suggesting a contribution from acetoclastic methane production. An increased relative abundance of *Methanosaeta* is identified. As evidenced by coupled analysis of $\delta^{13}C$ and δ^2H of CH_4, methane oxidation is important in large thermokarst lakes but is limited in peatland pore water.

Conclusions

Carbon cycling strongly evolves in discontinuous permafrost landscapes affected by permafrost degradation. Following thaw, permafrost carbon is partly mobilized as DOM and mineralized. Following permafrost thaw and the development of new peatlands, DOM origin and composition evolve towards recently metabolized origin. Methane production pathways shift from hydrogenoclastic to a greater contribution of acetoclatic production.

Acknowledgments

This research was conducted with the support of CNRS through the PEPS program, was part of the ERANET-LAC METHANOBASE project, and was supported by the GDRI "Car-Wet-Sib". Anatoly Pimov is greatly thanked for his support of field investigations.

References

Liebner, S., Ganzert, L. et al., 2015. Shifts in Methanogenic Community Composition and Methane Fluxes along the Degradation of Discontinuous Permafrost. *Frontiers in Microbiology* 6, 356.

McCalley, C. K., Woodcroft, B.J., et al. 2014. Methane dynamics regulated by microbial community response to permafrost thaw. *Nature* 514 (7523):478-81.

Persistence of permafrost after 55 years of climatic warming and fire disturbance in the sporadic discontinuous zone

Jean E. Holloway[1]
Antoni G. Lewkowicz[1]
[1]*Department of Geography, Environment and Geomatics, University of Ottawa, Canada*
jean.holloway77@gmail.com

Abstract

Ecosystem-protected permafrost is thought to be sensitive to environmental change, but peatlands may follow other trajectories because of the insulating properties of the substrate. This study examined 26 sites in the sporadic discontinuous zone in Canada, all of which had permafrost in 1962. Ten sites have subsequently undergone fire disturbance, and all sites have experienced climatic change. At each site, we investigated frost table depth, organic mat thickness, substrate, and used electrical resistivity tomography surveys to evaluate permafrost thickness. Our results show that permafrost has persisted at 65% of the sites, including six of the ten burned sites. These sites all had organic mat thicknesses of at least 60 cm and were underlain by fine-grained materials. Overall, our results suggest the importance of substrate for the persistence of warm permafrost after disturbance.

Keywords: Climate change; forest fire; discontinuous permafrost; peatland

Introduction

Effects of global climate change are being felt in all aspects of the cryosphere, and how permafrost will respond to these variations is of concern. Ecosystem-protected permafrost covers millions of square kilometres in the subarctic and is protected by forest vegetation from changes in air temperature. It is thought to be sensitive to environmental change as it is thin, discontinuous, and just below 0° C. However, peatlands may follow other trajectories because of the insulating properties of the substrate. This study examined 26 peatland sites in Canada along the Mackenzie Highway between Meander River, AB (59.05°, -117.72°) and Hay River, NT (60.82°, -115.79°) in August 2017 in order to evaluate current permafrost conditions. The sites all had permafrost when they were first examined in 1962 (Brown, 1964). All sites have experienced some form of disturbance over the last 55 years; ten of the sites have experienced forest fires and the entire region has warmed by 1.7° C.

Methods

Brown (1964) indicated site locations using milepost numbers and also showed them on a map at a scale of 1:650,000. This map was digitized and overlain on a GoogleEarth image to generate approximate site coordinates. In the field, 2 km sweeps of the highway were conducted, centered on the approximate coordinates, and locations were identified which best matched site descriptions of terrain, drainage, and vegetation. These locations were then probed using a 1.2 m long frost probe, starting at the approximate coordinates. If a frost table was identified, depth to frozen ground was measured at 10 points located 1 m apart. If no frost table was reached at the approximate coordinates, investigations proceeded at the next location until a frost table was located or it was established that no frozen ground was present in the area. Organic mat thickness and substrate were recorded at all transects, and soil samples taken within the active layer at permafrost sites. Electrical resistivity tomography (ERT) surveys were undertaken at four sites to evaluate permafrost thickness. This geophysical technique provides an image of the electrical properties of the ground to a depth of 25 m which can be interpreted as frozen and thawed zones.

Figure 1. Peatland which burned in 2007.

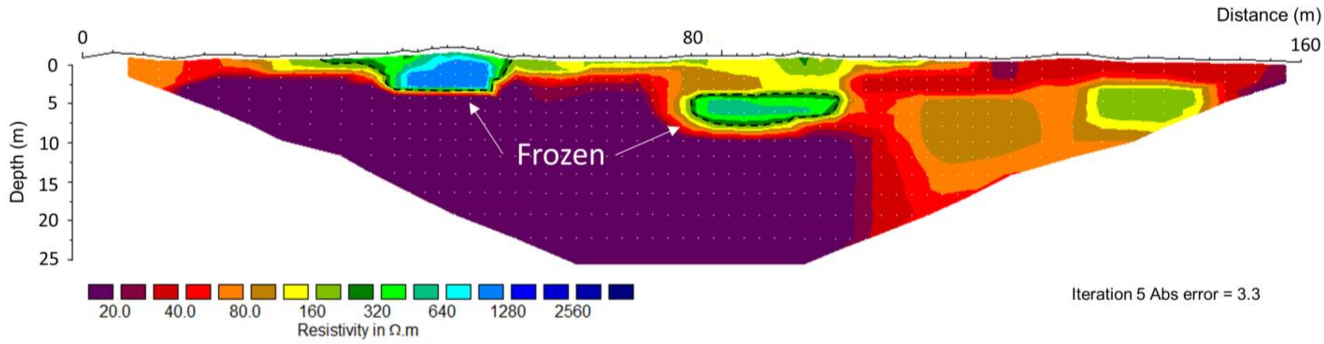

Figure 2. ERT profile of a site which burned in 2012, showing the persistence of approximately 8 m of permafrost. We have interpreted frozen ground being anything higher than 300 Ωm.

Results

Our results show that permafrost has persisted at 17 of the 26 (65%) sites investigated in 1962. These sites all have a sphagnum moss cover and an organic layer thickness of at least 60 cm. Sites which experienced permafrost loss are underlain by coarser-grained substrates (generally sand and gravel) whereas the sites where permafrost has persisted are mainly in fine-grained materials (silt and clay). Six of the ten burned sites still have permafrost, including sites which burned recently (in 2007 and 2012) and others which burned several decades ago (1971 and 1981). Frost tables were as shallow as 45 cm (on August 5) and the ERT surveys indicate permafrost thickness up to 8 m (Figure 2).

Conclusion

Overall, our results suggest the importance of substrate in post-fire trajectories for warm permafrost. Peatlands provide sufficient protection following disturbance to allow permafrost to be maintained. These results also indicate a much higher level of permafrost persistence than has been previously reported for the sporadic discontinuous permafrost in this part of the Mackenzie Highway (Kwong & Gan, 1994).

Acknowledgments

This research has been supported by the Natural Sciences and Engineering Research Council, the University of Ottawa, the Northern Scientific Training Fund, the W. Garfield Weston Foundation, and the Government of the Northwest Territories. We gratefully acknowledge ongoing collaboration with Jennifer Baltzer, Merritt Turetsky, Steve Cumming, Jill Johnstone, Michelle Mack, Xanthe Walker, Nicola Day, Catherine Dieleman, and Stephen Wolfe. We appreciate all the assistance in the field.

References

Brown, R.J.E., 1964. *Permafrost investigations on the MacKenzie highway in Alberta and MacKenzie district.* Technical Paper No.175, National Research Council, Ottawa, Canada.

Kwong, Y. J. & Gan, T. Y., 1994. Northward migration of permafrost along the Mackenzie Highway and climatic warming. *Climatic Change* 26(4): 399-419.

Dissolved organic carbon export and its contribution to the carbon budget in a boreal peat landscape undergoing rapid permafrost thaw

Julien Fouché[1]
Oliver Sonnentag[2]
Manuel Helbig[2]
Karoline Lillie[2]
Gabriel Hould Gosselin[2]
William Quinton[3]
Tim Moore[4]

[1]*Department Biosystem Engineering (BIOSE), Gembloux Agro-Bio Tech, University of Liège (ULg), 5030 Gembloux, Belgium, julien.fouche@tuta.io*
[2]*Département de géographie & Centre d'études nordiques, Université de Montréal, Montréal, QC, H3C 3J7*
[3]*Cold Regions Research Centre, Wilfrid Laurier University, Waterloo, ON, N2L 3C5*
[4]*Department of Geography, McGill University, Montréal, QC, H3A 0B9*

Abstract

In boreal lowlands with warm and thin isolated permafrost, increasing temperatures cause a thaw-induced expansion of permafrost-free wetlands at the expense of forested permafrost peat plateaus. Permafrost thaw associated with warming may enhance decomposition of soil organic matter but also modify dissolved organic carbon (DOC) export to aquatic systems, which may play a non-negligible role for the carbon budget. We quantified the DOC export from a boreal peat landscape in the southern Northwest Territories (Canada) and estimate its contribution to the net ecosystem carbon balance. DOC export ranged from 2.5 to 4.0 g C m^{-2} from April to August, which accounted for ~51% (2014), 25% (2015) and 16% (2016) of the annual net ecosystem exchange. Our findings suggest that thawing boreal peat landscapes along the southern limit of permafrost are currently carbon neutral and increased vegetation productivity may turn the site into a weak sink.

Keywords: Net Ecosystem Carbon Balance; Sporadic and Discontinuous permafrost; Climate Change; Dissolved Organic Matter; SUVA

Introduction

Northern permafrost soils store 1035 ± 150 Pg of organic carbon (C; Hugelius *et al.*, 2014). In boreal lowlands with warm and thin isolated, sporadic and discontinuous permafrost, increasing temperatures cause a thaw-induced expansion of permafrost-free wetlands at the expense of forested permafrost peat plateaus (Quinton *et al.*, 2011).

Permafrost thaw associated with warmer soils may enhance microbial decomposition of near-surface and deeper organic matter and modify dissolved organic carbon (DOC) export to aquatic systems (Schuur *et al.*, 2015). Recent studies suggest that, in a warmer climate, the current net carbon dioxide (CO_2) sink strength of boreal peat landscapes may decline over the next few decades, eventually turning them into net CO_2 sources (Helbig *et al.*, 2017). DOC export from these organic-rich landscapes undergoing rapid permafrost thaw may play a non-negligible role for the net ecosystem carbon balance (NECB) in a warmer climate.

Material and methods

In this study, we quantify the DOC export from a boreal peat landscape in the southern Northwest Territories (Canada). We use half-hourly discharge measurements and DOC concentrations sampled at the outlets of three small headwater catchments (~0.1-0.3 km^2) to quantify runoff and DOC export from April to August 2014, 2015 and 2016. UV-Vis absorbance properties ($SUVA_{254}$ and a_{254}:a_{365}) were used as a proxy of dissolved organic matter (DOM) composition. We estimate the DOC export contribution to NECB using concurrent eddy covariance measurements of net ecosystem CO_2 exchange (NEE) and CH_4 emission. DOC inputs through rainfall were estimated using a mean DOC concentration of 9 mg L^{-1} (Moore, 2003).

Results and discussion

We found linear relationships between DOC concentration and discharge only during the spring freshet periods. However, DOC concentration and discharge were positively correlated in 2015 and negatively correlated in 2016. These between-year differences highlight changes in DOC availability during the spring freshet, when most of the discharge occurs. The three small catchments experienced different hydrological regimes, ~70% of DOC was exported from mid-April to early May at the West and South catchments while only 25% of DOC was exported at the East catchment during the same period (table 1).

During the three years, total DOC export from the watershed ranged from 2.5 to 4.0 g C m^{-2} from April to August. For the same period, the cumulative CH_4 emission ranged from 5.4 to 7.5 g C-CH_4 m^{-2}. NECB was equal to + 1 g C m^{-2} y^{-1} in 2014 (i.e., source of C), -7.6 and -15.6 g C m^{-2} y^{-1} in 2015 and 2016, respectively (i.e., sink of C). Our findings suggest that Scotty Creek, which represents a thawing boreal peat landscape along the southern limit of permafrost, is currently carbon neutral and increasing vegetation productivity may turn the site into a weak sink. Between-year differences in NECB are largely controlled by differences in NEE. Warmer springs in 2015 and 2016 experienced higher net CO_2 uptake, which appear to increase the C sink strength.

Table 1. Comparison of the three headwater catchment characteristics, seasonal yields of discharge and DOC fluxes in 2014, 2015 and 2016.

	East	West	South
Total area [km^2, %]	0.328, 100	0.105, 100	0.099, 100
Forest [km^2, %]	0.170, 51.95	0.051, 48.56	0.055, 44.55
Bog [km^2, %]	0.143, 43.61	0.054, 51.43	0.044, 55.45
Fen [km^2, %]	0.001, 0.32	0, 0	0, 0
Mineral soil [km^2, %]	0.014, 4.12	0, 0	0, 0
Bog :forest ratio [-]	0.84	1.06	1.24
2014			
Runoff [mm]	64.78	12.55	73.85
DOC export [g m^{-2}]	3.34 (24.12)	0.50 (97.34)	2.72 (68.19)
2015			
Runoff [mm]	83.27	64.84	72.60
DOC export [g m^{-2}]	4.30 (25.26)	2.60 (65.40)	2.66 (73.65)
2016			
Runoff [mm]	-	87.21	104.86
DOC export [g m^{-2}]	-	3.22 (72.01)	3.11 (86.98)

Values of the spring freshet contribution to total DOC export are reported within the brackets.

DOC is an important component of NECB, in particular in a context of rapid shift from source to sink of carbon. Although primarily depending on discharge, DOC export was sustained during drier years. Our measurements most likely underestimated DOC since biogenic dissolved inorganic carbon (i.e., CO_2 and CH_4) and particulate organic carbon were not accounted for.

The absorbance properties of the DOM were similar among the three dominating landforms (i.e., forested permafrost peat plateau, collapse-scar bog, and collapse scar) and the catchments outlets. SUVA values were high (> 3 L mg^{-1} m^{-1}) illustrating high aromaticity of DOM. The export DOM is likely dominated by terrestrial plant sources such as coniferous vegetation litter and a minimal microbial processing along the water flow pathway.

Associated with a shift from a snow-controlled to a more rainfall-controlled runoff regime and an increase in water storage with permafrost degradation, changes in the magnitude and timing of DOC export with warming may affect the carbon budget in the southern boundaries of the permafrost region.

References

Hugelius, G. *et al.*, 2014. Estimated stocks of circumpolar permafrost carbon with quantified uncertainty ranges and identified data gaps. *Biogeosciences* 11: 6573-6593.

Quinton, W. L. *et al.*, 2011. Permafrost-thaw-induced land-cover change in the Canadian subarctic: implications for water resources. *Hydrological Processes* 25: 152-158.

Schuur, E. A. G. *et al.*, 2015. Climate change and the permafrost carbon feedback. *Nature* 520: 171-179.

Helbig, M. *et al.*, 2017. Direct and indirect climate change effects on carbon dioxide fluxes in a thawing boreal forest-wetland landscape. *Global Change Biology* 23 8: 3231-3248.

Microbial greenhouse gas production in permafrost peatlands of the Hudson Bay Lowlands, Canada

Adam H. Kirkwood[1]
Pascale Roy-Léveillée[1]
Nathan Basiliko[1]
Jim McLaughlin[2]
Maara Packalen[2]

[1]*Laurentian University, Vale Living with Lakes Center, Co-operative Freshwater Ecology Unit*
[2]*Ontario Forest Research Institute, Ministry of Natural Resources and Forestry*

Abstract

The Hudson Bay Lowlands (HBL) is an important yet understudied peatland that spans across continuous and discontinuous permafrost zones and contains 30 Pg of carbon. The objective of this research is to determine the amount and decomposability of organic matter in thawing permafrost features of the HBL. The field work component of this research took place in August 2017 near Peawanuck, Ontario, which is in the continuous permafrost zone. Samples collected in the field were incubated to determine the production potential of carbon dioxide (CO_2) and methane (CH_4); two powerful greenhouse gases. Preliminary results suggest that the initial off-gassing during the thaw period constitutes a significant contribution to greenhouse gas emissions linked to permafrost degradation. Samples from greater depths produce more CH_4 and less CO_2, whereas samples closer to the surface producer much higher amounts of CO_2, and thermokarst samples have also proved to be very prolific producers of CH_4.

Keywords: continuous permafrost; organic matter; decomposition; incubations; methanogens; climate change

Introduction

Peatlands are important in the global carbon cycle and climate system. They act as both long-term sinks and sources of atmospheric carbon dioxide (CO_2) and as a significant source of methane (CH_4). The role of north temperate and boreal peatlands in carbon cycling and responses to environmental changes has been investigated, but important knowledge gaps exist in the biogeochemical functioning of permafrost peatlands and their responses and feedbacks to current and future climate change (Schuur *et al.*, 2008).

The Hudson Bay Lowlands is also the world's second largest peatland complex, with ~30Pg of stored C in soil organic matter and spans across continuous and discontinuous permafrost zones (Packalen *et al.*, 2014). Despite its relatively low latitude, the Northernmost areas of Ontario have sub-arctic climates that are also warming rapidly due to changing sea-ice dynamics in Hudson Bay. As such, permafrost features in the Hudson Bay Lowlands (the lowest latitude continuous permafrost in North America) are at particular risk of rapid degradation (Pironkova, 2017).

Palsas are prominent features in the study area. Palsas are composed of peat deposits that have been raised by the formation of segregated ground ice. Upon completion of a palsa lifecycle, thawing of the segregated ground ice causes subsidence and increased surface water (Sepällä, 1986). Such an increase in surface water results in anoxic environments where methanogenesis may occur

In Far North Ontario, Canada, these features are very common but little is currently known about how they will respond to climate change in terms of microbial greenhouse gas feedbacks. This research investigates the quantity and decomposability of organic matter, and aims to characterize microbial CH_4 and CO_2 production potential responses to simulated climate warming across intact and degraded palsas in Northern Ontario.

Methods

Samples were taken from five sites in Polar Bear Provincial Park in August 2017, where cores of the active layer, permafrost, and adjacent thermokarst terrain were acquired. In the laboratory, cores were split into depth segments of 10 cm, and subsamples representative of each depth were assessed for thaw subsidence potential, organic content, and incubated at two different temperatures. Selected temperatures were 4°C and 14°C, and were incubated in identical bio-chambers to determine differences in production potential of GHGs. After off-gas measurements were taken, samples were mixed with water to ensure an anaerobic environment conducive to production of gases by methanogens. Gases were re-evacuated, and placed back into the bio-chambers, where they were allowed to decompose for a prolonged period of time.

Preliminary Results

There were substantial emissions of CO_2 and CH_4 associated with the thawing of organic rich peat materials. The amount of CO_2 released upon thaw was similar to what was produced after seven days of decomposition. However, there was considerably more methane released during thaw, compared to what was released during the first week of decomposition. Generally, CO_2 production from palsa and thermokarst active layer samples was greater than samples from near the top of permafrost. The opposite was observed for CH_4 production: as samples from the bottom of the active layer and top of permafrost produced much higher levels of the gas.

Acknowledgments

Thanks to the Ontario Ministry of Natural Resources' Applied Research and Development Branch and Far North Branch for research funding and field support. Additional support was provided by Northern Development Canada's Northern Scientific Training Program.

References

Packalen, M.S., Finkelstein, S.A., McLaughlin J.W., 2014. Carbon storage and potential methane production in the Hudson Bay Lowlands since mid-Holocene peat initiation. *Nature communications* 5: 4078.

Pironkova, Z., 2017. Mapping Palsa and Peat Plateau Changes in the Hudson Bay Lowlands, Canada, Using Historical Aerial Photography and High-Resolution Satellite Imagery. *Canadian Journal of Remote Sensing*: 1-13.

Seppälä, M., 1986. The origin of palsas. *Geografiska Annaler: Series A, Physical Geography* 68.3: 141-147.

Schuur, E., et al., 2008. Vulnerability of permafrost carbon to climate change: Implications for the global carbon cycle. *AIBS Bulletin* 58.8: 701-714.

Incorporating a carbon cycle in the permafrost model Cryogrid 3

Håvard Kristiansen[1]
[1]*University of Oslo, havard.kristiansen@geo.uio.no*

Abstract

We present model principles and preliminary results from our efforts for incorporating a carbon cycle in Cryogrid 3, which is a model for the temperature and water content of permafrost soil.

Keywords: modelling; permafrost; carbon, feedback; peat,

Permafrost ground contains vast amounts of carbon (C), and there is a well-known risk that increasing air temperatures and changes in precipitation can accelerate permafrost thaw and increase the decomposition of stored C. This may lead to increasing emissions of carbon dioxide (CO_2) and methane (CH_4) depending on the oxygen availability. Despite ongoing research efforts, the scale of this permafrost carbon feedback remains uncertain.

In this project, we incorporate biogeochemical processes into the land-surface model Cryogrid 3, which simulates the thermal state of permafrost, based on climate forcing and initial freeze-thaw conditions in the soil (Westermann *et al.* 2016). Our goal is to simulate the effects of surface temperature, precipitation, net primary production, carbon allocation and sedimentation on the rates of individual subsurface processes (e.g. heterotrophic respiration, methanogenesis and methanotrophy) and the resulting surface flux of CO_2 and CH_4.

The new model will simulate sedimentation and decomposition of organic carbon across the Holocene, in order to improve our understanding of the balance between permafrost formation and C sequestration and on the other hand the increasing decomposition driven by climate changes.

If the model is able to successfully reproduce local and/or regional carbon stocks, the resulting estimates can in the future be used as initial conditions for a simulation of the permafrost carbon feedback, given specific climate trajectories over the next century.

Because the project is in its beginning, we present model concepts and preliminary results.

Acknowledgments

This work forms a contribution to LATICE, which is a strategic research area funded by the Faculty of Mathematics and Natural Sciences at the University of Oslo.

References

Westermann, S., Langer, M., Boike, J., Heikenfeld, M., Peter, M., Etzelmüller, B. & Krinner, G. 2016. *Simulating the thermal regime and thaw processes of ice-rich permafrost ground with the land-surface model CryoGrid 3*. Geosci. Model Dev., 9, 523-546.

Modelling the thermal stability of peat plateaus and palsas in Northern Norway

Léo Martin[1]
Sebastian Westermann[1]
Kjetil Schanke Aas[1]
Bernd Etzelmüller[1]
[1]*Department of Geosciences, University of Oslo, P.O. Box 1047, Blindern, 0316 Oslo, Norway, leo.martin@geo.uio.no*

Abstract

Palsa and peat plateaus are geomorphological features often observed in zones of sporadic permafrost (Sollid and Sørbel, 1998). Their evolution shows a complex feedback with the climatic conditions, being both dependent on climatic parameters such as the mean annual air temperature and on local small scale evolutions of the topography and vegetation (Seppälä, 2011). As palsas characterize the warmest areas presenting permafrost, understanding their evolution is of critical importance to bring robust constraints on the permafrost-atmosphere interactions that may be expected in case of long term climate warming and large scale permafrost thawing (Koven *et al.*, 2011).

In Northern Norway, palsas and peat plateaus have shown a clear trend of degradation over the last 60 years (Borge *et al.*, 2016), giving the opportunity for process studies that can shed light in the evolution of vast permafrost peatlands e.g. in Siberia under a warmer climate. In 2015, around 200 loggers temperature were installed at the ground surface of four peat plateaus in Northern Norway to assess the spatial variability of the surface forcing and its driving factors. Changes in micro-topography over the investigated year were quantified using differential GPS, while thaw depth was obtained for each logger site by manual probing. Despite of recorded mean annual ground surface temperatures of up to +3 degree C, the palsas and peat plateaus were overall stable with ground subsidence restricted to localized spots.

Understanding the underlying processes and conceptualizing them in numerical frameworks is challenging, but these measurements provide an ideal benchmark dataset to guide model development. We use the permafrost model CryoGrid 3 (Westermann *et al.*, 2016) with input climate forcing data derived from meso-scale atmospheric modelling (WRF model, 3km resolution, see Aas *et al.*, 2015), which is a flexible scheme that can in principle be adapted to arbitrary locations. Based on 1D-realizations for different logger sites, we present a first analysis in how far the scheme is capable of reproducing the coexistence of permafrost and permafrost-free areas over distances of only a few meters. We test the importance of parameters such as the water balance, the snow cover build-up or the evolution of the micro-topography on the palsas stability. First results suggest a distinct role of the lateral fluxes in the water balance, affecting the spatial patterns of ground subsidence and thus the evolution of micro-topography.

Keywords: Peat plateaus; Palsas; Thermal stability; Ground temperature loggers; Numerical modelling; Water Balance.

References

Aas, K.S. et al. 2015. A Comparison between Simulated and Observed Surface Energy Balance at the Svalbard Archipelago. *Journal of Applied Meteorology and Climatology*, 54(5):1102–1119.

Borge, A.F. et al. 2016. Strong degradation of palsas and peat plateaus in northern Norway during the last 60 years. *The Cryosphere*, 11(1): 1-16.

Koven, C.D. et al. 2011. Permafrost carbon-climate feedbacks accelerate global warming. *Proceedings of the National Academy of Sciences*, 108(36): 14769–14774.

Seppälä, M. 2011. Synthesis of studies of palsa formation underlining the importance of local environmental and physical characteristics. *Quaternary Research*, 75(2): 366–370.

Sollid, J., and Sørbel, L., 1998. Palsa Bogs as a Climate Indicator. *Research for Mountain Area Development: Europe*, 27(4): 287–291.

Westermann, S. et al. 2016. Simulating the thermal regime and thaw processes of ice-rich permafrost ground with the land-surface model CryoGrid 3. *Geoscientific Model Development*, 9(2): 523–546.

Peatland and permafrost in Mongolia: management options for climate change mitigation and adaptation

Tatiana Minayeva[1,4]
Yamkhin Jambaljav[2]
Chultem Dugarjav[3]
Andrey Sirin[4]
Gansukh Tsogt-Erdene[2]
Tsogtbaatar Undrakhtsetseg[2]
Gennady Suvorov[4]
Ab Grootjans[5]
Thomas Spehs[6]
[1]1Care for Ecosystems UG, Germany, tania.minajewa@gmail.com
[2]Institute of Geography & Geoecology Mongolian Academy of Sciences, Mongolia
[3] Institute of General and Experimental Biology Mongolian Academy of Sciences, Mongolia
[4]Institute of Forest Science Russian Academy of Sciences, Russian Federation
[5]Radboud University Nijmegen, The Netherlands
[6]MonMap Ltd, Mongolia

Abstract

The spatial analyses and field investigations brought us to the fact that distribution and functioning of peatlands and permafrost in Mongolia are closely interconnected. Both peatlands and permafrost provide unique and highly demanded ecosystem services from one side and are rapidly disappearing from the other. The cause of this phenomenon is not only in climate change, but also dramatic land use change – mainly overgrazing and partly mining. The investigation demonstrates the level and speed of the degradation, predicts the consequences and suggests the solutions in the land management including ecosystem conservation and restoration.

Keywords: permafrost; peatlands; Mongolia; overgrazing; degradation; conservation; ecosystem restoration.

Peatlands used to cover almost 2 % of Mongolia (Minayeva et al., 2016). Permafrost used to be usual feature of Mongolian landscape covering more than 63 % of the country area, where half of the area was the continuous permafrost (fig. 1). Both those landscape features play crucial role in regulation of key natural processes in ecosystems and provide unique resources to maintain traditional way of life and livelihoods of herders (Minayeva et al., 2016). During the last decades, Mongolian peatlands severely degraded both due to the climate related events and due to overgrazing. The peat degradation causes significant losses of carbon store, GHG emissions and is followed by changes in permafrost status, water balance and water composition.

According to the latest inventory, the permafrost area had shrunk more than twice mostly due to the disappearance of the discontinuous permafrost and shift of the continuous permafrost to the discontinuous. Currently it covers 29 % of Mongolia only (Fig. 2).

Due to the spatial analyses of the historical and current data carried out recently we found out clear connection between permafrost and peatlands distribution, and hence – degradation of both landscape features. The detailed assessment of peatland losses during the last 50 years showed that as minimum within 10 pilot areas the area of peatlands reduced twice. The most permafrost thaw is in the areas where peatlands had degraded. Meanwhile the livestock increased more than 4 times. From this we did the preliminary conclusion that both peatlands and permafrost degradation are enhanced by the overgrazing factor.

The issue arises if there is any possibility to improve the situation by ecosystem management including ecosystem restoration in this arid and subhumid climate. Could it be considered as measure for climate change mitigation and adaptation? The first steps of the peatlands and permafrost management pilots demonstrated that restoration of peatlands ecosystems in the arid and subhumid climate is possible and could be even followed by restoration of the temperature regime, opening possibility for permafrost stabilization. Anyhow conservation of peatlands area as preventive measure to protect permafrost and other ecosystem features is much more effective and cheaper than their restoration.

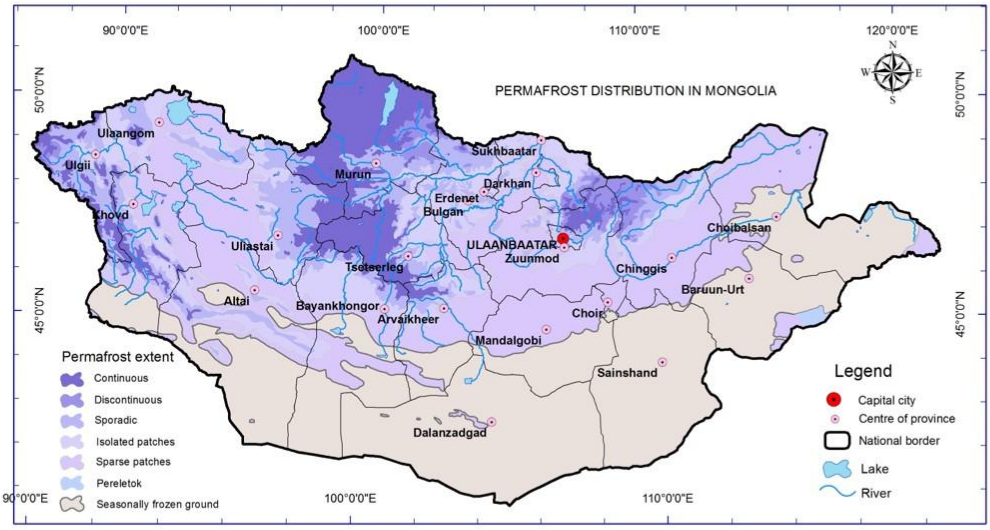

Fig.1 Permafrost distribution in Mongolia in year 1974 (Gravis et al., 1974)

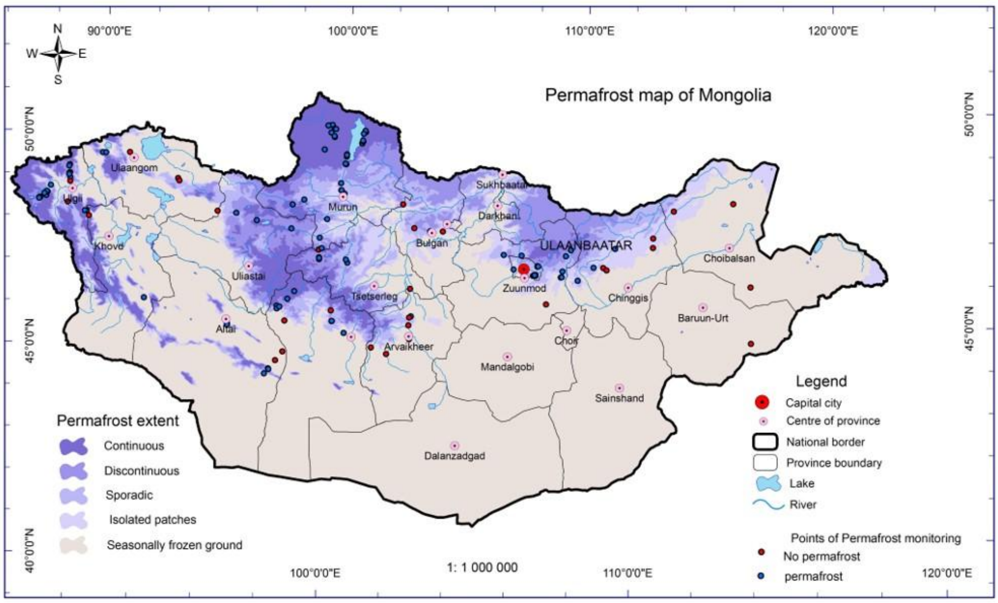

Fig. 2 Permafrost distribution in Mongolia in 2016 (Jambaljav, 2016)

Acknowledgments

We thank the members of long-term Russian-Mongolian Biological expedition and Asian Development Bank project with funding of the Government of Japan "Strategic Planning for Peatlands in Mongolia".

References

Gravis G.F. et al., 1974. *Geocryological conditions of Peoples Republic of Mongolia*. Melnikov P.I.(ed.) Joint Soviet-Mongolian research geological expedition. Proceedings. V. 10. Moscow: Nauka. 208 pp. (in Russian)

Minayeva, T., Sirin, A. and Dugarjav, C. 2016. Highland peatlands of Mongolia., 2016. In: Finlayson, C.M., Milton, G.R., Prentice, R.C. and Davidson, N.C. (Eds.). *The wetland book II: Distribution, description and conservation*. Springer Netherlands. 1–19.

Jambaljav Ya., Gansukh Ya., Temuujin X., Tsogt-Erdene G., Undrakhtsetseg Ts., Saruulzaya A., Amarbayasgalan Yo., Dashtseren A., Narangerel Sh., Permafrost Distribution Map of Mongolia, Ulaanbaatar: GAZRIIN ZURAG LLC. 2016.

Peat spots: hot centers of permafrost peatlands evolution

Olga Ogneva[1]
Matyshak George[1]
Department of soil science, Lomonosov Moscow State University (MSU), Moscow, Russia, Ogonlogin@gmail.com

Abstract

Peat spots – bare sites of permafrost peatlands without vegetation were studied in the northwest Siberia. Morphological characteristics, chemical properties and features of functioning of peat spots significantly differ from those in peatlands soils under the vegetation. Cryogenic processes and genesis of peat drive peat spots formation. Peat spots promote transformation of permafrost peatlands.

Keywords: permafrost peatlands soils; bare peat spots; cryogenesis; cryoturbations

Introduction

Permafrost Peatlands are common and often dominant landscape in Arctic region (Robinson *et al.*, 2003). Northern high-latitude peatlands store approximately 277 Pg of carbon (Tarnocai *et al.*, 2009), equivalent to 14% of the global soil carbon store (IPCC, 2000), that makes permafrost peatlands incredibly important to the global climate system. Climate change impact at northern latitudes leads to widespread changes in permafrost affected soils (Zubrzycki *et al.*, 2014), alters vegetation structure and composition, modify ecosystem functions (Callaghan *et al.*, 2002) and changes landscapes as a whole (Jorgenson *et al.*, 2001). Peatlands of contrasting boundaries landscapes such as forest-tundra transition zone are the most vulnerable to climate change impact. The unique soil formations "peat spots" develop there – sites of peatlands with bare surface, the vegetation on which is completely absent. The aim of research is to study peat spots (PS), their properties, features of formation and their role in permafrost peatlands evolution.

Materials and methods

PS were studied in the northwest Siberia in forest-tundra in the zone of discontinuous permafrost (Nadym region, N65°19', E72°53'). During field work soils of PS were studied in comparison with surrounding soils under vegetative cover.

Results and Discussion

Soil cover of permafrost peatlands is represented by a complex of Lithic Histoturbels and Typic Hemistels under sphagnum and lichen vegetation. Peat profile of these soils generally consist of two types of peat: top layer - more young oligotrophic peat and underneath layer – eutrophic peat. Soils of PS were classified as Typic Histoturbels, peat profile consist of homogenized highly decomposed eutrophic peat. PS have an oval form, diameter ranges from 0,5 to 5 m, and their surface is covered with the overdried peat crust. Morphological and chemical properties of PS are significantly differ from those of soils under vegetation. Decomposition degree of peat is higher in PS (50 ± 5 % PS and 40 ± 5% soils under vegetative cover), the active layer of PS is thicker (60-65 cm and 50-55, respectively). The content of total carbon in PS is higher (50.3 ± 2.1 % for PS and 45.7 ± 4.5 % for soils under vegetation), as well as the total nitrogen content (2.4 ± 0.4 and 1.5 ± 0.5 %, respectively). PS soils contain less nutrients such as potassium and iron.

CO_2 efflux from PS is lower (71,2 mg CO_2 $m^{-2}h^{-1}$ from PS, 155 mg CO_2 $m^{-2}h^{-1}$ from soils under vegetation). The average annual temperatures are higher in PS soils.

PS formation is driven by cryogenic processes (freeze-thaw and cryoturbations) and relict genesis of peat. Highly decomposed eutrophic peat after saturation with water is able to be subjected to cryoturbations. Under the pressure of these processes, peat acquires homogeneous structure and erupts on the peatlands surface. Plants cannot settle on PS because of repeated peat eruptions during autumn and spring seasons and because of peat chemical features (lack of mineral nutrition). Without any vegetation on the surface PS are very vulnerable to needle ice erosion. This ice forms develop on saturated bare peat surfaces, they are capped with a thin layer of peat, which has been heaved above the surface. When the needle ice melts this material is left as a layer of loose peat over the surface. This peat is readily removed by the wind or by subsequent rainfall.

Removing of peat leads to decrease of peat profile thickness and involve underneath mineral layers into soil formation processes.

Conclusions

Climate change predictions suggest that the frequency of soil freeze–thaw cycles and cryoturbations will increase in high-latitude regions (Kreyling *et al.*, 2008). In that case, PS will develop intensive and promote rapid transformation of permafrost peatlands soil cover and the landscape as a whole. Thus peat spots are "centers", "hot spots" of permafrost peatlands evolution.

References

Callaghan T.V., Crawford R.M., Eronen M., Hofgaard A., Payette S., Rees W.G., Skre O., Sveinbjörnsson B., Vlassova T.K. and Werkman B.R., 2002. The dynamics of the tundra-taigaboundary: an overview and suggested coordinated and integrated approach to research. *Ambio*, *Special Report* 12, 3–5.

IPCC. IPCC Special Report: Land use, land-use change, and forestry Summary for Policymakers, 2000. 1–9.

Jorgenson M.T., Racine C.H., Walters J.C., Osterkamp T.E., 2001. Permafrost degradation and ecological changes associated with a warming climate in central Alaska. *Climatic Change* 48(4): 551–579.

Kreyling, J., Beierkuhnlein C., Pritsch K., Schloter M. and Jentsch, A. 2008. Recurrent soil freeze–thaw cycles enhance grassland productivity. *New Phytologist*, 177: 938–945.

Robinson S.D., Turetsky M.R., Kettles I.M., and Wieder R.K., 2003. Permafrost and peatland carbon sink capacity with increasing latitude. In: *Proceedings of the 8th International Conference on Permafrost* [Phillips, M., S.M Springman, and L.U. Arenson (eds.)]. Zurich, Switzerland, 2, 965–970, Balkema Publishers, Lisse, The Netherlands.

Tarnocai C., Canadell J.G., Schuur E.A.G., Kuhry P., Mazhitova G., and. Zimov S., 2009. Soil organic carbon pools in the northern circumpolar permafrost region, *Global Biogeochem. Cycles*, 23, GB2023.

Zubrzycki S., Kutzbach L., and Pfeiffer E.M., 2014. Permafrost-affected soils and their carbon pools with a focus on the Russian Arctic, *Solid Earth*, 5, 595-609.

The permafrost peatlands ecosystem response to anthropogenic impact

Nataliia Petrzhik
Georgy Matyshak
Dmitry Petrov

Lomonosov Moscow State University, petrzhik.nat@mail.ru

Abstract

The Arctic has long-term anthropogenic impact. Significant transformation of the permafrost peatlands ecosystem along the pipelines has been established. It turned out that the maximum changes are in the zone with mechanical disturbances. The strongest changes are in vegetation - the height of a typical shrub increase 1.5-2 times. CO_2 emission grows 2 -3 times, the temperature of the soils increased from 2 to 10°C, the biological activity of soil reduces (DOC, MBC, BR) as compared with the natural plots. As a result of anthropogenic influence, we observe a tremendous response of the structure and functioning of the permafrost peatlands ecosystem.

Keywords: permafrost, soil, peatland, emission, Siberia, pipeline.

Introduction

The increasing of anthropogenic impact perturbs the natural permafrost peatlands ecosystems balance. Since 1960 the oil and gas industry grows in Russia. Especially in the North, where over 10 000 km of pipelines have been buried. The hydrocarbons can be transferred by pipelines only in the heated state. So, the permafrost is thawing, the soil is heated and the parameters of ecosystems change significantly.

The aim is to study permafrost peatlands ecosystems response to anthropogenic impact as a result of pipelines operation.

Location and objects

The study areas are located in Russia in the north of West Siberia in taiga with discontinues permafrost (N65°19'32.8" E72°51'52.4") and in tundra with continues permafrost (N67°29'37.2" E76°28'14.9"). Our object - vegetation and soil of the permafrost peatland ecosystems after the anthropogenic action of pipelines.

Methods

The areas with maximum effect in vegetative change and in mechanical disturbance were selected by remote sensing. Ten transects of 50 meters in length with sampling points every 5 meters from pipeline to undisturbed area were selected in august of 2015-2017. All measurements were carried out in 10 replicates. In every point the soil and vegetation were described, sampled, the thickness of organic horizon, soil moisture and CO_2 emission were measured.

In the laboratory, the content of dissolved organic carbon (DOC), microbial biomass carbon (MBC) and basal respiration (BR) were measured. (Brookes *et al.*,1985; Anderson & Domsch, 1973).

Transect analyzation

The area of anthropogenic impact has been identified within each transect:

1) mechanical disturbances zone - 0-5 m from the pipeline. It is maximum impact zone; the upper soil horizon was removed or disturbed. There is mechanical damage, partial or complete absence of upper organic horizons of soils and the spread of atypical vegetation.

2) warming zone – 10-25 m from the pipeline. There is no mechanical disturbance. Sharply differing from the background and altered vegetation cover. Thaw depth is more than 2 m.

3) control zone - 50 m from the pipeline, where the anthropogenic impact of pipeline was not fixed. A natural landscape with typical vegetation and thaw depth within 50-80 cm.

Results

The soil temperature in the control zone is 2.8°C in the taiga and 4°C in the tundra. The height of the typal shrubs is 35 cm. CO_2 is about 110 $mgCO_2/m^2 \times$ hour.

It was established that of all zones of pipelines exposure, the highest soil temperature (10.8°C in the taiga and 13.6°C in the tundra), and the lowest soil moisture (17%) in the mechanical zone. The height of shrubs is twice as large compared to the control zone (90 cm) and the CO_2 emission is maximal (363.7 and 200 $mgCO_2/m^2 \times$ hour).

The warming zone have average values of soil temperatures (5.8°C and 6.5°) and CO_2 emissions (280 and 210). The moisture differs slightly from the values in the control zone in both natural zones (30%).The height of shrub are 1.5 times more than in the control zone.

Laboratory investigations showed that in both anthropogenic zones, the content of DOC, MBC and BR decreased 2 times less than in the control zone.

Conclusion

Thus, the main effect of this anthropogenic impact is the active degradation of the permafrost in a strip up to 30 m wide on each side.

As we approach the construction, the depth of thawing increases 8 times or more, the soil temperature increases, the soil moisture decreases.

Substantial changes have been established for the biological activity of soils - as soon as they approach pipeline, CO_2 emissions increase, DOC, MBC, and BR decrease several fold.

In this case, the most striking regularities are noted in the zone of mechanical disturbances. Thus, as a result of long-term anthropogenic impact to permafrost peatland ecosystem, we found a permafrost degradation, significant feedback from structure and composition of vegetation, CO_2 efflux and biological activity of soils.

The areas of transformed permafrost peatland are huge, because of that we can observe significant effect of changing the Arctic.

References

Brookes, P.C., Kragt, J.F., Powlson, D.S., Jenkinson, D.S., 1985. Chloroform fumigation and the release of soil nitrogen: the effects of fumigation time and temperature. *Soil Biology & Biochemistry* 17, 831-835.

Anderson, J.P.E. & Domsch, K.H., 1973. Quantification of bacterial and fungal contributions to soil respiration. *Arch. Microbiol.,* 93, 113, 1973.

Recent changes in vegetation dynamics and hydrology in high-latitude and permafrost peatlands

Sanna (Riikka) Piilo[1]
Minna (Maria) Väliranta[1]
Hui Zhang[1]
Michelle Garneau[2]
Matthew Amesbury[3]

[1]*Ecosystems and Environment Research Programme, Faculty of Biological and Environmental Sciences, University of Helsinki, Finland, (sanna.piilo@helsinki.fi)*
[2]*Department of Geography, Université du Québec à Montréal, Canada*
[3]*Geography, College of Life and Environmental Sciences, University of Exeter, UK*

Abstract

Peatlands are globally significant ecosystems and landscape elements, which have important impacts on atmospheric geochemical cycles via vegetation-related changes. At high latitudes, climate is warming almost twice as fast as the projected global average. The subarctic permafrost ecotone is most sensitive to warming and permafrost landscapes are already under a state of change. Climate warming will result in changes in vegetation composition and hydrology and this will alter peatland carbon dynamics. Large uncertainties are still associated with the complex feedbacks related to e.g. peat accumulation, hydrology and vegetation changes. To better understand high-latitude peatland vegetation responses to climatic changes, such as the Little Ice Age (LIA) and recent warming, we apply high-resolution plant macrofossil and C/N analyses for a large set of circum-Arctic peat records. Proxy data are supplemented by robust radiocarbon (^{14}C) and lead (^{210}Pb) chronologies.

Keywords: permafrost peatlands; past climate changes; recent warming; vegetation dynamics.

Introduction

In high-latitudes, climate warming is expected to be the greatest (IPCC, 2013) and will likely have significant impacts on Arctic ecosystems. It has been speculated that warming may result in increase in plant primary productivity in lower latitude bogs (Charman *et al.*, 2013), thus creating a negative, cooling feedback mechanism in climate warming. However, comparable studies are largely missing from Arctic and subarctic peatlands. Field observations measuring permafrost peatland dynamics cover only the last decades. Accordingly, the measurement period is inadequately short to depict the response of these ecosystems to, for instance, post LIA warming (Swindles *et al.*, 2015), which could be considered an analogue for future warming in northernmost latitudes. In addition to post LIA warming, annual temperatures, since ca. 1980's, have increased notably in high-latitudes. Consequently thawing is already an ongoing process in the sporadic permafrost zone (e.g. Sannel *et al.*, 2016). However, there are hardly any observations for how Arctic peatland vegetation is responding to recent warming (Gałka et al., 2017 & 2018). As large vegetation- and hydrology-driven climate feedbacks can be expected, it is essential to understand these ecosystems better and to investigate potential climate response mechanisms.

Peat deposits form long-term palaeoecological archives that can be used to reconstruct former environmental conditions (e.g. Lamarre *et al.*, 2012; Väliranta *et al.*, 2007). In our study, plant macrofossil analysis is applied together with peat physical property analyses, carbon content measurements and chronological methods (^{14}C and lead ^{210}Pb) to reconstruct recent changes in peat accumulation and vegetation succession over the past centuries, with a particular focus on recent warming.

The research aim is to identify climate-induced changes in high-latitude peatland vegetation, possible associated changes in hydrology and their combined consequent influence on carbon dynamics from the past to the future decades.

Our approach is circum-Arctic and this allows spatio-temporal comparisons. The study sites are located in Fennoscandia, European Russia, Siberia, Eastern Canada and Svalbard. For each site, a set of peat cores is collected.

Preliminary results indicate high spatio-temporal variation, both between and within the study sites.

References

Charman, D. *et al.*, 2013. Climate-related changes in peatland carbon accumulation during the last millennium. *Biogeosciences* 10: 929-944.

Gałka, M. *et al.*, 2017. Vegetation Succession, Carbon Accumulation and Hydrological Change in Subarctic

Peatlands, Abisko, Northern Sweden. *Permafrost and periglacial processes*

Gałka, M. *et al.*, 2018. Response of plant communities to climate change during the late Holocene: Palaeoecological insights from peatlands in the Alaskan Arctic. *Ecological Indicators* 85: 525-536.

Intergovernmental Panel on Climate Change (IPCC), 2013. Annex I: Atlas of global and regional climate projections. In: Stocker T. F., Qin D., Plattner G.-K. *et al.,* (eds.) Climate Change 2013. The Physical Science Basis. Contribution of Working Group I to the Fifth Assessment Report of the Intergovernmental Panel on Climate Change. *Cambridge University Press*, Cambridge, New York, USA. 1311-1393.

Lamarre, A. *et al.*, 2012. Holocene paleohydrological reconstruction and carbon accumulation of a permafrost peatland using testate amoeba and macrofossil analyses, Kuujjuarapik, subarctic Québec, Canada. *Review of Palaeobotany and Palynology* 186: 131-141.

Sannel, A. B. K. *et al.*, 2016. Permafrost Warming in a Subarctic Peatland – Which Meteorological Controls are Most Important? *Permafrost and Periglac. Process* 27: 177-188.

Swindles, G. *et al.*, 2015. The long-term fate of permafrost peatlands under rapid climate warming. *Scientific Reports* 5: 17951.

Väliranta, M. *et al.*, 2007. High-resolution reconstruction of wetness dynamics in a southern boreal raised bog, Finland, during the late Holocene: a quantitative approach. *The Holocene* 17(8): 1093-1107.

Holocene development of subarctic permafrost peatlands in Finnmark, northern Norway

A. Britta K. Sannel[1,2]
Sofia Kjellman[1]
Pia Axelsson[1]
Bernd Etzelmüller[3]
Sebastian Westermann[3]

[1]*Department of Physical Geography, Stockholm University, 106 91 Stockholm, Sweden, britta.sannel@natgeo.su.se*
[2]*Bolin Centre for Climate Research, Stockholm University, 106 91 Stockholm, Sweden*
[3]*Department of Geosciences, University of Oslo, P.O. Box 1047, 0316 Oslo, Norway*

Abstract

Holocene peatland development and permafrost history have been studied at four peat plateau sites in Finnmark, northern Norway. Since peatland initiation during the early to mid-Holocene, permafrost-free wet fen conditions have been predominant. Permafrost aggradation, causing frost heave and a shift in the vegetation assemblage from wet fen to dry bog species, probably did not occur until c. 1000–800 cal yr BP during the onset of the Little Ice Age. The average long-term net carbon accumulation rate at the four study sites was 12 gC m^{-2} yr^{-1}, and the soil organic carbon storage was 97 kgC m^{-2}. If the permafrost thaws in a future warmer climate, previously frozen soil carbon can become available for decomposition and be emitted to the atmosphere either as carbon dioxide from expanding active layers or as methane from thermokarst lakes and fens.

Keywords: Peatland development, permafrost dynamics, peat plateau, carbon accumulation, subarctic Norway, Holocene.

Introduction and methods

Permafrost peatlands are widespread in subarctic lowland areas, and are important soil organic carbon reservoirs, storing approximately 300 Pg C (Hugelius *et al.*, 2014). In northern Fennoscandia peatlands started to develop around 10 000–8000 cal yr BP, soon after deglaciation of the Fennoscandian Ice Sheet (e.g. Weckström *et al.*, 2010). Previous studies suggest that northern Fennoscandian peatlands have remained permafrost-free throughout most of the Holocene, but they show some inconsistency concerning the timing of permafrost aggradation (e.g. Oksanen, 2006; Sannel *et al.*, 2017).

This study aims at increasing our understanding of Holocene peatland development and permafrost dynamics in subarctic peatlands in Finnmark. Analyses of plant macrofossils, bulk density, organic, carbon and nitrogen content, and AMS radiocarbon dating have been performed for profiles collected from four peat plateaus. An improved knowledge of peat properties and sensitivity to past climate changes in these environments can help us better predict future responses under warmer climatic conditions, and associated permafrost carbon feedbacks.

Study area

In Finnmark county in northern Norway approximately one fifth of the land surface is underlain by permafrost. In continental areas discontinuous mountain permafrost is found above c. 500 m a.s.l., whereas sporadic permafrost can occur in peatlands almost down to sea level (Gisnås *et al.*, 2017). For this study two continental peat plateau sites, Iskoras (69º20'27"N, 25º17'40"E; 381 m a.s.l.) and Suossjavri (69º23'2"N, 24º15'27"E; 337 m a.s.l.), and two coastal sites, Karlebotn (70º7'14"N, 28º28'30"E; 26 m a.s.l.) and Lakselv (70º7'15"N, 24º59'47"E; 50 m a.s.l.) were selected (Fig. 1). At the continental sites the MAAT (1961–1990) is c. -3 ºC. The coastal sites are warmer with a MAAT of c. 0 ºC. At all four locations the mean annual precipitation is around 350-400 mm yr^{-1} (MET, 2017).

Figure 1. Map showing the location of the four study sites in Finnmark county, northern Norway.

Results and conclusions

At the two continental sites peatland inception took place c. 9800–9200 cal yr BP. The later peatland initiation at the two coastal sites ~6200–5200 cal yr BP can at least partly be explained by a time lag between the deglaciation and land emergence by isostatic uplift. According to the plant macrofossil records all four studied peatlands remained wet fens without permafrost throughout most of the Holocene, and permafrost aggradation did not occur until c. 1000–800 cal yr BP (in Karlebotn and Iskoras) or as late as ~100 cal yr BP (in Lakselv and Suossjavri). The mean long-term net carbon accumulation rate at the four study sites was 12 gC m^{-2} yr^{-1}, and the soil organic carbon storage was 97 kgC m^{-2}. Having acted as long-term Holocene carbon sinks, these permafrost peatlands might at least temporarily turn into carbon sources if the ground thaws in a future warmer climate.

Acknowledgments

Financial support has been provided by The Swedish Research Council for Environment, Agricultural Sciences and Spatial Planning (214-2014-562), the Bolin Centre for Climate Research, COUP (JPI Climate), PERMANOR (Norwegian Research Council) and the Department of Geosciences, University of Oslo.

References

Gisnås, K., Etzelmüller, B., Lussana, C. *et al.*, 2017. Permafrost map for Norway, Sweden and Finland. *Permafrost and Periglacial Processes* 28: 359–328.

Hugelius, G., Strauss, J., Zubrzycki, S. *et al.*, 2014. Estimated stocks of circumpolar permafrost carbon with quantified uncertainty ranges and identified data gaps. *Biogeosciences* 11: 6573–6593.

MET, 2017. eKlima, http://sharki.oslo.dnmi.no

Oksanen, P.O., 2006. Holocene development of the Vaisjeäggi palsa mire, Finnish Lapland. *Boreas* 35: 81–95.

Sannel, A.B.K., Hempel, L., Kessler, A. *et al.*, 2017. Holocene development and permafrost history in sub-arctic peatlands in Tavvavuoma, northern Sweden. *Boreas*, doi:10.1111/bor.12276.

Weckström, J., Seppä, H. & Korhola, A., 2010. Climatic influence on peatland formation and lateral expansion in sub-arctic Fennoscandia. *Boreas* 39: 761–769.

Contribution of root and microbial respiration to soil CO_2 production

Anna Rubenovna Sefilian[1]
Olga Yurievna Goncharova[2]

[1] *Lomonosov Moscow State University, Department of Soil Science, Moscow, Russian Federation, annasefilyan@gmail.com*
[2] *Lomonosov Moscow State University, Department of Soil Science, Moscow, Russian Federation, goncholgaj@gmail.com*

Abstract

Permafrost-affected soils are one of the major sources of CO_2 pool. 65% of the Russian territory are in the permafrost zone. Soil respiration contains different sources. The knowledge about the contribution each of them are very important. It must be taken in the simulation of the carbon cycle and in the projecting of change in the intensity of the CO_2 release from the soil surface. Each component of the soil respiration has the different sensitivity to changing of biotic and abiotic factors, such as temperature, moisture, content and composition of biophilic elements in soils and substrate availability. Contribution of each components depends on different factors, such as method of determination, type of soils or ecosystems. Our results show that contribution of soil microbial respiration (only BSR) to the total soil respiration was 56–82%.

Keywords: root respiration, microbial respiration, peatlands, microbiological activity, permafrost, CO_2 efflux.

Introduction

Five main sources of the contribution to the total soil CO_2 efflux are allocated: 1) growth and respiration maintenance by roots (true root respiration), 2) rhizomicrobial respiration (microbial decomposition of rhizodeposits of living roots) 3) priming of soil organic matter decomposition by recent input of rhizodeposits, fresh plant residues, 4) decomposition of old soil organic matter (basal respiration (BSR)), 5) microbial decomposition of dead plant remains (Kuzyakov, 2006).

The purpose of the study was to estimate the contribution of individual components to the total respiration of permafrost peatland soil and assess the effect of vegetation and cryogenic processes on microbial activity.

The study area was located in the north of West Siberia (Russia) in discontinuous permafrost zone. The object of the study was peat soils under tundra vegetation and soils of peat spots without any vegetation cover for a long period (decades).

Methods

Two primary methods have been used to distinguish components of soil respiration: the comparison of vegetated and bared soils (without vegetation and living roots); the component integration method (Hanson *et al.*, 2000). The first method consists of comparison of the CO_2 emission values in two closely located areas: peat spots and soils under herbaceous vegetation and reindeer lichen. According to this method the contribution of soil microbial respiration (only BSR) to the total soil respiration was 56%.

We separately measured the root respiration of vascular plants (roots were washed to remove adhering humus) and the BSR. Input of each component was estimated as part of total respiration by means of the second method. The input of microbial respiration was 82%.

For bared peat spots and soils under vegetation some indicators of microbial activity were evaluated: labile soil carbon (Clab), microbial carbon (Cmic) and (BSR).

Results

The BSR and Cmic are three times less for soil of peat spots, than for soil under vegetation, Clab is approximately the same for both soils. This ratio can be caused by the impact of plants on the activity of biota. It's connected with root exudates and fresh plant residues. Furthermore, lower values for peat spots may be related to the cryogenic turbation.

Acknowledgments

Funding and research support were provided by RFBR grant 16-04-00808.

References

1) Hanson P.J., Edwards N.T., Garten C.T., Andrews J.A., 2000. Separating root and soil microbial contributions to soil respiration: A review of methods and observations. *Biogeochemistry 48: 115-146*.

2) Kuzyakov Y., 2006. Sources of CO2 efflux from soil and review of partitioning methods. *Soil Biol Biochem* 38:425–448.

Water and snow spatial distributions as drivers for simulated discontinuous permafrost formation and thaw

Ylva Sjöberg[1]
Britta Sannel[1]
Ethan Coon[2]
Ahmad Jan[2]
Scott Painter[2]

[1]*Department of Physical Geography and the Bolin Centre for Climate Research at Stockholm University, ylva.sjoberg@natgeo.su.se*
[2]*Climate Change Science Institute and Environmental Sciences Division, Oak Ridge National Laboratory*

Abstract

In this study, we explore the dynamics of discontinuous permafrost as controlled by variability in snow cover, soil moisture and surface water in a numerical modeling framework. We apply the Arctic Terrestrial Simulator modeling tool together with observed climate data from a permafrost-affected peatland to recreate observed distributions of permafrost, and use projected climate data to explore potential future thaw rates and processes. Our results highlight the sensitivity of discontinuous permafrost to small changes in snow distribution.

Keywords: discontinuous permafrost; hydrology; snow cover; modeling; palsa

Introduction

Discontinuous permafrost can be challenging to model at local scales due to complex interactions between different heat transfer processes in vertical and horizontal directions, which are not represented in most modeling tools. In warm permafrost areas the relative importance of snow cover, and hydrology and on permafrost distributions is stronger than in colder climates. An uneven snow cover and spatially variable soil moisture can determine where in the landscape permafrost is found and how it thaws. To understand the dynamics of permafrost in such areas we must apply models that capture these processes.

In this study we use the Arctic Terrestrial Simulator to model the dynamics of permafrost in a generalized palsa terrain (Painter *et al.*, 2016). By inducing topography-driven variability in snow cover and soil moisture across the domain, we examine the build-up and degradation of discontinuous permafrost. Our aim is to recreate observed distributions of permafrost in a palsa area in northern Sweden, and to examine potential thaw rates with warming.

Methods

The ATS couples heat transfer with freeze-thaw processes and surface and subsurface water fluxes in three dimensions, with models for surface energy balance and snow distribution. For our simulations we use a modeling domain that is 50 m deep and 50 m wide with a sine-shaped surface topography inspired by the palsa topography in the study area (Fig. 1). We test simulation scenarios with and without the presence of a shallow pond. The model is driven with air temperature, precipitation, wind speed, shortwave radiation and relative humidity data from the nearest available stations. Air temperature data were corrected for seasonal differences to data observed at the site between 2005-2014 (Sannel *et al.*, 2016). 100 year long time series were created by combining the full years of data for the air temperature, precipitation, and wind speed data in random orders for 100 years. For the other variables, daily averages were calculated and repeated for 100 years.

For simulations of future thaw, air temperature and precipitation output from simulations with the GFDL-ESM2M (2 × 2 km resolution) model for 2006-2100 for three scenarios (RCP2.6, RCP4.5, and RCP8.5) data were used to calculate warming trends. These trends were added to the observed air temperature and precipitation data series, described above.

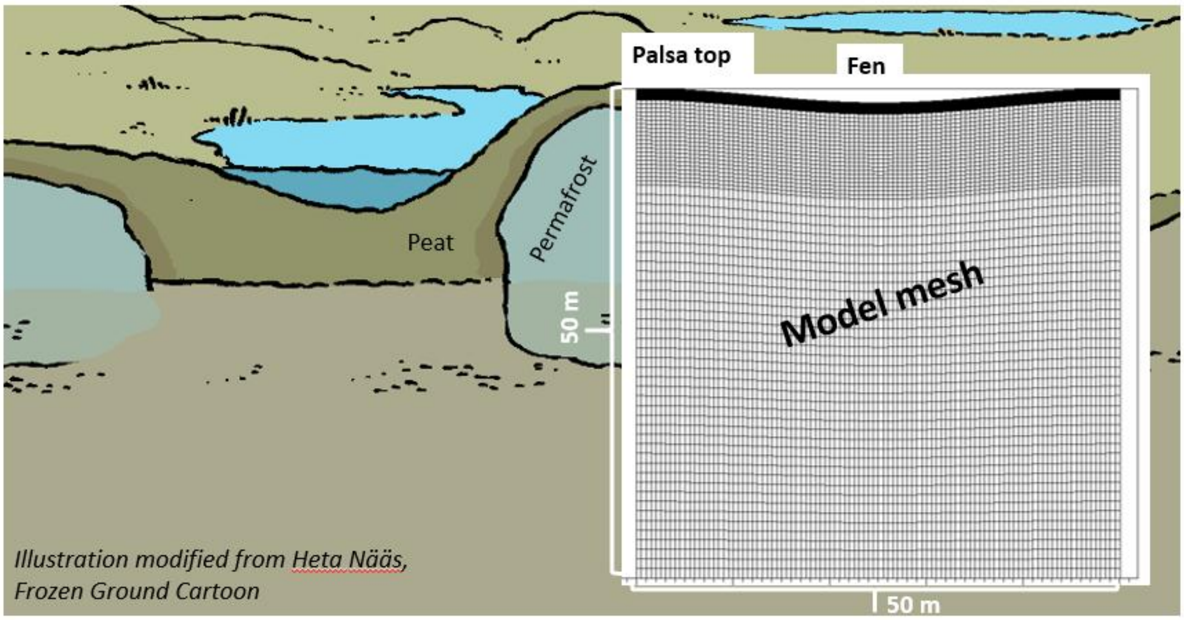

Figure 1. Conceptual sketch of a palsa peatland (modified from Nääs *et al.*, 2017) and the mesh used for the simulations.

Results

The simulated ground surface temperature is several degrees warmer at the fen/pond compared to the palsa (Fig. 1), and this difference is largest in the winter, due to the differences in snow cover across the domain. The soil moisture at the top of palsas varies between 4 % and 30 %, while the fen/pond is saturated year-round with approximately 10 cm of surface water year-round. The fen freezes to a depth of approximately 40 cm in winter. Permafrost forms immediately at the top of the palsas using the spinup climate data, with an active layer of similar thickness as the observed active layer on top of palsa at the field site. These simulated patterns in surface and ground temperature, snow cover and soil moisture mimic those observed at the field site. Simulations show that permafrost distributions are sensitive to variability in snow cover.

Acknowledgments

We are grateful for support from the Swedish Research Council for Environment, Agricultural Sciences and Spatial Planning (942-2015-790, 214-2014-562), the Bolin Centre for Climate Research and the Next-Generation Ecosystem Experiments (NGEE Arctic) project. The simulations were performed on resources provided by the Swedish National Infrastructure for Computing (SNIC) at Chalmers Technical University (C3SE).

References

Nääs, H., Ross, N., Bouchard, F. *et al.*, 2017. *Frozen-Ground Cartoons: An international collaboration between artists and permafrost scientists.* Potsdam: Bibliothek Wissenschaftspark Albert Einstein, 28 p.

Painter, S.L., Coon, E.T., Atchley, A.L. *et al.*, 2016. Integrated surface/subsurface permafrost thermal hydrology: Model formulation and proof-of-concept simulations. *Water Resources Research* 52: 6062-6077.

Sannel, A.B.K., Hugelius, G., Jansson, P. *et al.*, 2016. Permafrost warming in a subarctic peatland – Which meteorological controls are most important? *Permafrost and Periglacial Processes* 27: 177-188.

Carbon accumulation in Arctic permafrost peatlands: a special focus on the response to global warming

Hui Zhang[1, 2]
Minna Väliranta[1, 2]
Sanna Piilo[1, 2]
Matthew Amesbury[3]
Angela Gallego-Sala[3]
Dan Charman[3]

[1]*ECRU, Ecosystems and Environment Research Programme, University of Helsinki, Finland, hui.palaeo@gmail.com*
[2] *Helsinki Institute of Sustainability Science (HELSUS)*
[3]*Geography, College of Life and Environmental Sciences, University of Exeter, UK*

Abstract

High-latitude amplified warming and consequent permafrost thawing will inevitably influence permafrost peatland carbon (C) dynamics. In this study, we reconstructed C accumulation patterns of four permafrost peatlands in northeast European Russia and Finnish Lapland and tested their potential environmental drivers. We found that warmer climate during the Holocene Thermal Maximum stimulated apparent C accumulation rates (ACAR) while the Medieval Climate Anomaly did not show a similar pattern. During the Little Ice Age ACAR seem to be controlled more by other factors than cold climate. The differing peat core/peatland- specific patterns of ACAR reveal the complex nature of C accumulation dynamics in permafrost peatlands. Summer temperature and hydrology play significantly important roles.

Keywords: Carbon accumulation; permafrost peatlands; climate; global warming; last millennia.

Introduction

Warming may have profound impacts on carbon (C) accumulation patterns in high-latitude peatlands: partly because of increase in productivity (Charman *et al.*, 2013), but also due to changes in another important factors related to permafrost dynamics i.e. moisture, which also controls productivity (Pelletier *et al.*, 2017; Zhang *et al.*, 2018). Interlinked changes in temperature and moisture conditions may trigger shifts in vegetation composition (e.g., Zhang *et al.*, 2018) and consequently cause significant changes in C accumulation patterns (Treat *et al.*, 2016). Moreover, permafrost thaw may expose substantial quantities of stored organic C for decomposition, leading to release of carbon dioxide (CO_2) and/or methane (CH_4) to the atmosphere. This in turn forms a positive climate feedback effect (Hodgkins *et al.*, 2014). These divergent response patterns set challenges for estimations and models of future C dynamics (Schuur *et al.*, 2009; Jones & Yu, 2010). Will the end result be a positive or a negative feedback to global warming? To shed further light on this uncertainty, we selected four permafrost peatlands in northeast European Russia and Finnish Lapland to investigate the links between C dynamics and environmental variables.

Methods

Peat core analysis

Selected bulk peat samples were ^{14}C dated. The chronology of the top part of five cores was determined using ^{210}Pb dating. Bulk density (BD), percentage C and nitrogen (N) content were measured. For some cores, loss on ignition (LOI) was measured. Testate amoeba or/and plant macrofossil-based reconstructed water-table depth (WTD) was produced. Vegetation was grouped into plant functional types.

Apparent C accumulation rate (ACAR)

ACAR (g C m^{-2} yr^{-1}) was calculated by multiplying the BD of each depth increment by C content and by its accumulation rate of each sample.

Peat decay and modelling of C dynamics

We applied three models: (1) the exponential decay model (Clymo, 1984); (2) the C flux reconstruction model (Yu, 2011) and (3) a simplified peat decomposition model (Frolking *et al.*, 2001) to calculate accumulation rates over the deposition histories.

Preliminary results and Conclusions

In our study, the relatively large variations of ACAR for different cores in each peatland highlighted the need for a multiple core approach when studying peatland C dynamics. It was not possible to determine a single dominant driver for ACAR, though some environmental variables with explanatory power $p < 0.05$, showed correlations with ACAR, such as summer temperature (positive) and N% (negative).

Distinctly higher ACAR during the Holocene Thermal Maximum around 7000-6000 cal. BP corresponded to the reported long-term pattern for northern peatlands (Yu *et al.*, 2010). However, comparable rapid ACAR did not occur during the Medieval Climate Anomaly (MCA). Moreover, our study does not show a decline in ACAR from the MCA to the Little Ice Age (LIA) as found by Charman *et al.*, (2013); in contrast sometimes the pattern was opposite.

Peatlands are complex systems where C accumulation is controlled by multiple factors. Warming did trigger increase in C accumulation during the Holocene warm period, while the same pattern did not occur during the MCA. Cool climate during the LIA seems to have a weaker forcing on C accumulation rates. In addition to direct temperature influence, local vegetation, hydrology, N% as well as permafrost dynamics were also important. Our future work will concentrate on further investigating the role of recent warming on C accumulation in our study sites.

Acknowledgments

We acknowledge the financial support from the Academy of Finland, the University of Helsinki, and the China Scholarship Council (grant no. 201404910499).

References

Charman, D.J., Beilman, D.W., Blaauw, M., Booth, R.K., Brewer, S., Chambers, F.M., Christen, J.A., Gallego-Sala, A., Harrison, S.P., Hughes, P.D.M., Jackson, S.T., Korhola, A., Mauquoy, D., Mitchell, F.J.G., Prentice, I.C., van der Linden, M., De Vleeschouwer, F., Yu, Z.C., Alm, J., Bauer, I.E., Corish, Y.M.C., Garneau, M., Hohl, V., Huang, Y., Karofeld, E., Le Roux, G., Loisel, L., Moschen, R., Nichols, J.E., Nieminen, T.M., MacDonald, G.M., Phadtare, N.R., Rausch, N., Sillasoo, Ü., Swindles, G.T., Tuittila, E.-S., Ukonmaanaho, L., Väliranta, M., van Bellen, S., van Geel, B., Vitt, D.H., Zhao, Y., 2013. Climate related changes in peatland carbon accumulation during the last millennium. *Biogeosciences* 10: 929-944.

Clymo, R.S., 1984. The limits to peat bog growth. *Philosophical Transactions of the Royal Society of London. Series B, Biological Sciences* 303: 605-654.

Frolking, S., Roulet, N.T., Moore, T.R., Richard, P.J.H., Lavoie, M. & Muller, S.D., 2001. Modeling Northern Peatland Decomposition and Peat Accumulation. *Ecosystems* 4: 479-498.

Hodgkins, S.B., Tfaily, M.M., McCalley, C.K., Logan, T.A., Crill, P.M., Saleska, S.R., Rich, V.I. & Chanton, J.P., 2014. Changes in peat chemistry associated with permafrost thaw increase greenhouse gas production. *PNAS* 111: 5819-5824.

Jones, M.C. & Yu, Z.C., 2010. Rapid deglacial and early Holocene expansion of peatlands in Alaska. *PNAS* 107: 7347-7352.

Pelletier, N., Talbot, J., Olefeldt, D., Turetsky, M., Blodau, C., Sonnentag, O. & Quinton, W.L., 2017. Influence of Holocene permafrost aggradation and thaw on the paleoecology and carbon storage of a peatland complex in northwestern Canada. *The Holocene* 27: 1391-1405.

Schuur, E.A., Vogel, J.G., Crummer, K.G., Lee, H., Sickman, J.O. & Osterkamp, T.E., 2009. The effect of permafrost thaw on old carbon release and net carbon exchange from tundra. *Nature* 459: 556-559.

Treat, C.C., Jones, M.C., Camill, P., Gallego-Sala, A., Garneau, M., Harden, J.W., Hugelius, G., Klein, E.S., Kokfelt, U., Kuhry, P., Loisel, J., Mathijssen, P.J.H., O'Donnell, J.A., Oksanen, P.O., Ronkainen, T.M., Sannel, A.B.K., Talbot, J., Tarnocai, C. & Väliranta, M., 2016. Effects of permafrost aggradation on peat properties as determined from a pan-Arctic synthesis of plant macrofossils. *Journal of Geophysical Research: Biogeosciences* 121: 78-94.

Yu, Z.C., 2011. Holocene carbon flux histories of the world's peatlands: Global carbon-cycle implications. *The Holocene* 21: 761-774.

Yu, Z.C., Loisel, J., Brosseau, D.P., Beilman, D.W. & Hunt, S.J., 2010. Global peatland dynamics since the Last Glacial Maximum. *Geophysical Research Letters* 37: L13402.

Zhang, H., Piilo, S.R., Amesbury, M.J., Charman, D.J., Gallego-Sala, A.V. & Väliranta, M., 2018. The role of climate in regulating Arctic permafrost peatland hydrological and vegetation change over the last millennium. *Quaternary Science Reviews* 182: 121-130.

Changes in methane flux along a permafrost thaw sequence on the Tibetan Plateau

Guibiao Yang[1,2]
Yunfeng Peng[1]
David Olefeldt[3]
Yuanhe Yang[1,2*]
[1]*State Key Laboratory of Vegetation and Environmental Change, Institute of Botany, Chinese Academy of Sciences, Beijing 100093, China*
[2]*University of Chinese Academy of Sciences, Beijing 100049, China*
[3]*Department of Renewable Resources, University of Alberta, Edmonton, Alberta, Canada, T6G 2H1*

Abstract

Permafrost thaw may cause a positive feedback to climate warming through increased methane emissions. The current knowledge of methane emissions following thermokarst development is primarily based on expanding lakes and wetlands, while upland thermokarst has been studied less often. In this study, we monitored the methane emissions during the peak growing seasons along a thaw sequence within a thermo-erosion gully in a Tibetan swamp meadow. Both years had consistent results, with the early and mid-thaw stages (3 to 12 years since thaw) exhibiting low methane emissions that were similar to those in the undisturbed meadow, while the emissions from the late thaw stage (20 years since thaw) were 3.5 times higher. These findings differ from the traditional view that upland thermokarst could reduce methane emissions owing to the improvement of drainage conditions, suggesting that upland thermokarst development does not always result in a decrease in methane emissions.

Keywords: carbon cycle; climate feedback; methanogens; methanotrophs; permafrost thaw; thermokarst; methane

Introduction

Permafrost ground in high altitude and high latitude regions contains more than half the global soil organic carbon (C) (Abbott *et al.*, 2015; Ding *et al.*, 2016) and is considered vulnerable to climate warming. A warmer climate will cause widespread permafrost thaw, which can lead to land surface collapse and erosion, *i.e.*, thermokarst, in certain landscape settings.

Thermokarst often causes abrupt changes in soil environmental conditions and thus strongly influences the production rates of microbial greenhouse gases, including both carbon dioxide (CO_2) and methane (CH_4). Understanding the impacts of permafrost thaw on CH_4 emissions is particularly critical, considering the 25 to 30-fold greater warming potential of CH_4 compared to CO_2 over a 100-year horizon. Thermokarst is considered one of the key uncertainties in our understanding of future CH_4 emissions and the overall permafrost carbon feedback to climate change (Hugelius *et al.*, 2014; Koven *et al.*, 2011).

Methods

In this study, we conducted a two-year survey (2015 and 2016) of CH_4 emissions during the peak growing season in a thermo-erosion gully underlaid by discontinuous permafrost on the Tibetan Plateau. We also measured the biotic and abiotic parameters relevant to the processes of CH_4 production and consumption. Structural equation modeling (SEM) was used to evaluate the relative importance of various pathways that regulate CH_4 emissions. Overall, our current study aimed to 1) examine how the CH_4 emissions during peak growing season change along a thaw sequence; and 2) disentangle the biotic and abiotic regulating pathways of net CH_4 emission pattern along the thaw sequence.

Results

Variability in CH4 emissions along the thaw sequence

Our field observations showed that permafrost collapse had significant effects on CH_4 emissions, with consistent trends along the permafrost thaw sequence during the 2015 and 2016 peak growing season. In both years, significantly increased CH_4 emissions compared to the control were observed in only the late thaw stage, where surface collapse due to permafrost thaw had occurred 20 years prior (Fig. 1).

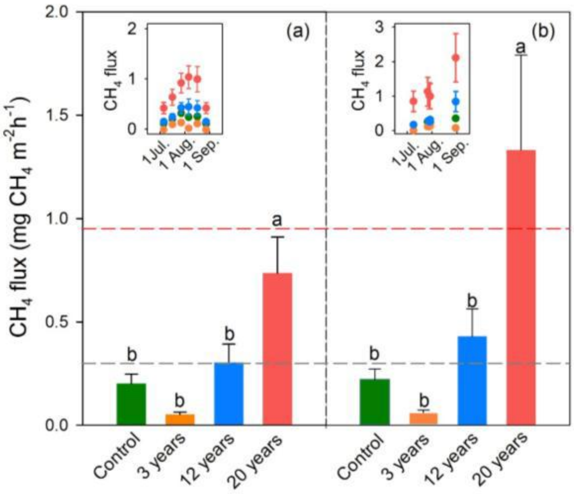

Figure 1. Changes in CH4 fluxes along the thaw sequence in 2015 (a) and 2016 (b). the error bars represent the standard error determined among replicates (n = 10). The colors correspond to the different collapse times. The gray line indicates the mean value of the CH4 flux in an arctic dry tundra, and the red line indicates the mean value of the CH4 flux in an arctic bog. Significant differences were denoted by different letters among the different stages since permafrost collapse (repeated-measures ANOVA, P < 0.05). The insert panels show the site-averaged CH4 fluxes for each sampling time during the entire sampling period, with the error bars representing the standard error determined among replicates.

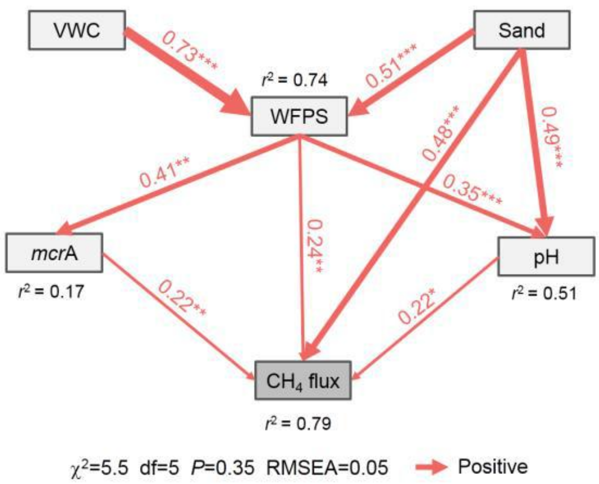

Figure 2. Final results of structural equation model (SEM) analysis examining the effects of edaphic and microbial properties on CH4 flux. In the model, square boxes indicate variables, and the abbreviations of the variables are explained in Table 1. The arrows connecting the boxes indicate the direction of causation. The red arrows denote positive relationships. The arrow widths are proportional to the standardized path coefficients, which reflect the importance of the factors in the model. The proportion of explained variance (r2) is below each response variable in the model. The final model fit was evaluated by a χ2 test and RMSEA value. * P < 0.05, ** P < 0.01, *** P < 0.001.

The SEM analysis

The combination of biotic (the abundance of the *mcrA* gene) and abiotic factors (sand content, VWC, WFPS and pH) explained 79% of the total variance in CH_4 emission along the permafrost thaw sequence (Fig. 2). Among the explanatory variables, sand content, WFPS, pH and the abundance of the *mcrA* gene had direct positive effects on CH_4 emissions, with standardized coefficients ranging from 22% to 48%, whereas VWC, WFPS and sand content had indirect positive effects, ranging from 18% to 32%. Specifically, sand content and VWC affected CH_4 emissions by modifying the WFPS, soil pH and *mcrA* gene copies. The WFPS regulated CH_4 emissions by altering the soil pH and the abundance of the *mcrA* gene. Of these biotic and abiotic variables, sand content was the most dominant factor responsible for the variations in the CH_4 fluxes along the permafrost thaw sequence.

References

Abbott B. W. & Jones J. B., 2015. Permafrost collapse alters soil carbon stocks, respiration, CH_4, and N_2O in upland tundra. *Glob Chang Biol,* 21: 4570-4587.

Ding, J. *et al*., 2016. The permafrost carbon inventory on the Tibetan Plateau: a new evaluation using deep sediment cores. *Global Change Biol*, 22: 2688-2701.

Hugelius, G. *et al*., 2014. Estimated stocks of circumpolar permafrost carbon with quantified uncertainty ranges and identified data gaps. *Biogeosciences*, 11: 6573-6593.

Koven, C. D. *et al*., 2011. Permafrost carbon-climate feedbacks accelerate global warming. *Proc. Natl. Acad. Sci. U. S. A*, 108: 14769-14774.

15 - The furthest frontier: Planetary Permafrost

Session 15

The furthest frontier: Planetary Permafrost

Conveners:

- **Antoine Séjourné**, Université Paris Sud, GEOPS, France (PYRN member)
- **Susan Conway**, Université Nantes, LPGN, France
- **Ernst Hauber**, Institute of Planetary Research, DLR, Berlin, Germany

Over the past decade, a multitude of high-resolution data sets from space missions have provided ever increasing evidence for dynamic processes involving ice and permafrost on Mars but also on the icy satellites, asteroids and recently comet.

This session aims to give an up-to-date insight of the study of ice and permafrost and resulting landforms on planetary bodies with an emphasis on the use of cold-climate environments on Earth as analogues for studying the other planets.

Presentations will be encouraged to discuss planetary periglacial and glacial processes and/or present analogies between terrestrial and planetary permafrost environments and can include fieldwork, remote sensing and laboratory studies. Scientists who are new to planetary science are particularly welcome.

Morphometrics evidence of glacial features in martian highlands: Dawes crater

Axel Bouquety [1]
Antoine Séjourné [1]
François Costard [1]
Sylvain Bouley [1]

GEOPS-Géosciences Paris Sud, Université Paris-Sud, CNRS, Université Paris-Saclay, 91405 Orsay, France, a.bouquety@gmail.com

Abstract

Several studies seem to tend towards a new model for Mars's climate, a cold model. First, a planetary geodynamic model showed that the formation of the Tharsis dome caused the tilting of the planet without changing its axis of rotation. Thus, the valley networks that were parallel to the equator are now in a southern tropical strip between 0° and 45°S (Bouley *et al.,* 2016). Secondly, climate modeling with the pre-Tharsis Martian conditions showed that, by fixing a Martian atmospheric pressure <1 bar for a 45° obliquity it was possible to reconstruct the martian climate during Noachian (Wordsworth *et al.*, 2013), ice is deposited and stable at latitudes below 60°S and in the same strip where are the valleys for an altitude >1000 m. The purpose of this study is to find geomorphologic evidence of this early cold climate to better constrain the climatic conditions. To achieve this, we will study geometry and the morphology of martian valleys and compare them with recent martian glacial and earthly morphologies.

Keywords: Morphometry; Dawes; Glaciation; Valley; Mars.

Introduction

The presence of branched valleys similar to Earth and phases of clay alterations (Bibring *et al.*, 2006) show that during the Noachian (4.5 to 3.7 Ga) a hydrosphere was active on the surface of Mars with relatively warm condition. Nevertheless, in recent years, several studies seem to tend towards a new cold model. Firstly, a planetary geodynamic model showed that the formation of the Tharsis dome caused the tilting of the planet without changing its axis of rotation (Bouley *et al.*, 2016). Thus, the valley networks that were parallel to the equator are now in a southern tropical strip between 0° and 45°S (Bouley *et al.*, 2016).

Secondly, climate modeling with the pre-Tharsis Martian conditions showed that, by fixing a Martian atmospheric pressure <1 bar for a 45° obliquity it was possible to reconstruct the Martian climate during Noachian (Wordsworth *et al.*, 2013). When pre-Tharsis parameters are applied for the current topography, ice is not deposited at latitudes below 60°S while it is possible to find traces of glacial activities at its latitudes, notably in Dorsa Argentea Formation. When pre-Tharsis parameters are applied but without taking into account the topography induced by Tharsis it can be seen that ice is deposited and stable at latitudes below 60°S and in the same strip where are the valleys for an altitude >1000m. Thus, the late Noachian climate is described by these models as "icy highlands" during which branched valley would have formed in a cold climate (Wordsworth *et al.*, 2013).

The purpose of this study is to find geomorphologic evidence of this early cold climate to better constrain the climatic conditions. To achieve this, we will study geometry and the morphology of martian valleys and compare them with recent martian glacial and earthly morphologies.

Data and Methods

To identify features, we used data from the Context Camera (CTX; 6 m/pixel) and to measure their geometry, we used data from High-Resolution Stereo Camera (HRSC; 10 m/pixel) with ArcGIS. The study area is located between 0° and 45°S where we tried to identify patterns of the glacial procession, especially glacial valleys. To characterize the valley, we used terrestrial valleys parameters like the « cross-section Law », glacial U-shapes VS V-shapes (Penck, 1905); width, length, depth, cumulative volume, elevation and the drainage area (Montgommery, 2002). Then, we studied the statistics by relating the parameters to each other and compared them with terrestrial and martian morphometric valley studies to deduce the erosive agent, namely water or ice. This new method allows us to compare all terrestrial and martian morphometric characteristics in the same way. 42 valleys and 70 cirques were identified in Dawes crater (37°7'5.387"E; 8°59'29.441").

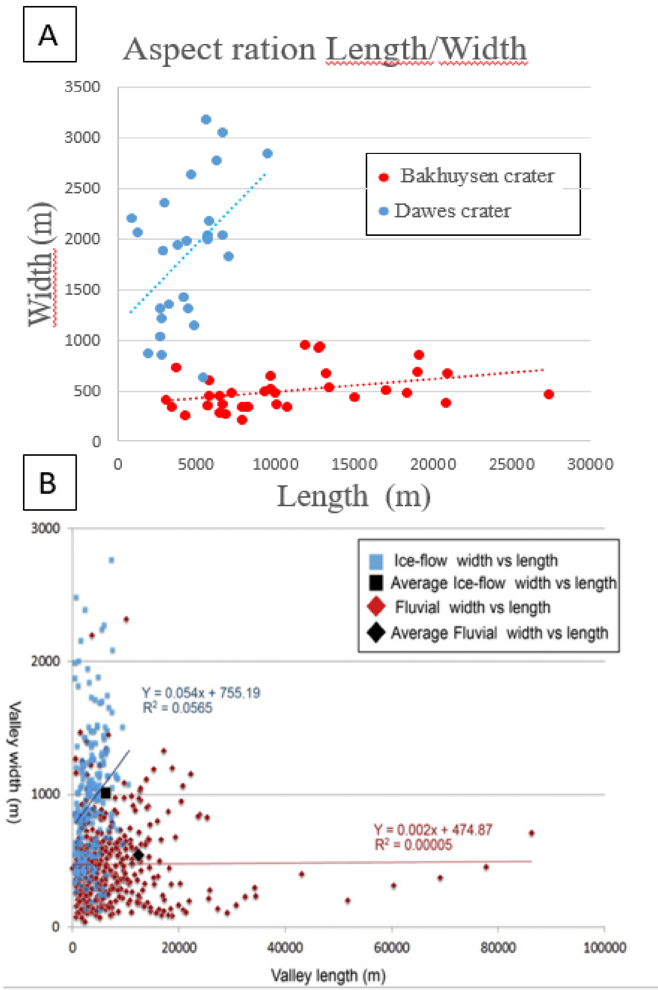

Fig 1: Aspect ratio length/ width for 2 cases
A: data from this study; B: Data from Crater valley

Morphometrics comparison

First we made a Mars/Mars comparison between Hobbs's results, Bakhuysen's fluvial morphology (Moore and Howard, 2005) and ours. Then an Earth/Mars comparison between (Penck, 1905; Montgommery, 2002; Livers & Wohl, 2014; Barr & Spagnolo, 2015)'s results and ours. We compared measurements between our study and Hobbs study (Mars/Mars comparison) (Fig. 1). Graphics (A) shows two trends. Crater Bakhuysen morphologies are much longer and wider than crater Dawes morphologies. Those ones are clearly wider than longer and are generally shorter than crater Bakhuysen valleys. When we compare trends in graphic (A) with graphic (B), we can see that crater Bakhuysen morphologies are similar to fluvial crater valley describe by Hobbs *et al.* (2016). Then the most interesting is that crater Dawes morphologies are following the trend of the Martian glacial valleys described by Hobbs which are relatively short and wide valleys.

Conclusion

This study allows us to create a new way to characterize Martian glacial valleys by a morphometrics analysis. In this study, we identify 77 cirques and 42 glacial valleys in Dawes crater. Morphologies studied have same morphometric characteristics and trends than terrestrial cirques and glacial valleys and Mars glacial valley. To conclude, that study strongly support glacial erosive agent at the origin of crater Dawes morphologies.

References

Bibring, J.-.P., Langevin, Y., Mustard J.F., Poulet, F., Arvidson, R., Gendrin, A., Gondet, B., Mangold, N., Pinet, P., & Forget, F., 2006. Global Mineralogical and Aqueous Mars History Derived from OMEGA/Mars Express Data. *Science* : Volume 312.

Bouley, S., Baratoux, D., Matsuyama, I., Forget, F., Séjourné, A., Turbet, M., & Costard, F., 2016. Late Tharsis formation and implications for early Mars. *Nature* : doi:10.1038/nature17171.

Wordsworth, R., Forget, F., Millour, E., Head, J.W., Madeleine, J.-B., & Charnay, B., 2013. Global modelling of the early Martian climate under a denser CO2 atmosphere: water cycle and ice evolution. *Icarus* 222 **:** 1–19.

Penck, A,. 1905. Glacial features in the surface of the Alps. *I. Geol.,* 13: 1-17.

Montgomery, D.R., 2002b. Valley formation by fluvial and glacial erosion. *Geology* 30 (11): 1047–1050.

Livers, B. & Wohl, E., 2015. An evaluation of stream characteristics in glacial versus fluvial process domains in the Colorado Front Range. *Geomorphology* 231 : 72–82.

Hobbs, S.W., Clarke, J.D.A. & Paull, D.J., 2016. Analysis of crater valleys, Noachis Terra, Mars: Evidence of fluvial and glacial processes. *Geomorphology* 261: 244–272.

Erosion of impact craters on Mars: the role of permafrost processes

Susan (J) Conway[1], Tjalling de Haas[2,3], Frances (EG) Butcher[4], Axel Deijns[3], Peter (M) Grindrod[5,6]
[1]*CNRS, UMR 6112 Laboratoire de Planétologie et Géodynamique, Université de Nantes, France. susan.conway@univ-nantes.fr*
[2]*Department of Geography, Durham University, South Road, Durham DH1 3LE, UK.*
[3]*Faculty of Geoscience, Universiteit Utrecht, The Netherlands.*
[4]*School of Physical Sciences, Open University, Milton Keynes, MK7 6AA, UK.*
[5]*Centre for Planetary Sciences at UCL/Birkbeck, University of London, UK*
[6]*Natural History Museum London, UK*

Abstract

The martian mid-latitudes are host to a suite of landforms that indicate significant geologically recent (10s – 100s Ma) surface-atmosphere exchanges of water ice. This study focuses on two of the most common landforms: martian gullies and viscous flow features which resemble debris covered glaciers on Earth. We examine the role they have played in landscape evolution over the last ten to hundreds of millions of years by using statistical analysis of topographic data.

Keywords: Mars; martian gullies, Viscous Flow Features, glacier-like-forms, erosion rate.

Introduction

The mid-to-high latitudes of Mars host assemblages of landforms reminiscent of a receding glacial landscape on Earth. These landforms are probably a result of dramatic changes in climate brought about by swings in Mars' orbital obliquity, which can vary between 15° and 35° on timescales of ~100,000 years (Laskar et al., 2004). At the highest obliquities it is thought that water ice is driven off the two permanent polar caps (which each have a mass equivalent to the Greenland icesheet) and redistributed to lower latitudes (e.g., Madeleine et al., 2009). Here, we report on the relationship of two suites of landforms: gullies and glacial landforms (Figure 1). Gullies are kilometre-scale erosion-deposition systems comprising a source alcove, a transportation channel and a deposition apron or fan (Conway et al., 2018; Malin and Edgett, 2000). The glacial landforms we describe here fall into two categories – extant viscous flow features wherein ice could still be present (e.g., Milliken et al., 2003; Plaut et al., 2009) and relicts of glaciation including arcuate ridges commonly interpreted as moraines (e.g., Arfstrom and Hartmann, 2005; Berman et al., 2005). Both gullies and glacial landforms are particularly common at the mid-latitudes and show similar trends in orientation with latitude – hinting at a common climatological origin. Our previous work has shown that dense concentrations of extant glacial forms are anti-correlated with dense gully-populations (Conway et al., 2017), yet gullies are found very commonly associated with relict glacial landforms. Other authors have already highlighted the possibility that this landscape assemblage could result from a similar suite of processes to that experienced in glacial environments on Earth (e.g., Hauber et al., 2011; Head et al., 2008).

Previous works noted that the crater rim immediately above arcuate ridges is often lower than the opposite one (Berman et al., 2005; Head et al., 2008). Hence in this work we sought to test whether glaciers could be responsible for erosion of the crater rim and if so how the other landforms were related to this erosion.

Glacial erosion

We found that disrupted bedrock was always found immediately upslope of what we will term "pasted on terrain" (Figure 1) and not on any other part of the crater rim. Pasted on terrain (Christensen, 2003) has also been described as "Latitude Dependent Mantle" (LDM) and martian gullies are often found incising into it (e.g., Dickson et al., 2015).

We used 1 m/pix digital elevation models derived from stereopairs of HiRISE images at 25 cm/pix to measure the slope of the bedrock at the crater rim both above pasted on terrain and where no such deposit is present. To obtain a baseline for the comparison we also measured the bedrock rim slopes of impact craters located near the equator distal to both gullies and glacial landforms.

We find that the disturbed bedrock above the pasted on terrain systematically has a lower slope than other bedrock exposures in the same crater and compared to bedrock exposed at the rim of equatorial impact craters. We attribute this slope-reduction to a retreat of ~50-100 m of the bedrock at the crater rim, commensurate with independent measures of glacial erosion on Mars (Levy et al., 2016).

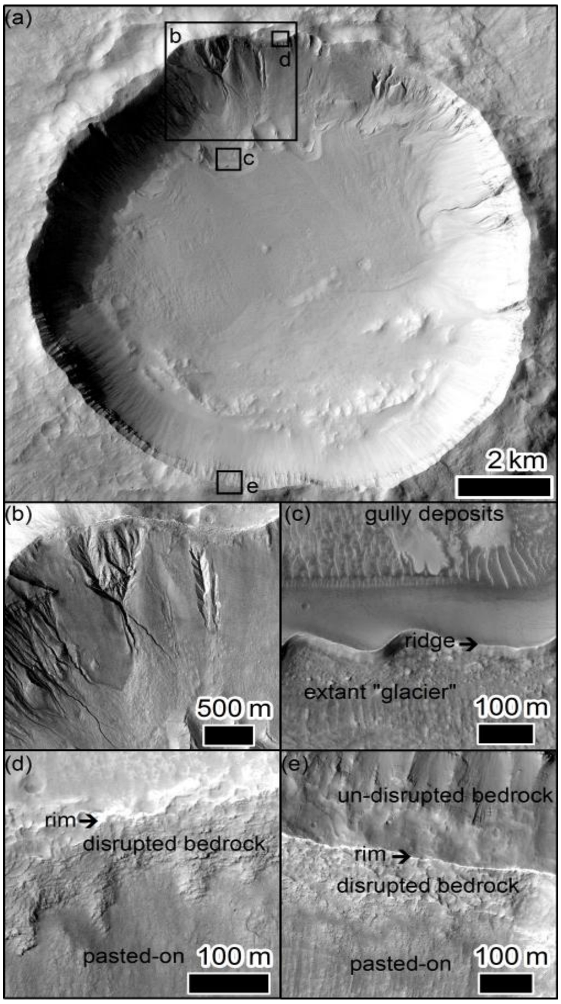

Figure 1. Crater Niquero on Mars with gullies and evidence of glaciation. (a) Overview in CTX image P03_002383_1417 with boxes indicating: (b) gullies, (c) aracuate ridge, (d) northern rim and (e) southern rim in HiRISE image ESP_030443_1410.

Therefore, the disturbed bedrock seems to be a reliable marker of glacial erosion and we raise the possibility that the pasted on terrain represents glacial deposits. Further, glaciotectonic deformation of sub-marginal and proglacial sediment may have contributed to formation of the arcuate ridges. Most of the gullies postdate the phase of glacial activity represented by the pasted on terrain, incising into it. Other authors have found evidence for gullies being buried by and exhumed from the pasted on terrain (Dickson et al., 2015) and others have found young (< 6.5Ma) gully systems without any evidence for pasted on terrain or arcuate ridges (de Haas et al., 2017, 2015). In these young systems gullies can erode up to 50 m into the bedrock at the crater rim, but in systems where pasted on terrain is present they erode mostly the pasted on terrain. Hence, erosion of mid-latitude crater walls can be achieved by both gully-erosion and glacial erosion.

References

Arfstrom, J., Hartmann, W.K., 2005. Martian flow features, moraine-like ridges, and gullies: Terrestrial analogs and interrelationships. Icarus 174, 321–335.

Berman, D.C., *et al.*, 2005. The role of arcuate ridges and gullies in the degradation of craters in the Newton Basin region of Mars. Icarus 178, 465–486.

Christensen, P.R., 2003. Formation of recent martian gullies through melting of extensive water-rich snow deposits. Nature 422, 45–48.

Conway, S.J., de Haas, T., Harrison, T.N., 2018. Martian gullies: a comprehensive review of observations, mechanisms and the insights from Earth analogues. Geol. Soc. Lond. Spec. Publ. 467.

Conway, S.J., *et al.*, 2017. New Slope-Normalised Global Gully Density and Orientation Maps for Mars. Geol. Soc. Lond. Spec. Publ. 467.

De Haas, T., *et al.*, 2017. Time will tell: temporal evolution of Martian gullies and paleoclimatic implications. Geol. Soc. Lond. Spec. Publ. accepted.

De Haas, *et al.*, 2015. Earth-like aqueous debris-flow activity on Mars at high orbital obliquity in the last million years. Nat. Commun. 6.

Dickson, J.L., *et al.*, 2015. Recent climate cycles on Mars: Stratigraphic relationships between multiple generations of gullies and the latitude dependent mantle. Icarus 252, 83–94. doi:10.1016/j.icarus.2014.12.035

Hauber, *et al.*, 2011. Periglacial landscapes on Svalbard: Terrestrial analogs for cold-climate landforms on Mars. Geol. Soc. Am. Spec. Pap. 483, 177–201.

Head, J.W., Marchant, D.R., Kreslavsky, M.A., 2008. Formation of gullies on Mars: Link to recent climate history and insolation microenvironments implicate surface water flow origin. Proc. Natl. Acad. Sci. U. S. A. 105, 13258–13263.

Laskar, J., *et al.*, 2004. Long term evolution and chaotic diffusion of the insolation quantities of Mars. Icarus 170, 343–364. doi:10.1016/j.icarus.2004.04.005

Levy, J.S., Fassett, C.I., Head, J.W., 2016. Enhanced erosion rates on Mars during Amazonian glaciation. Icarus 264, 213–219. doi:10.1016/j.icarus.2015.09.037

Madeleine, J.B., *et al.*, 2009. Amazonian northern mid-latitude glaciation on Mars: A proposed climate scenario. Icarus 203, 390–405.

Malin, M.C., Edgett, K.S., 2000. Evidence for recent groundwater seepage and surface runoff on Mars. Science 288, 2330–2335.

Milliken, *et al.*, 2003. Viscous flow features on the surface of Mars: Observations from high-resolution Mars Orbiter Camera (MOC) images. J Geophys Res 108, doi:10.1029/2002JE002005.

Plaut, J.J., *et al.*, 2009. Radar evidence for ice in lobate debris aprons in the mid-northern latitudes of Mars. Geophys. Res. Lett. 36, 02203.

Grid mapping of ice-related landforms in Acidalia Planitia, Mars

Ernst Hauber[1]
Csilla Orgel[2]
Dennis Reiss[3]
Stephan van Gasselt[4]
Andreas Johnsson[5]
[1]*German Aerospace Center (DLR), Institute of Planetary Research, Berlin, Ernst.Hauber@dlr.de*
[2]*Institut für Geowissenschaften, FU Berlin, orgel.csilla@fu-berlin.de*
[3]*Institut für Planetologie, WWU Münster, dennis.reiss@uni-muenster.de*
[4]*National Chengchi University, Taipei, Stephan.vanGasselt@gmail.com*
[5]*Dept.of Earth Sciences, University of Gothenburg, andreasj@gvc.gu.se*

Abstract

Many young landforms in mid- and high-latitudes on Mars are probably related to ice, but their exact distribution and origin are still poorly understood. In an attempt to determine their extent and identify possible spatial relationships and genetic links between them, we mapped their distribution across a N-S traverse across Acidalia Planitia, following a grid-mapping approach. The general characteristics of Acidalia are similar to that of Utopia Planitia and Arcadia Planitia, which are known to host large water ice reservoirs.

Keywords: Mars; permafrost; landforms; ice; climate; grid mapping.

Introduction

Large quantities of excess water ice reside in the upper parts of the Martian crust in the northern hemisphere (e.g., Plaut *et al.*, 2009; Stuurman *et al.*, 2016; Bramson *et al.*, 2015). Although it is believed that this ice was deposited during phases of different obliquities (e.g., Madeleine *et al.*, 2009), it does survive over geological time under current conditions (Bramson *et al.*, 2017) and does not seem to be in equilibrium with the atmosphere yet (Pathare *et al.*, 2018). Among the three prominent basins in the northern lowlands, ice reservoirs were detected by geophysical methods in Arcadia Planitia (Bramson *et al.*, 2015) and Utopia Planitia (Stuurman *et al.*, 2016). Morphological evidence for water ice is also observed in Arcadia Planitia (Viola *et al.*, 2015) and Utopia Planitia (e.g., Morgenstern *et al.*, 2007).

Various recent landforms in the Martian mid-latitudes have been hypothesized to be a result of freeze-thaw processes, with melting excess ice as a possible water source, analogous to landforms in periglacial climates on Earth. As the present climate of Mars physically prevents the formation of liquid water but in some extraordinary circumstances (e.g., deliquescence of salts), a major current debate focusses on the "wet" versus "dry" formation of such landforms (e.g., widespread patterned ground in Utopia Planitia; Séjourné *et al.*, 2011).

We aim at a better understanding of the distribution of possibly ice-related landforms in Acidalia Planitia, the third major lowland basin. Our goal is to identify latitude-dependencies of such landforms and their relation to each other as well as to external parameters such as topography, and thermal inertia.

Methods

We employ a grid mapping approach based on CTX images (Ramsdale *et al.*, 2017), which enables mapping large areas at small scales (Fig. 1). Our maps show a binary ("yes" or "no") distribution of specific landforms in each grid cell (~20 × 20 km), but allows for some ambiguity (one class is "possible", where no decision was possible). We also document where no data were available and where a landform is dominant. Examples of resulting maps are shown in Fig. 2.

Observations

We mapped individual landforms that may have formed in association with ice or water, including polygonal terrain, gullies, and mantling material (the full list of landforms is provided by Ramsdale *et al.* (2017). Our maps are very similar to corresponding maps of Utopia and Arcadia Planitiae that were produced by the same methods.

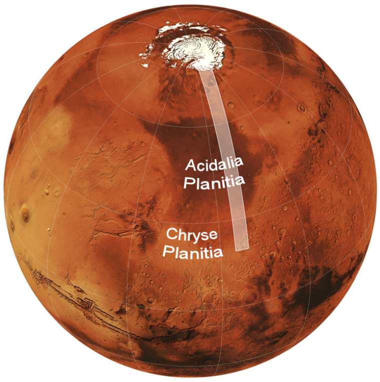

Figure 1. Location of traverse (300 km wide) across Acidalia Planitia (from 20°N to the margin of the north polar cap).

Acknowledgments

This work is a joint effort of an International Team sponsored by ISSI (International Space Science Institute) in Bern (CH).

References

Bramson, A. *et al.*, 2015. Widespread excess ice in Arcadia Planitia, Mars. *Geophys. Res. Lett.* 42(16): 6566–6574.

Bramson, A. *et al.*, 2017. Preservation of midlatitude ice sheets on Mars. *J. Geophys. Res. Planets* 122: doi: 10.1002/2017JE005357.

Madeleine, J.-B. *et al.*, 2009. Amazonian northern mid-latitude glaciation on Mars: A proposed climate scenario. *Icarus* 203: 390–405.

Morgenstern, A. *et al.*, 2007. Deposition and degradation of a volatile-rich layer in Utopia Planitia and implications for climate history on Mars. *J. Geophys. Res.* 112: E06010.

Pathare, A. *et al.*, 2018. Driven by excess? Climatic implications of new global mapping of near-surface water-equivalent hydrogen on Mars. *Icarus* 301: 97-116.

Plaut, J. *et al.*, 2009. Radar evidence for ice in lobate debris aprons in the mid-northern latitudes of Mars. *Geophys. Res. Lett.* 36: L02203.

Ramsdale, J. *et al.*, 2017. Grid-based mapping: A method for rapidly determining the spatial distributions of small features over very large areas. *Planet. Space Sci.* 140: 49–61.

Séjourné, A. et al., 2011. Scalloped depressions and small-sized polygons in western Utopia Planitia, Mars: A new formation hypothesis. Planet. Space Sci. 59: 412–422.

Stuurman, C. *et al.*, 2016. SHARAD detection and characterization of subsurface water ice deposits in Utopia Planitia, Mars. *Geophys. Res. Lett.* 43: 9484–9491.

Viola, D. *et al.*, 2015. Expanded secondary craters in the Arcadia Planitia region, Mars: Evidence for tens of Myr-old shallow subsurface ice. *Icarus* 248: 190–204.

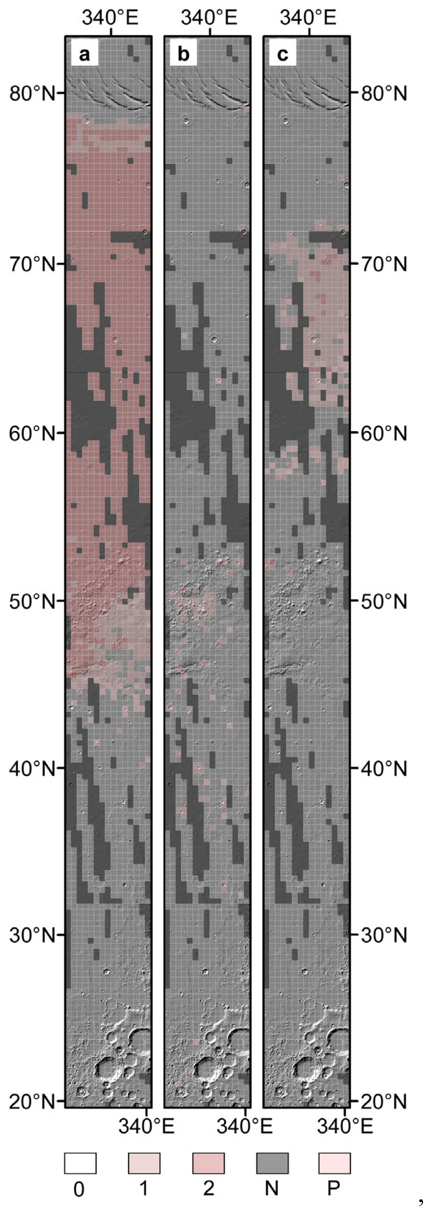

Figure 2. Selected grid maps with individual landforms. Colors indicate classification of grid cells (0=no color, just MOLA hillshade background: landform not present, 1: present, 2: dominant, N: no data, P: landform possibly present. (a) Mantling deposits. (b) Gullies. (c) Small-scale polygons.

Mapping the northern plains of mars: origins, evolution and response to climate change – a new overview of recent ice-related landforms in Utopia Planitia on Mars

A. Losiak[1], A. Séjourné[2], F. Costard[2], Z. M. Swirad[3]
[1]*Polish Academy of Sciences, Institute of Geological Sciences, Wroclaw, Poland, ania.losiak@twarda.pan.pl*
[2]*Univ. Paris-Sud, CNRS, Laboratoire GEOPS, UMR8148, Orsay, France*
[3]*Department of Geography, Durham University, Durham, UK.*

Abstract

The northern plains of Mars comprise several large overlapping sedimentary basins that contain near surface ground ice even at mid-latitude. However, no consensus about the nature of ground ice and formation of the planetary permafrost. An International Space Science Institute team project has been convened to study ice-related landforms in targeted areas in the northern plain of Mars: Acidalia, Arcadia, and Utopia Planitiae. Rather than traditional mapping with points, lines and polygons, we used a grid "tick box" approach to efficiently determine distribution of specific landforms by using grid of squares. Our results show that based on their spatial association, there are different assemblages of landforms. Their distribution is not only related to latitude but also on topography, geological context. Grid mapping provides an efficient and scalable approach to collecting data on large quantities of small landforms over large areas.

Keywords: Regional mapping, ice-related landforms, Climate change, Utopia Planitia

Introduction

The northern plains of Mars, topographically lower than the "cratered highlands" of the southern hemisphere, comprise several large overlapping basins that are filled by sediments. The region has been proposed to have hosted an ancient ocean and currently contains near surface ground ice even at mid-latitudes, (Table 1; Head et al., 2003; Feldman et al., 2004). However, no consensus about the nature of ground ice and formation of the planetary permafrost. The spatial distributions of ice-related landform at broad-scale and control by regional geology or climate is still not constrained. Improving the geological context of the northern plains will help constrain outstanding questions about martian geological evolution.

An International Space Science Institute (ISSI) team project has been convened to study ice-related landforms in targeted areas in the northern plain of Mars: Acidalia Planitia, Arcadia Planitia, and Utopia Planitia. Here, we describe our mapping of western Utopia Planitia along a strip from 25°N to 75°N latitude of 250 km wide. The goals are to: (i) map the geographical distribution of the surface ice-related landforms; (ii) identify their association with subtly-expressed geological units and; (iii) discuss what the distribution tell us about the ice-content, sediment types and environmental evolution in UP.

Tableau 1. Ice-related landforms mapped in the grid mapping

Landform type	Description
Basketball terrains	Etched terrain, includes linear, wrinkled and basketball sub-types
Viscous flow features	Comprises lineated valley and concentric crater fill (CCF), and lobate debris aprons
Scalloped depressions	Coalesced thermokarst-like depressions with concentric bands
100m scale polygons	Polygons of 100 m in diam. That are found in association with scalloped depressions
Pits	Thermokarst-like pits at the junction of 100 m polygons or along cracks inside km impact craters
High albedo Mounds	High albedo dome-like forms of 50 m to 1 km in diam. with summital pit
km scale polygons	High centred polygons of 1-5 km in diam.
Thumbprint Terrain	Ridges and chains of cones with an arcuate shape

Grid mapping strategy

Rather than traditional mapping with points, lines and polygons, we used a grid "tick box" approach to efficiently determine distribution of specific landforms by using grid of squares for each study area, each approximately 20×20 km. Over the region, ice-related landforms were identified and recorded as being either "present", "dominant", or "absent" in each sub-grid square displayed in a Cassini projection. The end result of the mapping is a "raster" showing the distribution of the various different types of landforms across the whole strip providing a digital geomorphological map.

Results

Our mapping shows that the scalloped depressions, pits and 100 m polygons occur over a broader area than previously shown (from 40°N to 65°N; Fig. 2)). Coalesced scalloped depressions of several km in diameter are concentrated near 50°N. The Viscous flow features are only observed inside impact craters (concentric crater fills) and have no preferential distribution. We also observed that the thumbprint terrains, high-albedo mounds of different diameter and km-scale polygons are mostly seen in the southern UP (from 30°N to 40°N; Fig. 2).

Based on their correlated distribution at regional scale but also at local scale where they are associated spatially, several assemblages of landforms can be defined. The scalloped depressions, pits and 100 m polygons are spatially associated at local scale because interrelated, pits cross-cut polygons that are degraded by scallops and at regional scale because same area between 40°N to 50°N. Scallops and pits being interpreted as due to sublimation of ground-ice and polygons due to thermal contraction, their distribution corresponds to an area where an ice-rich permafrost like on Earth (Séjourné et al., 2011).

Conclusion

Our knowledge of the distribution of ice-related landforms in UP was improved. Based on their spatial association, there are different assemblages of landforms. Their distribution is not only related to latitude but also on topography, geological context. Grid mapping provides an efficient and scalable approach to collecting data on large quantities of small landforms over large areas. The next step is to define unit: based on assemblage of landforms, albedo and/or crater counting. The differences/similarities of the three key regions in the northern plains reflect their complex geological history.

Acknowledgements

This work is a joint effort of an International Team sponsored by the International Space Science Institute.

References

Feldman, W. C. et al., 2004. Global distribution of near-surface hydrogen on mars. J. Geophys. Res. 59 (E9), E09006.

Head, J. W. et al., 2003. Recent ice ages on mars. Nature 426 (6968), 797–802.

Séjourné, A. et al., 2011. Scalloped depressions and small-sized polygons in western Utopia Planitia, Mars: A new formation hypothesis. PSS 59 (412-422).

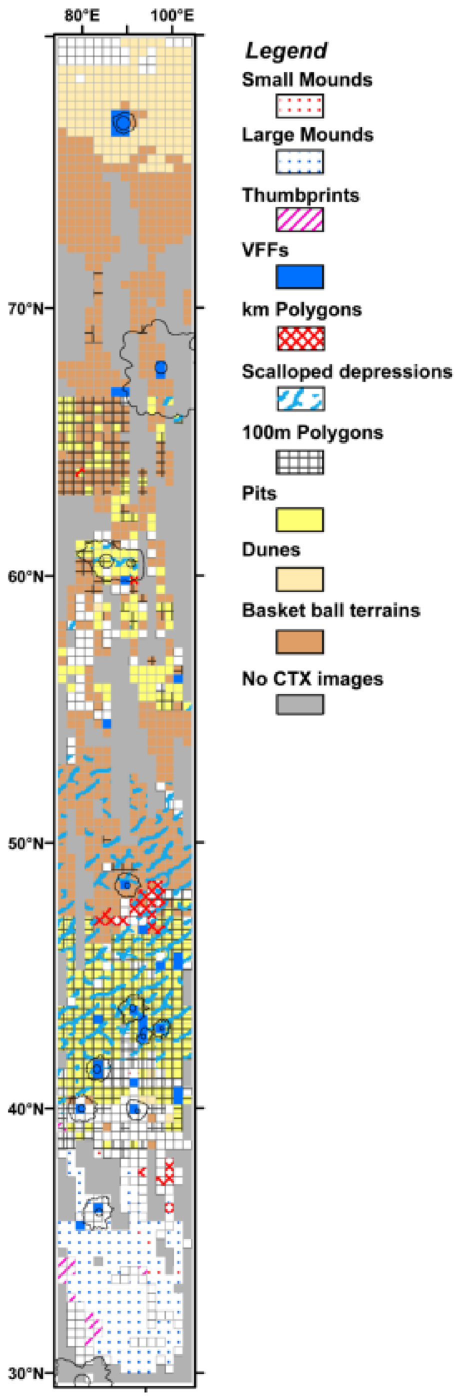

Figure 2. Geomorphological grid mapping of Utopia Planitia.

Shallow Permafrost Mapping on Mars using Seasonal Thermal Infrared Observations

Sylvain Piqueux[1]
David Kass[1]
Joshua Bandfield[2]
Christopher Edwards[3]

[1]*Jet Propulsion Laboratory, California Institute of Technology, USA, sylvain.piqueux@jpl.nasa.gov*
[2]*Space Science Institute, USA*
[3]*Northern Arizona University, USA*

Abstract

Mapping the presence and accessibility of subsurface water ice on Mars away from the poles has become an important task to support future human exploration, and also because H_2O ice is currently unstable and represents a relic of past climate conditions with great scientific value. We will present an update of our plans aiming at mapping very near surface water ice distribution at mid/low latitudes using thermal infrared data.

Keywords: Mars; Thermal Inertia; Permafrost; Ice; Temperature.

Introduction

Owing to the large thermal conductivity/inertia contrast between water ice and the dry Martian regolith, the analysis of surface temperature trends at polar and high latitudes indicates the presence of a widespread near-surface (i.e. cm to dm) permafrost. Little effort has focused on characterizing permafrost accessibility at mid to low latitudes, despite the significant interest incurred by future human exploration and the scientific interest of these deposits as relics of past climates. Here we present a plan to map subsurface permafrost properties at all latitudes.

Methods

Concept

Water ice has a distinctively high thermal conductivity (and therefore inertia) compared to the other dry loose Martian regolith, e.g., 2.0-4.4 J $m^{-1}K^{-1}s^{-1}$ [1] vs. 0.001-0.1 J $m^{-1}K^{-1}s^{-1}$ [2]. As a result, buried water ice (either in the form of massive ice or pore ice) under a layer of particulated regolith acts as a thermal capacitor, storing heat at specific seasons and releasing it at others. When the permafrost layer is located relatively close to the surface (i.e., with one or a few diurnal skin depths), seasonal surface temperatures are impacted and reflect both the depth to the permafrost layer as well as the thermophysical properties of the overlaying dry cover.

Repeated seasonal surface temperature observations can be used in conjunction with a thermal model to deconvolve the properties of the regolith, as model result show that unique temperature trends are associated with unique families of permafrost depth and top regolith inertias (Fig 1.).

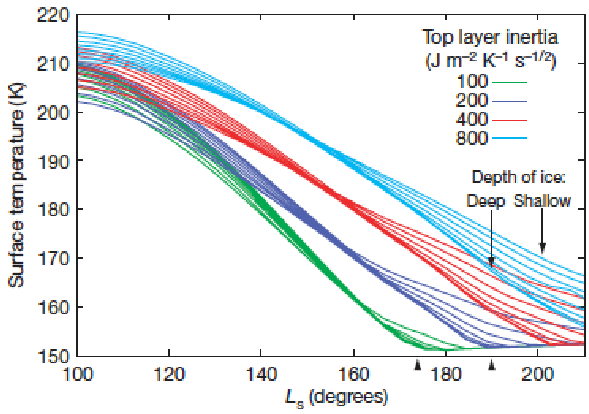

Fig. 1: Illustration of the effect of permafrost depth and top layer (dry) thermal inertia on nighttime seasonal surface temperatures at high latitudes on Mars. From [3].

Applications

Using TES data, [4] mapped the depth to the permafrost at high latitudes, as well as the dry regolith properties (Fig 2.). Similarly, but using only two pairs of strategically selected overlapping observations, [3] mapped the distribution and properties of water ice near the Phoenix Landing Site and found permafrost depth of a few cm, in excellent agreement with in situ observations [5].

Current/Planned Activities

Investigation #1: Global MCS Mapping

We are processing the MCS dataset to generate permafrost depth and top material thermal inertia maps at a spatial resolution of 1 pixel per degree (ppd). The new MCS-based map will be an improvement over the existing TES map for two reasons: 1) maps can be created at 2x the TES spatial resolution and 2) MCS generally has lower instrument noise. This map will be the most accurate product using existing data.

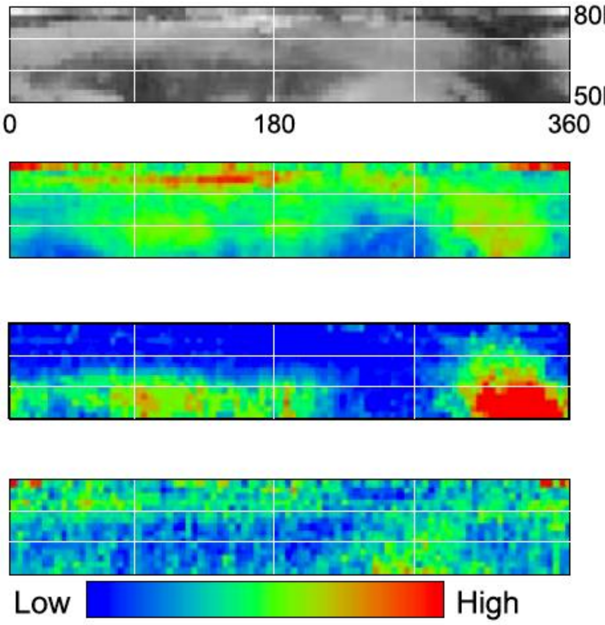

Fig. 2: Radiometric albedo (top), surface cover thermal inertia (2nd panel), permafrost depth (3rd panel), and RMS (bottom) from TES data (0.5 ppd), 0-360°E, 80°-50°N, [4]. See Fig. 3 for an estimation of the absolute permafrost depth in cm.

Investigation #2: MCS Observation Campaign

A key limitation to deriving quantitative permafrost depth is the availability of seasonal temperature data, i.e. frequent Summer/Fall observations for a given location. A dedicated observation campaign is allowing us to repeat observations necessary for the generation of a permafrost depth map at MCS native resolution (8 ppd, ~7.5km) and with the highest achievable confidence. We will present an update of this observation campaign.

Investigation #3: Regional THEMIS Mapping

We will expand the high spatial resolution (i.e., 100m/pixel) permafrost mapping work of [3] at all possible latitudes. Full coverage is not attainable because of data availability at adequate seasons, but global partial coverage is doable. A set of Maps similar to Fig. 3 will be generated.

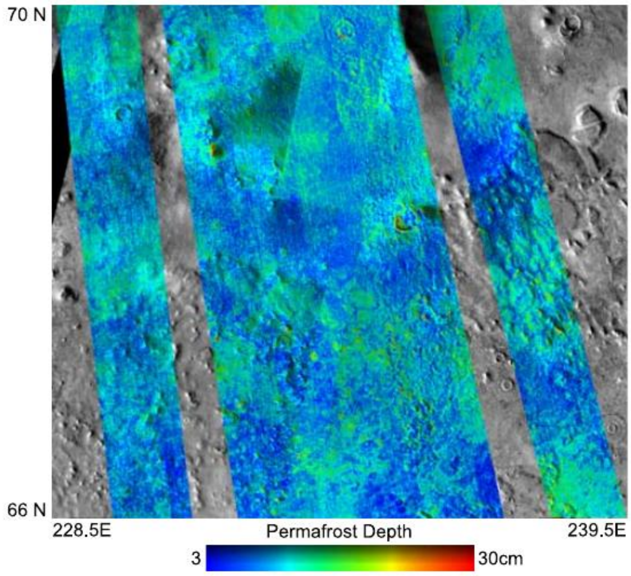

Fig. 3: 100m per pixel high latitude permafrost depth derived from an analysis of THEMIS seasonal data, from [4].

We will present the advancement and share the results of these investigations at the workshop.

Acknowledgments

Work at the Jet Propulsion Laboratory, California Institute of Technology was performed under a contract with NASA. US Government support acknowledged.

References

[1] Slack, G.A., 1980. Thermal Conductivity of Ice. *Physical Review B* 22 (6): 3065-3071.

[2] Presley, M.A., & Christensen, P.R., 1997. Thermal conductivity measurements of particulate materials, Part II: Results. *Journal of Geophysical Research* 102: 6551-6566.

[3] Bandfield, J.L., 2007. High-resolution subsurface water-ice distributions on Mars. *Nature* 447: 64-67.

[4] Bandfield, J.L., & Feldman, W.C., 2008. Martian high latitude permafrost depth and surface cover thermal inertia distributions. *Journal of Geophysical Research* 113 (E8).

[5] Mehta, M., Renno, N.O., Marshall, J., Grover, M.R., Sengupta, A., Rusche, N.A., Kok, J.F., Arvidson, R.E., Markiewicz, W.J., Lemmon, M.T., & Smith, P.H., 2011. Explosive erosion during the Phoenix landing exposes subsurface water on Mars. *Icarus* 211 (1): 172-194.

Interpretation of the first CaSSIS/TGO observations of circum-polar Martian regions by means of laboratory measurements on icy analogues

Antoine Pommerol[1]
Zuriñe Yoldi[1]
Victoria Roloff[1]
Nicolas Thomas[1]
Gabriele Cremonese[2]
and the CaSSIS team

[1]*Physikalisches Institut, University of Bern, NCCR PlanetS, Center for Space and Habitability, antoine.pommerol@space.unibe.ch*
[2]*INAF-Osservatorio Astronomicodi Padova, Vicolo Osservatorio 5, 35122 Padova, Italy*

Abstract

In April 2018, the Colour and Stereo Surface Imaging System of Exomars TGO will start acquiring data over Martian circum-polar regions with high temporal repeatability and variable local time over the seasons. This represents a unique opportunity to improve our understanding of processes related to volatiles cycles taking place in these regions known to host a shallow permafrost. In order to prepare for the operation of the instrument and the interpretation of the data, we have undertaken series of laboratory measurements to characterize the VIS-NIR reflectance properties of plausible icy analogues for Martian high-latitudes areas. Samples are prepared from water ice, carbon dioxide ice, and analogues for both dark and bright-red Martian soils. Hyperspectral cubes are acquired over the spectral range 0.4-2.4 µm, from which the CaSSIS signal through all four colour filters is simulated, allowing us to directly compare these results to actual CaSSIS images

Keywords: Mars, circum-polar regions, ice, remote-sensing, VIS-NIR reflectance, laboratory analogues

ESA's Exomars Trace Gas Orbiter (TGO) is the latest addition to the fleet of spacecraft scrutinizing the surface of Mars from a variety of orbits. The circular science orbit of TGO will be inclined by 74° and non Sun-synchronous, a particularity that will allow the four instruments on-board to observe all areas within the 60-75° latitude range at various local times through the seasons with very high repeatability. Within this range of latitude, large amounts of water ice are known to be present within the first meter below the surface, constituting the shallow Martian permafrost. Most of this ice is hidden from view by a thin layer of desiccated dust but the effects of its presence are still pervasive at the surface, in the form of geomorphological features such as polygons or because the different thermal properties of the frozen soil have noticeable effects on the seasonal condensation and sublimation of volatiles.

The Colour and Stereo Surface Imaging System (CaSSIS) of the TGO will provide a detailed dataset on these regions, unprecedented in terms of temporal coverage. In particular, it should provide new insights on how the peculiar activity associated with the sublimation of the seasonal ice in spring develops with season and local time. CaSSIS is particularly well suited to this task thanks to its four colour filters (500, 675, 836 and 937 nm), its high signal-to-noise (often >250) in a wide PAN filter and its ability to acquire nearly simultaneous stereo pairs in different colours.

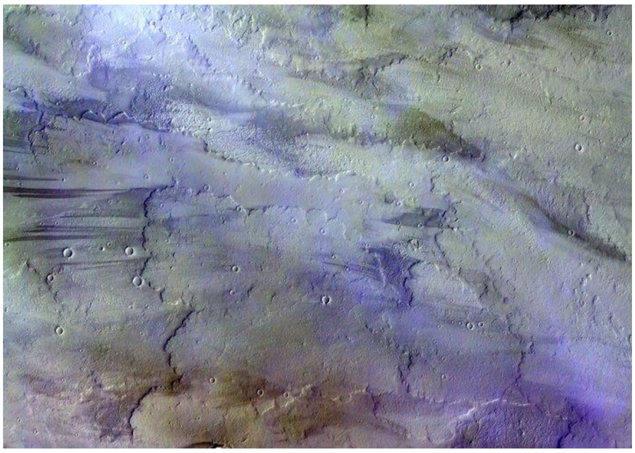

Fig. 1. NIR-RED-BLU colour composite CaSSIS image acquired on the 22nd of November 2016 as part of the first in-orbit commissioning campaign. Diffuse water-ice clouds are seen over lava flows (Image center: 131°W / 8.5°S). The ground resolution is 20.35 m/pixel, and the image is about 58 km across. ESA/Roscosmos/CaSSIS, CC BY-SA 3.0 IGO.

The instrument was tested for the first time in Martian orbit in November 2016 and the data collected during this commissioning phase confirm the excellent performances of the instrument. In addition, laboratory calibration prior to installation of the instrument on the spacecraft confirmed the expected spectral sensitivity of the instrument through all four filters. As commissioning data were acquired while the TGO was still on its initial elliptical capture orbit, only images of regions close to the Martian equator were acquired. The image in Fig. 1 shows lava flows 630 km west from the Summit of Arsia Mons. The image was acquired at Ls=266°, shortly before the summer solstice in the Southern hemisphere and early in the morning. Although this time of the year is the least favourable for the formation of clouds in the Tharsis region, CaSSIS reveals the presence of thin morning clouds that probably quickly dissipate as the atmosphere warms up during the course of the day.

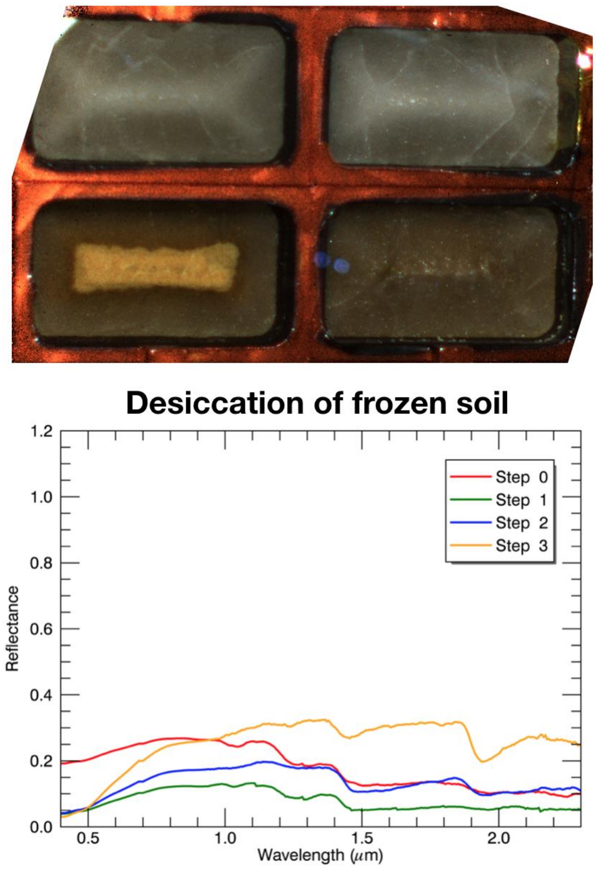

Fig. 2. (top) Example of a simulated CaSSIS colour (RED-PAN-BLU) image, built by applying CaSSIS spectral responses to a hyperspectral cube measured in the laboratory. The four samples are H_2O frozen soils made from dark basalt (top) or JSC Mars-1 (bottom). Over time, ice sublimates exposing ice-free soil (seen here at the centre on the lower-left sample). (bottom) Time series of VIS-NIR reflectance spectra of the desiccating frozen JSC Mars-1 soil analogue located in the lower-left corner of the image on the left.

In order to prepare for the operation of the instrument by optimizing the choice of observation modes and for the interpretation of the future data by providing reference data on well-characterized samples, we have undertaken series of laboratory measurements with analogues of Mars icy soils.

For this purpose, we have associated in different ways an analogue for bright and red Martian regions, JSC Mars-1, a dark basalt from Hawaii chosen as an analogue for dark terrains, and H_2O and CO_2 ices and frosts. Hyperspectral images of these samples were acquired and the hyperspectral data were processed to simulate the signal measured by CaSSIS through its four colour filters and to extract average reflectance spectra over the visible and near-infrared (up to 2.4 µm) spectral ranges. Among the various configurations tested, two series of measurements are particularly relevant for the topic of permafrost: the reflectance properties of frozen soils (i.e. water ice filling the porosity of the soil, Fig. 2) and the effects of the direct deposition of thin layers of frost on the cold surface.

At the time of writing, we are approaching the end of the aerobraking phase necessary to circularize TGO's orbit and preparing for the nominal science operations to start in April 2018. The first observations of circum-polar regions by CaSSIS and their interpretation based on the laboratory measurements described here will be presented at the meeting.

Acknowledgments

CaSSIS is a project of the University of Bern and funded through the Swiss Space Office via ESA's PRODEX programme. The instrument hardware development was also supported by the Italian Space Agency (ASI) (ASI-INAF agreement no.I/018/12/0), INAF/Astronomical Observatory of Padova, and the Space Research Center (CBK) in Warsaw. Support from SGF Ltd. (Budapest), the University of Arizona (Lunar and Planetary Lab.) and NASA are also gratefully acknowledged.

Some of this work has been carried out within the framework of NCCR-PlanetS supported by the Swiss National Science Foundation.

16 - Living with Permafrost: Community engagements and outreach products

Session 16

Living with Permafrost: Culture and Communities in Research and Outreach

Conveners:

- **Mathias Ulrich**, University of Leipzig, Institute for Geography, Leipzig, Germany (Coordinator)
- **Josefine Lenz**, Alfred Wegener Institute Helmholtz Centre for Polar and Marine Research, Periglacial Research Unit Potsdam, Germany; University of Alaska Fairbanks, Institute of Northern Engineering, Fairbanks, AK, USA (PYRN member)
- **Ylva Sjöberg**, Stockholm University, Department of Physical Geography, Stockholm, Sweden
- **Irina Streletskaya**, Moscow State University, Moscow, Russia

As awareness of permafrost continues to grow, and as communities continue to live with changing permafrost and socio-economic conditions, it is crucial to improve communication and collaboration between researchers in different disciplines, Arctic stakeholders, local residents, and the global community. For this session, the International Permafrost Association's (IPA) Standing Committee on Education and Outreach, and IPA's Action Group on Permafrost and Culture (PaC) in collaboration with an International Arctic Science Committee (IASC) Cross-Cutting Initiative, welcome contributions on outreach activities designed for the general public (through a variety of media and outlets) in indigenous, rural, mountainous and urban communities. In addition, we welcome contributions about how communities and individuals live, work, and play in permafrost landscapes, many of which are changing rapidly. For instance, research on interactions of permafrost, mobile pastoralism, land use, and animal husbandry illustrates some these complex relationships. We encourage participation from permafrost scientists as well as individuals from any organization striving to improve permafrost knowledge beyond the traditional educational framework, or those working with local communities to improve their understanding of permafrost.

After the Thaw: Permafrost, People and a new narrative approach to community engagement

Joaquin Alvarado, studiotobe

Abstract

The power of narrative storytelling has remerged with the podcasting and Netflix revolution. There is now more content from more sources than ever before. As a film and podcast executive producer I have been intensely committed to delivering fact based information to audiences in ways that will engage and inform them. ***After the Thaw*** is a new podcast and documentary series that will explore the people and places that are on the frontlines of the impact of climate change on Permafrost. This series will explore the science and social edges of this critical issue in ways that will combine the tension of a thriller with the power of an intimate podcast. Set in several countries across the arctic community, ***After the Thaw*** is set to go into production in the spring of 18 with a launch in Summer of 18. I would like to engage the scientific community attending the conference in creative exploration of themes and possible storylines to include in the series. My presentation will include select clips and scenes from the early production.

Keywords: Engagement ; Journalism ; Narrative ; Netflix ; Podcasts ; Communications

Introduction

Filmmakers, journalists, podcast producers and writers are finding new ways of engaging audiences in complex and compelling storytelling that is episodic and multi-platform. This project will test the potential for connecting these emerging narrative forms with critical climate change issues related to permafrost. By connecting storytellers to scientists and communities on the frontlines of research, mitigation and adaptation, ***After the Thaw*** will provide critical insights into community engagement and capacity building.

The After the Thaw Process

Aim

Connect audiences to important research and impacts of climate change on permafrost.

Research question submission

I have been reading the science and watching scientists working on permafrost over the last five years while developing the core concept and treatment for the show. I am interested in engaging the permafrost scientific community to help inform the design of production.

Results

In my presentation I'll share some basic findings on storylines characters and narrative threads for series.

Bakeapple picking in a changing physical and social landscape

Darya Anderson[1]
James Ford[2]
[1]McGill University, darya.anderson@mail.mcgill.ca
[2]Leeds University

Abstract

I describe the vulnerability of bakeapple picking to permafrost thaw in the context of concurrent social changes in a sub-Arctic Canadian Indigenous community. Using mixed methods, I identified the ecological changes that are impacting the abundance, quality, and ripening time of bakeapples and the interaction with socioeconomic changes, that advance or challenge families to go bakeapple pick. Warming temperatures and the resulting permafrost thaw and vegetation growth emerged as ecological changes that impact the growth of bakeapples. The closure of the fishery and resettlement emerged as key factors that have moved families farther from their traditional bakeapple picking grounds and make it harder to go bakeapple picking. Despite ecological and social changes, families still place a high cultural and nutritional value on bakeapples and use technological advances, like the speedboat, and financial incentives, like the market for bakeapples, to travel further and more quickly to go bakeapple picking.

Keywords: permafrost thaw; Indigenous communities; berry picking; bakeapples,

Introduction

Communities in the Canadian Arctic are already observing the impacts of permafrost thaw on infrastructure and traditional land based livelihoods (Ford et al., 2016). When permafrost thaws there are subsequent changes in soil moisture and vegetation and likely *Rubus chamaemorus* (bakeapples) growth, a berry with cultural and nutritional importance to Indigenous communities. The impacts of permafrost thaw on are exacerbated by concurrent socioeconomic changes and colonial legacies (Anisimov et al., 2007). This research will use a contextual vulnerability approach (Bennett et al., 2016) to consider how bakeapple picking has been impacted by permafrost thaw and added socioeconomic changes in a sub-Arctic Indigenous community.

Study Region

This study draws from data collected in and within 115 km of Cartwright, Labrador. Cartwright is located in southern Labrador on the coast. Cartwright was chosen as the case study community because community members and the NunatuKavut Community Council (NCC) expressed interest and support of the project, long term permafrost monitoring station in the region, and the importance of bakeapple berry picking in southern Labrador.

Methods

Vegetation surveys, satellite imagery analysis, long term weather data, interviews, a focus group, and participant observation were used to characterize the physical changes impacting bakeapple berry picking. Interviews and participant observation were used to characterize the socioeconomic changes that are impacting bakeapple berry picking.

I held one focus group activity with community members in Cartwright to inform where I went to collect data for my relevés (see below). I interviewed 18 individuals about changes in the season and weather that have impacted bakeapple berries and I supplemented this with historical Environment Canada temperature data, from a weather station in Cartwright.

For vegetation surveys, I used the relevé method to assess how the surface cover of bakeapple berries changes across a permafrost thaw gradient. For satellite imagery analysis, two multispectral and two panchromatic images from 2004 and 2016 were used to assess the changes in vegetation, surface water, and permafrost features over the 12-year period (Bouchard et al., 2014).

Preliminary Results and Discussion

Interviewees emphasized the importance of climate and weather on bakeapple growth. Interviewees observe that the bakeapples are ripening earlier due to warming temperatures in the spring. Historical weather data confirms that the late spring and early summer temperatures in the past 10 years are significantly warmer than the previous 74 years. This confirms interviewees observations.

Interviewees also observe that the vegetation is growing up in Cartwright, specifically in the "Big Marsh," a permafrost associated peatland where bakeapples are picked. This observation is confirmed by satellite imagery of the "Big Marsh" which shows an increase in vegetation by 21.5% over 12 years and in surface water by 66.4%. Interview participants observe that larger shrub and tree growth is constraining bakeapple growth.

Finally, relevé data shows that bakeapple abundance is dependent on the presence or absence of permafrost. Satellite imagery shows that permafrost extent has decreased by 64.5% in the "Big Marsh." Therefore, it is probable that permafrost thaw, and the resulting changes in soil moisture, have decreased the abundance of bakeapples in permafrost associated peatlands.

In addition to physical environmental changes, socioeconomic changes have impacted bakeapple pickers. Both resettlement and the transition from the in-land fishery to the off-shore fishery have ended the traditional use of both a summer and winter home. The semi-nomadic lifestyle between summer and winter home enabled people to bakeapple pick during the summer months. This component of sensitivity has parallels in other northern communities with land based livelihoods. Colonialization across the Canadian north has resulted in resettlement and resource extraction that has impacted the semi-nomadic lifestyle associated with land based livelihoods. Also, preliminary analysis indicates that both the speedboat and the value placed on culture heighten the adaptive capacity of community members. Technology and culture have both been noted as components of adaptive capacity in other Canadian northern communities. Even with these components of adaptive capacity, there are fewer young families bakeapple picking in Cartwright and across the Canadian north.

Conclusions

This research focuses on the climate and ecological related changes that are impacting bakeapple growth. Warming temperatures, decreases in permafrost extent and increased vegetation are relevant exposures for Indigenous communities who berry pick across the sub-Arctic. Despite these climate related changes, community members, in Cartwright, are not largely concerned about not having enough bakeapples because of ecological changes. Community members are more concerned about changes in their economic, social, and political situations that are making it harder to go bakeapple picking with their families and to pass knowledge about berry picking to younger generations.

Acknowledgments

Thank you to my supervisor, James Ford. Thank you to Leslie Hamel who was my field guide. Thank you to Robert Way who advised me and accompanied me in the field. Thank you to the NCC who facilitated the research process. Thank you to Judy Pardy who was my research coordinator. Thank you to all the research participants in Cartwright, Labrador. Ethics approval was received from the Ethics Review Board at McGill University and The NunatuKavut Community Council (NCC) in Happy Valley- Goose Bay Labrador. This research was funded by the Canadian Institute for Health Research (CIHR). The satellite imagery was provided by the Digital Globe Foundation.

References

Anisimov, O.A., D.G. Vaughan, T.V. Callaghan, C. Furgal, H. Marchant, T.D. Prowse, H. Vilhjálmsson and J.E. Walsh., 2007. Polar regions (Arctic and Antarctic). In M.L. Parry, O.F. Canziani, J.P. Palutikof, P.J. van der Linden and C.E. Hanson. (eds.), *Climate Change 2007: Impacts, Adaptation and Vulnerability. Contribution of Working Group II to the Fourth Assessment Report of the Intergovernmental Panel on Climate Change*, Cambridge: Cambridge University Press, 653-685.

Bennett, N. J., Blythe, J., Tyler, S., & Ban, N. C., 2016. Communities and change in the anthropocene: understanding social-ecological vulnerability and planning adaptations to multiple interacting exposures. *Regional Environmental Change* 4: 907–926.

Bouchard, F., Francus, P., Pienitz, R., Laurion, I., Feyte, S., 2014. Subarctic Thermokarst Ponds: Investigating Recent Landscape Evolution and Sediment Dynamics in Thawed Permafrost of Northern Québec (Canada). *Arctic, Antarctic, and Alpine Research* 1: 251–271. https://doi.org/10.1657/1938-4246-46.1.251

Ford, J., Bell, T., & Couture, N., 2016. Perspectives on Canada's North Coast Region. In D. S. Lemmen, F. J. Warren, T. S. James, & C. S. L. editors Mercer Clarke (eds.), *Canada's Marine Coast in a Changing Climate*. Ottawa: Government of Canada, 153–191.

Bibliometric analysis of permafrost studies in the world

Alexandra Bancheva[1]

[1]*Lomonosov Moscow State University, ban-sai@mail.ru*

Abstract

The paper is devoted to bibliometric analysis of permafrost and related to it studies for the period 2007-2016 (basing on data of SciVerse Scopus). Such indicators as the number of publications, it's dynamic for 10-years period and countries-leaders for each scientific area are identified.

Keywords: publication activity, assessment of scientific activity, scientific potential, trends in science

Introduction

Permafrost and related issues are actual subjects for scientific research. Due to such factors and conditions as climate change, economic development of the permafrost zone, indigenous land use etc. these research become more essential and frequent published. In this regard, the quantitative indicators of publication activity are considered important and presented in this research.

Methods

The bibliometric analysis method was used basing on data of edition Elsevier SciVerse Scopus (SCOPUS) with 10-years period (2007-2016). For the analysis, firstly, all issues related to permafrost were devided into smaller groups (for example, "monitoring of permafrost", "engineering in cryolithozone", "exploration of the resources", "indigenous people in permafrost zone" and others). Secondly, key words for these groups were formulated (for request in database). Thirdly, filters of request were indicated (type of publication, years etc.). In the result, the following indicators were analyzed: total number of publications for 10 years; 10-years dynamic; ranking of the countries in public activity in each group.

Results

Bibliometric analysis show that the number of publications in the scientific area "permafrost" is comparable with other scientific fields in environmental and Earth sciences and varies from several hundred publications per year to several thousand publications per year. For example such "classic" field as "air pollution" or "water pollution" have about 5-6 thousand papers per year, and such "relatively new" field as "green or sustainable transport" has about 5-6 hundred paper per year. In our case, for example, the group of issues that named "Climate change and the dynamics of cryosphere" has about 500 paper per year and +67% growth in the number of papers for 10-years period (Fig. 1, left). The group of issues that named "Geoengineering technologies" (incl. CCS technologies) has about 1500 paper per year and +141% growth in the number of papers for 10-years period (Fig. 1, right).

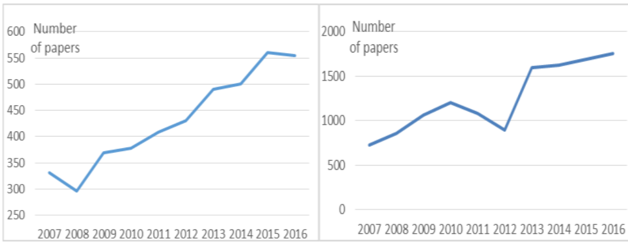

Fig. 1. Bibliometric characteristics for the group of issues "Climate change and the dynamics of cryosphere" (left) and bibliometric characteristics for the group of issues "Geoengineering technologies" (right)

As a result, the most published groups of issues and the most active countries were found out and classified according to the approach proposed by (Alekseeva, 2014).

References

Scopus official web-page https://www.scopus.com

Alekseeva N., Klimanova O., Margolina I., Toporina V. , 2014. Trends of Development of Applied Studies for Priority Area Rational Nature Management. *Ecology and Industry of Russia*, p. 34-38 [in Russian]

Beyond the cartoons: combining innovative permafrost comics with augmented reality

Frédéric Bouchard[1], Julie Sansoulet[2], the 'Frozen-Ground Cartoons' Team[3]

[1]*GEOPS/IPSL – UMR 8148 (UPS, CNRS), Université Paris-Saclay, Orsay, France*
[2]*Takuvik Joint International Laboratory, Université Laval (Canada) – CNRS (France)*
[3]*https://frozengroundcartoon.com/home/*

Abstract

Apart from people in cold region communities and the steadily growing scientific community, one knows very little about permafrost and the "whats", "whys", and "hows" of permafrost research. Our scientific outreach project called 'Frozen-Ground Cartoons' aims at making permafrost science accessible to children, youth, their parents, and teachers via a series of comic strips. Here we present the second phase of the project, which will involve a series of augmented reality (AR) material, such as maps, photos, videos and 3D drawings. AR material will be accessible by scanning the cartoons with a portable device (phone, tablet), generating complementary scientific information about permafrost. This project is part of the outreach program in the H2020 project Nunataryuk.

Keywords: outreach; education; science comics; augmented reality; permafrost; Arctic.

Introduction

Education and outreach is a fundamental component of scientific research activities. Especially for Arctic science, the involvement of local communities and the diffusion of scientific knowledge in schools is now an essential task on every researcher's to-do list. The International Permafrost Association (IPA) Action Group "A Frozen-Ground Cartoon" (2016-2018) aimed at filling the gap between indigenous knowledge, complex scientific results and outreach to the general public, especially children. These permafrost comics explain the impact of climate change in permafrost areas, its effects on local communities, wildlife and changing landscapes (Nääs *et al.*, 2017). The printed version has been released in target scientific events (Arctic Change, AGU), and several translation projects are completed, in progress or planned for the coming years (e.g., Inuktitut, French, Swedish, German, Japanese). Here we present the second phase of the project, which will involve complementary audio/visual material (e.g., maps, videos) collectively referred to as augmented reality (AR).

Applying AR tools to science cartoons

Comics are excellent ways to communicate messages in today's media landscape: they are graphic, funny and direct, and can be rapidly shared via social media. They can also provide scientific concepts from a different angle compared to traditional scientific literature. Our 'Frozen-Ground Cartoons' were designed to do just that, i.e. making permafrost science accessible to the general public, focusing on the younger generations (Fig. 1).

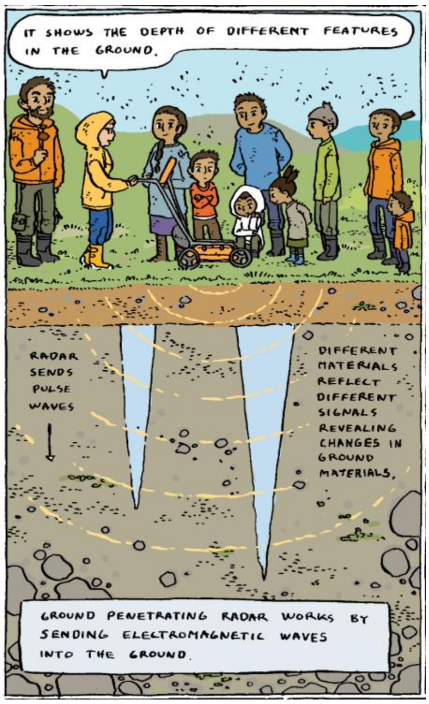

Figure 1. Explanation of how the GPR (ground penetrating radar) works in permafrost landscapes. From Nääs *et al.*, 2017.

Now that the cartoons have been printed and released, we plan to take them to another 'level of outreach' by providing complementary AR material. We will produce (or modify existing) maps, photos, videos and 3D drawings that will be readily available via smartphones and tablets. For example, the 'Circum-Arctic Map of Permafrost and Ground-Ice Conditions' (Brown *et al.*, 2002) could be used (or modified) in several places in the cartoons, as well as the numerous fieldwork photos generated by the science team through the recent years, giving a real-life glimpse of the activities done in the field. **Maps** will also allow the user to dynamically visualize in 3D why it is warmer in the Arctic and to understand land erosion and subsidence in local permafrost areas.

Furthermore, explanative **videos** will provide (i) information about permafrost physical properties and soil profile, (ii) examples of how data are collected in the field (e.g., permafrost drilling, active-layer probing) and in the laboratory (e.g., subsampling, mass-spectrometry), (iii) enlightenment about impact of climate change and solutions one can consider, and (iv) inputs on how Inuit and scientists collaborate to co-produce knowledge. Finally, **3D drawings** of permafrost properties and environment (e.g., sediment core, house adapted to the Arctic, thermokarst lakes) will provide an innovative way of presenting permafrost science elements to the general public - even to the specialists.

By pushing the limits of scientific outreach, specifically regarding international permafrost research, we wish to bring awareness to the sensitive Arctic regions to the general public and to political decision makers. Such an approach stems from an earlier international collaboration between early-career scientists that was targeted specifically to the permafrost science community (Fritz *et al.*, 2015). This project will be included in the Outreach program of Nunataryuk, an EU H2020 project investigating the impacts of thawing coastal permafrost on the global climate (www.nunataryuk.org).

Acknowledgements

This project would not have been possible without the support from the following organizations: International Permafrost Association (IPA), International Arctic Science Committee (IASC), Arctic Development and Adaptation to Permafrost in Transition (ADAPT), Permafrost Young Researchers Network (PYRN), Association of Polar Early Career Scientists (APECS), Climate and Cryosphere (CliC), Alfred Wegener Institute Helmholtz Centre for Polar and Marine Research (AWI), the Bolin Centre for Climate Research, and the IMPACT! Fund.

References

Brown, J., Ferrians, O., Heginbottom, J. A., Melnikov, E., 2002. *Circum-Arctic Map of Permafrost and Ground-Ice Conditions, Version 2*. Boulder: National Snow and Ice Data Center, online. http://nsidc.org/data/GGD318

Fritz, M., Deshpande, B. N., Bouchard, F., Högström, E., Malenfant-Lepage, J., Morgenstern, A., Nieuwendam, A., Oliva, M., Paquette, M., Rudy, A. C. A., Siewert, M. B., Sjöberg, Y., Weege, S., 2015. Brief Communication: Future avenues for permafrost science from the perspective of early career researchers. *The Cryosphere* 9: 1715-1720. doi:10.5194/tc-9-1715-2015.

Nääs, H., Ross, N., Bouchard, F., Deshpande, B., Fritz, M., Malenfant-Lepage, J., Nieuwendam, A., Paquette, M., Rudy, A., Siewert, M., Sjöberg, Y., Veillette, A., Weege, S., Harbor, J., Habeck, J. O., 2017. *Frozen-Ground Cartoons: An international collaboration between artists and permafrost scientists*. Potsdam: Bibliothek Wissenschaftspark Albert Einstein, 28 pp. doi: http://doi.org/10.2312/GFZ.LIS.2017.001.

Establishment of community-based permafrost observation network at the Upper Kuskokwim area as a model of interaction between scientists and indigenous people.

Alexander Kholodov[1]
Santosh Panda[1]
Teresa Hanson[2]
[1]*Geophysical Institute University of Alaska Fairbanks, alkholodov@alaska.edu*
[2]*Telida Village Council*

Abstract

Alaska's nature is undergoing a great upheaval induced by the climate changes that directly affects the tribal communities living in remote villages. Under these circumstances, local inhabitants have to have better information about environmental changes to facilitate safe subsistence. One of the ways to achieve it is the collaboration with scientists intends to build tribal capacity to monitor environmental changes. That might empower the tribal communities in assessing and responding to the natural changes. This report represents an example of such collaboration between UAF researchers and rural communities of Upper Kuskokwim aimed at the establishment of community-based observation system of the thermal state of permafrost. Data co-produced by scientists and residents of the village of Telida had been used for development of the village climate adaptation plan. But at the same time comprehensive mechanisms of implementation of scientific results to communities needs and concerns are still underdeveloped.

Keywords: Interior Alaska, permafrost, environmental changes, traditional knowledge, indigenous communities.

Introduction

Permafrost underlies about 80% of the territory of the state of Alaska (Jorgenson *et al.*, 2008). It undertakes sustainable increasing of the temperature (Arctic report card, 2016) and at some areas in the region of Interior Alaska it approached, the range of the intensive phase transition of soil moisture that makes permafrost in this region very vulnerable to climate variations or disturbance due to human activity. Permafrost degradation can affect humans life both direct (issues with construction stabilities or limitation of permafrost cellars usage) and indirect (changes in surface hydrology and vegetation) ways. The former is more typical for the area of ice-rich permafrost in the continuous zone, while the latter – within the discontinuous one. More than a half of Alaskans native communities are located in the permafrost extent (Figure 1) and soon might find themselves in front of face of dramatic environmental changes. Under these circumstances, local inhabitants have to have better information about environmental changes to facilitate safe subsistence. One of the ways to achieve it is the collaboration with scientists intends to build tribal capacity to monitor environmental changes. That might empower the tribal communities in assessing and responding to the natural changes.

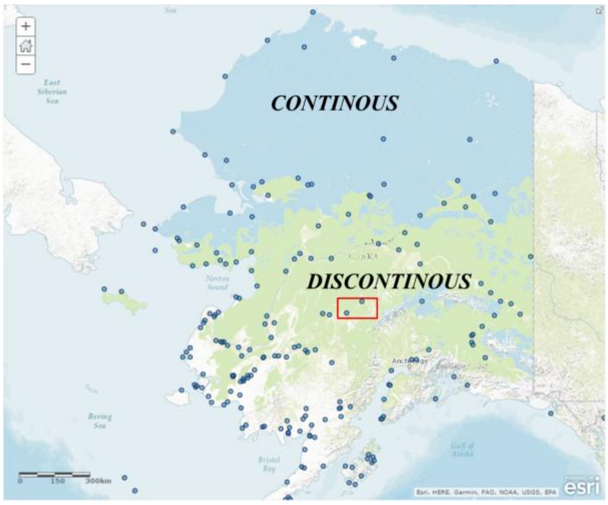

Figure 1. Zones of permafrost distribution and location of native communities in Alaska. Red box – villages of Nikolai and Telida, where observation network had been established.

This report represents an example of such collaboration between UAF researchers and rural communities of Upper Kuskokwim aimed at the establishment of community-based observation system of the thermal state of permafrost.

People's needs and concerns related to environmental changes

For better understanding of the environmental issues indigenous communities are suffering from in 2016 we conducted community survey among the residents of the villages Nikolai and Telida. Totally, we collected 50 responds. The gender ratio was 20 females and 30 males. The age of the most of respondents was 26 years and older, including 18 elders (older than 50 years) provides good time record. All of respondents use at least some kind of subsistence resources via fishing, hunting or berry picking. People are good aware about the climate changes and can observe it in their everyday life (29 people) or know about it from elders or family members (25). All respondents were familiar with the permafrost phenomena and gave clear definition of it.

In terms of the changes, affecting personal life two main concerns were identified: problems with transportation during winter season due to late rivers, lakes and swamps freezing and decreasing of berries productivity.

At the same time, some people noticed positive consequences of the climate warming, such as reduction of the heating costs.

Establishment of the observation network: approaches and first results

Members of Telida village council were involved in all our activities including site selection, equipment deployment, ecological, soil and snow surveys, data collection and instruments maintaining. The fact that some of them had some scientific skills doing sampling of berries, moss and fish tissues for the US Environmental Protection Agency programs was very useful. With the help of local residents, we identified location of observation points. The monitoring network covers all main ecotypes both around villages and in some undisturbed area as reference points. Currently network consists of 20 observation points. We had instrumented 12 sites (11 at the village of Telida and one more in Nikolai) in 2016 and 8 more (two in Telida and 6 in Nikolai) in 2017.

After the one year of observation we can make the conclusion, that permafrost in this area is close to the borderline. Mean annual temperature at the bottom of active layer varies from -1/-1.5°C at the undisturbed places to -0.2/-0.5°C at the areas recovered after low severity disturbance (fires or trees cutting). Within the areas, recovering after high severity fires mean annual ground temperature is positive.

Discussion

Results of our observations along with soil and ecological surveys allow us to identify dangerous areas, where land use activity can initiate permafrost degradation and development of thermokarst process. It might create amplify above-mentioned problems with transportation. It was reflected in the "Climate Adaptation Plan", Telida village council is working on now.

In general, establishment of the mechanisms of implementation of scientific results to the local community's needs and concerns was identified as one of the main problems of citizen science and coproduction of knowledge activity.

From the other side, we learned that involvement of indigenous people in scientific research could be a great benefit. Their traditional knowledge is a significant source of information about the area of investigations. In addition, participation of local residence can make long-term observations more sustainable, especially in remote areas, such us Upper Kuskokwim.

Thus, true coproduction of knowledge is only possible through the trusted and equal partnership with indigenous communities and a broad understanding of each other's mindset, needs and priorities.

Acknowledgments

We would like to appreciate all members of Telida and Nikolai communities for participation in survey, sharing their traditional knowledge and help in observation network establishment. We also want to acknowledge the National Science Foundation of the USA for support this research (project# 1503900).

References

Blunden, J. *et al.*, 2017. State of the Climate in 2016. *Bulletin of the American Meteorological Society* 98.8, 278 pp.

Jorgenson, M.T., Yoshikawa, K., Kanevskiy, M., Shur, Y., Romanovsky, V., Marchenko, S., Grosse, G., Brown, J. & Jones, B., 2008. Permafrost characteristics of Alaska. In *Proceedings of the Ninth International Conference on Permafrost*. University of Alaska, Fairbanks, June, Vol. 3: 121-122.

Meteosensitivity oil and gas workers in the negative impacts of climate and geographical conditions of the Arctic

Yana Korneeva
Northern (Arctic) Federal University named after M.V. Lomonosov, amazonkca@mail.ru

Abstract

The study was carried out as part of an expedition from March to April 2015, in which 70 employees of the oil and gas production company in the Nenets Autonomous District with ages between 24 and 60 (mean 38.5 ± 1.4) were questioned by means of questionnaires and subjected to psychological tests. Statistical analysis was carried out using descriptive statistics and step-by-step discriminant analysis within the SPSS 22.00 software package. As a result of the research, prevailing regulatory processes and mechanisms of psychological defenses (as parameters of a personal resource) were identified among workers operating on a shift method in the Arctic with low and high levels of situational meteorological response. The workers with a low level of situational meteorological reaction are characterized an average level of programming and a high level of evaluation of the results as regulatory processes.

Keywords: meteosensitivity; meteorological reaction; oil and gas workers; Arctic conditions; psychological protection; regulatory processes

Introduction

Climatic and weather events and factors have an adverse effect on human activities: they lead to disruptions in telecommunication and navigation systems, which violate the work of oil and gas equipment, railway transport, etc. (*Daglis, 2001*). Work on oil fields is carried out mainly in Arctic regions with extreme natural and climatic conditions of Arctic, which have moreover a strong impact on human health.

The revealed facts point to the need to pay special attention to the peculiarities of adaptation of oil and gas workers to the Arctic conditions (*Parkes, 1999*), one of which is the meteosensitivity (meteorological reaction) of a person. Meteosensitivity is defined as the ability of the body to coordinate life-supporting processes of the human body with cosmic, solar, planetary, geophysical, meteorological, field, and rhythmological processes in our environment (*Korneeva et al., 2013*).

According to our hypothesis, workers with different levels of meteosensitivity, use different mechanisms of regulation of their status, which corresponds to the different personal resources that allow them to overcome the negative impact of unfavorable climatic and geographical conditions.

Personal resources are represented by abilities and skills, as well as psychological qualities and personality traits, a combination of which is necessary and sufficient for the successful adaptation of a person in activity.

The research aim of this study was to identify the characteristics of the personal resource of oil and gas company workers to overcome the negative impact of climatic and geographical conditions in the Arctic.

Materials and Methods of Research

The study involved 70 employees of the oil and gas production company in the territory of the Nenets Autonomous Okrug, Russian Federation with shift durations of 30 days. Worker ages range between 24 and 60 (mean 38.5 ± 1.4 years). The shift work experience in the North of the surveyed workers varies from 0.5 to 31 years (mean 9.5 ± 1.1 years).

The study was conducted from March to April 2015 using questionnaires and psychological testing. Diagnostics of the level of situational meteorological reaction was carried out with the help of the original automated screening and assessment system for the disadaptive meteopathic and pathological conditions (SCRINMED; Hasnulin V.I., Makarenko A.A., reg.No. 970035 dated January 29, 1997; Hasnulin *et al., 1996*). A situational meteopatic reaction (situational meteorological reaction) is a painful reaction of the human body to the change in meteorogeophysical factors at a particular time.

The personal resource was studied using the following methods: 1) "The style of self-regulation of behavior" V.I. Morosanova (*Morosanova, 2004*); 2) method of psychological defense mechanisms "Life Style Index" (LSI) R. Plutchik, G. Kellerman, H.R. Conte in the adaptation of E.S. Romanova, L.R. Grebennikova (*Romanova et al., 1996*). Statistical analysis was carried out using descriptive statistics and step-by-step discriminant analysis. Analysis was performed using the SPSS 22.00 software package (license agreement № Z125-3301-14 (NArFU Lomonosov).

Research Results

With the help of SCRINMED, we determined two meteorological reaction indicators: situational and subjective. Differences in these two indicators are as follows, (i) situational meteorological reaction shows the body's objective reaction to weather events and is calculated on the basis of completed test tasks, and (ii) subjective meteorological reaction is calculated on the basis of a subjective assessment of the changes under examination of own status under the influence of weather phenomena.

Based on the results of diagnosing the situational meteorological reaction, all the surveyed workers were divided into two groups: 1) those with a low level (0-2 points) - 26.3%; 2) with a high level (3-5 points) - 73.7%.

We correlated the personal resource of workers with different levels of situational meteorological reactions. In this connection, we conducted step-by-step discriminant analysis, in which the low or high gradation of the *subjective* meteorological reactions level was chosen as the dependent variable. The independent variables were the parameters of "Style of self-regulation of behavior" in the first discriminant analysis; and the parameters of the "Life Style Index" (LSI) in the second discriminant analysis. A step-by-step variant of discriminant analysis was used, so in the final version there were variables that reached significant values of λ-Wilks (Table 1).

Table 1. Normed coefficients of canonical functions from the results of two discriminant analyzes.

Parameters	1	2	3	4
Programming	1,0	7,1±1,03	6,2±1,81	5-7
Compensation	-0,5	2,7±0,72	3,7±1,69	4,4
Projection	0,6	8,9±1,70	7,4±2,73	5,5
Rationalization	0,7	7,4±2,28	5,7±1,57	6,3

1 - The value of the canonical function

2 - The mean and standard deviation of parameters for group 1 - employees with a low level of *subjective* meteorological reaction

3 – The mean and standard deviation of parameters for group 2 - employees with a high level of *subjective* meteorological reaction

4 - The value of the norm according to the method

According to Tables 1, workers with a low level of subjective meteorological reaction are characterized by a higher level of programming as a regulatory process and a lower level of psychological defense mechanism «compensation» as well as high values of projection and rationalization. These employees differ in that they try in detail and deployed to think through the ways of their actions and behavior to achieve their goals. During difficult situations, they seek to solve the problem, to identify the true causes of it and to eliminate them, which leads to their success in activities and well-being. A characteristic feature of this group of workers is the use of projection as a mechanism of psychological defense. It unacceptable thoughts and feelings are attributed to surrounding people, as well as rationalization, i.e. "intellectual" way to overcome the conflict or situation without frustrating experiences. In other words, the personality suppresses the experiences caused by an unpleasant or subjectively unacceptable situation, by means of logical attitudes and manipulations, even if there is convincing evidence in favor of the opposite.

Conclusions

1. The results of the study showed that the majority of oil and gas workers in the Arctic conditions are characterized by a high level of expression situational (73.7%) meteorological reactions.
2. It is determined that the personal resource of oil and gas workers to overcome the adverse impact of climatic and geographic factors is a higher level of programming as a regulatory process, a low level of compensation as well as a higher level of projection and rationalization as mechanisms for psychological protection.

Acknowledgments

The study was sponsored by the Russian President's grant for state support of young Russian scientists - PhD (MK-6409.2018.6)

References

Korneeva, Ja.A., Simonova, N.N., Degteva, G.N., Dubinina, N.I., Fedotov, D.M., 2013. Psychophysiological and psychological indicators meteosensitivity working population of the Far North. *Proceedings of the Samara Scientific Center of the Russian Academy of Sciences*. T. 15. 2-2: 388-391.

Morosanova, V.I., 2004. *Questionnaire "style of self-regulation of behavior" (SMTA)*. Moscow. 44 p.

Romanova, E.S., Grebennikov, L.R., 1996. *Mechanisms of psychological protection Genesis, functioning, diagnostic*. Mytishchi. 144 p.

Hasnulin, V.I., 1996. Automated system of medical-ecological monitoring rapid assessment based on the error functions of the basic homeostatic systems with the rhythm of the changes meteorological and geophysical, social and technological factors - "Ecomed". *On the creation of a unified regional system of monitoring of environment and health of the population of Siberia*. Novosibirsk. 112p.

Parkes, K.R., 1999. Shiftwork, job type, and the work environment as joint predictors of health-related outcomes. *Journal Of Occupational Health Psychology*.4 (3): 256-68.

Space Storms and Space Weather Hazard., 2001. Ed. Daglis I.A., NATO Science Series. Vol. II/38, Kluwer Academic Publishers. Dordrecht. The Netherlands. 482 p.

Permafrost Research Priorities

Hugues Lantuit[1,2]
Ylva Sjöberg[3]
Michel Allard[4]
Mauro Guglielmin[5]
Margareta Johansson[6]
Gleb Kraev[7]
Michael Krautblatter[8]
Gerhard Krinner[9]
Edward (A. G.) Schuur[10]
Jenny Baeseman[11]
Karina Schollän[1]

[1]*Alfred Wegener Institute Helmholtz Centre for Polar and Marine Research, Germany, Hugues.Lantuit@awi.de*
[2]*University of Potsdam, Germany*
[3]*Stockholm University, Sweden*
[4]*Université Laval, Canada*
[5]*Insubria University, Italy*
[6]*Lund University, Sweden*
[7]*Centre for Forest Ecology and Productivity, Russian Federation*
[8]*Technical University of Munich, Germany*
[9]*LGGE Grenoble, France*
[10]*Northern Arizona University ,USA*
[11]*Scientific Committee on Antarctic Research, UK*

Abstract

The International Permafrost Association (IPA) and the Climate and Cryosphere project (CliC) recently completed the voting process of the Permafrost Research Priorities initiative. This project aimed at integrating priorities for forward-looking, collaborative, interdisciplinary Arctic research and observing. In this presentation, we introduce the outputs of the project and highlight the engagement of the permafrost community in the process.

Keywords: Permafrost, Climate Change, Future, Vision, Community engagement, Policy

Introduction

The International Permafrost Association (IPA) and the Climate and Cryosphere project (CliC) were invited to participate in the Third International Conference on Arctic Research Planning (ICARPIII) process, led by the International Arctic Science Committee (IASC). The ICARP III process aimed at integrating priorities for forward-looking, collaborative, interdisciplinary Arctic research and observing. The IPA and CliC, acknowledging that no consensus document existed at the international level to identify forward-looking priorities in permafrost research, decided to initiate a process by which such a document, focusing on permafrost research at large (i.e. including Arctic, Mountain, Antarctic and Sub-sea permafrost) would be published based on the engagement of the permafrost research community as a contribution to ICARP III. The product stemming from the effort should consist of a high level, but short benchmark publication listing and putting into context research priorities from 2017 to 2027.

The PRP Process

Aim

The aim of the Permafrost Research Priorities (PRP) process is to establish a concise set of ~10 research priorities as agreed on by researchers (primarily permafrost researchers) for the next ten years. The final number of research priorities might change during the process if input from the questionnaire and subsequent meetings deems it meaningful. The target audience of the exercise is three-fold: 1. The research community; 2. Funding agencies and 3. Policy-makers.

Research question submission

Participation to the online questionnaire was open to all and took place in 2014. The audiences targeted in the process were engaged through existing communication platforms and tools devised specifically for the exercise.

The announcement was circulated through partner organizations and through mailing lists relevant to the permafrost community. Additionally, target groups relevant to the policy arena and/or belonging to funding agencies were engaged in the process through targeted mailing. In order to reach out to the whole spectrum of permafrost research, a targeted search was conducted in Scopus to identify authors having published on permafrost over the past five years.

Question consolidation

Text is set in two columns. Do not add lines between paragraphs.

The submission process was very successful and as many as 359 researchers from 37 countries submitted research questions. The respondents were primarily active in the field of geomorphology, ecology, engineering and infrastructure. 79% of them had a PhD and 53.8% of them had more than 10 years of experience in permafrost research.

The core group consolidated the research questions and produced a consolidated list to submit for vote. The consolidation consisted in removing duplicate questions, merging questions with very similar foci, correcting the syntax and spelling of the questions and check that the questions answered the criteria put forward in the first phase of the process.

The result was a list of 347 questions organized in 20 categories.

Voting

The voting was opened on November 12th, 2017 until December 20th, 2017. It was performed using a professional survey platform ensuring full randomization of the questions. The participants were invited to vote on their category of expertise and to leave comments on the process.

Results

In this presentation, we'll introduce the results of the voting process and the subsequent consolidation performed by the core group. We'll also highlight basic statistics on the cohort of voters and report on lessons drawn from the process.

Acknowledgments

PRP is a process supported by the International Permafrost Association and the Climate and Cryosphere project (CliC). We thank the contribution of many individuals, including Stefanie Hohberg for support with the preparation of the online survey.

Best Practices in Collaborative Research with Northern Communities: A Synopsis from Early Career Researchers

Josefine Lenz[1,2], Louis-Philippe Roy[3], Kristina Brown[4], Emily Choy[5], Elena Kuznetsova[6], Robert Way[7], Richard Gordon[8], Anna Afanasyeva[9], Joachim Otto Habeck[10], Alevtina Evgrafova[11], Scott Zolkos[12]

[1]*Alfred Wegener Institute Helmholtz Centre for Polar and Marine Research, Periglacial Research Section, Potsdam, Germany Josefine.Lenz@awi.de*
[2]*University of Alaska Fairbanks, Institute of Northern Engineering, Fairbanks, AK, USA*
[3] *Yukon Research Centre/Northern Climate ExChange, Whitehorse, Yukon, Canada, presenting author*
[4] *Woods Hole Oceanographic Institution, Woods Hole, MA, USA*
[5] *University of Manitoba, Department of Biological Sciences, Winnipeg, Manitoba, Canada*
[6] *Norwegian University of Science and Technology, Department of Civil and Environmental Engineering, Trondheim, Norway*
[7]*Labrador Institute, Memorial University of Newfoundland, Happy Valley-Goose Bay, Canada*
[8] *Yukon Parks, Herschel Island Qikiqtaruk Territorial Park, Canada*
[9] *Centre for Sami Studies at the Arctic University of Tromsø, Norway*
[10] *University of Hamburg, Germany*
[11] *University of Bern, Switzerland and University of Koblenz-Landau, Germany*
[12] *University of Alberta, Edmonton, AB, Canada*

Abstract

Combining scientific and traditional knowledge is crucial to understanding environmental systems across circum-Arctic regions, where climate change is most impactful. However, building collaborative partnerships between visiting scientists and local, indigenous traditional knowledge holders in northern communities presents challenges. The workshop "Community-based Research: Do`s and Don`ts of Arctic Research" was organized as an IASC cross-cutting initiative at ICOP2016 in Potsdam, Germany, to facilitate dialogue between Early Career Researchers (ECRs) and northern residents. This workshop resulted in a diverse list of considerations and sustainable practices to improve traditional and scientific knowledge exchange, and collaborative northern research. An extensive list of positive (Do`s) and a few negative recommendations (Don`ts) was generated together with ECRs and Arctic representatives. Many good ideas on research design, active communication and community involvement developed from these fruitful discussions. This study provides an example of strategy development in order to enhance knowledge transfer between scientists and northern indigenous communities.

Keywords: science communication; community-based research; citizen science; Early Career Researchers; PYRN workshop; ICOP2016

Introduction

Research in Arctic and Subarctic environments presents unique challenges and obstacles, particularly when research is undertaken near indigenous communities by non-local, non-indigenous researchers. Non-local researchers may be less familiar with local norms, customs, social systems and protocols, commonly leading to challenges for both scientists and communities.

The Idea

Fellows of the International Arctic Science Committee (IASC) initiated an IASC cross-cutting activity to facilitate dialogue between Early Career Researchers (ECRs) and northern residents. A workshop session on "Community-based Research: Do`s and Don`ts of Arctic Research" was organized during the Permafrost Young Researchers Workshop on 18-19 June 2016, during the 11th International Conference on Permafrost 2016 (icop2016.org) in Potsdam, Germany.

Workshop Organization and Structure

Two 90-min sessions were held allowing up to 60 participants to partake in the workshop. Four experts were invited to discuss their background in the context of scientific activities in the Arctic: Richard Gordon who is Inuvialuit and Chief Ranger of Herschel Island Territorial Park (Inuvik, Canada); Anna Afanasyeva, a Russian Saami living in Norway and Indigenous Peoples Adviser at the International Barents Secretariat; Joachim Otto Habeck, a Professor at the Institute of Social and Cultural Anthropology at the University of Hamburg (Germany) and co-leader of the IPA Action Group "Permafrost and Culture" in the region of Sakha (Yakutia, Russia); and Robert Way, an Inuk (Nunatsiavut) and a PhD student at the University of Ottawa and part of the IASC Fellow organizing team.

The participants were then split into four smaller break-out groups which discussed their research experiences in Northern Communities together with one of the invited experts. Each group was moderated by an IASC fellow and was asked to create a list of Do`s and Don`ts for working with communities in Arctic research. These lists were then gathered and discussed with the overall group.

Results

A lively exchange between all workshop participants and experts resulted in a diverse list of Do`s and Don`ts of Arctic research. These included, considerations of: (1) the research design and early planning; (2) the contribution of science to northern communities; (3) the relationship of researchers and indigenous people; (4) communication and overall impression of visiting scientists; and (5) ways to include local people in the research process (Figure 1).

Conclusion

Representatives of several Arctic communities and student participants from across the globe participated in a collaborative and fruitful discussion which resulted in a set of best practices on how to maintain strong research partnerships with Northern Communities. Overall, this workshop was a great example of strategy development to enhance knowledge transfer between scientists and indigenous communities.

Acknowledgments

We would like to thank all workshop participants of the Permafrost Young Researcher Workshop at ICOP2016 who contributed their ideas and facilitated a fruitful discussion.

We gratefully acknowledge IASC for making this effort possible through their Fellowship program (granted to E. Kuznetsova, L.-P. Roy, E. Choy, R. Way, K. Brown, J. Lenz) and granting additional financial support through accepting an IASC cross-cutting proposal. The general workshop organization was enabled by support from the Alfred Wegener Institute (AWI), International Permafrost Association (IPA), BOLIN Centre for Climate Research, Potsdam Graduate School (PoGS), Climate and Cryosphere (CliC) and Permafrost Young Researchers Network (PYRN).

Figure 1. Word cloud created with *wordle* visualizing the most frequently mentioned terms in the lists of Do`s and Don`ts of Arctic Research.

Lessons learned from mapping permafrost vulnerability in northern communities

Louis-Philippe Roy
Katerine Grandmont
Cyrielle Laurent
Bronwyn Hancock
Fabrice Calmels

Northern Climate ExChange / Yukon Research Centre (Yukon College), Whitehorse, Yukon, Canada, lroy@yukoncollege.yk.ca

Abstract

Northern communities across Canada are concerned with permafrost thaw and its potential effects on their hunting and gathering areas, habitat, trails and traveling routes. They have been traveling on and living from these traditional lands for generations. Many community members are now worried that landscape changes will affect their ability to access traditional foods and interact with their land. Over the years, the NCE/YRC has worked on many projects on landscape vulnerability classification in northern communities of Yukon and NWT. These studies integrated science into decision-making by merging geoscience data and traditional knowledge to create an easily interpretable representation of vulnerability to potential future change. Inspired by our successful partnership with the communities, we here present examples of community-based permafrost vulnerability mapping. We hope the lessons learned during the development of these projects can serve as tools and examples for researchers and early career researchers who work with northern communities, to have a fruitful experience and increase resilience of northern communities.

Keywords: Community based research; Permafrost; Vulnerability mapping; Traditional knowledge; Food security

Introduction

Climate change is a significant challenge for northern communities, where the impacts of a warming climate are already having considerable and tangible effects. Many people living in small, often isolated communities are concerned about climate-related risks in their region. Because adverse impacts are a reality, it is important to implement climate change adaptation strategies. Since 2012, the Northern Climate ExChange (part of the Yukon Research Centre at the Yukon College, Yukon) has been involved in multiple community-based adaptation planning projects set in Yukon and the Northwest Territories. Eight communities (Figure 1) have been or are investigated and studied in collaboration with the community members to produce landscape vulnerability maps in relation to a changing climate, to orient community development and develop adaptation strategies.

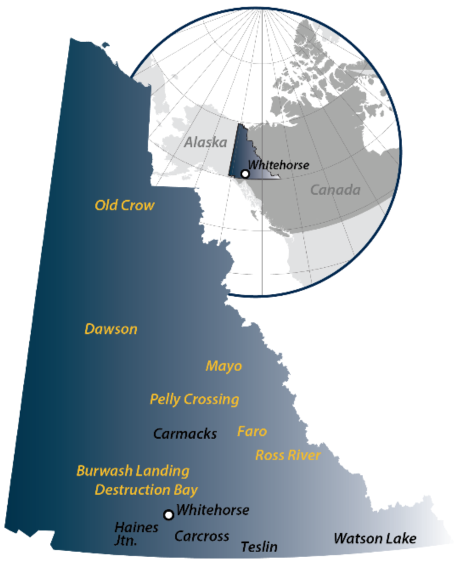

Figure 1. Location of investigated communities.

Community-based mapping - Project Development

In elaborating these projects, we made it a priority to involve the community members and build from their needs and knowledge. We developed an approach that incorporates local community concerns and infrastructure, traditional knowledge, land-disturbance history, permafrost distribution and characteristics, surficial geology conditions and hydrology.

The method we have elaborated for these studies in detailed in *Benkert et al. 2016*. The first stage involves conducting interviews with community members and leaders to define the areas of concern and determine the extent of the study area. We then integrate this information with a desktop analysis that incorporates existing data and newly gathered field data. Meetings with the community leaders are set to evaluate the results. Following validation, we present the final maps to the community and elaborate on our findings.

Lessons learned

Building on our experience working with Yukon and NWT communities over the years, here are some of the lessons we have learned.

- **Engaging First Nation communities in the early stages of the project**. Ideally, the community should take part in the elaboration of the project and be invited to participate in the submission of the funding proposal. If not, it is essential that they be involved in planning the schedule and project activities. The community then becomes an integral part of the project and can be actively involved in decision-making.

- **Employing community members as field assistant and community liaison**. By doing so you create links with a larger group of community members and provide inside knowledge of day-to-day activities and community operations. The community liaison will be your eyes on the ground outside of the field season. They could also help with fieldwork logistics, make arrangements for meetings and accommodation, and participate in report writing. The involvement of your research field assistant in the installation of monitoring sites and operation will allow them to keep the sites running and operating during and after the completion of the project and build capacity within the community.

- **Plan initial site visits with knowledgeable community members**. Ask them questions about their land in relation to your project to help narrow down your sites selection. The community may also have concerns or particular knowledge about some areas which will help prioritize the sites that should be studied and reflect the community's needs.

- **Offer training and/or workshops related to the project to build capacity in the community**. This can be for youth and/or other interested community members and can include: GPS training, field data collection, monitoring, basic mapping skills, and introduction to aerial photography interpretation. This helps raise awareness of the project on the particular topics that are studied in the community.

- **Organise a community dinner or lunch to communicate your results**. This is a nice gesture towards the community that welcomed you during your research. You can take the opportunity to display maps and posters about your project and discuss the results and findings of your research with the community.

We firmly believe that long-term projects can only benefit from the initial and ongoing involvement of the communities where they are set. Our approach is still evolving as we continue to find new ways to better work with the communities.

Acknowledgments

We would like to thank members of the Vuntut Gwichin, Ross River, Trondek Hwechin, Kluane, Selkirk Na-Cho Nyak Dun and Jean Marie River First Nation for supporting and participating in these projects and welcoming us on their lands and within their Traditional Territory.

References

Benkert, B.E., Kennedy, K., Fortier, D., Lewkowicz, A., Roy, L.-P., de Grandpré, I., Grandmont, K., Drukis, S., Colpron, M., Light, E., Williams, T. 2016. Old Crow landscape hazards: Geoscience mapping for climate change adaptation planning. *Northern Climate ExChange*, Yukon Research Centre, Yukon College. 136 p. and 2 maps.

Calmels, F., Laurent, C., Watertight Solution., Ireland, M., 2015. How Permafrost thaw may impact food security of Jean Marie River First Nation, NWY. *Proceedings of the Seventh Canadian Permafrost Conference*, Québec, Canada, September 20-23.

Jean Marie River First Nation, Calmels F., and Watertight Solutions ltd. Food Security Vulnerability Assessment Related to Permafrost Degradation in the JMRFN. Report 2014.

Flood zones delineation in Arctic river delta, Case study on Krasnoe settlement, Pechora river, Russian Federation

Alexey P. Vergun[1]
Pavel N. Terskii[2]
Mikhail O. Fatkhi[2]
Kirill K. Zhbakov[2]
Olga V. Gorelits[2]
Igor V. Zelmlianov[2]

[1]*Moscow State University, Laboratory of Geoecology of the North, alvergun@mail.ru*
[2]*Zubov State Oceanographic Institute*

Abstract

The research is focused on natural floods investigation based on hydrologicalal analysis and flood zones delination for arctic settlement in Pechora river delta (Russian Federation). Statistical approach to hydraulic calculations and field-based data allowed authors to produce reasonable applied flood zones delineation result.

Keywords: flood zones, water levels, Pechora, Arctic region of Russia

Introduction

The problem of periodic flooding is quite urgent in a number of localities on the territory of Russia In arctic regions access to people suffering by floods may be hardly limited due to undeveloped infrastructure and extreme natural conditions during spring flood period. Nowadays in Russia the state program on flood zone delineation for populated areas is carried out .

Krasnoe settlement is situated behind the Arctic Circle on the Pechora river delta (in Nenets province of Russian Federation). The settlement population count is 1470 people. This part of the Pechora river catchment refers to the Kaninsk-Timan geocryological region, to the discontinuous permafrost sub-zone and is located in relief depression. River valley and river bed are surrounded by through-type hydrogenic-radiative talic, saturated with pieces of frozen rocks. The village of Krasnoe is surrounded by water bodies on three sides connected to the Pechora River.

Methods

To determine the boundaries of flood zones, it is necessary to create a digital elevation model (DEM) and to calculate the maximum water levels with different probabilty.

DEM based on the georeferenced and digitized detailed-scale map of Krasnoe settlement using structure contours and height marks. The DEM was verified and updated using geodetic methods during field work session in 2017.

To calculate water levels along delta branches it requires initial water levels data at the top of the delta (Oksino hydrological gauging station). Water level distribution was calculated in two stages:

- Compilation of water surface longitudinal profiles in the defined orthometric height system from the data of several gauges.
- Respectively water level graphs are plotted using extremum values (minimum or maximum). So it should be used for longitudinal water level interpolation between gauging stations for extremum conditions.

The maximum water levels calculation for Krasnoe was carried out using water level measurement series for the Pechora River delta gauges (Oksino, Naryan-Mar, Oskolkovo). Empirical and analytical probability distribution curves were constructed with the use of the software complex "Hydrocalc" based on the gamma distribution of Kritsky-Menkel (Methodological…, 2005). The method of moments used to determine the parameters of the curves. Based on these curves, the values of maximum low probability water levels (with 1, 3, 5, 10, 20, 25 and 50% probability) were calculated. These values were correlated to the absolute elevations of the Baltic elevation system. Based on calculated maximum water levels, water surface profiles were created taking into account the distance between Krasnoe settlement and gauges in Pechora delta.

Flood zones caused by low probability water levels are delineated using special self-made software package called "Flood zones" developed by authors in Zubov State Institute of Oceanography. "Flood zones" package based on ESRI ArcGIS, QGIS, Hydrocalc, Python and C++ scripts and models meets the requirements of Russian hydrological regulatory acts (Terskii et.al, 2017).

Results

According to cadaster map of Russian Federation (RF) flooding affects 555 registered units of Krasnoe including 340 land plots, 80 buildings and 135 economic installations. Also flood zone covers 16 km of roads and dozens of electricity and pipe lines. According to General plan of settlement development until 2027 floodzone caused by 50% probability water level covers 80 different constructions in Krasnoe and 1% probability – 433.

Flood zones delineated for Krasnoe in 2017 are used for ground water short dynamics modeling and also to modify human activity legislation in Nenets administrative region.

Acknowledgments

We thank the Nenets province Department of Environmental Management and Krasnoe settlement administration head for assistance during field work session.

References

Methodological recommendations for determining the calculated hydrological characteristics in the presence of hydrometric observations. 2005. St. Petersburg, State Hydrological Institute, 103 p.

Krasnoe Settlement official webpage, www.pksovet.ru

Terskii, P.N., Fatkhi, M.O., Tsyplenkov, A.S., Zemlyanov, I.V., Gorelits, O.V., Pavlovskiy, A.E., 2017. Flood zones delineation for Moscow city rivers. *Georisk*, #3, p.20-29.

Living with Permafrost: Community engagements and outreach products

Kenji Yoshikawa[1]
Member of the Education and Outreach committee[2]
[1]*University of Alaska Fairbanks, kyoshikawa@alaska.edu*
[2]*International Permafrost Association*

Abstract

As awareness of permafrost continues to grow within the research community and the general public, and as permafrost communities continue to live with changing conditions, it is crucial to integrate citizen science, mass media, and outreach as an important part of our duties. We, the International Permafrost Association's (IPA) Standing Committee on Education and Outreach introduce on materials and activities designed for the general public in indigenous, rural, and urban communities. In addition, we welcome contributions about how communities and individuals live, work, and play in permafrost landscapes, many of which are changing rapidly. We are not limited to permafrost scientists as we encourage contributions from individuals from any organization striving to improve permafrost knowledge beyond the traditional educational framework and, it is also important to train local communities living on permafrost to improve their understanding of permafrost.

Keywords: Education and Outreach committee; local government; indigenous communities; rural communities; permafrost education; citizen science

Introduction

In November 2017, the permafrost archive book "*Permafrost in Our Time*, into a Russian version "*Мерзлота в наше время*" was released.

Figure 1. Russian (left) and English (right) version of permafrost temperature archive book "*Permafrost in Our Time*" for local governments and schools. Both editions covered all of the Arctic regions.

This was not simply a translation of the English-language, *Permafrost in Our Time*, but includes primarily examples from Siberian villages, many indigenous communities. This Russian version of Permafrost in Our Time covered many of the permafrost temperatures in Siberia and other Russian territories from Chukotka to the Kola Peninsula. We are visiting over 500 schools and communities in the Arctic (red dots on figure 2).

Figure 2. Visited schools and borehole sites

All Arctic communities visited in Eurasia are covered in Russian version book, and information about them is combined with information on Arctic communities visited in North America, reported in *Permafrost in Our Time* (in English).

Outreach example: Ice cellar design and temperature data

When we think of the Arctic indigenous people and permafrost connections, ice cellar would be a directly relationship for their life. Ice cellars (Lednik in Russian, Bulus in Sakha, Sigruaq in Inupiat) dug into the permafrost layer are a natural form of refrigeration for preserving block ice for drinking water, storing harvested food (fish, game meat, whale and livestock such as reindeer), and fermenting food. Ice cellars are traditionally used by indigenous Arctic people, such as Siberian Even, Evenk, Chukchi, Yukagir, Dolgan, and North American Inupiat, Yupik, Inuit. Though ice cellars are widely used in permafrost regions, these structures and the purpose for their use as well as the methods of maintenance are quite different among the communities and due to permafrost temperature conditions. Monitoring ice cellar temperatures and recording descriptions of ice cellars is important in the face of climate change in terms of permafrost studies and archiving traditional techniques of living with permafrost. We visited over 500 communities including Mongolian, Even, Evenk, Chukchi, Yukagir, Dolgan, Inupiat, Yupik, and Inuit, where we discussed local ice cellars with residents (Figure 3).

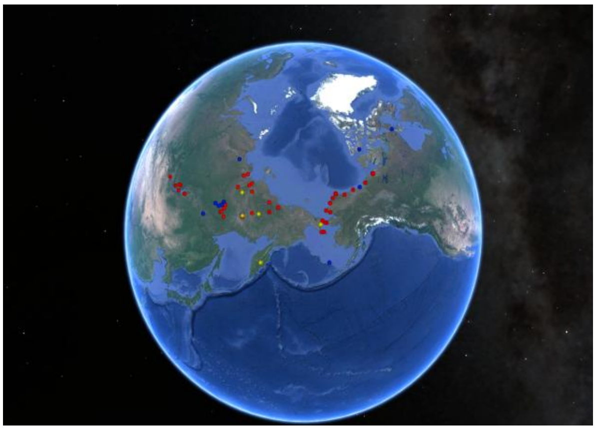

Figure 3. Ice cellar visited and temperature monitoring sites

Contemporary cellars in northern Sakha and North America regions are built primarily for the personal use of one or several families (such as a fishing/whaling crew and their dependents), and typically consist of a vertical shaft that leads to a small chamber or horizontal tunnel excavated into permafrost (Figure 4).

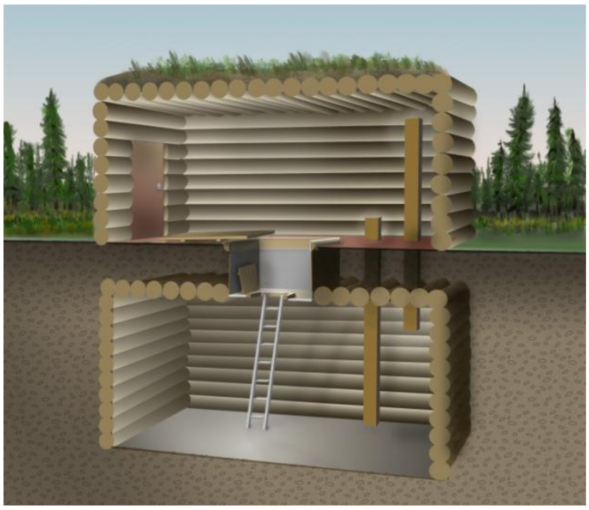

Figure 4. Vertical type cellar mainly used northern regions.

Older ice cellars or ones in southern permafrost areas are built primarily for personal use, and typically consist of a 15 to 20 degree declining tunnel entrance that leads to a small chamber excavated into permafrost or seasonally frozen soil (Figure 5).

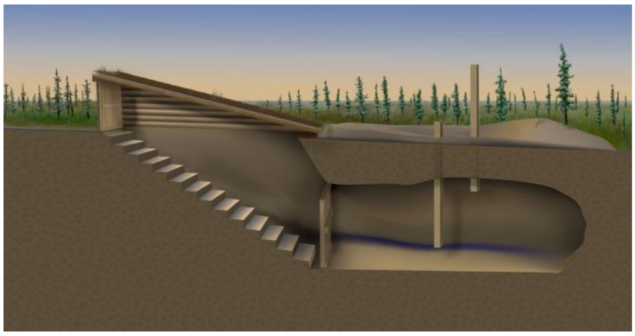

Figure 5. Horizontal type cellar mainly used southern regions or central yakutia.

The depth of the chamber is 1–3 m from the ground surface. This type of cellar is similar in design to European wine and food cellars or icehouses, and provides easy access and maneuvering of what has been stored.

Ice cellars are an important cultural and economic resource for residents of Arctic communities. Each community has its own problem of permafrost and usage of the cellar. Understanding of the cellar temperature, design and distribution aids future environmental adaptations.

17 - Subsea Permafrost Dynamics

Session 17

Subsea Permafrost Dynamics

Conveners:

- **Martin Stendel**, Danish Meteorological Institute, Climate and Arctic Research, Copenhagen, Denmark
- **Paul Overduin**, Alfred Wegener Institute, Helmholtz Centre for Polar and Marine Research, Potsdam, Germany
- **Matteo Puglini**, Max Planck Institute for Meteorology, Hamburg, Germany (PYRN member)

Large regions of the Arctic Shelf are underlain by permafrost. This permafrost formed during previous glacial cycles when low sea levels exposed the coastal plains. The marine transgression that followed the Last Glacial Maximum (from about 18 to 5 ka BP) resulted in the present-day coastal shelf and its relict terrestrial permafrost. These permafrost sediments contain organic carbon and greenhouse gases, some in gas hydrate form. Cold temperatures stabilize gas hydrates and limit bacterial turnover, and low diffusivities associated with frozen sediment trap gas below and within the permafrost. The warming that followed transgression and that results from ongoing climate change may therefore release large amounts of greenhouse gases to the overlying shelf sea, sea ice and atmosphere if the subsea permafrost thaws. Recent publications have broadened our knowledge of the arctic shelves and permafrost distribution, but observations are rare and unevenly distributed, and our process understanding is incomplete. Modelling of subsea permafrost and its potential degradation have produced a wide range of results.

In this session, we invite contributions that advance our understanding of the temporal evolution of subsea permafrost, both in past climates and under future climate change as well as contributions on observations of greenhouse gases and gas hydrates over the arctic shelves. Contributions are welcome that advance the development of models of subsea permafrost, including their parameterizations. New observation techniques and treatment of archive observations, measurements of gas fluxes or gas concentrations and studies of past and future climate including degradation of submarine permafrost are also welcome.

Geophysical surveys of sub-aquatic permafrost: talik dynamics and the influence of a freshwater to saltwater lake transition

Michael C. Angelopoulos[1,2], Pier Paul Overduin[1], Jens Strauss[1], Guido Grosse[1,2], Bennet Juhls[1]
Mikhail Grigoriev[3], Georgi Maximov[3]
[1]*Alfred Wegener Institute Helmholtz Centre for Polar and Marine Research, Potsdam, Germany*
[2]*Institute of Earth and Environmental Sciences, University of Potsdam, Potsdam, Germany*
[3]*Melnikov Permafrost Institute, Russian Academy of Sciences, Siberian Branch, Yakutsk, Russia*

Abstract

To investigate the fate of terrestrial thermokarst becoming flooded with saltwater, geophysical, thermal, and borehole activities were carried out at Polar Fox Lake on the Bykovsky Peninsula in the Laptev Sea. Polar Fox Lake is a former lake basin that became connected to the Laptev Sea through a natural drainage channel and was partially inundated by saltwater, forming the initial stage of a thermokarst lagoon. In the lake centre where no lake ice grounding occurs, winter borehole and temperature data from April 2017 show frozen sediment below salty unfrozen cryotic sediment. This hints that the talik might be very slowly re-freezing in the centre. Resistivity measured in July 2017 suggest that the talik is also re-freezing below a salt diffusion layer in shallow waters where lake ice grounding occurs in winter.

Keywords: Sub-aquatic permafrost, saline permafrost, talik, electrical resistivity, coastal, Siberia

Introduction

The degradation of sub-aquatic permafrost could release large quantities of methane into the atmosphere and impact offshore drilling. Sub-aquatic permafrost thaw depends on the duration of inundation, warming rate, the coupling of the bed to the atmosphere through bottom-fast ice, and brine injections into the sediments (Overduin et al., 2012). The impact of brine injections on permafrost degradation is dependent on salinity in the water column, which can vary seasonally. Due to the complex interplay of these processes and the lack of field observations, the fate of terrestrial thermokarst submerged with saltwater is uncertain (e.g. Shakhova *et al.,* 2017). The general hypothesis is that salty water depresses the freezing point and thus generates sub-zero water temperatures below the ice cover in winter, which could refreeze the talik if insufficient salt diffuses into the sediment. To test this hypothesis, two boreholes (27.5 m and 5.5 m deep below the lakebed) were drilled at the centre of a 3.4 m deep and 67 ha large saltwater lake (Polar Fox Lake) located within a partially drained freshwater lake basin connected through a drainage channel to the Laptev Sea on the Bykovsky Peninsula in Siberia (Fig. 2) in April 2017. Furthermore, a temperature chain was temporarily installed and sediment samples were collected for porewater chemistry tests. In July 2017, electrical resistivity surveys were undertaken to map unfrozen and frozen sediment beneath the lake and on the exposed portion of the basin separating the saltwater Polar Fox Lake from the northern freshwater lake.

Electrical resistivity tomography (ERT) has been shown to be effective at delineating unfrozen and frozen sediments, because there is an increase in electrical resistivity as water freezes to form ice (e.g. Kneisel et al., 2008). The resistivity of sub-aquatic permafrost soils is highly dependent on porosity, grain size, temperature, and porewater salinity, all of which affect unfrozen water content. We here present first data from ERT CTD, and temperature measurements at the Polar Fox Lake site.

Methods

For all six water resistivity surveys, apparent resistivity was sounded at 1 to 5 m intervals using an IRIS Syscal Pro Deep Marine (ISPDM). A 120 m cable with floating electrodes (each separated by 10 m) was towed behind a small inflatable boat. The ISPDM was equipped with a GPS and an echo sounder to record the position and water depth at the boat locations. In total, two current electrodes and 11 potential electrodes were used in a Reciprocal Wenner-Schlumberger array. On the land bridge, multiple soundings were carried out at 3 locations. These soundings were made with an IRIS Syscal Pro system, a 10 m electrode spacing, as well as both Reciprocal Wenner Schlumberger and Wenner arrays. The data was inverted with RES2DINV using a robust inversion, a 0.25 vertical to horizontal flatness filter ratio, and a fixed water resistivity of 12 ohm.m (Ω).

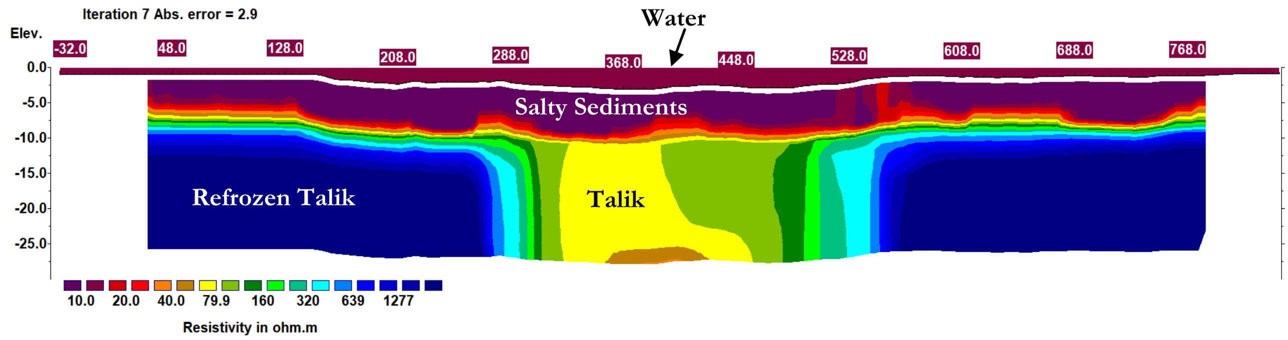

Figure 1. Southeast to northwest floating electrode resistivity survey at Polar Fox Lake.

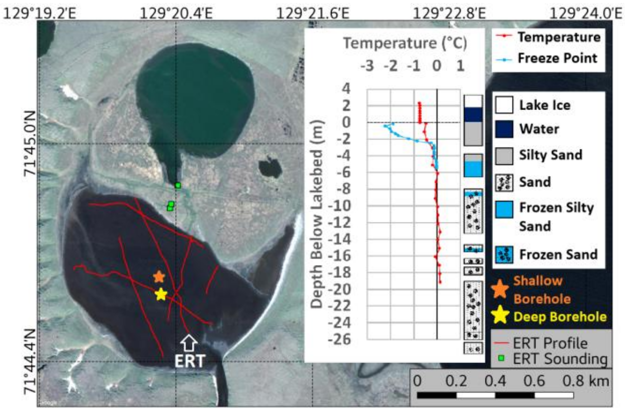

Figure 2. Polar Fox Lake borehole and resistivity survey locations and temperature data. While the southern part of the basin connects to the Laptev Sea through a drainage channel in the SE corner of Polar Fox Lake, the northern part of the basin remains a freshwater lake.

The deep borehole was drilled 27.5 m below the lakebed (BTLB). Then, a 19 m GeoPrecision temperature cable with an accuracy of 0.1 °C and a resolution of 0.01 °C was installed for 5 days. The cable contained 20 nodes each spaced by 1 m and the first node was located 0.1 m BTLB. The temperatures were corrected for drilling heat effects and sensor calibration. Water temperatures were measured with a conductivity, temperature, and depth (CTD) sensor. The shallow borehole was drilled 5.5 m BTLB and sediment cores were collected for porewater extraction and electrical conductivity tests to determine the freezing point.

Results

The deep borehole log shows silty sands in the upper 8 m of sediment overlying sands until the final depth (Fig 2). The log also shows frozen sediment between 4.7-6.6 m and 8.3-8.8 m below the lakebed. Water temperatures were near -0.8 °C and sediment temperatures increased until 10 m below the lakebed, below which temperatures were mostly above 0 °C. In the upper 2.3 m of sediment, the negative temperatures are well above the freezing point (derived from porewater electrical conductivity).

The summer resistivity profile in Fig. 1 shows four distinct regions: 1) a water layer with a resistivity of 12 Ω (measured with CTD), 2) a low resistivity zone (<20 Ω) above an elevation (el.) of 5 m, 3) a medium resistivity zone (70-100 Ω) from 288-528 m and <5 m el., and 4) two high resistivity zones (>1000 Ω) from both 0-288 m and 528-768 m at <5 m el. The low resistivity zone is likely salty sediments produced from salt diffusion into the lakebed. The medium resistivity zone is located in deeper waters (i.e. no ice grounding in winter) and is thus similar to the borehole conditions. This zone is likely a remnant of the talik from the original freshwater lake prior to the salty lake transition. Unlike the borehole, Fig.1 does not show thin frozen soil segments in the lake centre, possibly due to inadequate ERT resolution. However, the high resistivity zones could represent refrozen taliks. These zones are located in shallower waters (<= 1.5 m deep) where ice grounding can occur in winter and thus generate rapid cooling. The resistivity is the same order of magnitude of the land soundings, which show resistivities of >5000 Ω. The frozen sediment borehole observations suggest that talik refreezing might also be occurring in non-grounded ice zones, but at a much slower rate.

Acknowledgments

This study was additionally supported by ERC #335338.

References

Kneisel, C., et al., 2008. Advances in geophysical methods for permafrost investigations. *Permafrost Periglacial Processes* 19(2): 157-178.

Overduin, P.P., et al., 2012. Geoelectric observations of the degradation of nearshore submarine permafrost at Barrow (Alaskan Beaufort Sea). *J Geophys Res* 117.F2.

Shakhova, N., *et al.* 2017. Current rates and mechanisms of subsea permafrost degradation in the East Siberian Arctic Shelf. *Nature comm.* 8: ncomms15872.

Submarine permafrost development modelled at the circum-Arctic scale

Pier Paul Overduin, [1]
Thomas Schneider von Deimling[1]
Mikhail N. Grigoriev[2]
Bennet Juhls[3]
Hugues Lantuit[1]
Sebastian Westermann[4]
[1]*Alfred Wegener Institute Helmholtz Centre for Polar and Marine Research, paul.overduin@awi.de*
[2]*Mel'nikov Permafrost Institute, Siberian Branch, Russian Academy of Sciences*
[3]*Space Sciences Institute, Freie Universität Berlin*
[4]*Department of Geosciences, University of Oslo*

Abstract

Submarine permafrost is a key component of the permafrost-carbon climate feedback, but very poorly constrained. The current state and distribution of permafrost on the Arctic shelves are largely unknown, aside from regions for which industry data are available. Nor are there reliable estimates of the amount of organic matter and, more immediately important, greenhouse gas, below and within submarine permafrost. Both knowledge gaps stem from a paucity of observational data. An understanding of the dynamics of inundated terrestrial permafrost, however, would advance our understanding of the role submarine permafrost plays in the global climate system. Specifically, how resilient is submarine permafrost to shelf water warming and freshening and shifting sediment dynamics? And what are the implications for energy and mass fluxes from submarine permafrost under future changing conditons?

Keywords: subsea permafrost, Arctic, continental shelf, paleoclimate, numerical modelling.

Description of Work

Submarine permafrost has been mapped based on Last Glacial Maximum (LGM) ice extent, global sea level history and modern bathymetry. Marine regression and transgression histories determine relict subsea permafrost distribution at the circum-Arctic scale. The current map represents permafrost presence or absence, reflecting the probable distribution of cryotic sediments based on current oceanography. Improving our representation of submarine permafrost via consistent modelling of relevant physical processes at a circum-Arctic scale is the goal of this study.

We modelled submarine permafrost development for up to the past 450 ka using distributed reconstructions of air temperature and ice sheet dynamics from the CLIMBER 2 model, mapped geothermal heat fluxes and available sea level histories, combined with modern bathymetry and topography. The numerical model is a branch of the 1D heat flow CRYOGRID2 model. Sea level reconstructions and sedimentation history drove surface temperature histories. Assumed glacial, marine and terrestrial sedimentation rates provided the basis for shelf stratigraphy, but ignored the influence of coastal erosion, isostasy and neo-tectonics. Sediment freezing was included an osmotic potential term.

The resulting map provides a first order estimate of permafrost state and distribution that implies that much of the shelf can function as a cap on potential greenhouse gas stocks. We examine the evolution of permafrost in the Laptev, East Siberian, Beaufort and Barents seas, and in the Canadian Arctic Archipelago. The circum-Arctic dataset includes a map of the extent of cryotic sediment and the depth of cryotic sediment below the land or seabed. Relevant parameters such as ice saturation, which controls gas permeability and the thermal inertia of permafrost, and the enthalpy required to degrade permafrost completely, are also produced. Validation of the model includes comparison to existing sets of borehole and geophysical data.

Acknowledgments

An IPA Action Group award, a Helmholtz Joint Russian-German Research Grant (HGF-JRG100) and the EU H2020 Project *Nunataryuk: Permafrost thaw and the changing arctic coast: science for socio-economic adaptation* provide(d) support for this work.

Reactive-transport model on Arctic shelves: a focus on subsea permafrost affected sediments

Matteo Puglini[1,2]
Victor Brovkin[1]
Sandra Arndt[2]
[1]*Max Planck Institute for Meteorology, Hamburg (Germany). matteo.puglini@mpimet.mpg.de*
[2]*Université Libre de Bruxelles, Brussels (Belgium)*

Abstract

Arctic sediments are expected to contain a large quantity of methane and to be underlayered by subsea permafrost, a carbon stock whose extent is unknown and whose biogeochemical properties have not been explored yet. High methane concentrations (up to 500 nM) have been measured in the waters corresponding to the East Siberian Arctic Shelf [1], but its origin is still debated [2, 3], whether originating from methanogenetic degradation of organic matter stored in thawing subsea permafrost or from the destabilization of gas hydrates occurring below the Arctic shelves [4].

While some purely geophysical simulations of subsea permafrost vertical and lateral extent are available, no diagenetic biogeochemical model has been developed so far. Here we present the first setup of such a model: a version of the Biogeochemical Reaction Network Simulator (BRNS) [5] specifically tailored to simulate Arctic shelves and its typical processes. Our simulations aimed at describing such an environment: a sediment column threaded by an upgoing flow of water rich in methane nourishing a microbial community that is able to perform Anaerobic Oxidation of Methane (AOM). This last process, unlike the Aerobic Oxidation of Methane (AeOM) [6], increases alkalinity and, in an iron rich environment as the Arctic shelves, triggers a biogeochemical reaction network, which may lead to pyrite and authigenic carbonate precipitation. The latter is a distinguishing feature associated with methane seepage and can provide an indication of temporal dynamics of the AOM which, upon comparison with field samples, could serve as a proxy to reconstruct sediment diagenetic history or to validate the model itself. The version of BRNS we implemented goes beyond the simplification which describes AOM as a second order reaction, but envisages a kinetic as well as thermodynamic constraint on it [7].

We focused our attention on the effects that the presence of methane has on the biogeochemistry of the sediment column, assessing the efficiency of the AOM filter on oxidizing dissolved gas and testing how the explicit bioenergetic limitations affect the process. We will present how a methane release, *e.g.* as aftermath of thawing subsea permafrost, alters the benthic exchange fluxes of quantities like DIC and alkalinity. Transient and equilibrium states will be also presented to show the time scale needed for the microbial community to develop and adapt to change in methane flux from below.

Keywords: subsea permafrost; sediments; methane; AOM; reactive-transport model

References

1. Shakhova, N. *et al.,* 2014. Ebullition and storm-induced methane release from the East Siberian Arctic Shelf. *Nature Geoscience* 7.1: 64-70.
2. Sapart, C. J. *et al.,* 2017. The origin of methane in the East Siberian Arctic Shelf unraveled with triple isotope analysis. *Biogeosciences* 14.9: 2283.
3. Overduin, P. P., *et al.,* 2015. Methane oxidation following submarine permafrost degradation: Measurements from a central Laptev Sea shelf borehole. *Journal of Geophysical Research: Biogeosciences* 120.5: 965-978.
4. Ruppel, C. D. & Kessler, J.D., 2016. The interaction of climate change and methane hydrates. *Reviews of Geophysics*
5. Aguilera, D. R. *et al.*, 2005. A knowledge-based reactive transport approach for the simulation of biogeochemical dynamics in Earth systems. *Geochemistry, Geophysics, Geosystems* 6.7.
6. Biastoch, A. *et al.*, 2011. Rising Arctic Ocean temperatures cause gas hydrate destabilization and ocean acidification. *Geophysical Research Letters* 38.8
7. Dale, A. W. *et al.*, 2008. Methane efflux from marine sediments in passive and active margins: estimations from bioenergetic reaction-transport simulations. *Earth and Planetary Science Letters* 265.3: 329-344.

Subsea Permafrost Climate Modeling – From uncertainty estimates to estimates of future permafrost degradation

Christian B. Rodehacke[1,2]
Martin Stendel[2]
Dmitry J. Nicolsky[3]
Sergey Marchenko[3]
Jens Hesselbjerk Christensen[4,5]
Vladimir E. Romanovsky[3]
[1]Danish Meteorological Institute, Copenhagen, Denmark, cr@dmi.dk
[2]Alfred Wegener Institute for Polar and Marine Research, Germany
[3]Geophysical Institute, University of Alaska Fairbanks, USA
[4]Climate Physics, Niels Bohr Institute,University of Copenhagen, Denmark
[5]Uni Research Climate, Bergen, Norway

Abstract

Does increased methane release indicate wide-spread thawing of subsea permafrost over the East-Siberian-Arctic-Shelf? Since the physical properties of the ground largely determine this release, ground conditions are central. We simulate the East-Siberian-Arctic-Shelf's subsea permafrost reaction to changing climate conditions by extending an ensemble of simulations covering the last glacial-interglacial cycle into the future.

Only very few attempts to model the vulnerability of subsea permafrost have been made, because they require additional processes (eg. ocean transgression and forcing histories, freezing dependence on salt) beside common boundary conditions (eg. ground heat fluxes and water fraction in the sediments). We capture the complexity of these not well-constrained forcings and their combinations by running a large ensemble that are forced by plausible boundary conditions.

Since our ensemble map the multi-dimensional phase space, we can estimate the likelihood of future permafrost degradation and its timing depending on integrated uncertainties of past and present environmental conditions.

Keywords: Subsea permafrost; East Siberian Arctic Shelf; Permafrost Modeling; Projection

Introduction

Observations show increasing methane concentrations over the East Siberian Arctic Shelf (ESAS). Methane is currently trapped under permafrost at the bottom of the shelf sea. Does this release already indicate thawing of the ESAS subsea permafrost? If this is the case, a substantial fraction of the stored amount of carbon and methane could be released into the atmosphere, thus enhancing the greenhouse effect and leading to further permafrost degradation.

Since the physical properties of the ground largely determine the release and its timing, ground conditions are of prime interest to address questions about future conditions. We simulate the future fate of the ESAS subsea permafrost with regard to changing climate conditions by extending model simulations into the future that cover the last glacial-interglacial cycle until present-day.

Only very few attempts to address the vulnerability of subsea permafrost have been made and in contrast to land permafrost modeling, any attempt to model the future fate of subsea permafrost needs to consider several additional factors. In particular the dependence on different ocean transgression and forcing histories, variations in the salt content and its impact on the freezing temperature and other seabed properties have a decisive impact, beside the more common boundary conditions, such as ground heat fluxes and column amount of water in the sediments. We capture the complexity of these not well-constrained forcings and their combinations by running a large number of simulations that are forced by plausible numbers of these boundary conditions.

Here we present the results of this unique approach. The wide range of applied conditions allows us to draw a map in a multi-dimensional phase space. For this the complete ensemble space of physically meaningful simulations of the contemporary state is separated into those consenting with observations and physically unrealistic ensemble members that are in discrepancy with observations. We thus span up a phase space of physically meaningful simulations based on different combinations of the forcing factors which forms the basis of future scenarios of the fate of subsea permafrost. With this ensemble approach, we can estimate the likelihood of future permafrost degradation and its timing depending on integrated uncertainties of past and present environmental conditions.

Investigating current state and mechanisms of subsea permafrost degradation and associated methane emissions in the East Siberian Arctic Shelf

Natalia Shakhova[1,2], Igor Semiletov[1,2,3], Orjan Gustafsson[4], Valentin Sergienko[5], Leopold Lobkovsky[6], Oleg Dudarev[1,3], Vladimir Tumskoy1,[7,8], Michael Grigoriev[10], Alexey Mazurov[1], Denis Chernykh[1,3], Roman Ananiev[6], Andrey Koshurnikov[7], Denis Kosmach[1,3], Alexander Charkin[1,3], Nicolay Dmitrevsky[6], Victor Karnaukh[3], Alexey Gunar[7], Alexander Meluzov[6]

[1]*National Tomsk Research Polytechnic University, 30 Prospect Lenina, 634050, Tomsk, Russia*

[2]*University of Alaska Fairbanks, International Arctic Research Center, Akasofu Building, 99775-7320, Fairbanks, USA*
[3]*Russian Academy of Sciences, Pacific Oceanological Institute, 43 Baltiiskaya Street, 690041, Vladivostok, Russia*
[4]*Stockholm University, Department of Environmental Science and Analytical Chemistry, and the Bolin Centre for Climate Research, 10691, Stockholm, Sweden*
[5]*Russian Academy of Sciences, Institute of Chemistry, 100-Letiya Vladivostoka, 690022, Vladivostok, Russia*
[6]*Russian Academy of Sciences, P.P. Shirshov Oceanological Institute, 36 Nahimovski Prospect, 117997, Moscow, Russia*
[7]*Moscow State University, 1-12 Leninskie Gory, Moscow, 119991, Russia*
[8]*Russian Academy of Sciences, Institute of Geography, 29 Staromonetniy pereulok, Moscow, 119017, Russia*

Abstract

Methane (CH_4) release from thawing Arctic subsea permafrost and from failing coastal hydrates are two climate-related mechanisms that could substantially change projected greenhouse gas forcing within this century. Variability of CH_4 fluxes depends on the current state of subsea permafrost, which is undergoing destabilization caused by the long-lasting warming effect of inundation by seawater at the beginning of the Holocene. The observed range in CH_4 emissions associated with different degrees of subsea permafrost disintegration implies substantial and potent emission enhancement in the ESAS as the process of subsea permafrost thawing progresses coastward with time. Increasing storminess and rapid sea-ice retreat causing increased CH_4 fluxes from the ESAS are possible new climate-change-driven processes accelerating over time due to the current process of Arctic warming. The range of modern CH_4 emissions from the seafloor in the ESAS serves as a baseline for monitoring future dynamics in CH_4 fluxes from the Arctic shelf.

Keywords: Subsea permafrost, methane emissions, sea ice, new climate-change-driven processes, East Siberian Arctic Shelf

Introduction

Sustained CH_4 release to the atmosphere from thawing Arctic permafrost is a positive and likely significant feedback to climate warming (ACIA, 2005). Atmospheric venting of CH_4 from the East Siberian Arctic Shelf (ESAS) was recently reported to be on par with flux from the Arctic tundra and suggested to be determined by the current state of subsea permafrost, which contains large pre-formed CH_4 deposits within and underneath it (Shakhova *et al.*, 2014; 2015; 2017). However, the future scale of these releases remained unclear, because the current state of subsea permafrost and its future dynamics are largely unknown. Poor knowledge of the physical and chemical processes occurring within subsea permafrost, combined with a lack of observational data for model calibration, restricts further progress in subsea permafrost modeling, which remains the main source of data for prognostic scenarios about subsea permafrost degradation and associated CH_4 fluxes.

Mechanisms of subsea permafrost degradation

The following factors were suggested to determine the evolution of subsea permafrost after inundation: duration of submergence compared to duration of previous exposure above the sea surface; thermal state and thickness of permafrost before inundation; coastal morphology and hydro- and lithodynamics; shoreline configuration and retreat rate; pre-existing thermokarst accompanied by formation of thaw lakes; bottom water temperature and salinity; and sediment composition, including ice content (Overduin *et al.*, 2007).

The role of taliks

Interpretation of high-resolution seismic imagery suggested that submerged thaw-lake taliks may not freeze; instead, they may keep developing, creating pathways for ascending gas (Shakhova *et al.*, 2014, 2017). Such pathways propagating throughout the entire permafrost body could allow vigorous CH_4 venting, if over-pressured gas reservoirs beneath are unroofed. One possible mechanism for preventing taliks from freezing and/or causing talik formation could be groundwater flow through coastal sediments, especially in the areas underlain with the faults. This could cause formation of so-called tectono-genic taliks (Romanovskii 1983).

The role of ice-scouring

Another permafrost destabilization mechanism, specific to the shelf system, is ice scouring, which mechanically disintegrates the upper frozen and/or thawed sediment layers. Ice scouring was observed as a ubiquitous morphological feature, not only of the shallow part of the ESAS but also offshore (Shakhova *et al.*, 2017). Ice scouring is evidenced by a long, linear, relatively-straight furrow a few tens of meters wide extending for many tens of kilometers. In the ESAS, ice scouring penetrated as much as 10m into the sediments, and where surface sediments were underlain with free gas, strong ebullition to the water column through the scours was observed (Shakhova et al., 2017).

Rates of permafrost degradation

The first comprehensive scientific re-drilling to show that subsea permafrost in the near-shore zone of the ESAS has a downward movement of the ice-bonded permafrost table (IBPT) of ~14 cm yr^{-1} over the past 31-32 years. We calculated that IBPT deepening rates from the time of inundation until 1982-1983 varied from 3.9 to 8.5 cm yr^{-1} with a mean rate of 5.7 ± 2.8cm yr^{-1}, less than half as much as IBPT deepening rates observed during the last 31-32 years (Shakhova *et al.*, 2017).

Gas movement through sediments

In the marine environment, low-amplitude seismic anomalies, referred to as washed-out or semi-blanked zones, are associated with the presence of gas in sediments; in permafrost, these anomalies may also result from physical property variations or changes associated with talik development (Ramachandran, K. *et al.*, 2011). High-resolution seismic surveys along the same transect in two subsequent years allowed to record the top boundary of the observed acoustic anomaly moving upwards by ~5-7m in the course of just one year (Shakhova *et al.*, 2017).

Permafrost-associated CH_4 emissions

The recently reported range of modern CH_4 emissions from the seafloor in the ESAS serves as a baseline for monitoring future dynamics in CH_4 fluxes from the ESAS (Shakhova *et al.*, 2015). It was suggested that within the range of observed fluxes (2003-2017), the lowest fluxes are associated with an initial degree of subsea permafrost thawing, observed in the shallow shelf outside the areas affected by faults, rivers, and pre-existing thermokarst. The highest rates observed over the areas of hot spots are representative of local subsea permafrost disintegration that takes place in areas subjected to development of deep/open taliks due to increased fault-related geothermal flux and/or river heat-induced flux and/or thermokarst progression after submergence. Triple-isotope signature of CH_4, releasing in the different areas of the ESAS, varies significantly and reflects specific features of the sources (Sapart et al., 2017). The observed range in CH_4 emissions associated with different degrees of subsea permafrost disintegration implies substantial and potent emission enhancement in the ESAS as the process of subsea permafrost thawing progresses coastward with time.

References

1. Arctic Climate Impact Assessment (2005) Impacts of a Warming Arctic, Chapter 4: Future Climate Change: Modeling and Scenarios, Cambridge University Press, 99-150.
2. Shakhova, N., et al., 2014. Ebullition and storm-induced methane release from the East Siberian Arctic Shelf. *Nat. Geosci* 7, DOI:10.1038/NGEO2007.
3. Shakhova et al., 2015. The East Siberian Arctic Shelf: Towards further assessment of permafrost-related methane fluxes and role of sea ice. *Philos. T. R. Soc. A* **373**, 20140451.
4. Shakhova *et a*l., 2017. Current rates and mechanisms of subsea permafrost degradation in the East Siberian Arctic Shelf. *Nat. Commun*, 8, 15872, doi: 10.1038/ncomms15872
5. Overduin, P.P. et al., 2007. Hybberten, H.-W., Rachold, V., Romanovskii, N., Grigoriev, M., & Kasymskaya, M. in Coastline Changes: Interrelation of Climate and Geological Processes (eds Harff, J., Hay, W. W., and Tetzlaff, D. M. 426, 97-111..
6. Romanovskii, N.N., 1983. Undergound waters of cryolithozone (Moscow State University, Moscow..
7. Ramachandran, K. *et al.*, 2011. Imaging permafrost velocity structure using high resolution 3D seismic tomograph. *Geophysics* **76 (5)**, B187-B198.
8. Sapart et al., 2017. The origin of methane in the East Siberian Arctic Shelf unraveled with triple isotope analysis. *Biogeosciences,* 14, 9, 2283-2292

Organic matter composition across subsea permafrost thaw horizons

Birgit Wild[1,2]
Tommaso Tesi[3]
Hanna Joß[1]
Natalia Shakhova[4,5]
Oleg Dudarev[5,6]
Vladimir Tumskoy[7,8,9]
Igor Semiletov[4,5,6]
Örjan Gustafsson[1,2]

[1]*Department of Environmental Science and Analytical Chemistry, Stockholm University, Stockholm, Sweden, birgit.wild@aces.su.se*
[2]*Bolin Centre for Climate Research, Stockholm University, Stockholm, Sweden*
[3]*Institute of Marine Sciences, National Research Council (ISMAR-CNR), Bologna, Italy*
[4]*University of Alaska Fairbanks, International Arctic Research Center, Fairbanks, USA*
[5]*National Tomsk Research Polytechnic University, Tomsk, Russia*
[6]*Russian Academy of Sciences, Pacific Oceanological Institute, Vladivostok, Russia*
[7]*Moscow State University, Moscow, Russia*
[8]*Russian Academy of Sciences, Institute of Geography, Moscow, Russia*
[9]*University of Tyumen, Tyumen, Russia*

Abstract

Rapid thaw of subsea permafrost on the Arctic Ocean shelves might promote the degradation of vast amounts of organic carbon (OC) to the greenhouse gases CO_2 and CH_4. Based on three drill cores, we show that OC and lignin contents of subsea permafrost in the Buor Khaya Bay on the East Siberian Arctic Shelf are lower than of lacustrine and Ice Complex Deposits, but similar to fluvial deposits of similar age in the region. Organic C content and decomposition proxies (OC/TN ratios, $\delta^{13}C$ values, lignin phenol ratios) did not show systematic changes across the permafrost table that would indicate progressing decomposition upon thaw. We conclude that decomposition of thawing subsea permafrost organic matter in this region is likely slow. Nevertheless, subsea permafrost thaw might promote the escape of CH_4 from deeper deposits by providing new gas migration pathways.

Keywords: Subsea permafrost; organic matter decomposition; methane; biomarker; lignin; permafrost carbon feedback

Introduction

Subsea permafrost extends over large areas across the Arctic Ocean shelves and is rapidly thawing due to natural and anthropogenic climate warming. Recent observations from the Buor Khaya Bay on the East Siberian Arctic Shelf (ESAS) suggest a deepening of the ice-bonded permafrost table (IBPT) of on average 14 cm year^{-1} over the past three decades in this region (Shakhova *et al.*, 2017), highlighting the need to constrain the amount of organic carbon (OC) currently stored in subsea permafrost, and its fate upon thaw. Organic matter in subsea permafrost is protected from degradation while frozen, but might be converted to the greenhouse gases CO_2 and CH_4 when thawed, possibly inducing a positive feedback to global warming.

Aims and approach

This study focusses on organic matter and its degradation at the current thaw front of subsea permafrost. Based on OC and total N (TN) contents, $\delta^{13}C$ values of OC and lignin phenols measured at high depth resolution above and below the IBPT of three subsea permafrost cores from the Buor Khaya Bay, we (1) describe the content and decomposition state of organic matter in thawing subsea permafrost, (2) assess changes in organic matter properties across the IBPT, and thus (3) constrain the potential contribution of organic matter decomposition in thawed subsea permafrost to CH_4 production in the study area.

Organic matter properties and changes upon thaw

Subsea permafrost in the Buor Khaya Bay was characterized by low OC (0.7 ± 0.2 wt% mean ± standard deviation; n = 153) and lignin contents (6.5 ± 5.7 mg g^{-1} OC; n = 40), and low mineral surface area. Comparison with fluvial, lacustrine and Ice Complex Deposits of similar age at near-by sites (Schirrmeister *et al.*, 2011) might indicate a fluvial deposition regime.

High-resolution samples from above and below the current IBPT represent a continuum from OC that has been frozen since the Pleistocene, to OC that has been thawed during the most recent twenty years. OC contents and decomposition proxies (OC/TN ratios, $\delta^{13}C$ values, lignin phenol ratios) in our cores showed no systematic changes with depth that would indicate progressing decomposition upon thaw.

Conclusions

Our biomarker approach permits assessing the decomposition of thawing subsea permafrost under in situ conditions, for a time frame of up to twenty years. We conclude that decomposition is likely slow and might not contribute substantially to the high concentrations of CH_4 observed in ESAS waters. However, subsea permafrost thaw might promote the escape of CH_4 from deeper deposits by providing new gas migration pathways. Our study represents a first step towards a better understanding of subsea permafrost vulnerability upon thaw, and the potential contribution of organic matter decomposition in thawing subsea permafrost to greenhouse gas emissions of a warming Arctic.

References

Schirrmeister, L. *et al.*, 2011b. Fossil organic matter characteristics in permafrost deposits of the northeast Siberian Arctic. *J. Geophys. Res. Biogeosci.* 116: G00M02.

Shakhova, N. *et al.*, 2017. Current rates and mechanisms of subsea permafrost degradation in the East Siberian Arctic Shelf. *Nat. Commun.* 8: 15872.

18 - Deep permafrost - From local to global influences

Session 18

Deep permafrost - From local to global influences

Conveners:

- **Jens Strauss**, Periglacial Research Unit, Alfred Wegener Institute Helmholtz Centre for Polar and Marine Research, Potsdam, Germany (PYRN member)
- **Gustaf Hugelius**, Department of Physical Geography & Bolin Centre of Climate Research, Stockholm University, Stockholm, Sweden
- **Mathias Ulrich**, Institute for Geography, Leipzig University, Leipzig, Germany

Due to potential impacts and feedback mechanisms on the Earth system, deep ice-rich permafrost dynamics have become a focal point in sub-Arctic and Arctic research. For this session 'deep' includes permafrost from below the active layer down to approximately 50 m below surface. In these deposits, high ground-ice content (e.g. ice wedges and pore ice) and its associated vulnerability to surface subsidence may lead to landscape changes that impact local communities' livelihood and infrastructure. In addition to local human-permafrost interaction, large stocks of thaw-vulnerable frozen organic matter in deep permafrost deposits are expected to have a key influence on the global permafrost-climate feedback. Thus, there is an urgent need to (1) enhance the understanding of deep permafrost thawing and degradation processes, and (2) combine physical and social sciences in permafrost research. In this session, we aim to include studies about deep permafrost and its interactions with physical, ecological, and social- economic processes in a changing Arctic. This includes a variety of methods (e.g. sediment sampling, remote sensing, modelling, or community and traditional knowledge) and interdisciplinary studies on ground-ice origin, cryostratigraphy, modelling climatic sensitivity, mapping, paleopedology, and paleoclimatology for assessing local and regional impacts on northern communities, infrastructure, wildlife, as well as global influences like organic matter decomposition and release.

Soil carbon and nitrogen stocks in Arctic river deltas: New data for three Northwest Alaskan deltas

Matthias Fuchs[1,2], Guido Grosse[1,2], Josefine Lenz[1,3], Jens Strauss[1], Ingmar Nitze[1,2], Loeka L. Jongejans[1], Benjamin M. Jones[4], and Donald A. Walker[5]

[1] *Alfred Wegener Institute Helmholtz Centre for Polar and Marine Research, Potsdam, Germany, matthias.fuchs@awi.de*
[2] *Institute of Earth and Environmental Sciences, University of Potsdam, Potsdam, Germany*
[3] *Institute of Northern Engineering, University of Alaska Fairbanks, Fairbanks, USA*
[4] *U.S. Geological Survey, Alaska Science Center, Anchorage, USA*
[5] *Alaska Geobotany Center, Institute of Arctic Biology, University of Alaska Fairbanks, Fairbanks, USA*

Abstract

Arctic river deltas are dynamic and rapidly changing permafrost environments in a warming Arctic. Our study presents new data on permafrost carbon and nitrogen stocks from 26 soil permafrost cores collected from the Noatak, Kobuk and Selawik river deltas in Western Alaska. We analyzed 318 samples for total carbon (TC) and total nitrogen (TN). Average landscape-scale carbon storage is 50.1 ± 7.8 kg C (both organic and inorganic) and 2.4 ± 0.3 kg N m^{-2} (0-200 cm). This totals 67 ± 11 Mt C and 3.3 ± 0.6 Mt N in the first two meters of soil in the Noatak, Kobuk and Selawik deltas combined. Our findings demonstrate that Arctic river deltas are important regions of permafrost soil carbon storage and need to be considered in panarctic permafrost carbon estimations.

Keywords: Permafrost carbon, upscaling, deep deposits

Introduction

Arctic river deltas are dynamic and rapidly changing permafrost environments. In addition, they are long-term depositional environments that formed over the Holocene and therefore may contain a significant carbon and nitrogen pool in the circum-arctic permafrost region. So far, only limited data are available for the major arctic river deltas in the latest carbon estimation (91 +/- 52 Pg) for the permafrost region (Hugelius *et al.*, 2014). Small arctic river deltas are largely overlooked but likely contribute substantially to soil and nitrogen storage in arctic river deltas (e.g. Ping *et al.*, 2011; Fuchs *et al.*, in prep.).

This study aims to enlarge the carbon and nitrogen data from Arctic river deltas and enhance the understanding of the size of the carbon pool stored in deltaic deposits in permafrost regions. Here we present soil C and N data for the Noatak, Kobuk and Selawik river deltas in northwest Alaska.

Study sites and methods

The Noatak (67.04°N; 162.45°W), Kobuk (66.75° N; 161.29°W) and Selawik (66.58°N; 160.05°W) river deltas are located in Northwest Alaska close to the town of Kotzebue. The three deltas are characterized by continuous (Noatak and Kobuk) and discontinuous (Selawik) permafrost (Jorgenson *et al.*, 2008). Their surface areas are 190, 410, and 1260 km² for the Noatak, Selawik, and Kobuk river delta, respectively.

We collected 26 soil permafrost cores to a depth of 2 m in August 2016. The active layer was excavated, measured and sampled with a fixed volume cylinder prior to drilling the permafrost deposits with a SIPRE auger of 2 inch (5.08 cm) diameter. Soil cores were described, subsampled in the field, and transported cool to the laboratory.

In total, 318 individual soil samples were analyzed for total carbon and total nitrogen in the laboratory. Mean soil carbon (SC) and soil nitrogen (SN) stores were calculated for each permafrost core for the reference depths 0-30 cm, 0-100 cm, and 0-200 cm. Mean values for the different deltas were then calculated and later used to upscale SC and SN stocks for the three river deltas.

Results and discussion

Mean active layer depth, mean TC and TN, as well as mean volumetric ice content are presented in Table 1 for the three different Arctic river deltas. The high standard deviations indicate the wide spread of the data, especially in TC content which ranges from 0.6 to 55%.

Mean total soil carbon and soil nitrogen data indicate higher SC and SN values for the Noatak river delta compared with the two other deltas for all reference depths (Table 2 and 3).

Based on average carbon and nitrogen contents from each core and on the spatial extent of the river deltas, total study area stocks are 67 ± 11 Mt C and 3.3 ± 0.6 Mt N excluding water body areas from the analysis. This results in a landscape mean of 50.1 ± 7.8 kg C m^{-2} and of 2.4 ± 0.3 kg N m^{-2} for these small, but prominent northwest Alaska river deltas in the first two meter of soil.

Our study shows the importance of including small Arctic river deltas in future permafrost carbon and nitrogen estimations. The dynamic nature of river deltas and the high C and N values for 0-200 cm present a significant carbon and nitrogen pool, especially considering that Arctic deltaic deposits are significantly deeper than only two meters (Hugelius *et al.*, 2014). Therefore, besides additional soil cores, information on the depth of deltaic deposits would strongly enhance the carbon pool estimations for Arctic river deltas in future.

Table 1: Mean active layer (AL), total carbon (TC), total nitrogen (TN) and volumetric ice content (± standard deviation) for the three deltas

River delta	Mean AL depth [cm]	Mean TC [%]	Mean TN [%]	Vol. ice content [%]
Noatak	34 ± 2	11 ± 14	0.5 ± 0.6	55 ± 13
Kobuk	47 ± 16	11 ± 15	0.6 ± 0.9	56 ± 14
Selawik	47 ± 5	17 ± 17	0.6 ± 0.5	60 ± 12
Average	44 ± 13	12 ± 15	0.5 ± 0.6	56 ± 14

Table 2: Mean profile soil carbon in kg C m^{-2} (± standard deviation) for the reference depths 0-30 cm, 0-100 cm, 0-150 cm and 0-200 cm

River delta	0-30 cm	0-100 cm	0-150 cm	0-200 cm
Noatak	19 ± 5	41 ± 12	52 ± 14	63 ± 15
Kobuk	16 ± 3	34 ± 8	40 ± 8	49 ± 8
Selawik	12 ± 4	35 ± 7	40 ± 6	48 ± 5
Average	16 ± 4	36 ± 10	44 ± 11	54 ± 12

Table 3: Mean profile soil nitrogen in kg N m^{-2} (± standard deviation) for the reference depths 0-30 cm, 0-100 cm, 0-150 cm and 0-200 cm

River delta	0-30 cm	0-100 cm	0-150 cm	0-200 cm
Noatak	0.9 ± 0.3	2.1 ± 0.8	2.6 ± 0.9	3.0 ± 0.9
Kobuk	0.8 ± 0.2	1.8 ± 0.4	2.1 ± 0.4	2.5 ± 0.3
Selawik	0.3 ± 0.2	1.3 ± 0.4	1.6 ± 0.3	2.1 ± 0.3
Average	0.7 ± 0.3	1.8 ± 0.6	2.2 ± 0.7	2.6 ± 0.6

Acknowledgments

We thank the Nana Corperation and the US FWS staff in Kotzebue for supporting field work, Jim Kincaid from Northwestern Aviation and Jim Webster from Websters Flying Service for providing critical field logistics, and Paul Göckeritz and Dyke Scheidemann for help with sample processing. This study was supported by ERC Starting Grant #338335 and the Initiative and Networking Fund of the Helmholtz Association (#ERC-0013). M.F. was further supported by the Swiss National Science Foundation, Project Nr. P1SKP2_171784.

References

Fuchs, M., Grosse, G., Jones, B.M., Strauss, J., Baughman, C., & Walker, D.A., in prep. Carbon and nitrogen storage in two small permafrost-dominated Arctic river deltas in northern Alaska.

Hugelius, G., Strauss, J., Zubrzycki, S., Harden, J. W., Schuur, E. A. G., Ping, C.-L., Schirrmeister, L., Grosse, G., Michaelson, G. J., Koven, C. D., O´Donnell, J. A., Elberling, B., Mishra, U., Camill, P., Yu, Z., Palmtag, J., & Kuhry, P., 2014. Estimated stocks of circumpolar permafrost carbon with quantified uncertainty ranges and identified data gaps, *Biogeosciences* 11, 6573-6593, doi:10.5194/bg-11-6573-2014.

Jorgenson, M.T, Romanovsky, V., Yoshikawa, K., Kanevskiy, M., Shur, Y., Marchenko, S., Brown, J., & Jones, B., 2008. Permafrost characteristics of Alaska — a new permafrost map of Alaska. In: Hinkel K.M. (ed), *Proceedings of the 9th International conference on permafrost*. Institute of Northern Engineering, Fairbanks, University of Alaska: 121–122.

Ping, C.-L., Michaelson, G. J., Guo, L., Jorgenson, M. T., Kanevskiy, M., Shur, Y., Dou, F., & Liang, J., 2011. Soil carbon and material fluxes across the eroding Alaska Beaufort Sea coastline. *Journal of Geophysical Research*: 116,G02004, doi:10.1029/2010JG001588, 2011.

Organic carbon stored in a thermokarst affected landscape on Baldwin Peninsula, Alaska

Loeka L. Jongejans[1], Jens Strauss[1], Josefine Lenz[1,2], Francien Peterse[3], Kai Mangelsdorf[4], Matthias Fuchs[1,5] and Guido Grosse[1,5]

[1]Alfred Wegener Institute Helmholtz Center for Polar and Marine Research, Potsdam, Germany, loeka.jongejans@awi.de

[2]University of Alaska Fairbanks, Institute of Northern Engineering, Fairbanks, USA

[3]Utrecht University, Department of Earth Sciences, Utrecht, Netherlands

[4] Helmholtz Center Potsdam - German Research Center for Geosciences, Potsdam, Germany

[5] University of Potsdam, Institute of Earth and Environmental Sciences, Potsdam, Germany

Abstract

As Arctic warming continues and permafrost degrades, more organic carbon (OC) will be decomposed in high northern latitudes. Still, uncertainties remain in the quality and quantity of OC stored in permafrost. This study presents OC data from permafrost deposits on the Baldwin Peninsula, West-Alaska. We analyzed cryostratigraphical, biogeochemical and biomarker parameters of yedoma- and drained thermokarst lake basin (DTLB) deposits as well as thermokarst lake sediments to identify the size and quality of OC pools in ice-rich permafrost. Here we show that two thirds of soil OC in this region are stored in frozen DTLB deposits and that the lake sediments have the highest volumetric OC content. The n-alkane distribution shows, however, that OC stored in yedoma is of higher quality than that stored in DTLB deposits. These findings highlight the importance of molecular OC analysis for determining the potential future greenhouse gas emissions from thawing permafrost.

Keywords: Arctic, thermokarst lake development, organic carbon, biomarkers, biogeochemical cycling

Introduction

The Arctic region is especially vulnerable to climate change as it is warming twice as fast as the global mean (Overland et al., 2014). Rapid and large-scale permafrost degradation in ice-rich permafrost, such as late Pleistocene yedoma, may contribute additional positive feedbacks to atmospheric warming. With climate warming, previously freeze-locked OC can be decomposed resulting in increased greenhouse gas emissions into the atmosphere. It is therefore highly relevant to characterize the OC pools so that the vulnerability and amount of OC in thawing permafrost soils can be determined. By analyzing sediment samples from yedoma, drained thermokarst lake basins (DTLB), and thermokarst lakes we aim to estimate the size and quality of the subsurface OC stored in our study region.

Study sites and methods

The study site is located at the western coast of the Baldwin Peninsula, Northwest Alaska (66°40'N, 162°15'W). The Baldwin Peninsula is characterized by continuous permafrost and consists of a sequence of marine, glaciomarine and glacial sediments that are well exposed along coastal bluffs (Huston et al., 1990; Pushkar et al., 1999). During field reconnaissance in summer 2016 we identified several exposures with fine-grained, ice-rich permafrost deposits and large syngenetic ice wedges that we classified as typical yedoma. A large portion of the peninsula has been affected by severe permafrost degradation and multiple thermokarst lake basin generations are also visible in satellite imagery.

In order to characterize OC pools in the study area, field sampling of one yedoma coastal bluff, three DTLB coastal bluffs and coring of a thermokarst lake was carried out in summer 2016. In total, 81 samples have been collected. We analyzed the cryostratigraphy (absolute ice content, bulk density BD), biogeochemistry (total organic carbon TOC, total nitrogen TN, C/N, stable carbon isotopes $\delta^{13}C$) and biomarkers (*n*-alkanes) of the three different landscape units. We analyzed the CPI (carbon preference index), an n-alkane derived index, to assess the quality of OC. In addition, we estimated the OC budget by using deposit thickness and coverage, wedge-ice volume (WIV), BD and TOC (Table 1).

In a final step, a land cover classification map was made of Baldwin Peninsula in order to calculate the coverage for each landscape unit.

Table 1: Input organic carbon budget calculations per landscape unit. WIV from Ulrich et al. (2014).

Landscape unit	WIV[1] [vol%]	BD [10^3 kg m^{-3}]	TOC [wt%]
Yedoma	46.3	0.80	1.9
DTLB	8.9	0.78	9.9
Thermokarst lake	0	0.78	14.4

Table 2: Volumetric and absolute OC budget estimate per landscape unit.

Landscape unit	Vol. OC budget [kg m^{-3}]	Abs. OC budget [Mt]
Yedoma	8	17
DTLB	24	36
Thermokarst lake	113	5

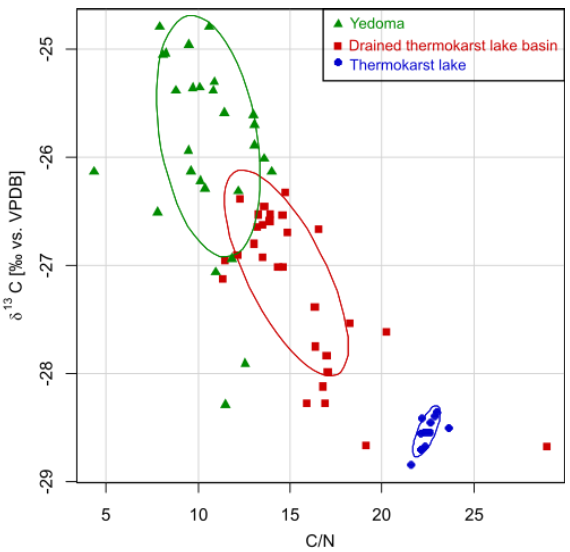

Figure 1: Scatterplot of C/N and δ¹³C per landscape unit.

Results and Discussion

We estimated the OC budget of the Baldwin Peninsula (~450 km²) (Table 2). Thermokarst lake sediments have the highest volumetric OC budget with 113 kg OC/m³ compared to yedoma deposits with only 8 kg OC/m³ and DTLB deposits with 24 kg OC/m³. These volumetric estimates fit well to previous estimates by Schirrmeister et al. (2011) and Strauss et al. (2013). Nevertheless, DTLB deposits store 70% of the OC, as they cover 65% of the area. The total OC budget of the frozen sediments on Baldwin Peninsula is 53 Mt.

An indication for the OC quality is presented in Figure 1, which shows the C/N in relation to δ^{13}C of the three landscape units. The plot shows a clear trend from low C/N and high δ^{13}C in yedoma, intermediate values for DTLB and high C/N and low δ^{13}C in the thermokarst lake sediments. We explain this trend by a combination of the origin and the state of degradation of the OC. Low C/N and high δ^{13}C in yedoma indicate low productivity and dry, cold conditions during accumulation (Schirrmeister et al., 2011). The high δ^{13}C in the thermokarst lake sediments corresponds to lake productivity (Meyers, 1994), and the high C/N reflects the freshness of the material. The intermediate values of the DTLB deposits indicate the mixed character of the heavily disturbed landscape due to thermokarst processes. The higher CPI in yedoma (mean: 11.6) compared to DTLB (mean: 8.8) indicates less degradation of OC in yedoma than in DTLB deposits. Therefore, the yedoma OC is of higher quality for future degradation.

Conclusions

The OC calculations show that two thirds of OC on Baldwin Peninsula are stored in frozen DTLB deposits and that the lake sediments have the highest volumetric OC content. However, OC stored in yedoma is of higher quality than that stored in DTLB deposits, as indicated by the CPI, indicating the higher potential of OC decomposition in yedoma deposits.

Acknowledgments

This study was carried out within the ERC PETA-CARB project (#338335). Special thanks are due to Dyke Scheidemann, Anke Sobotta and Cornelia Karger for analytical support in the lab.

References

Andersson, R.A., & Meyers, P.A., 2012. Effect of climate change on delivery and degradation of lipid biomarkers in a Holocene peat sequence in the Eastern European Russian *Arctic. Org. Geochem.* 53, 63–72.

Huston et al. 1990. Paleogeographic significance of middle Pleistocene glaciomarine deposits on Baldwin Peninsula, northwest Alaska. *Ann. Glaciol.* 14, 111–114.

Meyers, P.A., 1994. Preservation of elemental and isotopic source identification of sedimentary organic matter. *Chem. Geol.* 114, 289–302.

Overland et al., 2014. *Air Temperature,* in: Http://Arctic.Noaa.Gov/Report-Card.

Pushkar et al., 1999. Paleogeographic and paleoclimatic significance of diatoms from middle Pleistocene marine and glaciomarine deposits on Baldwin Peninsula, northwestern Alaska. *Palaeogeogr. Palaeoclimatol. Palaeoecol.* 152, 67–85.

Schirrmeister et al., 2011. Fossil organic matter characteristics in permafrost deposits of the northeast Siberian Arctic. *J. Geophys. Res. Biogeosciences* 116, 1-16.

Strauss et al., 2013. The deep permafrost carbon pool of the Yedoma region in Siberia and Alaska. *Geophys. Res. Lett.* 40, 6165–6170.

Ulrich et al., 2014. Quantifying Wedge-Ice Volumes in Yedoma and Thermokarst Basin Deposits. *Permafr. Periglac. Process.* 25, 151–161.

Deformation of permafrost strata with massive ice bodies

Anna N. Kurchatova[1, 2]
Victor V.Rogov[2, 3]
[1] *Tyumen Industrial University, Tyumen, Russia, kanni@tsogu.ru*
[2] *Institute of the Earth Cryosphere, Siberian Branch of the Russian Academy of Sciences, Tyumen, Russia*
[3] *Lomonosov Moscow State University, Moscow, Russia*

Abstract

Deformations of permafrost strata with massive ice bodies are considered from the point of view of their intrasedimental origin. Epigenetic freezing of coastal-marine sediments leads to the massive ice formation because of inversion of density and viscosity stratification with depth. Ice flows due to the gravitational instability in the direction of low pressure with changing of initially horizontal strata up to folds and intrusive stocks. The ice flow is accompanied by plastic and brittle deformation of crystalline structure and enclosing sediments. The mechanism of the process is determined by the thermodynamic conditions as well as by the tectonic activity.

Keywords: massive ice body, epigenetic freezing, rheological deformation, viscoplastic flow, thermodynamic conditions.

Introduction

Genesis of massive ice bodies is one of the greatest sources of debate in the geocryological researches. In the same case, the discordant relationship between the internal structure of the ice mass and the enclosing sediment is interpreted as buried glacier origin (glaciodislocations) and injection ice (Fortier et al., 2012). To explain the disturbances within permafrost strata researchers use the physical model of closed hydrogeological system with "huge" pressures during talik freezing. Deformations of permafrost strata with massive ice are considered in this study from the point of view of their intrasedimental origin because of inversion of density and viscosity with depth.

Study area and methods

Dislocations of permafrost strata with massive ice were studied at two key sites on the Yamal Peninsula (Western Siberia): the Marre-Sale and Bovanenkovo. The research was carried out at different scales:

Macro-level (tens of centimeters - hundreds of meters): the deformation of permafrost strata, cryogenic structures in coastal cliffs and river valleys. Meso-level (fractions of a millimeter - centimeters): the deformations of the cryogenic structure of sediments, the crystal structure of the thin sections of ice in polarized light. Micro-level (microns - fractions of a millimeter) - microstructure of sediments, cataclas of mineral grains, authigenic minerals, deformations of ice crystals (dislocations, twins) by electron microscopy and spectral microanalysis.

Results

In the sections of the marine terrace on the Yamal peninsula, the authors have established horizontal and complex massive ice bodies represented by folds, kink bands, intrusive stocks with shear cracks near the roof. Ice flow is confirmed by layers affected by boudinage and breccia. The crystal structure of ice varies regularly from laminated coarse-grained one in horizontal bodies and gentle folds to fine-grained cleavage in the vertical structures. The microstructure of ice also reflects the transition from plastic flow to brittle deformations by the appearance of crystal twins, cataclastically deformed mineral grains (Kurchatova & Rogov, 2015). The intrasedimental origin of the massive ice bodies is confirmed by the presence of marine diatoms, salt inclusions and authigenic minerals: carbonates (rhodochrosite and siderite), sulphides (marcasite), vivianite.

Discussion

Massive ice bodies form during the freezing of coastal-marine sediments characterized by interbeds of plastic-frozen clay and water-saturated sand. The increase in pore water pressure in sand leads to liquefaction under shear stress and the release of a layer of cooled water. The water freezing forms an "elementary layer" of the ice body. Freezing speed depends on water mineralization, gas saturation and influences the initial ice crystal size; shear deformation results in the layered texture (flow cleavage) that is the most common facie of the massive ice.

Stratification of the freezing sediments by ice layers (with the low density as compared with deposits) leads to the appearance of gravitational instability so ice flow in the direction of the pressure decrease, ultimately to the earth's surface, with the formation of folds and vertical structures of the type of salt and clay diapirs.

Dislocations of permafrost strata are one of the types of rheological deformation, i.e. the flow of rocks in the solid state (plastic, brittle-plastic, cataclastic, etc.). Rheological deformations of epigenetic permafrost in Western Siberia are genetically and spatially related to neotectonic structures of srike-slip deformations in the basement that determine the formation of permeability zones and vertical hydrocarbon migration (Gogonenkov & Timurziev, 2009).

Conclusion

The formation of the massive ice bodies occurs under shear stress due to the growth of pore pressure and the liquefaction of water-saturated sands during the freezing of coastal-marine sediments. The viscoplastic flow of the ground ice with the formation of complex ice bodies is due to inversion of density and viscosity stratification with depth.

The ice flow is accompanied by plastic and brittle (under the lower temperatures near the surface) deformations. Depending on the viscosity of the flow layer, the following types of movements are successively realized: plastic flow, intermittent slipping and brittle fracture.

The mechanism of the process is determined by the changing thermodynamic conditions as well as tectonic activity.

References

Fortier, D.; Kurchatova, A. N.; Jorgenson, M. T.; Godin, E.; M-Lepage, J.; Stephani, E.; Kanevskiy, M. Z.; Shur, Y. Origin of massive ice at Cape Marre-Sale, Yamal Peninsula, Siberia, Russia: contrasting views. *American Geophysical Union*, Fall Meeting 2012, abstract id. C13A-0605.

Kurchatova A.N. & Rogov V.V. Hydrocarbon seepage and formation of authigenic minerals in the permafrost of West Siberia. *Proceedings: GeoQuebec 2015,* Quebec, QC, September 20-23, 2015. http:// members. cgs.ca/documents/conference2015/GeoQuebec/papers /226.pdf.

Gogonenkov G., Timurziev A., 2009. Srike-slip deformations in the West Siberian basin and their impact of exploration and development of oil and gas reservoirs. *Central European Geology*, vol. 52. N 3: 359-390.

Distribution of mineral constituents in Yedoma permafrost: implications for Yedoma formation

Elisabeth Mauclet[1], Sophie Opfergelt[1], Arthur Monhonval[1], Jens Strauss[2], Guido Grosse[2], Matthias Fuchs[2], Lutz Schirrmeister[2]

[1]*Earth and Life Institute, Université catholique de Louvain, Louvain-la-Neuve, Belgium, sophie.opfergelt@uclouvain.be*
[2]*Alfred Wegener Institute Helmholtz Centre for Polar and Marine Research, Potsdam, Germany*

Abstract

Ice-rich permafrost deposits such as Yedoma are highly sensitive to thaw and given that they contain up to one third of the organic carbon content of the Northern circumpolar permafrost region, their degradation is considered to be a potential climate tipping point on Earth. Accurately predicting the impact of climate warming on the fate of organic carbon in Yedoma requires better constraints on the mineral element reserve in these deposits. This study provides evidence for the homogeneity of chemical composition and mineralogy of Yedoma deposits with depth. This suggests that upon deep thaw through thermokarst or thermo-erosion a high reserve in mineral nutrients is likely to be exposed also from deeper deposits.

Keywords: mineral constituents; Yedoma; thawing permafrost; Alaska; Siberia

Introduction

With thermokarst processes, Yedoma degradation not only exposes organic carbon but also mineral constituents. The exposure of a previously frozen reservoir of mineral nutrients may boost biological activity (Jansson & Tas, 2014), thereby modifying the balance between carbon input and output from these permafrost deposits. To predict more accurately the fate of organic carbon from Yedoma upon thawing, it is required to assess local variability of their mineral reserve and better understand the controlling factors on this local variability, i.e., the conditions of Yedoma formation. More specifically at the site scale, it is important to know how homogeneous the mineral reserve locked into Yedoma throughout its depositional history may be and thus how deep thaw may expose varying ranges of mineral constituents. Is the source of mineral grains in a deposit homogeneous over time? Is it a local source? This study provides preliminary data from the two major Yedoma domains in Alaska and Siberia, to contribute to answer these questions.

Study sites

Archived samples previously collected to study organic carbon stocks in Yedoma were gathered to characterize their mineral constituents. This includes samples from natural outcrops at the Colville River in North Alaska (Grosse, unpublished data), at the Itkillik River in North Alaska (Strauss *et al.*, 2012), at Buor-Khaya Peninsula in Northeast Siberia (Schirrmeister *et al.*, 2017), and from cores along a toposequence at Sobo Sise Island in the Lena Delta in Northeast Siberia (Fuchs *et al.*, 2017). A total of 117 samples were analysed in this study. The sites cover deposits from the Late Pleistocene until the early Holocene (55 000 - 8000 yr BP).

Results and discussion

Chemical composition of Yedoma

Based on the Total Reserve in Bases (TRB = total content [Ca + Mg + K + Na] measured by ICP-AES after alkaline fusion), the chemical composition of the deposits can be compared between sites. The TRB values are generally higher in Yedoma deposits from Alaska than in those from Siberia. More specifically, in Alaska, the TRB values are lower in Colville (299 to 441 $cmol_c.kg^{-1}$) than in Itkillik (460 to 579 $cmol_c.kg^{-1}$), and are dominated by Ca at ~66 % then by Mg at ~22 %. In Siberia, the two sites are characterized by TRB values in the same range (between 168 and 313 $cmol_c.kg^{-1}$), and are dominated by Na at ~32 % and Mg at ~29 %. These observations support that the chemical composition of Yedoma deposits is a local signal corresponding to the local environment of the site during deposition. The dominance of Na contribution in deposits from Siberia suggests that the sediment sources may include a marine contribution or a Na-rich mineral phase, by contrast with Yedoma from Alaska.

The evolution of the TRB with depth in the deposits corresponds to an evolution over time of deposition, knowing that the sites cover deposits from 55 000 - 8000 yr BP. The results indicate a higher variability of the TRB with depth in Yedoma from Alaska, than in those from Siberia. This could possibly be attributed to temporary changes in sediment sources during deposition in Alaska, or alternatively to post-depositional processes such as pedogenetic processes.

Implications of mineralogy for Yedoma formation

The mineralogical analyses indicate the presence of chlorite, mica, kaolinite, quartz, plagioclase in all Yedoma deposits studied, as illustrated for a Siberian site (Fig.1). Carbonates (calcite and dolomite) are detected only in deposits from Alaska, but not in those from Siberia. Together with the dominance of Ca (~66 %) in the TRB from Alaska, this observation suggests a strong contribution from carbonate sources to Yedoma deposits in Alaska, but not in Siberia.

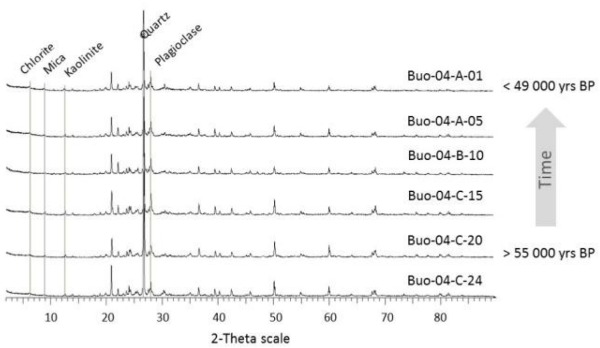

Figure 1. Mineralogy of a Yedoma deposit in Siberia, the profile Buo-04 in the site of Buor Khaya previously described and dated (Strauss *et al.* 2015).

In each deposit studied, the mineralogy is similar with depth, and hence over time (Fig.1). This observation supports the hypothesis that local sources of fine-grained material dominate contributions to the deposition. Sedimentological studies have highlighted different sediment facies types corresponding to contribution from both Aeolian and alluvial processes to Yedoma deposits (Strauss *et al.*, 2017). The homogeneous chemical composition and mineralogy observed in each site over time converge to support that the sources of fine-grained material for Aeolian and alluvial deposits are similar and are largely reflecting the local source materials and environmental conditions during Yedoma accumulation.

Conclusion

The data, at the site scale, support the homogeneity of the chemical composition and the mineralogy of Yedoma deposits with depth. This is an important parameter to take into account in the context of permafrost degradation. Given the high sensitivity of Yedoma deposits to thawing, thermokarst processes rapidly expose deep material to biogeochemical processes. This study supports that a high reserve in mineral nutrients, similar to that found at the surface, is present in deeper deposits and thus similar biogeochemical responses compared to near surface deposits maybe expected upon thawing.

Acknowledgments

Funding was received by S.O. from the European Research Council (ERC) under the European Union's Horizon 2020 research and innovation programme (ERC Starting Grant, WeThaw, grant agreement n°714617) as well as by G.G. through ERC PETA-CARB (#338335) and the Helmholtz Association's Initiative and Networking Fund (#ERC-0013).

References

Fuchs, M., Grosse, G., Strauss, J., Günther, F., Grigoriev, M., Maximov, G. M. & Hugelius, G., 2017. Carbon and nitrogen pools in thermokarst-affected permafrost landscapes in Arctic Siberia. *Biogeosciences Discuss*, doi.org/10.5194/bg-2017-173.

Jansson, J.K. & Tas, N., 2014. The microbial ecology of permafrost. *Nature Reviews Microbiolgy* 12: 414-425.

Schirrmeister, L., Schwamborn, G., Overduin, P. P., Strauss, J., Fuchs, M.C., Grigoriev M., Yakshina, I., Rethemeyer, J., Dietze, E. & Wetterich, S., 2017. Yedoma Ice Complex of the Buor Khaya Peninsula (southern Laptev Sea). *Biogeosciences* 14: 1261-1283.

Strauss, J., Schirrmeister, L., Grosse, G., Fortier, D., Hugelius, G., Knoblauch, C., Romanovsky, V., Schädel, C., Schneider von Deimling, T., Schuur, E.A.G., Shmelev, D., Ulrich, M. & Veremeeva, A., 2017. Deep Yedoma permafrost: A synthesis of depositional characteristics and carbon vulnerability. *Earth-Science Reviews* 172: 75-86.

Strauss, J., Shur, Y., Kanevskiy, M., Fortier, D., Bjella, K., Breen, A. & Johnson, C., 2012. Expedition Alaskan North Slope/Itkillik 2012, *Reports on polar and marine research – Expeditions to Permafrost 2012* Edited by Strauss, J. Ulrich, M. Buchhorn, M., Alfred Wegener Institute for Polar and Marine Research, Bremerhaven, Germany, ISSN 1866-3192, 3-28.

Strauss, J. Schirrmeister, L., Mangelsdorf, K., Eichhorn, L., Wetterich, S. & Herzschuh, U., 2015. Organic matter quality of deep permafrost carbon - a study from Arctic Siberia. *Biogeosciences* 12: 2227-2245.

Unfrozen liquid water content and long-term permafrost degradation

Dmitry Nicolsky[1]
Vladimir Romanovsky[1]

[1]*Geophysical Institute, University of Alaska Fairbanks, Fairbanks, AK 99709, djnicolsky@alaska.edu*

Abstract

Permafrost has been affected by climate warming and a wide spread of the permafrost responses is currently observed. In particular, at some locations rather slow rates of the permafrost degradations are noticed. We related this behavior to the presence of unfrozen water in frozen fine-grained earth material. We examine heat flux from the ground surface into the permafrost and discuss implications of the unfrozen liquid water content on the long-term thawing of permafrost. By conducting a series of numerical experiments, we demonstrate that the presence of fine-grained material with substantial unfrozen liquid water content at below 0°C temperature can significantly slow down the thawing rate and hence can increase resilience of permafrost to the warming events. This effect is highly nonlinear and a difference between the rates of thawing in fine- and coarse-grained materials is more drastic for lower values of the incoming into permafrost heat flux.

Keywords: unfrozen liquid water, heat flux, thawing, modeling

Introduction

Climate warming of the last half of a century resulted in many changes in all components of the Earth's system (IPCC, 2013), including the Cryosphere. Permafrost, as an important part of the Cryosphere, has been also strongly affected (Romanovsky *et al.,* 2010a, b; Vaughan *et al.,* 2013) by climate warming. Currently, a wide range of the permafrost responses is observed. Degradation of near-surface permafrost at some locations was observed as a result of climate warming (James *et al.*, 2013).

However, large ice wedges near the ground surface are commonly found at sites with undisturbed surface conditions during construction projects in the interior of Alaska where the mean ground temperature of permafrost is higher than −1°C, despite several decades of the climate warming. These ice wedges are of the Late Pleistocene age and they survived the Holocene Thermal Maximum occurred in Alaska about between 8 and 12 thousand years ago when the air temperature was by 1 or 2°C higher than now (Kaufman *et al.*, 2004; Renssen *et al.*, 2009). At other locations, where the natural or human surface disturbances occur, the permafrost first degrades relatively fast, but then its rate of thawing seems to decrease and becomes very small (Yoshikawa *et al.*, 2002). Recently Froese *et al.* (2008); Reyes *et al.* (2010) also implied on resilience of permafrost to degradation by reporting relict Middle Pleistocene ice wedges that were buried by volcanic tephra and consequently survived previous interglacial warming periods.

Unfrozen liquid water content conjecture

Romanovsky & Osterkamp (2000) related the lower rates of changes in relatively warm permafrost to the unfrozen water presence in frozen fine-grained earth material. However, we believe that an in-depth explanation of this phenomenon is warranted especially now when the changes in permafrost and specifically the rate of permafrost thawing were designated by (IPCC, 2013) as one of the major uncertainties in future climate projections.

The major driving force of permafrost warming and/or thawing is a long-term imbalance in incoming and outgoing heat fluxes at the upper boundary of permafrost integrated over a certain period of time (Williams, 1982). If more heat is coming in than going out, permafrost will be warming and eventually thawing. If the opposite is true, permafrost will be cooling, the active layer could be converting into permafrost from the permafrost table up and the thickness of permafrost may be increasing at the lower boundary of permafrost, although at a very slow rate. This heat imbalance at the permafrost table as well as the partial thawing of the interstitial ice inside the permafrost is partially responsible for a slow rate of talik formation; however, the partial thawing of interstitial ice is difficult to measure directly. Therefore, to investigate and explain the above-mentioned phenomena, we employ numerical modeling techniques and derive a semi-analytical solution to the generalized Stephan problem.

Results and Discussion

Results of our efforts show that the rate of deepening of the upper permafrost boundary in fine-grained materials could be significantly less than that for the coarse-grained materials, given all other factors are the same and the permafrost degradation just started. Furthermore, the rate is dramatically affected by the amount of the incoming heat flux. This effect is highly nonlinear and a difference between the rates of thawing in fine- and coarse-grained materials is more drastic for lower values of the incoming heat flux. For the high heat flux, the difference between these rates almost does not exist. Depending on a specific shape of the unfrozen water content curve in soil, permafrost thawing and a talik formation triggered by atmospheric warming may be delayed in fine-grained soils if compared to mineral soils of coarse-grain texture, such as sands or gravels.

We notice that while the interstitial ice may be actively thawing in the perennially frozen fine-grained sediments within a range of sub-zero temperatures (most typically between -1 and 0°C), the larger inclusions of pure ice, such as ice lenses, ice layers, and ice wedges, will not be melting at these temperatures, because their melting point is exactly at 0°C.

Since climate change history during the Holocene is represented by a series of warmer and colder periods with the duration of each less than a few centuries (Lavrushin & Alekseev, 2005, page 28), the Late Pleistocene Permafrost with massive syngenetic ice wedges imbedded into fine-grained silt sediment survived the time of the Holocene Optimum in many places around the Alaskan Interior.

Finally, we believe that representation of permafrost in global or regional climate models should include the thermal effects of unfrozen water in soils. Otherwise, the rates of permafrost thawing and degradation produced by these models will not be realistic.

Acknowledgments

We are grateful to Konstantin Khrulev and Edward Bueler (University of Alaska Fairbanks) for their advice and help with development of the analytical solution. This research was funded by the USGS award G14 AP00151, the NSF grant ARC-1304271, and by the State of Alaska.

References

Froese, D.G., Westgate, J.A., Reyes, A.V., Enkin, R.J., & Preece, S.J., 2008. Ancient permafrost and a future, warmer Arctic, *Science*, 321(5896):1648–1648.

IPCC, 2013. *Climate Change 2013: The Physical Science Basis. Contribution of Working Group I to the Fifth Assessment Report of the Intergovernmental Panel on Climate Change*, Cambridge University Press, [Stocker, T.F., D. Qin, G.-K. Plattner, M. Tig nor, S.K. Allen, J. Boschung, A. Nauels, Y. Xia, V. Bex & P.M. Midgley (eds.)], Cambridge, United Kingdom and New York, NY, USA, 1535 pp.

James, M., Lewkowicz, A., Smith, S., & Miceli, C., 2013. Multi-decadal degradation and persistence of permafrost in the Alaska Highway corridor, northwest Canada, *Environmental Research Letters,* 8(4):045013.

Lavrushin, Y., & Alekseev, M. 2005. The Arctic regions, In: Velichko, A.A. & Nechaev, V.P. (eds.) *Cenozoic climatic and environmental changes in Russia*, The Geological Society of America, Special Paper 382, 226 p.

Kaufman, D., *et al.,* 2004. Holocene thermal maximum in the western arctic (0-180°W), *Quaternary Science Reviews,* 23(56):529-560.

Renssen, H., Seppa, H., Heiri, O., Roche, D., Goosse, H., & Fichefet, T., 2009. The spatial and temporal complexity of the holocene thermal maximum, *Nature Geoscience*, 2:411-414.

Romanovsky, V., Smith, S., & Christiansen, H., 2010a. Permafrost thermal state in the polar northern hemisphere during the international polar year 2007-2009: a synthesis, *Permafrost and Periglacial Processes*, 21:106–116.

Romanovsky, V., *et al.,* 2010b. Thermal state of permafrost in Russia, *Permafrost and Periglacial Processes*, 21:136–155.

Romanovsky, V. & Osterkamp, T., 2000. Effects of unfrozen water on heat and mass transport processes in the active layer and permafrost, *Permafrost and Periglacial Processes*, 11:219–239.

Reyes, A.V., Froese, D.G., & Jensen, B.J., 2010. Permafrost response to last interglacial warming: field evidence from non-glaciated Yukon and Alaska, *Quaternary Science Reviews*, 29(2324):3256 – 3274.

Vaughan, D., *et al.,* 2013. Observations: Cryosphere. In: Stocker, T., *et al.,* (ed.), *Climate Change 2013: The Physical Science Basis. Contribution of Working Group I to the Fifth Assessment Report of the Intergovernmental Panel on Climate Change*, Cambridge University Press, Cambridge, United Kingdom and New York, NY, USA, 317–382.

Yoshikawa, K., Bolton, W., Romanovsky, V., Fukuda, M., & Hinzman, L., 2002. Impacts of wildfire on the permafrost in the boreal forests of interior Alaska, *Journal of Geophysical Research*, 107:8148.

Williams, P., 1982. *The Surface of the Earth: An Introduction to Geotechnical Science*, Longman, London, 224 pp.

The nitrogen stock of the ice-rich yedoma domain

Jens Strauss[1], Benjamin W. Abbott[2], Fabian Beermann[3], Christina Biasi[4], Matthias Fuchs[1,5], Guido Grosse[1,5], Marcus A. Horn[6] , Susanne Liebner[7] , Tina Sanders[8], Lutz Schirrmeister[1], Thomas Schneider von Deimling[1], Matthias Winkel[7], Sebastian Zubrzycki[3]

[1]*Alfred Wegener Institute Helmholtz Centre for Polar and Marine Research, Periglacial Research Unit, Potsdam, Germany, Jens.Strauss@awi.de*
[2]*Brigham Young University, Department of Plant and Wildlife Sciences, Provo, USA*
[3]*Universität Hamburg, Center for Earth System Research and Sustainability (CEN), School of Integrated Climate System, Germany* [4]*University of Eastern Finland, Department of Environmental Science, Kuopio, Finland*
[5]*University of Potsdam, Institute of Earth and Environmental Sciences, Potsdam, Germany*
[6]*Gottfried Wilhelm Leibniz Universität Hannover, Institute for Microbiology, Hannover, Germany*
[7]*GFZ German Research Centre for Geosciences - Helmholtz Centre Potsdam, Potsdam, Germany*
[8]*Helmholtz Centre Geesthacht, Centre for Materials and Coastal Research, Geesthacht, Germany*

Abstract

Recent studies on permafrost organic matter (OM) suggest that a portion of previously frozen carbon will enter the active carbon cycle as high latitudes warm. Less is known about the fate of other OM components, including nutrients such as nitrogen (N). The abundance and availability of N following permafrost thaw will regulate the ability of plants to offset carbon losses. Additionally, lateral N losses could alter aquatic food webs. There is growing evidence that some N is lost vertically as N_2O, a greenhouse gas 300 times stronger than CO_2 over 100 years. Despite broad recognition of its role regulating both carbon and non-carbon aspects of the permafrost climate feedback, estimates of permafrost N remain uncertain. To address this knowledge gap, we quantified N content for different stratigraphic units, including yedoma, Holocene cover deposits, refrozen thermokarst deposits, taberal sediments, and active layer soils. The resulting N estimates from this one permafrost region were similar in magnitude to previous estimates for the entire permafrost zone. We conclude that the permafrost N pool is much larger than currently appreciated and a substantial pool of permafrost N could be mobilized after thaw, with continental-scale consequences for biogeochemical budgets and global-scale consequences.

Keywords: Yedoma; permafrost; degradation; nitrogen pool; nitrogen cycle; climate feedback;

Introduction

Organic matter (OM) stored in permafrost constitutes a huge reservoir of carbon (C) and is an important subject in climate research. Multiple studies suggest the high potential for C release and incorporation into the active C cycle following permafrost thaw (Strauss et al., 2017). However, net ecosystem C balance in the permafrost zone depends on more than 'just' C. Many terrestrial ecosystems at high latitudes are nitrogen (N) limited, meaning that the availability of N during and after permafrost degradation could directly control the ability of plants to remove CO_2 from the atmosphere. Because many forms of N are hydrologically mobile, N liberated from permafrost could also be laterally transported to aquatic and estuarine ecosystems (Beermann et al., 2017), where it could alter food webs and productivity. Though some of these N effects could offset a portion of projected soil carbon losses, there are also risks of enhanced greenhouse gas emissions associated with great N availability. When permafrost thaws, changes in the soil profile including increased water content can create heterogeneous soil redox conditions favorable for microbial nitrification and denitrification, producing the potent greenhouse gas nitrous oxide (N_2O), as a side product of nitrification and denitrification (Elberling et al., 2010; Palmer et al., 2011; Repo et al., 2009). Despite its central importance to predicting local and global ecosystem feedbacks to climate change, relatively little is known about N stocks and composition in the permafrost zone (Keuper et al., 2012; Mack et al., 2004; Rustad et al., 2001). To address this knowledge gap, we quantified the abundance and distribution of N in the active layer and permafrost of the yedoma region of Siberia and Alaska.

Materials and methods

The yedoma domain comprises decameter thick ice-rich silts intersected by syngenetic ice wedges, which formed in late Pleistocene tundra-steppe environments, as well as other deposits resulting from permafrost degradation during the Holocene. Together, the deposits in this region constitute 7% of the total permafrost area but contain over 25% of total permafrost organic matter. Based on the most comprehensive data set of permafrost N (>1500 samples of total N content), our study aims to estimate the present pools of N in the different stratigraphic units of the yedoma domain. These are (1) late Pleistocene yedoma deposits; (2) in-situ thawed and diagenetically altered yedoma deposits (taberite); (3) Holocene thermokarst deposits; (4) Holocene cover deposits on top of yedoma and (5) the modern active layer of soils. We implemented statistical bootstrapping techniques, which resample observed values to estimate N stocks. The total mean pool size estimate was derived for each of the 10,000 bootstrapping runs, resulting in an overall estimate of mean and variance derived from 10,000 individual observation-based bootstrapping means. The conceptual formula for our nitrogen stock calculation:

$$m_{\text{TN, tot}} = \sum_{i=1}^{n} m_{\text{TN}, i} = \sum_{i=1}^{n} d_{\text{i}} \left(1 - f_{\text{wedge}, i}\right) \rho_{\text{b},i}\, c_{\text{TN},i}\, A_i$$

$m_{\text{TN, tot}}$: pool of total N in the included units,
$i = 1 \ldots n$: index numbers of the single unit considered for the N budgeting,
d_{i}: deposit thickness of unit *i*,
$f_{\text{wedge}, i}$: volume fraction of ice wedges in unit *i*,
$\rho_{\text{b},i}$: bulk density of deposits of unit *i*;
$c_{\text{TN},i}$: content of total nitrogen in deposits of unit *i*;
A_i: area of unit *i*

Results and discussion

The deposits of the yedoma domain store a much larger pool of N than previously recognized. Our estimates of permafrost N for the yedoma domain are similar in magnitude to previous estimates of N for the entire permafrost region, which were quantified with 40–60 Pg N (Harden et al., 2012; Weintraub and Schimel, 2003). This suggests that the permafrost N pool may be twice as large as currently estimated. A large portion of this nitrogen is expected to become mobilized after thaw, potentially affecting the recovery trajectory of local ecosystems and the overall magnitude and timing of the permafrost climate feedback. Possible effects of this N release include mitigation of the current nitrogen limitation of Arctic tundra ecosystems, substantial N delivery to freshwater and marine ecosystems, and additional greenhouse gas contributions from permafrost regions in the form of N_2O. In all cases, there is strong evidence that the permafrost-climate feedback will be affected by the amount and availability of this previously unquantified N.

Conclusion

The yedoma domain constitutes a large OM inventory storing several hundred Gt C, but are also known to be nutrient-rich environment due to rapid burial and freezing of plant remains. We found that the deposits of the Yedoma domain store a globally significant pool of N that may partially become activated following permafrost thaw. Future investigation of permafrost deposits should include the analysis of different nitrogen pools to clarify the potential climate feedback mechanisms of bioavailable nitrogen.

Acknowledgments

This project is integrated into the Action Group “The Yedoma Region” (funded by the International Permafrost Association (IPA). We acknowledge the support by the European Research Council (Starting Grant #338335), the German Federal Ministry of Education and Research (Grant 01DM12011 and CarboPerm: 03G0836A), and the Initiative and Networking Fund of the Helmholtz Association (#ERC-0013).

References

Beermann, F., et al, 2017. Permafrost thaw and liberation of inorganic nitrogen in eastern Siberia. *Permafrost and Periglacial Processes*, 28: 605-618.

Elberling, B., et al., 2010. High nitrous oxide production from thawing permafrost. *Nature Geoscience*, 3: 332-335.

Harden, J.W., et al., 2012. Field information links permafrost carbon to physical vulnerabilities of thawing. *Geophysical Research Letters*, 39: L15704.

Keuper, F., et al., 2012. A frozen feast: thawing permafrost increases plant-available nitrogen in subarctic peatlands. *Global Change Biology*, 18: 1998-2007.

Mack, M.C., et al., 2004. Ecosystem carbon storage in arctic tundra reduced by long-term nutrient fertilization. *Nature*, 431(7007): 440-443.

Palmer, K., et al., M.A., 2011. Contrasting denitrifier communities relate to contrasting N_2O emission patterns from acidic peat soils in arctic tundra. *The ISME Journal*, 6: 1058–1077.

Repo, M.E., et al., P.J., 2009. Large N_2O emissions from cryoturbated peat soil in tundra. *Nature Geoscience*, 2: 2189-192.

Rustad, L.E., et al., 2001. A Meta-Analysis of the Response of Soil Respiration, Net Nitrogen Mineralization, and Aboveground Plant Growth to Experimental Ecosystem Warming. *Oecologia*, 126: 543-562

Strauss, et al., 2017. Deep Yedoma permafrost: A synthesis of depositional characteristics and carbon vulnerability. *Earth-Science Reviews*, 172: 75-86.

Weintraub, M.N. & Schimel, J.P., 2003. Interactions between Carbon and Nitrogen Mineralization and Soil Organic Matter Chemistry in Arctic Tundra Soils. *Ecosystems*, 6: 0129-0143.

Vulnerability of Yedoma carbon to permafrost thaw – Insights from $^{14}CO_2$ analysis

Anja Wotte[1]
Philipp Wischhöfer[1]
Christian Knoblauch[2]
Janet Rethemeyer[1]
[1]*Institute of Geology and Mineralogy, University of Cologne, Cologne, Germany, Anja.Wotte@uni-koeln.de*
[2]*Institute of Soil Science, University of Hamburg, Hamburg, Germany*

Abstract

We performed in-situ radiocarbon (^{14}C) analysis of CO_2 respired from degrading Pleistocene aged permafrost deposits of the Siberian Arctic to evaluate the decomposability of the organic matter (OM) and to improve the prediction of CO_2 emissions during continuing thawing caused by global warming. We could show for the first time that up to 7,000 year BP old CO_2 is presently released from up to 31,000 year BP old deposits of the Siberian ice complex (Yedoma). The $^{14}CO_2$ data of permafrost deposits in which younger material is incorporated due to thermokarst and erosional processes reveals that a higher fraction of old organic carbon (OC) is degraded suggesting a positive priming effect. In contrast to previous studies, our CO_2 flux data do not indicate a higher carbon (C) release at sites with less decomposed OM.

Keywords: permafrost; respiration; radiocarbon; yedoma; CO_2; carbon.

Introduction

Pleistocene Yedoma deposits are characterized by massive syngenetic ice wedges and are widespread in Siberia and Alaska. Yedoma permafrost stores significant amounts of OC (83±12 to 129±30 Pg C; Strauss et al. 2017). Due to their high ice content, these permafrost deposits will be strongly affected by future climate change, but their vulnerability to microbial decomposition is poorly constrained (Strauss et al. 2017).

To improve predictions of C releases from these thawing deposits to the atmosphere, it is helpful to evaluate the degradability of the OM by determining fluxes as well as by identifying major OM sources of the released CO_2. Previous studies suggest that the OM in Yedoma deposits is relatively little decomposed plant material that became quickly freeze-locked and thus is expected to be easily degradable (Strauss et al., 2015).

We performed ^{14}C analysis of in-situ respired CO_2 collected from different sites on an exposed cliff of Pleistocene Yedoma deposits on Kurungnakh Island, Lena River Delta, NE Siberia. The outcrop along the river shoreline serves as a natural thermal erosional site and might provide an insight in how these ice complex deposits react towards increased global temperatures and thawing in the future.

Methods

We collected bulk sediment and CO_2 samples from different sites within the stratigraphic unit of the Pleistocene Yedoma deposits. The samples were taken from thermokarst mounds (K7 and KX), which were exposed due to thermal erosion of surrounding large syngenetic ice wedges (Fig. 1) and from sites between thermokarst mounds (K4) that consist of redistributed Pleistocene material mixed with Holocene

Figure 1. Study site on Yedoma deposits with massive syngenetic ice wedges on Kurungnakh Island.

sediments. The sites differ in bulk OM age and influences of thermokarst processes.

We determined bulk OM ^{14}C down to a depth of 45 cm and measured CO_2 fluxes using respiration chambers. The respired CO_2 was collected on molecular sieve cartridges for the subsequent ^{14}C analysis by accelerator mass spectrometry (Wotte et al. 2017). Different bulk geochemical parameters (TOC, C/N, $\delta^{13}C$) were analyzed to evaluate OM composition and stage of degradation.

Results and discussion

The oldest site is KX (up to 31 kyr BP), which is only little influenced by the input of Holocene OM in the top 10 cm (Fig. 2). K7 contains more Holocene aged OM, which is mixed into the sampled 15 cm thick layer of the thermokarst mound as reflected by younger ^{14}C ages (11–17 kyr BP). The youngest site investigated, K4 (~4 kyr BP), has the highest input of Holocene material (Fig. 2) and contains modern peat lenses at ~16 cm and ~32 cm depth. K4 has the highest TOC and C/N, and lowest ^{13}C values compared to the other sites.

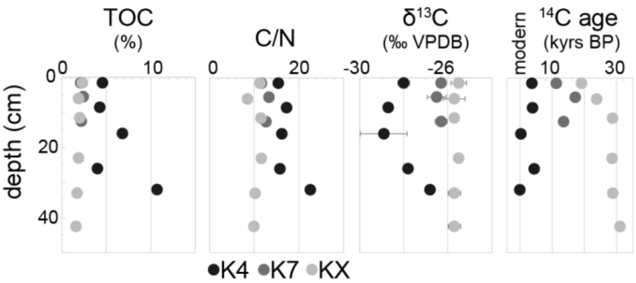

Figure 2: Profiles of TOC, C/N, $\delta^{13}C$ and ^{14}C-age.

Based on laboratory incubation experiments (Schädel et al., 2014) we expect the highest CO_2 flux at K4, the site containing the least degraded OM (highest C/N). However, we determined the highest CO_2 fluxes of 127 ± 37 µg CO_2 m^{-2} s^{-1} (n=3) at K7, which contains more strongly degraded OM as suggested by a lower C/N. Similar CO_2 fluxes of 49 ± 21 (n=6), 57 ± 5 µg CO_2 m^{-2} s^{-1} (n=5) were measured at sites K4 and KX. These results suggest that C/N alone is not sufficient to judge the degradability of the OM.

The ^{14}C age of respired CO_2 is younger than the bulk OM from which it derives: ~2.6 kyr BP at K4, 5.3 kyr BP at K7, and 5.6 kyr BP at KX. This indicates that young OM is preferentially respired by microbes. However, at the site with low degraded modern peat lenses, K4, the $^{14}CO_2$ signature is showing a higher contribution of the underlying mineral soil than at K7 and KX, which may suggest the enhanced decomposition of old OC by the input of easily degradable C (priming effect).

Overall, our results reveal that a significant fraction of old OM is released from Yedoma deposits.

References

Schädel C, Schuur EAG, Bracho R, Elberling B, Knoblauch C, Lee H, Luo Y, Shaver GR, Turetsky MR., 2014. Circumpolar assessment of permafrost C quality and its vulnerability over time using long-term incubation data. *Global Change Biology* 20:641-52.

Strauss J, Schirrmeister L, Grosse G, Fortier D, Hugelius G, Knoblauch C, Romanovsky V, Schädel C, Schneider von Deimling T, Schuur EAG, Shmelev D, Ulrich M, Veremeeva A., 2017. Deep Yedoma permafrost: A synthesis of depositional characteristics and carbon vulnerability. *Earth-Science Reviews* 172:75-86.

Strauss J, Schirrmeister L, Mangelsdorf K, Eichhorn L, Wetterich S, Herzschuh U., 2015. Organic-matter quality of deep permafrost carbon – a study from Arctic Siberia. *Biogeosciences* 12:2227-45.

Wotte A, Wischhöfer P, Wacker L, Rethemeyer J., 2017. $^{14}CO_2$ analysis of soil gas: Evaluation of sample size limits and sampling devices. *Nuclear Instruments and Methods in Physics Research Section B: Beam Interactions with Materials and Atoms* 413:51-6.

19 - Polar Coastlines in Transition: Arctic – Antarctic perspectives

Session 19

Polar Coastlines in Transition: Arctic – Antarctic perspectives

Conveners:

- **Matt C. Strzelecki**, University of Wroclaw, Poland (PYRN member)
- **Louise Farquharson**, University of Alaska Fairbanks, USA (PYRN member)
- **Boris Radosavljevic**, Alfred Wegener Institute, Germany (PYRN member)
- **Vladislav Isaev**, Moscow State University, Russia (PYRN member)

Polar coastlines make up over one third of the global total and are among the most dynamic in the world. Due to climate change polar coastlines are increasingly vulnerable to rapid change. Patterns of Arctic coastal change are mostly associated with decreased sea ice cover which is leaving coasts exposed to waves and storm action for longer each year. Additional influential factors include permafrost degradation, storm-surge flooding, and intensified sediment supply from glacierised catchments. These changes have wide-ranging impacts on circum-polar Arctic coastal communities through the destruction of culturally important sites, and modern infrastructure.

In the Antarctic region accelerated deglaciation has led to the exposure of new coastlines where permafrost-related processes and fluxes of sediments from paraglacially transformed glacial landforms control coastal dynamics.

In both regions climate warming has triggered extreme processes including accelerated permafrost thermoerosion, destabilization of coastal slopes by periglacial processes or landslides leading to formation of tsunami waves that profoundly change the functioning of fragile polar coastal environments.

This session invites submissions that will improve our understanding of polar (Arctic and Antarctic) coastal dynamics on local and regional scales. We encourage submissions focusing on both sub-aerial and sub-aqueous processes driving changes to coastal morphology, and are also interested in submissions which discuss rates of change and socio-economic impacts.

The objective of our session will be to raise interest in the topic and provide a platform for discussions on various aspects of coastal change and its impact on the resilience of polar environments and societies. We particularly encourage submission of contributions from members of ACD (Arctic Coastal Dynamics) and CACOON (Circum-Arctic Coastal Communities KnOwledge Network) groups.

Influence of massive ice beds on coastal dynamics of the Gulf of Kruzenshtern, Kara Sea

Alisa V. Baranskaya [1]
Anna V. Novikova [1]
[1]*Moscow State University, Laboratory of Geoecology of the North, alisa.baranskaya@yandex.ru*

Abstract

In the present study, we analyze dynamics of the Gulf of Kruzenshtern coasts, south-western Kara Sea, based on fieldwork data and multi-temporal satellite imagery. The influence of massive ground ice beds on coastal dynamics was also estimated. The coasts of the study area retreat mainly due to thermo-abrasion and thermo-denudation with the average rate of about 0.6 m/yr. On the segments, where massive ice beds outcrop, the rates of retreat increase to up to 1.6 m.yr^{-1}.

Keywords: coastal dynamics; thermo-erosion; massive ground ice; Kara Sea; Arctic.

Introduction

Due to wave erosion and thermal erosion, Arctic coasts composed of frozen deposits retreat with the average rates from 0.5 to 2 meters per year depending on lithology (Forbes, 2011).

Coastal dynamics are highly dependent on hydrometeorological parameters (such as, wind wave energy, as described in Ogorodov, 2011). Under the conditions of the global climate warming during the last decades, contribution of thermal and wave factors to the coastal processes has significantly grown. Increase of mean annual temperature, reduction of sea ice extent, increasing frequency of storms, and sea level rise enhance the retreat of the Arctic coasts.

Along with climatic factors, contents of permafrost and especially of ground massive ice plays a leading role in Arctic coastal dynamics. For example, it has been determined (Belova, 2015) that on the south-western coasts of the Kara Sea, coastal segments with exposed tabular ground ice retreats faster in comparison with the shorelines of adjacent areas.

Estimating rates of retreat of coasts with massive tabular ground ice outcrops in closed coastal water areas is an important fundamental task which helps to compare them with open coasts and assess the role of cryogenic structure and ground ice in velocities of coastal destruction. For such purposes, coasts of the Gulf of Kruzenstern, Western Yamal, are a perfect key area of studies.

The study area of the Gulf of Kruzenshtern is located in the southeastern part of the Kara Sea, in the west of Yamal Peninsula (Fig. 1). It is a relatively closed bay, protected from the influence of high waves of the Kara Sea by a chain of Sharapovy Koshki islands. The depth of the Gulf of Kruzenshtern does not exceed 2 m. There are several levels of topography: marine and lacustrine-alluvial terraces at the elevations of 20-35 m, 10-15 m, about 4 m and river deltas and tidal flats (laidas) at the heights up to 1.5 m.

The highest level at the altitude 20-35 m extends to the south of Mordiyakha river and near cape Yasalia (Fig. 1). It is consists of lacustrine-alluvial interbedded brown silts and badly washed fine-grained dark grey sands in its top part and of dark grey bluish non-laminated clays in its bottom part (probably glacial). The lower unit hosts massive ground ice. The ice is laminated with flowed upper contact, unconformly overlain by clays and silts. In the clays, numerous schlieres of ice up to 2 cm appear, both vertical and horizontal. The outcrops of the ground ice are up to 20-30 m long; their visible thickness reaches 2 m, which allows to classify them as massive ice beds. Similar ice has been described in the outcrops and boreholes of the near-lying Bovanenkovo area. The coasts of this terrace are mostly affected to thermo-abrasion.

Methods

The study is based on field data on geomorphology, Quaternary geology and cryogenic composition of the coasts collected in 2016 accompanied by interpretation of multi-temporal satellite imagery. To determine rates of coastal retreat, we analyzed Corona KH-4 satellite imagery (1967, spatial resolution ca. 3 m), and WorldView-1 (2010, 0.5 m). We orthorectified WV-1 image using ArcticDEM (https://www.pgc.umn.edu/data/arcticdem/).

The Corona images were referenced to WV-1 imagery and field GPS points. After that, we traced shorelines for 1967 and 2010 for abrasional segments (identifying the shoreline as the cliff top in this case) and compared them.

Results

Analysis of about 45 km of high coasts (20-35 m a.s.l.) in the Gulf of Kruzenshtern has revealed prevalent thermo-abrasion and abrasion. The average rate of retreat for the period of 1967-2010 for the whole key area was about 0.6 m/yr during. The greatest rates of retreat correspond to the coasts where we found massive ice during fieldwork – they reach up to 1.6 m/yr. Segments of thermoabrasional coasts have an average retreat rate of 0.9 m/yr.

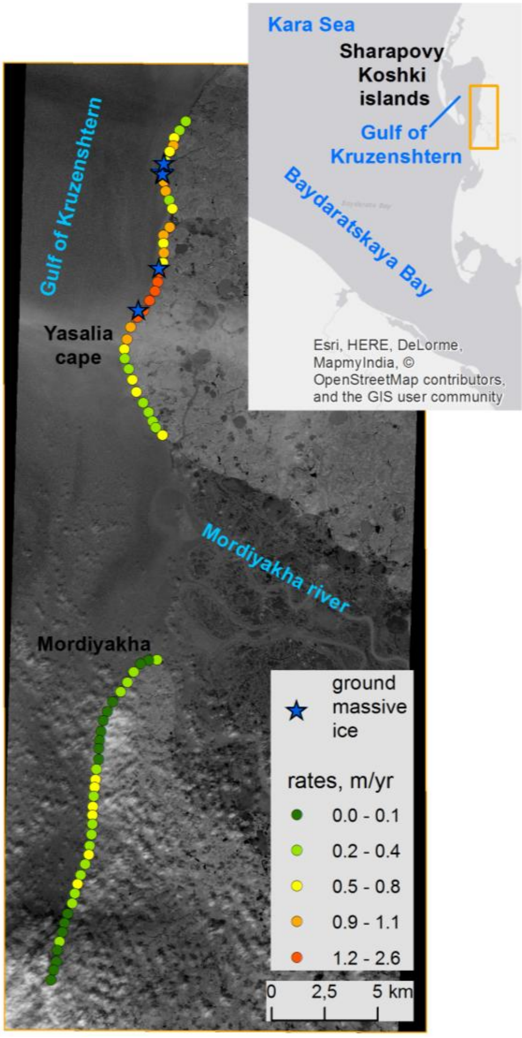

Figure 1. Retreat of the coasts of the Gulf of Kruzenshtern (base – World View-1, 2010). On the inset orange frame shows the study area.

Conclusions

The obtained rates of coastal retreat in the Gulf of Kruzenshtern (0.6 $m.yr^{-1}$) correspond to the rates typical for the Kara Sea in general (0.8-2 $m.yr^{-1}$ for open sectors and 0.2-0.7 $m.yr^{-1}$ for closed bays – according to Vasiliev *et al.*, 2006). We explain the difference in the values of retreat rates through the coast of the study area mainly by the diversity of cryogenic structure, presence of massive ice beds, and also by lithology and exposition of the coastline.

At the moment, rates of coastal retreat in the Gulf of Kruzenshtern are not catastrophic, but in case of even insignificant changes in climatic conditions, for example, with enhance of wind wave energy caused by reduction of sea ice coverage or with rise of sea level, these processes may intensify significantly.

Acknowledgments

The work was funded by the RSCF project 17-77-10130. We thank Digital Globe Foundation (http://foundation.digitalglobe.com/) for satellite imagery.

References

ArcticDEM https://www.pgc.umn.edu/data/arcticdem/

Belova, N., 2015. Massive ice of the western coast of the Baidaratskaya Bay of the Kara Sea. *Ice and snow* 130(2): 93-102 (in Russian).

Digital Globe Foundation http://foundation.digitalglobe.com/

Forbes, D.L. (ed.), 2010. *State of the Arctic Coast – Scientific Review and Outlook*. International Arctic Science Committee, Land-Ocean Interactions in the Coastal Zone, Arctic Monitoring and Assessment Programme, International Permafrost Association. Helmholtz-Zentrum, Geesthacht, Germany, 178 p. http://arcticcoasts.org

Ogorodov, S., 2011. *Role of sea ice in coastal dynamics*. Moscow University Publishing House, 173 p. (in Russian).

Vasiliev, A., Streletskaya, I., Cherkashev, G., Vanshtein, B., 2006. Dynamics of coasts of the Kara Sea. *The Cryosphere of the Earth* 910(2): 56 (in Russian).

Ground ice as a factor of coastal dynamics at south-western part of Kara Sea

Nataliya G. Belova
Daria M. Aleksyutina
Alisa V. Baranskaya
Anna V. Novikova
Stanislav A. Ogorodov
Natalia N. Shabanova

Laboratory of geoecology of the North, Faculty of Geography, Lomonosov Moscow State University, Russia

Abstract

For three key sections of the Kara Sea coast (Ural and Yamal coasts of Baydaratskaya Bay, Kharasavey Cape) the spatial variability of the of ground ice distribution (changes in ice content, massive ice occurrence) is traced. At the local level ground ice leads to high retreat rates compared to adjacent coastal segments. However, it is often difficult to distinguish between the contribution of ground ice and other parameters of coastal structure (such as fine-grained ice rich bluffs) to the resulting retreat rate. The maximum retreat rates of ice-rich coasts were observed in years with higher sum of positive air temperatures.

Keywords: coastal erosion; Kara Sea; ground ice; wedge ice; massive ground ice.

Introduction

The coasts of the southwestern part of the Kara Sea are composed of permafrost sediments (except for the rocky coasts of Yugorskiy Peninsula) and retreat with average annual rate 0.5 to 2 m per year (Vasiliev *et al.*, 2006; Lantuit *et al.*, 2012; Kritsuk *et al.*, 2014; Ogorodov *et al.*, 2016). As in other Arctic regions, retreat rates of permafrost coasts vary both spatially and temporally.

Ground ice as a factor of coastal retreat

Different types of ground ice are spred very uneven in the cryolithozone; the spatial distribution of ground ice is determined by the history of the development of the region's natural environment, including the conditions for the formation of permafrost. The contribution of ground ice to the rate of coastal erosion is also uneven and is determined not only by the total ice content but primarily by the structure of the coast. Researchers attempted to establish a correlation directly between the rates of retreat and the ice content of the coastal bluffs, it was assumed that the presence of ground ice would lead to an increase in the rates of retreat. However, in studies devoted to a particular region or to the Arctic shores as a whole (Héquette & Barnes, 1990, Lantuit et al., 2008), the correlation between ground ice content and the retreat rates was at best weak. The reason is that the studies analyzed the retreat rates of the coasts, which are extremely heterogeneous in terms of structure and hydrometeorological conditions. A wide range of factors contributes to coastal dynamics and the influence of an individual factor can only be traced locally (Konopczak *et al.*, 2014).

Key Sites at South-Western Coast of the Kara Sea

At three key sites (Fig.1) coastal dynamics have been investigated by researchers of Laboratory of geoecology on the North since the 1980s, including both field work and remote methods (analysis of aerial and satellite multitemporal imagery).

Kharasavey Cape, Western Yamal Peninsula

Cliffs 7–12 m in height are composed of permafrost deposits and retreat at an average annual rate of 1.1 m per year over a 52-year period (Belova *et al.*, 2017). The highest mean annual retreat rates (>2 m per year) are typical for coasts composed by very ice-rich fine silty clays; their cryogenic structure being the main factor of such fast retreat. In 2006–2016, average retreat rates increased to 1.2 m/year compared with the 1.0 m/year rate in 1964–2006, primarily due to the accelerated erosion rates of icy silty clays in the coastal cliffs. The impact of hydrometeorological forcing on Kharasavey coastal area increased in the late XX–early XXI centuries, causing faster coastal retreat.

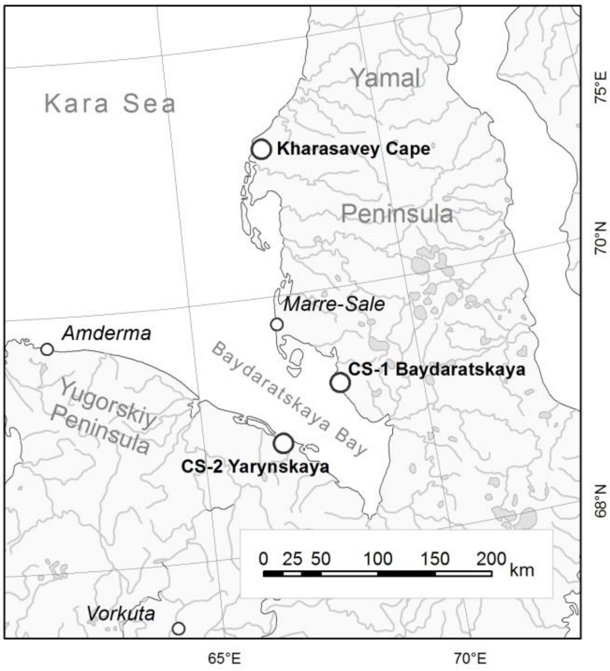

Figure 1. Research area.

Ural coast of Baydaratskaya Bay, Oyuyacha River mouth (CS-2 Yarynskaya)

The highest observed retreat rates were observed at laida (modern marine terrace up to 2 m height) with dense network of ice wedges. Along with ground ice, the factor of bluff height promotes accelerated coastal erosion. The segments of sandy bluffs 12-27 m height retreat with highest rates at sections with massive ice beds exposures (mean annual rate 2 m per year) due to thermocirques formation.

Yamal coast of Baydaratskaya Bay, Yarayacha River mouth (CS-1 Baydaratskaya)

Key site is characterized by low retreat rates (0.3-0.7 m per year) first of all due to the low ice content of sandy bluffs up to 30 m height. Local increase in retreat rates is due to anthropogenic impact.

Acknowledgments

The work has been supported by Russian Foundation for Basic Research, projects 16-35-60099 mol_a_dk.

References

Belova, N.G., Shabanova, N.N., Ogorodov, S.A., Kamalov, A.M., Kuznetsov, D.E., Baranskaya, A.V. & Novikova, A.V., 2017. Erosion of permafrost coasts of the Kara Sea near Kharasavey Cape, Western Yamal. *Earth's Cryosphere* 21 (6) (in print)

Héquette, A. & Barnes, P.W., 1990. Coastal retreat and shoreface profile variations in the Canadian Beaufort Sea. *Marine Geology* 91: 113–132.

Konopczak, A.M., Manson, G.K. & Couture, N.J., 2014. *Variability of coastal change along the western Yukon coast.* Geological Survey of Canada, Open File 7516, 81p.

Kritsuk, L.N., Dubrovin, V.A., Yastreba, N.V., 2014. Some results of integrated study of the Kara coastal dynamics in the Marre-Sale meteorological station area, with the use of GIS technologies. *Earth`s Cryosphere* 18(4): 52-62.

Lantuit H., Overduin P.P., Couture N., Ødegård R.S., 2008. Sensitivity of Coastal Erosion to Ground Ice Contents: An Arctic-Wide Study Based on the ACD Classification of Arctic Coasts. *Proceedings of the Ninth International Conference on Permafrost*, Fairbanks, Alaska, USA, June 29 -July3, Vol.2: pp. 1025-1029.

Lantuit, H., Overduin, P.P., Couture, N., Aré, F., Atkinson, D., Brown, J., Cherkashov, G., Drozdov, D., Forbes, D.L., Graves-Gaylord, A., Grigoriev, M., Hubberten, H.-W., Jordan, J., Jorgenson, T., Ødegård, R.S., Ogorodov, S., Pollard, W., Rachold, V., Sedenko, S., Solomon, S., Steenhuisen, F., Streletskaya, I., Vasiliev, A. & Wetterich, S., 2012. The Arctic Coastal Dynamics database: a new classification scheme and statistics on Arctic permafrost coastlines. *Estuaries and Coasts* 35: 383–400.

Ogorodov, S.A., Baranskaya, A.V., Belova, N.G. et al., 2016. Coastal dynamics of the Pechora and Kara Seas under changing climatic conditions and human disturbances. *Geography, Environment, Sustainability* 9 (3): 53–73.

Vasiliev, A.A., Streletskaya, I.D., Cherkashev, G.A. & Vanshtein, B.G., 2006. Coastal dynamics of the Kara Sea. *Earth's Cryosphere* 10(2): 56-67 (in Russian).

Rocky coasts evolution on the Brøgger peninsula (Spitsbergen): control and variability

Bourriquen Marine[1], Mercier Denis[2], Baltzer Agnès[3], Costa Stéphane[4], Fournier Jérôme[5]

[1] *University of Nantes, Laboratory LETG (CNRS - UMR 6554), Campus du Tertre BP 81 227, 44312 Nantes cedex 3, France, marine.bourriquen@univ-nantes.fr*

[2] *University Paris-Sorbonne, Laboratory ENec (CNRS - UMR 8185), 191 rue Saint-Jacques 75 005 Paris, France*

[3] *University of Nantes, Laboratory LETG (CNRS - UMR 6554), Campus du Tertre BP 81 227, 44312 Nantes cedex 3, France*

[4] *University of Caen, Laboratory LETG (CNRS - UMR 6554), Esplanade de la Paix, 14032 Caen, France*

[5] *National Center for Scientific Research, Marine Biological Station of the Museum of Natural History, Laboratory BOREA (CNRS - UMR 7208), France*

Abstract

The aim of this study is to identify and quantify the controlling factors of rocky coasts evolution on the north shore of the Brøgger peninsula, northwest Spitsbergen, from the Kvadehuken spit to the foot of the Haavimfjellet (fig. 1), in a context of climate change (Artic warming) and geomorphological transition (from glacial and periglacial to paraglacial and paraperiglacial systems). The study areas have been study using several methodologies. Aerial photographs from 1990 to 2010 have been used to quantify the evolution of top of the cliff and reveal a total loss area of -9752 m² with a retreat rate of -0,06 m/y. Schmidt hammer has been used to study the resistance variability on cliff faces and shows a lower resistance in the top of the cliff face on most studied sites. Evolution of the cliff face has been studied using photogrammetry from 2016 to 2017 and a thermal camera has been used to highlight facies variability and areas of weakness.

Keywords: Paraglacial; Coastal geomorphology; Kongsfjorden; Photogrammetry; Schmidt Hammer; Thermal camera.

Introduction

Although the Arctic coast represents 34% of global coastlines, only 1% has been studied in sufficient detail to allow a quantitative description of the processes involved in their evolution (Fritz *et al.*, 2017). Few studies have been conducted on Svalbard rocky coasts (Wangensteen *et al.*, 2007; Strzelecki, 2011; Strzelecki, 2016; Guégan & Christiansen, 2016; Strzelecki *et al.*, 2017; Swirad *et al.,* 2017).

Since the beginning of the 20th century, Spitsbergen has been concerned by a geomorphologic transition caused by a deglaciation context and characterized by paraglacial and paraperiglacial changes (Mercier, 2008). Temperature and precipitation increased in Ny-Ålesund by +4°C from 1969 to 2016 and + 190 mm from the decade 1969-1980 to 2011-2016. Rapid atmospheric warming in the Arctic has increased the action of geomorphological processes involved in Arctic coastal evolution such as permafrost degradation, the increase of sediment supplies from deglaciated catchments and the lengthening of the open-water season.

The aim of this study is to identify and quantify the controlling factors of rocky coasts evolution on the north shore of the Brøgger peninsula, northwest Spitsbergen in a context of climate change (Arctic warming) and geomorphological transition (from glacial and periglacial to paraglacial and paraperiglacial systems). The study area stretches from the Kvadehuken spit to the foot of the Haavimfjellet (fig. 1) and comprises several types of cliff environments: dynamic at the entrance of the fjord and calm in the fjord near Haavimfjellet foot. Active and fossil cliffs have been study using several methodologies. Cliffs are composed of sandstone or limestone. Aerial photographs from 1990 to 2010 have been used to quantify the evolution of top of the cliff and reveal a total loss area of -9752 m² with value of -5550 m² for sandstone formation and -3937 m² for limestone. Cliff top undergone a mean retreat of -0,06 m/y from 1990 to 2010. Schmidt hammer has been used to study the resistance variability on cliff faces. On most of the studied sites, lower and middle zone of the cliff are the most resistant and top of the cliff, concerned by periglacial weathering, is lower resistant. Evolution of the cliff face has been studied using photogrammetry from 2016 to 2017 and a thermal camera has been used to highlight facies variability and areas of weakness. The expected results will make it possible to discuss the respective role of structural factors like lithology (sandstone, limestone, layers thickness) and tectonic (fault and fracturing), paleo-environmental factors (glacial and paraglacial heritages, for example raised beach), and current processes (continental and marine processes) in the evolution of contemporary arctic cliff retreat.

Acknowledgments

The authors would like to thank the French Polar Institute (IPEV) for logistical support during the field work campaigns in 2016 and 2017 ("C3" Coasts under Climate Change in Kongsfjorden (Pr1172 IPEV – RIS-ID 10529)), and the Labex Mer for financial support.

References

Fritz, M., Vonk, J.E., and Lantuit, H., 2017. Collapsing Arctic coastlines. *Nature Climate Change* 7: 6-7.

Guégan, E.B.M., Christiansen, H.H., 2016. Seasonal Arctic Coastal Bluff Dynamics in Adventfjorden, Svalbard. *Permafrost et Periglacial Processes* 28: 18-31.

Mercier, D., 2008. Paraglacial and paraperiglacial landsystems: concepts, temporal scales and spatial distribution, Géomorphologie : relief, processus, environnement, 14 (4): 223-234. DOI: 10.4000/geomorphologie.7396

Strzelecki, M.C., 2011. Schmidt hammer tests across a recently deglacierized rocky coastal zone in Spitsbergen – is there a "coastal amplification" of rock weathering in polar climates? *Polish polar research* 32 (3): 239-252.

Strzelecki, M.C., 2016. The variability and controls of rock strength along rocky coasts of central Spitsbergen, HighArctic.*Geomorphology*.http://dx.doi.org/10.1016/j.geomorph.2016.06.014

Strzelecki, M.C. Kasprzak M., Limb, M., Swiradc Z.M., Jaskólski M., Pawłowski Ł., Modzel P., 2017. Cryo-conditioned rocky coast systems: A case study from Wilczekodden, Svalbard. Science of the Total Environment. 607-608: 443-453

Swirad, Z.M., Migon, P., Strzelecki, M.C., 2017. Rock control on the shape of coastal embayments of north-western Hornsund, Svalbard. *Zeitschrift für Geomorphologie.* doi: 10.1127/zfg/2017/0403

Wangensteen, B., Eiken, T., Ødegård, R., Sollid, J.L., 2007. Measuring coastal cliff retreat in the Kongsfjorden area, Svalbard, using terrestrial photogrammetry. *Polar Research* 26: 14-21

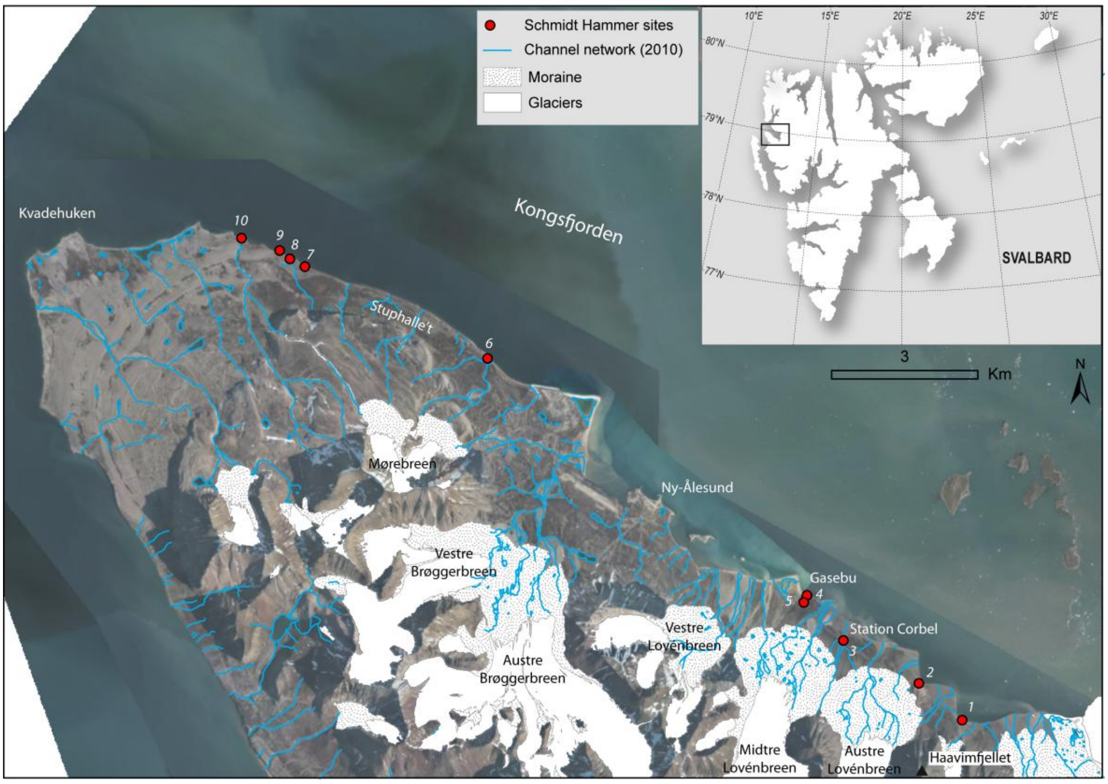

Figure 1. Localization of the study area, on the north shore of the Brøgger peninsula, from Kvadehuken spit (West) to Haavimfjellet foot (East).

Coastal responses to changing sea-ice regime: an Arctic mega-transect

Louise M. Farquharson[1]
Richard Buzard[1]
Daniel H. Mann[1]
Benjamin M. Jones[2]
Jacquelyn Overbeck[3]
[1] *Department of Geoscience, University of Alaska Fairbanks, Fairbanks, AK, USA*
(corresponding author email: lmfarquharson@alaska.edu)
[2] *U.S. Geological Survey Alaska Science Center, Anchorage, AK, USA*
[3] *Alaska Department of Natural Resources, Division of Geological & Geophysical Surveys*

Abstract

As the Arctic warms, the sea ice regime (phenology and extent) is changing rapidly. Sea ice influences coastal geomorphology by reducing wave fetch, and, in the case of shore-fast ice, by shielding shorelines from wave action, during autumn storms. In addition to changes in the sea ice regime, the temperature of the ground, air, and ocean are all increasing, and this is expected to contribute to permafrost degradation along coastlines. Here we describe the conceptual framework for a 1000-km transect in the Bering Sea region that spans a wide range of existing sea ice conditions. In most general terms, the purpose of this transect is to assess the potential for lower latitude sites to inform us about the future geomorphological trajectories of higher latitude coastlines as climate warms. Specifically, this mega-transect will quantify the effects of sea-ice regime on erosion rates along coastal bluffs.

Keywords: sea-ice; coastal geomorphology; permafrost bluff; barrier island; conceptual model.

Introduction

The Arctic as a whole contains over 100,000 km of ice-affected coastline (Lantuit et al. 2011). As the Arctic warms, the sea ice regime (phenology and extent) is changing. As the seasonal duration of sea ice continues to decline at up to 13 % per decade (NSIDC), we need a better understanding how coastal dynamics will respond.

The presence of sea ice influences coastal geomorphology by protecting the coast from wave action. It does this by simultaneously reducing fetch and increasing wind drag (Macklin, 1983), and, in the case of shorefast ice by protecting shorelines from wave action. Sea ice can also contribute to sediment movement onshore through processes of ice push (Kovacs and Sodhi 1980) and ice entrainment of sediment (Kempema et al. 1989).

How will changes in sea ice regime affect coastal geomorphology? To answer this question we established a latitudinal sea-ice transect composed of three study areas stretching from the southern Bering Sea to the Beaufort Sea along the western and northern coasts of Alaska (Figure 1).

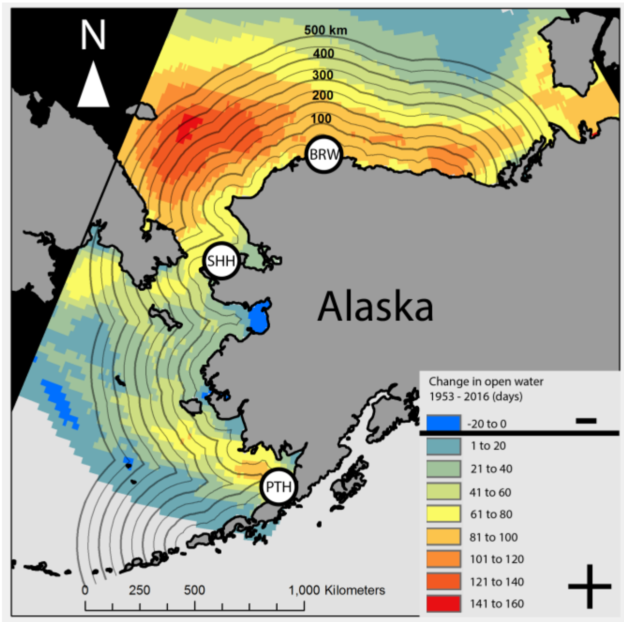

Figure 1. Study area map showing change in sea ice free days along the Alaska coast and at out sites: BRW = Barrow, SHH = Shishmaref. PTH = Port Heiden (data source: SNAP). The three study sites are circled.

Each of the three study sites has a similar fetch direction (N-NW) and are characterized by a combination of unconsolidated coastal bluffs, barrier islands, and lagoons (Figure 2).

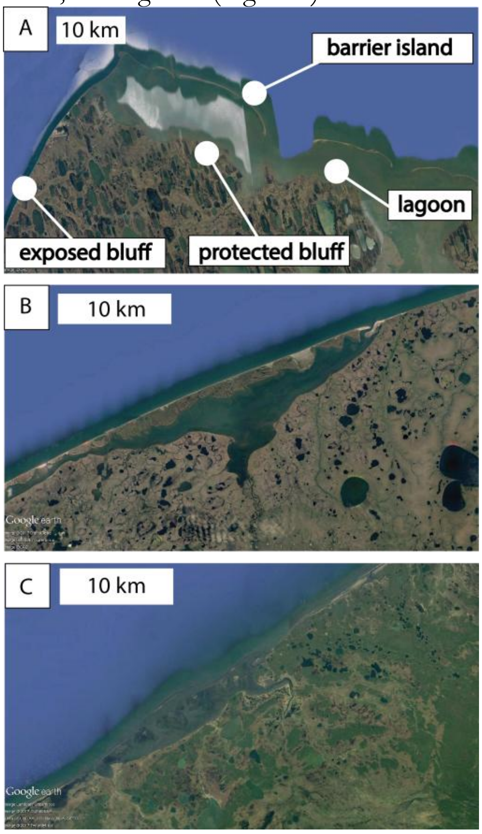

Figure 2. Examples of barrier islands, lagoons, and exposed coastal bluffs at each study site: A: the Barrow site, B: the Shishmaref site, C: the Port Heiden site.

Each study site experiences very different sea ice conditions, both in terms of seasonal sea-ice duration (for the period 1953-2013) and rate of sea-ice decline over recent years (Figures 1, 3). While sea ice currently is a major influence on limiting effective fetch (the point at which additional fetch has no effect on wave height) at the two northern sites, all three study sites will have similar effective fetches in the seasonally sea-ice free Arctic Ocean predicted to occur by 2030 (Wang and Overland, 2003).

We use these three sites to address the following research questions:

1) Is there a relationship between coastal geomorphology and sea-ice duration and extent?

2) How is sea-ice decline affecting the temporal and spatial patterns of wave fetch at each site?

3) How are these changes in fetch influencing coastal dynamics?

4) Most generally, is this analog-by-latitude approach useful in informing us about the potential geomorphological trajectories of higher latitude coastlines?

For Question 1, we will use high-resolution satellite imagery and digital elevation models to survey the length, height, and width of barrier islands, lagoons, tidal inlets, and bluffs along a 100 km stretch of coastline in each of our study sites. For Question 2, we will use available sea-ice concentration data to plot trends in changing wave fetch for each study site (Figure 3). For Question 3, we will use time series of remote sensing to compare rates of exposed bluff erosion over the last half a century at each site.

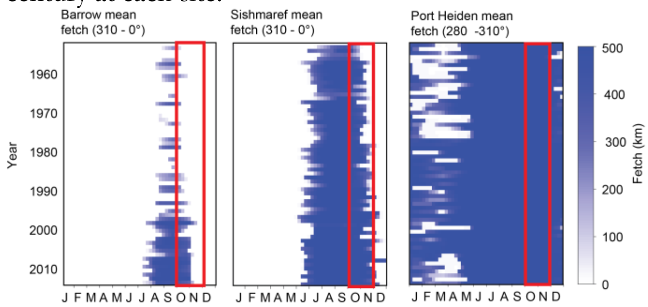

Figure 3. Changes in fetch between 1953 and 2013 for each study area (Data source: SNAP). Red boxes indicate fall storm season (Atkinson, 2005; Kinsman and Gould, 2014).

References

Atkinson, D.E., 2005. Observed storminess patterns and trends in the circum-Arctic coastal regime. *Geo-Marine Letters*, 25(2-3), pp.98-109.

Kempema, E.W., Reimnitz, E. and Barnes, P.W., 1989. Sea ice sediment entrainment and rafting in the Arctic. *Journal of Sedimentary Research*, 59(2).

Kinsman, N.E. and Gould, A., 2014. Contemporary shoreline retreat rates at Meshik in Port Heiden, Alaska. State of Alaska, *Department of Natural Resources, Division of Geological & Geophysical Surveys*.

Kovacs, A. & Sodhi, D.S. 1980. Shore ice pile-up and ride-up: Field observations, models, theoretical analyses. *Cold Regions Science and Technology* 2 : 210–288. DOI: 10.1016/0165-232X(80)90076-2

Lantuit, H., Overduin, P.P., Couture, N., Wetterich, S., Aré, F., Atkinson, D., Brown, J., Cherkashov, G., Drozdov, D., Forbes, D.L. and Graves-Gaylord, A., 2012. The Arctic coastal dynamics database: a new classification scheme and statistics on Arctic permafrost coastlines. *Estuaries and Coasts*, 35(2), pp.383-400.

Macklin, S.A., 1983. Wind drag coefficient over first‐ year sea ice in the Bering Sea. *Journal of Geophysical* Research: Oceans, 88(C5), pp.2845-2852.

Wang, M. and Overland, J.E., 2009. A sea ice free summer Arctic within 30 years?. *Geophysical research letters*, 36(7).

Long-term retreat of coastal permafrost bluffs, Barter Island, Alaska

Ann E. Gibbs[1]
Bruce M. Richmond[1]
Li H. Erikson[1]
Benjamin M. Jones[2]

[1]*U.S. Geological Survey Pacific Coastal and Marine Science Center, Santa Cruz, CA 95060, USA,* agibbs@usgs.gov
[2]*U.S. Geological Survey Alaska Science Center, Anchorage, AK 99672 USA*

Abstract

In contrast to most of the Arctic coast, a veritable treasure trove of historical imagery exists (n > 17) for Barter Island, Alaska, which allows for a detailed assessment of trends and patterns of coastal change over the past 70 years. Between 1955 and 2017, the 2.7 km long, the coastal permafrost bluffs retreated on average 93 m and maximum 142 m. The average long-term retreat rate of 1.5 ± 0.2 m/yr is punctuated by individual years with retreat rates up to 5 times higher. Evaluation of short-term bluff change rates show a steady increase in retreat over the last three decades and a best-fit polynomial trend suggests acceleration in retreat rates that is independent of large spatial and temporal variations observed on an annual basis.

Keywords: Arctic; coastal erosion; Alaska; Beaufort Sea

Introduction

Observed increases in the duration of the ice-free season and warming of land, air, and ocean temperatures in the Arctic over the past several decades (e.g. Barnhart *et al.*, 2014) will likely drive a related response in coastline behavior because of the linked mechanisms of shoreline change. Quantifying the response in coastal behavior on a regional scale is problematic, however, because historical data sets from which to compare change rates are rare. Along the north coast of Alaska, for example, temporally consistent, regional shoreline data exist for only four time-periods: 1940s, 1980s, 2000s, and 2010s. Shoreline change rates calculated using these data indicate the coast is dominantly erosional over the past 7 decades, however, no clear, statistically significant change in trend through time is observed (Gibbs & Richmond, 2017).

Barter Island, Alaska, is one of only a few locations in the Arctic where satellite and aerial photography were acquired on a near annual basis over the past two decades. In this study we capitalize on this relatively unique dataset to document and assess coastal change patterns and trends through time.

Study Site

Barter Island is located on the northeast coast of Alaska approximately 120 km west of the U.S.-Canadian border on the Alaskan Beaufort Sea coast. The village of Kaktovik and adjacent U.S. Air Force radar site sit on the north shore of the island near the eastern end of a nearly 3-km stretch of eroding permafrost bluffs. The bluffs range in height from a few meters to more than ten meters high and consist of a complex sequence of material ranging from dense clay, sand and gravel, and both massive and segregated ice. Broad, low-lying (< 2 m high) sand and gravel spits extend east and west from the topographically higher tundra hinterland of the island and beaches only intermittently front the coastal bluffs.

Methods

Seventeen bluff-edge positions were delineated from maps, aerial photographs, and satellite imagery acquired between 1955 and 2017. Change rates were calculated every 10-m alongshore using the Digital Shoreline Analysis System (Thieler *et al.,* 2009) for all time periods with available high-quality imagery. For details on methodology and uncertainty estimates see Gibbs & Richmond (2017).

Results

Barter Island's coastal bluffs retreated an average of 93 m (maximum 142 m) between 1995 and 2017. The average long-term (62 year) retreat rate of 1.5 ± 0.2 m/yr is punctuated by individual years with retreat rates up to 5 times higher. Evaluation of shorter-term (< 24 year) change rates show a steady increase in retreat over the last 3 decades and a best-fit 2nd-order polynomial trend suggests acceleration in retreat rates (Fig. 1). Very short-term (1- 5 years) retreat rates show large temporal and spatial variations, which is characteristic of most coastal environments but does not necessarily reflect persistent changes in forcing conditions.

Net long-term bluff retreat shows a westerly, ~500-m migration of the apex of the island, possibly caused by divergence in longshore transport due to changes in incident wave directions.

Data suggest the primary bluff failure modes are a combination of thermo-denudation and thermo-abrasion. Rates of retreat associated with thermo-denudation are on the order of 1 to 2 m/yr and contribute mostly to the long-term retreat rate. Higher retreat rates typically result from large storms that cause mechanical and thermal niching at the bluff toe, followed by rotational slumping and block collapse (Hoque & Pollard, 2016). We hypothesize the apparent acceleration in retreat rates at Barter Island may be related to increases in both thermo-denudation and the number of niche forming and block collapsing episodes associated with higher temperatures and longer ice-free conditions in the Beaufort Sea.

References

Barnhart, K.R, Overeem, I. & Anderson, R.S, 2014. The effect of changing sea ice on the physical vulnerability of Arctic coasts. *The Cryosphere*, 8, 1777-1799.

Gibbs, A.E., & Richmond, B.M., 2017. National assessment of shoreline change—Summary statistics for updated vector shorelines and associated shoreline change data for the north coast of Alaska, U.S.–Canadian border to Icy Cape. *U.S. Geological Survey Open-File Report 2017–1107*, 21 pp.

Hoque, M.A., & Pollard, W.H., 2016. Stability of permafrost dominated coastal cliffs in the Arctic. *Polar Science*, *10*(1), 79-88.

Thieler, E.R., Himmelstoss, E.A., Zichichi, J.L., & Ergul, A., 2009. The Digital Shoreline Analysis System (DSAS) version 4.0—An ArcGIS™ extension for calculating shoreline change (ver. 4.3.4730, April 2012): *U.S. Geological Survey Open-File Report 2008–1278,*

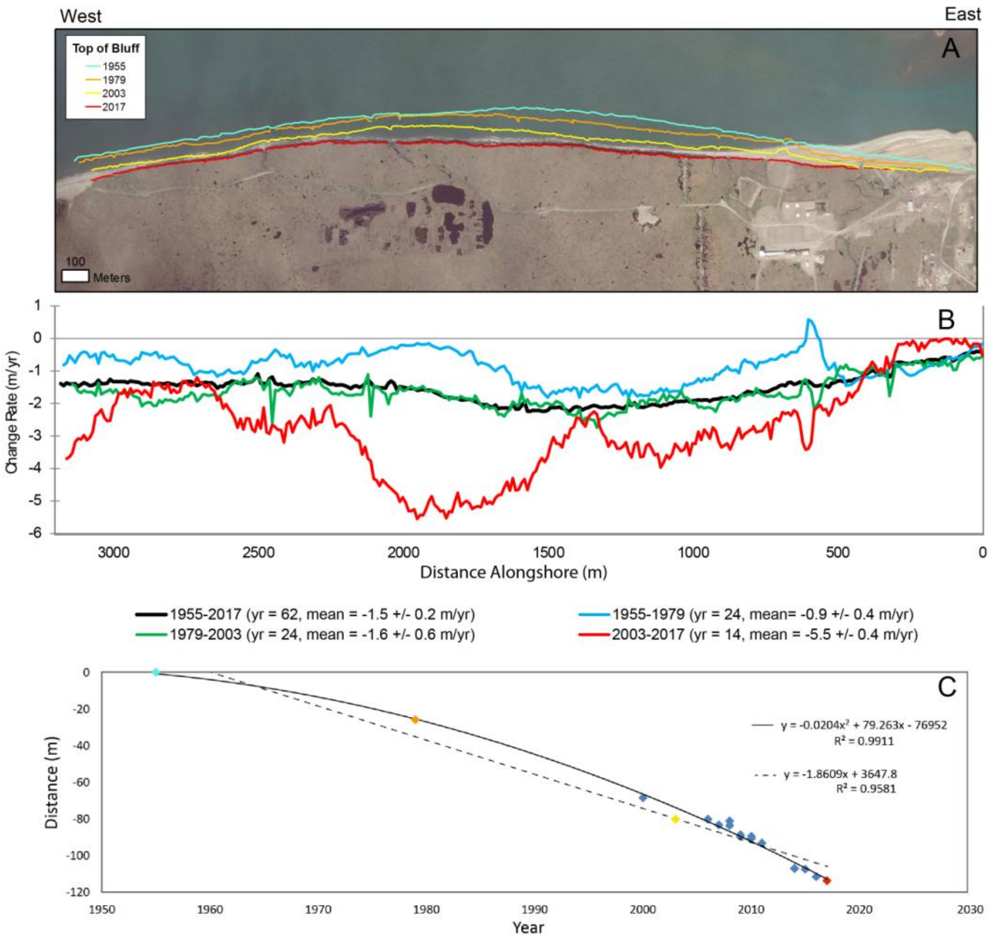

Figure 1. (A) Summary of historical shoreline position and (B) rates of change along the Barter Island bluff coast for multiple time-periods; (C) Example of shoreline change along one transect showing linear (dashed-line) and 2nd-order polynomial (solid line) trends through the data. Colored points correlate to years identified in panel A.

Integrated long-term research on Baydara Bay coastal line dynamic retreat (Kara sea)

Vladislav Isaev[1]
Andrey Koshurnikov[2]
Sergey Buldovich[3]
Darya Alexutina[4]
[1]*Lomonosov Moscow State University, Geological Department, isaev@geol.msu.ru*
[2]*Lomonosov Moscow State University, Geological Department*
[3]*Lomonosov Moscow State University, Geological Department*
[4]*Lomonosov Moscow State University, Geographic Department*

Abstract

The purpose of the research is integrated study and survey of coastline retreat for detection of main dependences between the lithology of the coastal deposits, heights of the coastal cliff and the retreat rates for this site with taking in account the climate changing and technogenic influence of pipeline construction.

Keywords: coastal retreat; thermal erosion; thermal abrasion; thermal denudation; temperature monitoring; DGPS mapping; geophysics survey.

Introduction

The coastal retreat is occurred due to thermal erosion which could consist of thermal denudation or/and thermal abrasion of the coastal deposits.

Thermal abrasion intensity depends on several main factors in the permafrost area, i.e.: the tidal activity mostly and ice regime, properties and composition of the seashore rocks, seawater temperature and its salinity. Thermal denudation depends on radiation-heat transfer to the surface of slope, mechanical properties of grounds, ice content in ground and lithology of deposits. It also influenced by the rate of debris transfer by seawater to the accumulation zone.

The ice activity of the sea effect significantly the retreat of the seashore (Are, 1980; Zachar, 1982; Dallimore *et al.*, 1996; Jones *et al.*, 2009; Arp *et al.*, 2011 et al). On the other hand, the most important phenomena are ice cover duration and ice coverage during the summer season. The easiest to erode are sand, loam clays and silty clay. These sediments are typical for marine and alluvial genetic types of Quaternary sediments on Kara seacoast. They often have high ice content represented by ice layers, ice wedges and massive ice texture of frozen ground (Badu *et al.*, 2013; Belova, 2014; Isaev *et al.*, 2016).

The debris transfer by the seawater is the considerable factor of the thermal abrasion activity as well as for the thermal denudation process.

The seawater temperature and its salinity do the influence on the seashore thermal erosion rate (Are, 1980).

Thermal denudation is spreading on coasts composed by frozen rocks with rich ice content (Gunter et al., 2013). It includes some exogenesis cryogenic gravitational processes (slumping, sliding, solifluction, erosion etc.) that are developped due to rock thawing as well as nivation (snow bank processes) which induces seashore destruction and material migration to the lower basis (beach). Thermal denudation impact on the water covering part of the littoral zone results in scarp flattening with their stability also is affected by abrasion (Melnikov & Spesivcev, 1995). Development of thermal denudation processes acquires some specific features in massive ice areas since on such areas these processes turn to be very intensive. Thermal cirques and thermal terraces are confining to massive ice exposure areas with the rate of their back land retreat much higher than the rate of thermal abrasion-inspired scarp retreat in the neighboring areas.

For evaluation of the rate of seashore retreats F.E. Are (Are *et al.,* 2004) suggested and implemented the method based on thermal terrace size measurements and their lifetime data. Thermal denudation resulting from snow melting and summer rains is more active in the areas without any vegetation. Vegetative ground cover induces block caving in the top of thermal cirques. Often it is a large block divided by ice wedges (Kizyakov & Leibman, 2008).

In accordance with the above-mentioned method, the complex scientific research of the coastal retreat was carried out on the western coast of Baydara Bay of Kara Sea. That works focused on detailed study of cryogenic destruction of seashore permafrost. That includes following activities: geocryological mapping, geodetic surveying, engineering-geocryological drilling, thermometric monitoring, geophysical fieldwork with radar and electrotomography methods as well as laboratory researches of ground samples in frost state on mechanical and physical properties determination.

The purpose of the research is integrated study and survey of coastline retreat for detection of main dependences between the lithology of the coastal deposits, heights of the coastal cliff and the retreat rates for this site with taking in account the climate changing and technogenic influence of pipeline construction. It is based on the 2013-2017 season observations (Fig.1).

Figure 1. DGPS profiles of western coastal line of Baydara bay from 2012 to 2017; lines of the coast section (red line); geophysics profiles (green lines); sites of parametric boreholes (yellow ring).

Acknowledgments

The research is supported by the SAMCoT WP6 (https://www.ntnu.edu/web/samcot/home)

References

Arp, C.D., Jones, B.M., Urban, F.E., Grosse, G. 2011. Hydrogeomorphic processes of thermokarst lakes with grounded-ice and floating-ice regimes on the Arctic coastal plain, Alaska//*Hydrological Processes*, Volume 25, 2422–2438.

Are, F.E. 1980. *Thermal abrasion of sea coasts*. Moscow: Nauka, 158 pp.

Are, F.E., Grigoriev, M.N., Rahol'd, F., Hubberten, H.GV. 2004. Measurement of the retreat rate of thermal abrasion coasts by the thermal terraces sizes // *Journal of Earth Cryosphere*, t. VIII, № 3, 52–56.

Badu, Yu.B., Gafarov, N.A., Podborny, E.E., 2013. Cryosphere of oil and gas condensate site of Yamal peninsula. Moscow: JSC "Gazprom expo", v.2, 424 pp.

Belova, N.G. 2014. Massive ice beds of south-western coast of the Kara sea, Moscow: Maxpress, 180 pp.

Dallimore, S. R., Wolfe, S.A., Solomon, S. M. 1996. Influence of ground ice and permafrost on coastal evolution, Richards Island, Beaufort Sea coast, N.W.T.// *Canadian Journal of Earth Sciences*, Volume 33, №5, 664-675.

Gunther, F., Overduin, P. P., Sandakov, A. V., Grosse, G., Grigoriev, M. N. 2013. Short- and long-term thermo-erosion of ice-rich permafrost coasts in the Laptev Sea region // *Biogeosciences*. v.10. 4297-4318

Isaev, V. Koshurnikov, A., Pogorelov, A., Amangurov, R., Podchasov, O., Sergeev, D, Kioka, A. 2016. *Field investigation and laboratory analyses; Baydaratskaya bay 2016*, SAMCoT report.

Kizyakov A.I., Leibman M.O., Perednya D.D. Destruktivnye reliefoobrazuyuschie processy poberezhiy Arkticheskih ravnin s plastovymi podzemnymi l'dami // *Kriosfera Zemli*, 2006, t. H, № 2, s. 79–89.

Jones, B. M., Arp, C. D., Beck, R. A., Grosse, G., Webster, J. M., Urban, F. E. 2009. Erosional history of Cape Halkett and contemporary monitoring of bluff retreat, Beaufort Sea coast, Alaska// *Polar Geography and Geology*. Volume 32, Issue 3-4, 129-142.

Melnikov, V.P., Spesivcev, V.I. 1995. Engineering-geological and geocryological conditions of Barents and Kara seashelfs. Novosibirsk: Nauka, 198 pp.

Zachar, D. 1982. *Soil erosion.* Elsevier Scientific Publishing Company. 547 pp.

Coastal changes in Greenland

Aart Kroon[1, 2]
Mette Bendixen[1, 2]
Priscila Emerich Souza[1]
Lars Nielsen[1]
Charlotte Sigsgaard[1]
[1]*Department of Geosciences and Natural Resource Management, University of Copenhagen, Denmark, ak@ign.ku.dk*
[2]*Center for Permafrost, University of Copenhagen, Denmark*

Abstract

Sedimentary coasts forms *ca.* 30 % of Greenland. The annual and decadal evolutions of the shorelines in these coastal environments show rapid changes, especially at deltas and along barriers. The main drives of these changes are the traditional coastal processes by waves and currents and the changing influx of sediments from the terrestrial, partly glaciated drainage basins.

Keywords: coastal change; delta; beach ridge plain; morphodynamics.

Motivation

Coasts are always on the dynamic interface between land and sea and rapid changes in these environments can occur in case of sedimentary shores. Normally, shoreline changes are mainly driven by coastal processes related to waves and tides, and to sediment availability. However, additional factors like ice, snow and freezing temperatures will heavily influence the dynamics along Arctic polar coasts. Coastal processes are only restricted to the ice-free periods of the open water and sea ice dynamics play a major role on the shores during the beak-up stages.

Many coasts in Greenland are on the fringe of mountainous terrestrial systems with alluvial valleys and fjords. The terrestrial sediment input of the partially glaciated drainage basins of these valleys play a major role in the sediment budget of coastal stretches. This can be sediments from the glaciers, eroded sediments of the mountains, or reworked sediment of alluvial, fluvial or glacial origin. Coastal processes, mainly driven by the waves and tides during the ice-free open water period at sea, shape the shores and may form for instance deltas, barriers and beaches.

A recent warming of the Arctic climate over the last decades induces many changes in terrestrial and open water systems and causes additional shoreline adaptations (Fig. 1). The changes include rising sea-level due to thermal expansion and increasing fresh water fluxes from glaciers and ice caps. At the same time, the open water periods extend due to a reduction in sea-ice coverage.

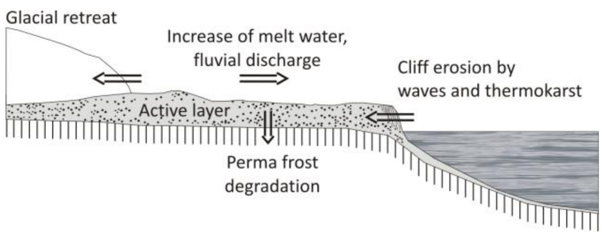

Figure 1. Changes in the Arctic coastal zone due to warming (after Kroon, 2014)

We give in this presentation a summary of different coastal environments in Greenland and will highlight coastal changes over the last years to decades with a special focus on deltas (Bendixen & Kroon, 2017; Bendixen *et al.*, 2017) and beach ridge plains (Nielsen *et al.*, 2017). We will present the main drivers for these changes and discuss the implication of a changing climate for these coastal environments

Acknowledgments

We gratefully acknowledge the financial support of CENPERM and the Danish Science Foundation.

References

Bendixen, M. & Kroon, A., 2017. Conceptualizing delta forms and processes in Arctic coastal environments. *Earth Surface Processes and Landforms* 42: 1227-1237.

Bendixen, M., Iversen, L.L., Bjørk, A.A., Elberling, B., Westergaard-Nielsen, A., Overeem, I., Barnhart, K., Kahn, S.A., Box, J.E., Abermann, J., Langley, K., Kroon, A., 2017. Delta progradation in Greenland driven by increasing glacial mass loss. *Nature* 550: 101-104.

Kroon, A., 2014. High-latitude coasts. In: Masselink, G. & Gehrels, R. (eds.), *Coastal Environments and Climate Change,* Wiley-Blackwell-Wiley, 338-355.

Nielsen, L., Bendixen, M., Kroon, A., Hede, M-U., Clemmensen, L.B., Wesseling, R. & Elberling, B., 2017. Sea-level proxies in Holocene raised beach ridge deposits (Greenland) revealed by ground-penetrating radar. *Scientific Reports* 7: 46460.

Microstructural organization and mineralogical aspects of pedogenesis in soils of Larsemann Hills (East Antarctica)

Aleksei V. Lupachev[1]
Tatiana V. Alekseeva[1]
Pavel I. Kalinin[1]
Lyubov E. Kurbatova[2]
Stanislav V. Gubin[1]
[1] *Institute of Physico-chemical and Biological Problems in Soil Science, RAS, Pushchino, Russia a.lupachev@gmail.com*
[2] *Botanical Institute, RAS, St.-Petersburg, Russia*

Abstract

Residual of the dominant parent rocks (granate-bearing quartz-feldspar paragneisses) with no plant cover and soils (mainly Hyperskeletic, Lithic and Nudilithic Leptosols), that are developed on the same rocks were studied (3 soil profiles (7 samples total) and 3 samples of rock residual). Main structural, physico-chemical features, bulk elements' and mineralogic composition of rock residual and soils were analyzed in order to find evidences of poor-expressed pedogenesis.

Keywords: soils, Antarctica, secondary minerals, initial pedogenesis.

Introduction

The main objective of the work was to determine the features of elements migration/accumulation, organo-mineral interaction, formation of the secondary minerals, which allow to characterize the material as "soil" and to more or less distinguish soils from the surrounding (and underlying) residual of the parent rocks.

Objects and methods

Larsemann Hills is the 50 km2 ice-free area on the seashore in the East Antarctica (S 69˚30', N 76˚20'). MAAT is -9,8°C (-15° - -18° in winter), MAP is around 250 mm. Daily summer temperatures are often higher than 4˚C, rock surfaces may be heaten up to 30-35˚C. Field soil descriptions followed the ANTPAS guide (Bockheim *et al.*, 2006)

Mosses are presented with *Bryum pseudotriquetrum, Bryum pseudotriquetrum, Bryoerythrophyllum antarcticum, Coscinodon lawianus, Ceratodon purpureus, Syntrichia sacroneurum, Cephaloziella varians*. Transformation of mineral material by sparse vegetation leads to forming of Leptosols (World Reference Base…, 2006): shallow but rich in total organic carbon.

Thin sections were examined using optical microscope Carl Zeiss Axiostar at 10X–50X magnification.

The mineral composition of different granulometric fractions was investigated by X-ray diffractometry using DRON-3 diffractometer (CuK radiation, with 0.1°step and 10 sec. scanning).

X-ray diagnostics of clay minerals was based on the results of the following tests: Mg^{+2} saturated in air-dry condition; Mg^{+2} saturated with ethylene glycol solvation for 24 hours; Mg^{+2} saturated and calcined at 350°C for 2 hours; Mg^{+2} saturated and calcined at 550°C for 2 hours.

Concentrations of the micro- and macroelements in the rocks and soils were measured on a Spectroscan Max-GV X-ray analyzer. Geochemical index (Ti/Al ratio) was used to estimate the degree of rock residual transformation by pedogenic processes.

Results

Micromorphological studying of soils of Larsemann Hills have shown some specific features of their structural organization some of which were mentioned earlier for other regions of Antarctica (Kubiena, 1970). Two main elements of soil microstructure here are coarse skeletal particles and pores. The dominant form of clay distribution in the fine earth is diffusive. Microzones of relatively stable structure were obtained within the mass of coarse particles. Despite the granular and agglomero-plasmic microstructure of the mineral material, microzones of clay accumulation were obtained. This clayish material is often optically oriented and has no features of iron accumulation. Rare particles have clayish coatings.

The well-expressed feature of organo-mineral interaction (besides the detritus accumulation on the mineral surfaces) is the formation of humic plasma on mineral particles that are in direct contact with mosses' rhisoidal sphere or with algae or lichen thalloms.

In soil samples (in contrast with rock residual) kaolinite clay is often obtained. In some cases the swelling smectite clays were detected, mainly in the lower parts of the soil profiles, and never detected in the material of rock residual. Organo-mineral material of the uppermost soil horizons is often enriched with organic acids (including humic components) and with X-ray-amorphous material. Coatings on the grains here contain hydrobiotite along with biotite itself, which may indicate among other reasons the regular change of redoximorphic conditions in soil profiles.

Bulk elements' content in the uppermost soil horizons and in the rock residual significantly differs. Organo-mineral horizons are characterized by leaching of the most of the elements (Na, Mg, Al, Si, K, Ti, Mn, Fe, Rb, Zr); only P and S (in some cases Ca) accumulate here due to high amount of soil organic matter, which (along with smectite presence) is the strong evidence of pedogenesis. Sometimes soils and rock residual are similar in Zr, Ti and Ti/Al ratio, which may indicate a low degree of pedogenesis intensity or, on the other hand, rock residual may be subjected to intense weathering in presence of liquid water.

Acknowledgments

Authors deeply thank management of the Russian Antarctic Expedition for logistical help during the fieldwork. The research was partially supported by RFBR (16-04-01050a). Laboratory analyses were carried out in Center of Common Facilities of the Institute of Physicochemical and Biological Problems in Soil Science.

References

Bockheim, J. G., Balks, M. R., & Mcleod, M. 2006. *ANTPAS Guide for Describing, Sampling, Analyzing and Classifying Soils of the Antarctic Region*. Earth. ANTPAS. 2006.

Kubiena W.L. 1970. Micromorphological investigations of Antarctic soils. *Antarctic J.* 5: 105-106.

World Reference Base for Soil Resources. 2006. 2nd edition World Soil Resources Reports No. 103. FAO, Rome: 133.

Complications of modelling coastal erosion in a permafrost environment

Brian J. Moorman[1]
Christopher Stevens[2]
Jenifer Bratsch[3]
Stephanie Lapka[4]
[1]*University of Calgary, Moorman@ucalgary.ca*
[2]*SRK Consulting (U.S.) Inc.*
[3]*Bayfield County Forestry & Parks*
[4]*Stantec*

Abstract

Modelling coastal erosion is difficult enough in southern environments. In the Arctic where permafrost must also be considered, it gets considerably more complicated. Research in the Mackenzie Delta in Canada on the distribution of the thermal and physical state of coastal terrain has elucidated some of the complications that permafrost adds to understanding coastal sedimentary processes in the Arctic. Working in a region of variable ground ice content, terrain morphology, thermal conditions and storm impact, two parameters are addressed specifically – excess ice distribution and the thermodynamics of the near shore zone. Various remote sensing and geophysical techniques were utilized to characterize the surface and subsurface properties on the terrestrial side of the shore as well as in the shallow water zone. The results illustrate the increased complexity in modelling arctic coastal erosion and provide some insights into how to take these complexities into account.

Keywords: shallow water zone, ground ice, thermal, coastal.

Introduction

The impact of costal erosion in the Arctic can be considerable given the effect it can have on communities, the terrestrial and marine environment. The influence of permafrost and excess ice on the strength and stability of the coast is a significant contributing factor to the character of coastal erosion. While permafrost initially "cements" coastlines the thermal erosion of wave action quickly melts the ice resulting in failure and shoreline retreat. In extreme ice content cases such as massive ice bodies, retrogressive thaw flows may result causing much faster coastal retreat. Some of the massive ice bodies extended below sea level and there are indications that the massive ice extends out into the shallow water zone where sea ice freezes to the bottom for an appreciable period of each winter.

Gaining a better understanding on these influences can lead to better coastal modelling, preservation and management. The objects of this research are to demonstrate effective ways to measure the spatial variability of thermal conditions and ground ice content, and to model the thermodynamics of the shallow water zone. This will aid in the prediction of coastal stability.

Study Area

The Mackenzie Delta in Northwest Territories, Canada provides and excellent location to study coastal erosion because of the variety of environments present from active lowland deltaic environments to ancient upland ice rich tundra environments. The permafrost varies from less than 100m to over 700 m thick. Ground ice content varies from unsaturated conditions to pure tabular massive ice bodies over 10 m thick. Because it is a delta, the coast is quite dynamic with zones of deposition, redistribution and erosion, with some of the eroding areas being tens of thousands of years old. The areas of greatest coastal erosion have been measured to retreat at over 10 m per year.

Methods

The focus of this research was not only to characterize the changing state of the coastal area but also to clarify the processes at work along the coast. As such, several techniques were utilized to image the surface and subsurface areas. Ground Penetrating Radar (GPR) and Electrical Resistivity Imaging (ERI) were used to map zones of permafrost with excess ice as well as imaging the thickness of massive tabular ice bodies on the landward side of the coast. Long time series LandSat imagery was utilized to map vegetation through time and the impact of storm surges. RadarSat imagery was used to determine the timing and extent of bottom-fast ice in the winter in order to create a dynamic detailed bathymetric map of the shallow water zones. The GPR was also used to map surface fresh water ice thickness, water depth, and sub bottom thermal structure to verify bathymetry maps and thermodynamic models. Finally, sub-bottom temperature cables were employed to calibrate shallow water thermal models.

Results

Mapping Ground Ice

Ground ice content directly controls how permafrost will react to erosional situations such as coastal erosion. Given similar situations, the character of coastal erosion is a function the amount and distribution of ground ice. Lower ice content permafrost coasts may just witness notching and block collapse while high ice content coasts are often characterized by retrogressive thaw flows and very rapid retreat.

Ground penetrating radar surveys were conducted along several sections of the coastline. Where the ground conditions were electrically resistive (i.e. not salty) the structure of the subsurface could be imaged to a depth of over 20 m with areas of massive ice having the best penetration. The depth of interfaces between frozen sediment, massive ice, and ice rich sediment were clearly distinguished with decimeter precision on the radar. Winter proved to be the best time to conduct GPR surveys as the electrical conductivity of the active layer is decreased when it is frozen. On land, the GPR surveys illustrated how ice content and the presence, size, and structure of massive ice were not correlated to ground surface topography, making it difficult predict the spatial variability without subsurface imaging or drilling. Thick massive ice bodies were mapped to extend below sea level. In retrogressive thaw flows it was also recognized that the massive ice body could become covered by sediment in the outflow zone before completely melting out. This could stabilize the thermal conditions and preserve the ice into the future. Because the ice bodies sometimes extended below sea level and the sediment flowing out from the retrogressive thaw flow made the near shore zone shallow enough for large areas of bottom-fast ice (leading to negative mean annual ground temperatures) to form subsea massive ice could be preserved

Thermodynamics

In deltaic environments, the coastal zone is heavily influenced by the flow of fresh water from of the river. In the shallow water zone of the Mackenzie Delta, the variability of the water depth and winter ice thickness varied greatly across distance and from year to year. This resulted in unpredicted winter river flow character and subaqueous channel development and spatially variable sub-bottom thermal conditions. The spatial variability was also seen to change quite rapidly from year to year.

Ground penetrating radar surveys conducted over fresh water ice in the delta enabled the imaging of snow and ice thickness, water depth and the thermal structure of the sub-bottom. This GPR data and direct sub-bottom ground temperature measurements demonstrated that the thermal structure of the ground was very sensitive to the duration that the floating ice is frozen to the bed. During this period of bottom-fast ice, the sub-bottom cools quickly enabling permafrost to aggrade. However, this only occurs when the water is shallow enough for the entire water column to freeze for an appreciable amount of the winter.

Spatial variability of sub-bottom permafrost

Because the dielectric contrast between water and ice is so great, while ice still has liquid water beneath it, there is a distinctive radar signature on satellite imagery compared to when it becomes bottom-fast. As a result, time-series radar satellite imagery could be used to map the seasonal evolution of bottom-fast ice across the delta. This data was then used to calculate "ice contact time", the length of time that an area was bottom fast, and model the thermodynamics and permafrost aggradation/degradation of the shallow water zone.

The thermodynamic stability of permafrost in the shallow water zone is a crucial element in the preservation of sub-bottom massive ice. Modelling shallow water thermodynamics by satellite greatly assists building process based models of coastal dynamics.

Conclusions

The results of this research have enabled a more thorough understanding of coastal conditions and processes in the Mackenzie Delta region. Both the distribution of massive ground ice and ice-rich permafrost on land, and the thermodynamics of the shallow water zone will lead to a better understanding of coastal processes and more robust modelling of coastal erosion.

Arctic Coastal Dynamics in the Area of Oil and Gas Development based on Satellite Imagery (a Case of Baydaratskaya Bay, the Kara Sea)

Anna V. Novikova, [1]
Stanislav A. Ogorodov[1]
Natalia G. Belova[1]
Alexey P. Vergun[1]

[1]*Moscow State University, Laboratory of Geoecology of the North, annamsu17@gmail.com*

Abstract

The coastal zone of the Arctic seas is extremely sensitive to human impact due to wide distribution of permafrost and under the conditions of global climate warming. In this research, we study coastal dynamics of Baydaratskaya Bay, the Kara Sea, and analyze factors of this dynamics, anthropogenic factor in particular.

Keywords: coastal dynamics; Kara Sea; Arctic coasts; human impact.

Introduction

The coasts of the Kara Sea are composed of permafrost sediments that provoke active cryogenic processes here. Among such processes, one of the most harmful for landuse is thermoabrasion. The global climate warming and induced by it reduction of sea ice extent, increasing frequency of storms, sea level rise coupled with human activities significantly enhance thermoabrasion and other natural hazards. In general, the average rates of coastal retreat in the Kara Sea are 0.8-2 m/yr for open sectors and 0.2-0,7 m/yr for closed bays (Vasiliev *et al.*, 2006). The maximum was observed on the eastern coast of Baydaratskaya Bay near Marre-Salye in 1989 and amounted to 3.5 m/yr (Vasiliev *et al.*, 2006).

In the region of our interest, the large gas pipeline Bovanenkovo-Uhta crosses Baydaratskaya Bay under water. Key areas of the study are sites on the Ural (western) and Yamal (eastern) coasts of the bay where the pipeline rises on the land. In these areas abrasion coasts predominate.

Methods

The study is based on the data of a long-term coastal monitoring and satellite imagery.

The monitoring of coastal zone at the key sites was carried out by the Laboratory of Geoecology of the North, Moscow State University, together with Zubov State Oceanographic Institute, for more than 30 years. It includes repeated topographic surveys along shore transects, every year from 1981 to 2016, and surveys of geomorphology, Quaternary geology and cryogenic composition. We also record and analyze hydrometeorological characteristics as parameters of wind-wave energy coming to the shores (Ogorodov, 2002). Moreover, we investigate coastal dynamics through interpretation of multi-temporal satellite imagery (from 1964 to 2016).

Results and Discussion

We analyzed coastal dynamics for two periods: 1) period of natural development of coastal processes – before the pipeline construction (1988-2009), 2) and for period of human impact – after the pipeline construction (2009-2016).

We calculated that abrasion coasts of the Ural site retreat with the average rate about 1.1 m/yr and on the Yamal site with about 0.2 m/yr before the beginning of the gas development. We explain faster retreat of Ural coasts by the higher contents of ice in sediments, presence of massive ground ice beds, diversity of lithology and exposure of the Ural coasts to stronger winds. The greatest retreat on the Ural coast (up to 90 meters per 40 years) was observed on the section of the high (about 15 m) terrace between Ngoyuyakha and Ngarko-Tombiakha rivers, where large massive ice beds outcrop.

After the beginning of active development, coastal dynamics in the key areas changed significantly. The construction of gas pipeline and infrastructure influences on the relief, structure and thermal regime of soils, sediment balance in the coastal zone. The combined effect has led to acceleration of retreat of abrasion segments and activation of retreat of segments stable or accumulative before. The average rate of retreat of Ural coast increased to 2.5 m/yr during the period of construction (2009-2013). The average rate of retreat of

Yamal coast increased to 0.7 m/yr during the period of 2005-2016. The contents of massive ice and highly iced loams in Ural coast provide lower resistance to anthropogenic stress compare with Yamal coast where massive ice were not found and sandy deposits are more common.

For the Ural area, we revealed the deceleration of coastal retreat after the completion of construction: the average rate of retreat in 2013-2016 is 0.7 m/yr.

Conclusions

It was found out that in natural conditions during the last decades abrasion coasts of Ural key area retreat with the average rate about 1.1 m/yr and abrasion coasts of the Yamal key area retreat with the average rate about 0.2 m/yr. During the period of underwater gas pipeline construction these rates increased twofold in Ural area, reaching 2.5 m/yr, and threefold in Yamal area, reaching 0.7 m/yr. After analysis of contribution of other factors, such as variations of wind wave energy and cryogenic composition, we consider that human impact was the main reason of the intensification of the coastal retreat.

Acknowledgments

The work was funded with the Russian National Foundation project No 16-17-00034. We thank Digital Globe Foundation for satellite imagery.

References

Ogorodov, S., 2002. Application of wind-energetic method of Popov-Sovershaev for investigation of coastal dynamics in the Arctic. In: Rachold et al. (ed.) *Reports on Polar and Marine Research*. Bremerhaven. Vol. 413, 37-42.

Vasiliev, A., Streletskaya, I., Cherkashev, G., Vanshtein, B. 2006. Dynamics of coasts of the Kara Sea. *The Cryosphere of the Earth* 910(2): 56 [in Russian].

Mechanisms controlling the evolution of rocky coasts in polar climates – examples from Arctic and Antarctic (Svalbard and South Shetland Islands)

Mateusz C. Strzelecki [1]
Michael Lim [2]
Marek Kasprzak [1]
Zuzanna Świrad [3]
Grzegorz Rachlewicz [4]
Piotr Migoń [1]
Marek Jaskólski [1]
Łukasz Pawłowski [1]
Piotr Modzel [1]

[1]*Institute of Geography and Regional Development, University of Wroclaw, Poland, mat.strzelecki@gmail.com*
[2]*School of Built Environment, Northumbria University, United Kingdom*
[3] *Department of Geography, Durham University, United Kingdom*
[4] *Cryosphere Research Department, Adam Mickiewicz University in Poznań, Poland*

Abstract

On the contrary to well-studied ice-rich permafrost coasts of Siberia, Alaska or NW Canada relatively little is known regarding the potential impacts of climate and sea-level change on polar rocky coast environments. Our work aimed to address this deficiency in understanding by quantifying the processes controlling the evolution and behavior of rock coasts evolving in polar climate based on representative examples from South Shetland Islands (Antarctic) and Svalbard (Arctic).

Keywords: rock coast evolution; periglacial weathering; paraglaciation; coastal permafrost; Arctic; Antarctic

Introduction

Up to 35% of the Arctic coastlines are rock-dominated and large parts of community and scientific infrastructure are located along rocky coasts, but few studies have focused specifically on this environment. In the Antarctica most of the recently exposed shorelines are also carved in bedrock. Previous works on polar rock coasts systems emphasized the role of icefoot, sea ice and snow cover as key controls of shore platform and cliff face geomorphology and rock coast thermal state (see Hansom et al. 2014 for a comprehensive review).

A notable exception to the deficit of research on rocky coasts in the polar regions is the Svalbard Archipelago, where one of the first ever investigation of the efficiency of rock coast erosional and weathering processes has been conducted (Jahn 1961). Rock coast studies in Svalbard have recently focused on detailed characteristics of rock coast weathering using Schmidt hammer rock tests (e.g. Strzelecki 2017). Swirad et al. (2017) analysed rock control on the geometry of northern Hornsund coastline. An important progress in understanding of Svalbard rock-dominated coastal systems was recently made by Strzelecki et al. (2017) who described the mosaic of processes and controls of rocky coast evolution along Wilczekodden, Hornsund.

Since the interesting insight into shore platform morphology by Hansom (1983) the processes controlling development of rock coasts in South Shetland Islands remain understudied.

We focused on changes in spatial distribution of coastal permafrost and the degree of rock surface weathering along landforms evolving in various lithologies. In this paper we summarize the results of our recent investigations into cryo-conditioned rock coast systems in Billefjorden and Hornsund (Svalbard) and Admiralty Bay (South Shetland Islands).

Methods

In our project we utilized a rigorous, coherent and novel suite of techniques to analyze the spatially and temporally diverse range of processes and responses controlling the polar rock coast environments:

-Schmidt Hammer Rock Tests (SHRT) of rock surface strength

-terrestrial laser scanning of rock cliffs in order to calculate their retreat rates

-traversing micro-erosion meter (TMEM) measurements of rock surface downwearing rates

-observations of seasonal changes in the state of permafrost using electrical resistivity tomography (ERT)

-monitoring of thermal state of the rocky coasts using network of thermistors

Selected findings

SHRTs, demonstrated strong spatial control on the degree of rock weathering (rock strength) along studied rock coasts. Elevation controlled geomorphic zones were identified and linked to distinct processes and mechanisms, transitioning from peak hardness values at the icefoot/sea-ice through the wave and storm dominated scour zones to the lowest values on the cliff tops, where the effects of periglacial weathering dominated. TMEM measurements indicated that significant changes in erosion rates occur at the junction between shore platform and the cliff toe, where rock erosion is facilitated by frequent wetting and drying and operation of nivation and sea ice processes. ERT surveys have been used to investigate frozen ground control on rock coast dynamics and revealed the strong interaction with marine processes in polar coastal settings. In South Shetland Islands the morphology of rocky coastal landforms borne traces of numerous environmental shifts that occurred in Antarctic region over the Holocene including storminess, relative sea-level and intensity of bioweathering associated with changes in bird colonies.

The results are synthesised to propose a new conceptual model of polar rock coast systems.

Acknowledgments

This is a contribution to the National Science Centre project UMO2013/11/B/ST10/00283: 'POROCO – Mechanisms controlling the evolution and geomorphology of rock coasts in polar climates'.

References

Hansom J.D., 1983. Shore-platform development in the South Shetland Islands, Antarctica. *Marine Geology* 53: 211-229.

Hansom, J.D., Forbes, D.L., Etienne, S., 2014. The rock coasts of polar and sub-polar regions. In: Kennedy, D.M., Stephenson, W.J., Naylor, L.A. (Eds.), Rock Coast Geomorphology: A Global Synthesis. 40. *Geological Society, London, Memoirs,* pp. 263–281.

Jahn, A., 1961. Quantitative analysis of some periglacial processes in Spitsbergen. *Zeszyty Naukowe Uniwersytetu Wrocławskiego* Seria B, nr 5. Geophys. Geogr. Geol. II 3–54.

Strzelecki, M.C., 2017. The variability and controls of rock strength along rocky coasts of central Spitsbergen. High Arctic. *Geomorphology* 293: 321-330.

Strzelecki M.C., Kasprzak M., Lim M., Swirad Z.M., Jaskólski M., Pawłowski Ł., Modzel P., Cryo-conditioned rocky coast systems: A case study from Wilczekodden, Svalbard. *Science of The Total Environment* 607-608:443-453.

Swirad, Z.M., Migoń, P., Strzelecki, M.C., 2017. Rock control on the geometry of coastal embayments of north-western Hornsund, Svalbard. *Z. Geomorphol.* 61: 11–28.

Features of frozen deposits in the Western Yamal low sea-coast plains, Russia

Nataliia Zadorozhnaia[1,2],
Irina Streletskaya[1],
Alexander Vasiliev[2,3],
Gleb Oblogov[2,3]

[1]*Lomonosov Moscow State University, Moscow, Russia, z.nataliia.95@gmail.com*
[2]*Earth Cryosphere Institute of Tyumen Scientific Center (ECI TSC) SB RAS, Tyumen, Russia*
[3]*Tyumen State University (TSU), Tyumen, Russia*

Abstract

Besides permafrost degradation under climate warming there are processes of permafrost aggradation in the low sea-coast plains, “laidas,” in the Arctic. Such coastal marshes are widespread along the Kara Sea strand (Western part of the Yamal peninsula, Russia). The low accumulative surfaces are favorable to syngenetic permafrost formation where freezing occurs synchronously with sedimentation. The marine sediments are characterized by high salinity, organic matter and water content on the low sea-coast plains have layered lithological and cryogenic structure. The layer alternation of frozen and cooled soils is due to sedimentation characteristics and climatic conditions, especially temperatures and storm surges regime. Combination of these factors on low accumulative surfaces lead to increase their heat capacity and affect the soil temperature. The depth of zero annual amplitude of ground temperature on the low sea-coast plain does not exceed 3-4 m where the temperature is around – 4.0 °C.

Keywords: permafrost aggradation; low sea-coast plains; syngenetic permafrost; Western Yamal; marine sediments.

Introduction

The permafrost degradation processes in the continental Arctic hold centre stage due to climate change according to latest publications. At the same time, processes of modern permafrost aggradation on the low surfaces have not been studied enough (Vasiliev *et al.*, 2017).

Modern permafrost aggradation

Modern low accumulative “laidas” (i.e. tidal flats) are relatively widespread along the Kara Sea coast. Low accumulative surfaces in areas of continuous permafrost are favorable to formation of syngenetic permafrost, which is formed synchronously with sedimentation. Sedimentation on shores of the northern seas depends on the amplitudes of the sea tides and ebbs, wind surges of seawaters. The freezing of soils in shallow waters and low sea-coast plains depends on changes of oceanic and climatic factors. Such conditions determine the heterogeneity of the geological section and the large water and ice saturation of sediments.

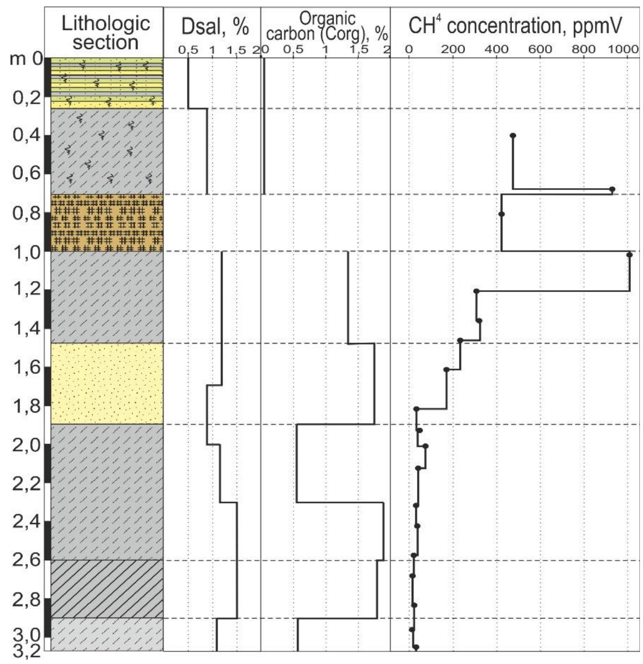

Figure 1. Generalized description of deposits on the sea laida near the Marre-Sale meteorological station (Western part of the Yamal peninsula, Russia).

Results

Description of site

The section of low sea-coast plain up to 3 meters consists of interbedding of Holocene saline sands, loams, sandy loams and clays with numerous organic matter inclusions of different decomposition degree (Fig. 1):

0-0.2 m – alternation of yellow and grey medium-fine-grained sand with rootlets of modern plants.

0.2-0.7 m – light gray sandy loam with roots of modern plants.

0.7-1.0 m – poorly decomposed dark brown peat.

1.0-1.5 m – dark gray sandy loam.

1.5-1.9 m – reddish-yellow medium-coarse-grained sand. Frozen. Cryotexture is massive with singular small ice crystals.

1.9-2.6 m – dark-gray sandy loam. Plastic-frozen. Cryotexture is massive with rare small ice crystals.

2.6-2.9 m – dark-gray loam. Plastic-frozen with a few small ice crystals.

2.9-3.2 m – dark-gray sandy loam. Frozen.

Organic-rich saline moistened sediments are favorable for methane formation on low accumulative sea-coast plain where it reaches 1000 ppmV. CH4 concentration was measured by headspace-equilibration, using KhPM-4 (Russia) gas chromatograph with flame ionization detector with hydrogen as a carrier gas (Pushchino, Russia).

Characteristics of syngenetic deposits

High salinity (up to 1.5% in loams, up to 1.2% in sands), high content of organic matter (up to 1.9% in loams, up to 1.8 % in sands) and high water content (up to 70%) leads to decrease of freezing temperature of studied sediments.

Permafrost aggradation occurs on the Western Yamal coast alongside with climate warming trend of 0.06 °C/year from 1970 to 2016 according to the Marre-Sale meteorological station data. The alternation of frozen and cooled deposits in the section was formed due to not harsh enough environmental conditions, i.e. the mean annual soil temperatures were close to the temperature of phase transitions (at the active-layer base) (Table 1).

Table 1. Mean annual air and ground temperatures at the active-layer base by years (Western Yamal, Russia).

Mean annual temperature, °C	2007	2008	2009	2010	2011	2012	2013	2014	2015
air	-5.4	-6.3	-8.9	-5.9	-3.6	-6.6	-7.4	-6.2	-3.9
deposits	-3.4		-4.7	-4.5	-3.2	-3.9		-3.4	-2.7

Conclusions

Permafrost on the low accumulative sea-coast plains is formed by syngenetic type (simultaneous sedimentation and freezing). Marine sediments include a large amount of poorly decomposed organic matter. Layered lithological and cryogenic structure of the section is due to climatic and sedimentation conditions during periodic storm surges.

Features of sedimentation, composition, ice content, salinity and organic carbon contents of sediments determine thermophysical properties and low mean annual temperature of soil with values from –3.5 to 5.5 °C. The depth of zero annual amplitude of ground temperature is small and does not exceed 3-4 m with the temperature is around– 4.0 °C on the observed low sea-coast. This is connected with increase in the heat capacity and the heat costs on phase transitions during the decrease of freezing temperature in saline sediments. Permafrost thickness varies from 5 to 10 meters.

Acknowledgments

The study was supported by grant 16-05-00612 from the Russian Foundation for Basic Research.

References

Vasiliev, A. & Oblogov, G. & Streletskaya I. et al., 2017. Thermal regime of the upper part of permafrost in the transition zone from land to sea, Western Yamal. *Earth's Cryosphere* v. 21, 4: 34-42.

21 - In situ permafrost sensing and monitoring technologies

Session 21

In situ permafrost sensing and monitoring technologies

Conveners:

- **Anna Wagner**, Cold Regions Research and Engineering Laboratory, Fairbanks, AK, USA
- **Nate Lindsey**, University of California, Berkeley, USA (PYRN member)
- **Jonathan Ajo-Franklin**, Lawrence Berkeley National Laboratory, Berkeley, USA

Permafrost degradation reroutes surface and groundwater flow, changes vegetation patterns, increases wildfire susceptibility, modifies topography, and releases carbon dioxide and methane to the atmosphere. The thermal, hydrological, and mechanical processes at play during degradation have been hypothesized to couple in complicated ways, but traditional single-point, ergodic, and remote sensing data collection campaigns are limited in their range and/or resolution in space and time. As a result, coupled multiphysics simulations have largely outpaced important calibration datasets. Meanwhile, recent efforts to generate in situ observations at the field-to-watershed scale using dense sensor deployments to capture transformations of permafrost are creating opportunities to test these hypotheses and numerical models. This session will explore novel advances in the field of in situ sensor technology including new sensing modalities, units, geometries, telemetry, data handling, and application domains with a focus on tracking the evolution of permafrost systems. We welcome case studies as well as relevant numerical and modeling studies used for guiding sensor design and installation.

Causes of altitudinal zonation of ground temperature in the Udokan ridge

Alexey Boyko[1]
[1]*Lomonosov State University, Department of Geocryology*

Abstract

The analysis of the geocryological monitoring in the Udokan Ridge and the Chara Basin (Sergeev *et al.*, 2016) shows vastly different thermal regimes in various altitudinal zones and relief elements. The altitude of the measurement points varies from 700 m. to 2035 m., and the mean annual ground temperature varies from -7.3°C to -0,6 °C. While the trend of annual temperatures seems to be constant, it is possible to apply the data of the old boreholes that are nowadays out of service (Romanovsky *et al.*, 1991) to identify dependencies between the spatial distribution of geocryological conditions, natural conditions and altitudinal zonation.

Keywords: Geocryological monitoring; temperature measurement; permafrost mapping.

Introduction

The area is located in Stanovoi plateau and includes mountain ridges and intermontains related to the Baikal rift zone (Romanovsky *et al.*, 1989). According to the data of the state meteorological observations over the last 50 years in Chara, the average rate of increase in the average annual air temperature approximately 0.03°C/year. Thus, it is known as the region with highly dynamic rate of warming. Despite this fact, the climate of the region is harsh: winters are long and cold, summers are short and warm. The formation of the permafrost layers of the Udokan ridge occurred under the influence of severe intracontinental climatic conditions and their periodic changes during the Quaternary period. Significant influence on the state and structure of permafrost within the limits of both mountain structures and depressions, was provided by semi-continental and alpine glaciations. Also the local climatic conditions are heavily influenced by a complex relief. There is a complex connection between annual air temperature and altitude. It rises with altitude due to the Balch effect on the range of heights from 700 to 900 m. On the altitude levels from 900-1100 m the temperature is maximum and stable (-6.5°C - -6.8°C). Above 1100 m it decreases with height.

The continuity of coverage of permafrost within the alpine elevation level (>1400 m) is continuous. The base depth of permafrost reaches 800-900 m and -8°C on the ranges of ridges with absolute heights of 2000-2200 m (Romanovsky *et al.*, 1989). There could be several reasons for formation of such an extended permafrost:

- larger surface area in comparison with gentle slopes;
- high drainage degree of rocks;
- high thermal conductivity and low heat capacity of rocks;
- low warming effect of snow cover on peaks and hilltops;
- altitudinal zonation of environmental conditions;
- wide presence of kurums.

Mountain (1200-1400 m) permafrost is discontinuous. Several thawed areas does exists within the river valleys such as Naminga, China, Apsat, Sakukan etc. Depth of permafrost varies from 100 to 200 m. Annual ground temperature varies from -2°C to -3°C. Lowland (800-1200 m) permafrost is also continuous with average depth of 100-350 m and annual ground temperature from -3°C to -5°C.

References

Romanovsky, N.N., Tyurin, A.I., Sergeev, D.O., Afonskaya, L.G., Boikov, S.A., Volvoka, V.P., Volchenkov, S.Yu., Zaycev, V.N., Klimov, I.V., Lisicina, O.M., Solovyev, V.P. & Yavelov A.V., 1989. Kurumi Gol'tsovogo Poyasa Gor. Novosibirsk Nauka: 30-33.

Romanovsky, N.N, Zaitsev, V.N., Volchenkov, S.Yu., Zagryazkin, D.D. & Sergeyev, D.O., 1991. Alpine permafrost temperature zonality, northern trans-Baikal region, U.S.S.R. *Permafrost and Periglacial Processes* 2 (3): 187-195.

Sergeev, D.O., Stanilovskaya, J.V., Perlshtein, G.Z., Romanovsky, V.E., Bezdelova, A.P., Alexutina, D.M., Bolotyk, M.M., Khimenkov, A.N., Kapralova, V.N., Motenko, R.G. & Maleeva, A.N., 2016. Back ground geocryological monitoring in northern Transbaikalia region. *Earth's Cryosphere* 20 (3): 24-32.

Monitoring and mitigation of the ground temperature regime of ice rich permafrost to stabilize highway foundations in Yellowknife, Canada.

Igor Egorov[1]
Dennis Krys[2]

[1]*National Research Council of Canada, Igor.Egorov@nrc-cnrc.gc.ca*
[2] *National Research Council of Canada, Dennis.Krys@nrc-cnrc.gc.ca*

Abstract

Numerous sections of Canadian highways are identified as high risk and are currently susceptible to climate change. The road foundation conditions are often ice rich permafrost with massive ground ice or thick segregated ice lenses. Thermokarst and thaw subsidence of such environment is critical to take into account for geotechnical investigations for roads design, maintenance or remediation. Monitoring and mitigation of ground temperature regime is also necessary to provide road stability and decrease maintenance costs. Increasing costs and greater risks of failure in the future have prompted NRC to evaluate permafrost monitoring and mitigation techniques and their effectiveness in improving highway performance and reducing operating costs. Several new passive and active cooling methods to moderate permafrost thaw are undergoing testing at NRC sites. New temperature probes are being used which eliminate the number of interfaces between the soil and temperature sensors. These probes are undergoing testing at a NRC site in Yellowknife.

Keywords: ground thermal regime; thermokarst; subsidence; monitoring; mitigation; ground temperature probe; discontinuous permafrost; thermal disequilibrium; Northwest Territories

Introduction

Construction of Highway 3 in Yellowknife and climate variations have caused thaw settlement of the road and adjacent areas in sections where the highway is underlined by ice-rich permafrost of lithalsas. It significantly increased the annual operating costs and maintenance of the highway. A thermokarst has developed on the both sides of the highway at the study location due to thaw of ice-rich soils of lithalsa. Climate warming will further intensify the thermokarst processes. National Research Council of Canada (NRC) and its partners have initiated a research project to evaluate permafrost mitigation techniques and their effectiveness in stabilizing highway and reducing operational costs. Previous studies assessed the susceptibility of the highway and described sensitive ice-rich permafrost areas estimated the potential impacts of the climate change on the similar permafrost ecotopes and Highway 3 in particularly where the highway is underlain by thaw sensitive permafrost (Wolfe *et al.*, 2015; Morse *et al.*, 2015, Gaanderse, 2015). NRC is proposing a conceptual solution and permafrost thaw remediation strategies using the findings in previous research of ice rich permafrost in the area as well as results from GSC and NRC sites (Wolfe *et al.*, 2015; Morse *et al.*, 2015; Gaanderse, 2015). The objectives of this research project are to: (i) evaluate the effectiveness of new methods of ground temperature investigations and monitoring; (ii) analyze the thermal gradients, lags and amplitudes together with mean annual ground temperature (MAGT) profiles to identify thermal properties of the soils and forecast thaw sensitivity of permafrost; (iii) establish field pilot tests for demonstration of new passive and active techniques moderating permafrost thawing and stabilizing highway.

Study Site

The study site is located near Boundary Creek within the Great Slave Lowlands 30 km from Yellowknife. Yellowknife has a continental climate with mean annual ground temperature -4.3 °C (Environment Canada http://www.climate.weather.gc.ca/). Mean total precipitation is 289 mm, rain is about 59%, and average maximum snow depth is 0.38 m (Wolfe *et al.*, 2015).

The site is located in discontinuous permafrost zone underlain by 50-90% of permafrost. Permafrost is associated mostly with peat deposits (Brown 1973) but also common in fined-grained unconsolidated ice rich sediments (Morse *et al.*, 2015). Permafrost is generally less than 50 m with MAGT >-2°C. The raised terrain site investigated is about 50 m from highway #3 (Fig. 1). Highway 3 was constructed during mid 1960s utilizing local silt and clay and during 2000s utilizing open-graded blast rock material with a chip-sealed surface treatment. Surface ponds often occurred along the embankment in thermokarst depressions. Change in drainage patterns resulting from highway construction pose significant challenge to stability of the highway in the future.

Fig. 1 Study site is located on the raised terrain, former lithalsa with ice rich silty clay sediments.

Methods

Ground temperature from natural settings was measured in 4 boreholes to depths up to 8.5 m with new advanced probes (Fig. 2). Ground temperature was recorded hourly by data loggers. Temperature are known to 0.05ºC with actual temperature change resolution 0.01ºC. We also examined ground temperature measured to 10 m depth reported in previous reports.

A new probe was developed to achieve more accurate ground temperature measurements. The probe was constructed out of 1 inch schedule 80 PVC pipe with 1x2 welding nipples connecting the sections of the PVC pipe. The welding nipple is a 1 inch ID and 2 inch long stainless steel tube with threads on both ends. The welding nipples were used at every location where there was a temperature sensor. The welding nipples were modified by welding fins onto them that would act as heat sinks for the temperature sensors. This was done to increase the surface area and to guarantee good contact with the soil around each temperature sensors.

Discussion

This work is aimed at evaluation of the effectiveness of new methods of ground temperature investigations in warm permafrost alongside of highway 3 in Yellowknife as well as monitoring and mitigation of thermokart thermal regime in a lithalsa ajustent to the highway. The research work analyzes the thermal gradients, lags and amplitudes together with mean annual ground temperature (MAGT) profiles to identify ground temperature trends, thermal properties of the soils, latent heat due to unfrozen water and forecast thaw sensitivity of warm ice rich permafrost. The work is also aimed to establish field pilot tests to demonstrate new passive and active techniques moderating permafrost thawing and stabilizing the highway.

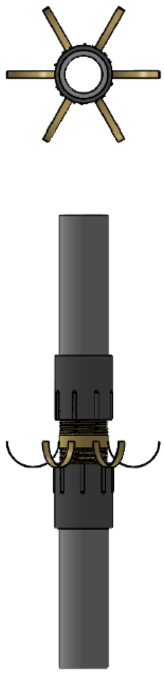

Fig. 2 Ground temperature probe with steel fins, heat sinks.

References

Morse, P. D., Wolfe, S. A., Kokelj, S. V., & Gaanderse, A. J. R., 2015. The Occurrence and Thermal Disequilibrium State of Permafrost in Forest Ecotopes of the Great Slave Region, Northwest Territories, Canada. *Permafrost and Periglac. Process 2015,* DOI: 10.1002/ppp.1858.

Wolfe, S.A., Morse, P.D., Hoeve, T.E., Sladen, W.E., Kokelj, S.V. & Arenson, L.U., 2015. Disequilibrium permafrost conditions on NWT Highway 3. *Proceedings of GeoQuébec-2015, 68th Canadian Geotechnical Conference and 7th Canadian Permafrost Conference.*

Gaanderse, A.J.R., 2015. *Geomorphic origin of a lithalsa in the Great Slave Lowlands, Northwest Territories, Canada*: Carleton University, 171 pp.

Automation in the field of geotechnical monitoring of especially dangerous industrial objects

M.V. Kasymskaya[1]
I.V. Prokopyuk[1]
A.A. Sharkov[1]
D.N. Krivov[1]
M.V. Kasymskaya[1]
M.Yu. Melyutin[1]
[1]*LLC Stroygazizyskaniya,* kasymskaya@sgiz.ru

Abstract

The development of fields' infrastructure in the permafrost region is necessarily accompanied by geotechnical monitoring. On the example of the test object the "SmartGTM" automated system is to be considered, which carries out a constant monitoring over any changes in the parameters of natural and geotechnical environment, and that predicts the condition of soil massif at the stages of any buildings and constructions' erection and operation.

Keywords: geotechnical monitoring, automated systems.

Most of the Russian oil and gas fields are located in the permafrost region. The buildings and constructions as being a part of the fields' infrastructure are exposed to a wide range of processes starting from the moment of their erection and further on during operation thereof, which adversely affect the stability, safety and efficiency of their use [1, 2].

Traditionally, geotechnical monitoring networks are to be used to monitor the condition of buildings and constructions, as well as their interaction dynamics with the natural and technical environment by using the classical "manual" method of data collection and processing. The frequency of observations of the main parameters, which characterize the construction's condition (foundation settlements, ground temperatures, ground-water levels) is one month (within the constructional period). At the same time, the development of many negative processes occurs much faster. In addition, the use of "manual" method of data collection often does not provide the required accuracy of taken measurements.

At present, we have developed some new technical solutions for organizing monitoring networks by using an automated method of data collection. The "SmartGTM" automated system is a hardware and software complex that includes the sensors for monitoring the parameters of the natural and technical environment (temperature, ground-water level, spatial position of constructions and etc.), communication systems, network and server equipment. This program also registers, stores, processes, visualizes and analyzes the results of such observations.

Approbation of the automated system was carried out on the real object of the Urengoy field. The study area refers to the zone of continuous permafrost with mean annual ground temperatures within the frames of minus 2.1 to minus 2.8 degrees Celsius. In the process of construction the natural landscapes were covered with a backfill with a thickness of 0.5 to 3.0 meters. The construction and operation of the facilities were planned with preservation of the frozen ground base and special measures for thermal stabilization.

Initially, data out of the survey data that is to be performed in natural environment, such as a topographic plan, geological sections, and mean annual ground temperatures for various landscapes were entered into the database of the system. Further, the database was supplemented with some design solutions (Fig.1) and the criterial parameters of the operational reliability of the buildings and constructions, namely the values of limiting deformations, the forecast mean annual temperatures of soils and etc.

In the process of construction, as monitoring network is to be arranged, the information was collected from the facilities, and geocryological and hydrogeological conditions were assessed for the area and depth at a given time period in comparison with the background values and project data (Fig. 2) in the remote mode. Thanks to the "SmartGTM" system the appeared zones of closed taliks that occurred under the erected construction and the soil massifs thawing on 0.5

to 1.0 degrees Celsius were discovered during the first six months. Timely received information allowed to give some recommendations for taking special measures to stabilize the temperature field.

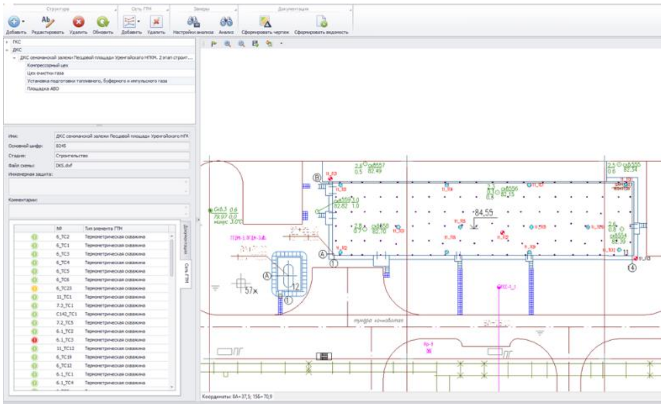

Figure 1. The fragment of a general plan of the project with design solutions (deformation marks, thermometric and hydrogeological holes and etc.)

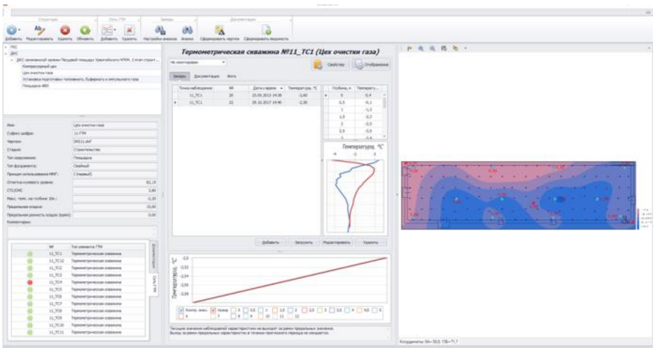

Figure 2. The results of thermometric observations and analysis of any soil temperature changes (left); The temperature field of the soil massif at a given time period and depth (right).

For the purpose of technical and economic optimization any observations by using the system can be carried out under various scenarios that are optimal for the conditions of a particular facility, such as monitoring with one key parameter (for example, monitoring of the temperature regime), or a comprehensive approach involving observations of all possible factors that affects the dynamics of natural and technical environment.

Based on the foregoing, the SmartGTM system has distinct advantages over the "manual" method, insofar as it increases operational and environmental safety, as well as an economic efficiency at all stages of the buildings and constructions life cycle.

References

Baulin, V, Aksenov, V.I., Dubikov, G.I., and *et al.* 1996. Engineering-geological monitoring of Yamal oil-and-gas fields. Tyumen. Institute of Northern Development Siberian Division Russian Academy of Sciences.

Chernyadiev, V.P., 1980. Forecast of the geocryological situation in connection with the violation of natural conditions. // Geocryological forecast and improvement of engineering surveys. Moscow. Stroyizdat.

Establishment of a complex ecological observation network in the discontinuous permafrost zone of Interior Alaska

Alexander Kholodov[1]
Susan Natali[2]
Michael Loranty[3]
Javier Fochesatto[1]
Vladimir Romanovsky[1]
[1]*University of Alaska Fairbanks, alkholodov@alaska.edu*
[2]*Woods Hole Research Center*
[3]*Colgate University*

Abstract

Permafrost is a crucial component in hydrological and ecological systems in Interior Alaska. Presence of a layer of frozen ground close to the surface controls the availability of water for vegetation as well as the processes of decomposition of soil organic material. At the same time, the presence of permafrost here is determined mostly by the ecosystems. This fact creates significant spatial variability in surface energy (and water) balance. This heterogeneity and the feedbacks between different components of the natural system make it increasingly difficult to model and integrate remote sensing data to develop an understanding of ongoing ecosystem changes in this region. Thus, coupled monitoring of ground temperature and soil moisture dynamics, radiation balance and biogeochemical processes combined with ecological surveys can provide advanced datasets for better description of these interacting processes. This research presents an example of establishment such complex observation system in the Fairbanks area.

Keywords: Permafrost, climate change, soil moisture, terrestrial ecology, radiation balance, monitoring.

Introduction

Interior Alaska is a region with dry continental climate. It belongs to the zone of boreal forest (Chapin et al., 2006). This is a region of discontinuous permafrost distribution. Under the current climate conditions, permafrost should not exist here and the reason for its presence is the cooling effect of the ecosystem on the heat transfer at the ground surface (Jorgenson et al., 2010). From the ecosystem perspective, presence of a frozen soil layer close to the ground surface controls the amount of water available for vegetation. The hydrological impact of permafrost is extremely important for the dry climate of this region. Thawing permafrost amplifies the low precipitation impact on the transpiration process (Cable et al., 2014). Thus, permafrost degradation can initiate dramatic ecosystem changes.

Research Site Characteristics

The research area is located in the city of Fairbanks, AK just north of the University of Alaska campus.

The observation network includes five sites located in different ecosystems. Three sites: Smith Lake (SL) 1, 2 and 3 are located in boreal forests dominated by black spruce (Picea mariana Mill B.S.P.) with high, medium, and low tree densities, respectively. Smith Lake 4 is a wetland with graminoid tussocks. The fifth site called Bicycle Bumps (BB) is located in an area where the original forest was demolished in 1908 (Pewe, 1954). It initiated permafrost thaw and formation of high-center polygons. It is now a deciduous forest with very uneven topography. Permafrost underlays the whole area except for BB. At SL3, deep seasonal thawing in 2006-2007 resulted in detachment of the active layer from permafrost and talik formation up to 2m depth.

The great variety of natural conditions in such a small area (the sites are separated by distances less than 1 km) makes this place an ideal location for intensive research on interactions between permafrost and ecosystems.

Methods

To understand the modern evolution of ecosystems in this area we combined ecological, soil and snow surveys with continuous measurements of air and ground temperature, air relative humidity, soil moisture, solar and photosynthetically active (PAR) radiation and soil organic matter (SOM) transformation. For the last component, we applied Tea Bag Index (TBI). This method allows estimates of both the rate of decomposition and the inhibiting effect of environmental conditions on the decay of labile fraction of SOM (Keuskamp et al., 2013).

Results and Discussion

Results of our research show that ground surface temperatures at all observation sites are well above the freezing point, with the exception of SL4 located within the tussock-dominated terrain (Table 1) due to shading effect of graminoid tussocks during summer, and snow redistribution at the beginning of winter. The warmest ground surface is at the BB site. SL4, which is also characterized by the lowest mean annual ground temperature (MAGT) at 1.5 m deep. Negative MAGT at the sites SL1 and SL2 is mostly caused by the thermal offset due to differences in thermal conductivity of frozen and unfrozen soil. The highest thermal offset occurs in peaty soil. Hence, the temperature gradient within active layer correlates with SOM content.

Table 1. Temperature regime at the observation sites in 2017.

Site ID	T at the ground surface	T at the 1.5 m	ΔTsurface during summer	ΔT in active layer
SL1	3.90	-0.39	-1.87	-4.29
SL2	2.55	-1.02	-0.94	-3.57
SL3	3.23	0.27	-4.83	-2.97
SL4	-0.78	-2.97	-16.45	-2.19
BB	4.71	1.77	-2.67	-2.93

Trees provide a shading effect during summer. The highest cumulative amount of solar radiation is received at the relatively open SL3 and SL4 sites, while the lowest at the high tree stand density: SL1 and BB. Similar pattern was noticed for PAR. The difference is that canopies of deciduous forest at BB site adsorb more radiation than spruce trees at SL1.

Soil moisture regime at the research sites largely depends on the presence of a frozen ground layer close to surface. At the boreal forest underlain by permafrost, the mineral soil is always fully. Water content in the organic layer fluctuates depending on precipitation, evapotranspiration and capillary rise. At the permafrost free BB site, soil saturation was reduced during the summer due to vertical drainage.

Differences in ground thermal and moisture regimes from site to site affect the process of SOM transformation. Rates of decomposition depend on ground surface temperature during summer and decreased from BB site to SL1. Stabilization factor, which indicates inhibition of decomposition of labile fraction of organic due to its partial recalcitrant, is mostly controlled by the soil moisture and reduces with increasing of saturation degree. Thus, warm but dry terrain of the BB site provides better conditions for freshly accumulated SOM stabilization.

Conclusion

Permafrost and ecosystems in Interior Alaska are strongly coupled to each other. Increasing biological productivity induced by climate warming may make permafrost more resilient. However, permafrost degradation will increase soil drainage and result in significant changes in vegetation and soil respiration processes. Small-scales spatial variability of natural conditions creates difficult condition for using remote sensing products for environmental monitoring in this region. A complex terrestrial observation network with dense sensor deployment provides an advanced platform to contribute to interpretation of remote sensing products and help modeling efforts to elucidate complex permafrost-ecosystem interactions and therefore provide further insights into natural changes.

Acknowledgments

Current research supported by the US National Science Foundation project #1417908.

References

Cable, J. M., Ogle, K., Bolton, W. R., Bentley, L. P., Romanovsky, V., Iwata, H., Welker, J. 2014. Permafrost thaw affects boreal deciduous plant transpiration through increased soil water, deeper thaw, and warmer soils. *Ecohydrology*, 7(3), 982-997.

Chapin, F.S., Oswood, M.W., Van Cleve, K., Viereck, L.A., Verbyla, D.L. eds., 2006. Alaska's changing boreal forest. Oxford University Press, 354 pp.

Jorgenson M.T., Romanovsky V., Harden J., Shur Y., O'Donnell J., Schuur E.A.G., Kanevskiy M., Marchenko S. 2010. Resilience and vulnerability of permafrost to climate change. *Canadian Journal of Forest Research-Revue Canadienne De Recherche Forestiere*, 40.

Keuskamp, J. A., Dingemans, B. J., Lehtinen, T., Sarneel, J. M., & Hefting, M. M. 2013. Tea Bag Index: a novel approach to collect uniform decomposition data across ecosystems. *Methods in Ecology and Evolution*, 4(11), 1070-1075.

Péwé, T. L., 1954: Effects of permafrost on cultivated fields, Fairbanks area, Alaska. In: *U.S. Geological Survey Bulletin*, 989- F, 315-351.

Hydro-chemical detection of dead ice and permafrost degradation

Sabine Kraushaar[1], Sarah Kamleitner[1], Verena Czarnowsky[2], Jan Blöthe[3], David Morche[4], Kay Knöller[5], Peter Steier[6], Johannes Lachner[6]

[1]*University of Vienna, Department of Geography and Regional Research, Vienna, Austria, contact: sabine.kraushaar@univie.ac.at*
[2]*Leipzig University, Institute for Geography, Leipzig, Germany*
[3]*University of Bonn, Institute for Geography, Bonn, Germany*
[4]*Martin-Luther-University Halle – Wittenberg, Institute of Geoscience and Geography, Halle, Germany*
[5]*Helmholtz Centre for Environmental Research – UFZ, Halle, Germany*
[6]*University of Vienna, Isotope Research and Nuclear Physics, Vienna, Austria*

Abstract

Perennial and episodic springs well from the lateral moraine deposits in the proglacial area of the Kaunertal valley and potentially indicate dead ice and permafrost thawing. The water samples origin could be differentiated in pre and post nuclear ice or no ice waters using stable isotope signatures δ^2H and $\delta^{18}O$, and the long-lived anthropogenic radionuclide ^{129}I. Results hint dead ice lenses and permafrost in subsurface areas below 2300m. Geo-electric measurements validate the existence of the ice and ablation measurements gave first insights into the volume loss during summer days. The late melt out of dead ice and permafrost up to 70 years after glacial retreat has potential significance for slope stabilities, image based erosion measurements and possibly the future water balance in Alpine valleys.

Keywords: *Permafrost; stable isotopes; radionuclides; thermal erosion*

Introduction

In recent years, the global climate change raised average temperatures in Austria by 1.5°C causing an acceleration in glacier retreat in the Alps and exposing lateral moraine deposits on the steep valley flanks (Warburton, 1990; Carrivick & Rushmer, 2009; Carrivick *et al.*, 2013; APCC, 2014). These unconsolidated sediments are presently eroding with visible gully features and landslides along the slopes (Dusik *et al.*, 2014; Baewert und Morche, 2014). In the Kaunertal Valley perennial and episodic springs well from these lateral moraines. We hypothesize that the springs indicate the melt out of dead ice lenses or permafrost in areas below 2500m, causing a potential significant volume loss of the matrix due to the melt out of ice and the drainage of the water. This could lead to a potential decrease of slope stability in the proglacial long after glacial retreat.

In this study, we aim to identify the spring waters origin using hydro chemistry analysis, ERT measurements, and ablation stakes to validate the chemical findings and quantify the volume loss due to the melt out.

Methods

Sampling

From May until October 2015 around 240 water samples were monthly derived from the various springs in altitudes between 2100 and 2330m. Additionally, monthly averaged precipitation samples, and samples from the Gepatschferner glacier were collected. Waters were analyzed on site for their pH, EC, and temperature and locations recorded.

Fieldwork

ERT measurements were implemented on five transects and 17 ablation stakes inserted in areas were ice lenses were visible in lateral moraine deposits, measuring 72 ablation days in total.

Laboratory analysis

Samples were analyzed at the Helmholtz Centre for Environmental Research in Halle for their stable isotope signatures of δ^2H and $\delta^{18}O$ by means of the Cavity Ring-Down Spectroscopy (Picarro, Danta Clara, CA, USA) and referenced against the Vienna Standard Mean Ocean Water (V-SMOW).

At the Nuclear Physics Department of the University of Vienna the long-lived anthropogenic radionuclide ^{129}I concentrations were examined following an iodine extraction scheme for AMS measurements modified after Szidat *et al.* (2000) and supplemented with additional analysis steps from Jabbar *et al.* (2011).

Results

Stable isotope signatures showed that glacier samples of melted ice had a significantly lighter isotopic composition than precipitation and water samples with long time surface exposure, such as impounded water reservoirs. Springs could be differentiated in two groups using cluster and discriminant analysis with one group being characterized by significantly lower temperatures, lower EC values and a lighter isotope signature.

The ^{129}I results showed a similar pattern of statistical significant differences between glacier and precipitation samples with the latter showing several magnitudes higher concentration values. Springs plotted along the full concentration gradient.

Discussion

The lighter isotopic cluster group with colder waters and a lower EC was interpreted as being melt waters from ice. However, it was not clear from the stable isotope signature alone if these melt waters originate from (i) recent ice, (ii) dead ice from the glacier or (iii) the active or passive layer of permafrost thawing. Thus, the relative dating of the spring's water with ^{129}I was helpful to determine a potential pre or post nuclear surface exposure of the waters (older or younger than 1950), assuming that low concentration point to dead ice or the passive layer of permafrost thawing (Herod *et al.*, 2016).

The combined method was assessed on three samples, where the origin was known: the glacier samples (pre nuclear ice), the impounded water reservoirs (post nuclear and no ice), and the precipitation samples (post nuclear no ice). The hydro chemical results validate all of these origins.

All but two springs indicating ice show a reasonable spatial pattern with their location on north and northwest exposed slopes. Some of them depict a pre nuclear origin and many mixed waters, possibly caused by a recent atmospheric ^{129}I contamination of the ice due to observed partial ice exposure by off sliding sediments on the slopes.

ERT transects validate the existence of subsurface ice in two out of three chosen areas and ablation stakes gave a first insight into potential daily thawing volume in summer month of 2.5±1.2cm.

Calculated on the area of the north exposed moraine this would amount to 850±407m^3 matrix volume loss on one summer day.

Conclusions

Stable isotope signatures and ^{129}I concentrations can hint the origin of spring waters in the proglacial. First estimated volume loss due to the melt out of dead ice or permafrost points to a potential significant amount when deriving sediment erosion volumes in proglacial areas with imaged based technologies such as LIDAR, TLS or SfM technologies. Furthermore, it is speculated that areas with springs indicating pre nuclear ice origin might face higher slope instabilities in the future.

Acknowledgments

The authors would like to express their great appreciation to laboratory staff, various field hands and the Austrian and German tax payer who financially made this research possible.

References

APCC - Austrian Panel on Climate Change, 2014. *Austrian assessment report 2014. AAR 14.* Österreichischer Sachstandsbericht zum Klimawandel, Wien.

Baewert, H., Morche, D., 2014. Coarse sediment dynamics in a proglacial fluvial system (Fagge River, Tyrol). *Geomorphology* 218: 88-97.

Carrivick, J.L., Rushmer, E.L., 2009. Inter- and intra-catchment variations in proglacial geomorphology: an example from Franz Josef Glacier and Fox Glacier, New Zealand. *Arctic, Antarctic, and Alpine Research* 41: 18-36.

Carrivick, J.L., Geilhausen, M., Warburton, J., Dickson, N.E., Carver, S.J., Evans, A.J., Brown, L.E., 2013. Contemporary geomorphological activity throughout the proglacial area of an alpine catchment. *Geomorphology* 188: 83-95.

Dusik, J., Heckmann, T., Neugirg, F., Hilger, L., Haas, F., Becht, M., 2014. The effect of rainfall events with changing frequency and magnitude on reworking conditions of proglacial moraines. *Geophysical research abstracts* Bd. 16: EGU2014-9781.

Jabbar, T., Steier, P., Wallner, G., Kandler, N., Katzlberger, C., 2011. AMS analysis of iodine-129 in aerosols from Austria. *Nuclear Instruments and Methods in Physics Research* B 269: 3183–3187.

Herod, M.N., Li, T., Pellerin, A., Kieser, W.E., Clark, I.D., 2016. The seasonal fluctuations and accumulation of iodine-129 in relation to the hydrogeochemistry of the Wolf Creek Research Basin, a discontinuous permafrost watershed. *Science of the Total Environment* 569–570: 1212–1223.

Szidat, S., Schmidt, A., Handl, J., Jakob, D., Botsch, W., Michel, R., Synal, H.-A., Schnabel, C., Suter, M., López-Gutiérrez, J., Städe, W., 2000. Iodine-129: Sample preparation, quality control and analyses of pre-nuclear materials and of natural waters from Lower Saxony, Germany. *Nuclear Instruments and Methods in Physics Research* B 172: 699–710.

Signals before subsidence: seismic waves slow down during permafrost thaw

Nathaniel J. Lindsey[1,2], Anna M. Wagner[3]
Stephanie R. James[4], Shan Dou[2], Ian Ekblaw[2], Art Gelvin[3]
Stephanie P. Saari[3], Jonathan Ajo-Franklin[2]

[1]*University of California, Berkeley, California, United States*
[2]*Lawrence Berkeley National Laboratory, Berkeley, California, United States*
[3]*U.S. Army Cold Regions Research and Engineering Laboratory, Ft. Wainwright, Alaska, United States,*
[4] *University of Florida, Gainesville, Florida, United States*

Abstract

How does permafrost thaw affect soil properties (e.g., density, permeability, hydraulic conductivity, saturation, bulk and shear modulus, etc.)? How do soil properties feedback into the style, rate, and timing of the permafrost thaw process? This paper studies the in situ evolution of soil properties undergoing thaw, using a network of >4000 distributed acoustic sensors (DAS) and both active and passive seismic sources. We conduct our time-lapse seismic experiments during a field-scale permafrost warming experiment in Fairbanks, AK. Using these data, we explore how seismic energy (5 – 80 Hz) propagating through the subsurface changes velocity and amplitude as permafrost warms. Our hypothesis is that melting ground ice decreases elastic wave velocity due to decreasing shear modulus, and causes attenuation effects related to partial melting and changes in scattering.
Keywords: geophysics, seismology, permafrost thaw

Introduction

When surface temperatures increase, ice-rich permafrost thaws, often resulting in surface subsidence. Our lack of understanding about the involved thermo-hydro-mechanical couplings is important because of the infrastructure hazard and feedbacks to biogeochemical processes. Alaska will spend more than $2 billion addressing and responding to near-surface permafrost thaw this century (Melvin et al., 2016). The UN Environmental Program has identified permafrost thaw as one of the most significant yet least studied environmental hazards (Schaefer et al., 2014). We are exploring the geophysical signals of permafrost thaw to understand the physical process and potentially aid in development of a thaw subsidence early warning system.

Recently, we artificially thawed a zone of discontinuous permafrost in a field-scale warming experiment (Wagner et al., this volume) to explore how seismic wave propagation is modified during permafrost thaw at the fieldscale. A novel distributed fiber-optic seismic recording method called Distributed Acoustic Sensing (DAS) was used to make dense array recordings in a continuous fashion (Daley et al., 2016). In this paper we describe preliminary seismic observations from this experiment.

Methodology & Seismic Data

Beginning in early August 2016, a 20m x 30m area at the permafrost table (~4m depth) in Fairbanks, AK was warmed using 121 resistive heaters (60W/heater). Over the next 60 days, a dense (1 sensor/m) fiber-optic distributed acoustic sensing (DAS) seismic array comprised of 4,000 sensing points in a rectilinear grid captured continuous passive recordings of local traffic noise (2 – 40 Hz) and a controlled-source orbital vibrator (30 – 80 Hz). By the end of the warming experiment the permafrost table directly below the array deepened by about 1m and the ground surface subsided 10 cm.

During each day of warming ambient seismic was analyzed (Park and Miller, 2008; Dou et al., 2017; Viens et al., 2015) to recover a stationary, 6-hour coherency estimate of the Green's Function between any two seismic sensors (4,000 x 4,000 = 16,000 potential raypaths).

Results

Using two colinear fibers separated by the warming plot (see example geometry in Figure 1), we find a seismic phase that slows down after August 31, resulting in a relative delay of >9% by early October (Figures 2 and 3).

This phase is hypothesized to be a relatively long period surface wave for the vehicular energy considered, or a refracted body wave (S-wave) energy, which has sensitivity to the permafrost thaw zone. These observations are compared with control raypaths that sampled permafrost outside the heated zone. These observations track the warming experiment's evolution within the permafrost volume as observed by temperature sensors and LiDAR.

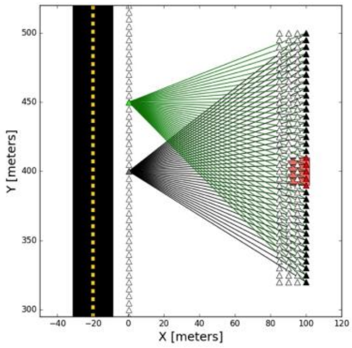

Figure 1. Example ambient noise source-receiver geometry with respect to Farmer's Loop Road (at left). Triangles represent 10% of the DAS sensing points recorded. Lines between triangles (length=100m) indicate raypaths used. The red rectangle is the artificial warming site.

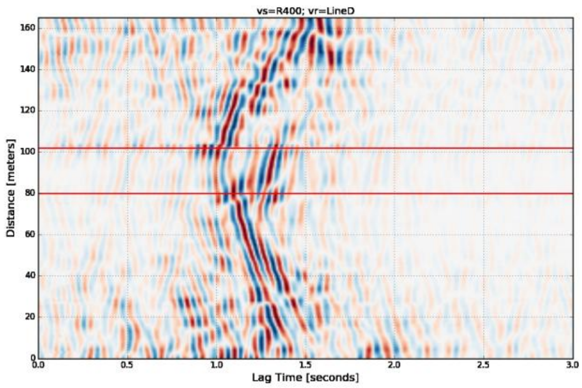

Figure 2. Virtual shot gather for October 10, 2016 representing an estimate of the Green's Functions shown as green raypaths in Fig. 1. Only the causal (positive time lags) sides of the coherency functions, after 6 hours of stacking 1 minute noise records, are shown. The warming zone is indicated by the red lines.

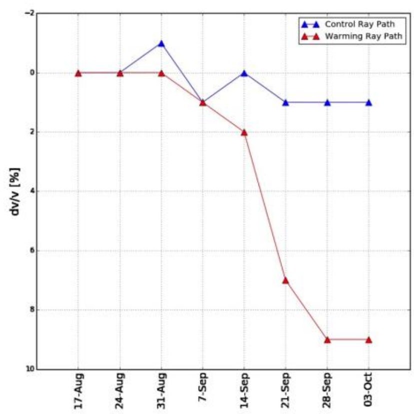

***Figure 3.** Traveltime changes during the permafrost warming experiment as observed using refracted seismic energy. The maximum change in velocity is 9.2% for the red raypath that traverses the warming experiment.*

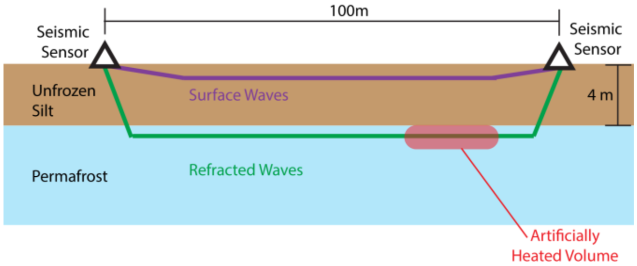

***Figure 4.** Cartoon diagram of the hypothetical seismic refraction moving through the heated volume (section view), which is found to be less sensitive to the shallow unfrozen zone compared with surface waves.*

Acknowledgments

This effort was primarily supported by the US Department of Defense through the Resource Conservation section of the Strategic Environmental Research and Development Program (SERDP) as grant RC-2437 (PIs J. Ajo-Franklin & A. Wagner). Eileen Martin was supported under a DOE CSGF fellowship grant under contract DE-FG-97ER25308. Nate Lindsey was supported through the National Science Foundation Graduate Research Fellowship Program. The authors would like to acknowledge the efforts of CRREL employees Ann Staples, Andrew Balser, Gary Larsen, and Chris Williams. We would also like to acknowledge early infrastructure development at the site by Stan Wullschleger and colleagues, funded by U.S. Department of Energy Office of Science, Biological and Environmental Research as well as Oak Ridge National Laboratory (LDRD program).

References

Daley, T.M., Freifeld, B.M., Ajo-Franklin, J., Dou, S., Pevzner, R., Shulakova, V., Kashikar, S., Miller, D., Goetz, J., Henninges, J., Lueth, S., 2013. Field testing of fiber-optic distributed acoustic sensing (DAS) for subsurface seismic monitoring. *The Leading Edge*, p.699-706.

Dou, S., Lindsey, N., Wagner, A.M., Daley, T.M., Freifeld, B., Robertson, M., Peterson, J., Ulrich, C., Martin, E.R. and Ajo-Franklin, J.B., 2017. Distributed Acoustic Sensing for Seismic Monitoring of The Near Surface: A Traffic-Noise Interferometry Case Study. *Scientific Reports*, *7*, p.11620.

Melvin, A. M., Larsen, P., Boehlert, B., Nuemann, J. E., Chinowsky, P., Espinet, X., Martinish, J., Baumann, M. S., Rennels, L., Bother, A., Nicolsky, D. J., & Marchenko, S. S. (2016), Climate change damages to Alaska public infrastructure and the economics of proactive adaptation. *Proceedings of the National Academy of Sciences*: p.201611056.

Park, C.B., Miller, R.D. and Xia, J., 1999. Multichannel analysis of surface waves. *Geophysics*, *64*(3), pp.800-808.

Schaefer, K., Lantuit, H., Romanovsky, V., & Schuur, E. A. G. (2014). Policy Implications of Warming Permafrost (United Nations Environment Programme, 2012).

Viens, L., Miyake, H. and Koketsu, K., 2015. Long-period ground motion simulation of a subduction earthquake using the offshore-onshore ambient seismic field. *Geophysical Research Letters*, *42*(13), pp.5282-5289.

High precision temperature, pressure, profile and inclinometer logger

Aleksey Markov [1]
Pavel Talalay [2]
Mikhail Sysoyev [2]
Youhong Sun [3]
Rusheng Wang [2]

[1] *Polar Research Center, Jilin University, Changchun, China, email: am100@inbox.ru*
[2] *Jilin University, Changchun, China*
[3] *Polar Research Center, Jilin University, Changchun, China*

Abstract

The integrated borehole logger are designed for high-accuracy Measuring the temperature, pressure, diameter, angle of inclination and azimuth of the borehole axis in ice sheets and in permafrost.

Keywords: borehole logger, ice sheets, permafrost.

High-accuracy measurements in the boreholes with extremely low temperatures less than -35 °C are substantially complicated because of the limitation of the minimum operating temperature for electronic components.

The developed integrated borehole logger (and its separate parts) are designed for high-accuracy research in borehole in ice sheets and in permafrost (Fig.1, Fig2).

Pressure-temperature logger

Fig.1. Pressure-temperature logger

The developed pressure-temperature logger was designed for precise measurement of temperature down to -60 °C and pressures up to 35 MPa due to local heating of the chips inside pressure chamber. To prevent the influence of the local heating of the chips on the accuracy of temperature measurements the following design decisions were incorporated: 1) pressure chamber was thermally isolated and temperature-stabilized; 2) temperature sensor was remote from the heat source using extension tube; 3) extension tube was produced from Caprolon®, material with a low thermal conductivity. As the result, the logger can measure temperature with accuracy of 0.01 °C and pressure within ± 0.23% error.

The developed borehole profile meter is designed to measure the radius of the borehole in 12 directions (Fig.2).

Profile meter and inclinometer

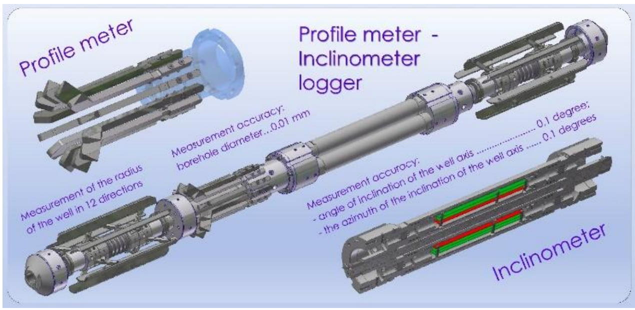

Fig.2. Profile meter and inclinometer

The measurement are made with strain gauges, which record the bending of the measuring "leg" depending on the diameter of the borehole.

The range of the measured borehole diameter from 118 mm to 144 mm (range can be changed with little alteration of the device).

The sensitivity of measuring the diameter of the borehole is 0.01 mm.

The developed tilt angle meter (from the vertical) and the azimuth of the borehole axis (inclinometer) (Fig.2) is used to determine the position of the borehole.

The measurement are made with microelectromechanical accelerometers and micromagnetoresistive three-component "compasses".

The range of the measured angle of inclination (from the vertical) of the borehole axis is from 0 to 20 degrees, the sensitivity of measuring the angle of inclination of the boreholel axis is 0.1 degrees.

The range of measured borehole azimuth from 0 to 360 degrees, the sensitivity of measuring the azimuth of the boreholel axis is 0.1 degree.

Function

Measuring the temperature, pressure, diameter, angle of inclination and azimuth of the borehole axis can be concatenated into an integrated device for measuring in borehole.

The integrated device allows for complex measurements in borehole drilled in ice sheets or permafrost.

These complex measurements make it possible to produce:

- control of the technical condition of the borehole;

- determine the parameters of the environment near the borehole;

- monitor changes in the environment around the borehole.

Multi-scale site evaluation of thermokarst potential in a High Arctic landscape

Michel Paquette[1]
Ashley C.A. Rudy[2]
Scott F. Lamoureux[3]

[1]*Department of Geography, Universite de Montreal, Montreal, QC, Canada*
[2]*Cold Regions Research Centre, Dept. of Geography, Wilfrid Laurier University, Waterloo ON, Canada, arudy@wlu.ca*
[3]*Department of Geography and Planning, Queen's University, Kingston, ON, Canada*

Abstract

Warming climate has resulted in widespread permafrost degradation and increased thermokarst activity. Detection by remote sensing can provide a combination of both relatively fine-scale spatial resolution with broader landscape coverage, but work has often been carried out without extensive ground controls. Differential interferometric synthetic aperture radar (DInSAR), is a technique for determining vertical ground displacements associated with the accumulation and thaw of ground ice. It can detect the thaw of shallow ice as surface changes, providing detailed spatial coverages and temporal resolutions during thermokarst assessment. Here, we present a case-study of combined field and DInSAR assessment of subsurface ice content in the Canadian High Arctic. We compare DInSAR data with permafrost coring and ground penetrating radar data obtained during a field season. This work demonstrates the utility of DInSAR in identifying complex ground ice conditions in comparatively uniform landscape conditions, aiding research focused on hydrological and thermokarst landscape change.

Keywords: DInSAR, ground penetrating radar, thermokarst, ground ice, active layer detachment

Introduction

Thermokarst remains one of the key concerns of a changing permafrost environment, with implications for hazards, environmental degradation and hydrological and ecosystem impacts (Liljedahl *et al.*, 2016, Rowland *et al.* 2010, Wrona *et al.*, 2016). Researchers have taken a wide range of approaches to estimate the susceptibility of permafrost degradation, including permafrost core analysis (Stephani *et al.*, 2014), terrain and geomorphic mapping (Holloway *et al.*, 2016; Kokelj *et al.*, 2017), geostatistical modeling (Rudy *et al.*, 2016), geophysical investigations and satellite measurements such as differential interferometric synthetic aperture radar (DInSAR, Rudy *et al.* 2018). These approaches provide a wide range of insights into the potential for thermokarst at different spatial scales and contribute to our understanding of the landscape-scale controls over thermokarst activity. However, each approach usually provides limited connection between field-scale processes and landscape-scale thermokarst susceptibility. Remote sensing offers the potential to provide a combination of both relatively fine-scale spatial resolution with broader landscape coverage, but is often performed without extensive ground control. One remote sensing methodology in particular, DInSAR, has shown potential for determining landscape vertical displacements that can be associated with the accumulation and thaw of ground ice. The technique depends on repeated acquisitions of the same area at different times, with changes in phase converted to displacement measurements on the order of centimeters to decimeters. Applications in several northern settings reveal coherent patterns related to inferred subsurface ice content in different landscape units. Given the compelling need for ice content information to assess local and regional thermokarst potential, improving the integration of ground-based approaches with remotely sensed DInSAR analyses represents a key opportunity to improve available ice content information and thermokarst potential. In this study, we present a combined field and DInSAR assessment of subsurface ice content from the Cape Bounty Arctic Watershed Observatory (CBAWO) in the

Canadian High Arctic. We compared ground ice contents measured by ground-based permafrost coring and ground penetrating radar (GPR) surveys with DInSAR data, providing a measure of similarity between field conditions and remote sensing measurements. This comparison is very useful to research focused on hydrological changes and thermokarst modifications of the landscape.

Results and Conclusions

A prominent area of subsidence that was observed in 2013 and 2015 DInSAR displacement measurements was investigated in the summer of 2016 using ground penetrating radar and permafrost core analysis. Permafrost coring and GPR surveys demonstrated the proximity of ice-rich cryofacies to the soil surface, from sediment rich ice (50 to 75 % volumetric ice content) to massive ice (> 90 % volumetric). These layers extended throughout the surveyed area, in a spatial pattern consistent with the DInSAR subsidence. These results also suggest that the potential for localized thermokarst is influenced by the complex geometry of near-surface massive ice. This area of substantial subsidence is associated with an older (c. 65+ years) active layer detachment (ALD) scar and indicates ongoing adjustment to this earlier disturbance.

This work demonstrates the utility of DInSAR in identifying complex ground ice conditions in relatively uniform landscapes. It also provides a framework for developing site-specific investigations of thermokarst potential and the integration of available remote sensing, geophysical and field sampling methods to link larger scale thermokarst indicators to physical processes. This framework is suitable for both downscaling landscape-scale remote sensing data sets, and for improving interpretations of thermokarst potential. Together with recent landscape modelling efforts, this study provides new insights into thermokarst potential and prediction in changing permafrost landscapes.

References

Holloway, J.H., Lamoureux, S.F., Montross, S.N., Lafrenière, M.J. 2016. Climate and Terrain Characteristics Linked to Mud Ejection Occurrence in the Canadian High Arctic. *Permafrost and Periglacial Processes* 27(2): 2014-218.

Kokelj, S.V., Lantz, T.C., Tunnicliffe, J., Segal, R. and Lacelle, D. 2017. Climate-driven thaw of permafrost preserved glacial landscapes, northwestern Canada. *Geology* 45: 371-374.

Liljedahl, A.K., Boike, J., Daanen, R.P., Fedorov, A.N., Frost, G.V., Grosse, G., Hinzman, L.D., Iijma, Y., Jorgenson, J.C., Matveyeva, N., Necsoiu, M., Raynolds, M.K., Romanovsky, V.E., Schulla, J., Tape, K.D., Walker, D.A., Wilson, C.J., Yabuki, H. and Zona, D. 2016. Pan-Arctic ice-wedge degradation in warming permafrost and its influence on tundra hydrology. *Nature Geoscience* 9: 312.

Rowland, J.C., Jones, C.E., Altmann, G., Bryan, R., Crosby, B.T., Hinzman, L.D., Kane, D.L., Lawrence, D.M., Mancino, A., Marsh, P., Mcnamara, J.P., Romanvosky, V.E., Toniolo, H., Travis, B.J., Trochim, E., Wilson, C.J. and Geernaert, G.L. 2010. Arctic Landscapes in Transition: Responses to Thawing Permafrost. *Eos, Transactions American Geophysical Union* 91: 229-230.

Rudy, A.C.A., Lamoureux, S.F., Treitz, P., Ewijk, K.V., Bonnaventure, P.P. and Budkewitsch, P. 2016. Terrain Controls and Landscape-Scale Susceptibility Modelling of Active-Layer Detachments, Sabine Peninsula, Melville Island, Nunavut. *Permafrost and Periglacial Processes* 28: 79-91.

Rudy, A.C.A., Lamoureux, S.F., Treitz, P., Short, N. and Brisco, B. 2018. Seasonal and multi-year surface displacements measured by DInSAR in a High Arctic permafrost environment. *International Journal of Applied Earth Observation and Geoinformation* 64: 51-61.

Stephani, E., Fortier, D., Shur, Y., Fortier, R. and Doré, G. 2014. A geosystems approach to permafrost investigations for engineering applications, an example from a road stabilization experiment, Beaver Creek, Yukon, Canada. *Cold Regions Science and Technology* 100: 20-35.

Wrona, F.J., Johansson, M., Culp, J.M., Jenkins, A., Mård, J., Myers-Smith, I.H., Prowse, T.D., Vincent, W.F. and Wookey, P.A. 2016. Transitions in Arctic ecosystems: Ecological implications of a changing hydrological regime. *Journal of Geophysical Research: Biogeosciences* 121: 650-674.

Permafrost station at Sommeiller Pass (NW Italy): from the monitoring to reference site and methods

Luca Paro[1*], Mauro Guglielmin[2], Andrea Merlone[3], Graziano Coppa[3], Chiara Musacchio[3], Francesca Sanna[3]

[1] *Agenzia Regionale Protezione Ambiente (ARPA) Piemonte, Torino (Italy), l.paro@arpa.piemonte.it*
[2] *Università dell'Insubria, Varese (Italy)*
[3] *Istituto Nazionale di Ricerca Metrologica (INRiM), Torino (Italy)*

Abstract

The Sommeiller Pass permafrost monitoring station, at about 3000 m of altitude, is the key site of the regional network installed in 2009 during the European Project *PermaNET* in the Piedmont Alps (NW Italy). The station consists of 3 vertical boreholes 5, 10 and 100 m deep with different characteristics, equipped with thermometric chains for a total of 34 Pt100 sensors. Due to infiltration and freezing of water inside the instrumentation and boreholes, the station became operational in 2011 after recovering. The collected data shows a constant active layer 8-9 m of thickness, while the permafrost temperature curves show a degradation of the base at approximately 65 m of depth since 2014. In order to verify this variation (about 0.4 °C), considering the station history, a sensor calibration was carried out in laboratory and on site aimed to understand the reliability of the measurements in progress.

Keywords: permafrost monitoring, sensor calibration, reference methods, reference site

Introduction

Up to about 10 years ago, knowledge on permafrost in the Piedmont Alps was rather poor, limited to a few localized rock glacier studies in the Maritime Alps. Since 2006, ARPA Piemonte, in collaboration with the Insubria University, started a regional study aimed to improve knowledge on relations among alpine permafrost and climate change, natural hazards and water resources. These activities increased during the European project *PermaNET - Long-term monitoring network* (2008-2011) [1], thanks to which 5 permafrost monitoring stations were established in the Piedmont Alps, from 2,500 m to more than 3,000 m of altitude, including the Sommeiller Pass station. Since 2009, the activity on "Permafrost Monitoring" has became an institutional service of ARPA Piemonte, allowing the maintenance and implementation of the study and monitoring of the permafrost and periglacial environment in Piedmont Alps [2].

Permafrost monitoring station of the Sommeiller Pass

Site characterization

The Sommeiller permafrost monitoring station is the key site of the regional network, located at about 3,000 m a.s.l. in high Susa Valley (NW Italy), near the France border. The station consists of 3 boreholes 5, 10 and 100 m deep vertically drilled in the bedrock, a few meters from each other, equipped with Pt100 thermometric chains (Pt107 Campbell Sci.). The 5 m borehole is equipped with two sensors placed directly in the uncovered hole filled with cuttings. The 10 m and 100 m boreholes are equipped with 12 and 20 sensors respectively, placed in both cases in a ∅50 mm HDPE tube. The 100 m borehole is equipped with a metal covering for the first 10 m due to drilling problems, with head buried under about 70 cm of debris. Data are collected in the datalogger (CR1000 Campbell Sci.) and manually downloaded once a year.

In addition, a weather station equipped with thermo-hygrometer and nivometer has been installed in the same site. Since 2009, the site was also subjected to other surveys such as geoelectric and Bottom Temperature of the Snow (BTS) measures.

The history of the station

The station was initially planned completely underground to reduce environmental impact, vandalism and lightning events. In 2009, data loggers and batteries were placed in metal and concrete manholes and the head of boreholes in plastic manholes, all below ground surface. Unfortunately, water infiltrations flooded the manholes and boreholes, damaging dataloggers irreparably and blocking the thermistor chains in the ice.

Therefore, in 2011 a recovering station has been completed with datalogger, solar system and head of boreholes raised above ground surface. The ice-locked thermometers in the boreholes have been released through a hot water recirculation system and boreholes emptied from the water with high-pressure air.

Preliminary data

The available dataset covers the period summer 2011-summer 2017, with valid elaboration for the years 2012 to 2016, for only 32 sensors in boreholes 10 and 100 m deep (the 2 sensors in the 5 m deep borehole were activated in summer 2017).

From the elaborations it is noted that the active layer and the Zero Annual Amplitude (ZAA) are approximately constant respectively 8-9 m thick and about 13-14 m deep. The thermal state of permafrost indicates temperature close to 0 °C with a few tenths of degrees in the negative temperature range. Permafrost conditions were present at least for 100 m of depth until 2013. Since 2014, a positive temperature transition (+ 0.2 °C) has occurred at about 65 m of depth indicating a degradation of the permafrost base.

Sensor calibration activity

In the framework of EURAMET project MeteoMet [3,4], an in-situ calibration campaign was planned in 2016, in cooperation with Istituto Nazionale di Ricerca Metrologica (INRiM), for the permafrost temperature sensors hosted at the Sommeiller station. The campaign was carried out in a week in August 2017, when reference temperature sensors, along with a thermostatic bath, a high-accuracy readout bridge, two power generators and a light shelter were brought to the site (Fig. 1).

Figure 1 - The mobile calibration facility at Sommeiller Pass during the 2017 campaign.

Thirteen out of the 34 total sensors were calibrated in the alcohol-powered thermostatic baths at 5 temperature points close to the freezing point of water (-7 °C, -3 °C, 0 °C, +3 °C, +7 °C and repeated 0 °C calibration to check for stability-hysteresis), in order to maximize the calibration accuracy in the temperature range most important for permafrost studies and minimize the interpolation uncertainties.

Towards reference methods and reference site

In February 2017, a workshop was held within the activities of the MeteoMet project. Among the topics, permafrost temperature measurements methods and accuracy, high mountains climate research sites, metrology for the cryosphere, reference grade measurements for glaciology were discussed.

The workshop underlined the need to discuss and agree on common approach, best practice and uncertainty evaluation on the numerous measurements made in glacial and periglacial areas, including methods to measure permafrost temperature profiles. Together with the experience achieved during the calibration campaign at the Sommeiller pass, and the issues encountered during laboratory calibration of different typologies of thermometers, the need is now fully defined and studies can be started towards definition of reference methods and reference observation sites. This initiative is expected to also benefit the GCW[1] station network, due to the primary interest of WMO[2] initiatives and GCOS[3] networks [5], towards measurement traceability and comparability and for identifying reference sites from baseline networks.

References

[1] http://www.permanet-alpinespace.eu/home.html

[2] Paro, L. & Guglielmin, M., 2013. *Neve e valanghe* 80: 50-59

[3] Merlone, A. *et al.* 2015. *Meteorological Application* 22: 820–829.

[4] Merlone, A. *et al.* 2017, *Meas. Sci. Tech.*, https://doi.org/10.1088/1361-6501/aa99fc in press

[5]http://gosic.org/content/gcos-terrestrial-ecv-permafrost

[1] Global Cryosphere Watch
[2] World Meteorological Organization
[3] Global Climate Observing System

Systematic derivation of anchoring forces in permafrost affected bedrock

Regina Pläsken[1, 2]
Michael Krautblatter[1]
Markus Keuschnig[2]
[1]*Technical University Munich, Landslide Research, regina.plaesken@tum.de*
[2]*GEORESEARCH Forschungsgesellschaft mbH*

Abstract

Warming rate in the European Alps is twice the average global rate since the 19th century. Warming-related permafrost degradation is closely linked to changes in mechanical system behavior of rock slopes in high alpine regions. These affect slope stability itself as well as structures built on permafrost-affected bedrock in a potentially stability-relevant manner. It is, however, very difficult to gain insight in the in-situ mechanical system behavior of such permafrost-affected bedrock. However, despite the frequent use of anchoring systems, very little long-term monitoring data on the mechanical behavior of rock anchors in permafrost-affected bedrock and annual changes is available. This study uses measurements of forces on rock anchors in combination with borehole temperature data of different depths to deduce determining factors for mechanical system behavior.

Keywords: high alpine permafrost; rock anchors; mechanical system behavior; infrastructure.

Motivation

Climate warming has considerable consequences for sensitive high-alpine environments. In the European Alps warming has been twice as high as the global average rate (EEA 2009), affecting bedrock properties, and potentially altering the stability of high-alpine constructions. However, mechanical system behavior and the magnitude of stability-relevant changes is widely unexplored (Fischer et al., 2006). The overall aim of this study is to identify the predominating factors of the mechanical system by using continuous measurements of anchoring forces and temperatures.

Study site

The study site is located around the summit station of the Kitzsteinhorn cable car (3029 m a.s.l., Austria). Its immediate vicinity is home to an interdisciplinary Open-Air Lab (OpAL), where the consequences of climate change, based on a long-term surface, subsurface and atmospheric monitoring are investigated (Hartmeyer et al., 2012). It encompasses the north-oriented rock wall of the Kitzsteinhorn, which consists of calcareous micaschists. The foliation of the micaschists is inclined roughly in line with the slope, at angles between 39° and 52°. Until the mid-20th century most parts of the rock wall were covered by a permanent ice face. However, the current surface of the glacier is now located approximately 100 m lower. The summit station first built in 1965/66, has since been reconstructed twice.

Data and methods

Site investigations

Near-surface properties of the rock wall were investigated during the geotechnical mapping of the study site (Geoconsult ZT GmbH 2010).

Load Cells, Anchoring Forces

Two rows of 15 pre-stressed rock anchors were installed directly beneath the summit station in November 2015. The 25 m long anchors were drilled with an inclination of around 3° and a grouted section of 7 m length. Three of these rock anchors were equipped with continuously measuring anchor load cells.

Boreholes, Temperatures

Within the framework of OpAL two deep boreholes (22m & 30 m) are providing continuous rock temperature time series in 11 depth steps in close vicinity to the rock anchors (Fig 1.).

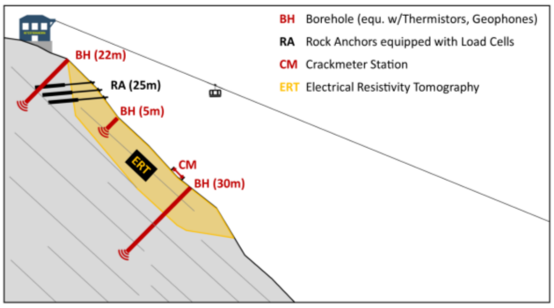

Figure 1. Existing monitoring OpAL (Hartmeyer et al., 2017).

Results

Anchor loads significantly vary between summer and winter. During the entire measuring period of two years, load values reach their maximum around December and stagnate until the end of May. From May on values decrease on average by 120 kN (22%) below their maximum. Specific load values are shown in Table 1.

Table 1. Anchor Load Values.

Load cell	Min	Max	Variability abs	Variability perc
#9	400	585	185	32%
#12	386	492	106	21%
#15	506	580	74	13%

Combining datasets on load values and temperature at anchor head and different depth steps in boreholes an annually recurring pattern is clearly discernible (Fig. 2.).

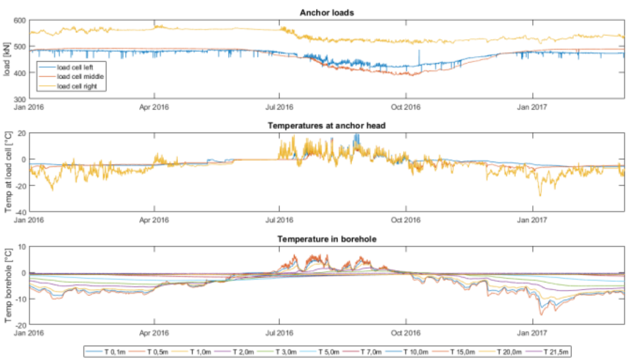

Figure 2. anchor loads and temperatures.

Discussion

Annual changes in anchor loads correlate with temperatures at anchor head and borehole temperatures. To determine plausible physical explanations for observed annual changes, an engineering model of the mechanical system, based on information on joint sets obtained from geological mapping as well as logs on anchor drilling comprising anchor and surrounding rock, was set up (Fig. 3).

Measuring load variations at the anchor head is tantamount to integrating relative displacement over the volume of influence of the anchor (free stressing length). Steel and the bedrock clearly exhibit similar coefficients of thermal expansion, which is why differential thermal strain can be rejected as reason for relative displacements. With known stress-strain behavior of steel and free stressing length a requisite displacement for the measured differential loads is determined. Resulting displacements can therefore be assumed to result from joints only. Regarding water and ice content in joints, ice segregation appears to be the primary driving force within the rock-anchor-joints system.

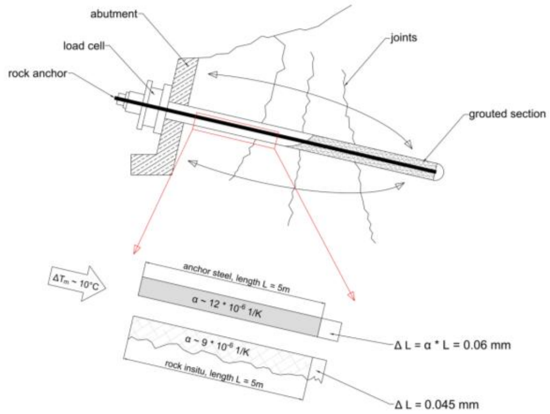

Figure 3. System sketch engineering model.

Conclusion and outlook

This is the first study to demonstrate systematic variations in anchoring forces in permafrost rocks. Ice segregation seems to have the greatest influence on mechanical system behavior. Thus, integrating these findings in the understanding of cyclic anchoring stress variations is crucial to a better design of high alpine infrastructure in future.

Reference list

European Environment Agency, 2009. Regional climate change and adaption. The Alps facing the challenge of changing water resources. Luxembourg.

Fischer L, Kääb A, Huggel C, Noetzli J. 2006. Geology, glacier retreat and permafrost degradation as controlling factors of slope instabilities in a high-mountain rock wall: the Monte Rosa east face. *Natuaral Hazards and Earth System Sciences 6*: 761 – 772.

Geoconsult ZT GmbH. 12.12.2010. Kartierung Gipfelstation. Salzburg. Austria.

Hartmeyer I., Keuschnig, M., Schrott L. (2012): Long-term monitoring of permafrost-affected rock faces – A scale-oriented approach for the investigation of ground thermal conditions in alpine terrain, Kitzsteinhorn, Austria. *Austrian Journal of Earth Science*, Vol. 105/2, 128-139.

Hartmeyer I., Keuschnig, M., Krautblatter M., Helfricht K., Leith K., Otto J., GlacierRocks – Glacier-Headwall Interaction and its Influence on Rockfall Activity. *EGU2017-14921, Vol. 19*, EGU General Assembly 2017.

Thermal Monitoring of Frozen Wall Thawing at Petrikov Mine

Aleksei Pugin[1]
Lev Levin [2]
Yuri Klukin[3]
Plekhov Oleg[4]

[1]*Mining Institute Ural Branch Russian Academy of Sciences, dr.alexpugin@gmail.com*
[2,3]*Mining Institute Ural Branch Russian Academy of Sciences*
[4]*Institute of Continuous Media Mechanics Ural Branch Russian Academy of Sciences*

Abstract

Shaft sinking through water-saturated soils requires special techniques of mining and monitoring. Traditionally, an artificial ground freezing method is applied to prevent shaft flooding. We construct thermal monitoring system based on optical fiber measurements in boreholes, which provides the safety of the Petrikov mine sinking. The innovative technique allows data collecting continuously in time (1Hz frequency) with high resolution (0.25 m). It is very important to investigate the thawing of the frozen wall around the shaft, so the novelty of the new system consists in the optical fiber branch inside the shaft to monitor the frozen soil state within the freeze pipe contour beyond lining. It permits the precise reconstructing of temperatures within the rock mass under freezing or thawing and the daily estimation of the frozen wall thickness and completeness. The system plays a key role to organize the mining (grouting especially) correctly.

Keywords: shaft sinking; artificial ground freezing; frozen wall; thawing; thermal monitoring; optical fiber

Introduction

Shaft sinking through water-saturated soils requires special techniques to prevent flooding. One of them is artificial ground freezing. The creation of a frozen wall around the shaft needs powerful equipment and highly reliable methods for its state monitoring. Specific freezing pipes surround the shaft and the refrigeration plant cools a heat transfer agent and circulates it through the pipes extracting heat from soils. The brine ($CaCl_2$) is generally used as the heat transfer agent.

Physical Conditions

Many different factors influence the process and define the possibility of freezing such as geology, filtration activity, natural and technogenic thermal conditions, mechanical parameters and others.

Geology of the Petrikov potash mine considered here has water-saturated siltstones, argillites and chalk down to the depth ~265 m. Clay separate aquifers and the solid clay underlay groundwater. There are no regional faults, but small disjunctive dislocations exist. Groundwater has low infiltration rate.

In accordance with the laboratory examination, Soils at the Petrikov area freeze at the temperature between 0^0 C and -1^0 C – except for clay which contains 60% more water being -5^0 C. Some rocks have extremely high or low thermal characteristics: heat conductivity and capacity.

Thermal Monitoring System

Traditionally, mining engineers carry out thermal logging in boreholes periodically to know the state of freezing or thawing soil. Initially, boreholes are drilled both inside and outside a freeze pipe contour, but inner boreholes are destroyed later due to shaft sinking. It allows collecting outer data only while shaft sinking and doesn't provide information about inner part of the frozen wall.

Short inner boreholes are drilled through special technological holes in the tubbing lining to inject grout when shaft walls have already lined. A thermometer is put in some boreholes and logs temperatures. The refrigeration plant turns off and the frozen wall around the shaft begins to thaw at this period. This operational period requires strong levels of safety because grout injecting requires 0.5-1 m soil thawed from the lining side, but frozen wall must be complete.

Although many researchers have been investigating the frozen soils for a long time (Frivik, 1981), each shaft sinking produces new issues because of incomplete information. It is hard to collect necessary data putting the thermometer periodically. Currently, the optical fiber is often applied to measure temperature in boreholes continuously in time. However, thermal logging with thermometers are still carried out in short boreholes through the lining to investigate the thawing.

In our investigation, we modernized thermal monitoring system at the Petrikov mine (Republic of Belarus) and set optical fiber into 2 m length boreholes through the lining at different depths determined geologically. It provides the opportunity to study frozen wall thawing inside and outside continuously in time. The scheme of the thermal monitoring system is shown in figure 1.

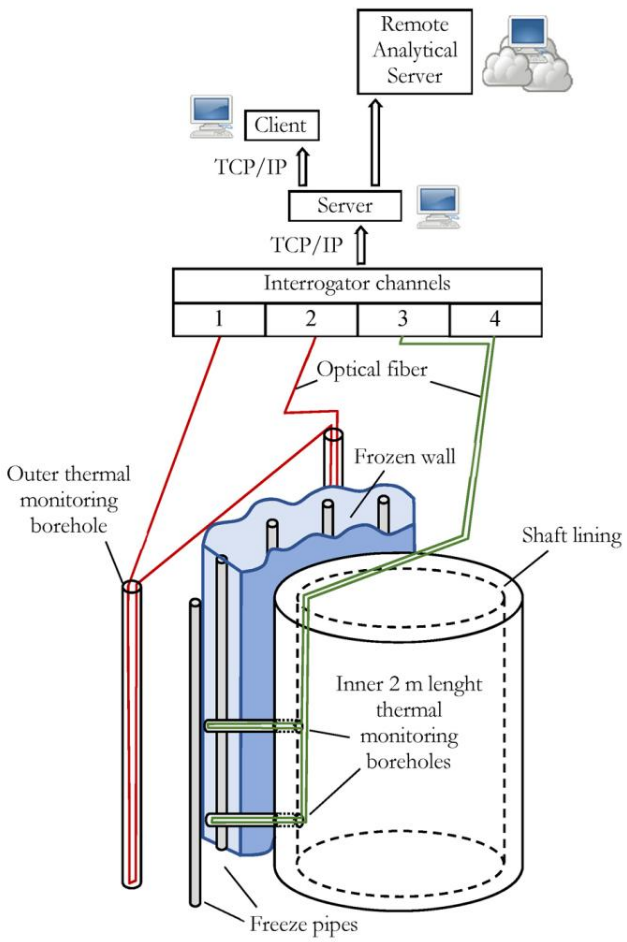

Figure 1. The scheme of the monitoring thermal system

The brine continued the circulation through freeze pipes when the refrigeration plant had turned off and the monitoring of its temperature provided with additional information.

Data Application

Optical fiber data were analyzed and interpreted in real time. The previous investigation was used for the initial point (Levin *et al*, 2017). Information continuously measured in time inside and outside the contour of freeze pipes allows precise reconstruction of temperatures in the rock mass and daily estimation of the frozen wall thickness and completeness.

Artificial ground freezing in situ provided the understanding of processes within the rock mass. The new system created the opportunity for miners to organize grouting works correctly.

Summary

Optical fiber thermal logging helps to investigate freezing and thawing processes in artificially frozen soils while the shaft is sinking and to understand several unusual occurrences. The optical fiber technology, the same as mentioned above, can be applied to investigate the state of permafrost in the real time.

Acknowledgments

The authors thank Ivan I. Golovaty, Director General of “Belaruskali” Company, for continuous cooperation in mining investigations.

This research was supported by 17-11-01204 project (Russian Science Foundation).

References

Frivik, Per E., 1981. State-of-the-art report. Ground freezing: thermal properties, modelling of processes and thermal design. Engineering Geology 18: 115–133.

Levin, L.Yu., Semin, M.A., Parshakov, O.S., Kolesov, E.V., 2017. Metod resheniya obratnoy zadachi Stefana dlya kontrolya sostoyaniya ledoporodnogo ograzhdeniya pri prohodke shahtnyih stvolov (Method for solving inverse Stefan problem to control ice wall state during shaft excavation). Perm Journal of Petroleum and Mining Engineering 16 (3): 255–267.

Modern photogrammetric methods to assess vegetation change in relation to air and soil temperature and ALT trends (1995-2017), Toolik Lake, Alaska, USA

Brianna J. Rick[1]
Anna E. Klene[1]
Nikolay I. Shiklomanov[2]

[1]*University of Montana, Department of Geography, Missoula MT, brianna.rick@umontana.edu*
[2]*George Washington University, Department of Geography, Washington, DC, USA*

Abstract

The Circumpolar Active Layer Monitoring (CALM) Project has been monitoring a 1 ha plot at Toolik Lake on the Alaskan North Slope since 1995. This site is located in the Arctic foothills physiographic province. Air temperature and soil-surface temperature are measured *in-situ* daily, and active layer thickness (ALT) is measured annually during maximum thaw (August). Over time (1995-2017) there has been a slight increase in mean summer (July-August) air temperatures and a slight decrease in mean soil-surface temperatures. Such an increase in the difference between air and soil-surface temperatures may be related to changing vegetation properties. Color-infrared aerial photograph pairs from peak greenness in 1995 and 2017 were analyzed using modern photogrammetric techniques to quantify vegetation change. This research complements coarser remote sensing efforts as well as plot-level biomass measurements showing Arctic greening in this region.

Keywords: Alaska; Circumpolar Active Layer Monitoring; vegetation; climate; surface temperature; remote sensing

Introduction

The National Science Foundation's (NSF) Arctic Systems Science's (ARCSS) Flux Study established 1-hectare plots along the North Slope of Alaska where soil, vegetation, active-layer, ecological, and microclimatic characteristics were inventoried (Weller *et al.*, 1995; Reeburgh *et al.*, 1998; Walker *et al.*, 1998). NSF's Circumpolar Active Layer Monitoring (CALM) Project continued monitoring eight of these plots along a latitudinal gradient, and time series of soil-surface and air temperatures, as well as active layer thickness (ALT), are available from 1995-2017. These sites provide a uniquely long data set on the North Slope, enabling time-series analysis.

The time series at each of the plots reveal an increasing trend in mean summer (July-August) air temperatures, yet a shallower increase or slight decreasing trend in mean summer soil-surface temperatures (Klene *et al.*, 2015). This growing difference between air and soil-surface temperatures raises the question of the driving force behind the decoupling of these variables. Annual measurements at these sites have included active-layer thickness (depth of the seasonally thawed surface layer); however, no vegetation measurements have been taken since their establishment in 1995.

Study Site

While eight 1 hectare (100 m × 100 m) CALM sites on the Alaskan North Slope have been monitored since 1995, this paper focuses specifically on CALM site U12B (ARCSS Flux Study Plot 6) at Toolik Lake. A description of the study site can be found in Walker and Bockheim (1995). CALM site U12B is a moist acidic tundra and water-track complex in the Arctic foothills province, near the University of Alaska-Fairbanks' Toolik Field Station.

The purpose of this study is to investigate vegetation change at Toolik Lake on the Alaskan North Slope, and its relationship to the observed air, soil-surface temperature, and active-layer thickness trends over the past 23 years. This is the first study to use differential stereopair analysis to quantify vegetation change at one of the CALM sites, and is an attempt to better understand the micro-scale influence of climate and vegetation on permafrost.

Methods

Within CALM site U12B, five 2-channel data loggers collect hourly temperature time series, 9 soil-surface and one air temperature. Soil-surface temperatures were averaged when reporting SST for the plot (Figure 1).

Active layer thickness measurements are collected every summer during maximum thaw (August) at 5 m intervals along 3 transects. ALT measurements were also averaged when reporting maximum thaw at the site (Figure 2).

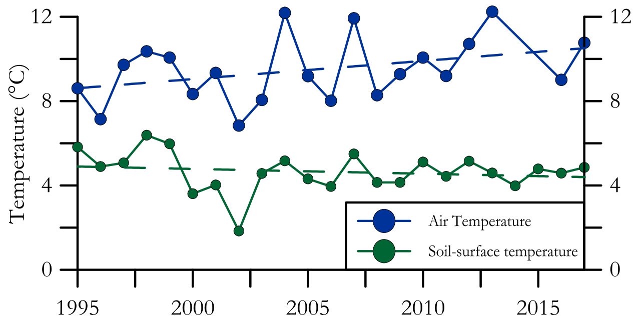

Figure 1. Time-series plot for CALM site U12B showing trends in mean July-August air and soil-surface temperatures from 1995-2017.

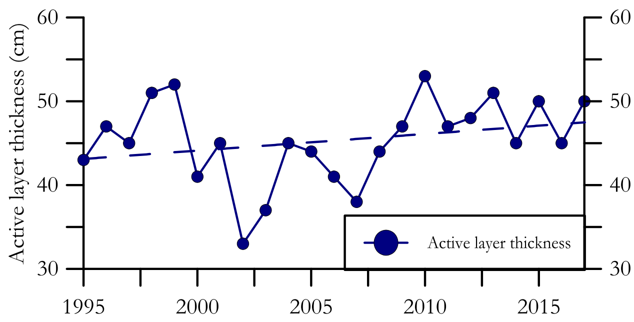

Figure 2. Time-series plot of active layer thickness for CALM site U12B from 1995-2017.

Remote-sensing techniques show promise for quantifying vegetation change over time by comparing historical and current aerial photographs. Color-infrared (CIR) aerial photographs of CALM site U12B at Toolik Lake were obtained at 1:3000 resolution in 1995, as well as a thorough vegetation survey (Walker & Bockheim, 1995). In 2017, UAS imagery (red, green, blue and red, green) of the plot was flown by the GIS office at the Toolik Field Station during peak vegetation (August) to capture the full extent of vegetation growth.

Agisoft Photoscan (Agisoft LLC, St. Petersburg, Russia) was used to create a point cloud, digital surface model (DSM), and digital terrain model (DTM) from stereopairs for 1995 and 2017. By differencing the models, vegetation can be quantified, leading to assessment of changes in vegetation both spatially and temporally.

Preliminary Results

Time series between 1995 and 2017 reveal an overall increase in mean summer (July-August) air temperatures and a slight decrease in mean soil-surface temperatures (Figure 1). Trends in ALT show a slight increase despite cooler soil temperatures (Figure 2). There are complex feedback loops associated with an increase in vegetation, increasing summer soil-surface insulation and increasing winter insulation (trapped snow). Another possibility that needs further exploration is a reduction in the ALT trend due to subsidence (Shiklomanov, *et al.*, 2013).

Acknowledgments

We thank the many people who have assisted with the data collection over the years. This research was supported by the U.S. National Science Foundation (grants OPP-0095088, OPP-0352958, OPP-0856421, and OPP-1304555). Any opinions, findings, conclusions, or recommendations expressed in this study are those of the authors and do not necessarily reflect the views of the NSF.

References

Klene, A.E., F.E. Nelson, K.E. Nyland, N.I. Shiklomanov, D.A. Streletskiy, & Q. Yu., 2015. Comparison of soil-surface temperatures with satellite trends of increasing phytomass in northern Alaska. *AGU Fall Meeting*, San Francisco, CA, December 14.

Reeburgh, W.S., J.Y. King, S.K. Regli, G.W. Kling, N.A. Auerbach, & D.A. Walker, 1998. A CH_4 emission estimate for the Kuparuk River basin, Alaska. *Journal of Geophysical Research* 103(D22): 29,005-29,013.

N.I. Shiklomanov, D.A. Streletskiy, J.D. Little, & F.E. Nelson, 2013. Isotropic thaw subsidence in undisturbed permafrost landscapes. *Geophysical Research Letters* 40:6356-6361. DOI10.1002/2013GL058295.

Walker, D.A. & Bockheim, J.G. 1995: Vegetation-Soil Characterization at the 12 Flux Tower Sites. *ARCSS/LAII/Flux Study*. LAII Science Management Office, University of Alaska Fairbanks, Fairbanks, AK.

Walker, D.A., N.A. Auerbach, J.G. Bockheim, F.S. Chapin III, W. Eugster, J.Y. King, J.P. McFadden, G.J. Michaelson, F.E. Nelson, W.C. Oechel, C.L. Ping, W.S. Reeburg, S. Regli, N.I. Shiklomanov, & G.L. Vourlitis, 1998. Energy and trace-gas fluxes across a soil pH boundary in the Arctic. *Nature* 394: 469-472.

Weller, G., F.S. Chapin, K.R. Everett, J.E. Hobbie, D. Kane, W.C. Oechel, C.L. Ping, W.S. Reeburgh, D. Walker, & J. Walsh, 1995. The Arctic Flux Study: a regional view of trace gas release. *Journal of Biogeography* 22: 365-374.

Monitoring of arctic infrastructure in Svalbard

Anatoly Sinitsyn[1]
Pavel Kotov[2]
Arne Aalberg[3]
Katharina Beutner[3]
[3]*SINTEF Building and Infrastructure, anatoly.sinitsyn@sintef.no*
[2]*Lomonosov Moscow State University, Geocryology department*
[3]*The University Centre in Svalbard*

Abstract

A settlement monitoring campaign for building foundations in the small cities of Longyearbyen, Barentsburg, Svea, and Pyramiden in Svalbard was initiated in summer 2017. Permafrost exists to a depth of hundred meters or more at these locations. Reference points were established on the foundations of selected buildings, and a survey was conducted by differential leveling. Existing older buildings and recent buildings were selected for the study, with different bearing structures and different types of foundations. Recent time-series observations and climate model predictions show that significant climate warming will occur in Svalbard in the 21st century. The objective of the monitoring campaign is to document the conditions of the selected foundations and to provide a basis for repeated surveying of settlements in a 10-20 years perspective. Combined with long-term data series of air and ground temperatures at several sites in Svalbard, the survey may provide valuable information on settlement rate of various buildings and foundations, useful for decision making for maintenance of existing structures and selection of foundation materials and design of future constructions.

Keywords: permafrost, settlement of foundations, climate change, frozen ground, foundations in permafrost.

Introduction

Climate change is considered one of the major global challenges for humanity in 21st century. Projected climate changes are most pronounced in the polar regions. It is believed that the impacts on permafrost conditions in the arctic may lead to significant damage to infrastructure. As pointed out by (Instanes, 2003) and (Anisimov & Vaughan 2007), the effects of construction and maintenance of infrastructure may also significantly affect the ground thermal regime locally in the permafrost ground, and may add to problems related to stability of foundations.

Long-term field measurements are useful for the design and documentation of performance of foundations. The results of systematic monitoring of vertical positions of foundations, in conjunction with records of hydro-meteorological parameters and maintenance history of a building, may help to identify the primary factors causing severe damage to foundations or decrease of building serviceability.

Svalbard is well suited for the present study because several building types and foundation systems are easily accessed at the four geographical locations, and at the same time climate projections suggest significant climate warming towards year 2100 (Benestad *et al* 2016) and (Forland *et al* 2011). Consequences of warming of permafrost and increase in the active layer thickness and subsequent soil strength loss and settlements is thus quite likely. In order to provide data on a range of foundation solutions, the survey covers new and old buildings, supported on shallow plate and strip foundations, as well as deeper pile foundations. Quite significant settlements were observed for some of the buildings, while others were mostly without deformations.

Methods

The initial heights of the reference points on the building foundations were determined by performing a standard manual differential leveling. This basic method is widely used due to a number of advantages, which include high accuracy and rapid measurements, simple and inexpensive equipment, and allowing measurements under difficult conditions. Requirements for such works are found in standards for monitoring of infrastructure.

The Digital level *Leica Sprinter 250 M* instrument and a barcode staff *Leica GSS 111* rod were used for the survey. Leveling was performed in forward and reverse directions using approximately equal distances, and in closed paths around each building with two repetitions.

The following works were carried out in 2017:

1) Identification and/or establishment of reference points (fixed ground points) in the vicinity of the buildings. As far as possible these were points that could be assumed to not develop significant vertical movement

in a long-term (decades) perspective, e.g., massive piled concrete foundations.

2) Installation of fixed bolts on the base or foundation structure of the buildings, in easily accessible positions. Bolts were installed on the corners of the buildings and at points closely spaced along the building sides, drilled and hammered into piles or characteristic foundation points at every 4-5 meters.

3) Leveling of the marked points.

The precision of a level run is described in terms of a maximum allowable error of the closed path. The survey was conducted in accordance with the allowable errors defined in [5].

Description of surveyed buildings

Longyearbyen

The apartment building UNIS Guest House and the hotel "Elvesletta Byggetrinn 1" under construction were surveyed. The first is a two-story wooden module building, standing on wooden piles deployed in the ground to a depth of ca. 9 m. Crawl space protected by decorative planks allows air flow below the building (sun shelter in summer, cooling in winter). The building is in plan approximately 15 by 70 m. The building was constructed in 2009–2011. The second building is a three-story wooden building, founded on 140 by 140 mm square hollow steel sections deployed to a depth of ca. 18 m. Crawl space is also sheltered by decorative planks. The building is approximately 16 by 30 m, and is due to be finished in early 2018.

Barentsburg

The three-story building "Komplex GRZ", constructed in 1975–1978, was selected for the survey. The building is approximately 50 by 15 m. The building is constructed of concrete beams and columns, with infill and exterior brick walls, and is supported on concrete piles. The piles have an estimated length of 10 meters. The opening under the building provides free flow of air. Some observed damage is most likely caused by previous settlements, visible as surface cracks on the southern wall.

Pyramiden

A multi-purpose garage built in 1981–1983 was selected for the survey. The building has brick walls and is supported on pillars on concrete piles. It is believed that the piles are 10 m long. The space below the building permits free airflow in the crawl space. Cracks were observed on the western wall of the building.

Svea

In the mining city of Svea, the two-story barrack building "New green barrack" and a multi-purpose garage were surveyed. The first was constructed in 2010, from prefabricated wooden modules supported on a beam frame on wooden piles. Standard ventilated space and cover planks allows air flow below the building. Small deformations are visible on the South-East and East side, likely caused by foundation movements. The building is shaped in a horizontal angle (equal legs), total length of north side is 80 m, southern side is 90 m, and the width of the building body is 11 m. The multi-purpose garage for material storage is a light.weight structure comprising a steel framework and sandwich steel façade walls, on a concrete slab with integrated closely spaced ventilation cooling ducts, supported directly on the ground. Duct ends are to be manually closed/opened in summer/winter.

Results

Elevation data for monitoring points on the buildings were collected, these data establish a present ("as-today") dataset for each building. Data are stored in the project archive, which will be publically available at a later stage from the Research-In-Svalbard (RiS) database.

Acknowledgments

The authors would like to thank The Research Council of Norway for the economic support through the POLARPROG programme (246757/E10), and for the contributions by the project partners Lomonosov Moscow State University, Longyearbyen Lokalstyre, Trust Articugol, Store Norske Spitsbergen Grubekompani AS, The University Centre in Svalbard, and SINTEF Building and Infrastructure.

References

Instanes, A., 2003. Climate change and possible impact on Arctic infrastructure. Proceedings of the 8th *International Conference on Permafrost.* Zurich, Switzerland, July 21-26: 461-466

Anisimov, O.A. and Vaughan D.G., 2007. Polar Regions, in Climate Change impacts, adaptation, and vulnerability. *Contribution Working group II to the Fourth Assessment Report of the Intergovernmental Panel on Climate Change*: 654-685.

Benestad, R.E., et al. 2016. Climate change and projections for the Barents region: what is expected to change and what will stay the same *Environ. Res. Lett.*: 1-8.

Forland, E.J., et al., 2011. Temperature and Precipitation Development at Svalbard 1900-2100. *Advances in Meteorology:* 1-14.

Geophysical monitoring of an artificially heated permafrost site

Anna M. Wagner[1]
Nathaniel J. Lindsey[2, 3]
Arthur B. Gelvin[1]
Jonathan Ajo-Franklin[2, 3]

[1]*U.S. Army Cold Regions Research and Engineering Laboratory, United States, Anna.M.Wagner@usace.army.mil*
[2]*University of California, Berkeley, California, United States*
[3]*Lawrence Berkeley National Laboratory, Berkeley, California, United States*

Abstract

The combination of distributed measurement, low cost, and performance in harsh environments makes fiber optic sensing an ideal tool for monitoring arctic infrastructure. In this study, we performed a controlled-warming experiment in Fairbanks, Alaska where we investigated the potential utility of fiber optic distributed sensing technologies (seismic, strain, and temperature) as an early detection system for permafrost thaw. We present the experimental design and heating method, the multidisciplinary data types, results from this active heating experiment, and thermo-hydro-mechanical coupling implications for other in situ permafrost experiments, both natural and artificial. This experiment demonstrates a viable approach for both simulating deep permafrost thaw and densely measuring the resulting soil property evolution.

Keywords: Fiber optic; geophysical measurements; LiDAR; permafrost; subsidence;

Introduction

Small thermal perturbations can have dramatic impacts on structural stability ranging from foundation settling to catastrophic failure of roads, bridges, and runways due to thermokarst generation. The non-linear coupling of future changes in air temperature, surface insolation, and surface/subsurface hydrology to soil mechanics, generates a high degree of uncertainty as to the environmental changes which existing infrastructure will actually experience. In this paper, we present a new methodology using fiber optics as an early detection monitoring technique.

Methods

In 2016, an artificial permafrost warming experiment took place at the Permafrost Research Station, Fairbanks, Alaska using 121 60-Watt vertical heaters. The heaters installed covered an area of about 140 m^2 where the distance between each heater was about 1.2 m. Throughout the site we installed about 5 km of fiber optic cable horizontally in shallow trenches (20 cm depth).

This experiment involved a variety of measuring techniques to capture changes in the subsurface. Electronic Distance Measurement (EDM), GPS, time-lapse photogrammetry, LiDAR, and fiber optic distributed strain sensing recorded the deforming surface topography. Prior to starting the heating experiment, a terrestrial based LiDAR scanner captured the initial ground topography. The LiDAR surveys were collected using a Leica ScanStation C10 and were performed approximately once a week.

Passive ambient vehicular traffic and a surface orbital vibrator (SOV) active source recorded by geophone, broadband, and fiber optic distributed acoustic sensing instruments, enabled measurement of changes in relative shear wave speed and dispersive surface wave propagation.

Several thermistor strings throughout the site captured changes in temperatures during the experiment. The monitored temperatures supported thermal modeling of the heating soil temperatures using a 3D finite element model (SVOffice5).

Results

The experiment began on August 5, 2016 and continued through November 11, 2016. The depth to permafrost at the heating site was initially between 4 – 4.5 m below the surface. At the center of the heated plot, the depth to the permafrost table increased by about 1 m during the heating process based on estimates of the change in temperature versus time, as measured nearest the thaw-freeze interface using the temperature sensors in the borehole. Figure 1 shows soil temperatures during and following the heating period from the center of the heated area.

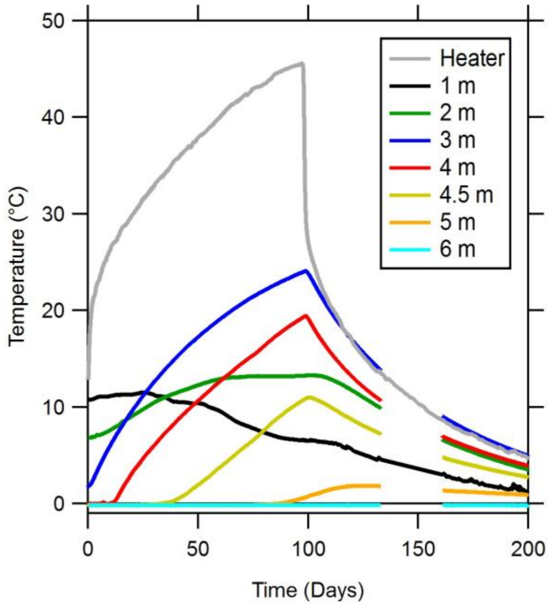

Figure 1. Heater temperature at the heating element (gray) and soil temperatures at different depths approximately 0.5 m from the heater.

The deformation of the ground surface using a combination of traditional surveying techniques and LiDAR scanning (Fig. 2) showed an area with the greatest amount of subsidence to be between 0.04 to 0.10 m of change.

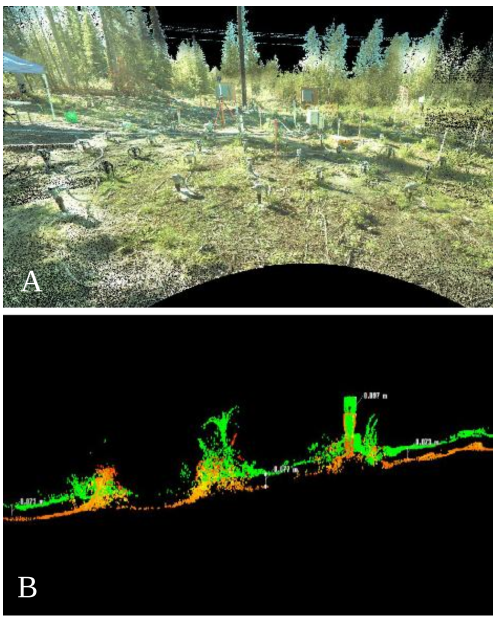

Figure 2. LiDAR point clouds of the (a) site and (b) a slice from August 5 (green) and October 7 (orange).

Simulations of soil temperatures using a finite element model over a total of 200 days closely matched the measured soil temperatures at depth (Fig. 3). This suggests that the assumed soil parameters (dry density of 800 kg/m^3; volumetric water content of 40%; thermal conductivity of 0.55 W/mK) were reasonable, and that conduction, not advection, drives thermal degradation of the permafrost.

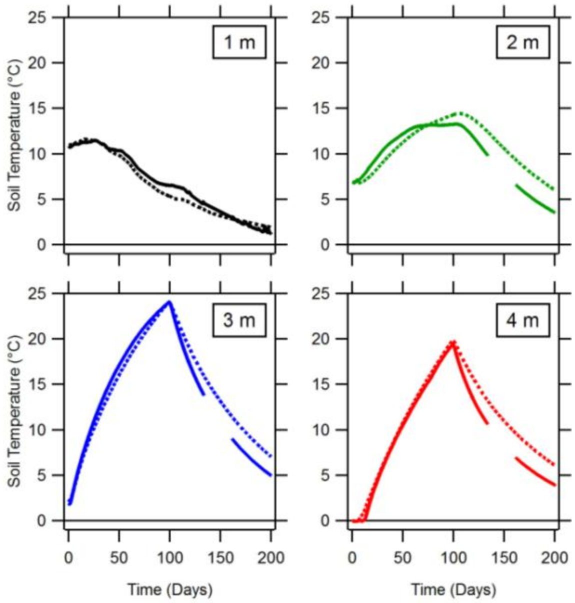

Figure 3. Measured (solid) and modeled (dashed) soil temperatures approximately 1 m from the heater.

Our experiment demonstrates a viable approach for simulating both deep permafrost thaw and the resulting surface subsidence, an integrated platform for testing sensor systems targeting such processes.

Acknowledgments

This effort was primarily supported by the US Department of Defense through the Resource Conservation section of the Strategic Environmental Research and Development Program (SERDP) as grant RC-2437. Nate Lindsey was supported through the National Science Foundation Graduate Research Fellowship Program. The authors would like to acknowledge the efforts of Andrew Balser, Shan Dou, Ian Ekblaw, Stephanie Ewing, Gary Larsen, Stephanie Saari, Ann Staples, Craig Ulrich, and Chris Williams. We also acknowledge early infrastructure development at the site by Stan Wullschleger and colleagues, funded by U.S. Department of Energy Office of Science, Biological and Environmental Research as well as Oak Ridge National Laboratory (LDRD program).

22 - Frost at the margins of permafrost / Frost related phenomena in non permafrost areas

Session 22

Frost at the margins of permafrost / Frost related phenomena in non permafrost areas

Conveners:

- **Reynald Delaloye**, Université de Fribourg, Fribourg, Switzerland
- **Vincent Jomelli**, LGP, CNRS, Meudon, France
- **Cecile Pellet**, Université de Fribourg, Fribourg, Switzerland (PYRN member)

Frost related phenomena concern not only the continuous and discontinuous permafrost zones, but also seasonal frost, freeze/thaw cycles, and patchy permafrost due to specific local conditions (like cold scree slopes, or ice caves). Periglacial geomorphology covers the whole range of frost effects. In mountain ranges, processes linked to seasonal frost and freeze/thaw cycles form what French geographers call the « infraperiglacial belt ».

All these phenomena will be affected by climate change, and seasonal frost has been defined by WMO as an Essential Climate Variable. The knowledge on the distribution, driving factors and evolution of these phenomena is however very limited. Very little is known for instance on the spatial/altitudinal distribution of seasonal frost and on its recent evolution. Very few studies exist on patchy permafrost: are they relics of ancient more continuous permafrost or original spots due to local conditions? Are they very sensitive or resilient systems regarding climate change?

This session aims at promoting research and exchanges on subjects related to seasonal frost, freeze/thaw cycles, patchy permafrost, cold scree slopes, etc. It will accept contributions on monitoring, process studies, ecological studies, or modeling, in mountain as well as arctic context.

Spatiotemporal mapping of the evolution of ground temperature on a cold scree slope at Pellafol, Devoluy, Isère, France

Joseph Drevon-Planchot[1]
Philippe Schoeneich[1]
Marco Marcer [1]
Simon Meynier[2]
Antoine Carriot [1]

[1]*Université Grenoble Alpes, Institut de Géographie Alpine, PACTE, Grenoble France, drevonjo@gmail.com*
[2]*IRSTEA, Grenoble, France*

Abstract

Cold scree slopes induce the presence of very local permafrost patches at low altitude in mountain ranges. Alternating seasonal ventilation induces an overcooling of the lower part of the slope. The Pellafol scree slope in the French Alps was instrumented with 58 temperature data loggers, on a 10x6 regularly spaced grid. Data acquisition was set to a 2 h time-step. The data allow the mapping of the spatial temperature distribution and its evolution through time. The time lapse temperature maps show the seasonal variations of the temperature pattern, as well as short time variations due to meteorological factors.

Keywords: cold scree slope ; spatio-temporal mapping ; temperature ; patchy permafrost; Alps

Introduction

Cold scree slopes are micro-geo-ecosystems found below the permanent permafrost inferior limit, from mountain to sub-alpine belts.

They form on coarse and porous debris or scree deposits, which permit an internal air circulation. This circulation is characterized by its thermal role in the formation of an over-cooled patch at the bottom part of cold scree slopes. Thus cold scree slopes represent patchy permafrost occurrences at low altitude.

The seasonal thermal regime shows 4 phases (Morard 2011), opposing 2 different states/direction of ventilation for summer and winter, with transition occurring over spring and autumn. During summer phases of descending air circulation, fresh air flows out at the bottom of the scree, cooling the near-vents' zones while accumulating warmer air by the top. During winter phases of ascending air circulation, warmer air flows out at the top of the slope, while cold air flows in by the foot, even through the snow cover.

The lower part of the system is therefore always cold. This over-cooling of the soil induces the presence of local "cold" ecosystems characterized by dwarf trees, abundant moss and lichen cover and raw humus. They are called "abyssal ecosystems", since they correspond to climate conditions usually found much higher in altitude (Huc et al. this conference).

The monitoring of these systems is motivated by two opposite hypotheses regarding climate change: they may be either very sensitive due to their low altitude, or very resilient due to the ventilation system. Also, some sites have been spotted near forest paths, arising the question of their protection.

At this moment, studies which surround those interests are relatively new, thus poor in number, but they show high technical support. (Morard 2011, Schwindt 2013). In the French Alps, research is conducted within the Abys 38 project (funded by the biodiversity research hub of the Isère department), a multidisciplinary project involving ecologists, geographers and foresters. The present communication will focus on one of the research sites of this project, the Pellafol cold scree.

The aim of this communication is to propose a method allowing the visualization of the infra-site temperature evolution year round. One of the expected result is the characterization of the spatial temperatures distribution and its evolution, at different time scales, from seasonal temperatures phases, to infra-phases typology or differences between day/night circulation.

Study site

The Pellafol cold scree slope is located in the Northern part of the Devoluy massif in the French Alps (Lat 44.787°N; Long 5.890°E), between 1200 and 1300 m a.s.l. It is an inactive scree composed of limestone.

Materials and Methods

The Pellafol cold scree slope is equipped since 2012, with first data series starting on the 31/07/12, up to 04/06/15. Four I-button temperature loggers were placed at 4 different positions as air (2m from the ground), bottom (in an identified vent), middle (foot of a tree, actually still in the over-cooled part of the slope) and top part of the cool zone (foot of a tree). This first set allowed the characterization of the thermal regime (Gautron 2014).

In order to map the spatial temperature distribution, a new set of 58 sensors (I-button) was set as a grid of 10x6 measurement points. The lowest line A contains only 4 sensors, lines B-J 6 sensors each. Spacing is 10 m horizontally and 15 m in the slope direction, corresponding to ca. 10-12 m in horizontal projection. The acquisition started on the 23/05/16, with 3 intermediary data download on 06/01/17, 22/06/17 and the last 22/11/17. As the time-step for acquisition was set to 2h, this leads us to 58 series of up to 6500 values. Some sensors appeared to be defect, which leads to gaps in the spatial coverage.

The mapping of temperature fields was automated on R, in order to produce an interpolated temperature map for each time-step. The intepolation method was set to inverse distance weight. Time series were then assembled to produce time lapse animations.

For seasonal variations, daily means and running means were used in order to reduce noise. For the analysis of shorter time windows, the full 2 h time resolution was used. Time series of selected sensors were used for the analysis of the thermal regime (figure 1).

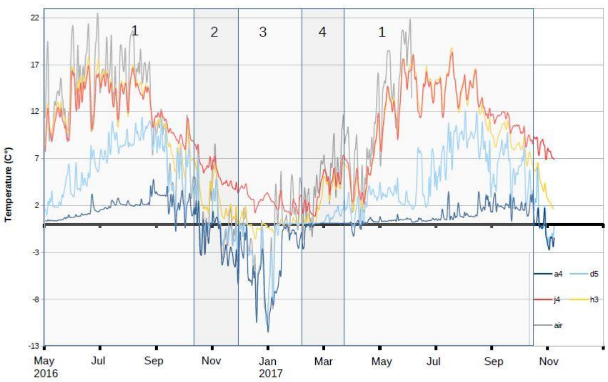

Figure 1: Thermal regimes of 4 selected sensors: a4 and d5 lower cold zone, h3 and j4 upper warm zone.

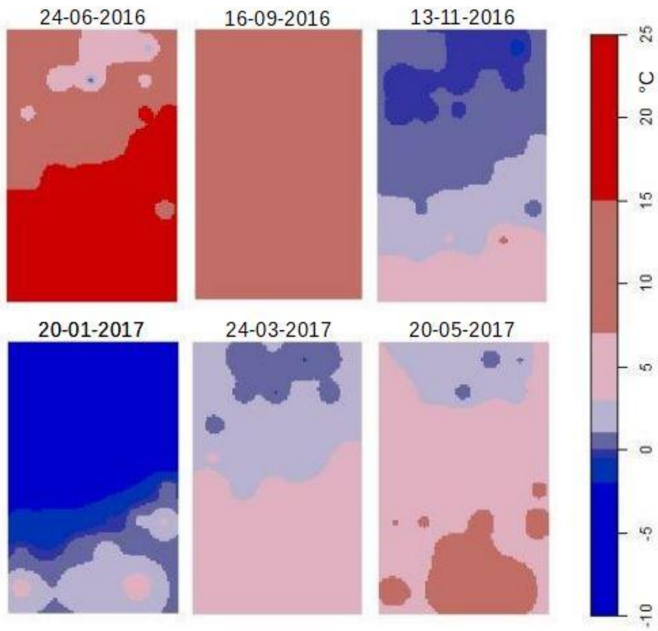

Figure 2: Interpolated temperature field at chosen dates

Results

Six examples of interpolated temperature maps are shown in figure 2, illustrating the main seasonal phases. The time series shows contrast intensity variations related to the thermal regime, as well as variations in the extent and location of cold/warm areas. Some varaitions seem to be due to the exhaustion of the cold/warm reservoirs during the season (see sensor h3 on figure 1). The temperature patterns allow also a finer inteprretation of the vegetation zones.

Acknowledgments

The present research was initiated during the Abys38 project, funded by the Pole biodiversité Isère (Isère department) and the Zone Atelier Alpes (CNRS).

References

Gautron, C., 2014. *Caractérisation des éboulis froids français, Secteur alpes jura, Eléments pour une approche thermique*. Master thesis, Université Grenoble Alpes

Morard, S., 2011. *Effets de la circulation d'air par effet de cheminée dans l'évolution du régime thermique des éboulis froids de basse et moyenne altitude*. PhD, Université de Fribourg (Suisse), 224p.

Schwindt, D., 2012. *Permafrost in ventilated talus slopes below the timberline, A multi-methodological study on the ground thermal regime and its impact on the temporal variability and spatial heterogeneity of permafrost at three sites in the Swiss Alps*. PhD, Universität Würzburg.

Cryogenic earth hummocks developed in mineral substrates

Stuart A. Harris[1]

[1]*Department of Geography, University of Calgary, Canada,* harriss@ucalgary.ca

Abstract

Cryogenic earth hummocks consist of mounds up to 1m high by 2.5 m long, formed by the local accumulation of seasonal ice in the soil. They differ from active sorted and non-sorted patterned ground by the absence of seasonal circulatory soil movements. Four different kinds are described from maritime mid-latitude climates to dry, cold High Arctic deserts. *Oscillating hummocks* develop in the boreal forest, persisting until fires cause their collapse. They redevelop as the permafrost recovers under the new trees, and are characterized by blocks of peat in the frozen core. *Thufurs* grow in cold maritime climates such as Iceland by movement of silt with water to the freezing plane in winter. *Silt-cycling hummocks* have been reported from New Zealand and Dartmoor, though their exact mechanism of formation remains to be confirmed. *Niveo-aeolian hummocks* occur in the dry, cold High Arctic deserts as a result of aeolian action.

Keywords: Cryogenic earth hummocks; Oscillating hummocks; Thufurs; Silt-cycling hummocks; Niveo-aeolian hummock

Introduction

Cryogenic hummocks are those in which the accumulation of localized seasonal ice lenses often accompanied by sand or silt in the upper soil layers is involved. This localized accumulation of sediment causes the upwards growth of the hummock.

They consist of mounds up to 1 m high and less than 2.5 m in length, developed on slopes or horizontal surfaces. They are usually circular in outline and do not show complete mixing of the sediment within them. On slopes, they may be somewhat elongate. Earth hummocks differ from non-sorted circles by the absence of a seasonal circulatory movement in the soil producing the landform as in mudboils. They occur in a variety of cold climates varying from the maritime humid situations with seasonal frost, *e.g.*, Iceland, to the taiga and boreal forests of somewhat elongate. In North America and Asia where they are underlain by permafrost. This paper discusses the origin of the main forms not produced by burrowing animals that have been adequately described so far (Table 1).

Table 1: Summary of the different kinds of cryogenic earth hummocks developed in mineral soil

Type of hummock	Permafrost Zone	Vegetation	Process
Oscillatory	Continuous and Discontinuous	Taiga	Buildup of ice lenses alternating with collapse after periodic forest fires
Thufers	Sporadic/Seasonal	Cool, Perhumid Meadow	Movement of silt to the freezing plane, with soil moisture in stratified salt
Silt-cycling	Humid Temperate	Wet Moors	Movement of silt with moisture to the frozen sides and top of the hummock. Formed in homogenous silt loams.
Niveo-aeolian	High Arctic Desert	Tundra	Winter movement of sand from the top of the hummocks downwind with snow.

Oscillating hummocks

These consist of vegetated mounds 20-100 cm high with a basal diameter of 50-150 cm occurring primarily in the boreal forest and taiga over permafrost. In cross-section, they show mixed-up blocks of surface sediment and/or organic material with the host sediment. The mounds gradually increase in height as ice accumulates each winter. Zoltai (1975) found that the trees on the sides of the hummocks tilted once every 25 years on average, indicating continued growth. Eventually the hummocks collapse when a forest fire occurs, spreading laterally over the surrounding organic top-soil by lateral flowage as the ice melts. When the vegetation cover rejuvenates, ice lenses start to form in the collapsed material, and upward growth commences (Pettapiece, 1974; Kokelj *et al.*, 2007). Radiocarbon dating of the buried organic matter produces dates back to before 11 ka with the bulk of the included buried material dating from after 5 ka (Tarnocai & Zoltai, 1978), *i.e.* during the cold humid Neoglacial events.

Oscillating hummocks have been reported from the discontinuous and continuous permafrost zones of Canada, the forest margins of Mongolia, Russia, and the alpine tundra of northern Europe and China.

Thufurs

These are small mounds that grow in farmer's fields in cold humid climates, often in volcanic tephra. They are similar in size to oscillating hummocks, but show discrete layers in cross-section. However, there is a distinct thickening of the silt in the layers in the middle of the mound. Grain sizes are essentially coarse silt with fine sand but less than 30% clay.

Corte (1996) demonstrated that silt particles can move with liquid water to the freezing plane through the spaces between the coarser mineral grains. Schunke (1977) invoked this mechanism to explain the thickening of the layers in the mounds in Iceland. There the mounds can reform in 10 years after being bulldozed flat. These mounds are limited to areas of discontinuous to seasonal frost under meadow vegetation.

Silt-cycling hummocks

Mark (1994) and others have explained hummocks in homogenous silt loam sediments in temperate humid climates such as New Zealand as resulting from the seasonal freezing of the tops and sides of mounds but not the troughs. There, they occur in tussock grasslands above tree line. Movement of soil water from the troughs to the freezing plane is invoked to carry silt with it to gradually enlarge the height of the mounds. Eventually the increase in silt in the mound is equal to the gravity-induced processes moving silt down the sides resulting in an equilibrium height but with potential lateral enlargement. In Cornwall, Killingbeck & Ballantyne (2012) have shown their growth in 3ka on Dartmoor, but they are absent on adjacent sandy sediments. Their exact geographic range remains to be determined.

Niveo-aeolian hummocks

Lewkowicz & Gudjonsson (1992) and Lewkowicz (2011) have described "slope hummocks" from the Fosheim Peninsula on Ellesmere Island in the Canadian Arctic as being decimeter-scale mounds on slopes of 8-27° overlying permafrost developed in stratified silty sand. They exhibit a >75% vegetation cover with limited signs of cryoturbation, and occur on north-facing slopes with a thin active layer. In winter, the tops are exposed above the snow pack and undergo wind erosion, the eroded material being redeposited on the down-slope side of the mounds in the snow. Modelling suggests that the hummocks move 20-40 m down-slope in about 2-4 ka, based on C^{14} dates obtained from buried organic matter in the soil since emergence from the sea together with actual measured rates of gelifluction. They are probably limited to the cold dry, high Arctic Archipelago. The hummocks described by Kojima (1994) may be similar. The initial development of these hummocks is unknown.

Similar-looking mounds of uncertain origin

Although there have been numerous descriptions of cryogenic earth hummocks in mineral soil in the literature, most lack enough information to determine their precise mode of formation. With the development of better field equipment and techniques (see Jelinski *et al.,* 2017), it is to be hoped that this will change in the future.

References

Corte, A.E., 1966. Particle sorting by repeated freezing and thawing. *Builetyn Peryglacjalny* 15: 175-240.

Jelinski, N.A., Yoo, K. & Klaminder, J., 2017. Utilizing a suite of isotopic and elemental tracers to constrain cryoturbation rates and patterns in non-sorted circles. *Permafrost and Periglacial Processes* 28(4): 634-648.

Killingbeck, J. & Ballantyne, C.K., 2012. Earth hummocks in West Dartmoor, S.W. England: Characteristics, age and origin. *Permafrost and Periglacial Processes* 23(2): 152-161.

Kojima, S., 1994. Relationships of vegetation, earth hummocks and topography in the high arctic environment of Canada. *Polar Biology* 7: 256-269.

Kokelj, S.V., Burn, C.R. & Tarnocai, C., 2007. The structure and dynamics of earth hummocks in the Subarctic Forest near Inuvik, Northwest Territories, Canada. *Arctic, Antarctic and Alpine Research* 39(1): 99-109.

Lewkowicz, A.G., 2011. Slope hummock development, Fosheim Peninsula Ellesmere Island, Nunavit, Canada. *Quaternary Research* 75: 334-346.

Lewkowicz, A.G. & Gudjonsson, K.A., 1992. Slope hummocks on Fosheim Peninsula, Northwest Territories. *Geological Survey of Canada, Current Research, Part B* Paper 92-1B: 97-102.

Pettapiece, W.W., 1974. A hummocky permafrost soil from the Subarctic of northwestern Canada and some influences of fire. *Canadian Journal of Soil Science* 54(4): 343-355.

Schunke, E., 1977. Zur Ókologie der Thufer Islands. *Ber. A. d Forschungsstelle "Nedri Ar".* 26. Hveragerdi, Iceland, 26p

Tarnocai C. & Zoltai, S.C., 1978. Earth hummocks of the Canadian Arctic and Subarctic. *Arctic and Alpine Research* 10: 581-594.

Zoltai, S.C., 1975. Tree ring record of soil movements on permafrost. *Arctic and Alpine Research* 7: 331-340.

Plant species indicative of cold screes at low altitudes in the French Alps

Stéphanie Huc[1]
[1] *Conservatoire botanique national alpin, Gap, s.huc@cbn-alpin.fr*

Abstract

This study deals with cold screes in the French Alps. Vegetation is used as indicator of morpho-dynamic changes. 10 sites are monitored. 12 species appear as "characteristics".

Keywords: cold screes; bio-indicator; climate change; monitoring.

Introduction

Below the timberline, some North Slope forests shelter special periglacial formations: abyssal ecosystems on cold scree. These openwork block formations are characterized by the presence of a negative thermal anomaly in summer in the lower part and a positive thermal anomaly in winter in the upper part (Delaloye *et al.*, 2003). The openwork system provides an internal air circulation mechanism. The presence of perennial ice lenses at the bottom of scree slopes is the only occurrence of patchy sporadic permafrost at low altitude (900-1300 m above sea level) (Gude *et al.*, 2003). We observe abyssal plant species and dwarf trees on the cold areas representing original paleo refuges (Růžička *et al.*, 2012). This natural habitat is a European priority under the term "Pine communities with *Pinus mugo subsp. uncinata* and *Picea abies* on frozen scree" (code 9430). In the context of climate change, we wonder about this environment: resilient or sentinel system? We know that plant species can be used to indicate dynamics and evolutions (Huc, 2008).

To assess the evolution of vegetation in time and space in relation to possible modification in air circulation due to climate change, we propose two goals: 1- To identify the characteristic plant species in the cold zone and the margins and 2- To test a simple monitoring protocol in the coldest zone and in the control area.

To appreciate the potential changes, this ecological study makes the connection with the study of humus (Meynier & Brun 2017) and microclimatic monitoring (Schoeneich, 2017). Finally, 10 cold screes are studied along a latitudinal gradient at the scale of the French Alps.

Methods

From the vegetation surveys carried out in the cold screes of the Alps (Database Flora (version 2), 2017), we have selected species that meet 3 criteria: a frequency of occurrence >30%, a vegetation cover >15% and an altitudinal shift (their natural range is generally located at a higher altitude) or a possible dwarfism of trees. Identified species are then monitored in time and space. The protocol consists in identifying the presence of characteristic species in 30 plots of 1 on 0.5 m (Fig. 1) along transects in the cold zone and in the control area for temporal monitoring and along a transverse transect that cuts the cold zone and the control area for spatial monitoring.

Figure 1. Sampling with 30 plots of 1 on 0.5 m along transect.

Results

With the first results obtained in 2016 and 2017 we test the validity of the species chosen for monitoring. The species previously identified as "characteristic" of the coldest zone are significantly more present in the coldest zone than in the control area (p-value<0.01) (Fig. 2). In the coldest zone, 14 species share frequency of occurrence from 11 to 61.7%. Among these species, only 2 species do not have a specific cryophilic character

(*Rubus saxatilis* and *Vaccinium myrtillus*). 12 species identified as indicators of the cold zone are mainly located in the cold scree, like *Salix retusa*, *Salix reticulata*, *Dryas octopetala, Cladonia arbuscular* and *rangifera, Cetraria islandica*). Four other share equivalent frequencies in the cold zone and in the control zone.

Other non-characteristic species will also be monitored in the case of the thermal dynamics would be disturbed with appearance of new species in the cold zone or with a modification of the frequencies for the species already present.

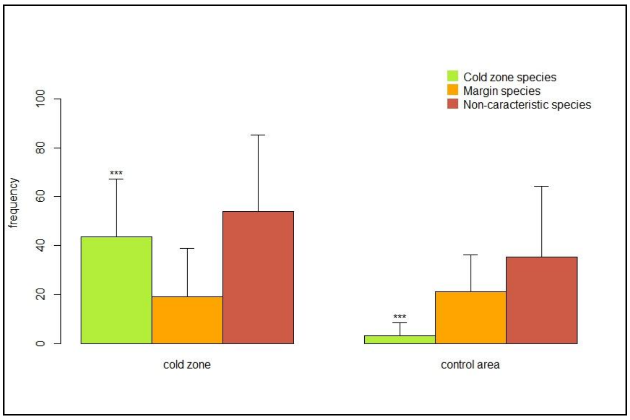

Figure 2. Comparison between cold zone and control area for the « characterictic » species. *** p-value<0.001

Conclusion

The monitoring protocol will be renewed in 2019 and 2020 in order to assess the evolution of the vegetation. It will be put into perspective with the results of thermal monitoring carried out in the same areas.

Acknowledgments

This program is financially supported by Europe (POIA) and the PACA and AURA regions.

References

Database Flora (version 2). 2017. CBNA. F – 05000 Gap

Delaloye, R., Reynard, E., Lambiel, C., Marescot, L., Monnet, R., 2003. Thermal anomaly in a cold scree slope (Creux du Van, Switzerland). *Proceedings 8th international Conference on permafrost*, Zürich: 175-180.

Gude, M., Dietrich, S., Mäusbacher, R., Hauck, C., Molenda, R., Ruzicka, V., Zacharda, M., 2003. Probable occurence of sporadic permafrost in non-alpine scree slopes in central Europe, *Proceedings 8th international Conference on permafrost*, Zürich: 331-336.

Huc, S., 2008. Scree mobility above the treeline in the eastern Pyrenees (France): morphodynamic and biological indicators. *Géomorphologie: relief, processus, environnement* 2: 99-112.

Meynier, S., Brun, J.-J., 2017. Humus forms pathways in low-elevation cold scree slopes: Tangel or Mor? *Applied Soil Ecology*.

Růžička, *V., Zacharda, M., Nemcova, L., Smilauer, P., Nekola, J.,* 2012. Periglacial microclimate in low-altitude scree slopes supports relict biodiversity, *Journal of Natural History*, 46, 35-36: 2145-2157.

Schoeneich, P., Huc, S., Brun, J.J., Meynier, S., Desplanque, C., 2017. *Ecosystèmes forestiers abyssaux : une opportunité pour la gestion durable des forêts de montagne en Isère*, Conseil Général d'Isère, Institut de géographie alpine, 61p.

Multi-method investigation of a patchy permafrost occurrence in the eastern Swiss Alps

Christof Kneisel[1]
Franziska Losert[1]

[1]*Physical Geography, Institute of Geography and Geology, University of Wuerzburg, Germany,*
kneisel@uni-wuerzburg.de

Abstract

At a subalpine site with permafrost below the timberline in the eastern Swiss Alps the complex interrelationship between different environmental factors was investigated by applying an integrated approach that combines two-dimensional and three-dimensional near-surface geophysics and surface and subsurface temperature monitoring. The objectives of this approach were to explore the 3D extension of isolated permafrost bodies and to characterize the site-specific thermal regime and frozen ground conditions in this subalpine environment dominated by seasonal frost. The focus of the present research was to detect the subsurface structure and composition of the scree slope around two boreholes instrumented with temperature sensors and to analyze the temperature records from the boreholes as well as surface loggers in order to evaluate the sensitivity of the patchy permafrost to climate change.

Keywords: frozen ground conditions; seasonal frost; cold scree slope; 3D electrical resistivity imaging; thermal regime; organic layers.

Introduction

Permafrost is a common phenomenon in cold alpine environments that are characterized by extreme climatic conditions. Discontinuous permafrost distribution in the Swiss Alps usually appears at north-exposed sites above an altitude of 2400 m asl, and on south-facing sites above 3000 m asl, respectively. Below the timberline, at very shaded sites and under special environmental conditions isolated permafrost can exist.

In the Bever Valley, Upper Engadine (eastern Swiss Alps), such patchy permafrost at low altitude has been confirmed and characterised (Kneisel et al., 2000). The studied scree slopes represent one of the few sites in the Alps where isolated permafrost at low altitude could be verified. Other sites with scree slopes with thermal anomalies and patchy permafrost are described in Delaloye et al., 2003 and Stiegler et al., 2014.

Recent research at the Bever site aimed at discovering the reasons for the spatial variability of frozen ground with the differing surface conditions (Kneisel et al., 2015). Aim of the present study was to detect the subsurface structure and composition of the scree slope in more detail around two boreholes instrumented with temperature sensors and to analyze the temperature records from the boreholes as well as surface loggers in view of the potential impact of atmospheric warming.

Study Site and Methods

The study area is located in the Bever Valley, a tributary of the main wide valley of the Upper Engadine, in the eastern Swiss Alps. The regional climate is continental having a fairly low precipitation and a comparatively high temperature range. Mean annual precipitation is 1050 mm and the mean annual air temperature is +1°C. At present, the upper timberline is between 2200 m asl and 2300 m asl. Larch (Larix decidua) and Swiss stone pine (Pinus cembra) are the dominant tree species of the forest. The studied scree slopes are having an elevation of 1780 m asl at the foot of the slopes.

Two-dimensional (2D), quasi-3D and three-dimensional (3D) electrical resistivity imaging (ERI) surveys were performed using a Syscal Pro Switch resistivity-meter. Different arrays and electrode spacings (1-3 m) were applied. For the additional seismic refraction surveys we used a Geode Seismograph, a sledge hammer as source of the seismic signal and a geophone spacing of 3 m.

The first borehole was drilled in autumn 2006 to a depth of 8 m and a thermistor string having eight sensors was inserted. The second borehole was drilled in autumn 2015 to a depth of 10 m and instrumented with a thermistor string consisting of 15 sensors.

Results

The results of the different geophysical measurements confirm isolated permafrost occurrences consisting of several thin permafrost lenses at shallow depth (down to 20 m) with a comparatively thin active layer (1–3 m). The detected high resistive anomalies can be interpreted as frozen ground since additional 2D seismic refraction surveys showed P-wave velocities between 1700 and 4300 m/s. As those values are indicative of ground ice, air cavities as the sole reason for the high resistivity values can be excluded, as they would result in much smaller P-wave velocities.

Figure 1 shows a 2D ERI tomogram from the lower parts of the scree slope, the blue colors represent frozen ground. The small and shallow permafrost patch at the foot of the slope highlighted with the arrow is the area where the new borehole was drilled in 2015 and one of the 3D ERI grids was placed around the borehole location covering different surface conditions (see Fig 2.)

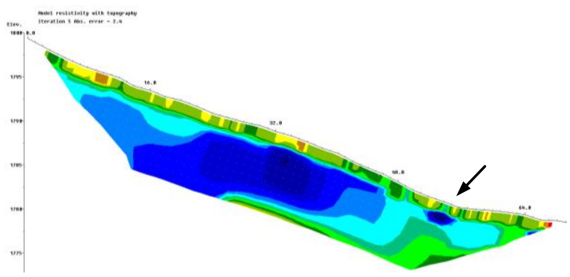

Figure 1. ERI survey along the scree slope

Figure 2. Photograph of the 3D ERI setup

The 3D approach enabled a spatial imaging of the variation of the properties of the subsurface. These properties could then be correlated to terrain parameters and surface characteristics. When the surface characteristics (esp. humus forms) are compared with the resistivity images of the subsurface, a spatial coincidence of the areas having a moss layer and the high resistivity anomalies can be seen. However, other humus forms could also be identified in areas having permafrost. The organic surface layers are known to play an important role in insulating the subsurface and thus controlling the ground thermal regime.

The super-cooling of the scree slope due to the chimney effect is a fundamental process that explains the presence of permafrost. Although climate warming is well acknowledged for the last decades in the Alps and the mean annual air temperature at the site is above 0°C, frozen ground conditions in the investigated scree slope do not seem to have changed greatly.

References

Delaloye, R., Reynard, E., Lambiel, C., Marescot, L., Monnet, R., 2003. Thermal anomaly in a cold scree slope (Creux du Van, Switzerland). *Proceedings of the 8th International Conference on Permafrost*, 21–25 July 2003, Zürich, Switzerland: 175–180.

Kneisel, C., Hauck, C., Vonder Mühll, D., 2000. Permafrost below the timberline confirmed and characterized by geoelectrical resistivity measurements, Bever Valley, eastern Swiss Alps. *Permafrost and Periglacial Processes* 11: 295-304.

Kneisel, C., Emmert, A., Polich, P., Zollinger, B., Egli, M., 2015. Soil geomorphology and frozen ground conditions at a subalpine talus slope having permafrost in the eastern Swiss Alps. *Catena* 133: 107-118.

Stiegler, C., Rode, M., Sass, O., Otto, J.-C., 2014. An undercooled scree slope detected by geophysical investigations in sporadic permafrost below 1000 m asl, Central Austria. *Permafrost and Periglacial Processes* 25: 194-207.

Cold scree slopes environments: unusual ecological processes highlighted by humus forms

Simon Meynier
Jean-Jacques Brun

Univ. Grenoble Alpes, Irstea, France, Simon.Meynier@univ-grenoble-alpes.fr

Abstract

Cold scree slopes are characterized by the *chimney effect*, an internal air circulation, causing a strong negative anomaly of temperature in their lower part. It may result in the formation of underlying permafrost lenses at strikingly low elevation. Consequently, cold screes harbor boreo-arctic environments, remarkable at such low altitude and/or latitude. While thermal mechanics of cold screes have recently raised interest from geomorphologists, their ecological processes remain barely studied. Humus forms, considered as ecological integrators, were studied in five cold screes in the French Alps. Only one in four humus forms we observed displayed morphological and chemical characteristics consistent with those usually found under such cold conditions. Our results suggest that the underlying abiotic conditions (bedrock, soil temperature and moisture) of cold scree slopes outweigh vegetation and atmospheric climate as dominant drivers of the ecosystem functioning. It may lead them to diverge from regular ecological pathways.

Keywords: cold scree slope; humus form; patchy permafrost; ecological processes; boreo-arctic environment

Cold scree slopes are porous debris accumulation governed by a curious ventilation phenomenon called *chimney effect*. This complex internal air circulation leads to the warming of the upper part of the scree in winter, while the bottom area is constantly and strongly undercooled all year long (Delaloye et al., 2003). It can even cause the formation of perennial ice lenses far below the regular lower limit of permafrost.

This unusual abiotic context result in the occurrence of boreo-arctic environments, typically characterized, among other things, by the presence of dwarf trees, alpine and subalpine vegetation, and a thick raw humus with great organic matter accumulation. These environments, remarkable at such a low altitude and/or latitude, are thus considered as abyssal ecosystems. Moreover, cold scree slopes act as refugia for many species and communities unable to live outside the specific conditions they provide. In the context of climate change, they might play a key role by sheltering species otherwise doomed to disappear, especially in medium-sized mountains. But, overall, ecological properties of these atypical ecosystems have been poorly investigated so far.

We aimed to explore ecological processes of five cold screes in the French Alps through the investigation of their humus forms. Humus form is the part of the topsoil that is strongly influenced by organic matter. It is determined according to the various organic and organo-mineral horizons types, thickness, and stacking. Humus layers are shaped by the varying size and proportion of dropping accumulation of pedofauna, and/or the stacking of remains and humic components fragmented by fungi or other non-faunal processes. They directly depend on both biotic and abiotic context, thus representing an ecological integrator that synthesizes their climatic, geological and biological conditions of formation (Zanella et al., 2011).

In Europe, terrestrial humus forms are known to follow two paths, shifting from Mull in favorable context (temperate climate; neutral conditions) to Moder and then Mor (acidic conditions) or Amphi and then Tangel (calcareous conditions) in colder climate (Ponge et al., 2010).

We tested whether humus forms of cold screes are consistent with those regular pathways. To that end, we studied morphological, chemical and spectral (i.e. through FT-IR spectroscopy analysis) characteristic of humus forms within the five cold screes we studied. Moreover we analyzed humus forms under ericaceous shrubs, bryophytes, and under mixed ericaceous-bryophytes communities to take heed of vegetation on humus processes.

Our observations were somewhat surprising. Among the four humus forms we found, three were clearly unusual (intermediate Tangel/Mor humus in calcareous context plus peculiar Tangel and Histomor) while only one was fully consistent with those usually recorded under such cold conditions (Mor humus in acidic context)(see Fig.1).

Furthermore, we did not detect any vegetation influence on humus forms nor event soil organic matter. Every major difference between humus forms we recorded stood out in their subjacent layer, which is lying between scree boulders. It may reflect a decoupling of plant-soil feedback within cold screes. This decoupling seems to be due to various phenomena:

(i) The ventilation system of cold screes (causing cold temperature, moisture, intense and longer frost period) outweigh vegetation and atmospheric climate as the main drivers of humus formation.

(ii) These peculiar abiotic conditions have an even stronger impact on subjacent than on upper humus horizons.

(iii) In addition, the presence or absence of perennial ice lenses among cold screes could be a major feature of their ecosystem functioning by governing, through direct and indirect effects, the overlying pedoclimate.

Hence, the atypical abiotic context of cold screes may lead abyssal ecosystems they host to diverge from usual ecological processes, resulting in these curious humus forms. Our study highlights that cold scree slopes environments are plenty of surprises for ecologist scientists. Due to their presumed crucial role as refugia for many communities, further studies are needed for a better understanding of their singular ecological patterns.

References

Delaloye, R., Reynard, E., Lambiel, C., Marescot, L., Monnet, R., 2003. Thermal anomaly in a cold scree slope (Creux du Van, Switzerland), in: Phillips, M., Springman, S.M., Arenson, L.U. (Eds.), *Proceedings of the 8th International Conference on Permafrost. Presented at the 8th International Conference on Permafrost*, A a Balkema Publishers, Zürich, pp. 175–180.

Meynier, S., Brun, J.-J., 2017. Humus forms pathways in low-elevation cold scree slopes: Tangel or Mor? *Appl. Soil Ecol.* In press

Ponge, J.-F., Zanella, A., Sartori, G., Jabiol, B., 2010. Terrestrial humus forms: ecological relevance and classification.

Zanella, A., Jabiol, B., Ponge, J.F., Sartori, G., De Waal, R., Van Delft, B., Graefe, U., Cools, N., Katzensteiner, K., Hager, H., Englisch, M., 2011. A European morpho-functional classification of humus forms. *Geoderma* 164, 138–145.

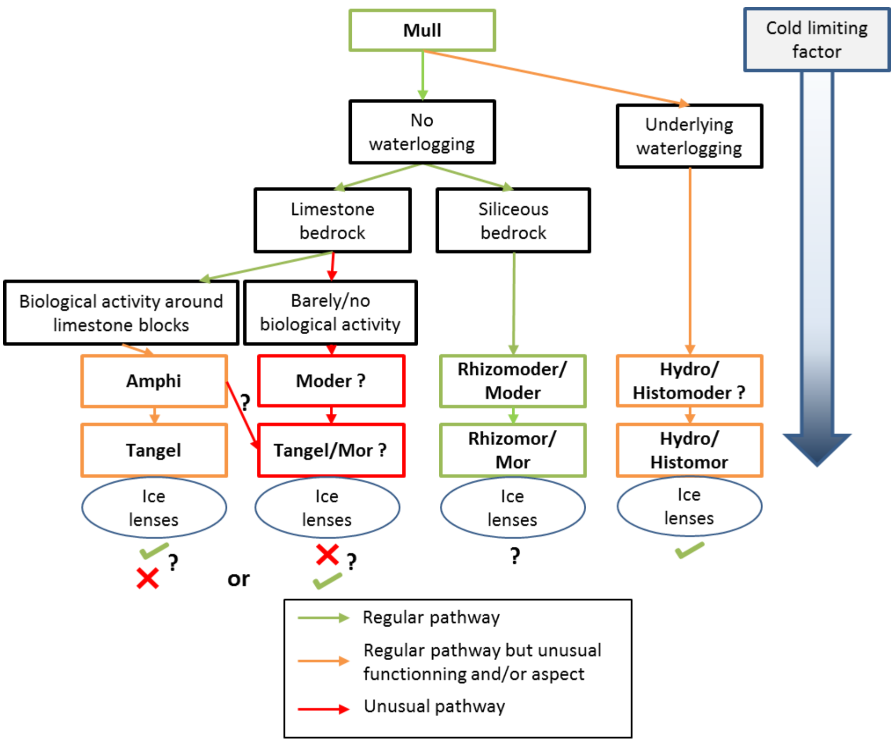

Figure 1. Humus forms recorded in cold scree slopes. Only one follows the usual pathway known in Europe under cold conditions (Meynier & Brun, 2017).

Fillings freeze and countermeasures used for a dam core construction in seasonal frost region, SW China

Yanhu Mu[1], Qihao Yu[1], Pan Yue[2], Xinbing Wang[1]

[1]*State Key Laboratory of Frozen Soil Engineering,* Chinese Academy of Sciences, muyanhu@lzb.ac.cn
[2]*Yalong River Hydropower Development Company, Ltd.*

Abstract

In seasonal frost region, dam construction is facing some challenges posed by cold climate and cyclic freeze-thaw. In this paper, fillings temperature of impervious core of a dam in Sichuan province, southwest China was measured in a wintertime. The results showed that freeze could occurred within shallow depths of the compacted fillings in the nighttime. The duration of the freezing were less than 24 h as the frozen fillings could be thawed rapidly after the sunrise. To prevent this daily freeze-thaw, thermal insulations made by nonwoven geotextile and LDPE geomembrane were used to cover the impervious core in the nighttime and downtime. While fill and compaction of the impervious core were only conducted in the daytime. With the insulation, no freeze occurred in the compacted fillings.

Keywords: Dam construction; core fillings; cyclic freeze-thaw; seasonal frost region

Introduction

In seasonal frost region, dam construction is facing some challenges posed by cold climate and cyclic freeze-thaw. On the one hand, freeze under subzero environment temperatures will make fillings compaction more difficult. To reach the required compaction degree, more roller compaction work will be needed. On the other hand, seasonal and/or daily freeze-thaw actions will exert negative impacts on compacted fillings. As a weathering process, cyclic freeze-thaw can change the mechanical properties of compacted fillings considerably (Qi *et al.*, 2012). For example, the hydraulic permeability often increases by one to two orders of magnitude after freeze-thaw (Chamberlain EJ & Gow, 1979; Eigenbrod, 1996). Thus, freeze or freeze-thaw of compacted fillings are generally forbidden for dam construction in seasonal frost region.

In this paper, fillings freeze-thaw characteristics of impervious core of a dam in seasonal frost regions, Sichan Province, southwest China is reported based on field-measured temperature data. Thermal insulations used to prevent fillings freezing is also introduced, as well as its insulation effect.

Study site and method

The studied dam is an earthen-rock dam located at the Yajiang country (3000 m a.s.l.) in west of Sichuan province and east margin of the Qinghai-Tibet Plateau and, southwest China. Fillings of impervious core of the dam includes gravelly soil and clay. The mean annual air temperature of the dam location is about 10.9 °C, and the lowest air temperature can reach to -15.9 °C. The lowest mean month air temperature is 1.4 °C in January.

Thermal insulations made by nonwoven geotextile and LDPE geomembrane were used in the nighttime and downtime to prevent compacted fillings of the impervious core from freeze in winter times. To gain the fillings freeze characteristics, a path of thermal insulation were uncovered. Soil temperatures were measured with a string of thermistors and collected by a datalogger (Fig. 1). Along the string, nine thermistors was buried at 0.5, 3, 6, 9, 12, 34, 56, 78, 100 cm depths, respectively, to gain thermal regime of compacted fillings in 1 m depth without insulation.

Figure 1. Photos of dam core and soil temperature monitoring system.

Results and analysis

Fig. 2 shows surface temperature (0.5 cm depth) of compacted fillings without thermal insulation in winter times of 2016-2017. It can be found that subzero temperature occurred in compacted fillings, and the lowest temperature could reach to -5.0 °C. After freeze, visible pore ice can be identified in compacted fillings. The freezing of compacted fillings without insulation generally started freezing at wee hours. Then, the freeze front advanced downwards slowly with time. At about 10 a.m. (sunrise is generally at 8 a.m.) of the second day, the frozen fillings started thawing and the thaw process are very rapidly. The duration of the fillings freeze were all less than 24 h in the monitored winter (Fig. 4).

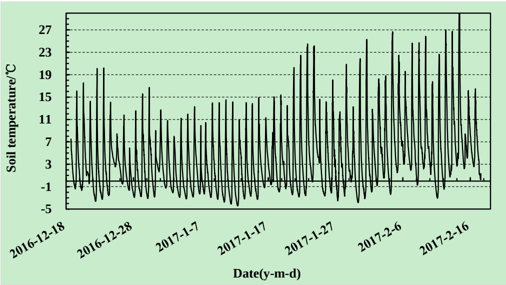

Figure 2. Time series of surface temperature of compacted fillings without thermal insulations at dam core.

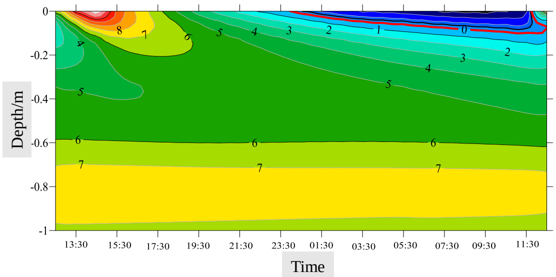

Figure 3. Freeze-thaw process of gravel soil at dam core on 21 October, 2016.

The above monitored results indicated that without thermal insulation the compacted fillings would freeze in the nighttime and thaw in the day time, experiencing daily freeze-thaw cycles. Thus, to prevent filling freeze, thermal insulations made by nonwoven geotextile and LDPE geomembrane were used in the nighttime and downtime (Fig. 4). While, in the daytime, the insulations were uncovered and the impervious core was filled normally. The coverage and uncovering of the insulation were done manually.

Figure 4. Dam core covered with thermal insulations made by nonwoven geotextile and LDPE geomembrane.

With the thermal insulation, there was almost no freeze occurring in the compacted fillings (Fig. 5). Moreover, with thermal insulation, amplitude of surface temperature of compacted fillings decreased considerably. The lowest surface temperature with thermal insulations was about 3.5 to 5 °C higher than that without thermal insulations.

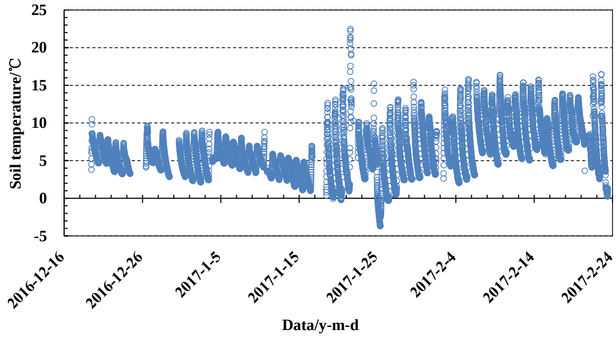

Figure 5. Time series of surface temperature of compacted fillings without thermal at dam core.

Conclusions

Compacted fillings temperatures of impervious core of a dam in seasonal frost regions, Sichan Province, southwest China was measured during the wintertime of 2016 to 2017. Measurements showed that the compacted fillings would freeze in the nighttime and thaw in the daytime, with the duration of freeze less than 24 h. The maximum freezing depth could be greater than 10 cm. Considering the negative impacts of daily freeze-thawing on engineering properties of the compacted fillings of dam core, thermal insulations made by nonwoven geotextile and LDPE geomembrane were used in the nighttime and downtime. With thermal insulation, there were almost no freeze occurs in the compacted fillings and the impervious core were filled and compacted only in the daytime.

Acknowledgments

This work is supported by Science Program of Yalongjiang River Hydropower Development Company, Ltd.

References

Qi, J.L., Vermeer, P.A., Cheng, G.D., 2006. A review of the influence of freeze-thaw cycles on soil geotechnical properties. *Permafrost and Periglacial Process* 17: 245-252.

Chamberlain, E.J. & Gow, A.J., 1979. Effect of freezing and thawing on the permeability and structure of soils. *Engineering Geology* 13(1-4): 73-92.

Eigenbrod K.D., 1996. Effects of cyclic freezing and thawing on volume changes and permeability of soft fine-grained soils. *Canadian Geotechnical Journal* 33(4): 529-537.

Seasonal frost in the French Alps

Philippe Schoeneich[1]
Laetitia Lazizi[1]
Philippe Choler[2]
Jean-Paul Laurent[3]
Samuel Morin[4]
Thomas Morin[5]
[1]*Université Grenoble Alpes, Institut d'Urbanisme et de Géographie Alpine, PACTE, Grenoble, France, philippe.schoeneich@univ-grenoble-alpes.fr*
[2]*Station Alpine Joseph Fourier, CNRS, Grenoble, France*
[3]*Université Grenoble Alpes, IGE, CNRS, Grenoble, France*
[4]*Météo-France, CNRM-CEN, Grenoble, France*
[5]*ROMMA, France*

Abstract

Seasonal frost is defined by WMO as an essential climate variable. Only few monitoring data exist however. The communication presents a compilation of available soil temperature data in the French Alps, coming from meteorological stations, ecological monitoring plots as well as a few sites especially equipped for seasonal frost monitoring. The analysis shows that seasonal frost is highly variable in occurrence, intensity and duration, and that there is no simple altitudinal gradient. The main driving factor is the onset date of the snow cover in early winter.

Keywords: seasonal frost; Alps; monitoring; snow cover.

Introduction

Seasonal frost is defined by WMO as an essential climate variable, together with permafrost temperature, active layer thickness and other cryospheric variables. Only few monitoring data exist however. Most monitoring efforts have been put on permafrost, and seasonal frost appears as a neglected phenomenon.

Seasonal frost will be affected by climate change, and some geomorphological processes driven by it will evolve too. Ecologists consider that the upper soil temperature and seasonal frost are control factors for the vegetation. Thus changes in the soil thermal regime could induce changes in the vegetation cover.

Data sets

The following datasets are used:

- The longest soil temperature series in the French Alps is measured since 1993 at the MeteoFrance station of Col de Porte, at 1320 m a.s.l. (Lat. 45.2951°; Long. 5.7655°). It measures soil temperature at 10, 20 and 50 cm depth. The site is the reference station for snow cover monitoring, so that snow cover data are available too.
- Around Col du Lautaret (Lat. 45.0354°; Long. 6.4050), the Station Alpine Joseph Fourier installed over 100 ecological monitoring plots at altitudes ranging from 2000 to 2800 m a.s.l.. 30 of them are equipped since 2007 for subsurface soil temperature monitoring, at 5 cm depth;
- Five additional measurement sites were installed in 2013 in the Roche Noire valley above Col du Lautaret, from 2200 to 2650 m a.s.l., on ecological plots, and equipped for soil temperature monitoring at 10, 30 and 50 cm depth;
- Several data sets could be retrieved from the PermaFrance permafrost monitoring network, from sensors placed close to monitored rockglaciers but outside of the permafrost area;
- Three soil temperature monitoring sites were installed on Hauts Plateaux du Vercors natural reservation (Lat. 44.9686°; Long. 5.4769°) in 2004, between 2350 and 2740 m a.s.l.;
- The CREA participative netowrk runs ecological observation stations distributed all over the French Alps. Some of them measure subsurface soil temperature, together with meteorological parameters.

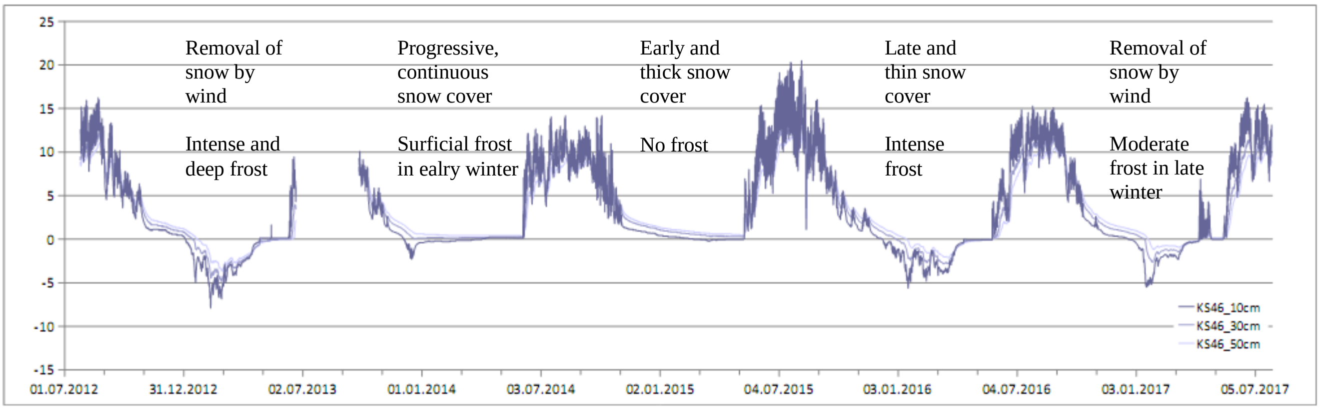

Figure 1. Soil temperature at 10, 30 and 50 cm depth, from July 2012 to July 2017, at site KS46 at 2650 m a.s.l.. The record shows very different thermal regimes from one winter to the other, depending on the snow cover history.

Except at the Col de Porte station, using a central logger, most other sites use autonomous mini-data-loggers of various types. Accuracy and resolution are however comparable.

The analysis is based mainly on soil temperature profiles including several measurement depths. Subsurface data are used as additional data for the analysis of spatial patterns.

Satellite data are used for reconstructing snow cover extent.

Results

First of all, frost occurrence is discontinuous in time. At middle mountain ranges, winter soil frost is rare: at Col de Porte, frost depth at 10 cm only occurred once in 20 years. On the Hauts Plateaux du Vercors, seasonal frost only occurred some years. Even as high as 2650 m a.s.l., seasonal frost does not occur every year (figure 1).

It is highly variable in space too: at the same altitude, some sites can be deep frozen, whereas others remain unfrozen. There can be very strong interannual and spatial differences in intensity: at a given site, the minimal winter soil temperature can range from -5 or -10°C to 0°C or even slightly positive values.

Soil thermal regimes appear therefore to be very variable, even on a given site (Schoeneich et al. 2016).

The main driving factor appears to be the snow cover and its insulation effect from air temperature. The most important factor is the onset date of a sufficient thick and continuous snow cover. In case of early snow cover, the soil is still warm and can remain above 0°C until end of winter, even at high altitude (as in winter 2014-15, figure 1). In case of late snow cover onset, the soil will cool down and reach very negative temperatures.

Windblow episodes, uncovering the soil, will also induce strong cooling (as in winter 2012-13, figure 1).

Conclusions and outlook

Simple thinking leads to the hypothesis that seasonal frost should follow an altitudinal gradient, and that frequency, duration, intensity and depth should increase with altitude, up to the lower limits of permafrost. Data show that this assumption is wrong ! There is no obvious dependancy of seasonal frost on altitude. Local conditions are largely predominant. These include aspect, exposition to wind, the tendency to accumulate snow and in some cases atmospheric inversion layers.

Moreover, there is no simple relationship with climate change. The absence of seasonal frost at high altitude in recent winters is not due to warm air temperatures, but to an early onset of a thick snow cover. On the opposite, very strong cooling is linked to late or shallow snow cover. It appears that the precipitation regime will most probably be the main driving factor for the future evolution of seasonal frost.

References

Schoeneich, P., Choler, P., Morin, T., Kenny, D., 2015. Ground thermal regimes of seasonal frost. *Eleventh International Conference on Permafrost,* Potsdam.

Frost protection of roads and railways

Elena (Kuznetsova) Scibilia[1]
Karlis Rieksts[1]
Benoit Loranger[1]
Inge Hoff[1]
Guy Dore[2]
Jean Côté [2]
Jostein Aksnes[3]

[1]*Department of Civil and Environmental Engineering, Norwegian University of Science and Technology, Trondheim, Norway, elena.kuznetsova@ntnu.no*

[2]*Department of Civil and Water Engineering, Laval University, Quebec city, Canada*

[3] *Norwegian Public Roads Administration, Trondheim, Norway*

Abstract

Norwegian road construction practice has changed significantly during the last 40 years due to the replacement of gravel by crushed rock materials in the granular layers of pavements. However, most of the classifications (e.g. frost susceptibility, thermal conductivity) used in the current specifications are based on the research within the former project Frost i Jord (1970 - 1976). Different materials were used in granular layers of roads at that time (gravel instead of crushed rock). Complex approach is required to develop new design guidelines for pavements in cold climate conditions. Optimization of the properties of crushed rock material (gradation, water content, mineralogy) is needed to adapt existing design procedure to climate change. The research project "Frost protection of roads and railways" (2015-2019) was initiated with the objective to increase the understanding within this complex area and provide scientific basis for new design guidelines.

Keywords: conduction, convection, crushed rock, frost heave, frost protection, radiation.

Introduction

"Frost Protection of Roads and Railways" (FROST) is an international research project, primary supported by the Research Council of Norway (RCN). The key objective of this project is to build new knowledge on behavior of crushed rock materials and subgrade soils, used in road and railway construction, under cold climate conditions. Research is conducted based on three main aspects: laboratory investigations, field observations, and numerical analyses to simulate different climate conditions, thickness of structures and material combinations. The project focuses on two main areas: (1) heat transfer mechanisms in granular layers, and (2) frost susceptibility of pavement materials.

Laboratory experiments

In laboratory, three kinds of tests have been conducted: (1) small-scale and (2) large-scale experiments to measure heat transfer properties for different gradation curves, and (3) frost heave test to measure segregation potential of granular materials.

Small scale: thermal conductivity

Small-scale laboratory experiments implies testing various mineral materials for their thermal conductivity as a function of water content and dry density (Fig. 1). The sample size is limited to 75 mm in height and 100 mm in diameter. This allows testing materials with particle size up to 16 mm having various mineralogy and degree of saturation. Tests are performed in both, frozen and unfrozen states (Rieksts et al., 2017a).

Figure 1. Setup for small-scale experiment (Rieksts et al., 2017a)

Large scale: convection, conduction and radiation

Large-scale laboratory test is used to test the main heat transfer mechanisms of crushed rock aggregates ranging between 0-200 mm (Fig. 2). The setup allows testing material with a total volume of 1 m^3. By applying different temperature gradient, it is possible to perform the tests in two modes, imposing upward or downward heat flow (Rieksts et al., 2017b). By comparing heat flux from both modes, it is possible to assess the contribution of convection and radiation. Apart from testing coarse aggregates, large-scale experiments are used to assess the thermal properties of insulation material Leca® and Glasopor®.

Figure 2. Setup for large scale experiment: A-A – vertical and B-B – horizontal cross-sectional view (Rieksts et al., 2017b)

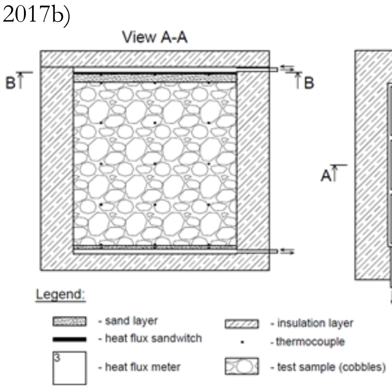

Frost susceptibility of pavement materials

In Norway, frost susceptibility of natural soils and crushed rock granular materials are mostly based on grain size criterion. As a part of the FROST project, frost susceptibility of materials is going to be measured based on mineralogy and particle shape of fine fraction (<63 µm). A frost heave test apparatus designed by Le Laboratoires des Chaussées (Quebec Government, Canada) is used to conduct a series of tests using the theory of the segregation potential to quantify materials' frost susceptibility.

Field experiments

During the fall of 2016, a full-scale field test site was built allowing to acquire temperature distribution throughout a year (Loranger et al., 2017). The test site includes six sections (6m x 8m) for roads and four sections for railways (Fig. 3). Three road section have various gradations of material used for the frost protection layer: coarse open-graded, fine dense-graded and "typical" grading. The other three road sections have different layer of insulation material (Leca® or Glasopor®) while the frost protection layer have a fixed gradation. The four railway sections have a varying subballast layer constructed with two different gradations and mineralogy. All test sections are equipped with thermocouples placed in every layer of construction. In addition, test sections are equipped with moisture sensors and linear variable differential transformers (LVDT) to monitor frost heave actions.

Figure 3. Aerial view of site's dimension and sub-section divisions and names (Loranger et al., 2017)

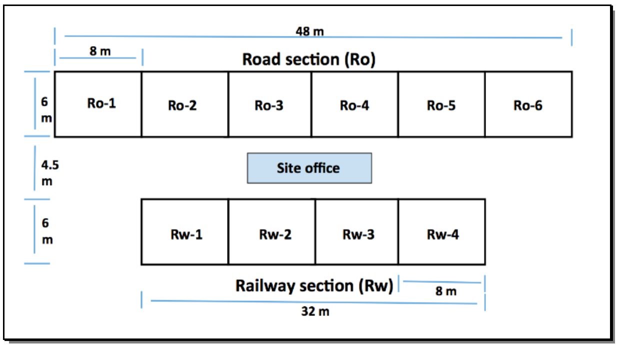

Conclusions

After 2 years of running the FROST project, three laboratory tests have been established to test crushed rock granular material: small and large-scale experiments on heat transfer mechanisms, and another test on segregation potential. In addition, the full-scale test site was built in 2016 and so far temperature data for 2 winters have been recorded. As a next step, data from laboratory and field experiments will be used for validating and calibrating numerical models.

Acknowledgments

This research was supported by the Norwegian Research Council (NRC) under grant 246826/O70.

References

Loranger, B., Kuznetsova, E., Hoff, I., Aksnes, J., & Skoglund, K. A., 2017. Evaluation of Norwegian gradation based regulation for frost susceptibility of crushed rock aggregates in roads and railways. *Tenth International Conference on the Bearing Capacity of Roads, Railways and Airfields.*

Rieksts, K., Hoff, I., Kuznetsova, E., & Côté, J., 2017a. Laboratory investigations of thermal properties of crushed rock materials. *Tenth International Conference on the Bearing Capacity of Roads, Railways and Airfields.*

Rieksts, K., Hoff, I., Kuznetsova, E., & Côté, J., 2017b. Laboratory investigations on heat transfer of coarse crushed rock materials. *70th Canadian Geotechnical Conference.*, GeoOttawa, Ottawa, Canada, October 1-3.

Sporadic permafrost on the Kola Peninsula to the south of the Arctic circle

Fedor A. Romanenko [1]
Alisa V. Baranskaya [1]
Nikolay N. Lugovoy [1]
Natalya N. Shabanova[1]
Olga A. Shilovtseva [1]
[1]*Moscow State University, Faculty of Geography, faromanenko@mail.ru*

Abstract

In the conditions of global climate change, observations of the geographic position of the southern boundary of permafrost are of high importance for estimation of its changes and possible shift northwards as a result of current warming. We revisited sites in the south of the Kola Penisula, where sporadic permafrost had been found in the 1930s by M.A. Lavrova. It has been determined that permafrost still exists in peatlands of the region; however, we documented it only at some of the points described back in the 1930s. For the preservation of insular permafrost, thickness of peat deposits plays a crucial role: for peatlands thicker than 2 m, permafrost persists and remains relatively stable through time.

Keywords: sporadic permafrost, peatlands, Kola Peninsula, southern boundary of permafrost, climate change

Introduction

Determining the position of the southern limit of permafrost is of high interest in the conditions of the modern climate change. It can be generally assumed that during warming, this boundary should gradually shift northwards, and rare islands of frozen sediments should decrease and disappear. At Kola Peninsula, where sporadic and insular permafrost occupies large areas, this process has to be especially well expressed.

Objectives, methods and previous studies

To test this assumption, we conducted fieldwork on the Terskiy coast of the White Sea (southern part of Kola Peninsula, situated far to the south of the Northern Arctic Circle) in September 2015 and 2017. The main objective was to reveal the presence of preserved insular permafrost.

In 1934, M.A. Lavrova (Lavrova, 1935) found such sporadic permafrost near fishermen villages of Chavanga, Tetrino and Strelna on the Terskiy coast, in the southernmost part of the Kola Peninsula, during geological surveys. Frozen peat mounds of complicated shape up to 70 m wide were divided by deep hollows filled by liquid peat mass.

Results

In 2015, we observed the same conditions in a swamp 1 km to the north of Chavanga village. Peat mounds up to 1.5 m high are "floating" in the thawed peat with thickness of up to 3 m, which started forming about 8 ^{14}C kA BP. The depth of the active layer didn't exceed 0.6-0.7 m; the frozen sides of the mound dropped down abruptly. In this way, the width of the contact between the frozen and thawed peat, seen from above, didn't exceed 1 m.

In 2017, similar palsa with frozen peat mounds were found near Pialitsa village and Nikodimskiy lighthouse (80 and 60 km to the east of Chavanga, accordingly). The depth of the active layer didn't exceed 0.8 m either; edges of the mounds dropped into unfrozen peat up to 5 m thickness. Between Chavanga and Nikodimskiy lighhouse, near Strelna and Tetrino villages (where permafrost had been described by M.A. Lavrova in the 1930s), no frozen peatlands were found. However, there are abundant traces of permafrost degradation in swamps, seen from above as a net of relic polygons.

Therefore, permafrost has generally been found in the region, although not at all key areas. The peatlands where permafrost has been preserved and similar ones where it has degraded are in very similar climatic conditions, therefore we consider that the most important factor which allowed the preservation of permafrost to the south of the Arctic circle is the presence of peat deposits of more than 2 m thickness. In such areas, sediments have stayed in frozen condition due to the fact that the warming is mostly expressed in the winter period when air temperatures still remail low, and a "storage of cold" forms.

Analysis of ground air temperature at the stations of the southern part of Kola Peninsula starting from the end of the XIX century has revealed its quasi-cyclic changes with the period of about 70 years, characterized by a distinctly seen linear trend of average mean annual air temperature increase with the rate of about 1.0°C in 100 years. In all seasons, the linear air temperature trend is positive; in winter it is the most significant.

At the beginning of the XXI, positive anomalies of ground air temperature were observed almost constantly. In 2000-2009, the greatest average anomalies were observed in winter (1.8°C) and the lowest ones - in summer (0.75°C).

The modern warming has an uneven distribution, increasing from Gulf of Kandalaksha towards the Gorlo Strait of the White Sea: in Kandalaksha it is almost unseen, while on Sosnovets Island it becomes statistically significant. Multiannual trends of precipitation fluctuations at Kola Peninsula in the second half of XX-beginning of XXI centuries are statistically insignificant. A positive linear trend indicating slight increase of humidity can only be noticed.

The main reason for such cycles are fluctuations of the general atmospheric circulation.

Conclusions

Areas of the southern Kola Peninsula where sporadic permafrost had been found back in the 1930s, were revisited in 2015 and 2017. It has been found that preservation of permafrost mainly depends on peat thickness: in large and thick peatlands where it exceeds 2 m, frozen peat is well preserved through the XX-beginning of XXI century. However, in palsa with smaller peat thickness, no permafrost was found, while traces of its former presence and degradation (polygons) are observed. The climatic conditions which allowed preservation of sporadic permafrost are mainly characterized with greater air temperature increase during the winter months, allowing frozen deposits to remain preserved. In summer, air temperature increase exists as well, however, it is smaller than during the cold season.

Acknowledgments

Fieldwork was executed as part of the State Research Topic of the department of Geomorphology and Palaeogeography (№ AAAA-A16-11632810089-5) and Laboratory of geoecology of the North (№ AAAA-A16-116032810055-0) of the Faculty of Geprgaphy, MSU; cameral work and meteorologic parameters' analysis were executed with the support of the Russian Science Foundation (project № 14-37-00038).

References

Lavrova M.A., 1935. A note about found permafrost on the southern coast of Kola Peninsula. *Procceedings of the Commission on permafrost studies*. Vol. IV. [in Russian].

Five years of monitoring rock glaciers ground surface temperature in Southern Carpathians

Flavius Sirbu[1]
Alexandru Onaca[1]
Florina Ardelean[1]
Brigitte Magori[1]
Petru Urdea[1]
[1] *West University of Timisoara, Romania, flavius.sirbu@gmail.com*

Abstract

The mean annual ground surface temperature of four rock glaciers in the Southern Carpathians was monitored, using 20 sensors, for a period of five years. The gathered data is presented and put into context with regard to air temperature, snow cover and the specific topography of the study area, in order to reveal the current state of rock glaciers and permafrost conditions as well as the most important topographical factors that influence their existence.

Keywords: Permafrost; Rock glaciers; snow cover; airflow; MAGST; iButton

Introduction

Rock glaciers (RG) are characterized by a typical topology of furrows and ridges and represent defining landforms of periglacial environments. They are also one of the most valuable indicators for climate conditions from the period they were developed, when they indicated permafrost condition. They can also be used as a proxy to evaluate the changing environment and local climate conditions (Frauenfelder & Kaab, 2000). In the Southern Carpathians just a few rock glaciers still maintain a permafrost and/or an interstitial ice core (Onaca *et al.*, 2017) and are still dynamically active (Necsoiu *et al.*, 2016), but in marginal conditions.

This study presents the 5-year data record of rock glaciers ground surface temperature in the Southern Carpathians and its relations with air temperature and snow cover.

Study Area

The Southern Carpathians are located in the median part of the temperate zone and have a length of 250 km from west to east. With the highest peaks towering well over 2500m (Moldoveanu, 2544 m, Negoiu, 2535 m, etc.), the Southern Carpathians are characterized by a periglacial environment (rock glaciers, block fields, etc.) at altitudes above 1800m, with a mean annual air temperature (MAAT) as low as -2°C at Omu meteorological station (2500m a.s.l.). In the Southern Carpathians there are a number of 306 RGs, with a total area of 12.7 km², from which 227 were classified as talus RG and 79 as debris RG (Onaca *et al.*, 2017).

Methodology

The ground surface temperature (GST) was measured using 20 iButton miniature sensors (iButton Digital Thermometers DS 1922L) located in four rock glaciers, with different characteristics (e.g. exposition, size, shape, etc.). The iButton sensors were set to record temperatures at a 4h interval with a 0.065°C resolution and a precision of ±0.5°C. Also for one of the rock glaciers snow cover duration and thickness was measured for three years, between august 2012 and august 2015.

Because there is no close weather station that can provide relevant climate data, the air temperature was recorded using two UTL 3 Scientific Dataloggers. They were set to record the air temperature at an hourly interval with a resolution of 0.1°C and a precision of ±0.1°C.

Results and discussions

Based on the data gather in this period, a few general conclusions can be drawn:

i) The thermal regime of the rock glaciers in the Southern Carpathians differs significantly even between parts of the same RG or neighboring RGs. In the Judele RG, for example, for an area of about 3ha the differences in mean annual ground surface temperature

(MAGST) between neighboring sensors are up to between 4°C to 5°C

ii) Permafrost appears likely at those sites, where a strong cooling occurs in the early winter due to ground airflow (convection, advection).

iii) The measured data demonstrates that within the Southern Carpathians, permafrost conditions are favored mostly by shading, terrain surface roughness and cooling effect of the blocky surface than by altitude.

References

Frauenfelder, R., Kaab, A., 2000. Towards a palaeoclimatic model of rock-glacier formation in the Swiss Alps. In: K. Steffen (Ed.), *Annals of Glaciology*, Vol 31, 2000. Annals of Glaciology. Int Glaciological Soc, Cambridge, pp. 281-286.

Necsoiu, M., Onaca, A., Wigginton, S., Urdea, P., 2016. Rock glacier dynamics in Southern Carpathian Mountains from high-resolution optical and multi-temporal SAR satellite imagery. *Remote Sens. Environ.*, 177, 21-36.

Onaca, A., Ardelean, F., Urdea, P., Magori, B., 2017,. Southern Carpathian rock glaciers: inventory, distribution and environmental controlling factors. *Geomorphology*, 293(2017), 391-404.

23 - New developments and applications of geophysical techniques in permafrost terrain

Session 23

New developments and applications of geophysical techniques in permafrost terrain

Conveners:

- **Hauck Christian**, Department of Geosciences, Université de Fribourg, Fribourg, Switzerland
- **Halla Christian**, Department of Geography, University of Bonn, Germany (PYRN member)
- **Thomas Ingeman-Nielsen**, Center for Arctic Technology, Technical University of Denmark, Denmark

Geophysical methods, including e.g. electrical, electromagnetic, seismic and gravimetric techniques, are one of the standard methods in permafrost research for detecting, quantifying and monitoring frozen ground and ground ice occurrences. Recent studies show also a high potential of these methods for multi-scale approaches in combination with point-scale in-situ measurements, upscaling techniques in combination with remote sensing data and detailed process studies in combination with energy balance and thermo-hydraulic modelling.

We welcome all kind of studies focusing on new or improved approaches using geophysical techniques, their application in permafrost terrain, innovative combinations with complementary data sets and models, and studies showing the potential of using geophysical techniques for process studies and permafrost monitoring.

Application of geophysical methods to estimate mechanical properties of frozen saline soils (based on experimental data)

Ivan Agapkin
Pavel Kotov
Andrey Koshurnikov
[1] *Lomonosov Moscow State University, Geocryology department, 15331533@mail.ru*

Abstract

The research is aimed at establishing interrelations (functional and correlation) between electrical, acoustic and strength properties frozen saline soil. Testing were conducted on two soil types (fine sand, lean clay), different salinity (from 0.07% to 1.42%), temperature (-2 ^{o}C, -4 ^{o}C,-6 ^{o}C) and water content. Strength properties determined by uniaxial compression and spherical template indenter test A total of 110 tests were conducted. As a result of generalization, the regression equation of the dependence of the strength on the wave velocity was obtained. The coefficients of this equation are functions of temperature. Factor analysis showed that the specific electrical resistance is inversely proportional to the concentration of the pore solution. With increasing salinity, electrical properties change more intensively than wave velocities.

Keywords: frozen saline soil, mechanical properties, velocity of ultrasonic waves, electrical resistivity

Introduction

One of the most important investigations in geophysics is estimation of the stress-strain state of frozen soils in the massif. Today engineering geology and geotechnics are successfully applied for this purpose (drilling, sampling, laboratory and field testing). As a result of these investigations there is a geological section which divided into engineering-geological elements with a set of physical and mechanical properties of soils. These characteristics are used to calculate the stress-strain state. However these methods are very laborious, require high material costs and in some cases are difficult to implement. The characteristics of soils obtained during the tests are discrete and do not take into account the spatio-temporal variability of the properties and conditions of frozen soils. Therefore it is important to use geophysical methods for forecasting and monitoring the properties of frozen soils. Although this estimate is indirect and less accurate than direct testing, it can characterize the massif in its natural form and provide long-term monitoring of the change in its stress-strain state. The scientific significance lies in establishing the basic dependencies used in the transition from geophysical parameters to physical and mechanical. Simultaneous use of electrical and acoustic characteristics to evaluate the same parameters of the composition and structure of the soil can significantly improve the reliability of the results obtained (Wu, 2017). Of particular interest from the point of view of increasing the informativeness of geophysical methods is the establishment of the dependence of strength on geophysical parameters that are connected in correlation with the modulus of deformation. Therefore, special studies were made of the relationship between strength and geophysical properties (electrical and acoustic)

Research methodology

The studies were conducted on two artificial samples (fine sand, lean clay). Artificial soil belonged to non-saline. Solutions with different concentrations of NaCl were mixed to set different degrees of salinity (fine sand – 0,1%, 0,23%, 0,6%, lean clay - 0,3%, 0,6% 1%) We have prepared samples of a given water content (sand - 9%, 15% and 20%, lean clay – 20%, 30% and 36%). The density was set by layering compaction in special forms. All samples had massive cryogenic texture.

Spherical template indenter test and uniaxial compression were carried out according to GOST 12248-2010 at temperatures of -2°C;-4 °C;-6 °C. All tests were carried out with a fourfold repetition. A total of 110 experiments were conducted.

Acoustic and electrical properties were determined on the samples before and after the tests. Measurements of the electrical properties of soils were carried out on a low-frequency alternating current by a four-electrode installation. Measurements were made with a set of equipment "Spectrum 1", developed by LLC "MSU-Geophysics". Measurements of the acoustic properties of soils were carried out using UD4-130 equipment and a set of acoustic sensors with a center frequency of 60 kHz. The choice of such a frequency range was associated with the need to obtain clear first arrivals, provided that the ratio of the wavelength and the geometric parameters of the sample are preserved. For the measurement of the velocities of the passage of elastic waves, the X-ray method was used. The speed of passage of elastic vibrations is defined as the ratio of the base of transmission to the time of propagation of these waves.

Results

Temperature is a significant factor influencing the value of strength of frozen soils. Unfrozen water content has strong relationship with strength and it mainly depends on temperature. Velocity of ultrasonic waves depends on temperature too because of velocity increases in ice or mineral part. The ultrasonic wave velocities and electric resistivity dramatically increased as the temperature chanced from -2 ^{o}C to -6 ^{o}C.

This relationship is more noticeable in lean clay because there is far less unfrozen water in sand. So we can see that lean clay under -6 ^{o}C have maximum velocity and maximum strength with a increasing in temperature row unfrozen water content increase too and values of velocity and strength reduce. Salinity is important factor which increase a freezing temperature. In salty samples electrical resistivity decreases cause salt water is good conductor. The samples with maximum salinity have more unfrozen water which decrease strength and geophysics characteristics.

Regressive equations were obtained for the dependence of strength and deformation characteristics as a function of salinity, wave velocity, limiting electrical resistance for each soil type. The coefficients of this equation are functions of temperature. Factor analysis showed that the specific electrical resistance is inversely proportional to the concentration of the pore solution. With increasing salinity, electrical properties change more intensively than wave velocities.

References

GOST 12248-2010, 2011. *Soils. Laboratory methods for determining the strength and strain.* Standartinform,. 109 pp.

Y. Wu et al. Electrical and seismic response of saline permafrost soil during freeze - Thaw transition / Journal of Applied Geophysics 146 (2017) 16–26

The technology of spatial radio wave researches for monitoring the thawing of permafrost. The case study of investigation on oil and gas field in Western Siberia

Artem Cherepanov[1]
Vyacheslav Istratov[2]
[1]*Russian State Geological Prospecting University, cherepanov_a_o@yahoo.com*
[2]*"Radionda" Ltd*

Abstract

Currently the priority is the control of the permafrost rock mass condition on the different objects of oil and gas sector, located in the Far North regions. We present the technology of spatial radio wave researches (RWGI) and new experience of monitoring at a multiple-well platform of an oil field in Western Siberia.

Keywords: permafrost, geophysical monitoring, radio wave researches, oil and gas fields.

Introduction

Currently the priority is the control of the permafrost rock mass condition on the different objects of oil and gas sector, located in the Far North regions. The oil development is carried out by multiple drilling method. The heads of the production and the injection wells are tightly grouped on the small territory in a close proximity to each other which are named multiple well platform. . Injection wells participate in the production cycle. Heated solution with the temperature of 120 ^{0}C is pumped through their wellheads. Thermal interaction between permafrost rocks and injection well occurs during exploitation of the object. This results in formation of a thawing zone that can transform into a thermokarst pit. Merging of such zones around production wells is a special hazard, as this is an extremely adverse factor for stability and long service life of the multiple well platform facilities. The development dynamics of thawing area of permafrost rock mass depends on lots of factors, such as the climatic and geocryological conditions at a specific site, the construction of thermal protection, and the temperature of the fluid at the wellhead. The changes of permafrost rock mass on the multiple well platform are estimated according to regime thermometric observations. A significant disadvantage of the borehole thermometry is the locality of the study, only the limited area of the borehole environment is studied. The linear interpolation of borehole thermometry does not characterize the array of permafrost rock mass in general, because of the complex structure of the upper part of the section. Electrical parameters of rocks - electrical resistivity (ϱ) and permittivity (ε) are more sensitive to changes in physical and mechanical properties of permafrost rock massif comparing with temperature data.

Methods

The technology of spatial geoelectric monitoring has been developed and experimentally tested for the early diagnosis of frozen-thawed state variations of the in-site rocks. (Cherepanov, 2013, 2014) The technology is based on modern radio wave methods of borehole geophysics: Radio wave geo-introscopy (RWGI) and Multi-frequency one-well radio wave profiling (ORWP) (Istratov &. Frolov, 2003).

Radio wave methods are based on the study of the intensity of radio wave energy absorption by rocks, located on the path of wave propagation from the emitter to the field's receiver. Rocks with low values effective electrical resistivity (ϱ_{eff}) and effective permittivity (ε_{eff}) are characterized by high absorption of radio waves.

Radio wave geo-introscopy of inter-well space (RWGI) - way of «visualization» of an internal structure of geological media in space between wells. RWGI researches are conducted on a special network of observation wells and characterized by high density of research. Algorithms and data processing programs permit to obtain volume distribution of ϱ_{eff} and ε_{eff} of rocks in the inter-wellbore space. Method ORWP-MF is high-frequency electromagnetic method of resistivity logging, which permit to determine the ϱ_{eff} and ε_{eff} of rocks near the well.

Results

The report describes the experience of using new technologies at the stages of engineering design, construction and production time of the multiple well platforms of oil and gas fields in Western Siberia. The variety and complexity of the geocryological situation are illustrated. The development of the thawing area around the injection well has been demonstrated for the current multiple-well platform of one of the fields for several years.

The technology of spatial geoelectric monitoring makes it possible to determine the geoelectric structure of the research site, to classify the state of the rocks into three main categories: 1 – frozen rocks, which are in an unchanged state, 2 - rocks in the thawing state, when the process of phase transition of ice into water began; 3 - completely thawed rocks, in which the phase transition has been completed.

References

Cherepanov, A.O., 2013. Borehole geophysics methods for studying permafrost rocks at the multiple well platforms of the oil and gas fields in Western Siberia.. *Geophysical Research* 13: 38-47. (In Russian).

Cherepanov, A.O., 2014. Spatial geoelectric monitoring of permafrost state near injection wells by the example of an oil field in Western Siberia. *Geophysical Research* 12: 18-24. (In Russian).

Istratov, V.A., &. Frolov, A.D. 2003. Radio wave borehole measurements to determine *in situ* the electric property distribution in a massif. *J. Geophys. Res. – Planets*, Vol. 108, No E4: 8038-8043.

3D inversion of resistivity and induced polarization on an alpine rock glacier supporting unstable cable-car

Pierre-Allain Duvillard [1,2], André Revil [3], Abdellahi Soueid Ahmed [3], Youzheng Qi[3], Ludovic Ravanel [1]

[1] EDYTEM lab., University Savoie Mont-Blanc - CNRS, Le Bourget-Du-Lac, France, pierre-allain.duvillard@univ-smb.fr
[2] IMSRN, Parc Pré Millet – 680, rue Aristide Bergès, 38330 Montbonnot, France
[3] ISTerre lab., University Savoie Mont-Blanc - CNRS, Le Bourget-Du-Lac, France

Abstract

Electrical Resistivity Tomography is widely used nowaday to investigate the subsurface conditions of loose deposits in mountain permafrost environments. At the same time, induced Polarization, a geoelectrical method, is rarely used in permafrost studies. Here, we performed 16 profiles (16 ERT including 10 IP profiles) on Thorens rock glacier in Val thorens (Vanoise, France), supporting an unstable cable-car pylon. A 3D inversion of the ERT and IP data was performed using a homemade code. Chargeability and resistivity calibration of rock and deposit samples with temperature will allow analyzing more accurately the geophysical images.

Keywords: Induced polarization; Electrical resistivity; 3D inversion; rock glacier; infrastructure; Vanoise massif.

Introduction

Geophysical methods such as Electrical Resistivity Tomography (ERT) are widely used today to investigate the subsurface conditions in loose deposits in mountain permafrost environments. Electrical survey enables to assess the subsurface properties, *e.g.* to distinguish frozen and unfrozen areas (Scapozza & Laigre, 2014). This information can be used for geotechnical and geomorphological analysis. Contrary to ERT, Induced Polarization (IP) is a geoelectrical method rarely used in permafrost studies (Kneisel *et al.*, 2008). The interest of this method is to provide additional information, particularly in terms of clay content and degree of fracturing / porosity of the ground (Revil, 2012).

3D investigations are sparse in the field of periglacial geomorphology. Early works exist with graphically combined results from 2-D ERT surveys on 3D diagrams (Scapozza & Laigre, 2014). Then, some studies dealt with inversion in 3D on a data set including multiple intersecting 2-D ("quasi-3-D" approach), which enabled a horizontal mapping of resistivity variations (Emmert & Kneisel, 2017).

In this study, we performed 16 profiles, resulting in 6267 resistance measurements in ERT and 2021 in IP. In order to have a more realistic and accurate characterization of the subsurface structures, we performed a 3D inversion of the ERT and IP data, using a using a homemade code written in Matlab (in development).

Study site

Thorens rock glacier

Thorens rock glacier is located in Val Thorens ski resort (Vanoise massif), on the north of the Col du Bouchet (2993 m a.s.l.). It is composed of debris materials from sedimentary rocks (sandstone and shale with clay of Houiller). It is shaped of two tongues of approximately 60 m × 250 m. The Permafrost Favourability Index map (Marcer *et al.*, 2017), which describes the spatial distribution of permafrost in the French Alps, indicates a PFI of 0.95, which means the rock glacier has "permafrost in all conditions". The occurrence of permanently frozen ground in the rock glacier was also reported by feasibility and geotechnical studies in 2008 and 2010 (Fabre *et al.*, 2015). These studies helped in the choice of the implantation of the foundations of the Thorens cable car.

Thorens cable-car

The Thorens cable-car was built during the summer 2011. It is composed of 4 pylons among which 3 are most probably installed on permafrost (Duvillard *et al.*, 2015). The P2 pylon was built on the right lobe of the rock glacier after a geotechnical diagnosis (Fabre *et al.*, 2015).

P2 underwent a major movement between its implantation in 2011 and July 2016 with a displacement of the foundations of 25 cm laterally and 55 cm vertically, more noticeable for the western foundations, because of a thermokarstic subsidence. This movement generated a side shift of approximately 1.5 m at the top of the pylon.

Methods

Data acquisition and 3D inversion

ERT and IP field campaigns were realized in September 2016 and July 2017 with a total of 16 ERT profiles and 10 IP profiles (Table 1). In both cases, the measurements were carried out using an ABEM SAS4000 and the coordinates of each electrode were measured using a dGPS.

Table 1. Details on ERT and IP surveys.

	ERT 2016	ERT 2017	IP 2017
Acquisition dates	1-2 Sept.	24-27 July	24-27 July
Number of 2-D profiles collected	5	11	10
Array type	Wen 64	Wen 32	Grip64
Spacing	2 /2.5 m	5 m	5 m
Number of electrodes	320	635	315
Number of data points for inversion	2004	4263	2021

Laboratory calibration

While the temperature-resistivity relationship in the permafrost area has already been studied in the laboratory for rock slope environment (Krautblatter *et al.,* 2010), chargeability calibration on rock and deposit sample will allow analyzing more accurately the geophysical images. Calibration between resistivity and chargeability was done using a laboratory water bath between -5 °C to +5°C.

Results

The 3D ERT inversion allows to state that: (i) the resistivity are quite low (10 - 100 kΩm) and seems to correspond to a "temperate" permafrost, *i.e.* close to the melting temperature with a high liquid water content; (ii) the rock glacier seems to be divided into two parts: a left tongue with permafrost and a right lobe without where the pylon is located, probably under the talik effect of the nearby lake.

Conclusion

3D inversion and the combination of ERT and IP data have never been carried out on a rock glacier before. At this stage, only the 3D ERT are processed but it already allows discussing the permafrost distribution in a rock glacier. First result of ERT and 3D IP inversion will also highlight the permafrost depth and the porosity of the ground.

Acknowledgments

The authors gratefully acknowledge the SETAM (Société d'Exploitation des Téléphériques Tarentaise Maurienne) for the collaboration and all the geotechnicals information given. Thanks to M. Marcer, K. Génuite, G. Heller and A. Ollive for their valued help on the field.

References

Duvillard, P-A., Ravanel, L., & Deline, P., 2015. Risk assessment of infrastructure destabilisation due to global warming in the high French Alps. *J. Alp. Res.* 103-2.

Emmert, A., & Kneisel, C., 2017. Internal structure of two alpine rock glaciers investigated by quasi-3-D electrical resistivity imaging. *The Cryosphere,* 11: 841-855.

Fabre, D., Cadet, H., Lorier, L., & Leroux, O., 2015. "Detection of Permafrost and Foundation Related Problems in High Mountain Ski Resorts," in *Eng. Geol. for Soci. and Terri. - V1: Climate Change and Engineering Geology*, 321-324.

Kneisel, C., Hauck, C., Fortier, R., & Moorman, B., 2008. Advances in geophysical methods for permafrost investigations. *Permafr. Periglac. Process*. 19: 157–178.

Krautblatter, M., Verleysdonk, S., Flores-Orozco, A., & Kemna, A., 2010. Temperature-calibrated imaging of seasonal changes in permafrost rock walls by quantitative electrical resistivity tomography (Zugspitze, German/Austrian Alps). *J. Geophys. Res. Earth Surf.* 115.

Marcer, M., Bodin, X., Brenning, A., Schoeneich, P., Charvet, R., & Gottardi, F., 2017. Permafrost favourability index : spatial modelling in the French Alps using rock glaciers inventory. *Front. Earth Sci.* 5: 1-17.

Revil, A., 2012. Spectral induced polarization of shaly sands: Influence of the electrical double layer. *Water Resour. Res.* 48:1–23.

Scapozza, C., & Laigre, L., 2014. The contribution of Electrical Resistivity Tomography (ERT) in Alpine dynamics geomorphology: case studies from the Swiss Alps. *Géomorphologie Relief Process. Environ.* 20: 27–42.

Application of multidimensional geophysical surveying for investigations on the internal structure of palsas

Adrian Emmert[1,2]
Christof Kneisel[1]

[1] *Institute of Geography and Geology, University of Wuerzburg, adrian.emmert@uni-wuerzburg.de*
[2]*Chair of Landslide Research, Technical University of Munich*

Abstract

We performed numerous 2-D and 3-D Electrical Resistivity Imaging and 2-D and 3-D Ground-Penetrating Radar surveys to map permafrost distribution and investigate the internal structure of palsa landforms in Central Iceland. In a comparative approach, palsas of different size and shape were investigated and different electrode setups and antenna frequencies were applied to find optimal settings for the respective issues. Results show a patchy permafrost distribution and a varying thickness of the active layer between the different palsas. It indicates that the investigated palsas represent different stages of development. While the radar surveys suffer from a loss of energy in the water-saturated surface layer, results of the resistivity surveys provide valuable information also on deeper layers.

Keywords: Palsa; Permafrost; Internal Structure; Ground-Penetrating Radar; Electrical Resistivity Imaging.

Introduction

A detailed knowledge on the internal structure of palsas is important to understand the dynamics of palsa formation and decay. It can help to improve conceptual models and assist for calculations of heat fluxes or other subsurface processes.

Through field campaigns in 2015 and 2017, we performed numerous two- and three-dimensional Electrical Resistivity Imaging (ERI) and Ground-Penetrating Radar (GPR) surveys to investigate permafrost distribution, active layer thickness (ALT), frost table topography and permafrost thickness. To assess information on palsa dynamics, surveys were performed on morphologically different palsas.

Study Site

The occurrence of palsas in the surrounding of Lake Orravatn (65.05° N, 18.32° W) is described in detail by Saemundsson *et al.* (2012). Due to the mineral substrate, the term 'lithalsa' may also be used appropriately. We investigated palsas of four different phenotypes: large-scale palsas surrounded by water (Palsa01), a deeply cracked medium size palsa (Palsa02), a rather flat uplift area (Palsa03) and a smaller frost mound surrounded by shallow water logs (Palsa04) (Table 1).

Table 1. Investigated Palsas.

	Palsa01	Palsa02	Palsa03	Palsa04
Height [m]	2.4	1	1	0.5
Size [m²]	1090	40	240	30
Description	Large Palsa	Deeply cracked	Uplift area	Shallow water logs

Methods

GPR surveys were performed using a PulseEKKO PRO device with two unshielded antennas in bistatic mode and an odometer wheel for signal triggering. For the 3-D GPR approach, data from closely separated parallel lines was collated. ERI surveys were performed using a Syscal Pro (2015) and a Syscal Junior (2017) device, respectively. A rectangularly shaped grid of electrodes was set up for the 3-D ERI approach. Various antenna frequencies (50MHz–200MHz) and electrode spacings (0.5m–3m) were applied in the different surveys. In addition to the geophysical techniques, frost-probing with a 1.2m long steel rod was performed to validate the results.

Results

Permafrost distribution and ice content

Based on a threshold value of 0.6kΩm that was derived from comparing results of 3-D ERI and manual frost-probing, a widespread but patchy permafrost distribution is present in the palsa mire. Similar results are derived from GPR, where the course of a strong reflector below the palsas mounds corresponds well to the manually detected frost table. In a combined radar and resistivity profile, areas of lower resistivity values correspond to the appearance of a rather moderate linear reflection pattern (Fig. 1).

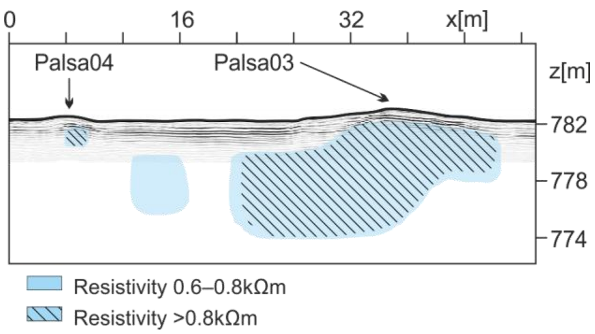

Figure 1. Combined radar and resistivity profile

A basic qualitive assignment of ice content through a positive correlation with resistivity values shows highest values for Palsa01 where maximum resistivity values are higher than 60kΩm. Lower resistivity values between 1kΩm and 10kΩm at the other palsas indicate lower values of ice content.

Frost table topography and permafrost thickness

ALT varies between the different palsas. It is around 0.5m at Palsa01 and Palsa02 and exceeds 1m at Palsa03 and Palsa04. At Palsa02, results from ERI show that the frost table is cracked at positions corresponding to deep cracks on the palsa surface.

Thickness of the frozen layer could only be assessed by ERI. Like thickness of the active layer, it differs strongly between the different palsas. It ranges from 9m (Palsa01) over 7m (Palsa03) and 2m (Palsa04) to 1.5m (Palsa02).

Methodological approach

Comparing results of frost-probing and 3-D surveying shows that both geophysical techniques produce results that are in high accordance with the manually detected frost table. However, with our measurement setup, ERI results did not reach the same level of accuracy.

Due to wet surface conditions and the consequently low velocity of wave propagation (ca. 0.04m/ns), penetration depth of GPR was strongly reduced. Depending on the applied electrode spacing, ERI can reach a deeper penetration depth and provide additional information on ice content.

The striking differences observed within the palsas' structures emphasize the dynamic state of environmental conditions, as indicated by Kneisel (2010). Although the high ice content of Palsa01 indicates stable conditions, initial cracks are visible on the palsa surface. In contrast to the deep surface cracks of Palsa02, they are not reflected in the geophysical models and likely represent a less advanced stage of degradation. At Palsa03, a far-reaching frozen area that exceeds the recent palsa points towards new palsa formation (Fig. 1). Palsa04 shows a similar ratio between active layer and permafrost thickness as Palsa01 which points towards a similar stage of development.

Acknowledgments

We are grateful to Julian Trappe and Felix Schmidt for assistance in the field. C. Kneisel thanks the German Research Foundation (DFG) for financial support (KN542/13-1).

References

Kneisel, C., 2010. The nature and dynamics of frozen ground in alpine and subarctic periglacial environments. *The Holocene*, 20(3): 423-445.

Saemundsson, T., Arnalds, O., Kneisel, D., Jonsson, H.P. & Decaulne, A., 2012. The Orravatnsrustir palsa site in Central Iceland—Palsas in an aeolian sedimentation environment. *Geomorphology,* 167-168: 13-20.

Monitoring the active layer using Electrical Resistivity Tomography: daily, weekly and monthly variability at Crater Lake, Deception Island, Antarctica.

Mohammad Farzamian [1]
Gonçalo Vieira [2]
Borhan Yaghoobi Tabar [3]
Fernando A. Monteiro Santos [1]
Christian Hauck [4]
Ivo Bernando [1]
Maria Catarina Paz [1]
Miguel Ramos [5]
Miguel Angel de Pablo [5]
[1] IDL, Universidade de Lisboa, Portugal; mohammadfarzamian@fc.ul.pt
[2] Centre for Geographical Studies, IGOT, Universidade de Lisboa, Portugal
[3] School of Mining, Petroleum and Geophysics, Shahrood University of Technology, Iran
[4] Department of Geosciences, University of Fribourg, Switzerland
[5] Universidad de Alcalá de Henares, Spain

Abstract

We installed an automatic Electrical Resistivity Tomography (ERT) and temperature monitoring system under the Circumpolar Active Layer Monitoring (CALM) program in order to study the active layer in the Crater Lake site at Deception Island during 2010. The Western Antarctic Peninsula region is one of the hot spots of climate change and one of the most ecologically sensitive regions of Antarctica, where permafrost is near its climatic limits. Apparent resistivity data were processed and inverted to image the daily, weekly and monthly subsurface resistivity variations and in order to investigate the dynamics of the active layer in space and time.

Keywords: Active layer; Deception Island; ERT monitoring; Virtual borehole analysis

Introduction

The CALM program is a network of permafrost observatories distributed over both Polar regions and selected mid-latitude mountain ranges. CALM is an international global-change monitoring program concerned with active layer dynamics and the shallow permafrost environment. Low altitude permafrost temperatures are slightly below 0 °C in the Crater Lake CALM site in Deception Island (South Shetlands, Antarctic Peninsula), showing that the region is near its climatic boundary (Ramos et al., 2016; Ramos and Vieira, 2009). This fact reinforces the importance to study the evolution of permafrost and active layer in the region. Ashes and pyroclasts compose the soils with high porosity and high water content, with an active layer of about 30-40 cm (Ramos et al. 2016).

Material and methods

The Crater Lake CALM-S site consists of a 100 × 100 m grid with 121 nodes at 10 m intervals (Fig. 1). Air temperatures at 1.60 m above the surface; ground temperatures in shallow boreholes down to 1.60 m (node 3,3), 1.60 m (node 7,7) and 4.50 m (node 2,5); and snow thickness were monitored during 2010.

An automatic ERT monitoring system using a 4POINTLIGHT_10W device was installed in the vicinity of the ground temperature sensors in the borehole S3,3. ERT surveys were performed using the Wenner electrode configuration for the best signal-to-noise ratio. 20 electrodes with an electrode spacing of 0.50 m were used and a total of 56 data points were collected for each image. The ERT measurements started at the beginning of 2010 and repeated each 4 hours during one year. Consequently, a total of 2,200 datasets were obtained during the experiment.

Under the assumption that general conditions (e.g. lithology, pore space) remain unchanged during the year of observations, repeated resistivity measurements can provide a mean for evaluation of freezing or thawing processes (Hauck, 2002).

The apparent resistivity data was processed and then inverted using the full 4D inversion algorithm within

RES2DINV software. The robust inversion as well as the mesh refinement to the half of the electrode spacing was applied to better resolve expected strong contrast in subsurface resistivity. A virtual borehole analysis (Hauck, 2002) was also performed to investigate the dynamics of the active layer in more detail during 2010.

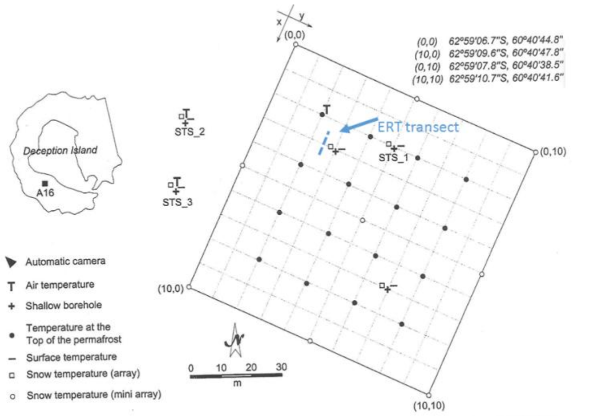

Fig. 1: Instrumentation setting at the Crater Lake site.

Results and Discussion

Fig. 2(a) shows the ground temperature variations during the ERT monitoring observed for the borehole S3,3, located within the ERT profile and Fig. 2(b) presents the corresponding virtual resistivity models taken from the inverted tomograms for January to December 2010. Specific events with brief surficial refreezing and thawing during the experiment are highlighted in Fig. 2(a).

The temperature below zero is delineated by the yellow to red colors, which indicate that the active layer has an approximate thickness of 40 cm in the borehole S3,3. The temperature of the active layer falls below 0 ºC at the end of April and stays below 0 ºC until the beginning of November.

An investigation of the virtual resistivity section in Fig. 2(b) reveals a sharp resistivity increase when the active layer temperature falls below zero. The resistivity variations during the freezing cycle are probably related to the temporal variations of the unfrozen water content.

The resistivity variations during the events A and B are shown in Fig. 3 to examine how well the brief surficial refreezing and thawing events are resolved with the ERT. From the shown sections, we see that the ERT can successfully resolve the events. A continuous resistivity increase is evident during the brief surficial refreezing event in the resistivity sections. On the other hand, the brief surficial thawing causes a sharp and continuous resistivity decrease during May 2010.

Conclusion

The preliminary results of automated and continuously measured ERT datasets at the Crater Lake site reveal that the temporal resistivity changes can be well resolved using the ERT method and demonstrate the high potential of remote monitoring in the polar permafrost environments.

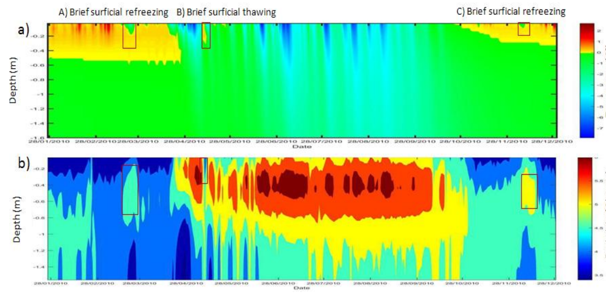

Fig.2 (a) Temperature evolution in borehole S3,3(b) Temporal evolution of resistivity in virtual borehole S3,3

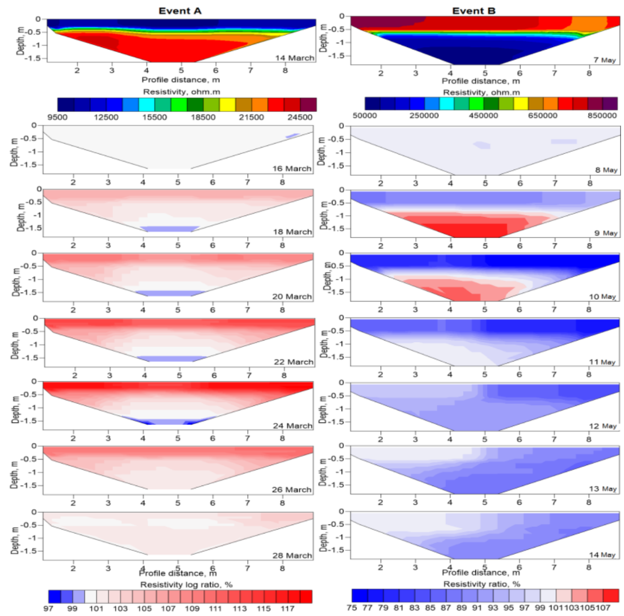

Fig. 3. (Left) percentage change in resistivity during the brief active layer freezing in March 2010 (Event A). (Right) percentage change in resistivity during the brief active layer thawing in May 2010 (Event B).

Acknowledgments

This publication is supported by FCT- project UID/GEO/50019/2013 – IDL.

References

Hauck C., 2002. Frozen ground monitoring using DC resistivity tomography. Geophysical Research Letters 29.

Ramos, M., Vieira, G., 2009. Evaluation of the ground surface enthalpy balance from bedrock shallow borehole temperatures (Livingston Island, Maritime Antarctic). Cryosphere 3, 133–145.

Ramos, M., Vieira, G., de Pablo, M.A., Molina, A., Abramov, A., Goyanes, G., 2017. Recent shallowing of the thaw depth at Crater Lake, Deception Island, Antarctica (2006–2014). Catena 149 (2), 519–528.

GPR measurement of active layer thickness on CALM-S site, James Ross Island, Antarctic Peninsula

Filip Hrbáček[1]
Zbyněk Engel[2]
Michaela Kňažková[1]
Jana Smolíková[2]
Jan Kavan[1]

[1]*Department of Geography, Masaryk University, Brno, Czech Republic, hrbacekfilip@gmail.com*
[2]*Department of Physical Geography and Geoecology, Faculty of Science, Charles University, Praha, Czech Republic*

Abstract

In this work we present the preliminary results of active layer thickness measurement using ground-penetrating radar and soil probe on CALM-S JGM site on James Ross Island in the Antarctic Peninsula region. Our results showed only 2 cm difference in mean active layer thickness when comparing results obtained by probing and the radar. Very close results were also found comparing minimum (62 and 63 cm) and maximum (85 and 89) values recorded by both approaches. The radar was further tested in braid plain area, where the active layer thickness of 120 cm were detected beneath small streams. Despite it being not possible to clearly detect a boundary between active layer and permafrost, the use of ground-penetrating radar on James Ross Island was found a useful method. It may eliminate the limits of probing in coarse ground as well as cover larger areas.

Keywords: GPR, active layer thickness, CALM, Antarctica,

Introduction

Circumpolar active layer monitoring (CALM) method is a standard approach for the active layer thickness (ALT) and temperature monitoring. The CALM sites are widespread across the northern hemisphere, while in Antarctica total number of the CALM-S (south) sites is limited to about 15 sites, mostly in Antarctic Peninsula region. The main limitation of CALM-S is usually very coarse ground, which prevent the soil probing or makes it very hard with unconvincing results. One of the way to surpass the probing limitation can be the utilization of geophysical methods. The ground-penetrating radar (GPR) measurement of the ALT has been successfully used in Arctic (e.g. Westerman et al., 2010) or Alpine regions (e.g. Klug et al., 2017), but it has been used sparsely in Antarctica (e.g. Schwamborn et al., 2008). In this work, we present the initial results of ALT probing complemented with GPR survey applied on CALM-S JGM site on the northern part of James Ross Island, Antarctica in the thawing season 2016/17.

Methods

CALM-S JGM is located near to Johann Gregor Mendel station, about 200 m far from a shoreline. The monitoring area of 80 x 70 m is situated at an elevation of 7-11 m a.s.l on flat surface (< 4°) gently inclined to the north. A Holocene marine sediments form the northern part of the test site whereas cretaceous sediments of Whisky Bay fm. prevail in its southern part. The ALT was measured on 12 February 2017 in 10 m distant nodes using soil probe. The GPR survey was realized in transverse and longitude profiles across the CALM-S nodes and in small (45 x 25 m) site in Bohemian Stream braid plain. The GPR measurement was performed with a RAMAC CU-II control unit (MALÅ) with a shielded 500 MHz antenna. The GPR equipment allowed measurement to depths of ~2.5 m with the longitudinal (depth) resolution of 0.05 m. GPR data were processed using REFLEXW software (Sandmeier, 2012). The depth axis of profiles was converted from the time axis using a wave velocity of 0.095 m ns^{-1}. The velocity was determined from the ALT measured in eight points with the core sampler and from the position of the relevant reflector in obtained GPR scans. The scans allowed the determination of ALT along measured profiles including the CALM-S grid nodes. In some parts, it was not possible to clearly detect boundary between active layer and permafrost. These parts were excluded from analyses and the study area was limited to 50 x 50 m.

Preliminary results

Mean ALT measured by probing on the selected 50 × 50 m area of CALM-S reached 75 cm; minimum thickness was 62 cm, while the maximum thickness was 85 cm. The mean ALT detected by GPR reached 73 cm, it varied between 63 cm and 89 cm. Comparing probing, and GPR we found the similar pattern of the depth distribution along CALM-S with the prevailing differences of measurement ±5 cm. These values correspond to the depth resolution of GPR, thus it can be consider as valid. In the stream site, the ALT varied between 70 and 120 cm, with the maximum values beneath small streams.

Conclusions

In this study we found the GPR a potentially useful approach for ALT monitoring on James Ross Island. It provides detailed information about the ALT along tested profiles, which is consistent with probe values measured at the study site grid nodes. The application of GPR method may eliminate the limits of probing in coarse ground and it also allows to cover larger areas, than soil probing. Anyway, our surveying showed also some limitation of the GPR survey. In some sections the reflections that correspond to permafrost table are weak or identifiable, which makes impossible to extract useful information from the data. The signal attenuation may be caused by clay or soil water content variation in the CALM-S grid.

Acknowledgments

Research was supported by Ministry of Education, Youth and Sports of the Czech Republic projects LM2015078 and CZ.02.1.01/0.0/0.0/16_013/0001708 and by the Masaryk University project MUNI/A/1419/2016.

References

Hrbáček, F., Kňažková, M., Nývlt D., Láska, K., Mueller, C.W., Ondruch, J., 2017. Active layer monitoring at CALM-S site near J.G.Mendel Station, James Ross Island, Eastern Antarctic Peninsula. *Sci.Total.Environ.,* 601–602: 987–997.

Klug C., Rieg L., Ott P., Mössinger M., Sailer R., Stötter J., 2017. A Multi-Methodological Approach to Determine Permafrost Occurrence and Ground Surface Subsidence in Mountain Terrain, Tyrol, Austria. *Permafr. Periglac. Process.,* 28(1): 249-265.

Sandmeier K.J., 2012. REFLEXW Version 7.0. Karlsruhe, K.J. Sandmeier.

Schwamborn, G., Wagner, D., Hubberten, H.W., 2008. The use of GPR to detect active layer in young periglacial terrain in Livingston Island, Maritime Antarctica. *Near Surface Geophysics*, 6: 327 – 332.

Westerman, S., Wollschläger, U., Boike, J., 2010. Monitoring of active layer dynamics at a permafrost site on Svalbard using multi-channel ground-penetrating radar. *The Cryosphere,* 4: 475–487.

Measurements of the Induced Polarization effect in alpine permafrost using Transient Electromagnetic and Complex Resistivity methods

Adrian Flores Orozco[1]
Theresa Maierhofer[1]
Lukas Aigner[1]
Christin Hilbich[2]

[1]*Geophysics Research Division, Department of Geodesy and Geoinformation, TU-Wien, Austria, flores@tuwien.ac.at*
[2]*Department of Geosciences, University of Fribourg, Switzerland*

Abstract

We investigate the applicability of the Transient Electromagnetic (TEM) and Complex Resistivity (CR) methods to quantify the Induced Polarization (IP) effect in alpine permafrost

Keywords: Electrical resistivity induced polarization; transient electromagnetic; active layer; rock glacier; frozen rocks.

Introduction

Subsurface investigations in alpine regions with high spatial and temporal resolution are critical to quantify the impact of atmospheric events on the thermal status in permafrost, as well as their effect in the water balance. Geophysical imaging methods have emerged as suitable monitoring techniques as they provide quasi-continuous information about subsurface properties and temporal variations (Hauck & Kneisel, 2008). In particular, the electrical resistivity tomography (ERT) has become a popular method considering the distinctive response of water, ice and geologic media (e.g., Supper et al., 2014); as well as its sensitivity to temperature changes, permitting the quantification of permafrost degradation (Krautblatter et al., 2010).

Nevertheless, ERT measurements in winter can be challenging due to the poor contact between the electrodes and the ground, which significantly reduces the signal-to-noise ratio (S/N), or may even hinder the conduction of ERT surveys. Moreover, measurements in alpine fractured media may also bias the interpretation of the ERT results, considering the impossibility to differentiate the highly resistive response associated with air- and ice-filled fractures.

To overcome the limitations mentioned above, here we investigate the applicability of the Transient Electromagnetic (TEM) and Complex Resistivity (CR) methods to quantify the Induced Polarization (IP) effect in alpine permafrost. The IP is a measure of the electrical polarization (i.e., capacitive) properties of the subsurface, which can help in the interpretation of ERT for an improved lithological characterization. Moreover, the frequency-dependence of the IP effect has shown a clear dependence on the textural and thermal properties of rocks (Kemna & Weigand, 2014); thus it may permit an improved ice quantification in alpine investigations.

The application of TEM soundings alleviates the necessity of galvanic coupling, permitting the collection of data in coarse-blocky, snow- or ice-covered surfaces. Hence, we investigate the application of TEM measurements to permit a fast assessment on changes in the electrical resistivity of extensive areas, including locations not easily accessible for ERT and CR. We also investigate the applicability of TEM measurements to quantify changes in the active layer.

Material and methods

As a first step, we aimed at the collection of an extensive database of TEM and CR measurements to evaluate the applicability of both methods in alpine permafrost investigations. Selected sites comprise a broad range of morphological features: coarse blocky talus, rock glaciers, bedrock slopes and plateaus, as well as varying ground ice contents. Measurements are planned within Austria (A) and Switzerland (CH), at sites where ERT data is available for validation.

TEM measurements were collected using a single loop configuration, with 24 readings collected in the early times (4 – 238 μs) using a square loop of 25 m x 25 m and a current of 4 Amp. CR measurements were performed in the frequency-domain, in frequency range between 0.1 and 100 Hz, using 64 electrodes, with separation between electrodes varying between 1 m and 3 m for the different study areas to permit a fair comparison with existing ERT data.

Results and discussions

Collection of CR data at a broad frequency bandwidth, in both summer and winter, has been only possible at the Schilthorn rock slope (CH), where a thick debris soil layer and relative low ground ice content permit the injection of high current densities and enhanced S/N. However, CR measurements in other sites, such as the Hoher Sonnblick (A) - characterized by fractured rock and high ground ice content -, have resulted only in poor current injections (<50 mA), limiting data collection. The CR imaging results reveal anomalies with high variability in the IP effect as expected due to pore-space variations in textural parameters and ice content. Moreover, imaging results reveal a significant frequency-dependence in the IP effect. To illustrate this, Figure 1 shows representative IP spectra extracted from the inverted models for data collected at Schilthorn. Although promising, the increase in the IP effect at higher frequencies (>50 Hz) may indicate the contamination of the data with capacitive coupling associated to variations in the contact resistances between electrodes.

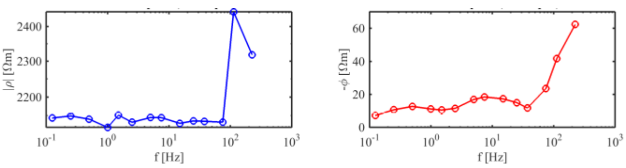

Figure 1. Frequency dependence of the CR in terms of its magnitude (left) and phase-shift (right) for shallow model parameters extracted from Schilthorn imaging results.

TEM measurements revealed in general relatively good data quality for measurements in the earlier times (~100 μs), which is related to the low S/N for "deeper" measurements in the resistive environments, as expected. Yet, the information contained in the early times permits to invert for models with variations in the electrical resistivity within the first 15-30 m.

Contrary to the previous observation, measurements collected in rock glaciers revealed higher quality for the later readings, permitting deeper investigations. Furthermore, most of the measurements revealed a signal reversal, such as the one presented in Figure 2 for measurements collected at Schafberg rock glacier (CH). Such negative values in the readings have been attributed to IP effects, for instance due to the polarization of ice (Marchant et al. 2014). In Figure 2 we present the measured voltage in TEM sounding as well as the inverted resistivity model. For validation, Figure 2 also shows the ERT results, where the anomaly with high resistivity values indicates the occurrence of ice-rich permafrost.

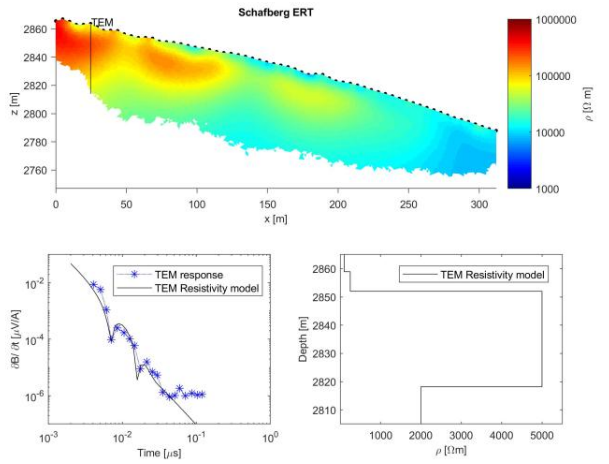

Figure 2. Resistivity model for ERT (top) and TEM (bottom) data collected in the Schafberg rock glacier.

Conclusions

The CR measurements reveal high spatial variability in the IP effect, which may permit an improved quantification of ice-content. Yet collection of high frequency CR data (>100 Hz) requires the correction for possible capacitive coupling effects in the data. Moreover, CR surveys require improved field methodologies to enhance the S/N. The TEM method is well suited for alpine permafrost investigations, yet further investigations are required to (1) improve the modeling in the early times, and (2) to understand the signal reversal observed and its interpretation with the IP due to ice.

Acknowledgments

The ATMOperm project funded by the Austrian Academy of Sciences (ÖAW).

References

Hauck, C. & Kneisel, C., 2008. *Applied geophysics in periglacial environments*. Cambridge University Press.

Marchant, D., Haber, E., & Oldenburg, D., 2014. Three-dimensional modeling of IP effects in time-domain electromagnetic data. *Geophysics* 79(6): E303-314.

Kemna A. & Weigand, M., 2014. *4th European Conference on Permafrost*, Évora, Portugal, June: 328

Krautblatter, M., Verleysdonk, S., Flores- Orozco, A., & Kemna, A., 2010. Temperature- calibrated imaging of seasonal changes in permafrost rock walls by quantitative electrical resistivity tomography (Zugspitze, German/Austrian Alps). *JGR: Earth Surface*: 115(F2).

Supper, R., Ottowitz, D., et al., 2014. Geoelectrical monitoring of frozen ground and permafrost in alpine areas: field studies and considerations towards an improved measuring technology. *Near Surface Geophysics*, 12(1): 93-115.

Geophysical investigations of permafrost ground as a basis for hazard mitigation planning in Longyearbyen, Svalbard

Kjersti (Gleditsch) Gisnås[1]
Jürgen Scheibz[2]
Regula Frauenfelder[2]
Helgard Anschütz[2]
Asgeir (Olaf Kydland) Lysdahl[2]
Arni Jónsson[3]
[1]*Norwegian Geotechnical Institute, Kjersti.Gisnas@ngi.no*
[2] *Norwegian Geotechnical Institute*
[3]*Hnit Consulting Engineers*

Abstract

Distribution of active layer thickness (ALT), ice content and depth to bedrock are among the key variables in construction planning in permafrost areas. In areas difficult to access for drilling campaigns, geophysical investigations provide cost-effective and useful data. Here we show how geophysical data (ERT and GPR) was used in a consultancy job in Longyearbyen, Svalbard, in the context of the planning of mitigation measures against avalanches and debris flow from the Sukkertoppen mountain. The data are used as supplement to drillings performed in the accessible part of the area, and provide important information about the steep parts of the field area. The study demonstrates the usefulness of combining techniques in order to improve data quality and to reduce the costs for such investigations.

Keywords: Geophysical investigations, Longyearbyen, Svalbard, ERT, GPR.

Introduction

On Saturday 19th of December 2015, an avalanche hit the village of Longyearbyen (78°13'N 15°38'E) in Svalbard, ten houses were damaged and two lives were lost. On 21st of February 2017 a new avalanche hit the village in the same area, and houses were again destroyed. Luckily, no lives were lost.

It is now decided to build mitigation measures to reduce the risk for the buildings and people in Longyearbyen. Detailed, spatially distributed information on ground properties, including ALT and ice content, are necessary to plan the constructions. However, due to steep terrain, permafrost conditions at the site and, consequently an instable surface layer during the thaw season, direct ground-investigations, such as drillings, are difficult and very expensive.

In order to lower the costs and increase the spatial distribution of information, geophysical investigations comprising Electrical Resistivity Tomography (ERT) and ground penetrating radar (GPR) were conducted.

Field investigations in Longyearbyen

An arctic maritime snow climate

Longyearbyen is among the places in the world that have warmed fastest in the latest decades. Mean annual air temperature at Svalbard airport raised from -6.7°C to -4.6°C between the periods 1960-1990 and 1980-2010 (Førland et al., 2011).

The island has an Arctic maritime snow climate, and snow typically covers the town from November to May. The climate in Longyearbyen is dry and the snow cover shallow. Due to the dry snow conditions and the harsh weather, the redistribution of snow due to wind drifting can be extreme.

Longyearbyen is situated in the continuous permafrost zone, with ALT around 1 m in the valley bottoms. However, the thaw depths vary due to variations in snow cover, water drainage and ground material. Thawing season normally lasts from June to September.

The field investigations were conducted in the period 12th–19th of September 2017. This was approximately at the timing of observed maximum thaw depth, and the ground surface started to freeze by the end of the period.

Geophysical investigations

The investigation comprised nine profiles of ERT profiles and 11 GPR profiles (Figure 1). The profiles varied in length from 160 to 400 m, and covered partly steep slopes of 30–45° (red shading). An ABEM Terrameter LS 2 was used for the ERT-measurements. Electrode spacing was 2 and 3 m, and the investigation depth was approximately 35 m.

For the GPR soundings, we used a GSSI-SIR 4000 instrument with center antennae frequencies of 100 MHz and 400 MHz. The profiles were measured along the same profiles as the ERT measurements, but also along to additional profiles (yellow lines, Figure 1).

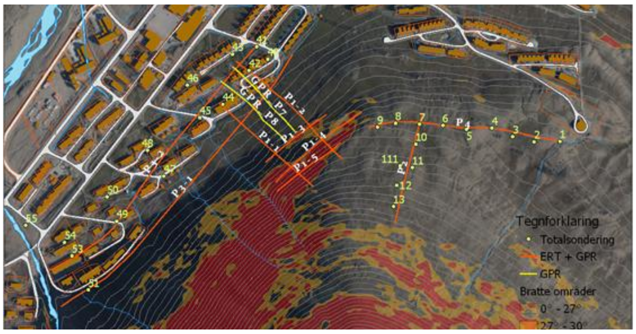

Figure 1: The field site with the ERT and GPR profiles (orange lines), and only GPR profiles (yellow lines).

Due to fine grained sediments, the penetration depth of the 400 MHz antennae was limited to 1-1.5 m, and therefore the 100 MHz data was used for interpretation. Due to steep slopes and difficult surface conditions, parts of the acquired data showed difficult reflection patterns which could not be correlated to subsurface structures.

Ground drillings (numbered green points, Figure 1) were performed at several locations along the accessible parts of the profiles in the weeks after the geophysical investigations. Depth to permafrost and bedrock as well as grain distribution curves were recorded from all drilling locations, and were used as reference for the analysis of the geophysical data.

Preliminary results

All ERT-profiles show a constant top layer with low resistivity, with depths from 1.5 to 3.5 m (Figure 2). This is interpreted as the ALT. The data deviates from this general finding in the southwesterly parts of P1-1, P1-4 and P1-5. In these areas, the layer of lower resistivity reaches much deeper, 9-13 m in some areas. This is unrealistic ALTs, and the bedrock is visible near the area. A drainage channel is located south of this area, and the ground material may therefore be drier and, consequently, has a lower resistivity.

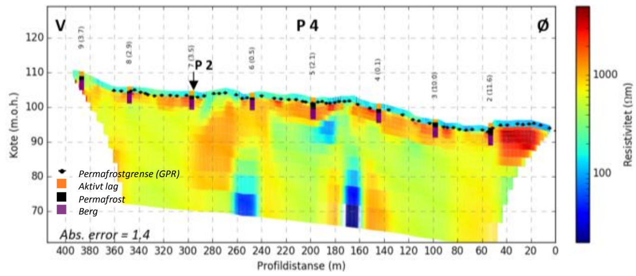

Figure 2: Resistivity values from ERT-profile P4 with the boundary layer from GPR (black dots) interpreted as the permafrost table. Observed ALT and depth to bedrock from drilling are shown in orange, black and purple colors.

Below the low-resistivity layer there is a layer with higher, but variable resistivity, in some areas up to 10 000 Ωm. The highest values are found close to the buildings and in the lower parts of the western slope.

The geophysical results correlate well with the boundary layers observed in the drilling data, showing ALT of 1.5–2.0 m, and varying depths to competent bedrock of 2–8 m. The drilling data shows several boundaries between more or less porous bedrock, but no clear boundary to the bedrock.

Concluding remarks

Geophysical ground investigations have proved to be a cost-effective method to obtain spatially distributed information on ALT, particularly in areas inaccessible for, e.g., drillings. The ERT data show a clear transition from unfrozen to frozen ground in most profiles, and provide information on relative ice content in the area. Because of the very coarse surface material and the steep slopes, the GPR results were difficult to use in parts of the field area.

Acknowledgments

This consultancy work was financed by the Norwegian Water and Energy Directorate (NVE), and coordinated by Stian Bue Kanstad (NVE) and Øyvind Skeie Hellum in Longyearbyen Lokalstyre. We thank the mentioned institutions and persons for the collaboration and for their permission to share our findings with the scientific community.

References

Førland E.J., Benestad R., Hanssen-Bauer I., Haugen J. E., & Skaugen T. E., 2011. Temperature and Precipitation Development at Svalbard 1900–2100. Adv. in Meteorology, vol. 2011. doi:10.1155/2011/893790

Contribution of electrical resistivity tomography measurements in the Study permafrost: Examples from the Altai Mountains

Anastasya Goreyavcheva[1]
Vladimir Olenchenko[2]
[1]*Novosibirsk State University, Lapkovskaya.a.a@gmail.com*
[2]*Institute of Petroleum Geology and Geophysics, SB RAS, Novosibirsk*

Abstract

Inversion and interpretation of electrical resistivity tomography data of permafrost in Altai Mountains are presented. Geoelectrical investigations is a useful tool to investigate thawing and freezing processes. A result of the studies on the geoelectric section, the following types of permafrost distribution were identified: Continuous, Discontinuous, Isolated. There is a conclusion that the method of Electrical resistivity tomography allows to determine the thickness of the permafrost, allocate a thaw zone in geological section.

Keywords: Mountains; electrical resistivity tomography; permafrost.

Introduction

The study of the features of permafrost propagation is one of the main tasks of geocryology. To determine the morphology of the frozen bed, geophysical methods are used along with drilling. One of the most informative methods for studying cryolithozone is a modern modification of vertical electric sounding - electro tomography (Hilbich *et al*, 2009; Hauck *et al*, 2003).

Permafrost rocks are typical for high latitudes, but it also occur at low latitudes in high mountain regions. On the territory of Russia, the permafrost is widely manifested in the Altai Mountains.

In this paper some results of the study of the distribution of frozen rocks in the territory of the Gorny Altai (Russia) are presented. The main tasks of this study - determination of the thickness of the permafrost, the layer of seasonal thawing, and determination of the boundaries of permafrost distribution. The work area is located in the Kosh-Agach region of the Republic of Gorny Altai. The measurements were carried out on the southern slope of the Kuraisky range, 8 km north-west of the village Kuray.

Field Site Characteristics and fieldwork technique

The work area is located in the Kosh-Agach region of the Republic of Gorny Altai. The measurements were carried out on the southern slope of the Kuraisky range, 8 km north-west of the village Kuray.

The technology of electrical resistivity tomography (ERT) is based on two-dimensional data inversion and multielectrode measurements. As a result of measurements, we obtain the distribution of the resistivity of rocks in a section, according to which the geological structure of the massif can be assumed (Loke, 2009).

The high spatial density of observations and the two-dimensional approach make it possible to use the method of electro tomography to study complex geological sections, such as media with permafrost rocks.

To carry out measurements we used such equipment as Multi-electrode all-in-one resistivity meter «Skala-48». The measurements were made using the Schlumberger installation, with a electrode spacing equal to 5 m. The lower elevation of the profile is 1705 m, the upper one - 2583 m.

A significant elevation (878 m) makes it possible to study in detail the effect of altitudinal zonality on the distribution of permafrost on the profile which was chosed for the study.

Results

As a result of the studies on the geoelectric section, the following types of permafrost distribution were identified: continuous, discontinuous, isolated. According to the data obtained, it can be concluded that the effect of high-altitude zonation on permafrost propagation is well traced on geoelectric sections (with increasing altitude and decreasing average annual temperatures, the continuity and thickness of permafrost rocks increases, resistance increases and the thickness of the seasonally thawed layer decreases).

The parameters obtained for each type of permafrost distribution are presented in Table 1.

Table 1. Permafrost parameters according to ERT.

Type of permafrost distibution	Resistivity, Om·m	Permafrost thickness,m	Seasonal thaw depth,m
Continuous	>4500	20-?	0.5-1
Discontinuous	2000-5000	5-30	2-3
Isolated	1500-3000	3-15	3-5

The results show the high value of the method of electrical resistivity tomography as a technique for investigating the characteristics of the distribution of permafrost.

References

Loke, M.H. 2009, Electrical imaging surveys for environmental and engineering studies. A practical guide to 2-D and 3-D surveys, RES2DINV *Manual*, IRIS Instruments.

Hilbich, C., Marescot, L., Hauck, C., Loke, M. H., & Mäusbacher, R., 2009. Applicability of electrical resistivity tomography monitoring to coarse blocky and ice-rich permafrost landforms. *Permafrost and Periglacial Processes*, 20(3), 269-284.

Hauck, C., & Mühll, D. V., 2003. Inversion and interpretation of two-dimensional geoelectrical measurements for detecting permafrost in mountainous regions. *Permafrost and Periglacial Processes*, 14(4), 305-318.

Volumetric ice content in active rock glaciers derived from geophysical modeling (Central Andes of Argentina)

Christian Halla[1]
Jan Henrick Blöthe[1]
Carla Tapía Baldis[2]
Christian Hauck[3]
Lothar Schrott[1]

[1]*Department of Geography, University of Bonn, christian.halla@uni-bonn.de*
[2]*Instituto Argentino de Nivología, Glaciología y Ciencias Ambientales. CCT CONICET Mendoza, Argentina*
[3]*Department of Geosciences, University of Fribourg, Switzerland*

Abstract

Active rock glaciers potentially constitute significant reservoirs and sources of water in the dry Central Andes. However, volumetric ice and water contents of Andean rock glaciers are largely unknown. In this study, the so-called four-phase model (4PM) is applied in order to quantify the material composition of the talus-derived rock glacier Dos Lenguas and the large rock glacier complex Morenas Coloradas. The 4PM is based on different porosity models for ice-rich permafrost bodies and on geoelectric and refraction seismic tomography that were conducted in the root zone, middle part and on the tongues of both rock glaciers. The spatial distributions of ice and water contents show a heterogeneous pattern. Ice-oversaturated permafrost and massive ground ice with ice contents of 50 up to 90 vol. % are two to three times higher in root zones of both rock glaciers compared to lower lying rock glacier tongues containing 20 to 30 vol. %.

Keywords: active rock glacier, permafrost, ice content, internal structure, geophysics, Central Andes

Introduction

The extensive periglacial belt in the semiarid to arid Andes hosts one of the highest rock glaciers concentrations in the world. Active rock glacier permafrost is generally considered as ice-rich due to cohesive flow (Barsch, 1996). Therefore, active rock glaciers potentially constitute significant water reservoirs in the dry Central Andes of Argentina. However, the overall water storage capacities are largely unknown.

Previous studies on rock glaciers in different environments indicate that volumetric ice contents can vary between 10-90 % (Arenson & Jakob, 2010). Thus, large uncertainties exist for the assessment of the ice content of rock glaciers. Out of this started the controversial scientific debate about the hydrological significance of rock glaciers and ground ice in the dry Andes (Arenson & Jakob, 2010).

In this study, we aim to detect the internal structure, the material composition and its spatial distribution at the talus-derived rock glacier Dos Lenguas and the giant rock glacier complex Morenas Coloradas. Water and ice contents of active layer and permafrost were estimated in the root zones, middle parts, and tongues during summer in 2016 and 2017. Both rock glaciers are among the few locations where data from borehole temperatures (Trombotto & Barzotta, 2009) and geophysical properties of the active layer and permafrost are available (Schrott, 1996).

Methods

2D Electrical resistivity tomography (ERT) and refraction seismic tomography (RST) were conducted and identical longitudinal and cross profiles were measured in the root zone, middle part and on the tongues of both rock glaciers.

ERT and RST serve as input data for the four-phase model (4PM; Hauck *et al.*, 2011). The 4PM estimates the volumetric fractions of liquid water, ice and air within the pore space of the rock fraction. Four scenarios with different porosity models were used to assess the ice fraction: Scenario 1 is based on 30 % porosities that allows saturation with interstitial ice of the frozen sandy soil matrix; Scenario 2 and 3 allow ice-oversaturated permafrost conditions using porosities of 50 % and 70 %, respectively; Scenario 4 includes differing porosities of known or assumed material properties (*e.g.*

~30 % porosity for sandy active layer, 90 % for massive ground ice). Based on the Scenarios 1-4 reasonable ranges of volumetric ice content were evaluated.

Results & Conclusions

Volumetric ice content of permafrost in the active talus rock glacier Dos Lenguas range from 20 to 50 vol. % from lower to upper parts based on the most reasonable modeling results. The depth of active layer is heterogeneous (4-10 m) and increases towards lower parts of Dos Lenguas as well as underneath surface depressions with saturated water conditions.

Modeling results of Morenas Coloradas reveal massive ground ice (90 vol. %) and ice-oversaturated permafrost (70 vol. %) in the central root zone and upper parts of the rock glacier complex. The lowest tongue of the rock glacier complex, called Balcon I, shows increased active layer depths (>10 m) containing higher water contents above ice-saturated permafrost conditions (<30 vol. %).

To conclude, volumetric ice contents are 2-3 times higher in root zones of both rock glaciers than in the lower lying rock glacier tongues. Volumetric ice contents are higher in the Morenas Coloradas complex than in the talus-derived rock glacier Dos Lenguas.

The spatial distribution of ice and water contents show a heterogeneous pattern. High water contents and saturated subsurface conditions are identified underneath surface depression and furrows indicating water pathways. Increased active layer depths and dissected permafrost bodies indicate the influence of thermal erosion on the internal structure of both rock glaciers.

Acknowledgments

This research has been funded by the German Research Foundation (DFG; Schr 648/3-1). We further thank D. Trombotto, E. Bottegal, J. Götz, F. Miesen, J. Isigkeit, L. Banzer,T. Höser for their help in the Andes.

References

Arenson, L.U. & Jakob, M., 2010. The significance of rock glaciers in the dry Andes - A discussion of Azócar and Brenning (2010) and Brenning and Azócar (2010). *Permafrost and Periglacial Processes* 21: 282–285.

Barsch, D., 1996. *Rockglaciers: indicators for the present and former geoecology in high mountain environments*. Springer, 331 p.

Hauck, C., Bottcher, M., Maurer, H., 2011. A new model for estimating subsurface ice content based on combined electrical and seismic data sets. The *Cryosphere* 5(2): 453-468.

Schrott, L., 1996. Some geomorphological-hydrological aspects of rock glaciers in the Andes (San Juan, Argentina). *Z Geomorph NF* 104: 161-173.

Trombotto, D. & Borzotta, E., 2009. Indicators of present global warming through changes in active layer-thickness, estimation of thermal diffusivity and geomorphological observations in the Morenas Coloradas rockglacier, Central Andes of Mendoza, Argentina. *Cold Regions Science and Technology* 55: 321-330.

Influence of pore space reduction upon freezing on the electrical and seismic properties of permafrost

Christian Hauck[1]
Sarah Morard[1]
Coline Mollaret[1]
Cécile Pellet[1]
Christin Hilbich[1]

[1]*Department of Geosciences, University of Fribourg, Switzerland, christian.hauck@unifr.ch*

Abstract

We extended an existing geophysical 4-phase model based on electric and seismic data sets to calculate volumetric fractions of ground ice and water content in permafrost areas to its time-lapse variant and improved its electrical mixing rule formulation. In time-lapse formulation, the model is not anymore dependent on time-invariant properties such as porosity, pore water resistivity (if assumed constant), cementation exponent and P-wave velocity of the rock material. Temporal ground ice content changes can then be calculated from repeated electrical resistivity and seismic P-wave velocity data sets. In addition, the electrical mixing rule for the frozen state was improved by taking into account the reduced pore space available for ionic conduction to take place. The time-lapse and improved 4-phase model formulation should now be able to quantify more accurately the loss of ground ice in the context of ongoing climate change. Examples from several mountain permafrost sites will be shown where ground truth data are available.

Keywords: geoelectrics; seismic refraction; ground ice content; 4-phase model; time-lapse; resistivity

Introduction

Electrical Resistivity Tomography (ERT) and Refraction Seismic Tomography (RST) are often used to characterize permafrost occurrences and monitor the ground ice content changes as the different elastic (seismic) and electric (geoelectrics) properties of ice, water, air and soil/rock enable to differentiate between the different material compositions. In principle, they can be combined to estimate the volumetric ice content and its spatial variability using the so-called 4-phase model (4PM, Hauck et al. 2011). This model is based on two petrophysical relationships (mixing rules) for electrical resistivity and seismic P-wave velocity and uses inverted ERT and RST data to calculate ice-, water and air content for a given porosity model. This model has so far been applied successfully to several mountain permafrost sites in the European Alps, the Andes and Maritime Antarctica and has been validated/calibrated with borehole data where available.

Methodology

The major drawback up to now has been the need to prescribe a realistic porosity model along the tomographic domain, which is often difficult due to the strong heterogeneity especially in mountainous terrain (Pellet et al. 2016). Here, we want to present an improved model formulation based on time-lapse ERT and RST data, which allows calculating ice content changes independent of porosity. In addition, the porosity formulation in the electrical mixing rule (Archie's Law) of the standard 4PM is improved by taking into account the reduced pore space available for ionic conduction upon freezing. The two new model approaches are tested using synthetic data sets (cf Mewes et al. 2017) and data from field sites in the Swiss Alps, where long-term geophysical monitoring has been established since 1999 (Hilbich et al. 2008, Mollaret et al. 2017).

The time-lapse approach uses coincident ERT and RST measurements at two different moments in time t_1 and t_2 as input data, and calculates the change in ice content Δf_i using time-dependent versions of the resistivity and P-wave velocity mixing rules as follows (Hauck et al. 2017; indices $_1$ and $_2$ denote in the following measurements/volumetric fractions at time t_1 and t_2, respectively):

$$\rho_1 = \rho_2 \left(\frac{f_{w2}}{f_{w1}} \right)^n \quad (1)$$

$$\frac{1}{v_1} - \frac{1}{v_2} = \frac{f_{i1} - f_{i2}}{v_i} + \frac{f_{w1} - f_{w2}}{v_w} + \frac{f_{a1} - f_{a2}}{v_a} \quad (2)$$

$$f_{i1} - f_{i2} = \Delta f_i = f_{w2} - f_{w1} + f_{a2} - f_{a1} \quad (3)$$

with the electrical resistivity ρ, the seismic P-wave velocity v, the Archie saturation exponent n and the volumetric fractions of the different materials f. The subscripts *i*, *a* and *w* denote ice, air and water, respectively. If the initial estimate of f_{w1}, the saturation exponent n and the (known) P-wave velocities of water, ice and air (v_i, v_w, v_a) are prescribed, the change in ice content can be calculated from the measured change in resistivity and P-wave velocity. It has to be noted that in the original formulation of the 4PM the usually unknown pore water resistivity ρ_w, the cementation exponent m, the P-wave velocity of the rock/soil material v_r and the porosity Φ have to be prescribed as well.

Finally, we propose a new formulation of the electrical mixing rule based on Archie´s Law (Archie, 1942). In the standard 4PM version, Archie's second law is used as follows:

$$\rho = \rho_w \Phi^{-m} S^{-n} \quad (4)$$

where S is the water saturation, which can also be written as $S = f_w / \Phi$ and $\Phi = 1\text{-}f_r$. Figs. 1a,b show the conceptual model for the situation in unfrozen and partly frozen state. The brown areas denote the rock/soil fraction of the subsurface (f_r), the dark blue the water (f_w), the light blue the ice (f_i) and the white areas the air/unsaturated parts (f_a). In the new electrical formulation (Eq. (5)), the ice is considered explicitly as reduction of pore space, by this linking the electrical mixing rule with the ice content, which was not the case in the standard Archie's law formulation of 4PM.

$$\rho = \rho_w (\Phi - f_i)^{-m} \left(\frac{f_w}{\Phi - f_i}\right)^{-n} \quad (5)$$

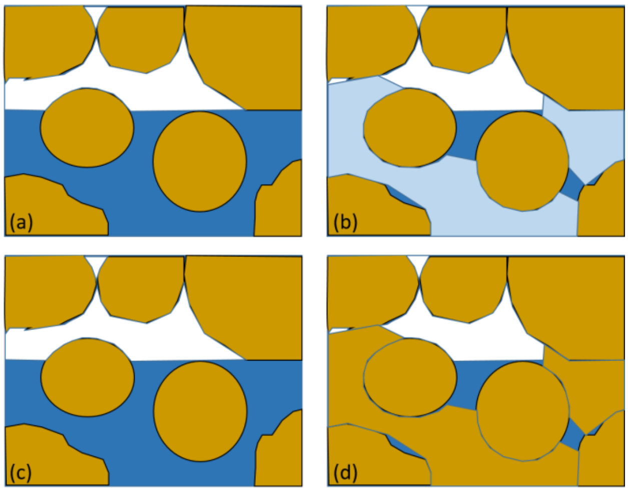

Figure 1. Conceptual model for (a) the seismic mixing rule in unfrozen state, (b) the seismic mixing rule in partly frozen state, (c) the electrical model in unfrozen state and (d) the Archie-type electrical model in partly frozen state.

References

Archie, G. E., 1942. The electrical resistivity log as an aid in determining some reservoir characteristics. *Petrol. Trans. Am. Inst. Min. Metallur. Eng.* 146, 54–62.

Hauck, C., Böttcher, M. & Maurer, H, 2011. A new model for estimating subsurface ice content based on combined electrical and seismic data sets. *The Cryosphere*, 5, 453–468.

Hauck, C., Hilbich, C. & Mollaret, C., 2017. A Time-lapse Geophysical Model for Detecting Changes in Ground Ice Content Based on Electrical and Seismic Mixing Rules. In 23rd European Meeting of Environmental and Engineering Geophysics, DOI: 10.3997/2214-4609.201702024.

Hilbich, C., Hauck, C., Hoelzle, M., Scherler, M., Schudel, L., Völksch, I., Vonder Mühll, D. & R. Mäusbacher, 2008. Monitoring mountain permafrost evolution using electrical resistivity tomography: A 7-year study of seasonal, annual, and long-term variations at Schilthorn, Swiss Alps, *J. Geophys. Res.,* 113, F01S90, doi:10.1029/2007JF000799.

Mewes, B., Hilbich, C., Delaloye, R. & Hauck, C., 2017. Resolution capacity of geophysical monitoring regarding permafrost degradation induced by hydrological processes. *The Cryosphere*, 11(6), 2957-2974.

Mollaret, C., Hilbich, C. & Hauck, C., 2017. Analysis Procedures of an ERT Monitoring Network to Assess Mountain Permafrost Degradation Rate. In 23rd European Meeting of Environmental and Engineering Geophysics. DOI: 10.3997/2214-4609.201701997.

Pellet C, Hilbich C, Marmy A & Hauck, C., 2016. Soil moisture data for the validation of permafrost models using direct and indirect measurement approaches at three alpine sites. *Front. Earth Sci.* 3:91. doi: 10.3389/feart.2015.00091.

Using GPR spectral signal analysis to search for taliks in the Shestakovka River basin in the continuous permafrost zone

Ivan Khristoforov[1], Liudmila Lebedeva[1], Paul Overduin[2], Kirill Bazhin[1], Kencheeri Danilov[1]
[1]*Melnikov Permafrost Institute, Siberian Branch, Russian Academy of Sciences, ivankhristoforov@mpi.ysn.ru*
[2]*Alfred Wegener Institute Helmholtz Centre for Polar and Marine Research*

Abstract

Water bodies, such as rivers and lakes, create different conditions for permafrost distribution than below surrounding terrain. GPR offers a means of detecting changes in the liquid water and ice content of the ground, and thus for measuring the shape of unfrozen region associated with rivers or lakes. We studied the displacement of the spectra of electromagnetic pulses in the frequency range from 75 to 375 MHz in situ in homogeneous sands in the Shestakovka River catchment. Results showed a correlation of the change of the frequency characteristics of the spectrum of the transmitted signal with the presence of shallow taliks, suggesting that spectral signal analysis can help to detect permafrost distribution.

Keywords: Ground Penetrating Radar (GPR), signal spectrum, talik, permafrost, hydrology.

Introduction

The integration of geophysical methods in hydrogeology has recently been widely used for the study of taliks in permafrost conditions. (e.g. Yanhui *et al.*, 2017). The use of GPR in hydrology in particular, for example to identify liquid water and taliks, is well known. However, the potential benefits of spectral analysis of GPR signals in the study of taliks in the permafrost zone has not received much attention.

We address this gap with comprehensive field work that included GPR and ERT methods, thermometric monitoring and boreholes with sampling for sediment water content, at the well-studied Shestakovka river site, located 20 km southwest of Yakutsk (Anisimova, 1980). The subsurface at the site is sandy sediment of fine and medium fractions of quartz-feldspar and is characterized by a specific gravity of 2.55-2.65 g/cm^3 and a porosity of 30-40%. The supra-permafrost subaerial water-bearing taliks have a discrete distribution. Permafrost at this site reaches a depth of 400 m (Boitsov, 2011).

Research methods

We present one profile measured across the seasonally frozen layer (SFL) adjacent to the Shestakovka river in April 2016. The profile was 152 m long on a horizontal surface at an altitude of 214 m above sea level. Our GPR measurements were made with an OKO-2 georadar system (from the company *OOO Logis-GEOTECH*) with an antenna block with central frequencies of 150 and 250 MHz. The measurements were conducted with transmitter and receiver in contact with the frozen ground in profiling mode with a scan duration of 200 ns.

Transitions from one phase state of water to another result in a phase change of the signal reflected from the boundaries between regions, based on changes in the dielectric permittivity at the phase change interface. Therefore, the GPR method can clearly define the boundaries of thawed and frozen soils (Khristoforov, *et al.*, 2016).

The amplitude-frequency spectrum was determined using a windowed Fourier transform applied separately for transmitted and received electromagnetic signals. An algorithm for procedure is available in the specialized program GeoScan32 (also from *OOO Logis-GEOTECH*). A Garmin map64 GPS was used to georeference more than 10 GPR transects crossing taliks. In addition, a borehole drilled about 200 m from the profile in April 2016 provides information on the presence of frozen and unfrozen layers and values of total sediment water content (borehole № 3/16).

Results

Dielectric permittivity of the sediment was measured around the time of maximum annual freezing (Fig. 1). On the left side of the central graphic (showing the GPR profile, Fig. 1), the timeline of the arrival of the reflected the electromagnetic wave from the boundaries is given in nanoseconds, while, on the right side depth are given based on an assumed constant dielectric constant of 6. A water-saturated talik with a total moisture content of 8 % was encountered in the borehole (not shown) between 2 and 7 m below the surface.

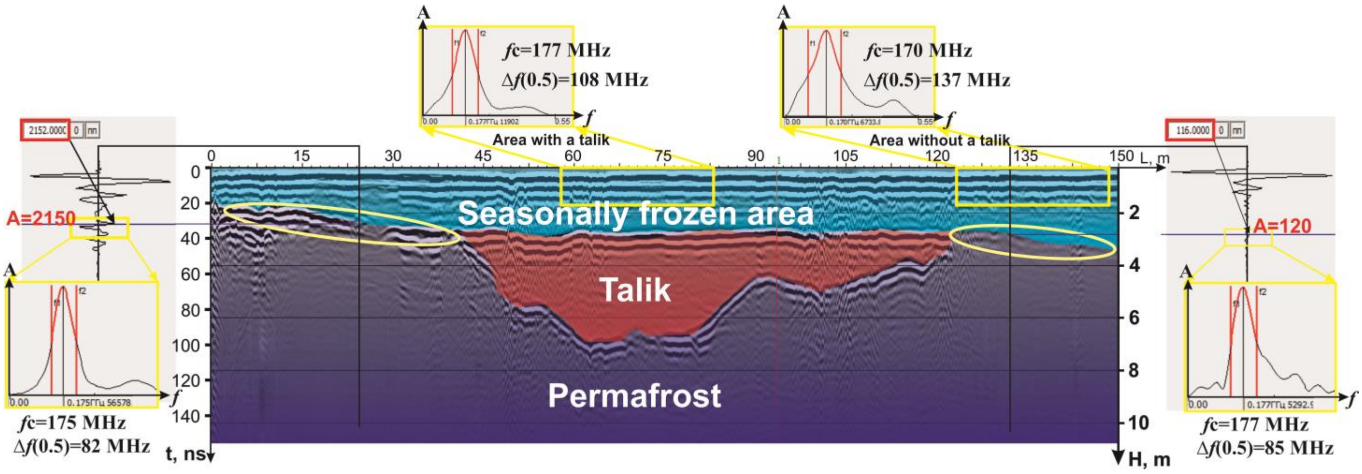

Figure 1. Frequency characteristics of spectrum in the detection of the talik. A GPR profile is shown with coloration added to indicate interpreted units. The lateral length of the profile is 152 m.

For different regions of the profile, we determined the spectral characteristics of the transmitted signal: the central frequency (fc) of the amplitude-frequency spectrum, and the width of the spectrum (Δf) at energy level 0.5. In areas with a talik located approximately 3 m below the surface, the width of the spectrum (at the energy 0.5, indicated by red lines) of the probing signal is slightly narrower where there is an underlying talik than where there is no talik. In our case, by almost 29 MHz (about 20%). Also when considering probing signals from many profiles, there is a slight shift downward in average frequency when sounding in areas where there are no taliks.

The amplitude of GPR signals at the interface between the SFL and permafrost at the beginning of the profile and at the end (in the figure indicated by the yellow ovals) are different. The average difference of the amplitude values of the reflected signals varies by a factor of 15 to 20 (Fig. 1). The frequency characteristics of the spectra may indicate the presence of a water-saturated boundary layer at low values of the amplitudes of the reflected electromagnetic signals. However, the spectra of the signals reflected from these boundaries are almost identical.

Conclusions

Using GPR surveys with a device in contact with the frozen environment, we observed a reduction in the width of the spectrum at the energy 0.5 (approximately 20%) of the transmitted GPR signal at frequencies from 75 to 375 MHz. This reduction indicated the presence of a shallow talik down to 5-6 m below the frozen surface layer. In spite of the large difference in the amplitude values of the reflected signals, the amplitude-frequency spectra of the reflected signals were similar at the same depth in the absence of large taliks. Our work provides an example of the use of spectral analysis of GPR data to gain information on talik distribution in permafrost.

Acknowledgments

The study was partially supported by the Russian Foundation for Basic Research (RFBR, grants № 16-31-60082_mol_a_dk & № 17-05-00926) and via an Ulla Johansen DAAD scholarship (№ 0000716550).

References

You Y., Yu Q., Pan X., Wang X. & Guo L., 2017. Short communication geophysical imaging of permafrost and talik configuration beneath a thermokarst lake, *Permafrost and Periglacial Process*. 28: 470–476 doi: 10.1002/ppp.1938

Anisimova, N., Golovanova, T., Zhigalova, O., Lebedeva, T., Shepelev, V., 1980. *Feeding conditions, level regime and chemical composition of the suprapermafrost and surface water in the area of the Malaya Chabyda lake*. Yakutsk: Melnikov Permafrost Institute Press, 261 pp.

Boitsov, A., 2011. *Geocryology and groundwater in permafrost zone*. Tyumen: Publishing House of TSOGU, 177 pp.

Khristoforov, I., Olenchenko V., Gagarin L., Omelyanenko A., 2016. Geophysical Forecasting of the formation of Thermal Suffosion Depressions in Central Yakutia. *Proceedings of XI International Conference on Permafrost*, Potsdam, Germany, June 20–24: 864-867, doi:10.2312/GFZ.LIS.2016.001

Two- and three-dimensional geophysical investigation of a thrust moraine in the glacier forefield Muragl, eastern Swiss Alps

Julius Kunz[1]
Christof Kneisel[1]

[1]*Physical Geography, Institute of Geography and Geology, University of Würzburg, Germany,*
julius.kunz@stud-mail.uni-wuerzburg.de

Abstract

The genesis of thrust moraines in high alpine environments like the European Alps is still poorly explored. In this study a coarse blocky thrust moraine in the forefield of the Muragl glacier was investigated by two-dimensional electrical resistivity imaging and two- and three-dimensional ground-penetrating radar surveys. Aim of the study was to detect the internal structure and composition of the moraine complex in order to develop a conceptual model of moraine formation including the impact of permafrost and potential pre-existing glacier-permafrost relationships.

Keywords: thrust moraine; permafrost; glacier-permafrost relationships; ground-penetrating radar; electrical resistivity imaging.

Introduction

Permafrost distribution and glacier-permafrost interactions within the glacier forefield Muragl, eastern Swiss Alps, have been investigated using different methodological approaches. Results of these investigations showed very high electrical resistivity values in some parts of the thrust moraine pointing to a massive ice core with a polygenetic origin within the moraine body (Kneisel, 2004; Kneisel & Kääb, 2007).

Aim of the present study was to detect the internal structure and composition of the moraine complex in more detail in order to develop a conceptual model of glacier-permafrost interactions and thrust moraine formation, respectively.

We used an integrative approach combining two-dimensional electrical resistivity imaging (2D ERI) and ground-penetrating radar (GPR) to map the present-day extent of the massive ice core in the lower parts of the thrust moraine and to detect the boundaries between the areas with different grain sizes in the subsurface of the moraine body. On the surface, these boundaries between zones with fine substrates and those zones with coarse blocky substrates are clearly visible. In theory this boundaries are the effect of glaciotectonic deformation and the thrusting of different substrates. The use of GPR should enable the detection of these boundaries and the shear zones as it was shown by Monnier et al. (2011) on Thabor rock glacier.

Methods

The ERI surveys were performed using a Syscal Pro Switch resistivity imaging system and a Wenner-Schlumberger array with an electrode spacing of 5 m. GPR surveys were performed using a PulseEKKO Pro device with two unshielded antennas with 50 MHz.

In a small area, where the 2D GPR profiles indicated boundaries between the different substrates very clearly, a 3D GPR grid was performed additionally (Fig. 1). These measurements should help to investigate the three-dimensional structure of the dipping reflectors of the substrate boundaries.

Figure 1. 3D GPR-measurements on the thrust moraine in the glacier forefield Muragl in May 2017 (Photo: C. Kneisel).

On the remnant of the Muragl glacier several GPR-measurements with 100 MHz-antennas were undertaken to map the ice thickness and the glacier bed morphology. The present-day extent of the partially debris covered ice body could be identified by these surveys.

Preliminary Results

First insights into the results of the 2D GPR-measurements are shown in Fig. 2. Especially in the upper meters the contrasts between grainsizes of the different substrates are visible. The black line at the right side of the profile indicates the bedrock below the moraine complex, which is verified by dipping bedrock near the western margin of the moraine. The dotted lines near the surface are interpreted as the boundaries between the different substrates. The structure of these reflectors show the typical dipping to the proximal side of the moraine as it is characteristic for the formation of a moraine complex influenced by glacier-permafrost interactions (cf. Bennet 2001; Benediktsson et al. 2015).

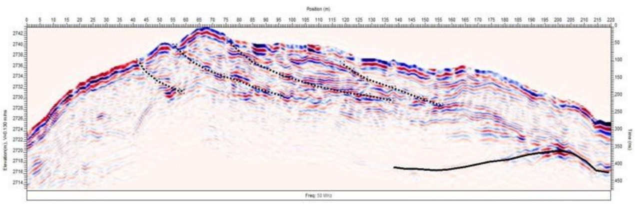

Figure 2. GPR-cross section of the thrust moraine.

Similar dipping reflectors could also be verified by the 3D GPR measurements. The extent and course of the reflectors is another indication, that these reflectors could be shear zones of glaciotectonic deformation.

In contrast to the GPR data the ERT results do not reveal the substrate-boundaries in the subsurface (Fig. 2). However, with the ERT surveys, which are applied at the same survey locations, an anomaly with very high resistivity values on the proximal side of the moraine could be detected (blue colors in Fig. 3). This anomaly is interpreted as a massive ice body. The range of resistivity values points to a polygenetic origin of the ice.

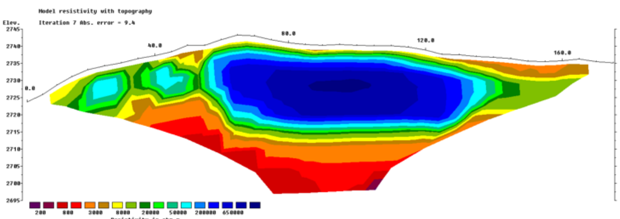

Figure 3. ERT-cross section of the thrust moraine.

In comparison to results of earlier surveys perfomed in 1997 the results of the measurements on the surface ice body in the upper part of the cirque showed a distinct reduction of the ice thickness. Additionally, the results of the GPR measurements indicate polythermal conditions within the ice remnant.

The integrative approach using GPR and ERT showed promising results about the internal structure of the thrust moraine and the present-day existence of ground ice within it. Further investigations will include ERT measurements with a smaller spacing to optimize the model resolution in the upper few meters.

References

Benediktsson, I.Ö., Schomacker, A., Johnson, M.D., Geiger, A.J., Ingolfsson, O, Gudmundsdottir, E.R. 2015. Architecture and structural evolution of an early Little Ice Age terminal moraine at the surge-type glacier Mulajökull, Iceland. *Journal of Geophysical Research: Earth Surface* 120: doi:10.1002/2015JF003514.

Bennet, M.R., 2001. The morphology, structural evolution and significance of push moraines. *Earh-Science Reviews* 53: 197-236.

Kneisel, C., 2004. New Insights into Mountain Permafrost Occurrence and Characteristics in Glacier Forefields at High Altitude through the Application of 2D Resistivity Imaging. *Permafrost and Periglacial Processes* 15: 221-227.

Kneisel, C., Kääb, A., 2007. Mountain permafrost dynamics within a recently exposed glacier forefield inferred by a combined geomorphological, geophysical and photogrammetrical approach. *Earth Surface Processes and Landforms* 32: 1797-1810.

Monnier, S., Camerlynck, C., Rejiba, F., Kinnard, C., Feuillet, T., Dheaied, A., 2011. Structure and genesis of the Thabor rock glacier (Northern French Alps) determined from morphological and ground-penetrating radar surveys. *Geomorphology* 134: 269-279.

Petrophysical approach of ERI data interpretation for various salinity deposits in permafrost areas

Dina Kvon [1]
Evgeny Zerkal [2]
Igor Modin[2]
Vladimir Shevnin[2]
Aleksey Skobelev[2]
Dmitry Makarov[2]
[1]*Research Center Geoscan LLC, Moscow, kvonchik@mail.ru*
[2]*Lomonosov Moscow State University*

Abstract

In this paper are presented the results of electrical resistivity imaging (ERI) survey performed in several areas of the Yamal Peninsula. The objective of the study was to use geophysical approach with petrophysical and statistical analysis to distinguish spatial distributions of various lithological units and characterize permafrost properties including soil salinity and ice content.

Keywords: petrophysical modelling; saline permafrost; near surface geophysics; unfrozen water content.

Introduction

In this study we investigated a near-surface cross section in the north-west part of the Yamal peninsula using ERI. According to the borehole data, each site was composed of 10-20 m of loams in the subsurface followed by 10-20 m of sands and loams in underlying area.

Here simultaneous ERI data statistical processing and petrophysical modelling were used to distinguish and map the deposits of various lithology and to characterize such properties as salinity and volumetric ice content in the permafrost.

Statistical analysis and petrophysical approach

Resistivity histograms (Fig. 1) show that there are different effective electrical resistivity intervals at different sites, while borehole data gives the same lithology (view details in discussion).

Petrophysical modeling was performed in PetroWin program (Matveev & Ryzhov, 2006) which allows to calculate electrical resistivity for each type of soil material, taking into account porosity, ice, clay and unfrozen water content, temperature, cation exchange capacity, porous brine salinity etc., since resistivity of frozen ground is known to depend on such parameters (Dafflon *et al.*, 2016).

Based on core analysis, previous surveys data and borehole logging we confined petrophysical properties within total ice content of 12-68%, unfrozen water content 2-20% for -4^{0}C temperature for frozen loams and ice content 24-49%, 1-7% unfrozen water content for -4^{0}C temperature and 41-49% porosity for frozen sands.

The model of unfrozen ground was limited in porosity (40-60% for loams and 35-50% for sands) and moisture content (40-60% for loams, 10-50% for sands). Also, for resistivity models pore water salinity varied from 0.1 to 40 g/l for all types of modeled soils.

Discussion

The main results of petrophysical modelling are assumed in Figure 2. According to histograms, as compared with petrophysical modelling, for site 1 resistivity values 10^3-10^4 Ohm·m correspond to relatively high ice content (~50%) in subsurface loams and sands at the bottom; comparatively low resistivity values 10^2-10^3 Ohm·m in the middle part of the cross-section are related to conductive heterogeneities in sands with increased unfrozen water content.

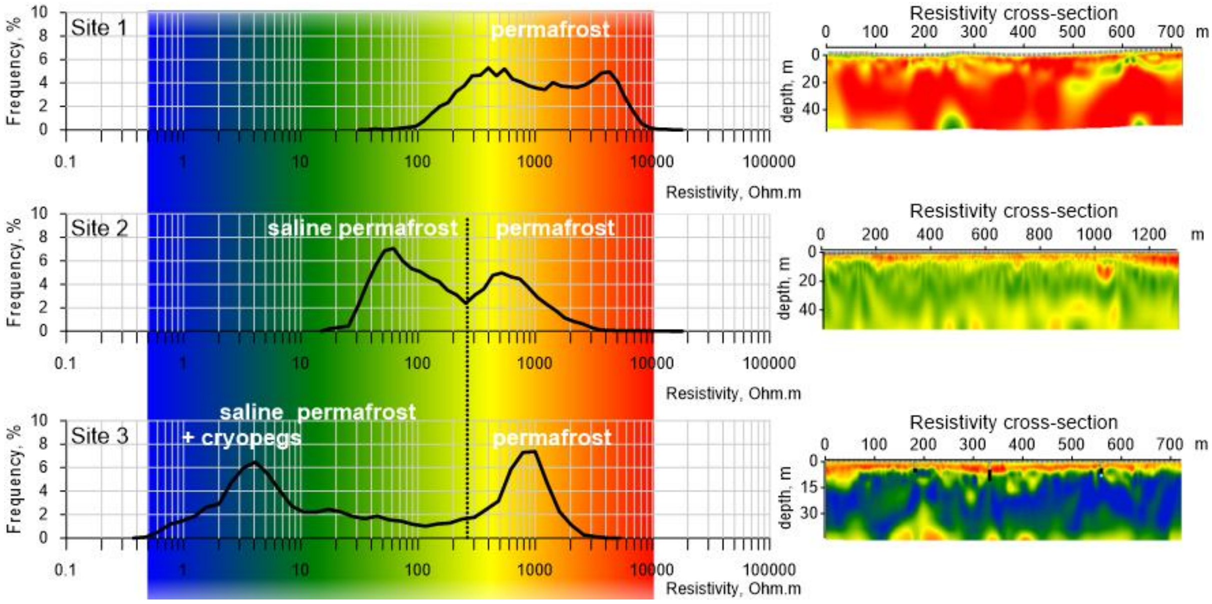

Figure 1. ERI histograms and cross-sections at different sites.

In the upper parts of the cross-sections on sites 2 and 3, resistivity values about 10^3 Ohm·m coincide with frozen loams with ice content ~30% and low total dissolved salts, which is confirmed by numerous studies (Badu, 2015). The middle part of site 2 cross-section is presented by 10-300 Ohm·m resistivity layer interpreted as frozen loams and sands with salinity and unfrozen water content increasing with depth.

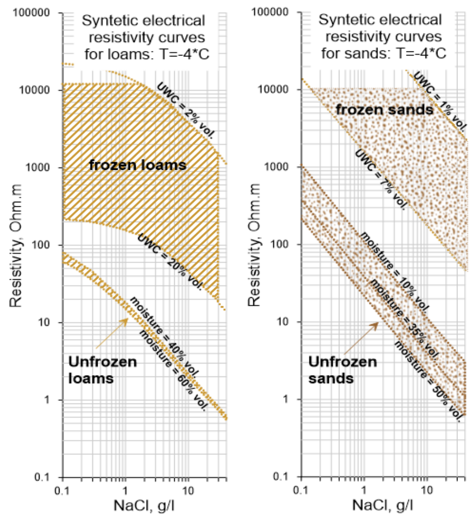

Figure 2. Calculated resistivity models for frozen and unfrozen material.

In the middle part of site 3 cross section a low resistivity area 0.4-100 Ohm·m corresponds to unfrozen permafrost caused by progressively elevated soil salinity in underlying deposits. Gradual increment of resistivity values (10^1-10^3 Ohm·m) is attributed to total ice content elevation.

Conclusions

Through the simultaneous ERI data statistical processing and advanced petrophysical modelling we distinguished and mapped deposits with various lithology and characterized such properties as salinity and ice content in selected permafrost areas.

This study improves understanding and quantifies relations between electrical resistivity in this permafrost and such parameters as porosity, ice, clay content, temperature, cation exchange capacity and unfrozen water properties that provide an essential input in electrical resistivity values.

References

Badu, Yu. B., 2015. Ice content of cryogenic strata (permafrost interval) in gas-bearing structures, Northern Yamal. *Kriosfera Zemli*, vol. XIX, No. 3, pp. 9–18.

Dafflon, B., Hubbard, S., Ulrich, C., Peterson, J., Wu, Y., Wainwright, H., Kneafsey, T. J., 2016. Geophysical estimation of shallow permafrost distribution and properties in an ice-wedge polygon-dominated Arctic tundra region. *Geophysics*, Vol. 81, No. 1; P. WA247–WA263

Matveev, B.C. and Ryzhov, A.A., 2006. Geophysical support of regional hydrogeological, engineering-geological, geocryological, and geoecological studies. *Razved. I Okhr. Nedr*, no. 2, pp. 50–57.

Multi-scale geophysical mapping of deep permafrost change after disturbance in interior Alaska, USA

Burke J. Minsley, Benjamin R. Bloss, Brian Ebel, David Rey, Michelle Walvoord[1]
Dana R.N. Brown[2]
Ronnie Daanen, Abraham Emond[3]
Andy Kass[4]
Neal Pastick, Bruce Wylie[5]

[1] *U.S. Geological Survey, Denver, CO, USA, bminsley@usgs.gov*
[2]*University of Alaska Fairbanks, Fairbanks, AK, USA*
[3]*Alaska Division of Geophysical and Geological Surveys, Fairbanks, AK, USA*
[4]*Aarhus University, Aarhus, Denmark*
[3]*U.S. Geological Survey, Sioux Falls, SD, USA*

Abstract

Disturbance related to fire or hydrologic processes can cause degradation of deep (greater than 1 m) permafrost. These changes in deep permafrost have the potential to impact landscapes and infrastructure, alter the routing and distribution of surface water or groundwater, and may contribute to the flux of carbon to terrestrial and aquatic ecosystems. However, characterization of deep permafrost over large areas and with high spatial resolution is not possible with traditional remote sensing or surface observations. We make use of multiple ground-based and airborne geophysical methods, as well as numerical simulations, to better understand the distribution of permafrost and how it has changed after disturbance. Together, these geophysical datasets help to fill a critical gap in understanding permafrost landscapes and their response to disturbance.

Keywords: geophysics; disturbance; deep permafrost

Introduction

Geophysical methods fill a unique role in permafrost observation, enabling the mapping of deep permafrost and soil characteristics over large areas and with high spatial resolution that cannot be achieved with remote sensing, drilling, or other direct observations (Hauck, 2013). Subsurface mapping techniques are critical for understanding the deep belowground changes that can occur after disturbance related to fire or hydrologic processes, and the potential impacts on landscapes and infrastructure. Here, we summarize data collected from multiple ground-based and airborne geophysical campaigns (Fig. 1) aimed at mapping deep permafrost characteristics and the impacts of disturbance (Minsley et al., 2016; Minsley et al., 2012; Minsley et al., 2017; Kass et al., 2017).

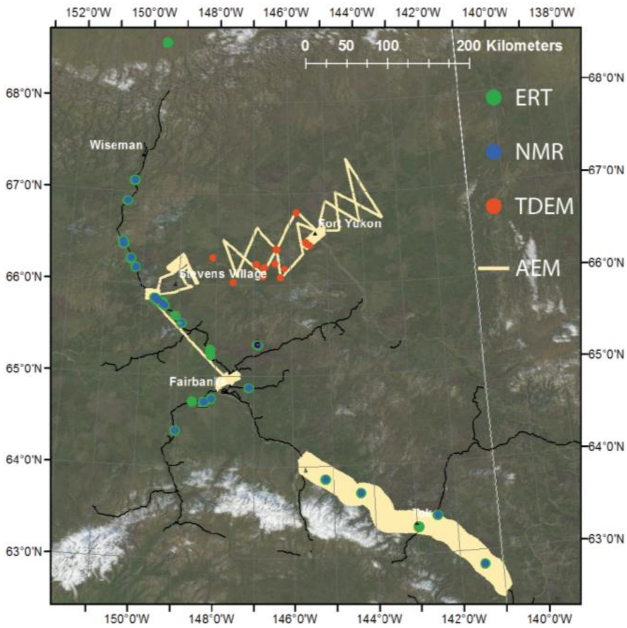

Figure 1. Ground-based and airborne geophysical datasets acquired from 2010 – 2017 in interior Alaska, USA.

Select Results

Electrical Resistivity Tomography (ERT) Transects

At the local scale, electrical resistivity tomography (ERT) measurements are used to identify changes in permafrost characteristics to depths of up to 15 m along more than 40 100-200 m-long transects collected in interior Alaska. These data have identified deep thaw features and reforming permafrost many years after fire (Fig. 2A), permafrost beneath small streams and on adjacent hillslopes (Fig. 2B), and significant thaw at depth beneath thermokarst bogs (Fig. 2C).

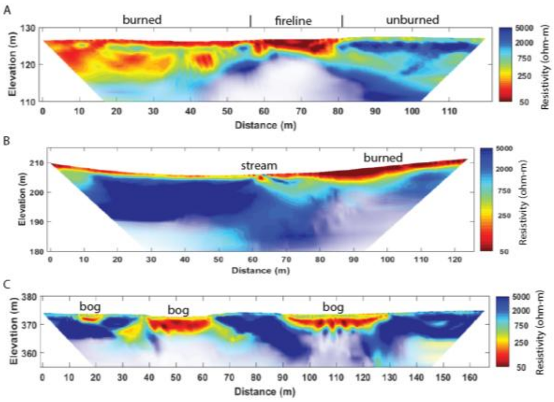

Figure 2. ERT transects across (A) a fireline that divides burned and unburned black spruce forest, (B) a small stream and adjacent hillslopes, and (C) a thermokarst bog site.

Nuclear Magnetic Resonance (NMR)

At select locations along the ERT profiles, measurements of downhole nuclear magnetic resonance (NMR) were made to depths of 2 m belowground in order to quantify *in situ* unfrozen water content and soil texture that help to constrain ERT interpretations. Being able to quantify the amount of unfrozen water in sediments that are at or just below 0° C is important for quantifying warm permafrost that may be vulnerable to further degradation, and that may be biogeochemically active zones where carbon degradation occurs.

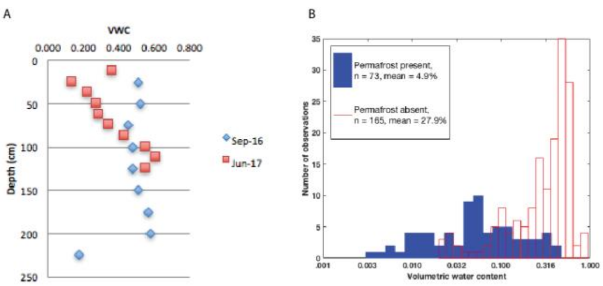

Figure 3. (A) NMR data show seasonal changes in unfrozen water content with depth. (B) Summary of unfrozen water content for more than 200 NMR measurements at sites where frozen ground was (blue) and was not (red) detected with a frost probe.

Regional mapping

At the regional scale, airborne electromagnetic (AEM) data have been acquired along more than 2,000 km of flight lines in the Yukon Flats to characterize the distribution of permafrost beneath and surrounding the many surface water features in the region to depths of 100 m or more (Fig. 4). To complement the AEM surveys, ground-based EM data were collected on top of 16 frozen lakes in order to better constrain sublacustrine thaw depths.

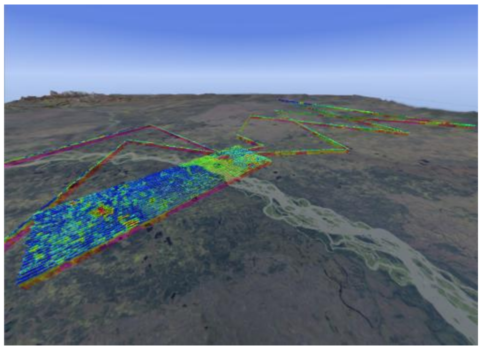

Figure 4. Airborne electromagnetic data collected over parts of the Yukon Flats captures the complex distribution of permafrost surrounding lakes and rivers.

Acknowledgments

This work is supported by the USGS LandCarbon Program, and the NASA Terrestrial Ecology Program under ABoVE project 14-TE14-0012.

References

Hauck, C., 2013, New Concepts in Geophysical Surveying and Data Interpretation for Permafrost Terrain: *Permafrost and Periglacial Processes.*

Kass, M.A., Irons, T.P., Minsley, B.J., Pastick, N.J., Brown, D.R.N., and Wylie, B.K., 2017, In situ nuclear magnetic resonance response of permafrost and active layer soil in boreal and tundra ecosystems: *The Cryosphere*, v. 11, no. 6, p. 2943–2955.

Minsley, B.J., Abraham, J.D., Smith, B.D., Cannia, J.C., Voss, C.I., Jorgenson, M.T., Walvoord, M.A., Wylie, B.K., Anderson, L., Ball, L.B., Deszcz-Pan, M., Wellman, T.P., and Ager, T.A., 2012, Airborne electromagnetic imaging of discontinuous permafrost: *Geophysical Research Letters*, v. 39, p. L02503.

Minsley, B.J., Emond, A., and Rey, D.M., 2017, Airborne electromagnetic and magnetic survey data, Western Yukon Flats, Alaska, February 2016:

Minsley, B.J., Pastick, N.J., Wylie, B.K., Brown, D.R.N., and Andy Kass, M., 2016, Evidence for nonuniform permafrost degradation after fire in boreal landscapes: *Journal of Geophysical Research: Earth Surface*,, p. 2015JF003781.

Ice and liquid water saturations jointly inverted from electrical and refraction seismic datasets in mountain permafrost

Coline Mollaret[1]
Florian Wagner[2]
Christin Hilbich[1]
Christian Hauck[1]

[1]*Departement of Geosciences, University of Fribourg, Switzerland, coline.mollaret@unifr.ch*
[2]*Departement of Geophysics, University of Bonn, Germany*

Abstract

The non-uniqueness and limited resolution of inverse problems may result in misinterpreted inversion solutions. The improvement of the inversion and its quality check are consequently a basic and crucial step in geophysical data processing. Electrical resistivity tomography (ERT) and refraction seismic tomography (RST) bring complementary information regarding the water and ice contents in permafrost areas, as elastic and electric properties are markedly different for ice, water and air. We believe that a joint inversion of ERT and RST can help significantly to reduce the uncertainties and will improve the interpretability of the subsurface model. In this contribution, liquid water, ice and air saturations are jointly inverted for a synthetic soil model to validate the approach, as well as for ice-poor and ice-rich (rock glacier) mountain permafrost sites.

Keywords: geophysics; joint inversion; mountain permafrost; ERT; refraction seismic.

Introduction

Electrical Resistivity Tomography (ERT) is one of the most commonly used geophysical methods for permafrost monitoring (Hauck & Kneisel, 2008). Ice can be indeed well distinguished from liquid water due to its different electrical properties. However, this method has also limitations as it requires to solve an inverse problem which is usually under-determined and has no unique solution. To reduce the uncertainties and improve the interpretability of the inversion model, geophysical methods are usually combined with ground truth measurements or other geophysical methods.

Moreover, ice and air are both characterized by very high electrical resistivity and are consequently hard to distinguish using ERT alone. Ice can, however, be well distinguished from air from their P-wave velocity properties (3500 m/s vs 330 m/s). Hilbich (2010) showed how refraction seismic monitoring alone can successfully characterize ground ice gain and loss. This is why Refraction Seismic Tomography (RST) is an optimal second geophysical method to be combined with ERT to assess ice or liquid water content and their respective spatio-temporal variabilities.

Method

Joint inversion

To fully exploit two geophysical datasets to improve the reliability of the results, several possibilities to combine the independent datasets have been successfully achieved. Hellman *et al.* (2017) described to what extent two pairs of datasets can be coupled: (i) joint interpretation of two datasets, (ii) one common parameter (water saturation, porosity, etc) can be jointly inverted from two separate datasets and (iii) joint inversion, where each dataset constrains the other one. In this contribution, we jointly invert for the liquid water, ice and air saturations using petrophysical relationships.

Petrophysical relationships

A petrophysical joint inversion for the liquid water, ice and air saturations is applied using the general framework for joint inversions provided in pyGIMLI (Rücker *et al.*, 2017). The saturation models are constrained between 0 and 1. The porosity is an unknown parameter, which need to be computed as well or prescribed. In the first instance, several porosity models (homogeneous soil and porosity model derived from boreholes information) are applied.

The commonly used Archie's law (Archie, 1942) links the electrical resistivity to the water saturation.

A combination of the equations by Wyllie *et al.* (1956) and Timur (1968) links the P-wave velocities with the air, water and ice contents.

Datasets

In a first step, we apply the joint inversion scheme to synthetic datasets, representing different soil types (low/high porosity, low/high ice content), to validate the general applicability of our approach.

In a second step, the saturations are jointly inverted from field data which span a large range of conditions from ice-rich permafrost (rock glacier) to ice-poor permafrost sites.

Discussion

Comparison with other water estimates

The results are then discussed and compared with complementary approaches such as the 4-phase-model (4PM) approach (Hauck *et al.*, 2011), which uses individual ERT and RST inversions and petrophysical relationships to estimate ice, water and air contents. Finally, the sensitivities of the different parameters are analyzed.

Comparison with ground truth

Several field sites are equipped with boreholes where temperature data are available. Calculated water and ice content are discussed in relation with the active layer thickness and temperature dataset.

Conclusion

Permanently frozen soils are a very sensitive climate indicator in mountain terrains. Commonly, only soil temperatures are monitored in permafrost research. Indirect geophysical methods are applied to cover a 2nd or 3rd dimension. Jointly interpreting two distinct geophysical datasets is a common procedure for a better ground characterization. Here, we jointly invert the ice and water saturations from two geophysical datasets to reduce the uncertainties and improve the interpretability of the subsurface. We particularly focus on the individual importance of the parameters on the results and potential improvement of the joint inversion results compared with standard individual inversions.

References

Archie, G. E., 1942. The electrical resistivity log as an aid in determining some reservoir characteristics. *Petrol. Trans. Am. Inst. Min. Metallur. Eng.* 146, 54–62.

Hauck, C., & Kneisel, C., 2008. *Applied Geophysics in Periglacial Environment.* Cambridge: Cambridge University Press.

Hauck, C., Böttcher, M., & Maurer, H., 2011. A new model for estimating subsurface ice content based on combined electrical and seismic datasets. *Cryosphere,* 5, 453–468.

Hellman, K., Ronczka, M., Günther, T., Wennermark, M., Rücker, C., & Dahlin, T., 2017. Structurally coupled inversion of ERT and refraction seismic data combined with cluster-based model integration. *Journal of Applied Geophysics*, *143*, 169-181.

Hilbich, C., 2010. Time-lapse refraction seismic tomography for the detection of ground ice degradation, *The Cryosphere*, 4, 243–259.

Rücker, C., Günther, T. & Wagner, F.M., 2017. pyGIMLi: An open-source library for modelling and inversion in geophysics. *Computers and Geosciences*, 109, 106-123.

Timur, A., 1968. Velocity of compressional waves in porous media at permafrost temperatures. *Geophysics* 33, 584–595.

Wyllie, M. R., Gregory, A. R., & Gardner, G. H. F., 1956. An experimental investigation of factors affecting elastic wave velocities in porous media, *Geophysics*, 23(3), 459–493.

Overcoming data scarcity of active layer thicknesses using geophysics

Albane Saintenoy[1], Eric Pohl[2], Christophe Grenier[2], Antoine Séjourné[1], Ivan Khristoforov[3], Pavel Konstantinov[3], Kencheeri Danilov[3], Kirill Bazhin[3], Alexander Fedorov[3]

[1]*GEOPS/IPSL, UMR 8148 UPS-CRNS Univ. Paris Saclay, albane.saintenoy@u-psud.fr*

[2]*LSCE/IPSL, UMR8212 CEA/CNRS/UVSQ Univ. Paris-Saclay*

[3]*Melnikov Permafrost Institute, Siberian Branch, Russian Academy of Sciences*

Abstract

The thermal imprint of a typical river in the continuous permafrost of Central Yakutia (Siberia, Russia) is studied by active layer thickness measurements along six cross sections, either directly or with geophysical methods. Ground-Penetrating Radar (GPR) and Electrical Resistivity Tomography (ERT) measurements provide permafrost depths comparable to direct measurements acquired in boreholes and pits when available. Geophysical data interpretations complement non-instrumented cross-sections and show that the unfrozen/frozen interface is deeper below the riverbed for all studied cross sections and depends on the local river width. GPR data provide depths of 1 to 2 m with a sampling step as small as 5 cm when the riverbed width is less than 8 m. Where riverbeds are wider, ERT data are more adapted than GPR in imaging the unfrozen layer. ERT data indicates a permafrost boundary as deep as 6 m for the wide river cases, compared to less than 2 m for the narrower ones. The geophysical data enabled us to reveal an exceptional spatial variability in active layer depths that could not be attributed with *in situ* measurements before.

Keywords: Ground-Penetrating Radar; Electrical Resistivity Tomography; Active Layer; River Influence.

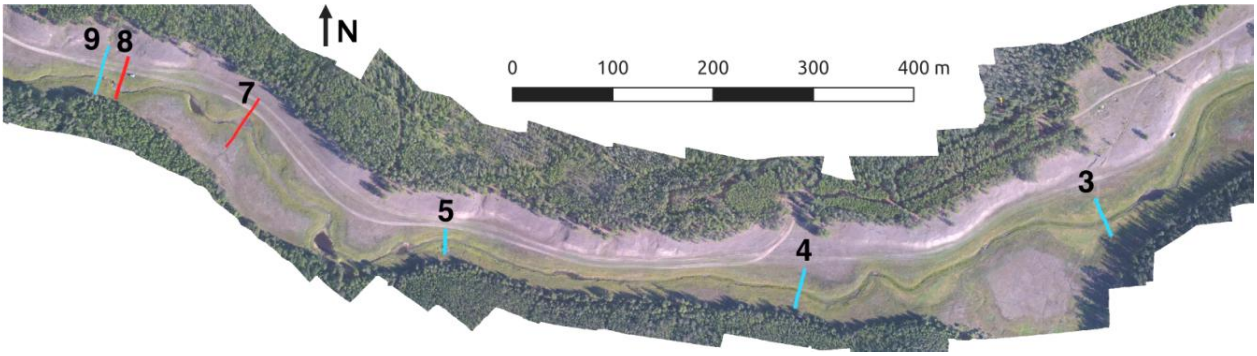

Figure 1 : Positions of the six studied cross-sections (CS3, CS4, CS5, CS7, CS8 and CS9) along a river close to Syrdakh (Central Yakutia). Blue (red) lines are CS with a river width of less (more) than 8 m.

Introduction

Typical landscape features in Yakutia are small rivers that connect thermokarstic lakes within Alas valleys. Due to latent heat effects, rivers create a warmer soil below the riverbed compared to the surroundings. They influence the thermal equilibrium of the soil and the depth to permafrost in their vicinity. Here, we focus on a small river in a valley 100-km East of Yakutsk, close to Syrdakh village. The river is flowing from E to W, resulting in a S-facing right bank and a N-facing left bank, the latter largely covered with forest. The river width varies along its course from 2.5 m up to 15 m when the river forms larger water pools (Fig. 1). In September 2017, exceptional conditions occurred because of two consecutive very dry years. The river had mainly dried out and facilitated access to the riverbed allowed us to apply Ground-Penetrating Radar (GPR) and Electrical Resistivity Tomography (ERT) in order to measure detailed permafrost depth variations in 6 cross sections along the river (Fig. 1). Recently, Léger *et al.* (2017) successfully combined these two techniques to quantify the active layer depths in Arctic soil.

Geophysical data

GPR data were acquired using the Russian OKO system using two sets of antennas with nominal frequencies of 250 and 150 MHz. Measurements were acquired while walking at a constant speed, taking marks every 1 or 2 m. Traces were evenly interpolated every 5 cm in between each marks. The parameter settings of the GPR measurements were adjusted depending on the antenna size, using a time window from 100 ns down to 300 ns.

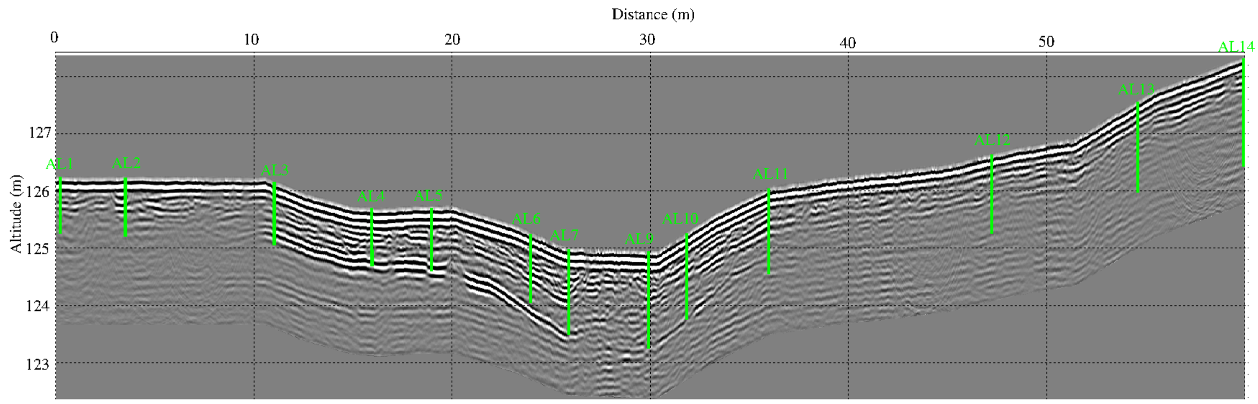

Figure 2 : GPR profile (250 MHz) acquired on CS9 from S to N. Green bars localize boreholes with permafrost depths.

One cross-section, CS9, is intensively equipped with 11 piezometers and 14 boreholes down to the permafrost as described in Pohl *et al.* (companion submission). These measurements were used to calibrate geophysical data (Fig. 2). In addition, four pits were dug after GPR data were acquired over a test profile (not shown here). Diffraction hyperbolas analysis and adjusting depth measured *in situ* of the unfrozen/frozen interface with reflection arrival time observed on radargrams, give an estimated electromagnetic wave velocity of 0.052 m/ns. All radargrams were migrated using Stolt's method (1978) using this velocity.

ERT data were acquired along CS7 and CS9 using a 16-channel instrument SibER-64 system (made in Novosibirsk) with 64 electrodes and a 0.5-m spacing between electrodes, using Schlumberger and gradient protocols. Data were inverted using three different softwares (Res2Dinv, ZondRes2D and BERT).

Results

Permafrost depths are estimated from GPR data and ERT data acquired in September 2017 (Fig. 3). All permafrost depths estimated from geophysical data are in reasonable ranges compared with those estimated from boreholes. The influence of the river on these depths is visible on all CS. GPR data suggest that for river channels narrower than 8 m, permafrost below the river is at least 0.5 m deeper than 10 m away. Insolation differences between right and left bank are also visible at some CS (*e.g.* CS3 and CS9), which are not completely shadowed by the forest (*e.g.* CS5). When the riverbed is wider than 8 m, electromagnetic loss is too strong for clearly resolving permafrost depth below the river with GPR data. ERT data acquired on CS7 show a high conductivity zone as deep as 6 m below the river (Fig. 3). Even though the limits of this zone are subject to some uncertainty and depend on the inversion software, ERT provides first order estimates where GPR cannot resolve the permafrost interface.

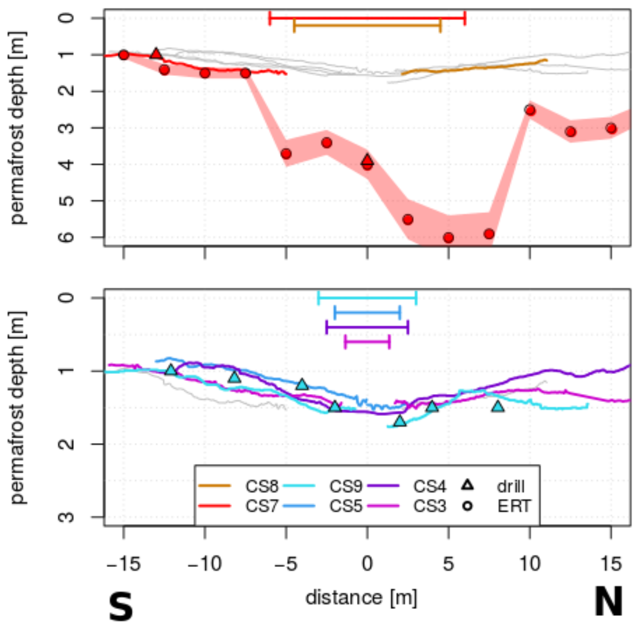

Figure 3 : Summary of permafrost depths from boreholes, GPR and ERT profiles (bottom: narrower riverbed, top: larger riverbed). River widths are provided on top of each graphics.

Acknowledgments

We gratefully acknowledge funding from Univ. Paris-Saclay SPU Carbon Fate Emerging Project, Labex-IPSL and RFBR grants N°16-31-60082-mol-a-dk. We thank E. Léger for BERT inversions.

References

Léger, E. *et al.*, 2017. Quantification of Arctic Soil and Permafrost Properties Using GPR and ERT Datasets. *IEEE Journal of Selected Topics in Applied Earth Observations and Remote Sensing* 10: 1-5.

Stolt, R., 1978. Migration by Fourier Transforms. *Geophysics* 43: 23-48.

Permafrost mapping within Pechora-river delta (European North) with seismic and ground penetrating radar

Marat Sadurtdinov[1]
Andrei Tsarev[2]
Andrei Skvortsov[3]
Maria Sudakova[4]
Galina Malkova[5]

[1]*Earth Cryosphere Institute SB RAS, Tyumen, mr_sadurtdinov@mail.ru*
[2]*Earth Cryosphere Institute SB RAS, Tyumen*
[3]*Earth Cryosphere Institute SB RAS, Tyumen*
[4]*Earth Cryosphere Institute SB RAS, Tyumen, Lomonosov Moscow State University, Moscow*
[5]*Earth Cryosphere Institute SB RAS, Tyumen*

Abstract

In this study we present results of geophysical investigations for permafrost mapping on the site within the delta of Pechora river (European North). For identification of frozen rocks it is necessary to use seismic methods. At the same time with ground penetrating radar (GPR) it is possible to investigate internal structure of geocryological section in details. The main result of our studies is a permafrost distribution map on river bank and near the Kashin island (CALM R24A-1 area).

Keywords: GPR, geophysics, permafrost, monitoring, active layer.

Introduction

The delta of the Pechora river mainly consists of unfrozen rocks. Only in some of it parts and on the coastal islands there are small areas of discontinuous permafrost. In this region, scientists from the Earth Cryosphere Institute of the SB RAS conducts geocryological studies on the Kashin and Kumzha islands included in the CALM program.

Since 2011 geophysical investigations is being carried out in these areas as well as engineering and geocryological studies. Geophysical investigations include seismic, electromagnetic and GPR research. The goal of geophysical studies is permafrost mapping and detection of permafrost features.

Methods

In the process of research, general principles for the integration of seismic and GPR methods have been developed. Seismic methods are considered as reference, especially in the absence or lack of drilling data. They provide a reliable geological interpretation and depth of reflective and refractive boundaries. GPR field research is relative simple and can significantly increase the amount of received information, and provide imaging of thin layers and fine features of permafrost. We used seismic refraction and reflecrion methods and GPR profiling.

Results

On the Kashin site investigations was carried out on land and in the coastal part of the water area at a distance of 300 m from the coastline. It was found that at high elevations of the island within undisturbed areas permafrost lies directly under active layer at depths from 1 to 1.5 m, and in places of eluvial sand bodies permafrost table dives down to 6 m depth.

There is no permafrost in the low peat areas. On the beach of the southern and most parts of the north-west coast, permafrost is absent as well. Here permafrost thin out in the middle part of shore slope. In the middle part of the north-western coast of Kashin island there is a permafrost area more than 550 m length and 200 m width (Fig. 1). At with area permafrost table depth is from 6 m at the island bank to 11-12 m in water at 200 m distance from shoreline. The permafrost thickness within the island by seismic and electromagnetic data is 30-35 m. According to geophysical data, a map of permafrost distribution in this area was constructed (Fig. 1).

At the Kumzha site, the permafrost table depth is from 2 to 9 m. This is partly due to a strong technogenic change in landscape conditions. At such depths, the determination of the permafrost table position is impossible with the metal probe and labor-consuming with the drilling.

In this situation, permafrost imaging and detection of permafrost features was made with using of seismic methods and GPR. Within the site at the CALM site GPR monitoring surveys were made in 2015-2017, which recorded significant active layer depth changes.

Conclusion

The results of geophysical studies in these areas made it possible to obtain a large amount of data on the features of permafrost in the area of discontinuous permafrost distribution.

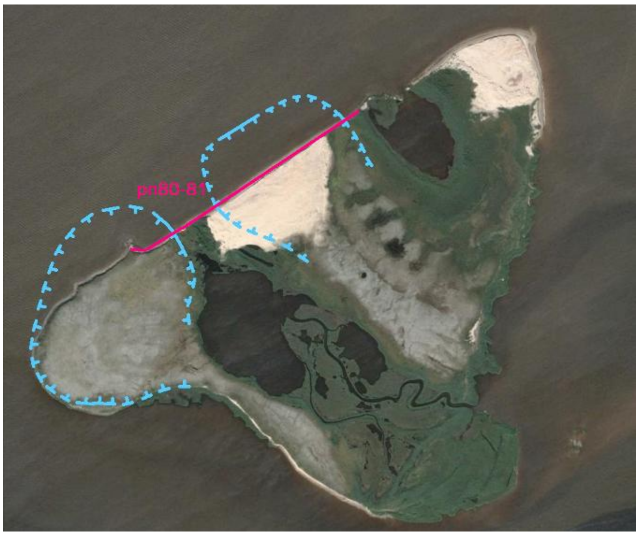

Fig. 1. Permafrost distribution (light blue line) map at Kashin island (Pechora river delta, European North, Russian Federation).

Acknowledgments

This work was supported by the international projects CALM and TSP, RSF grant 16-07-00102.

One decade of permafrost monitoring at the Zugspitze (Germany/Austria)

Tanja Schröder[1]
Michael Krautblatter[1]
[1] *Technical University of Munich, Chair of Landslide Research, Tanja.Schroeder@tum.de*

Abstract

Mechanical and thermal properties of frozen rock slopes hence permafrost degradation determine its stability and impose an increasing risk on people and infrastructure in high mountain regions. Electrical resistivity tomography (ERT) became the dominating tool for temporal and spatial permafrost monitoring. Here we present results from one decade of ERT-based permafrost monitoring at the Zugspitze. We hypothesize a link between seasonal and long-term climate variability and permafrost temperature development and its spatial variability. External climate forcings affect permafrost rock temperatures with a signal propagation time of ca. 2 - 6 months. Short term influences through cleft and pore water via convective heat transport cause abrupt local changes of the temperature regime.

Keywords: Permafrost rock walls; geophysical monitoring; electrical resistivity tomography (ERT); rock slope failure.

Introduction

Degradation of alpine permafrost due to changed thermal and mechanical properties of rock and ice are key process trigger for rock slope instabilities in high mountain areas (Krautblatter *et al.*, 2013), imposing a significant risk on people and infrastructure instalments.

Geoelectric measurements, such as electrical resistivity tomography (ERT) provide a simple and detailed inside into the spatial - temporal variability of permafrost occurrence in high mountain regions. Electric resistivity of frozen rock is highly temperature sensitive and can differentiate between frozen and unfrozen conditions (Krautblatter *et al.*, 2013; Keuschnig *et al.*, 2017). Here we present results from one decade of ERT-based permafrost monitoring at the Zugspitze, assessing monthly spatial variations of permafrost distribution and quantitative information on frozen rock temperature.

Study Area

The Zugspitze, Germany's highest mountain (summit: 2962 m asl.) is located at the German-Austrian border. Geologically it is part of the Northern Calcareous Alps, built up by 800 m of decameter bedded Triassic limestone, dipping NW-ENE at the north face (Miller, 1961; Krautblatter *et al.*, 2010; Ulrich & King, 1993). According to Ulrich & King (1993) permafrost is present above 2500 m asl. Borehole temperature data below the Zugspitze summit indicate permafrost temperatures between -2 °C and -4 °C (LfU 2017). Meteorological data recorded at the summit DWD station monitor a warming trend of MAAT (mean annual air temperature) since the late 1980s (Krautblatter *et al.*, 2010).

Methods

ERT-measurement are conducted in the Kammstollen along the north face. Three electrode arrays are used for optimal spatial resolution: Wenner configuration with 61 electrodes (a = 4.6 m) along the main gallery, two Wenner-Schlummberger arrays with 41 electrodes each (a = 1.53 m) perpendicular thereto in the side gallery, resulting in ~1100 data points (Krautblatter *et al.*, 2010). First measurements were carried out from February to September 2007, since 2014 a continuous monthly monitoring is executed. Data acquisition is conducted using the ABEM Terrameter SAS1000 or LS device. ERT-inversion is accomplished using the 2-D smoothness-constraint inversion algorithm CRTomo by Kemna (2000) (Krautblatter *et al.*, 2010). ERT-temperatures are based on laboratory calibration of electric resistivities to rock temperature for Wetterstein limestone by Krautblatter *et al.* (2010).

First results & interpretation

Along the side gallery a high-resistivity body appears between 50 – 150 m and from 240 – 276 m, reaching resistivity values $\geq 10^{4.5}$ Ωm (≅ –0.5 °C), indicating frozen rock displaying a core section with resistivities $\geq 10^{4.7}$ Ωm (≅ –2 °C) (Fig. 1) (Krautblatter *et al.*, 2010). Seasonal variability is seen by laterally aggrading and degrading marginal sections (Krautblatter *et al.*, 2010). The "permafrost lens", defined as the perennial $>10^{4.5}$ Ωm rock body, shows an areal alternation between ~1,500 to >3,000 m². Highly fractured zones allow the breakthrough of water passage in the core section from summer forward accounting for warming of the adjacent rock mass.

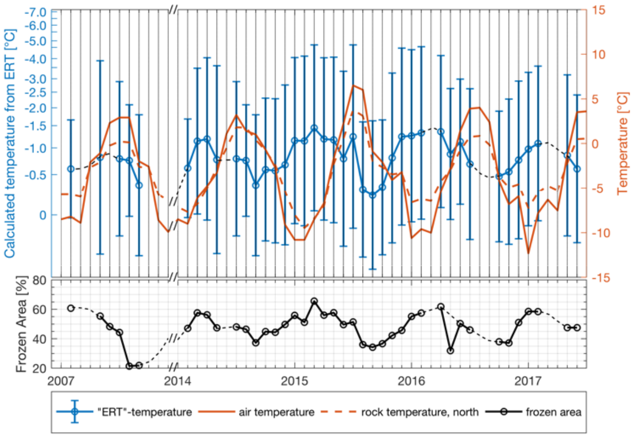

Figure 2: Calculated temperatures from ERT-measurements (mean value, standard deviation), combined with air temperature and north face rock temperatures, as well as relative frozen area. Missing values due to data acquisition errors. Dashed lines are interpolated values.

Calculated temperatures from ERT-data show a phase shift of ~2 (past T_{max}) to ~6 month (past $T_{0°C}$) in comparison to measured air temperatures (Fig. 2). This time span equates the time needed by the climate signal to propagate through the rock wall via convective energy transport resulting in recession and readvance of the zero-curtain in rock (Krautblatter *et al.*, 2010). Further quantitative analysis linking ERT and climate parameters to be executed.

Acknowledgments

Special thanks to the Bayerische Zugspitzbahn AG and the Bayerisches Landesamt fuer Umwelt (LFU) for their friendly support. Biggests thanks to Riccardo Scandroglio, Max Wittmann, Verena Stammberger, Christoph Körner and Saskia Eppinger for being a major important part of data acquisition in the field.

References

Kemna, A., 2000. Tomographic inversion of complex resistivity – Theory and application. Ph.D. thesis, Ruhr-Univ., Bochum, Germany.

Keuschnig, M., Krautblatter, M., Hartmeyer, I., Fuss, C. & Schrott, L., 2017. Automated Electrical Resistivity Tomography Testing for Early Warning in Unstable Permafrost Rock Walls Around Alpine Infrastructure. *Permafrost Periglac. Proc.* 28: 158-171.

Krautblatter, M., Verleysdonk, S., Flores-Orozco, A. & Kemna, A., 2010. Temperature-calibrated imaging of seasonal changes in permafrost rock walls by quantitative electrical resistivity tomography (Zugspitze, German/Austrian Alps). *J. Geophys. Res.* 115: F02003.

Krautblatter, M., Funk, D. & Günzel, F.K., 2013. Why permafrost rocks become unstable: a rock-ice-mechanical model in time and space. *Earth Surf. Proc. & Landforms* 38: 876-887.

LfU, 2017. https://www.lfu.bayern.de/geologie/permafrost/zugspitze/doc/temperaturentwicklung.pdf

Miller, H., 1961. Der Bau des westlichen Wettersteingebirges. *Z. Dtsch. Geol. Ges.* 113, 409-425.

Ulrich, R. & King, L., 1993. Influence of mountain permafrost on construction in the Zugspitze mountains, Bavarian Alps, Germany. *6th Int. Conf. on Permafrost, Chinese Soc. Glaciol. & Geocryl.,* Beijing.

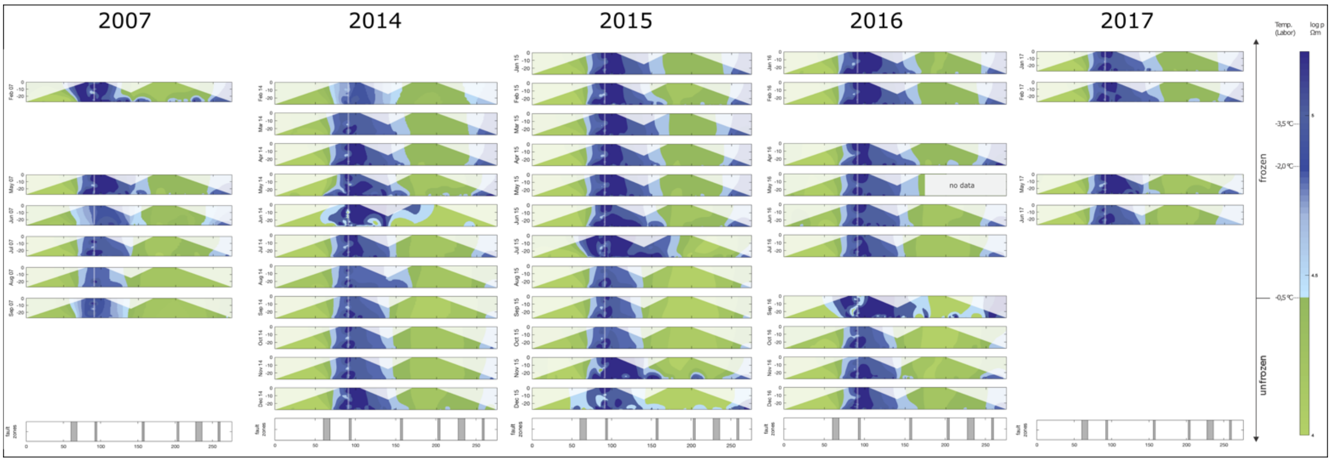

Figure 1: Monthly ERT-results from 2007 & 2014 - 2017. Shaded areas indicate extrapolated values. Last bar shows fracture zones with joint apertures > 2 mm (ref.: Krautblatter *et al.* 2010)

CHAMONIX Mont-Blanc 23 June - 1st July 2018 EUCOP5

3D refraction seismic tomography investigations in alpine permafrost at Hoher Sonnblick (Austria)

Matthias Steiner[1]
Theresa Maierhofer[1]
Werner Chwatal[1,2]
Georg Heinrich[3]
Stefan Pfeiler[4]
Adrian Flores-Orozco[1]

[1]*TU-Wien, Department of Geodesy and Geoinformation, Research Group Geophysics, Vienna, Austria, matthias.steiner@geo.tuwien.ac.at*
[2]*Pöyry-Infra GmbH, Salzburg, Austria*
[3]*University of Graz, Department of Geography and Regional Science, Graz, Austria*
[4]*Geological Survey of Austria, Department of Geophysics, Vienna, Austria*

Abstract

Between 2015 and 2017, different geophysical methods have been applied at the summit of Hoher Sonnblick, Austria, to characterize temporal and spatial variations of the active layer thickness. Here, we present the results obtained from Refraction Seismic Tomography (RST) for data collected using a 3D survey layout including borehole geophones. For the inversion of the RST dataset, an initial model was constructed based on structural information obtained from complementary geophysical methods and borehole temperature measurements, which permitted to reduce the uncertainty in the inversion. The results reveal changes in the seismic P-wave velocity related to variations in the porosity due to unfrozen and frozen rocks. Our results show that the active layer depth varies between 2 and 6 m, which is consistent to previous observations at the study area. Yet our results present the first 3D model with enhanced resolution of the active layer geometry over the entire summit area.

Keywords: refraction seismic; 3D tomography

Introduction

The Sonnblick Observatory at the summit of Hoher Sonnblick (3106 m.a.s.l.) facilitates research activities in various fields, including atmospheric and cryospheric studies. To permit an improved characterization of permafrost processes, such as spatial and temporal variations of the active layer thickness, different geophysical campaigns have been conducted.

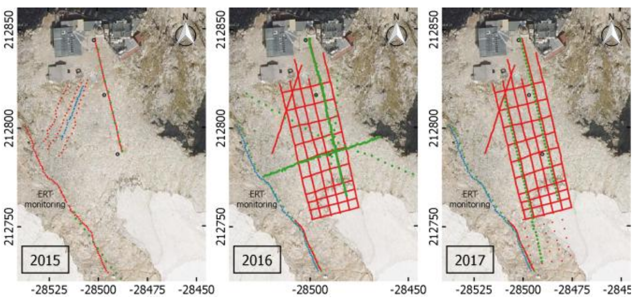

Figure 1. Orientation of the profiles for RST (green), GPR/EMI (red) and IP (blue) measurements. Black circles indicate the positions of the boreholes.

Such campaigns aim at gaining information of different physical properties by means of different methods to improve the quantitative interpretation of the inversion results. In particular, surveys have consisted of: Refraction Seismic Tomography (RST), Ground Penetrating Radar (GPR), Electromagnetic Induction (EMI), Induced Polarization (IP), and Transient Electromagnetic (TEM). Furthermore, monitoring Electrical Resistivity Tomography (ERT) datasets are collected on a daily-basis in a permanently installed profile (see Fig. 1).

Table 1. Campaigns conducted since August 2015.

	15			16					17		
	08	06	07	08	09	11	05	06	07	09	10
RST	X			X			X			X	
GPR	X	X	X	X	X	X	X			X	
EMI	X	X		X	X	X	X				
SIP	X		X		X	X	X	X	X	X	X
TEM							X			X	

Field work

Starting in August 2015, eleven campaigns have been conducted, each with a particular focus on a given objective and geophysical methods (Table 1). Measurements in 2015 permitted to define the best protocols and settings to collect data with enhanced resolution and signal-to-noise ratio (SNR). The recollection of data with such settings in 2016 and 2017 aimed at the characterization of the active layer with high spatial resolution for the entire summit (Fig. 1).

3D Refraction Seismic Tomography

Seismic methods permit to solve variations in the velocity of seismic waves, typically related to lithological interfaces. In particular, the contrasting P-wave velocities (V_p) for frozen and unfrozen materials allow the quantification of the active-layer (Draebing, 2016).

In 2016, a 3D seismic survey was conducted deploying 41 surface geophones (4 m separation; two perpendicular lines) together with 15 geophones placed at depths of 1, 2, 5, 10 and 20 m in three boreholes (Fig. 2). First break travel time picks were inverted using the algorithm by Hole (1992) and the commercial software Rayfract. To improve the results from the seismic tomography structural information obtained from GPR and EMI imaging results was used to refine the initial model for the inversion. Uncertainty in the inversion of the seismic data was quantified by statistical analysis of the inversion results obtained using an ensemble of different initial models.

Results

The obtained seismic P-wave velocities (V_p) presented in (Fig. 3) show a near-surface layer characterized by low V_p velocities (< 2000 m/s), which corresponds to unconsolidated and unfrozen rocks. The interface between the active layer and the permafrost layer is defined initially by post-processed and error-corrected borehole temperature data (Heinrich, 2017) which corresponds to seismic velocities (V_p) of ~ 2800 m/s. The active layer depth varies in a range from 2 to 6 m within the summit area, yet the results in proximity to the boreholes show agreement with previous studies (Schöner *et al.*, 2012). ERT monitoring data further allowed for a validation and an enhanced quantitative interpretation of the RST imaging results.

Acknowledgments

The ATMOperm project is funded by the Austrian Academy of Sciences (ÖAW). We thank the team at the Sonnblick observatory for supporting this project.

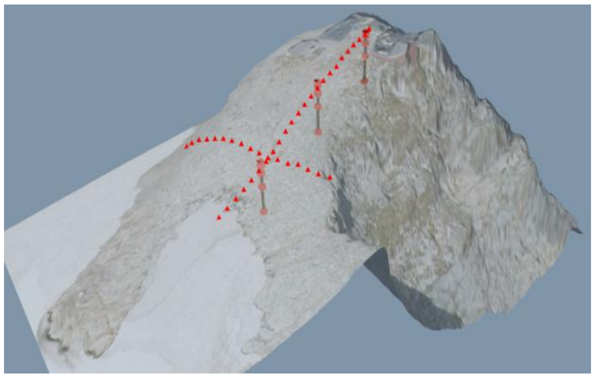

Figure 2. Locations of the 3D RST survey surface (red triangles) and borehole (red cubes) geophones.

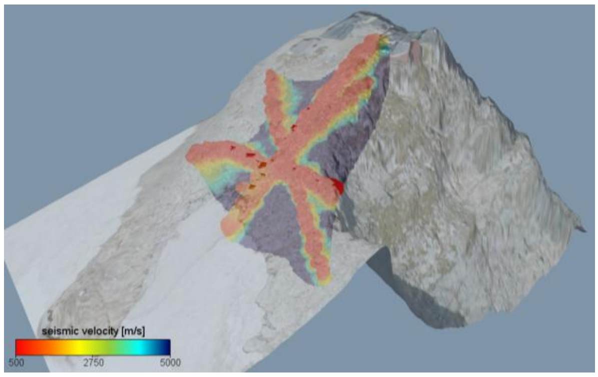

Figure 3. 3D image of seismic P-wave velocities in the summit area obtained from tomographic inversion.

References

Heinrich, G., 2017. *Borehole temperature and active layer variability at Hoher Sonnblick, Austria*. Diploma thesis. Graz: University of Graz, 130 pp.

Hole, J.A., 1992. Nonlinear high-resolution three-dimensional seismic travel time tomography. *Journal of Geophysical Research: Solid Earth*, *97*(B5), pp.6553-6562.

Draebing, D., 2016. Application of refraction seismics in alpine permafrost studies: A review. *Earth-Science Reviews*, *155*, pp.136-152.

Schöner, W., Boeckli, L., Hausmann, H., Otto, J.C., Reisenhofer, S., Riedl, C. and Seren, S., 2012. Spatial patterns of permafrost at Hoher Sonnblick (Austrian Alps)-extensive field-measurements and modelling approaches. *Austrian Journal of Earth Sciences, 105/2,* pp.154-168.

Spectral Induced Polarization Surveys to Infer Ground Ice in a Peatland and a Lithalsa in Warm Permafrost Near Yellowknife, Canada

David E. Stillman[1]
Robert E. Grimm[1]
Stephan Gruber[2]
[1]*Planetary Science Directorate, Southwest Research Institute, Boulder, CO, USA, dstillman@boulder.swri.edu*
[2]*Carleton University, Ottawa, Canada*

Abstract

Quasi-static ("DC") electrical resistivity measurements are commonly applied to infer ground-ice content in permafrost. This has, however, considerable ambiguity because dry and frozen materials have similar signatures. By contrast, Spectral Induced Polarization (SIP) has been demonstrated to detect ice in the lab and in relatively controlled field settings. This study applied SIP in warm permafrost with the aim to infer subsurface ice content. The tomographic SIP profiles show an ice signature at depth. This signature has clear differences from the results obtained by quasi-static electrical resistivity alone. Analysis of drill cores will provide further support for interpretation. We hope that this and further testing of SIP in field experiments will establish a better understanding of the opportunities that this method may offer as well as the practical limitations that it will have.

Keywords: Spectral induced polarization, geophysics, ice content, lithalsa, peatland, dielectric characteristics

Introduction

Geophysical methods have the potential to fill a critical gap by providing spatial context or by replacing studies requiring core sampling (see reviews by Scott *et. al.*, 1990; Hauck, 2013). Their main strength has been to identify frozen vs. unfrozen ground, e.g., delineating the active layer and the base of permafrost. Electrical and electromagnetic methods have been widely applied because the quasi-static ("DC") resistivity of ice is very high compared to soils containing unfrozen water. Unfortunately, both dry materials and totally frozen ice-rich materials have high DC resistivity, so there is substantial ambiguity about ice content.

There is, however, a unique property of frozen ground that heretofore has not been exploited: its electrical polarizability. Ice has a large and diagnostic dielectric relaxation, which is manifested as a decrease in electrical resistivity from ~10^2 to ~10^5 Hz at temperatures near 0ºC. A first field detection of the dielectric relaxation of ice (Grimm & Stillman, 2015) was performed in the Permafrost Tunnel in Fox, AK, USA. Laboratory measurements indicated that ice content was correlated with normalized magnitude of the high/low-frequency resistivity difference, which allowed relating impedance measurements to ice content with an accuracy <20%.

This initial test and success of SIP for permafrost studies took place in an environment with widespread excess ice and temperatures around -3ºC. Its applicability to permafrost with lower and more variable ice content as well as a higher temperature and content of liquid water remains to be fully evaluated. As a first step in this direction, this study investigates two sites in discontinuous permafrost near Yellowknife, aiming to infer patterns of relative subsurface ice content. Ground temperature just below 0ºC, silt/clay soils, and wet subsurface conditions make this a non-trivial test.

Methods and Data

We used the Fuchs SIP III to perform SIP field measurements. The system has 20-kHz bandwidth, high input impedance, transmits signals from the receiver electrodes by fiber-optic cable, and incorporates a remote-reference electrode for noise reduction. SIP field surveys are geometrically identical to classical DC resistivity or Electrical Resistivity Tomography (ERT). The apparent resistivities between each transmitter-receiver pair are converted to true resistivity through standardized inversion procedures (Loke & Barker, 1996; see RES2DINV). We use the images at 10 Hz and 20 kHz to assess ice content via the Resistivity Frequency Effect (RFE), which is the difference between the low- and high-frequency resistivities normalized by the low-frequency value.

Auxiliary temperature and compositional data inform and constrain the SIP results. Temperature measurement near the surface (10 cm) have an accuracy of 0.1 ºC, in the borehole of 0.02ºC. Drilling and recovery of frozen cores of 10 cm diameter was performed in July 2017.

Results

White Truck Peatland (W114.5318° N62.4562°)

The 38 m long profile was measured in a peatland with ~1.2 m of peat overlying glaciolacustrine silt/clay on Nov. 6, 2017. At the time, the peatland was between 0.0°C (near-surface) and -0.6°C (1.15 m) based on three loggers at 10 cm depth and a short thermistor chain.

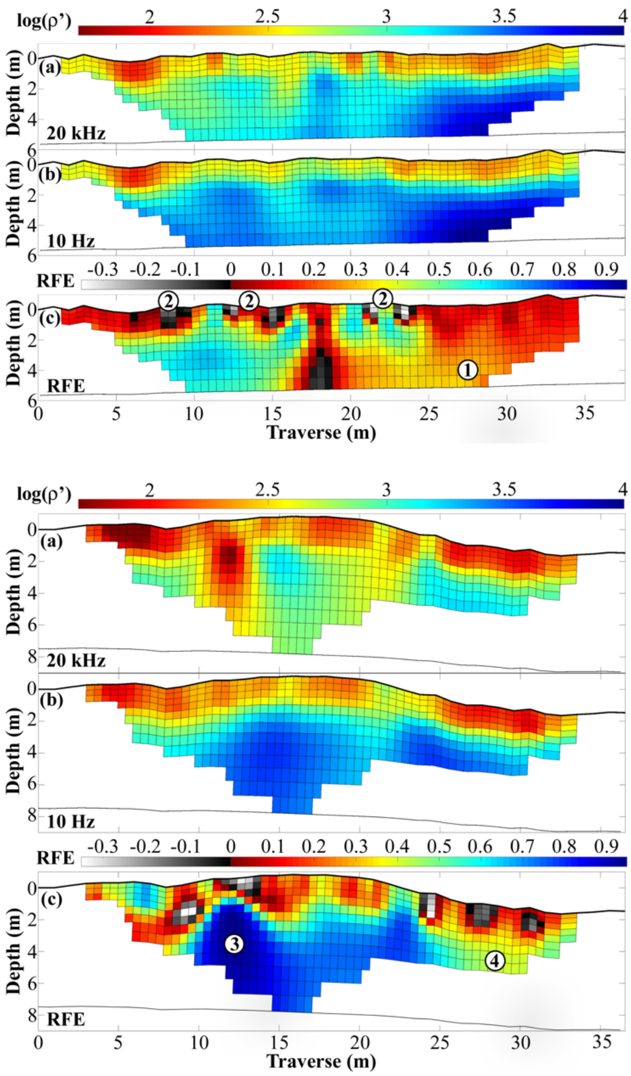

Figure 1: Survey results for the White Truck peatland (top three panels) and for the Birch Syrup lithalsa (bottom three panels).

The partially thawed unfrozen layer ~1 m is highly conductive at both low and high frequencies (Fig. 1). Negative IP artifacts (marked 2) are produced by under-resolving high contrast anomalies in the unfrozen layer. This can likely be corrected in future surveys by adjusting the survey geometry for more uniform coverage.

Below the active layer, high RFE (>0.5) points to the presence of excess ice on the left but not the right part (marked 1) of the profile, which could be misinterpreted as ground ice if only the high resistivity at 10 Hz—analogous to an ERT survey—were used.

Birch Syrup Lithalsa (W114.2768° N62.5071°)

The 36 m long profile was measured on Nov. 8, 2017. The lithalsa material is silt/clay of similar origin as that at the White Truck site. The dry top of the lithalsa (profile start) has tall birch forest and temperatures were between -8.2°C and -5.7°C (3 locations, 10 cm) while the foot (profile end) was in a moist spruce forest with temperatures between -0.0°C and -0.3°C (3 locations, 10 cm).

Beneath the crest of the lithalsa (marked 3) the largest RFE points to high ice content as expected based on drilling results from previous work on similar locations, nearby. Again, the 10 Hz result shows highly resistive ground at depth across the entire section but RFE indicates waning ice content to right (marked 4).

Discussion and Conclusion

SIP at these warm permafrost locations produced results that agree with site knowledge. RFE shows more detail, which is expected to be strongly related to subsurface ice content, than the low-frequency results alone.

Surface and core samples will be analyzed in the lab to derive the constitutive relations for RFE as a function of ice content at these sites. Permafrost with the highest and lowest ice contents inferred from SIP will be targeted for confirmation by drilling.

Acknowledgments

This work was supported by Southwest Research Institute (DES, REG) and by ArcticNET, NSERC and the Canada Foundation for Innovation and ArcticNET (SG).

References

Grimm, R.E., Stillman, D.E., 2015. Field test of detection and characterization of subsurface ice using broadband spectral-induced polarization. *Permafrost and Periglac. Proc.* 26: 28–38.

Hauck, C., 2013. New concepts in geophysical surveying and data interpretation for permafrost terrain. *Permafrost and Periglac. Proc.* 24: 131–137.

Loke, M.H., Barker, R.D., 1996. Practical techniques for 3D resistivity surveys and data inversion. *Geophysical Prospecting* 44: 499–523.

Scott W.J., Sellman P.V., Hunter J.A. 1990. Geophysics in the study of permafrost. In Ward, S.H. (ed.), *Geotech. and Environ. Geophys., Vol 1, Invest. Geophys.*, 5, Soc. Explor. Geophys., Tulsa, pp. 355–384.

Coupled thermo-geophysical inversion for permafrost monitoring

Soňa Tomaškovičová[1]
Thomas Ingeman-Nielsen[2]
[1]*Department of Civil Engineering, Technical University of Denmark, soto@byg.dtu.dk*
[2] *Department of Civil Engineering, Technical University of Denmark*

Abstract

We describe an approach to calibrating the thermal parameters of a ground undergoing cycles of freezing and thawing using exclusively time-lapse geoelectrical measurements collected from the ground surface. The method links a heat conduction model with a ground resistivity model in a fully coupled optimization approach. The data used for model calibration come from a high-latitude permafrost monitoring site in Ilulissat, West Greenland. Parameters calibrated on time-lapse geoelectrical data reproduce the calibration dataset with an accuracy comparable to that of a calibration on borehole temperature data, and reproduce the observed borehole temperatures to within ±0.6 °C. Given the under-determined nature of the inverse problem and the simplicity of the heat model, the parameter values are non-uniquely determined in both calibration approaches. Nevertheless, the method offers the possibility of gaining an outlook of ground thermal conditions over a larger area, at lower cost and with reduced impact on the fragile arctic environment.

Keywords: geoelectrical monitoring, coupled inversion, permafrost, time-lapse ERT, heat transfer

Introduction

Surface geophysical measurements potentially provide an attractive way of informing permafrost (thermal) models. Studies by Hauck et al. (2008) and Krautblatter et al. (2010) demonstrate that there is a quantitative link between electrical and thermal properties of geological materials. However, until now, geophysical data have not been used in a fully coupled optimization scheme to constrain estimations of ground thermal parameters.

We test an approach to calibrating ground thermal properties using surface time-lapse geoelectrical measurements. Electrical properties of the ground depend mainly on the amount of unfrozen water available to conduct the current. This unfrozen water content is temperature-depended, and the temperature at any depth depends on the ground surface temperature and the thermal properties of the ground. A quantitative comparison between ground temperature timeseries and resistivity timeseries over complete freeze (thaw) cycles is expected to support calibration of the petro-physical relationship that can be further exploited for predictions of ground reaction to changes in surface temperature forcing.

Method

The coupled inversion approach is an optimization/inversion algorithm. It aims to estimate soil properties (thermal and electrical) which will, with sufficient accuracy, reproduce observed resistivity timeseries, given a certain surface temperature variation.

The coupled model consists of two, essentially standalone, modules: a heat transfer model and an electrical resistivity model. The 1D heat conduction model calculates the temperature distribution in the subsurface given a set of initial and boundary conditions, forcing ground surface temperatures and thermal parameters. The calculated temperature distribution is translated into a 1D multi-layer geoelectrical model. This is done by dividing the model into many equally spaced layers. For each layer of the resistivity model, the layer-representative temperature is found by interpolating between the nearest grid points of the heat model. For each layer-representative temperature, fractions of water, ice and rock are found using an relation describing unfrozen water content in soils at subfreezing temperatures. The effective bulk soil resistivity for the given model layer is calculated from specific resistivities of the respective ground constituents using a resistivity mixing rule. From the geoelectrical model, the forward apparent resistivity response is calculated by the CR1Dmod program (Ingeman-Nielsen & Baumgartner, 2006) using the same electrode configurations as on the field site. The calculated apparent resistivities are then compared to the field geoelectrical measurements. The difference is minimized by adjusting the thermal parameters of the heat model from which the forward resistivities are calculated. The final heat model calibration is validated by comparing the simulated ground temperature distribution to borehole temperature timeseries from the location of the time-lapse ERT acquisitions.

The fundamental characteristic of our approach is the use of apparent resistivities for calibration, instead of inverted resistivities. The reason for using the apparent resistivities is the expectation that they introduce less additional uncertainty to the calibration in form of inherent inversion assumptions and artifacts. Most importantly, the relationship translating a certain ground electrical composition into apparent resistivity is unique and governed by equations for conservation of charge, Ohm's law and the geometry of the electrode configurations used to collect the resistivity data. As opposed to that, any inverted resistivity model is only one of a number of possible realizations that explain the measured apparent resistivity data acceptably well. The non-unique nature of the inverted resistivity model thus provides a less solid basis for the quantitative calibration of a thermal model.

The modeling and optimization framework is implemented in Matlab, with the heat equation solver implemented in Python.

Field site and data

The data used for model development and validation were collected between September 2012 and October 2015 at a permafrost monitoring site near Ilulissat, West Greenland (69° 14' N, 51° 3' W, 33 m.a.s.l.). The on-site conditions and instrumentation were detailed in Tomaskovicova & Ingeman-Nielsen (2016). We use the freezing season 2014/2015 (September 1st to February 28th) for calibration, and freezing seasons 2012/2013 and 2013/2014 for validation of the model.

Resistivity mixing relationship

A resistivity mixing relationship that correctly translates the ground phase composition into a ground resistivity model is a crucial component of the coupled modeling approach. We evaluate two commonly used mixing relationships against field resistivity data: the geometric mean (Guéguen & Palciauskas, 1994) and the Archie's law (Archie, 1942). We found Archie's law to better reproduce resistivity variations associated with freezing and thawing. Additionally, the coupled model was more sensitive to Archie parameters than to the geometric mean parameters. Consequently, we continue to use the Archie's law in the resistivity model.

Coupled *vs.* thermal modeling

The two modules of the coupled framework were first calibrated/validated individually, before attempting the coupled approach.

The heat model reproduces ground temperature variation with a mean error of 0.55 °C when calibrated on borehole temperature data from the freezing season 2014/2015. The calibrated model predicts temperature variations in two previous freezing seasons 2012/2013 and 2013/2014 within 0.63 °C and 0.32 °C respectively. The heat model calibrated exclusively on time-lapse apparent resistivities showed a similar performance.

The apparent resistivity data constrained calibration of thermal parameters so that the resulting temperature field fits the training dataset within 0.60 °C and the validation datasets within 0.37 °C and 0.30 °C respectively. The uniqueness of parameter determination is not significantly improved by the coupled approach. However, a number of possible improvements in both heat and resistivity modules was identified and may improve model performance when implemented (?).

Thanks to the predictive value of the coupled thermo-geophysical model, we see application of the method in describing permafrost thermal conditions in remote areas where use of traditional geotechnical site investigations would be challenging both logistically and financially.

References

Archie, G. E., 1942. The electrical resistivity log as an aid in determining some reservoir characteristics. In: *Transactions of the AIME* 146.01: 54–62.

Guéguen, Y. and Palciauskas V., 1994. *Introduction to the physics of rocks.* Princeton University Press.

Hauck, C., Bach, M. and Hilbich, C., 2008. A 4-phase model to quantify subsurface ice and water content in permafrost regions based on geophysical datasets. *Proceedings of the Ninth International Conference on permafrost,* Fairbanks, Alaska, June: 675 - 680.

Ingeman-Nielsen, T. and Baumgartner, F., 2006. CR1Dmod: A Matlab program to model 1D complex resistivity effects in electrical and electromagnetic surveys. *Computers and Geosciences* 32(9): 1411 - 1419.

Krautblatter, M., Verleysdonk, S., Flores-Orozco, A. and Kenna, A., 2010. Temperature-calibrated imaging of seasonal changes in permafrost rock walls by quantitative electrical resistivity tomography (Zugspitze, German/Austrian Alps). *Journal of geophysical research: Earth Surface*, 115(F2).

Tomaskovicova, S. & Ingeman-Nielsen, T., 2016. Automated long-term time lapse ERT monitoring of high-latitude permafrost – results of 3 years of monitoring and modeling study. In: *Proceedings of the XI. International Conference on Permafrost:* 990-991.

Magnetic prospecting of ice wedge polygons: the case of Kurungnakh ice complex in Lena delta

Leonid Tsibizov[1,2]
Alina Grigorevskaya[1,2]
Alexey Fage[1,2]

[1]*Novosibirsk state university, tsibizov.lv@gmail.com*
[2]*Trofimuk Institute of Petroleum Geology and Geophysics of Siberian Branch of Russian Academy of Sciences (IPGG SB RAS)*

Abstract

Ice wedges produce negative magnetic anomalies due to their negligible magnetic susceptibility against frozen ground. High-precision magnetic survey allows to efficiently determine ice wedge distribution in permafrost. The case study was conducted on selected objects on the ice complex on Kurungnakh Island in Lena delta. Alongside the magnetic survey a ground penetrating radar was used within some study areas. Obtained results were mapped on the high-resolution aerial imagery and digital elevation model. Observed total magnetic field anomalies come up to 10 nanoteslas and distinctly show a polygonal pattern of the ice complex structure. GPR data generally agrees with magnetic one and also indicates some local features such as wet zones. Polygonal structure in some cases is hardly observable both on aerial photo and in topography due to vegetation inhomogeneity, solifluction or upper layers, which cover the ice wedges.

Keywords: permafrost, ground ice, magnetic survey, magnetometry.

Introduction

Ice wedge polygons play an important role in permafrost landscape change (Liljedahl *et al.*, 2016). Estimation of permafrost ice content requires reliable data on ice-wedge geometry and distribution. Thermoerosion driven by thawing of hidden massive ice wedges (Fortier *et al.*, 2007) can also become a hazard for infrastructure in northern regions.

Geophysical techniques are widely used in ice-wedge polygons mapping and yield a detailed permafrost upper layer structure including ice-wedges (Dafflon *et al.*, 2016; Munroe *et al.*, 2007). Magnetic survey has a great potential in this field due to its features: rapidness, absence of contact with the surface and independence from temperature and salinity of frozen ground. Magnetic anomalies above ice wedges were noted in archaeomagnetic studies (Hodgetts *et al.*, 2011). Nevertheless there has been no systematic research of ice-wedge polygons using this method. In order to proceed on the subject a high-presicion magnetic survey was conducted on selected objects at the ice complex on Kurungnakh Island in Lena delta. The research based on the filed data obtained in 2016-2017 (Tsibizov *et al.*, 2017), some results of data processing were published in the paper (Tsibizov, Rusalimova, 2017).

Methods

Ground based high-precision magnetic survey was conducted using quantum and proton magnetometers at the elevation about 1 m above the surface. Results were enhanced by means of ground penetrating radar technique and sampling on some of the areas. High-resolution aerial imagery (3-5 cm/pix.) and digital elevation model (DEM) constructed using photogrammetry allowed to improve data interpretation.

Results

Polygonal pattern is distinctly observed in anomalous magnetic field on each study area. Results obtained on some of selected objects are shown in Figures 1, 2 and 3.

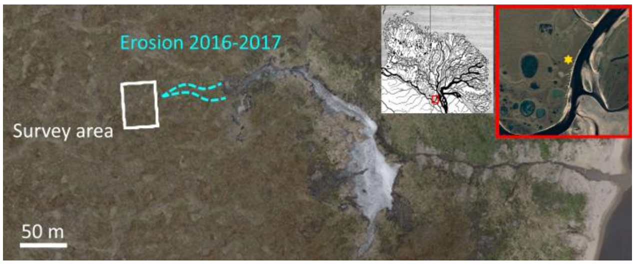

Figure 1. July 2016 aerial photo: blue dotted line marks thermoerosional gully progress since 2016.

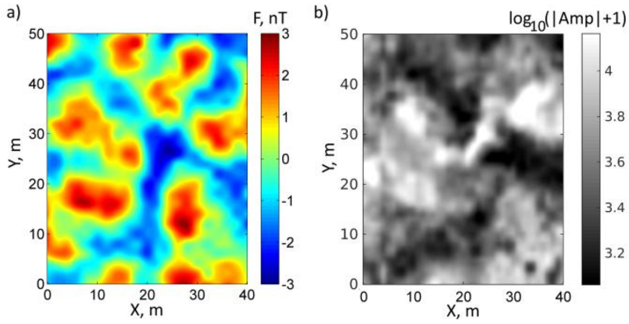

Figure 2. Anomalous total magnetic field at 1 m height (a) and radargram amplitude slice on 4 m depth (b). Negative magnetic anomalies (a) amount up to several nanoteslas and correspond to ice wedges. Thick wedges correspond to low amplitude (b). Wet zone related to degrading permafrost is probably marked by areas with the highest amplitude (b), their location follows the direction of valley propagation.

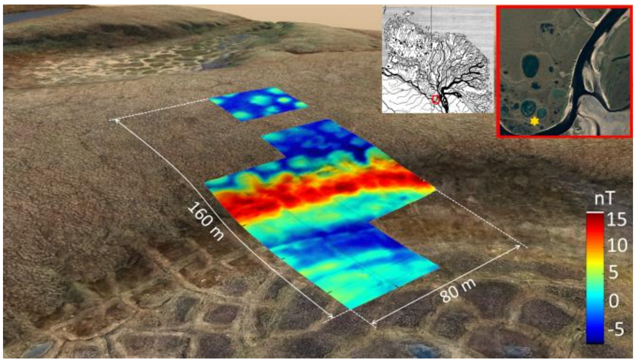

Figure 3. Magnetic anomalies on the alas slope at the elevation 1 m: polygonal pattern of the anomalies is observed on the slope (polygons are not visible on the surface due to solifluction), positive anomaly crossing the slope is presumably linked with sediment accumulation area.

The study found that magnetic survey as rapid and nonimpact method could be widely used in permafrost research for ice wedges mapping and permafrost ice content estimation. It could significantly improve the complex of methods which is conventionally used for such goals. The method has a great potential in tundra conditions: vast wet areas, which make ground-based survey quite difficult, are coupled with absence of trees and smooth relief - supportive environment for UAV-based magnetic systems.

References

Dafflon, B. et al., 2016. Geophysical estimation of shallow permafrost distribution and properties in an ice-wedge polygon-dominated Arctic tundra region. *Geophysics* 81(1): 247-263.

Fortier, D. et al., 2007. Observation of rapid drainage system development by thermal erosion of ice wedges on Bylot Island, Canadian Arctic Archipelago. *Permafrost and Periglacial Processes* 18(3): 229-243.

Hodgetts, L. et al., 2011. Archaeological magnetometry in an Arctic setting: a case study from Maguse Lake, Nunavut. *Journal of Archaeological Sciences* 38: 1754–1762.

Liljedahl, A. K. et al., 2016. Pan-Arctic ice-wedge degradation in warming permafrost and its influence on tundra hydrology. *Nature Geoscience* 9(4): 312-318.

Munroe, J. S. et al., 2007. Application of ground- penetrating radar imagery for three- dimensional visualisation of near- surface structures in ice- rich permafrost, Barrow, Alaska. *Permafrost and Periglacial Processes* 18(4): 309-321.

Tsibizov L. et al., 2017. Integrated non-invasive geophysical-soil studies of permafrost upper layer and aerial high-resolution photography. Russian-German Cooperation: Expeditions to Siberia in 2016, Berichte zur Polar- und Meeresforschung = *Reports on polar and marine research, Bremerhaven, Alfred Wegener Institute for Polar and Marine Research* 709: 56-69.

Tsibizov, L. & Rusalimova, O., 2017. Magnetic imaging of the Kurungnakh Island ice complex upper layer structure, Lena Delta, Russia. *Near Surface Geophysics* 15(5): 527-532.

Wetterich, S. et al., 2008. Palaeoenvironmental dynamics inferred from late Quaternary permafrost deposits on Kurungnakh Island, Lena Delta, northeast Siberia, Russia. *Quaternary Science Reviews* 27: 1523–1540.

Application of 3D interpretation technologies to solving foundation monitoring problems at hydroprojects in permafrost regions

Sergey A. Velikin
Vilyui Permafrost Research Station, Melnikov Permafrost Institute SB RAS, Chernyshevsky, Russia, frozen@mirny.sakha.ru

Abstract

For many permafrost foundation monitoring problems, spatial representation of the temporal changes in geophysical sections is important to monitor the development of natural and human-induced processes in the zones where engineering structures interact with permafrost which is highly sensitive to anthropogenic disturbances. This paper demonstrates the applicability of 3D data processing technologies to permafrost foundation monitoring at dams and other hydroprojects.

Keywords: permafrost; geophysics; electrical resistivity tomography; hydroproject; seepage.

Introduction

The most serious problems for stability of foundations of dams and other hydraulic structures are caused by permafrost degradation. The thawing of permafrost is generally accompanied by changes in physical properties, including electrical properties which are most sensitive to the phase change of ice to water.

Electrical resistivity methods, particularly electrical resistivity tomography (ERT), are therefore most promising for detecting and tracing seepage flows, as well as for mapping permafrost degradation areas (Velikin & Shesternev, 2015).

Background

The applicability of ERT in foundation monitoring is complicated by a number of natural and man-made effects. This is especially true for hydraulic structures where measurements are interfered by numerous sources, such as machinery, power lines, pipelines, and ground freezing pipes, as well as by the dam itself and its reservoir nearby.

Further difficulties to ERT monitoring are caused by field problems at the hydroproject sites, such as possible small relative shifts in the transmitter-receiver array when using access roads and changes in electrical conductivity in the upper part of the resistivity section (the active layer). In order to reduce the effects of these factors, the present author has used a 3D procedure for processing geoelectrical sections obtained from monitoring observations using the COSCAD 3D statistical and spectral correlation analysis software and other computer programs for layer-by-layer interpolation and filtering of input data.

Applications

The spatiotemporal interpolation 3D technologies for processing of geophysical monitoring data, which use their temporal periodicity as an additional coordinate, provide a reliable means to detect early indicators of adverse geocryological processes in the industrial areas where sources of natural and cultural noise are inevitably present (Velikin & Marchenko, 2016).

At the Vuilyui Hydroelectric Power Station, this interpretation technique allowed us to identify resistivity changes caused by seepage in the dam abutment against the background of seasonal variations and water-level changes in the nearby reservoir.

Time-lapse resistivity inversion was applied at the Sytykan Reservoir Scheme to determine seepage direction and rates in the abutment seepage zone. In this method, the initial data set is used to constrain the inversion of the later time data sets so as to minimize changes in the model resistivity values that are unlikely to be due to actual changes. Then, the data obtained were processed using COSCAD 3D (Petrov *et al.,* 2007).

The results of the interpretation revealed an area of increased electrical conductivity. The rate of seepage was determined to be 288 m/hr, much higher than the estimate from previous studies of less than 100 m/hr.

This technique of using the time coordinate for 3D processing has also proven effective for geothermal observations at the hydroprojects where extrapolated temperature sections are used to predict thaw advance in the areas of abutment seepage. Solving this problem is difficult because temperature in boreholes penetrating the seepage zone depends on seepage flow temperature which, in turn, depends on water temperature in the reservoir subject to seasonal variations. This can result in significant error in thaw front extrapolation. With 3D processing it is possible to reveal a general trend in temperature dynamics and to reduce noises due to small shifts of temperature cables, thus making predictions of seepage flow (or thaw front) advancement more reliable.

The 3D technologies are also applicable in open-pit diamond mining to the problem of assessing and predicting the dome location and migration rates of injected brines, helping reduce the measurement noise level (failure or clogging of observation wells, difficulties with level measurements at depths, human error, etc.) and reveal the basic trends.

This technique was used to determine the brine distribution patterns in frozen carbonate rocks at the Oktyabrsky disposal site (Fig. 1), where injection of diamond mine wastes is characterized by dome development near the injection well succeeded by depression after reaching a critical level. The patterns revealed will be useful in optimizing the brine injection regime.

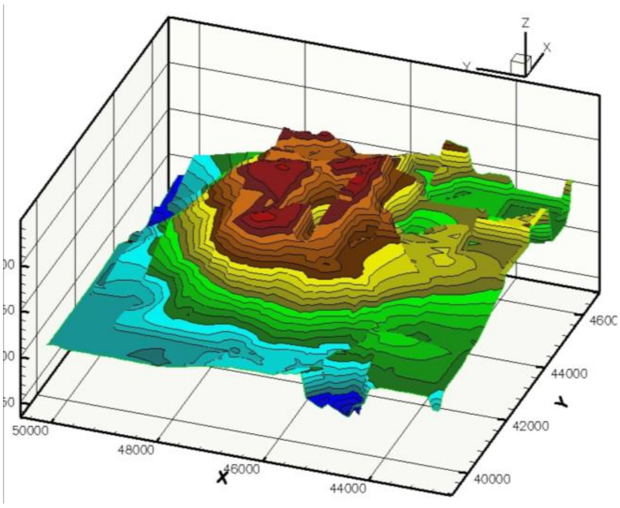

Figure 1. Dome of injected brine, Octyabrsky disposal site.

Conclusion

The spatiotemporal interpolation 3D technologies for processing of geophysical monitoring data, which use their temporal periodicity as an additional coordinate, provide a reliable means to detect early indicators of adverse geocryological processes in the industrial areas where sources of natural and cultural noise are inevitably present.

The interpretation technique has proven especially effective for abutment conditions when measurement units cannot be placed along the dam (across the abutment seepage pathway) and roads along the abutments have to be used.

References

Petrov, A.V., Nikitin, A.A. & Zinovkin, S.V., 2007. Development of statistical techniques for geophysical field processing and interpretation in the COSCAD 3D computer technology. *Geologiya I Razvedka* 7: 68-74.

Velikin, S.A. & Marchenko, Y.L., 2016. Scientific-methodological foundations of geophysical monitoring of hydraulic and mining projects in the Yakutian permafrost region. *Proceedings of the 5th Conference of Russian Geocryologists "Geotechnics in Permafrost"*, Moscow, Russia, June 14-16, vol. 1, part 4: 305-311.

Velikin, S.A. & Shesternev, D.M., 2015. Scientific-methodological basis for geophysical monitoring of hydro- and mining projects on permafrost in the Yakutsk Diamond Province. *Proceedings of the EAGO International Conference and Exhibition, "Engineering, Coal and Mining Geophysics-2015"*, Sochi, Russia, September 28-October 2: 184-196.

ERI surveys of embankment dam with petrophysical aspects of data interpretation

Evgeny Zerkal[1]
Dina Kvon[2]
Igor Modin[3]
Vladimir Shevnin[3]
Aleksey Skobelev[3]
Mikhail Marchenko[3]
[1]*Lomonosov Moscow State University, zerkal.eugene@gmail.com*
[2]*Research Center Geoscan LLC, Moscow*
[3]*Lomonosov Moscow State University*

Abstract

In order to delineate frozen rocks and taliks within the rock embankment dam body, situated on fractured rock foundation in presence of continuous permafrost, the electrical resistivity imaging survey along with water electrical conductivity and temperature measurements were performed. The goal was achieved by applying the advanced petrophysical approach when interpreting the data acquired.

Keywords: electrical resistivity imaging, electropetrophysical modelling, talik, tailing, permafrost.

Introduction

Dams are among the most important development infrastructures in any country, and are used for many different purposes including irrigation, water supply, flood control, electricity production and storage of mine wastes (Vallejo & Mercedes, 2011).

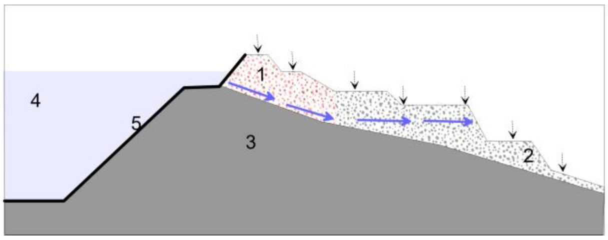

Figure 1. Dam scheme: 1 – thawed rockfill material; 2 – frozen rockfill material; 3 – frozen foundation; 4 – tailing; 5 – damp-proof membrane; black arrows – ERI profiles.

The object of the study is an embankment dam with a rock foundation on fractured andesites and tuffaceous sandstones of continuous permafrost (Figure 1). The dam is composed of coarse-grain material about 20-30 m in thickness.

Taliks and frozen rocks were detected and delineated through geophysical surveys (specifically, electrical resistivity imaging (ERI), water electrical conductivity and temperature measurements).

Petrophysical modelling and statistical analysis

Petrophysical modelling was accomplished by means of PetroWin program (Matveev & Ryzhov, 2006). For thawed rock fill material (Fig. 2) the model was fixed with porosity and temperature, according to core sample analysis and thermometry in surface water seepages and boreholes. Other properties, such as water content and brine conductivity, were varied within the values observed, corresponding to the sample analysis and water electrical conductivity measurements.

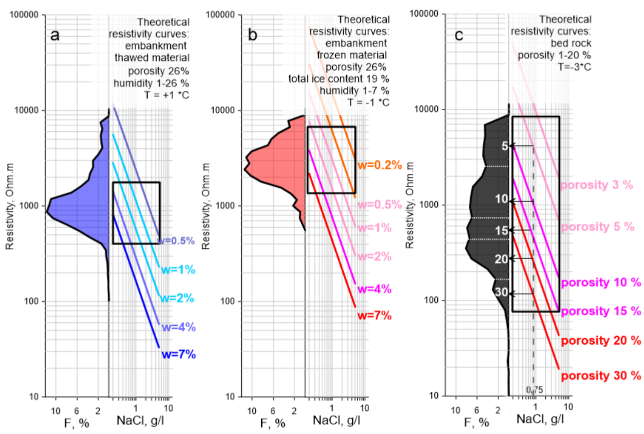

Figure 2. Electrical resistivity histograms combined with petrophysical modelling: a – thawed rockfill material; b – frozen rockfill material; c – foundation (bedrock).

In case of frozen rock fill material (Fig. 2), the model was corrected due to ice occurrence: the initial volumetric porosity was reduced by the total ice content.

In the upper part of the geological cross-section (Fig. 3) the frozen rockfill material is observed along almost all ERI profiles except for the middle part of the profile closest to the tailing where the talik is located and for the bigger part of the lower profile.

Petrophysical modelling of bedrocks was performed with fixing temperature and supposing that all voids in rocks are fully filled with water. Such parameters as effective porosity and brine mineralization correspondingly varied between 3-30% and 0.2-7 g/l.

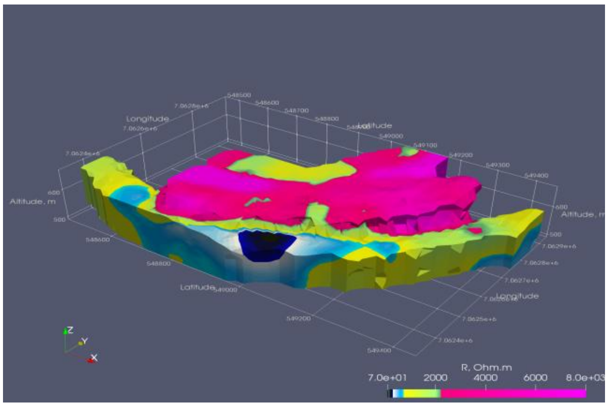

Figure 3. Upper part of the cross-section.

According to the histogram, the electrical resistivity of bedrock lies between 70 and 9000 Ohm·m. Furthermore, modelling shows a huge variety of bedrock porosity (3–30%). As is known a massive or slightly fractured igneous rocks are generally watertight. This statement is compatible with 0-5% porosity interval for bedrocks (>2200 Ohm·m). Porous sandstones and certain volcanic rocks are generally not watertight. This type of material collates with 5-10% (700-2200 Ohm·m) and 10-30% (<700 Ohm·m) effective porosity intervals.

The lower part of the cross-section (Fig. 4) shows that a half of the survey plot can be qualified as massive rocks with high resistivity values (>2200 Ohm·m), and the other half can be divided into permeable semi porous rocks (700-2200 Ohm·m) and huge low-resistivity taliks (<700 Ohm·m).

Conclusions

The combination of ERI with thermometry and water conductivity measurements is an effective method to delineate between frozen ground and talik zones.

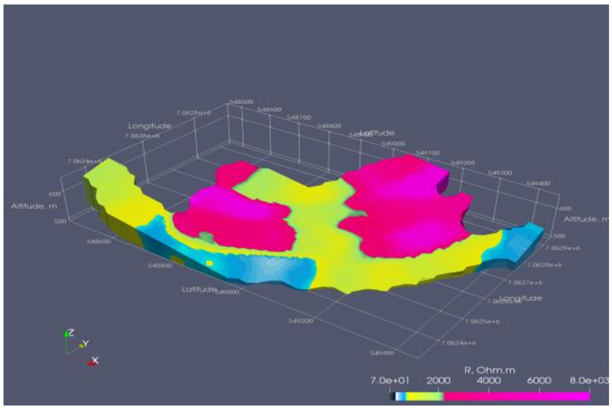

Figure 4. Lower part of the cross-section.

Using petrophysical modelling combined with statistical analysis we divided the cross-section into frozen and unfrozen parts, separated massive and porous units in bedrocks and traced three-dimensional heterogeneities in dam body and footing.

The presence of a detected 3D complicated permeable structure in the axial region may mean that the seepage from the storage reservoir flows in between the rockfill and foundation or dives into the lower part of the cross-section. This may lead to erosion processes which can affect the stability of the foundation with the negative expected results.

References

De Vallejo, L.G. and Ferrer, M., 2011. *Geological engineering*. CRC Press, London, UK, 700 pp.

Matveev, B.C. and Ryzhov, A.A., 2006. Geophysical support of regional hydrogeological, engineering-geological, geocryological, and geoecological studies. *Razved. Okhr. Nedr,* no. 2, pp. 50–57.

On geophysical monitoring of geocryological processes in permafrost foundations of hydroprojects

Rudolf V. Zhang
Sergei A. Velikin
Yuri G. Ivanov
Yulia L. Marchenko
Artem A. Yakimov
Melnikov Permafrost Institute SB RAS, Yakutsk, Russia, rvzhang@mpi.ysn.ru

Abstract

The authors present the results of long-term geophysical monitoring of the permafrost environment of the Vilyui Hydroelectric Station. The investigations are combined into a monitoring system which makes it possible to control the condition of hydraulic structures under changing permafrost conditions. The case study demonstrates the capabilities of geophysical methods to monitor thermal and hydrological processes in the dam embankment, foundation and abutments.

Keywords: permafrost; geophysics; hydroproject; seepage.

Introduction

Construction and operation of hydroprojects on permafrost produce significant changes to the geocryological conditions on which the structures rely for support and stability. Global climate change observed in the 20th and early 21st centuries also has a strong influence on the processes within the upper lithosphere which is subject to annual temperature variations and hosts the structures whose stability depends on the thermal state of the ground (Zhang *et al.,* 2017). Under these circumstances, monitoring studies (geophysical monitoring) which detail the environment and monitor the performance of hydraulic structures have attained greater importance.

Importance of geophysical monitoring for hydroprojects on permafrost

The development of geocryological processes, latent or detectable, may be comparable in duration with the life of the hydroproject. Foundation materials are often pervious to seepage and permafrost serves to provide an impervious barrier. Degradation of permafrost due to project operations leads to rapid exogeneous geocryological processes, which develop dynamically and chaotically, and uncertainty in their development over time requires continuous observations.

If no careful attention is given to the dynamics of geocryological processes, a catastrophic situation may occur at any time during the construction or operation phases of the project.

In order to prevent the development of dangerous processes in the foundations of hydraulic structures, long-term observation systems using instrumentation and integrated geophysical monitoring should be used to control and predict the condition of the foundation (Velikin & Marchenko, 2016).

A standard observation program for hydroprojects on permafrost commonly includes measurements of temperature changes, piezometric levels and water pressures in dams and foundations, as well as geodetic measurements of displacements and settlements. Practice has shown, however, that in many cases such programs are not sufficient to resolve the problems associated with difficult geotechnical and permafrost conditions.

Statistical data describing the present condition of the northern hydroprojects suggest that about 80 percent of the existing structures are subject to active adverse factors.

Seasonal and perennial ground temperature variations, as well as technogenic processes related to project operations cause the physical properties of foundation materials to change spatially and temporally over a wide range. This is due to the complex physicochemical processes which are primarily related to phase changes. The change of state of the soil from frozen to thawed or vice versa has a significant impact on its stability and may take place over a wide range of temperatures, depending on its salinity and gravimetric moisture content.

Therefore, thermometry alone becomes insufficient for assessing the condition of foundations, while geodetic and piezometric measurements can not serve as predictive tools, because they usually can detect irreversible events, such as dam breaks, landslides or abutment seepage (Velikin, 2013).

The main advantage of geophysical monitoring is that it provides a means for detecting human- and climate-induced permafrost degradation in the early stages, because the process of degradation is associated with spatiotemporal changes in electrochemical activity, electrical conductivity values and mechanisms, elasticity, viscosity, strength and other physical properties.

In summary, with the general trend of permafrost degradation beneath and near the hydraulic structures due to the impact of the latter there are changes in the physical properties of the originally frozen foundation and abutment materials. The necessity of using geophysical methods is thus apparent.

Research subject and results

The present authors have been involved in long-term investigations conducted at the Vilyui Hydroelectric Station in western Yakutia, Russia (Fig. 1). The station is the first large hydroproject constructed in the continuous permafrost zone.

Figure 1. Vilyui Hydroelectric Station-1,2. General view.

The research was initiated because of the seepage problems in the right abutment of the headworks. These long-term investigations have resulted in the development of an integrated geophysical monitoring program for hydroprojects in permafrost regions. It includes electrical resistivity tomography, electromagnetic induction profiling and ground penetrating radar.

The results obtained indicate that the integrated observation and control system in the zones where the dam and reservoir actively interact with the environment should be established by combining the required observation network at the key sites with the existing standard instrumentation network. This will increase its information capability in general, as well as owing to the integrated, multi-purpose use of observation boreholes and sites.

It is suggested that modern digital multi-component systems be used in the instrumentation network. Among their advantages is the comprehensive character of information provided and the flexibility of measurement frequency setting with remote control under rapidly changing geocryological conditions.

Conclusion

The results of the study indicate that geophysical methods are effective in monitoring permafrost degradation processes beneath and around water retaining structures due to the high level of detail and the two basic requirements met: continuity and integration.

The first requirement ensures the necessary completeness of data and timely detection of adverse geocryological processes around the hydraulic structure, while the second requirement identifies (locates) the physical form in which these adverse processes develop.

Finally, it should be noted that, with all the "standardization" of geophysical integration, an individual geophysical monitoring complex should be developed for each hydroproject in the permafrost zone depending on the geotechnical and permafrost conditions at the project site.

References

Velikin, S.A. & Marchenko, Y.L., 2016. Scientific-methodological foundations of geophysical monitoring of hydraulic and mining projects in the Yakutian permafrost region. In: *Geotechnics in permafrost*. Vol. 1, Part 4. Moscow: Universitetskaya Kniga, 305-311.

Velikin, S.A., 2013. Possibilities of using geophysical methods to investigate the state of a hydroengineering structure in the permafrost zone. *Inzhenernye Izyskania* 9: 52-59.

Zhang, R.V., Velikin, S.A. & Shesternev, D.M., 2017. Temperature-cryogenic regime of the Vilyui Hydroelectric Station-1,2: geocryological monitoring. *Gidrotekhnicheskoe Stroitel'stvo* 6: 10-23.

24 - Permafrost hazards in high mountains

Session 24

Permafrost hazards in high mountains

Conveners:

- **Michael Krautblatter**, Technical University of Munich, Germany
- **Christian Huggel**, University of Zurich, Switzerland
- **Markus Keuschnig**, GEORESEARCH, Austria (PYRN member)

Permafrost change in high mountains increasingly causes rock and soil slope instability, changes in the hydrological systems, enhanced debris flow and rock avalanche activity as well as widespread subsidence. These processes pose a significant risk to high mountain infrastructure, mountain communities and individuals living and travelling in high mountains.

(i) This session invites contributions that investigate potentially hazardous permafrost change in high mountains using observation, monitoring and modelling techniques using meteorological, geotechnical, geophysical, geological, geomorphological and geomechanical techniques.

(ii) We also welcome complementary contributions that focus on the imposed hazard and risk and assess the vulnerability of individual, communities and infrastructure.

A Technical Guidance Document for the Assessment of Glacier and Permafrost Hazards in Mountain Regions

Simon Allen[1]
Holger Frey[1]
Christian Huggel[1]
Michael Krautblatter[2]
Wilfried Haeberli[1]
Marta Chiarle[3]
Marten Geertsema[4]

[1] *Department of Geography, University of Zurich, Switzerland*
[2] *Technische Universität München, Germany*
[3] *Consiglio Nazionale delle Ricerche (CNR), Istituto di Ricerca per la Protezione Idrogeologica (IRPI), Italy*
[4] *Ministry of Forests, Lands, and Natural Resource Operations, and Rural Development, Prince George, BC, Canada*

Abstract

Hazards relating to glaciers and permafrost are a threat to lives and livelihoods in many mountain regions. In view of rapid global warming and related changes in the mountain cryosphere, landscapes are evolving and new threats are emerging. Coupled with ongoing expansion of people and their infrastructure into high mountain valleys there is an increasing potential for societal losses and far-reaching disasters. Recognizing the need for a structured and comprehensive approach to hazard assessment underpinned by latest scientific understanding, the Joint Standing Group on Glacier and Permafrost Hazards in High Mountains (GAPHAZ) of the International Association of Cryospheric Sciences (IACS) and the International Permafrost Association (IPA) has produced a technical guidance document as a resource for international and national agencies, responsible authorities and private companies. The document provides guidance on susceptibility assessment, impact modelling, and hazard mapping for a range of catastrophic mass flows and onsite hazards.

Keywords: susceptibility; impact; scenarios; hazard mapping; assessment

Introduction

In the context of a warming and evolving mountain landscape, this technical guidance document focusses on hazards that are directly conditioned or triggered by contemporary changes in mountain glaciers and permafrost. Emphasis is given to catastrophic mass flows that can travel far downstream or downslope, potentially leading to cascading processes and impacts (Fig 1). This includes ice avalanches and other glacier instabilities, rock or mixed rock-ice avalanches, para- or periglacial debris flows, and outburst floods from glacial lakes. In addition, we address glacier- and permafrost-related hazards that produce on-site threats, such as land subsidence and deep instabilities.

Two core components were distinguished within an assessment framework:

1. Susceptibility and stability assessment: Identifying where from, and how likely hazard processes are to initiate.
2. Impact assessment: Identifying the potential threat from the hazard for downslope and downstream areas, and providing the scientific basis for decision making and planning.

Susceptibility and stability assessment

We provide guidance for a wide-ranging assessment of the atmospheric, cryospheric, and geotechnical factors that condition and trigger a hazard event. Conditioning factors encompasses static and inherent characteristics of the site, but also those dynamic factors that gradually increase the susceptibility of a site over time. Triggering factors are reserved for those processes that directly initiate movement or transform a site from a stable to unstable state. How relevant certain factors are for susceptibility or stability will vary from one region to another, and expert judgement is needed to determine whether or not more weighting should be applied to some factors in the local assessment of susceptibility.

Conditioning and triggering factors inform not only about where and how likely an event is to initiate, but also provide insight on possible magnitudes that may be involved. Hence, the susceptibility and stability assessment provides a basis for identifying and prioritizing where subsequent impact studies will be focused (e.g. focusing on highly susceptible or unstable slopes), while the information gathered during this stage will also feed directly into the scenario development and hazard modeling within the impact assessment phase.

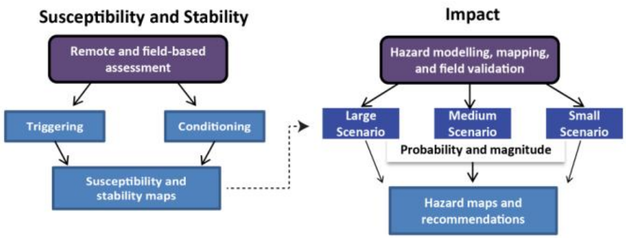

Figures 1. Simplified version of the framework for glacier and permafrost hazard assessment (after GAPHAZ 2017).

Impact assessment

Where critical situations are identified, hazard modelling and mapping is likely to be undertaken. Hazard mapping, in the context of the guidance document, refers strictly to the assessment of hazard as defined on the basis of the probability that an event will occur, and the expected intensity of the given event (also termed magnitude). Hazard mapping typically draws upon historical records to establish frequency – magnitude relationships that can then be used as a basis for scenario development and hazard modelling. However, for hazards originating in high mountain environments, the ability to establish reliable frequency – magnitude relationships are generally limited, not least because glaciers and permafrost are changing rapidly and in many cases conditions are already beyond any historical precedence. Hence, a semi-qualitative approach to scenario development is recommended whereby scenarios of three different magnitudes (e.g., small, medium, and large) are linked to corresponding best estimates of the likely probability of occurrence (e.g., low, medium, high). A scenario is inherently forward looking but does not necessarily consider a comprehensive set of future drivers of hazards, such as climate change and related impacts on glaciers and permafrost. If the scenario is intended to be valid over longer time periods (several decades), one needs to appropriately consider the respective future climatic changes which can themselves be based on different climate scenarios (e.g., as related to low and high greenhouse gas emissions).

We specifically highlight the importance of including a worst-case scenario, i.e., the largest magnitude event that is anticipated. Particularly for the anticipation of new or emerging threats under a changing climate, worst-case scenarios provide a conservative approach with which to capture the various sources of uncertainty inherent in future projections. A toolbox of physical-numerical models can then simulate for each scenario the potential downslope/downstream hazard event, providing key parameters such as flow heights, impact pressures, and velocities, as required for intensity mapping and hazard classification (after Raetzo et al. 2002).

The guidance document provides illustrative examples from the Peruvian Andes (after Schneider et al. 2014), demonstrating how the assessment framework can be applied in the case of cascading, chain reaction events. It is meant as a tool for experts in charge of hazard evaluations, reflecting current scientific state-of-the-art, but does not intend to replace the knowledge and experience required for such assessments. In view of the rapidly changing cryosphere, leading, e.g., to increasing potential for large rock avalanches from degrading permafrost slopes triggering an outburst flood event and/or downstream debris flow events, this is particularly timely.

Acknowledgments

The guidance document was elaborated within the framework of the “Proyecto Glaciares+”, promoted and funded by the Swiss Agency of Development and cooperation (SDC).

References

GAPHAZ, 2017. *Assessment of Glacier and Permafrost Hazards in Mountain Regions. Technical Guidance Document.* IACS/IPA Standing Group on Glacier and Permafrost Hazards (GAPHAZ), 72 pp.

Raetzo, H., Lateltin, O., Bollinger, D. & Tripet, J. P., 2002. Hazard assessment in Switzerland - Codes of Practice for mass movements. *Bulletin of Engineering Geology and the Environment* 61: 263–268.

Schneider, D., Huggel, C., Cochachin, A., Guillén, S. & García, J., 2014. Mapping hazards from glacier lake outburst floods based on modelling of process cascades at Lake 513, Carhuaz, Peru. *Advances in Geosciences* 35: 145–155, doi:10.5194/adgeo-35-145-2014.

Modeling permafrost occurrence, glacier-bed topography and possible future lakes for assessing changing hazard conditions in cold mountain regions

Wilfried Haeberli[1]
Florence Magnin[2,3]
Andreas Linsbauer[1,4]
[1]*Geography Department, University of Zurich, 8057 Zurich, Switzerland*
[2]*Department of Geosciences, University of Oslo, Blindern, 0316 Oslo, Norway*
[3]*EDYTEM Lab, Université Savoie Mont Blanc, CNRS, 73376 Le Bourget du Lac, France*
[4]*Department of Geosciences, University of Fribourg, 1700 Fribourg, Switzerland*

Abstract

The rapid transformation of glacial into periglacial mountain landscapes under conditions of continued global warming can cause new and locally severe changes in hazard and risk conditions. A special focus must be on systematically increasing risks due to far-reaching flood waves or debris flows caused by rock/ice avalanches into new lakes at the foot of steep slopes with decreasing stability due to permafrost degradation and/or glacial de-buttressing. Modeling permafrost occurrence and glacier-bed topography provides important information for anticipating critical future situations.

Mis en forme : Justifié

Keywords: global warming, mountain permafrost, glacier beds, new lakes, rock/ice avalanches, natural hazards.

Under conditions of continued global warming in cold mountains, most glaciers tend to disappear within decades while the degradation of permafrost on exposed slopes can take centuries. Glacial landscapes are therefore rapidly and for extended future time periods transforming into periglacial landscapes with permafrost still existing but in strong thermal disequilibrium. Modeling such new landscapes is an important emerging research field (Haeberli, 2017). One key aspect relates to changing hazard conditions related to decreasing slope stability due to permafrost degradation and glacial de-buttressing, possibly causing impact/flood waves from rock/ice avalanches into new lakes (Haeberli *et al.*, 2017). Anticipation of critical future situations requires permafrost and glacier-bed modeling (Colonia *et al.*, 2017; Linsbauer *et al.*, 2016; Magnin *et al.*, 2017). Figure 1 shows an example from an ongoing study in the Mont Blanc region. Rock wall temperature was mapped based on a statistical model fitted with rock surface temperature measurements from the entire Alpine range (Boeckli *et al.*, 2012) implemented with high-resolution (4 m) topography and local air temperature data (Magnin *et al.*, 2015). Glacier-bed topography was calculated using the GlabTop model (Linsbauer *et al.*, 2012) with a 20 m resolution DEM (upscaled 4 m DEM) and digitized branch lines drawn within glacier outlines mapped by Gardent *et al.* (2014). Modeled overdeepenings were checked against morphological criteria (slope change, crevasse patterns, lateral narrowing; Frey *et al.*, 2010). It can be seen that possible future lakes will not only form at the foot of large and steep permafrost slopes, for instance at Aiguille Verte and Les Droites, but also close to oversteepened and glacially de-buttressed lateral glacier-bed slopes.

Mis en forme : Justifié

New lakes exposed to potential rock/ice avalanches are multipliers of hazard and risk in the region. Possible catastrophic process chains including impact waves and secondary phenomena such as far-reaching flood waves and debris flows must be considered using corresponding sequences of numerical models (Schneider *et al.*, 2014, Somos-Valenzuela *et al.*, 2016, Worni *et al.*, 2014). The probability of catastrophic events cannot be quantified but undoubtedly increases with further glacier retreat and related formation of new lakes in the valley, and with continued permafrost degradation and stability reduction in the surrounding icy peaks. Reflection about possible protective measures should better start now than later, because simple solutions may not exist and major investments and efficient engineering work such as retention structures may be difficult and take time. Aspects of landscape protection and options for hydropower production, water supply and tourism should also be considered. A matrix-type analyses of potential synergies but also of potential conflicts as part of participative planning can be recommended (Haeberli *et al.* 2016).

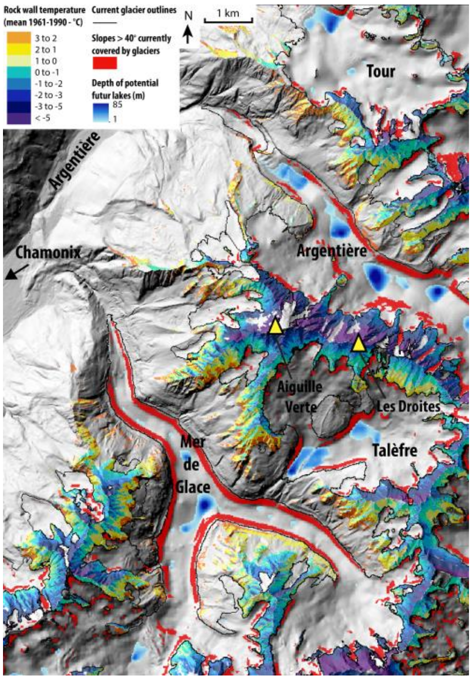

Figure 1: Mer de Glace, Glacier d'Argentière and surroundings in the Mont Blanc region, French Alps: Model calculation of present rock-wall temperatures, glacier-bed topography with oversteepened and overdeepened parts of glacier beds. With the vanishing of the glacier ice, the oversteepened parts of the glacier beds will become de-buttressed and glacier-bed overdeepenings may transform into possible future lakes when becoming exposed.

Acknowledgments

We thank M. Gardent for providing glacier outlines and related information.

References

Boeckli, L., Brenning, A., Gruber, S. & Noetzli, J. 2012. Permafrost distribution in the European Alps: calculation and evaluation of an index map and summary statistics. *The Cryosphere* 6: 807–820. doi:10.5194/tc-6-807-2012

Colonia, D., Torres, J., Haeberli, W., Schauwecker, S., Braendle, E., Giraldez, C. & Cochachin, A., 2017. Compiling an inventory of glacier-bed overdeepenings and potential new lakes in de-glaciating areas of the Peruvian Andes: Approach, first results, and perspectives for adaptation to climate change. *Water* 9, 336. doi:10.3390/w9050336.

Frey, H., Haeberli, W., Linsbauer, A., Huggel, C. & Paul, F., 2010. A multi level strategy for anticipating future glacier lake formation and associated hazard potentials. *Natural Hazards and Earth System Science* 10: 339-352. doi:org/10.5194/nhess-10-339-2010

Gardent, M., Rabatel, A., Dedieu, J.-P. & Deline, P. 2014. Multitemporal glacier inventory of the French Alps from the late 1960s to the late 2000s. *Global and Planetary Change* 120: 24-37. doi.org/10.1016/j.gloplacha.2014.05.004

Haeberli, W., 2017. Integrative modelling and managing new landscapes and environments in de-glaciating mountain ranges: An emerging trans-disciplinary research field. *Forestry Research and Engineering: International Journal* 1(1). doi: 10.15406/freij.2017.01.00005 442.

Haeberli, W., Buetler, M., Huggel, C., Lehmann Friedli, Th., Schaub, Y. & Schleiss, A.J., 2016. New lakes in deglaciating high-mountain regions – opportunities and risks. *Climatic Change* 139(2): 201-214. doi:10.1007/s10584-016-1771-5

Haeberli, W., Schaub, Y. & Huggel, C., 2017. Increasing risks related to landslides from degrading permafrost into new lakes in de-glaciating mountain ranges. *Geomorphology* 293: 405-417. doi:10.1016/j.geomorph.2016.02.009

Linsbauer, A., Frey, H., Haeberli, W., Machguth. H., Azam, M.F. & Allen, S., 2016. Modelling glacier-bed overdeepenings and possible future lakes for the glaciers in the Himalaya–Karakoram region. *Annals of Glaciology* 57 (71): 119-130. doi:10.3189/2016AoG71A627

Linsbauer, A., Paul, F. & Haeberli, W., 2012. Modeling glacier thickness distribution and bed topography over entire mountain ranges with GlabTop: Application of a fast and robust approach. *Journal of Geophysical Research* 117: F03007. doi:10.1029/2011JF002313

Magnin, F., Brenning, A., Bodin, X., Deline, P. & Ravanel, L. 2015. Modélisation statistique de la distribution du permafrost de paroi : application au massif du Mont Blanc. *Géomorphologie : relief, processus, environnement* 21 : 145-162, doi.org/10.4000/geomorphologie.10965

Magnin, F., Josnin, J.-Y., Ravanel, L., Pergaud, J., Pohl, B. & Deline, Ph., 2017. Modelling rock wall permafrost degradation in the Mont Blanc massif from the LIA to the end of the 21st century. *The Cryosphere* 11: 1813–1834. doi:org/10.5194/tc-11-1813-2017

Schneider, D., Huggel, C., Cochachin, A., Guillén, S. & García, J., 2014. Mapping hazards from glacier lake outburst floods based on modelling of process cascades at Lake 513, Carhuaz, Peru. *Advances in Geosciences* 35: 145–155. doi:10.5194/adgeo-35-145-2014

Somos-Valenzuela, M.A., Chisolm, R.E., Rivas, D.S., Portocarrero, C. & McKinney, D.C., 2016. Modeling glacial lake outburst flood process chain: The case of Lake Palcacocha and Huaraz, Peru. *Hydrology and Earth System Sciences* 20: 2519–2543. doi:10.5194/hess-20-2519-2016

Worni, R., Huggel, C., Clague, J.J., Schaub, Y. & Stoffel, M., 2014. Coupling glacial lake impact, dam breach, and flood processes: a modeling perspective. *Geomorphology* 224: 161–176. doi.org/10.1016/j.geomorph.2014.06.031

Mis en forme : Espagnol (Espagne)

Do deformation patterns and initial failure timing of rock-slope instabilities in Norway relate to permafrost dynamics?

Paula Hilger[1,2]
Reginald L. Hermanns[1,3]
Bernd Etzelmüller[2]
Kristin Sæterdal Myhra[4]
Florence Magnin[2]
John C. Gosse[5]

[1]*Geological Survey of Norway, Trondheim, paula.hilger@ngu.no*
[2]*Department of Geosciences, University of Oslo, Norway*
[3]*Norwegian University of Science and Technology, Trondheim, Norway*
[4]*Western Norway University of Applied Science, Sogndal, Norway*
[5]*Department of Earth Sciences, Dalhousie University, Halifax, Canada*

Abstract

Deep-seated and slow moving rock-slope instabilities are common in the Norwegian valley and fjord system. While many sudden rock-slope failures happened shortly after deglaciation, there is still a number of recently deforming unstable rock slopes. We have dated several slip surfaces using cosmogenic nuclide exposure dating, which provides the duration of time that a rock surface has been exposed to cosmic rays. The chronologies reveal that rock-slope deformation can be active during most of the Holocene, and that creep velocities have varied during this period. The principal objective is to evaluate the reason of these velocity variations, including if thermal processes in the rock slopes may have influenced the rock slope dynamics.

Keywords: Rock-slope instabilities; TCN-dating; deformation pattern; thermal processes; permafrost.

Introduction

More than 300 active rock slopes demonstrating post glacial deformation are mapped in Norway (Oppikofer et al., 2015). Seven are classified as high-risk objects because of the advanced deformation of the rock mass, the sliding rates and other parameters checked in the norwegian hazard and risk classification for unstable rock slopes, e.g. potential loss of life (Hermanns *et al.,* 2013a; Blikra *et al.,* 2016).

In addition to post-glacial stress increase, we expect water pressure and altitudinal permafrost dynamics to significantly impact these gravity driven slope processes along complex pre-existing bedrock structures. In this presentation we discuss the possible reasons for the different deformation patterns along unstable rock-slopes.

Methods and study sites

High energy cosmic ray particles will interact with atoms in exposed minerals on the rock surface to produce terrestrial cosmogenic nuclides (TCN). The concentration of a specific nuclide, such as ^{10}Be, ^{21}Ne, or ^{36}Cl, can therefore be used to calculate the apparent exposure duration of the surface (Gosse & Phillips, 2001). This can be used to reproduce the movement history of unstable rock slopes, gradually exposing the sliding surface (fig. 1).

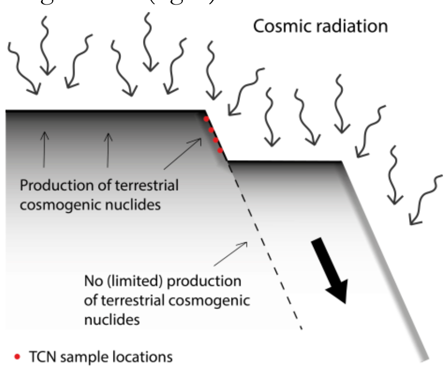

Figure 1. Schematic illustration of TCN production on the cross section of a mountain plateau and slope with a gravitationally moving block. Theoretical sample locations are indicated in red.

We present updated ages and slip rates for two rockslides in western Norway: Skjeringahaugane slide in Sogn og Fjordane (Hermanns *et al.,* 2012), and the Oppstadhornet rockslide in Møre og Romsdal (Hermanns *et al.,* 2013b). The former is a complex instability, where the unstable slope is broken up with several secondary sliding surfaces. In addition to these recalculations, we sampled along vertical transects over the sliding surfaces of three different active rock-slope instabilities. While one is located ca. 5.5 km SE of Oppstadhornet in western Norway, two adjacent instabilities are located at Revdalsfjellet in the Troms county in northern Norway.

Preliminary results and discussion

Preliminary TCN ages of the Mannen and Revdalsfjellet 2 instabilities suggest that sliding started close to the Holocene Thermal Maximum (HTM), when mountain permafrost presence was at a minimum. This indicates that permafrost thawing may have contributed to the timing of these rock-slope instabilities. The preliminary results of Revdalsfjellet 1, which is an adjacent but independently moving rock body to Revdalsfjellet 2, suggest a movement onset during strong temperature fluctuations in the mid Holocene.

The new results of the Skjeringahaugane rock-slope instability differ greatly from the ages published previously and imply ages affected by inheritance. While the main sliding surface indicate early deformation following deglaciation, deformation at a secondary sliding surface started during the mid Holocene. The onset of Oppstadhornet seems to coincide with the local deglaciation.

Deformation measurements at the Mannen rockslide, compared to the dating results, indicate a recent acceleration of deformation. This could be influenced by late stage permafrost thawing at the lower boundary of altitudinal permafrost. The different timing of the initial failure and deformation velocities at the two adjacent instabilities at Revdalsfjellet demonstrate the importance of local settings. Although the instabilities at present lie below the lower boundary of continuous altitudinal permafrost in the area, thermal processes under specific local conditions (isolated permafrost) cannot be excluded, as demonstrated at the nearby Jettan rock-slope instability, where thermal processes and permafrost in open cracks are monitored in connection with recent deformation (Blikra & Christiansen, 2004).

Acknowledgments

This research was carried out within the CryoWALL project (243784/CLE), which is mainly funded by the Research Council of Norway with co-financing by the Geological Survey of Norway (NGU) and the Department of Geosciences, University of Oslo.

References

Blikra, L.H. & Christiansen, H.H., 2014. A field-based model of permafrost-controlled rockslide deformation in northern Norway. *Geomorphology* 208: 34-49.

Blikra L.H., Majala, G., Anda, E., Hallvard, B., Eikenæs, O., Helgås, G., Oppikofer, T., Hermanns, R.L. & Böhme, M. 2016. Fare- og risikoklassifisering av ustabile fjellparti. *NVE-Rapport nr 77-2016* 47.

Gosse, J.C. & Phillips, F.M., 2001. Terrestrial in situ cosmogenic nuclides: theory and application. *Quaternary Science Reviews* 20: 1475-1560.

Hermanns, R.L., Redfield, T.F., Bunkholt, H.S.S., Fischer, L. & Oppikofer, T., 2012. Cosmogenic nuclide dating of slow moving rockslides in Norway in order to assess long-term slide velocities. In: Eberhardt et al. (eds.), *Landslides and Engineered Slopes: Protecting Society through Improved Understanding.* Taylor & Francis Group, London, 849-854.

Hermanns, R.L., Oppikofer, T., Anda, E., Blikra, L.H., Böhme, M., Bunkholt, H., Crosta, G.B., Dahle, H., Devoli, G., Fischer, L., Jaboyedoff, M., Loew, S., Sætre, S. & Yugsi Molina, F., 2013a. Hazard and risk classification system for large unstable rock slopes in Norway. In: Genevois R. & Prestininzi A., (eds.) *International conference on Vajont - 1963-2013. Italian Journal of Engineering Geology and Environment, Book series 6,* Rome, Italy, 245-254.

Hermanns, R.L., Oppikofer, T., Dahle, H., Eiken, T., Ivy-Ochs, S. & Blikra, L.H., 2013b. Understanding long-term slope deformation for stability assessment of rock slopes: The case of the Oppstadhornet rockslide, Norway. In: Genevois R. & Prestininzi A., (eds.) *International conference on Vajont - 1963-2013. Italian Journal of Engineering Geology and Environment, Book series 6,* Rome, Italy, 255–264.

Oppikofer, T., Nordahl, B., Bunkholt, H., Nicolaisen, M., Jarna, A., Iversen, S., Hermanns, R.L., Böhme, M., & Molina, F.X.Y., 2015. Database and online map service on unstable rock slopes in Norway - From data perpetuation to public information. *Geomorphology* 249: 69-81.

Thermal and mechanical modelling of massive rock slope failure following fjord deglaciation

Benjamin Jacobs[1]
Kristin S. Myhra[2]
Johannes (Michael) Leinauer[1]
Michael Krautblatter[1]
[1]*Technical University of Munich, Chair of Landslide Research, Benjamin.jacobs@tum.de.*
[2]*Western Norway University of Applied Science.*

Abstract

During the last decade, more than 300 unstable rock walls have been systematically identified throughout Norway, of which five are classified as high-risk instabilities with respect to high hazard scores and anticipated casualties. At these five sites long-term permafrost degradation following glacial retreat seems to significantly influence large-scale rock instability. Here we combine thermal and mechanical modelling of extreme fjord topographies over the Pleniglacial / Lateglacial / Holocene to demonstrate how permafrost degradation controls long-term rock slope failure. The reduction of rock mass strength upon thaw was evaluated using samples from site for rock mechanical testing. To gain information on Holocene rock wall temperatures and thermal coevolution of landslide scarps we use a transient heat flow model (CryoGrid2D) and temperature-calibrated 3D electrical resistivity tomography respectively. Additionally, 2D electrical resistivity tomographies combined with field mapping reveal hydraulic forcing on a slope scale as surface features can be attributed to zones of increased infiltration.

Keywords: Mechanical Modelling; Thermal Modelling; Permafrost Rockwalls; Massive Rock Slope Failure.

Introduction

Massive rock slope failures in formerly glaciated mountain ranges are often attributed to glacial debuttressing and oversteepening, however, a frequently observed lag-time between glacial retreat and the occurrence of instabilities is yet to be explained (McColl, 2012). Developing a rock-ice-mechanical model for rock slope failure, Krautblatter *et al.* (2013) suggest a compelling link between thermal and mechanical processes resulting in a decrease of rock-slope stability upon thaw.

Here, we use outputs of a transient heat flow model and temperature-controlled rock mechanical testing to set up a long-term mechanical model for steep fjord topographies in Norway to evaluate the development of massive rock slope failures throughout the Pleniglacial / Lateglacial / Holocene, hereafter referred to as Deglaciation. We hypothesize, that the thermal regime and permafrost degradation is a crucial factor controlling the lag-time between glacial retreat and large-scale slope instability.

Study Area

This study focusses on two test sites in southwestern Norway: Skjerdingstindane and Ramnanosi. Both sites are situated in areas of both Early and Mid-Holocene landslide activity and have a similar geological setting exposing granite and granitic gneiss from the Precambrian basement and the Caledonian Orogen. However, both areas have a very distinct deglaciation history resulting in different rock wall temperature regimes throughout the Holocene.

In a later stage of this study, stability analysis will be extended to two of Norway's high-risk slope instabilities at Mannen and Gamanjunni.

Methods

To model rock wall temperatures at the test sites during Deglaciation, we used the transient heat flow model CryoGrid 2D which describes the transfer of energy by heat conduction and the phase transition of water/ice (Myhra *et al.*, 2015). This model was applied on a simplified, typical Norwegian, slope geometry consisting of a flat plateau adjacent to steep slopes, and forced by local ambient air temperatures as well as a geothermal heat flux.

The spatio-temporal permafrost distribution modelled with CryoGrid 2D was transferred in a multi-stage mechanical model. Under the assumption that on a large scale, such as a cross profile of a whole fjord, the rock mass can be mechanically described as a continuum, we used a continuum-mechanical model to assess stress distribution and potential massive rock slope failure at the test sites.

Critical rock strength parameters, such as uniaxial compressive strength and tensile strength, were tested in frozen and unfrozen conditions using standard rock mechanical tests. Seismic testing derived elasticity parameters in frozen and unfrozen conditions. All test were conducted on in-situ samples or analogue samples from Norway.

shows three general phases of rock wall stability during Deglaciation: (i) mechanically stable, glacier-covered and unfrozen rock wall, (ii) mechanically stable, deglaciated and frozen rock wall and (iii) mechanically unstable and partially thawed rock wall. This suggests glacier-induced normal stress and post-glacial permafrost condition to have a stabilizing effect on steep fjord topographies, whereas permafrost degradation of a critically stressed rock wall reduces stability below a critical level, thus producing a time-lag between deglaciation and massive rock slope failure.

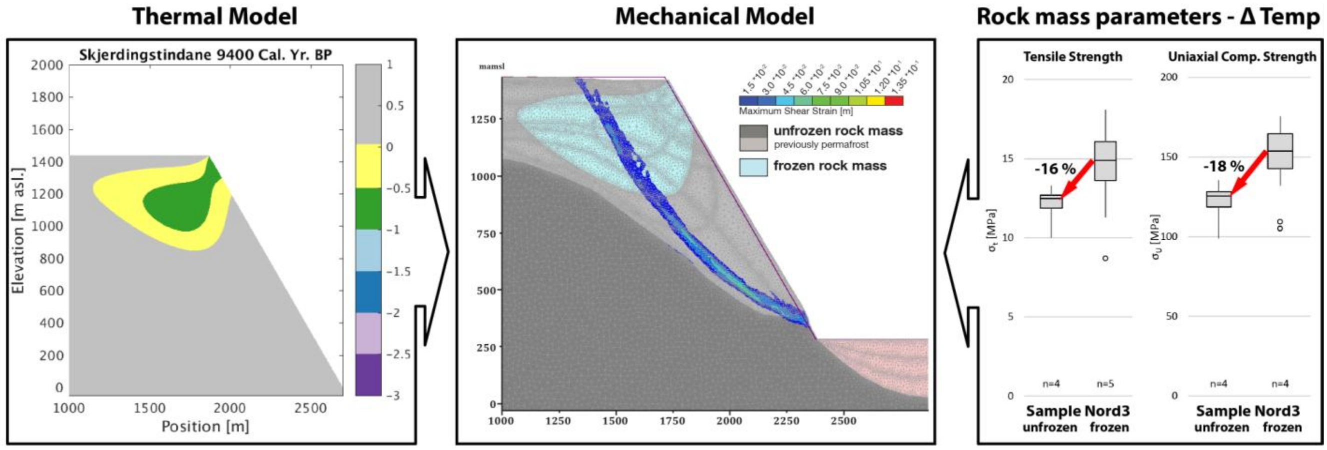

Figure 1. Methodological setup and first results of the thermal model (left), rock mechanical testing (right) and mechanical model for an exemplary fjord topography at Skjerdingstindane.

First results and interpretation

Thermal modelling of the rock wall temperatures shows a distinct pattern of permafrost development and degradation during Deglaciation. Assuming warm based glacier conditions towards the end of the Pleistocene, CryoGrid 2D reveals an intense cooling of the rock wall and extensive advancement of permafrost distribution following glacial retreat (max. permafrost extend at 12 ka BP). Due to rising ambient air temperatures during the Holocene, the model shows drastic permafrost degradation with a minimum spatial extend at ca. 7.7 ka BP, followed by a fluctuating extent of the permafrost lens until today.

Rock mechanical testing of five samples consisting of 108 specimens shows a clear decrease of rock strength upon thaw. Uniaxial compressive strength and tensile strength decrease by 5 to 20 % and 13 to 25 % respectively. Young's modulus is reduced by 38 to 79 %, whereas the Poisson ratio remains unchanged.

Both the results from transient thermal modelling and rock mechanical testing were fed into a continuum mechanical model (Figure 1). This mechanical model

Acknowledgments

This research is conducted within the Project CryoWall (NRF Project Number 243784) funded by the Norwegian Research Council. We express our gratitude to P. Hilger, B. Etzelmüller, T. Oppikofer, K. R. Jogerud and S. Westermann for support regarding fieldwork and logistics.

References

McColl, S.T., 2012. Paraglacial rock-slope stability. *Geomorphology* 153-154: 1-16:

Myhra, K.S., Westermann, S. & Etzelmüller, B., 2015. Modelled Distribution and Temporal Evolution of Permafrost in Steep Rock Walls Along a Latitudinal Transect in Norway by CryoGrid 2D. *Permafrost and Periglacial Processes* 28: 172-182.

Krautblatter, M., Funk, D. & Günzel, F.K., 2013. Why permafrost rocks become unstable: a rock-ice-mechanical model in time and space. *Earth Surface Processes and Landforms* 38: 876-887.

A temperature- and stress-controlled failure criterion for ice-filled permafrost rock joints

Philipp Mamot [1]
Samuel Weber[2]
Michael Krautblatter[1]
[1]*Chair of Landslide Research, Technical University of Munich, Munich, 80333, Germany, philipp.mamot@tum.de*
[2]*Department of Geography, University of Zurich, Zurich, 8057, Switzerland*

Abstract

Most of the currently observed failures in permafrost-affected rock walls are likely triggered by the degradation of bedrock permafrost and ice-filled joints which may evolve into potential shear planes that support destabilisation and failure. The failure of ice-filled rock joints in particular has only been observed in a small number of experiments often using concrete as a rock analogue. Here, we present a systematic study of the brittle failure of rock-ice interfaces under relevant stress conditions ranging from 100 to 800 kPa, i.e. 4–30 m rock overburden and at temperatures ranging from -10 to -0 °C, typical for recently documented rock slope failures in alpine permafrost. In 140 shear experiments, we demonstrate that both, warming and unloading of ice-filled rock joints lead to a significant drop in the shear resistance. We introduce a Mohr-Coulomb failure criterion for rock-ice interfaces that demonstrates friction and cohesion change with temperature, which applies to more than 90 % of the recently observed final failures in permafrost rock walls.

Keywords: Bedrock permafrost; rock slope failure; ice-filled rock joints; brittle failure; shear strength.

Introduction

Rock slope failures influenced by permafrost degradation have increased in the recent past and are expected to respond to a warming climate by more frequent events. The majority of failures in permafrost-affected rock frequently expose ice-filled joints as potential shear and detachment planes (Gruber & Haeberli, 2007; Ravanel et al., 2010). Mechanical processes leading to failure are still poorly understood. The failure of ice-filled permafrost rock joints in particular has only been observed in a small number of experiments mostly using concrete as a rock analogue (Davies et al., 2000; Krautblatter et al., 2013).

Here we present a systematic series of 140 constant strain-rate shear tests on sandwich-like rock-ice-rock samples (i) to study the brittle failure of ice and rock-ice interfaces along ice-filled permafrost shear planes and its dependence on warming and changes in rock/ice overburden, (ii) to develop a new brittle failure criterion and (iii) to apply it to real-world permafrost rock slope destabilisation (Mamot et al., submitted to The Cryosphere).

Methods

Tests were performed with Wetterstein limestone collected at the permafrost-affected Zugspitze summit, Germany, 2962 m a.s.l., and ground to international rock mechanical standard roughness. Ice-filled rock joints were simulated by a sandwich composed of two rock cylinders (diameters 15 cm, height 8 cm) and a thin ice layer (2.5 cm) in between (Fig. 1).

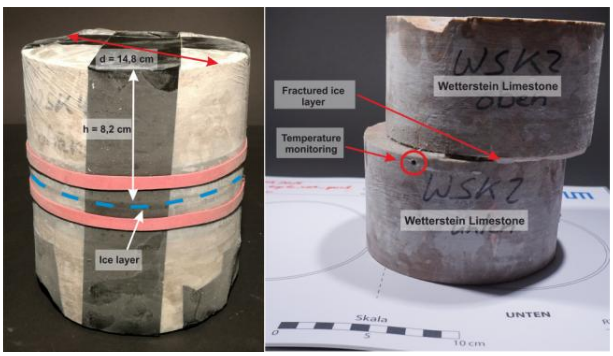

Figure 1. Sandwich samples before (left) and after (right) shearing (Mamot et al., submitted to The Cryosphere).

Fracturing of ice and rock-ice-interfaces occur i) at strain rates > 10^{-3} s^{-1} (Sanderson, 1988) and ii) mainly below a rock overburden of 20–30 m (Krautblatter et al., 2013). Hence, the brittle failure of ice and rock-ice-contacts increasingly controls the accelerating final failure along predefined slip planes (Krautblatter et al., 2013) and dominates rock failure volumes ≤ 30.000 m³ where all ice-filled failure planes are ≤ 20–30 m deep. Normal stress levels of 100, 200, 400 and 800 kPa (i.e. 4–30 m rock overburden) and a mean strain rate of 0.7 * 10^{-3} s^{-1} were applied.

The experiments were conducted at temperatures between -0.5 and -10 °C, typical for recently documented rock slope failures in alpine permafrost. Rock temperature was monitored during shearing (Fig. 1) and the onset and behaviour of failure was controlled by acoustic emission sensors fixed at the top of the upper specimen ring.

Results and discussion

The onset of AE hit increase occurs when 65 % of the time between shear start and failure has passed. With temperature increase from -10 °C to -0.5 °C, the shear stress at failure reduces by 75–85 % for 100 and 400 kPa. At a given temperature, the shear resistance of rock-ice interfaces significantly decreases with decreasing normal stress from 800 to 100 kPa.

We use the linear and stress-dependent Mohr-Coulomb failure criterion to develop a shear strength description of ice-filled permafrost rock joints. Both the cohesion and friction angle decrease by 86 % and by 60 % respectively when approaching the melting point (each with R^2 = 0.85). The temperature-dependent shear stress at failure for ice-filled rock joints can be described by $\tau[kPa] = \sigma' * (0.03 - 0.17 * T) + (181 - 63 * T)$ where σ' is the effective normal stress (in kPa) and $(\sigma' * (0.03 - 0.17 * T))$ and $(181 - 63 * T)$ are the friction and the cohesion respectively.

The new derived model shows a robust fit with the measured values (Fig. 2). Best accordance between the means of the measured peak shear stress values and the calculated regression lines is achieved for temperatures -8 and -0.5 °C (coefficients of variation 4–18 %) whereas mean absolute errors do not exceed 200 kPa, except at -6 °C. The validation data sets (-5, -3 and -1 °C) lie well within the calculated error margin.

For the first time, we develop a failure criterion that (i) includes the fracturing of ice infillings, rock-ice interfaces and a combination of both, along ice-filled permafrost rock joints, (ii) is based on Mohr-Coulomb and contains both a temperature dependent friction angle and cohesion and (iii) applies to temperature and stress conditions of more than 90 % of the recently documented final failures in permafrost rock walls.

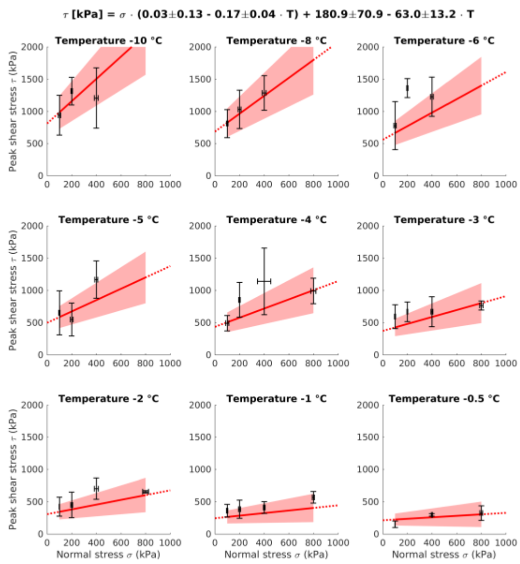

Figure 2. Validation test for the new failure criterion for ice-filled rock joints, including temperatures -1, -3 and -5 °C, which were not used in the model development. Red areas represent the error ranges of the regression lines.

Results clearly show a shear strength decrease with decreasing normal stress and increasing temperature. Thus, as soon as a first slab has detached from a rock slope, further slabs below may subsequently be destabilized by progressive thermal warming and by sudden unloading.

References

Davies, M. C. R., Hamza, O., Lumsden, B. W. and Harris, C., 2000. Laboratory measurement of the shear strength of ice-filled rock joints. *Annals of Glaciology* 31: 463-467.

Gruber, S. and Haeberli, W., 2007. Permafrost in steep bedrock slopes and its temperature-related destabilization following climate change. *Journal of Geophysical Research* 112: 1–10.

Krautblatter, M., Funk, D. and Günzel, F. K., 2013. Why permafrost rocks become unstable: a rock-ice-mechanical model in time and space. *Earth Surface Processes and Landforms* 38: 876-887.

Mamot, P., Weber, S., Schröder, T. and Krautblatter, M. A temperature- and stress-controlled failure criterion for ice-filled permafrost rock joints. *Submitted to The Cryosphere.*

Ravanel, L., Allignol, F., Deline, P., Gruber, S. and Ravello, M., 2010. Rock falls in the Mont Blanc Massif in 2007 and 2008. *Landslides* 7: 493-501.

Sanderson, T. J. O., 1988. *Ice Mechanics. Risks to offshore structures*. Graham & Trotman, 253 pp.

Spatial footprint of degrading permafrost in the French Alps using destabilized rock glacier inventory and susceptibility modeling

Marco Marcer[1,2], Charlie Serrano[1,2], Xavier Bodin[2], Jason Goetz[3], Philippe Schoeneich[1]
[1]*Université Grenoble Alpes, PACTE, Institut d'Urbanisme et de Geographie Alpine, Grenoble, France. marco.marcer@univ-grenoble-alpes.fr*
[2]*Laboratoire EDYTEM, CNRS, Universite Savoie-Mont Blanc, Bourget le Lac, France*
[3]*Department of Geography, Friedrich Schiller University Jena, Jena, Germany*

Abstract

Emerging hazards related to mountain permafrost degradation have been threatening the alpine community for the past few decades. In the present study, we propose an exploratory methodology to evaluate the spatial extent of the phenomena in the French Alps. Rock glaciers showing recurrent morphological features (e.g. crevasses and scarps) were exhaustively inventoried and used in order to identify destabilized landforms. The typical topo-climatic conditions where destabilizations occur were modelled using a Generalized Additive Model. A permafrost degradation susceptibility map was computed under the assumption that rock glacier destabilization is a representative process for permafrost degradation. Results suggest that destabilized rock glaciers are common in the region (~10% of the active rock glaciers). The GAM performances are encouraging and the susceptibility map shows patterns coherent with the observed destabilized rock glaciers, suggesting that the method is consistent with its aim.

Keywords: Permafrost degradation; destabilized rock glacier; rock glacier inventory; susceptibility map; statistical modelling.

Introduction

In the past decades, permafrost degradation-related processes have been observed in a wide range of contexts, from rockwall failure to borehole temperature rise (Bodin *et al.*, 2015). In particular, permafrost degradation in rock glaciers can compromise their typical creeping behavior, resulting in a series of processes, as great velocities, basal sliding and crevasses development, generally defined as destabilization (e.g. Bodin *et al.,* 2016).

The present study aims to quantify the spatial footprint of degrading permafrost in the French Alps using mapped destabilized rock glaciers as evidence for permafrost degradation. This is done by taking inspiration from novel methodology experimented in the Canadian Arctic (Rudy *et al.*, 2017), which consists of two steps: (i) an inventory of destabilized rock glaciers is compiled and (ii) this inventory is used as a database to realize a permafrost degradation susceptibility map.

Methodology

Destabilized rock glacier inventory

Destabilized rock glaciers have been observed to present a variety of geomorphological signs, here grouped into four categories: crevasses, scarps, cracks and debris flow channels. Using the rock glacier inventory of the French Alps (Marcer *et al.*, 2017) and high resolution aerial orthoimagery, rock glaciers with geomorphological evidences of destabilization were retrieved and mapped. After cross-validation of observed features between several operators, rock glaciers were classified according to a destabilization index, varying from 0 (stable rock glaciers) to 3 (severely destabilized rock glaciers) according to the amount and severity of the destabilization signs.

Susceptibility Modeling

The spatial footprint of degrading permafrost was modeled using a statistical approach inspired from Rudy *et al.* (2017). The destabilized rock glacier inventory was used as dependent variable, under the assumption that rock glacier destabilization is a representative process for permafrost degradation. Severely destabilized rock glaciers were considered as evidence of degrading permafrost, while stable rock glaciers as evidence of non-degrading permafrost. Topoclimatic variables derived from a 25-m DEM were sampled at the rock glacier locations and used as predictor variables. The correlations between dependent and predictor variables were modeled using a Generalized Addictive Model (GAM) and extrapolated to a susceptibility map.

Results

The inventory contains about 50 severely destabilized rock glaciers, i.e. 10% of the active rock glaciers in the area. About 30-40% of the active rock glaciers present some evidence of destabilization (categories 1 and 2). Although many cases of severe destabilization are very evident and undisputable, we emphasize that the inventory presents some degree of uncertainty due to subjective interpretations and orthoimagery distortions.

The strong performances of the GAM indicate that the methodology is consistent to model the link between topo-climatic settings and rock glacier destabilization. Rock glacier destabilization is more likely to occur in an altitudinal range between 2500 and 2700 m.s.l.. North facing, moderate slopes up to 35° with convex profiles seem to favor destabilization.

The model is used to compute a susceptibility map (Fig. 1), which displays the likelihood for the occurrence of rock glacier destabilization. The map manages to reproduce well most of destabilization patterns identified on rock glaciers, suggesting that its use may be of interest in land use planning and risk assessment.

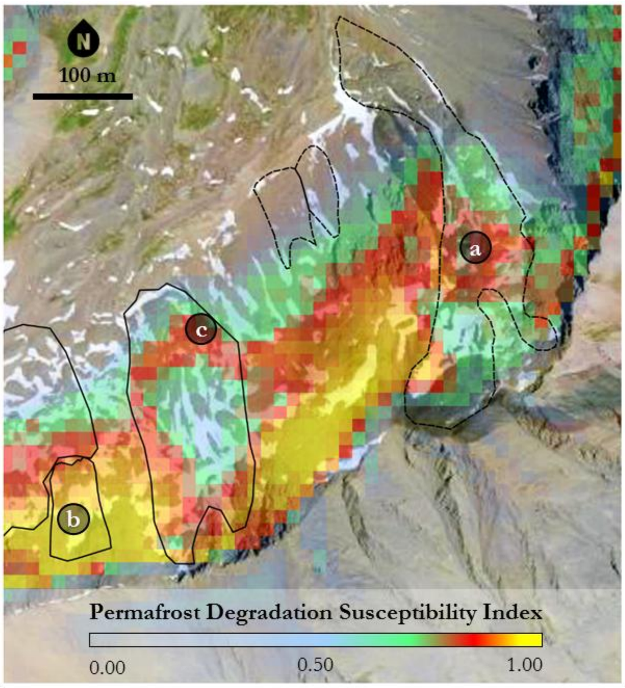

Figure 1. Example of Permafrost Degradation Susceptibility map, successfully identifying (a) the collapse zone of the Bérard rock glacier (Bodin *et al.,* 2016), (b) a destabilized active lobe and (c) a frontal debris flow gully on active rock glacier. Notice that the significance of the map outside rock glaciers is limited by the hypothesis that rock glacier destabilization is a significant process for degrading permafrost.

Conclusions

The present study reveals that rock glacier destabilization is a widespread phenomenon in the French Alps. Susceptibility modeling appears to be a consistent method to estimate the spatial footprint of degrading mountain permafrost that, according to our results, may interest about 20% of the periglacial belt. The present study therefore provides an exploratory methodology that can assess the spatial footprint of degrading permafrost in mountain areas, and the resulting susceptibility map can be of interest for land use planning and risk assessment.

Acknowledgments

This study is part of the PhD project PERMARISK, funded by the region Auvergne-Rhone Alpes, and the project PermaRisk, funded by the FEDER POIA program.

References

Bodin, X., Schoeneich, P., Deline, P., Ravanel, L., Magnin, F., Krysiecki, J. M., & Echelard, T. (2015). Mountain permafrost and associated geomorphological processes: recent changes in the French Alps. *Journal of Alpine Research*, 103-2, URL : http://rga.revues.org/2885; DOI : 10.4000/rga.2885.

Bodin, X., Krysiecki, J., Schoeneich, P., Roux, O., Lorier, L., Echelard, T., Michel Peyron, & Walpersdorf, A. (2016). The 2006 Collapse of the Bérard Rock Glacier (Southern French Alps). *Permafrost and Periglacial Processes*. DOI: 10.1002/ppp.1887

Marcer, M., Bodin, X., Brenning, A., Schoeneich, P., Charvet, R., & Gottardi, F. (2017). Permafrost Favorability Index: Spatial Modeling in the French Alps Using a Rock Glacier Inventory. *Frontiers in Earth Science* 5. DOI: 10.3389/feart.2017.00105

Rudy, A., Lamoureux, S., Treitz, P., Van Ewijk, K., Bonnaventure, P., & Budkewitsch, P. (2017). Terrain Controls and Landscape-Scale Susceptibility Modelling of Active-Layer Detachments, Sabine Peninsula, Melville Island, Nunavut. *Permafrost and Periglacial Processes*, 28, 79–91. DOI: 10.1002/ppp.1900

Rockfalls in the *Grand Couloir du Goûter* (Mont-Blanc massif) An interdisciplinary monitoring system

Jacques Mourey[1]
Pierre-Allain Duvillard[12]
Marco Marcer[3]
Guilhem Marsy[14]
Ludovic Ravanel[1]
Antoine Rabatel[5]

[1] *Univ. Grenoble Alpes, Univ. Savoie Mont Blanc, CNRS, EDYTEM, 73000 Chambéry, France,* jacques.mourey@univ-smb.fr
[2] *IMSRN, Parc Pré Millet - 680 Rue Aristide Bergès, 38330 Montbonnot, France*
[3] *Univ. Grenoble Alpes, Institue de Géographie Alpine, CNRS, PACTE, 38041 Grenoble, France*
[4]*Univ. Grenoble Alpes, Univ. Savoie Mont Blanc,* LISTIC Polytech Annecy-Chambéry, France
[5] *Univ. Grenoble Alpes, CNRS, IRD, Grenoble INP, IGE, UMR 5001, 38000 Grenoble, France*

Abstract

Permafrost degradation in the Alps implies more frequent and intense rockfalls. These rockfalls may represent a serious risk for people frequenting high mountain areas. This risk is very high in the *Grand Couloir du Goûter,* located on the most popular route to the summit of Mont-Blanc (4809 m a.s.l.) and numerous accidents and fatalities occur each year. In order to better understand the geomorphological conditions in which rockfalls are occurring and to better quantify the vulnerability, a monitoring system has been implemented including rock surface temperature loggers, automatic camera, terrestrial LiDAR and frequentation sensor. This interdisciplinary monitoring allows a vulnerability assessment and the identification of specific behaviors leading to accidents.

Keywords: permafrost degradation, snow cover, mountaineering, monitoring, Mont-Blanc massif.

In the context of global warming (IPCC, 2014), high alpine environments are affected by significant changes such as glacial retreat and permafrost degradation (Deline *et al.*, 2015). The latter is one of the main factors triggering rock slope instabilities at high elevations and implies more frequent and voluminous rockfalls (Ravanel *et al.,* 2017). Degrading permafrost thus represents a direct risk for mountaineers.

This risk is very important on the classic climbing route (the "*Royale*" route) to the summit of the Mont-Blanc (4809 m a.s.l.) – which is probably one of the most frequented mountaineering route in the world (about 15 000 person/yr). Before climbing up to the *Aiguilles du Goûter* (3863 m a.s.l.; Fig. 1), the route crosses the *Grand Couloir du Goûter* at 3270 m a.s.l., where rockfalls are very frequent especially between 10 am and 4 pm (AlpeIngé, 2012). As a consequence, between 1990 and 2011, and mainly due to rockfalls, 256 accidents occurred in this sector with 74 fatalities and 180 injured persons. On average, there are 3 fatalities and 8 injured persons per summer season (Descamps & Estachy, 2012).

Despite the volume and frequency of the rockfalls and the dangerousness of this route, very few studies have been carried out e.g. AlpeIngé (2012), Descamps & Estachy (2012) and Lemarchal (2011). Thus, there is a lack of data to understand and characterize the geomorphological conditions that control rockfalls.

Therefore, two monitoring methods have been implemented: (i) 4 rock surface temperature loggers have been installed in July 2016 at 10 cm deep in the rock at 3345, 3460, 3665 and 3830 m a.s.l. to characterize the local permafrost conditions; (ii) an automatic camera, installed in June 2016 is taking 4 pictures a day, allowing to study the snow cover and its control on permafrost and more generally on the rockfalls occurrence. A 3D model acquired by long range terrestrial laser scanning in 2016 allowed a precise study of the snow cover surfaces; another one is planned for the next summer to quantify the location and volume of the rockfalls occurred between the 2 scans. Moreover, a weather station located 600 m away from the couloir, at 3180 m a.s.l., is providing air temperature measurements. Pooled together, these data allow a better understanding of the geomorphological conditions that led to rockfalls during the summer 2016 and 2017.

At the same time, in order to quantify and characterize the attendance of the routes by mountaineers, in June 2017 a frequentation sensor has been installed on the track, before the couloir (Fig. 1). It measures the number and the walking direction of the mountaineers, allowing to quantify and characterize the vulnerability. As a result, it is estimated that 50 % of the 29.182 couloir crossings during the summer 2017 occurred between 10 am and 4 pm, *i.e.* when rockfalls are the more frequent.

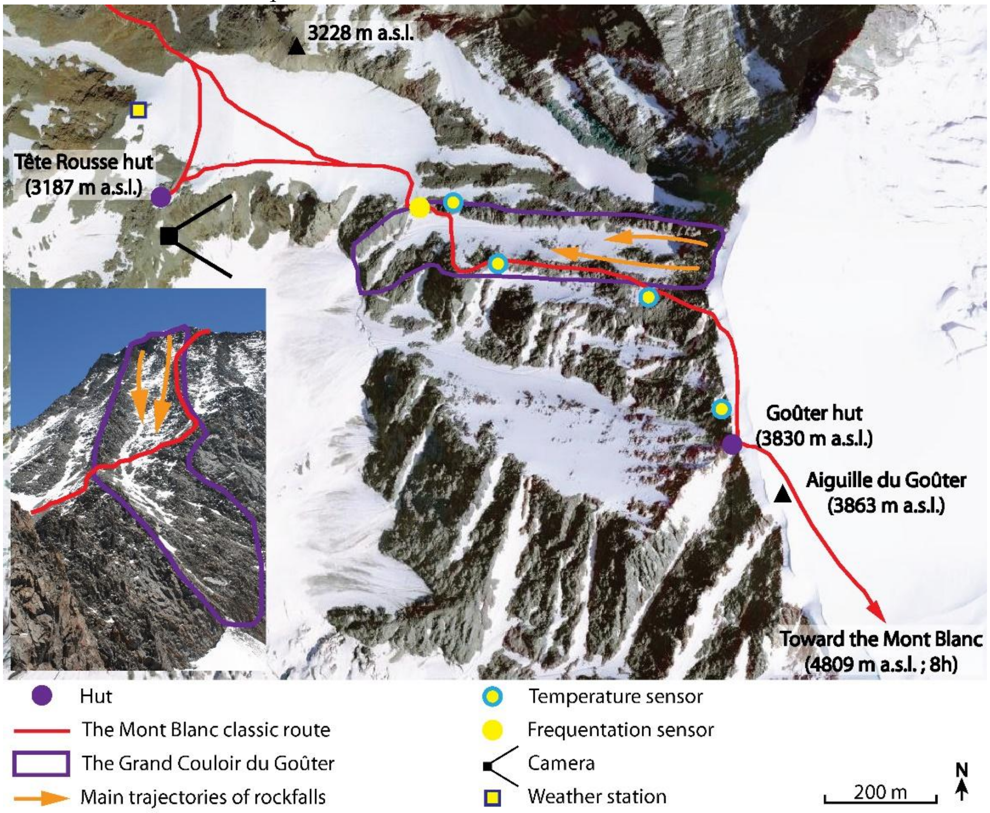

Figure 1. The monitoring system at the *Grand couloir du Goûter,* on the classic route to the Mont-Blanc.

First results are encouraging, suggesting that this interdisciplinary monitoring system will lead to a better vulnerability assessment and to the identification of behaviors not adapted to the local risk of rockfalls. On this basis, adaptation and prevention strategies can be proposed.

Acknowledgments

The authors thank the *Compagnie du Mont-Blanc* for facilitating access to the study site and the municipality of Saint-Gervais for allowing this study to set up. This study is part of the EU ALCOTRA *PrévRisk Haute Montagne* and *AdaPT Mont Blanc* projects.

References

Alpes Ingé., 2012. Couloir du Goûter, Suivi et analyse des chutes de blocs et de la fréquentation pendant l'été 2011. Rapport final. Fondation Petzl, 37 p.

Deline, P. Gruber, S. Delaloye, R. Fischer, L. Geertsema, M. Giardino, M. Hasler, A. Kirkbride, M. Krautblatter, M. Magnin, F., *et al.*, 2015. Ice loss and slope stability in high-mountain regions. Haeberli, W. Whiteman, C. and Shroder, J.F., (eds.), *Snow and Ice-Related Hazards, Risks, and Disasters*, Elsevier Science, Saint-Louis, p. 521-561.

Descamps & Estachy, 2012. Accidentologie dans le couloir du Gouter et sur la voie normale au Mont-Blanc, Étude des secours organisés sur l'itinéraire du glacier de Tête Rousse au refuge du Goûter, entre 1990 et 2011. Peloton de gendarmerie de haute montagne, Fondation Petzl, 28 p.

IPCC., 2014. Climate Change 2014: Impacts, Adaptation and Vulnerability. Part A: Global and Sectoral Aspects. Contribution of Working Group II to the Fifth Assessment Report of the Intergovernmental Panel on Climate Change, *Cambridge University Press, Cambridge-New York.*

Lemarchal, D., 2011. Traversée du grand couloir. Etude de faisabilité et avant-projet de sécurisation. EURL Meige, Fondation Petzl, 85 p.

Ravanel, L. Magnin, F. Deline, P., 2017. Impacts of the 2003 and 2015 summer heat waves on permafrost-affected rockwalls in the Mont Blanc massif. *Science of the Total Environment* 609:132–143. Doi: 10.1016/j.scitotenv.2017.07.055.

Modelling late Pleistocene and Holocene permafrost conditions in steep rock walls in Norway

Kristin Sæterdal Myhra[1]
Bernd Etzelmüller[2]
Sebastian Westermann[2]
Paula Hilger[3]

[1]*Western Norway University of Applied Sciences, Sogndal, Norway, kristism@hvl.no*
[2] *Department of Geosciences, University of Oslo, Norway*
[3]*Geological Survey of Norway, Trondheim, Norway*

Abstract

Stress redistribution following glacier retreat is often proposed as the main triggering mechanism of post-glacial rock slope failures in Norwegian mountain areas, but dated rock avalanche deposits indicate that slope failure events occurred regularly through the post-glacial period. Aiming for an improved understanding of post-glacial permafrost conditions, we have modelled the potential evolution of ground temperatures in Norwegian rock walls from the fully glaciated situation in the *Weichselian* (c. 20 000 cal. Yr. BP) until present with a two-dimensional heat conduction model. Our results indicate that the deglaciation dynamics controlled the permafrost conditions through the *Pleistocene*, while the glacial dependence relaxed through the *Holocene*. Though the modelling results imply that permafrost persisted more or less continuously in high elevation rock walls through the *Holocene*, oscillating temperature conditions in the steep rock walls may have influenced rock wall stability conditions and contributed to post-glacial failure mechanisms.

Keywords: numerical modelling; steep rock walls; slope stability

Introduction

The large climatic changes from the *late Pleistocene* until present have had pronounced effects on glacier dynamics, frozen ground conditions and the interaction between them. The investigation of rock wall permafrost is of high relevance for geohazard assessment as its changes over time can cause slope instability and trigger rock falls. Studies indicate that rock slope failure events in western Norway were in particularly numerous in the early *Holocene* (before 10 000 cal. Yr. BP) and clustered in certain time intervals through the *Holocene*, in particular between 3000 – 2000 cal. Yr. BP (Hermanns *et al.,* 2017). An improved understanding of temperature conditions in Norwegian rock walls through Weichselian deglaciation and the climatic variations in the post-glacial period are therefore of major interest within studies of permafrost and rock wall stability. Through this study, we aimed to test the hypothesis that the *Weichselian* deglaciation chronology influenced rock wall permafrost conditions through the post-glacial period. For this, we modelled the evolution of bedrock temperatures from the *Weichselian maximum in Scandinavia* (c. 20 000 cal. Yr. BP) until present for four rock slope sites in western Norway located along the fjord landscape.

The modelling study was performed with CryoGrid 2D (Myhra *et al.*, 2015), a process-based permafrost model in which the heat conduction equation with material and temperature dependent thermal parameters is solved. The potential post-glacial bedrock temperatures were modelled for simplified geometries representing a number of rock wall sites in western Norway with site-specific deglaciation dynamics. The forcing data were derived from the Greenland Ice Core temperature data (GISP2) shifted to fit the climatic conditions in western Norway. Deglaciation stages in Norway for different sites were evaluated based on Hughes *et al., 2016*.

Results and discussion

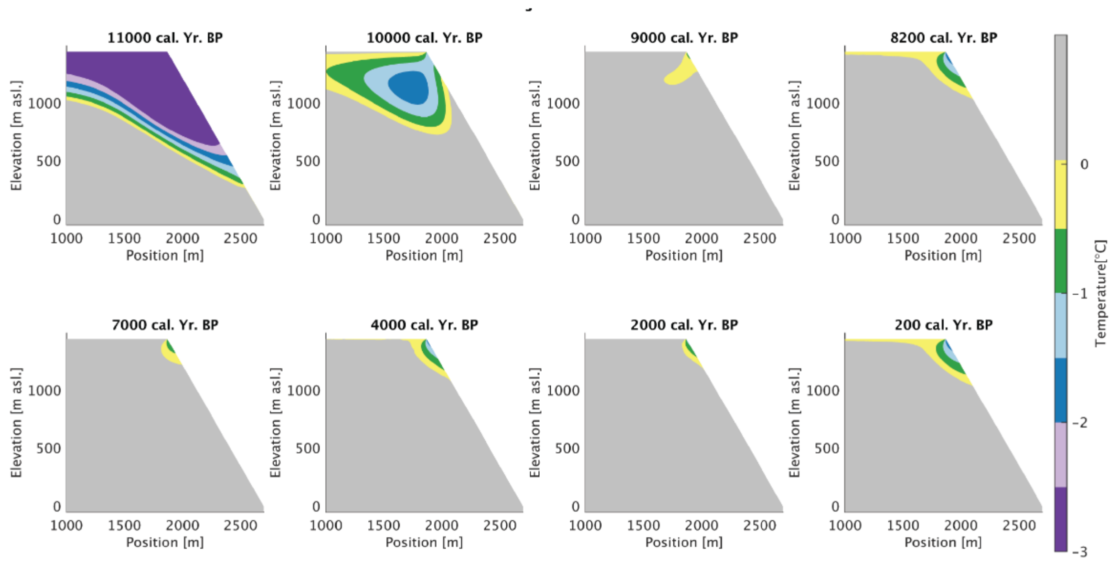

Figure 1. *Modelled ground temperature conditions for one of the chosen sites from the late Pleistocene and through the Holocene. Colors indicate frozen ground conditions*

According to our simulations, glacier dynamics and large climatic variations have induced significant bedrock temperature variations through the post-glacial period (Fig. 1). Our model results indicate rapidly warming ground temperature conditions through the late *Pleistocene* and early *Holocene*, followed by thermal oscillations through the *Holocene*. Further, our modelled ground temperature conditions indicate distinct different permafrost distribution, conditioned by varying deglaciation chronologies in southern Norway.

It is well accepted that changing ground temperatures may influence rock wall stability through increasing ice- and hydrostatic pressures in bedrock discontinuities and alter the shear strength along rock-ice interfaces through changing friction conditions, creep of ice and rock fracturing (Krautblatter *et al.*, 2013).

From our analysis it is evident that permafrost aggregated in many steep rock walls following glacier retreat, especially if rock walls became ice-free before the Younger Dryas. These large modelled permafrost bodies thawed towards the Holocene Thermal maximum. Several dated rock avalanche events in Norway occurred several thousand years after the deglaciation in periods with thawing permafrost conditions. This delay between deglaciation and rock avalanche events indicates that mechanisms other than glacial debuttressing have influenced the rock wall stability in addition.

Acknowledgements

This research was carried out within the CryoWALL project (243784/CLE), which is mainly funded by the Research Council of Norway. Funding was provided by the Department of Geosciences, University of Oslo and Western Norway University of Applied Sciences.

References

Hermanns, R. L., Schleier, M., Böhme, M., Blikra, L. H., Gosse, J., Ivy-Ochs, S., & Hilger, P. 2017. Rock-Avalanche Activity in W and S Norway Peaks After the Retreat of the Scandinavian Ice Sheet. In *Workshop on World Landslide Forum* (pp. 331-338). Springer, Cham.

Hughes, A. L., Gyllencreutz, R., Lohne, Ø. S., Mangerud, J., & Svendsen, J. I. 2016. The last Eurasian ice sheets–a chronological database and time- slice reconstruction, DATED- 1. *Boreas*, *45*(1), 1-45.

Krautblatter M, Funk D, Günzel FK. 2013. Why permafrost rocks become unstable: a rock–ice- mechanical model in time and space. *Earth Surface Processes and Landforms* 38: 876-887.

Myhra KS, Westermann S, Etzelmüller B. 2015. Modelled Distribution and Temporal Evolution of Permafrost in Steep Rock Walls Along a Latitudinal Transect in Norway by CryoGrid 2D. *Permafrost and Periglacial Processes.* 28(1):172-182.

Progresses in the investigation of the relation between climate and slope instability processes at high-elevation

Roberta Paranunzio[1]
Marta Chiarle[1]
Francesco Laio[2]
Guido Nigrelli[1]
Laura Turconi[1]
Fabio Luino[1]

[1]*Consiglio Nazionale delle Ricerche – Istituto di Ricerca per la Protezione Idrogeologica (IRPI), Torino Italy, roberta.paranunzio@irpi.cnr.it*
[2]*Politecnico di Torino, Torino, Italy*

Abstract

The ongoing debate about the effects of global warming in glacial and periglacial areas implies a lack of knowledge about the role of climate elements on the cryosphere dynamics. Slope instability processes are one of the major indicators of a changing climate at high elevation, but we know little about the relation between climate and slope instability processes. In this work, we briefly introduce our activities and developments on this issue. We collected more than 440 slope failures events at high-elevation sites in the Italian Alps from year 2000 on. By means of a statistical-based method, we detect the possible anomalies of the climate variables at the date when slope instability events occurred. Based on the preliminary outcomes of this work, we expect to be able to identify the variables which acted as potential triggers/drivers of slope instability processes in (peri)glacial and permafrost areas.

Keywords: Italian Alps, Climate change, Temperature, Rainfall, Statistical method, Slope instability.

Introduction

Climate is changing, this is unequivocal. This is even more evident in (peri)glacial areas, which are among the most sensitive environments to global warming (Chiarle *et al.*, 2017). Cryosphere/permafrost degradation and mass-wasting processes, could be considered as terrestrial indicators of changing climate (Gariano & Guzzetti, 2017). Slope instability processes could be triggered by a number of factors, including climate, seismic and anthropic activities. In this context, understanding how climate variables could effectively impact on initiation mechanisms is a key issue. Recent studies started to focus on the effects of air and rock temperature on rock mass stability (Nigrelli *et al.*, 2017; Weber *et al.*, 2017). Is it possible to quantitatively assess the role of the climate variables in the initiation mechanisms? A statistical-based method aimed to detect anomalous values in the climate variables at the date of occurrence of a slope failure at high-elevation has been proposed by Paranunzio *et al.*, 2015. Afterwards, Paranunzio *et al.* (2016) focused on the role of temperature in the initiation of high elevation rockfalls, thus concentrating on events without a clear rainfall, seismic, or anthropic trigger. For the present work, we inventoried all documented events at high elevation in the Italian Alps, from year 2000 on, including rainfall-induced events and types of slope instabilities which were not considered in Paranunzio *et al.*, 2016 (e.g., debris flows). We are also working on improving the method of Paranunzio *et al.*, 2015, to better characterize the trigger mechanisms behind the processes considered. Further developments on this issue will be the object of future works.

Characterization of the dataset

So far, our catalogue includes 443 slope instability events, occurred in the period 2000-2016 on the Italian Alps, above the elevation of 1500 m a.s.l. Data included in the inventory are mainly based on documentation coming from IRPI archives, Italian regional agencies and local/national newspapers. Fig. 1 illustrates the distribution of the events by process type.

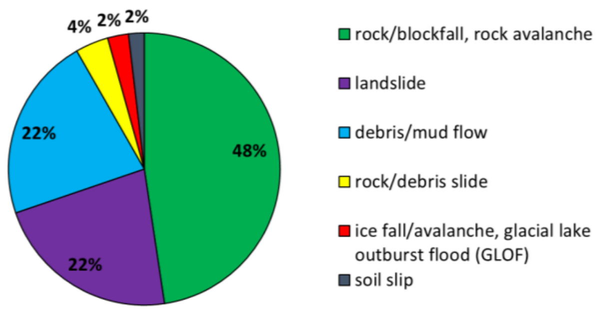

Figure 1. Type and sample size of the instability process included in the catalogue.

Fig. 2 shows the season of occurrence, elevation and slope aspect of the considered events. Based on the preliminary results of our analysis, the events mainly occur in summer in the lower (1500-2400 m a.s.l.) and medium (2400-3300 m a.s.l.) ranges of elevation, whereas spring and autumn events are concentrated at the lowest elevations. A frequency distribution analysis pointed out that the detachments areas are distributed across slopes of all aspects, with a major concentration on slopes facing from SE to SW.

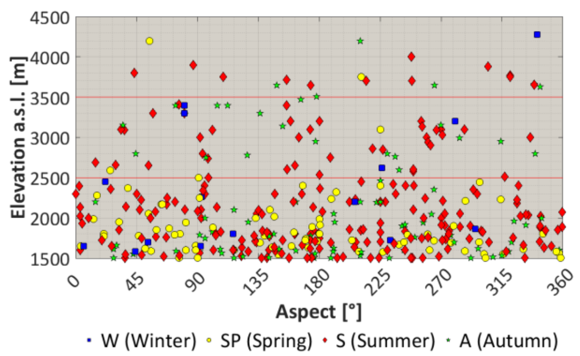

Figure 2. Season of occurrence of slope instabilities across aspects and elevation ranges.

Work in progress

For the analysis of this slope instability catalogue, we collected and organized climate data obtained from more than 230 weather stations, pertaining to different networks in the Italian Alps. We considered (i) mean, minimum, and maximum daily air temperature and (ii) daily cumulated precipitation. Data fragmentation entails inhomogeneity in information accuracy, thus only 363 out of the 443 case studies of the catalogue were selected for climatic analysis.

For the analysis of these 363 case studies, we aim to improve the method proposed by Paranunzio *et al.* (2015). Based on previous works (Paranunzio *et al.*, 2016) and on the preliminary outcomes of this study, we expect to catch a possible climatic signal (i.e. heavy precipitation and/or extreme temperatures) at different time scales that could be related to slope failure initiation. Our purpose is to summarize the variables that could be more impacting for the different process typologies considered. This approach could represent a further attempt towards a better characterization of the relation between climate warming and slope failure activity.

References

Chiarle, M. Cat Berro, D. *et al.* 2017. Slope instabilities occurred at high elevation in the Italian Alps in 2016: regional landscape fragility and meteorological framework. *Geophysical Research Abstracts*, Vol. 19, EGU2017-8498.

Gariano, S. L. & Guzzetti, F. 2016. Landslides in a changing climate. *Earth-Science Reviews*, 162, 227-252.

Nigrelli, G. Fratianni, S. *et al.* 2017. The altitudinal temperature lapse rates applied to high elevation rockfalls studies in the Western European Alps. *Theoretical and Applied Climatology* Online first.

Paranunzio, R., Laio, F. *et al.* 2015. A method to reveal climatic variables triggering slope failures at high elevation. *Natural Hazards*, 76(2), 1039-1061.

Paranunzio, R., Laio, F. *et al.* 2016. Climate anomalies associated with the occurrence of rockfalls at high-elevation in the Italian Alps. *Natural Hazards and Earth System Sciences*, 16(9), 2085-2106.

Weber, S., Beutel, J. *et al.* 2017. Quantifying irreversible movement in steep, fractured bedrock permafrost on Matterhorn (CH). *The Cryosphere*, 11(1), 567.

Contribution of the *PrévRisk Haute Montagne* project to knowledge and management of risks related to alpine permafrost

Ludovic Ravanel[1], Pierre-Allain Duvillard[1,2], Florence Magnin[3,1], Grégoire Guillet[1], Philip Deline[1]
Fabrizio Troilo[4], Elena Motta[4], Claudio Lucianaz[4]
Umberto Morra di Cella[5], Paolo Pogliotti[5], Edoardo Cremonese[5]
Luca Paro[6]

[1]*Univ. Grenoble Alpes, Univ. Savoie Mont Blanc, CNRS, EDYTEM, 73000 Chambéry, France, ludovic.ravanel@univ-smb.fr*
[2]*IMSRN, Montbonnot, France*
[3]*University of Oslo, Department of Geosciences, Oslo, Norway*
[4]*Fondazione Montagna sicura, Courmayeur, Aosta valley, Italy*
[5]*ARPA VdA, Saint Christophe, Aosta valley, Italy*
[6]*ARPA Piemonte, S.S. Monitoraggi e Studi Geologici, Italy*

Abstract

In the current context of climate change, with huge effects on high mountain areas, knowledge of emerging natural hazards as well as information and awareness policies on such hazards are priorities for local authorities who must manage these risks. Thus, with the objective of improving the resilience of mountain communities facing emerging risks, the Interreg V-A ALCOTRA n°342 *PrévRisk Haute Montagne* project - which brought together 6 Italian and French partners (and a Swiss participant) between 2016 and 2017 - has developed a large number of awareness and knowledge actions on risks related to permafrost, in particular through data networking.

Keywords: Permafrost, rockwalls, rock glaciers, risks, networking.

Introduction

The overall objective of actions on permafrost within the *PrévRisk Haute Montagne* project was to consolidate knowledge of high alpine permafrost in order to improve the associated risk analysis, capitalizing on the results and tools developed in previous projects (*PERMAdataROC*, *PermaNET*, *RiskNat*).

Data sharing on permafrost and related risks

This activity has enabled the update of the APD platform (www.alpine-permafrostdata.eu ; Cremonese *et al.*, 2011) which aims in particular to provide an operational tool for information on permafrost to managers and technicians working in this field. The database contains (i) the location, (ii) the characteristics and (iii) the related data of 436 evidences (Dec. 2017) of presence of permafrost in the Alps. These evidences are high elevation sites where permafrost-related slope instabilities have occurred, soil temperature monitoring sites or periglacial surface velocities, and sites where the presence of permafrost has been attested by geophysics, geomorphology, or building.

The action also enabled the reactivation and improvement of data collection activities on high-altitude rockfalls in the Mont Blanc massif (MBM; Ravanel & Deline, 2013), which are crucial for understanding this permafrost-related process. Operational since 2007, a network of observers (mountain guides, hut keepers, mountaineers, rescue teams) is supported since 2014 by the *Alp-Risk* app, newly replaced by the *Obs-Alp* app. More than 150 rockfalls, from 100 to 44 000 m^3, were documented during the project, especially during the 2017 summer heatwave (*cf.*: Ravanel *et al.*, 2017a). The largest one occurred during the night of 28-29 September 2017 at Eperon Tournier, in the north face of the Aiguille du Midi (3842 m a.s.l.). A few days later, ice was extracted from the rockfall scar and is currently being analyzed (dating, structure). An analysis of the dataset collected in the APD as well as by the network of observers is underway.

Advanced monitoring methods for permafrost-related risk analysis

The aim was to develop monitoring methods - often experimental - for the analysis and understanding of permafrost-related risks. The methods used were mainly focused towards the identification of surface movements (creep, block and fracture movements in rock masses) and the characterization of the internal structure of rock glaciers and rock slopes.

Drone photogrammetry and terrestrial laser scanner (LiDAR) measurements have enabled the construction of digital terrain models (DEMs) with centimeter resolution over several rock glaciers (*e.g.* Gran Sometta and Pointe d'Arpisson active rock glaciers in Aosta Valley, Italy) and ~ 12 rockwalls in the MBM (*cf.*: Ravanel *et al.*, 2012). The comparative analysis of the DEMs resulting from each flight or LiDAR survey makes it possible to obtain, for each pixel/point, in a chronological series, the surface movements and, consequently, an extremely detailed dynamic surface description of the slope movements.

Geophysical methods, such as electrical resistivity tomography (Magnin et al., 2015a), made possible to complete the understanding of the study areas, in particular to determine areas with degrading permafrost (sometimes below infrastructure, including the Grands Montets cable-car and the Cosmiques refuge in the MBM). Each partner has made available to others their expertise and tools to share techniques and methods of acquisition, processing, and analysis of the data.

Development of key permafrost monitoring sites

In order to ensure the long-term viability of the instruments present in several major permafrost monitoring sites or to develop new sites, the project has enabled the maintenance, replacement and installation of new sensors (Ravanel *et al.*, 2017b). Visits and field activities common to all the partners helped to enhance the partnership nature of the project.

The monitoring has been optimized at Cime Bianche (*cf.*: Pogliotti *et al.*, 2015), Gran Sommetta, Cervino (Aosta Valley), and completed at Grands Montets, Aiguille du Midi (*cf.*: Magnin *et al.*, 2015b) and Cosmiques (MBM). The site of the new Goûter refuge (3835 m a.s.l.) has also been instrumented (MBM). In Piemonte (Italy), a multi-parameter station comprising a 30-m-deep borehole equipped with DMS – including 30 inclinometers, 30 temperature sensors and 2 accelerometers – was set up on the southern ridge of Mount Rocciamelone (3538 m a.s.l.; https://youtu.be/yGRi5InYKMI), affected by major gravitational process that is accelerating over the last 15 years (Paro *et al.*, 2016).

Finally, a new field of research has been developed about the evolution and the role of ice/snow covers on permafrost-affected rockwalls: two boreholes were drilled in the MBM at the Tour Ronde (3792 m a.s.l.) and Mont Blanc du Tacul (4248 m a.s.l.) to measure the temperature inside the ice and at its base.

References

Cremonese, E. *et al.*, 2011. An inventory of permafrost evidence for the European Alps. *The Cryosphere* 5: 651-657.

Magnin, F., Krautblatter, M., Deline, P., Ravanel, L., Malet, E. & Bevington, A., 2015a. Determination of warm, sensitive permafrost areas in near-vertical rockwalls and evaluation of distributed models by electrical resistivity tomography. *Journal of Geophysical Research* 120: 745-762.

Magnin, F., Deline, P., Ravanel, L., Noetzli, J. & Pogliotti, P., 2015b. Thermal characteristics of permafrost in the steep alpine rock walls of the Aiguille du Midi (Mont Blanc Massif, 3842 m a.s.l). *The Cryosphere* 9: 109-121.

Paro, L., Re Fiorentin, G. & Ronchi, C., 2016. Monitoraggio geotechnico e termico della cresta sud del Monte Rocciamelone. *Neve e Valanghe* 87:4-15.

Pogliotti P., Guglielmin M., Cremonese E., Morra di Cella U., Filippa G., Pellet C. & Hauck C., 2015. Warming permafrost and active layer variability at Cime Bianche, Western European Alps. *The Cryosphere* 9: 647-661.

Ravanel, L. & Deline, P., 2013. A network of observers in the Mont Blanc massif to study rockfalls from high alpine rockwalls. *Geografia Fisica e Dinamica Quaternaria* 36: 151-158.

Ravanel, L., Deline, P., Lambiel, C. & Vincent C., 2012. Instability of a highly vulnerable high alpine rock ridge: the lower Arête des Cosmiques (Mont Blanc massif, France). *Geografiska Annaler A* 95: 51-66.

Ravanel, L., Magnin, F. & Deline P. (2017a). Impacts of the 2003 and 2015 summer heat waves on permafrost-affected rockwalls in the Mont Blanc massif. *Science of the Total Environment* 609: 132-143.

Ravanel, L., Malet, E., Duvillard, P.-A., Magnin, F., Deline, P., Guillet, G., Troilo, F., Pogliotti, P., Morra di Cella, U., Beutel, J. & Gruber S. (2017b). Instrumentation thermique et cinématique des parois à permafrost du massif du Mont Blanc. *Collection Edytem* 19: 27-38.

Permafrost Degdradation as Key Factor for Process Chains and Prediction of Climate Change induced Mass Movements

Daniel Tobler[1]
Isabelle Kull[2]
George Gotziridse[3]
Mikheil Elashvili [2]

[1]*Geotest Ltd, Zollikofen, Switzerland, daniel.tobler@geotest.ch*
[2] *Geotest Ltd, Zollikofen, Switzerland*
[3] *Geographic Ltd., Tbilisi, Georgia*
Ilia State University, Tbilisi, Georgia

Abstract

Climate change affects the cryosphere in a strong way. Since 2012 different studies concluded that there is high confidence that changes in heat waves, glacial retreat and/or permafrost degradation will have a strong on high mountain phenomena such as slope instabilities, mass movements and glacial lake outburst floods (GLOF). The overall frequency of debris flows may decrease in absolute terms, but the magnitude of events may increase. Permafrost degradation mainly stands at the beginning of the different process chains. The precise prediction of permafrost development using downscaling methods is one of the major key factors to create high quality input data in sophisticated mass movement simulation tools. The results are presented in a so-called periglacial hazard indication map visualizing endangered areas in the future for mass movement processes. It is a useful instrument for the authorities to identify potential hot spots of future hazard areas and the basis for a specific hazard management in high mountain regions. Devastating events and ongoing case studies from Switzerland and Georgia emphasize the needs of such products.

Keywords: permafrost degradation, downscaling, glacier retread, high mountain, climate change, prediction

Introduction

After the exceptional rock fall occurrence throughout the Alps during the unusually hot summers of 2003 (Gruber et al. 2004) and 2017, slope instabilities from the periglacial environment became the focus of various research activities, especially in the highly populated European Alps. Based on the observed clustering of large rock slope failures in high mountain areas around the world in recent years, Huggel et al. (2013) present approaches that can be potentially used to detect changes in landslide activity in high mountains. The approaches include the analysis of slope failure inventories, case histories and trigger mechanisms, and Huggel et al. (2013) concluded that these are promising avenues for detection studies. Gruber (2012) notes the difficulties of understanding low frequency and high-magnitude events, such as landslide hazards in cold regions that may be intensified by progressive and nonlinear changes in the periglacial environment.

Geohazard trigger mechanism from permafrost-underlain terrain, such as rock fall and debris flow, usually include some effect of water. Slope instabilities leading to a debris flow may be initiated by the reduction in effective stress at the permafrost table in combination with seepage pressure. Rock fall is often related to the formation of hydrostatic pressures or expansion pressures from the freezing of water in unfavorably oriented joint sets. Two key meteorological parameters can affect these triggering mechanisms due to climate warming: (i) increase in air temperatures; and (ii) increase in precipitation type, intensity and duration. Higher air temperatures result in a thickening of the active layer and likely changes in the frequency of freeze-thaw cycles.

Changes in precipitation regime can alter seepage pressures in the active layer or the hydrostatic pressure within a fractured bedrock system. For example, a change towards higher rainfall intensities may lead to accelerated transient pore water pressure increases and subsequent slope failure. The combination of such changes may influence the geohazard potential. When evaluating these parameters, it is important to not just consider changes in average values but take into account projected extremes, since risk assessments need to account for the full range of possible geohazard scenarios.

In the end process chains from the beginning (thawing permafrost) to the very end down in the valley (debris flow and flood processes) have to be considered for the hazard management as well as the risk assessment.

Downscaling Permafrost Data

Thawing permafrost and retreating glaciers stand at the beginning of the process chains. Gruber (2013) developed a high-resolution map of the permafrost area over most part of the world, based on DTM and climate data with a resolution of < 1 km. These data are freely available. To detect areas where permafrost degradation can increase the disposition for hazard processes like rock avalanches and debris flows or where sediment supply can be augmented drastically this resolution is still too coarse, especially in mountainous areas. A procedure has been developed to downscale the permafrost zonation index. Based on the detailed permafrost zonation index map, the classified ground surface material and the aspect areas, where climate change induced permafrost degradation can cause higher sediment mobilisation.

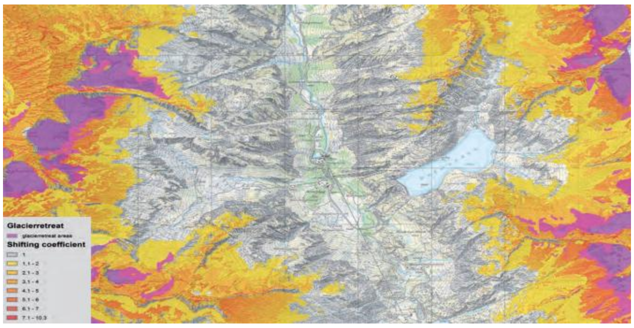

Figure 1: Permafrost indication map downscaled to use as input for process simulations (Tobler et al., 2015).

Periglacial Hazard Indication Map

The prediction of periglacial processes and their consequences is an interdisciplinary question. Meteorological scenarios for the future derived from climate change scenarios stand at the beginning of the decision chains. The susceptible periglacial areas which act as starting zones for mass movements or new sediment sources can be calculated through sophisticated permafrost and glacier retreat models. Well established simulation tools allow to predict the process extensions in the mountain valleys. The results are presented in a so-called periglacial hazard indication map visualizing endangered areas in the future for mass movement processes as well as other natural hazards like floods or subglacial lake outburst (Tobler et al. 2015). Such a map provides a basis for answering further-reaching planning, policy and financial questions regarding the evolution of natural hazards in the study area. It is a useful instrument for authorities to identify potential hot spots of future hazard areas and the basis for a specific hazard management in high mountain regions. The new developed methodology has to be calibrated by events and other studies.

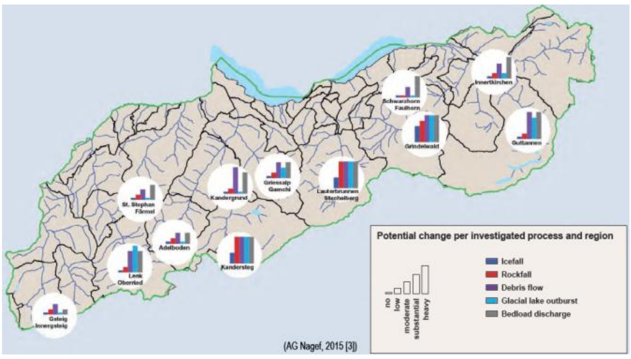

Figure 1: Prospective natural hazard potential in the Bernese Oberland, Switzerland (AG Nagef, 2015).

Case Studies Switzerland / Georgia

The first study for a detailed periglazial hazard indication map has been elaborated in Switzerland. Further similar permafrost based studies have been carried out at Jungfraujoch, Top of Europe (Dalban et al., 2018) and Schilthorn. A new will in Georgia. The mountainous tourist areas of Mestia and Mt. Kazbeg are prone to periglacial hazard processes. This has been demonstrated by climate change induced flood events in September 2017 in Mestia and different glacial debris flow events at Devdoraki valley since 2014. The ongoing assessment of periglacial hazard situation and the following prediction of possible process chains and process areas in the two major tourist regions will give the Georgian authorities the possibility to develop their areas with respect to the future hazard situation.

References

-AG Nagef (2015): Klimawandel und Naturgefahren
- Gruber S., Haeberli W. and Hoelzle M., (2004): Permafrost thaw and destabilization of Alpine rock walls in the hot summer of 2003. Geoph. research letters, Vol. 31, L13504, doi:10.1029/2004GL020051, 2004
- Huggel C., Korup O., Gruber, S. (2013): Landslides and climate change. In: Shroder, Jr J.F.(ed.), Treatise on Geomorphology. Academic Press, , vol. 13, 288-301.
- Tobler D., Riner R., Mani P., Haehlen N., Raetzo H. (2015): Prediction of climate change forced mass movement processes induced in periglacial areas. In G.Lollino et al.(eds.), Engineering Geology for society and Territory, Springer.
- Gruber, S. (2012): A global view on permafrost in steep bedrock, Proceedings of the 10th International Conference on Permafrost, 25–29 June 2012, Salekhard, Russia, 131–136.
- Dalban P., Ryter U., Tobler D., Badoux V., Roth G. (2018): Combined rock temperatures modelling and glaciological survey on the Jungfraujoch (Switzerland). EUCOP 2018, Conference Proceedings (in press)

Acoustic and micro-seismic signal of rockfall on Matterhorn

Samuel Weber[1]
Jan Beutel[2]
Jérome Failletaz[1]
Matthias Meyer[2]
Andreas Vieli[1]

[1]*Department of Geography, University of Zurich, Switzerland*
[2]*Computer Engineering and Networks Laboratory, ETH Zurich, Switzerland*

Abstract

Despite substantial technical advances in the instrumentation of steep rock slopes, our ability to detect precursor events of rock slope instability remains limited. In this study, we investigate the acoustic and micro-seismic signal of fracture and rockfall events at Matterhorn. A rockfall event with a volume of 2 to 3 m³ was recorded by crackmeter and micro-seismic measurements on 14 August 2015 UTC 20:10 with high energy concentration below 100 Hz. The acoustic emission (higher frequency range) did not capture the rockfall event itself, but occurs coincidently with preceding irreversible fracture displacements. In the lower frequency range, we clearly capture the rockfall event, but to our surprise the wave amplitude and energy during the rockfall event was not higher than in the preceding ten days.

Keywords: bedrock permafrost; acoustic and micro-seismic; rock fall; Matterhorn

Introduction

Understanding of processes and factors affecting slope stability is essential for detecting and assessing the stability of potentially hazardous slopes. Despite substantial technical advances in the instrumentation of steep rock slopes, our ability to detect precursor events of rock slope instability remains limited. This study investigates the acoustic emissions (AE) and micro-seismic (MS) signal emitted by a rockfall event (2-3 m³) in steep, structured bedrock permafrost on Matterhorn Hörnligrat (Fig. 1) on 14 August 2015.

Field Site and Methodology

The Hörnligrat field site is located at an elevation of 3500 m a.s.l. on the North-East ridge of Matterhorn in the Swiss Alps (Weber *et al.*, 2017). Several rockfall events were observed in spring 2015 using a time-lapse camera. Consequently, the existing fracture observation have been complemented by continuous broadband AE/MS monitoring. AE and MS signals are elastic waves generated by the rapid release of energy within a material (Hardy, 2003). AE refers to waves with a frequency in the range 10^4-10^6 Hz while MS signals are in the range 1-10^3 Hz (Amitrano *et al.*, 2012). The instrumentation required to cover the frequency range 1-10^5 Hz consists of three different transducer types: piezoelectric sensors for capturing AE, accelerometer and seismometers for MS range.

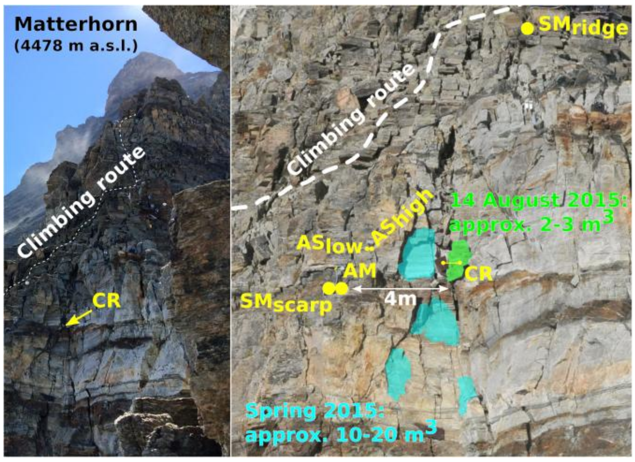

Figure 1. Instrumentation measuring fracture kinematics (CR), AE (AS) and MS (SM and AM) is indicated in yellow.

Results

The rockfall event investigated in this study was detected on 14 August 2015 UTC 20:10.32. A preceding fracture displacement of 13.2 mm was measured 10 h previously and a much smaller of only 0.15 mm occurred on 9 August 2015 (red arrows in Fig. 2a).

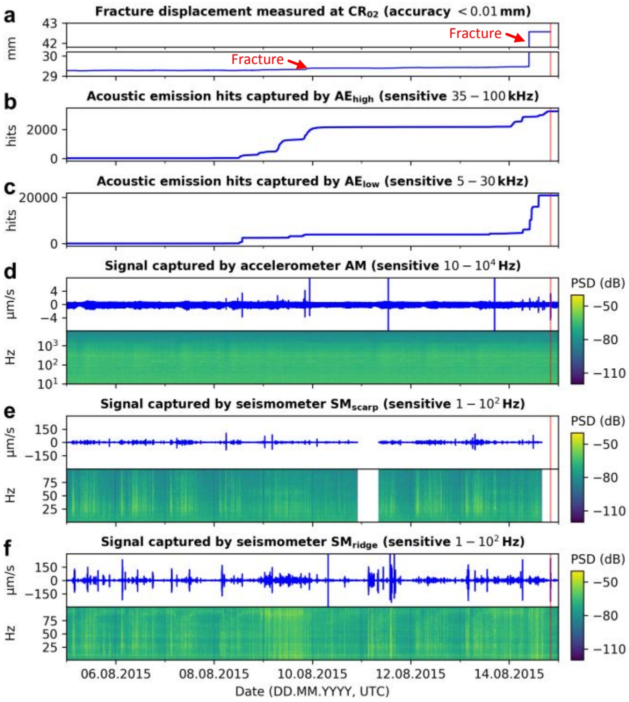

Figure 2. Crackmeter and AE/MS records during a ten-day period preceding the rockfall event on 14 August 2015 UTC 20:10 (indicated with vertical, red line).

Most of the threshold triggered AE events were captured before or at these previous fracture displacements, but none during the failure event itself (Fig. 2b+c). On the contrary, the waveforms measured at the accelerometer and seismometers show several times high amplitude values, which are asynchronous of the measured fracture displacement (Fig. 2d-f).

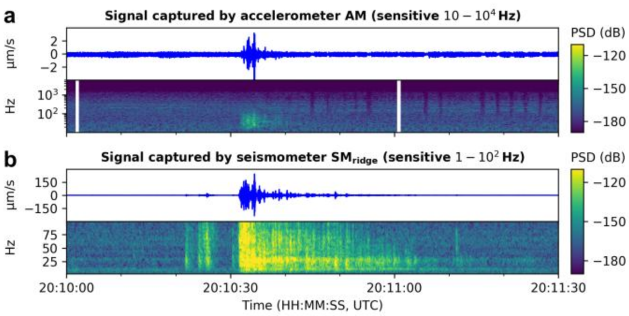

Figure 3. Waveform and spectrograms over the period of the rockfall event on 14 August 2015 measured by the accelerometer in the scarp and the seismometer on the ridge.

However, there are amplitude peaks in the MS range coincident with the failure and the two preceding displacements, but with lower amplitudes. Figure 3 shows the measured MS response to the failure at the accelerometer (AM) and the seismometer on the ridge (SM_{ridge}), indicating high power concentration below 100 Hz and a post-event seismic tremor.

Discussion

AE/MS signals recorded during a ten-day period preceding a rockfall event shows (i) the ability of MS to capture failure events and (ii) an increase in AE activity likely linked to irreversible fracture displacement. However, no AE events were emitted during the finale failure itself. A main challenge in AE/MS analysis is separating signal by progression of damage from environmental (wind, hail, etc.) and anthropogenic noise (mountaineers, helicopters, etc.). Therefore, it remains unclear whether the increased AE activity relates to the irreversible fracture displacement or to a noise source. Further, recognition of small failure events turned out to be difficult, because the MS records of the failure are not clearly distinguishable from other events although irreversible fracture displacement is often related to snowmelt or in-situ measured rainfalls periods.

References

Amitrano, D., Gruber, S. & Girard, L., 2012. Evidence of frost-cracking inferred from acoustic emissions in a high-alpine rock-wall. *Earth Planet. Sci. Lett.* 341–344: 86–93.

Hardy, H. R., 2003. *Acoustic Emission/Microseismic Activity*. The Netherlands. Sets & Zeitlinger B.V., 270 pp.

Weber, S., Beutel, J., Faillettaz, J., Hasler, A., Krautblatter, M. & Vieli, A., 2017. Quantifying irreversible movement in steep, fractured bedrock permafrost on Matterhorn (CH), *The Cryosphere* 11: 567-583.

25 - Open session on mountain permafrost

Session 25

Open session on mountain permafrost

Conveners:

- **Martin Hoelzle**, Department of Geosciences, Université de Fribourg, Fribourg, Switzerland
- **Sebastian Vivero**, Institute of Earth Surface Dynamics (IDYST), University of Lausanne, Lausanne, Switzerland (PYRN member)

This session is related to permafrost as an important variable of the mountain cryosphere. We are expecting all different sorts of research contributions related to interactions of permafrost with the climate and corresponding impacts on the natural and human systems in mountain permafrost environments.

This session is thought to complement the more specific sessions proposed at the conference. We are looking forward to receive a large number of contributions reflecting different fields ranging from theory to applied approaches at diverse geographic locations. We would like to stimulate especially contributions and discussions about near surface processes, theoretical concepts, measurement technologies, monitoring strategies, different model approaches on different scales and the related uncertainties.

Improved sensitivity analysis of permafrost models to projected changes in continentality, Yukon, Canada

Philip P. Bonnaventure[1], Antoni G. Lewkowicz[2] & Robert G. Way[3]
[1]*Department of Geography, University of Lethbridge, Philip.bonnaventure@uleth.ca*, [2]*Department of Geography, Environment and Geomatics University of Ottawa,* [3]*Labrador Institute, Memorial University of Newfoundland*

Abstract

The effects of continentality (defined as large shifts between winter and summer air temperature) have been examined in the high-latitude mountains of the Yukon in western Canada to examine the impact on the future (RCP 8.5, 2100) distribution of permafrost. This study involved the generation of a high-resolution mean annual air temperature (MAAT) model with input data from almost 60 local stations as well as field observations of surface lapse rate (SLR). These data were then used to interpret permafrost probability using a logistic regression model with nearly 800 observations of permafrost presence/absence. The MAAT field was recalculated using temperature increases corresponding to (1) downscaled spatially variable GCM scenarios, and (2) downscaled GCM scenarios adjusted for changes to local SLRs associated with reduced annual temperature range due to enhanced warming in winter. The MAAT fields calculated with variable SLRs exhibited above-average warming, and loss of permafrost, in the valley bottoms and lesser amounts at high elevations.

Keywords: Mountain Permafrost, Continentality, Surface Lapse Rate (SLR), Yukon, AR5, Sensitivity.

Introduction

The distribution of permafrost in the mountain ranges of the Yukon differs from those in mid-latitudes because temperature dependence on elevation is non-linear and spatially variable (Bonnaventure et al., 2012). Permafrost may be present below treeline due to the high frequency of near-surface air temperature inversions which alter Surface Lapse Rates (SLRs), especially in winter. Prior work has linked inversion frequency and strength to temperature amplitude (continentality), defined as the difference in the mean temperatures between the warmest and coldest months, and land cover type (Lewkowicz & Bonnaventure, 2011). Correspondingly, regional-scale SLRs can be estimated from temperature amplitudes and land cover products for historical and future climate scenarios across the region. Incorporation of the magnitude and sign of SLRs for climate scenarios into empirical statistical permafrost modelling allows spatial trends in mountain permafrost distribution to be predicted for the present day and into the future. SLRs and inversions also control how the permafrost distribution is expected to change as climate warms and a new equilibrium is established. Previous modelling of permafrost change for future climate scenarios has been based on uniform changes in mean annual air temperature (MAAT) (e.g. +1 to +5°C) (Bonnaventure & Lewkowicz, 2013). However, GCM predictions for the region indicate that the magnitude of warming will be seasonally and spatially variable.

Our hypothesis is that changes to temperature amplitude (i.e. continentality) will be associated with alterations to the pattern and magnitude of SLRs. Radiosonde records from Whitehorse (1958-2003) support this interpretation and show a clear link between climate warming and reduced temperature amplitudes. This study examines the impact of changes in continentality on high-latitude mountains through an improved analytical framework that incorporates more climate stations than prior work and is based on downscaled predictions from the IPCC fifth assessment report (AR5).

Study region

The study region extends from 59 °N to 65 °N and from the Yukon/NWT border to the Yukon/Alaska border, covering an area of approximately 400 000 km² (Figure 1).

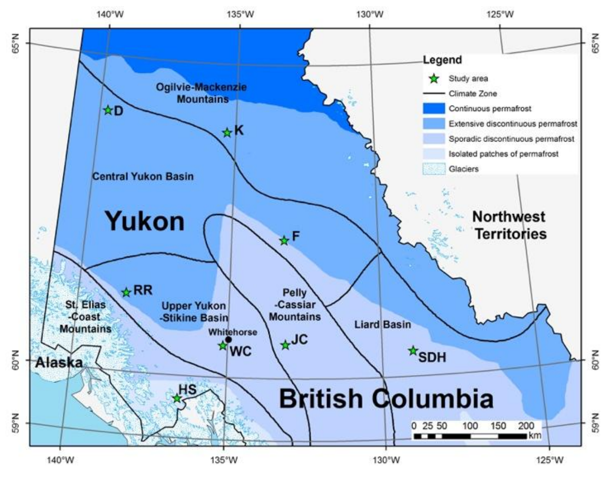

Figure 1. Study area map including locations field observation.

The region is part of the Cordilleran orogen geological grouping, comprising large mountain belts of deformed and metamorphosed sedimentary and volcanic rocks, mainly of the Phanerozoic and Proterozoic ages (Wahl et al., 1987). Elevations range from 250 m a.s.l. in the Yukon River valley to higher than 5000 m a.s.l. in the St. Elias Mountains. With the exception of glaciated portions, the entire region falls within the Boreal Cordillera ecozone. The climate of the region is mainly subarctic continental, with long, cold winters and short, warm summers, varying with elevation and aspect. MAAT currently ranges from about 5 °C in the extreme southwest to <-10 °C on the highest mountain peaks (Lewkowicz et al., 2012).

Methods

Permafrost probability across the mountainous regions of the southern Yukon and northern British Columbia was generated at a high spatial resolution (30 m). This model was produced for current climate conditions (2001-2015) using logistic regression driven by climate data (MAAT) from approximately 60 stations in Yukon, British Columbia, NWT and Alaska and field observations of SLR and interpolated using known relations between temperature amplitude and SLR. The model was calibrated against nearly 800 physical observations of permafrost presence or absence. The MAAT field was then recalculated for the current period using temperature increases corresponding to (1) downscaled spatially variable GCM scenarios according to Representative Concentration Pathway (RCP) scenarios from AR5 (shown here RCP 8.5 for 2100), and (2) downscaled RCP scenarios with adjustments for changes to local SLRs due to reduced annual temperature range caused by asymmetrical seasonal warming (Table 1).

Table 1. Subset of station data used to calculate new SLRs for stations in the study region.

Station n = 58	MAAT (°C) 2001-15	Amplitude (°C) 2001-15	SLR (°C km-1) 2001-15	Amplitude (°C) RCP 8.5 2100	SLR (°C km-1) RCP 8.5 2100
Atlin	1.26	24.30	-4.49	23.68	-4.70
Dawson	-3.66	40.49	1.00	37.97	0.14
Fort Good Hope	-5.28	43.46	2.01	38.90	0.46
Fort Nelson	0.05	36.06	-0.50	34.94	-0.88
Haines Junction	-1.71	29.56	-2.70	28.10	-3.20
Mayo	-1.78	36.80	-0.24	34.25	-1.11
Norman Wells	-4.70	42.20	1.57	37.98	0.15

Results

The MAAT fields calculated with variable SLRs exhibited above-average warming in the valley bottoms and lesser amounts at high elevations. The different methods used to model MAAT affected both the total permafrost extent at the regional scale and the pattern of permafrost change in relation to the topography. The model taking into account continentality revealed greater spatial change of permafrost in valley bottoms in continental areas where warming was modelled to be amplified in comparison to adjacent mountain tops. We conclude that predictions of future permafrost probabilities for purposes such as infrastructure planning or rapid mass movement modelling should incorporate the impact of alterations to the elevational pattern of air temperature change, as well as the magnitude of change.

Acknowledgments

The authors are grateful for the support of the National Science and Engineering Council of Canada (NSERC) as well as the Yukon Fire Network for providing station data.

References

Bonnaventure P.P., Lewkowicz A.G., Kremer M. and Sawada M.C. 2012. A Permafrost Probability Model for the Southern Yukon and Northern British Columbia, Canada. *Permafrost and Periglacial Processes.* 23: 52-68, doi: 10.1002/ppp.1733.

Bonnaventure P.P. & Lewkowicz A.G. 2013. Impacts of mean annual air temperature change on a regional permafrost probability model for the southern Yukon and northern British Columbia, Canada. The Cryosphere, 7: 935-946. doi: 10.5194/tcd-6-4517-2012.

Lewkowicz A.G. & Bonnaventure P.P. 2011. Equivalent Elevation: A New Method to Incorporate Variable Surface Lapse Rates into Mountain Permafrost Modelling. Permafrost and Periglacial Processes*,* 22: 153-162, doi: 10.1002/ppp.720.

Lewkowicz, A.G., Bonnaventure, P.P., Smith, S.L., and Kuntz, Z. 2012. Spatial and thermal characteristics of mountain permafrost, Northwest Canada. *Geografiska Annaler,* 94, 195-213, DOI: 10.1111/j.1468-0459.2012.00462.x

Wahl H.E., Fraser D.B., Harvey R.C. and Maxwell J.B. 1987. *Climate of Yukon.* Canadian Government Publishing Centre.

Transient modelling of permafrost distribution in Iceland

Justyna Czekirda[1]
Sebastian Westermann[2]
Bernd Etzelmüller[2]
Tómas Jóhannesson[3]
[1]*Department of Geosciences, University of Oslo, Oslo, Norway, justync@student.geo.uio.no*
[2]*Department of Geosciences, University of Oslo, Oslo, Norway*
[3]*Icelandic Meteorological Office, Reykjavík, Iceland*

Abstract

The ground thermal regime of the potential permafrost area in Iceland in the period 1960-2015 is modelled by employing a transient permafrost model, CryoGrid 2, which is forced by the gridded data sets of air temperature and snow depth series derived from precipitation data using a degree-day based algorithm. The model validation is based on ground temperature measurements, ground surface temperature loggers along with occurrence of permafrost-related landforms such as rock glaciers.

Keywords: Iceland; transient permafrost modelling; permafrost mapping; maritime permafrost; permafrost dynamics

Introduction

Globally, the distribution of mountain permafrost has been mapped and monitored mainly in locations with relatively continental climates characterized by a stable snow cover and low winter temperatures. In contrast, there is a paucity of systematic ground temperature investigations from maritime mountain areas such as Iceland. Knowledge of the present distribution and thermal characteristics is crucial for assessing the response of permafrost to climate change and its geomorphological and geotechnical impact. The importance of permafrost degradation for slope processes in Iceland has been exemplified in 2011 when a large landslide containing ice-cemented debris within the deposits was observed for the first time in Iceland. Since then two such events also occurred in the other regions of the country (Sæmundsson *et al.*, 2017).

Iceland has wide-spread discontinuous mountain permafrost, roughly above 800 m a.s.l., and sporadic permafrost related to palsa areas in the central part of the island. Since 2004 four boreholes monitor ground temperatures in central and eastern Iceland (Etzelmüller *et al.*, 2007), showing an increase in ground temperatures especially since 2012, and the possible development of taliks at the borehole sites (Etzelmüller *et al.*, this volume).

In order to assess the temporal and spatial changes of permafrost distribution in Iceland, we implemented the transient permafrost model CryoGrid 2 for entire Iceland, as a first step between 1960 and 2015 and at a resolution of 1 km². This model is used to evaluate recent ground temperature changes, and forms the basis for future predictions of permafrost change.

Methods and data

CryoGrid 2 model

In the CryoGrid 2 model, the snow and ground temperature profiles for every spatial grid cell are calculated from the one-dimensional heat conduction equation, assuming that the lateral heat transfer between the adjacent 1 km² cells is negligible. Furthermore, the total latent heat released/absorbed during the ground freezing/thawing is accounted for in the model. The thermal conductivity and specific heat capacity of a given soil layer are computed as functions of the thermal properties of the individual soil constituents like water, ice, air, minerals and organic matter, and their respective volumetric fractions. The snowpack is considered as one homogenous layer with constant thermal conductivity and capacity.

Model input

The snow water equivalent is computed on a daily basis from a degree–day based model developed by the Norwegian Meteorological Institute (“seNorge”; Saloranta 2012), which is forced by data provided by the Icelandic Meteorological Office: gridded air temperature data set (Crochet & Jóhannesson, 2011) and two gridded precipitation data sets, a data set based on the linear model of orographic precipitation (Crochet *et al.*, 2007) between 1960 and 1979 and a data set derived from the numerical weather prediction model HARMONIE (Bengtsson *et al.*, 2017) between 1980 and 2015. In order to decrease the execution time per cell, the transient permafrost model forcing consists of weekly averaged air temperature and snow depth series.

Results and future work

The model produces a realistic image of permafrost spatial distribution, including many of the palsa areas (Fig. 1). The runs also display realistic ground temperature changes as observed in the boreholes. Problems are related to snow cover, which partly is overestimated, and wind drift is not included in the calculations. We therefore will improve the current model implementation by performing multiple runs for varying snow depths. Furthermore, we will show the results of further sensitivity tests and model validation for Iceland.

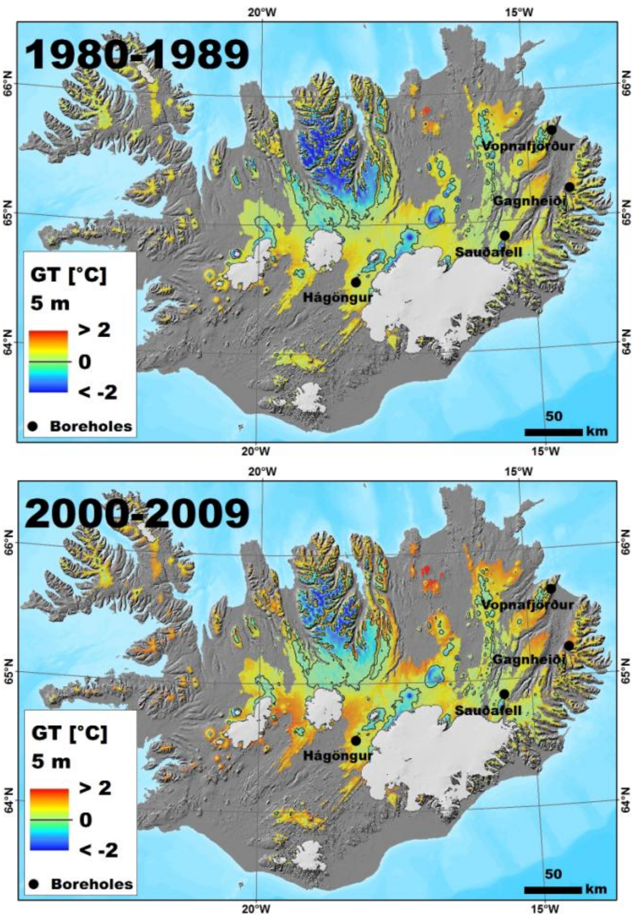

Figure 1. Average modelled ground temperature (GT) at 5 m depth for the periods 1980-1989 and 2000-2009.

References

Bengtsson, L., Andrae, U., Aspelien, T., Batrak, Y., Calvo, J., de Rooy, W., Gleeson, E., Hansen-Sass, B., Homleid, M., Hortal, M., Ivarsson, K.-I., Lenderink, G., Niemelä, S., Nielsen, K. P., Onvlee, J., Rontu, L., Samuelsson, P., Muñoz, D. S., Subias, A., Tijm, S., Toll, V., Yang, X., & Ødegaard Køltzow, M., 2017. The HARMONIE-AROME model configuration in the ALADIN-HIRLAM NWP system. *Monthly Weather Review* 145: 1919–1935.

Crochet, P. & Jóhannesson, T., 2011. A data set of gridded daily temperature in Iceland, 1949–2010. *Jökull* 61: 1–17.

Crochet, P., Jóhannesson, T., Jónsson, T., Sigurðsson, O., Björnsson, H., Pálsson, F. & Barstad, I., 2007. Estimating the spatial distribution of precipitation in Iceland using a linear model of orographic precipitation. *Journal of Hydrometeorology* 8: 1285–1306.

Etzelmüller, B., Farbrot, H., Guðmundsson, Á., Humlum, O., Tveito, O. E., & Björnsson, H. 2007. The regional distribution of mountain permafrost in Iceland. *Permafrost and Periglacial Processes* 18: 185-199.

Etzelmüller, B., Lilleøren, K. S. & Westermann, S., this volume. Permafrost dynamics observed in Norway and Iceland.

Saloranta, T. M., 2012. Simulating snow maps for Norway: description and statistical evaluation of the seNorge snow model. *The Cryosphere* 6: 1323–1337.

Sæmundsson, Þ., Morino, C., Helgason, J.K., Conway, S.J., Pétursson, H.G., 2017. The triggering factors of the Móafellshyrna debris slide in northern Iceland: Intense precipitation, earthquake activity and thawing of mountain permafrost. *The Science of The Total Environment,* in press.

Combined rock temperatures modelling and glaciological survey on the Jungfraujoch (Switzerland)

Pierre Dalban Canassy[1]
Ursula Ritter[2]
Vincent Badoux[2]
Daniel Tobler[2]
Gabriel Roth[3]
[1]*Geotest Ltd, Zollikofen, Switzerland, pierre.dalban@geotest.ch*
[2] *Geotest Ltd, Zollikofen, Switzerland*
[3] *Jungfraubahnen AG, Interlaken, Switzerland*

Abstract

The Jungfraujoch touristic site is located at 3454 m a.s.l inside a rocky ridge at the top of Aletschgletscher (Bernese Oberland, Switzerland). The site is composed of several buildings and tunnels dug into the rock, whose conception required intensive geological studies. Part of them are related to rock stability and rockfall hazard, which become evermore significant due to the retreat of glaciers and mountain permafrost in the context of current climate change. In this contribution, we present the results of a 3D modelling study of the rock temperatures in the southeast part of Jungfraujoch between 1933 and 2100. Based on changes in air temperatures and glacier extent, the modelling results show that changes in the permafrost distribution arise in close relation with the increase of the air temperature and the anthropogenic heat influx as well as the extension of the ice-free areas, indicating that the rock stability may be affected.

Keywords: rock temperatures, permafrost, glaciers, rock stability, numerical modelling, anthropogenic heat input

Introduction

The Jungfraujoch railway station is located at 3454 m a.s.l at the top of the Aletschgletscher (Bernese Oberland, Switzerland). Since 1912, the station is connected to the valley with a rack-railway operated by the Jungfraubahnen Ltd. Nowadays, Jungfraujoch offers a large variety of touristic facilities distributed in the numerous galleries and buildings as well as on the Aletschgletscher, and is visited by several thousands of people per day.

The development of the station within the rocky massif and at the surface has been made possible through very demanding construction works, in which Geotest Ltd has been deeply involved as consulting geologist since the 1980s. In addition to the feasibility and stability issues inherent to the construction of new buildings and tunnels, specific problematics related to the high mountain environment, like rockfall hazards or the preservation of the mountain permafrost, have to be addressed. In the past, this latter point was mostly tackled by limiting the effects of anthropogenic heat by means of innovative building solutions. However, in the context of current climate change (IPCC, 2014), the impact of permafrost retreat on the rock stability is shown to become more and more significant at high altitude (Ravanel & Deline, 2011). As a consequence, potential changes of rock temperatures have to be taken into account at a large scale for the planning of future constructions.

In this contribution, we present the results of a 3D modelling study of the rock temperatures in the southeast part of Jungfraujoch (Fig.1), combined with a glaciological survey. Considering changes in air temperatures and glacier extent since 1933, the survey aims at determining the future evolution of the local mountain permafrost from now until 2100, with the final goal of predicting long-term alteration of the rock stability. The study was carried out on behalf of the Jungfraubahnen Ltd.

Study site

The Jungfraujoch is located on a rocky ridge bordering the Aletschgletscher to the south and the valley of Lauterbrunnen to the north. On the north side, the ridge is predominantly covered by hanging glaciers, whereas the south face exhibits very steep rocky cliffs culminating 170 m above the glacier and rapidly diving below the ice at the bergschrund (Fig.1). The rocky massif has been intensively excavated due to the building of numerous galleries and cavities.

Figure 1: Topographic map of the Jungfraujoch and study area in red (source swisstopo).

Data

The input data of the study are the following:

- Air temperature time series 1933-2017 recorded at the station Jungfraujoch (Meteoswiss)
- Air temperature changes scenarios from the Swiss climate Change Scenarios (CH2011, 2011)
- Rock surface temperature measurements from PermaSense network (Beutel *et* al, 2009)
- Modelled ice thickness changes on Aletschglestcher (VAW, 2017)
- Borehole measurements of rock temperature (Geotest, Jungfraubahnen)
- Digital elevation model (DEM) (swisstopo)
- Ice thickness measurements using radar investigation and hot water drilling (Geotest)

Methods

The spatial and temporal evolution of the rock temperatures is modelled using the finite element code FEFLOW. The 3D mesh (Fig.2) is based on a DEM of the bedrock derived from the swisstopo data and our radar- and hot water drilling measurements. It distinguishes ice free and englaciated surfaces and is constrained by the location of the galleries.

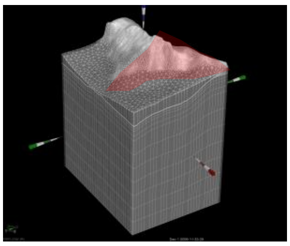

Figure 2: 3D mesh as implemented in FEFLOW. The investigated domain is in red.

The boundary conditions are defined as time varying fixed temperatures and distinguish the elevation, the orientation and the ice cover. On the south and north faces as well as inside the tunnels, they are derived from rock- and air-temperature measurements using the method described by Magnin *et al.* (2014). At the interface of englaciated surfaces, they are defined as temperate in the south face and negative below the hanging glaciers in the north face. The temporal evolution of the rocky surface exposed to the air is derived from a modelling survey of the ice thickness performed at location close to the study site (VAW, 2017). The model calibration is achieved on the 2007-2016 time-period, based on air temperatures and borehole rock temperature measurements. The scenarios CH2011 were used to assess the temperature changes in the future.

Results

The rock temperatures modelled in the calibration period point out both spatially and temporally a good agreement with the borehole measurements. This allows us to consider the retained boundary conditions as valid for the modelling until 2100. Results of the calibration also highlight the following points: first, strong seasonal variations of the rock temperatures; second, a significant cooling effect from the north face; third, the high sensitivity with respect to the surface rock temperatures applied inside the tunnels, which confirms the strong effect of the anthropogenic heat influx in the model.

Between 2017 and 2100, preliminary results indicate that changes in the permafrost distribution arise in close relation with the increase of the air temperature and the extension of the ice-free areas. More particularly, rock temperatures modelled in the late 2090s show that only a narrow band of permafrost in the north face may subsist. Changes in the rock stability may therefore be expected.

References

IPCC, 2014. Climate change 2014: Impact, Adaptations, and Vulnerability.

Ravanel, L. & Deline, P., 2011. Climate influence on rockfalls in high-Alpine steep rockwalls: The north side of the Aiguilles de Chamonix (Mont Blanc Massif) since the end of the 'Little Ice Age', *The Holocene* 21.2

CH2011, 2011. *Swiss Climate Change Scenarios,* CH2011,published by C2SM, MeteoSwiss, ETH, NCCR Climate, andOcCC, Zurich, Switzerland, 88 pp. ISBN: 978-3-033-03065-7

Beutel, J., Gruber, S., Gubler, S., Hasler, A., Keller, M., Lim, R., Talzi, I., Thiele, L., C. Tschudin C. & Yücel, M., 2009. The PermaSense Remote Monitoring Infrastructure, in *International Snow Science Workshop Davos*

VAW, 2017. Bericht Nr 7911.21.5.2017

Magnin, F., Deline, P., Ravanel, L., Noetzli, J. & Pogliotti, P., 2014. Thermal characteristics of permafrost in the steep alpine rock walls of the Aiguille du Midi (Mont Blanc Massif, 3842 m a.s.l), *The Cryosphere* 9, 109-121.

CTS-PB and GS-PT as two surfaces integrating glacial and periglacial permafrost

Wojciech Dobiński[1]
[1]University of Silesia WNoZ Sosnowiec, Poland, wojciech.dobinski@us.edu.pl

Abstract

Geophysical surveys conducted using ground penetrating radar (GPR) on the Storglaciären, northern Sweden allow to identify the cold-temperate transition Surface (CTS) inside the glacier. The electroresistivity tomogrpahy (ERT) research that accompany them on the glacier forefield allow to identify the permafrost table (PT) and permafrost base (PB) on the glacial forefield encompassed by permafrost. CTS-PB surfaces form an continuous axis between glacier and its forefield combining *glacial* and *periglacial permafrost base.* Analogically the PT surface together with the surface of the glacier (GS) in the ablation season create an analogous axis (GS-PT) on the surface of this *glacial-periglacial permafrost table.* Both surfaces are continuous and are subject to dynamic variability along with climate evolution.

Keywords: glacial permafrost; periglacial permafrost; ERT; GPR;

Permafrost is a thermophysical phenomenon that encompass the lithosphere, maintaining its negative temperature for at least two consecutive years. Because ice is classified as a mineral and occurs commonly on the surface of the Earth and other planets in the form of a monomineral rock, it should also be classified as a component of the lithosphere (Dobrowolski 1931). Although the inclusion of ice in the permafrost is obvious by definition (Washburn 1973), the inclusion of ice into the lithosphere is a prerequisite for the presence of permafrost in it.

Periglacial permafrost includes traditionally understood rock. It may be frozen or not, but it remains at or below 0°C. It forms a thermal layer, which is contained between permafrost table (PT) occurring on its surface at 0°C and above, and the surface of permafrost base (PB), where 0°C is replaced by a positive temperature. In special cases, as it can happen at very high altitudes in equatorial regions, the active layer may not exist. This is because of the negative mean annual air temperature (MAAT), and lack of seasonal variability of the climate, which allows the negative temperature of the ground to start directly from the surface (Gorbunov 2003).

The term *Glacial permafrost* has recently found its place in the scientific circulation (Dobiński 2006). It encompass any type of ice whose durability is at least 2 years. Glaciers and ice-sheets are adequately long-lasting to meet the definition requirements. Glacial permafrost also has no active layer because it is replaced by the size of the seasonal glacier ablation.

However, because freezing is not a condition *sine qua non* for the permafrost existence, and the cryotic state is its synonym, the pressure melting point (PMP), which always has a negative temperature, meets the requirements of the definition of permafrost as well.

With some exception (eg. low latitudes), glaciers usually end up in an area where prevail suitable conditions for the permafrost development. This is especially true in areas where MAAT is lower than -1°C. Then even the retreating glacier leaves space for permafrost aggradation in the forefield.

The thermal structure of the polythermal glacier allows to discriminate two 0°C surfaces that occur at and within it. First is its upper limit (ie. glacier surface - GS) during the ablation period. Its location changes together with the ablation of the glacier. Its counterpart on the cold glacial forefield encompassed by permafrost occurrence is the permafrost table (PT). Together both 0°C surfaces creates a specific environmental axis that we can call GS-PT axis.

The second characteristic 0°C surface inside the polithermal glacier is cold-temperate transition surface (CTS) (Petersson et al. 2003). It is the surface separating cold and temperate ice at PMP. Its continuation on the glacial forefield is permafrost base (PB). These surfaces are separated from each other by a layer of permafrost remaining at a negative temperature (usually in frozen state), the thickness of which decreases as the altitude decreases in a mountain environment. Ultimately, both surfaces combine with each other at the site of the disappearance of permafrost. The surface of the CTS in the glacier can be detected using GPR, while on the glacial forefield the thickness of traditional permafrost can be detected by means of ERT (Dobiński et al. 2017).

The coexistence of these surfaces is dynamic. Their course and range changes even seasonally with the change of the glacier's range and temperature, change of active layer thickness on the glacial foreland etc. These surfaces, however, are interdependent and exist as long as the glacier and its frozen forefield, ie: glacial permafrost and periglacial permafrost, both, in the mountain environment and beyond.

Acknowledgments

The work is one of the results of a research funded by the National Science Centre, Poland (NCN) DEC-2012/07/B/ST10/04268, and UMO-2016/21/B/ST10/02509.

References

Dobrowolski, A. B., 1931. La glace au point de vue petrographique (Essai de classification des roches de glace), *Bulletin de la Société Française de Minéralogie* 54 (1-2): 5-19.

Dobiński, W., 2006. Ice and environment: A terminological discussion. *Earth Science Reviews* 79: 229-240.

Dobiński, W. Grabiec, M. & Glazer, M., 2017. Cold – temperate transition surface and permafrost base (CTS-PB) as an environmental axis in glacier–permafrost relationship, based on research carried out on the Storglaciären and its forefield, northern Sweden. *Quaternary Research*, 88 (3): 551–569.

Gorbunov, A.P., 2003. *Wietchnaya merzlota gor. Ot ekvatora do poliarnych shirot.* Al'.maty 122 pp.

Pettersson, R. Jansson, P. & Holmlund P., 2003. Cold surface layer thinning on Storglaciären, Sweden, observed by repeated ground penetrating radar surveys. *Journal of Geophysical Research* 108, F1, 6004.

Washburn, A.L., 1973. *Periglacial processes and environments*. Edward Arnold, 320.

Complex model simulations of permafrost in remote regions improved by data assimilation using a particle batch smoother

Joel Fiddes[1]
Sebastian Westermann[1]
Kristoffer Aalstad[1]
[1] *University of Oslo, Norway*, *joelfiddes@gmail.com*

Abstract

The mountain cryosphere is undergoing significant changes globally, yet these changes are in many cases poorly constrained, particularly in remote regions where data is sparse. We present a modeling toolkit that couples a subgrid method, downscaling scheme and data assimilation tools which allows efficient ensemble, large area transient simulations at high-resolution. The approach reallocates order of magnitude computational gains from the subgrid method to treatment of uncertainty in driving meteorological variables, which has the potential for significant improvements in modelling the ground thermal regime. Additionally, the model chain uses only globally available inputs and therefore is a globally consistent method and allows for first order assessments at high resolution in remote regions. We present results from validation in the European Alps and test applications in the Nepalese Himalaya together with new results from the latest ECWMF reanalysis ERA5.

Keywords: data assimilation; uncertainty; ensemble simulations; subgrid; remote regions; downscaling

Introduction

The mountain cryosphere is undergoing significant changes globally, yet these changes are in many cases poorly constrained, particularly in remote regions where data is sparse. Previously developed methods for downscaling driving meteorology (Fiddes and Gruber 2014) and a subgrid scheme (Fiddes and Gruber 2012) have proven to be promising approaches to large area transient simulations of permafrost in remote areas due to order of magnitude efficiency gains. However, major sources of uncertainty still remain in the meteorological forcing, particularly precipitation which features high spatio-temporal variability and is heavily modulated by local topographic effects. Additional complexity arises due to the inherent uncertainty in precipitation observations, especially in the solid phase. Solid precipitation is an important target variable to accurately quantify as it is a key control on the ground thermal regime. To address these issues we employ an ensemble data assimilation scheme, based on the particle batch smoother, that assimilates MODIS fractional snow cover observations into the modelling framework. Efficiency gains in the underlying framework, due to the downscaling and subgrid scheme, make this approach particularly suited for the treatment of uncertainty through ensemble simulations and data assimilation.

Methods and data

We use the particle batch smoother data assimilation method (Margulis et al., 2015, Aalstad et al., 2017) to assimilate MODIS fSCA into the numerical model GEOtop (Endrizzi et al. 2014). This is coupled to a subgrid scheme (Fiddes and Gruber, 2012) based on a high resolution DEM (SRTM) and a downscaling scheme (Fiddes and Gruber, 2014) that scales reanalysis meteorological variables from ERA-Interim to DEM resolution.

Results and discussion

The approach has produced promising results based on the limited validation that has been conducted so far. The assimilation successfully constrains the ensemble spread and pushes the median towards observations (Fig. 1). We are now in the process of running a comprehensive validation exercise. The strength of this combined approach is that order of magnitude computation gains of the subgrid method can be directed to the additional resources required for ensemble simulations. Computational resources are essentially redirected from repetitive explicit 2D simulation to the treatment of uncertainty which is likely a more efficient allocation of resources in the modelling process. Additionally, the model chain uses only globally available inputs and therefore is a globally consistent method and allows for first order assessments at high resolution in remote regions.

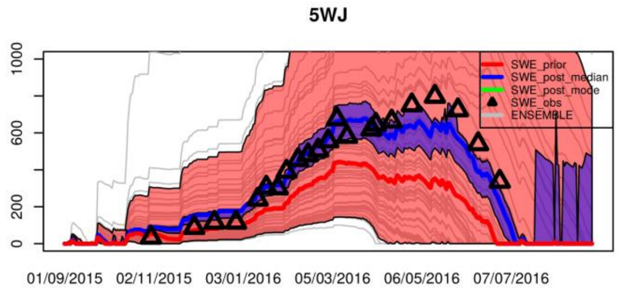

Figure 1. Example ensemble simulation of snow water equivalent (mm) at the Weissfluhjoch research site. Red/blue shaded area is prior/posterior 90th percentile range. Bold line is the respective median values. Black triangles are manual snow profile observations.

Acknowledgments

We acknowledge funding by Swiss National Science Foundation Post-doc Mobility project number P2ZHP2_165435.

References

Aalstad, K., Westermann, S., Schuler, T. V., Boike, J., Bertino, L.: Ensemble-based assimilation of fractional snow covered area satellite retrievals to estimate snow distribution at a high Arctic site, *The Cryosphere*, https://doi.org/10.5194/tc-2017-109, accepted, 2017.

Endrizzi, S., Gruber, S., Dall'Amico, M., & Rigon, R. 2014. GEOtop 2.0: simulating the combined energy and water balance at and below the land surface accounting for soil freezing, snow cover and terrain effects, *Geoscientific Model Development*, 7(6), 2831-2857.

Fiddes, J. & Gruber, S., 2012. TopoSUB: a tool for efficient large area numerical modelling in complex topography at sub-grid scales, *Geoscientific Model Development* 5: 1245–1257

Fiddes, J. & Gruber, S., 2014. TopoScale: a tool for efficient large area numerical modelling in complex topography at sub-grid scales, *Geoscientific Model Development* 5: 1245–1257

Margulis, S. A., Girotto, M., Cortés, G., & Durand, M., 2015. A particle batch smoother approach to snow water equivalent estimation, *Journal of Hydrometeorology,* 16(4), 1752-1772.

Fracture kinematics in steep bedrock permafrost, Aiguille du Midi (3842 m a.s.l., Chamonix Mont-Blanc, France)

Grégoire Guillet[1]
Ludovic Ravanel[1]
Jan Beutel[2]
Philip Deline[1]

[1] *Univ. Grenoble Alpes, Univ. Savoie Mont Blanc, CNRS, EDYTEM, 73000 Chambéry, France, gregoire.guillet@univ-smb.fr*
[2] *Computer Engineering and Networks Laboratory, ETH, Zurich, Switzerland*

Abstract

Permafrost-affected rockwalls can suffer from mechanical fatigue related to thermo-cryogenic processes. However, these processes, the rock slope kinematics, and the links between both remain largely unclear. This study reports five years of crackmeter measurements at 2-hours resolution from six of the main perennially ice-filled rock clefts at the Aiguille du Midi (3842 m a.s.l., Mont Blanc massif). Seasonal and inter-annual variations as well as response of fracture kinematics to thermo-cryogenic process are analyzed.

Keywords: permafrost, fracture kinematics, thermo-cryogenic processes, irreversible displacement, extensometry, Mont Blanc massif.

Introduction

In the current context of climate change, permafrost-affected rockwalls are increasingly affected by rockfalls (Ravanel *et al.*, 2017a) but processes that control climate-dependent rockfalls from these rockwalls are still poorly understood (Draebing *et al.*, 2017). In this study, we analyze crackmeter measurements installed in 2012 in the steep rockwalls of the Aiguille du Midi (AdM, 3842 m a.s.l.) within a Wireless Sensor Network (Ravanel *et al.*, 2017b), and their relationship with air temperature.

Study site

The AdM is located on the NW side of the Mont Blanc massif. This part of the massif is formed by an inclusion-rich, porphyritic granite and is bounded by a wide shear zone. The highest area of the AdM is steep, with few large fractures. The lower parts are gentle and more fractured. The AdM consists of three granite peaks (Piton Nord, Piton Central, and Piton Sud).

We chose the AdM as a monitoring site because: (i) permafrost is largely present; (ii) thermal monitoring (at surface and depth) is carried out since 2005; (iii) peaks offer a large range of aspect, slope angle and fracture density; (iii) its easy access by cable car from Chamonix and the availability of services (*e.g.* electricity) at the summit station; (iv) the possible easy data transmission; and (v) the risk related to permafrost for the infrastructure.

Monitoring system

The two main peaks have been equipped with crackmeters in 2012. Four crackmeters have been placed inside four major fractures at the Piton Nord, and two crackmeters have been installed along a major fracture at the Piton Central, equipped with three 10-m-deep boreholes with 15 temperature sensors since 2009. Data transmission is carried out thanks to a Wireless Sensor Network (Beutel *et al.*, 2009).

First outcomes

Common patterns can be identified throughout the dataset with a partly reversible seasonal displacement. In order to analyze crackmeter data, the methods proposed by Weber *et al.* (2017) were used.

First, a regression analysis between temperature and facture displacement is performed. Crackmeter measurements are divided into groups of 70 days where temperature variations must be of at least 8°C. For each group, the absolute value of the Pearson coefficient is computed.

The regression analysis between temperature and fracture displacement shows that every crackmeter record exhibits reversible displacement due to thermo-elastic strains related to annual temperature variations. Highest negative correlations between displacement and temperature mostly occur at the end of winter and the beginning of spring. In order to estimate timing and amplitude of plastic strain-induced irreversible displacement, we subtract the reversible component from the recorded displacement. From the irreversible displacement, we compute the irreversibility index (Weber *et al.*, 2017), that quantifies irreversibility within fracture kinematics.

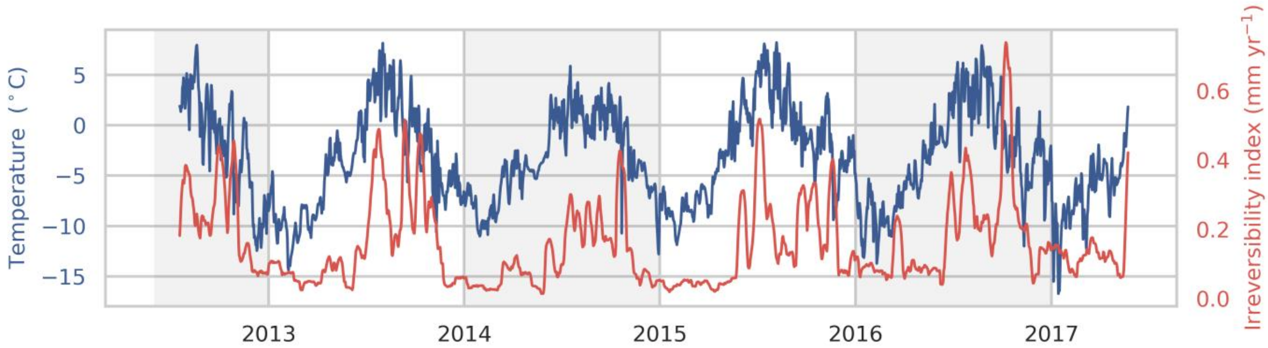

Figure 1: Irreversibility index for one of the crackmeters installed at the Piton Nord (South Face, Aiguille du Midi) and local air temperature (2012–2017)

First results show onset of highest irreversibility index when air temperature becomes > 0°C. This increase in irreversibility index seems related to increase in temperature and highlights thawing-related processes as the main generators of irreversible displacement.

During winter, lower peaks of irreversibility index are observed, widely contributing to overall annual irreversible displacement, and appear to be linked to rapid variations of local temperature conditions. Ice thermal expansion and contraction processes are thought to be responsible for the onset of such irreversible displacement.

Some sensors record high peaks of irreversibility index during autumn, when air temperature is lowering below 0°C. These peaks are the result of ice formation within the clefts.

In a next step, every crackmeter recording will be compared to temperature measured in the boreholes in order to better understand the scale variance of thermo-cryogenic processes affecting high alpine permafrost.

Acknowledgments

This research is part of the Swiss *PermaSense,* French ANR *VIP Mont-Blanc*, and ALCOTRA *PrévRisk Haute Montagne* and *AdaPT Mont Blanc* projects. We thank the Compagnie du Mont Blanc for allowing access to the site.

References

Beutel, J. *et al.*, 2009. The PermaSense remote monitoring infrastructure. *In: Proceedings of the International Snow Science Workshop Davos 2009*, pp. 187-191.

Draebing, D., Krautblatter, M. & Hoffmann, T., 2017. Thermo-cryogenic controls of fracture kinematics in permafrost rockwalls. *Geophysical Research Letters* 44: 3535–3544.

Ravanel, L., Magnin, F. & Deline, P. 2017a. Impacts of the 2003 and 2015 summer heat waves on permafrost-affected rockwalls in the Mont Blanc massif. *Science of the Total Environment* 609: 132-143.

Ravanel, L., Malet, E., Duvillard, P.-A., Magnin, F., Deline, P., Guillet, G., Troilo, F., Pogliotti, P., Morra di Cella, U., Beutel, J. & Gruber, S., 2017b. Instrumentation thermique et cinématique des parois à permafrost du massif du Mont Blanc. *Collection EDYTEM* 19: 27-38.

Weber, S., Beutel, J., Faillettaz, J., Hasler, A., Krautblatter, M. & Vieli A., 2017. Quantifying irreversible movement in steep, fractured bedrock permafrost on Matterhorn (CH). *The Cryosphere* 11: 567-583.

Debris size classification of alpine landforms using high-resolution images

Elisa Giaccone[1]
Christophe Lambiel [1]
Grégoire Mariéthoz[1]
[1]*University of Lausanne, Institute of Earth Surface Dynamics, Lausanne, Switzerland, elisa.giaccone@unil.ch*

Abstract

This research is focused on the development of a method to estimate debris size distribution (DSD) of alpine landforms using high-resolution images. To this end, a new image analysis technique has been employed. This method is split in 2 phases. First, the high-resolution orthomosaic, obtained by Unmanned Aerial Vehicle (UAV), was processed in a software which identify the grain size on the basis of the two-axis diameters of grain. Second, mobile median and standard deviation were computed to realize the debris size classification map.

Keywords: debris size classification; granulometry; high-resolution images; UAVs.

Introduction

In alpine environment, debris size is an important factor for permafrost development because it influences the micro-topography and consequently the ground temperatures (eg. Gruber & Hoelzle, 2008; Rödder & Kneisel, 2012).

To estimate the DSD of a rock glacier or other landforms, accurate punctual measurements of the two or three axis of debris typically have to be carried out. However, on large surfaces, manual data acquisition is time-consuming. Another method is based on the analysis of high-resolution DEMs from which information regarding the surface roughness is extracted (Grohmann *et al.*, 2011; Otto *et al.*, 2012). Nevertheless, the mathematical solutions to quantify the surface roughness smooth the real topography and don't allow knowing accurately the debris size.

In this study, we are developing a methodology to determine the DSD based on optical high-resolution images. Our approach is applied to the Martinets rock glacier, located in the Western Swiss Alps (2300-2440 m a.s.l.). Images were acquired using the Sensefly eBee RTK UAV. The acquired images were processed in the Pix4D software to produce a high-resolution orthomosaic (5.75 cm/pixel).

Methodology

1) Grain detection

The orthomosaic (Fig. 1A) has been uploaded in the Basegrain software (created by ETH Zürich, Switzerland; Detert & Weitbrecht, 2013), a Matlab-based automatic software tool that allows to estimate the granulometry by analyzing digital photographs. The software is constituted by five step algorithms that detects interstices and edges and obtains the properties of each grain.

Basegrain was originally designed to analyze the granulometry of fluvial gravel beds from top-view photographs. Here we use this approach to analyze drone images covering wide surfaces.

In our case the detected minimum grain size was 20 cm (Fig. 1B). The final output is a list of all detected grains, their size and their position in the image (x-y coordinates).

2) Debris size classification

In the second step we want to estimate the density of grain size. Therefore, we represented graphically in a new grid the x-y position of each detected grain (Fig. 1C). Then, for each point, mobile median (Fig. 1D) and standard deviation (Fig. 1E) of the grain size were computed with a coarsening of 40 px and a radius of 100 px. The final outputs are a map of DSD (Fig. 1D) and a map of the variability of debris size (Fig. 1E).

This new method has been validated for now with visual criteria: the areas with bigger grain size correspond between orthomosaic and DSD map in most of the cases, but vegetation patches are confused with smaller debris. To avoid that, a mask for the vegetation and snow will be added before the Basegrain elaboration. The variability map can be used to identify the homogeneous or inhomogeneous areas.

Furthermore, the validation has to be enhanced to improve the processing with manual measurements.

Acknowledgments

This research is developed in the framework of the project "Integrating spatial predictions of vegetation, soils, geomorphology and hydrology for improved assessment of ecosystem services under climate change", supported by the Swiss National Science Foundation (project N° CR23I2_162754 / 1).

References

Detert, M. & Weitbrecht, V., 2013. User guide to gravelometric image analysis by BASEGRAIN. Advances in River Sediment Research, Fukuoka et al. (Eds) © 2013 Taylor & Francis Group, London, ISBN 978-1-138-00062-9, 1789–1796.

Grohmann, C.H., Smith, M.J., Riccomini, C., 2011. Multiscale analysis of topographic surface roughness in the Midland Valley, Scotland. *IEEE Transactions on Geoscience and Remote Sensing*, 49: 1200–1213.

Gruber, S. & Hoelzle, M., 2008. The cooling effect of coarse blocks revisited: a modeling study of a purely conductive mechanism. *9th International Conference on Permafrost*, Fairbanks, Alaska, 29 June - 03 July: 557–561.

Otto, J.-C., Keuschnig, M., Götz, J., Marbach, M., Schrott L., 2012. Detection of mountain permafrost by combining high resolution surface and subsurface information – an example from the Glatzbach catchment, Austrian Alps. *Geografiska Annaler*: Series A, Physical Geography, 94: 43–57.

Rödder, T. & Kneisel, C., 2012. Influence of snow cover and grain size on the ground thermal regime in the discontinuous permafrost zone, Swiss Alps. *Geomorphology*, 175-176: 176–189.

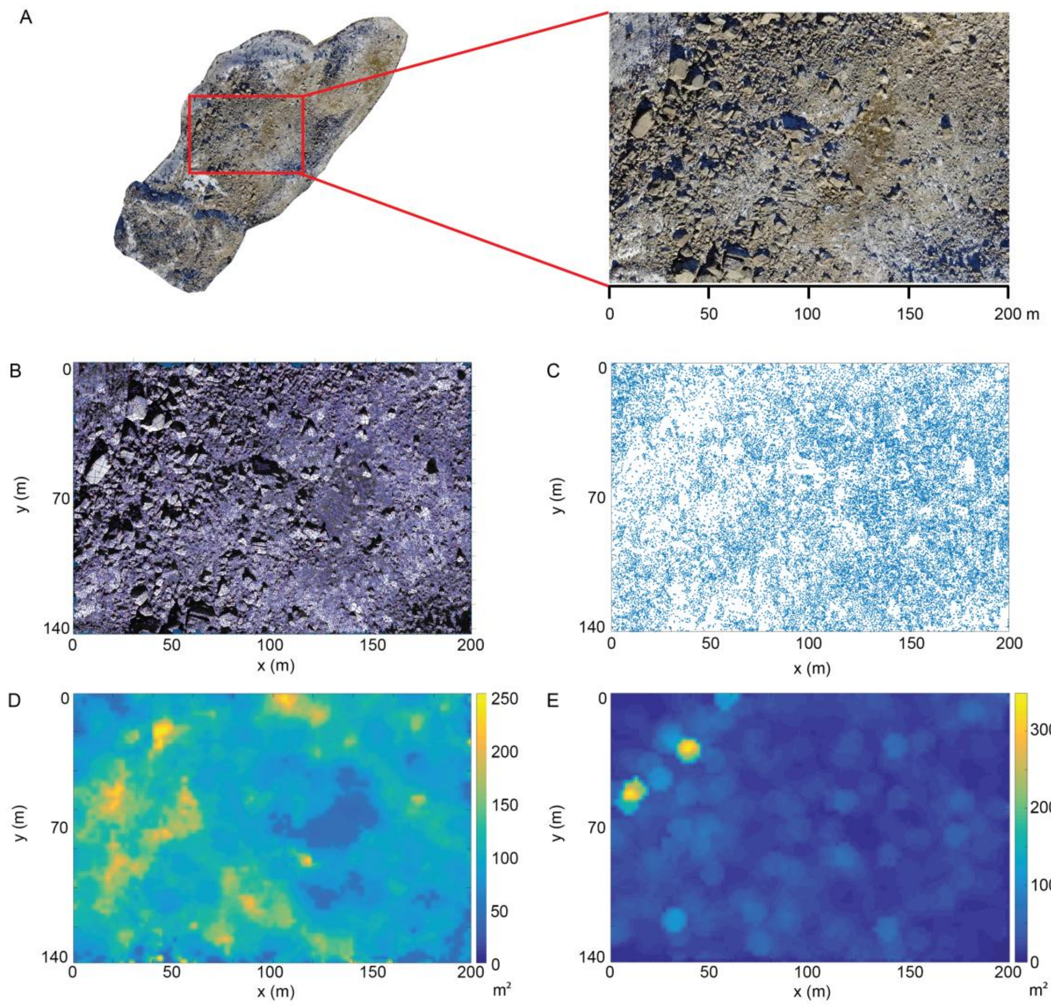

Figure 1. A – Orthomosaic of the rock glacier and analyzed detail. B – Basegrain processing and detection of two axis diameters of the debris. C – x-y position of detected elements. D – Area of detected debris in m². E – Standard deviation of debris size in m².

Influences of snow on the temperature regime of steep frozen rock walls

Anna Haberkorn[1], Marcia Phillips[1], Robert Kenner[1], Nander Wever[2], Michael Lehning[1,3], Martin Hoelzle[4]

[1]*WSL Institute for Snow and Avalanche Research SLF, haberkorn@slf.ch*
[2]*University of Colorado Boulder*
[3]*CRYOS, School of Architecture, Civil and Environmental Engineering, EPFL Lausanne*
[4]*Department of Geosciences, Unit of Geography, University of Fribourg*

Abstract

Observations show that up to 2 m of snow can accumulate in steep, rough rock walls like the Gemsstock ridge (Switzerland), despite the common presumption that only intermittent and thin snow covers exist in steep slopes. The heterogeneously distributed snow cover significantly affects the surface energy balance and hence the thermal regime of frozen rock walls. The snow influence was investigated with measurements and spatially distributed modelling, comparing a snow-covered model scenario with a snow-free one. Mean annual near-surface rock temperature increases were both measured and modelled as a consequence of a thick, long lasting snow cover. Rock temperatures were 1.3-2.5 °C higher in the shaded and sunny rock walls, when comparing snow-covered to the snow-free simulations. In rock wall thermal modelling a part of the energy balance of steep bedrock is thus only poorly described if a lack of snow in terrain exceeding 50° is assumed.

Keywords: distributed energy balance modelling; impact of snow on rock thermal regime; rock wall temperature; steep frozen rock walls; snow distribution

Introduction

The highly variable spatial and temporal distribution of the snow cover strongly influences the thermal regime of steep, rough rock faces. A warming effect of the snow cover on mean annual ground surface temperature (MAGST) was observed by Haberkorn *et al.* (2015) and Magnin *et al.* (2015) in shaded rock walls, whilst in moderately inclined sun-exposed rock walls Hasler *et al.* (2011) suggest a reduction of MAGST due to snow persistence during summer months. Thus, accounting for the varying snow cover is necessary for realistic modelling of the spatial permafrost distribution in steep rock. The potential effect of snow on steep bedrock temperatures has been simulated, changing snow depths arbitrarily in one- (Pogliotti, 2011) and two-dimensional (Myhra *et al.*, 2015) numerical model runs. Both showed a considerable influence of snow on rock temperatures, but did not verify their results with measurements.

We combine observations and distributed modelling of the influence of snow on the surface energy balance and thus on near-surface rock temperatures (NSRT) in steep, rough rock walls.

Study site

The Gemsstock mountain ridge is located on the main divide of the central Swiss Alps, at the lower fringe of mountain permafrost. We focus on a specific area on the N and S facing rocky flanks of the ridge, consisting of Gotthard paragneiss and granodiorite. The 40 m high slopes (2890–2930 m a.s.l.) are 40° to 70° steep, with vertical to overhanging (>90°) sections. The steep to vertical N facing scarp slope is intersected by a series of 0.3 to 3 m wide horizontal ledges. In contrast, the S facing dip slope is smooth.

Methods

To assess the spatial and temporal small-scale variability of snow depth in rugged rock faces the snow cover was observed using high resolution (0.2 m) winter terrestrial laser scans (TLS) and time-lapse photographs, as well as from in-situ snow pit investigations. The thermal impact of the snow on the rock was investigated between 2012-2014, combining continuous NSRT measurements (0.1 m depth) distributed over the N and S facing rock walls (Fig. 1) and borehole temperature measurements in the ridge.

In parallel, the effects of the snow on the surface energy balance and thus on rock temperatures were modelled at selected points in and over the rugged, steep rock walls. The distributed, physics-based Alpine3D model was used. The distribution of the snow cover in the steep terrain was provided using a precipitation scaling approach based on a combination of snow depth measurements from the on-site automatic weather station and snow depth distribution data obtained using TLS. The influence of snow on rock temperatures was investigated by comparing a snow-covered model scenario (precipitation input provided by precipitation scaling) with a snow-free (zero precipitation input) one.

Results and discussion

Observations

Rock wall micro-topography strongly determines snow depth distribution. Around 2 m of snow can accumulate on slopes up to 75° due to ledges. However, a thermal insulation of the ground already starts with snow depths exceeding 0.2 m in the steep rock faces. This is 0.4 to 0.6 m less snow than previously observed in flatter, blocky terrain. At the rock wall scale the accumulation of a thick, long lasting snow cover smooths contrasts in mean annual rock surface temperature (MANSRT) between N and S facing slopes. Differences are less than 4 °C. However, over the rock walls, small-scale heat fluxes between adjacent snow-covered and snow-free locations are pronounced due to strongly varying micro-topography and micro-climate. This results in daily NSRT variations of up to 10 °C within a few metres.

Modelling

The heterogeneously distributed snow cover was moderately well reproduced by Alpine3D with mean absolute errors ranging between 0.47 and 0.77 m. However, snow cover duration was reproduced well and so NSRT were modelled convincingly. Uncertainties in rock temperature modelling were around 1.6 °C.

MANSRT were up to 2.5 °C higher in the shaded and up to 2.3 °C higher in the sun-exposed rock walls when comparing the modelled snow-covered scenario to the snow-free one (Fig. 1), due to the thick long-lasting snow cover. As snow reduces ground heat loss in winter, it has an overall warming effect on both N and S facing rock walls, despite the fact that it provides protection from solar radiation in early summer.

Conclusions

The strong controlling effect of a seasonal snow cover on rock temperatures in steep, rugged rock walls was observed and modelled. The temporal snow cover evolution controls the presence or absence of permafrost. The spatially distributed physics-based model Alpine3D realistically models the influence of the heterogeneously distributed snow cover on the rock thermal regime. The correction of winter precipitation input using a precipitation scaling method based on TLS greatly improved snow cover and thus also rock temperature simulations. A strong increase in MANSRTs in both the shaded and sun-exposed steep rock walls induced by a thick long-lasting snow cover were both measured and modelled.

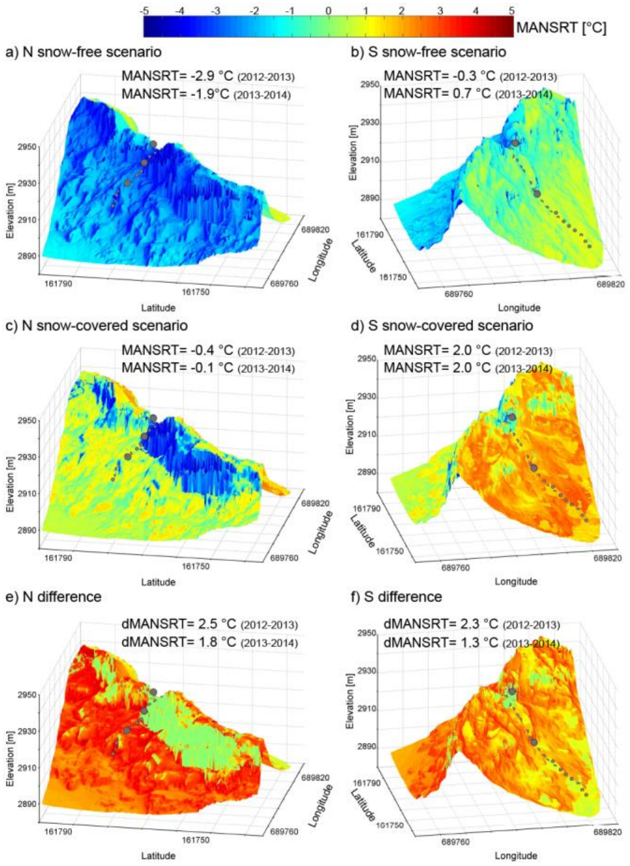

Figure 1. Modelled MANSRT distribution in the N (left) and the S (right) facing slopes for the snow-free scenario (top) and the snow-covered one (middle), and their differences dMANSRT (bottom; snow-covered – snow-free) shown for 2012-2013. MANSRT and dMANSRT are averaged over the individual N/S facing rock walls, and given for 2012-2013 and 2013-2014. Grey dots: NSRT locations.

References

Haberkorn, A., Hoelzle, M., Phillips, M. & Kenner, R., 2015. Snow as driving factor of rock surface temperatures in steep rough rock walls. *Cold Reg. Sci. Technol.* 118: 64-75.

Hasler, A., Gruber, S. & Haeberli, W., 2011. Temperature variability and offset in steep alpine rock and ice faces. *Cryosphere* 5: 977-988.

Magnin, F., Deline, P., Ravanel, L., Noetzli, J. & Pogliotti, P., 2015. Thermal characteristics of permafrost in the steep alpine rock walls of the Aiguille du Midi (Mont Blanc Massif, 3842 m a.s.l.). *Cryosphere* 9: 109-121.

Myhra, K.S., Westermann, S. & Etzelmüller, B., 2015. Modelled Distribution and Temporal Evolution of Permafrost in Steep Rock Walls Along a Latitudinal Transect in Norway by CryoGrid 2D. *Permafr. Periglac. Process.* 28: 172-182.

Pogliotti, P., 2011. *Influence of Snow Cover on MAGST over Complex Morphologies in Mountain Permafrost Regions.* Ph.D. thesis, University of Torino, 79 pp.

A distributed temperature sensing approach to mapping mountain permafrost

Jordan S. Harrington[1, 2]
Masaki Hayashi[1]
[1]*Department of Geoscience, University of Calgary, Calgary, AB, Canada; jordan.harrington@ucalgary.ca*
[2]*BGC Engineering Inc., Vancouver, BC, Canada*

Abstract

This study presents an application of distributed temperature sensing (DTS) to delineate the presence of permafrost using the BTS (bottom temperature of snowpack) method at an alpine site where previous investigations have found permafrost patches. The performance of the DTS approach was evaluated using conventional discrete temperature loggers and geophysical imaging surveys. The DTS data suggest that the distribution of permafrost at the site may be controlled by the variation in grain (block) size of surficial sediments. Furthermore, DTS can be a useful tool for the measurement of the BTS and permafrost mapping at high spatial resolution.

Keywords: DTS; bottom temperature of snowpack; BTS; rock glacier; Canadian Rockies.

Introduction

The distribution of mountain permafrost has implications for geomechanical and hydrogeological processes in mountainous environments. Mountain permafrost exhibits strong heterogeneity, driven by large contrasts in topography, climate, and geology. Mapping its distribution in areas of non-continuous permafrost remains challenging (Haeberli *et al.*, 2010).

Distributed temperature sensing

Distributed temperature sensing (DTS) is a method that measures temperature at high spatial resolution (*i.e.* < 1 m) along a fibre-optic cable. DTS has been used in diverse environments such as wellbores, dams, soils, snowpacks, groundwater, streams, lakes, pipelines, sewers, and the atmosphere (*e.g.* van de Geisen *et al.*, 2012). Recently, Roger *et al.* (2015) used DTS to monitor permafrost under road embankments in Nunavik.

The objective of this study is to use DTS to measure the bottom temperature of snowpack (BTS) at high spatial resolution for the delineation of mountain permafrost. This research was conducted at a rock glacier in the Canadian Rockies (52°N, 116°W; Figure 1), where previous investigations found evidence of permafrost patches (Harrington *et al.*, in review).

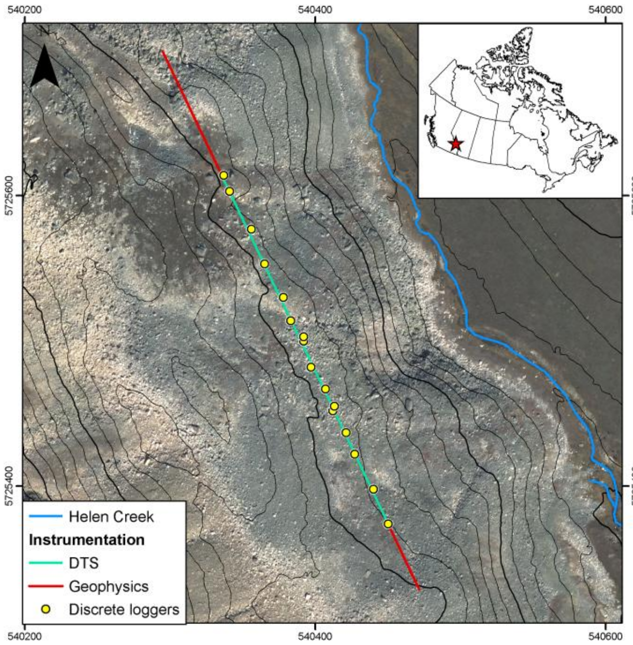

Figure 1. Study area satellite imagery (courtesy Parks Canada) and topography showing instrumentation (5 m contour interval; coordinates in UTM Zone 11U, NAD 83).

Methods

A fibre-optic cable was installed on the surface of the rock glacier along a previous geophysical imaging transect (Figure 1). Sixteen discrete temperature loggers (Maxim iButton DS1921Z, Onset HOBO Water Temp Pro v2) were placed along the fibre-optic cable at 15-25 m intervals (Figure 1).

A DTS unit (Sensornet Oryx OX4-SR) was used to measure the temperature at 1 m intervals along the fibre-optic cable. Forward and reverse measurements were integrated over 300 s intervals, and averaged over an hour.

Results

The discrete temperature loggers showed that on average a late-winter plateau in the BTS occurred in March (data not shown). Due to logistical and access issues in the wintertime, the DTS unit was selectively operated in late March. On this date, a snow survey along the DTS transect verified that snow depths were > 0.9 m. The DTS data are shown in Figure 2. From 150-290 m, the BTS are within the classical ranges of 'possible' and 'probable' permafrost, *i.e.* < –2°C (Haeberli, 1973).

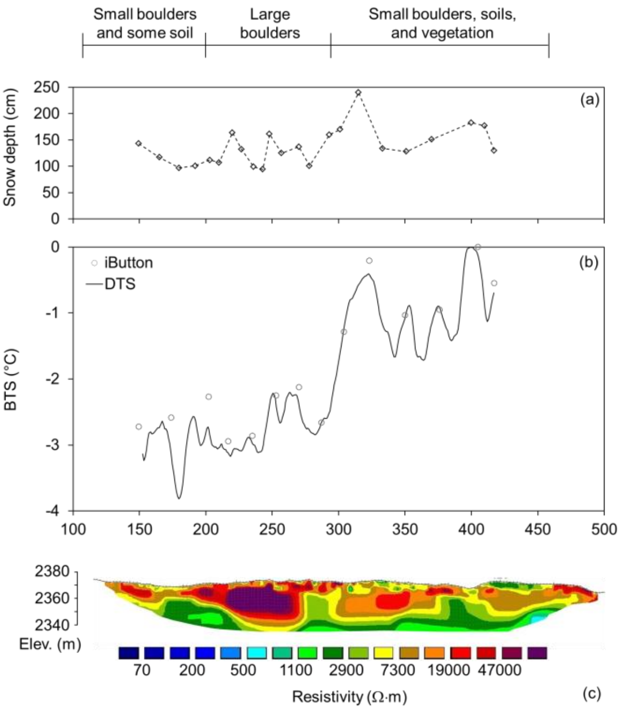

Figure 2. (a) Snow depth, (b) discrete and distributed BTS, and (c) electrical resistivity tomography image (courtesy A. Mozil).

Discussion and conclusions

The distinct transition in temperature measured by the DTS unit *ca.* 300 m is coincident with a transition from coarse blocky surficial materials to finer-grained surface sediments. Previous research has found that ground temperatures are commonly lower in coarse blocky media, due to a variety of convective and conductive heat transfer processes (*e.g.* Harris & Pedersen, 1998).

This study has shown that DTS can provide high spatial resolution measurements of the BTS, which can assist in the interpretation of permafrost presence. Specifically, the high resolution improves the identification and understanding of spatial trends in the BTS. Recent developments in automated DTS show promise for future studies to collect data from remote sites at higher temporal frequency (*e.g.* Kurth *et al.*, 2013).

Acknowledgments

This study was funded by the Natural Sciences and Engineering Research Council of Canada through a Discovery Grant and a Climate Change and Atmospheric Research Grant (Changing Cold Regions Network).

References

Haeberli, W., 1973. Die basis-temperatur der winterlichen schneedecke als möglicher indikator für die verbreitung von permafrost. *Zeitschrift für Gletscherkunde und Glazialgeologie* 9: 221-227.

Haeberli, W. *et al.*, 2010. Mountain permafrost: development and challenges of a young research field. *Journal of Glaciology* 56: 1043-1058.

Harrington, J.S., Mozil, A., Hayashi, M., Bentley, L.R., in rev. Groundwater flow and storage processes in an inactive rock glacier. *Hydrological Processes* HYP-17-0895.

Harris, S.A., & Pedersen, D.E., 1998. Thermal regimes beneath coarse blocky materials. *Permafrost and Periglacial Processes* 9: 107-120.

Kurth, A.-M., Dawes, N., Selker, J., Schirmer, M., 2013. Automated distributed temperature sensing for long-term heated applications in remote areas. *Geoscientific Methods and Data Systems* 2: 71-77.

Roger, J., Allard, M., Sarrazin, D., L'Hérault, E., Doré, G., Guimond, A., 2015. Evaluating the use of distributed temperature sensing for permafrost monitoring in Salluit, Nunavik. *68th Canadian Geotechnical Conference and 7th Canadian Permafrost Conference*, 8 pp.

van de Geisen, N., Steele-Dunne, S.C., Jansen, J., Hoes, O., Hausner, M.B., Tyler, S., Selker, J., 2012. Double-ended calibration of fibre-optic Raman spectra distributed temperature sensing data. *Sensors* 12: 5471-5485.

Towards accurate quantification of ice content in permafrost of the Central Andes – results from geophysical campaigns in 3 different regions

Christin Hilbich[1]
Reynald Delaloye[1]
Christian Hauck[1]
Coline Mollaret[1]
Laura Niggli[1]

[1]*University of Fribourg, Department of Geosciences, christin.hilbich@unifr.ch*

Abstract

The significance of permafrost occurrences in the Central Andes for the hydrological cycle is currently being discussed in a controversial way. Given the lack of comprehensive field measurements and quantitative data on the local variability of internal structure, ground ice content and their hydrological contribution of different permafrost landforms, this contribution aims to provide field-based data from several extensive geophysical campaigns since 2011 in three different high-altitude regions of the Central Andes. Besides a qualitative interpretation, we also use the quantitative 4-phase model to estimate the ground ice content and its spatial distribution for numerous ice-rich and ice-poor permafrost landforms.

Keywords: permafrost; Andes; ground ice content; geophysics; 4-phase model.

Introduction

The presence of permafrost is widespread in the Central Andes of South America, and both permafrost in general and especially rock glaciers, are considered key stores of frozen water (e.g., Rangecroft et al. 2015). Within the context of the projected water shortage in arid mountain regions as consequence of continued climate change, the significance of permafrost occurrences in the Central Andes for the hydrological cycle is currently being discussed in a controversial way (e.g., Brenning 2008, Duguay et al. 2015). Numerous publications highlight the need for field observations regarding thickness, internal structure and ground ice content of permafrost, and especially rock glaciers (Duguay et al. 2015, Rangecroft et al. 2015, Azócar & Brenning 2010, Perucca & Angillieri 2011, Croce & Milana 2002), but studies based on direct measurements are still rare (e.g. Croce & Milana, 2002, Arenson et al. 2010, Monnier & Kinnard 2013). In addition, most studies regarding the water/ice content of rock glaciers are still entirely based on rough estimates of rock glacier thickness (e.g., Rangecroft et al. 2015) or empirical volume-area correlations (Brenning 2005).

To improve this lack of comprehensive field measurements and quantitative data on the local variability of ground ice content within rock glaciers as well as ice-poor permafrost occurrences, we conducted extensive geophysical measurement campaigns in different high-altitude regions of the Central Andes.

We here present geoelectric (Electrical Resistivity Tomography, ERT) and seismic (Refraction Seismic Tomography, RST) data from several permafrost sites in the Chilean Andes with different geomorphologic settings, including numerous ice-rich and ice-poor permafrost occurrences.

Data Set

Between 2011 and 2018, five 2-4 week long geophysical campaigns have been conducted and more than 35 ERT and approximately 20 RST profiles were acquired to characterize permafrost conditions within three different areas.

In addition to their qualitative interpretation, the combination of ERT and RST data allows for estimating the ground ice content along 2-dimensional profiles using the so-called 4-phase model (4PM, Hauck et al. 2011, Pellet et al. 2016, Mewes et al. 2017). For sites with a sufficient data coverage, the 4PM in principle enables a quantitative estimate of the total ground ice content within an entire landform.

More than 20 coinciding ERT and RST profiles were subsequently used for the estimation of the ground ice content and its spatial variability with the 4PM. The methodological approach could be validated through the availability of core drillings and ground temperature records as well as numerous test pits within many of the profile lines.

Results

Our results show that estimated ground ice contents from combined electrical and seismic measurements match well with available ground truth data from geotechnical boreholes and test pits, thus enabling the spatial analysis of ground ice occurrence and its quantification.

Ground ice is present in nearly all profiles, with ice contents ranging from a few percent by volume to clearly supersaturated conditions within various rock glaciers. At sites with shallow sediment cover (ice-poor) small ice lenses are frequently present.

Ice-rich rock glaciers are hereby characterized by a considerable spatial heterogeneity (cf. Fig. 1 for an example), which can often not be assessed from surface-based analysis alone. Care has therefore to be taken regarding up-scaling approaches for quantitative estimates of the total ground ice content of a rock glacier. The corresponding uncertainties will be discussed, also with respect to the inherent uncertainties of both, the geophysical inversions of ERT and RST, and the 4PM (cf. Mewes et al. 2017).

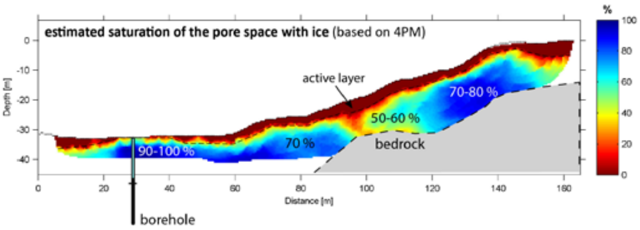

Figure 1. Typical 4PM result for a rock glacier in the Chilean Andes. Values are given as estimated ice saturation of the pore space.

Acknowledgments

The acquisition of this comprehensive data set would not have been possible without the valuable support and hard work of numerous field helpers from Switzerland and Chile.

References

Arenson, L.U., Pastore, S., Trombotto, D., Bolling, S., Quiroz, M. A., and Ochoa, X. L., 2010. Characteristics of two rock glaciers in the Dry Argentinean Andes based on initial surface investigations. *Geo2010*, Calgary.

Azócar, G.F. & Brenning, A., 2010. Hydrological and geomorphological significance of rock glaciers in the Dry Andes, Chile (27°–33°S). *Permafrost & Periglacial Processes* 21: 42–53.

Brenning, A., 2005. *Climatic and Geomorphological Controls of Rock Glaciers in the Andes of Central Chile: Combining Statistical Modelling and Field Mapping.* Ph.D. thesis, Humboldt-Universität zu Berlin.

Brenning, A., 2008. The impact of mining on rock glaciers and glaciers: examples from central Chile. *In* Orlove, B. S., Wiegandt, E., and Luckman, B. (eds.), *Darkening Peaks: Glacier Retreat, Science and Society.* Berkeley: University of California Press, 196–205.

Croce, F.A. & Milana, J.P., 2002. Internal structure and behaviour of a rock glacier in the arid Andes of Argentina. *Permafrost & Periglacial Processes* 13: 289–299.

Duguay, M.A., Edmunds, A., Arenson, L.U. & Wainstein, P. 2015. Quantifying the significance of the hydrological contribution of a rock glacier - A review. GeoQuébec 2015.

Hauck, C., Böttcher, M., & Maurer, H. 2011. A new model for estimating subsurface ice content based on combined electrical and seismic data sets. *The Cryosphere* 5(2): 453-468.

Mewes, B., Hilbich, C., Delaloye, R., & Hauck, C. 2017. Resolution capacity of geophysical monitoring regarding permafrost degradation induced by hydrological processes. *The Cryosphere* 11: 2957-2974.

Monnier, S. & Kinnard, C. 2013. Internal structure and composition of a rock glacier in the Andes (upper Choapa valley, Chile) using borehole information and ground-penetrating radar. *Annals of Glaciology* 54(64): 61–72.

Pellet, C., Hilbich, C., Marmy, A. & Hauck, C. 2016. Soil moisture data for the validation of permafrost models using direct and indirect measurement approaches at three alpine sites. *Front. Earth Sci.* 3:91.

Perucca, L. & Angillieri M.Y.E. 2011. Glaciers and rock glaciers distribution at 28° SL, Dry Andes of Argentina, and some considerations about their hydrological significance. *Environ Earth Sci* 64: 2079-2089.

Rangecroft, S., Harrison, S. & Anderson K. 2015. Rock Glaciers as Water Stores in the Bolivian Andes: An Assessment of Their Hydrological Importance. *Arctic, Antarctic, and Alpine Research* 47(1): 89-98.

Tibetan permafrost change during the past five decades

Duoying Ji[1]
Wenbin Sun[1]
[1]*College of Global Change and Earth System Science, Beijing Normal University, Beijing 100875, China, duoyingji@bnu.edu.cn*

Abstract

Permafrost is a climatologically important feature of the Tibetan Plateau, and it has been treated as an indicator of climate change and is highly sensitive to climate changes. Changes in permafrost are likely to influence local energy exchanges, hydrological processes and carbon budgets and hence global climate system. In this study, we analyze Tibetan Plateau permafrost change simulated by six offline land surface models participated in Permafrost Carbon Network Model Intercomparison Project (PCN-MIP). We diagnose the permafrost extent, active layer thickness and soil organic carbon budget changes. The land surface models participated in PCN-MIP adopt varying parameterization schemes on permafrost thermal-hydrological physics and soil carbon dynamics, such as representations on surface organic layer, soil column depth, and vertical resolving on soil organic carbon dynamics. We study how these different parameterizations affect the simulated permafrost change during the past five decades.

Keywords: Tibetan Plateau; Permafrost; Soil Carbon

Introduction

Permafrost contains a large amount soil organic carbon of 1330-1580PgC and it's the largest soil organic carbon stocks in the terrestrial ecosystem. The significant climate-permafrost carbon feedback will enhance the future climate warming. The Tibet Plateau has the largest permafrost region in the middle and low latitudes, which is of 1.35×10^6 km^2 with the average elevation of about 4000 m, and contains about 160±87PgC soil organic carbon, which account for about 10% of global permafrost soil organic carbon, while it occupies about only 5% of global permafrost extent.

Data and Methods

We use six land surface models (CLM4.5, ISBA, JULES, LPJ-GUESS, ORCHb and UW-VIC) participated in Permafrost Carbon Network Intercomparision Project (PCN-MIP), all models are driven by offline atmospheric forcing datasets and the simulations focus on northern hemisphere permafrost regions during the period of 1960-2009 (McGuire et al., 2016). The study region of Tibet Plateau is between 26°N-44°N and 64.5°E-107.5°E. We use −2°C isotherm of mean annual air temperature (MAAT) to derive the Tibetan permafrost extent.

Preliminary results

Most of models analyzed in this study simulated a degrading trend of Tibetan permafrost extent during the past five decades (Figure 1). A sparking declining period occurs around 1998 for all six models, which is consistent with near surface air temperature change at the same period. The soil temperatures at 3m depth show a different amplitude of warming for all six models around the following year of 1999 (not shown). All models show a significant increasing trend of Tibetan permafrost extent during the first decade simulation. Among the six models, UW-VIC is the most sensitive model to surface air temperature forcing in terms of 3m soil temperature change, which shows larger interannual variation and decreasing tendency over the first decade than other models.

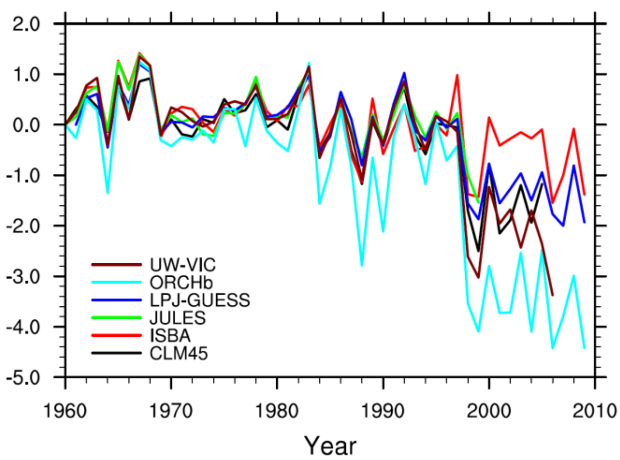

Figure 1. Tibetan permafrost extent ($10^5 km^2$) change during the period of 1960-2009.

References

McGuire, A. D. and Coauthors, 2016. Variability in the sensitivity among model simulations of permafrost and carbon dynamics in the permafrost region between 1960 and 2009, *Global Biogeochemical Cycles* 30(7): 1015-1037.

Distinguishing ice-rich and ice-poor permafrost to map ground temperatures and -ice content in the Swiss Alps

Robert Kenner[1]
[1]WSL Institute for Snow and Avalanche Research SLF, kenner@slf.ch

Abstract

A clear improvement in the prediction of mountain ground temperatures and permafrost distribution could be achieved by distinguishing ice-poor/free and ice-rich permafrost in the modelling process. Separating the referencing data into these two classes, a very strong correlation (CC: 0.99; SE: 0.19 °C) of ground temperatures with elevation and potential incoming solar radiation could be demonstrated for ice-poor and ice-free ground by a linear regression analysis. Based on this, a countrywide permafrost distribution map of Switzerland was created. While temperatures and distribution of ice-poor permafrost were defined using the regression results, the distribution of ice-rich permafrost was defined by modelling mass wasting processes and the burial of snow and ice caused by them. The map represents the occurrence of permafrost in 3 clearly defined classes: permafrost, permafrost sporadically possible and potential ice-rich permafrost. Next to permafrost presence, the map also indicates permafrost temperature and ice-content.

Keywords: Map; ground ice; ground temperatures; Switzerland; mountain permafrost; permafrost distribution

Introduction

Permafrost distribution maps are useful products applied in different fields of practice and research. They are used to plan construction work in alpine terrain, to evaluate local slope instability or to estimate large scale permafrost frequency for scientific purposes. Previous mapping approaches in Switzerland (i.a. Gruber et al., 2006; Boeckli et al., 2012; Deluigi et al., 2017) have in common that they represent a statistically based permafrost likelihood. This has the advantage that uncertainties in the mapping of permafrost become clearly evident. However, the probability classes are difficult to interpret and a clear conclusion on permafrost occurrence is seldom possible.

The permafrost and ground ice map (PGIM) of Switzerland presented here uses a different approach, based on the distinction of ice-rich and ice-poor permafrost. Ice-rich permafrost (permafrost containing excess ice) was considered as being mainly caused by the burial of snow and ice into the ground, i.e. permafrost occurrence as a result of ground ice formation. Ice-poor permafrost (permafrost without excess ice) was focused on as being controlled by atmospherically driven thermal processes and solar radiation, i.e. occurrence of small amounts of ground ice as a result of permafrost.

This approach allowed a considerably higher permafrost prediction accuracy and so a totally different mapping approach: In contrast to other permafrost maps, PGIM does not represent an empirically defined permafrost likelihood of occurrence, but analytically defined ground temperatures and areas with potentially high ground ice content. This type of approach could so far not be implemented by any other permafrost mapping study, due to the apparently too high complexity of permafrost distribution.

Methods

The permafrost and ground ice map PGIM of Switzerland consists of 3 zones: Permafrost (Zone 1), permafrost sporadically possible (Zone 2) and potential ice-rich permafrost (Zone 3). Zone 3 includes all forms of ice-rich permafrost such as rock glaciers, ice-rich talus slopes or ice-bearing moraines and was defined in ERSI ArcGIS. The deposition areas of rock falls and snow avalanches below slopes steeper than 40° and the further creep paths of the ice saturated mass were calculated. These zones were then reduced considering terrain parameters and the surface coverage.

Zones 1 and 2 of the PGIM were derived from modelled ground temperatures. Zone 1 includes all areas with modelled negative ground temperatures. Zone 2 includes the areas with ground temperatures ranging between 0°C and 1°C and is intended as a buffer zone. The ground temperatures were calculated based on a linear regression analysis using the explanatory variables potential incoming solar radiation and elevation (as proxy for mean annual air temperature).

Results

Predicting the ground temperatures of 10 ice-poor boreholes based on elevation and potential incoming solar radiation yields a correlation coefficient of 0.99 and a standard error of 0.19°C. This very strong connection highlights the rather simple dependency of ice-poor permafrost on these two factors and its high predictability (Fig. 1). The PGIM was validated using 92 reference sites. Twenty of 22 validation sites representing ice-poor permafrost are located in Zone 1, one in Zone 2 and one site outside the permafrost zonation. In turn, 0 of 49 sites devoid of permafrost are located in Zone 1 and 4 in Zone 2. Zone 3 (potential ice-rich permafrost) includes 18 sites indicating permafrost and 11 indicating permafrost absence. Zone 3 furthermore includes 95.5% of a validation rock glacier inventory. At the time of abstract submission a further improvement of Zone 3 was still in process.

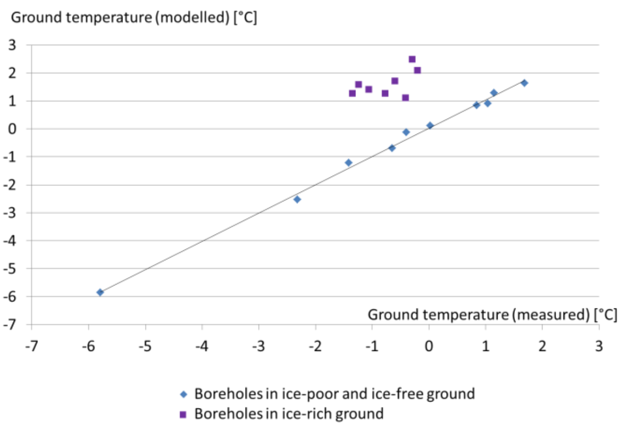

Figure 1. Measured ground temperatures (PERMOS; BAFU; Uni. Lausanne, Uni. Fribourg) against ground temperatures modeled using the explanatory variables solar radiation and elevation.

Discussion

In contrast to other maps, the PGIM only has 3 zones, which are easy to interpret: Two zones (1 and 2) represent modelled ground temperatures and the third one specifies areas with potentially high ground ice content. This improves mapping accuracy and reduces uncertainty.

The uncertainty can be measured by the validation points, which are clearly attributed by the map as permafrost or not. Compared to previous permafrost maps, the PGIM can attribute clearly the most validation points to a definitive class (Permafrost/No permafrost). Despite this low ambiguity, the mapping accuracy, measured by the number of validation points wrongly attributed to a definitive class, is nevertheless as good as in the most accurate permafrost probability maps.

A strength of the PGIM compared to former maps is the reproduction of permafrost free areas. This refers in particular to the phenomenon of 'elevational permafrost 'gaps'. A common permafrost distribution in the Alps shows thermally induced permafrost in the upper parts of a rock wall, a 'permafrost gap' below and ice-rich permafrost at the base of the underlying talus slope (Fig. 2). Mapping based on thermal influences only is not able to reproduce the gap.

Zone 3 of the PGIM had initially a relatively high uncertainty. Although, there is very little ice-rich permafrost outside this zone, it includes approximately 1/3 of permafrost free areas. These problems refer mainly to a missing distinction between bedrock and talus as well as to the correct reproduction of rock glacier creep paths and are currently being solved.

Next to ice content, the zonation of the PGIM also allows an estimation of the permafrost temperature, as Zones 1 and 2 indicate ground temperatures and the ice-rich permafrost of Zone 3 usually has a temperature close to 0°C. The localization of ice-rich and warm permafrost is particularly important for engineering purposes as it affects the ground stability and bearing capacity strongest.

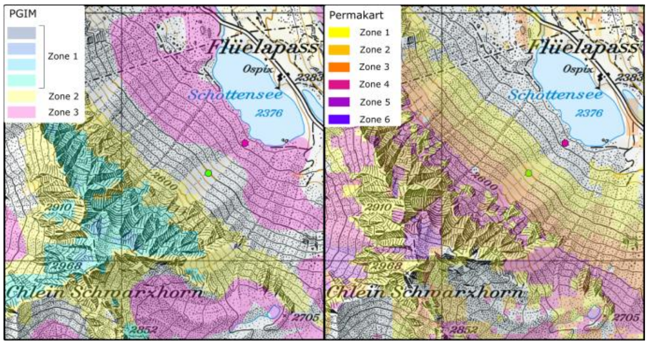

Figure 2. Left: PGIM, showing a well-known "permafrost gap". Right: Potential Permafrost distribution map (Gruber et al., 2006)

References

Boeckli L, Brenning A, Gruber S, Noetzli J 2012. Permafrost distribution in the European Alps: calculation and evaluation of an index map and summary statistics. The Cryosphere 6(4): 807-820.

Deluigi N, Lambiel C, Kanevski M 2017. Data-driven mapping of the potential mountain permafrost distribution. Sci. Total Environ 590: 370-380.

Gruber S, Haeberli W, Krummenacher B, Keller F, Mani P, Hunziker G, Hölzle M, Vonder Mühll D, Zimmermann M, Keusen H-R, A. G, Rätzo H, 2006. Erläuterungen zur Hinweiskarte der potentiellen Permafrostverbreitung in der Schweiz 1:50'000. Swiss Federal Office for the Environment (FOEN)

Difference in surface temperatures and their influences on permafrost temperatures on the Qinghai-Tibet Plateau

Dongliang Luo[1]
Huijun Jin[1]
[1] *State Key Laboratory of Frozen Soil Engineering, Northwest Institute of Eco-Environment and Resources, Chinese Academy of Sciences, Lanzhou 730000, China, luodongliang@lzb.ac.cn*

Abstract

Surface temperatures, which differ in near-surface air temperature (T_a), land surface temperature (LST), and ground surface temperature (GST), are critical to the simulation of permafrost to climate change. We compared the hourly, seasonally and yearly T_a, LST, GST, and ground temperatures, as well as the freezing and thawing indices, the N-factors, and the surface and thermal offsets derived from these temperatures on the Qinghai-Tibet Plateau. Furthermore, we employed the GIPL model to simulate the dynamics of ground temperature driving by T_a, LST, and GST, respectively. Results demonstrated that GST was a reliable driving indicator for the thermal regime of frozen ground. However, great biases of mean annual ground temperatures were induced on the basis of simulations with LST and T_a when the thermal effect of surface characteristics was neglected. Quantitative calculating the thermal effect of surface characteristics on GST is indispensable for permafrost simulations based on the T_a and LST datasets.

Keywords: Near-surface air temperature (T_a); land surface temperature (LST); ground surface temperature (GST); mountainous permafrost; Qinghai-Tibet Plateau (QTP).

Introduction

The ground surface is considered as a thermal boundary other than a physical boundary of permafrost, on which complex heat and water exchange takes place with atmosphere and lithosphere (Riseborough *et al.*, 2008; Smith & Riseborough, 2002). The complex interplay between GST and Ta is simplified as surface offset and N-factors (Lunardini, 1978; Riseborough *et al.*, 2008). However, a number of model practices, especially when applied in vast regions, define the upper boundary conditions with the easily obtained Ta. Moreover, few practices had been conducted to compare the results from different modeling or simulations based on varied upper boundary conditions. Therefore, there is a pressing need that the surface temperatures undergoing an inspection of comparisons before applying at a finer or local scale.

In this study, we compared the hourly, seasonally and annually differences between these surface temperatures. We aim at comparing the difference in surface temperatures and providing some implications for simulating ground temperature and further contribute to the quantitatively accurate mapping permafrost at the rugged topographical environments of the QTP.

Methods

We calculated and compared the freezing and thawing indices, surface offset, and thermal offset based on varied surface temperatures (Luo *et al.*, 2017b). To compare the influence of Ta, LST, and GST on the thermal regimes of the ground, we used the Geophysical Institute Permafrost Laboratory (GIPL) model to simulate the ground temperature based on different driving surface temperatures. Thermophysical properties of the soils (soil water content, unfrozen water curve parameters, heat capacity and thermal conductivity, and the thickness of soil layers, etc.) were maintained the same so as to consider the sole influence of different surface temperatures. The GIPL model was originally designed to simulate the dynamics of ground temperature based on the consideration of the thermal effect of snow-cover and vegetation layer by solving 1D nonlinear heat equation with phase change numerically.

Results and discussions

Half-hourly averaged T_a, LST, and GST in the study region are significantly different in the amplitude of temperature. Due to the sunlight exposure, the undulation of the LST is markedly wider than the T_a, and the peak and valley value of the LST appears different from the T_a. The heat-dampening of surface cover reduces the amplitude of the GST as well. There is a consistent tendency that the minimum half-hourly LST is smaller than that of the half-hourly T_a and GST, and the maximum half-hourly LST is larger than that of the half-hourly T_a and the half-hourly GST.

The differences between MAAT and MAGST (*i.e.*, the surface offset) for the study sites are all within 3.5 °C, which are comparable to those sites in the interior plateau lies to the west of the SAYR (Pan *et al.*, 2016), but markedly lower than those in the Arctic and Subarctic regions such as Franklin Bluffs and Deadhorse in Alaska, where the surface offset could amount to 6.8 °C (Romanovsky & Osterkamp, 1995). This indicates a smaller effect of surface characteristics especially the snow cover on the thermal regime of the ground on the QTP than those in the Arctic and Subarctic regions. Although snow cover exerts both warming and cooling effect and its effect on GST varies daily, monthly and annually, the insulating or warming of snow on the ground surface in the Arctic and Subarctic regions could be greater than that on the QTP due to much thicker of snow thickness and longer duration of snow cover are presented in the Arctic and Subarctic regions. While the strong solar radiation may be responsible for the short preservation of unstable snow cover on the QTP.

The simulations based upon the GST are in good agreement with measured values, while large data biases are induced by simulations based upon both the T_a and LST especially for shallower depths at all sites (Figure 1).

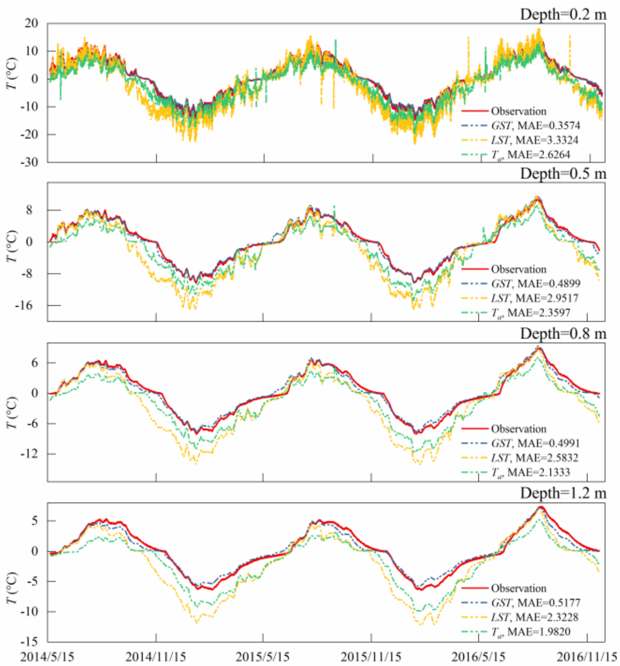

Figure 1. Comparisons of simulated results based on GST, LST and T_a.

Conclusions

Simulated results based on the GLPL model demonstrated that the GST (0-5 cm subsurface) is a reliable driving parameter to simulate the permafrost temperatures even without considering the thermal effect of surface characteristics. Simulations based on LST or T_a by ignoring the thermal effect of surface characteristics result in the mean annual values between the simulations and observations being as large as 3 °C. Therefore, the consideration of the thermal effect of surface characteristics to T_a and the LST remote sensing products are essential to simulate the thermal regime of permafrost. In some cases, the N-factors, ratio of GST to Ta, could be indirectly replaced to obtain the GST to simulate the thermal regime of permafrost, especially for the rugged topography. In the future, ongoing efforts to investigate the thermal effects of surface characteristics on the ground surface should improve the modeling or mapping of permafrost on the QTP.

Acknowledgments

This research is supported by National Natural Science Foundation (NSF) of China (41671060, 41301068), the Key Research Program of Chinese Academy of Sciences (CAS) (No. KZZD-EW-13).

References

Smith, M.W. & Riseborough, D.W., 2002. Climate and the limits of permafrost: a zonal analysis. *Permafrost and Periglacial Processes* 13: 1-15.

Riseborough, D., Shiklomanov, N., Etzelmuller, B., Gruber, S., Marchenko, S., 2008. Recent advances in permafrost modelling. *Permafrost and Periglacial Processes* 19(2): 137-156.

Luo DL, Jin HJ, Marchenko SS, et al., 2018. Difference between near-surface air, land surface and ground surface temperatures and their influences on the frozen ground on the Qinghai-Tibet Plateau. *Gerderma* 312: 74-85.

Pan, X., Li, Y., Yu, Q., Shi, X., Yang, D., Roth, K., 2016. Effects of stratified active layers on high-altitude permafrost warming: a case study on the Qinghai–Tibet Plateau. *The Cryosphere* 10(4): 1591-1603.

Romanovsky, V.E. & Osterkamp, T.E., 1995. Interannual variations of the thermal regime of the active layer and near-surface permafrost in northern Alaska. *Permafrost and Periglacial Processes* 6: 313-335.

Lunardini, V.J., 1978. Theory of n-factors and correlation of data, *Proceedings of the Third International Conference on Permafrost*, Edmond, Alberta, Canada, July: 40-46.

Monitoring and statistical modelling of permafrost in steep slopes of Norway

Florence Magnin[1]
Bernd Etzelmüller[1]
Sebastian Westermann[1]
Paula Hilger[1,2]
Cristian Lussana[3]
Ketil Isaksen[3]
Reginald Hermanns[2,4]

[1] *Department of Geosciences, University of Oslo, P.O. Box 1047, Blindern, 0316 Oslo, Norway, florence.magnin@geo.uio.no*
[2] *Geohazard and Earth Observation Group, Geological Survey of Norway, 7491 Trondheim, Norway*
[3] *Norwegian Meteorological Institute, 0313 Oslo, Oslo, Norway*
[4] [3]*Norwegian University of Science and Technology, Trondheim, Norway*

Abstract

Permafrost can become a crucial factor of steep slope stability, and knowing the distribution of permafrost in steep terrain is a prerequisite when evaluating slope stability in such areas. However, permafrost distribution in such terrain is poorly known. In this study, we present a very first effort in modelling steep slopes permafrost at the nation-scale of Norway. This study is based on a multi-years dataset of 26 rock-surface temperature measurement points covering various aspects, elevations and latitudes. These measurements allow for statistical modelling of rock surface temperature that is then used to map permafrost probability. In this presentation, we present the measurement settings, the rock surface temperature data, the modelling approach and first results of the permafrost mapping.

Keywords: Permafrost; steep slopes; Norway; statistical modelling; mapping.

Introduction

The Norwegian fjords and valleys are characterized by steep mountain flanks lying above human settlements and infrastructures, the sea or lakes. These settings are a main source of risk. The destabilizations of steep slopes endanger the human lives and activities because they can (i) directly hit houses and infrastructures, (ii) dam the valley bottom, disturbing human activities and transports, which also provokes (iii) modifications in the water streams creating new lakes susceptible to outburst, and can also (iv) hit existing water bodies and trigger displacement waves. Such mass movements and their secondary effects have caused hundreds of fatalities in the Norwegian history (Hermanns *et al.,* 2012).

While geological and paraglacial processes have been extensively studied to understand steep slope destabilizations in Norway, the possible influence of permafrost has been less emphasized. However, recent studies in various mountain ranges, especially in the European Alps, have pinpointed that permafrost degradation is a major factor of steep slope stability (Gruber & Haeberli, 2007). Many unstable steep slopes lie in a possible permafrost range in Norway and an estimation of its distribution is required as a first step to better understand its role in these destabilizations. A first map of rock wall permafrost distribution in Norway has been proposed by Steiger *et al.* (2015) based on general assumptions on the link between permafrost and air temperature. In this presentation, we present a preliminary estimation of permafrost distribution based on a statistical model fitted with 24 rock surface temperature (RST) times series and a preliminary estimation of permafrost distribution.

Methods and preliminary results

Rock surface temperature measurements

During summers 2015, 2016 and 2017, 22 RST loggers were installed along a latitudinal profile from 60°50'N to 69°46'N. They complete 4 loggers installed in 2010 in Jotunheimen (Hipp et al., 2014). Measurements points cover all aspects and range from 215 to 2320 m asl.

Statistical modelling approach

In fall 2017, the available time series yield 54 mean annual rock surface temperature (MARST) points available for statistical modelling. Possible predictors of

MARST are determined based on multi-collinearity tests and by analyzing their statistical significance. As evidenced in other mountain ranges, mean annual air temperature (MAAT) and the potential incoming solar radiation (PISR) are the most important predictors of MARST. The statistical model is then implemented in a GIS to map permafrost probability on a 10-m-resolution DEM (released by the Norwegian Mapping Authority).

Permafrost probability mapping

Permafrost is mapped based on the 1961-1990 MAAT data released by the Norwegian Meteorological Institute (SeNorge v2; Lussana *et al.,* 2017), downscaled from 1 km to 10 m resolution using a regional lapse rate. PISR is mapped using GIS tools and assuming an atmospheric transmissivity of 100%. MARST is then mapped using the parameters of the statistical model and the permafrost probability is expressed as a probability of the MARST to be ≤ 0°C. The permafrost probability is classified based on standard classification with isolated (0 to 10%), sporadic (10 to 50%), discontinuous (50 to 90%) and continuous (>90%) permafrost (Fig. 1).

Preliminary results

Continuous permafrost (MARST ≤ to 0°C) is likely above 1200 m a.s.l. in North faces and above 1600 m a.s.l. in the South faces of the South-Western Norway. In Northern Norway, the lower limit of continuous permafrost rather lies at around 600 m in North faces and 900 m in South faces. This preliminary estimation already shows that many of the unstable steep slopes of Norway lie within the range of discontinuous-continuous permafrost, such as the Mannen (1294 m asl.) rock slide (up to 30Mm^3, depending on the scenario) in SW Norway (Fig.1).

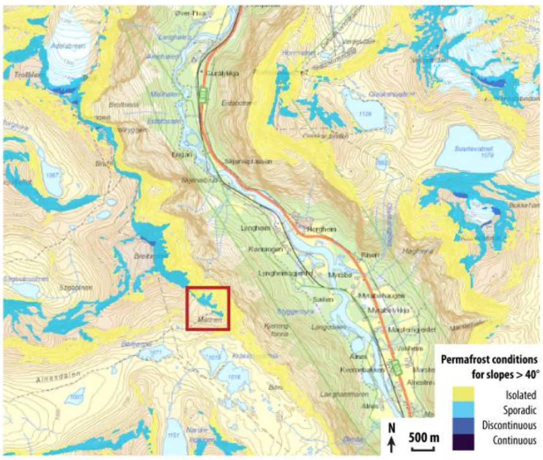

Figure 1. Example of the permafrost distribution map in the steep slopes of Romsdalen. The Mannen rock slide (red square) lies in the sporadic permafrost zone.

Outlooks

Using the 1961-1990 normal MAAT results in permafrost overestimation. The model will be also implemented with the MAAT of 1981-2010 to better represent current conditions.

The resulting MARST map can be used to setup a transient numerical model such as those from Myhra *et al.* (2015). In the frame of this project, transient models of steep slope thermal regime are coupled with mechanical models to better assess the role of permafrost in steep slope destabilization.

Acknowledgments

This study was mainly funded by the Research Council of Norway (CryoWALL - 243784/CLE), in addition to the Geological Survey of Norway (NGU) and the Department of Geosciences, University of Oslo.

References

Gruber S. & Haeberli W., 2007. Permafrost in steep bedrock slopes and its temperature-related destabilization following climate change. *Journal of Geophysical Research: Earth Surface*, 112: F02S18.

Hermanns, R., Hansen, L., Sletten, K., Böhme, M., Bunkholt, H.S.S., Dehls, J.F., Eilertsen, R.S., Fisher, L., L'Heureux, J.-S, Høgaas, F., Nordahl., B., Oppikofer, T., Rubensdotter., L., Solberg, I.-L., Stalsberg, K., & Yugsi Molina, F.X., 2012. Systematic geological mapping for landslide understanding in the Norwegian context. In E. Eberhardt, C. Froese, A.K: Turner & S. Leroueil (eds.), *Landslide and Engineered Slopes: Protecting Society through Improved Understanding,* Taylor & Francis Group: London, 265-271.

Hipp, T., Etzelmüller, B. & Westermann, S., 2014. Permafrost in Alpine Rock Faces from Jotunheimen and Hurrungane, Southern Norway', *Permafrost and Periglacial Processes*, 25(1): 1-13.

Lussana, C., Tveito, O. E. & Uboldi, F. 2017. "Three-dimensional spatial interpolation of two-meter temperature over Norway", accepted for publication on the Quarterly Journal of the Royal Meteorological Society

Myhra, K.S., Westermann, S., & Etzelmüller, B., 2015. Modelled Distribution and Temporal Evolution of Permafrost in Steep Rock Walls Along a Latitudinal Transect in Norway by CryoGrid 2D. *Permafrost and Periglacial Processes*, 28: 172-182, doi:10.1002/ppp.1884,

Steiger, C., Etzelmüller, B., Westermann, S., & Myhra, K.S., Modelling the permafrost distribution in steep rock walls in Norway, *Norwegian Journal of Geology*, 96(4): 329-341.

Rock glaciers of the Balkan Peninsula

Brigitte Magori[1]
Petru Urdea[1]
[1]*West University of Timisoara, brigitte.magori@gmail.com*

Abstract

Being one of the defining alpine features, rock glaciers are spread and studied in high mountains around the world, but the scale and level at which they are analyzed differs greatly across the continents. In the Balkan region, the research of the permafrost relates landform is at its beginnings, with a limited number of studies being conducted until now. We present an overview of the main characteristics of rock glaciers in the Balkan Peninsula based on their morphometric features and basic statistical analysis. Our results show a relation between the latitude of rock glaciers and their size and altitude, especially interesting being the fact that rock glaciers size tends to increase at lower latitudes.

Keywords: rock glaciers; permafrost; morphometric characteristics; Late Glacial; Balkan Peninsula.

Introduction

Rock glaciers (RG) are rock-mantled ice bodies widespread in the alpine environment of the Balkan Peninsula and elsewhere. Because they transport both rock and ice down-valley due to the deformation of the ice within (Haeberli, 2000) they are characterized by a distinct surface microrelief of longitudinal or transversal ridges and furrows (Barsch, 1996). These features are morphological indicators for mountain permafrost occurrence and for periglacial conditions. In the current study, we present an overview of the rock glaciers from the Balkan Peninsula by analyzing their geomorphometric characteristics and their geographic location

Until now the presence of rock glaciers has been inventoried, at a local scale, for the Rila (Gikov & Dimitrov, 2010), Pirin (Dimitrov & Gikov, 2011), Pindus (Hughes *et al.*, 2003; Palmentola & Stamatopoulos, 2006) or Dinaric Mountains (Milivojević *et al.*, 2008; Palmentola *et al.*, 1995) and has just been suggested for the Parnassus mountain range (Pechoux, 1970).

Methodology and Results

We analyzed 196 rock glaciers located in six different high mountains of the Peninsula (Table 1) spread over about three degrees of latitude. The morphometric parameters were extracted using ArcGIS from a 30m resolution DEM and the statistical analysis (correlations, t test) were performed using the software R.

Out of the total number of RGs, 149 (76%) are tongue shaped and the rest are lobate. The tongue shaped are also located at higher altitudes ($t=4.98$, $p<0.05$) and have a greater area ($t=5.05$, $p<0.05$) than the lobate RGs.

Table 1. Rock glaciers in the Balkan Peninsula

Mountains	Coordinates	Nr. of RG	Mean elevation of the RG front (m)
Prokletije	42°26'30"N 19°48'45"E	42	1992
Rila	42°06'00"N 23°33'00"E	39	2348
Korab	41°47'28"N 20°32'52"E	8	2233
Pirin	41°45'49"N 23°23'58"E	83	2339
Tymphi	39°58'54"N 20°48'54"E	8	1932
Tzoumerka	39°29'00"N 21°12'00"E	16	1748
Parnassus	38°32'09"N 22°37'27"E	1	1890

The results show that 70% of rock glaciers have a northern aspect and they are spread at altitudes between 1748-2447 m, with the highest rock glaciers situated in the Rila Mountains, Bulgaria and the lowest in Tzoumerka Mountains, Greece. The rock glaciers slope ranges from 9^{o} to 28^{o}, with a mean of around 17^{o} for all the mountain ranges.

The average area is 12.4ha, with the biggest RG being in the Prokletije mountains with an area of 89.7ha.

Conclusions

The analysis of the rock glacier characteristics reveals the following conclusions:

The Tzoumerka are the southernmost mountains with a significant number of rock glaciers and have the lowest most altitude at which they form.

The results show that the size of the rock glaciers increases with the decrease of the latitude.

This overview is a necessary first step in our propose to reconstruct the permafrost conditions from the Late Glacial and Holocene in the Balkan Peninsula.

References

Barsch, D., 1996. *Rockglaciers. Indicators for the present and former geoecology in high mountain environments*. Springer, Berlin.

Dimitrov, P. & Gikov, A., 2011. Relict rock glaciers identification and mapping in Pirin Mountain using aerial and satellite images. *Proceeding of the Seventh Scientific Conference SPACE, ECOLOGY, SAFETY.*

Gikov, A. & Dimitrov, P., 2010. Identification and mapping of the relict rock glaciers in the Rila Mountain using aerial and satellite images. *Proceeding of the Sixth Scientific Conference SPACE, ECOLOGY, SAFETY.*

Haeberli, W., 2000. Modern research perspectives relating to permafrost creep and rock glaciers: a discussion. *Permafrost Periglacial Process*., 11(4), 290-293.

Hughes, P., Gibbard, P., Woodward, J., 2003. Relict rock glaciers as indicators of Mediterranean palaeoclimate during the Last Glacial Maximum(Late Wuermian) in northwest Greece. *J. Quat. Sci*., 18(5), 431-440.

Milivojević, M., Menković, L., Ćalić, J., 2008. Pleistocene glacial relief of the central part of Mt. Prokletije (Albanian Alps). Quat. Int., 190(1), 112-122.

Palmentola, G., Baboci, K., Gruda, G., Zito, G., 1995. A note on rock glaciers in the Albanian Alps. *Permafrost Periglacial Process*., 6(3), 251-257.

Palmentola, G. & Stamatopoulos, L., 2006. Preliminary data about sporadic permafrost on Peristeri and Tzoumerka massifs (Pindos chain, Northwestern Greece). *Revista de Geomorfologie*, 8, 17-23.

Pechoux, P., 1970. Traces of glacial action in the Mountains of Central Greece. *Revue de Géographie Alpine*, 58, 211-224.

Modelling of Ground Penetrating Radar in alpine Permafrost at Hoher Sonnblick Summit

Theresa Maierhofer[1]
Matthias Steiner[1]
Werner Chwatal[1,2]
Wolfgang Schöner[3]
Adrian Flores-Orozco[1]
[1]*TU Wien, Department of Geodesy and Geoinformation, Research Group Geophysics, Vienna, Austria, tm@as-m.at*
[2]*Pöyry-Infra GmbH, Salzburg, Austria*
[3] *University of Graz, Department of Geography and Regional Science, Graz, Austria*

Abstract

In frame of the ATMOperm project, we conducted a series of Ground Penetrating Radar (GPR) surveys at Hoher Sonnblick Summit. The objective was to determine the internal structures and distribution of mountain permafrost and associated changes due to seasonal variations in temperature. To achieve this, 3D GPR surveys were repeated between 2015 and 2017 at different times. Besides the processing of the raw data, modelling of electrical properties for the computation of synthetic radargrams was carried out to permit a better interpretation of the observed changes in GPR results.

Keywords: Ground Penetrating Radar, synthetic modelling, monitoring

Introduction

Current permafrost research focuses on understanding the effect of atmospheric events, such as climate change in the degradation of alpine permafrost.

To better understand subsurface processes, here we present geophysical imaging results for data collected at the Hoher Sonnblick Summit. This is located in the Austrian Central Alps, 3106 m above sea level, where a permanently installed monitoring array (Fig. 1) permits the collection of electrical resistivity tomography (ERT) being a standard method in permafrost investigations (Krautblatter et al., 2008). However, ERT measurements might be limited in winter due to the low current injections taking place in surfaces covered by snow and ice. To overcome such limitation, we performed monitoring measurements with GPR, a contactless method based on the propagation of electromagnetic waves, which has been successfully applied in previous studies in permafrost environments (Hauck & Kneisel, 2008; Moorman *et al*, 2007).

The final objective of our investigations is to obtain a 3D subsurface model of the electrical properties at the Hoher Sonnblick Summit for an improved characterization of the active layer and lithological contacts and discontinuities (e.g., fractures). Aiming at improving the quantitative interpretation, the synthetic response was numerically modelled taking into account the resistivity distribution in the subsurface as derived from ERT monitoring data and information from supplementary geophysical surveys.

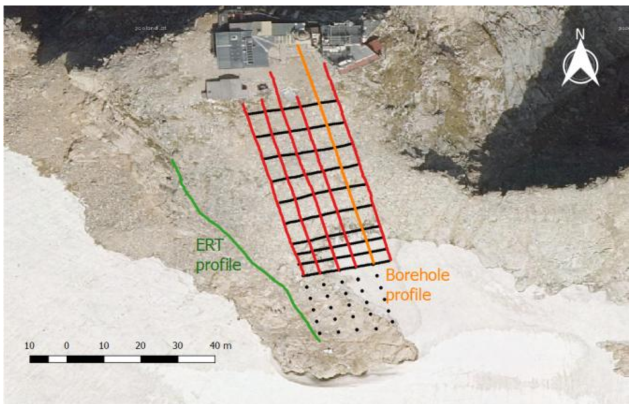

Figure 1: Orientation of the GPR profiles defined by six long profiles (red), 13 transverse profiles (black) and ERT monitoring profile (green).

Field Work

A total of eight GPR campaigns were organized between August 2015 and September 2017. In those campaigns GPR datasets were collected using a SIR 3000 unit in a common offset configuration, mainly with 200 and 400 MHz antennas. Results presented here refer to a campaign in winter 2017 collected along 6 long profiles and 13 perpendicular shorter profiles (Fig. 1) covering an area of ca. 25 x 100 m using a 200 MHz antenna.

Results

GPR raw data were analyzed using REFLEXW software, based on the application of standard filter routines and topographic correction. Results obtained for an exemplary dataset clearly reveal interfaces between materials with different electrical properties (Fig. 2). The first interpretation of the radargrams took into account amplitude information and the propagation velocity of the radar waves derived by hyperbola analysis. To validate such interpretation, we perform numerical modelling after assigning electrical values to the different materials based on GPR- and ERT-measurements and those reported in literature (Hauck & Kneisel, 2008; Moorman *et al*, 2007).

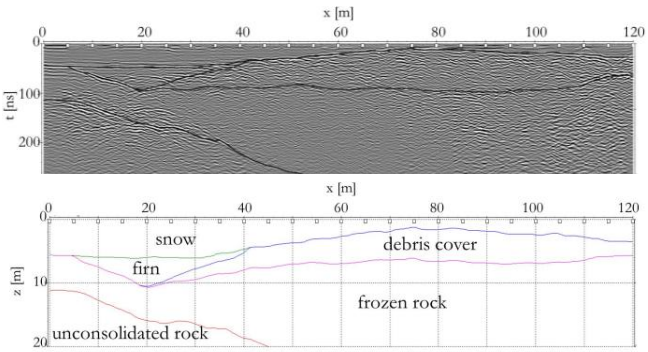

Figure 2: Radargram of borehole profile using a 200 MHz antenna (top) and corresponding interpreted model (bottom).

Since the reflection of GPR signals is related to variations in both the electrical permittivity (ε) and conductivity (σ) of the medium, our modelling included variations in the contrasts between those parameters and the geometry of the interfaces. Hence, the analysis of different numerical models permits us to adjust the synthetic radargram to approximate the actual measured data (Fig. 3). Fractures were added representing the debris cover to reconstruct the patterns observed in the measured data. Moreover, further structural information in the models has been obtained through results from seismic P-wave velocity information and transient electromagnetic soundings.

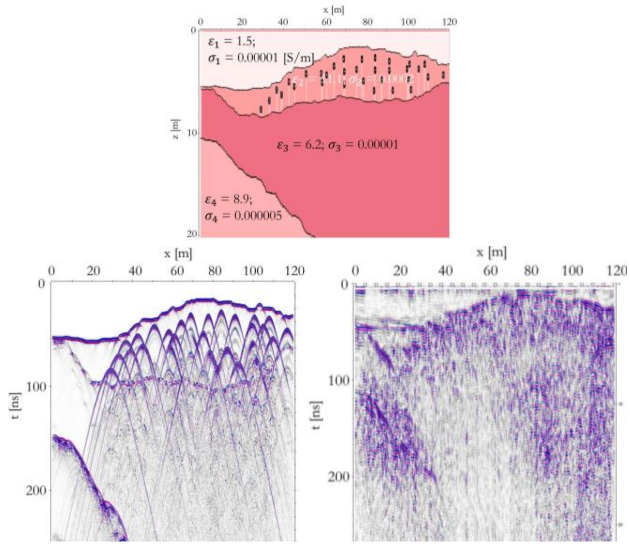

Figure 3. Comparison of synthetic (left) and measured (right) radargram representing the heterogeneous debris-covered mountain environment at the Hoher Sonnblick.

As expected due to the complexity of alpine permafrost soils, the models need to take into account the large number of discontinuities observed in the GPR data. Thus, careful data processing is required to permit the identification of the active layer and improve the quantitative meaning of the deviated electrical models. Future research will focus on the integration of borehole temperature data for the improved modelling of GPR.

Acknowledgments

The ATMOperm project is funded by the Austrian Academy of Sciences (ÖAW). We thank the team at the Sonnblick observatory for supporting this project and Stefan Reisenhofer, Martin Mayr and Jakob Gallistl for their help in the field surveys.

References

Hauck, C., & Kneisel, C. (2008). *Applied geophysics in periglacial environments* (Vol. 240). Cambridge: Cambridge University Press.

Krautblatter, M., Verleysdonk, S., Flores-Orozco, A., & Kemna, A. (2010). Temperature-calibrated imaging of seasonal changes in permafrost rock walls by quantitative electrical resistivity tomography (Zugspitze, German/Austrian Alps). *Journal of Geophysical Research: Earth Surface*, *115*(F2).

Moorman, B., Robinson, S., & Burgess, M. (2007). Imaging near-surface permafrost structure and characteristics with Ground-Penetrating Radar. *CSEG Recorder J*, *32*(2), 23-30.

Monitoring rock glacier by optical stereoscopic "time-lapse" device

Guilhem Marsy[1, 2, 3]
Xavier Bodin, Emmanuel Malet[2]
William Castaings[3]
Flavien Vernier, Héla Hadri, Emmanuel Trouvé[1]
[1] *LISTIC Polytech Annecy-Chambéry, Univ. Savoie Mont Blanc, guilhem.marsy@univ-smb.fr*
[2] *Univ. Grenoble Alpes, CNRS, Univ. Savoie Mont-Blanc, Environment Dynamics and Territories of Mountains (EDYTEM), 73000 Chambéry, France*
[3] *TENEVIA 38240 Meylan, France*

Abstract

Classical methods to monitor rock glacier's dynamics rely on repeated *in situ* field campaigns to evaluate the evolution of the glacier surface. Methods such as photogrammetry (structure from motion) with drone or from a set of images allow to get a dense spatial resolution, up to the pixel size, but are limited in terms of time repeatability. On the other hand, continuous GPS measurement on the glacier surface can capture seasonal changes but with a poor spatial resolution. To get both spatial and time resolution we developed an optical stereoscopic time lapse device. The system, made with two fixed reflex cameras, placed at different viewpoints and taking several images per day, is able to acquire the 3D surface of the glacier over time and thus producing time series of spatial data at high resolution in space and time (4D).

Keywords: Rock glacier kinematics; Surface displacement monitoring; Time-lapse stereo-photogrammetry.

Introduction

Rock glacier, mainly situated in dry mountains and area of discontinuous permafrost, are creeping mixtures of ice and debris (Haeberli, 1985). Due to the high thermal inertia of permafrost, the monitoring of rock glacier flow can highlight climatic trends. The Laurichard rock glacier, situated in the southern French Alps, has been studied for several decades, with the use of different methods : LiDAR surveys, repeated GPS surveys of marked blocks, geoelectric campaigns and continuous ground temperature measurements (Bodin et al, 2009). Regarding velocity surface monitoring, these methods lack of time repeatability and/or spatial resolution. On the other hand (Hadhri et al, 2017) have proposed a solution based on monoscopic time lapse imagery, to compute dense velocity surface field of slow moving surfaces, such as glacier, with high temporal resolution. We propose to extend this work by using a second camera to get velocity field in meters and not only in pixels coordinates and apply it in the Laurichard rock glacier context.

Methods

Study site

The Laurichard rock glacier is situated at an altitude between 2400 and 2700-m asl, surrounded by high rock faces, and is 500-m long and between 80 and 200-m wide. The typical mean velocity is around 25-cm/year at the glacier roots and front, and can reach more than one meter on the median steepest part.

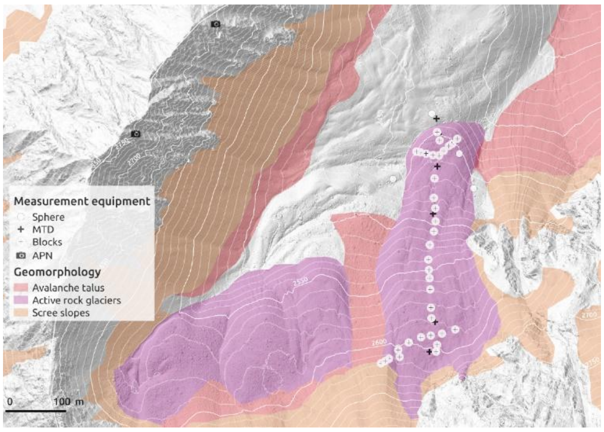

Figure 1 Field installations on the Laurichard rock glacier: cameras, spheres, marked blocks, temperature sensors.

Two Nikon D800 with a 85mm focal lens are situated 300-m away from the glacier and the baseline between the camera is 200-m. Five spheres, with a diameters of 35-cm are situated around the glacier and are used as fixed ground control points (one sphere located on the tongue of the rock glacier). Figure 1 gives an overview of the field installations.

Data processing

The outdoor conditions are really challenging for photogrammetric measurements: fog, snow cover, cast shadows, illuminations changes, lens flare, can affect the quality of the output velocity vector field. That is why several images are taken per day to maximize the probability to have a pair of stereo images that can be further processed. The first step is to identify the best images of the day and discard the images that cannot be processed.

Even though the cameras are fixed to solid rock, unwanted shifts of the images often occur, related to the thermally-controlled differential dilatation/retraction of the various parts of the device (camera itself, lens, case...). The second step is to register all the images such that fixed ground stays still in the images, this is done estimating an homography transformation from extracted corresponding points on stable areas of the scene.

Then sparse correspondences between images taken at different dates are extracted to get velocity vector field in pixels. Figure 2 shows the extracted displacement between October 2013 and October 2016.

To convert velocities from pixels to meters vectors, the cameras need to be calibrated. The calibration is done by identifying feature points in the images with known 3D coordinates, then a nonlinear optimization algorithm estimates the intrinsic and extrinsic parameters of the cameras (Hartley and Zisserman 2003).

From this calibration, it is possible to convert a velocity vector in pixels to a vector in meter if the vector can be identified in the two stereo pair of images (Hartley and Zisserman 2003).

Further processing can be done to improve the results, such as snow detection to restrict correspondences extraction in time to snow free area.

Figure 2 Surface vector velocity field in pixels of the Laurichard rock glacier between September 2013 and September 2016.

References

Bodin X., Thibert E., Fabre D., Ribolini A., Schoeneich P., Francou B., Reynaud L., Fort M., 2009. Two Decades of Responses (1986–2006) to Climate by the Laurichard Rock Glacier, French Alps. *Permafrost and Periglacial Processes* 20, 331–344.

Haeberli, W., 1985. Creep of Mountain Permafrost: Internal Structure and Flow of Alpine Rock Glaciers. Mitteilungen der VAW, ETH: Zürich; 142 pp.

Hadhri, H., Vernier, F., Atto, A., & Trouvé, E. (2017, June). Inverse Formulation of Temporal Closure and Proposed Solutions for Offset Tracking of Natural Scenes. In *MultiTemp 2017*.

Hartley, Richard, and Andrew Zisserman. *Multiple view geometry in computer vision*. Cambridge university press, 2003.

Reconstruction of mean annual ground surface temperature in discontinuous permafrost region, northern Mongolia

Munkhdavaa Munkhjargal[1]
Gansukh Yadamsuren[2]
Jambaljav Yamkin[2]
Lucas Menzel[1]
[1] Department of Geography, Heidelberg University, Heidelberg, Germany, munkhjargal@uni-heidelberg.de
[2] Institute of Geography and Geoecology, Mongolian Academy of Science, Ulaanbaatar, Mongolia

Abstract

Mean annual ground surface temperature (MAGST) for 2016-2017, including complete thawing and freezing periods, has been estimated with 30m resolution to determine the spatial distribution of permafrost presence over Sugnugur valley, northern Mongolia. The key findings were; i) a north-south surface temperature difference of 3-4°C and the relationship between surface and lower air temperature decreased as elevation increased; ii) smaller surface offsets existed on rock and bare ground surfaces relative to vegetated surface types, and consistent snow-induced freezing and distinct thawing n-factors were observed; iii) MAGST was estimated with a RMSE of ±1.4°C and r^2 of 0.68 with greater errors on steep slopes; iv) wildfire severity affected the intensity of active layer lowering and altered the hydrological regime; v) micro-climate, topographic factors and surface characteristic influenced the presence of permafrost. These findings suggest that the stability of permafrost in this region is very vulnerable to global warming and fire-induced effects.

Keywords: discontinuous permafrost, surface temperature, air temperature, potential radiation, wildfire

Introduction

The study area is located in a semi-arid Siberian discontinuous permafrost region with -1°C of mean annual air temperature (MAAT) and has rough topography. The seasonal relations between air (Ta) and surface (Ts) temperatures based on in situ measurements and empirically projected MAAT from potential solar radiation (PSR) were considered as the driving parameters for the estimation. The results indicate that the approximation of MAAT might be derived from PSR using least linear regression analyses (with R^2=0.98) after several adjustments (Fig. 1). Relative consistent snow-insulated freezing n-factor nF of about 0.5 at different altitudes including mountain top was observed, while thawing n-factor nT notably varies, ranging from 0.8-1.2 depending on surface characteristics (Table 1).

Table 1. The observed surface offset and n-factors

Sites	SO	nF	nT	SD (cm)	Surface characteristic
Xoxoo	4	0.52	1.2	24	Short grassland
Eislager	3.5	0.6	1.05	20	Poorly vegetated
Bärental	4	0.53	1.16	25	Short grassland
Mtn. top	1.5	0.52	0.8	NA	Rock surface

SO, nF, nT and SD denote surface offset, freezing n-factor, thawing n-factor and snow depth, respectively

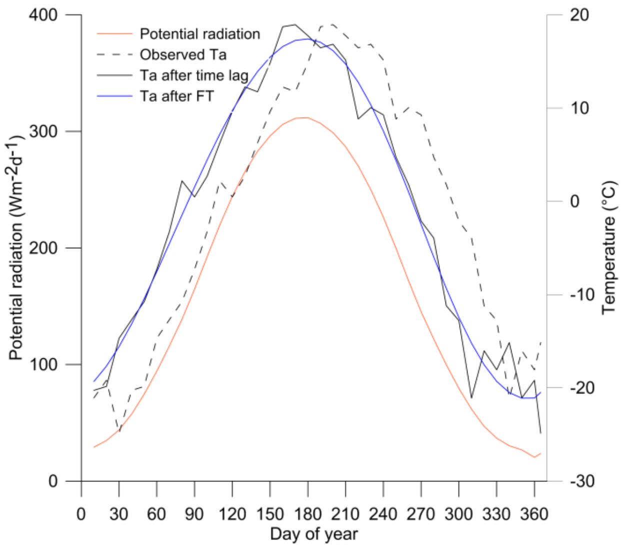

Figure 1. The distribution curves of daily mean PSR, observed and adjusted air temperatures at Bärental site on 10 day running averages. Fourier transform (FT) and 30-day time lag adjustments were applied to remove time variances

The vegetation and snow covers were observed using remote sensing images and during field campaigns. South-facing slopes were observed to be 3–4°C warmer than north-facing slopes on annual average and were mostly snow free due to high sublimation and prevailing winds. No winter precipitation gradient has been observed and the depth of snow cover on north-facing slopes and the valley bottom were similar except for the relative thin snow cover under dense forest.

The winter freezing degree-days (FDD) in surface temperature were similar on both slopes, showing rapid decrease and increase on snow-free south-facing slopes compared to north-facing slopes and bottom of the valley with thick snow cover as well. In contrast, thawing degree-days (TDD) correlated to the impact of vegetation cover and ambient air temperature during summer months play a notable role in the spatial distribution of MAGST. The correlation coefficient between Ta and Ts decreased as elevation increased, which could be explained by extended snow cover.

The MAGST is initially warmer than MAAT, with surface offsets ranging from +1.5°C on rock surface to +4°C on short grasslands. Surface temperature at 5cm depth and snow depth measurements at our permanent meteorological station (since 2012) in the lower part of the valley reveal that MAGST in 2016-2017 was about 2°C warmer than the average value of previous years (Table 2).

Table 2. Mean and max snow depth (cm) with air and surface temperatures (Ta and Ts, °C) and incoming solar radiation (ISR, Wm^{-2}) in winters since 2012.

	2012/13	*2013/14*	*2014/15*	*2015/16*	*2016/17*
Mean	0.25	0.19	0.12	0.15	0.19
Max	0.41	0.26	0.25	0.26	0.29
Ts	-12.3	-10.9	-12.3	-11	-9.8
Ta	-23.7	-19.7	-18.5	-21.2	-18.7
ISR	78.8	88.8	83.5	79.6	86.9

It was caused by the occurrence of hot and dry summer 2017 (not shown here) and relative thick snow cover during winter 2016/17, leading to warmer mean surface temperature.

This may have led to 1-2°C warmer MAGST in the study region during the investigated period. The RMSE of the estimated MAGST (Fig. 3) was ±1.4°C, with greater anomaly on north-facing slopes due to low PSR allocation. Additionally, the impacts of wildfire in the active layer were discussed based on soil temperature and moisture data recorded in three boreholes under severely burned, partly burned and unburned forests. The preliminary analysis indicate that the recent wildfire has altered both the hydrological and temperature regimes (Fig. 2) of the active layer significantly, leading to increase in active layer thickness and potential permafrost degradation in this semi-arid climate.

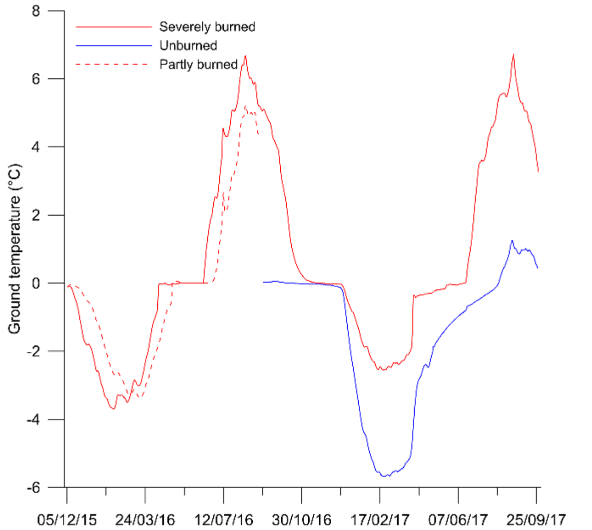

Figure 2. Temperature variabilities at 100cm depth in severely burned, partly burned and unburned forests. The fire intensity affects the magnitude of seasonal thaw depth.

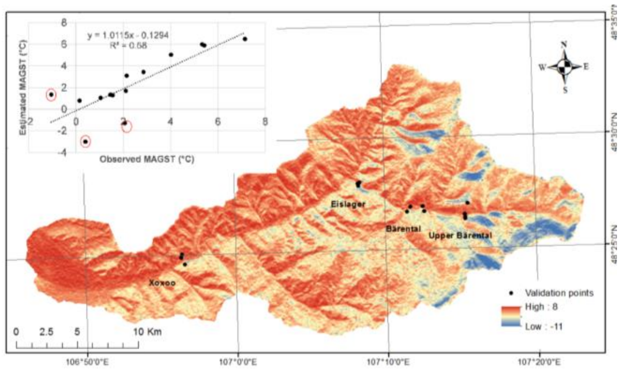

Figure 3. Estimated surface temperature in Sugnugur valley for 2016-2017. Red circles in the upper-left figure show the outliers with greater standard error. Black dots represent the locations of the validation site.

The further investigations will focus on the relationship between air and surface temperatures on different slopes including various exposures and below forest canopy to improve the accuracy of the estimation.

Seasonal and inter-annual variability of soil moisture in permafrost terrains

Cécile Pellet[1]
Coline Mollaret[1]
Christian Hauck[1]
[1]*Department of Geosciences, University of Fribourg, Switzerland, cecile.pellet@unifr.ch*

Abstract

Soil moisture is a key factor controlling the energy and mass exchange processes at the soil-atmosphere interface. In permanently frozen ground it strongly affects the thermal behavior of the ground by influencing its physical properties such as ice content, thermal conductivity and heat capacity. Using a unique combination of long-term borehole temperatures, meteorological data and geophysical datasets, we characterize the seasonal and inter-annual variability of soil moisture at three alpine permafrost sites. Seasonally, the evolution of soil moisture can be distinguished into three stages consistent with temperature and electrical resistivity.

Keywords: Soil moisture; Mountain permafrost, Geophysics

Introduction

Soil moisture is a key factor influencing the energy and mass exchange processes at the soil-atmosphere interface. In frost-affected terrains, soil moisture is of particular relevance given its impact on the physical properties of the subsurface such as the thermal and hydraulic conductivity as well as the ice content, the heat capacity or the electrical conductivity. Several modelling studies confirmed the influence of soil moisture on the thermal regime of frozen ground (e.g. Boike *et al.*, 2008; Hinkel *et al.*, 2001; Scherler *et al.*, 2010). However, measurement-based studies are lacking due to the scarcity of operational soil moisture monitoring stations at high elevation.

In a first attempt to assess the role of water content on the thermal regime of the ground in mountainous terrains, a soil moisture monitoring network has been established in 2013 along an altitudinal gradient spanning from middle to high elevation in Switzerland (SOMOMOUNT network see Pellet & Hauck, 2017). Two stations have been installed in collaboration with the Swiss permafrost monitoring network PERMOS in the vicinity of well-established long-term permafrost monitoring sites: Schilthorn (Hilbich *et al.*, 2011) and Stockhorn (Gruber *et al.,* 2004). Similar datasets are also available in the Italian Alps at the Cime Bianche monitoring site (Pogliotti *et al.*, 2015).

Using this unique combination of data, this contribution aims at 1) quantifying and characterizing the seasonal and inter-annual variations of soil moisture in mountain permafrost terrain and 2) comparing these variations with measured in-situ ground temperatures, meteorological data and geophysical datasets.

Table 1. Summary of all the data available at each site.

	Schilthorn	Cervinia	Stockhorn
Soil moisture	2007-2017	2007-2017	2014-2017
Borehole temperature	1999-2017	2006-2017	2000-2017
Meteorological data	1999-2017	2006-2017	2002-2017
Geophysics (ERT)	1999-2017	2013-2017	2005-2017

Methodology and Results

The datasets available at Schilthorn, Stockhorn and Cervinia (see Tab.1) constitute state of the art measurements in mountain permafrost areas and have been used to analyze the thermal state and evolution of permafrost in several studies (e.g. Hilbich *et al.*, 2011; PERMOS, 2016; Pogliotti *et al.,* 2015). In addition, operational soil moisture measurements have been initiated at Schilthorn and Cervinia in 2007 and at Stockhorn in 2014.

Seasonally, liquid soil moisture (LSM) exhibits variations consistent with the measured temperatures and resistivity at comparable depth (Fig.1). Three typical stages can be identified: the frozen stage (lowest LSM and temperatures, smallest variability), the zero-curtain period (temperatures constant near the freezing point and marked LSM increase as well as resistivity decrease) and the unfrozen stage (high LSM and temperature variability controlled by meteorological forcing). This evolution is observed at the three field sites with differences in onsets and duration of the stages due to site specific factors.

In addition to being spatially highly variable, the LSM evolution is also temporally variable. Thus, the inter-annual variation of LSM during the summer was analyzed and related to the meteorological conditions, ground temperature and resistivity. The two contrasting years 2014 (wet) and 2015 (warm-dry) have been especially analyzed to understand LSM behavior under very different atmospheric forcing.

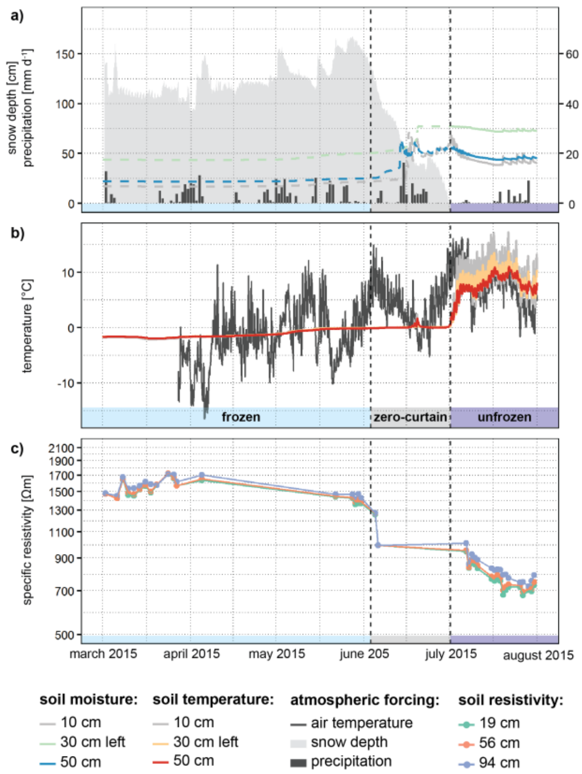

Figure 1. Temporal evolution of near surface liquid soil moisture (a), soil temperature (b) and soil resistivity (c) at Schilthorn. Air temperature, precipitation sum and snow depth are also displayed as well as the thermal state of the ground. (Figure adapted from Pellet & Hauck, 2017)

Acknowledgments

The soil moisture data at Schilthorn and Stockhorn have been collected within the SOMOMOUNT project funded by the Swiss National Science Foundation (project no. 143325). The geophysical data at Cervinia are the fruit of the collaboration between the University of Fribourg and the regional environmental protection agency of Val d'Aosta (ARPA). We also thank our colleagues from ARPA for providing the monitoring data from the Cervinia field site and the PERMOS network for the data collected within this network at Schilthorn and Stockhorn.

References

Boike, J., Wille, C. & Abnizova, A., 2008. Climatology and Summer Energy and Water Balance of Polygonal Tundra in the Lena River Delta, Siberia *Journal of Geophysical Research-Biogeosciences* 113:G03025.

Gruber, S., King, L., Kohl, T., Herz, T., Haeberli, W. & Hoelzle, M., 2004. Interpretation of Geothermal Profiles Perturbed by Topography: The Alpine Permafrost Boreholes at Stockhorn Plateau, Switzerland *Permafrost and Periglacial Processes* 15:349–57.

Hilbich, C., Fuss, C. & Hauck, C., 2011. Automated Time-Lapse ERT for Improved Process Analysis and Monitoring of Frozen Ground *Permafrost and Periglacial Processes* 22:306–19.

Hinkel, K. M., Paetzold, F., Nelson, F. E. & Bockheim. J. G., 2001. Patterns of Soil Temperature and Moisture in the Active Layer and Upper Permafrost at Barrow, Alaska: 1993-1999 *Global and Planetary Change* 29: 293–309.

Scherler, M., Hauck, C., Hoelzle, M., Staehli, M. & Voelksch, I., 2010. Meltwater Infiltration into the Frozen Active Layer at an Alpine Permafrost Site *Permafrost and Periglacial Processes* 21:325–34.

Pellet, C. & Hauck, C., 2017. Monitoring Soil Moisture from Middle to High Elevation in Switzerland: Set-up and First Results from the SOMOMOUNT Network *Hydrolgy and Earth System Sciences* 21:3199–3220.

PERMOS, 2016. Permafrost in Switzerland 2010/2011 to 2013/2014 *Glaciological Report (Permafrost) of the Cryospheric Commission of the Swiss Academy of Sciences* 12-15.

Pogliotti, P., Guglielmin, M., Cremonese, E., Morra di Cella, U., Filippa, G., Pellet, C. & Hauck, C., 2015. Warming Permafrost and Active Layer Variability at Cime Bianche, Western European Alps *The Cryosphere* 9:647–661.

Preliminary assessment for mountain frozen ground distribution (33°S, 70°W)

Ruiz Pereira, S.[1], Fernandez, H.[1,2], Moskalenko, F.[3], García, J.L. [1], Marquardt, C. [4], Lambert, F. [1]
[1]*Geography Institute, Pontifical Catholic University of Chile*, ***spruiz@uc.cl***
[2]*Christian Humanism Academy, Santiago de Chile.* [3]*Pontifical Catholic University of Chile*
[4] *Department of Mining Engineering and Geosciences group, Pontifical Catholic University of Chile*

Abstract

Semi-arid (27-32°S) Andean range possesses a wide variety of cryoforms, which are slightly assessed in terms of their impact relative to human access to water. 33°S and southwards, the ratio of covered/uncovered glaciers decreases. Glacierized sub-catchments of the Aconcagua basin, Juncal Norte (terminus at 3000m ASL) and Alto Del Plomo/Monos de Agua (terminus at 3800m ASL), have not been assessed in terms of their recent process dynamic. To approach this gap, sub-catchments were analyzed by remote and direct observations. Relict cryoforms (such as ice-cored moraines) coexist with preserved ones as result of differential ablation and hence the onset of paraglacial dynamic.

Keywords: Mountain frozen ground; glacier; ice-cored moraine; Andes.

Introduction

A knowledge gap where process spatial distribution is crucial to integrate catchment runoff (Pellicciotti et al., 2014) in areas where permafrost types remain present in the most arid conditions (Garcia et al., 2017), difficult to assess because of tome varying relative contributions (Rodriguez et al., 2016). Differential landscape evolution between two deglacierizd areas might account on paraglacial transition processes therein.

Methods

Study area is Juncal-Norte Glacier (JNG, Fig. 1), calculated ELA at 4,500m ASL (Ayala et al., 2017), and Monos de Agua (Fig. 2) sub-catchments. Satellite imagery (Landsat 1-8) and field mapping were utilized to assess cryoforms.

Results

The present retreat at JNG does not resemble the paraglacial evolution at Monos de Agua (MAG). Nevertheless, in between them, isolated ice-bodies and covered-glaciers were attested (Fig.1 a & b).
Ice-cored lateral moraines should persist in both settings while facing south/south-west. While moraine at JNG (Fig. 1.a) ranges from clasts to boulders, in MAG has lower sizes, and thermokarst lakes (Fig. 2) on surface.

a

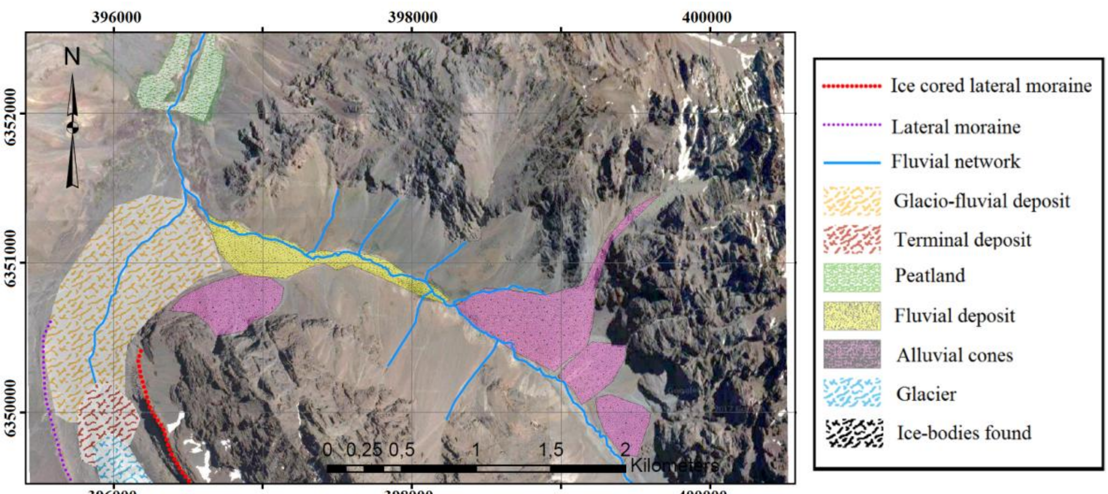

(Figure continues)

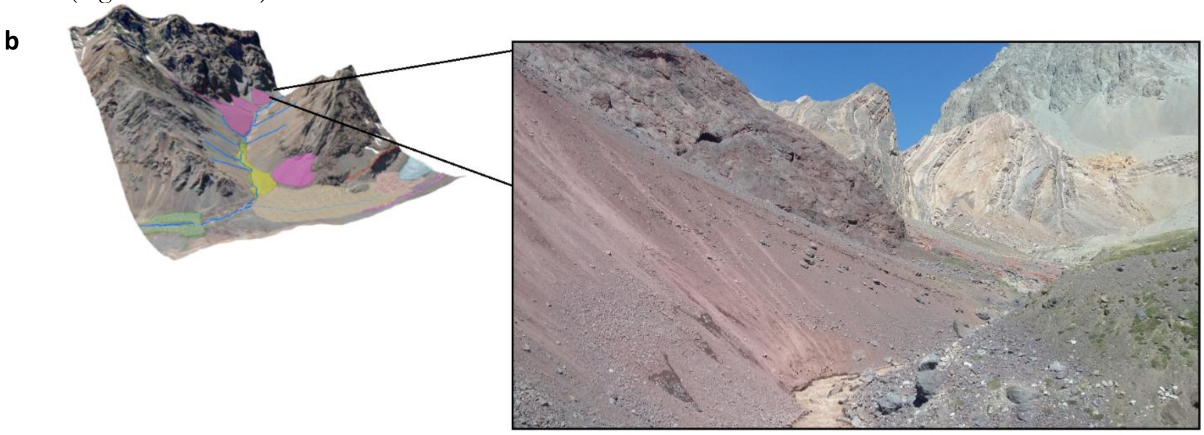

Figure 1. Monos de Agua sub-catchment, 3000-3300m ASL. Altitude in (a) increasing eastwards. Glacier in lower-left corner is Juncal Norte. Zoom in (b) shows ice-containing elements in late warm season 2016.

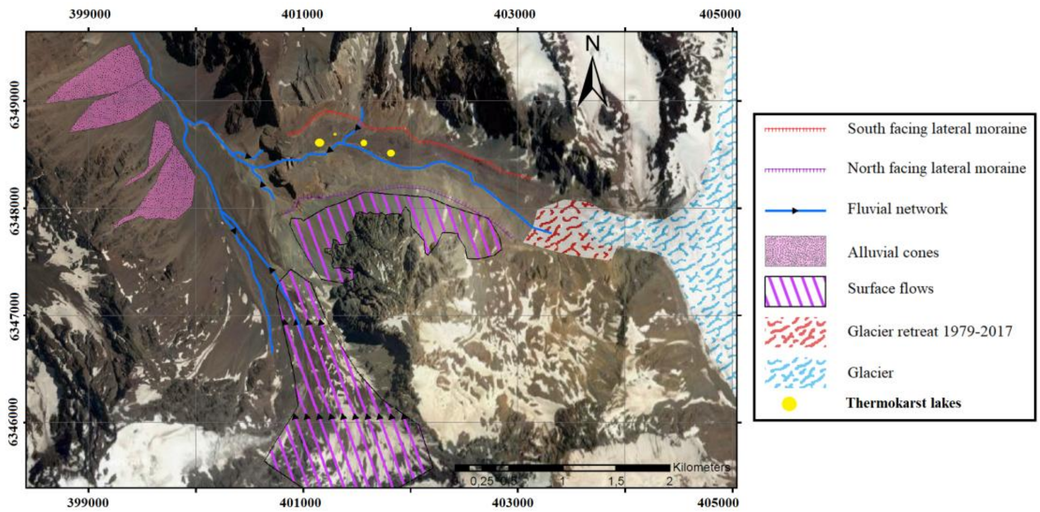

Figure 2. Monos de Agua sub-catchment, 3300-4000m ASL. Easternmost border (with Argentina) at 4000m ASL. Glaciar Alto del Plomo's terminus falling westwards & Monos de Agua falling southwards.

In the case of MAG a likely persistent kilometric ice cored lateral moraine, a process assumed to occur between 1979-1989 from L1 & L4 images. Coalescent, now paraglacial taluses on the south-facing lateral moraine (Fig. 2) are considered of protalus-rampart origin and non-embryonal rock-glaciers due their steep slope and southward exposition. Fig. 2 also shows in the lower-center a distinctive gelifluction form with color-differentiated gullies running downslope over 1 mile.

Conclusions

Cryoforms between both catchments outline dominating factors of deglacierization processes and landscape transition at the central Chilean Andes.

Although deglacierization obeys contemporary climate, comparison of sediments cover thicknesses and hydrological processes would allow determining main variables in the proglacial and later paraglacial process.

References

Ayala, A., Pellicciotti, F., Peleg, N., & Burlando, P. (2017). Melt and surface sublimation across a glacier in a dry environment: distributed energy-balance modelling of Juncal Norte Glacier, Chile. *Journal of Glaciology*, *63*(241), 803-822.

Pellicciotti, F., Ragettli, S., Carenzo, M., & McPhee, J. (2014). Changes of glaciers in the Andes of Chile and priorities for future work. *Science of the Total Environment*, *493*, 1197-1210.

Rodriguez, M., Ohlanders, N., Pellicciotti, F., Williams, M. W., & McPhee, J. (2016). Estimating runoff from a glacierized catchment using natural tracers in the semi-arid Andes cordillera. *Hydrological Processes*, *30*(20), 3609-3626.

Quantifying erosion rates of steep bedrock hillslopes in glacial landscapes with cosmogenic nuclides – A case study from the Chhota Shigri Glacier, India

Dirk Scherler[1]
David L. Egholm[2]

[1] GFZ German Research Centre for Geosciences, Telegrafenberg, D-14473 Potsdam, Germany, scherler@gfz-potsdam.de
[2] Department of Geoscience, Aarhus University, 8000 Aarhus, Denmark, david@geo.au.dk

Abstract

How fast do steep bedrock hillslopes in glacial landscapes erode? And how sensitive are erosion rates in these environments to temperature changes? These are fundamental questions related to past and present climate change, but they are difficult to answer. Here, we present erosion rate estimates from steep bedrock hillslopes above the Chhota Shigri Glacier, Indian Himalaya. Our estimates are based on the ^{10}Be inventory of debris that is exposed in medial moraines. Results suggest rock wall retreat rates of ~0.6-1.3 mm yr^{-1}. We find a relatively consistent pattern of increasing ^{10}Be concentrations (decreasing erosion rates) downglacier, which cannot be explained by ice-surface residence alone. We use a numerical ice flow model that includes debris production and transport to assess potential explanations for the observed trend. Preliminary results yield a modeled glacier that reasonably reproduces observed patterns of debris exposure.

Keywords: supraglacial debris, cosmogenic nuclides, erosion rates, frost cracking, debris-covered glaciers

Introduction

Debris-covered glaciers are widespread in the Himalaya and other steep mountain ranges. They testify to active erosion of ice-free bedrock hillslopes that tower above valley glaciers, sometimes more than a kilometer high. It is well known that supraglacial debris cover significantly reduces surface ablation rates and thereby influences glacial mass balances and runoff. However, the dynamic evolution of debris cover, along with climatic and topographic changes, is poorly understood. Here, we present ice-free hillslope erosion rates from the catchment of the Chhota Shigri Glacier, Indian Himalaya. We follow the approach of Ward and Anderson (2010), and use an ablation-dominated medial moraine as a sampler for ^{10}Be-derived erosion rates of glacier valley walls. We combine our empirical, field-based approach with a numerical model of frost-related sediment production and glacial debris transport to (1) assess patterns of ice-free hillslope erosion that are permissible with observed patterns of debris cover, and (2) explore the coupled response of glaciers and ice-free hillslopes to climatic changes.

Study area

The Chhota Shigri Glacier is located in the North Indian state of Himashal Pradesh, in a small basin that drains into the Chandra River. The northerly oriented glacier has a length of ~9 km, covers an area of 15.7 km^2, and ranges from ~4200 m to ~6100 m elevation.

The medial moraine currently originates at the base of a bedrock ridge that protrudes above the surrounding ice. Its width increases from ~5 m near the junction of the two main branches of the glacier to several 10s of meters closer to the glacier terminus.

Results

^{10}Be concentrations and erosion rates

We collected five samples from the medial moraine of the Chhota Shigri Glacier between 4638 m and 4773 m elevation. The sample locations are separated by approximately 500 m along the glacier. All samples consist of an amalgamation of >1000 surface clasts with grain sizes between ~1 and ~30 mm, yielding samples of ~5 kg weight. The clasts were randomly taken from surface patches of approximately 5 m by 5 m, which were centered on the medial moraine. Measured ^{10}Be concentrations increase downglacier from ~3×10^4 to ~6×10^4 atoms (g quartz)$^{-1}$ yielding hillslope erosion rates of ~1.3-0.6 mm yr^{-1}.

Numerical modeling

We used the ^{10}Be-derived hillslope erosion rates to define a debris supply rate of 1 mm yr^{-1} from ice-free bedrock hillslopes in the numerical ice and landscape evolution model iSOSIA (Egholm *et al.*, 2011). Based on available mass balance and ice thickness data, the calibrated model reproduces the medial moraine of the Chhota Shogri Glacier quite well, although uncertainties exist due to the transient disequilibrium of the glacier, i.e., the current debris cover was fed into the glacier during the Little Ice Age (LIA), and thus under different boundary conditions.

Discussion & Conclusions

The accumulation of ^{10}Be during debris residence on the ice surface can only account for a small fraction (<20%) of the downglacier increase. Other potential explanations include heterogeneous source areas with different average productions rates and/or erosion rates, and temporally variable erosion rates. We currently perform transient experiments during warming and cooling periods for testing models of frost-related and temperature-sensitive debris production, and for assessing the coupled sensitivity of hillslopes and glaciers to climate change.

Acknowledgments

We thank J. Mey for help during fieldwork and P. Eugster for helping in the lab.

References

Egholm, D.L., Knudsen, M.F., Clark, C.D., Lesemann, J. E., 2011. Modeling the flow of glaciers in steep terrains: The integrated second-order shallow ice approximation (iSOSIA). *J. Geophys. Res.* 116: F02012, doi: 10.1029/2010JF001900, 2011

Ward, D.J. & Anderson, R.S., 2010. The use of ablation-dominated medial moraines as samplers for 10Be-derived erosion rates of glacier valley walls, Kichatna Mountains, AK. *Earth Surface Processes and Landforms* 36: 495-512, doi: 10.1002/esp.2068.

Present and future runoff regimes at Murtèl-Corvatsch rockglacier

Martin Scherler [1]
Martin Hoelzle [1]
Matthias Huss [1, 2]
Christian Hauck [1]
[1]*Department of Geosciences, University of Fribourg, Fribourg, Switzerland, martin.scherler@unifr.ch*
[2]*Laboratory of Hydraulics, Hydrology and Glaciology (VAW), ETH Zurich, Zurich, Switzerland*

Abstract

As glaciers are expected to continue to retreat during the 21st century due to climate change, an important source of water will be diminishing, especially during the summer months. Hence, other sources of water, such as meltwater from permafrost, will become more important to the runoff regime and the total runoff. This study aims at modelling the melt of ground ice in permafrost bodies with regard to total runoff from a small hydrological basin. We compare the results of two different models for simulating the hydrologic behavior of Murtèl-Corvatsch rockglacier from 1991 to 2100. One model is a physically based 1D heat and mass transfer model (COUP), the other a spatially distributed glacio-hydrological model (GERM). We present the simulated runoff regimes of both models for the periods 1991-2020 and 2061-2090. Significant differences of the contributions of the different reservoirs to runoff are identified and discussed.

Keywords: rockglaciers, runoff, modelling, permafrost evolution.

Introduction

As glaciers are expected to retreat substantially during the 21st century due to a warming climate, an important source of water will be diminishing, especially during the summer months. In turn, water from other sources such as permafrost will become more important in the runoff regime. This water might serve as a valuable fresh water source for agricultural needs, hydropower production or direct human consumption in mountain areas. Therefore, it is of great interest to know the origin and the amount of runoff coming from rockglaciers and slopes underlain by permafrost.

This study investigates the amount of fresh water available on a sustainable basis from such regions. In case of a disequilibrium of summer melt and winter refreezing there will be a constant or even accelerated loss of ice volume stored in permafrost and a peak in runoff. Two different models are used to gain insight into these processes. The models are applied to the well-studied site of the Murtèl–Corvatsch rockglacier in the Upper Engadin, Switzerland. The ice-rich rockglacier reaches from 2850 to 2620 m a.s.l. and is 400 m long and 200 m wide, facing north-northwest. The Murtèl study site has been the subject of numerous studies including borehole logging, energy balance measurements, geophysical surveys and numerical modelling in the past (Mittaz *et al.*, 2000, Vonder Mühll & Haeberli, 1990). It is also part of the PERMOS monitoring network (PERMOS, 2016).

Methodology and Results

Methods

We compare the results of two different models for simulating the hydrological behavior of Murtèl-Corvatsch rockglacier from 1991 to 2100. On the one hand, we use a physically based 1D heat and mass transfer model (Coup Model; Jansson & Karlberg, 2011), on the other hand a spatially distributed highly parameterized glacio-hydrological model (GERM; Huss *et al.*, 2011). Both models account for the conductive and latent heat exchange between the atmosphere and the sub-surface and are able to resolve the mass balance of ground ice. We present the simulated runoff regimes of both models for the periods 1991-2020 and 2061-2090. The contributions of the different runoff components are presented for both models. The models are driven by climate scenario data (ENSEMBLES; MPI).

Results

The results of the models are shown in Figures 1 and 2. In the case of GERM, the runoff components are derived directly from the different water reservoirs in the model. In COUP, the components have to be calculated from the model results of all model layers.

Comparing the water fluxes computed by the two models it can be noted that the total runoff according to COUP is significantly higher during spring for both the present and the future periods. The runoff regimes in the period 1991-2020 are characterized by a snowmelt-induced peak a constant decrease until December. In the future period (2061-2090), a period of lower constant runoff is projected by both models lasting from July through to October. The contribution of permafrost storage change is significantly higher than in the present-day situation in both models. Following GERM mass gain can be expected in spring and a continuous mass release in late summer and autumn. COUP projects ice mass losses in all months except in April and September.

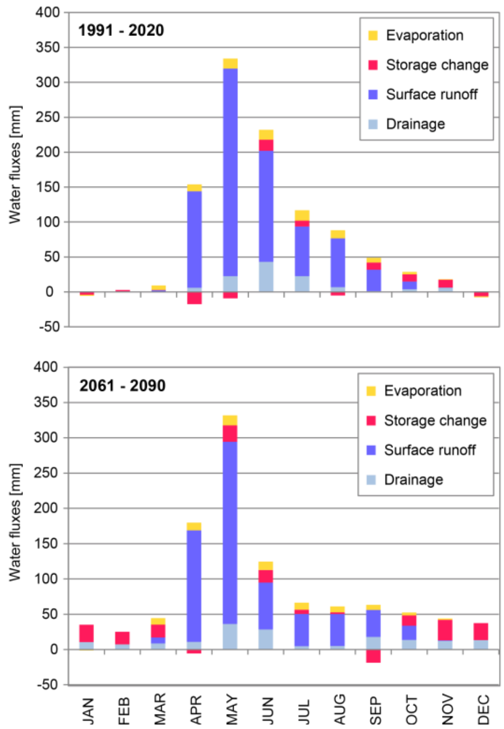

Figure 1. Mean monthly water fluxes in COUP for the time periods 1991 - 2020 and 2061 - 2090.

Conclusions

Although the model structures and complexities are quite different, similar annual runoff regimes are simulated for both the present-day situation and the future. An increase in the contribution of permafrost ice melt to runoff can be seen in both models.

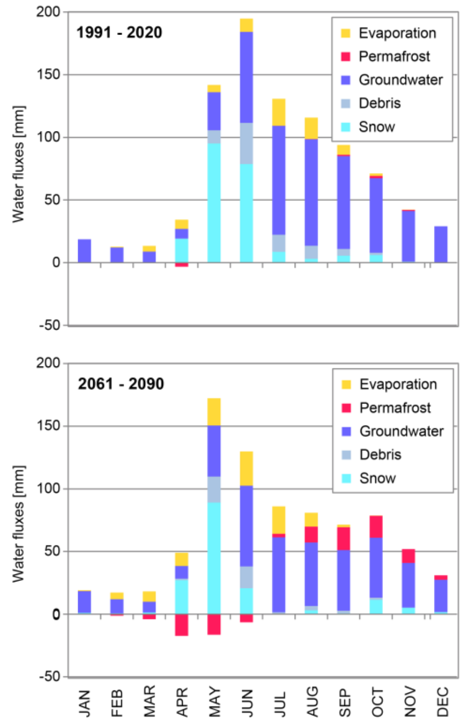

Figure 2. Mean monthly water fluxes in GERM for the time periods 1991 - 2020 and 2061 - 2090.

References

Huss, M., Scherler, M., Schneider, S., Hoelzle, M. & Hauck, C. 2011. Future water yield from melting mountain permafrost: A fully distributed modeling approach. *Geophysical Research Abstract*, EGU2011-11466.

Jansson, P.-E. & Karlberg, L., 2011. Coup manual. Coupled heat and mass transfer model for soil–plant–atmosphere systems. *Royal Institute of Technology: Stockholm*; 435.

Mittaz, C., Hoelzle, M. & Haeberli, W. 2000. First results and interpretation of energy-flux measurements of Alpine permafrost. *Annals of Glaciology* 31:275-280.

Scherler, M., Hauck, C., Hoelzle, M., & Salzmann, N. 2013. Modeled sensitivity of two alpine permafrost sites to RCM- based climate scenarios. *Journal of Geophysical Research: Earth Surface*, 118(2), 780-794.

PERMOS., 2016. Permafrost in Switzerland 2010/2011 to 2013/2014. Noetzli, J., Luethi, R., and Staub, B. (eds.), *Glaciological Report (Permafrost) No. 12-15 of the Cryospheric Commission of the Swiss Academy of Sciences*, 85 pp.

Vonder Mühll, D. & Haeberli, W., 1990. Thermal characteristics of the permafrost within an active rock glacier (Murtèl/Corvatsch, Grisons, Swiss Alps). *Journal of Glaciology*, 36(123):151-158

Frozen ground, periglacial processes and mountain permafrost in the Monte Perdido-Tucarroya massif (The Pyrenees)

Enrique Serrano[1]
Juan Ignacio López Moreno[2]
Raúl Martín-Moreno[3]
Manuel Gómez-Lende[4]
Alfonso Pisabarro[1]
María González-García[1]
Ibai Rico[5]
Esteban Alonso-González[2]
[1]*Dpto. Geography. Universidad de Valladolid, Spain., email. serranoe@fyl.uva.es*
[2] *Instituto Pirenaico de Ecología (CSIC), Spain.*
[3] *Dpto. Didácticas Específicas, Universidad Autónoma de Madrid, Spain.*
[4] *PANGEA, Universidad de Valladolid. Spain*
[5] *Dpto. Geography, Universidad del País Vasco, Spain.*

Abstract

The work studies the distribution of periglacial landform, seasonal frozen ground and permafrost in the high mountain of the Monte Perdido massif, Ordesa-Monte Perdido National Park. The ground thermal regimen, BTS, and geomorphological mapping of periglacial landforms and processes permit to know the distribution and activity of the ice in the ground. In the Tucarroya Cirque and Monte Perdido massif between 2500 and 2800 m the ground can remain free of ice whole year round. Between 2650 and 2780 are found seasonal frozen ground and landforms as gelifluction lobes and patterned ground, the most common periglacial feature in the studied area. Above 2760 permafrost possible appear in the North slope alternating with seasonal frozen grounds, where frost mounds are present. Finally, above 2885 the permafrost probable is developed.

Keywords: Mountain permafrost, seasonal frozen ground, periglacial, Pyrenees.

Introduction

The study area is in the Ordesa-Monte Perdido National park, in the Monte Perdido massif (3335 m) and the Tucarroya glacial cirque. It is a high valley placed between 2450 and 2800 m, a glacial area, where today exist the Monte Perdido glacier, of 37,7 Ha, the second one by extension of the Pyrenees, and moraine complexes of the Younger Dryas and the Little Ice Age. The main goal is to know the distribution of seasonal frozen grounds, mountain permafrost and current periglacial processes.

Methods

The method is based in four techniques. The mapping of periglacial shapes and processes at 1: 10,000 scale permits to know the presence and distribution of landforms and processes linked to ground ice. BTS measurements show the winter thermal conditions. 18 data-loggers (i-buttons models DS1922L and DS1921G) installed in the study area during the period 2014-2016 have permits us to know the ground thermal regime. The annual average ground temperature, the average winter ground temperature, the freeze index and the thaw index have been also calculated. Solar Radiation Rate have been modelled in whole study area.

Results

The geomorphological indicators of the possible presence of frozen grounds, permanent or seasonal, and the thermal indicators allow to establish an altitudinal zonation of seasonal frozen ground or permafrost (Figure 1). Landforms associated with permafrost are very scarce and reduced in both surface and altitudinal extension. There are no rocky glaciers or protalud lobes, as they do exist in other cirques in the Pyrenees at the same altitudes. The presence of frozen bodies of metric to decametric sizes, gelifluction lobes and frost mounds, have been detected above 2770 m, and up to 3020, always in North slopes, indicating the possible existence of permafrost. These altitudes and orientations are adjusted to those obtained from the thermal regime. BTS measures denote possible permafrost above 2765 m. In Tucarroya, three types of thermal regimes have been detected, showing the variation of temperatures and the possible presence of frozen ground.

1. Ground thermal regimes linked to atmospheric temperature. The ground remains free of ice whole year round, or can be developed seasonal frozen grounds.

2. Ground thermal regimes linked to the snow cover. It clearly indicates the absence of seasonal frozen grounds and permafrost in a wide altitudinal range between 2585 and 2970 m.

3. Thermal regimes with frozen grounds, where the ground temperature remains below 0^{0}C, between 2650 and 3020 m. This regime denotes the existence of seasonal frozen grounds or permafrost. From 2980 m the ground thermal conditions indicate likely permafrost, interrupted in walls and hills, where topoclimatic conditions prevent their presence. The thermal conditions for the mountain permafrost development, sporadic or discontinuous, show up from 2760 m in Tucarroya and surroundings of Monte Perdido.

In the studied area, three geomorphological environments have been mapped: without ice in the ground; seasonal frozen grounds; and possible or likely permafrost. The presence of permafrost in Tucarroya is determined by the shading factors and, to a lesser degree, the altitude, so that it develops mainly on the northern slope. The largest extension of frozen grounds is represented by the seasonal frozen grounds, characterized by their annual freezing and thawing. They are kept frozen between 1 and more than 4 months and constitute the most effective geomorphological action. Gelifraction and gelifluction processes and patterned grounds are linked to the seasonal frozen grounds and scattered between 2650 and 3000 m. Patterned grounds are the most widespread periglacial landforms, join the gelfluction lobes, the last one located mainly at low altitudes. Between 2650 and 2780 are found seasonal frozen ground and landforms as gelifluction lobes and patterned ground, the most common periglacial feature in the studied area. Above 2760 permafrost possible appear in the North slope alternating with seasonal frozen grounds, where frost mounds are present, and above 2885 m the permafrost probable is developed. Finally, there are ice-free areas up to 2800 m, from this altitude the ice is always present in the ground.

Altitude	Ground temperature or landfroms	Orientation	Indicador			
3075	-7,5	--	Seasonal frozen ground			
3030	Gelifluction lobes	N	Permafrost	Probable permafrost		
3020	-5,9	N	Permafrost probable			
3000	-3,4	S	Permafrost probable			
2967	0,5	--	No permafrost*			
2960	L.G.	N	Permafrost			
2920	L.G.	N	Permafrost			
2896	-3.9	S	Permafrost Probable			
2886	Gelifluction lobe	N	Permafrost			
2878	-1.0	S	Seasonal frozen ground	?	Seasonal frozen ground	
2865	-1.4	S	Seasonal frozen ground			
2853	L.G.	N	Permafrost			
2850	Frost mounds	N	Permafrost			
2849	-1.4	SE	Seasonal frozen ground			
2849	-2.0	S	Posible Permafrost	Possible permafrost		
2818	-0.9	S	Seasonal frozen ground			
2810	L.G.	N	Permafrost			
2800	4,5	--	No permafrost			No ice in the ground
2796	-0.9	N	Seasonal frozen ground			
2788	-2.3	S	Possible Permafrost			
2785	-1,5	S	Seasonal frozen ground			
2780	Gelifluction lobes	N	Permafrost			
2773	4,9	--	No permafrost			
2772	-2.5	N	Possible Permafrost			
2770	-2.6	N	Possible Permafrost			
2764	-2.1	N	Possible Permafrost			
2761	-0.3	N	Seasonal frozen ground			
2760	M.H.	N	Permafrost			
2760	-1.5	N	Seasonal frozen ground			
2757	-0.9	S	Seasonal frozen ground			
2755	0	S	No permafrost			
2753	0,3	N	No permafrost			
2748	-0.9	N	Seasonal frozen ground			
2739	-0.6	S	No permafrost			
2737	-0.8	N	No permafrost			
2730	-0,7	N	Seasonal frozen ground			
2717	-1.2	SE	Seasonal frozen ground			
2711	-1.7	S	Seasonal frozen ground			
2699	-0.4	S	No permafrost			
2692	-1.7	N	Seasonal frozen ground			
2688	-1.9	N	Seasonal frozen ground			
2676	-1.9	N	Seasonal frozen ground			
2650	-0,1	N	Seasonal frozen ground			
2620	0	N	No permafrost			
2585	2,8	S	No permafrost			

Figure 1. Indicators of frozen ground distribution in the Tucarroya and Monte Perdido.

Permafrost probability model for debris surfaces in the Central Andes (29º to 33º SL, Argentina).

Carla Tapia Baldis[1]
Dario Trombotto Liaudat[1]
Christian Halla[2]

[1]*Ianigla (Argentine Institute of Snow Research, Glaciology and Environmental Sciences), CCT Conicet, Mendoza, Argentina, ctapia@mendoza-conicet.gob.ar*
[2]*Department of Geography, University of Bonn, Germany*

Abstract

A regional-extension permafrost distribution model was achieved, including locally adjusted data. It discriminates between permafrost in debris or loose sediments from rock permafrost and ice bodies. The final model is a combination of two separate occurrence probability models: a) mean annual air temperature-terrain ruggedness model and, b) mean annual air temperature-potential incoming solar radiation model. Possible permafrost, in coarse debris, is expected between 4200 to 5700 m asl (MAAT from -3º to -18ºC) and covers a surface of aprox. 1200 km2 in the Andes.

Keywords: Central Andes, mountain permafrost, probability model, debris surfaces.

Introduction

In the Central Andes of Argentina (28º to 33º SL/71º to 69º WL) different permafrost occurrence models were applied in the last years but only over reduced areas.. On the other hand, Gruber's PZI global model (2012), locally displays biased data and due to its coarse resolution. Our approach aims to obtain a regional permafrost distribution model, including locally adjusted data that discriminates between permafrost below debris or loose sediments from rock permafrost and surface ice.

Study area

The study area comprises high altitude mountain ranges (Mercedario peak: 6770 masl), low precipitation rates (ca. 200-300 mm/yr from 30º to 33º SL and aprox. 100-150 mm/yr from 28º to 30º SL) with high solar radiation rates. Precipitation occurs mostly during the austral cold-season and the snow layer does not remain yearly outside protected niches. From a geomorphological point of view, Andean landscape is the result of different glacial, periglacial, paraglacial, alluvial and fluvial systems. Quaternary glacial stages modeled the landscape however; periglacial features dominate over the former ones today. The periglacial environment is expected above 3500 to 3800 m asl, while both active and inactive rock glaciers are located approximately the same limit. At 3500 m asl, mean annual air temperature (MAAT) is about 1.3ºC.

Methodology

An empiric-static model was used to estimate regional mountain permafrost distribution, using a logistic regression method. A similar approach was previously used by Brenning and Trombotto (2006) and Azócar *et al.* (2017). Predictive variables include mean annual air temperature (MAAT, ºC), terrain ruggedness index (TRI) and potential incoming solar radiation (PISR, W/m2). The final model is a combination of two separate occurrence probability models: a) MAAT-TRI model and, b) MAAT-PISR model. As both models are independent, wholesome probability is equal to Model "A" Probability * Model "B" Probability.

The MAAT was previously modeled using the period from 1979 to 2010 gridded data from NCEP-CSFR reanalysis series, compared to the available, yet scarce, data from meteorological stations. As heat-transfer processes differ from coarse or blocky surfaces compared to cohesive rock outcrops, both should be discriminated as suggested by Boeckli et al. (2012). TRI values, obtained using the homonymous algorithm in SAGA GIS® with an ASTER-GDEM base are suitable for this task. PISR was calculated in SAGA GIS® using a time-lapse of 1 hour each 5 days during one year;

yearly values were then averaged for the period 1979-2010

The complete geomorphological characterization of the Bramadero river basin, chosen as calibration area, and the geomorphometric data from every single kind of landform (2344 units over 150 km²), were used to set the permafrost predictive categories. The first category (presence) includes geoforms that certainly indicate permafrost, such us; active rock glaciers, inactive rock glaciers, protalus ramparts, cryoplanation surfaces and perennial snow patches. The second category (absence) includes geoforms without permafrost (relict or fossil rock glaciers, bedrock, glacial abrasion surfaces, debris/mud flows and Andean peatlands). It includes as well geoforms where the presence of permafrost could not be certainly assessed such us, frozen and unfrozen talus slopes, glaciers and covered glaciers, moraines and morainic complexes, drift deposits, debris/snow avalanches, rock avalanches and rock slides and thermokarst depressions.

Results

MAAT-TRI model correctly displays the differences between coarse debris surfaces and bedrock while the MAAT-PISR model reflects more precisely temperature ranges for permafrost occurrence in the area, even though it overestimates its extension. Combining both models, realistic results in terms of permafrost distribution-patterns and temperature trends were achieved. Statistics of each model are displayed in Table 1. Results were cross-validated with the Argentine rock glacier inventory and with field work inspections.

Table 1. Logistic regression statics for MAAT-PISR and MAAT-TRI models.

	MAAT-PIRS model	MAAT-TRI model
Observations	7463	7463
-2 Log	9485	7389
R^2 (Cox and Schnell)	0.80	0.85
R^2 (Nagelkerke)	0.85	0.9
AIK	9491	7395
AUROC	0.68	0.84

Possible permafrost, in coarse debris, is expected between 4200 to 5700 m asl (MAAT from -3º to -18ºC) and covers a surface of approx. 1200 km² in the Andes. Likely permafrost is expected at 3400 to 4200 m asl (MAAT from 1.5º to -8ºC) and cover a surface of ca. 6150 km². Besides, the Precordillera, displays 35 km² of likely permafrost.

Conclusions

The present probability model predict permafrost occurrence in debris surfaces for the study area, with good correlation with former rock glaciers inventories and professional expertise. However, it does not predict ice ground content or permafrost thermal state.

Acknowledgments

This study is part of the PhD thesis of C. Tapia Baldis. Funds come from the project PIP 1222015-0100913 (2015-2017) leader by Dr. Dario Trombotto.

References

Azócar, G.F., Brenning, A. & Bodin, X., 2017. Permafrost distribution modelling in the semi-arid Chilean Andes. *The Cryopshere* 11: 877-890.

Boeckli, A., Brenning, A., Noetzli, J. & Gruber, S., 2012. A statistical approach to modelling permafrost distribution in the European Alps or similar mountain ranges. *The Cryosphere* 6(1): 125-140.

Brenning, A. & Trombotto, D., 2006. Logistic regression modeling of rock glacier and glacier distribution: Topographic and climatic controls in the semi-arid Andes. *Geomorphology* 81: 141-154.

Gruber, S., 2012. Derivation and analysis of a high-resolution estimate of global permafrost zonation. *The Cryosphere* 6(1): 221-223.

Frozen ground in the cold-arid Himalaya: a case study from upper Ganglass catchment, Leh

John (Mohd) Wani[1]
Renoj (J.) Thayyen[2]
C.S.P. Ojha[1]
Stephan Gruber[3]
Dorothea Stumm[4]
[1]*Department of Civil Engineering, Indian Institute of Technology, Roorkee, India-247667, johnn.nith@gmail.com*
[2]*National Institute of Hydrology, Roorkee, India-247667*
[3]*Carleton University, Ottawa, Canada*
[4] *International Centre for Integrated Mountain Development (ICIMOD), Kathmandu, Nepal*

Abstract

Long-term data series of ground temperatures in high elevation cold-arid regions are important to improve understanding of seasonally frozen ground and permafrost. In 2016, the National Institute of Hydrology (NIH), Roorkee, established ground temperature monitoring network in the cold-arid trans-Himalayan region of Ladakh. This network consists of 26 ground temperature (sub-surface) data loggers placed at a depth of 10 cm at elevations of 4700–5600 m a.s.l. recording data every 20 minutes. For installation of data loggers, the selection of plots was done with focus to cover the influence of topographic variables such as slope, aspect and elevation, and finally the ground cover types. In September 2017, one year of data from 24 loggers was retrieved. The database generated will provide an understanding of the near-surface ground thermal regime and potential permafrost occurrence. In this study, first results from the measurement campaign are presented.

Keywords: cold-arid region; data loggers; frozen ground; Himalayas; Ladakh

Introduction

Permafrost is a rarely studied (but likely important) component of high elevation cold-arid mountain systems. An initial assessment estimates the permafrost area in the Hindu Kush Himalaya (HKH) region to be 1 ±0.5 million km² (Gruber *et al.,* 2017). A remote-sensing study of rock glaciers suggest their occurrence in the region at an elevation of 3500–5500 m a.s.l. (Schmid *et al.,* 2015). Allen *et al.,* (2016) made a spatial simulation of permafrost in the Kullu district of Himachal Pradesh, India. To better understanding ground thermal regimes, permafrost distribution, and their changes, long-term ground-temperature measurements can prove cost effective. So far, however, such data is not available in the Indian Himalayas. We started the first measurement campaign by installing miniature temperature data (MTD) loggers. Their data can provide information about the duration of snow-cover, start of snow melt, zero-curtain period, mean annual ground temperatures (MAGT), and period of ground freezing and thawing, etc. (Hoelzle *et al.,* 2003). These results provide a basis for monitoring of change over time, as well as for further efforts to simulate (*e.g.*, Fiddes *et al.,* 2015) and map permafrost distribution and characteristics. The aim of this study is to investigate ground temperature, seasonal freezing/thawing, and the presence of permafrost in the upper Ganglass catchment.

Methods

Logger installation

In August 2016, we installed 26 MTDs (24 M-Log5W simple in soil/debris and 2 M-Log5W cable in bedrock, manufactured by GeoPrecision) at 10 cm depth in ten different plots as distinguished by ground cover and topography. These were at elevations of 4700–5600 m in the upper Ganglass catchment (34.25–34.29°N 77.55–77.65°E) Leh, Ladakh. The data is available from September 2016 to August 2017.

Data analysis

The variability of MAGT is investigated at two scales by following the approach of Gubler *et al.* (2011):

(a) The coarse scale in which we analyze the inter-plot variability of the mean MAGT (μ_p), which in plot p is defined as the mean of the mean of each time series within that plot:

$$\mu_p = \frac{1}{n_p}\sum_{i=1}^{p} \mu_{p,i}$$

Where n_p is the number of loggers inside that plot and μ_p is the MAGT of each logger within the plot.

(b) Fine scale, in which we analyse the intra-plot variability of MAGT (x_p) and is defined by the range of MAGT inside that plot:

$$\xi_p = \max_{i=1,\dots,n_p} (\mu_{p,i}) - \min_{i=1,\dots,n_p} (\mu_{p,i})$$

The length of zero-curtain period was estimated by following the procedure of Schmid *et al.* (2012).

Results

The instantaneous ground temperatures recorded by all soil/debris loggers during study period are between 20.2 to -22.7°C recorded at an elevation of 4700 and 5600 m a.s.l. respectively. The ground temperatures of the two bedrock loggers at an elevation of 5075 m a.s.l. vary between 29.2 and -21.2°C. The average MAGT for all the sites during the study period was -3.03°C. The typical ground temperature data recorded by a logger located in a fine material stripe is shown in Fig. 1.

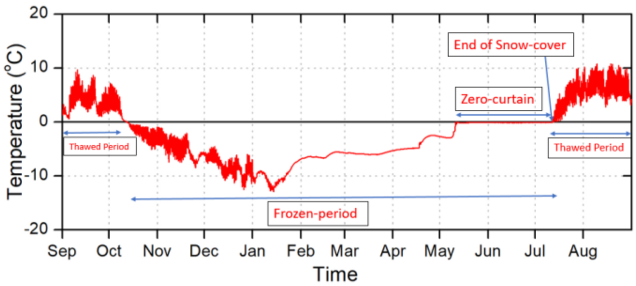

Figure 1. Typical ground temperature data recorded by a miniature data logger from one of the sites in upper Ganglass catchment, Leh during the period Sep-2016 to Aug-2017.

The inter-plot range of MAGT is 10.5ºC, ranging from -8.4 to 2.1°C, whereas the intra-plot variability ranges from 0.04 to 3.4°C. The MAGT data recorded were compared with slope, aspect and elevation (not shown). The relationship of MAGT was strong with elevation followed by slope and aspect. The elevation displayed strongest correlation with MAGT ($R^2 = 0.78$). The slope angle exhibits the second highest correlation ($R^2 = 0.70$). Slope aspect exhibits the weakest correlation with MAGT ($R^2 = 0.13$). Future work will analyse the influence of solar radiation.

The mean annual air temperature (MAAT) at all the logger sites ranges from -8.9 to -2.6°C with average MAAT of -5.7°C. The surface offset estimated at all the sites is between -1.1 to 5.1°C, with most sites having values near 2.7°C.

At all the logger sites, the frozen period varies between 131 to 217 days during the study period. The snow cover melt-out dates for all the loggers vary from 12th May 2017 to 8th Aug 2017.

Conclusions

From the MTD data, 21 out of 24 loggers have MAGT below 0°C. The elevation of the highest logger with positive MAGT is 4727 m a.s.l. and the elevation of the lowest logger with negative MAGT is 4934 m a.s.l. However, there is an exception with MAGT of 0.01°C recorded at 5075 m a.s.l. by one of the loggers installed in bedrock. Even if there are some inter-annual fluctuations, the ground temperatures observed are a reliable indication of having permafrost in this catchment. Hence, these sites will be our focus to further investigate the presence and characteristics of Himalayan permafrost.

Acknowledgments

John Mohd Wani acknowledge the Ministry of Human Resource Development (MHRD) Government of India (GOI) fellowship for carrying out his Ph.D. work. Renoj J. Thayyen thank National Institute of Hydrology (NIH) Roorkee and SERB (Project No. EMR/2015/000887) for funding the instrumentation in the Ganglass catchment. The assistance of ICIMOD is also highly acknowledged.

References

Allen, S. K., Fiddes, J., Linsbauer, A., Randhawa, S. S., Saklani, B., Salzmann, N. 2016. Permafrost studies in Kullu district, Himachal Pradesh. *Current Science* 11: 257-260.

Fiddes, J., Endrizzi, S., Gruber, S., 2015. Large-area land surface simulations in heterogeneous terrain driven by global data sets: application to mountain permafrost. *The Cryosphere* 9: 411–426.

Gruber, S., Fleiner, R., Guegan, E., Panday, P., Schmid, M. O. *et al.*, 2017. Inferring permafrost and permafrost thaw in the mountains of the Hindu Kush Himalaya region. *The Cryosphere* 11: 81-99.

Gubler, S., Fiddes, J., Keller, M., Gruber, S., 2011. Scale-dependent measurement and analysis of ground surface temperature variability in alpine terrain. *The Cryosphere* 5: 431–443.

Hoelzle, M., Haeberli, W., Stocker-Mittaz, C., 2003. Miniature ground temperature data logger measurements 2000-2002 in the Murtèl-Corvatsch area, Eastern Swiss Alps, in: *Proceedings of the Eighth International Conference on Permafrost*, Zurich, Switzerland, 20-25 July: 25.

Schmid, M. O., Gubler, S., Fiddes, J., Gruber, S., 2012. Inferring snowpack ripening and melt-out from distributed measurements of near surface ground temperatures. *The Cryosphere 6:* 1127-1139.

Schmid, M. O., Baral, P., Gruber, S., Shahi, S., Shrestha, T., Stumm, D., Wester, P., 2015. Assessment of permafrost distribution maps in the Hindu Kush Himalayan region using rock glaciers mapped in Google Earth. *The Cryosphere* 9: 2089-2099.

Convective Heat Transfer in Coarse Permafrost Substrate: A Numerical Model Study in the Swiss Alps

Jonas Wicky[1]
Christian Hauck[1]
[1]*University of Fribourg, Department of Geosciences, Alpine Cryosphere and Geomorphology Group (jonas.wicky@unifr.ch)*

Abstract

In an Alpine permafrost setting the coarse blocky terrain (talus slopes, rock glaciers etc.) is often very porous. The high permeability of such landforms allows air to circulate within the soil, which influences ground temperature and therefore permafrost conditions. Recently, a numerical model approach realistically simulated this internal air circulation, which takes place under free convection conditions as result of density differences between warm and cold air with no additional forcing. The resulting seasonally reversing (chimney-type-) circulation leads to a substantial cooling in the lower part of a talus slope. The present study shows that the type of convection and therefore the influence on the ground thermal regime strongly depends on the slope angle and the permeability.

Keywords: Mountain permafrost; convection; talus slope; numerical model; heat transfer

Introduction

Thermal modelling is important for a better understanding of the ground thermal regime in Alpine permafrost. The presented modelling approach makes use of common concepts in engineering sciences (FE-modelling) to represent and quantify convective heat transfer in air in coarse permafrost substrate. Many observation-based studies addressed the effect of convective heat transfer in air (e.g., Delaloye *et al.*, 2003). Modelling approaches are still rare and often limited to one dimension (Scherler *et al.*, 2014; Luethi *et al.*, 2017), which neglects lateral heat transfer. Previous results from a 2-D model showed that convective heat transfer leads to a substantial cooling in the lower part of a talus slope (Wicky & Hauck, 2017). We now extend this modelling approach to a parametric sensitivity study on different slope angles and permeabilities.

Model

The model consists of a numerical domain representing a schematical talus slope divided in two subdomains, one for bedrock and another one for porous substrate (Fig. 1). The lower thermal boundary condition is set to 0.6°C (borehole observation) and the upper boundary is the median from a ground surface temperature (GST) logger time series at Lapires talus slope in Valais Alps, Switzerland (Permos, 2016). Slope angle varies from 0° – 40° and permeability from 1e-7 to 8.89e-5 m^{-1} (Goering & Kumar, 1996; Herz, 2006). The model solves for heat transfer accounting for convection and for air circulation (Darcy's law with Boussinesq approx.) and is set up within the software package Comsol Multiphysics.

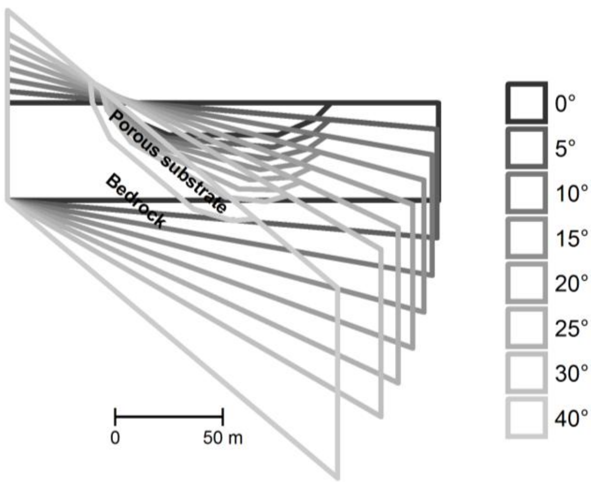

Figure 1. Different geometries used to model different slope angles.

Results

The air velocity within the porous domain increases with increase of slope angle and permeability. Ground temperature (GT) shows a more complex behavior. The different behaviors are explained by different circulation patterns. Depending on the parameter set, three different circulation patterns may take place: Multicellular vertical convection, lateral advection cells and unidirectional downflow (Fig. 2). These circulation patterns have an influence on the GT: Seasonally reversing lateral advection (chimney-type circulation) leads to a pronounced cooling in the lower part of the domain, multicellular convection leads to uniformly colder GT and unidirectional downflow mainly leads to a fast propagation of the surface boundary temperature into the ground. Lateral advection leads to the coldest GT, multicellular convection to a uniform cooling, whereas unidirectional downflow results in warmer GT compared to a setting without convective heat transfer (conduction only).

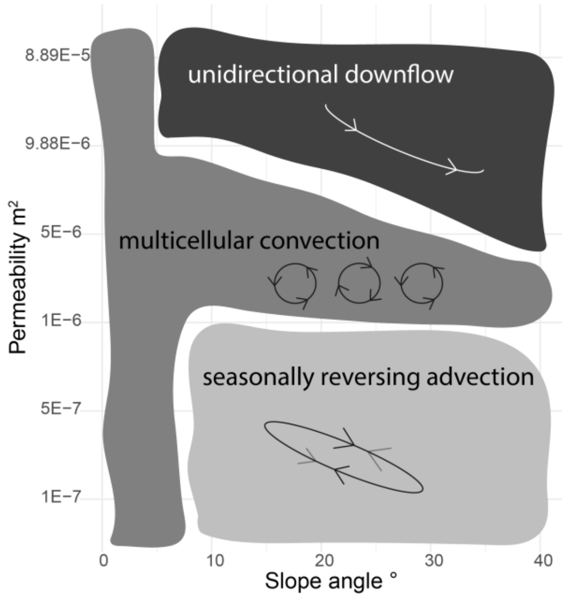

Figure 2. Sketch of different circulation patterns relative to slope angle and permeability.

Conclusion

We modelled successfully convective circulation within porous permafrost substrate and we are able to show the influence of slope angle and permeability on the circulation pattern and thus the ground thermal regime. Our results help to explain isolated permafrost occurrences and thermal anomalies within continuous permafrost. The improved process understanding may be integrated in permafrost mapping or long-term permafrost modelling projects.

Acknowledgments

This study was conducted within the MODAIRCAP project funded by the SNF (n° 200021_169499). We are thankful to PERMOS for the temperature data.

References

Delaloye, R., Reynard, E., Lambiel, C., Marescot, L. & Monnet, R., 2003. Thermal anomaly in a cold scree slope (Creux du Van, Switzerland). *Proceedings of the 8th International Conference on Permafrost*, Zurich, Switzerland, July 21-25.

Goering, D.J. & Kumar, P., 1996. Winter-time Convection in Open-Graded Embankments. *Cold Regions Science and Technology*, 24: 57–74.

Herz, T., 2006. *Das Mikroklima grobblockiger Schutthalden der alpinen Periglazialstufe und seine Auswirkungen auf Energieaustauschprozesse zwischen Atmosphäre und Lithosphäre.* Giessen: Universitätsbibliothek, 224pp.

Luethi, R., Phillips, M. & Lehning, M., 2017. Estimating Non-Conductive Heat Flow Leading to Intra-Permafrost Talik Formation at the Ritigraben Rock Glacier (Western Swiss Alps). *Permafrost and Periglacial Processes*, 28(1): 183-194.

PERMOS, 2016. PERMOS Database. *Swiss Permafrost Monitoring Network*, Fribourg, Switzerland.

Scherler, M., Schneider, S., Hoelzle, M. & Hauck, C., 2014. A two-sided approach to estimate heat transfer processes within the active layer of the Murtèl–Corvatsch rock glacier. *Earth Surface Dynamics*, 2(1): 141-154.

Wicky, J. & Hauck, C., 2017. Numerical modelling of convective heat transport by air flow in permafrost talus slopes. *The Cryosphere*, 11(3), 1311-1325.

26 - Open session on permafrost hydrology

Session 26

Open session on permafrost hydrology

Conveners:

- **William L. Quinton**, Cold Regions Research Centre, Wilfrid Laurier University, Waterloo, Ontario, Canada
- **Ryan F. Connon**, Wilfrid Laurier University, Yellowknife, NT, Canada (PYRN member)
- **Chris Spence**, Environment and Climate Change Canada, Saskatoon, SK, Canada

Permafrost hydrology seeks to understand the flux and storage of water and energy in earth systems where temperatures are at or below 0°C for at least two consecutive years. The supra-permafrost layer includes the active layer, a zone that freezes and thaws annually, and may also include a perennially thawed (i.e. talik) layer. By impounding and re-directing surface and subsurface water, permafrost influences both the nature of hydrological flowpaths and the partitioning of hydrological input into runoff and storage. Permafrost also promotes high moisture contents in the overlying layers by limiting infiltration, and by providing structural support to the overlying terrain, permafrost strongly influences the nature of the supported ecosystems, including their hydrological characteristics. Most hydrological processes and pathways occur above the permafrost, both within the supra-permafrost layer, and above the ground surface. Permafrost thaw and the resulting ground surface subsidence and ecosystem change has the potential to alter hydrological processes from local to regional scales. Understanding the interdependence of permafrost, hydrology and ecosystems is critical to understanding not just the flux and storage of water in permafrost terrains, but also how such systems might change in response to climate and anthropogenic disturbance.

Characterization of Runoff Within a Periglacial Micro-Watershed of the Andes Containing Rock Glaciers

Lukas U. Arenson[1]
Pablo A. Wainstein[2]
Jordan S. Harrington[3]
Holly A. Miller[4]
[1]*BGC Engineering Inc. Vancouver BC, Canada, larenson@bgcengineering.ca*
[2]*BGC Engineering Inc., Calgary, AB, Canada*
[3]*BGC Engineering Inc., Vancouver, BC, Canada*
[4]*University of Colorado, Boulder, CO, USA*

Abstract

Water chemistry and isotope analysis, together with surface runoff and groundwater level measurements, were conducted in a small watershed containing rock glaciers in the Central Andes of South America. Preliminary results indicated that the temporal and spatial differences in the water chemistry and isotopic signatures are likely related to the thaw front penetrating the active layer, and that there is no discernible contribution from rock glacier ground ice melt to the runoff. However, the results currently available are preliminary and additional data from this ongoing study are required to confirm these initial findings.

Keywords: Rock Glacier; Runoff; Water Chemistry

Introduction

The hydrology of mountain systems in the arid Central Andes of South America is of great interest to the scientific community, but also project developers, regulators, NGOs and local stakeholders, because of the need for fresh, clean water for industrial, domestic and agricultural use in the region (Viviroli & Weingartner, 2004; Viviroli *et al.*, 2007; Arenson & Jakob, 2010). Past research studies on mountain hydrology primarily focused on headwater catchments dominated by snowmelt runoff and glaciated terrain (Duguay *et al.*, 2015; Cowie *et al.*, 2017). However, our understanding of the contributions from and the role of ground ice in mountain permafrost terrain, and specifically from rock glaciers, to the hydrology of these mountain regions is less well known and a quantitative accounting of the hydrologic role of rock glaciers remains mainly unresolved (Duguay *et al.*, 2015; Arenson & Jakob, 2010).

The majority of currently available rock glacier research focuses on their dynamics and morphology (Barsch, 1996; Williams *et al.*, 2006; Arenson *et al.*, 2016). One reason for this focus is the difficulty in collecting hydrologic and geochemical information about rock glaciers due to their location and structure. The higher percentage of rocks in rock glaciers compared to ice in glaciers presents extra difficulties in collecting ground ice samples through boreholes, and the logistics of collecting melting ground ice water in high alpine regions are challenging (Williams *et al.*, 2006; Leopold *et al.*, 2011; Thies *et al.*, 2013).

Thermal and morphologic properties of rock glaciers are significantly different than those of glaciers (Barsch 1996), which results in radically different hydrologic responses. For example, rock glaciers are slower to respond to long-term (climate) and seasonal changes due to the thermal protection of the thick and coarse-grained active layer (Duguay *et al.*, 2015). In addition, the morphology and dynamics of rock glaciers do not depend on annual mass balances driven by accumulation and ablation, as is the case for glaciers.

We present preliminary results of the first year of analyzing water chemistry and isotopes as indicators for the origin of surface water collected within a micro-watershed containing rock glaciers.

Preliminary Results

Lower proportion of sodium and higher proportion of sulfate were measured at the bottom of the watershed containing the rock glacier compared to nearby stations, producing a unique geochemical signature. These geochemical differences are caused by interactions of water with the local geology.

Stable naturally occurring water isotopes, δ18O and δD, are used to identify the contributions of source waters to the hydrologic system, which is the results of a mixture of groundwater, surface water, snow and ground ice melt. The isotopic signature of the runoff directly downstream of the rock glacier (Station A5 (squares) in Figure 1) shifts from a uniquely enriched signal in February towards a depleted signal in December relative to other waters in the watershed. December is the beginning of summer. The enrichment in the samples in the late melting period may indicate the presence of meltwater coming from the seasonally frozen ground within the active layer from higher bounds of the watershed, where the freezing and thawing cycles are stronger and as such the water´s isotopic signature gets enriched as more phase changes occur.

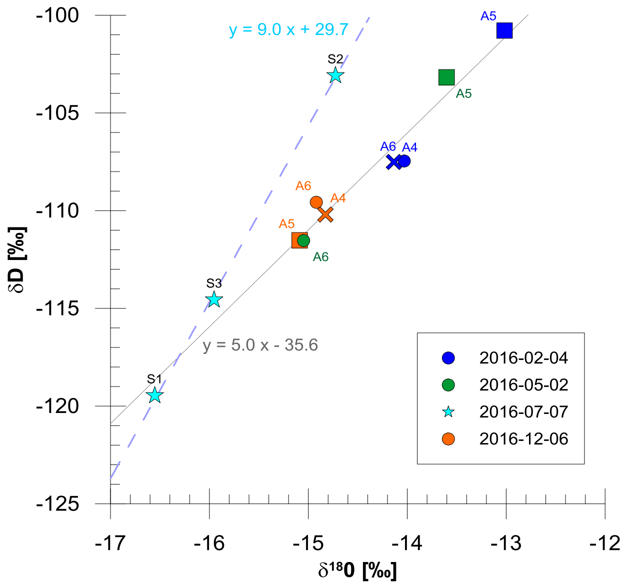

Figure 1. Isotopic composition of samples in the micro-watershed measured at various times. Samples from July 2016 are snow samples.

Preliminary Conclusions

Water chemistry and isotope analysis, together with surface runoff and ground water level measurements show that there are differences in the origin of the water in the watershed containing a rock glacier compared to runoff from non-rock glacier containing areas. The differences are, however, most noted during the summer when the thaw front penetrates the active layer releasing seasonally frozen water. Towards the end of the summer, when the thaw front reaches the permafrost table (~April), no significant differences were noted, which would be indicative of an absence in contribution of rock glacier ground ice melt to the runoff.

The results presented herein are preliminary and are currently being complemented with additional sampling and analysis to help support the aforementioned, initial conclusion.

References

Arenson, L.U. & Jakob, M., 2010. The significance of rock glaciers in the dry Andes - A discussion of Azócar and Brenning (2010) and Brenning and Azócar (2010). *Permafrost and Periglacial Processes* 21: 282–285.

Arenson, L.U., Kääb, A., & O'Sullivan, A. 2016. Detection and Analysis of Ground Deformation in Permafrost Environments. *Permafrost and Periglacial Processes* 27: 339–351.

Barsch, D. 1996. *Rockglaciers: Indicators for the Present and Former Geoecology in High Mountain Environments.* In Springer Series in Physical Environment. Springer-Verlag, Berlin Heidelberg.

Cowie, R.M., Knowles, J.F., Dailey, K.R., Williams, M.W., Mills, T.J. & Molotch, N.P., 2017. Sources of streamflow along a headwater catchment elevational gradient. *Journal of Hydrology* 549: 163–178.

Duguay, M.A., Edmunds, A. & Arenson, L.U., 2015. Quantifying the significance of the hydrological contribution of a rock glacier – A review. *Proceedings of GEOQuébec 2015. 68th Canadian Geotechnical Conference and 7th Canadian Permafrost Conference*: 8 p.

Leopold, M., Williams, M.W., Caine, N., Völkel, J. & Dethier, D., 2011. Internal structure of the Green Lake 5 rock glacier, Colorado Front Range, USA. *Permafrost and Periglacial Processes* 22: 107–119.

Thies, H., Nickus, U., Tolotti, M., Tessadri, R., & Krainer, K. 2013. Evidence of rock glacier melt impacts on water chemistry and diatoms in high mountain streams. *Cold Regions Science and Technology* 96: 77–85.

Viviroli, D., Dürr, H.H., Messerli, B., Meybeck, M. & Weingartner, R., 2007. Mountains of the world, water towers for humanity: Typology, mapping, and global significance. *Water Resources Research* 43: W07447.

Viviroli, D. & Weingartner, R., 2004. The hydrological significance of mountains: from regional to global scale. *Hydrology and Earth System Sciences* 8: 1016–1029.

Williams, M.W., Knauf, M., Caine, N., Liu, F., Verplanck, P.L., 2006. Geochemistry and source waters of rock glacier outflow, Colorado Front Range. *Permafrost and Periglacial Processes* 17: 13–33.

High Arctic Sediment Yield Responses to Geomorphic and Permafrost Change in a Transitioning Climate

Casey R Beel[1]
Scott F Lamoureux[1]
John F Orwin[1,2]

[1]*Department of Geography and Planning, Queen's University, Kingston ON Canada K7L 3N6, 15cb29@queensu.ca*
[2]*Environmental Monitoring and Science Division, Alberta Environment and Parks, Calgary AB Canada T3L 1S4*

Abstract

That the Arctic is changing is no longer in question. How much it will change and how that change is propagated through geomorphic systems are important questions as surface air temperatures and precipitation patterns continue to change in the foreseeable future. In the first long-term High Arctic sediment investigation we demonstrate the response of a fluvial system to an episode of permafrost disturbance.

Keywords: High Arctic, Permafrost, Geomorphic Change, Suspended Sediment Transfer, Connectivity, Cape Bounty Arctic Watershed Observatory

Introduction

Enhanced climatic warming in the High Arctic has led to an increase in the occurrence of landscape disturbances in recent decades. Landscape disturbances that connect with channel networks may have a substantial impact on suspended sediment transfer dynamics. However, the impact and recovery of disturbance on the fluvial geomorphic system is poorly understood due to a dearth of long-term monitoring sites in these settings. Similarly, the linkages between climatic drivers, discharge generation and suspended sediment transfer remains poorly understood for much of the Arctic because of this lack of available data.

Long-term records of suspended sediment transfer are important for understanding how landscapes are responding to enhanced climatic warming and permafrost change. This is because suspended sediment transfer is a sensitive indicator of landscape change, since it is broadly supply controlled. Channel suspended sediment flux has been monitored in paired watersheds at the Cape Bounty Arctic Watershed Observatory (CBAWO), Melville Island, Nunavut (Figure 1) since 2003 (excluding the years 2011, 2013, and 2015 due to logistical constraints) and represents the longest High Arctic record in existence. In 2007, both watersheds were impacted by extensive permafrost disturbances on slopes and along the channels. Disturbances on slopes resulted in the formation of new slope tributary streams and significantly increased slope erosion. As a result, our records provide us with a unique dataset that allow us to investigate the long-term geomorphic responses to landscape disturbances. The objectives of this research was to (i) identify the main controls on discharge generation and suspended sediment transfer, (ii) investigate the long-term geomorphic responses to landscape disturbances, and (iii) to consider the stability and evolution of High Arctic landscapes in a transitioning climate.

Our long-term results indicate prominent decoupling between climatic drivers and geomorphic energy in the fluvial system. Annually, discharge generation and suspended sediment transfer are not a function of summer climate, but driven by snow availability for melt and by geomorphic controls. Short-term geomorphic disturbances, coupled with hydroclimatic change, should increase the intensity of downstream sediment flux. However, our results show a significant decrease in downstream sediment flux post-2007 landscape disturbances. These results suggest that short-term geomorphological disturbances compete with hydroclimatic change in these watersheds. We hypothesize that this is also largely a result of weak landscape connectivity, and that fluvio-geomorphic connectivity is the tipping point to Arctic landscape change.

An experimental study of permafrost restoration under the seismic line in the wetland-dominated zone of discontinuous permafrost, Northwest Territories, Canada

Michael Braverman [1,2]
William Quinton[1]
[1]Cold Regions Research Centre, Wilfrid Laurier University, Waterloo, ON
[2]GHD Canada, Waterloo, ON

Abstract

Thermosyphons are closed-system heat extraction devices. They extract heat from the ground, contributing to cooling of frozen ground and maintaining temperature below zero and as such are useful for preserving permafrost. Two types of thermosyphons are used: passive and hybrid systems. Passive one does not require any external power to operate. The hybrid installation combines the passive system with a refrigeration compressor so that negative soil temperatures are maintained during summer. The most common type of thermosyphon uses a carbon dioxide filled vessel under a pressure varying from about 2100 to 4800 kPa. Thermosyphon technology is successfully used for stabilizing building foundations, dams and pipelines. While passive thermosyphons do not require extensive maintenance they do require specially trained personal for installation. Also the high cost of thermosyphons limit their extensive use below linear infrastructure. Liquid based thermosyphons were developed and tested as an inexpensive alternative to carbon dioxide system. This paper presents and discussed the technical aspects of liquid-filled thermosyphons and demonstrates their application in a region of degrading permafrost at Scotty creek, NW, Canada.

Keywords: Seismic line, permafrost, thermosyphons.

Introduction

Surface disturbance of ice rich soils in permafrost regions results in permafrost degradation, reduction of ground bearing capacity and slope stability problems. Preventing permafrost thaw is a serious concern for the construction industry. One of the most popular methods of maintaining permafrost in its natural state is the use of thermosyphons. Thermosyphons have been used for stabilizing foundations in continuous and discontinuous permafrost areas since 1960 Richardson, (1979). There are two types of thermosyphons: passive and hybrid Johnston, (1981). Passive thermosyphons contain no moving parts. These sealed pipes are usually filled with carbon dioxide at a high pressure of 2-5 MPa. Pipe pressure should be adjusted during installation to ensure that carbon dioxide located below ground is maintained in liquid form. Vaporization of the liquid carbon dioxide results in a heat transfer from the lower part, the evaporator, of the thermosyphon to the upper part, the condenser, where it condenses in winter time and trickles back down to the evaporator. Passive thermosyphons work only in the winter time and remain dormant while the air temperature is higher than the ground temperature. Hybrid thermosyphons are designed to keep the ground frozen in the summer as well as the winter time, but this process involves an active refrigeration system.. While ground freezing with thermosyphons can be considered as a "last line of defence" when any other methods for foundation stabilization are not available or are not feasible due to geotechnical conditions or high costs, this technology is nonetheless very expensive. According to the Government of the Northwest Territories, Department of Transportation, climate change may affect the quality of Highway 3, the main highway of the NWT, which is already under extensive maintenance every summer. However, thermosyphon technology is not applied in this case because of associated costs, among other factors. The complex installation process of thermosyphons is another factor which limits their use. Heuer, (1979) noted that installation of heat pipes affects construction timing, as it requires special knowledge and skills, which are often not available within general drilling contractor crews.

Thermosyphons are an effective, but expensive technology for the prevention of permafrost thaw. The cost of this technology limits its application under linear structures such as roads. In some cases, it is more prudent to invest in road maintenance, rather than the prevention of permafrost thaw. The proposed thermosyphon system can easily overcome the above mentioned problems due to the simplicity of its design and its low cost. This system does not require any special training or licencing for its operation, although the need for some maintenance may limit use in remote, regions.

Site location

The Scotty Creek basin is located approximately 50 km SE of Fort Simpson, NT. (Figure 1)
The average annual temperature in the region is -3.20 C. (1964-2013). The average temperatures for July and January are 17.10 C and -25.90 C, respectively. This area belongs to the continental climate zone and is situated in the region of discontinuous permafrost. The soil layer of interest is 100% saturated peat with a porosity of ~ 80%. The testing of performance was done during the winter of 2016-2017. The test site was equipped with temperature monitoring stations in August 2014.

Description and Principals of Operation

Liquid based thermosyphons were developed and tested as an inexpensive alternative to carbon dioxide system.
The proposed thermosyphon consists of two coaxial pipes. The external is aluminum pipe and had a length of 3 m and a diameter of 75 mm. The maximum snow thickness for the experiment was ~50 cm. Thus, only 50 cm of the thermosyphon was exposed to open air. The thermosyphon was equipped with a low power consumption (0.8 W) submersible pump to circulate the coolant. The outflow from the submersible pump was directed through 12.5 mm internal pipe to the bottom of the thermosyphon. The operational rate of the pump was between 40 and 120 L hr-1, depending on the performance of the solar panel. The power line was equipped with a mechanical thermal switch, which connected the power supply to the pump when air temperatures dropped below zero. Four thermistors were placed around the thermosyphon at various distances and depths. An additional thermistor was placed close to the bottom of the thermosyphon at a depth of 199 cm. Figure 1 demonstrates test results for Case B.

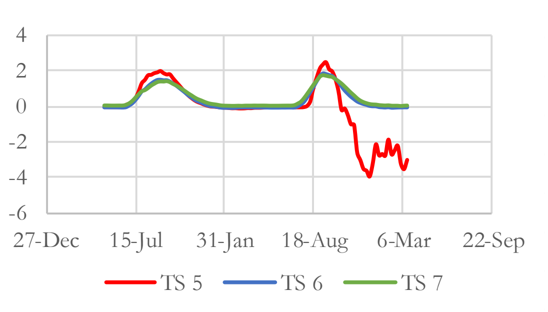

Figure 1. Temperature distribution around thermosyphon #5 recorded by thermistors # 5,6 and 7

As shown in Figure 1, the soil in close proximity of the thermosyphon was frozen to an average temperature of ~ -30C. Radius of freezing reached ~ 20 cm with average temperature ~-0.5°C.

Conclusions

This paper presents the results of an experimental study of liquid filled thermosyphons with forced circulation. With recent developments in energy-conserving technologies and renewable energy sources, the system presented here is an economically feasible alternative to traditional two phase passive thermosyphons. According to data obtained from the field experiment, the proposed thermosyphon can transfer sufficient thermal energy to freeze the saturated peat layer within a diameter of at least 50 cm around, even with a relatively short above-ground section. The low power consumption submersible pump can maintain a below 0oC temperature in the frozen layer throughout the cold season, while operating exclusively on a renewable energy source, such as a solar panel or a small wind turbine generator.
Data obtained from field experiments shows that even with a relatively short above-ground section, which is exposed to cold air, the proposed thermosyphon can transfer sufficient thermal energy to freeze the saturated peat layer at a diameter of at least 0.4 m around a 3 inch thermosyphon. It should be noted that only one thermosyphon was tested in this experiment. A cluster of thermosyphons can be expected to yield much better result.

The content of this paper has patent pending status

References

Heuer, C. E. 1979. The application of heat pipes on the Trans-Alaska Pipeline. Directorate of Military Programs Office, Chief of Engineers. Hanover, NH: US Army Cold Regions Research and Engineering Laboratory.

Holubec, I. 2008. Flat loop thermosyphon foundations in warm permafrost. Government of the Northwest Territories Asset Management Division of Public Works and Services and the Climate Change Vulnerability Assessment of the Canadian Council of Professional Engineers.

Richardson, P., 1979. Tough Alaska conditions prove new pile design's versatility. Alaska Construction and Oil, February: 20–28.

Government of the Northwest Territories, Department of Transportation Engineers, Canada Public Infrastructure, Engineering Vulnerability Committee, Climate Change Vulnerability Assessment for NWT Highway 3, Final Report, Project No: 0836-002, August 10, 2011

Rock glacier outflows: a distinct alpine stream type?

Stefano Brighenti[1,3]
Michael Engel[2]
Monica Tolotti[3]
Maria Cristina Bruno[3]
Francesco Comiti[2]
Walter Bertoldi[1]

[1]*Department of Civil, Mechanical and Environmental engineer University of Trento, Italy, stefano.brighenti@unitn.it*
[2]*Faculty of Science and Technology, Free University of Bolzano (BZ, Italy)*
[3] *Research and Innovation Centre, Edmund Mach Foundation, S. Michele all'Adige, Italy*

Abstract

Alpine glaciers are predicted to significantly decrease their water contribution to European Alps ecohydrology, while rock glaciers may become increasingly important due to their slower ice loss. Different alpine stream habitat types can be distinguished according to water source. However, despite the large amount of literature available for glacier-, groundwater- and snowmelt/precipitation-fed habitats, very little is known on rockglacier-fed streams. We describe the habitat parameters of two rockglacier outflows during summer 2017, compared to streams with different water origin (two groundwater-fed, two glacier-fed, one mixed origin) in the upper Solda Valley (Eastern Italian Alps). The Solda rockglacier stream is characterized by high channel stability, low turbidity, high electrical conductivities and high Ca, Mg, PO_4, Sr, As and Ba concentrations. The water chemistry of the Zay rock-glacial stream resembles the stream of mixed origin. Results suggest a potential hydroecological role of rockglacier-fed streams in the context of Alpine deglaciation.

Keywords: Deglaciation, rock glacial streams, Alpine hydroecology, habitat conditions

Introduction

Rockglaciers are one of the most evident forms of permafrost in mountain areas such as in the European Alps, where they often feed streams or lakes (e.g Mair et al., 2015). Since deglaciation proceeds at quicker rates for glaciers than for permafrost (Haeberli et al., 2016), valley glaciers are expected to lose their key role of hydrological drivers in Alpine catchments over the next decades. Rock glacier outflows might become increasingly important in deglaciating Alpine areas, especially in the forecasted enhanced precipitation stochasticity (Milner *et al.,* 2009) and earlier summer snowmelt (Stewart, 2009). Water origin is fundamental for shaping the hydroecology of Alpine streams, since it determines the geomorphological, physical and chemical conditions that influence biotic communities (Ward, 1994; Brown *et al.,* 2003). Even if little studied so far, rockglacier-fed streams are characterized by distinctive habitat conditions (Mair *et al.,* 2015; Colombo *et al.,* 2017), and thus they can potentially host peculiar biotic communities.

Research aims and methods

This study aims at identifying key habitat characteristics of rock glacial streams. The study area is located in the Solda valley (Ortles-Cevedale massif, Italian Alps), with sampling stataions in the upper Solda and Zay subcatchments (2105-2833 m a.s.l.) draining metamorphic gneiss bedrocks (Province of Bolzano, 2017). We compared the physical and chemical features (Table 1) of 7 streams with different water source (2 fed by rockglacier, 2 by groundwater, 2 by glacier, 1 with mixed source), sampled in June, August, and September 2017.

Table 1. List of habitat variables used in the analysis

Habitat feature	Variables
Water origin	δ^2H, $\delta^{18}O$ stable isotopes
Channel instability	Pfankuch index (Bottom component)
Physical parameters	Turbidity, Temperature
Anions and cations	Electrical conductivity, Ca, Mg, SO_4, SiO_2
Nutrients	NO_3, PO_4, DOC
Trace elements	Al, As, Ba, Pb, Cd, Fe, Mn, Sr, U, Zn

Water origin was verified by analyzing δ²H and δ¹⁸O in stream waters using mixing models with snowmelt, precipitation, and glacier ice melt as potential end-members. A Principal Component Analysis (PCA) was applied to the environmental variables of all samples collected in summer 2017. The same method was applied only to trace elements.

Results and discussion

Temperature profiles (measured with dataloggers) showed only very small diel oscillations for both rock glacial streams, compared to the other stream types.

The Solda rock glacial stream (SRG) was separated from all the other stations (Fig. 1) based on its clear waters (NTU<3), low temperatures (<1.2°C), stable channel (PFAN=19), higher electrical conductivity (376-630 μS cm^{-1}) and Ca (47.5-73.5 mg L^{-1}), Mg (12.5-15 mg L^{-1}), PO_4 (3.8-5 μg L^{-1}) and SO_4 (107.3-170 mg L^{-1}) concentrations, which increased over summer. The Zay rock glacial stream (ZRG) resembles the mixed origin station (Fig. 1). This is likely due to the infiltration of glacial waters into the upstream rock glacier margin (personal observation), thus smoothing the permafrost signal. Glacier-fed streams are characterized by high seasonality, with higher turbidity (NTU=43-132) and lower conductivity (EC=9-72 μS cm^{-1}) in June and August than in September (EC=79-270 μS cm^{-1}, NTU=32-60), when flow was almost exclusively subglacial, due to the low air temperatures.

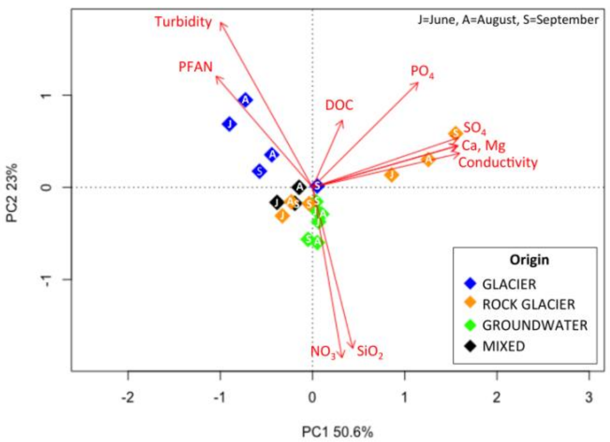

Figure 1. PCA biplot of habitat variables of the streams sampled in summer 2017.

Temperature profiles along with results for trace elements, and δ²H and δ¹⁸O isotopes, currently under analysis, will be shown in the presentation.

Conclusions

Our results show that rockglacial streams, in agreement with information in literature, represent peculiar habitats, according to a set of physical and chemical parameters. However, the similarity of Zay rock glacial stream with non-glacial streams underscores that hydrological complexity must be taken in consideration when assessing the hydroecological peculiarity of rock glacier fed headwaters. These results confirm that rockglacier fed streams deserve more attention in relations to effects of global warming on Alpine hydrology.

Acknowledgments

This work was carried out within the Erasmus Mundus Joint Doctorate Program SMART (Science for the Management of Rivers and their Tidal Systems) funded with the support of the EACEA of the European Union. We thank Werner Tirler and Giulio Voto at EcoResearch l.t.d. (Bolzano) for trace element analyses.

References

Brown, L. E., Hannah, D. M. & Milner, A. M., 2003. Alpine stream habitat classification: an alternative approach incorporating the role of dynamic water source contributions. *Arctic, Antarctic and Alpine Research*, *35*(3): 313-322.

Colombo, N., Salerno, F., Gruber, S., Freppaz, M., Williams, M., Fratianni, S. & Giardino, M., 2017. Impacts of permafrost degradation on inorganic chemistry of surface fresh water. *Global and Planetary change*, accepted

Haeberli, W., Schaub, Y. & Huggel, C., 2016. Increasing risks related to landslides from degrading permafrost into new lakes in de-glaciating mountain ranges. *Geomorphology*, 293: 405-417.

Mair V., Lang K., Tonindandel D., Thaler B., Alber R., Lösch B., … Tolotti M., 2015. *Progetto Permaqua – Permafrost e il suo effetto sul bilancio idrico e sull'eologia delle acque di alta montagna*. Provincia Autonoma di Bolzano, Bolzano, Italy: Ufficio geologia e prove dei materiali.

Milner, A. M., Brown, L. E. & Hannah, D. M., 2009. Hydroecological response of river systems to shrinking glaciers. *Hydrological Processes*, *23* (1): 62–77

Provincia di Bolzano, 2017. Carta Geologica d'Italia 1:100000 layer. Online Geobrowser

Stewart, I. T. (2009). Changes in snowpack and snowmelt runoff for key mountain regions. *Hydrological Processes, 23* (1): 78–94.

Ward, J. V. (1994). Ecology of alpine streams. *Freshwater Biology*, *32*(2): 277–294.

High frequency data reveals new insights into hydrological and biogeochemical processes in a discontinuous permafrost watershed

Sean K. Carey[1]
Nadine J. Shatilla[1]
Weigang Tang[1]
[1]*School of Geography and Earth Sciences, McMaster University, Hamilton, ON, Canada, careysk@mcmaster.ca*

Abstract

Conceptual models of alpine watersheds underlain with permafrost have developed over the last 50 years based on careful field measurements and observations. Furthermore, the importance of permafrost soils in catchment biogeochemistry has more recently received scrutiny. In recent years, new water quality sensors (fluorometers, multi-parameter sondes) provide an opportunity to both test and enhance our understanding of coupled water and biogeochemical cycling in headwater systems. In this paper, multi-year multi-parameter high frequency data sets from the Wolf Creek Research Basin, Yukon, Canada, will be utilized to assess the influence of active layer development, permafrost and seasonality on runoff generation processes and catchment connectivity. We utilize 15-minute salinity and coloured dissolved organic matter (CDOM) measurements to generate seasonal and event-based hysteresis loops with discharge. The magnitude and direction of these loops reflects flow pathways and wetness-induced catchment connectivity.

Keywords: Hydrology; alpine environments; discontinuous permafrost; runoff generation; high-frequency data.

Introduction

The influence of permafrost, active layer development and frozen ground on runoff hydrology has been well characterized with decades of research (Woo, 2012). Permafrost acts as an aquitard, whereas the seasonal development of the active layer is an important control on runoff pathways (Carey & Woo, 2001). As the active layer develops, relatively deeper and slower runoff pathways predominate, affecting both the rate and volume of runoff along with stream chemical signatures. In areas with discontinuous permafrost, there is considerable variability in hydrological processes due to the partitioning between relatively rapid near-surface runoff processes and deeper drainage.

Over the past decade, there has been an advancement of in-stream instrumentation that allow high-frequency measure of water quality parameters (e.g. temperature, salinity, pH, coloured dissolved organic matter (CDOM)). Considering that stream chemistry in headwater alpine watersheds is largely a reflection of terrestrial hydrological processes and water-soil-rock interaction, an opportunity exists to advance our understanding of these systems through new data.

The objective of this paper is to utilize high frequency (15-minute) discharge (Q), salinity (SpC) and CDOM data to assess whether water quality information can provide additional insights into runoff generation processes. This will be completed by examining hysteresis in Q-SpC and Q-CDOM at seasonal and event time scales.

Study Site and Methods

Study site

Granger Basin (60°31’N, 135°18’W) is a 7.6 km2 headwater catchment located within the long-term Wolf Creek Research Basin, Yukon Territory, Canada. Granger Basin ranges in elevation from 1,310 to 2,250 masl and has a continental subarctic climate with mean annual precipitation ~400 mm (40% snow) and a mean annual temperature of -3°C. The geology is primarily sedimentary overlain by a glacial till and ~70% of the basin is underlain with permafrost (Lewkowicz & Ednie, 2004), with low-elevation southerly exposures permafrost-free. Vegetation consists of low-lying grasses, herbs and shrubs such as dwarf birch and willow (McCartney *et al.,* 2006).

Field methods

For this paper, 15-minute data from 2016 is analyzed throughout the ice-free season. Discharge was calculated using a stage-discharge relationship. Salinity was measured using a Hobo U24 conductivity logger and corrected for temperature. CDOM was collected using a Turner C3 submersible fluorimeter.

Analysis

The HydRun toolkit (Tang & Carey, 2017) was used to extract rainfall-runoff events from the annual hydrograph and match them with the salinity and CDOM data. Hysteresis indices were calculated after Lloyd et al. (2016).

Results

Seasonal patterns in 2016

Discharge began in early May in response to snowmelt, with two main temperature-driven events, and peaked in mid-June following a large rain event when the active layer was relatively shallow. There is a general seasonal recession with precipitation event responses and an increase in flows beginning in late August when conditions were very wet (Figure 1). SpC in general declined when flows increased, yet as the season progressed, there is an overall decline in SpC for any given Q (Figure 2). CDOM was greatest in early spring and declined throughout the season, yet increased when flows rose in response to precipitation. There were periods when both SpC and CDOM were not measured because of instrument problems.

Figure 1. Runoff, specific conductance and CDOM for Granger Basin, 2016

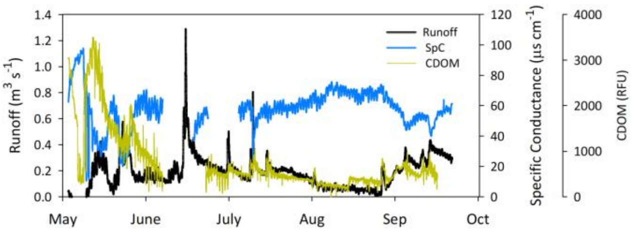

Figure 2. Runoff versus specific conductance at 15 minute intervals for Granger Basin in 2016.

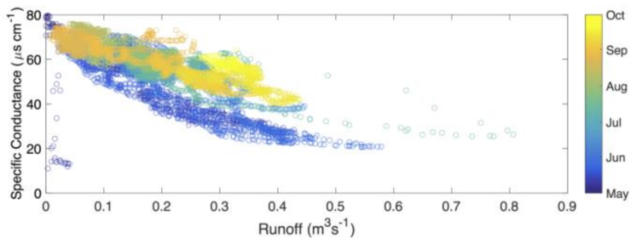

Figure 3. Runoff versus CDOM (relative fluorescence units) at 15 minute intervals for Granger Basin in 2016.

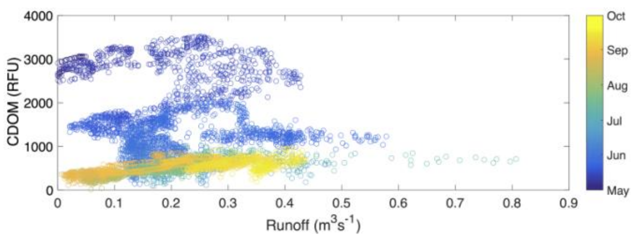

Event delineation and hysteresis Loops

The HydRun toolkit extracted 16 distinct runoff events in 2016 that had Q-SpC pairs. Of the Q-SpC events, 12 were clockwise (CW), 3 were counter-clockwise (CCW) and 1 was unresolvable. For the Q-CDOM events, 4 were CW, 10 were CCW and 2 were unresolvable. There were no distinct seasonal patterns to the direction and the openness of the loops.

Discussion

High frequency water quality data provides new insight into runoff generation processes in Granger Basin. There is a strong seasonal increase in conductivity for given flows superimposed on the high-frequency hysteresis (Figure 2). This seasonal increase in SpC is a result of deeper runoff pathways later in the season as the active layer thickens connecting to the stream and greater opportunity for water-soil contact. The general clockwise hysteresis for Q-SpC curves indicates lower salinity on the falling limb of the hydrograph and some dilution, however is it more likely that this reflects water reporting from more dilute near-surface horizons later in the event. Q-CDOM shows a strong seasonal clockwise pattern with distinct CCW event patterns. As a proxy for dissolved organic matter, this represents a general flushing throughout the year. However, on event time scales, CDOM CCW loops indicate a rise after the peak Q, which at event scales does not suggest a flushing but a mobilization mechanism. It is important to note that the loops for Q-CDOM are less well defined that the Q-SpC loops highlighting the complexity of DOM dynamics.

Acknowledgments

We wish to acknowledge funding through the Natural Sciences and Engineering Research Program, the Changing Cold Regions Research Network, and Yukon Environment, Water Resources for logistical support.

References

Carey, S.K. & Woo, M-K., 2001. Slope runoff processes and flow generation in a subarctic, subalpine catchment. *Journal of Hydrology* 253: 110-119.

Lewkowicz, A.G. & Ednie. M., 2004. Probability mapping of mountain permafrost using the BTS method, Wolf Creek, Yukon Territory, Canada. *Permafrost and Periglacial Processes* 15: 67-80.

McCartney. S., Carey, S.K., & Pomeroy, J.W., 2006. Intra-basin variability of snowmelt water balance calculations in a subarctic catchment. *Hydrological Processes* 20: 1001-1016.

Tang, W. & Carey, SK., 2017. HydRun: A MATLAB toolbox for rainfall-runoff analysis. *Hydrological Processes* 31: 2670-2682.

Woo, M-K., 2012. Permafrost Hydrology. Sprenger 563 pp.

Monitoring the Hydrogeochemical Evolution of Groundwater in a Small Watershed in a Discontinuous Permafrost Zone, Québec, Canada

Marion Cochand[1]
John Molson[2]
Johannes A.C. Barth[3]
Robert van Geldern[3]
Jean-Michel Lemieux[2]
Richard Fortier[2]
René Therrien[2]
[1] *Département de géologie et de génie géologique et Centre d'études Nordiques, Université Laval, Québec, QC, Canada, marion.cochand.1@ulaval.ca*
[2] *Département de géologie et de génie géologique et Centre d'études nordiques, Université Laval, Québec, QC, Canada*
[3]*GeoZentrum Nordbayern, Friedrich-Alexander-Universität Erlangen-Nürnberg, Germany*

Abstract

In northern regions such as Nunavik, Québec, Canada, the impacts of climate change are already apparent. However, the impacts of climate warming and permafrost degradation on groundwater dynamics and quality are still not well understood. This study aims to improve our understanding of hydrogeological interactions in degrading permafrost environments using hydrogeochemical characterization of groundwater. A small 2-km² catchment in a discontinuous permafrost zone close to the Inuit community of Umiujaq, on the eastern shore of Hudson Bay in northern Québec, Canada, was studied using hydrogeochemical tracers. Major ions, water stable isotopes, dissolved and particulate carbon, their stable carbon isotopes, and dating tracers were analyzed in order to characterize groundwater in this changing environment. The results have provided a better understanding of groundwater origin, evolution and residence time in the catchment. Linking this hydrogeochemical characterization to numerical modelling of groundwater flow and heat transfer at the watershed and permafrost mound scales is improving our knowledge on hydrogeological interactions in degrading permafrost environments.

Keywords: Groundwater hydrogeochemistry; permafrost; climate change; cold regions hydrogeology.

Introduction

One consequence of global warming already being felt in northern Québec (Canada) is permafrost degradation. Although its influence on groundwater resources is still largely unknown, it will probably lead to increased groundwater recharge and changing flow dynamics (Michel & Van Everdingen, 1994; Quinton & Baltzer 2013). This study aims to improve knowledge on changing hydrogeological conditions in degrading permafrost environments using hydrogeochemical characterization of groundwater.

Study site

This study is being conducted in a small 2-km² watershed, located close to Umiujaq, on the eastern shore of Hudson Bay in northern Québec, Canada, in the discontinuous permafrost zone.

Two aquifers are currently being investigated using monitoring wells: 1) an unconfined shallow sandy aquifer located in the upper part of the watershed, and 2) a deeper confined aquifer in sands and gravels located below silty sediments invaded in part by permafrost (Fig. 1) (Lemieux et al., 2016).

Results and Interpretation

Groundwater, precipitation, stream and surface water as well as ice-rich permafrost were sampled during field investigations from 2013 to 2016 and were analyzed for major ions, water and carbon stable isotopes, carbon phases and tritium.

Results indicate that groundwater has a Ca-HCO3 composition with a low total dissolved solids content, typical for young and poorly-evolved water, and tritium values are close to 8.5 TU. Groundwater evolution can be explained by short residence times (evidence of modern recharge with tritium data), slow reaction rates due to the cold environment as well as low levels of dissolved CO_2 (low organic soils with $PCO_2 = 10^{-2.5}$ atm

(Clark & Fritz, 1997)). Dissolved inorganic carbon (DIC)Dissolved organic carbon concentrations are very low in groundwater and have a $\delta^{13}C$ signature typical of C3-type vegetation.

Stream chemical composition is influenced by groundwater exfiltration at the base of permafrost mounds in the lower part of the watershed. DIC and its $\delta^{13}C$ signature provide evidence of CO_2 degassing along the stream.

Ice lenses in permafrost have a water stable isotope composition close to modern precipitation and groundwater. This could indicate that the groundwater feeding the ground ice formation during permafrost aggradation was similar to modern groundwater and/or that permafrost warming-cooling cycles have drawn modern water into the permafrost mounds.

Conclusions

This study has allowed delineating groundwater evolution in a catchment containing discontinuous permafrost in Nunavik, Québec, Canada. Using various hydrogeochemical tracers, groundwater appears to be young and relatively poorly evolved. Tracers also highlight that the stream is fed by groundwater discharge at the base of permafrost mounds. Isotopic signatures of ice-rich permafrost lenses down to five meters deep are close to modern groundwater, which suggests influence of modern water. Linking this hydrogeochemical characterization to groundwater and thermal modelling can help to improve our knowledge on hydrogeological interactions in degrading permafrost environments

Acknowledgments

The authors acknowledge funding from a NSERC Strategic Project Grant, the Québec Ministry of Sustainable Development, Environment and Fight against Climate Change (MDDELCC) and the Québec Research Fund – Nature and Technology (FRQNT). We also thank the local community of Umiujaq for their help and collaboration on this project.

References

Clark, I. D. & Fritz, P., 1997. *Environmental Isotopes in Hydrogeology*. CRC Press.

Lemieux, J.-M., Fortier, R., Talbot-Poulin, M.-C., Molson, J., Therrien, R., Ouellet, M., Banville, D., Cochand, M. and Murray, R., 2016. Groundwater occurrence in cold environments: examples from Nunavik, Canada. *Hydrogeology Journal* 24, 1497-1513.

Michel, F. A. & Van Everdingen, R. O., 1994. Changes in hydrogeologic regimes in permafrost regions due to climatic change. *Permafrost and Periglacial Processes*, 5(3), 191–195.

Quinton, W. L. & Baltzer, J. L., 2013. The active-layer hydrology of a peat plateau with thawing permafrost (Scotty Creek, Canada). *Hydrogeology Journal*, 21, 201–220.

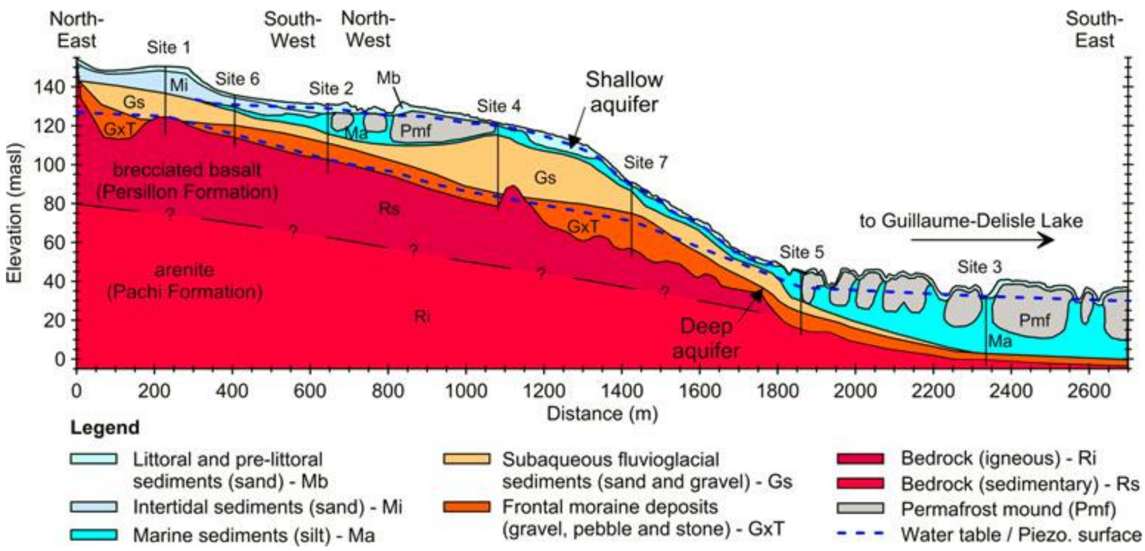

Figure 1: Cross-section of the study site showing the sampling sites, deep and shallow aquifers, the Quaternary sediments and the geology (Lemieux et al., 2016)

New insights into snowfall and snow accumulation trends and patterns across the Northwest Territories

Connon, R.F.[1], Coles, A.E.[1], Kokelj, S.A.[2], and Quinton, W.L.[1]

[1]*Wilfrid Laurier University, Yellowknife, NT, rfconnon@gmail.com*
[2]*Environment and Natural Resources, Government of the Northwest Territories, Yellowknife, NT*

Abstract

It is unclear whether snow water equivalent (SWE) in the Northwest Territories of Canada has changed in the past several decades in response to climate warming. This is in part due to the paucity of continuous, long-term snow water equivalent (SWE) datasets in the region. Further, there appear to be inconsistent long-term precipitation trends, depending on the use of adjusted SWE data, non-adjusted SWE data, or snowpack accumulation data. Accurate snowfall and snow cover data are important for parameterizing hydrological and permafrost distribution models. It is suggested that errors in snow depth calculations are artificially inflating adjusted SWE values, such as shown here for Fort Simpson, NWT - one of the few long-term climate stations in the territory. On the ground historical (1980 – present) snow survey data are used to demonstrate the spatial distribution of SWE across the NWT.

Keywords: Snow, SWE, Permafrost

Introduction

Climate warming in northwestern Canada is occurring at one of the fastest rates on Earth. There is significant uncertainty as to how climate warming may affect snow accumulation, redistribution and melt patterns in this region (Shi *et al.*, 2015). Quantifying total end-of-winter snow-water equivalent (SWE) is important for anticipating spring water level conditions and annual water balance computations in this area dominated by nival regime hydrology Understanding how (and if) snowfall is changing is also necessary to parameterize hydrological models to predict future streamflow under different warming scenarios. Furthermore, given that snowfall is an effective insulator of permafrost, understanding and predicting the timing and magnitude of snow accumulation is essential to anticipate future permafrost conditions. In the Northwest Territories (NWT), there is a lack of long term, spatially distributed snow measurements. As a result, there is often a reliance on adjusted and/or gridded data when trying to forecast future conditions. Widely used adjusted datasets may show poor agreement with ground-based measurements (*i.e.* snow surveys), in part arising from the small number of measurement stations. The objectives of this study are to: 1) synthesize and assess various sources of snowfall data and trends from across the NWT; and 2) to compare the findings to a comprehensive analysis of end-of-season SWE based on historic ground survey data.

Methodology

Where available, the Environment and Climate Change Canada (ECCC) Adjusted and Homogenized SWE datasets (Mekis and Vincent, 2011) were compared to gauged precipitation data and ground-based snow measurements across the NWT to assess if this dataset is a valid representation of field conditions. These trends were also compared against trends from GlobSnow, a satellite-based daily SWE product from which end-of-season SWE was derived.

To facilitate trend analysis of long-term datasets, the ECCC adjusted SWE data is calculated by:

$$SWE = D \times \rho_{fresh} \times \rho_{swe}$$

where: SWE (m); D is snow depth (m); ρ_{fresh} is the assumed density of fresh snow (100 kg m^{-3}); and ρ_{swe} is the spatially-variable SWE adjustment factor. This calculation is dependent on snow depth data and uses a constant snow density. However, beginning in the mid-1960s, weighing precipitation gauges were implemented at ECCC climate stations, providing a direct measure of SWE. Here, we use the non-parametric Mann-Kendall test to compare the Adjusted SWE dataset against gauged SWE data in the NWT.

This study also analyses long-term, historical on the ground snow survey data collected by academic and government institutions. Typically, the snow survey data were obtained by measuring snow depth with a wooden ruler and/or a depth-integrated snow density using a snow tube and calibrated SWE scale.

Results

The data presented here are from Fort Simpson, NWT, located on the southern edge of discontinuous permafrost. Fort Simpson climate records span over 100 years (1898 – present). Over the available 114year record, the adjusted dataset indicates that SWE is significantly increasing ($p < 0.001$) at a rate of 12 mm/decade, however the non-adjusted dataset increases at a significant ($p = 0.03$) rate of only 3.5 mm/decade (Figure 1).

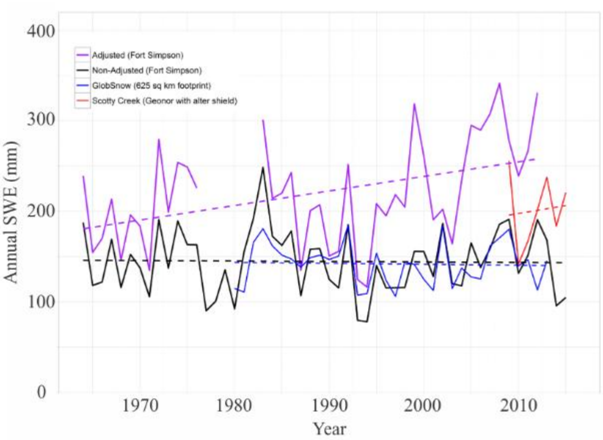

Figure 1. Differences between annual SWE measured near Fort Simpson, NWT.

The station was re-located in 1964, after which the adjusted dataset shows significant increases ($p < 0.001$) of 17.9 mm/decade, whereas the non-adjusted dataset decreases at a non-significant ($p = 0.356$) rate of 0.5 mm/decade. The GlobSnow dataset (1980 – present) displays similar trends to the non-adjusted data and also has a small, non-significant ($p = 0.339$) decreasing trend of 2.7 mm/decade (Fig 1).

Recent annual SWE values in the adjusted dataset have also been much higher than those measured on the ground. For example, during a high snowfall year in 2008, total adjusted SWE was 342 mm, whereas non-adjusted SWE was 186 mm, GlobSnow SWE was 171 mm and SWE measured on the ground at Scotty Creek was 176 mm.

It is suggested that the large differences in SWE are the result of errors in depth measurements originating after 1995. Prior to 1995, the depth measurements and non-adjusted SWE measurements approximated the 10:1 ratio, where 10 mm of fresh snow equals approximately 1 mm of SWE. However, after 1995, the relationship is no longer clear (Fig 2) and snow depths appear to be exaggerated. It is proposed that this is likely due to the change to an automated snow depth instrument (*i.e.* SR50, *Campbell Scientific*) that is not recording accurate data. A similar trend was found at the Hay River climate station, where a strong increasing trend in SWE was observed in the adjusted dataset, without a concomitant increase in the non-adjusted or GlobSnow datasets. Ongoing work will be conducted to analyze trends at other stations in the NWT, as well as to use on the ground snow survey data to compile a comprehensive data set for SWE across the territory.

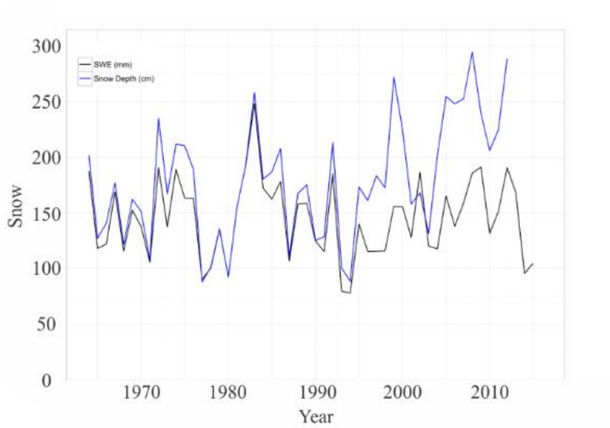

Figure 2. Comparison of snow depth (cm) and SWE (mm) at Fort Simpson A climate station.

Conclusions

It appears that the adjusted and homogenized SWE data for some climate stations in the NWT suggest increasing trends that are not corroborated with on the ground observations. It is important to accurately characterize these trends to:

1) Predict how spring runoff events will change under different warming scenarios
2) Calculate over-winter energy loss from permafrost systems, given that snow is a very effective insulator.

References

Mekis, E., and Vincent, L. 2011. An overview of the second generation adjusted daily precipitation dataset for trend analysis in Canada, *Atmos-Ocean*, 49:2, 163-177.

Shi, X., Marsh, P., and Yang, D. 2015. Warming spring air temperatures, but delayed spring streamflow in an Arctic headwater basin, *Environ. Res. Lett.*, 10, 1-10.

Quantifying the Interactions Between Subsurface Hydro-Thermal Characteristics, Permafrost Distribution, Soil Physical Properties and Landscape Structure in an Arctic Watershed

Baptiste Dafflon[1], Emmanuel Léger [2], Yves Robert [2], John Peterson [2], Craig Ulrich [2], Sébastien Biraud [2], Anh Phuong Tran [2], Bhavna Arora [2], Haruko Wainwright [2], Vladimir Romanovsky [3], Susan Hubbard [2]

[1] *Lawrence Berkeley National Laboratory, Berkeley California, bdafflon@lbl.gov*

[2] *Lawrence Berkeley National Laboratory, Berkeley California*

[3] *University of Alaska Fairbanks, Fairbanks Alaska*

Abstract

Understanding the link between soil physical properties (incl. fraction of soil constituents, bedrock depth, permafrost characteristics), thermal behavior, hydrological conditions and landscape properties is particularly challenging yet is critical for predicting the storage and flux of water, carbon and nutrient in a changing climate in the Arctic permafrost environment. In this study we investigate the characteristics of and controls on deep permafrost processes in a watershed on the Seward Peninsula AK. A variety of ground-based and aerial measurements are integrated together to identify the various subsurface hydro-thermal behavior in the watershed and to evaluate the multi-dimensional relationships between subsurface and surface properties. The various datasets allow us to distinguish shallow permafrost from deep permafrost with overlying talik. In addition, several interactions are identified between the subsurface permafrost/soil characteristics, the topography and the snow thickness and plant distribution. We use numerical models to reproduce some of the identified behavior.

Keywords: Permafrost; Talik, Discontinuous; Geophysics; Hydrology; Co-variability.

Introduction

Improving understanding of Arctic ecosystem functioning and parameterization of process-rich hydro-biogeochemical models require advances in quantifying ecosystem properties, from the bedrock to the top of the canopy (Jorgenson et al., 2010). In Arctic regions having significant subsurface heterogeneity, understanding the link between soil physical properties (incl. fraction of soil constituents, bedrock depth, permafrost characteristics), thermal behavior, hydrological conditions and landscape properties is particularly challenging yet is critical for predicting the storage and flux of water, carbon and nutrient in a changing climate. In this study we investigate the distribution of various hydro-thermal behavior in an Arctic watershed with discontinuous permafrost, and we investigate the relationships between the subsurface soil properties and the landscape structure.

Field Site and Data

This study, which is part of the Next Generation Ecosystem Experiment (NGEE-Arctic), takes place in a watershed between Nome and Teller AK on the Seward Peninsula. The watershed is characterized by an elevation gradient, shallow bedrock, and discontinuous permafrost. At this site, the top of permafrost cannot be easily identified with a tile probe (due to rocky soil and/or large thaw layer thickness). As such, we developed a technique using vertically resolved thermistor probes to directly sense the temperature regime at multiple depths and locations (Fig. 1). These measurements complement electrical resistivity tomography imaging, seismic refraction and point-scale data for identification of the various thermal behavior and soil characteristics. In addition, we used a Unmanned Aerial Vehicle (UAV)-based aerial imaging platform to measure surface properties including a digital surface model (DSM), the plant distribution and vigor, and the estimation of snow thickness (e.g., Wainwright et al., 2017). The surveys are performed at a 150 x 300 m scale to understand the interactions between a shallow permafrost zone and surrounding deeper permafrost, as well as along long 2 km long transects from the bottom to the top of the watershed to understand watershed-scale permafrost and hydrological characteristics. Finally, we also initiated the monitoring of the co-variability between surface and subsurface properties along a 130 m long transect using a coincident above/below ground monitoring strategy following the approach developed earlier at another Arctic site (Dafflon et al., 2017).

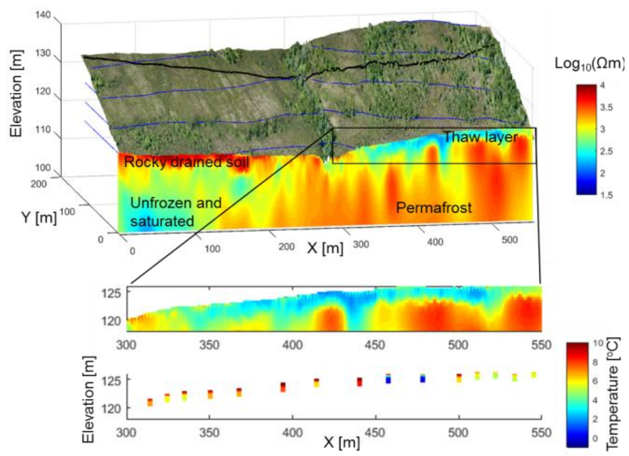

Figure 1. (top) Electrical Resistivity Tomography (ERT) and UAV-inferred mosaic and digital surface elevation model. (bottom) Zoom in of shallow ERT and vertically resolved temperature profiles. Presence of unfrozen channels observed from ERT is confirmed by higher soil temperature values.

Method

A statistical data analysis is performed to understand the multi-dimensional relationships between the various subsurface and surface properties. In particular, we evaluate linkages between the soil physical-thermal properties and the surface hydrological conditions, geomorphic characteristics, snow thickness and vegetation distribution. The data integration and analysis is supported by numerical approaches that simulate hydrological and thermal processes. Various scenarios are simulated to evaluate and explain various hydrological-thermal behavior observed in the field data.

Results and Discussion

Results show significant spatial co-variability between permafrost characteristics, vegetation, and geomorphology (ie, between above-, at- and below-ground characteristics). The permafrost distribution influences the distribution of shallow soil moisture and the geometry of surface and subsurface drainage paths. The transition zones between shallow and deeper or no permafrost zones show sharp changes in thermal behavior involving very distinct trends in vertically resolved soil temperature profiles and strong lateral variations over a few meters. We observe association between various thermal behaviors and hydrological conditions, as well as soil properties and vegetation types. Potential preferential flow paths in the subsurface have also been identified.

Further, winter subsurface thermal behaviors show the presence of taliks at several locations and potentially year-round flow and transport with highest accumulation of unfrozen water at the bottom of hillslope. Numerical models parameterized based on the field data enable us to investigate various conceptual model and improve the understanding of the present and future of such system.

Overall, this study illuminates the watershed structure and the interactions between various subsurface and landscape properties in a representative Arctic watershed with discontinuous permafrost. These interactions are of significant interest, as they are critical for understanding the evolution of the landscape and the permafrost distribution. The obtained information is expected to be useful for improving predictions of Arctic ecosystem feedbacks to climate.

Acknowledgments

The Next-Generation Ecosystem Experiments (NGEE Arctic) project is supported by the Office of Biological and Environmental Research in the DOE Office of Science. This NGEE-Arctic research is supported through contract number DE-AC0205CH11231 to Lawrence Berkeley National Laboratory. The authors thank Drs. C. Ruecker and T. Guenther for providing 2D complex resistivity imaging codes, and the NGEE PI Dr. S. Wullschleger for his support.

References

Dafflon, B.; Oktem, R.; Peterson, J.; Ulrich, C.; Tran, A. P.; Romanovsky, V.; Hubbard, S. S., 2017. Coincident aboveground and belowground autonomous monitoring to quantify covariability in permafrost, soil, and vegetation properties in Arctic tundra. *Journal of Geophysical Research: Biogeosciences*, 122 (6), 1321-1342.

Jorgenson, M. T.; Romanovsky, V.; Harden, J.; Shur, Y.; O'Donnell, J.; Schuur, E. A. G.; Kanevskiy, M.; Marchenko, S., 2010. Resilience and vulnerability of permafrost to climate change. *Canadian Journal of Forest Research-Revue Canadienne De Recherche Forestiere*, 40 (7), 1219-1236.

Wainwright, H. M.; Liljedahl, A. K.; Dafflon, B.; Ulrich, C.; Peterson, J. E.; Gusmeroli, A.; Hubbard, S. S., 2017. *Mapping snow depth within a tundra ecosystem using multiscale observations and Bayesian methods*. The Cryosphere, 11 (2), 857-875.

Taliks, a tipping point in permafrost degradation

Élise Devoie[1]
James R. Craig[1]
William L. Quinton[2]
Ryan F. Connon[2]
Erfan A. Amiri[1]
[1]*Universty of Waterloo, Waterloo, ON, egdevoie@uwaterloo.ca*
[2]*Wilfrid Laurier University, Waterloo, ON*

Abstract

Permafrost thaw is modelled in peatlands in the discontinuous permafrost region in northern Canada using a 1-D thermodynamic model of annual freeze-thaw cycles. The effects of thermal conductivity, soil moisture, advection, and snow cover are considered when modelling overwinter re-freeze depths. Conditions are identified under which insufficient energy is removed from the system to re-freeze the soil column entirely, forming a confined talik between the active layer and the permafrost table. These conditions are found to be very similar to measured soil conditions at Scotty Creek, NWT. The modelled data is compared to field measurements, and is used to determine the relative contribution of various factors to permafrost thaw, as well as quantifying anticipated thaw rates in different parts of the landscape. The model is easily extended to mineral soil systems to make predictions elsewhere.

Keywords: Permafrost; Climate Change; Hydrology; Modelling; Active Layer Evolution.

Introduction

Rapid climate warming in northern Canada is resulting in permafrost loss (Payette *et al., 2014)*. At the southern limit of permafrost, thaw is observed in peatlands as a loss in extent of permafrost-supported peat plateau (Quinton *et al.*, 2011). The precursor to loss of permafrost is proposed to be linked to the formation of confined taliks. Sub-active layer taliks form when the net ground heat flux is positive, i.e. more energy is gained by the soil during the summer than can be lost through the winter. Under these conditions, the entire soil column is unable to refreeze, and a thawed region is left between the base of the active layer and the top of the frozen permafrost table (Connon *et al.*, 2018). The presence of this talik affects the hydrology of the system, especially over winter when the system was historically quiescent. More importantly in this context, the formation of taliks is thought to be a tipping point in permafrost thaw.

Methodology

A one-dimensional thermodynamic model of active layer evolution in saturated porous media including conductive, sensible, and latent heat has been developed. This model is used to simulate soil columns initially with and without a confined talik. Annual freeze-thaw cycles are applied to these hypothetical soil columns for several possible climate scenarios, and soil conditions, to determine the evolution of the soil columns with and without a talik. Results are compared to representative talik characterization data collected form the Scotty Creek Research Station (SCRS), located in discontinuous permafrost peatlands of the southern Northwest Territories, Canada.

Fig. 1: Measured and modelled soil temperature

Results

Simulated soil temperatures determined by a representative boundary heat flux at the surface are compared to field data collected at SCRS. The stable ground heat flux condition is generally consistent with observed soil temperatures, but deviates in the winter months. A comparison of modelled and measured soil temperatures at a depth of 20cm is shown in Fig. 1. The summer soil temperature is relatively well represented, however the timing of thaw progression through the soil profile as well as the over-winter temperature are not, resulting in an over-estimation of refreeze depths. This is expected since hypothetical net ground heat flux was used to force the simulation instead of measured data.

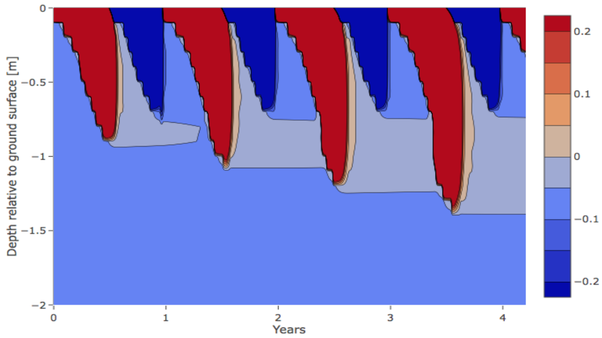

Figure 2: Talik formation under observed ground heat flux

Thermal conductivity, unsaturated soil and changes in snow cover are investigated as factors influencing depth of thaw and refreeze, and are compared to field data for various years and soil columns. Model results are sufficiently close to field data to act as a proxy of the system for sensitivity analysis and hypothesis evaluation. Conditions consistent with recently observed soil temperature data result in talik formation in areas with a sparse canopy (Fig. 2). Under soil heat flux conditions consistent with stable permafrost, a system including a talik does not necessarily recover, in fact slight degradation of permafrost can be observed at the base of the soil profile.

Taliks have many impacts on the hydrology, thermodynamics, ecology and topography of the landscape. Taliks can from a conduit for water when they connect adjacent wetland features. This increases the hydrologic connectivity of the landscape, resulting in smaller non-contributing or isolated areas, higher basin outflow (Fig. 3), and increased winter baseflows.

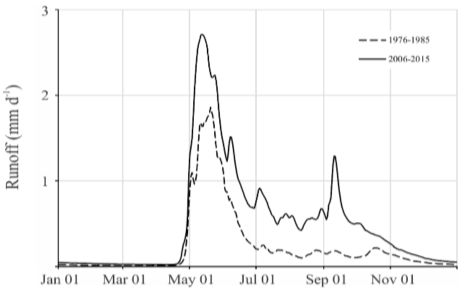

Fig. 3: Increase in streamflow due to increased hydrologic connectivity resulting from permafrost thaw

Water moving through confined talik pathways carries heat energy with it, driving advective thaw, here treated as a heat flux only in the liquid water region. Advective thaw can drastically accelerate permafrost degradation rates, as shown in Fig. 4. These results are used to explain the observed accelerated thaw in filed sites with taliks.

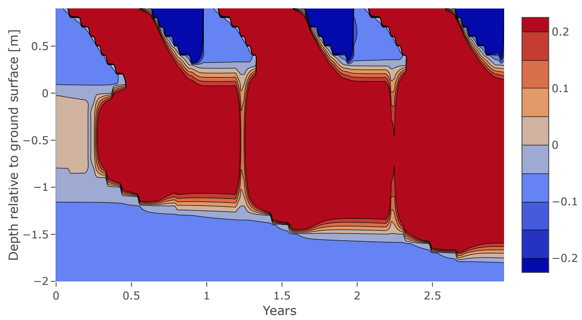

Fig. 4: Accelerated thaw due to advection in connected talik

Taliks are observed in different locations in the field, and serve different functions in each of these locations, as determined by pressure and temperature gradients. Slow-evolving isolated taliks likely act mainly as storage features, and are not subject to advection-driven thaw. Taliks connecting adjacent features can convey water and heat year-round, and may exhibit accelerated thaw. Taliks have been found along the borders of wetland features. Taliks bordering fens can store water throughout the winter, increasing in pressure until thaw occurs, when they drain into the adjacent fen over the course of the summer. Taliks bordering bogs exhibit a gradient reversal over winter, indicating a transition from contributing to receiving storage feature.

Thaw rates adjacent to bogs and fens are estimated from the thermodynamic thaw model using field data. It is found that taliks adjacent to fens are expanding more quickly than those adjacent to bogs. This is validated using historic and current aerial imagery of permafrost extent. Thaw rate data will be used to predict landscape evolution in the discontinuous permafrost peatlands system in future research.

References

Connon, R.F., Devoie, É., Quinton, W.L., & Hayashi, M., 2018. A thinning active layer ´ in a warming climate. *Journal of Geophysical Research*.

Payette, S., Delwaide, A., Caccianiga, M., & Beauchemin, M., 2004. Accelerated thawing of subarctic peatland permafrost over the last 50 years. *Geophysical Research Letters*, 31:18.

Quinton, W. L., Hayashi, M., & Chasmer, L. E., 2011. Permafrost-thaw-induced land-cover change in the Canadian subarctic: Implications for water resources. *Hydrological Processes*, 25:152–158.

Multi-tracer approach for characterizing rock glacier outflow

Michael Engel[1]
Stefano Brighenti[2, 3]
Maria Cristina Bruno[3]
Monica Tolotti[3]
Francesco Comiti[4]
[1]*Free University of Bozen-Bolzano, Italy, Michael.Engel@unibz.it*
[2]*University of Trento, Italy*
[3]*Fondazione Edmund Mach - Research and Innovation Center, San Michele all'Adige, Italy*
[4]*Free University of Bozen-Bolzano, Italy*

Abstract

The present study used a multi-tracer approach (water stable isotopes, electrical conductivity (EC), and major, minor, and trace elements) to identify the impact of rock glacier outflow on water quality. Springs and streams/creeks fed by rock-glaciers were selected in the Upper Sulden and Zay catchment, South Tyrol (Eastern Italian Alps). Preliminary results indicate that all waters sampled in the study area derived from Atlantic water vapour as water source. Melt waters emerging from rock glaciers showed typical ice melt isotopic signatures (δ^2H: -91 to -105‰) and relatively high EC (380 to 611µS cm^{-1}). Preliminary results indicate that EC, Sr, and As concentrations could be used to differentiate rock glacier melt waters from stream waters.

Keywords: permafrost thawing; water stable isotopes; heavy metals; ecological communities; alpine rivers; glacierized catchment

Introduction

Current warming in high mountains leads to increased melting of snow, glacier ice and permafrost. In particular rock glaciers, as a common form of mountain permafrost, may release contaminants such as heavy metals into the stream during summer (Thies *et al.*, 2007). Permafrost thawing may have strong impacts on both water quantity and quality of fresh water resources, with potential consequences on alpine stream ecology. However, only few rock glacier studies using multi-tracer approaches were carried out in the Alps. At the regional scale (South Tyrol, Eastern Italian Alps), high concentrations of Ni were found in meltwater from the Lazaun rock glacier in the southern Ötztal Alps (Krainer *et al.*, 2015; Mair *et al.*, 2011) or lake water in contact with Rasass rock glacier in Vinschgau valley (Thies *et al.*, 2007). These observations call for characterizing rock glacier outflows by means of hydrochemical characteristics. For example, Carturan *et al.* (2016) used spring water temperature as significant indicator to identify permafrost distribution.

Material and methods

Study area

The present study was located in the glacierized Sulden catchment (130 km²) in South Tyrol (Italy). The site ranges in elevation between 1110 and 3905 m a.s.l. and has a glacier extent of about 17.7 km² (14 % of the catchment). Geologically, the study area belongs to the Ortler-Campo-Cristalin (Mair *et al.*, 2007). Permafrost and rock glaciers are most probably present in this region at elevations higher than 2600–2800m a.s.l. (Boeckli *et al.*, 2012). Two active rock glaciers feeding two springs at 2600 m a.s.l. (0.09 km²) were selected in the Upper Sulden in 2015 and one rock glacier at 2718 m a.s.l. (0.08 km²) were chosen in the Upper Zay catchment in 2017, an eastern sub-catchment within the main Sulden stream Valley. Meteorological data were measured by an Automatic Weather Station at 2825 m a.s.l. of the Hydrographic Office (Autonomous Province of Bozen-Bolzano).

Water sampling

Initially, we carried out a monthly sampling of two springs and one stream station as reference draining the rock glaciers in the Upper Sulden catchment from July to October 2015 (Engel *et al.*, 2017a). We resumed the study from June to September 2017 and added the two springs and one stream stations in the Zay sub-catchment. In addition, we sampled potential runoff components such as snowmelt, glacier melt, and precipitation. While all types of melt waters were sampled as grab samples of dripping meltwater from snow patches and the glacier surface, precipitation was taken from bulk collectors placed in proximity to the rock glaciers.

Water analysis

Electrical conductivity and water temperature were measured by a portable conductivity meter WTW 3410 (WTW GmbH, Germany) with a precision of +/- 0.1 µS cm^{-1} (nonlinearly corrected by temperature compensation at 25 °C). Isotopic analysis was conducted by laser spectroscopy (L2130-i, Picarro Inc., USA) at the Free University of Bozen-Bolzano. Major, minor, and trace elements were analyzed by Inductively Coupled Plasma Mass Spectroscopy (ICP-MS ICAP-Q, Thermo Fischer) at EcoResearch l.t.d. (Bozen).

Results: tracer-based melt water characterization

Results from 2015 show that water from the two springs and the stream in the Upper Sulden catchment fell along the global meteoric water line, indicating Atlantic water vapor as water source. Melt water from rock glaciers showed typical ice melt isotopic signatures (δ^2H: -91 to -105‰) and relatively high EC (380 to 611µS cm^{-1}). Preliminary results indicate that EC, Sr, As and K concentration could be used to discriminate rock glacier melt waters from stream waters for the Sulden sub-catchments in 2015. The important role of EC, Sr, and As as indicators was confirmed in 2017 for spring waters from both sub-catchments. Notably, As concentrations exceeded thresholds for drinking water both in the Sulden and Zay springs from summer to autumn.

Conclusions

The multi-tracer approach based on stable water isotopes, EC, and major, minor, and trace elements proved to be useful to initially characterize rock glacier melt waters in the study area. While isotopic data revealed that all different water types in the catchment derived from Atlantic origin, some hydrochemical parameters (EC, Sr, and As) showed distinct characteristics when comparing rock glacier fed-spring water and reference stream waters (*i.e.* not fed by permafrost). Similarly, these element concentrations also characterized high-elevation spring water in the Matsch Valley, a neighbouring valley of the study area (Engel *et al.*, 2017b). Further work is needed to fully elaborate the tracer dataset obtained and to carry out additional water sampling during the following years, corroborating the present findings.

Acknowledgments

This research is part of the GLACIALRUN project and funded by the foundation of the Free University of Bozen-Bolzano, and part of an Erasmus Mundus Joint Doctorate Program SMART funded by the Education, Audiovisual and Culture Executive Agency (EACEA) of the European Commission. We thank Werner Tirler and Giulio Voto at EcoResearch l.t.d. (Bozen/Bolzano) for the element analysis.

References

Boeckli, L., Brenning, A., Gruber, S., Noetzli, J., 2012. A statistical approach to modelling permafrost distribution in the European Alps or similar mountain ranges. *The Cryosphere* 6: 125-140.

Carturan, L., Zuecco, G., Seppi, R., Zanoner, T., Borga, M., Carton, A., Dalla Fontana, G., 2016. Catchment-Scale Permafrost Mapping using Spring Water Characteristics. *Permafrost and Periglacial Processes* 27: 253–270.

Engel, M., Penna, D., Tirler, W., Comiti, F., 2017a. Tracer-based identification of rock glacier thawing in a glacierized Alpine catchment. *Geophysical Research Abstracts European Geosciences Union*, Vienna, Austria, 23-28 April.

Engel, M., Penna, D., Tirler, W., Comiti, F., 2017b. Multi-Parameter-Analyse zur Charakterisierung von Landschaftsmerkmalen innerhalb eines experimentellen Messnetzes im Hochgebirge. *In*: M. Casper *et al.* (Eds.): *Den Wandel Messen – Proceedings Tag der Hydrologie 2017, Forum für Hydrologie und Wasserbewirtschaftung* 38: 293-299.

Krainer, K., Bressan, D., Dietre, B., Haas, J. N., Hajdas, I., Lang, K., Mair, V., Nickus, U., Reidl, D., Thies, H., Tonidandel, D., 2015. A 10,300-year-old permafrost core from the active rock glacier Lazaun, southern Ötztal Alps (South Tyrol, northern Italy). *Quaternary Research* 83: 324-335.

Mair, V., Nocker, C., Tropper, P., 2007. Das Ortler-Campo Kristallin in Südtirol. *Mitteilungen der Österreichischen Mineralogischen Gesellschaft* 153: 219-240.

Mair, V., Zischg, A., Lang, K., Tonidandel, D., Krainer, K., Kellerer-Pirklbauer, A., Deline, P., Schoeneich, P., Cremonese, E., Pogliotti, P., Gruber, S., Böckli, L., 2011. *PermaNET - Permafrost Long-term Monitoring Network. Synthesis report*. INTERPRAEVENT Journal series 1, Report 3. Klagenfurt.

Thies, H., Nickus, U., Mair, V., Tessadri, R., Tait, D., Thaler, B., Psenner, R., 2007. Unexpected response of high Alpine lake waters to climate warming. *Environmental Science & Technology* 41: 7424-7429.

Variability of the hydrology of the Middle Lena River (Siberia) since 1937

Emmanuele Gautier[1], François Costard[2], Alexander Fedorov[3]
Thomas Depret[1], Delphine Grancher[1], Clément Virmoux[1] and Daniel Brunstein[1]

[1]*LGP, Université Paris 1, Meudon, France, emmanuele.gautier@lgp.cnrs.fr*
[2]*GEOPS, Geosciences Paris Sud, Université Paris Saclay, Orsay, France,*
[3]*Permafrost Institut, Russian Academy of Science, Yakutsk, Russia*

Abstract

The main aim of this study is to determine the hydrologic and morphodynamic response of the Lena River in Eastern Siberia to ongoing climate change. The hydrologic variability of the Middle Lena River indicates a net hydrologic change with an increase in the intensity and duration of floods in the two decades ending in 2012. The recent occurrence of storms in summer and the early autumn is probably the main cause of the "multi-peak" hydrograph we identified in the decade preceding 2012. Both erosion of the banks and the thickness of deposits were correlated with the duration of flooding

Keywords: permafrost, Siberia, flood, Lena, climatic change

Introduction

Recent observations indicate that over the last decades, climate change has increasingly influenced the frequency, intensity and duration of extreme climatic and hydrologic events. In Eastern Siberia, permafrost temperature already underwent an increase up to 1 °C over the course of the 20th century (Fedorov and Konstantinov, 2003) and an increase in warming has been observed since the beginning of the 21st century (Fedorov et al., 2014). The fluvial regime of the Arctic rivers is immoderate with very low flow during winter and a spring flood characterized by a steep rising limb and a peak discharge that can exceed by ten times the winter discharge. The frozen islands in the Lena River are much more sensitive to thermal erosion than the channel banks (Are 1983, Gautier et al., 2008). During floods, the combination of the increase of discharge and the increase of the temperature of the stream, explains the rapid bank retreat (Costard et al., 2003 and 2007).

The main aim of this study is to determine the hydrologic and morphodynamic response of the Lena River in Eastern Siberia to ongoing climate change. We examine the influence of the different parameters of hydrologic functioning on erosion and sedimentation. To this end, we also analyze the morphological and sedimentary response of the river using data from instrumented sites that were surveyed from 2008 to 2012.

Study area

The study area (61° 4'N and 129° 3'E) is located upstream of Yakutsk city near the the Tabaga gauging site. In the middle valley, upstream of Yakutsk city, the Lena floodplain is 25 km wide. In that area, the Lena floodplain consists of a large number of shallow and wide channels that are between several hundred meters and three kilometers in width

From October to the end of April, the river Lena goes through a long low water stage, and is covered by ice between 200 and 250 days. The great majority of flood peaks occurs in May and June, associated with the flood wave coming from the upper basin and with the local break-up. Secondary peaks may be registered in summer, mostly due to rainstorms.

Data and methods

We used monthly and daily hydrologic data for 76 years at Tabaga gauging site for the 1937-2012 period. First, we calculated the mean monthly discharge, particularly for the spring and summer seasons (May-September) and we calculate high water level and the flooding period. The thermo-buttons were installed on different trees, at 0.5 m intervals from the soil surface to a height of 4 m; the temperature was recorded at 3 hourly intervals from the end of April until October. We estimated the effect of hydrologic events on erosion and sedimentation with high resolution analysis on different islands.

Results

Mean monthly discharges have increased significantly in recent decades. Winter discharges (November-April) were characterized by a significant increase after the late 1980s. Positive anomalies were recorded for monthly discharge in May; except 2003 & 2004. The recent hydrologic change is also reflected in the increased frequency of positive anomalies.

Two periods were characterized by frequent high floods. First, the 1957-1966 period was an active period. Second, after the 1980s, the frequency of floods greater than 40 000 m3s-1 increased progressively (Fig. 1).

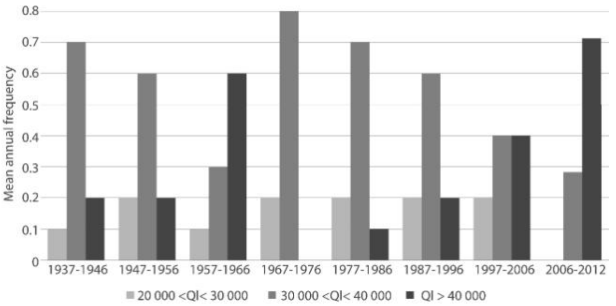

Figure 1: Mean annual frequency of maximum water discharge (per decade between 1937 and 2012).

Hydrologic changes can also be detected by analyzing the duration of the different classes of discharge. Discharges higher than 40 000 m^3s^{-1} rarely exceeded a few days. After 2004, longer durations became more frequent: 9 days in 2004, a historic maximum of 21 days in 2006, and 8 days in 2012.

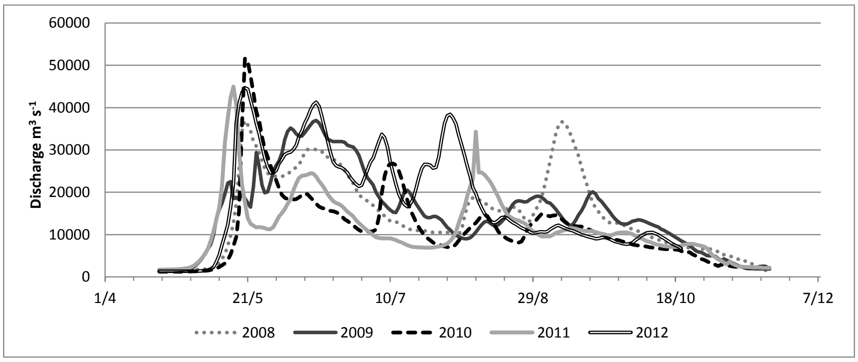

Figure 2: Recent floods with secondary peaks

Erosion and sedimentation were also measured on different river islands in the hydrologic years 2008-2012. Both erosion of the banks and the thickness of deposits were correlated with the duration of flooding and the period of flooding also influenced the bank retreat.

Conclusion

Spring monthly discharge has undergone a net increase caused by longer bar-full and bank-full water levels. Flood peaks are also more frequent. The hydrologic change is not only expressed by the flood intensity but also -and mainly- by the increasing duration of the discharges. The efficiency of the water discharges is reinforced by the increase in water temperature: later and longer hydrologic processes are combined with much warmer stream temperatures. Thus, the mobility of the channels and islands threatens numerous activities: navigation, and river infrastructure are destabilized

Examination of discharge between 1936 and 2012 confirmed that high variability is an intrinsic feature of the hydrologic functioning of the Lena River. The Central Yakutia was hardly affected by Arctic warming (1935-1945). An increase in the thawing index was evidenced from 1988 to 1995, and the increase was much more pronounced after 2005 (Fedorov et al., 2013).

The recent occurrence of storms in summer and the early autumn is probably the main cause of the "multi-peak" hydrograph we identified in the decade preceding 2012 (Fig. 2). At Tabaga, there is no clear correlation between the occurrence of a secondary flood peak in August or September and the precipitation. Thus the great majority of the secondary summer peaks mainly corresponds to a flood wave coming from the upper basin. In those areas, rainfall events can create a secondary flood in the summer (August or September) with a water discharge a little above 20 000 m^3s^{-1}. These events are more frequent from the beginning of the 21st century.

Acknowledgments

Financial support from Agence Nationale de la Recherche ANR-07-VULN- (002 CLIMAFLU), the GDR 3062 "Mutations Polaires.

References

- Are F. 1983. Thermal abrasion on coasts, Proceedings, *Fourth International Conference on Permafrost,* 24-28.
- Costard et al. 2007. Impact of the global warming on the fluvial thermal erosion over the Lena river in Central Siberia. *Geophys. Res. Lett.*, 34, (14).
- Gautier et al., 2008. Proceedings *9th International Permafrost Conference.* 493-498.
- Fedorov and Konstantinov, 2003. *Proceedings of International Permafrost Conference*, Zurich, 239-243.
- Gautier et al. 2018. Hydrologic response of Middle Lena River reach (Siberia) to the climate variability and change. *J. of Hydrology*, in press.

Identification of patterns in hydrological conditions governing flow in an unregulated river basin in the Northwest Territories, and implications for downstream hydroelectric power generation

Jennifer Hickman[1]
Michael English[2]
Phil Marsh[2]
[1]*Wilfrid Laurier University, Global Water Futures, jhickman@wlu.ca*
[2]*Wilfrid Laurier University, Cold Regions Research Centre*

Abstract

Located in the discontinuous permafrost zone of the Northwest Territories, Canada, the Snare River hydroelectric power system supplies power to the Territory's capital city, Yellowknife, and surrounding communities. Recent low water levels in the Snare River have intermittently reduced and/or eliminated the possibility of generating hydroelectric power, resulting in significant expenditure by NTPC on diesel fueled generators as an alternative power source. Of significant concern is whether low-flow conditions will become more frequent in the future, and result in a potentially non-sustainable expense. The objective of this study is to understand how antecedent climatic and hydrological conditions in an unregulated basin influence flow patterns, specifically the conditions that result in low discharge contributions to hydroelectric reservoirs. By identifying patterns among the various controls on flow, it may be possible to provide a predictive capacity for stakeholders of the Snare River hydroelectric system to aide in decision-making surrounding the generation of power.

Keywords: hydrology; subarctic; hydroelectric power; antecedent conditions

Study site and methods

The Snare River, located in the Northwest Territories, Canada, is used for generating hydroelectric power for the Territory's capital city of Yellowknife and several smaller communities. Low river flow during the last two decades, and most recently between 2013-2015, has intermittently reduced and/or eliminated the possibility of generating hydroelectric power, resulting in the expenditure of approximately $30 million on diesel fuel as an alternative power source. Of significant concern to stakeholders is whether low flow and drought conditions will become more frequent in the future, resulting in a potentially non-sustainable expense.

The objective of this study is to understand how antecedent climatic and hydrological conditions in a large unregulated portion of the Snare basin influences flow patterns, specifically identifying those conditions that result in low recharge contributions to hydroelectric reservoirs. Identifying patterns among the variables controlling flow may provide a predictive capacity for stakeholders of the Snare River hydroelectric system, which may aide in decision-making regarding the future of power generation in the NWT.

As with many isolated northern river basins there is very little climatic or hydrological data available, and little research is undertaken upon which to base any predictive capacity. In the Snare watershed, aside from river flow data from Water Survey of Canada, very little usable data exists. Consequently, numerous extrapolation techniques using data external to, but within reasonable proximity to the basin, are utilized to quantify an annual hydrological mass balance. This includes employing remote sensing platforms for estimating snowpack water equivalent, and methods for estimating rainfall and evapotranspiration with storage solved as the residual in the mass balance equation. These calculations are complicated by the size and physical nature of the watershed, comprised of a dense network of interconnected lake catchments with shallow till underlain by widespread discontinuous permafrost. These terrain characteristics coupled with the large number of lake reservoirs complicates our understanding of storage.

For this study, a 17-year period, 1999-2015, was selected, providing us with a suitable range of hydrological and climatic conditions appropriate for ascertaining how antecedent conditions may play a role in subsequent years basin hydrology. It has become clear that particular combinations of watershed conditions heavily influence the total outflow, and thus the ability to generate hydroelectric power downstream. In particular, this work highlights the common misconception that high water inputs from snow and rain will result in high water output at the basin outlet.

Results and discussion

The relationship between water inputs and outputs from this system are significantly governed by the timing and intensity of the most significant annual hydrological event; the spring freshet. By examining the slope of the cumulative flow curve during the thaw season, it is possible to identify which years experienced the most intense snowmelt (Fig. 1). Comparing these slope values to the overall basin efficiency confirms the importance of a rapid snowmelt (Fig. 2). For example, 2006 experienced a rapid snowmelt period, as indicated by the steep cumulative flow curve (Fig. 1), which resulted in a high basin efficiency (Fig. 2) and ultimately high river discharge at the basin outlet.

It is possible that a prolonged melt that occurs later in the thaw season is susceptible to higher losses to storage, as then the active layer has thawed to a greater depth in turn influencing storage potential. It is the combination of conditions like these that govern flow at the basin outlet, and ultimately determines the extent to which hydroelectric reservoirs will be filled.

While examining relationships among mass balance variables provides us with year to year insight into what potentially controls discharge from the unregulated portions of the Snare basin, it is also of interest to see if larger scale climatic events play a role in the future hydrological patterns in the Snare system. To do this we examined the long-term pattern of Arctic Oscillations (AO) and related this to annual peak snowpack water equivalent in the basin as determined from Globsnow. The AO record extends from 1949 to the present time. Over this period of time there is a slow but significant change from a dominance of negative AO to a positive AO, most pronounced over the past two decades (Fig.3). A somewhat weak but statistically significant positive relationship between AO index and SWE also exists (Fig.4). As we shift towards winters dominated by positive AO there is a tendency for increasing SWE.

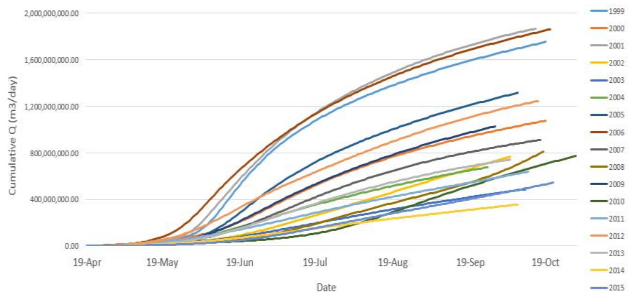

Figure 1. Thaw season cumulative Q 1999-2015

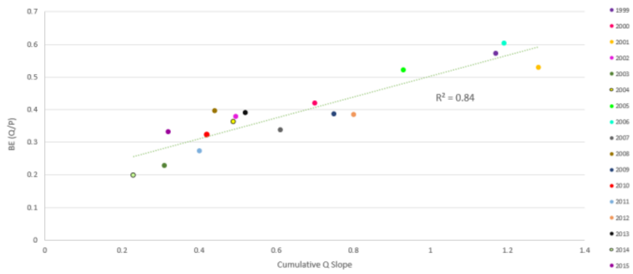

Figure 2. Cumulative Q slope vs. basin efficiency

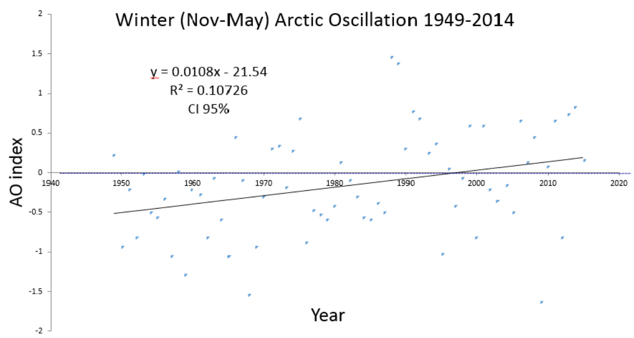

Figure 3. AO index change over time

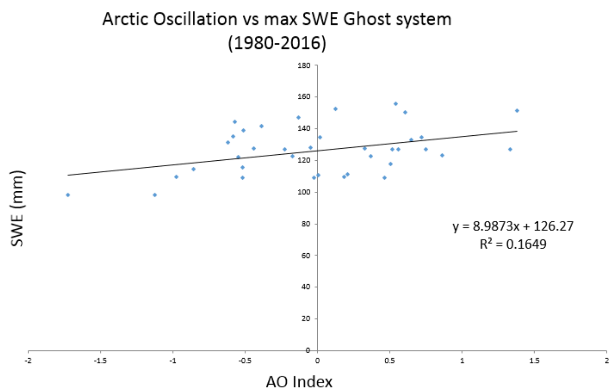

Figure 4. AO index vs. SWE

Using Snowmelt Peak Flows Drivers to Estimate Peak Flows on Alaska's North Slope

Alexa Marion Hinzman[1]
Ype van der Velde[2]
Svetlana Stuefer[3]

[1]*Vrije Universiteit Amsterdam, a.m.h.hinzman@vu.nl*
[2]*Vrije Universiteit Amsterdam*
[3]*University of Alaska Fairbanks*

Abstract

Historic drivers of peak flows can be used to predict future peak flows with the help of linear regression. Using historic data from four watersheds on the North Slope of Alaska, linear regression equations were created for individual watersheds and combined watersheds to identify independent physiographic and climatic variables that statistically predict future peak flows accurately. Snow water equivalent and antecedent soil moisture storage was determined to be strongest correlated variables in individual watersheds while area of the watershed was found to be the highest correlated variable when all watersheds where combined.

Keywords: Alaska; Snowmelt; Soil moisture; Peak flows.

Introduction

Snowmelt peak discharges in Alaska can cause flooding of roads and structures and millions of dollars of damage every year. Underestimating peak flows lead to more cases of flooding and more damage to infrastructure and the inability to reach remote locations. With a fast changing Arctic climate, to understand changes in peak flows it is important to identify the controlling factors.

Peak discharges on the North Slope of Alaska are accurately predicted through linear regression equations with independent meteorological and physiographic variables collected from four watersheds, verified through recorded snowmelt peaks. Terrestrial Environmental Observation Network (TEON) was initiated to monitor the North Slope of Alaska and continue historic data collection.

Study area

Each of the watersheds used in the study are somewhat unique. The Putuligayuk River watershed is located on the coastal plain of Alaska. The Upper Kuparuk River is the upper headwaters of the Kuparuk Watershed. Imnavait Creek abuts the Upper Kuparuk and has the longest historic data collection. Roche Moutonnée Creek is the most southern watershed and has the greatest slope. It has had peak flows collected since 1976, however climatic data collection by TEON researchers was started in 2015.

Table 1. Watershed Comparisons.

Name of Watershed	Area (km^2)	Slope (km/km)	Record Length (years)	Storage Data Available?
Putuligayuk River	471	0.0015	17	Yes
Upper Kuparuk River	142	0.045	21	No
Imnavait Creek	2.2	0.027	31	Yes*
Roche Moutonnée Creek	84	0.164	25	No

*Partial Record

Methods

This paper compares frequently used flood frequency analysis techniques, and produces linear regression equations to predict peak flows for each watershed as well as all watersheds combined. Bulletin 17B was utilized as the first flood frequency analysis technique (U.S. Interagency Advisory Committee on Water Data, 1982). U.S. Geological Survey used a least square regression approach to create regional sets of equations to predict peak flows (Curran *et al.*, 2016). This method was also compared to the linear regression equations.

Discussion

From five linear regression equations created, three found snow water equivalent (SWE) to be the most significant predictor of peak flows. The first attempt to estimate peak flows for all watersheds used area and had a high R^2 value of 0.72. The second equation for all watersheds included area and SWE as the meteorological independent variable. It was interesting to note the soil moisture storage was not indicative of peak flow magnitudes for each individual watershed.

Conclusion

While the evidence presented is quite promising that modeling can be useful in estimating peak flows in ungauged arctic watersheds, the limitations of using only four watersheds to determine the equations call for further analysis and verification. More validation studies are needed to demonstrate that viable equations may be applied to all watersheds on the North Slope of Alaska or to other regions.

Acknowledgments

This study was funded by Arctic Landscape Conservation Cooperative (ALCC) through Terrestrial Environmental Observation Network (TEON).

I thank Janet Curran and the USGS Alaska Science Office, as well as the USGS researchers who helped collect historic peak flow data for the Putuligayuk River and Roche Moutonnée Creek.

I thank the WERC faculty, staff and students at the University of Alaska Fairbanks for collecting and processing data over the years, specifically Rob Gieck, Emily Youcha, and other researchers who collected the historic data. I also thank the professors, Svetlana Stuefer, Chris Arp and David Barnes.

References

Curran, Janet H, Nancy A Barth, Andrea G Veilleux & Robert T Ourso., 2016. Estimating Flood Magnitude and Frequency at Gaged and Ungaged Sites on Streams in Alaska and Conterminous Basins in Canada, Based on Data through Water Year 2012. *Scientific Investigations Report*: 1-47.

U.S. Interagency Advisory Committee on Water Data. 1982. *Guidelines for Determining Flood Flow Frequency*, Bulletin 17B of the Hydrology Subcommittee. Edited by U.S. Geological Survey. Reston, Virginia: Office of Water Data Coordination, 183pp.

Hydrologic connectivity is a key control on the impacts of permafrost disturbance on fluvial fluxes

Melissa J. Lafreniere[1]
Scott F. Lamoureux[2]
[1]*Department of Geography and Planning, Queen's University, Kingston, ON, Canada, Melissa.lafreniere@queensu.ca*
[2]*Department of Geography and Planning, Queen's University, Kingston, ON, Canada*

Abstract

This study reviews research on the impacts of changing permafrost conditions on the fluvial exports in a High Arctic permafrost setting. This body of research highlights the importance of hydrological connectivity in regulating the response of watershed biogeochemical fluxes to physical and thermal disturbance of permafrost. The research identifies that the impacts of permafrost disturbances on fluvial biogeochemical fluxes are the result of hydrologic connectivity between affected landscapes and streams, which is primarily a function of i) the surface exposure of excess ice and solute-rich permafrost, and ii) late summer rainfall. An improved understanding of biogeochemical flux response of watersheds to permafrost disturbances requires better knowledge of the key characteristics and processes that establish hydrological connectivity in permafrost watersheds, such as the distribution of ice in the upper permafrost, and the physical characteristics of the active layer that control infiltration and runoff generation.

Keywords: permafrost disturbance, permafrost hydrology, fluvial fluxes, hydrologic connectivity

Introduction

Climate change is simultaneously altering permafrost conditions and hydrological regimes in Arctic watersheds (AMAP, 2017). Deep thaw and permafrost disturbances, including active layer detachments (ALDs), thermo-erosion features, and retrogressive thaw slumps generate important downstream hydrological and biogeochemical responses (Abbott *et al.*, 2015; Lafrenière *et al.*, 2017; Roberts *et al.*, 2017).

This paper examines the magnitude and persistence of the impact of permafrost change on the fluvial export of material (including particulates, inorganic ions, nutrients and dissolved organic matter (DOM)) as reported in research conducted at the Cape Bounty Arctic Watershed Observatory (CBAWO). Specifically, this synthesis examines how the impacts of permafrost perturbations (e.g. deep thaw and physical disturbance) on the fluxes of important water quality components are related to processes that establish hydrological connectivity between the landscape and streams.

Permafrost disturbances

We identify two dominant mechanisms of permafrost perturbation that impact fluvial exports: physical disturbance and thermal perturbations (Lafrenière & Lamoureux, 2013). Physical disturbances result in the fracture, displacement and/or complete removal of the organic rich surface soil horizon, and the exposure of previously buried mineral soils. These disturbances are spatially constrained, but can have pronounced impacts on the surface morphology of the landscape, and thus influence the storage and surface water flow pathways.

Thermal perturbation occurs when thaw extends beyond the usual depth of the active layer, into the transition zone, or shallow permafrost. Increasing the depth of thaw increases potential soil water storage, introduces new flow pathways, and liberates previously frozen mobile solutes and nutrients (Lamhonwah *et al.*, 2017). These thermal perturbations do not have visible geomorphic impacts, yet they are spatially extensive, affecting the active layer across the entire catchment.

Flux Response and Hydrologic connectivity

Impacts of disturbance type on flux response

Various studies from CBAWO demonstrate that the physical disturbance, in the form of ALDs, enhance the fluvial fluxes of sediment (Lamoureux *et al.,* 2014), inorganic solutes and nitrogen (Lamhonwah *et al.,* 2017; Lafrenière *et al.,* 2017), and decrease the flux of DOM (Fouché *et al.,* 2017). These changes in fluxes were not related to the extent of the disturbed area, but rather to the degree of channelization of the disturbances, which is a measure of hydrologic connectivity. (Lafrenière & Lamoureux, 2013; Lamoureux et al. 2014). The impacts on fluxes were both more prominent and more persistent in watersheds where incised channels, and/or continued disturbance, exposed fresh sediment (Lamoureux *et al.*, 2014). Hence, the magnitude and persistence of disturbance impacts on fluxes are a function of the degree to which freshly exposed or disturbed material is flushed and/or eroded.

Thermal perturbations have also been shown to substantially increase solute fluxes, even in absence of physical disturbance (Lafrenière & Lamoureux, 2013). The composition of water stable isotopes and ions in permafrost cores support that the thawing of the ice rich and ion rich transition zone was the likely the source of the water and ions during these periods of deep thaw (Lamhonwah *et al.,* 2017). These findings demonstrate that deep thaw can hydologically connect this subsurface ice and solute-rich zone to the channel system. This hydrological connection involves a limited extent of the active layer, and minimal flow volumes, however, the impacts can be important as thaw can conceivably hydrologically- connect the entire catchment.

Water inputs are also key to establishing hydrologic connectivity. Until recently, snow was considered the most important water input, and the extensive hydrologic connectivity established during snowmelt was considered the primary control on fluvial fluxes in permafrost watersheds. However, recent studies at CBAWO documents that late summer rainfall, especially in combination with deep thaw and physical disturbances, can provide a larger flux of solute and sediment than the nival runoff period (Lewis *et al.,* 2012; Lafrenière & Lamoureux, 2013). The significant impact of summer rainfall on material fluxes is likely because rainfall establishes spatially extensive hydrologic connectivity at a time when sediment and solutes at the surface of disturbances or deep in the active layer are readily mobilized.

Conclusions

This body of research indicates that the impacts of permafrost disturbances on fluvial biogeochemical fluxes are the result of hydrologic connectivity between affected landscapes and streams, which is primarily a function of i) the thaw and disturbance of unconsolidated ice rich material, and ii) late summer rainfall.

Our findings support that an improved understanding of biogeochemical response and recovery of watersheds to permafrost disturbances requires better knowledge of i) the distribution of ice in the upper permafrost, ii) physical characteristics of the active layer that control infiltration and generation of subsurface flow and rainfall runoff, and iii) the processes controlling the stabilization of disturbances. Knowledge of these parameters would facilitate the development of metrics that can be used do model the hydrological connectivity, and thus biogeochemical response of watersheds to permafrost and climate change.

Acknowledgments

We acknowledge the efforts of all the students and postdoctoral fellows who have contributed to research at CBAWO. Research funding has been provided by NSERC, ArcticNet, the Government of Canada International Polar Year program, and Environment and Climate Change Canada. The Polar Continental Shelf Programme has supported our field logistics.

References

Abbott, B.W., Jones, J.B., Godsey, S.E., Larouche, J.R. & Bowden, W.B. 2015. Patterns and persistence of hydrologic carbon and nitrogen export from collapsing upland permafrost. *Biogeosciences* 12: 3725-3740.

AMAP 2017. *Snow, Water, Ice and Permafrost in the Arctic (SWIPA) 2017*, Arctic Monitoring and Assessment Programme (AMAP), Oslo, Norway, 269 pp.

Fouché, J., Lafrenière, M.J., Rutherford, K. & Lamoureux, S.F., 2017. Seasonal hydrology and permafrost disturbance impacts on dissolved organic matter composition in High Arctic headwater catchments. *Arctic Science* 3(2): 378-405.

Lafrenière, M.J. & Lamoureux, S.F., 2013. Thermal perturbation and rainfall runoff have greater impact on seasonal solute loads than physical disturbance of the active layer. *Permafrost and Periglacial Processes* 24, 241-251.

Lafrenière, M.J., Louiseize, N.L. & Lamoureux, S.F., 2017. Active layer slope disturbances affect seasonality and composition of dissolved nitrogen export from High Arctic headwater catchments. *Arctic Science* 3(2): 429-450.

Lamhonwah, D., Lafrenière, M.J., Lamoureux, S.F. & Wolfe, B.B. (2017) Multi-year impacts of permafrost disturbance and thermal perturbation on High Arctic stream chemistry. *Arctic Science* 3(2), 254-276.

Lamoureux, S.F., Lafrenière, M.J. & Favaro, E., 2014. Erosion dynamics following localized permafrost slope disturbances. *Geophysical Res. Lett.*41: 2014GL060677R.

Lewis, T., Lafrenière, M.J. & Lamoureux, S.F., 2012. Hydrochemical and sedimentary responses of paired High Arctic watersheds to unusual climate and permafrost disturbance, Cape Bounty, Melville Island, Canada. *Hydrological Processes* 26(13):2003-2018.

Roberts, K.E., Lamoureux, S.F., Kyser, T.K., Muir, D.C.G., Lafrenière, M.J., Iqaluk, D., Pieńkowski, A.J. & Normandeau, A., 2017. Climate and permafrost effects on the chemistry and ecosystems of High Arctic Lakes. *Scientific Reports* 7(1), 13292.

Distribution of suprapermafrost taliks in the Shestakovka River catchment, continuous permafrost zone

Liudmila Lebedeva
Ivan Khristoforov
Kirill Bazhin
Melnikov Permafrost Institute Siberian Branch Russian Academy of Sciences, Yakutsk, Russia, lyudmilaslebedeva@gmail.com

Abstract

GPR and ERT measurements at sandy slopes covered by sparse pine forest within the Shestakovka river catchment (Central Yakutia, Russia) showed that there are water-saturated suprapermafrost taliks at eight profiles out of fifteen. Pine forest covers 47% of the watershed area. We conclude that 20-25% of the watershed area could be occupied by taliks in continuous permafrost environment. It suggests possible importance of groundwater pathways for the runoff generation even for the small rivers that do not have any channel flow during the cold season.

Keywords: talik; suprapermafrost groundwater; permafrost; Electrical resistivity tomography; Ground Penetrating Radar.

Introduction

In hydrology, continuous permafrost is usually considered as impermeable frozen ground. Surface flow and flow in the shallow seasonally thawing layer are often main sources of river flow in permafrost river catchments. Suprapermafrost taliks are known in Eastern Siberia in the Lena and Vilyuy rivers terraces. They are usually found on the well-drained gentle sandy slopes covered by sparse pine forests. Although existence of taliks is acknowledged, their distribution, genesis, evolution and role in surface-subsurface water interactions remain unresolved issues.

Geophysical techniques could provide spatially and vertically distributed information about permafrost, taliks and groundwater that cannot be obtained from drilling data alone. The study aims at estimation of talik distribution in the Shestakovka research watershed by combination of Electrical Resistivity Tomography (ERT) and Ground Penetrating Radar (GPR) techniques.

Study site

The Shestakovka River watershed with area 170 km² is located in 20 km to south-west of Yakutsk within the erosion-denudational slope of the ancient accumulative plain with absolute elevation of 150-280 m. The permafrost thickness is 200-400 m. The upper 40 m of the section are represented by quartz-feldspar sands with rare inclusions of silty sandy loam and loam. The climate is cold and dry with mean annual air temperature -9.5°C, precipitation 240 mm/year (1950-2015). Mean annual river flow depth is 24 mm/year (1951-2015). Dominant landscapes are pine (47% of the watershed area) and larch (38%) forests. Mires and bogs cover rest of the watershed. Active layer (AL) thickness in the pine forest could reach 3-4 m. Larch forests are characterized by cold permafrost with AL thickness up to 1 m.

Methods

Overall approach

Boitcov (2011) revealed that in Central Yakutia taliks could be found when three factors meet: i) bare soil or soil sparsely covered with organic layer ii) sandy deposits iii) hilly relief. Fifteen key sites within the Shestakovka catchment were chosen that meet the above-mentioned criteria. 300 m-long GPR profiles were measured at every key site in early May 2017. Six profiles were selected for more time-consuming ERT measurements that were performed in later May and September 2017. There are boreholes at two key sites that allow verification of geophysical results.

Electrical Resistivity Tomography

16-channel ERT and IP instrument SibER-64 produced by "Siber-instruments" (Novosibirsk, Russia) was used for ERT measurements. Two cables consisting of 32 copper wires were employed. Ground connection was performed by means of steel rods 300 mm long.

Unit electrode spacing varied from 1 to 5 m depending on required level of detail and studied depth. Dipole-dipole array, gradient array and Schlumberger array with four electrodes were used for measurements. Data processing and interpretation were performed using RiPPP and ZondRes2d software packages.

Ground Penetrating Radar

GPR measurements were made with an OKO-2 georadar system (from the company *Logis-GEOTECH Ltd.*) with an antenna block with central frequencies of 150 and 250 MHz. The measurements were conducted with transmitter and receiver in contact with the frozen ground in profiling mode with scan duration of 200 ns.

Results

GPR measurements showed that there are water-saturated suprapermafrost taliks at eight profiles out of fifteen. Landscape scheme, "talik" and "non-talik" profiles are shown at the Figure 1. Typical talik thickness is from 2 to 10 m. Talik extent varies from 30-40 to more than 500 m. If assume that selected key site are representative for pine forest of the watershed we conclude that 20-25% of the watershed area could be occupied by taliks. The high fraction of taliks containing suprapermafrost groundwater suggests possible importance of groundwater pathways for the river runoff generation even for the small watershed in continuous permafrost zone.

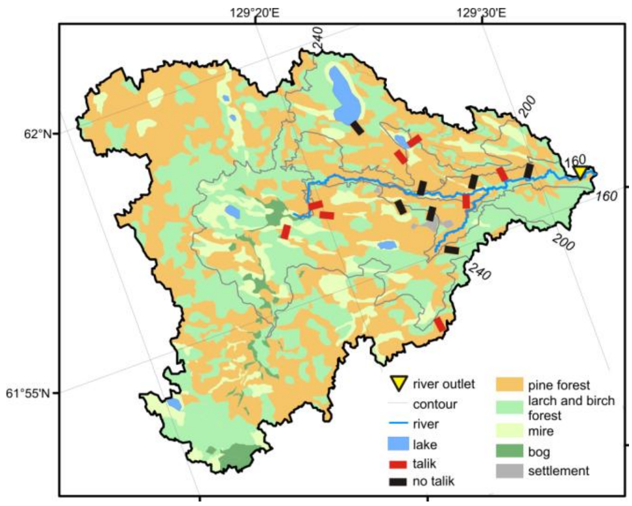

Figure 1 Landscape scheme of the Shestakovka catchment and results of the geophysical survey

Six profiles (five with taliks and one without) were selected for more time-consuming ERT measurements. ERT results confirmed talik presence at five profiles and absence at one.

Good agreement between GPR and ERT measurements increase reliability of the interpretation of geophysical data. Borehole drilling is planned for the spring 2018.

Conclusions

GPR and ERT measurements showed that 2-10 m deep suprapermafrost taliks are abundant phenomena at sandy gentle slopes covered by pine forests in continuous permafrost environment in Central Yakutia, Russia. 20-25% of the Shestakovka watershed area could be occupied by taliks. The high fraction of taliks containing suprapermafrost groundwater suggests possible importance of groundwater pathways for the river runoff generation even for the small watershed in continuous permafrost zone. Understanding of groundwater storages could advance concepts of runoff generation that underlay hydrological, hydrogeological and permafrost modelling strategies and future projections.

Acknowledgments

The study is partially supported by the Russian Foundation for Basic Research, grants № 17-05-00926 and № 16-31-60082_mol_a_dk.

References

Boitcov A.V. 2011. *Geocryology and underground water of the cryolithozone*. Tyumen: Tyumen State Oil and Gas University Press, 177 pp.

Hydraulic behaviour of a liquid through thawing soil in a geotechnical centrifuge

Patrick Nadeau[1]
Ryley Beddoe[1]
Sarah Creber[1]
[1]*Royal Military College of Canada, Kingston, Ontario*

Abstract

Understanding how hydrology in cold regions is affected by long-term seasonal freeze-thaw cycles can be a challenge, especially on a large scale. Remoteness and logistical challenges make long-term research of in-situ hydrology in these regions an expensive endeavour. In this study, a geotechnical centrifuge was used to examine soil-water interactions during a thawing cycle, by taking advantage of centrifuge scaling laws that allow one to simulate this cycle within a few days or even hours. The dimension scale effect allows us to simulate the behaviour of large prototype areas using benchtop sized models. This study presents the development of an in-flight climate chamber, allowing for thawing of the sample. The ability to simulate a freeze-thaw cycle in the centrifuge can provide us with the means of creating physical models for frost heave, thaw settlement, hydrogeology and contaminant transport in cold regions, such as Canada's Arctic.

Keywords: Freeze-thaw; geotechnical centrifuge; contaminant transport.

Introduction

Centrifuge

Geotechnical centrifuge modelling can be used to understand and solve complex engineering problems. The basic concept of geotechnical centrifuge modelling is to enhance the gravitational field of a 1/N scaled model to replicate the stresses at prototype or field conditions (e.g. Mudabhushi, 2015). A 1.5m diameter Broadbent geotechnical centrifuge (Fig. 1), recently acquired by the Royal Military College of Canada, was used for these simulations. In the centrifuge, the scaling law for seepage velocity is: Model/Prototype = N. The scaling law for time is 1/N, since these tests were dynamic in nature (Madhabushi, 2015).

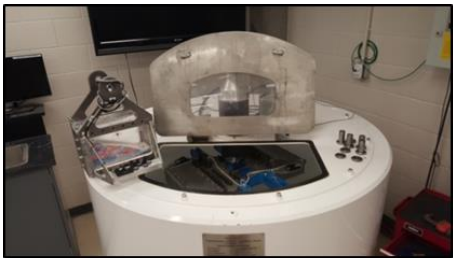

Figure 1. Broadbent geotechnical centrifuge.

Goal

The goal of this research is to establish the methodology to best replicate, in the centrifuge, the annual freeze-thaw cycles to which Canada's Artic is subject. However, there are several challenges associated with conducting freeze-thaw processes in a geotechnical centrifuge, and as such there have been limitations on this technique being widely used by the permafrost and cold regions research communities. In these preliminary tests, a climate chamber was used to establish environmental conditions within the centrifuge cradle. The hydraulic boundary conditions for different particle-sized soils were then observed while it thawed during flight.

Methodology

Test 1

The first test (Fig. 2) consisted of a frozen layer of saturated Kaolin clay. The thickness of the model was 60 mm which represents a 1.8 m thick soil layer. Ice pucks were placed at the top of the sample to simulate the leaching of an initially frozen contaminant in the spring. The puck on the left was mixed with black food dye while the other was mixed with potassium permanganate. The sample was subject to 30g acceleration for 95 minutes. In order to promote thawing, room-temperature air was blown across the air surface above the soil layer throughout the test.

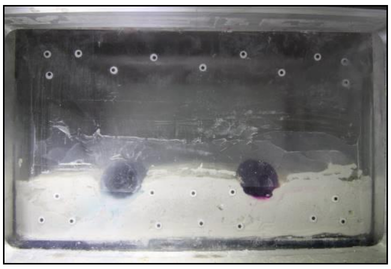

Figure 2. Initial conditions for Test 1.

Test 2

The second test (Fig. 3) consisted of a frozen 60 mm layer of saturated Aqua Quartz #20 pool filter sand superposed by a frozen 30 mm layer of dry sand of the same type which would represent 1.8 m and 0.9 m layers respectively. Three frozen pucks of water and potassium permanganate were placed in a line in the middle of the sample. After 10 minutes, two pucks were moved to new locations. The sample was subject to 30g acceleration for 60 minutes.

Figure 3. Initial conditions for Test 2.

Results

Test 1

This test simulated the movement of dyed water through saturated Kaolin clay over a 48 hour period. It was observed that the water dyed with potassium permanganate was more easily visualized, which is why it was used exclusively for Test 2. The dyed water moved vertically through the clay and even moved laterally when it encountered large voids filled with water (Fig. 4). The consolidation and subsequent drainage of the clay throughout thawing was also observed.

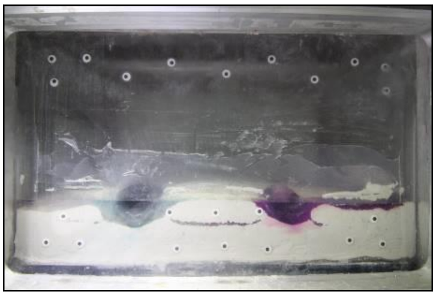

Figure 4. Movement of dyed water through clay.

Test 2

This test was a simulation of the movement of dyed water through a layer of unsaturated sand and a layer of saturated sand over a 30 hour period. Interestingly, the water table dropped approximately 1 cm when the centrifuge started rotating. As expected, the dyed water moved through the sand faster than it did in the clay. Once the water reached the water table, it dispersed laterally throughout the saturated layer of sand (Fig. 5). It appears that there is a hydraulic gradient towards the small exit port at the bottom left of the cradle.

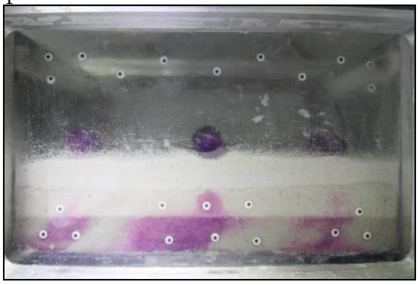

Figure 5. Movement of dyed water through sand.

Conclusion

With these tests, it has been shown that it is possible to simulate thawing soil in the centrifuge and to observe the hydraulic behaviour of an initially frozen liquid during the thawing process. Eventually, the goal is to simulate several freeze-thaw cycles in a single test by building a climate controlled cradle, which would use vortex tubes and insulation (e.g. Stone *et al.*, 1995; Clark & Phillips, 2003), as well as the means to monitor temperature throughout the sample while in flight. Another goal is to monitor the movement of different contaminants through soil undergoing freeze-thaw cycles. In that case, the water in the soil could not act as a conduit for diffusion (Biggar *et al.*, 1998), which might slow the vertical movement and eliminate the lateral movement through the soil.

References

Biggar, K.W., Nahir, N., Haidar, S., 1998. Migration of petroleum contaminants into permafrost. *Proceedings of the Seventh International Conference on Permafrost*, Yellowknife, Canada, 23-27 June: 43-49.

Clark, J.I. & Phillips, R. 2003.Centrifuge modelling of frost heave of arctic gas pipelines. *Proceedings of the Eighth International Conference on Permafrost*, Zürich, Switzerland, 21-25 July: 151-156.

Madabhushi, G., 2015. *Centrifuge Modelling for Civil Engineers*. CRC Press, 292 pp.

Stone, K.J.L., Smith, C.C. & Schofield, A.N, 1995. Technical Report No: CUED/D-SOILS/TR296. A Thermally controlled test chamber for centrifuge and laboratory experiments. *Cambridge University Engineering Department*.

Assessment of aufeis role in hydrological regime of the North-Eastern Russia

Nataliia Nesterova[1,2]
Olga Makarieva[1,3,4]
Andrey Ostashov[1]
Andrey Shikhov[5]
[1]*St. Petersburg State University, St. Petersburg, Russia, nnesterova1994@gmail.com*
[2]*State Hydrological Institute, St. Petersburg, Russia*
[3]*Gidrotehproekt Ltd, St. Petersburg, Russia*
[4]*Melnikov Permafrost Institute, Yakutsk, Russia*
[5]*Perm State University, Perm, Russia*

Abstract

The goal of the research is the development and verification of mathematical modelling methods for assessing and predicting the role of aufeis in hydrological regime of the rivers of the North-East of Russia in current and future climate. Three catchments with available historical data on the location and characteristics of the aufeis and runoff observations with basin areas from 400 to 8290 km² and aufeis share from 6 to 113 km² in mountainous area of North-East are chosen for the study. The method of Sokolov was adapted to the Hydrograph model for calculating aufeis runoff. Historical information on aufeis locations and their features from the Aufeis Cadaster (1958) was corrected with the use of topographic maps and satellite images. The values of the aufeis flow vary from 9 to 13 % of the average annual river flow for the Suntar and Charky rivers accordingly, which puts aufeis on the one level with the glaciers in the sense of their impact on hydrological regime in studied region.

Keywords: aufeis; river runoff; hydrological modelling; Hydrograph model; the North-East of Russia.

Introduction

Hydrological processes occur in specific conditions in the mountains of the North-Eastern Siberia. The aufeis are the indicators of the complex interconnection of river and groundwater in permafrost environment (Sokolov, 1975) and play an important hydrological role in that region. In winter, they reduce the river and underground runoff, and in warm season melted aufeis waters form additional source of rivers flow. Under the changing climate conditions, understanding the role of aufeis in runoff formation processes is an important task. In most cases, the share of the aufeis component of annual river runoff is about 3-7% (Reedyk *et al.*, 1995; Sokolov, 1975). At the same time, water consumption from melting aufeis (based on the data from Alaska and Canada) can be 1.5-4 times higher than the water discharge of groundwater forming it (McEven & Marsily, 1991). Most significant flow from melting aufeis is observed in May-June. In some river basins with exceptionally large aufeis, the proportion of this runoff can reach 25-30% (Sokolov, 1975).

Approach

Up to this point, there are no hydrological models that take into account the role of aufeis in rivers flow formation in an explicit form. In this study we aimed to update the Hydrograph model with such additional algorithm.

The Hydrograph model (Vinogradov *et al.*, 2011) describes hydrological processes in different permafrost environments including the dynamics of ground thaw/freeze. In this model the processes have a physical basis and certain strategic conceptual simplifications. The level of model complexity is suitable for a remote, sparsely gauged region such as Arctic domain as it allows for a priori assessment of the model parameters (Semenova *et al.*, 2013).

The method of Sokolov (1975) to estimate the aufeis flow was adapted for modelling aufeis input to river runoff in the Hydrograph model. The method makes it possible to calculate the hydrograph of aufeis-runoff for a long period and specific years, at basin scale and for an individual aufeis. The method requires following data:

daily air temperature at aufeis, maximum area of aufeis before spring melt; the altitude of individual or grouped aufeis. The other conceptual parameters that for example account for share of aufeis destruction due to air temperature, solar radiation and thermal erosion by river flow were estimated by Sokolov (1975) based on the field data obtained in 1960s.

By Sokolov (1975) the ice volume in aufeis is calculated depending on the area (1):

$$W=0{,}96F^{1{,}094} \quad (1)$$

where W – ice volume of aufeis, thousand km^3; F – area of aufeis, thousand km^2.

Initial information on aufeis locations and their characteristics within the catchments was taken from the Cadaster of the aufeis of the North East Siberia of the USSR (1958) and corrected by topographic maps and satellite images. Satellite imagery were used also to assess the inter-annual and seasonal dynamics of aufeis within the period of 1999 to 2017 in chosen catchments.

The correction of the input meteorological information according to the climatic change trends would allow assessment of changes of the aufeis share runoff in total river flow in the future.

Study objects

Three catchments with available historical data on the location and characteristics of the aufeis and runoff observations were chosen for the study: the Charky river (03474), the Suntar river (03499) and the Anmangynda river (01604) belonging to the Yana, Indigirka and Kolyma Rivers basins correspondingly (Table 1, Fig.1).

Preliminary comparison of the Cadaster and satellite data at the Charky river basin has shown that some large aufeis are absent in the Cadastre and some historical aufeis are absent at modern satellite images. This may indicate the dynamics of aufeis processes in this region, which will be studied together with climate data.

Table. 1 Study objects

River (gauge code)	Period	Area, km^2	Aufeis area, km^2 (%)	Annual river runoff, mm	Calculated aufeis runoff, mm (%)
03474	1949-2007	8290	113 (1.4)	239	32 (13)
03499	1959-2015	7680	58 (0.8)	189	17 (9)
01604	1962-1992	400	6 (1.5)	301	*24 (8)**

* *from Sokolov (1975)*

First results

The aufeis flow was estimated for the period 1965-2012 for two rivers using historical meteorological information. It accounted for about 13 % (32 mm) of average annual flow at the Charky river and about 9 % (17 mm) at the Suntar river. The preliminary results suggest that aufeis flow may be much more significant than one from the glaciers.

The modelling approach, the results of satellite imagery analysis and aufeis flow assessment will be presented.

References

Cadastre to the map of aufeis of the North East Siberia of the USSR. 1958. Scale 1:2000000. Shilnikovskaya Z.G./Central complex thematic expedition of the North-Eastern Geological Administration. Magadan

McEwen, T., & Marsily, G.de. 1991. *The potential significance of permafrost to the behavior of a deep radioactive waste repository* (SKI-TR - 91-8). Sweden

Reedyk, S., Woo, M.K., Prowse T.D. 1995. Contribution of icing ablation to flowflow in a discontinuous permafrost area. *Canadian Journal of Earth Science* 32: 13-20

Semenova, O., Lebedeva, L., Vinogradov Yu. 2013. Simulation of subsurface heat and water dynamics, and runoff generation in mountainous permafrost conditions, in the Upper Kolyma River basin, Russia. *Hydrogeology Journal* 21(1): 107–119 DOI: 10.1007/s10040-012-0936-1

Sokolov B.L. 1975. *Aufeis and river runoff*. Leningrad: Gidrometeoizdat, 190 pp.

Vinogradov, Yu.B., Semenova, O.M., Vinogradova, T.A. 2011. An approach to the scaling problem in hydrological modelling: the deterministic modelling hydrological system. *Hydrological Processes*. 25: 1055–1073, doi:10.1002/hyp.7901.

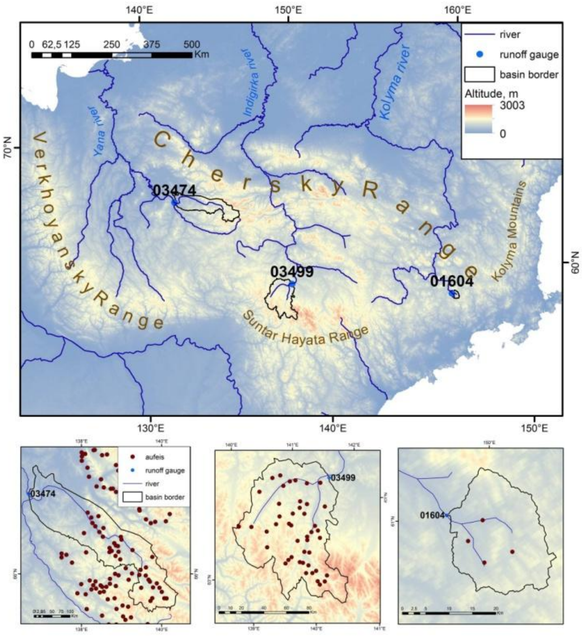

Figure 1. The study basins, red dots are aufies locations (without scale).

Hydrological change trajectories in the southern Taiga Plains, Canada

William Quinton[1], Michael Braverman[1], Ryan Connon[1], James Craig[2], Élise Devoie[2], Kristine Haynes[1]

[1]*Wilfrid Laurier University, Waterloo, Ontario, Canada, wquinton@wlu.ca*
[2]*University of Waterloo, Waterloo, Ontario, Canada*

Abstract

Climate warming in the southern Taiga Plains ecoregion of northwestern Canada has led to unprecedented rates of permafrost thaw and a myriad of land-cover changes with uncertain impacts on hydrology. Consequently there is growing uncertainty in regards to the future availability of water resources in this region. This paper synthesises key findings of recent hydrological field studies and remote sensing analyses of land-cover change in the southern Taiga Plains. The purpose of this synthesis is to improve the understanding of the trajectory of land-cover change in this region and how this change could influence water flow and storage processes.

Keywords: Permafrost thaw, landcover change, peatlands, Boreal, hydrology.

Introduction

This study is focussed on the southern Taiga Plains ecoregion in northwestern Canada (Figure 1a), and draws mainly from studies conducted at Scotty Creek (61°18' N, 121°18' W), a 152 km^2 drainage basin 50 km south of Fort Simpson, Northwest Territories (NWT) (Figure 1b). Scotty Creek basin is underlain by discontinuous permafrost and is covered by peatland complexes typical of the 'continental high boreal' wetland region. The peat thickness at Scotty Creek ranges between 2 and 8 m below which lies a thick clay/silt-clay glacial till deposit of low permeability. Most of the Scotty Creek basin is a heterogeneous mosaic of forested peat plateaus underlain by permafrost, and treeless, permafrost-free wetlands (Figure 1c), typical of the southern fringe of discontinuous permafrost (Helbig *et al.*, 2016). Fort Simpson has an average annual air temperature of -2.8° C, and receives 388 mm of precipitation annually, of which 38% is snow. This paper draws on numerous published and unpublished studies involving both hydrometric field observations and aerial/satellite image analysis. Collectively these studies are used to inform conceptualisations of hydrological change.

There are strong indications that permafrost thaw and the resulting land-cover changes have affected basin water balances, as suggested by rising river flows throughout the border region. Most notably, the total annual runoff from all gauged rivers in the lower Liard River valley of the NWT has steadily risen since the mid-1990s (Connon *et al.*, 2014). Rising flows from subarctic rivers are often attributed to 'reactivation' of groundwater systems, but the very low hydraulic

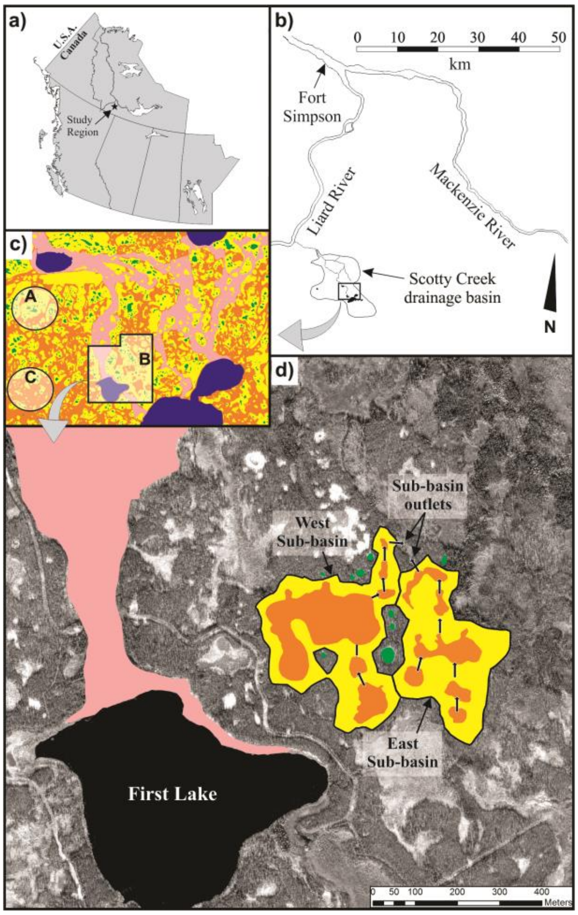

Figure 1: a) study region and b) Scotty Creek; c) peat plateaus (yellow), isolated (green) and connected (orange) bogs, channel fens (pink); d) enlargement of "B" showing cascade bogs.

conductivity of the glacial sediments below the peat, precludes appreciable groundwater input. Permafrost thaw-induced changes to basin flow and storage processes offers a more plausible explanation for rising river flows in this region (Connon *et al.*, 2015).

Field observations and image analyses (suggest that plateaus contain two distinct runoff source areas separated by a break in slope approximately 10 m inland from the fen-plateau edge. Primary runoff drains from the sloped edges of plateaus directly into the basin drainage network (*i.e.* a channel fen). Field measurements suggest that the entire primary area supplies runoff to the fen throughout the thaw season. Secondary runoff drains into the interior of the plateau toward the topographic low often occupied by a bog. If the receiving bog is hydrologically isolated, the runoff it received will remain in storage, evaporate or recharge the underlying aquifer. If the receiving bog is part of a bog cascade, and if its storage capacity is exceeded, then the secondary runoff it receives will be routed toward the channel fen via the down slope bog or bogs. Secondary runoff is therefore, neither direct nor continuous. The rate of secondary runoff is greatest during periods of high moisture supply and minimal ground thaw when the hydrological connection among the bogs of a cascade, and between individual bogs and their contributing "bog-sheds" is maximised. As the active layer thaws and drains, the contributing area shrinks and secondary runoff decreases. Large rain events can temporarily reverse this decrease.

Over a period of decades, the plateaus conducting primary and secondary runoff are transformed by permafrost thaw. Three general stages can be seen from Figure 1c. In chronological sequence, the area indicated by "A" represents an early stage of permafrost thaw where bogs are mostly hydrologically-isolated, and as such, drainage into the fen is supplied only by primary runoff from the margins of the plateaus. "B" represents an intermediate stage of permafrost thaw where primary runoff is augmented by secondary runoff from the ephemeral bog cascades. The activation of secondary runoff arises from the greater hydrological connectivity of land-cover "B" than "A". As a result, a greater proportion of the snowmelt and rainfall arriving on land-cover "B" is converted to runoff than in the previous stage. Because B is transitional between A and C, some bogs are hydrologically connected (via surface or near surface flow and/or talik flow), while other bogs remain hydrologically isolated. "C" represents an advanced stage, where the shrinking peat plateaus occur as islands within an expansive bog complex. Interestingly, this stage is a near mirror image of "A" where it is the bogs that occur within an extensive plateau complex. By stage "C", plateau diameters are on the order of a few tens of metres and as such contain no secondary runoff and no interior bogs.

As the land-cover transitions from the isolated bog (A) to the plateau islands (C) stages, the way in which peat plateaus generate runoff changes dramatically, with direct consequences on their runoff pattern and rate. For each stage, water (snowmelt or rainfall) arriving in the channel fen is conducted directly to the basin outlet. Likewise, water arriving on a plateau but not within a bog catchment (*i.e.* bogshed) is routed directly to the adjacent fen. Water arriving directly into bogs or their bogsheds is prevented from reaching channel fens in stage A, but can reach the latter in stage B depending upon the degree of hydrological connectivity in the bog cascades. Activation of secondary runoff therefore increases the amount of runoff between stages A to B. Primary runoff may also increase between these two stages since the fragmentation of plateaus increase can increase the length of the overall plateau-fen edge. Water arriving onto plateaus in stage C is neither stored nor routed as secondary runoff through bog cascades and as such this stage provides the most direct runoff response. However, stage C has the lowest plateau runoff since it is capable only of generating primary runoff, and this runoff is generated from the relatively small total surface area of the remaining plateaus.

Acknowledgments

We wish to thank the Natural Sciences and Engineering Research Council of Canada (NSERC) and the Dehcho First Nation, Liidlii Kue First Nation and the Jean Marie River First Nation for their continued support of the Scotty Creek Research Station (SCRS).

References

Connon, R., Quinton, W., Hayashi M. & Craig, J. 2014. The effect of permafrost thaw on rising stream flows in the lower Liard River valley, NWT, Canada. Hydrological Processes. pp. 4163–4178. DOI: 10.1002/hyp.10206

Connon, R., Quinton, W., Craig, J., Hanisch, J., Sonnentag, O. 2015. The hydrology of interconnected bog complexes in discontinuous permafrost terrains. Hydrological Processes, DOI: 10.1002/hyp.10604.

Helbig M., Wischnewski K., Kljun N., Chasmer L., Quinton W., Detto M., Sonnentag, O. 2016. Regional atmospheric cooling and wetting effect of permafrost thaw-induced boreal forest loss. Global Change Biology, doi:10.1111/gcb.13348.

First insights in bacteria diversity in headwaters emerging from Alpine rock glaciers.

Monica Tolotti[1]
Davide Albanese[1]
Leonardo Cerasino[1]
Claudio Donati[1]
Massimo Pindo[1]
Michela Rogora[2]
Roberto Seppi[3]
[1] *Edmund Mach Foundation, Via E. Mach 1, S. Michele all'Adige, Italy email: monica.tolotti@fmach.it*
[2]*CNR Institute of Ecosystem Study (ISE), Largo Tonolli 50, Verbania-Pallanza, Italy*
[3]*Department of Earth and Environmental Sciences, University of Pavia, Via Ferrata 1, Pavia, Italy*

Abstract

Global warming exerts particularly pronounced effects on the European Alps. As the thawing rates of mountain permafrost ice is lower than for glacier ice, a shift from glacial/periglacial to paraglacial/periglacial dynamics is predicted for Alpine landscapes during the 21st century in relation to deglaciation. Poor knowledge exists on chemical and biological features of waters emerging from Alpine rock glaciers. A set of glacial- or permafrost-fed headwaters was investigated in the Eastern Italian Alps, aiming at exploring bacterial community composition and diversity in epilithic biofilm and sediments. Bacterial assemblages show significant differences according to water and sample type, and to catchment geology. Rock glacier-fed waters show enhanced conductivity and trace element concentrations, and their highly diverse bacterial assemblages significantly differ only from those of glacial streams. Further research will better outline the role of environmental features in modulating bacterial diversity of Alpine headwaters affected by progressing deglaciation.

Keywords: Alpine permafrost, glaciers, water chemistry, bacterial finger-printing, biofilm, surface sediment.

Introduction and Methods

Glacier retreat is a major effect of current global warming and 80-100% of the Alpine glaciers is predicted to vanish in the next few decades (Zemp *et al.*, 2006). As the thawing rate of permafrost ice is 10-100 times lower than for glacier ice, more subsurface permafrost ice will remain than surface glacier ice, and a shift from "glacial/periglacial to paraglacial/periglacial dynamics" is predicted for mountain landscapes in the next few decades (Haeberli *et al.*, 2017). Although rock glaciers (RG) are a common landform of mountain permafrost, both chemical and biological features of waters emerging from them are still poorly known (Thies *et al.*, 2013).

This work aims at characterizing the bacterial diversity in biofilm and sediments of Alpine headwaters directly affected by active RGs, and at exploring possible differences respect to headwaters of different origin. A headwater set (2027-2900 m a.s.l.) was surveyed in autumn 2016 (during base-flow conditions) in three metamorphic catchments of the Eastern Italian Alps (EIA, Table 1). The water samples were analyzed for temperature, turbidity, pH, major ions, nutrients, and trace elements. Environmental DNA from epilithic biofilm (EPI), surface and deep sediment (SS: 0-2 cm depth, SD: ~5-10 cm) was extracted and analyzed by high throughput sequencing (MiSEQ Illumina) using the specific variable region V4 of 16S rRNA gene. Bioinformatic analyses were performed using the MICCA pipeline (Albanese *et al.*, 2015).

Table 1. Location, dominant geology, and number of headwaters sampled in the EIA in autumn 2016.

Range	Sub-catchment	Geology	nGL	nREF	nRG
Ortler	SU	Sc, Gn	2	0	2
Cevedale	MR	Gn, Sc	1	2	4
Presanella	AM	Gr	1	1	3

SU, MR, AM: Sulden, la Mare, Amola Valley, resp.: Sc, Gn, Gr: scists, orthogneiss, granite, resp. nGL, nREF, nRG: number of glacier-, rock glacier- and mainly precipitation-fed waters, resp.

Results and Discussion

RG-fed headwaters in MR and SU stand out for their low water temperature (≤1°C), low turbidity (<10 NTU) and higher electrical conductivity (118-516 µS cm^{-1} 20°C) with respect to GL and REF waters in the same catchments (means 26 and 106 µS cm^{-1}, respectively). All AM waters show very low conductivity (11-19 µS cm^{-1}) in relation to the granitic bedrock. All waters are poor in reactive P (2-5 µg L^{-1}), while NO_3-N and SiO_2 are very low in the GL waters (<100 µgL^{-1} and <1 mgL^{-1}, resp.). All GL streams show high levels of total P (70-428 µg L^{-1}) and N (up to ~4 mg L^{-1}), and varying levels of Fe (17-250 µg L^{-1}) and Al (19-255 µg L^{-1}). RG waters of MR and SU are enriched in Sr (82-315 µg L^{-1}), Ni (12-60 µg L^{-1}), As (6-31 µg L^{-1}).

The α-diversity of the bacterial assemblages in terms of number of observed OUT and Shannon index (Fig. 1a-b, respectively) is much higher in both the SD and SS samples of the RG and REF streams. On the contrary, the epilitic samples do not show significant differences in bacterial diversity. The first three principal coordinates (PCo) based on weighted UniFrac distances outline significant differences (Wilcoxon rank-sum test with Bonferroni correction, $p<0.001$) in 16S bacterial composition according to substrate type (PCo1), water origin (PCo2), and, to less extent, geographical location (PCo3, Fig. 1c).

The GL bacterial peculiarity is due to the co-dominance of Proteobacteria and Actinobacteria, followed by Bacterioidetes. Acidobacteria replace the last two phyla in RG samples. Epilithc samples from all water types show higher abundance in Cyanobacteria, while the geographical separation only produces rearrangements in the abundances of a few ubiquitous major phyla. Preliminary correlation analyses revealed significant relations between the abundance of several bacteria taxa and water turbidity, NO_3-N, SiO_2, and metal concentrations.

The absence of significant differences between bacterial assemblages of RG-fed and mainly precipitation-fed REF waters suggests that chemical traits of RG-fed waters are not sufficient to select specific bacterial assemblages. In addition, further environmental variables need to be considered in future investigations of Alpine headwaters affected by permafrost degradation.

Acknowledgments

The research was financially supported by the Edmund Mach Foundation. A special thank goes to Stefano Brighenti for his precious help during the field work.

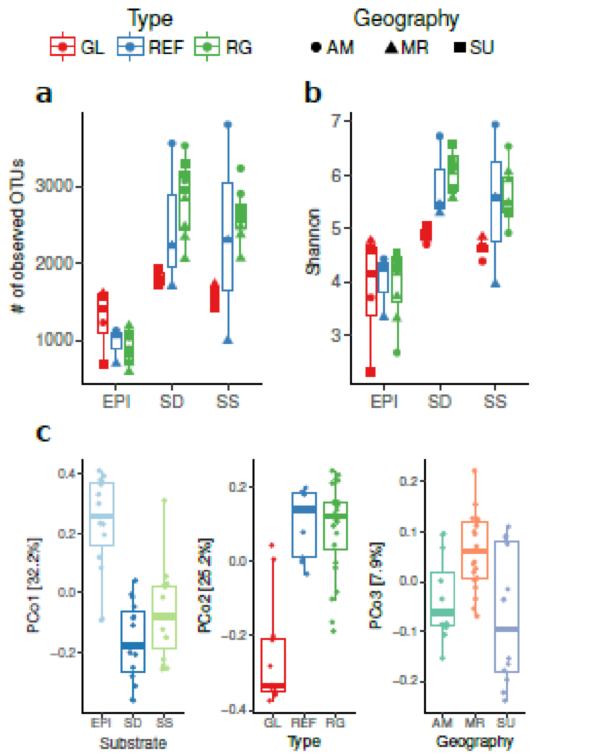

Figure 1. Number of observed bacterial OTUs (a) and Shannon Index values (b) in the sample collected from the headwater studied. (c) The first three principal coordinates (PCo) based on the weighted UniFrac distances outline differences in 16S bacterial composition between different substrates, water types, and sampling sites. Abbreviations as in Table 1.

References

Albanese, D., Fontana, P., De Filippo, C., Cavalieri, D. & Donati, C., 2015. MICCA: a complete and accurate software for taxonomic profiling of metagenomics data. *Scientific Reports* 5:9743.

Haeberli, W., Schaub, Y. & Huggel, C., 2017. Increasing risks related to landslides from degrading permafrost into new lakes in de-glaciating mountain ranges. *Geomorphology* 293: 405-417.

Thies, H., Nickus, U., Tolotti, M., Tessadri, R. & Krainer, K., 2013. Evidence of rock glacier melt impacts on water chemistry and diatoms in high mountain streams. *Cold Regions Science and Technology* 96: 77-85.

Zemp, M., Haeberli, W., Hoelzle, M. & Paul, F., 2006. Alpine glaciers to disappear within decades? *Geophysic Resources Letters* 33: 1-4.

Author Index

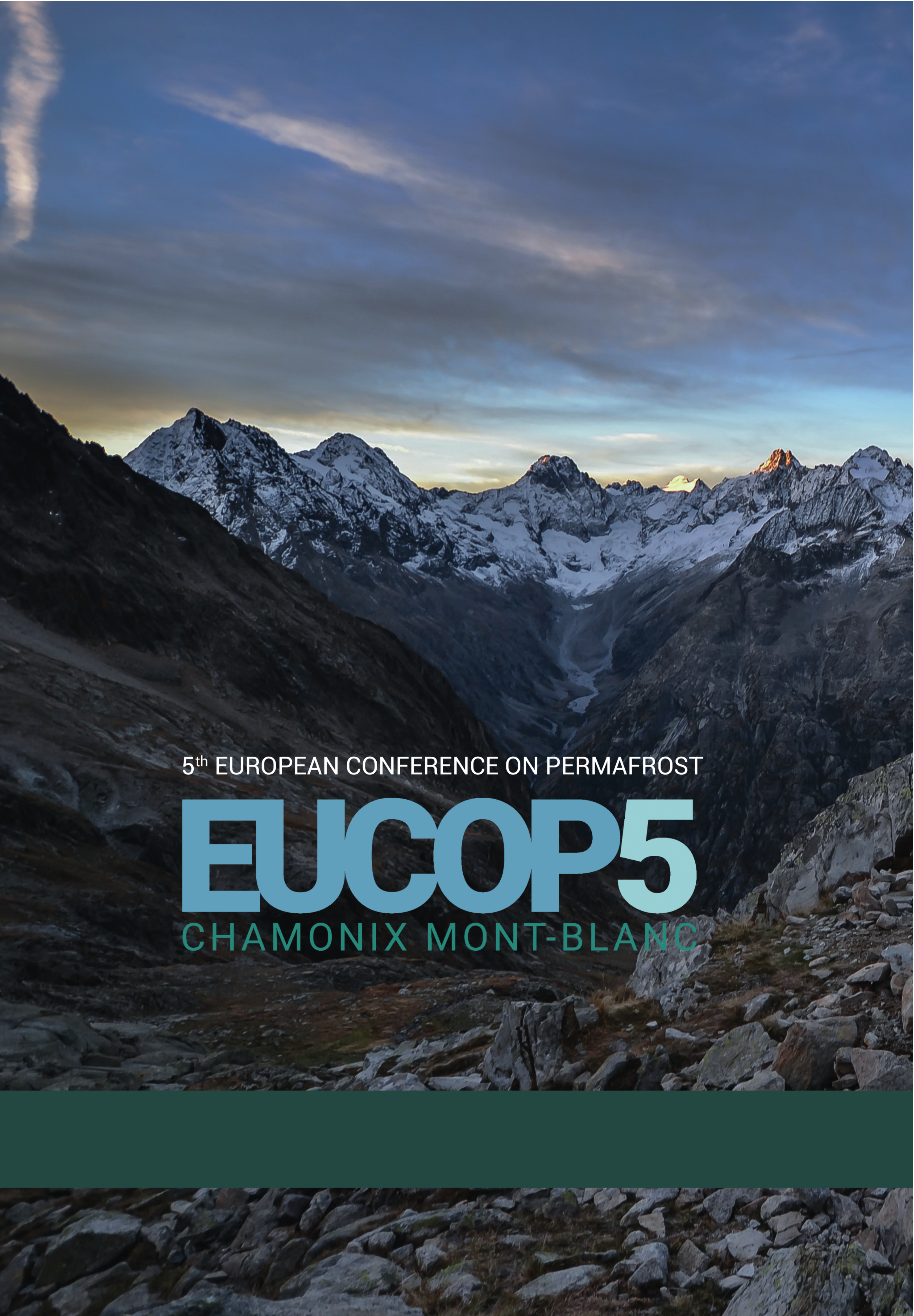
5th EUROPEAN CONFERENCE ON PERMAFROST
EUCOP5
CHAMONIX MONT-BLANC